IUPS 2013

21–26 July 2013 Birmingham, UK

Programme

#IUPS2013
on Twitter

Scan and download
MyItinerary
for IUPS 2013

L1

Physiology moves back onto centre stage: a new synthesis with evolutionary biology

D. Noble

Physiology, Anatomy and Genetics, University of Oxford, Oxford, UK

New developments in evolutionary biology and molecular genetics have far-reaching consequences for physiological science since they imply major extensions or even replacement of the Modern Synthesis (Neo-Darwinism) [1, 2, 3, 4, 5]. The Modern Synthesis was a mid-twentieth century gene-centric view of evolution, based on random mutations accumulating to produce gradual change through natural selection. Any role of physiological function in influencing genetic inheritance was excluded. The organism became a mere carrier of the real objects of selection: its genes. We now know that genetic change is far from random and often not gradual. Molecular genetics and genome sequencing have deconstructed this unnecessarily restrictive view of evolution in a way that reintroduces physiological function and interactions with the environment as factors influencing the speed and nature of inherited change. Acquired characteristics can be inherited, and in a few but growing number of cases that inheritance has now been shown to be robust for many generations. The twenty-first century can look forward to a new synthesis that will reintegrate physiology with evolutionary biology. This lecture will outline the key features of the new synthesis and why it could bring physiology back onto centre stage in biology. “It is hard to think of a more fundamental change for physiology, and for the conceptual foundations of biology in general.” [1]

Noble, D., Physiology is rocking the foundations of evolutionary biology. Experimental Physiology, 2013 http://ep.physoc.org/content/early/2013/04/12/expphysiol.2012.071134.full.pdf+html

Noble, D., Neo-Darwinism, the Modern Synthesis, and Selfish Genes: are they of use in physiology? Journal of Physiology, 2011. 589: p. 1007-1015.

Gissis, S.B. and E. Jablonka, eds. Transformations of Lamarckism. From Subtle Fluids to Molecular Biology. 2011, MIT Press: Cambridge, Mass

Pigliucci, M. and G.B. Müller, Evolution - The extended synthesis, 2010, Cambridge, Mass: MIT Press.

Shapiro, J.A., Evolution: a view from the 21st century, 2011, Upper Saddle River, NJ: Pearson Education Inc.

Work in the author’s laboratory is supported by EU Framework 7 grants for the Virtual Physiological Human

Where applicable, the authors confirm that the experiments described here conform with The Physiological Society ethical requirements.

L2

Pathological development of brain microvasculature

E. Dejana

IFOM, FIRC Institute of Molecular Oncology and Department of Biosciences, University of Milan, Milan, Italy

Brain microvasculature constitute a highly specialized and selective vascular barrier between blood and the central nervous system, called blood brain barrier (BBB). In these vessels endothelial cells present a highly developed system of tight junctions (TJs), absence of fenestration and low pinocytotic activity. Cells of the brain parenchyma, the astrocytes, contribute to the BBB-coverage with their foot processes, which constitute about the eighty percent of the basal aspect of the vessels. As a consequence, circulating solutes do not readily enter the brain parenchyma unless through specific endothelial “transporters”. Thus, BBB also limits the passage of anticancer drugs from the blood to the brain. Therefore, it would be therapeutically useful to develop systems to modulate BBB permeability. To this aim it is important to define the molecular mechanisms that regulate the establishment and maintenance of BBB properties.

Data from our laboratory suggest a key role of the Wnt/β-catenin signaling pathways in the induction, regulation and maintenance of the BBB characteristics during embryonic and post-natal development. In endothelial cells, Wnt signaling induces barrier differentiation by increasing the stabilization and the transcriptional activity of β-catenin. On the contrary, inactivation of β-catenin causes significant downregulation of junctional proteins, and consequent BBB breakdown.

Besides β-catenin, other three proteins, CCM1, CCM2 and CCM3, expressed by brain endothelial cells, are emerging as key modulators of the organization and function of the BBB. Indeed, mutations occurring in any of the genes encoding these proteins, leads to Cerebral Cavernous Malformation (CCM), a pathology characterized by brain vascular malformations. The endothelium in the lesions presents very few tight junctions and gaps are observed between endothelial cells. In addition, the vascular basal lamina is disorganized and the astrocytes do not take contact with the endothelial wall. The structural alterations of the BBB observed in CCM lesions are associated with severe clinical manifestations, such as cerebral haemorrhages and stroke. Additional data point to a possible link between inflammatory cytokines and the function of CCM proteins in the regulation of BBB stability. These data open new therapeutic opportunities for this so far incurable disease

Where applicable, the authors confirm that the experiments described here conform with The Physiological Society ethical requirements.

L3

3R’s: Reproductive Regulation Revised

I. Clarke

Physiology, Monash University, Melbourne, VIC, Australia

The last decade has seen remarkable advances in our understanding of the control of reproduction. In particular, neuroendocrine systems have been discovered that significantly alter the way that we view central control of gonadotropin releasing hormone (GnRH) secretion and action. The recognition that kisspeptin is a potent stimulator of GnRH neurons was a seminal advance. Kisspeptin cells are now seen as the sex-steroid responsive cells that relay feedback information to GnRH cells. In addition, in seasonal breeders, the function of kisspeptin cells is altered in a predictable way between breeding and non-breeding seasons. The finding that kisspeptin cells of the arcuate nucleus also produce neurokinin B and dynorphin add another layer of control of reproduction and this has led to the development of new tools for the manipulation of reproduction. The kisspeptin cells also interact with appetite regulating neurons in the brain and this has furthered our understanding of how metabolic state can influence reproductive function. The question as to whether kisspeptin cells

are the sought after 'pulse generators' for GnRH cells will be discussed.
Another newcomer on the reproductive neuroendocrine stage is gonadotropin inhibitory hormone (GnIH) and the extent to which this is important has been investigated in a variety of species. Compelling data for an inhibitory role in the regulation of reproduction has been obtained in studies on sheep and this will be reviewed.
With the expansion of our knowledge of the reproductive neuroendocrine system, revision of our textbooks is in progress. Kisspeptin provides us with the conduit for communication from the gonads to the GnRH cells and GnIH may play a lesser role as a modulator of GnRH function. In addition, the modulatory role of other neuropeptides, such as the melanocortins, is now appreciated and allows us to formulate models for the multimodal regulation of reproduction by the brain.

Where applicable, the authors confirm that the experiments described here conform with The Physiological Society ethical requirements.

L4

Health-promoting effects of exercise in diabetes and obesity: from molecular mechanisms to clinical action

J.R. Zierath

Karolinska Institutet, Solna, Sweden

Insulin resistance is a characteristic feature of Type 2 diabetes mellitus and obesity. Although defects in glucose homeostasis have been recognized for decades, the molecular mechanisms accounting for impaired whole body glucose uptake are still incompletely understood. This lecture will focus on the sites of insulin resistance in Type 2 diabetes and mechanisms by which exercise enhances glucose uptake in skeletal muscle. Epigenetic modifications are thought to play an important role in the development of metabolic diseases. DNA methylation is one form of epigenetic modification linking environmental factors to the control of insulin sensitivity. The first part of this lecture will focus on the role of DNA methylation and insulin sensitivity in type 2 diabetes and obesity. Thereafter, the role of DNA methylation as a regulatory mechanism for gene expression changes in response to exercise will be discussed. Given the importance of lifestyle factors in the development of metabolic disorders, DNA methylation provides a mechanism by which environmental factors, including diet and exercise, play a role on the pathogenesis of skeletal muscle insulin resistance and risk for Type 2 diabetes.

Where applicable, the authors confirm that the experiments described here conform with The Physiological Society ethical requirements.

L5

Neuronal calcium channels and migraine

D. Pietrobon

Biomedical Sciences, University of Padova and CNR Institute of Neuroscience, Padova, Italy

It is generally recognized that the primary cause of migraine lies in the brain and that cortical spreading depression (CSD) is the neurophysiological correlate of migraine aura. In animal studies, a single CSD can lead to prolonged activation of meningeal nociceptors and central trigeminovascular neurons, suggesting that CSD may also initiate the headache mechanisms. Gain-of-function mutations in the CaV2.1 (P/Q-type) calcium channel and loss-of-function mutations in the alpha2 Na/K-ATPase cause a rare subtype of migraine with aura: familial hemiplegic migraine (FHM1 and FHM2, respectively). Cav2.1 channels are located in presynaptic terminals and somatodendritic membranes throughout the brain and play a prominent role in initiating action potential-evoked neurotransmitter release at central nervous system synapses. The alpha2 Na/K ATPase is expressed primarily in neurons during embryonic development and at time of birth but almost exclusively in astrocytes in the adult brain. Knockin (KI) mouse models carrying FHM1 or FHM2 mutations show a lower threshold for CSD induction and a higher velocity of CSD propagation. In this lecture I summarize our studies in FHM1 KI mice that reveal the functional consequences of FHM1 mutations on i) the neuronal Ca current in different cortical and trigeminal ganglion (TG) neurons, ii) the unitary synaptic transmission and short-term synaptic plasticity at the main synapses of the cortical microcircuit involving pyramidal cells, fast spiking interneurons and somatostatin-expressing interneurons, iii) the balance between the total excitatory and inhibitory synaptic drive in individual cortical neurons during spontaneous cortical network activity, and iv) CGRP release in the TG and dura. The insights into the pathophysiology of migraine obtained from these studies will be discussed. In general, our data strengthen the view of CSD as a key migraine trigger and point to episodic disruption of the excitatory-inhibitory balance and neuronal hyperactivity as the basis for vulnerability to CSD ignition in migraine.

D.P. is supported by grants from University of Padova (Strategic Project: Physiopathology of Signaling in Neuronal Tissue), Fondazione Cariparo (Excellence Project: Calcium Signaling in Health and Disease) MIUR (PRIN 2010JFYFY2_005) and acknowledges the support from Telethon-Italy (GGP06234).

Where applicable, the authors confirm that the experiments described here conform with The Physiological Society ethical requirements.

L6

Brown adipose tissue: the mammalian prerogative

B. Cannon

Stockholm University, Stockholm, Sweden

During most of the eons when life has existed on earth, living organisms have been controlled in their activity not by their own needs but rather by the environment, in the simple way that life is based on chemical reactions; thus, with decreasing temperatures, activity decreases. The evolutionary advantages of a system that allows organisms to maintain a high and constant body temperature and thus to control their activity in accordance with their own demands is obvious, and different advanced species have attempted to approach this state.
A major breakthrough occurred when development of the true mammals started. In an evolutionarily extremely rapid process, an existing mitochondrial transporter – with an unknown function – was completely changed so that it gained the ability, in a controlled manner, to allow for (the equivalent) of proton transport over the mitochondrial membrane. This allows for the release of the energy accrued by mitochondrial oxidation in the form of heat, instead of transferring it into ATP. Apparently, this development opposes the general concept of life as a system to conserve energy rather than utilize it, but this trans-

formation of a proto-UCP1 to the mammalian UCP1 (uncoupling protein) provided the developing mammals with a totally new mechanism for gaining extra heat: that of nonshivering thermogenesis. We can only imagine that the intention to maintain a high and stable body temperature developed first and that initially the necessary extra heat could only be obtained through shivering, but those (pre)mammals that developed nonshivering thermogenesis obtained the ability to produce the extra heat in a comfortable way, that allowed them to do other things while heat was being produced imperceptibly in their bodies. In our opinion, no other mechanism for nonshivering thermogenesis exists in mammals except for that derived from the activity of UCP1 residing in the dedicated brown adipose tissue – and, to some extent, in certain nominally white adipose tissue depots (brite or beige adipose tissues).

Possession of nonshivering thermogenesis allowed mammals to inhabit niches which were earlier closed for active life: the cold nights, the cold areas of the world, and thus gave them evolutionary advantages. Additionally, brown adipose tissue may have bestowed upon mammals the ability to perform so-called facultative diet-induced thermogenesis, a process in which some of the energy of the food eaten is combusted in an apparently meaningless way, but the process may allow mammals to extract important nutrients from rather low-quality food.

As members of the mammalian group, we as humans share the ability to produce heat through brown adipose tissue activity. Until recently, this ability was thought to be restricted to newborn babies, but the present opinion is that brown adipose tissue is found and is active (when necessary) in a majority of adult humans as well. Thus, it may be said that the development of brown adipose tissue was what gave the developing mammals their evolutionary advantage, and that we still today as humans, even adults, are beneficiaries of this mammalian prerogative of possessing brown adipose tissue.

Where applicable, the authors confirm that the experiments described here conform with The Physiological Society ethical requirements.

L7

Teaching and research in physiology in Sub Saharan Africa – achievements and challenges

O. Sofola

Physiology, College of Medicine, University of Lagos, Nigeria, Lagos, Nigeria

Sub Saharan Africa (SSA) is the land mass extending below the Sahara desert excluding countries in the North of Africa and Sudan, according to the World Bank. There are about 52 countries with a population of about 874 million.

The history of teaching of physiology in many medical schools is fairly recent, the earliest possibly in the University of Cape Town (Republic of South Africa – RSA)in 1912, Pretoria (RSA) in 1943, Makerere (Uganda) in 1924, University College Ibadan,(Nigeria) in 1948, and Zimbabwe in 1952. There are about 74 Medical Schools in SSA (1), 26 in Nigeria and 8 in the Republic of South Africa. Teaching of physiology has traditionally been domiciled in Medical schools with majority using the traditional face-to-face method due largely to limited resources. One notable exception is the republic of South Africa, which we call 'European country located in Africa'. Teaching largely utilizes the white board and overhead/multimedia projectors. Many schools are beginning to incorporate some ICT components for teaching. However, we can claim some achievements as several physiologists have been trained in SSA. In addition, we have contributed to the training of several doctors as well as record modest achievements in training of PhDs. South Africa however has staff that is world class. Most universities in sub Saharan Africa depend virtually on government for funding. It is only recently that some universities started charging high tuition fees (2).

Other issues related to teaching challenges include:

- Limited number of PhD holders and low wages.
- Low lecturer : student ratio
- Outdated textbooks
- Limited ICT/ Internet facilities
- Outdated curricula

As for Research, with the exception of South Africa, the research output from the region is very low. It is estimated that SSA contributes less than 0.9% to published work with over 50% from South Africa (3). An analysis of university rankings bears this out as the highest ranked university from SSA is University of Cape Town at 133 (4). Only 5 African universities are in the world's top 1,000. The obvious reason is poor funding and thus less resource for acquiring top equipment for research. This is reflected in the low quality of articles in some regional journals that publish papers with little or no cellular or sub-cellular mechanisms. On the other hand publications from South Africa are top class. However, efforts are being made to play 'catch up'. For example, our laboratory has studied the effects of high salt diet on vascular mechanisms, using rat aortic rings. Our results were confirmed using the pressurized mesenteric artery preparation (5) during the author's tenure as British Heart Foundation Fellow at Leeds University. However, on return to Nigeria, such facility was not available but we are still publishing using the ring preparation (6). Subsequent studies have been on investigating the role of the Epithelial Sodium Channel (ENaC) in hypertensive Nigerians (Dr Elias, PhD thesis, Lagos, 2012) while collaborating with foreign laboratories for DNA sequencing and identification of genetic polymorphisms. We hope that this foray will open new grounds and attract more graduate students to genetic and molecular aspects of physiology.

Other challenges relating to research include:

- Heavy teaching load.
- Low PhD production in addition to in-breeding and inadequate mentoring
- Outdated equipment and little availability of reagents and consumables
- Lack of or limited access to journals
- Brain drain from SSA (3).

This brings up the point of how we in SSA (except perhaps South Africa) can leverage on the superb research facilities in the developed countries. It will also involve the exposure of our staff to research at cellular and sub-cellular levels including cell signaling etc, in line with current trends.

Thus, an appeal is being made to the IUPS to come to the aid of SSA. As the way forward, some suggestions are;

- Provision of sabbaticals for nationals of SSA to laboratories in the developed countries.
- Provision of laboratory space for research training and skills acquisition by our younger colleagues to increase their research capabilities
- A mechanism for equipment transfer through donation of 'surplus to requirement' but useful equipment to universities in SSA. For example, establishing a ' warehouse' system in the IUPS etc for donation of equipment and transfer of such to interested laboratories in SSA.

The thematic of these and other suggestions is assistance to SSA physiologists to boost teaching and research capabilities

and thereby improve on the present dismal situation. This is to arrest the brain drain and make competent and willing researchers to remain in their country and contribute meaningfully to global scientific enterprise.

List of Medical Schools in Africa: http//en.wikipedia.org/windex.php

Medical Schools in sub Saharan Africa. Lancet, 377: 113 - 21, 2011

Funding Tertiary Education in Africa . UNESCO, 2009

Times Higher Education (THE). World Fanking of Universities, 2012 - 13

Sofola OA, Knill A, Hainsworth R, Drinkhill M. J Physiol 543: 255 - 60, 2002

Oloyo A, Nair RP, Anigbogu CN, Sofola OA. Can J Physiol Pharmacol, 90: 1647 - 51, 2012

Support from IUPS/ AD Instruments is acknowledged

Where applicable, the authors confirm that the experiments described here conform with The Physiological Society ethical requirements.

L8

The Rhythms of Life – What your body clock means to you from eye disease to jet lag

R.G. Foster

University of Oxford, Oxford, UK

We all have embedded within our biology a body clock or "circadian system". The circadian system is used to anticipate the 24 hour day/night cycle so that physiology and behavior can be fine-tuned and adapted to the varying demands of activity and rest. In anticipation of wake, while we are still asleep, body temperature, metabolism and alertness begin to rise in preparation for the activity ahead. And in the same way, in anticipation of sleep, the body begins to slow-down, blood pressure drops, alertness falls and core body temperature declines. The internal clock driving these daily rhythms is not exactly 24 hours, in most of us it is a little longer. As a result, to keep the entire circadian system synchronized, the body clock is adjusted on a daily basis by the changes in light intensity around dawn and dusk. Without this daily re-setting of the clock, 24 hour body rhythms of sleep and wake would rapidly become desynchronized with the real world and lose their adaptive value.

The master clock is located within the base of the brain in a small paired structure called the suprachiasmatic nuclei – abbreviated to the SCN. The SCN are located just above where the optic nerves enter the brain and they contain around 50,000 cells, all of which contain their own individual molecular clock. The SCN cells work together to generate a near 24 signal throughout the body. Small changes in the genes that generate the molecular clock have been associated with the tendency to be a "morning" or "evening" person. Until recently, It was thought that only the SCN contains clock cells, but we now know that all cells of the body contain their own molecular clock. As a result the SCN coordinates the 24h rhythmic activity of billions and billions of cells throughout the body. The SCN receives a direct projection from the eye which adjusts all the cells in the SCN to the light/dark cycle. In addition to the rod and cone photoreceptors of the eye which provide us with our sense of vision, the eye contains a recently discovered 3rd class of light-sensitive cell called a "photosensitive retinal ganglion cell". There are relatively few of these cells within the eye but they are critical for the measurement of environmental brightness, and hence adjustment of the SCN to dawn and dusk.

In parallel with our increased understanding of the neuroscience of circadian rhythms, there is a growing appreciation of the severe consequences of ignoring the impact of these rhythms on diverse areas our health and quality of life. For example, the discovery of the pRGCs within the eye has transformed our understanding of blindness. We now appreciate that eye diseases which result in rod and cone photoreceptor death need not result in the loss of pRGC light detection. In these cases if a visually blind individual retains pRGC function they should be encouraged to expose their eyes to sufficient day-time light to maintain normal circadian regulation and sleep-wake timing. Even without sight, these eyes should be preserved at all costs as their loss will plunge an individual into a world without any sense of time; Additionally, individuals with eye diseases of the inner retina, which result in retinal ganglion cell death (e.g. glaucoma), are at particular risk of circadian rhythm disruption. Such individuals would be strong candidates for treatment with appropriately timed medications that help consolidate sleep timing. Until recently, sleep and circadian rhythms have rarely been addressed in clinical departments of ophthalmology, yet worldwide there are over 50 million people classified as blind and perhaps a further 300 million with severe visual loss. The quality of life and health of many of these individuals would be improved if there were a greater understanding by ophthalmologists of how the eye regulates our internal time.

Jet-lag represents another example where the circadian system becomes uncoupled from the environment, but in this case because of travel across multiple time-zones. Upon exposure to the new light/dark cycle it takes the circadian system days to readjust to local time. Furthermore, the timing of the multiple cellular clocks throughout the body becomes uncoupled for variable periods of time before adjustment. The net result is a body that is poorly adapted to function in the new time-zone. Insomnia, fatigue, impaired cognition, depression, metabolic and gastrointestinal problems all persist until the circadian system has adapted fully to the new light/dark cycle. The number of people affected by jet-lag is rising rapidly, but little is done to address the problems suffered by these individuals.

This presentation will consider the remarkable discoveries of how our circadian rhythms are generated and regulated by light. The second part of the talk will consider how a knowledge of this physiology is having a major impact upon both medicine and in the way we structure and our society.

Where applicable, the authors confirm that the experiments described here conform with The Physiological Society ethical requirements.

L9

Calcium signal mechanisms in secretory cells: physiology and pathology

O.H. Petersen

Biosciences, Cardiff University, Cardiff, UK

More than forty years ago, I showed that acetylcholine (ACh) evokes fast release of Ca^{2+} from intracellular stores in exocrine glands, delayed influx of Ca^{2+} from the extracellular solution and activation of Ca^{2+} extrusion (Nielsen & Petersen 1972). The now established basic elements of cellular Ca^{2+} homeostasis in electrically non-excitable cells, namely messenger-mediated opening of Ca^{2+} channels in intracellular stores, store-

operated Ca^{2+} entry and Ca^{2+} pump – mediated extrusion of Ca^{2+} into the extracellular solution (Petersen & Tepikin 2008) were thus identified in the 1972 paper (Nielsen & Petersen 1972). The first measurements of the cytosolic Ca^{2+} concentration ($[Ca^{2+}]i$) in exocrine gland cells were performed using the Ca^{2+}-activated K+ channel as an intrinsic Ca^{2+} sensor. Combining results of single-channel current recordings in excised inside-out membrane patches, at different well-defined Ca^{2+} concentrations in solutions in contact with the membrane inside, with cell-attached single channel recordings from intact acinar cells in the resting state, as well as after stimulation, showed that resting $[Ca^{2+}]i$ was between 50 and 100 nM and that stimulation caused a significant rise in this level (Maruyama et al 1983). Later imaging studies, employing fluorescent Ca^{2+}-sensitive dyes and patch clamp electrophysiology, showed that stimulation with physiologically relevant hormone concentrations did not evoke a sustained elevation of $[Ca^{2+}]i$, but repetitive short-lasting spikes and that these were mostly confined to the apical granular part of the pancreatic acinar cells (see Petersen & Tepikin 2008). These local Ca^{2+} transients stimulated the exocytotic secretion process of digestive enzymes. Indeed every single Ca^{2+} transient evokes a transient exocytotic response (Petersen & Tepikin 2008). The continued generation of repetitive local Ca^{2+} signals, evoked by continuous stimulation with a physiological hormone level, relies on the Ca^{2+} tunnel function of the endoplasmic reticulum, the concentration of Ca^{2+} release channels in the apical granular area and the peri-granular mitochondrial belt, functioning as a Ca^{2+} firewall (see Petersen & Tepikin 2008). A sustained elevation of $[Ca^{2+}]i$ in the pancreatic acinar cells, evoked by hyperstimulation, only causes an initial transient secretory response but then, in contrast to what happens with physiological stimulation, activates intracellular proteases. This protease activation is initiated in the apical granular area and at the same time transformation of the normally electron-dense zymogen granules into empty looking vacuoles begins. Both intracellular protease activation and vacuolization can be prevented by intracellular Ca^{2+} chelation (Raraty et al 2000). These processes are characteristic of what happens in the human disease acute pancreatitis, which is mostly caused by alcohol abuse or gallstone complications. Surprisingly, we found that ethanol – even at extraordinarily high and unrealistic concentrations – had very little effect on Ca^{2+} homeostasis in intact pancreatic acinar cells, whereas fatty acid ethyl esters (FAEEs) – non-oxidative products of ethanol and long chain fatty acids – are very effective releasers of stored Ca^{2+} in pathophysiologically relevant concentrations (Gerasimenko et al 2009,2011). The surprisingly weak effect of ethanol itself is due to an intrinsic protective effect of calmodulin (CaM). In permeabilized acinar cells, ethanol – even at a modest concentration – did evoke significant Ca^{2+} release from internal stores, as well as trypsinogen activation, but these effects could be markedly suppressed by adding CaM to the external solution, which in these experiments was in direct contact with the cytosol (Gerasimenko et al 2011). Remarkably, a Ca^{2+}-like peptide (CALP-3) completely suppressed trypsinogen activation induced even by a very high ethanol concentration (Gerasimenko et al 2011). Since the Ca^{2+} releasing effect of FAEEs is much stronger than that of ethanol alone, the mechanism of action has been explored in some detail. Knock-out of IP3 receptors of types 2 and 3 markedly reduced both the Ca^{2+} release and the trypsinogen activation induced by FAEEs to very low levels, indicating that most of the Ca^{2+} release occurs through the very same receptors that also serve normal stimulus-secretion coupling (Gerasimenko et al 2009). Under physiological conditions the IP3 receptor activation is moderate, whereas under pathological conditions maximal opening of these channels occurs, with the result that the stores are completely emptied. Overall, our results indicate that even a small, but sustained, rise in $[Ca^{2+}]i$, while not in itself necessarily causing damage, sensitizes cells to noxious stimuli, for example oxidative stress, markedly increasing the risk for necrosis (Ferdek et al 2012).

Ferdek, P.E., Gerasimenko, J.V., Peng, S., Tepikin, A.V., Petersen, O.H. and Gerasimenko, O.V. (2012) A novel role for Bcl-2 in regulation of cellular calcium extrusion. Curr. Biol. 22, 1241-1246.

Gerasimenko, J.V., Lur, G., Sherwood, M.W., Ebisui, E., Tepikin, A.V., Mikoshiba, K., Gerasimenko, O.V. & Petersen, O.H. (2009) Pancreatic protease activation by alcohol metabolite depends on Ca2+ release via acid store IP3 receptors. Proc. Natl. Acad. Sci. USA (PNAS) 106, 10758-10763.

Gerasimenko, J.V., Lur, G., Ferdek, P., Sherwood, M.W., Ebisui, E., Tepikin, A.V., Mikoshiba, K., Petersen, O.H. and Gerasimenko, O.V. (2011) Calmodulin protects against alcohol-induced pancreatic trypsinogen activation elicited via Ca2+ release through inositol trisphosphate receptors. Proc. Natl. Acad. Sci. USA (PNAS) 108, 5873-5878.

Maruyama, Y., Petersen, O.H., Flanagan, P. & Pearson, G.T. (1983). Quantification of Ca2+-activated K+ channels under hormonal control in pig pancreas acinar cells. Nature 305, 228-232.

Nielsen, S.P. & Petersen, O.H. (1972). Transport of calcium in the perfused submandibular gland of the cat. J. Physiol. 223, 685-697.

Petersen, O.H. & Tepikin, A.V. (2008) Polarized calcium signaling in exocrine gland cells. Annu. Rev. Physiol. 70, 273-299.

Raraty, M., Ward, J., Erdemli, G., Vaillant, C., Neoptolemos, J.P., Sutton, R. & Petersen, O.H. (2000). Calcium-dependent enzyme activation and vacuole formation in the apical granular region of pancreatic acinar cells. Proc. Natl. Acad. Sci. USA (PNAS) 97, 13126-13131.

Supported by MRC Programme Grant. Ole Petersen is an MRC Professor.

Where applicable, the authors confirm that the experiments described here conform with The Physiological Society ethical requirements.

L10

Stem cell biology for vascular medicine

T. Asahara

Tokai University, Isehara, Kanagawa, Japan

The finding that Endothelial progenitor cells (EPCs) can home to sites of neovascularization and differentiate into endothelial cells in situ is consistent with “vasculogenesis”, a critical paradigm well described for embryonic neovascularization, but recently also proposed for the adult organism in which a reservoir of progenitor cells contributes to post-natal neovascular formation. The discovery of EPCs has therefore drastically changed our understanding of adult blood vessel formation. Furthermore, people noticed the valuable capability to translate EPC potential to improve the clinical applicability in the fight against cardiovascular diseases. Many groups involved in clinical trials have demonstrated that EPC therapy is safe and feasible for the treatment of critical limb ischemia and cardiovascular diseases. However, many issues in the field of EPC biology, especially in regards to the proper and unambiguous molecular characterization of these cells still remain unresolved, hampering not only basic research but also the effective therapeutic use and widespread application of these cells.

In this presentation, I introduce the recent concept of EPC identification in terms of hematopoietic and non-hematopoietic

EPCs along with the development of EPC biology research. Furthermore, I define the role of circulating EPCs in post-natal neovascularization to illustrate the future direction of EPC therapeutic applications.
I overview candidate cells for cardio- and peripheral- vascular diseases, introduce the practical example of therapeutic application of cells to ischemic disease patients and discuss the future direction.

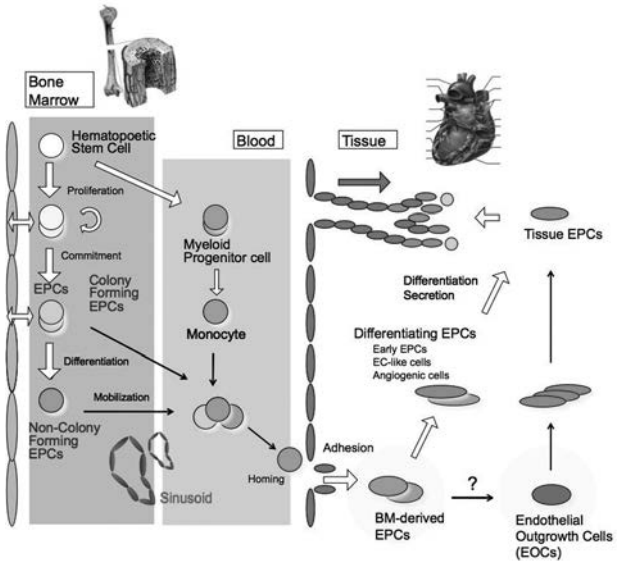

Asahara T, Murohara T, Sullivan A, Silver M, van der Zee R, Li T, Witzenbichler B, Schatteman GIsner J M. Isolation of putative progenitor endothelial cells for angiogenesis. Science, 1997. 275:964-7.

Takahashi T, Kalka C, Masuda H, Chen D, Silver M, Kearney M, Magner M, Isner J M, Asahara T. Ischemia- and cytokine-induced mobilization of bone marrow-derived endothelial progenitor cells for neovascularization. Nat Med, 1999. 5:434-8.

Kawamoto A, Katayama M, Handa N, Kinoshita M, Takano H, Horii M, Sadamoto K, Yokoyama A, Yamanaka T, Onodera R, Kuroda A, Baba R, Kaneko Y, Tsukie T, Kurimoto Y, Okada Y, Kihara Y, Morioka S, Fukushima M, and Asahara T. Intramuscular Transplantation of Granulocyte Colony Stimulating Factor-Mobilized CD34-Positive Cells in Patients with Critical Limb Ischemia: A Phase I/IIa, Multi-Center, Single-Blind and Dose-Escalation Clinical Trial. Stem Cells, 2009. 27:2857-64.

Masuda H, Alev C, Akimaru H, Ito R, Shizuno T, Kobori M, Horii M, Ishihara T, Isobe K, Isozaki M, Itoh J, Itoh Y, Okada Y, McIntyre B A, Kato S, and Asahara T. Methodological development of a clonogenic assay to determine endothelial progenitor cell potential. Circ Res, 2011. 109:20-37.

Asahara T, Kawamoto AMasuda H. Concise review: Circulating endothelial progenitor cells for vascular medicine. Stem Cells, 2011. 29:1650-5.

Where applicable, the authors confirm that the experiments described here conform with The Physiological Society ethical requirements.

L11

Local protein synthesis

E. Schuman

c/o MPI Biophysics, Max Planck Institute for Brain Research, Frankfurt, Germany

An individual neuron in the brain possesses approximately 10,000 synapses, many of which are hundreds of microns away from the cell body, which can process independent streams of information. During synaptic transmission and plasticity, remodeling of the local proteome occurs via the regulated synthesis of new proteins. I will discuss previous and current studies aimed at understanding how the local transcriptome, obtained with deep sequencing, and the local proteome might influence synaptic transmission and plasticity.

Where applicable, the authors confirm that the experiments described here conform with The Physiological Society ethical requirements.

L12

Vascular metabolism: principles and strategies

P. Carmeliet

Laboratory of Angiogenesis and Neurovascular link, Vesalius Research Center, VIB - KU Leuven, Leuven, 3000 Leuven, Belgium

Angiogenesis, the growth of new blood vessels, plays a crucial role in numerous diseases, including cancer. Anti-angiogenesis therapies have been developed to deprive the tumor of nutrients. Clinically approved anti-angiogenic drugs offered prolonged survival to numerous cancer patients. However, the success of antiangiogenic VEGF-targeted therapy is limited in certain cases by intrinsic refractoriness and acquired resistance. New strategies are needed to block tumor angiogenesis via alternative mechanisms. We are therefore exploring whether targeting endothelial metabolism can be a possible alternative therapeutic strategy for anti-angiogenic therapy.

Where applicable, the authors confirm that the experiments described here conform with The Physiological Society ethical requirements.

L13

Gastrointestinal hormones and the dialogue between gut and brain

G. Dockray

Cell and Molecular Physiology, University of Liverpool, Liverpool, UK

The landmark discovery by Bayliss and Starling in 1902 of the first hormone, secretin, was based in part on the observation that a response (pancreatic secretion) following a stimulus (intestinal acidification) occurred after section of the relevant afferent nerve pathway. With the subsequent discovery of many more hormones, numerous examples of interactions between endocrine and autonomic efferent pathways emerged. But it was to be nearly 80 years before it was discovered that visceral afferent neurons could themselves also be targets for gut and other hormones. Signalling from gut to brain by gut hormones acting on vagal afferent neurons is now recognised to be an early step in the activation of vagovagal reflexes regulating gastric acid secretion and in controlling nutrient delivery to the intestine by modulating gastric emptying. Importantly, gut hormones acting on vagal afferent neurons also influence food intake and interest in these mechanisms has grown rapidly in view of the alarming global increase in obesity. Several of the gut hormones released by nutrients (cholecystokinin, CCK; PYY3-36; glucagon-like peptide-1, GLP-1) excite vagal afferent neurons to activate an ascending pathway via the brainstem and hypothalamus leading to inhibition of food intake. Conversely others eg ghrelin, that are released in the inter-digestive period, inhibit vagal

afferent neurons leading to increased food intake. Moreover, the vagal afferent neurons targeted by gut hormones are now emerging as integrators of several different types of peripheral signal. Thus, (a) leptin stimulates these neurons and potentiates the effects of CCK indicating mechanisms that integrate adipose- and gut-derived signals. (b) Nutrient status determines the neurochemical phenotype of vagal afferent neurons and in particular regulates a switch between states that emphasise orexigenic or anorexigenic signalling; for example food withdrawal increases the expression of receptors (eg cannabinoid, CB1, receptor) and a putative neuropeptide transmitter (melanin concentrating hormone, MCH) that are associated with stimulation of food intake, while refeeding increases the expression of a receptor (Y2) and neuropeptide transmitter (cocaine and amphetamine regulated transcript, CART) associated with satiety signalling. (c) The gut luminal and tissue environments modulate vagal sensitivity to gut hormones through mechanisms that vary with different regions of the gut. Thus small intestinal infection, and proinflammatory cytokines, potentiate vagal afferent responses to CCK leading to loss of appetite; in the stomach, however, infection and inflammation can be regarded as physiological states, and here expression of plasminogen activator inhibitor (PAI)-1 is increased by inflammation and depresses vagal afferent sensitivity to CCK, thereby protecting nutrient intake. Finally, (d) shifts in the gut microbiota that occur in obesity are associated with leptin insensitivity in vagal afferent neurons, and therefore insensitivity to CCK as well, which appears to develop before leptin-insensitivity in hypothalamic neurons. Together these observations indicate a hitherto unsuspected level of sophistication in the signalling between gut to brain that underlies homeostatic mechanisms controlling nutrient intake. They also suggest new opportunities to develop treatments for obesity and feeding disorders.

Where applicable, the authors confirm that the experiments described here conform with The Physiological Society ethical requirements.

L15

Physiological insights into the developmental origins of non-communicable disease

M. Hanson

Human Development and Health, University of Southampton, Southampton, UK

Non-communicable diseases (NCD) including cardiovascular disease, diabetes, chronic lung disease and some forms of cancer now pose an increasing threat to global health and the economies of both developed and developing countries, where they are now overtaking communicable diseases (1). Not simply diseases of affluence, attempts to reduce their incidence through adult lifestlye are not succeeding (2). Risk of such disease is set in part during early life, when environmental influences including mother's diet, body composition and exposure to stress, affect the development of her fetus and newborn, establishing its responses to later environmental challenges such as an obesogenic lifestyle. Paternal lifestyle can also produce developmental effects via the sperm. Such parental effects may confer fitness advantage by enabling rapid phenotypic response to an environmental change (3). If the cues which the developing embryo and fetus detect are inaccurate, e.g. unbalanced maternal diet or because nutritional transition occurs between generations through migration or rapid economic improvement, offspring's responses are mismatched to later environmental challenges, leading to greater risk of NCD. Whilst undernutrition remains an enormous problem throughout the developing world, in both developing and developed societies adverse consequences of over- and undernutrition co-exist (4). The resulting risk can be transmitted down multiple generations. The consequences affect many aspects of the lifecourse including reproductive health, behavioural, cognitive problems, osteoporosis, sarcopenia and some allergic conditions. Epidemiological, human clinical and basic science research has now indicated underlying mechanisms, many of which involve epigenetic processes (5, 6). These can thus serve as early markers of later risk and they are in principle reversible by dietary, endocrine or pharmacological means. They include DNA methylation, but also changes in histone protein structure and small non-coding RNAs. New evidence is revealing how such processes, which extend beyond imprinted genes, can modify the effects of transcription factors on gene expression and thus responses to later challenges (7). The specific patterns of CpGs methylated can be important, and the regions of importance are not solely in CpG-rich islands. These physiological insights indicate the opportunity for complex social interventions before conception to reduce NCD risk in the next generation.

See comments and articles in The Global Burden of Disease Study 2010. The Lancet 380. Dec 15, 2012

Gluckman P, Hanson M (2012). Fat, Fate and Disease. Oxford University Press

Gluckman PD, Hanson MA, Spencer HG (2005). Predictive adaptive responses and human evolution. Trends in Ecology and Evolution 20(10): 527-533

Hanson MA, Gluckman PD (2011). Developmental origins of noncommunicable disease: population and public health implications. Am J Clin Nutr 94:1754s-8s

Michels KB, Waterland RA (2012), The Role of Epigenetics in the Developmental Origins of Health and Disease. In Epigenetic Epidemiology. Ed K B Michels pp105-116, DOI: 10.1007/978-94-007-2495-2_7

Relton, C. (2010) Epigenetics and Developmental Origins of Health and Disease. Epigenetics 5: 516-526

Gluckman PD, Hanson MA, Beedle AS (2007). Non-genomic transgenerational inheritance of disease risk. Bioessays 29(2):145-154

MAH is supported by the British Heart Foundation

Where applicable, the authors confirm that the experiments described here conform with The Physiological Society ethical requirements.

L16

Mitochondrial superoxide flashes

H. Cheng and X. Wang

State Key Laboratory of Biomembrane and Membrane Biotechnology, Peking University, Beijing, China

Respiratory mitochondria spontaneously undergo quantal, brief bursts of superoxide production, named "superoxide flashes". A property common to all species and cell types examined, generation of superoxide flashes is coupled to transient opening of mitochondrial membrane permeability transition pore (mPTP) and depends on the functional integrity of electron transfer chain (ETC). Unitary properties of superoxide flashes (amplitude, duration) appear to be stereotypical, at levels from isolated mitochondria to whole organs (e.g. beating heart) and even to live animals. Functionally, superoxide flashes act as elemental reactive oxygen species (ROS) signaling events ("signaling ROS") that participate in diverse cellu-

lar processes, whereas constitutive electron leakage from the ETC to molecular oxygen produces the bulk of ROS for the regulation of redox homeostasis ("homeostatic ROS"). In particular, superoxide flash incidence provides a digital readout to gauge the glucose- and insulin-stimulated mitochondrial metabolism in live animals, and a novel biomarker of the oxidative stress in hyperosmotic stress and ischemia-reperfusion injury. These findings support the notion that ROS act as second messengers in physiological and pathophysiological contexts, and demonstrated the paramount importance of spatiotemporal organization of ROS signals in determining their signaling efficiency and modality.
Keywords: Reactive oxygen species (ROS); Superoxide flash; Local ROS signaling; Mitochondrial permeability transition pore; Mitochondria

Where applicable, the authors confirm that the experiments described here conform with The Physiological Society ethical requirements.

L17

T-type calcium channels, thalamic firing modes, and control of consciousness and cognition

H. Shin

Center for Cognition and Sociality, Institute for Basic Science, Daejeon, Republic of Korea

The thalamocortical circuit has long been considered important in control of consciousness. Series of works utilizing mice with genetic modifications of the alpha1G T-type Ca2+ channel have helped to settle the long held issue on the critical role, in vivo, of T-type channels in control of neuronal firing mode and consciousness. These have been shown by studies on absence epilepsy, sleep, and alcohol-induced loss of consciousness. As we explore further into the structure and function of the thalamocortical circuit, especially in relation to other brain regions, we begin to find that the thalamus has critical roles in other fundamental brain functions, i.e. in cognition and emotion control. Thus, we showed that the thalamus is deeply involved in control of empathy fear by the anterior cingulate cortex and in extinction of fear memory by the amygdala and prefrontal cortex. In the latter case, we began our studies with a mutant mouse for the phospholipase Cbeta4 gene, a signaling molecule downstream to mGluR1. Using gene manipulation, pharmacology, lesion, single-unit recording via tetrodes, and intracranial electrical stimulations, we found that the mediodorsal thalamus plays a critical switch function in extinction of fear memory through two different firing patterns, burst vs tonic. The demonstration of the opposite functions, suppression vs enhancement, of the two firing modes on extinction of fear memory clearly shows the distinctive physiological roles of the two firing modes of the thalamus in control of cognition, in addition to their roles in control of consciousness. Current studies on this issue will be discussed.

Where applicable, the authors confirm that the experiments described here conform with The Physiological Society ethical requirements.

L18

Role of ATP-regulated potassium channels in pancreatic alpha- and beta-cells

P. Rorsman

Radcliffe Department of Medicine, University of Oxford, Oxford, UK

Insulin and glucagon are the body's principal gluco-regulatory hormones. They are secreted by the pancreatic β- and α-cells in response to hyperglycaemia and hypoglycaemia, respectively. The metabolic regulation of insulin secretion is well understood: glucose-induced closure of ATP-sensitive potassium channels (KATP-channels), which are spontaneously active at low glucose, results in membrane depolarization, initiation of Ca2+-dependent electrical activity and stimulation of insulin granule exocytosis. An increase in plasma glucose leads to inhibition of glucagon secretion. Surprisingly, glucagon-secreting α-cells are equipped with KATP-channels of exactly the same molecular composition as those found in the β-cells. The role of the KATP-channels in α-cells remains enigmatic. How can closure of KATP-channels result in stimulation of insulin secretion from β-cells but inhibition of glucagon secretion from the α-cells?
Our recent studies on α-cells in freshly isolated intact islets have established that the KATP-channels are active in α-cells exposed to 1mM glucose (a condition associated with stimulation of glucagon secretion) and that they close when glucose is increased to 6mM. This results in ~10mV membrane depolarization and <2-fold increase in action potential frequency. Yet, glucagon secretion measured in parallel from the same batch of pancreatic islets was inhibited by ~50%. The KATP-channel blocker tolbutamide mimicked the effects of glucose on electrical activity and glucagon secretion. Importantly, the depolarizing effect of glucose or tolbutamide was associated with a 10-15mV reduction of action potential peak voltage. The sodium channel blocker TTX and the P/Q-type calcium channel inhibitor agatoxin mimicked the effects of glucose on glucagon secretion/electrical activity. These data suggest that KATP-channel closure exert dual effects on secretion/electrical excitability depending on the complements of voltage-gated ion channels. In cells in which action potential firing depends on ion channels that do not undergo much voltage-dependent inactivation (as exemplified by the β-cell), membrane depolarization will stimulate secretion. In cells in which action potential firing instead involves ion channels that exhibit voltage-dependent inactivation (like the α-cell), membrane depolarization, via reduced action potential height and less activation of P/Q-type calcium channels, results in inhibition rather than stimulation of secretion.
These data may help to explain why glucagon secretion is increased in diabetic patients (exacerbating the hyperglycemia due to the lack of insulin). Potential therapeutic implications of these findings will be discussed.

Supported by the Wellcome Trust

Where applicable, the authors confirm that the experiments described here conform with The Physiological Society ethical requirements.

L19

Sifting circuits for motor control

T.M. Jessell

HHMI, Kavli Institute for Brain Science, Depts. Neuroscience, Biochemistry and Molecular Biophysics, Columbia University, New York, NY, USA

This talk will examine two aspects of the organization of spinal circuits devoted to the control of limb movement – the logic of circuit assembly, and the link between circuit wiring and motor behavior. The application of molecular genetic methods to problems of neuronal diversity and connectivity has begun to emphasize the importance of neuronal settling position as an adjunct to cell recognition in driving the assembly of motor microcircuits. Through this analysis it has become evident that the detailed wiring of local motor circuits differs systematically, as a function of limb muscle position and the biomechanical demands of individual joints. Molecular appreciation of the vast diversity of spinal motor neuron and interneuron subtypes has also permitted more precise ways of perturbing, genetically, the function of individual spinal neuronal subsets and examining the consequences of such manipulations for motor behavior. Examples of the way in which this general approach can be applied to questions of local inhibitory control, and the internal representation of motor output, will be discussed.

Funded by HHMI, NINDS, ProjectALS, Mathers Foundation

Where applicable, the authors confirm that the experiments described here conform with The Physiological Society ethical requirements.

L20

Structure and function of voltage-gated sodium channels at atomic resolution

W.A. Catterall

Pharmacology, University of Washington, Seattle, WA, USA

Voltage-gated Na+ channels initiate action potentials in excitable cells and are important targets for drugs. Recent research gives new insight into the structural basis for permeation, drug-block, and voltage-dependent gating. Voltage-sensing depends on the S4 segments, which move outward through a gating pore via a 'sliding-helix' mechanism. Outward movement of S4 is coupled to pore-opening by tilting and rotation of the S6 segments. A structural model reveals conformational changes underlying activation and pore-opening, and disulfide locking of substituted cysteines demonstrates voltage-dependent formation of ion pairs during channel activation, as in the sliding-helix model. Sodium channel blocking drugs bind to a conserved receptor site in the inner pore, and binding is enhanced by repetitive opening of the pore and inactivation of the channel. A three-dimensional view of these structural components is provided by a high-resolution structure of a voltage-gated Na+ channel from Arcobacter butzleri (NavAb) captured in a closed-pore conformation with four activated voltage-sensors at 2.7 Å resolution. The arginine gating charges make multiple hydrophilic interactions within the voltage-sensor, including unanticipated hydrogen bonds to the protein backbone. Comparisons to previous open-pore Kv channel structures suggest that the voltage-sensor domains and the S4-S5 linkers dilate the central pore by pivoting around a hinge at the base of the pore. The NavAb selectivity filter is short, ~4.6 Å wide, and water-filled, with four acidic glutamate side-chains surrounding the narrowest part of the ion-conduction pathway. This unique structure presents a high-field-strength anionic coordination site, which confers Na+ selectivity through partial dehydration via direct interaction with glutamate side-chains. Multiple sodium binding sites are observed in crystals and in molecular dynamics simulations, supporting a 'knock-on' model of permeation. The local anesthetic site is located in the central cavity of the pore. Fenestrations in the sides of the pore are unexpectedly penetrated by fatty-acyl chains that extend into the central cavity, and these portals are large enough for entry of small, hydrophobic pore-blocking drugs. Determination of the crystal structure of NavAb in two similar inactivated states suggests asymmetric pore collapse as the mechanism of slow inactivation of NavAb channels and reveals dramatic conformational change in its drug receptor site that might underlie preferential voltage-dependent block of inactivated sodium channels.

Where applicable, the authors confirm that the experiments described here conform with The Physiological Society ethical requirements.

L21

New insights in the fetal origins of adult cardiometabolic disease

S. Davidge, C. Rueda-Clausen, J. Morton, V. Dolinsky and J. Dyck

Women and Children's Health Research Institute, University of Alberta, Edmonton, AB, Canada

Cardiovascular disease causes the greatest mortality in the world today. It is now recognized that the quality of the fetal environment during early development is important for cardiovascular health in later life. Understanding the consequences of a poor *in utero* environment leading to cardiometabolic disease creates an exciting window of opportunity to diagnose, intervene and ultimately reduce the development of cardiovascular disease.

Fetal hypoxia is one of the most common consequences of complicated pregnancies worldwide. Intrauterine hypoxia is associated with a variety of maternal, placental and fetal conditions, such as chronic maternal pulmonary disease, heart disease, acute respiratory infections, preeclampsia as well as placental insufficiency and hypoxic environments. Our studies use a model of chronic maternal hypoxia (rats housed at 11.5% oxygen for their last third of pregnancy) that leads to intrauterine growth restriction (referred to here as IUGR).

For our vascular studies, we hypothesized that exposure to prenatal hypoxia would cause changes in vascular function that would impair vasodilation later in life in an age- or sex-dependent manner. We found that flow-induced vasodilation was unaffected at a young age (3 months old) but was significantly reduced in aging (12 months) IUGR animals compared to aging controls. Interestingly, nitric oxide (NO)-mediated vasodilation was significantly reduced in both young and aging IUGR males and females (1), suggesting altered pathways of vasodilation in offspring exposed to prenatal hypoxia for both sexes. Overall, our data suggest that a change in the mechanisms of vasodilation occurring at an earlier age in IUGR offspring may predispose them to adult cardiovascular diseases. In regard to cardiac function, we have used *in vivo* echocardiographic techniques that demonstrated that hypoxia-induced IUGR is associated with the development of chronic car-

diopulmonary dysfunction (such as diastolic dysfunction and pulmonary hypertension) in offspring as the age (2). Moreover, cardiac tolerance to ischemia/reperfusion injury is reduced in hypoxic offspring by 4 months of age. Furthermore, we identified a mismatch in glucose metabolism leading to proton accumulation in the postischemic myocardium of offspring born IUGR as a potential mechanism involved (3). We further identified that in only the male offspring, IUGR was associated with an increase in myocardial oxidative stress as evidenced by an increased GSSH/GSH ratio (4).

We further expanded our studies to address the impact of prenatal hypoxia on indices of metabolic syndrome. In IUGR offspring fed a high fat (HF)-diet, there was a relative increase in intra-abdominal fat deposition and size, as well as an increase in fasting plasma concentrations of leptin, triglyceride and free fatty acids by 3 months of age that was not evident in the control group. These changes were accompanied by *in vivo* insulin resistance and impaired glucose tolerance (5). Interestingly, we showed a synergistic effect of prenatal hypoxia and postnatal high fat diet to reduce the capacity for recovery from cardiac ischemia/reperfusion injury (6). Thus offspring exposed to prenatal hypoxia do not appear to have reserve against secondary insults such as high fat diet or aging. We next addressed a potential intervention strategy. Since resveratrol (Resv), the polyphenol produced by plants, exerts insulin-sensitizing effects, we tested whether Resv could prevent deleterious metabolic effects of being born IUGR. We showed that in only the IUGR offspring, feeding a HF diet supplemented with Resv for 9 weeks, from the time of weaning, prevented intra-abdominal fat deposition, improved the plasma lipid profile and ameliorated insulin resistance and glucose intolerance (7). Our results suggest that early, postnatal intervention can alleviate HF-diet induced pathologic metabolic phenotypes in young, adult offspring born from a complicated pregnancy associated with prenatal hypoxia.

Overall, our laboratory has demonstrated that prenatal hypoxia leads to intrauterine growth restriction and impairs later life endothelial-dependent vascular function and decreases cardiac tolerance to ischemia/reperfusion injury. We have also noted that compromised offspring do not have the reserve to accommodate a secondary stress such as consuming a high fat diet. Understanding the impact of different interventions such as Resv will improve our knowledge of mechanisms and address potential strategies for early intervention for children at risk due to their prenatal history.

Morton JS et al. (2011). *J App Physiol* **110**, 1073-1082

Rueda-Clausen CF et al. (2009). *Cardiovasc Res* **81**, 713-722

Rueda-Clausen CF et a.l (2011). *Cardiovasc Res* **90**, 285-294

Rueda-Clausen CF et al. (2012). *JDOHaD* **3**, 350-357

Rueda-Clausen CF et al. (2011). *Diabetes* **60**, 507-516

Rueda-Clausen CF et al. (2012). *Am J Physiol* **303**, R418-426

Dolinsky VW et al. (2012). *Diabetes* **60**, 2274-2284

This work is funded by grants from the Canadian Institutes of Health Research (CIHR) and the Women and Children's Health Research Institute of the University of Alberta. SDavidge is a Canada Research Chair in Women's Cardiovascular Health and is an AIHS-funded Scientist.

Where applicable, the authors confirm that the experiments described here conform with The Physiological Society ethical requirements.

L22

An overview of Physiome activities

P. Hunter

University of Auckland, Auckland, New Zealand

Multi-scale models of organs and organ systems, based on model encoding standards, are being developed under the umbrella of the IUPS Physiome Project and the Virtual Physiological Human (VPH) project funded by the European Commission. These computational physiology models deal with multiple physical processes (coupled tissue mechanics, electrical activity, fluid flow, etc) and multiple spatial and temporal scales. They are intended both to help understand physiological function and to provide a basis for diagnosing and treating pathologies in a clinical setting. A long term goal of the project is to use computational modeling to analyze integrative biological function in terms of underlying structure and molecular mechanisms. Web-accessible databases, based on the standards, have been established for models and model-related data at the cell, tissue, organ and organ system levels. This talk will discuss recent developments in the IUPS Physiome Project.

Hunter, P.J. and Borg, T.K. Integration from proteins to organs: The Physiome Project. Nature Reviews Molecular and Cell Biology. 4, 237-243, 2003.

Hunter, P.J. and Nielsen, P.M.F. A strategy for integrative computational physiology. Physiology. 20,316-325, 2005.

Bassingthwaighte, J., Hunter, P.J. Noble, D. The Cardiac Physiome: perspectives for the future. Experimental Physiology, 94(5):597-605, 2009.

De Bono, B. and Hunter, P.J. Integrating knowledge representation and quantitative modelling in physiology. Biotechnol. J. 7:958–972, 2012. DOI 10.1002/biot.201100304

Coveney, P.V., Diaz-Zuccarini, V., Graf, N., Hunter, P., Kohl, P., Tegner, J. and Viceconti, M. Integrative approaches to computational biomedicine. Interface Focus. 2013 3 20130003; doi:10.1098/rsfs.2013.0003

Hunter, P.J., et al. Discussion: A vision and strategy for the virtual physiological human: 2012 update. Interface Focus. 2013 3 20130004; doi:10.1098/rsfs.2013.0004

Where applicable, the authors confirm that the experiments described here conform with The Physiological Society ethical requirements.

L23

Integration and modulation of intercellular signalling underlying blood flow control

S.S. Segal

Med Pharm Physiology, University of Missouri, Columbia, MO, USA and Dalton Cardiovascular Research Center, Columbia, MO, USA

Blood flow control in the microcirculation requires coordinated interplay among the multiple branches of vascular resistance networks. These branches include arterioles embedded within the tissue parenchyma and their upstream feed arteries located external to the tissue. Vasoactive stimuli arising from cellular activity at discrete locations within a tissue (e.g., skeletal muscle fibres of motor units) activate receptors and ion channels of both smooth muscle cells and endothelial cells. The ensuing chemical and electrical signals must be integrated among vessel branches to effectively increase local perfusion in accord with local nutritive requirements of metabolic demand.

Ascending vasodilatation is an intrinsic property of the resistance vasculature that enables signals initiated at discrete sites to spread from cell to cell along and among network branches. As demand (e.g., exercise intensity) increases, dilatation originating in distal arterioles governing capillary perfusion spreads upstream into intermediate and proximal arterioles that control the distribution and magnitude of tissue blood flow. Ascending dilatation of feed arteries coordinately governs total flow entering the microcirculation. The axial orientation of endothelial cells and their robust coupling to each other through gap junctions underscores the effectiveness of the endothelium as a cellular pathway for transmitting signals along vessel walls. In turn, heterocellular coupling through myoendothelial gap junctions enables radial signalling from the endothelium into consecutive smooth muscle cells to coordinate their relaxation and the spread of vasodilatation. Through altering cell-to-cell coupling, the regulation of gap junction expression and patency (e.g., by phosphorylation, nitrosylation and accessory proteins) can modulate both longitudinal and radial signalling in resistance networks. Intercellular signalling is also modulated by ion channels in plasma membranes. For example, the fall in membrane resistance upon activating small- and intermediate- Ca^{2+} activated K^+ channels (SK/IK) along the endothelium promotes the dissipation of electrical signals, thereby "tuning" the effective distance of transmission. Inherent to myoendothelial coupling is that variations in the size, number and functional channels of smooth muscle cells further modulate longitudinal signalling. In addition to their intimate coupling to the endothelium, smooth muscle cells throughout resistance networks are enmeshed by a plexus of perivascular nerves coursing along the adventitia. Upon physical stress, increased sympathetic nerve activity promotes vasoconstriction that competes against vasodilator signals arising from both skeletal muscle and endothelium. In turn, the activation of adrenergic receptors on smooth muscle cells generates second messengers (e.g., inositol trisphosphate and Ca^{2+}) that can diffuse through myoendothelial gap junctions to signal endothelial cells reciprocally. Independent of autacoid production, the opening of SK/IK (i.e., endothelium-dependent hyperpolarization) can thereby modulate vasoconstriction along the network while attenuating the efficacy of electrical conduction. Thus, irrespective of gap junctions, regulating ion channels in plasma membranes can govern local perfusion by modulating ascending vasodilatation. Such dynamic interactions between parenchymal cells, vascular cells and perivascular nerves effectively coordinate vasomotor activity throughout resistance networks to ensure perfusion according to local needs. Vasodilatation predominates in distal and intermediate arterioles, where sympathetic vasoconstriction is overridden as metabolic demand increases (i.e., "functional sympatholysis"). At the same time, resistance is maintained in proximal arterioles and feed arteries, where sympathetic neuroeffector signalling suppresses ascending vasodilatation via complementary actions on both smooth muscle and endothelium. While restricting dilatation of proximal vessels limits maximal tissue perfusion, the negative modulation of ascending vasodilatation maintains peripheral resistance and arterial perfusion pressure. In doing so, the integration of intercellular signalling underlying blood flow control ensures the ability to support the elevated demands of intense physical activity. Ongoing investigations focus on understanding how such key signalling events are altered by aging and disease.

Bagher P & Segal SS (2011). *Acta Physiol* **202**, 271-284.

Behringer EJ & Segal SS (2012). *J Physiol* **590**, 6277–6284.

Haug SJ & Segal SS (2005). *J Physiol* **563**, 541–555.

Segal SS (2005). *Microcirculation* **12**, 33-45.

Socha MJ, Segal SS *et al.* (2012). *Microcirculation* **19**, 715-770.

VanTeeffelen JWGE & Segal SS (2003). *J Physiol* **550**, 563-574.

Westcott EB & Segal SS (2013). *J Physiol* **591**,1251-1263.

Research support: Grants R37-HL041026 and R01-HL086483 from the National Institutes of Health, United States Public Health Service.

Where applicable, the authors confirm that the experiments described here conform with The Physiological Society ethical requirements.

L24

The renin-angiotensin system: new concepts and perspectives

R.A. Santos

Physiology and Biophysics, Federal University of Minas Gerais, Belo Horizonte, Minas Gerais, Brazil

It is well known that the renin-angiotensin system (RAS) is a key regulator of the cardiovascular system and the hydro-electrolyte balance. The classical concept of the RAS in which the octapeptide angiotensin II was the only biologically active end product has undergone important changes In the past years. The biological actions of this system are now considered to be performed by two main axes: ACE/Ang II/AT1R and ACE2/Ang-(1-7)/Mas. Resembling Ang II, Ang-(1-7) has pleiotropic actions in the body. However, in many instances the effectors of these two arms produce opposite effects. One of the most remarkable differences between Ang II and Ang-(1-7) is their opposite effect in blood vessels: Ang II is a potent vasoconstrictor while Ang-(1-7) is vasodilator. In the brain both peptides modulates the autonomic system activity producing similar effects in some regions (rostro-ventrolateral medulla for example) and opposite effects in others. Central administration of Ang-(1-7) increases the baroreflex control of arterial pressure while Ang II produces an opposite effect. Ang-(1-7) is importantly involved in cardiac function (inotropism, rhythmicity), modulation of regional vascular resistance and endothelial function, favoring the production of NO. It appears to be a key player in reproduction, acting both on ovarian and testicular function. Ang-(1-7) also influences glucose and lipid homeostasis. One of the most prominent actions of Ang-(1-7) is its anti-fibrotic effect which was demonstrated in the heart, lungs, liver, kidney and tumors. The widespread physiological influence of Ang-(1-7) in many organs and systems appears to be dependent of its stimulatory effect on AKT activity which plays a central role in molecular signaling. However, recent phosphoproteomic data indicate that in parallel to the Ca+2-independent activation of the PI3K/AKT pathway, Ang-(1-7) activates potent intra-cellular anti-proliferative pathways which may explain its anti-angiogenic/anti-tumoral activity. Recently studies have addressed the therapeutic potential of the ACE2/Ang-(1-7)/Mas axis. The results obtained with Mas stimulation or ACE2 activation in conditions such as myocardial infarction, hypertension, trombogenesis, heart fibrosis and stroke suggest that the relevance of angiotensin-(1-7) could go beyond its role in physiology. Recently we have identified a novel component of the RAS, the heptapeptide alamandine, which can be formed from angiotensin A by ACE2 and from Ang-(1-7) by decarboxilation of the aspartate residue . Alamandine produces effects resembling those of Ang-(1-7), including vasodilation and central cardiovascular effects at the

ventro-lateral medulla. However, differently from Ang-(1-7) it acts independent of Mas. Alamandine binds to the Mas-related protein G-Protein receptor, MrgD. These novel findings expanded our understanding of the RAS and opens new perspectives for further exploring its physiological significance and therapeutic possibilities.

CNPq, CAPES, FAPEMIG

Where applicable, the authors confirm that the experiments described here conform with The Physiological Society ethical requirements.

L25

TRPV1 channels: from molecules to physiology

T. Rosenbaum

Neurodevelopment and Physiology, Instituto de Fisiología Celular, Universidad Nacional Autónoma de México, Mexico, Mexico

Transient receptor potential (TRP) channels were first described in Drosophila, where photoreceptors carrying trp gene mutations exhibited a transient voltage response to continuous light (Cosens and Manning, 1969). Since that time the TRP channel family has grown to include at least 20 members. TRP channels exhibit a wide variety of functions: invertebrate phototransduction, responses to painful stimuli and to moderate temperature changes, regulation of intracellular calcium stores, receptor mediated excitation and modulation of the cell cycle. Despite the clear physiological importance of TRP channels, little is known about what regulates their function or about their structure.

One type of TRP channel, TRPV1, is a polymodal receptor that integrates a number of painful stimuli. These stimuli include: noxious heat,,extracellular acidification, with a pKa of about 5.3, anandamide and other arachidonic acid metabolites and capsaicin, a pungent extract from plants in the Capsicum family (Rosenbaum and Simon, 2007). A combination of electrophysiological, molecular biology and biochemical techniques has allowed us to study the structural and functional properties of the TRPV1 channel and we have determined important regions for its function. For example, by constructing several TRPV1- channel mutants in which cysteine residues were substituted for other amino acids and by using cysteine-modifying compounds, we have found a single cysteine residue located at the second ankyrin repeat of the N-terminus (C157) of TRPV1, which is solely responsible for activation of this channel by allicin, a pungent compound found in plants such as onions and garlic (Salazar et al., 2008).

We have also engineered a functional cysteineless-TRPV1 in which all 18 native cysteines were substituted for other amino acids and used it to perform experiments with cysteine-modifiers. These experiments have allowed us to locate the gate that controls ion fluxes through the TRPV1 channel to an intracellular region in the S6 transmembrane domain near residue Y671 as well as to identify a constriction in the pore (near residue L681), which impedes the passage of larger molecules to the pore (Salazar et al., 2009).

More recently, we have identified a new endogenous bioactive lipid that functions as a direct agonist of TRPV1, lysophosphatidic acid, and we have shown that this lisyolipid binds to residue K710 in the proximal C-terminus of TRPV1 that results in an increase of the open probability of the channel (Nieto-Posadas et al., 2012).

Although the field of TRP-channel study has observed important advances, further studies are still needed to fully comprehend how these proteins are gated.

Cosens, D.J., Manning, A., 1969. Abnormal electroretinogram from a Drosophila mutant. Nature 224(5216), 285-287.

Nieto-Posadas, A., Picazo-Juarez, G., Llorente, I., Jara-Oseguera, A., Morales-Lazaro, S., Escalante-Alcalde, D., Islas, L.D., Rosenbaum, T., 2012. Lysophosphatidic acid directly activates TRPV1 through a C-terminal binding site. Nature chemical biology 8(1), 78-85.

Rosenbaum, T., Simon, S.A., 2007. TRPV1 Receptors and Signal Transduction, in: Liedtke, W.B., Heller, S. (Eds.), TRP Ion Channel Function in Sensory Transduction and Cellular Signaling Cascades, Boca Raton (FL).

Salazar, H., Jara-Oseguera, A., Hernandez-Garcia, E., Llorente, I., Arias, O., II, Soriano-Garcia, M., Islas, L.D., Rosenbaum, T., 2009. Structural determinants of gating in the TRPV1 channel. Nature structural & molecular biology 16(7), 704-710.

Salazar, H., Llorente, I., Jara-Oseguera, A., Garcia-Villegas, R., Munari, M., Gordon, S.E., Islas, L.D., Rosenbaum, T., 2008. A single N-terminal cysteine in TRPV1 determines activation by pungent compounds from onion and garlic. Nature neuroscience 11(3), 255-261.

This work was supported by grants 58038 and CB-129474 from CONACyT, IN200308-3 and IN294111-3 from PAPIIT and by Fundación Miguel Alemán.

Where applicable, the authors confirm that the experiments described here conform with The Physiological Society ethical requirements.

L26

Purinergic signalling: the discovery and current developments

G. Burnstock

Autonomic Neuroscience Centre, University College London, London, UK

The talk will begin with a description of the discovery in the early 1970's of purinergic neurotransmission (i.e. ATP acting as a neurotransmitter) and the struggle we had for the next 20 years to establish this hypothesis. It is now recognised that the purinergic signalling system is one of the most ancient and widespread intercellular signalling systems in living tissue. The major conceptual steps leading to our current understanding of purinergic signalling will be described, including ATP as a cotransmitter, cloning and characterisation of P1 (adenosine), P2X (ATP) ion channel and P2Y (ATP, ADP, UTP, UDP) G protein-coupled receptors, physiological release of ATP by mechanical deformation of cells, identification of ectonucleotidases and both fast and long-term (trophic) purinergic signalling. Reference will be made to some of the key scientists who have influenced its development. Finally, some of the exciting areas of current interest will be considered, including in particular the pathophysiology of purinergic signalling and its therapeutic potential.

Where applicable, the authors confirm that the experiments described here conform with The Physiological Society ethical requirements.

L27

The molecular mechanisms of signaling at chemical synapses

E. Gouaux

Oregon Health & Science University, Oregon, OR, USA

Rapid signal transduction at chemical synapses involves calcium-dependent neurotransmitter release from presynaptic neurons, binding of transmitter to ligand-gated ion channels located primarily on the postsynaptic membrane, and subsequent uptake of transmitter by way of sodium-coupled neurotransmitter transporters. Chemical synapses can be defined by the released neurotransmitter and the class of receptor activated by the transmitter. The major classes of neurotransmitter receptors are, on the one hand, cation-permeable excitatory receptors and, on the other hand, anion-permeable inhibitory receptors. Whereas tetrameric ionotropic glutamate receptors that include AMPA, kainate and NMDA receptors are the primary neurotransmitter receptors that mediate fast excitatory neurotransmission, the pentameric, Cys-loop GABA and glycine receptors encompass the major group of receptors that participate in fast inhibitory neurotransmission. There are additional Cys-loop receptors, however, that are selective for cations, and these include the excitatory acetylcholine and serotonin receptors. Trimeric ATP-gated P2X receptors, together with the similarly trimeric yet amino acid sequence disparate acid-sensing ion channels define a final class of cation permeable receptors present in the central nervous system.
To resolve fundamental questions of receptor architecture and molecular mechanism, my research group has embarked on studies of neurotransmitter receptors using x-ray crystallographic, electrophysiological and biochemical methods. We are particularly interested in understanding the mechanism by which agonist binding leads to receptor activation, the molecular principles that underlie receptor desensitization or inactivation, and the chemical and structural basis for ion selectivity, ion channel block and allosteric modulation of receptor activity. Over the past several years we have elaborated the atomic structures of intact trimeric acid sensing ion channels and ATP-gated P2X receptors, tetrameric AMPA receptors and pentameric Cys-loop receptors in multiple conformational states and in complexes with a wide array of agonists, antagonists, toxins, ions and allosteric modulators. Here I will define the overall architectures of these receptors and provide molecular mechanisms for their activities at chemical synapses that are grounded in experimental structural data at atomic resolution.

Where applicable, the authors confirm that the experiments described here conform with The Physiological Society ethical requirements.

L28

How are memories represented and recollected by the human brain?

E.A. Maguire

Wellcome Trust Centre for Neuroimaging, University College London, London, UK

We are endlessly fascinated with memory – we desire to improve it and fear its loss. While it has long been recognised that brain regions such as the hippocampus are vital for supporting memories of our past experiences, we still lack fundamental knowledge about the mechanisms involved. This is because studying the neural signatures of memories in vivo in humans presents a significant challenge. However, recent developments in high-resolution structural and functional magnetic resonance imaging coupled with advanced analysis methods now permit access to hippocampal processing that has hitherto been precluded in humans. In this talk I will describe how the application of 'decoding' techniques to brain imaging data is now beginning to disclose how individual memory representations develop and change, while also illuminating why some people have clearer memories than others, and why confusion about past experiences characterises normal aging and pathological states.

Supported by the Wellcome Trust.

Where applicable, the authors confirm that the experiments described here conform with The Physiological Society ethical requirements.

L29

Rho proteins in cardiovascular physiology and diseases

G. Loirand

Inserm UMR_S1087, Nantes, France

Small G proteins exist in eukaryotes from yeast to human and constitute the Ras superfamily comprising more than 100 members. This superfamily is structurally classified into five families: the Ras, Rho, Rab, Arf and Ran families that control a wide variety of cell and biological functions through highly coordinated regulation processes. Among them, proteins of the Rho family are initially described as master regulators of the actin and microtubule cytoskeletons, thus regulating numerous cellular functions, including migration, membrane trafficking, adhesion, polarity and cell shape changes. However, increasing evidence has accumulated to identify Rho proteins and their regulators as key players of the cardiovascular physiology that control a large panel of cardiac (heart rhythm, contraction, hypertrophy) and vascular functions (angiogenesis, vascular permeability, vasoconstriction).
Indeed, basal Rho protein activity is required for homeostatic functions in physiological conditions, but sustained over-activation of Rho proteins or spatiotemporal dysregulation of Rho signalling pathways has pathological consequences in the cardiovascular system. Both pharmacological studies, genetic approaches in human, mouse models with targeted mutations in Rho proteins or regulators genes enabled the analysis of Rho protein functions in vivo, demonstrating their involvement in the pathogenesis of several diseases, including hypertension, coronary vasospasm, stroke, atherosclerosis, heart failure and diabetes. Accordingly, Rho protein signalling pathway and Rho proteins effectors such as Rho kinases are considered as important new pharmacological targets for the next generation of therapeutic agents in cardiovascular medicine. The primary object of this lecture is to provide a comprehensive overview of the current progress in our understanding of the role of Rho proteins and their regulators in cardiovascular physiology and pathologies and describing challenges for the future.

Where applicable, the authors confirm that the experiments described here conform with The Physiological Society ethical requirements.

L30

Sensing, signaling and sorting pathways in kidney epithelial cells

D. Brown, T.G. Paunescu, R. Bouley, S. Breton and H.A. Lu

Center for Systems Biology and Division of Nephrology/Program in Membrane Biology, Massachusetts General Hospital and Harvard Medical School, Boston, MA, USA

Maintaining tight control over body fluid and acid/base homeostasis is essential for human health and is a major function of the kidney. This presentation will briefly outline new findings that have emerged over the past 2 or 3 years related to the function of two distinct cell types in the kidney collecting duct that are highly specialized to regulate water reabsorption (principal cells) and acid/base balance (intercalated cells) (1). Our work addresses the cell biological and signaling mechanisms that allow these cells to maintain systemic homeostasis by responding to physiological variations in plasma osmolality/volume and pH.

Principal cells: The antidiuretic hormone vasopressin (VP) and its receptor, the V2R, play a central role in regulating the urinary concentrating mechanism by stimulating accumulation of aquaporin 2 (AQP2) water channels in the plasma membrane of collecting duct principal cells (1). This increases epithelial water permeability and allows osmotic water reabsorption to occur. Knowledge of the basic V2R signaling pathways and their effect on AQP2 trafficking in epithelial cells is critical for the development of new therapeutic strategies for diseases such as nephrogenic diabetes insipidus, in which VP signaling is defective. We will summarize efforts to bypass defective V2R signaling in principal cells to induce AQP2 plasma membrane accumulation with agents such as sildenafil citrate and statins, and with the hormone calcitonin. A novel chemical screening assay is currently being used to identify new compounds that may be useful to regulate AQP2 trafficking in the context of urinary concentrating disorders. Finally, the potential role of AQP2 in renal development via an interaction with integrins will be discussed (3).

Intercalated cells: Urinary acidification due to the activation of intercalated cells is also critical to organ function, and defects lead to several pathological conditions in humans. We are striving to understand how these “professional” proton secreting cells respond to cellular and environmental cues, and some key work in this area was summarized in a recent review (2). One potential signaling pathway that intercalated cells might use to detect acid/base imbalances involves the soluble adenylyl cyclase, sAC, which could function as a luminal bicarbonate sensor in renal tubules to regulate acid/base homeostasis (6). By generating cAMP in response to elevated tubular bicarbonate, this pathway results in apical plasma membrane accumulation of the vacuolar H+ATPase (V-ATPase) (7), which increases acid secretion in an attempt to reduce systemic acidosis caused by inappropriate bicarbonate excretion. Other stimuli for proton secretion in these cells include, but are not limited to, aldosterone and angiotensin II.

As part of this work, we generated mice that express EGFP in their intercalated cells, driven by the promoter of the B1 V-ATPase subunit (5), as well as mice that lack specific V-ATPase subunits. These animal models, as well as intercalated cells isolated from our EGFP-expressing mice by fluorescence activated cell sorting are being used for various studies, including proteomic (4) and gene expression analysis, cell specific signaling studies, kidney function analysis, and differentiation pathways. Some of this recent and ongoing work will be addressed in this presentation.

Brown D, Bouley R, Paunescu TG, Breton S, and Lu HA: New insights into the dynamic regulation of water and acid/base balance by renal epithelial cells. Am J Physiol Cell Physiol 2012.

Brown D, and Wagner CA: Molecular mechanisms of acid-base sensing by the kidney. J Am Soc Nephrol 23: 774-780, 2012.

Chen Y, Rice W, Gu Z, Li J, Huang J, Brenner MB, Van Hoek A, Xiong J, Gundersen GG, Norman JC, Hsu VW, Fenton RA, Brown D, and Lu HA: Aquaporin 2 promotes cell migration and epithelial morphogenesis. J Am Soc Nephrol 23: 1506-1517, 2012.

Da Silva N, Pisitkun T, Belleannee C, Miller LR, Nelson R, Knepper MA, Brown D, and Breton S: Proteomic analysis of V-ATPase-rich cells harvested from the kidney and epididymis by fluorescence-activated cell sorting. Am J Physiol Cell Physiol 298: C1326-1342, 2010.

Miller RL, Zhang P, Smith M, Beaulieu V, Paunescu TG, Brown D, Breton S, and Nelson RD: V-ATPase B1-subunit promoter drives expression of EGFP in intercalated cells of kidney, clear cells of epididymis and airway cells of lung in transgenic mice. Am J Physiol Cell Physiol 288: C1134-1144, 2005.

Paunescu TG, Da Silva N, Russo LM, McKee M, Lu HA, Breton S, and Brown D: Association of soluble adenylyl cyclase with the V-ATPase in renal epithelial cells. Am J Physiol Renal Physiol 294: F130-138, 2008.

This work was supported by NIH grants DK73266 (TGP), DK42956 (DB), DK97124 and HD40793 (SB). We thank all of our many colleague who contributed to the work outlined in this presentation.

Where applicable, the authors confirm that the experiments described here conform with The Physiological Society ethical requirements.

L31

Cortical HCN channels: function, trafficking and plasticity

M.M. Shah

UCL School of Pharmacy, London, UK

The hyperpolarization-activated cyclic nucleotide gated (HCN) channels are voltage-gated ion channels that are active at rest and are important for determining the intrinsic membrane properties of neurons. Four HCN subunits (HCN1-4) have been cloned, with HCN1 predominantly expressed in the cortex. These subunits are abundant in cortical pyramidal neuron dendrites but can also be located in synaptic terminals and axons. In this lecture, I will highlight work on the involvement of these channels in dendritic excitability, synaptic release and epileptogenesis in the entorhinal cortex (EC), an area of the brain involved in normal physiological processes such as spatial navigation and cognition as well as pathophysiological conditions such as epilepsy. I will also present work on the distinct molecular mechanisms underlying trafficking of these channels to dendritic and pre-synaptic compartments. This lecture should, thus, provide an insight into the role of these channels in regulating cortical neuronal function and the potential consequences of this for cognition and epilepsy.

Funded by the European Research Council, Medical Research Council, Wellcome Trust and Royal Society

Where applicable, the authors confirm that the experiments described here conform with The Physiological Society ethical requirements.

L32

Respiratory and neural consequences for fish of a warmer and more carbonated future

G.E. Nilsson

Department of Biosciences, University of Oslo, Oslo, Norway

Average sea-surface temperature and the amount of CO_2 dissolved in the ocean are rising due to increasing concentrations of atmospheric CO_2. Many coral reef fishes appear to be living close to their thermal optimum, and for some of them, even relatively moderate increases in temperature (2 - 4°C) lead to significant reductions in aerobic scope (i.e. the difference between resting and maximum rates of oxygen uptake). Reduced aerobic capacity could affect population sustainability since less energy can be devoted to feeding and reproduction. Coral reef fish seem to have limited capacity to acclimate to elevated temperature as adults, but recent research shows that developmental and transgenerational plasticity occur, which might enable some species to adjust to rising ocean temperatures. A mayde even greater worry is that, even at maintained water temperatures, predicted future rises in ocean CO_2 levels have been found to alter sensory responses and behaviour of marine fishes. Changes include increased boldness and activity, loss of behavioural lateralization, altered auditory preferences and impaired olfactory function. It has been found that impaired olfactory function makes larval coral reef fish attracted to odours they normally avoid, including ones from predators and unfavourable habitats. These behavioural alterations have significant effects on mortality that may have far-reaching implications for populations. However, the underlying mechanism linking high CO_2 to these diverse responses has been unknown until recently. I will present results showing that abnormal olfactory preferences and loss of behavioural lateralization exhibited by two species of larval coral reef fish exposed to high CO_2 can be rapidly and effectively reversed by treatment with an antagonist of the GABA-A receptor. GABA-A is a Cl- / bicarbonate channel and a major neurotransmitter receptor in the vertebrate brain. These results indicate that high CO_2 interferes with brain ion-balance and thereby neurotransmitter function, a hitherto unrecognized threat to marine populations and ecosystems. Given the ubiquity and conserved function of GABA-A receptors, this predicts that rising CO_2 levels could cause sensory and behavioural impairment in a wide range of marine animals.
See Munday et al. (2012) and Nilsson et al. (2012) for further reading.

Munday PL, McCormick MI & Nilsson GE (2012). Impact of global warming and rising CO2 levels on coral reef fishes: what hope for the future? *J. Exp. Biol.* **215**, 3865-3873.

Nilsson GE, Dixson DL, Domenici P, McCormick MI, Sorensen C, Watson SA & Munday PL (2012). Near-future carbon dioxide levels alter fish behaviour by interfering with neurotransmitter function. *Nature Clim. Change* **2**, 201-204.

Supported by the University of Oslo and the Scandinavian Physiological Society

Where applicable, the authors confirm that the experiments described here conform with The Physiological Society ethical requirements.

SA1

Regulation of tonic inhibition in the hippocampus

M. Walker[1], I. Pavlov[1], A.C. Linthorst[2] and A. Semyanov[3,4]

[1]UCL Institute of Neurology, London, UK, [2]Henry Wellcome Laboratories for Integrative Neuroscience and Endocrinology, University of Bristol, Bristol, UK, [3]RIKEN Brain Science Institute, Wako-shi, Japan and [4]Nizhny Novgorod State University, Nizhny Novgorod, Russian Federation

Activation of GABA(A) receptors (GABARs) produces two forms of inhibition: phasic inhibition generated by the rapid, transient activation of synaptic GABARs by presynaptic GABA release, and tonic inhibition generated by the persistent activation of perisynaptic or extrasynaptic GABARs, which can detect extracellular GABA. Tonic GABAR-mediated currents are present in multifarious neuronal subtypes in the hippocampus, but are predominantly mediated by alpha5 subunit-containing and delta subunit-containing GABA(A) receptors.

These tonic currents have a profound effect upon neuronal excitability, and can be regulated over different time scales through receptor expression, receptor modulation and changes in extracellular GABA concentrations. This talk will present recent evidence on the regulation of extracellular GABA in the hippocampus and its impact on tonic inhibition, and on how extrasynaptic GABA(A) receptor characteristics contribute to the their computational role.

In vivo, GABA concentrations in the hippocampus (measured using microdialysis) under resting conditions are of the order of 100 nM, and even lower concentrations are detected by principal neurons. The tight regulation of extracellular GABA is maintained by effective GABA transporters: GAT1 which mainly regulates GABA originating from the synaptic pool, and GAT3 which predominantly regulates GABA originating from the extrasynaptic pool. GAT3 can also contribute to regulation of synaptically released GABA when GAT1 is blocked or when network activity increases.

The low concentration of GABA during resting condition means that a substantial proportion of the tonic current is mediated by spontaneously opening GABARs. These spontaneously opening GABARs maintain a lower limit to tonic inhibition and permit regulation through modulators even when GABA is not being detected. Spontaneously opening receptors also have a different pharmacology from openings due to GABA binding.

Increases in synaptic activity can raise the extracellular GABA; during seizure-like activity, the GABA can rise 3-4 fold. This results in increases in tonic currents, both through direct activation of GABARs and also through GABA(B) receptor-dependent enhancement of extrasynaptic GABAR function. This increase in tonic currents generally inhibits neurons, but can have biphasic effects in interneurons in which the GABAR reversal potential is depolarizing relative to resting membrane potential.

The computational effect of increasing extrasynaptic GABR activation is partly dependent upon the current-voltage characteristics of the receptors, which show marked outward rectification. This results in a shunting effect of tonic inhibition at spiking threshold with a much lesser effect on noise at resting membrane potential. The consequence of this outward rectification is that tonic currents in pyramidal cells affect offset of the input-output function of neurons without affecting gain. In contrast, synaptic inhibition affects both offset and gain.

In temporal lobe epilepsy, in which there is a shift from phasic to tonic inhibition, the input-output functions of neurons would be expected to have maintained off-set but increased gain. We hypothesize that such a change results in network instability, contributing to the sporadic occurrence of seizures.

Wlodarczyk AI, Sylantyev S, Herd MB, Kersanté F, Lambert JJ, Rusakov DA, Linthorst AC, Semyanov A, Belelli D, Pavlov I, Walker MC. GABA-Independent GABAA Receptor Openings Maintain Tonic Currents.J Neurosci. 2013;33(9):3905-14

Kersanté F, Rowley SC, Pavlov I, Gutièrrez-Mecinas M, Semyanov A, Reul JM, Walker MC, Linthorst AC. A functional role for both GABA transporter-1 and GABA transporter-3 in the modulation of extracellular GABA and GABAergic tonic conductances in the rat hippocampus. J Physiol. 2013 (in press)

Pavlov I, Savtchenko LP, Kullmann DM, Semyanov A, Walker MC. Outwardly rectifying tonically active GABAA receptors in pyramidal cells modulate neuronal offset, not gain. J Neurosci. 2009;29(48):15341-50.

Song I, Savtchenko L, Semyanov A. Tonic excitation or inhibition is set by GABA(A) conductance in hippocampal interneurons. Nat Commun. 2011 Jul 5;2:376

Scimemi A, Semyanov A, Sperk G, Kullmann DM, Walker MC.Multiple and plastic receptors mediate tonic GABAA receptor currents in the hippocampus.J Neurosci. 2005;25(43):10016-24

Pavlov I, Walker MC. Tonic GABA(A) receptor-mediated signalling in temporal lobe epilepsy.

Neuropharmacology 2013 (in press)

Semyanov A, Walker MC, Kullmann DM. GABA uptake regulates cortical excitability via cell type-specific tonic inhibition. Nat Neurosci. 2003;6(5):484-90.

Wellcome Trust, Medical Research Council (UK), Epilepsy Research UK and European Integrated Project "EPICURE" (EFP6-037315).

Where applicable, the authors confirm that the experiments described here conform with The Physiological Society ethical requirements.

SA2

The role of GABAergic interneurons in controlling information flow through the cerebellar cortex

B. Stell

C.N.R.S., Paris, France and Université Paris Descartes, Paris, France

The coordinated simple spike activity of neighboring Purkinje cells has been studied extensively using electrophysiological techniques in both awake animals and cerebellar slices (Person and Raman, 2012). However, electrophysiological recordings have restricted the spatial extent to which this coordination has been examined. We demonstrate that fluorescent calcium indicators can be used as a highly effective readout of simple spike activity, and allow the monitoring of this activity in many Purkinje cells simultaneously. By imaging multiple Purkinje cells, a degree of spatial information is retained and it becomes possible to probe components of the cerebellar circuit and view how information flows out of the cerebellar cortex via these cells. Using this method to examine spontaneous Purkinje cell activity, we find highly coordinated pauses between cells that is dependent upon GABA-A receptor activation. Furthermore, activation of molecular layer interneurons with either electrophysiological or channelrhodopsin stimulation, induces pauses that are coordinated between neighboring Purkinje cells. These coordinated pauses are likely play a large role in controlling spiking of the deep cerebellar

nuclear cells which in turn output the information from the cerebellum.

Person, A., and Raman, I. (2012). Synchrony and neural coding in cerebellar circuits. Frontiers in neural circuits, 6(December), 1–15. doi:10.3389/fncir.2012.00097

Where applicable, the authors confirm that the experiments described here conform with The Physiological Society ethical requirements.

SA3

Metabolic hormones turn-on GABA-A channels that generate tonic inhibition

B. Birnir, Z. Jin and S. Korol

Department of Neuroscience, Uppsala University, Uppsala, Sweden

The hippocampus is an established center for memory and learning but it is less well known that it also governs body physiology. It is, therefore, not surprising that the hippocampus can sense physiological parameters and robustly expresses a number of receptors for a variety of molecules including metabolic hormones (1). We, nevertheless, know relatively little about how the metabolic hormones modulate hippocampal neuronal function. Do the hormones modulate the excitatory or the inhibitory system or both? Or, when there is too much or too little of these molecules e.g. insulin or glucagon-like peptide-1 (GLP-1), do these hormones then contribute to or even cause disease states, like decreased memory formation, increased seizure frequency or strength or even neuronal death like can occur in dementia, Alzheimer disease, epilepsy, diabetes and multiple sclerosis? We have studied the effects of insulin and GLP-1 on GABA-activated currents in rat hippocampal pyramidal neurons. The insulin receptor is prominently expressed in the hippocampus suggesting that insulin regulates hippocampal function (1). We have identified a molecular target of insulin signaling in the CA1 pyramidal neurons, the output neurons of the hippocampus (2). In acute hippocampal brain slices, physiological concentrations of insulin (1 nM) "turn-on" new, extrasynaptic GABA-A receptors in the CA1 pyramidal neurons. These channels are activated by more than a million times lower GABA concentration (EC50 17 + 4 pM) than the synaptic channels and generate tonic currents. The channels are inhibited by GABA-A receptors antagonists and have novel pharmacology as flumazenil and zolpidem are inverse agonists. The results are consistent with the channels containing at least $\alpha5\beta\gamma2$ GABA-A receptor subunits. Activation of the channels results in decreased action potential firing. Importantly, our results show that tonic rather than synaptic conductances regulate basal neuronal excitability when significant tonic conductance is expressed. GLP-1, another metabolic hormone, is secreted by intestinal L cells. Application of GLP-1 (10 pM – 10 nM) or its analog exendin-4 (10 - 100 nM) evoked tonic currents and increased the frequency of synaptic GABA-activated currents as compared to control in the rat hippocampal CA3 pyramidal neurons. The neuronal membrane potential hyperpolarized upon GLP-1 application and the action potential frequency decreased. When GLP-1 was removed, the membrane potential depolarized back to the initial value and the action potential frequency recovered (n = 5). Our findings demonstrate an unexpected hormonal control of GABA-A receptor subtypes and excitability of hippocampal neurons. The results have implications for not only normal function but also diseases of the hippocampus.

1. Lathe R (2001) Hormones and the hippocampus. J Endocrinol 169: 205-231.

2. Jin Z, Jin Y, Mendu SK, Degerman E, Groop L, Birnir B (2011) Insulin reduces neuronal excitability by turning on GABA-A channels that generate tonic current. PLoS One 6: e16188.

Where applicable, the authors confirm that the experiments described here conform with The Physiological Society ethical requirements.

SA4

Tipping the balance between cortical excitation and inhibition

O. Yizhar

Weizmann Institute of Science, Rehovot, Israel

Excitation and inhibition in neocortical circuits are finely tuned and the balance between them is tightly regulated. Multiple lines of evidence, from psychiatric disease patients and animal models of psychiatric disease, have led to the hypothesis that changes in the cellular balance between excitation and inhibition (E/I balance) could lead to the severe behavioral deficits associated with diseases such as epilepsy, autism and schizophrenia. To evaluate this hypothesis experimentally, we developed several new optogenetic tools that allow simultaneous modulation of neocortical excitatory and inhibitory neurons. Microbial opsin-based optogenetic tools allow genetically-encoded, light-based control of neural circuits in vivo. The use of microbial opsins as optogenetic tools requires robust delivery of the opsin gene products to the plasma membrane of targeted neurons, efficient modulation of targeted cells through in vivo light delivery and readout strategies for recording the electrophysiological and behavioral outcomes of optical manipulation. We created a set of engineered channelrhodopsins with distinct spectral and temporal properties and targeted these optogenetic tools to cortical excitatory or inhibitory neurons. With this approach, we bidirectionally modulated the cellular excitation-inhibition balance in the prefrontal cortex of awake, behaving mice. We found that elevation, but not reduction, of the cellular E/I balance within the medial prefrontal cortex leads to profound impairment in cellular information processing and is associated with both specific behavioral deficits and increased high-frequency power in the 30–80 Hz range. Our results demonstrate the utility of new optogenetic tools in modulating neural activity and provide support for the cellular E/I balance hypothesis in neuropsychiatric disease.

Where applicable, the authors confirm that the experiments described here conform with The Physiological Society ethical requirements.

SA5

Inflammation and GABA-A receptors

B. Orser

Physiology and Anesthesia, University of Toronto, Toronto, ON, Canada

Inflammation causes deficits in learning and memory deficits through mechanisms that remain poorly understood. I will present evidence that memory loss associated with inflammation involves the same receptors that mediate the memory blocking properties of a variety of drugs, including anesthetics and benzodiazepines. Our results show that key pro-inflammatory cytokines including interleukin-1β (IL-1β)

increase the activity of α5 subunit-containing γ- aminobutyric acid type A (α5GABAA) receptors. This increase in receptor activity reduces long-term potentiation, a synaptic correlate of memory, in hippocampal slices from wild-type mice. Further, IL-1β induced memory deficits were observed in WT but not Gabra5-/- mice. Collectively, the results show that α5GABAA receptor activity increases during inflammation and this increase is critical for inflammation-induced memory deficits.

Where applicable, the authors confirm that the experiments described here conform with The Physiological Society ethical requirements.

SA7

Interplay between molecules of adaptive homeostasis and their interaction with hypobaric hypoxia

Q. Pasha

CSIR-Institute of Genomics and Integrative Biology, Delhi, India

High-altitude (HA), the elevation above 8,000 feet, is responsible for low partial pressure of air and as a consequence reduced blood arterial oxygen saturation (SaO2) in the body. Out of many characteristic features of the HA environment, it is the hypobaric hypoxia that has the main effect on living beings and is the chief driving force for major acclimatization and adaptive processes. When exposed to this environment body undergoes various physiological changes so as to maintain the O2 availability to the tissue.

The HA natives because of generations of inhabitation have acquired unique phenotypes. Compared to the HA natives, the lowland population when exposed to a similar environment reacts differentially. There are sojourners with no signs of discomfort whereas few of them experience discomfort and develop mountain disorders. Among the various mountain disorders, HA pulmonary edema (HAPE) is a unique disorder of concern especially to sojourners. It is a multi-factorial trait characterized by hypoxic pulmonary vasoconstriction, endothelial dysfunction and intra-vascular fluid retention that are contributed effectively and equally by genetic and epigenetic factors. Hence, any kind of perturbation in the regular O2 supply of the body disturbs pathways maintaining vascular and adaptive homeostasis resulting in organ dysfunction. As a consequence, the genes of these pathways become obvious candidates and hence, *Apelin (APLN), Apelin receptor (APLNR), Endothelial nitric oxide synthase (NOS3)* and *HIF-prolyl hydroxylase 2 (EGLN1)* have been elucidated in HAPE pathophysiology and adaptation. The human ethical committees of Institute of Genomics and Integrative Biology and SNM hospital have approved the study.

In a comparative study of healthy highlanders (HLs) and sojourners i.e. HAPE-free controls (HAPE-f) and HAPE-patients (HAPE-p), the distribution of alleles, haplotypes, interacting genotypes, epigenetic regulations and their association with clinical and biochemical parameters provided some interesting insights. The healthy HLs and HAPE-f had significantly higher level of SaO_2 compared to HAPE-p (P<0.0001). Likewise, pulmonary arterial systolic pressure (PASP) was also significantly lower in these healthy subjects. The higher SaO2 and lower PASP levels clearly signify better physical capabilities in health and vice versa in diseased state. Analysis of genotype distribution revealed significant differences in the SNPs of *EGLN1, APLN, APLNR* and *NOS3* with respect to adaptation and HAPE. The 4.55-fold upegulated *EGLN1* expression in HAPE-p (P=0.0084) when compared with HAPE-f suggested that this upregulation caused dysfunctioning of HIF1α prohibiting downstream genes from maintaining cellular O2 homeostasis. Furthermore, the risk variants rs1538664A, rs479200T, rs2486729A, rs2790879G, rs480902C, rs2486736A, and rs973252G and the respective haplotypes A-T-A-G-C-A-G, G-T-A-G-C-A-G, and G-T-G-T-C-G-A, which were over-represented in HAPE, correlated with decreased SaO2 level and increased EGLN1 expression.

The 11.7 Kb long APLN sequencing showed the presence of CpG islands. The significantly higher percentage of methylation in these islands in HAPE-p seems to be responsible for downregulation of APLN expression (P>0.05). The *APLN* and *APLNR* expression was down-regulated by 3.52- and 2.35-fold in HAPE-p (P=0.003 and 0.068). Similarly, the APLN-13 levels were down-regulated in the patients compared to HAPE-f and HLs (P<0.0001). Further, analysis of risk variants *APLN* rs3761581G, rs2235312T and *APLNR* rs11544374A revealed association with decreased APLN levels and gene expression (P<0.05). As APLN-APLNR system brings its effect through activation of NOS3; therefore, the role of NOS3 was perceptible. *NOS3* expression was upregulated by 5.2-fold in HLs (P=0.0015) when compared to HAPE-f and NO levels were 57.67 ±35.5 μmol/L, 73.75 ±49.9 μmol/L and 122.45 ±103.3 μmol/L in HAPE-p, HAPE-f and HLs (P<0.0001). The significant down-regulation of APLN and NO suggested the disruption of APLN-APLNR system in HAPE. Of note, the genotypes interactions between the genes depicted few best disease pre¬dicting models in HAPE (P<0.05).

To conclude, the association of EGLN1 SNPs rs1538664, rs479200, rs2486729, rs2790879, rs480902, rs2486736, and rs973252 with SaO2 levels and *EGLN1* expression, *APLN* SNPs rs3761581, rs2235312 and *APLNR* SNPs rs11544374 with APLN levels and *APLN* expression and *NOS3* SNPs rs7830, rs1799983 and 4b/4a with NO levels and *NOS3* expression portrayed the functional consequences of these variants at HA. In addition, this extreme environment influences the epigenetic regulation as is evident through higher methylation of *APLN*.

Where applicable, the authors confirm that the experiments described here conform with The Physiological Society ethical requirements.

SA6

Mild hypoxia regulate the property/function of neural stem cells *in vitro*

L. Zhu, X. Huang and M. Fan

Department of Cognitive Sciences, Institute of Basic Medical Sciences, Beijing 100850, China, Beijing, China

Neural stem cells(NSCs) exist widely in the developing and adult mammalian brain, which are self-renewing and can differentiate into neurons, astrocytes or oligodendrocytes in vitro. The proliferation of NSCs in vitro has been reported to be regulated by various factors. However, growing studies by the use of oxygen microelectrodes show that the mammalian embryo developed in uterus with a hypoxic environment and neural stem or progenitor cell in the brain are also with hypoxic niche. The mean oxygen concentration is about 1-5% in tissues. To date, in vitro studies using NSCs have primarily been done under atmospheric conditions of 20% oxygen as the standard culture system. This indicates that traditional oxygen concentration in cell culture system may be a hyperoxia environment but not a condition of “physiological hypoxia” to most of cells in situ. Herein, we performed a series of experiments to testify whether the exogenous hypoxia could impact the

growth of NSCs and their function? How hypoxia regulates the property of NSCs? And then what's the molecular involved in this process?

Firstly, we compared the different exogenous oxygen content on the NSCs' growth in vitro. The embryo-derived neural stem cells were cultured under the 3%,10% and 20% oxygen concentration. There are about 2- to 5- fold increases in the number of NSCs cultured after exposure to hypoxia condition compared to normal condition. Especially, mild hypoxia dramatically promotes the proliferation of NSCs and decreases its apoptosis. The above results were further confirmed in both mouse and human-derived neural stem cells from embryo and adult, which revealed that neural stem cells in vitro prefer 1 to 10% oxygen culture environment. Thus, Mild hypoxia (1-10% oxygen) is a much more potent trigger to promote the proliferation of adult stem cells than normoxia (20% oxygen), suggesting mild hypoxia is a novel method for expansion of various adult stem cells in vitro.

We further examine the differentiation ability of NSCs expanded under hypoxia conditions in vitro. The NSCs cultured in hypoxia (3% O2) displayed an increase in the percentage of neurons. Especially the percentage of TH-positive neurons differentiated from NSCs in lowered oxygen increased significantly. Dopamine (DA) content in supernatant of culture hypoxia group was the double of that in the normoxia group. This study may also offer a new approach to yield DA neurons by using a physical factor.

The data above demonstrate that low oxygen significantly promotes the proliferation of NSCs and supports the property of self-renewal in vitro. However, the molecular mechanisms underlying this hypoxia-driven proliferation are unknown. To address this question, a cDNA microarray containing 5704 rat genes was used to characterize the gene expression pattern during hypoxia-driven proliferation of NSCs. Of the 5704 genes examined, 49 were down-regulated less than 0.5-fold and 22 were upregulated more than twofold at 24 h. At 72 h, 60 genes were upregulated and 11 were downregulated. Among the 71 differentially expressed genes identified at 24 h, the greatest number were involved in glycolysis and metabolism (36%), followed by transcriptional regulation (15%) and cell organization and biogenesis (10%). The NSCs under low oxygen consumed more glucose and produced energy by glycolysis. The information gained from gene expression and metabolic changes of NSCs under low oxygen conditions will provide new approaches for the evaluation of NSCs as potential in vivo cellular therapeutics.

Without doubt, Hypoxia-inducible factor (HIF)-1, which is one of the key transcription factors under hypoxia, play an important role mediating a variety of adaptive cellular and systemic responses to hypoxia by regulating the expression of more than 50 different genes. The hypoxia-induced Small non-coding RNA (ncRNA) was investigated and shown involved in regulation of NSC proliferation. Results revealed that 15 small RNAs were up-regulated at least threefold and 11 were down-regulated in NSCs after subjected to hypoxic conditions. Especially, MiR-210 was observed to be highly expressed in NSCs in a time- and oxygen-dependent manner, and is directly regulated by HIF-1a. Hypoxia-induced expression of miR-210 may be involved in regulating apoptosis and proliferation of NSCs under hypoxia.

In summary, our studies demonstrate that mild hypoxia not only promote the self-renew ability of NSCs in vitro, but also increase their differentiation ability into neurons. Therefore, via expansion of NSCs in vitro or modification of it's' property in situ, mild hypoxia could become a potential approach for allograft cell transplantation. We hope these findings will aid in the transplantation of NSCs to treat neural degenerative diseases such as Parkinson's disease and brain trauma.

Where applicable, the authors confirm that the experiments described here conform with The Physiological Society ethical requirements.

SA9

Andean, Tibetan and East African patterns of adaptation to high-altitude hypoxia

C.M. Beall

Case Western Reserve University, Cleveland, OH, USA

Low ambient partial pressures of oxygen at high altitudes result in low alveolar and arterial partial pressures that stress physiological oxygen delivery systems. People moved onto high-altitude plateaus in three areas of the world in the past 10,000 or more years, resulting in independent natural experiments in adaptation and evolution. Unexpectedly, the high-altitude native populations of the Andean, Tibetan and East African plateaus have different suites of adaptive traits and their genomes show different signatures of natural selection despite the common stress. This talk presents aspects of the three patterns of adaptation, their relative costs and benefits, and evidence that they result from evolutionary processes. The variety of responses to the same stress expands our understanding of oxygen homeostasis.

Where applicable, the authors confirm that the experiments described here conform with The Physiological Society ethical requirements.

SA8

Work capacity and selected physiological factors by ethnicity and residential altitude – cross-sectional studies of 9- to 10-year-old children in Tibet

B. Bianba

Tibet University Medical College, Lhasa, China and University of Oslo, Oslo, Norway

The objective of the present study is to compare work capacity (maximal power output) and selected physiological factors (arterial oxygen saturation and heart rate at rest and during maximal exercise, hemoglobin concentration and forced vital capacity) in groups of native Tibetan children living at different residential altitudes (3,700 vs. 4,300 m above sea level) and across ethnicity (native Tibetan vs. Han Chinese children living at the same altitude of 3,700 m). The maximal power output was 2.68 ±0.49 W/kg in native Tibetans at 3,700 m, which was 3.5% higher than Han Chinese at 3,700 m (2.59 ±0.48 W/kg), and 19.6% higher than native Tibetans at 4,300 m (2.24 ±0.56 W/kg). The superior work capacity in native Tibetans vs. Han Chinese may reflect a better adaptation to life at high altitude. Tibetans at a lower residential altitude of 3,700 m demonstrate a better work capacity than residents at a higher altitude of 4,300 m. The associations between residential altitude and ethnicity with maximal power output could not be fully explained by the measured physiological factors. However, several physiological parameters explained the variance in work capacity, including higher arterial oxygen saturation and higher forced vital capacity.

Where applicable, the authors confirm that the experiments described here conform with The Physiological Society ethical requirements.

SA10

Mechanisms of thermo- and chemosensing in TRP channels

T. Voets

Laboratory of Ion Channel Research, KU Leuven, Leuven, Belgium

The ability to sense environmental temperatures and to avoid noxious heat or cold is crucial for the survival of all organisms. In mammals, sensory neurons from dorsal root and trigeminal ganglia convey thermal information from the skin, mouth and nose to the central nervous system. Recent evidence has established that thermoTRPs, a subset of the TRP superfamily of cation channels, act as primary temperature sensors in cold- and heat-sensitive neurons. The gating of these thermoTRPs exhibits strong temperature dependence, leading to steep changes in inward current upon heating or cooling. Moreover, several natural or synthetic compounds act as ligands of thermoTRPs, thereby creating sensations of cold or hot independent of actual changes in temperature.
In this presentation, I will present our latest insights in how these channels detect and integrate thermal and chemical stimuli, and discuss the in vivo consequences of thermoTRP gating .

Our work on thermoTRPs is supported by grants from the Belgian Federal Government (IUAP P7/13), the Research Foundation-Flanders (F.W.O.) (G.0565.07), and the Research Council of the KU Leuven (GOA 2009/07 PF-TRPLe).

Where applicable, the authors confirm that the experiments described here conform with The Physiological Society ethical requirements.

SA11

Physiological functions of melastatin TRPs in the heart

Z. Yue, J. Xie, X. Qin, B. Sun, Y. Zhang, J. Du, B. Liang and L. Yue

Cardiology/Cell Biology, University of Connecticut Health Center, Farmington, CT, USA

The transient receptor potential channels (TRP) play important roles under various physiological/pathological conditions. In the heart, several members of TRPC channel subfamily have been demonstrated to play a role in hypertrophy and heart failure. In the TRPM subfamily, TRPM7, TRPM4, and TRPM2 have been shown to be functionally expressed in the heart. Patients carrying TRPM4 mutations develop A-V block. We have demonstrated previously that TRPM7 mediated Ca2+ plays an important role in fibrogenesis and human atrial fibrillation. Here we show that in transverse aortic constriction (TAC) induced hypertrophy and heart failure mouse model, TRPM7 is highly up-regulated. Deletion of Trpm7 significantly increases heart performance in comparison with the wild type (WT) mice after TAC. The ejection fraction is significantly larger and the ratio of heart versus body weight is much smaller in TRPM7-KO mice compared to WT mice after TAC. Moreover, depletion of Trpm7 significantly decreases collagen production and fibrosis formation in TAC induced heart failure mice. Taken together, deletion of Trpm7 can protect against TAC induced heart failure.

Where applicable, the authors confirm that the experiments described here conform with The Physiological Society ethical requirements.

SA12

Allosteric models and thermo sensitivity in TRPM8 channels

R. Latorre[1], C. Gonzalez[2], D. Baez-Nieto[3] and N. Raddatz[4]

[1]Centro Interdisciplinario de Neurociencia, Universidad de Valparaiso, Valparaiso, Chile, [2]Centro Interdisciplinario de Neurociencia, Universidad de valparaiso, Valparaiso, Chile, [3]Centro Interdisciplinario de Neurociencia, Universidad de Valparaiso, Valparaiso, Chile and [4]Centro Interdisciplinario de Neurociencia, Universidad de Valparaiso, Valparaiso, Chile

TRPM8 channels are a polymodal receptors activated by voltage, low temperatures and agonists. The structural data suggests that the distal C-terminus (1064–1104 amino acid residues) form a coiled-coil motif. Our aim was to investigate the importance of this structure in the thermo-sensitivity of TRPM8. TRPM8 wild type and deletion mutants of the coiled-coil region of this channel were cloned and expressed in Xenopus oocytes. Macroscopic currents were recorded by patch-clamp technique in cell-attached configuration at different temperatures (10°C- 40°C). An analysis of the conductance-voltage curves determined from tail currents showed that values of the voltage at which the open probability is 0,5 (V1/2) saturate at high and low temperatures. These results and limiting slope analysis of the open probability–voltage curves demonstrated that TRPM8 channel gating is best explained using an allosteric gating model for both voltage and temperature dependence. On the other hand, gradual deletions of the coiled-coil region (from 1064 to 1104 residues) promoted a gradual decrease in the temperature sensitivity of TRPM8 channel, without affecting the voltage dependence. The decrease in the enthalpy promoted by gradual deletions of the distal C-terminus suggests that coiled-coil region is a structural determinant of the thermo sensitivity in TRPM8 channels. Our results also indicate that the voltage and temperature sensors are localized in different structural domains.

Supported by FONDECYT grants 1110430 to R.L, CONICYT AT-24100020 to N.R. CINV is a Millennium Scientific Institute.

Where applicable, the authors confirm that the experiments described here conform with The Physiological Society ethical requirements.

SA13

Transient receptor potential channels in sperm physiology

C.L. Trevino

Genetica del Desarrollo y Fisiologia Molecular, Instituto de Biotecnoligía, Universidad Nacional Autonoma de Mexico, Cuernavaca, Morelos, Mexico

Fertilization is a fundamental biological process that produces a new and unique individual, enabling species preservation and evolution through sexual reproduction. Sperm cells are uniquely equipped to reach, recognize and fuse with the egg. To perform such diverse tasks, spermatozoa must be prepared to face the challenges presented by their constantly changing surroundings. Thus, sperm cells heavily rely on sophisticated signal transduction mechanisms to swim in a directed fashion, and to adjust to changing environmental conditions.

Ion-mediated signal transduction is particularly important in sperm cells, as they essentially lack the protein synthesis capabilities required for signaling mechanisms normally available to other cell types. Accordingly, fluctuations in intracellular Ca^{2+} concentrations ($[Ca^{2+}]_i$) trigger and/or regulate some of the main sperm functions involved in fertilization. These include motility, capacitation (a process that confers fertilization capability), and the acrosome reaction or AR (a Ca^{2+}-dependent exocytotic event required for fertilization). The extent of participation and the specific roles of the many putative Ca^{2+} channels thought to mediate sperm functions still remain to be elucidated. Based on studies conducted on various other cell types, Transient Receptor Potential (TRP) channels are known to be a functionally diverse family of Ca^{2+} channels; they modulate $[Ca^{2+}]_i$ in response to various thermal, chemical or mechanical stimuli. Members of the M (Melastatin) subfamily (TRPM) participate in sensory physiology, both at the cell and organismal levels. For example, they are responsible for sensing, among other stimuli, changes in temperature, osmolarity, voltage and/or pH. Importantly, these channels are often sensitive to more than one stimulus and are thus regarded to function as signal integrators. While this particular feature is conceivably of great value for sperm cells embarking on their adventurous journey towards the egg, the involvement of TRPM channels in sperm physiology has not been established. We therefore centered this work on the characterization of TRPM8 –a Ca^{2+} channel known to open upon temperature decrease– both in mouse (CD-1 strain) and in human sperm. Using specific antibodies, we first show that TRPM8 immunolocalizes to the head and to the flagellum in both species (n=3); the expression of this channel was confirmed by Western blot analyses (n=3) in both species. We then studied the functionality of sperm TRPM8 by: (a) measuring $[Ca^{2+}]_i$ using fluorescent dyes; (b) measuring AR induction using standard methodologies for mouse (1) and human (2) sperm; and (c) measuring ion currents making use of the recently established sperm patch clamping technique (3), which is performed on a unique cytoplasmatic extension of sperm cells known as the cytoplasmic droplet. We found that menthol (a TRPM8 agonist) elevates$[Ca^{2+}]_i$ inducing the AR in a dose-dependent manner both in human and mouse sperm (IC_{50} = 300 and 500 μM, respectively). BCTC (N-(4-t-Butylphenyl)-4-(3-Chloropyridin-2-yl) tetrahydropyrazine-1(2H)-carboxamide) and capsazepine (two TRPM8 antagonists) inhibit the menthol-induced AR in both species (n=3). In human sperm these inhibitors did not interfere with the AR induced by two of the physiological inductors, namely ZP3 (zona pellucida protein 3) and progesterone, suggesting that TRPM8 activation triggers the AR through a different signaling pathway than these physiological inductors (2). The effect of low temperature was also tested in mouse sperm, where it induced an increase in $[Ca^{2+}]_i$. However, in this species, BCTC and capsazepine did inhibit –at least partially– the ZP3- and progesterone-induced AR (n=3). Consistently, we found that spermatozoa from TRPM8 knockout mice do not undergo the menthol-induced AR that is sensitive to TRPM8 antagonists (n=3). Patch clamp experiments were exclusively conducted in testicular mouse spermatozoa, revealing currents triggered by menthol, icilin (another TRPM8 agonist), and low temperature. These currents were inhibited by BCTC and capsazepine (n=3), confirming they are due to TRPM8 activity (1). Further studies are needed to elucidate the precise roles that TRPM8 channels may play during fertilization, but the present confirmation of their expression and functionality in sperm cells places them as likely signal integrators in Ca^{2+}-mediated signaling. As such, these channels become attractive subjects of investigation as plausible participants in chemotaxis and thermotaxis –two processes whose involvement in fertilization is still awaiting confirmation.

Martinez-Lopez, P., Trevino, C. L., de la Vega-Beltran, J. L., De Blas, G., Monroy, E., Beltran, C., Orta, G., Gibbs, G. M., O'Bryan, M. K., and Darszon, A. (2011) TRPM8 in mouse sperm detects temperature changes and may influence the acrosome reaction. J Cell Physiol 226(6), 1620-1631

De Blas, G. A., Darszon, A., Ocampo, A. Y., Serrano, C. J., Castellano, L. E., Hernandez-Gonzalez, E. O., Chirinos, M., Larrea, F., Beltran, C., and Trevino, C. L. (2009) TRPM8, a versatile channel in human sperm. PLoS ONE 4(6), e6095

Kirichok, Y., Navarro, B., and Clapham, D. E. (2006) Whole-cell patch-clamp measurements of spermatozoa reveal an alkaline-activated Ca2+ channel. Nature 439(7077), 737-740

This work was supported by Consejo Nacional de Ciencia y Tecnología (CONACyT-Mexico) (99333 and 128566 to CT); Dirección General de Asuntos del Personal Académico/ Universidad Nacional Autónoma de México (IN202212-3 to CT). Special thanks go to Dr. Marcela B. Trevino for valuable input and editing work.

Where applicable, the authors confirm that the experiments described here conform with The Physiological Society ethical requirements.

SA14

Role of TRPA1 in gastrointestinal motility

H. Ito, K. Nozawa, H. Doihara, R. Kojima, E. Kawabata-Shoda, Y. Keto and T. Yokoyama

Pharmacology Research Labs., Drug Discovery Research, Tsukuba, Ibaraki, Japan

Transient receptor potential ankyrin1 (TRPA1) is a non-selective cation channel activated by cold stimuli under 17 °C, mechanosensation, and pungent irritants such as allyl isothiocyanates (AITC) and cinnamaldehyde (CA). TRPA1 is located in the sensory terminals of nociceptive fibers in their target organs, such as urinary bladder and the small intestine, and the activation of TRPA1 elicited contractile responses in these organs. However, little is known about the functional role of TRPA1 in non-neural tissues, especially in the gastrointestinal tract.

We demonstrated that TRPA1 is highly expressed in enterochromaffin (EC) cells in enteric mucosa, and that TRPA1 stimulation with agonists evokes the release of 5-hydroxytryptamine (5-HT) from EC cells.[1)] This could produce contraction of guinea-pig ileum by stimulating serotonergic mechanisms. The release of 5-HT from the mucosa and the stimulation of $5\text{-}HT_3$ receptors located in the myenteric plexus may contribute to the TRPA1 agonist-induced contractions in guinea pig ileum. Gastrointestinal (GI) dysmotility and visceral pain/discomfort are the main symptoms of irritable bowel syndrome (IBS). The neurotransmitter 5-HT has been shown to be involved in the pathophysiology of IBS. Especially, postprandial plasma level of 5-HT in patients with IBS with constipation (IBS-C) has been reported to be lower than that in healthy subjects.

As mentioned above, we originally found that TRPA1 receptors were expressed on EC cells in GI tract, which are 5-HT releasing cells.[1)] Therefore, TRPA1 receptor is expected to be involved in GI motility and to be a novel target of the drug for IBS-C.

ASP7663 has been newly synthesized in Astellas Pharma Inc. as a novel selective TRPA1 receptor agonist. The compound activated human, rat, and mouse TRPA1 receptors with EC_{50} values of 0.51(0.40-0.66), 0.54(0.40-0.72), and 0.50(0.41-0.63)

μM, respectively. We examined the effect of ASP7663 on constipation using an experimental rodent model of IBS-C.[2] Further, the effect of ASP7663 on visceral pain response was also examined. ASP7663 showed anti-constipation effects in Loperamide-induced delay of colonic transit in mice, and analgesic effect in colorectal distension-induced visceral pain responses in rat.[3] Consequently, ASP7663 is expected to be a novel and promising therapeutic agent for IBS-C with substantial efficacy in relieving on both constipation and visceral pain symptoms Our results indicate that TRPA1 acts as a sensor molecule for EC cells and may regulate the gastrointestinal function. TRPA1 activation by ingested food containing pungent ingredients, such as mustard oil and cinnamon oil, could promote gastrointestinal motility through these mechanisms. Furthermore, in case of functional GI disorder, such as IBS, TRPA1 receptor agonists hold promise as a beneficial treatment.
In addition, our research on the QGP-1 cell line, a new model for the investigation of TRPA1 function in the human EC cell,[4] and functional role of TRPA1 in GI motility in dog[5] would also be mentioned.

Nozawa K *et al.* (2009). *Proc Natl Acad Sci USA* **106**, 3408-3413

Kojima R *et al.* (2009). *Pharmacology* **84**, 227-233

Keto Y *et al.* (2012). *DDW2012* Tu1375-2012 AGA

Doihara H *et al.* (2012). *Mol. Cell. Biochem* **331**, 239-245

Doihara H *et al.* (2009). *Eur. J. Pharmacol* **617**, 124-129

Where applicable, the authors confirm that the experiments described here conform with The Physiological Society ethical requirements.

SA15

Vascular senescence and organ fibrosis

J. Maizel, R. Vasko, S. Xavier, J. Chen, J. Cao and M.S. Goligorsky

Medicine, Pharmacology, Physiology, New York Medical College, Valhalla, NY, USA

Multiorgan fibrosis commonly occurs in ageing mammals and its causes are not apparent. We have previously established a colony of mice with endothelial deletion of sirtuin 1 (SIRT1; SIRT1endo-/- mice) and noticed that these mice spontaneously develop traces of fibrosis in the kidneys and the heart and mount an exaggerated fibrotic response after challenge with stressors. Taking into the account the fact that SIRT1 becomes depleted in ageing, these findings raised the possibility of its participation in fibrosis of ageing. To address this possibility, we characterized the animal model of SIRT1endo-/-. Data showed that endothelial and endothelial progenitor cells exhibit higher levels of premature senescence, apoptosis, and reduced resistance to stressors, along with the impaired angiogenesis and reduced endothelium-dependent vasorelaxation. Morphologic examination of the heart and kidneys from these mice did not reveal any pathological changes in heterozygote animals, but showed a spontaneously developing mild patchy interstitial fibrosis in SIRT1endo-/- mice already at the age of 12 weeks. Quantitative PCR data demonstrated significantly higher expression of collagen I and a slightly increased collagen III under basal conditions. Echocardiography studies showed development of a mild diastolic dysfunction in 30 week-old SIRT1endo-/- mice. Applying a selection pressure on angiogenic and regenerative processes, we next examined adriamycin-induced cardiomyopathy and folate-induced nephropathy models. Data showed that trichrome staining, collagen I and III mRNA expression, as well as the short/long ratio of endoglin isoforms, a marker of senescence, were all elevated in SIRT1endo-/- mice. Folic acid-treated SIRT1endo-/- mice exhibited microvascular rarefaction, which was undetectable under basal conditions. It was previously reported that SIRT1 inhibition reduces MMP-14 mRNA abundance in cultured endothelial cells. We were able to reproduce these findings and showed that SIRT1endo-/- mice exhibited a 5-fold decrease in MMP-14 staining intensity compared to control animals and SIRT1 inhibition reduced MMP-14 protein abundance and matrylitic activity. Next, we examined other putative targets of MMP-14, endoglin and tissue transglutaminase (both normally cleaved by MMP-14), over-expression of both potentially contributing to pro-fibrotic program via type II TGF-β receptor and matrix proteins cross-linking, respectively. Inhibition of SIRT1 in HUVEC resulted in accumulation of endoglin Similarly, expression of cell-associated tissue transglutaminase was elevated in cells treated with SIRT1 inhibitor. Collectively, these findings confirmed that MMP-14 represents a novel target for SIRT1 and that depletion of the latter reduces MMP-14 expression with the resulting loss of proteolytic matrix-degrading properties of endothelial cells and subsequently decreased cleavage of endoglin and tissue transglutaminase. ConA has been previously shown to induce MMP-14. We confirmed this activity of ConA in vitro and showed that ConA effect was independent on the expression of SIRT1. Therefore, we next treated wild-type B6;129 mice with highly specific SIRT1 inhibitor III together with weekly intravenous injections of ConA, and compared those with mice receiving SIRT1 inhibitor III treatment alone. To validate the efficacy of this model, we performed quantitative real-time PCR and immunoblot analysis, which showed suppression of renal MMP-14 in the inhibitor-treated mice and its induction in ConA co-treated animals. In these mice, ConA treatment resulted in the reduction of proteinuria and significant prevention of fibrosis, as demonstrated by Masson's trichrome staining. The mRNA synthesis of collagen I and III did not differ between SIRT1 inhibitor III-treated and SIRT1 inhibitor III/ConA-treated mice, demonstrating that ConA does not directly affect synthesis of extracellular matrix (ECM), but rather stimulates the cleavage of ECM excess through induction of MMP-14. Moreover, the angiogenic sprouting and matrilytic activity of aortic rings cultured in 3D matrigel, both suppressed in mice receiving SIRT1 inhibitor alone, showed a dramatic increase in ConA-treated animals. This data confirms the pathogenetic role of suppressed MMP-14 in exaggerated fibrotic response of SIRT1endo-/- mice. It also suggests that SIRT1 depletion with ageing and propensity toward fibrosis are linked via this novel MMP-14 mechanism.

Where applicable, the authors confirm that the experiments described here conform with The Physiological Society ethical requirements.

SA16

Role of sirtuins in endothelial cell senescence

A. Cardús[1,2], A. Uryga[1] and J. Erusalimsky[1]

[1]Cardiff Metropolitan University, Cardiff, UK and [2]Universitat de Lleida, Lleida, Spain

Members of silent information regulator (Sir) proteins regulate lifespan in multiple models organism. The most studied sirtuin is sir2 in yeast, an NAD+- dependent deacetylase that remove acetyl groups from another protein, thereby regulating the biological function of their targets. In addition Sir2 appears to be a limiting component in yeast ageing. Due to their established role in controlling lifespan in lower organism,

there is growing interest in determining the effect of sirtuins in mammal cells. Like their yeast homologs, the mammalian sirtuins (SIRT1-7) were originally described as deacetylase proteins (class III HDAC) requiring NAD+ as a cofactor to deacetylate substrates ranging from histones to transcriptional regulators (Blander et al, 2004). Based in the phylogenetic analysis mammalian sirtuins can be divided into four classes: SIRT1-SIRT3 belongs to class I, SIRT4 to class II, SIRT5 to class III and SIRT6 and SIRT7 to class IV (Frye et al, 2000). Also, it is described that mammalian sirtuins have diverse cellular localization and target multiple substrates, consequently affecting a broad range of cellular functions. Specifically, SIRT6 is in the nucleus where promotes DNA repair and protect against genomic instability (Michishita et al, 2008). Moreover, it's described that SIRT6 could modulate telomeric chromatin and regulates genomic stability on the cellular level and ageing-associated pathologies at the organismal level (Mostoslavsky et al, 2006). On the other hand, a recent paper has demonstrated that SIRT6 binds to the NF-κB subunit RelA and attenuates Nf-κB signalling by modifying chromatin at NF-κB target genes (Kawahara et al, 2009). NF-κB family is considered an emerging modulator of ageing-related pathways in mammals that controls the activity of genes involved in apoptosis, cell senescence, inflammation, and immunity.

Ageing and hypertension represent two major independent risk factors for cardiovascular disease. Many of the cardiovascular complications associated with both ageing and hypertension are attributable, at least in part, to endothelial dysfunction. The pathophysiology of endothelial dysfunction is complex and involves multiple mechanisms. One potential trigger for endothelial dysfunction is inflammation (Clapp et al, 2004) and recently it has been increasingly linked to cellular senescence process (Erusalimsky, 2009). The aim of this study was to investigate whether SIRT6 has an effect in endothelial cells senescence and dysfunction and the model of action. In this presentation we will show that SIRT6 is expressed in endothelial cells, mRNA expression (n=3-6) analysis of SIRT1 and SIRT6 was measured by quantitative polymerase chain reaction using Taqman probes. SIRT6 expression was higher in differentiated endothelial cells compared to hematopoietic progenitor cells and presented similar levels to SIRT1 in mature endothelial cells. Furthermore, comparing early and late passages of endothelial cells showed a decreased of SIRT6 expression due to replicative senescence, in both, mRNA (n=3) and protein levels (n=3) measured by western blot. SIRT6 depletion by RNA interference induced a decrease in endothelial cells proliferation quantified by BrdU immunofluorescence assay (n=4), increased senescence-associated-b-galactosidase positive cells (n=4) and diminished ability of the cells to form tubule networks on Matrigel coating (n=5-6), all features of cell senescence. Consistent with this notion, SIRT6-depleted cells presented higher levels of intercellular-adhesion-molecule-1 (ICAM-1) in both, mRNA (n=9) and protein levels (n=3) analysed by flow cytometry. Also showed an increase of PAI-1 mRNA levels (n=9) and lower levels of eNOS mRNA (n=9) and protein (n=3). On the other hand, we examined the accumulation of γH2AX foci by immunofluorescence in SIRT6 depleted cell (n=3). We detected a significant increase in γH2AX foci and in the co-localization with TRF-1, meaning that SIRT6 attenuates DNA damage and telomere dysfunction. Finally, we studied the downstream mechanism by which senescence is induced in SIRT6 depleted cells, higher levels of p21, a cyclin-dependent kinase, was present in SIRT6-depleted cells compared to controls (n=4). These data demonstrate that SIRT6 is highly expressed in endothelial cells where it confers protection from both genomic DNA damage and telomere dysfunction. Besides, our finding that SIRT6 depletion induces senescent phenotype suggests that increasing the activity of this sirtuin may be a relevant approach to delay vascular ageing.

Blander G, Guarente L (2004). The Sir2 family of protein deacetylases. Annu Rev Biochem. 73:417-35.

Clapp BR, Hingorani AD, Kharbanda RK, Mohamed-Ali V, Stephens JW, Vallance P, MacAllister RJ (2004). Inflammation-induced endothelial dysfunction involves reduced nitric oxide bioavailability and increased oxidant stress. Cardiovasc Res. 64(1):172-8.

Erusalimsky JD (2009). Vascular endothelial senescence: from mechanisms to pathophysiology. J Appl Physiol. 106(1):326-32.

Frye R (2000) Phylogenetic classification of prokaryoti and eukariotic Sir2-like proteins. Biochem Biophys Res Commun. 273:793-798.

Kawahara TL, Michishita E, Adler AS, Damian M, Berber E, Lin M, McCord RA, Ongaigui KC, Boxer LD, Chang HY, Chua KF (2009). SIRT6 links histone H3 lysine 9 deacetylation to NF-kappaB-dependent gene expression and organismal life span.

Cell. 136(1):62-74.

Michishita E, McCord RA, Berber E, Kioi M, Padilla-Nash H, Damian M, Cheung P, Kusumoto R, Kawahara TL, Barrett JC, Chang HY, Bohr VA, Ried T, Gozani O, Chua KF (2008). SIRT6 is a histone H3 lysine 9 deacetylase that modulates telomeric chromatin. Nature. 452:492-496

Mostoslavsky R, Chua KF, Lombard DB, Pang WW, Fischer MR, Gellon L, Liu P, Mostoslavsky G, Franco S, Murphy MM, Mills KD, Patel P, Hsu JT, Hong AL, Ford E, Cheng HL, Kennedy C, Nunez N, Bronson R, Frendewey D, Auerbach W, Valenzuela D, Karow M, Hottiger MO, Hursting S, Barrett JC, Guarente L, Mulligan R, Demple B, Yancopoulos GD, Alt FW (2006). Genomic instability and aging-like phenotype in the absence of mammalian SIRT6. Cell. 124(2):315-29.

Where applicable, the authors confirm that the experiments described here conform with The Physiological Society ethical requirements.

SA17

Endothelial cell senescence: molecules and mechanisms

P. Jansen-Dürr

Research Institute for Biomedical Aging Research, University of Innsbruck, Innsbruck, Austria

The free radical theory of aging suggests that reactive oxygen species (ROS) are a driving force of the aging process. In many postmitotic tissues with high mitochondrial activity, the mitochondria are considered as main sources of ROS, which arise as by-products of oxidative metabolism. However, in recent years it has been shown that depending on the tissue type also nonmitochondrial enzymes, such as NADPH oxidases and other oxidative enzymes, can contribute significantly to the cellular load of ROS. The emerging picture suggests that various sources of ROS contribute in a different way to aging phenotypes in various tissues. Using senescence of human endothelial cells as a model system, we reported previously that endogenous levels of NADPH oxidase Nox4 are major drivers of human endothelial cell senescence, by inducing a DNA damage response (Lener et al., 2009). We have addressed molecular mechanisms by which Nox4 may induce DNA damage and found an unanticipated link to the mitochondria, which seem to act as important signal amplifiers. We also found that the hydrogen sulphide (H_2S)-producing enzyme cystathione beta-synthase (CBS) regulates senescence of human endothelial cells (Albertini et al., 2012); the role of H_2S in cellular senescence will be discussed.

Lener B, Koziel R, Pircher H, Hütter E, Greussing R, Herndler-Brandstetter D, Hermann M, Unterluggauer H, Jansen-Dürr P. The NADPH oxidase Nox4 restricts the replicative lifespan of human endothelial cells. Biochem J. 2009 Oct 12;423(3):363-74

Albertini E, Koziel R, Dürr A, Neuhaus M, Jansen-Dürr P. Cystathionine beta synthase modulates senescence of human endothelial cells. Aging (Albany NY). 2012 Oct;4(10):664-73.

Where applicable, the authors confirm that the experiments described here conform with The Physiological Society ethical requirements.

SA18

Endothelial senescence in smokers and COPD patients

K.E. Paschalaki[1,2], R.D. Starke[2], Y. Hu[4], N. Mercado[1], A. Margariti[4], V.G. Gorgoulis[3], P.J. Barnes[1] and A.M. Randi[2]

[1]Airway Disease Section, National Heart & Lung Institute, Imperial College London, London, UK, [2]Vascular Sciences, National Heart and Lung Institute, Imperial College London, London, UK, [3]Department of Histology and Embryology, University of Athens, Athens, Greece and [4]Cardiovascular Division, King's College London, London, UK

Introduction: Cardiovascular disease (CVD) is a major cause of death in smokers, particularly in patients with chronic obstructive pulmonary disease (COPD), an obstructive lung inflammatory disorder affecting approximately 20% of smokers. Even though numerous studies describe evidence of endothelial dysfunction in young healthy smokers and COPD patients, the molecular pathways that link cigarette smoke and CVD remain unclear.

Increased DNA damage and cellular senescence have been recognized as important contributors to CVD. DNA damage, caused by factors such as oxidative stress, activates ataxia-telangiectasia mutated (ATM) kinase, a key player in the DNA damage response (DDR), and results in cell cycle arrest, senescence or apoptosis. Senescent vascular cells exhibit dysfunctional characteristics and have been shown to contribute to accelerating vascular aging and atherosclerosis.

Circulating endothelial progenitor cells (EPC) are required for endothelial homeostasis, and their dysfunction also contributes to CVD. Blood outgrowth endothelial cells (BOEC, also called endothelial colony forming cells - ECFC), are a well characterized endothelial cell population with robust clonal proliferative potential and ability to form de novo vessels *in vivo*. This population has recently attracted considerable interest as a potential cell-based therapy for vascular regeneration, and as a tool to study endothelial dysfunction in patients.

Our aim was to investigate whether EPC from smokers and COPD patients are dysfunctional due to increased DNA damage imposed by cigarette smoke-oxidative stress, which could contribute to the development of CVD, and to elucidate the pathways involved in this process.

Methods: To investigate EPC dysfunction in smokers, we isolated and expanded BOEC from peripheral blood samples of healthy non-smokers, healthy smokers and COPD patients. The mononuclear fraction was placed in culture in the presence of endothelial growth factors and BOEC colonies appeared between days 7 and 24. BOEC colonies were expanded and used at passages 4 to 6 for all experiments. Endothelial senescence was measured by senescence-associated β-galactosidase (SA-β-Gal) activity. Expression of sirtuin (SIRT)-1, p16, p21, γ-H2AX and 53BP1 were measured by Western blotting and/or immunofluorescence confocal microscopy. SIRT1 activity was measured using a SIRT1 fluorescent activity assay kit. To investigate angiogenesis *in vivo*, BOEC were labelled with Vybrant DiI Cell-Labelling Solution, mixed with Matrigel and injected subcutaneously into the back of NOD.CB17-Prkdcscid/NcrCrl mice. Seven days later, the mice were sacrificed and the plugs were harvested and cryosectioned.

Results: *In vitro*, BOEC from smokers and COPD patients showed increased DNA double-strand breaks (measured by γ-H2AX, 53BP1) and senescence (senescence associated-β-galactosidase activity, p16 and p21 levels) compared to non-smokers. Senescence negatively correlated with expression and activity of sirtuin-1 (SIRT1), a protein deacetylase that inhibits DNA damage and cellular senescence. Inhibition of DNA damage response by silencing of ATM kinase resulted in up-regulation of SIRT1 expression and decreased senescence. Interestingly, treatment of BOEC from COPD patients with the SIRT1 activator resveratrol or a selective ATM inhibitor rescued the senescent phenotype. Using the *in vivo* Matrigel plug assay, BOEC from COPD patients displayed reduced ability to form capillary-like structures and increased DNA damage, senescence and apoptosis (measured by 53BP1, p16, TUNEL and cleaved-caspase 3 staining) compared to non-smokers.

Conclusions: This study provides evidence of epigenetic alterations in endothelial progenitors from smokers, linked to cigarette smoke-oxidative stress, namely reduced SIRT1 expression via activation of the DNA damage response / ATM pathway. We demonstrated that progenitor cells of the endothelial lineage in smokers and COPD patients show reduced angiogenesis *in vivo* and display increased DNA damage and senescence, associated with reduced SIRT1 expression. These defects may contribute to endothelial dysfunction and cardiovascular events in smokers and COPD patients and could potentially constitute therapeutic targets for intervention.

Dr Anna M. Randi and Professor Peter J. Barnes share senior authorship.

Where applicable, the authors confirm that the experiments described here conform with The Physiological Society ethical requirements.

SA19

Smooth muscle cell senescence in atherosclerosis

M. Bennett

Division of Cardiovascular Medicine, University of Cambridge, Cambridge, UK

Background: Despite the historical focus on cell proliferation in atherosclerosis, advanced plaques are characterized by vascular smooth muscle cell (VSMC) senescence, apoptosis, persistent DNA damage and activation of the DNA damage response (DDR).

Methods and Results: Using a series of mouse models, we find that VSMC senescence is regulated by DNA damage and repair, and promotes features of vulnerable plaques, including reduced fibrous cap thickness and expansion of the necrotic core. VSMC senescence may also promote medial degeneration, aneurysm formation and ongoing inflammation. We show that oxidative stress regulates both telomere dependent and independent senescence, and senescence is inhibited by DDR proteins and sirtuins. Mitochondrial DNA damage occurs early in atherosclerosis, and can also promote both VSMC senescence and atherosclerosis.

Conclusions: VSMC senescence directly promotes atherosclerosis and medial degeneration, mediated through nuclear and mitochondrial DNA damage

Gorenne, I, Kumar, S, Gray, K, Figg, N, Yu, H, Mercer, J, Bennett, MR. Vascular Smooth Muscle Cell Sirtuin 1 protects against DNA damage and inhibits atherosclerosis. Circulation. 2013;127(3):386-96

Aging and Atherosclerosis: Mechanisms, functional consequences, and potential therapeutics for cellular senescence. Circ Res 2012;111:245-59.

Mercer, J, Cheng, KK, Figg, N, Gorenne, I, Mahmoudi, M, Griffin, J, Vidal-Puig, A, Logan, A, Murphy, MP, Bennett, MR. DNA damage links mitochondrial dysfunction to atherosclerosis and the metabolic syndrome. Circ Res 2010;107;1021-1031

This work was funded by British Heart Foundation grants FS/08/003 (to IG), RG08/009/25841 and PG/09/071 (to MRB), and the NIHR Cambridge Biomedical Research Centre.

Where applicable, the authors confirm that the experiments described here conform with The Physiological Society ethical requirements.

SA20

Reactive oxygen species signalling in microvascular permeability

P. Fraser

BHF Centre of Research Excellence, Cardiovascular Division, King's College London, London, UK

The brain endothelium constitutes a barrier to the passive movement of substances from the blood into the cerebral microenvironment, and disruption of this barrier after a stroke or trauma has potentially fatal consequences. Reactive oxygen species (ROS), which are formed during these cerebrovascular accidents, have a key role in this disruption. ROS are formed constitutively by mitochondria and also by the activation of cell receptors that transduce signals from inflammatory mediators, e.g., activated phospholipase A_2 forms arachidonic acid that interacts with cyclooxygenase and lipoxygenase to generate ROS. Endothelial NADPH oxidase, activated by cytokines, also contributes to ROS. There is a surge in ROS following reperfusion after cerebral ischemia and the interaction of the signaling pathways plays a role in this. ROS are transiently generated during reperfusion following cerebrovascular ischaemia, which results in the initial disruption of the blood-brain barrier. This allows plasma proteins into the brain substance that leads to gliosis and subsequent destruction of brain tissue. We have investigated the source of this reperfusion injury-generated ROS in single venular capillaries on the cortical surface of the brain in young anaesthetized rats. The permeability to sulforhodamine dye (588 Da) of single venular capillaries of rats (anaesthetized with pentobarbitone: 60 $mg.kg^{-1}$ ip, an overdose of which was administered to kill humanely) was measured by the occlusion technique. Cerebral ischaemia-reperfusion was instigated by infusing into the internal carotid artery 40 μm starch microspheres that subsequently dissolve due to the action of plasma amylase. This produced a blockage of the middle cerebral artery territory and we found that the permeability of previously tight venules increased with the duration of the ischaemia. This permeability increase was sensitive to blocking the bradykinin B2 receptor, but was an order of magnitude greater than the maximum permeability response to acutely applied bradykinin. Acutely applied bradykinin itself results in a free radical scavenger sensitive and calcium entry dependent permeability response. The source of this ROS was shown to be both cyclooxygenase and lipoxygenase activated by arachidonic acid released by phospholipase A_2 activated in response to the applied bradykinin. Prolonged application of bradykinin did not itself increase the response, but permeability did increase after 30 min, and this was blocked by inhibiting the interleukin-1 receptor. We also found that interleukin-1β (IL-1β) application before applying bradykinin resulted in a large potentiation of the response. Furthermore, the early component of the potentiated response was shown to be sensitive to inhibiting NOX-2 assembly (Fig. 1). The vascular permeability response to the starch microsphere injection was also measured in the whole of the affected hemisphere by using escape of horseradish peroxidase (HRP) into the tissue. 50 μm thick sections were incubated with diaminobenzidine (DAB) and the rate of development of the reaction product was used to calculate the concentration of HRP in the tissue by comparison with brains soaked in HRP standard solutions. The PS product was calculated after 30 minutes reperfusion from the time averaged plasma HRP concentration according to the Crone-Renkin equation. PS increase depended on the duration of the blockage of the circulation and was greatest on the pial surface and radial veins draining the cortex. These experiments confirmed that the permeability increase on reperfusion lasted for less than 1h, and could be much reduced by preventing the formation of the hydroxyl radical by treating the animal with desferrioxamine which chelates the ferrous ion, so preventing the Fenton reaction.

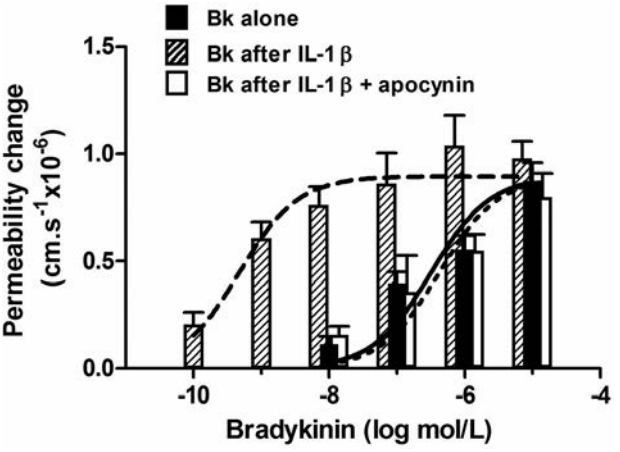

Figure1. Concentration–response curves for bradykinin before and after treatment with IL-1β in the presence of cycloheximide to prevent protein synthesis thought to be responsible for the later permeability increase. Apocynin co-applied with IL-1β, and removed with it, completely blocked the potentiation.

Where applicable, the authors confirm that the experiments described here conform with The Physiological Society ethical requirements.

SA21

Regulation of endothelial barrier by Rho GTPases

M. Aslam[2,1], C. Hamm[2] and D. Guenduez[2]

[1]Institute of Physiology, Justus Liebig University, Giessen, Germany and [2]Cardiology and Angiology, Justus Liebig University, Giessen, Germany

Introduction: Endothelial barrier dysfunction is associated with many types of vascular diseases (e.g. atherosclerosis, inflammation and ischemia/reperfusion). Endothelial barrier function is mainly regulated by cell-cell adhesions and endothelial contractile machinery. Rho family of GTPases particularly RhoA and Rac1 are the main regulators of both endothelial cell-cell

adhesions and contractile machinery. The activity of Rho GTPases is regulated by different mechanisms including by post-translational prenylation. Prenylation of both RhoA and Rac1 is regulated by farnesyltransferase and geranylgeranyltransferase, and dysregulation of their activity may influence the activity of RhoA and Rac1. In the present study, the effect of RhoA and Rac1 prenylation on endothelial permeability was analysed.
Methods: The study was performed on isolated human umbilical vein endothelial cells (HUVECs). Endothelial barrier function was analysed by measuring flux of labeled albumin through HUVEC monolayers. RhoA and Rac1 activity was measured by pulldown assay. Thrombin was used as an inflammatory mediator.
Results and Conclusion:
In this presentation, we will present the data showing how interfering with the activities of farnesyltransferase and geranylgeranyltransferase can differentially affect the activities of Rho GTPases and thus influence endothelial permeability both positively and negatively. Moreover, the data on the influence of statins, which also inhibit protein prenylation, on Rho GTPases and thus endothelial barrier function will be discussed.

The technical support by S. Schäfer, D. Reitz, and H. Thomas is gratefully acknowledged.

Where applicable, the authors confirm that the experiments described here conform with The Physiological Society ethical requirements.

SA22

Role of calcium signaling on cyclic nucleotide regulation of vascular permeability

D. Mehta

Pharmacology, University of Illinois, Chicago, IL, USA

The vascular endothelium interfacing between the blood and vessel wall has the vital functions of regulating tissue fluid balance and supplying the essential nutrients needed for the survival of the organism. It is known that loss of this function results in tissue inflammation, the hallmark of inflammatory diseases such as the Acute Respiratory Distress Syndrome. Dynamic interaction between adherens junctions and cell-matrix attachments plays a primary role in regulating endothelial permeability. However, counter-adhesive forces generated by actinomysin molecular motors activated upon inflammatory mediators such as thrombin, bradykinin, histamine, VEGF, and others upon binding to their receptors, disrupt the organization of adherens junctions and cell-matrix complexes, thereby opening the junctional barrier.
An increase in cytosolic Ca2+ has been established as the initial pivotal signal that precedes endothelial cell shape change and opening of adherens junctions resulting in barrier dysfunction. Following cell stimulation with inflammatory mediators, an increase in cytosolic Ca2+ concentration is apparent. There is an initial transient peak as the result of Ca2+ release from endoplasmic reticulum (ER) stores, which is followed by more sustained response secondary to Ca2+ entry via plasmalemma channels. Ca2+ entry refills ER stores and sustains Ca2+ signaling. Proteins of the transient receptor channel (TRPC) family are non-selective cation channels present in endothelial cells that increase intracellular Ca2+, and play an important role in regulating actin-myosin motor activity and endothelial barrier function. Human pulmonary endothelial cells highly expressed TRPC1 and TRPC6, whereas TRPC3, TRPC4, and TRPC7 are expressed only weakly. TRPC1, TRPC4, and TRPC5 are activated by depletion of ER stores, and are therefore called store-operated channels (SOCs), whereas TRPC3 and TRPC6 are activated independently of store depletion, and are referred to as receptor-operated channels (ROC). SOCs and ROCs provide the primary structures by which Ca2+ enters endothelial cells. Both SOC and ROC have been shown to induced actin-myosin induced endothelial cell contraction and thereby endothelial permeability.
In contrast to Ca2+, an increase in the concentration of cAMP is known to stengthen endothelial barrier function such that it prevents increased permeability in response to known permeability-increasing mediators in endothelial cells and intact microvessels. Evidence indicates that increased levels of cAMP can be endothelial barrier protective through the cAMP-dependent kinase, PKA as well as modulation of adherens junctions and cell-matrix attachemnets. Cyclic AMP response element binding (CREB) protein is a nuclear transcriptional factor that regulates several cellular functions such as inflammation, cell proliferation, differentiation, adaptation and survival. We have shown that CREB plays a pivotal role in regulating endothelial barrier function by restricting endothelial contraction through regulating the expression of p190RhoGAP. These findings indicate that TRPC and cAMP-mediated signaling mechanisms must intersect with each other to regulate endothelial permeability. My objectives in this presentation will be to discuss the data from genetic, physiological, cellular, and morphological studies whether TRPC- and cAMP-mediated signaling intersects and how this intersection plays a role in regulating endothelial barrier function.

Mehta D and Malik AB. Physiol. Rev. 86 (1): 279-367, 2006.

Chava K et al. Blood 2012 119(1):308-19.

Tauseef M et al. J. Exp Med 2012, 209(11):1953-68.

Patterson CE et al. Endothelium. 2000;7(4):287-308.

This work was supported by National Institute of Health grants HL71794, HL84153, HL060678.

Where applicable, the authors confirm that the experiments described here conform with The Physiological Society ethical requirements.

SA23

Sphingosine-1-phosphate regulation of endothelial cytoskeleton

J.G. Garcia

Office of the Vice President for Health Affairs, University of Illinois Hospital and Health Sciences System, Chicago, IL, USA

Effective therapies to limit the profound vascular leakage in inflammatory injury are severely limited. Our early translational investigations first suggested sphingosine 1-phosphate (S1P), a multifunctional lipid mediator and angiogenic factor, as an effective therapy for reducing vascular leakage in inflammatory lung injury. We have shown that S1P rapidly stimulates a Rac GTPase-driven signaling cascade leading to reorganization of the vascular endothelial cell cytoskeleton and enhanced junctional integrity, biophysical events which ultimately strengthen the EC barrier and decrease vascular permeability. Importantly, S1P administration to mice with endotoxin (LPS)-induced lung injury or to dogs in a lung injury model induced by intrabronchial LPS instillation, markedly improves oxygenation and reduces alveolar edema formation. As S1P is found in nano-micromolar quantities in plasma, the expres-

sion and dynamic responses of G-protein-coupled S1P receptors (S1PRs) serve to coordinate cellular responses to S1P. S1PR1, S1PR2, and S1PR3 are highly expressed in lung vascular endothelium, however, only ligation of S1PR1 reduces murine lung vascular permeability in response to LPS, ischemia/reperfusion, ventilator–induced injury and ionizing radiation. Furthermore, S1PR1 is critical to hepatocyte growth factor-, hyaluronan- and activated protein C-mediated EC barrier enhancement via S1PR1 transactivation. In contrast, ligation of S1PR3 induces Rho GTPase signaling to the cytoskeleton and increased lung permeability. We recently investigated the role of specific S1P/S1PR responses in inflammatory lung injury including dose- and delivery route-dependent (intratracheal vs intravenous) effects of S1P and selective S1PR receptor agonists and antagonists on vascular leakage in wild type and genetically-engineered mice in relevant murine models of inflammatory lung injury. We determined that direct intratracheal (IT) or intravenous (IV) administration of S1P, or a selective S1PR1 agonist (SEW- 2871) produces highly concentration-dependent barrier-regulatory responses in the murine lung. IT or IV administration of S1P or SEW-2871 at <0.3 mg/kg was protective against LPS-induced murine lung inflammation and permeability, however, IT delivery of S1P at 0.5 mg/kg (2hrs) resulted in significant alveolar-capillary barrier disruption (42% increase in BAL inflammatory protein) and produced rapid lethality when delivered at 2 mg/kg. Despite greater S1PR1 selectivity, IT-delivered SEW-2871 at 0.5 mg/kg also resulted in significant alveolar-capillary barrier disruption but was not lethal at 2 mg/kg. Consistent with S1PR1 regulation of alveolar/vascular barrier function, wild type mice pretreated with a S1PR1 antagonist, SB-649146, or S1PR1+/- mice exhibited loss of S1P/SEW-2871-mediated barrier protection following LPS challenge. Finally, our gene resequencing studies identified novel SNPs in genes involved in sphingolipid metabolism, S1P-mediated vascular signaling, and S1P-mediated barrier regulation which are potentially involved in susceptibility to ALI. These studies, which underscore the potential therapeutic effect of highly selective S1PR1 receptor agonists in reducing inflammatory lung injury, highlight the critical role of S1P delivery route, S1PR1 agonist concentration, and S1PR1 expression in target tissues.

Where applicable, the authors confirm that the experiments described here conform with The Physiological Society ethical requirements.

SA24

Brown and white adipose tissues: functional significances

J. Nedergaard and B. Cannon

The Wenner-Gren Institute, Stockholm, Sweden

Whereas we earlier thought about the existence of just two different adipose tissues – heat-producing brown and energy-storing white – we now see a much broader spectrum of tissues and cells; - and whereas we earlier thought that brown and white adipose tissues were closely related tissues, as the names imply, we now realize that brown adipose tissue is really developmentally a kind of muscle tissue – and although we do not really know the developmental origin of white adipose tissue, it is clearly not of muscle origin. These different developmental backgrounds are highly reflected in the character of metabolism in the tissues. To this should be added that certain cells (presently called brite or beige) within certain white adipose tissue depots may be able to express the (earlier considered) unique protein of brown adipose tissue: UCP1. The functional significances of the tissues for thermogenesis is strongly related to their ability to express sufficiently high levels of UCP1 to allow them to play a role in systemic metabolism. Whereas the issue of functional significance of the brown and white adipose tissue was earlier an issue mainly of academic interest – as it was thought that brown adipose tissue was not found in adult humans – the present understanding that brown fat exists and is active in adult humans has lifted the issue of the functional significance of the brown adipose tissue to being an enticing and possibly important issue in human metabolic research.

Where applicable, the authors confirm that the experiments described here conform with The Physiological Society ethical requirements.

SA25

Regulation of brown adipose tissue development: Progenitors, BMPs and beyond

T.J. Schulz

Adipocyte Development, German Institute of Human Nutrition, Nuthetal, Germany and Integrative Physiology and Metabolism, Joslin Diabetes Center, Boston, MA, USA

Obesity develops due to an imbalance of increased energy intake over decreased energy expenditure. A sedentary lifestyle in combination with readily available, energy-dense food sources have led to a pandemic spread of obesity in modern societies that represents a significant challenge to medical care systems. Excess calories from food are stored as triglycerides within the white adipose tissue (WAT), exacerbating a number of diseases associated with pathological overweight, such as diabetes, cardiovascular complications, and dyslipidaemias. Brown adipose tissue (BAT) is a specialized fat tissue that is dedicated to body temperature regulation. Due to its remarkable capacity for thermogenesis and its demonstrated presence in adult humans, BAT holds great promise for the treatment of obesity and the metabolic syndrome [1]. Two distinct types of brown fat cells have recently been described in mammalians: the constitutive or classical BAT (cBAT), which is of embryonic origin and anatomically located in the interscapular region of mice; and the so called recruitable BAT (rBAT), that has alternatively been termed brite (brown-in-white) or beige fat, due to its predominant anatomical distribution within WAT. While a common set of progenitor cells may give rise to white adipocytes and rBAT (within WAT), cBAT derives from a developmental lineage that is more closely related to skeletal muscle. Accordingly, recent findings have not only established that cBAT-progenitors are marked by a myogenic gene expression signature, but also that myogenic transcription factors, such as Myf5 and Pax7, are expressed in a common lineage of embryonic progenitors that give rise to cBAT in addition to skeletal muscle [2-4].

Morphogens have been implicated as instructive signals in the lineage determination of brown adipogenic progenitors. In this line, we were recently able to show that bone morphogenetic protein (BMP)-7 regulates the formation of brown adipocytes in multipotent progenitor cells, whereas loss of BMP7 resulted in a marked paucity of embryonic cBAT [5]. Interestingly, emerging evidence has also implicated BMP7 and BMP8b in the control of thermogenic capacity of mature BAT, altogether highlighting the central role of this pathway in brown fat physiology.

Taking advantage of these observations, we generated a knockout mouse model with conditional ablation of the type 1A BMP

receptor, BMPR1A, which functions as a major receptor for BMP7. Loss of BMPR1A in cells of the common muscle/cBAT-lineage severely impairs the formation of cBAT but not skeletal muscle during embryogenesis, thereby leading to reduced body temperature in new-born mice. Adult knockout mice, however, display an unexpected normalization of body temperature and overall thermogenic capacity. Importantly, knockouts are able to resume normal body temperature following prolonged exposure to cold, indicating that compensatory mechanisms are in place to counter the defect in thermoregulation induced by cBAT-paucity. Indeed, knockout mice show a greater propensity to recruit brown adipocytes within their classical WAT-depots, a process that is associated with increased sympathetic input to WAT. This previously unknown compensatory mechanism, aimed at restoring total brown-fat-mediated thermogenic capacity in the body, is sufficient to maintain normal temperature homeostasis and resistance to diet-induced obesity. These data suggest an important physiological cross-talk between constitutive and recruitable brown adipocytes involving cBAT-to-brain and brain-to-WAT communications and that is at least partially mediated by the sympathetic nervous system. This regulatory mechanism of body temperature may participate in the control of energy balance and metabolic disease and could provide a novel target for therapeutic approaches aimed at shifting the energy balance to a beneficial proportion [6].

Nedergaard J et al. (2007). Am J Physiol.Endocrinol Metab 293, E444-E452.

Petrovic, N et al. (2009). J Biol Chem 285, 7153-7164.

Seale P et al. (2008). Nature 454, 961-967

Wu J et al. (2012). Cell 150, 366-376

Tseng YH et al. (2008). Nature 454, 1000-1004

Schulz TJ et al. (2013). Nature, doi:10.1038/nature11943

Mary K Iacocca Foundation

German Research Foundation

Where applicable, the authors confirm that the experiments described here conform with The Physiological Society ethical requirements.

SA26

Turning off the furnace: downregulation of BAT function during lactation in mice

E. Krol

Institute of Biological and Environmental Sciences, University of Aberdeen, Aberdeen, UK

It has been proposed that the performance of lactating animals is limited by the capacity of the female to dissipate body heat – the heat dissipation limit (HDL) theory (Król and Speakman 2003, Speakman and Król 2010). This theory predicts that milk production might be constrained not by intrinsic properties of the mammary glands but rather by competitive heat production such as thermogenesis in brown adipose tissue (BAT). To test this prediction, we measured the expression of genes linked to thermogenesis in BAT of lactating laboratory mice. The applicability of BAT gene expression to reflect thermogenic activity of BAT was confirmed by a positive relationship between expression levels of several BAT genes (summarised by the first principal component following principal component analysis) and daily energy expenditure in virgin mice. Milk production at peak lactation was strongly and negatively associated with the expression of thermogenic genes in BAT (Fig. 1). Downregulation of these genes during lactation was correlated with low levels of circulating leptin and high levels of circulating prolactin (Fig. 2). We used path analysis to further examine associations between hormone levels, BAT activity (reflected by the PC1 scores) and milk production in lactating mice. Low levels of circulating leptin were correlated with and may contribute to the increase in milk production by reducing BAT activity and by BAT-independent mechanisms. High levels of circulating prolactin were correlated with increased milk production via associations with the activity of BAT rather than by BAT-independent mechanisms, but the relationships with prolactin were weaker than those with leptin. Our results are consistent with the prediction of the HDL theory that downregulation of BAT thermogenesis reduces competitive heat production, permitting greater production of lactogenic heat within the overall heat dissipation capacity limit. However, we cannot discount an alternative explanation that the causality in the associations is the reverse, i.e. that greater milk production, directly via thermogenic mechanisms alone (Cannon and Nedergaard 2004) or via endocrine and physiological processes, reduces BAT activity. The highly coordinated downregulation of thermogenic genes in BAT during lactation provides a new model system to investigate molecular pathways involved in switching on and off BAT activity and function.

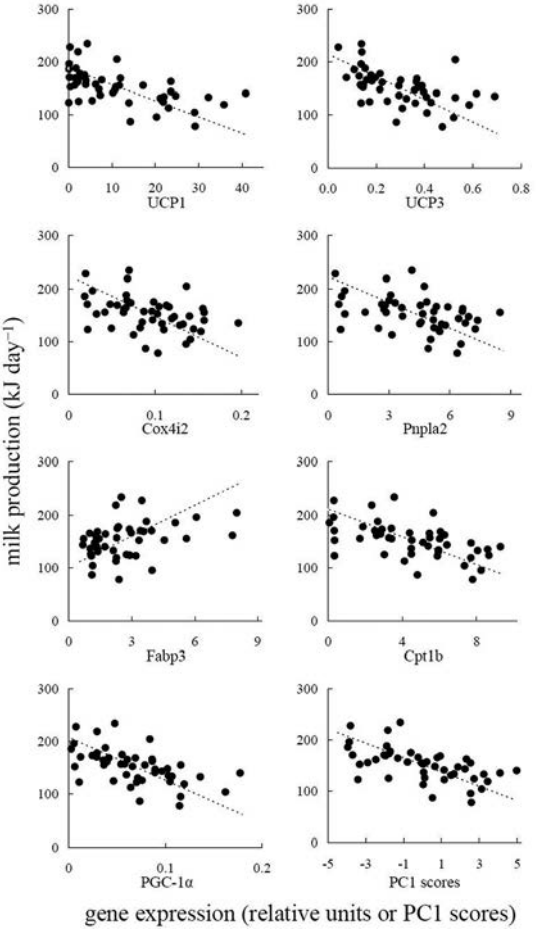

Fig. 1. Milk production plotted against the expression of several genes in brown adipose tissue (BAT) of lactating mice (N=47). Gene expression is normalized against the expression of housekeeping genes and presented in relative units. PC1 scores summarise the expression levels of thermogenic genes in BAT of lactating mice. All associations are significant (P<0.05) and fitted with the lines that represent reduced major axis regressions.

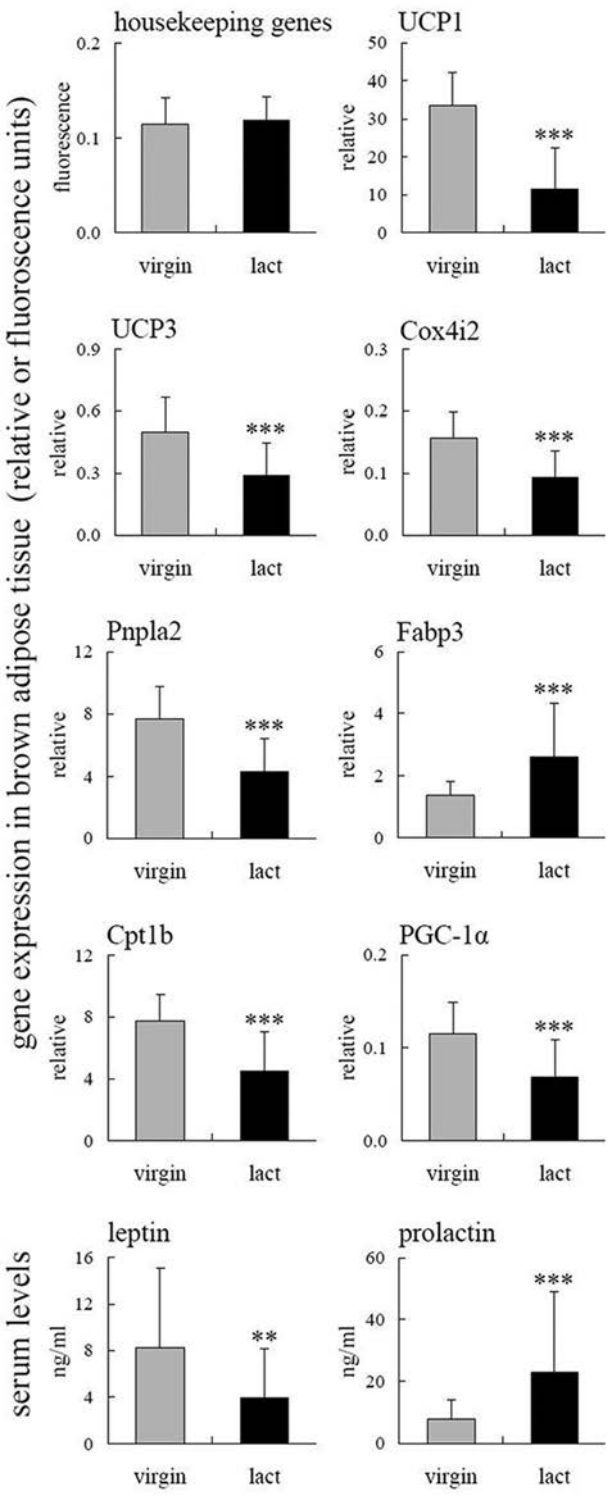

Fig. 2. Expression of genes in brown adipose tissue and corresponding levels of circulating leptin and prolactin in lactating (N=47) and virgin female (N=16) mice. Expression of housekeeping genes (geometric mean expression of β-actin and Rpl13a) is in arbitrary fluorescence units; expression of thermogenic genes is normalized against the expression of housekeeping genes and presented in relative units. Bars represent mean + 1 standard deviation. **P<0.01, ***P<0.001.

Król, E. and Speakman, J. R. (2003). Limits to sustained energy intake VI. Energetics of lactation in laboratory mice at thermoneutrality. J. Exp. Biol. 206, 4255-4266.

Speakman, J. R. and Król, E. (2010). Maximal heat dissipation capacity and hyperthermia risk: neglected key factors in the ecology of endotherms. J. Anim. Ecol. 79, 726-746.

Cannon, B. and Nedergaard, J. (2004). Brown adipose tissue: function and physiological significance. Physiol. Rev. 84, 277-359.

Where applicable, the authors confirm that the experiments described here conform with The Physiological Society ethical requirements.

SA27

Browning of adipose organ

S. Cinti

University of Ancona, Via Tronto 10a 60020 Ancona, Italy

Most of white and brown adipocytes, in spite of their well known different functions: i.e. storing energy (white) and thermogenesis (brown), are contained together in visceral and subcutaneous depots (adipose organ) in all mammals including humans. A growing body of evidence suggests that the reason for this anatomical mixture could reside in the fact that adipocytes have peculiar plastic properties allowing them to convert directly each other under appropriate stimuli. Under chronic cold exposure white convert into brown to support the need for thermogenesis and under obesogenic diet brown convert into white to satisfy the need of energy storing.
We recently showed that both white and brown adipocytes originate from endothelium of capillaries in adipose tissues. Differentiation imply a transformation of poorly differentiate cells that progressively assume structural and functional properties determining a specific phenotype. Electron microscopy defines specific steps of differentiation for white and brown adipocytes development. White and brown adipogenesis can occur in adipose organ of adult mammals under specific environmental requirements such as obesity (whitening) or cold adaptation (browning). The cytological modifications during whitening and browning of adipose organ are quite different from those of white or brown ontogenesis and suggest a direct conversion of mature adipocytes into a different phenotype (transdifferentiation). Morphometric and BrdU data obtained from the analysis of most depots of adult adipose organ in different strains of mice confirmed that this plasticity is mainly due to transdifferentiation. By lineage tracing and graft experiments we also showed that white adipocytes are able to reversibly transdifferentiate into milk-secreting epithelial cells in mammary glands of pregnant and lactating mice. Thus, transdifferentiation is a plastic phenomenon that can occur physiologically in the adipose organ of adult mammals with important implications for the therapeutic control of widely diffuse pathologies because the brown phenotype of the adipose organ is associated with obesity resistance and drugs inducing the brown phenotype curb obesity and T2 diabetes.

Where applicable, the authors confirm that the experiments described here conform with The Physiological Society ethical requirements.

SA28

CFTR activation by specific regions of the R domain

J. Chen[1] and M.J. Welsh[2]

[1]Department of Physiology, University of Hong Kong, Hong Kong, China and [2]Internal Medicine, University of Iowa, Iowa City, IA, USA

Cystic fibrosis transmembrane conductance regulator (CFTR) is an anion channel activated by PKA-dependent phosphorylation on its regulatory domain (R domain). Previous studies have demonstrated that the R domain controls phosphoryla-

tion-dependent CFTR activation by multiple effects including inhibition and stimulation on channel activity. However, it is unclear whether specific regions in the R domain are account for these mechanisms controlling CFTR activation. To test this hypothesis by screening the function of different R domain regions, we constructed a variety of R domain deletions over the region from residue 708 to 835 in CFTR. We studied the single-channel activity and PKA-independent constitutive Cl^- currents of these CFTR constructs. Our data indicate that deleting region 784-835 generated little constitutive Cl^- currents in the presence of 1 mM ATP alone, but reduced greatly CFTR channel activity after PKA phosphorylation. Further studies on small deletions in this region suggest that whole region 784-835 regulates the closing rate of the CFTR channel, whereas region 829-835 also modulates the channel opening rate. Therefore, the C-terminal part of the R domain is required for normal CFTR activity. Conversely, deletions of region 708-759 and region 760-783 had small effects on channel activity. Moreover, deleting region 760-783 or subregions 760-769 and 770-776 produced large constitutive Cl^- currents. These data suggest that region 760-776 may form an inhibitory motif that prevents CFTR activation. Taken together, our data suggest that the small R domain regions in different locations may form functional motifs that either inhibit or stimulate the channel activity of CFTR.

Where applicable, the authors confirm that the experiments described here conform with The Physiological Society ethical requirements.

SA29

3D structural models of CFTR

J. Mornon[1], B. Hoffmann[1], P. Lehn[2] and I. Callebaut[1]

[1]UMR7590, CNRS, Université Pierre et Marie Curie, Paris, France and [2]INSERM U1078, Université de Bretagne Occidentale, Brest, France

Cystic Fibrosis Transmembrane conductance Regulator (CFTR) is a chloride channel belonging to the large family of ABC exporters. The onset of the first experimental 3D structure, at atomic resolution, of a member of the ABC exporter family has permitted to perform homology modeling of the whole 3D structure (except for the regulatory R domain, which appears less structured). Presently, seven experimental structures of ABC exporters are known, in outward- and inward-facing conformations, having allowed to propose several models of the open and closed states of the ion channel, respectively.
These models, together with the results coming from several molecular dynamics studies, have been widely used to better understand the molecular basis of the CFTR functions, which intimately depend on the intricate interactions between the different subunits.
Recently, based on the improved knowledge we acquired from the experimental 3D structures, we made a new model of the open form of the CFTR channel, always based on the Sav1866 structure but refined in the Membrane Spanning Domains, which share very low levels of sequence identity with the ABC exporters templates. Moreover, we made a comprehensive analysis of the available 3D structures of ABC exporters, in order to define the conformational transition pathway followed between outward- and inward-facing conformations. This provide a new vision of the CFTR pore, both for the open and closed forms, the latter one being characterized by a more limited dissociation of the two Nucleotide-Binding Domains (NBDs) than for classical ABC transporters.
Altogether, the whole set of models of the 3D structure of human CFTR in different conformations open the door to a search of specific molecules, which may be able to fix the assembly of the different domains of the protein, a major cause of the low ability of CFTR to reach and remain at the membrane.

This work is supported by the French Association Vaincre La Mucoviscidose (Paris).

Where applicable, the authors confirm that the experiments described here conform with The Physiological Society ethical requirements.

SA30

CFTR's degenerate nucleotide binding site 1 probably moves during channel gating

L. Csanády[2], C. Mihályi[2], A. Szollosi[2], B. Töröcsik[2] and P. Vergani[1]

[1]Neuroscience, Physiology and Pharmacology, University College London, London, UK and [2]Medical Biochemistry, Semmelweis University, Budapest, Hungary

The CFTR ion channel belongs to the ATP binding cassette (ABC) protein superfamily. All ABC proteins share a similar domain organization with a "core" functional unit comprising two cytosolic nucleotide binding domains (NBDs) and two transmembrane domains (TMDs) (Fig. 1A). NBDs bind and hydrolyze ATP. Structurally they comprise a RecA-like subdomain ("head"), and a helical subdomain ("tail"). In the presence of ATP, NBDs can associate to form a tight "head-to-tail" dimer with two composite ATP binding sites at the interface (Fig. 1B). The ATP molecules provide crucial molecular contacts that stabilize the dimer. It is generally believed that NBD dimerization - driven by ATP binding - and dimer disengagement - following ATP hydrolysis - couple ATPase cycles to functionally important conformational changes in the TMDs. Most ABC proteins are transporters while CFTR, alone, is an ion channel. However, it was proposed that CFTR gating is "driven" by ATP binding and hydrolysis employing the molecular mechanisms used by transporters: ATP binds to NBD1 and NBD2 which associate to form an intramolecular "dimer" with composite sites 1 and 2 buried at the interface; ATP at site 2 is then hydrolyzed, triggering dimer dissociation; NBD dimer formation and dissociation are sensed by the TMDs where they result in opening and closing, respectively, of the pore (Fig. 1C).
In CFTR, consensus motifs involved in ATP binding and hydrolysis are conserved only in site 2. In site 1, non-conservative substitutions at key residues result in tight ATP binding, but no efficient hydrolysis. Non-canonical substitutions in the same key positions, presumably resulting in reduced or absent hydrolysis at one composite site, are also seen in other important human (e.g. TAP1/TAP2 and SUR) as well as in numerous yeast and prokaryotic transporters. The latter group includes TM287/288, a heterodimeric transporter whose high resolution structure has been very recently solved [1]. At site 1 in this crystal, an ATP molecule is bound and NBDs maintain contact but dimer interface is largely solvent accessible. Early biochemical studies revealed that ATP remains bound, unhydrolyzed, at CFTR's site 1 for periods of time much longer than a channel gating cycle (~1 s). This finding was confirmed in a recent functional study [2]. The high-affinity ATP analogue N6-(2-phenylethyl)-ATP (P-ATP) was found to speed up opening and to slow down closing of CFTR channels. The onset of these two effects, following sudden replacement of ATP with P-ATP,

followed distinct time courses. Whereas the effect on opening rate appeared immediately, likely reflecting P-ATP binding to the rapid-turnover site 2, the onset of slowed closure was delayed by 30-50 s, consistent with an action of P-ATP at slow-turnover degenerate site 1. Furthermore, because nucleotide exchange rate at site 1 was affected by mutations in the tail of NBD2, the authors suggested that composite site 1 remained associated in closed channels. Our thermodynamic studies [3], examining state-dependent changes in energetic coupling between pairs of residues on opposing faces of site 1, supported this idea. A lack of change in energetic coupling for three such pairs was interpreted to be consistent with the interface around composite site 1 remaining "closed" throughout the gating cycle.

A more detailed analysis of the changes in gating kinetics caused by two site 1 perturbations has, however, lead us to question this initial interpretation. We focused on the effects of P-ATP dependent on site-1 occupancy and of the H1348A mutation in the NBD2 tail. Both site-1 perturbations had similar effects on gating: a 2-3 fold decrease in the non-hydrolytic closing rate (k-1, Fig. 1C) and in the rate of the O1→O2 transition (k1), consistent with the changes in site 1 causing a selective stabilization of state O1 with respect to both posthydrolytic O2 and closed C1. The pore-closing O2→C2 step was not affected. Could the lack of histidine/presence of phenylethyl moiety in site 1 be altering the energetics of other parts of the protein (e.g. TMDs and site 2) without site 1 actually moving during opening and hydrolysis? This interpretation would require that the site 1 perturbations (which cause an increase in the energetic barriers the channel must overcome to exit the O1 state) have different effects on the O1 ground state and on the transition states of the opening and hydrolysis steps. It is difficult to envisage how such differential allosteric effects could occur if the region around the perturbation remained static. A simpler interpretation of the data is that the physicochemical environment around the 1348 histidine side chain and around the N6 group on the adenine is not identical in O1 and in those transition states. In other words, this region of site 1 moves during opening and coincident with hydrolysis at the active site 2.

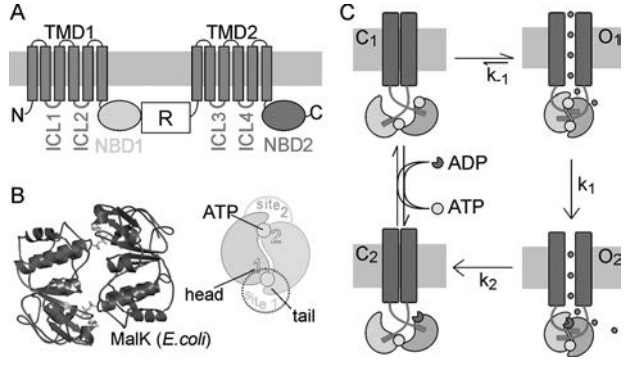

Fig. 1 A: Topology of CFTR. B: NBDs form head-to-tail dimers, with two ATP molecules at the interface. C: While ATP remains bound, unhydrolysed, at site 1 (lower composite site) ATP binding and hydrolysis at site 2 are coupled to CFTR pore opening and closing, respectively.

Hohl, M et al (2012). Nat Struct Mol Biol 19:395-402

Tsai, MF et al (2010). J Gen Physiol. 135: 399-414

Szollosi, A et al (2011). J Gen Physiol. 137: 549-562

Where applicable, the authors confirm that the experiments described here conform with The Physiological Society ethical requirements.

SA31

Employing chemical biology to define the molecular defects caused by the major Cystic Fibrosis mutant, F508del-CFTR

C. Bear, P.D. Eckford, M. Ramjeesingh and C. Li

The Hospital for Sick Children, Toronto, ON, Canada

Cystic Fibrosis is caused by loss of function mutations in the Cystic Fibrosis Transmembrane Conductance Regulator Gene: CFTR and is associated with severe airway disease. Loss of CFTR channel function on the surface of epithelial cells leads to mucus obstruction with recurrent infection. Drug discovery efforts have identified a "potentiator" drug (Ivacaftor or VX-770) that partially repairs the defective channel activity exhibited by the rare CF causing mutation: G551D and leads to improved lung function. Now, there is an urgent need to find a compound (or compounds) to rescue the defects caused by the major CF causing mutation: F508del present on at least one allele in 90% of CF patients. The F508del mutation causes the CFTR protein to misfold, leading to its retention in the endoplasmic reticulum and degradation. "Corrector" compounds have been identified that improve folding and trafficking of F508del-CFTR to the surface of cultured cells. However, the lead corrector: VX-809, failed to show efficacy in clinical trials of patients homozygous for this mutation. A recent press release reported promising, yet variable results for Phase 2a clinical trials of the combination: VX-809 plus VX-770. Most patients exhibited a relatively modest increase in FEV1 -highlighting the requirement for further drug development. The discovery of better modulators of mutant CFTR protein will be enabled by understanding the mechanism of action of these existing compounds. We hypothesize that these compounds bind directly to modulate CFTR folding and function and tested this hypothesis in novel in-vitro assays, using purified and reconstituted Wt and mutant CFTR.

Our in-vitro studies show that the potentiator VX-770 directly modified the channel activity of purified and reconstituted purified CFTR proteins. Channel activity of purified protein was evaluated using both a proteoliposomal flux assay and in planar lipid bilayer studies. Regardless of the CFTR genotype, ie. Wt, F508del or G551D-CFTR, we observed an increase in channel activity of PKA phosphorylated CFTR protein in the presence of its natural activating ligand, ATP. Interesting, we also found that VX-770 enhanced channel activity of phosphorylated CFTR in the nominal absence of ATP, suggesting that it acts via a canonical pathway to modify the channel gate. Currently, we are employing chemical analogues of VX-770 to gain insight into the structural properties of the VX-770 binding site and the mechanism underlying ATP independent channel activity.

Interestingly, we found that the two corrector compounds: VX-809 (in clinical trial) and C18 (an analog of VX-809) also bind directly to Wt-CFTR, F508del-CFTR and G551D-CFTR. The binding of C18 led to enhanced ATP-independent channel activity in all three of these genotypes, suggesting that it may share a similar binding site as the VX-770 or its binding leads to similar conformational changes. In the case of the purified mutant, F508del-CFTR, the binding of VX-809 or C18 also induces a more stable protein conformation, with a reduced propensity to aggregate. This latter observation, likely accounts for the partial "rescue" effect of these compounds on the misfolding of F508del-CFTR. As in our studies of VX-770, we are employing chemical analogues of C18 to probe the properties of its binding site on mutant CFTR. We anticipate that these binding studies will report the structural defects caused by the

F508del-CFTR mutation and enable discovery of more efficacious corrector compounds.
Together, these studies support the use of small chemical molecules in probing the structural basis for folding and function of CFTR.

These studies were supported by Operating grants awarded to C.E.B. from the Canadian Institutes of Health Research and Cystic Fibrosis Canada

Where applicable, the authors confirm that the experiments described here conform with The Physiological Society ethical requirements.

SA32

Relating genotypes to phenotypes

S.W. Omholt

Norwegian University of Science and Technology, Trondheim, Norway

One uses DNA information in at least four explanatory settings: as a pure marker where we do not make a direct link to any particular phenotype; when we by statistical means establish an association between one or more chromosomal regions and phenotypic variation; when we can document that a particular DNA variation (natural or imposed) does indeed cause a phenotype; and finally in a causally cohesive setting where we can also explain how the genetic variation causes the observed phenotype in terms of biophysical mechanism at the cell, tissue and organ system levels. Even though there are several challenges associated with the first three types of explanation, they are all dwarfed by those facing us in connection with the fourth type. But these are the ones to be overcome if we are to bridge the gap between the genotype and the phenotype with real understanding, and thus realize the disciplinary goals of both genetics (Bateson, 1906 p.190) and physiology (Gove, 1981).
The relation between genotype and phenotype can be conceptualized as a genotype-phenotype map (GP map), assigning a phenotype to each possible genotype. The concept is highly instrumental for physiological research and concords well with the disciplinary goals of physiology as they are laid out in the standard definition of the discipline: "the study of the functions and activities of living matter (as of organs, tissues, or cells) as such and of the physical and chemical phenomena involved" (Webster's Third New International Dictionary). Fulfilling these goals demands an understanding of the mechanisms underlying the GP map.
The GP map concept applies to any time point in the ontogeny of a living system and it is an abstraction of a relation that is the outcome of very complex dynamics that include environmental effects. The concept does not imply that DNA has a privileged place in the chain of causality authorizing the current zoo of anthropomorphic concepts we attribute to it (Omholt, 2012; Noble, 2012). As advocated by Omholt (2012), DNA allows a system to induce perturbations of its own dynamics as a function of its own system state or phenome. Thus there is no direct causal arrow from genotype to phenotype in the sense that DNA is responsible for exerting a direct effect as a sub-system on the system dynamics. The causality flows from the system state through a change in use of DNA (as an inert system component) that results in a change in the production of RNA and protein, which in turn perturbs the system's dynamics. In those cases where variations in DNA cause changes in the perturbation regime it may lead to different system dynamics and thus physiological variation. This way of perceiving the function of DNA in a GP map context brings physiology back as the major arena for understanding the manifestation and propagation of genetic variation.
The talk will elaborate on the above concepts and show how computational physiology is the key to combine genetics and physiology. Starting out from simple illustrations on how to analyse genetic concepts within a systems dynamics framework, the talk will present current work to link genetics with mechanistic multiscale and multiphysics model descriptions of high-dimensional phenotypes by use of so-called causally cohesive genotype to phenotype models (cGP models). It will be shown how this approach is capable of providing a direct link between genetic variation, molecular regulatory biology and phenotypic variation. It can therefore be used to build theory about heredity phrased in terms of regulatory principles, something which standard genetic concepts and approaches are incapable of.

Where applicable, the authors confirm that the experiments described here conform with The Physiological Society ethical requirements.

SA33

Cross-species cloning: influence of cytoplasmic factors on development

Y. Sun

Institute of Hydrobiology, CAS, Wuhan, China

The crosstalk between naive nucleus and maternal factors deposited in egg cytoplasm before zygotic genome activation is crucial for early development of vertebrates. However, it is difficult to clarify the relative roles of zygotic and cytoplasmic factors in normal developing embryos, in which both types of factors were derived from the same species. Cross-species nuclear transfer provides an ideal system to study the relative role and crosstalk between egg cytoplasm and zygotic nucleus in development.
In most studies of nuclear transplantation, the cloned animals were obtained by intraspecies nuclear transfer and are phenotypically identical to their nuclear donors. In fishes, however, cross-species nuclear transplantation could be achieved in quite a few species. By transferring nuclei from transgenic common carp (Cyprinus carpio) into enucleated eggs of goldfish (Carassius auratus), we generated seven cross-genus cloned transgenic fish. Nuclear genomes of the cloned fish were exclusively derived from the nuclear donor species, common carp, whereas the mitochondrial DNA from the donor carp gradually disappeared during the development of nuclear transfer (NT) embryos. The somite development process and somite number of nuclear transplants were consistent with the recipient species, goldfish, rather than the nuclear donor species, common carp. This resulted in a long-lasting effect on the vertebral numbers of the cloned fish, which belonged to the range of goldfish. These demonstrate that fish egg cytoplasm not only can support the development driven by transplanted nuclei from a distantly related species at the genus scale but also can modulate development of the nuclear transplants.
Although cross-species NT could be used to retain the genetic viability of a species near extinction, most embryos produced by cross-species NT were unable to develop to later stages due to incompatible nucleo-cytoplasmic interactions between the donor nuclei and the recipient cytoplasm from different species. To study the early nucleo-cytoplasmic interaction in

cross-species NT, two laboratory fish species, zebrafish (Danio rerio) and Chinese rare minnow (Gobiocypris rarus), from different subfamilies were used to generate cross-subfamily NT embryos. Suppression subtractive hybridization (SSH) was performed to screen out differentially expressed genes from the forward and reverse subtractive cDNA libraries. After dot blot and real-time PCR analysis, 80 of 500 randomly selective sequences were proven to be differentially expressed in the cloned embryos. Among them, 45 sequences shared high homology with 28 zebrafish known genes, and 35 sequences were corresponding to 22 novel expressed sequence tags (ESTs). Based on functional clustering and literature mining analysis, the up- and down-regulated genes in the cross-subfamily cloned embryos were mostly found to be relevant to transcription and translation initiation, cell cycle regulation, protein binding, etc. Therefore, it is concluded that the fish egg cytoplasm could not only support the division and development of nuclei from another species, but also exert impact on the cellular homeostasis of the cross-species clones at different levels of biological processes.

Zebrafish and Chinese rare minnow were also utilized to produce mutual crossbred embryos, zebrafish ♀ X Chinese rare minnow ♂ (ZR) and Chinese rare minnow ♀ X zebrafish ♂ (RZ), and to examine the impact of cytoplasm from different species on a common type of nucleus. Although these two types of crossbred embryos originated from common nuclei of the same genetic materials, various developmental capacities were gained due to different origins of the egg cytoplasm. Using cDNA amplified fragment length polymorphism (cDNA-AFLP), we compared transcript profiles between the mutual crossbred embryos at two developmental stages (50%- and 90%-epiboly). Three thousand cDNA fragments were generated in four cDNA pools with 64 primer combinations. All differentially displayed transcript-derived fragments (TDFs) were screened by dot blot hybridization, and the selected sequences were further analyzed by semi-quantitative RT-PCR and quantitative real-time RT-PCR. Compared with ZR embryos, 12 genes were up-regulated and 12 were down-regulated in RZ embryos. The gene fragments were subjected to BLASTN analysis. The sequences encoded various proteins which functioned at various levels of proliferation, growth, and development. One gene (ZR6), dramatically down-regulated in RZ embryos, was chosen for loss-of-function study. The knockdown of ZR6 gave rise to the phenotype resembling that of RZ embryos.

All these evidences reveal that fish nucleus developing in the circumstance of egg cytoplasm could be largely influenced by the cytoplasmic factors. Therefore, developmental process should be interpreted in a systematic way rather than in a way that solely focuses on the role of nuclear genome.

Where applicable, the authors confirm that the experiments described here conform with The Physiological Society ethical requirements.

SA34

The Read-Write (RW) genome

J.A. Shapiro

Dept. of Biochemistry and Molecular Biology, University of Chicago, Chicago, IL, USA

The genome is traditionally treated as a Turing tape or Read-Only Memory (ROM) subject to change by copying errors. This default assumption of accidental mutation arose from the inevitable ignorance of the mechanisms of genome change in the 19th and early 20th Centuries. It contributed to the historical divorce between physiology, homeostasis and regulation, on the one hand, and studies of genetics and evolution, on the other.

In contrast to early assumptions about genomic accidents, research dating back to the 1930s has shown that genetic change is the result of cell-mediated processes, not simply damage to the DNA. McClintock's study of X-ray mutagenesis found that this mode of induced genome change arose because ionizing radiation caused chromosome breakage and cells have the capacity to detect, mobilize and join broken ends together, generating chromosome rearrangements (McClintock 1984; McClintock 1987). In other words, X-ray mutagenesis resulted from a physiological response to genome damage.

This cell-active view of genome change applies to all scales of variation, from point mutations to large-scale genome rearrangements and whole genome duplications (WGDs) (Shapiro 2011). As with X-rays, we now recognize all mutagen-induced change to result from the action of error-prone repair processes. The smallest "point mutations" involve the action of so-called "trans-lesion mutator polymerases" (Napolitano, Janel-Bintz et al. 2000; Goodman 2002).

Larger chromosome changes involve biochemical repair of double-strand breaks by "non-homologous end-joining" (NHEJ) complexes (Lieber, Gu et al. 2010) or the action of mobile genetic elements (Kazazian 2004; Nakayashiki 2011). Many large changes, including whole genome duplication (WGD), occur because of epigenetic modifications in response to stress conditions, chemical stimuli, or breeding between different species (http://shapiro.bsd.uchicago.edu/ExtraRefs.CellularRegulationNaturalGeneticEngineering.shtml, http://shapiro.bsd.uchicago.edu/ExtraRefs.WholeGenomeDoublingCriticalStagesEvolution.shtml, http://shapiro.bsd.uchicago.edu/TableII.7.shtml, http://shapiro.bsd.uchicago.edu/TableII.8.shtml, and http://shapiro.bsd.uchicago.edu/TableII.10.shtml). Moreover, cell-mediated changes to the genome can be targeted to particular locations in the genome by well-established molecular mechanisms (http://shapiro.bsd.uchicago.edu/TableII.11.shtml). It is possible, therefore, to begin understanding the genome evolutionary process as a sophisticated physiological response to ecological modifications and disruptions.

The take-home lesson of this lecture is that DNA changes are biological (biochemical, physiological) and not accidental in origin. Consequently, it is necessary to revise our concept of genome storage to accommodate the potentials of a Read-Write (RW) storage system. The evolutionary implications of this conceptual change are profound. Cell inscriptions on the genome, like all biochemical and physiological activities, are subject to regulation by control circuitry, in particular epigenetic controls. The interactions between these control circuits and the environment make it possible to begin a detailed experimental investigation of the relation between ecological and genomic changes in evolution.

Goodman, M. (2002). "Error-prone repair DNA polymerases in prokaryotes and eukaryotes." Ann Rev Biochem 71: 17-50. http://www.ncbi.nlm.nih.gov/pubmed/12045089.

Kazazian, H. H., Jr. (2004). "Mobile elements: drivers of genome evolution." Science 303(5664): 1626-1632. http://www.ncbi.nlm.nih.gov/pubmed/15016989.

Lieber, M. R., J. Gu, et al. (2010). "Nonhomologous DNA end joining (NHEJ) and chromosomal translocations in humans." Subcell Biochem 50: 279-296. http://www.ncbi.nlm.nih.gov/pubmed/20012587.

McClintock, B. (1984). "The significance of responses of the genome to challenge." Science 226(4676): 792-801. http://www.ncbi.nlm.nih.gov/pubmed/15739260.

McClintock, B. (1987). Discovery And Characterization of Transposable Elements: The Collected Papers of Barbara McClintock New York, Garland.

Nakayashiki, H. (2011). "The Trickster in the genome: contribution and control of transposable elements." Genes Cells 16(8): 827-841. http://www.ncbi.nlm.nih.gov/pubmed/21722269.

Napolitano, R., R. Janel-Bintz, et al. (2000). "All three SOS-inducible DNA polymerases (Pol II, Pol IV and Pol V) are involved in induced mutagenesis." Embo J 19(22): 6259-6265. http://www.ncbi.nlm.nih.gov/pubmed/11080171.

8. Shapiro, J. A. (2011). Evolution: A View from the 21st Century. Upper Saddle River, NJ, FT Press Science. .

Where applicable, the authors confirm that the experiments described here conform with The Physiological Society ethical requirements.

SA35

Computational biology as a tool for reverse engineering genotype-phenotype relations

C. Cha[1,2], Y. Himeno[2], T. Shimayoshi[3], Y. Nakamura[4], E. Santos[2], A. Amano[2] and A. Noma[2]

[1]OCDEM, University of Oxford, Oxford, UK, [2]Bioinformatics, Ritsumeikan University, Ritsumeikan, Japan, [3]ASTEM Research Institute of Kyoto, Kyoto, Japan and [4]Diabetes and Clinical Nutrition, Kyoto University, Kyoto, Japan

Electrically excitable cells generate time-dependent change in transmembrane potential (action potential), which arises from complex interactions among ion channels and transporters expressed in the membrane. To understand how the excitable cell regulates its function, it is important to elucidate the role of individual channels in generating particular shape of action potentials. Conventionally, inhibition or knock-out methods have been used in experimental or even in mathematical modelling studies. However, inhibition of one kind of channel always induces unintended modification of the rest of channels through the complex interaction, and then the response cannot be considered as the effect of the channel of interest. We developed a new analytical method- lead potential analysis, which can be applied to any electrophysiological cell models and calculate contribution of each cellular component to membrane potential change in a quantitative way, not interfering with normal cellular condition. In this presentation, I demonstrate the recent studies to apply lead potential analysis, in which the electrical mechanisms were successfully elucidated in cardiac sinoatrial node cell and pancreatic beta cell.

Where applicable, the authors confirm that the experiments described here conform with The Physiological Society ethical requirements.

SA36

The modern synthesis: extension or replacement?

G.B. Müller

Department of Theoretical Biology, University of Vienna, Vienna, Austria

Since the time of the last major theoretical integration in evolutionary biology, the Modern Synthesis of the 1930s and 1940s, the biosciences have made significant advances, and today's evolutionary biology operates with numerous concepts that were not part of the original synthesis. Since the retrospective subsumption of these novel concepts under the well defined Synthesis framework is impossible, propositions for a new and extended evolutionary synthesis are on the rise. One characteristic feature of such revised models is the shift from the population dynamic emphasis, favored by the traditional approach, towards a causal-mechanistic explanation of phenotypic complexity. The integration, for instance, of organizing relations between genes, cells, and tissues in development, as well as the interactions of these processes with physiological and environmental factors, entails a revised understanding of the evolutionary role of natural selection. It will be argued that not only the kind and number of theory elements have increased, but their inclusion also modifies the formal structure of evolutionary theory and expands its explanatory capacity.

Where applicable, the authors confirm that the experiments described here conform with The Physiological Society ethical requirements.

SA37

Generating and regenerating blood and the cardiovascular system

R. Patient

University of Oxford, Headington, UK

Blood cells are turned over rapidly and we carry a relatively modest number of stem cells to regenerate them. One of the key properties to understand is how these cells stably maintain the undifferentiated state. To study this, we have taken the approach of determining how these cells are programmed. We have lineage traced the cells in Xenopus and zebrafish embryos to determine their history and the niches that they occupy. We have then searched these niches for the signals that programme the cells. We have also begun to identify the nuclear responses to these signals that lead to the establishment of a stable networks of transcription factors that specify cell fate. We have taken a similar approach to the myocardium, and more recently have begun to compare normal development with regeneration. We are attempting to identify the cells, signals and transcriptional networks involved in this process, an understanding of which could inform regenerative strategies in the human heart.

MRC, BHF, Wellcome Trust and CardioCell EU FP7

Where applicable, the authors confirm that the experiments described here conform with The Physiological Society ethical requirements.

SA38

The fate of mesothelial cells and their role in tissue homeostasis

T. Benameur[1,2], W. Qing[2], A. Thornburn[2], P. Hohenstein[2], N. Hastie[2] and B. Wilm[1]

[1]Cellular and Molecular Physiology, University of Liverpool, Liverpool, UK and [2]MRC Human Genetics Unit MRC IGMM, MRC IGMM University of Edinburgh, EDINBURGH, UK

Mesothelium consists of a monolayer of specialized cells known as mesothelial cells that form during embryonic development over internal organs and line peritoneal, pleural and pericardial cavities. Mesothelial cells have been shown to undergo

epithelial-mesenchymal transition (EMT) and during embryonic development differentiate into a variety of cells including vascular smooth muscle cells in the heart, lungs and intestine, fibroblast cells and cardiomyocytes. Recent studies have shown that the mesothelium of the heart, the epicardium, contributes to the coronary vasculature during embryonic development and is involved in repair mechanisms in injury models of the heart and liver.
In order to determine which tissues and organs mesothelial cells contribute to during embryonic development and how they maintain adult tissue homeostasis, we have established a lineage tracing strategy using a mesothelial-specific Cre (Recombinase) mouse line.
In order to demonstrate a stem/progenitor cell role of mesothelial cells, Tamoxifen was administrated to pregnant or adult mice carrying the mesothelial-specific CreERT2 construct, in combination with a Rosa26-based reporter, for short and long term pulse-chase experiments. Our results indicate that mesothelial-derived cells contribute to a range of tissues in the developing embryo and in the adult. Specifically, in embryos, mesothelial cells contributed to the formation of vascular structures in developing kidneys. Furthermore, in adult mice, our analysis revealed that Tamoxifen pulse induced recombination is dose and route of administration dependent, leading to significant recombination of reporter alleles which can be detected weeks after Tamoxifen injection. As a consequence of mesothelial-specific lineage tracing, we found clonal distribution of labelled cells in the mesothelium of all internal organs, including the heart, lungs, intestine, spleen, and kidney.
Here, we will present our current understanding of the dynamics of mesothelial cell contribution to tissue maintenance and regeneration. Further, we will discuss that duration and route of Tamoxifen administration are important parameters that need to be considered during Tamoxifen-induced lineage tracing studies.

You Ying Chau; Allyson Ross; Paul Perry; Mathiew Pearson; Katie Gibson; Lynn McLaughlyn; Pamela Pask; Andrew Houghton

Where applicable, the authors confirm that the experiments described here conform with The Physiological Society ethical requirements.

SA39

HIFs, metabolism, and tumor progression

M.C. Simon

Cell and Developmental Biology, University of Pennsylvania, Philadelphia, PA, USA

Solid tumors exhibit heterogeneous microenvironments, often characterized by limiting concentrations of oxygen (O2), glucose, and other nutrients. How oncogenic mutations alter stress response pathways, metabolism, and cell survival in the face of these challenges is incompletely understood. Here, we report that constitutive mTORC1 activity renders hypoxic cells dependent on exogenous desaturated lipids, as levels of de novo synthesized unsaturated fatty acids are reduced under low O2. Specifically, we demonstrate that hypoxic Tsc2-/- cells deprived of serum lipids exhibit a magnified UPR response, but fail to appropriately expand their ER, leading to IRE1-dependent cell death that can be reversed by the addition of unsaturated lipids. UPR activation and apoptosis were also detected in Tsc2-deficient kidney tumors. Importantly, we observe this phenotype in multiple human cancer lines and suggest that cells committed to unregulated growth within ischemic tumor microenvironments are unable to balance lipid and protein synthesis due to a critical limitation in desaturated lipids.

Where applicable, the authors confirm that the experiments described here conform with The Physiological Society ethical requirements.

SA40

Notch signals and intestinal stem cells: from crypt homeostasis to colon cancer

S. Fre

Developmental Biology and Genetics, Institut Curie, PARIS, France

In adult organisms, tissues are maintained and repaired by stem cells, which divide and differentiate to generate more specialized progeny. The mechanisms that control the balance between self-renewal and differentiation promise fundamental insights into the origin and design of multi-cellular organisms. A tissue that is particularly suited to approach these questions is the intestinal epithelium, as it consists of a monolayer of epithelial cells that endlessly divide, migrate while differentiating and are replaced to ensure continuous and fast cell renewal throughout adult life. In this tissue, somatic stem cells represent crucial elements that govern tissue remodeling and homeostasis and the combined work of several laboratories has provided evidence for the existence of at least two different stem cell populations in the small intestinal crypt. In this program, we focus on the Notch signaling pathway as a new promising marker to study gut stem cell physiology. Our observations indicate that the Notch1 receptor is expressed in both crypt stem cell populations, implying that it can mark either one of the two in vivo and providing a precious tool to dissect the hierarchy between these different stem cells.
Notch signaling plays an evolutionarily conserved role in metazoans, which basically consists in mediating cell coordination in development and during adult tissue homeostasis, through the profound effects it has on stem cells. The precise identity of the cells in which Notch signaling is active is still unclear, mainly due to the lack of reliable tools to investigate Notch expression in vivo. For this purpose, we have recently developed and characterized a novel roster of unique transgenic mice that permit to assess Notch expression and activation in vivo in an unprecedented fashion. Thanks to these novel mice, we have been able to formally show that the expression of the Notch1 receptor and of its transcriptional target Hes1 identifies crypt stem cells. We are now using these mouse models to dissect the hierarchy between stem cell populations in the small intestine, while expanding our knowledge on colonic stem cells, that remain poorly studied. In addition, we study the dynamic behavior of stem cells during regeneration upon injury.
The critical role played by Notch signaling in intestinal renewal and differentiation, as well as in tumorigenesis in this tissue, is exemplified by the vast number of reports on this topic appeared in recent years (i.e. [1-6]). In the past five years, the Notch signaling pathway has emerged as an essential regulator of intestinal homeostasis; indeed Notch signals can control the segregation of each mature lineage from undifferentiated progenitor cells, and they are instrumental for maintaining the proliferating intestinal cell pool. When Notch signaling is inhibited, all crypt cells cease to proliferate and differentiate into secretory cells [4]. Reciprocally, we have shown that gain of Notch function in the developing intestinal epithe-

lium dramatically impairs cell differentiation and increases the proportion of dividing cells [2]. The role of Notch in promoting intestinal proliferation requires Wnt signals, whereas it specifies cell fate independently of Wnt [5]. Importantly, our work has shown that Notch acts in synergy with the Wnt pathway to induce intestinal polyps [5]. The accumulated evidence in both systems supports a role for Notch in expanding a potentially malignant cell population and hence increasing the chances of a tumorigenic event. It is indeed widely accepted that the primary events in tumourigenesis are linked to stem cell transformation: the process of tumor development is thought to initially affect normal stem cells or closely related early progenitors. In order to establish the identity of Notch1-expressing cells within a tumor and to follow their fate in vivo, we have crossed N1-CreERT2/GFP mice to Apc heterozygous animals, which give rise to intestinal tumors by stochastic loss of heterozygosity (LOH) at the Apc locus. Our novel genetic fate-mapping system will consent to identify which cells within a tumor express the Notch1 receptor, as well as to follow the progeny of the Notch-expressing tumor cells. Our preliminary results show that only a small fraction of tumor cells expresses the N1cre-driven GFP reporter. These experiments will allow us to highlight in vivo which and how many cells within a tumor present Notch activity.

Our research aims at understanding the molecular features of adult stem cells, as well as the mechanisms by which Notch signaling controls the fate of specific cell populations during regeneration and tumourigenesis. We believe that the identification of common organizational principles of tissue architecture is an essential step in order to develop safe and efficacious applications of stem cells in regenerative medicine.

Fre, S., et al., Notch lineages and activity in intestinal stem cells determined by a new set of knock-in mice. PLoS One, 2011. 6(10): p. e25785.

Fre, S., et al., Notch signals control the fate of immature progenitor cells in the intestine. Nature, 2005. 435(7044): p. 964-8.

Pellegrinet, L., et al., Dll1- and Dll4-mediated Notch signaling is required for homeostasis of intestinal stem cells. Gastroenterology, 2011.

van Es, J.H., et al., Notch/gamma-secretase inhibition turns proliferative cells in intestinal crypts and adenomas into goblet cells. Nature, 2005. 435(7044): p. 959-63.

Fre, S., et al., Notch and Wnt signals cooperatively control cell proliferation and tumorigenesis in the intestine. Proc Natl Acad Sci U S A, 2009. 106(15): p. 6309-14.

Fre, S., et al., Notch signaling in intestinal homeostasis across species: the cases of Drosophila, Zebrafish and the mouse. Exp Cell Res, 2011.

Where applicable, the authors confirm that the experiments described here conform with The Physiological Society ethical requirements.

SA41

CD133+ progenitors and regeneration of the renal tissue: from cells to vesicles

B. Bussolati

Dept of Molecular Biotechnology and Health Sciences, University of Torino, Torino, Italy

The tubular compartment of the nephron displays a high regenerative ability. We previously isolated CD133+ stem/progenitor cells in the tubular compartment of the human kidney(1-3). However, their possible contribution to repair is unknown. We here evaluated the possible modulation of CD133+ cells by the hypoxic environment, the molecular mechanisms involved and their possible involvement in renal regeneration.

CD133+ progenitors cultured under hypoxia (1%O2) showed increased proliferation and clonogenic ability. When injected in vivo, CD133+ hypoxic progenitors showed ability to differentiate in structures resembling the different segments of the nephron. Moreover, hypoxia up-regulated Oct-4 isoforms in CD133+ cells via regulation of the Oct4 promoter. In parallel, hypoxia downregulated microRNA-145, known to act as an Oct4 transcriptional repressor. Epithelial differentiation increased microRNA-145 and reduced Oct4 level, suggesting a balance between Oct4 and microRNA-145. Labelled CD133+ progenitors localized into the injured kidneys in a model of acute renal damage and promoted renal functional regeneration. In addition, modulation of the HIF pathway through PHD2 inhibitors increase EPO production by CD133+ cells. These results suggest that hypoxia may direct CD133+ progenitors toward a more stem phenotype via Oct4A/miR145 balance. The plasticity of renal CD133+ cells could be exploited in renal regeneration after hypoxic damage. Among the mechanisms that may be involved in the regenerative properties of CD133+ cells, release of growth factors and of microvescicles were investigated. Results show that hypoxic CD133+ cells release microvescicles enriched in microRNA and that exosome injection may directly mediate their in vivo effect in a model of acute kidney injury.

Bussolati B, Bruno S, Grange C, Buttiglieri S, Deregibus MC, Cantino D,

Camussi G. Isolation of renal progenitor cells from adult human kidney. Am J

Pathol. 2005 Feb;166(2):545-55.

Bussolati B, Moggio A, Collino F, Aghemo G, D'Armento G, Grange C, Camussi G.

Hypoxia modulates the undifferentiated phenotype of human renal inner medullary

CD133+ progenitors through Oct4/miR-145 balance. Am J Physiol Renal Physiol. 2012

Jan 1;302(1):F116-28.

Bussolati B, Collino F, Camussi G. CD133+ cells as a therapeutic target for

kidney diseases. Expert Opin Ther Targets. 2012 Feb;16(2):157-65. doi:

10.1517/14728222.2012.661417.

Where applicable, the authors confirm that the experiments described here conform with The Physiological Society ethical requirements.

SA42

Pathophysiology of human heart failure: importance of skeletal muscle myopathy and reflexes

M.F. Piepoli[1] and A. Crisafulli[2]

[1]Heart Failure Unit, Cardiac Dept, G. da Saliceto Hospital, AUSL Piacenza, Italy and [2]Department of Medical Sciences, Sports Physiology Lab, University of Cagliari, Cagliari, Italy

The origin of symptom of exercise intolerance is still considered one of the major challenges among scientists and clinicians involved in the care of patients with chronic heart failure (CHF). In contrast to the traditional vision that saw a malfunction of the heart as a pump as the leading cause, in the last 20 years there has been mounting evidence that the complex pathophysiology of CHF begins with an abnormality

of the heart as a "*primum movens*", but involves adaptive changes in many body parts, including the cardiovascular, musculoskeletal, renal, neuroendocrine, haemostatic, immune, and inflammatory systems. These systems' changes are playing key roles in the HF expression and progression. Alterations in skeletal muscle mass are also of importance in limiting peak functional capacity in patients with CHF, as reduced physical activity (disuse and immobilisation in advanced stages) plays some part in the muscle alterations in CHF. On the whole, these abnormalities resemble those induced by physical deconditioning. A great bulk of evidence, originally from our Lab., has pointed towards the existence of a reflex network that becomes hyperactive secondary to skeletal muscle alterations due to peripheral modification including early occurrence of acidosis, early depletion of high energetic metabolic factors, particularly in the skeletal muscle. The overactivation of signals originating from skeletal muscle receptors (mechano-metaboreceptors) is an intriguing hypothesis proposed to explain the origin of symptoms and the beneficial effect of exercise training in the CHF syndrome. These reflexes may contribute to sympathetic overactivation, to exercise intolerance, and to the progression of CHF syndrome. The so called metaboreflex has been demonstrated to be hyperactive in CHF and to be responsible for paradoxical increase in systemic vascular resistance and decrease in cardiac output whenever activated in these patients. Recently, it was found in heart transplant recipients that, after transplant, despite improved cardiac function, re-setting of metaboreflex-induced cardiovascular adjustments to exercise requires months in these patients, thereby suggesting that this reflex was dys-regulated before transplant.

Where applicable, the authors confirm that the experiments described here conform with The Physiological Society ethical requirements.

SA43

Skeletal muscle dysfunction in heart failure and its reversal by exercise training

P.C. Brum

School of Physical Education and Sport, University of Sao Paulo, São Paulo, São Paulo, Brazil and Circulation and Medical Imaging, Norwegian University of Science and Technology, Trondheim, Norway

Skeletal myopathy plays a prominent role in heart failure (HF) symptoms since skeletal muscle myopathy worsens with HF progression and parallels exercise intolerance observed in HF individuals. HF-induced skeletal muscle myopathy includes morphological and functional changes along with derangements in skeletal muscle metabolism and autonomic function. We have demonstrated that autonomic dysfunction, such as sympathetic hyperactivity, contributes to the skeletal myopathy in HF. Mice with sympathetic hyperactivity-induced HF (Brum et al 2002) display skeletal myopathy characterized by exercise intolerance, skeletal muscle pro-oxidant state (marked by decreased redox balance and increased lipid hydroperoxidation) and skeletal muscle wasting (Bacurau et al 2009, Bueno et al 2010). The latter is associated with increased proteolysis by the ubiquitin-proteasome system (Cunha et al 2012).
Aerobic exercise training is a powerful tool counteracting skeletal muscle myopathy. We have observed reduced muscle noradrenaline levels and oxidative stress associated with improved exercise capacity and re-established muscle mass in HF (Bacurau et al 2009). The mechanism by which aerobic exercise training prevents/attenuates skeletal muscle atrophy is unclear. Recent data from our group suggest that aerobic exercise training improves protein synthesis by increasing skeletal muscle IGF-1/PI3K/Akt signaling pathway in HF mice (Bacurau et al, unpublished results). Interestingly, we have also demonstrated that aerobic exercise training reduces protein catabolism. Aerobic exercise training decreased mRNA levels of the main skeletal muscle atrophic genes (MuRF and Atrogin-1/MAFbx) and reestablished proteasome activity in both mice and humans with HF (Cunha et al 2012).
Collectively, our studies suggest that aerobic exercise training promotes remarkable adaptations in skeletal muscle in HF that counteract skeletal myopathy. Regarding skeletal muscle wasting, aerobic exercise training prevents atrophy leading to a better balance between protein synthesis and degradation. Therefore, aerobic exercise training is a powerful non-pharmacological therapy for HF.

Bacurau AVN, Jardim MA, Ferreira JC, Bechara LR, Bueno Junior CR, Alba-Loureiro TC, et al. Sympathetic hyperactivity differentially affects skeletal muscle mass in developing heart failure: role of exercise training. J Appl Physiol 2009; 106:1631-40.

Bueno CR, Jr., Ferreira JC, Pereira MG, Bacurau AV, Brum PC. Aerobic exercise training improves skeletal muscle function and Ca2+ handling-related protein expression in sympathetic hyperactivity-induced heart failure. J Appl Physiol 2010;109:702-9.

Brum PC, Kosek J, Patterson A, Bernstein D, Kobilka B. Abnormal cardiac function associated with sympathetic nervous system hyperactivity in mice. Am J Physiol Heart Circ Physiol 2002;283:H1838-45.

Cunha TF, Bacurau AV, Moreira JB, Paixão NA, Campos JC, Ferreira JC, et al. Exercise training prevents oxidative stress and ubiquitin-proteasome system overactivity and reverse skeletal muscle atrophy in heart failure. PLoS One. 2012;7(8):e41701

FAPESP, CAPES and CNPq

Where applicable, the authors confirm that the experiments described here conform with The Physiological Society ethical requirements.

SA44

Modifiers of heart and muscle function: where genetics meets physiology

E.M. McNally

University of Chicago, Chicago, IL, UK

Many single gene disorders are associated with a range of symptoms that cannot be explained by the primary genetic mutation. In humans, this is clearly seen in individuals with the identical loss of function mutation in Sgcg, the gene encoding the dystrophin associated protein gamma-sarcoglycan. Like their human counterparts, Sgcg mice develop progressive muscle wasting and weakness along with dilated cardiomyopathy. To identify genetic regions that modify outcome in muscular dystrophy and cardiomyopathy, we used an intercross strategy. Sgcg mice in the DBA2/J or 129T2/SvEmsJ were intercrossed, representing severe and mild forms of disease, respectively. Nearly 200 mice were analyzed using echocardiography in vivo, and ex vivo analysis of muscle and heart for mass, hydroxyproline content and Evans blue dye uptake as indicators of muscle fibrosis and damage. Genomewide profiling was conducted and identified 40 suggestive QTLs and 12 significant QTLs. A second intercross using the Sgcg allele in the DBA2/J background was generated with the superhealing MRL background. Genomewide analysis identified a locus on chromosome 2 that regulates cardiopulmonary function. These data indicate that mouse models of muscular dystrophy

and cardiomyopathy can be used to identify modifier loci that correlate with outcome. The identification of the genes responsible for these QTLs will help define the pathological defects of cardiopulmonary dysfunction.

Heydemann A, et al.. Neuromuscul Disord. (2005) 15:601-9.

Heydemann A et al. J Clin Invest. (2009) 119:3703-12.

Swaggart KA et al. Physiol Genomics. (2011) 43:24-31.

Heydemann AH et al. Skeletal Muscle (2012) 2:26.

Supported by the NIH.

Where applicable, the authors confirm that the experiments described here conform with The Physiological Society ethical requirements.

SA45

Autonomic, locomotor and cardiac abnormalities in a mouse model of muscular dystrophy: targeting the renin angiotensin system

R. Sabharwal

Internal Medicine, University of Iowa, Iowa City, IA, USA

Muscular dystrophies are a heterogeneous group of genetic muscle diseases characterized by muscle weakness and atrophy. Mutations in sarcoglycans and other subunits of the dystrophin-glycoprotein complex cause muscular dystrophy and dilated cardiomyopathy (DCM) in animals and humans [1]. Aberrant autonomic signaling is recognized in several neuromuscular disorders. Antagonists of the renin angiotensin system (RAS) have been shown to attenuate skeletal muscle pathology in mouse models of muscular dystrophy [2]. Furthermore, treatment with an angiotensin converting enzyme inhibitor and β-adrenergic receptor blocker has been shown to reduce symptoms of congestive heart failure in Duchenne muscular dystrophy [3].

Thus, we hypothesized that activation of the RAS contributes to skeletal muscle and autonomic dysfunction in mice deficient in sarcoglycan-δ (Sgcd) at a young age; and this early autonomic dysfunction contributes to later development of left ventricular (LV) dysfunction and increased mortality. We measured cardiac function (echocardiography); blood pressure (BP), heart rate (HR) and locomotor activity (radiotelemetry); spontaneous baroreflex sensitivity (BRS, sequence technique); cardiac sympatho-vagal tone (HR responses to propranolol and atropine, respectively); and survival (Kaplan-Meier) in conscious Sgcd-/- and control mice.

We demonstrated that young, 10 wk old Sgcd-/- mice exhibit histopathological features of skeletal muscle dystrophy (fibrosis, centralized nuclei), oxidative stress, decreased locomotor activity and severe autonomic dysregulation, but normal cardiac function [4]. Autonomic function continued to deteriorate in Sgcd-/- mice with age and was accompanied by LV dysfunction and DCM at older ages (>50 wks) [5]. Autonomic dysregulation at a young age predicted later development of LV dysfunction and high mortality in Sgcd-/- mice [5].

Angiotensin II (AngII) acting via type 1 receptors (AT1R) causes oxidative stress, fibrosis, and cardiovascular and autonomic dysfunction, while Ang[1-7] acting via Mas receptors counteracts these deleterious actions [6]. Subgroups of control and Sgcd-/- mice were treated with either the AT1R blocker losartan (10 mg/ml, drinking water) or Ang[1-7] (2.5mg/kg/day, osmotic pump) for 8 wks beginning at 3 wks of age. Both losartan and Ang[1-7] decreased AT1R expression, oxidative stress, and fibrosis in skeletal muscle, increased locomotor activity, and prevented autonomic dysfunction in Sgcd-/- mice without affecting these measures in control mice.

Summary: We conclude that activation of RAS, at a young age, contributes to skeletal muscle and autonomic dysfunction in muscular dystrophy. We speculate that the latter is mediated via abnormal sensory nerve and/or cytokine signaling from dystrophic skeletal muscle to brain, and contributes to age-related LV dysfunction, DCM, arrhythmias and premature death. Therefore, correcting the early autonomic dysregulation may provide a novel therapeutic approach in muscular dystrophy.

Ervasti JM et al. (1991) Cell 66,1121-1131.

Cohn RD et al. (2007) Nat Med 13, 204-210.

Jefferies JL et al. (2005) Circulation 112, 2799-2804.

Sabharwal R, Weiss RM, Chapleau MW (2009) FASEB J 23, 1008.11.

Sabharwal R, Weiss RM, Zimmerman K, Chapleau MW (2010) Clin Auton Res 20, 300.

Ferreira AJ et al. (2005) Braz J Med Biol Res 38, 499-507.

Where applicable, the authors confirm that the experiments described here conform with The Physiological Society ethical requirements.

SA46

Maintaining skeletal muscle mass: lessons learned from hibernation

R.D. Cohn

Paediatrics, The Hospital for Sick Children, University of Toronto, Toronto, ON, Canada

Maintaining skeletal muscle mass is essential for general health and prevention of disease progression in various neuromuscular conditions. Here we provide an innovative approach to evaluate the mechanisms underlying muscle preservation in a naturally occurring hibernating animal that is protected from muscle atrophy despite prolonged periods of immobilization and starvation. We find that absence of proteolysis and autophagy accompanied by increased protein synthesis during hibernation is regulated independent of Akt. These observations challenge the current paradigm that Akt is the major determinant and regulator of skeletal muscle mass and homeostasis. Instead, we demonstrate that serum- and glucocorticoid-inducible kinase, SGK, represents a novel mediator of skeletal muscle homeostasis and function in hibernating and non-hibernating mammals. Our results thus identify a novel therapeutic target to combat loss of skeletal muscle mass in a variety of conditions associated with muscle atrophy and degeneration. Furthermore, we will demonstrate how these pathways are regulated in cardiac muscle during hibernation and thus emphasize the versatility of biological protection of numerous tissues during prolonged periods of decreased blood flow and metabolism.

Where applicable, the authors confirm that the experiments described here conform with The Physiological Society ethical requirements.

SA47

Extracellular matrix remodeling in the post-myocardial infarction aging heart

A. Yabluchanskiy[1,3], Y. Ma[1], Y. Jin[2] and M. Lindsey[1,3]

[1]Physiology & Biophysics, Univ MS Medical Center, Jackson, MS, USA, [2]Electrical and Computer Engineering, UTSA, San Antonio, TX, USA and [3]Research Service, G.V. (Sonny) Montgomery Veterans Affairs Medical Center, Jackson, MS, USA

Aging impairs the ability of the left ventricle (LV) to respond to stress or injury. Cardiac aging is characterized by increased inflammation, an accumulation of extracellular matrix (ECM), and the development of diastolic dysfunction. Matrix metalloproteinases (MMPs) are key enzymes that regulate ECM turnover, and in particular MMP-9 deletion has been shown to attenuate LV dysfunction and remodeling post-myocardial infarction (MI) in young mice, by coordinating inflammatory and ECM responses. MMP-9 levels rise with age, in both the LV and plasma. The increase in cardiac MMP-9 is due to an accumulation of macrophages, which contribute to the increase in inflammation and ECM. Aging, therefore, gradually resets the cardiac environment. This talk will discuss the outcomes when myocardial infarction (MI) is superimposed on a cardiac aging background, focusing on changes to the inflammatory response that coordinate infarct scar formation and how MMP-9 deletion regulates these changes in the aging setting.

We acknowledge support from NIH/NHLBI HHSN 268201000036C (N01-HV-00244) for the San Antonio Cardiovascular Proteomics Center and R01 HL075360 and from the Biomedical Laboratory Research and Development Service of the Veterans Affairs Office of Research and Development Award 5I01BX000505 to MLL.

Where applicable, the authors confirm that the experiments described here conform with The Physiological Society ethical requirements.

SA48

Lysyl oxidase, collagen cross-linking, and cardiac dysfunction

J.D. Gardner, J.M. Bradley and M.C. El Hajj

Physiology, LSU Health Sciences Center, New Orleans, LA, USA

Heart failure develops when compensatory mechanisms fail to overcome injury and hemodynamic stress that can be caused by myocardial infarction, pressure and volume overload, or hypertension. Increased stress on the heart results in a reorganization of the myocardial extracellular collagen matrix (ECM), leading to fibrosis and dysfunction. Lysyl oxidase (LOX) is critical for the enzymatic cross-linking necessary for normal collagen processing, yet over-activation of LOX is associated with fibrosis. LOX is significantly elevated in failing human hearts, but it is not known if excess LOX activity accelerates cardiac failure. Using a rodent model of heart failure, we assessed the role of LOX activity in the progression of cardiac dysfunction and adverse ECM alterations. Statistical analyses were performed using one-way ANOVA with Dunnett's post test, and considered significant at $p<0.05$. Surgically induced volume overloaded and sham-operated rats were studied at 14 wks post-surgery (n=5 to 7 per group). To assess the role of LOX in disease progression, rats were treated with a LOX inhibitor (BAPN; 100 mg/kg/d) starting 2 wks post-surgery. LOX inhibitor or vehicle saline was delivered using Alzet osmotic minipumps implanted in the abdominal cavity. Echocardiography was used to evaluate cardiac function and progression of left ventricular (LV) remodeling. LV LOX expression and activity were determined by Western blot and Amplex red assay, respectively. Extracellular collagen assays included: interstitial fibrosis by picrosirius red staining of LV sections; cross-linking by pyridinoline content; and collagen type I and III expression by western blot. Volume overload (VO) caused significant ventricular dilatation (43% increase) and dysfunction (26% decrease, %FS) by 14 wks post-surgery versus Sham. LOX protein expression was increased (65%; $p<0.05$ vs Sham) by VO with concomitant increases in LOX activity. These increases in LOX were associated with significantly elevated interstitial collagen, cross-linking, and type I/III ratio ($p<0.05$ vs Sham). LOX inhibition prevented the development of cardiac dysfunction and blocked the VO-induced changes in LV collagen. LOX inhibition normalized LV collagen staining, cross-linking, and expression to levels comparable to age-matched Sham. Our findings indicate that LOX inhibition was cardioprotective in the volume overload stressed heart. Further studies are warranted to determine the cellular mechanisms responsible for increased LOX expression and LOX-dependent damage in the stressed heart.

Funding for these studies was provided in part by the American Heart Association Greater Southeast Affiliate #11GRNT7700002 (jdg) and NIH/NCRR #P20RR016456 (Kapusta; subproject jdg).

Where applicable, the authors confirm that the experiments described here conform with The Physiological Society ethical requirements.

SA49

G-protein coupled receptor signaling in the diseased heart

U. Mende

Medicine/Cardiology, Rhode Island Hospital & Brown University, Providence, RI, USA

Signal transduction via G protein-coupled receptors (GPCRs) is essential for the regulation of cardiovascular function, including heart rate, growth, contraction, and vascular tone. Pertubations in GPCR signaling have pathophysiological consequences and are major contributors to cardiac disease. Regulators of G protein Signaling (RGS proteins) belong to a diverse protein family that was originally discovered for their ability to accelerate signal termination in response to GPCR stimulation, thereby reducing the amplitude and duration of GPCR effects. Interaction of their common RGS domain with some $G\alpha$ subunits of heterotrimeric G proteins mediates their biologic regulation of GPCR signaling by limiting the interactions between $G\alpha$-GTP and $G\beta\gamma$ with intracellular or membrane effectors or ion channels. Additional functional domains in some RGS protein isoforms can facilitate protein-protein and protein-lipid interactions that confer additional regulatory functions. Several RGS proteins are expressed in the heart and have been implicated in the cardiac remodeling response and heart rate regulation. Changes in RGS protein expression and/or function are believed to participate in the pathophysiology of cardiovascular diseases including hypertrophy, failure, arrhythmias and hypertension.

Our investigations have focused primarily on RGS2, a member of the RGS R4 subfamily. RGS2 distinguishes itself from other

closely related RGS isoforms by its susceptibility to regulation and signaling specificity. Expression studies in isolated adult rat ventricular cardiomyocytes (CM) and cardiac fibroblasts (CF) revealed that - among the cardiac RGS isoforms - RGS2 is most susceptible to regulation and that this is a highly dynamic process. Short-term activation of the Gq/11 signaling pathway transiently up-regulates RGS2 mRNA in both CM and CF, which likely represents a negative feedback mechanism. Acute β-adrenergic or forskolin stimulation also markedly increases RGS2 mRNA, which points to potential crossregulation and desensitization between Gs- and Gq/11-mediated signaling pathways. Importantly, in contrast to acute stimulation, marked RGS2 down-regulation was discovered in vivo in ventricles subjected to pressure overload, CM from mice expressing constitutively active Gαq as well as CM and CF from rats subjected to prolonged Angiotensin II infusion, which has been implicated in exacerbating cardiac remodeling in stressed or injured hearts. Functionally, using a gain-of-function approach (adenoviral infection), we show that RGS2 is a potent negative regulator of Gq/11 signaling in both CM and CF but has no effect on sympathetic or parasympathetic regulation of adenylate cyclase (AC) or AC itself (as reported for other cell types). Using a loss-of-function approach (RNA interference), we demonstrate that endogenous RGS2 is a functionally important negative regulator of Gq/11-mediated CM hypertrophy and function as well as CF proliferation and collagen production.

It was previously shown that mice with generalized targeted deletion of RGS2 display enhanced hypertrophy and fibrosis in response to pressure overload (Takimoto et al., 2009), which is mediated in large part via Gq/11 signaling (Wettschureck et al., 2001). We generated a mouse model with α-myosin heavy chain promoter-driven RGS2 expression to investigate whether RGS2 overexpression in CM can be used to attenuate Gq/11 signaling and hypertrophy in vivo. Transgenic RGS2 was highly functional in negatively regulating Gq/11 signaling in atrial appendages and to a much lesser extent in ventricles. In ventricles (but not atrial appendages), RGS2-mediated modulation of Gq/11 signaling was absent after pressure overload induction by transverse aortic constriction (TAC), which may account for the lack of anti-hypertrophic effect we observed in transgenic mice. Importantly, TAC-induced RGS2 expression changes (down-regulation) did not underlie the functional differences we observed between atria and ventricles. Random insertion effect and changes in the expression of other RGS proteins were excluded as well.

Interestingly, our findings suggest that RGS2 function is differentially regulated in atria and ventricles in vivo, which could include differences in posttranslational modifications (such as phosphorylation and palmitoylation) that can modulate the effectiveness of RGS2 in exerting regulatory effects on GPCR signaling. Since transgenic overexpression of RGS2 was associated with highly effective inhibition of Gq/11 signaling in the atria, the new model can be utilized to advance understanding of atrial signaling and to mitigate Gq/11 signaling in the atrium for potential therapeutic purposes. The in vivo role of RGS2 in regulating CF signaling and function in both atria and ventricles under both physiological and pathophysiological conditions also remains to be explored.

Takimoto E et al. (2009). J Clin Invest 119, 408-420.

Wettschureck N et al. (2001). Nat Med 7, 1236-1240.

Supported by the NHLBI and AHA

Where applicable, the authors confirm that the experiments described here conform with The Physiological Society ethical requirements.

SA50

Genetic modulation of heart failure progression

F. Sheikh

University of California-San Diego, La Jolla, CA, USA

Cardiovascular disease is the leading cause of death in developed countries. It is now clear that many cardiomyopathies leading to the progression of heart failure result from genetic mutations or alterations in the cytoskeletal network/basic structural components of the cardiac muscle. For the last five decades, the simplistic obligatory step of calcium binding to actin bound regulatory proteins (eg., troponin-tropomyosin complex) has contributed to the prevailing view that the control of calcium cycling and actin-bound regulatory proteins (thin filament proteins) dominates regulation of muscle contraction as well as underlie the dysregulation of contractile dynamics in heart failure. Several studies have shown that dysregulation of myosin regulatory proteins (thick filament proteins), such as myosin light chain-2 (MLC2), via dephosphorylation is associated with human cardiomyopathies and heart failure; however, mechanistic insights into its underlying role in cardiac muscle and heart disease remain poorly understood. Using integrative gene-targeted mouse and multi-scale computational models, we identify the mechanisms underlying an indispensable role for ventricular MLC2 (MLC2v) phosphorylation in regulating cardiac myosin cycling kinetics, which directly control actin-myosin interactions, while also surprisingly, feeding back to cooperatively influence calcium-dependent activation of the thin filament. Loss of these mechanisms uncovers previously unrecognized early cardiac muscle defects in the rates of twitch relaxation and ventricular torsion, which strikingly precede the left ventricular dysfunction of heart disease and failure in a novel non-phosphorylatable MLC2v mouse model. We show that in contrast to conventional views, there is a direct and early role for MLC2 phosphorylation in regulating actin-myosin interactions in striated muscle contraction and that dephosphorylation of MLC2 and loss of these mechanisms play a critical role in heart failure progression.

Where applicable, the authors confirm that the experiments described here conform with The Physiological Society ethical requirements.

SA51

Early epigenetic modulation of the diseased heart

L.M. Delbridge

Department of Physiology, University of Melboune, Melbourne, VIC, Australia

There is now an abundance of evidence to support the proposition that perinatal growth influences have long term impact on defining adult health status - cardiovascular health in particular. These investigations have highlighted the role that tissue modeling processes enacted in the early postnatal period play in setting the scene to ensure long term appropriate growth responses. Although the phenomenology of early disease 'origins' is generally accepted, understanding of the mechanisms involved is limited. The emphasis has been primarily on aspects of the gestational environment which influence fetal growth – ie nutritional state and other factors associated with uteroplacental insufficiency. Less is understood about how offspring genetic/epigenetic factors can operate inde-

pendently during the perinatal period to define subsequent tissue and organ growth.
The switch from proliferative (ie mitotic) to hypertrophic cellular growth occurs in the perinatal period as myocytes exit from the cell cycle, and beyond this period the myocardium is considered to be largely a terminally differentiated tissue. Thus, the myocyte population is essentially fixed at this time point, defining the non-replaceable pool of cells available to support ongoing maturational growth of the heart. As a highly metabolically active tissue, the heart is particularly vulnerable to substrate 'starvation' stress in the perinatal period, during transition from placental to lactational nutrition. To support energy homeostasis, autophagic activity is upregulated in multiple tissues during the neonatal starvation period – and particularly in the heart. A high level of autophagic activity can be lethal, and cell death by autophagy is recognized as a distinctive, non-apoptotic type of programmed cell death. Thus, myocyte loss through autophagy during the perinatal period has the potential to significantly deplete the heart cell population.
Recently, using novel experimental animal models, it has been possible to demonstrate a link between reduced cardiac myocyte population in the neonatal heart due to upregulated autophagy and abnormal cardiac enlargement in the adult. An interaction between angiotensin II/G-protein-coupled-receptor and IGF1/PI3Kinase-dependent signaling pathways is implicated in this neonatal growth suppression and autophagy induction. Furthermore there is emerging evidence that autophagy pre-disposition and the cross-talk between these signalling pathways is different in male and female hearts, and new findings that microRNA molecules (miR) are the key to sex-specific programming patterns of gene expression which have long-term tissue modeling influence on cardiac pathophysiology. Understanding the early epigenetics of disease predisposition has become an exciting and high priority research pursuit which will yeild important information about the mechanisms of sex difference in adult cardiac disease outcomes.

Where applicable, the authors confirm that the experiments described here conform with The Physiological Society ethical requirements.

SA52

Interactive pedagogies in physiology education

J. Kibble

Medical Education, University of Central Florida, Orlando, FL, USA

Population theorists have described different generations according to their demographics and the key life events they grew up with. Accordingly, these collective life experiences result in particular attitudes and behaviors that may characterize a generation. The Millennial generation was born from 1981 to 1999. Key events in their formative years include 9-11 and a decade of international wars. Millennial students have been shaped by immersion in technology, and by the nurturing of overprotective ("helicopter") parents. This generation of students is said to be optimistic, generous, open-minded and team-oriented. They value association to others, have high expectations of technology and are accustomed to structured environments, and to receiving regular feedback. Their challenges may include a lack of experience with unplanned environments and a tendency to worry (1,2).
At the University of Central Florida we have built a new medical school that has graduated its first class and received full accreditation in 2013. This has been a rare opportunity to design a new curriculum and build new facilities. Our curriculum has three phases: 1) Foundations, 2) Systems-based study of disease, 3) Translation to practice. The first two phases are comprised of integrated instructional modules that precede clinical clerkships. Our pedagogic approach seeks to maximize opportunities for active and independent learning and to be congruent with the traits of the current generation of learners.
To support the required knowledge base, all our students receive an iPad that is loaded with interactive textbooks and have access to a fully electronic medical library. They are given training in the use of medical databases and reference organization early in the curriculum. We make extensive use of online "self-learning modules" to prepare students for formal classroom activities. Our research on these online modules has identified successful characteristics to include learner control, adherence to instructional design principles in the use of visuals, and the inclusion of self-tests. When compared against segments of the curriculum without such online modules, student performance was shown to significantly increase (3).
Our classroom instruction emphasizes co-operative learning to leverage the purported acumen of Millennial students in this kind of learning. The use of team-based learning, case-based learning, simulations and other approaches where group work occurs has the overall goal of using classroom time to engage higher order learning. We have developed software to deploy virtual laboratory classes and also use ADInstruments LabTutor software to author and present case-based learning materials. In both cases students work in groups to solve problems and upload their collective solutions online, giving the opportunity for faculty feedback. Our qualitative research in this area suggests that students are highly accepting of the organizational structure and quality of content but also appreciate how the software supports group process, co-operative learning and that it allows self-monitoring (4). However, when comparing generic feedback to group-specific feedback we found a significant decline in student acceptance for this specific component.
Formative assessment provided during the learning process has long been considered an important component of curricula. The need for rich feedback is also a trait associated with Millennial students. We provide extensive formative assessment by giving not-for-credit online quizzes every week throughout the first two years in addition to self-testing embedded in online instructional materials and feedback about cases. Our research in this area shows that the degree of participation in voluntary quizzes is a good indicator of student success in summative assessment. Despite sharing this information with students during orientation, a significant fraction of students still opt not to take online quizzes in a timely manner. In an in-depth interview study we have discovered that fear of judgment, time management, quality of questions and quality of feedback are the major barriers to quiz use. Despite the availability of a lot of formative assessment we find that improving the quality of feedback remains a challenge to satisfy the present generation of students.

Borges NJ, Manuel RS, Elam CL, Jones BJ. 2010. Differences in motives between Millennial and Generation X students. Med Edu 44(6):570-6

Twenge JM. 2009. Generational changes and their impact in the classroom: Teaching Generation Me. Med Educ 43(5):398-405

Khalil MK, Nelson LD, Kibble JD. 2010. The use of self-learning modules to facilitate learning of basic science concepts in an integrated medical curriculum. Anat Sci Educ 3:219-226

Khalil MK, Kirkley DL, Kibble JD. 2013. Development and evaluation of an interactive electronic laboratory manual for cooperative learning of medical histology. Anat Sci Educ, In Press

Mohammed Khalil - co-investigator; Dale Voorhees - educational techologist; Nadine Dexter - medical librarian.

Where applicable, the authors confirm that the experiments described here conform with The Physiological Society ethical requirements.

SA53

Use of the moodle platform to create an effective online learning site

B. Ramirez

University of Santiago, Santiago, Chile

Moodle is a platform for teaching, available free in the web. It can be used in totally virtual courses (e-learning) or as support in classic courses (b-learning). It offers multiple possibilities for interactive learning, since it supports wikis, forums, tests, data-bases and others, than can be accessed on line by the students. Teachers can also offer there a copy of the powerpoints and documents in different formats, to be accessed at all time by the students.
I will show here tips for using moodle both, for e-learning and for b-learning.

Where applicable, the authors confirm that the experiments described here conform with The Physiological Society ethical requirements.

SA54

Strategic directions and collaborations for teaching physiology in the new millennium

P. Poronnik

School of Medical Sciences, The University of Sydney, Sydney, NSW, Australia

Physiology teaching in the new millennium is well placed to embrace not only the new technological affordances but also the significant paradigm shift that is emerging in the bioinformatics / systems biology revolutions. However, adapting to these changes means that we will have to revisit traditional academic roles.
In terms of technologies, MOOCs and classroom inversion are emerging as very real factors that will influence the way in which academics and students interact and require, in some instances, re-articulation of the purpose of a campus based experience. Mobile computing devices are also a clear game changer, a revolution in which we are already caught up. The new affordable and compact tablet PCs are the most recent player, bringing the capacity for each student to connect directly to and run sophisticated data acquisition equipment. This allows the student in effect to "own" the experiment and their data.
In the context of physiology teaching, the proliferation of mobile wireless personal monitoring devices as well as increasingly affordable genetic and proteomics screening are significant points of leverage. This rapid shift to personalized medical data gathering presents multiple opportunities for students to contextualize learning to themselves – making these data very authentic. One significant challenge is how best to position the core physiology content while optimizing student engagement. The possibility of having student cohorts collect large data sets opens up "cloud-sharing" to compare population parameters across local and national boundaries in new ways. This enables a deeper appreciation of how the cultural and environmental surrounds effect human physiology.
Gamification / augmented reality can also be powerful tools to enhance student learning when implemented in appropriate ways. Quality on-line resources such as laboratory modules, simulations and patient / case studies are also critical in the mobile world. Our students live, however, in a world of expecting high production values and achieving this comes with significant labour and cost implications.
We have already entered this very exciting era. It is the speed of change and our capacity to adapt to and resource these changes that are our greatest challenges. There is an urgency to develop strategies that connect the innovators and early adopters with the broader physiology community in a unity of purpose around the new ways of teaching.
The most effective means to facilitate a community approach is through the formation of collaborative leadership networks. Such networks can serve to (i) provide the critical mass needed to identify, address and solve the central challenges that face us in delivering a forward looking and sustainable curriculum and (ii) maximize the efficiency of development, dissemination and adoption of innovative physiology teaching. This critical mass is also essential to seek new the funding opportunities required to support innovation and sustainability. In a complex international environment, such a network can serve to aggregate, filter and connect ideas and information with the appropriate teams of people to achieve effective, transferable and sustainable solutions. There are some examples of local networks, however, these are issues that required collaboration at an international level. IUPS is well positioned to play a central role in such an extended network.

Where applicable, the authors confirm that the experiments described here conform with The Physiological Society ethical requirements.

SA55

Experiences in using online courses

A.K. Vidanapathirana

Department of Physiology, University of Colombo, Colombo 8, Sri Lanka and Department of Physiology, Brody School of Medicine, East Carolina University, Greenville, NC, USA

With the advancement of e-learning, online instruction is becoming a significant component of graduate education. This presentation is based on experiences in the Professional Skills Training Online Course: Abstract Writing for Scientific Meetings conducted by the American Physiological Society. Insights gained following discussions with colleagues who followed several other online courses in various disciplines and in different formats are also included.
Online courses are more conducive in the global e-leaning environment. Compared to live courses covering similar material, the online courses have the unique advantages of being convenient, time and cost effective for both organizers and participants. The retention of knowledge through these online courses was largely dependent on the format of delivery, relevance and applicability. Well defined objectives and a tutorial on the course design with technical support at the beginning of the course greatly enhanced the knowledge gain. However, online only courses have the disadvantage of limited face-to face interactions and discussions which impedes the peer learning and professional interactions. The blended course design (i.e. a combination of live and online course components) was perceived as a more effective method of teach-

ing in the current graduate education. The overall efficiency of learning through online courses was determined by the course content, context, incentives and commitment of the participants. Students who are self-motivated and prefer a self-learning approach in contrast to didactic teaching benefit more from these courses.
The meticulous selection of topics and content is crucial in designing online courses as all subject matter and skills cannot be conveyed or conceived online. Expanding the opportunities for live interactions within the course will increase the overall appeal and success of online courses. The characteristics and the prerequisites of the target student population also need to be considered in designing, implementing and evaluating graduate level online courses. Well defined guidelines and measures of quality-control for online courses will greatly facilitate the sustainability of online education.

Where applicable, the authors confirm that the experiments described here conform with The Physiological Society ethical requirements.

SA56

Development and evaluation of online courses and resources

D. Dewhurst

Learning Technology, Edinburgh University, Edinburgh, UK

Physiology teaching has a history of being at the forefront in the use of technology-enhanced learning methods. This presentation will cover the use of technology-enhanced learning in physiology from multimedia CALs in the 1980s and 1990s, virtual learning environments, open educational resource initiatives and learning object repositories in the early 2000s, and more recently web-based courses delivered entirely online and Massive Open Online Course (MOOCs) initiatives.
Early use of technology in physiology teaching focused on learning materials such as multimedia resources, largely developed to support student-centred learning. Typically such resources made effective use of features such as high-quality graphics, animation, video and audio bringing a range of media together into a single package and delivering it on CDROM. Some were developed to support teaching of practical physiology providing students with activities and self-assessments built around data from laboratory experiments on either human or animal subjects. In a virtual laboratory students might sit at a computer and be required to 'design' experiments, collect data from the computer screen, analyse and report their results in much the same way as they would in the real laboratory. Built-in self-assessment questions would test accuracy of data collection, data interpretation skills and knowledge of underlying physiological principles. Students could use the virtual labs to better prepare themselves for a real laboratory teaching session or they might use them to collect additional data outside the laboratory session. In some instances the 'simulations' might replace a real laboratory session and this practice has become more common as the 'cost' of providing real laboratory experiences for students has increased. Other multimedia resources focused on supporting lectures, presenting factual information on specific topics and structuring this alongside student activities and self-assessments in an interactive format which went beyond the traditional textbook approach. Students would commonly have 24/7 access to such resources with tutors often embedding the resources into the curriculum. Numerous evaluations of the educational effectiveness of both virtual labs and interactive tutorials have been carried out, most suggesting that the computer-based learning materials can address many of the learning objectives very effectively, and data from some of these studies will be presented.
The last ten years has seen the growth of Internet resources many of which are openly accessible, some provided by institutions as 'open courseware', others provided by individuals. It is now possible for students to access teaching materials, e.g. an online video lecture, from a world expert on a particular topic; they have access to online textbooks, online wikis, e-books and more and more universities are putting their course content online. Teachers can now provide their students with prior access to a wide range of high-quality factual information, generated by themselves and/or others and utilize face-to-face teaching sessions in a more interactive way to, for example, diagnose learning difficulties, better explain curriculum topics which students find difficult, or contextualise the factual information through problem-based or scenario-based learning approaches. Audio-responses systems are often cited as an effective way of making such sessions more engaging and promoting peer learning. This 'flipped-classroom' approach has been found to be effective in supporting student learning. While there may be some questions around the quality of open-access resources there is little doubt that students will continue to use the web as their first port of call for factual information and we need to ensure that students are provided with resource discovery skills and the ability to properly critique and quality-assure those resources.
More recently some universities have started to offer online courses in which all student – tutor interactions take place online. These may be credit-bearing courses (e.g. University certificate, diploma or Masters degree), or they be short non-credit bearing courses, such as MOOCs, which typically offer certificates of completion rather than educational credits. There is no doubt that the flexibility such courses offer is highly beneficial to and highly valued by many learners particularly those in developing countries where access to high quality learning resources can be problematic for many. The presentation will look at some examples of online distance learning courses and MOOCs and give some institutional perspective of their development, sustainability and how they might be evaluated.

Where applicable, the authors confirm that the experiments described here conform with The Physiological Society ethical requirements.

SA57

Aging and DNA methylation: A role in fetal origins of adult disease?

C. Sapienza and S. Song

Fels Institute for Cancer Research, Philadelphia, PA, USA

Age-associated differences in site-specific DNA methylation have been observed in both humans and animal models. We, and others, have also observed longitudinal changes in DNA methylation in humans, with an average interval between samples of more than a decade. Our published data indicate that it is likely that both genetic and environmental factors are involved with these changes. The absolute magnitude of the observed changes in humans is small but, by extrapolation from data in the mouse, may be considerably larger in some tissues. Moreover, we have observed that even small differences in DNA methylation can be associated with much larger differences in transcript level. Nevertheless, whether such age-

related differences are a cause or a consequence of aging is a matter for discussion. Multiple epidemiological studies have identified maternal age as an additional factor influencing the longevity of offspring, with those offspring born to younger mothers living longer than offspring born to older mothers. We have examined site-specific DNA methylation in the offspring of mothers whose ages vary by more than 20 years. A number of genes exhibit maternal age-related differences in DNA methylation. Our observations indicate a potential role of maternal age-related methylation differences in the health and lifespan of offspring.

Research supported by NIH R01 HD048730; U54 HD068157

Where applicable, the authors confirm that the experiments described here conform with The Physiological Society ethical requirements.

SA58

The ageing brain; effects on DNA repair and DNA methylation in mice

S.A. Langie[1,2], K.M. Cameron[3], G. Ficz[4], D. Oxley[4], B. Tomaszewski[2], J.P. Gorniak[2], L.M. Maas[5], R.W. Godschalk[5], F.J. van Schooten[5], W. Reik[4], T. von Zglinicki[3] and J.C. Mathers[2]

[1]Environmental Risk and Health unit, Flemish Institute of Technological Research (VITO), Mol, Belgium, [2]Centre for Brain Ageing and Vitality, Human Nutrition Research Centre, Institute for Ageing & Health, Newcastle University, Campus for Ageing and Vitality, Newcastle upon Tyne, UK, [3]Centre for Integrated Systems Biology of Ageing and Nutrition, Institute for Ageing and Health, Newcastle University, Campus for Ageing and Vitality, Newcastle upon Tyne, UK, [4]Laboratory of Developmental Genetics and Imprinting, The Babraham Institute, Cambridge, UK and [5]Department of Toxicology, Maastricht University, Maastricht, Netherlands

DNA repair systems such as base excision repair (BER) may become less effective with ageing resulting in accumulation of DNA lesions, genome instability and altered gene expression that contribute to cellular and tissue dysfunction and increase the risk of age-related degenerative diseases. The brain is particularly vulnerable to accumulation of oxidative DNA lesions and proper functioning of DNA repair mechanisms is thus important for neuronal survival. Although the mechanism(s) of age-related decline in DNA repair capacity is unknown, growing evidence suggests that epigenetic events, including aberrant DNA methylation, contribute to the ageing process and may be functionally important through dysreguledexpression of DNA repair genes.

We hypothesise that oxidative stress modulates DNA repair, specifically BER, in the ageing brain and that epigenetic mechanisms are involved in mediating age-related effects. Brains from C57/BL male mice were isolated at 3-32 months of age. Using pyrosequencing, we observed significantly increased methylation of the promoter region of the BER gene *Ogg1* with ageing, which correlated inversely with *Ogg1* expression. The reduced *Ogg1* expression correlated with enhanced expression of methyl-CpG binding protein 2 (MeCP2) and of ten-eleven translocation enzyme 2 (Tet2). The functional consequence, if any, of the latter association is unclear since Tet enzymes can convert 5-methylcytosine to 5-hydroxy-methylcytosine and play a role in further active DNA demethylation. On this basis, one would have anticipated an inverse correlation between expression of *Ogg1* and of *Tet2*. MeCP2 is a methyl-CpG binding protein that can suppress transcription. In adult brain, MeCP2 binds to methylated DNA across the genome and plays a crucial role in normal brain functioning. We also observed a significant inverse correlation between gene methylation and expression observed for *Neil1*, which is another BER gene. During ageing, there was a trend towards decreased expression of *Mutyh* and *Xrcc1*, in parallel to slightly higher gene methylation levels. The corresponding phenotype i.e. BER-related incision activity in brain was reduced significantly, which was associated with significantly increased 8-oxo-7,8-dihydro-2'-deoxyguanosine levels. These data indicate that *Ogg1* and *Neil1* expression can be epigenetically regulated and that this may play a role in the adverse effects of ageing on DNA repair in mammalian brain.

In conclusion, this study has provide evidence that through altered expression of BER genes, epigenetic mechanisms - i.e. increased promoter methylation as well as the involvement of TET enzymes and MeCP2 - can reduce capacity for neuronal DNA repair during ageing. This reduced capacity for DNA repair may contribute to the accumulation of oxidative DNA damage and mutations across the whole genome, causing genome instability and increasing the risk of age-related neurodegenerative diseases.

The Centre for Brain Ageing & Vitality is funded through the Lifelong Health and Wellbeing cross council initiative by the MRC, BBSRC, EPSRC and ESRC. This work was further supported by the Centre for Integrated Systems Biology of Ageing and Nutrition funded by the BBSRC and EPSRC. We thank Hoffmann-La Roche (Basel) for supplying Ro 19-8022 and Sofia Lisanti for providing us the primer sequences for the qRT-PCR reference genes. We also like to thank Adele Kitching, Satomi Miwa, Liz Nicolson and Julie Wallace for care of the animals and assistance with dissections.

Where applicable, the authors confirm that the experiments described here conform with The Physiological Society ethical requirements.

SA59

Genome-wide epigenetic changes during ageing

M.F. Fraga

IUOPA, Universidad de Oviedo, Oviedo, Spain

Genomic DNA methylation is not stable during development and aging. Recent works, mainly focused in blood, show that DNA hypermethylation in aging preferentially occurs at sequences associated with bivalent chromatin domains in embryonic stem cells that are also frequently hypermethylated in cancer. In my talk, I will comment recent work of our laboratory in which we compare the genome wide DNA methylation status of adult stem cells obtained from healthy individuals of different ages. Using this approach we identified a set of genes showing specific DNA methylation changes in aged stem cells. In addition, by crossing these genes with previously published genome-wide data on chromatin modifications, we identified a global epigenetic signature of aging.

Where applicable, the authors confirm that the experiments described here conform with The Physiological Society ethical requirements.

SA60

Epigenetic regulation of retrotransposable elements by TET enzymes

M. Branco

Epigenetics Programme, The Babraham Institute, Cambridge, UK and Centre for Trophoblast Research, University of Cambridge, Cambridge, UK

DNA methylation or 5-methylcytosine (5mC) is crucial for embryonic development and plays important roles in the control of gene expression, genome stability and silencing of transposable elements. It was recently shown that the TET family of enzymes can oxidize 5mC to 5-hydroxymethylcytosine (5hmC) as part of a potential demethylation pathway. We and others have shown that TET1 and 5hmC help to maintain the pluripotency network in mouse embryonic stem (ES) cells by preventing methylation of pluripotency-associated genes. We also found that LINE1 retrotransposons are enriched for 5hmC at their 5' end in ES cells and more recently confirmed this using a quantitative technique for single-base mapping of 5hmC. TET targeting to LINE1 elements maintains them in a hypomethylated state and consequently transcriptionally active. TET enzymes may therefore be involved in controlling retrotransposon mobility and thus implicated on the impact that these potentially mutagenic elements have on the genome. We are currently investigating the role of these epigenetic mechanisms in controlling LINE-1 mobility in ES cells, neural stem cells and during ageing, where increased retrotransposon mobility may contribute to the etiology of neurodegenerative diseases.

Where applicable, the authors confirm that the experiments described here conform with The Physiological Society ethical requirements.

SA61

Epigenetic regulation of fetal growth and healthy aging

R. John and S. Tunster

Cardiff, Cardiff, UK

A defining feature of mammals is the development in utero of the fetus supported by the constant flow of nutrients from the mother (John and Hemberger, 2012). Poor growth in utero combined with rapid post natal catch up growth is known to predispose to the development of metabolic diseases in adult humans, including type 2 diabetes. A significant proportion of human low birth weight infants exhibit elevated placental expression of the imprinted PLECKSTRIN HOMOLOGY-LIKE DOMAIN, FAMILY A, MEMBER 2 (PHLDA2/IPL/TSSC3) gene (McMinn et al., 2006).
We have engineered this specific alteration in a mouse model system and found that elevated expression of Phlda2 drives severe placental defects alongside asymmetrical fetal growth restriction (Tunster et al., 2010). The low birth weight offspring rapidly catch up growth with their littermates but develop glucose intolerance and show increased adiposity as adults. Using another genetic model, we are able to rescue both fetal growth restriction and glucose intolerance thus assigning the adult phenotypes to the in utero growth restricting properties of Phlda2. We are also able to demonstrate that Phlda2 is a nutrient responsive gene in the placenta. These data support the idea that factors manipulating epigenetic processes early in life can influence the aging process. Furthermore, our data suggest that low birth weight human infants with high PHLDA2 expression may be predisposed to develop type 2 diabetes and other diseases linked to fetal programming.

John, R. and Hemberger, M. (2012). A placenta for life. Reprod Biomed Online 25, 5-11

McMinn, J., Wei, M., Schupf, N., Cusmai, J., Johnson, E. B., Smith, A. C., Weksberg, R., Thaker, H. M. and Tycko, B. (2006). Unbalanced placental expression of imprinted genes in human intrauterine growth restriction. Placenta 27, 540-549

Tunster, S. J., Tycko, B. and John, R. M. (2010). The imprinted Phlda2 gene regulates extraembryonic energy stores. Mol Cell Biol 30, 295-306

Where applicable, the authors confirm that the experiments described here conform with The Physiological Society ethical requirements.

SA62

Regulation of ENaC by external cues

T. Kleyman

Medicine, University of Pittsburgh, Pittsburgh, PA, USA

Epithelial Na channels (ENaCs) reside in the apical membrane of principal cells in the aldosterone-sensitive distal nephron, where they transport Na and have key roles in extracellular volume homoeostasis and blood pressure control. Specific proteases activate ENaC, a trimer composed of three structurally related subunits, by liberating inhibitory tracks imbedded in the extracellular regions of the alpha and gamma subunits. Extracellular Na inhibits ENaC by binding to sites within the extracellular regions of ENaC subunits, leading to a reduction in channel open probability. Recent findings regarding sites within ENaC subunits where inhibitory peptides and Na bind, and how these binding events affect channel gating will be reviewed.

Support by grants from NIDDK.

Where applicable, the authors confirm that the experiments described here conform with The Physiological Society ethical requirements.

SA63

Activation of the epithelial sodium channel by plasmin and cathepsin-S

S. Haerteis, M. Krappitz, A. Diakov, A. Krappitz, R. Rauh and C. Korbmacher

Institut für Zelluläre und Molekulare Physiologie, Friedrich-Alexander-Universität Erlangen-Nürnberg, Erlangen, Germany

Proteolytic channel activation is a unique feature of the epithelial sodium channel (ENaC). Cleavage at specific sites in the extracellular domains of α-, δ-, and γENaC is essential for channel activation [1; 2]. However, the (patho-)physiologically relevant proteases and molecular mechanisms involved in proteolytic channel activation remain to be determined. Inappropriate ENaC activation by proteases may be involved in sodium retention and the pathogenesis of arterial hypertension in the context of renal disease. Recently, we and others reported that the serine protease plasmin can proteolytically activate ENaC which may contribute to renal sodium retention in nephrotic syndrome [3; 4]. In mouse γENaC a puta-

tive plasmin cleavage site (K194) has been reported [4]. For human ENaC, the relevant cleavage site(s) for plasmin remain to be determined. In addition to serine proteases, cathepsin proteases may activate ENaC. Cathepsin proteases belong to the group of cysteine proteases and play a pathophysiological role in inflammatory diseases. Under pathophysiological conditions cathepsin-S (Cat-S) may reach ENaC in the apical membrane of epithelial cells. Our aims were (a) to identify functionally relevant plasmin cleavage sites in human γENaC [5] and (b) to investigate the effect of Cat-S on human ENaC [6].

Mutant human γENaC constructs were generated by site-directed mutagenesis. Human wild-type or mutant αβγENaC was expressed in *Xenopus laevis* oocytes. Amiloride-sensitive whole-cell currents (ΔI_{ami}) were determined by two-electrode voltage-clamp before and after 30 min incubation of the oocytes in human plasmin (10 μg/ml), chymotrypsin (2 μg/ml) or Cat-S (1 μM). Biotinylated cell surface γENaC cleavage products were detected by western blot analysis using a γENaC antibody.

(a) Sequence alignment revealed a putative plasmin cleavage site in human γENaC (K189) that corresponds to a plasmin cleavage site (K194) in mouse γENaC. We mutated this site to alanine (K189A) and expressed human wild-type αβγENaC and αβγK189AENaC in oocytes. The γK189A mutation reduced but did not abolish activation of ENaC whole-cell currents by plasmin. Mutating a putative prostasin site (γRKRK178AAAA) had no effect on the stimulatory response to plasmin. In contrast, a double mutation (γRKRK178AAAA;K189A) prevented the stimulatory effect of plasmin. We conclude that in addition to the preferential plasmin cleavage site K189 the putative prostasin cleavage site RKRK178 may serve as an alternative site for proteolytic channel activation by plasmin. Interestingly, the double mutation delayed but did not abolish ENaC activation by chymotrypsin. The time-dependent appearance of cleavage products at the cell surface nicely correlated with the stimulatory effect of chymotrypsin on ENaC currents in oocytes expressing wild-type or double mutant ENaC. This indicates a causal link between proteolytic cleavage and channel activation. Delayed proteolytic activation of the double mutant channel with a stepwise recruitment of so-called near silent channels was confirmed in single-channel recordings from outside-out patches. Interestingly, mutating two phenylalanines (γFF174) adjacent to the prostasin cleavage site prevented proteolytic activation by chymotrypsin. This indicates that the two phenylalanines constitute a preferential cleavage site for ENaC activation by chymotrypsin.

(b) We demonstrated that Cat-S activates ΔI_{ami} in ENaC-expressing oocytes. ENaC stimulation by Cat-S was associated with the appearance of a γENaC cleavage fragment at the plasma membrane indicating proteolytic channel activation. Mutating two valine residues (V182 and V193) in the critical region of γENaC prevented proteolytic activation of ENaC by Cat-S. The stimulatory effect of Cat-S on ENaC activity and the concomitant appearance of a γENaC cleavage product at the cell surface were prevented by the Cat-S inhibitor LHVS (morpholinurea-leucine-homophenylalanine-vinylsulfone-phenyl). In contrast, LHVS had no effect on ENaC activation by the prototypical serine proteases trypsin and chymotrypsin. To our knowledge, this is the first report that the cysteine protease Cat-S can activate ENaC which may be relevant under pathophysiological conditions.

In this study, we identified cleavage sites in a region critical for proteolytic channel activation in the γ-subunit of human ENaC with functional importance for its proteolytic activation by plasmin, chymotrypsin and Cat-S. The fact that γENaC contains several different cleavage sites in this region is likely to have physiological implications. Indeed, it may provide a mechanism for differential ENaC regulation by tissue-specific proteases.

Rossier BC & Stutts MJ (2009). Annu Rev Physiol **71**, 361-79.

Kleyman TR et al. (2009). J Biol Chem **284**, 20447-51.

Svenningsen P et al. (2009). J Am Soc Nephrol **20**, 299-310.

Passero CJ et al. (2008). J Biol Chem **283**, 36586-91.

Haerteis S et al. (2012). J Gen Physiol **140**, 375-89.

Haerteis S et al. (2012). Pflügers Arch **464**,353-65.

This work was supported by the Interdisziplinäres Zentrum für Klinische Forschung (IZKF) and by the ELAN program of the Medical Faculty of the Friedrich-Alexander-Universität Erlangen-Nürnberg.

Where applicable, the authors confirm that the experiments described here conform with The Physiological Society ethical requirements.

SA64

Regulation of the epithelial Na^+ channel (ENaC) by kinases

A. Dinudom, I. Lee, S. Song and D.I. Cook

Discipline of Physiology, Sydney Medical Scool, The University of Sydney, Sydney, NSW, Australia

Activity of the amiloride-sensitive Na^+channel (ENaC) expressed in the distal nephron and respiratory epithelium has a profound impact on Na^+ homeostasis, the regulation of blood pressure and respiratory surface fluid volume. Dysfunction of ENaC underlies human diseases such as Liddle's syndrome, pseudohypoaldosteronism type 1 and cystic fibrosis. The activity of ENaC is tightly controlled by an array of physiological factors that exert their effect on transcription, trafficking and gating of the channel via multiple cellular signalling pathways. Hydrogen peroxide (H_2O_2) is one of the reactive oxygen species produced in response to oxidative stress, and it modulates a variety of physiological events. H_2O_2 exerts its effects via redox-sensitive proteins including transcription factors, protein tyrosine kinases and small G proteins. Previous studies suggested that H_2O_2 plays an important role in the regulation of ENaC, implicating it in the pathophysiology of pulmonary edema and acute lung injury. Consistent with this notion, exogenous H_2O_2 inhibits transepithelial ion transport and suppresses baseline expression of the α-subunit of ENaC in alveolar epithelial cells. In agreement with these reports, we found that H_2O_2 has a profound inhibitory effect on the amiloride-sensitive current in mouse collecting duct (M1) cells and on exogenous ENaC expressed in Fisher Rat Thyroid (FRT) cells. This inhibitory effect of H_2O_2 is attenuated in cells over-expressing a dominant-negative mutant of apoptosis signal-regulating kinase 1 (ASK-1), a ubiquitously expressed MAP kinase kinase kinase that is activated in response to cytotoxic stress. Our data further suggest that H_2O_2 inhibits the activity of ENaC via the ASK-1/p38 MAP kinase signalling cascade by a mechanism that interferes with proteolytic activation of ENaC subunits. H_2O_2 is also known to be an activator of the proto-oncogene tyrosine-protein kinase (Src), a non-receptor membrane-associated tyrosine kinase that plays an important role in cytoskeletal organization and cell proliferation, tyrosine phosphorylation of many cellular signalling molecules and is involved in the cellular signalling pathway by which endothelin-1 inhibits activity of ENaC. We found that Src mediates the inhibitory effect of platelet-derived growth factor (PDGF) on ENaC. Unlike ASK-1, Src alters total ENaC protein expression and the abundance of ENaC at the

cell membrane, but has no effect on proteolytic cleavage of the channel subunits. The inhibitory effect of Src requires caveolin-1, suggesting that the effector molecules that are involved in the Src-mediated signalling system that regulates ENaC may be organised in the cholesterol-rich lipid raft sub-membrane domain.

Where applicable, the authors confirm that the experiments described here conform with The Physiological Society ethical requirements.

SA65

Multiple COMMD proteins alter the trafficking of the epithelial sodium channel, ENaC

F.J. McDonald[1], Y. Liu[1], M. Swart[1], K. Ly[1] and E. Burstein[2]

[1]Physiology, University of Otago, Dunedin, New Zealand and [2]Internal Medicine and Molecular Biology, University of Texas Southwestern Medical Center, Dallas, TX, USA

The epithelial sodium channel (ENaC) has an important role in maintaining salt and water balance, and in long-term blood pressure control. Multiple proteins interact with ENaC to control its forward movement along the protein secretion pathway to the cell surface, and ENaC endocytosis and trafficking to the lysosome or recycling endosome (reviewed in Butterworth 2010). For example, the E3 ubiquitin ligase Nedd4-2 catalyses covalent attachment of ubiquitin moieties onto ENaC subunits to promote endocytosis and trafficking to the lysosome. Nedd4-2 action is mitigated upon its phosphorylation by the aldosterone-stimulated kinase SGK1. The regulation of ENaC in the kidney by Nedd4-2 and SGK1 appears to be a key pathway by which ENaC Na+ transport is controlled. We discovered that the Copper Metabolism Murr1 Domain-containing protein 1 (COMMD1) interacts with ENaC (Biasio et al., 2004), and reduces amiloride-sensitive short circuit current (Isc-amil) in Fischer rat thyroid (FRT) epithelia expressing ENaC. COMMD1 appears to form a complex with SGK-Nedd4-2 resulting in a decrease in the ENaC population at the cell surface (Ke et al., 2010). COMMD1 is the founding member of a ten-member family of proteins (COMMD1-10) sharing a C-terminal COMM domain (Burstein et al., 2005). Although COMMD1 has pleiotropic roles in copper, chloride transport, NF-κB transcriptional downregulation, and regulation of the HIF1α complex, roles for other COMMD proteins have not been described. To investigate whether other COMMD proteins also regulate ENaC we used co-immunoprecipitation and showed that COMMD1-10 all interact with ENaC. Using immunohistochemistry we found that COMMD1, 3, and 9 were widely expressed in rat kidney including collecting duct cells, and showed colocalisation with ENaC. COMMD1, 3, and 9 individually inhibited Isc-amil in ENaC-expressing FRT epithelia. These COMMD proteins appear to have unique roles in inhibiting ENaC because COMMD3 and 9 retained their ability to reduce Isc-amil in ENaC-expressing FRT epithelia when COMMD1 expression was reduced using siRNA knockdown. COMMD1, 3, and 9 all decreased cell surface expression of ENaC, therefore they likely affect trafficking of ENaC to or from the cell surface. Another family member, COMMD10, was found to regulate forward trafficking of proteins in the secretory pathway. Thus multiple COMMD family members negatively regulate ENaC, but may act at different locations in the protein trafficking pathway.

Biasio W, Chang T, McIntosh CJ, McDonald FJ. 2004. Identification of Murr1 as a regulator of the human delta epithelial sodium channel. J. Biol. Chem. 279(7):5429-5434.

Burstein E, Hoberg JE, Wilkinson AS, Rumble JM, Csomos RA, Komarck CM, Maine GN, Wilkinson JC, Mayo MW, and Duckett CS. 2005. COMMD proteins, a novel family of structural and functional homologs of MURR1. J. Biol. Chem. 280: 22222-22232.

Butterworth MB. 2010. Regulation of the epithelial sodium channel (ENaC) by membrane trafficking. Biochim. Biophys. Acta 1802(12):1166-1177.

Ke Y, Butt AG, Swart M, Liu YF, McDonald FJ. 2010. COMMD1 downregulates the epithelial sodium channel through Nedd4-2. Am. J. Physiol. Renal Physiol. 298(6):F1445-1456.

Funding: Marsden Fund Council, University of Otago PhD stipend to YFL, Department of Physiology MSc stipend to MS, and Department of Physiology Aim funding to KL.

Where applicable, the authors confirm that the experiments described here conform with The Physiological Society ethical requirements.

SA66

***In vivo* regulation of ENaC by the ubiquitin ligase Nedd4L in lung and intestinal epithelia**

D. Rotin

Hospital for Sick Children, Toronto, ON, Canada

The amiloride-sensitive Epithelial Na+ Channel (ENaC) plays a pivotal role in regulating salt and fluid transport in salt absorbing epithelia in the kidney, lung, intestine and other tissues, and is involved in controlling blood pressure. An important regulator of ENaC stability at the plasma membrane is the ubiquitin ligase Nedd4L (Nedd4-2), which promotes ENaC ubiquitination and endocytosis, thus downregulating the channel by targeting it for lysosomal degradation. In vivo, knockout of Nedd4L in mouse kidney was shown (by the Staub and Yang groups) to increase abundance of both ENaC and the Na+/Cl- co-transporter, leading to salt-induced hypertension. The in vivo role of Nedd4L in the lung was not known. To investigate the role of Nedd4L in the lung, we knocked it out specifically in lung epithelia (in SPC-expressing Type II and airway epithelial cells). Our results show that these mice developed cystic fibrosis-like lung disease, with airway mucus obstruction, goblet cell hyperplasia, massive inflammation, fibrosis and death by 3-weeks of age. Cystic fibrosis is caused by impaired ion transport due to mutated CFTR, accompanied by elevated activity of ENaC. These effects of Nedd4L loss in the lung were likely caused by enhanced ENaC function, as reflected by increased ENaC protein levels, increased lung dryness at birth, amiloride-sensitive dehydration of lung explants, and elevated ENaC currents in primary alveolar-Type II cells analyzed by patch clamp recordings. Moreover, the lung defects could be rescued with administration of amiloride into the lungs of young knockout pups via nasal instillation. Our results therefore suggest that the ubiquitin ligase Nedd4L normally opposes the onset of cystic fibrosis symptoms by inhibiting ENaC in lung epithelia. More recently, we have begun investigating the role of Nedd4L in the intestine, by knocking out Nedd4L specifically in intestinal epithelium (in Villin-expressing cells). The results of these studies will be presented.

Cystic Fibrosis Canada and the Canadian Institute of Health Research (CIHR)

Where applicable, the authors confirm that the experiments described here conform with The Physiological Society ethical requirements.

SA67

Human and small animal studies of maternal obesity and weight gain

L. Poston

Women's Health, King's College London, London, UK

Mother-child cohort studies suggest an association between maternal BMI/ excessive gestational weight gain and offspring risk of cardiovascular and metabolic disease. Investigations are however complicated by inevitable confounding influences of postnatal factors which cannot always be accounted for in statistical analysis, and assumption of causality must be cautious.Randomised controlled trials (RCTs) of intervention studies in pregnant women which aim to ameliorate the metabolic influences of maternal obesity on the developing child can obviate some of these issues. The EU funded EarlyNutrition project brings together several relevant RCTs to address the influence of maternal interventions on childhood obesity and health, including the UK UPBEAT trial of a complex (dietary and physical activity) intervention in obese pregnant women. Protocols have been standardised between studies, and children will be investigated at the age of 3 and 5. Detailed measurement of body composition, breast feeding history, diet, and physical activity, as well as health, social and environmental factors will be obtained. With knowledge the maternal body composition, weight, diet and physical activity from women in intervention and control arms of the studies, these studies should provide valuable information on maternal/child obesity relationships, as well as other childhood health outcomes. Mechanistic insight will also be gained but for practical reasons this cannot be of equivalent depth to that achievable in animal models, which have provided convincing evidence for influences of maternal obesity on offspring health. Models of maternal obesity in rodents, performed under UK Home Office legislation have provided information on the mechanisms leading to offspring obesity and hypertension in the offspring, including a central role for hypothalamic centres of energy balance and autonomic pathways of blood pressure control. The offspring also demonstrate a hepatic disorder very similar to non-alcoholic fatty liver in man. These studies have led to testable hypotheses in the children of obese women, which we have now incorporated into studies of children in a mother-child cohort study (SCOPE) and from the UPBEAT trial.

Maternal Obesity. Eds Gillman M and Poston L. Cambridge University Press. 2012. ISBN 978-107-00396-5

Samuelsson A-M, Morris A, Igosheva N, Kirk SL, Pombo JMC, Coen CW, Poston L, Taylor PD. Evidence for sympathetic origins of hypertension in juvenile offspring of obese rats. Hypertension published online Nov 9, 2009; DOI: 10.1161/HYPERTENSIONAHA.109.139402.

Mouralidarane A, Soeda J, Visconti-Pugmire C, Samuelsson AM, Pombo J, Maragkoudaki X, Butt A, Saraswati R, Novelli M, Fusai G, Poston L, Taylor PD, Oben JA. Maternal obesity programs offspring non-alcoholic fatty liver disease via innate immune dysfunction in mice. Hepatology. 2013 Jan 12. doi: 10.1002/hep.26248. [Epub ahead of print]

We are grateful to the following funding bodies;the National Institute of Health Research (NIHR RP-PG-0407-10452), the British Heart Foundation (FS/10/003 and PG/06/067/21009) and the EU (Framework 7; Grant no 289346).

Where applicable, the authors confirm that the experiments described here conform with The Physiological Society ethical requirements.

SA68

Offspring of mothers on a high fat diet show altered circadian biology and fatty liver

K.D. Bruce[1,2], D. Szczepankiewicz[2], K.K. Sihota[2], M. Ravindraanandan[2], M.A. Hanson[2], C.D. Byrne[2] and F.R. Cagampang[2]

[1]Metabolism and Aging, The Scripps Research Institute, Jupiter, FL, USA and [2]Human Development and Health, University of Southampton, Southampton, Hampshire, UK

Perturbations in circadian rhythms are associated with a range of metabolic disorders including obesity, type 2 diabetes and fatty liver disease. We have previously shown that high fat (HF) exposure during early life primes adult onset of severe fatty liver in the offspring. Recent findings show that hepatic lipid homeostasis is maintained by a cell autonomous transcriptional feedback loop composed of the transcription factors CLOCK and BMAL1 and their target genes many of which are transcription factors with roles in lipogenesis (e.g REVERB, SREBP1c). Therefore, the precise timing of clock gene expression is critical for optimal hepatic metabolism. The "clock" proteins are regulated by the NAD+ dependent deacetylase SIRT1, and thus are themselves influenced by nutrition and cellular metabolism. To date, the effect of HF exposure during early life on the circadian clock network and hepatic metabolism in the offspring in later life is unknown. We used our mouse model of developmentally primed fatty liver disease to demonstrate that offspring exposed to HF diets during development and adulthood exhibit the most severe fatty liver phenotype in later life. These offspring also show a reduction in cellular NAD+ and SIRT1 expression. We show that the circadian pattern of core clock genes, and protein expression, is disrupted in response to a HF diet a perturbation that is exacerbated in offspring exposed to a maternal HF diet during development. Moreover, expression of clock target genes involved in lipogenesis (REVERB, SREBP1c) is up-regulated in offspring from HF fed mothers, which may further contribute to fat accumulation in the liver. Our results suggest that early HF exposure causes persistent changes in cellular redox status, SIRT1 reduction, clock gene imbalance, and up-regulated lipogenic transcription factors, developmentally priming the onset of fatty liver in later life.

Supported by BBSRC

Where applicable, the authors confirm that the experiments described here conform with The Physiological Society ethical requirements.

SA69

Programming metabolic and psychological diseases: effects of maternal obesity and diet

K. Grove

ONPRC/OHSU, Beaverton, OR, USA

Childhood obesity is associated with increased risk of metabolic diseases later in life; however, it is also associated with a broad spectrum of behavior/psychological disorders including depression, anxiety, poor learning, and attention deficient disorder. Maternal obesity, diabetes and high fat diet (HFD) consumption during pregnancy, which is highly prevalent in the United States, has a high association with early onset obe-

sity. Using a nonhuman primate (NHP) model our group is investigating the relative impact of maternal metabolic health and diet on the development of hypothalamic systems involved in the regulation of energy homeostasis as well as stress and anxiety behaviors. To date, we have observed that fetal offspring of animals consuming the HFD develop early onset fatty liver as well as abnormalities in the development of pancreatic islets and in brain circuits involved in the regulation of appetite and stress responsiveness. A likely causal factor for these developmental abnormalities is placental insufficiency and an increase in circulating cytokines (originating from the placenta) during critical periods of fetal development, as well as the activation of local inflammatory systems within the brain. Importantly, most of these developmental programming effects were independent of the maternal metabolic phenotype, as they were observed in both obese and lean animals consuming the HFD. Infant offspring of animals consuming the HFD have a higher rate of growth during the postnatal period resulting in a doubling of body fat and insulin resistance, as well as pancreatic islet hyperplasia and fatty liver at weaning. Furthermore, female, but not male, infant offspring also display increased anxiety-like behavior. This sexual dimorphism in anxiety-like behavior is consistent with human clinical studies demonstrating that the behavior/psychological disorders associated with childhood obesity are more prevalent in young girls. However, both male and female HFD offspring displayed increased appetite, food preferences for palatable foods and social behavior abnormalities, that were not reversible by post-weaning diet reversal. Overall, these results suggest that chronic consumption of a HFD during pregnancy alone can cause significant abnormalities in the development of critical metabolic system in the fetal offspring. Many of the changes appear to be due to the high lipid environment leading to the activation of the proinflammatory cytokines both within the placenta as wells as the brain. This lipotoxicity may also have broad negative impact on the neural systems involved in social behavior as well as learning and memory.

Acknowledgements: NIH grants DK79194, DK090954 and OD011092

Where applicable, the authors confirm that the experiments described here conform with The Physiological Society ethical requirements.

SA70

Periconceptional overnutrition and maternal weight loss effects on offspring obesity and metabolism in sheep

L.M. Nicholas[1], L. Rattanatray[1,2], S.M. MacLaughlin[1], S.E. Ozanne[3], D.O. Kleemann[4], S.K. Walker[4], J.L. Morrison[1], S. Zhang[1], B.S. Muhlhausler[1], M.S. Martin-Gronert[3] and I.C. McMillen[1]

[1]Sansom Institute for Health Research, School of Pharmacy and Medical Sciences, University of South Australia, Adelaide, SA, Australia, [2]Discipline of Physiology, School of Molecular and Life Sciences, University of Adelaide, Adelaide, SA, Australia, [3]Institute of Metabolic Science-Metabolic Research Laboratories, University of Cambridge, Cambridge, UK and [4]Turretfield Research Centre, South Australian Research and Development Institute, Rosedale, SA, Australia

The obesity epidemic has resulted in more women entering pregnancy overweight or obese. Offspring of obese women have increased risk of obesity and impaired glucose tolerance in childhood and adult life. It has therefore been proposed that there is an 'intergenerational cycle' of obesity and insulin resistance. Studies have shown that changes in the abundance of insulin signalling molecules in skeletal muscle and adipose tissue precede the development of insulin resistance and type 2 diabetes (1,2). It is not clear, however, whether exposure to maternal obesity results in insulin resistance in her offspring as a consequence of the impact of increased adiposity on insulin sensitive tissues (3,4) or as a consequence of the programming of specific changes in the abundance of insulin signalling molecules in these tissues (2,5). It has previously been shown in sheep that exposure to maternal obesity around the time of conception alone led to increased adiposity in female lambs at 4 months of age and that dietary restriction in the obese ewe during the periconceptional (PC) period abolished this effect (6). While dieting before pregnancy may have metabolic benefits for the offspring, there are also potential metabolic and endocrine costs for the offspring (7). The pathways and critical periods during which the metabolic consequences of maternal obesity or dietary restriction are transduced from mother to the offspring are, however, not known. Moreover, there is a paucity of knowledge on the possible epigenetic mechanisms that are recruited in the oocyte/early embryo, which could contribute to such changes.

We used an embryo transfer model in sheep to investigate the effects of maternal obesity and of dietary restriction during the PC period on insulin signalling in liver and skeletal muscle of the offspring. Furthermore, we also investigated the role of miRNAs in regulating hepatic insulin signalling in these offspring. Donor ewes were allocated to 1 of 4 groups & were fed the following diets in the PC period: 100% metabolisable energy requirements (MER) for ≥ 20wks (CC); 100% MER for ≥ 16wks & then 70% MER for 4wks (CR); ~180% MER for ≥ 20wks (HH); ~180% MER for ≥ 16wks & then 70% MER for 4wks (HR). This continued for 1wk post-conception before single embryos were transferred into recipient ewes of normal weight. At 16wks after birth, liver and skeletal muscle samples were collected to determine insulin signalling gene expression (by qRT-PCR) and protein abundance (by Western Blotting) and expression of key miRNAs (by qRT-PCR) in the offspring. The effects of PC nutrition and sex on protein abundance and miRNA expression were determined using a two-way ANOVA. A Duncan's post hoc test was used to determine significant differences between groups.

We found decreased insulin receptor (IR) ($P<0.05$), Akt2 (female lambs) ($P<0.05$), phospho-Akt ($P<0.01$) and phospho-FoxO1 ($P<0.01$) abundance and in contrast, an increased Caveolin-1 ($P<0.05$) abundance in the liver of HH lambs. There was a parallel increase in miR-29b ($P<0.05$), miR-103 ($P<0.01$) and miR-107 ($P<0.05$) expression in these lambs. Maternal dietary restriction abolished some of the effects of maternal obesity. The abundance of Akt2, however, remained low (female lambs) and Caveolin-1 and miR-103 remained increased in HR lambs. Furthermore, there was decreased hepatic PDK1 gene expression ($P<0.01$) and phospho-PDK1and aPKCζ protein abundance ($P<0.05$) in CR and HR lambs. In contrast to the liver, maternal obesity resulted only in decreased GLUT4 abundance in muscle of female lambs. There was, however, increased IR abundance and decreased aPKCζ, phospho-AS160 and GLUT4 abundance in both CR and HR lambs.

We have found that exposure of the oocyte/early embryo to maternal obesity leads to differential changes in gene expression and protein abundance of key insulin signalling molecules in liver and muscle in postnatal life. Our results also suggest that miRNAs may be potential epigenetic regulators that are sensitive to programming by the maternal metabolic/nutritional environment and may play a key role in transducing the metabolic consequences of maternal obesity from the mother

to her offspring. Importantly, we also found that in most instances, dietary restriction was unable to ablate the effects of maternal obesity in both liver and skeletal muscle of lambs. Instead, exposure to dietary restriction itself irrespective of whether the ewes were previously on a normal or high plane of nutrition led to changes in a different suite of molecules within both liver and skeletal muscle of the offspring. These results suggest that maternal metabolic response to weight loss around conception, irrespective of her pre-pregnancy body weight has long lasting metabolic consequences for the offspring, which may contribute to the emergence of insulin resistance in later life.

Jensen CB, Martin-Gronert MS, Storgaard H, Madsbad S, Vaag A, Ozanne SE. Altered PI3-Kinase/Akt signalling in skeletal muscle of young men with low birth weight. PLoS ONE 2008;3.

Ozanne SE, Olsen GS, Hansen LL, et al. Early growth restriction leads to down regulation of protein kinase C zeta and insulin resistance in skeletal muscle. Journal of Endocrinology 2003;177:235-41.

Greenfield JR, Campbell LV. Insulin resistance and obesity. Clinics in Dermatology 2004;22:289-95.

Savage DB, Petersen KF, Shulman GI. Disordered lipid metabolism and the pathogenesis of insulin resistance. Physiol Rev 2007;87:507-20.

Li X, Monks B, Ge Q, Birnbaum MJ. Akt/PKB regulates hepatic metabolism by directly inhibiting PGC-1a transcription coactivator. Nature 2007;447:1012-6.

Rattanatray L, MacLaughlin SM, Kleemann DO, Walker SK, Muhlhausler BS, McMillen IC. Impact of maternal periconceptional overnutrition on fat mass and expression of adipogenic and lipogenic genes in visceral and subcutaneous fat depots in the postnatal lamb. Endocrinology 2010;151:5195-205.

Zhang S, Rattanatray L, MacLaughlin SM, et al. Periconceptional undernutrition in normal and overweight ewes leads to increased adrenal growth and epigenetic changes in adrenal IGF2/H19 gene in offspring. FASEB Journal 2010;24:2772-82.

Where applicable, the authors confirm that the experiments described here conform with The Physiological Society ethical requirements.

SA72

Role of muscle afferents in the ventilatory and circulatory response to endurance exercise

M. Amann

Department of Medicine, University of Utah, Salt Lake City, UT, USA

Ventilatory and cardiovascular responses to exercise are primarily regulated by two largely separate systems. The first, a feed-forward mechanism termed 'central command', elicits cardiovascular and ventilatory responses to exercise. The second, a feedback mechanism, reflexly changes ventilation and circulation as a consequence of limb muscle contraction. The focus here is on the latter.

Numerous animal and human studies have suggested a key role for muscle afferents in evoking cardiovascular and ventilatory responses during exercise. Specifically, non-nociceptive Group III/IV muscle afferents, the so-called 'ergoreceptors', are thought to depict the afferent arm of the cardiovascular and ventilatory reflexes, which are mediated via neural circuits in the nucleus tractus solitarius and the ventrolateral medulla. Recent human studies using local anaesthetics (lumbar epidural space) to block the central projection of Group III/IV muscle afferents during whole-body endurance exercise (leg cycling) found attenuated, similar or even increased cardiovascular and ventilatory responses when the identical exercise was performed with blocked muscle afferents. Although some of these studies conform to the idea that continuous afferent feedback is necessary for adequate ventilatory and circulatory responses, others are contradictory, leaving the exact role of muscle afferents in the cardioventilatory control during endurance exercise controversial. At least some of these conflicting findings may be explained by the use of local anaesthetics, which attenuate efferent as well as afferent nerve activity. The effects of local anaesthetics on efferent nerves cause a drug-induced 'muscle weakening', which inevitably requires an increase in central command in order to work at and/or maintain a given external workload. More recent studies designed to circumvent the confounding impact of local epidural anaesthetics now provide valuable insights into the effects of muscle afferents on the circulatory and ventilatory response to whole-body endurance exercise. By using lumbar intrathecal fentanyl, a selective μ-opioid receptor agonist, we were able to inhibit the central projection of Group III/IV muscle afferents without affecting the muscle's force-generating capacity and therefore without affecting central command during the exercise. The outcome of these studies clearly shows that when Group III/IV muscle afferents from the lower limbs are blocked during endurance exercise of various intensities, ranging from mild to heavy, circulation and pulmonary ventilation are substantially compromised. This not only causes arterial hypoxaemia and attenuates both perfusion pressure and blood flow, which eventually reduces O2 delivery to the working muscles, but also facilitates ventilatory and metabolic acidosis, all of which combine to accelerate the development of peripheral locomotor muscle fatigue during exercise. These findings suggest that continuous sensory feedback from working skeletal muscle may depict a vital component in providing a high capacity for rhythmic endurance exercise because controlled muscle perfusion and O2 delivery determine the fatigability of skeletal muscle and thus affect its performance.

Where applicable, the authors confirm that the experiments described here conform with The Physiological Society ethical requirements.

SA73

Separating central command, muscle mechano and metaboreflex mediated cardiorespiratory responses to exercise in man

L.C. Vianna

Physiology and Pharmacology, Fluminense Federal University, Niterói, Rio de Janeiro, Brazil

The cardiovascular and hemodynamic adjustments to exercise are primarily mediated by alterations in parasympathetic and sympathetic neural activity. These changes in autonomic neural outflow are mediated via three distinct neural control mechanisms: central command, exercise pressor reflex (EPR) and the arterial baroreflex. Central command is a feedforward mechanism that, through signals originating in higher brain centers, activates cardiovascular and somatomotor systems in parallel. The EPR is a feedback peripheral neural drive originating in skeletal muscle. The arterial baroreflex provides further modulation via tonically active baroreceptors, located in the carotid and aortic arteries. As such, the alterations in autonomic outflow during physical activity are carefully controlled by these neural inputs to induce changes in heart rate, stroke volume and total peripheral resistance and evoke increases in arterial blood pressure (BP) appropriate for the metabolic demands of the exercising muscle. Although all three neural

mechanisms are important for cardiovascular regulation during exercise, considerable attention has been given to the EPR due to its importance determining the magnitude of sympathoexcitation during exercise. The sensory component of the EPR is comprised of group III and IV skeletal muscle afferents that respond to both mechanical (i.e., muscle mechanoreflex) and metabolic (i.e., muscle metaboreflex) stimuli. It should be noted, however, that both type III and IV afferents show a degree of polymodality and may readily respond to either mechanical or metabolic provocation. The muscle mechanoreflex can be activated by mechanical stretch in humans, however its effects on cardiovascular responses appear small and transient. As a result, the evoked hemodynamic consequences to passive stretch of leg or arm muscles are limited in humans. In contrast, the muscle metaboreceptors are paramount in generating the reflex increases in sympathetic outflow during isometric exercise in normal physiological states. In humans, muscle metaboreflex activation can be isolated by means of circulatory arrest of the active limb just before the cessation of exercise. During this maneuver, metabolic by-products of muscle contraction are trapped in skeletal muscles and stimulate metabolically sensitive afferents fibers. Stimulation of these afferents results in an elevated blood pressure achieved in part by sympathetically-mediated increases in systemic vasoconstriction, with elevations in heart rate playing a minor role. Importantly, this maneuver isolates the muscle metaboreflex from central command and muscle mechanoreflex. Overall, while it is well established that the EPR is one of the principal mediators of the cardiovascular response to exercise, the receptors activating the group III and IV fibers that are important to EPR function remains unclear. Recent animal studies have reported that either capsaicin balm or infusion of capsazepine attenuates the pressor response to muscle contraction, indicating the transient receptor potential vanilloid1 (TRPv1) receptor (localized on the group IV afferent neuron) as an important mediator of the EPR via its metabolic component (named muscle metaboreflex). Whether these findings can be extended to human remains to be determined. Based on humans studies performed in our laboratory, I will provide evidence that capsaicin-based analgesic balm effectively attenuates BP (photoplethysmography), sympathetic outflow (peroneal microneurgraphy) and vasconstrictory (Doppler Ultrasound) responses evoked by metabolically sensitive skeletal muscle afferents in humans. These data are consistent with the concept that TRPv1 receptors contribute to the EPR in humans, via its metabolic component.

Supported by CAPES, CNPq, FAPERJ, FINEP.

Where applicable, the authors confirm that the experiments described here conform with The Physiological Society ethical requirements.

SA74

Spinal control of human inspiratory motoneurones

S. Gandevia[2,1], A. Hudson[1,2] and J. Butler[1,3]

[1]University of New South Wales, Neuroscience Research Australia, Randwick, NSW, Australia, [2]University of New South Wales, Neuroscience Research Australia, Randwick, NSW, NSW, Australia and [3]University of New South Wales, Neuroscience Research Australia, Randwick, NSW, Australia

Evolution is certain to have ensured optimal strategies to drive inspiratory muscles to produce pulmonary ventilation, a function which is essential for survival. However, the neural underpinnings for such strategies are little studied. We have examined the recruitment of single human motoneurones in obligatory inspiratory muscles, particularly the diaphragm and inspiratory intercostal muscles (e.g. Butler & Gandevia, 2008), in an attempt to find common strategies that may underlie their recruitment in different tasks. These include volitionally-driven inspiration and inspiration driven by chemical drive, presumably from pontomedullary respiratory centres.

During quiet breathing, inspiratory activity in the parasternal intercostal muscles is measured for populations of single units. There is earlier and greater activity in those muscle portions with a greater mechanical advantage for inspiration (e.g. De Troyer et al 2005; Gandevia et al 2006). This ensures efficient matching between neural drive and ventilation. This principle of 'neuromechanical matching' represents a recruitment strategy superimposed on the well-known Henneman size principle. During highly volitional breathing this strategy is preserved in the intercostal muscles (Hudson et al 2011). We have proposed that this common neuromechanical matching is mediated at a premotoneuronal level via a 'spinal distribution network' for inspiratory drive. Unfortunately, the human studies do not reveal whether such a network exists at a spinal level, or whether pontomedullary, or even motor cortical circuits are involved. However, recent studies in dogs spinalised at C2 show that intercostal motor unit firing preserves the usual neuromechanical matching of spontaneous breathing even when ventilation is evoked by thoracic spinal cord stimulation (DiMarco & Kowalski, 2010; 2011). This represents evidence for a spinal distribution network which can impose neuromechanical matching on intercostal motor output. There is also other evidence for respiratory propriospinal neurones (e.g. Saywell et al 2011). A spinal distribution network makes sense from an evolutionary perspective: axial muscles would first have been driven by reticulospinal paths, then also by bulbospinal paths as lung breathing developed, and then finally by corticospinal paths. Such a network would ensure efficient muscle use with a range of descending drives for different tasks.

Butler JE, Gandevia SC. 2008. The output from human inspiratory motoneurone pools. J Physiol 586: 1257-64

De Troyer A, Kirkwood PA, Wilson TA. 2005. Respiratory action of the intercostal muscles. Physiol Rev 85: 717-56

DiMarco AF, Kowalski KE. 2010. Intercostal muscle pacing with high frequency spinal cord stimulation in dogs. Resp Physiol Neurobiol 171: 218-24

DiMarco AF, Kowalski KE. 2011. Distribution of electrical activation to the external intercostal muscles during high frequency spinal cord stimulation in dogs. J Physiol 589: 1383-95

Gandevia SC, Hudson AL, Gorman RB, Butler JE, De Troyer A. 2006. Spatial distribution of inspiratory drive to the parasternal intercostal muscles in humans. J Physiol 573: 263-75

Hudson AL, Gandevia SC, Butler JE. 2011. Common rostrocaudal gradient of output from human intercostal motoneurones during voluntary and automatic breathing. Resp Physiol Neurobiol 175: 20-8

Saywell SA, Ford TW, Meehan CF, Todd AJ, Kirkwood PA. 2011. Electrophysiological and morphological characterization of propriospinal interneurons in the thoracic spinal cord. J Neurophysiol 105: 806-26

Where applicable, the authors confirm that the experiments described here conform with The Physiological Society ethical requirements.

SA75

Central and peripheral contributions to tremor – essentially we don't know

M. Lakie

University of Birmingham, Birmingham, UK

Pubmed shows that the annual total of papers mentioning physiological tremor has grown steadily from ~ 200 to ~ 400 over the last twenty years. One particular interest is the idea that a centrally generated, approximately 10 Hz component plays an important role in tremor generation. The concept of an autonomous central "tremor generator" is nearly as old as the discovery of the alpha rhythm. The discovery of a brain rhythm which had about the same frequency as tremor lead quickly to the idea that it "must" be the cause. This was quickly shown to be false, but the idea of a central generator is persistent. Work by Elble and colleagues established the central tremor generator ("an oscillating system of neurones located within the CNS", Elble and Koller (1990)). It is now common to divide tremor into "central" and "mechano-reflex" components. More recently, the central oscillator theory has been invoked to explain the approximately 10 Hz tremor-like discontinuities that can be observed during movement (for example, Vallbo and Wessberg (1993)). This has suggested that all slow movements are executed on a pulsatile basis. The idea of obligatory pulsatile control is actually quite old (Travis 1929, Tiffin and Westhafer, 1940)) but has recently been reworked (Bye and Neilsen, 2010; the BUMP theory). There are at least two difficulties with the idea of a central generator. First, how many such generators are there? One per motor unit, one per muscle, one per movement or one per person? Second, central generators operating at ~ 10 Hz during posture and movement have not been confidently identified.

The other half of the tremor story (the "mechano-reflex component") has also been studied. The "mechano" part is the resonant properties of the limbs. It may be augmented by appropriately phased "reflex" activity (Lippold, 1970). Resonance results from the interaction of the stiffness of the muscles and the inertia of the moving parts of the limb. In recent work, we have shown that the complete spectrum of tremor can be economically explained by resonance. A simple way to demonstrate this is to see if a specific form of EMG is necessary to generate tremor, or whether a realistic tremor can be created by an entirely random neural input. In one approach we compared real tremor to that produced by a simple resonant model. The resonant model recreated the tremor spectrum when driven by real EMG or by an entirely random artificial input. We concluded that the contribution of any central component must therefore be minimal (Lakie et al 2012). In the second approach we drove relaxed limbs with random artificial excitation and again showed that a realistic tremor resulted.

One of the key planks of the division of tremor into central and mechano-reflex components was that they occupied distinct and identifiable parts of the frequency spectrum. For some time, however, it has been known that the resonant frequency of a limb cannot be described by a single value. Skeletal muscles are thixotropic so that they decrease their stiffness with movement (Lakie et al 1984). We have shown that this feature can also be captured very well by a simple resonant model. Fig 1 shows hand tremor acceleration spectra recorded from a postural (static) and slowly moving (dynamic) limb. During movement the tremor size greatly increases (by approximately an order of magnitude) and decreases in frequency. This behaviour is also recreated by our simple resonant model using appropriately sized random inputs or recorded EMG.

For finger tremor the resonant frequency is thought to be higher than the wrist – usually greater that 20 Hz. Recent work leads us to question this assumption, because the frequency of finger resonance will reduce very considerably with movement. The tremor spectrum with its two peaks is usually thought to represent coexisting and distinguishable central and mechano-reflex mechanisms. We alternatively suggest that the two peaks may both represent resonance. The high frequency peak occurs when the finger is stationary and the muscles are stiff and the lower frequency occurs during movement when the muscle stiffness is much decreased.

We suggest that the finger tremor frequency is related to the speed of movement. When quasi-stationary, (postural), stiffness and resonant frequency are high and during movement both are reduced. Our conclusion is that as far as physiological tremor is concerned the role of a central component is negligible. Peripheral factors are extremely important and mechanical resonance is fundamental. It is possible that the resonant properties are complemented by reflex activity. One caveat is that the situation for pathological tremor is clearly different. Central oscillators are clearly involved in the genesis of Parkinsonian tremor and at least some forms of essential tremor.

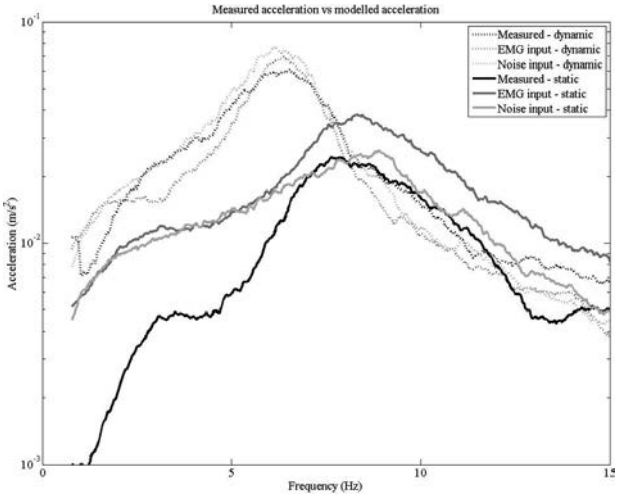

Bye RT, Neilson PD. (2010) The BUMP model of response planning: intermittent predictive control accounts for 10 Hz physiological tremor. Hum Mov Sci 29(5):713-36

Elble RJ, Koller WC (1990) Tremor. Johns Hopkins University Press Ltd. Baltimore

Lakie M, Walsh EG, Wright GW. (1984) Resonance at the wrist demonstrated by the use of a torque motor: an instrumental analysis of muscle tone in man. J Physiol.353:265-85.

Lippold OCJ (1970) Oscillation in the stretch reflex arc and the origin of the rhythmical 8-12 c/s component of physiological tremor. J. Physiol. 206:359-382

Tiffin J, Westhafer FL (1940) The relation between reaction time and temporal location of the stimulus on the tremor cycle. J Exp Psychol 27 (3):318-324

Travis LE (1929) The relationship of voluntary movement to tremors. J Exp Psychol 12:515-524

Vallbo AB, Wessberg J. (1993) Organization of motor output in slow finger movements in man. J Physiol. 469:673-91.

Where applicable, the authors confirm that the experiments described here conform with The Physiological Society ethical requirements.

SA76

Pattern control of human locomotion

Y. Ivanenko

Laboratory of Neuromotor Physiology, Fondazione Santa Lucia, Rome, Italy

Interaction of central and peripheral factors in the control of human posture and locomotion is a long standing topic. As Sherrington so accurately expresses in the statement "posture follows movement like a shadow," this highlights the interrelation of posture and movement . Tonogenic circuitry is a component of several, diverse supraspinal structures, including rostral ward, for example, the reticular formation, vestibular nuclei, the cerebellum, and selected mesodiencephalic nuclei. Here the two aspects of the locomotor circuitry functioning will be discussed: importance of muscle tone and development of locomotion in humans. Any reflection on the nature of human bipedalism should include a consideration of the mechanisms determining the choice of unconscious habitual posture. Disturbances in postural tone may also result in the emergence of quadrupedal gait in humans. Human stepping movements emerge in utero and show several milestones during development to independent walking. We examined the development of the spinal motor output by identifying the basic patterns of lumbosacral motoneuron activity from multimuscle recordings and by mapping the distribution of motoneuron activity in the lumbosacral spinal cord in stepping newborns, toddlers, preschoolers and adults. Muscle activity during human locomotion is accounted for by a combination of few basic patterns, each one timed at a different phase of the gait cycle. In particular, the two basic patterns of stepping neonates are retained through development, augmented by two new patterns first revealed in toddlers. The alternating spinal motor output is consistent with a simpler organization of neuronal networks in neonates. The development of human locomotion from the neonate to the adult starts from a rostrocaudal excitability gradient and involves a gradual functional reorganization of the pattern generation circuitry.

Where applicable, the authors confirm that the experiments described here conform with The Physiological Society ethical requirements.

SA77

Pulmonary vascular mechanics: Important contributors to increased right ventricular afterload of pulmonary hypertension

Z. Wang and N.C. Chesler

Biomedical Engineering, University of Wisconsin, Madison, WI, USA

Chronic hypoxia causes pulmonary vasoconstriction and vascular remodeling, which lead to hypoxic pulmonary hypertension (HPH). HPH is associated with living at high altitudes and is a complication of many lung diseases, including chronic obstructive pulmonary disease, cystic fibrosis, and obstructive sleep apnea. Pulmonary vascular changes that occur with HPH include stiffening and narrowing of the pulmonary arteries that appear to involve all vascular cell types and sub-layers of the arterial wall. Right ventricular (RV) changes that occur with HPH include RV hypertrophy and RV fibrosis, often with preserved systolic and diastolic function and ventricular-vascular coupling efficiency. Both vascular stiffening and narrowing are important contributors to RV afterload via increases in oscillatory and steady ventricular work, respectively. The increased blood viscosity that occurs in HPH can be quite dramatic and is another important contributor to RV afterload. However, the viscosity, vascular mechanics and ventricular changes that occur with HPH are all reversible. Furthermore, even with continued hypoxia vascular remodeling does not progress to the obliterative, plexiform lesions that are seen clinically in severe pulmonary hypertension. In animal models, the RV changes appear adaptive, not maladaptive. In summary, HPH-induced vascular mechanical changes affect ventricular function but both are adaptive and reversible, which differentiates HPH from severe pulmonary hypertension. The mechanisms of adaptation and reversibility may provide useful insight into therapeutic targets for the clinical disease state.

Supported by NIH HL086939.

Where applicable, the authors confirm that the experiments described here conform with The Physiological Society ethical requirements.

SA78

The TGFbeta-BMP signalling pathway in pulmonary vascular homeostasis and disease

P.D. Upton, L. Long, A. Crosby, R.J. Davies, X. Yang, T. Tajsic, M. Southwood and N.W. Morrell

Medicine, University of Cambridge, Cambridge, UK

Germ-line mutations in the bone morphogenetic protein type II receptor (BMPR-II) gene cause the majority of heritable pulmonary arterial hypertension (PAH) cases. PAH is a subset of the spectrum of pulmonary hypertension (PH) disorders, including hypoxia-related lung diseases.

BMPR-II belongs to the Transforming Growth Factor beta (TGFβ) receptor superfamily. Bone morphogenetic proteins (BMPs), via BMPR-II, activate the canonical Smad1/5/9 pathway to induce target genes, such as ID1-4. TGFβs (TGFβ1-3), signalling via the ALK5 receptor, regulate various cellular processes through the canonical Smad2/3 pathway. Dysregulated TGFβ1 signalling is pathogenic in fibrotic kidney and lung diseases. Our studies have addressed whether BMPR-II loss is a common feature of PH and if it correlates to enhanced TGFβ1 signalling in PH. This question has been addressed via studies of interaction between the BMP and TGFβ pathways in animal PH models and human pulmonary artery smooth muscle cells (PASMCs).

PH can be induced in rats by injecting the plant alkaloid, monocrotaline, resulting in progressive disease (MCT-PAH), or exposure to chronic normobaric hypoxia (FiO2 10% O2). In our studies, both hypoxic PH and MCT-PAH were associated with reduced lung BMPR-II protein and mRNA (1). However, significant increases in TGFβ1 and decreased Smad/ID responses were only observed in MCT-PAH(1). To investigate the role of TGFβ1 further, we administered a pharmacological inhibitor of the TGFβ type I receptor, ALK5. This inhibitor prevented disease progression in the MCT-PAH model, but not in hypoxia (1).

In vitro studies have also been performed using PASMCs from donor lungs and BMPR-II mutation positive PAH PASMCs. The mutation-bearing PASMCs exhibit reduced BMP4 responsiveness(2). TGFβ1 attenuated BMP4-mediated ID1/2 induction and activation of a Smad-dependent luciferase reporter, yet did not alter Smad phosphorylation. Conversely, BMP4 did not

alter TGFβ1-mediated responses. The inhibitory effect of TGFβ1 upon BMP4 responses was reversed by ALK5 inhibition and by Smad3 siRNA, but was unaffected by Smad2 siRNA.
In conclusion, our studies have shown that BMPR-II loss is common to the hypoxic and MCT PH models, but systemic ALK5 inhibition is only effective in the MCT model, highlighting a specific role for TGFβ1 in vascular remodelling in MCT-PAH. On the background of reduced BMPR-II, TGFβ1 exerts a potential pathogenic role via inhibition of the BMP-Smad transcriptional pathway through a Smad3-dependent mechanism. Therefore, intravenous anti-TGFβ1 therapy may be more effective in PAH, particularly related to BMPR-II mutations, rather than hypoxic PH.

Long, L., Crosby, A. et al. (2009). Circulation 119, 566-576.

Yang, J. et al. (2008) Circ Res. 102, 1212-1221

Where applicable, the authors confirm that the experiments described here conform with The Physiological Society ethical requirements.

SA79

Pulmonary hypertension and the right ventricle in hypoxia

R. Naeije

Erasme University Hospital, Brussels, Belgium

Hypoxia causes pulmonary vasoconstriction. Regional hypoxic vasoconstriction improves the matching of perfusion to alveolar ventilation. Global hypoxic vasoconstriction increases right ventricular afterload. The hypoxic pulmonary pressor response is universal in mammals and in birds, but with considerable inter-species and inter-individual variability. Chronic hypoxia induces pulmonary hypertension in proportion to initial vasoconstriction. Chronic hypoxia also is associated with an increase in red blood cell mass, which aggravates pulmonary hypertension by an increased blood viscosity. Hypoxic vasoconstriction is a quasi-immediate response followed by vascular remodeling after a as soon as after 6-8 hours to become largely irreversible with supplemental oxygen after 24 to 48 hours of hypoxic exposure. Hypoxic pulmonary hypertension in humans is usually mild to moderate, but pulmonary vascular pressure-flow relationships are steep, which corresponds to a substantial afterload on the right ventricle during exercise. This limits aerobic exercise capacity be a decrease in maximum right ventricular flow output. A partial recovery of maximum oxygen uptake has been reported with intake specific pulmonary vasodilating interventions in hypoxic subjects. While there are very few reported measurements of cardiac function during exercise, resting echocardiographic examinations disclose subtle deteriorations in both systolic and diastolic function, with right ventricular predominance. These findings are more pronounced in patients with chronic mountain sickness, but their clinical significance remains incompletely understood.

Where applicable, the authors confirm that the experiments described here conform with The Physiological Society ethical requirements.

SA80

Systems medicine of neurogenic hypertension

J. Schwaber

Thomas Jefferson University, Philadelphia, PA, USA

High-throughput data are extremely variable. The variability is such that it does not appear to represent deviation around a mean, with samples drawn from a single distribution - it appears more consistent with multiple distinct subtypes or states within the population. “Precision medicine” requires we treat this variability and complexity “not as a glitch but as a feature”. In this regard we view the genome, and thus cell phenotype, as highly adaptive, dynamic in response to changing environment. Our approach is to use the transcriptome, defined as RNA and RNA regulatory proteins, as a surrogate for phenotype, and to both analyze and drive the variability in neuronal phenotype. We take the transcriptome as a summary record of the unique experience of the organism, and indeed of each cell, over its history in the environment – and as not an end state but as highly malleable, including responses leading to disease. Thus, our goal is to develop a molecular physiology that incorporates variability.
We study the neural regulation of visceral homeostasis and take regional, pooled cell, and single cell samples in the central neural control system involved. We assay these neural samples at rest and in response to elevated blood pressure. Analysis of the resulting high-dimensional dataset reveals a remarkable complexity and heterogeneity of the samples and of their response to changes in blood pressure. These results demonstrate differential expression modules for each anatomically distinct neuronal group and neuronal type. We have been able to analyze the variability in a way that connects it to higher-level neurophysiological and neuroanatomical features of the system. The results suggest a novel concept of neuronal regulation of cardiovascular homeostasis arising from variability in the molecular physiology.
Our view is this approach may now enable a mechanistic molecular physiology of neural function and disease, involving constrained gene regulatory network models and multiscale models. Our multiscale models include the several cell types comprising brain tissue as they interact in innate neuroimmune inflammatory responses during the development of hypertension. We are developing the approach with the aim of discovering the adaptive responses involved in the development of neurogenic hypertension, thought to underlie the vast majority of all hypertension.

Where applicable, the authors confirm that the experiments described here conform with The Physiological Society ethical requirements.

SA81

Peptide modulation of cardiac autonomic transmission

N. Herring

Burdon Sanderson Cardiac Science Centre, Department of Physiology, Anatomy and Genetics, University of Oxford, Oxford, UK

Beta-blockers are known to improve mortality post myocardial infarction and in chronic congestive heart failure where sympathetic drive to the heart is high. However, the release of additional sympathetic co-transmitters can have deleteri-

ous consequences for cardiac parasympathetic neurotransmission even in the presence of these medications. Stimulation of the cardiac vagus reduces heart rate, lowers myocardial oxygen demand, improves coronary blood flow and independently raises ventricular fibrillation threshold. Methods used to assess vagus function in humans have demonstrated that higher nerve activity is a protective prognostic indicator in several cardiovascular disease states. This presentation will discuss recent data demonstrating a direct action of the sympathetic co-transmitters neuropeptide-Y and galanin on the ability of the vagus to release acetylcholine (1, 2), as well a strong correlation between plasma neuropeptide-Y levels and coronary microvascular function in patients with ST-elevation myocardial infarctions being treated by primary percutaneous coronary intervention (3). Targeting neuropeptide-Y receptors pharmacologically may therefore be a useful therapeutic strategy both acutely during myocardial infarction and also during chronic heart failure. Such medications would be expected to act synergistically with beta-blockers and implantable vagus nerve stimulators to improve patient outcome.

Herring N, Lokale MN, Danson EJ, Heaton DA, Paterson DJ. Neuropeptide Y reduces acetylcholine release and vagal bradycardia via a Y2 receptor-mediated, protein kinase c-dependent pathway. J Mol Cell Cardiol 2008;44:477-485.

Herring N, Cranley J, Lokale MN, Li D, Shanks J, Alston EN, Girard BM, Carter E, Parsons RL, Habecker BA, Paterson DJ. The cardiac sympathetic co-transmitter galanin reduces acetylcholine release and vagal bradycardia: Implications for neural control of cardiac excitability. J Mol Cell Cardiol 2012;52:667-676.

Cuculi F, Herring N, De Caterina AR, Banning AP, Prendergast BD, Forfar JC, Choudhury RP, Channon KM, Kharbanda RK. Relationship of plasma neuropeptide Y with angiographic, electrocardiographic and coronary physiology indices of reperfusion during ST elevation myocardial infarction. Heart 2013 DOI 10.1136/heartjnl-2012-303443

NH is a British Heart Foundation Centre of Research Excellence Intermediate Fellow at the University of Oxford. This work is supported by projects grants from the BHF and an Oxford Health Services research grant.

Where applicable, the authors confirm that the experiments described here conform with The Physiological Society ethical requirements.

SA82

Novel insights into cardiac vagal ganglion transmission *in situ*

L.M. Salo[1], R.M. McAllen[2], J.F. Paton[1] and A.E. Pickering[1]

[1]School of Physiology & Pharmacology, Bristol Heart Institute, University of Bristol, Bristol, UK and [2]Florey Neuroscience Institutes, University of Melbourne, Melbourne, VIC, Australia

Vagal drive to the heart is a key determinant of resting heart rate and respiratory sinus arrhythmia. Cardiac vagal tone is an important indicator of cardiovascular health, and loss of cardiac vagal tone is a feature of many cardiovascular disorders, including hypertension and heart arrhythmias. The cardiac ganglia are an important site for regulation of vagal drive to the heart, where depression of transmission may translate to loss of vagal tone. Attenuated ganglionic transmission has been shown in models of heart failure (1) and hypertension (2).

As cardiac vagal postganglionic neurons (CVNs) are located in a ganglionic plexus on the surface of the beating heart, it has hitherto been difficult to investigate how CVNs process ongoing and reflex evoked vagal activity. We have extended the working heart-brainstem preparation (WHBP, 3) and developed a model whereby we can make stable, intracellular recordings from CVNs. To begin to address any deficit in cardiac ganglionic transmission in disease states we first characterised how CVNs respond to ongoing cardiac vagal tone and activation of a number of vagally-mediated cardiorespiratory reflexes in Wistar rats (4).

Male Wistar rats (P18-32, n=39) were anaesthetised with 5% Halothane (until decerebration) for surgical set up of the working heart-brainstem preparation. The atria were opened, stabilised and the cardiac vagal ganglia exposed. Intracellular recordings were made from CVNs with sharp microelectrodes (65-170MΩ, 0.5M KCl). CVNs were classified as tonic or phasic depending on whether they produced tonic firing or single spikes in response to depolarising current pulses (500ms, 0.3Hz, 1-10nA), respectively. CVN responses to activation of chemo- (50μl, 0.03% NaCN i.a.), baro- (+20-50mmHg perfusion pressure ramps), diving (100μl, ~10°C aCSF to the nose) and von Bezold-Jarisch (phenylbiguanide; PBG, 200μg i.a.) reflexes were assessed. Examples of phasic (n=6) and tonic (n=6) CVNs were filled with biocytin (4%), fixed in 4% formaldehyde and then incubated with Streptavidin conjugated to Alexa Fluor 594 (red) dye (1:1000, 12-24hr). The cells were then morphologically characterised using fluorescence microscopy.

Stable intracellular recordings were made from 61 cardiac vagal ganglion cells with preserved central connections. Cardiac ganglion cells with vagal synaptic inputs (spontaneous, n=21; or electrically evoked from the vagus, n=3) were identified as principal neurones and showed tonic firing responses to injected current pulses as described previously (5). Cells lacking vagal inputs (n=37, presumed interneurones) were quiescent but showed phasic firing responses to depolarising current pulses. In principal cells the ongoing action potentials and EPSPs exhibited respiratory modulation, with peak frequency in post-inspiration. Action potentials arose from unitary EPSPs and autocorrelation of those events showed that each ganglion cell received inputs from a single active preganglionic neurone. Peripheral and cardiac chemoreceptor, arterial baroreceptor and diving response activation all evoked high frequency synaptic barrages in these cells, as well as a concomitant bradycardia. Principal cells responded to activation of all reflexes indicating a convergence of reflex pathways. EPSP amplitudes showed frequency dependent depression, leading to more spike failures at shorter inter-event intervals. Marked temporal summation of EPSPs occurred only during activation of an intense von Bezold-Jarisch reflex response where EPSP frequency was so high (151Hz) that they summated to produce a depolarising envelope (+10mV). All imaged cells had identifiable processes, which were divided into three classes: monopolar (5/12), dipolar (4/12) and multipolar (3/12). Most cells had a long, recognisable axon (9/12), and none had extensive dendritic arrangements. Morphometrically, there was no significant difference between tonic and phasic cells as assessed by their mean soma area, length or diameter.

These data show that activation of vagally-mediated reflexes excite a common pool of vagal postganglionic neurones shared by numerous cardiorespiratory reflexes, with no evidence of recruitment of ganglionic interneurons during reflex activation. There do not appear to be marked morphological differences between 'tonic' (putative principal ganglion neurones) or 'phasic' (putative interneurones) cells, despite markedly different synaptic and intrinsic electrophysiological properties. These findings indicate that rather than integrating convergent inputs, cardiac vagal postganglionic neurones can gate preganglionic inputs, so regulating the proportion of central

parasympathetic tone that is transmitted on to the heart. We plan to assess how this is altered in cardiovascular disease states.

1. Bibevski S & Dunlap ME (1999). *Circulation* **99**, 2958-2963.

2. Heaton DD et al. (2007). *Hypertension* **49**, 380-388.

3. Paton JF (1996). *J Neurosci Methods* **65**, 63-68.

4. McAllen RM et al. (2011). *J Physiol* **589**, 5801-5818.

5. Edwards FR et al. (1995). *J Physiol* **486**, 453-471.

Funded by the BHF.

Where applicable, the authors confirm that the experiments described here conform with The Physiological Society ethical requirements.

SA83

Causes and benefits of respiratory sinus arrhythmia

A. Ben-Tal[1], S.S. Shamailov[1] and J.F. Paton[2]

[1]INMS, Massey University, Auckland, New Zealand and [2]School of Physiology & Pharmacology, University of Bristol, Bristol, UK

Respiratory sinus arrhythmia (RSA) is a phenomenon where heart-rate (HR) varies with respiration. It is widely accepted that the loss of RSA is a prognostic indicator for cardiovascular disease and that the prominent presence of RSA indicates a healthy cardiac system, yet the reasons for this are still being debated (Larsen et al. 2010). One controversy is over the main mechanism that gives rise to RSA. While most investigators agree that RSA is mainly due to direct central respiratory modulation of the parasympathetic cardiac signal, others argue that RSA is mediated by the baroreflex responding to blood pressure oscillations triggered by the abdominal thoracic pump (Eckberg 2009). Another controversy is over the physiological function of RSA. Hayano et al. (1996) hypothesized that the physiological function of RSA is to match ventilation and perfusion in the lungs and thus optimize oxygen (O2) uptake and carbon dioxide (CO2) removal. Recently, using mathematical models, we showed that RSA may serve to minimize the energy expenditure of the heart while keeping arterial CO2 levels at physiological tensions (Ben-Tal et al. 2012); our theoretical study did not support Hayano's hypothesis.

Our study was performed using different mathematical techniques and different models. First, the optimal HR was calculated using techniques from optimal control theory in a simplified model of gas exchange. We found that the calculated HR was remarkably similar to RSA and that this became more profound under slow and deep breathing. Second, the HR function was prescribed and the cardiac work, as well as the volumes of O2 and CO2 taken up or removed by the blood respectively were calculated in a more detailed model of gas exchange. We found that cardiac work was minimized for RSA-like HR functions when the blood partial pressure of CO2 was controlled, most profoundly under slow and deep breathing and that although gas exchange efficiency improved with slow and deep breathing and with increased mean heart rate, this was unrelated to RSA. Third, we tested the two hypotheses using a newly developed minimal model for the neural control of HR in which RSA appears naturally and found similar results. The newly developed minimal model for the neural control of HR assumes that the heart period is affected primarily by the parasympathetic signal, with the sympathetic signal taken as a constant. We included the baroreflex, mechanical stretch-receptor feedback from the lungs, and central modulation of the cardiac vagal tone by the respiratory drive, but we omitted the chemoreflex. Our model mimics a range of experimental observations and provides several new insights. Most notably, the model can mimic the growth in the amplitude of RSA with decreasing respiratory frequency which then decreases at frequencies below 7 breaths per minute (for humans) and predicts that the decrease in the amplitude of RSA at low breathing frequencies is due to the baroreflex (we show this both numerically and analytically with a linear baroreflex). Another new prediction of the model is that the gating of the baroreflex leads to the dependency of RSA on mean vagal tone. These findings provide new insights into potential reasons and benefits of RSA under physiological conditions.

Ben-Tal, A., Shamailov, S. S., and Paton, J. F. R. (2012), 'Evaluating the physiological significance of respiratory sinus arrhythmia: looking beyond ventilation-perfusion efficiency', The Journal of physiology, 590.8, 1989-2008.

Eckberg, D. L. (2009), 'Point: Counterpoint: Respiratory sinus arrhythmia is due to a central mechanism vs. respiratory sinus arrhythmia is due to the baroreflex mechanism', Journal of applied physiology, 106 (5), 1740-1750.

Hayano, J., et al. (1996), 'Respiratory sinus arrhythmia. A phenomenon improving pulmonary gas exchange and circulatory efficiency', Circulation, 94 (4), 842-847.

Larsen, P. D., et al. (2010), 'Respiratory sinus arrhythmia in conscious humans during spontaneous respiration', Respiratory Physiology & Neurobiology, 174 (1-2), 111-118

The research was partly supported by NIH Grant R01 NS069220.

Where applicable, the authors confirm that the experiments described here conform with The Physiological Society ethical requirements.

SA84

Inhibitory synaptic plasticity of GABAergic synapses in the hippocampus

M. Woodin

University of Toronto, Toronto, ON, Canada

The hippocampus plays a central role in memory formation in the mammalian brain. Its ability to encode information is thought to depend on the plasticity of synaptic connections between neurons. Pyramidal neurons from the CA3 produce monosynaptic excitatory postsynaptic potentials (EPSPs) followed rapidly by feedforward (disynaptic) inhibitory postsynaptic potentials (IPSPs). Long-term potentiation (LTP) of glutamatergic EPSPs is the leading model of synaptic plasticity, in part due to its dependence on NMDA receptors (NMDARs), which are also required for spatial and temporal learning in intact animals. Using whole-cell recording in hippocampal slices from adult rats, we find that the efficacy of synaptic transmission from CA3 to CA1 can be enhanced without the induction of glutamatergic LTP. We show that the induction of GABAergic plasticity at feedforward inhibitory inputs results in the reduced shunting of excitatory currents, producing a long-term increase in the amplitude of Schaffer collateral-mediated postsynaptic potentials. This GABAergic plasticity weakens inhibition due to a depolarization of the reversal potential for GABAA receptor currents (EGABA) through a decrease in the function of the neuron-specific K+-Cl- cotransporter KCC2. This form of inhibitory synaptic plasticity is termed disinhibition-mediated long-term potentiation (LTP). We found that disinhibition-mediated LTP is not restricted to the paired pathway, but rather is expressed to the same extent at

unpaired control pathways. However, the overall strength of GABAergic transmission is maintained at the unpaired pathway by a heterosynaptic increase in GABAergic conductance. The pairing-induced depolarization of EGABA at the paired and unpaired pathways required Ca2+-influx through both the L-type voltage-gated Ca2+ channels and NMDA receptors. However, only Ca2+-influx through L-type channels was required for the increased conductance at the unpaired pathway. As a result of this increased GABAergic conductance, disinhibition-mediated LTP remains confined to the paired pathway and thus is synapse specific, suggesting it may be a novel mechanism for hippocampal-dependent learning and memory.

Where applicable, the authors confirm that the experiments described here conform with The Physiological Society ethical requirements.

SA86

GABAergic synaptic plasticity in the developing spinal cord

P. Wenner

Emory University, Atlanta, GA, USA

Homeostatic plasticity refers to the mechanisms that a cell or network are thought to employ, in order to homeostatically maintain a set level of spiking activity. Such a process would be critical for ensuring that networks do not become too active or inactive. Homeostatic plasticity is studied by perturbing activity levels and identifying mechanisms that could contribute to the restoration of the original activity levels. These mechanisms include compensatory changes in excitatory and inhibitory synaptic strength, as well as changes in intrinsic cellular excitability. For instance, when spiking activity was blocked for 2 days in cultured neural networks, glutamatergic synaptic strength increased and GABAergic synaptic strength decreased. Homeostatic plasticity is typically studied in vitro at a stage when GABA or glycine are inhibitory. I will discuss the expression of homeostatic plasticity in the living embryonic spinal cord at an early developmental stage when both glutamate and GABA are depolarizing and excitatory. When spiking activity is blocked for 2 days in the living embryo, compensatory increases in excitatory GABAergic and glutamatergic synaptic strength are observed. Interestingly, GABAergic synaptic strength is increased through dramatic increases in intracellular chloride, thereby enhancing the driving force for these chloride-mediated currents. We are currently working to understand how this occurs. Not only are the compensatory changes in GABAergic synaptic strength mediated by changes in chloride levels, but it appears that the chloride-mediated GABAergic currents are involved in triggering homeostatic plasticity. When GABAa receptors were blocked in the embryo for 2 days, increases in GABAergic and glutamatergic synaptic strength were observed, and were even larger than following activity blockade. GABAergic synaptic strength was again increased through chloride accumulation. We believe that activity blockade reduces the release of GABA, thereby reducing GABAa receptor activation, which then triggers changes in GABAergic and glutamatergic synaptic strength. This places the GABAa receptor, and possibly the depolarizing chloride current, as part of the sensing machinery that triggers homeostatic plasticity.

Gonzalez-Islas, C., Wenner, P., (2006) Spontaneous network activity in the embryonic spinal cord regulates AMPAergic and GABAergic synaptic strength. Neuron. 49: 563-575.

Wilhelm, J., Wenner, P., (2008) GABAA transmission is a critical step in the process of triggering homeostatic increases in quantal amplitude. PNAS, 105(32):11412-7.

Gonzalez-Islas, C., Chub, N., Garcia-Bereguiain, M.A., and Wenner, P., (2010) GABAergic synaptic scaling in embryonic motoneurons is mediated by a shift in the chloride reversal potential. J. Neuroscience 30(39): 13016-13020.

Where applicable, the authors confirm that the experiments described here conform with The Physiological Society ethical requirements.

SA87

Alterations in KCC2 compromise GABAergic control of the HPA axis

J. Maguire

Neuroscience, Tufts University School of Medicine, Boston, MA, USA

Effective GABAergic inhibition requires the maintenance of the chloride gradient, which is primarily accomplished by the K+/Cl- co-transporter, KCC2, in the adult brain. Alterations in KCC2 expression and function have been demonstrated under pathological conditions and in specific cell types under physiological conditions, including following stress. The body's physiological response to stress is mediated by the hypothalamic-pituitary-adrenal (HPA) axis. Corticotropin-releasing hormone (CRH) neurons in the paraventricular nucleus (PVN) of the hypothalamus are at the apex of HPA axis control and these neurons are tightly regulated by robust GABAergic inhibition. In response to a stressful event, the inhibitory control over CRH neurons, arising from multiple brain regions and mediated by numerous receptor subtypes, must be very rapidly lifted. Here we demonstrate that following acute restraint stress in mice, there is a dephosphorylation of KCC2 residue Ser940, which regulates the surface expression and function of KCC2, and downregulation of total KCC2 expression in the PVN. In addition, we demonstrate excitatory actions of GABA following acute restraint stress on CRH neurons. Our data suggest that collapsing the chloride gradient, by dephosphorylation and downregulation of KCC2, alleviates the inhibitory GABAergic control of CRH neurons which is necessary to mount the physiological response to stress. In contrast, following acute restraint stress in mice, we do not observe alterations in KCC2 expression in the hippocampus. Interestingly, following chronic restraint stress, there is a dephosphorylation of KCC2 residue Ser940 and a downregulation of KCC2 in the hippocampus, associated with a shift in EGABA and increased excitability of CA1 pyramidal neurons. These alterations in KCC2 expression may play a role in mediating the known increased neuronal excitability in the hippocampus following chronic stress. These data demonstrate rapid changes in KCC2 function and dynamic changes in GABAergic inhibition in a brain region-specific manner following both acute and chronic stress. Furthermore, alterations in KCC2 may have implications for stress-related disorders, including epilepsy and depression.

The authors would like to thank Dr. Steve Moss for the generous gift of the phospho-specific KCC2 Ser940 antibody.

Where applicable, the authors confirm that the experiments described here conform with The Physiological Society ethical requirements.

SA88

Ionic plasticity of GABAergic synapses by rapid regulation of the K-Cl cotransporter KCC2

P. Blaesse

Laboratory of Neurobiology, University of Helsinki, Helsinki, Finland and Institute of Physiology I, University of Münster, Münster, Germany

Cation-chloride cotransporters exert a major influence on the neuronal intracellular chloride concentration. Thereby, they are crucial for the Cl-dependent signalling mediated by $GABA_A$ and glycine receptors. Short-term and long-term changes in $[Cl^-]_i$ based on changes in the activity of the chloride transporters lead to ionic plasticity, i.e. quantitative and qualitative changes in the action of GABA and glycine. Such changes in inhibitory signalling occur during development, when a shift from relatively high intracellular Cl^- levels towards lower levels is seen in most central neurons. In addition, such changes may also contribute to pathological neuronal activity, e.g., epilepsy (Kahle et al., 2008; Blaesse et al., 2009).

KCC2, a K-Cl cotransporter, is the main Cl^- extruder in central neurons and responsible for an inwardly-directed Cl^- electrochemical gradient that is required for classical hyperpolarizing GABAergic inhibition. Numerous studies have shown that posttranslational modifications play a pivotal role in the short-term regulation of the transporter under physiological and pathophysiological conditions.

Mimicking certain aspects of human epilepsy in animal models and in vitro revealed new molecular mechanisms involved in the fast regulation of KCC2. In contrast to the known down-regulation of KCC2 by increased neuronal activity in mature neurons, a single seizure episode led to a rapid activation of KCC2 in the neonatal rat hippocampus, when KCC2 is not yet active under control conditions (Khirug, Ahmad et al., 2010). The activity-dependent functional up-regulation of KCC2 in immature neurons was paralleled by an increase in KCC2 surface expression. Signalling via the TrkB tyrosine kinase was essential for the activity-induced changes in KCC2-mediated Cl^- transport and KCC2 trafficking. Interestingly, TrkB signalling is also crucial for the activity-dependent down-regulation of KCC2 in the more mature system, pointing to a developmental sign change within the TrkB-KCC2 signalling cascade.

In addition to changes in trafficking, activity-dependent cleavage of KCC2 by the plasticity-associated protease calpain has been identified as a new mechanism for the fast functional down-regulation of KCC2 (Puskarjov, Ahmad et al., 2012). The application of the glutamate receptor agonist NMDA or the induction of interictal-like activity led to a fast reduction of KCC2 protein level and of KCC2-mediated Cl^- transport in hippocampal CA1 neurons. Both effects were blocked by inhibitors of the calcium-activated protease calpain.

The role of the different mechanisms and of the resulting ionic plasticity of GABAergic signalling under physiological (e.g., in learning-associated synaptic plasticity) and pathological conditions will be discussed.

Blaesse P, Airaksinen MS, Rivera C, Kaila K (2009) Cation-chloride cotransporters and neuronal function. Neuron, 61:820-838.

Kahle KT, Staley KJ, Nahed BV, Gamba G, Hebert SC, Lifton RP, Mount DB (2008) Roles of the cation-chloride cotransporters in neurological disease. Nat Clin Pract Neurol, 4:490-503.

Khirug S, Ahmad F, Afzalov R, Khiroug L, Kaila K, Blaesse P (2010) A single seizure episode leads to rapid functional activation of KCC2 in the neonatal rat hippocampus. J Neurosci, 30:12028-35.

Puskarjov M, Ahmad F, Kaila K, Blaesse P (2012) Activity-dependent cleavage of the K-Cl cotransporter KCC2 mediated by calcium-activated protease calpain. J Neurosci, 32:11356-64.

Where applicable, the authors confirm that the experiments described here conform with The Physiological Society ethical requirements.

SA89

Hydrogen sulfide in the vascular system: an overview of its roles and mechanisms

R. Wang

Lakehead University, Thunder Bay, ON, Canada

"Hydrogen sulfide, a lethal gas best known for smelling like rotten eggs, turns out to play key roles in the body – a finding that could lead to new treatment for heart attack victims and others" (Scientific American, 302: 66-71, 2010). Research over the last decade has revealed critical biomedical implications of hydrogen sulfide (H2S), a gasotransmitter produced in almost every type of cells with cysteine and homocysteine as substrates. Cystathionine gamma lyase (CSE) plays the most important role in cardiovascular system for the endogenous production of H2S. It is localized in the cytosol of vascular smooth muscle cells (SMCs) under resting conditions. H2S produced in the cytosol of SMCs stimulates KATP channels, leading to vascular relaxation. CSE can be transported into mitochondrion upon the sustained elevation of intracellular calcium level to produces H2S inside mitochondria. The mitochondria-produced H2S decreases ATP production under nomoxia condition but increases it under hypoxia condition. This oxygen-sensitive mitochondrial production of H2S may be important for regulation of vascular remodeling and proliferation. On the other hand, H2S is produced in vascular endothelial cells (ECs) via a calcium/calmodulin-dependent mechanism. Deficiency in endothelium production of H2S leads to delayed wound healing, suppressed endothelial proliferation and migration, vulnerability of endothelium to hyperglycemia damage, abolished endothelium-dependent vasorelaxation, and age-dependent development of hypertension. Micro-electrode recording of the membrane potential changes in endothelium-intact peripheral vascular tissues has provided direct evidence that H2S is an endothelium-derived hyperpolarizing factor (EDHF). As an EDHF, H2S induces greater hyperpolarization of SMCs from female mouse mesenteric arteries than that from male ones. In conclusion, the production of hydrogen sulfide in cardiovascular system is mediated by different mechanisms in different types of cells. By regulating mitochondrial functions and by acting on KATP channels in vascular SMCs and small to medium conductance KCa channels in ECs (as an EDHF), H2S differentially modulates the proliferation of SMCs and ECs and induces vasorelaxation.

Supported by Natural Sciences and Engineering Research Council of Canada and Canadian Institutes of Health Research.

Where applicable, the authors confirm that the experiments described here conform with The Physiological Society ethical requirements.

SA90

Role of H2S balancing oxidative stress and antioxidant pathways and modulating vascular tone

D. Henrion

Vascular Biology, INSERM -CNRS, Angers, France

The microcirculation is sensitive to small changes in pO2 and pCO2 as well as to gasotransmitter such as nitric oxide (NO) and carbon monoxide generated by the vascular endothelium [1, 2]. Resistance arteries, located upstream the microvasculature control local blood flow in part through their myogenic reactivity [3], Hydrogen sulfide (H2S), is a potent environmental toxic gas, which has recently been described as a gasotransmitter, similar to nitric oxide or carbon monoxide. Endogenous synthesis of H2S has been documented in both physiological and pathological conditions. In the vasculature, H2S is synthesized from cysteine by cystathionine-γ-lyase in smooth muscle cells and 3-mercaptopyruvate sulfuresterase and cystathionine-γ-lyase in the endothelial cells [4]. Depending on the pathophysiological condtions, H2S has been reported to exhibit pro- and anti-inflammatory properties. H2S has been shown to induce contraction at low doses through the inhibition of the conversion of citrulline into arginine by eNOS and relaxation at high doses through by activation of K+ATP channels in the rat and mouse aorta. More recent investigations have shown that H2S induces a "suspended animation-like" state leading to a better protection of animals against lethal hypoxia. Similarly, the pre-treatment of rats with H2S (intravenous injection or inhalation) prevents death after controlled but unresuscitated hemorrhage.
Recent studies have shown that NaHS is protective against the effects of ischemia reperfusion induced by controlled hemorrhage in rats. NaHS was also able to improve cardiovascular homeostasis in the early resuscitation phase after hemorrhagic shock, most probably through a reduction of oxidative stress [5]. Consequently, the use of NaHS represents a promising therapeutic perspective in limiting the consequences of ischemia reperfusion. The role of H2S in the balance between pro- and antioxidant mechanisms in the vasculature will be detailed.

Henrion, D., Pressure and flow-dependent tone in resistance arteries. Role of myogenic tone. Arch Mal Coeur Vaiss, 2005. 98(9): p. 913-21.

Freidja, M.L., et al., Heme oxygenase-1 induction restores high-blood-flow-dependent remodeling and endothelial function in mesenteric arteries of old rats. J Hypertens, 2010. 29(1): p. 102-12.

Kauffenstein, G., et al., Emerging role of G protein-coupled receptors in microvascular myogenic tone. Cardiovascular Research, 2012. 95(2): p. 223-232.

Paul, B.D. and S.H. Snyder, H(2)S signalling through protein sulfhydration and beyond. Nat Rev Mol Cell Biol, 2012. 13(8): p. 499-507.

Ganster, F., et al., Effects of hydrogen sulfide on hemodynamics, inflammatory response and oxidative stress during resuscitated hemorrhagic shock in rats. Crit Care, 2010. 14(5): p. R165.

This work was supported by the National Institut for Health and Medical research (INSERM, France)

Where applicable, the authors confirm that the experiments described here conform with The Physiological Society ethical requirements.

SA91

Homocysteine to hydrogen sulfide: *in vitro*, *ex vivo* and *in vivo*

S.C. Tyagi

University of Louisville, Louisville, KY, USA

Hydrogen sulfide (H(2)S) is identified as a regulator of various physiological events, including the hypertension, H(2)S is produced as a metabolite of homocysteine (Hcy) by cystathionine β-synthase (CBS), cystathionine γ-lyase (CSE), and 3-mercaptopyruvate sulfurtransferase (3MST). Although Hcy is recognized as vascular risk factor at an elevated level [hyperhomocysteinemia (HHcy)] and contributes to vascular injury leading to hypertension, the exact mechanism was unclear. To determine whether conversion of Hcy to H(2)S mitigates hypertension. Ex vivo renal artery culture with CBS, CSE, and 3MST triple gene therapy generated more H(2)S in the presence of Hcy, and these arteries were more responsive to endothelial-dependent vasodilation compared with nontransfected arteries treated with high Hcy. Cross section of triple gene-delivered renal arteries immunostaining suggested increased expression of CD31 and VEGF and diminished expression of the antiangiogenic factor endostatin. In vitro endothelial cell culture demonstrated increased mitophagy during high levels of Hcy and was mitigated by triple gene delivery. Upregulated matrix metalloproteinases-13 and downregulated tissue inhibitor of metalloproteinase-1 in HHcy were normalized by overexpression of triple genes. Together, these results suggest that H(2)S plays a key role in hypertension during HHcy.

Where applicable, the authors confirm that the experiments described here conform with The Physiological Society ethical requirements.

SA92

Transient receptor potential ankyrin 1 receptors mediate hydrogen-sulphide-induced calcitonin-gene-related-peptide release and cutaneous vasodilatation

Z. Hajna, G. Pozsgai, T. Bagoly, M. Boros, . Kemény, Z. Helyes, J. Szolcsányi and E. Pintér

Department of Pharmacology and Pharmacotherapy, University of Pécs, Faculty of Medicine, Pécs, Hungary

Introduction: Capsaicin-sensitive sensory neurons express Transient Receptor Potential Ankyrin 1 (TRPA1) and Vanilloid 1 (TRPV1) receptors. TRPA1 can be activated by several chemical stimuli, such as allylisothiocyanate (AITC), the pungent agent of mustard oil, resulting in the release of vasoactive inflammatory neuropeptides like calcitonin-gene-related-peptide (CGRP). The gaseous mediator hydrogen-sulphide (H2S) has been recently suggested to act on capsaicin-sensitive sensory neurons. Therefore, the aim of our present study was to investigate the involvement of TRPA1 receptors in H2S-evoked CGRP-release from sensory nerves in vitro and microcirculatory changes in vivo.
Methods: In vitro experiments were performed on isolated tracheae of male and female Wistar rats (200–250 g). Tracheae were removed in deep anaesthesia (sodium thiopentone, 100 mg/kg, i.p.). Sensory nerve terminals of the isolated rat tracheae were stimulated by increasing concentrations of AITC or the H2S-donor NaHS and CGRP-release was measured by radioimmunoassay. The effects of the TRPA1 antagonist HC-

030031 and the TRPV1 antagonist BCTC were tested on this response.
In vivo experiments were carried out on Balb/c mice for testing pharmacological inhibition by HC-030031, while TRPA1 (TRPA1-/-) and TRPV1 gene-deficient (TRPV1-/-) mice were compared to their wild types (WTs, 25-30 g). Measurements were performed under ketamine (100 mg/kg, s.c.) and xylazine (5 mg/kg, s.c.) anaesthesia. Vasodilatation of the murine ear was evoked by AITC (15 μl, 2%) or NaHS (15 μl, 5%) and skin blood flow was measured by laser Doppler imaging for 30 minutes in case of AITC-, and for 50 minutes in case of NaHS-application.
Results: Both AITC and NaHS elicited concentration-dependent release of CGRP in the rat tracheae. CGRP-release induced by AITC amounted to 1.46±0.31 fmol/mg, which was only 0.14±0.06 fmol/mg in the presence of 100 μmol/l of HC-030031. NaHS-evoked CGRP-release reached 0.47±0.09 fmol/mg, which was only 0.0008 fmol/mg when HC-030031 (100 μmol/l) was applied. In the presence of BCTC, NaHS-induced CGRP-release amounted to 0.52±0.05 fmol/mg.
AITC evoked an increased skin blood flow with a maximum value of 27.87%±2.31% above baseline at 6 minutes. 30 or 100 mg/kg of HC-030031 inhibited AITC-evoked vasodilation by 54.5% and 53.6%, respectively. NaHS increased cutaneous microcirculation with a peak value of 67.42%±4.87% above baseline at 48 min. 30 and 100 mg/kg of HC-030031 inhibited NaHS-induced vasodilatation by 24.6% and 51.4%, respectively.
In wild type mice, maximum value of blood flow amounted to 17.36%±4.1%. In the TRPA1-/- animals it reached only -1.69%±4.17%, while in the TRPV1 knockouts it peaked at 17.77%±5.28%. In WTs, NaHS caused a 44.18%±3.19% increase of microcirculation. In the TRPA1-/- mice it reached only 23.75%±4.09%, while in the TRPV1-/- animals it peaked at 35.73%±3.29%.
Conclusion: Similarly to the effect of AITC, NaHS also evoked a concentration-dependent CGRP-release, which was inhibited by HC-030031, but not by BCTC. Likewise AITC, NaHS also increased cutaneous microcirculation in the mouse ears, and this vasodilatory response to NaHS could be ameliorated by HC-030031. Blood flow of TRPA1-/-, but not the TRPV1-/- mice showed significantly smaller increase in response to NaHS compared to the wild types.
Activation of TRPA1 receptors plays an important role in H2S-induced CGRP-release and cutaneous vasodilatation in the murine ear, while TRPV1 receptors are not involved in these processes. Our results highlight that TRPA1 receptor activation should be minded as a potential mechanism of vasoactive effects of H2S.

Support: OTKA K-81984, Baross Gábor Program, SROP 4.1.2.B-10/2/KONV-20/0-0002 and SROP-4.2.2/B-10/1-2010-0029

Where applicable, the authors confirm that the experiments described here conform with The Physiological Society ethical requirements.

SA93

Mitochondria-targeted slow release hydrogen sulfide donors: a novel link to an old 'tail'?

M. Whiteman

University of Exeter Medical School, Exeter, UK

Hydrogen sulfide (H2S) has recently been identified as an endogenous redox active gaseous mediator and proposed as an endogenous regulator of nitric oxide (NO) bioavailability, vascular tone and inflammation. Novel slow release H2S donor (SRHD) molecules such as GYY4137 [1,2] have been shown to regulate blood pressure in experimental and genetically induced hypertension and to inhibit tissue damage, oedema, cell death and inflammatory signalling [3-5] in sepsis and arthritis [6]; conditions well known to involve perturbed mitochondrial function and oxidative stress. In this study we have synthesised a series of compounds containing a mitochondria-targeting moiety (triphenylphosphonium), a C2-C18 'linker' and H2S releasing moieties containing either a dithiolethione or thiohydroxybenzamide 'tail' (mitochondria-targeted SRHDs; mtSRHDs).
To investigate H2S-mediated cytoprotection in vitro, we exposed human microvascular endothelial cells (HMEC) to oxidative injury with H2O2, 4-hydroxynonenal (4-HNE) and SIN-1 (or a cocktail of oxidants) in the presence or absence of either mitochondria-targeted H2S donors (< 100nM) or non-targeted SRHDs (GYY4137, AP67, AP72; < 200μM) for comparison. Oxidant induced cellular toxicity was assessed using standard metabolic assays, mitochondrial membrane depolarisation assays, ATP content, phosphatidylserine externalisation, caspase activation and activity etc. Intracellular oxidant production was estimated using intracellular fluorescent probes, DCF-DA, mitosoxRed and dihydroethidium. We also determined the effects on of SRHDs/mtSRHDs systemic blood pressure, heart and breathing rates in spontaneously hypertensive and L-NAME-treated rats.
Preliminary experiments showed a C10 linker to optimal and AP39 (dithiolethione) and AP123 (hydroxythiobenzamide) were chosen for further study. Treatment of HMEC with SIN-1, H2O2 (100μM) 4-HNE (10μM) for 18h resulted in significant cytotoxicity (ANOVA,$p<0.01$). The toxicity of individual oxidants or oxidants used in combination to achieve similar effects (e.g. 50μM SIN-1/H2O2 with 2μM 4-HNE) was significantly inhibited by non-targeted SRHDs (100μM; $p>0.01$ all treatments). However, in each cytotoxicity assay the potency was substantially increased by targeting H2S delivery to mitochondria (AP39/123, 100nM; $p<0.01$). In spontaneously hypertensive and L-NAME (30mg/kg) treated rats, AP39 (1μM/kg) induced a rapid and sustained decrease in blood pressure and heart rate; an effect more pronounced than non-targeted SRHDs AP67 (30μM/kg) or GYY4137 (133μM/kg) [1].
These data suggest SRHDs can inhibit and / or reverse oxidative stress-mediated vascular cell injury and regulate vascular tone. Furthermore, strategies which increase H2S bioavailability, and in particular target mitochondria, represent a new therapeutic opportunity to limit mitochondrial and endothelial dysfunction.

Li et al., Characterization of a novel, water soluble hydrogen sulfide-releasing molecule (GYY4137): New insights into the biology of hydrogen sulfide. Circulation 2008;117:2351-2360.

Li et al., GYY4137, a novel hydrogen sulfide-releasing molecule, protects against endotoxic shock in the rat. Free Radic. Biol. Med. 2009;47:103-113.

Whiteman et al., Emerging role of hydrogen sulfide in health and disease: critical appraisal of biomarkers and pharmacological tools. Clin. Sci. (Lond). 2011;121:459-488.

Fox et al., Inducible hydrogen sulfide synthesis in chondrocytes and mesenchymal progenitor cells: Is H2S a novel cytoprotective mediator in the inflamed joint? J Cell. Mol. Med. 2011: 16:896-910

Whiteman et al., The effect of hydrogen sulfide donors on lipoloysaccharide-induced formation of inflammatory mediators in macrophages. Antiox. Redox Signalling. 2010;12:1147-1154.

Li et al., The complex effects of the slow releasing hydrogen sulfide donor GYY4137 in human cartilage cells and in a murine model of acute joint inflammation. J Cell Mol. Med. In Press. doi: 10.1111/jcmm.12016.

Dr. Mark E. Wood and Dr. Alexis Perry, Bioscience, University of Exeter. Ms. Sophie Le Trionairre, MRC-funded PhD student, University of Exeter Medical School, Prof. Karol Ondrias, Slovak Academy of Sciences. Dr. Jacqueline L. Whatmore and Dr. Bridget Fox, University of Exeter Medical School.

Where applicable, the authors confirm that the experiments described here conform with The Physiological Society ethical requirements.

SA94

JAM'S in inflammation and vascular disease

B. Imhof

dept pathology and Immunology, CMU / university geneva, Genève 4, Switzerland

We investigate the roles of junctional adhesion molecules (JAMs) in pathology of leukocyte migration, inflammatory diseases and angiogenesis. Simultaneously with other laboratories we discovered the vascular adhesion molecules JAM-B and JAM-C. Expression and production of recombinant JAMs enabled the development of a large panel and monoclonal and polyclonal antibodies, and we produced transgenic mice overexpressing JAM-C in the vasculature and JAM-C and JAM-B deficient mice. Using these reagents and the gene modified animals we showed JAM-C involved in immune responses against microorganisms preventing pneumonia and studied the role of this moleculkes in immunity against Leishmaniasis . Furthermore, antibodies against JAM-C reduced the severity of acute and chronic inflammatory pathologies such as pancreatitis, peritonitis, rheumatoid arthritis. These effects of JAM-C seem to be due to its role in leukocyte transendotheial migration. The molecules form a vascular barrier for tissue leukocytes returning back to the blood i.e. it contributes to the one-way traffic observed during leukocyte homing. In collaboration with Sussan Nourshargh, London we visualized neutrophils and monocytes reverse, polarised transendothelial migration. These events were detected by blocking JAM-C in vitro and in vivo using 3D intravital microscopy of inflammation following ischemia/reperfusion injury.
(JAM-C) is expressed by vascular endothelium and also by human but not mouse B lymphocytes. Together with Thomas Matthes, Geneva we recently described that the level of JAM-C expression defines B cell differentiation stages and allows the classification of marginal zone (JAM-C positive) and germinal center (JAM-C negative) B cell lymphomas. Now we found a role for this lymphocyte JAM-C in migration of human B cells, using a xenogeneic NOD/SCID human/mouse model. Treatment with anti-JAM-C antibodies reduced homing of normal and malignant human, JAM-C expressing B cells to bone marrow, lymph nodes and spleen. Blocking spleen homing is remarkable as most other anti-adhesion antibodies reduced homing of B cells only to bone marrow and lymph nodes but not to spleen. Plasmon resonance studies identified JAM-B as the major vascular ligand for JAM-C while homotypic JAM-C interactions remained at background levels. Accordingly, anti-JAM-C antibodies blocked adhesion of JAM-C expressing B cells to blood vessels in human and mouse lymphoid organs. In particular, JAM-B is highly expressed by the spleen vasculature.
We will review our work on JAM-C and JAM-B and compare it to the roles of JAM-A, the first molecule discovered and belonging to the JAM family.

Where applicable, the authors confirm that the experiments described here conform with The Physiological Society ethical requirements.

SA95

Monocyte influx supports the proliferation of angiogenic microvessels under ischemic and inflammatory conditions

A. Woodfin, B. Ma and S. Nourshargh

William Harvey Research Institute, Barts and The London School of Medicine, Queen Mary University of London, London, UK

Angiogenesis is a common feature of chronic inflammatory and ischemic conditions, and is both driven by, and contributory to, the eventual pathological outcomes. An example of this can be seen in the development of atherosclerotic plaques, where neovascularisation facilitates monocyte infiltration into lesions, a process that contributes to plaque instability and eventual rupture, leading to thrombosis and vascular occlusion. Yet despite the tremendous interest in the role of angiogenesis in these disorders surprisingly little is known about the profile, dynamics and mechanisms of inflammation within angiogenic tissues. A major limiting factor here has been the lack of availability of suitable in vivo models for direct investigations of inflammatory events in angiogenic vessels.
We have developed a model of ischemic angiogenesis in the mouse cremaster, which is amenable to in vivo confocal imaging with high temporal and spatial resolution. This imaging system has been employed to characterise the angiogenic profile of this model and to investigate the link between immune cell infiltration and new vessel growth. At one week post induction of chronic ischemia, tissues exhibit a high density of small diameter, PECAM-1 expressing microvessels, with a functional lumen but a characteristically disordered morphology. A significant tissue infiltration of CX3CR1-eGFP+ cells of a monocytic lineage were noted at this time point, often forming close associations with angiogenic vessels.
Further analysis of the time course of infiltration and phenotype of these CX3CR1-eGFP+ cells has revealed that a large influx of GR1high/F4/80low M1 type monocytes is seen within one day of induction of ischemia. Subsequently these cells migrate within the tissue and undergo morphological and phenotypic changes, adopting a GR1low/F4/80high M2 like macrophage phenotype by one week post ischemia. Depletion of blood monocytes prior to induction of ischemia significantly inhibits the angiogenic response, demonstrating a role for these cells in vasculogenesis.

The present study into the relationship between myeloid cells and the induction and maintenance of chronic inflammation and angiogenesis aims to identify potential opportunities for therapeutic interventions in the context of chronic inflammatory and ischemic disorders.

A.W. is a British Heart Foundation Research Fellow

Where applicable, the authors confirm that the experiments described here conform with The Physiological Society ethical requirements.

SA96

Role of cholesterol in determining macrophage phenotype

T.J. Van Berkel, J. Kuiper and M. Van Eck

LACDR - Biopharmaceutics, Leiden University, Leiden, Netherlands

High plasma lipid levels form a prerequisite for the development of atherosclerosis. The recruitment of monocytes to the arterial wall is initiated by the local environment which must be modulated by lipidomic factors. Once monocytes in the arterial wall are converted to macrophages, deposition of excessive amounts of cholesteryl esters, leading to foam cell formation can be considered as a key event in the progression of atherogenesis. Macrophage cholesterol homeostasis involves a delicate balance between lipid influx and lipid efflux. Macrophages are incapable of limiting the uptake of lipids via scavenger receptors and therefore largely depend on cholesterol efflux pathways to maintain cellular lipid homeostasis. Important mediators of macrophage cholesterol efflux are ABCA1, which mediates the efflux of cholesterol to lipid-poor apo A-I. Furthermore ABCG1 and SR-BI can efflux cholesterol to mature HDL. As a consequence of compensatory mechanisms, the single ABCA1, ABCG1 or SR-BI deficiency in macrophages only leads to moderate effects on cholesterol efflux and atherogenesis. Combined deletion of ABCA1 and ABCG1 leads to massive lipid accumulation and foam cell formation of tissue macrophages, while massive foam cell formation, atherosclerotic lesion development and inflammation is also observed by combined deletion of macrophage ABCA1 and SR-BI. The combined macrophage deletions of ABCA1, ABCG1 and/or SR-BI show the essential function of these cholesterol transporters in macrophage foam cell formation and atherosclerotic lesion development. An enhancement of sytemic inflammation markers does accompany the extend of foam cell formation and the interaction between lipid accumulation and the inflammatory status might form an important factor for the pathological events during atherogenesis.

Where applicable, the authors confirm that the experiments described here conform with The Physiological Society ethical requirements.

SA97

Role of adaptive immunity in foam cell inflammatory phenotype

K. Ley

La Jolla Institute for Allergy & Immunology, La Jolla, CA, USA

Macrophage-derived foam cells are a defining feature of atherosclerotic lesions. Vulnerable plaques contain more foam cells and larger necrotic cores. However, when foam cells are generated in vitro (Cho,H. et al. Physiological Genomics 29:149-160, 2007) or in mice (Spann,N.J. et al., Cell. 151:138-152, 2012), their overall phenotype is anti-inflammatory, not pro-inflammatory. Yet, in atherosclerotic lesions foam cells show a pro-inflammatory phenotype, based on phenotyping by immunofluorescence and other methods. This apparent discrepancy suggests that an additional factor not present in reductionist systems drives foam cell inflammation. We propose that this additional factor are CD4 T cells that provide pro-inflammatory cytokines including IFN-γ, IL-17 and TNF-α. Multiphoton microscopy of Apoe-/- mouse aortas show that CD11cYFP antigen-presenting cells become rounded and less motile, consistent with conversion to foam cells. We show that adoptive transfer of antigen-experienced CD44hiCD62L- CD4 T cells induces production of IFN-γ, IL-17 and TNF-α. IFN-γ is very efficient at increasing uptake of oxidized low density lipoprotein (oxLDL) in macrophages in culture. Our experiments suggest that both antigen-experienced T cells and a suspected autoantigen are present in Apoe-/- mice. These data also suggest that modulating the autoimmune response might be effective in preventing or treating atherosclerosis.

Where applicable, the authors confirm that the experiments described here conform with The Physiological Society ethical requirements.

SA98

Recruitment of Ly6Chigh monocytes is required for the enhancement of anti-inflammatory (M2) macrophage phenotype *in vivo* in atherosclerosis regression in mice

E.A. Fisher, Y. Vengrenyuk, N. Girgis and P. Loke

Medicine/Cardiology, New York Univ. Sch. of Med., New York, NY, USA

Blocking the progression of atherosclerotic lesions and inducing their regression are important clinical goals. We've reported several mouse models of atherosclerosis regression in which an improvement of plasma lipoprotein profiles results in a rapid reduction lesion macrophage content. Another common feature was a dramatic phenotypic enrichment of plaque CD68+ cells (macrophages) in markers of the anti-inflammatory (M2) state. Here, we investigate the origin of M2 macrophages in regressing lesions by modifying our original aortic transplantation model to include recipients whose monocytes lack the major receptors responsible for their recruitment into tissues. Aortic arch segments containing an atherosclerotic lesion from an apoE-/- mouse were transplanted into CCR2-/-, CX3CR1-/-, or CCR5-/- mice, in addition to WT and apoE-/- controls. Macrophage marker CD68+ area quantification data showed that the lack of CCR2 or CX3CR1 in transplant recipients completely blocked regression despite the reversal of dyslipidemia, while CCR5 deficiency had no effect. Since inflammation-prone Ly6Chigh monocytes require both CCR2 and CX3CR1 receptors to enter atherosclerotic lesions, our results suggest that the recruitment of new Ly6Chigh inflammatory monocytes is required for regression. Furthermore, CCR2-/- and CX3CR1-/- recipients lacked M2 macrophages in atherosclerotic lesions, suggesting that the M2 macrophages in regressing lesions are derived from the recruitment of inflammation-prone Ly6Chigh monocytes. Finally, we tested whether the M2 enrichment in regression follows the classical Il/4-STAT6 signaling pathway by using STAT6-/- mice as transplant recipients. The lack of STAT6 not only prevented upregulation of M2 markers, but also resulted in impaired lesion regression. In conclusion, we showed that newly recruited Ly6Chigh monocytes give rise to the anti-inflammatory M2 macrophages under regression conditions in a STAT6-dependent manner, and that both the recruitment of new cells and a functioning STAT6 pathway are also required for atherosclerosis regression. The results argue against the possibility that M1 macrophages in progressing lesions repolarize to the M2 phenotype under regression conditions in vivo and support the notion that regression is not a rewinding of progression, but requires the participation of newly recruited inflammation-prone monocytes that in this context promote the resolution of inflammation.

In the aortic transplantation procedure, mice are administered ketamine and xylazine.

Where applicable, the authors confirm that the experiments described here conform with The Physiological Society ethical requirements.

SA99

What do we mean by competency-based education and how does it apply to professional curricula?

W.R. Galey

Science Education, Howard Hughes Medical Institut, Bethesda, MD, USA

Although there is general consensus across the medical education community that graduates should be competent in the sciences there is little agreement as to what is meant by "competency". Many nations are moving to "competency-based" or competency influenced education. This symposium will explore how "competency" is being interpreted and implemented in various educational venues around the world. One such venue is the United States.
In 2007 Howard Hughes Medical Institute (HHMI) the largest philanthropy in the United States dedicated to biomedical research and science education partnered with the Association of American Medical Colleges (AAMC) to convene a group dedicated to defining the core science that should be mastered by students by the time of their graduation from medical school. The committee was charged with not only establishing the graduating scientific abilities for physicians but also defining the science students should have mastered by the time they matriculate into medical school.
The committee composed of clinical, medical school basic science and premedical science teachers met over a period of 18 months. The report of the committee published in 2009 titled Scientific Foundations for future Physicians (SFFP) https://www.aamc.org/students/download/302644/data/hhmi.pdf 1) established competencies as the goal of medical science education, 2) defined eleven overarching principles for science in medical education and 3) set eight science competencies for graduating physicians and eight competencies that all students should have mastered on matriculation to medical school. For each competency, Learning Objectives and Examples were given to guide the establishment of expectations as to the appropriate depth and application at which the competencies should be accomplished by learners.
It was recognized by the SFFP Committee that the growing knowledge of the natural world, especially the biological sciences, precludes the mastery of all science knowledge. Hence some information while important in particular disciplines or certain realms of endeavor are less important to understanding human biology, pathophysiological processes and the treatment of disease and should not be required. Further, recognizing that certain important concepts are shared across the natural science disciplines, the committee suggested that integration of learning might be more efficient than the separated learning of a concept in multiple disciplines. Acknowledging the increasing need to understand and apply quantitative information to medical practice the SFFP committee emphasized a need for a greater mastery of mathematical concepts statistics and computational sciences.
The SFFP Report and the Report of the MR5 Committee which reviewed the content and structure of the Medical College Aptitude Test (MCAT) used by most US medical schools to evaluate the preparedness of students wishing to enter medical school have influenced the nature of the revised MCAT to be initiated in 2015 https://www.aamc.org/students/applying/mcat/mcat2015/.
These reports are stimulating US colleges and Universities to examine how competencies in the sciences might be more effectively learned. Furthermore many medical schools are reexamining their admission requirements, the structure of their curricula and the methods of instruction.

Where applicable, the authors confirm that the experiments described here conform with The Physiological Society ethical requirements.

SA100

Competency based education: a European perspective

C. Karatzaferi

PE & Sports Science, University of Thessaly, Trikala, Greece

Competency based education (CBE) focuses on students acquiring knowledge and skills, called competencies, required for a particular course/degree. Mature students seem to be particularly suited for CBE, as they enter a course of study with variable backgrounds of knowledge and skills, usually aiming for a professional qualification. However, CBE is gaining ground in undergraduate courses as well. In truth, CBE core elements (such as laboratory experience, skills, problem solving, team work, ethics, student research and enquiry) pre-existed the formulation of CBE in the modern era. Nowhere is this so true than the medical sciences field. Physiology always played a key role in the curricula of medical studies and of health allied professions. However CBE implementation is fragmented and varied in Europe. In Greece the importance of physiology for the acquisition of medical/health allied competencies has been recognized almost from the beginning of the University system. This talk will discuss the implementation of CBE in Greece and will draw comparisons with European-wide examples.

Where applicable, the authors confirm that the experiments described here conform with The Physiological Society ethical requirements.

SA101

Aligning competencies in undergraduate and professional programs

D.U. Silverthorn

Integrative Biology, University of Texas, Austin, TX, USA

The move to competency-based education in the United States is gaining momentum, but there are still many institutions, particularly at the undergraduate level, that are hesitant to move away from traditional courses. Recent changes proposed for the testing and admission process for American medical schools have now focused attention on the premedical curriculum and its rigid course requirements in biology, chemistry, physics, and mathematics. Some universities are beginning to explore the use of competency-based education to condense these course requirements, thereby creating space in the curriculum for more behavioral science and liberal arts classes.
In 2009 the Association of American Medical Colleges partnered with the Howard Hughes Medical Institute (HHMI) and issued a report, Scientific Foundations for Future Physicians (SFFP, available at www.hhmi.org/grants/pdf/08-209_AAMC-

HHMI_report.pdf). The SFFP report called for the substitution of competencies in place of rigid course requirements for admission to medical school, and it described eight broad competencies that were fundamental background for beginning specialized medical education. Some of the intent of the SFFP report was to open the door for development of creative interdisciplinary curricula and for collaboration between disciplines. To support this objective, HHMI created the NEXUS project (www.hhmi.org/grants/office/nexus). For example, as part of NEXUS, an interdisciplinary team from the University of Maryland developed a physics course for life science students that emphasizes basic scientific competencies and uses biological examples to teach physical principles.
In the medical and academic institutions of the University of Texas System, a pilot project called Transformation in Medical Education (TIME) aims to shorten the time between high school and completion of the medical degree by using competencies to eliminate redundancies in the undergraduate and medical curricula. To accomplish this, we first created sets of competencies from those required for physician graduates. Now we are mapping competencies onto existing courses and using the map looking for opportunities to combine traditional courses, such as those in physics and physiology. This talk will show how this work has progressed and will discuss some of the obstacles to implementation.

Where applicable, the authors confirm that the experiments described here conform with The Physiological Society ethical requirements.

SA102

The development of competency-based curriculum and quality assurance in Indonesian medical education

M. Irfannuddin Misbach

Physiology, University of Sriwijaya, Palembang, South Sumatra, Indonesia

The recent reformation of medical curriculum in Indonesia was stimulated by public concern about the quality of health care officers. The content-based curriculum produced graduates who were not able to follow advances in science and technology, and who lacked the technical and communication skills needed to effectively serve the community.
In 2006, the Indonesian Medical Council adopted seven categories of competencies as the main outcomes of the competency-based curriculum for physicians: communication, clinical skills, medical scientific foundation, health problem management, information management, self awareness, and professional ethics. The Council determined that rather than follow a core curriculum, Indonesian institutions must implement Ron Harden's SPICES curriculum design strategy.(1)
At the beginning, implementation of the reforms was slowed by resistance to student-centered and integration approaches, concerns that a problem based learning approach was incompatible with Asian culture, and gaps in institutional capability. The changes accelerated after the government involved professional medical associations and obtained support from foreign grants. However, faculty members still had difficulty matching new competencies to existing learning objectives and learning strategies, particularly for generic competencies.
As part of the reform, the Council implemented a national board examination and applied a quality assurance system to ensure graduates were able to meet the national minimum competencies. The results from the exam show that there are still weaknesses in the areas of communication, professional ethics, information management and clinical skills.(2)
Our internal survey also revealed dissatisfaction of faculty alumni and staff on the competence of recent graduates in the areas of communication, biomedical sciences, information management and clinical skills.(3)
In 2012, the Council revised the competency standards to emphasize generic skills and the foundation of biomedical sciences. The revision also added detailed learning objectives. This led to some institutions revising their curriculum to strengthen the biomedical sciences and generic skills.(4)
Quality assurance system is implemented through both an internal and external approach. Only few well-established medical schools have implemented an internal quality assurance system. Most schools use the external quality assurance coordinated by the National Agent of Accreditation. Currently, only 16 of the 76 medical schools in Indonesia have achieved the highest accreditation grade.(5)
Although there is still dissatisfaction with the curriculum changes among several physiology teachers, physiology has proven more adaptable other branch of biomedical sciences. Most institutions have adopted an organ-system curriculum design, where the physiological concepts of integration, control and feedback are strongly represented in the competency based curriculum.
Key words: Competency-based curriculum, quality assurance, implementation.

Konsil Kedokteran Indonesia. Standar kompetensi dokter. Jakarta: Konsil Kedokteran Indonesia; 2006

Komite Bersama Uji Kompetensi Dokter Indonesia. Laporan hasil ujian kompetensi dokter Indonesia, tahun 2011. Jakarta: KB-UKDI-KKI; 2012. Letter Report

Unit Pendidikan Kedokteran FK-Unsri. Laporan evaluasi program pendidikan dokter FK-Unsri. Palembang: FK-Unsri; 2012. 20p. Report

Kelompok Kerja Standar Pendidikan Dokter Indonesia. Draft revisi: Standar kompetensi dokter Indonesia. Jakarta: Asosiasi Institusi Pendidikan Kedokteran Indonesia (AIPKI); 2012.

Badan Akreditasi Nadional Perguruan Tinggi. Daftar akreditasi program studi pendidikan dokter dan dokter gigi. [Internet]. 2012 [cited 2012 Nov 15]. Available from: http://www.ban-pt.kemdiknas.go.id/pencarian-direktori.php

Where applicable, the authors confirm that the experiments described here conform with The Physiological Society ethical requirements.

SA103

Is competency-based education the way forward in the Middle East?

M.M. Subhan

Physiology, Arabian Gulf University, Manama, Bahrain

The Middle East comprises of approximately 15 nations and refers to the area between Arabia and India, mainly the nations of the Persian Gulf. Although a form of competency-based medical education was present centuries ago in this region, this discussion will cover recent information about modern physiology and medicine in this region.
The oldest centre for modern medical training in the Middle East was started in 1867 in Lebanon, and this is now known as the American University of Beirut. Within the six Gulf Cooperative Council (GCC) states, Saudi Arabia has the oldest medical college, King Saud University (KSU, 1967). The current levels of competency-based physiology education in the curricula at KSU and the Arabian Gulf University; a regional GCC uni-

versity based which started in Bahrain in 1982, and other universities in the Middle East will be presented.
Around 2002, the Accreditation Council for Graduate Medical Education (ACGME) in the USA identified six general competencies to assess resident competence. The World Federation for Medical Education endorsed these. The World Federation for Medical Education has produced a document 'Basic Medical Education WFME Global Standards for Quality Improvement'. It was produced in 2003 and revised in 2012, with an aim to set international standards to all medical schools and also encourage reform. The present state of physiology education will be discussed in the light of these standards.
More specific to the Middle East, the Arab Knowledge Report 2009, although positively showing a consistent decline in illiteracy in the region, also paints a worrying picture for universities in the region. This report was co-produced by the Mohammed bin Rashid Al Maktoum Foundation and the United Nations Development Programme/Regional Bureau for Arab States.
Whether competency-based education (CBE) in physiology and other medical sciences will improve or worsen the situation described by the Arab Knowledge Report 2009 will be discussed. This matter is also complicated by the fact there has been an exponential establishment and growth by 400 % of Departments of Physiology in the Middle Eastern region over the last 2 decades. Due to this expansion, CBE has taken a back seat in terms of present teaching priorities for physiologists and administrators in the region. Eventually, physiologists have to match student competencies with the needs of patients and stakeholders, in a new era of globalization and interdependence.

Where applicable, the authors confirm that the experiments described here conform with The Physiological Society ethical requirements.

SA104

The evolution of the vertebrate heart: functional and phylogenetic insights

J.W. Hicks[1] and T. Wang[2]

[1]Ecology and Evolutionary Biology, University of California Irvine, Irvine, CA, USA and [2]Department of Bioscience - Zoophysiology, Aarhus University, Aarhus, Denmark

The emergence of the four-chambered heart and its underlying substructures was a critical event in vertebrate evolution, appearing at least twice independently; once in the vertebrate group that gave rise to crocodilians and birds (archosaurs), and once in the ancestral group of mammals (synapsids). A fully divided ventricle provides for the ability to maintain high cardiac outputs and systemic arterial blood pressures, while simultaneously keeping low blood pressures within the pulmonary circulation. Low pulmonary blood pressures allow for a thinner blood-gas barrier within the lungs, an important component of overall higher pulmonary diffusion capacity and hence more efficient gas exchange. In addition, a fully divided ventricle also avoids the mixture of oxygen-rich and oxygen-poor blood within the heart. These characteristics are both necessary for supporting increased rates of metabolism, which is directly linked with the rapid expansion and success of mammals and birds (Hicks and Wang, 2012).
Inferences about cardiac evolution result from studies investigating comparative cardiac morphology and function in extant species. Although extant reptiles (turtles, lizards, snakes and crocodilians) are only distantly related to modern mammals and birds, this clade provides the best group of animals for investigating and ultimately understanding the evolution of the four-chambered heart.
The heart of non-crocodilian reptiles has two anatomically divided atria, and a single ventricle. Between the many species of reptiles, the internal morphology of the ventricle exhibits a large degree of variability, with many folds and septae. Regardless of the anatomical variability within the ventricle, a functional characteristic of the heart within all non-crocodilian reptiles is the potential for the mixing of oxygen rich blood and oxygen poor blood (cardiac shunting). Cardiac shunting is defined by its directionality, with right-to-left shunts (R-L) being defined as a portion of systemic venous blood bypassing the lungs and reentering the systemic circulation. Alternatively, a left-to-right (L-R) shunt represents pulmonary venous blood (oxygen rich) recirculating back to the lungs. Emerging from the single ventricle are the three great vessels; the pulmonary artery, the left aortic arch (LAo) and right aortic arch (RAo) (Hicks and Wang, 2012).
It is interesting to note that crocodilians evolved a four-chambered heart, similar to birds and mammals. However, even in these animals, the separation of the pulmonary and systemic circulations is not absolute. Crocodilians retain the ancient phenotype of dual aortae (LAo and RAo), with the LAo emerging from the right ventricle, along with the pulmonary artery. The RAo exits the left ventricle. This unique anatomical arrangement results in the capacity for portion of the systemic venous blood to bypass the lungs and reenter the systemic circulation (right-to-left shunt) (Hicks and Wang, 2012).
In the latter half of the 20th century, many comparative cardiovascular physiologists argued that cardiac shunts were an adaptive trait in non-avian reptiles. Basically it was reasoned; why would reptiles maintain such a unique cardiac morphology and shunting capacity if such traits were not adaptive? This view resulted in a number of hypotheses about the adaptive advantages of cardiac shunting (see Hicks and Wang, 2012 for review). However experimental support for an adaptive significance of cardiac shunting in non-avian reptiles has been lacking.
For physiological or morphological trait to be considered adaptive it is important to provide evidence that the absence of the trait actually reduces physiological performance and/or reproductive fitness. Lacking such evidence, it is just as likely, that the unique features and functions of the reptilian heart is simply an embryonic or ancestral character; a character that does not negatively impact overall animal fitness and therefore has not been selected against. However, quantifying genetic fitness in reptiles is nearly impossible. Consequently the "adaptiveness" of cardiac shunts and determining the factors that drove the evolution of the four chambered heart and its characteristic structures, must be inferred by using a strategy that takes advantage of a variety of analytical and experimental approaches. Several of these approaches will be discussed in this symposium.

Hicks, JW and Wang, T (2012) The functional significance of the reptilian heart: new insights into an old question. In: Ontogeny and Phylogeny of the Vertebrate Heart. ed. D. Sedema and T. Wang, Springer-New York, pg. 207-227.

Where applicable, the authors confirm that the experiments described here conform with The Physiological Society ethical requirements.

SA105

Transcription factors regulate cardiac septum formation in the vertebrate evolution

K. Koshiba-Takeuchi[1], S. Kawakami[1], H. van Weerd[1,2], N. Yokota[1], Y. Moriyama[1] and J.K. Takeuchi[1]

[1]IMCB, The University of Tokyo, Tokyo, Japan and [2]University of Amsterdam, Amsterdam, Netherlands

Vertebrates have been modified cardiac morphologies and abilities to adapt terrestrial life with the use of lung for breathing in the evolution. The hearts morphologies have been more sophisticated and complicated from fish to mammals; fish have simple two-chambered heart (one atrium and one ventricle), amphibians have three-chambered (two atria and one ventricle), and crocodilian, birds, and mammals have four-chambered (two atria and two ventricles) heart. Interestingly at early stages mammalian heart forms a turning tube like as fish heart. Then we thought that to know the molecular mechanism of heart evolution leads to elucidation of developmental mechanism of cardiac septal formation and of congenital disease occurred in cardiac septa.
Non-crocodilian reptiles hold a unique place in the evolution of the heart, as their ventricle chambers are apparent intermediates between three-chambered heart and four-chambered heart. The previous study indicated that a steep and correctly positioned Tbx5 gradient is important for ventricular septum formation by using reptiles and the transgenic mice in which Tbx5 expressions like as reptiles. Sarcopterygians, including lungfish and coelacanth, also sit on the unique position between two-chambered heart (fish) and three-chambered heart (amphibian), suggesting that sarcopterygian is quite useful for studying about atrial septum formation. We constructed 3D images of lungfish and coelacanth hearts to observe the inside structure in detail. As a result, coelacanth heart is still similar to the fish, but lungfish has very sophisticated septated heart both in atria and ventricles. In this session we want to present when and how atrial septum is formed in vertebrate evolution via lungfish heart development comparing fish and amphibians.

Where applicable, the authors confirm that the experiments described here conform with The Physiological Society ethical requirements.

SA106

Development of the cardiac building plan

A.F. Moorman

Anatomy, Embryology & Physiology, AMC, Amsterdam, Netherlands

Molecular and genetic studies around the turn of this century have revolutionized the field of cardiac development. We now know that the primary heart tube, as seen in the early embryo contains little more than the precursors for the left ventricle, whereas the precursor cells for the remainder of the cardiac components are continuously added, to both the venous and arterial pole of the heart tube, from a single centre of growth outside the heart. While the primary heart tube is growing by addition of cells, it does not show significant cell proliferation, until chamber differentiation and expansion starts locally in the tube, by which the chambers balloon from the primary heart tube. The transcriptional repressors Tbx2 and Tbx3 locally repress the chamber-specific program of gene expression, by which these regions are allowed to differentiate into the distinct components of the conduction system. Molecular genetic lineage analyses have been extremely valuable to assess the distinct developmental origins of the various component parts of the heart, which currently can be unambiguously identified by their unique molecular phenotype.

Moorman AFM, Christoffels VM. 2003. Cardiac chamber formation: development, genes and evolution. Physiological Reviews 83: 1223-1267.

Where applicable, the authors confirm that the experiments described here conform with The Physiological Society ethical requirements.

SA107

Evolution of the building plan of the heart

B. Jensen[1,2], B.J. Boukens[2], T. Wang[1], A.F. Moorman[2] and V. Christoffels[2]

[1]Biosciense, Aarhus University, Aarhus C, Denmark and [2]University of Amsterdam, Amsterdam, Netherlands

In the hearts of mammals and birds, a system of nodes and fast-conducting tissues govern the activation pattern that induces myocardial contractions. We have previously shown that the atrioventricular conduction axis, consisting of the atrioventricular junction and the ventricles, is evolutionary conserved. From fish to man, the embryonic heart is patterned into compartments by the same genes. It has a muscular and slow conducting atrioventricular canal (Tbx2/3 positive) and a spongy ventricle (Cx40 and Anf positive) that serves the dual purpose of fast conduction and contraction. This design is maintained in fishes, amphibians and reptiles, whereas mammals and birds develop a fibrous insulating plane, thick compact ventricular walls and septum and, hence, form a discrete ventricular (His-Purkinje) conduction system from the embryonic spongy ventricle. Our understanding of the cardiac pacemaker, seen as a sinus node in mammals, is less clear. Most vertebrates have myocardium upstream of the right atrium (atrium in fishes) called the sinus venosus. It remains disputed if the dominant pacemaker of the heart is a property of the sinus venosus in entirety or of a specialised subset of sinus venosus myocardium. In the anole lizard the sinus venosus consists of three sinus horns that together equal the size of the right atrium. We investigated the electrical activation of the sinus venosus with optical mapping. Activation was earliest in the posterior sinus horn and then spread to the anterior sinus horns both of which are guarded by valves at the sinus-venous border. Later, the atria were activated from the dorsal sinu-atrial border, where the sinus node of mammals and birds is located. This region expressed the conserved sinus node markers Isl1 and Tbx3. We conclude that chambers and border regions of the vertebrate heart have highly similar patterns of gene expression and phenotypes, and that the cardiac conduction system simply follows from this building plan. Consequently, modifications rather than novelties characterise cardiac evolution.

Where applicable, the authors confirm that the experiments described here conform with The Physiological Society ethical requirements.

SA108

The evolving role of the cardiac sarcoplasmic reticulum

H. Shiels

Life Sciences, University of Manchester, Manchester, UK

The fundamental principles of excitation-contraction coupling are highly conserved between vertebrate species. However, the role of one organelle in particular, the sarcoplasmic reticulum (SR), is highly variable among species, tissue-type, age and environmental conditions, and has been linked to heightened cardiac performance and numerous cardiac pathologies. The SR is a specialised form of endoplasmic reticulum found in muscle cells that provides an intracellular reservoir of calcium. SR calcium can be rapidly mobilised and released from the SR for contraction, and re-sequestered back into the SR for relaxation. In mammals, this intracellular calcium flux pathway is essential for normal cardiomyocyte excitation-contraction coupling. The role of the SR is more contentious in non-mammalian vertebrates with some species recruiting little or no calcium from the SR during excitation-contraction coupling. While most studies suggest athletic ectotherms rely more strongly on SR calcium cycling, phylogenetic investigations suggest other factors may be important, and environmental conditions are also major determinants. This talk will discuss the enigmatic role of the SR during the evolution of the four-chambered heart drawing on comparative studies across vertebrates.

Where applicable, the authors confirm that the experiments described here conform with The Physiological Society ethical requirements.

SA109

The Hawaiian bobtail squid as a model organism for studying host/microbe interactions

S. Nyholm

Molecular and Cell Biology, University of Connecticut, Storrs, CT, USA

The establishment and maintenance of the light organ symbiosis between the Hawaiian bobtail squid Euprymna scolopes and the bioluminescent bacterium Vibrio fischeri depends on selection of V. fischeri and exclusion of non-symbiotic bacteria from the environment. Successful colonization of the host and cell-cell signaling between the partners triggers a morphogenetic program that leads to maturation of the association. Subsequent physical, biochemical and immunological mechanisms help to ensure that host-symbiont specificity is maintained. Current evidence suggests that the host's cellular innate immune system, in the form of macrophage-like hemocytes, assists in mediating host tolerance of V. fischeri. To further understand the role of hemocytes in this association, we have used both transcriptomic and proteomic analyses of this cell type. We have identified a number of pattern receptors involved with the recognition of microbe-associated molecular patterns. Among these was a complete open reading frame to a novel peptidoglycan recognition protein (EsPGRP5) with conserved residues for predicted amidase activity. Other transcripts and proteins identified included members of the conserved NF-κB signaling pathway, predicted members of a complement-like pathway, the carbohydrate binding protein galectin and a putative cephalotoxin. Quantitative PCR of complement-like genes, cephalotoxin, EsPGRP5, and a nitric oxide synthase showed differential expression in circulating hemocytes isolated from adult squid with colonized light organs compared to those from cured hosts. These data suggest that light organ colonization influences gene expression of the cellular innate immune system of the host. Studies are currently underway to determine how hemocytes distinguish between V. fischeri and non-symbiotic bacteria in both juveniles and adults. In addition to the light organ symbiosis, female squid have, as part of their reproductive system, an accessory nidamental gland (ANG) that houses a bacterial consortium within epithelia-lined tubules. We have used a number of microscopy and molecular techniques to identify dominant members, including the Rhodobacterales (Phaeobacter spp.) and Verrucomicrobia. 16S rRNA fluorescent in situ hybridization revealed that many ANG tubules were dominated by specific bacterial taxa, such as Rhodobacterales, Verrucomicrobia or Cytophaga-Flavobacteria-Bacteroidetes. Our data also suggest that bacteria from the ANG are deposited directly into the jelly coat of freshly laid eggs. To begin to explore the function of the ANG bacterial consortium, we conducted a series of experiments whereby development of egg clutches (with and without antibiotic treatment) was monitored over a four-week period. Treated eggs developed a thick fungal biofilm that resulted in the death of the embryos. A fungal culture was isolated from this biofilm and morphological characterization and multi-locus sequence typing suggest that it is a haplotype of the Fusarium solani species complex, a group that includes pathogens of marine animals. Taken together, these data suggest ANG bacteria may protect developing squid embryos from fungal biofilms, similar to what has been described for bacterial egg protection of other marine invertebrates. Overall, E. scolopes offers the unique opportunity to study both a binary (light organ) and consortial (ANG) bacterial association in the same host.

This work was supported by National Science Foundation IOS-0958006 and the University of Connecticut Research Foundation to SVN.

Where applicable, the authors confirm that the experiments described here conform with The Physiological Society ethical requirements.

SA110

Genomic evidence for the evolution of physiological robustness in coral-algal symbiosis

M. Weber[1,2], R. Iglesias-Prieto[2], H. Kitano[3] and M. Medina[1]

[1]School of Natural Sciences, UC Merced, Merced, CA, USA, [2]Unidad de Sistemas Arrecifales Instituto de Ciencias del Mar y Limnología, UNAM, Puerto Morelos, Q. Roo, Mexico and [3]Systems Biology Institute, Tokyo, Japan

We explored coral gene expression patterns and the physiological response of their dinoflagellate symbionts (*Symbiodinium*) to temperature stress. Fragments of *Montastraea faveolata* were field-collected in the Mexican Caribbean during summer (2012) and winter (2011) seasons. For each seasonal experiment, the corals were acclimated to 28degC under controlled tank conditions. Half of the fragments were kept in the controlled 28degC conditions and half were increased to 32degC for ten days. Subsequently the treatment corals were returned to 28degC and allowed to recover for up to six weeks. The same protocol was used for two different experiments in winter and summer. After ten days of thermal stress, we

observed break down of symbiosis (bleaching) in the summer experiment. The symbiosis was robust in corals collected for the winter experiment, despite exposure to equivalent stress.
We analyzed host transcriptome response to temperature stress. Several cellular pathways appeared to contribute to holobiont robustness. Corals differentially express a variety of enzymes that react with reactive oxygen species produced by stressed algal symbionts. Genes with functions attributed to calcium ion regulation and cell-cell adhesion are also differentially expressed before activation of the cell death pathways that cause symbiosis breakdown. We measured clear physiological differences in resident *Symbiodinium* populations between winter vs. summer experiments suggesting that the regulation of dinoflagellate physiology also contributed to holobiont robustness. We will discuss the host transcriptome response, organismal performance and the evolution of holobiont tolerance to thermal stress associated with these physiological differences. We will use this case study to discuss a theoretical model of biological robustness for the coral-algal holobiont.

Where applicable, the authors confirm that the experiments described here conform with The Physiological Society ethical requirements.

SA111

Role of light and multiple scattering on the establishment of mutualistic relationship with photosynthetic organisms

S. Enríquez

Unidad Académica de Sistemas Arrecifales Puerto Morelos, Universidad Nacional Autónoma de México, Cancún, Quintana Roo, Mexico

On the pigment-protein complexes, antenna, of the photosynthetic membranes relies the capacity of the primary producers to collect solar radiation and to transfer the excitation energy to the reaction centre of the two photosystems, where takes place its transformation into chemical energy. In order to favour an efficient excitation transfer and a continuous flow of electrons, evolution has generated a large diversity of antenna collectors, which also must photoprotect the photosynthetic apparatus from the excess of energy absorbed through the formation of "quenchers". Efficient excitation transfer has been achieved at expenses of reducing pigment ability to collect light. A phenomenon called "packaging effect" identified first for oceanographers while describing the variability in the inherent optical properties of phytoplankton, has found that photosynthetic pigments organized in alive structures are very inefficient to collect light due to self-shading. Multiple scattering of light has allowed counterbalancing the packaging effect, thanks to the enhancement in pigment absorption produced by the enlargement of the photon optical path. Multiple scattering, then, has mediated the design of a large biological diversity of solutions all of them led to the generation of efficient solar energy collectors. The establishment of mutualistic relationships with non-photosynthetic organisms able to supply scatting structures can also be explained by the capacity of multiple scattering to increase the photosynthetic performance of the new holobiont optimizing the use of the limiting resources. Here are presented a few examples of successful symbiotic relationships between invertebrates and algae, where the ability of (1) the highly reflective aragonite surfaces of the coral skeleton, or (2) the sponge silica spicula have allowed the appearance of the most efficient light collectors in nature, and explains the evolutionary and ecological success of these extremely efficient symbiotic relationships. This comparative study also highlights the capacity of multiple scattering to explain the origin itself of multicellularity in photosynthetic organisms.

Duysens LNM (1956) Biochem Biophys Acta 19, 1-12

Morel A, & Bricaud A (1981) Deep-Sea Res 28, 1375-1393

Osborne BA & Geider RJ (1989) Mar Biol 100, 151-159

Rühle W & Wild A (1979) Planta, 146, 551-557

Enríquez S, Méndez ER, & Iglesias-Prieto R (2005) Limnol Oceanogr 50, 1025-1032

Enríquez S & Sand-Jensen K (2003) Int J Plant Sci 164, 125-136

Enríquez S, Ávila E, & Carballo JL (2009) Journal of Phycology 45, 81-90

Monica Medina is acknowledged for her kind invitation to participate in this meeting and Roberto Iglesias-Prieto is also acknowledged for his always stimulating discussion and the opportunity given to dive into the coral reef world

Where applicable, the authors confirm that the experiments described here conform with The Physiological Society ethical requirements.

SA112

Individuality and temporal stability of the human gut microbiome

S. Sunagawa[1], S. Schloissnig[1], M. Arumugam[1], M. Mitreva[2], J. Tap[1], A. Zhu[1], A. Waller[1], D.R. Mende[1], J.R. Kultima[1], J. Martin[2], K. Kota[2], S. Sunyaev[3], G.M. Weinstock[2] and P. Bork[1]

[1]EMBL, Heidelberg, Germany, [2]The Genome Institute, Washington University School of Medicine, St Louis, MO, USA and [3]Harvard Medical School, Boston, MA, USA

The human body typically harbors about 100 trillion cells of microbial origin - commonly referred to as the human microbiome - the vast majority of which resides in the gastrointestinal tract (Savage 1977). While studying the extent of human genetic variation, for example in the 1,000 genomes project (The 1000 Genomes Project Consortium, 2010), and the understanding of its practical impact have advanced rapidly, the genetic variation of the human microbiome has remained largely unexplored. One of the reasons is attributed to the difficulty in cultivating the multitude of microbial species that inhabit our intestines. The possibility to high-throughput sequence DNA directly isolated from the environment has revolutionized the study of microbial communities, but analyzing single nucleotide polymorphisms (SNPs) in mixed microbial populations has remained a challenge. We therefore developed a methodological and statistical framework for metagenomic variation analysis and applied it to published sequencing data derived from 252 faecal samples of 207 European and North American individuals (The Human Microbiome Project Consortium 2012 and Qin et al. 2010). Exploiting the information generated by aligning 7.4 billion Illumina reads to 101 reference species, we detected 10.3 million single nucleotide polymorphisms (SNPs), almost as many as have been identified in humans so far.
Population variation of gut microbial communities with accompanying changes in species abundances over long time periods have not been studied yet in large cohorts. It has been unclear if host-specific strains are retained over time or constantly replenished via the environment. To address this question, we used 88 gut metagenomes collected from 43 healthy

subjects that were sampled at least twice over time intervals of up to 1 year and measured population similarities of dominant gut species using fixation indices (FST). The most striking result was that subjects sampled at varying time intervals exhibited individuality and temporal stability of SNP variation patterns, despite considerable composition changes of their gut microbiota. This indicates that individual-specific strains are not easily replaced and furthermore, that an individual may have a unique metagenomic genotype, which may also imply gut physiological individuality and consequences for personalized diet or drug intake.

Savage DC (1977). Annu Rev Microbiol. 31, 107.

The 1000 Genomes Project Consortium (2010). Nature 467, 1061–1073.

The Human Microbiome Project Consortium (2012). Nature 486, 215–221.

Qin,J.et al. (2010). Nature 464, 59–65.

Schloissnig et al. (2013). Nature 493, 45-50.

The research leading to these results has received funding from EMBL, the European Community's Seventh Framework Programme via the MetaHIT (HEALTH-F4-2007-201052) and IHMS (HEALTH-F4-2010-261376) grants as well as from the National Institutes of Health grants U54HG003079 and U54HG004968.

Where applicable, the authors confirm that the experiments described here conform with The Physiological Society ethical requirements.

SA113

Endophytic bacteria in plant meristems: a new type of mutualistic symbiosis

A. Pirttilä, J.J. Koskimäki and J. Pohjanen

Biology, University of Oulu, Oulu, Finland

We have identified a unique symbiotic plant-endophyte association in the meristematic tissue of Scots pine buds, where *Methylobacterium* spp. are the dominant species. These microbes are found in the cells of the apical meristem, needle and scale primordia, and around the resin ducts. Throughout the year they are associated with growing tissues (Pirttilä *et al.* 2000, 2005). Infection of pine seedlings by the endophytic strain *Methylobacterium extorquens* sp. DSM13060 induces expression of several PR-like genes, along with genes associated with development and signaling, such as *HYL1* and *ALE2*, a receptor protein kinase, and *CYP71*. A group of genes associated with development and apoptosis such as *AMP1*, *MERI5*, *AGL8*, *COW1*, plantacyanin, and chlorophyllase are down-regulated in the *M. extorquens* -infected seedlings. We have isolated endophytic products that increase viability of pine tissue *in vitro* (Pirttilä *et al.* 2004) and characterized some of them as antioxidants. When *M. extorquens* sp. DSM13060 was tagged with fluorescent proteins expressed by endophyte-specific promoters, the colonization with respect to specific metabolic processes could be observed in Scots pine seedlings. Furthermore, we saw that *M. extorquens* sp. DSM13060 specifically enters the plant through the plant epiderm by the crack entry and/or active penetration and forms infection pockets, resembling rhizobial infection. Unpublished data indicates that meristem-associated endophytes likely exist in other plant species. The shoot meristems can be considered among the most important tissues of the plant, responsible for growth and development of new leaves and stems. The finding of bacterial endophytes in these tissues suggests that a balanced interaction is essential for their proper function. As endophytes have been occupying the plant interior for more than 400 million years (Krings *et al.* 2007), mutual evolution must have driven ways to subsist, adapt, and eventually refine the interaction to a balanced state.

Pirttilä AM *et al.* (2000) *Appl. Environ. Microbiol.* 66, 3073-3077.

Pirttilä AM *et al.* (2004) *Physiol. Plant* 121, 305-312

Pirttilä AM *et al.* (2005) *Tree Physiol.* 25, 289-297

Krings M *et al.* (2007) *New Phytol.* 174, 648–657.

Academy of Finland

Where applicable, the authors confirm that the experiments described here conform with The Physiological Society ethical requirements.

SA114

Muscle protein and strength retention by bears during winter fasting and starvation

H.J. Harlow

Zoology & Physiology, University of Wyoming, Laramie, WY, USA

In the 1960s Cahill defined fasting in 3 phases with Phase II as fat using and protein conserving which is extended by animals adapted to long-term fasts without detrimental effects. Hibernation is a form of extreme fasting and black bears, Ursus americanus, undergo 5 months where they do not eat, drink, urinate or defecate while the body temperature is maintained only 5°C below normal. To accomplish this, they have a high hypothalamic set-point for fall hyperphagia and large fat reserve with a high proportion of polyunsaturated fatty acids. During transition to phase II there is elevated leptin, enhanced gut flora, decreased thyroxin and declining urea:creatinine ratios which together represent a period of fall "walking hibernation". The inhibitory effect of leptin on neuropeptide Y from the arcuate nucleus may initiate the onset of anorexia and the bear's entrance into their winter den. Bears are relatively unique in that they undergo pregnancy and lactation while fasting. There is 47% greater fat and 26% greater protein deposition for reproductive bears in the fall to offset their greater rate of mass and energy loss during denning. Long-term fasting in obese humans results in cardiac muscle protein loss and dysfunction, however, echocardiographic images of bears revealed no left ventricular resculpturing or reduced thickness during winter inactivity and chronic hypotension. Bears showed dramatic respiratory sinus arrhythmia with long pauses between breaths and profoundly depressed heart rates as low as 4 bpm. Accelerated heart rate during inhalation enhances oxygen transport within the heart tissue while the period of dramatically reduced heart rate acts to minimize energy expenditure and conserve cardiac protein. Skeletal muscle biopsies were taken from the biceps femoris, gastrocnemius and vastus lateralis during early and late denning. There was no loss of number, cross sectional area of fibers or marked transition of SO to FG fibers. Denning bears lost only about 0.03% protein/day, a value that is an order of magnitude below that reported for rats and humans, perhaps due to high ketone body inhibition of gluconeogenesis associated with a low thyroid activation of proteolysis and low urea:creatine ratio. This conservation of morphology and protein is atypical of starvation or disuse-induced skeletal muscle atrophy models. Bears underwent a period of skeletal muscle protein accretion with synthesis rates 1.4 times higher than degradation during the

summer. Rates of synthesis and breakdown decreased 60-70% from summer to fall during the "walking hibernation" transition period with a concomitant 30-60% drop in RNA, a decreased ratio of RNA to DNA and an elevated δ 15N value in skeletal muscles. But all parameters then remained unchanged throughout the 5 months of denning without food or water. However, not all muscle behaves identically during fasting. There was a 4-11% loss of protein from the gastrocnemius and biceps femoris muscle by lactating bears but no loss from the vastus lateralis. Protein synthesis could occur in a selected muscle if amino acids are made available by the marginal degradation of other skeletal muscles in concert with proteolysis of organs, collagen and smooth muscle. The collagen metabolites hydroxyproline and glycine were elevated in denned bears. In addition, proteolysis of kidney tissue releases large amounts of serine that was high in late winter. The gastrointestinal tract may also be a labile protein source as seen in an elevation of blood alpha amino acids. Winter protein demands during the Phase II fast are further reduced by: 1) no winter arousal bouts, 2) delayed implantation for pregnant females, 3) no fur growth and 4) urea nitrogen salvaging (UNS) to avoid urinary nitrogen loss. Bears recycle almost 100% of their urea, perhaps due to UTB urea transporters in the bladder and intestines which salvage urea for microbial hydrolysis in the intestine. The resulting ammonia is transported to the liver where it is reamminated into new amino acids and muscle protein. UNS is upregulated in hibernators 10-40 fold during fasting and torpor as shown by 15N labeled urea studies. Bears exhibit subtle EMG patterns throughout the denning period with peripheral vasodilation which may disperse heat and facilitate wound healing. As a result of conserved protein, fiber morphology and isometric/isotonic contraction patterns, bears during 150 days of confinement and complete food deprivation exhibit only marginal loss of strength. Muscle performance measured both in vivo and in vitro declined only 23% from early to late winter compared to a 70% loss predicted for humans confined to a hospital bed (inactive but well fed) for 150 days. Bears are truly adapted long-term fasters.

Where applicable, the authors confirm that the experiments described here conform with The Physiological Society ethical requirements.

SA115

Direct measurements of substrate oxidation using 13CO2 breath testing reveals shifts in fuel mix during starvation

M.D. McCue

Biological Sciences, St. Mary's University, San Antonio, Texas, UK

Fasting animals are believed to sequentially switch from utilizing one metabolic substrate to another in the order of carbohydrates, to lipids, then to proteins. The timing of these physiological transitions are traditionally estimated using indirect measures of substrate oxidation including, changes in RER, blood metabolites, or respiratory enzyme activities. Here we show that the oxidation of distinct nutrient pools in the body (lipids, proteins, and carbohydrates) that are gradually enriched in 13C can be directly quantified using 13CO2-breath testing. Seventy-two Swiss Webster mice were raised to adulthood on diets supplemented with 13C-1-L-leucine, 13C-1-palmitic acid, 13C-1-D-glucose, or no tracer. Mice were then fasted for 72 hours during which VO2, VCO2, δ13CO2, body temperature (Tb), and blood metabolites (i.e., glucose, ketone bodies, and triacylglycerides) were continually measured. The fasting mice exhibited reductions in Tb (4.6°C), body mass (29%), BMR (24%), and RER (0.18), and significant changes in blood metabolites, but these responses were not useful to clearly identify specific changes in fuel mixture. Direct measurements of endogenous nutrient oxidation by way of 13CO2-breath testing revealed a rapid crash in the rate of oxidation of carbohydrates from 47% to 27% of the total energy expenditure during the first 6 hours without food. This response was mirrored by a coincidental increase in rate of endogenous lipid oxidation from 31% to 52%. A final transient peak in carbohydrate oxidation occurred between 8-18 hours indicating the transition between Phase I and II. A period of protein sparing between 8-12 hours was observed where endogenous protein oxidation accounted for as little as 9% of the total energy expenditure. Thereafter, protein oxidation continually increased accounting for as much as 25% of the total energy expenditure by 72 hours, suggesting that these mice exhibit a gradual, not an abrupt, transition from Phase II to III. This study demonstrates that direct measurements of substrate oxidation address a gap in our understanding of the timing and magnitude of sequential changes in substrate oxidation that occur during prolonged fasting and starvation.

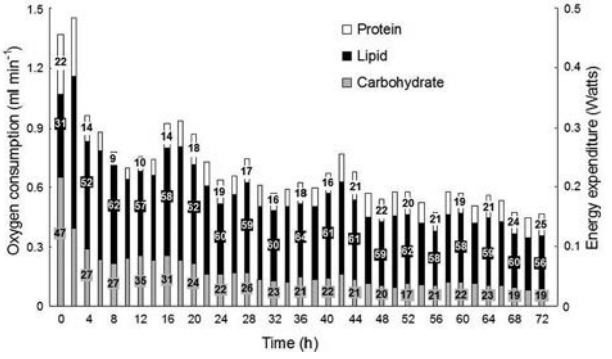

How a mouse oxidizes different types of endogenous nutrients to meet its energy demands during prolonged fasting.

Where applicable, the authors confirm that the experiments described here conform with The Physiological Society ethical requirements.

SA116

Differential mobilization and use of fatty acids during fasting

T.G. Valencak[1,2] and E.R. Price[3]

[1]University of Veterinary Medicine Vienna, Vienna, Austria, [2]Institute of Genetics and Developmental Biology, Chinese Academy of Sciences, Beijing, China and [3]University of Wisconsin - Madison, Department of Forest and Wildlife Ecology, Madison, WI, USA

Fatty acids and particularly, polyunsaturated fatty acids are essential constituents of biological membranes. Apart from this, they fulfil functions as signalling molecules, anti- freezing compounds and energy storage. While a lot of research has been conducted on the changes in lipid content that occur during fasting, only few studies have focused on changes in the quality of body lipids.

During fasting and any extended period of diminished energy intake such as starvation, the fatty acid composition of the lipids is altered: fat mobilisation, transport and oxidation all work together and induce an apparent "fasting fatty acid response" with saturated fatty acids being largely retained whereas monounsaturated and polyunsaturated fatty acids

are largely mobilised and thus decreased in stored triacylglycerols.
In the presentation, this pattern will be explained in more detail in a variety of animals in the light of the existing literature on the subject. We will examine changes in whole- animal, adipose and muscle fatty acid composition that occur during fasting/starvation. We will also discuss the selective retention of C 18:2 n-6 in white adipose tissue of hibernating animals that seems to be related to physiological heterothermy and not starvation per se.
We conclude that the observed changes in fatty acid composition are unlikely to represent an adaptive "starvation response". While triacylglycerols seem to change in an unregulated manner in response to fasting and starvation, membrane fatty acid composition is changed more systematically when an animal is restricted calories. Future research might shed light on this subject and should emphasise the separation of lipid fractions (triacylgylcerols vs. phospholipids) in the various tissues.

Price ER, Valencak TG (2012) Changes in fatty acid composition during starvation in vertebrates: mechanisms and questions. In: "Comparative Physiology of Fasting, Starvation and Food limitation" edited by M.D. McCue, Springer- Verlag Berlin Heidelberg 2012. DOI: 10.1007/978-3-642-29056-5_15

Where applicable, the authors confirm that the experiments described here conform with The Physiological Society ethical requirements.

SA117

Alternate day fasting: a novel dietary restriction regimen for weight loss in humans

K.A. Varady

Kinesiology and Nutrition, University of Illinois, Chicago, Chicago, IL, USA

Background: The ability of modified alternate day fasting (ADF) (i.e. consuming 25% of energy needs on the fast day, and ad libitum fed on feed day) to facilitate weight loss and lower vascular disease risk in obese individuals remains unknown. Objective: This study examined the effects of ADF, administered under controlled versus self-implemented conditions, on body weight and coronary heart disease (CHD) risk indicators in obese adults. Design: Sixteen obese subjects (12 women/4 men) completed a 10-week trial, consisting of 3 phases: 1) 2-week control phase, 2) 4-week weight loss/ADF controlled feeding phase, and 3) 4-week weight loss/ADF self-selected feeding phase. Results: Dietary adherence remained high throughout the controlled feeding phase (86% days adherent), and the self-selected feeding phase (89% days adherent). Rate of weight loss remained constant during controlled feeding (0.67 ± 0.1 kg/week) and self-selected feeding phases (0.68 ± 0.1 kg/week). Body weight decreased ($P < 0.001$) by 5.6 ± 1.0 kg (5.8% ± 1.1%) after 8 weeks of diet. Percent body fat decreased ($P < 0.01$) from 45 ± 2% to 42 ± 2%. Total cholesterol, LDL cholesterol, and triacylglycerol concentrations were lowered ($P < 0.01$) by 21 ± 4%, 25 ± 10%, 32 ± 6%, respectively, after 8 weeks of ADF, while HDL cholesterol remained unchanged. Systolic blood pressure decreased ($P < 0.05$) from 124 ± 5 mm Hg to 116 ± 3 mm Hg. Conclusions: These findings suggest that ADF is a viable diet option to help obese individuals lose weight and decrease CHD risk.

Where applicable, the authors confirm that the experiments described here conform with The Physiological Society ethical requirements.

SA118

Thermoregulatory adaptations to starvation and cold in birds

E. Hohtola

Department of Biology, University of Oulu, Oulu, Finland

As endothermic animals, birds allocate a significant part of their energy intake for maintaining homeothermy, especially in cold environments. Their body temperatures and metabolic rates are typically higher than in mammals of similar body mass. Therefore, food shortage and starvation pose a true energetic challenge for maintaining homeothermy in birds (McCue 2010). As most birds are small, their energy reserves in relation to metabolic rate are limited, which together with high surface-to-volume ratios exacerbates the effects of starvation.
During food shortage, energy can be saved if the need for active thermogenesis can be reduced. Such a hypometabolic state can be achieved by increasing thermal insulation beyond the level found in fed birds or by reducing body temperature in a regulated manner or by combining the two mechanisms. Even in fed state, birds increase their insulation during the rest phase of the daily cycle. This is done mainly by ptiloerection and postural adjustments and there is probably not very much extra insulation available by these mechanisms in fasting birds. However, a significant decrease in heat loss can be achieved by regional heterothermia, where peripheral parts of the body are allowed to cool and only the core parts are held normothermic. Although this phenomenon is known from other physiological situations, it has not been studied extensively in fasting or food-restricted birds.
A general decrease in core body temperature will naturally decrease the metabolic burden of homeothermy. More and more evidence for a capability to a regulated decrease of body temperature (rest-phase hypothermia, shallow torpor) during starvation in birds is accumulating (McKechnie & Lovegrove 2002). The decline of body temperature in shallow torpor is typically 3–10°C. While deep torpor triggered by starvation or even without energetic stress has been recognized for a long time in some avian groups (e.g., in humming-birds and swifts), recent studies show that basically all avian groups can save energy by entering starvation-induced shallow torpor during the rest-phase of their daily cycle. In deep torpor, birds lose their responsiveness to environmental stimuli, whereas in shallow torpor the react to external disturbances, which has implications ion vigilance and predator avoidance. So far, deep or shallow torpor has been found in at least 11 avian orders and 29 families.
The metabolic savings in shallow torpor are obviously smaller than in deep torpor. The reduction in metabolic rate is, however, often larger than predicted by the decline in deep-body temperature (Hohtola 2012). This suggests that fasting birds are able to recruit otherwise unused insulative mechanisms. Regional heterothermy in peripheral tissues is one possibility, although it has not been studied in detail. It would save energy by two mechanisms: 1) By making the temperature gradient between body core and the environment less steep (resulting in lower conductance) and 2) By lowering thermostatic costs of the peripheral parts at lower tissue temperature.

The thermoregulatory adjustments during fasting are tuned to the amount of remaining energy reserves. Thus, nocturnal hypothermia is deeper in birds that roost at lower body mass (Reinertsen 1996) and hypothermia is deeper on each successive fasting day during prolonged fasting (see Hohtola 2012). How starvation is translated to a neurohumoral thermoregulatory signal that results in a lower regulated body temperature and metabolic savings is, however, not known. These mechanisms, together with the observed large energy savings ensuing from the relatively small decline in body temperature warrant further studies on fasting-induced thermoregulatory adaptations.

Hohtola E (2012). In: McCue M (ed.) Comparative Physiology of Fasting, Starvation, and Food Limitation. New York, Springer, pp. 155-170.

McCue MD (2010) Comp Biochem Physiol A 156, 1-18.

McKechnie AE & Lovegrove BG (2002) Condor 104: 705-724.

Reinertsen R (1996) In: Carey C (ed.) Avian energetics and nutritional ecology. New York, Chapman & Hall, pp. 125-157.

Supported by the Academy of Finland and Thule-Institute (University of Oulu)

Where applicable, the authors confirm that the experiments described here conform with The Physiological Society ethical requirements.

SA119

The adventitia: a dynamic interface containing resident progenitor cells

M. Majesky[1,4], X. Dong[4], V. Hoglund[4] and W. Mahoney[2,3]

[1]Pediatrics, University of Washington, Seattle, WA, USA, [2]Pathology, University of Washington, Seattle, WA, USA, [3]Institute for Stem Cell & Regenerative Medicine, University of Washington, Seattle, WA, USA and [4]Seattle Children's Research Institute, University of Washington, Seattle, WA, USA

Recent observations suggest that the outer layer of blood vessel walls, the adventitia, exhibits properties of a stem/progenitor cell niche. Stem cell antigen-1 (Sca1)/CD34-positive progenitor cells have been isolated from the adventitia of both murine and human arteries and veins with potentials to form smooth muscle cells (SMCs), pericytes, macrophages, osteogenic cells and adipocytes. These progenitors cluster at or near the border zone between the outer media and inner adventitia. In the mouse this border zone region corresponds to a localized site of sonic hedgehog (Shh) signaling in the artery wall. The onset of Shh signaling corresponds to termination of SMC layer formation in developing arteries and the appearance of adventitial Sca1-positive (AdvSca1) cells around E15.5. Shh acts as a mitogen and survival factor for AdvSca1 cells ex vivo and many fewer Sca1-positive cells are found in the adventitia of Shh-null embryos in vivo. AdvSca1 cells form pericytes and macrophages in matrigel implant angiogenesis assays in vivo. The role of AdvSca1 cells in growth, remodeling and disease of blood vessels and surrounding tissues will be discussed.

Support: NIH Grant HL-93594.

Where applicable, the authors confirm that the experiments described here conform with The Physiological Society ethical requirements.

SA120

Enhancing stem cell recruitment within the microcirculation - chemokines, chemicals and caveats

D.P. Kavanagh, A.I. Yemm, R.L. White and N. Kalia

College of Medical and Dental Sciences, University of Birmingham, Birmingham, West Midlands, UK

Considerable interest surrounds the use of stem/progenitor cells (SCs) in tissue regeneration and repair. A variety of potential therapeutic cell types have been identified, including adult bone marrow (BM)-derived haematopoietic (HSC) and mesenchymal stem cells (MSC). Experimental studies suggest that HSCs and MSCs are able to alleviate inflammation and subsequently contribute to tissue repair. Local recruitment of injected SCs by the microcirculation of injured tissue is a likely prerequisite for repair. Limited recruitment of SCs subsequent to systemic infusion has been partly used to explain the poor clinical success of cellular therapy. The molecular adhesive mechanisms that underpin SC recruitment and retention in injured tissue remain poorly understood. Understanding these mechanisms may allow identification of strategies that can enhance SC recruitment and may improve the efficacy of SC-based therapies.

HSCs express a variety of surface adhesion molecules (e.g. CD49d, CD18, CD44) that are important in mediating their recruitment to injured tissues. Our intravital microscopy studies, conducted on different murine organs, demonstrate tissue-specific recruitment of HSCs to the injured microvasculature. For instance, recruitment of HSCs in ischemically injured liver is dependent on the integrin sub-unit CD49d, while recruitment of HSCs in ischemically injured gut is dependent on the integrin sub-unit CD18. Additionally, a role for the non-integrin glycoprotein CD44 appears critical in mediating HSC recruitment to injured kidney. Since these adhesion molecules are essential for stem-endothelial cell interactions, modification of their surface expression, affinity for endothelial counterligands or avidity (clustering) may facilitate or impede recruitment of HSCs into specific tissues.

In addition to direct manipulation of adhesion molecules, chemokine pre-treatment strategies have promise in enhancing HSC recruitment to injured tissues. HSC pre-treatment with chemokines such as CXCL12 (SDF-1α) or KC (murine functional IL-8 homologue) significantly enhances their recruitment into the microvasculature of the ischemically injured intestine. Pre-treatment of HSCs with either CXCL12 or the reactive oxygen species, hydrogen peroxide (H_2O_2), can increase cell adhesion in the ischemically injured intestine. Crucially, these factors are released into the local microenvironment following ischemic tissue injury. Pre-treatment strategies may enhance adhesion via a number of mechanisms, including enhanced integrin clustering. Indeed, we have demonstrated that our HSC pre-treatment strategies are able to enhance surface integrin clustering. For instance, H_2O_2 (100μM; 1hr) significantly increases surface clustering of integrins CD18 and CD49d without affecting HSC viability or function (still capable of differentiation into mature hematopoietic cells). Interestingly, pre-treatment strategies may also modify SC kinetics through non-adhesion molecule related mechanisms. For instance, we have data to show that CXCL12 pre-treatment increases HSC deformability, as demonstrated using a micropipette aspiration method. This has important clinical implications as non-specific entrapment is considered a major obstacle for systemic SC delivery. Non-specific entrapment may reduce the pool of circulating transplanted SCs available for recruitment.

An additional biological approach to enhancing SC recruitment involves utilising platelet-derived microparticles (PMPs). PMPs are the predominant subtype of microparticle found in peripheral blood, with numbers increased in patients with inflammatory disorders. PMPs can 'coat' neutrophils and increase leukocyte-endothelial interactions. Based on this phenomena, we demonstrated that coating HSCs with PMPs prior to infusion in mice enhanced their recruitment in chronically injured colitis colon. We have recently performed parallel intravital studies to investigate the kinetics of MSC homing in vivo. Preliminary studies suggest distribution of MSCs post-infusion is not increased in injured tissue compared to healthy controls – this differs from HSC data.
Our understanding of the molecular mechanisms underlying SC homing to sites of injury is increasing and allowing us to develop strategies that can modulate their adhesion. Our ongoing studies have demonstrated that enhancing HSC presence confers a greater anti-inflammatory effect within the local microcirculation. While it is easy to presume that enhanced SC recruitment may be beneficial in models of injury, we should be wary that an "over-recruitment" may have deleterious effects. Certainly, MSCs can behave pro-fibrotically and may worsen the local tissue milieu in conditions of injury. Whether enhancing local MSC presence proves beneficial or detrimental is currently being investigated.
Supported by the British Heart Foundation

Where applicable, the authors confirm that the experiments described here conform with The Physiological Society ethical requirements.

SA121

Identification of resident c-kit expressing vascular endothelial stem cells on the adult blood vessel wall

S. Fang, J. Wei, N. Pentinmikko, H. Leinonen and P. Salven

Department of Pathology, Haartman Institute,University of Helsinki, Helsinki, Finland

Angiogenesis is essential many physiological and pathological events, for instance in wound repair and tumor progression. The origin of newly-formed blood vessel endothelial cells in adults is not known. Here we identified and isolated c-kit+ vascular endothelial stem cells (VESCs) by the phenotype lin-CD31+CD105+Sca1+CD117+, a small subpopulation residing on the vessel wall. A single transplanted VESC is able to generate functional blood vessels in connection with the host circulation and maintain a long-term self-renewal capacity in vivo. Further, we showed that a genetic deficit in endothelial c-kit expression remarkably decreases total colony-forming VESCs, indicating a functional role of c-kit in VESCs. A deficit in c-kit expression also resulted in impaired angiogenesis and growth retardation in tumor. Thus, VESCs would provide a novel cellular target to inhibit pathological angiogenesis in cancer therapies. Isolated VESCs could also be utilized in therapies to restore tissue vascularization in many diseases.

Where applicable, the authors confirm that the experiments described here conform with The Physiological Society ethical requirements.

SA122

Pericytes for cardiovascular repair: a roadmap towards first-in-man trial

P. Madeddu

Bristol Royal Infirmary, Bristol, UK

Pericytes for cardiovascular repair: a roadmap towards first-in-man trial Paolo Madeddu, Prof. MD FAHA University of Bristol Recent studies have highlighted the regenerative potential of progenitor cells from human vasculature. This presentation will address the protocol for isolation, expansion and preclinical testing of human pericytes from saphenous veins of elderly cardiovascular patients in view of a first in human clinical trial. We have so far isolated pericytes from more than 70 venous samples and characterized variability of preparations and we are now introducing clinical grade reagents, including the use of immunomagnetic beads for separation of antigenically defined cells and serum free media.
We have also obtained initial epigenetic hits that predict preclinical therapeutic activity and indicate safety of the cell product.

Where applicable, the authors confirm that the experiments described here conform with The Physiological Society ethical requirements.

SA123

Perivascular adipose tissue as a determinant of organ perfusion

E.C. Eringa

Department of Physiology, Institute for Cardiovascular Research, VU University Medical Centre, Amsterdam, Netherlands

Accumulation of ectopic fat is strongly related to risk of type 2 diabetes and cardiovascular disease. One of the most important fat depots in this context is perivascular adipose tissue (PVAT), which is situated around most blood vessels with a diameter >100 microns. In organs such as adipose tissue, muscles and the heart, PVAT associates with resistance arteries, suggesting a role in (dys)regulation of perfusion of these tissues. As perfusion is a determinant of local glucose metabolism, PVAT control of tissue perfusion may also contribute to regulation of insulin sensitivity. In recent years, PVAT around resistance arteries has been found to induce vasodilatation by direct relaxing effects on smooth muscle and enhancement of vasodilatation induced by insulin and acetylcholine. These vasodilator properties of PVAT are mediated by a variety of bioactive substances (adipokines) such as adiponectin and inflammatory mediators. In human and experimental obesity, hypertension and Western diet exposure, impaired vasodilator properties of PVAT have been observed. This is triggered by infiltration of inflammatory cells such as macrophages in PVAT and, in muscle, associates with reduced perfusion. In conclusion, vasoregulation in resistance arteries by PVAT contributes to regulation of local perfusion and metabolism, and impairment of this function of PVAT may be a novel mechanism underlying insulin resistance and target organ damage in type 2 diabetes.

Where applicable, the authors confirm that the experiments described here conform with The Physiological Society ethical requirements.

SA124

Adipokine signaling and angiogenesis

A. Bouloumie

INSERM U1048, Toulouse, France and University Paul Sabatier, Toulouse, France

The adipose tissue plays a major role in energy homeostasis as the main tissue of energy reserve but also as source of adipokines involved in the control of metabolic fluxes. Among them, many adipokines exhibit pro-angiogenic activities including leptin (1), the family of vascular endothelial growth factors, the angiopoietins, hepatocyte growth factor, angiopoietin like factor 4, apelin, visfatin, the families of fibroblast growth factors and of matrix metalloproteinases (2). Anti-angiogenic factors such as thrombospondins, Secreted Protein Acidic and Rich in Cysteine, osteopontin, resistin, the metalloproteases inhibitors and plasminogen activator inhibitor 1 are also produced by TA (2). The global angiogenic status of the human AT is modulated mainly by the adiposity degree and the AT location. Indeed, a global increase in AT angiogenic status is found with obesity. This effect might be related to the accumulation of immune-inflammatory cells within AT including macrophages shown to stimulate angiogenesis in AT (3) . Hypoxia, that may be consecutive to the increased size of adipocytes (or hypertrophy), is a condition that will increase the production of pro-angiogenic adipokines in AT (4). Distinct angiogenic statuses are described according to the fat mass location, visceral AT being considered more proangiogenic than subcutaneous fat mass (5). Angiogenesis within AT is a key event in the cellular homeostasis during fat mass development and most of the approaches to lower angiogenesis have been shown to interfere with AT growth and whole energy expenditure (6). This key mechanism may become pathological under too strong local angiogenic pressure leading to accelerated aging of endothelial cells (5) and ultimatively to endothelial cell dysfunction. Therefore the link involving adipokines in the communication between adipocytes and endothelial cells is of great interest to better understand the link between obesity and associated pathologies.

Leptin, the product of Ob gene, promotes angiogenesis.

Bouloumié A, Drexler HC, Lafontan M, Busse R.

Circ Res. 1998 Nov 16;83(10):1059-66.

Angiogenesis in adipose tissue.

Bouloumié A, Lolmède K, Sengenès C, Galitzky J, Lafontan M.

Ann Endocrinol (Paris). 2002 Apr;63(2 Pt 1):91-5.

Remodeling phenotype of human subcutaneous adipose tissue macrophages.

Bourlier V, Zakaroff-Girard A, Miranville A, De Barros S, Maumus M, Sengenes C, Galitzky J, Lafontan M, Karpe F, Frayn KN, Bouloumié A.

Circulation. 2008 Feb 12;117(6):806-15.

Effects of hypoxia on the expression of proangiogenic factors in differentiated 3T3-F442A adipocytes.

Lolmède K, Durand de Saint Front V, Galitzky J, Lafontan M, Bouloumié A.

Int J Obes Relat Metab Disord. 2003 Oct;27(10):1187-95.

Adipose tissue endothelial cells from obese human subjects: differences among depots in angiogenic, metabolic, and inflammatory gene expression and cellular senescence.

Villaret A, Galitzky J, Decaunes P, Estève D, Marques MA, Sengenès C, Chiotasso P, Tchkonia T, Lafontan M, Kirkland JL, Bouloumié A.

Diabetes. 2010 Nov;59(11):2755-63.

Cao Y Adipose tissue angiogenesis as a therapeutic target for obesity and metabolic diseases. Nat Rev Drug Discov. 2010 9: 107-15

Research is supported by “the fondation pour la recherche médicale”, Clarins and INSERM

Where applicable, the authors confirm that the experiments described here conform with The Physiological Society ethical requirements.

SA125

PVAT function in obesity: mechanisms and therapy

A. Heagerty

The University of Manchester, Manchester, UK

There is now clear evidence that adipocytes are engine rooms producing a large number of factors which can have profound influences upon adjacent tissues. In particular, perivascular fat can influence arterial tone and healthy adipocytes secrete a number of vasorelaxing molecules. Recent evidence has suggested that one of these playing a prominent role is adiponectin and the bioavailability of this adipokine is lost when subjects become obese and develop maturity on-set diabetes or the metabolic syndrome. Adiponectin appears to be released by the stimulation of beta-adrenor receptors located on adipocyte plasma membranes and its actions involve nitric oxide both in the endothelium and in the adipocyte itself. Crucial to the normal functioning of this pathway is the BKCa channel and knockout mice demonstrate no vasorelaxing activity of perivascular fat. In the obese state there is adipocyte hypertrophy and activation of recruited macrophages. Evidence suggests that without the macrophage there is no loss of perivascular vasodilator activity and our most recent data following up patients who have undergone bariatric surgery suggest that this intervention is associated with a loss of inflammation and the restoration of normal perivascular fat function.

Where applicable, the authors confirm that the experiments described here conform with The Physiological Society ethical requirements.

SA126

Cardiac t-tubules as a specialised microdomain for trans-sarcolemmal Ca flux and its regulation in health and disease

C. Orchard, S. Bryant and A. James

School of Physiology and Pharmacology, University of Bristol, Bristol, UK

The transverse (t-) tubules of mammalian cardiac ventricular myocytes are invaginations of the surface membrane that form a complex network within the cell. The function of many of the key proteins involved in cardiac excitation-contraction coupling occurs predominantly at the t-tubules: acute detubulation results in an ~80% decrease of L-type Ca current (I_{Ca}), an ~65% decrease of Na-Ca exchange current (I_{NCX}), and complete loss of Ca extrusion via the sarcolemmal Ca ATPase (see Orchard *et al*., 2009 for review; Chase & Orchard, 2011). Thus the majority of trans-sarcolemmal Ca influx and efflux occurs across the t-tubule membrane, which ensures that both activation and relaxation occur rapidly throughout the cell.
Cell signalling is also different at the t-tubule and surface membranes: the β-adrenergic agonist isoprenaline causes greater stimulation of I_{Ca} at the t-tubules than at the surface mem-

brane, suggesting better coupling of the β -adrenergic pathway to I_{Ca} at the t-tubules (Brette *et al*., 2004), and recent work suggests that localisation of I_{Ca} and I_{NCX} to the t-tubules is due, in part, to localised stimulation of these currents at the t-tubules by basal activity of protein kinase A (PKA; Chase *et al*., 2010; Chase & Orchard, 2011). Since β_2 adrenoceptors occur predominantly in the t-tubules in normal ventricular myocytes (Nikolaev *et al*., 2010), it seems possible that tonic activity of the β_2 adrenergic pathway underlies this localisation.

To investigate further the mechanisms underlying this localisation, we have used a membrane-permeable peptide representing the scaffolding domain of Caveolin-3 (Cav-3; MacDougall *et al*., 2012). This peptide (C3SD) reduced basal I_{Ca} and inhibited the stimulatory effects of the β_2-adrenergic agonist zinterol on I_{Ca}. The PKA inhibitor H-89 also reduced basal I_{Ca}; however, the inhibitory effects of H-89 and C3SD on basal I_{Ca} were not summative, suggesting that they share a common pathway involving PKA. Thus Cav-3 appears to play an important role in facilitating stimulation of I_{Ca} by basal PKA activity and in response to β_2-adrenoceptor stimulation, consistent with the hypothesis that basal activity of the β_2-adrenergic pathway underlies stimulation of I_{Ca}, to which it is coupled via Cav-3.

T-tubules may also play an important role in pathological conditions. Changes in t-tubule morphology have been reported in both human heart failure (HF) and in animal models of HF, with t-tubule structure becoming disordered, with consequent changes in the synchrony of Ca release. Changes in cell signalling also occur: H-89 has a greater inhibitory effect on basal I_{Ca} in myocytes isolated 16 weeks after coronary artery ligation than in those from sham operated controls, suggesting greater stimulation by PKA, as shown previously. However, C3SD does not decrease I_{Ca} significantly in the ligation model (Bryant *et al*., 2013), suggesting that the coupling of PKA activity to I_{Ca} by Cav-3 described above is already disrupted. Although the role of the t-tubules in these changes is still being elucidated, it is interesting that HF is associated with redistribution of β_2 adrenoceptors from the t-tubules to the surface membrane, and a change from localised to diffuse cAMP signalling in response to β_2 adrenoceptor stimulation (Nikolaev *et al*., 2010), making it tempting to speculate that loss of Cav-3 coupling plays a role in these changes.

Thus the t-tubules appear to form a specialised domain for trans-sarcolemmal Ca flux and its regulation, and thereby play a key role in physiological and pathophysiological cell function.

Brette F *et al*. (2004). *J Mol Cell Cardiol* **36**, 265–275.

Bryant S *et al*. (2013). Abstract, this meeting.

Chase A *et al*. (2010). *Mol Cell Cardiol* **49**, 121–131.

Chase A & Orchard CH (2011). *J Mol Cell Cardiol* **50**, 187-193.

MacDougall DA *et al*. (2012). *J Mol Cell Cardiol* **52**, 388–400.

Nikolaev VO *et al*. (2010). *Science* **327**, 1653–1657.

Orchard CH *et al*. (2009).*Exp Physiol* **94**, 509-519.

The authors would like to thank the BHF for its support.

Where applicable, the authors confirm that the experiments described here conform with The Physiological Society ethical requirements.

SA127

Optical recording of action potential propagation in transverse-axial tubular system

L. Sacconi[1,3], C. Crocini[1], C. Ferrantini[2], R. Coppini[2], C. Tesi[2], E. Cerbai[2], C. Poggesi[2] and F.S. Pavone[1,3]

[1]European Laboratory for Non-Linear Spectroscopy, Sesto Fno, Italy, [2]University of Florence, Sesto F.no, Italy and [3]National Institute of Optics, Florence, Italy

T-tubules are invaginations of the plasma membrane that conduct the electrical depolarization to the cardiomyocyte core, allowing a fast and synchronous Ca2+ release. We have recently developed an ultrafast random access multi-photon (RAMP) microscope that, in combination with a customly synthesized voltage-sensitive dye (VSD), is used to simultaneously measure action potentials (APs) at multiple sites within the sarcolemma with submillisecond temporal and submicrometer spatial resolution in real time. We found that the tight electrical coupling between different sarcolemmal domains is guaranteed only within an intact tubular system. In fact, we found that AP propagation into the pathologically remodeled tubular system frequently fails and may be followed by local spontaneous electrical activity (Sacconi et al. PNAS 2012). To clarify the link between tubular abnormalities and Ca2+-dependent arrhythmias, we combine the advantage of RAMP microscope with a double staining approach to optically record tubular AP and, simultaneously, the corresponding local Ca2+ transient. Isolated rat cardiomyocytes were co-loaded with the VSD and a green calcium indicator. Although the calcium and voltage probes can be excited at the same wavelength, the large Stokes shift of the VSD emission allows us to use spectral unmixing to resolve the voltage and calcium responses. The capability of our technique in probing spatiotemporal relationship between Ca2+ and electrical activity was explored in a model of acute detubulation in which failure to conduct AP in disconnected t-tubules causes local delay of Ca2+ transient rise.

Sacconi L, Ferrantini C, Lotti J, Coppini R, Yan P, Loew LM, Tesi C, Cerbai E, Poggesi C, Pavone FS; Action potential propagation in transverse-axial tubular system is impaired in heart failure; Proc Natl Acad Sci U S A. 2012; 109(15):5815-9.

The research leading to these results received funding from the European Union Seventh Framework Programme (FP7/2007–2013) under Grant Agreement 241526. This research project was also supported by Human Frontier Science Program Research Grant RGP0027/2009 and the Flagship Nanomax Project.

Where applicable, the authors confirm that the experiments described here conform with The Physiological Society ethical requirements.

SA128

Plasticity of cardiomyocyte t-tubules

O.M. Sejersted[1,2] and W.E. Louch[2,1]

[1]Univ of Oslo, Oslo, Norway and [2]Oslo University Hospital Ullevaal, Oslo, Norway

T-tubules are extensive tubular invaginations of the sarcolemma mostly located at the Z-line in cardiomyocytes. With membrane staining the t-tubules are seen to form a regular striation pattern with a sarcomere distance between the trans-

verse lines. However, the tubules are highly interconnected and wrap around the myofibrils. Here they come in close contact with the junctional part of the sarcoplasmic reticulum (SR) to form dyads where calcium induced calcium release occurs. In these specialized regions, L-type calcium channels and Na,Ca-exchangers in the t-tubule membrane, and ryanodine receptors of the SR are closely clustered. Hence efficient transmission of the action potential in the t-tubular system will provide a rapid calcium release that is synchronized throughout the cardiac cell with a short lag of a few ms (1). In failing hearts the t-tubules become disorganized and some longitudinal tubules start to appear. This reshaping of the t-tubular system contributes to dyssynchronous calcium release because a larger fraction of ryanodine receptors will be outside the dyads and calcium will have to diffuse a longer distance to activate them (1, 2). Thus, time to peak of the calcium transient becomes longer, and contraction slower. However, t-tubule disorganization can only explain part of the dyssynchrony. In failing hearts, the basic calcium release "quantum" – the spark – is altered. About 20% of sparks have a markedly slower rise time and some are quite prolonged. This variability in spark kinetics contributes to dyssynchrony of the calcium transient (3). The reason for this variability seems to be that in some dyads the ryanodine receptors become rearranged. Dyssynchrony can be partly offset by increased SR calcium content and/or increased ryanodine receptor sensitivity to calcium (2). Prolongation of the action potential in failing hearts could also contribute to dyssynchronous calcium release, but this effect seems to be offset by increased sensitivity of the ryanodine receptors (4). If the SR function is dramatically decreased by removing the calcium-pump (SERCA2) in a conditional, cardiac specific knock-out mouse model, calcium for contraction is provided across the sarcolemma (5). In these hearts t-tubules proliferate and grow longitudinally in the cell. Dyads are formed at the A-band midway between the Z-lines (6). Interestingly, in these new dyads L-type calcium channels seem to be absent, whereas Na,Ca-exchangers are found opposite the ryanodine receptors. Thus, we believe that calcium entry via Na,Ca-exchange can trigger calcium release, indicating that the growth of new longitudinal T-tubules is compensatory. Thus, existing data show that T-tubules are highly plastic structures that can grow, shrink or become disorganized in the adult cardiac cells. This has important functional consequences for the formation of dyads and the efficiency and synchrony of calcium release throughout the cell.

W. E. Louch et al., J. Physiol. (Lond) 574, 519 (2006)

L. Øyehaug et al., Biophys. J. In press, (2013)

W. E. Louch et al., J. Mol. Cell. Cardiol. (2013)

W. E. Louch et al., Biophys. J. 99, 1377 (2010)

K. B. Andersson et al., J. Mol. Cell. Cardiol. 47, 180 (2009)

F. Swift et al., Proc. Natl. Acad. Sci. U. S. A. 109, 3997 (2012)

This study was supported by The Research Council of Norway, the KG Jebsen Foundation, Anders Jahre's Fund for Promotion of Science and South-Eastern Norway Regional Health Authority

Where applicable, the authors confirm that the experiments described here conform with The Physiological Society ethical requirements.

SA129

Functional significance of atrial t-tubules: effects of heart failure

K. Dibb, J. Clarke, D. Eisner and A. Trafford

University of Manchester, Manchester, UK

T-tubules are deep invaginations of the cellular surface membrane containing a host of ion channels known to be important in excitation contraction coupling in the heart. While an important functional role for ventricular t-tubules has been well defined it has been generally assumed that the atria lacks these important structures. More recently our lab and others have demonstrated the existence of t-tubules in the atria of a number of large mammalian species including human. In cells where t-tubules are absent (small mammalian atrial myocytes) triggered release of Ca^{2+}, responsible for initiating cellular contraction, occurs only at the cell periphery. The presence of atrial t-tubules is associated with triggered Ca^{2+} release in the cell interior.

Ventricular t-tubules are decreased in heart failure, playing an important role in the pathophysiology of the disease. Using a sheep rapid paced model of heart failure (instrumented under anaesthesia with 1-4% isoflurane and analgesia provided by 0.25mg/kg meloxicam) we have shown atrial t-tubules to be virtually absent at the point of heart failure. Loss of atrial t-tubules in heart failure is associated with a reduction in the L-type Ca^{2+} current, the loss of triggered Ca^{2+} release in the cell interior and, significantly, a decrease in Ca^{2+} transient amplitude. It is therefore important to understand if t-tubules can be restored to the failing atria in order to restore function.

Following termination of rapid pacing sheep were allowed to recover from heart failure. Recovery was associated with the restoration of atrial t-tubules although these structures were extremely disordered. Preliminary data however suggests despite this disorder recovery of t-tubules may restore functional properties to the atria. Thus atrial t-tubules are not only important in normal excitation contraction coupling but also play a significant role in the pathophysiology of disease.

Where applicable, the authors confirm that the experiments described here conform with The Physiological Society ethical requirements.

SA130

Towards understanding the mechanism of T-tubule remodeling in cardiac disease

L. Song

Department of Internal Medicine, University of Iowa, Iowa City, IA, USA

The highly organized transverse (T)-tubule network is critical for rapid electric excitation and synchronous triggering of sarcoplasmic reticulum (SR) Ca2+ release, and, therefore, coordinated and efficient excitation-contraction coupling function in working ventricular myocytes. Because of the critical roles played by T-tubules, T-tubule architecture has recently become an area of considerable research interest in the cardiovascular field. Early studies from us and others have shown that the regularly arrayed T-tubule system undergoes disruptive remodeling, leading to aberrant intracellular Ca2+ release and compromised myocyte contractility, in failing myocytes from animal models and human patients. Recently, using in situ

confocal imaging technique, we showed that in a pressure overload rat cardiomyopathy model the remodeling of T-tubules starts much earlier in the disease spectrum, even prior to echocardiographically-detectable left ventricular (LV) systolic dysfunction. The T-tubule system in the LV undergoes progressive deterioration from compensated hypertrophy through early heart failure to advanced heart failure. Moreover, the integrity of T-tubule system highly correlates with cardiac ejection fraction of diseased hearts, indicating T-tubule integrity is a crucial determinant of cardiac function, and that maladaptive T-tubule remodeling is a causal event that drives the transition from compensated hypertrophy to heart failure. In more recent work, we have dissected the molecular mechanisms underlying T-tubule remodeling in heart disease, in particular the importance of junctophilin-2 (JP2), a structural protein spanning T-tubules and the SR membrane. JP2 is severely downregulated in multiple heart failure models as well as in failing human hearts. Furthermore, loss of JP expression correlates with the extent of T-tubule damage. In cultured myocytes, knockdown of JP2 using lentivirus containing a JP2 shRNA caused T-tubule disorganization. Transgenic expression of a JP2 shRNA in mice induced T-tubule structural damage, dyssynchronous and blunted Ca2+ release, and acute heart failure. These data provide compelling evidence that JP2 is a key mediator of myocyte T-tubule remodeling in cardiac disease.

Song LS, Sobie EA, McCulle S, Lederer WJ, Balke CW, and Cheng H. Orphaned RyRs in the failing heart. PNAS 2006; 103:4305-4310

Wei S, Guo A, Chen B, Kutschke W, Xie YP, Zimmerman K, Weiss R, Anderson ME, Cheng H, Song LS. T-tubule remodeling during transition from hypertrophy to heart failure. Circulation Research 2010; 107:520-531

Chen B, Li Y, Jiang S, Xie YP, Guo A, William Kutschke, Kathy Zimmerman, Robert Weiss, Francis Miller, Anderson ME, Song LS. Beta-adrenergic receptor antagonists ameliorate myocyte T-tubule remodeling following myocardial infarction. FASEB Journal 2012; 26:2531-2537

Guo A, Zhang CM, Wei S, Chen B, Song LS. Emerging mechanisms of T-tubule remodeling in heart failure. Cardiovascular Research, 2013 (May)

van Oort RJ, Garbino A, Wang W, Dixit SS, Landstrom AP, Gaur N, De Almeida AC, Skapura DG, Rudy Y, Burns AR, Ackerman MJ, Wehrens XH. Disrupted junctional membrane complexes and hyperactive ryanodine receptors after acute junctophilin knockdown in mice. Circulation. 2011;123(9):979-88

Funding support from NIH R01-090905.

Where applicable, the authors confirm that the experiments described here conform with The Physiological Society ethical requirements.

SA131

Development of CO_2 chemoceptive respiratory circuits in the mouse embryo: Insights into congenital central hypoventilation syndrome?

G. Fortin

Neurobiology & Development, CNRS, Institut de Neurobiologie Alfred Fessard, Gif sur Yvette, France

We breathe roughly half a billion times in a lifetime, generally in an effortless and even unconscious manner owing to activity of a respiratory central pattern generator (CPG) located in the hindbrain. The respiratory CPG relies on the coupling of two prominent rhythmogenic sites located in the medulla, the pre-Bötzinger Complex (preBötC) and the retrotrapezoid nucleus/para-Facial Respiratory Group (RTN). Working in the mouse embryo, we have identified the emergence of embryonic versions of these two oscillators using developmental genetics tools, electrophysiological and optical recordings. We have recently defined molecular and functional signatures for cells composing each oscillator. The talk will focus on the embryonic version of the RTN, an Egr2- (also known as Krox20-) derived, Lbx1-/Atoh1- and Phox2b-expressing group of cells located at the ventral surface of the brainstem below the facial motor nucleus.

Mutations in the neuron type-specific homeogene *Phox2b* are causative for central congenital hypoventilation syndrome (CCHS). Introducing one of the most common human mutations (*Phox2b*^{27Ala}) in mouse leads to a CCHS-like respiratory syndrome, including apneas, arythmia, and unresponsiveness to a hypercapnic challenge —and neonatal death. This mutation preserves many *Phox2b*-positive neural structures, but destroys the retrotrapezoid nucleus (RTN). Similarly, Atoh1 null mutants feature a disrupted RTN and die at birth. Electrophysiological studies have implicated the RTN in central CO2 sensitivity and perinatal entrainment of the preBötC and downstream inspiratory outputs. We have confirmed this at embryonic stages using an optogenetic approach and patterned light photostimulation targeting RTN neurons. Altogether, these data point to the RTN as a major culprit in CCHS pathogenesis. However, we also found that spatially limited expression of the *Phox2b*^{27Ala} allele can be compatible with life, while nevertheless destroying the RTN and abolishing the perinatal hypercapnic response. Thus, the central chemoreflex is dispensable for neonatal life and defects in *Phox2b*-expressing neurons outside the RTN contribute to the full CCHS-like syndrome in mouse.

Work supported by CNRS, INSERM, ANR and FRM grant to GF.

Where applicable, the authors confirm that the experiments described here conform with The Physiological Society ethical requirements.

SA132

Do the carotid bodies modulate heart rate variability and baroreflex control of blood pressure in humans?

E.A. Wehrwein[1,2], J.L. Taylor[2], A. Basu[3], T. Curry[2], R. Basu[3] and M.J. Joyner[2]

[1]Physiology, Michigan State University, East Lansing, MI, USA, [2]Anesthesia Reserach, Mayo Clinic, Rochester, MN, USA and [3]Endocrine Reserach, Mayo Clinic, Rochester, MN, USA

Hypoglycemia impacts baroreflex control of blood pressure and cardio-vagal tone. The carotid bodies are sensitive to low glucose and mediate hypoglycemic counterregulation. Peripheral chemoreceptors in the carotid body also regulate respiration, sympathetic outflow, and blood pressure by serving as multi-modal physiological sensors. We hypothesized that desensitization of the carotid bodies by hyperoxia during hypoglycemia would blunt baroreflex control of blood pressure and cardio-vagal tone. Ten young healthy adults were exposed to normoxia [PaO2 122 ± 3 mmHg] or hyperoxia [PaO2 424 ± 39] (to blunt cellular activation of the carotid body glomus cells) during a hyperinsulinemic-hypoglycemic clamp (2 mU/kg FFM/min; 3.33 mmol/L). Two 180 min hyperinsulinemic-hypoglycemic clamps were performed on each subject one week apart, randomized to either normoxia or hyperoxia ($p<0.05$). Blood pressure was monitored continuously via a brachial arterial catheter. Cardio-vagal tone was assessed via the high fre-

quency (HF) component of heart rate variability from 5 min periods of 5-lead ECG recording under baseline (euglycemia) and hypoglycemia. Mean blood pressure during hypoglycemia was significantly lower with hyperoxia than with normoxia (delta reduction from baseline: -5.4 ± 3.4 mmHg normoxia vs. -13.8 ± 1.9 mmHg hyperoxia, $p<0.05$). The typical baroreflex-mediated rise in heart rate and sympathetic activity with lower blood pressure did not occur when the carotid bodies were silenced. Area under the curve values (expressed as % normoxia response) for catecholamines during hypoglycemia were significantly suppressed by hyperoxia (norepinephrine -50.7 ± 5.2%, epinephrine -62.6 ± 3.3%, $p<0.05$ vs normoxia). HF values decreased significantly from baseline during hypoglycemia, however this reduction was attenuated under hyperoxia (Normoxia: -69% vs. Hyperoxia: -41%, $p=0.04$). Heart rate increased significantly during hypoglycemia (Normoxia: 59.7 bpm ± 2.4 vs. 71.9 ± 4.0; Hyperoxia: 60.6 bpm ± 1.9 vs. 68.5 ± 3, $p<0.001$), however, this increase was not different between normoxia and hyperoxia despite differences in cardio-vagal tone, heart rate variability, and blood pressure. These data indicate that the carotid body chemoreceptors may be partially responsible for the reduction in cardio-vagal tone associated with hypoglycemia, and they provide evidence for a role of the carotid body chemoreceptors in parasympathetic tone to the heart and sympathetic mediation of the baroreflex. Together, these data support the idea that the carotid bodies play a role in heart rate variability and baroreflex control of blood pressure in humans.

Where applicable, the authors confirm that the experiments described here conform with The Physiological Society ethical requirements.

SA133

Central chemoreceptors in developing heart failure

A. Gourine[1] and S. Kasparov[2]

[1]University College London, London, UK and [2]University of Bristol, Bristol, UK

Heart failure may lead to hypoperfusion and hypooxygenation of tissues and this is often exacerbated by central and obstructive sleep apnoeas associated with recurrent episodes of systemic hypoxia and hypercapnia/hypocapnia. Astrocytes residing in the rostral ventrolateral medulla oblongata (RVLM) may function as specialized brain chemoreceptors. They sense PCO2/pH changes and via release of ATP impart these changes on neurones of the ventral respiratory column triggering adaptive increases in the respiratory activity. We used in vitro and in vivo models to determine whether selective activation of RVLM astrocytes leads to the release of ATP, and via release of ATP increases the activity of sympathoexcitatory (pre-sympathetic) RVLM neurones. We also explored whether ATP actions in the RVLM contribute to maladaptive and detrimental sympathoexcitation in heart failure.

It was found that optogenetic activation of RVLM astrocytes transduced to express light-sensitive channelrhodopsin-2 activates sympathoexcitatory RVLM neurones in ATP-dependent manner. In anaesthetized rats in vivo, optogenetic stimulation of RVLM astrocytes increases sympathetic renal nerve activity, arterial blood pressure and heart rate. To interfere with ATP-mediated signalling by promoting extracellular breakdown of ATP, we developed a lentiviral vector to express a potent ectonucleotidase - transmembrane prostatic acid phosphatase (TMPAP) on the cellular membranes. In rats with myocardial infarction-induced heart failure, expression of TMPAP bilaterally in the RVLM led to a lower plasma noradrenaline concentration, maintained left ventricular (LV) end diastolic pressure, attenuated decline in dP/dT(max) and shifted the LV pressure-volume relationship curve to the left.

These results demonstrate that activated RVLM astrocytes are capable of increasing the activity of the brainstem sympathoexcitatory neuronal circuits while facilitated breakdown of ATP in the RVLM reduces sympathetic tone, attenuates the progression of LV remodelling and heart failure secondary to myocardial infarction. Our data provide the first experimental evidence suggesting that altered glial activity leading to higher level of "ambient" ATP in the brainstem might be responsible for the increases in sympathetic tone and by doing so contribute to the development and progression of heart disease associated with increased activity of the sympathetic nervous system.

The research in our laboratories referred to in this abstract was funded by The Wellcome Trust and the British Heart Foundation.

Where applicable, the authors confirm that the experiments described here conform with The Physiological Society ethical requirements.

SA134

Significance of the carotid body in insulin resistance and hypertension

S.V. Conde[1], M.J. Ribeiro[1], J.F. Sacramento[1], C. Gonzalez[2], A. Obeso[2] and G.P. Maria[1]

[1]Pharmacology, CEDOC, Faculdade Ciencias Médicas, Universidade NOVA, Lisboa, Portugal and [2]Bioquimica, Biologia Molecular e Fisiologia, Universidad de Valladolid, Facultad de Medicina. Instituto de Biología y Genética Molecular, CSIC. Ciber de Enfermedades Respiratorias, CIBERES, Instituto de Salud Carlos III, Valladolid, Spain

Increased sympathetic activity is a well-known pathophysiological mechanism in insulin resistance (IR) and hypertension (HT). The carotid bodies (CBs) are arterial chemoreceptors being PO2, PCO2/pH sensors-efectors which upon a decrease in PO2 or a PCO2/[H+] increase, release neurotransmitters that regulate the firing rate in the sensory fibres of the carotid sinus nerve (CSN). CSN activity is integrated in the brain stem to induce a fan of respiratory reflexes aimed, primarily, to normalize the altered blood gases via hyperventilation (Gonzalez et al.1994) and to regulate blood pressure and cardiac performance via sympathetic nervous system activation (Marshall 1994). The CB directly activates the adrenals via increased sympathetic drive and also increases sympathetic vasoconstrictor outflow to muscle, splanchnic, and renal beds (Marshall 1994; Cao & Morrison 2001). Recently, the CB was proposed to be a glucose sensor (Pardal & López-Barneo 2002) and implicated in energy homeostasis control (Koyama et al. 2000). However, to date no studies have anticipated its role in the development of IR. The aim of this work was to investigate the role of the CB in the pathogenesis of IR and HT.

Experiments were performed in Wistar rats (200–420 g) of both sexes, aged 3 months. Two diet-induced IR and HT animal models were used: the rat submitted to a high-fat (HF) diet, a model that combines obesity, IR and HT and the rat submitted to a high-sucrose (HSu) diet, a lean model of combined IR and HT. To test the hypothesis that CB activity is increased in IR and HT animal models we compared HF and HSu with control group. To evaluate the contribution of CB to the gen-

esis of IR and HT, bilateral resection of CSN was performed 5 days prior to submitting the animals to standard or hypercaloric diets. These procedures were performed in aseptic conditions under ketamine (30mg/kg)/xylazine (4mg/kg) anaesthesia and brupenorphine (10microg/kg) analgesia. Additionally, rats fed with standard diet were used to investigate if insulin triggers CB activation. All measurements were performed with animals under sodium pentobarbital (60 mg/kg i.p.) anaesthesia.

We demonstrated that CB activity was increased in diet-induced animal models of IR and HT. CB-mediated basal ventilation and ventilation in response to ischemic hypoxia were increased in the pathological models tested, as well as the CB chemoreceptor cell function - assessed both as hypoxia induced-release of dopamine and as tyrosine hydroxilase expression. We have also observed that CSN bilateral resection totally prevented diet-induced IR and HT, as well as increased fasting glicemia, fasting insulinemia, free fatty acids and systemic sympathoadrenal overactivity. Moreover, we showed that insulin triggers CB, highlighting a new role for hyperinsulinemia as a stimulus for CB-overactivation. We demonstrated that insulin receptors are present in the CB and that its phosphorylation increases in response to insulin. Additionally, we showed that insulin was capable of initiating a neurosecretory response measured as the increase in intracellular Ca2+ and the release of the neurotransmitters, ATP and dopamine, that is transduced into an increase in ventilation.

We propose that CB is implicated in the pathogenesis of metabolic and hemodynamic disturbances through sympathoadrenal overactivation and may represent a novel therapeutic target in these diseases.

Gonzalez C, Almaraz L, Obeso A, Rigual R.. Carotid body chemoreceptors: from natural stimuli to sensory discharges. Physiol Rev 1994; 74: 829-98.

Marshall JM. Peripheral chemoreceptors and cardiovascular regulation, Physiol Rev 1994; 74:543-94.

Cao WH, Morrison SF. Differential chemoreceptor reflex responses of adrenal preganglionic neurons. Am J Physiol Regul Integr Comp Physiol 2001; 281: R1825-32.

Pardal R, López-Barneo J. Low glucose-sensing cells in the carotid body. Nat Neurosci 2002; 5:197-8

Koyama Y, Coker RH, Stone EE et al.. Evidence that carotid bodies play an important role in glucoregulation in vivo. Diabetes 2000; 49:1434-42

Supported by Portuguese Foundation for Science and Technology PTDC/SAU-ORG/111417/2009 and by 2009 L'Oreal Medals of Honour for Women in Science.

Where applicable, the authors confirm that the experiments described here conform with The Physiological Society ethical requirements.

SA135

Noradrenergic neurons and control of the central and peripheral chemoreflex

L. Gargaglioni

Animal Morphology and Physiology, Sao Paulo State University, Jaboticabal, Sao Paulo, Brazil

The noradrenergic cell groups provide neural inputs to almost all brain areas including the respiratory network. Developmental dysfunctions in these neurons are linked to pathological conditions such as Rett syndrome and Sudden Infant Death, which can impair the control of the cardio-respiratory system and coordination of the sleep-waking cycle. We have been evaluating the involvement of A5 and A6 (locus coeruleus - LC) cell groups in the cardiorespiratory response to central (7-10% CO_2 in air) and peripheral (7-10% O_2) chemoreflex stimulation. A reduction of approximately 80% of noradrenergic (NA) neurons of LC is associated with a large decrease in the respiratory response to CO_2 of approximately 64%, indicating that this nucleus exerts a profound effect on the CO_2-drive to breathe, but no effect is observed during low O_2 conditions (Biancardi et al., 2008; 2010). These data suggests the specific role of LC NA neurons in the ventilatory response to high CO_2 rather than to hypoxia. Many neurotransmitters/neuromodulators have been demonstrated to be involved in the modulation of the LC response, such as serotonin, orexin, glutamate, ATP and also the GAP junctions (Gargaglioni et al., 2010). As to cardiovascular response, chemical lesion of the LC with 6-hydroxydopamine (6-OHDA) does not affect mean arterial pressure and heart rate during normocapnia and hypercapnia, indicating that noradrenergic LC neurons are unlikely to play a significant role in the control blood pressure and heart rate. However, lesion of LC using substance P-saporin conjugate (SP-SAP), that kills NK-1 immunoreactive (NK1R-ir) neurons, increase the heart rate during hypercapnia, suggesting that NK1R-ir neurons in the LC, probably the GABAergic ones, may modulate heart rate during CO2 exposure, since Glutamic Acid Decarboxylase immunoreactivity decreases after SP-SAP lesion (de Carvalho et al., 2010). Regarding A5 region, the role of this NA group in central and peripheral chemoreflex is strongly dependent on the state of the animal, anesthetized or unanesthetized. In unanesthetized animals, A5 noradrenergic neurons exert an excitatory modulation on the ventilatory response to hypoxia but do not affect cardiorespiratory control during CO_2 exposure. However, in urethane-anesthetized animals, A5 noradrenergic neurons contribute to the sympathoexcitation and the increase in phrenic nerve activity produced by raising the end-expiratory CO_2 (Taxini et al., 2011). In addition, under anesthesia, these noradrenergic neurons are not involved in autonomic regulation elicited by peripheral chemoreflex activation.

Biancardi V, Bícego KC, Almeida MC, Gargaglioni LH. Locus coeruleus noradrenergic neurons and CO2 drive to breathing. Pflugers Arch. 455(6):1119-28, 2008.

Biancardi V, da Silva LT, Bícego KC, Gargaglioni LH. Role of locus coeruleus noradrenergic neurons in cardiorespiratory and thermal control during hypoxia. Respir Physiol Neurobiol. 170(2):150-6, 2010.

Gargaglioni LH, Hartzler LK, Putnam RW. The locus coeruleus and central chemosensitivity. Respir Physiol Neurobiol. 173(3):264-7, 2010.

de Carvalho D, Bícego KC, de Castro OW, da Silva GS, Garcia-Cairasco N, Gargaglioni LH. Role of neurokinin-1 expressing neurons in the locus coeruleus on ventilatory and cardiovascular responses to hypercapnia. Respir Physiol Neurobiol. 172(1-2):24-31, 2010.

Taxini CL, Puga CC, Dias MB, Bícego KC, Gargaglioni LH. Ionotropic but not metabotropic glutamatergic receptors in the locus coeruleus modulate the hypercapnic ventilatory response in unanesthetized rats. Acta Physiol (Oxf). 2013 Feb 15. doi: 10.1111/apha.12082.

Taxini CL, Takakura AC, Gargaglioni LH, Moreira TS. Control of the central chemoreflex by A5 noradrenergic neurons in rats. Neuroscience.199:177-86, 2011.

Financial Support: FAPESP, CNPq and INCT of Comparative Physiology

Where applicable, the authors confirm that the experiments described here conform with The Physiological Society ethical requirements.

SA136

Perception and the expectation of reward

K. Krug

Physiology, Anatomy & Genetics, Oxford University, Oxford, UK

The effect of reward is thought to be pervasive. It affects our motor actions and our sensory judgements. We have investigated the influence of reward on perceptual decision-making at multiple levels in humans and macaque monkeys. We set up a behavioural paradigm that could be employed with both species. The perceptual decision-making task involved reporting the direction of rotation of a structure-from-motion cylinder made up of two transparent sheets of random dots. Cylinder rotation could be disambiguated by applying binocular disparity to separate the front and back surface of the cylinder. This allowed us to present a range of stimuli in each experiment, including the case of an ambiguous cylinder stimulus whose direction of rotation could either be perceived as clockwise or counterclockwise on a given trial.

Two Rhesus macaques were each implanted with a headpost, eye coils and a recording chamber under general anaesthesia (7-8 mg/kg/hr alfaxalone/alfadolone acetate i.v. or 1-3% isoflurane gas, to effect) (Dodd et al 2001; Read and Cumming 2003). They were trained to report the direction of rotation of the cylinder by making a saccade to one of two choice targets. They received a fluid reward for a correct decision; for ambiguous stimuli they received a fluid reward on 50% of randomly selected trials. The amount of fluid they received increased in a predictable fashion after two and then four consecutive, correct choices. We used electrical microstimulation in extra-striate visual area V5/MT to distinguish the separate roles of sensory neural signals arriving in V5/MT (and therefore not influenced by microstimulation) from the combined neuronal signals downstream of V5/MT (which are influenced by microstimulation). Electrical stimulation of a cluster of neurons selective for a particular direction of cylinder rotation biased visual perception. Psychometric functions for discrimination of cylinder rotation were consistently shifted, with the animal making more choice in the preferred direction of cylinder rotation at the stimulation site. Importantly, the size of this electrical microstimulation effect on the psychometric function was different when the reward available at the end of a trial was large or small (Wilcoxon signed-rank test: $p<0.001$, $n = 48$ stimulation sites). This result suggests that reward affected sensory signals separately from the artificially introduced electrical signal rather than simply acting upon the combined neural signal downstream of V5/MT. When we fitted psychometric functions with a simplified drift diffusion model, the best fitting model required a significant change in drift rate as well as a change in bound, indicating that reward affects both the early sensory stages and the later decision-related stages of cortical processing.

Further evidence for this conclusion comes from a study with six human participants carrying out the same perceptual task under different reward conditions, in which the reward is points converted into money at the end of the experiment. Preceding each trial, human participants were cued to indicate whether both choices were rewarded equally or one higher than the other (8 versus 1 point). Only correct responses were rewarded; for ambiguous stimuli, half the trials were rewarded at random. Feedback of points scored was given at the end of every trial and the cumulative score was given at regular intervals during the experiment. Under these conditions, participants showed a consistent behavioural response bias towards more highly rewarded choices for the same cylinder stimulus. Analysis with a drift diffusion model again implicated changes in drift rate to account for the effect of reward, the stimulus parameter that represents the strength of the sensory evidence being integrated to the decision (Model fit t-test comparison across individuals, $p<0.05$). Human magnetoencephalography (MEG) recordings with a beamformer analysis showed that after the cue onset but prior to stimulus onset, there was activation for biased reward conditions over balanced reward in both V5/MT at around 475 msec and dorsolateral prefrontal cortex (dPFC) at 590 msec. When the cylinder stimulus on a given trial had a direction of rotation that was highly not lowly rewarded, we found cortical activation in the precuneus in visual cortex at 85 msec after stimulus onset followed by dPFC at 125 msec and other prefrontal areas during stimulus presentation.

These results, obtained with humans and monkeys, show that signals in visual cortex are affected by the reward available on a given trial. This suggests that in perceptual decision tasks, one mechanism by which reward could influence behaviour might be through biasing of signals in the visual processing areas of the brain.

Dodd JV, Krug K, Cumming BG, Parker AJ (2001) J Neurosci 21, 4809-21.

Read JC, Cumming BG (2003) J Neurophysiol 90, 946-60.

My insightful collaborators are Nela Cicmil, Andrew Parker and Bruce Cumming. This work was supported by Royal Society, Wellcome Trust and NIH.

Where applicable, the authors confirm that the experiments described here conform with The Physiological Society ethical requirements.

SA137

Reconciling rapid neuronal and perceptual adaptation to motion

N. Price

Physiology, Monash University, Clayton, VIC, Australia

Prolonged exposure to an "adapting" visual stimulus improves our ability to detect and discriminate subsequently viewed "test" stimuli that have similar properties to the adaptor. These changes in perceptual sensitivity are often accompanied by reductions in the firing rates and shifts in the tuning curves of sensory neurons. Adaptation may help reduce the redundancy of neural codes, improving how the brain represents prevailing stimulus conditions. It allows a dynamic trade-off between the range of stimuli that can be represented by a neuron's firing rate and the minimum detectable difference between stimuli. The best functional example of adaptation comes from the retina, where ganglion cells can encode luminance over many orders of magnitude, but adaptation can shift the sensitivity of individual neurons to optimally represent the prevailing conditions. However, the links between neuronal and perceptual adaptation remain poorly understood for even basic stimulus properties such as colour, shape and motion. In particular, while adaptation is well characterised at the level of single neurons, few studies have examined how adaptation affects the responses of populations of neurons. This is important, because perception depends on both the firing rates, and structure of response correlations, across a population of neurons. To better understand how adaptation affects sensory encoding by neuronal populations, we implanted multi-electrode arrays in a range of visual cortical areas in anaesthetised mar-

mosets. The marmoset is an ideal model for array recordings because its smooth cortical surface ensures most brain areas are readily accessible with electrode arrays. We recorded visual-evoked spiking activity at up to 128 sites in V1, V2 and the dorso-medial area (DM). We used two main stimulus sets: first, direction tuning was characterised in an unadapted case using moving gratings; second, direction tuning was characterised after adaptation to 1-2 seconds of sustained exposure to motion in a single direction. In addition, we characterised the receptive field locations of all neurons.

At the single neuron level, the effects of adaptation depended on the cortical area. In all areas, neuronal gain, or the peak firing rate evoked by a test stimulus, was reduced following adaptation, regardless of the relationship between a neuron's preferred direction and the adaptation direction. In V1/V2, adaptation produced "repulsive" changes in tuning, such that the post-adaptation preferred direction was shifted away from the adaptation direction. Surprisingly, in DM, no consistent changes in direction tuning were observed following adaptation.

To characterise effects at the population level, we determined spike-count correlations (rSC). For each pair of neurons, rSC is the Pearson correlation between the spike counts evoked by multiple repetitions of an identical stimulus. Before adaptation, rSC between a pair of neurons was highest when the neurons had similar preferred directions and had the greatest level of overlap in their receptive fields. This is expected from previous work, and reflects the larger proportion of inputs shared between neurons with similar sensitivity. After adaptation, average rSC across the population remained constant, but the structure of correlations changed in a tuning-dependent manner. rSC decreased for neurons with similar direction preferences, leading to a smaller range of correlations across the population.

We argue that this decorrelation is a way of optimising sensitivity to the prevailing stimulus conditions, consistent with Barlow's original hypothesis that adaptation decorrelates the activity of a neuronal population to reduce redundancy. However, the tuning-dependence of the decorrelation suggests that adaptation is only able to affect a limited range of inputs to a population of neurons, notably those that are shared locally, between neurons with similar preferences, rather than those that are globally shared across all neurons in an area. The implications of this tuning-dependent correlation for perception are captured in a population decoding model.

HFSP - Career Development Award

NHMRC - Project Grant APP1008287

Where applicable, the authors confirm that the experiments described here conform with The Physiological Society ethical requirements.

SA138

Perception and action in three-dimensional vision

P. Janssen

KU Leuven, Leuven, Belgium

The visual analysis of three-dimensional (3D) shape relies on a network of cortical areas in the primate ventral (Janssen et al., 2000) and dorsal (Srivastava et al., 2009) visual stream. Previous studies have emphasized that distinct neural representations of disparity-defined 3D shape exist in the inferior temporal cortex (ITC), the posterior parietal cortex (area AIP) and even in the premotor cortex (area F5a). Here I will review a series of studies that relate the neural selectivity in these cortical areas to perception and action. Using a combination of single-cell recordings, fMRI, electrical microstimulation and reversible inactivation in behaving macaque monkeys (Maccaca mulatta), I will argue that the extensive processing of 3D shape subserves different behavioral goals. Specifically, neural activity in ITC correlates with perceptual choice (Verhoef et al., 2010), and microstimulation in ITC predictably alters the categorization of convex and concave 3D shapes and accelerates the time to decision (Verhoef et al., 2012). In contrast, 3D-shape selective neurons in the parietal (AIP) and premotor cortex (F5a) are also active during grasping of 3D objects (Theys et al., 2012; Theys et al., 2013), and reversible inactivation of clusters of 3D-shape selective neurons in AIP produces a strong grasping deficit but no perceptual deficit. Furthermore microstimulation of AIP produces weak effects on 3D-shape categorization and generally prolongs the decision time (Verhoef et al., in preparation). Finally, microstimulation of 3D-shape selective AIP neurons during fMRI reveals the functional connectivity of these neurons: consistent with the known anatomical connectivity, AIP microstimulation selectively activates F5a in the ventral premotor cortex and area CIP in the posterior Intraparietal sulcus. Thus a combination of research techniques and behavioral tasks can clarify how 3D shape processing is related to both perception and action.

Janssen P, Vogels R, Orban GA (2000) Three-dimensional shape coding in inferior temporal cortex. Neuron 27:385-397.

Srivastava S, Orban GA, De Maziere PA, Janssen P (2009) A distinct representation of three-dimensional shape in macaque anterior intraparietal area: fast, metric, and coarse. J Neurosci 29:10613-10626.

Theys T, Pani P, van LJ, Goffin J, Janssen P (2012) Selectivity for three-dimensional shape and grasping-related activity in the macaque ventral premotor cortex. J Neurosci 32:12038-12050.

Theys T, Pani P, van LJ, Goffin J, Janssen P (2013) Three-dimensional Shape Coding in Grasping Circuits: A Comparison between the Anterior Intraparietal Area and Ventral Premotor Area F5a. J Cogn Neurosci 25:352-364.

Verhoef BE, Vogels R, Janssen P (2010) Contribution of inferior temporal and posterior parietal activity to three-dimensional shape perception. Curr Biol 20:909-913.

Verhoef BE, Vogels R, Janssen P (2012) Inferotemporal cortex subserves three-dimensional structure categorization. Neuron 73:171-182.

Supported by the FWO Vlaanderen (G.0713.09), ERC-StG-260607, Programmafinanciering PFV10/008, Geconcerteerde Onderzoeksacties GOA 10/19

Where applicable, the authors confirm that the experiments described here conform with The Physiological Society ethical requirements.

SA139

The neural mechanisms involved in finding objects and switching between targets

N.C. Rust

Psychology, University of Pennsylvania, Philadelphia, PA, USA

Finding specific objects and switching between targets requires the flexible integration of visual and task-specific information. To investigate how the brain solves a target-switching task, we recorded neural responses in perirhinal cortex (PRH) and its primary input, inferotemporal cortex (IT) as subjects performed a task that required finding different targets in different blocks of trials. Our results suggest that visual and

target information are initially combined within or before IT in a "tangled" or nonlinearly separable manner, followed by "untangling" computations in PRH that reformat this information such that it is more accessible via a linear read-out. These computations culminate in a subpopulation of "bingo neurons" in PRH that fire whenever a target is currently in view, across changes in target identity.

This work was supported by the National Eye Institute (R01EY020851)

Where applicable, the authors confirm that the experiments described here conform with The Physiological Society ethical requirements.

SA140

Progression of target-to-gaze command coding in superior colliculus and frontal eye fields during head unrestrained gaze shifts

D. Crawford

Psychology, York University, Toronto, ON, Canada and Centre for Vision Research, York University, Toronto, ON, Canada

The most fundamental question in sensorimotor physiology is, 'how do neurons transform sensory information into motor commands'? Take for example the case of visuospatial transformations for gaze control (where gaze is the product of both eye and head movement). The input is clearly target location relative to the retina, and the output is clearly muscular commands for eye rotation relative to the head and head rotation relative to the body, but the intermediate transformations are difficult to pinpoint. Distinguishing between different intermediate codes is made difficult by their relative similarity (e.g., target angle, gaze angle, eye and head rotation) relative to the variability of behavior and neural noise.

Our solution to this has been to develop a method that allows one to map visual and motor response fields (RFs) relative to different possible representations (i.e., target position, gaze, eye, and head displacement or final position) in various frames of reference, i.e., relative to eye, head, or space (see figures). This allows a number of 'model fits', whereby we determine the best fit to be the one that produces the least residuals of raw neural data to the model (Keith et al. 2009). In our first application of this method (DeSouza et al. 2011), we found that the bursts of neural activity in the superior colliculus (SC) during head unrestrained gaze shifts made directly to briefly flashed visual targets dominantly code the location of the target relative to initial eye orientation, rather than the detailed parameters of the gaze, eye, or head movement.

Here, we performed similar experiments on the SC and frontal eye fields (FEF) in two rhesus monkeys, the key structures involved in outputting early visual signals and gaze commands to the brainstem. To isolate the question of visual-motor transformation we used a delayed memory task where animals were required to continue fixating briefly for a variable time between seeing the target and shifting their gaze. Target positions were varied throughout the RF of each neuron tested, and initial gaze fixations were varied (along with natural animal-selected variations of initial eye and head position) to allow us to separate the spatial frame of the neural code. Three-dimensional (3-D) eye and head orientations were recorded so that we could account for small torsional 'twists' of the eye around the line of site, and for correct mathematical analysis.

For the SC (Sadeh et al. 2012), we found that the visual response (to the appearance of the target) of all of the neurons we tested gave the best fit to target relative to initial eye orientation (Te). Perhaps surprisingly, in 'visuomotor' neurons that showed both a visual response and a motor response during the gaze shift, the motor response also coded for Te. It was only in cells that did not have any visual response that the motor response fit best to a motor parameter: final gaze position relative to initial eye orientation (Ge; or the mathematically similar gaze displacement model Gd). Note that these gaze models were spatially separable from target models because we allowed monkeys to be somewhat 'sloppy' with their final gaze positions around each target.

For the FEF (Sajad et al. 2012), a similar picture emerged, especially in the visual responses, but in FEF cells all motor responses preferred Ge over Te (see Figures). Since many FEF cells showed both visual responses (fitting Te) and motor responses (fitting Ge), we also looked at the memory delay activity between them, and found a gradual progression of activity fitting best along the continuum between Te and Ge, leading up to the gaze shift. In none of our 71 SC neurons or 64 FEF neurons did we observe a response that significantly preferred an individuated motor effector (eye or head) or a non-eye-centered frame of reference.

These results show that –although the SC and FEF show subtle differences in our paradigm— they both employ similar eye-centered codes for vision and gaze. This finding suggests that such codes are only worked out a later stage of the visuomotor transformation- most likely in the brainstem. More interestingly, we have shown that both of these structures are involved with intrinsic transformations of target-based spatial codes to gaze motor codes, not only between different cell and response types, but within some cortical neurons, across time for different aspects of the task. Since these are fundamental properties of neural coding, one expects similar principles to apply to the early stages of other sensorimotor transformations.

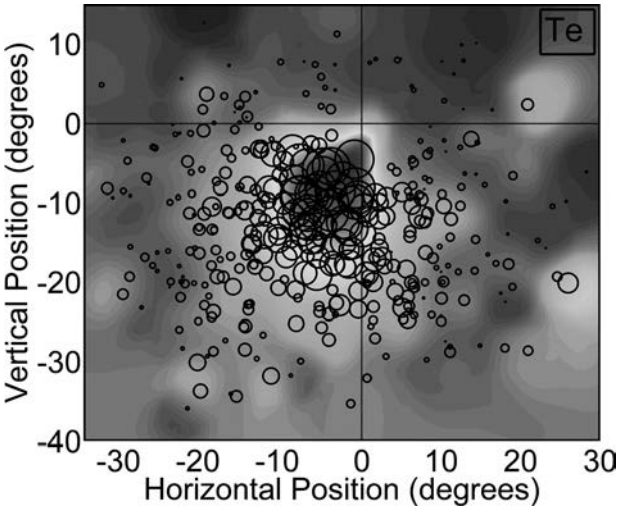

Visual response field (RF) for a frontal eye field (FEF) neuron. Circle size indicates number of action potentials evoked by (80-180ms after) target presentation during individual trials. The grey scale indicates a non-parametric fit to these individual trials. Data are plotted in the coordinates that gave the lowest residuals between individual trials and the fit: angle of target position relative to initial 3-D eye orientation (Te).

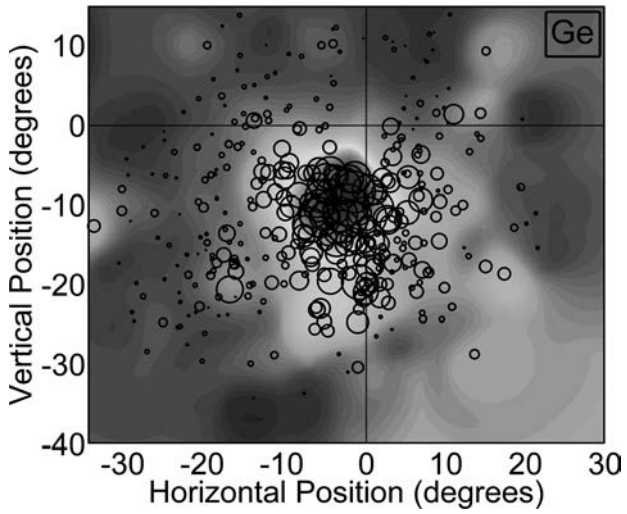

Motor response field (RF) for the same frontal eye field (FEF) neuron. Circle size indicates number of action potentials occurring during the gaze shift for individual trials. The grey scale indicates a non-parametric fit to these individual trials. Data are plotted in the coordinates that gave the lowest residuals between individual trials and the fit: angle of final gaze position relative to initial 3-D eye orientation (Ge).

Keith et al. (2009) J Neurosci Meth 180, 171-84.

DeSouza et al. (2011) J Neurosci 31, 18313-18326.

Sadeh et al. (2012) Soc Neurosci Abst 419.10.

Sajad et al. (2012) Soc Neurosci Abst 419.01.

This work is funded by the Canadian Institutes of Health Research. J.D. Crawford is supported by a Canada Research Chair.

Where applicable, the authors confirm that the experiments described here conform with The Physiological Society ethical requirements.

SA141

Nutrient sensing of Group C GPCRs

H. Bräuner-Osborne

Department of Drug Design and Pharmacology, University of Copenhagen, Copenhagen, Denmark

G protein-coupled receptors (GPCRs) are divided into Group A, B and C receptors based on phylogenetics. The majority of Group C GPCRs consist of a large extracellular 'Venus Flytrap' domain and Cystein-rich domain followed by a 7-transmembrane domain. The 'Venus Flytrap' domain is homologous to periplasmic binding proteins which act as amino acid and nutrient transporters in bacteria. Likewise, human Group C GPCRs have been shown to binds amino acids, cations and sugars and thus potentially act as nutrient sensors in mammals [1]. We have paid particular interest to the Group C receptor entitled GPRC6A, which will be the focus of the present talk. In 2004 we reported the cloning and tissue expression of the GPRC6A receptor [2]. Using a variety of pharmacological assays at the human, mouse and rat receptor orthologs expressed in Xenopus laevis oocytes and mammalian cell lines, we have shown that the receptor is Gq coupled and promiscuously activated by L-amino acids of which the basic L-amino acids L-Arg, L-Lys and L-ornithine are the most potent [3-4]. In addition, we have shown that the receptor is co-activated by divalent cations such as calcium [4-5]. Unfortunately, these endogenous agonists also act on a range of other targets, which decreases their use as pharmacological tool compounds. Novel tools are thus warranted to study the physiological function of the receptor including its potential role as nutrien sensor. To this end, we recently reported the first GPRC6A selective negative allosteric modulators (NAMs). The NAMs, based on so-called privileged structures containing a 2-phenyl-indole scaffold, were inferred from family A receptors using chemogenomics [6]. Another strategy has been to develop a GPRC6A knockout mouse where exon 6 containing the entire 7TM domain was removed. We have shown that the GPRC6A knockout mice had wild-type-like growth rate [7] body composition and glucose metabolism [8] when fed a regular chow diet. However, when the mice are fed a 60% high fat diet the knockout mice become more obese than their wild-type littermates and show impaired glucose metabolism [9]. Given that the GPRC6A receptor is expressed in the islets of Langerhans and that L-amino acids such as L-Arg are known to increase insulin secretion, we hypothesized that the impaired glucose metabolism could be caused by decreased L-amino acid insulin secretion. However, both ex vivo experiments on isolated islets and in vivo experiments demonstrate that the GPRC6A knockout mice demonstrate wild-type-like L-Arg mediate insulin release [8]. Collectively, these studies of our GPRC6A knockout mice indicate a role as nutrient sensor. However, further studies are needed to delineate the precise mechanisms of the observed phenotype.

References:

1. Wellendorph et al. Mol. Pharmacol. 2009; 76: 453-465.
2. Wellendorph and Bräuner-Osborne, Gene 2004; 335: 37-46.
3. Wellendorph et al. Mol. Pharmacol. 2005; 67: 589-597.
4. Wellendorph et al. Gene 2007; 396: 257-267.
5. Christiansen et al. Br. J. Pharmacol. 2007; 150: 798-807.
6. Gloriam, Wellendorph, Johansen et al. Chem. Biol. 2011; 18: 1489-1498.
7. Wellendorph et al. J. Mol. Endocrinol. 2009; 42: 215-223.
8. Smajilovic et al. Amino Acids. 2013; 383-390.
9. Clemmensen, Smajilovic et al. Submitted.

Where applicable, the authors confirm that the experiments described here conform with The Physiological Society ethical requirements.

SA142

Dietary programming of hypothalamic nutrient-sensing

N. Balthasar, M. Wherlock, H. Weir, A. Simpson and L. Dearden

School of Physiology and Pharmacology, University of Bristol, Bristol, UK

How do dynamically modulated neuronal transcriptomes underpin long-term adaptive changes that lead to positive processes, such as learning, or negative adaptations, like failure to sense metabolic state? This is a core question in neurobiology and ultimately CNS-mediated disease and my lab is using hypothalamic nutrient-sensing as a model to investigate the programmes supporting such neuronal plasticity.

Hypothalamic nutrient-sensing is critical for maintenance of appropriate body weight and glucose homeostasis. However, in clinical situations such as obesity and type 2 diabetes, but also recurrent hypoglycemia in type 1 diabetes, hypothalamic nutrient-sensing fails and adjustment of metabolic balance is lost. In addition to a continued rise in obesity and diabetes in an adult population, early life events are major determinants of obesity and diabetes risk with in utero exposure being of particular importance. With an increasing number of obese,

diabetic mothers, maternal programming of offspring metabolic homeostasis adds momentum to the 'obesity epidemic'. Our recent data investigate the neuroadaptive mechanisms underpinning neuronal responses to metabolic state. Indeed, many neuroadaptative responses are downstream of the induction of transcription factors and subsequent regulation of gene expression, which can have long-lasting effects on neuronal function. We have recently described a mechanism linking hypothalamic glucose-sensing with CRE-gene transcription via activation of a CREB co-activator and linked the subsequently induced transcriptome to the regulation of food intake. In addition, we demonstrate that maternal diet has significant effects on offspring hypothalamic transcriptome regulation and subsequently metabolic balance.
By combining the use of neuronal subpopulation-specific genetically modified mouse models with genome-wide transcriptomics and epigenomics approaches we are in the process of identifying mechanisms in environmental- and disease-mediated modifications of neuronal transcriptomes causing neuronal dysfunction.

Where applicable, the authors confirm that the experiments described here conform with The Physiological Society ethical requirements.

SA143

Brain lipid sensing and nervous system control of energy balance

B.E. Levin

Neurology Service (127C), VA Medical Center, East Orange, NJ, USA

Energy homeostasis is regulated by a constant dialogue between metabolic and hormonal sensors in the periphery and the brain. Long chain fatty acids (LCFA) provide an important metabolic substrate that is sensed by specialized receptors and transporters located on metabolic sensing neurons that are widely distributed throughout the brain. These neurons alter their activity in response to a variety of other metabolic substrates and hormones. The LCFA receptor/transporter CD36 regulates LCFA sensing in more than half of the ventromedial hypothalamic (VMH) metabolic sensing neurons. Depletion of rat VMH CD36 alters body weight, food intake, carcass fat deposition, insulin sensitivity and linear growth depending upon the strain and age of rat used. But neuronal FA sensing is also markedly influenced by astrocyte-produced ketone bodies, especially in the face of high fat diet intake. This ketone production overrides the CD36-mediated FA sensing pathway and thereby alters food intake. Thus, neuronal FA sensing plays an important role in regulating energy homeostasis and is markedly influenced by dietary fat content.

Levin, B. E., et al. (2011). "Metabolic Sensing and the Brain: Who, What, Where, and How?" Endocrinology 152(7): 2552-2557.

Le Foll, C., et al. (2009). "Characteristics and mechanisms of hypothalamic neuronal fatty acid sensing." Am J Physiol Regul Integr Comp Physiol 297(3): R655-664.

Le Foll, C., et al. (2009). "Effects of maternal genotype and diet on offspring glucose and fatty acid sensing ventromedial hypothalamic nucleus neurons." Am J Physiol Regul Integr Comp Physiol 297(5): R1351-R1357.

This work was funded by the Research Service of the Veterans Administration and the National Institute of Diabetes, Digestive and Kidney Diseases.

Where applicable, the authors confirm that the experiments described here conform with The Physiological Society ethical requirements.

SA144

Neural circuitry organizing behavioral responses to nutrient and electrolyte availability

G.L. Yosten

Pharmacological and Physiological Science, Saint Louis University, Saint Louis, MO, USA

Although the brain is capable of sensing a variety of nutrient signals, it must integrate those signals and generate an appropriate behavioral response. The Central Melanocortin System, composed of proopiomelanocortin (POMC)/alpha-MSH-producing neurons originating in the arcuate nucleus of the hypothalamus or the nucleus of the solitary tract, is perfectly positioned to integrate nutritional signals of both peripheral and central origin. Several neural systems have been implicated as downstream effectors of melanocortin actions; however, the organization and order of activation of those systems is only now becoming understood. Using pharmacological approaches in whole animal models, we have confirmed the association of the Central Melanocortin System with downstream activation of central corticotropin releasing hormone (CRH) receptors and the central oxytocin system. Furthermore, we have delineated the organization of this essential circuit, in that activation of CRH receptors occurs after stimulation of POMC neurons, which in turn leads to the activation of the central oxytocin system. Interestingly, although this circuit appears to be important for the regulation of feeding behavior, an alternative and as yet unknown circuit underlies the cardiovascular actions of the central melanocortin system. These findings may have important implications for the pathogenesis of obesity and its associated complications, including obesity-associated diabetes and hypertension.

Where applicable, the authors confirm that the experiments described here conform with The Physiological Society ethical requirements.

SA145

Physiological biased signaling by the actions of Ca^{2+}_o or L-amino acids on the calcium-sensing receptor

A.D. Conigrave

University of Sydney, Sydney, NSW, Australia

The calcium-sensing receptor (CaSR) is a nutrient-sensing receptor that mediates feedback regulation of systemic calcium homeostasis in fetal and postnatal life, and also plays key roles in cell fate determination (survival, proliferation and differentiation) acting to support complex development programs for diverse organs including the CNS and lung (1). In this respect the receptor provides a 'switch' function that arises firstly from its expression in the presence of activating concentrations of Ca^{2+} and other nutrients, and secondly from local or systemic modulation of nutrient levels.
The CaSR's more general role in nutrient sensing arises from its membership of the taste receptor sub-group of GPCR class C. This it senses not only Ca^{2+} and Mg2+ ions but also L-amino acids (review: (2)) by which it plays roles in coordinating gastrointestinal responses to ingested dietary protein e.g., via

stimulating the release of enteric hormones including gastrin, cholecystokinin, GLP, GIP and PYY.

To achieve these diverse roles the CaSR exhibits ligand-directed (biased) signaling by which certain but not all ligands are restricted in their access to specific signaling pathways. The most striking comparison is between Ca^{2+} and L-Phe. Ca^{2+} activates all known pathways downstream of the receptor and its interactions with $G_{q/11}$, $G_{i/o}$ and $G_{12/13}$. L-Phe, on the other hand, activates a restricted set of signaling pathways downstream of $G_{q/11}$ and $G_{i/o}$ that appear to limit its actions primarily to the acute control of peptide hormone secretion.

The mechanisms that underlie these physiologically important restrictions on L-amino acid-dependent signaling are starting emerge and appear to include not only the adoption of ligand-specific receptor conformations but also posttranslational modifications such as PKC-dependent phosphorylation of CaSR residue T888.

The physiological significance of amino acid dependent signaling is being revealed in transgenic mice in which the CaSR's sensing functions for L-amino acids and Ca^{2+}_o have been dissociated.

Riccardi D, Kemp P. The calcium-sensing receptor beyond extracellular calcium homeostasis: conception, development, adult physiology, and disease. Annu Rev Physiol. 2012;74:271-297.

Conigrave AD, Hampson DR. Broad-spectrum amino acid-sensing class C G-protein coupled receptors: molecular mechanisms, physiological significance and options for drug development. Pharmacol Therap. 2010;127:252-260.

Where applicable, the authors confirm that the experiments described here conform with The Physiological Society ethical requirements.

SA146

The growth of academic physiology in Britain, 1860-1930

S. Jacyna

Centre for the History of Medicine, UCL, London, UK

This paper gives an account of the development of physiology as an academic discipline in Great Britain between the mid-nineteenth century and the early decades of the twentieth century. It pays particular attention to the movement of key individuals from Scotland to the new London University (subsequently renamed University College London) in the early part of the period. It then considers how individuals trained at UCL went on to found major schools of physiology in such other centres as Cambridge, Oxford and Edinburgh.

Where applicable, the authors confirm that the experiments described here conform with The Physiological Society ethical requirements.

SA147

Early physiology in Birmingham, c.1870-1930

J. Reinarz

University of Birmingham, Birmingham, UK

This paper emerges from a Wellcome-funded, comparative history of five English provincial medical schools between c.1825 and 1939. Among other things, it considers the establishment of the first provincial schools in England, the evolution of the curriculum, as well as the emergence of something that more closely resembles modern medical science. In many ways, the new scientific method in medicine was epitomised by physiology; this paper will therefore examine the rise of physiology and the emergence of provincial research schools of physiology. Given the local setting of this conference, this paper will explore the emergence of academic physiology (c.1870) in Birmingham and its development over approximately half a century. Among other things, it will discuss the first instructors, who were usually clinicians, which goes some way towards explaining the practical nature of the earliest classes. It also follows the development of physiology instruction, including the appointment of full-time professors and research laboratories. While it has been suggested that provincial schools often led those in the metropolis in their willingness to embrace courses such as physiology, they also had considerable difficulties first establishing programmes that would satisfy the demands of existing regulatory bodies.

Where applicable, the authors confirm that the experiments described here conform with The Physiological Society ethical requirements.

SA148

The prevention and the treatment of frostbite in the early twentieth century

L.J. Howarth

Population, Socities and Humanities, University of Birmingham, Birmingham, UK and School of Medicine, University of Birmingham, Birmingham, UK

'Those who approached the fires, sufficiently near, to warm frozen feet and hands, were attacked by gangrene…these fatal occurrences mutilating the majority of our soldiers, threw them into the power of the enemy'. These words, spoken by Baron Larrey the chief surgeon to the French army in the Napoleonic wars, sound as horrific now as they did exactly 200 years ago. The soldiers expected warmth to heal their frostbitten sores; yet, it hastened their injuries to an irreversible gangrenous state. It is with Larrey the history of modern frostbite management and pathophysiology commenced. The history of frostbite has been briefly covered, but never in great depth or encompassing both previous military and exploration (polar and high-altitude) experiences together. This presentation offers a more general history of the prevention and the treatment of frostbite in the twentieth century. It covers the British experiences of frostbite from exposure in cold, hostile territories of the exploration campaigns and military operations. Discussed will be frostbite in the polar explorations (1910 - 1917), military frostbite (1914 – 1918) and finally Everest expeditions (1921 – 1938). Although different experiences, demonstrated is a progression in our understanding of frostbite and its management.

I would like to thank Dr. Jonathan Reinarz, the University of Birmingham Population, Societies and Humanities team, Dr. Vanessa Heggi and Dr. John Holden for their much valued time in helping me complete this research.

Where applicable, the authors confirm that the experiments described here conform with The Physiological Society ethical requirements.

SA149

The Silver Hut Expedition: A seminal research expedition into high altitude medicine

R. Rabbitts

Yeovil District Hospital, Yeovil, UK and University of Birmingham, Birmingham, UK

The Himalayan Scientific and Mountaineering Expedition of 1960/61 remains one of the most ambitious and successful high altitude expeditions ever undertaken. Innovatively thought up by Sir Hilary and Dr Pugh, both well known figures in the field of high altitude research, it comprised of a team of physiologists who themselves would winter over at extreme altitude, a concept borrowed from the Trans-Antarctic Expeditions [1]. Significantly, this was the first attempt to look at the long term physiology behind acclimatisation and the effects of extreme altitude on the human body [2]. After spending the winter at extreme altitude the team, joined by some fresh members, would move to Mt. Makalu for an attempt on the summit. The attempt on Mt. Makalu allowed the scientists to see whether 'super-acclimatization' was possible. Observations conclusively showed that the wintering party were not at any advantage, apart from very initially [3]. The Silver Hut succeeded in removing variables commonly encountered on previous mountaineering expeditions to extreme altitude.

One of the physiologists; Dr James Milledge has been generous enough to share his personal recollections of the expedition in detailed personal interview which allows a more humane and practical side when discussing the expedition, highlighting the role he played within the expedition. Milledge was responsible for several experiments during the expedition. He looked at ventilation and showed that even after three months of living at 5800m, the primary respiratory drive was still caused by hypoxia [4]. Two important changes in the control of ventilation were confirmed. Firstly, there was an increase in carbon dioxide sensitivity, which took three to five weeks to develop. Importantly, Milledge showed that there was no further increase in carbon dioxide sensitivity after the initial month, this had not been demonstrated before [5]. The second change was a significant reduction in the threshold response to carbon dioxide [6]. Additionally, it had been previously been proposed that the hypoxic sensitivity would decrease when ascending to high altitudes. For the first time, it was shown that there was no change in hypoxic sensitivity when ascending to high altitude [7].

The expedition was extraordinarily successful and the scientific return was extensive. There were many publications emanating from the expedition, twenty of the thirty six articles were published in per reviewed journals. These results portray just what an enormous undertaking the expedition really was. It not only required immense organisation of every aspect of the expedition by the leaders, Pugh and Hillary, but also relied on the dedicated team of physiologists willing to partake in both performing the investigations and also being the subjects for the other team members' experiments. It was by far the most ambitious high altitude research expedition of its time. Remarkably, the legacy of the Silver Hut expedition is still stimulating further research today. The 2007 Caudwell Xtreme Everest expedition can trace its routes back to the Silver Hut and AMREE expeditions. It is significant that none of the scientific return has been disproven, and only a few findings superseded, much is still very relevant in present research.

Ward, Michael P and Milledge, James S. Times Past. Griffith Pugh, Pioneer Everest Physiologist. High Altitude Medicine And Biology. Vol. 3, (No. 1), 2002: 77-87.

Ward, Michael. Mountain Medicine- A clinical study of cold and high altitude. London, Crosby Lockwood Staples, 1975. p. 16.

Milledge, James. S. The "Silver Hut" Expedition- a Commentary 40 Years Later. Wilderness and Environmental Medicine: Vol. 13, (No. 1), 2002: 55-56.

Pugh L.G.C.E. Physiological and Medical Aspects of the Himalayan Scientific and Mountaineering Expedition, 1960-61. Br Med J. (No. 2), 8 Sept 1962: 621-627.

Milledge, James S. The Silver Hut Expedition. In: Sutton, J.R., Jones, N.L., Houston C.S. Eds. Hypoxia: Man At Altitude. New York, Thieme Stratton Inc, 1982: 113-117.

Pugh LGCE. Physiological and Medical Aspects of the Himalayan Scientific and Mountaineering Expedition, 1960-61. Br Med J. (No. 2), 8 Sept 1962: 621-627.

Milledge, James S. The Silver Hut Expedition. In: Sutton, J.R., Jones, N.L., Houston C.S. Eds. Hypoxia: Man At Altitude. New York, Thieme Stratton Inc, 1982: 113-117.

Many thanks to Dr James Milledge.

Where applicable, the authors confirm that the experiments described here conform with The Physiological Society ethical requirements.

SA150

Historical aspects of the physiology of high altitude

J.B. West

Medicine-Physiology, University of California, San Diego, La Jolla, CA, USA

The centenary of the Anglo-American high altitude expedition to Pikes Peak in 1911 provides an opportunity to look at the development of high altitude physiology before and since then. A watershed event was the publication of *La Pression Barométrique* by Paul Bert in Paris in 1878. This clearly implicated the low PO_2 in the air as the critical variable. A few years later the first high altitude research laboratory was erected on Mont Blanc at an altitude of 4350 m. Shortly thereafter Angelo Mosso from Turin arranged for the Capanna Margherita to be placed at an altitude of 4559 m on the Monte Rosa. This was the site of extensive physiological studies carried out by a burgeoning international high altitude physiology community. This included Nathan Zuntz from Berlin who organized an international expedition to the Alta Vista Hut, altitude 3350 m, on Tenerife, Canary Islands. The Pikes Peak expedition led by J. S. Haldane from Oxford and Y. Henderson from Yale had a classical design with measurements first at sea level, then on the summit, altitude 4300 m, for five weeks, and then back at sea level. Extensive studies of cardiorespiratory physiology were carried out which laid the basis of much of what we know today. More recently the first measurements of human physiology on the summit of Mt. Everest, altitude 8848 m, were made in 1981, a simulated ascent of Everest in a low-pressure chamber took place in 1985, and very recently arterial blood samples were taken near the summit. A dramatic advance has been the discovery of a genetic change in Tibetans with extensive implications for the oxygen transport system. High altitude physiology is one of the most colorful and fast moving areas of environmental physiology.

Where applicable, the authors confirm that the experiments described here conform with The Physiological Society ethical requirements.

SA151

OCTs: quintessential multidrug transporters

S.H. Wright

Physiology, University of Arizona, Tucson, AZ, USA

The kidney and liver secrete a diverse array of positively charged organic molecules, including many widely prescribed drugs. Although one characteristic of the suite of transporters that mediate this process is their (necessary) multiselectivity, it includes the potential for unwanted drug-drug interactions (DDIs) at the point of secretion, interactions that can influence a drug's clinical or toxicological profile. In addition, interactions at the level of renal (and hepatic) drug transport can influence drug accumulation within these organs, with concomitant effects on drug toxicity. Thus, predicting the occurrence of DDIs is a major focus of work on OC transport.

The cellular model of OC secretion by renal proximal tubule (RPT) cells, hepatocytes, and other barrier epithelia involves the sequential activity of an OC 'entry step,' from blood to cell across the basolateral membrane (BLM), via an electrogenic organic cation transporter; followed by an apical 'exit step,' from cell to the adjacent fluid-filled compartment (e.g., renal tubular filtrate or bile), mediated by electroneutral OC/H^+ exchange. Whereas apical 'exit' appears to be dominated by one or more members of the MATE family of transporters (Multidrug And Toxin Extrusion; SLC2247), OC 'entry' is mediated by one or more members of the Organic Cation Transporter family (SLC22A). This presentation focuses on these OCTs, with particular emphasis on the following issues:

(i) Site of OCT expression. OCT1 in humans is primarily expressed in the sinusoidal membrane of hepatocytes (with some in apical membrane of RPT cells and BLM of enterocytes). In rodents, Oct1 is expressed in BLM of RPT cells, as well as in the liver. OCT2 in humans and rodents is primarily expressed in BLM of RPT cells. In contrast, OCT3 has a very broad tissue distribution.

(ii) Molecular/structural properties. The human OCTs (554-556 amino acids) have 12 transmembrane helices (TMHs) and a protein fold that includes N- and C-terminal halves of 6 TMHs each, separated by a large water-filled cleft (the substrate translocation pathway) with an extensive, putative binding surface. An extracellular loop between TMHs 1 and 2 influences OCT-OCT interaction, including formation of functional multimers.

(iii) Energetics and kinetics. Although OCTs support electroneutral OC/OC exchange, the prominent physiological mode of operation is electrogenic uniport. Consequently, the inside negative membrane potential of RPT cells and hepatocytes is the principal driving force for OC^+ entry. Transport follows Michaelis-Menten kinetics with apparent K_m values that range from sub-μM to well above 1 mM. Substrates with low affinity frequently display comparatively large maximal rates, resulting in transport efficiencies ('V_{max}/K_m') that permit high flux even for 'low affinity' substrates.

(iv) Selectivity. The OCTs typically transport molecules that share little in common structurally except cationic charge, modest hydrophobicity, and one or more hydrogen donor/acceptor sites. Although the several pharmacophores developed to define the structural determinants of ligand interaction with OCT1 and OCT2 generally include these features, their 3D locations differ, perhaps reflecting use of structurally distinct substrates as the marker of OCT transport activity, i.e., a consequence of 'substrate-dependent' ligand interactions. Consistent with this possibility, the kinetics of ligand interaction (of both substrates and inhibitors) include competitive, noncompetitive and mixed-type mechanisms. Taken with current views of OCT structure (see above), it is likely that ligand binding to OCTs involves a large surface with multiple interaction sites.

(v) Regulation. The long cytoplasmic loop between TMHs 6 and 7 of all three OCTs contains multiple consensus phosphorylation sites potentially available for acute modulation of transport activity. Consistent with this observation, OCT1 and OCT2 respond to kinase activation (e.g., PKA and PKC), although there are substantial species differences in the resulting effect on transport. Sex steroids exert substantial influence on long-term expression of OCT2.

(vi) Impact on drug clearance. Elimination of Oct1 and Oct2 in mice eliminates TEA secretion, and decreases its accumulation in kidney and liver, supporting the view that OCTs mediate the entry step in OC secretion. The common (~15%) OCT2 polymorphism, A270S, alters metformin transport and has been correlated with changes in metformin PD and PK. However, whereas elimination of Oct1/2 decreases metformin clearance and tissue accumulation in mice (as expected), metformin PD effects were not diminished, complicating the link between OCT activity and drug PD.

It is clear that OCTs play a central role in drug clearance. But the field still falls short of the goal of predicting clinically relevant DDIs and the influence of genetic variation on OCT activity.

Where applicable, the authors confirm that the experiments described here conform with The Physiological Society ethical requirements.

SA152

Cellular processing of organic cation transporters (OCT)

B. Hirsch[1], S. Brast[1], A. Grabner[1], C. Albiker[1], E. Schlatter[1], L. Florin[2] and G. Ciarimboli[1]

[1]Department of Internal Medicine D, University Hospital Münster, Münster, Germany and [2]Institut für Medizinische Mikrobiologie und Hygiene, Johannes Gutenberg-Universität, Mainz, Germany

OCT are membrane proteins involved in the transport of endogenous (e.g. the biogenic amines dopamine and histamine) and of exogenous organic cations. OCT are highly expressed in excretory organs (kidney, liver) and also in the brain. For this reason, OCT have a crucial importance in modulating cerebral and renal dopaminergic activity and dopamine clearance from the blood. OCT determine also the efficacy and toxicities of drugs such as biguanides, platin derivatives, and tyrosine kinase inhibitors. OCT have been assigned to the SLC22A family. This family can be divided into various subgroups according to substrates and transport mechanisms. Three OCT subtypes (OCT1, OCT2, and OCT3) with specific organ distribution have been identified. In this work, we focused on human OCT2 (hOCT2), the renal subtype of OCT. Since one of the factors determining transporter function and regulation is the building of complexes with other proteins or with itself, we searched for interaction partners of OCT and investigated the functional role of such a complex.

For these investigations, a mating-based split-ubiquitin-yeast-two-hybrid system (mbSUS), fluorescence resonance energy transfer (FRET), Western blot analysis, crosslinking experiments, immunofluorescence, and uptake measurements of the fluorescent organic cation 4-4-(dimethylamino)styryl)-N-methylpyridinium (ASP) were applied to HEK293 cells stably

transfected with hOCT2 and partly also in freshly isolated human proximal tubules.
Since the quaternary structure of transmembrane proteins plays an essential role for their cellular trafficking and function, we investigated whether hOCT2 forms oligomeric complexes and if so which part of the transporter is involved in the oligomerization. The role of cysteines for oligomerization and trafficking to the plasma membranes was investigated in cysteine mutants of hOCT2. The mbSUS, FRET, and Western blot analysis shows that hOCT2 forms oligomers both in the HEK293 expression system and in native human kidneys. The cysteines of the large extracellular loop are important to enable correct folding, oligomeric assembly, and plasma membrane insertion of hOCT2. Mutations of the first and the last cysteines of the loop at positions 51 and 143 abolished oligomer formation. Thus, the cysteines of the extracellular loop are important for a correct trafficking to the plasma membrane and for oligomerization. Other than with itself, hOCT2 also interacts with the lysosomal associated protein transmembrane 4 alpha (LAPTM4A) as demonstrated by mbSUS, FRET, and pull-down experiments. LAPTM4A is an intracellular localized membrane protein associated to lysosomes and late endosomes. Functionally, overexpression of LAPTM4A significantly decreased ASP uptake in HEK293 cells stably transfected with hOCT2, suggesting a negative regulation of hOCT2 mediated transport. Furthermore, overexpression of LAPTM4A led to a significantly decreased hOCT2 plasma membrane expression in surface biotinylation experiments. Significant expression of LAPTM4A in human kidney was demonstrated by immunoblotting and immunofluorescence. The interaction hOCT2-LAPTM4A may give origin to a tandem structure, where organic cations, binding at the plasma membrane to hOCT2, are immediately directed by LAPTM4A to lysosomes, where they accumulate. Alternatively, the interaction leads to recruitment of OCT in an endocytotic compartment, where the complex hOCT2-LAPTM4A is digested.
Another direct interaction partner identified by mbSUS and confirmed by pull-down and also by FRET-FACS analysis is the tetraspanin CD63. Tetraspanin CD63 is a ubiquitously expressed protein of the endosomal system which also moves to the cell surface. Overexpression of CD63 significantly decreased organic cation transport in HEK293 cells stably transfected with hOCT2, while its down-regulation by siRNA stimulated it, suggesting a negative regulation of hOCT2 mediated transport by CD63. Furthermore, overexpression of CD63 significantly decreased hOCT2 plasma membrane localization in surface biotinylation experiments. Total interne reflection resonance experiments showed CD63-hOCT2 interaction in the plasma membrane but stronger in vesicular compartments. Expression and colocalization of CD63 with hOCT2 was demonstrated in human kidneys by immunohistochemistry. As functional consequences of CD63 knockout in mice we observed that hOCT2 lost its specific basolateral localization in the kidney, appearing to be widespread distributed in the cell with a significantly decreased transport rate. In conclusion, CD63 regulates in a physiologically relevant fashion the function of hOCT2. We speculate that CD63 influences its trafficking to/from the cell membrane and processing via the intracellular sorting machinery and that this processing depends on polarization behaviour of the cells.
Supported by the Deutsche Forschungsgemeinschaft (DFG CI 107/4-1 to 2).

Where applicable, the authors confirm that the experiments described here conform with The Physiological Society ethical requirements.

SA153

An "Omics" view of Oats and Octs: the remote sensing and signaling hypothesis

S.K. Nigam

Pediatrics, Univ. of Calif., San Diego, La Jolla, CA, USA

Systems biology analyses of metabolomics and transcriptomics data from various SLC 22 transporter knockouts suggests a broad role in metabolism. Furthermore, classical signaling molecules (eg. prostaglandins, cyclic nucleotides, odorants and steroid conjugates) are among the best ligands for several original and more recently identified SLC22 family members. This, together with interesting tissue expression patterns in barrier epithelia under normal and perturbed conditions, as well as during organ development, has led to the hypothesis that these and other so-called drug transporters function as part of a "Remote Sensing and Signaling System" critical in the maintenance of local and systemic concentrations of rate-limiting metabolites and signaling molecules. This Remote Sensing and Signaling System involving SLC and ABC "drug" transporters may be important for inter-organ remote communication, functioning in parallel with other regulatory systems (eg. endocrine, growth factor, autonomic) as well communication between organisms (eg. gut microbiome-human).

Where applicable, the authors confirm that the experiments described here conform with The Physiological Society ethical requirements.

SA154

Exploring OCT physiological functions in the bronchial epithelium

M. Mukherjee[1], J. Lewis[1,2], L. Shemiss[1], A. Brown[1], I. Sayers[2], D.I. Pritchard[1] and C. Bosquillon[1]

[1]School of Pharmacy, University of Nottingham, Nottingham, UK and [2]School of Clinical Sciences, University of Nottingham, Nottingham, UK

The five main isoforms of the human Organic Cation Transporters (OCT), i.e., OCT1, OCT2 OCT3, OCTN1 and OCTN2 have been detected in the pulmonary tissue (1, 2) and there is published evidence these transporters impact on the absorption of inhaled drugs across the airway epithelium (2,3). In contrast, their physiological roles in the lungs have hardly been explored. It has been reported that OCT1 and OCT2 mediated the release of the non-neuronal acetylcholine from bronchial epithelial cells into the lung fluid (4) and that the OCT1-3 genes were dysregulated in the lungs of rodents following an acute ovalbumin challenge (5). However, the pathophysiological implications have not been investigated to date.
Since the airway epithelium is the primary protection barrier in the lungs, we initially assessed how environmental insults associated with chronic inflammatory pulmonary diseases affected OCT expression in bronchial epithelial cells. Layers of the human bronchial epithelial cell line Calu-3 cultured on permeable filters at an air-liquid interface for 21 days were used as a physiologically relevant in vitro model of the bronchial epithelium. Similarly to normal human bronchial epithelial cell layers, these expressed OCT1, OCT3, OCTN1 and OCTN2 while OCT2 could not be detected (6). Calu-3 layers were exposed to lipopolysaccharide (LPS), a common pro-inflammatory stim-

ulant, for 48h or to the aeroallergen house dust mite (HDM) for 8h twice over 48h. In parallel, they were also 'scrape' wounded using a pipette tip and allowed to recover for 48h. Changes in OCT gene and protein expression were measured by quantitative polymerase chain reaction (qPCR) or 'In-cell' Western, respectively. All three epithelial insults caused fold increases in the expression of OCT1, OCT3 and OCTN2 while OCTN1 was exclusively upregulated upon exposure to HDM at a concentration that compromised the integrity of the cell layer tight junctions (TJ). Interestingly, a non TJ disruptive concentration of the allergen only enhanced the expression of OCTN2.

Subsequently, the alveolar epithelial cell line A549 was used to evaluate the potential roles of OCT1 and OCTN2 in the mechanism of epithelial healing after injury as well as in airway protection against inflammation. The gene of the two transporters was successfully knocked down in the cell line using targeted siRNA. Knocked down layers grown on tissue culture plates were either scratched or challenged with LPS for 6h. Cell recovery after wounding was monitored by time lapse microscopy and by the Presto Blue® cell viability assay while the production of reactive oxygen species (ROS) upon LPS stimulation was measured using the dichlorofluorescein diacetate dye. In contrast to wild type cells, both OCT1 and OCTN2 knocked down layers failed to repair within 48h. In addition, low expression of the two transporters resulted in an increase in ROS formation following cell exposure to LPS.

Our data demonstrated that OCT expression in airway epithelial cells is affected by a pro-inflammatory stimulus, an allergen abuse and physical damage, with possible consequences in chronic inflammatory respiratory diseases. They also suggest OCT1 and OCTN2 participate in the repair of the airway epithelium after injury and might play a role in the control of oxidative stress during airway inflammation. The underlying mechanisms remain however to be investigated.

Bleasby K et al. (2006). Xenobiotica 36, 963-988

Bosquillon C. (2010). J Pharm Sci 99, 2240-55

Nakamura T et al. (2010). Mol Pharm 7, 187-95

Lips KS et al. (2005). Am J Respir Cell Mol Biol 33, 79-88

Lips KS et al. (2007) Life Science 80, 2263-9

Mukherjee M et al. (2012) Int J Pharm 426, 7-14

This work was supported by the University of Nottingham and the Royal Society of Great Britain (Research Grant RA26D1).

Where applicable, the authors confirm that the experiments described here conform with The Physiological Society ethical requirements.

SA155

Organic cation transporter 2 controls response and vulnerability to stress

S. Gautron

UMRS952/UMR7224, Paris, France

In higher organisms, the response to stress plays an important role in optimizing the reactions and behavioral strategies in terms of perception, risk assessment and decision-making in the face of potential threats. However, the repeated solicitation of the biological systems underlying this response also imposes a negative burden on mental health by promoting mood-related disorders such as depression. The polyspecific organic cation transporters (OCTs) were shown previously to be sensitive to the hormone corticosterone in vitro in cultured cells, suggesting they might play a role in the physiological response to stress. In a recent study, we examined the implication of organic cation transporter 2 (OCT2) in the response to stress. We found that OCT2 is expressed in several stress-related circuits in the brain and along the hypothalamo-pituitary-adrenal (HPA) axis. Genetic deletion of OCT2 in mice strikingly enhanced the hormonal response to acute stress. As a consequence, OCT2–/– mice were potently more sensitive to the effects of chronic stress on depressive-like behaviors. The functional state of the GSK3β intracellular signaling pathway, highly responsive to acute and chronic stress, was altered in the hippocampus of OCT2–/– mice. In vivo pharmacology and Western blot experiments argue for increased serotonin tonus as a main mechanism for impaired Akt/GSK3 signaling in OCT2–/– mice brain. Our findings identify OCT2 as an important determinant of the response to stress in the brain, suggesting that in humans OCT2 mutations or blockade by diverse drugs may interfere with mood-related central functions and enhance vulnerability to repeated adverse events leading to depression.

Where applicable, the authors confirm that the experiments described here conform with The Physiological Society ethical requirements.

SA156

TRPC, Orai1 and STIM1 in physiological and pathological Ca2+ influx

S. Muallem

NIH, Bethesda, MD, USA

A critical component of the receptor-evoked Ca2+ signal is Ca2+ influx mediated by the TRPC and Orai channels and is regulated by the ER luminal Ca2+ sensor STIM1. Ca2+ influx is essential for all cell functions, yet excess Ca2+ influx is highly toxic and is involved in numerous cellular pathologies. A key question is how STIM1 interacts and open these channels. Most aspects of STIM1 interaction with the TRPC and Orai channels have been studied in model system, while the behavior of the native proteins is not known, in particular in polarized cells. We used model system and gene deletion in mice to study regulation of Orai and TRPC channels by STIM1. We identified several critical domains in STIM1 that are required for regulation of the channels. In particular, the STIM1 SOAR domain mediates interaction of STIM1 with both channel type. The newly discovered CTID domain downstream of SOAR regulates access of the inhibitor SARAF to SOAR. SOAR also mediates interaction of STIM1 with the C terminus of TRPC channels to present the basic lysine-rich domain of STIM1 to the TRPC channels to gate them. The localization of the native Orai1, TRPCs and STIM1 in polarized cells provide further clues as to the regulation and potential role of TRPC channels in cellular pathology. Finally, deletion of TRPC channels in mice markedly affect acinar cells receptor and store mediated Ca2+ influx and protects the cells from Ca2+-mediated toxicity brought about by cell stress.

Where applicable, the authors confirm that the experiments described here conform with The Physiological Society ethical requirements.

SA157

Protective role of calmodulin in pancreatic toxicity

J. Gerasimenko

Cardiff School of Biosciences Cardiff University, Cardiff, UK

The most frequent causes of acute pancreatitis are either gallstones or heavy alcohol consumption. Recurrent episodes of acute pancreatitis often result in progression of the disease to chronic pancreatitis and increase the risk of pancreatic cancer. The pathogenesis of inflammation in acute and chronic pancreatitis is tightly linked to the induction of necrosis and apoptosis. There is currently no specific therapy for pancreatitis; however, latest findings allow hope for future progress. Single pancreatic acinar cells and clusters of two or three acinar cells were isolated from the mouse pancreas. The mice were humanely killed according to the UK Schedule 1 regulation of the Animal (Scientific Procedures) Act, 1986. Cells were loaded with calcium sensitive dye Fluo-5N AM followed by permeabilization using a short pulse of high intensity two-photon laser beam. BZiPAR was used to continuously measure the activity of trypsin by adding the substrate to the perfusion chamber after cell permeabilization. Measurements of fluorescence were performed using Leica multi-photon SP5 system.
Recently we have shown that the calcium sensor calmodulin provides a protective mechanism, regulating the sensitivity of the calcium release process. Activation of calmodulin using Ca2+-like peptide 3 (CALP-3) abolished the pathological calcium release and trypsinogen activation evoked by ethanol as well as its non-oxidative metabolite palmitoleic acid ethyl ester (POAEE) in intact and permeabilized cells. We have experimentally compared a number of ways to reduce calcium overload inflicted by known pancreatitis inducing factors (alcohol, fatty acid ethyl esters, bile acids, high concentration of cholecystokinin) including inhibition of calcium release, inhibition of calcium entry, potentiation of calcium recovery and activation of calcium regulation mechanisms. Our data suggest that activation of calcium regulation and inhibition of calcium entry (or possibly combination of both) reduces calcium overload as well as necrosis, bringing hope for new therapeutic approaches.

Where applicable, the authors confirm that the experiments described here conform with The Physiological Society ethical requirements.

SA158

Pancreatic Stellate Cells (PSCs): a starring role in pancreatitis and pancreatic cancer

M. Apte

Pancreatic Research Group, University of New South Wales, Liverpool, NSW, Australia

While the morphology and function of most of the cells of the exocrine and endocrine pancreas have been well described over several centuries, one important cell type in the gland, the pancreatic stellate cell (PSC), was first described only as recently as 30 years ago. Furthermore, it was to be another 16 years before the biology of these cells could begin to be studied because it was only in 1998 that methods were developed to isolate and culture PSCs from rodent and human pancreas. PSCs are now known to be key players in pancreatic fibrosis, a predominant histological feature of two major diseases of the pancreas - chronic pancreatitis and pancreatic cancer.
In health, PSCs are in their quiescent phase and are characterised by abundant vitamin A storing lipid droplets in their cytoplasm. The cells are responsible for maintaining normal pancreatic architecture via regulation of the synthesis and degradation of extracellular matrix (ECM) proteins. Recently, PSCs have also been implicated in other functions as progenitor/stem cells, as immune cells and as intermediaries in exocrine pancreatic secretion in humans. During pancreatic injury, PSCs change to an activated, myofibroblast-like phenotype, characterised by loss of the vitamin A stores and the synthesis of excessive amounts of ECM proteins resulting in the fibrosis of chronic pancreatitis and pancreatic cancer. An ever increasing number of factors that stimulate and/or inhibit PSC activation via paracrine and autocrine pathways are being identified. Furthermore, the signalling pathways and second messengers mediating the effects of exogenous or endogenous factors on PSC function are being increasingly characterized. Importantly, it has now been clearly demonstrated, using both in vitro and in vivo approaches, that PSCs interact closely with pancreatic cancer cells to promote local tumour growth as well as distant metastasis. PSCs from primary tumours in the pancreas have also been shown to travel to distant metastatic sites where they likely facilitate the seeding and subsequent proliferation of cancer cells. In view of the central role of PSCs in both chronic pancreatitis and pancreatic cancer, current research is focussed on novel therapeutic strategies to inhibit/retard PSC activation and to interrupt their interaction with cancer cells so as alleviate chronic pancreatitis and/or inhibit tumour growth. The challenge that remains is to translate these pre-clinical developments into clinically applicable treatments for patients with chronic pancreatitis and pancreatic cancer.

Where applicable, the authors confirm that the experiments described here conform with The Physiological Society ethical requirements.

SA159

The effects of pancreatitis-inducing factors on calcium signaling in pancreatic ductal cells

P. Hegyi[1], V. Venglovecz[1], P. Pallagi[1], J. Maléth[1], M.A. Gray[2] and Z. Rakonczay Jr.[1]

[1]First Department of Medicine, University of Szeged, Szeged, Hungary and [2]Institute for Cell & Molecular Biosciences, Newcastle University, Newcastle upon Tyne, UK

Excessive ethanol (EtOH) consumption and biliary tract diseases are the most common etiological factors of acute pancreatitis. In vivo pancreatitis animal models have revealed that not only acinar cells, but most probably the pancreatic ductal epithelial cells (PDEC) are also involved in the pathogenesis of acute pancreatitis (ref.1). One of the main aims of our workgroup is to understand the role of PDEC in acute pancreatitis. In recent years we have characterized the effects of different bile acids, ethanol, ethanol-metabolites and activated proteases on PDEC function.
Both EtOH and bile acids have dual effects on pancreatic ductal bicarbonate secretion. Low concentrations of these toxic factors stimulate, whereas high concentrations, inhibit the secretory process. Importantly, the stimulatory effects of both toxic factors are calcium dependent. EtOH and bile acids induce an oscillatory calcium elevation which can be blocked by BAPTA-AM, caffeine, xestospongin C and the phospholipase C

inhibitor U73122, but not by the lack of extracellular calcium (ref.2). Administration of high concentrations of EtOH, bile acids and fatty acids induce a sustained calcium elevation. This sustained calcium elevation is caused by (1) calcium release from the endoplasmic reticulum, via IP3 and ryanodine receptor activation;(2) by inhibiting the endoplasmic reticulum calcium ATPase and (3) by stimulating extracellular calcium influx. Blocking this sustained calcium elevation by BAPTA-AM prevents the inhibitory effects of EtOH and fatty acids, but not that caused by bile acids. The inactive protease trypsinogen has no effect on calcium, however, trypsin induces calcium elevation via activation of PAR2. Inhibiting this calcium elevation, either by trypsin inhibitor, a PAR antagonist or BAPTA-AM totally blocks the inhibitory effect of trypsin (ref.3).
These results indicate that pancreatitis-inducing factors strongly and differentially modulate intracellular calcium, which interferes with the secretory activity of PDEC. Understanding the calcium transporters/channels involved in these pathophysiological mechanisms may lead to more specific therapies for acute pancreatitis.

Czako et al. Pancreatic fluid hypersecretion in rats after acute pancreatitis (1997). Dig Dis Sci 42:265-72.

Venglovecz V. et al. (2008). Effects of bile acids on pancreatic ductal bicarbonate secretion in guinea pig. Gut 57:1102-12.

Pallagi P et al. (2011). Trypsin reduces pancreatic ductal bicarbonate secretion by inhibiting CFTR Cl- channels and luminal anion exchangers. Gastroenterology 141:2228-2239

This study was supported by National Development Agency grants (TÁMOP-4.2.2.A-11/1/KONV-2012-0035, TÁMOP-4.2.2-A-11/1/KONV-2012-0052 and TÁMOP-4.2.2.A-11/1/KONV-2012-0073), the Hungarian Scientific Research Fund (NF105758 to Z.R. and NF100677)

Where applicable, the authors confirm that the experiments described here conform with The Physiological Society ethical requirements.

SA160

Calcium signaling and pancreatic stellate cell function

D.I. Yule

Pharmacology and Physiology, University of Rochester, Rochester, NY, USA

The exocrine pancreas is comprised of three prominent cell types. While the roles of the acinar and ductal cells in physiology and disease are reasonably well defined, a third cell type, the pancreatic stellate cell (PSC) is far less studied. PSC are present in a periacinar and periductal localization. In common with hepatic stellate cells they are characterized as retinol/lipid storing cells expressing a variety of intermediate filament proteins including desmin and glial fibrillary acid protein. Under physiological conditions, stellate cells appear to be quiescent and relatively little is known regarding their contribution to the normal function of the gland. However, in culture, PSC undergo a phenotypic transformation from a quiescent state to a myofibroblast-like phenotype. This is believed to parallel the induction of an activated state observed in chronic pancreatitis and pancreatic cancer. Activated PSCs are highly proliferative, migratory and secrete large amounts of extracellular matrix. These properties are thought to contribute to the pathogenesis of pancreatic disease. The goal of the present study was to define the role of changes in intracellular Calcium concentration ([Ca2+]i) in mouse PSC function. We have utilized a variety of techniques, including pharmacological agents and adenoviral constructs which buffer [Ca2+] and Inositol 1,4,5-trisphosphate in specific cellular compartments and used these approaches to probe the contribution of Ca2+ release and Ca2+ influx for PSC function. For example, data will be presented which suggests that Ca2+ signaling does not appear to play a major role in the activation of quiescent PSC. Nevertheless, following activation, an increase in [Ca2+] within the nucleus is required for proliferation. This appears to be dependent on Ca2+ release, because blockade of Ca2+ influx is without effect on growth. In contrast, migration of activated stellate cells is attenuated in the absence of Ca2+ influx. These data suggest that Ca2+ signaling plays multiple roles in PSC function and further that manipulation of this signal may be a promising future target for clinical intervention.

Work was supported by the NIH grants DK054568, DE014756 and DE19245.

Where applicable, the authors confirm that the experiments described here conform with The Physiological Society ethical requirements.

SA161

Altered excitability of dorsal horn neurons

J.A. Lopez-Garcia

Physiology, University of Alcala, Alcala de Henares, Madrid, Spain

The mechanisms underlying central sensitization following peripheral injury of inflammatory or neuropathic nature are the centre of an intense scientific debate. Potential mechanisms have been classified into 4 categories including synaptic mechanisms, membrane excitability changes, phenotypical changes and morphological reorganization (Sandkühler et al, 2000). We have studied changes in membrane excitability of deep dorsal horn neurones induced by peripheral inflammation. We expected to find enhanced membrane excitability in sensitized neurons.
Intraplantar injections of carrageenan produce clear signs of pain hypersensitivity in mice and rats. Spinal cords from these hyperalgesic animals maintained *in vitro* show significant signs of potentiated segmental reflexes which is interpreted as a sign of central sensitization (Hedo et al 1999). Therefore, we have used the mouse isolated spinal cord *in vitro* coupled to intracellular techniques to compare the excitability of neurons extracted from naïve and inflamed animals. Cords were always extracted under urethane anaesthesia (2 g/kg, i.p.) following approved protocols.
Neurons from treated animals showed large synaptic responses shortly after inflammation (1h) and developed further after a long term inflammation (20h). In contrast, these treated neurones showed biphasic changes in membrane excitability with an increase shortly after inflammation and a decrease in the longer term.
These observations lead to the conclusion that membrane excitability plays a complex role in central sensitization. Whereas an increased excitability may be a fast means to boost central sensitization, longer term decreases in excitability may represent a homeostatic correction of an abnormal state of synaptic activity.
This new framework opens a window for the study of particular ionic currents and specific ion channels in the dynamic shaping of cell excitability during sensitization. We have shown the contribution of transient and sustained potassium currents to this changing excitability (Rivera-Arconada & Lopez-Garcia 2010). Recently we have also investigated a potential role for

the mixed Ih current carried by HCN channels (Rivera-Arconada et al, 2013). Additional evidence from the laboratory suggests that the potassium M current may be involved in shaping excitability during sensitization. These experimental studies will be discussed within the presentation.

Sandkühler J et al. (2000). Prog Brain Res 129, 81-100

Hedo G et al. (1999). Neurosci 92, 309-18

Rivera-Arconada I & Lopez-Garcia JA (2010). J Neurosci 30, 5376-83

Rivera-Arconada I et al. (2013). Neuropharmacol 70C, 148-55

Supported by the Spanish Government (BFU 2012-37905)

Where applicable, the authors confirm that the experiments described here conform with The Physiological Society ethical requirements.

SA162

Mitochondrial dysfunction in chemotherapy-induced neuropathy

S. Flatters

Wolfson Centre for Age-Related Diseases, King's College London, London, UK

Painful peripheral neuropathy is the major dose-limiting side effect of several first-line, highly effective chemotherapeutic agents. Currently there is no effective therapy for the prevention or treatment of chemotherapy-induced painful peripheral neuropathies (CIPPN). Furthermore, several analgesics with established efficacy in other painful neuropathies have failed to show any efficacy in double-blind, placebo-controlled RCTs of patients with CIPPN. Therefore understanding the causal mechanisms for CIPPN is essential to enable analgesic development in this area of substantial unmet clinical need. Several reports using rodent models of CIPPN have indicated evidence for mitochondrial dysfunction and reactive oxygen species (ROS) to be contributory factors to this pain syndrome. Our research team at King's College London, is examining the contribution of mitochondrial function before, during and at the resolution of paclitaxel-induced painful peripheral neuropathy to correlate cellular mechanisms to whole animal behaviour. During this talk, I will discuss some of our latest data on ROS and mitochondrial function during paclitaxel-induced painful peripheral neuropathy.

Where applicable, the authors confirm that the experiments described here conform with The Physiological Society ethical requirements.

SA163

Microglia causing neuropathic pain after nerve injury

K. Inoue

Kyusyu University, Fukuoka, Japan

Neuropathic pain is a highly debilitating chronic pain that occurs after nerve injury and is resistant to currently available treatments. We reported that activated microglia overexpressed P2X4 receptors after nerve injury which release brain-derived neurotrophic factor (BDNF) evoking a collapse of their transmembrane anion gradient and the subsequent neuronal hyper-excitability (Nature, 2003 & 2005). Recently, we found that a single intrathecal administration of IFN-γ to normal animals produces a long-lasting tactile allodynic behavior and activation of microglia in the spinal cord. The expression of IFN-γ receptor mRNA in the spinal cord is localized predominantly in microglia. IFN-γ evoked P2X4 up-regulation through Lin-kinase activation in microglia. Furthermore, IFN-γ receptor-deficient mice (ifngr-/-) exhibited a striking reduction in nerve injury-induced tactile allodynia and activation of microglia. We also found that CCL2, ligands for CCR2, increased P2X4R expression in microglial surface fraction. These findings suggest that IFN-γ signaling through IFN-γR plays as a crucial trigger of microglia activation after nerve injury and the subsequent tactile allodynia through P2X4 stimulation, and that CCR2 signaling may increase the P2X4R expression on the surface membrane of microglia.

Microglia become activated by multiple types of damage in the nervous system, and play essential roles in neuronal pathologies. However, how microglia transform into reactive phenotypes is poorly understood. Then, we identified the transcription factor interferon-regulatory factor 8 (IRF8) as a critical regulator of reactive microglia. IRF8 expression was markedly upregulated in microglia, but not in neurons or astrocytes, after nerve injury. IRF8 overexpression in cultured microglia promoted the transcription of genes associated with reactive states; conversely, IRF8 deficiency prevented these gene expressions in the spinal cord following PNI. Furthermore, IRF8-deficient mice were resistant to neuropathic pain, and transferring IRF8-overexpressing microglia spinally to normal mice produced pain. Therefore, IRF8 may activate a program of gene expression that transforms microglia into a reactive phenotype.

Where applicable, the authors confirm that the experiments described here conform with The Physiological Society ethical requirements.

SA164

BDNF-induced plasticity before and after SCI

S.M. Garraway

Psychology, Texas A & M University, College Station, TX, USA

For nearly two decades, much research has focused on brain-derived neurotrophic factor (BDNF), an important member of the neurotrophin family. Results from these studies show that BDNF exerts numerous modulatory actions within the central nervous system; actions ranging from cellular and molecular to behavioral. In the spinal cord, BDNF is identified as a critical mediator of central sensitization and spinal nociception that underlie the development of pain hypersensitivity. In addition to these actions, BDNF has also been implicated in beneficial effects such as promoting functional recovery following spinal cord injury (SCI). The existence of both adaptive and maladaptive spinal effects of BDNF has led us to propose that BDNF functions in a state dependent manner; that its specific actions are determined by whether or not a SCI exists.

To affirm this proposal, we conducted studies that utilized several experimental designs to investigate the effects of BDNF on spinal plasticity in naïve and spinal cord injured subjects. In the first set of studies, we used spinal cord slices in juvenile rats to examine the effect of exogenously administered BDNF on dorsal root-evoked synaptic currents in lamina II neurons. The results showed that in naïve subjects, BDNF produces a prolonged synaptic facilitation that requires post-synaptic NMDA receptors, protein kinase C and increases in intracellular calcium, indicating a pro-nociceptive role for BDNF. However, BDNF fails to induce facilitation of the evoked synaptic

responses in the injured spinal cord. The second set of experiments used a simple instrumental learning paradigm to assess the interaction between controllable shock and BDNF in adult rats with a complete spinal transection. Previous studies had shown that controllable shock to the hindlimb promotes adaptive plasticity and facilitates subsequent spinal learning through BDNF-dependent mechanisms (Gómez-Pinilla et al., 2007; Neuroscience 148:893-906). Supporting this, we demonstrated that controllable shock significantly increases the expression of BDNF and its receptor, TrkB, primarily in the spinal dorsal horn. Our third set of experiments assessed the relationship between spinal BDNF levels and the detrimental effects of intermittent nociceptive stimulation (~0.5Hz) in adult subjects with a moderate contusion injury. Previous observations showed that this stimulation paradigm induces a learning deficit and undermines functional recovery following SCI (Crown et al., 2002; Behav. Neurosci. 116:1032-1051). We now show that noxious stimulation shortly after SCI significantly increases the onset and maintenance of mechanical allodynia in adult rats with a moderate spinal cord contusion injury. Surprisingly, this pro-nociceptive response is accompanied by a decrease in the spinal expression of BDNF, TrkB and associated downstream signaling kinases, ERK1/2 and CAMKII.
Together, these observations suggest that injury alters how BDNF affects spinal nociceptive processing. In the absence of SCI, BDNF promotes central sensitization and spinal nociception. In contrast, after injury BDNF appears to have a protective effect that attenuates the effect of nociceptive stimulation.

Supported by: UNCF-Merck Fellowship to S.M. Garraway; Christopher Reeve Paralysis Foundation grant (Consortium on Spinal Injury), NINDS R01 NS-16996 and NIH P01 NS39420 to L.M. Mendell; NINDS NS41548 and NICHD HD058412 to J.W. Grau.

Where applicable, the authors confirm that the experiments described here conform with The Physiological Society ethical requirements.

SA165

Altered inhibition in dorsal horn circuits and strategies for pharmacological restoration

H. Zeilhofer

Dept of Pharmacology, University of Zurich, Zurich, Switzerland

Peripheral nerve damage and inflammation induce alterations in synaptic inhibition in neuronal circuits of the spinal dorsal horn through a variety of different processes, including changes in the transmembrane chloride gradient of dorsal horn neurons, changes in the synthesis of neurotransmitters and alterations in the function of neurotransmitter receptors (for a review see Zeilhofer et al., 2012). Such impaired inhibition commonly leads to pathologic pain syndromes manifesting in the development of hyperalgesia and allodynia, and possibly also in compromised spinal motor control. During the last five years our group has worked on the identification of pharmacological targets that would allow to restore compromised neuronal inhibition without the typical unwanted effects of typical GABAergic compounds such as the classical benzodiazepines. Using a series of GABA-A receptor point mutated mice we could demonstrate that the selective activation of GABA-A receptors containing alpha2 subunits can alleviate sensory symptoms of impaired spinal synaptic inhibition without inducing sedation (Zeilhofer et al., 2009). Other at present still underexplored possibilities may include the pharmacological potentiation of inhibitory glycine receptors (Yevenes & Zeilhofer, 2011). Recent work indicates that certain structural analogues of endocannabinoids act as allosteric modulators of inhibitory glycine receptors. Evidence from different groups suggests that such compounds also reverse pathological pain syndromes in different rodent models.

Zeilhofer HU, Benke D, Yévenes GE (2012) Chronic pain states: pharmacological strategies to restore diminished inhibitory spinal pain control. Ann Rev Pharmacol Toxicol 52:111–133

Zeilhofer HU, Möhler H, Di Lio A (2009) GABAergic Analgesia – New Insights from Mutant Mice and Subtype-Selective Agonists. Trends Pharmacol Sci 30, 397-402.

Yévenes GE, Zeilhofer HU (2011) Molecular sites for the positive allosteric modulation of glycine receptors by endocannabinoids. PLoS one, 6:e23886

The work of the authors is currently supported by grants from the European Research Council, the Swiss National Science Foundation, and by the Swiss Contribution of the Swiss Federal Government.

Where applicable, the authors confirm that the experiments described here conform with The Physiological Society ethical requirements.

SA166

Regulation and roles of the $Na^+HCO_3^-$ cotransporter NBCn1 (SLC4A7) and the Na^+/H^+ exchanger NHE1 (SLC9A1) in breast cancer

S.F. Pedersen

Department of Biology, University of Copenhagen, Copenhagen, Denmark

Within the last decade it has become increasingly clear that dysregulated expression, splicing, and/or function of ion transporters and channels occurs in all cancers and contributes importantly to cancer development (1,2). Being linked to essentially all of the widely accepted hallmarks of cancer, ion transporters and channels represent novel therapeutic, diagnostic and prognostic targets. Our research group has focused in particular on dysregulation of pH regulatory ion transport in breast cancer. A fundamental property of solid tumors is a markedly altered pH-profile compared to normal tissues, with acidic extracellular, and often alkaline intracellular pH (pH_i). This at least in part reflects their upregulated glycolytic metabolism, necessitating increased acid extrusion to maintain survival.
Whereas the Na^+/H^+ exchanger NHE1 (SLC9A1) has until recently received the majority of the attention in the context of pH (dys)regulation in cancer, our recent findings indicate that the $Na^+HCO_3^-$ cotransporter NBCn1 (SLC4A7) may be of substantial importance in this context. Expression of a constitutively active, truncated form of the ErbB2/HER2 receptor (ΔNErbB2) greatly increased pH regulatory capacity in MCF-7 human breast cancer cells, in a manner mediated by NHE1 and NBCn1 (3). After ΔNErbB2 expression or stimulation of wild-type ErbB receptors, NBCn1 was strongly upregulated at the mRNA and protein levels, and NHE1 was phosphorylated at Ser703, a known target for the 90 kDa Ribosomal S6-Kinase (p90RSK). The regulation of the NBCn1 promoter by ErbB2 signaling involves Src, Extracellular Signal Regulated Kinase (ERK), and Phosphatidyl-Inositol-3 Kinase (PI3K)-Akt signaling, as well as the transcription factor Krüppel-like 4 (KLF4), which has

been assigned important and context-dependent pro- and anti-oncogenic roles in various cancers.
In 2D cultures of MCF-7 cells NHE1 localized strongly to invadopodial rosettes, where it colocalized with the invadopodial markers cortactin, F-actin and phospho-Tyr416-Src, as well as with its known binding partners, ezrin and radixin (4). NHE1 inhibition or siRNA-mediated NHE1 knockdown potently sensitized ΔNErbB2-MCF-7 cells to cisplatin-induced apoptosis and enhanced their adhesion and 2D migration on collagen-I (3,4).
Using 2D- and 3D cell culture models mimicking various aspects of the tumor microenvironment we show that the regulation and localization of NHE1 and NBCn1 are dependent on different microenvironmental factors, and that the role of NBCn1 may become more prominent in 3D culture. Finally, using matched sets of patient tissue we show that NHE1 and NBCn1 are upregulated in primary breast carcinomas and lymph node metastases compared to normal breast tissue, and we demonstrate that $Na^+HCO_3^-$ cotransport is a major determinant of pH_i regulation in freshly dissected human breast tumors (5).
In conclusion, expression and activity of the two major pH regulatory ion transporters NBCn1 and NHE1 are altered in human breast cancer, resulting in altered pH regulation. NBCn1 expression is strongly sensitive to ErbB receptor activity, and NHE1 regulates chemotherapy sensitivity and cell motility. We suggest that NHE1 and NBCn1 are potential targets in breast cancer diagnosis and/or treatment.

Pedersen SF & Stock CM (2013) *Cancer Res* **doi** 10.1158/0008-5472.CAN-12-4188

Boedtkjer E *et al.* (2012) *Curr Pharmacol Des* **18**(10):1345-71

Lauritzen G *et al.* (2010) *Exp Cell Res* **316**:2538-2553

Lauritzen G *et al.* (2012) *Cancer Letters* **317**(2):172-83

Boedtkjer E *et al.* (2013) *Int J Cancer* **132**(6):1288-99

We gratefully acknowledge funding from the Danish Cancer Society, the Novo Foundation, the Danish National Research Council, and the Lundbeck Foundation.

Where applicable, the authors confirm that the experiments described here conform with The Physiological Society ethical requirements.

SA167

Physiological role of Na+-coupled HCO–3 transporters deduced from knockout studies

A. Sinning[1,2], L. Liebmann[1] and C.A. Huebner[1]

[1]Human Genetics, University Hospital Jena, Mainz, Germany and [2]Physiology and Pathophysiology, University Hospital Mainz, Mainz, Germany

Cellular ion homeostasis and pH regulation critically depend on the activity of ion exchangers. This is of special importance in the brain, where pH modulates neuronal excitability and neuronal activity in turn can cause changes in pH. The objective of our studies were the investigation of the physiological function of the Na+-coupled anion-exchanger Slc4a8 in the mammalian brain, as well as a comparative analysis of the closely related transporter Slc4a10 with the help of knockout mouse models.
Both anion exchanger are expressed broadly in neurons. Supporting an important role of Slc4a8 for neuronal pH regulation, cultured hippocampal neurons of mice with a targeted disruption of Slc4a8 showed a reduced steady-state pHi and recovered more slowly from an acute acid load. In accordance with enrichment of Slc4a8 in presynaptic nerve endings of pyramidal neurons, the electrophysiological analysis revealed a pH-dependent presynaptic defect with impaired glutamate release. Whereas, release of the inhibitory neurotransmitter GABA was not affected. The decrease of hippocampal excitability in Slc4a8-/- slices in vitro was reflected by an increased seizure threshold in vivo. Accordingly, these results of our studies propose that Slc4a8 in the brain modulates glutamate release and thus synaptic strength in a pH-dependent way.
In contrast, Slc4a10 shows a distinct neuronal expression, partly overlapping but mostly amendatory to Slc4a8. The newest results of our group suggest a crucial role of Slc4a10 for GABAergic inhibition.
Thus, these results suggest important roles of Slc4a8 and Slc4a10 for brain function and support their importance as possible targets for clinical applications e.g. in the future treatment of epilepsy.

Sinning A et al. (2011). J Neurosci 31, 7300-7311

Leviel F et al. (2010). J Clin Invest 120, 1627-1635

Jacobs S et al. (2008). Proc Natl Acad Sci U S A 105, 311-316

Dr. L. Liebmann (Human Genetics, University Hospital, Jena)

Prof. Dr. C.A. Huebner (Human Genetics, University Hospital, Jena)

Where applicable, the authors confirm that the experiments described here conform with The Physiological Society ethical requirements.

SA168

Role of exofacial carbonic anhydrase, Na-HCO_3 co-transport, and connexin channels in the spatial control of intracellular pH in multicellular tumour cell growths and myocardial tissue

R.D. Vaughan-Jones[1], P. Swietach[1], C. Garciarena[1], A. Moreno[2], A. Hulikova[1] and K.W. Spitzer[2]

[1]Department of Physiology Anatomy & Genetics, 1 Burdon Sanderson Cardiac Science Centre, Oxford, UK and [2]Cardiovascular Research & Training Institute, Salt Lake City, UT, USA

A sufficiently high intracellular pH (Ph_i) is permissive for cell survival, growth, function and proliferation. High metabolic production of H^+ ions is compensated for by acid extrusion on ion transport proteins such as Na/H exchange (NHE) and Na-HCO_3 co-transport (NBC). This helps to regularise pH_i in individual cells. In addition, H^+-ion cross-talk between adjacent cells helps to co-ordinate pH_i throughout the tissue. The talk will contrast two different pH_i-co-ordination strategies. One is common in poorly vascularised developing tumours and relies on the activity of exofacial carbonic anhyrase enzymes, notably HIF-activated CAIX, which facilitates the venting of cellular CO_2. The other, which is common in the heart, is the buffer-shuttling of acid via histidyl dipeptides (HDPs) and CO_2/HCO_3^- between cells, through gap junctions (predominantly Cx43 channels in the myocardium).
Extracellular CAIX operates in concert with membrane HCO_3^- influx on NBC. CAIX up-regulation in hypoxic zones is associated with down-regulation of cytoplasmic CAs such as CAII. NBCs are constitutively expressed at high basal activity in a wide range of tumour cell-lines, unlike NHE1 that can be at either high or low functional level. By facilitating CO_2 diffusion out of cells, CAIX raises pH_i and reduces pHo, producing the functional hall-mark of aggressive cancer. Down regulation of CAIX activity, either by genetic manipulation or by pharma-

cological inhibition, typically results in a more acidic core pH_i in 3-D spheroid growths (eg. RT112; HCT116), a more heterogeneous spatial pH_i distribution, and a more alkaline pH in the restricted extracellular spaces.
Gap-junctional channels tend to be repressed in developing tumours, but they are commonly expressed in most healthy tissues. Cx43 channels in the myocardium mediate high passive H^+ flux whenever $[H^+]_i$ differences are presented across junctional regions. High H^+-flux is achieved by reversible binding to intrinsic HDPs (carnsoine, anserine, homocarnosine) that are present in cytoplasm (~15mM), and which readily permeate the junction. HCO_3 anion flux through the channels also enhances cell-cell H^+ transmission. The H^+ and HCO_{3-} flux is gated by moderate $[H^+]_i$ and high $[H^+]_i$ which increases and reduces Cx43 channel permeability respectively. These are acute channel-gating phenomena, also observed for Cx43 channels stably transfected into Hela or N2A cell-pairs. Because buffer permeation of Cx43 channels is high, so is cell-cell H^+ ion transmission. The system provides for spatial H^+ communication and permits slow H^+ diffusive equilibration of pH_i in tissue, resulting in a pH_i syncitium that regularises cell function. H^+-gating of cell-cell H^+ flux (autoregulation) is absent when the cytoplasmic tail of Cx43 sub-units is truncated. The talk will compare the kinetics and spatial outreach of CAIX and Cx43 mediated pH_i control, highlighting the potential advantages of each mechanism.

Where applicable, the authors confirm that the experiments described here conform with The Physiological Society ethical requirements.

SA169

Should I stay or should I go? – Regulating Orai function

D. Alansary, K. Doerr, T. Kilch, C. Peinelt, I. Bogeski and B.A. Niemeyer

Biophysics, Saarland University, Homburg, Germany

Ca2+ release-activated Ca2+ (CRAC) channels were originally identified as store-operated highly selective Ca2+ channels in primary rat mast cells and Jurkat T cells (Hoth & Penner, 1992; Zweifach & Lewis, 1993), but have since been identified in many cell types. While STIM1 and Orai1 constitute the main subunits of CRAC channels in lymphocytes, other cell types contain different combinations/ratios of Orai1, Orai2 or Orai3 and STIM1 or STIM2. We are interested in physiological and pathophysiological regulation of CRAC channels by environmental factors such as oxidation, as well as by posttranslational alterations of their glycosylation status. We have shown that Orai1 channels but not Orai3 channels are inhibited by extracellular applied ROS and that C195 is mainly responsible for mediating this effect (Bogeski et al, 2010). But how does oxidation of C195 affect function? What if the channels are heteromers between Orai1 and Orai3? Current studies investigate these questions by analyzing diffusional properties (FRAP), clustering (TIRF) and heteromerization of Orai channels. In addition to functional regulation by extracellular ROS, we are interested to find out if and how T-cell function controlled by CRAC is regulated by altered glycosylation patterns. Changes in the extracellular composition of T-cell glycans are likely involved in physiological and pathophysiological dysregulation of T-cell function during ageing and in certain diseases, e.g. diabetes. Both STIM proteins are predominantly ER resident proteins showing basal glycosylation patterns. Mutations of the N-glycosylation sites of STIM1 regulate Ca2+ influx by altered oligomerization of STIM1 and by destabilization of the Ca2+ channel Orai1 (Kilch et al, 2013). In contrast, Orai1 is a complex glycosylated protein. We show that Orai1 glycosylation is cell-type specific and that given the correct repertoire of specific glycosyltransferases the glyco-fingerprint of Orai1 can affect localization and function in calcium signaling.

Bogeski I, Kummerow C, Al-Ansary D, Schwarz EC, Koehler R, Kozai D, Takahashi N, Peinelt C, Griesemer D, Bozem M, Mori Y, Hoth M, Niemeyer BA (2010) Differential redox regulation of ORAI ion channels: a mechanism to tune cellular calcium signaling. Science Signaling 3: ra24

Hoth M, Penner R (1992) Depletion of intracellular calcium stores activates a calcium current in mast cells. Nature 355: 353-356

Kilch T, Alansary D, Peglow M, Dorr K, Rychkov G, Rieger H, Peinelt C, Niemeyer BA (2013) Mutations of the Ca2+-sensing Stromal Interaction Molecule STIM1 Regulate Ca2+ Influx by Altered Oligomerization of STIM1 and by Destabilization of the Ca2+ Channel Orai1. J Biol Chem 288: 1653-1664

Zweifach A, Lewis RS (1993) Mitogen-regulated Ca2+ current of T lymphocytes is activated by depletion of intracellular Ca2+ stores. Proc Natl Acad Sci U S A 90: 6295-6299.

Where applicable, the authors confirm that the experiments described here conform with The Physiological Society ethical requirements.

SA170

Physiological functions of store-operated calcium entry

J. Putney and N. Steinckwich-Besancon

NIEHS, Research Triangle Park, NC, USA

Our laboratory has been investigating the functions of store-operated Ca2+ entry (SOCE) in various physiological contexts by a combined strategy employing cell lines together with genetically modified mouse models. We disclosed significant roles for store-operated channels in the development and function of bone cells, both osteoclasts and osteoblasts; in lacrimal gland function; in differentiation of keratinocytes as well as in their role in wound healing. In this presentation, I will discuss our recent work on the role of store-operated Ca2+ channels in chemotaxing neutrophils.
Chemotaxis is essential for neutrophils to locate sites of inflammation. The formylated chemotactic peptide, fMLF, is an agonist for FRPR1 receptors through which it activates phospholipase C and induces Ca2+ release from intracellular endoplasmic reticulum stores. We first investigated the Ca2+ dependence of chemotaxis in the differentiated HL-60 cell model. Using a transwell assay, we determined that chemotaxis, but not undirected movement, is completely lost in the absence of extracellular Ca2+ or in the presence of the SOCE inhibitor, Gd3+. In many cell types, STIM1, a Ca2+ sensor protein resident in the endoplasmic reticulum, detects the extent of Ca2+ depletion and communicates this to plasma membrane Orai calcium channels to activate SOCE. In addition, STIM1 is known to play a role in organizing the organellar structure of cells through an interaction with the microtubule network. Down regulation by siRNA of STIM1 or its channel partner, Orai1, revealed that both proteins are required for chemotaxis. We over-expressed an eYFP-tagged STIM1, which augmented fMLF-induced Ca2+ signaling, as well as fMLF-induced chemotaxis. We followed the localization of eYFP-STIM1 by confocal microscopy. Chemotaxing cells polarize and move in a crawling way to a target which in this study was a micro-pipette releasing fMLF. During chemotaxis, STIM1 cellular localization was not homogeneous but rather STIM1 accumulated in the rear of migrating cells, the uropode.

We analyzed the effect of STIM1 knock out in neutrophils, in vivo, in a conditional STIM1fl/fl LyzM+/+ knockout mouse model. Treatment of mice with imiquimod cream induced a psoriasis-like skin condition and induced neutrophil migration into the skin. STIM1fl/fl LyzM+/+ knockout mice had significantly less infiltrated neutrophils in the epidermis than control mice. Together, our results suggest that Ca2+ signaling, involving SOCE, is necessary for chemotaxis in vitro and in vivo. STIM1, and by inference SOCE, may play a role in the spatiotemporal dynamics of the uropode. These findings provide new insights to our understanding of how intracellular Ca2+ changes orchestrate the cellular behavior underlying chemotactic directional movement.

Where applicable, the authors confirm that the experiments described here conform with The Physiological Society ethical requirements.

SA171

Decoding calcium signalings for cancer progression

Y. Chen[1], Y. Chen[2], W. Chiu[2] and M. Shen[1,3]

[1]Pharmacology, National Cheng Kung University, Tainan City, Taiwan, [2]Biomedical Engineering, National Cheng Kung University, Tainan, Taiwan and [3]Obstetrics and Gynecology, National Cheng Kung University Hospital, Tainan, Taiwan

The remodeling of Ca^{2+} homeostasis has been suggested as an important event in driving the expression of the malignant phenotypes, such as proliferation, migration, invasion, and metastasis. Store-operated Ca^{2+} entry (SOCE) is a predominant Ca^{2+} entry pathway in epithelial cells. Stromal-interaction molecule 1 (STIM1) is an endoplasmic reticulum (ER) Ca^{2+} sensor that triggers SOCE. The functional significance of STIM1-dependent Ca^{2+} signalings in cancer development and progression has been emerged from studies on breast and cervical cancers. STIM1 overexpression in tumor tissue was noted in 71% cases of early-stage cervical cancer. Tumor expression level of STIM1 was significantly associated with the risk of metastasis and survival, suggesting a diagnostic and prognostic value of STIM1. STIM1-dependent Ca^{2+} signalings are important for cervical cancer growth, migration, and angiogenesis. Interference with STIM1 expression or blockade of SOCE activity inhibited tumor growth and angiogenesis in animal models, confirming the crucial role of STIM1-mediated Ca^{2+} influx in aggravating tumor development *in vivo*. Mechanistic investigations revealed that STIM1 regulates the production of vascular endothelial growth factor (VEGF), a critical stimulator for tumor angiogenesis, from cervical cancer cells. Because of an increase of p21 protein levels and a decrease of Cdc25C protein levels, STIM1-silencing in cervical cancer cells significantly inhibited cell proliferation by arresting the cell cycle at the S and G2/M phases. SOCE activities as well as STIM1 expression were required for epidermal growth factor (EGF)-stimulated cancer cell migration. EGF could stimulate the aggregation and translocation of STIM1 towards to the Orai1-containing regions to mediate SOCE. STIM1-dependent SOCE was necessary for the activation of Ca^{2+}-regulated protease calpain and Ca^{2+}-regulated cytoplasmic kinase Pyk2, which regulated the focal-adhesion dynamics of migratory cervical cancer cells. STIM1 silencing also inhibited the recruitment and association of active focal adhesion kinase (FAK) and talin at focal adhesions, indicating the blockade of force transduction from integrin signaling. EGF-induced phosphorylation of myosin II regulatory light chains and actomyosin formation were dependent on STIM1-mediated Ca^{2+} entry. The direct measurement of cell traction forces revealed that STIM1-dependent Ca^{2+} signaling regulated the traction force generation at cell adhesions. Taken together, these results highlight the potential role of STIM1-dependent signaling as a target to interfere with cancer malignant behaviors.

Where applicable, the authors confirm that the experiments described here conform with The Physiological Society ethical requirements.

SA172

STIM proteins, Ca2+ oscillations and gene expression

P. Kar and A. Parekh

Oxford University, Oxford, UK

Stimulation of cells with physiological concentrations of calcium-mobilising agonists often results in the generation of repetitive cytoplasmic Ca2+ oscillations. Although oscillations arise from regenerative Ca2+ release, they are sustained by store-operated Ca2+ entry through CRAC channels. Ca2+ nanodomains near CRAC channels that open during the oscillatory cycle recruit local signalling pathways that lead to activation of NFAT transcription factors and increased expression of genes including c-fos and tumour necrosis factor-α. Stores communicate with CRAC channels through the ER Ca2+-sensing proteins STIM1 and STIM2. In this talk, we will describe our recent experiments that address the relative roles of STIM1 and STIM2 in maintaining Ca2+ oscillations and gene expression in mast cells. Our results reveal that different agonists utilise different STIM proteins to support Ca2+ signals and subsequent downstream responses. We will also compare gene knockdown strategies with pharmacological block of STIM proteins to address their relative contributions to physiological levels of Ca2+ signalling.

Work in our laboratory is supported by the MRC.

Where applicable, the authors confirm that the experiments described here conform with The Physiological Society ethical requirements.

SA173

Native neuronal Kv4-encoded channels function in macromolecular protein complexes

J.M. Nerbonne

Developmental Biology, Washington University Medical School, St. Louis, MO, USA

Voltage-gated K+ (Kv) channels are key determinants of membrane excitability in the peripheral and in the central nervous systems, functioning to control the resting membrane potentials, the waveforms of action potentials and the repetitive firing properties of individual neurons. In addition, by influencing presynaptic neurotransmitter release and the postsynaptic responses to neurotransmitters, Kv channels regulate the integrative properties of neurons and modulate synaptic potentiation and depression. Electrophysiological studies have distinguished multiple types of Kv currents, based on differences in kinetic, voltage-dependent and/or pharmacological properties, both central and peripheral neurons. Indeed, in most neurons, multiple types of Kv channels with unique time- and voltage-dependent properties, as well as with distinct cellular and subcellular distribution patterns and functional roles, are co-expressed. Consistent with the apparent functional diversity of native neuronal Kv channels, multiple subfamilies of Kv channel pore-forming (α) subunits, as well as numerous putative Kv channel accessory subunits and regulatory proteins, have been identified and shown to be differentially expressed in neurons, as well as in other cell types. Rapidly activating, inactivating and recovering Kv currents, typically referred to as A-type Kv currents (IA), for example, have been shown to be expressed in many peripheral and central neu-

rons and to regulate input resistances, action potential durations, repetitive firing rates and the back-propagation of action potentials into dendrites, and to modulate the responses to synaptic inputs and influence synaptic plasticity. Interestingly, Kv currents with very similar biophysical properties, referred to as Ito,f (fast transient outward Kv currents), have been identified in mammalian cardiac myocytes and shown to control the early phase of myocardial action potential repolarization. Interestingly, a number of recent studies have demonstrated critical roles for pore-forming (α) subunits of the Kv4 subfamily, particularly Kv4.2 and Kv4.3, but also Kv4.1, in the generation of native neuronal IA channels, as well as in the generation of native cardiac Ito,f channels. Studies in heterologous cells have also suggested potential functional roles for a number of transmembrane and cytosolic Kv channel accessory proteins, including members of the minK/MiRP (minimal K+ channel), KChIP (K+ channel interacting protein) and DPP (dipeptidyl peptidase) subfamilies of Kv channel accessory subunits, in the generation of Kv4-encoded channels. Although the results of recent studies using targeted "knockdown" and "knockout" strategies to define directly the physiological role(s) Kv4 channel accessory subunits in determining the functional cell surface expression and the biophysical properties of native Kv4-encoded neuronal IA (and myocardial Ito,f) channels are consistent with some of the results obtained in heterologous overexpression studies, novel physiological roles have also been revealed. In addition, the application of quantitative mass spectrometry-based proteomic analysis as a rapid and unbiased approach to identify the components of native Kv4-encoded neuronal IA (and myocardial Ito,f) channel macromolecular protein complexes has, in addition to confirming association between Kv4 α subunits and the KChIPx and DPPx accessory subunits in brain, also identified a number of novel Kv channel accessory/regulatory proteins. Multiple experimental approaches, exploited in parallel to define the physiological roles of newly identified, putative channel accessory and regulatory subunits in the generation of native neuronal IA channels, will also be discussed.

Where applicable, the authors confirm that the experiments described here conform with The Physiological Society ethical requirements.

SA174

Dynamic aspects of the subunit stoichiometry of the KCNQ/KCNE channel complex

K. Nakajo[1,2] and Y. Kubo[1,2]

[1]Div Biophys & Neurobiol, National Institte for Physiological Sciences, Okazaki, Aichi, Japan and [2]Dept Physiol Sci, Graduate Univ for Advanced Studies, Hayama, Kanagawa, Japan

KCNQ1 is a voltage-gated potassium channel α subunit. KCNQ1 forms a tetramer and gives rise to K^+ conductance in many tissues such as heart, inner ear, kidney, intestine and pancreas. Biophysical properties of KCNQ1 are dynamically modulated by the presence of KCNE proteins. KCNE1, for example, increases KCNQ1 current amplitude, slows down the activation and deactivation kinetics and greatly shifts the conductance-voltage (G-V) curve in the positive (depolarizing) direction. This KCNQ1-KCNE1 complex underlies the slowly-activating K^+ current called I_{Ks} in the heart, and regulates the excitability of cardiac myocytes. KCNE3, co-expressed with KCNQ1 in the intestine, makes KCNQ1 channel constitutively-active. Therefore, the subunit organization of KCNQ1-KCNE complex is essential for the ion channel properties and the physiological functions of KCNQ1.

One of the fundamental questions for KCNQ1 channel is the stoichiometry of KCNQ1-KCNE complex. Previous works indicate the stoichiometry of KCNQ1 and KCNE1 is fixed at 4:2; two KCNE1 proteins bind to a tetrameric KCNQ1 channel. We recently applied the subunit counting method using single GFP molecule imaging to address this question (Nakajo et al. 2010). KCNE1-GFP fusion protein was co-expressed with KCNQ1 channels in *Xenopus* oocytes. Using a total internal reflection microscope, a single bleaching event from a single GFP molecule tagged to KCNE1 protein was observed as a step-wise reduction of fluorescence. The number of KCNE1 proteins in a single ion channel complex can be estimated by the number of bleaching events from a single optical spot. By counting the number of KCNE1 proteins, we found that some of the KCNQ1 ion channel complexes contain four KCNE1 proteins. This result indicates that "4:4" channel (four KCNQ1 subunits with four KCNE1 subunits) does exist. Interestingly, the number of KCNE1 proteins in KCNQ1 channel complex was not fixed but variable. More KCNE1 proteins are expressed, more "4:4" channels are produced. Because "4:4" channel showed slower activation kinetics compared to "4:2" channel, an increase in KCNE1 expression may elevate the excitability of cardiac myocytes.

Our results imply that the dynamic interaction between KCNQ1 and KCNE proteins may occur on the plasmamembrane. If that is the case, KCNQ1 channels expressed on the plasmamembrane can be directly regulated by the association and dissociation of KCNE proteins. To investigate this possibility, we examined electrophysiological properties of series of tandem constructs of KCNQ1 and KCNE1 with various linker lengths. If the stoichiometry of KCNQ1-KCNE1 complex is flexible and dynamically changeable on the plasmamembrane, KCNQ1 channel properties would depend on the linker length between KCNE1 and KCNQ1. KCNE1-KCNQ1 constructs (producing "4:4" channel) showed a linker-length dependent change; as linker length increased, G-V curves were shifted to hyperpolarizing direction. On the other hand, KCNE1-KCNQ1-KCNQ1 constructs (producing "4:2" channel) showed no apparent linker-length dependent change in the G-V curves. These results suggest that 1st and 2nd KCNE1 proteins firmly bind to KCNQ1 channel while 3rd and 4th KCNE1 proteins may bind loosely. 3rd and 4th KCNE1 might dynamically regulate "4:2" channel by association/dissociation on the plasmamembrane. Further experiments are needed to prove the dynamic interaction between KCNQ1 and KCNE proteins on the plasmamembrane.

It is also important to understand how KCNE proteins regulate KCNQ1 channels. Growing evidences from different groups including us indicate that KCNE proteins give influence on the movement of the voltage-sensing domain (VSD; S1-S4 segments) of KCNQ1 channel. By using cysteine-modifying MTS reagents, we showed that the accessibility of S4 segment was significantly changed by the presence of KCNE proteins (Nakajo and Kubo, 2007). As longer depolarization was required to be modified by MTSES, we concluded that the VSD of KCNQ1 was stabilized in the "down" state. On the other hand, KCNE3 stabilized the VSD in the "up" state and that is the reason why KCNE3 makes KCNQ1 a constitutively-open channel. By comparing the amino acid sequence of human KCNQ1 to that of Ci-KCNQ1 (KCNQ1 ortholog from marine chordate *Ciona Intestinalis*), we successfully identified S1 segment of KCNQ1 as a binding site for KCNE3 protein (Nakajo et al. 2011). KCNE1 also interacts with the VSD and modifies its movement. Because KCNQ1-KCNE channel complex can form different stoichiometries, it is important to know how each

VSD is modified by KCNE proteins towards further understanding the modulation of KCNQ1 channel by KCNE proteins.

Nakajo K & Kubo Y (2007) *J Gen Physiol* **130**, 269-81

Nakajo K et al. (2010) *PNAS* **107**, 18862-7

Nakajo K et al. (2011) *J Gen Physiol* **138**, 521-35

Where applicable, the authors confirm that the experiments described here conform with The Physiological Society ethical requirements.

SA175

Gated motions and assembly modalities of the IKS potassium channel complex

M. Dvir[1], D. Shaham[2], I. Ben-Tal Cohen[1], R. Strulovitz[2], Y. Haitin[1], J. Hirsch[2] and B. Attali[1]

[1]Physiology, Tel Aviv University, Tel Aviv, Israel and [2]Biochemistry, Tel Aviv University, Tel Aviv, Israel

Kv7 channels (KCNQ) represent a family of voltage-gated K+ channels, which plays a prominent role in brain and cardiac excitability. Their physiological importance is underscored by the existence of mutations in human Kv7 genes, leading to severe cardiovascular and neurological disorders such as the cardiac arrhythmias and neonatal epilepsy. In the heart, the assembly of Kv7.1 with KCNE1 produces the IKS potassium current that is crucial for the late repolarization of the cardiac action potential. Mutations in either Kv7.1 or KCNE1 genes produce the long QT or short QT syndromes, which are genetically heterogeneous cardiovascular diseases, characterized by ventricular or atrial arrhythmias. The scaffolding A-kinase anchoring protein Yotiao (AKAP9) brings together PKA, PP1, PDE4D3, AC9, and the IKS channel complex to achieve regulation following β adrenergic stimulation. Kv7 channels exhibit some structural and functional features that are distinct from other Kv channels. Notably, the Kv7 family lacks the T1 tetramerization domain and it does not associate with the Kvβ subunit. Rather, it has a large intracellular C-terminal (CT) domain, ranging from 320 to 500 residues in size, bound constitutively to calmodulin. This domain is responsible for channel tetramerization, proper channel trafficking, and gating properties. Here we provide a brief overview of current insights and yet unsettled issues about the gated motions and assembly modalities of the IKS potassium channel complex. Proximal helices A and B form the site for calmodulin (CaM) binding, while distal coiled-coil helices C and D are important for channel tetrameric assembly and protein interactions. We studied the interactions and voltage-dependent motions of IKS channel intra-cellular domains, using fluorescence resonance energy transfer combined with voltage-clamp recording and in-vitro binding of purified proteins. The results indicate that the KCNE1 distal C-terminus interacts with the coiled-coil helix C of the Kv7.1 tetramerization domain. This association is important for IKS channel assembly rules as underscored by Kv7.1 current inhibition produced by a dominant-negative C-terminal domain. Upon channel opening, the C-termini of Kv7.1 and KCNE1 come close together. Co-expression of Kv7.1 with the KCNE1 long QT mutant D76N abolished the K+ currents and gated motions. Thus, during channel gating KCNE1 is not static. Instead, the C-termini of both subunits experience molecular motions, which are disrupted by the D76N causing disease mutation. We investigated the structure of the membrane proximal CT module in complex with CaM by x-ray crystallography. The results show that CaM intimately hugs a two helical-bundle. Biochemical data, structure-based mutagenesis of this module in the context of concatemeric channels and functional analysis lead us to conclude that one CaM binds to one individual protomer, without crosslinking subunits and that this configuration is required for proper channel expression. Molecular modeling of the CT/CaM complex in conjunction with small-angle X-ray scattering and electrophysiology suggest that the membrane proximal region, with a rigid lever arm is a critical gating module. We examined the effect of long QT mutations located at the C-terminal interface of the two subunits. Our results suggest that the distal KCNE1 C-terminus, probably via its interaction with the coiled-coil helix C, is a crucial determinant for the functional modulation of Kv7.1 by Yotiao-mediated PKA phosphorylation.

This study was supported by a DIP-DFG grant, the Israel Science Foundation (ISF 488/09) and the Ministry of Health (MOH:3-6273)

Where applicable, the authors confirm that the experiments described here conform with The Physiological Society ethical requirements.

SA176

The regulation of KCNQ channels by phosphoinositides

S.C. Harmer

William Harvey Heart Centre, Queen Mary University of London, London, UK

Membrane phosphoinositides, and in particular phosphatidylinositol (4,5)-bisphosphate (PIP_2), have been shown to be important for the function of the five members of the KCNQ channel family (KCNQ1-5). In general, our studies have primarily focussed on their actions on KCNQ1. KCNQ1 combines with the auxiliary subunit KCNE1 to form a heteromultimeric channel complex which underlies the cardiac delayed rectifier current I_{Ks}. The activity of this channel can be regulated through $G_{q/11}$-coupled receptors and downstream phospholipase-C (PLC) activation. The activation of PLC leads to I_{Ks} channel inactivation and it is now thought that this occurs due to the hydrolysis of plasma membrane bound PIP_2. In detail, the depletion of PIP_2 leads to channel inactivation by acting to slow the rate of channel activation and increase the rate of channel deactivation and these effects combine to result in a large shift in the voltage dependence of channel activation ($V_{0.5}$) towards depolarised potentials. Although PIP_2 acutely modulates I_{Ks} channel function, the nature of the molecular interactions and the specific residues involved in the binding of PIP_2 to this channel had not been established. Using a combination of biochemical and electrophysiological techniques we have identified that a cluster of basic residues (Lys-354, Lys-358, Arg-360 and Lys-362), located just after the S6 domain in the proximal C-terminus, are crucial for the binding of a range of anionic phospholipids, including PIP_2. The mutation of these charged residues to alanine, singly or in combination, results in a loss of binding to anionic phospholipids and acts to mimic the electrophysiological effects of PIP_2 depletion on channel function by causing a positive shift in the $V_{0.5}$. Our data also suggest that the two middle residues (Lys-358 and Arg-360), which form the core of the charge cluster, appear to be particularly important as their mutation in combination results in a complete loss of binding to PIP_2 (and a range of other phosphoinositides) and a dramatic shift (~+60 mV) in the $V_{0.5}$. Given that the charged residues we have identified in KCNQ1 appear in general to be well conserved in homologous positions in the other members of the KCNQ family it

raises the possibility that the effects of PIP_2 on these channels could also be mediated through similarly located charge clusters. To investigate this possibility we have recently, in collaboration, analysed whether the mutation, to alanine, of homologous residues in KCNQ2 acts to alter this channels response to PIP_2. Interestingly, the mutation of Arg-325 (which is homologous to Arg-360 in KCNQ1) results in a ~60% reduction in current density, without change in the $V_{0.5}$, and an approximately eight-fold reduction in the sensitivity of the channel to activation by an exogenously applied water soluble derivative of PIP_2. In summary, we have identified that charged residues located in the proximal C-terminus of KCNQ1 and in a homologous region in KCNQ2 are involved in regulating the response of these channels to PIP_2. Whether the actions of PIP_2 on the remaining members of the KCNQ family are mediated through similarly located charge clusters remains to be determined.

Where applicable, the authors confirm that the experiments described here conform with The Physiological Society ethical requirements.

SA177

Role of KCNQ4 K+ channels in sensory biology

T.J. Jentsch

FMP/MDC, Berlin, Germany

Human pathologies associated with KCNQ channels include cardiac arrhythmias, deafness, and epilepsy. We have shown previously that the KCNQ4 K+ channel underlies a form of dominant human hearing loss (1) and have generated mouse models which showed that this pathology is owed to a degeneration of cochlear sensory outer hair cells (OHCs) that depolarize in the absence of KCNQ4 (3). KCNQ4 localizes to the base of OHCs and is also found at calyx synapses of type vestibular hair cells and selected tracts and nuclei of the brainstem (2). In contrast to cochlear hair cells, KCNQ4 is expressed postsynaptically at vestibular hair cell synapses, where it may contribute to remove K+ from the synaptic cleft (4). Mice lacking KCNQ4 show discrete vestibular symptoms which have also been observed in some humans with KCNQ4-related hearing loss.

The expression of KCNQ4 in trigeminal ganglia (2) prompted us to examine its expression in dorsal root ganglia (DRGs). Indeed, we found KCNQ4 to be expressed in a subset of large diameter DRG neurons (5). These innervate a subset of rapidly adapting skin mechanoreceptors, where they localize to sensory nerve endings. Both our Kcnq4 mouse models, as well as patients with KCNQ4 mutations, showed altered skin mechanoreception (5). KCNQ4 tunes the response of mechanoreceptors to their optimal frequencies. KCNQ4 has multiple, rather unrelated roles in sensory biology.

Kubisch C., Schroeder B.C., Friedrich T., Lütjohann B., El-Amraoui A., Marlin S., Petit C., Jentsch T.J. (1999). KCNQ4, a potassium channel expressed in sensory outer hair cells, is mutated in dominant deafness. Cell 96: 437-446.

Kharkovets T., Hardelin J.P., Safieddine S., Schweizer M., El-Amraoui A., Petit C., Jentsch T.J. (2000). KCNQ4, a K+-channel mutated in a form of dominant deafness, is expressed in the inner ear and in the central auditory pathway. Proc. Natl. Acad. Sci. U.S.A. 97: 4333-4338.

Kharkovets T., Dedek K., Maier H., Schweizer M., Khimich D., Nouvian R., Vardanyan V., Leuwer R., Moser T., Jentsch T.J. (2006). Mice with altered KCNQ4 K+ channels implicate sensory outer hair cells in human progressive deafness. EMBO J. 25, 642-652.

Spitzmaul G., Tolosa L., Winkelman B.H.J., Heidenreich M., Frens M.A., Chabbert C., de Zeeuw C.I., Jentsch T.J. (2013). Vestibular role of KCNQ4 and KCNQ5 K+ channels revealed by mouse models. J. Biol. Chem., electr. prepub.

Heidenreich, M., Lechner S.G., Vardanyan V., Wetzel C., Cremers C.W., De Leenheer E.M., Aránguez G., Moreno-Pelayo M.A., Jentsch T.J.*, Lewin G.R.* (2012). KCNQ4 K+ channels tune mechanoreceptors for normal touch sensation in mouse and man. Nature Neurosci. 15, 138-145.

Where applicable, the authors confirm that the experiments described here conform with The Physiological Society ethical requirements.

SA178

Therapeutic potential of endothelial growth factors and receptors

K. Alitalo

Wihuri Research Institute, Helsinki, Finland and Translational Cancer Biology Research Program, University of Helsinki, Helsinki, Finland

Cancer and cardiovascular diseases are the leading causes of morbidity and mortality in the developed countries. Current cardiovascular and cancer therapies are often insufficient, unsuccessful or not suitable for all patients, thus novel therapies are urgently needed. Inhibition of angiogenesis is already used in the clinics, but with limited success. On the other hand, stimulation of the growth of blood vessels, angiogenesis, and of arteriogenesis has been unsuccessfully tried for the treatment of tissue ischemia in humans. The elucidation of disease-related functions of endothelial growth factors and their signal transduction in cancer and cardiovascular disease should help in development of improved therapy for these diseases. Possible new therapy requires on solid knowledge of the biology of vascular endothelial growth factors, angiopoietins, angiogenesis and lymphangiogenesis.

Where applicable, the authors confirm that the experiments described here conform with The Physiological Society ethical requirements.

SA179

Distinguishing neuropilin signalling in angiogenesis, arteriogenesis and vascular permeability

C. Ruhrberg

UCL, London, UK

Vascular morphogenesis requires the complementary processes of vasculogenesis, angiogenesis and arteriogenesis. All three processes are VEGF-A dependent, but how VEGF-A signalling is regulated to selectively stimulate each one at the appropriate time is poorly understood. The VEGF-A isoform specific receptor neuropilin 1 (NRP1) contributes to both angiogenesis and arteriogenesis and has additionally been implicated in vascular permeability. We find that mice expressing solely a truncated form of NRP1 lacking the cytoplasmic domain have normal angiogenesis. In contrast, they show reduced arteriogenesis, similar to mice lacking synectin/GIPC1, which binds the NRP1 cytoplasmic domain. Tissue culture studies linked the arteriogenic defect to impaired VEGFR2 endocytosis downstream of VEGF-A activation, which increased dephosphorylation of the VEGFR2 site that activates ERK1/2

signalling. Mice lacking the NRP1 cytoplasmic tail also showed reduced VEGF-A induced vascular permeability, but, synectin was not required for the permeability response. Taken together, these findings suggest that the membrane-anchored extracellular domain of NRP1 is sufficient for angiogenesis, whilst arteriogenesis and vascular permeability additionally require the NRP1 cytoplasmic tail, with a differential dependence on synectin.

Where applicable, the authors confirm that the experiments described here conform with The Physiological Society ethical requirements.

SA180

Formation of microvascular networks: role of stromal interactions directing endothelial growth

J.B. Hoying[1], U. Utzinger[2] and J.A. Weiss[3]

[1]Cardiovascular Therapeutics, Cardiovascular Innovation Institute, Louisville, KY, USA, [2]Biomedical Engineering, University of Arizona, Tucson, AZ, USA and [3]Bioengineering, University of Utah, Salt Lake City, UT, USA

In the adult, angiogenesis leads to an expanded microvascular network as new vessel segments are added to an existing microcirculation(1). This necessarily means that growing neovessels must navigate through tissue stroma as they locate and grow towards other neovessels and/or existing vessels of the parent network. We have a growing body of evidence demonstrating that angiogenic neovessels reciprocally interact with the stromal environment (interstitial matrix and stromal cells) resulting in persistent and directed neovascular growth during angiogenesis(2-4). Given the malleability of matrix elements and the viscoelastic properties of collagen gels, neovessel guidance by the stroma is likely due to perpendicular compressive forces arising from active tissue deformation. These similar stromal influences can also control the final network topology of the new microcirculation, including the distribution of arterioles, capillaries and venules(5). In this case, stromal-derived stimuli must be present during the post-angiogenesis remodeling and maturation phases of neovascularization in order to have this effect. Interestingly, the pre-existing organization of vessels prior to the start of angiogenesis has no lasting influence on the final, new network architecture. Additionally, we have new evidence that tissue stromal cells enable the invasion of growing neovessels across interstitial matrix interfaces during angiogenesis through a paracrine-dependent process. Importantly, stromal cells need to be spatially near the growing neovessels suggesting a local, but as of yet undefined, interaction. Combined, the evidence describes interplay between angiogenic neovessels and stroma that is important in directed neovessel growth and invasion. This dynamic is also likely a mechanism by which global tissue forces influence vascular form and function.

Leblanc AJ, Krishnan L, Sullivan CJ, Williams SK, and Hoying JB. Microvascular Repair: Post-Angiogenesis Vascular Dynamics. Microcirculation 19(8):676-95 2012.

Kirkpatrick ND, Andreou S, Hoying JB, and Utzinger U. Live imaging of collagen remodeling during angiogenesis. AmJPhysiol Heart CircPhysiol 292: H3198-H3206, 2007.

Krishnan L, Hoying JB, Nguyen H, Song H, and Weiss JA. Interaction of angiogenic microvessels with the extracellular matrix. AmJPhysiol Heart CircPhysiol 293: H3650-H3658, 2007.

Krishnan L, Underwood CJ, Maas S, Ellis BJ, Kode TC, Hoying JB, and Weiss JA. Effect of mechanical boundary conditions on orientation of angiogenic microvessels. CardiovascRes 78: 324-332, 2008.

Chang CC, Krishnan L, Nunes SS, Church KH, Edgar LT, Boland ED, Weiss JA, Williams SK, and Hoying JB. Determinants of microvascular network topologies in implanted neovasculatures. Arterioscler Thromb Vasc Biol 32: 5-14, 2012.

Supported by USA NIH grants EB007556 and HL077683

Where applicable, the authors confirm that the experiments described here conform with The Physiological Society ethical requirements.

SA181

The intermediate filament cytoskeleton plays a key role in endothelial sprout initiation

K.J. Bayless[1], H. Kang[1], C.L. Duran[1], C.A. Abbey[1], H. Kwak[1], J.M. Dave[1], R.R. Kaunas[2] and S.A. Maxwell[1]

[1]Molecular & Cellular Medicine, Texas A&M Health Science Center, College Station, TX, USA and [2]Biomedical Engineering, Texas A&M University, College Station, TX, USA

Endothelial cells normally line the vasculature and remain quiescent. However, these cells can be rapidly stimulated to initiate new blood vessel formation given the proper cues. This study reports a new mechanism for initiating angiogenic sprout formation that involves vimentin, the major intermediate filament protein in endothelial cells. We utilized two models to stimulate endothelial sprouting responses into three-dimensional collagen matrices, where sphingosine 1-phosphate (S1P) was combined with either growth factors (GF) or wall shear stress (WSS). Initial studies confirmed vimentin was required for both S1P + GF- and S1P + WSS-induced endothelial cell invasion. We also observed that vimentin was cleaved by calpains during invasion. Calpains were predominantly activated by GF and were required for sprout initiation. Because others have reported membrane type 1 – matrix metalloproteinase (MT1-MMP) is required for endothelial sprouting responses, we tested whether vimentin and calpain acted upstream of MT1-MMP. Both calpain and vimentin were required for successful MT1-MMP membrane translocation in both invasion systems, which shared a common activation by S1P. In addition, vimentin complexed with MT1-MMP in a manner that required both the cytoplasmic domain of MT1-MMP and calpain activation, which increased the soluble pool of vimentin in endothelial cells. Altogether, these in vitro data indicate that pro-angiogenic signals converge to activate calpain-dependent vimentin cleavage and increase vimentin solubility, which act upstream to facilitate MT1-MMP membrane translocation, resulting in successful endothelial sprout formation in three-dimensional collagen matrices. To confirm these data in an in vivo model, wound healing studies were conducted in mice anesthetized with a ketamine/xylazine cocktail in an acceptable plane of anesthesia. Mice were treated with FTY720, a pharmacological antagonist of S1P or vehicle control. Compared to vehicle, FTY720 treatment significantly reduced vascular density at 9 days of wound healing. In addition, mice lacking vimentin exhibited reduced angiogenic responses compared to wild-type littermates. These data help reinforce a requirement for S1P in angiogenic responses in vivo, as well as a critical role for vimentin in angiogenic responses during wound healing. In addition, these findings help explain why S1P synergizes with GF and WSS to stimulate robust sprouting in 3D collagen matrices.

This work was supported by Public Health Service grant HL-095786 from the National Heart Lung and Blood Institute (KJB).

Where applicable, the authors confirm that the experiments described here conform with The Physiological Society ethical requirements.

SA182

Recruitment and role of platelets and leukocytes in models of infection and immunity

P. Kubes

Physiology and Pharmacology, University of Calgary, Calgary, AB, Canada

The hemocyte plays the role of both platelets and leukocytes in invertebrates. In mammals, two separate cell types exist including the platelet which has been assigned the role of hemostasis and the neutrophil which is an innate immune cell involved in fighting infection. However this separation is somewhat artificial and probably does not accurately represent the function of platelets and neutrophils. In fact the platelet likely contributes to both sterile inflammation and in host response to infections. In sterile injury in for example the liver the platelet arrives at sites of injury in seconds plugging sinusoids. This occurs via certain integrins and functions to permit the neutrophil to gain access to the site of injury. In infection in the liver, the platelet also contributes meaningfully. In fact, we have identified a novel patrolling mechanism for platelets in the sinusoids where a touch and go interaction continuously occurs with the intravascular macrophage of the liver, the Kupffer cell. When a bacterium is caught by Kupffer cells, the platelets touch but don't let go and form an encapsulation around the microbe and prevent dissemination. If the microbe persists in the vasculature, the platelet also binds neutrophils and induces the formation of Neutrophil Extracellular Traps in the vasculature thereby helping to catch intravascular free-flowing bacteria. In fact the trapping can be improved 4-fold above the constitutive Kupffer cell trapping of bacteria. Clearly the platelet contributes to neutrophil recruitment to sites of sterile injury as well as to neutrophil and macrophage function to help eradicate infections.

Where applicable, the authors confirm that the experiments described here conform with The Physiological Society ethical requirements.

SA183

Leukocyte recruitment during angiogenesis

M. Phillipson

Medical cell biology, Uppsala University, Uppsala, Sweden

Blood vessel growth, angiogenesis, is a tightly regulated process involving not only endothelial cells, but also several different cell types. Leukocytes are known to accumulate at sites of hypoxia and were recently identified as key players in the process of vessel neo-formation. Recognition of leukocyte involvement in angiogenesis has unlocked a new research area especially focusing on tumor vascularization, but the dynamics of leukocyte involvement in angiogenesis, as well as their exact pro-angiogenic actions are still largely unknown. To address this, we developed a model that allows for in vivo visualization and tracking of leukocytes at the site of angiogenesis.
Isolated pancreatic islets are transplanted to the cremaster muscle of genetically identical recipient mice. Leukocytes, endothelial cells and blood flow at the site of islet transplantation are studied in parallel at different time points following transplantation using high-speed in vivo confocal microscopy. We found that isolated islets transplanted to striated muscle rapidly regained their dense, glomeruli-like capillary network. Neutrophils were crucial for initiation of this process and islets transplanted to neutropenic mice did not become revascularized. In fact, a distinct neutrophil subset with proangiogenic actions was recruited from the circulation to the site of hypoxia by islet-derived vascular endothelial growth factor A (VEGF-A), the main angiogenic factor. Proinflammatory neutrophils were not recruited by VEGF-A and expressed distinct lower levels of the chemokine receptor CXCR4 compared to the proangiogenic subset. Proangiogenic neutrophils delivered highly active MMP-9 (matrix metalloproteinase 9) known to be important for angiogenesis to the site of islet transplantation. The role of neutrophil-derived MMP-9 was demonstrated by transplanting islets to MMP-9 deficient mice, which resulted in severely delayed development of the intra-islet capillary network as well as an altered vascular network at later time points following transplantation. Further, our data imply the existence of two separate neutrophil lineages already in circulation based on the levels of CXCR4. These different neutrophil subsets did not change phenotype by in vitro stimulation with MIP-2 (CXCL2) or VEGF-A. Not only neutrophils exert proangiogenic actions, and ongoing studies in my laboratory address both neutrophil and monocyte recruitment to sites of hypoxia, as well as the different roles of neutrophils and macrophages for vessel neoformation and maturation. We also track the migration pattern and cellular interactions of the different cell types to understand the respectively driving force and actions during angiogenesis.
Thus, by using a new in vivo imaging model for studying the behavior and actions of different leukocyte populations during angiogenesis, important information of their identities and actions are gained. We found that neutrophils and macrophages have very different, but profound roles and effects on the revascularization of transplanted pancreatic islets.

These studies were supported by the Swedish Research Council, the Swedish Diabetes Association, the Novo Nordisk foundation, the Diabetes Wellness foundation and the Ragnar Söderberg foundation. Mia Phillipson is a Wallenberg Academy fellow.

Where applicable, the authors confirm that the experiments described here conform with The Physiological Society ethical requirements.

SA184

Regulation of endothelial junctions in leukocyte extravasation

D. Vestweber

Max Planck Institute for Molecular Biomedicine, Muenster, Germany

The formation of endothelial junctions and their regulation in patho-physiological processes is regulated by complex mechanisms that modulate the actomyosin based cytoskeleton and cell adhesion activities at endothelial contacts. The stability of endothelial junctions is centrally dependent on the adhesive function of VE-cadherin. We have recently shown that knock in mice expressing a fusion protein consisting of VE-cadherin and α-catenin instead of wt VE-cadherin are strongly impaired

in VEGF- or histamine-induced vascular permeability and in cytokine-induced recruitment of leukocytes into various inflamed tissues. These results demonstrate that both processes require in vivo interference with the adhesive function of VE-cadherin.

In vitro studies have suggested that the phosphorylation of certain tyrosine residues in VE-cadherin is involved in the induction of transendothelial permeability and transmigration of leukocytes through cultured endothelial cell layers. In agreement with this, we found that the endothelial specific receptor type protein tyrosine phosphatase, VE-PTP, associates with VE-cadherin and supports its adhesive function. We showed recently that the dissociation of VE-PTP from VE-cadherin is in vivo necessary for leukocyte extravasation and induction of vascular permeability.

To analyze the relevance of tyrosine phosphorylation of VE-cadherin for the regulation of endothelial junctions in vivo we have generated knock in mice where certain tyrosine residues in VE-cadherin were replaced by phenylalanines. In addition, we generated specific antibodies for each of these different phosphorylated tyrosines within VE-cadherin. Surprisingly, we found differential regulation of the phosphorylation of these residues in vivo. Furthermore, analysis of the induction of vascular permeability and leukocyte recruitment in the different knock in mice revealed distinct roles for different tyrosine residues.

Schulte D, Küppers V, Dartsch N, Broermann A, Li H, Zarbock A, Kamenyeva O, Kiefer F, Khandoga A, Massberg S, Vestweber D. Stabilizing the VE-cadherin catenin complex blocks leukocyte extravasation and vascular permeability. EMBO J. 30: 4157-4170 (2011)

Broermann A, Winderlich M, Block H, Frye M, Rossaint J, Zarbock A, Cagna G, Linnepe R, Schulte D, Nottebaum AF, Vestweber D. Dissociation of VE-PTP from VE-cadherin is required for leukocyte extravasation and for VEGF-induced vascular permeability in vivo. J. Exp. Med. 208:2393-2401 (2011)

Vestweber D. Novel insights into leukocyte extravasation. Curr. Opin. Hematol. 19: 212-217 (2012)

Where applicable, the authors confirm that the experiments described here conform with The Physiological Society ethical requirements.

SA185

Mode and dynamics of neutrophil transmigration *in vivo*

S. Nourshargh

William Harvey Research Institute, Barts and The London Medical School, Queen Mary University of London, London, UK

Migration of leukocytes to sites of injury or inflammation is a critical component of both innate and adaptive immunity. To penetrate venular walls, leukocytes must migrate through multiple barriers, endothelial cells (EC), the pericyte sheath and the venular basement membrane (BM) 1, 2. Although there is increasing interest and understanding of the mechanisms that mediate transendothelial cell migration (TEM), the relative contribution of individual molecules requires further clarification 1, 2. Within our group we aim to investigate the mode and mechanisms of leukocyte transmigration through imaging of inflamed tissues by multiple methods, including the application of high resolution confocal intravital microscopy. With this approach we have noted previously unreported physiological responses (eg ICAM-1-mediated sub-endothelial cell crawling 3) and also potential pathological events such as "disrupted" modes of neutrophil TEM 4. The latter includes the first direct observation of in vivo neutrophil reverse TEM (rTEM) within a mammalian system, a response that we have associated with reduced expression of JAM-C from EC junctions, indicating a key role for JAM-C in regulation of polarised luminal to abluminal neutrophil TEM 4.

In investigating the pathophysiological relevance of rTEM we noted that this response was most prevalent following ischemia-reperfusion (I-R) injury and was associated with the presence of a subset of functionally primed neutrophils within the pulmonary vasculature which correlated with the development of acute lung inflammation 4. As loss of EC JAM-C from a primary site of injury/inflammation appears to be instrumental in turning a local inflammatory response to a systemic multi-organ phenomena, on-going works have aimed to elucidate the prevalence of this event and its associated mechanisms.

Overall, through rigorous analysis of leukocyte-vessel wall interactions by direct real-time imaging of inflamed tissues, our findings provide novel insights into the cellular and molecular mechanism via which leukocytes breach venular walls in vivo, findings that are likely to identify novel and disease-specific phenomena. Collectively, our findings have contributed to the developing concept that neutrophils have a broader role in inflammation, immunity and pathogenesis of inflammatory disorders than conventionally considered, emphasising the need for greater insight into the mode, mechanisms and implications of neutrophil trafficking in vivo.

Nourshargh,S., Hordijk,P.L., & Sixt,M. Breaching multiple barriers: Leukocyte motility through venular walls and the interstitium. Nat Rev Mol Cell Biol 11, 366-378 (2010).

Ley,K., Laudanna,C., Cybulsky,M.I., & Nourshargh,S. Getting to the site of inflammation: the leukocyte adhesion cascade updated. Nat Rev Immunol 7, 678-689 (2007).

Proebstl,D. et al. Pericytes support neutrophil subendothelial cell crawling and breaching of venular walls in vivo. J Exp Med 209, 1219-1234 (2012).

Woodfin,A. et al. The junctional adhesion molecule JAM-C regulates polarized transendothelial migration of neutrophils in vivo. Nat Immunol 12, 761-769 (2011).

Funded by the Wellcome Trust

Where applicable, the authors confirm that the experiments described here conform with The Physiological Society ethical requirements.

SA186

Molecular correlates of pain in the anterior cingulate cortex

L. Wu

Department of Cell Biology and Neuroscience, Rutgers University, Piscataway, NJ, USA and Department of Physiology, University of Toronto, Toronto, ON, Canada

Glutamatergic transmission and plasticity in the brain are critical for behaviors, such as memory, addiction, and chronic pain. In the anterior cingulate cortex (ACC), a brain area related to persistent pain, peripheral inflammation caused functional alterations in NMDA receptors and glutamate release (Wu et al., 2005; Zhao et al., 2006). The mechanism underlying the regulation of glutamatergic transmission remains elucidated. Among many possible candidate molecules, cyclic AMP (cAMP) is a key second messenger for synaptic plasticity and chronic pain in the ACC. We have found impaired synaptic plasticity in the ACC (Liauw et al., 2005) and attenuated behavioral sensitization in various chronic pain models in mice lacking calmodulin-stimulated adenylyl cyclase (AC) 1 and AC8 (Wei

et al., 2002). Moreover, cAMP pathway is involved in both postsynaptic and presynaptic alterations in the ACC after chronic pain (Wu et al., 2005; Xu et al., 2008; Zhao et al., 2006). However, the dissection of the relative contributions of pre- and postsynaptic components to chronic pain in the brain is difficult. Particularly, it is unclear if changes in presynaptic glutamate release related to cAMP pathway may be sufficient to cause behavioral nociceptive responses.

In order to address this question, we took advantage of transgenic mice heterologously expressing an Aplysia octopamine receptor (Ap oa1) (Isiegas et al., 2008). This G protein coupled receptor selectively activates the cAMP pathway after binding of its natural ligand, octopamine (Chang et al., 2000), in the forebrain. Using whole cell recording of pyramidal neurons in the ACC, we found that activation of Ap oa1 by octopamine enhanced glutamatergic synaptic transmission (127.5±6.8% of control, n=11, P<0.01, paired t-test). The facilitatory effects was mediated activation of Ap oa1 at presynaptic site, as octopamine increased the frequency of miniature excitatory postsynaptic currents (from 3.9±0.9 Hz to 5.6±1.1Hz, n=8, P<0.01, paired t-test) and decreased paired pulse facilitation (1.48±0.09 to 1.28±0.06, n=14, P<0.05, paired t-test). Bilateral microinjection of octopamine into the ACC significantly facilitated behavioral responses to inflammatory pain (the formalin test, F(1,286) = 5.46, P<0.037, two-way ANOVA) but not acute pain. The present study provides the first evidence linking enhanced presynaptic glutamate release in the ACC to behavioral sensitization caused by peripheral inflammation.

Chang, D.J., Li, X.C., Lee, Y.S., Kim, H.K., Kim, U.S., Cho, N.J., Lo, X., Weiss, K.R., Kandel, E.R., and Kaang, B.K. (2000). Activation of a heterologously expressed octopamine receptor coupled only to adenylyl cyclase produces all the features of presynaptic facilitation in aplysia sensory neurons. Proc Natl Acad Sci U S A 97, 1829-1834.

Isiegas, C., McDonough, C., Huang, T., Havekes, R., Fabian, S., Wu, L.J., Xu, H., Zhao, M.G., Kim, J.I., Lee, Y.S., et al. (2008). A novel conditional genetic system reveals that increasing neuronal cAMP enhances memory and retrieval. J Neurosci 28, 6220-6230.

Liauw, J., Wu, L.J., and Zhuo, M. (2005). Calcium-stimulated adenylyl cyclases required for long-term potentiation in the anterior cingulate cortex. J Neurophysiol 94, 878-882.

Wei, F., Qiu, C.S., Kim, S.J., Muglia, L., Maas, J.W., Pineda, V.V., Xu, H.M., Chen, Z.F., Storm, D.R., Muglia, L.J., et al. (2002). Genetic elimination of behavioral sensitization in mice lacking calmodulin-stimulated adenylyl cyclases. Neuron 36, 713-726.

Wu, L.J., Toyoda, H., Zhao, M.G., Lee, Y.S., Tang, J., Ko, S.W., Jia, Y.H., Shum, F.W., Zerbinatti, C.V., Bu, G., et al. (2005). Upregulation of forebrain NMDA NR2B receptors contributes to behavioral sensitization after inflammation. J Neurosci 25, 11107-11116.

Xu, H., Wu, L.J., Wang, H., Zhang, X., Vadakkan, K.I., Kim, S.S., Steenland, H.W., and Zhuo, M. (2008). Presynaptic and postsynaptic amplifications of neuropathic pain in the anterior cingulate cortex. J Neurosci 28, 7445-7453.

Zhao, M.G., Ko, S.W., Wu, L.J., Toyoda, H., Xu, H., Quan, J., Li, J., Jia, Y., Ren, M., Xu, Z.C., et al. (2006). Enhanced presynaptic neurotransmitter release in the anterior cingulate cortex of mice with chronic pain. J Neurosci 26, 8923-8930.

Dr. Long-Jun Wu is supported by Scientist Development Grant from American Heart Association (11SDG7340011).

Where applicable, the authors confirm that the experiments described here conform with The Physiological Society ethical requirements.

SA187

Maladaptive brain plasticity in pain: amygdala and prefrontal cortex

V. Neugebauer

Neuroscience & Cell Biology, Univ. of Texas Medical Branch, Galveston, TX, USA

The amygdala is generally considered a brain center for emotions. In pain models, synaptic plasticity develops in a network of lateral (LA), basolateral (BLA) and central (CeA) nuclei. The resulting hyperactivity of CeA neurons drives amygdala-dependent pain behaviors such as emotional-affective responses (vocalizations) and anxiety. Hyperactivity of BLA neurons inhibits processing in the medial prefrontal cortex (mPFC) through “feedforward inhibition”, resulting in cognitive deficits such as impaired decision-making. Counteracting abnormal inhibition of mPFC output neurons mitigates cognitive deficits and also inhibits pain behaviors. At least part of this beneficial effect involves cortical inhibition of amygdala neurons, suggesting that strategies to restore cortical control may have therapeutic value.

Neugebauer, V., Galhardo, V., Maione, S. and Mackey, S.C. Forebrain Pain Mechanisms. Brain Res. Rev. 60:226-242, 2009

Ji, G., Sun, H., Fu, Y., Li, Z., Pais-Vieira, M., Galhardo, V. and Neugebauer, V. Cognitive impairment in pain through amygdala-driven prefrontal cortical deactivation. J. Neurosci. 30: 5451–5464, 2010

Sun, H. and Neugebauer, V. mGluR1, but not mGluR5, activates feedforward inhibition in the medial prefrontal cortex to impair decision-making. J. Neurophysiol. 106:960-973, 2011

Ji, G. and Neugebauer, V. Modulation of medial prefrontal cortical activity using in vivo recordings and optogenetics. Mol. Brain 5:36-45, 2012

Kiritoshi, T., Sun, H., Ren, W., Stauffer, S.R., Lindsley, C.W., Conn, P.J. and Neugebauer, V. Modulation of pyramidal cell output in the medial prefrontal cortex by mGluR5 interacting with CB1. Neuropharmacology 66:170–178, 2013

Supported by NIH grants R01NS38261, P01NS11255, RR029876

Where applicable, the authors confirm that the experiments described here conform with The Physiological Society ethical requirements.

SA188

Central neuronal mechanisms underlying the central post stroke pain

B. Shyu

Institute of Biomedical Sciences, Taipei, Taiwan

Approximately 8-14% of stroke victims suffer central post-stroke pain (CPSP) and such a cause of pain affects a large number of people, many of whom are not referred for proper medical evaluation or treatment. Studies that addressed the detailed mechanisms of CPSP are not well established, thus resulting in presently inadequate therapies (Bowsher, 2001). CNS inflammation arises from initial insults of ischemic and traumatic brain injuries such as stroke may give rise to increased levels of extracellular nucleotides. These extracellular nucleotides and their metabolites may activate a variety of cell surface purinergic receptors, influence the inflammatory activities among responding cells. Many of these activities are mediated through P2X receptors, and in particular, through

the activation of the subtype, P2X7 receptor (Wang X. et al., 2004). P2X7 receptors have been highly postulated to be associated with nociceptive transmission and chronic neuropathic pain. However, it still unclear is whether P2X7 receptors directly participate in pain signaling in the CPSP.

Proliferation of microglia and glia cells in dorsal root ganglia was reported in neuropathic pain induced by spinal cord injury or peripheral injury. Over expression of brain-derived neurotrophic factor (BDNF) by proliferated microglia or glia cell in dorsal root ganglia after injury was a factor related to neuropathic pain (Zhang. et al., 2011). Expression of KCC2 and NKCC1 channels of mature neuron cell could be changed after the over expression of BDNF and intracellular chloride concentration would be in an unbalance state that could cause an abnormal excitation (Jolivalt et al., 2008).

In the present study, we tested the hypothesis that persistent CPSP is caused by P2X7 receptor activation and BDNF over expression after thalamic tissue damage and subsequent elevations in inflammatory cytokines, such as IL-1β. A CPSP rat model was utilized to elucidate the characteristics of CPSP. Male Sprague-Dawley rats (300–400 g) were housed in an air-conditioned room with free access to food and water. All experiments were carried out in accordance with the guidelines of the Academia Sinica Institutional Animal Care and Utilization Committee. Type 4 collagenase (0.125U/0.5 μl) was injected into rats' lateral thalamic area. Significant hyperalgesia to mechanical and thermal pain stimulation were developed beginning 1 week after surgical CPSP induction, which persisted for at least 5-6 weeks compared with their contralateral unaffected side. P2X7 receptors and inflammatory cytokines were found highly elevated in the thalamus under CPSP conditions. Induced CPSP rats with early treatment of P2X7 antagonist exhibited reduction of hyperalgesia and hyper neuronal excitability. Early treatment with P2X7 receptor antagonist also blocked the enrichment of microglia aggregation and elevated P2X7, TNF-α, IL-6, and I-L1β but not BDNF levels. Activity of medial thalamus was enhanced after repeated noxious stimuli in CPSP animal and this enhancement could be blocked by acute TrKB-FC (an extracellular scavenger of BDNF) infusion. Medial thalamic spontaneous oscillatory activities could be suppressed by GABAA receptor agonist in control rats but that was enhanced in CPSP rats. Compared to control group, the expression of BDNF in medial thalamus was increased in CPSP. But expressions of GABAA channel and KCC2 channel were decreased in CPSP group. Expressions of TrKB receptor and NKCC1 channel were not different between two groups.

Our results suggested that differential mechanisms involved glutamatergic and GABAergic neurotransmission were mediated by P2X7 receptor activation and BDNF over expression respectively after CPSP development. Targeting P2X7 receptors and BDNF may be bi-effectively therapeutic as a treatment for CPSP, as a pain blocker and immunosuppressant that inhibits inflammatory damage to brain tissue which will be widely beneficial for the recovery of central pain of patients suffered from stroke.

Bowsher D. Stroke and central poststroke pain in an elderly population. J Pain. 2001;2(5):258-61.

Wang X, Arcuino G, Takano T, Lin J, Peng WG, Wan P, et al. P2X7 receptor inhibition improves recovery after spinal cord injury. Nat Med. 2004;10(8):821-7.

Zhang X, Wang J, Zhou Q, Xu Y, Pu S, Wu J, Xue Y, Tian Y, Lu J, Jiang W, Du D. Brain-derived neurotrophic factor-activated astrocytes produce mechanical allodynia in neuropathic pain. Neuroscience. 2011;199:452-60.

Jolivalt CG, Lee CA, Ramos KM, Calcutt NA. Allodynia and hyperalgesia in diabetic rats are mediated by GABA and depletion of spinal potassium-chloride co-transporters. Pain. 2008;140(1):48-57.

The authors thank Dr. Daniel Kai-Yuan Hsu and Ms. Hong-Ann Ting from GlycoCore for technical advice and assistance with RT-PCR and the Common Equipment Core Facility of the IBMS, Academia Sinica for imaging processing advices. The present study is supported by the IBMS, Academia Sinica Taiwan, and a National Science Council grant to Dr. Bai-Chuang Shyu (NSC# 99-2811-B-001-072).

Where applicable, the authors confirm that the experiments described here conform with The Physiological Society ethical requirements.

SA189

Functional changes in entorhinal-hippocampal circuits may contribute to pain-associated object recognition memory impairment

J. Chen

Institute for Biomedical Sciences of Pain, The Fourth Military Medical University, Xi'an, China

Entorhinal-hippocampal (EC-HIP) circuits are major synaptic organizations involved in episodic memory that is acquired, stored and retrieved through its auto-association network. Neurons in layer II of the entorhinal cortex send their direct projections to dentate gyrus, while the EC layer III neurons send their fibers directly to CA1, through perforant path. The EC-HIP synaptic connections have been believed to be responsible for object recognition memory (ORM) in animals. In this report, ORM test was first used to examine whether, if any, how pain can influence upon recollection of episodic memory? Then multi-electrode array recording technique and 2D-current source density imaging were used to check whether there are spatial and temporal changes in EC-HIP circuits in the hippocampal slices? Finally, the possible mechanisms underlying nociception-associated spatial and temporal changes in EC-HIP circuits were studied. Our major results are as follows: (1) rat's OBM could be impaired by both acute inflammatory pain and chronic neuropathic pain although there was a time difference in onset. (2) peripheral blockade or morphine suppression of nociceptive afferent impulses could prevent OBM from impairing in inflammatory pain model, but not in neuropathic pain model, suggesting a difference in the underlying mechanisms. (3) when checking the induction of long-term potentiation (LTP) and long-term depression (LTD) between inflammatory and neuropathic pain states, it was surprisingly shown that higher LTP induction was accompanied by lower LTD induction in inflammatory pain model, whereas, lower LTP induction was accompanied by higher LTD induction in neuropathic pain model. Moreover, spatial enlargement of EC-HIP synaptic network was commonly observed in both types of pain models. In conclusions: (1) persistent or chronic pain impairs episodic memory recollection in rats regardless of etiology; (2) spatially and temporally functional alterations of EC-HIP circuits may contribute to pain-associated object recognition memory impairment; (3) nociceptive pain enhances LTP with blocking LTD, whereas, neuropathic pain, like stress, enhances LTD with blocking LTP. This pain etiology-specific temporal plasticity in the hippocampal formation may shed new light on the brain mechanisms of pain comorbidities such as amnesia, anxiety and depression.

Yassa M & Stark CEL (2011). Trends Neurosci 34,515-525.

Apkarian AV et al. (2011). Pain 152, S49-64.

Liu MG & Chen J (2009). Neurosci Bull 25, 237-266.

Liu MG et al. (2012). Neurosci Bull 28, 409-422.

Zhao XY et al. (2009) Mol Pain 5, 55.

Liu MG et al. (2011). Brain Res 1382, 57-69.

Liu MG et al. (2012). Neurosci Lett 507, 38-42.

This work was supported by grants from the MOST (2013CB853100, 2013BAI04B04), the NSFC (81070899, 81171049) and the military project (AWS12J004) to JC.

Where applicable, the authors confirm that the experiments described here conform with The Physiological Society ethical requirements.

SA190

Maternal environment, placental phenotype and fetal growth

A.L. Fowden

Physiology, Development and Neuroscience, University of Cambridge, Cambridge, UK

Human epidemiological and experimental animal studies have shown that the pattern of intrauterine growth is an important determinant of adult physiology with impacts on health, disease risk and, ultimately, lifespan. In particular, low birth weight is associated with adult dysfunction and overt disease of the cardiovascular, metabolic and endocrine systems in human populations (1). In experimental animals, changes in adult physiological phenotype occur after intrauterine growth restriction induced by a range of sub-optimal environmental conditions such as maternal under- or over-nutrition, hypoxia overexposure to stress hormones and administration of alcohol, caffeine and nicotine (2). Even when birth weight is unaffected by these conditions, there can be abnormalities in the subsequent functioning of physiological systems that impair the responses to environmental challenges later in life. The maternal environment during pregnancy, therefore, has an important role in controlling the development of individual fetal tissues and organ systems with physiological consequences long after birth.

This epigenetic regulation of development is determined, in part, by the placenta, the primary source of the nutrients and oxygen required for intrauterine growth (2). Growth of the placenta *per se* is impaired by many of the environmental conditions known to restrict fetal growth and program adverse physiological outcomes later in life. However, the placenta is not just a passive conduit for nutrients and oxygen. It also regulates the bioavailability of hormones with direct and indirect effects on fetal growth and can adapt its transport characteristics in response to environmental signals to help maintain fetal growth, even when its own growth is restricted. Recent studies in rodents have shown that placental phenotype in late gestation is affected by natural variations in litter size and by maternal restriction of calories and/or protein, dietary composition, particularly of fat and sugar, and by overexposure to toxins, such as alcohol and caffeine, and to natural and synthetic glucocorticoids. These adaptations in placental phenotype are both morphological and functional and involve changes in the placental imprintome, nutrient transporter abundance and the intracellular signalling pathways involved in growth and nutrient sensing. They may also vary with the sex of the offspring and with gestational age at the time of the insult. Particularly when the placenta is growth restricted, there is often an increase in the relative proportion of the labyrinthine zone responsible for nutrient uptake and a thinning of the barrier between the maternal and fetal circulations, both of which will improve transplacental transfer of nutrients and oxygen. Similarly, small placentae frequently have a greater abundance of glucose and System A amino acid transporters which increases transport of these nutrients to the fetus per gram placental mass. These changes lead to a shift in maternal resource allocation in favour of fetal growth, despite poor maternal nutrient availability in certain circumstances (3).

Changes in placental transport phenotype induced by sub-optimal environmental conditions are often associated with altered expression of several imprinted genes known to regulate placental development such *Igf2, H19, Grb10* and *Phlda2*. Indeed, deletion of these genes causes alterations in placental nutrient transport and, in some instances, abolishes the adaptive response of the placenta to environmental challenges like undernutrition. In addition, there are changes in placental expression of proteins in the PI3K, MAPK and mTOR signalling pathways in response to maternal under- and over-nutrition and to deletion of the *Igf2P0* transcript which suggests that that these pathways have a central role in mediating the effects of nutrient availability on placental phenotype. Comparison of the different genetically and environmentally induced placental phenotypes has led to the concept that the placenta may respond to fetal demand signals for nutrients, particularly when there is a mismatch between the fetal drive for growth and the materno-placental ability to supply the required nutrients. Thus, the environmentally induced changes in placental phenotype are likely to reflect a combination of signals arising from the nutritional status of the mother and fetus and from the ensuing degree of feto-placental compromise. By altering the amount and relative proportions of specific nutrients supplied to the fetus, these changes in placental phenotype can program development long after the original insult with adverse physiological consequences later in life (2,3).

Barker D.J.P. (1994) Mother, babies and disease in later life. BMJ Publishing Group

Vaughan, O.R., Sferruzzi-Perri A.N. Coan, P.M. & Fowden, A.L. (2012). Environmental regulation of placental phenotype: implications for fetal growth. Reprod. fert. Develop. 24 80-94.

Burton G.J. & Fowden A.L. (2012) The placental and developmental programming: balancing fetal nutrient demands and maternal resource allocation. Placenta 33 Suppl A Trophoblast Research S23-S27.

Funded by the BBSRC

Where applicable, the authors confirm that the experiments described here conform with The Physiological Society ethical requirements.

SA191

An integrated approach to amino acid transfer and its regulation

J.K. Cleal

Institute of Developmental Sciences, University of Southampton, Southampton, UK

Amino acid transfer across the placenta is an important determinant of fetal growth and fetal growth restriction is associated with impaired amino acid transport.

Transfer of amino acids across the placenta requires transport of amino acids across the apical microvillous (MVM) and basal (BM) membranes of the placental syncytiotrophoblast. Individual amino acids are transported across membranes by specific amino acid transport proteins. However for the placenta to take up all the different amino acids it requires and to transfer them to the fetus it requires interaction between different classes of amino acid transporter. On the MVM accumulative transporters and exchangers must interact to mediate uptake of all the amino acids required by the placenta. On the basal membrane amino acid exchangers must interact with facilitated transporters to transfer amino acids into the fetal circulation. The interaction between different amino acid transporters creates complex interdependencies which mean that it is not easy to predict how changes in one amino acid transporter will affect the activity of the system as a whole.
Amino acid transporters can be regulated by a range of maternal signals including plasma nutrients and hormones. Within the placenta these signals are mediated via intracellular signaling mechanisms such as mTOR or by epigenetic regulation such as DNA methylation and microRNAs. The activity of amino acid transporters may be regulated by multiple regulatory signals. An important area of research is to determine whether transporters are regulated coordinately or whether they are regulated independently within the placenta.
Understanding amino acid transfer and its regulation will therefore require an integrated approach not only to the mechanisms mediating the transport but also to multiple regulatory signals which determine the activity of amino acid transporters.

Where applicable, the authors confirm that the experiments described here conform with The Physiological Society ethical requirements.

SA192

Maternal obesity and placental function

T. Powell, S. Lager, I. Aye, F. Gaccioli, R. Fredrick and T. Jansson

Obstetrics and Gynecology, University of Texas Health Science Center San Antonio, San Antonio, TX, USA

Nearly two-thirds of American women enter pregnancy overweight or obese and the prevalence of maternal overweight and obesity is increasing rapidly in many other countries, including the UK. The obese mother is at higher risk for many pregnancy complications and fetal overgrowth is common in these pregnancies. Fetal overgrowth increases the risk for perinatal complications and predisposes the child for obesity, diabetes and hypertension later in life. The mechanisms underlying increased fetal growth in overweight and obese women are poorly understood. Since fetal growth largely depends on the transfer of nutrients across the placenta, we hypothesize that altered placental function in obese women may lead to fetal overgrowth and its' associated long term health consequences. We are exploring the role of altered maternal metabolism associated with obesity in regulating placental nutrient transport. The placenta, uniquely juxtapositioned between the maternal and fetal blood supplies, must integrate both maternal supply and fetal demand signals. In cases of maternal obesity the signals impinging on the placenta are diverse and include high levels of macronutrients (glucose, amino acids, fatty acids), hyperinsulinemia, elevated adipokines (leptin, TNF-alpha, IL1-beta) and low levels of adiponectin. We evaluated alterations in placental nutrient transport capacity and multiple placental signaling pathways including 1) Toll Like Receptor 4 (TLR4), 2) insulin/IGF-I 3) mammalian target of rapamycin and 4) PPARs in term placentas from women of varying pre-pregnant body mass index (BMI). We found mTOR and inflammasome pathway activation, decreased PPARgamma activation and increased expression of amino acid and fatty acid transporters in placentas of high BMI women. Additionally, we developed a model of obesity without diabetes in mice based on feeding a highly palatable high-fat and high-sugar diet. The maternal metabolic phenotype resembles that of obese women with increased leptin and decreased adiponectin. Our model results in increased fetal growth and the placentas of obese mice were found to have an activation of insulin/IGF-I and mTOR signaling and a greater nutrient transport capacity.
We used cultured primary human trophoblast cells to directly study regulation of placental nutrient transporters and demonstrated that saturated and monounsaturated fatty acids stimulate trophoblast System A amino acid uptake in a TLR4 dependent manner while omega3 long chain polyunsaturated fatty acids inhibit amino acid uptake by System A. Insulin, leptin and pro-inflammatory cytokines also increased trophoblast amino acid uptake. These data suggest that in obese mothers with high leptin, insulin resistance, and chronic pro-inflammatory activation, the placenta is stimulated by the maternal metabolic environment to deliver excess nutrients to the fetus. Adiponectin is insulin sensitizing in some tissues however elevated adiponectin, a feature of lean women, inhibits placental insulin signaling at the level of IRS-1 in cultured trophoblast cells. This would tend to decrease amino acid uptake in normal healthy pregnancies. In contrast, low adiponectin, which is associated with obesity, would promote insulin stimulated amino acid transfer across the placenta. Our experiments in cultured trophoblast cells indicate that adiponectin treatment leads to PPARalpha and p38 MAPK activation and increased ceramide biosynthesis, resulting in decreased insulin sensitivity. Additionally, we performed chronic infusion of full-length adipoenctin in normal mice and found an inhibition of placental insulin/IGF-I and mTOR signaling along with decreased fetal growth (-20%).
These studies have identified mechanistic links between the perturbed maternal metabolism in pregnancies complicated by obesity and changes in placental signaling and nutrient transport capacity that likely lead to increased nutrient delivery to the fetus. We have discovered that adiponectin constitutes an endocrine link between maternal adipose tissue and placental function, supporting our hypothesis that the maternal metabolic environment is of key importance in regulating placental function. The role of the placenta in integrating signals from both the mother and fetus involves a complex interaction of extrinsic signals such as hormones, cytokines, maternal nutrient and energy levels with intrinsic placental signaling pathways for nutrient sensing, inflammation, and growth. Understanding the complex placental signaling pathways that lead to alterations in fetal growth will allow for the development of strategies to prevent short- and long-term health consequences of pathological fetal growth.

This work was supported by grants from the National Institutes of Health DK89989 and HD065007.

Where applicable, the authors confirm that the experiments described here conform with The Physiological Society ethical requirements.

SA193

Targeted delivery of drugs to the placenta to improve treatment of pregnancy pathologies

L.K. Harris

Maternal and Fetal Health Research Centre, University of Manchester, Manchester, UK

More than ten percent of pregnant women develop serious complications such as pre-eclampsia and fetal growth restriction (FGR), which cause significant morbidity and mortality. Despite the ability to identify women at risk of these conditions and detect reduced fetal growth and impaired utero-placental blood flow mid gestation, current treatment options are limited to induction of labour, early delivery and neonatal intensive care. In the short term, affected infants are at high risk of developing respiratory distress syndrome, retinopathy of prematurity, cerebral palsy and infection. Moreover, small size at birth is associated with an increased risk of elevated serum cholesterol, cardiovascular disease, stroke, type II diabetes, adiposity and osteoporosis in later life.
The primary causes of pre-eclampsia and FGR are poor placental growth or impaired placental function. Several potential therapies that enhance placental function, alleviate maternal symptoms and improve fetal growth in animal models have recently been identified; however, drug trials in human pregnancy are rare because the pharmaceutical industry fears expensive lawsuits associated with adverse side effects and teratogenicity. To address this issue, we have developed novel nanocarriers for targeted delivery of drugs to the placenta, as a means of improving drug efficacy and minimizing side effects in maternal and fetal tissues. We have identified a series of "placental homing peptides" which when intravenously injected, selectively bind to the uterine spiral arteries and surface of the mouse placenta, but do not bind to the vascular beds of other organs. These peptides also bind to, and are retained within, the outer syncytial layer of human placental tissue cultured in vitro. To create biocompatible nanoparticles into which drugs can be packaged, we have synthesized liposomes that display placental homing peptides on their surface. The principles of targeted drug delivery, the design and validation of peptide-decorated liposomes and the potential for this technology improve treatment strategies for pregnancy complications will be discussed.

This research was funded by a BBSRC David Phillips Fellowship to LKH

Where applicable, the authors confirm that the experiments described here conform with The Physiological Society ethical requirements.

SA194

Diabetes mellitus and the placenta: The key role of maternal and fetal insulin

G. Desoye

Obstetrics and Gynaecology, Medical University of Graz, Graz, Austria

Owing to its position the placenta is exposed to metabolic and hormonal diabetes-associated derangements of both mother and fetus, and one can expect some impact of the diabetic intrauterine environment on the placenta. One of its key functions is to provide the developing fetus with an adequate amount of nutrients, which are derived from the mother. This transport across the placenta has to be carefully regulated, because over- and undersupply may result in fetal growth disturbances. The fetus and newborn of diabetic pregnancies are characterized by excessive fat accumulation independent of the birth weight and the fetal fat associates with childhood obesity thus contributing to the obesity epidemic. Understanding the role of the maternal-placental-fetal interactions in determining fat accumulation in the fetus may thus have important implications for health care systems and the society at large.
According to the Pedersen hypothesis maternal hyperglycaemia leads to fetal hyperglycaemia with ensuing fetal hyperinsulinism. Collective evidence suggests that placental glucose transport is flow limited, and changes at the transporter level, if at all, will not affect fetal glucose levels in maternal diabetes. Thus, maternal-to-fetal glucose flux is determined by the maternal-fetal glucose concentration gradient, which itself is also regulated by fetal insulin. Fetal insulin is a main driver for fetal fat deposition, and also correlates with the risk for childhood obesity. Because of the high density of insulin receptors on the placental villous endothelium in the third trimester of pregnancy, fetal hyperinsulinism regulates some processes also in the placenta such as glycogen deposition and vascularization of the villi, both altered in maternal diabetes.
Diabetes mellitus is often associated with maternal hyperinsulinism either because of beta-cell compensation of insulin resistance or because of insulin administration to the mother. Early in gestation insulin receptors are located primarily on the microvillous membrane of the syncytiotrophoblast. Maternal insulin may then stimulate trophoblast proliferation and thereby drive placental growth. Moroever, insulin also stimulates matrixmetalloproteinases, which are implicated in extracellular matrix degrading, villous remodelling and angiogenesis. Thus, hyperglycaemia-associated maternal hyperinsulinism will modify placental growth and development in this critical period of gestation and thus have long lasting effects also on fetal development. Associations of maternal hyperglycaemia in the first trimester of pregnancy with fetal birth weight support this concept. Therefore, the main therapeutic goal in pre-gestational and gestational diabetes must be to avoid hyperinsulinism from occurring in both mother and fetus.

Where applicable, the authors confirm that the experiments described here conform with The Physiological Society ethical requirements.

SA195

Effects of muscle fatigue and exercise on the way in which the nervous system drives the muscles during voluntary contractions

J.L. Taylor

Neuroscience Research Australia, Sydney, NSW, Australia and University of New South Wales, Sydney, NSW, Australia

Sustained or repetitive use of skeletal muscles leads to muscle fatigue. For human exercise, muscle fatigue can be defined as a decrease in maximal voluntary force or power of a muscle or muscle group. This definition implies that not just the muscle itself but also the nervous system has a role in exercise-related fatigue. During fatiguing exercise, the central nervous system can compensate for some weakness and slowness of the muscle to allow continued performance of a task, but

may also become "fatigued" and contribute to a fall in maximal voluntary force.

Twitch interpolation has been used to demonstrate central fatigue by showing that fatigue increases the increment in force evoked by electrical stimulation of a muscle during the performance of a maximal voluntary contraction. This interpretation has been challenged by studies in mouse muscle fibres (Place *et al.* 2008). These studies suggested that changes in the intracellular force-Ca^{2+} relationship could provide a peripheral mechanism by which interpolated twitches could grow in size with fatigue. However, interpolated twitches do not grow in human adductor pollicis when the muscle is fatigued by a sustained contraction evoked by constant frequency stimulation of the ulnar nerve (Gandevia *et al.* 2013). Rather, the twitches diminish, in part because of failure of the muscle fibre action potential. Therefore, at least for sustained maximal efforts, growth of the interpolated twitch can only occur with a reduction in neural drive to the muscle and so reflects a central component of fatigue.

The motoneurones are one site at which central fatigue may impair motor output. Our recent studies have shown that the responses of motoneurones to single corticospinal volleys are reduced during fatiguing maximal and submaximal isometric contractions (McNeil *et al.* 2009, 2011a). The reduction was most pronounced when descending voluntary drive was transiently interrupted but some reduction was also seen when voluntary drive was ongoing. These changes are unlikely to be the result of altered muscle spindle or small-diameter muscle afferent feedback (McNeil *et al.* 2011b). Furthermore, during submaximal contractions, smaller responses were more affected than larger responses. This differential effect suggests that not all of the motoneurones in the pool become less responsive but that it is mainly the motoneurones that are active during the contraction. The altered input-output relationship of the motoneurones may contribute to the mismatch between perceived effort and the level of voluntary EMG that occurs during sustained submaximal efforts.

The firing of small-diameter muscle afferents is perceived as muscle pain and/or fatigue and causes reflex cardiorespiratory responses to exercise. For the elbow flexor muscles, the ability of subjects to drive the muscle maximally in isometric maximal voluntary efforts remains low after a fatiguing contraction if the firing of fatigue-sensitive muscle afferents is maintained by block of blood flow to the fatigued muscle. Thus, these afferents contribute to central fatigue. However, this influence appears to be at a supraspinal level (Gandevia *et al.* 1996). Indeed, the motoneurones of the elbow flexors are facilitated by the afferent firing (Martin *et al.* 2006). Recent experiments have shown that the supraspinal influence of small-diameter afferent firing is not confined to the fatigued muscle. Block of blood flow to the elbow extensor muscles when they were fatigued resulted in impaired voluntary drive to the non-fatigued elbow flexors, as did maintained firing of small-diameter muscle afferents from the hand. Therefore, afferent feedback from fatigue of one muscle in a limb can alter drive to other muscles in the same limb. This is likely to be important in the development of central fatigue in most coordinated actions.

Multiple mechanisms at multiple levels of the nervous system contribute to central fatigue. They include repetitive activity, which creates a specific deficit at the motoneurone level, and sensory feedback from fatigued muscles, which has wider effects on the motoneurones and supraspinally, as well as on autonomic responses to exercise.

Gandevia SC *et al.* (1996) *J Physiol* **490**, 529-536.

Gandevia SC *et al.* (2013) *J Physiol* Jan 2 [online ahead of print]

Martin PG *et al.* (2006) *J Neurosci* **26**, 4796-4802

McNeil CJ *et al.* (2009) *J Physiol* **587**, 5601-5612

McNeil CJ *et al.* (2011a) *J Physiol* **589**, 3533-3544.

McNeil CJ *et al.* (2011b) *J Physiol* **589**, 3731-3738.

Place N *et al.* (2008) *J Physiol* **586**, 2799-2805.

JLT is supported by a Fellowship from the National Health and Medical Research Council of Australia.

Where applicable, the authors confirm that the experiments described here conform with The Physiological Society ethical requirements.

SA196

A model of motoneuron behavior and muscle-force generation for sustained isometric contractions

P. Contessa[1,2] and C.J. De Luca[1,3]

[1]NeuroMuscular Research Center, Boston University, Boston, MA, USA, [2]Department of Information Engineering, University of Padova, Padova, Italy and [3]Department of Electrical and Computer Engineering, University of Padova, Boston University, MA, USA

The control of motor units and the regulation of muscle force during sustained isometric contractions are still subject to debate. We have developed a model to simulate the behavior of motoneurons and the generation of muscle force in the first dorsal interosseous (FDI) and vastus lateralis (VL) muscles. The model sheds light on the mechanisms of muscle force regulation during isometric tracking tasks sustained to the endurance limit, on the changes in motor unit firing behavior and on the cause of increased force fluctuation with fatigue.

The input to the model consists of an excitatory signal representing the sum of all excitatory and inhibitory inputs to the muscle. The input excitation is common to all the motor units in the pool of the muscle following the "common drive" concept, which states that all motor units are modulated by a common source [1]. The model describes a non-linear relation between the input excitation to the motoneuron pool and the firing rates of motor units [2], to which synaptic noise is added [3]. Motor unit firing rates follow the "onion skin" principle [4], which describes a hierarchical relationship between recruitment threshold and firing rates, with later-recruited motor units having progressively lower firing rates than earlier-recruited motor units. The model generates the motor unit mechanical responses (force twitches) [5], whose amplitude is altered with contraction time to replicate the initial increase (as a result of muscle potentiation) and subsequent decrease (as a result of muscle fatigue) in force generating capacity reported during sustained muscle activation [6-7]. The force contributions of the active motor units are computed by convolving each motor unit firing train with their respective force twitch, and are summed to obtain the simulated muscle force. A feedback loop adjusts the value of the input excitation so that the simulated muscle force is maintained at a value similar to that of a target force, mimicking the performance of force-tracking tasks.

We modeled the force produced by the FDI and VL muscles during a series of repeated force contractions sustained at 50% and 20% MVC until the endurance limit, i.e., until the force could no longer be maintained at the target level. The model behavior was validated by comparing the simulated motor unit firing rate and force output with experimental evidences derived from a similar protocol of repeated contractions [6-7]. For both muscles, the model predicts the initial decrease and

subsequent increase in motor unit firing rates which occur during sustained muscle activation as motor unit force twitches vary. A greater number of motor units are progressively activated as the simulation approaches the endurance limit. Increasing force fluctuations are observed as fatigue develops, likely due to the recruitment of higher-threshold higher-twitch amplitude motor units. Throughout the contraction series, the force produced by the VL muscle is smoother than that produced by the FDI muscle, probably due to the different mechanical characteristics of the two muscles.
The results of the simulations reproduce the motor unit firing rate behavior and the increase in force fluctuations observed in previous empirical data during a similar protocol of repeated contractions [6-7]. Motor unit twitch force is the only parameter allowed to change with contraction time in the model. These results strongly suggest that, during voluntary isometric contractions, the excitation to the motoneuron pool is adjusted to compensate for the varying muscle-force generating capacity.

De Luca CJ et al. (1982). J Physiol 329: 129-142.

De Luca CJ & Contessa P (2012). J Neurophysiol 107: 178-195.

Fuglevand AJ et al. (1993). J Neurophysiol 70: 2470-2288.

De Luca CJ & Erim Z (1994). Trends Neurosci 17: 299-305.

Raikova RT & Aladjov HTs (2002). J Biomech 35: 1123-1135.

Adam A & De Luca CJ (2005). J Appl Physiol 99: 268-280.

Adam A & De Luca CJ (2003). J Neurophysiol 90: 2919-2927.

The work was supported by grant NS-058250 from NINDS NIH; by grant HD-050111 from NCMRR NIHD/NIH; by MIUR (Italy); and by Fondazione Ing. A. Gini (Italy).

Where applicable, the authors confirm that the experiments described here conform with The Physiological Society ethical requirements.

SA197

What experiments with intact single muscle fibres tell us about the role of calcium in muscle fatigue in mammalian skeletal muscle

J. Bruton

Physiology & Pharmacology, Karolinska Institute, Stockholm, Sweden

In humans and other mammals extended bouts of dynamic or isometric exercise result in a failure to produce the force that was possible at the start of the exercise (i.e. fatigue). Experimental results from non-invasive measurements in exercising human subjects clearly indicate that mechanisms located within the muscle are important determinants of fatigue. But it is difficult to follow the dynamics of fatigue in intact human muscle fibres *in vivo*. Muscle biopsies, NMR recordings and blood samples obtained during exercise have identified factors that potentially affect contractile function. These factors have been subsequently studied in isolated single intact fibres to determine how they affect force production and the likely mechanisms. Overall, these experiments indicate that increased inorganic phosphate and possibly ROS depress contractions resulting in fatigue, whereas increased extracellular [K^+] and reduced intracellular pH are less important. This overview uses data from isolated intact single muscle fibres from both rodents and humans to illustrate and explain the mechanisms underlying the changes in intracellular calcium and the decreased force production seen during various types of exhaustive exercise.

Research was funded by Swedish Research Council, the Swedish National Center for Sports Research, and Funds at the Karolinska Institutet.

Where applicable, the authors confirm that the experiments described here conform with The Physiological Society ethical requirements.

SA198

Weaving laboratory data into true stories from patients and their families

T. Macknight

ADInstruments, Dunedin, New Zealand

The majority of students coming into Physiology programs are doing so because they are curious about how the human body works in health and in disease, so it makes sense to build your curriculum around people and their stories. But what worries us all, is that this can sound like a plan to dilute the essential basic sciences and result in a course that is high in 'good intentions' but low in rigor. But this needn't be so. Used properly, case-based teaching can motivate students, encourage self-directed learning and enhance knowledge and understanding of basic physiological concepts.
Most courses where cases are used rely on paper cases. Here is a tyical example:
"Mrs M is a 74 year old lady who has become increasingly breathless over a number of years. She is now very limited in what she can do because of this. She was admitted to hospital with acute respiratory symptoms on three occasions over the last two years. She has a past history of cigarette smoking. On examination, Mrs M is a rather thin woman. Her face is a dusky color, and her lips have a bluish tinge. Her breathing is quiet but labored. Her chest movements are poor but symmetrical with a lot of activity in her accessory inspiratory muscles and expiratory effort as well. Listening to her chest reveals very quiet breath sounds. There are occasional crepitations and scattered rhonchi. Her heart rate is 82 bpm. Her heart sounds are normal."
The difficulty with paper cases is that we don't see the people as 'real'. The students always think that we have 'created' the person to provide a good example of the condition that we wish them to understand the basic physiology of. And certainly, with a paper case, there is a temptation to manipulate the story and the data to remove the complexities of real life. And, because the students don't really see the 'patient' as a person, they are not really concerned for him or her.
With modern computers and fast internet, it is now possible to replace these paper cases with videos. To make compelling videos what we need are co-operative patients. But we also need to be sure that the videos that we produce are of professional quality, for the students watch professional videos every day and are never happy to see 'amateur' efforts. My experience is that the most difficult part of the production is sound recording. But lighting is another problem at times. Most importantly, the format of the videos needs to be considered. Should these be filmed as interviews or should the patient speak directly to the audience? The latter seems to be the more effective in involving students in the patients and their problems.
It is also appropriate to video interviews with family and with health care professionals (doctors, nurses, physiotherapists,

occupational therapists, dieticians, etc) involved with the patient. These interviews provide students with a broader perspective about the patient's problems and their professional management.
Video cases can be used to illustrate points during lectures, as part of case-based tutorials, to reinforce laboratory work and also as part of on-line learning. They are very effective used as an introduction to the study of a new topic, for they can arouse interest in the topic and provide motivation to study it. They are also very suitable for use in group work where you wish to encourage student collaboration. During the talk, I shall provide several examples of video cases and how they can be used to motivate students, increase the relevance of laboratory time and reinforce the understanding of basic physiological concepts.

These video cases would not be possible without the informed consent of the patients to have their stories used to enhance the education of health and life science students throughout the world. We are grateful for the assistance and contributions of staff of the University of Otago School of Medicine and the Southern District Health Board.

Where applicable, the authors confirm that the experiments described here conform with The Physiological Society ethical requirements.

SA199

Anecdotes in the learning of physiology

A.P. Arikawe

Department of Physiology, College of Medicine of the University of Lagos, Lagos, Lagos, Nigeria

Anecdote is a short narrative account of an amusing, unusual, revealing, and interesting event about a real incident or a person. A good anecdote must have a single and definite point. Its setting, dialogue, and characters must usually be subordinate to the point of the story. Uses of anecdotes include clarify abstract points, humanize individuals and to create a memorable image in the reader's mind.
Rudy Roden was a 17-year old medical student in Eastern Europe when the Germans invaded. He and his family were detained and sent to a concentration camp. When asked his occupation, Rudy said, "I'm a baker," and he was sent to work in the kitchens. When he was transferred to a new camp, he noticed construction going on, so he said he was a bricklayer. Rudy survived 4 different camps by being observant and making himself into whatever was needed.
After liberation from Auschwitz, Rudy Roden immigrated to Canada and became first a family physician, then a psychiatrist. Lesson from Rudy's life: if you want to survive, you have to take an active role in your future. Look around and see what is needed, what needs to be done and then figure out how you can be the one to fill that need. As Physiology educators we need to adapt and evolve. We must teach students how to do this.
During my third year Physiology undergraduate Practical session, the technical staff and students struggled for over 2 hours to anaesthetize a dog for animal experiment. A Professor of Physiology from a neighbouring institution walked into the laboratory at this point (coincidence), offered to assist and within few minutes the animal (dog) was fully sedated and unconscious! For most of the students, this was magic at the highest level
As the Physiology professor walked out of our Laboratory in Lagos 15 years ago, I quietly made a promise to work under him for MSc and PhD degrees. These were achieved in 2003 and 2012 respectively. In between these years (2008), I got the MB.BS degree! As Physiology educators we must inspire, encourage and assist our students to seek graduate admission.

Muow DR. (1981). New directions for teaching and learning, Vol 1981 (7): 27 – 30.

Westerhof N. (2011). Acta Physiologica, 202: 601 – 603.

Naftalin, RJ. (2011). Physiology News, 83: 8 – 11.

Silverthorn DU. (2011). The Physiologist, 54 (6): 233, 238 – 243.

Where applicable, the authors confirm that the experiments described here conform with The Physiological Society ethical requirements.

SA200

Enlivening physiology teaching with African folklore

F.B. Mojiminiyi

Physiology, Usman Danfodio University, Sokoto, Nigeria

African folklore is awash with tales and proverbs e.t.c. about everyday living in Africa. These are used to teach morals and principles. Each tale or proverb is indelibly associated with a moral or principle which is easily recalled once the former is recounted. This suggests that the power of stories/proverbs in teaching is well recognized by our forbears. Folklores elsewhere share these attributes. A classical example is the so called Ondine's curse in German mythology. This tale may be used to teach the separation of voluntary from involuntary respiration (1). In addition, the National Institutes of Health (NIH) of the United States of America has been reported to have hired a professional story teller to help teach her scientists on how best to explain their research findings to others especially students and the general public. Thus the power of tales/proverbs in enhancing teaching is becoming more recognized. However this tool has either not been used at all or rarely used in the teaching of Physiology to African students. This work will present the use of African folklore in teaching physiological principles including righting reflexes, ageing, respiratory adjustments to high altitude and other aspects of physiology. This may hopefully stimulate others to explore this powerful tool in teaching physiology or communicating their research findings to colleagues, students and the public.

Ganong WF (2003) A Review of Medical Physiology, twenty first edition, Lange Medical Books.

Support from the IUPS and the Physiological Society London are gratefully acknowledged

Where applicable, the authors confirm that the experiments described here conform with The Physiological Society ethical requirements.

SA201

A narrative of the Facebook-PhysBook learning community

H.M. Cheng

Physiology, University of Malaya, Kuala Lumpur, Malaysia

Engaging and connecting with students learning Physiology is a primary focus of all Physiology educators. A Facebook open group was started in 2011 (PhysBook011) to exploit the ver-

satility of this social media to foster interactions, discussions and enjoyment in learning Physiology. The PhysBook group now numbers about 1,400 members, mainly students and several educators. The platform has been used for Physiology updates, Quizzes, Test sample analyses, Learning aids, Creative Physio-songs and is also open for students to pose questions and think through Physiology together. A description of some of these PhysBook learning components will be shown during this IUPS teaching enhancement session.

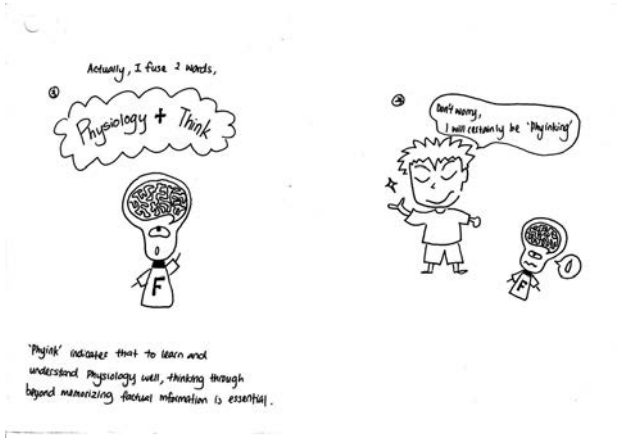

Where applicable, the authors confirm that the experiments described here conform with The Physiological Society ethical requirements.

SA202

Using everyday situations to teach integrative physiology

P. Hansen

Memorial University of Newfoundland, Blaketown, NF, Canada

Research on learning and teaching has shown that learning is often more enjoyable, memorable, and meaningful when knowledge and concepts are organized around descriptions of human situations familiar to students. The evidence for this is clear and compelling, yet many physiologists are unaware of its potential for improving their students' learning. Narratives familiar to students from their everyday lives pique their interest in physiology and allow them to relate their new knowledge to what they already know. Skiing at high altitude, jogging, donating blood, having sex, and experiencing jet lag are some examples of familiar situations students can relate to. Such stories can be designed to reflect specific cultures, and to place physiology in the context of other biological sciences, social sciences, and ethics. Some situations can lead naturally to pathophysiology and clinical conditions. For example, the physiology of eating a meal is a foundation for learning about nutrition, obesity, and diabetes. Normal sexual function and pregnancy could lead to study of erectile dysfunction or infertility. This talk will articulate the theoretical and research background for using everyday stories and provide examples of their successful use in undergraduate, graduate, and health professional physiology education.

Where applicable, the authors confirm that the experiments described here conform with The Physiological Society ethical requirements.

SA203

An inhibitory connectome controls the respiratory rhythm in vivo

D.W. Richter

Neuro- and Sensory Physiology, University of Goettingen, Goettingen, Germany and Molecular Physiology of the Brain, DFG Research Center, Goettingen, Germany

The neuronal network controlling breathing under in vivo conditions is a distributed throughout the lower brainstem and the pons. Responsible for the respiratory rhythm generation is a core micro-circuitry formed within the pre-Bötzinger Complex (pre-BötC) and the Bötzinger complex (BötC) regions. A basic process is executed by glycinergic neurons forming a distinct inhibitory connectome between early-inspiratory, post-inspiratory and also late-expiratory neurons. It generates an effective control of endogenous bursting activity and allows a dynamic adjustment of breathing to behavioral and cortical commands. Disturbances of this neural management may become dangerously life threatening as they can lead to an abnormally prolonged inspiration (apneusis) producing enduring breath-holdings and also to complete cessation of breathing (apnea). Comparable defects of glycinergic inhibition were identified in several diseases, such as in Rett Syndrome, Hyperekplexia, Olivo-ponto-cerebellar atrophy (OPCA) and also Brainstem infarction.
The systemic processes underlying such disorder of respiratory activity will be explained by a comparative analysis of the effects of modulation or depression of glycinergic inhibition on single cell responses and computational modeling of complex network reactions.

Supported by the Cluster of Excellence and DFG Research Center Nanoscale Microscopy and Molecular Physiology of the Brain (CNMPB).

Where applicable, the authors confirm that the experiments described here conform with The Physiological Society ethical requirements.

SA204

Purinergic modulation of preBötzinger complex inspiratory rhythm generating networks

J. Zwicker[1], S. Pagliardini[1], V. Rajani[1], S. Kasparov[2], A. Gourine[3] and G. Funk[1]

[1]Physiology, University of Alberta, Edmonton, AB, Canada, [2]Physiology and Pharmacology, University of Bristol, Bristol, UK and [3]Neuroscience, Physiology and Pharmacology, University College London, London, UK

ATP actions on central inspiratory networks are determined by a 3-part signaling system comprising: i) the excitatory actions of ATP at P2 receptors (Rs) ii) ectonucleotidases that degrade ATP into ADP and adenosine (ADO), and iii) the inhibitory actions of ADO at P1Rs. During hypoxia, an initial increase in ventilation is followed by a secondary depression that is life threatening in premature infants. The release of ATP in respiratory networks, including the preBötzinger Complex (preBötC, important site of inspiratory rhythm generation) attenuates this secondary ventilatory depression. The degree of this attenuation, however, will be determined in part by the complement and density of local ectonucleotidases. Degra-

dation of ATP to ADP, a P2YR agonist, could enhance the attenuation while degradation to ADO by different enzymes could exacerbate the depression. My thesis research has explored the significance of this 3-part signaling system for preBötC networks in rodents using primary cultures of preBötC glia, rhythmically-active medullary slices from rats and mice, and anesthetized adult rats. My objective is to use these various reduced preparations to understand the mechanisms by which ATP acts when it is released endogenously within the preBötC. In rhythmic medullary slices from neonatal rats in vitro, injection of ATP into the preBötC evokes a 2-4 fold increase in frequency via a P2Y1R mechanism that involves both neurons and glia. Analysis of cultured preBötC astrocytes suggests that the glial mechanism is mediated through phospholipase C, the release of Ca2+ from intracellular stores and the release of excitatory gliotransmitters, including glutamate, that in turn excite inspiratory neurons. In contrast to rats, however, injection of ATP into the preBötC of rhythmic slices from neonatal mice has no effect on rhythm. However, ATP does evoke a P2Y1R-mediated frequency increase if A1 ADORs are blocked, suggesting that in mice ATP is rapidly broken down into ADO, which acts via A1 ADORs to counteract the excitatory actions of ATP at P2Y1Rs. Consistent with this, ADO inhibits preBötC frequency in mice but not rats. To assess whether differential expression of ectonucleotidases might also contribute to the varied ATP responses in rats vs mice, we analyzed mRNA from preBötC punches using real time PCR to reveal that TNAP, an enzyme that degrades ATP to ADO, is the main ectonucleotidase in mice but NTPDase2, which degrades ATP to ADP (a P2Y1R agonist) is the main ectonucleotidase in rats.

The significance of these purinergic signaling mechanisms for mature preBötC networks in vivo was examined in three ways. First, injection of a P2Y1R agonist into the preBötC of urethane anesthetized rats evoked a 40% increase in respiratory frequency. Second, comparing hypoxic ventilatory responses of urethane anesthetized rats revealed that compared to control saline injections, the hypoxic ventilatory depression was much greater following unilateral injection of a P2Y1R antagonist into the preBötC. Finally, the importance of endogenous ATP in establishing the dynamics of the hypoxic ventilatory response was examined by increasing ectonucleotidase activity in the preBötC via local injection of a lentivirus that caused increased expression of the enzyme TMPAP. Compared to rats injected with a control virus, TMPAP-injected animals with elevated ectonucleotidase activity showed a much greater secondary hypoxic ventilatory depression.

Data indicate that the effects of ATP on the preBötC network of neonatal rodents are determined by a delicate balance between the excitatory actions of ATP and ADP at P2Rs and the inhibitory actions of P1R actions (on neurons and glia), and that the local subtype and concentration of ectonucleotidase is a key factor in setting this balance. In neonatal rat, the balance favours excitation. In mouse, (at least under conditions of exogenous ATP application) the excitatory actions of ATP and inhibitory actions of ADO are balanced, providing a valuable model to explore how purinergic signaling might be manipulated to tip the balance in favour of excitation to counteract respiratory instabilities as seen in apnea of prematurity. The same appears to apply to adult preBötC networks under conditions of endogenous ATP release during hypoxia where disruption the balance by increasing ectonucleotidase expression significantly alters response dynamics.

Supported by CIHR, WCHRI, AIHS.

Where applicable, the authors confirm that the experiments described here conform with The Physiological Society ethical requirements.

SA205

Role of synaptic inhibition for respiratory rhythm and pattern formation

A.P. Abdala[1], J.M. Bissonnette[2], J.C. Smith[3] and J.F. Paton[1]

[1]School of Physiology and Pharmacology, University of Bristol, Bristol, Avon, UK, [2]Ob/Gyn & Cell & Develop Biol, Oregon Health and Science University, Portland, OR, USA and [3]Cellular and Systems Neurobiology Section, National Institute of Neurological Disorders and Stroke (NINDS), National Institutes of Health (NIH), Bethesda, MD, USA

The current accepted model for respiratory rhythm and pattern formation dictates that a medullary inhibitory circuitry is crucial for normal breathing; however this topic is still an area of great contention. We demonstrated that the mechanisms essential for breathing combine both intrinsic cellular properties and dynamic synaptic interactions, with a major emphasis on reciprocal inhibition. With this arrangement, the central pattern generator can produce different modes of oscillatory respiratory behaviour and the circuitries pertaining to each of them can operate independently when disconnected experimentally. This not only confers the robustness and flexibility necessary for operation, but allows network reconfiguration when responding to changes in state (metabolic, arousal) or patho-physiological situations ensuring that ventilation persists. It also implies that failure in inhibitory circuitry would result in rhythm irregularity and central apnoeas. One example is the respiratory pathology featured in patients with Rett Syndrome (RTT), an autism spectrum disorder caused by mutations in the gene that encodes the DNA binding protein methyl-CpG-binding protein 2 (MeCP2). Included in the phenotype are frequent apnoeas, breathing irregularities and periodic breathing. The deficiency in MeCP2 function has been shown to affect synaptic transmission (including GABA) on multiple levels. In a mouse model of Rett syndrome, we found that insufficiency of GABAergic synaptic transmission in discrete brainstem loci was key for generating the RTT respiratory phenotype with important therapeutic implications. More recently, we generated novel viral vectors that allow us to genetically target GABAergic and glycinergic neurones providing further insight into the crucial functional role and connectivity of brainstem inhibitory neurone subpopulations. Using transgenic animals, genetic targeting of respiratory inhibitory neurones and optogenetics, I will demonstrate the essential role of synaptic inhibition within both pontine and ventral medullary respiratory regions in the generation of the eupnoeic breathing pattern.

This work was supported by the International Rett Syndrome Foundation, Newlife Foundation for Disabled Children and NIH grants R01 NS057815 and R01 NS069220.

Where applicable, the authors confirm that the experiments described here conform with The Physiological Society ethical requirements.

SA206

Electrophysiological properties of the brainstem respiratory neurones in rats submitted to chronic intermittent hypoxia

D.J. Moraes

Physiology, School of Medicine of Ribeirao Preto, Ribeirao Preto, Sao Paulo, Brazil

We hypothesized that active expiration following chronic intermittent hypoxia (CIH) exposure is dependent on alterations in the electrophysiological properties of expiratory neurones in the Bötzinger Complex (BötC), in which are an important part of the complex respiratory network. Using simultaneous recordings of respiratory nerves and whole cell path-clamp of respiratory neurones of ventrolateral medulla, we evaluated the mechanisms underlining CIH-induced active expiration in juvenile rats. In CIH rats, the decrease in the frequency discharge of post-inspiratory (post-I) neurons reduced the post-I activity of cervical vagus nerve. As consequence, the firing frequency of augmenting-expiratory neurones (aug-E) and the abdominal activity in the second half expiration (active expiration) were enhanced in CIH rats. However, CIH produced changes in the input resistance and excitability, independent of synaptic transmission, only in BötC post-I neurones. These changes were due to increased potassium-mediated leak current in post-I neurones, with no changes in the currents mediated by calcium-activated large conductance potassium channels or low voltage-activated calcium channels. In addition, the increase in the potassium-mediated leak current in response to acute hypoxia (10% O2) was higher in post-I neurons from CIH than control rats. With these precise electrophysiological approaches, we are describing the mechanisms underlying active expiration in CIH rats, which critically depend on changes of ionic currents in BötC post-I neurones. Possible implications of changes in the post-I neurones electrophysiological properties in the respiratory control of upper airway resistance and in the sympathetic over activity and hypertension in CIH rats will be also discussed.

Financial Support: FAPESP, CAPES and CNPQ.

Where applicable, the authors confirm that the experiments described here conform with The Physiological Society ethical requirements.

SA207

Emergence and maturation of the respiratory oscillator during embryonic development

M. Thoby-Brisson

INCIA, CNRS, Univ Bordeaux2, Bordeaux, France

Breathing is a rhythmic motor act generated and controlled by hindbrain neuronal networks. An essential component of this generator is the pre-Bötzinger oscillator that produces and paces inspiration. In order to ensure survival at birth, the respiratory generator must be anatomically and functionally established during the prenatal period. Indeed, respiratory-like movements that play an important role in the proper maturation of the lungs, respiratory motoneurons and muscles, are already present during the ultimate stages of fetal development.

Over the last decade we have sought insights into the mechanisms underlying the emergence and maturation of respiratory function during embryonic development, mainly by using electrophysiological and optical recordings of neuronal activities from reduced in vitro preparations from the mouse embryo, together with anatomical investigations. Here, I will first present some of the earlier work that has enabled 1), determining the time of inception of pre-Bötzinger circuit operation during embryonic development, 2), defining several genetic components required for the proper specification of the constitutive neuronal elements, and 3), describing some of the network properties expressed by the embryonic pre-Bötzinger oscillator. For example, we have found 1), that rhythmically organized, respiratory-related activity emerges at embryonic day 15 (E15) in the mouse (gestation lasting 18 to 19 days), 2), the homeobox gene Dbx1 is required for the specification of glutamatergic interneurons involved in respiratory rhythmogenesis, 3), intra-network synchronization relies upon glutamatergic synapses, and 4), some of the major neuronal membrane properties found at postnatal stages, including pacemaker properties, are already present before birth.

Furthermore, because respiratory-related rhythmic activity is first detectable at the beginning of the last third of gestation (E15), and since important changes have been proposed to occur elsewhere in the CNS between E15 and birth, we are currently exploring the maturational processes that the pre-Bötzinger complex undergoes during this terminal prenatal period. In this context, I will present recent preliminary data on the functional maturation of the respiratory network associated with changes both in inhibitory synaptic signaling the properties of the population of respiratory neurons exhibiting pacemaker properties.

In a translational perspective, finally, developmental anomalies in central respiratory neural control contribute significantly to human newborn mortality. Therefore, elucidating the cellular, molecular and genetic mechanisms involved in the formation and function of the respiratory generator during mammalian prenatal development is of particular importance to improving the understanding of pathologies and potentially to a better adaptation of therapeutical approaches to treating young babies suffering from respiratory distress.

Where applicable, the authors confirm that the experiments described here conform with The Physiological Society ethical requirements.

SA208

Using transgenic animal models to understand the role and regulation of the gastrointestinal surface pH microclimate

U.E. Seidler

Gastroenterology, Hannover Medical School, Hannover, Germany

The gastrointestinal epithelia secrete and absorb large amounts of solvents and fluid, while being exposed to harsh conditions, such as very low pH, high CO2 tensions, food products, detergents, bacteria and their products, as well as noxious agents released by the immune cells of the organism itself. Protective properties of the gastrointestinal mucus layer have been postulated more than a decade ago, but it was clear to investigators that the mucus layer had to be traversed from the epithelium to the lumen by the very same products that it needed to be protected from, such as the gastric acid. What was actually going on directly at the epithelial surface?

Researchers from Europe, Japan and the US pioneered the study of gastrointestinal surface pH measurements more than 3 decades ago, by advancing pH- and voltage-sensitive dual-barreled electrodes through the mucus layer of chambered

isolated mucosa, and later also through the mucus of exteriorized vascularly perfused stomach of live rodents. The small intestine was probed in a similar fashion. The disadvantage was that the advancement of the microelectrode potentially disturbed the unstirred layer within the mucus. This problem was overcome two decades later, when the use of pH-sensitive fluorescent dyes and multiphoton imaging allowed dynamica monitoring of the pH immediately adjacent to the surface of the gastric mucosa. When adapting this method to other parts of the gastrointestinal tract, other pH-sensitive dyes need to be used, because of the rather small pH range within which these dyes change their emission intensities proportionally to changes in pH.

Using the above methods, it became clear that pH- gradients formed within the unstirred fluid layer in the mucus between the acidic lumen and the neutral-slightly alkaline oH of the epithelial cell layer in the upper segments of the GI tract. In the jejunum, the surface microclimate was acidic compared to the neutral lumen and enterocyte pH values. What factors allow the buildup and stability of such pH-gradients? In order to understand the regulation of the surface microclimate in a segment of the gastrointestinal tract, it has to be amenable to experimental manipulation. For the study of gastric pH gradients, acid secretion was easy to stimulate or inhibit in rodents. It was found that the stimulation of acid secretion enhanced the alkalinity of the surface pH above the mucous surface cells, possibly caused by the “alkaline tide”, the HCO3- that is exported via the parietal cell basolateral membrane and enters the capillaries that bring blood to the surface regions of the gastric epithelium. However, the opposite, the stimulation and inhibition of HCO3- secretion, was far more difficult to achieve. Thus, gene-manipulated mice were used that lacked either important transporters or important regulatory molecules for HCO3- secretion. In the stomach, this allowed the dynamic assessment of the alkaline halo adjacent to a microscopic wound and its role in protecting the wounded epithelium from acid damage. In the jejunum, changes in epithelial surface pH were found to accompany and modify the nutrient and electrolyte absorptive processes. In the colon, alterations in surface pH, brought about by deletion of the major apical Cl-/HCO3- exchanger Slc26a3 (DRA), are associated with changes in the mucus layer quality, an altered microbiome composition, an increase susceptibility to damage, and even slight inflammatory changes in the nonchallenged colonic mucosa. A combination of fluorescent markers, applied as dyes, fluorescent bacteria, or genetically expressed in the epithelial layer, allows the simultaneous assessment of tight junction integrity, mucus layer permeability, as well as of some physiological states of the cell layer below. In summary, advances in electrophysiological and imaging techniques have allowed to study dynamic changes of the surface pH microclimate during physiological digestive processes and pathological derangements. The use of transgenic animals allows, to some extent, to tentatively establish causal relationships. The development of new fluorescent markers and transgenic animal models, as well as a combination of optical and electrophysiological techniques, will likely allow an simultaneous assessment of more qualities of the surface microclimate and the underlying mucosa.

The author would like to thank her team for the many difficult experiments that allowed her to give this presentation, and the many collaborators that made knockout mice and technical knowhow available. She thanks the DFG, the Volkswagen Stiftung, the Mukoviszidose e.V. Stiftung, the Ministry of Lower Saxony, and the BMBF for financial support.

Where applicable, the authors confirm that the experiments described here conform with The Physiological Society ethical requirements.

SA209

SLC26A8 and CFTR cooperation in the regulation of anions exchanges during sperm motility and activation

A. Toure

Development, Reproduction & Cancer, Institut Cochin. INSERM U1016, CNRS UMR8104, Paris, France

Ion fluxes play an essential role in the control of sperm motility and capacitation (a maturation event occurring in the female genital tract and required for fertilization); in particular, calcium, chloride and bicarbonate are essential for both processes by activating cAMP-PKA-dependent phosphorylation pathways (1). We previously described SLC26A8, also known as Testis Anion Transporter 1 (SLC26A8), as a male germ cell-specific member of a large family of anion transporters (or sulfate permeases) known as SLC26 (Solute Linked Carrier 26) proteins (2).

Most SLC26 proteins display transport activity towards monovalent and/or divalent anions (including sulfate, chloride, bicarbonate, iodide, oxalate) and in humans, genetic abnormalities of SLC26A2, SLC26A3, SLC26A4, and SLC26A, have been causally associated with diastrophic dysplasia, chloride diarrhea, Pendred syndrome and deafness respectively (3).

We have previously shown that homozygous deletion of Slc26A8 in the mouse leads to male sterility due to the total lack of sperm motility, impairment of sperm capacitation and severe structural defects of the flagellum (midpiece disorganization, hairpin-like bending of the flagellum and atrophy of the annulus). (4). Consistent with this phenotype, SLC26A8 in mature sperm localizes at the equatorial segment of the head and at the annulus, a ring shape structure at the junction between the midpiece and the principal piece of the flagellum (4).

In various epithelia, members of the SLC26 family (SLC26A3, A4, A5, A6 and A9) complex with the Cystic Fibrosis Transmembrane conductance Regulator, the chloride/bicarbonate channel mutated in cystic fibrosis, and are able to regulate CFTR transport activity (5). Interestingly, the CFTR channel has been shown to localize at the equatorial segment of the head and at the flagellum (midpiece) of mature sperm, and to be required for sperm motility and capacitation (6,7). We will report our recent findings about SLC26A8 and CFTR functional cooperation and the consequences of SLC26A8 mutations in human male fertility.

Visconti, P.E., Westbrook, V.A., Chertihin, O., Demarco, I., Sleight, S. and Diekman, A.B. (2002) Novel signaling pathways involved in sperm acquisition of fertilizing capacity. J Reprod Immunol, 53, 133-150.

Toure, A., Morin, L., Pineau, C., Becq, F., Dorseuil, O. and Gacon, G. (2001) Tat1, a novel sulfate transporter specifically expressed in human male germ cells and potentially linked to rhogtpase signaling. J Biol Chem, 276, 20309-20315.

Everett, L.A. and Green, E.D. (1999) A family of mammalian anion transporters and their involvement in human genetic diseases. Hum Mol Genet, 8, 1883-1891.

Toure, A., Morin, L., Pineau, C., Becq, F., Dorseuil, O. and Gacon, G. (2001) Tat1, a novel sulfate transporter specifically expressed in human male germ cells and potentially linked to rhogtpase signaling. J Biol Chem, 276, 20309-20315.

Ko, S.B., Zeng, W., Dorwart, M.R., Luo, X., Kim, K.H., Millen, L., Goto, H., Naruse, S., Soyombo, A., Thomas, P.J. et al. (2004) Gating of CFTR by the STAS domain of SLC26 transporters. Nat Cell Biol, 6, 343-350.

Xu, W.M., Shi, Q.X., Chen, W.Y., Zhou, C.X., Ni, Y., Rowlands, D.K., Yi Liu, G., Zhu, H., Ma, Z.G., Wang, X.F. et al. (2007) Cystic fibrosis transmembrane conductance regulator is vital to sperm fertilizing capacity and male fertility. Proc Natl Acad Sci U S A, 104, 9816-9821.

Hernandez-Gonzalez, E.O., Trevino, C.L., Castellano, L.E., de la Vega-Beltran, J.L., Ocampo, A.Y., Wertheimer, E., Visconti, P.E. and Darszon, A. (2007) Involvement of cystic fibrosis transmembrane conductance regulator in mouse sperm capacitation. J Biol Chem, 282, 24397-24406.

This work was supported by the Ministère de l'Education Nationale et de la Recherche Scientifique, Institut National de la Santé et de la Recherche Médicale, Centre National de la Recherche Scientifique, Université Paris Descartes, Agence Nationale de la Recherche (ANR-07-JCJC-0099; ANR-12-BSV1-0011-01 MUCOFERTIL) and Association Vaincre la Mucoviscidose (RF20110600465).

Where applicable, the authors confirm that the experiments described here conform with The Physiological Society ethical requirements.

SA210

Airways surface liquid pH: regulation of ion transport by novel acid-sensitive soluble mediators

R. Tarran

University of North Carolina, Chapel Hill, NC, USA

Mucus clearance is an important aspect of the mammalian lung's innate defense system. During normal mucus clearance, inhaled pathogens become trapped in the mucus layer and are expelled before they can colonize the airways. The mucus layer is kept away from underlying epithelia by the presence of a ~7 μm periciliary liquid layer (PCL), which acts as a lubricant for the mucus. Together, these layers make up the airway surface liquid (ASL). The rate of mucociliary clearance is strongly influenced by the hydration state of the ASL. ASL volume hydration is largely maintained by Cl^- secretion through CFTR, with Na^+ and H_2O following by osmosis. However, as ASL moves up the respiratory tract, due to a reduction in surface area as airways converge, excess ASL is absorbed when needed via isotonic Na^+-led ASL absorption, which is mediated by the epithelial Na^+ channel (ENaC). Our experimental data indicate that ASL volume and ion transport regulation are in dynamic equilibrium, and that either a reduction in CFTR-mediated Cl^- secretion or an increase in ENaC-mediated Na^+ absorption will lead to ASL/PCL depletion and mucus dehydration. ENaC is highly sensitive to both membrane attached and soluble extracellular proteases which can cleave and activate ENaC. In addition, soluble volume sensing reporter molecules are present in the ASL and can bind to ENaC when ASL volume is low, removing ENaC from the plasma membrane, thus favouring secretion. These reporter molecules act as feedback sensors to modulate ASL volume. Importantly, these reporter molecules are contained within the ASL and are lost when cultures are mounted in Ussing chambers or following other experimental protocols that require flooding of the mucosal surface. The study of normal and CF airway epithelia under thin film conditions is essential to understanding the regulation of CFTR and ENaC and studies of airway epithelia under flooded conditions may produce aberrant results. In contrast, thin film studies correlate well with the increased cleavage pattern seen with ENaC in CF airways biochemically. We have recently identified the short palate lung nasal epithelial clone 1 (SPLUNC1) as one such ASL volume-sensing molecule. SPLUNC1 acts as a potent negative regulator of ENaC that serves to prevent excessive volume absorption when ASL volume is at optimum levels. Removal or dilution of SPLUNC1 leads to increased ASL absorption and temporary ENaC hyperactivity in normal airway cultures – until SPLUNC1 level rise again. For reasons that are currently under investigation, SPLUNC1 is present in CF ASL but is unable to regulate ENaC in CF airway cultures. To better understand defective SPLUNC1 regulation in CF, we identified the ENaC inhibitory domain of SPLUNC1 and further proteomic analysis suggested that this domain may be functionally deficient in CF airways in vivo. In addition to being a Cl- channel, CFTR is also permeable to bicarbonate, and CF airways are hypothesized to have a reduced ASL pH due to a lack of bicarbonate secretion through CFTR. This reduction in pH may be minimized by the backflow of bicarbonate through the paracellular pathway. Nonetheless, differences in pH in excess of 0.5 pH unit difference have been detected between normal and CF airway epithelia. In this talk, we will discuss how the interaction between soluble reporter molecules such as SPLUNC1 and ENaC are affected by pH. Furthermore, many extracellular proteases are pH-sensitive and their impact on ENaC and ASL volume will also be discussed.

Where applicable, the authors confirm that the experiments described here conform with The Physiological Society ethical requirements.

SA211

Luminal pancreatic ductal acid-base microclimate and pancreatic disease

V. Venglovecz[1], Z. Rakonczay Jr.[2], J. Maléth[2] and P. Hegyi[2]

[1]Department of Pharmacology and Pharmacotherapy, University of Szeged, Szeged, Hungary and [2]First Department of Medicine, University of Szeged, Szeged, Hungary

Clinical and experimental observations suggest that acidic environment in the pancreatic lumen may increase the risk of developing acute pancreatitis. The luminal pH is mainly regulated by both acinar and ductal cells. Acinar cells secrete digestive enzymes and protons which leads to acidification in the acinar lumen (Behrendorff et al., 2010). The high proton concentration inside the lumen can distrupt intercellular junctional links which may be involved in the initiation or development of acute pancreatitis. In contrast to acinar cells, ductal cells secrete a bicarbonate-rich alkaline solution (Argent, 2006) which neutralizes the stomach acidic chyme. It has been recently highlighted that this alkaline fluid is responsible for the neutralization of the extracellular pH in the acinar lumen as well (Freedman et al., 2001). The luminal proton, secreted by acinar cells may act as a paracrine messenger on the ductal cells and stimulate ductal bicarbonate secretion via acid-sensing ion channels (ASICs) (Holzer et al., 2007). The defect in ductal bicarbonate secretion, which occurs in certain pancreatic diseases (such as cystic fibrosis) can increase the risk to pancreatitis (Hegyi et al., 2011). Recent studies on ductal cells suggest that toxic factors, such as bile acids (Venglovecz et al., 2008) or ethanol (Yamamoto et al., 2003) also inhibit pancreatic ductal bicarbonate secretion which acidifies the lumen of the ducts and slows down the washout of the digestive enzymes. In summary, characterization of the ductal acid sensing mechanisms is essential to understand the acinar-ductal functional unit and may improve our knowledge in the pathomechanism of pancreatitis.

Argent, B. (2006). "Cell physiology of pancreatic ducts," in Physiology of the Gastrointestinal Tract, 4th Edn, Vol. 2, ed. L. R. Johnson (San Diego: Elsevier), 1376–1396.

Behrendorff, N., Floetenmeyer, M., Schwiening, C., and Thorn, P. (2010). Protons released during pancreatic acinar cell secretion acidify the lumen and contribute to pancreatitis in mice. Gastroenterology 139, 1711–1720.

Freedman, S. D., Kern, H. F., and Scheele, G. A. (2001). Pancreatic acinar cell dysfunction in CFTR–/– mice is associated with impairments in luminal pH and endocytosis. Gastroenterology 121, 950–957.

Hegyi, P., Pandol, S., Venglovecz, V., and Rakonczay Z. Jr. (2011). The acinar-ductal tango in the pathogenesis of acute pancreatitis. Gut 60, 544–552.

Holzer, P. (2007). Taste receptors in the gastrointestinal tract. V. Acid sensing in the gastrointestinal tract. Am. J. Physiol. Gastroint. Liver Phys. 292, G699–G705.

Venglovecz, V., Rakonczay, Z. Jr., Ózsvári, B., Takács, T., Lonovics, J., Varró, A., Gray, M. A., Argent, B. E., and Hegyi, P. (2008). Effects of bile acids on pancreatic ductal bicarbonate secretion in guinea pig. Gut 57, 1102–1112.

Yamamoto, A., Ishiguro, H., Ko, S. B. H., Suzuki, A., Wang, Y. X., Hamada, H., Mizuno, N., Kitagawa, M., Hayakawa, T., and Naruse, S. (2003). Ethanol induces fluid hypersecretion from guinea-pig pancreatic duct cells. J. Physiol. (Lond.) 551, 917–926.

Supported by grants from the Hungarian Scientific Research Funds (PD78087, NF105758, NF100677), National Development Agency grants (TAMOP-4.2.2.A-11/1/KONV-2012 -0035, -0073, -0052) and Bolyai Postdoctoral Fellowships (00334/08/5, 00174/10/5)

Where applicable, the authors confirm that the experiments described here conform with The Physiological Society ethical requirements.

SA212

Unraveling secreted mucins by luminal HCO_{3-} ions

J. Yang[1], G. Flores[1], A.K. Shamsuddin[1] and P.M. Quinton[1,2]

[1]Department of Pediatrics, University of California San Diego, San Diego, CA, USA and [2]Biomedical Sciences, University of California, Riverside, CA, USA

Mucus coating epithelia is one of the most critical components of innate defense against injury and infection of internal organs. To become protective, however, mucins, which are the longest, largest molecules in biology, must unravel from intensely condensed structures inside intracellular granules to occupy volumes 3 orders of magnitude larger as extracellular molecular 'mucus'. Impressively, the transformation occurs within seconds at most. Having found that the formation of "mucus' is critically dependent on the presence of HCO_{3-} (1) (2), we now address the properties of mucin / HCO_{3-} interactions and secretions. We surmise that HCO_{3-} effects mucus unraveling largely by competing away Ca2+ that divalently bridges the innumerable anionic sites fixed to the mucin peptide polymers, but other binding may also be involved. Using pH stat and transepithelial electrical measurements of HCO_{3-} flux, we show that HCO_{3-} is secreted in the intestines, airways, and reproductive tracts. Using histochemical staining of mucus (3) with morphometry, we determine relative losses of mucin from goblet cells. By applying selective inhibitors (GlyH-101, DIDS, acetazolamide) and agonists (Isoproterenol, Forskolin/IBMX, PGE2, Carbachol, UTP, VIP) in the presence and absence of HCO_{3-}, we illustrate the impact of HCO_{3-} secretion on mucin exocytosis and mucus discharge in these systems. These results indicate that secretion of gel forming mucins and HCO_{3-} secretion are regulated independently and in separate cells. It appears that exocytosis of gel forming mucins from goblet cells is largely under Ca2+ mediated control, while HCO_{3-} secretion derives from surrounding secretory cells is largely under cAMP mediated control of CFTR. Thus, even though HCO_{3-} may affect the exocytosis of mucins, the luminal secretion of HCO_{3-} appears to be required to support normal mucus maturation and formation. The relevance of these results to pathogenesis will be considered.

Quinton, P. M. (2010) Role of epithelial HCO3 transport in mucin secretion: lessons from cystic fibrosis. Am J Physiol Cell Physiol 299, C1222-1233

Gustafsson, J. K., Ermund, A., Ambort, D., Johansson, M. E., Nilsson, H. E., Thorell, K., Hebert, H., Sjovall, H., and Hansson, G. C. (2012) Bicarbonate and functional CFTR channel are required for proper mucin secretion and link cystic fibrosis with its mucus phenotype. J Exp Med 209, 1263-1272

Muchekehu, R. W., and Quinton, P. M. (2010) A new role for bicarbonate secretion in cervico-uterine mucus release. J Physiol 588, 2329-2342

Where applicable, the authors confirm that the experiments described here conform with The Physiological Society ethical requirements.

SA213

Homeostatic responses fail to correct defective amygdala inhibitory circuit maturation in Fragile X syndrome

M. Huntsman

Pharmaceutical Sciences and Pediatrics, University of Colorado, Aurora, CO, USA

Fragile X Syndrome (FXS) is a debilitating neurodevelopmental disorder thought to arise from disrupted synaptic communication in several key brain regions including the amygdala - a central processing center for information with emotional and social relevance. Recent studies reveal defects in both excitatory and inhibitory neurotransmission in mature amygdala circuits in Fmr1-/y mutants, the animal model of FXS. However, whether these defects are the result of altered synaptic development or simply faulty mature circuits remains unknown. Using a combination of electrophysiological and genetic approaches, we show the development of both pre- and postsynaptic components of inhibitory neurotransmission in the FXS amygdala is dynamically altered during critical stages of neural circuit formation. Surprisingly, we observe that there is a homeostatic correction of defective inhibition, which, despite transiently restoring inhibitory synaptic efficacy to levels at or beyond those of control, ultimately fails to be maintained. Using inhibitory interneuron-specific conditional knockout and rescue mice, we further reveal that Fragile X Mental Retardation Protein (FMRP) function in amygdala inhibitory microcircuits can be segregated into distinct pre- and postsynaptic components. Collectively, these studies reveal a previously unrecognized complexity of disrupted neuronal development in FXS and therefore have direct implications for establishing novel temporal and region-specific targeted therapies to ameliorate core amygdala-based behavioral symptoms.

Olmos-Serrano JL, Paluszkiewicz SM, Martin BS, Kaufmann WE, Corbin JG, Huntsman MM (2010) Defective GABAergic neurotransmission and pharmacological rescue of neuronal hyperexcitability in the amygdala in a mouse model of fragile X syndrome. J Neurosci 30: 9929-9938.

This work was supported by grants from NIH/NINDS (R01 NS053719), Autism Speaks, and FRAXA. Dr. Joshua G. Corbin (Children's National Medical Center) is a co-corresponding author on this work.

Where applicable, the authors confirm that the experiments described here conform with The Physiological Society ethical requirements.

SA214

Abnormal thalamocortical activation of somatosensory cortex in the young Fmr1-KO mouse model of Fragile X Syndrome

A. Domanski[1,2], J.T. Isaac[2,3] and P.C. Kind[1]

[1]Biomedical Sciences, University of Edinburgh, Edinburgh, Midlothian, UK, [2]NINDS, National Institutes of Health, Bethesda, MD, USA and [3]Eli Lilly and Company, Erl Wood, Surrey, UK

Fragile X Syndrome (FXS) is the most common heritable form of intellectual disability, affecting 1:4-6000 children, and a prominent genetic cause of Autism. Symptoms include cognitive impairment, seizures, and deficits in sensory processing including tactile hypersensitivity. Dissecting sensory cortical pathophysiology in FXS offers insight into both sensory dysfunction and higher cognitive impairment. Studies in the Fmr1-KO mouse model of FXS display developmental and lasting abnormalities in cortical neuronal physiology. In particular, altered plasticity at thalamocortical (TC) synapses, the principal cortical input for ascending sensory information, was shown in somatosensory cortex during the first 10 postnatal days. During this early critical period in wild-type (WT) mice, the temporal resolution of TC inputs undergoes coordinated developmental refinement to selectively promote cortical responsiveness to high frequency TC synaptic activity essential for high fidelity tactile coding and activity-dependent refinement of intracortical circuitry.

Hypothesizing that abnormal presentation of sensory inputs at the first stage of cortical processing could both affect juvenile sensory perception in FXS and impair the maturation of cortical circuits, we examined TC input responses in the juvenile Fmr1-KO somatosensory cortical Layer 4 (L4) circuit. Synaptic integration, L4 connectivity and evoked network activity were investigated using whole-cell and Multi-Electrode Array electrophysiology in a TC brain slice preparation. Relative to WTs, Fmr1-KO L4 excitatory neurons displayed elevated intrinsic excitability, increased feed-forward inhibitory drive and altered TC synaptic kinetics. Intracortical connectivity between excitatory/excitatory and excitatory/inhibitory neurons was broadly reduced in Fmr1-KOs. Computational simulations of TC input integration informed by in vitro data suggested dynamic re-tuning of TC processing in Fmr1-KOs by distributed circuit mechanisms but an uncompensated hypersensitivity to high frequency stimulation. As predicted, thalamorecipient excitatory neurons in Fmr1-KO slices showed altered temporal resolution of TC inputs following thalamic stimulation with behaviourally relevant patterns. Significantly exaggerated voltage summation could be achieved in L4 excitatory neurons following burst stimulation at 20-50Hz, with abnormal recruitment of reverberant L4 network activity possible following 5-20Hz stimulation. Quantifying L4 network activity in Fmr1-KO slices demonstrated pronounced reductions in population response sparsity, spike rate and trial-to-trial fidelity in Fmr1-KOs, with reduced spatial spread of network activity.

Together, these data demonstrate cortical hypersensitivity to TC inputs and abnormal recruitment of network activity by critical period Fmr1-KO somatosensory cortical circuits. The hyperresponsiveness and reduced fidelity of intracortical circuitry following behaviourally salient stimuli demonstrated in the present study may underlie tactile hyperexcitability and abnormal sensory discrimination in FXS patients, and likely contribute to deleterious cortical development.

Where applicable, the authors confirm that the experiments described here conform with The Physiological Society ethical requirements.

SA215

Altered vesicle dynamics and neuronal synchrony in a mouse model of mental retardation

A.D. Powell, P. Saintot, K.K. Gill and J.G. Jefferys

School of Clinical & Experimental Medicine, University of Birmingham, Birmingham, UK

Mental retardation (MR) is a common disorder affecting 2-3% of the general population; a leading cause of moderate to severe MR is mutations of genes located on the X-chromosome. One gene implicated in X-linked mental retardation (XLMR) is the OPHN1 (*Ophn*-1 in mice) gene which encodes oligophrenin-1, a RhoGAP protein. Loss of function mutations upregulate Rho GTPase-dependent signalling pathways leading to altered actin cytoskeleton dynamics which are important in vesicle dynamics and dendritic spine structure. In addition to its function in regulating actin dynamics, oligophrenin-1 regulates the kinetic efficiency of clathrin-mediated endocytosis of synaptic vesicles leading to reduced repetitive activation in inhibitory synapses.

As neuronal synchrony in the hippocampus plays a role in encoding and retrieving episodic memory and attention, we hypothesised that alterations in synaptic vesicle availability will alter neuronal synchronisation and could underlie the reduced cognitive performance of *Ophn*-1 null mice. *Ophn*-1 mice (male 15-30g, 3-10 weeks old) were anaesthetised by I.P. injection of medetomidine (1mg/kg) and ketamine (76mg/kg). Values are expressed as mean±S.E.M, compared by ANOVA or Student's t-test.

Initial experiments tested if oligophrenin-1 functioned as a regulator of vesicle availability in hippocampal CA3 synapses. Whole cell patch-clamp recordings from CA3c pyramidal neurons revealed that the frequency of spontaneous EPSCs and IPSCs (excitatory postsynaptic currents and inhibitory postsynaptic currents) was lower in *Ophn*-$1^{-/y}$ than *Ophn*-$1^{+/y}$ neurons (sEPSCs: 1.67±0.37 Hz, n=9; 6.91±1.50 Hz n=8, p=0.003; sIPSCs: 8.78±0.81 Hz, n=7; 12.63±0.76 n=7, p=0.009, respectively). Consistent with reduced spontaneous transmission, evoked IPSCs were significantly smaller in *Ophn*-$1^{-/y}$ neurons than *Ophn*-$1^{+/y}$ neurons (1573.3±172.5 pA, n=15 and 2316.9±278.6 pA, n=13, respectively; p=0.02).

As neuronal synchrony is dependent on the ability of inhibitory synapses to follow repetitive activation, we examined whether secretory vesicle availability was altered in *Ophn*-1 null slices at frequencies relevant to cognition. Inhibitory synapses were stimulated at 33 Hz; IPSCs built up with successive stimuli, reaching a steady level within 10 stimuli in *Ophn*-$1^{+/y}$ neurons; IPSC facilitation was much weaker in *Ophn*-$1^{-/y}$ neurons (p=0.001). We tested whether this inability to follow repetitive stimulation was a result of a reduced readily releasable pool (RRP) of synaptic vesicles. The RRP was smaller in *Ophn*-$1^{-/y}$ than *Ophn*-$1^{+/y}$ synapses (513.8±100.9 pA, n=7 and 1466.2±307.7 pA, n=5, respectively, p=0.005), corresponding to a smaller number of vesicles in the RRP (12±2 and 35±7, respectively).

Gamma oscillations can be generated *in vitro* in the CA3 region of the hippocampus by tonic activation of kainate receptor or can occur spontaneously. Spontaneous gamma activity was

smaller in *Ophn*-1$^{-/y}$ slices than in *Ophn*-1$^{+/y}$ slices (27.5±7.6 μV^2, n=8 and 66.0±13.7 μV^2, n=10, respectively, p=0.03). Superfusion of KA (50 nM) increased CA3 network activity throughout its application in both *Ophn*-1$^{+/y}$ and *Ophn*-1$^{-/y}$ slices. KA-induced gamma oscillations were significantly smaller in *Ophn*-1$^{-/y}$ slices than in *Ophn*-1$^{+/y}$ slices (2910.1±521.3 μV^2, n=21 and 5906.2±936.9 μV^2, n=30, respectively, p=0.02).

We have previously shown that the synaptic deficits in *Ophn*-1$^{-/y}$ neurons are reversed by acute inhibition of Rho-kinase (ROCK) activity. Application of the ROCK inhibitor, Y–27632 (10 μM, for 20 minutes) significantly increased spontaneous oscillations in *Ophn*-1$^{-/y}$ slices (vehicle 71.5±19.2 μV^2, Y–27632 215.8±51.8 μV^2, p=0.005). In *Ophn*-1$^{+/y}$ slices, Y–27632 did not affect spontaneous oscillations (vehicle 137.5±20.9 μV^2, Y–27632 180.8±40.9 μV^2, p=0.32).

In the present study, we investigate the role of oligophrenin-1 in neuronal network activity; particularly spontaneous- and kainate-induced gamma oscillations using the *Ophn*-1 mouse model of intellectual disability. We demonstrate that hippocampal inhibitory synapses are unable to function at frequencies necessary for higher cognitive function, due to a substantial decrease in the readily releasable pool (RRP) of synaptic vesicles. We propose that these synaptic changes underlie the deficits in gamma oscillations. The rescue of the emergent neuronal network activity by small molecule pharmacological inhibition of the downstream signalling pathway of oligophrenin-1, raises the possibility of a pharmacotherapy to treat affected individuals.

This work was supported by a Wellcome Trust grant to JGRJ (074771/Z/04/Z).

Where applicable, the authors confirm that the experiments described here conform with The Physiological Society ethical requirements.

SA216

Troubled translation in Fragile X

E. Osterweil[1], S. Chuang[2], A.A. Chubykin[1], M. Sidorov[1], R. Bianchi[2], R.K. Wong[2] and M.F. Bear[1]

[1]Picower Institute for Learning and Memory, MIT, Cambridge, MA, USA and [2]The Robert F. Furchgott Center for Neural and Behavioral Science, State University of New York Downstate Medical Center, Brooklyn, NY, USA

A major single-gene cause of autism is fragile X syndrome (FXS), a developmental disorder associated with intellectual disability and a high incidence of epilepsy. FXS develops due to silencing of the *FMR1* gene and subsequent loss of FMRP, a potent repressor of translation. The long-term depression of synaptic strength (LTD) induced by metabotropic glutamate receptor 5 (mGluR5) activation is enhanced in the FXS mouse model (*Fmr1* KO), and it has been suggested that the protein synthesis downstream of mGluR5 significantly contributes to the synaptic pathophysiology of the disorder. Consistent with this, we find that hippocampal protein synthesis is excessive in the *Fmr1* KO, and that acute pharmacological inhibition of either mGluR5 or the ERK1/2 signaling pathway is sufficient to normalize protein synthesis to WT levels. This correction is specific to the ERK1/2 pathway, as inhibition of the mTOR pathway does not normalize protein synthesis in the *Fmr1* KO.

Interestingly, it had been shown that a mild reduction of ERK1/2 activity can be achieved by disrupting the post-translational maturation of the upstream activator, Ras using the HMG-CoA reductase inhibitor, lovastatin. Based on these findings, we tested the efficacy of lovastatin for correcting pathological phenotypes in the *Fmr1* KO. Remarkably, we find that lovastatin, a drug in widespread use and approved to treat hypercholesterolemia in children, decreases Ras-ERK1/2 signaling, normalizes excessive protein synthesis, corrects exaggerated hippocampal mGluR-LTD, eliminates hippocampal epileptiform activity, normalizes neocortical hyperexcitability, and significantly ameliorates audiogenic seizures (AGS) in the *Fmr1* KO mouse. These data suggest that lovastatin is potentially disease modifying, and could be a viable prophylactic treatment for FXS.

Osterweil, EK et al. (2013). *Neuron* 77, 243-50.

Osterweil, EK et al. (2010). *J Neurosci* 30, 15616-27.

We are grateful for support from HHMI, FRAXA, NIH/NICHD, and the Simons Foundation.

Where applicable, the authors confirm that the experiments described here conform with The Physiological Society ethical requirements.

SA217

Synaptic alterations in animal models of Rett syndrome

T. Pizzorusso[1,2], E.M. Boggio[2,3], G. Della Sala[1], M. Giustetto[3], G. Lonetti[2] and E. Putignano[2]

[1]NEUROFARBA, Universty of Florence, Pisa, Italy, [2]Inst Neuroscience, CNR, Pisa, Italy and [3]Neuroscience, University of Turin, Turin, Italy

There is mounting evidence showing that the structural and molecular organization of synaptic connections is affected both in human patients and in animal models of neurological and psychiatric diseases. As a consequence of these experimental observations, it has been introduced the concept of synaptopathies, a notion describing brain disorders of synaptic function and plasticity. A close correlation between neurological diseases and synaptic abnormalities is especially relevant for those syndromes including also mental retardation in their symptomatology, such as Rett syndrome (RS). RS (MIM312750) is an X-linked dominant neurological disorder that is caused in the majority of cases by mutations in methyl-CpG-binding protein 2 (MeCP2). We will discuss recent data characterizing synaptic alterations in animal models of RS and their regulation by environmental and molecular factors.

This work was supported by Telethon projects 2009 and 2010, the EU 7th Framework Programme [FP2007-2013] under grant agreements no 223326 and 223524, the EXTRAPLAST IIT project, Regione Toscana (CANESTRO project), Epigenomics Flagship Project EPIGEN MIUR-CNR, and Associazione italiana sindrome di Rett. The authors declare no competing financial interests.

Where applicable, the authors confirm that the experiments described here conform with The Physiological Society ethical requirements.

SA218

Selected scientific topics on synthetic biology

F. Képès

institute of Systems & Synthetic Biology, Genopole®, CNRS, Evry, France

Synthetic Biology is the engineering of biology: the deliberate (re)design and construction of novel biological and biologically based systems to perform new functions for useful purposes, that draws on principles elucidated from biology and engineering (source: ERASynBio). Synthetic Biology is an emerging and promising research area with the potential to have a strong impact on future innovation and technological progress that is beneficial for the economy and for society as a whole. Synthetic Biology is at the intersection of engineering, bioscience, chemistry, and information technology. It provides concepts and toolboxes that open the way to a wide range of biotechnological applications in health, environment, bioenergy and fine chemical synthesis. It also allows to ask some fundamental questions in a new and sometimes more efficient way.
This lecture will provide a multifocal definition of Synthetic Biology and of its scientific contents. It will discuss of the epistemological conditions of its recent emergence. It will finally cover a wide ground of applications of Synthetic Biology through specific examples.

SA219

Legal knowledge gaps and constructs in synthetic biology - a comparative review of the state of the art

D. Milius

Department of Human Genetics, Faculty of Medicine, McGill University, Montreal, QC, Canada and Department of Commercial Law, Faculty of Law, University of Cape Town, Cape Town, Western Cape, South Africa

Gene systems and organisms constructed using synthetic biological techniques will have their origins in the human mind and imagination, and as such, will not be the products of nature. Though isolated and purified sequences are patentable, with recent controversies noted, they must satisfy the patentability criteria in addition to satisfying the usual statutory subject matter requirement. Should controversy over the patentability of isolated human genes persist, the value of synthetic genes to scientists will markedly rise. But even then there exist legal gaps, and with their more recently proposed solutions, the suggestion is to develop new legal constructs to adapt the law to newer modes of doing new things in biology. For instance, the implications for copyright's threefold requirement of original authorship, of enabling expression in a fixed medium, and of the work being capable of reproduction (so far narrowly understood), make it an attractive intellectual property right to consider though there are others that might also apply as scientists develop more capable "biological software". Trademarks and trade secrets are other potentially lucrative options that might be balanced by more open synthetic biology modes of production, which essentially take a non-proprietary approach to innovation in biotechnology. This presentation will include a discussion of syn-agriculture and of third-to-fourth-generation biofuels in order to help draw a map of the contours of the legal certainties, as well as to identify the perceived gaps and their current conceptual boundaries. It is hoped that evaluating the extent to which the proposed solutions address these uncertainties will help identify opportunities for the effective regulation and management of synthetic biology as a tool with the potential to improve food resources and energy production for the foreseeable bio-future.

Where applicable, the authors confirm that the experiments described here conform with The Physiological Society ethical requirements.

SA220

Who owns living organisms issued from synthetic biology?

C. Rhodes

University of Manchester, Manchester, UK

This presentation focuses on synthetic organisms in the sense of the biological 'parts' that are developed and the microorganisms in which they are combined in the field of synthetic biology. Starting from the basis of looking at approaches that can be taken to the ownership of genetic resources (the definition of which includes those of synthetic origin), it examines which of these approaches might be appropriate for synthetic organisms and whether the products of synthetic biology should be treated any differently from other genetic resources in this regard. Approaches that have been taken to ownership of genetic resources include: free access; common heritage; intellectual property rights; state sovereign rights; and the rights of farmers, local groups and indigenous peoples. Application of state sovereign rights and availability of intellectual property rights protection are the current dominant approaches (the latter being particularly controversial). The presentation will argue that these approaches are inappropriate on both practical and ethical grounds, and recommend a shift towards a (modified) common heritage approach to synthetic organisms (and genetic resources more generally).

Where applicable, the authors confirm that the experiments described here conform with The Physiological Society ethical requirements.

SA221

Biotechnology and use of living: a public matter

D. Browaeys

VIVAGORA, Paris, France

Nanotechnology: « manipulate atoms » is a slogan which responds now to a more ambitious project: "Life manufacturing". After molecular biology permitting to spell out the genetic code and more especially analyze the genetics programs, we are now thinking about rewrite them to obtain shaped organisms. This dreaming project stimulates the imagination of all the pioneers of synthetic biology. They promise to transform the coal in methane thanks to reprogrammed bacteria, resurrect mammoths and, why not, humans... After mechanical industries and chemical industries, are we going to see a new industrial age, the age of biological machine? These promises are they credible? If it's the case, what are the dangers of these new technologies and how to control it? Is this biology really conforming to our cultural and ethical values? And is that the biology we want for our society? The bioeconomy of the 21st century aims to increase the capabilities

of energy, foods, drugs and materials productions... Synthesis biology is not simply the processing of few microbes, plants, animals in productive factories but the commoditized production of unreleased organisms with which we had to live and not without socials, economics and ecological consequences. Indeed, what happens to our judgment concerning the distinction between artificial and natural, living and inanimate? How do we control the spread of "animated tools" we build? Who take the responsibilities for these autonomous products? Today it is a necessity to think about the issues of these new technologies and explore their strengths, limitations and alternatives. Face to these questions, VivAgora has implemented since 2009 many reflections about synthesis biology through a first cycle of events and purchase this approach with a workshop scenario and a seminar called "Les Assises du Vivant" in 2012. Furthermore, Bernadette Bensaude-Vincent and Dorothée Benoit-Browaeys co-authored in 2009 the book "Fabriquer la vie: Où va la biologie de synthèse?" In 2013, VivAgora became part of the "Observatory synthetic biology" steering committee. Who is VivAgora? Vivagora is an NGO involved in organizing debates on societal issues raised by scientific and technological innovations. By promoting the expression and inclusion of all stakeholders, and exploring the diversity of their views and goals, it seeks to build trust and promote a new culture of innovation. In a world where risks and uncertainties are increasing, VivAgora want to make sure that scientific and technological development benefits the community at large. Its goals: Help citizens understand issues raised by technological developments Create opportunities for stakeholders with conflicting interests to discuss their perspectives, support dialogue between stakeholders in order to explore responsible innovation practices and facilitate the inclusion of all stakeholders in scientific and technical decision-making bodies. Competences: Since 2003, VivAgora has implemented many cycles of public debates focused on health, environment, nanotechnologies, synthetic biology, neurosciences...It has developed an extensive expertise on the analysis and elaboration of engagement processes. It has initiated a Citizen Alliance on the challenges of nanotechnologies supporting the website: http://nano.acen-cacen.org/AccueiL. VivAgora is also mobilized on pluralist expertise and its process called COEXnano is devoted on nanocoating (supported by the Ministry for environment). The NGO has developed regional activities to encourage the creation of citizens groups concerned by nanotechnologies' programs. Those groups expressed themselves within the Nanoforum meetings in Paris (supported by the Ministry of health). Stopped in 2009, the forum will come back in 2013 with several meeting focused on "accountable practises". VivAgora gathers both public and private professionals involved in scientific and technological innovation, in open innovation events. VivAgora's website [www.vivagora.fr] presents current debates and news (quarterly Vivagoveille), as well as public engagement processes in France and worldwide. Accessible to anyone, it offers a wide variety of in-depth articles, alerts on emerging issues, a calendar of public events, and VivAgora activities.

Where applicable, the authors confirm that the experiments described here conform with The Physiological Society ethical requirements.

SA222

Role of microRNAs in vascular inflammation and proliferation in response to mechanical stress

S. Chien

Departments of Bioengineering and Medicine, and Institute of Engineering in Medicine,, University of California San Diego, La Jolla, CA, USA

Vascular endothelial cells (ECs) play significant roles in regulating circulatory homeostasis. The shear stress resulting from circulatory flow modulates EC functions by activating mechano-sensors, signaling pathways, and gene and protein expressions. Sustained shear stress with a clear direction (e.g., the pulsatile shear stress, PS, in the straight part of the arterial tree) down-regulates the molecular signaling of pro-inflammatory and proliferative pathways. In contrast, shear stress without a definitive direction (e.g., the disturbed or oscillatory flow, OS, at branch points and other regions of complex geometry) causes sustained molecular signaling of pro-inflammatory and proliferative pathways. The EC responses to directed mechanical stimuli involve the remodeling of EC structure to minimize alterations in intracellular stress/strain and elicit adaptive changes in EC signaling in the face of sustained stimuli; these cellular events constitute a feedback control mechanism to maintain vascular homeostasis and are athero-protective. Such a feedback mechanism does not operate effectively in regions of complex geometry, where the mechanical stimuli do not have clear directions, thus placing these areas at risk for atherogenesis. The differential modulation of EC functions by various flow patterns involves intricate interplays of signaling pathways and gene regulation, with the participation of microRNA (miR). For example, miR-23b mediates the PS-induced inhibition of EC proliferation by causing RB hypophosphorylation, and miR-21 mediates the OS-induced monocyte adhesion to ECs by enhancing the expression of adhesion molecules such as vascular cell adhesion molecule-1 and monocyte chemotactic protein-1. miR-92a exerts an inhibitory effect on the transcription factor KLF2, which is anti-inflammatory and anti-proliferative. The athero-protective effect of PS is mediated by the inhibition of miR-92a and the atherogenic effect of OS is mediated by the activation of miR-92a. There is also evidence that ECs can release miR-126 to modulate the gene expression and functions of vascular smooth muscle cells via a paracrine mechanism. These experimental studies on miR, in combination with the in silico approaches in systems biology, provide new insights on the mechanism of the fine tuning of gene regulation in response to differential flow patterns in health and disease.

Where applicable, the authors confirm that the experiments described here conform with The Physiological Society ethical requirements.

SA223

The role of nuclear matrix on proliferation and apoptosis of vascular cells modulated by mechanical strain

Y. Qi, Y. Han and Z. Jiang

Institute of Mechanobiology & Medical Engineering, Shanghai Jiao Tong University, Shanghai, China

Background: Arterial wall is exposed to three main hemodynamic forces in vivo: shear stress, caused by the dragging fric-

tional force of blood flow; transmural pressure, caused by the hydrostatic forces of blood within the blood vessel; and cyclic strain, defined as the repetitive deformation of the cells as the arterial wall rhythmically distends and relaxes with the cardiac cycle [1]. It had been proved that pathophysiological mechanical states of vascular cells, i.e. endothelial cells (ECs) and vascular smooth muscle cells (VSMCs), contribute to vascular disorder resulting from atherosclerosis, hypertension, bypass graft occlusion, et al [1, 2]. Nucleus is the largest and stiffest organelle in the cell, where is the site of transcriptional regulation, and contains the genome [3]. Nuclear matrix acts as the skeleton structure of the nucleus, but its role in mechanosensing and gene-expression-regulating is still unclear.
Methods and Results: The co-culture parallel-plate flow chamber system was used to mimics the shear stress, and FX-4000T Strain Unit to mimics the cyclic strain, respectively. We demonstrated the effects of three kinds of nuclear matrix proteins, i.e. Nesprin2, SUN1 and LaminA, in proliferation and apoptosis of vascular cells modulated by shear stress and cyclic strain. Our results indicated that both shear stress and cyclic strain application significantly modulated the expressions of Nesprin2, SUN1 and LaminA, but in different ways. Physiological shear stress (15 dyne/cm2) and pathological shear stress (5 dyne/cm2) revealed similar repressed effect on expressions of nuclear matrix in comparison with the static control. Physiological cyclic strain (5% elongation) increased, but pathological (15% elongation) decreased the expressions of nuclear matix proteins. By using target siRNA and overexpression plasmid transfection in ECs and VSMCs respectively, it revealed that nuclear matrix proteins participated in regulation of apoptosis and proliferation. Furthermore, the activations of transcription factors were detected by Protein/DNA array after both suppressing and increasing nuclear matrix proteins expressions. TFIID, regulated by Nesprin2, Stat-1, 3, 5 and 6, regulated by LaminA, were remarkably changed in vascular cells transfected with target siRNA and overexpression plasmid respectively.
Conclusion: Our study revealed that nuclear matrix proteins might be the novel mechanical-sensitive molecules in vascular cells, which and may play a crucial role in cell functions.

Haga JH, Li YS, Chien S. Molecular basis of the effects of mechanical stretch on vascular smooth muscle cells. J Biomech. 2007; 40(5): 947-60.

Chien S. Mechanotransduction and endothelial cell homeostasis: the wisdom of the cell. Am J Physiol Heart Circ Physiol. 2007; 292(3): H1209-24.

Caille N, Thoumine O, Tardy Y, Meister JJ. Contribution of the nucleus to the mechanical properties of endothelial cells. J Biomech. 2002; 35(2): 177-87.

This research was supported by grants from the National Natural Science Foundation of China, Nos. 10972140 and 11222223, and Shanghai Rising-Star Program, No. 11QA1403200.

Where applicable, the authors confirm that the experiments described here conform with The Physiological Society ethical requirements.

SA224

Atheroprotective effects of shear stress through the regulation of the renin-angiotensin system

S. Lehoux

Lady Davis Institute, McGill University, Montreal, QC, Canada

Atherosclerosis develops primarily at arterial bifurcations or curvatures, where flow is oscillatory, whereas vascular segments exposed to shear stress are protected. We showed that local, endothelial-specific angiotensin type 1 receptor (AT1R) expression may be pathologically significant: 1) endothelial expression of AT1Rs, which transduce most known effects of AngII, localizes to low flow, plaque-prone sites in the aorta, and 2) in vitro, endothelial AT1R expression is downregulated by shear stress. Recent data has allowed us to define how shear stress regulates AT1R expression acutely, through interaction with caveolin-1 and internalization. This process is important for shear stress-dependent activation of ERK1/2. We have also found that the hemodynamic environment may influence the expression of other components of the renin-angiotensin system, pointing to a localized tissue regulation of angiotensin II release and activity. Our findings illustrate the many levels at which shear stress orchestrates vascular function.

Where applicable, the authors confirm that the experiments described here conform with The Physiological Society ethical requirements.

SA225

Regulation of proinflammatory signalling pathways by shear stress in vascular endothelial cells

M. Zakkar

Cardiothoracic surgery, St Georges Hospital, University of London, London, UK and Cardiovascular medicine, Imperial college, London, UK

Atherosclerosis is a chronic inflammatory disease. Several pro-inflammatory mediators
including (LPS and TNFα) activate EC by simultaneously activating dual NF-KB and MAP kinase signalling pathways. The activity of p38 and JNK MAP Kinases is tightly controlled in EC by several negative regulators including MAPK phosphatase-1 (MKP- 1) and the transcription factor Nrf2.
Blood flow exerts several mechanical forces on endothelial surfaces including pressure,
circumferential stretch, and shear stress (mechanical drag). It is widely believed that shear stress plays a central role in the pathogenesis of atherosclerosis as lesions predominate at regions exposed to disturbed flow that is associated with low shear stress while regions exposed to high shear stress are protected.
MKP-1 is a central mediator of the anti-inflammatory effects of shear stress. Studies using cultured human umbilical vein EC (HUVEC) revealed that MKP-1 is induced by prolonged high shear stress. In-vivo studies of murine aortae by en face staining showed that MKP-1 is expressed at atheroprotected sites which are exposed to high shear stress but not at atherosusceptible sites. The assessment of the functional role of MKP-1 in-vivo was carried out by comparing wild type and MKP-1-/- C57BL/6 mice which revealed that MKP-1 is necessary for the suppression of p38 and JNK activity, and VCAM-1 expression

at atheroprotected sites as the genetic deletion of MKP-1 can lead to the loss of protection at these sites.
The c-Jun N-terminal kinase (JNK) is activated constitutively in EC at atherosusceptible sites but is inactivated at atheroprotected sites. The identification of transcriptional programs regulated by JNK by applying a specific pharmacological inhibitor to cultured EC and assessing the transcriptome using microarrays and subsequent validation by gene silencing revealed that JNK positively regulates the expression of numerous proapoptotic molecules. Analysis of aortae of wild-type, JNK1(-/-), and MKP-1(-/-) mice revealed that EC at an atherosusceptible site express proapoptotic proteins and are primed for apoptosis and proliferation in response to lipopolysaccharide through a JNK1-dependent mechanism, whereas EC at a protected site expressed lower levels of proapoptotic molecules and were protected from injury by MKP-1.
Nrf2 is also essential for the suppression of endothelial activation by high shear. The activation of Nrf2 at atherosusceptible sites of murine aortae by sulforaphane (a dietary antioxidant that acts as a potent activator of Nrf2) suppressed p38 activation and VCAM-1 expression in cultured EC. In-vivo studies showed that the administration of sulforaphane increased Nrf2 activity and reduced p38 activation and VCAM-1 expression at the atherosusceptible sites of wild type but had no effect on Nrf2-/- C57BL/6 mice.

Prof. P Evans

Prof. D Haskard

Dr. H Chaudhury

Where applicable, the authors confirm that the experiments described here conform with The Physiological Society ethical requirements.

SA226

Athero-susceptibility of the stressed endothelium

P.F. Davies[1,2], M. Civelek[2,6], Y. Fang[1,7], E. Manduchi[4], P. Islam[3], Y. Zhang[5] and Y. Jiang[1]

[1]Pathology & Laboratory Medicine, University of Pennsylvania, Philadelphia, PA, USA, [2]Bioengineering, University of Pennsylvania, Philadelphia, PA, USA, [3]Chemistry, University of Pennsylvania, Philadelphia, PA, USA, [4]Center for Bioinformatics, University of Pennsylvania, Philadelphia, PA, USA, [5]Biomedical Graduate Studies, University of Pennsylvania, Philadelphia, PA, USA, [6]Medicine, UCLA, Los Angeles, CA, USA and [7]Medicine, University of Chicago, Chicago, IL, USA

Endothelial phenotype heterogeneity plays an important role in the susceptibility of the cardiovascular system to pathogenesis. Arteries (and heart valves) are susceptible to chronic inflammatory disease in regions of blood flow disturbance, implicating hemodynamic forces and transport characteristics as prominent influences upon pro-pathological endothelial phenotype.
Our studies are focused on the normal and hypercholesterolemic domestic swine (Sus scrofa), an animal model close to human physiology and pathology, and are complemented by mechanistic in vitro studies of human arterial endothelial cells. All animal procedures were conducted under FDA and University of Pennsylvania IACUC approved protocols
Microarrays and next generation sequencing combined with systems analyses were used to identify differential expression of genes, small regulatory RNAs and epigenetic modifications in atherosusceptible endothelium. Data obtained from such high throughput 'omics' (discovery science) measurements in cells freshly harvested from the in vivo environment 'informed' the design of in vitro experiments (reductionist science). Where possible, the robustness of new mechanisms discovered in vitro was further tested in vivo to complete a cycle.
The association of chronic low level endoplasmic reticulum (ER) stress in endothelium in regions of flow disturbance was identified in atherosusceptible sites of aorta, carotid, renal, and coronary arteries as an important adaptive biomarker of susceptible phenotype. ER stress is linked to proinflammatory and oxidative stress pathways. Examples of microRNA and transcription factor mechanisms involved in site specific endothelial phenotype heterogeneity and pro-inflammatory/susceptible status in vivo will be presented.
We propose endothelial atherosusceptibility as a systems imbalance of multiple interrelated pathways that sensitizes the cells to pathological change. However, by adjusting the balance of cellular pathways the endothelium may respond to risk factor perturbation with surprisingly protective as well as pathological outcomes, reflecting the resilient nature of endothelial adaptation to the physical and chemical environment.
Research supported by the National Heart Lung and Blood Institute of the US National institutes of Health and the American Heart Association.

Davies PF. 2009, Hemodynamic Shear Stress and the Endothelium in Cardiovascular Pathophysiology. Nature Clin. Pract. Cardiovasc. Med. 6:16-26.

Civelek, M., Manduchi, E., Riley, R., Stoeckert, C.J., Davies, P.F. 2009, Chronic endoplasmic reticulum (ER)-stress activates unfolded protein response (UPR) in arterial endothelium in regions of susceptibility to atherosclerosis. Circ. Research, 105:453-461

Fang, Y., Shi, C., Manduchi, E., Civelek, M., Davies, P.F. 2010, MicroRNA-10a regulation of pro-inflammatory phenotype in athero-susceptible endothelium in vivo and in vitro. Proc. Natl. Acad Sci. USA. 107:13450-13455

Civelek, M., Manduchi, E., Riley, R.J., Stoeckert CJ, Jr., Davies PF. 2011, Coronary artery endothelial transcriptome in vivo: Identification of ER-stress and enhanced ROS by gene connectivity network analysis. Circulation: Cardiovascular Genetics. 4:243-252.

Fang, Y., Davies, P.F. 2012. Site-specific MicroRNA-92a regulation of Kruppel-like Factors 4 and 2 (KLF4; KLF2) in athero-susceptible endothelium. Arterio. Thromb. Vasc. Biol. 32:979-987.

Where applicable, the authors confirm that the experiments described here conform with The Physiological Society ethical requirements.

SA227

TRP channels in cerebral arteries

S. Earley

Colorado State University, Fort Collins, CO, USA

The mammalian transient receptor potential (TRP) superfamily of cation channels consists of 28 members divided among six subfamilies based on sequence homology. The function of many TRP channels present in the vasculature remains unknown. A goal of my laboratory is to elucidate the physiological significance of the sole member of the ankyrin (A) TRP subfamily, TRPA1, in endothelium-dependent regulation of cerebral arteries. TRPA1 is a Ca2+-permeable non-selective cation channel activated by noxious and pungent electrophilic compounds, such as allyl isothiocyanate (AITC), a substance derived from mustard oil and allicin, a compound present in garlic. The structure of the channel is distinguished by the ~14-

19 ankyrin repeat (AR) domains present in the intracellular amino terminus. TRPA1 is thought to be involved in diverse physiological processes including nociception, mechanotransduction, and thermal and oxygen sensing. We find that TRPA1 is present in the endothelium of cerebral, but not coronary, mesenteric, renal, or skeletal muscle arteries. Furthermore, AITC-induced activation of TRPA1 causes endothelium-dependent dilation of cerebral arteries. These observations suggest that TRPA1 channels may play a critical but unknown role in the regulation of the cerebral vasculature. Physiological activators of the channel in this tissue are not known. We tested the hypothesis that lipid peroxidation products (LPP) generated by reactive oxygen species produced by NADPH oxidase (NOX) stimulate TRPA1 channels in the endothelium in an autocrine manner. We found that the LPP 4-hydroxy-nonenal (4-HNE) caused concentration-dependent cerebral artery dilation (EC50 = 8.4 μM) that was abolished by the selective TRPA1 antagonist HC-030031. Using total internal reflection fluorescent microscopy (TIRFM) to record TRPA1 Ca2+ sparklets (unitary TRPA1-mediated Ca2+ influx events), we found that the NOX substrate NADPH increased TRPA1 Ca2+ sparklet frequency in primary cerebral artery endothelial cells. This response was blocked by HC-030031. NADPH also dilated isolated and pressurized (80 mmHg) cerebral arteries with pre-developed myogenic tone in a concentration-dependent manner (EC50 = 1.2 μM). Pre-treatment with HC-030031 diminished NADPH-induced dilation, suggesting involvement of TRPA1 channel activity in this response. Significantly, 4-HNE and NADPH-induced dilation were absent from novel, endothelial cell-specific TRPA1 knockout (eTRPA1-/-) mice. Furthermore, immunolabeling studies and proximity ligation assays using primary cerebral artery endothelial cells and isolated cerebral arteries demonstrate co-localization of TRPA1, NOX2, and 4-HNE within myoendothelial junction (MEJ) sites. Together, these data indicate that NOX-derived LPP dilate cerebral arteries by activating TRPA1 in myoendothelial junctions, demonstrating a novel mechanism for the regulation of cerebral blood flow. Our findings suggest that TRPA1 channels may be a suitable target for the development of new therapies for cerebrovascular diseases associated with endothelial dysfunction, such as stroke.

Supported by R01HL091905 (NHLBI) and a Monfort Excellence Award (Monfort Family Foundation).

Where applicable, the authors confirm that the experiments described here conform with The Physiological Society ethical requirements.

SA228

Pressure-sensing by TRPC5-containing channels in aortic baroreceptor

C. Wong[1,2], B. Shen[1], O. Lau[1] and X. Yao[1]

[1]School of Biomedical Sciences, The Chinese University of Hong Kong, Hong Kong, Hong Kong and [2]Integrative Biology and Pharmacology, UT Health, Houston, TX, USA

Arterial baroreceptors contain mechanosensors that detect the change in blood pressure, and transduce the mechanical signal into electrical signal transmitted via sensory neurons. The molecular identities of the baroreceptor mechanosensor are not fully understood, however, mechanosensitive ion channels are ideal candidates due to their ability to alter membrane potential. By mechanically stimulating the aortic baroreceptor neurons isolated from rat, we recorded a cation channel current comprising TRPC5. The baroreceptor TRPC5-containing channels were directly activated by membrane stretch on the soma and the neurite terminal. The channel activity was potentiated by Gd^{3+}, but was abrogated by an anti-TRPC5 blocking antibody T5E3 and by expressing a dominant-negative TRPC5 construct T5DN. Calcium imaging and single-channel electrophysiology confirmed the mechanosensitivity of heterologously expressed mouse TRPC5 in cell lines. Disruption of TRPC5 function in rat baroreceptor neurons by lentivirus mediated delivery of T5DN cDNA impaired the high blood pressure-induced firing frequency increase of the aortic depressor nerve, and it also impaired the baroreceptor-mediated reflex control of heart rate. In TRPC5 knockout (*trpc5*$^{-/-}$) mice, the pressure-induced firing frequency increase was markedly attenuated, and the baroreflex responses were also impaired. TRPC5 thus forms a stretch-activated channel participating in the mechanotransduction at the aortic baroreceptor.

Where applicable, the authors confirm that the experiments described here conform with The Physiological Society ethical requirements.

SA229

Lipid-sensing TRPC channels in cardiovascular health and disease

D. Beech

University of Leeds, Leeds, UK

Transient Receptor Potential Canonical (TRPC) proteins assemble to form channels that enable influx of calcium and sodium ions. There are six TRPC proteins in humans but more than six TRPC channels may arise because of heteromers amongst TRPCs and other TRP proteins. The proteins are widely expressed and have multiple functions throughout the peripheral and central systems of the body. Modulators of the channels include lipids, redox factors, and agonists at G-protein-coupled and tyrosine kinase receptors. My research addresses fundamental understanding of how and why cells control calcium ion entry in vascular biology; particularly in adaptive processes, human disease, and therapeutics. TRPC channels are an important but not singular aspect of these calcium entry mechanisms (Beech 2013 Circ J published on-line). They are expressed throughout the vasculature and probably in all cell types of the vasculature. These channels appear to have most significance as drivers of change when there is strain or insult in physiology or disease. Intriguingly, many, but not all, of the TRPC channel modulators are lipids or lipid-soluble substances; there are 10 known lipid modulators of the TRPC5 subtype and 9 of the TRPC6 subtype. These observations suggest that TRPC channels are lipid-sensing ion channels. Some of the lipid factors act directly, others indirectly (e.g. via lipid-sensing G-protein-coupled receptors). Our recent work has identified TRPC channels in perivascular and other adipocytes, which are key cell types in the control and storage of lipids and which play primary roles in cardiovascular health. The functional significance of these channels arises through negative regulation of adiponectin, a pivotal anti-inflammatory adipokine (Sukumar et al 2012 Circ Res 111, 191-200). The work identified dietary omega-3 fatty acids as inhibitors of these adipocyte TRPC channels and revealed the striking finding that the stimulatory effect of these fatty acids on adiponectin secretion is completely abrogated by in vivo genetic disruption of TRPC ion channel function. These and other recent findings will be discussed.

The research is supported by the Wellcome Trust and British Heart Foundation.

Where applicable, the authors confirm that the experiments described here conform with The Physiological Society ethical requirements.

SA230

TRPA1 channels and and cutaneous blood flow

A.A. Aubdool[1], R. Graepel[1], X. Kodji[1], E.S. Fernandes[1], S. Bevan[2] and S.D. Brain[1]

[1]BHF Centre of Cardiovascular Excellence and Centre of Integrative Biomedicine, King's College London, London, UK and [2]Wolfson CARD Centre, King's College London, London, UK

Cold-induced vasodilatation was first described by Lewis (1930) and remains an important phenomenon in protecting against cold-induced injury. Although this field of research has been extensively studied, the mechanisms involved in cold-induced vasodilatation currently remains unclear. The non-selective cation channel, transient receptor potential ankyrin 1 (TRPA1) is expressed in a subset of sensory neurons and was initially reported to sense noxious cold temperature. Although several studies have previously investigated its role as a cold sensor in the study of pain, its influence in cold-induced vascular responses is unknown. We have investigated the influence on peripheral vascular responses to environmental cold exposure in skin in vivo. Using non-invasive laser Doppler flowmeter techniques, peripheral blood flow was measured in anaesthetised mice before (5-10 min:baseline) and after local cold exposure of the mice hindpaw (30 min). Results were analysed as area under the response curve (AUC), expressed as mean + S.E.M. in arbitrary flux units (x1000 flux units) and analysed by 2-way ANOVA + Bonferroni's test. Cold treatment caused the expected reduction in skin blood flow, followed by a dilator response that was monitored for the following 30 min in WT mice. This response was substantially reduced in TRPA1 KO mice compared to respective age-matched WT mice (245.1 + 39.6 vs 86.1 + 11.0, x 1000 flux units, AUC, n=6, $p<0.01$) and antagonised by the TRPA1 antagonist HC030031 (100mg/kg, i.p., n=5, $p<0.001$). The cold-induced response was also shown to be significantly reduced in WT mice pre-treated with the calcitonin gene related peptide (CGRP) receptor antagonist, CGRP8-37 (400nmol/kg, i.v., n=7, $p<0.001$) and the substance P neurokinin-1 receptor antagonist SR140333 (480nmol/kg, i.v. n=5, $p<0.001$), suggesting a prominent role of neuropeptides in the cold-induced vascular responses. These results provide novel evidence of a major involvement of TRPA1 in local cold-induced vascular responses in vivo, with findings indicating a role for TRPA1-dependent neurogenic vasodilation as a key component of this response.

Lewis T (1930). Heart 15, 177-208.

This study was supported by a BBSRC-led IMB capacity building award.

Where applicable, the authors confirm that the experiments described here conform with The Physiological Society ethical requirements.

SA231

TRP channels as regulators of blood pressure and cardiac hypertrophy

M. Freichel

Institute of Pharmacology, Heidelberg University, Heidelberg, Germany

In the last few years, the large family of transient receptor potential (TRP) channels has been associated with the development of several cardiovascular diseases. 28 mammalian TRP-related proteins have been cloned, which are divided in 6 subfamilies: the classical TRPs (TRPC1–7); the vanilloid receptor TRPs (TRPV1–6); the melastatin TRPs (TRPM1–8); the mucolipins (TRPML1–3); the polycystins (TRPP1–3); and ankyrin transmembrane protein 1 (TRPA1). The proteins of the TRP family exhibit a 6-transmembrane domain architecture and form cation channels activated by, among others, temperature, receptor stimulation, chemical agonists, or possibly mechanical forces. In this way, they may contribute directly to transplasmalemmal Ca2+ influx and/or influence intracellular Ca2+ concentration ([Ca2+]i) indirectly by setting the membrane potential or regulating Ca2+ release from intracellular organelles. Depending on the cell type, TRP channel–mediated changes in cellular Ca2+ homeostasis can lead to alterations in vascular and cardiac contractility, neurotransmitter release, secretion of vasoactive hormones, mineral absorption, and body fluid balance to regulate blood pressure. In the heart, neuroendrocrine stimuli like noradrenaline, adrenaline and Angiotensin II lead to activation of G-protein-dependent signaling pathways that evoke Ca2+ entry and Ca2+-dependent processes, e.g. activation of Calcineurin/NFAT, CaM-Kinase and protein kinase C leading to the development of myocyte growth and cardiac hypertrophy. Although this represents an adaptive response preserving cardiac function initially, the persistent activation of this pathway during long-term cardiac stress may lead to cardiac failure in many cardiovascular disease entities including hypertension, ischemic or valvular heart disease. A specific pharmacology is still lacking for most TRPs. Therefore, studies to unravel the roles of TRP channels currently rely on experiments using transgenic animals and our findings about the role of individual TRP proteins for blood pressure regulation and development of cardiac hypertrophy using TRP-deficient mice will be presented.

Where applicable, the authors confirm that the experiments described here conform with The Physiological Society ethical requirements.

SA232

Functions of the C1 neurons: a synthetic overview

P.G. Guyenet

Pharmacology, University of Virginia, Charlottesville, VA, USA

The C1 neurons reside in the rostral ventrolateral medulla (RVLM). They use glutamate as fast transmitter and synthesize catecholamines plus various neuropeptides. Only a third of the C1 neurons are presympathetic i.e. innervate sympathetic preganglionic neurons. These C1 cells include several subgroups that are organized in roughly viscerotopic manner and regulate the circulation in concert with other types of RVLM bulbospinal neurons. Other subsets of C1 cells control the parasympathetic outflow and the hypothalamic pituitary

axis including the secretion of vasopressin, oxytocin and corticotrophin releasing factor via direct projections to the dorsal motor nucleus of the vagus and the paraventricular nucleus of the hypothalamus respectively. C1 cells are variously activated by hypoglycemia, infection or inflammation, hypoxia, nociception and hypotension. Optogenetic stimulation of the C1 cells increases breathing and activates brainstem noradrenergic neurons including the locus coeruleus. Based on the various effects attributed to the C1 cells, their axonal projections and what is currently known of their synaptic inputs, we propose that subsets of C1 cells are differentially recruited by pain, hypoxia, infection/ inflammation, hemorrhage and hypoglycemia to produce a repertoire of stereotyped autonomic, metabolic and neuroendocrine responses that help the organism survive physical injury and its associated cohort of acute infection, hypoxia, hypotension and blood loss.

Where applicable, the authors confirm that the experiments described here conform with The Physiological Society ethical requirements.

SA233

Respiratory modulation of sympathetic nerve activity: insights from human studies

J.P. Fisher

College of Life and Environmental Sciences, University of Birmingham, Birmingham, UK

It has been known since the earliest direct recordings that postganglionic sympathetic nerve activity shows a respiratory modulation in humans. Sympathetic outflow to the skeletal muscle vasculature reaches a nadir at peak inspiration and peaks during expiration. This pattern of activity is the net result of a complex integration of central neuronal circuits and modulatory feedback signals from cardiorespiratory sensory afferents, including lung-stretch receptors, baroreceptors, central and peripheral chemoreceptors. There is accumulating evidence from animal models and patient populations indicating that pathophysiological alterations in the respiratory modulation of sympathetic nerve activity can occur. Simms et al. (2009) reported that an altered coupling between respiration and sympathetic nerve activity is a causative factor in the elevated vascular resistance and blood pressure observed in the spontaneously hypertensive rat. We have observed an attenuation of the normal cyclical inhibition of muscle sympathetic nerve activity burst incidence during respiration in our preliminary studies of patients with essential hypertension (Fisher et al. 2011). Similar findings have been reported in patients with chronic heart failure, where a diminished sympathoinhibitory effect of the lung inflation reflex has been closely related to heightened muscle sympathetic nerve activity (Goso et al. 2001). Interestingly, acute slow deep breathing transiently reduces muscle sympathetic nerve activity in patients with hypertension (Oneda et al. 2010). Ongoing studies in our laboratory are examining the effects of a home-based training device which guides slow deep breathing (8 weeks, 15 min daily) on resting sympathetic nerve activity and its respiratory modulation in patients with hypertension.

Fisher et al. (2011) FASEB J. 25:1076.2.

Goso et al. (2001) Circulation. 104:418-423.

Oneda et al. (2010) Hypertens Res. 33:708–712.

Simms et al. (2009) J Physiol. 587(Pt 3):597-610.

Supported by the British Heart Foundation (PG/11/41/28893)

Where applicable, the authors confirm that the experiments described here conform with The Physiological Society ethical requirements.

SA234

Inhibitory regulation of sympathetic outflows

A.K. Goodchild[1], B.R. Bowman[1], P.G. Burke[1,2], S.F. Hassan[1], N.N. Kumar[1,2] and L.M. Parker[1]

[1]The Australian School of Advanced Medicine, Macquarie University, Sydney, NSW, Australia and [2]Department of Pharmacology, University of Virginia, Charlottesville, VA, USA

The destination of the sympathetic outflow which arises from sympathetic preganglionic neurons located in the thoracolumbar spinal cord is a myriad of target organs that include the vasculature, the adrenal gland, the viscera and brown adipose tissue. Much work has been directed at determining what areas of the brain influence which of these functional outflows and how this is regulated. For example, we have demonstrated that somatostatin inhibits, by way of somatostatin 2A receptors, a select population of neurons in the rostral ventrolateral medulla that regulate vasomotor tone by way of a fast conducting spinal pathway (1,2). We have combined a functional approach with anatomical analysis to investigate the neurochemicals used to control these neuronal pathways. A wide range of neurotransmitters/neuromodulators are found in presympathetic pathways that control sympathetic preganglionic neurons and in the preganglionic neurons themselves. These neurochemicals include amino acids, short lived gases and peptides. This presentation will discuss the role of inhibitory neuropeptides in the control of the sympathetic outflows named above. We have identified how specific outflows are influenced by a range of inhibitory neuropeptides in the spinal cord. The use of specific physiological stressors has permitted the identification of the neurons activated and retrograde tracing techniques allow target organ destination of neurons to be identified. Using such approaches we have defined the neurochemical codes for neurons activated by glucoprivic and hypotensive stimuli. The role of neuropeptides in particular and the colocalisation of multiple neurotransmitters in general will also be addressed.

Burke PG, Neale J, Korim WS, McMullan S, Goodchild AK. Patterning of somatosympathetic reflexes reveals nonuniform organization of presympathetic drive from C1 and non-C1 RVLM neurons. Am J Physiol Regul Integr Comp Physiol. 2011 Oct;301(4):R1112-22. doi: 10.1152

Burke PG, Li Q, Costin ML, McMullan S, Pilowsky PM, Goodchild AK. Somatostatin 2A receptor-expressing presympathetic neurons in the rostral ventrolateral medulla maintain blood pressure. Hypertension. 2008 Dec;52(6):1127-33. doi:10.1161

Funds supporting this work include NHMRC 1028183, ARCDP120100920

Where applicable, the authors confirm that the experiments described here conform with The Physiological Society ethical requirements.

SA235

Central respiratory-sympathetic coupling and sympathetic overactivity after chronic intermittent hypoxia

D. Zoccal

Physiology and Pathology, School of Dentistry of Araraquara, São Paulo State University, Araraquara, SP, Brazil

Chronic exposure to intermittent hypoxia (CIH) introduces significant neural plasticity in the respiratory and sympathetic networks. As a consequence, substantial changes in the mechanisms controlling respiratory and sympathetic activities can be observed in rats exposed to CIH. These include exaggerated respiratory and sympathetic chemoreflex responses, enhanced respiratory long-term facilitation and baseline sympathetic overactivity. The latter has been pointed out as an important factor contributing to the development of arterial hypertension in rats submitted to CIH. In our studies, we have been exploring the hypothesis that the enhanced sympathetic drive following CIH exposure is, at least in part, dependent on alterations in the respiratory network and its interaction with the sympathetic nervous system. We found that juvenile rats exposed to 10 days of CIH exhibited a pattern of active expiration with recruitment of abdominal muscles during late expiratory phase (late-E) in conditions of normoxia/normocapnia. Correlated with the emergence of late-E bursts in abdominal activity, we verified that sympathetic nerve of CIH rats also displayed novel bursts of activity during late-E, which were eliminated with the reduction of the central respiratory drive with hypocapnia. The abdominal and sympathetic late-E activities of CIH rats were recorded in the absence of peripheral feedback information and were associated with changes in the neuronal activity of expiratory neurons of ventral surface of medulla. Altogether, our data suggest that strengthened interactions between expiratory and sympathetic neurons contribute to elevate baseline sympathetic activity of CIH rats. These observations put forward the central respiratory-sympathetc coupling mechanisms as a novel player for the development of neurogenic hypertension.

FAPESP and CNPq

Where applicable, the authors confirm that the experiments described here conform with The Physiological Society ethical requirements.

SA236

Oxygen sensing and hypertension

J.F. Paton

Physiology & Pharmacology, University of Bristol, Bristol, UK

Many organs contain neural sensors detecting the chemical milieu. These sensors include those sensing oxygen and/or blood perfusion. They feed back afferent signals to the central nervous system triggering reflex responses that bring about appropriate homeostatic adjustment. Typically, this involves activation of the sympathetic nervous system to raise perfusion pressure in an attempt to restore adequate tissue oxygenation and blood flow within the organ from which the afferent signal originated.
Hypertension is a condition characterized by high vascular resistance, elevated sympathetic activity, T-lymphocyte vascular infiltration and inflammation, and vascular hypertrophy. These symptoms all hamper organ blood flow and oxygenation. Our working hypothesis is that the organs that are most sensitive to restriction in blood flow and reduced oxygenation (i.e. hypoperfusion) are likely to be critical for life and contribute greatest to reflexly evoked increases in sympathetic activity and hypertension. These organs are the brain and carotid body chemoreceptors. After all, carotid body function in ensuring adequate oxygenation of the brain may be the most important one they possess.
The relative contribution of brainstem hypoperfusion, carotid body activation and the interaction between these organs in hypertension will be discussed. My presentation will include reciprocating translational studies between animal models with hypertension and hypertensive patients. I will present data revealing elevated cerebral vascular resistance in hypertension that occurs prior to the onset of the hypertension. I will report on a novel intra-cranial detector system that when activated by cerebral hypoperfusion produces sustained hypertension. As a putative transduction mechanism for the detection of cerebral hypoperfusion, and resultant sympathoexcitation, I will discuss the role of TRPV4 channels. An issue with cerebral perfusion in hypertension may be due to a paucity of parasympathetic vasodilator fibre innervation and poor functional hyperaemic responses: I shall provide evidence describing such changes. I will also show that carotid body chemoreceptors not only have heightened reflex sensitivity but also tonicity in hypertension. Although it is well known that repeated stimulation of the carotid body triggers hypertension and increases in sympathetic nerve activity, we have found that this is, in part, mediated via an adrenomedullin mediated mechanism in the rostral ventrolateral medulla and enhanced central respiratory-sympathetic coupling. Our recent results show that hypertension and excessive sympathetic nerve activity can be alleviated by removing carotid body afferent feedback, which reduces the excitatory synaptic coupling of respiratory cells innervating pre-sympathetic motoneurones. Based on these results, I will discuss novel therapeutic interventional approaches to treat drug-resistant hypertension in humans.

British Heart Foundation and Cibiem funded research

Where applicable, the authors confirm that the experiments described here conform with The Physiological Society ethical requirements.

SA237

Neuronal voltage-gated calcium channels: the role of auxiliary $\alpha 2\delta$ subunits in channel trafficking and in neuropathic pain

A.C. Dolphin

Neuroscience Physiology and Pharmacology, University College London, London, UK

The $\alpha 2\delta$ auxiliary subunits of voltage-gated calcium channels enhance calcium currents and affect their properties, but their mechanism of action is not well understood. We have recently shown that $\alpha 2\delta$ subunits are glycosyl phophatidyl inositol (GPI)-achored proteins (Davies et al., 2010), and this is essential for their function, and explains their localization in lipid raft fractions (Davies et al., 2006). The anti-epileptic and anti-nociceptive drugs gabapentin (GBP) and pregabalin (PGB) are known to bind to $\alpha 2\delta$-1 and $\alpha 2\delta$-2, and the $\alpha 2\delta$-1 target is essential for the antihyperalgesic action of this drug (Field et al., 2006). We have found that acute application of GBP does

not affect calcium currents in several different systems. However, chronic application of GBP to cultured cells reduces both calcium currents and cell-surface expression of heterologously expressed α2δ and α1 subunits (Hendrich et al., 2008), and PGB also affects α2δ trafficking in vivo (Bauer et al., 2009). This process involves an inhibition of trafficking through the recycling endosomes (Tran-Van-Minh & Dolphin, 2010). Our evidence indicates that gabapentinoid drugs act chronically to impair the trafficking function of α2δ subunits and the associated α1 calcium channel subunits.

Evidence from numerous studies has identified an important role for α2δ-1 in neuropathic pain. The mRNA and protein for α2δ-1 are up-regulated in dorsal root ganglion (DRG) neurons following spinal nerve ligation (SNL), a model of neuropathic pain, an increase which correlates with the onset of mechanical hypersensitivity (Bauer et al., 2009). In a recent study, we have examined the role of α2δ-1 in sensory neuron function by examining sensory processing and the development of experimental neuropathic pain in α2δ-1 knockout mice (Fuller-Bicer et al., 2009). We have found that α2δ-1 gene deletion results in reduced baseline sensitivity to cold and mechanical stimuli, and a marked delay in the onset of mechanical hypersensitivity following nerve injury. This is coupled with a reduction in the proportion of DRG neurons sensitive to menthol in α2δ-1 knockout mice, suggesting defects in specific sensory modalities and that α2δ-1 is essential for the rapid development of behavioural hypersensitivity following nerve damage

Bauer CS et al. (2009) J Neurosci 29, 4076-4088

Davies A et al. (2006) J Neurosci 26, 8748-8757

Davies Aet al. (2010) Proc Natl Acad Sci U S A 107, 1654-1659.

Field MJ et al. (2006) Proc Natl Acad Sci USA 103, 17537-17542

Fuller-Bicer GA et al. (2009). Am J Physiol Heart Circ Physiol 297, H117-H124.

Hendrich J et al. (2008) Proc Natl Acad Sci USA 105, 3628-3633.

Tran-Van-Minh A & Dolphin AC (2010). J Neurosci 130, 12856-12867

We thank Wellcome Trust and MRC for support. The work on α2δ-1 knockout mice is a collaboration with Prof A Schwartz and Prof AH Dickenson.

Where applicable, the authors confirm that the experiments described here conform with The Physiological Society ethical requirements.

SA239

Neuronal dysfunction in genetic prion diseases: mutant prion protein impairs delivery of voltage-gated calcium channels to the presynaptic membrane

R. Chiesa

Neuroscience, Mario Negri Institute for Pharmacological Research, Milan, Italy and Dulbecco Telethon Institute, Milan, Italy

How mutant prion protein (PrP) leads to neurological dysfunction in genetic prion diseases is unknown. Tg(PG14) mice synthesize a misfolded mutant PrP which is partially retained in the neuronal endoplasmic reticulum (ER). As these mice age, they develop ataxia and massive degeneration of cerebellar granule neurons. We report that motor behavioral deficits in Tg(PG14) mice emerge before neurodegeneration and are associated with defective glutamate exocytosis from granule neurons due to impaired calcium dynamics. We found that PrP interacts with the voltage-gated calcium channel α2δ-1 subunit which promotes the anterograde trafficking of the channel. Owing to ER retention of mutant PrP, α2δ-1 accumulates intracellularly, impairing delivery of the channel complex to the cell surface. Thus mutant PrP disrupts cerebellar glutamatergic neurotransmission by reducing the number of functional channels in cerebellar granule neurons. These results link intracellular PrP retention to synaptic dysfunction, indicating new modalities of neurotoxicity and potential therapeutic strategies.

Senatore A., Colleoni S., Verderio C., Restelli E., Morini R., Condliffe S.B., Bertani I., Mantovani S., Canovi M, Micotti E., Forloni G, Dolphin A.C., Matteoli M., Gobbi M., and Chiesa R. (2012) Mutant PrP suppresses glutamatergic neurotransmission in cerebellar granule neurons by impairing membrane delivery of VGCC α2δ-1 subunit. Neuron, 74: 300-313

Where applicable, the authors confirm that the experiments described here conform with The Physiological Society ethical requirements.

SA240

CRMPs curb calcium channels for cessation of chronic pain: an old target engages a new partner

R. Khanna

Pharmacology and Toxicology and Biochemistry and Molecular Biology, Indiana University School of Medicine, Indianapolis, IN, USA and Program in Medical Neurosciences, Paul and Carole Stark Neurosciences Research Institute, Indiana University School of Medicine, Indianapolis, IN, USA

The use of N-type voltage-gated calcium channel (CaV2.2) blockers in pain therapeutics is limited by numerous physiologic side-effects. Here we report suppression of inflammatory and neuropathic hypersensitivity by inhibiting binding of collapsin response mediator protein 2 (CRMP-2) to CaV2.2, thus reducing channel function. A peptide of CRMP-2 fused to the HIV TAT protein (TAT-CBD3) decreases neuropeptide release from sensory neurons and excitatory synaptic transmission in dorsal horn neurons, reduces meningeal blood flow, reduces nocifensive behavior induced by formalin injection or corneal capsaicin application, and reverses neuropathic hypersensitivity produced by an antiretroviral drug. TAT-CBD3 was mildly anxiolytic without affecting memory retrieval, sensorimotor function, or depression. At doses 10-fold higher than that required to reduce hypersensitivity in vivo, a transient episode of tail kinking and body contortion was observed. By preventing CRMP-2-mediated enhancement of CaV2.2 function, TAT-CBD3 alleviates inflammatory and neuropathic hypersensitivity, an approach that may prove useful in managing chronic pain. Remarkably, sympathetic-associated cardiovascular activity is not affected by TAT-CBD3. Peptide analgesics, such as TAT-CBD3 and its derivatives, with restricted access to the CNS represent a completely novel approach to the treatment of severe pain with an improved safety profile.

This work was supported, in part, by grants from the Indiana Clinical and Translational Sciences Institute funded, in part by a Project Development Team Grant Number (RR025761) from the National Institutes of Health, National Center for Research Resources, Clinical and Translational Sciences Award, the Indiana State Department of Health – Spinal Cord and Brain Injury Fund (A70-9-079138 to R.K.), a National Scientist Development from the American Heart Association (SDG5280023 to R.K.), a Neurofibromatosis New Investigator Award from the Department of Defense Congressionally Directed Military Medical Research and Development Program (NF1000099 to R.K.), a Ralph W. and Grace M. Showalter Foundation grant (to R.K.), the Indiana University Biomedical Committee – Research Support Funds (to R.K), and a Research Inventions and Scientific Commercialization grant (to R.K.) from the Indiana CTSI. R.K. is a co-founder of Sophia Therapeutics, LLC.

Where applicable, the authors confirm that the experiments described here conform with The Physiological Society ethical requirements.

SA241

Ca^{2+} channel subunits $\alpha_2\delta2$ and $\alpha_2\delta3$ are essential for normal hearing in mice

J. Engel[1], B. Fell[1], A. Pirone[2], S. Kurt[3], A. Zuccotti[2], L. Rüttiger[2], P. Pilz[4], D. Brown[5], C. Franz[2], M. Schweizer[6], M.B. Rust[7], N. Brandt[1], V. Scheuer[1], G.J. Obermair[9], J. Dlugaiczyk[8], D. Hecker[8], R. Rübsamen[5], B. Schick[8], E. Friauf[7] and M. Knipper[2]

[1]Dept. of Biophysics, Saarland University, Homburg, Germany, [2]Tuebingen Hearing Research Centre, University of Tuebingen, Tuebingen, Germany, [3]Institute of Neurobiology, University of Ulm, Ulm, Germany, [4]Institute of Neurobiology, University of Tuebingen, Tuebingen, Germany, [5]Institute of Neurobiology II, University of Leipzig, Leipzig, Germany, [6]Center for Molecular Neurobiology, University of Hamburg, Hamburg, Germany, [7]Dept. of Biology, University of Kaiserslautern, Kaiserslautern, Germany, [8]Dept. of Otolaryngology, Saarland University, Homburg, Germany and [9]Dept. of Physiology and Medical Physics, Innsbruck Medical University, Innsbruck, Austria

The ascending auditory pathway consists of the auditory periphery, including mechanosensitive hair cells in the cochlea, spiral ganglion neurons forming the auditory nerve, and at least five stations until sound reaches the auditory cortex. All synapses along this pathway require proper expression and function of presynaptic Ca^{2+} channels for triggering transmitter release. Voltage-gated calcium channels (VGCCs) are protein complexes composed of an α_1 pore-forming subunit and auxiliary subunits β and $\alpha_2\delta$. VGCCs of cochlear inner hair cells (IHCs) are mainly composed of the α_1 subunit $Ca_v1.3$ (contributing to ~90% of I_{Ca}; refs. 1,2) and $\beta2$ (contributing to ~70% of I_{Ca}; ref. 3), and lack of $Ca_v1.3$ or $\beta2$ causes deafness.

Auxiliary subunits assist in trafficking and membrane surface expression of VGCCs and modulate their biophysical properties. Recently, novel roles for $\alpha_2\delta$ in synapse development have been suggested (refs. 4,5). So far, expression and contribution of the four $\alpha_2\delta$ subunits $\alpha_2\delta1$-4, and their specificity for the pore-forming α_1 and auxiliary β subunits are still unknown.

Because quantitative PCR revealed the expression of $\alpha_2\delta2$ in IHCs at pre-hearing and hearing age, we here analyzed hearing and IHCs of ducky mice ($\alpha_2\delta^{du/du}$), a mouse line with a mutation in the *cacna2d2* gene encoding a non-functional $\alpha_2\delta$ protein. Auditory brainstem response (ABR) click thresholds were increased by 18.3 dB in the mutants, and frequency ABR showed a significant elevation of hearing thresholds by about 20 dB between 11.3 and 22.6 kHz ($n \geq 11$ ears). Distortion-product otoacoustic emission (DPOAE) amplitudes were slightly larger in $\alpha_2\delta^{du/du}$ compared with wild-type animals, indicating normal outer hair cell (OHC) function. Synaptic morphology, as assessed by immunolabelling, revealed normal expression of presynaptic $Ca_v1.3$ and $\beta2$ as well as postsynaptic GluR2/3-proteins in close apposition with synaptic ribbons in IHCs of $\alpha_2\delta^{du/du}$ mice. However, both peak Ca^{2+} and peak Ba^{2+} current densities of $\alpha_2\delta^{du/du}$ IHCs were reduced by 29 % ($n \geq 11$). Moreover, the voltages for half-maximum activation of Ca^{2+} and Ba^{2+} currents were shifted to more positive potentials by 5 mV and 7 mV, respectively, whereas the voltage sensitivities (steepness of the activation curves) were unaffected. Inactivation of Ca^{2+} and Ba^{2+} currents over 300 ms depolarization steps was unchanged.

These results are in accordance with the classical role of $\alpha_2\delta$ subunits in surface expression and gating modulation of VGCCs. In wild-type IHCs, $Ca_v1.3$ and $\beta2$ appear to co-assemble with $\alpha_2\delta2$. Lack of $\alpha_2\delta2$ cannot be fully compensated, because of reduced IHC Ca^{2+} currents causing a moderate hearing impairment.

We detected another form of hearing impairment in a mouse line carrying a targeted deletion of $\alpha_2\delta3$ ($\alpha_2\delta3^{-/-}$; ref. 6). ABR hearing thresholds were slightly but significantly higher in $\alpha_2\delta3^{-/-}$ mice by 5 dB and 8-19 dB for click and pure tone stimuli, respectively, compared with wild-type littermates. Additionally, ABR waveforms showed a reduction in the amplitude of wave II and distortion of waves III and IV in $\alpha_2\delta3^{-/-}$, suggesting impaired signal transmission along the auditory pathway. In behavioral experiments, $\alpha_2\delta3^{-/-}$ mice learned to discriminate pure tones but completely failed to discriminate temporally structured amplitude-modulated tones, as demonstrated by an aversive go/no-go shuttle-box paradigm. IHCs of $\alpha_2\delta3^{-/-}$ mice had robust Ba^{2+} currents through Ca^{2+} channels and normal numbers of $Ca_v1.3$-immunopositive spots, which were co-localized with synaptic ribbons. Together with normal DPOAE amplitudes in $\alpha_2\delta3^{-/-}$ mice, these data suggest that deletion of $\alpha_2\delta3$ does not impair IHC and OHC function. $\alpha_2\delta3$ expression was predominant in spiral ganglion neurons and in auditory brainstem nuclei. Impaired synaptic transmission from auditory nerve fibers to bushy cells was confirmed by juxtacellular in-vivo recordings of sound-evoked activity, which revealed shallower rate-level functions and increased latencies at these synapses in $\alpha_2\delta3^{-/-}$ mice. Sizes of auditory nerve fiber synaptic boutons, which terminate at the somata of bushy cells, were significantly smaller in mutants, and the level of $Ca_v2.1$ channel immunoreactivity was reduced. These results identify a novel role for the $\alpha_2\delta3$ auxiliary subunit in establishing and maintaining the morphology and function of specific synapses

in the mammalian auditory pathway and identify the $\alpha_2\delta 3$ gene as a potential candidate gene for an auditory processing disorder.

Platzer J et al. (2000). Cell 102, 89-97.

Brandt A et al. (2003). J Neurosci 23, 10832-10840.

Neef J et al. (2009). J Neurosci 29, 10730-10740.

Kurshan PT et al. (2009). Nat Neurosci 12, 1415-1423.

Dolphin AC (2012). Nature reviews Neuroscience 13, 542-555.

Neely GG et al. (2010). Cell 143, 628-638.

Supported by EU-CAVNET MRTN-CT-2006-035367, RIMB (University of Kaiserslautern), DFG SFB 894, DFG PP1608, Studienstiftung Saar and ZHMB (Saarland University).

Where applicable, the authors confirm that the experiments described here conform with The Physiological Society ethical requirements.

SA242

Pharmacological relevance of intestinal drug transporters

I. Tamai

Kanazawa University, Kanazawa, Ishikawa, Japan

Although there are many suggestions for the contribution of efflux transporters in intestinal secretion/barrier of drugs mediated by ABC transporter, information on the absorptive/influx transporter molecules responsible for the intestinal absorptive process is limited. Organic anion transporting polypeptides (OATP; SLCO) family is expressed in various tissues including intestine and liver (1). OATP1B1 and OATP1B3 are selectively expressed in liver basolateral membrane thereby contributing in hepatic uptake of xeno- and endo-biotics such as bile acids and conjugated metabolites of bilirubin and steroids hormones. Those OATPs accept clinically used drugs such as statins and others. Effect of genetic polymorphism of OATP1B1, which cause altered activity, on pharmacokinetics of its substrate drugs clarified in vivo significance of OATP1B1(1). Accordingly, based on such a pharmacological relevance, OATPs are well recognized as physiologically and pharmacologically important transporters. OATP molecules are expressed in intestine and we tried to clarify its role in intestinal absorption of drugs. OATP2B1 (OATP-B, SLCO2B1) is expressed at the apical membrane of human intestinal epithelial cells and accepts similar compounds with hepatic OATPs as substrates (2,3). Accordingly, it is possible that OATP2B1 may drug absorption due to its broad substrate selectivity, while it is not easy to demonstrate its in vivo relevance to intestinal absorption. We found that genetic variant SLCO2B1*3, which has mutation c.1457>T that causes the amino acid change S486F, showed a decreased transport activity of estrone-3-sulfate (E3S), which is a physiological substrate of OATP2B1 (3). Fexofenadine (FEX), an anti-allergic agent is a substrate of OATP2B1, and OATP2B1 was thought to be the mechanism of its intestinal absorption, while there was no evidence of in vivo contribution of OATP2B1. Accordingly, we tested effect of genotype, SLCO2B1*3 (c.1457>T), on intestinal absorption of FEX after oral administration (3). As the results AUCs in individuals with genotype TT showed lowest plasma exposure of FEX, demonstrating in vivo contribution of OATP2B1 in the drug absorption. Another evidence of in vivo relevance of OATP2B1 was obtained by interaction of FEX absorption with fruit juices (FJ). When taking drugs orally with grapefruit juice (GFJ) and apple juice (AJ), plasma concentrations of substrate drugs of OATP2B1, including FEX and beta-adrenergic receptor antagonist talinolol, are affected (3). When examined inhibitory effect of those FJ on OATP2B1 by in vitro OATP2B1-expressing cultured cells, all FJs decreased apparent uptake of E3S via OATP2B1 at diluted concentration lower than 10% (4). These in vitro FJ effects strongly suggest that OATP2B1 is responsible for drug absorption. Further studies suggested that the responsible components in GFJ as inhibitors include naringin, hesperidin and others, while it was not clear in AJ. However, by uptake studies using in vitro OATP2B1-expressed cells, naringin showed differential inhibitory effect depending on used substrates, demonstrating substrate selective inhibitory effect. In addition, concentration dependence in E3S uptake by OATP2B1 showed biphasic kinetics. Therefore, it is possible that there are multiple binding sites (MBS) on OATP2B1 which show different substrate and inhibitor selectivity (5). MBS may cause dose/concentration dependence by mainly contributing binding sites on OATP2B1. Accordingly, MBS hypothesis may explain apparently discrepant in vitro and in vivo observations as well as broad substrate selectivity of OATP2B1. More interestingly, AJ but not GFJ decreased OATP2B1 activity even by only preincubation without co-existence during uptake measurement, namely long-lasting effect (6). Although the mechanism of long-lasting effect of AJ is not clear, it is known that OATP2B1 protein is internalized by protein-kinase C activation, thereby showing reduction of apparent uptake activity (7). When we exposed OATP2B1-expressing cultured cells with AJ and analyzed protein localization using antibody, intracellular localization was apparently changed by exposing with AJ. Accordingly, AJ effect might be explained by altered intracellular localization of OATP2B1 protein.

In conclusion, OATP2B1 should be responsible for absorption of various compounds including clinically used drugs. MBS may contribute to a broad substrate specificity of OATP2B1. In addition, clinical observation in OATP2B1-mediated absorption and interaction may be complex due to MBS and change in trafficking of OATP2B1 proteins by any co-administered drugs or food/juice. Most of information on OATP2B1, especially in vivo observation, came from the studies using drugs. According utilization of clinically used drugs as probes to monitor transporter activity is useful.

Nakanishi T and Tamai I. Drug Metab. Pharmacokinet. 27: 106-121 (2012).

Tamai I. et al. Biochem. Biophys. Res. Commun. 273: 251-260 (2000).

Tamai I. Adv. Drug Delivery Rev. 64: 508-514 (2012).

Shirasaka Y. et al. J. Pharm. Sci. 102: 280-288 (2013).

Shirasaka Y. et al. Drug Metab. Pharmacokinet. 27: 360-364 (2012).

Shirasaka Y. et al. Drug Metab. Dispos. 41: 615-621 (2013).

Kock K. et al. Am. J. Physiol. 285: 11336-11347 (2010).

Where applicable, the authors confirm that the experiments described here conform with The Physiological Society ethical requirements.

SA243

Polyspecific transporters as powerful pharmacological targets: the case of PEPTs (*SLC15*) and OCTs (*SLC22*)

M. Sala-Rabanal

Department of Cell Biology & Physiololgy, and CIMED, Washington University, St. Louis, MO, USA

The proton-dependent oligopeptide transporters (PEPTs, *SLC15*) and the organic cation transporters (OCTs, *SLC22*), two

mechanistically very distinct families within the Major Facilitator Superfamily (*Transporter Classification Database*, www.tcdb.org), share a common thread: a broad substrate selectivity, which in recent years has been subject to intense scrutiny, driven by the prospect of using these carriers for the delivery of drugs and prodrugs. Their relatively tolerant recognition and binding requirements, together with their localization to barrier epithelia and organs of drug disposition, make the PEPTs and the OCTs prime candidates for rational drug design, but these same properties can lead to competitive drug-drug interactions or toxicity in non-target organs. Pharmacological, structural and computational studies contribute to the refinement of existing pharmacophore models, towards improved targeting strategies and the prevention of undesired side effects.

PEPT1 (*SLC15*A1) and PEPT2 (*SLC15*A2) are mainly expressed, respectively, in the brush-border membrane of enterocytes, and in the apical membrane of renal proximal tubular cells, the lung epithelium and the choroid plexus, where they mediate the absorption, reabsorption and accumulation of all di- and tripeptides resulting from the hydrolysis of dietary and endogenous protein. In addition, they have been shown to recognize a broad spectrum of pharmacologically active compounds, both peptidomimetic, such as the β-lactam antibiotics, and non-peptidic. By means of biochemical and electrophysiological assays in *Xenopus* oocytes, we showed that the widely-prescribed antibiotics ampicillin, amoxicillin, cephalexin, cefadroxil, and the antineoplastics bestatin and δ-aminolevulinic acid are transported by human PEPT1 and PEPT2, and we established the alternating-access mechanism by which both oligopeptides and xenobiotics are translocated (Sala-Rabanal, Loo et al. 2006, Sala-Rabanal, Loo et al. 2008). The drugs, however, were transported with much lower efficiency than the natural substrates, and our findings suggest that the presence of physiological concentrations of dietary peptides in the gut may reduce or delay the absorption of oral delivery drugs, which should thus be taken in an empty stomach.

In humans, OCT1 (*SLC22*A1) and OCT2 (*SLC22*A2) are predominantly expressed in hepatocytes and proximal tubular cells, whereas OCT3 (*SLC22*A3) is found in placenta, bronchial and intestinal epithelium, and astrocytes. OCTs interact with many natural and xenobiotic monovalent cations and have been reported to transport dicationic compounds, including the short polyamine putrescine. In a recent study, we used *Xenopus* oocytes expressing mammalian OCT1, OCT2, or OCT3 to demonstrate that spermidine, which is longer and carries an additional positive charge, is also transported by the OCTs; and that, as for monovalent cations, hydrophobicity is a major requirement for recognition in polyvalent OCT substrates and inhibitors (Sala-Rabanal, Li et al. 2013). The identification of OCTs as relevant polyamine exchange systems may contribute to further our understanding of the physiological roles of polyamines, and aid in the design of polyamine-like OCT-targeted drugs: carcinogenesis and tumor growth have been associated with increased intracellular polyamine levels, and thus the OCTs might be targeted for the delivery of cytotoxic polyamine analogs or polyamine-conjugated imaging probes.

Sala-Rabanal, M., D. D. Loo, B. A. Hirayama, E. Turk and E. M. Wright (2006). Molecular Interactions Between Dipeptides, Drugs and the Human Intestinal H+ -Oligopeptide Cotransporter hPEPT1. J Physiol 574: 149-166

Sala-Rabanal, M., D. D. Loo, B. A. Hirayama and E. M. Wright (2008). Molecular Mechanism of Dipeptide and Drug Transport by the Human Renal H+/Oligopeptide Cotransporter, hPEPT2. Am J Physiol Renal Physiol 294: F1422-F1432

Sala-Rabanal, M., D. C. Li, G. R. Dake, H. T. Kurata, M. Inyushin, S. N. Skatchkov and C. G. Nichols (2013). Polyamine Transport by the Polyspecific Organic Cation Transporters OCT1, OCT2 and OCT3. Mol Pharm., In press

Where applicable, the authors confirm that the experiments described here conform with The Physiological Society ethical requirements.

SA244

The role of folate transporters in folate homeostasis and the targeted delivery of pharmacological agents to cancer cells

I. Goldman

Medicine and Molecular Pharmacology, Albert Einstein College of Medicine, Bronx, NY, USA

The folates (vitamin B9) are a family of one-carbon donors required for biosynthetic processes in mammalian cells. Their absorption in the gut, transport to systemic tissues and across epithelia is mediated by three specific processes: (i) The proton-coupled folate transporter (PCFT-SLC46A1) mediates folate absorption across the apical brush-border membrane of the proximal small intestine and across the blood:choroid plexus:cerebrospinal fluid barrier. This process is electrogenic and optimal at pH ~5.5. As the pH increases the influx Kt increases and the Vmax decreases. (ii) The reduced folate carrier (RFC-SLC19A1) is ubiquitously expressed and is the major route of transport of folates into systemic tissues. RFC functions optimally at pH 7.4 and is an organic phosphate antiporter that produces large electrochemical-potential differences for folates across cell membranes. (iii) Folate receptors (FRα & FRβ) are GPI-anchored membrane glycoproteins that transport folates by an endocytic process. FRα is expressed at the apical (luminal) membrane of the renal proximal tubules, retinal pigment epithelial cells and the choroid plexus. FRβ is expressed in cells of hematopoietic origin. All the transporters are expressed in placenta; however, the absence of any one of these transporters, 00alone, does not impair placental function. There are gene-targeted mouse models for these transporters. RFC -/- is embryonic lethal; however, if the dams are folate-supplemented, the pups are normal at birth but die within two weeks due to atrophy of the hematopoietic organs. The FRβ -/- mouse has no phenotype. The FRα -/- mouse is embryonic lethal but when the dams are folate-supplemented pups are normal and their requirement for supplementation does not persist. Adult animals are fertile with a normal phenotype save for a slight folate deficiency. PCFT -/- mice are normal at birth but subsequently develop severe folate deficiency and neurological defects. The human counterparts include: (i) hereditary folate malabsorption, due to loss-of-function mutations in the PCFT gene, is characterized by signs and symptoms of severe systemic and neural folate deficiency, (ii) cerebral folate deficiency due to mutations in FRα resulting in neurological defects that, unlike in FRα -/- mice, manifest several years after birth.

All three transporters are expressed in human cancers and have a role in cancer therapeutics. The classical antifolate, methotrexate - a dihydrofolate reductase inhibitor that causes tetrahydrofolate depletion, is transported via RFC with an influx Kt of ~ 5 μM. Resistance to this drug has been associated with loss-of-function mutations in, or loss of expression of, RFC. Recently, a second-generation much more potent antifolate of this class, pralatrexate, was approved for cancer treatment, with an influx Kt of 0.05 μM. Pemetrexed is another recently

approved antifolate which, in its active (polyglutamate) forms synthesized in cells, is a direct inhibitor of one-carbon utilization in thymidylate and purine synthesis. While this agent has an affinity for RFC somewhat greater than MTX, its PCFT-mediated transport is better preserved than most other folates at neutral pH so that the drug's antitumor activity is sustained even in the absence of RFC.

A major emphasis of contemporary drug development in cancer therapeutics is on (i) identifying intracellular targets that drive proliferation of malignant cells and (ii) the development of "targeted" agents that selectively block these processes. Another approach involves the development of agents that utilize specific transporters that are primarily expressed and/or are functional in cancer, but not normal, cells. Since RFC is the major route of transport into normal tissues, it plays a major role in antifolate toxicity. On the other hand, while PCFT is ubiquitously expressed, it does not play an important role in the delivery of folates or antifolates into normal tissues at physiological pH. Drugs are being developed that have a very low affinity for RFC but a very high affinity for PCFT which operates more efficiency in the acid microenviroment of solid tumors. Folate receptors are highly expressed in a variety of epithelial tumors (FRα) and hematological malignancies (FRβ). In a different approach antineoplastics, structurally unrelated to folates, are coupled to folic acid through linkers that include a cleavable sulfhydryl bond. The complex is endocytosed and, when the reducing potential of the endosome is increased, the bond is broken and the drug, which must be lipid soluble, diffuses out of the endosome to reach its intracellular target. A similar strategy is being used to ablate macrophages, which express FRβ, for the treatment of inflammatory diseases.

Qiu, A., Jansen, M., Sakaris, A., Min, S., Chattopadhyay, S., Tsai, E., Sandoval, C., Zhao, M.,Akabas, M.H., and Goldman, ID. Identification of an intestinal folate transporter and the molecular basis for Hereditary Folate Malabsorption. Cell, 127:917-928, 2006

Zhao R, Diop-Bove N, Visentin M, and Goldman ID. Mechanisms of Membrane Transport of Folates into Cells and Across Epithelia. Annual Review of Nutrition. 31:177-201, 2011.

Goldman ID, Chattopadhyay S and Moran R. The Antifolates: Evolution, New Agents in the Clinic, and How Targeting Delivery via Specific Membrane Transporters is Driving Development of a Next Generation of Folate Analogs. Current Opinion in Investigational Drugs. 11:1409-23, 2010.

Leamon CP, Jackman AL. Exploitation of the folate receptor in the management of cancer and inflammatory disease. Vitam Horm. 2008;79:203-33, 2008. PMI:18804696

Desmoulin SK, Hou Z, Gangjee A, Matherly LH. The human proton-coupled folate transporter: Biology and therapeutic applications to cancer.

Cancer Biol Ther. 13:1355-73, 2012

This research is support by a grant, CA82621, from the National Institutes of Health.

Where applicable, the authors confirm that the experiments described here conform with The Physiological Society ethical requirements.

SA245

Regulated trafficking of concentrative nucleoside transporters (CNTs) to the plasma membrane: a key event in nucleoside-derived drugs action

P. Fernández-Calotti[1,2] and M. Pastor-Anglada[1,2]

[1]Department of Biochemistry and Molecular Biology. Institute of Biomedicine (IBUB), University of Barcelona, Barcelona, Spain and [2]Centro de Investigación Biomédica en Red-Enfermedades Hepáticas y Digestivas (CIBER EHD), Barcelona, Spain

Nucleoside analogues (NA) constitute an important class of pro-apoptotic antimetabolites used in the treatment of hematological malignancies, solid tumors, and infectious diseases such as AIDS and hepatitis (1, 2). These therapeutic compounds include various pyrimidine and purine analogues (1) that mimic physiological nucleosides in terms of uptake into the cell and metabolism. Nucleosides and nucleoside derived drugs are hydrophilic molecules and diffuse slowly across cell membranes, thus, specific membrane proteins mediate their translocation from the extracellular milieu into the cytoplasm and, in some cases, from the cytoplasm towards the extracellular milieu. This cellular uptake occurs via nucleoside-specific membrane transporters (NT), belonging to the solute carrier families SLC28 and SLC29, encoding the concentrative (hCNT), which are Na+-dependent, and equilibrative (hENT), which are Na+-independent transporters, respectively. NA entrance into cells contribute to drug bioavailability and hence to cytotoxicity or antiviral capacity of nucleoside-derived drugs.

Among NT, hCNT proteins mediate concentrative high-affinity nucleoside influx by coupling substrate translocation to the inwardly directed electrochemical sodium gradient. This family comprises three members: hCNT1, hCNT2, and hCNT3. hENT proteins mediate facilitated, sodium-independent nucleoside-derived drug translocation. hENT1 and hENT2 are major determinants of equilibrative drug transport across the plasma membrane.

Resistance to NA treatments is usual in clinics. A key event in resistance is drug availability and entrance into the cells through NT. This is why the expression and activity of those molecules at the plasma membrane are essential.

Regulation of nucleoside transport activity in an isoform-specific manner is a suitable approach to modulate nucleoside-derived drug bioavailability. In this sense, it was shown that hCNT3 protein is retained intracellularly in a subpopulation of chronic lymphocytic leukemia (CLL) cases, showing that those patients with elevated levels of intracellular hCNT3 achieved a lower complete response rate after the purine analog fludarabine therapy (3). We have recently reported that all-trans retinoic acid (ATRA) induces hCNT3 trafficking to the plasma membrane, causing an increase in hCNT3 transporter activity and consequently fludarabine entrance in all fludarabine-resistant CLL samples analyzed (4). This effect was partially mediated by TGF-β1 by a mechanism that was dependent on the activation of the mitogen-activated protein (MAP) kinases p38 and ERK1/2 (5). Moreover, a reversion of fludarabine insensitivity was achieved in fludarabine-resistant CLL samples after ATRA or TGF-β1 treatment.

We have also found that induced traffic of NT to the plasma membrane seems to be involved in the combination therapy involving interferon α (IFNα) and the broad spectrum antiviral ribavirin, a purine nucleoside derivative drug. IFNα was shown to significantly increase the effect of ribavirin over the viral load (6). Although in basal conditions hENT1 is the main ribavirin transporter (7), no studies have evaluated the role

of hCNT2, a putative ribavirin good transporter, in the presence of IFNα. We recently demonstrated that IFNα induces a transient increase in hCNT2 activity within 15 minutes in HHL5-hepatocytes cells. This increase seems to be dependent on the translocation of hCNT2 containing vesicles to the plasma membrane by an ERK1/2 activation and microtubule integrity (Pinilla-Macua, Fernández-Calotti and Pastor-Anglada, submitted).

It is clear that NT expression is variable and that the available evidence supports a putative role for NT in nucleoside-derived drug bioavailability and responsiveness. NT expression pattern analysis might be useful as a biomarker of drug metabolism and action or as a predictor of response to therapy and patient outcome. Thus, major efforts should be made to determine the biological basis for the specific regulatory properties of NT trafficking as a way to improve cancer and viral therapies.

Errasti-Murugarren E, Pastor-Anglada M. Drug transporter pharmacogenetics in nucleoside-based therapies. Pharmacogenomics. 2010;11(6):809-41.

Minuesa G, Huber-Ruano I, Pastor-Anglada M. et al. Drug uptake transporters in antiretroviral therapy. Pharmacol & Ther. 2011;132(3):268-79.

Mackey J.R, Galmarini C.M, Graham K.A, et al. Quantitative analysis of nucleoside transporter and metabolism gene expression in chronic lymphocytic leukemia (CLL): identification of fludarabine-sensitive and -insensitive populations. Blood. 2005;105(2),767–774.

Fernández-Calotti PX, Lopez-Guerra M, Colomer D and Pastor-Anglada M. Enhancement of fludarabine sensitivity by all-trans-retinoic acid in chronic lymphocytic leukemia cells. Haematologica. 2012;97(6):943-51.

Fernandez Calotti P and Pastor Angada M. Alltrans- retinoic acid promotes trafficking of human concentrative nucleoside transporter- 3 (hCNT3) to the plasma membrane by a TGF-beta1-mediated mechanism. J Biol Chem. 2010;285(18):13589-98.

Jain M. K. and Zoellner C. Role of ribavirin in HCV treatment response: now and in the future. Expert Opin Pharmacother. 2010;11(4):673-683.

Fukuchi Y, Furihata T. et al. Characterization of ribavirin uptake systems in human hepatocytes. J Hepatol. 2010;52(4):486-492.

Where applicable, the authors confirm that the experiments described here conform with The Physiological Society ethical requirements.

SA246

Physiological and pharmacological insights from OATP uptake transporter knockout mice

A.H. Schinkel

Molecular Oncology, The Netherlands Cancer Institute, Amsterdam, Netherlands

Organic anion transporting polypeptides (OATPs, gene name SLCO) are uptake transporters for a broad range of endogenous compounds and xenobiotics. To investigate the physiological and pharmacological roles of Oatp1a/1b transporters, we generated and analyzed mice lacking all Slco1a/1b genes, and humanized transgenic rescue mice overexpressing human OATP1B1 and OATP1B3 in the liver. Slco1a/1b$^{-/-}$ mice were viable and fertile but suffered from marked conjugated hyperbilirubinemia, likely due to impaired hepatic (re-)uptake of bilirubin-glucuronide (Van de Steeg et al, 2010). These mice also displayed increased plasma levels of unconjugated bile acids. Using Oatp1a/1b and Abcc3 knockout mice and the OATP1B1 and OATP1B3 transgenic mice, we could show that in normal liver Oatp1a/1b, OATP1B1, OATP1B3, and the multispecific sinusoidal export pump Abcc3 drive a detoxification-enhancing liver-blood shuttling loop for bilirubin glucuronide. Within liver lobules, this shuttle allows flexible transfer of bilirubin- and probably also drug-conjugates formed in upstream hepatocytes to downstream hepatocytes. This likely helps to prevent saturation of further detoxification processes (e.g., biliary excretion) and subsequent hepatocyte toxic injury in the upstream hepatocytes. In close collaboration with Dr. M. Jirsa (Charles University, Prague), we subsequently demonstrated that the human Rotor syndrome, a benign hereditary conjugated hyperbilirubinemia, is a two-gene disorder, caused by impaired hepatocellular (re-)uptake of bilirubin glucuronide and other compounds owing to complete deficiencies of OATP1B1 and OATP1B3 (Van de Steeg et al, 2012). Since even partial OATP1B1 deficiencies cause life-threatening drug hypersensitivities in humans, the newly identified OATP1B1 and OATP1B3 null mutations likely confer substantial drug toxicity risks. Slco1a/1b$^{-/-}$ mice not only showed decreased hepatic uptake and increased systemic exposure of the anionic drug methotrexate, but also of the bulky hydrophobic anticancer drug paclitaxel. Humanized OATP1B1 and OATP1B3 could mostly rescue these phenotypes, suggesting a similar functional importance of these proteins in humans (Van de Steeg et al, 2013). Some Oatp1a/1b proteins are also expressed in the small intestine and thought to contribute to the intestinal uptake of orally administered drugs. However, despite extensive efforts, we have so far been unable to demonstrate any effect of the Oatp1a/1b knockout on the intestinal uptake of methotrexate, fexofenadine, or pravastatin (Van de Steeg et al, 2010; Iusuf et al, 2013). In conclusion, variation in OATP1A/1B activity due to genetic variation and pharmacological inhibition, or differences in tumor-specific expression levels might affect plasma, tissue, and tumor levels of these drugs in patients, and hence their therapeutic efficacy. The developed mouse models will provide excellent tools to study such questions.

Iusuf *et al*. (2013). *Mol Pharm* **9**, 2497-2504.

Van de Steeg *et al*. (2010). *J Clin Invest* **120**, 2942-2952.

Van de Steeg *et al*. (2012). *J Clin Invest* **122**, 519-528.

Van de Steeg *et al*. (2013). *Clin Cancer Res* **19**, 821-832.

This work was supported in part by grant NKI 2007-3764 of the Dutch Cancer Society

Where applicable, the authors confirm that the experiments described here conform with The Physiological Society ethical requirements.

SA247

Development of the cardiac conduction system

V. Christoffels

Anatomy, Embryology and Physiology, Academic Medical Center, Amsterdam, Netherlands

The contraction pattern of the cardiac chambers is controlled by myocytes of the pacemaker and the conduction system. In the developing heart all cardiac myocytes initially possess pacemaker properties. However, the majority of the embryonic myocytes differentiates into working myocardium, and only a small population of these cells will form the sinus node and the atrioventricular (AV) node and bundle. The development of these nodal regions is achieved by highly localized suppression of working muscle differentiation and stimulation of the pacemaker gene programs. Key transcription factors that

control this process have been identified, including T-box transcription factors Tbx3 and Tbx5.
During development, the AV canal myocardium is responsible for the AV conduction delay. This type of myocardium is highly evolutionary conserved in vertebrates and will form the AV node in higher vertebrates like birds and mammals. Recently, we identified a distinctive sinus node cell population in the fish heart, revealing deep conservation of these cells as well.
Despite the electrophysiological similarities between myocytes of the sinus node and the AV node and conduction system, their molecular programs show striking differences. For example, Tbx18, Shox2 and Isl1 uniquely control sinus node development, whereas Tbx2 and Nkx2-5 control AV canal formation.
In this presentation, I will show experimental findings on the molecular mechanisms of differentiation and morphogenesis of the pacemaker tissues of the heart, and discuss how misregulation of AV canal development can lead to formation of accessory pathways and ventricular preexitation.

Where applicable, the authors confirm that the experiments described here conform with The Physiological Society ethical requirements.

SA248

Optical mapping of the sinus and atrioventricular nodes

V.V. Fedorov

Physiology and Cell Biology, The Ohio State University, Dublin, OH, USA

Since Keith and Flack's anatomical discovery of the Sino-Atrial Node (SAN), the primary pacemaker of the human heart, the question of how such a small SAN structure can pace the entire heart has remained for a large part unanswered. There is a paucity of information regarding physiological function of the SAN in normal and diseased human heart at the cellular, tissue, and organ levels. Recent advances in optical mapping technology have made it possible to unambiguously resolve the origin of excitation and conduction within the animal and human atrial pacemaker complexes including SAN. The combination of high-resolution optical mapping and histological structural analysis reveal that the human SAN and atrioventricular (AVN) are functionally insulated from the surrounding atrial myocardium, except for several critical conduction pathways. Indeed, the atrial pacemaker clusters including SAN and AVN require anatomical (fibrosis, fat, and blood vessels) and/or functional barriers (paucity of connexins), in order to protect them from the hyperpolarizing influence of the surrounding atrium. The presence of conduction barriers and pathways may help explain how a small cluster of pacemaker cells in the atrial pacemaker complex manages to depolarize different, widely-distributed areas of the right atria as evidenced functionally by exit points and breakthroughs. The autonomic nervous system and humoral factors can further regulate conduction through these pathways, affecting pacemaker automaticity and ultimately heart rate. Moreover, the conduction barriers and multiple pathways can form substrates for reentrant activity and thus lead to atrial flutter and fibrillation.

Where applicable, the authors confirm that the experiments described here conform with The Physiological Society ethical requirements.

SA249

HCN channelopathies and sinus node arrhythmias

D. DiFrancesco

Dept Biosciences, University of Milano, Milano, Italy

It is generally agreed that the major role played by the funny current in the heart relates to the generation of normal, physiological pacemaker activity in the cardiac pacemaker region, the sinoatrial node (SAN), and to the control of heart chronotropism, although the exact degree by which funny channels contribute to govern pacemaking within the framework of the more complex set of partecipating mechanisms is still strongly debated. Several experimental and theoretical results provide evidence for the role of If in pacemaking. Among these results, of practical impact are applications of the concept of funny channel-based pacemaking of clinical relevance; starting from molecular/cellular properties, these applications translate the concept to the more integrated level of cardiac health in a clinical setting.
In a first example, the correlation between expression of funny channels, or more specifically of their molecular correlates HCN channels, and spontaneous activity is the basis for proof-of-concept development of "biological pacemakers". In cell-based models, it has been shown that spontaneously beating ESC-derived myocytes, known to express If, can pace cultures of neonatal rat cardiac myocytes and generate ectopic rhythms when injected in the ventricle of animal models after ablation of the AV node (Rosen et al., 2011). The aim of these protocols is to develop potential alternatives to electronic pacemakers.
In a second example, a most important clinical exploitation of funny channel properties relates to the pharmacological control of heart rate. Many funny channel-targeted drugs have been developed so far, among which ivabradine, the only drug marketed today for use in chronic stable angina and heart failure. Ivabradine is a specific blocker of funny channels, a property leading to a therapeutically useful "pure" heart rate slowing action (DiFrancesco & Camm, 2004). Ivabradine-induced block of funny channels has been analyzed in detail and shown to be characterized by a marked "use dependence", which may favour increased drug efficiency, as a rate-reducing agent, at high heart rates (tachycardia).
In a third example, several studies have shown recently that mutations in HCN4, the HCN isoform most highly expressed in pacemaker tissue, are associated with inheritable forms of arrhythmias and have provided growing evidence for a role of dysfunctional funny channels in rhythm disorders. Reported HCN4 mutations are associated with asymptomatic and symptomatic sinus bradycardia, tachycardia-bradycardia syndrome, AV node block, atrial fibrillation and contribute to more complex arrhythmias (Baruscotti et al., 2010).
The above studies, together with evidence from studies of HCN knockout mice (Bucchi et al., 2012) and data from the clinical use of ivabradine (Cappato et al., 2012), indicate that the role of funny channels need not be confined to control of physiological pacemaker activity of the SAN, but can also be relevant to maintenance of normal rhythmic activity in a broader context.
If has a recognized pathophysiological role in heart failure, since transcription of HCN channels increases in hypertrophied ventricles of failing hearts and predisposes to enhanced ventricular automaticity. Also, reduction of funny channel expression in pacemaker cells of cardiac-specific, inducible HCN4 KO mice eventually leads to lethal AV block, as well as to the

expected slowing of SAN rate, suggesting a previously unsuspected role of HCN4 in AV node activity and stimulus conduction (Baruscotti et al., 2011). Finally, ectopic beats originating in pulmonary veins are recognized sources of atrial arrhythmias and can initiate AF. It is interesting to note that funny channel-expressing pacemaker cells are present in pulmonary veins, and can contribute to ectopic beat generation and arrhythmogenesis (Chen et al., 2009). This implies that dysfunctional funny channels and/or altered If tissue distribution may also contribute to atrial arrhythmias and AF.
My talk will be devoted to review recent reports illustrating how candidate gene screening of the Hcn4 gene in families with arrhythmias has identified several causative HCN4 mutations in different types of rhythm disorders, and to discuss the perspective of future research in this area.

-Baruscotti M et al. (2010). Pflugers Arch 460, 405-415

-Baruscotti M et al. (2011). Proc Natl Acad Sci U S A108(4), 1705-1710

-Bucchi A et al. (2012). Frontiers Physiol 3, 240

-Cappato R et al. (2012). J Am Coll Cardiol 60, 1323-1329

-Chen YC et al. (2009). J Cardiovasc Electrophysiol 20, 1039-1045

-DiFrancesco D & Camm JA (2004). Drugs 64, 1757-1765

-Rosen MR et al. (2011). Nat Rev Cardiol 8, 656-666

Partially supported by a grant from the Italian Ministry of Research PRIN2010BWY8E9

Where applicable, the authors confirm that the experiments described here conform with The Physiological Society ethical requirements.

SA250

Modulation of atrioventricular node cell activity: endothelin-1 and acetyl-choline

S.C. Choisy[1], H. Cheng[1], G.L. Smith[2], A.F. James[1] and J.C. Hancox[1]

[1]Cardiovascular Research Laboratories, Bristol Heart Institute, School of Physiology and Pharmacology, University of Bristol, Bristol, UK and [2]Cardiovascular Physiology, University of Glasgow, Glasgow, UK

The activity of the atrioventricular node (AVN) is established to be modulated by the autonomic nervous system. By contrast, whilst receptors for the peptide hormone endothelin-1 (ET-1) are known to be present in the AVN (e.g. Molenaar et al, 1993), until recently there has been little information on ET-1 modulation of AVN electrophysiology. Accordingly, we have studied effects of ET-1 on rabbit AVN cellular electrophysiology (Choisy et al, 2012a). For this investigation, adult male New Zealand White rabbits were killed in accordance with UK Home Office legislation and AVN cells were isolated by enzymatic and mechanical dispersion. Whole-cell voltage-clamp was performed at 37ºC using a standard Tyrode's solution and K^+-based pipette solution (Choisy et al, 2012a). Application of 10 nM ET-1 to spontaneously active AVN cells led to a rapid cessation of spontaneous action potentials (APs), accompanied by a marked membrane potential hyperpolarization that partially 'relaxed' in the presence of ET-1 (Choisy et al, 2012a). Under voltage-clamp, ET-1 reduced L-type calcium current and rapid delayed rectifier K^+ current, whilst during hyperpolarising voltage steps it activated a tertiapin-Q (TQ; 300 nM) sensitive inwardly rectifying current with properties similar to the muscarinic (GIRK) K^+ current, $I_{K,ACh}$ (Choisy et al, 2012a). This response showed some time-dependent decline. When spontaneous APs were recorded in the presence of TQ, AP magnitude progressively declined and the maximum diastolic potential depolarised. Thus, in the absence of TQ, ET-1 activation of $I_{K,ACh}$ was the dominant response (Choisy et al, 2012a).
Since our results with ET-1 were suggestive of some time-dependent decline of ET-1 activated $I_{K,ACh}$, this phenomenon was studied further in experiments using either ET-1 (10 nM) or acetyl-choline (ACh; 1 μM or 100 nM), together with repetitive application of brief voltage-ramps (Choisy et al, 2012b). In these experiments, ACh application activated a large TQ-sensitive $I_{K,ACh}$ via M2 muscarinic receptors. This response showed rapid bi-exponential 'fade' (Choisy et al, 2012b). Comparative experiments with ET-1 using the same protocol demonstrated 'fade' of ET-1-activated $I_{K,ACh}$, though with a different (mono-exponential) time-course. 'Fade' rate did not correlate with initial response (i.e. K^+ flux) magnitude. Sequential application of ACh (1 μM) and ET-1 (10 nM) showed heterologous desensitization of the ET-1 response by ACh. These results suggest that ET-1 and ACh act on a common pool of GIRK channels and that $I_{K,ACh}$ 'fade' involves desensitization that may occur down-stream of receptor activation. Internal application of GDPβS (3 mM) to rabbit AVN cells via diffusion from the patch-pipette led to a reduction in the extent of desensitization of $I_{K,ACh}$, consistent with an involvement of the G-protein cycle in rapid 'fade' of $I_{K,ACh}$ (*cf* Leaney et al, 2004). 'Fade' of $I_{K,ACh}$ was also observed in AVN myocytes isolated from a difference species (C57BL6J mice).
Collectively, the results of these studies indicate that both ET-1 and ACh activate $I_{K,ACh}$ in AVN myocytes and that the response exhibits rapid desensitization. Some previous studies on anaesthetized dogs (Martin, 1983) and rabbit isolated atrial preparations (Salata and Jalife, 1985) have provided evidence for 'fade' of the response to vagal stimulation. Our findings raise the possibility that this may be attributable to desensitization-induced 'fade' of AVN $I_{K,ACh}$.

Molenaar P, O'Reilly G, Sharkey A, Kuc RE, Harding DP, Plumpton C, Gresham GA, Davenport AP (1993). Characterization and localization of endothelin receptor sub-types in the human

atrioventricular conducting system and myocardium. *Circ Res* **72**, 526–538.

Choisy SC, Cheng H, Smith GL, James AF, Hancox JC (2012a). Modulation by endothelin-1 of spontaneous activity and membrane currents of atrioventricular node myocytes from the rabbit heart. *PLoS One* **7**, e33448.

Choisy SC, James AF, Hancox (2012b). Acute desensitization of acetylcholine and endothelin-1 activated inward rectifier K^+ current in myocytes from the cardiac atrioventricular node. *Biochem Biophys Res Comm* **423**, 496-502.

Leaney JL, Benians A, Brown S, Nobles M, Kelly D, Tinker A (2004). Rapid desensitization of G-protein gated inwardly rectifying K^+ currents is determined by G protein cycle. *Am J Physiol* **287**, C182-C191.

Martin P (1983). Secondary AV conduction responses during tonic vagal stimulation. *Am J Physiol* **245**, H584-H591.

Salata JJ and Jalife J (1985). "Fade" of hyperpolarizing responses to vagal stimulation at the sinoatrial and atrioventricular nodes of the rabbit heart. *Circ Res* **56**, 718-727.

This work was funded by the British Heart Foundation (PG/08/104 and PG/11/97).

Where applicable, the authors confirm that the experiments described here conform with The Physiological Society ethical requirements.

SA251

Purkinje fibers and arrhythmias

P. Boyden

Columbia University, Columbia, NY, USA

Much new information has evolved about the role of Purkinjes in Arrhythmia initiation and perpetuation. Several examples of such and the reasons for this will be discussed. In addition important new information about the macromolecular makeup of Purkinje "pacemaking" machinery will be explored.

Where applicable, the authors confirm that the experiments described here conform with The Physiological Society ethical requirements.

SA252

The future of medicine: putting the individual where she should be

H.V. Westerhoff

Synthetic Systems Biology, SILS, NISB, the University of Amsterdam, Amsterdam, Netherlands and Manchester Centre for Integrative Systems Biology, University of Manchester, Manchester, UK

Airplanes and motorways are repaired successfully when broken. Humans suffering from one of the many multifactorial diseases are rarely so; at best, their diseases are managed. Yet, mankind has been able to put a man onto the moon and to get him back healthily. It is not that we haven't spent the same amount of money towards understanding and finding cures for these diseases. And it is not that we are linearly progressing towards curing these diseases: most new publications add more issues than they resolve. Lack of progress may be due both to the excessive complexity of the topic at hand, to a crisis in the handling of information and communication in the life sciences and health care, and to a reluctance to see the forest for the trees.

By organizing the plethora of biomedical information into a new type of dynamic framework, more of the information that is acquired will work towards the understanding of health and disease. The basis of this framework will be a molecule based, structured model of the human. I will discuss the potential that Recon2, the March 2013 consensus reconstruction of genome-wide human metabolism, may already offer. Important here is the ready generation of millions of metabolic maps, one for each sequenced individual. I will also give examples of how conjunction of such a genomics driven approach with an equally individualized physiological approach may lead to new strategies of dealing with truly individualized medicine: differential network-based drug design, transcription clocks, drug detoxification and biomarkers thereof.

Where applicable, the authors confirm that the experiments described here conform with The Physiological Society ethical requirements.

SA253

Microvascular systems biology

S. Peirce

Biomedical Engineering, Univ. of Virginia, Charlottesville, VA, USA

The growth and adaptation of microvascular networks are essential processes in development, tissue homeostasis, and responses to disease. The signaling networks and cellular behaviors that underpin the establishment and remodeling of microvessels are complex, dynamic, and spatially heterogeneous. Computational modeling approaches have enabled otherwise intractably difficult experiments to be performed in silico with high throughput hypothesis testing and generation. Computational and mathematical models at nearly every relevant level of biological scale (gene-to-tissue) have offered new insights. Increasingly, multiscale models that bridge phenomena at one level of scale to another, have been created and deployed to understand how perturbations within and around individual cells in a tissue affect vessel structure and overall organization of the network. Close integration with in vitro or in vivo experimental analogs, typically afforded by endothelial cell culture models or various thin vascularized tissues in small animal models (e.g. retina, subcutaneous tissue, ear, thin muscles), facilitates model specification and independent validation. Collaborative partnerships, which are often highly interdisciplinary, have emerged to fuel linkages between different modeling approaches and close coupling of models with experiments. Our group has recently partnered with other modeling groups and with experimental biologists to develop a novel multiscale model of sprouting angiogenesis (Figure 1). We have coupled agent-based modeling (ABM) with receptor-ligand kinetics modeling to explore how signaling inputs from neighboring cells (e.g. NOTCH/Dll4) and extracellular cues (e.g. VEGF) coordinate capillary sprouting and microvascular network patterning. Cellular functions including mitosis, migration, and phenotype regulation are explicitly modeled in the ABM, while a coupled partial differential equations model predicts extracellular gradients of growth factor, as well as membrane-bound and soluble receptor-ligand binding in and around the cell membrane. We demonstrate that when key parameters that are impossible to measure empirically (e.g. extent of the VEGF gradient across the length of a single cell) are varied within certain ranges, our multiscale model can accurately predict locations of capillary sprout emergence from a parent vessel that are consistent with independent experimental observations obtained using the embryoid body model of vasculogenesis. Sensitivity analyses further suggest that initial geometry is key to determining the location of sprout initiation while chemotactic gradients principally govern the rate of sprout extension. As with any model — experimental or computational — the true test of its utility is the ability to uncover new understanding that advances the field. To this end, we are deploying our multiscale model in an iterative model-experiment-model cycle in order to probe the fundamental mechanisms of sprout initiation, extension, maturation, and network patterning in the context of sprouting angiogenesis.

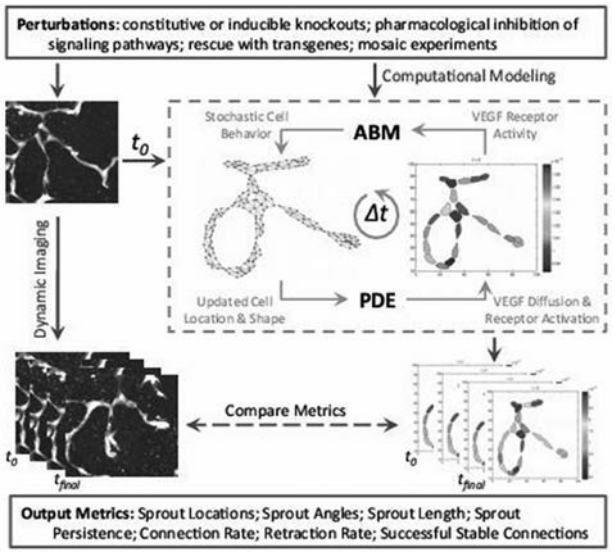

Figure 1. Multiscale computational model of capillary angiogenesis combines agent-based modeling with partial differential equations modeling to predict sprout emergence, extension, and connection. Confocal images of early-stage embryoid body networks specify the initial network configuration for the computational model at t=0. Quantitative analysis of dynamic images at subsequent time points provides independent validation for in silico predictions of emergent patterning outcomes. (Project collaborators: Dr. Vicki Bautch & Dr. John Chappell, University of North Carolina; Dr. Feilim Mac Gabhann, Johns Hopkins University)

Collaborators, Dr. Vicki Bautch and Dr. John Chappell (Univ. of North Carolina) for their contribution of experimental data; Dr. Feilim Mac Gabhann (Johns Hopkins University) for his contribution to the signaling kinetics model.

Where applicable, the authors confirm that the experiments described here conform with The Physiological Society ethical requirements.

SA254

Multi-scale modeling of cardiac excitation-contraction coupling

N. Smith, S.A. Niederer, J. Lee, D. Nordsletten and P. Lamata

King's College London, London, UK

The diversity and quantity of currently available experimental and imaging data, including measurements of single cells, cardiac wall motion, chamber flow patterns, coronary perfusion and electrical mapping, presents a significant opportunity to improve both physiological understanding and ultimately clinical care for cardiovascular disease.

However, the clinical practice of using population-based metrics derived from separate image sets often indicates contradictory treatment plans due to both a lack of integrative mechanistic understanding and inter-individual variability in pathophysiology. Thus, despite measurement advances, determining optimal treatment strategies for cardiac patients remains problematic. To exploit the full value of measurement technologies, and the combined information content they produce, requires the ability to integrate multiple types of anatomical and functional data into a consistent framework.

An exciting and highly promising strategy for contributing to this integration is through the development of bio-physically based mathematical models. However, despite these advances there remains a significant translational barrier to applying and customising models to interpret specific experimental data or for human clinical application. This is because the vast majority of cardiac models are currently developed and validated using data collected from heterogeneous measurements in animal populations. These models are useful for the demonstration of proof of concept function and development of mechanistic concepts. However, there are inherent limitations to such model developments specifically with respect to quantitatively mimicking function in health and disease. Moreover, the relevance of insights gained from such models to human health remains difficult to determine.

To address these issues, we present recent developments in both murine and clinically relevant human models that cover the coupling and simulation of cardiac fluid flow, mechanics, perfusion and electrical excitation.

At the heart of computational modelling. Niederer SA, Smith NP. J Physiol. 2012 Mar 15;590(Pt 6):1331-8. doi: 10.1113

Cardiac cell modelling: observations from the heart of the cardiac physiome project. Fink M, Niederer SA, Cherry EM, Fenton FH, Koivumäki JT, Seemann G, Thul R, Zhang H, Sachse FB, Beard D, Crampin EJ, Smith NP. Prog Biophys Mol Biol. 2011 Jan;104(1-3):2-21. doi: 10.1016/j.pbiomolbio.2010.03.002

An analysis of deformation-dependent electromechanical coupling in the mouse heart.

Land S, Niederer SA, Aronsen JM, Espe EK, Zhang L, Louch WE, Sjaastad I, Sejersted OM, Smith NP. J Physiol. 2012 Sep 15;590(Pt 18):4553-69. doi: 10.1113/jphysiol.2012.231928.

Calcium dynamics in the ventricular myocytes of SERCA2 knockout mice: A modeling study.

Li L, Louch WE, Niederer SA, Andersson KB, Christensen G, Sejersted OM, Smith NP. Biophys J. 2011 Jan 19;100(2):322-31. doi: 10.1016/j.bpj.2010.11.048.

The multi-scale modelling of coronary blood flow. Lee J, Smith NP. Ann Biomed Eng. 2012 Nov;40(11):2399-413. doi: 10.1007/s10439-012-0583-7. Epub 2012 May 8.

This work was funded by the United Kingdom Engineering and Physical Sciences Research Council (EP/GOO7527/1), the Centre of Excellence in Medical Engineering funded by the Wellcome Trust and the EPSRC under grant number WT 088641/Z/09/Z)

Where applicable, the authors confirm that the experiments described here conform with The Physiological Society ethical requirements.

SA255

Modeling the pulmonary physiome: integration of clinical data with multi-scale analysis

M. Tawhai

Auckland Bioengineering Institute, University of Auckland, Auckland, New Zealand

Achieving effective gas exchange in the mammalian lung requires coordinated matching of ventilation and perfusion, both of which are sensitive to the branching structure of the lung's airway and vascular trees, hydrostatic pressure, and gravity acting to deform the lung within the chest wall. Virtually all pathology of the lung impairs gas exchange by disrupting ventilation-perfusion (V/Q) matching, but because of the complexity of the integrated respiratory system it is not always possible to predict how impairment to a single mechanism will affect the function of the system as a whole. To understand the emergence of asthmatic bronchoconstriction and variable patient response to acute pulmonary embolism (APE) we have developed computational methods that exploit

volumetric computed tomography – from normal volunteers, clinical subjects with suspected APE, and animal validation studies – and pulmonary function testing, to derive structure-based models for predicting function in the individual. These data-driven multi-scale models include the pathways for ventilation and perfusion and their interaction at the gas exchange surface, and calcium signaling for smooth muscle force development. Multi-scale analysis reveals synergistic interactions between deep inspirations and smooth muscle fluidization during bronchoconstriction, which may contribute to different responses in normals and asthmatics; and that the cardio-respiratory response to mitigate hypoxia in APE is dependent on the location of embolus, with our model predicting V/Q disruption in regions that are distant from the embolus, and the severity of predicted response tightly correlated with clinically identified right ventricular dysfunction.

Where applicable, the authors confirm that the experiments described here conform with The Physiological Society ethical requirements.

SA256

Stochastic multiscale modelling of the neuro-musculoskeletal system

M. Viceconti

INSIGNEO Institute for in silico medicine, University of Sheffield, Sheffield, UK

Introduction

The socioeconomic burden imposed by osteoporosis is growing exponentially in every economically developed country [1]. The ability to predict subject at high risk of bone fracture is necessary to modulate the therapies but also to motivate necessary restrictions to the life style. Such risk is usually predicted with epidemiology-based models, the most popular being the FRAX system developed at the University of Sheffield. However, these models show in various studies limited predictive accuracy (expressed as area under the Receiver Operating Characteristic curve (AUC)), typically around 0.65 [2]. The primary reason for this moderate accuracy is that while the main cause of osteoporotic bone fractures is the loss of mechanical strength due to the increased porosity of bone tissue, another important cause is the tendency for elders to fall and overload the skeleton more frequently than normal healthy, a factor that can be modelled only as a stochastic process.

In the VPHOP project we developed a multiscale model of the neuromusculoskeletal system that can be individualised using patient data from clinical, imaging, and instrumental observation, capable of predicting the risk of bone fracture in a patient as a function of her degree of osteoporosis, of her propensity to fall, and of the expected progression of the disease over time without or with pharmacological treatment.

In this work we present such multiscale model, describe its current limitations, and show how a subset of it was validated over multiple restrospective cohorts, and confirmed with population studies.

Materials and methods

A complete body-organ-tissue-cell multiscale model of the skeletal biomechanics for the prediction of the hip and spine fractures have been realised by the VPHOP consortium, along the lines proposed in [3]. The multiscale model describes the skeletal loading as a stochastic process identified over a large database of musculo-articular forces during physiological and pathological activities, as predicted by an individualised whole body musculoskeletal dynamics model. Such loading spectra are applied, within a Monte Carlo scheme, to a individualised finite element model of the hip and of the spine, which predicts for each load instance if the bone would fracture or not in that condition; since those skeletal sites under those loading conditions fail both in fragile and ductile mode, a full anisotropic elastic-viscoplastic constitute equation was used. The bone constitutive equation is defined at the tissue scale, and homogenised at the continuum level. A bone-remodelling algorithm predicts the changes over time of the tissue morphology due to the cellular activity, which change the constitutive equation, and thus the strength of the bone.

The full multiscale model required 62,055 core hours to be solved, which makes it unpractical for large scale clinical use at this point in time. While we expect that in five years the computational cost will be reduced on 20 times only with the improvement of the computational resources, at the present it was decided to conduct the clinical validation using a subset of the multiscale model. This reduced model retrains the body and organ models, uses a linear-elastic failure criterion (accurate for the fragile fractures observed at the hip), and replace the tissue-cell models, with a phenomenological model that predicts the changes of the bone density at the continuum level as a function of time, removing the need to solve repeatedly tissue-scale finite element models involving over 20 million degrees of freedom.

Results

Various retrospective cohorts were investigated to assess the predictive accuracy of the reduced multiscale model. Here we present the results on a cohort originally investigated at the University of Sheffield, formed by 50 post-menopause women with a femoral neck fracture, and 50 non-fractured post-menopause women age, height, and weight matched. On this cohort the FRAX algorithm showed an AUC of 0.64, whereas the VPHOP model showed an AUC of 0.75, an improvement usually considered sufficient enough to justify the adoption of a new technology in the clinical practice. Comparable results were obtained in other studies conducted by our consortium, over two additional retrospective cohorts in Reykjavik and in Bologna.

In order to obtain a confirmation, the same multiscale model was used to conduct three public health studies where entire populations were modelled, using statistical distributions of input values derived from the literature for the specific population being modelled. In all three cases good agreement was found [4-6].

Ström O, et al. Arch Osteoporos. 2011 Dec;6(1-2):59-155

Bolland MJ, et al. J Bone Miner Res. 2011 Feb;26(2):420-7

Viceconti M, et al. Clin Biomech. 2008 Aug;23(7):845-52

Viceconti M. Multiscale Modeling of the Skeletal System. Cambridge Press, 2012a; pp. 205.

Viceconti M, et al. J Biomech. 2012b 45(4): S476

Viceconti M, et al. J Biomech. 2012c 45(3):421-6

This study was partially funded by the ICT for Health Unit of the European Commission as part of the VPHOP project (FP7-2008-ICT-224635).

Where applicable, the authors confirm that the experiments described here conform with The Physiological Society ethical requirements.

SA257

Regulators of spine density as targets for the treatment of psychiatric disease

M. Milenkovic, C. Mielnik, R. Ruddy and A. Ramsey

Pharmacology and Toxicology, University of Toronto, Toronto, ON, Canada

There is a growing body of literature correlating changes in spine density and morphology with changes in brain function and behavior. Altered spine density has been reported in many disease states including schizophrenia and depression. Therefore, spine density could be a useful index to measure the therapeutic profile of psychoactive drugs. In the same way, the signal transduction systems that induce synaptogenesis and maintain spine density represent promising targets for the development of new treatments for mental illness.
Our laboratory has studied the role of the NMDA-type glutamate receptor in the regulation of spine density, with a focus on the mechanisms by which altered spine density could translate into psychiatric disease states. NMDA receptors have been implicated in a number of psychiatric diseases as a causal agent or a target for therapeutic intervention. For example, NMDA receptor hypofunction is thought to contribute to the symptoms of schizophrenia, a disease in which reductions in spine density have been reported. Using a genetic mouse model, we have discovered that sustained NMDA receptor dysfunction causes an age-dependent reduction in spine density. Our findings show that NMDA receptor signaling is more important for synapse maintenance than synapse formation. Furthermore we found a temporal developmental correlation between spine loss and several behavioral abnormalities. We sought to determine the molecular mechanisms by which NMDA receptor dysfunction leads to spine loss. Our investigation revealed reductions in the levels of the Rho GTPase Rac1 and its downstream effectors. Therefore, RhoGTPase signaling represents a novel pathway to modulate spine density and improve psychiatric conditions.

This work was supported by an operating grant from CIHR and a NARSAD Young Investigator Award.

Where applicable, the authors confirm that the experiments described here conform with The Physiological Society ethical requirements.

SA258

Synaptic signaling scaffolds and autism spectrum disorders

E. Kim

Center for Synaptic Brain Dysfunctions, Institute for Basic Science (IBS), Daejeon, Republic of Korea and Department of Biological Sciences, Korea Advanced Institute of Science and Technology (KAIST), Daejeon, Republic of Korea

A growing number of synaptic proteins have recently been associated with diverse neuropsychiatric disorders including autism spectrum disorders (ASDs), schizophrenia, attention deficit hyperactivity disorder (ADHD), and mood disorders. ASDs represent a group of neurodevelopmental disorders with a prevalence of ~1% and are characterized by core symptoms including impaired social interaction, impaired social communication, and restricted/repetitive behaviors and interests. Although a large number of ASD-related genes and mutations have been identified, a few of them have been verified by approaches including mouse genetics. In addition, neural mechanisms underlying the development of ASDs remain largely unknown, explaining the lack of efficient medications for the treatment of autism. Synaptic scaffolding proteins at excitatory synapses interact with various synaptic proteins including receptors and signaling molecules, and promote the physical and functional coupling of receptor activation with downstream signaling events. In this presentation, I will discuss how defects in synaptic signaling scaffolds affect synaptic transmission, signaling, and plasticity, and how these defects are associated with ASD-like behavioral abnormalities in mice.

This work was supported by the Institute for Basic Science.

Where applicable, the authors confirm that the experiments described here conform with The Physiological Society ethical requirements.

SA259

Glutamate receptor surface dynamics: regulation in brain pathophysiology

L. Groc

CNRS - Université de Bordeaux, Bordeaux, France

Glutamate, the major excitatory neurotransmitter in brain, activates diverse subtypes of receptors. The NMDA receptor type (NMDAR) play critical roles in both synaptic integration and plasticity. The subunit composition of these receptors, typically GluN2A and/or GluN2B containing, is controlled both by development and activity. This composition plays a crucial role in fine-tuning receptor function. Recent studies have made substantial progress in understanding the cellular and molecular underpinnings of the dynamic behavior of glutamate receptors such as NMDAR and their role in disease. Using high-resolution nanoparticle imaging we recently track single NMDAR at the surface of live neurons. This revealed that the surface distribution and dynamics of NMDAR is locally regulated by salient neuronal stimulation and, interestingly, such surface trafficking plays an instrumental role in synaptic adaptations. In models of neuropsychiatric disorders, characterised by a known altered glutamate transmission, we uncovered an altered surface dynamics of the glutamate receptors (e.g. NMDAR), opening new avenues of research for our comprehension of the glutamate receptor dysfunction in brain diseases and for future therapeutical strategies.

Where applicable, the authors confirm that the experiments described here conform with The Physiological Society ethical requirements.

SA260

Effect of disease causing mutations on NMDA receptor function

H. Yuan[1], T. Pierson[3], S. Undiagnosed Disease Program[2] and S.F. Traynelis[1]

[1]Pharmacology, Emory University School of Medicine, Atlanta, GA, USA, [2]Undiagnosed Disease Program, NIH, Bethesda, MD, USA and [3]Pediatrics and Neurology, Cedars-Sinai Medical School, Los Angeles, CA, USA

NMDA receptors are ligand-gated cation-selective channels that mediate a slow, Ca2+-permeable component of the excitatory postsynaptic current. These receptors are involved in a wide range of important functions in the central nervous system, including synaptic plasticity and development. In addition, these receptors have been implicated in several neurological diseases, including depression, schizophrenia, Parkinson's disease, and epilepsy. We have, in collaboration with the NIH Undiagnosed Disease Program, investigated de novo mutations that have been found to arise in patients with varying neurological disorders, including seizures or developmental delay. Next generation high throughput whole exome sequencing of patients, parents, and relatives together with unique de novo analysis routines has identified a single candidate mutation within NMDA receptor subunits GRIN2A and GRIN2B for each patient. These mutations were subsequently introduced into recombinant human NMDA receptor cDNAs encoding the GluN2A and GluN2B subunits, which were studied in heterologous expressions systems using voltage clamp recordings to assess their effects on channel function. We utilized two electrode voltage recordings from Xenopus laevis oocytes injected with cRNA transcribed in vitro to study pharmacological properties of mutant human GluN1/GluN2 NMDA receptors. These experiments were complemented with patch clamp recordings in HEK 293 cells transfected with cDNA encoding the human GluN1/GluN2 NMDA receptor subunits. The goal of these functional studies was to determine whether the changes in receptor properties produced by these mutations were potentially disease-causing. In both cases the mutations had strong functional effects that were highly suggestive of these mutations being disease-causing. The location of the mutation implicated a key residue in the glutamate binding domain of GluN2B and S2-M4 GluN2A linker. The loss of function GluN2B mutation showed dramatically lower sensitivity to glutamate (50-fold higher EC50) without a change in glycine potency, and was associated clinically with severe developmental delay. The GluN2A gain-of-function mutation increased both glutamate and glycine potency 8-fold and increased open probability, leading to hyperactive NMDA receptors. The overactivation of NMDA receptors may account for frequent seizures. Experiments with memantine showed that it remained an effective antagonist against mutant NMDA receptors, suggesting a therapeutic course of action, which when implemented improved the patient's condition. We are currently expanding our search for potential disease causing mutations in the glutamate receptor family. Identification and characterization of such mutations provides an opportunity both to better understand glutamate receptor function, as well as the role of glutamate receptors in human disease.

This work was supported by the NIH-NINDS

Where applicable, the authors confirm that the experiments described here conform with The Physiological Society ethical requirements.

SA261

Computations performed by theta LFP oscillations in the hippocampal formation

J. O'Keefe

University College London, London, UK

The rodent hippocampal formation constructs a spatial representation of the local environment which can be used to identify the animal's current location, to remember events that happened there in the past, and to navigate to desirable locations in that environment. Spatial cells found in the hippocampal formation represent the animal's location (place cells), its current heading direction (head direction cells), the metric of the environment (grid cells), and the animal's distance from boundaries of the environment (boundary vector cells). These cells provide two ways of identifying the animal's location, first on the basis of its relationship to environmental landmarks, and second on the basis of path integration signals which update this location on the basis of interoceptive cues from the vestibular, proprioceptive and motor systems. All of the cells use firing rate as the code for spatial representation. In addition, however place and grid cells use a timing code. This timing code takes the form of the phase of spike firing relative to the ongoing theta - local field potential (LFP) wave. The sinusoidal theta rhythm is a prominent feature of the hippocampal LFP which ranges between 6 - 11 Hz in the rat, the rate varying as a function of the animal's running speed. We have suggested that theta-LFP is an integral part of one of the mechanisms by which the hippocampus carries out spatial computations. A key idea here is that there is not one but several theta -like oscillations of differing frequencies which produce oscillatory interference patterns which can account for many of the properties of place and grid cell firing. I will describe these ideas and discuss recent experiments which provide evidence in favour of and against them.

Where applicable, the authors confirm that the experiments described here conform with The Physiological Society ethical requirements.

SA262

Network dynamics in entorhino-hippocampal circuits during exploratory behaviour

A. Sirota

Center for Integrative Neuroscience, University of Tuebingen, Tuebingen, Germany

Population representation of spatial memories in hippocampus exhibits complex spatio-temporal dynamics. It is likely that understanding mechanistic origin of this dynamics and link to animal behaviour is the key to understanding the code. To this end we investigate the role of gamma synchronization dynamics across entorhino-hippocampal system and ongoing exploratory behaviour of the rat as dynamics contributors to the population coding in hippocampus. We show how dynamic changes in gamma synchronization and exploratory behaviour affect hippocampal activity.

Where applicable, the authors confirm that the experiments described here conform with The Physiological Society ethical requirements.

SA263

Cell-type specific regulation of hippocampal microcircuits

I. Soltesz

Anatomy & Neurobiology, University of California Irvine, Irvine, CA, USA

Distinct interneuronal subtypes have evolved in cortical circuits to deliver GABA to specific spatial domains of principal cells at particular times during behaviorally relevant network oscillations. The precise spatiotemporal control of populations of principal cells by the GABAergic system is a critically important yet incompletely understood process that is compromised in several other major neurological and psychiatric disorders. A significant gap in our understanding of the GABAergic control of chronocircuits has been the lack of precise information about the interneuronal firing patterns during network oscillations in the anesthesia-free brain. We will discuss recent results from awake, head-restrained animals that demonstrate the differential, highly specific spike timing of perisomatic and dendritically projecting, rigorously identified hippocampal interneuronal subtypes during theta, gamma, epsilon and ripple oscillations. The results reveal a novel form of frequency-independent temporal ordering of interneuronal discharges during network oscillations in the hippocampus. In addition, we will also discuss how the close integration of experimental findings with large-scale, data-driven computational simulations of hippocampal networks offers a powerful tool towards the identification of key circuit parameters that may be particularly effective in controlling chronocircuit behavior. These closely integrated experimental and computational approaches allows a better understanding of the mechanisms underlying neuronal oscillatory circuit functions in control animals and chronocircuit dysfunction in neurological and psychiatric disorders.

Supported by the NIH (NS35915 to IS).

Where applicable, the authors confirm that the experiments described here conform with The Physiological Society ethical requirements.

SA264

Optogenetic dissection of oscillatory circuits

I. Oren[1,2], M. Cano-Jaimez[2] and D.M. Kullmann[2]

[1]Centre for Cognitive and Neural Systems, University of Edinburgh, Edinburgh, UK and [2]Department of Clinical and Experimental Epilepsy, UCL Institute of Neurology, London, UK

The hippocampal CA1 network supports gamma oscillations of variable frequencies, with fast (~80Hz) and slow (~40Hz) gamma occurring on different phases of the theta cycle (Colgin et al., 2009). It has been suggested that the fast and slow components are generated through distinct excitatory pathways, namely, perforant path and Schaffer collaterals respectively. However, the functional local circuitry that is recruited by the inputs to generate these gamma frequency bands remains to be determined.
In order to investigate the local circuit mechanisms of oscillatory responses to variable excitatory drive, we induced oscillations in acute hippocampal slices in vitro. Mice (3 weeks) were transfected with the red-shifted depolarising opsin C1V1 (Yizhar et al., 2009) by stereotactic intrahippocampal injection (under isofluorane anaesthesia) of an adeno-associated virus with a Camk2α promoter. The virus was left to express for 4 weeks. Mice were sacrificed by transcardial perfusion with an N-Methyl-D-Glucamine based saline solution and acute horizontal slices prepared. We delivered variable intensity ramps of light to slices and simultaneously recorded the local field potential and whole-cell intracellular currents.
Light ramps induced gamma frequency oscillations in the CA1 pyramidal cell layer (range=34 – 51 ±2 Hz, n=5. Means ± SEM. Recorded at 32^{o}C). Phasic excitatory and inhibitory synaptic currents occurred in both principal cells and interneurons. Synaptic currents were superimposed on a direct C1V1-mediated current that was prominent in pyramidal neurons. Blocking glutamatergic synaptic transmission profoundly attenuated oscillations. Increasing the drive to the network increased oscillation frequency, and shifted the oscillation from an inhibition-dominant to an excitation-dominant regime.
These findings suggest that differential recruitment of pyramidal cells and interneurons by CA1 afferents may contribute to the emergence of fast and slow gamma in vivo.

Colgin LL *et al*. (2009) Nature **462**:353–357.

Yizhar O *et al*. (2011) Nature **477**:171–178.

We thank the European Research Council for supporting this work.

Where applicable, the authors confirm that the experiments described here conform with The Physiological Society ethical requirements.

SA265

Cortical properties of human slow wave sleep

I. Ulbert

RCNS HAS, Budapest, Hungary

The slow wave is a fundamental cortical rhythm that emerges in deep non rapid eye movement sleep. It is thought to underlie essential restorative processes and facilitate the consolidation of declarative memories. Animal studies show that slow wave activity is composed of rhythmically recurring phases of widespread, increased cortical cellular and synaptic activity, referred to as active- or up-state, followed by cellular and synaptic inactivation, referred to as silent- or down-state. However, its neural mechanisms in humans are poorly understood. To elucidate the intracortical neuronal mechanisms of slow wave activity in humans, laminar microelectrodes were chronically implanted into the cortex of patients with focal epilepsy undergoing cortical mapping for seizure focus localization.
We found that slow wave activity in humans reflects a rhythmic oscillation between widespread cortical activation and silence. Cortical activation was demonstrated as increased wideband spectral power including virtually all bands of cortical oscillations, increased multiple and single unit activity, and powerful inward trans-membrane currents, mainly localized to the supragranular layers. Neuronal firing in the up-state was sparse and the average discharge rate of single cells was less than expected from animal studies. Action potentials at up-state onset were closely synchronized across all cortical layers, suggesting that any layer could initiate firing at up-state onset.
These findings provide experimental evidence that slow wave activity in humans is characterized by hyperpolarizing currents associated with suppressed cell firing, alternating with high levels of oscillatory synaptic/trans-membrane activity associated with increased cell firing. Our finding that slow wave activ-

ity and corresponding high frequency rhythms including spindle, alpha, beta, gamma and ripple oscillations mainly involve supragranular layers is consistent with the massive cortical expansion of neuronal number and increased apical dendritic complexity observed in humans.
The strong supragranular oscillatory activity in sleep may be beneficial for the local, higher order processing of previous sensory experience, since these layers are interconnected by dense cortico-cortical projections forming fine-scale functional networks to perform integrative functions. The weaker infragranular activity may reflect the relatively suppressed cortical executive, output functions, which may prevent effective connectivity between distant cortical areas from developing in slow wave sleep.

Supported by Hungarian Scientific Research Fund OTKA 81357, National Office for Research and Technology NKTH-ANR, Neurogen and Multisca, European Union FP7 NeuroSeker and TÁMOP-4.2.1.B-11/2/KMR-2011-0002

Where applicable, the authors confirm that the experiments described here conform with The Physiological Society ethical requirements.

SA266

The efferent olivocochlear system and protection from acoustic trauma

A.B. Elgoyhen

Institute for Research in Genetic Engineering and Molecular Biology, CONICET, Buenos Aires, Argentina

Sound-induced acoustic injury is one of the most common causes of hearing loss and tinnitus. Although prevention from exposure to intense sound would be the obvious way to keep our inner ear healthy, finding alternatives to increase resistance to damage is a research field of great interest. The medial olivocochlear (MOC) pathway provides inhibitory feedback, through the release of acetylcholine (ACh) from brainstem neurons onto outer hair cells (OHCs) of the cochlea, reducing their ability to amplify sounds, and thus reducing cochlear sensitivity. Although many possible roles for this pathway have been proposed, understanding remains incomplete. We have explored the MOC pathway's function by generating a strain of genetically modified mice carrying a mutation in the nicotinic acetylcholine receptor (nAChR) subunit expressed by OHCs. We tested the effect of the mutation by recording signals from hair cells in cochlear preparations in vitro. Mutant hair cells exhibited greater sensitivity to exogenous ACh and the synaptic currents were prolonged in comparison to wild type preparations, indicating that the mutation enhanced nAChR function. To determine the consequences of this enhanced receptor function for cochlear responses, we measured auditory brainstem responses and distortion product otoacoustic emissions. The threshold levels of sound required to evoke these responses were elevated in the mutant mice, suggesting that the baseline inhibitory effect of the MOC pathway was enhanced. Furthermore, suppression of OHC-mediated amplification produced by stimulating the MOC pathway electrically was enhanced and dramatically prolonged in mutant mice. Surprisingly, mutant mice had a greater resistance to permanent acoustic injury resulting from exposure to 100 dB sounds, indicating that activation of the MOC feedback can protect the inner ear from noise-induced damage. Thus, the efferent pathway provides a promising target for pharmacological prevention of inner ear pathologies derived from acoustic injury, such as hearing loss and tinnitus. Finding drugs that mimic the effect of the mutation would be the developmental path to follow.

This work was supported by an HHMI International Scholar Grant, NIH and CONICET

Where applicable, the authors confirm that the experiments described here conform with The Physiological Society ethical requirements.

SA267

Effect of myelin loss on synaptic function in the auditory brainstem

S. Kim[1], C. Kushmerick[2] and J. Kim[1]

[1]Department of Physiology, University of Texas Health Science Center, San Antonio, TX, USA and [2]Departamento de Fisiologia e Biofisica, Universidade Federal de Minas Gerais, Belo Horizonte, Minas Gerais, Brazil

Myelination of axons greatly increases the conduction velocity and fidelity of impulse propagation in the mammalian CNS. The auditory brainstem is a useful model to test the importance of proper myelination because its circuits rely on very fast, precise, and reliable synaptic relays to process auditory information. To determine the fundamental role of myelination in auditory brainstem function, we recorded the sound evoked auditory brainstem response (ABR) from Long Evans Shaker (LES) rats, which lack myelin due to a genetic deletion of myelin basic protein. Control and LES rats were anesthetized and maintained with 2 % isoflurane (1 L/min O2 flow rate) during ABR recording. In control, the ABR evoked by a click consisted of five well-defined waves (denoted wave I-V), whereas in LES rats waves II and III could not be distinguished and the latency to wave I and IV was greatly increased. In addition, the sound threshold of the ABR was increased in LES rats using tone stimulations of 8 kHz or higher. The central conduction time of the auditory pathway increased significantly in the LES rats, while control showed a significant reduction of conduction time during development. To identify mechanisms by which central demyelination impairs the transmission of auditory signals, alterations in synaptic transmission were explored using whole-cell patch clamp at the synapse formed by the calyx of Held nerve terminal in the Medial Nucleus of the Trapezoid Body (MNTB) in the auditory brainstem. In LES rats, postsynaptic neurons from the MNTB displayed a delayed action potential and an increase in the number of action potential failures during high frequency stimulation when compared to controls. Voltage clamp experiments revealed that the size of the EPSC and the degree of EPSC depression during high frequency stimulation was similar in control and LES MNTB, but both the conduction delay and the synaptic delay were increased in LES rats. Taken together our results suggest that the defects observed in evoked auditory potentials in LES rats is related to the reduction in the temporal fidelity and the reliability of synaptic transmission, which is critical for the accurate processing of sound signals in auditory brainstem involved in sound localization.

This work was supported by an NIDCD R03 grant (R03 DC011140) and AHA (11BGIA7430033) to J.H. Kim

Where applicable, the authors confirm that the experiments described here conform with The Physiological Society ethical requirements.

SA268

Cellular mechanism of sound localization

M. van der Heijden[1], J.A. Lorteije[1,3], A. Plauska[1], M.T. Roberts[2], N.L. Golding[2] and J.G. Borst[1]

[1]Neuroscience, Erasmus MC, Rotterdam, Netherlands, [2]Section of Neurobiology and Center for Learning and Memory, University of Texas at Austin, Austin, TX, USA and [3]Vision & Cognition, Netherlands Institute for Neuroscience, Amsterdam, Netherlands

Neurons in the medial superior olive (MSO) enable sound localization by their remarkable sensitivity to submillisecond interaural time differences (ITDs). Each MSO neuron has its own "best ITD" to which it responds optimally. A difference in physical path length of the excitatory inputs from both ears cannot fully account for the ITD tuning of MSO neurons. As a result, it is still debated how these inputs interact and whether the segregation of inputs to opposite dendrites, well-timed synaptic inhibition, or asymmetries in synaptic potentials or cellular morphology further optimize coincidence detection or ITD tuning. Using in vivo juxtacellular and whole-cell recordings, we find that ITD tuning of MSO neurons is determined by the timing of their excitatory inputs. The inputs from both ears sum linearly, whereas spike probability depended nonlinearly on the size of synaptic inputs. This simple coincidence detection scheme thus makes accurate sound localization possible.

This work was supported by an FP6 European Union grant (EUSynapse) and by SenterNovem, The Netherlands (NeuroBasic).

Where applicable, the authors confirm that the experiments described here conform with The Physiological Society ethical requirements.

SA269

What does a cochlear implant do to your brain? Plastic changes in the primary auditory cortex with long-term deafness and cochlear implant use

J.B. Fallon

Bionics Institute, East Melbourne, VIC, Australia and University of Melbourne, Melbourne, VIC, Australia

Sensorineural hearing loss initiates a cascade of anatomical and functional changes within the auditory system. The secondary loss of spiral ganglion neurones, the target cells of cochlear implants, is the most critical peripheral change; and there are a range of atrophic changes within the central auditory pathway. However, equally important are the functional changes, particularly the degradation in spatial (spectral) and temporal processing, that occur within the central auditory system.

Over the past decade, we have focussed on the changes in the response of the primary auditory cortex in the cat to intracochlear electrical stimulation with long-term, ototoxically induced, profound deafness. The most striking effect is a complete loss of the normal cochleotopic organisation seen in normal hearing animals. We have also examined the effects of chronic environmentally derived intracochlear electrical stimulation, delivered by a cochlear implant, on central auditory processing. Specifically, chronic cochlear implant use can drive the cochleotopic organisation of primary auditory cortex, both in young and mature animals. The effects of cochlear implant use can be observed after as little as one month of chronic use, highlighting the importance of early (re)habilitation following implant activation in a clinical setting.

The excellent performance of cochlear implant recipients has also led to a relaxation of the criteria for candidacy for implantation. Initially only implanted in patients with no useful hearing in either ear, patients with significant amounts of low-frequency hearing are now routinely implanted, who previously would only have been treated with hearing aids. These patients have access to information from both acoustic hearing (via their remaining low-frequency hearing) and electric hearing (via their cochlear implant stimulating the more basal, high frequency region of the cochlea). However, it is unclear how the central auditory system represents and integrates the two modalities of stimulation. Therefore, we have begun examining the representation of both acoustic and electric activation of the cochlea in ototoxically partially deafened animals, some of whom have received a cochlear implant.

This work was funded by NIDCD (HHS-N-263-2007-00053-C) and the NHMRC (1002430). The Bionics Institute acknowledges the support it receives from the Victorian Government through its Operational Infrastructure Support Program.

Where applicable, the authors confirm that the experiments described here conform with The Physiological Society ethical requirements.

SA270

Optimizing VNS-directed neural plasticity for the treatment of chronic tinnitus

M. Kilgard[1], M. Borland[1], P. Beall[1], E. Buell[1], S. Vanneste[2,1], D. De Ridder[2], A. Sloan[1] and R. Rennaker[1]

[1]Behavioral and Brain Sciences, University of Texas at Dallas, Richardson, TX, USA and [2]University Hospital, Antwerp, Belgium

Pathological neural plasticity plays a major role in the genesis and maintenance of chronic tinnitus. Reversal of aberrant plasticity is therefore a promising approach to the treatment of tinnitus.We have developed a novel method to direct highly specific and long lasting neural plasticity (Engineer, 2011). Brief bursts of vagus nerve stimulation (VNS) trigger release of neuromodulators that direct brain changes specific to associated neural activity patterns. Pairing VNS with tones is sufficient to powerfully shape responses in the central auditory system. We have demonstrated that this therapy can be therapeutic in an animal model of tinnitus and in human patients. We are now optimizing the clinical parameters through parallel studies in humans and preclinical studies in animals. We will present evidence suggesting that with further study VNS-directed plasticity may be optimized to become a reliable, safe, and long-lasting therapy for chronic tinnitus.

Reversing pathological neural activity using targeted plasticity, Engineer ND, Riley JR, Seale JD, Vrana WA, Shetake JA, Sudanagunta SP, Borland MS, Kilgard MP, Nature, 470:101-4, 2011.

Where applicable, the authors confirm that the experiments described here conform with The Physiological Society ethical requirements.

SA271

Ghrelin: an orexigenic gut - brain reward signal

S.L. Dickson, R.H. Shirazi and K.P. Skibicka

Institute of neuroscience and Physiology, The Sahlgrenska Academy at the University of Gothenburg, Gothenburg, Sweden

Obesity has reached global epidemic proportions and there is therefore much need to understand mechanisms underlying excessive and uncontrolled food intake. Ghrelin, the only known circulating orexigenic hormone, stimulates feeding behavior via its CNS actions. In addition to its role in "metabolic hunger", ghrelin potently increases food reward behavior (1,2). The neurochemical circuitry that links ghrelin to the mesolimbic reward system and to the increased food reward behavior remains unclear (3). Ghrelin receptors can be found on the ventral tegmental area (VTA) dopamine neurons (4) and ghrelin injection to the VTA is sufficient to drive food motivated behavior (5). It is, however, unknown which dopaminergic projections are relevant for ghrelin's effects on reward, since VTA dopamine neurons send projections to several brain areas relevant for reward behavior including the nucleus accumbens (NAc), amygdala and prefrontal cortex. Here we examine whether VTA-NAc dopaminergic signalling is required for the effects of ghrelin on food reward and intake. To measure food motivation/reward behavior, rats were trained in a progressive ratio sugar-induced operant behavior schedule. Chow intake was measured subsequent to the operant behavior test. A D1-like or a D2 receptor antagonist was injected into the NAc in combination with ghrelin microinjection into the VTA to investigate whether this blockade attenuates ghrelin-induced food reward behavior. VTA injection of ghrelin significantly increased food reward behavior and chow intake. Pretreatment with either a D1-like or D2 receptor antagonist into the NAc, completely blocked the reward effect of ghrelin, leaving chow intake intact. We also found that this circuit is potentially relevant for the effects of endogenously released ghrelin as both antagonists reduced fasting (a state of high circulating levels of ghrelin) elevated sucrose-motivated behavior but not chow hyperphagia. Taken together our data identify the VTA to NAc dopaminergic projections, along with D1-like and D2 receptors in the NAc, as essential elements of the ghrelin-responsive circuits controlling food reward behavior. Interestingly the results also suggest that food reward behavior and the intake of chow are controlled by divergent circuitry, where NAc dopamine plays an important role in food reward but not in food intake. The idea that ghrelin's effects on food intake and food reward behavior engage different reward circuitry is also supported by previous studies in which we were able to parse ghrelin's effects these behaviors pharmacologically using mu-preferring opioid receptor antagonist or an NPY Y1 receptor antagonist (6).

Egecioglu E, Jerlhag E, Salomé N, Skibicka KP, Haage D, Bohlooly-Y M, Andersson D, Bjursell M, Perrissoud D, Engel JA, Dickson SL. Ghrelin increases intake of rewarding food in rodents. Addict Biol. 2010, 15:304-311.

Skibicka KP, Hansson C, Egecioglu E, Dickson SL. Role of ghrelin in food reward: impact of ghrelin on sucrose self-administration and mesolimbic dopamine and acetylcholine receptor gene expression. Addict Biol. 2012, 17:95-107.

Skibicka KP, Dickson SL. Ghrelin and food reward: the story of potential underlying substrates. Peptides. 2011, 32:2265-2273.

Abizaid A, Liu ZW, Andrews ZB, Shanabrough M, Borok E, Elsworth JD, Roth RH, Sleeman MW, Picciotto MR, Tschöp MH, Gao XB, Horvath TL. Ghrelin modulates the activity and synaptic input organization of midbrain dopamine neurons while promoting appetite. J Clin Invest. 2006, 116:3229-3239.

Skibicka KP, Hansson C, Alvarez-Crespo M, Friberg PA, Dickson SL.Ghrelin directly targets the ventral tegmental area to increase food motivation. Neuroscience. 2011, 180:129-37.

Skibicka KP, Shirazi RH, Hansson C, Dickson SL.Ghrelin interacts with neuropeptide Y Y1 and opioid receptors to increase food reward. Endocrinology. 2012, 153:1194-205.

GRANTS/FELLOWSHIPS: The research was supported by the Swedish Research Council for Medicine (2009-S266, 2012-1758), European Commission 7th Framework (FP7-HEALTH-2009-241592; FP7-KBBE-2009-3-245009 and FP7-KBBE-2010-4-266408), FOU/ALF Göteborg (ALFGBG-138741), NovoNordisk Fonden, the Swedish Foundation for Strategic Research to Sahlgrenska Center for Cardiovascular and Metabolic Research (A305-188) and the Swedish Institute.

Where applicable, the authors confirm that the experiments described here conform with The Physiological Society ethical requirements.

SA272

Reciprocal interactions between the stress response and hedonic food reward after prenatal stress

J. Menzies

University of Edinburgh, Edinburgh, UK

Stress can increase or decrease food intake and, consequently, body weight. However, in animal models of stress, rats often selectively increase palatable high-energy food intake and put on weight. There is a parallel in human behaviour – comfort eating, a widespread behaviour where people who feel anxious or stressed seem motivated to consume palatable food. The mechanisms underlying this stress-induced change in behaviour are unknown. Here we use a model of prenatal stress in rats to examine palatable food consumption and the reciprocal effect of palatable food rewards on the acute stress response.

Prenatally stressed (PNS) rats were generated by exposing their mothers to repeated social stress during the latter part of pregnancy. These rats show an enhanced acute stress response as adults, reflected in increased plasma levels of ACTH and corticosterone (CORT; Brunton and Russell, 2010). We hypothesised that this enhanced acute stress response could be suppressed by consumption of palatable high-energy food prior to the acute stressor. To test this we gave a group of PNS rats twice-daily time-restricted access to a condensed milk reward for 14 days and monitored their feeding behaviour (n = 7). A group of unrewarded PNS rats (n = 7) and two groups of control rats (one rewarded, one unrewarded, both n = 8) acted as comparisons.

Both PNS and control rats quickly learned to consume the reward in the allotted time. In control rats the latency to start eating had reduced from 237±66 sec (mean±sem) to 16±3 sec by day 4. However, the latency in PNS rats remained high and variable (233±154 sec on day one, 76±31 sec on day 14) indicating that PNS rats may have a reduced motivation to consume rewarding foods. Next we tested the effect of reward access on the acute stress response. At the end of the reward period all rats were subjected to a 30 min acute restraint and blood was taken before, during and after to measure plasma CORT by RIA. All rats showed an increase in CORT during the

restraint stress that returned to baseline levels 4 h after the stress. Unrewarded PNS rats showed an enhanced stress response compared to unrewarded control rats. Rewarded PNS rats showed an increased stress response compared to unrewarded PNS rats, though this increase was superimposed on a higher baseline CORT secretion after reward consumption. Moreover, access to reward appeared to reduce the duration of the CORT response in control but not PNS rats. Hence, intake of palatable food can influence the HPA axis response to acute stress.

Brunton P & Russell J (2010). J Neuroendocrinol 22, 258-271

Funded by the European Community's 7th Framework Programme under grant agreement 245009 (NeuroFAST) and 266408 (Full4Health).

Where applicable, the authors confirm that the experiments described here conform with The Physiological Society ethical requirements.

SA273

In vivo neural responses to changes in energy balance, leptin and ghrelin

G. Van der Plasse, R. van Zessen, M. Luiendijk, G. Ramakers and R. Adan

UMCU, Utrecht, Netherlands

The mesolimbic dopamine (mesDA) system is known for its role in associative learning, reward-seeking, and signaling of reward-related information. As such, increased activity of mesDA neurons drives motivated behavior and promotes operant responding for food. What remains unclear is the nature of mesDA's role in energy balance. Given the fact that ventral tegmental area (VTA) dopamine (DA) neurons are sensitive to feeding-hormones like leptin and ghrelin (that signal information about the current metabolic state), this system may be important in the regulation of food intake.
To investigate how energy balance affects reward-signaling by mesDA neurons, in vivo electrophysiological recordings were made of (putative) DA neurons in the ventral tegmental area (VTA) during the execution of a behavioural task. Neuronal activity was subsequently related to cue-presentation and the delivery of food rewards. To manipulate energy balance, animals were either food-deprived or free-fed preceding the recording session. In addition, the effect of peripheral injections of leptin and ghrelin on reward-encoding was measured. Elucidation of how hunger, leptin and ghrelin signaling affect mesDA neurons in feeding behavior provides important insights into the role of this neural circuit in obesity and anorexia nervosa

This work was supported by FP7 EU project Full4 Health

Where applicable, the authors confirm that the experiments described here conform with The Physiological Society ethical requirements.

SA274

Dissecting the neural and behavioral processes linking leptin and reward

S. Fulton

Nutrition, University of Montreal, Montreal, QC, Canada and Montreal Diabetes Research Center, Montreal, QC, Canada

The adiposity hormone leptin is a critical modulator of energy balance. Apart from its hypothalamic actions, leptin regulates neural circuits controlling reward, motivation and emotion. Leptin has been shown to inhibit motivated behavior for rewarding electrical brain stimulation and palatable food. Dopamine (DA) neurons of the midbrain ventral tegmental area (VTA) are an essential component of the neural circuitry regulating motivation and reward. Via the long-form of its receptor (LepRb) leptin targets the VTA to inhibit feeding, food-motivated behavior, locomotion, and anxiety. Stat3 is the predominant signal whereby leptin regulates gene expression and leptin induces Stat3 phosphorylation in dopamine (DA) and GABA neurons of the VTA. We generated DA-specific Stat3 knockout (KO) mice to determine the contribution of LepRb-Stat3 signaling in midbrain DA neurons. While showing a similar anorectic response to leptin, KO mice exhibit marked impairments in food-motivated operant learning. In addition to large increases in ambulatory activity and voluntary running in male KO mice, the rewarding aftereffects of running are significantly elevated. These behavioral changes are accompanied by decreases in DA biosynthesis and D1 receptor protein expression in the nucleus accumbens. Our findings suggest an important role for leptin in attenuating running reward that are mediated via LepRb-Stat3 signaling in midbrain DA neurons and changes in DA tone. We posit that leptin acts in mesolimbic brain reward circuitry as a signal-of-plenty to dampen the motivational and rewarding effects of several behaviors that serve to replenish energy stores.

Supported by a grant from the Canadian Institutes of Health Research

Where applicable, the authors confirm that the experiments described here conform with The Physiological Society ethical requirements.

SA275

Opioid orchestration of feeding behavior

C. Dieguez

Department of Physiology, University of Santiago de Compostela, Santiago de Compostela, Spain

The relevance of opioids in reward processes leading to addictive behavior such as self-administration of opioids and drugs of abuse including nicotine and alcohol is widely recognized. Data gleaned in recent years have uncovered the importance of the endogenous opioid system modulating feeding behavior and other parameters that are crucial for the regulation of energy balance in both prelinical and clinical settings. The effects of endogenous opioid tone in food intake appears to be exerted by the three main families of opioid receptors. Data obtained from transgenic knockout mice for the different receptors subtypes indicates that the complete lack of MOR and KOR causes important alterations in energy balance, particularly when mice are fed on fat-enriched diets . Adminis-

tration of selective μ-agonists into the NAcc of rodents induces feeding even in satiated animals, while administration of μ-antagonists reduces food intake. Using pharmacological and gene silencing approaches, it was recently shown that ghrelin utilizes a hypothalamic κ-opioid receptor (KOR) pathway to increase food intake in rats. Pharmacological blockade of KOR decreases the acute orexigenic effect of ghrelin. Inhibition of KOR expression in the hypothalamic arcuate nucleus is sufficient to blunt ghrelin-induced food intake. By contrast, the specific inhibition of KOR expression in the ventral tegmental area does not affect central ghrelin-induced feeding. This new pathway is independent of ghrelin-induced AMP-activated protein kinase activation, but modulates the levels of the transcription factors and orexigenic neuropeptides triggered by ghrelin to finally stimulate feeding. These data implicate hypothalamic KOR signaling in the orexigenic action of ghrelin. Whether other orexigenic signals act through this pathway or whether this effect is specific for ghrelin is under investigation.

Where applicable, the authors confirm that the experiments described here conform with The Physiological Society ethical requirements.

SA276

The "ins and outs" of Ca^{2+} sparks

M.B. Cannell

Physiology & Pharmacology, Bristol University, Bristol, UK

In cardiac muscle, depolarization of the sarcolemma initiates Ca2+ release by activating sarcolemmal L-type Ca2+ channels, providing a small increase in cytoplasmic calcium concentration in the junctional space of the dyad. This initiates [Ca2+]-dependent activation of the sarcoplasmic reticulum (SR) Ca2+ release channels known as ryanodine receptors (RyRs). The subsequent release of calcium from the SR further increases the [Ca2+] in the junctional space and leads to regenerative RyR activation, in a process called calcium-induced calcium release (CICR)(1). In such a regenerative process, the larger SR Ca2+ flux should prevent subsequent control by the surface membrane as well as SR Ca2+ store depletion. However, the quantity of Ca2+ released from the SR has a graded dependence on the magnitude of the Ca2+ influx across the sarcolemma and the SR releases only ~50% of its total content (e.g. (2)). The discovery of Ca2+ sparks (3) provided a solution to this problem by showing that graded responses can result from the spatio-temporal summation of individual Ca2+ release sites which are spatially uncoupled to limit regenerative behaviour. However, local regeneration in CICR during Ca2+ sparks might still prevent reliable Ca2+ spark termination.
Using computer modelling to recover the flux associated with a Ca2+ spark places limits on (for example) the number of RyRs involved in their generation as well as SR release time course. Our work shows that RyR closure appears to occur more slowly than the SR release flux, suggesting that local depletion of the SR store may be key to termination. In addition, by incorporating measured RyR gating (from planar lipid bilayer experiments) we find that the termination of SR release can be explained by a process we call induction decay(4). Induction decay provides robust termination of SR Ca2+ release because the falling RyR single channel current (as the local SR depletes) leads to a rapid increase in RyR closed time. This prevents RyRs reopening before an open RyR closes, thereby breaking the regenerative feedback during CICR. This is essentially the reversal of Ca2+ release inducing process within CICR (which prompted our naming it induction decay).
Therefore after 30 years of work, the mechanisms that activate and terminate Ca2+ sparks (and the whole cell Ca2+ transient) are gradually becoming clearer, although fine details such as the role of RyR gating modulation remain to be clarified. In addition, the possible remodelling of the junction between the surface membrane and SR in disease may also contribute to the development of dyssynchrony in Ca2+ release (e.g. 5). Recent developments in ultra high resolution imaging (e.g. 6) may provide the much needed structural information to explain such effects with more anatomically accurate computer models.

Fabiato, A. 1983 Am. J. Physiol. 245: C1–14.

Picht, E. et al. 2011 Circ. Res. 108: 847–856.

Cheng, H. et al.1993 Science. 262: 740–744

Laver D.R. et al., 2013 J. Mol. Cell. Cardiol. 10.1016/j.yjmcc.2012.10.009

Litwin S.E. et al., 2000 Circ. Res. 24;87(11):1040–1047.

Jayasinghe I.D. et al. 2012 Biophys. J. 102(5):L19–21.

The Royal Society for grant support

Where applicable, the authors confirm that the experiments described here conform with The Physiological Society ethical requirements.

SA277

Subcellular alterations in RyR activation in a sheep model of atrial fibrillation

N. MacQuaide[1], I. Lenaerts[1], P. Holemans[1], R. Willems[2] and K.R. Sipido[1]

[1]Experimental Cardiology, Department of Cardiovascular Sciences, KU Leuven, Leuven, Belgium and [2]Cardiology, Department of Cardiovascular Sciences, KU Leuven, Leuven, Belgium

In sheep atrial myocytes, a moderate density of t-tubular structure has been described, which was further reduced as a result of remodeling in a model of atrial pacing induced persistent atrial fibrillation (AF). A concomitant reduction in ICaL and triggered Ca^{2+} release was observed, as well as attenuation of β-receptor responsiveness. In the current study, we have examined the effect of proximity of TTs to RyR on diastolic RyR activity (spontaneous Ca^{2+} sparks) and how this changes after induction of AF. The role of CaMKII in this situation is further investigated.
Ca^{2+} transients were recorded in fluo-4 loaded cells using confocal linescan microscopy (CLSM). Whole cell voltage clamp was used to elicit Ca^{2+} release induced by depolarizing pulses at 2Hz. 3-D distance mapping was used to correlate time to half maximal release of the fluorescence from triggered Ca^{2+} release with TT proximity. Release sites were localized and categorized as coupled (≤0.5 μm) and non-coupled (≥2 μm). After 2 minutes, stimulation was stopped and spontaneous Ca^{2+} sparks were measured for a period of 15 seconds and assigned to their cellular locations. SR content was assessed by integrating the sodium calcium exchange current after rapid application of caffeine (10 mM).
In CTRL myocytes (N=6, n=21), non-coupled sites regions had less frequent sparks (-32.7±11.1%) than coupled regions. These had similar amplitude and width, but the mean half-maximal duration was reduced by 16.5±7.8 %. After AF no change in SR content was observed (N=6, n=23). The most striking difference was observed as a reversal of the regional frequency

relationship: sparks were more frequent in non-coupled (+99±16%) vs. coupled regions in atrial myocytes from AF animals. Addition of AIP (5μM) caused a normalization in both AF and CTRL, with no change in SR content.
To further activate CaMKII, but in the absence of PKA activation, isoproterenol (100 nM) and PKI (5 μM) was added. This led to the initiation of Ca^{2+} waves in 50% of CTRL cells and 93% of AF cells.

This works was funded by an FP7 Marie Curie fellowship (PIEF-GA-2009-255264) to NM, the Fund for Cardiosurgery to R.W. and FP7 grant (HEALTH-F2-2009-241526, EUTrigTreat) to K.R.S.

Where applicable, the authors confirm that the experiments described here conform with The Physiological Society ethical requirements.

SA278

Termination of Ca sparks: role of cytosolic and intra-luminal Ca

A.V. Zima

Department of Cell and Molecular Physiology, Loyola University Chicago, Maywood, IL, USA

The majority of Ca that initiate cardiac contraction is released from the sarcoplasmic reticulum (SR), via the process of Ca-induced Ca release (CICR)[1] mediated by ryanodine receptors (RyRs). Since CICR by definition is a self-regenerating, SR Ca release would be expected to continue until the SR Ca pool is fully exhausted. However, compelling experimental evidence shows that CICR ends when intra-SR Ca ($[Ca]_{SR}$) is only partially depleted[2-4]. Thus, a robust termination mechanism must exist to counteract the positive feedback of CICR. Despite a significant effort, the CICR termination mechanism remains unclear. This is significant because abnormal SR Ca release termination has been linked to Ca-dependent arrhythmias during cardiac pathologies such as heart failure (HF)[5].
In cardiac myocytes, SR Ca release occurs at specialized release sites that contain clusters of RyRs. Spontaneous elementary SR Ca release events, called sparks6, arise from the concerted opening of several RyRs at one release site. Sparks are measured as non-propagating local increases in cytosolic [Ca] ($[Ca]_i$). The corresponding local $[Ca]_{SR}$ depletion can be measured and is called a Ca blink[2, 4]. To explore mechanisms that control CICR termination, we simultaneously monitored local changes of $[Ca]_i$ (spark) and $[Ca]_{SR}$ (blink) in permeabilized rabbit ventricular myocytes. In addition, single cardiac RyR activity was studied after reconstruction of the channel into lipid bilayers We analyzed Ca sparks and corresponding blinks over a wide range of SR Ca loads. To decrease SR Ca load, cells were treated with the SR Ca pump inhibitor thapsigargin. Upon thapsigargin application, SR Ca load and spark frequency progressively decreased until sparks ceased when load had declined to 60% of its starting value. We also found that irrespective of SR Ca load blinks terminate at a relatively fixed level of $[Ca]_{SR}$ (60% of initial $[Ca]_{SR}$). Our data indicate that release during a spark reduces $[Ca]_{SR}$ to a critical level where RyRs in a cluster become inactive. A fall in local $[Ca]_{SR}$ may terminate a spark by two different mechanisms. First, $[Ca]_{SR}$ depletion can drive unbinding of Ca from an intra-SR RyR regulatory site and thus promote RyR closing[7,8]. Second, local $[Ca]_{SR}$ depletion can terminate a spark by reducing the unitary RyR current, decreasing $[Ca]_i$ around a cluster and thus breaking the local positive feedback of CICR[9].
The contribution of the latter mechanism to CICR termination has not been systematically explored. We studied effects of Mg and caffeine (compounds which change RyR sensitivity to $[Ca]_i$) on Ca spark termination. Cytosolic Mg (0.7 mM) decreased RyR activity by 80%, whereas caffeine (0.2 mM) increased it by 110%. We found that RyR inhibition by Mg decreased spark amplitude, width and Ca release flux. Moreover, Ca sparks terminated at 85% of the initial $[Ca]_{SR}$, much higher than for blinks observed in the absence of RyR inhibition (60%). On the other hand, RyR $[Ca]_i$ sensitization by caffeine had the opposite action on Ca spark termination. Caffeine (0.2 mM) increased Ca spark amplitude and decreased the $[Ca]_{SR}$ level at which sparks terminated (by 20%). We also explored how changes in cytosolic Ca buffering affect Ca spark termination. No substantial changes in single RyR function were observed in the presence of cytosolic BAPTA (a fast Ca buffer) if free [Ca] was kept constant. However, the same cytosolic [BAPTA] added to permeabilized myocytes significantly suppressed Ca spark activity. This BAPTA effect on sparks was not due to decrease in SR Ca load. Moreover, the fast cytosolic Ca buffer caused faster CICR termination at higher $[Ca]_{SR}$. In contrast, lowering cytosolic Ca buffering (by decreasing [EGTA]) drastically increased Ca spark frequency and width, leading to generation of multifocal (or propagating) sparks. By enhancing local CICR, a low [EGTA] solution decreased the termination $[Ca]_{SR}$ level for Ca sparks.
Finally, we studied if Ca spark termination was altered in myocytes from failing hearts, where remodeling processes lead to RyR malfunction. Recordings of RyR activity revealed that the channel sensitivity to $[Ca]_i$ is significantly increased in rabbit HF myocytes. In cells, this alteration of RyR function in HF causes termination of global Ca transients and local Ca sparks at significantly lower $[Ca]_{SR}$ compared to that in non-failing myocytes. We suggest that increased RyR sensitivity to $[Ca]_i$ allows HF myocytes to maintain systolic SR Ca release of nearly normal size even at a depleted SR Ca load. However, this RyR modification contributes to enhanced SR Ca leak and increased propensity of arrhythmogenic Ca waves.
Collectively, our results indicate that cardiac Ca sparks terminate when $[Ca]_{SR}$ fall to a certain critical level, supporting the existence of a functional link between partial $[Ca]_{SR}$ depletion and CICR termination. This functional link likely involves falling single RyR Ca flux and Ca unbinding from an intra-SR RyR Ca regulatory site as local $[Ca]_{SR}$ falls. We conclude that multiple $[Ca]_{SR}$-dependent termination mechanisms likely co-exist to ensure a stability of cardiac Ca cycling.

Fabiato A. Calcium-induced release of calcium from the cardiac sarcoplasmic reticulum. Am J Physiol 1983 July;245(1):C1-14.

Brochet DX, Yang D, Di Maio A, Lederer WJ, Franzini-Armstrong C, Cheng H. Ca2+ blinks: rapid nanoscopic store calcium signaling. Proc Natl Acad Sci U S A 2005 February 22;102(8):3099-104.

Shannon TR, Guo T, Bers DM. Ca2+ scraps: local depletions of free [Ca2+] in cardiac sarcoplasmic reticulum during contractions leave substantial Ca2+ reserve. Circ Res 2003 July 11;93(1):40-5.

Zima AV, Picht E, Bers DM, Blatter LA. Termination of cardiac Ca2+ sparks: role of intra-SR [Ca2+], release flux, and intra-SR Ca2+ diffusion. Circ Res 2008 October 10;103(8):e105-e115.

Belevych AE, Terentyev D, Terentyeva R, Nishijima Y, Sridhar A, Hamlin RL, Carnes CA, Gyorke S. The relationship between arrhythmogenesis and impaired contractility in heart failure: role of altered ryanodine receptor function. Cardiovasc Res 2011 June 1;90(3):493-502.

Cheng H, Lederer WJ, Cannell MB. Calcium sparks: elementary events underlying excitation-contraction coupling in heart muscle. Science 1993 October 29;262(5134):740-4.

Jiang D, Chen W, Wang R, Zhang L, Chen SR. Loss of luminal Ca2+ activation in the cardiac ryanodine receptor is associated with ventricular fibrillation and sudden death. Proc Natl Acad Sci U S A 2007 November 13;104(46):18309-14.

(8) Terentyev D, Kubalova Z, Valle G, Nori A, Vedamoorthyrao S, Terentyeva R, Viatchenko-Karpinski S, Bers DM, Williams SC, Volpe P, Gyorke S. Modulation of SR Ca release by luminal Ca and calsequestrin in cardiac myocytes: effects of CASQ2 mutations linked to sudden cardiac death. Biophys J 2008 August;95(4):2037-48.

(9) Guo T, Gillespie D, Fill M. Ryanodine receptor current amplitude controls Ca2+ sparks in cardiac muscle. Circ Res 2012 June 22;111(1):28-36.

Where applicable, the authors confirm that the experiments described here conform with The Physiological Society ethical requirements.

SA279

Slow Ca^{2+} sparks de-synchronize Ca^{2+} release in failing cardiomyocytes

W.E. Louch[1,2], J. Hake[3,4] and O.M. Sejersted[1,2]

[1]Institute for Experimental Medical Research, Oslo University Hospital Ullevål and University of Oslo, Oslo, Norway, [2]KG Jebsen Cardiac Research Center and Center for Heart Failure Research, University of Oslo, Oslo, Norway, [3]Simula Research Laboratory, Lysaker, Norway and [4]Department of Bioengineering, University of California San Diego, La Jolla, Norway

Systolic heart failure has been widely reported to involve reduced contraction magnitude of individual cardiomyocytes. However, accumulating data indicate that contraction is also slowed in this condition, which contributes to a reduced power of the heartbeat [1]. We and others have identified that a slowed rising phase of the Ca^{2+} transient is a critical underlying mechanism [1-3]. Although Ca^{2+} entry through Ca^{2+} channels is generally reported to be unaltered in failing cells, triggered release of Ca^{2+} from the sarcoplasmic reticulum (SR) via ryanodine receptors (RyRs) is de-synchronized and slowed [2,3]. This results, at least in part, from altered structure of T-tubules, which are invaginations of the surface sarcolemma. T-tubules become lost and/or disorganized during heart failure, which effectively removes some Ca^{2+} channels from their dyadic junctions with clusters of RyRs [2,3]. Thus, a significant proportion of RyRs are "orphaned" during heart failure, and Ca^{2+} release is delayed at these sites, as it is dependent on Ca^{2+} diffusion following release from intact dyads. However, we previously reported that irregular gaps between T-tubules and the formation of orphaned RyRs accounted for only a fraction of the overall slowing of the Ca^{2+} transient in this condition [2]. Thus, we presently hypothesized that alterations in RyR function also contribute to slowing of Ca^{2+} release in a mouse model of congestive heart failure (CHF) following myocardial infarction. Myocardial infarction was induced by left coronary artery ligation in anaesthetized (2.5% isoflurane inhalation) 8-10 week old C57BL/6 mice. SHAM-operated mice served as controls. Using echocardiography, animals which had developed CHF at 1 week following surgery were distinguished from non-failing animals by increased left atrial diameter (>2.0 mm) and infarct size >40% of the total left ventricular circumference. CHF was then allowed to progress until 10 weeks post-infarction when animals were sacrificed. Cardiomyocytes were isolated from viable regions of the septum. Field-stimulated Ca^{2+} transients (fluo-4 AM) rose markedly slower in CHF than SHAM myocytes as indicated by longer time to peak values (CHF=152±12% of SHAM, n_{cells} =22, 23 in SHAM, CHF, P<0.05). The rise time of Ca^{2+} sparks was also increased in CHF (SHAM=9.6±0.6 ms, CHF=13.2±0.7 ms, n_{sparks}= 89, 254 in SHAM, CHF, P<0.05), due to a sub-population of sparks (≈20%) with markedly slowed kinetics. Importantly, these slow sparks were distinct from prolonged, plateau-like Ca^{2+} release events, known to result from RyR subconductance states [4]. Regions of the cell associated with slow spontaneous sparks also exhibited slowed Ca^{2+} release during the action potential. Thus, greater variability in spark kinetics in CHF promoted less uniform Ca^{2+} release across the cell. As expected, dyssynchronous Ca^{2+} transients in CHF additionally resulted from T-tubule disorganization, as indicated by fast Fourier transforms. However, simultaneous imaging of T-tubules and Ca^{2+} indicated that slow sparks were not associated with orphaned RyRs. We instead hypothesized that an altered spatial configuration of RyRs could account for slow sparks. Western blotting revealed reduced RyR expression in CHF and, using an extended version of the sticky cluster model [5], we observed that reducing RyR density in the dyad could slow the rate of rise of the Ca^{2+} sparks. More dramatic slowing of Ca^{2+} release was modeled by distributing RyRs into sub-clusters, as there was a time delay inherent in the propagation of Ca^{2+} between sub-clusters. Adjusting other parameters in the model such as the physical coupling ("stickiness") of RyRs, junctional SR volume, cytosolic and SR [Ca^{2+}], and RyR triggering threshold did not produce slow sparks. Thus, our results suggest that altered configuration of dyadic RyRs can produce abnormally slow Ca^{2+} sparks in CHF. In combination with disrupted T-tubule structure, these alterations promote slowed, dyssynchronous Ca^{2+} transients in this condition.

Mørk et al., Am J Physiol Heart Circ Physiol 2009; 296: H1069-H79.

Louch WE et al., J Physiol 2006; 574: 519-33.

Song et al., Proc Nat Acad Sci USA 2006; 103: 4305-10.

Zima AV et al., Biophys J 2008; 94: 1867-79.

Sobie EA et al., Biophys J 2002; 83: 59-78.

The authors thank Professor Eric A. Sobie for sharing the code for the sticky cluster model.

Where applicable, the authors confirm that the experiments described here conform with The Physiological Society ethical requirements.

SA280

A modified local control model for Ca transients in cardiomyocytes

J. Bridge

CVRTI, University of Utah, Salt Lake City, UT, USA

It is widely accepted that Ca transients in ventricular heart cells are produced by the summation of locally controlled release events. These release events are produced by couplons that reside in junctions. However we have recently shown that in isolated rabbit ventricular cells t-tubules are lost during the isolation procedure. This creates a significant number of RyR clusters that are non junctional and no longer exists as part of the couplon but are still able to release Ca (1). These non-junctional RyRs are far less numerous in tissue.. We studied mechanisms by which Ca is release is locally controlled from both couplons and non-junctional RyR clusters. Since t-tubules are known to be lost in various pathological conditions isolated rabbit cells provide a convenient model to study the nature of Ca transients in disease states. We have already established that, provided intracellular Na is present local release

events are produced with a probability approaching 100%(2). We therefore investigated a possible mechanism that could explain this. With action potential shaped voltage clamp pulses we measured a significant Na current and an accompanying Ca transient using epiflourescence (3). However if the clamp pulse was preceded by a ramp, which inactivated all Na current the Ca transient, was reduced by 27%. We next investigated trans membrane Ca flux in isolated cells in which SR release flux was blocked. There was little difference in trans membrane Ca flux with and without the Na current. We therefore conclude that Ca current carries the majority of the flux. It therefore appears that a very small Ca flux mediated by NCX can have a large effect on SR Ca release if the SR is functioning. We further investigated this with a hypothesis first proposed by Maier et al (4). That Ca release can be mediated by a brain type (TTX sensitive Na channels). We measured SR release flux in the presence of 100 nM TTX and observed a 33 % reduction in release flux (similar to that produced by elimination of all Na currents). To explain this we propose that TTX sensitive Na currents are activated upon membrane depolarization and that that this primes the junctional cleft with Na. This Na in turn causes reverse NCX, which in turn primes the junction with Ca without triggering SR Ca release. Since we expect the relationship between SR Ca release and junctional Ca concentration to be sigmoid we imagine that priming the junction causes junctional Ca to increase along the foot of this sigmoid curve. Therefore when Ca currents are activated thy act on the steep portion of this curve which increases their coupling fidelity (5). Thus we view junctional priming as a mechanism that increases the coupling fidelity of Ca currents during an action potential. This ensures a high probability of activation of couplons and at least in part can account for the fact that local release events are observed to occur at high probability during action potentials in rabbits. We next investigated Ca transients in two dimensions using a Zeiss live 5 rapid scan head. We accomplished this by labeling cell membranes with di-8 anepps and using the Ca indicator fluo 4. Two-dimensional scans can be completed in 3.64 ms. Couplons were activated early and fairly synchronously. However Ca spread to non-junctional regions in a manner that was both temporarily and spatially inhomogeneous. In an attempt to understand whether the spread of Ca was simply due to diffusion from couplons or was due to activation of non-junctional release units we compared the spread of Ca in two dimensions with a model based on a reaction diffusion equation. The results suggested that non-junctional release units within 1 micron of the membrane (including t-tubules) were activated (presumably triggered by efflux from couplons). Beyond this distance we could not determine the extent to which non-junctional release unit were activated. These inhomogeneous Ca transient are expected to produce inhomogeneous sarcomere shortening with considerable weakening of contraction. Presumably this provides at least one explanation for the failure of contraction in end stage heart disease. We suggest therefore that local control of couplons does not simply occur by activation of Ca currents within the couplon but also involves Ca priming of the junctional cleft. Non-junctional RyRs are controlled by activation of local couplons but this control is more spatially extended. Moreover we suggest that a high probability of activation of couplons ensures optimal activation of non-junctional release units.

Torres NS, Rock A, Savio-Galimberti E, Sachse FB, Bridge JHB. Occurrence of spontaneous sparks in ventricular myocytes from junctional and non-junctional RyR clusters. Biophys J. 2010;98:106a

Ca2+ sparks in rabbit ventricular myocytes evoked by action potentials: involvement of clusters of L-type Ca2+ channels. Inoue M, Bridge JH. Circ Res. 2003 Mar 21;92(5):532-8. Epub 2003 Feb 27.

Na+ currents are required for efficient excitation-contraction coupling in rabbit ventricular myocytes: a possible contribution of neuronal Na+ channels. Torres NS, Larbig R, Rock A, Goldhaber JI, Bridge JH. J Physiol. 2010 Nov 1;588(Pt 21):4249-60.

An unexpected requirement for brain-type sodium channels for control of heart rate in the mouse sinoatrial node. Maier SK, Westenbroek RE, Yamanushi TT, Dobrzynski H, Boyett MR, Catterall WA, Scheuer T. Proc Natl Acad Sci U S A. 2003 Mar 18;100(6):3507-12

Nature. 2001 Mar 29;410(6828):592-6. Ca2+ signalling between single L-type Ca2+ channels and ryanodine receptors in heart cells. Wang SQ, Song LS, Lakatta EG, Cheng H.

The Nora Eccles Harrison Treadwell Foundation funded this work

Where applicable, the authors confirm that the experiments described here conform with The Physiological Society ethical requirements.

SA281

Mechanisms of vascular ageing and calcification

C. Shanahan

King's College London, London, UK

Vascular calcification is a serious and ubiquitous clinical problem in ageing and is set to become increasingly prevalent as populations age. It is an independent risk factor for cardiovascular (CV) mortality and emerging evidence suggests that calcification is directly causal in the induction of CV events. Calcification of the vessel media is particularly prevalent in aged populations leading to vascular stiffening and a progressive rise in after-load stress, myocardial workload and changes in diastolic perfusion that predispose to ischemia, heart failure and arrhythmia. Vascular calcification is orchestrated by vascular smooth muscle cells (VSMCs), which undergo maladaptive osteo/chondrocytic differentiation and this, combined with cell death and vesiculation, act to promote mineral deposition in the vessel wall.

Vascular calcification is also prevalent in patients with premature ageing disorders such as Werner's Syndrome and Hutchison-Gilford Progeria Syndrome, which are caused by defects in the nuclear lamina protein, Lamin A. In these patients the accumulation of a defective form of unprocessed lamin A acts to drive VSMC degeneration and patients die prematurely of myocardial infarct or stroke within the second decade. Importantly, aged VSMCs also acquire nuclear lamina defects characterized by the accumulation of prelamin A, the immature, unprocessed form of lamin A. Prelamin A accumulation drives DNA damage and premature senescence in VSMCs and this occurs concomitantly with induction of osteo/chondrocytic differentiation and upregulation of the bone-associated proteins Runx2 and alkaline phosphatase. siRNA knockdown or chemical inhibition of key proteins regulating DNA damage signalling, such as ATM/ATR, can block VSMC osteo/chondrocytic differentiation and mineralization. Evidence suggests that prelamin A acts to promote DNA damage by interfering with the nuclear translocation of key DNA damage response proteins to sites of double strand breaks. However the factors that link DNA damage to osteo/chondrocytic differentiation remain unclear. One possibility is that aged/senescent VSMCs activate an inflammatory cytokine storm, called the senescence associated secretory phenotype (SASP), and release procalcific factors such as BMP2 and IL6 which drive osteo/chondrocytic differentiation. However other more direct mechanisms may also be involved.

Taken together emerging data has begun to highlight a key role for the nuclear lamina and DNA damage signalling in promoting VSMC ageing and calcification. These pathways should provide novel therapeutic targets for the amelioration of this detrimental age associated vascular pathology.

Ragnauth CD, Warren DT, Liu Y, McNair R, Tajsic T, Figg N, Shroff R, Skepper J, Shanahan CM. Prelamin A acts to accelerate smooth muscle cell senescence and is a novel biomarker of human vascular aging. Circulation. 2010 May 25;121(20):2200-10.

British Heart Foundation

Where applicable, the authors confirm that the experiments described here conform with The Physiological Society ethical requirements.

SA282

miRNA-125b and their targets in cardiovascular calcification

C. Goettsch

Center for Interdisciplinary Cardiovascular Sciences Brigham and Women's Hospital/Harvard Medical School, Boston, MA, USA

Cardiovascular calcification is a prominent feature of chronic inflammatory disorders — such as chronic kidney disease (CKD), type 2 diabetes (T2D), and atherosclerosis — that associate with significant morbidity and mortality. The concept that similar pathways control both bone remodeling and vascular calcification is widely accepted, but the precise mechanisms of calcification remain largely unknown. Micro-RNAs (miRNAs) are a large class of evolutionarily conserved, small, endogenous, non-coding RNAs serving as essential post-transcriptional modulators of gene expression that play a crucial role in normal physiology. The central role of microRNAs (miRNA) as fine-tune regulators in the cardiovascular system and bone biology has gained acceptance and has raised the possibility for novel therapeutic targets. Additionally, circulating miRNAs have been proposed as biomarkers for a wide range of cardiovascular diseases, but knowledge of miRNA biology in cardiovascular calcification is very limited. However, we recently provided the first miRNA-dependent mechanism in the progression of vascular calcification by demonstrating that miR-125b dysregulation leads to the transition of human coronary arterial smooth muscle cells (HCASMC) into osteoblast-like cells. Osteogenic transition of HCASMC was induced by osteogenic medium and led to matrix mineralization. Increased expression of miR-125b was time-dependent in HCASMC and diminished during osteogenesis. After 21 days in the osteogenic environment, miR-125b was significantly reduced (-42%) compared with HCASMC cultured in control medium. The expression of two miR-processing enzymes that are essential for SMC function, RNase III endonucleases DICER1 and DROSHA, were reduced in calcified HCASMCs. Furthermore, inhibition of endogenous miR-125b promoted alkaline phosphatase activity and matrix mineralization *in vitro*. Correspondingly, in vivo observations indicate that miR-125b is decreased in calcified aortas of apolipoprotein-deficient (Apoe) mice fed a high fat diet for 26 weeks compared to those sacrificed after 10 weeks. *In silico* and expression analyses revealed the osteoblast transcription factor SP7 (osterix) as a target of miR-125b. Our results suggest that miR-125b is involved in vascular calcification *in vitro* and *in vivo*, at least partially by targeting SP7. As cardiovascular calcification and bone remodeling share common mechanisms, we need an in-depth understanding of miRNA function and their association with the molecular pathogenesis of osteoporosis and vascular calcification. This knowledge will be critical for the developing of a more specific therapy for cardiovascular calcification that does not adversely affect physiological bone homoeostasis.

Where applicable, the authors confirm that the experiments described here conform with The Physiological Society ethical requirements.

SA283

Arterial calcification in chronic kidney disease (CKD): role of phosphate and phosphate transporters

C. Giachelli

Bioengineering, University of Washington, Seattle, WA, USA

Vascular calcification contributes to the high risk of cardiovascular mortality in CKD patients. Dysregulation of mineral metabolism, in particular elevated serum phosphate levels with associated abnormalities in phosphate-regulating hormones, is common in CKD patients, and is thought to drive vascular calcification. In this talk, I will review current concepts in the pathogenesis of vascular calcification in CKD, and highlight our recent experimental findings directed at understanding the mechanisms by which elevated phosphate promotes vascular calcification. The effects of elevated phosphate on vascular cell differentiation, apoptosis, and matrix degradation will be reviewed. We have identified sodium-dependent phosphate cotransporters as important mediators of vascular smooth muscle cell calcification in response to elevated phosphate, and data on their roles in these processes, including phosphate uptake-dependent and –independent pathways, will be presented. Unravelling the complex pathways involved in vascular calcification will ultimately provide novel targets and therapies to limit the deleterious effects of vascular calcification in CKD patients.

Where applicable, the authors confirm that the experiments described here conform with The Physiological Society ethical requirements.

SA284

Calcium phosphate crystals and cell death

D. Proudfoot[1], Y. Dautova[1], D. Kozlova[2], M. Epple[2], J.N. Skepper[3] and M.D. Bootman[1,4]

[1]Signalling, Babraham Institute, Cambridge, Cambridgeshire, UK, [2]Inorganic Chemistry, University of Duisburg-Essen, Essen, Germany, [3]Department of Physiology, Development and Neuroscience, Universtiy of Cambridge, Cambridge, Cambridgeshire, UK and [4]Life, Health and Chemical Science, Open University, Milton Keynes, UK

Calcium phosphate (CaP) crystals are a natural component of bone, but are also commonly found in other tissues in association with ageing and several diseases including atherosclerosis, medial calcification (Mönckeberg's sclerosis), arthritis and cancer. The amount of CaP crystals deposited in arteries correlates positively with atherosclerotic plaque rupture and myocardial infarction but whether the crystals actively participate in driving the disease is unclear. The damaging effect of nano- and microparticulate CaP crystals in arthritic joints has been known for some time, and small CaP crystals occur in regions of atherosclerotic plaque stress and rupture. Since vascular smooth muscle cells (VSMCs) have a protective role

in plaque rupture, we investigated whether CaP crystals could affect VSMC function.
Adding either synthetic CaP crystals or calcified particles extracted from human atherosclerotic plaques to human aortic VSMCs in culture induced cell death, with the synthetic crystals being more potent than the plaque-extracted crystals. To investigate the mechanism of cell death, intracellular calcium ion levels were measured using video imaging of Fura-2-loaded cells. CaP crystals caused rapid rises in intracellular calcium ion concentration preceding cell death. Both effects were inhibited when lysosomal acidification was blocked with bafilomycin A, implicating lysosomal involvement in calcium signalling and cell death.
Video imaging of VSMCs indicated that CaP crystals induce the formation of large plasma membrane blebs prior to cell death, suggesting focal sites of plasma membrane damage. Transmission electron microscopy revealed that CaP crystals adhered to the plasma membrane within 5 minutes of addition of crystals, with crystals individually aligning with the membrane or grouped in clusters at sites of profound plasma membrane fragmentation. VSMCs did not die until approximately 30 minutes after addition of CaP crystals (measured using propidium iodide uptake), which implies that the initial plasma membrane damage does not kill cells, but rather that cells make an attempt to repair/extrude damaged components. However, continued exposure to crystals overwhelms repair and calcium homeostatic mechanisms resulting in cell necrosis.
Further studies suggest that CaP-binding proteins such as fetuin and albumin, that are known to bind to CaP crystals *in vivo*, may dampen the toxic effects of CaP on VSMCs. The coating of plaque-derived CaP crystals by these proteins could explain why they are less potent than synthetic CaP crystals in causing VSMC death. Uncovering how CaP crystals bind to VSMCs, induce damage, activate repair mechanisms, induce calcium signalling and involve key cellular organelles to result in necrosis may provide strategies to limit their damaging effects in the vessel wall.

This work is funded by the British Heart Foundation (FS/11/21/28691, D. Proudfoot).

Where applicable, the authors confirm that the experiments described here conform with The Physiological Society ethical requirements.

SA285

Pro-inflammatory aspects of cardiovascular calcification: insights from molecular imaging

E. Aikawa

Cardiovascular Medicine, Brigham and Women's Hospital, Harvard Medical School, Boston, MA, USA

The collective global impact of the spectrum calcific cardiovascular diseases is serious but underappreciated health problem in the developed and rapidly developing regions of the world. Cardiovascular calcification is an independent risk factor for cardiovascular morbidity and mortality. Ectopic mineralization mainly affects the aorta, coronary arteries, peripheral arteries, and aortic valves, with fully-formed bone observed in atherosclerotic plaques and stenotic aortic valves. This disease of dysregulated metabolism is no longer viewed as a passive degenerative disorder, but instead as an active process triggered by pro-inflammatory cues. Hypercholesterolemia, metabolic syndrome, end-stage renal disease, diabetes mellitus and increased age accelerate cardiovascular calcification.
Traditional imaging modalities such as computed tomography, although perfectly adept at identifying and quantifying advanced calcification, cannot detect the early stages of this disorder and offer limited insight into the mechanisms of mineral dysregulation. Here we present optical molecular imaging as a promising tool that simultaneously detects pathobiological processes associated with inflammation and early stages of calcification *in vivo* at the (sub)cellular levels.
Research into treatment of cardiovascular calcification is lacking, as shown by clinical trials that have failed to demonstrate the reduction of calcific aortic stenosis. Hence the need to elucidate the pathways that contribute to cardiovascular calcification and to develop new therapeutic strategies to prevent or reverse calcification has driven our investigations.
We previously showed that early calcification/microcalcification associates with macrophage accumulation in vulnerable atherosclerotic plaques. Chronic renal disease (CRD) and mineral imbalance accelerates calcification and the subsequent release of matrix vesicles (MVs) — precursors of microcalcification. We tested the hypothesis that macrophage-derived MVs contribute directly to microcalcifications, which in turn may contribute to plaque rupture.
We showed that macrophages associated with regions of calcified vesicular structures in human carotid plaque samples (n=136 patients). *In vitro*, macrophages released MVs with high calcification and aggregation potential. MVs expressed exosomal markers (CD9 and TSG101), and contained S100A9 and annexin V (Anx5). Silencing S100A9 *in vitro* and genetic deficiency in S100A9$^{-/-}$ mice reduced MV calcification, while stimulation with S100A9 increased calcification potential. Externalization of phosphatidylserine (PS) after Ca/P stimulation, and interaction of S100A9 and Anx5, indicated that a PS–Anx5–S100A9 membrane complex facilitates hydroxyapatite nucleation within the macrophage-derived MV membrane. These results supported the novel concept that macrophages release calcifying MVs, enriched in S100A9 and Anx5, which contribute to accelerated formation of microcalcification in CRD.
This presentation will discuss studies that have used molecular imaging methods to advance knowledge of cardiovascular calcification, focusing in particular on the inflammation-dependent mechanisms of arterial and aortic valve calcification.

Where applicable, the authors confirm that the experiments described here conform with The Physiological Society ethical requirements.

SA286

Deciphering dead-end docking of large dense core vesicles in chromaffin cells

S. Hugo[1], E. Dembla[1], M. Halimani[1], U. Matti[2], J. Rettig[1] and U. Becherer[1]

[1]Institut für Physiologie, Universität des Saarlandes, Homburg, Germany and [2]CBB - Ries Group, European Molecular Biology Laboratory, Heidelberg, Germany

Calcium-dependent exocytosis of large dense core vesicles (LDCVs) comprises several steps: docking of the vesicles to the plasma membrane (PM), priming to render the vesicles release-competent and fusion with the PM. Total internal reflection fluorescence microscopy (TIRFM) enables the real-time visualization of LDCVs near the PM as they undergo changes from

one functional state to the other (Nofal et al., 2007). We used this technique in combination with patch-clamp electrophysiology to study the secretion of LDCVs in bovine chromaffin cells (Becherer et al., 2007) stimulation of the cells for 5 minutes with 6 μM [Ca2+]i induced maximal secretion and a large reduction of the LDCVs density at the plasma membrane. However, 14.1 ± 1.5% of the LDCVs were visible at the plasma membrane throughout experiments, indicating they were permanently docked. We defined these vesicles as dead end vesicles. Overexpression of Munc18 2 or SNAP-25 reduced the pool size of these vesicles. Conversely, expressing open-Syntaxin increased this pool. These results indicate that the unproductive target Soluble NSF Attachment Protein Receptor acceptor complex composed of 2:1 syntaxin–SNAP-25 exists in vivo. More importantly, they define a novel function for this acceptor complex in mediating dead end docking.

Becherer U, Pasche M, Nofal S, Hof D, Matti U, Rettig J. (2007) Quantifying exocytosis by combination of membrane capacitance measurements and total internal reflection fluorescence microscopy in chromaffin cells. PLoS One. 2(6):e505.

Nofal S, Becherer U, Hof D, Matti U, Rettig J. (2007) Primed vesicles can be distinguished from docked vesicles by analyzing their mobility. J Neurosci. 27:1386-95.

We thank L. Wirtz and U. Kazmaier for synthesizing the FFN511; M. Klose, M. Schneider, K. Sandmeier, C. Bick and A. Ludes for expert technical support. This work was supported by local funding (HOMFOR, Universität des Saarlandes) and by grants from the Deutsche Forschungs¬gemeinschaft SFB 530 and 894 (to J.R. and U.B.).

Where applicable, the authors confirm that the experiments described here conform with The Physiological Society ethical requirements.

SA287

DOC2B and Munc13-1 differentially regulate neuronal network activity

A. Lavi, A. Sheinin, R. Shapira, D. Zelmanoff and U. Ashery

Neurobiology, Tel Aviv University, Tel Aviv, Israel

Alterations in the levels of synaptic proteins affect synaptic transmission and synaptic plasticity. However, the precise effects on neuronal network activity are still enigmatic. Here, we utilized microelectrode array (MEA) to elucidate how manipulation of the presynaptic release process affects the activity of neuronal networks. By combining pharmacological tools and the genetic manipulation of synaptic proteins we show that overexpression of DOC2B and Munc13-1, proteins known to promote vesicular maturation and release, elicits opposite effects on the activity of the neuronal network. Although both cause an increase in the overall number of spikes, the distribution of spikes is different. While DOC2B enhances, Munc13-1 reduces the firing rate within bursts of spikes throughout the network; however, Munc13-1 increases the rate of network bursts. DOC2B's effects were mimicked by Strontium that elevates asynchronous release but not by a DOC2B mutant that enhances spontaneous release rate. This suggests for the first time that increased asynchronous release on the single-neuron level promotes bursting activity in the network level. This innovative study demonstrates the complementary role of the network level in explaining the physiological relevance of the cellular activity of presynaptic proteins and the transformation of synaptic release manipulation from the neuron to the network level.

Where applicable, the authors confirm that the experiments described here conform with The Physiological Society ethical requirements.

SA288

Activity-mediate expansion of the secretory fusion pore is regulated by a calcineurin-dependent dynamin-syndapin signaling pathway in neuroendocrine mouse adrenal chromaffin cells

C. Smith and P. Samasilp

Physiology and Biophysics, Case Western Reserve University, Cleveland, OH, USA

Neuroendocrine chromaffin cells release a variety of transmitter molecules into the circulation as a specific function of sympathetic activation. Activity-dependent release of transmitter single species or classes of transmitters is controlled through regulation of the secretory fusion pore. Under sympathetic tone, basal synaptic activity drives chromaffin cells to secrete modest levels of catecholamine through a restricted secretory fusion pore. In contrast, elevated sympathetic firing, as evoked by environmental stress or injury, results in the expansion of the fusion pore for maximal catecholamine release. Pore expansion also facilitates release of co-packaged peptide transmitters from the dense granule core. Therefore, fusion pore expansion is a regulatory step for the activation of the sympatho-adrenal stress response. Despite the physiological impact and importance of this process, the molecular mechanism by which pore expansion is regulated remains unresolved. Here we employ fluorescence imaging in combination with electrophysiological and electrochemical-based measurements to test the role of dynamin I in the regulation of activity-mediated fusion pore expansion in mouse adrenal chromaffin cells (Samasilp et al., 2012). We show that under elevated electrical stimulation, dynamin I is dephosphorylated at Ser-774 by the protein phosphatase, calcineurin. We also demonstrate that disruption of dynamin I binding to syndapin, a step regulated by calcineurin-dependent dynamin dephosphorylation, inhibits fusion pore expansion. Lastly, we show that pharmacologic block of N-WASP function (a syndapin binding partner) limits activity-dependent expansion of the fusion pore. Our results suggest that fusion pore expansion is regulated by a calcineurin-dependent dephosphorylation of dynamin I. Dephosphorylated dynamin I acts via a syndapin/N-WASP signaling cascade, leading to pore expansion.

Samasilp P, Chan SA, Smith C (2012) Activity-dependent fusion pore expansion regulated by a calcineurin-dependent dynamin-syndapin pathway in mouse adrenal chromaffin cells. J Neurosci 32:10438-10447.

Where applicable, the authors confirm that the experiments described here conform with The Physiological Society ethical requirements.

SA289

Studies of a cyclic nucleotide regulated potassium channel

J. Morais Cabral

IBMC, Porto, Portugal

The superfamily of cyclic nucleotide regulated cation channels includes the eukaryotic hyperpolarization-activated cyclic nucleotide-gated (HCN) and cyclic nucleotide gated (CNG)

channels as well as a family of bacterial cyclic nucleotide regulated potassium channels. All of these channels are tetramers, with each subunit having 6 trans-membrane helices and a C-terminal cytosolic cyclic nucleotide binding (CNB) domain. The major difference between the eukaryotic and bacterial channels is the presence, in the eukaryotic membrane proteins, of a long linker (the C-linker) between the channel regions and the CNB domain. Despite this major difference, structural studies of the MlotiK1 bacterial channel (1,2,3) have provided general insights into the ligand-dependent conformational changes occurring in the CNB domains and about the structural properties of cation channels with 6 trans-membrane helices, such as voltage-gated potassium channels. This bacterial channel also displays specific properties that are very different from the properties of the eukaryotic channels (4). Interestingly, the recently determined structures of CNB-like domains from eukaryotic EAG channels have raised the possibility of novel molecular mechanisms of regulation by domains with this fold (5,6).

Clayton GM et al. (2004) Cell 119, 615-27

Clayton GM et al. (2008) PNAS 105, 1511-5

Altieri SL et al. (2008) J Mol Biol. 381, 655-69

Mari SA et al. (2011) PNAS 108, 20802-7

Marques-Carvalho MJ et al. (2012) J Mol Biol. 423, 34-46

Brelidze TI et al. (2012) Nature 481, 530-3

Support for this work was provided by EMBO (Installation grant) and by NIH (1R01NS081320).

Where applicable, the authors confirm that the experiments described here conform with The Physiological Society ethical requirements.

SA290

Structure and regulation of the CorA magnesium channel

J. Payandeh

Structural Biology, Genentech, Inc., South San Francisco, CA, USA

The magnesium ion (Mg^{2+}) is the most abundant intracellular divalent cation and plays an essential role in a myriad of biochemical processes. Proper Mg^{2+} homeostasis has been correlated with physiological well-being and Mg^{2+} deficiency is associated with pathological states including cardiac syndromes, immunodeficiency, epilepsy, migraine, muscular dysfunction and bone wasting. Despite its impact on human health, relatively little is known about the molecular mechanisms that regulate Mg^{2+} transport and storage. I will describe a series of recent crystal structures of the CorA Mg^{2+} channel from *Thermotoga maritima* that have provided the first structural insights into the gating and selectivity mechanisms operating in this unique channel superfamily. CorA is revealed to be a funnel-shaped homopentamer containing a large intracellular regulatory domain linked through an extended alpha-helix to a membrane-embedded ion pore. Functional analysis and molecular dynamics simulations confirm that CorA contains an intrinsic and elaborate Mg^{2+}-sensor which couples cellular Mg^{2+} status to the regulation of its ion pore. The CorA pore appears to be sealed by at least two gates in its closed state, which suggests that cellular Mg^{2+} transport is well guarded and very tightly regulated.

Where applicable, the authors confirm that the experiments described here conform with The Physiological Society ethical requirements.

SA291

Activation and inhibition of prokaryotic pentameric ligand-gated ion channels

R. Dutzler

Dept. of Biochemistry, University of Zurich, Zurich, Switzerland

The pentameric ligand-gated ion channels (pLGICs) are ionotropic neurotransmitter receptors that mediate electrical signaling at chemical synapses. The X-ray structures of two prokaryotic homologues have provided first insight into the detailed architecture of the family at high resolution [1]. The structure of GLIC, a proton-activated channel from the cyanobacterium Gloebacter violaceous shows an open conformation of the pore [2]. The channel conducts cations with similar properties as the nicotinic acetylcholine receptor (nAChR). The transmembrane pore is funnel-shaped with a wide hydrophobic entrance at the extracellular side that narrows to a hydrophilic intracellular opening. In this region conserved residues coordinate ions which have lost a large part of their hydration shell [3]. The structure of ELIC, a pLGIC from the plant pathogen Erwinia chrysanthemi, shows a non-conducting conformation that was obtained in the absence of ligands [4]. In its structure the extracellular half of the pore is occluded by bulky hydrophobic residues that likely prevent ion conduction. ELIC is activated by a set of primary amines that include the neurotransmitter GABA [5]. The protein forms cation selective channels with large conductance that slowly desensitize in the presence of ligands. Both proteins were used to study distinct mechanisms of channel inhibition. Ion conduction in GLIC is inhibited by the same set of open channel blockers that also act on nAchRs [3]. In ELIC acetylcholine acts as competitive inhibitor, which binds to the agonist site and stabilizes the closed conformation of the channel. Divalent cations, in contrast, are allosteric modulators, which bind to a site distant from the agonist binding site where they interfere with gating [6]. The strong structural similarity to their eukaryotic counterparts make ELIC and GLIC important model systems for the pLGIC family that will ultimately allow a detailed comprehension of mechanistic properties that are still poorly understood.

Hilf, R. J. & Dutzler, R. A prokaryotic perspective on pentameric ligand-gated ion channel structure. Current opinion in structural biology 19, 418-424, (2009).

Hilf, R. J. & Dutzler, R. Structure of a potentially open state of a proton-activated pentameric ligand-gated ion channel. Nature 457, 115-118, (2009).

Hilf, R. J. et al. Structural basis of open channel block in a prokaryotic pentameric ligand-gated ion channel. Nature structural & molecular biology 17, 1330-1336, (2010).

Hilf, R. J. & Dutzler, R. X-ray structure of a prokaryotic pentameric ligand-gated ion channel. Nature 452, 375-379, (2008).

Zimmermann, I. & Dutzler, R. Ligand activation of the prokaryotic pentameric ligand-gated ion channel ELIC. PLoS Biol 9, (2011).

Zimmermann, I., Marabelli, A., Bertozzi, C., Sivilotti, L. G. & Dutzler, R. Inhibition of the prokaryotic pentameric ligand-gated ion channel ELIC by divalent cations. PLoS Biol 10, (2012).

Where applicable, the authors confirm that the experiments described here conform with The Physiological Society ethical requirements.

SA292

Comparison of the structure of a potassium channel in both 2D and 3D crystals

R. De Zorzi[2], L. Bannwarth[1], W. Nicholson[2] and C. Venien-Bryan[1,2]

[1]IMPMC, UMR 7590, CNRS-UPMC-IRD, UPMC, Paris6, Paris, France and [2]Biochemistry, University of Oxford, Oxford, UK

Inwardly-rectifying potassium (Kir) channels regulate membrane electrical excitability and K+ transport in many cell types where they control such diverse processes as heart rate, vascular tone, insulin secretion and salt/fluid balance. Their physiological importance is highlighted by the fact that genetically inherited defects in Kir channels are responsible for a wide-range of channelopathies. To elucidate how channel function becomes defective in the disease state requires a detailed understanding of channel structure in both the open and closed states. Here for the first time, we report the structure of a KirBac potassium channel with an open bundle crossing indicating a mechanism of channel gating determined by X-ray crystallography at 3Å resolution. In this model, the rotational twist of the cytoplasmic domain is coupled to opening of the bundle-crossing gate via a network of inter- and intra-subunit interactions [1]. In addition, we have also used EM analysis of 2D crystals of the same Kir channel trapped in an open state and compared these results with the 3D structure.

Intriguingly, the projection maps from the EM experiments suggest a larger opening of the pore in the 2D crystal form compared to that observed in the 3D crystal structure [2]. The organization of these two crystal forms is different and suggests that the 2D crystals may permit stabilisation of an open state structure that is not compatible with 3D crystallisation. These results not only have major implications for our understanding of the open state structure of the Kir channel, but more importantly they demonstrate the general utility and importance of methods such as electron microscopy and 2D crystallography for the study of membrane protein structure.

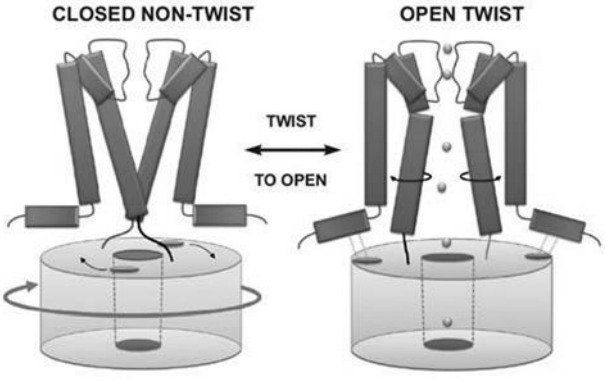

Cartoon of gating model

[1] Bavro VN, De Zorzi R, Schmidt MR, Muniz JR, Zubcevic L, Sansom MS, Vénien-Bryan C, Tucker SJ Nature Structural & Molecular Biology Structure of a KirBac potassium channel with an open bundle crossing indicates a mechanism of channel gating 7, 158–163 (2012).

[2] Rita De Zorzi,William V. Nicholson, Jean-Michel Guigner, Françoise Erne-Brand, Henning Stahlberg, and Catherine Vénien- Bryan Growth of large and highly ordered 2D crystals of a K+ channel, structural role of lipidic environement. submitted

THis work was supported by grants from the BBSRC, the Wellcome Trust and CNRS. RdZ was supported by a Marie Curie intra-European Fellowship

Where applicable, the authors confirm that the experiments described here conform with The Physiological Society ethical requirements.

SA293

Structure of sodium channel pore - implications for ion permeation and gating

D. Minor

UCSF Cardiovascular Research Institute, San Francisco, CA, USA

Voltage-gated sodium channels (NaVs) are central to cellular excitation and are important drug targets. We have determined the structure of a closed conformation of a pore only bacterial NaV (BacNaV) that provides insight into both of these fundamental properties. Our findings underscore commonalities between BacNaVs and eukaryotic voltage gated channels and provide a framework for understanding gating and ion permeation in this superfamily.

Where applicable, the authors confirm that the experiments described here conform with The Physiological Society ethical requirements.

SA294

Biomechanical control of the SMC phenotype during arteriogenesis

T. Korff

Institute of Physiology and Pathophysiology, Heidelberg University, Heidelberg, Germany

Arteriogenesis is an important adaptive remodeling process which involves the enlargement and thickening of arterioles running in parallel to an occluded artery, and is capable of partially compensating the consequences of peripheral artery disease by creating natural bypasses. The arteriolar remodeling is orchestrated by changes in the biomechanical forces to which the vessel wall is exposed to. Based on Poiseuille's equation, progressive stenosis of the main artery will lead to an increase in resistance hence to a significant drop in pressure distal to the site of occlusion. As a consequence, the pressure difference between both ends of the collateral arterioles is enhanced resulting in an increased flow and, as a consequence, an increase in shear stress.

Laminar shear stress is thought to be responsible for the initial dilation of the collateral arterioles through activation of endothelial cell nitric oxide synthase. Moreover, the NO-mediated dilation decreases the wall thickness and thus - according to the Laplace equation - results in an increase in circumferential wall stress. While the impact of shear stress on collateral growth has been extensively studied, the role of circumferential wall stress in the early phase of arteriogenesis is less well defined. To this end, our studies indicate that wall stress or biomechanical stretch activates the transcription factor AP-1 in endothelial and smooth muscle cells and controls the expression of MCP-1 - an important determinant of arteriogenesis. Furthermore, this biomechnical force promotes the activation of smooth muscle cells by imparing the function of myocardin - a crucial regulator of the contractile capacity of these cells - and acts in concert with shear stress to reprogram G-protein signaling cascades in smooth muscle cells.

Collectively, our findings suggest that biomechanical stress controls rate-limiting mechanisms during the remodeling of

collateral arterioles and contributes to a mechanosensitive gene expression in vascular smooth muscle cells during arteriogenesis.

Where applicable, the authors confirm that the experiments described here conform with The Physiological Society ethical requirements.

SA295

Inhibition of individual 14q32 microRNAs drastically increases neovascularization and blood flow recovery after ischemia

S.M. Welten[1,2], A.J. Bastiaansen[1,2], A.A. Hellingman[1], R.C. de Jong, M.R. de Vries, H.A. Peters, E.R. Kandimalla, P.H. Quax and A.Y. Nossent[1]

[1]Department of Vascular Surgery, Leiden University Medical Center, Leiden, Netherlands, [2]Einthoven Laboratory for Experimental Vascular Medicine, Leiden University Medical Center, Leiden, Netherlands and [3]Idera Pharmaceuticals, Cambridge, MA, USA

Background. Neovascularization, i.e. angiogenesis and arteriogenesis is a multifactorial process. As microRNAs can regulate expression of up to several hundred target genes, we set out to identify microRNAs that target genes in all pathways of neovascularization. Using www.targetscan.org, we performed a reverse target prediction on a set of 197 genes involved in neovascularization. We found enrichment of binding sites for 27 miRs in a single microRNA gene cluster. MicroArray analyses showed that 14q32 microRNAs were down-regulated during neovascularization in mice subjected to single femoral artery ligation.
Methods and Results. Novel microRNA-inhibitors, Gene Silencing Oligonucleotides (GSOs), were used to inhibit four 14q32 microRNAs, miR-487b, miR-494, miR-329 and miR-495 one day prior to double femoral artery ligation. Blood flow recovery was followed by Laser Doppler Perfusion Imaging. All 4 GSOs clearly improved blood flow recovery after ischemia. Mice treated with GSO-495 or GSO-329 showed increased perfusion already after 3 days (30% perfusion vs. 15% in control) and those treated with GSO-329 showed a remarkable full recovery of perfusion after 7 days (vs. 60% in control). Increased collateral artery diameters (arteriogenesis) were observed in adductor muscles of GSO-treated mice, as well as increased capillary densities (angiogenesis) in the ischemic soleus muscle. In vitro, treatment with GSO-329, GSO-495 and GSO-487 led to increased arterial endothelial cell activation whereas treatment with GSO-494 led to increased arterial fibroblast proliferation.
Conclusions. Inhibition of 14q32 miRs leads to drastic increases in post-ischemic blood flow recovery in vivo and may offer an alternative to growth factors in therapeutic neovascularization.

Where applicable, the authors confirm that the experiments described here conform with The Physiological Society ethical requirements.

SA296

Vasomotor properties of collateral arteries: effects of exercise training

M.H. Laughlin

Biomedical Sciences, University of Missouri, Columbia,, MO, USA

The purpose of this paper is to characterize the vasomotor properties of collateral vessels and summarize knowledge of the impact of exercise training/physical activity (EX) on these properties. The focus is on vasomotor properties of collateral vessels that provide blood flow to cardiac and skeletal muscle because this is my experience.
Vasomotor Properties of Collaterals: In response to occlusive vascular disease inadequate blood flow is provided downstream of the occlusion which chronically stimulates a number of adaptations that help restore blood flow toward normal. Structural enlargement of collateral vessels is well characterized in animal models (Laughlin et al. 2012). There is relatively less appreciation of the importance of vasomotor reactivity of collateral vessels but it is known that vasomotor properties of collateral arteries differ from those of normal arteries. Compared to normal arteries, the constrictor response to ET-1, U46619, KCl, thromboxane A2, are reported to be blunted in collateral arteries (Angus et al.1991). Dilator responses to adenosine SNP and cromakalin are normal or increased in collaterals. In contrast, endothelium-dependent dilation (EDD) is generally reported to be blunted in peripheral collateral arteries (Taylor et al. 2008) and collateral dependent coronary arteries and arterioles (Griffin et al. 1999 & 2001). Peripheral collateral arteries exhibit unaltered constrictor responses to phenylephrine (Taylor et al. 2008).
It is possible that these EDD is blunted due to decreased intravascular pressure downstream of arterial occlusion (EDD is blunted when normal arteries are evaluated at the low pressures comparable to those reported in collateral vessels.) On the other hand, the low luminal pressure caused by upstream obstruction also modifies flow distribution to enhance blood flow through the collateral circuit in a nitric oxide (NO)-dependent manner. When exercise is imposed on the collateral circuit, it may result in an increased shear stress and thereby contribute to the enlargement of, and increased EDD of, the collateral vessels.
Flow-induced dilation, an EDD response, is blunted in collateral arteries. Indeed, peripheral collateral arteries exhibit a modest dilation at low shear stress and then a significant vasoconstriction with increasing shear stress whereas similarly sized arteries simply demonstrate dilation. Colleran et al (2010) suggested this may be the result of an interaction of NO with reactive oxygen species (ROS) producing peroxynitrite which stimulates vasoconstriction via thromboxane A2 production through the COX pathway.
Effects of exercise training: Several investigators have tested the hypothesis that, since shear stress is increased during exercise (due to the increased blood flow), chronic EX would stimulate adaptations in vasomotor control of collateral vessels including an enhanced EDD (Laughlin et al. 2012). In addition, it appears that EX can modify the responses of vascular smooth muscle in collateral arteries as evidenced by an EX-induced reversal of the modest reduction in vasodilator responsiveness to sodium nitroprusside (Colleran et al. 2010). Colleran et al also reported that EDD responses were significantly greater to both ACh and intravascular flow in collateral arteries of EX rats. Neither blockade of COX with indomethacin nor block-

ade of endothelial nitric oxide synthase with NG-nitro-L-arginine methyl ester eliminated the increased EDDs.
The coronary literature does not consistently indicate enhanced growth of collateral arteries in models of coronary artery disease (CAD) or in patients with CAD after EX. However, it appears that EX has beneficial effects on the vasomotor reactivity of collateral arteries and/or vasomotor control of resistance in collateral-dependent myocardium. For example, it is reported that collateral-dependent coronary arteries exhibited improved EDD and improved adenosine-induced vasodilation in EX animals. EX also improved bradykinin-induced EDD in arterioles from collateral-dependent myocardium and VEGF165-induced EDD was reported to be enhanced in collateral-dependent arterioles. Fogarty et al. (2004) also reported that the enhanced VEGF-induced EDD was mediated principally via increased NO bioavailability.
EX appears to increase myogenic tone in arterioles isolated from collateral-dependent zones of models of CAD in a manner similar to that reported for arterioles from normal EX hearts (Laughlin et al. 2012). EX is also reported to enhance endothelin-1-mediated contractile responses in collateral-dependent resistance arteries and to exhibit increased basal tone, and increased K+ channel activity (Laughlin et al. 2010).

Angus et al. (1991). Cir Res 69:1340-1352.

Colleran et al. (2010) J Physiol; 588:1293-1307.

Fogarty et al. (2004) Circ. 109:664-670.

Griffin et al. (1999) J. Appl. Physiol. 87:1948-1956.

Griffin et al. (2001) Circ. 104:1393-1398.

Laughlin et al. (2012) Am J Physiol Heart Circ Physiol. 302:H10-H23

Taylor, et al. (2008) J Physiol. 586:5983-5998.

The author's work is supported by NIH grant # HL36088.

Where applicable, the authors confirm that the experiments described here conform with The Physiological Society ethical requirements.

SA297

Constraint-based analysis of energy metabolism in mitochondrial diseases

E. Marchiori and W. Megchelenbrink

Radboud University, Nijmegen, Netherlands

Genome-scale metabolic networks can be reconstructed using a constraint-based modeling approach. The stoichiometry of the network and the physiochemical laws still enable organisms to achieve certain objectives -such as biomass composition- through many various pathways. This means that the system is under-determined and many alternative solutions exist. A recent popular method used to reduce the number of alternative pathways is Flux Balance Analysis (FBA), which tries to optimize a given biological objective function. FBA does not always find a correct solution and for many networks the biological objective function is simply unknown. As a consequence researchers may have to measure certain fluxes. In this talk we discuss a method that combines a sampling approach with a greedy algorithm for finding a small given number of fluxes that, if measured, are expected to reduce as much as possible the solution space towards the true flux distribution. The method can be used for guiding the biologists to perform experimental analysis of metabolic networks. We will also shortly review studies that focus on constraint-based models of normal and malfunctioning mitochondria.

W. Megchelenbrink, M. Huynen and E. Marchiori.

Flux Measurement Selection in Metabolic Networks.

IAPR Conference on Pattern Recognition in Bioinformatics (PRIB), Lecture Notes in Computer Science, Vol. 7036, pp. 214-224, 2011.

Sangar V, Eddy JA, Simeonidis E, Price ND.

Mechanistic modeling of aberrant energy metabolism in human disease.

Front Physiol. 2012;3:404. doi: 10.3389/fphys.2012.00404.

This work has been partially funded by the Netherlands organization for scientific research (NWO) and the Netherlands organization for health research and innovation in healthcare (ZonMW).

Where applicable, the authors confirm that the experiments described here conform with The Physiological Society ethical requirements.

SA298

Detecting gene-gene interactions in genome-wide association studies of complex diseases

H.J. Cordell

Institute of Genetic Medicine, Newcastle University, Newcastle upon Tyne, UK

Over the last 5 to 6 years, genome-wide association studies (GWAS) have proved enormously successful for the detection of genomic regions that harbour genes associated with complex diseases and quantitative traits. However, moving from a replicable association signal to determination of the underlying causal genetic variant and an understanding of its mechanism has proved more challenging. The variants detected in GWAS generally confer modest effects (odds ratios of 1.5 or less), making them of limited use for risk prediction, and do not generally account for a large proportion of the observed heritability (the additive genetic contribution to the overall trait variance), suggesting there are many additional, possibly interacting, genetic contributors to be found. From a biological perspective, interactions between genes (epistasis) are expected to be ubiquitous, as complex biological phenotypes are likely to result from complex combinations of genetic (and non-genetic) factors rather than from such factors operating in isolation. In this talk I will discuss the statistical challenges involved in, and some possible strategies for, detecting and modelling gene-gene interactions using GWAS data. I will focus on some recent work carried out by ourselves and others to develop tests that show high power over a wide range of scenarios while maintaining an acceptable false positive rate.

Where applicable, the authors confirm that the experiments described here conform with The Physiological Society ethical requirements.

SA299

Molecular programming of cell and vessel phenotypes during neurovascular formation

D. Ryan, B. Long, R. Rekhi, A. Abrego, B. Zaunbrecher, A. Mahadevan and A.A. Qutub

Bioengineering, Rice University, Houston, TX, USA

Brain hypoxia affects hundreds of thousands of people annually, leading to perinatal brain injury, complications of ischemic

strokes, vascular dementia, and neurodegeneration. Despite this, there are no FDA approved drugs specifically targeting brain hypoxia. Regeneration of capillaries, or therapeutic angiogenesis, is a strategy to treat patients with brain hypoxia. One way to accomplish this is by enhancing or mimicking the body's own angiogenic response. A challenge lies in understanding this response with the mechanistic-detail needed to develop effective therapeutic strategies.
Methods: Two main growth factors that regulate angiogenic sprouting in the brain are vascular endothelial growth factor (VEGF) and brain-derived growth factor (BDNF). We present an integrated computational-experimental strategy to characterize human endothelial cell-cell interactions as a function of these proteins. We introduce a 3D "rules-as-agents" model of cell movement that allows rapid testing and comparison of multiple hypotheses to in vitro angiogenesis experiments. Endothelial cells are represented as machines that transition between finite behavior states, and their properties are explored by a genetic search algorithm. We rank and quantify differences between competing hypotheses about cell behavior during the formation of unique capillary phenotypes. We validated the 'state-machine' paradigm through in vitro assays. In vitro assays included 3D angiogenic spheroid assays and the 2D classification of primary human umbilical vein endothelial cell (HUVEC) states as a function of varying concentrations and combinations of BDNF and VEGF (control; 25 ng/ml VEGF; 50 ng/ml VEGF; 25 ng/ml VEGF, 25 ng/ml BDNF; 25 ng/ml VEGF, 50 ng/ml BDNF; 50 ng/ml VEGF, 100 ng/ml BDNF; 50 ng/ml BDNF; 100 ng/ml BDNF), at 6, 12, 24 and 48 hrs of stimulation. Hierarchical and k-means cluster analysis coupled to molecular imaging identified similarities between stimulated HUVEC based on 7 main categories including intracellular cytoskeletal regulation, actin fiber alignment, and network connectivity.
Results: Our best adaptive state machine models of endothelial cell behavior as a function of BDNF and VEGF predicted novel in vitro results within a standard deviation of all measurements (22% of models). Cluster analysis of >10,000 endothelial cells revealed a set of dominant morphological phenotypes and cell-cell connectivity. These results show that VEGF and BNDF can reproducibly induce unique frequencies of behavior; morphological angiogenic states; and cell-cell connectivity in 2D and 3D. Ongoing work involves delineating the effect of these identified endothelial cell phenotypes and networks on neural function. This work offers the ability to understand – and ultimately control – human cell behavior at the microvasculature level. Applications of these technologies include guiding regenerative therapies targeting the neurovasculature.

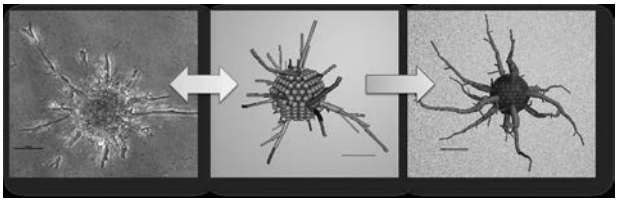

Figure 1. From in vitro observations, a framework for controlling endothelial cell behavior c(x,t) as a function of BDNF and VEGF can be created to produce a specific capillary phenotype p(x,t).

Ryan, D., Long, B., Zaunbrecher, B., Hu, J., and Qutub, A. A. (2013) A Network Analysis of Endothelial Cell Patterning. Submitted

Ryan, D., Long, B., Zaunbrecher, B., Hu, J., and Qutub, A. A. (2013) Predicting Endothelial Cell Phenotypes in Angiogenesis. Proceedings of the ASME

Long, B. L., Rekhi, R., Abrego, A., Jung, J., and Qutub, A. A. (2012) Cells as state machines: Cell behavior patterns arise during capillary formation as a function of BDNF and VEGF. J Theor Biol, in press

Schweller, R. M., Zimak, J., Duose, D. Y., Qutub, A. A., Hittelman, W. N., and Diehl, M. R. (2012) Multiplexed in situ immunofluorescence using dynamic DNA complexes. Angew Chem Int Ed Engl 51, 9292-9296

Qutub, A., Gabhann, F., Karagiannis, E., Vempati, P., and Popel, A. (2009) Multiscale models of angiogenesis. IEEE Eng Med Biol Mag 28, 14-31

Qutub, A. A., and Popel, A. S. (2009) Elongation, proliferation & migration differentiate endothelial cell phenotypes and determine capillary sprouting. BMC Syst Biol 3, 13

Qutub, A. A., and Popel, A. S. (2006) A computational model of intracellular oxygen sensing by hypoxia-inducible factor HIF1 alpha. J Cell Sci 119, 3467-3480

We thank our collaborators Michael Diehl (Rice) and Gabor Balazsi (M.D. Anderson Cancer Center), and the following funding sources: NSF CAREER Award, National Academies Keck Future Initiatives Grant, Hamill Innovation Award.

Where applicable, the authors confirm that the experiments described here conform with The Physiological Society ethical requirements.

SA300

Remembrances of things past, and the epigentic origins of phenotypic variation and disease risk

J.H. Nadeau

Pacific Northwest Research Institute, Seattle, WA, USA

Both humans and animal models provide many examples of highly heritable traits where the disease-causing genetic variants elude discovery. In these cases, heritability is often high but the explained genetic variance is low. The usual explanation involves undetected genetic variants with weak and heterogeneous actions in affected individuals. This explanation is reasonable given the limited statistical power in most genetic studies. However, we recently found several examples of heritable epigenetic changes, through the germline, suggesting that modes of inheritance other than DNA can also be transmitted across generations to affect phenotypic variation and disease risk. In each case, genetic variants in ancestral generations lead to phenotypic variation in subsequent generations. These effects can be as common and strong as those resulting from conventional inheritance, and they can persist for multiple generations. Transgenerational inheritance affects cancer, metabolic diseases, behaviors and many other traits. The effects are usually specific to one germ-lineage, with examples of transmission through the female germ-lineage and others through the paternal germ-lineage. The identity of the genes that mediate these effects implicate aspects of RNA biology including RNA editing, demethylation, translation control, and regulation of miRNA biology. These transgenerational effects challenge our understanding of inheritance and the origins of phenotypic variation and disease risk.

Where applicable, the authors confirm that the experiments described here conform with The Physiological Society ethical requirements.

SA301

Sphingolipid-induced nutrient transporter loss as a mechanism for growth control

A. Edinger

Developmental and Cell Biology, University of California Irvine, Irvine, CA, USA

All rapidly growing cells must take up extracellular nutrients at an accelerated rate to support the anabolism required to double cell mass. Restricting nutrient access will thus limit cell proliferation. Moreover, because the mutations that occur in cancer cells make them metabolically inflexible, nutrient deprivation will be more detrimental to transformed than non-transformed cells. When nutrient limited, normal cells become quiescent and catabolic, entering a hibernation-like state. Cancer cells, in contrast, cannot respond adaptively to starvation and continue to try to grow, forcing themselves into a bioenergetic crisis. As a result of these differences in metabolic wiring, a therapeutic compound that triggers nutrient transporter loss would likely be an effective and selective cancer therapy. Sphingolipids have an evolutionarily conserved role as regulators of nutrient transporter surface expression. In heat stressed stressed yeast, sphingolipids cause nutrient permease down-modulation that protects cells by slowing growth. We found that ceramide and the sphingosine-like drug FTY720 trigger the rapid down-regulation of nutrient transporter proteins in a variety of mammalian cell types. Restricting nutrient access in this way is indeed more toxic to cancer cells than to normal cells. To better understand which oncogenic mutations confer sensitivity and resistance to sphingolipid-induced nutrient transporter loss, we compared the sensitivity of TSC2 wildtype and knockout fibroblasts to ceramide. TSC2-/- cells have constitutively high mTORC1 activity. The mTORC1 kinase complex is active in most cancer cells where it drives protein translation, glycolysis, and lipid synthesis. TSC2 is a critical negative regulator of mTORC1 under unfavorable growth conditions. Because they cannot reduce anabolism, TSC2-/- cells are hypersensitive to glucose withdrawal. Surprisingly, we found that TSC2-/- cells were resistant to death induced by sphingolipids. Although amino acid and glucose transporters were initially down-regulated, TSC2-/- cells mounted an exaggerated adaptive response to nutrient stress exhibiting a dramatic, mTORC1-dependent up-regulation of new transporter proteins. Patients heterozygous for inactivating mutations in TSC1 or TSC2 develop benign hamartomatous growths and we propose that this loss of tissue homeostasis might be due in part to the ability of TSC1/2 deficient cells to overcome nutrient or ceramide enforced limits on growth. Interestingly, these hamartomas do not progress to malignant disease. Consistent with this, we found that introducing the potently transforming H-RasV12 mutant reversed the survival advantage of TSC2-/- MEFs, apparently by increasing nutrient demand. These results support the idea that fully transformed cancer cells will be susceptible to drugs targeting transporter proteins. Along these lines, we are developing new analogs of FTY720. FTY720 is effective in multiple animal models of cancer, but cannot be used in human patients because it causes profound bradycardia by affecting sphingosine-1-phosphate receptors 1 and 3. We have found that FTY720's effects on S1P receptors and nutrient transporter proteins are separable and unrelated. FTY720 analogs designed to lack S1P activity are effective anticancer agents both in vitro and in vivo. Moreover, these compounds show striking synergy with other compounds targeting the metabolic changes associated with cancer including mTORC1 activation. Together, these studies suggest that these novel compounds targeting multiple nutrient transporters simultaneously could prove to be safe and effective anti-cancer therapies.

Where applicable, the authors confirm that the experiments described here conform with The Physiological Society ethical requirements.

SA302

Cellular nutrient sensing in cancer

D.C. Goberdhan

Physiology, Anatomy and Genetics, University of Oxford, Oxford, Oxon, UK

The fundamental cellular roles of mechanistic (formerly mammalian) Target of Rapamycin Complex 1 (mTORC1) activity are evident from the wide range of major human diseases in which it is misregulated, including the majority of human cancers, neurodegenerative disorders, cardiovascular disease, diabetes, obesity and other age-related disorders. mTORC1 is a key signalling hub that controls cellular homeostasis by responding to a diverse range of physiological inputs, like endocrine insulin/insulin-like growth factors (IGFs), energy levels (ATP:AMP ratio), oxygen levels, and local amino acid (AAs) to modulate cellular metabolism and growth (reviewed in Malik et al., 2012 [epub]). There are, however, still significant gaps in our understanding of local AA regulation of mTORC1, which takes place at the surface of late endosomes and lysosomes (LELs; reviewed in Durán and Hall 2012). Intracellular AAs have been highlighted as playing a key role in activating mTORC1, via two very different, but not necessarily mutually exclusive mechanisms. The first involves sensing of cytosolic leucine and the second the sensing of AA within late endosomes and lysososomes (LELs).

Charged Leucyl tRNA Synthetase (LRS) seems to act as a direct sensor of cytosolic leucine levels, leading to interaction with the Rag GTPases on LELs and subsequent activation of mTORC1. However, the proposed mechanism differs significantly between human cells and yeast, and a key residue involved in the human mechanism is not conserved in fly LRS (reviewed in Durán and Hall 2012).

Unbiased screening in flies and subsequent analysis in human cells led us to identify the Proton-assisted Amino acid Transporter (PAT/SLC36) family located at the surface of LELs, as central players in AA-dependent mTORC1 activation (Heublein et al., 2010; Ögmundsdóttir et al., 2012). Our studies have focused on the two ubiquitous human PAT transporters, PAT1 and PAT4. While modest overexpression of PAT1 leads to mTORC1 activation and increased cell growth and proliferation (Ögmundsdóttir et al., 2012, higher levels reduce tissue growth and mTORC1 signalling (Goberdhan et al., 2005; Zoncu et al., 2011), most likely due to a dominant negative effect. The discovery that LEL-located PAT1 interacts with Rags and is required to activate mTORC1 and promotes cell proliferation, together with a substantial amount of work from the Sabatini lab, has highlighted a multi-protein complex that we have called the 'nutrisome', located on the LEL surface. The nutrisome appears to respond to the intraluminal pool of AA within LELs, reflects LEL extracellular AA levels (for details see Figure 1; reviewed in Malik et al., 2012 [epub]).

Aggressive tumour cells are able to survive and grow even when poorly vascularised with limited access to growth factors and nutrients. These microenviromental stresses lead to the induction of autophagy, resulting in the build-up of AA

within autolysosomes. The PAT1-containing nutrisome (Figure 1) is well placed to utilise these luminal nutrients to maintain a residual level of mTORC1 activity and maintain homeostasis within the cell until conditions improve (reviewed in Goberdhan, 2010). We have previously shown in vivo in flies that when PI3K signalling is increased, as is the case in the majority of human cancers, the growth-promoting properties of the PATs are enhanced. PATs, which are normally distributed between intracellular membranes and the cell surface, become more intracellular in these conditions, a trafficking process that is required for increased growth (Ögmundsdóttir et al., 2012). I will present data showing that PI3K is also involved in PAT regulation in colon cancer cell lines, particularly under stress conditions.

I will also discuss the analysis we have performed using IPTG-inducible shRNA constructs targeting PAT4 in HCT116 tumours using in vitro and xenograft models. Combined with expression studies in human tumour samples, this work suggests a role for PAT4 in tumour progression.

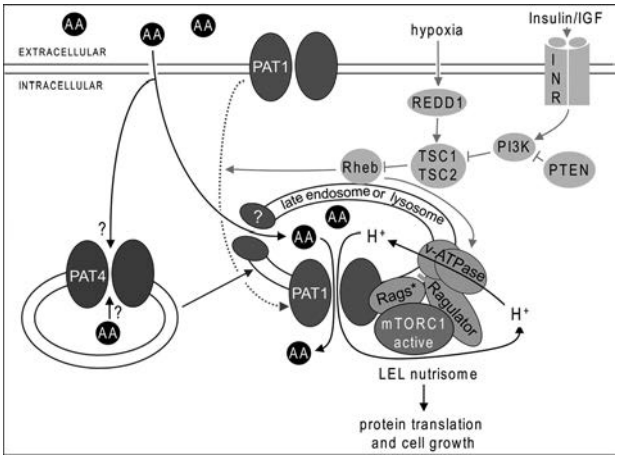

Figure 1 | Schematic model shows the PAT1 protein complex that we have identified in HEK-293 cells and dubbed the 'nutrisome'. This is formed on LELs following stimulation of cells with extracellular amino acids (AAs). AA stimulation also leads to the rapid build-up of AA within LELs via an unknown mechanism. Components of the nutrisome, namely the activated Rag heterodimer (Rags*), pentameric Ragulator, PAT1 and v-ATPase proton pump are required for mTOR to shuttle to LELs to form active mTORC1 and promote cell growth. Cycling of protons through the nutrisomal engine or binding of AA to PAT1 may lead to conformational changes in the complex that activate mTORC1. PI3K/Akt/Rheb signalling regulates endocytosis of the PATs in flies and may also regulate PAT1 (dotted arrow) subcellular localisation. PAT4, like PAT1, is required for AA-stimulated mTORC1 activation and cell proliferation, but its subcellular localisation is currently unclear.

Malik AR, Urbanska M, Macias M, Skalecka A, Jaworski J Beyond control of protein translation: What we have learned about the non-canonical regulation and function of mammalian target of rapamycin (mTOR). Biochim Biophys Acta 2012 Dec 29. doi:pii: S1570-9639(12)00290-7. 10.1016/j.bbapap.2012.12.010. [Epub ahead of print]

Durán RV, Hall MN (2012) Leucyl-tRNA synthetase: double duty in amino acid sensing. Cell Res 22, 1207-9.

Heublein, S, Kazi, S, Ögmundsdóttir, MH, Attwood, EV, Kala, S, Boyd, CAR, Wilson, C and Goberdhan, DC (2010) Proton-assisted amino-acid transporters are conserved regulators of proliferation and amino-acid-dependent mTORC1 activation. Oncogene 29, 4068-79.

Ögmundsdóttir, MH, Heublein S, Visvalingam, SM, Reynolds, B, Kazi, S, Shaw, M, Goberdhan, DC (2012) Proton-Assisted amino acid transporter PAT1 complexes with Rag GTPases and activates TORC1 on late endosomal and lysosomal membranes. PLoS ONE 7, e36616.

Goberdhan, DC, Meredith, D, Boyd, CAR and Wilson, C (2005) PAT-related amino acid transporters regulate growth via a novel mechanism that does not require bulk transport of amino acids Development 132, 2365-75.

Zoncu R, Bar-Peled L, Efeyan A, Wang S, Sancak Y, Sabatini DM (2011) mTORC1 senses lysosomal amino acids through an inside-out mechanism that requires the vacuolar H-ATPase. Science 334, 678-83.

Goberdhan, DC (2010) Intracellular amino acid sensing and mTORC1 regulated growth; new ways to block an old target? Curr Opin Invest Drugs 11, 1360-7.

This work was supported by funding to DCIG from Cancer Research UK (CR-UK) grant numbers C19591/A6181, C19591/A9093, C7713/A6174 and also C38302/A12278, through the Oxford Cancer Research Centre Development Fund.

Where applicable, the authors confirm that the experiments described here conform with The Physiological Society ethical requirements.

SA303

The role of heterodimeric transporters in cancer cell growth

Y. Kanai

Division of Bio-system Pharmacology, Department of Pharmacology, Osaka University Graduate School of Medicine, Osaka, Japan

Heterodimeric transporters belong to SLC7 cationic amino acid transporter/glycoprotein-associated family. They are composed of single membrane-spanning glycosylated heavy chains and non-glycosylated multiple membrane-spanning light chains. The light chains are catalytic subunits responsible for substrates transport, whereas the heavy chains are accessory subunits that form complexes with the light chains via a disulfide bond and assist the membrane localization of the heterodimeric complexes. In addition to the roles in membrane sorting of the transporters, one of the heavy chains 4F2hc (4F2 heavy chain; CD98hc; SLC3A2) is involved in multiple protein-protein interactions and generates growth signals presumably through the interactions with integrins. The substrates of such heterodimeric transporters are in general amino acids. Among the heterodimeric transporters, LAT1 (SLC7A5) and xCT (SLC7A11), both of which form heterodimers with 4F2hc, have been demonstrated to be upregulated in cancers. LAT1, as described bellow, mediates uptake of the large neutral amino acids for cellular nutrition and mTOR signaling, whereas xCT is responsible for the uptake of cystine for cellular glutathione production to protect cells from oxidative stress. The upregulation of xCT in cancer stem cells has been reported to be responsible for the resistance to drug and radiation therapy.

In terms cellular metabolism, amino acid transporters mediate cellular uptake of amino acids for cells to growth and survive. They are regulated to keep up with the metabolic status so that living cells take up amino acids depending on the metabolic requirements. In tumor cells, amino acid transporters are upregulated to support massive protein synthesis for continuous growth and proliferation. Among amino acid transporters expressed in tumor cells, system L transporters have been proposed to be crucial to supply tumor cells with large neutral amino acids including many essential amino acids. Among them, LAT1 (L-type amino acid transporter 1) is highly expressed in human malignant tumors. In contrast, cells in normal tissues express other amino acid transporters including the other isoform of system L transporter LAT2. We have found

that the high expression of LAT1 in tumors is correlated with poor prognosis. Thus, LAT1 can be a molecular target for the diagnosis of cancers. In fact, many radiolabeled amino acid probes used for bio-imaging and diagnosis of cancers are the substrates of LAT1. Among them, 18F-FAMT (L-[3-18F]-alpha-methyltyrosine) is selective for LAT1 and an excellent probe in positron emission tomography (PET) for the diagnosis of cancers. Different from 18F-FDG (fluorodeoxy glucose) conventionally used for PET diagnosis of cancers, 18F-FAMT is specific to cancers and not accumulated in non-cancerous legions. Additionally, 18F-FAMT can be applied to brain tumors because the brain background is low in 18F-FAMT PET.

Because LAT1 is upregulated in tumor cells to support continuous growth and proliferation, the inhibition of LAT1 is expected to suppress cancers. We have examined the effect of inhibition of LAT1 on tumor growth and found that a classical system L inhibitor, 2-aminobicyclo-(2,2,1)-heptane-2-carboxylic acid (BCH), and an antisense oligonucleotide designed against LAT1 inhibits the proliferation of tumor cells and suppressed the growth of tumors subcutaneously inoculated to nude mice. In agreement with this, the inhibition of LAT1 by BCH and the antisense oligonucleotide prolongs the survival of tumor-bearing mice. In order to design the LAT1-specific high-affinity inhibitors, we examined the properties of substrate recognition by LAT1. We found that LAT1 relies on the ionic interaction with alpha-carboxyl group and alpha-amino group and on the hydrophobic interaction with the substrates. Based on this, we designed chemical compounds and obtained LAT1 inhibitors with an affinity ~1,000 fold higher that that of BCH. They effectively suppressed tumor growth in vivo and in vitro at lower doses compared with those for BCH. These observations conclude that LAT1 is essential for cancer cell growth and progression of cancers. Additionally, it is proposed that the inhibition of LAT1 could be a new rationale to anti-tumor therapy.

In cancer cells, LAT1/4F2hc forms further molecular complexes with other membrane proteins such as integrins, CD147 and amino acid transporter ASCT2. ASCT2 mediates the influx of glutamine and assists the influx of essential amino acids including leucine through LAT1 via exchange mechanism. Such "transportsome" is essential for the activation of mTOR signaling in cancer cells. In the lecture, the role of LAT1/4F2hc heterodimeric complex in cancer cell growth will be discussed in terms cellular signaling originated from both LAT1 and 4F2hc.

Where applicable, the authors confirm that the experiments described here conform with The Physiological Society ethical requirements.

SA304

The role of monocarboxylate transporters in cancer microenvironment

F. Baltazar

Life and Health Sciences Research Institute (ICVS), School of Health Sciences, University of Minho, Braga, Portugal and ICVS/3B's - PT Government Associate Laboratory, Braga/Guimarães, Portugal

One essential hallmark of tumour cells is altered metabolism (1). Most tumour cells exhibit high rates of glycolysis, even in the presence of oxygen ("Warburg effect"), resulting in increased production of lactate, which is transported out of the cells, contributing to the acidic microenvironment encountered in tumours. The acidic microenvironment has been associated with invasive behaviour, mutagenesis as well as radio- and chemoresistance (2). More recently, several authors have proposed a metabolic complementarity between tumour and stroma. If the tumour is glycolytic, the associated stroma is more oxidative and vice-versa. The latter process is known as the "reverse Warburg effect" (3).

Monocarboxylate transporters (MCTs), by performing the plasma membrane efflux of lactate coupled with a proton, especially the isoforms 1 (MCT1) and 4 (MCT4), play an important role in the maintenance of the metabolic phenotype of tumours and associated stroma. MCT1 has been more associated with cells exhibiting an oxidative phenotype, being involved in lactate uptake, while MCT4 has been associated with the glycolytic phenotype, being responsible for lactate efflux (4).

Our group has been studying the expression of these MCT isoforms as well as their chaperone, CD147, essential for MCT activity and plasma membrane expression, in several series of human cancers (5). We found upregulation of MCT1 and MCT4 colorectal cancer, upregulation of MCT1, MCT4 and CD147 in cervical cancer, upregulation of MCT1 in breast cancer and upregulation of MCT1 and CD147 in glioblastomas, compared to the corresponding non-neoplastic tissues. On the other hand, there was downregulation of MCT4 in gastric cancer and downregulation of MCT1 in prostate cancer. We also found important associations between MCT overexpression and the clinicopathological data of the cases, mostly with aggressiveness parameters. Due to their role in the maintenance of tumour metabolism, MCTs are considered promising targets in cancer therapy. Thus, we are also studying the effects of MCT inhibition using different tumour models. In general, MCT inhibition in glycolytic tumour cells leads to a decrease in lactate production, cell proliferation, migration and invasiveness (6).

In summary, MCT activity is essential for the maintenance of the metabolic phenotype of tumours, playing a key role in the crosstalk between tumour cells and microenvironment. However, MCTs are differentially expressed among the solid tumours and future strategies of MCT inhibition in cancer treatment should take this fact into account.

Hanahan D & Weinberg RA (2011). Cell 144, 646-674.

Gatenby RA & Gillies RJ (2004). Nat Rev Cancer 4, 891–899.

Pavlides S et al. (2009). Cell Cycle. 8, 3984-4001.

Sonveaux P et al. (2008). J Clin Invest 118, 3930–3942.

Pinheiro C et al. (2012). J Bioenerg Biomembr 44, 127-139.

Miranda-Gonçalves V et al. (2013). Neuro Oncol 15, 172-188.

This work was partially supported by FCT grant ref. PTDC/SAU-FCF/104347/2008, under the scope of ''Programa Operacional Temático Factores de Competitividade'' (COMPETE) of ''Quadro Comunitário de Apoio III'' and co-financed by Fundo Comunitário Europeu FEDER.

Where applicable, the authors confirm that the experiments described here conform with The Physiological Society ethical requirements.

SA305

SLC6A14 as a drug target for cancer therapy

V. Ganapathy, M. Thangaraju, P.D. Prasad, V. Coothankandaswamy and Y. Bhutia

Biochemistry and Molecular Biology, Georgia Regents University, Augusta, GA, USA

"Starve the tumor cells to death" - A novel therapeutic approach with a logical basis: Rapid growth is a hallmark of cancer, a feature that places increased demand for nutrients. Entry of nutrients into tumor cells is enhanced by upregulation of specific transporters; these transporters have potential as drug targets for cancer therapy. If we can interfere with the entry of essential nutrients into tumor cells, we should be able to starve these cells to death. If the transporters that are specifically induced in tumor cells compared to normal cells are identified, blocking the function of the induced transporters would have potential as a logical therapeutic strategy for cancer treatment. Since normal cells don't depend on these transporters for survival, cell death induced by such a strategy would be tumor-specific, with little off-target effects.

Amino acid nutrition in cancer: Tumor cells have an increased need for amino acids to support protein/nucleotide synthesis. Mammalian cells cannot synthesize essential amino acids; they must obtain these amino acids via specific transporters. Glutamine, though a non-essential amino acid, is critical for tumor cells. Tumor cells are addicted to glutamine ("glutamine addiction") and metabolize glutamine through a novel pathway known as "glutaminolysis" (1). Amino acids are also coupled to cell signaling via the mammalian target of rapamycin (mTOR), which integrates signals from growth factors, energy status, and amino acid nutritional status, and coordinates these signals with cell growth (2). Inhibitors of mTOR are in clinics for cancer treatment. Amino acid deprivation in tumor cells would also be expected to interfere with mTOR signaling.

SLC6A14 as a novel drug target for treatment of cancer: Mammalian cells express ~40 amino acid transporters that are expressed in different combinations in a cell type-specific manner. Among them, one transporter stands out as unique based on its functional features. It is SLC6A14 (3). It transports all essential amino acids as well as glutamine. It is exceptionally concentrative, coupled to a Na+ gradient, a Cl- gradient, and membrane potential. It is expressed at low levels in normal tissues, but is induced in colon cancer (4), cervical cancer (5), estrogen receptor (ER)-positive breast cancer (6), and pancreatic cancer. Tumor cells upregulate SLC6A14 to meet their increased demand for essential amino acids and glutamine, indicating that SLC6A14 drives their "glutamine addiction." Therefore, blocking the function of this transporter would starve these tumor cells to death. We have shown that this indeed is the case. Down-regulation of SLC6A14 in colon cancer cells, ER-positive breast cancer cells, and pancreatic cancer cells with shRNA suppresses the growth of these cells in mouse xenografts. We have also identified α-methyl-L-tryptophan (α-MLT) as a selective blocker of SLC6A14. α-MLT induces amino acid starvation and death in SLC6A14-positive cancer cells in vitro and inhibits their growth in mouse xenografts. The growth of SLC6A14-negative cancer cells is not affected under similar conditions, demonstrating lack of off-target effects. The blockade of SLC6A14 induces cell death in SLC6A14-positive tumor cells by three different mechanisms: it prevents the entry of essential amino acids, it targets the "glutamine addiction" behavior, and it inhibits mTOR (7). We have recently generated Slc6a14-null mouse. The mouse is viable and fertile, suggesting that SLC6A14 is not essential for normal tissues. Since cancer cells selectively induce SLC6A14 to meet their increasing demands for amino acids, we predicted that deletion of Slc6a14 would provide protection against cancer. This indeed is the case.

α-MLT could be used as a drug in clinical trials for treatment of colon cancer, pancreatic cancer, cervical cancer, and ER-positive breast cancer. It can also serve as a lead compound for development of new and more potent anti-cancer drugs targeting SLC6A14. Another strategy is to develop monoclonal antibodies against SLC6A14 with ability to block the transporter function. Such biologicals would also be effective in the treatment of SLC6A14-positive tumors in a manner similar to the currently used cancer therapies with monoclonal antibodies targeting EGF receptor, VEGF receptor, and HER2.

SLC6A14 is not a universal drug target for all cancers. Some cancers, e.g., ER-negative and triple-negative breast cancers, do not upregulate SLC6A14 and therefore will not respond to blockers of the transporter. But success of our studies demonstrating SLC6A14 as a viable drug target for colon cancer, cervical cancer, pancreatic cancer, and ER-positive breast cancer provides a rational basis for identification of new amino acid transporters as drug targets for other types of cancers because the SLC6A14-negative cancer subtypes must upregulate some other amino acid transporters to support their growth.

Wise, D. R., and Thompson, C. B. (2010) Glutamine addiction: a new therapeutic target in cancer. Trends Biochem. Sci. 35: 427-433.

Ganapathy, V., Thangaraju, M. and Prasad, P. D. (2009) Nutrient transporters in cancer: Relevance to Warburg hypothesis and beyond. Pharmacol. Ther. 121: 29-40.

Ganapathy, M. E., and Ganapathy, V. (2005) Amino Acid Transporter ATB0,+ as a delivery system for drugs and prodrugs. Curr. Drug Targets Immune Endocr. Metabol. Disord. 5: 357-364.

Gupta, N., Miyauchi, S., Martindale, R. G., Herdman, A. V., Podolsky, R., Miyake, K., Mager, S., Prasad, P. D., Ganapathy, M. E., and Ganapathy, V. (2005) Upregulation of the amino acid transporter ATB0,+ (SLC6A14) in colorectal cancer and metastasis in humans. Biochim. Biophys. Acta 1741: 215-223.

Gupta, N., Prasad, P. D., Ghamande, S., Martin, P. M., Herdman, A. V., Martindale, R. G., Podolsky, R., Mager, S., Ganapathy, M. E., and Ganapathy, V. (2006) Upregulation of the amino acid transporter ATB0,+ (SLC6A14) in carcinoma of the cervix. Gynecol. Oncol. 100: 8-13.

Karunakaran, S., Umapathy, N. S., Thangaraju, M., Hatanaka, T., Itagaki, S., Munn, D. H., Prasad, P. D. and Ganapathy, V. (2008) Interaction of tryptophan derivatives with SLC6A14 (ATB0,+) reveals the potential of the transporter as a drug target for cancer chemotherapy. Biochem. J. 414: 343-355.

Karunakaran, S., Ramachandran, S., Coothankandaswamy, V., Elangovan, S., Babu, E., Periasamy-Thandavan, S., Gurav, A., Gnana-Prakasam, J., Singh, N., Schoenlein, P. V., Prasad, P. D., Thangaraju, M., and Ganapathy, V. (2011) SLC6A14 (ATB0,+), a highly concentrative and broad-specific amino acid transporter, is a novel and effective target for treatment of estrogen receptor-positive breast cancer. J. Biol. Chem. 386: 31830-31838.

Where applicable, the authors confirm that the experiments described here conform with The Physiological Society ethical requirements.

SA306

Behavioural ecology of the gut

T. Piersma, A. Dekinga, A. Bijleveld, T. Oudman and J.A. van Gils

Marine Ecology, NIOZ Royal Netherlands Institute for Sea Research, Den Burg, Netherlands

We look at the gut as the biggest interface between an organism and its environment. Guts are responsive to many external conditions (food availability, pathogen pressure and nutritional demands), whilst at the same time serving internally orchestrated seasonal fitness functions. In our work on the ecology and evolution of shorebirds, i.e. seasonal migrants that travel the length and with of the globe but with distinct habitat preferences, we have taken the gut as a consequential and fully integrated part of the organism-environment interaction. We will review how different parts of the gut respond to changes in food quality and demand, even representing strategic design solutions to challenges and habitats encountered next. Our prime example are molluscivore specialists (especially red knots, Calidris canutus) that in some conditions trade a hard-shell-processing against a food-toxin constraint. A novel level of organismal integration is suggested by the finding that personality differences between individuals correlate with gut size in seemingly adaptive ways.

Piersma, T. & van Gils, J.A. (2011). The flexible phenotype. A body-centred integration of ecology, physiology, and behaviour. Oxford: Oxford University Press.

Where applicable, the authors confirm that the experiments described here conform with The Physiological Society ethical requirements.

SA307

Flexibility of the gut during the neonatal period: does it have consequences later in life?

G. Boudry

INRA UR 1341 ADNC, St-Gilles, France

Early life nutrition impacts durably several physiological and metabolic functions and is a risk factor for the development of metabolic disease in adults (obesity, type 2 diabetes, hypertension, ...). This theory of nutritional imprinting or Developmental Origin of Health and Disease established by Barker in the late 80's (1) has been reinforced by experimental data on organs and tissues directly involved in the pathophysiology of the metabolic syndrome (liver, adipose tissue, pancreas...) (2). The gut has got little attention in this context so far. Yet, evidences for a role of the gut in the pathophysiology of metabolic diseases in adults, especially with gut microbiota and barrier function maladaptation to a high fat diet, have emerged (3-4). The structure of the gut microbiota is established and the mucosal immune system programed in early life. This postnatal development is not hard-wired and is influenced by environmental and nutritional factors. Man can hypothesize that this flexibility in acquisition of the microbiota and education of the gut immune system in early life would be long-lasting and induce distinct response to a high fat diet later in life. There are already several evidences that early life environmental factors including stress such as maternal deprivation or chemical contaminants such as bisphenol A dramatically impact adult response to gut inflammation or visceral painful stimuli in models of inflammatory bowel disease and irritable bowel syndrome. Recently, evidences have also emerged that nutritional factors, including energy, fat and fatty acids, protein, and micronutrients imbalances during early life have remnant effects of gut function in adults with alterations in microbiota, intestinal barrier function and/or defense systems. Examples of such long-term effects on the gut will be provided, focusing on piglet model and adaptation to a high fat diet. Those emerging data challenges neonatal nutrition which, apart from its traditional role as a supplier of building blocks for growth, may play another, yet potentially crucial role in shaping the individual's future life, impinging on the risk of disease decades later on.

Barker et al. (1989) Lancet, 2:577-80

Hales et al. (1991) BMJ, 303:1019-22

Cani & Delzenne (2009) Curr. Pharm. Des. 15:1546-1558

Turnbaugh et al. (2006) Nature, 444:1027-31

Where applicable, the authors confirm that the experiments described here conform with The Physiological Society ethical requirements.

SA308

Diverse feeding regimes and gut flexibility in ectotherms

S. Secor

Department of Biological Sciences, University of Alabama, Tuscaloosa, AL, USA

Animals exhibit a wide diversity of feeding habits, within which exists a broad continuum of feeding frequencies and feeding patterns. At one end of the continuum are small endotherms that seemingly are continuously digesting to maintain their high metabolic rates, whereas at the opposite end of the spectrum are large ectotherms that as a function of their foraging habits and low energy demands, feed relatively infrequently. In addition, many animals experience each year an extended period of fasting due to the lack of food, harsh conditions, or the conflicting demands of reproduction. Driven by very predictable long episodes of digestive quiescence and the elevated cost of maintaining an active gut, selection would favor the down regulation of GI performance during such fasting periods. Consequently, such an adaptive response would require the capacity to rapidly upregulate GI function with feeding. While such examples of phenotypic flexibility are prevalent across vertebrate taxa, the most striking cases are observed for ectotherms, especially snakes. Studies with snakes have identified a remarkable adaptive interplay between feeding habits and the capacity to regulate intestinal form and function. Species of snakes that feed infrequently in the wild (e.g., pythons, boas, and rattlesnakes) experience with the completion of digestion the downregulation of intestinal hydrolase and transporter activities and atrophy of the intestinal epithelium. Feeding triggers the immediate upregulation of intestinal function and rapid hypertrophy of the epithelium. In contrast, snakes that feed relatively frequently in the wild (i.e., many colubrids) experience only modest regulation of intestinal form and function with feeding and fasting. These snakes, as is the case for many other vertebrates, maintain an active gut between meals. Significant modulation of intestinal structure and function with fasting and feeding have likewise been observed for fishes and amphibians, the latter best exemplified by species that aestivate during dry seasons. The cellular mechanism largely responsible for this dichotomy in intestinal response resides with the extent that the microvilli

modulate their surface area. Fasting triggers a rapid shortening of the intestinal microvilli for infrequently feeding snakes, with is reversed with feeding. The 5-fold changes in microvillus length and surface area with fasting and feeding match the magnitude of change of intestinal function. Frequently feeding snakes do not alter microvillus length with feeding, and hence do not experience any significant change in function. Examined for the Burmese python is that feeding triggers a very rapid genomic response; evident by the more than 2000 intestinal genes whose expression are significantly regulated with feeding. A close examination of the adaptive interplay between snake feeding habits and gastrointestinal regulation reveal two caveats, that feeding habits of snakes are highly phylogenetically conserved and that feeding frequency is spread over a broad continuum. Hence, modes of digestive response may be dictated by phylogeny, rather than as adaptations, and species with intermediate feeding habits or that exhibit interpopulation variation in feeding habits, may experience intermediate or alternative mechanisms of digestive response. Preliminary data for boas suggest that feeding habits trumps phylogeny in determining the mode of intestinal response to feasting. Early exploration of the intestinal response of the generalist feeding viperid, the water moccasin (*Agkistrodon piscivorus*), has found modest regulation of intestinal morphology across populations. Driven by the fitness-based selection of optimizing energy, animals have evolved the integrative machinery to alter gastrointestinal performance based on the periodicity and magnitude of digestive demand.

Support for this research was provided by the National Institutes of Health, the National Science Foundation, and the University of Alabama.

Where applicable, the authors confirm that the experiments described here conform with The Physiological Society ethical requirements.

SA309

Assessing the interplay between digestive flexibility and community structure in a Neotropical fish assemblage

N. Vidal, N. Zaldúa, A. D'Anatro and D. Naya

Universidad de la Republica, Montevideo, Uruguay

Phenotypic plasticity has been suggested as the main mechanism for species persistence under a global environmental change scenario (e.g., Charmentier et al. 2008; Deutsch et al. 2008). However, standard models aimed to predict the effect of climatic change on species distribution do not allow for the inclusion of differences in plastic responses among populations. This is mainly because we still lack quantifications of plasticity for several traits in several populations for each species to be modelled. An encouraging pathway that could bring closer our ability to made realistic predictions on species persistence with the pace of current environmental changes, is the identification of general patterns in phenotypic plasticity, which could be easily incorporated into the models (Molina-Montenegro and Naya 2012). In line with this, several studies analyzing latitudinal patterns in phenotypic plasticity have been published in the recent years (Naya et al. 2008; Kellerman et al. 2009; Molina-Montenegro and Naya 2012). However, very few studies have evaluated phenotypic plasticity at the local community level, considering, for example, plastic responses in an entire species assemblage (but see Peacor et al. 2012). In addition, no one of them has addressed the relationship between phenotypic plasticity and basic community structure attributes, such as species trophic habits, body mass and relative abundance. Within this context, here we assessed seasonal flexibility and flexibility during short-term fasting in digestive organs size for an entire fish assemblage, comprising ten species, four trophic levels, and a 37-fold range in body mass. Specifically, we were aimed to test the following hypothesis: (1) Given that species occupying lower trophic levels mainly consume resources that are abundant all year round (e.g., detritus, periphyton), while species occupying higher trophic levels typically predate on resources that markedly change in abundance between seasons f(e.g., insects, fish larvae); we predict a positive relationship between seasonal digestive flexibility and trophic position; (2) Given that food intake rates scale with body mass with an exponent lower than one (typically between 0.66 and 0.75), while organs size scale with body mass isometrically; we predict a negative relationship between digestive flexibility during fasting and body size; (3) Given the potential impact of digestive flexibility on organisms' fitness, we predict that more flexible species, both in a seasonal and short-term basis, should have greater relative abundances than less flexible species. In agreement with our predictions, we found that: (1) Seasonal flexibility in intestinal length was correlated with species trophic position, as could be expected from seasonal changes in species diet composition and energetic demands; (2) Flexibility during fasting in intestine and liver dry masses were inversely correlated with body size, as expected from scaling relationships; (3) Flexibility in intestinal mass, both seasonal and during fasting, was positively correlated with species relative abundance. In summary, our study identified three interesting trends in digestive flexibility in relation to community structure attributes, which represent an encouraging departure point in the search of general patterns in plasticity at the local community scale. The fact that rare species were the less flexible is, however, worrisome under the current scenario of global environmental change.

Charmentier A, McCleery RH, Cole LR, Perrins C, Kruuk LEB, Sheldon BC. 2008. Adaptive phenotypic plasticity in response to climate change in a wild bird population. Science 320:800-803.

Deutsch CA, Tewksbury JJ, Huey RB, Sheldon KS, Ghalambor CK, Haak DC, Martin PR. 2008. Impacts of climate warming on terrestrial ectotherms across latitude. Proc. Natl. Acad. Sci. USA 105:6668-6672.

Kellerman V, van Heerwaarden B, Sgro CM, Hoffmann AA. 2009. Fundamental evolutionary limits in ecological traits drive Drosophila species distributions. Science 325:1244-1246.

Molina-Montenegro MA, Naya DE. 2012. Latitudinal patterns in phenotypic plasticity and fitness-related traits: assessing the climatic variability hypothesis with an invasive plant species. PLoS ONE: e47620.

Naya DE, Bozinovic F, Karasov WH. 2008. Latitudinal trends in physiological flexibility: testing the climatic variability hypothesis with data on the intestinal length of rodents. Am. Nat. 172:E122-E134.

Peacor SD, Pangle KL, Schiesari L, Werner E.E. 2012. Scaling-up antipredator phenotypic responses of prey: impacts over multiple generations in a complex aquatic community. Proc. R. Soc. Lond. B 279: 122-128.

Where applicable, the authors confirm that the experiments described here conform with The Physiological Society ethical requirements.

SA310

Host-gut microbe symbioses and adaptation to dietary change

H.V. Carey

Comparative Biosciences, University of Wisconsin, Madison, WI, USA

The vertebrate gut is home to trillions of microbes that have evolved complex, mutualistic relationships with their hosts. The microbiota has profound and diverse effects on animal development and physiology (McFall-Ngai et al., 2013), perhaps best exemplified in the gastrointestinal tract which has been shaped through evolution to achieve a tolerant, cooperative relationship with gut symbionts. Host diet is a major factor that influences the diversity and abundance of the microbiota. To meet their metabolic needs, most gut microbes (in non-ruminant animals) utilize dietary components that have escaped small intestinal digestion and absorption. Certain host-derived substrates, such mucin glycans and nutrients in shed epithelial cells, can also be metabolized. Our recent studies have focused on the role of gut microbiota in shaping seasonal flexibility in gastrointestinal structure and function in hibernating mammals. As in other seasonal hibernators, 13-lined ground squirrels undergo a distinct annual cycle that prepares them for the physiological extremes that occur during the winter months. After emergence in spring when body mass is at a nadir, ground squirrels fatten through summer and fall, and then gradually reduce food intake and activity until emergence into burrows. Food intake ceases once hibernation begins and metabolism shifts to a primary reliance on lipids for fuel. Although periods of extended fasting are a normal and necessary component of the annual hibernation cycle, they have the potential to compromise gastrointestinal integrity. The absence of enteral nutrients, particularly in species that do not fast on a regular basis, can reduce expression of brush border enzymes and nutrient transporters and increase intestinal permeability, which elevates the risk of bacterial translocation. In contrast, species that hibernate display a remarkable degree of adaptive flexibility in gut structure and function that minimizes adverse changes during winter fasting. Seasonal cycles of feeding and fasting can also impact the relationship between hibernators and their resident gut microbes. In 13-lined ground squirrels, the microbiota associated with luminal contents undergoes seasonal restructuring during the hibernation season that reflects shifts in taxonomic groups that rely to varying degrees on dietary vs. host-derived substrates (Carey et al., 2013). Although microbial metabolism is largely suppressed during the low body temperatures of winter torpor, periodic arousals to euthermia provide sufficient time for microbial degradation of endogenous substrates, resulting in production of short-chain fatty acids that can be utilized by the host. Seasonal flexibility in host characteristics likely contributes to maintenance of a mutually beneficial, tolerant state. For example, several features of the intestinal immune system, which is the primary sensor of gut microbes and their metabolites, are modified during hibernation in a manner indicative of altered host-microbe signaling in the absence of inflammation or pathologic immune cell infiltration (Kurtz and Carey, 2007). Enterocytes in hibernating squirrels increase expression of the tight junction protein occludin, which may help to restrict paracellular movement of bacterial metabolites in the setting of a "leakier" gut (Carey et al., 2012). Mucin protein expression also rises shortly after hibernation begins, which is important because the mucus layer both protects the host epithelium from microbial invasion and provides metabolizable substrates for microbial proliferation. Mucus production in the hibernator gut may be particularly important for the mucosa-associated microbiota, a population that resides adjacent to the epithelium in the mucus layer. Our recent studies indicate that the mucosal microbiota undergoes some of the same seasonal trends as seen in the luminal population, e.g., reductions in relative abundance of Firmicutes taxa and increases in abundance of Bacteroidetes and Betaproteobacteria. Phylogenetic diversity across the annual cycle is highest and lowest in microbiotas of spring and late winter squirrels, respectively. Together, these studies emphasize that investigation of gastrointestinal flexibility in animals should incorporate the potential contributions of gut microbes, which can have profound effects on their hosts beginning at birth and extending into adulthood through recurring seasonal events that affect the host-microbial symbiosis.

Carey, H.V., Pike, A.C., Weber, C.R., Turner, J.L., Visser, A., Beijer-Liefers, S.C., Bouma, H.R., and Kroese, F.G.M. (2012). Impact of hibernation on gut microbiota and intestinal barrier function in ground squirrels. In Living in a Seasonal World: Thermoregulatory and Metabolic Adaptations, T. Ruf, C. Bieber, A. Arnold, and E. Millesi, eds. (Heidelberg: Springer).

Carey, H.V., Walters, W.A., and Knight, R. (2013). Seasonal restructuring of the ground squirrel gut microbiota over the annual hibernation cycle. Am J Physiol Regul Integr Comp Physiol 304, R33-42.

Kurtz, C.C., and Carey, H.V. (2007). Seasonal changes in the intestinal immune system of hibernating ground squirrels. Dev Comp Immunol 31, 415-428.

McFall-Ngai, M., Hadfield, M.G., Bosch, T.C., Carey, H.V., Domazet-Loso, T., Douglas, A.E., Dubilier, N., Eberl, G., Fukami, T., Gilbert, S.F., et al. (2013). Animals in a bacterial world, a new imperative for the life sciences. Proc Natl Acad Sci USA 110, 3229–3236.

Where applicable, the authors confirm that the experiments described here conform with The Physiological Society ethical requirements.

SA311

Architecture and dynamics of native AMPA receptors in the mammalian brain - insights from functional proteomics

B. Fakler

University of Freiburg, Freiburg, UK

AMPA-type glutamate receptors (AMPARs) are central players in the mammalian brain crucial for a variety of processes including fast excitatory neurotransmission, synapse development and activity-dependent synaptic plasticity that underlies learning and memory.

As a key to this pronounced diversity in physiological functions, we have recently provided the first comprehensive analysis of architecture and composition of native AMPARs using novel high-resolution proteomic technologies. Thus, AMPARs in the adult rodent brain are multi-protein complexes of previously unanticipated complexity that are assembled from a pool of 34 different constituents. The majority of these constituents, mostly secreted proteins or transmembrane proteins of different classes, have not yet been related to AMPAR function.

Using the newly building blocks of native AMPARs we have started to analyze the significance of this molecular framework for the complex role of AMPARs in excitatory synaptic transmission.

Where applicable, the authors confirm that the experiments described here conform with The Physiological Society ethical requirements.

SA312

TARP interplay and the regulation of Ca^{2+}-permeable AMPA receptors: lessons from *stargazer* mice

C. Bats[1], D. Studniarczyk[1], D. Soto[1,2], M. Farrant[1] and S.G. Cull-Candy[1]

[1]Neuroscience, Physiology and Pharmacology, University College London, London, UK and [2]Laboratori de Neurobiologia – IDIBELL, Barcelona, Spain

While GluA2-containing calcium-impermeable AMPA receptors (CI-AMPARs) are widely expressed in the central nervous system, the expression of GluA2-lacking calcium-permeable AMPA receptors (CP-AMPARs) is more restricted - they are only found in a subset of neuronal and glial cells or at specific developmental stages. These CP-AMPARs play an important role in the physiology of the brain. Not only do they contribute to basal transmission, but they are also essential to normal development and synaptic plasticity. On the other hand, the over activation or upregulation of CP-AMPARs, has been linked to diverse neurological disorders, including hypoxic/ischemic damage to neurons and glia, chronic pain and drug addiction. As the relative contribution of CP-AMPARs to synaptic transmission is critical in both physiological and pathological processes, it is of interest to understand the molecular mechanisms underlying their regulation. Transmembrane AMPAR regulatory proteins (TARPs) enhance both AMPAR expression and channel function. With this in mind, we asked whether these auxiliary subunits play a role in the differential trafficking of CP- and CI-AMPARs.

Much of our knowledge of TARP/AMPAR interactions comes from work on cerebellar granule cells, neurons that normally express only CI-AMPARs. Like granule cells, cerebellar stellate cells express TARPs γ-2 and -7, but contain both CP- and CI-AMPARs. We have examined AMPAR subtype distribution in these two cell types, using patch-clamp recording. In particular, we have considered which TARPs are involved in the synaptic and extrasynaptic expression of different AMPAR subtypes, using the spontaneous mutant mouse *stargazer*.

Experiments on *stargazer* played a central role in the discovery of TARPs as essential components of the native AMPAR complex. These ataxic mice lack TARP γ-2 and display a characteristic loss of AMPAR-mediated currents at mossy fiber-to-granule cell synapses. This is associated with a near complete absence of surface AMPARs. Closer examination has demonstrated that, γ-2 not only promotes the delivery of AMPARs to the plasma membrane, but also enables the clustering of surface AMPARs at synapse by specifically interacting with PDZ-containing proteins of the postsynaptic scaffold (PSD-95). Six functional TARPs have been identified, according to their ability to rescue AMPAR-mediated EPSCs in *stargazer* granule cells - TARPs γ-3, -4, -and -8 (which are closely related to γ-2), and the atypical TARPs, γ-5 and -7. The latter interact physically and functionally with AMPARs but fail to restore synaptic transmission in *stargazer* granule cells. Each of these six TARPs displays distinct, partially overlapping, patterns of expression in the brain. However, it has generally been assumed that only one TARP subtype is present within a given AMPAR complex. TARP γ-2 and -7 are enriched within the cerebellum, where they co-cluster at synaptic contacts **[1]**. Importantly, no other TARP is expressed in cerebellar granule cells, which would explain why these neurons are particularly susceptible to the loss of γ-2 in *stargazer* mice.

Unlike granule cells, stellate cells in *stargazer* mice still display AMPAR-mediated EPSCs. However, we find that the contribution of CI-AMPARs to these synaptic currents is dramatically decreased **[2]**. This implies that CP-AMPARs, unlike CI-AMPARs, can cluster at synapses in the absence of γ-2, or any other typical TARPs. Surprisingly, while functional γ-7-associated CP-AMPARs are present at the surface of *stargazer* stellate cells, EPSCs are mediated by TARPless CP-AMPARs. Whereas it was believed that γ-7 simply fails to compensate for the lack of γ-2 in *stargazer* granule cells, we show that γ-7 prevents AMPAR surface expression and synaptic clustering, as knocking-down γ-7 rescues synaptic currents. Our observations indicate that the loss of surface AMPARs in *stargazer* granule cells lacking γ-2 is caused by the absence of CP-AMPARs and a suppressive effect of γ-7 .

Together our results suggest that the relationships between AMPARs and TARPs, and between typical and atypical TARPs, are more complex than originally thought, and that there is still much to learn from *stargazer* mice about AMPAR trafficking.

Yamazaki M *et al*. (2010). *Eur J Neurosci* **31**, 2204-2220.

Bats C *et al*. (2012). *Nat Neurosc* **15**, 853-861.

We thank all members of the Mark Farrant / Stuart G Cull-Candy laboratory for invaluable help and discussions. This work was supported by a Wellcome Trust Programme Grant (S.G.C.-C. and M.F.), a Medical Research Council Programme Grant (S.G.C.-C. and M.F.) and a Marie Curie Intra-European Fellowship (C.B.).

Where applicable, the authors confirm that the experiments described here conform with The Physiological Society ethical requirements.

SA313

TARPs as major molecular determinants for expression and heterogeneity in synaptic AMPA receptors

M. Watanabe

Anatomy, Hokkaido University Graduate School of Medicine, Sapporo, Japan

To ensure reliable synaptic transmission, AMPA receptors are anchored in the postsynaptic density via PSD-95 and transmembrane AMPA receptor regulatory proteins (TARPs). The TARP family comprises six isoforms: four classical (g-2, g-3, g-4, and g-8) and two atypical (g-5 and g-7) TARPs. Their spatial distributions are distinct in the brain, but multiple TARPs are expressed in given neural regions (Fukaya et al., 2005). We have so far studied synaptic expression of individual TARPs, and pursued their roles in AMPA receptor expression by using mutant mice defective in TARP genes. In the cerebellum, TARPg-2 and g-7 are the major isoforms in two major cerebellar neurons, i.e., granule cells and Purkinje cells. They are selectively localized on the postsynaptic membrane of excitatory synapses, and synergistically promote synaptic expression of AMPA receptors. Most notably, GluA2 and GluA3 subunits are severely lost at Purkinje cell synapses in g-2/g-7-double knockout mice, and AMPA receptor-mediated currents at climbing fiber synapses are reduced to 10% of the wild-type levels (Yamazaki et al., 2010). TARPg-7 is also expressed in Bergmann glia, and substantial loss of GluA1 and GluA4 expressions occurs in Bergmann glia of g-7-knockout mice. These observations indicate that TARPs are the major

molecular determinants for expression of neuronal and glial AMPA receptors. It should be noted that synaptic expression of AMPA receptors undergoes target cell type-dependent and input source-dependent regulation. This is best known in the hippocampus, where TARPg-8 is the major TARP with additional expression of TARPg-2 and g-3 (Fukaya et al., 2006). To specify the role in the target cell type-dependent regulation, we have recently tested three types of Schaffer collateral synapses in the hippocampal CA1, i.e., perforated and non-perforated synapses on pyramidal cell spines and dendritic synapses on parvalbumin-positive interneurons. In the symposium, we will present our molecular-anatomical data suggesting that TARPg-2 is more potent than TARPg-8 in producing the heterogeneity of AMPA receptor contents among the Schaffer collateral synapses.

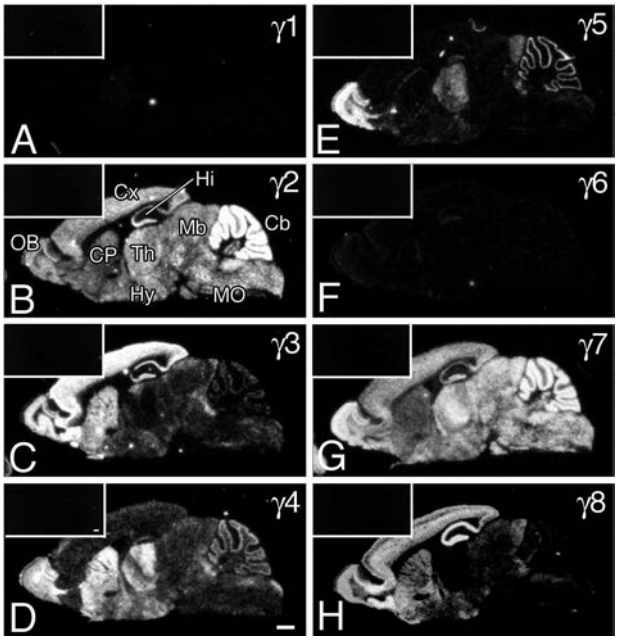

Fukaya M, Yamazaki M, Sakimura K, Watanabe M: Spatial diversity in gene expression for VDCCγ subunit family in developing and adult mouse brains. Neurosci. Res. 53:376-383, 2005.

Fukaya M, Tsujita M, Yamazaki M, Kushiya E, Abe M, Akashi K, Natsume R, Kano M, Kamiya H, Watanabe M, Sakimura K: Abundant distribution of TARP γ-8 in synaptic and extrasynaptic surface of hippocampal neurons and its major role in AMPA receptor expression on spines and dendrites. Eur. J. Neurosci. 24:2177-2190, 2006.

Yamazaki M, Fukaya M, Hashimoto K, Yamasaki M, Tsujita M, Itakura M, Abe M, Natsume R, Takahashi M, Kano M, Sakimura K, Watanabe M: TARPs g-2 and g-7 are essential for AMPA receptor expression in the cerebellum. European J. Neurosci..31:2204-222, 2010.

Where applicable, the authors confirm that the experiments described here conform with The Physiological Society ethical requirements.

SA314

Modulation of AMPA receptor function by CamKII and stargazin

A. Kristensen

Drug Design & Pharmacology, Københavns Universitet, København Ø, Danmark, UK

AMPA-selective glutamate receptors are ligand-gated cation channels that mediate fast excitatory neurotransmission in the brain and thus mediate many aspects of brain function including cognition, movement, learning and memory. The function and number of postsynaptic AMPA receptors is dynamically regulated by a number of cellular mechanisms to control synaptic strength, a key feature of cellular models of learning and memory such as long-term potentiation. The function, trafficking and synaptic signaling of AMPA receptors containing the GluA1 subunit is tightly regulated by phosphorylation. Ca2+/calmodulin-dependent kinase II (CaMKII) phosphorylates the GluA1 AMPA receptor subunit at Ser831 to increase single-channel conductance. We show that CaMKII increases the conductance of native AMPA receptors in mouse hippocampal neurons through phosphorylation of Ser831 located in the intracellular C-terminal domain. Dissection of the molecular mechanism underlying CamKII modulation of conductance reveal that transmembrane AMPA receptor regulatory proteins (TARPs) play an critical role for allowing for phospho-Ser831 to increase conductance of heteromeric GluA1-GluA2 receptors; a main AMPA receptor subtype in hippocampal neurons. Phosphorylation of Ser831 increases the efficiency with which each subunit can activate, thereby increasing the likelihood that more receptor subunits will be simultaneously activated during gating. The molecular basis for this regulation is currently unknown. Present work evaluating the mechanism by which GluA1 phosphorylation influences AMPA receptor function include studies of intra- or interprotein interactions in AMPA receptor C-terminal that may be modulated by TARPs and GluA1 phosphorylation.

Where applicable, the authors confirm that the experiments described here conform with The Physiological Society ethical requirements.

SA315

A nanoscale view into the dynamic of AMPA receptor organization in synapses

D. Choquet

IINS, Bordeaux, France

Ionotropic AMPA glutamate receptors (AMPAR) mediate fast excitatory synaptic transmission in the central nervous system. Using a combination of high resolution single molecule imaging techniques and video-microscopy, we have previously established that AMPARs are not stable in the synapse as thought initially, but undergo continuous entry and exit to and from the post-synaptic density through lateral diffusion.
Single molecule approaches give access to the full distribution of molecule behaviors and overcome the averaging intrinsic to bulk measurement methods. They allow access to complex processes where a given molecule can have heterogeneous properties over time. We will present some recent developments in single molecule imaging technologies and their application to track single molecules in live neurons.
We have recently found a new function for this fast diffusion in controlling fast synaptic transmission. Upon consecutive synaptic stimulation at high frequency, synaptic transmission is depressed. This depression shapes the frequency dependent adaptation of individual synapses. AMPAR lateral diffusion allows fast exchange of desensitised receptors with naïve functional ones within or nearby the post-synaptic density. This participates to the recovery from depression in the tens of millisecond time range, in parallel with recovery from desensitization.
In addition, we now show that the Ca2+/Calmodulin-dependent protein kinase II (CaMKII), which is critically required for the synaptic recruitment of AMPA-type glutamate receptors

(AMPARs) during both development and plasticity, induces the synaptic trapping of AMPARs diffusing in the membrane. Furthermore, this CaMKII dependent AMPAR immobilization regulates short term plasticity. Thus, NMDA dependent Ca2+ influx in the post-synapse trigger a CaMKII and Stargazin dependent decrease in AMPAR diffusional exchange at synapses that controls synaptic function.

1. Heine, M., Groc, L., Frischknecht, R., Beique, J.C., Lounis, B., Rumbaugh, G., Huganir, R.L., Cognet, L., and Choquet, D. (2008). Surface mobility of postsynaptic AMPARs tunes synaptic transmission. Science 320, 201-205.

2. Bats, C., Groc, L., and Choquet, D. (2007). The interaction between Stargazin and PSD-95 regulates AMPA receptor surface trafficking. Neuron 53, 719-734.

3. Ehlers, M.D., Heine, M., Groc, L., Lee, M.C., and Choquet, D. (2007). Diffusional Trapping of GluR1 AMPA Receptors by Input-Specific Synaptic Activity. Neuron 54, 447-460.

4. Groc, L., Lafourcade, M., Heine, M., Renner, M., Racine, V., Sibarita, J.B., Lounis, B., Choquet, D., and Cognet, L. (2007). Surface trafficking of neurotransmitter receptor: comparison between single-molecule/quantum dot strategies. J Neurosci 27, 12433-12437.

5. Triller, A., and Choquet, D. (2005). Surface trafficking of receptors between synaptic and extrasynaptic membranes: and yet they do move! Trends Neurosci 28, 133-139.

6. Groc, L., Heine, M., Cognet, L., Brickley, K., Stephenson, F.A., Lounis, B., and Choquet, D. (2004). Differential activity-dependent regulation of the lateral mobilities of AMPA and NMDA receptors. Nat Neurosci 7, 695-696.

7. Tardin, C., Cognet, L., Bats, C., Lounis, B., and Choquet, D. (2003). Direct imaging of lateral movements of AMPA receptors inside synapses. Embo J 22, 4656-4665.

Where applicable, the authors confirm that the experiments described here conform with The Physiological Society ethical requirements.

SA316

Activity patterns and synaptic development in the mammalian retina

D. Kerschensteiner

Washington University School of Medicine, Saint Louis, MO, USA

The developing retina generates spontaneous waves of activity that propagate up to primary visual cortex and guide the synaptic refinement of early visual circuits. Across several species, retinal waves mature in three stereotypic stages (I – III), in which different circuit mechanisms give rise to activity patterns with unique spatiotemporal properties. In the final stage (III), glutamate release from bipolar cells drives retinal waves that sequentially recruit neighboring retinal ganglion cells with opposite light responses (ON and OFF RGCs). I will discuss recent insights from our group into the circuit mechanisms of stage III waves. Using systematic combinations of dual patch clamp recordings we reconstructed the sequence of neuronal activation during stage III waves, identified intersecting lateral excitatory and vertical inhibitory networks that propagate and pattern this activity, and characterize the mechanisms of communication among neurons in these circuits. In addition, I will describe our findings on the influence of glutamatergic activity on the synaptic development of bipolar cells, highlighting novel cell-type-dependent and retrograde plasticity mechanisms.

NIH, Sloan Foundation, Whitehall Foundation, Mallinckrodt Foundation, Research to Prevent Blindness Foundation

Where applicable, the authors confirm that the experiments described here conform with The Physiological Society ethical requirements.

SA317

Signal from noise: properties and homeostasis of retinal waves

M.H. Hennig

School of Informatics, University of Edinburgh, Edinburgh, UK

Neural activity in the neonatal mouse retina consists of spontaneous, correlated bursts originating from neighbouring retinal ganglion cells (RGCs), resulting in propagating waves. It is well established that the properties of retinal waves change during the course of development as the retinal network slowly assembles. Through computational modelling, we have recently found that early-stage waves (around P5 in the mouse), which depend on cholinergic synaptic transmission, reflect a very specific network state that maximises the variability of the activity patterns. I will present new recordings of mouse retinal waves at near-cellular resolution with a 4,096-channel multielectrode array, which confirm the predicted high variability of early-stage waves, and also reveal relatively low RGC recruitment. The recordings also show that waves become slower and smaller when GABAergic signalling matures (P6-7). Glutamatergic waves (P10 onwards), in contrast, are denser and begin to show repetitive trajectories confined to few localized hotspots that gradually tile the retina. Finally, I will show that some key properties of early-stage waves are under homeostatic control, but not after GABAergic signalling has matured. Taken together, these findings suggest that the role of retinal waves may change over development. Early-stage waves are very robust and appear well suited to signal broad topographic order and drive eye-specific segregation in RGC target areas, while late-stage waves appear to activate neurons in a more compact and localised manner.

Supported by BBSRC grant BB/H023569/1 and MRC Fellowship G0900425

Where applicable, the authors confirm that the experiments described here conform with The Physiological Society ethical requirements.

SA318

From how to make a hair cell tick to orchestrating auditory development: action potentials in the immature cochlea

C.J. Kros

School of Life Sciences, University of Sussex, Brighton, UK and Dept of Otorhinolaryngology, UMCG, Groningen, Netherlands

In the mature cochlea, inner hair cells (IHCs) signal the reception of sound by means of graded receptor potentials with rapid kinetics. Before the onset of hearing, which occurs at about postnatal day 12 in small altricial rodents such as mice, rats and gerbils, the IHCs fire spontaneous action potentials with mean frequencies in the order of one Hz instead (Kros et al 1998; Johnson et al 2011). Developmental changes in ion channel expression along the basolateral membrane of the IHCs, mainly the replacement of a slow delayed-rectifier potassium current, $I_{K,neo}$, with a fast BK current, $I_{K,f}$ and changes in the Ca^{2+}-dependence of neurotransmitter release, underlie this switch in function (reviewed by Kros 2007).

Speculation about the possible roles for these spontaneous action potentials includes that they may be important for the correct maturation of the IHCs and their innervation, which undergoes considerable change between birth and the onset of hearing. Another potential function is that spontaneous activity may be required for the refinement of tonotopic maps to enable frequency analysis, in the IHCs themselves or further along the auditory pathway. A number of recent findings is beginning to provide some evidence. The action potential pattern is found to vary as a function of location of the IHCs along the cochlea, so that immature apical IHCs fire action potentials in bursts, whereas basal IHC fire more randomly (Johnson et al 2011). Within the bursts of the apical IHCs the frequency of the action potentials is similar to that of the randomly firing action potentials in the base, but the overall mean frequency is lower in the apex. This might in principle serve as a signal that could be used to set up a tonotopic gradient. The bursts in the apical-coil IHCs depend on release of acetylcholine (ACh) by the efferent terminals hyperpolarizing the IHCs via SK2 channels closely coupled to the ACh receptors, whereas the firing of the basal-coil IHCs depends on hyperpolarization by ATP, again via SK2 channels coupled to P2X receptors (Johnson et al 2011). ATP is released in waves in the immature postnatal cochlea from supporting cells situated to the modiolar side of the IHCs (Tritsch et al 2007).

Another useful finding is that, at least in the second postnatal week, action potential firing is inferred to depend on the mechano-electrical transducer current that flows when the hair bundle is at rest (Johnson et al 2012), i.e. in the absence of sound stimulation (which does not reach the inner ear yet at this stage of development). This may explain why IHCs of mice with mutations that affect the function of proteins in the mechanosensitive hair bundle, such as myosin 6 and myosin 7a, fail to mature into fully functional auditory hair cells (myosin 6: Roux et al 2009; myosin 7a: Roberts, Ranatunga and Kros in preparation). The absence of a resting transducer current might prevent action potential activity in these cases, leading to a failure of maturation of the IHCs.

Challenging questions remain. For example, what causes the developmental failure of outer hair cells (OHCs), which in the myosin 7a mutants fail to express their characteristic KCNQ4 potassium current $I_{K,n}$ (Roberts, Ranatunga and Kros in preparation)? OHCs are not generally thought to fire spontaneous action potentials during development. Would this developmental programme have to be repeated if fully functional mature hair cells are to be regenerated in the mammalian cochlea? Since spiral ganglion cells already exhibit intrinsic spontaneous activity at embryonic day 14 (E14) in mice (Marrs and Spirou 2012), well before that of the IHCs starts at E17.5 in the base and E18.5 in the apex, it would be interesting to investigate their respective roles in the functional maturation of the auditory pathway.

Johnson SL et al (2011) Nat Neurosci 14:711-717.

Johnson SL et al (2012) J Neurosci 32:10479-10483.

Kros CJ (2007) Hear Res 227:3-10.

Kros CJ et al (1998) Nature 394:281-284.

Marrs GS & Spirou GA (2012) J Physiol 590:2391-2408.

Roux I et al (2009) Hum Mol Genet 18:4615-4628.

Tritsch NX et al (2007) Nature 450:50-55.

Research in the Kros lab is supported by the MRC and the BBSRC.

Where applicable, the authors confirm that the experiments described here conform with The Physiological Society ethical requirements.

SA319

Characterization of efferent inputs to the inner hair cells before hearing onset

I. Roux

Otolaryngology - Head and Neck Surgery, The Johns Hopkins School of Medicine, Baltimore, MD, USA

In vivo recordings show that cochlear afferent neurons fire bursts of action potentials from P0 on (1), about two weeks before hearing onset in rats. This 'spontaneous' activity of the auditory nerve fibers is driven by glutamate release from inner hair cells (IHCs), that themselves can fire spontaneous calcium action potentials. By analogy to retinal development, it has been suggested that such a spontaneous activity may promote the survival and functional maturation of auditory neurons and guide the refinement of synaptic connections in the auditory brainstem (for review see (2)). Different mechanisms have been shown to contribute to IHCs depolarization. Those include the release of ATP from supporting cells, which drive bursts of action potentials in auditory nerve fibers for most of the postnatal, pre-hearing period (3). Resting level of activation of the mechanotransduction channels, present in the sensory cells from post natal day 1 to post natal day 3 (P1/P3) on, may also contribute to the IHCs depolarization. Interestingly, P0 is also the age at which the cholinergic efferent axons originating in the superior olive complex, are first observed in close vicinity to the IHCs and seem to make initial contact ((4), for review see (5)). Here, I will present recent results obtained using *ex vivo* whole cell recordings, immunohistochemistry and imaging, which demonstrate a 'developmental switch' whereby the hair cell's cholinergic response changes from excitatory to inhibitory during synapse formation. Thus, as in vertebrate skeletal muscle, the nicotinic acetylcholine receptors (nAChRs), most likely formed by α9 and α10 nAChRs subunits (6), are functional and present in the sensory hair cell plasma membrane before synapses are formed. Then, in a second step, nAChRs clustering, coupling to calcium-dependent small conductance potassium channels (SK2) and synaptic currents appear, suggesting that efferent synaptic function is contemporaneous with, and may require, SK2 channel expression, a hypothesis consistent with the lack of functional efferent activity reported in SK2 knockout IHCs (7).

Tritsch NX et al. (2010) *Nat Neurosci* **13**,1050–1052.

Blankenship AG & Feller MB. (2010) *Nat Rev Neurosci* **11**, 18-29.

Tritsch NX & Bergles DE (2010) *J Neurosci* **30**, 1539 –1550.

Bruce LL et al. (2000) *J Comp Neurol* **423**, 532–548.

Simmons DD (2002) *J Neurobiol* **53**, 228–250.

Elgoyhen AB et al. (2001) *Proc Natl Acad Sci U S A* **98**, 3501–3506.

Kong JH et al. (2008) *J Physiol* **586**, 5471–5485.

Supported by the NOHR Foundation Research Award 2010 and HHF Emerging Research Grant 2012 to IR and NIDCD R01DC006476 to Elisabeth Glowatzki.

Where applicable, the authors confirm that the experiments described here conform with The Physiological Society ethical requirements.

SA320

Calcium signalling in the developing cochlea: insight from mouse models of deafness

F. Mammano

Venetian Institute of Molecular Mediicine, Foundation for Advanced Biomedical Research, Padua, PD, Italy and Department of Physics and Astronomy, University of Padua, Padua, PD, Italy

Cellular rhythms are ubiquitous at all levels of biological organization and involve biochemical oscillations that modulate the concentration of key metabolic substrates and second messengers. Among these, rhythmic variations in the cytosolic free calcium concentration have been shown to arise spontaneously or after stimulation by hormones or neurotransmitters. In the developing cochlea, ATP-dependent calcium oscillations occur in non-sensory cells of the lesser epithelial ridge either as a consequence of intercellular calcium wave propagation or due to sustained ATP stimulation in the submicromolar range [1]. Spontaneous calcium oscillations in the lesser epithelial ridge are rarely observed in cochlear organotypic cultures at room temperature, but their frequency is drastically increased upon blockade of ectonucleotidases, a manipulation that highlights the tonic release of ATP from these cells [2]. On the contrary spontaneous calcium transients are always observed in the greater epithelial ridge, in a class of non-sensory cells (first described by Koelliker) which transiently populate the sensory epithelium from the spiral limbus to the inner hair cells. Spontaneous calcium transients in these cells have been attributed to release of ATP through connexin hemichannels [3, 4]. We recently demonstrated that cochlear non-sensory cells of the lesser and the greater epithelial ridge share the same PLC- and IP_3R-dependent signal transduction cascade activated by ATP. Furthermore, we found that: (a) phosphatidylinositol phosphate kinase type 1γ is primarily responsible for the synthesis of the PIP_2 pool in the cell syncytia that support auditory hair cells; (b) spatially graded impairment of this signalling pathway in cochlear non-sensory cells causes a selective alteration in the acquisition of hearing [5]. Previous studies had noted that ATP-dependent calcium oscillations in non-sensory cells of the cochlea feed-back on connexin expression and participate in the coordinated regulation of connexin 26 and connexin 30 through NF-κB (nuclear factor kappa-light-chain-enhancer of activated B cells). We extended those findings demonstrating that connexin 26 and connexin 30 are both targets and effectors of calcium signalling in the developing cochlea. Altogether, these experiments have highlighted a crucial link in cochlear non-sensory cells between the expression and function of connexin 26 and connexin 30, ATP release, calcium waves, periodic calcium transients and NF-κB signalling networks, but other calcium-dependent transcription factors used by non-excitable cells may be involved. Clarifying the pathogenesis of sensorineural hearing loss and deafness due to connexin dysfunction (DFNB1, DFNA3; http://hereditaryhearingloss.org/) is just one aspect of the problem. The other critical issue is discovering appropriate treatments. Gene delivery with vectors derived from recombinant adeno-associated viruses has been successfully explored as a means to restore connexin expression and rescue intercellular coupling and calcium signalling in cochlear organotypic cultures from connexin-knockout mice with defective expression of connexin 26 and connexin 30 [6, 7]

Mammano F. (2013). ATP-dependent intercellular Ca^{2+} signaling in the developing cochlea: Facts, fantasies and perspectives. Seminars in cell & developmental biology 24, 31-39. DOI: 10.1016/j.semcdb.2012.09.004.

Anselmi F, Hernandez VH, Crispino G, Seydel A, Ortolano S, Roper SD, Kessaris N, Richardson W, Rickheit G, Filippov MA, Monyer H & Mammano F. (2008). ATP release through connexin hemichannels and gap junction transfer of second messengers propagate Ca^{2+} signals across the inner ear. Proceedings of the National Academy of Sciences of the United States of America 105, 18770-18775. DOI: 10.1073/pnas.0800793105

Tritsch NX, Yi E, Gale JE, Glowatzki E & Bergles DE. (2007). The origin of spontaneous activity in the developing auditory system. Nature 450, 50-55. DOI: 10.1038/nature06233

Schutz M, Scimemi P, Majumder P, De Siati RD, Crispino G, Rodriguez L, Bortolozzi M, Santarelli R, Seydel A, Sonntag S, Ingham N, Steel KP, Willecke K & Mammano F. (2010). The human deafness-associated connexin 30 T5M mutation causes mild hearing loss and reduces biochemical coupling among cochlear non-sensory cells in knock-in mice. Human molecular genetics 19, 4759-4773. DOI: 10.1093/hmg/ddq402

Rodriguez L, Simeonato E, Scimemi P, Anselmi F, Cali B, Crispino G, Ciubotaru CD, Bortolozzi M, Ramirez FG, Majumder P, Arslan E, De Camilli P, Pozzan T & Mammano F. (2012). Reduced phosphatidylinositol 4,5-bisphosphate synthesis impairs inner ear Ca^{2+} signaling and high-frequency hearing acquisition. Proceedings of the National Academy of Sciences of the United States of America 109, 14013-14018. DOI: 10.1073/pnas.1211869109

Ortolano S, Di Pasquale G, Crispino G, Anselmi F, Mammano F & Chiorini JA. (2008). Coordinated control of connexin 26 and connexin 30 at the regulatory and functional level in the inner ear. Proceedings of the National Academy of Sciences of the United States of America 105, 18776-18781. DOI: 10.1073/pnas.0800831105

Crispino G, Di Pasquale G, Scimemi P, Rodriguez L, Galindo Ramirez F, De Siati RD, Santarelli RM, Arslan E, Bortolozzi M, Chiorini JA & Mammano F. (2011). BAAV mediated GJB2 gene transfer restores gap junction coupling in cochlear organotypic cultures from deaf $Cx26^{Sox10Cre}$ mice. PLoS ONE 6, e23279. DOI:10.1371/journal.pone.0023279

Supported by Telethon grant GGP09137and MIUR PRIN grant n. 2009CCZSES to F.M.

Where applicable, the authors confirm that the experiments described here conform with The Physiological Society ethical requirements.

SA321

Mechanism and regulation of DHHC S-acyltransferases

M. Linder, B.C. Jennings and J. Lai

Molecular Medicine, Cornell University, Ithaca, NY, USA

Protein S-palmitoylation is a reversible posttranslational modification of proteins with palmitate or other long-chain fatty acids. In the last five years, improved proteomic methods have increased the number of proteins identified as substrates for palmitoylation from tens to hundreds. Palmitoylation regulates protein membrane interactions, activity, trafficking, and stability and can be constitutive or regulated by signaling inputs. A family of protein acyltransferases or PATs is responsible for modifying proteins with palmitate or other long-chain fatty acids on the cytoplasmic face of cellular membranes. The signature feature is a DHHC (Asp-His-His-Cys)-cysteine rich domain that is the catalytic center of the enzyme. The biomedical importance of members of this family is underscored by their association with intellectual disability, Huntington's Disease, and cancer in humans and raises the possibility of the enzymes as targets for therapeutic intervention. Accordingly, elucidating the mechanism and regulation of the DHHC pro-

teins is important for understanding how palmitoylation manifests in physiology and pathophysiology.
Our recent work has focused on the enzymology of DHHC PATs, addressing the mechanism of palmitate transfer to substrate and the quaternary structure of the enzymes. DHHC proteins acylate themselves upon incubation with palmitoyl-CoA, a process termed autoacylation. Both autoacylation and transfer of palmitate to substrate are dependent upon the cysteine within the DHHC motif. It has been suggested that autoacylation of the enzyme represents a transient acyl-enzyme transfer intermediate. To directly test this hypothesis, we performed single turnover assays with DHHC2 and DHHC3 and demonstrated that a radiolabeled acyl group on the enzyme transferred to the protein substrate, consistent with a two-step ping-pong mechanism. Enzyme autoacylation and acyltransfer to substrate displayed the same acyl-CoA specificities, further supporting a two-step mechanism.
Evidence suggests that mutation of the catalytic cysteine within the DHHC motif results in a protein that acts as a dominant negative (Fukata M. et al. (2004); Fang C. et al. (2006). However, the mechanism by which the mutation interferes with the function of the wild type protein is unknown. One hypothesis is that DHHC proteins function as oligomers and that mixed oligomers of wild type and mutant enzyme are inactive. Support for this argument comes from coimmunoprecipitation experiments that suggest that DHHC3 forms homomultimers and heteromultimers with DHHC7 (Fang C. et al. (2006). We sought to determine whether DHHC proteins oligomerize in cells and in vitro. Bioluminescence resonance energy transfer experiments revealed that DHHC2 or DHHC3 self-associate when expressed in HEK-293 cells. Purified DHHC3 resolved as a monomer and dimer on blue native polyacrylamide gels. In intact cells and in vitro, catalytically inactive DHHC proteins displayed a greater propensity to form dimers. BRET signals were higher for the catalytically inactive DHHC2 or DHHC3 than their wild type counterparts. DHHC3 BRET in cell membranes was decreased by the addition of palmitoyl-CoA, a treatment that results in autoacylation of the enzyme. Cross-linking of purified DHHC2 reversibly inhibited its activity in vitro. The correlation of enzyme activity with the monomeric species suggests that oligomerization may represent a mechanism to regulate enzyme activity.

Fang, C., Deng, L., Keller, C. A., Fukata, M., Fukata, Y., Chen, G., and Luscher, B. (2006) GODZ-mediated palmitoylation of GABA(A) receptors is required for normal assembly and function of GABAergic inhibitory synapses. J Neurosci 26, 12758-12768

Fukata, M., Fukata, Y., Adesnik, H., Nicoll, R. A., and Bredt, D. S. (2004) Identification of PSD-95 palmitoylating enzymes. Neuron 44, 987-996

This work has been supported by NIH grant GM51466.

Where applicable, the authors confirm that the experiments described here conform with The Physiological Society ethical requirements.

SA322

Palmitoylation and the control of cardiac ion transporters

W. Fuller

Cardiovascular Division, University of Dundee, Dundee, UK

In excitable tissues, the activity of plasmalemmal ion transporters is vital for the maintenance of normal electrical activity and ion gradients. In cardiac muscle, the transarcolemmal Na gradient established by the ubiquitous Na/K ATPase (Na pump) is essential not only for generating the rapid upstroke of the action potential but also for driving a number of ion exchange and transport processes critical for normal cellular function, ion homeostasis and the control of cell volume (1). The cardiac sodium calcium exchanger (NCX1), which is functionally coupled to the Na pump, similarly plays a vital role in the regulation of trans-sarcolemmal Ca fluxes in cardiac muscle, because it is the principal route by which Ca leaves the cell during diastole (2). Inappropriate NCX1 function contributes to cardiac contraction abnormalities and heart failure: reduced NCX1 activity reduces Ca removal and impairs relaxation, whereas overactive NCX1 unloads the intracellular Ca stores and impairs systolic function.
Curiously, a common feature of regulation of both the Na pump and NCX1 is controversy regarding the roles and targets of protein kinases in their regulation. Phosphoregulation of NCX1 is an unresolved controversy. In the heart, phosphoregulation of the Na pump is now established to be through phosphorylation of the accessory protein phospholemman (PLM). Unphosphorylated PLM inhibits the Na pump, and phosphorylation by PKA (at S68) or PKC (at S63, S68 and T69) activates the pump (1).
As well as being phosphorylated, PLM is palmitoylated at two cysteines, C40 and C42 in an intracellular α-helix adjacent to its transmembrane domain. Palmitoylation of PLM inhibits the Na pump, but intriguingly palmitoylation of PLM is promoted by its phosphorylation at S68 by PKA (3). Hence one post-translational modification of PLM that activates the Na pump promotes a second, which inhibits it. Although the DHHC-PAT(s) that palmitoylate PLM (or any pump subunits - see below) are yet to be identified, another important regulator of the palmitoylation status of PLM is the redox state of the cell. Cellular glutathione status is linked to PLM palmitoylation state by the anti-oxidant protein peroxiredoxin 6, which depalmitoylates PLM in a glutathione dependent manner. In addition, mitochondrial redox stress leads to a reduction in PLM palmitoylation, with a concomitant increase in its glutathionylation at C42. The presence of PLM (or other members of the FXYD gene family to which it belongs, which are also palmitoylated) in the Na pump enzyme complex therefore provides a means to link pump activity to cellular redox / metabolic state, through a balance between its phosphorylation, palmitoylation, and glutathionylation. Interestingly, we find palmitoylation of PLM is reduced in a mouse model of cardiac hypertrophy induced by ligation of the thoracic aorta, highlighting that the contribution of ion transporter palmitoylation to the development of cardiovascular diseases is a research area of considerable promise.
We have recently undertaken proteomic profiling of protein palmitoylation in ventricular muscle. A considerable number of cardiac ion channels, transporters and ion transport regulators are palmitoylated, including NCX1 and the plasma membrane Ca ATPase PMCA1 (the two routes for Ca efflux during diastole), the Na pump catalytic α and regulatory β subunits, voltage gated Na channel pore-forming and regulatory subunits, and voltage gated Ca channel pore-forming and regulatory subunits. Although the sites and functional effects of palmitoylation of these transporters are still to be fully defined, it is strikingly significant that every route of entry and exit of Na and Ca into and out of cardiac myocytes is palmitoylated. Since palmitoylation may directly regulate spatial organisation as well as ion channel / transporter activity, the role of palmitoylation in the acute and long term co-ordination of cardiac sarcolemmal Na and Ca fluxes, and therefore excitation-contraction coupling and cardiac contractility may prove as significant as any post-translational modification investigated to date.

Fuller W et al (2013). Regulation of the Cardiac Sodium Pump. *Cell Mol Life Sci.* In Press.

Bers DM (2002). Cardiac excitation-contraction coupling. *Nature* **415**, 198-205.

Tulloch LB et al (2011). The inhibitory effect of phospholemman on the sodium pump requires its palmitoylation. *J Biol Chem.* **286**, 36020-31.

This work was supported by grants from the British Heart Foundation (reference numbers PG/10/92/28650, PG/12/6/29366 & RG/12/4/29426)

Where applicable, the authors confirm that the experiments described here conform with The Physiological Society ethical requirements.

SA323

Direct imaging of palmitoylated PSD-95 in neurons

M. Fukata and Y. Fukata

National Institute for Physiological Sciences, Okazaki, Japan

Precise regulation of protein assembly at specialized membrane domains is essential for diverse cellular functions including synaptic transmission. However, it remains unclear how protein clustering at plasma membranes is initiated and controlled. Protein palmitoylation, a common reversible lipidation, regulates protein targeting to plasma membranes. Such modified proteins are enriched in these membrane domains. To enable visualization of this dynamic process, we selected a recombinant antibody that specifically recognizes the palmitoylated conformation of PSD-95, a major postsynaptic scaffold protein. When used as a GFP-tagged antibody in living neurons, it revealed that endogenous palmitoylated PSD-95 is partitioned into multiple discrete clusters in a dendritic spine. Membrane-inserted PSD-95 palmitoyltransferase, DHHC2, catalytically generates and maintains these subspine membrane domains, which serve as anchoring positions for AMPA-type glutamate receptors. Thus, the palmitoylating enzyme at plasma membranes creates highly localized hotspots of protein palmitoylation and directly marks sites where specific proteins concentrate to organize membrane domains.

Where applicable, the authors confirm that the experiments described here conform with The Physiological Society ethical requirements.

SA324

Palmitoylation and trafficking of peripheral membrane proteins

L.H. Chamberlain

SIPBS, University of Strathclyde, Glasgow, UK

Palmitoylation, the attachment of fatty acids (predominantly palmitate) onto cellular proteins, has emerged as a widespread post-translational modification of both transmembrane and peripheral membrane proteins. Recent breakthroughs in the palmitoylation field came with the discovery of the "DHHC" protein family that collectively regulate cellular palmitoylation dynamics; at least 24 of these DHHC proteins are encoded in the human genome. I will discuss how the interaction of specific DHHC isoforms with peripheral membrane protein substrates is encoded. In addition, I will discuss how multiple palmitoylation of individual peripheral membrane proteins affects their intracellular trafficking and dynamics in normal and disease states.

Where applicable, the authors confirm that the experiments described here conform with The Physiological Society ethical requirements.

SA325

Human circadian rhythms, melatonin and metabolism

D.J. Skene[1], J.E. Ang[2], K. Ackermann[3], M. Kayser[3], B. Middleton[1], S. Davies[1], V.L. Revell[1], A.E. Thumser[1], J.D. Johnston[1] and F.I. Raynaud[2]

[1]Faculty of Health and Medical Sciences, University of Surrey, Guildford, UK, [2]Cancer Research UK Cancer Therapeutics Unit, Division of Cancer Therapeutics, The Institute of Cancer Research, Sutton, UK and [3]Department of Forensic Molecular Biology, Erasmus MC University Medical Center Rotterdam, Rotterdam, Netherlands

The circadian timing system drives the cyclic processes observed in most physiological processes including sleep/wake and metabolic function. The mammalian circadian system comprises a master clock located in the hypothalamic suprachiasmatic nuclei (SCN) and peripheral clocks found in most body tissues. For optimal functioning correct temporal coordination between the central SCN clock and peripheral clocks is maintained via feedback/feed forward neuroendocrine and autonomic mechanisms. The environmental light/dark cycle is the primary time cue synchronising the human circadian timing system to 24 h.

Recent research has demonstrated links between circadian clocks and metabolism, and between sleep deprivation/sleep restriction, circadian desynchrony and metabolic disorders. Our current studies aim to investigate the mechanisms underlying these interactions between circadian timing, sleep and metabolism. Measuring the human circadian timing system has traditionally relied on assessment of circadian rhythms driven by the central SCN clock, such as melatonin, cortisol and core body temperature. Of these SCN-driven rhythms, the timing of the melatonin rhythm is considered the most reliable marker of circadian phase and numerous studies have used the melatonin profile to assess circadian rhythmicity and phase in healthy and diseased individuals in laboratory and field studies.

Studying circadian regulation of metabolism and assessing the relative importance of photic and non-photic time cues (e.g. food, exercise, sleep/wake behaviour) for entrainment, however, also requires reliable markers of peripheral clocks in humans. For example, it might be that food is a major entrainer of peripheral clocks in humans, as has been demonstrated in animals.Early studies reported clock gene expression in peripheral blood cells and buccal tissue. Gene expression in peripheral blood mononuclear cells (PBMCs) shows 24 h rhythms which are driven by the circadian clock1 and can be phase shifted by appropriately timed light2. Our recent data show that the core clock mechanism in peripheral leucocytes is compromised during acute sleep deprivation3. During one night of total sleep deprivation expression of the clock gene BMAL1 was suppressed and the heat shock gene HSPA1B expression was induced. Some clock gene rhythms showed reduced amplitude during sleep deprivation (CRY1, CLOCK, DBP) while other high-amplitude clock gene rhythms (e.g. PER1-3, REV-ERBα) remained unaffected.

For metabolism-clock studies, serial sampling of human adipose tissue offers promise. We have recently demonstrated

robust 24 h rhythms in gene expression in this metabolically active tissue in three experimental groups: lean, obese-non-diabetic and obese-Type 2 diabetic groups4. Nocturnal plasma melatonin concentrations were significantly higher in obese-non-diabetic subjects compared to weight-matched Type 2 diabetic subjects ($p < 0.01$) and lean controls ($p < 0.05$), whereas there was no difference in the amplitude or timing of leptin rhythms between the three experimental groups5.

Elucidation of the mechanisms linking metabolic disease and circadian clock misalignment, however, will require a global "systems" approach in order to identify the metabolites, genes and proteins driving endogenous circadian rhythms and how factors such as sleep/wake, light/dark, food and posture impact on these. Metabolomics is the untargeted investigation of small molecule metabolite profiles that provides a novel and powerful tool, which may provide a better representation of functional phenotype than changes in DNA, RNA and proteins. We have recently established an untargeted liquid chromatography–mass spectrometric (LC-MS) method to measure metabolite rhythms in human plasma6. In healthy volunteers, a total of 1069 metabolite features were detected and 203 (19%) showed significant time of day variation. Of these, 34 metabolites were identified using a combination of accurate mass, tandem MS, and online database searches. These metabolites include corticosteroids, bilirubin, amino acids, acylcarnitines, and lysophospholipids. Defining time of day variation in the human metabolome, in addition to increasing our understanding of daily metabolic pathways, will be crucial for the future applied use of metabolomics in the detection and treatment of human disease.

Viola, A.U., Archer, S.N., James, L.M., Groeger, J.A., Lo, J.C.Y., Skene, D.J., von Schantz, M. and Dijk, D-J. PER3 polymorphism predicts sleep structure and waking performance. Current Biol. (2007) 17, 613-618.

Ackermann, K., Sletten, T.L., Revell, V.L., Archer, S.N. and Skene, D.J. Blue-light phase shifts PER3 gene expression in human leukocytes. Chronobiology Int. (2009) 26, 769-779.

Ackermann, K., Plomp, R., Lao, O., Middleton, B., Revell, V.L., Skene, D.J. and Kayser, M. Effect of sleep deprivation on rhythms of clock gene expression and melatonin in humans. Chronobiol. Int. (2013) in press.

Otway, D.T., Mäntele, S., Bretschneider, S., Wright, J., Trayhurn, P., Skene, D.J., Robertson, M.D. and Johnston, J.D. Rhythmic diurnal gene expression in human adipose tissue from individuals who are lean, overweight and have type 2 diabetes. Diabetes (2011) 60, 1577-1581.

Mäntele, S., Otway, D.T., Middleton, B., Bretschneider, S., Wright, J., Robertson, M.D., Skene, D.J. and Johnston, J.D. Daily rhythms of plasma melatonin, but not plasma leptin or leptin mRNA, vary between lean, obese and type 2 diabetic men. PLoS One (2012) 7, e37123.

Ang, J.E., Revell, V., Mann, A., Mäntele, S., Otway, D.T., Johnston, J.D., Thumser, A.E., Skene, D.J. and Raynaud, F. Identification of human plasma metabolites exhibiting time-of-day variation using an untargeted liquid chromatography-mass spectrometry metabolomics approach. Chronobiol. Int. (2012) 29, 868-881.

Where applicable, the authors confirm that the experiments described here conform with The Physiological Society ethical requirements.

SA326

Molecular and cellular circuits underlying circadian rhythms of behavior

A. Sehgal

University of Pennsylvania, Philadelphia, PA, USA

We use the fruit fly, Drosophila melanogaster, as a model to understand the molecular underpinnings of behavior and physiology. Like mammals, Drosophila have a sleep state that is controlled by circadian and homeostatic mechanisms. The homeostatic system drives the need to sleep while the circadian system ensures that sleep occurs with a ~24 hour rhythm. The molecular and cellular networks underlying these two types of regulation are distinct and yet they also intersect. Over the year, we and others have identified molecular components of the clock and also molecules required to transmit time-of-day signals form the clock to produce rhythmic sleep:wake. We have also identified genes that regulate sleep, and the cellular site of action of some of these genes. In recent work, we have been mapping the cellular circuits that give rise to rhythmic behavior. Cells that are part of the central clock have been well-studied, but those that receive signals from clock cells and transmit time-of-day signals to produce the overt behavioral rhythm are not known. Using a combination of genetic and anatomical approaches, we have identified some of these cells, and are addressing the connections between them. Together these studies are expected to lead to an understanding of how circadian and homeostatic regulation are integrated to produce sleep:wake cycles.

Funded by the HHMI and the NIH

Where applicable, the authors confirm that the experiments described here conform with The Physiological Society ethical requirements.

SA327

Systems and synthetic biology of biological timings

H.R. Ueda

Laboratory for Systems Biology and Functional Genomics Unit, Center for Developmental Biology, RIKEN, Kobe, Hyogo, Japan and Laboratory for Synthetic Biology, Quantitative Biology Center, RIKEN, Kobe, Hyogo, Japan

The logic of biological networks is difficult to elucidate without (1) comprehensive identification of network structure, (2) prediction and validation based on quantitative measurement and perturbation of network behavior, and (3) design and implementation of artificial networks of identified structure and observed dynamics.

Mammalian circadian clock system is such a complex and dynamic system consisting of complicatedly integrated regulatory loops and displaying the various dynamic behaviors including **i**) endogenous oscillation with about 24-hour period, **ii**) entrainment to the external environmental changes (temperature and light cycle), and **iii**) temperature compensation over the wide range of temperature. In this symposium, I will take a mammalian circadian clock as an example, and introduce the systems- and synthetic-biological approaches for understanding of biological timings.

Ukai-Tadenuma M. et al, *Nat Cell Biol.* 10, 1154-63 (2008).

Minami Y. et al, *PNAS* 106, 9890-5 (2009).

Isojima Y. et al, *PNAS* 106, 15744-49 (2009).

Masumoto KH. et al, *Curr Biol.* 20, 2199-206 (2010).

Ukai-Tadenuma M. et al, *Cell* 144, 268-81 (2011).

Hogenesch JB, Ueda HR. *Nature Rev. Genet.* 12, 407-16 (2011).

Jolley CC, Ode KL, Ueda HR. *Cell Reports* 2, 938-50 (2012).

Where applicable, the authors confirm that the experiments described here conform with The Physiological Society ethical requirements.

SA328

Circadian rhythms and seasonal adaptation

D. Weinert

Institute of Biology/Zoology, Martin-Luther-University, Halle, Germany

Seasonal acclimation is associated with various behavioral and physiological changes, allowing animals to cope with different climatic conditions and food availability. These changes are timed by the annual photoperiodic cycle. In some species, it entrains an endogenous circannual rhythm to a period of 1 year. In other species, the photoperiodic cycle directly drives the seasonal changes in a given function (or at least one of the transitional phases of this function). Whatever the underlying mechanism is, it enables the organism to prepare for rather than merely react to cyclic events in the environment.
Most organisms use circadian oscillators to measure length of day and, in mammals, the suprachiasmatic nuclei (SCN) play a crucial role. These structures receive photic stimuli via the retino-hypothalamic tract and encode information about photoperiod via modification of clock gene expression and reorganization of neuronal networks. The resulting signal, in turn, regulates pineal melatonin synthesis and release. It is mainly the duration of the melatonin signal that provides the information about photoperiod and the direction (lengthening or shortening) of its change. This hormone is secreted at night and transported to various target sites where the signal is "decoded". The duration of secretion is inversely related to day length.
In Djungarian hamsters (Phodopus sungorus) of our breeding stock, a certain number of animals show a delayed activity onset (DAO) which is caused by a diminished ability to photic synchronization. Other hamsters show arrhythmic activity patterns (AR) because the SCN as the main circadian oscillator does not generate a circadian signal. Since, a functional circadian system is a prerequisite for photoperiodic time measurement the question arose, what consequences these deteriorations may have for seasonal adaptation.
When animals of the different rhythmic phenotypes were transferred to short day (SD) conditions (L:D = 8:16 h), none of the DAO and AR hamsters displayed any SD trait. Only wild type (WT) hamsters did respond properly. Their activity time expanded, body mass and testes size decreased, and fur coloration changed from summer to winter pelage. Only a small number of hamsters did not respond, a phenomenon that has been described before. Possibly, this is of adaptive significance, as these animals may reproduce late in the year if the environmental conditions are suitable. Non-responding hamster, we also found under natural lighting and temperature conditions. Moreover, these animals did not display daily torpor, a state that was regularly observed in responders. This way, hamsters do save energy under conditions of low outdoor temperature. The times of torpor onset and offset are under circadian control.
When DAO hamsters were kept in constant darkness (DD), they exhibited typical short-day traits like lengthening of activity time, reduction of body mass and testes size, and change of fur coloration. Since, under these conditions, non-parametric light effects inducing phase responses are absent, activity-onset and activity-offset (~evening and morning oscillators) may change according to the oscillators' intrinsic period lengths. Both are >24 h, but the period of the evening oscillator is shorter than that of the morning oscillator, and this is the reason for the expansion of activity time in DD. The decompression may cause a longer melatonin signal and, subsequently, the short-day traits that were obtained. By contrast, AR animals did not display any SD response even after 14 weeks in DD. Obviously they are incapable of measuring photoperiodic time due to a complete disruption of circadian rhythmicity. Their SCN do not generate a circadian rhythm.
The results show physiological mechanisms necessary for seasonal adaptation are working in DAO hamsters and that it is the inadequate interaction of the LD cycle with the SCN that prevents the photoperiodic reaction. The signal released by the SCN and sent to the pineal is not consistent with the photoperiod. As a consequence of this disruption in the circadian system, the pattern of melatonin synthesis does not reflect the length of night appropriately. We have shown that the circadian melatonin rhythm in DAO hamsters kept under long day conditions correlates with their delayed activity-onset; a similar pattern might be expected when these hamsters are kept in SD.
In summary, one may conclude that only animals with a functional circadian system, the WT hamsters, can respond properly to changes of the photoperiod and, thus, adapt to seasonal variations in the environment. Hamsters of the other two phenotypes not only lack the ability to synchronize with the 24-h day, but also the capability of photoperiodic time measurement.

Where applicable, the authors confirm that the experiments described here conform with The Physiological Society ethical requirements.

SA329

Circadian rhythms in hypometabolic models – lessons learnt from an animal with unique wintering strategies

O. Thalmann[1], D. Wegmann[2], S. Hasan[1], T.A. Pulikotial[3], H. Lohi[3], S. Saarela[4] and K. Herzig[4]

[1]Department of Biology; Genetics, University of Turku, Turku, Finland, [2]University of Fribourg, Fribourg, Switzerland, [3]University of Helsinki, Helsinki, Finland and [4]University of Oulu, Oulu, Finland

Unraveling the various mechanisms that facilitate adaptive processes in nature is a pivotal challenge uniting evolutionary biologists, physiologists, ecologists and scientists from many diverse fields. While over the past decades, we have acquired comprehensive knowledge about the physiological, immunological or morphological modifications that allow species to adapt and thrive in natural environments, their underlying genetic mechanisms remain mostly unknown. With recent advances in molecular technologies we are now - for the first time - able to investigate genetic changes that play key-roles in these fundamental evolutionary processes. Moreover, the rapidly growing number of completely sequenced genomes allows us to find and compare variation in genes, which might represent examples of parallel evolution acting in many diverse taxa.
Here we present preliminary data investigating the adaptive genetic changes in an unusual, hypometabolic model – the raccoon dog (Nyctereutes procyonoides). The raccoon dog is the only member of dog-like mammals (family Canidae) that adopts a passive wintering strategies (shallow winter sleep) in order to survive harsh seasonal weather conditions. By doing so, the animal reduces its metabolic rate to a minimum and relies upon its stored energy resources, which it mostly gained before transforming into the hypometabolic state. Vast metabolic changes are required to undergo the physiological fluctuations associated with this wintering strategy and identify-

ing the genetic mechanisms underlying these processes has importance for our understanding of winter sleep and hibernation in endothermic mammals in general.
We utilized high-throughput sequencing of the raccoon dog's transcriptome to identify genes responsible for the species' unique metabolism. The sampling consisted of normalized cDNA extracted from a pool of diverse tissues such as liver, brain, kidney and fat tissue of one female and one male raccoon dog. The millions of sequenced nucleotides were assembled into approx. 26,000 contigs and mapped against all protein coding genes extracted from the fully sequenced genome of a close relative, the dog. Subsequently, we generated a multispecies alignment of orthologous genes present in seven different species: raccoon dog, dog, three hibernators (bat, hedgehog and squirrel) and two non-hibernating control species (human, cow). We developed a model that utilizes the genetic distances between a quartet of species including one hibernator, the raccoon dog, the dog and a non-hibernating outgroup to identify genes that show more similarity between the raccoon dog and any of the hibernators than to its evolutionary relative the dog. Our model identified a suite of candidates that might play a key-role in metabolic processes facilitating wintering strategies of endothermic mammals and we currently investigate those genes in more depth by means of analyzing the patterns of selection acting upon them and characterizing the causal mutations.
Notably, our model is also generally applicable to future projects that aim at testing other traits or genes for signals of parallel evolution.

Where applicable, the authors confirm that the experiments described here conform with The Physiological Society ethical requirements.

SA330

The renin-angiotensin system in cardiovascular progenitor cells

A. Roks

Internal Medicine, Erasmus Medical Center Rotterdam, Rotterdam, Netherlands

Modulation of the renin-angiotensin system, in particular of the function of the hormones angiotensin II and angiotensine-(1-7), is an important target for pharmacotherapy in the cardiovascular system. In the classical view, such modulation affects cardiovascular cells to decrease hypertrophy, fibrosis, and endothelial dysfunction, and improves diuresis. In this view, excessive stimulation of angiotensin II type 1 receptors fulfills a detrimental role, as it promotes cardiovascular pathogenesis, and this is opposed by stimulation of angiotensin II type 2 and the angiotensin-(1-7) receptor coded by the Mas proto-oncogene. In recent years, this view has been broadened with the observation that the renin-angiotensin system regulates bone marrow stromal cells and stem cells, thus involving hematopoiesis and tissue regeneration by progenitor cells. This change of paradigm has enlarged the field of perspectives for therapeutic application of existing as well as newly developed medicines that alter angiotensin signaling, and now stretches beyond cardiovascular therapy. In the present lecture the role of angiotensin II and angiotensin-(1-7) and their respective receptors in hematopoietic and mesenchymal stem cells is reviewed and the latest findings with respect to Ang-(1-7) are discussed as well as possible pharmacotherapeutical implications.

Where applicable, the authors confirm that the experiments described here conform with The Physiological Society ethical requirements.

SA331

The (Pro)renin receptor in neurogenic hypertension

W. Li[1], H. Peng[1], A. Ichihara[2] and Y. Feng[1]

[1]Tulane University, New Orleans, LA, USA and [2]Medicine II, Tokyo Women's Medical University, Tokyo, Japan

The brain renin-angiotensin system plays an important role in blood pressure (BP) regulation. However, the origin of brain Ang II remains unknown due to the low brain renin activity. We previously reported that prorenin and (pro)renin receptor (PRR) is present in the brain. To test our hypothesis that prorenin mediates Ang II formation in the brain via binding to PRR, the neuron-specific PRR knockout (Nefh-PRRKO) and wild type (WT) mice (n=5/group) were implanted with telemetric probes and intracerebroventricular (ICV) cannulas. BP was recorded in conscious mice during ICV infusion (0.3μl/min) for ten minutes. ICV infusion of Ang II (100ng/μl) increased BP (ΔMAP, mmHg) in both WT (48±5) and Nefh-PRRKO (40±2)mice; and this effect was blocked by AT1 receptor blocker (Losartan) indicating that the AT1R is functionally intact in Nefh-PRRKO mice. ICV infusion of mouse prorenin (100ng/μl) induced a pressor response in WT mice (42.3±5.7), and this response was completely blocked by Losartan or Captopril suggesting that prorenin induced Ang II-dependent pressor response in WT mice. Interestingly, the pressor response to mouse prorenin was abolished in Nefh-PRRKO mice (5±1; $P<0.05$), indicating that prorenin mediates pressor response via binding to PRR. To determine whether PRR contributes to the development of brain RAS-dependent hypertension, Nefh-PRR and WT littermates (N=8/group) were treated with 50mg of deoxycorticosterone acetate (DOCA) subcutaneously, plus 0.9% NaCl drinking water for 21 days. The baseline BP was similar between Nefh-PRR (101 ± 2) and WT (101 ± 3) mice. BP was increased in WT mice (132 ± 6) by DOCA-salt treatment, while Nefh-PRR mice remained normotensive (108 ± 3). In summary, prorenin via PRR mediates AngII/AT1R-dependent pressor response in the brain. Neuron-specific PRR deletion attenuates the development of DOCA-salt hypertension likely due to the lack of Ang II/AT1R activation. We conclude that prorenin/PRR may be the key factors to initiate the brain RAS and play an essential role in neurogenic hypertension.

Where applicable, the authors confirm that the experiments described here conform with The Physiological Society ethical requirements.

SA332

(Pro)renin receptor functions

G. Nguyen

Early Development and Pathologies", Collège de France, 75231 Paris, France

Since the discovery of the (pro)renin receptor (PRR) much effort was made to establish its role in pathology, hoping to optimize the blockade of the renin-angiotensin system with a PRR blocker. In spite of a positive correlation between a polymorphism of the PRR gene called *ATP6AP2* and higher blood pressure in Japanese and Caucasian subjects, experimental

models failed to clearly establish a link between PRR, hypertension and organ damage. Because complete ablation of the *PRR/ATP6AP* led to embryonic lethality in mice, contrary to all other components of the RAS, more essential cellular function of PRR were suspected. These functions are related to the vacuolar H^+-ATPase (V-ATPase), the ATP-dependent proton pump that acidifies intracellular vesicles lysosome, endosomes and to the Wnt signalling pathways. Indeed, conditional knock-out of PRR in cardiomyocytes and podocytes revealed an essential role of PRR in the assembly and the function of the V-ATPase, leading to impaired vesicles acidification and endocytosis, increased autophagy, cell apoptosis and rapid death of the animal. Moreover, PRR is involved in the Wnt/beta-catenin and Wnt/Planar Cell Polarity signalling pathways that are absolutely critical during embryonic development. It is important to stress that the functions of PRR in the V-ATPase and in Wnt signalling are totally independent of renin and prorenin.
PRR is cleaved intracellularly by furin to generate a soluble form (sPRR) actively secreted in plasma and in urine. sPRR is able to bind renin and prorenin and to activate prorenin. Our results of sPRR determination in plasma show that it is not correlated with age, gender, plasma renin or prorenin.
Altogether, these results indicate that PRR has much broader functions than binding renin and prorenin and they question the role of PRR in patho-physiological states related to the activation of the renin angiotensin system.

Where applicable, the authors confirm that the experiments described here conform with The Physiological Society ethical requirements.

SA333

Vasoprotective axis of the RAS- a novel target against diabetic retinopathy

Q. Li, A. Verma, P. Zhu, P. Shil, T. Prasad and M. Raizada

University of Florida, Gainesville, FL, USA

Diabetic retinopathy (DR) is the most common diabetic vascular complication. Despite recent advances in therapeutics and management, DR remains the leading cause of severe vision loss in people under age of sixty and there is no cure currently. Existing evidence suggests that hyperactivity of the vasoconstrictive, proliferative, pro-inflammatory, and fibrotic axis [angiotensin-converting enzyme (ACE)/angiotensin II (Ang II)/angiotensin type I receptor (AT1R)] of the renin-angiotensin system (RAS) plays a central role in the pathogenesis of DR. Diabetes induced hyperactivity of RAS contributes to development and progression of diabetic retinopathy by increasing oxidative stress, vascular inflammation and endothelial dysfunction. Nevertheless, inhibitors of this axis have not proven to be effective in the treatment and prevention of DR in several clinical trials. This is likely due to local activation of Ang II formation independent of circulating Ang II, as well as Ang II-independent activation of RAS within ocular tissue that is not affected by classic RAS inhibitors. This is supported by overwhelming evidence that all components of RAS are expressed in various cell types of the retina and the ocular Ang II levels are much higher in vitreous fluids than plasma in patients with proliferative diabetic retinopathy. The recently established vasoprotective axis involving ACE2/Ang-(1-7)/Mas counteracts the traditional proliferative, fibrotic, proinflammatory and hypertrophic effects of the ACE/Ang II/AT1R axis of the RAS. We have shown that all genes of the RAS are locally expressed; establishing the existence of an intrinsic retinal RAS; and DR is associated with impaired balance of local retinal RAS. Increased expression of ACE2/Ang-(1-7) using AAV-mediated gene delivery overcomes this imbalance and confers protection against DR; and these beneficial effects of gene transfer occur without influencing the systemic hyperglycemic status. Thus, strategies enhancing the protective ACE2/Ang-(1-7) axis of RAS could serve as a novel therapeutic target for DR.

Supported by American Diabetes Association, American Heart Association, Research to Prevent Blindness, NIH grants EY021752 and EY021721.

Where applicable, the authors confirm that the experiments described here conform with The Physiological Society ethical requirements.

SA334

ACE2/Ang (1-7) in ischemic and hemorrhagic stroke

R.W. Regenhardt[1], A.P. Mecca[1], D.A. Bennion[1], M. Liu[1], L.L. Donnangelo[1], D.A. Pioquinto[1], N.A. Patel[1], J.A. Ludin[1], D. Greenstein[1], F. Desland[1], M.K. Raizada[1], M.J. Katovich[2] and C. Sumners[1]

[1]Department of Physiology and McKnight Brain Institute, University of Florida, Gainesville, FL, USA and [2]Department of Pharmacodynamics2, University of Florida, Gainesville, FL, USA

Stroke is a leading cause of death throughout the world, and angiotensin II (Ang II) acting via its type 1 receptors (AT1R) is well known to exert harmful effects in both the ischemic and hemorrhagic forms of this disease. In several cardiovascular diseases, the angiotensin converting enzyme 2/angiotensin-(1-7)/Mas (ACE2/Ang-(1-7)/Mas) axis of the renin-angiotensin system exerts beneficial actions, often in opposition to the deleterious actions of Ang II/AT1R. Therefore we have investigated the potential beneficial actions of the ACE2/Ang-(1-7)/Mas axis in both ischemic and hemorrhagic stroke. Ischemic stroke was induced in Sprague-Dawley (SD) normotensive rats by intracranial injection of endothelin-1 (ET-1; 3 ul of 80 uM) to elicit middle cerebral artery occlusion (MCAO). For this and all other surgical procedures anesthesia was induced using a mixture of oxygen and isoflurane (4%), and was maintained during the procedure with oxygen/isoflurane (2%). Following the surgeries, before waking, rats were administered the analgesic buprenorphine (0.05 mg/kg). Intracerebroventricular (icv) infusion of Ang-(1-7) [1.1 nM; 0.5 ul/h] via osmotic minipumps prior to and during ET-1 induced MCAO elicited significant neuroroprotection, as indicated by a >50% reduction in infarct size and improved performance on behavioral tests. Similar neuroprotection was elicited by icv infusion of the ACE2 activator diminazine aceturate (DIZE; 5 ug/0.5 ul/h) as above. These beneficial effects of Ang-(1-7) and DIZE were abolished by central infusion of the Mas receptor blocker A-779 (1.14 nM; 0.5 ul/h). Importantly, DIZE exerted similar neuroprotective actions when administered systemically post-ischemic stroke. For example, intraperitoneal (IP) injection of DIZE (0.75-7.5 mg/kg) at 4, 24 and 48 h post ET-1-induced MCAO produced significant (~40%) decreases in cerebral infarct size and behavioral deficits, effects that were reversed by icv administered A-779 (1.14 nM; 0.5 ul/h). In stroke prone spontaneously hypertensive rats (spSHR), an animal model of hemorrhagic stroke, icv infusion of Ang-(1-7) as above elicited a significant reduction in the number of striatal hemorrhages and increased the lifespan of these rats. With respect to mechanism, these protective actions of Ang-(1-7)/DIZE were not associated with either altered blood pressure, cerebral

blood flow or (in the case of ischemic stroke) attenuation of ET-1 action. However, Ang-(1-7) administered icv as above exerts anti-inflammatory effects, reducing the increased levels of pro-inflammatory cytokines and microglial activation within cerebral infarct zone following ischemic stroke, and reducing the numbers of microglia within the striatum of spSHR. In vitro studies using microglia isolated from rat cerebral cortex and striatum indicate that Ang-(1-7) (100 nM) decreases activation of these cells and reduces the levels of pro-inflammatory cytokines, confirming an anti-inflammatory action of this peptide. In summary our data indicate that induction of the ACE2/Ang-(1-7)/Mas axis produces powerful anti-stroke actions, and may represent a novel therapeutic avenue for both ischemic and hemorrhagic stroke.

Where applicable, the authors confirm that the experiments described here conform with The Physiological Society ethical requirements.

SA335

Epigenetics and non-coding RNAs in the regulation of macrophage gene expression

C.K. Glass

Dept. of Cellular & Molecular Medicine, University of California, San Diego, La Jolla, CA, USA

Our recent studies have utilized a combination of genome-wide and genetic approaches to define the molecular mechanisms that underlie the development of classically activated and alternatively activated macrophage phenotypes. These studies suggest a relatively simple model of hierarchical interactions between lineage-determining and signal-dependent transcription factors that are required to select functional cis-active regulatory elements. The majority of these interactions occur at enhancer-like elements that are distant from target promoters. The discovery that these enhancer elements themselves generate transcripts referred to as 'eRNAs' raises a number of interesting new questions regarding the mechanisms underlying enhancer function and therapeutic approaches to modulate macrophage phenotypes.

Where applicable, the authors confirm that the experiments described here conform with The Physiological Society ethical requirements.

SA336

microRNAs and epigenetic control

A. Zernecke

Department of Vascular Surgery, Technische Universität München, München, Germany

Atherosclerosis is widely appreciated to represent a chronic inflammatory disease of the vessel wall. As part of the inflammatory infiltrate, monocytes/macrophages contribute to the pathogenesis of atherosclerosis. Given the functions of microRNAs as key regulators of cellular functions, such as proliferation, differentiation and cytokine responses, it is conceivable that miRNAs expressed in inflammatory cells would also control disease progression, and circulating miRNAs detected in blood, apoptotic bodies and microvesicles may affect plaque cells and be useful as disease biomarkers. In addition, also epigenetic mechanisms contribute to the regulation of gene expression. We have characterized the expression profile of miRNAs in human plaque tissue and circulation monocyte subsets, and have investigated DNA methylation and corresponding methyltransferases in early and advanced human atherosclerotic carotid lesions and serum of patients with high grade carotid artery stenosis in comparison to healthy individuals. Given the importance of the delicately orchestrated immune response in atherosclerosis, miRNAs expressed in immune cells and epigenetic modifications will likely have profound effects during the evolution of lesion formation and constitute possible targets for therapeutic interventions.

Where applicable, the authors confirm that the experiments described here conform with The Physiological Society ethical requirements.

SA337

Epigenetics and biomechanical stress responses in cardiac cell biology and disease

F. Sheikh

University of California-San Diego, La Jolla, CA, USA

The biomechanical environment is an important epigenetic factor. Little is known of how biomechanical stress is sensed by the cardiomyocyte sarcomere to transduce intracellular hypertrophic signals and how dysfunction of these pathways may lead to disease. We demonstrate that four and a half LIM domain protein-1 (FHL1) is part of a novel complex within the cardiomyocyte sarcomere, which serves to sense biomechanical stress-induced responses important for cardiac hypertrophy. Fhl1 deficiency in cardiac muscle resulted in a blunted response to hypertrophy and beneficial functional response to pressure overload, induced by transverse aortic constriction. A link to the Galpha-q signaling pathway is shown when Fhl1 deficiency prevents the cardiomyopathy observed in Galpha-q transgenic mice. Mechanistic studies demonstrate that FHL1 plays an important role in the mechanism of pathological hypertrophy by sensing biomechanical stress responses via the stretch sensor domain (titin N2B), which leads to changes in titin and MAPK mediated responses, important for sarcomere extensibility and intracellular signaling. We demonstrate that FHL1 can affect titin N2B expression and mediate changes in muscle compliance that are dependent on titin N2B phosphorylation. We further identify titin N2B as a novel target of ERK2 and demonstrate that a dose-dependent increase in FHL1 interferes with ERK2-mediated titin N2B phosphorylation. These studies identify a novel complex within the cardiomyocyte sarcomere that is critical for biomechanical stress responses in hypertrophy.

Where applicable, the authors confirm that the experiments described here conform with The Physiological Society ethical requirements.

SA338

Simultaneous optical recording of membrane potential and calcium signals

M. Canepari

Inserm U836, Grenoble, France

Combining voltage and Ca2+ imaging allows correlation of electrical and chemical activity at sub-cellular level. We developed and commercialised an imaging system designed to obtain simultaneous voltage and Ca2+ measurements with

high signal-to-noise ratio from sites as small as a few microns. Using the combination of the commercial voltage sensitive dye JPW1114 and of a UV excitable Ca2+ indicator, these measurements can be obtained with negligible optical cross-talk between the two signals and negligible photo-damage of the preparation. More recently, we started using the recently developed voltage sensitive dye Di-2-ANBDQ(F)PTEA emitting in the IR. This dye can be combined with blue excitable calcium indicators (Calcium Green, Oregon Green or Fluo) permitting the use of simultaneous UV illumination for uncaging. In this presentation I will start showing published results using commercial indicators demonstrating the capability to obtain single-trial resolution from sites as small as 2 microns. I will then present some novel results using a new fast CCD camera permitting acquisitions of both voltage and Ca2+ wavelengths at high speed (up to 20 kHz). This high speed is particularly relevant when using Ca2+ indicators with equilibrium constant > 10 μM which are able to follow Ca2+ signals in less than a millisecond. Thus, using these indicators, it is possible to follow the fast rise time of Ca2+ currents associated with an action potentials and correlate them with local changes of membrane potential. The problem of calibrating optical signals will be also addressed in detail. In summary, the experimental approach presented here opens the gate to many novel physiological investigations requiring simultaneous measurement of voltage and Ca2+ signals.

Where applicable, the authors confirm that the experiments described here conform with The Physiological Society ethical requirements.

SA339

Voltage imaging from axons and dendritic spines

M. Popovic

Cellular and Molecular Physiology, Yale University School of Medicine, New Haven, CT, USA

A central question in neuronal network analysis is how the interaction between individual neurons produces behavior and behavioral modifications. This task depends critically on how exactly are signals integrated by individual nerve cells functioning as complex operational units. Regional electrical properties of branching neuronal processes which determine the input-output function of any neuron are extraordinarily complex, dynamic, and, in the general case, impossible to predict in the absence of detailed measurements. To obtain such measurements one would, ideally, like to be able to monitor, at multiple sites, subthreshold events as they travel from the sites of origin (synaptic contacts on dendritic spines) and summate at particular locations to influence action potential (AP) initiation. It became possible recently to carry out this type of measurements with sub-millisecond and sub-micrometer resolution using multisite recording of membrane potential changes with intracellular voltage-sensitive dyes (Vm imaging). Our method is based on pioneering work on voltage-sensitive molecular probes that report membrane potential changes in transmission and fluorescence light intensity measurements (Cohen and Salzberg, 1978). Many aspects of the initial technology have been continuously improved over several decades (Canepari et al., 2010).

The spatial pattern of Na(+) channel clustering in the axon initial segment (AIS) plays a critical role in tuning neuronal computations, and changes in Na(+) channel distribution have been shown to mediate novel forms of neuronal plasticity in the axon. We took advantage of a critical methodological improvement in the high sensitivity membrane potential imaging technique to directly determine the location and length of the spike trigger zone (TZ) as defined in functional terms. The results show that in mature axons of mouse (postnatal day 18-30) cortical layer 5 pyramidal cells in acute brain slices, action potentials initiate in a region ~20 μm in length centered between 20 and 40 μm from the soma. From this region, the AP depolarizing wave invades initial nodes of Ranvier within a fraction of a millisecond and propagates in a saltatory fashion into axonal collaterals without failure at all physiologically relevant frequencies. We further demonstrate that, in contrast to the saltatory conduction in mature axons, AP propagation is non-saltatory (monotonic) in immature axons prior to myelination in mouse postnatal day 5-9.

The evidence for an important hypothesis that cortical spine morphology might participate in modifying synaptic efficacy that underlies plasticity and possibly learning and memory mechanisms is inconclusive. Both theory and experiments suggest that the transfer of excitatory postsynaptic potential (EPSP) signals from spines to parent dendrites depends on the spine neck morphology and resistance. Furthermore, modeling of signal transfer in the opposite direction predicts that synapses on spine heads are not electrically isolated from voltages in the parent dendrite. To provide direct evidence for the specific question of the transfer of dendritic signals to spine synapses, we further advanced the V(m) imaging technique (Popovic et al. 2012; fig 1) and carried out optical measurements of electrical signals from 4 groups of spines in mouse cortical layer 5 pyramidal cells with different neck length and simultaneously from parent dendrites. The results show that spine neck does not filter membrane potential signals as they spread from the dendrites into the spine heads. The improved Vm imaging technique enabled characterization the transfer of unitary EPSPs from spine synapses across the spine neck to the parent dendrite. A series of measurements showed that the spine/dendrite EPSP amplitude ratio varied from 1 to 4 in different spines.

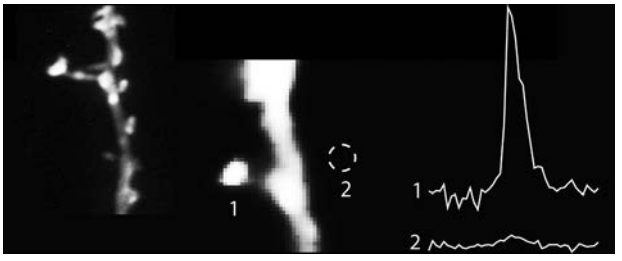

Improved Vm imaging enables high signal to noise ratio and high spatio-temporal resolution

Cohen LB, Salzberg BM (1978), Rev Physiol Biochem Pharmacol.,83:35-88.

Canepari M, Willadt S, Zecevic D, Vogt KE (2010), Biophys J., 98(9):2032-40

Popovic MA, Gao X, Carnevale NT, Zecevic D.(2012), Cereb Cortex. 2012 Oct 10. [Epub ahead of print]

This work was supported by National Institute of Health (NS068407 to Dejan Zecevic), National Science Foundation (IOS-0817969 to Dejan Zecevic), and by the Kavli Institute for Neuroscience at Yale (to Dejan Zecevic).

Where applicable, the authors confirm that the experiments described here conform with The Physiological Society ethical requirements.

SA340

Membrane potential investigated with voltage sensitive dyes

C. Petersen

EPFL, Lausanne, France

Increasingly deep understanding of the organization of the mouse brain has been facilitated by advances in genetics, electrophysiology and optical techniques together with development of awake head-restrained behaviors. Here, I will present voltage-sensitive dye imaging data correlating neocortical activity with sensorimotor behavior in awake head-restrained mice. In addition, I will discuss optogenetic manipulations specifically perturbing neural activity to gain causal insight. Our data shed new light on the functional organization of sensorimotor cortex, including a surprising direct role for sensory cortex in motor control in the whisker system.

Where applicable, the authors confirm that the experiments described here conform with The Physiological Society ethical requirements.

SA341

Teasing apart biophysical unpinnings of CNS axon spike kinectics

A.J. Foust

CNRS UMR8154, Université Paris Descartes, Paris, France

The shape of action potentials invading presynaptic terminals, which can vary significantly from spike waveforms recorded at the soma, may critically influence the probability of synaptic neurotransmitter release. Revealing conductances that determine spike shape in presynaptic boutons could bear insights into how dynamic axonal electrochemical milieux modulate synaptic strength, but the small diameter of CNS axon collaterals has prevented direct characterization with traditional electrode recordings.

Voltage imaging has long shown promise for overcoming the low spatial resolution of patch electrode recording; however, low sensitivity previously precluded investigation of phenomena too rapid or too complex to be elucidated with extensive averaging. A recent modification to the fluorescence excitation approach (Holthoff et al., 2010) now enables high signal-to-noise ratio (SNR), single-trial recordings from axons and axon collaterals (Foust et al., 2010, 2011; Popovic et al. 2011).

Utilizing the improved sensitivity of single cell voltage sensitive dye (VSD) imaging, we characterized action potentials propagating through small diameter axon collaterals of pyramidal neurons and interneurons in mouse cortical brain slices with high spatial (1-4 μm) and temporal (0.05-0.1 ms) resolution in single trials. Averaging small numbers of trials (4-8 trials) generated SNRs appropriate for comparing the kinetics of action potentials in different types of cortical neurons. Importantly, the action potentials in the axons of parvalbumin-positive fast spiking interneurons repolarized more quickly than in SOM-positive Martinotti interneurons or excitatory pyramidal neurons. Furthermore, we found that prolonged subthreshold somatic depolarization of layer 5 pyramidal neurons elicited action potential broadening in collaterals and boutons in a distance dependent fashion (Foust et al. 2011).

Lastly, by combining single-cell VSD imaging with pharmacological manipulations, we discovered that Kv1 subunit containing ion channels are important for repolarizing action potentials in cortical pyramidal axon collaterals and en passant presynaptic terminals. Moreover, the spike broadening with depolarization was blocked with Kv1 antagonists, indicating that D-current could play an important role in local graded synaptic transmission (Foust et al., 2011).

Together these findings represent a small sample of new insights to be gained into axonal action potential characteristics and plasticity with high sensitivity single cell voltage imaging.

Holthoff K, Zecevic D, and Konnerth A (2010). J Physiol 588, 1085-1096.

Foust AJ, Popovic M, Zecevic D, McCormick DA (2010). J Neurosci 30(20):6891-6902.

Foust AJ, Yu Y, Popovic M, Zecevic D, McCormick DA (2011). J Neurosci 31(43):15490-15498.

Popovic M, Foust AJ, McCormick DA, Zecevic D (2011). J Physiol 589(17):4167-4187.

This research was generously supported by a graduate research fellowship from the National Science Foundation (2007-2010), a pre-doctoral NRSA fellowship from the National Institutes of Health: National Institute of Neurological Disorders and Stroke (NIH/NINDS F31 NS070368-02), and an NIH/NINDS grant R01NS060135-04 awarded to Dr. David McCormick.

Where applicable, the authors confirm that the experiments described here conform with The Physiological Society ethical requirements.

SA342

Membrane potential imaging during functional development of neuronal circuits in vertebrate embryos

Y. Momose-Sato[1] and K. Sato[2]

[1]Department of Health and Nutrition, Kanto Gakuin University, College of Human Environmental Studies, Yokohama, Japan and [2]Department of Health and Nutrition Sciences, Komazawa Women's University, Faculty of Human Health, Tokyo, Japan

Investigating the developmental organization of the embryonic nervous system has been one of the major challenges in neuroscience. Despite their significance, functional studies of the vertebrate embryonic CNS have been hampered, since conventional electrophysiological means have some technical limitations. First, early embryonic neurons are small and fragile, and the application of microelectrodes is often difficult. Second, the simultaneous recording of electrical activity from multiple sites is limited, and as a consequence, spatio-temporal patterns of neural network responses cannot be assessed. The advent of optical techniques using voltage-sensitive dyes has enabled the non-invasive monitoring of electrical activity in living cells and also facilitated the simultaneous recording of neural responses from multiple regions. Using optical recording techniques, it is now possible to follow the functional organization of the embryonic nervous system and to image the spatio-temporal dynamics of the neural network's formation. Here, we present recent progress in optical studies on the embryonic nervous system with special emphasis on methodological considerations and the study of neuronal circuit formation, which demonstrates the utility of fast voltage-sensitive dye imaging as a powerful tool for elucidating the functional organization of the embryonic CNS.

Where applicable, the authors confirm that the experiments described here conform with The Physiological Society ethical requirements.

SA343

Coronary microvascular network adaptation in a rabbit model of developing heart failure: insights from 3D cryomicrotome imaging

J.P. van den Wijngaard, M.G. van Lier, P. van Horssen, J.A. Spaan and M. Siebes

Biomedical Engineering and Physics, Academic Medical Center, Univ of Amsterdam, Amsterdam, Netherlands

Background: Collateral formation by adaptive microvascular remodeling during chronic myocardial ischemia may ameliorate the development of heart failure. However, little quantitative information is available about potentially protective vascular changes in chronic ischemia leading to heart failure. In this study, we aimed to quantify adaptive changes in chronically ischemic rabbit hearts using high-resolution 3D imaging of the microvascular network. The rabbit heart is known for its lack of innate collateral vessels, while its intermediate size allows assessment of changes in coronary vasculature and transmural perfusion resulting from gradual coronary occlusion.
Methods and Results: New Zealand White rabbits (n=5, male, 2,5-3kg) were anesthetised with a mixture of ketamine (15mg/kg) and dexmedetomidine (0.2mg/kg) with buprenorphine (0.03mg/kg) for analgesia, all i.m.. Anesthesia was maintained by 1.5-3% isoflurane. Regional myocardial ischemia was induced in rabbits by a left thoracotomy and placement of an ameroid constrictor on a side branch of one of the major coronary arteries. Progressive occlusion within 7-10 days produced distal tissue ischemia. A sham-operated animal served as control. Cardiac function was monitored with echocardiography. Post operative, animals received carprofen (4mg/kg i.m.)
After 8 weeks, the animals were sacrificed, the heart was excised and the coronary arteries were filled with fluorescent replica material. Each heart was frozen and alternately cut and block-face imaged at 14 μm slice thickness using a custom-developed imaging cryomicrotome (Spaan et al., 2005). The microvascular structure is clearly visible in the unprocessed image stacks (Fig. 1 A) and replica material can be detected in transmural arteries of up to 50 μm diameter.
Subsequent image processing of the raw images is performed by application of a Hessian based vesselness enhancing algorithm (Sato et al. 1998). Thereby removing the halo around the large coronary arteries and enhancing the small arteriolar structures with low brightness, figure 1B. From the enhanced structure, a topologically representative vascular tree can be reconstructed following the application of a peeling algorithm (Palagyi et al. 1998) reducing the tubular structures to the centerline pixels. From the analysis of the vascular tree skeleton, vascular diameters and collaterals can be obtained, figure 1C (van den Wijngaard et al. 2010).
No signs of myocardial infarction were observed in ischemic hearts, although left ventricular wall thinning was present as compared to the control heart. Computer analysis of the segmented vascular tree identified coronary collateral formation in the ischemic hearts, with collateral connections ranging 50-100 micron between well-perfused territories and the perfusion territory distal to the ameroid constrictor. Few innate collateral anastomoses were detected in the sham operated heart.
Conclusion: With use of 3D episcopic cryomicrotome imaging, coronary microvascular adaptation in ischemic rabbit hearts was demonstrated. Future studies employing fluorescent microspheres will serve to assess regional myocardial blood flow across the ventricular wall in relation to collateral development between the normally perfused and ischemic territories.

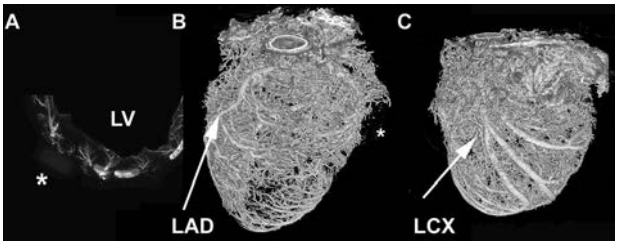

Figure 1. A; Short axis view of a 2.8mm thick maximum intensity projection of coronary vasculature of the left ventricle wall (LV) with an ameroid constrictor (*). B,3D computer reconstruction of coronary vasculature in an ischemic heart and constrictor (*) showing left anterior descending artery (LAD) perfusion territory, ischemic territory is between the LAD and LCX branch. C; 3D orientation as in B showing vascular tree with reduced opacity and a subset of coronary collaterals.

Palagyi, K., Kuba, A., A 3D 6-subiteration thinning algorithm for extracting medial lines. Patt Recog Lett. 1998;19:613–627.

Sato Y, Nakajima S, Shiraga N, Atsumi H, Yoshida S, Koller T, et al. Three-dimensional multi-scale line filter for segmentation and visualization of curvilinear structures in medical images, Med Image Anal. 1998;2:143-168.

Spaan JAE, ter Wee R, van Teeffelen JWGE, Streekstra G, Siebes M, Kolyva C, et al. Visualisation of intra-mural coronary vasculature by an imaging cryomicrotome suggests compartmentalisation of myocardial perfusion areas. Med Biol Eng Comput. 2005;43:431–435.

van den Wijngaard, J.P., van Horssen, P., ter Wee, R., Coronel, R., de Bakker, J.M., de Jonge, N, et al. Organization and collateralization of a subendocardial plexus in end-stage human heart failure. AJP-H. 2010;298,H158–162.

This work is supported in part by a Veni grant from the Netherlands Organization for Scientific Research (ZonMw 91611171) to JPHM van den Wijngaard.

Where applicable, the authors confirm that the experiments described here conform with The Physiological Society ethical requirements.

SA344

Generation of microvascular networks: a biological patterning problem

T.W. Secomb[1,2], J.P. Alberding[2], M.W. Dewhirst[3] and A.R. Pries[4]

[1]Department of Physiology, University of Arizona, Tucson, AZ, USA, [2]Arizona Research Laboratories, University of Arizona, Tucson, AZ, USA, [3]Department of Radiation Oncology, Duke University Medical Center, Durham, NC, USA and [4]Department of Physiology and CCR, Charité - Universitätsmedizin Berlin, Berlin, Germany

Formation of functionally adequate vascular networks by angiogenesis presents a problem in biological patterning. Generated without predetermined spatial patterns, networks must develop hierarchical tree-like structures for efficient convective transport over large distances, combined with dense space-filling meshes for short diffusion distances to every point in the tissue. Moreover, networks must be capable of restructuring in response to changing functional demands without interruption of blood flow. We hypothesize that the problem of vascular patterning is 'solved' by over-abundant stochastic

sprouting angiogenesis in response to a growth factor generated in hypoxic regions (e.g. vascular endothelial growth factor, VEGF), coupled to structural reactions (growth, regression, elimination) of each vessel to mechanical and biochemical stimuli. According to this hypothesis, angiogenesis results in networks with disordered structures, which organize themselves into functional networks through structural adaptation and pruning.
To test this hypothesis and analyze the relations between biological mechanisms and system properties, we developed a theoretical model that integrates simulations of network blood flow, convective and diffusive oxygen transport, generation and diffusion of VEGF, stochastic sprouting angiogenesis, structural adaptation and vessel elimination by pruning. The simulation of structural adaptation of vessel diameters includes information transfer by conducted responses along vessel walls, which is needed for proper flow distribution and avoidance of functional shunts. The model is based on experimental observations of network structure and hemodynamics in rat mesentery, a thin sheet-like tissue.
The model results show that the combination of stochastic angiogenesis stimulated by a growth factor, structural adaptation and pruning in response to hemodynamic and metabolic stimuli is capable of solving the 'problem' of vascular patterning and can generate hierarchical networks with low diffusion distances. To establish and maintain such networks, the following mechanisms are essential: (i) generation of a diffusible vessel growth factor in hypoxic tissue regions; (ii) formation of vessel sprouts in response to above-threshold levels of growth factor; (iii) maintenance of sprouts without pruning before they connect to other vessels; (iv) ability of sprouts to connect with other vessels forming patent flow pathways; (v) diameter adaptation of flowing vessels to hemodynamic and metabolic stimuli and upstream conducted responses; (vi) elimination of redundant vessels by pruning. The model allows assessment of the roles of individual mechanisms in the patterning process and changes resulting from their modification, as may occur in pathological conditions such as tumor growth. Resulting insights may stimulate further experimental investigations of angiogenesis and development of novel therapeutic approaches.

Where applicable, the authors confirm that the experiments described here conform with The Physiological Society ethical requirements.

SA345

A microvascular origin of the systemic arterial pressure level

J.B. Jacobsen[1], C.B. Poulsen[2], B.O. Hald[1], N. Holstein-Rathlou[1] and M. Damkjær[3]

[1]University of Copenhagen, Copenhagen, Denmark, [2]Department of Cardiology, Aarhus University Hospital, Aarhus, Denmark and [3]Department of Paediatrics, Kolding Hospital, Kolding, Denmark

The mean arterial pressure (MAP) is relatively invariant across numerous mammalian species despite variation in body mass spanning many orders of magnitude. This suggests that the origin of the MAP-level may be found in structures or circumstances that are invariable among the species, such as the conditions set by the physics of the system.
In most instances, the circulatory system per se does not contribute directly to the main function of a given tissue, e.g. force development in muscle tissue. In addition there is a certain metabolic cost of maintaining a distributing system, i.e. of vessel walls and of the blood itself, increasing with the volume occupied by the system. Arguably therefore, distribution systems such as vascular networks, should occupy as little space as possible within the parenchyma. On the other hand, the distribution system must reach within a sufficiently small distance from every point in the tissue to overcome the limitations set by diffusion properties of substances necessary to sustain tissue metabolism. Different networks with vessels of different dimensions can full-fill the latter requirement however, more narrow vessels requires a larger pressure-volume work pr. volume blood delivered to the tissue. Hence, a balance must exist between not occupying to much space on one hand and not requiring too much energy for the pressure-volume work on the other hand. This balance may be central in determining the MAP.
Although blood cells are flexible, the smallest vessels, i.e. the capillaries, must have a size that allows for their passage. Given that capillaries has a certain smallest possible diameter and with capillary length and density being set, average capillary flow velocity must have a size ensuring that the diffusion field of the different species satisfies the surrounding tissues. The question is therefore: which perfusion pressure is needed to deliver blood that has a certain flow-velocity in the capillary bed? Obviously this problem does not have a unique solution since an infinity of combinations of different perfusion pressures and different network structures may give rise to a specific capillary flow-velocity. However, if the physics of the system, i.e. capillary dimensions and a "cost" of increasing the volume of the network sets constraints on the network structure, then one of the two unknowns are fixed and perfusion pressure may converge towards a specific level.
To access this problem we present a simple network model composed of a large number of individual vessels. Except for the capillaries, whose dimensions are maintained constant, every vessel in the network is allowed to adapt structurally as regards both lumen diameter and wall-thickness. It is required that each vessel adapts dynamically to a disturbance so as to regain a certain homeostatic state. Homeostasis in this regard means the effect on the vessel wall of transmural pressure and luminal flow. The basic vasomotor mechanisms sensitive to these entities are the myogenic response and the flow-dependent mechanism operating via circumferential wall stress and endothelial shear stress respectively. Whereas these mechanisms set the basic level of vascular tone, they are subject to modulation by other mechanisms such as local metabolism and vascular conducted responses. Eventually all mechanisms feed into a common activation function that determines vascular diameter both acutely (through changes in tone) and chronically (through changes in structure). Simultaneously with these processes, perfusion pressure is allowed to change freely.
On performing full-scale simulations of the model each vessel eventually settles in a homeostatic state. At this point networks with realistic structural and hemodynamic properties have emanated. Furthermore, the network perfusion pressure eventually settles at a specific value.
The present very simple model indicate that perfusion pressure may be determined by structure and diffusion properties at the lowest level of the system, i.e. the capillary bed, and that the upstream resistance network and the downstream venoular network can adapt so as to ensure a sufficient capillary perfusion while each vessel at the same time remain in homeostasis as regards wall stress and activation.

Where applicable, the authors confirm that the experiments described here conform with The Physiological Society ethical requirements.

SA346

Microvascular network assessment in the clinic

D. De Backer

Intensive Care, Erasme University Hospital, Brussels, Belgium

Tissue perfusion assessment at bedside in critically ill patients still depends largely on measurement of global hemodynamic variables such as arterial pressure, cardiac output and mixed venous oxygen saturation (SvO2). However, alterations in distribution of regional perfusion and, even more importantly, alterations in microcirculatory perfusion often occur and impair tissue perfusion even when global perfusion is preserved.
How can we measure the microcirculation? Recently developed tools to assess the microcirculation include small hand held microscopes, such as orthogonal polarization spectral (OPS)/sidestream dark field (SDF) imaging (primarily in the sublingual region). These allow direct visualization of red blood cell flowing in the microcirculation, and hence are particularly useful to evaluate perfusion and in particular density of perfused vessels and heterogeneity in perfusion. Of note, white blood cells and platelets are hardly detected. These microscopes can be applied of tissues covered by a thin epithelial layer. In humans it was mostly used in the sublingual area. In the operating field, it can be directly applied to the heart, but great caution should be used to minimize motion artifact and to discard bloody secretions. The use of near-infrared spectroscopy (NIRS), can also be useful but it requires performance of a transient vascular occlusion test to evaluate microvascular reactivity. Hence, it is used in primarily in the thenar eminence. Measurement of tissue oxygenation with actual tools, including NIRS, without performance of vascular occlusion test is of limited interest. Indeed, this is a regional measurement of oxygen saturation but this measurement aggregates multiple vessels O2 saturation and fails to evaluate microcirculatory perfusion especially when perfusion is eterogeneous. Extensive discussion of the different techniques can be found in a recent review paper [1].
In humans, it has been shown that microcirculatory alterations occur in patients with severe sepsis [2] and in patients with severe heart failure [3]. These alterations were no related with systemic hemodynamic variables [4]. These alterations are characterized by heterogeneity of perfusion with capillaries with stop flow in close vicinity to well perfused capillaries. Different mechanisms have been implicated in the development of these alterations including loss of communication between vascular segments, impaired endothelial vasoreactivity, alterations in red and white blood cells rheology, alteration in endothelial glycocalyx, platelet aggregation and microthrombosis.
What are the consequences of theses alterations in microvascular perfusion? The presence of stop flow capillaries favours development of zones of tissue hypoxia, even though total perfusion to the organ is preserved. Heterogeneity in perfusion is a crucial problem, leading to inadequate matching of flow to metabolism. In critically ill patients, the severity of microvascular alterations are independently associated with outcome [2;3;5-7].
How can these alterations be influenced? The first point is of course to minimize the factors leading or contributing to their development. Increasing flow without recruiting the microcirculation is ineffective. The role of fluids, transfusions, inotropic agents is quite variable. The use of vasodilatory agents has been proposed but there is still insufficient evidence to support their use. In particular, due to their absence of selectivity, these can also dilate already perfused vessels and lead to a steal phenomenon. Other agents such as anticoagulant agents, vitamin C and statins may improve the microcirculation.

De Backer D, Ospina-Tascon G, Salgado D, Favory R, Creteur J, Vincent JL. Monitoring the microcirculation in the critically ill patient: current methods and future approaches. Intensive Care Med 2010; 36:1813-25.

De Backer D, Creteur J, Preiser JC, Dubois MJ, Vincent JL. Microvascular blood flow is altered in patients with sepsis. Am J Respir Crit Care Med 2002; 166:98-104.

De Backer D, Creteur J, Dubois MJ, Sakr Y, Vincent JL. Microvascular alterations in patients with acute severe heart failure and cardiogenic shock. Am Heart J 2004; 147:91-9.

De Backer D, Creteur J, Dubois MJ, Sakr Y, koch M, Verdant C, et al. The effects of dobutamine on microcirculatory alterations in patients with septic shock are independent of its systemic effects. Crit Care Med 2006; 34:403-8.

Sakr Y, Dubois MJ, De Backer D, Creteur J, Vincent JL. Persistant microvasculatory alterations are associated with organ failure and death in patients with septic shock. Crit Care Med 2004; 32:1825-31.

den Uil CA, Lagrand WK, van der EM, Jewbali LS, Cheng JM, Spronk PE, et al. Impaired microcirculation predicts poor outcome of patients with acute myocardial infarction complicated by cardiogenic shock. Eur Heart J 2010; 31:3032-9.

De Backer D, Donadello K, Sakr Y, Ospina-Tascon GA, Salgado DR, Scolletta S, et al. Microcirculatory alterations in patients with severe sepsis: impact of time of assessment and relationship with outcome. Crit Care Med 2013; 41:791-9.

Where applicable, the authors confirm that the experiments described here conform with The Physiological Society ethical requirements.

SA347

Compartmentation of nitric oxide synthase regulates $^{Ca2+}$ signaling in heart

Y. Zhang

Department of Physiology, Seoul National University, College of Medicine, Seoul, Republic of Korea and Yan Bian University Hospital, Yanji, China

Cardiac neuronal nitric oxide synthases (NOS1 or nNOS) has been well documented to regulate myocardial contraction and relaxation by targeting specific $^{Ca2+}$ handling proteins, protein kinase- or phosphatase-dependent phosphorylation/dephosphorylation and redox homeostasis. Specif$_{ICa}$lly, in left ventricular (LV) myocytes from healthy heart, NOS1 modulates myocardial inotropy and the amplitude of $^{Ca2+}$ transient by limiting $^{Ca2+}$ influx via attenuating L-type $^{Ca2+}$ channel activity ($_{ICa}$) through protein phosphatase 2A (PP2A)-dependent dephosphorylation of $_{ICa}$ and by increasing $^{Ca2+}$ leak following s-nitrosylation of RyR (increase subconductance of RyR). On the other hand, NOS1 facilitates myocardial lusitropy by promoting sarcoplasmic $^{Ca2+}$-ATPase activity and $^{Ca2+}$ reuptake through increasing PKA-dependent (and cGMP/PKG-independent) phospholamban phosphorylation at serine 16 (PLN-Ser^{16}) secondary to PP2A inhibition. Furthermore, NOS1 inhibits superoxide production from both XOR and NADPH oxidase. These compelling evidences show that NOS1 interacts with molecules in different subcellular compartments and exerts different effects in the heart.
Importantly, the protein expression and the activity of NOS1 are increased in hypertrophic and failing myocardium and NOS1 up-regulation is associated with cardiac protection from

oxidative stress, injury and arrhythmia. Under these conditions, NOS1 has been shown to traffic away from RyR to caveolin 3 in sarcolemma, suggesting that nNOS may target distinctive $^{Ca2+}$ handling molecules from healthy conditions under stress. So far, our understandings of the upstream or downstream mechanisms mediating NOS1 transcription and NOS1 regulation of cardiac function in the heart under stress are sparse. Recently, we have demonstrated that the pathogenic stimulator, angiotension II (Ang II) is the upstream stimulator of NOS1 protein expression and activity. Our results demonstrated that type 1, type 2 Ang II receptors and Mas receptor (in the absence of Ang 1-7) mediated Ang II stimulation of NOS1 in LV myocytes, which *in turn*, inhibited NADPH oxidase activity and facilitated LV myocyte relaxation. Unexpectedly, NOS1 up-regulation was associated with unchanged $_{ICa}$ and myocyte contraction. In addition, NOS1 increased PLN-Ser^{16} through cGMP/PKG-dependent mechanism (independent of PKA, CaMKII or peroxynitrite signaling). Similarly, NOS1 was up-regulated in cardiac myocytes from Ang II-induced hypertensive hearts, facilitated LV myocyte relaxation and decay kinetics of $^{Ca2+}$ transients (tau) and increased PLN-Ser16. Again, myocyte contraction and $_{ICa}$ were remained unaltered. Surprisingly, increased PLN-Ser16 and tau were ineffective to NOS1 inhibition; in contrast, NOS1 were shown to modulate myofilament $^{Ca2+}$ sensitivity by regulating the phosphorylation of key proteins in sarcomere.

Collectively, these results suggest that NOS1 shifts its target proteins for effective regulation of cardiac function in the myocardium under stress. This novel mechanism is important in better understanding of the endogenous cardiac protective mechanisms of NOS1 during disease progression.

Where applicable, the authors confirm that the experiments described here conform with The Physiological Society ethical requirements.

SA348

Spatial coupling between pH and Ca^{2+} in the ventricular myocyte

P. Swietach[1], J. Youm[1], N. Saegusa[2], C. Leem[3], K.W. Spitzer[2] and R.D. Vaughan-Jones[1]

[1]Department of Physiology, Anatomy and Genetics, Oxford University, Oxford, UK, [2]Nora Eccles Harrison Cardiovascular Research and Training Institute, University of Utah, Salt Lake City, UT, USA and [3]Department of Physiology, University of Ulsan College of Medicine, Ulsan, Republic of Korea

Most cells are exquisitely responsive to calcium (Ca^{2+}) (1) and hydrogen (H^+) ions (i.e. pH) (2). In cardiac myocytes, Ca^{2+} ions trigger contraction and control growth and development (3), whereas H^+ ions, which are generated or consumed metabolically, are potent modulators of virtually all biological processes (4). By acting on Ca^{2+}-handling proteins directly or via other molecules, H^+ ions exert both inhibitory and excitatory effects on Ca^{2+} signaling. Due to slow diffusion and common buffering, changes in cytoplasmic $[Ca^{2+}]$ or $[H^+]$ ($[Ca^{2+}]_i$, $[H^+]_i$) can become compartmentalized, leading potentially to complex spatial Ca^{2+}/H^+ coupling.

We investigated the relationship between intracellular pH (pH_i) and diastolic or resting $[Ca^{2+}]_i$ by fluorescence-imaging of rat ventricular cardiac myocytes loaded with reporter-dyes for Ca^{2+} (Fluo3) or pH (cSNARF1). An increase in $[H^+]_i$, produced by superfusion of 80mM acetate (salt of membrane-permeant weak acid), evoked a 47±2% $[Ca^{2+}]_i$-rise, independent of sarcolemmal Ca^{2+}-influx (replacing extracellular Na^+ with N-methyl-D-glucamine and Ca^{2+} with EGTA), electrical pacing (2Hz field stimulation) or release from mitochondria (10 μM ruthenium-360), sarcoplasmic reticulum (10 μM thapsigargin or 10 mM caffeine) or acidic-stores (5 μM bafilomycin or 100 μM glycyl-L-phenylalanine 2-naphthylamide). Photolytic H^+-uncaging from the membrane-permeant donor 2-nitrobenzaldehyde also raised $[Ca^{2+}]_i$. The $[Ca^{2+}]_i$-rise evoked by H^+-uncaging or superfusion with acetate was absent in cells that were loaded with the pH-insensitive exogenous Ca^{2+}-buffer BAPTA, either as the membrane-permeant acetoxymethyl ester or as the membrane-impermeant salt via patch-pipette (confirming that the H^+-evoked $[Ca^{2+}]$-rise is cytoplasmic). Inhibition of mitochondrial respiration with FCCP (1-5 μM), rotenone (10 μM), myxothiazole (10 μM), or of glycolysis with deoxyglucose (2 mM), reduced the H^+-evoked $[Ca^{2+}]_i$-rise in a manner that correlated with the decline of [ATP] (determined by luciferase assay). H^+-uncaging into buffer-mixtures in-vitro demonstrated that Ca^{2+}-unloading from proteins, histidyl-dipeptides (HDPs; e.g. carnosine) and ATP can underlie the H^+-evoked $[Ca^{2+}]_i$-rise. Raising $[H^+]_i$ tonically at one end of a myocyte (regional exposure to 80 mM acetate using dual-microperfusion) evoked a local $[Ca^{2+}]_i$-rise in the acidic microdomain, which did not dissipate spatially but, instead, was maintained for as long as $[H^+]_i$ was compartmentalised. Activating membrane-bound acid-extruding and acid-loading transporter-proteins on either end of the cell using dual microperfusion also produced standing pH_i and $[Ca^{2+}]_i$ gradient. These results are consistent with uphill Ca^{2+}-ion transport into the acidic-zone via Ca^{2+}/H^+-exchange on diffusible HDPs and ATP molecules, energized by the spatial $[H^+]_i$-gradient. Ca^{2+}-recruitment to a localized acid-microdomain was greatly reduced during intracellular Mg^{2+}-overload (superfusion with 30 mM Mg^{2+} in the absence of Na^+ and Ca^{2+}) or by metabolic inhibition (rotenone and deoxyglucose), maneuvers that reduce the Ca^{2+}-carrying capacity of HDPs (displacement of buffer-bound Ca^{2+} by Mg^{2+}) and deplete ATP-levels. By exchanging Ca^{2+} for H^+, diffusible cytoplasmic Ca^{2+}/H^+ buffer-molecules act like local 'pumps', producing uphill Ca^{2+}-movement within cytoplasm, in response to H^+-ion gradients.

We conclude that cytoplasmic HDPs and ATP underlie spatial Ca^{2+}/H^+ coupling in the cardiac myocyte, by providing ion exchange and transport on common buffer-sites. Cytoplasmic histidyl-dipeptides and ATP thus act like a *biological 'pump' without a membrane*. Moreover, the involvement of Ca^{2+}-bound ATP confers metabolic sensitivity to the cytoplasmic H^+-Ca^{2+} interaction. Results indicate that cytoplasmic pH_i-microdomains, formed during membrane H^+- or weak acid transport will generate Ca^{2+}-microdomains. These may help to compensate for the reactive effects of H^+-ions on Ca^{2+}-dependent protein function. Given the abundance of cellular HDPs and ATP, spatial Ca^{2+}/H^+ coupling is likely to be of general importance in cell signaling.

Clapham DE (2007) Calcium signaling. *Cell* 131(6):1047-1058.

Boron WF (2004) Regulation of intracellular pH. *Adv Physiol Educ* 28(1-4):160-179.

Bers DM (2002) Cardiac excitation-contraction coupling. *Nature* 415(6868):198-205.

Vaughan-Jones RD, Spitzer KW, & Swietach P (2009) Intracellular pH regulation in heart. *J Mol Cell Cardiol* 46(3):318-331.

Supported by the British Heart Foundation, National Institutes of Health and Royal Society.

Where applicable, the authors confirm that the experiments described here conform with The Physiological Society ethical requirements.

SA349

Orchestration of signaling microdomains in heart by cytoskeleton and protein scaffolds

J.J. Saucerman, E.C. Greenwald and R. Polanowska-Grabowska

Biomedical Engineering, University Of Virginia, Charlottesville, VA, USA

There is growing evidence that subcellular compartmentation allows signaling pathways to perform multiple functions while maintaining input-output specificity. For example, cyclic AMP signaling in the heart regulates contractility, metabolism, apoptosis and hypertrophy in a receptor-specific manner. Quantitative models and experimental approaches are needed to understand precisely how subcellular compartmentation of signaling is achieved, and how such compartmentation affects specificity and other signaling properties. I will discuss two examples of how we have combined computational models and live-cell imaging to elucidate mechanisms and consequences of signaling compartmentation.

Compartmentation of cyclic AMP signaling is widely recognized to be regulated by localized degradation by phosphodiesterases. However computational models by our group and others have predicted that phosphodiesterases are not sufficient: physical barriers are also required to quantitatively explain cyclic AMP compartmentation. We have developed a new technique to directly assess the role of physical barriers in cyclic AMP compartmentation. Fluorescently labeled (and phosphodiesterase resistant) cyclic AMP was microinjected into live cardiac myocytes. By both FRAP and kymograph analysis of diffusing fluorescent cyclic AMP, we measured substantially reduced diffusion than expected from its molecular weight alone. Disrupting microtubule or especially actin cytoskeleton accelerated cyclic AMP diffusion, indicating that cytoskeletal structures help restrict cyclic AMP diffusion.

Formation of protein complexes provides another major mechanism for signaling compartmentation. A-kinase anchoring proteins (AKAPs) localize protein kinase A and other signaling proteins to discrete locations, and AKAPs have been shown to regulate the specificity of both cardiac hypertrophy and contractile signaling. While most mathematical models assume free diffusion of signaling proteins, we propose a new "scaffold state switching" model of signaling within a protein complex. Using the tethering of protein kinase C (PKC) to AKAP7α as an example, we predicted and then experimentally validated acceleration and amplification of PKC signaling by AKAP7α. Further, the model predicted that AKAP7α insulates PKC from ATP- and substrate-competitive inhibitors, but not activation-competitive inhibitors. These model predictions were validated experimentally as well. The generality of the predicted amplification, acceleration and insulation by AKAPs was examined using model sensitivity analysis.

Overall, these two examples illustrate how mathematical modeling can be integrated with live-cell imaging to determine the mechanisms and functional consequences of subcellular signaling compartmentation.

Where applicable, the authors confirm that the experiments described here conform with The Physiological Society ethical requirements.

SA350

Caveolae contribute to spatial control of cAMP within the cardiac cell

S. Calaghan

University of Leeds, Leeds, UK

Cyclic AMP production within the cardiac cell is highly compartmentalised allowing different receptors which increase cAMP to produce distinct cellular responses. Our recent work has shown that the organisation of signal components within microdomains of the cell membrane makes a significant contribution to spatial cAMP control [1,2]. Lipid rafts are liquid-ordered domains of the membrane enriched in cholesterol and sphingolipids. Caveolae ('little caves') are invaginated rafts defined by the presence of caveolin (Cav) and cavin proteins. Clustering of elements of particular signal cascades within a caveola promotes efficiency and fidelity of signalling, and caveolin provides additional control through its regulatory interaction with many protein partners via a 20 residue caveolin scaffolding domain (CSD). Although caveolae and non-caveolar rafts co-exist, evidence suggests that most proteins are clustered by caveolae in the cardiac cell [3].

In the adult rat ventricular myocyte, stimulation of β1- and β2-adrenoceptors (AR) and the type E prostaglandin receptor (EPR) increases total cellular cAMP (indexed using a cytosolic FRET cAMP biosensor based on Epac2). However activation of these receptors produces diverse functional responses. β1-AR stimulation increases $I_{Ca,L}$ and $[Ca^{2+}]_i$ and has pronounced positive inotropic and lusitropic effects. By contrast, β2-AR stimulation has a minimal impact on these parameters and EPR stimulation is without effect. Clearly, the cAMP signal produced by stimulation of these 3 receptors has access to different subcellular sites. The inotropic and lusitropic response to β1-AR stimulation can be directly linked with a large and sustained increase in cAMP seen specifically in regions where protein kinase A (PKA) type RII is tethered to A kinase anchoring proteins (assessed using a PKA-based sensor). Only transient changes in cAMP were recorded in this compartment following β2-AR and EPR stimulation. Disruption of caveolae with the cholesterol-depleting agent methyl-β-cyclodextrin (MBCD) enhanced PKA probe responses to β1- and β2-AR (but not EPR) stimulation but was without effect on Epac2 probe responses. Again, the change in PKA probe response with MBCD was directly correlated with functional changes: enhanced inotropic and lusitropic responses to stimulation of both β-AR subtypes were seen. As β2-AR are predominantly caveolar, β1-AR are found in both caveolar and non-caveolar fractions, whereas EPR are excluded from caveolar fractions, these data suggest that disruption of caveolae selectively promotes production of cAMP in a PKA RII domain through effects on receptors located in caveolae (i.e. all β2-AR and a subset of β1-AR). A simple explanation for this is that MBCD removes the normal inhibitory effect of Cav3 on adenylyl cyclase (AC) thereby promoting cAMP production.

Interestingly, the cAMP signal revealed by caveolar disruption has access to different sites depending on the β-AR receptor activated. With β1-AR stimulation MBCD treatment increases $I_{Ca,L}$ and hastens relaxation and $[Ca^{2+}]_i$ transient decay, consistent with targeting of both the Ca2+ channel and phospholamban (PLB) by the enhanced cAMP signal. By contrast, the nascent β2-AR cAMP signal seen following MBCD treatment only targets PLB; no increase in $I_{Ca,L}$ or phosphorylation of TnI or RyR are observed. The marked increase in phosphorylation of PLB (pPLB) evoked by β2 AR stimulation in MBCD-

treated cells is mimicked by selective disruption of Cav3 binding using a cell-permeable Cav3 CSD peptide, consistent with a caveolae-specific effect of MBCD. Although AC activity may increase if the inhibitory influence of Cav3 is removed, our data suggest that the main factor contributing to the caveolar compartmentation of β2-AR signalling is facilitation of coupling of the β2-AR with Gi which inhibits cAMP production [4]. However, this does not explain the selective control of pPLB. We believe that this can be accounted for by the fact that phosphorylation of PLB is selectively restrained by PP1 tethered along with its inhibitor I-1 to AKAP18δ [5]. The sustained (and propagating) cAMP signal seen when β2-AR-Gi coupling is severed by caveolar disruption acts as a switch to turn off PP1 by PKA-phosphorylation of I-1, thereby allowing phosphorylation of PLB to be maintained.
In summary, our work shows that compartmentation of cAMP signalling can be explained, in part, by the organisation of proteins in membrane microdomains. Cavaolae normally act to restrain the cAMP signal specifically in PKA RII domains following stimulation of caveolar β1- and β2-ARs. Given this, we predict that alterations in caveolae seen in disease (e.g. heart failure) and with treatment for disease (e.g. statins) will make a significant contribution to spatial control of cAMP and cardiac function during sympathetic stimulation.

[1] MacDougall DA et al (2012) *J Mol Cell Cardiol* **52**:388-400 [

[2] Agarwal SR et al (2011) *J Mol Cell Cardiol* **50**:500-509

[3] Morris JB et al (2006) *J Mol Cell Cardiol* **41**:17-25

[4] Calaghan S & White E (2006) *Cardiovasc Res* **69**:816-824.

[5] Singh A et al (2011) *Mol Pharmacol* **79**:533-540.

This work was supported by the MRC, NIH and BHF.

Where applicable, the authors confirm that the experiments described here conform with The Physiological Society ethical requirements.

SA351

Imaging brain activity from capillaries

S. Charpak

Paris Descartes University, Paris, France

The need for a non-invasive technique to monitor oxygen *in vivo*, in 3D and in both tissue and vessels, have stimulated more than two decades of research, based on the phosphorescent quenching method. Using two-photon phosphorescence lifetime microscopy (2PLM), we have performed depth-resolved micron-scale measurements of the oxygen partial pressure (P_{o2}) in both the neuropil and the vessels of the rodent olfactory bulb. In capillaries of glomeruli, 2PLM has also allowed simultaneous measurements of P_{o2} and blood flow, and revealed the presence of erythrocyte-associated transients (EATs), i.e. P_{o2} fluctuations associated with each individual erythrocyte. We have then investigated the extent to which EAT properties in capillaries could report local neuronal activity. We find that at rest, P_{o2} at EAT peaks overestimates the mean P_{o2} by 35 mm Hg. P_{o2} between two EAT peaks is at equilibrium with, and thus reports, P_{o2} in the neuropil. During odor stimulation, a small P_{o2} decrease is detected in capillaries prior to functional hyperaemia, demonstrating that the P_{o2} initial dip, controversial in the field of fMRI, is present at the level of capillaries. We conclude that imaging oxygen dynamics in capillaries provides a unique and non-invasive approach to finely map brain activity.

Where applicable, the authors confirm that the experiments described here conform with The Physiological Society ethical requirements.

SA352

Astroglial hemichannels modulate UP and DOWN states in the olfactory bulb

L. Roux[1,2], A. Madar[1], M. Lacroix[3,4], K. Benchenane[3,4] and C. Giaume[1]

[1]Collège de France, CIRB, CNRS UMR 7241, INSERM U1050, MEMOLIFE, Université Paris 6 ED158, Paris, France, [2]Neuroscience Institute, NYU Langone Medical Center, New York, NY, USA, [3]MOBs team, Laboratory of Neurobiology, ESPCI - ParisTech, Paris, France and [4]UMR 7637, CNRS, Paris, France

While the role played by astrocytes in synaptic transmission has now largely been documented, their contribution to network activities only starts to be appreciated. A typical feature of astrocytes is their high rate of connexin expression (Cx43 and Cx30), the molecular basis for gap junctional communication and hemichannel (HC) formation. Even though connexin-formed HCs have been shown to be permeable to several neuroactive compounds, their role in physiological conditions has largely been unexplored. We thus question whether the function of Cx-based HCs in astrocytes has an impact on neuronal network behaviors in the mouse olfactory bulb (OB).
In OB acute slices, we observed that the membrane potential of mitral cells (MCs) alternates between a DOWN (hyperpolarized, silent) and an UP (depolarized, spiking) state at a slow frequency (~0.2Hz), resembling slow oscillations observed in cortical neurons during slow-wave sleep. Such alternations were inhibited by a pharmalogical blockage of glutamatergic transmission and correlated with the local field potential monitored within the corresponding glomerulus, highlighting a network effect. Interestingly, this spontaneous neuronal activity induced the opening of Cx HCs in astrocytes as shown by ethidium bromide uptake assays. We then asked whether such astroglial HC activity can in turn impact on the slow network activity, using knock-out (KO) mice for astroglial Cxs. In absence of Cx43, but not Cx30, MCs showed significant decrease in UP state amplitude compared to control. This alteration was mimicked by a blockage of Cx43 HCs, pointing out the role played by Cx43 HC function in the modulation of MC UP and DOWN states. Importantly, we found that this effect requires the activation of adenosine A1 receptors, likely via ATP release by astrocytes through Cx43 HCs. These results suggest that Cx43 HC function in astrocytes is promoted by neuronal activity, and in turn modulates neuronal network activity. Such bidirectional neuroglial interactions could play an important role in olfactory information processing.
Supported by the ANR-12-BSV4-0013-01

Where applicable, the authors confirm that the experiments described here conform with The Physiological Society ethical requirements.

SA353

Astrocytes control release of noradrenaline in the locus coeruleus via a novel signalling mechanism

A.G. Teschemacher[1], F. Tang[1], S. Lane[1], A. Korsak[2], A.V. Gourine[2] and S. Kasparov[1]

[1]Physiology and Pharmacology, University of Bristol, Bristol, UK and [2]Physiology, Pharmacology and Neuroscience, UCL, London, UK

Astroglia is now accepted as an active player in information processing in the central nervous system, playing a role in a variety of vital functions. Astrocytes may influence activity of adjacent neurons via a number of mechanisms, including release of signalling molecules, such as ATP, D-serine and glutamate. In addition, according to the 'astrocyte-to-neuron lactate shuttle' hypothesis, astrocytes generate L-Lactate (LL) from glucose or glycogen and deliver it to the extracellular space from where it may be taken up by neurones and consumed as preferred energy substrate (Suzuki et al., 2011).

We used optogenetics to stimulate astrocytes in rat organotypic cultured slices containing the locus coeruleus (LC), the largest group of brain noradrenergic (NAergic) neurones. Optogenetic actuators ChR2(H134R) or the rhodopsin-β2-adrenoceptor chimaera Opto-β2-AR (Airan et al., 2009) were introduced with adenoviral vectors and expressed by a transcriptionally enhanced, compact glial fibrillary acidic protein promoter (Liu et al., 2008) to ensure astrocyte-selective expression. We then measured electrophysiological responses in adjacent noradrenergic neurones by patch clamp, or monitored noradrenaline (NA) release using fast-scan cyclic voltammetry.

We found that that optogenetic activation of astrocytes leads to excitation of LC neurones. Depolarisations were suppressed by treatment with the glycogen metabolism blocker 1,4-dideoxy-1,4-imino-D-arabinitol (DAB; 500μM) or co-application of D-lactate (2 mM), but not by treatment with the monocarboxylate transporter blocker 4-CIN (100uM). This suggests that the excitation may be triggered by LL, released by activated astrocytes, and acting on a substrate located on the extracellular side of the cell membrane of LC neurones. Exogenously applied LL (0.2 – 20 mM) was also excitatory to LC neurones. These effects were not due to pH or caloric effects of LL as intracellular LL (2 mM), or extracellular pyruvate were ineffective.

Using fast scan cyclic voltammetry, we found powerful NA release in response to optogenetic activation of astrocytes or application of LL. These responses were also sensitive to DAB and D-lactate.

Microinjection of LL into the LC of urethane (i.p.) anaesthetised rats *in vivo* caused an increase in arterial blood pressure and changes in EEG qualitatively similar to those of L-glutamate, an established excitatory transmitter.

Together, these effects of LL may not be explained by its value as an energy substrate for LC neurons but are consistent with its role as an inter-cellular signalling molecule operating between astrocytes and NAergic neurones. Moreover, they imply an existence of as yet unknown receptor for this new "glio-transmitter".

Airan RD, Thompson KR, Fenno LE, Bernstein H, & Deisseroth K (2009). Temporally precise in vivo control of intracellular signalling. Nature 458, 1025-1029.

Liu B, Paton JF, & Kasparov S (2008). Viral vectors based on bidirectional cell-specific mammalian promoters and transcriptional amplification strategy for use in vitro and in vivo. BMC Biotechnology 8, 49.

Suzuki A, Stern SA, Bozdagi O, Huntley GW, Walker RH, Magistretti PJ, & Alberini CM (2011). Astrocyte-neuron lactate transport is required for long-term memory formation. Cell 144, 810-823.

This work was supported by the British Heart Foundation and the Wellcome Trust.

Where applicable, the authors confirm that the experiments described here conform with The Physiological Society ethical requirements.

SA354

Brain and mind reading

G. Rees

Institute of Cognitive Neuroscience, UCL, London, UK

Everything we know about the world comes to us through our brain. Yet for each of us our own conscious mental world of thoughts and feelings is isolated and private. Despite several centuries of research on the brain, communication through language or gesture remains the only way we can discover the conscious thoughts and experiences of others. But if thoughts and feelings arise from patterns of neural activity in the brain, then it should be possible to directly decode such conscious experiences from brain activity alone. Recent advances in brain imaging technology raise just such a possibility, by showing that it is possible to accurately decode a person's conscious experience based only on non-invasive measurements of their brain activity. Moreover, recent research demonstrates that there is substantial variability in how different people experience the same physical environment and that this can be indexed by structural and functional imaging of the human brain. Such 'brain reading' abilities may transform our understanding of the brain and provide important new medical insights, but also raise important ethical issues concerning the privacy of personal thought and behavioral predispositions.

I know what you're thinking: brain imaging and mental privacy. Eds Richmond S, Rees G & Edwards SJL. Oxford University Press 2012

The Wellcome Trust funded this work

Where applicable, the authors confirm that the experiments described here conform with The Physiological Society ethical requirements.

SA355

The Brain Imaging Dialogue: navigating the politics of science and technology

O. Escobar

School of Social and Political Sciences, University of Edinburgh, Edinburgh, UK and Public Policy Network, Academy of Government (University of Edinburgh), Edinburgh, UK

This presentation addresses a fundamental issue at stake in this symposium: Notwithstanding whether brain imaging is an ethical time bomb or not, who should deal with it in policy terms and how? Firstly, I will briefly outline lessons learned from the Brain Imaging Dialogue process that took place in Scotland during 2010, and which brought together a range of participants including scientists, technicians, health prac-

titioners, legal experts, social scientists, policy makers and members of the public to discuss the social and policy implications of current and future non-medical uses of brain imaging.
Secondly, I will argue that, in a democracy, the appropriate way to deal with an issue of this nature is through substantial public engagement. In other words, it is no longer enough that expert and policy elites shape the way we govern an array of technologies that bring with them such fundamental ethical, social and political challenges. Insofar we are talking about values and good practice, considered judgement by citizens must be at the heart of any process that seeks to legitimately address those challenges in policy terms.
Accordingly, I will conclude by proposing the use of democratic innovations such as deliberative 'mini-publics' (e.g. consensus conferences, citizen juries, planning cells, citizen assemblies, deliberative polls) in order to address this issue and make informed policy through meaningful public engagement.

I would like to thank the organisers of the Brain Imaging Dialogue programme "What are you thinking? Who has the right to know? Brain imaging and its impact in society", which took place at the Scottish Universities Insight Institute in Glasgow during 2010. I am deeply indebted to them for letting me be part of that process and supporting my research.

Where applicable, the authors confirm that the experiments described here conform with The Physiological Society ethical requirements.

SA356

The business of brain imaging – a commercial perspective

G. Calvert

Marketing, Nanyang Technological University, Singapore, Singapore

Traditional market research relies on measuring consumers' explicit responses via questionnaires, surveys or focus groups in order to predict how brands, new products or messages will fare in the marketplace. However, with approximately 80% of all new products failing within their first year to market despite millions of dollars spent on explicit pre-testing, companies have been looking into alternative ways to find out with greater accuracy what consumers really want. Enter the rapidly expanding field of "neuromarketing" – the application of state-of-the-art brain imaging tools and methods from psychology and neuroscience to understand consumer behaviour at a much deeper level than has been possible previously.
Neuroscientists now agree that a great deal of human behaviour is driven by brain processes that operate below the level of conscious awareness and that emotions rather than rational deliberations are, more often than not, determinants of choices. So market research that relies solely on explicit conscious responses offers only a partial picture of the multitude of brain processes (predominantly subconscious) that shape consumer behaviour. Over the past two decades, neuroscientific methods such as functional MRI and EEG have been used to study and define these explicit and implicit neural mechanisms. Companies too have conducted a substantial amount of research using the full gamut of neuroscientific approaches to understand, and ultimately predict, consumer behaviour with far more accuracy than has been permitted by reliance on spoken feedback. Areas of specific commercial interest include finding out the extent to which marketing messages or campaigns are encoded into long-term memory, whether key frames within a television commercial have been absorbed and whether changing certain parameters of a new product alters the extent to which it stimulates the brain's reward areas. The range of human emotions that manufacturers are now able to measure is considerable: trust, anticipation of price, brand loyalty and empathy are just a few.
For years, manufacturers have sought a closer alliance with their customers, recognising that including them in the design and manufacturing process not only delivers superior products but also enhances the customer experience and builds loyalty to the brand. And while not a panacea – the human brain is an extraordinarily complicated organ and neuroscientists have some way to go before they understand it completely – there is little doubt that neuromarketing offers manufacturers a more objective and scientific framework for the study of consumer behaviour. But should consumers be concerned that the ability to see inside our heads and capture our subconscious responses will allow marketers to manipulate us into making purchasing decisions that we otherwise would not?
In this talk, I will examine some of the issues that are at the forefront of the neuromarketing debate including issues of infringement of privacy, scientific integrity and ethical standards. Such factors must be considered in the light of the substantial benefits to global industry and consumers (less wastage and improved product satisfaction through more accurate understanding of what consumers really want) that can be offered by applied neuroscience.

Where applicable, the authors confirm that the experiments described here conform with The Physiological Society ethical requirements.

SA357

The promises and perils of brain imaging technology: an ethical perspective

L.Y. Cabrera

Inst. Biomedical Ethics, University of Basel, Basel, Switzerland

One area of incredible advances and promises within neurotechnology has been brain imaging technologies (BIT). But great promises often come along with great perils. In addition, given that BIT is not confined any more to the clinical setting the different ethical issues it can bring to the fore go beyond those that are regularly discussed in the medical context. For instance, who should see or have access to our brain image? Should neuroimages be used as evidence in court? Or for commercial issues? Here I will explore from a neuroethics perspective some of the promises and perils surrounding the uses of BIT outside the medical and research arenas.
BITs are generally seen as technologies to monitor brain function. Among BIT one of the most portrayed in the media and public discourse is functional Magnetic Resonance Imaging (fMRI), but there are other imaging technologies, such as Positron emission Tomography (PET) and electroencephalography EEG. BIT has unique capabilities inasmuch as it can help us to understand the brain in detail and depth that previous technologies and methods have not enabled us to achieve before. It can also help us to understand how the brain develops, changes and wires itself, which in turn can shed light into our understanding of human behavior and cognition. So among the promises of BIT we found claims related to it helping us to better monitor and diagnose neuro-related diseases and conditions, which could have a positive impact for society. However, we should bear in mind that at present BIT is

far from being perfect, and its reliability is often questioned, being charged with issues related to overinference, neuroaesthetics, confirmation bias, and trait state confusion (Farah, 2010, Wolpe et al, 2005).

There is another source of concern, namely the way neuroimaging results are interpreted. Some people have seen the potential of BITs to tell us something about mental states which can then be used for: neuromarketing, lie detection (brain reading), and assessment of potential dangerousness. Others have seen it as the analogous to genotyping, in which through our brainotype we will be able to measures, for instance how personality traits are reflected in the brain's functional architecture and as such determine the kind of persons we are or how different brain areas at work can tell us about morally relevant intuitions and those that are not (Levy, 2011). However, it is questionable the ability of brain imaging to provide an objective interpretation of complex social behavior (Phelps and Thomas, 2003), such as whether someone is lying (Wolpe and Foster, 2005), likely to show dangerous behavior or about our morality (Cabrera, 2011). It is one thing to use BIT to predict the likelihood of someone developing a certain neurological condition and another thing to say that we can use BIT to predict dangerousness. Imaging technologies can tell us that certain mental activity correlates with activity in certain brain region, but not whether the activity is actually the result the mental activity itself. Now, even if we ever developed a BIT with which we feel comfortable to use for assessing whether someone has committed or not a crime, or whether that someone shows a 'dangerous brain' and as such it is unsuitable for release, it will not make much sense to use it for such purposes unless we already have a program in place to deal with the positive cases we might encounter.

We have to remain cautious in the ways we use neuroimaging technologies but also in the way we interpret neuroimages. The new understandings that BIT promise to give us can certainly help us to capture the dynamic and complex ways of our mental life, including our intuitions, beliefs, desires as they tell us about their neural/psychological bases and the way they are influenced by reasoning, emotion, and social influences; but these new understandings could also reduce complex human behaviors to just certain brain activities while stigmatizing other important resources and elements of our mental processes (Cabrera, 2011). As Martha Farah (2010) has put it "some of the most profound ethical challenges from neuroscience come not from new technologies but from new understandings". Thus, if we want to ensure that these technologies are used for the benefit of our society, then we have to start questioning ourselves about the practical value of neuroscientific knowledge and how we should best realize it.

Cabrera, L. 2011. 'Neuroethics: A New Way to Do Ethics or a New Understanding of Ethics?', AJOB Neuroscience, 2: 2, 25 — 26

Farah, M., ed. 2010. Neuroethics: An introduction with readings. Cambridge, MA: MIT Press.

Levy, N. 2011. Neuroethics: A new way of doing ethics. AJOB Neuroscience 2(2): 3–9.

Phelps, E. A., and L. Thomas. 2003. Race, behavior, and the brain: The role of neuroimaging in understanding complex social behaviors. Political Psychology 40(4): 747–758.

Wolpe, P. R., K. R. Foster, and D. D. Langleben. 2005. Emerging neurotechnologies for lie-detection: Promises and perils. American Journal of Bioethics 5(2): 39–49.

Where applicable, the authors confirm that the experiments described here conform with The Physiological Society ethical requirements.

SA358

Society meets neuroimaging – likely tensions

H. Greely

Stanford University, Stanford, CA, USA

As neuroimaging and neuroscience tell us more about how the human brain works, this knowledge inevitably will have both medical and non-medical implications for society. Many of those implications will be based on accurate understandings of the new science; others will stem from misunderstandings – and some of them the result of willful exaggeration. Whether the science is accurate or not, the social effects may be substantial.

This talk will survey six areas where new neuroscience results are likely to affect society beyond solely medical consequences: prediction, mind-reading, responsibility, treatment, enhancement, and culture. Neuroimaging will improve our ability to predict future mental health, neurological conditions, and behavior. It will allow us, in some circumstances, to do make better inferences about what a person's mental states, whether that involves deception, pain, or more general communication. Responsibility – criminal, civil, and moral – is not likely to be revolutionized by neuroimaging, but neuroimaging will make its assignment, in at least some cases, more difficult. Funding for neuroimaging comes largely from hopes of finding prophylaxis, treatment, or even cures for mental or neurological illnesses, but improved understanding of brain processes may allow "treatment" for non-disease behaviors, such as criminal activity, which would raise its own set of ethical questions. Neuroscience, guided by neuroimaging, may also allow not just the ill but also the healthy to enhance their cognitive abilities. And, finally, neuroimaging may (but, I suspect, probably will not) have broader cultural consequences by affecting people's understanding of free will.

In each of these cases, many "breakthroughs" will be claimed, but few will actually occur. We need to maintain, and educate the public to, an appropriate skepticism about whether these breakthroughs really do work – and, if they work, how well. At the same, we should benefit from considering just how our societies will be affected by real progress in understanding the workings of human brains.

Where applicable, the authors confirm that the experiments described here conform with The Physiological Society ethical requirements.

SA359

Molecular insights into the regulation of T cell signalling

K. Gaus

Centre for Vascular Research, University of New South Wales, Sydney, NSW, Australia and Australian Centre for Nanomedicine, University of New South Wales, Sydney, NSW, Australia

T cell activation begins with the formation of signalling complexes at the cell surface involving the T cell antigen receptor (TCR), the Src family kinase Lck and the adaptor protein, linker for activation of T cells (LAT). How early TCR signalling events are regulated to prevent inopportune signalling in resting T cells but efficient activation upon receptor ligation is poorly understood. We have established localization microscopy to determine how TCR engagement reorganizes signalling proteins on the molecular scale. Imaging single molecules in intact

cells has provided new insights into the mechanisms of Lck clustering (Rossy et al. Nat Immunol 2013) and LAT recruitment (Williamson et al. Nat Immunol 2011) upon TCR activation. We are now extending this work to elucidate how the membrane environment affects protein interactions (Owen et al. Nat Commun 2012) to better understand the molecular principles of TCR signalling regulation.

Williamson D, Owen DM, Rossy J, Magenau A, Wehrmann M, Gooding JJ, Gaus K. (2011) Pre-existing clusters of the adaptor Lat do not participate in early T cell signaling events. Nature Immunol, 12, 655-662.

Rossy J. Owen DM, Williamson D, Yang Z, Gaus K. (2013) Conformational states of Lck regulate clustering in early T cell signalling. Nature Immunol, 14, 82-9

Owen DM, Williamson D, Magenau A, Gaus K. (2012) Sub-resolution lipid domains exist in the plasma membrane and regulate protein diffusion and distribution. Nat Commun. 4;3:1256

Where applicable, the authors confirm that the experiments described here conform with The Physiological Society ethical requirements.

SA360

Nano-resolution fluorescence electron microscopy

S. Watanabe and E.M. Jorgensen

Biology, University of Utah, Salt Lake City, UT, USA

To fully characterize the biology of a cell, we must know where proteins are located relative to sub-cellular structures. A fluorescence tagging approach is a very robust way to localize proteins at a sub-cellular level, but the lack of cellular context in fluorescence images and the resolution of fluorescence microscopy limits the ability to localize proteins to sub-cellular structures[1]. On the other hand, immuno-electron microscopy (immuno-EM) has high resolution, but it is limited by sample preparation and availability of antibodies[1]. The strengths of fluorescence microscopy (all proteins can potentially be tagged with fluorescent proteins) and immuno-EM (resolution of sub-cellular structures) are complementary, and thus many correlative fluorescence and electron microscopy techniques have been developed. However the precision of protein localization is limited with the currently available methods.

In the last few years, new light-based microscopy techniques have been developed with almost one hundred-fold better resolution than conventional microscopes. Photo-activated localization microscopy (or PALM)[2] is one example. With this approach, individual fluorescent proteins can be localized with 10 nm resolution. The resolution of the image is comparable to that of an image acquired with electron microscopy. However, the localization of proteins relative to the sub-cellular structures is limited despite the improvement in resolution. To add subcellular context, we developed a method to preserve fluorescence in the sample embedded in plastic for electron microscopy while preserving the cellular morphology[1]. We performed super-resolution imaging on thin sections of tissues and correlated the signals to the subcellular structures revealed by electron microscopy. Using this method, we localized histones, TOM-20, and liprin to the expected organelles: the nucleus, mitochondrial membrane, and dense projection, respectively[1]. Nano-resolution fluorescence electron microscopy (nano-fEM) can be readily used to reveal the location of proteins within a cell.

Watanabe, S. et al. Protein localization in electron micrographs using fluorescence nanoscopy. Nat. Methods 8, 80–84 (2011)

Betzig, E. et al. Imaging Intracellular Fluorescent Proteins at Nanometer Resolution. Science 313, 1642–1645 (2006)

Where applicable, the authors confirm that the experiments described here conform with The Physiological Society ethical requirements.

SA361

Seeing the forest, tree by tree - Single molecule superresolution microscopy of multiprotein complexes

H. Ewers

UZH | ETH Zurich, Zurich, Switzerland

Single molecule localization-based superresolution microscopy methods such as PALM or STORM, have been breakthrough techniques of the last years. Until now however, they require special fluorescent proteins to be cloned or high-affinity antibodies to be generated for specific labeling. On the other hand, many laboratories will have most of their constructs in GFP form and entire genomes are available as functional GFP-fusion proteins.

Here, we report a method that makes all these constructs available for superresolution microscopy by targeting GFP with tiny, high-affinity antibodies coupled to blinking dyes. It thus combines the molecular specificity of genetic tagging with the high photon yield of organic dyes and minimal linkage error. Direct STORM on microtubules labeled with our novel antibodies showed that indeed the linkage error was minimal, whereas the large size of standard antibodies resulted in an additional error of >10 nm in immunolabeling. The brightness of our labels enabled us to perform rapid time-lapse dSTORM and sptPALM on living neurons expressing the outer membrane protein GPI-GFP. Three-dimensional dSTORM on microtubules using the biplane approach allowed us to distinguish overlapping microtubules with an axial separation of ~100 nm. Using a budding yeast GFP-tag genomic library we could readily image several GFPtagged proteins targeted to specific intracellular locations.

In summary, targeting of GFP-labeled constructs with tiny antibodies provides fast and simple access to superresolution microscopy of virtually any known protein in cells. Since for several organisms the entire genome is available as GFP-tagged constructs, all these proteins are immediately accessible without the requirement for cloning or the generation of antibodies. Finally, due to a simple one-step labeling protocol, our technique opens the door to highthroughput localization analysis of entire genomes at the nanoscopic level in cells.

Where applicable, the authors confirm that the experiments described here conform with The Physiological Society ethical requirements.

SA362

High-speed hyperspectral nanoscopy for studying dynamic protein interactions below the diffraction limit

K. Lidke

University of New Mexico, New Mexico, NM, USA

Many cellular signaling processes are initiated by dimerization or oligomerization of membrane proteins. However, since the spatial scale of these interactions is below the diffraction limit of the light microscope, the dynamics of these interactions have been difficult to study on living cells. We have developed

a novel high-speed hyperspectral microscope (HSM) to perform single particle tracking of up to 8 spectrally distinct species of quantum dots (QDs) at 30 frames per second. The distinct emission spectra of the QDs allows localization with ~ 10 nm precision even when the probes are clustered at spatial scales below the diffraction limit. The capabilities of the HSM are demonstrated by application of multi-color single particle tracking to observe membrane protein behavior, including: 1) resolving antigen induced aggregation of the high affinity IgE receptor, FcεR1 ; 2) dynamic formation and dissociation of Epidermal Growth Factor Receptor dimers; 3) four color QD tracking while simultaneously visualizing GFP-actin; and 4) high-density tracking for fast viscosity mapping of the cell membrane.

Where applicable, the authors confirm that the experiments described here conform with The Physiological Society ethical requirements.

SA363

Conformational changes during the CLC transport cycle

A. Accardi, D. Basilio, K. Noack and A. Picollo

Anesthesiology, Weill Cornell Medical College, New York, NY, USA

The CLC proteins catalyze transport of chloride ions (Cl-) through cellular membranes in muscle, kidney, bone, and neurons. While some CLCs are ion channels others are H+-coupled secondary active transporters mediating the stoichiometric exchange of 2 Cl- for 1 H+. The exchange mechanism of the CLCs is unclear. Extensive structural and functional work suggests that the only conformational change taking place during transport is the movement of a conserved glutamate side chain in and out of the Cl- permeation pathway. However, other indirect lines of evidence suggest that regions distal to the Cl- pathway might also be involved in transport.
To test whether transport entails only local or also global rearrangements we used the crystal structure of CLC-ec1, a prokaryotic CLC homologue, to introduce crosslinks at the contact points of helices J, O, P and Q. These helices do not line the Cl- or H+ pathways. We hypothesized that if exchange involves movement of these helices then these constraints should inhibit transport. In a cys-less background we introduced pairs of cysteines at different locations in this 4-helix bundle and used Hg2+ to crosslink them. All unreacted proteins mediated Cl-/H+ exchange at rates comparable to that of the WT. Reaction with Hg2+ results in a striking pattern: constraining residues facing the extracellular side has no effect, while targeting pairs towards the intracellular side induces progressively a more drastic reduction of activity. Finally, constraints placed close to the intracellular side results in inactive transporters. This reduction is not due to a Hg2+-induced distortion of the Cl- pathway, as the structure of the "locked-shut" protein is virtually identical to that of WT CLC-ec1. Removal of either gate removes the inhibitory effect of the crosslinks, suggesting that this conformational change is part of the allosteric coupling of the two gates rather than directly control the movement of a single gate. In conclusion, our results demonstrate that the CLC exchange cycle entails a conformational rearrangement of helices outside of the Cl- transport pathway that control the coupling between the two gates.

Funding from the NIH and the Hirschl Trust is gratefully acknowledged.

Where applicable, the authors confirm that the experiments described here conform with The Physiological Society ethical requirements.

SA364

The mechanics of Na+/H+ antiport

D. Drew[1,2], C. Lee[1], H. Kang[1], C. von Ballmoos[2], S. Newstead[1,4], P. Uzdavinys[2], S. Iwata[3,4], O. Beckstein[5] and A. Cameron[3,4]

[1]Molecular Biosciences, Imperial College London, London, UK, [2]Biochemistry and Biophysics, Stockholm University, Stockholm, Sweden, [3]Membrane Protein Laboratory, Diamond Light Source, Harwell, UK, [4]Research Complex at Harwell Rutherford, Appleton Laboratory, Harwell, UK and [5]Department of Physics, Arizona State University, Tempe, AZ, USA

Na+/H+ antiporters finely tune intracellular concentrations of salt and pH by rapidly exchanging sodium ions with protons across the cell membrane. In humans these integral membrane proteins play an important role in physiology and their dysfunction is associated with a number of different diseases, eg, postischemic myocardial arrhythmias, cancer, heart disease and hypertension, the latter a major disorder affecting 1 in 4 adults in the United States. Here, I will discuss new structural insights into the mechanics of Na+/H+ antiport that has enabled us to have a better understanding of how they function at the atomic level.

This work was funded by grants from the Medical Research Council, the Swedish Research Council and the BBSRC. We are grateful for the use of the Membrane Protein Laboratory funded by the Wellcome Trust at the Diamond Light Source Limited and The Centre of Biomembrane Research, supported by the Swedish Foundation for Strategic Research. Computer simulations were partially run on XSEDE resources. C.L. was a recipient of a BBSRC-funded PhD scholarship, H.K. a Human Frontiers Postdoctoral fellowship, and D.D. acknowledges the support from The Royal Society through the University Research Fellow (URF) scheme.

Where applicable, the authors confirm that the experiments described here conform with The Physiological Society ethical requirements.

SA365

Dance lessons for proteins: the dynamics of the glutamate transporter homologue

O. Boudker

Physioogy and Biophysics, Weill Cornell Medical College, New York, NY, USA

Glutamate transporters are integral membrane proteins that catalyze neurotransmitter uptake from the synaptic cleft into the cytoplasm of glial cells and neurons. To pump their substrates against steep concentration gradients, they utilize the energy stored in the form of electro-chemical gradients of ions, primarily sodium. Their mechanism involves transitions between extracellular- (outward-) and intracellular- (inward-) facing conformations, whereby substrate binding sites become accessible to the opposite sides of the membrane. Our crystallographic studies on a bacterial homologue of glutamate transporters suggest that this process entails trans-membrane movements of three discrete transport domains within a trimeric scaffold. Using single-molecule fluorescence resonance

energy transfer imaging, we have directly observed large-scale transport domain movements. We find that individual transport domains alternate between periods of quiescence and periods of rapid transitions, reminiscent of bursting patterns first recorded in single ion channels using patch-clamp methods. We suggest that the switch to the dynamic mode in glutamate transporters is due to separation of the transport domain from the trimeric scaffold, which precedes domain movements across the bilayer. This spontaneous dislodging of the substrate-loaded transport domain is approximately 100-fold slower than subsequent trans-membrane movements and may be rate determining in the transport cycle. In addition, by means of X-ray crystallography, we have uncovered smaller local conformational transitions associated with substrate and ion binding in the outward- and inward-facing states of these transporters.

Where applicable, the authors confirm that the experiments described here conform with The Physiological Society ethical requirements.

SA366

Structural physiology of PepT1, the mammalian proton coupled peptide transporter

S. Newstead

Biochemistry, University of Oxford, Oxford, UK

The mammalian peptide transporter, PepT1, is a member of the Proton-coupled Oligopeptide Transporter (POT) superfamily of integral membrane proteins. The POT family function by coupling the bulk uptake of short chain peptides to the inwardly directed proton motive force present across the plasma membrane in eukaryotes and inner membrane of prokaryotes. POT family of transporters range in size from ~45 – 75 kDa and contain either 12 or 14 transmembrane helices. The smaller members of the family, which are mostly found in prokaryotes, consist almost entirely as a hydrophobic bundle of helices that reside within the membrane. The larger members of the family are mammalian in origin and whilst still maintaining the same conserved transmembrane core of 12 helices, have an additional polar domain that sits on the outside of the membrane.

Substantial progress has recently been made in determining the crystal structures of the bacterial members of the POT family, in particular understanding how they bind and transport peptides across the membrane. However, the role of the extra cellular domain, found only in PepT1 and PepT2, still remains unresolved. We have recently determined the crystal structure for this domain from PepT1 at 2.2 Å enabling the construction of a hybrid model of the mammalian PepT1 transporter. Combined with in vivo functional data, a role for this domain in transport is proposed, revealing intriguing mechanistic insights into the difference between the bacterial and mammalian POT family transporters with important implications for understanding peptide transport in mammalian cells.

Where applicable, the authors confirm that the experiments described here conform with The Physiological Society ethical requirements.

SA367

From crystallographic snapshots towards a mechanism for secondary transport

C.M. Ziegler

Structural Biology, MPI, Frankfurt, Hessen, Germany

The molecular understanding of secondary transport, in particular how transport activity is regulated, is one of the cutting-edge questions in biological science (1). A number of secondary transporters show regulation of transport activity, which plays an important role in nearly all stress-induced cellular responses. Transport activity can be regulated in response to various external stimuli, which often are difficult to identify. Therefore, only a few regulated transporters are described to date; one of the best characterized amongst them is the Na+-coupled betaine symporter BetP from Corynebacterium glutamicum (2). In the last five years several atomic structures of trimeric BetP were solved in different conformational states and under active and inactive conditions (3). First insights into a molecular mechanism of regulated transport in BetP were obtained by the combination of X-ray and electron crystallography data, functional measurements, spectroscopy and bioinformatics. Thereby, the transport cycle of BetP was described in molecular detail. The key towards crystallizing different conformational state was found in a combination of rational mutagenesis of residues involved in substrate-coupling and purification methods that consider strongly the stabilizing effects of lipids.

1. Forrest LR, Krämer R, Ziegler C. The structural basis of secondary active transport mechanisms. Biochim Biophys Acta. 2011 1807(2):167-88.

2. Ziegler C, Bremer E, Krämer R. The BCCT family of carriers: from physiology to crystal structure. Mol Microbiol. 2010 78(1):13-34.

3. Perez C, Ziegler C. Mechanistic aspects of sodium-binding sites in LeuT-like fold symporters. Biol Chem. 2013 Jan 29 [Epub ahead of print].

Reinhard Krämer and Lucy Forrest

Where applicable, the authors confirm that the experiments described here conform with The Physiological Society ethical requirements.

SA368

Time to translate? Overview of myometrial contractility

S. Wray

University of Liverpool, Liverpool, UK

The focus of my presentation will be to review our understanding of myometrial contractility, how it is brought about and controlled, to highlight emerging topics of interest, and ask if we are getting closer to having new drugs to help prevent preterm or slow labours.

I will focus on recent insights into the role of the sarcoplasmic reticulum in the myometrium to illustrate how we have to study the myometrium, not other smooth muscles or cell lines, if we are to understand the uterus. I will then describe what insights may be gained from studying different patient groups, e.g. women who are obese or diabetic, pregnant with twins or going beyond their due dates. Do we now have the tools to understand the impact of these conditions on the underlying myometrial physiology? What contributions can modelling,

medicinal plants and studies of extracellular matrix and electrophysiology, make? How can we make all of this synergise so that we can bear down on being able to translate from the basic science to women in labour?

Where applicable, the authors confirm that the experiments described here conform with The Physiological Society ethical requirements.

SA369

From genome-wide screens to computational modelling: finding novel targets to manipulate uterine function

A. Blanks

University of Warwick, Coventry, UK

Clinical conditions commonly associated with abnormal uterine activity are preterm labour (PTL), dysfunctional labour and post partum haemorrhage (PPH). Preterm birth is the biggest cause of neonatal mortality and morbidity. Dysfunctional labour leads to operative vaginal and abdominal delivery with its inherent maternal risks, and PPH is a major global cause of maternal morbidity and mortality accounting for around 25% of deaths in postpartum mothers in developing nations. PTL, PPH and dysfunctional labour have complex, multi-factorial aetiologies and it is unrealistic to assume that all cases will be treated by a single approach. None-the-less a greater understanding of the underlying principles of uterine contractions offers the prospect of discovering novel therapeutics for these disorders. We have established a research programme combining molecular biology, computational modeling, in vitro and in vivo physiology, and drug discovery to increase basic understanding and discover new treatments. In this presentation I shall argue that such an approach has enormous potential by using our discovery of a novel inwardly rectifying potassium channel as an exemplar.

To identify novel targets we started by using laser capture micro dissection to isolate mRNA from pure myometrial (MSMC) and vascular smooth muscle cells (VSMC) present in uterine samples taken at cesarean section. mRNA was then amplified and sequenced by RNAseq. Gene lists of all expressed ionic conductances were constructed and analysed for significant differences between MSMC and VSMC. Identified candidates were then subjected to a 'virtual' screen by computationally modeling the effect of changing channel densities/activity based on known biophysics (Aslanidi et al. 2011). One candidate, Kir7.1 was taken forward as a potential modifier of resting membrane potential and uterine excitability during gestation. qRT-PCR and western blot analysis demonstrated that Kir7.1 expression is regulated at the mRNA and protein level during gestation in mouse and human. Knockdown of Kir7.1 protein, in vitro, by lentiviral miRNA resulted in profoundly increased contractions when compared to scrambled control. Over expression of hKir7.1 resulted in inhibition of phasic contractions. Microelectrode recordings of phasic contractions in knockdown and overexpressing strips demonstrated that the observed phenotypes were mediated by a change in membrane potential. In vivo, mice injected with lentiviral miRNA demonstrated significantly increased intrauterine pressure and preterm delivery when compared to scrambled control. To explore potential therapeutic avenues at this protein target we tested the effect of the novel Kir7.1/ROMK inhibitor VU590 and VU590 (Lewis et al. 2009) like derivatives on whole cell current under voltage clamp conditions combined with current clamp recordings of in vitro contracting myometrial strips. VU590 dose dependently inhibits a Kir7.1 like current in native mouse and human MSMC, whilst addition of VU590 to contracting myometrial strips leads to rapid depolarization of resting membrane potential followed by long-lasting tonic contractions that are reversible on washout. To test whether physiological activity was specific to Kir7.1 we manufactured chemical derivatives that lost Kir7.1 activity but retained ROMK activity. These derivatives failed to affect contractions or membrane potential.

I shall conclude that genomic screening of laser-dissected tissues, taken under different physiological conditions, and combined with RNAseq is an effective means of surveying mRNA profiles. Such profiles, when combined with accurate biophysical information and computational models can lead to a rapid, predictive, focusing down on potential targets with desirable physiological phenotypes. Once identified, in vitro knockdown of targets using lentiviral delivery vectors provides an excellent first means to assess whether subsequent investment of time and resources in a drug discovery programme is worthwhile.

Aslanidi, O. et al., Prog Biophys Mol Biol 107(1), 183 (2011)

Lewis, LM. et al., Mol Pharmacol. Nov;76(5), 1094-103 (2009)

Work presented was funded by:

1. Medical Research Council grant number G0901801
2. Medical Research Council Centenary Award to Dr Blanks
3. Medical Research Council Technologies

Where applicable, the authors confirm that the experiments described here conform with The Physiological Society ethical requirements.

SA370

The importance of the smooth muscle cytoskeleton for preterm labor

K. Morgan

Boston University, Boston, MA, USA

Myometrial stretch and increases in wall tension have been implicated clinically in the initiation of labor and the etiology of preterm labor. We have taken a biomechanical and biochemical approach, using human tissues and rodent models to investigate the molecular mechanisms involved. Together with our collaborators, we have found, firstly, that the intracellular Ca requirement for activation of the contractile filaments increases during gestation. The decreased Ca sensitivity correlates with an increase in the expression of caldesmon, an actin binding protein and inhibitor of myosin activation, during pregnancy. In late pregnancy we observed an increase in ERK-mediated caldesmon phosphorylation, which appears to reverse this inhibitory effect during labor.

Force generated by the myometrial contractile filaments is communicated across the plasmalemma and to the uterine wall through the focal adhesions. Using phosphotyrosine screening and mass spectrometry of stretched myometrial samples, we identified 3 stretch-activated focal adhesion proteins, FAK, p130Cas, and alpha actinin. FAK-Y397, which signals integrin engagement, is constitutively phosphorylated in term human myometrium whereas FAK-Y925, which signals downstream ERK activation, is phosphorylated during stretch. This Src mediated signaling appears to provide a tunable tension sensor in the myometrial cell.

We have recently identified smooth muscle Archvillin (SmAV) as a new ERK scaffolding protein. A newly produced SmAV-

specific antibody demonstrates gestation-specific increases in SmAV protein levels and stretch-specific increases in SmAV association with focal adhesion proteins. Thus, whereas increases in caldesmon levels suppress human myometrium contractility during early pregnancy, stretch-dependent focal adhesion signaling, and ERK activation contribute to subsequent myometrial activation.

In parallel, biophysical measurements of smooth muscle compliance at both the cellular and tissue levels suggest that decreases in cellular compliance due to changing interactions of the actin cytoskeleton with the focal adhesions may also promote increases in uterine wall tension. Thus these results, taken together, suggest that focal adhesion proteins and their interaction with the cytoskeleton may present a new mode of regulation of uterine contractility.

Li Y, Je HD, Malek S, Morgan KG. Role of ERK1/2 in uterine contractility and preterm labor in rats. Am J Physiol Regul Integr Comp Physiol 2004; 287(2):R328-35.

Li Y, Gallant C, Malek S, Morgan KG. Focal adhesion signaling is required for myometrial ERK activation and contractile phenotype switch before labor. J Cell Biochem, 2007; 100:129-140.

Wu X, Morgan KG, Jones CJ, Tribe RM, Taggart MJ. Myometrial mechanoadaptation during pregnancy: implications for smooth muscle plasticity and remodeling. JCMM 2008; 12:1360-73.

Li YP, Reznichenko M, Tribe R, Hess P, Taggart MJ, Kim HR, Gangopadhyay S, Morgan KG. Gestation-Dependent Stretch Activates Focal Adhesion Signaling and Modulates Human Myometrial Activation. PLoS ONE 2009 4(10):e7489

Min J, Reznichenko M, Poythress P, Gallant C, Vetterkind S, Li Y, Morgan KG. Src Modulates Contractile Vascular Smooth Muscle Function via Regulation of Focal Adhesions. J Cell Physiol. 2012 227: 3585-92.

Where applicable, the authors confirm that the experiments described here conform with The Physiological Society ethical requirements.

SA371

Finding new agent and mechanisms in medicinal plants

S. Kupittayanant, P. Munglue, W. Lijuan, W. Proprom and N. Buddhakala

Physiology, Suranaree University of Technology, Muang, Nakhon Ratchasima, Thailand

Since ancient times medicinal plants have had an important place in preventing and treating disease. Many conventional drugs originate from plant sources, including aspirin (from willow bark), the heart drug digoxin (foxglove), and morphine (opium poppy). Scientific and modern pharmaceutical interest in medicinal plants is largely due to the need for new, safe drugs, but they remain important to many people in the developing world who do not have access to modern medicines. Several medicinal plants have been used for uterine proposes in the developing world (Gruber & O'Brien, 2011). However, the mechanisms of action of such the plants have never been elucidated. The aims of the studies in my laboratory are therefore to investigate the effects of some medicinal plants on myometrial physiology. Plant extracts were prepared from botanical sources, standardized and validated. Phytochemical screening of the crude extracts was analysed using gas chromatography–mass spectrometry. All separated compounds were identified from the recorded mass spectra by comparison with the mass spectra from the NIST and Wiley libraries. Animal cares, environmental conditions, and uses followed the guidelines of Laboratory Animal Resources and the procedures of the experiment were approved by the Institutional Animal Care and Use Committee. Rats were humanly killed. The uteri were removed and the strips of longitudinal myometrium isolated. Isometric force was measured in organ baths and vehicle and time controls were always performed. The effects of plant extracts on spontaneous and agonist-induced contraction in the uterus were investigated, and the dose response range determined. Using a pharmacological approach, the parts of the myometrial excitation contraction pathway which were affected by the extracts, were dissected. This approach provided a good amount of mechanistic information. The results showed that some of the plant extracts are potent inhibitors (Buddhakala et al, 2008; Munglue et al, 2012) whereas others are potent stimulators (Promprom et al, 2010; Lijuan et al, 2011) for the uterus. The parts in the pathways affected were extract specific and reveal many therapeutic targets, including calcium entry and sarcoplasmic reticulum release, and stimulating the NO-cyclic guanosine monophosphate relaxant pathway. Taken together, these data will give us a better understanding of how medicinal plants work on the uterus and the results of these findings can be applied in other areas of smooth muscle physiology, as well as pharmacy and medicine.

Buddhakala N, Talubmook C, Sriyotha P, Wray S & Kupittayanant S (2008). Inhibitory effects of ginger oil on spontaneous and $PGF_{2\alpha}$-induced contraction of rat myometrium. *Planta Med*74(4), 385-391.

Gruber CW & O'Brien M (2011). Uterotonic plants and their bioactive constituents. *Planta Med*77(3), 207-220.

Lijuan W, Kupittayanant P, Chudapongse N, Wray S & Kupittayanant S (2011). The effects of wild ginger (*Costus speciosus* (Koen) Smith) rhizome extract and diosgenin on rat uterine contractions. *Reprod Sci*18(6), 516-524.

Munglue P, Eumkep G, Wray S & Kupittayanant S (2012). The Effects of Watermelon (*Citrullus lanatus*) Extracts and L-Citrulline on Rat Uterine Contractility. *Reprod Sci*; DOI: 10.1177/1933719112459223.

Promprom W, Kupittayanant P, Indrapichate K, Wray S & Kupittayanant S (2010). The effects of pomegranate seed extract and beta-sitosterol on rat uterine contractions. *Reprod Sci*17(3), 288-296.

I gratefully acknowledge the National Research Council of Thailand, the Office of the Higher Education Commission (Thailand), Suranaree University of Technology (Thailand), and the Physiology Society (London) for financial support.

Where applicable, the authors confirm that the experiments described here conform with The Physiological Society ethical requirements.

SA372

A tale of two channels-Kv7 and ERG in myometrial regulation

I.A. Greenwood

St George's, London, UK

Regulation of smooth muscle contractility is crucial aspect of uterine physiology. This is highlighted by the developmental switch that the myometrium undergoes as gestation progresses into labour. However, little is known about the molecular mechanisms that govern the change in contractile phenotype and how these mechanisms are affected in pathological scenarios. Potassium channels are integral to the control of myometrial contraction and various types of potassium channel have been identified in rodent and human myometrial smooth muscle. Our collaborative work has focussed upon the expression and functional impact of two types of voltage-gated potassium channels previously associated with neuronal and

cardiac excitability namely KCNQ- and ether-a-go-go (KCNH) genes. This talk will be give an overview of our work on these channels showing the expression of different KCNQ and KCNH isoforms in uterus from non-pregnant and pregnant animals as well as human tissues. It will also highlight the different impact of these potassium channels in myometrial contractility with ERG channels losing functional impact as gestation develops whereas KCNQ channels remain a robust and therapeutically viable target through-out pregnancy. These data have provided mechanistic insight into uterine physiology and provide new possible targets for therapeutic intervention.

Work in Dr Greenwood's laboratory is supported by the BBSRC, Action Medical Research and the British Heart Foundation with further support from NeuroSearch A/S

Where applicable, the authors confirm that the experiments described here conform with The Physiological Society ethical requirements.

SA373

The role of miRNAs in cardiovascular ageing

R. Boon

Institute for Cardiovascular Regeneration, Goethe University, Frankfurt, Germany

Aging is the major risk factor for developing cardiovascular complications like endothelial dysfunction, aneurysm formation, acute myocardial infarction and heart failure. The mechanisms involved in cardiovascular aging are poorly understood, but microRNAs (miRNAs) have emerged as key biological regulators. We have identified that age-induced miR-29 has a causal role in aneurysm formation by regulating the expression of extracellular matrix proteins in the aorta. Furthermore, we recently described the crucial role for miR-34a in cardiac aging, which regulates cardiomyocyte apoptosis and telomere length by targeting the protein phosphatase nuclear targeting subunit PNUTS. Current studies in the laboratory focus on determining the role of miRNAs, their targets and their transcriptional regulators in aging of the endothelium and how these affect organ homeostasis and cellular metabolism.

Where applicable, the authors confirm that the experiments described here conform with The Physiological Society ethical requirements.

SA374

The role of miRNA in vascular remodeling

A. Baker

Institute of Cardiovascular and Medical Sciences, University of Glasgow, Glasgow, UK

MicroRNAs (miRNAs) are short non-coding RNAs, which post-transcriptionally regulate gene expression. miRNAs are important in governing cell differentiation, development and disease. Our work spans the role of miRNA in the development of vascular pathologies associated with remodeling and with the vascular regenerative strategies in ischaemic conditions. We have focused on miRNA in the development of pulmonary arterial hypertension and vein graft disease. In consideration of the role played by miRNAs in cell proliferation and vascular remodeling, we evaluated the involvement of the smooth muscle cell-associated miRNAs miR-143 and miR-145 in the development of PAH, as well as the role of miRNA-21 which is more widely expressed. Significant dysregulation of these miRNAs in PAH and VG disease has been observed in animal models and in pathological samples and manipulation has been shown to the beneficial in prevention of pathological remodelling. Manipulation of miR-21 and miR-145 may therefore represent a novel strategy to prevent the development of these pathologies that have substantial unmet clinical need. Strategies to efficiently delivery these therapeutics to the vessel wall will also be discussed.

Where applicable, the authors confirm that the experiments described here conform with The Physiological Society ethical requirements.

SA375

microRNAs, transforming growth factor beta-1 and tissue fibrosis

R.H. Jenkins

Institute of Molecular and Experimental Medicine and Central Biotechnology Services, School of Medicine, Cardiff University, Cardiff, UK

microRNAs are small, endogenous, post-transcriptional regulators of gene expression. A single microRNA may potentially regulate several hundred protein-coding genes, and recent estimates suggest approximately 60% of human protein-coding genes are regulated by microRNAs. Changes in microRNA expression patterns are linked to profound effects on cellular phenotype and microRNAs have an emerging role in diverse physiological and pathological processes. This presentation will describe the regulation of microRNA expression by Transforming Growth Factor Beta-1, a key cytokine with pivotal roles in cellular proliferation, differentiation, motility and adhesion. Consistent with these roles, Transforming Growth Factor Beta-1 expression is a frequent observation in fibrosis-driven pathology. In this context, I will discuss data from our laboratory focusing on the role of miR-192 in the pathogenesis of acute and chronic kidney disease.

Jenkins RH, Davies LC, Taylor, PR, Akiyama H, Phillips AO, Bowen T, Fraser DJ. microRNA-192 mediated induction of G2M growth arrest in aristolochic acid nephropathy. Am. J. Pathol. (in submission)

Bowen T, Jenkins RH, Fraser DJ. MicroRNAs, Transforming Growth Factor Beta-1, and Tissue Fibrosis. J. Pathol. 2013 229(2) 274-85

Jenkins RH, Martin J, Phillips AO, Bowen T, Fraser DJ. Transforming growth factor-β1 represses proximal tubular cell microRNA-192 expression via decreased hepatocyte nuclear factor binding. Biochem. J. 2012 443(2) 407-16

Martin J, Jenkins RH, Bennagi R, Phillips AO, Bowen T, Fraser DJ. Post-transcriptional regulation of transforming growth factor-β1 by microRNA-744. PLoS One 2011 6 (10), e25044

Krupa A, Jenkins RH, Luo DD, Lewis A, Phillips AO, Fraser, DJ. Loss of miR-192 promotes fibrogenesis in diabetic nephropathy. J. Am. Soc. Nephrol. 2010 21(3), 438-47

This work was supported by Kidney Research UK [RP24/2009]

Where applicable, the authors confirm that the experiments described here conform with The Physiological Society ethical requirements.

SA376

Role of miRNAs in mitochondria and genetic disease

A. Henrion-Caude

Imagine Institute, Inserm U781, Paris, France

MicroRNAs (miRs) are most often depicted as fine-tuners of gene expression, and more occasionally as genetic switches. Still few examples delineate their contributions as phenotypic modulators. We reasoned that browsing their contribution to genetic disease could provide a framework for understanding some of the requirements to devise miRNA-based therapy strategies. Here we will browse through what appeared as a mitochondrial view of miRs. We will provide examples showing that miRs may be crucial in the regulation of mitochondrial components, such as in the case of Friedreich ataxia. Conversely, we will present the rationale that supports their involvement within the mitochondrion.

We thank the AFAF for their financial support.

Where applicable, the authors confirm that the experiments described here conform with The Physiological Society ethical requirements.

SA377

Type 1 angiotensin receptors in the kidney and the control of blood pressure

S.B. Gurley, J. Stegbauer, M.A. Sparks, D. Chen, M. Herrera and T.M. Coffman

Duke University Medical Center, Durham, NC, USA

The renin-angiotensin system (RAS) is a key regulator of blood pressure (BP), with angiotensin II (ang II) acting as a major effector molecule via its receptors which are broadly expressed in a variety of tissues. Previous and ongoing work from our lab has demonstrated the significance of the type 1 angiotensin receptor in the kidney for BP homeostasis. We have taken the approach of gene-targeting in mice to study the role of the AT1A receptor in BP regulation and hypertension pathogenesis. Mice completely deficient in AT1A receptors had profound reductions (>20 mm Hg) in systolic blood pressure. Following this, we next used a kidney cross-transplantation approach to identify the kidney as a tissue with a distinct role in BP regulation by the RAS. Kidney AT1A KO mice had lower baseline BPs and were resistant to angiotensin II hypertension. Our more recent studies have investigated the function of the AT1A receptor in BP control in individual cell lineages in order to dissect the role of the RAS in specific regions of the kidney. To accomplish this, we utilized a *cre*-loxp approach for cell-specific gene targeting using a mouse line we generated with a conditional *Agtr1a* allele. We have systematically examined the role of the AT1A receptor in BP regulation in the renal proximal tubule, distal nephron and renal vasculature. Our studies have identified critical segments in the kidney for baseline blood pressure homeostasis, salt sensitivity, and regulation of hypertension. Together, our data suggest that type 1 angiotensin receptors in the kidney play a complex role in the integrated control of blood pressure.

Where applicable, the authors confirm that the experiments described here conform with The Physiological Society ethical requirements.

SA378

Sympathetic vasomotor control by oxidative stress in renovascular hypertension

E.B. Oliveira Sales[1], R.R. Campos[1] and J.F. Paton[2]

[1]Physiology, Federal University of Sao Paulo, Sao Paulo, Brazil and [2]Physiology, University of Bristol, Bristol, UK

There is mounting evidence that increased oxidative stress and sympathetic nerve activity play important roles in renovascular hypertension. In the present study, we tested whether enhanced superoxide signaling in RVLM of 2 kidney-1 clip rats (2K-1C) contributes to the chronic hypertension via sympathetic activation in conscious rats. In our previous studies, we identified an increase in AT1 angiotensin II receptor expression and in oxidative markers within the RVLM of 2K1C rats. Furthermore, tempol or vitamin C acute administration into the RVLM or systemically reduced blood pressure and renal sympathetic activity in 2K-1C but not in control rats. Thus, in this study, we enhanced superoxide scavenging into the RVLM by overexpressing cytoplasmically targeted superoxide dismutase enzyme using an adenoviral vector (Ad-CMV-CuZn-SOD) in Wistar rats (male, 150 to 180 g) in which the left renal artery was occluded partially 3 weeks earlier. Hypertension was documented using 24 hour radio-telemetry recording of arterial pressure (AP) and heart rate (HR) in conscious freely-moving rats. Hey Presto software (Waki et al, 2006) was used to calculate indices of autonomic function from the AP and HR variability by spectral analysis. Renovascular hypertension elevated both serine phosphorylation of p47phox subunit of NADPH and superoxide levels within the RVLM. The elevated superoxide levels were normalized by expression of CuZnSOD in the RVLM. Moreover, the hypertension produced in the 2K-1C rats was reversed 1 week after viral-mediated expression of CuZnSOD. This antihypertensive effect was maintained and associated with a decrease in the low-frequency spectra of systolic blood pressure variability, suggesting reduced sympathetic vasomotor tone. The expression of CuZnSOD was localized in the RVLM neurons, of which some contained tyrosine hydroxylase (C1 neurons). None of the above variables changed in control rats receiving Ad-CMV-eGFP in the RVLM. In renovascular hypertension, superoxide signaling in the RVLM plays a major role in the generation of increased sympathetic vasomotor tone and the chronic sustained hypertension.

Waki H et al (2006). Exp Physiol, 91,201-13.

Supported by CAPES and British Heart Foundation.

Where applicable, the authors confirm that the experiments described here conform with The Physiological Society ethical requirements.

SA379

Mice with selective angiotensin type 1A receptor deletion from catecholaminergic neurons show altered angiotensin II-dependent hypertension

A.M. Allen[1], N. Jancovski[1], J.K. Bassi[1], A.A. Connelly[1], J. Brandi[1], E.A. Stevens[1] and G.A. Head[2]

[1]Physiology, University of Melbourne, Parkville, VIC, Australia and [2]Neuropharmacology, Baker IDI Research Institute, Melbourne, VIC, Australia

Background: Angiotensin II (AngII) acts via several tissues, including the brain to exert its well established roles in the regulation of blood pressure (BP) and fluid and electrolyte regulation. Manipulation of brain AngII can also induce metabolic changes including lean phenotype and increased metabolic rate possibly via modulation of the sympathetic nervous system. These actions are mediated via activation of the AngII type 1A receptor (AT1AR). In addition, chronic low dose infusion of Ang II induces hypertension via activation of the AT1AR. Whilst the involvement of AT1AR in specific cells of the kidney has been demonstrated in AngII-dependent hypertension it is not clear whether other tissues are involved. The present study aimed to investigate whether targeted deletion of AT1ARs from the catecholaminergic cells affects the baseline metabolic parameters and blood pressure (BP) and the response to sustained infusion of AngII. Methods: All experiments were approved by the University of Melbourne Animal Experimentation Ethics Committee in accordance with guidelines of the Australian National Health and Medical Research Council. Mice (C57Bl/6 background) with cell-selective deletion of the AT1AR from catecholaminergic cells were generated by crossing AT1AR floxed (AT1ARfl/fl) mice with mice expressing cre-recombinase (Cre) under the control of the tyrosine hydroxylase (TH) promoter. Two different genotypes AT1ARfl/fl;TH-Cre+/- (knockouts) and AT1ARfl/fl;TH-Cre-/- (controls) were used in this study. In vitro autoradiography was performed to confirm the loss of AT1R binding from catecholaminergic cells. All surgical procedures were performed under surgical anesthesia (loss of pedal withdrawal reflex) using either isoflurane delivered by a gas mask (~2% in oxygen) or ketamine/xylacine i.p. (75 mg/kg:10 mg/kg). All animals received a long-acting, non-steroidal anti-inflammatory agent at the start of the surgical procedure (caroprofen 5 mg/kg). Telemetry devices were used to record baseline BP and heart rate (HR). For the metabolic studies, mice were housed individually in metabolic cages with free access to food and water. After 1 day acclimatization 24 hour urine output and food and water intake were recorded. AngII-dependent hypertension was induced by subcutaneous implantation of mini-osmotic pumps designed to infuse Ang II (500 ng/kg/min) for 4 weeks. Results: AT1R binding was completely absent in the adrenal medulla and thoracic sympathetic ganglia of the AT1AR fl/fl;TH-Cre+/- mice. Basal systolic BP and HR were not different between the groups (mean±SEM; 109± 1mmHg vs. 108 ± 2 mmHg and 553± 10 bpm vs. 573 ± 10 bpm). Body weight, water intake, and 24 h urine volumes were also not different between groups. Infusion of Ang II in AT1ARfl/fl;TH-Cre-/- induced a gradual pressor response that was increased above baseline by day 5 of infusion. The maximal change in BP occurred at day 13. After day 17 BP gradually decreased toward baseline. The trajectory of BP increase was less in the AT1A fl/fl;TH Cre+/- mice throughout the infusion with a significant decrease in the maximal response at day 13 of infusion (150± 3 mmHg vs. 133 ± 2 mmHg; $P<0.05$). The reduced pressor response was associated with reduced fluid and electrolyte retention, reduced activation of the sympathetic nervous system and loss of superoxide formation in key brain cardiovascular nuclei. Conclusions: AT1AR knockout from catecholaminergic cells does not elicit changes in metabolic state, baseline systolic BP or HR but expression of the receptor by these cells is essential for the full development of AngII hypertension.

Funded by the Australian NHMRC

Where applicable, the authors confirm that the experiments described here conform with The Physiological Society ethical requirements.

SA380

Contributions of vascular inflammation in the brainstem for neurogenic hypertension

H. Waki

Physiology, Wakayama Medical University School of Medicine, Wakayama, Japan

Essential hypertension is idiopathic; however, it is accepted as a complex polygenic trait with underlying genetic components that remain unknown. Our supposition is that the pathogenesis of primary hypertension involves the activation of the sympathetic nervous system. In this symposium, I will summarize our findings obtained from experimental animal models of hypertension and introduce new mechanisms of neurogenic hypertension.

One pivotal region controlling the arterial pressure set point is the nucleus tractus solitarii (NTS). Since bilateral microinjection of $CoCl_2$, a non-selective blocker of neurotransmission, into the NTS of an animal model of human hypertension (the spontaneously hypertensive rat: SHR) resulted in an attenuated pressor response compared to normotensive Wistar Kyoto (WKY) rats (H. Waki, unpublished data). We therefore propose that alterations in the electrical excitability state of neurons in the NTS could be involved, at least in part, in the mechanisms underlying neurogenic hypertension in the SHR.

By performing whole-genome expression profiling on NTS tissues, we found that pro-inflammatory molecules, such as junctional adhesion molecule A (JAM-A) and leukotriene B4 (LTB4), were over-expressed in the NTS in SHRs compared to WKY rats [1, 2]. We also observed the accumulation of endogenous leukocytes inside capillaries within the NTS of SHRs and JAM-A- and LTB4-over-expressing rats [1, 2]. We also confirmed functionally that high levels of JAM-A and LTB4 may, in part, contribute to the development of neurogenic hypertension, and are not secondary to hypertension [1, 2]. Importantly, recent findings further confirmed that JAM-A may be involved in the etiology of not only SHRs but also other animal models of hypertension [3] and essential hypertension in humans [4].

The next question we addressed was how these high levels of pro-inflammatory molecules in the NTS can cause neurogenic hypertension. Despite the specific inflammatory state in the NTS of SHRs, which may be genetically programmed, the transcripts of some inflammatory molecules, such as chemokine (C–C motif) ligand 5 (Ccl5) and its receptors, chemokine (C–C motif) receptor 1 and 3, were down-regulated in the NTS of SHRs compared to WKY rats [5]. This may be a compensatory mechanism to avoid further strong inflammatory activity. Supporting this hypothesis, we found that a high level of LTB4 in the NTS could reduce Ccl5 transcript levels [5]. More importantly, we found that down-regulation of Ccl5 in the NTS of SHRs may be pro-hypertensive, since microinjection of Ccl5

into the NTS of SHRs decreased arterial pressure, but was less effective in WKY rats [5]. Since Ccl5 receptors are involved in the modulation of glutamate transmission from glutamate nerve endings, we hypothesize that the down-regulation of Ccl5 in the NTS may directly affect NTS neurons and hence result in the development of neurogenic hypertension in the SHR.

In addition to the above theory for the etiology of hypertension, we hypothesized that localized hypoxia in the NTS may also have a role in neurogenic hypertension [6]. The accumulation of leukocytes in the NTS microvasculature may induce an increase in vascular resistance and hypoperfusion within the NTS; the latter may trigger focal hypoxia, which may affect central neural cardiovascular activity. Therefore, we explored whether increased vascular resistance, low blood perfusion, and low oxygen delivery localized to the NTS can increase arterial pressure. We measured cardiovascular parameters before and after specific branches of the superficial dorsal medullary veins were occluded; we assumed these were drainage vessels from the NTS and their occlusion would produce stagnant hypoxia [7]. Following vessel occlusion, blood flow in the dorsal surface of the medulla oblongata, including the NTS region, showed an ~60% decrease and was associated with hypoxia in neurons located predominantly in the caudal part of the NTS, as revealed by using Hypoxyprobe-1, which is a marker for cellular hypoxia [7]. Arterial pressure increased and this response was significantly pronounced in both magnitude and duration when baroreceptor reflex afferents were sectioned [7]. These results suggest that localized hypoxia in the NTS increases arterial pressure. We propose that this represents a protective mechanism whereby the elevated systemic pressure is a compensatory mechanism to enhance cerebral perfusion. We assumed that this physiological mechanism may also be involved in the pathogenesis of neurogenic hypertension [6, 7].

All told, we suggest that vascular inflammation within the brainstem leads to elevated sympathetic nerve activity by multiple pathways in neurogenic hypertension.

Waki H, et al., Hypertension, 2013, 61: 194-201

Waki H, et al., Hypertension, 2007, 49: 1321-1327

Xu H,et al., Cardiovasc Res, 2012, 96: 552-560

Ong KL, et al., Am J Hypertens, 2009, 22: 500-505

Gouraud SS, et al., J Hypertens, 2011, 29: 732-740

Paton JF, et al., Exp Physiol, 2009, 94: 11-17

Waki H, et al., J Hypertens, 2011, 29: 1536-1545.

Supported by the British Heart Foundation and KAKENHI (19599022, 19-07458, 21300253)

Where applicable, the authors confirm that the experiments described here conform with The Physiological Society ethical requirements.

SA382

Advent of the coronary circulation: Comings and goings among most of the world's vertebrates

T. Farrell, G. Cox, N. Farrell and H. Jourdan

University of British Columbia, Vancouver, BC, Canada

The embryonic development of a coronary circulation in birds and mammals occurs in concert with myocardial compaction, likely in response to myocardial hypoxia and the work of a cardiac chamber. Whether similar driving forces featured prominently during the evolution of the coronary circulation among chordates remains a mystery, in part because the arrangements for supplying oxygen to fish hearts are far more diverse than a simple coronary supply to compact myocardium. Indeed, it may be that the majority of fish species do not have a coronary circulation! As evident from extant cyclostome fishes, the archetype chambered, myogenic heart probably had no coronary circulation; a spongy ventricular myocardium receives its oxygen supply from systemic venous blood. Instead, the coronary circulation likely made its first appearance with the appearance of a jaw and a vertebral column advent in the elasmobranch fishes. While all elasmobranchs have compact myocardium in variable amounts in their ventricle, all boney fishes (teleosts) do not have a coronary circulation, suggesting an evolutionary loss of this cardiac oxygen supply route, a feature that persists in extant amphibians. Molecular phylogenies have shown where losses have occurred. Thus, many fish do not need a coronary circulation, even if the heart's oxygen supply is precariously dependent on oxygen-depleted venous blood. Thus, beyond the highly developed coronary circulations of endothermic sharks, salmonids and tunas, cardiac evolution showed movement away from coronary dependence, beginning perhaps with the cyprinid lineage and persisting at least through to the amphibians. . The degree of ventricular compaction in boney fishes, in part, is tied to athleticism, as shown by salmon and tunas, suggesting a close tie between the degree of compaction and cardiac workload. Nevertheless, salmon can survival and swim after coronary artery ligation, which suggests only a facultative dependence under certain situations. In fishes, the fact remains that a coronary circulation is always associated with compact myocardium and this is true for cardiac muscle of the ventricle as well as the cardiac muscle of the outflow tract, the conus arteriosus. Where the greatest mystery lies is with the forerunners of the tetrapod lineage, the lungfishes and coelocanths, and with the extant species of basal teleosts, many of which breathe air as well as water. Often these fishes lack compact myocardium in their ventricle, but possess a coronary circulation, which raises the question of coronary vascularity in the spongy myocardium. While the evolution of air breathing in fishes certainly increased the security of the cardiac oxygen supply by bringing better-oxygenated blood to spongy myocardium, it clearly did not supplant the need for a coronary circulation. Curiously, the early evolution of cardiac compaction and a coronary circulation also introduced the possibility of coronary arteriosclerosis since it is very prevalent in migratory salmon.

Farrell, A.P., N.D. Farrell, H. Jourdan, and G.K. Cox. 2012. A Perspective on the evolution of the coronary circulation in fishes and the transition to terrestrial life. In: Ontogeny and Phylogeny of the Vertebrate Heart. Eds. D. Sedmera and T. Wang, New York, Springer. pp. 75-102.

Davie, P.S. and A.P. Farrell. 1991. The coronary and luminal circulations of the myocardium of fishes. Can. J. Zool. 69: 1993-2001.

Saunders, R.L., A.P. Farrell and D.E. Knox. 1992. Progression of coronary arterial lesions in Atlantic salmon (Salmo salar) as a function of growth rate. Can. J. Fish. Aquat. Sci. 49: 878-884.

Steffensen, J.F. and A.P. Farrell. 1998. Swimming performance, venous oxygen tension and cardiac performance of coronary-ligated rainbow trout, Oncorhynchus mykiss, exposed to progressive hypoxia. Comp. Biochem. Physiol. A 119: 585-592.

APF is supported by a Canada Research Chair and NSERC Canada.

Where applicable, the authors confirm that the experiments described here conform with The Physiological Society ethical requirements.

SA383

Cardiovascular function in fish: consequences from life in a chronically heated environment

E. Sandblom[1], A. Ekström[1], T. Aho[3], F. Sundström[2] and F. Jutfelt[1]

[1]Dept of Biological and environmental sciences, University of Gothenburg, Gotheburg, Sweden, [2]Dept of Animal Ecology, Uppsala University, Uppsala, Sweden and [3]Institute of Coastal Research, Swedish University of Agricultural Sciences, Öregrund, Sweden

Global climate change is predicted to continue with increasing average temperatures and more frequent temperature extreme events. This will have a profound impact on ectothermic animals such as fish where the body temperature and metabolism is directly determined by the ambient temperature. Current prevailing hypotheses suggest that insufficient oxygen transport is a primary limitation for ectothermic animals at elevated temperature, but knowledge about the adjustments to the cardiorespiratory system in fish during long-term warming (i.e. via acclimation and genetic adaptation) is still limited. Results from a recently launched research project on cardiovascular and respiratory function in Eurasian perch (Perca fluviatilis) that live and reproduce in the chronically heated 'Biotest enclosure' in the Baltic Sea off the nuclear power plant in Forsmark in Sweden will be presented and discussed. Cooling water from the nearby nuclear reactors has been directed to the 90 hectare enclosure since 1980 keeping water temperatures 5-10°C above ambient for over 30 years, but at otherwise the same abiotic conditions as the surrounding archipelago. Thus, this experimental facility presents a unique opportunity to study the physiological responses to chronic warming in a wild fish population. Preliminary results reveal that fish from the Biotest enclosure have smaller hearts relative to their body mass, and they are considerably more tolerant to acute temperature increase and better able to maintain cardiac function during acute thermal challenges. In addition, they have a depressed metabolic rate and a lower resting heart rate due to a higher cholinergic tone and a reduced intrinsic cardiac pacemaker rate relative to fish from outside the enclosure when compared at the same temperature.

Where applicable, the authors confirm that the experiments described here conform with The Physiological Society ethical requirements.

SA384

Control of pacemaker HCN channel function by cAMP and voltage

E. Accili

University of British Columbia, Vancouver, BC, Canada

Pacemaker HCN channels contribute to pacing in the mammalian sinoatrial node (SAN) (1), a region of the heart that determines natural beating rate, as well as in other species such as frog (2) and even the most basal chordates (3,4). Pacemaker channels are unusual in that they are opened by hyperpolarization and bind cAMP, which facilitates opening. Here, I discuss recent findings on how this channel is unusually modified by cyclic nucleotides and voltage.

D. DiFrancesco. Pacemaker mechanisms in the heart. Annu Rev Physiol. 1993;55:455-72.

Pacemaker mechanisms in cardiac tissue.

Champigny G, Lenfant J. Block and activation of the hyperpolarization-activated inward current by Ba and Cs in frog sinus venosus. Pflugers Arch. 1986 Dec;407(6):684-90.

A. Hellbach, S. Tiozzo, J. Ohn, M. Liebling, A.W. De Tomaso. Characterization of HCN and cardiac function in a colonial ascidian. J Exp Zool A Ecol Genet Physiol. 2011 Oct 1;315(8):476-86. doi: 10.1002/jez.695. Epub 2011 Jul 18.

Wilson CM, Farrell AP. Pharmacological characterization of the heartbeat in an extant vertebrate ancestor, the Pacific hagfish, Eptatretus stoutii. Comp Biochem Physiol A Mol Integr Physiol. 2013 Jan;164(1):258-63. doi: 10.1016/j.cbpa.2012.09.013. Epub 2012 Sep 23.

Funding from the Canadian Institutes of Health Research and the Natural Sciences and Engineering Council of Canada.

Where applicable, the authors confirm that the experiments described here conform with The Physiological Society ethical requirements.

SA385

Take a deep breath: cellular adaptations for life without oxygen

G.L. Galli

Faculty of Life Sciences, The University of Manchester, Manchester, England, UK

For most animals, oxygen is essential for the continual function of cellular processes. The absence of oxygen, termed anoxia, is associated with a number of pathological states such as ischemia, stroke, angina and cancer. Remarkably, certain vertebrates have evolved to live without oxygen for days, weeks and even months. Anoxia tolerance in these animals is derived from a wide array of physiological adaptations. As the study of ectothermic physiology advances, the cellular mechanisms underlying these adaptations are becoming resolved. Mitochondrial function is of particular interest, as it is the final arbitrator of life and death during oxidative stress. In particular, regulation of the F1F0 ATPase (Complex V of the electron transport chain) is emerging as a fundamental component of mitochondrial and cellular anoxia survival across vertebrates. A reduction in Complex V activity serves to preserve precious ATP supplies during acute anoxia and may protect against reactive oxygen species generation. Recent data suggests a down-regulation of Complex V is also characteristic of long term anoxic survival. Importantly, this anoxic survival strategy has been identified in all classes of vertebrates, which suggests fundamental mechanisms have been conserved throughout the animal kingdom to endure periods without oxygen.

Where applicable, the authors confirm that the experiments described here conform with The Physiological Society ethical requirements.

SA386

Gaining control, the role of the contractile element in the evolution of muscle function

T. Gillis

University of Guelph, Guelph, ON, Canada

Evolutionary processes have increased the complexity and functional capability of the vertebrate heart. This includes the transformation of the single chambered found in tunicates heart to the teleost heart with one ventricle and one atrium to the four-chambered organ found in mammals and birds. Associated with these anatomical changes was a parallel increase in heart rate that enabled increased cardiac output. What is the same, however, in all myocardium is that contraction is generated using a similar collection of component proteins. Muscle contracts when intracellular Ca increases and binds to the contractile element via cardiac troponin C (cTnC). The activation of cTnC triggers a series of conformational changes through the components of the thin filament that results in the generation of force by the myocyte. While all muscle contraction is powered by this mechanism, comparison of contractile function between vertebrate species reveals significant variation. This includes differences in the rate of myocyte contraction and relaxation, in the strength of contraction as well as in functional response following the activation of protein kinases with β-adrenergic stimulation. This seminar will examine the functional basis for these differences and how these have evolved within the vertebrate heart. Specific focus will be placed on cardiac troponin I (cTnI) and cardiac myosin binding protein C (cMyBP-C) and how these proteins have evolved to regulate contractile function in the vertebrate heart. Both cTnI and cMyBP-C are targets for phosphorylation following β-adrenergic stimulation in the mammalian heart. The influence of the evolution of endothermy on the function of the contractile element is also considered, as is the ability of hearts from specific species to function over a variety of physiological conditions. This analysis is completed through the integration of functional studies that have examined the role of specific proteins in regulating cardiac function with studies that have utilized phylogenetic approaches to examine the evolution of specific proteins and how this relates to key functional traits. It is generally found that as the heart became more complex in both anatomy and functional capacity, changes in protein sequence enabled improved control of the contractile reaction. In addition, the evolution of endothermy appears to have driven changes in the function of specific proteins including cTnC, cTnI and cMyBP-C. It is hoped that this integration of functional and phylogenetic studies will provide new insight into the role that the contractile element plays in regulating cardiac function and how this has evolved in vertebrates.

Where applicable, the authors confirm that the experiments described here conform with The Physiological Society ethical requirements.

SA387

Plasma membrane estrogen receptors and the biology of estrogen action

E.R. Levin

University of California, Irvine and the Long Beach VA, Irvine, CA, USA

Estrogen receptors exist in many cellular pools throughout most organs. This is true for the alpha and beta isoforms that are responsible for the actions of the sex steroid on normal organ development and function, and both opposing and promoting organ pathophysiology. Although many additional proteins have been speculated to act as estrogen receptors, scant evidence supports this role. In contrast, classical ERα and ERβ are found in multiple cellular pools, and only the complete knockout of these receptors produces a profound series of phenotypes that define the important functions of these sex steroid receptors. However, total deletion of the classical receptors does not inform us of the contributions of each cellular pool. We therefore have made transgenic mice, representing the selective loss of the nuclear receptor pool (membrane-only ERalpha (MOER) mice) or loss of the membrane pool (nuclear-only,NOER) mice. Using these mice, we have defined unique phenotypes, novel gene regulatory mechanisms, and metabolic signatures. For most complex organ development and biological functions, both membrane and nuclear ERα are generally required but in specific ways.

Where applicable, the authors confirm that the experiments described here conform with The Physiological Society ethical requirements.

SA388

Membrane initiated estrogen actions on the cytoskeleton

M. Kampa, V. Pelekanou, G. Notas and E. Castanas

Laboratory of Exp.Endocrinology, School of Medicine, Univesity of Crete, Heraklion, Crete, Greece

During the last decade our knowledge on estrogen action has been highly enriched by new data on their ability to exert rapid effects that are initiated at the membrane and activate a number of membrane related kinases and subsequently modify intracellular signaling cascades. One of the major targets of membrane initiated action of estradiol in a variety of cell types is actin cytoskeleton. Cytoskeletal modifications are of great importance since they can lead to changes in a wide range of cellular functions. More specifically estradiol has been shown to induce endothelial remodeling (Simoncini et al, 2006), axonal growth (Sanchez et al, 2009) and modulate cell migration of both normal (e.g. endometrial stromal cells) (Flamini et al, 2011) and cancerous (e.g. breast cancer cells) (Kampa et al, 2008, Sanchez et al, 2010) cells. Indeed in breast cancer, estrogens have been reported to induce actin cytoskeleton redistribution that favors cell migration which is required for cancer cell invasion and metastasis. Their action occurs through membrane estrogen receptors that trigger specific signaling events, involving G proteins, small GTPases, src, FAK, cdc42 and N-WASP. Even though the nature of membrane estrogen receptor has not been fully elucidated, it has been shown both biochemically (Sanchez et al, 2010) and verified by our group by a transcriptome analysis that the membrane receptor involved in this cytoskeletal action is ERα (Kampa et al, 2012).

Interestingly, this is not the only role for ERα, which has in its sequence an interesting motif (P295-T311) that is located between the D- (hinge) and E- (Ligand Binding Domain) regions, in the autonomous activation function AF-2a, and is considered as an important platform for various post-translational modifications and calmodulin binding. In fact a peptide corresponding to this motif (ERα17p) that could be liberated after the proteosomal degradation of ERα, we have equally found to induce rapid actin cytoskeleton re-arrangements and affect cell migration independently of the presence of ERα (Kampa et al, 2011) . This finding is very interesting since ERα bearing cells can affect the migration of ER negative cells and modulate one of the major problems of breast cancer, metastasis.

Simoncini T et al. (2006). Mol Endocrinol 20,1756-1771.

Sanchez AM et al. (2009). Mol Endocrinol 23, 1193-1202.

Flamini MI et al. (2011). Fertil Steril 95, 722-726.

Kampa M et al. (2008). Steroids 73, 953-960.

Sanchez AM et al. (2010). Mol Endocrinol 24, 2114-2125.

Kampa M et al. (2012). Steroids 77, 959-967.

Kampa M et al. (2011). J Cell Biochem 112, 3786-3796

Where applicable, the authors confirm that the experiments described here conform with The Physiological Society ethical requirements.

SA389

The G-protein-coupled estrogen receptor GPER in health and disease

M. Barton

Molecular Internal Medicine, University of Zurich, Zurich, Switzerland

Estrogens importantly contribute to physiological homeostasis and exert their effects through genomic and non-genomic ("rapid") actions [1, 2]. Rapid signaling of estrogen, which has been first reported in the 1960s [3-5] involves membrane estrogen receptors (ERs), including membrane subpopulations of ERalpha and ERbeta. In the early 1990s, rapid increases in cyclic AMP in response to estrogen were reported in human coronary arteries as well as in mammary and uterine cells [6, 7]. Shortly thereafter, several laboratories independently reported the cloning of an orphan G protein-coupled receptor from vascular and cancer cells that was named GPR30 [8-11]. Research published between 2000 and 2005 provided evidence that GPR30 binds and signals via estrogen indicating that this intracellular receptor is involved in rapid, non-genomic estrogen signaling [12-14]. The receptor has since been designated as the G protein-coupled estrogen receptor (GPER) by the International Union of Pharmacology [15]. The availability of genetic tools such as different lines of GPER knock-out mice, as well as GPER-selective agonists and antagonists has advanced our understanding, but also added some confusion about the new functions of this receptor (reviewed in [16]). Research of the past decade has provided evidence that GPER is critically involved in the regulation of vascular tone and blood pressure, metablic control [17], inflammation, and reproductive biology, among others. It is important to note that GPER not only binds estrogens but also other substances, including SERMs, SERDs, and environmental ER activators (endocrine disruptors; xenoestrogens) and also interacts with other proteins [18]. The current knowledge and unresolved questions about GPER-dependent signaling and function in health an disease will be discussed, as well as controversies that have complicated our understanding of GPER function, including interactions with human ERa-36 and aldosterone as a potential ligand [18].

1 Mendelsohn ME, Karas RH: Molecular and cellular basis of cardiovascular gender differences. Science 2005;308:1583-1587.

2 Levin ER: Rapid signaling by steroid receptors. Am J Physiol Regul Integr Comp Physiol 2008;295:R1425-1430.

3 Szego CM, Davis JS: Adenosine 3',5'-monophosphate in rat uterus: acute elevation by estrogen. Proc Natl Acad Sci U S A 1967;58:1711-1718.

4 Szego CM, Davis JS: Inhibition of estrogen-induced elevation of cyclic 3',5'-adenosine monophosphate in rat uterus. I. By beta-adrenergic receptor-blocking drugs. Mol Pharmacol 1969;5:470-480.

5 Pietras RJ, Szego CM: Endometrial cell calcium and oestrogen action. Nature 1975;253:357-359.

6 Mugge A, Riedel M, Barton M, Kuhn M, Lichtlen PR: Endothelium independent relaxation of human coronary arteries by 17 beta-oestradiol in vitro. Cardiovasc Res 1993;27:1939-1942.

7 Aronica SM, Kraus WL, Katzenellenbogen BS: Estrogen action via the cAMP signaling pathway: stimulation of adenylate cyclase and cAMP-regulated gene transcription. Proc Natl Acad Sci U S A 1994;91:8517-8521.

8 Owman C, et al.: Cloning of human cDNA encoding a novel heptahelix receptor expressed in Burkitt's lymphoma and widely distributed in brain and peripheral tissues. Biochem Biophys Res Commun 1996;228:285-292.

9 Carmeci C et al.: Identification of a gene (GPR30) with homology to the G-protein-coupled receptor superfamily associated with estrogen receptor expression in breast cancer. Genomics 1997;45:607-617.

10 Takada Y, et al.: Cloning of cDNAs encoding G protein-coupled receptor expressed in human endothelial cells exposed to fluid shear stress. Biochem Biophys Res Commun 1997;240:737-741.

11 O'Dowd BF, et al.: Discovery of three novel G-protein-coupled receptor genes. Genomics 1998;47:310-313.

12 Filardo EJ, Qet al.: Estrogen-induced activation of Erk-1 and Erk-2 requires the G protein-coupled receptor homolog, GPR30, and occurs via trans-activation of the epidermal growth factor receptor through release of HB-EGF. Mol Endocrinol 2000;14:1649-1660.

13 Revankar CM, et al.: A transmembrane intracellular estrogen receptor mediates rapid cell signaling. Science 2005;307:1625-1630.

14 Thomas P, Pang Y, Filardo EJ, Dong J: Identity of an estrogen membrane receptor coupled to a G protein in human breast cancer cells. Endocrinology 2005;146:624-632.

15 Alexander SP, Mathie A, Peters JA: Guide to Receptors and Channels (GRAC), 5th edition. Br J Pharmacol 2011;164 Suppl 1:S1-324.

16 Prossnitz ER, Barton M: The G-protein-coupled estrogen receptor GPER in health and disease. Nat Rev Endocrinol 2011;7:715-726.

17 Tiano JP, et al.: Estrogen receptor activation reduces lipid synthesis in pancreatic islets and prevents beta cell failure in rodent models of type 2 diabetes. J Clin Invest 2011;121:3331-3342.

18 Barton M: Position paper: The membrane estrogen receptor GPER—Clues and questions. Steroids 2012;77:935-942.

Where applicable, the authors confirm that the experiments described here conform with The Physiological Society ethical requirements.

SA390

Estrogen regulation of KCNQ1:KCNE3 channels in intestinal secretion

R. Rapetti-Mauss, V. Urbach and B.J. Harvey

Department of Molecular Medicine, Royal College of Surgeons in Ireland, Dublin, Ireland

Estrogen, 17-βestradiol (E2), rapidly reduces cAMP-dependent intestinal Cl^- secretion by inhibiting K^+ recycling (1). KCNQ1:KCNE3 is the rate-limiting K^+ channel involved in Cl^- secretion in the colon (2) and E2 rapidly inhibits KCNQ1 current in the female rat distal colon by a gender-specific mechanism (3). Regulation of KCNQ1 surface density has been shown to play a role in the control of KCNQ1 activity. Recently we demonstrated that estrogen rapidly uncouples KCNQ1 from its regulatory beta subunit KCNE3 causing a decrease in channel conductance (4). The aim of this study was to determine if membrane trafficking plays a role in the E2 inhibition of KCNQ1 function in the human colonic cell line, HT29cl19A. Ussing chamber ion transport measurements, biotinylation assays and immuno-staining have been used to study the effect of 10nM E2 treatment on KCNQ1 current and protein cellular localization. Protein expression was determined by Western blotting assay. All results are given as the mean ± S.E.M. Statistical significance was established using one-way ANOVA followed by a Tukey's post hoc test or a Student t test where relevant.

E2 (10 nM) reduced both forskolin-induced Cl^- secretion (30 ± 6 % n=6 $p<0.05$) and KCNQ1 activity (45 ± 8 % n=4 $p<0.05$) in HT29 cells monolayer. KCNQ1 was removed from the plasma membrane and internalized in cytosolic pools after 15 min E2 treatment (n=5). A biotin internalization assay confirmed this observation (internalized KCNQ1 after E2 treatment = 200 ± 9.9 % of control, n=5, $p<0.001$). Our results suggested that KCNQ1 internalization is clathrin and dynamin dependent since chlorpromazine and dynasore reversed E2 mediated KCNQ1 internalization as shown by immunofluorescence (n=4). Fluorescence co-localization studies indicated that KCNQ1 rapidly co-localized with the clathrin adaptor AP2 μ2 (Adaptor Protein 2 sub-unit μ2) 10 min after E2 treatment (overlap coefficient (O.C.) = 0.28 ± 0.04, control – 0.77 ± 0.01 E2, n=4). Following internalization, a subset of KCNQ1 appeared to accumulate in early endosomes (EE), (EE marker, EEA-1; O.C. with KCNQ1 = 0.30 ± 0.07% control, 0.60 ± 0.04 E2, n=4, $p< 0.05$). Further experiments revealed that KCNQ1 is recycled to the membrane rather than degraded. Following E2 exposure KCNQ1 rapidly co-localized with Rab4 (O.C. = 0.31 ± 0.02, control, 0.64 ± 0.02 E2 15 min), but Rab11 co-localization was only observable after 120 min (O.C. = 0.3 ± 0.03 control, 0.67 ± 0.01, E2) suggesting that KCNQ1 is sorted from the EE to the recycling endosomes. After 240 min exposure to E2, 70 ± 5 % (n=6, $p<0.001$) of internalized KCNQ1 was recycled back to the membrane as shown by the biotin recycling assay. Following E2 treatment, PKCδ (287 ± 51 % n=4, $p<0.05$) and AMPK (232 ± 24%, n=5, $p<0.05$) phosphorylation were increased within 2 min exposure to E2. Immuno-staining and biotinylation experiments revealed that E2 failed to induced KCNQ1 endocytosis in HT29cl19A cells when pre-treated with BIS1 a general PKC inhibitor, rottlerin a potent PKCδ inhibitor or Compound-C a AMPK inhibitor (n=4). Interestingly, we also demonstrated that KCNQ1 rapidly associates with Nedd4.2, an ubiquitin ligase, in response to estrogen treatment (346 ± 56% n=3, $p<0.001$). The last results suggest that E2 induces KCNQ1 ubiquitination to stimulate channel internalization.

This study establishes a role for E2 in the regulation of KCNQ1 cell surface abundance. In conclusion, we propose that the internalisation of KCNQ1 is a rapid estrogen response in modulating intestinal secretion.

Condliffe SB. et al J Physiol. 2001 1; 530(Pt 1):47-54.

Preston P. et al J Biol Chem. 2010; 5; 285(10):7165-75.

O'Mahony F. et al J. Biol. Chem. 2006; 282:24563-73.

Alzamora R. et al J Physiol. 2011 ; 589.21 5091-5107

This work was supported by NBIP Ireland and the Higher Education Authority (HEA) PRTLI Cycle 4.

Where applicable, the authors confirm that the experiments described here conform with The Physiological Society ethical requirements.

SA391

Oestrogen receptor beta: a new target for type 2 diabetes treatment

P. Alonso-Magdalena[1], A.B. Ropero[1], M. García-Arévalo[1], S. Soriano[1], I. Quesada[1], S.J. Muhammed[3], A. Salehi[3], J. Gustafsson[2] and A. Nadal[1]

[1]Universidad Miguel Hernandez de Elche, Elche (Alicante), Spain, [2]University of Houston, Houston, TX, USA and [3]University of Lund, Malmö, Sweden

The estrogen receptor beta (ERbeta) is emerging as an important regulator of pancreatic beta cell function (Soriano et al, 2009). Here we have evaluated the role of the ERbeta selective agonist, WAY200070, as an insulinotropic molecule and its antidiabetic actions in CB57 mice. We have demonstrated that it enhances glucose-stimulated insulin secretion (GSIS) both in mouse and human islets of Langerhans. In vivo experiments showed that a single-administration of WAY 200070 leads to an increase in plasma insulin levels with a concomitant improved response to a glucose load. Two-week treatment increased GSIS, pancreatic beta-cell mass and improved glucose and insulin sensitivity. In addition, streptozotocin-nicotinamide-induced diabetic mice treated with WAY200070 exhibited a significant improvement in plasma insulin levels and glucose tolerance as well as a regeneration of pancreatic beta-cell mass. Studies performed in db/db mice demonstrated that this compound restored first-phase insulin secretion, enhanced pancreatic beta-cell mass and favored the control of body weight. We conclude that ERbeta agonists should be considered as new targets for the treatment of diabetes (Alonso-Magdalena et al, 2013).

Soriano S, Ropero AB, Alonso-Magdalena P, Ripoll C, Quesada I, Gassner B, Kuhn M, Gustafsson JA, Nadal A. (2009) Rapid Regulation of KATP Channel Activity by 17beta-Estradiol in Pancreatic beta-Cells Involves the Estrogen Receptor beta and the Atrial Natriuretic Peptide Receptor. Molecular Endocrinology. 23: 1973-1982.

2.Alonso-Magdalena P, Ropero AB, Garcia-Arevalo M, Soriano S, Quesada I, Muhammed SJ, Salehi A, Gustafsson JA, Nadal A. (2013) Antidiabetic actions of an ERβ selective agonist. Diabetes. in press.

This work was supported by grants Ministerio de Ciencia e Innovacion grant BFU2008-01492, Ministerio de Economia y Competitividad grant BFU2011-28358, Generalitat Valenciana grants PROMETEO/2011/080, Swedish Cancer Fund and Emerging Technology Fund of Texas.

Where applicable, the authors confirm that the experiments described here conform with The Physiological Society ethical requirements.

SA392

Long non-coding RNA & cancer

S. Diederichs

German Cancer Research Center, Heidelberg, Germany and Dept. of Pathology, University of Heidelberg, Heidelberg, Germany

The last decade introduced a paradigm shift in molecular biology towards the recognition of non-protein-encoding RNA molecules as functionally important players in physiological and pathological processes. These transcripts are frequently deregulated in tumors and may also exert tumor suppressive or oncogenic functions. Our research aims at elucidating the expression, regulation and function of long non-coding RNAs in lung, liver and breast cancer.
In detail, I will present our discovery of the lncRNA MALAT1 as a biomarker for lung cancer metastasis and the generation of a novel loss-of-function model in human cells unraveling the active function of MALAT1 as a regulator of gene expression governing lung cancer metastasis.
We also provide the first global comprehensive map of long ncRNA expression in a broad range of human tumor and normal tissue samples and discovered many new lncRNAs associated with cancer as well as tissue-, histology- and prognosis-specific ncRNA signatures. First data shed light onto the important functions of these newly discovered lncRNAs at the cellular and molecular level.

T Gutschner, M Hämmerle, M Eissmann, J Hsu, Y Kim, G Hung, AS Revenko, G Arun, M Stentrup, M Gross, M Zörnig, AR MacLeod, DL Spector, S Diederichs: "The non-coding RNA MALAT1 is a critical regulator of the metastasis phenotype of lung cancer cells" Cancer Research (2013) 73: 1180-1189

T Gutschner, M Baas, S Diederichs: "Non-coding RNA gene silencing through genomic integration of RNA destabilizing elements using zinc finger nucleases" Genome Research (2011) 21: 1944-1954

P Ji*, S Diederichs*, W Wang, S Böing, R Metzger, PM Schneider, N Tidow, B Brandt, H Buerger, E Bulk, M Thomas, WE Berdel, H Serve, C Müller-Tidow: "MALAT-1, a novel non-coding RNA, and Thymosin b4 predict Metastasis and Survival in early-stage Non-Small Cell Lung Cancer" Oncogene (2003) 22: 8031-8041

T Gutschner, S Diederichs: "The Hallmarks of Cancer: A long non-coding RNA point of view" RNA Biology (2012) 9: 703-719

Where applicable, the authors confirm that the experiments described here conform with The Physiological Society ethical requirements.

SA393

Human nuclear dicer restricts accumulation of endogenous double strand RNA

M. Gullerova

University of Oxford, Oxford, UK

Dicer is a central enzymatic player in RNA interference (RNAi) pathways that acts to regulate gene expression in nearly all eukaryotic cells. In mammals, the well documented cytoplasmic role of Dicer in generating small interfering (si) and micro (mi)RNA, is known to lead to the selective degradation and translational repression of messenger (m)RNA. The view persists that mammalian Dicer has no direct nuclear function, even though in other eukaryotes such as plants, drosophila, C. elegans5 and some yeast the nuclear role of Dicer in transcriptional gene silencing (TGS) through siRNA formation is well established. More recent analysis of potential mammalian nuclear RNAi has revealed that it is possible to induce TGS by nuclear RNAi pathways and also that loss of Dicer can directly impact on genic and intergenic transcriptional activity. Here we show unequivocally that Dicer is present in both the nucleus and cytoplasm, but that its nuclear levels are tightly regulated. In its nuclear manifestation Dicer interacts with RNA polymerase II (Pol II) at actively transcribed gene loci. Loss of Dicer causes the immediate appearance of endogenous dsRNA leading to induction of the interferon response pathway and consequent cell death. Our results suggest that Pol II associated Dicer restricts endogenous dsRNA formation, presumably from overlapping non-coding RNA transcription units (natural antisense RNA). Failure to do so has catastrophic effects on cell function. Taken together, we present here a miRNA independent role for human nuclear Dicer.

Where applicable, the authors confirm that the experiments described here conform with The Physiological Society ethical requirements.

SA394

RNA regulation in male germline

N. Kotaja

Department of Physiology, Institute of Biomedicine, University of Turku, Turku, Finland

Germ cells are unique in their capability to give rise to a new organism. In addition to genetic information, the epigenetic status of cells is inherited, which emphasizes the importance of securing both genetic integrity and correct epigenetic marks in the germline. The alarming decline in the semen quality and reproductive health in Western countries has unveiled the necessity of understanding the genetic, epigenetic and environmental factors governing male reproductive functions. Male germ cell differentiation is orchestrated by accurate, spatially and temporally controlled gene expression patterns. Male germ cells express outstanding amount of different non-coding RNAs, including both small RNAs and yet poorly characterized long non-coding RNAs. Small non-coding RNAs are important regulators of gene expression that mainly function at the post-transcriptional level. Small RNAs produced by the male germline include Dicer-dependent microRNAs (miRNAs) and endogenous small interfering RNAs (endo-siRNAs), and Dicer-independent piwi-interacting RNAs (piRNAs).
The goal of our research is to clarify the roles of non-coding RNAs and the mechanisms of post-transcriptional gene control during male germ cell differentiation. We have shown that Dicer-dependent pathways are required for normal spermatogenesis and male fertility by analyzing a knockout mouse model to delete Dicer1 gene specifically in early postnatal male germ cells. Our results demonstrate that Dicer is crucial for the correct nuclear polarization and chromatin condensation of developing spermatids. piRNAs that are expressed predominantly in the germline form a big, complex and functionally diverse group of small RNAs. piRNA expression is known to be greatly induced in late meiotic cells and round spermatids, and interestingly, we have shown that in these cells, piRNAs accumulate in an intriguing male germ cell -specific cytoplasmic ribonucleoprotein granule, a chromatoid body (CB). We have isolated CBs from mouse testis and identified its molecular composition by mass spectrometric analysis and RNA sequencing to better understand its functions in haploid cells. The CB appears to act as a central RNA regulation platform as it accumulates a multitude of different RNA-binding

and RNA-processing proteins as well as several RNA species including piRNAs, mRNAs and long non-coding RNAs. All the results indicate that the CB has an important role in the regulation of meiotic and post-meiotic processes. Many of the CB components are essential for normal spermatogenesis in mouse, which highlights the significance of this structure in maintaining male fertility.

Where applicable, the authors confirm that the experiments described here conform with The Physiological Society ethical requirements.

SA395

Spontaneous activity patterns in the developing mouse visual cortex

C. Lohmann

Synapse and Network Development, Netherlands Institute for Neuroscience, Amsterdam, Netherlands

The developing brain generates spontaneous activity even before our senses are activated. This spontaneous activity is transmitted along neuronal pathways and is required for setting up precise connections between nerve cells. How specific activity patterns are translated into precise patterns of connectivity is currently unknown. To start addressing this question, we are investigating the patterns of spontaneous activity in the developing visual cortex using in vivo calcium imaging and electrophysiology. We discovered two types of spontaneous activity that are characterized by low and high levels of synchronization between neurons: L- and H-events, respectively. Manipulating peripheral spontaneous activity, i.e. retinal waves shows that L-events are largely driven by retinal inputs. In contrast, H-events are centrally generated. Here, I will discuss the characteristics of these activity patterns from the synaptic to the network level and propose ideas about how these activity patterns may guide the development of specific connections in the developing visual system.

Where applicable, the authors confirm that the experiments described here conform with The Physiological Society ethical requirements.

SA396

Structural correlates of visual cortex plasticity

T. Keck

MRC Centre for Developmental Neurobiology, King's College London, London, UK

Sensory experience is widely thought to drive activity levels in the cortex. In adult animals, chronic modifications of sensory activity, such as visual deprivation, lead to compensatory changes in synaptic strength. The postsynaptic mechanisms that underpin modifications of synaptic strength have been studied in great detail. In contrast, the presynaptic mechanisms that are altered following a change in cortical activity are less well understood. Here we study presynaptic axonal boutons of excitatory axons in superficial layers of the adult mouse primary visual cortex following enucleation. We found greater bouton turnover at excitatory axons in the cortex of mice with reduced visually driven activity (deprived). Persistent boutons fluctuated in a size dependent manner; so that large boutons became smaller whilst smaller boutons became bigger. This shift in the synaptic 'weighting' of individual boutons was balanced so that the population average remained constant. Functional analysis of the paired pulse ratio was consistent with a remapping of synaptic weights so that synaptic dynamics shifted from largely depression to a combination of weak depression and facilitation. One mechanism that might account for regulation of this process is the sharing of a finite pool of local presynaptic machinery. We propose that this is a form of presynaptic homeostasis.

Where applicable, the authors confirm that the experiments described here conform with The Physiological Society ethical requirements.

SA397

***In vivo* imaging of coordinated excitatory and inhibitory synaptic dynamics on pyramidal cell dendrites**

K.L. Villa[1,2], K.P. Berry[1,2], J.L. Chen[1,2], J. Cha[3], P.C. So[3,4] and E. Nedivi[1,5]

[1]Picower Institute for Learning and Memory, Massachusetts Institute of Technology, Massachusetts, MA, USA, [2]Department of Biology, Massachusetts Institute of Technology, Massachusetts, MA, USA, [3]Department of Mechanical Engineering, Massachusetts Institute of Technology, Massachusetts, MA, USA, [4]Department of Biological Engineering, Massachusetts Institute of Technology, Massachusetts, MA, USA and [5]Department of Brain and Cognitive Sciences, Massachusetts Institute of Technology, Massachusetts, MA, USA

A critical feature of brain plasticity is the capacity to dynamically adapt in response to the environment by remodeling connections between neurons. Inhibitory neurons are known to play a vital role in defining the window for critical period plasticity during development, and it is increasingly apparent that they continue to exert powerful control over experience-dependent cortical plasticity in adulthood. Recent *in vivo* imaging studies demonstrate that long-term plasticity of inhibitory circuits is manifested through structural rearrangements. Changes in sensory experience drive this structural remodeling of inhibitory interneurons in a cell type and circuit specific manner. We recently found that inhibitory synapse formation and elimination occurs with a great deal of spatial and temporal precision, and is often locally coordinated with excitatory synaptic changes on the same dendrite, largely clustered within a 10 um distance. Yet, the nature of the clustered inhibitory and excitatory synaptic dynamics remains temporally unresolved in terms of whether the two events occur simultaneously or if one of the two events drives the change, while the other adjusts to it. Does the presence of a dynamic inhibitory synapse destabilize neighboring spines, or do excitatory synaptic changes drive inhibitory synapse dynamics? Are the valence changes of coordinated events weighed in the same direction, or are they compensatory? I.e. does excitatory synapse loss drive formation or loss of an inhibitory synapse? To further probe the nature of 'coordination' between inhibitory and excitatory synaptic dynamics we triple-labeled L2/3 pyramidal neurons in the mouse visual cortex via *in utero* electroporation using YFP as a cell fill, PSD95-mcherry to label excitatory synapses, and Teal-Gephyrin to label inhibitory synapses. Upon reaching adulthood, these mice were implanted with cranial windows and labeled cells in binocular visual cortex were imaged *in vivo* at short intervals using spectrally resolved two-photon microscopy.

Where applicable, the authors confirm that the experiments described here conform with The Physiological Society ethical requirements.

SA398

The emergence of functional microcircuits in visual cortex

S. Hofer

University College London, London, UK and Biozentrum, University Basel, Basel, Switzerland

The ability of the brain to extract meaning from sensory stimuli depends on the computational capabilities of precisely connected neuronal networks in the cerebral cortex. Despite variations between cortical areas and species, neurons receiving similar inputs or sharing similar response properties often aggregate into fine-scale functional networks. In the mature visual cortex (V1), for example, neurons are not randomly connected, but form specific local and long-range circuits, which may influence the neuronal selectivity for different features of visual scenes, such as their orientation, direction and position. How such fine-scale functional circuits emerge during postnatal development from an immature neuronal network remains a fundamental question in neuroscience.
We are addressing this question in mouse V1 by directly relating patterns of excitatory synaptic connectivity to visual response properties of neighbouring layer 2/3 pyramidal neurons at different postnatal ages, using two-photon calcium imaging in vivo in anaesthetized mice and multiple whole-cell recordings in vitro. Our previous work revealed that pyramidal neurons connect preferentially if they respond similarly to visual stimuli. At eye-opening, although neural responses were already highly selective for visual stimuli, neurons responding to similar visual features were not yet preferentially connected, indicating that the emergence of feature selectivity does not depend on the precise arrangement of local synaptic connections. After eye opening, local connectivity reorganised extensively, as more connections formed selectively between neurons with similar visual responses, and connections were eliminated between visually unresponsive neurons, while the overall connectivity rate did not change. We propose a unified model of cortical microcircuit development based on activity-dependent mechanisms of plasticity: neurons first acquire feature preference by selecting feedforward inputs before the onset of sensory experience, after which patterned input drives the formation of functional subnetworks through a redistribution of recurrent synaptic connections.

Where applicable, the authors confirm that the experiments described here conform with The Physiological Society ethical requirements.

SA399

How sensory deprivation and learning change neuronal responses in mouse visual cortex

M. Hübener

Max Planck Institute of Neurobiology, Martinsried, Germany

Neuronal response properties in the brain are not static over time. They can change during development, after deprivation, and following learning. We study such functional plasticity with two-photon calcium imaging, using orientation selectivity in the mouse visual cortex as a model.

One way to alter orientation tuning in the visual cortex is stripe rearing, where animals are exposed to contours of only one orientation for a certain period. Earlier studies have shown that stripe rearing causes a relative overrepresentation of neurons in visual cortex tuned to the experienced orientation. It is not clear, however, whether these changes are merely due to a permissive effect, causing cells tuned to the non-experienced orientations to lose responsiveness, or whether the experienced orientation acts in an instructive fashion, such that some cells actively change their tuning. The main reason for this uncertainty is that with conventional methods it is difficult to assess the proportion of unresponsive cells. This problem can be overcome by two-photon calcium imaging, where all neurons are labeled, thereby allowing for an unbiased determination of the fraction of unresponsive cells.
We have raised juvenile mice for three weeks with cylinder lens goggles limiting visual experience to only one orientation. Following this period, orientation preference in the visual cortex was determined with two-photon calcium imaging. Stripe rearing changed the distribution of preferred orientations such that more cells responded to the experienced orientation than to the orthogonal orientation. The fraction of responsive neurons was lowered, but this effect could not fully account for the changes observed in the distribution of preferred orientations.
The magnitude of the stripe rearing effect increased with cortical depth: the distributions of preferred orientations changed only modestly in upper layer 2/3, but we noted a pronounced drop in the fraction of responsive cells. In contrast, neurons deeper in layer 2/3 did not change their overall responsiveness, but we found a clear shift towards the experienced orientation. Thus, diverse mechanisms contribute to the changes in preferred orientation following stripe rearing, but the effect is at least partially mediated by an instructive process, by which individual neurons change their orientation preference.
We next asked the question whether orientation tuning in the visual cortex also shows plasticity under behaviorally relevant conditions. During active vision, the visual cortex is subject to extensive feedback signaling and top-down modulations. However, in which way and to what extent the visual cortex is involved in visual perceptual learning remains highly controversial. We used repeated two-photon calcium imaging in anaesthetized mice over twelve days with the genetically encoded calcium indicator GCaMP3. Applying this technique, we quantified changes in orientation tuning in individual neurons in the visual cortex before, during and after orientation discrimination learning. While overall orientation preference was not affected, tuning width and response amplitude changed during learning in neurons with specific differential preferred orientations (with regard to the rewarded orientation). Strikingly, these changes were correlated with task performance. Moreover, we found a pronounced gain in the number of orientation-selective neurons in mice that performed well in the orientation discrimination task. These neurons were mostly tuned to the rewarded or the orthogonal orientation, pointing to an enhanced neuronal responsiveness to these orientations. These data support, in line with previously proposed theories, a reweighting of visual information during visual perceptual learning.

Where applicable, the authors confirm that the experiments described here conform with The Physiological Society ethical requirements.

SA400

Calcium dynamics in nano-junctions between the sarcoplasmic reticulum (SR), plasma-membrane and other organelles in vascular smooth muscle

C. van Breemen[1], N. Fameli[1], M. Esfandiarei[1] and A. Evans[2]

[1]Department of Anesthesiology, Pharmacology & Therapeutics, University of British Columbia, Vancouver, BC, Canada and [2]Centre for Integrative Physiology, University of Edinburgh, Edinburgh, UK

Physiological selection between different modes of cell function is based on the segregation of Ca^{2+} transients in different locations of the cytoplasm. Evidence in the literature suggests that in smooth muscle such segregation is effected by a large variety of specialized SR-organelle nano-junctions, each controlling the [Ca^{2+}] in a nano-space near Ca^{2+} sensitive enzymes, channels, pumps and exchangers (Pan-Junctional SR). If different parts of the Pan-Junctional SR generate different localized [Ca^{2+}], then it is likely that the SR itself is compartmentalized. However, it has been shown that the SR luminal Ca^{2+} concentration can be independently regulated via PM-SR junctions and that there is structural continuity throughout the SR and nuclear envelope. The answer to this paradox could be resolved by assuming that the SR lumen is irregular, has spatially separated clusters of sarco/endoplasmic reticulum Ca^{2+} ATPases (SERCA), inositol 1,4,5-trisphosphate receptors (IP_3R) and ryanodine receptors (RyR) and exhibits areas of restricted diffusion. Therefore, the nanospaces bordering both surfaces of the SR are critical in defining the specificity of the Ca^{2+} signals. In this presentation, we propose that the typical make-up of the Pan-junctional SR determines the smooth muscle type and pose the question of how to formulate a quantitatively testable hypothesis describing Ca^{2+} transport mechanism in junctions between the membranes of the SR and other organelles, including the plasma-membrane (PM).
All vascular smooth muscles respond to physiological stimulation with Ca^{2+} oscillations, but three different types of Ca^{2+} oscillations have been reported for various blood vessels:
1. Waves of Ca^{2+} induced Ca^{2+} release (CICR) involving IP_3R initiated by elevation of IP_3.
2. Waves of CICR involving RyR, initiated by nicotinic acid adenine dinucleotide phosphate (NAADP)-mediated lysosomal Ca^{2+} release.
3. Non wave-like Ca^{2+} oscillations paced by periodic SR Ca^{2+} release.
Since Ca^{2+} release channels exhibit Ca^{2+} sensitivity on both their cytoplasmic and luminal terminals, fluctuations in regional luminal Ca^{2+} can also function as pacemakers to determine the frequency of SR Ca^{2+} release waves and that of non-wave-like Ca^{2+} oscillations.
How do we test these provocative hypotheses?
At present, specific hypotheses borne out of experimental observations often yield only cartoon models and can hardly be verified by conventional experimental methods. We argue that realistic quantitative modeling of the stochastic processes characterizing ion transport in the junctions is a necessary tool on the one hand for testing of such hypothesis and on the other to generate further testable predictions on SR junction mechanisms.
We briefly overview a quantitative modeling approach that integrates the available experimental evidence into a realistic reproduction of two specific vascular smooth muscle SR junctions: (1) the PM-SR junction, which appears to be at the base of CICR wave phenomena originating from IP_3R Ca^{2+} release from the SR upon adrenergic stimulation; (2) the lysosome-SR junction, in which NAADP-mediated Ca^{2+} release from two pore segment channels type 2 (TPC2) seems to originate Ca^{2+} bursts, which cause cell-wide CICR at RyR.
Finally, we address the general question of how this approach could further our understanding of the coordinated regulation of such diverse processes as vaso-motor tone, metabolism and nuclear transcription.

Where applicable, the authors confirm that the experiments described here conform with The Physiological Society ethical requirements.

SA401

Acidosis dilates brain parenchymal arterioles by reshaping spontaneous calcium signals to activate BK_{Ca} channels

F. Dabertrand[1], M.T. Nelson[1,2] and J.E. Brayden[1]

[1]Pharmacology, University of Vermont - College of Medicine, Burlington, VT, USA and [2]Institute of Cardiovascular Sciences, Manchester, UK

Acidosis is a powerful vasodilator signal in the brain circulation. However, the mechanisms by which this response occurs are not well understood, particularly in the cerebral microcirculation. Ryanodine receptors (RyRs) are Ca^{2+} permeable channels in the sarcoplasmic reticulum. They dilate cerebral (pial) arteries by activation of large-conductance, calcium-sensitive potassium (BK_{Ca}) channels by local Ca^{2+} signals (Ca^{2+} sparks). This mechanism is clearly demonstrated by the non-additive constrictions induced by RyR or BK_{Ca} channel blockers in pressurized pial arteries. Nevertheless, these blockers have little effect on the diameter of pressurized parenchymal arterioles (PAs) from the brain, even though functional BK_{Ca} channels and RyRs are present. To determine the mechanism by which acidosis dilates brain PAs and to elucidate the roles of RyRs and BK_{Ca} channels in this response, internal diameter and vascular smooth muscle cell Ca^{2+} signals were measured in isolated pressurized murine PAs, using imaging techniques. At physiological pH (7.4) vascular smooth muscle cells exhibited largely Ca^{2+} waves but not Ca^{2+} sparks. Reducing external pH from 7.4 to 7.0 in both normocapnic and hypercapnic conditions decreased Ca^{2+} wave activity, and dramatically increased Ca^{2+} spark activity. Acidic pH caused a dilation of PAs which was inhibited by about 60% in a non-additive manner by BK_{Ca} channel blocker (1 μM paxilline) or RyR blocker (ryanodine 10 μM). Similarly, dilator responses to acidosis were reduced by nearly 60% in arterioles from BK_{Ca} channel knockout mice. Dilations induced by acidic pH were unaltered by inhibitors of K_{ATP} channels (1 μM glibenclamide) or nitric oxide synthase (100 μM L-NAME). These results support the novel concept that acidification, by converting Ca^{2+} waves to sparks, leads to the activation of BK_{Ca} channels to induce dilation of cerebral PAs.

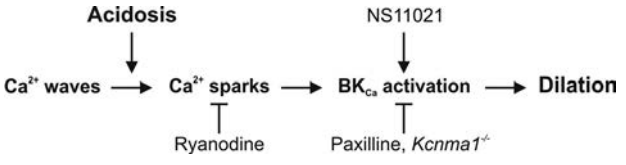

Proposed mechanism for ryanodine receptors (RyRs)- and calcium-sensitive potassium (BK_{Ca})-dependent, acidosis-induced dilation of brain parenchymal arterioles. By decreasing the open probability of RyRs in vascular smooth muscle cells, protons reshape intracellular Ca^{2+} signaling from waves to sparks which activate BK_{Ca} channels and then cause dilation.

This work was supported by National Institutes of Health grants RO1 HL44455, RO1 HL58231, and PO1 HL095488, Totman Trust for Medical Research, and a postdoctoral fellowship from the American Heart Association 09POST2290090 to Fabrice Dabertrand.

Where applicable, the authors confirm that the experiments described here conform with The Physiological Society ethical requirements.

SA402

From contraction to gene expression: function-specific calcium signals are delivered by the strategic positioning of calcium pumps and release channels within membrane-membrane nanojunctions of the sarcoplasmic reticulum

A. Evans

Centre for Integrative Physiology, University of Edinburgh, Edinburgh, UK

Pulmonary arterial hypertension is driven by smooth muscle contraction and by the switch from a contractile to a migratory-proliferative smooth muscle phenotype(s), which requires changes in gene expression. These processes are selected, in part, by calcium signals, but how different calcium signals are generated to select each function is enigmatic.

We have previously shown that SERCA2b and RyR1 are preferentially targeted to the sarcoplasmic reticulum (SR) proximal to the plasma membrane (PM) in pulmonary arterial smooth muscle cells (PASMCs; Clark et al., 2010); i.e. to the superficial buffer barrier formed by PM-SR nanojunctions (van Breemen et al., 2013). Here they may support vasodilation in response to β-adrenoceptor activation. Induced increases in SERCA2b activity may thus remove calcium from the deeper cytoplasm to the superficial SR, from which calcium sparks may be released into the PM-SR junction via RyR1 to activate PM resident BKCa channels, driving hyperpolarisation (Boittin et al., 2003), removal of calcium from the cell by forward mode NCX activity and ultimately vasodilation (Boittin et al., 2003; Clark et al., 2010).

In marked contrast, SERCA2a is entirely restricted to the deep, perinuclear SR (Clark et al., 2010) and may function to recycle calcium into this sub-compartment in support of vasoconstriction (Dipp & Evans, 2001; Dipp et al., 2001; Kinnear et al., 2004; Clark et al., 2010). Importantly, differrent subtypes of RyR are also strategically positioned here. RyR3 is preferentially targeted to the perinuclear SR and associated lysosome-SR nanojunctions (Kinnear et al., 2004, Kinnear et al., 2008), while the distribution of RyR2 is more widespread and extends from this region to the wider cell (Kinnear et al., 2008; Clark et al., 2010). We therefore proposed that perinuclear clusters of RyR3 may act as an initiation site for propagating calcium waves and contraction (Dipp & Evans, 2001; Kinnear et al., 2008). Thereafter, by calcium-induced calcium release, RyR2 may carry propagating calcium waves away from perinuclear clusters of RyR3 and across the myofilaments to enhance myocyte contraction (Kinnear et al., 2008; Clark et al., 2010).

We have now identified a third subtype of SERCA pump in PASMCs, namely SERCA1, which together with RyR1 preferentially lines the nucleoplasmic reticulum (nSR). By contrast, we find no evidence of similar nSR labeling for other SERCA or RyR. It seems likely, therefore, that a variety of calcium pumps and release channels, with different kinetics and affinities for calcium, are strategically positioned within and serve to demarcate different nanojunctions of the SR and their respective cytoplasmic nanodomains. Function-specific calcium signals may thus arise to provide for selective modulation of smooth muscle contraction and gene expression.

Boittin FX, Dipp M, Kinnear NP, Galione A & Evans AM. (2003). Vasodilation by the calcium-mobilizing messenger cyclic ADP-ribose. The Journal of biological chemistry 278, 9602-9608.

Clark JH, Kinnear NP, Kalujnaiab S, Cramb G, Fleischer S, Jeyakumar LH, Wuytack F & Evans AM. (2010). Identification of Functionally Segregated

Dipp M & Evans AM. (2001). Cyclic ADP-ribose is the primary trigger for hypoxic pulmonary vasoconstriction in the rat lung in situ. Circulation research 89, 77-83.

Dipp M, Nye PC & Evans AM. (2001). Hypoxic release of calcium from the sarcoplasmic reticulum of pulmonary artery smooth muscle. Am J Physiol Lung Cell Mol Physiol 281, L318-325.

Kinnear NP, Boittin FX, Thomas JM, Galione A & Evans AM. (2004). Lysosome-sarcoplasmic reticulum junctions. A trigger zone for calcium signaling by nicotinic acid adenine dinucleotide phosphate and endothelin-1. The Journal of biological chemistry 279, 54319-54326.

Kinnear NP, Wyatt CN, Clark JH, Calcraft PJ, Fleischer S, Jeyakumar LH, Nixon GF & Evans AM. (2008). Lysosomes co-localize with ryanodine receptor subtype 3 to form a trigger zone for calcium signalling by NAADP in rat pulmonary arterial smooth muscle. Cell calcium 44, 190-201.

van Breemen C, Fameli N & Evans AM. (2013). Pan-Junctional Sarcoplasmic Reticulum in Vascular Smooth Muscle: Nanospace Ca2+ transport for Site- and Function-specific Ca2+ signalling. The Journal of physiology, DOI jphysiol.2012.246348 [pii] 10.1113/jphysiol.2012.246348

This work was supported by a British Heart Foundation Programme Grant to AME (RG/12/14/29885)

Where applicable, the authors confirm that the experiments described here conform with The Physiological Society ethical requirements.

SA403

Targeted STIM deletion impairs calcium homeostasis, NFAT activation, and growth of smooth muscle cells

S. Mancarella, S. Potireddy, Y. Wang, H. Gao, R. Gandhirajan, M. Autieri, R. Scalia, H. Wang, M. Madesh, S. Houser and D. Gill

Temple University School of Medicine, Philadelphia, PA, USA

Stromal interaction molecule (STIM1) and its isoform (STIM2) are single span sarco/endoplasmic (SR) transmembrane proteins that function as powerful SR Ca2+ sensors. When the SR Ca2+ content decreases STIM proteins migrate in proximity of the plasma membrane to tether and activate the Orai channels initiating the so called store operated Ca2+ entry (SOCE). In non-excitable cells STIM mediates Ca2+ entry that is required for regulating cell proliferation and migration. Smooth muscle cells (SMC) can exist as non-excitable cells, known also as the “proliferative” phenotype, or as excitable cells, known as the “contractile” phenotype. Furthermore, SMC can interchange their phenotype in response to environmental stimuli; Ca2+ signaling plays a crucial role in regulating this transition. However, very little is known about the role of STIM in SMC. Because isolated primary SMC quickly lose their contractile phenotype when placed in culture, the role of STIM proteins in SMC has been eluded. To overcome this limitation we used the Cre-lox technology approach to generate SM-specific STIM1-, STIM2-, and STIM1/STIM2- knockout (KO) mice, this model allowed us to systematically analyze the physiological role of STIM in SMC.

SM-STIM1-KO mice survival rate was only about 50% within the first 30 days after birth. In addition, SM-STIM1-KO mice showed

a consistent reduced body weight when compared to control mice. While the SM-STIM1/STIM2 double-KO phenotype was perinatally lethal, the SM-STIM2-KO was without a detectable phenotype. However, in the SM-STIM1 KO mice the STIM2 expression is enough to rescue the otherwise lethal phenotype, revealing that also STIM2 plays an important role in the SMC. Smooth muscle containing organs, such as intestine and aorta harvested from SM-STIM1-KO mice revealed morphological abnormalities when compared with organs harvested from control mice. Vascular reactivity analyzed using wire myography revealed that while depolarization-induced aortic contraction was unchanged, phenylephrine-mediated contraction was reduced by 26%, and store-dependent contraction was almost eliminated in aortas isolated from SM-STIM1-KO mice. Neointima formation induced by partial carotid artery ligation was suppressed by 54%. Consistently, in vitro PDGF-induced SMC proliferation was also reduced by 79% in STIM1-KO SMC. Notably, the Ca2+ store-refilling rate in STIM1-KO SMCs was substantially reduced, and sustained PDGF-induced Ca2+ entry was abolished. This defective Ca2+ homeostasis prevents PDGF-induced NFAT activation in both contractile and proliferating SMCs. In conclusion, our data show that STIM1-regulated Ca2+ homeostasis is crucial for NFAT-mediated transcriptional control required for induction of SMC proliferation, development, and growth during physiological as well as pathophysiological conditions.

This work was supported by U.S. National Institutes of Health grant AI058173 (to D.L.G.), and U.S. National Heart, Blood, and Lung Institute postdoctoral fellowship HL105066 (to S.M.). The authors thank Dr. Anjana Rao (La Jolla Institute for Allergy and Immunology, La Jolla, CA, USA) and Dr. Masatsugu Ohhora (Tokyo Medical and Dental University, Tokyo, Japan) for generously providing the floxed STIM mouse lines.

Where applicable, the authors confirm that the experiments described here conform with The Physiological Society ethical requirements.

SA404

NFAT-dependent excitation-transcription coupling in smooth muscle

M.F. Gomez

Lund University, Malmö, Sweden

Patients with diabetes have a much more widespread and aggressive form of atherosclerosis in the coronary arteries, lower extremities and extracranial carotid arteries, causing nearly 80% of all deaths and much of the disability in these patients (1). Diabetes type 1 and 2 are independent risk factors for myocardial infarction, peripheral vascular disease and stroke, also worsening their early and late outcomes, increasing the risk of recurrence and leading to poorer prognosis following surgical revascularization procedures. Despite the vast clinical experience linking diabetes and atherosclerosis, very little is understood about the molecular mechanisms connecting hyperglycemia to atherosclerosis.

The nuclear factor of activated T-cells (NFATc1-c4) are a family of Ca^{2+}/calcineurin-dependent transcription factors first characterized in T-lymphocytes as inducers of cytokine gene expression. Since then, NFAT proteins have been shown to play various roles outside immune cells, including in the cardiovascular system (2). We have previously shown that modest elevations of extracellular glucose effectively activate NFATc3 in vascular smooth muscle cells (VSMC) of large arteries (aorta and cerebral) and in small (retinal) microvessels in mice, both *ex vivo* and *in vivo* (3; 4). This effect involves the local release of extracellular nucleotides, such as UTP and UDP, acting on purinergic-2Y receptors, leading to increased $[Ca^{2+}]_i$ and subsequent activation of calcineurin and NFATc3. In addition to promoting NFATc3 nuclear translocation, high glucose also reduces nuclear export of NFAT by inhibiting GSK-3β and JNK, providing additional mechanisms for glucose-induced NFAT activation. Once activated, NFAT promotes the expression of osteopontin (OPN). Diabetic mice showed increased expression of OPN in the ascending and thoracic aorta, vascular segments particularly prone to development of atherosclerosis and this was prevented by *in vivo* treatment with the NFAT inhibitor A-285222 or by lack of NFATc3 protein in arteries from $NFATc3^{-/-}$ mice. Additional experimental evidence supports a role for NFAT as a regulator of genes able to promote vascular dysfunction and potentially, a pro-atherogenic vascular phenotype. NFAT promotes VSMC proliferation and migration, and plays a role in neointima formation and in the regulation of cyclooxygenase 2 (Cox2) and RCAN1 expression after vascular injury (5). NFAT contributes to the development of angiotensin II-induced hypertension, via down-regulation of potassium channel expression (6). Moreover, NFAT controls the alternative splicing of allograft inflammatory factor-1 (AIF-1), resulting in products differentially associated to parameters defining human plaque phenotype and stability (7).

Together, these observations led us to hypothesize that NFAT may act as a glucose-sensor in the vessel wall, translating changes in Ca^{2+} signals into changes in gene expression that lead to macrovascular disease in diabetes. To more directly test this hypothesis and in the context of an atherosclerosis-prone experimental model, we investigate the effects of NFAT-signaling inhibition on atherosclerotic plaque formation and inflammatory burden in diabetic and non-diabetic apolipoprotein (Apo)E deficient mice. We found that inhibition of NFAT-signaling completely suppresses the diabetes-induced aggravation of atherosclerosis, also effectively reducing the expression of OPN, MCP-1, IL-6, ICAM-1 and tissue factor in the arterial wall. This effect was independent of changes in plasma glucose or lipid levels, and not due to systemic immunosuppression. These findings suggest that NFAT may play a role in the development of atherosclerosis in diabetes and identifies this signaling pathway as a novel therapeutic target for the treatment of diabetic macrovascular complications.

Rahman S *et al.* (2007). *Diabetes Obes Metab* **9**: 767-780.

Nilsson LM *et al.*(2008). *Curr Opin Lipidol* **19**: 483-490.

Nilsson J *et al.* (2006). *Arterioscler Thromb Vasc Biol* **26**: 794-800.

Nilsson-Berglund LM *et al.* (2009). *Arterioscler Thromb Vasc Biol* **30**: 218-224.

Lee MY *et al.* (2009). *Hum Mol Genet* **19**: 468-479.

Nieves-Cintron M *et al.* (2007). *J Biol Chem* **282**: 3231-3240.

Berglund LM *et al.*(2011). *Cardiovasc Res* **93**: 414-423.

Support: Swedish Research Council (#2009-4120; #2011-3900), Lund University Diabetes Centre, Exodiab (#2009-1039) and FP7 IMI-JU SUMMIT project (#115006)

Where applicable, the authors confirm that the experiments described here conform with The Physiological Society ethical requirements.

SA405

Has the continuing relevance of comparative physiology "gone missing" in biomedical research?

M.J. Joyner

Anesthesiology, Mayo Clinic, Rochester, MN, USA

Biomedical research relies on limited animal models to address questions related to human health. The limitations of inbred or genetically modified rodent models has become especially clear recently based on a number of high profile publications showing limited animal to human translation. Historically, many key discoveries have been generated by studies on a range of animals adapted to unusual environments. For example major advances in the understanding of the microcirculation continue to come from studies of the bat wing. In this context, the goal of this symposium is to explore what might be described as the "re-emergence" of comparative physiology to address important questions in human health and disease. It will also highlight sex differences in blood pressure regulation in humans.
This talk will provide a brief historical overview of the issues outlined above and also highlight areas such as hypoxia tolerance, and maintenance of bone and muscle mass during extreme inactivity where there are comparative "solutions" to problems with high relevance to human health and disease.

Where applicable, the authors confirm that the experiments described here conform with The Physiological Society ethical requirements.

SA406

Sex, nerves and blood pressure: a comparative analysis of the role that sex plays in blood pressure modulation

E.C. Hart[1], N. Charkoudian[2], G. Wallin[4] and M. Joyner[3]

[1]Physiology and Pharmacology, University of Bristol, Bristol, UK, [2]US Army Research Institute of Environmental Medicine, Natick, MA, USA, [3]Mayo Clinic and Foundation, Rochester, MN, USA and [4]Institute of Neuroscience and Physiology, University of Goteborg, Goteborg, Sweden

Sex hormones are essential in the development of the biological and physiological sexual characteristics of males and females. However, it is well known that they also play an important role in modulating cardiovascular regulation, particularly with regard to regulation of arterial pressure. Recent comparative examinations of blood pressure regulation in healthy men and women have increased our understanding regarding normal blood pressure control and how sex /sex hormones might influence the development of cardiovascular diseases such as hypertension. Previous studies have shown that, under the age of 40, men and women do indeed regulate resting blood pressure differently. The sympathetic nervous system is central to blood pressure regulation in humans; despite this, basal levels of muscle sympathetic activity (MSNA, an estimate of central sympathetic outflow) are not related to resting blood pressure in either men or women. How can this be when MSNA causes vasoconstrictor tone? Interestingly, in young men MSNA is positively related to peripheral vascular resistance but inversely related to cardiac output. Consequently, men with high MSNA have a high vascular resistance but a lower cardiac output. This balance negates the effect of MSNA on resting blood pressure in men; so men with high MSNA can have a normal resting blood pressure. However, this balance does not exist in young women. In young pre-menopausal women, MSNA is not related to total peripheral resistance or cardiac output. Thus, it appears that basal levels of MSNA contribute little to resting peripheral vasoconstrictor tone. Importantly, this difference between men and women appears to change with age and menopausal status. In postmenopausal women, MSNA becomes directly related to peripheral vascular resistance and blood pressure. This provides strong evidence that sex and sex hormones might modulate how MSNA affects resting blood pressure.

Where applicable, the authors confirm that the experiments described here conform with The Physiological Society ethical requirements.

SA407

Maintaining homeostasis despite deadly physiological extremes: lessons from a natural expert

S. Martin[1,2], A. Hindle[1] and K. Grabek[1,2]

[1]Department of Cell and Developmental Biology, University of Colorado School of Medicine, Aurora, CO, USA and [2]Human Medical Genetics and Genomics Program, Univ of Colorado School of Medicine, Aurora, CO, USA

Hibernating ground squirrels survive physiological deviations so removed from the mammalian norm that they inevitably lead to death in non-hibernators. In 13-lined ground squirrels and other circannual, or obligate, hibernators, a season of homeothermy that begins with reproduction and ends with obesity is segregated from a season of hibernation. Hibernation is characterized by cycles between extended (~2 weeks) bouts of torpor, punctuated by short (12 hr) arousals to typical euthermic conditions that are superimposed upon months of continuous fasting and inactivity. In torpor, the hibernating mammal exhibits profound drops in heart rate from a few hundred to a few beats/min, metabolic rate to a few percent of active, and core body temperature from 37°C to near zero. Remarkably, the physiological depressions are spontaneously reversed without harm during each arousal. Moreover, at the end of hibernation, the animal returns to homeothermy with surprisingly little muscle, gut or bone disuse atrophy. Clearly, numerous features of the hibernation phenotype would be beneficial if they could be harnessed and applied to humans. Because superimposition of hibernating species on the mammalian phylogeny implies that the common ancestor of all mammals was a hibernator (6), the possibility of deriving useful therapies that mimic various aspects of the hibernation phenotype is within the realm of science, and not merely science fiction. The first step towards achieving this goal is to define the molecular pathways and mechanisms used during natural hibernation to orchestrate and manage their remarkable phenotypic plasticity. Because hibernation's varied phenotypes are so distinctive, it is unlikely that hypothesis-driven work based on understanding of non-hibernators will provide the transformative data needed to understand hibernation at a molecular level. Our approach to this problem is to interrogate a precisely timed set of samples from 13-lined ground squirrels representing hibernation's major physiological phenotypes for biochemical differences. Our working hypothesis is that hibernation is a cycle-within-a-cycle, with the torpor-arousal cycles being embedded within a summer-winter seasonal cycle. This model predicts a resetting of baseline physiology between the summer and winter modes that leads to tissue protection and that it is only in the protected winter

state that torpor can be elicited. To test the predictions of this hypothesis and identify the underlying molecular mechanisms, we have collected an extensive tissue bank representing multiple timepoints throughout the year that represent key transitions in both cycles together. These samples are being examined with high-throughput 'omics' methodologies to identify the metabolites, proteins and transcripts in multiple organs that are candidates to support and drive the remarkable physiological transitions of hibernation. Early data support our model of an altered baseline physiology that separates winter from summer animals and reveal a surprising degree of tissue-specific variation that reflects unique aspects of organ function in the changes observed (1-5).

Epperson LE, Karimpour-Fard A, Hunter LE, and Martin SL. Metabolic cycles in a circannual hibernator. Physiol Genomics 43: 799-807, 2011.

Grabek KR, Karimpour-Fard A, Epperson LE, Hindle AG, Hunter LE, and Martin SL. Multistate proteomics analysis reveals novel strategies used by a hibernator to precondition the heart and conserve ATP for winter heterothermy. Physiol Genomics 43: 1263-1275, 2011.

Grabek KR, and Martin SL. Theme and variation: proteomic changes across three organs in hibernation cycles of the 13-lined ground squirrel. In: Living in a Seasonal World: Thermoregulatory and Metabolic Adaptations, edited by Ruf T, Bieber C, Arnold W, and Millesi E. Heidelberg: Springer, 2012, p. 423-432

Hindle AG, Karimpour-Fard A, Epperson LE, Hunter LE, and Martin SL. Skeletal muscle proteomics: carbohydrate metabolism oscillates with seasonal and torpor-arousal physiology of hibernation. Am J Physiol Regul Integr Comp Physiol 301: R1440–R1452, 2011.

Jani A, Orlicky DJ, Karimpour-Fard A, Epperson LE, Russell RL, Hunter LE, and Martin SL. Kidney proteome changes provide evidence for a dynamic metabolism and regional redistribution of plasma proteins during torpor-arousal cycles of hibernation. Physiol Genomics 44: 717-727, 2012.

Srere HK, Wang LCH, and Martin SL. Central role for differential gene expression in mammalian hibernation. Proc Natl Acad Sci U S A 89: 7119-7123, 1992.

Funding from NIH HL089049 and DK095180

Where applicable, the authors confirm that the experiments described here conform with The Physiological Society ethical requirements.

SA408

Comparative physiology in regenerative medicine

H. Lauridsen

MR-Research Centre, The Institute of Clinical Medicine, Aarhus University, Aarhus N, Denmark

Advances in stem cell research and tissue engineering in recent decades have led, i.a., to the generation of induced pluripotent stem cells and biocompatible artificial scaffolds, inspiring hope for future regenerative therapies. Progress in the field of regenerative medicine is, however, inevitably difficult applying the mammalian model organisms traditionally used in biomedical research, owing to the lack of tissue regenerative potential in these organisms. In contrast, urodele amphibians possess impressive regenerative capabilities at both tissue, organ, and structural level, and are apt models for regenerative biology and medicine, exemplified in the iconic Mexican axolotl (Ambystoma mexicanum). In this talk I will present the axolotl as an important comparative model for unraveling the mechanisms of intrinsic tissue regeneration in general and in particular as a model for tissue regeneration following myocardial infarction as well as a model for stem cell tracking using MRI for non-invasive evaluation of future regenerative therapies.

The axolotl heart has been described to recover completely following partial ventricular amputation of the apex, serving as a model for regeneration in a relatively simple structure in the sense of only a few different tissues involved. Removal of heart tissue in the form of partial amputation is, however, not a very clinically relevant situation, on the other hand regeneration following myocardial infarction is highly clinically relevant. We have developed an axolotl myocardial infarction model that allows for description and discovery of regenerative events in the process of heart repair. In this talk I will present our latest discoveries of basic molecular and cellular mechanism that are activated at the initiation of heart regeneration in the axolotl.

One fundamental challenge of future stem cell therapies will be the ability to monitor the progress of therapy in the sense of being able to track injected stem cell. The technique to accomplish this has to be non-invasive - there is no point in regenerating tissue, if this is destroyed by biopsies later on to ensure that regeneration has in fact taken place. Additionally, cell tracking technology will have to be safe and repetitive to allow for follow up evaluations. Ultrasmall superparamagnetic iron oxide particles (USPIO), nanoparticles containing an iron oxide core and a biocompatible coating, have been suggested and applied for non-invasive and safe stem cell tracking in preclinical studies, as cells labeled with these particles can be detected with MRI due to their ferrous core. We have developed a fluorophore conjugated USPIO detectable with MRI and optical imaging and tested the tracking methodology in the axolotl, in this situation serving as a model of intrinsic regeneration.

Where applicable, the authors confirm that the experiments described here conform with The Physiological Society ethical requirements.

SA409

Comparative physiology of temperature regulation: of brains and different sized bodies

S.K. Maloney[1], A. Fuller[2] and D. Mitchell[2]

[1]Anatomy Physiology and Human Biology, University of Western Australia, Crawley, WA, Australia and [2]Physiology, University of the Witwatersrand, Johannesburg, Gauteng, South Africa

We discuss the relevance of comparative physiology to aspects of temperature regulation, and the problems of extrapolating from animal models to humans. Students of comparative physiology learn detail of size scaling laws in animal energetics, including laws that describe the effect of body size on heat exchange and on the thermoneutral zone. Much of the research on animal models of human disease, including genetic risk models, is done on rodents maintained at 22-23°C, a temperature well below a rodent's thermoneutral zone. In some disease domains this experimental anomaly may not matter, but the increase in metabolism and decrease in RQ (indicative of increased fat oxidation) that occurs below the thermoneutral zone may confound extrapolations to humans in any disease with a metabolic component. Another medical issue topical currently is whether isolated cooling of the traumatized human brain is feasible, the study of which is confounded by the difficulty of measuring deep brain temperature in healthy humans. Based on studies of many other species, we show that capacity for selective brain cooling depends on the carotid rete, a structure that humans and other

primates do not possess, rendering it improbable that humans can implement selective brain cooling. The primary determinant of brain temperature is the temperature of the blood reaching it. If the temperature of blood destined for the brain is manipulated, isolated cooling of the brain is possible. Cooling the head without cooling the blood destined for the brain does not result in isolated brain cooling.
e-mail: shane.maloney@uwa.edu.au

Where applicable, the authors confirm that the experiments described here conform with The Physiological Society ethical requirements.

SA410

Role of myocardial reactive oxygen species (ROS) signalling in post-operative and non-surgical atrial fibrillation

B. Casadei

University of Oxford, Oxford, UK

Atrial fibrillation (AF) is common and is associated with significantly increased morbidity and mortality (mostly due to heart failure and stroke). A striking feature of AF is the ability of this arrhythmia to sustain itself. It is accepted that, by increasing atrial rate, AF leads to electrical and structural remodelling of the atria, which, in turn, promotes AF maintenance and increases vulnerability to relapse. There is considerable interest in developing treatment and prevention strategies that target mechanisms upstream of ion channels modifications (e.g., myocardial redox state and metabolism); however, whereas changes in ion channels conductance are the common denominator of virtually all types of AF, the myocardial signalling upstream of atrial electrical and structural remodelling may differ with the stage and substrate of AF, demanding a more refined ad hoc approach to the prevention and management of this arrhythmia. For example, we have shown that a gp91phox-containing NADPH oxidase (NOX2) is the main source of reactive oxygen species (ROS) in human atrial myocytes, and that atrial NOX2 activity is independently associated with an increased risk of developing AF and other postoperative complications in patients undergoing cardiac surgery. We have also established that short term treatment (3 days) or ex vivo tissue incubation with HMG CoA reductase inhibitors (statins) increases NO bioavailability and reduces vascular and cardiac NOX2 activity in patients undergoing coronary revascularization by inhibiting one of the key components of the oxidase complex (i.e., the small G protein Rac1), before any change in LDL cholesterol can be detected. Together, these findings suggest that NOX2 inhibition with statins may help prevent the new onset of AF after cardiac surgery and, possibly, in other disease states characterized by inflammation. However, whether NOX2 inhibition may also be beneficial in the secondary prevention of AF or in conditions where atrial structural remodeling provides the arrhythmic substrate remains a matter of debate. To address this issue, we investigated the time-dependent changes in the expression and activity of atrial oxidase systems in the atrial myocardium of goats with pacing-induced AF (2 weeks and 6 months) or atrial structural remodeling secondary to atrioventricular block, and in human atrial samples. We found that NOX2 and Rac1 activity and the protein level of the cytochrome-forming subunits of the oxidase (NOX2 and p22phox) are significantly increased in the left atrial myocardium of goats after 2 weeks of AF and in atrial samples from patients in sinus rhythm who develop AF after cardiac surgery. By contrast, the increase in ROS production observed in longstanding AF or in the presence of atrioventricular block (i.e., in the presence of atrial structural remodeling) is due to mitochondrial oxidases and NOS "uncoupling" (a phenomenon whereby the catalytic electron flow within the enzyme is uncoupled from NO synthesis and diverted to molecular oxygen to yield superoxide), secondary to a reduction in the atrial content of the NOS co-factor BH4 and an increase in arginase activity.
Ex vivo atorvastatin causes a mevalonate-reversible inhibition of atrial Rac1 and NOX2 activity in patients who develop AF after cardiac surgery, but it does not affect atrial ROS production, NOS uncoupling or BH4 content in patients with permanent AF.
Taken together, these data demonstrate that the mechanisms responsible for the NO-redox imbalance in the fibrillating atrial myocardium change with the duration of AF and the development of atrial structural remodeling and suggest that a shift in the atrial sources of ROS with the duration of AF may influence the antiarrhythmic efficacy of statins.

Where applicable, the authors confirm that the experiments described here conform with The Physiological Society ethical requirements.

SA411

Changes in spatio-temporal pattern of Ca2+ release in tachycardia-induced atrial remodelling

M. Greiser[1,2] and U. Schotten[1]

[1]Maastricht University, Maastricht, Netherlands and [2]University of Maryland, Baltimore, MD, USA

Atrial fibrillation (AF) is characterized by sustained high atrial activation rates and cellular Ca2+ signaling instability, which is thought to contribute to atrial arrhythmogenesis. How high rate and arrhythmogenic Ca2+ instability may be related, however, is poorly understood. We have characterized the effect of sustained high atrial activation rates on sub-cellular Ca2+ signaling in a rabbit model. L-type Ca2+ current and whole cell [Ca2+]i transient were reduced as was ryanodine receptor (RyR2) expression (by 77%) with a 7fold increase in RyR2 phosphorylation (Ser2809). Ca2+ release in the myocyte center was blunted due to increased [Ca2+] buffering strength. The spatial distribution of junctional and central SR sites was unchanged. Surprisingly, SR Ca2+ content, characteristics and rates of Ca2+ sparks and -waves were unchanged. Computational estimates of Ca2+ signaling suggest that the observed behavior arises from a higher Ca2+ leak rate per RyR2 associated with less RyR2s per SR cluster. Additionally, lower total Ca2+ release per [Ca2+]i transient, due to failed Ca2+ wave propagation to the myocyte center and the higher Ca2+ buffering strength contribute. Sustained high atrial rates produce "Ca2+ signaling silencing" and not Ca2+ instability. Ca2+ signaling silencing serves as an adaptive response to rapid myocyte activation and this hampers the development of Ca2+ dysregulation-based arrhythmogenic mechanisms

Where applicable, the authors confirm that the experiments described here conform with The Physiological Society ethical requirements.

SA412

Chasing tails: clinics and C-termini

F. Karet

University of Cambridge, Cambridge, UK

It is well recognized that the C-terminal domains of many proteins are important for directing them to heir correct cellular destination. Molecular genetic and cellular investigations of patients with a variety of inherited conditions that result from trafficking and targeting abnormalities have provided insights into the normal behaviour of membrane and other compartment residents.
This talk will illustrate a range of such mechanisms that are of particular importance in the kidney, set in the context of a specialist multidisciplinary clinical service.

Where applicable, the authors confirm that the experiments described here conform with The Physiological Society ethical requirements.

SA413

The role of Tmem27 and ACE2 on renal neutral amino acid transport

S.M. Camargo

University of Zurich, Zurich, ZH, Switzerland

The interaction of amino acid transporters with accessory proteins guarantees their insertion in the membrane and may modulate the activity or the supply of substrate. Neutral amino acid transporters of the SLC6 family have been shown to rely on the expression of Tmem27 and the angiotensin-converting enzyme 2 (ACE2), two members of the renin-angiotensin system (RAS). ACE2 and Tmem27's role as a partner protein of amino acid transporters was revealed by gene ablation and co-expression in heterologous system. The *tmem27* knock-out mice presented generalized neutral aminoaciduria, while *ace2* knock-out animal had normal amino acids excretion. The amino acid transport in the kidneys of *tmem27* and intestine of *ace2* knock-out animals is reduced, moreover Slc6 family amino acid transporters expression is affected. In the kidney of *tmem27* mice the expression of B^0AT1, B^0AT3 (*Slc6a19* and *18*) and the imino transporter SIT1 (*Slc6a20*) were abolished or strongly reduced. In the *ace2* knock-out mice the renal expression of B^0AT1 was normal, while it was absent in the small intestine. B^0AT1 is the major neutral amino acid transporter in the kidney and intestine, and has two tissue specific accessory proteins, Tmem27 in the kidney and ACE2 in intestine. Mutations in the gene (*SLC6A19*) encoding the B^0AT1, but not in the genes encoding the accessory proteins, are the cause of Hartnup disorder. Hartnup disorder patients present aminoaciduria, and may also additionally develop symptoms resembling pellagra, including light-sensitive dermatitis and diarrhea that manifests under conditions of stress and malnutrition. Pellagra like symptoms is thought to result from defective intestinal absorption of L-tryptophan, the precursor of niacin. The ablation of B^0AT1 in the intestine of *ace2* knock-out mice leads to a decreased L-tryptophan absorption, increased susceptibility to intestinal infection, but not to dermatitis-like symptoms. These results suggest that B^0AT1 ablation in intestine may contribute to the development of symptoms different from aminoaciduria observed in the Hartnup disorder subjects. The phenotype of Hartnup patients has been shown to vary due to nutritional status, environment, and high frequency of compound heterozygous. Additionally, mutated transporter can interact differentially with tissue specific accessory proteins, and might contribute to the phenotypic heterogeneity among individuals with Hartnup disorder. The work on amino acid transporters of the SLC6 family and their tissue-specific partner proteins has provided critical information concerning the modulation of amino acid transporter function, however several questions are still waiting to be solved such as the mechanism guiding the selection of the partner protein in kidney, regulation of the expression and function of the transporters and their accessory proteins by diet, gender, hormones, age and diseases are crucial and are just starting to be investigated.

Essential role for collectrin in renal amino acid transport. Danilczyk U, Sarao R, Remy C, Benabbas C, Stange G, Richter A, Arya S, Pospisilik JA, Singer D, Camargo SM, Makrides V, Ramadan T, Verrey F, Wagner CA, Penninger JM. Nature. 2006; 444(7122):1088-91.

Tissue-specific amino acid transporter partners ACE2 and Collectrin differentially interact with Hartnup mutations. Simone M. R. Camargo, Dustin Singer, Victoria Makrides, Katja Huggel, Klaas M. Pos, Carsten A. Wagner, Keiji Kuba, Ursula Danilczyk, Flemming Skovby, Robert Kleta, Josef M. Penninger, and François Verrey. Gastroenterology, 2009 Mar;136(3):872-82.

Orphan transporter SLC6A18 is renal neutral amino acid transporter B0AT3. Singer D, Camargo SM, Huggel K, Romeo E, Danilczyk U, Kuba K, Chesnov S, Caron MG, Penninger JM, Verrey F.J Biol Chem. 2009; 284(30):19953-60.

Defective intestinal amino acid absorption in Ace2 null mice. Singer D, Camargo SM, Ramadan T, Schäfer M, Mariotta L, Herzog B, Huggel K, Wolfer D, Werner S, Penninger JM, Verrey F. Am J Physiol Gastrointest Liver Physiol. 2012;303(6):G686-95.

ACE2 links amino acid malnutrition to microbial ecology and intestinal inflammation. Hashimoto T, Perlot T, Rehman A, Trichereau J, Ishiguro H, Paolino M, Sigl V, Hanada T, Hanada R, Lipinski S, Wild B, Camargo SM, Singer D, Richter A, Kuba K, Fukamizu A, Schreiber S, Clevers H, Verrey F, Rosenstiel P, Penninger JM. Nature. 2012 Jul 25;487(7408):477-81.

Where applicable, the authors confirm that the experiments described here conform with The Physiological Society ethical requirements.

SA414

Disorders of neutral amino acid transport

S. Broer

Research School of Biology, Australian National University, Canberra, ACT, Australia

The proximal tubule is endowed with a variety of neutral amino acid transporters to ensure efficient reabsorption of this large group of metabolites. Molecular cloning efforts have successfully identified apical transporters for amino acids. The major transporter for neutral amino acids (SLC6A19 or B0AT1) mediates the uptake of all neutral amino acids. Mutations in this transporter cause Hartnup disorder. Surface expression of B0AT1 requires expression of collectrin (TMEM27) in the kidney or of angiotensin converting enzyme 2 in the intestine. Complete reabsorption of proline and glycine requires additional transporters, namely SLC6A20 (SIT1) and SLC36A2 (PAT2). Mutations in these transporters cause iminoglycinuria and glycinuria, two benign aminoacidurias, which are however interesting from a genetic point of view. Combination of different alleles can cause similar phenotypes in homozygotes,

but present differently in heterozygotes. In mice neutral amino acid reabsorption is different from humans making use of SLC6A18 (B0AT3) instead of PAT2. Human SLC6A18 is an inactive protein, which is still expressed in the proximal tubule but does not appear to have a functional role. B0AT3 also requires collectrin or ACE2 for surface expression, but its expression mainly overlaps with collectrin. A mouse model lacking SLC6A19 in the intestine and kidney shows reduced body weight and cannot control body weight on diets of different protein content. On a high-fat diet the animals gain less weight than wild-type litter mates. Insulin sensitivity and glucose tolerance are improved compared to wildtype mice. The mechanisms underlying these physiological changes are currently under investigation.

Broer, S. and Palacin, M. (2011) The role of amino acid transporters in inherited and acquired diseases. Biochem J. 436, 193-211

Broer, A., Juelich, T., Vanslambrouck, J. M., Tietze, N., Solomon, P. S., Holst, J., Bailey, C. G., Rasko, J. E. and Broer, S. (2011) Impaired Nutrient Signaling and Body Weight Control in a Na+ Neutral Amino Acid Cotransporter (Slc6a19)-deficient Mouse. J Biol Chem. 286, 26638-26651

Vanslambrouck, J. M., Broer, A., Thavyogarajah, T., Holst, J., Bailey, C. G., Broer, S. and Rasko, J. E. (2010) Renal imino acid and glycine transport system ontogeny and involvement in developmental iminoglycinuria. Biochem J. 428, 397-407

Broer, S., Bailey, C. G., Kowalczuk, S., Ng, C., Vanslambrouck, J. M., Rodgers, H., Auray-Blais, C., Cavanaugh, J. A., Broer, A. and Rasko, J. E. (2008) Iminoglycinuria and hyperglycinuria are discrete human phenotypes resulting from complex mutations in proline and glycine transporters. J Clin Invest. 118, 3881-3892

Research in the laboratory of SB is supported by grants from the National Health and Medical Research Council (NHMRC) and Sanofi.

Where applicable, the authors confirm that the experiments described here conform with The Physiological Society ethical requirements.

SA415

Tubular defects leading to renal stones

J.A. Sayer

Institute of Genetic Medicine, University of Newcastle, Newcastle upon Tyne, UK

Renal stone disease may be seen as clinical symptom of an underlying pathological process predisposing to crystallization within the renal tract.
Molecular genetics has allowed significant progress to be made in our understanding of renal tubular salt handling which underlies certain stone forming conditions. The molecular defect underlying these inherited tubular disorders often contributes to a significant metabolic risk factor for stone formation. In contrast, idiopathic renal stone formation relates to the interplay of environmental, dietary and genetic factors, with hypercalciuria being the most commonly found metabolic risk factor. The pathophysiological and genetic basis underlying familial hypercalciuria and calcium stone formation remains elusive.
Here I will discuss known molecular players in the pathogenesis of hypercalciuria and the need for novel insights into why the majority of hypercalciuria remains unexplained

Sayer JA. (2011) Renal stone disease. *Nephron Physiol* 118, 35-44.

This work is supported by Kidney Research UK and the Northern Counties Kidney Research Fund.

Where applicable, the authors confirm that the experiments described here conform with The Physiological Society ethical requirements.

SA416

Uromodulin-associated kidney diseases

O. Devuyst

Institute of Physiology, University of Zürich, Zürich, Switzerland

Uromodulin (Tamm-Horsfall protein) is the most abundant protein excreted in the urine under physiological conditions. It is exclusively produced in the kidney and secreted into the urine via proteolytic cleavage. Its biological function is still not fully understood. Uromodulin has been linked to water/electrolyte balance and to kidney innate immunity. Studies in knockout mice demonstrated that it has a protective role against urinary tract infections and renal stone formation. Mutations in the *UMOD* gene encoding uromodulin lead to rare autosomal dominant diseases, collectively referred to as uromodulin-associated kidney diseases. They are characterized by progressive tubulointerstitial damage, impaired urinary concentrating ability, hyperuricemia, renal cysts, and progressive renal failure. Novel in vivo studies point at intracellular accumulation of mutant uromodulin as a key primary event in the disease pathogenesis. Recently, genome-wide association studies identified uromodulin as a risk factor for chronic kidney disease (CKD) and hypertension, and suggested that the level of uromodulin in the urine could represent a useful biomarker for the development of CKD. These investigations emphasize the scientific and clinical interest for this long discovered molecule.

Where applicable, the authors confirm that the experiments described here conform with The Physiological Society ethical requirements.

SA417

Translational spectral electroencephalographic markers in the European PharmaCog project: a new resource for drug discovery for Alzheimer's disease

C. Babiloni[1,2], F. Infarinato[3], J.F. Bastlund[4], B. Clausen[4], G. Forloni[5], A. Frasca[5], M. Bentivoglio[6], P.F. Fabene[6], G. Bertini[6], J. Kelley[7], S. Dix[8], J.C. Richardson[9], W. Drinkenburg[7] and C. Del Percio[3]

[1]University Sapienza, Rome, Rome, Italy, [2]University of Foggia, Foggia, Italy, [3]IRCCS San Raffaele Pisana, Roma, Italy, [4]Lundbeck, Valby, Denmark, [5]Mario Negri Institute, Milano, Italy, [6]University of Verona, Verona, Italy, [7]Janssen, Beerse, Belgium, [8]Eli Lilly, Basingstoke, UK and [9]GSK, Brentford, UK

In the IMI PharmaCog project (2010-2014) we showed that the electroencephalographic (EEG) rhythms related to eyes opening as a condition of cortical arousal are abnormal in patients with mild cognitive impairment and Alzheimer's disease (AD; Babiloni et al., 2010, JAD). Towards a back-translation we evaluated whether EEG rhythms related to motor activity change across physiological aging in wild type (WT) mice, as well as in Tg models of AD such as PDAPP and TASTPM mice. For the physiological aging, EEG data were recorded in 19 young (4.5-6 months), 12 middle age (12-14 months), and 15 old (24 months) male WT mice. For the pathological aging, EEG data were recorded in 15 WT vs. 10 PDAPP male mice (24

months), as well as in 14 WT mice (12-14 months) vs. 15 TASTPM mice (12-14 months). Artifact-free EEG segments during wake active state (gross movements, exploratory movements or locomotor activity) and passive state (no sleep) were used as an input for EEG power density analysis. Results showed that (1) 1-2 and 2-4 Hz power density during the passive state was greater in old WT than in young and middle age WT mice ($p<0.05$); (2) 6-8 Hz power density during the active state was greater in these old mice ($p<0.05$); (3) 8-10 Hz power density during the active state was greater in young than in middle age mice ($p<0.05$); (4) 2-4 and 4-6 Hz power density during the passive state was lower in PDAPP compared to WT mice ($p<0.05$); (5) 8-10 Hz power density during the active state was lower in PDAPP compared to WT mice ($p<0.05$); (6) 2-4 and 4-6 Hz power density during the passive state was lower in TASTPM compared to WT mice ($p<0.05$); and (7) 10-12 Hz power density during the active state was lower in TASTPM compared to WT mice ($p<0.05$). The present results suggest that the EEG markers of motor activity are useful to unveil neurophysiological mechanisms of cortical neural synchronization characterizing the physiological aging in WT mice, as well as the pathological cortical neural synchronization in Tg mice.

Babiloni C, Lizio R, Vecchio F, Frisoni GB, Pievani M, Geroldi C, Claudia F, Ferri R, Lanuzza B, Rossini PM.

Reactivity of cortical alpha rhythms to eye opening in mild cognitive impairment and Alzheimer's disease: an EEG study. J Alzheimers Dis. 2010;22(4):1047-64. doi: 10.3233/JAD-2010-100798.

The activity leading to the present review has received funding from the European Community's Seventh Framework Programme (FP7/2007-2013) for the Innovative Medicine Initiative under Grant Agreement No. 115009 (Prediction of cognitive properties of new drug candidates for neurodegenerative diseases in early clinical development, PharmaCog). For further information on the PharmaCog project, please refer to http://www.pharmacog.org.

Where applicable, the authors confirm that the experiments described here conform with The Physiological Society ethical requirements.

SA418

Cortical gamma oscillations and mitochondrial dysfunction: food for thought in neurodegeneration?

M.O. Cunningham

Institute of Neuroscience, The Medical School, University of Newcastle upon Tyne, Newcastle Upon Tyne, UK

Mitochondria are a cell organelle responsible for the production of energy for cellular activities. This is done mainly by the formation of ATP through oxidative phosphorylation via the mitochondrial respiratory chain. Since neurons are highly active cells, it is not surprising that neurons depends highly on optimal mitochondrial function for their survival and a broad range of physiological activities. Increasingly, neurodegenerative disorders are being identified as having secondary mitochondrial dysfunction. These include Alzheimer's disease (AD), Parkinson's disease (PD) and Huntington's disease (HD). In all of these conditions, cognitive dysfunction is a core symptom with limited effective nootropic therapies currently available.

In attempting to understand the role of mitochondrial dysfunction and the implications of this for cognitive processes we have utilized in vitro brain slice preparations. Using this technique, patterns of cortical network activity associated with cognitive processes can be reproduced. In particular, we have examined oscillatory activity in the range of 30-80 Hz, termed the gamma frequency oscillation. This approach also affords sufficient access and manipulation to probe their network, cellular and synaptic underpinnings.

Using this approach, data from studies using rodent and human brain slices will be presented which illustrate that the cortical gamma frequency oscillation depends largely on mitochondrial energy formation and highly sensitive to mitochondrial dysfunction, especially complex I inhibition1. We will also provide evidence that within this context, our results suggest that the decline in gamma oscillation power seen with inhibitors of the mitochondrial respiratory chain results primarily from effects on these fast spiking interneurons.

These findings may offer insight into pathophysiology of cortical dysfunction in neurodegenerative conditions in which secondary mitochondrial dysfunction is implicated.

Whittaker RG, Turnbull DM, Whittington MA, Cunningham MO (2011). Brain 134(Pt 7):e180

Where applicable, the authors confirm that the experiments described here conform with The Physiological Society ethical requirements.

SA419

Neuron-glia crosstalk under pathological condition of Alzheimer's disease

I. Mook-Jung

Biochemistry & Biomedical Sciences, Seoul National University College of Medicine, Seoul, Republic of Korea

Alzheimer's disease (AD) is a progressive and irreversible neurodegenerative disorder that leads to cognitive dysfunction, memory impairment and emotional disturbance in elderly persons. Activated microglia and reactive astrocytes are commonly found in and around the senile plaques that are the central pathological hallmark of AD. Beta-amyloid peptide (Abeta) accumulates in these plaques. Astrocytes respond to neuronal activity through the release of gliotransmitters such as glutamate, d-serine and adenosine 5'-triphosphate (ATP). How gliotransmitters regulate neuronal activity, however, is not well defined and even controversial. Also, astrocyte secreted several proteins to the synapse, which modulate synaptic function including synaptogenesis and neurogenesis directly or indirectly to the neurons. In the present study, we examined the effect of one of gliotransmiitters, ATP on neurons damaged by Abeta42 peptides in both primary astrocytes and U373 astrocyte cell line. We found that exogenous ATP protects against Abeta42-mediated reduction in synaptic molecules, such as NMDA receptor 2A, PSD-9ATP5 and synaptophysin, through purinergic receptor P2X in primary hippocampal neurons. ATP also prevented Abeta42-induced spine reduction and impaired long-term potentiation in the hippocampal neurons. Our findings suggest that Abeta-induced gliotransmitter ATP plays a protective role against Abeta42-mediated synaptic plasticity disruption. As an astrocyte-secreted protein, thrombospondin-1 (TSP-1) was examined in vitro and in AD animal model (5XFAD mice). The release of TSP-1 from astrocytes was decreased by Abeta42 in vitro, and the reduced level of TSP-1 was observed in brains of AD animal models. Synaptic pathology caused by Abeta42 such as decreased dendritic density, impaired synaptic activity, and reduced long-term potentiation (LTP) were prevented by co-incubation with TSP-1 and

Abeta. TSP-1 is a potential therapeutic component against the damaging effects caused by Abeta42 in AD pathogenesis.

McKhann G, Drachman D, Folstein M, Katzman R, Price D, Stadlan EM (1984) Clinical diagnosis of Alzheimer's disease: report of the NINCDS-ADRDA Work Group under the auspices of Department of Health and Human Services Task Force on Alzheimer's Disease. Neurology 34:939-944.

Jung ES, An K, Hong HS, Kim JH, Mook-Jung I. (2012) Astrocyte-originated ATP protects Ab(1-42)-induced impairment of synaptic plasticity.

National Research Foundation (2009-0081673); World Class University-Neurocytomics

Where applicable, the authors confirm that the experiments described here conform with The Physiological Society ethical requirements.

SA420

Understanding physiological roles of microtuble binding protein tau

D. Whitcomb

University of Bristol, Bristol, Bristol, UK

Tau is a microtubule binding protein and has been identified as a key molecule in Alzheimer's disease (AD), as well as other tauopathies (Ballatore et al., 2007). Though tau is primarily located in axons, the entirety of its physiological roles are yet to be clearly defined. Given the dysregulation of the synapse in AD pathology (Selkoe, 2002), we investigated a possible physiological synaptic function of tau. We studied synaptic plasticity in the rat hippocampus, and found a selective deficit in long-term depression (LTD) as a result of RNAi knockdown of tau in vitro. Furthermore, we found that the induction of LTD is associated with the phosphorylation of tau, and this is required for the activation of key AMPA receptor internalisation mechanisms. These findings demonstrate that tau has a critical function in AMPA receptor trafficking during LTD and suggest that tauopathies may result from an aberrant form of LTD in the CNS.

Ballatore, C. et al. Tau-mediated neurodegeneration in Alzheimer's disease and related disorders. Nature Reviews Neuroscience 8, 663-672 (2007).

Selkoe, D. J. Alzheimer's disease is a synaptic failure. Science 298, 789-791 (2002).

Where applicable, the authors confirm that the experiments described here conform with The Physiological Society ethical requirements.

SA421

Gender specific differences in muscle protein metabolism

B. Mittendorfer

Geriatrics And Nutritional Sciences, Washington University School of Medicine, St Louis, MO, USA

Sexual dimorphism in body composition and muscle mass is well recognized. The mechanisms responsible for this phenomenon and how a person's sex affects the response to anabolic and catabolic stimuli are not completely understood. Several studies indicate that there is no difference in the basal rate of muscle protein synthesis or muscle protein breakdown or the anabolic responses to nutritional stimuli and resistance exercise in young and middle-aged adult men and women. Nevertheless, recent evidence suggests that aging affects muscle protein turnover differently in men and women. The basal rate of muscle protein synthesis is greater in old women than in old men; in addition, both old women and old men are resistant to the anabolic effects of exercise and nutrition and old women appear to be more resistant than old men. This suggests that differences in muscle protein turnover between men and women might be most apparent when muscle mass is changing (i.e., during aging vs. young and middle-adulthood when muscle mass is steady) and suggests a possible role of changes in the hormonal milieu with aging, in particular at the onset of menopause in women.

Where applicable, the authors confirm that the experiments described here conform with The Physiological Society ethical requirements.

SA422

Metabolic and molecular regulation of skeletal muscle in older age

P.J. Atherton

School of Graduate Entry Medicine and Health, University of Nottingham, Derby, UK

Physical activity in the form of exercise or increasing the plasma availability of essential amino acids (EAA) by exogenous supply (orally or intravenously) or via oral protein sources stimulates skeletal muscle anabolism. Mechanistically, EAA-induced increases in muscle protein synthesis (MPS) are initiated after AA-transportation into the muscle cell whereupon leucine indirectly activates the mechanistic target of rapamycin complex-1 (mTORc1), independent of proximal insulin signaling (phosphatidylinositol 3-kinase (PI3K)) pathways. Similarly, exercise also stimulates mTORc1 signaling via mechano-mediated routes, again largely independent of proximal insulin signalling. Subsequent downstream mTORc1 signaling enhances translational initiation via activation of mTORc1 substrates (e.g. p70S6K1, 4EBP1) culminating in ribosomal assembly, polyribosome formation and increased MPS. In terms of kinetics, skeletal muscles are receptive to the anabolic effects of EAA for only a short period, equating to ~2 h in the rested state (even after ~50 g EAA-rich protein), thereafter becoming refractory despite continued EAA availability and mTORc1 signalling. This phenomenon has been termed "muscle-full", whereby muscles intrinsically sense "excess" EAA and divert them toward oxidation. Episodes of physical activity (i.e., exercise) are able to delay the "muscle-full" signal to facilitate muscle adaptation (e.g. cellular remodelling/ hypertrophy) in accordance to the demands of the exercise activity imposed e.g. resistance vs. endurance. Intake of nutrition also provides a second route for muscle anabolism via suppression of muscle protein breakdown (MPB). This occurs independently to direct effects of EAA on MPB since EAA supply under insulin clamped conditions (postabsorptive ~5μU.ml-1) is insufficient to suppress MPB. Instead, the release of insulin in response to nutrition causes suppression of MPB (~15μU.ml-1 provides ~50% suppression). On this basis, the robust insulin secretagogue properties of EAA are likely sufficient to increase plasma insulin enough to supress MPB, and maximise nutrient-driven muscle anabolism even in the absence of carbohydrates. To facilitate delivery of AA and insulin to the myocellular-capillary interface, nutrients also modulate peripheral vascular function. Indeed, while insulin is known to increase blood flow to skeletal muscle, certain AA (e.g. arginine, the precursor for nitric

oxide) can also enhance muscle microvascular flow. Therefore, an appreciation of the co-ordination between endocrine pancreas, peripheral vasculature, and muscle cells is needed to understand the anabolic effects of AA and the nature of any interactions with exercise in terms of muscle protein anabolism. In terms of ageing, it has been demonstrated that the transient anabolic effects of exercise and/or EAA are blunted in older age (vs. younger groups) providing evidence for the existence of so-called 'anabolic resistance'. While this phenomenon has been proven in both pre-clinical and clinical scenarios as an "all-cause" mechanism of skeletal muscle atrophy, how much this relates to inactivity in older-aged individuals remains to be definitively determined. Nevertheless, this has lead to suggestion that strategies aimed at increasing dietary EAA-intake or enhancing the anabolic effects of exercise/nutrition represent important foci in treating sarcopenia. To summarise, optimal nutritional strategies for older individuals need to be viewed in the context of the gut-vascular-pancreas-muscle axis and in terms of interactions with physical activity; only comprehension of all these facets will afford full exploitation of the anabolic efficacy of nutrition and exercise in sarcopenia. Finally, a better comprehension of the metabolic and molecular basis of other facets of ageing muscles, beyond those occurring in protein metabolism (e.g. ectopic lipids, satellite cells dysfunction), are needed to generate a more holistic appreciation of the effects of ageing on skeletal muscle in relation to deleterious functional and metabolic outcomes.

Where applicable, the authors confirm that the experiments described here conform with The Physiological Society ethical requirements.

SA423

Muscle insulin resistance, immobilisation and remobilisation

F. Dela

Xlab - Center for Healthy Aging, University of Copenhagen, Copenhagen, Denmark

A family history of type 2 diabetes (e.g. first degree relatives, FDR) and low birth weight (LBW) are risk factors of type 2 diabetes and predisposes to type 2 diabetes via genetically and environmental susceptibility, respectively. Severe physical inactivity could purposely unmask their predisposal and reveal a larger vulnerability to physical inactivity than those without preexisting risk factors. Furthermore, comparisons between FDR and LBW in the response to alterations in the daily physical activity level may exemplify the relative influence of genes and environmental factors. We have studied such groups before and after a ten-day bed rest intervention study, which was followed by a four wk re-training program. Thirteen FDR (age: 26 ± 1 yr; body weight 80 ± 3 kg; BMI: 25 ± 1; VO2max: 39 ± 1 ml/min/kg), twenty LBW (age: 26 ± 1 yr; body weight 72 ± 3 kg; BMI: 23 ± 1; VO2max: 44 ± 3 ml/min/kg) and twenty healthy controls (CON) (age: 25 ± 1 yr; body weight 78 ± 2 kg; BMI: 24 ± 1; VO2max: 44 ± 1 ml/min/kg) was included in the study (Sonne et al., 2010). Insulin secretion and action, endothelial function, inflammation, and muscle transcriptional and translational changes was studied in a comprehensive experimental program.
Aging per se does not lead to skeletal muscle insulin resistance (Dela et al., 1996b;Dela et al., 1996a), but with age physical inactivity may develop. Data from a study on how one-legged immobilization for 2 wks with subsequent 6 wks rehabilitation may change markers on insulin sensitivity in young and old men will be reported.

Dela F, Mikines KJ, Larsen JJ, & Galbo H (1996a). Glucose clearance in aged trained skeletal muscle during maximal insulin with superimposed exercise. J Appl Physiol 87, 2059-2067.

Dela F, Mikines KJ, Larsen JJ, & Galbo H (1996b). Training-induced enhancement of insulin action in human skeletal muscle: The influence of aging. J Gerontol 51A, B247-B252.

Sonne MP, Alibegovic AC, Hojbjerre L, Vaag A, Stallknecht B, & Dela F (2010). Effect of 10 days of bedrest on metabolic and vascular insulin action: a study in individuals at risk for type 2 diabetes. J Appl Physiol 108, 830-837.

Where applicable, the authors confirm that the experiments described here conform with The Physiological Society ethical requirements.

SA424

Ageing, inactivity and rehabilitation

C. Suetta

Glostrup Hospital, Copenhagen, Denmark and University of Copenhagen, Copenhagen, Denmark

Skeletal muscle atrophy is a common debilitating condition associated with human immobilisation and ageing resulting in a reduced muscle function. In animal models, loss of muscle mass with immobilisation or unloading has been suggested primarily to occur through an accelerated degradation of myofibrillar proteins via the ubiquitin-proteasome pathway, although rapid decreases in protein synthesis also has been shown. Somewhat in contrast, studies in young human individuals have suggested that a decline in protein synthesis rather than accelerated protein breakdown is responsible for the muscle loss observed with disuse. With aging, muscle loss is suggested to be associated with increased inflammation, decreased anabolic signalling, increased apoptosis, impaired myogenic responsiveness as well as decreased mitochondrial function. Moreover, aging has been found to affect signalling pathways that regulate myogenic growth factors and myofibrillar protein turnover in skeletal muscle of rodents. However, very little is known about how immobilisation and skeletal muscle disuse affects ageing muscle. We therefore set to investigate some of the cellular and molecular mechanisms suggested being responsible for the age-related changes in skeletal muscle with disuse and re-growth, including the differential involvement and time course of such signalling pathways.
Recent data from our group indicate that, although immobility induces muscle atrophy in both young and old individuals, the loss in muscle mass is more pronounced in young. Yet, the elderly, compared to young individuals, required a prolonged recovery phase in order to return to initial muscle mass levels following short-term immobilisation. An age-specific regulation of the signalling pathways orchestrating the initiation and time-course of human disuse muscle atrophy was therefore hypothesized and a range of genes from signalling pathways previously demonstrated to play a central role in the regulation of skeletal muscle atrophy and hypertrophy in a variety of animal models was profiled. Collectively, our findings indicate that the time-course and regulation of human skeletal muscle atrophy is age-dependent, leading to an attenuated loss in aging skeletal muscle when exposed to longer periods of immobility-induced disuse. Moreover, age-specific differences may exist for the ability of human skeletal muscle to regenerate after immobility-induced muscle atrophy.

Where applicable, the authors confirm that the experiments described here conform with The Physiological Society ethical requirements.

SA425

Maximising muscle protein synthesis: influence of nutrition and resistance training modalities

S.M. Phillips

Kinesiology, McMaster University, Hamilton, ON, Canada

Muscle proteins are constantly and simultaneously being synthesized and degraded. This 'turnover' provides for a mechanism of constant maintenance and greater potential for changes in protein pool size. The two most potent stimuli for enhancing muscle protein synthesis (MPS) are exercise and provision of protein. While protein feeding and exercise are independent stimulators of MPS they are additive in their effect and when combined over longer periods of time sum to result in expansion of a protein pool, the most obvious example of which is muscle fibre hypertrophy with resistive exercise (Phillips et al., 2005). The traditional dichotomy for the phenotypic adaptation induced by exercise is that endurance exercise does not lead to hypertrophy but instead results in expansion of the mitochondrial protein pool. On the other hand resistance exercise leads to muscle fibre hypertrophy (i.e., expansion of the myofibrillar protein pool) and does not change mitochondrial content. Our work has shown that in the untrained state the response to exercise is, however, rather generic and that both protein pools expand, at least acutely (Wilkinson et al., 2008). With increased specificity and time spent training with one particular exercise mode the response is 'honed' and the protein pools that are synthesized become specific (Wilkinson et al., 2008). With a focus on resistive exercise, since it is a potent countermeasure to atrophy even in small doses and an effective countermeasure to sarcopenic muscle loss, we have shown that various paradigms of resistance exercise that are non-traditional are actually effective in stimulating MPS (Burd et al., 2010;Burd et al., 2012a) and also in promoting hypertrophy (Mitchell et al., 2012). In combination with our work on optimal sources of protein to promote MPS (Tang et al., 2009;Burd et al., 2012b) we are now beginning to formulate strategies for older persons and persons with limited mobility to restore muscle mass as effectively as possible. In short, rapidly digested high-leucine content proteins such as whey protein are remarkably effective in stimulating MPS (Tang et al., 2009;Burd et al., 2012b); The figure below is a schematic representation of the 'leucine trigger' hypothesis showing how the rise in intramuscular free leucine, likely through mTOR signalling, stimulates MPS. Noteworthy is the fact that slowly digested or lo leucine-containing proteins are ineffective in stimulating MPS. We have begun to use the information we have gathered in young men in older persons with compromised muscle mass who embody a condition known as 'anabolic resistance'. Anabolic resistance in aging describes a condition in which older persons have an impaired ability to mount a robust anabolic response to usually anabolic stimuli like protein/amino acid feeding and resistance exercise. The reasons for anabolic resistance are not completely clear but likely involve defects in protein signalling, reductions in microvascular perfusion, and potentially a number of molecular-level maladaptative age-related changes. Data from our lab shows that older persons become anabolically resistant with even small periods of relative inactivity and that such periods are more common in aging and likely contribute to the sarcopenic muscle loss. something that is prevalent with aging and with muscle disuse. Strategies to effectively combine exercise and protein ingestion will be discussed and new data presented on how this applies to aging and disuse.

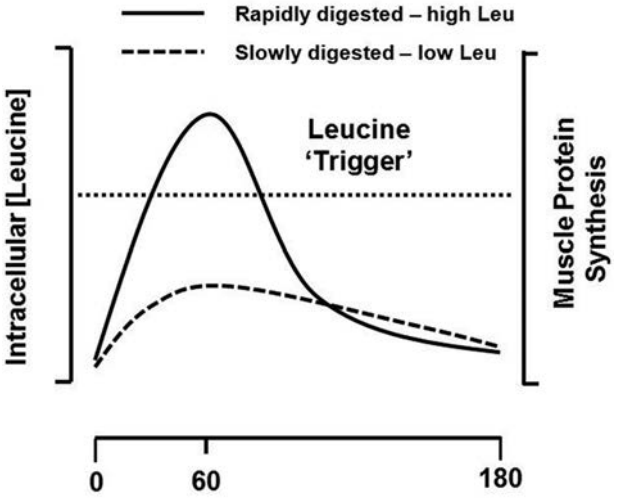

A schematic illustration of the 'leucine trigger' thesis: the rise in intracellular leucine is an initiating and crucial event in the stimulation of muscle protein synthesis (MPS). Rapidly digested and high leucine-content proteins are effective stimulators of MPS, whereas slowly digested proteins or those that contain low leucine are not as effective.

Burd NA et al. (2012a). Muscle time under tension during resistance exercise stimulates differential muscle protein sub-fractional synthetic responses in men. J Physiol 590, 351.

Burd NA et al. (2010). Low-Load High Volume Resistance Exercise Stimulates Muscle Protein Synthesis More Than High-Load Low Volume Resistance Exercise in Young Men. PLoS ONE 5, e12033.

Burd NA et al. (2012b). Greater stimulation of myofibrillar protein synthesis with ingestion of whey protein isolate v. micellar casein at rest and after resistance exercise in elderly men. Br J Nutr 108, 958.

Mitchell CJ et al. (2012). Resistance exercise load does not determine training-mediated hypertrophic gains in young men. J Appl Physiol 113, 71.

Phillips SM et al. (2005). Dietary protein to support anabolism with resistance exercise in young men. J Am Coll Nutr 24, 134S.

Tang JE et al. (2009). Ingestion of whey hydrolysate, casein, or soy protein isolate: effects on mixed muscle protein synthesis at rest and following resistance exercise in young men. J Appl Physiol 107, 987.

Wilkinson SB et al. (2008). Differential effects of resistance and endurance exercise in the fed state on signalling molecule phosphorylation and protein synthesis in human muscle. J Physiol 586, 3701.

Funding for this work was provided by The Natural Science and Engineering Research Council (NSERC) of Canada and the Canadian Institutes for Health Research (CHIR) to the author; both funding sources are gratefully acknowledged.

Where applicable, the authors confirm that the experiments described here conform with The Physiological Society ethical requirements.

SA426

Beta-adrenergic signalling in Takotsubo cardiomyopathy

S.E. Harding, H. Paur, P. Wright, M. Tranter, M. Sikkel, J. Gorelik and A. Lyon

NHLI, Imperial College, London, UK

There has been a rapid growth of individual case reports and larger series describing a new syndrome of acute and severe,

but reversible, heart failure – Takotsubo cardiomyopathy (TC). This syndrome usually follows an identifiable emotional, psychological or physical stress and mimics symptoms of acute myocardial infarction. It is characterised by regional wall motion abnormalities, classically an apical ballooning due to a hypercontractile base of the heart but poorly contracting or "stunned" apex. However, its most surprising characteristic is the rapid (days to weeks) recovery of many patients, usually from severe impairment to full health with subsequent good prognosis. For such a profound depression of contraction, deaths are relatively infrequent (1-3%) and, in that small percentage of patients in which the syndrome recurs, recovery is again complete. It is this ability to recover which makes the syndrome of such interest, since equivalent changes in chronic heart failure would be considered end-stage. This begins to lead us to the hypothesis that the cardiodepression is linked to some physiological strategy of benefit to the organism.
Evidence points to adrenaline as the precipitating factor. Catecholamine levels in TC patients 1-2 days after presentation are higher than those MI: adrenaline falls back to MI levels only after 7-9 days. Particularly, the reproduction of the signs of TC by accidental administration of adrenaline (including single intramuscular 1mg doses from an 'Epi-pen') is most indicative of its central role. Adrenaline activates beta2AR as well as beta1ARs and the beta2AR is pleiotropic, having the potential to couple through Gs-AC-cAMP (like the beta1AR) but also though Giapha, Gbetagamma and non-G-protein pathways. The ability of different agonists to drive the beta2AR towards one or other coupling partners is known as biased agonism or stimulus trafficking. We had found in other circumstances that adrenaline at high concentrations could show biased agonism towards Gi coupling, with switch from a positive to negative inotropic response, and hypothesised that this was underlying the depression of contraction.
In order to investigate this hypothesis and the underlying pathophysiological mechanisms, we have developed a model of TC in which an anaesthetised rat receives an intravenous (jugular) bolus of adrenaline (equivalent to ~5mg in an adult human) (Paur et al Circulation 2012). Intravenous bolus delivery was selected to mimic the human physiological response to sudden high stress. Adrenaline bolus triggered a marked decrease in cardiac contraction initiating at 15 min and reversing within an hour: this was localised to apex and mid-LV, a hallmark of TC. We showed that isolated apical cardiomyocytes demonstrated an increased beta2:beta1 ratio and greater beta2AR-specific contractile responses compared to paired basal cardiomyocytes isolated from the same heart. Importantly noradrenaline, which has a lower affinity at the beta2AR and is far weaker at producing beta2AR -Gi signalling, did not reproduce the effect of adrenaline. The negative effect of adrenaline was completely abolished by pertussis toxin, providing strong evidence for a Gi-dependent mechanism of action. Importantly, beta-blockers which demonstrate biased agonism of the beta2AR to Gi have an additive negative inotropic effect when added at the peak of the adrenaline-induced cardiodepression. The downstream mediator of negative inotropism appeared to be through p38 MAP kinase. We found evidence that the Gi/p38 negative inotropic signalling was cardioprotective as well as cardiodepressant, since blocking beta2AR or p38 MAPK precipitated a significantly increased incidence of sudden death in the adrenaline-treated animals.
In summary, we have evidence that Takotsubo Cardiomyopathy is a result of beta2AR biased agonism to Gi pathways at high adrenaline levels. We hypothesise that this is part of a protective strategy to prevent catecholamine damage but that transient cardiodepression can be a consequence in particular individuals.
.

Where applicable, the authors confirm that the experiments described here conform with The Physiological Society ethical requirements.

SA427

Spatio-temporal dynamics of cAMP-dependent protein kinase in cardiac myocytes

G. Vandecasteele

Inserm UMR-S 769 / Labex LERMIT, University Paris Sud, Châtenay-Malabry, France

β-adrenergic receptors enhance cardiac contractility by increasing cAMP levels and activating the cAMP-dependent protein kinase (PKA). PKA phosphorylates several key excitation-contraction coupling proteins, including L-type Ca^{2+} channels at the plasma membrane. However, PKA regulates numerous other effectors in cardiac myocytes, and notably nuclear effectors ultimately leading to hypertrophic remodelling and heart failure. In the last few years, our group has contributed to the recognition that physiological cAMP signaling is confined in specific subcellular domains and identified cyclic nucleotide phosphodiesterases (PDEs) as crucial regulators of compartmentalized cAMP signals and local PKA activity. This presentation will briefly summarize published data regarding the regulation of L-type Ca^{2+} current by type 4 phosphodiesterases (PDE4) and the implication for cardiac arrhythmias. It will then focus on the regulation of cytoplasmic *versus* nuclear PKA activity in cardiac myocytes, visualized by FRET-based A-kinase activity reporters targeted to these compartments. The role of PDEs as well as Ser/Thr phosphatases in the differential integration of the PKA response to β-adrenergic stimulation will be discussed.

Where applicable, the authors confirm that the experiments described here conform with The Physiological Society ethical requirements.

SA428

Targeting β-AR signalling in heart disease through G-protein receptor kinases

P. Most

Department of Internal Medicine III, University of Heidelberg, Heidelberg, Germany

Abnormal β-adrenergic receptor (β-AR) signalling is considered a hallmark of congestive heart failure driving its progression towards contractile failure and lethal tachyarrhythmias. Although advanced understanding of underlying molecular abnormalities has been gleaned from experimental research, β-AR blockade remains to date the only therapeutic intervention that shields the heart from noxious sympathetic overdrive. The aim of this paper is to discuss therapeutic innovations targeting dysfunctional G-protein-coupled receptor kinase (GRK) activity beyond β-AR blockade and highlight translational strategies that embark on proof-of-concept studies in small and large animal HF models for therapeutic modulation of the GRK2- and Gbγ-protein dependent signalling.

Where applicable, the authors confirm that the experiments described here conform with The Physiological Society ethical requirements.

SA429

Compartmentalized beta-adrenergic receptor signalling to cAMP in healthy and failing cardiomyocytes

V. Nikolaev

Heart Research Center Göttingen, Götttingen, Germany

The ubiquitous second messenger cAMP is an important regulator of cardiac function and disease. In cardiomyocytes, cAMP signalling is organized in discrete subcellular microdomains which are often involved in calcium cycling and lead to temporal and spatial segregation of subcellular cAMP responses. To directly visualize cAMP dynamics in such microdomains, we generated two novel targeted fluorescence resonance energy transfer (FRET)-based biosensors and expressed them in cardiomyocytes of transgenic mice under the alpha-myosin heavy chain promoter. The first sensor reports local cAMP dynamics associated with the sarcolemmal T-tubular microdomains and the second one can visualize cAMP directly at the sarcoplasmic reticulum calcium ATPase 2 (SERCA2)
Echocardiography, immunostaining and cell fractionation analysis confirmed the absence of any adverse cardiac phenotype and the proper localization of the sensors in transgenic mouse hearts. Local cAMP signals were measured in single freshly isolated adult ventricular myocytes and compared to cAMP dynamics in the bulk cytosolic compartment. FRET measurements revealed the predominant role of phosphodiesterase type 4 (PDE4) in the regulation of basal cAMP levels in the SERCA2 compartment and PDE3 in the regulation of the beta2-adrenergic receptor stimulated cAMP pools at the T-tubules. In failing cardiomyocytes, isolated from mouse hearts 8 weeks after transverse aortic constriction, these local PDE4 and PDE3 activities were severely reduced which led to specific subcellular changes in cAMP compartmentation
In conclusion, through generation of novel FRET biosensors and transgenic models, we were able to get direct insights into localized cAMP signaling in various subcellular microdomains and to unravel its changes in a cardiac disease model.

Where applicable, the authors confirm that the experiments described here conform with The Physiological Society ethical requirements.

SA430

Cyclic nucleotides, physiology and function in heart disease

M. Zaccolo

University of Oxford, Oxford, UK

Catecholamine-dependent cAMP signalling is a key regulator of excitation-contraction coupling and the incorrect activation of this pathway is a hallmark of disease states such as cardiac hypertrophy and heart failure (HF). In addition to β-adrenergic receptors (β-AR), several other types of Gs-coupled receptors signal in the heart through the generation of cAMP. Cardiac signalling of different cAMP-elevating hormones has long been known to result in distinct functional outputs. This observation has led to the recognition that mechanisms must be in place that allow for specificity of response and that alterations of such mechanisms may result in cardiac disease, although the nature of such mechanisms and the disease-associated changes are poorly defined. The question of how cAMP signalling fidelity is achieved is therefore of fundamental importance for understanding cardiac function in health and disease. Spatial control of cAMP signal propagation has emerged as a key mechanism responsible for specificity of response. That is, activation of individual GPCRs generates spatially restricted pools of cAMP within distinct subcellular compartments, leading to the activation of selected subsets of the cAMP effector, protein kinase A (PKA). PKA subsets are clustered on a scaffold of A-kinase anchoring proteins (AKAPs) into microdomains together with other key downstream elements of the signalling cascade and in the vicinity of specific effectors such as receptors, phospholamban, and ion channels. Based on this model, contractility is affected by changes in cAMP levels in a defined subcellular compartment whereas cAMP changes in other compartments may affect gene transcription or apoptosis, for example.
Although HF is characterized by down regulation of cAMP signals, elevation of cAMP via activation of the adrenergic system in HF patients correlates directly with shortened survival. This apparent paradox may be explained by failure to achieve the necessary spatial accuracy when manipulating bulk cAMP levels through β-AR activation, resulting in deleterious, off-target effects. Therefore a detailed understanding of the molecular mechanisms that regulate compartmentalised cAMP signalling may help developing novel strategies for the treatment of heart disease.
We are using a combination of real-time imaging, biochemical and genetic approaches to study the spatio-temporal dynamics of cAMP in intact living cells. We aim at understanding the architectural and regulatory principles by which intracellular cAMP signalling networks achieve the plasticity and context-sensitivity necessary for a cardiac myocyte to function and we are dissecting how alterations of these networks may be responsible for the development of cardiac disease.

Where applicable, the authors confirm that the experiments described here conform with The Physiological Society ethical requirements.

SA431

Interaction of endothelial connexins: Can they mutually replace each other at the functional level?

C. de Wit

Institut für Physiologie, Universität Lübeck, Lübeck, Germany and DZHK (German Centre for Cardiovascular Research), partner site Hamburg/Kiel/Lübeck, Lübeck, Germany

Connexin40 (Cx40) is a crucial component in gap junctions (GJ) with a strong impact on cardiovascular and renal physiology since Cx40-deficient mice exhibit pronounced hypertension, altered negative feedback of renin secretion causing an increased plasma renin activity, and impaired conduction of endothelium-dependent dilations. Cx40 is expressed abundantly in endothelial and renin-producing cells and we assessed the effects of cell-specific Cx40 deletion. Expectedly, lack of Cx40 in renin-producing cells led to hypertension that was renin-dependent since low-salt diet and blockade of angiotensin-converting enzyme abrogated the enhanced arterial pressure. In contrast, deletion of Cx40 in endothelial cells did not elevate arterial pressure but strongly reduced the conduction of endothelium-dependent dilations in the microcirculation similar to global Cx40-deficient mice. Such attenuation was not present in hypertensive mice being deficient for

Cx40 in renin-producing cells. Thus, a vascular and a renal phenotype can be well distinguished. Notably, the expression of the second connexin that is found abundantly in endothelial cells (Cx37) is strongly reduced in conducting arteries and lacking in arterioles in global Cx40-deficient hypertensive mice. This altered expression of Cx37 is not related to the hypertension, but solely due to the lack of Cx40 because it was also observed in normotensive endothelial-cell specific but not in hypertensive renin-producing cell specific Cx40-deficient mice. These findings raise the question if the defect in the conduction of dilatory signals along arterioles is indeed related to the lack of Cx40 or if the combined deletion of Cx40 and Cx37 is required to produce this effect. Hitherto, we studied animals carrying a mutated non-conducting Cx40 identified in humans (Ala96->Ser, A96S). In these animals, the conduction of endothelium-dependent dilation is similarly impaired despite the fact that the non-conducting mutated Cx40 as well as Cx37 was identified in endothelial cell membranes in arterioles by immunohistochemistry. This suggests that Cx37 cannot support the conduction of dilatory signals in arterioles in the absence of a functional Cx40. Moreover, animals carrying this mutated Cx40 were also hypertensive suggesting similar mechanisms with regard to Cx40 function in renin-producing cells. Thus, we conclude that Cx40 is the most important connexin in cardiovascular and kidney physiology.

Where applicable, the authors confirm that the experiments described here conform with The Physiological Society ethical requirements.

SA432

Role of Pannexin 1 in the regulation of blood pressure

M. Billaud[1,2], T. Parpaite[1], Y. Chiu[3], A.W. Lohman[1,2], S.M. Mutchler[2], J.K. Sandilos[3], D.A. Bayliss[3] and B.E. Isakson[1,2]

[1]Department of Molecular Phyiology and biological Physics, University of Virginia, Charlottesville, VA, USA, [2]Robert M Berne Cardiovascular Research Center, University of Virginia, Charlottesville, VA, USA and [3]Department of Pharmacology, University of Virginia, Charlottesville, VA, USA

We demonstrated that pannexin1 (Panx1) channels are expressed in the smooth muscle cells of small arteries where they participate in α1D adrenergic receptor (α1DAR)-mediated vasoconstriction[1]. In this paper, we also showed that ATP is released from vascular smooth muscle cells via Panx1 channels upon phenylephrine (PE) stimulation. Since the α1DAR-mediated constriction as well as ATP signaling are key in the regulation of peripheral resistance and blood pressure, we hypothesized that Panx1 could participate in blood pressure regulation. Therefore, we created an inducible conditional KO mouse model where Panx1 is deleted specifically in smooth muscle cells by breeding smooth muscle myosin heavy chain (SMMHC) - $CreER^{T2+}$ mice with $Panx1^{fl/fl}$ mice. After 10 days of tamoxifen injections, the expression of Panx1 in arterial smooth muscle cells was abolished and the vasoconstriction of small arteries in response to PE was significantly reduced. Using radiotelemetry, we measured a reduction in the mean arterial pressure in these mice after tamoxifen injections. Because Panx1 is activated by the α1DAR signaling cascade and because the channel and the receptor are closely located at the plasma membrane of arterial smooth muscle cells, we hypothesized that disruption of the Panx1/α1DAR signaling pathway would alter vasoconstriction. In order to specifically inhibit Panx1 activation by the α1DAR, we designed a peptide mimicking the intracellular loop (IL) region of Panx1, which is enriched in proline, making this region more susceptible to interact with protein partners for intracellular signaling. When treated with the IL peptide, pressurized small arteries exhibited decreased vasoconstriction to PE. In parallel, we performed electrophysiology on HEK cells co-transfected with Panx1 and α1DAR plasmids and confirmed PE-induced Panx1 activation in vitro by measuring an increase of Panx1 current and ATP release upon PE stimulation. The PE-induced Panx1 activation was also altered by Panx1 IL peptide. To further investigate the key amino acids of Panx1 intracellular loop in PE-induced Panx1 activation, we created specific mutants of Panx1 in the region mimicked by the IL peptide and cotransfected these mutants in HEK cells along with the α1DAR plasmid. Both ATP release and Panx1 currents were decreased when the amino acids YLK in position 198 to 200 were mutated to alanine, showing their essential role in PE-induced Panx1 activation. In summary, our results show that Panx1 plays an essential role in the α1DAR-mediated constriction by releasing ATP and thus in the regulation of blood pressure. Furthermore, we have identified a key region in Panx1 intracellular loop that is essential in the PE-induced activation of Panx1. This work provides the basis for a novel understanding of blood pressure control by the sympathetic nervous system.

[1] Billaud M et al. (2011). Circ Res 109, 80-85

Where applicable, the authors confirm that the experiments described here conform with The Physiological Society ethical requirements.

SA433

Cellular mechanisms mediated by connexin channels involved in the control of blood pressure

J. Haefliger

medicine, CHUV, Lausanne, Vaud, Switzerland

Connexins (Cxs) form connexons within the plasma membrane to create domains referred as gap junctions. The intercellular channels established by the pairing of two connexons allow for the diffusion of ions and molecules between adjacent cells. Vascular Cxs play a role in the contractility of the vessel wall by allowing the exchange of signaling molecules to coordinate the activity of the smooth muscle cells (SMCs) and the endothelial cells (ECs). In the vascular wall, four Cxs are mostly expressed: Connexin37 (Cx37) and Cx40 in ECs and Cx43 and Cx45 in SMCs. To investigate the effects of chronic hypertension on vascular Cxs in the aorta, Wild-type (WT) mice and mice lacking Cx40 (Cx40-/-), a genetic model of renin-dependent hypertension were subjected to either a two-kidney, one-clip (2K1C) procedure associated with elevated angiontensinII levels (AngII) or to N-nitro-l-arginine-methyl-ester (L-NAME) treatment, which induce renin-dependent and -independent hypertension, respectively. All hypertensive mice featured a thickened aortic wall, increased levels of Cx37 and Cx45 in SMCs, and of Cx40 in ECs (except in Cx40-/- mice). Cx43 was up-regulated only in the SMCs of renin-dependent models of hypertension. Blockade of the renin-angiotensin system of Cx40-/- mice normalized blood pressure and prevented both aortic thickening and Cx alterations. Ex vivo exposure of WT aortas, carotids, and mesenteric arteries to physiologically relevant levels of AngII increased the levels of Cx43, but not of other Cxs. In the aortic SMCs line A7r5, AngII activated kinase-dependent pathways and induced binding of the nuclear factor-kappa B (NF-kappaB) to the Cx43 gene promoter, increasing Cx43 expression. These data suggest that Cx43 is selectively

increased in renin-dependent hypertension via an AngII activation of the extracellular signal-regulated kinase and NF-kappaB pathways.
Upon agonist stimulation, ECs trigger smooth muscle relaxation through the release of relaxing factors such as nitric oxide (NO). We investigated the link between the expression of endothelial Cxs (Cx40 and Cx37) and endothelial nitric oxide synthase (eNOS) expression and function in the mouse aorta. We demonstrated that acetylcholine (ACh)- and ATP-induced endothelium-dependent relaxations solely depend on NO release in both WT and Cx40-/- mice, but are markedly weaker in Cx40-/- mice. Consistently, both basal and ACh- or ATP-induced NO production were decreased in the aorta of Cx40-/- mice. Altered relaxations and NO release from aorta of Cx40-/- mice were associated with lower expression levels of eNOS in the aortic endothelium of Cx40-/- mice. We further demonstrate that eNOS, Cx40, and Cx37 tightly interact with each other at intercellular junctions in the aortic endothelium of WT mice, suggesting that the absence of Cx40 in association with a marked decrease of Cx37 levels in ECs from Cx40-/- mice participate to the decreased levels of eNOS. To investigate changes in vascular Cxs and eNOS during hypertension in mice aorta, WT mice and Cx40-/- were subjected to either one-kidney, one-clip (1K1C; volume overload model) or 2K1C surgery procedure. Mean blood pressure was 10% higher in the 1K1C Cx40-/- mice compared to the other hypertensive models (Cx40-/-, 2K1C Cx40-/-, 2K1C WT and 1K1C WT), due to the association of a renin-dependent and -independent hypertension. eNOS phosphorylation was specifically increased in the aortic endothelium of 1K1C Cx40-/- mice showing that the increased mechanical forces impinging on the aortic wall were elicited by the association of renin-dependent and independent hypertension, further suggesting a compensatory mechanism associated with decreased eNOS levels in the Cx40-/- mice. Finally, to investigate the role of Cx40 in the propagation of Ca2+ waves in the endothelial cells of the mouse aorta, we performed Ca2+ imaging on intact aortic endothelium from both WT and Cx40-/- mice. ACh induced Ca2+ signaling in a fraction of ECs expressing the M3 muscarinic receptors. Inhibition of intercellular communication using carbenoxolone or octanol fully blocked the propagation of ACh-induced Ca2+ transients toward adjacent cells in WT and Cx40-/- mice. As compared to WT, Cx40-/- mice displayed a reduced propagation of ACh-induced Ca2+ waves, indicating that Cx40 contributes to the spreading of Ca2+ signals. These findings provide evidence that 1) different types of hypertension are associated with a differential regulation of Cxs expression in SMC and ECs layers; 2) ECs Cxs play a role in the regulation of eNOS expression and function in response to hypertension; 3) Cx40 and Cx37 contribute to the propagation and amplification of the Ca2+ signaling triggered by ACh in ECs expressing the M3 muscarinic receptors.

Where applicable, the authors confirm that the experiments described here conform with The Physiological Society ethical requirements.

SA434

Connexins in ischemia-reperfusion injury

S. Morel[1], V. Braunersreuther[2], E. Sutter[1], G. Pelli[1], B. Foglia[1], F. Mach[2] and B. Kwak[1,2]

[1]Department of Pathology and Immunology, University of Geneva, Geneva, Switzerland and [2]Department of Internal Medicine – Division of Cardiology, University of Geneva, Geneva, Switzerland

Intercellular channels formed by connexins (Cx) have been shown to play a critical role in cardiovascular disease. For instance, vascular Cx43 influences atherosclerosis development and plaque stability, and cardiac Cx43 may determine the development of arrhythmias after myocardial infarction. In the heart, Cx40 is expressed in atrial cardiomyocytes, the conduction system and in endothelial cells, whereas Cx37 is only found in the endothelium. Here, we investigated the implication of the two endothelial connexins during ischemia and reperfusion in mice.
For this purpose, we used the Cre-loxP system to create a mouse line in which Cx40 is deleted from the endothelium only. Immunostainings on TIE2-Cre+Cx40fl/flApoE-/- mice confirmed the absence of Cx40 in the endothelium, whereas the protein was normally expressed in the atria and cardiac conduction system. Moreover, Cx40 was normally expressed in the endothelium, atria and conduction system of TIE2-Cre+Cx40wt/wtApoE-/- and TIE2-Cre-Cx40fl/flApoE-/- control mice. Sixteen-week-old mice were subjected to in vivo left coronary artery occlusion for 30 minutes and sacrificed 24-hours after reperfusion for analysis of infarct size and infiltration of inflammatory cells. Myocardial surface areas at risk and infarcted areas were measured from computed images using NIH Image software. Areas at risk, normalized to total left ventricle surface areas, were similar between the experimental groups, i.e TIE2-Cre+Cx40wt/wtApoE-/-: 29.2±1.2% (N=11), TIE2-Cre-Cx40fl/flApoE-/-: 33.7±3.7% (N=9), and TIE2-Cre+Cx40fl/flApoE-/- 31.7±2.2% (N=11, n.s.). Interestingly, the infarct area, normalized to areas at risk, was significantly increased in TIE2-Cre+Cx40fl/flApoE-/- (20.2±3.1%, P<0.05) mice as compared to controls (10.1±2.0% and 11.3±1.8%). Moreover, we performed immunofluorescent stainings against Ly6G to detect neutrophils in the infarcted heart. We showed that neutrophil infiltration was significantly higher in TIE2-Cre+Cx40wt/wtApoE-/- mice (24.2±3.1%, P<0.01, N=4) in comparison with controls (9.8±1.8%, N=5 and 8.5±1.7%, N=5). In a previous study, we demonstrated that endothelial-specific deletion of Cx40 promotes atherosclerosis by increasing CD73-dependent leukocyte adhesion to the endothelium. To determine whether this interaction also plays a role in ischemia-reperfusion injury, CD73-/-ApoE-/- mice have been submitted to in vivo ischemia-reperfusion. Whereas the area at risk in this group of mice was similar to those measured in the previous groups (31.3±3.6%, N=8), the infarcted area was significantly increased in comparison with control mice (18.2±1.6%, P<0.01). Treatment of TIE2-Cre+Cx40wt/wtApoE-/- mice with methotrexate, a CD73 activator, significantly reduced the infarcted area (8.5±1.3%, P<0.05, N=10) as compared to TIE2-Cre+Cx40wt/wtApoE-/- mice without treatment. Finally, hearts from TIE2-Cre+Cx40wt/wtApoE-/- mice and control mice have been submitted to ex vivo ischemia-reperfusion by using a Langendorff perfusion system. Areas at risk and infarct size were similar between the three groups. To investigate the possible implications of another endothelial connexin in myocardial infarction, Cx37-/-ApoE-/- mice were submitted to the same protocol of in vivo ischemia-reperfusion. Areas at risks were

similar between Cx37-/-ApoE-/- and control ApoE-/- mice, and the infarcted area appeared also not affected by the deletion of Cx37 (Cx37-/-ApoE-/-: 13.8±1.3%, ApoE-/-: 14.7±2.7%, N=12, n.s.).
We conclude that endothelial Cx40, but not Cx37, is implicated in resistance of the heart to ischemia-reperfusion injuries, such as cell death and inflammatory infiltration, by a CD73-dependent pathway. These findings may point towards a specific novel therapeutic target to limit the cardiac injury after coronary interventions.

Where applicable, the authors confirm that the experiments described here conform with The Physiological Society ethical requirements.

SA435

Gap junctions in the pulmonary artery: from physiology to pulmonary hypertension

C. Guibert

Centre de Recherche Cardio-Thoracique de Bordeaux, INSERM U1045, Bordeaux, France and Centre de Recherche Cardio-Thoracique de Bordeaux, Université Bordeaux Segalen, Bordeaux, France

Intercellular channels or gap junctions (GJ) are formed by connexin (Cx) proteins, transmembrane proteins that play a pivotal role in the direct movement of ions and larger cytoplasmic solutes between vascular endothelial cells (EC), between vascular smooth muscle cells (SMC), and between endothelial and smooth muscle cells (myoendothelial junctions). GJ are clusters of intercellular channels resulting from the connection of two hexameric assembly of Cx (hemichannels). Hemichannels are localized on the membrane of two adjacent cells and arranged with identical or different Cx (21 isoforms in human) with various possible combinations. Such process has functional consequences and provides an efficient cellular strategy to finely regulate cell-to-cell communication in the vascular wall. The expression of different GJ proteins is dynamically regulated throughout different types of vascular bed in healthy vessels and in vascular disease states such as atherosclerosis, systemic and pulmonary hypertension (PH) and diabetes. Our studies focus on the role of intercellular communications (Cx) in the physiology and pathophysiology of the pulmonary arterial vascular bed.
In the pulmonary circulation, endothelial control of smooth muscle tone is of critical importance to maintain low pressure and low resistance. In this connection, most of the medical treatments used in PH (e.g., NO, prostacyclin…) mimic and amplify the physiological control of EC on SMC. Myoendothelial junctions may thus potentially participate in this process. We demonstrated that Cx 37, 40 and 43 are expressed and functional in small intrapulmonary arteries (IPA) from rat. Interestingly, resistance vessels are very important for blood flow regulation and the incidence of myoendothelial gap junctions is higher in resistance than in conduit arteries. We also showed that 5-HT, a potent vasoconstrictor whose concentration is increased in PH, produces superoxide anion ($O_2^{\bullet-}$) in the smooth muscle and NO in the endothelium. $O_2^{\bullet-}$ passes through the myoendothelial junctions to decrease endothelial NO production and thus strengthen pulmonary vasoreactivity (Billaud M *et al.*, 2009). Unlike 5-HT, endothelin-1 (ET-1) and phenylephrine (Phe, an α1 adrenoceptor agonist) do not produce $O_2^{\bullet-}$ in IPA. We investigated the signalling pathways involved in 5-HT-induced $O_2^{\bullet-}$ production in rat IPA by focusing on the sources of reactive oxygen species (ROS), the role of intra and extracellular calcium and the role of caveolae. This 5-HT-induced production of $O_2^{\bullet-}$ is mediated by 5-HT2A receptors, is dependent on the complex I of the mitochondrial respiratory chain and NADPH oxidases and extracellular calcium influx plays an important role in this process (Khoyrattee N *et al.*, 2012). We also demonstrated that the main candidates involved in this signaling pathway are localized within/close to caveolae. This is the first time that a negative control of the endothelial NO function by the smooth muscle is demonstrated.
PH is a multifactorial disease characterized by a progressive increase in pulmonary vascular resistance caused by vasoconstriction, vascular cell proliferation and obliteration of pulmonary microvasculature. These processes lead to right heart failure and ultimately to death. PH occurs in a variety of clinical situations and is associated with a broad spectrum of histological patterns and molecular abnormalities. Because of this diversity, early diagnosis is difficult and efficient treatments are still lacking. The recent revision of the classification of PH distinguishes five groups. Among these groups, the category 1 PH also known as pulmonary arterial hypertension (PAH) includes idiopathic PAH, familial PAH and acquired PAH, the latter of which being associated with other diseases such as HIV or connective tissue diseases. The non-category 1 PH previously known as secondary PH includes the category 3 which is a widely distributed PH secondary to alveolar hypoxia as a result of lung disease such as chronic obstructive pulmonary disorder (COPD). Although, PH has progressively evolved from a fatal to a chronic disease, none of the currently available therapies is curative. Despite intensive research, PH remains an important medical challenge and a better knowledge of the underlying molecular and cellular mechanisms remains crucial for the development of new or additional innovative therapies. By using different rat models of PH (category 1 and 3) and heterozygous knock-out mice for Cx43, we highlighted Cx43 was overexpressed in PH rats and Cx have some role in the contractile response to stimuli, already known to be involved in PH, namely 5-HT, ET-1, Phe and depolarising solutions (high potassium solutions) (Billaud M *et al.*, 2011; Khoyrattee N *et al.*, 2012).
Future directions will be thus to consider Cx as new therapeutic targets and strategies in pulmonary hypertension.

Billaud M *et al.* (2009). *PLoS ONE* **4**, e6432.

Billaud M *et al.* (2011). *Respir Res* **12**, 30.

Khoyrattee N *et al.* (2012). *Archives of cardiovascular diseases*, **3 (suppl 1)**, 19.0068.

Where applicable, the authors confirm that the experiments described here conform with The Physiological Society ethical requirements.

SA436

A new take on uptake: neurotransmitter transporters and the cellular mechanisms of amphetamine action

S.G. Amara

National Institute of Mental Health, National Institutes of Health, Bethesda, MD, USA

Neurotransmitter transporters present at the plasma membrane contribute to the clearance and recycling of neurotransmitters and have a profound impact on the extent of receptor activation during neuronal signaling. These carriers also are the primary targets for psychostimulant drugs of abuse, antidepressant medications, and drugs such as

methylphenidate and amphetamines, which are used to treat attention deficit disorders in children. In recent studies we have observed that once amphetamine-like drugs enter dopamine neurons they activate multiple intracellular signaling pathways to trigger changes in the cellular trafficking of the dopamine transporter and other neuronal membrane proteins. Within the cell amphetamines activate the small GTPases, Rho and Rac1 and trigger endocytosis of the dopamine transporter (DAT) by a RhoA- and dynamin-dependent pathway. We have also found that increases in cAMP and PKA activity mediated by D1/D5 dopamine receptors or by amphetamine itself, serve as a break on DAT internalization, revealing interplay between PKA and RhoA signaling in the regulation of DAT activity. This work implies that amphetamine-like drugs not only block monoamine transport and potentiate neurotransmitter action, but also act on specific cytoplasmic targets that regulate protein trafficking and many other cellular activities. Although several key steps in the process remain to be defined, this novel intracellular mode of amphetamine action has major implications for the mechanisms of neuroplasticity and neurotoxicity associated with psychostimulant use and suggests novel drug targets for modulating the actions of amphetamines.

This work was supported by ARRA funds and NIH grants DA07595 and MH80726.

Where applicable, the authors confirm that the experiments described here conform with The Physiological Society ethical requirements.

SA437

Dendritic inhibition by DAT-mediated dopamine-release

B. Falkenburger

Neurology, RWTH University, Aachen, Germany

Neurotransmitter transporters take up neurotransmitter secreted by exocytosis. I will discuss our published work indicating that the dopamine transporter may, in addition, secrete dopamine from dendrites of dopaminergic neurons when glutamatergic inputs are activated. Similar phenomena may occur for further transmitters. Since this finding has remained controversial, I will include descriptions of transporter-mediated neurotransmitter release by other groups.

Where applicable, the authors confirm that the experiments described here conform with The Physiological Society ethical requirements.

SA438

Molecular physiology and pathophysiology of glutamate transporter-associated anion channels

C. Fahlke

Institue of Complex Systems, Zelluläre Biophysik (ICS-4), FZ Jülich, Jülich, Germany

Excitatory amino acid transporters (EAATs) do not only mediate secondary-active glutamate transport, but also anion-selective currents. EAAT anion currents are small in the absence and increase upon application of L-glutamate due to substrate-dependent gating of EAAT anion channels. At present, neither the molecular basis nor the physiological importance of the EAAT anion conductance is sufficiently understood. Anion channel gating can be described by a kinetic scheme that is based on the glutamate transport cycle and in which anion channel opening is associated with certain states. All voltage- and substrate-dependent conformational changes of EAAT anion channels are linked to transitions within the transport cycle, and there are no indications for additional substrate—dependent anion channel opening and closing transitions. To account for the substrate dependence of macroscopic currents different transporter states might either exhibit distinct unitary conductances or distinct anion channel open probabilities. Macroscopic current recordings and noise analysis revealed a single channel conductance of 1 pS at symmetrical NO3- for EAAT4 anion channels in the absence as well as in the presence of glutamate (Kovermann et al., 2010). All our experimental data are consistent with opening of a defined anion conduction pathway that opens with different open probability for separate substrate conditions. Although there are marked differences in macroscopic EAAT anion currents, the underlying single channel amplitudes are very similar among different isoforms (Torres-Salazar & Fahlke, 2007; Winter et al., 2012), indicating that the anion conduction pathway is well conserved. All EAAT anion channels exhibit a lyotropic selectivity sequence (Wadiche & Kavanaugh, 1998; Melzer et al., 2003), indicating that selectivity between anion is determined by anion dehydration rather than by association to defined binding sites. These functional data suggest a rather hydrophobic pore with low electrostatic potential.

The physiological importance of EAAT anion channels is illustrated by episodic ataxia (EA), a human genetic disease characterized by paroxysmal cerebellar incoordination. There are several genetically and clinically distinct forms of this disease, and one of them, episodic ataxia type 6, is caused by mutations in the gene encoding a glial glutamate transporter, the excitatory amino acid transporter (EAAT) 1. We examined the effects of a disease-associated point mutation, P290R, on glutamate transport, anion current as well as on the subcellular distribution of EAAT1 using heterologous expression in mammalian cells (Winter et al., 2012). P290R reduces the number of EAAT1 in the surface membrane and impairs EAAT1-mediated glutamate uptake. Cells expressing P290R EAAT1 exhibit larger anion currents than WT cells in the absence as well as in the presence of external L-glutamate, despite a lower number of mutant transporters in the surface membrane. Noise analysis revealed unaltered unitary current amplitudes, indicating that P290R modifies opening and closing, and not anion permeation through mutant EAAT1 anion channels. These findings identify gain-of-function of EAAT anion conduction as pathological process in episodic ataxia. Increased EAAT1 anion currents might modify intracellular anion concentrations and thus affect GABAergic transmission. These data illustrate possible functional roles of EAAT anion channels also under physiological conditions.

Kovermann P, Machtens JP, Ewers D & Fahlke Ch. (2010). A conserved aspartate determines pore properties of anion channels associated with excitatory amino acid transporter 4 (EAAT4). J Biol Chem 285, 23676-23686.

Melzer N, Biela A & Fahlke Ch. (2003). Glutamate modifies ion conduction and voltage-dependent gating of excitatory amino acid transporter-associated anion channels. J Biol Chem 278, 50112-50119.

Torres-Salazar D & Fahlke Ch. (2007). Neuronal glutamate transporters vary in substrate transport rate but not in unitary anion channel conductance. J Biol Chem 282, 34719-34726.

Wadiche JI & Kavanaugh MP. (1998). Macroscopic and microscopic properties of a cloned glutamate transporter/chloride channel. J Neurosci 18, 7650-7661.

Winter N, Kovermann P & Fahlke Ch. (2012). A point mutation associated with episodic ataxia 6 increases glutamate transporter anion currents. Brain 135, 3416-3425.

This work was supported by the Deutsche Forschungsgemeinschaft (FA301/9).

Where applicable, the authors confirm that the experiments described here conform with The Physiological Society ethical requirements.

SA439

GABA transporters, GABA release and opioid dependence

E. Bagley

Pharmacology, University of Sydney, University of Sydney, NSW, Australia

Neurotransmitter transporters can affect neuronal excitability indirectly via modulation of neurotransmitter concentrations or directly via transporter currents. A physiological or pathophysiological role for transporter currents has not been described. We found that GABA transporter 1 (GAT-1) cation currents directly increased GABAergic neuronal excitability and synaptic GABA release in the periaqueductal gray (PAG) during opioid withdrawal in rodents. In contrast, GAT-1 did not indirectly alter GABA receptor responses via modulation of extracellular GABA concentrations. Notably, we found that GAT-1-induced increases in GABAergic activity contributed to many PAG-mediated signs of opioid withdrawal. Together, these data support the hypothesis that GAT-1 activity directly produces opioid withdrawal signs through direct hyperexcitation of GABAergic PAG neurons and nerve terminals, which presumably enhances GABAergic inhibition of PAG output neurons. These data provide, to the best of our knowledge, the first evidence that dysregulation of a neurotransmitter transporter current is important for the maladaptive plasticity that underlies opiate withdrawal.

Supported by the National Health & Medical Research Council of Australia (project 512390, Fellowship to MJC 511914) and the Intramural Research Program of the National Institutes of Health, National Institute on Drug Abuse.

Where applicable, the authors confirm that the experiments described here conform with The Physiological Society ethical requirements.

SA440

Bath salts interactions with the human dopamine transporter

L.J. De Felice

Physiology and Biophysics, Virginia Commonwealth University, Richmond, VA, USA

Action potentials (APs) release dopamine (DA) via voltage gated ion channels that de-polarize the presynaptic membrane, open Ca++ channels, and increase the probability of vesicle fusion and DA release. The dopamine transporter (DAT) transports DA back into the presynaptic membrane where it is repackaged into synaptic vesicles. Presynaptic membrane depolarization is thus the trigger for neurotransmitter release. We will argue that abused drugs (such as amphetamine, AMPH, methamphetamine, METH, and certain structurally related cathinones present in bath salts) bypass the normal AP-generated DA release mechanism. Present theories to explain drug-induced DA release rely on DAT reverse transport and include AMPH-DA exchange, phosphorylation-induced efflux, channel-mode efflux, or AMPH-induced vesicular depletion. An alternative mechanism for drug-induced DA release requires a departure from the traditional model of Na-coupled transport (the fixed stoichiometry alternating access model) and proposes another model of co-transport (the flux coupled channel model). We have recorded electrical currents mediated by hDAT expressed in Xenopus laevis oocytes and HEK cells exposed to DA, METH, a known hDAT stimulant and DA releaser, mephedrone (MEPH), methylenedioxypyrovalerone (MDPV), MEPH + MDPV, or cocaine, a known hDAT inhibitor (1). DA, METH, and MEPH induce an inward depolarizing current when cells are held near rest (-60 mV), therefore acting as excitatory hDAT substrates. Structurally analogous MDPV induces an outward hyperpolarizing current under the same conditions, similar to cocaine, and therefore acts as an inhibitory non-substrate blocker. Two common components of bath salts, MEPH and MDPV, thus produce opposite effects at hDAT that are comparable to METH and cocaine, respectively. In our assay MEPH is nearly as potent as METH; however, MDPV is 35X more potent than cocaine and its effect as a blocker lasts much longer. When applied in combination, MEPH exhibits faster kinetics than MDPV; namely, the MEPH depolarizing current occurs seconds before the slower MDPV hyperpolarizing current. Bath salts are not a defined combination of drugs; however, those that contain MEPH (or a similar drug) and MDPV might be expected initially to release DA and subsequently to prevent its reuptake via hDAT. The channel mode of dopamine transporters is thus crucial to understand how AMPH-like drugs including synthetic cathinones can affect the integration of inputs to dopaminergic neurons to modify excitability, activate voltage-gated channels, and regulate synaptic signaling. Our central hypothesis states that AMPH-like drugs (including certain synthetic cathinones present in bath salts) induce depolarizing currents in excitable cells that increase the probability of Ca++ entry, vesicular fusion, and DA release from the presynaptic terminal. In addition, wherever hDAT is located (for example on the cell body), drug-induced depolarization via the channel mode of transporters may increase excitability (2). The powerful positive feedback mechanism of AMPH-like drugs on dopaminergic neurons may generalize to drugs that interact with serotonin or norepinephrine transporters. Conversely, transporter blockers such as cocaine, MDPV, or fluoxetine may have a negative feedback on endogenous or induced currents mediated via transporters, thus lowering the probability of transmitter release. The contribution of transporters to the electrical profile of neurons depends on a more complete picture of synapses than we have at present. In particular, the setting of transporters in the context of voltage-gated ion channels would be essential to understand fully the contribution of transporter channels to neurotransmitter release. However, evidence is growing that AMPH, and by inference AMPH-like drugs, may release DA via vesicle fusion mechanisms (3, 4). In summary, bath salts that contain both DA releasers (mephedrone, methylone, etc.) and a reuptake inhibitor (MDPV) act synergistically on hDAT, which may explain the powerful effect of this drug combination on bath salts abusers. We will discuss how drug interactions with transporters modify electrical signaling for nerve cell communication that is important for brain physiology and pathology.

Cameron KN, Kolanos R, Solis, E, De Felice LJ, Glennon. Bath salts components mephedrone and methylenedioxypyrovalerone (MDPV) act synergistically at the human dopamine transporter (2013). British Journal of Pharmacology Accepted manuscript online: 21 Nov 2012 DOI: 10.1111/bph.12061

Ingram SL, Prasad BM, Amara SG.. Dopamine transporter-mediated conductances increase excitability of midbrain dopamine neurons (2002), Nat Neurosci 10:971-978

Ramsson ES, Howard CD, Covey DP. Garris PA. High doses of amphetamine augment, rather than disrupt, exocytotic dopamine release in the dorsal and ventral striatum of the anesthetized rat (2011). J. Neurochem 119:1162-1172

Daberkow DP, Brown HD, Bunner KD, Kraniotis SA, Doellman MA, Ragozzino ME, Garris PA, Roitman MF. Amphetamine Paradoxically Augments Exocytotic Dopamine Release and Phasic Dopamine Signals. The Journal of Neuroscience 33: 452– 463

This work is supported by NIH NIDA 5R01DA033930.

Where applicable, the authors confirm that the experiments described here conform with The Physiological Society ethical requirements.

SA441

Dorsal-ventral differences in HCN channel function and expression in hippocampus

D. Johnston[1], K. Dougherty[1] and D. Nicholson[2]

[1]Center for Learning and Memory, University of Texas at Austin, Austin, TX, USA and [2]Department of Neurological Sciences, Rush Univ. Med. Center, Chicago, IL 60612, ID, USA

The rodent hippocampus can be divided into dorsal and ventral domains based on distinct anatomical, biochemical, and behavioral phenotypes associated with each region. Recently, we explored the cellular properties of CA1 pyramidal neurons in these two regions, and found that CA1 neurons from the ventral region are intrinsically more excitable than their dorsal counterparts. Among the many possible differences in ion channel expression and function that could account for these different cellular properties, we have initially focused on the hyperpolarization-activated cation-nonselective current (Ih). Measurement of Ih using cell-attached patches along the somatodendritic axis revealed a significant distant-dependent depolarizing shift in the $V_{1/2}$ of activation for h-channels in ventral, but not dorsal neurons. Ultrastructural immuno-localization of HCN1 and HCN2 h-channel subunits revealed a similar distant-dependent shift in the HCN1/HCN2 ratio for ventral, but not dorsal neurons. These observations suggest that a shift in the expression of HCN1 and HCN2 drives functional changes in I_h for ventral neurons, and could thereby significantly alter dendritic integration in neurons from these two regions.

Where applicable, the authors confirm that the experiments described here conform with The Physiological Society ethical requirements.

SA442

The cellular basis of sensory hyperexcitability in the Fmr1 knockout mouse model of Fragile X Syndrome

A. Frick[1], Y. Zhang[1], A. Bonnan[1], M. Ginger[1], I. Ferezou[2], J. Rossier[3] and B. Oostra[4]

[1]Neurocentre Magendie, INSERM U862, Bordeaux, France, [2]CNRS UPR 3293, Gif-sur-Yvette, France, [3]CNS UMR7637, Pariz, France and [4]Erasmus MC, Rotterdam, Netherlands

Increased sensitivity to sensory stimuli is a prominent feature of Fragile-X Syndrome (FXS) and other Autism Spectrum Disorders (ASD), but its underlying mechanisms are poorly understood. We found that deletion of the Fmr1 gene results in somatosensory hyper-excitability in a mouse model for FXS. Fmr1 knockout (Fmr1KO) mice required significantly less tactile information for haptic exploration, and touch-evoked whisker representations in the primary somatosensory cortex (S1) spread with increased velocity in Fmr1KO mice compared to wild-type control. At the cellular level, dendrites of S1 pyramidal neurons were hyper-excitable, facilitating the coupling of synaptic input to the generation of action potential output in these neurons. This defect was, at least in part, attributable to a dysfunction of h-channels and BKCa channels and was partially rescued by pharmacological activation of BKCa channels. These findings argue for a novel and critical role for channelopathies in the expression of sensory hyper-excitability in FXS and ASD.

FRAXA Research Foundation, INSERM, Max-Planck-Society, Region of Aquitaine, and DFG SFB 870

Where applicable, the authors confirm that the experiments described here conform with The Physiological Society ethical requirements.

SA443

Dendritic computation *in vivo*

S.L. Smith, I.T. Smith, T. Branco and M. Häusser

Wolfson Institute for Biomedical Research, University College London, London, UK

The computational power of dendrites has long been predicted using modeling approaches, but actual experimental examples of how dendrites solve computational problems are rare. We have addressed this question by performing direct patch-clamp recordings from the dendrites of pyramidal cells in mouse primary visual cortex during sensory processing. Visual stimulation triggered regenerative events in the dendrites of layer 2/3 pyramidal cells, including high-frequency bursts of dendritic spikes. These events were orientation tuned and suppressed by either hyperpolarization or intracellular NMDA receptor blockade. Both these manipulations also decreased the selectivity of subthreshold orientation tuning measured at the soma, thus linking dendritic regenerative events with somatic orientation tuning. These results suggest that dendritic spikes triggered by visual input contribute to a fundamental cortical computation: enhancing orientation selectivity in visual cortex.

Where applicable, the authors confirm that the experiments described here conform with The Physiological Society ethical requirements.

SA444

Sensory-evoked calcium signaling in dendrites and spines of cortical neurons *in vivo*

A. Konnerth

TU Munich, Munich, Germany

Neurons in cortical sensory regions receive modality-specific information through synapses that are located on their dendrites. The use of two-photon microscopy combined with whole-cell recordings has helped identify visually-evoked dendritic calcium signals in mouse visual cortical neurons in vivo. The calcium signals were restricted to small dendritic domains ('hotspots') and represented visual synaptic inputs that were highly-tuned for orientation and direction (Jia et al., Nature, 2010). A new variant of two-photon imaging with an improved sensitivity for fluorescence signaling and a reduced risk of phototoxicity, termed LOTOS (= low power temporal oversampling), allowed the detection of sensory-evoked calcium transients in dendritic spines of mouse neurons in the auditory (Chen et al., Nature, 2011). Individual spines on the same dendrite were functionally heterogeneous. Even neighboring spines were often tuned to different sound frequencies. In line with these observations, we found in the vibrissal cortex that stimulation of different whiskers activated distinct spines on the same dendrite (Varga et al., PNAS, 2012). Some spines were activated uniquely by single whiskers, but many spines were activated by multiple whiskers. These shared spines indicate the existence of presynaptic 'feeder' neurons that integrate and transmit activity arising from multiple whiskers. Together, our results suggest that in different cortices (visual, auditory, vibrissal), afferent sensory inputs to layer 2/3 neurons are widely distributed throughout the entire dendritic tree in a 'salt-and-pepper'-like manner and that the 'computational units' in the dendrites layer 2/3 neurons in vivo are highly tuned individual spines.

Jia H, Rochefort N, Chen X and Konnerth A (2010) Dendritic organization of sensory input to cortical neu-rons in vivo. Nature 464, 1307-1312.

Chen X, Leischner U, Rochefort NL, Nelken I and Konnerth A (2011) Functional mapping of single spines in cortical neurons in vivo. Nature 475, 501-505.

Varga Z, Jia H, Sakmann B and Konnerth A (2011) Dendritic coding of multiple sensory inputs in single cortical neurons in vivo. Proc Nat Acad Sci USA 108, 15420-15425.

Where applicable, the authors confirm that the experiments described here conform with The Physiological Society ethical requirements.

SA445

Altered spatial and temporal microvascular perfusion heterogeneity in metabolic syndrome

J. Frisbee

Physiology and Pharmacology, West Virginia University HSC, Morgantown, WV, USA and Center for Cardiovascular and Respiratory Sciences, West Virginia University HSC, Morgantown, WV, USA

A key clinical outcome for non-atherosclerotic peripheral vascular disease (PVD) in patients is a progressive decay in skeletal muscle performance and its ability to resist fatigue with elevated metabolic demand. This study builds on previous work to evaluate in situ arteriolar hemodynamics in cremaster muscle of obese Zucker rats (OZR) model of the metabolic syndrome, manifesting a non-atherosclerotic PVD, to integrate existing knowledge into a greater understanding of impaired skeletal muscle perfusion and performance. In OZR cremaster muscle, perfusion distribution at microvascular bifurcations (γ) was consistently more heterogeneous than in controls. However, while consistent, the underlying mechanistic contributors were spatially divergent as altered adrenergic constriction was the major contributor to altered γ at proximal microvascular bifurcations, with a steady decay with distance, while endothelial dysfunction was a stronger contributor in distal bifurcations with no discernible role proximally. Using measured values of γ, simulations predict that successive alterations to γ in OZR caused more heterogeneous perfusion distribution in distal arterioles than in controls; an effect that could only be rectified by combined adrenoreceptor blockade and improvements to endothelial dysfunction. To minimize this negative outcome in spatial perfusion heterogeneity, a likely compensatory mechanism against an increased γ should be an increased temporal switching at arteriolar bifurcations to minimize downstream perfusion deficits. Using the identical in situ cremaster muscle preparation, we determined that temporal activity (the cumulative sum of absolute differences between successive values of γ, taken every 20 seconds) was lower in OZR than in control animals, and this difference was present in both proximal (1A-2A) and distal (3A-4A) arteriolar bifurcations. While adrenoreceptor blockade (phentolamine) improved temporal activity in 1A-2A arteriolar bifurcations in OZR, this was without impact in the distal microcirculation, where only interventions against oxidant stress (TEMPOL) and thromboxane A2 activity (SQ-29548) were effective. Analysis of the attractor for γ indicated that it was not only elevated in OZR as compared to LZR, but also exhibited severe reductions in range. Taken together, these results suggesting that the ability of the microcirculation to respond to any imposed physiological or pathological challenge becomes highly restricted with metabolic syndrome, and may represent the major contributors to the manifestation of poor muscle performance at this age in OZR.

National Institutes of Health and American Heart Association

Where applicable, the authors confirm that the experiments described here conform with The Physiological Society ethical requirements.

SA446

The role of pericytes in microvascular network pattern formation

W.L. Murfee

Biomedical Engineering, Tulane University, New Orleans, LA, USA

Quantitative approaches for studying the microcirculation include computational methods and integrative experimental models. This presentation will provide examples of applying both approaches to better understanding the causes and effects of microvascular network pattern formation. The first objective will be to highlight the use of a computational method for gaining new insight into the relationship between network patterns and resistance in hypertension. Microvascular rarefaction, defined by a loss of vessels, is a common characteristic of hypertension and has been linked to elevated microvascular resistance. However, vessel loss in mesenteric microvascular networks from adult spontaneously hyperten-

sive rats (SHRs) versus age-matched normotensive Wistar-Kyoto (WKY) controls is accompanied by an increase in low resistance arterial-venule shunts. Using a computational model that can account for intact network patterns, the total resistances were compared in SHR versus WKY networks. For simulations with uniform vessel diameter and with the diameters based on reported intra-vital measurements, SHR resistance was not increased compared to the WKY level. This result challenges the paradigm that microvascular networks experience increased resistance during hypertension. Still, a question remains – What causes the vessel loss and pattern alterations in the SHR? An answer might be vascular pericytes. SHR networks also display altered pericyte expression of neuron-glia antigen 2 (NG2) implicating them as a critical cell type. The second objective of the presentation will be to introduce the rat mesentery culture model as a novel experimental tool for determining the effect of NG2 inhibition on microvascular network growth. After 3 days in culture with minimum essential media, Wistar mesenteric microvascular networks remain viable and intact. More importantly, growth factor induced endothelial cell sprouting can be inhibited by antibody blocking of NG2 on pericytes. This result confirms the importance of NG2 as a functional regulator of capillary sprouting and establishes the rat mesentery culture model as a novel tool for mechanistic studies investigating pericyte-endothelial cell interactions at specific locations within a microvascular network. Overall, the use of computational modelling and the rat mesentery culture model in these studies emphasizes the value of integrating a quantitative and systems level perspective in microvascular research.

This work was funded by the the Tulane Center for Aging (NIH P20GM103629-01A1) and the Tulane Hypertension and Renal Center of Excellence (NIH P20RR017659-10).

Where applicable, the authors confirm that the experiments described here conform with The Physiological Society ethical requirements.

SA447

Insights from numerical simulations of brain blood flow regulation in large anatomical networks

S. Lorthois

IMFT, CNRS, Toulouse, France

Blood micro-circulation plays a central role in the local adaptation of cerebral blood flow to neural activity (neuro-vascular coupling). A growing body of evidence indicates that neurons, glia, and cerebral blood vessels, acting as an integrated unit, have a crucial role in mediating the activation-induced changes in blood flow. In particular, the smooth muscle cells surrounding the arterioles, and possibly pericytes, at capillary level, convert the bio-chemical signals that originate from this integrated unit into changes in vascular diameter, thus regulating blood flow by modulating vascular resistance [1].
However, the relative role of arterioles and capillaries in the control of cerebral blood flow is still controversial [1]. In particular, it is at present not clear whether the capillary dilatation experimentally observed in vivo by several groups is a passive consequence of upstream arteriolar dilatation via an alteration in perfusion pressure or the result of an active regulation of the capillary diameter via contraction/relaxation of pericytes [1].
Answering this question is of importance in the context of functional neuroimaging. The spatial resolution and specificity of hemodynamically based functional imaging techniques (including fMRI and PET) are indeed bound to the density and localization of the blood flow regulating structures [2].
However, using experimental means for that purpose is extremely challenging. For example, the penetration depth of the most recent intravital two-photon microscopy techniques (typically ~500 μm) does neither allow to investigate the cortical layers of highest capillary density, which are located approximately in the middle third of the cortex [3] nor those where the fastest capillary dilation occurs [4].
By contrast, several authors [1,5] have pointed out that modelling using anatomically accurate representations of the intracortical vascular network allows a better and more quantitative understanding of cerebral blood flow control. In particular, such an approach can be valuable for generating predictions as to the likely impact of pericyte-mediated capillary diameter regulation [1].
Our group has recently performed the first numerical simulations of blood flow in an anatomically accurate large human intra-cortical vascular network (~ 10000 segments), using a 1D non-linear model taking into account the complex rheological properties of blood flow in microcirculation (i.e. Fahraeus, Fahraeus-Lindquist and phase separation effects) [6]. This model predicts blood pressure, blood flow and hematocrit distributions, volumes of functional vascular territories, regional flow at local, voxel and network scales, etc.
Using this approach, we have studied the flow re-organizations induced by arteriolar vasodilations, highlighting the hemodynamic component of various functional neuroimaging techniques [7].
In the present paper, the variations in cerebral blood flow induced by global or localized capillary vasodilations are studied and compared to these previous results, demonstrating that pericyte-mediated regulation of blood flow at capillary level would be efficient for neuro-vascular coupling. By contrast to a regulation situated at the level of arterioles [7], the changes in blood volume can be highly localized in space, with the potential to be as close as possible of areas of neuronal activation. However, the changes in blood flow are much more diffuse. This imposes limits on the ultimate spatial resolution of hemodynamically based brain functional imaging techniques, whatever the localization of the blood flow regulating structures.

Hamilton NB et al., Pericyte-mediated regulation of capillary diameter: a component of neurovascular coupling in health and disease. Front. Neuroenergetics, 2, 1-14 (2010).

Harel N et al., Frontiers of brain mapping using MRI. J. Magn. Reson. Imaging 23, 945–57 (2006).

Lauwers F et al., Morphometry of the human cerebral cortex microcirculation: general characteristics and space-related profiles. Neuroimage, 39, 936-48 (2008).

Tian P, et al., Cortical depth-specific microvascular dilation underlies laminar differences in blood oxygenation level-dependent functional MRI signal. PNAS, 107, 15246-51 (2010).

Weber B et al., The microvascular system of the striate and extrastriate visual cortex of the macaque. Cereb. Cortex 18, 2318–30 (2008).

Lorthois S et al., Simulation study of brain blood flow regulation by intra-cortical arterioles in an anatomically accurate large human vascular network: Part I : Methodology and baseline flow, Neuroimage, 54, 1031-42 (2011).

Lorthois S et al., Simulation study of brain blood flow regulation by intra-cortical arterioles in an anatomically accurate large human vascular network: Part II : Flow variations induced by global or localized modifications of arteriolar diameters, Neuroimage, 54, 2840-53 (2011).

Where applicable, the authors confirm that the experiments described here conform with The Physiological Society ethical requirements.

SA448

The spatio-temporal dynamics of vascular plexus regeneration are related to vessel function

M. Machado[1], M. Watson[3], A. Devlin[2], M. Chaplain[4], S. McDougall[3] and C. Mitchell[2]

[1]MVRL, University of Bristol, Bristol, UK, [2]CMB, University of Ulster at Coleraine, Coleraine, UK, [3]Institute of Petroleum Engineering, Heriot-Watt University, Edinburgh, UK and [4]Division of Mathematics, University of Dundee, Dundee, UK

The structure of the microvascular network within the murine *panniculus carnosus* is highly anisotropic and adapted to the functional requirements of the tissue. To assess the rate of wound closure and functional characteristics of the regenerating vascular plexus, dorsal skinfold chambers (dsc) were implanted in adult mice enabling the use of intravital microscopy. As a result of heat-induced injury to the tissue, a non-perfused area defined as wound was created. Three days after wounding, vasodilatation of the surviving vessel segments was noted even in more distal areas of the plexus, with a peak in vessel junction density at day 6 (indicative of the period of active sprouting), and partial recovery of functional vessel density by day 9.

Having established a longitudinal model of wound healing-induced angiogenesis, we sought to test the influence of different parameters in the progression of blood vessel growth. TNP-470 was the first anti-angiogenic agent to undergo clinical trials in human tumours. The main complication of anti-angiogenic therapy for tumours is its unavoidable effect on physiological processes such as wound healing. TNP-470 covalently binds and inhibits the metalloprotease methyonine aminopeptidase metAP-2 (Sin *et al.*, 1997), which is enriched in endothelial cells, effectively arresting the cell cycle. Injection of TNP-470 led to a significant delay in wound closure with both the extent of vessel sprouting and recovery of tissue perfusion inhibited compared to vehicle-injected mice. Thus, in this experimental model, increase in functional vessel density depends upon endothelial cell proliferation (Machado *et al.*, 2011).

Blind-ended vessels (BEVs) at the leading edge of an expanding vascular plexus were recognized as major regulators of the structure of the developing network (Guerreiro-Lucas *et al.*, 2008). Plasma leakage into the surrounding extracellular matrix occurring from BEVs could play an important role in preparing hypoxic tissue for vascular invasion. As such, plasma flux across the vessel wall was quantitated through the use on *in vivo* Fluorescence Recovery After Photobleaching (FRAP). Determination of time elapsed from bleaching until recovery of fluorescence intensity to half of baseline average ($t_{1/2}$) revealed that the permeability of newly formed vessel segments (both flowing and blind-ended) is greater than that of pre-existing vessels between days 5-7 after injury. Furthermore, TNP-470 reduces macromolecular flux across the vessel wall of BEVs at the leading edge of the advancing vascular plexus, while increased FITC-dextran leakage was observed from pre-existing vessels after treatment with TNP-470 ($p<0.05$), consistent with induction of transient vascular damage, (Machado & Mitchell, 2011). This evidence contradicts previous reports where quiescent endothelium is not affected by TNP-470 (Kruger & Figg, 2000). Using *in vivo* FRAP in the dsc, these studies demonstrate the relationship between temporal changes in microvascular macromolecular flux and the morphology of maturing vascular segments. The combination of techniques used to characterize the morphology and function of the newly-formed blood vessels in this experimental model provided spatially and temporally resolved data, which is amenable for use within mathematical modeling approaches. The predictive power of these data-driven models will enable us to test for unwanted side effects of anti-angiogenic drugs, such as the increased leakiness of pre-existing vasculature.

Sin M *et al.* (1997). PNAS **94**: 6099-6103.

Machado MJ *et al.* (2011). Microcirculation **18**: 183-197.

Guerreiro-Lucas LA *et al.* (2008). Microvascular Research **76**: 161-168.

Machado MJ & Mitchell CA (2011).The Journal of Physiology **589**: 4681-4696.

Kruger EA & Figg WD (2000). Exp. Opin. Invest. Drugs **9**: 1383-1396.

Invaluable help in the interpretation of FRAP data was offered by Prof Axel Pries and Prof Tim Secomb, for which we are most grateful.

Where applicable, the authors confirm that the experiments described here conform with The Physiological Society ethical requirements.

SA449

Insights from structure based imaging, analysis and computational modelling of coronary microcirculation

N. Smith[1], A. Goyal[1], T. Sochi[1], J. Spaan[2], M. Siebes[2], J. van den Wijngaard[2] and J. Lee[1]

[1]King's College London, London, UK and [2]Medical Physics, Amsterdam Medical Center, Amsterdam, Netherlands

Coronary microcirculatory flow is governed by a number of determinants including network anatomy, systemic afterload and the mechanical interaction with the myocardium throughout the cardiac cycle. The range of spatial scales and multi-physics nature of coronary perfusion highlights a need for a multi-scale framework that captures the relevant details at each level of the network. Using a data driven structural based approach we have developed a set of novel methods to reconstruct three-dimensional coronary vasculature from images, comprised of two distinct sets of data – fluorescent microsphere beads and anatomically vasculature. Current state-of-the-art radii estimation methods and a model-based method were applied on whole-organ porcine data that was automatically reconstructed. Using this anatomical model blood flow simulations were performed to obtain blood flow rate, calculated using the conductance and pressure drop across each branch in the tree throughout the whole vasculature. The results from this blood flow simulation were compared to regional microsphere perfusion distribution.

At each branch in the arterial tree, the number of microspheres that passed through it in the vasculature was counted. Shortest path tracing also revealed the main source coronaries for every branch in the arterial tree and the myocardial perfusion regions of these main coronaries. The regional microsphere distribution (number of microspheres counted going through a branch, normalized by the total number of microspheres counted in the entire perfused region of myocardium) was compared to the regional flow (flow rate in a branch normalized by the total flow rate in the root artery). To analyze the discrepancy observed between the microsphere perfusion and flow model, we studied the distribution of microspheres at

bifurcations. Using this data we have constructed a model of this error parameterised by the branching angle and daughter-to-parent ratio of the vessel cross-sectional area is shown to more accurately predict the biased distribution of the microspheres. Incorporating the disproportionate microsphere distribution model at bifurcating segments with the largest branch angles, ranging from 100- 120 degrees, reduced the error from 24 to 7 percent error in between the fraction of flow predicted by the model and the fraction of microspheres.

Ann Biomed Eng. 2012 Nov;40(11):2399-413. doi: 10.1007/s10439-012-0583-7. Epub 2012 May 8. The multi-scale modelling of coronary blood flow. Lee J, Smith NP

Model-based vasculature extraction from optical fluorescence cryomicrotome images.

Goyal A, Lee J, Lamata P, van den Wijngaard J, van Horssen P, Spaan J, Siebes M, Grau V, Smith NP.IEEE Trans Med Imaging. 2013 Jan;32(1):56-72. doi: 10.1109/TMI.2012.2227275

This work was funded by the United Kingdom Engineering and Physical Sciences Research Council (EP/GOO7527/1), the Centre of Excellence in Medical Engineering funded by the Wellcome Trust and the EPSRC under grant number WT 088641/Z/09/Z)

Where applicable, the authors confirm that the experiments described here conform with The Physiological Society ethical requirements.

SA450

Role of tight junction claudins in biological systems – more than a simple paracellular barrier in inflammation and metabolism

S. Tsukita

Laboratory of Biological Science Graduate School of Frontier Biosciences and Graduate School of Medicine, Osaka University, 2-2, Yamadaoka, Suita, Japan

The tight junction (TJ) system is primarily responsible for establishing the paracellular barrier function of epithelial cell sheets. The TJ is a supramolecular complex containing transmembrane proteins associated with membrane-scaffolding proteins such as ZO-1/2 and cingulin that allows the dynamic regulation of ion and solute passage across the paracellular space. Among the TJ transmembrane proteins, claudins are specifically required to form the TJ strands that organize the paracellular barrier structure. The multi-gene claudin family has at least 27 members in human and mouse. Although claudins are paracellular barrier-forming proteins, certain “ion leaky” claudins specify which ions can cross the barrier. A remarkable characteristic of claudin family proteins is their distinct tissue-dependent expression patterns. In our laboratory, some claudins such as claudins 2,15,18 have recently been intensively studied with regard to their biological roles in processes such as inflammation and nutrient absorption. These studies highlight the functions of claudin beyond that of a simple barrier.

Suzuki H et al., *Nat Commun* In press

Wada M et al., *Gastroenterology* In press

Hayashi D et al., (2012) *Gastroenterology* **142**, 292-304.

Tamura A et al., (2011) *Gastroenterology* **1403**, 913-923.

Where applicable, the authors confirm that the experiments described here conform with The Physiological Society ethical requirements.

SA451

Elucidating the molecular organization of tight junction strands and design of claudin-modulators

J. Piontek

Leibniz-Institut für Molekulare Pharmakologie; Institut für klinische Physiologie, Charité, Berlin, Germany

The paracellular barrier in epithelia and endothelia is formed by tight junctions (TJ). They limit and regulate the paracellular permeation of ions, solutes and proteins. The barrier properties of TJs in different tissues are mainly determined by the claudin composition of the heteropolymeric TJ-strands. To analyze the molecular organization of TJ, these strands were reconstituted by claudin-transfection of TJ-free HEK293-cells. A single claudin-construct was expressed to obtain defined homomeric TJ-strands. In addition, another claudin subtype or a member of the TJ-associated marvel domain protein family was expressed to obtain defined heteromeric TJ-strands. The ability to form strands and their morphology was investigated by freeze fracture electron microscopy or single molecule fluorescence nanoscopy. The barrier function of the TJ-strands was demonstrated by tracer exclusion imaging. cis-Interactions of claudin molecules were investigated by cellular fluorescence resonance energy transfer (FRET)- and native PAGE. trans-Interactions were detected by confocal cell-cell contact enrichment scanning. The mobility of claudins in the membrane was measured by fluorescence recovery after photobleaching (FRAP). This approach was used to characterize heterophilic compatibility of claudins. In addition, to elucidate mechanistic details of the claudin assembly, the blood brain barrier relevant Cld5 and Cld3 that differ in assembly properties were analyzed in more detail. Generation and investigation of Cld3/Cld5 chimeric mutants revealed protein segments and residues differentially involved in the assembly of claudin oligomers and TJ-strands. Futhermore, the domain III of Clostridium perfringens enterotoxin (cCPE), a high affinity ligand of a subset of claudins was used as a probe to gain information about the structure of the extracellular loop 2 of classic claudins. The experimental data was combined with schematic and molecular homology modeling of Cld3 and Cld5. The results provide novel molecular insights into subtype-specific assembly of classic claudins, paracellular barriers and the potential of pharmacological claudin-modulation, e.g. for paracellular drug delivery or treatment of claudin-overexpressing tumors.

Where applicable, the authors confirm that the experiments described here conform with The Physiological Society ethical requirements.

SA452

Identifying proteins and protein networks of the tight junction

J. Anderson and C.M. Van Itallie

National Institutes of Health, Bethesda, MD, USA

The proteins and functional protein networks of the tight junction remain incompletely defined. Among the currently known proteins are barrier forming proteins like occludin and the claudin family, scaffolding proteins like ZO-1 and some cytoskeletal, signaling and cell polarity proteins. To define a more complete list of proteins and investigate their functional

implications, we identified the proteins which are within molecular dimensions of ZO-1 by fusing biotin ligase to either its N- or C-terminus, expressing these fusion proteins in MDCK epithelial cells and purifying and identifying the resulting biotinylated proteins by mass spectrometry. Out of a predicted proteome of ≈ 9000 we identified more than 300 proteins tagged by biotin ligase fused to ZO-1, with both identical and distinct proteins near the N- and C- terminal ends. Those proximal to the N-terminus were enriched in transmembrane tight junction proteins and those proximal to the C-terminus were enriched in cytoskeletal proteins. We also identified many unexpected, but easily rationalized proteins. In addition, functional networks of interacting proteins were tagged, such as the basolateral but not apical polarity network. These results provide a rich inventory of proteins and potential novel insights into functions and protein networks that should catalyze further understanding of tight junction biology. This approach is being extended to identify proteins which are near occludin and claudins with the goal of defining subjunctional protein compartments.

This work is supported by the Division of Intramural Research, National Institutes of Health, USA

Where applicable, the authors confirm that the experiments described here conform with The Physiological Society ethical requirements.

SA453

Patch clamp recordings reveal paracellular claudin-2 channels

C. Weber

Pathology, The University of Chicago, Chicago, IL, IL, USA

There are a large number of intestinal disorders in which tight junction barrier defects are associated with changes in the expression and/or localization of tight junction proteins. In particular, claudin-2 has been shown to be upregulated in a number of disease states, including inflammatory bowel disease. Expression of claudin-2 has been demonstrated to increase paracellular Na^+ permeability without increasing permeability to large molecules. This finding has contributed to the hypothesis that claudin-2 forms paracellular size and charge selective pore-like structures. However, available measures to study barrier function of epithelial monolayers cannot resolve function of individual pores. To overcome this limitation, patch clamp recordings were used to define claudin-2 function at a single channel level.
Tight junction patch clamp recordings reveal single claudin-2 channel openings. Claudin-2 expression reduces global measures of transepithelial resistance and induces a corresponding increase in the frequency, but not size of claudin-2 opening events detected in patch clamp recordings. Opening events were not detectable when electrodes were sealed on apical cell membranes away from tight junctions. Ion substitution analyses demonstrate that claudin-2 openings are cation selective and permeable to methylamine$^+$ (radius 1.9 Å), but have low permeability to tetramethylammonium$^+$ (radius 2.8 Å). Claudin-2 channel openings are blocked by cysteine derivatization of I66, a residue within the first extracellular loop of claudin-2, known to be an important determinant of claudin-2 pore properties. Similarly application of lanthanum, a known claudin-2 blocker blocks all single channel openings. These data show that claudin-2 size and charge selectivity are explained by the average behavior of a population of claudin-2 channels present in the tight junction. Furthermore, these data suggest frequency and duration of tight junction channel openings as potential mechanism whereby tight junction barrier function may be regulated in health and disease.

Jerrold Turner; Deborah Nelson; Alan Yu; Guohua Liang; K08 DK088953; S&R Foundation Ryuji Ueno Award for Ion Channels and Barrier Function Research

Where applicable, the authors confirm that the experiments described here conform with The Physiological Society ethical requirements.

SA454

Towards understanding tight junction functions and signalling

M. Balda

University College London, London, UK

Tight junctions are key componet of cell-cell junctional complexes in epithelial and endothelial cells. Tight junction proteins participate in the control of the diffusion of molecules through the paracellular pathway, act as an intramembrane diffusion barrier for lipids between the apical and basolateral cell surface domains, as well as function in the regulation of cell proliferation and gene expression. We have identified and characterized several TJ-associated signalling complexes that contain different types of signalling proteins, such as ZONAB, a ZO-1-interacting nucleic acid binding protein, RhoGTPase activators such as GEF-H1 and p114RhoGEF, and the Rho GAP SH3BP1. Results will be discussed that disclose further molecular mechanisms on how tight junctions regulate paracellular permeability, cell proliferation and survival, as well as transcriptional and postranscriptonal modes of gene expression.

MRC, The Wellcome Trust, Fight for Sight, BBSRC

Where applicable, the authors confirm that the experiments described here conform with The Physiological Society ethical requirements.

SA455

Maternal obesity and the developmental programming of hypertension; a role for Leptin

P.D. Taylor

Women's Health, King's College London, London, UK

The prevalence of maternal obesity has more than doubled in the past two decades with approximately 1 in 5 UK pregnant women now obese [1]. Maternal obesity and excessive gestational weight gain (GWG) constitute some of the most common obstetric risk factors and have direct implications for pregnancy outcome [2]. However, recent evidence suggests that maternal obesity may also have deleterious consequences for the cardiovascular health of the next generation. Mother-child cohort studies have established that both pre-pregnancy BMI and GWG are independently associated with cardio-metabolic risk factors in young adult offspring, including systolic and diastolic blood pressure [3, 4]. Animal models in sheep and non-human primates provide further evidence for the influence of maternal obesity on offspring cardiovascular function, whilst our recent studies in rodents have shown that fetal exposure to the metabolic milieu of maternal obesity may permanently

change the regulatory pathways in the hypothalamus that contribute to cardiovascular homeostasis.
Leptin plays an important role in the central control of appetite, and is also involved in activation of efferent sympathetic pathways to both thermogenic and non-thermogenic tissues, such as the kidney, and is therefore implicated in obesity-related hypertension. Leptin is also thought to have a neurotrophic role in the development of the hypothalamus and we have recently reported that altered neonatal leptin profiles secondary to maternal obesity were associated with evidence of permanently altered hypothalamic structure and function. Hyperphagia and increased adiposity in the adult offspring of obese rodents is associated with region specific hypothalamic leptin resistance in the appetite regulatory pathways of the arcuate nucleus[5]. We have recently reported compelling evidence from our rodent model that maternal obesity confers persistent sympathoexcitatory hyper-responsiveness and hypertension acquired in the early stages of development. Juvenile offspring develop hypertension as early as 30 days of age and, importantly, prior to the onset of obesity. Hypertension in the offspring of obese rats results from persistent sympathoexcitatory hyper-responsiveness[6] with enhanced cardiovascular stress reactivity, an increase in low/high frequency ratio of heart rate variability (HRV), and increased pressor response to exogenous leptin, all evidence of increased sympathetic tone. Disturbed sympathetic control of blood pressure has not previously been reported as a consequence of maternal obesity. The baroreflex response was also abnormal in OffOb rats (90days) and may also represent a primary programmed defect secondary to maternal obesity.
To investigate the role of neonatal hyperleptinaemia in offspring cardiovascular dysfunction, we have treated naive rats with exogenous leptin on postnatal days 9-14. At 1 month of age leptin-treated rats displayed increased mean arterial pressure (MAP) compared to saline treated controls which continued into adulthood. These data provide proof of principle that hyperleptinaemia during a critical window of hypothalamic development may directly lead to adulthood hypertension.
These data add to increasing evidence for developmental plasticity in the central efferent pathways of the autonomic nervous system, and further implicates a central role for an acquired selective leptin resistance and 'hardwiring' of the developing hypothalamus for a hyperphagic and hypertensive offspring phenotype in offspring of obese rodents. Insight from these animal models raises the possibility that early life exposure to leptin in humans leads to early onset essential hypertension. On-going mother-child cohort and intervention studies in obese pregnant women provide a unique opportunity to address associations between maternal obesity and offspring cardiovascular function.

Heslehurst N, Rankin J, Wilkinson JR, Summerbell CD. A nationally representative study of maternal obesity in england, uk: Trends in incidence and demographic inequalities in 619 323 births, 1989-2007. Int J Obes (Lond). 2009

Poston L, Harthoorn LF, Van Der Beek EM. Obesity in pregnancy: Implications for the mother and lifelong health of the child. A consensus statement. Pediatr Res. 2011;69:175-180

Mamun AA, O'Callaghan M, Callaway L, Williams G, Najman J, Lawlor DA. Associations of gestational weight gain with offspring body mass index and blood pressure at 21 years of age: Evidence from a birth cohort study. Circulation. 2009;119:1720-1727

Hochner H, Friedlander Y, Calderon-Margalit R, Meiner V, Sagy Y, Avgil-Tsadok M, Burger A, Savitsky B, Siscovick DS, Manor O. Associations of maternal prepregnancy body mass index and gestational weight gain with adult offspring cardiometabolic risk factors: The jerusalem perinatal family follow-up study. Circulation. 2012;125:1381-1389

Kirk SL, Samuelsson AM, Argenton M, Dhonye H, Kalamatianos T, Poston L, Taylor PD, Coen CW. Maternal obesity induced by diet in rats permanently influences central processes regulating food intake in offspring. PLoS One. 2009;4:e5870

Samuelsson AM, Morris A, Igosheva N, Kirk SL, Pombo JM, Coen CW, Poston L, Taylor PD. Evidence for sympathetic origins of hypertension in juvenile offspring of obese rats. Hypertension. 2010;55:76-82

This work was supported by the British Heart Foundation (FS/10/003/28163) and the BBSRC (BBD5231861).

Where applicable, the authors confirm that the experiments described here conform with The Physiological Society ethical requirements.

SA456

Epigenetic mechanisms in the developmental programming of cardiovascular and metabolic disease

T. Plosch

University Medical Center Groningen, Groningen, Netherlands

An overwhelming body of evidence links fetal (mal)nutrition to the development of chronic diseases at adult age (DOHaD hypothesis, Developmental Origins of Health and Disease). Several explanations for the various observed facets of the long-term consequences of fetal (under)nutrition are currently under investigation.
In recent papers, epigenetic mechanisms like DNA methylation or histone modifications have been proposed to be involved in metabolic programming: CpG islands, CG-dinucleotide-rich regions in the promoter of a gene, have been shown to be of crucial importance for the transcriptional activity of particular promoters. In general, transcription of a gene is blocked when the CpG island is methylated. A second layer of complexity is added by the fact that methylated areas of DNA attract methyl-DNA binding proteins and acquire histone modifications which also affect the accessibility of the DNA for transcription. Together, the interaction of DNA methylation and histone modification can regulate the activity of a DNA region. New technologies (pyrosequencing, next generation sequencing) now enable us to measure DNA methylation and the active/silent areas of chromatin in a genome-wide way and correlate it with physiological observations.
Embryonic development proceeds as a complex set of interdependent and precisely integrated biological programmes, initiated by selective transcription of specific genes at specific points of time and regulated by a controlled maternal supply of nutrients. With the current state of knowledge of molecular regulation of cholesterol and lipid metabolism, it is possible to generate a network of metabolic events in the embryo and the fetus that may underlie programming. Nuclear receptors (PPARs, LXRs, FXR) provide the vehicles through which nutrients interact with the (epi)genome. Expression of these nuclear receptors is at least partially under control of CpG islands.
Disturbances in this complex network of interactions represent key events in metabolic programming of insulin resistance, hyperlipidemia and cardiovascular disease and are the focus of my work. I will discuss some of the early epigenetic modifications we observed in animal models and human samples and try to link them to metabolic and cardiovascular disease in later life.

Torsten Plösch is supported by the Dutch Heart Foundation (grant 2004T4801) and the Netherlands Organisation for Health Research and Development (ZonMW TOP grant).

Where applicable, the authors confirm that the experiments described here conform with The Physiological Society ethical requirements.

SA457

Early life stress-induced mechanisms of cardiovascular disease

J.S. Pollock, C. De Miguel, D.H. Ho, D.M. Pollock and A.S. Loria

Experimental Medicine, Georgia Regents University, Augusta, GA, USA

Maternal separation (MatSep) is a model of behavioral stress during early life in rodents. This model of early life stress has been extensively studied with respect to behavioral outcomes in adulthood. MatSep induces a pro-anxiety phenotype in adult rats. We hypothesized that MatSep may also promote vascular dysfunction and/or overt cardiovascular disease. MatSep was performed in male Wistar Kyoto rats 3 hs/day from day 2 to 14 of life. Non-separated littermate rats (NS) were used as control. For all experiments described with ex vivo tissues, we utilized intraperitoneal injection of 65mg/kg sodium pentobarbital to terminate the rats for dissection of tissues. We reported that MatSep induces an exaggerated angiotensin II (AngII)-induced aortic constriction ex vivo in adult male rats. The exaggerated AngII-mediated aortic constriction was specific to the AngII pathway because other vasoconstrictor mediators (ET-1, phenylephrine, KCl) did not elicit an exaggerated response in the MatSep rats. We found that MatSep induces a dysfunction in AngII-mediated signaling specifically in the endothelium, such that NOS activation was impaired and NO buffering was reduced. AngII receptors, AT1 and AT2, function was determined. Vascular AT2 activation was impaired, while AT1 appeared to be intact. Moreover, vascular AT2 expression was significantly reduced. AT1 receptor and other known AngII pathway genes were shown to have similar expression levels in MatSep and NS rats. We hypothesized that MatSep would induce an AngII-sensitive phenotype in vivo. We anesthetized rats with 2% isoflurane gas by inhalation and inserted radiotelemetry devices to monitor blood pressure chronically. In vivo, MatSep rats elicit exacerbated AngII-induced hypertension mediated via a loss of NO buffering capacity as elucidated with L-NAME (NOS inhibitor) in the drinking water. AngII infusion induced a significant increase in AT1 receptor expression in the renal cortex of MatSep rats, while in NS rats a decrease in AT1 receptor expression was found. AngII infusion in the MatSep rats enhanced increased T cell and macrophage infiltration to the endothelium and the peri-vascular adventitia of the aorta; as well as T cell infiltration was shown to be exaggerated in the renal cortex by immunohistochemical techniques. Remarkably, AngII-induced renal damage was exaggerated exclusively in the interstitial arteries of MatSep rats by histological analyses. These data indicate that MatSep sensitizes AngII responses via increased activation of AT1 receptors, leading to an increased hemodynamic response associated with an enhanced T cell activation. To further elucidate the immune response of the MatSep rats, we exposed NS and MatSep rats to an acute (12 hr) exposure of lipopolysaccharide (LPS) injected intraperitoneally. No differences were found in the number of circulating or renal T cells at baseline or in LPS-treated rats. Renal tissue from LPS-treated MatSep rats showed a 4 to 16 fold increase in levels of cytokines (IL-16, CCL3, CCL4, IFNg), chemokine receptors (CCR3, CCR4, CXCR4) and activation markers (CD40, CD40Ig) compared to LPS-treated NS rats indicating that MatSep sensitizes T cell activation. These results indicate that MatSep enhances pro-inflammatory activation of circulating and renal T cells, which most likely leads to promotion of pathological cardiovascular responses. Our findings provide new insights in the mechanisms of developmental programming of cardiovascular disease and new risk factors associated to an adverse postnatal environment.

Loria, A.S., D.M. Pollock, J.S. Pollock. Early life stress sensitizes rats to angiotensin II-induced hypertension and vascular inflammation in adult life. Hypertension, 55: 494-9, 2010.

Loria AS, Kang K-T, Pollock DM, Pollock JS. Early life stress enhances angiotensin II-mediated

vasoconstriction by reduced endothelial NO buffering. Hypertension, 58(4):619-26, 2011.

Loria AS, Yamamoto T, Pollock DM, Pollock JS. Early life stress induces renal dysfunction in adult male but not female rats. Am J Physiol: Regulatory, Integrative, Comparative, in press, 2013.

NIH NHLBI Program Project Grant Stress Related Hypertension Risk

Where applicable, the authors confirm that the experiments described here conform with The Physiological Society ethical requirements.

SA458

The roles of 11β-hydroxysteroid dehydrogenase type 2 in placenta and fetus in developmental programming

E. Cottrell[1], M.C. Holmes[2], J.R. Seckl[2] and C.S. Wyrwoll[3]

[1]Institute of Human Development, University of Manchester, Manchester, UK, [2]University/BHF Centre for Cardiovascular Science, University of Edinburgh, Edinburgh, UK and [3]The University of Western Australia, Perth, WA, Australia

Fetal growth restriction (FGR), reflective of an adverse intrauterine environment, confers a significantly increased risk of perinatal mortality and morbidity. In addition, low birth weight associates with adult diseases including hypertension, metabolic dysfunction and behavioural disorders. Glucocorticoids are critical for fetal development, however exposure of the fetus to excess glucocorticoids reduces fetal growth and can permanently alter organ structure and function, predisposing to disease in later life.

Fetal glucocorticoid exposure is regulated, at least in part, by the enzyme 11β-hydroxysteroid dehydrogenase type 2 (11β-HSD2), which catalyzes the intracellular inactivation of glucocorticoids. This enzyme is highly expressed within the placenta at the maternal-fetal interface, limiting passage of glucocorticoids to the fetus. Expression of 11β-HSD2 is also high in fetal tissues, particularly within the developing central nervous system (CNS). Down-regulation or genetic deficiency of placental 11β-HSD2 is associated with significant reductions in fetal growth and birth weight, and programmed outcomes in adulthood.

We have shown that in addition to reducing the passage of glucocorticoids, 11β-HSD2 plays a key role in regulating placental function through modulation of local glucocorticoid levels, affecting placental vascularization, blood flow and transport capacity. Endogenous placental 11β-HSD2 activity can also be modulated by maternal stressors (such as poor diet), suggesting that regulation of glucocorticoid metabolism may play a part in feto-placental adaptation to adverse conditions. The question still remains as to whether it is placental or fetal 11β-HSD2 that are key to subsequent programmed outcomes. A recently developed knockout of 11β-HSD2 specifically within

the CNS during development suggests that neural 11β-HSD2 does indeed have a role in protecting the developing brain and thus determining adult behavioural outcomes. This may prove to be a partial role (additive to that of 11β-HSD2 in the placenta), as the phenotype appears more subtle than the global 11β-HSD2 knockout. Thus, alterations in 11β-HSD2 within both fetal and placental tissues affects growth and development during the perinatal period, and influences the life-long health of an individual.

Studies were supported by a Wellcome Trust project grant (to M.C.H. and J.R.S.) and a Human Frontier Science Program grant (RGP0039/2006-C) to J.R.S.

Where applicable, the authors confirm that the experiments described here conform with The Physiological Society ethical requirements.

SA459

Sex differences and programming of hypertension

B.T. Alexander

Physiology, Univ Miss Med Ctr, Jackson, MS, USA

Hypertension is a multi-factorial disorder thought to result from both genetic and environmental factors. Numerous epidemiological studies report an association between birth weight and blood pressure. This association is observed in a variety of populations from around the world and is further supported as elevations in blood pressure are also found in low birth weight children Thus, the inverse relationship between birth weight and blood pressure suggests that factors present in the fetal environment which affect fetal growth are responsible for the developmental programming of blood pressure control. Recent experimental studies suggest that developmental programming occurs in response to adverse environmental influences during fetal life resulting in permanent adaptive responses that lead to structural and physiological alterations and the subsequent development of cardiovascular disease and hypertension. Sex differences in response to fetal insult are observed in many animal models of developmental programming with phenotypic outcome linked to the severity of the insult. In general, phenotypic outcome is more severe in male offspring relative to females (1). Although the exact mechanisms that mediate the sexual dimorphism in programmed blood pressure are unclear, experimental studies suggest that sex-specific programming of blood pressure involves a key role for the kidney (1), the renin angiotensin system (2), oxidative stress (3), and sex steroids (4). Whether a sex difference in blood pressure is present in low birth weight men relative to low birth weight women has not been clearly established. However, one study indicates that blood pressure is higher in low birth weight boys relative to low birth weight girls during childhood (5). Other studies indicate that men demonstrate a strong association between birth weight and blood pressure in young adulthood (6), whereas hypertension is not present until age 60 in low birth weight women (7). Thus, these studies suggest that the association between birth weight and blood pressure amplifies with age. Moreover, age may adversely impact the protective role of the female sex on programming of later chronic health. It is well established that aging is a critical mediator of age-related increases in blood pressure. Yet, few experimental studies have examined the impact of aging on sex differences in programmed hypertension. Thus, susceptibility to developmental programming of hypertension is sex-specific. However, age-dependent changes may serve as a secondary influence following fetal insult implicating a need for further studies to investigate the impact and the mechanisms involved in age-dependent increased cardiovascular risk in low birth weight men and women.

Grigore D, Ojeda NB, Alexander BT. Sex differences in the fetal programming of hypertension. Gend Med. 2008;5 Suppl A:S121-32..

Moritz KM, Cuffe JS, Wilson LB, Dickinson H, Wlodek ME, Simmons DG, Denton KM. Review: Sex specific programming: a critical role for the renal renin-angiotensin system. Placenta. 2010;31 Suppl:S40-S46.

Ojeda NB, Hennington BS, Williamson DT, Hill ML, Betson NE, Sartori-Valinotti JC, Reckelhoff JF, Royals TP, and Alexander BT. Oxidative stress contributes to sex differences in blood pressure in adult growth-restricted offspring. Hypertension 2012;60: 114-122.

Ojeda NB, Grigore D, Robertson EB, Alexander BT. Estrogen protects against increased blood pressure in postpubertal female growth restricted offspring. Hypertension. 2007;50:679-685.

Jones A, Beda A, Osmond C, Godfrey KM, Simpson DM, Phillips DI. Sex-specific programming of cardiovascular physiology in children. Eur Heart J. 2008;29:2164-2170.

Jarvelin MR, Sovio U, King V, Lauren L, Xu B, McCarthy MI, Hartikainen AL, Laitinen J, Zitting P, Rantakallio P, Elliott P. Early life factors and blood pressure at age 31 years in the 1966 northern Finland birth cohort. Hypertension. 2004;44:838-846.

Andersson SW, Lapidus L, Niklasson A, Hallberg L, Bengtsson C, Hulthen L. Blood pressure and hypertension in middle-aged women in relation to weight and length at birth: a follow-up study. J Hypertens. 2000;18:1753-1761

Dr. Alexander is supported by NIH grants HL074927 and HL51971.

Where applicable, the authors confirm that the experiments described here conform with The Physiological Society ethical requirements.

SA460

Heterothermy in Afrotropical birds: phylogenetic and ecological patterns

A. McKechnie

University of Pretoria, Hatfield, South Africa

In comparison to mammals, relatively little is known about the ecology and phylogenetic distribution of heterothermy in birds. Reviews of avian hetereothermy have not so far revealed any clear links with climatic variables, but instead suggest heterothermy is most pronounced in phylogenetically older taxa that feed on spatially and temporally unpredictable diets such as nectar, aerial insects, or fruit. Africa's avifauna offers rich opportunities to investigate phylogenetic and ecological correlates of heterothermy, and here I review recent work in this area.

Mousebirds (Coliiformes) are a phylogenetically ancient order endemic to the Afrotropics, and have long been considered one of the avian taxa in which torpor is most pronounced. However, work on both captive and free-ranging mousebirds reveals that the ecological significance of torpor in this group needs to be viewed in the context of its interaction with communal roosting behaviour; whereas mousebirds readily enter torpor when housed individually, when roosting communally they maintain body temperatures (T_b) similar to typical avian normothermic values. Torpor is probably rare in wild mousebirds. Two other non-passerine taxa whose phylogenetic position, body mass and ecological traits suggest they might have evolved the capacity for pronounced heterothermy are barbets (Piciformes: Lybiidae) and small owls (Strigidae). Two species of barbets held in outdoor aviaries in mid-winter

showed small decreases in rest-phase T_b, but not the large reductions characteristic of torpor. In a study of thermoregulation in two small owl species in the Kalahari Desert of southern Africa, free-ranging African Scops-owls (*Otus senegalensis*) regularly reduced skin temperature (T_{skin}) by up to 8.6 °C below normothermic levels, but Pearl-spotted Owlets (*Glaucidium perlatum*) remained normothermic throughout the study period. These findings emphasise the variation in heterothermy that can exist in related species at a single site.

Patterns of heterothermy can also vary substantially within species. Among Freckled Nightjars (*Caprimulgus tristigma granosus*) in the more mesic eastern part of southern Africa, torpor was used frequently by some individuals, but was not correlated with lunar phase. In contrast, torpor in conspecifics (*C. t. lentiginous*) at a desert site was strongly linked to lunar cycles, becoming progressively deeper around new moon and shallower around full moon. These intraspecific differences likely reflect variation between sites in terms of both aridity and rainfall seasonality.

In contrast to some phylogenetically older orders, passerines appear to possess a very limited capacity for torpor. Laboratory data for a small granivorous finch from the southern African arid zone supports this view, with only small decreases in T_b occurring during periods of restricted energy supply. Body temperatures approaching those associated with deep torpor have been reported in sunbirds (Nectariniidae), although the relationship between metabolic rate, T_b and air temperature in these cases suggest a modified form of shallow hypothermia, rather than classic torpor.

The overall picture that emerges from studies of avian heterothermy is that many birds that *a priori* would seem good candidates to use pronounced torpor and/or hibernation apparently do not do so. One key factor that may select against torpor use is predation risk; the lethargic, non-responsive state characteristic of torpor likely significantly increases the risk of predation for many species. The notion that predation risk is a major evolutionary determinant of avian heterothermy is supported by recent findings that African Green-pigeons (*Treron calvus*) apparently do not enter torpor, whereas an ecologically similar species restricted to an island with no native predators does. Columbid birds, on account of their spectacular diversification on islands, potentially represent a very useful model taxon for testing hypotheses regarding the role of predation risk in the evolution of torpor in birds.

McKechnie AE & Lovegrove BG (2002). *Condor* **104**, 705-724.

McKechnie AE & Lovegrove BG (2003). *J Comp Physiol* **173**, 339-346.

McKechnie AE et al. (2004). *Condor* **106**, 144-150.

McKechnie AE et al. (2007). *J Avian Biol* **38**, 261-266.

McKechnie AE & Smit B (2010). *Ostrich* **81**, 97-102.

Smit B & McKechnie AE (2010). *Physiol Biochem Zool* **83**, 149-156.

Smit B et al. (2011). *J Biol Rhythms* **26**, 241-248.

The work presented here reflects a series of productive and enjoyable collaborations, and I thank Ben Smit, Justin Boyles, Mark Brigham, Matt Noakes, Robert Ashdown, Murray Christian, Gerhard Körtner, Barry Lovegrove, and Blair Wolf.

Where applicable, the authors confirm that the experiments described here conform with The Physiological Society ethical requirements.

SA461

Mechanisms of mitochondrial metabolic suppression in hibernation

J.F. Staples

Biology, University of Western Ontario, London, ON, Canada

In winter mammalian hibernators, such as the 13-lined ground squirrel (*Ictidomys tridecemlineatus*), enter a state of torpor where metabolic rate is suppressed by ca. 90%, and body temperature (T_b) subsequently declines towards freezing. These changes are fully reversed during arousals, which occur spontaneously every 5-14 days throughout the winter. Arousals return animals to full euthermia for ca. 1 day before they enter another bout of torpor. This cycle is apparently driven by endogenous signals, and offers an excellent natural model to study plasticity of many physiological functions, including mechanisms of metabolic.

The reversible suppression of whole-animal metabolism in hibernation is mirrored by some aspects of mitochondrial oxidative phosphorylation. In liver mitochondria isolated from torpid animals, state 3 (phosphorylating) respiration, fueled by succinate oxidation, is ca. 70% lower than in euthermic animals, even when measured at the same *in vitro* temperature (37ºC)[1]. Torpid suppression of mitochondrial respiration may conserve endogenous fuels and minimize damage by ROS, but it is not evident in all tissues, including cardiac muscle and forebrain. Moreover this suppression depends on several factors, including oxidative substrate and *in vitro* assay temperature. For example, in mitochondria isolated from skeletal muscle, respiration is suppressed in torpor by ca. 35%, but only with succinate as substrate, and only when measured at 37ºC[2]. Although not universal, the plasticity of oxidative phosphorylation seen in some hibernator tissues provides valuable information about the regulation of mitochondrial metabolism. In liver mitochondria suppression of state 3 respiration occurs early during entrance into torpor, declining by 70% within the short time it takes for T_b to fall from 37ºC to 30ºC[3]. Conversely, reversal of this suppression during arousal occurs only gradually, and even after T_b rises from 5ºC to 30ºC, respiration is only ca. 50% of values from fully aroused, euthermic animals[4]. This "fast in, slow out" pattern suggests that acute and temperature-sensitive mechanisms are responsible for the reversible suppression of mitochondrial metabolism, and our recent research seeks such mechanisms.

Mitochondrial membranes are remodeled during entrance and arousal, with changes in both phospholipid classes and fatty-acyl chain saturation. These membrane changes, however, are transient and do not correlate with mitochondrial respiration[5]. In torpor, both intact mitochondria and succinate dehydrogenase (SDH) have higher apparent affinity for succinate, but SDH is inhibited by ca. 25%[2]. The inhibition of SDH is probably caused by oxaloacetate (OAA), a Krebs cycle intermediate, and the apparent affinity of SDH for OAA increases in torpor. Reversal of OAA inhibition (by preincubation with isocitrate) restores SDH activity, but it does not fully "rescue" state 3 respiration to euthermic levels[4]. Our recent phosphoproteomic analysis revealed seasonal (i.e. summer vs. winter) differences in the phosphorylation state of several mitochondrial proteins, but no differences within winter (i.e. torpid vs. aroused), when the rapid and reversible suppression of oxidative phosphorylation is most evident. Future experiments will examine potential inhibition of oxidative phosphorylation complexes by measuring their redox state in intact mitochondria using rapid-scanning optical spectrometry. We will also examine

changes in mitochondrial protein acetylation state using immunoblot analysis, and inhibition of substrate transport, especially by the dicarboxylate carrier which is responsible for succinate transport.

Muleme HM *et al.* (2006). *Phys Biochem Zool* **79**, 474-483

Brown JCL *et al. J Exp Biol* in press

Chung D *et al.* (2011) *J Comp Physiol B* **181**, 699-711

Armstrong C & Staples JF (2010) *J Comp Physiol B* **180**, 775-783

Armstrong C *et al.* (2011) *Phys Biochem Zool* **84**, 438-449

Funding courtesy of the Natural Sciences and Engineering Research Council, Canada

Where applicable, the authors confirm that the experiments described here conform with The Physiological Society ethical requirements.

SA462

Translating drug-induced hibernation to therapeutic hypothermia

K.L. Drew, V.M. Combs and T.R. Jinka

Institute of Arctic Biology, University of Alaska Fairbanks, Fairbanks, AK, USA

Hibernation is a fully reversible condition characterized by hypometabolism and deep hypothermia. Core body temperature (Tb) in hibernating ground squirrels decreases to within 1 or 2°C of ambient temperature (Ta) and can fall to as low as -3°C (Barnes, 1989). In recent work, we showed that the arctic ground squirrel enters hibernation through activation of CNS adenosine A1 receptors (A1AR) (Jinka et al., 2011), in a manner consistent with the inhibition of thermogenesis. Similarly, A1AR agonists in nonhibernating species mediate a hypothermic response through effects on the CNS (Anderson et al., 1994).

Several aspects of the hibernation phenotype have therapeutic implications (Drew et al., 2001). Here we harness mechanisms hibernating animals use to cool during onset of torpor for therapeutic hypothermia (TH). TH is the only treatment known to improve prognosis for cardiac arrest patients (Hypothermia-after-Cardiac-Arrest-Study-Group, 2002). Thermoregulatory responses such as shivering, however, complicate cooling in comatose cardiac arrest patients and limit efficacy of TH in conscious stroke patients (Zgavc et al., 2011). Stimulating CNS A1AR to suppress thermogenesis mimics the process hibernating animals use to cool during onset of hibernation. Here we describe a strategy of targeted temperature management based on principles of CNS control of hibernation. All work on animals was approved by the UAF IACUC.

In these experiments the A1AR agonist ^{6}N-cyclohexyladenosine (CHA) was administered to rats (male, 69-75 days old; 250-350g, n=6) at a Ta of 16°C to lower body temperature. 8-(p-Sulfophenyl)theophylline (8-SPT), a nonselective adenosine receptor antagonist that does not cross the blood brain barrier was administered prior to CHA to mitigate direct effects of CHA on the heart. Asphyxial cardiac arrest was performed as before (Dave et al., 2006). Rats were anesthetized with 4% isoflurane and a 30:70 mixture of O_2 and N_2O followed by endotracheal intubation and mechanical ventilation. Vecuronium (1mg/kg) was injected iv and apnea induced by disconnecting the ventilator from the endotracheal tube to induce cardiac arrest. Adequacy of isoflurane anesthesia was assessed prior to onset of neuromuscular blockade and maintained at this level for less than 10 min before cardiac arrest induced a comatose state. Resuscitation was initiated after 8 min of apnea. Rats resuscitated within 120 sec were screened for additional inclusion criteria and randomly allocated to TH or normothermic control (NC) treatment groups. Subcutaneous body temperature was monitored using IPTT-300 transponders (Biomedic Data Systems, Inc., USA).

Treatments: The TH group was administered 8-SPT (25mg/kg,ip) 15min prior to CHA 1mg/kg,ip. This drug combination was administered 6 times at 4h intervals to rats held at a Ta of 16°C. The NC group was administered 8-SPT vehicle (saline) 15 min prior to CHA vehicle (0.1M phosphate buffer) in the same manner as 8-SPT/CHA and held in a neonatal incubator set to 29°C. Treatment commenced 70min after restoration of spontaneous circulation (ROSC) and continued for 24h. The final injection of CHA was administered at 20h and rats rewarmed at 24h by returning to the home room at a Ta of 20°C.

Histology: 7 days after ROSC rats were perfused as before (Dave et al., 2006) and hippocampal CA1 regions examined for histopathology.

Results: Mean ± SEM Tb was 33.5°C±0.07 and 33.5°C±0.14 in the NC and TH groups at onset of treatment. Tb in all 3 NC rats increased to 36.5-36.8 within 15 min of placement at 29°C and remained between 36.2 and 37.3°C until death. Only 1 rat in the NC group survived to 7 days. The remaining 2 rats died between 13-18h after ROSC. Tb in the 3 rats treated with TH decreased to 31.0 to 31.6°C within 3h of CHA injection and remained between 31.8 and 29.2°C for 24h before rewarming. Rats rewarmed within 5h after transfer to a Ta of 20°C, 4h after the last injection of CHA. Qualitative assessment of CA1 histopathology in TH treated rats indicated an absence of pathology; the CA1 in TH treated rats appeared similar to CA1 in naïve rats. Quantitative analysis by an observer unaware of treatment indicated that the number of healthy neurons in CA1 of TH treated rats was not statistically different from naïve rats, p=0.154, n=3-5.

Conclusion: Activation of CNS A1AR in animals exposed to a thermal gradient (Ta of 16°C) is a simple and effective means of inducing TH. Animals cooled in this manner survived cardiac arrest better than control treated animals and showed no evidence of histopathology in CA1 when compared to naïve rats. These results suggest that by mimicking mechanisms used by hibernating animals to cool it will be possible to administer therapeutic hypothermia in a highly effective, noninvasive and reversible manner.

Anderson, R., Sheehan, M. J. and Strong, P. (1994). Characterization of the adenosine receptors mediating hypothermia in the conscious mouse. Br J Pharmacol 113, 1386-90.

Barnes, B. M. (1989). Freeze avoidance in a mammal: body temperatures below 0 degree C in an Arctic hibernator. Science 244, 1593-5.

Dave, K. R., Prado, R., Raval, A. P., Drew, K. L. and Perez-Pinzon, M. A. (2006). The Arctic ground squirrel brain is resistant to injury from cardiac arrest during euthermia Stroke 37(5) 1261-5.

Drew, K. L., Rice, M. E., Kuhn, T. B. and Smith, M. A. (2001). Neuroprotective adaptations in hibernation: therapeutic implications for ischemia-reperfusion, traumatic brain injury and neurodegenerative diseases. Free Radic Biol Med 31, 563-73.

Hypothermia-after-Cardiac-Arrest-Study-Group. (2002). Mild therapeutic hypothermia to improve the neurologic outcome after cardiac arrest. N Engl J Med 346, 549-56.

Jinka, T. R., Toien, O. and Drew, K. L. (2011). Season primes the brain in an arctic hibernator to facilitate entrance into torpor mediated by adenosine A(1) receptors. J Neurosci 31, 10752-8.

Zgavc, T., Ceulemans, A. G., Sarre, S., Michotte, Y. and Hachimi-Idrissi, S. (2011). Experimental and clinical use of therapeutic hypothermia for ischemic stroke: opportunities and limitations. Stroke Res Treat 2011, 689290.

Supported by NIH R15NS070779 and P20GM103395.

Where applicable, the authors confirm that the experiments described here conform with The Physiological Society ethical requirements.

SA463

Waking to drink: rates of evaporative water loss determine arousal frequency in hibernating bats

M. Ben-Hamo and B. Pinshow

Mitrani Department of Desert Ecology, Ben-Gurion University of the Negev, Midreshet Ben-Gurion, Israel

Hibernation is an adaptive strategy in bats that facilitates coping with low ambient temperatures (T_a) and scarce food during winter. The decline in metabolic rate (MR) and body temperature (T_b) of a bat during hibernation brings about a significant reduction in nutrients and water use, enhancing the probability of survival (Geiser and Koertner, 2010). However, hibernation is not a constant state of reduced T_b and MR, rather it comprises bouts of torpor interspersed with periods of arousal, when the animal returns to its normothermic T_b and MR (French, 1985). Although, bats arouse for only 5-10% of the time that they hibernate, arousals can account for over 85% of a hibernating bat's energy expenditure (Wang, 1978). Many different hypotheses attempting to explain periodic arousals have been proposed (Thomas and Geiser, 1997); all relate arousals to processes, such as metabolism and water loss, that vary in the same direction with T_b and T_a. Consequently, they give rise to the same prediction, namely that torpor bout length (TBL) is negatively correlated with T_a and T_b. This correlation alone cannot establish a causal link between arousal and the proposed processes, and, in addition, it introduces a difficulty in distinguishing between the hypotheses. We tested the "water balance" hypothesis, first proposed by Fisher and Manery (1967) that asserts that hibernating animals continuously lose water through evaporation while hibernating, and the ensuing dehydration initiates arousals, during which the animal rehydrates by drinking (Thomas and Geiser, 1997).

We tested our hypothesis in groups of a small bat, Kuhl's pipistrelle (*Pipistrellus kuhlii*), that were all maintained at constant T_a and constant absolute humidity. We assumed that at constant T_a, bats have similar T_bs and MRs, and that water vapor density at the skin surface is saturated at skin temperature. We manipulated the difference in water vapor density (e_w) between the skin surface (e_s) and the adjacent ambient air (e_a) by changing e_a, and measured water loss in Kuhl's pipistrelles in both dry and humid air, at constant T_a.

We found that TBL and TEWL were significantly related in hibernating Kuhl's pipistrelles, independent of MR and/or T_a, supporting the water balance hypothesis, while distinguishing it from other hypotheses that relate processes correlated with MR, T_a, or both. We also found that arousal frequency during hibernation was positively related with the amount of body mass (m_b) lost during this period, suggesting that bats with higher rates of TEWL that awoke more frequently lost more m_b and thus end hibernation with smaller fat reserves. These results demonstrate the importance of TEWL in survival of overwintering bats. Most, if not all, temperate zone bats in both suborders, the Yangochiroptera and Yinpterochiroptera, are hibernators (Altringham, 2011). Therefore, due to the similarities in the ecological and behavioral characteristics of these animals, the possibility exists that what we found in *P. kuhlii*, a vespertilionid bat, may occur in other hibernating bat species of different families.

Altringham, J. D. (2011). Bats: from evolution to conservation. New-York: Oxford University Press.

Fisher, K. C. and Manery, J. F. (1967). Water and electrolyte metabolism in heterotherms. In Mammalian Hibernation, vol. 3 eds. K. C. Fisher A. R. Dawe C. P. Lyman and E. Schonbaumn), pp. 235-279. Edinburgh: Oliver & Boyd.

French, A. R. (1985). Allometries of the durations of torpid and euthermic intervals during mammalian hibernation - a test of the theory of metabolic control of the timing of changes in body-temperature. J. Comp. Physiol. B-Biochem. Syst. Environ. Physiol. 156, 13-19.

Geiser, F. and Koertner, G. (2010). Hibernation and daily torpor in Australian mammals. Australian Zoologist 35, 204-215.

Thomas, D. W. and Geiser, F. (1997). Periodic arousals in hibernating mammals: is evaporative water loss involved? Functional Ecology 11, 585-591.

Wang, L. C. H. (1978). Energetic and field aspects of mammalian torpor: The richardson's ground-squirrel. In Strategies in the cold, eds. L. C. H. Wang and J. W. Hudson), pp. 109-141. New York: Academic Press.

We thank Paloma Larrain for her laboratory and field assistance and all the laboratory members who were quiet and patient while the bats were in torpor close by. This research was done under permit 37066 from the Israel Nature and National Parks Protection Authority and under permit IL-71-12-2010 from the Ben-Gurion University committee for the ethical care and use of animals in experiments.

Where applicable, the authors confirm that the experiments described here conform with The Physiological Society ethical requirements.

SA464

Remodeling of cardiac excitation-contraction coupling in hibernation: comparison with heart failure

S. Wang

State Key Lab of Biomembrane and Membrane Biotechnology, Peking University College of Life Sciences, Beijing, China

Hibernating mammals survive winter season by periodically lowering their body temperature down to the freezing point. The hibernation regulation therefore means a great challenge to their cardiovascular systems. To elucidate the underlying adaptation, we compared the excitation-contraction (E-C) coupling in ventricular cardiomyocytes from hibernating (HGS) and awake (AGS) ground squirrels. Whole-cell voltage clamp showed that the current through L-type Ca2+ channels (LCC) was down-regulated in HGS compared with that in AGS. However, simultaneous recording of fluo-4 fluorescence revealed that the Ca2+ transient triggered by LCC current was not decreased. The gain of Ca2+-induce Ca2+ release (CICR) was thus enhanced remarkably in hibernation. To seek the molecular mechanisms, we investigated the intermolecular signaling between a single LCC and ryanodine receptors (RyRs). Loose-patch confocal imaging showed that the LCC-RyR coupling exhibited shortened latency and increased chance-of-hit in HGS. The enhancement of LCC-RyR signaling efficiency was not attributable to any difference in the Ca2+ contents in the sarcoplasmic reticulum (SR). Realtime PCR and western blot both revealed that the expression of junctophilin-2, a protein anchoring the RyR-residing SR to the LCC-residing T-tubules, was up-regulated in HGS. These data indicated hibernation comes with a regulation that enhances the efficiency of E-C coupling in heart cells. This molecular and functional remod-

eling is exactly opposite to that occurring in failing hearts, and thus provides an ideal research model for seeking new strategies against heart failure.

Where applicable, the authors confirm that the experiments described here conform with The Physiological Society ethical requirements.

SA465

Characterization and engineering of natural photoreceptors for optogenetic applications

G. Nagel

Univ. Wuerzburg, Wuerzburg, Germany

In order to study functioning of cells it is often helpful to disturb the cellular equilibrium and to analyze the consequences. Ideally this is achieved non-invasively and in a living organism. Light is an ideal medium for this purpose in translucent organisms but can also easily be applied via thin fibres in non-translucent animals. Light-sensitive proteins (photoreceptors) from one organism might render another one light-sensitive if expressed in specific cells. Photoreceptors from archaea, bacteria, and green algae were molecularly identified in recent years. We could show that some of them are ideal tools to manipulate animal cells by illumination. We showed that the Channelrhodopsins from the unicellular green alga C. reinhardtii are Light-gated cation channels which allow fast light-induced depolarization of the plasma membrane (1,2). Mutations led to a slower photocycle and therefore to Channelrhodopsins with higher light sensitivity. Neuronal expression of Channelrhodopsin-2 (ChR2) yields Light-induced action potentials and Light-manipulated behaviour in C. elegans (3) and other transgene animals. We demonstrated that the Light-activated chloride pump halorhodopsin (HR) from the archaeum Natronomonas pharaonis efficiently hyperpolarizes the plasma membrane and allows Light-induced silencing of neurons (4). These two antagonistic rhodopsins may even be expressed in the same cell and still specifically be light-activated with 460 nm for ChR2 and 580 nm for HR. Photoactivated Adenylyl Cyclases (PAC) from Euglena gracilis (5,6) or Beggiatoa spec. (7) are flavoproteins which quickly elevate cytoplasmic cyclic AMP by illumination with blue light in cultured cells and living animals or plants. Recently we identified and characterized a further bacterial PAC with high cAMP production.

Nagel G., D. Ollig, M. Fuhrmann, S. Kateriya, A.M. Musti, E. Bamberg, P. Hegemann (2002). Channelrhodopsin-1: a light-gated proton channel in green algae. Science 296: 2395-2398

Nagel, G, T. Szellas, W. Huhn, S. Kateriya, N. Adeishvili, P. Berthold, D. Ollig, P. Hegemann, E. Bamberg. (2003) Channelrhodopsin-2, a directly Light-gated Cation-selective Membrane Channel. Proc Natl Acad Sci U.S.A. 100:13940-13945

Nagel, G., M. Brauner, J.F. Liewald, N. Adeishvili, E. Bamberg, A. Gottschalk (2005) Light-activation of Channelrhodopsin-2 in excitable cells of Caenorhabditis elegans triggers rapid behavioral responses. Current Biology 15(24):2279-84.

Zhang F., L.-P. Wang, M. Brauner, J.F. Liewald, K. Kay, N. Watzke, P.G. Wood, E. Bamberg, G. Nagel, A. Gottschalk, and K. Deisseroth (2007) Multimodal fast optical interrogation of neural circuits. Nature 446:633-639

Schröder-Lang, S., M. Schwärzel, R. Seifert, T. Strünker, S. Kateriya, J. Looser, M. Watanabe, U. B. Kaupp, P. Hegemann, G. Nagel (2007) Fast manipulation of cellular cAMP level by light in vivo. Nat Methods 4(1):39-42

Looser J, Schröder-Lang S, Hegemann P, Nagel G. (2009) Mechanistic insights in light-induced cAMP production by photoactivated adenylyl cyclase alpha (PACalpha). Biol Chem. 390(11):1105-11

Stierl M, Stumpf P, Udwari D, Gueta R, Hagedorn R, Losi A, Gärtner W, Petereit L, Efetova M, Schwarzel M, Oertner TG, Nagel G, Hegemann P. (2011) Light-modulation of cellular cAMP by a small bacterial photoactivated adenylyl cyclase, bPAC, of the soil bacterium Beggiatoa. J Biol Chem. 286(2):1181-8

Funded by the German Research Society (DFG). I am indebted to my collaborators and coworkers, especially Ernst Bamberg (MPI Biophysik Frankfurt/M.), Karl Deisseroth (Stanford Univ.), Alexander Gottschalk (Univ. Frankfurt/M.), Ronnie Gueta (Univ. Würzburg), Peter Hegemann (Humboldt Univ. Berlin), Jens Looser (Univ. Würzburg), and Saskia Schröder-Lang (MPI Biophysik Frankfurt/M.).

Where applicable, the authors confirm that the experiments described here conform with The Physiological Society ethical requirements.

SA466

Towards the Dynamictome

A. Vaziri

Research Institute of Molecular Pathology (IMP) & Center for Molecular Biology, University of Vienna, Vienna, Austria

Knowledge on structural connectivity in neuronal circuits is necessary for understanding information representation and processing in local circuits. However, as some examples of well-characterized neuronal architectures illustrate, structural connectivity alone it is not sufficient to predict how input stimuli are mapped onto activity patterns of neuronal populations and how the collective dynamics of all neurons in the network leads to behavior. Addressing this challenge has been hampered by lack of appropriate tools and methods that allow parallel and spatiotemporally specific application of excitation patterns onto neuronal populations while capturing the dynamic activity of the entire network at high spatial and temporal resolution. I will discuss how the combination of new optical excitation techniques, optogenetics and imaging are providing new opportunities to address this challenge and move towards a dynamic map of neuronal circuits, the "Dynamictome".

Where applicable, the authors confirm that the experiments described here conform with The Physiological Society ethical requirements.

SA467

The use of optogenetics to probe the role of spontaneous rhythmic activity and cyclic AMP transients during in-vivo spinal motor circuit development

L.T. Landmesser, K.K. Kastanenka and Y. Maeno-Hikichi

Neurosciences, Case Western Reserve University, Cleveland, OH, USA

Developing spinal cords of birds and mammals exhibit rhythmic waves of spontaneous electrical activity during initial motor axon outgrowth. In chick embryos electroporated channelrhodopsin-2 can be activated in-ovo to chronically drive waves at different frequencies, avoiding the complication of altering frequency by drugs that affect different neurotrans-

mitter systems, as carried out in previous experiments. Motor axon pathfinding was found to be highly sensitive to the frequency of such waves, as modest decreases in frequency selectively affected the binary dorsal-ventral pathfinding decision and the expression of molecules involved in this guidance choice, while modest increases selectively disrupted the subsequent motoneuron pool-specific pathfinding choice. The ability to precisely control in-vivo wave frequency non-invasively by light should facilitate the elucidation of the intracellular signaling pathways underlying these divergent pathfinding choices and the extent to which the frequency versus the pattern of the waves is important. This approach should also aid in the discovery of other activity dependent aspects of spinal cord development. In the retina and spinal cord waves trigger Ca2+ transients which in turn generate transients of cAMP. To explore the role of cAMP transients we have used a light activated bacterial adenylyl cyclase to cause cAMP transients in cultured motoneurons and in intact spinal cords in-ovo. Such transients affected growth cone behavior of cultured motoneurons and generated spontaneous waves in isolated spinal cords and in intact embryos in-ovo. While additional experiments are needed these optogenetic tools should prove valuable in further characterizing the roles of Ca2+ and cAMP transients and their possible interactions in motor axon pathfinding and circuit development.

This work was supported by NIH grant R21 NS074199

Where applicable, the authors confirm that the experiments described here conform with The Physiological Society ethical requirements.

SA468

Optogenetical approach to reveal the regulatory mechanism of instinctive behaviors by the hypothalamic neurons

A. Yamanaka and T. Tsunematsu

Research Institute of Environmental Medicine, Nagoya University, Nagoya, Japan

IInstinctive behaviors, such as sleep/wakefulness, feeding and sexual behaviors are regulated by the hypothalamic neurons. Recent research revealed that the hypothalamic neurons containing neuropeptides are implicated in the regulation of these instinctive behaviors. It is essential to study neural regulatory mechanisms of these instinctive behaviors using a whole animal since these instinctive behaviors are exhibited only therein. Optogenetics enable control of the activity of specific type of neurons in the whole body animal using light. We apply optogenetics to Orexin/hypocretin-producing neurons (orexin neurons). Orexin neurons are located in the hypothalamus but project their efferents throughout the brain. Intriguingly, mice lacking the prepro-orexin gene showed behavioral characteristics similar to human sleep disorder "Narcolepsy", that is a fragmentation of sleep/wakefulness and sudden muscle weakness. Human clinical studies also showed that orexin neurons are specifically degenerated in the narcoleptic patient's brain. These results suggest that the orexin neurons play a critical role in the regulation of sleep/wakefulness. Previous studies using electrophysiological in vitro techniques have identified potential neuronal pathways or networks connecting orexin neurons with other neurons which are known to be involved in sleep/ wakefulness regulation. To apply optogenetics to orexin neurons, we generated transgenic mice in which specifically express halorhodopsin or Archaerhodopsin-3, a light driven neural silencer. In these mice brain more than 90% of orexin neurons express halorhodopsin or Archaerhodopsin-3. Acute inhibition of orexin neurons (~1hr) using optogenetics induced fragmentation of sleep/wakefulness in the early dark period (Figure), but not cataplexy-like behavioral arrest, which is characteristic symptom in narcoleptic patient. This result might suggest that chronic inhibition of orexin neurons might be caused to trigger cataplexy-like behavioral arrest. Our current research involves applying optogenetics in the hypothalamic peptide-containing neurons to reveal regulatory mechanisms of these instinctive behaviors.

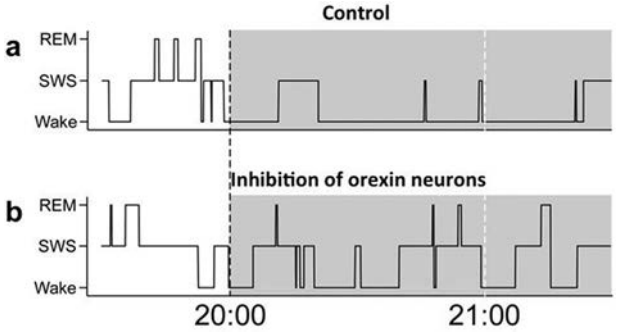

Tsunematsu, T. et al. Acute optogenetic silencing of orexin/hypocretin neurons induces slow-wave sleep in mice. J Neurosci 31, 10529-39 (2011).

This study was supported by the JST PRESTO program, Grant-in-Aid for Scientific Research on Innovative Areas "Mesoscopic Neurocircuitry" (23115103), Grant-in-Aid for Scientific Research (B) (23300142) (A.Y.).

Where applicable, the authors confirm that the experiments described here conform with The Physiological Society ethical requirements.

SA469

Optogenetic delivery of touch sense into peripheral and central nervous systems

H. Yawo[1,2], T. Honjoh[1,2], Z. Ji[1,2], Y. Yokoyama[1,2], A. Sumiyoshi[3], S. Ito[1,2], T. Ishizuka[1,2], R. Kawashima[3], H. Ohta[4] and Y. Fukazawa[5]

[1]Developmental Biology and Neuroscience, Tohoku University Graduate School of Life Sciences, Sendai, Japan, [2]JST, CREST, Sendai, Japan, [3]Institute of Development, Aging and Cancer, Tohoku University, Sendai, Japan, [4]Department of Physiology, National Defense Medical College, Tokorozawa, Japan and [5]Department of Anatomy and Molecular Cell Biology, Nagoya University Graduate School of Medicine, Nagoya, Japan

All knowledge about the world is perceived through our sensory systems which consist of peripheral sensory organs, sensory nerves and central nervous system (CNS). In principle a sensation is classified according to its modality, a kind of energy inducing physiological transduction in a specific group of sensory organs. For example, in the somatosensory systems, each mode of touch-pressure, temperature or pain is sensed by independent sensory endings of primary afferent neurons and conducted to the specific cortical locus as nerve impulses, but integrated thereafter as a whole. Although it has been anticipated that the peripheral sensory nerve endings would become photosensitive with the ectopic expression of photoreceptive molecules, it has never been proved with the mammalian systems. Could the animal sense light on its skin if the peripheral sensory nerve endings are photosensitive? In one of trans-

genic rat lines which express channelrhodopsin-2 (ChR2), one of algal photoreceptive molecules (1, 2), the light is sensed by skin through the touch-pressure sensitive nerve endings. We provided evidences for the first time that the sensory modality of the somatosensory system can be modified so as to be also reactive to light even in the rat.

We have previously generated several lines of transgenic rats which express ChR2 under regulation of Thy1.2 promoter (3). The transgene expression was variable from line to line, being dependent on the integration sites in chromosomes and/or the number of inserted copies (4). In one of these transgenic rat lines, W-TChR2V4, ChR2 was specifically expressed in a subpopulation of mechanoreceptive neurons in the dorsal root ganglion (DRG) but not in the small-sized neurons which are involved in nociception. Furthermore, ChR2 is also expressed in their peripheral nerve endings such as those innervating Merkel corpuscles and Meissner corpuscles, which are involved in the touch sense. Indeed, this transgenic rat showed a sensory-evoked behavior in response to blue flash light on their plantar skin as if it were touched by something. However, it ignores red light that is not sensed by ChR2. It is thus concluded that the rat has acquired an unusual sensory modality that it senses light at skin (5).

We also identified the expression of ChR2 in the peripheral endings of trigeminal mechanoreceptive neurons which innervate whisker follicles. Is a whisker-related sensory perception induced by the photostimulation of their follicles? To test this, the barrel cortex responses were examined using electrophysiological recordings and functional magnetic resonance imaging (fMRI). Under anesthesia with urethane, the whiskers were trimmed and connected with optic fibers of which other endings were connected to LEDs. Pulsative irradiation of blue LED light was used as a test and that of red LED light as control.

We found that the blue light irradiation of whisker follicles evoked enhanced unit activities as well as a local field potential in the barrel field of contralateral somatosensory cortex whereas the red light did not. The blue light irradiation also induced blood oxygenation level-dependent (BOLD) and cerebral blood volume (CBV) responses in the barrel field of contralateral somatosensory cortex. It is suggested that the optogenetic whisker stimulation could activate the whisker-barrel cortical pathway of mechanoreceptive signaling.

The light-evoked somatosensory would facilitate the study how the complex tactile perception such as form, movement, size and texture is generated. The various and reproducible patterned tactile stimulations could be easily made by the patterned illuminations on the whisker pad without using any mechanical instruments. Since our rat system does not express ChR2 in the nociceptive pathway, it enables one to do in vivo experiments without ethical problems. It would particularly beneficial for the researches using fMRI because the illumination system would not influence the magnetic fields. The light-evoked somatosensory perception should facilitate study of how the complex tactile sense emerges in the brain.

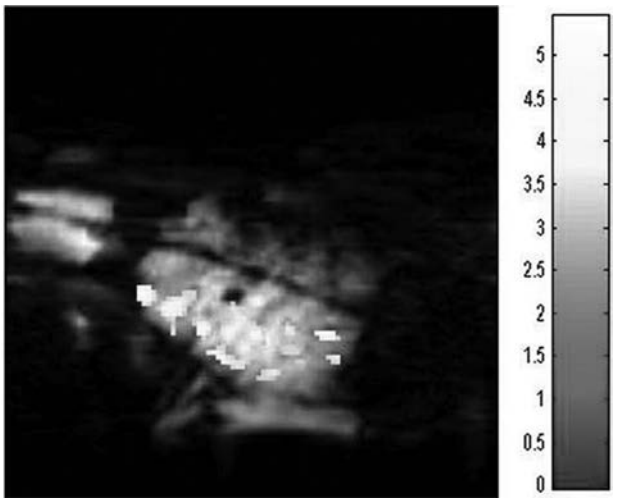

Nagel G, et al. (2003) Channelrhodopsin-2, a directly light-gated cation-selective membrane channel. Proc. Natl. Acad. Sci. USA 100:13940–13945.

Ishizuka T, et al. (2006) Kinetic evaluation of photosensitivity in genetically engineered neurons expressing green algae light-gated channels. Neurosci. Res. 54:85-94.

Tomita H, et al. (2009) Visual properties of transgenic rats harboring the Channelrhodopsin-2 gene regulated by the Thy-1.2 promoter. PLoS One 4: e7679.

Araki et al. (2005) Transgenic mouse lines expressing synaptopHluorin in hippocampus and cerebellar cortex. genesis 42:53–60.

Ji Z-G, et al. (2012) Light-evoked somatosensory perception of transgenic rats which express channelrhodopsin-2 in dorsal root ganglion cells. PLoS ONE 7:e32699.

Where applicable, the authors confirm that the experiments described here conform with The Physiological Society ethical requirements.

PCA001

Xanthohumol reduces transcription of pro-inflammatory markers TNF-α, IL-1β, NFκB2, and HO1 in the lung of senescence-accelerated prone mice (SAMP8)

S. Paredes[1], A. Carrasco[2], L. Rancan[2], R. Kireev[1], E. Vara[2] and J. F. Tresguerres[1]

[1]Department of Physiology, Complutense University of Madrid, Madrid, Spain and [2]Department of Biochemistry and Molecular Biology III, Complutense University of Madrid, Madrid, Spain

Lungs are highly vascularised organs directly exposed to atmospheric oxygen. Consequently, they are an important source of reactive species that seem to be involved in local defense against pathogens. With age, increased production of free radicals, together with a reduced antioxidant defense activity, may surpass the antioxidative capability of lungs, leading to lung damage and increasing susceptibility to other pathologies. Xanthohumol, the major prenylated chalcone found in hops, has been shown to present anti-inflammatory and antioxidant properties in several organs, including liver, brain, and at the level of the reproductive system. Its effect on the aging lung has yet to be elucidated. For this reason, the aim of the present study was to evaluate the possible anti-inflammatory role of xanthohumol on a model of male senescence-accelerated prone mice (SAMP8). Young and old animals, aged 2 and 10 months respectively, were maintained under a 12:12 h light-dark cycle in an environmentally-controlled room and fed ad libitum. They were divided into 4 experimental groups: Young non-treated, old non-treated, old treated with 1 mg/kg/day xanthohumol, and old treated with 5 mg/kg/day xanthohumol. Young and old non-treated male senescence-accelerated resistant mice (SAMR1) were used as controls. Xanthohumol was dissolved in ethanol and added to the drinking water. Only ethanol was administered to the water of non-treated animals. After 30 days of treatment, animals were sacrificed and lungs were collected and immediately frozen in liquid nitrogen. mRNA expression of tumor necrosis factor-alpha (TNF-α), interleukin-1 beta (IL-1β), nuclear factor NF-kappa-B p100 subunit (NFκB2), and heme oxygenase 1 (HO1) was measured by means of RT-PCR using the SYBR Green PCR Master Mix (Applied Biosystems, Warrington, UK) and 300 nM concentrations of specific primers. For the normalization of cDNA loading in the PCR reaction, the amplification of 18S rRNA for every sample was used. Relative changes in gene expression were calculated using the 2-ddCt method. Mean values were analyzed by ANOVA. Compared to the young animals, old non-treated SAMP8 mice presented significantly elevated ($P<0.05$) mRNA levels of TNF-α, IL-1β, NFκB2, and HO1. SAMR1 mice showed significantly decreased ($P<0.05$) mRNA levels of these pro-inflammatory markers in comparison with the old non-treated SAMP8 group. Treatment with xanthohumol was able to decrease significantly ($P<0.05$) the age-induced elevation at any of the doses administered. Supplementing the diet with foodstuffs containing xanthohumol may be used as a potential tool for counteracting inflammation and oxidative stress in the aging lung.

Where applicable, the authors confirm that the experiments described here conform with The Physiological Society ethical requirements.

PCA002

Melatonin decreases the expression of inflammation and apoptosis markers in the lung of a senescence-accelerated mice model

A. Puig[1], L. Rancan[1], S. Paredes[2], G. Yoldi[2], R. Kireev[2], E. Vara[1] and J. F. Tresguerres[2]

[1]Department of Biochemistry and Molecular Biology III, Complutense University of Madrid, Madrid, Spain and [2]Department of Physiology, Complutense University of Madrid, Madrid, Spain

Aging is associated with an increase in oxidative stress and inflammation. Aging lung is particularly affected to this damage since alveolar epithelial cells are continuously exposed to environmental oxidants and antioxidant machinery seems to be weakened with age. Melatonin is a potent free radical scavenger and broad spectrum antioxidant that has been shown to counteract inflammation and apoptosis in healthy cells. Its effect on aging lung is, however, not yet fully understood. Thus, the aim of the present study was to investigate the effect of the exogenous administration of melatonin on the mRNA expression of inflammation markers tumor necrosis factor-alpha (TNF-α), interleukin-1 beta (IL-1β), nuclear factor NF-kappa-B p100 subunit (NFκB2), heme oxygenase 1 (HO1) and apoptosis parameters Bcl-2-associated death promoter (BAD) and apoptosis inducing factor (AIF) in male senescence-accelerated prone mice (SAMP8). Young and old animals, aged 2 and 10 months respectively, were maintained under a 12:12 h light-dark cycle in an environmentally-controlled room and fed ad libitum. They were divided into 4 experimental groups: Young non-treated, old non-treated, old treated with 1 mg/kg/day melatonin, and old treated with 10 mg/kg/day melatonin. Young and old non-treated male senescence-accelerated resistant mice (SAMR1) were used as controls. Melatonin was dissolved in ethanol and added to the drinking water. Only ethanol was administered to the water of non-treated animals. After 30 days of treatment, animals were sacrificed and lungs were collected and immediately frozen in liquid nitrogen. mRNA expression was measured by means of RT-PCR using the SYBR Green PCR Master Mix (Applied Biosystems, Warrington, UK) and 300 nM concentrations of specific primers. For the normalization of cDNA loading in the PCR reaction, the amplification of 18S rRNA for every sample was used. Relative changes in gene expression were calculated using the 2-ddCt method. Mean values were analyzed by ANOVA. Old non-treated SAMP8 animals showed significantly increased ($P<0.05$) levels of TNF-α, IL-1β, NFκB2, and HO1 with respect to the values obtained in the young group. SAMR1 mice showed significantly decreased ($P<0.05$) mRNA levels of these pro-inflammatory markers in comparison with the old non-treated SAMP8 group. Melatonin treatment with either dose tested was able to reverse significantly ($P<0.05$) the aging-derived augmentation of these inflammatory markers. In addition, BAD and AIF expression rose with aging, the effect being significantly counteracted ($P<0.05$) with melatonin administration. Melatonin treatment may modulate the inflammatory and apoptosis status of the aging lung, exerting a protective effect on age-induced damage.

Where applicable, the authors confirm that the experiments described here conform with The Physiological Society ethical requirements.

PCA004

Ageing is associated with changes in structure and ion channel expression within the atrioventricular conduction axis

Y. Saeed, Z. Borbas, I. Temple, A. Atkinson, J. Yanni, M. Boyett, C. Garratt and H. Dobrzynski

Cardiovascular Research Group, University of Manchester, Manchester, UK

Introduction:The inferior nodal extension (INE), compact atrioventricular (AV) node and penetrating/His bundle (PB) form the AV conduction axis and are responsible for delay and propagation of the action potential from the atria to the ventricles. With ageing, dysfunction in these tissues results in prolongation of the PR interval and first, second and third degree AV block. The only treatment is implantation of permanent pacemakers, which are known to be associated with various complications. Previous studies have described age-related structural and functional changes in the AV conduction axis, but detailed examination of morphological changes (fibrosis and hypertrophy) as well as changes in ion channel expression with ageing have not been investigated.
Methods: We have compared the regions of the AV conduction axis (INE, compact AV node, CN, proximal PB, PPB and distal PB, His bundle) from 3 (n=9) and 24 (n=8) months old male rats (humanely killed in accordance with UK Animals Scientific Procedures Act 1986). From the survival curve, 3 months old rats correspond to 20 years old humans, whereas 24 months old rats correspond to ~70 years old humans. Morphological characteristics of these tissues were studied using serial cryosections and Masson's trichrome (MT) and picrosirius red (PR) histological stains and light and polarised microscopy. The expression of the ion channel HCN4 (responsible for pacemaking) and the gap junction channels Cx43 and Cx40 (responsible for electrical coupling between cardiac cells) was studied using immunofluorescence and confocal microscopy. Qualitative signal intensity of these channels was measured using Volocity software. Statistical analysis was performed using independent t test with SPSS version 20.1.
Results: At the structural level, we observed significant changes with ageing. MT staining showed that the cells of INE, CN, PPB and His bundle are more loosely packed and irregularly arranged in older animals. Age-dependent cellular hypertrophy was confirmed by a statistically significant increase in cell size across all regions of the AV junction. With ageing, total collagen content estimation showed a statistically significant increase in thin (but not in thick) collagen fibres in the CN, PPB and His bundle. Immunohistochemistry revealed a decrease in Cx43 expression in the INE (P=0.003), PPB (P=0.005), His bundle (P=0.02), but an increase in Cx40 expression in the INE (P=0.01) and CN (P=0.005) with ageing. There was also trend to downregulation of HCN4 expression especially in the His bundle (P=0.051).
Conclusion: Ageing is associated with structural changes of the AV junction tissues, which include fibrosis, hypertrophy and changes in Cx43 and Cx40 and possibly HCN4 expression. Our current findings may explain the prolongation of the PR interval with ageing observed in our previous study.1

1. Tellez et al. (2011) Experimental Physiology 96,1163–1178

Where applicable, the authors confirm that the experiments described here conform with The Physiological Society ethical requirements.

PCA005

Ageing has heterogeneous effects within the left ventricle and between genders on mRNA expression for key calcium-regulatory proteins

L.T. Cheah, K. Rostron, J. Wilkinson and M.K. Lancaster

School of Biomedical Sciences, University of Leeds, Leeds, UK

Progressive ageing associates with an increasing incidence of cardiac dysfunction and arrhythmias. Such problems are likely to be contributed to by changes in cardiac intracellular calcium regulation but findings are often inconsistent possibly due to a mix of sample types, ages, species and genders studied.
This study used quantitative PCR (qPCR) to assess expression of mRNA for proteins involved in cellular calcium regulation across the wall of the left ventricle (LV) in both genders at three age points: young (6 months), adult (12 months) and old (24 months). C57Bl6 mice (n=6 for each gender at each age) were euthanised by cervical dislocation and samples from the sub-endocardial (endo) and sub-epicardial (epi) LV free wall dissected. Following mRNA isolation, samples were subjected to qPCR with results normalised to GAPDH mRNA abundance. Data were assessed by Pearson correlation or ANOVA.
The effects of ageing on key transcripts are summarised in Table 1. The combined data showed significant negative correlations between age and mRNA expression for the L-type Ca^{2+} channel, D-type Ca^{2+} channel, the cacna1h isoform of the T-type Ca^{2+} channel, ryanodine receptors (RYR), phospholamban (PLB) and calcium-calmodulin dependent protein kinase 2 (CAMK2D). Analysing individual genders these age-associated declines were common to males and females for PLB but all other correlations were significant in males only, aside for that of the D-type Ca^{2+} channel decline which correlated with age only in females.
No regional heterogeneity of changes was observed in females. In contrast in males the cacna1h isoform of the T-type Ca^{2+} channel, and CAMK2D fell significantly with age in endo only, whilst a rise in calsequestrin mRNA was unique to this region. RYR mRNA fell in both endo and epi whilst PLB mRNA fell significantly only in epi. SERCA2a mRNA remained unchanged, as did that for the cacna1g isoform of the T-type Ca^{2+} channel, sarcolemmal Ca^{2+} pumps (PMCA1 and 4), sodium-calcium exchanger and sodium-potassium pump α1 isoform.
In conclusion, ageing has heterogeneous effects on mRNA transcript abundance for key regulatory proteins dependent on gender and ventricular region. The majority of changes were observed in the male heart alone where increasing heterogeneity of expression across the LV wall may predispose to dysfunction and arrhythmias.

Table 1: Percentage Change in mRNA Abundance with Ageing

	L-type Ca^{2+} channel	T-type Ca^{2+} channel (Cacna1h)	T-type Ca^{2+} channel (Cacna1g)	RYR	PLB	SERCA2a	CAMK2D
Combined	-17.7±14.5*	-45.5±26.0*	+4.7±25.2	-28.5±12.5*	-26.4±4.7*	-1.8±8.3	-17.5±8.2*
Male	-22.4±13.2	-50.4±22.5*	+1.4±9.9	-42.6±10.0*	-30.9±4.2*	+7.5±7.6	-18.7±13.6*
Female	-12.8±16.1	-34.8±15.4	+8.2±14.3	-11.1±8.8	-21.3±5.7*	-7.2±9.5	-16.1±11.1
Male-endo	-19.6±11.9	-56.1±17.1^	+62.1±18.4	-37.0±13.4^	-12.1±39.5	+18.3±4.7	-23.5±4.9^
Male-epi	-24.4±14.8	-32.3±41.3	-7.4±12.3	-46.6±10.3^	-46.6±10.6^	+3.6±13.9	-13.0±6.5

Data are mean ± standard deviation

* = significant correlation with age ($p<0.05$), ^ = significant difference from young ($p<0.05$)

Where applicable, the authors confirm that the experiments described here conform with The Physiological Society ethical requirements.

PCA007

The effects of velocity and temperature on swimming performance in rainbow trout (Oncorhynchus mykiss)

A. Keen, E. John, H. Shiels and R. Nudds

Faculty of Life Sciences, University of Manchester, Manchester, UK

The reproductive success of many salmonid species relies on successful migration to natal spawning grounds. Energy efficient locomotion, dictated by cost of transport (COT), may be an important selection pressure for completion of migratory routes. In addition, climate change poses further difficulties for migration due to elevated temperatures and varying water velocities. To explore how temperature affects efficiency of locomotion, rainbow trout (Oncorhynchus mykiss) were subjected to a modified critical swimming speed (UCrit) test, while oxygen consumption (MO2) and swimming form were recorded, at acclimation (11°C) and high (20°C) temperature. Calculation of strouhal numbers (St) enabled gait change to be assessed in terms of swimming efficiency and performance. Increasing temperature from 11-20°C gave a large increase in oxygen consumption (Q10 = 1.67). Incremental increase in swimming speed (from 1 Bl s-1 to UCrit) resulted in further increases in oxygen consumption (349.942 ± 53.02 and 423.185 ± 51.5 1mg O2 kg-1 h-1 for controls and high temperature, respectively). However, the rate of MO2 increase with increasing water velocity was not different between the two temperature groups, or at different gaits. As previously shown, tail beat frequency and amplitude increased to accommodate greater speed, up to the onset of burst and glide gait, but at high speeds tail beat amplitude alone was modulated. Rainbow trout swum within the strouhal number range for optimum propulsive efficiency (0.2 < St < 0.4), as seen in numerous animals. Increased velocity and gait change did not affect strouhal numbers at low temperature. However, at high temperature strouhal number increased with speed, due to an augmented tail beat frequency at high temperature. This result suggests a higher muscle twitch rate at high temperature, in agreement with previous muscle physiology data.

Where applicable, the authors confirm that the experiments described here conform with The Physiological Society ethical requirements.

PCA008

Anemia in medical students and its relationship with heart rate variability

K. Agrawal[1], B.H. Paudel[1], R. Khadka[1], N. Upadhyay[1], S.K. Dev[1] and S.N. Majhi[1,2]

[1]Physiology, BPKIHS, Dharan, Nepal, Dharan, Nepal and [2]Biochemistry, B.P. Koirala Institute of Health Sciences, Dharan, Nepal

Anemia is prevalent in pregnant ladies. It is also common in college girls and other age groups of female. Anemia has been found to be associated with low heart rate variability (HRV) indicating increased cardiac risk. Medical students are under stress, which may affect both the hemoglobin level and HRV. Thus, we aimed to assess the hemoglobin, iron status, and HRV. A cross-sectional comparative study was conducted on 40 unmarried female medical students of age 18-30 years. They were divided into three groups based on hemoglobin (Hb) level following WHO guidelines: normal Hb group (Hb≥12g/dl), mild anemia (Hb<11.9-10.0g/dl) and moderate anemia (Hb 9.9-7.0g/dl). Their mean corpuscular volume, RBC counts and ferritin levels were measured. Short-term heart rate variability and cardio-respiratory variables were recorded in all subjects after 15 min of supine rest and compared among the groups. The relationship between HRV and blood parameters was studied using Spearman's Rank correlation. Kruskal Wallis followed by multiple comparisons was applied to compare the variables of blood and HRV among the groups. According to Hb level, 17.5% students were moderately anemic, 50% were mild anemic and 32.5% were with normal Hb level. They were comparable in terms of their age, BMI, diastolic blood pressure and heart rate. However, systolic blood pressure [92(90.0-110.0) mmHg vs. 110(108.5-112) mmHg, p=0.022] and respiratory rate [18(16-18) per minute vs. 20(19-22) per minute p= 0.001] were lower in moderate anemic group compared to normal group. Also systolic blood pressure [92(90.0-110.0) mmHg vs. 110(102-110) mmHg, p= 0.042] was lower in moderate anemic group than mild anemic group. The Hb level, RBC count, MCV, and ferritin levels { [9.2 (9.0-9.8) g/dl vs. 11.0 (10.17-11.45) g/dl vs. 12.4(12.0-12.65) g/dl, p= 0.001], [3.7(3.5-3.7) per mm3 vs. 4.0(3.9-4.1) per mm3 vs. 4.2(4.11-4.36) per mm3, p= 0.001], [77.94(77.29-82.97) fl vs. 85(78.76-88.7) fl vs. 90.06(86.33-92.54) fl, p= 0.01] and [7.9(6.5-19.4) ng/ml vs. 18.85(15.85-38.0) ng/ml vs. 28.9(17.3-44.7) ng/ml p=0.01]} respectively were lower in moderate anemic group than mild anemic and normal groups. However, there were no significant differences in HRV parameters among the groups, and no significant correlations were obtained between HRV and blood parameters. Moderately anemic female medical students had lower systolic BP and respiratory rate compared to mildly anemic female medical students. However, there were no significant differences in HRV parameters among the groups. It indicates mild and moderate anemia may not have effect on cardiac autonomic modulation in this female age group.

All the students, junior residents, computer staff and all who helped me directly or indirectly.

Where applicable, the authors confirm that the experiments described here conform with The Physiological Society ethical requirements.

PCA009

Stimulation of M2-cholinoreceptors increases the outward current of sodium-calcium exchanger in fish atrial myocytes

D.V. Abramochkin[1,2], S.V. Tapilina[1] and M. Vornanen[3]

[1]Department of Human and Animal Physiology, Moscow State University, Moscow, Russian Federation, [2]Department of Fundamental and Applied Physiology, Russian National Research Medical University, Moscow, Russian Federation and [3]Department of Biology, University of Eastern Finland, Joensuu, Finland

Sodium-calcium exchanger (NCX) plays crucial role in regulation of cardiac calcium homeostasis and provides a key ionic current (I_{NCX}) involved into pacemaker activity of sinoatrial cardiomyocytes. However, modulation of I_{NCX} by autonomic neurotransmitters, which contribute to regulation of cardiac performance, still remains questionable. The present study provides the first evidence for direct modulation of I_{NCX} via muscarinic receptors. In atrial cardiomyocytes of crucian carp (*Carassius carassius L.*) and rainbow trout (*Oncorhynchus mykiss W.*) muscarinic agonist carbacholine (Cch, 10^{-6}-10^{-4}M) produced a strong increase of the outward I_{NCX} without any

changes in the inward I_{NCX}. A selective blocker of I_{NCX}, KB-R7943 (10^{-5} M), abolished the basal I_{NCX} (both inward and outward current), which was registered in the absence of Cch, as well as the Cch-induced outward I_{NCX}. In ventricular myocytes from both studied species even the high concentration of Cch (10^{-4} M) was completely ineffective due to the putative absence of muscarinic receptors. On the contrary, in the atrial cells muscarinic antagonist atropine (10^{-6} M), which blocks M-receptors without any subtype selectivity, completely eliminated the response of outward I_{NCX} to Cch, but did not affect the basal I_{NCX}. A selective antagonist of M2 cholinoreceptors, AF-DX 116 (2×10^{-7}M) and a M3 antagonist, 4-DAMP (10^{-9} M), decreased Cch-induced current by 84.4% and 16.6% respectively. Pertussis toxin, which irreversibly inhibits G_i-protein coupled to M2 receptors, reduced the Cch-induced I_{NCX} by 95%, when applied into the pipette solution. The present results indicate a vectorial cholinergic stimulation of I_{NCX} in fish atrial myocytes, predominantly mediated by M2 cholinoreceptors. We conclude that the selective stimulation of the outward component of I_{NCX} by M2 cholinoceptors represents a new molecular target for the cardiac parasympathetic innervations, which is present at least in fish myocardium.

This work was supported by the Academy of Finland to MV (project No. 14795), the Russian Foundation for Basic Research [12-04-31737] and the Russian Ministry of Education and Science [State Contract 12.741.12.0151] to DA. The authors thank Anita Kervinen for skillful technical assistance.

Where applicable, the authors confirm that the experiments described here conform with The Physiological Society ethical requirements.

PCA010

Oral contraceptive-induced impaired glucose tolerance is associated with elevated plasma uric acid, triglyceride/high-density lipoprotein-cholesterol ratio but not with high C-reactive protein levels in female rats

L.A. Olatunji[1], S.A. Biliaminu[2], A.A. Safiriyu[1], O.A. Adeyanju[1], T.M. Abiodun[1] and A.O. Soladoye[1]

[1]Physiology, University of Ilorin, Ilorin, Kwara, Nigeria and [2]Chemical Pathology & Immunology, University of Ilorin, Ilorin, Kwara, Nigeria

Women are exposed to estrogen and/or progestogen through several means such as hormonal contraceptives and hormone replacement therapies. The cardiometabolic effects of using oral contraceptive (OC) in particular are still inconclusive (1). High C-reactive protein (C-RP), uric acid (UA) as well as triglycerides (TG)/high-density lipoprotein cholesterol (HDL-C) ratio are now widely accepted as salient atherosclerotic risk indicators, independently predicting future cardiovascular events (2-4). The present study therefore sought to determine the effects of combined OC steroids on C-RP, UA and TG/HDL-C ratio in a female rat model with impaired glucose tolerance. Twelve female Wistar rats weighing between 120 and 180g were randomly allotted to OC-treated (n=6) and vehicle-treated (n=6) groups. OC-treated rats received a combination of OC steroids (15.0 μg norgestrel and 1.5 μg ethinyl estradiol/rat; NEE, p.o.) while vehicle-treated rats were given distilled water (0.3ml/rat, p.o.) daily for 6 weeks. Rats had unrestricted access to food and water. An oral glucose tolerance test was performed after 12-hour overnight fast, and glucose tolerance was expressed as a function of the area under the tolerance curve (AUC). Values are means ± S.E.M., compared by independent t-test. When compared with the vehicle-treated rats, OC treatment led to significant decreases in glucose tolerance (AUC: 288.8±12.5 vs. 398.5.4±10.2mg/dl, $p<0.05$), circulating 17β-oestradiol (13.1±0.2 vs. 4.8±0.8pg/ml, $p<0.05$) and testosterone (0.38±0.02 vs. 0.11±0.03ng/ml $p<0.05$). On the other hand, there were significant increases in plasma UA (181.6±11.2 vs. 483.0±14.9μmol/L, $p<0.05$), TG (89.2±7.3 vs. 156.1±11.2mg/dl, $p<0.05$), TG/HDL-C ratio (1.8±0.2 vs. 3.2±0.1, $p<0.05$) with OC treatment. However, fasting blood glucose, plasma total cholesterol (TC), low-density lipoprotein-cholesterol (LDL-C), HDL-C, TC/HDL-C ratio, C-RP, total protein and albumin levels were not significantly affected by OC treatment. These results demonstrate that OC-induced impaired glucose tolerance is associated with high plasma UA and TG/HDL-C ratio, but not with increased plasma C-RP level. The findings imply that dyslipidemia associated with OC-induced impaired glucose tolerance may promote atherosclerotic complications, and that plasma level of UA but not that of C-RP may be an important factor to be monitored during OC use.

Grimes D.A. and Lobo R.A. Obstet Gynecol 2002, 100: 1344–1353.

Ridker P.M. Circulation 2001, 103: 1813–1818.

Bos M.J., Koudstaal P.J., Hofman A., Witteman J.C. and Breteler M.M. Stroke 2006, 37: 1503–1507.

Zoppini G., Targher G., Negri C., Stoico V., Gemma M.L. and Bonora E. Atherosclerosis 2010, 212: 87–291.

The authors appreciate the laboratory assistance of Mrs Dipe Olawale-Bello.

Where applicable, the authors confirm that the experiments described here conform with The Physiological Society ethical requirements.

PCA011

The effects of blood components modulation on load-dependent cardiac function during an acute hemodilution

S. Chatpun[1] and P. Cabrales[2]

[1]Institute of Biomedical Engineering, Prince of Songkla University, Hatyai, Songkhla, Thailand and [2]Bioengineering Department, University of California, San Diego, La Jolla, CA, USA

Modulation of blood components, both red blood cells and plasma, particularly affects on circulatory system. This study investigated the load-dependent cardiac function and systemic changes after normovolemic hemodilution with four different transfusion fluids in anesthetized Golden Syrian hamsters. The investigation was performed in anesthetized 60–70 g male Golden Syrian hamsters. Animal handling and care followed the US National Institute of Health Guide for Care and Use of Laboratory Animals. Twelve hamsters were randomly divided into 4 groups (n=3 for each group). Anesthesia was induced by intraperitoneal injection of sodium pentobarbital (50 mg/kg) and core body temperature was maintained using a heating pad. Animal surgical preparation included: (i) left jugular vein for transfusion fluid injection, (ii) right common carotid artery for a pressure-volume conductance catheterization, (iii) left femoral artery for blood withdrawal, and (iv) tracheotomy with polyethylene-90 tube to facilitate spontaneous breathing. Normovolemic hemodilution was performed by the exchange of 40% of the animal's blood volume with transfusion fluid. Four different transfusion fluids included 3-week stored blood, dextran 70 kDa (viscosity 3.0 cP), low viscosity plasma volume expander (LVPE; 2% dextran 2000 kDa, viscosity

2.2 cP), and high viscosity plasma volume expander (HVPE; 6% dextran 2000 kDa, viscosity 6.4 cP). Left ventricular cardiac systolic function was quantitatively assessed with a pressure-volume conductance catheter. Values are means ± S.D., compared by ANOVA. Plasma viscosity after hemodiluted with HVPE was 2.12±0.10 CP after hemodilution while other groups were 1.01±0.10 (stored blood), 1.27±0.03 (dextran 70 kDa) and 1.21±0.05 cP (LVPE). Cardiac output at the end of experiment increased from baseline in the group hemodiluted with HVPE (10.35±2.38 ml/min at baseline vs 13.10±4.02 ml/min at the end of experiment) and dextran 70 kDa (10.685±2.62 ml/min at baseline vs 12.49±1.64 ml/min at the end of experiment). On the other hand, cardiac output in the group hemodiluted with LVPE was less than baseline (13.11±0.49 ml/min at baseline vs 10.96±0.91 ml/min at the end of experiment) that was similar to the group exchanged with stored (8.40±3.49 ml/min at baseline vs 6.76±2.85 ml/min at the end of experiment). Stroke work relative to baseline in the group hemodiluted with HVPE significantly increased compared to those in the group hemodiluted with LVPE (HVPE: 1.23±0.14 vs. LVPE: 0.81±0.15, $p<0.05$). These data suggest that modulation of plasma expander viscosity affects load dependent cardiac function. Stored blood reduces load dependent cardiac function when compared to baseline condition.

The authors thank Cynthia Walser for the surgical preparation of the animals.

Where applicable, the authors confirm that the experiments described here conform with The Physiological Society ethical requirements.

PCA012

Effects of class III anti-arrhythmic agents with hERG channel block and facilitation on cardiac action potential: a simulation study

K. Furutani, K. Tsumoto, I. Chen and Y. Kurachi

Department of Pharmacology, Osaka University Graduate School of Medicine, Suita, Osaka, Japan

Potassium channels encoded by human ether-a-go-go-related gene (hERG) underlie the rapidly activating component of the delayed rectifying potassium current (IKr) in heart and play an important role in terminating the cardiac action potential (AP) (Sanguinetti & Tristani-Firouzi, 2006). hERG channel has been shown to be the target of class III anti-arrhythmic agents. It has also become clear that hERG channel is blocked by compounds with high pro-arrhythmic risk. The unintended block of hERG channel causes an acquired form of QT interval prolongation, worsens transmural dispersion of repolarization and forms the substrate for generation of life-threatening cardiac arrhythmias, including torsades de pointes. Recently, we have experimentally demonstrated a dual effect of some anti-arrhythmic agents, such as nifekalant, on hERG channel (Hosaka et al., 2007; Furutani et al., 2011). Besides blocking hERG channel, these compounds can facilitate its activation. To assess the clinical relevance of hERG channel modulations by compounds, we conducted simulations of cardiac AP in a modified Luo-Rudy model with hERG channel block and facilitation, using our experimental data of nifekalant. Then, we found that the hERG channel block prolonged action potential duration (APD) in the block conditions both with and without facilitation. In addition, the refractory period in both conditions equally increased from control condition so that the ectopic cell excitation is suppressed, suggesting that even if hERG channel blocker has facilitation effect, anti-arrhythmic efficacy of the drug is equivalent to that of pure blocker. As in our simulation, we could observe an early afterdepolarization (EAD) when both IKr and the slowly activating component of the delayed rectifying potassium current (IKs) were blocked. Importantly, facilitation mechanism prevents hazardous prolongation of APD and the induction of EAD by accelerating the repolarization rate via an increase in IKr during prolonged phase 3. Therefore, anti-arrhythmic agents that has both block and facilitation effects on hERG channel may have a lower risk for inducing EADs and triggered activity and thus be more suitable for the treatment of arrhythmias than pure hERG blocker.

Sanguinetti MC and Tristani-Firouzi M (2006). Nature 440, 463-469.

Hosaka Y et al. (2007). Channels 1, 198-208.

Furutani K et al. (2011). Biochem Biophys Res Commun 415: 141-146.

Where applicable, the authors confirm that the experiments described here conform with The Physiological Society ethical requirements.

PCA013

Ischemia-induced subcellular remodeling of sodium channels as a mechanism of ventricular proarrhythmia by class-I antiarrhythmic drug

K. Tsumoto[1], T. Ashihara[2], R. Haraguchi[3], K. Nakazawa[3] and Y. Kurachi[1]

[1]Osaka University, Suita, Japan, [2]Shiga University of Medical Science, Otsu, Japan and [3]National Cerebral and Cardiovascular Center Research Institute, Suita, Japan

Background: Na channel blockade has a long history used for the treatment of symptomatic ventricular premature contractions and tachycardia. However, the Cardiac Arrhythmia Suppression Trial (CAST) in patients with old myocardial infarction showed that class-I antiarrhythmic drugs have proarrhythmic effects, resulting in poor prognoses. So far, the arrhythmogenic mechanisms by the Na channel blockade are not well-known. Methods: To clarify this issue, we conducted simulations of action potential propagation in a myofiber model incorporating the electric field mechanism (taking into account the intercellular cleft potentials). Since it is recently reported that Na channels are confined to intercalated discs of surviving myocytes (lack of Na channels in lateral cell membrane) in the ischemic border zone, we incorporated the intracellular remodeling of Na channels into the model.
Results: We found that the intracellular remodeling of Na channels in myocytes located at ischemic border zone contributed to conduction slowing. In addition, conduction block tended to occur in the ischemic border zone when numerically administered Na channel blockade to the myofiber model, but this was not the case when the Na channels were distributed over the entire cell membrane.
Conclusion: Ischemia-induced intracellular remodeling of Na channels might be partly responsible for the proarrhythmic effects of Na channel blockade in patients with old myocardial infarction.

Where applicable, the authors confirm that the experiments described here conform with The Physiological Society ethical requirements.

PCA015

Cardiac-targeted deletion of Cα subunit of PP2A in mice caused dilated cardiomyopathy with electrical remodeling

D. Dong[1], J. Liu[1], Z. Zhu[1], W. Chen[1], P. Gu[2], X. Gao[2] and Z. Zhang[1]

[1]Jiangsu the Key Laboratory for Molecular and Medical Biotechnology, College of Life Science, Nanjing Normal University, Nanjing, Jiangsu, China and [2]Model Animal Research Center, Nanjing University, Nanjing, Jiangsu, China

Reversible phosphorylation governed by kinases and phosphatases is a crucial post-translational modifications of the protein functions. Dysregulation of protein phosphorylation has been linked to a host of dysfunctional and arrhythmic heart diseases(1, 2). We have previously observed that the mice with cardiac-tagerted deletion of Cα subunit of PP2A (KO) generated with C57BL/6J mice by Gu et al(3), developed dilated cardiomyopathy at the postnantal day 11 and died around the day 13. The goal of present study was to analyse patterns of cardiac electrical remodeling in KO mice. The mice at 9 to 11 days after birth were anaesthetised with avertin (240 mg/Kg, i.p.) or phenobarbitol sodium (40mg/Kg, i.p.) for echocardiographic meaurements (n=3 respectively, for each group) or for the heart dessection. Values are means ± S.E.M, compared by Student's paired *t*.-test or ANOVA followed by a *q*. test. As compared to control, cardiac hypertrophy was evidenced by the increases in left ventricle to body weight ratio and left ventricle mass, by the significant elevation of mRNA expression for ANP, BNP and β-MHC, by the increase in both end of diastolic and end of systolic volumes for left ventricles as well as by the decrease in the fractional shortening and ejection fraction in KO mice ($P<0.05$). In addition to morphological changes observed in HE staining, notable ultrastructural alterations in KO myocytes were illustrated in TEM analysis. Moreover, electriophysiological recordings indicated that the duration of APs in KO myocytes were markedly prolonged as compared with those in control ($P<0.01$ KO vs control, n=9 and 7 cells, respectively, from at least 3 to 4 mice for each group). In contrast, no changes were observed in RPs and other parameters of APs. Consequently, a significant reduction of transient outward K^+ currents and intermediate increase of L-type Ca^{2+} currents were documented in KO myocytes ($P<0.05$ KO vs control, n=7 and 5 respectively). In consistence with changes in ion currents, an upregulation of Cav1.2, whereas down-regulations of Kv4.2, Kv4.3, Kv1.4 and KChIP2 proteins co-accembling α and β subunites of transient outward K^+ channel were detected by western blot analysis (from 3 independent expreiments). Importantly, the increased phosphorylation of Cav1.2 Ca^{2+} channels in KO mice was demonstrated by immunohistochemistry and western blot analysis in comparasion with those of control (n=3 for each, $P<0.05$). Taken together, these findings are indicative of the fundamental role of PP2A in the mouse heart and imply that loss of PP2A may disturbant Cav1.2 phosphorylation and intracellular Ca^{2+} concentration and then, causes cardiomyopathy along with electrical remodeling.

Dai S, Hall DD & Hell JW (2009). *Physiol Rev* .89:411-452.

Olsen JV *et al.*. (2006). *Cell*.127:635-648

Gu P *et al.*. (2012).).*Genesis*. 50:429–436

This project was supported by 973 Program (2006CB943503), NSFC (30871228, 31171302) and PAPD (164320H106).

Where applicable, the authors confirm that the experiments described here conform with The Physiological Society ethical requirements.

PCA017

The role of fibre orientation in cardioversion of chronic atrial fibrillation: a simulation study

S.R. Kharche[1], T. Stary[1], I.V. Biktasheva[2], H. Zhang[3] and V.N. Biktashev[1]

[1]Department of Applied Mathematics, College of Engineering, Mathematics and Physical Sciences, University of Exeter, Exeter, UK, [2]Department of Computer Science, University of Liverpool, Liverpool, UK and [3]Department of Physics, University of Manchester, MANCHESTER, LANCS, UK

Fiber orientation anisotropy in the human atria influences the success of electrical cardioversion. This computational study quantifies the effectiveness of a feedback controlled cardioversion method [1] using a novel cardiac simulation environment, BeatBox [2].

A biophysical human atrial cell model [3] was adopted to simulate Control and chronic atrial fibrillation (CAF) action potentials (APs). Electrophysiological alterations due to CAF were simulated as described previously [4]. The cell model was combined with human atrial geometry with fiber orientation to construct a 3D realistic human atrial model. Scroll waves were initiated using a phase distribution method and allowed to evolve for 10 s. The cardioversion parameters [1] of threshold stimulus and low energy stimulation strength required for scroll wave termination were evaluated. Scroll waves were initiated at two sites to elicit the effects of scroll wave location. The obtained results were compared a previous isotropic case study [5].

CAF reduced the AP from 306 ms to 120 ms (Fig 1, A). Scroll waves were initiated at two locations and the electrical activity registered at a point registration electrode (Fig 1, B). Under CAF isotropic conditions, the scroll waves became pinned (Fig 2, A). In contrast, anisotropy caused the scroll wave to degenerate into multiple scrolls with each scroll evolving erratically or pinning to anatomical defects (Fig 2, A). Recurrence cycle maps (Fig. 2, B) show that under CAF isotropy leads to a monomorphic tachycardia while with anisotropy gives rise to a polymorphic tachycardia. The single shock stimulation threshold to eliminate CAF scroll waves was found to be 4.5 pA/pF. For CAF scroll waves initiated at location L1 (Fig 1, B), a series of small amplitude global stimuli of strength 0.4 pA/pF were sufficient in terminating the scroll waves. However CAF scroll waves initiated at L2 required a minimum stimulation strength of 2 pA/pF for termination within 10 s. In all CAF simulations, the localized pacing at the registration electrode was approximately 8 Hz.

Inherent atrial anisotropy plays an important role in atrial electrical properties. The low energy stimulus strength has a strong correlation to the scroll wave location. The low energy stimulation strength was always lower than the threshold stimulus. Anisotropy aggravates CAF and leads to high frequency erratic propagations. The efficacy of cardioversion is significantly affected by anatomical defects as well as anisotropy. The novel multifunction simulation package, BeatBox, is an ideal simulation environment that facilitates such extensive large scale simulation studies.

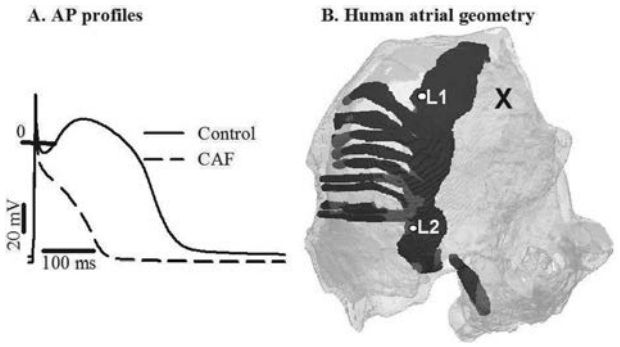

Fig 1. A: Human atrial AP profiles. B: Atrial geometry with isotropic tissue (translucent), and conduction pathways with fiber orientation (black). The initiation sites (L1 and L2) and the registration electrode location (marked by "X") are also shown.

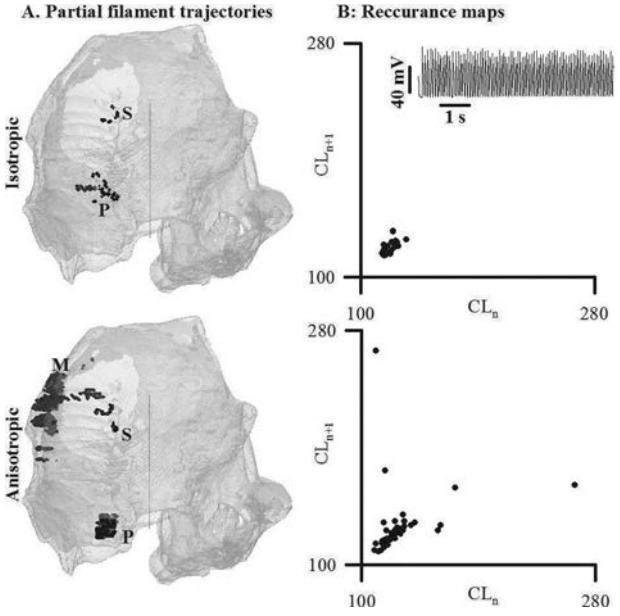

Fig. 2. Filament traces of CAF scroll waves with isotropic in the top row and anisotropic in the bottom row. A: Filament trajectories at the initial (S), meandering (M) and pinned (P) stages of the 10 s simulations. B: Recurrence maps of simulations shown in A. Representative AP recording is shown inset.

Biktashev VN & Holden AV. (1994). *J Theor Biol*, **169**, 101-112.

McFarlane R &Biktasheva IV (2008) *Visions of Computer Science— BCS International Academic Conference.* pp. 99-109.

Courtemanche M et al. (1998). *Am J Physiol.* **275 (1)**, H301-H321.

Morgan SW et al. (2009). *Biophys J*, **96**, 1364-1373.

Kharche SR et al. (2012). *Computing in Cardiology* **39**, 133-136.

EPSRC (EP/I029664/1, EP/I029826/1, EP/I030158/1), EU PRACE Introductory HPC Access (PRPB09, 2012).

Where applicable, the authors confirm that the experiments described here conform with The Physiological Society ethical requirements.

PCA018

Simulating cell apoptosis induced sinus node dysfunction

S.R. Kharche[1], T. Stary[1], I.V. Biktasheva[2], H. Zhang[3] and V. Biktashev[1]

[1]CEMPS, University of Exeter, Exeter, UK, [2]Computer Science, University of Liverpool, Liverpool, UK and [3]Physics, University of Manchester, MANCHESTER, LANCS, UK

Sinus node dysfunction (SND) is a known cause of bradycardia, sinus arrest, and sinus pause, and leads to subnormal atrial pacing. Experimental evidence shows that SND is correlated to the pacemaker sinoatrial node (SAN) cell apoptosis [1]. The effect of such a dysfunctional SAN on electrical propagation into neighboring atrial tissue remains under explored. A novel computational cardiology simulation environment, BeatBox [2], which provides a versatile computational tool to develop and construct simulation models and was used in this study.

The computationally efficient Fenton-Karma (FK) model [3] was extended to simulate mouse SAN and atrial cell action potentials (APs). To simulate atrial AP, the basal model parameters [3] were altered. Further, a hyperpolarisation activated current was incorporated into the basal model, and then the parameters altered to simulate the SAN pacemaking AP. The cell models were incorporated into a 2D model consisting of a central SAN region surrounded by atrial tissue. In each 2D simulation, 10 s of electrical activity were simulated. First, the basal size of mouse SAN pacemaking region was estimated using the 2D model. Then in multiple simulations, SAN cell apoptosis was simulated by randomly eliminating a proportion of SAN cells from the pacemaking region. The effects of an increasing proportion of apoptotic pacemaker cells on atrial tissue pacing were simulated and quantified.

The modified FK model that reproduces SAN and atrial APs as well as validation with experimental observations is shown in Fig. 1. The SAN size that gave a basal mouse atrial cycle length (ACL) of 295 ms was found to be 0.6 mm in radius. In the simulations where pacemaker cell apoptosis was considered (Fig. 2), a more dramatic effect was seen. At low pacemaker cell apoptosis proportion, there was a drastic increase of ACL. At modest increase in the number of apoptotic cells, bradycardia was observed. The incidence of sinus arrest was also found to be high. When the numbers of apoptotic cells were 10% of the total number of pacemaking cells, all pacemaking was arrested. Our computational findings agree with recent experimental results [1].

Novel phenomenological models have been developed to facilitate the study of mouse atrial electrophysiology as well as tissue behaviour. The results show the significance of cell apoptosis as a major mechanism of SND. Novel computational modules in the simulation environment were developed to enable this study. BeatBox is an ideal computational environment to conduct such large scale studies.

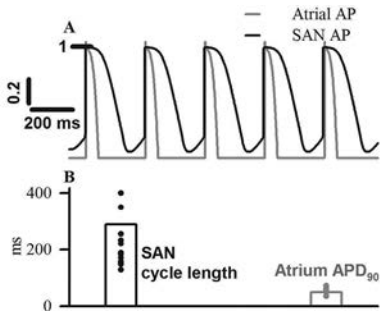

Fig 1. Simulated APs using the modified FK models. A: AP profiles of mouse SAN (solid line) and mouse atrial (gray line) cell types. B: Validation of SAN cycle length and atrial APD90. Symbols show experimental data and bars show simulation results. The experimental data was taken from a previous study [4].

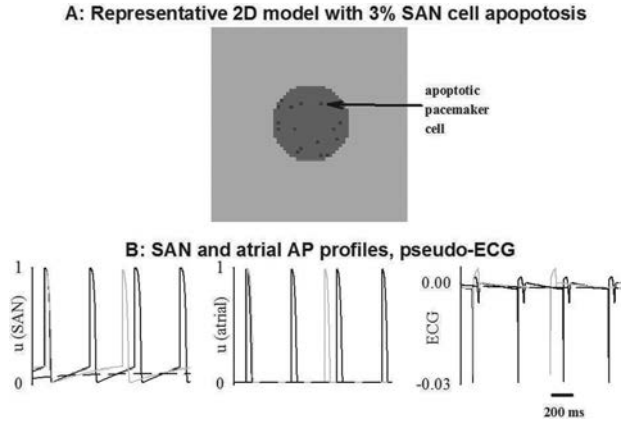

Fig. 2. A: Atrial (light gray), SAN (dark gray), and apoptotic cells (black) in the 2D idealized model. B: Representative SAN APs (left panel), atrial APs (middle panel), and pseudo-ECG profiles from the 3% apoptosis simulation. Out of the 50 run population, the APs shown are ACL = 400 ms (black lines in all 3 panels), ACL = 800 ms (gray lines), and a SAN arrest case (dashed black lines).

Swaminathan PD. (2011) *J Clin Invest* 121, 3277-3288.

McFarlane R & Biktasheva IV (2008). Visions of Computer Science—BCS International Academic Conference

Fenton F & Karma A, (1998). *Chaos*, 8, 20-47.

Kharche SR et al. (2011). *Am J Physiol***301 (3)** H945-H963.

UK EPSRC (EP/I029664/1, EP/I029826/1, EP/I030158/1), PRACE Intro. HPC Access (PRPB09, 2012).

Where applicable, the authors confirm that the experiments described here conform with The Physiological Society ethical requirements.

PCA019

Effects of diabetes mellitus and exercise training on expression of mRNA, contraction and calcium transport in the adult Goto-Kakizaki rat heart

F.C. Howarth[1], K.A. Salem[1], M.A. Qureshi[1], V. Sydorenko[1], K.A. Parekh[1], P. Jayaprakash[1], T. Iqbal[2], J. Singh[2], M. Oz[3] and T.E. Adrian[1]

[1]Physiology, UAE University, Al Ain, United Arab Emirates, [2]School of Pharmacy & Biomedical Sciences, University of Central Lancashire, Preston, UK and [3]Pharmacology, UAE University, Al Ain, United Arab Emirates

The prevalence of diabetes mellitus (DM) in the United Arab Emirates is among the highest in the world. Hearts of diabetic patients are frequently in a compromised condition. A variety of diastolic and systolic dysfunctions have been reported in patients with type 2 diabetes mellitus (T2DM). Although, several novel forms of intervention aiming at newly identified therapeutic targets are being developed for T2DM it is well established that physical exercise continues to be one of the most valuable forms of non-pharmacological therapy. An abundance of evidence exists for prescribing exercise therapy in the treatment of various diseases including metabolic syndrome-related disorders, heart and pulmonary diseases. Physical activity has been reported to influence several aspects of DM including blood glucose concentrations, insulin action and cardiovascular risk factors and long-term exercise has been repeatedly associated with lower rates of T2DM. The effects of DM and exercise training on expression of mRNA encoding cardiac muscle proteins and on ventricular myocyte contraction and intracellular Ca2+ transport in the adult Goto-Kakizaki (GK) type 2 diabetic rat was investigated. Experiments were performed in GK and control rats aged 10-11 months following 2-3 months of treadmill exercise training. Expression of mRNA was assessed in ventricular muscle with real-time RT-PCR. Shortening, intracellular free Ca2+ and L-type Ca2+ current were measured in ventricular myocytes with video edge detection, fluorescence photometry and whole cell patch clamp techniques. Non-fasting blood glucose was elevated in GK compared to age-matched controls and exercise slightly reduced blood glucose in control and more so in GK rats. Expression of mRNA encoding cardiac muscle, intercellular, cell membrane transport, calcium and potassium channel proteins were variously altered in GK and control rats and with exercise. Expression of Tpm2, Gja4, Atp1b1, Cacna1g, Cacnb2, Hcn2, Kcna3 and Kcne1 were up-regulated and Gja1, Kcnj2 and Kcnk3 were down-regulated in heart of GK rats compared to sedentary controls. Gja1, Cav3 and Kcnk3 were up-regulated and Hcn2 was down-regulated in hearts of exercise trained GK compared to sedentary GK controls. Amplitudes of shortening, Ca2+ transients and L-type Ca2+ current were not significantly altered in ventricular myocytes from GK rats compared to sedentary controls or by exercise training. Despite alterations in the profile of expression of mRNA encoding a variety of cardiac muscle proteins in the GK rat and as a result of exercise training, ventricular myocyte shortening and Ca2+ transport were generally well preserved in the adult GK diabetic rat heart.

Grants from the UAE University and Emirates Foundation. Research in

our laboratory is also supported by LABCO, a partner of Sigma-Aldrich.

Where applicable, the authors confirm that the experiments described here conform with The Physiological Society ethical requirements.

PCA020

AT1 receptor blockade by irbesartan attenuates hyposmostic-induced increase of IKs current and prevents shortening of APD in guinea-pig atrial myocytes

J. Wu[1,3], W. Ding[2], J. Dou[1], H. Matsuura[2] and M. Horie[3]

[1]Medical School of Xi'an Jiaotong University, Xi'an, Shaanxi, China, [2]Physiology, Shiga University of Medical Science, Otsu, Shiga, Japan and [3]Cardioascular and Respiratory Medicine, Shiga University of Medical Science, Otsu, Shiga, Japan

The shortening of action potential duration (APD) and effective refractory period (ERP) are generally regarded as pivotal factors for the occurrence of reentry-based atrial fibrillation (AF). During AF, impaired atrial contraction causes the atria to dilate or stretch and induce the secretion of Ang II from cardiomyocytes. Stretch of the atrial membrane up-regulates the slow component of delayed rectifier K+ current (IKs). Blockade of angiotensin II subtype 1 receptors (AT1R) attenuates this increase in IKs. The present study aimed to examine effects of irbesartan, a selective AT1R blocker (ABR), on both the enhancement of IKs and the shortening of action potential duration (APD) induced by stretching atrial myocytes for exploring the mechanisms underlying the prevention of AF by ABR. Adult female Hartley guinea pigs (weighing 250-350g) were anaesthetized with pentobarbital sodium (80 mg kg-1, I.P.) and single atrial myocytes were enzymatically dissociated from the hearts of using a retrograde Langendorff perfusion method. Hyposmotic solution (Hypo-S) was used to stretch guinea pig atrial myocytes. IKs and APD were recorded using the whole-cell patch-clamp technique. Values are means ± S.E.M., compared by one-way ANOVA with Newman-Keuls post-hoc test. The result shows that therapeutically-relevant concentrations of irbesartan (1-50 μM) attenuated the Hypo-S-induced increase (but not baseline) levels of atrial IKs and shortening of APD90. Hypo-S increased the IKs by 113.4±9.96% (n = 18), whereas Hypo-S + 1 μM irbesartan and Hypo-S + 50 μM irbesartan only increased the IKs by 74.5±8.49% (n = 10; $p < 0.05$ vs. Hypo-S) and 70.3± 9.34% (n = 16; $p < 0.05$ vs. Hypo-S), respectively. In addition, Hypo-S shortened the APD90 by 19.03±1.36% (n = 17), whereas Hypo-S + 1 μM irbesartan and Hypo-S + 50 μM irbesartan shortened the APD90 by 12.05 ± 1.38 (n = 9; $p < 0.01$ vs. Hypo-S) and 12.0 ± 1.46 (n = 14; $p < 0.01$ vs. Hypo-S), respectively. The above data suggest that actions of irbesartan on electrical changes induced by stretching atrial myocytes are associated with blocking AT1R and may be beneficial for treating AF that is accompanied by atrial dilation and prolongation of the effective refractory period.

Where applicable, the authors confirm that the experiments described here conform with The Physiological Society ethical requirements.

PCA021

Implication of myocardial connexin-43 and PKC signaling in cardio-protective effects of melatonin in spontaneously hypertensive rats

N. Tribulova[1], T. Benova[1], C. Viczenczova[1], J. Radosinska[1], B. Bacova[1], V. Knezl[2], V. Dosenko[3] and M. Zeman[4]

[1]Institute for Heart Research, SAS, Bratislava, Slovakia, [2]Institute for Experimental Pharmacology, SAS, Bratislava, Slovakia, [3]Bogomoletz Inst. of Physiology, Kiyv, Ukraine and [4]Faculty of Natural Sciences Comenius University, Bratislava, Slovakia

Background and Purpose: Experimental and human studies indicate that melatonin may regulate blood pressure and suggest the potential use of melatonin as adjunct antihypertensive therapy. However, melatonin levels have been shown decreased in patients treated with beta-adrenergic blockers as well as in spontaneously hypertensive rats (SHR). We aimed to examine whether treatment with melatonin will affect propensity of SHR heart to malignant arrhythmias and electrical coupling protein, connexin-43 (Cx43).
Design and Methods: SHR and healthy Wistar rats fed a standard rat chow received orally melatonin (40 mikrog/ml) for 4 weeks and were compared with untreated rats. Systolic blood pressure (BP), plasma cholesterol (CH), triglycerides (TG) and blood glucose (BG) were registered at the end of experiment. Myocardial Cx43 mRNA level was determined by real time PCR, while the expression of Cx43 protein, protein kinase C (PKC) epsilon and delta by western blots. Isolated Langendorff-perfused heart was used to test its susceptibility to electrically inducible ventricular fibrillation (VF).
Key Results: Melatonin significantly reduced BP (180+24 vs 206+10 mmHg) and normalized TG but did not affect body, heart and left ventricular weights in SHR. Compared to healthy rats the threshold to induce sustained VF was lower in SHR (18.7+2 vs 29.0+5 mA, $p<0.05$) and significantly increased in melatonin-treated SHR to 33.0+4 mA. Myocardial Cx43 mRNA levels did not differ from healthy rats but total Cx43 protein was decreased in SHR heart left ventricle. In contrast, melatonin treatment resulted in a significant increase of both Cx43 protein and mRNA in SHR as well as healthy rats. Moreover, melatonin normalized myocardial PKC-delta expression and enhanced PKC-epsilon in SHR as well as healthy rat hearts.
Conclusions: Results indicate antiarrhythmic effects of melatonin in hypertensive rats that can be, in part, attributed to up-regulation of myocardial Cx43 and PKC signaling. Findings support monitoring of melatonin levels and its supplementation in patients with CVD.

This work was supported by VEGA 2/0046/12 and SKS grants.

Where applicable, the authors confirm that the experiments described here conform with The Physiological Society ethical requirements.

PCA022

Left ventricle structural remodelling in the streptozotocin-induced type 1 diabetic rat

J. Singh[1], A. D'Souza-[2], T. Iqbal[3], E. Adeghate[4], F.C. Howarth[5] and K.A. Bidasee[6]

[1]School of Pharmacy and Biomeduical Sciences and School of Forensic and Investigative Sciences, University of Central Lancashire, Preston, Lancashire, UK, [2]School of Forensic and Investigative Sciences, University of Central Lancashire, Preston, Lancashire, UK, [3]School of Pharmacy and Biomedical Sciences, University of Central Lancashire, Preston, Lancashire, UK, [4]Human Anatomy, United Arab Emirates University, Al-Ain, Abu Dhabi, United Arab Emirates, [5]Physiology, United Arab Emirates University, Al-Ain, Abu Dhabi, United Arab Emirates and [6]Pharmacology and Experimental Neurosciences, University of Nebraska Medical Centre, Omaha, NE, USA

Heart failure in diabetes mellitus (DM) is a major cause of premature morbidity and mortality but the underlying mechanisms are elusive and treatment remains empirical. Previously, we reported significant voltage-dependent decreases in force of contraction and L-type calcium current channel activities in the streptozotocin (STZ)-induced diabetic heart. This study now investigated how DM via hyperglycaemia (HG) can induce histopathological changes in the left ventricle (LV) of STZ-treated type 1 diabetic male Wistar rats compared to age-matched controls, six-eight weeks following STZ-administration (60 mg/kg body weight). The study was approved by the Home Office and UCLAN Ethics Committee. A portion of the LV underwent processing for histological studies employing the Haematoxylin and Eosin stain, labelling with FITC-conjugated Lectin and the Masson's trichrome stain for determination of myocyte size and quantitative assessment of fibrosis, respectively. Immunohistochemical studies were conducted to assess the contribution of diabetes towards activation of apoptotic pathways governed by caspase-3.
STZ-treated rats presented with significantly (Student's t-test; $p<0.01$) higher blood glucose values (305.86± 7.48 mg/dl, n=6) relative to controls (89.51±3.56 mg/dl, n=6) and significantly ($P<0.05$) reduced body (232.33±11.07 g) and heart (0.55±0.03 g) weights compared to controls (301.20±16.31 g for body and 0.94±0.05±0.05 g for heart, n=6). Similarly, heart to body mass ratio (g/100 g body weight) was significantly ($P<0.05$) less in the diabetic animals (0.24± 0.02, n=6) compared to control (0.31± 0.02, n=6). LV morphology was also severely altered by DM. Morphometric analysis indicated significant ($P<0.05$) increments in fibrous tissue proliferation (5.05±0.44% vs 3.51±0.44%, n=6) and smaller myocyte transverse diameter in the diabetic heart compared to control. The heart was also atrophied and STZ-treated animals presented with lower heart weights and heart weight to body weight ratios relative to controls ($p<0.01$). In STZ-treated LV, the pathology frequently manifested as focal scarring, myofibrillar loss, vacuolisation and large clusters of cells showing histological signs of apoptosis. Activity of cleaved caspase-3 was also significantly ($p<0.01$) increased in the STZ-treated group. The results indicate that STZ-induced type-1 DM results in the development of a cardiac disease characterised by LV histopathological changes consistent with a dominant influence of HG and underlying alterations in insulin action.

Where applicable, the authors confirm that the experiments described here conform with The Physiological Society ethical requirements.

PCA023

Fibrosis and downregulation of Ca^{2+}-handling proteins as an underlying cause of cardiac repolarisation alternans and sudden cardiac death in the human

J. Yanni[1], P. Lambiase[2], M. Orini[3], B. Hanson[3], H. Dobrzynski[1], X. Jie[3], M. Boyett[1], M.P. Hayward[3] and P. Taggart[3]

[1]Institute of Cardiovascular Sciences, University of Manchester, Manchester, UK, [2]Cardiology Department, Heart Hospital, London, UK and [3]Department of Medicine, University College London, London, UK

Repolarisation alternans has been found to be predictive of or precede lethal ventricular arrhythmias in cardiac patients, as well as in the laboratory. Alternans is believed to cause arrhythmias by enhancing the regional physiological heterogeneities within normal cardiac tissue, to the point where functional conduction blocks develop, to initiate re-entrant arrhythmias. Using qPCR, immunohistochemistry and western blot (to confirm the specificity of antibodies), this study investigated the expression of ion channels and extracellular matrix (mRNAs and proteins) in areas of ventricular tissue displaying cardiac alternans & non-alternans sites. Epicardial samples were obtained from 19 patients who were undergoing elective surgery primarily for ischaemic heart disease. During the surgery, the patient's heart was mapped using an epicardial sock which contained 256 electrodes. The heart was then paced at fixed cycle lengths to induce alternans. Activation Recovery Intervals (ARI), a surrogate for action potential duration (APD), was estimated and repolarisation alternans was quantified by an index incorporating both extent and persistence of beat-to-beat variations in ARI. Two myocardial biopsies were taken for mRNA analysis, each from sites of maximum and zero repolarisation alternans. The criterion for alternans was ≥ 6 consecutive beats of alternans with a steady state drive train of ventricular pacing at between 600-350 ms cycle length for 30 seconds each (50 ms reduction in cycle length between drive trains). Vimentin mRNA, which is a fibroblast marker, and collagen type 1 mRNA, which constitutes ~80% of total collagen mRNA, showed positive correlations with repolarisation alternans (R^2 of 0.76 and 0.86 for vimetin and collagen type I, respectively). KChIP2 mRNA showed a positive correlation with repolarisation alternans (R^2=0.82), whereas SERCA2 mRNA showed a negative correlation with repolarisation alternans (R^2=0.82). A possible explanation is that there are areas of micro-infarction in the ventricle and this causes fibrosis accompanied by a downregulation in KChIP2 and SERCA2 which contribute to the production of repolarisation alternans. These micro-infarcts may, therefore, be responsible for arrythmogenesis.

Where applicable, the authors confirm that the experiments described here conform with The Physiological Society ethical requirements.

PCA024

Cardioprotection of Hydrogen sulfide post-conditioning against ischemia reperfusion injury involved in ATF6 activated endoplasmic reticulum stress -induced apoptosis

X. Yan, J. Deng, T. Chen, Y. Wang, Z. Wang and Y. Ding

Department of Physiology, Wuhan University school of basic medical sciences, Wuhan, China

Endogenous hydrogen sulfide (H2S) was involved in myocardial ischemia postconditioning and alleviated ischemia-reperfusion (I/R) injury, and exogenous H2S postconditioning has a protective effect on the isolated heart I/R injury. Myocardial I/R can induce endoplasmic reticulum stress (ERS), and excessive ERS will induce apoptosis and increase the myocardial injury. Recently, studies have shown that ATF6 is activated in myocardiaocytes by ER stress. In the present study, we determined whether H2S post-conditioning protection myocardium from I/R injury involved in ATF6 activated ERS. Sprague-Dawley rats (male, 250-300g) were anaesthetised with urethane (1g kg-1 i.p.) and were randomly divided into 5 groups (n= 12 in each): Sham group, I/R group, I/R+NaHS groups (H2S post-conditioning group), I/R+TUDCA (Tauro Ursodesoxy Cholic Acid, an ERS blocker) group and I/R+TUDCA+NaHS group. NaHS 14μmol/kg and TUDCA 25mg/kg were injected i.p. after 30min of myocardial ischemia and within reperfusion 10 min. The myocardial I/R rats were subjected to ischemia by 30 min of coronary artery branch of left anterior descending occlusion followed by 2 h of reperfusion. At the end of the reperfusion, myocardial infarct size was examined by triphenyltetrazolium chloride (TTC) staining, serum concentration of H2S was determined with a spectrophotometer, myocardial apoptosis was detected by TUNEL and the protein levels of ATF6, GRP78, PDI, and CHOP were assayed by western blotting. At the end of reperfusion, the average myocardial infarct size was 37.41±3.3%. Compared with the Sham group, the H2S concentration in the serum of the I/R group was significantly decrease (24.98±0.69 vs 44.56±0.86μmol/L, P<0.01); the myocardiaocytes apoptotic rate were significantly increased (84.28±3.03% vs 0.50±0.29%, P<0.01); the endoplasmic reticulum stress related proteins ATF6, GRP78, PDI and CHOP expression level in myocardial tissue were significantly increased (P<0.01). Compared with I/R group, serum H2S concentrations of I/R+NaHS group were significantly increased (43.48±2.31 vs 24.98±0.69μmol/L, P<0.01). Administration of exogenous H2S into rat /H2S post-conditioning could decrease myocardial infarct size (18.69±1.87% vs 37.41±3.3%, P<0.01) and myocardiocytes apoptotic rate (34.23±2.92% vs 84.28±3.03%, P<0.01) significantly. The decrease of ATF6, PDI, GRP78 and CHOP protein level in I/R could be partly reversed by H2S post-conditioning (P<0.05). Using TUDCA to block ER stress could also attenuate I/R injury; compared with I/R+TUDCA group, I/R+NaHS group had even stronger protecting effect on myocardial infarct size and apoptosis rate. This finding suggested that cardioprotection of H2S postconditioning may involve inhibiting apoptosis caused by ATF6 activated excessive ERS induced by myocardiac I/R.

Yong QC et al. (2008). Am J Physiol Heart Circ Physiol. 295(3):H1330-40

Ji Y et al. (2008). Eur J Pharmacol. 587(1-3):1-7

Minamino T et al. (2010). Circ Res. 107(9):1071-1082

Martindale JJ et al. (2006). Circ. Res. 98: 1186-1193

Doroudgar S et al. (2009). J Biol Chem. 284(43):29735-29745

This study was supported by the National Natural Science Foundation of China (No.31071005)

Where applicable, the authors confirm that the experiments described here conform with The Physiological Society ethical requirements.

PCA026

An extra-mitochondrial domain rich in carbonic anhydrase activity improves myocardial energetics

M.A. Schroeder[1], M.A. Ali[1], A. Hulikova[1], C.T. Supuran[2], K. Clarke[1], R.D. Vaughan-Jones[1], D.J. Tyler[1] and P. Swietach[1]

[1]Department of Physiology, Anatomy and Genetics, Oxford University, Oxford, UK and [2]Dipartimento di Scienze farmaceutiche, Università degli Studi di Firenze, Florence, Italy

The heart's intensive pumping activity is powered by a uniquely high rate of mitochondrial respiration. This generates vast quantities of the waste-product CO_2, which must be removed efficiently from mitochondria. Carbonic anhydrase (CA) enzymes, expressed at various sites in ventricular myocytes, may affect mitochondrial CO_2-clearance by catalyzing CO_2 hydration (to H^+ and HCO_3^-) thereby changing the gradient for CO_2 venting. In this study, we measured CA activity in cardiac myocytes, and investigated the effects of CA inhibition on cardiac energetics and function.

CA activity in the cytoplasm of isolated ventricular myocytes was measured by fluorescence imaging of cells loaded with the pH reporter dye, cSNARF1 (10 μM, AM-loading for 5 min). Rapid exposure to CO_2-containing solution evoked CO_2 entry and its intracellular hydration which was only modestly accelerated by CA activity (2.7±0.3[SEM]-fold above spontaneous kinetics determined in the presence of the broad-spectrum CA inhibitor acetazolamide, ATZ, 100 μM). A similar experiment performed on isolated ventricular mitochondria demonstrated negligible intra-mitochondrial CA activity. CA activity was also investigated in intact hearts by ^{13}C magnetic resonance spectroscopy (MRS) from the rate of $H^{13}CO_3^-$ production from $^{13}CO_2$ released specifically from mitochondria by pyruvate dehydrogenase-mediated metabolism of hyperpolarized [1-^{13}C]pyruvate. Under these conditions, the steady-state between de novo production and capillary wash-out produces a gradient of $^{13}CO_2$ from mitochondria to the sarcolemma. CA activity measured upon [1-^{13}C]pyruvate infusion was 11.4±0.9 fold above spontaneous kinetics (i.e. four-fold higher than the cytoplasm-averaged value).

A fluorescent CA-ligand (fluorescein-thioureido-homosulfanilamide) co-localized with the mitochondrial marker TMRE (Pearson's coefficient 0.735±0.06), indicating that mitochondria are near a CA-rich domain. Based on immunoreactivity, this domain comprises the nominally cytoplasmic CAII and sarcoplasmic reticulum-associated CAXIV. Inhibition of extra-mitochondrial CA activity with ATZ acidified the matrix by up to 0.1 unit (pH 7.73±0.03 to 7.62±0.02 measured by fluorescence imaging of permeabilized myocytes and isolated mitochondria by flow cytometry), impaired cardiac energetics (phosphocreatine-to-ATP ratio decreased from 2.02±0.13 to 1.58±0.14, measured by ^{31}P-MRS of perfused hearts) and reduced contractility (developed pressure in perfused hearts decreased by 18±5%). These data provide evidence for a functional domain of high CA activity around mitochondria to support CO_2-venting, particularly during elevated and fluctuating respiratory activity. Aberrant distribution of CA activity may therefore reduce the heart's energetic efficiency.

Schroeder et al, (2013) Proc Natl Acad Sci [published ahead of print February 19, 2013, doi:10.1073/pnas.1213471110]

Supported by the British Heart Foundation, Royal Society and Wellcome Trust.

Where applicable, the authors confirm that the experiments described here conform with The Physiological Society ethical requirements.

PCA027

A new experimental approach reveals a high Ca^{2+} sensitivity of TRPM4 channel and its significant implications in arrhythmogenicity

R. Inoue, Y. Hu, Y. Duan, R. Kurahara-Hai and J. Ichikawa

Department of Physiology, Fukuoka University School of Medicine, Fkuoka, Fukuoka, Japan

TRPM4 is a molecular correlate for Ca^{2+}-activated monovalent cation selective channels ubiquitously expressed in both excitable and non-excitable tissues. Recent investigations have revealed that increased expression of this channel protein may be the main causes for certain types of familial atrio-ventricular blocks and other arrhythmogenic propensity associated with cardiac remodeling. However, the apparent Ca^{2+} sensitivity of this channel evaluated in heterologous systems is almost out of physiological range (typically >10μM), so that it remains still puzzling how exactly it could contribute to arrhythmogenicity. In this study, we re-evaluated the Ca^{2+} sensitivity of TRPM4 channels in both expression systems and immortalized atrial cardiomyocyte cell line HL-1, and explored their roles in inducing arrhythmic changes by means of mathematical model simulations.
In cell-free conditions, the Ca^{2+} sensitivity of human TRPM4 channels expressed in HEK293 cells rapidly declined requiring more than several-hundred μM Ca^{2+} for half maximal activation (K_d) near the resting membrane potential. However, a much higher Ca^{2+} sensitivity was observed when cells were maintained as intact as possible and intracellular Ca^{2+} concentration was changed via ionomycin-mediated Ca^{2+} influx (K_d: ~ 0.5μM). A similar estimate of K_d was obtained in experiments evaluating the relationship between the integral of voltage-dependent Ca^{2+} influx and the magnitude of tail cationic current in HEK cells coexpressing TRPM4 and voltage-dependent Ca^{2+} channels (VDCC) subunits (α1C/β2/α2δ). Furthermore, repetitive activation of VDCC at high frequencies induced the development of sustained TRPM4 current at -80mV. 4-5 day treatment of HL-1 myocytes with angiotensin II resulted in enhanced expression of TRPM4 channel protein and current density, and induced spontaneous action potentials (APs) with prolongation of AP duration, which could be abolished by a relatively selective concentration (10μM) of a TRPM4 channel blocker, 9-phenanthrol. In silico simulation of cardiac action potentials (APs) based on 2000 Luo-Rudy or Nygren models which incorporated the Ca^{2+}- and voltage-dependent kinetics of TRPM4 channel reproduced the late phase-3 AP prolongation and moderate basal depolarization when increasing the expression level of TRPM4 by several fold.
These results suggest that the intact Ca^{2+} sensitivity of TRPM4 channel would be sufficiently high to induce arrhythmic changes, when the channel expression or function is up-regulated.

This work is supported by Grants-in-aid to R.I. from Scientific Research on Innovative Areas (No. 22136008).

Where applicable, the authors confirm that the experiments described here conform with The Physiological Society ethical requirements.

PCA028

Intrinsic left atrial histoanatomy as the basis for reentrant excitation causing atrial fibrillation/flutter in rats

T. Matsuyama[2,1], H. Tanaka[1], T. Adachi[1], Y. Jiang[1], H. Ishibashi-Ueda[2] and T. Takamatsu[1]

[1]Pathology and Cell Regulation, Kyoto Prefectural University of Medicine Graduate School of Medical Science, Kyoto, Japan and [2]Pathology, National Cerebral and Cardiovascular Center, Osaka, Japan

In contrast to the pulmonary veins as a well-accepted site for triggering paroxysmal atrial fibrillation/flutter (AF/AFL), little is known about the intrinsic basis for reentrant excitation in persistent AF/AFL. To explore histoanatomic substrates for reentrant AF/AFL in atria, we conducted functional and histoanatomic studies of the whole atria of rats by combining optical imaging of impulse propagation with histologic examination. After sufficient general anaesthesia applied to male Wistar rats (n=19, 11-14 weeks, 290–430 g) by single intraabdominal injection of sodium pentobarbitone (19 mg/100g), hearts with bilateral lungs were excised and were quickly perfused in a Langendorff manner. Spatiotemporal patterns of impulse propagation were visualized optically on the posterior surface of the atria stained with di-4ANEPPS at 32 °C with cytocholasin D (4 μmol/L). AF/AFL was evoked by single extra stimulation (S2) after 5-Hz consecutive pacing (S1) at the right atrium (RA). After the optical imaging we quantified regional differences in 3 histological determinants for conductivity, i.e., myocardial density, myofibre orientation, and distribution of gap junctional (connexin 43) proteins (n = 10). The myocardial density was evaluated by Masson's trichrome staining, and other two parameters were assessed by confocal immunohistochemistry. Quantitative data (mean±SD) were analysed by paired t-test or one-factor ANOVA. Burst (S1-S2) pacing at the RA provoked AF/AFL in 15 of 19 hearts, and most cases developed by organized reentrant excitation through the coronary sinus (CS) and left atrium (LA) roof, with non-organized irregular propagation in 3 cases. The reentrant circuit developed along 2 directions of propagation in the LA: a slower one at the LA roof and a faster one along the CS, with conduction velocities of 42.4±16.6 cm/s and 53.3±9.2 cm/s, respectively ($p<0.005$). Upon S2 stimulus the impulse at the LA roof propagated retrogradely from the CS, resulting in reentrant propagation that mediated through the CS and the LA roof. Histologic quantification revealed significantly lower myocardial density in the posterior LA and the septum than in the remainder of the atria, suggesting a possible electrical obstacle. Moreover, myocytes in the LA roof were significantly of lower density ($p<0.005$) and arranged more randomly in the direction of conduction than those in the CS. Connexin 43 plaques were distributed randomly over the entire cell membrane in the LA roof (slower pathway), whereas those in the CS (faster pathway) were located in orderly fashion. We identified an intrinsic histoanatomic basis in the LA, especially the posterior LA, septum and LA roof, for formation of reentrant propagation in the atria. These regional heterogeneities observed in the LA would constitute a pro-reentrant substrate for perpetuating AF/AFL.

Where applicable, the authors confirm that the experiments described here conform with The Physiological Society ethical requirements.

PCA029

Altered thyroid status affects myocardial connexin-43 and PKC expression in male and female Wistar rats: effect of antioxidant-rich red palm oil intake

B. Bacova[1], C. Viczenczova[1], J. Radosinska[2], J. Zurmanova[3], S. Pavelka[4], T. Soukup[4], J. van Royen[5] and N. Tribulova[1]

[1]Institute for Heart Research, SAS, Bratislava, Slovakia, [2]Institute of Physiology, Faculty of Medicine, Comenius University, Bratislava, Slovakia, [3]Faculty of Science, Charles University in Prague, Prague, Czech Republic, [4]Institute of Physiology, v.v.i., AS CR, Prague, Czech Republic and [5]Cape Peninsula University of Technology, Bellville, South Africa

Background and purpose: The cardiovascular system is modulated by thyroid hormones and their deficiency or excess in hypo- (HY) or hyperthyroid (TH) status may affect both cardiac function and arrhythmogenesis. We hypothesized that intercellular communication via connexin-43 (Cx43) channels might be implicated. The goal of this study was to explore myocardial Cx43 and PKC expression in rats with altered thyroid status as well as the effects of antioxidant-rich red palm oil (RPO) intake.
Design and Methods: Male and female 4-month-old Wistar euthyroid rats (EU); HY rats (treated with 0.05% methimazole); TH rats (treated with T3/T4, 5/25 μg/100g b.w./day) fed with RPO (100 microL/100g b.w./day) for six weeks were compared with untreated rats. Left ventricular tissue was taken for Cx43 and PKC-epsilon mRNA and protein analysis using Real Time PCR and immunoblotting.
Key Results: Heart and left ventricular weights were significantly increased in male and female TH and decreased in HY rats compared to EU rats. Cx43 mRNA level was increased in male, but not in female TH rats and decreased in HY rats regardless of sex. In contrast, Cx43 protein and its functional phosphorylated (P) forms were increased in HY, but decreased in TH rats of both sexes. PKC-epsilon gene expression did not change in male, but decreased in female TH rats whereas it increased in male, but not in female HY rats. PKC-epsilon protein expression was decreased in male, but not in female TH rats and increased in HY rats regardless of sex. RPO intake reduced heart and left ventricular weight in TH rats; partially normalized Cx43 mRNA as well as protein expression and its P forms in male and female TH and HY rats; normalized PKC-epsilon protein expression in male TH rats.
In conclusion, our findings indicate sex-related differences in Cx43 and PKC-epsilon gene expression due to altered thyroid status. In general, there is a down-regulation of myocardial Cx43 and PKC-epsilon in hyperthyroidism, while up-regulation in hypothyroidism. RPO intake attenuated abnormalities of Cx43 and PKC-epsilon expression.

This work was supported by VEGA 0046/12, APVV-SK-CZ-0027-11, MSM0021620858, MSCT-CR 7AMB12SK158 and RVO 67985823 (AV0Z 50110509) grants.

Where applicable, the authors confirm that the experiments described here conform with The Physiological Society ethical requirements.

PCA030

Spermine reduced no-reflow size induced by ischemia-reperfusion through regulating autophagy

H. Liping, Y. Linbo, S. Yangping and S. Jundan

Physiology, Wenzhou Medical College, Wenzhou, China

Background: No-reflow (NR) phenomenon is a risk factor which severely compromises the benefits of coronary revascularization in patients with acute myocardial infarction. It has been found that autophagy increased after IR, and it seems that modest levels of autophagy appear to be protective. Our previous researches showed that the myocardial IR caused significant change of polyamine metabolism, and exogenous spermine protected the neonatal rat cardiomyocytes against anoxia-reoxygenation injury (ARI). The present study was undertaken to see whether exogenous spermine had protective effects against acute myocardial IR injury in vivo rat model, whether it reduced the myocardial no-reflow size and whether autophagy were involved in the protective effect.
Methods: Thirty SD rats weighing 250-300g were equally randomized to three groups: Sham control group, where the rats were treated with thoracotomy only; ischemia reperfusion (IR) group, where the rats were treated with ischemia for 40 min and reperfusion for 60 min; and spermine (SP) group, where 0.5mmol/L spermine (2ml/kg, i.v.) were given just 15min before reperfusion. The cardiac troponin I (cTnI) and creatine kinase isoenzyme (CK-MB) activities in serum were determined. NR size of the myocardium was measured by using Evan's blue and thioflavin S staining. Inflammatory response was detected by myocardial tissue myeloperoxidase (MPO) assay. And autophagy function was detected by measuring expression of Beclin-1 through Western blot.
Results: Spermine decreased serum cTnI and CK-MB levels, and reduced the IR-induced NR size of the left ventricle. Tissue MPO assay showed that myocardial inflammatory response was attenuated by spermine compared with IR. Western blot showed that Beclin-1 was up-regulated by spermine compared with IR group.
Conclusion: By up-regulating autophagy, exogenous spermine attenuated inflammatory response during myocardial IR, which contributed to reduce IR-associated NR size. Therefore, exogenous spermine or induce endogenous spermine might be a promising approach to prevent NR in patient with acute myocardial infarction (AMI) underwent reperfusion.
Animal care
All animal experiments were approved by the Animal Research Ethics Committee of the Wenzhou Medical College, Wenzhou, China. The investigation conformed with the guide for the care and use of laboratory animals published by the US National Institutes of Health. The whole procedures were performed under anaethesia.

Jaffe R, Charron T, Puley G, Dick A, Strauss BH: Microvascular obstruction and the no-reflow phenomenon after percutaneous coronary intervention. Circulation 2008, 117: 3152-3156.

Beth L, Guido K: Autophagy in the Pathogenesis of Disease. Cell 2008, 132: 27-42.

Wang RC, Wei Y, An Z, Zou Z, Xiao G, Bhagat G, White M, Reichelt J, Levine B: Akt-mediated regulation of autophagy and tumorigenesis through Beclin 1 phosphorylation. Science 2012, 338:956-959.

Jansen HJ, van Essen P, Koenen T, Joosten LA, Netea MG, Tack CJ, Stienstra R: Autophagy activity is up-regulated in adipose tissue of obese individuals and modulates proinflammatory cytokine expression. Endocrinology 2012, 153:5866-5874.

This work was supported by the National Nature Science Foundation of China (No. 81100138) and the Nature Science Foundation of Zhejiang Province, China (No. Y2100028).

Where applicable, the authors confirm that the experiments described here conform with The Physiological Society ethical requirements.

PCA031

Generation of reentrant arrhythmias by spatially non-uniform gap-junction connection with myofibroblasts in rat cultured myocyte monolayers

T. Adachi, Y. Jiang, H. Tanaka, E. Hashimoto and T. Takamatsu

Department of Pathology and Cell Regulation, Kyoto Prefectural University of Medicine, Kyoto, Japan

Cardiac myofibroblasts (MFs) have recently been regarded as important in arrhythmogenesis. There is growing evidence that coupling of cardiomyocytes (CMs) with MFs in vitro alters impulse propagation via electrotonic effect by MFs. However, exact initiating mechanisms of the MF-mediated arrhythmia remain elusive because studies on the arrhythmogenesis have been conducted mostly on mixed co-cultured monolayers of CMs with MFs. **On the hypothesis** that spatially non-uniform coupling of CMs with MFs is requisite for reentrant arrhythmogenesis, we analysed spatiotemporal changes in impulse propagation of the CM monolayer cultured on a filter membrane (25-mm diameter; pore diameter, 8 μm; pore density, $6x10^5$ /mm^2) with culture of either MFs or CMs on the reverse side. CMs and MFs were obtained from neonatal rat hearts excised under generalised anaesthesia by i.p. injection of sodium pentobarbitone (0.2mg/g body wt). CMs ($2x10^5$ cells/cm^2) were plated on the upper membrane layer, and either CMs ($2x10^5$ cells/cm^2, CM/CM model) or MFs ($2x10^4$ cells/cm^2, CM/MF model) were plated on the reverse side. After 5-day culture, spatiotemporal changes in fluo-4-fluorescence (11x7mm, 192x128 pixels, 200 frames/s) were imaged on the confluent CM monolayers on the upper side at 33°C. Data (mean±SD), statistically analysed by ANOVA, were considered as significant at $p<0.05$. **We found** that during 2-Hz pacing at the margin of the upper layer, CMs exhibited uniform wavefronts from the pacing site in the CM/CM model with CV of 76.6±10.9mm/s (n=20), whereas those in the CM/MF model exhibited irregular wavefronts with slower CV (51.8±12.2mm/s, n=23, $p<0.01$). Gap-junction coupling between the upper and lower layers was demonstrated by calcein-dye transfer and its inhibition by heptanol. During 3-Hz pacing CM monolayers exhibited reentrant arrhythmias with greater induction rate in CM/MF models (67.4%, n=43) than that in the CM/CM models (22.2%, n=27, $p<0.01$). In contrast, high-K^+ (8mM) perfusion in the CM/CM models, which slowed CV (41.3±7.6mm/s) equivalent to that in the CM/MF models under control K^+ (4mM) perfusion, barely induced arrhythmias (10.0%, n=10). In confocal immunofluorescence analysis for connexin 43 (Cx43) plaques at the membrane pores, the CM/MF model revealed denser distribution (35.5±3.5%, n=6) in the reentrant cores than in the surroundings (24.6±5.0%, n=6, $p<0.01$), suggesting greater electrotonus of MFs to CMs on the core than the surroundings. However, the CM/CM models that failed to induce arrhythmia showed no regional difference in Cx43 density (n=6). **In conclusion**, heterocellular coupling of CM monolayer with MFs depresses CV, but spatial non-uniformity in the coupling is requisite for reentrant arrhythmogenesis.

Where applicable, the authors confirm that the experiments described here conform with The Physiological Society ethical requirements.

PCA032

Arterial hypertension promotes atrial remodelling and fibrillation in pigs

G. Antoons[1], M. Schwarzl[1], G. Jin[1], D. Zweiker[1], S. Huber[2], J. Verderber[1], A. Alogna[1], P. Schoenleitner[1], P. Wakula[1], A. Lueger[3], F.R. Heinzel[1], B. Pieske[1] and H. Post[1]

[1]Cardiology, Medical University Graz, Graz, Austria, [2]Cardiac Surgery, Medical University of Graz, Graz, Austria and [3]Internal Medicine, Medical University of Graz, Graz, Austria

Arterial hypertension is an independent risk factor for atrial fibrillation (AF). The occurrence of AF is related to atrial dilation and extracellular matrix remodelling, shortening of atrial refractory period (AERP), and disturbed Ca^{2+} handling. In this study, we investigate if chronic hypertension in a porcine model induces structural and electrical changes in the atria, including Ca^{2+} homeostasis, and whether these changes enhance susceptibility to AF.

To induce hypertension, 8 landrace pigs received subcutaneous DOCA-pellets (aldosterone analogon, 90-day release) and high-lipid/salt diet for 12 weeks. Eight weight-matched pigs served as controls. AERP was determined at different cycle lengths, S0, followed by a premature extrastimulus with 5 ms decrements. To test for AF susceptibility, a separate group of pigs (N=16) was instrumented with a telemetry-controlled pacemaker. Surgical procedures and in vivo interventions were performed under anesthesia (1.0 % isoflurane, 35 μg/kg/h fentanyl, 1 mg/kg/h midazolam, and 0.2 mg/kg/h pancouronium). A number of 5/16 pigs received DOCA/salt starting 2 weeks before the onset of rapid atrial pacing (600 bpm). After 2 weeks pacing, spontaneous atrial rhythm was monitored in unsedated pigs. AF susceptibility was defined as no detectable sinus rhythm for > 1h.

Atrial myocytes were isolated from 12 w-treated DOCA (N=3) and control pigs (N=4), from left (LA) or right atrium (RA). Calcium transients (CaT) and cell shortening were measured during field stimulation using Fura-2 AM (0.5 – 2 Hz, 37°C). Data are expressed as mean ± s.e.m.

After 12 w DOCA, systolic blood pressure was 139±11, vs 95±6 mmHg in control pigs ($P<0.05$, tail-cuff-method). LA area was enlarged (12.4±0.3 vs 9.7±0.6 cm^2 in control, $p<0.05$, echocardiography). Interstitial fibrosis was reduced (14.8±1.8 vs 20.5±1.7% in control, $p<0.05$, expressed as % stained area by Sirius Red). AERP was significantly shortened in DOCA (fig 1). In single atrial myocytes, CaT amplitude was comparable in DOCA and control, in LA and RA. In LA, but not in RA, diastolic Ca^{2+} levels were lower (0.54±0.02 $F_{340/380}$, n=5, N=1, vs 0.81±0.01 in control, n=7, N=2, 0.5 Hz), and Ca^{2+} decline was faster (RT_{50} 81±24 ms, vs 197±21 ms in control, 0.5 Hz). While unchanged in RA, in LA cells, cell shortening was increased from 2.3±0.8% in control (n=3, N=2) to 5.4±0.5% in DOCA (n=8, N=1, 0.5 Hz). DOCA pigs were more susceptible to AF. After 2 w of rapid pacing, sustained AF (>1h) occurred in 4/5 DOCA pigs, vs 2/11 control pigs ($p<0.05$).

In conclusion, although sinus rhythm is maintained, hypertensive pigs develop left atrial dilation and reduced electrical refractoriness, which was related to enhanced AF susceptibility. At the myocyte level, faster Ca^{2+} kinetics and increased contractility may reflect compensatory mechanisms that primarily occur in the left atria during chronic hypertension.

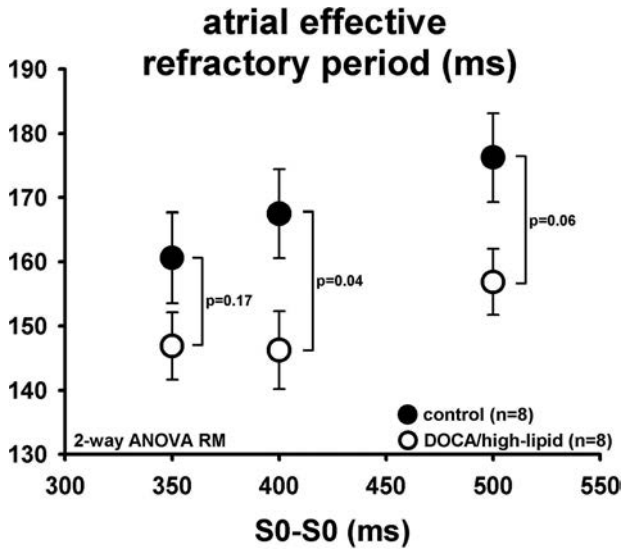

Where applicable, the authors confirm that the experiments described here conform with The Physiological Society ethical requirements.

PCA033

NADH and FAD kinetics reveal altered mitochondrial function in right ventricular heart failure

R.C. Wüst[1], M. Helmes[1,2] and G.J. Stienen[1]

[1]Department of Physiology, VU Medical Center, Amsterdam, Netherlands and [2]IonOptix llc, Milton, MA, USA

Purpose. In chronic heart failure, alterations occur in cardiac metabolism, enzyme content calcium handling and mitochondrial function. However, little is understood about the influence of alterations in mitochondrial function on energy metabolism during the transition from cardiac hypertrophy (CH) to failure (HF). A photometry-based technique (cf. 1) was used to simultaneously measure contractile function and autofluorescence of NADH (reduced nicotinamide adenine dinucleotide; electron donor to complex I) and FAD (oxidized flavin adenine dinucleotide; product after supplying electrons to complex II) in thin cardiac trabeculae.
Methods. Three groups (n=6 in each) were studied: CH (monocrotaline (MCT) injection s.c.: 40 mg.kg^{-1}) or HF (MCT: 60 mg.kg^{-1}) and CON (saline). After 23±1 days, hearts were dissected from isoflurane-anaesthetised male Wistar rats. Right ventricular trabeculae were excised, attached to a force transducer at optimal length and superfused with oxygenated tyrode with both 1 and 0.5 mM Ca^{2+}. Autofluorescence of both NADH (excitation: 340 nm; emission: 460 nm) and FAD (ex: 450 nm; em: 525 nm) were recorded using an inverted microscope during transitions in pacing frequency between 0.5 and 3 Hz at 27 °C.
Results. Upon an increase in pacing frequency from 0.5 to 3 Hz, force-time integral increased less in CH and HF compared to CON (4.0±1.4 and 3.2±0.2 vs. 5.6±1.4 fold, respectively). NADH autofluorescence dropped abruptly upon an increase in pacing frequency. Larger changes were observed in HF compared to CON, with CH showing intermediate responses. In CON, steady-state NADH concentration after 3 min of stimulation at 3 Hz was lower than steady state values at 0.5 Hz. In contrast, steady state NADH concentration was higher than at 0.5 Hz in CH and this increase was larger in HF. FAD responses showed a mirror image. The amplitudes of the responses of NADH and FAD were more pronounced in 1 mM compared to 0.5 mM Ca^{2+}.
Conclusions. Despite a smaller increase in the force-time-integral, the initial changes in NADH and FAD were more pronounced in CH and HF than in CON, indicating a larger deviation in metabolic homeostasis in CH and HF. Lower NADH and higher FAD throughout the 3 Hz contractions confirm net oxidation upon an increase in ATP demand in CON (1). In contrast, the higher steady-state NADH and lower FAD concentration in CH and HF point towards net NADH and $FADH_2$ production in CH, which is exacerbated in HF. These results are suggestive of a mismatch between dehydrogenase activity and oxidative phosphorylation, and reveal an altered mitochondrial function in CH and HF.

Brandes et al. Circ Res 82, 1189, 1998

Where applicable, the authors confirm that the experiments described here conform with The Physiological Society ethical requirements.

PCA034

Conduction of excitation in the rabbit and rat pulmonary veins myocardium under normal conditions and parasympathetic stimulation

V.S. Kuzmin, Y.V. Egorov and L.V. Rosenshtraukh

Laboratory of Heart Electrophysiology, Russian Cardiologic Research and Production Complex, Moscow, Russian Federation

Much attention is paid to the pulmonary veins (PVs) myocardium as a region responsible for atrial fibrillation (AF) triggering. It has been recognized re-entrant circuits and anisotropic conduction in the human PVs myocardial sleeves, that, probably, responsible for the onset of AF. However, the electrophysiologic properties of the PVs in laboratory animals have not been well characterized.
The aim of the present study is to investigate excitation wave conduction in rabbit and rat PVs myocardium with use of optical mapping technique.
Rabbits (male, 2.6-3.2 kg) and rats (male, 250-300 g) were anaesthetized with an urethane (1.5 g/kg i.v. and 2 g/kg i.p, respectively), preparations consisting of left atrium (LA) and PVs of left lung lobe were dissected. All procedures accorded with current Russian guidelines for the use of experimental animals.
Tyrode superfused isolated preparations were treated with potential sensitive dye di-4-ANEPPS (5 μM) in presence of 2,3-butanedione monoxime (1 g/l). Optical signals were captured with use of high speed CCD camera (WuTech Instruments). Cardioplex software (RedShirtImaging) was applied for conduction velocity and action potentials duration (APDs) estimation, isochronic maps reconstruction.
Rabbit PVs characterized by a very short zone (2-3 mm), which conduct excitation and by an abrupt transition to unexcitable nonmyocardial regions. Maximal conduction velocity (θ) in the conducting zone of rabbit PVs does not demonstrate significant difference with LA (65±7 and 69±6 cm/s, respectively, n=8, P>0.1). Also, no differences were seen for wavelength (55±6 and 58±6 mm, n=8) estimated with use of APDs. No conduction slowing, disturbances or blocks were observed in rabbit PVs at various patterns of stimulation or acetylcholine (ACh) application (5 μM).
Conduction of excitation was observed in distal and even intrapulmonary regions of rats PVs. Rat LA and PV myocardium also demonstrated weak differences in the conduction velocity.

Maximal θ in LA - 84 ± 14 cm/s, the same parameter in PVs was 71 ± 11 cm/s (n=12, P>0.1). Wavelength for rat LA - 37 ± 5, and for PVs 43 ± 7 mm (n=12, P>0.05).
Regions, that characterized by conduction slowing and blocks, were shown in rat PVs, but not in LA myocardium. Marked decreasing of conduction velocity and inexcitability were demonstrated in the rat PVs after periods (5 min) of quiescence (absence of stimulation). Application of ACh (5 μM, n=6) restore excitability and conduction velocity to the normal level. These data suggest functional similarity LA and PVs myocardium and PVs nonsusceptibility to conduction abnormalities in rabbits in contrast to rats. Significant distinction of conduction in PVs may be critical to experimental data interpretation in AF investigation.

This work supported by Russian Foundation for Basic Research grant 11-04-00712_a.

Where applicable, the authors confirm that the experiments described here conform with The Physiological Society ethical requirements.

PCA035

Chaotic excitation spread during tachycardia-like excitation in the rat isolated atrium revealed by optical mapping studies

T. Sakai[1] and K. Kamino[2]

[1]Department of Systems Physiology, Graduate School and Faculty of Medicine, University of the Ryukyus, Nishihara, Japan and [2]Tokyo Medical and Dental University, Tokyo, Japan

We have been carrying out experiments that involve the mapping of excitation spread in the isolated rat atrial preparation using multiple-site optical recording methods [1, 2]. When the tetanus stimulation was applied to the preparation, long-lasting rhythmical excitation with high frequency, which looks like tachycardia, occurred. We call this phenomenon as "tachycardia-like excitation" [3 - 5]. We found the chaotic excitation spread during this event. Adult rats were anesthetized by inhalation of ether, and the hearts were removed quickly. The isolated atrial preparations were stained with a fast voltage-sensitive merocyanine-rhodanine dye (NK2761). The preparation chamber was mounted on the stage of a microscope equipped with 16 X 16 or 12 X 12 -element photodiode array. Optical action potentials were recorded from 256 or 144 adjacent areas of the preparation simultaneously. Then, maps of excitation spread were made. From the spatio-temporal patterns of excitation spread on the map, the characteristics of "tachycardia-like excitation" are summarized as follows.

1. Tachycardia-like excitation is the generation of (or "transition to") a new pattern of excitation spread evoked by perturbing the "normal" pattern.
2. During its generation, transitional unstable complex (so called "chaotic") patterns of excitation spread, with blocked areas and ectopic foci, are observed.
3. After this phase, a new quasi-stable pattern appears. It is "quasi-stable" because the newly emerged pattern often returns to the original "normal" pattern spontaneously.
4. Event-to-event variations are always observed. Furthermore, preparation-to-preparation variations are also observed. During the event of tachycardia-like excitation, cycle-to-cycle variations (for circus movement) and/or site-to-site variations (for ectopic focus, i.e. spatial sift of the focus) are also observed. Based on the evidences shown above, we consider that tachycardia-like excitation is an example of a functional "self organizing system", although the physiological background is still unclear. Especially, the event-to-event variations seem to result from physiologically trivial difference(s) of the initial conditions. This characteristic of a "complex system" strongly supports this idea. We consider the quasi-stable state observed here as the "physiology-specific attractor". This study was carried out in accordance with Act on Welfare and Management of Animals of Japan, and approved by the Animal Care and Use Committee, Tokyo Medical and Dental University.

Kamino K (1991) Optical approaches to ontogeny of electrical activity and related functional organization during early heart development. Physiol Rev 71:53-41.

Sakai T, Kamino K (2001) Optical mapping approaches to cardiac electrophysiological functions. Jpn J Physiol 51:1-18.

Sakai T, Hirota A, Momose-Sato Y, Sato K, Kamino K (1997) Optical mapping of conduction patterns of normal and tachycardia-like excitations in the rat atrium. Jpn J Physiol 47:179-188.

Sakai T (2003) Optical mapping of the spread of excitation in the isolated rat atrium during tachycardia-like excitation. Pflügers Arch - Eur J Physiol 447:280-228.

Sakai T (2008) Optical mapping analysis of the spatiotemporal pattern of experimental tachyarrhythmia in improved isolated rat atrium preparation. J Physiol Sci 58:87-97.

We are most grateful to B. M. Salzberg for reading the manuscript and his useful comments. We also thank L. B. Cohen for the lesson on the concept of "event-to-event variations". This work was supported in part by Grants from the Ministry of Education, Culture, Sports, Science and Technology of Japan.

Where applicable, the authors confirm that the experiments described here conform with The Physiological Society ethical requirements.

PCA036

Early growth response 1 acts as an early signal to induce Cav3.2 T-type calcium channels during cardiac hypertrophy in mice

S. Hsu[1,2] and C. Chen[1]

[1]Institute of Biomedical Sciences, Academia Sinica, Taipei, Taipei, Taiwan and [2]Institute of Biochemistry and Molecular Biology, National Yang-Ming Univ, Taipei, Taiwan

Voltage-gated T-type Ca2+ channels (T-channels) are highly expressed in embryonic but undetectable in adult ventricular myocytes. Interestingly, T-channels are reexpressed in hypertrophied or failing hearts. It has been shown that Cav3.2 T-channel is involved in the pathogenesis of cardiac hypertrophy via the activation of calcineurin/nuclear factor of activated T cells (NFAT) pathway (Chiang et al, 2009). However, it is unclear when and how Cav3.2 is induced during cardiac hypertrophy. Because the mRNA re-expression is mainly through the transcriptional regulation in the promoter or enhancer conserved in different species, we hypothesized that the evolutionary conserved promoter (ECP) of Cav3.2 carries important binding sites for transcription factors that regulate its re-expression in the hypertrophic hearts. In this study, we obtained the ECP of Cav3.2 by aligning Cav3.2 genes from different species. By fusing mouse ECP with the reporter gene firefly luciferase, we showed that the ECP drove high luciferase activity in the cells expressing endogenous Cav3.2 but not in the one without Cav3.2. To further validate ECP in vivo, we generated transgenic mice expressing luciferase reporter driven by Cav3.2 ECP (Tg-Cav3.2-Luc). Analysis of the Tg-Cav3.2-Luc

mice showed that ECP confers the reporter expression similar to the endogenous Cav3.2 in the tissue distribution, development of hearts, and most importantly, the inducibility of hypertrophic stimulation. The left ventricular luciferase activity can be induced as early as 3 days after pressure overload created by trans-aortic banding (TAB) surgery (Chiang et al, 2009). By injecting reporters driven by different truncated promoters followed by TAB surgery, the hypertrophic regulatory element was located within -420 bp relative to the transcription start site (TSS) of Cav3.2. We searched the putative TF binding sites within the proximal 420 bp of mouse Cav3.2 5'-flanking sequence (Cav3.2-420) using the TFSEARCH and confirmed that early growth response 1 (Egr1) is the important transcription factor to enhance Cav3.2 gene expression. We showed the Egr1 could bind to the -81 to -41 bp upstream of Cav3.2 TSS using MESA and Chip assays. The protein level of Egr1 in left ventricle was also upregulated at 3 days after TAB, the same time point when the Cav3.2-Luc was induced in Tg-Cav3.2-Luc. To demonstrate that Egr1 indeed regulates Cav3.2 expression after hypertrophic stimulation, we showed that knockdown of Egr1 using siRNA prevented the phenylephrine (PE)–induced upregulation of Egr1, Cav3.2 and cellular hypertrophy in H9C2 cells. Furthermore, overexpression of Cav3.2 in Egr1 knockdown cells restored the PE-induced hypertrophy. In conclusion, our results demonstrate that Egr1 regulates the expression of Cav3.2 T-type calcium channel in cardiac hypertrophy.

Chiang CS, Huang CH, Chieng H, Chang YT, Chang D, Chen JJ, Chen YC, Chen YH, Shin HS, Campbell KP, Chen CC. The ca(v)3.2 t-type ca(2+) channel is required for pressure overload-induced cardiac hypertrophy in mice. Circulation research. 2009;104:522-530

Where applicable, the authors confirm that the experiments described here conform with The Physiological Society ethical requirements.

PCA037

Modulation of Ca^{2+} uptake by changing of SERCA activity in mouse myocardium did not alter Ca^{2+} leak from sarcoplasmic reticulum in physiological condition

S. Morimoto[1], K. Hongo[1], M. Kawai[1], J. O-Uchi[3], Y. Kusakari[2], K. Komukai[1], M. Yoshimura[1] and S. Kurihara[2]

[1]Division of Cardiology, Department of Internal Medicine, The Jikei University School of Medicine, Tokyo, Japan, [2]Department of Cell Physiology, The Jikei University School of Medicine, Tokyo, Japan and [3]Department of Medicine, Thomas Jefferson University, Philadelphia, PA, USA

Introduction Intracellular Ca^{2+} handling in cardiac muscle plays an important role in cardiac contraction and relaxation. Recently, increased Ca^{2+} leak from sarcoplasmic reticulum (SR) through ryanodine receptor has been reported to decrease cardiac contraction. It has been also reported that there were more heart failure patients with preserved cardiac contractility than we expected in clinical field. Heart failure with preserved contractility presents diastolic dysfunction, which may be caused by impaired relaxation due to decreased Ca^{2+} uptake into SR. However, the relationship between Ca^{2+} uptake and leak in SR has not been fully investigated. In the present study, we investigated the relationship between Ca^{2+} leak from SR through ryanodine receptor and Ca^{2+} uptake into SR by SR Ca^{2+}-ATPase (SERCA). **Methods** We used the mice hearts with overexpression of SERCA (SERCA-TG) or sarcolipin (SLN-TG) which suppresses SERCA activity. The hearts were quickly removed from mice anesthetized with sodium pentobarbital (300 mg/kg intraperitoneal administration). We used saponin-treated thin trabeculae and papillary muscles obtained from these mice hearts. Each SR function of these mice hearts was estimated by measuring the Ca^{2+} content in SR by using caffeine (50 mM) and fluo-3 when SR was loaded in the solution with various Ca^{2+} concentrations (pCa 8-5.6) and loading time (10-300 sec). Ca^{2+} transient and tension in twitch contraction of intact papillary muscles from mice were also measured. To estimate the effect of the beta-adrenergic stimulation on myocardium in SERCA-TG and SLN-TG, isoproterenol (100 nM) was applied to papillary muscles obtained from mice hearts. **Results** At short Ca^{2+} loading time, Ca^{2+} content in SR was larger in SERCA-TG (159%) and smaller in SLN-TG (50%) compared to each control myocardium. Ca^{2+} leak from SR in SERCA-TG and SLN-TG did not differ from each NTG. In SERCA-TG heart, the peak of Ca^{2+} transient increased and the time course of Ca^{2+} transient was accelerated. In SLN-TG heart, the peak of Ca^{2+} transient decreased and the time course of Ca^{2+} transient was slowed. In the papillary muscle preparation from control, isoproterenol increased Ca^{2+} transient and tension and accelerated time courses of both signals. In the papillary muscle preparation from SERCA-TG, Ca^{2+} transient and tension were not increased and time courses of both signals were not altered by isoproterenol treatment. In papillary muscles preparation from SLN-TG, Ca^{2+} transient and tension were significantly increased and time courses of both signals were significantly altered by isoproterenol treatment (e. g. Asahi *et al*. (2004)). **Conclusion** Selective modulation of Ca^{2+} uptake into SR influenced time course of Ca^{2+} transient, however, it did not influence Ca^{2+} leak from SR.

Where applicable, the authors confirm that the experiments described here conform with The Physiological Society ethical requirements.

PCA038

The Langendorff perfused heart and cardiac tissue slices, a comparison study

K. Wang[1], P. Lee[2], D. Gavaghan[1], P. Kohl[1,3] and C. Bollensdorff[3,4]

[1]Department of Computer Science, Oxford University, Oxford, UK, [2]Physics Department, Oxford University, Oxford, UK, [3]Heart Science Center, Imperial College London, London, UK and [4]Qatar Cardiovascular Research Center, Doha, Qatar

Several studies have shown that cardiac tissue slices are a good candidate for drug testing [1-4]. Furthermore cardiac slices as pseudo 2D preparations of heart muscle are a good experimental model to study patho-physiological mechanisms. However, similarities and differences of cardiac slices as compared to whole heart electrophysiological parameters have not yet been investigated in detail. We established a new method to compare action potential (AP) properties of intact whole-heart and cardiac tissue slices from the same heart.

Whole Langendorff-perfused hearts from female guinea pigs (300-400g) were bolus loaded with di-4-ANBDQPQ (15μL, 19mg/mL Ethanol). For AP mapping an EMCCD camera (~500fps) was used. A blue LED (CBT90, Luminus) was used [5] to minimize penetration depth, while being efficient to evoke a sufficiently strong signal, weighted towards the subsurface of the left ventricle (LV). The hearts were perfused with modified Krebs buffer containing 10μM blebbistatin. The solution was bubbled with carbogen and recirculated (8mL/min). The heart was held in a mould and the perfusion cannula was fixed to the specimen holder of a microtome. For whole heart

stimulation two platinum electrodes where placed about 0.5 cm away from the heart (40V, 2 to 5ms, bipolar) in the bath surrounding the tissue. Several cardiac tissue slices (400μm) were cut tangentially to the LV surface (microtome 7000smz, advance speed 0.02mm/s, blade frequency 80Hz). While the whole heart was imaged in the bath before each section, the cardiac slices were transferred to a special slice imaging station. The bath temperature in both set ups was kept at 35±2oC. The solution of the slice bath was also bubbled with carbogen between measurements, and continuously circulated for additional bubbling.

Living tissue slices could successfully obtained from the Langendorff heart, perfused at body temperature, avoiding the need to section from tissue wedges in ice-cold solution. Tissue slices differ from LV tissue in many ways, including mechanical load, electrical source-sink relations, and activation pathways. Slices do deform after sectioning, due to the lack of mechanical strain from neighbouring tissue. Therefore the exact AP pattern in a slice is different from a corresponding tissue area in whole heart. However, slices preserve several key characteristics of the AP, such as overall APD distribution, AP shape, and response to variation in stimulation rate. Therefore, within limits, cardiac tissue slices may be a useful model for exploration of cardiac electrophysiology in relation to identifiable underlying tissue sources, and may be particularly useful for differential studies involving before/after investigations, such as for the study of drug effects.

Bussek A, Schmidt M, Bauriedl J, Ravens U, Wettwer E, Lohmann H (2012) Cardiac tissue slices with prolonged survival for in vitro drug safety screening. J Pharmacol Toxicol Methods 66:145-51 DOI Electronic Resource Number

Camelliti P, Al-Saud SA, Smolenski RT, Al-Ayoubi S, Bussek A, Wettwer E, Banner NR, Bowles CT, Yacoub MH, Terracciano CM (2011) Adult human heart slices are a multicellular system suitable for electrophysiological and pharmacological studies. J Mol Cell Cardiol 51:390-8 DOI Electronic Resource Number

Bussek A, Wettwer E, Christ T, Lohmann H, Camelliti P, Ravens U (2009) Tissue slices from adult mammalian hearts as a model for pharmacological drug testing. Cell Physiol Biochem 24:527-36 DOI Electronic Resource Number

de Boer TP, Camelliti P, Ravens U, Kohl P (2009) Myocardial tissue slices: organotypic pseudo-2D models for cardiac research & development. Future Cardiol 5:425-30 DOI Electronic Resource Number

Lee P, Bollensdorff C, Quinn TA, Wuskell JP, Loew LM, Kohl P (2011) Single-sensor system for spatially resolved, continuous, and multiparametric optical mapping of cardiac tissue. Heart Rhythm 8:1482-91 DOI Electronic Resource Number

This work was supported by the British Heart Foundation (P.K., C.B.), Microsoft Research (fellowship to K.W.) and the Qatar Foundation (C.B.)

Where applicable, the authors confirm that the experiments described here conform with The Physiological Society ethical requirements.

PCA039

Low Na increases ventricular gap junction resistivity and phosphorylation levels of connexion43-serine 368: Possible synergistic interaction between calcineurin and protein kinase C

A. Waheed, S.C. Salvage, A. Orlowski, C.C. Fry and R.I. Jabr

Biochemistry and Physiology, University of Surrey, Surrey, UK

Ventricular arrhythmias are initiated by abnormal action potential (AP) conduction partially caused by an increased gap junction (GJ) resistivity (R_j). Alterations in ventricular GJ electrical properties may result from either raised $[Ca^{2+}]_i$ and/or changes in the phosphorylation state of GJ proteins, connexin 43 (Cx43). In particular, the phosphorylation of the serine residue at 368 site (Cx43-pS368) by protein kinase C (PKC). We have reported that the slowed AP conduction velocity induced by raised $[Ca^{2+}]_i$ was reversed by cyclosporin A (CsA), an inhibitor of the Ca^{2+}/calmodulin serine-threonine dependent protein phosphatase, calcineurin (Cn). In this study we tested the hypothesis that raised $[Ca^{2+}]_i$ increases R_j as a result of increased Cx43-pS368 levels caused by a possible interaction between Cn and PKC.

Guinea-pig left ventricular papillary muscles were dissected in Tyrode's solution (total [Na]=147.4mM; 24mM $NaHCO_3$, 5%CO_2, 37°C). Tissue impedance (Z) was measured over a range of frequencies (0.02-100kHz) using the oil gap technique. R_j was calculated from Z values in control and low Na Tyrode's solutions (29.4 mM Na, used to increase $[Ca^{2+}]_i$) in the absence/presence of Cn inhibitors (CsA, 5μM and Cn-autoinhibitory peptide,CAIP, 50μM) or PKC inhibitor (chelerythrine, CHE, 2μM). The protein expression of total Cx43 (T-Cx43) as well as Cx43-pS368 was determined from whole tissue lysates using western blotting. Cx43- pS368 bands were in turn normalised to their corresponding T-Cx43 (Cx43-pS368/T-Cx43). Data are means ± SEM, compared by ANOVA, the null hypothesis rejected at $p<0.05$.

R_j was significantly increased by low Na (608 ± 104Ω.cm) when compared to control (403 ± 62Ω.cm; n=7; $p<0.001$). Such an effect was reversed by CsA (475±100 Ω.cm; n=7;$p<0.001$) which alone had no effect. Similar effects were observed with CAIP. Combination of low Na and CHE partially inhibited the rise in R_j induced by low Na alone (control:232.5Ω.cm; low Na:397.5Ω.cm; low Na and CHE: 316.6 Ω.cm; n=2). Moreover, T-Cx43 protein expression was unchanged during all interventions when compared with control. However, there was a significant increase of the Cx43-pS368/T-Cx43 in low Na (0.90±0.64; n=6; $p< 0.05$) when compared to control (0.05±0.02;n=6). Such an increase was reversed by CsA (0.15±0.04; n=6; $p<0.001$) or CHE (0.03±0.01; n=3; $p<0.001$) in the presence of low Na solution.

Raised $[Ca^{2+}]_i$ in ventricular myocardium is associated with CsA and CHE-sensitive increase in R_j caused by increased Cx43-pS368 protein levels. This site is known to be targeted by PKC and lowering Cx43 gap junction conductance. In conclusion, we propose a possible synergistic interaction between Cn and PKC evoked by raised $[Ca^{2+}]_i$ slowing AP conduction a mechanism known to be proarrhythmogenic.

Where applicable, the authors confirm that the experiments described here conform with The Physiological Society ethical requirements.

PCA040

Exercise training in doxorubicin induced cardiomyopathy

C. Matsuura[1], C. Peres[1], E.M. Carvalho[1], V.N. Rocha[1], J.J. Carvalho[2], A. Mendes-Ribeiro[1,3] and T.M. Brunini[1]

[1]Pharmacology, State University of Rio de Janeiro, Rio de Janeiro, Rio de Janeiro, Brazil, [2]Histology and Embriology, State University of Rio de Janeiro, Rio de Janeiro, Rio de Janeiro, Brazil and [3]Physiological Sciences, Federal University of the State of Rio de Janeiro, Rio de Janeiro, Rio de Janeiro, Brazil

Introduction One of the most serious adverse effects of doxorubicin (DOX) chemotherapy is the development of cardiomyopathy. Here we sought to investigate whether exercise

training would ameliorate structural cardiac damage after the development of DOX-induced cardiomyopathy.
Methods 48 male Sprague Dawley rats (220-250 g) received intraperitoneal injections of DOX (1 mg.kg-1.day-1, total 10 mg.kg-1) or 0.9% saline (SAL). Four weeks after injections, they were further divided into exercise (EX) or sedentary (SED) groups. EX groups exercised on a treadmill (30 min.d-1, at 60% of maximal velocity, 5 d.wk-1, for 6 wk). Forty eight hours after the last exercise bout, rats were anesthetized with thiopental (50 mg.kg-1, i.p.), and the heart was removed after KCl intracardiac injection. Fragments of the left ventricle were fixed at 2.5% glutaraldehyde in a 0.1 M cacodylate buffer and post-fixed in 1% osmium tetroxide with 0.8% potassium. Thereafter, fragments were dehydrated in acetone and embedded in Epon. Semithin sections were cut and stained with toluidine blue and observed with a light microscope. Ultrathin sections were obtained from selected areas with ultramicrotome, counterstained with uranyl acetate and lead citrate, and examined with a Zeiss EM 906 transmission electron microscope at 80 Kv. All experimental procedures were approved by the Institutional Animal Care and Use Committee (CEA/051/2009).
Results Before starting training, cardiac dysfunction was confirmed by echocardiography in DOX rats, which showed significant reduction of 24 ± 4% in shortening fraction, and enlarged end-diastolic and end-systolic diameters. An elevated mortality rate was observed in both DOX/groups, but it was significantly lower in DOX/EX (33%) than in DOX/SED (67%) assessed by log rank test (P<.05). Ultrastructural analysis of the heart showed myocardial damage in both DOX/SED and DOX/EX (Fig.1C and 1D) when compared to the SAL/SED and SAL/EX groups (Fig. 1A and 1B). These changes consisted of mitochondria damage with degeneration or loss of cristae and intramitochondrial vacuoles. Moreover, we observed an increase in the mitochondrial matrix caused by mitochondrial loss and intense disarray and fragmentation of myofilaments.
Fig.1. Electron micrographs of cardiac specimens. A, saline/sedentary; B, saline/exercised; C, doxorubicin/sedentary; D, doxorubicin/exercise. Bars 2 μm.
Conclusion The increased survival observed in the DOX/EX group cannot be attributed to an improved myocardial structure. We had previously reported that exercise training led to an improvement in vascular smooth muscle relaxation,1 and therefore we believe that despite the absence of changes in the heart structure, the reduced afterload could contribute to a reduced myocardial oxygen demand.

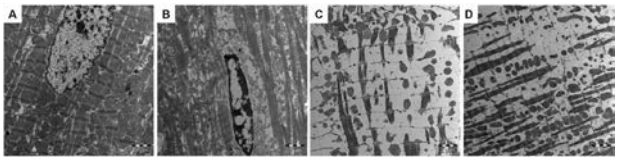

1 Matsuura C et al. J Am Soc Hypertens 4(1):7-13, 2010

Financial support: FAPERJ and CNPq grants

Where applicable, the authors confirm that the experiments described here conform with The Physiological Society ethical requirements.

PCA041

The effect of Mudanpi and its main active component on cardiac ischemia and ion channels

Y. Ma, P.J. Noble, S. Lee, R. Wilkins, C. Ellory and D. Noble

Department of Physiology, Anatomy and Genetics, University of Oxford, Oxford, UK

Mudanpi, a herbal medicine prepared from the root bark of Paeonia Suffruticosa, was traditionally used for thousands of years to 'remove pathogenic heat from blood'. Previous studies showed that Mudanpi has a significant cardioprotective effect against cardiac ischemia (Ma et al 1984), and its active component, paeonol, inhibits the pacemaker potential of cultured myocytes (Ma et al 1986) suggesting that paeonol might influence the activity of cardiac ion channels. Further studies indeed showed that paeonol has a significant effect on the ion channels of cardiac myocytes (Ma et al 2006). We present here the findings obtained over many years from the East to the West; data were collected from heart ischemic model to ion channel activities of the isolated cardiac myocytes using patch clamp electrophysiological method.
The cardiac ischemic model was established by coronary artery occlusion in canines; extract of mudanpi was infused intravenously. The epicardial ECG were recorded by applying 30 electrodes to predetermined epicardial sites. The electrodes were connected to an amplifier, and the epicardial ECG recorded. The elevation of S-T segments were used as a measure of the degree of ischemia. Aterial pressure, heart rate and heart oxygen consumption were recorded. The actions of paeonol on ionic channel were studied using the standard whole-cell configuration of the patch-clamp technique in isolated guinea-pig ventricular myocytes. The effects of paeonol on the action potential (AP) and a variety of ion channels were studied, and the possible mechanisms underlying the alteration of ion channel function were analysed.
The results showed that Mudanpi had a significant protective effect against acute ischemic injury by reducing myocardial oxgen comsumption, reducing cardiac arrhythmic risk, lowering blood pressure and heart rate. The main effect of paeonol on the ventricular myocytes was to shorten the AP duration, suppress the AP upstroke velocity and amplitude, actions associated with the blockade of the voltage-gated, fast sodium current. The shortening effect of paeonol on the AP duration was independent of the blockade of the fast sodium current, and the blockage of calcium current, nor did it activate ATP-sensitive potassium current or chloride current. However, paeonol did block the slowly inactivating sodium current, and blockade of this current is known to result in AP shortening. Using the Noble Heart computational model (Noble et al 1998) we predicted that paeonol inhibits ADP of the AP, a strong indication of antiarrythmic action.
These findings suggest that paeonol, and therefore Mudanpi, may possess antiarrhythmic activity, which may confer their cardioprotective effects.

Ma, YL., Bates, S. & Gurney, A.(2006). European Journal of Pharmacology. 545:87-92

Noble, D., Varghese, A., Kohl, P. and Noble, P. (1998). Can J Cardiol, 14: 123-134.

Ma Yu-ling, Li Lian-da at al. (1986). Chinese J. Integrated Traditional and Western Medicine. 6(5):.292-294

Ma Yu-ling, Li Lian-da et al. (1984). Shan Xi Medical and Pharmaceutical J. 18(4):.212-214

We thank Professor Lian-da Li and Professor Alison Gurney for supervising Yu-Ling's MSc and PhD studies in making the findings presented here.

Where applicable, the authors confirm that the experiments described here conform with The Physiological Society ethical requirements.

PCA043

Opioid receptors involved in cardioprotection of chronic intermittent hypobaric hypoxia in rats through a PKC/ERS signaling pathway

Y. Zhang[1], F. Yuan[1], L. Zhang[2] and S. Wang[1]

[1]Hebei Medical University, Shijiazhuang, China and [2]The third Hospital, Hebei Medical University, Shijiazhuang, China

Background: Chronic intermittent hypobaric hypoxia (CIHH) protects myocardium against ischemia/reperfusion injury. This study aimed to investigate whether opioid receptors participate in cardioprotection of CIHH rats for the first time.
Methods: Adult male Sprague-Dawley (SD) rats were exposed to hypoxia(simulated 5000m altitude)for 28 days, 6 hours per day. The hearts were subjected to 30 min ischemia and 60 min ensuing reperfusion using Langendorff technique. Cardiac function, infarct size, and active of lactate dehydrogenase (LDH) were measured. Expression of opioid receptors and endoplasmic reticulum stress (ERS) molecular chaperones (GRP78, CHOP and caspase-12) was revealed by Western blot analysis.
Results: In CIHH rats after I/R, the recovery of left ventricular function was improved, infarct size and activity of LDH was decreased, expression of and κ opioid receptors was up-regulated, and over-expression of GRP78, CHOP and caspase-12 was inhibited (P< 0.05). All above-mentioned effects of CIHH were abolished respectively by the nonselective opioid receptor antagonist Naloxone, the selective κ-opioid receptor antagonist BNI and the selective δ-opioid receptor antagonist NTI.However,the nonselective opioid receptor agonist morphine, the selective κ-opioid receptor agonist U50488H, and the selective δ-opioid receptor agonist DADLE exerted a protective effect on heart against I/R, and decreased over-expression of GRP78, CHOP and caspase-12 in I/R myocardium of control rats (P<0.05).The cardioprotection of CIHH and opioid agonists was inhibited by CHE, a PKC blocker. The inhibitory effects of CIHH on ERS were also blocked by CHE.
Conclusions: CIHH protects heart against I/R injury through activating opioid receptors and via a PKC/ERS pathway in rats.

Zhu WZ, Wu XF, Zhang Y, Zhou ZN. Proteomic analysis of mitochondrial proteins in cardiomyocytes from rats subjected to intermittent hypoxia. Eur J Appl Physiol 2012 Mar;112(3):1037-46.

Zhang Y, Zhou ZN. Cardioprotective Effect of Chronic Intermittent Hypobaric Hypoxia. Science 2012; suppl (1238-39):38-9.

Zhang Y, Zhong N, Gia J, Zhou Z. Effects of chronic intermittent hypoxia on the hemodynamics of systemic circulation in rats. Jpn J Physiol 2004; 54(2):171-4.

Maslov LN, Barzakh EI, Krylatov AV, Chernysheva GA, Krieg T, Solenkova NV, Lishmanov AY, Cybulnikov SY, Zhang Y. Opioid peptide deltorphin II simulates the cardioprotective effect of ischemic preconditioning: role of delta(2)-opioid receptors, protein kinase C, and K(ATP) channels. Bull Exp Biol Med 2010 Oct;149(5):591-3.

Teng X, Song J, Zhang G, Cai Y, Yuan F, Du J, Tang C, Qi Y. Inhibition of endoplasmic reticulum stress by intermedin(1-53) protects against myocardial injury through a PI3 kinase-Akt signaling pathway. J Mol Med (Berl) 2011 Dec;89(12):1195-205.

This study was supported by National Basic Research Program of China (No. 2012CB518200),National Natural Science Foundation of China (No. 31071002,81100229,31211120166),Natural Science Foundation of Hebei province(No. C2012206001,C2012206063), Science and Technology program of Hebei Province (No.12276104D40), and Medical Research Key Project of Hebei Province Health Bureau (No. 20090319).

Where applicable, the authors confirm that the experiments described here conform with The Physiological Society ethical requirements.

PCA044

Post-transcriptional regulation of human ether-a-go-go-related gene potassium channel protein by AT1 receptor stimulation

Y. Cai, Y. Wang, X. Zuo and Y. Xu

Hebei Medical University, Shijiazhuang, China

There is increasing evidence that angiotensin II (Ang II) is associated with the cardiac electrical remodeling and thus the occurrence of ventricular arrhythmias under pathological conditions. Human ether-a-go-go-related gene (hERG) encodes the pore forming subunit of the channel underlying IKr, which is crucial for the repolarisation of cardiac action potentials. Our previous study has shown that Ang II produces an acute inhibitory effect on IKr/hERG currents via AT1 receptors in guinea pig ventricular myocytes. The present study was designed to investigate the post-transcription regulation of hERG channel protein by chronic stimulation of AT1 receptors in heterologous expression system. An HEK 293 cell line stably expressing hERG channels was established and human AT1 receptor was transiently co-transfected. Western-blot analysis showed that Ang II decreased the abundance of mature hERG protein (155-kDa) in a time- and dose-dependent manner without affecting the level of immature hERG protein (135-kDa). The relative intensity of mature 155-kDa band as control was 68 ± 4% after incubation of Ang II at 100 nM for 24 hours (P<0.01, n=6). Values are means ± S.E.M. of n experiments, compared by two-tailed Student's t test. To investigate the effects of Ang II on degradation of mature hERG channels, we blocked forward trafficking with a Golgi transit inhibitor brefeldin A (BFA, 10 μM). Ang II significantly enhanced the time-dependent reduction of mature hERG channels. A proteasomal inhibitor lactacystin (5 μM) significantly inhibited Ang II-mediated reduction of the mature protein (from 67 ± 4% to 89 ± 3%, P<0.05, n=3), but the lysosomal inhibitor bafilomycin A1(1 μM) had no significant effect on the role of Ang II. It indicated that Ang II accelerated channel protein degradation, primarily through the proteasome pathway. The protein kinase C inhibitor bisindolylmaleimide I antagonized the reduction of mature 155-kDa proteins by Ang II, suggesting that the effect of Ang II was mediated by intracellular PKC signaling pathway. In conclusion, the chronic incubation of Ang II reduced the mature hERG channel protein by accelerating channel degradation through a PKC pathway. The findings suggest a potential mechanism by which elevated levels of Ang II may be involved in the hERG channel remodeling in heart diseases.

This work was supported by the National Natural Science Foundation of China (30871010).

Where applicable, the authors confirm that the experiments described here conform with The Physiological Society ethical requirements.

PCA045

Pharmacological and pH modulation of sodium-dependent background current in rabbit atrioventricular node cells

H. Cheng[1], M.R. Boyett[2], C.H. Orchard[1] and H.C. Jules[1]

[1]School of Physiology and Pharmacology, University of Bristol, Bristol, UK and [2]Institute of Cardiovascular Sciences, University of Manchester, Manchester, UK

The atrioventricular node (AVN) plays a critical role in normal cardiac conduction and can also take over pacemaking of the ventricles should the sinoatrial node fail. The cellular electrophysiological basis of AVN pacemaking is incompletely understood, although it is likely to involve multiple ionic conductances (Inada *et al*., 2009). The potential importance of a background inward conductance in sinoatrial node cells has long been recognised (Hagiwara *et al*., 1992), and we recently presented preliminary evidence for a sodium-dependent background current ($I_{B,Na}$) in rabbit AVN cells (Cheng *et al*., 2012). The present study was designed to investigate further the characteristics of $I_{B,Na}$ from rabbit AVN cells. Adult male New Zealand White rabbits were killed in accordance with UK Home Office legislation and AVN cells were isolated as described previously (Cheng *et al*., 2009). Whole-cell voltage-clamp using voltage-ramp protocols was used to record the background current, after the Ca^{2+}, K^+, Na^+-K^+ pump and Na^+-Ca^{2+} exchange (NCX) currents were inhibited by appropriate blockers (Hagiwara *et al*., 1992). Values are means±SEM, compared by ANOVA or *t*-test. Since $I_{B,Na}$ is Na^+-dependent, in order to preclude the involvement of NCX current (I_{NCX}), Ni^{2+} was applied at a concentration (10 mM) which produces profound block of I_{NCX} (Hinde *et al*., 1999). 10 mM Ni^{2+} caused only a small decrease in the amplitude of $I_{B,Na}$ at -100 mV, from -1.27±0.11 pA/pF (in 2 mM Ni^{2+}, which was present in all solutions and substantially inhibits the NCX; Hagiwara *et al*, 1992; Hinde *et al*, 1999) to -0.98±0.06 pA/pF (P<0.05, n=6 and7). $I_{B,Na}$ also persisted following application of a second NCX inhibitor (KB-R7943; 5 μM). These data demonstrate that $I_{B,Na}$ in rabbit AVN cells cannot be attributed to I_{NCX}. Amiloride (1 mM), which was reported to produce partial inhibition of $I_{B,Na}$ in sinoatrial node cells (Hagiwara *et al*., 1992), produced a modest reduction in $I_{B,Na}$ (-0.91±0.11 vs. -1.52±0.13 pA/pF in control at -100 mV, P<0.01, n=8). In contrast, changing extracellular solution pH from 7.4 to 6.3 markedly decreased $I_{B,Na}$ (to -0.43±0.08 pA/pF from -1.11±0.12 pA/pF at -100 mV, P<0.01, n=12). The sensitivity of $I_{B,Na}$ to extracellular acidosis is consistent with the notion that modulation of $I_{B,Na}$ is likely to contribute to previously reported effects of pH on AVN cell electrophysiology (Cheng *et al*., 2009).

Cheng H, Smith GL, Orchard CH, Hancox JC (2009). Acidosis inhibits spontaneous activity and membrane currents in myocytes isolated from the rabbit atrioventricular node. *J Mol Cell Cardiol* 46, 75-85.

Cheng H, Orchard CH, Boyett MR, Hancox JC (2012). Sodium-dependent background current in cells from the rabbit atrioventricular node. *University of Manchester, a themed meeting (CR) of the Physiological Society*, PC41.

Hagiwara N, Irisawa H, Kasanuki H, Hosoda S (1992). Background current in sinoatrial node cells of the rabbit heart. *J Physiol* 448, 53-72.

Hinde AK, Perchenet L, Hobai IA, Levi AJ, Hancox JC (1999). Inhibition of Na/Ca exchange by external Ni in guinea-pig ventricular myocytes at 37°C, dialysed internally with cAMP-free and cAMP-containing solutions. *Cell Calcium* 25, 321-331.

Inada S, Hancox JC, Zhang H, Boyett MR (2009). One-dimensional mathematical model of the atrioventricular node including atrio-nodal, nodal and nodal-His cells. *Biophys J* 97, 2117-2127.

This work was funded by the British Heart Foundation (PG/11/24/28818).

Where applicable, the authors confirm that the experiments described here conform with The Physiological Society ethical requirements.

PCA046

Investigation of the influence of hERG 1b on hERG channel pharmacology

A. EL Harchi[1], D. Melgari[1], H. Zhang[2] and J.C. Hancox[1]

[1]School of Physiology and Pharmacology, University of Bristol, Bristol, UK and [2]School of Physics and Astronomy, The University of Manchester, Manchester, UK

hERG channels mediating the rapid delayed rectifier K^+ current (I_{Kr}) are important for normal ventricular repolarisation. In native cardiac tissues, the hERG 1a subunit co-assembles with a subunit encoded by an alternate transcript, "ERG1b" which has a shorter N-terminus and influences current kinetics (Jones et al, 2004). There is some evidence that hERG 1b may confer altered pharmacological properties on hERG 1a/1b compared to hERG 1a alone (Sale et al, 2008; Abi-Gerges et al, 2011). Some of this evidence derives from automated patch-clamp at room temperature (RT). As hERG kinetics show a complex temperature dependence (Vandenberg et al, 2006), we have sought to investigate comparative pharmacology of hERG 1a and hERG 1a/1b using manual patch clamp at physiological temperature and for some drugs at room temperature. HEK-293 cells stably expressing either hERG 1a alone or transiently co-transfected with hERG 1a and hERG 1b plasmid constructs were utilised. Effects of chloroquine and fluoxetine on hERG tail currents recorded at -40 mV (I_{hERG}) carried either by hERG 1a or hERG 1a+1b were assessed using a standard voltage clamp protocol (every 12s a 2-s depolarising step to +20mV followed by a repolarising step to -40mV to elicit tail currents were applied). Most experiments were performed at 37ºC; for fluoxetine (previously reported to be more potent against hERG 1a/1b than hERG 1a with automated patch clamp at room temperature (RT) (Abi-Gerges et al, 2011)), we compared RT and 37ºC. For concentration–response relations for drug inhibition of I_{hERG} tail at – 40 mV, four different concentrations of chloroquine and fluoxetine were tested (n=4 to 7 cells per concentration). We also examined the effect of a single concentration close to IC_{50} value for hERG 1a inhibiton by fluoxetine on I_{hERG}1a and I_{hERG}1a/1b elicited with a ventricular action potential voltage command at 37ºC. At 37ºC the sensitivity of I_{hERG} tails to each of chloroquine and fluoxetine did not differ between I_{hERG}1a and I_{hERG}1a/1b. At 25ºC the deactivation kinetics of both I_{hERG}1a and I_{hERG}1a/1b were slowed compared to 37ºC. This was accompanied by a ~2.1 fold decrease in sensitivity to fluoxetine for I_{hERG}1a/1b tails versus ~1.4 for I_{hERG}1a tails at 25ºC compared to 37ºC. We also observed a marked temperature dependence of the time-course of I_{hERG}1a inhibition by fluoxetine but this was not the case for I_{hERG}1a/1b. Finally, we did not observe any difference in I_{hERG}1a and I_{hERG}1a /1b sensitivity to 1 μM fluoxetine at 37ºC under AP clamp. Our

data are consistent with modest differences between I_{hERG}1a and I_{hERG}1a/1b pharmacology. These differences vary between drugs and experimental temperatures.

Jones EM, Roti Roti EC, Wang J, Delfosse SA, Robertson GA. Cardiac I_{Kr} channels minimally comprise hERG 1a and 1b subunits. J Biol Chem 2004; 79(43):44690-4

Sale H, Wang J, O'Hara TJ, Tester DJ, Phartiyal P, He JQ, Rudy Y, Ackerman MJ, Robertson GA. Physiological properties of hERG 1a/1b heteromeric currents and a hERG 1b-specific mutation associated with Long-QT syndrome. Circ Res. 2008 Sep 26;103(7):e81-95.

Abi-Gerges N, Holkham H, Jones EM, Pollard CE, Valentin JP, Robertson GA. hERG subunit composition determines differential drug sensitivity. Br J Pharmacol. 2011 Sep;164(2b):419-32.

Vandenberg JI, Varghese A, Lu Y, Bursill JA, Mahaut-Smith MP, Huang CL. Temperature dependence of human ether-a-go-go-related gene K^+ currents. Am J Physiol Cell Physiol. 2006 Jul;291(1):C165-75. Epub 2006 Feb 1.

This work was supported by the British Heart Foundation (PG/10/96).

Where applicable, the authors confirm that the experiments described here conform with The Physiological Society ethical requirements.

PCA047

Detecting diffusion barriers in rat cardiomyocytes with extended raster image correlation spectroscopy

P. Simson, N. Jepihhina, P. Peterson and M. Vendelin

Laboratory of Systems Biology, Institute of Cybernetics, Tallinn University of Technology, Tallinn, Estonia

A series of kinetic experiments show the existence of considerable ADP and ATP diffusion restrictions in rat cardiomyocytes (1,2). As an alternative method to estimate diffusion, we have extended raster image correlation spectroscopy — RICS (3) — - to study diffusion in anisotropic media, such as heart muscle cells (4). On the basis of the measurements on two different dyes, our analysis suggests that the diffusion restrictions are localized in certain areas of the cell (5). However, their location, physiological role, and the intracellular structures responsible for these restrictions are still unclear. We hypothesize that diffusion restrictions in cardiomyocyte are in the form of membrane-like barriers, and present a theoretical foundation for the use of RICS to determine the presence and the locations of such barriers. With a Gaussian point spread function of the microscope, the pair correlation function (PCF) for an impermeable membrane is calculated analytically, thus giving a convenient theoretical basis for the interpretation of microscopy data. We demonstrate that, in the proximity of the membrane, the PCF is not symmetric, as opposed to the case of homogeneous media. As a result, this property of PCF can be used to detect barriers. Indeed, our preliminary experimental results support this theory. We recorded fluctuations in fluorescence within the permeabilized rat cardiomyocyte along a line that was partially in the cell and partially in the solution. Paired-correlation RICS analysis shows that in the cell region the symmetry of the correlation function is modulated, but not in the solution. These results can be interpreted as an evidence that periodic diffusion barriers exists in rat cardiomyocytes.

Sepp M, Vendelin M, Vija H, and Birkedal R. ADP compartmentation analysis reveals coupling between pyruvate kinase and ATPases in heart muscle. Biophys J. 2010;98:2785-2793.

Jepihhina N, Beraud N, Sepp M, Birkedal R, and Vendelin, M. Permeabilized rat cardiomyocyte response demonstrates intracellular origin of diffusion obstacles. Biophys J. 2011;101(9):2112-2121.

Digman M.A, Brown C.M, Sengupta P, Wiseman P.W, Horwitz A.R, and Gratton E. Measuring fast dynamics in solutions and cells with a laser scanning microscope. Biophys J. 2005;89(2):1317–1327.

Vendelin, M and Birkedal, R. Anisotropic diffusion of fluorescently labeled ATP in rat cardiomyocytes determined by raster image correlation spectroscopy. Am J Physiol Cell Physiol. 2008;295:C1302-C1315.

Illaste A, Laasmaa M, Peterson P, and Vendelin M. Analysis of Molecular Movement Reveals Latticelike Obstructions to Diffusion in Heart Muscle Cells. Biophys J. 2012;102(4):739-748.

This work was supported by Wellcome Trust International Senior Researcher Fellowship (WT081755) and European Union through the European Regional Development Fund.

Where applicable, the authors confirm that the experiments described here conform with The Physiological Society ethical requirements.

PCA048

Assay of the perfused rat heart during cardiac ischemia with Rb Electron Probe Microanalysis

V. Pogorelova and A. Pogorelov

Institute of Theoretical and Experimental Biophysics RAS, Pushchino, Russian Federation

Cardiac ischemia is followed by the potassium deficiency in cardiomyocyte [1-2]. The intracellular potassium concentration is an integrative result of active influx through Na^+/K^+-ATPase and passive transport via K^+ channels and anti- and symporters. Therefore the intensive potassium release may mask the pump activity. As Rb^+ is assumed to be a biological congener of K^+, and extracellular medium is modified to contain rubidium ions, ^{87}Rb NMR have been developed to mark K^+ fluxes between extracellular space and tissue [3]. Electron Probe Microanalysis (EPMA) allows the determination of elemental contents in cellular cytoplasm and this was utilized for Rb analysis in the neural and cardiac cells [4-5]. We applied EPMA to compare the kinetic parameters of potassium influxes at normoxic and ischemic conditions.

After decapitation the heart from 300-350 g male Wistar rat was perfused in the Langendorff mode with Tyrode's solution at a constant pressure of 70 mm Hg and the myocardial temperature was maintained at 38°C. Normoxic conditions were created with 95% O_2 + 5% CO_2 aeration of Tyrode. Ischemia was employed using glucose free solution equilibrated with 100% argon. Following 6 minutes of equilibration, hearts were perfused 5 min, 30 min, 45 min and 60 min at normoxic or ischemic conditions. Then papillary muscles were excised from the heart for EPMA technique [1]. Freshly isolated papillary muscle was frozen immediately by plunging into liquid propane (90°K) and cut in cryostat (240°K). Tissue cryosections were picked up and freeze-dried for 12 hours in a high vacuum. Freeze-dried cryosections were mounted on aluminium grids and intracellular rubidium content was examined in a scanning electron microscope JEOL JSM-U3 equipped with wavelength dispersive spectrometers. The section was viewed in the STEM mode at an accelerating voltage of 25 kV, a beam current of 1-5 nA and a probe diameter about 0.1 μm. EPMA data obtained are summarised in Table 1.

Experimental data of Rb EPMA allowed us to estimate the kinetic parameters [5]. Thus EPMA provides a method of determining uni-directional K fluxes in the cardiac myocell of perfused rat heart.

Table1. Changes of rubidium concentration (mM) in myocells of isolated rat heart during normoxic and ischemic Langendorff's perfusion with solution containing 2,5 mM Rb^+ and 2,5 mM K^+ *

Time of perfusion	Normoxic perfusion	Ischaemic perfusion
15 min	33±2	11±1
30 min	59±3	20±1
45 min	66±3	23±1

* EPMA data are presented as means ± S.E.M. for 100 myocells from 4 animals

Pogorelov AG *et al.* (1991). *J Microsc* **12**, 24-38.

Pogorelov AG *et al.* (2002). *Biophysics* **47**, 691-698.

Allis JI *et al.* (1989). *FEBS Letters* **242**, 215-217.

Saubermann AJ *et al.* (1992). *Brain Research* **577**, 64-72.

Pogorelov AG *et al.* (2012). *Biophysics* **57**, 640–643.

Where applicable, the authors confirm that the experiments described here conform with The Physiological Society ethical requirements.

PCA049

HIP-55 inhibits isoproterenol-induced cardiac remodeling through negatively regulating p38 MAPK

Z. Li

Institute of Vascular Medicine, Peking University Third Hospital, Beijing, China and Key Laboratory of Cardiovascular Molecular Biology and Regulatory Peptides, Ministry of Health, Beijing, China

Cardiac remodeling is a common pathophysiological process shared by many cardiovascular diseases and is crucial in the transition of cardiac function from compensated to decompensated stage. It is closely related to the occurrence, development and prognosis of these diseases. The excessive activation of sympathoadrenal system(especially activation of β-ARs) is an important cause of cardiac remodeling and heart failure,while β-ARs blockers can observably improve the prognosis for patients. In our previous research, HIP-55 was found as a novel protein involeved in isoproterenol (ISO) induced cardiac remodeling by using proteomics approaches. Here, we induced cardiac remodeling in HIP-55 transgenic or knockout C57BL/6 mice with injection of isoproterenol hydrochloride (ISO) for 7 days[5 mg/(kg*d)]. The cardiac remodeling was inhibited in transgenic mice and aggravated in knockout mice, suggesting that HIP-55 can inhibit the ISO induced myocardial remodeling. Further mechnism research showed that p38 MAPK inhibitor SB203580 obviously reduced ISO induced myocardial remodeling in neonatal rat ventricular cardiomyocytes and cardac fibroblasts with western blot, realtime PCR and BRDU proliferation assay. While HIP-55 can inhibit the phosphorylation and kinase activation of P38, which were decreased in HIP-55 over-expressed cardiomyocytes and cardiofibroblasts and increased in HIP-55 knock-down cells.Thus, those results indicates that HIP-55 can obviously inhibit the ISO induced myocardial remodeling, and that the mechanism is through negtively regulating p38 MAPK signaling pathway.

This work was supported by the the National Natural Science Foundation of China (81270157 and 810700781) and the Beijing Municipal Natural Science Foundation (7102158).

Where applicable, the authors confirm that the experiments described here conform with The Physiological Society ethical requirements.

PCA050

Effects of detubulation on spatiotemporal properties of Ca transients in sheep atrial myocytes

M.A. Richards, G. Kirkwood, J.D. Clarke and K.M. Dibb

Institute of Cardiovascular Sciences, University of Manchester, Manchester, UK

Transverse (t-) tubules are essential for facilitating the synchronous increase in cytosolic calcium during excitation-contraction coupling in mammalian ventricular myocytes. It has recently been established that atrial cells of large mammals, including humans, also possess substantial t-tubule networks[1]. Here we investigate the functional significance of t-tubules for synchronous Ca release in sheep atrial myocytes.

Myocytes from adult sheep were enzymatically isolated from the left atrial appendage. Formamide was used to detubulate the cells[2]. Cells were bathed in Tyrode's solution and stimulated via patch pipette. Confocal microscopy was used to obtain xy scans of a single z-plane of atrial myocytes using the Ca indicator Fluo-5F AM. Images were sampled at 50Hz and merged to produce pseudo-linescans. T-tests were used for statistical analysis.

Pseudo-linescans showed triggered Ca release in control myocytes was synchronous, with a rapid rise at both sarcolemmal and central regions of the cell. In contrast, detubulated cells showed a rapid Ca rise at sarcolemmal sites and a slow Ca rise at central regions. To quantify the synchronicity of Ca release, rates of Ca rise for each region were plotted as a function of distance from the sarcolemma and fitted with a linear regression. The mean gradient was flat for control cells but was steep for detubulated cells (0.0015 ± 0.0085 vs. -0.075 ± 0.014, n=8-10; P<0.001) indicating a high degree of dyssynchrony. This resulted in a steep gradient for time to peak in detubulated cells (0.0006 ± 0.0014 vs. 0.0232 ± 0.0053, n=8-10; P<0.01). The difference in time to peak between central and sarcolemmal regions was significantly slower in detubulated than control cells (2.1 ± 14.5ms vs. 215.8 ± 39.5ms, n=8-9; P<0.001). Detubulated cells showed a marked latency in central Ca rise (6.4 ± 5.3ms vs. 68 ± 22.5ms, n=8-9; P<0.05). On exposure to isoprenaline (100nM) detubulated cell Ca transients from central regions showed a rapid Ca rise similar to those at the sarcolemmal regions. The steep gradient of dyssynchrony seen in detubulated cells was flattened in the presence of isoprenaline (-0.075 ± 0.014 vs. 0.009 ± 0.02, n=4; P<0.01). However, in spite of an increase in synchronicity of Ca release, the latency of Ca rise was still present (68 ± 22.5ms vs. 57.4 ± 8.6ms, n=4; P>0.05).

These data show that Ca transients of sheep atrial myocytes result from synchronous Ca release at all regions of the cell. Acute loss of t-tubules resulted in dyssynchrony, increased latency and time to peak of Ca transients at central regions of the myocytes. β-adrenoceptor activation improves synchronicity of Ca release in detubulated myocytes but latency of Ca transients at the central regions persists due to the reliance of Ca wave propagation in the absence of t-tubules.

Richards et al. (2011) Am J Physiol Heart Circ: 301, H1996-H2005

Brette et al. (2002) Am J Physiol Heart Circ: 283: H1720-H1728

This work was supported by the British Heart Foundation

Where applicable, the authors confirm that the experiments described here conform with The Physiological Society ethical requirements.

PCA051

Membrane nanotubes as a novel long distance intercellular connectivity between Cardiomyocytes and Cardiofibroblasts

Y. Zhang

Institute of Vascular Medicine, Peking University Third Hospital, Beijing, China and Key Laboratory of Cardiovascular Molecular Biology and Regulatory Peptide, Ministry of Health, Beijing, China

Background: Intercellular interactions between cardiomyocytes (CMs) and cardiofibroblasts (FBs) are important in the physiological and pathophysiological heart. Understanding such interactions is important for developing effective therapies for heart disease. However, little is known about these interactions until recently. Membrane nanotube (MNT) is a novel structure connecting the mammalian cells over long distance. The classical view is that paracrine and gap junctions are the only forms of "communication" between MCs and FBs. Methods and Results: By membrane dye staining, we observed long, thin membrane nanotubular structures containing actin and microtubules that connected neonatal rat ventricular CMs and FBs. The mean length of WGA-stained membrane nanotubes between CMs and FBs was 13.9±10.4 mm (n=73 of 39 pairs of cells). By single-particle tracking, we observed vehicles moving between CMs and FBs within the membrane nanotubes. By dual colour staining, confocal imaging and flow cytometry, we observed mitochondria exchange between CMs and FBs in a coculture system. By combined atomic force microscopy (AFM) and confocal microscopy, we observed calcium signal propagation from AFM-stimulated CM or FB to unstimulated FB or CM via membrane nanotubes. By membrane and cytoskeleton staining, we observed similar nanotubular structures in adult mouse heart tissue, which suggests their physiological relevance. Conclusion: Our study posts a challenge to the classical "cardiac communication" theory, and suggests that MNT is an important structure for long distance "communication" between cardiac cells.

This work was supported by the National Key Basic Research Program of People's Republic of China (2007CB935601) and the Natural Science Foundation of China (81030001, 30821001).

Where applicable, the authors confirm that the experiments described here conform with The Physiological Society ethical requirements.

PCA052

Palmitoylation of the Na pump catalytic subunit

K. Wypijewski[1], J. Howie[1], L. Reilly[1], L. Tian[2], M.J. Shipston[2], M.L. Ashford[1] and W. Fuller[1]

[1]Division of Cardiovascular & Diabetes Medicine, College of Medicine Dentistry & Nursing, University of Dundee, Dundee, UK and [2]Centre for Integrative Physiology, University of Edinburgh, Edinburgh, UK

Acute regulation of the cardiac Na pump by extracellular stimuli is crucial in allowing the heart to match its output to systemic requirements. The Na pump not only plays a critical role in a plethora of transmembrane transport process, electrical excitability and cell volume control but also, by setting intracellular Na, is a primary determinant of cardiac contractility because it determines the set-point for the sarcolemmal sodium-calcium exchanger.

S-palmitoylation is a reversible covalent post-translational attachment of the fatty acid palmitic acid to the thiol group of cysteine, via an acyl-thioester linkage. Palmitoylation can alter enzymatic / ion channel activity, stability or subcellular localisation of the target protein, and this is usually achieved by the recruitment of the palmitoylated cysteine to the lipid bilayer. As such, palmitoylation has the potential to induce substantial changes in protein secondary structure and thus function, through the recruitment of intracellular loops to the inner surface of the membrane bilayer.

We investigated palmitoylation of the catalytic α subunit of the Na pump in ventricular myocytes isolated from adult male Wistar rats. Palmitoylated proteins were purified by resin-assisted capture, and palmitoylation sites identified by differential alkylation of palmitoylated and non-palmitoylated cysteines, followed by analysis by LC-MS/MS against inclusion lists. Cys 374 in the α1 subunit of the Na pump was found palmitoylated. Located within the P (phosphorylation) domain of the α1 subunit which is transiently phosphorylated during the reaction cycle of the pump, C374 lies only 2 amino acids from the central catalytic aspartate (376), the site of this transient phosphorylation, meaning its palmitoylation is highly likely to influence pump activity.

In order to determine which acyl palmitoyl transferase (DHHC-PAT) palmitoylates the Na pump α1 subunit, all 25 mammalian DHHC-PATs were individually transiently overexpressed in HEK-293 cells, and palmitoylation of the endogenous Na pump α1 subunit assessed by immunoblotting after resin-assisted capture. Only expression of DHHC15 significantly increased palmitoylation of the α1 subunit (4.6±1.8 fold over mock transfected control, n=5, mean±SEM $p<0.05$, t-test), implicating this DHHC-PAT in pump α subunit palmitoylation.

DHHC15 is a Golgi-localised DHHC-PAT. We therefore propose that α subunit palmitoylation occurs early in the lifetime of the cardiac Na pump complex, and may represent a mechanism to inhibit futile ATP hydrolysis and / or Na-loading of intracellular compartments by the Na pump during it passage through the secretory pathway. The control of α subunit depalmitoylation upon delivery to the surface membrane may therefore represent a crucial step in controlling the number of active Na pumps at the cell surface.

This work was supported by a grant from the British Heart Foundation, reference PG/12/6/29366

Where applicable, the authors confirm that the experiments described here conform with The Physiological Society ethical requirements.

PCA053

Simultaneous measurement of cytoplasmic and SR calcium during modulation of ryanodine receptor open probability in canine ventricular myocytes

D.J. Greensmith[1], G.L. Galli[1], M.J. Morton[2], C.E. Pollard[2], A.W. Trafford[1] and D.A. Eisner[1]

[1]Unit of Cardiac Physiology, The University Of Manchester, Manchester, UK and [2]Safety Pharmacology, Safety Assessment UK, AstraZeneca R&D, Macclesfield, UK

We have previously shown in rat ventricular myocytes that modulation of ryanodine receptor (RyR) open probability using low concentrations of caffeine has no *maintained* effect on the amplitude of systolic Ca (Trafford *et al*, 2000). We suggested

that the increased RyR open probability was compensated for as the initial increase in systolic Ca enhanced sarcolemmal Ca efflux thus reducing SR Ca content. Here we present data that address two outstanding issues. (1) Are similar results seen in a large animal model? (2) We wished to measure SR Ca content directly rather than, as in our previous work, inferring it from sarcolemmal Ca fluxes.

Canine ventricular myocytes were loaded with Fluo-3 for cytoplasmic Ca measurement or co-loaded with Fluo-3 and the low-affinity Ca indicator, Mag-Fura-2 for cytoplasmic and intra SR Ca measurement respectively and paced at 0.5 Hz under voltage or current clamp.

Under voltage clamp, application of 0.5 mM caffeine initially increased the amplitude of systolic Ca by 115 %. This was associated with a 19 % decrease in Ca influx on the L-type Ca current and a 145 % increase in sarcolemmal Ca efflux. However, within 3 or 4 beats in caffeine, all these parameters recovered to control levels. Upon caffeine washout, we observed an under shoot in the amplitude of systolic Ca which subsequently recovered to control levels. In the steady state, 0.5 mM caffeine reduced SR Ca content (quantified by application of 10 mM caffeine) by 47 % which subsequently recovered during washout.

To directly measure beat by beat SR Ca, myocytes were co-loaded with Fluo-3 and Mag-Fura-2 and paced under current clamp. Upon caffeine application, a 154 % potentiation of systolic Ca was associated with a 755 % increase in the magnitude of systolic SR Ca depletion. Both these parameters rapidly recovered to control levels during caffeine application, coinciding with a beat by beat reduction of SR Ca to 84 % of control. Upon washout, an initial 41 % decrease in systolic Ca was associated with a 55 % decrease in the magnitude of systolic SR Ca depletion. Both these parameters and SR Ca content subsequently recovered to control levels.

These data demonstrate that in a large animal model, modulation of RyR open probability has no maintained effect on the amplitude of systolic Ca. Increasing RyR open probability initially increases systolic Ca leading to reduced Ca influx and enhanced Ca efflux and so a net loss of Ca from the cell. This results in a beat by beat loss of SR Ca to a level that compensates for the increased RyR open probability, at which point the amplitude of systolic Ca is restored. The converse is true during the relative decrease of RyR open probability during wash.

Trafford AW *et al*. (2000). *J Physiol* **522**, 259-270

Where applicable, the authors confirm that the experiments described here conform with The Physiological Society ethical requirements.

PCA054

Regulation of I_{Ca} by basal protein kinase A activity and its facilitation by caveolin-3 are altered in heart failure in rat ventricular myocytes

S. Bryant[1], C.H. Kong[1], M. Suleiman[2], A.F. James[1] and C.H. Orchard[1]

[1]School of Physiology & Pharmacology, University of Bristol, Bristol, UK and [2]School of Clinical Sciences, University of Bristol, Bristol, UK

The transverse (t-) tubules of cardiac ventricular myocytes show marked changes in structure during heart failure (HF), which lead to decreased synchrony of Ca release and Ca transient amplitude. We have previously shown that stimulation of L-type Ca current (I_{Ca}) by basal protein kinase A (PKA) activity occurs predominantly in the t-tubules and is facilitated by caveolin-3 (Cav-3). However, the effect of HF on such regulation is unknown. We have, therefore, investigated Cav-3 and PKA mediated regulation of I_{Ca} in a rat model of HF.

Myocardial infarction was induced in male Wistar rats (~250g) by ligation of the left anterior descending coronary artery (LAD) under surgical anaesthesia (Ketamine 75 mg/kg, Medetomidine 0.5 mg/kg, *i.p.*) with appropriate analgesia (Buprenorphine 0.05 mg/kg, *s.c.*). Left ventricular myocytes were isolated from ligated (HF) or sham animals 16 weeks after surgery, following removal of the heart under Pentobarbitone (140 mg/kg *i.p.*) anaesthesia. All animal procedures were approved by the University of Bristol ethics committee and conducted in accordance with UK legislation. I_{Ca} was recorded using whole-cell patch-clamp at room temperature. Incubation with TAT-tagged C3SD peptide was used to disrupt normal Cav-3 protein binding (MacDougall et al., 2012); non-incubated cells were used as controls (Con). Cells stained with di-8-ANEPPS were imaged using confocal microscopy. T-tubule regularity was quantified using FFT analysis by plotting the amplitude of the first harmonic as a function of total intensity (TT power). Data are expressed as mean±SEM (n). Statistical significance at $p<0.05$ was determined using Student's t-test or analysis of variance with the appropriate Bonferroni *post hoc* test.

Animals that underwent LAD ligation had significantly increased heart:body weight (Sham 3.3±0.2 (9) vs HF 4.6±0.2 (7) g/kg, $p<0.001$) and lung:body weight (Sham 3.2±0.1 (9) vs HF 3.7±0.1 (7) g/kg, $p<0.05$). HF myocytes had increased cell capacitance (Sham 285±12 (31) vs HF 348±18 (21) pF, $p<0.01$ and reduced TT power (Sham 70.6±9.8 (48) vs HF 35.4±4.7 (58) a.u., $p<0.002$).

Under basal conditions I_{Ca} density was not different between Sham and HF (Sham -6.1±0.2 (31), HF -5.8±0.3 (21) pA/pF, ns). However, after inhibition of basal PKA activity using H-89 (20 μM) I_{Ca} density was lower in HF (Sham -3.0±0.1 (18), HF -2.3±0.1 (14) pA/pF, $p<0.05$). I_{Ca} was reduced by C3SD in sham cells (Sham -6.5±0.4 (16), Sham+C3SD -4.9±0.3 (16) pA/pF, $p<0.01$) but was not affected by C3SD in HF cells (HF –5.6±0.4 (14), HF+C3SD -5.8±0.5 (15) pA/pF, ns).

These data suggest that in HF, under basal conditions, there is increased stimulation of I_{Ca} by basal PKA activity but that the normal coupling of PKA activity to I_{Ca} by Cav-3 is disrupted.

MacDougall DA, Agarwal S, Stopford E, Chu H, Collins J, Longster A, Colyer J, Harvey R & Calaghan S (2012). J Mol Cell Cardiol 52, 388-400.

This work was supported by the British Heart Foundation

Where applicable, the authors confirm that the experiments described here conform with The Physiological Society ethical requirements.

PCA055

Loss of myocardial nNOS in atrial fibrillation (AF) affects action potential duration: Implications for AF-induced electrical remodelling

X. Liu[1], S. Reilly[1], A. Bueno-Orovio[2], R. Carnicer[1], A. Recalde[1], R. Jayaram[1], B. Rodriguez[3] and B. Casadei[1]

[1]Cardiovascular Medicine, University of Oxford, Oxford, UK, [2]Oxford Centre for Collaborative Applied Mathematics, University of Oxford, Oxford, UK and [3]Computer Science, University of Oxford, Oxford, UK

Rationale: Reduced action potential duration (APD) and lack of APD rate dependent-adaptation are hallmarks of AF-induced electrical remodelling of the atrial myocardium. Understanding the mechanism underlying atrial electrical remodelling in AF is of fundamental importance for the prevention and treatment of AF. We have recently found that nitric oxide synthase (NOS) activity is dramatically reduced in atrial myocytes from goats and patients with AF. Whether loss of NOS activity contributes to the AF-induced atrial electrical remodelling remains to be established.
Methodology: The whole cell current patch clamp technique was used to measure the AP in human and murine isolated atrial myocytes (N: number of patients or mice; n: number of myocytes). AF was induced in mice in vivo by using transoesophageal electrical stimulation. The protein content of constitutive NOSs (nNOS and eNOS) was assessed by Western blotting in atrial lysates. NOS activity was measured by the L-arginine to citrulline assay. Simulations were performed to evaluate the role of decreased nNOS activity in rotor stability in mouse right/left atrial (RA/LA) tissue models.
Results: We found that decreased atrial NOS activity in patients with AF was associated with a significant reduction in nNOS protein expression (by 62%) whereas eNOS was unchanged. To evaluate the role of nNOS on atrial electrical properties, we examined the effects of the nNOS inhibitor, S-methylthiocitrulline (SMTC), or nNOS gene deletion on APD. SMTC induced 38%, 39% and 30% reduction in APD20, APD50 and APD90 respectively in RA myocytes from patients in Sinus Rhythm (SR) (N=8, n=38 control vs. N=8, n=31 cells perfused and dialyzed with SMTC, $p<0.001$) and suppressed the APD rate dependent-adaptation. In murine RA myocytes, inhibition and gene deletion of nNOS reduced APD by 38% and 22%, respectively (N=9, n=35 from $nNOS^{-/-}$ & N=6, n=11 wild type, WT, cells plus SMTC vs. N=10, n=28 control WT cells, $p<0.001$). SMTC had no effect on APD in atrial myocytes from $nNOS^{-/-}$ mice. nNOS inhibition and gene deletion also abolished the physiological RA to LA gradient in APD. In silico simulation indicated that lack of atrial APD gradient promotes rotor stability at the RA/LA junction which may contribute to increased AF propensity. In agreement with these findings, nNOS-deficient mice displayed a 2-fold increase in AF inducibility in response to stimulation ($p<0.05$ vs. WT littermates, N=18 in each group).
Conclusions: In mammalian atrial myocytes, nNOS plays an important role in determining APD, its rate-adaptation and the physiological RA/LA electrical gradient. These findings suggest that the marked loss of nNOS protein and activity in the fibrillating atrial myocardium has potentially important implication for AF-induced electrical remodelling.

Where applicable, the authors confirm that the experiments described here conform with The Physiological Society ethical requirements.

PCA056

A molecular modeling approach for understanding mechanism of disease causing mutations in domain C1 of cardiac myosin binding protein C

N. Krishnamoorthy[1], P. Gajendra Rao[1], H.S. Kassem[2], S. Moharem-Elgamal[2], F. Cecchi[3], I. Olivotto[3] and M.H. Yacoub[1,4]

[1]Qatar Cardiovascular Research Center, Qatar Foundation, Doha, Qatar, [2]BA-HCM National Programme, Aswan Heart Centre, Aswan, Egypt, [3]Referral Center for Myocardial Diseases, Careggi University Hospital, Florence, Italy and [4]National Heart and Lung Institute, Imperial College London, London, UK

Hypertrophic cardiomyopathy (HCM) is an inherent heart disease that dysregulate cardiac muscle contraction and several mutations in sarcomeric proteins are reported to be associated with HCM. Recently, in Egypt, we identified three disease causing mutations in cardiac myosin binding protein C (cMyBP-C), which is one of the sarcomeric proteins with multiple-domains (C0-C10). However, structure-function relationship for the mechanism of disease is largely unknown. Here, we describe structural consequences of the three HCM causing mutations, Arg177His, Ala216Thr and Glu258Lys, in domain C1 using molecular modeling techniques (Poornima et al., in press, PLOS ONE). Molecular dynamics simulations and stability analyses showed that the mutations affect the following structural properties of domain C1 i) rigidity, ii) intra-molecular interactions, iii) secondary structural elements and iv) surface electrostatics. The described structural changes (Figure) in domain C1 could distract binding of cMyBP-C to other sarcomeric proteins such as actin and/or myosin and thereby influence Ca2+ signalling and energy supply for contractile function to produce energy depletion. This study provides possible explanations to understand the relationship between structural change and molecular mechanism of the disease.

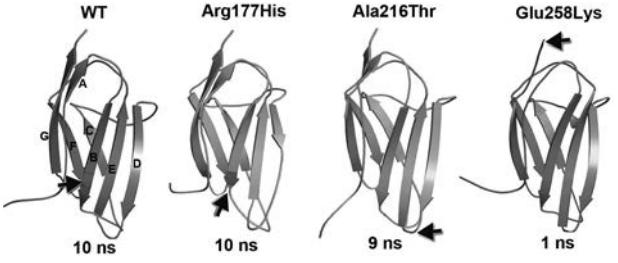

We thank Dr. Sophia N. Yaliraki, Department of Chemistry, Imperial College London for advice and suggestions throughout this work. We extend our thanks to Texas A&M University in Qatar (TAMUQ) for providing supercomputing facility.

Where applicable, the authors confirm that the experiments described here conform with The Physiological Society ethical requirements.

PCA057

Properties of pro-arrhythmic Ca^{2+} waves in rat ventricular myocytes are altered globally and locally by changes in intracellular pH

K.L. Ford[1], E.L. Moorhouse[1], M. Bortolozzi[1,2] and R.D. Vaughan-Jones[1]

[1]Physiology, Anatomy and Genetics, University of Oxford, Oxford, UK and [2]Department of Physics and Astronomy G. Galilei, University of Padua, Padua, Italy

Intracellular acidosis is a feature of both myocardial ischaemia, where it has been linked to ischaemia-reperfusion injury[1], and heart failure[2]. A decrease in pH_i has been shown to have multiple effects on the calcium handling apparatus[3], leading to the hypothesis that acidosis may drive myocardial pathology via effects on calcium. Here, we show that altering pH_i globally and locally affects multiple parameters of spontaneous Ca^{2+} waves, which may be an arrhythmogenic risk factor. pH_i was altered globally by superfusing with 20-80 mM acetate (acidosis) or 20 mM trimethylamine (alkalosis). Spontaneous Ca^{2+} waves, induced by raising superfusate Ca^{2+}, were linescan-imaged at 37°C in rat isolated ventricular myocytes AM-loaded with fluo-3. Parallel pH_i measurements were made using AM-loaded SNARF-1. Data are mean±SE, *P* values calculated using a paired Student's *t* test. Intracellular acidosis increased spontaneous wave frequency up to 360±62% of control (*P*=0.0002, n=18). This effect was prevented by inhibiting the sarcolemmal Na^+/H^+ exchanger (NHE) with 30 μM 5-(N,N-dimethyl)amiloride, demonstrating Na^+-coupling to intracellular Ca^{2+} dynamics. Under these conditions, waves were suppressed relative to control (to 61±22% of control; *P*=0.0023, n=11), indicating that H^+ may have cardioprotective properties. Intracellular alkalosis also decreased wave frequency to 60% of control after 60 seconds (*P*=0.0048, n=10). Decreasing pH_i increased wave velocity up to 140±3% of control (*P*<0.0001, n=17), while an intracellular alkalosis decreased velocity to 80% of control (*P*<0.0001, n=12). Analysis over a range of pH_i values demonstrated a linear relationship between pH_i and wave velocity. Computational modelling[4] suggests that this may be due to a decrease in cytoplasmic Ca^{2+} buffering; consistent with this, inhibiting NHE had no further significant effect during acidosis. It is likely that pH_i in the ischaemic heart is heterogeneous, therefore to investigate whether differences in pH_i affect local Ca^{2+} properties, we induced a stable pH_i gradient (pH_i 6.6-7.3) in single ventricular myocytes by superfusing two parallel microstreams perpendicular to the cell, one containing normal Tyrode, the other 80 mM acetate[5]. With NHE inhibited, wave initiation was inhibited in the acidic microdomain (31±7% of control;*P*<0.05, n=13) and stimulated in the more alkaline microdomain (164±25%; *P*<0.05, n=13), while wave velocity was increased in the acidic microdomain and decreased in the more alkaline microdomain. Other effects on Ca^{2+} dynamics, including wave decay, also mapped on to the pH_i gradient. We conclude that pH_i locally regulates Ca^{2+} handling and dynamics, and thus pH_i heterogeneity may provide a substrate for aberrant Ca^{2+} signalling in cardiac pathology.

Avkiran M. (1999) *Am J Cardiol* **83**:10-18

Li L, Louch WE, Niederer SA, Aronsen JM, Christensen G, Sejersted OM, Smith NP. (2012) *Biophys J* **102**:2039-2048

Choi HS, Trafford AW, Orchard CH, Eisner DA. (2000) *J Physiol* **529**:661-668

Swietach P, Spitzer KW, Vaughan-Jones RD. (2010) *Front Biosci* **15**:661-680

Spitzer KW, Ershler PR, Skolnick RL, Vaughan-Jones RD. (2000) *Am J Physiol Heart Circ Physiol* **278**:H1371-H1382

Funded by the BHF and Wellcome Trust.

Where applicable, the authors confirm that the experiments described here conform with The Physiological Society ethical requirements.

PCA058

The effects of repaglinide on cardiac action potential and ion channels

H. Lee, S. Park and K. Kim

Next-generation Pharmaceutical Research Center, Korea Institute of Toxicology, Daejeon, Republic of Korea

Unfortunately, many non-cardiac drugs have also been reported to cause cardiac events including QT prolongation and/or life-threatening Tosade de points (TdP). Recent reports are shown that the diabetic patients with more pronounced QT abnormalities and cardiovascular complications. Repaglinide is well-known antidiabetic drug. Therefore, it is important that the evaluation of the potential effects of repaglinide on cardiac repolarization.

In the present study, we examined the in vitro action potential (AP) assay with isolated rabbit Purkinje fiber (New Zealand White rabbits, 2.5-3 kg) to predict the potential of repaglinide to induce these undesirable adverse effects on the heart. Furthermore, we examined the effects of repaglinide on the major cardiac ion channels transiently transfected with the hERG(IKr), KCNQ1/KCNE1(IKs), KCNJ2(IK1) and SCN5A(INa) cDNA in HEK293 cells and the native voltage-gated Ca2+ channels in rats (Sprague-Dawley, 250-350 g, male) ventricular myocytes using the whole-cell patch clamp technique. Pooled data are expressed as means ± S.E.M., and compared by ANOVA followed by Dunnett's test. According to the results, repaglinide at 30 μM significantly prolonged the action potential duration at 50% levels of repolarization (APD50, from 156.2 ± 4.3 to 179.1 ± 4.3 ms, n=4, P<0.05) and the action potential duration at 90% levels of repolarization (APD90, from 241.6 ± 7.4 to 278.9 ± 4.5 ms, n=4, P<0.01). According to ion channel studies, these effects could be induced by K+ channels blocking especially hERG and IKs. However, repaglinide at 100 μM significantly shortened the APD50 (156.2 ± 4.3 to 120.0 ± 7.9 ms, n=4, P<0.01) and APD90 (from 241.6 ± 7.4 to 190.9 ± 8.6 ms, n=4, P<0.01). In addition, the 100 μM repaglinide caused decrease of the maximum velocity of phase 0 (Vmax) from 269.2 ± 13.1 to 179.8 ± 9.1 V/s (n=4, P<0.01). These effects could be induced by the blocking of depolarizing currents for Na+ and Ca2+ channels. In the ion channel studies, repaglinide did inhibit the all of the tested ionic currents in a concentration-dependent manner except IK1. Among these ion channels, the voltage-gated Ca2+ channel was the most susceptible to repaglinide.

The drug-induced shortening of the QT interval could potentially increase the ventricular tachycardia and the ventricular fibrillation risk of sudden death. Therefore, all patients taking this drug should be more carefully monitored for cardiac events.

Veglio M et al. (2002). Diabetes Care 25, 702-707.

Rajeev K et al. (2004). Br J Diabetes Vasc Dis 4, 146-150.

Watters K et al. (2012). Diabet Med 2, 290-292.

Garberoglio L et al. (2007). Electrocardiol 40, 43-46.

Where applicable, the authors confirm that the experiments described here conform with The Physiological Society ethical requirements.

PCA059

Structural characteristics of the sinus node and surrounding atrial tissue in the goat heart

Z. Borbas, J. Caldwell, A. Vohra, A. Hoschtitzky, M.R. Boyett, C.J. Garratt and H. Dobrzynski

Cardiovascular Research group, University of Manchester, Manchester, UK

Introduction: Sinus node (SN) dysfunction is a common clinical condition that is accounted for 50% of permanent pacemaker implantation. In order to examine the value of the goat as a model of human SN function and dysfunction we examined the structure of the SN and the surrounding right atrium in this species.
Method: Right atria were harvested from 4 humanely killed goats. Under 3% Isoflurane anaesthesia, two of the 4 animals underwent an incremental protocol of epicardial SN ablation, sufficient to cause at least a 50% fall in heart rate, in order to determine the functional extent of the SN. All preparations were frozen, serially sectioned at 1 mm intervals and stained for histology using Masson trichrome technique. The extent and morphology of the native and ablated SN were determined. For verification of the histology, immuno-staining for Connexin43 (Cx43; a negative marker for the SN) and Na/Ca exchanger (NCX, a membrane-bound ion channel protein; positive marker for of all cardiomyocytes) was used on selected tissue sections. Images were taken with light and confocal microscopy.
Results: The goat SN was located in the intercaval region (ICR) parallel to the crista terminalis (CT) and extended 2/3 of its length in the long axis. In the short axis, the centre of the SN occupied the full thickness (2mm) of the intercaval region (panel A). The SN, as in other species, consisted of cells which were small, lightly stained (compared to atrial myocytes) and embedded in a network of connective tissue (panel B, C) [1,2]. All myocytes expressed NCX but not Cx43 unlike atrial myocytes.
We also observed a transitional zone (TZ), (panel D) arising on the endocardial side of the CT (Panel A) which extended caudally beyond the SN. The morphology of TZ was intermediate to nodal and atrial tissue; conaining atrial as well as nodal cells..In addition, TZ contained an intermediate cell-type which histologically was similar to atrial myocytes, but lacked expression of Cx43; similarly to the novel paranodal area recently described in the human heart[3] .
In the experimental goats, the size and location of the ablated area corresponded to that of the healthy SN in the control group, but it spared an area caudal to the SN and did not involve the TZ.
Conclusions: The SN in the goat is associated with an extensive adjacent region of transitional cells, similar to that recently described in the human. The natural function of this region is currently unknown but may provide a useful target for novel methods of "biological pacemaking" currently in development.

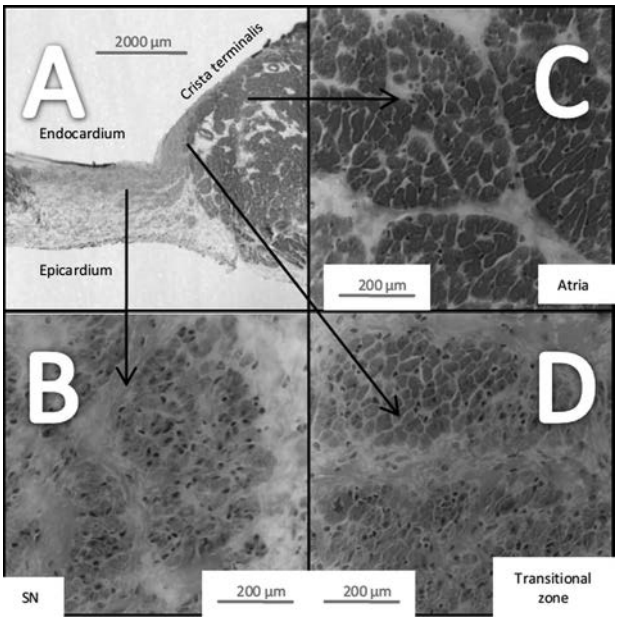

Figure 1: Sinus node in the goat

Panel A: low power image of a section through the SN Panels B-D: High power images through SN, atrium and TZ

Boyett, M R et al., 2006 Advances in Cardiology, 42, pp.175–197

Dobrzynski, H. et al., 2006.Journal of Molecular and Cellular Cardiology, 41(5), pp.855–867

Chandler, Natalie J et al., 2009 Circulation, 119(12), pp.1562–1575

Where applicable, the authors confirm that the experiments described here conform with The Physiological Society ethical requirements.

PCA060

Angiotensin II receptor blocker and PPAR-gamma agonist, telmisartan, delayed inactivation of cardiac Nav1.5: A novel drug mechanism

H. Kim, J. Youm, S. Lee, K. Ko, B. Rhee, N. Kim and J. Han

National Research Laboratory for Mitochondrial Signaling Laboratory, Department of Physiology, College of Medicine, Cardiovascular and Metabolic Disease Center, Inje University, Busan, Republic of Korea

Telmisartan is an angiotensin II receptor blocker and partial peroxisome proliferator-activated receptor gamma agonist that modulates the renin-angiotensin-aldosterone system. It is used primarily to manage hypertension, diabetic nephropathy, and congestive heart failure. Recent studies have reported that myocardial infarction (MI) has occurred in telmisartan-treated patients.The purpose of the study was to investigate the specific conditions and underlying mechanisms that may result in telmisartan-induced MI. We evaluated the effect of telmisartan on whole hearts, cardiomyocytes, and cardiac sarcolemmal ion channels. Hearts of 8-week-old male Sprague–Dawley rats were perfused with 3, 10, 30, or 100 μM telmisartan or losartan, or normal Tyrode's solution (control) for 3 hours. We found that telmisartan induced myocardial infarction, with an infarct size of 21% of the total at 30 μM ($P<0.0001$) and 63% of the total area at 100 μM ($P<0.001$). Telmisartan also induced cardiac dysfunction (e.g., decreased heart rate, diminished coronary flow, hypercontracture, and arrhythmia). Confocal microscopy demonstrated that 30 μM telmisartan significantly elevated intracellular Ca2+ level lead-

ing to hypercontracture and cell death. Patch clamp analysis of isolated cardiomyocytes revealed that telmisartan induced Na+ overload by slowing the inactivation of voltage-gated Na+ current (INa), activating the reverse-mode of Na+-Ca2+ exchanger activity, and causing Ca2+ overload. Telmisartan significantly delayed inactivation of the voltage-gated Na+ channel causing cytosolic Na+ overload, prolonged action potential duration, and subsequent Ca2+ overload. Above 30 μM, telmisartan may potentially cause cardiac cell death and MI.

Fig. 7

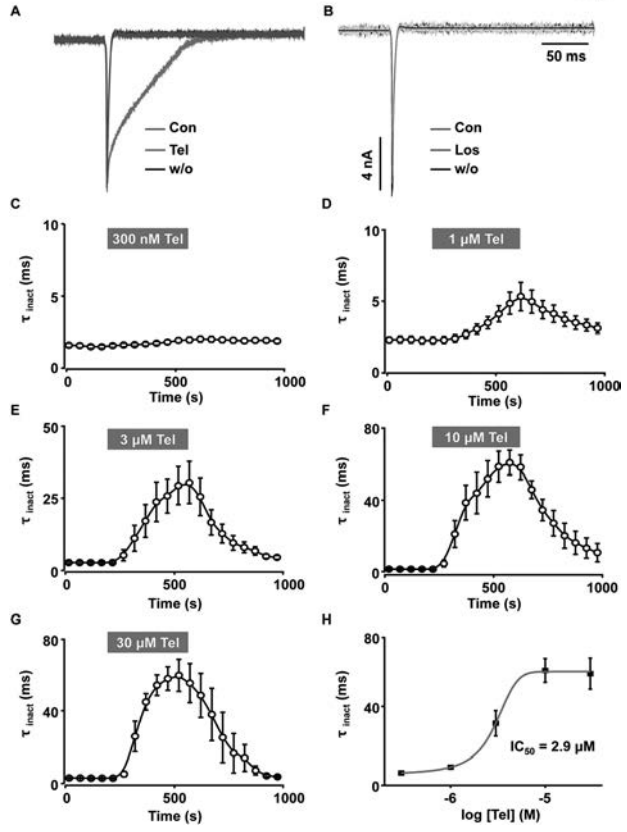

Telmisartan delays inactivation of voltage-dependent Na+ channels in ventricular myocytes. Effect of 30 μM telmisartan (A, red) and 30 μM losartan (B, green) on INa. Cells were held at -80 mV, and step pulses to -50 mV were applied every 10 s to activate INa. Telmisartan (30 μM) delayed inactivation of the inward current without affecting rate of activation or amplitude (n=21), whereas the same concentration of losartan affected neither time course nor amplitude of the inward current (n=3). The prolonged INa fully recovered by switching to NT solution. C–G, Time course of INa inactivation during telmisartan perfusion (300 nM, n=6; 1 μM, n=6; 3 μM, n=11; 10 μM, n=7; 30 μM, n=4). H, The data fit well to the Hill equation (EC50=2.94±0.07 μM).

Where applicable, the authors confirm that the experiments described here conform with The Physiological Society ethical requirements.

PCA061

Bisphenol A decreases *in vitro* atrial contractility and also attenuates Phenylbiguanide evoked reflexes after chronic exposure in anaesthetized rats

J. Pant, P. Ranjan, M.K. Pant and S.B. Deshpande

Physiology, Institute of Medical Sciences, Banaras Hindu University, Varanasi, Uttar Pradesh, India

Bisphenol A (BPA), an endocrine disruptor, is used in the manufacturing of plastics. BPA is reported to produce a number of reproductive defects and is even associated with behavioural abnormality, diabetes and deranged liver enzymes. However, the knowledge on toxic effects of BPA on cardiovascular system is limited. Therefore the present study was performed to examine the effects of BPA on spontaneously beating rat right atrial preparation *in vitro* as well as to see the changes after chronic exposure to BPA in *in vivo* conditions. The experiments were performed using adult female rats of Charles Foster strain weighing 150-200 grams after obtaining clearance from the ethical clearance committee of the institute. The study was divided in two groups. In group 1, *in vitro* isometric contractions of rat right atria were recorded. Effect of cumulative concentration of BPA on atrial contractions was obtained in the absence or presence of antagonists. BPA (0.1–100 μM) decreased the rate and the force of atrial contractions in a concentration dependent manner. The BPA-induced changes were blocked after pretreatment with N- ω- nitro-L- arginine methyl ester (L- NAME, a nitric oxide synthase inhibitor) or methylene blue (a guanylyl cyclase inhibitor) whereas atropine (muscarinic receptor blocker) did not block the BPA-induced changes in atria.

In group 2, to study the effect of chronic exposure of BPA, the animals were ingested pellets with BPA (2 μg/kg body weight/day) or without BPA (time-matched control) for 30 days. Further, the animals were anaesthetized with urethane (1.5 gm/kg bw; i.p.) and prepared for recording blood pressure, ECG and respiratory excursions. Phenylbiguanide (PBG) 10 μg/kg body weight was injected through jugular vein to evoke cardio-pulmonary reflexes in these animals. Thereafter, the rats were killed using excess dose of urethane and the lungs and heart were excised and processed for histopathological examination. In time-matched control rats, PBG produced bradycardia, hypotension and tachypnoea over a period of time. In BPA treated group, the PBG-induced heart rate and respiratory frequency changes were attenuated significantly. The histological findings of the lungs revealed emphysematous and consolidative changes in BPA treated group whereas in case of heart, there was rupture of myofibrils with edematous changes.

The present results indicate that BPA produces cardiac toxicity by producing acute and chronic changes. Acute changes were seen as decreased atrial contractility *in vitro* involving NO-dependent G-cyclase signaling mechanisms. The chronic changes manifested as lowered blood pressure and heart rate along with attenuation of cardio-respiraory reflexes. In addition there were degenerative changes in lungs and heart to produce the effects of chronic exposure.

Where applicable, the authors confirm that the experiments described here conform with The Physiological Society ethical requirements.

PCA062

Myofilament basis analyses of afterload dependent increasing in crossbridge formation in ejecting rat heart

Y. Tamura[1], K. Horiuchi[2], T. Miyasaka[3] and J. Shimizu[2]

[1]Thoracic and Cardiovascular Surgery, Nara Medical University, Kashihara, Nara, Japan, [2]Clinical Radiology, Hiroshima International University, Higashi-Hiroshima, Hiroshima, Japan and [3]Health Care Science, Himeji Dokkyo University, Himeji, Hyogo, Japan

Myofilament basis mechanism of afterload-dependent increase in contractile force is still remained unclear (1). The purpose of this study is to investigate whether increasing afterload cor-

relate with myosin head proximity to actin filaments and presumably crossbridge activated during contractions. We used eight male Wistar rats anesthetized by pentobarbital (50mg/kg, ip). We used x-ray diffraction analyses of beat-to beat contractions in spontaneously beating rat hearts under open-chest conditions simultaneous with recordings of left ventricular (LV) pressure and volume(2, 3). Aortic occluder was placed at descending aorta to increase afterload. We recorded x-ray diffraction patterns of the LV anterior free wall before and after aortic occlusion to determine the change in intensity ratio (I1,0/1,1) and myosin filament lattice spacing (D1,0). We found significant change neither in end-diastolic I1,0/1,1 nor D1,0, indicating that the proportion of myosin heads in proximity to actin filaments and myosin filament lattice spacing were unchanged by increasing afterload. Peak systolic I1,0/1,1 decreased significantly more after aortic occlusion than before aortic occlusion. Increase in D1,0 during contraction was significantly reduced after aortic occlusion than before aortic occlusion. A significant increase in myosin head proximity to actin filaments with increasing afterload correlated with increase in LV end-systolic pressure. A significant reduction in changes of D1,0 between diastole and systole with increasing afterload correlated with decrease in LV stroke volume. Since sarcomere length of cardiomyocyte related inversely with D1,0 because of constant cellular volume, reduced D1,0 change during contraction means prevention of sarcomere shortening with increasing afterload. These findings support a role of arterial resistance in determining LV stroke volume as the cardiovascular interaction.

Shimizu J, Todaka K, Burkhoff D.,Load dependence of ventricular performance explained by model of calcium-myofilament interactions., Am J Physiol Heart Circ Physiol. 2002 Mar;282(3):H1081-91.

Yagi N, Shimizu J, Mohri S, Araki J, Nakamura K, Okuyama H, Toyota H, Morimoto T, Morizane Y, Kurusu M, Miura T, Hashimoto K, Tsujioka K, Suga H, Kajiya F., X-ray diffraction from a left ventricular wall of rat heart.,Biophys J. 2004 Apr;86(4):2286-94.

Pearson JT, Shirai M, Ito H, Tokunaga N, Tsuchimochi H, Nishiura N, Schwenke DO, Ishibashi-Ueda H, Akiyama R, Mori H, Kangawa K, Suga H, Yagi N., In situ measurements of crossbridge dynamics and lattice spacing in rat hearts by x-ray diffraction: sensitivity to regional ischemia., Circulation. 2004 Jun 22;109(24):2976-9.

Where applicable, the authors confirm that the experiments described here conform with The Physiological Society ethical requirements.

PCA064

Stimulation of I_{Ca} by protein kinase A in the t-tubules of rat cardiac ventricular myocytes is facilitated by caveolin-3

S. Bryant, T. Kimura-Wozniak, C.H. Orchard and A.F. James

School of Physiology & Pharmacology, University of Bristol, Bristol, UK

In cardiac ventricular myocytes many of the key proteins involved in excitation-contraction coupling, including L-type calcium channels (LTCC), are located predominantly at the transverse (t-) tubules. Protein kinase A (PKA)-mediated stimulation of L-type Ca current (I_{Ca}) also occurs predominantly at the t-tubules. Caveolin-3 (Cav-3) has been implicated in the localization of PKA activity to macromolecular complexes. We have, therefore, investigated whether Cav-3 plays a role in the stimulation of I_{Ca} by PKA in the t-tubules of rat ventricular myocytes.

Ventricular myocytes were isolated from the hearts of male Wistar rats (250-300 g) killed either by cervical dislocation or under pentobarbitone (140 mg/kg *i.p.*) anaesthesia in accordance with UK legislation. I_{Ca} was recorded using the whole-cell patch-clamp technique. From a holding potential of -80 mV, a 100 ms step depolarisation to -40 mV was used to inactivate I_{Na}, followed by a 500 ms step depolarisation (to voltages between -50 and +80 mV) to activate I_{Ca} (0.2 Hz; room temperature). Standard immunohistochemical techniques were used in conjunction with confocal microscopy to determine the localization of Cav-3, total LTCC (tLTCC) and phosphorylated LTCC (pLTCC). Incubation with TAT-tagged C3SD peptide (C3SD) was used to disrupt normal Cav-3 protein binding (MacDougall et al., 2012). Scrambled peptide (Scram) and non-incubated cells (Con) were used as controls. β_2-adrenoceptor stimulation was achieved using zinterol (1-10 μM) applied to cells pre-exposed to atenolol (10 μM). Detubulation (DT) was achieved by exposing cells to 1.5M formamide (Kawai et al., 1999). Data are expressed as mean±SEM (n cells). Statistical analysis was performed by analysis of variance (1 or 2 way) with the appropriate Bonferroni *post hoc* test; significance was taken at $p<0.05$.

In control cells, I_{Ca} density was significantly reduced by C3SD and unaffected by Scram peptide (Con -7.6±0.3 (11), Scram -8.0±0.4 (9), C3SD -5.4±0.2 (15) pA/pF, $p<0.0001$ C3SD vs Scram). However, in detubulated cells C3SD did not decrease I_{Ca} (DT -4.7±0.2 (5), DT+C3SD -4.2±0.4 (6) pA/pF, ns). C3SD had no effect on the distribution of staining of Cav-3 or tLTCC but significantly altered the distribution of pLTCC staining.

The PKA inhibitor H-89 decreased I_{Ca} by 53±3% in Con, but by only 28±10% in the presence of C3SD ($p<0.001$), to a level that was not significantly different from in the presence of H-89 alone (Con -3.6±0.5 (5), C3SD -3.7±0.3 (5) pA/pF, ns). The increase of I_{Ca} induced by zinterol was inhibited in cells incubated with C3SD.

These data are consistent with the notion that Cav-3 plays an important role in mediating the localised stimulation of t-tubular I_{Ca} by basal PKA activity and in response to β_2-adrenoceptor stimulation.

MacDougall DA, Agarwal S, Stopford E, Chu H, Collins J, Longster A, Colyer J, Harvey R & Calaghan S (2012). J Mol Cell Cardiol 52, 388-400.

Kawai M, Hussain M, Orchard CH (1999). Am. J. Physiol. 277, H603-H9.

This work was supported by the British Heart Foundation

Where applicable, the authors confirm that the experiments described here conform with The Physiological Society ethical requirements.

PCA066

Cardiomyocytes from creatine deficient AGAT mice show no changes in mitochondrial organization and cellular compartmentation

S. Kotlyarova[1], M. Mandel[1], N. Sokolova[1], D. Aksentijevic[2], C.A. Lygate[2], S. Neubauer[2], M. Vendelin[1] and R. Birkedal[1]

[1]Laboratory of Systems Biology, Institute of Cybernetics at TUT, Tallinn, Estonia and [2]Department of Cardiovascular Medicine at Wellcome Trust Centre for Human Genetics, University of Oxford, Oxford, UK

In cardiac muscle, the creatine kinase (CK) system temporally buffers ADP and ATP concentrations near sites of ATP production and consumption. It has also been suggested to be an important spatial buffer facilitating the transport of ADP and ATP. This was corroborated by a study of CK knockout mice,

where cardiac fibers exhibited changes in mitochondrial organization and functional compartmentation – potentially to diminish diffusion distances between mitochondria and ATPases. However, a recent study on cardiomyocytes from creatine-deficient guanidinoacetate methyltransferase (GAMT) knockout mice showed no effect on mitochondrial organization and compartmentation. It has been suggested that in GAMT-/- mice, accumulated guanidinoacetate can be used as a substrate instead of creatine. Therefore, we studied the same parameters in L-arginine:glycine amidinotransferase (AGAT) mice, which are also creatine-deficient, but do not accumulate guanidinoacetate. Mice received an i.p. injection of 250U heparin, and were anesthetized with ketamine/dexmedetomidine mixture (150 mg/kg and 0.5mg/kg, i.p.respectively). Three-dimensional mitochondrial organization at whole cell level was assessed by confocal microscopy. Kinetic measurements on permeabilized cardiomyocytes included the affinity of oxidative phosphorylation to exogenous ADP and ATP, competition between mitochondria and pyruvate kinase for ADP produced by ATPases, ADP-kinetics of endogenous pyruvate kinase and ATP-kinetics of ATPases. Tibial length of AGAT-/- mice was similar to that of AGAT+/+ mice, but body weight was significantly lower. Our results show surprisingly little difference between cardiomyocytes of AGAT-/- and AGAT+/+ mice. We did find that the protein content of AGAT-/- cardiomyocytes was approximately two times lower than that of AGAT+/+ cardiomyocytes. However, visual inspection of mitochondrial organization suggests no essential difference. Also, when respiration is related to the number of cardiomyocytes, there is no difference in the kinetics of respiration and ATPases. Thus, our data so far suggest no differences in cardiomyocyte mitochondrial organization and cellular compartmentation between AGAT-/- and AGAT+/+ mice. We conclude that the lack of compensatory changes in mitochondrial organization and cellular compartmentation in AGAT as well as GAMT mice raise questions regarding the importance of the CK system as a spatial buffer.

This work was supported by Wellcome Trust (Fellowship No. WT081755), Estonian Science Foundation (Grant No. 8041) and European Union through the European Regional Development Fund.

Where applicable, the authors confirm that the experiments described here conform with The Physiological Society ethical requirements.

PCA067

Phospholamban ablation reduces the propensity for triggered activity in CPVT transgenic heart cells despite increased SR Ca^{2+} load

K. Gusev[1] and S.E. Lehnart[1,2]

[1]Department of Cardiology & Pulmonology, University of Göttingen, DZHK, Göttingen, Germany and [2]BioMET, University of Maryland, Baltimore, MD, USA

The cardiac ryanodine receptor (RyR2), the principal Ca^{2+} release channel of the heart, is affected by patient mutations and catecholaminergic stress causing defective channel closure, irregular Ca^{2+} triggered action potentials (tAPs), and a ventricular arrhythmia syndrome (CPVT). Based on results obtained in heterologous overexpression models of CPVT mutant RyR2 channels, other groups suggested that catecholaminergic stimulation may lead to triggered activity by reducing the threshold for store overload-induced Ca^{2+} release. We have previously shown that heterozygous RyR2-R2474S ($RyR2^{RS}$) knock-in mice reproduce the characteristic patient phonotype of CPVT. To clarify the physiological arrhythmia mechanism, we evaluated phospholamban deficient ($PLN^{-/-}$;$RyR2^{RS}$) cells with constitutive sarcoplasmic reticulum (SR) Ca^{2+} store overload.

Double transgenic model: heterozygous $RyR2^{RS}$ knock-in mice were crossed with $PLN^{-/-}$ mice to produce $RyR2^{RS}$;$PLN^{-/-}$ mice established in the C57Bl6 background. Electrophysiology: in vivo ECG as well as current-clamp combined with intracellular Ca^{2+} imaging of isolated ventricular myocytes (37C, fluo-3) was used to evaluate the influence of SR Ca^{2+} load on arrhythmogenic behavior. Comparing $RyR2^{RS}$;$PLN^{-/-}$ vs. $RyR2^{RS}$;$PLN^{+/+}$ mice showed for PLN deficient RS cells: (1) significant QT interval shortening (60±2 ms vs. 68±2 ms, respectively; $p<0.05$); (2) significant action-potential shortening (APD90: 89±4 ms vs. 117±8 ms, respectively; $p<0.05$); (3) significantly accelerated Ca^{2+} transient decay (28±2 ms vs. 69±5 ms, $p<0.001$); and (4) significantly increased SR Ca^{2+} load ($\Delta F/F0$: 9.7±1.6 vs. 5.3±1.4, respectively; $p<0.001$). (5) As expected, acute β-adrenergic stimulation with 30 nM isoproterenol resulted in no further increase of SR Ca^{2+} load in $PLN^{-/-}$ ($\Delta F/F0$: $RyR2^{RS}$;$PLN^{-/-}$ 8.1±2.7 vs. $RyR2^{RS}$;$PLN^{+/+}$ 7.0±1.7; n.s.). (6) Despite maximal, constitutive SR Ca^{2+} loading in $RyR2^{RS}$;$PLN^{-/-}$ cardiomyocytes, the occurrence of tAPs during β-adrenergic stimulation was significantly decreased in $RyR2^{RS}$;$PLN^{-/-}$ cells ($RyR2^{RS}$;$PLN^{+/+}$: 9 out of 12 cells (75%); $RyR2^{RS}$;$PLN^{-/-}$: 1 out of 10 cells (10%) had tAP; $p<0.05$).

In summary, our data suggest that maximal upregulation of SERCA2a activity in $PLN^{-/-}$ (1) leads to increased SR Ca^{2+} load and accelerated cytosolic Ca^{2+} removal, which shortens the APD and the QT interval in vivo; and (2) decreases the propensity for tAPs in the context of a highly arrhythmogenic CPVT model with significantly increased diastolic SR Ca^{2+} leak. This suggests that, contrary to expectation, increased SR Ca^{2+} per se, at levels occurring during catecholaminergic stress, may not trigger APs under physiological conditions. An increased susceptibility of $RyR2Ca^{RS}$ cells for tAPs might be blunted by accelerated SR Ca^{2+} uptake and altered diastolic Ca^{2+} handling dynamics.

Where applicable, the authors confirm that the experiments described here conform with The Physiological Society ethical requirements.

PCA068

Biochemical phenotype of a human phospholemman mutation

J. Walker[1], E. Johnston[1], J. Howie[1], H. Parry[1], A. Cassidy[2], M. Shattock[3], C. Palmer[1] and W. Fuller[1]

[1]Division of Cardiovascular & Diabetes Medicine, University of Dundee, Dundee, UK, [2]Human Genetics Unit, University of Dundee, Dundee, UK and [3]Cardiovascular Division, King's College London, London, UK

Phospholemman (PLM) regulates the cardiac Na pump. Unphosphorylated PLM inhibits the pump, and PLM phosphorylation at S63 and T69 (by PKC), and S68 (by PKA or PKC) causes pump activation. Abnormal phosphorylation of PLM is well established in cardiac hypertrophy and failure. We investigated whether genetic polymorphisms in PLM underlie left ventricular hypertrophy (LVH) by sequencing PCR-amplified PLM exons from anonymised genomic DNA from the Go-DARTS database. Inclusion criteria were age <55, systolic blood pressure <140mmHg, BMI <30kgm^{-2}, and moderate-severe LVH

according to echocardiography. 2 out of 43 individuals possessed the same non-synonymous missense coding variant: a C to T transition in position 1 of the codon encoding arginine 70 in PLM exon 7, resulting in the mutation R70C.
The R70C PLM phenotype was investigated by expressing wild type (WT) and R70C PLM in HEK293 cells. Phosphorylation induced by activating PKA (10μM forskolin) and PKC (300nM PMA) was measured by phosphospecific immunoblotting, and expressed relative to WT or R70C-expressing cells treated with vehicle. Phosphorylation of WT and R70C PLM by PKA at PLM-S68 was unchanged (2.0±0.3 fold increase over vehicle-treated for WT, 1.8±0.1 fold increase for R70C, mean±SEM, n=4). PKC-induced phosphorylation of PLM-S63 was also unchanged, but R70C PLM was phosphorylated less than WT at S68 following activation of PKC (1.8±0.2 for WT, 1.0±0.2 for R70C, n=4, $p<0.05$, t-test), suggesting mutation of the arginine at position +2 to S68 had altered this consensus PKC phosphorylation site. We also measured cell surface localisation (membrane-impermeable biotinylation reagents) and palmitoylation (resin-assisted capture of acylated proteins) of WT and R70C PLM. A greater fraction of R70C PLM than WT was found at the cell surface (R70C 3.8±2 fold more enriched than WT, n=3), suggesting a proposed ER retention motif in PLM was also disrupted. A greater fraction of R70C PLM was palmitoylated than WT (53±10% vs 29±5%, n=4, $p<0.05$), possibly due to this enhanced traffic to the cell surface.
Rs61753924, the single nucleotide polymorphism (SNP) underlying PLM R70C, occurs at 0.1% frequency in the 1000 Genomes Project. We investigated the frequency of this SNP in LVH case and non-LVH controls: 19 out of 393 LVH cases (4.8%) and 10 out of 266 (3.7%) controls were positive for rs61753924 (odds ratio = 1.14, $p>0.05$).
In conclusion, PLM R70C shows reduced phosphorylation at S68 by PKC. In vivo PLM is significantly phosphorylated at rest by PKC, so the reduced phosphorylation and enhanced cell surface localisation and palmitoylation of R70C PLM may lead to reduced Na efflux via the pump. Preliminary analysis indicates that the presence of SNP rs617539241 is not a risk factor for the development of LVH, but is enriched in the local population.

Supported by grants from British Heart Foundation (RG/12/4/29426), and Ninewells Hospital Anonymous Trust

Where applicable, the authors confirm that the experiments described here conform with The Physiological Society ethical requirements.

PCA069

Popdc genes and cardiac pacemaking: The molecular basis of genetic redundancy

S. Simrick[1], R. Schindler[1], R. Kreutzer[2], M. Krüger[3], T. Braun[3], C. Terracciano[1], L. Fabritz[2] and T. Brand[1]

[1]National Heart and Lung Institute, Imperial College London, London, UK, [2]Cardiovascular and Respiratory Sciences, University of Birmingham, Birmingham, UK and [3]Max Planck Institute for Heart and Lung Research, Bad Nauheim, Germany

Popeye domain containing (Popdc) genes encode a novel class of cAMP-binding proteins. Functional analysis of *Popdc1* and *-2* genes in mice indicate a potential role in the chronotropic response to β-adrenergic signalling, with single null mutants displaying a stress-induced bradycardia.[1] The overlapping phenotype in both mutants is age-dependent, suggesting the presence of genetic redundancy. Here we report our preliminary analysis of *Popdc1;Popdc2* double knockout (P12dKO) mice and the functional interactions of Popdc1 and -2 at the protein level.
Popdc1;Popdc2 double heterozygous (P12dHET), P12dKO, and wild type (WT) age-matched control male mice were subjected to telemetric ECG analysis at rest and during physical stress (6min swim, 15min recovery). In accordance with our single null mutant analysis, no significant difference was observed in the heart rates of 3 month old mice at rest (WT 514±34bpm, n=7; P12dHET 547±36bpm, n=5, two-tailed t-test p=0.14; P12dKO 552±36bpm, n=3, two-tailed t-test p=0.20). However, in contrast to the single null mutants where the stress-induced bradycardia was not observed until 5.5 months of age, the 3 month old P12dKO mice had a blunted response to physical stress (WT 39% increase in heart rate, n=7; P12dHET 32%, n=5, two tailed t-test p=0.35; P12dKO 18%, n=3, two-tailed t-test p=0.01). A blunted increase in heart rate in response to physical stress is consistently seen in P12dKO older mice (>9 months), although not exacerbated compared to P1KO mice (WT 719±14bpm, n=5; P1KO 593±39bpm, n=5; P12dKO 665±24bpm, n=6, WT vs P12dKO two-tailed t-test $p<0.01$), which suggests that during early postnatal development the two Popdc genes can functionally compensate each other and act in the same functional context since the loss of either gene is causing a pacemaker deficiency and phenotypic severity does not increase if both Popdc genes are missing.
Immunohistochemistry revealed that both Popdc1 and -2 proteins are expressed throughout the heart, with enhanced expression in the cardiac conduction system. At the single cell level both proteins are located at the plasma membrane, intercalated disks and in T-tubules. To identify new interaction partners for Popdc proteins, we performed co-immunoprecipitation followed by mass spectrometry. By this screen Ankyrin-G and -B and the Na^+/Ca^{2+} exchanger NCX1 were identified and subsequently confirmed by Western Blot as interacting proteins. Furthermore, we were able to demonstrate an interaction of Popdc1 and 2, suggesting that members of the Popdc family are interacting with each other and thereby acting in the same functional context. This may explain the overlapping phenotypes of *Popdc1* and *-2* mutants and the earlier manifestation of the bradycardia in P12dKO mice. Further analysis at the protein, cell, and organismic level, will help to define the role of Popdc proteins in cardiac stress adaptation.

[1]Froese A et al (2012) Popeye domain containing proteins are essential for stress-mediated modulation of cardiac pacemaking in mice. J Clin Invest. 122, 1119-30.

Where applicable, the authors confirm that the experiments described here conform with The Physiological Society ethical requirements.

PCA070

Potential antiarrhythmic effects of paeoniflorin and paeonol extracted from the paeoniaceae family

S. Lee[1,2], P.J. Noble[1], Y. Ma[1], Y. Earm[3] and D. Noble[1]

[1]Department of Physiology, Anatomy and Genetics, University of Oxford, Oxford, UK, [2]Department of Physiology, College of Korean Medicine, Sangji University, Wonju, Republic of Korea and [3]Department of Physiology, College of Medicine, Seoul National University, Seoul, Republic of Korea

Paeoniflorin and paeonol are major components found in the Paeoniaceae family such as *Paeonia lactiflora* Pallas and *Paeonia suffruticosa* Andrews. *Paeonia lactiflora* Pallas has traditionally been used to relieve spasmodic abdominal pain as well

as muscle stiffness and *Paeonia suffruticosa* Andrews has been used to enhance blood flow and to relieve joint pain in Korea, China and Japan. Current research has shown that paeoniflorin has protective effects in acute myocardial ischemia *via* improving coronary blood flow and blocking the L-type calcium channels. It has also been reported that paeonol blocked the voltage-gated sodium channels. However, there is lack of research to reveal the relationship between cardiac function and blockade of ion channels by both compounds.
In this study, therefore, we aim to investigate whether paeoniflorin and paeonol have antiarrhythmic effects *via* modulating cardiac ion channels. We collated the effects of paeoniflorin and paeonol on multiple ion channels such as the fast sodium channel, the L-type calcium channel, and the rectifying potassium channel from published papers. To incorporate the information on multi-channel block, we computed the effects using the mathematical cardiac model of guinea-pig ventricular cell (Noble 1998 model) and induced early afterdepolarizations (EADs) to simulate what would be an arrhythmia in the whole heart. We then showed that both paeoniflorin and paeonol enabled recovery of the cardiac ventricular action potential from EADs through blocking of the cardiac L-type calcium channel and sodium channel effectively.
This finding, therefore, suggests that paeoniflorin and paeonol possess antiarrhythmic activity and they and their original herbs can be potential candidates as antiarrhythmic drugs. .

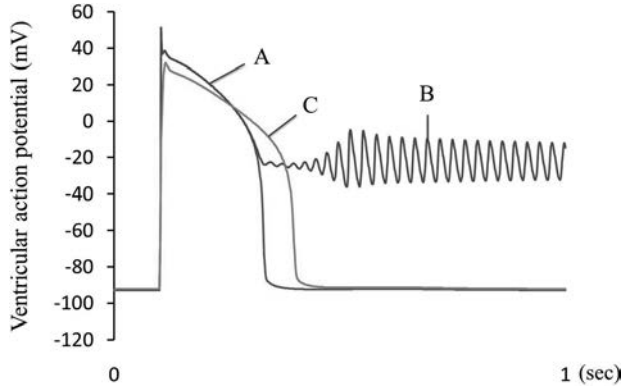

Figure 1. Effect of paeoniflorin on the recovery from EADs. A, normal ventricular action potential; B. action potential with induced EADs; C. recovered action potential from EADs with application of 100 μM of paeoniflorin.

Noble D, Varghese A, Kohl P, Noble P. Improved guinea-pig ventricular cell model incorporating a diadic space, IKr and IKs, and length- and tension-dependent processes. Can J Cardiol. 1998;14(1):123-34.

Wang RR, Li N, Zhang YH, Ran YQ, Pu JL. The effects of paeoniflorin monomer of a Chinese herb on cardiac ion channels. Chinese Medical Journal. 2011;124(19):3105-11.

Zhang GQ, Hao XM, Chen SZ, Zhou PA, Cheng HP, Wu CH. Blockade of paeoniflorin on L-type calcium channel in isolated rat ventricular myocytes. Chinese Pharmacol Bull. 2003;19(8):863-6.

Ma Y, Bates S, Gurney AM. The effects of paeonol on the electrophysiological properties of cardiac ventricular myocytes. Eur J Pharmacol. 2006;545:87-92.

This work was supported by the National Research Foundation of Korea Grant funded by the Korean Government (NRF-2012-013-2012S1A2A1A01031775).

Where applicable, the authors confirm that the experiments described here conform with The Physiological Society ethical requirements.

PCA071

Principles of Membrane and Protein Network Organization in Health and Disease

T. Kohl[1,2], E. Wagner[1,2], S. Brandenbúrg[1,2], U. Parlitz[3,2], J.W. Lederer[4] and S.E. Lehnart[1,5]

[1]Dept. of Cardiology and Pneumology, University Medical Center Göttingen, Germany, Goettingen, Germany, [2]Heart Research Center Goettingen, Göttingen, Germany, [3]Biomedical Physics Group, Max Planck Institute for Dynamics and Self-Organization, Göttingen, Germany, [4]Center fo Biomedical Engineering and Technology, University of Maryland, Baltimore, MD, USA and [5]DZHK (German Center for Cardiovascular Research), site Göttingen, Germany

In heart muscle cells both longitudinal and transversal architectures along the main cell axises represent important building principles that overcome challenging local conditions considering cell size versus cellular metabolic, proteomic and energetic needs. Furthermore, the specific cell volume is occupied by myofilaments that are aligned with mitochondria and the endo/sarcoplasmic reticulum network (SR), which is tightly associated with a highly branched internal sarcolemmal membrane network, the T-tubules (TT). TTs distribute electrochemical signals and nutrients to intracellular Ca2+ release nanodomains and organelles that involve the junctional SR (jSR).
Here we present fundamental properties of the highly branched T-tubule (TT) network as revealed by STED microscopy in isolated mouse cardiomyocytes. Healthy myocytes exhibit longitudinal and transversal components at similar frequencies. Yet, after myocardial infarction the specific micro-scale organization of TT membranes changes leading to a significant increase of longitudinal components and increased network branching, and overall to increased network complexity and spatial dysfunction.
In addition, it remains unclear how TTs interface with the microtubule (MT) system and whether MTs contribute to the TT membrane remodeling described above. MTs have been functionally associated with the organization of SR terminal cisternae and sub-membrane scaffolds (in skeletal muscle) and CaV1.2 targeting to T-tubules (in heart). Therefore, we further examined the MT network architecture and pathological changes. We found predominantly longitudinal MT components with more complex network patterns in the periphery of cells (cortex) as compared to deep internal MTs. Our data suggest, that MT branching occurs at major functional points where dispersed Golgi organelles can be locally identified. Moreover we compare microtubule (MT) networks before and after myocardial remodeling after gradient-controlled aortic banding, which will be presented.
In conclusion, quantitative analysis of membrane and protein networks showed important properties of spatial organization and suggest local mechanisms of remodeling that may contribute to intracellular Ca2+ release heterogeneity.

Where applicable, the authors confirm that the experiments described here conform with The Physiological Society ethical requirements.

PCA072

Simvastatin's effects on muscle are temporally defined and tissue specific

D.A. MacDougall, S.D. Pugh, A. Schorah, W. Rennie and S. Calaghan

School of Biomedical Sciences, University of Leeds, Leeds, UK

Cellular cholesterol is regulated by uptake, *de novo* synthesis, storage and efflux. Statins are inhibitors of HMG CoA reductase, an enzyme governing the rate limiting step in cholesterol synthesis. Statin treatment will initially decrease free cellular cholesterol but this in turn will promote expression of proteins responsible for cholesterol uptake (LDL receptors) and synthesis (HMG CoA reductase) and decrease expression of proteins involved in its storage as cholesteryl esters (acyl CoA cholesterol transferase) and efflux (caveolin) *via* sterol regulatory elements (SRE) in promoter regions. It has recently been shown that cholesterol efflux pathways are the main means by which (neonatal) cardiac myocytes regulate their cholesterol (Reboulleau *et al*., 2012).

We have compared the effect of acute and chronic statin treatment on cardiac and skeletal muscle. In adult rat ventricular myocytes exposed to 10 μM simvastatin for 48 h in culture, cholesterol levels were reduced by 30%, and a corresponding decrease in caveolin 3 expression was seen (cells from n=3-4 hearts; P<0.05; Student's t-test). By contrast, myocardium from adult rats treated with 40 mg/kg simvastatin by oral gavage daily for 2 weeks showed no change in cholesterol (0.38 ± 0.01 *vs*. 0.38 ± 0.02 μg/mg total protein; n=6 hearts; P>0.05). Despite this, caveolin 3 expression was reduced by 40% in statin-treated animals (P<0.05). These data are consistent with the concept that, following 2 weeks of statin treatment, SRE-dependent decreases in caveolin 3 expression act to return cellular cholesterol to normal levels by attenuating efflux pathways. However, normalisation of cholesterol at this time point is not common to all muscle. In *gastrocnemius* type II skeletal muscle from the same group of animals, cholesterol levels were lowered by 70% (P<0.05), despite an equivalent reduction in caveolin 3 expression (P<0.05). This indicates that skeletal muscle lacks the ability to regulate cholesterol homeostasis to the extent observed in cardiac muscle.

Our data suggest that the effects of statins are temporally defined, with acute statin treatment *in vitro* providing a snapshot of early cardiac statin effects before SRE-dependent changes in caveolin expression are able to normalise cholesterol by attenuating its efflux. Skeletal muscle lacks the cholesterol homeostatic mechanisms of cardiac muscle and is therefore more susceptible to statin-induced damage by long term cholesterol depletion. The marked decrease in both cholesterol and caveolin, two essential elements of caveolae, in statin-treated skeletal muscle may be a mechanism underlying statin-induced myopathy.

Reboulleau A *et al*. (2012) *J Mol Cell Cardiol* **53**:196-205

This work was funded by the British Heart Foundation.

Where applicable, the authors confirm that the experiments described here conform with The Physiological Society ethical requirements.

PCA073

Localization of atrial natriuretic peptide and impact of acute stressors on its expression in rat heart

J. Slavikova[1], M. Chottova Dvorakova[1,2], S. Hynie[2], P. Sida[2], E. Mistrova[1] and V. Klenerova[2]

[1]Department of Physiology, Faculty of Medicine in Plzen Charles University Prague, Plzen, Czech Republic and [2]Institute of Medical Biochemistry, First Faculty in Medicine Charles University Prague, Prague, Czech Republic

Atrial natriuretic peptide (ANP) which is produced by mammalian cardiomyocytes is involved in the regulation of blood pressure and fluid homeostasis. The peptide induces suppression of the renin-angiotensin as well as the sympathetic nervous systems to protect cardiovascular homeostasis, which is also deteriorated by the stress. The present study was designed to detect ANP and to examine expression of ANP mRNA in all heart compartments. Additionally, we investigated whether ANP distribution and ANP mRNA expression in the heart could be affected by the stress. We used male Sprague-Dawley (SD) rats (200g). Treatment of animals was in accordance with the Declaration of Helsinki Guiding Principles on Care and Use of Animals [DHEW Publication, NHI 80-23]. The study was approved by the Ethical Review Committee, First Faculty of Medicine, Charles University in Prague. A restraint stressor (immobilization, IS) and IS combined with partial immersion of rats into water (ICS) were applied to animals for one hour. One or three hours after the stress termination, the rats were decapitated, hearts were removed, and each atrium and ventricle were examined separately. Thus, all studies were performed in five groups of animals: in controls, IS1, IS3, ICS1, and ICS3 (n=4-6 per group). ANP localization in sections of preparations was identified by indirect immunohistochemistry with the use of specific commercial antibody. Expression of ANP mRNA was detected by real-time qRT PCR in all heart chambers by comparing their threshold cycle values (CT) to CT of reference gene β-actin. The relative expression ratios were calculated using Mann-Whitney test. Values are means ± S.E.M. In control rats, ANP-immunopositivity was strongly expressed in the left (LA) and right (RA) atrium in coarse granules within the cytoplasm (n=3 per group). No immunofluorescence was observed in the left (LV) and right (RV) ventricle in both control and stressed animals. ANP mRNA expressions were much higher in atria than in ventricles. In control rats, rank order of the gene expression was: LA = 138.8 (p<0,005) > RA = 39.2 (p<0,005) > RV = 10.1 (p<0,005) > LV = 1. The stress exposition led to increased expression of ANP mRNA by 56% (1.56±0.18, p<0.05) in RA, 22% (1.22±0.09, p<0.05) in LA, and 90% (1.90±0.37, p<0.05) in LV after IS1. The increase was also observed after IS3 in the same compartments, by 53% (1.53±0.14, p<0.05) in RA, 49% (1.49±0.21, p<0.05) in LA, and 134% (2.34±0.20, p<0.05) in LV. Combined stress (ICS3) caused the increase of ANP mRNA expression by 67% (1.67±0.22, p<0.05) in LA and by 187% (2.87±1.0, p<0.05) in LV. In conclusion, restraint stressors induced changes in expression of ANP mRNA in cardiomyocytes of atria and left ventricles; these effects may have relevance to ANP induced cardioprotection.

This work was supported by the Charles University Research Fund (project number P36), the project ED2.1.00/03.0076 from European Regional Development Fund, PRVOUK–25/LF1/2, MSM 0021620806.

Where applicable, the authors confirm that the experiments described here conform with The Physiological Society ethical requirements.

PCA074

Ischemia modified albumin: a sensitive and reliable marker of cardioprotection during on-pump cardiac operations

I.Z. Solak Gormus[1], A. Kiyici[2], M. Kayrak[3], N. Gormus[4] and N. Ergene[1]

[1]Physiology, Meram Medical School, Konya, Turkey, [2]Biochemistry, Meram Medical School, Konya, Turkey, [3]Cardiolgy, Meram Medical School, Konya, Turkey and [4]Cardiovascular Surgery, Meram Medical School, Konya, Turkey

Problem statement: The evaluation of myocardial protection during on-pump cardiac operations is of great importance. Creatinin kinase, cardiac troponin I, myoglobin, fatty-acid-binding proteins are well known markers for investigation of ischemia (1). Ischemia modified albumin is a reliable, new marker in cardiac ischemia investigations (2). In our prospective study we would like to investigate of our cardioprotective strategies during on-pump cardiac operations with ischemia modified albumin.
Methods: Fifty patients who needed coronary artery bypass operations according to AHA/ACC guidelines were taken to this study. All of the patients were elective cases and the operations were performed with standard cardiopulmonary bypass technique. During the cardiac arrest cold blood cardioplegia solution was used every 20 minutes (10 ml per kilogram) with antegrade technique through an aortic root cannula. Blood samples were taken before and at the end of operations. Cardiac troponin I, albumin, and ischemia modified albumin were investigated in these samples.
Results: There were no deaths after the cardiac operations. The preoperative and postoperative echocardiographic evaluation of ejection fraction were in normal ranges and there were no significant changes. The ischemia modified albumin levels were significantly increased after the cardiac operations ($p < 0.05$), while cardiac troponin I levels did not show any statistically significant difference. The albumin levels were significantly decreased after the operations.
Conclusions: Ischemia modified albumin is a sensitive and reliable marker of ischemia during on-pump cardiac operations. This marker can be used with all other markers in order to evaluate the optimal cardioprotective strategy.

Demographic data of operations and mean ischemia modified albumin and albumin results.

Mean Cardiopulmonary bypass time	75 min
Mean EF (%)	40
Mean number of vessels revascularized	3
IMA preoperative	0.34
IMA postoperative	0.55
Alb preoperative (g/dl)	3.4
Alb postoperative (g/dl)	2.3

Birdi I, Angelini GA, Bryan AJ. Biochemical markers of myocardial injury during cardiac operations. Ann Thorac Surg 1997;63:879-84.

2. Hueb W, Gersh BJ, Rezende PC, Garzillo CL, Lima EG, Vieira RD, Garcia RM, Favarato D, Segre CA, Pereira AC, Soares PR, Ribeiro E, Lemos P, Perin MA, Strunz CC, Dallan LA, Jatene FB, Stolf NA, Hueb AC, Dias R, Gaiotto FA, da Costa LM, Oikawa FT, de Melo RM, Serrano CV Jr, de Ávila LF, Villa AV, Filho JR, Nomura C, Ramires JA, Filho RK; MASS-V Study Group. Hypotheses, rationale, design, and methods for prognostic evaluation of cardiac biomarker elevation after percutaneous and surgical revascularization in the absence of manifest myocardial infarction. A comparative analysis of biomarkers and cardiac magnetic resonance. The MASS-V Trial. BMC Cardiovasc Disord. 2012 Aug 16;12:65. doi: 10.1186/1471-2261-12-65.

Where applicable, the authors confirm that the experiments described here conform with The Physiological Society ethical requirements.

PCA075

Mapping of repolarisation gradients in the canine left ventricular free wall using myocardial slices

P. Camelliti[1], S. Al-Ayoubi[1], J. Cartledge[1], P. Dias[1], M. Yacoub[1], A. Sridhar[2] and C. Terracciano[1]

[1]National Heart and Lung Institute, Imperial College, London, UK and [2]David Jack Centre for Research and Development, GlaxoSmithKline, Ware, UK

Introduction: Studies on isolated cardiomyocytes and ventricular wedges have shown contradicting data on the presence of transmural repolarization gradients in the left ventricle (LV). Here, we investigate electrophysiological heterogeneities of the canine LV free wall, using myocardial slices.
Methods: Vibratome-cut myocardial slices (300 μm thick) were prepared from transmural LV biopsies (10x10x9 mm; n=4 hearts), tangentially to the wall surface. Multiphoton microscopy was used to visualise muscle fiber orientation. Multi-electrode arrays (60 microelectrodes, total area 4.9x4.9 mm) were used to map electrophysiological parameters. Preparations were paced at cycle lengths (CL) ranging from 1 to 4s. Values are means ± S.E.M.
Results: Slices had longitudinal muscle fiber orientation, independent from transmural location. Activation-recovery intervals (ARI; Fig) correlated with transmural site at all pacing CL ($p<0.001$; ANOVA), with the longest values found in a 1.2 mm layer of the deep midmyocardium (4.8 to 6 mm from the epicardial surface; total LV thickness 9 mm). Longer pacing CL heterogeneously prolonged ARI (Fig) and increased transmural repolarization gradient from 63±7 to 106±3 ms (1s versus 4s CL; $p<0.01$ t-test). In plane ARI dispersion ranged from 9±1 to 18±3 ms, and was independent from transmural location and CL ($p>0.05$; ANOVA), suggesting the presence of electrophysiologically homogeneous and well coupled cells in each slice.
Conclusion: The deep midmyocardium contains a well-defined homogeneous region of prolonged ARI, which may contribute to repolarisation gradients in the canine LV.

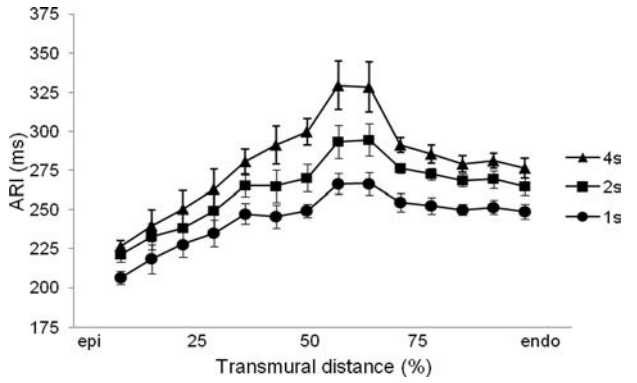

Figure: Transmural activation-recovery interval (ARI) profile measured at pacing CL ranging from 1 to 4s.

Where applicable, the authors confirm that the experiments described here conform with The Physiological Society ethical requirements.

PCA076

Histological and immunohistochemical study of the myocardial sleeves of the extensive pulmonary vein network of the rat

Y. Xiao[1,2], X. Cai[1], A. Atkinson[1], S. Logantha[1], G. Hart[1], M. Boyett[1], Z. Shui[1] and H. Dobrzynski[1]

[1]University of Manchester, Manchester, UK and [2]Cardiovascular Surgery, Union Hospital, Huazhong University of Science and Technology, Wuhan, China

Atrial fibrillation is the most common clinical cardiac arrhythmia and is associated with cardiac dysfunction and stroke. It is believed to be triggered by ectopic electrical activity originating in the myocardial sleeves surrounding the pulmonary veins. Despite their importance, the processes within the pulmonary veins that lead to cardiac arrhythmias are unknown. The aim of this study was to investigate the architecture of the pulmonary veins. Male Sprague-Dawley rats (~450 g) were heparinized and humanely sacrificed in accordance with the UK Animals Scientific Procedures Act 1986. The hearts were perfused with phosphate buffered saline to flush out blood and then embedded in freezing medium and frozen in isopentane cooled in liquid N2. Cryosections of 20 μm thickness were cut in the coronal, sagittal and transverse planes from the whole hearts. From each heart, 16 sections (at intervals of 400 μm) were stained with Masson's trichrome. At levels containing the pulmonary veins, sections were double immunolabelled for connexin43 (major gap junction protein in the working myocardium of the heart; Cx43) and caveolin3 (cardiac-specific isoform of the caveolin family) or alternatively Cx43 and HCN4 (major isoform responsible for the pacemaker current If in nodal tissues). The best view of the pulmonary veins was from sections cut in the transverse plane; it was possible to view the majority of the pulmonary veins in one section. Sections cut in the coronal plane were the best for showing the right superior pulmonary vein, as well as the sinoatrial and atrioventricular nodes. An example of a transverse section through the pulmonary veins immunolabelled for Cx43 and HCN4 is shown in Fig. 1. The marker of cardiac myocytes, caveolin3, was expressed throughout the atria (data not shown). It was also expressed in the myocardial sleeves of the pulmonary vein and its many branches (data not shown). The marker of working myocardium, Cx43, was also expressed throughout the atria (except for the sinoatrial and atrioventricular nodes) as well as the myocardial sleeves of the pulmonary vein and its branches (Fig. 1). In contrast, the nodal marker HCN4 was only expressed in the sinoatrial and atrioventricular nodes; it was not expressed in the working myocardium and it was not expressed at any point in the myocardial sleeves of the pulmonary vein and its branches (Fig. 1). HCN4 is, therefore, unlikely to be responsible for the ectopic activity of the pulmonary veins. In conclusion, it has been shown that the myocardial sleeves of the pulmonary veins can be identified by immunolabelling and the myocardial sleeves extend for many millimetres in the extensive pulmonary vein network of the rat. This is consistent with the work of Logantha et al. (1), who have shown cardiac action potentials can be recorded from intrapulmonary branches of vein.

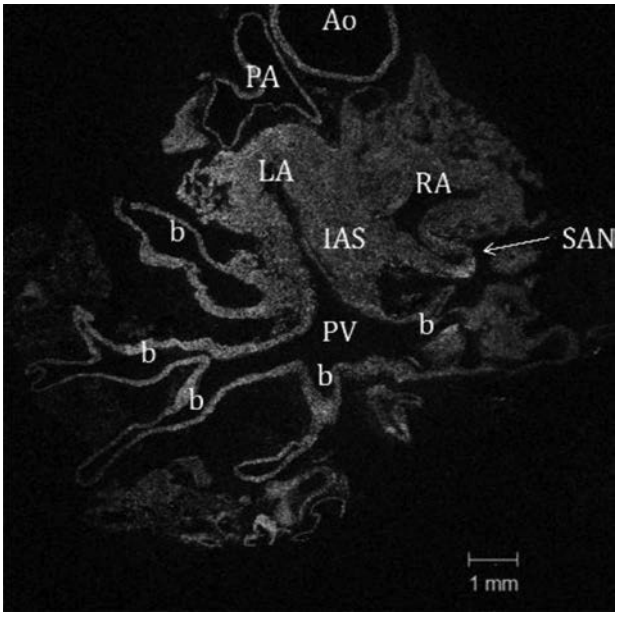

Fig1. Immunolabelling for Cx43 and HCN4 in transverse section at the level of the pulmonary veins. RA, right atrium; LA, left atrium; PV, pulmonary vein; b, branch of pulmonary vein; Ao, aortic artery; PA, pulmonary artery; IAS, interatrial septum; SAN, sinoatrial node.

Logantha SJ, Drummond RM, Rowan EG. (2007) Proceedings of the British Pharmacological Society at http://www.pA2online.org/abstracts/Vol5Issue2abst097P.pdf

Where applicable, the authors confirm that the experiments described here conform with The Physiological Society ethical requirements.

PCA077

Steep APD restitution in rat failing right ventricular myocytes

M.E. Hardy[1], O. Bernus[2,1] and E. White[1]

[1]School of Biomedical Sciences, University of Leeds, Leeds, UK and [2]Inserm U-1045 Universite de Bordeaux 2, Bordeaux, France

Pulmonary artery hypertension causes the right ventricle (RV) to become hypertrophied and fail. During this process the RV undergoes electrophysiological remodeling with resultant changes in action potential duration (APD). This study evaluated the effects of removing intracellular calcium (thus preventing forward-mode sodium-calcium exchanger (NCX) current) on the altered APD restitution in hypertrophied RV rat myocytes. Additionally experiments were performed using

ranolazine to assess the effects of the late sodium current ($I_{Na,late}$) on APD restitution in these cells.
Male Wistar rats were given a single i.p. injection of monocrotaline (60 mg/kg) or an equivalent volume of saline. When clinical symptoms of heart failure became apparent (3-4 weeks later) animals were euthanized and the hearts excised. RV myocytes were enzymatically isolated and used for measurements of APD at pacing rates between 1 and 9 Hz. Both sham and failing cells were either left untreated, loaded with BAPTA-AM (5 μM for 15 min), or perfused with 5 μM ranolazine. Some cells treated with BAPTA were also used under discontinuous (4 kHz) action potential (AP) clamp to impose the AP recorded at 1 Hz at pacing rates of 1, 2, 5 and 7 Hz.
Myocytes from the failing RV had a steeper APD_{90} restitution curve and significantly longer APD between 1 and 9 Hz compared to sham cells at all pacing rates ($p < 0.01 – 0.0001$, 2 Way ANOVA, Tukeys post-test, n = 5-6 cells). Despite this greater APD shortening, under AP clamp, compensation currents in failing myocytes were smaller in amplitude as pacing frequency increased (at 7 Hz, $p < 0.05 – 0.0001$ at -40 to 0 mV, n = 5-7). However, integrating the currents showed that in failing cells (which had a longer APD), greater positive charge was passed ($p < 0.05 – 0.0001$ at -40 to -25 mV, n = 3-7).
Failing RV cells that were preloaded with BAPTA had no significant change in APD_{90}. However, at APD_{25}, BAPTA increased the gradient of the restitution curve causing significant increases in duration at slower pacing frequencies ($p < 0.05 – 0.001$ at 1-2 Hz, n = 5 cells). Under AP clamp, BAPTA caused increases in positive charge passed at more positive membrane potentials, compared to untreated hypertrophied cells.
Inhibition of $I_{Na,late}$ using 5 μM ranolazine had no effect on either the APD_{90} or APD_{25} in either sham or failing RV myocytes (n = 6-9).
These data show that cells isolated from the monocrotaline treated RV have a longer APD and steeper APD restitution than those from sham animals. Additionally, our results suggest that steeper APD restitution in failing RV myocytes is not caused by either forward mode NCX or $I_{Na,late}$. Steeper restitution with decreased currents recorded under AP clamp is consistent with an increase in membrane resistance in failing cells. This may be caused by downregulation of K^+ currents. We are currently investigating this possibility.

Funded by the MRC.

Where applicable, the authors confirm that the experiments described here conform with The Physiological Society ethical requirements.

PCA078

Functional characterization of stem cell-derived cardiomyocytes: a comparative study

I.C. Marcu[1], P. Heuking[2], M. Jaconi[2] and N.D. Ullrich[1]

[1]Department of Physiology, University of Bern, Bern, Switzerland and [2]Department of Pathology and Immunology, University of Geneva, Geneva, Switzerland

Cardiovascular diseases represent the number one cause of death globally, and high prevalence of atherosclerosis in coronary vessels is paving the way for the development of ischemic heart disease and myocardial infarction. The low regenerative potential of the human heart cannot prevent the detrimental remodelling after cardiac injury, and therefore, the use of stem cells (SCs) for cardiac repair has gained great interest in recent years. In spite of ongoing preclinical and clinical trials using SCs in the heart, only little is known about the basic functional properties of these newly generated heart cells, and recent advances in reprogrammation of somatic cells into cardiomyocytes add to the need of thorough characterization of these cells, before functional integration of these cells into the myocardium can be advised.
The aim of this study was to characterize the electrical properties of SC-derived cardiomyocytes of different sources and to investigate intercellular coupling between cell pairs. For our comparison, we used mouse embryonic and induced pluripotent SC-derived cardiomyocytes (ESCs, iPSCs) and assessed their function relative to native neonatal cardiomyocytes and cultured HL-1 cells.
Parallel electrophysiological measurements using the patch clamp technique and confocal Ca2+ imaging with fluo-3 allowed us to study electrical parameters of the cells and excitation-contraction coupling. In order to study intercellular communication between neighboured myocytes, expression of gap junction proteins was confirmed in immunocytochemical assays and the gap junction permeant fluorescent dye calcein was used to measure metabolic coupling between cells.
In differentiated SC-cardiomyocytes, we have identified two distinct populations of cardiomyocytes, spontaneously active and silent but excitable cells, as reflected by the shape of their action potentials. They functionally express the pacemaking HCN channel in spontaneously active cells and cardiac-specific voltage-dependent Na+, L- and T-type Ca2+ channels, as confirmed by current properties and pharmacology. Immunocytological examination revealed strong expression of the cardiac gap junction protein connexin-43. Functional tests of intercellular coupling confirmed electrical coupling between SC-cardiomyocytes. However, permeation kinetics of dye transfer in SC-cardiomyocytes were similar to HL-1 cells, but significantly reduced in comparison with neonatal cells.
In conclusion, we provide a clear physiological profile of single and coupled SC-cardiomyocytes of different origin and evaluate their functional similarities with native cardiomyocytes and HL-1 cells. Despite strong electrophysiological parallels, the disparities in metabolic communication need to be carefully considered for future use of these cells in cardiac regenerative therapy.

SNF-Ambizione

Where applicable, the authors confirm that the experiments described here conform with The Physiological Society ethical requirements.

PCA079

An investigation into the effects of single point mutations found in patients with hypertrophic cardiomyopathy upon Junctophilin-2 structure and stability

H. Bennett, B. Davenport, A.W. Trafford, C. Pinali and A. Kitmitto

Faculty of Medical and Human Sciences, The University of Manchester, Manchester, UK

Excitation contraction coupling in cardiac muscle requires a precise spatial organisation of the L-type voltage-gated calcium channel (LTCC), on the t-tubule (t-t) membrane, and the ryanodine receptor (RyR2) localised to the junctional sarcoplasmic reticulum (jSR)[1]. In the heart, Junctophilin-2 (JP2) is thought to act as a scaffold to bridge, and stabilise, the gap between the two membranes forming the dyadic cleft. JP2 is believed to be tethered to the SR, via a C-terminal transmem-

brane domain, span the cytosol, and bind to the inner leaflet of the t-t via the N-terminal region. Genetic defects in JP2 have been associated with hypertrophic cardiomyopathy (HCM), which is the most common cause of sudden cardiac death in young people[2]. Several single amino acid mutations have been discovered within JP2 in HCM patients (S101R, S165F, Y141H, G505S) significantly, these carriers did not have any mutations of the Z-disc or contractile proteins typically associated with HCM[3]. The mechanisms by which these mutations lead to disease are still not understood. In order to investigate how the introduction of single point mutations influence the function of JP2 we have expressed and purified wild-type and mutant JP2 proteins from *E. coli*. Using fluorescence spectroscopy, exploiting the presence of instrinsic tryptophan residues within the JP2 amino acid sequence, we examined the thermal denaturation profiles of each protein. Slit widths were set at 5 nm, the excitation wavelength at 280 nm and the emission collected at 280 nm, 330 nm and 350 nm. The temperature was increased at a rate of 0.5ºC min^{-1} (20 - 80ºC). The transition temperature (T_m), the temperature at which 50% of the protein is denatured, was determined for wild-type and mutant JP2 by plotting the ratio of the emission intensity F_{330}/F_{350}. Guanidine hydrochloride was employed to study the effects of chemical denaturation and secondary structure analysis was conducted using circular dichroism (CD). Thermal and chemical denaturation experiments revealed the mutations had no overall effect on protein stability and the T_m for each protein was 52ºC. CD revealed that JP2 is comprised of 38% α-helix, 16% β-sheet, 18% turns and 28% random coil, correlating with predicted secondary structure analysis. However, the S101R and Y141H mutants exhibited changes to the secondary structure profile with a reduction to the overall helical content and increase in random coil. These results indicate the JP2 mutations do not appear to effect the stability of the protein but lead to a modification of the structure which may alter the t-t binding properties and/or disrupt potential protein interactions between JP2 and dyadic cleft proteins involved in calcium homeostasis.

Bers DM (2002). *Nature* **415**, 198–205.

Garbino, A *et al.* (2009). *Physiol. Genomics* **37**, 175–186

Landstrom, AP *et al* (2007). *J. Mol. Cell Cardiol* **42**, 1026–1035

We acknowledge and thank the British Heart Foundation for funding this work (RG/11/2/28701).

Where applicable, the authors confirm that the experiments described here conform with The Physiological Society ethical requirements.

PCA080

Increased cytosolic [Na] despite increased sodium potassium pump activity during early development of heart failure in beta1 adrenergic receptor overexpressing mice

P. Schoenleitner[1], G. Antoons[1], S. Khan[1], G.J. Unterer[1], P. Wakula[2], S. Engelhardt[3], B. Pieske[2,1] and F.R. Heinzel[2,1]

[1]Cardiology, Medical University Graz, Graz, Austria, [2]Ludwig Boltzmann Institute for Translational Heart Failure Research, Graz, Austria and [3]Pharmacology&Toxicology, Technische Universitaet Muenchen, München, Germany

Chronic stimulation of the β1-adrenergic pathway leads to cardiac hypertrophy and heart failure (HF). In mice overexpressing the β1-adrenergic receptor (β1), changes in Ca2+ handling precede the development of structural hypertrophy at an early stage of remodelling (8-12w). The Na+/K+ ATPase (NKA) is an important regulator of [Na+]i, and indirectly of Ca2+ homeostasis. Therefore we investigated putative changes in NKA activity, regulation and expression as well as mechanisms linked to the regulation of Na+ and Ca2+ in an early stage of HF.

Single left ventricular myocytes were isolated from 8-12 weeks old male β1 mice and wild-type littermates (WT). For Na+-measurements, myocytes were loaded with SBFI-AM. Relaxation of Ca2+ transients (CaT, fluo-3 AM) was measured as the time constant of decay by exponential fitting (time constant tauStim for CaT during 0.5Hz stimulation; and tauCaff for caffeine-induced transients, 20 mM). For NKA pump current measurements (Ip) a Cs-Asp based pipette solution with 10 mM Na+ was used. To measure maximal Ip, Cs-Asp was replaced with Na-Asp to a final concentration of 100 mM [Na+]pip. Cells were superfused with normal Tyrode solution with additional, in mM: 2 BaCl2, 2 NiCl2 (pH=7.4 with NaOH), at 37°C. Ip was measured as the difference in outward current, at 0 mV, after rapid solution switch to K+-free solution. Currents were normalized to cell capacitance. Protein expression of NKA subunit α1 and α2, NHE 1, TRPC 1/3/6, PLM and PLM phosphorylation were determined using Western blotting in whole ventricle homogenates. Protein densities were normalized to GAPDH.

In β1 myocytes, CaT showed a slower decline (tauStim 232±27ms in β1 vs. 180±17 ms in WT;mean±S.E.;n≥11/group;P<0.05). Ca2+ removal via forward NCX was significantly slowed. Cytosolic [Na+] was increased in resting cells (24.3±4.5 vs. 14.2±2.5 mM), and during stimulation (1Hz: 27.6±5.1 vs. 17.6±3.5 mM; 3 Hz:28.6±5.4 vs. 19.7±4.4 mM;n=14 and 8 respectively; all P<0.05). Protein levels of the NKA α1 subunit, NHE 1, TRPC 1,3 and 6 were unchanged, whereas the α2 subunit was reduced. Phospholemman (PLM), an inhibitory subunit of NKA, showed increased phosphorylation at Ser68 and the total amount was reduced in β1 mice. With [Na+]pip=10 mM, Ip density was significantly increased in β1 myocytes. Maximal Ip density was unchanged. In β1 mice, the slower Ca2+ removal via NCX is related to increased cytosolic [Na+]i.

Proteins related to Na+ influx, NHE 1, TRPC 1/3 and 6, are not differentially regulated at this early stage of cardiac remodeling. At physiological [Na+]i, NKA current is increased, consistent with the higher phosphorylation degree of PLM, thus rather acting as a compensatory mechanism for the high Na+ levels during early remodeling in heart failure.

Where applicable, the authors confirm that the experiments described here conform with The Physiological Society ethical requirements.

PCA081

Conduction defects and fibrosis in aged hearts with long QT syndrome 3

F. Syeda[1], D. Kucerova[2], I. Piccini[2], L. Fortmueller[2], G. Riley[1], M. Schaefers[3], M. Kuhlman[3], P. Kirchhof[1,2] and L. Fabritz[1,2]

[1]University of Birmingham, Birmingham, UK, [2]University Hospital Muenster, Muenster, Germany and [3]European Institute for Molecular Imaging, Muenster, Germany

Background and objectives: Altered sodium channel expression and function can cause sudden death. A knock-in mouse model with increased late sodium current, mimicking long QT syndrome 3 (δ-KPQ-SCN5A), was used to study effects of ageing on ventricle-ventricle conduction.

Methods: Electrophysiology-Hearts were removed from δ-KPQ-SCN5A (dKPQ) and their wildtype (WT) littermates under terminal anaesthesia with urethane (2mg/kg), and immediately perfused on a modified upright Langendorff apparatus, where monophasic action potentials were recorded using custom-made Ag-AgCl electrodes. Interventricular activation times were measured during right ventricular pacing at 100ms fixed-rate cycle length, in three age groups (very young: 2-5 months, young: 6-9 months, and old: 18-24 months).
Histology- 4μm-thick sections of paraffin-embedded hearts were stained with picrosirius red/haematoxylin. Collagen deposition was quantified using NIS Elements imaging software (Nikon) and Image J (National Institutes of Health, USA). Fibrosis was expressed as % of connective tissue relative to the total tissue inside the region of interest.
Results: In old WT mice (18-24 months) there was no significant increase in activation time, compared with very young mice (2-5 months, 11±1, n=11 vs. 13±1, n=8). Conduction times were consistently longer in dKPQ mice in older mice (very young: 11±1, n= 11 vs. 13±1, n=8; young: 10±1, n= 7 vs. 16±1, n=7*; old: 13±1, n= 8 vs. 17±1, n=9*). Consistent with the subtle conduction defect, there was subtle ventricular fibrosis in old dKPQ hearts and upregulation of several genes involved in fibrosis and structural remodelling, compared with old WT hearts.
Conclusion: A selective increase of the late sodium current may adversely affect ventricular conduction and this may be linked with ventricular fibrosis.
All values are expressed as mean±SEM, *p<0.05.

Where applicable, the authors confirm that the experiments described here conform with The Physiological Society ethical requirements.

PCA082

Life with "arrhythmia": peculiarity of pacemakering in ascidia's heart myoepithelial cells

V. Golovko and M. Gonotkov

Institute of Physiology, Syktyvkar, Russian Federation

Despite the considerable interest and a big amount of studies on various aspects of the electrophysiology of cells that initiation heart rhythm, the understanding of the mechanisms underlying their electrogenesis is insufficient. The main goal of this work is to analyze the effects of blockers of K +, Na + and Ca2 + channels on the configuration of the phases of the action potential and to determine which of the currents is pivotal. Method. The experiments were performed on spontaneously contracting heart of ascidia Styela rustica (n = 13) using microelectrode technique. Isolated heart was perfused with aerated sea (White See) water (mmol): 280 NaCl; 6 KCl; 36 MgCl2; 7 CaCl2; 19 Na2SO4; pH ~ 8.1 (Kuzmin et al., 2012).
Results. Action potentials of the myoepithelial cells in the heart were divided into two types: the action potential with slow diastolic depolarization (SDD; pacemaker) and without diastolic depolarization (working or contractile). Cells without SDD generated AP with a higher amplitude 96 ± 11 mV, and dV / dtmax 7 ± 1 V / sec (n = 12) comparing to the pacemaker type cells 71 ± 6 mV and 1.6 ± 0.3 V / sec (n = 4). All ascidia heart cells exhibited as episodes with burst from 7-16 action potentials. Then there was a pause for about a minute, after which there was a burst of APs on the other, turned to the stomach, side of the heart. On average, the frequency of action potential generation was 11 ± 4 pulses per min, without counting the time of "silence" or pause. Lidocaine (1 mM) decreased the dV / dt max in the contractile cells from 4.9 ± 0.3 V / sec up to 3.7 ± 0.4 V / sec (n = 5; 21%), and lengthed prolonged the action potential at 20 % of repolarization, APD 20 from 75 to 120 ms compared to the control . In pacemaker cells 4-aminopyridine (4AP; 5 mM) increased APD20 three times and decreased the upstroke velocity dV / dt max by more than 50% compared with the control. The period of the action potential generation in this burst did not changed. The increasing of the amount of APs in bursts, the decrease of the time of pauses in two-three times, the increasing of action potentials duration at 90 % of repolarization by 51% compared to the control were registered after the 30 minutes exposure to EGTA (5 mM).
The data indicate that K-currents play a pivotal role in the generation of pacemakering of ascidia's heart myoepithelial cells.

Suppoted by the Russian FBR12-0-32288jr (M.G.) and Ural's Division RAS projects 1054; 1022.

Where applicable, the authors confirm that the experiments described here conform with The Physiological Society ethical requirements.

PCA085

Unambiguous rapid sarcomere length measurements using remote focussing microscopy

R.B. Burton[1], A. Corbett[2], E.J. Botcherby[2], C.W. Smith[2], C. Bollensdorff[3], T. Wilson[2], M. Booth[2] and G. Bub[1]

[1]Department of Physiology, Anatomy and Genetics, University of Oxford, Oxford, UK, [2]Department of Engineering Science, University of Oxford, Oxford, UK and [3]National Heart and Lung Institute, Imperial College London, London, UK

Introduction: Sarcomere length (SL) is an important indicator of cardiac mechanical function, but current imaging modalities cannot unambiguously measure and characterize SL at the cell level in intact, living tissue(1). We have developed a method for measuring SL and tissue orientation using remote focusing microscopy, an emerging imaging modality that can capture 2-photon fluorescence from oblique planes.
Methods: The illumination spot in a microscope can be translated along the z-axis by illuminating the objective lens with a non-parallel light beam, however this introduces significant optical aberrations. To obtain diffraction-limited performance and fast z-scanning, we use an axial scan unit (ASU) consisting of a second, matched objective that compensates for aberrations introduced by the imaging objective and a lightweight mirror. We have demonstrated that rates of up to 2.7 kHz are achievable with our system, due to the low weight of our scanning mirror. The scan speed in the z-direction is therefore comparable with galvanometer scan rates in the xy-plane(2).
All experiments conformed to the Guide for the Care and Use of Laboratory Animals published by the Animals (Scientific Procedures) Act 1986 (UK). Hearts were isolated from female Sprague-Dawley rats, swiftly perfused via the aorta in Langendorff mode, loaded with membrane dye di-4-ANEPPS, transferred to a custom built cradle and imaged. We measure cell orientation from user selected cells in a field of view by imaging sarcomere structure on two oblique sub-planes that share a common major axis with the cell, at +45° and -45° to the image plane.
Results: Our methods captured a wide range of tissue angles, ranging from 0 to 26 degrees over 8 experiments. SL correction using the angle data calculated from the arbitrary planes resulted in an average reduction of SL standard deviation of

7%, and in one experiment the standard deviation for SLs decreases from 0.071 μm to 0.055 μm after correction, a 23% reduction.
Discussion: Remote focusing microscopy can unambiguously measure cell orientation in complex two photon data sets without capturing full z-stacks. The techniques presented here will allow rapid assessment of SL in healthy and diseased heart experimental preparations.

1) Bub G, Camelliti P, Bollensdorff C, et al. Am J Physiol Heart Circ Physiol. 2010 May;298(5):H1616-25.

2) Botcherby EJ, Smith CW, Kohl MM, et al. Proc Natl Acad Sci U S A. 2012 Feb 21;109(8):2919-24.

This work was supported by Oxford's BHF CRE, the EPSRC, and the BHF. RABB is an EP Abraham Cephalosporin JRF of Linacre college, Oxford.

Where applicable, the authors confirm that the experiments described here conform with The Physiological Society ethical requirements.

PCA086

Individual microvascular units are critical to cardiac performance

S. Egginton[1,2], D. Hauton[1,3], J. Winter[1,4], A. Al Shammari[5], E. Gaffney[5] and R. Evans[6]

[1]Physiology, University of Birmingham, Birmingham, UK, [2]Biomedical Sciences, University of Leeds, Leeds, UK, [3]Applied Medicine, University of Aberdeen, Aberdeen, UK, [4]Cardiovascular Sciences, University of Leicester, Leicester, UK, [5]Mathematical Institute, University of Oxford, Oxford, UK and [6]Physiology, Anatomy & Genetics, University of Oxford, Oxford, UK

High cardiac energy demand relies on lipid & glucose oxidation, depending on oxygen availability [1]. The relative importance of functional capillary supply or ability to switch between substrates to preserve cardiac performance is currently unclear, but may be critically important in conditions such as diabetes that are characterized by a reduced metabolic flexibility through the loss of insulin sensitivity [2]. The role of arteriole perfusion in selection of substrates was established before and after infusion of polystyrene microspheres (mean diameter 15.0±0.2μm) to mimic capillary rarefaction due to microvascular disease. The effect of acute loss of functional capillary supply on palmitate and glucose metabolism together with function was determined in normal working hearts from male rats. Random blockade of coronary arterioles by microspheres decreased rate-pressure product (RPP; R^2=0.82) in a dose-dependent manner, and halved peak developed pressure (P<0.01), in perfused-working hearts [3] from control and STZ-diabetic rats. Palmitate oxidation halved (P<0.001) with a similar increase in glucose oxidation (P<0.01) for control hearts, but in diabetic hearts palmitate oxidation was 2.5-fold higher (P<0.001) with unchanged glucose oxidation (ns). Arteriole occlusion decreased the density of patent capillaries by 40% (P<0.001) and increased capillary supply area by 60% (P<0.01). There was a more heterogeneous distribution of functional capillaries in the myocardium following microsphere infusion (CV=19.15% untreated vs. 25.80% occluded). Calculated myocardial PO^2 was sensitive to occlusion of arterioles leading to a decrease in oxygen consumption, and an increase in the fractional area of hypoxic regions. Graded loss of arteriole supply thus led to a reduction in both coronary flow and cardiac work, and metabolism was also decreased as a consequence. Interestingly, hearts demonstrate the capacity to switch between substrates, from palmitate to glucose, to maximise oxygen efficiency and sustain cardiac work. Our data suggests that the decline in performance noted for the heart in chronic diabetes may not be metabolic in origin but could result from the secondary consequence of diabetes, namely capillary rarefaction and microvascular disease leading to a regional inadequacy in oxygenation of the myocardium. This supports the importance of preventing arteriole loss as a consequence of microvascular disease.

Stanley WC, Recchia FA, Lopaschuk GD (2005) Physiol Rev 85:1093-1129

Pitkänen OP et al. (1998) Diabetes 47:248-254

Hauton D, Bennett MJ, Evans RD (2001) Biochim Biophys Acta 1533:99-109

The authors wish to thank the University of Birmingham Research Development Committee for supporting this work.

Where applicable, the authors confirm that the experiments described here conform with The Physiological Society ethical requirements.

PCA087

Effects of cannabinoid-1 receptor blockade in diabetic cardiomyopathy

S. Batkai[1], M. Rajesh[2], P. Mukhopadhyay[2], B. Horvath[2], R. Cinar[2], L. Liaudet[3], K. Mackie[4], G. Hasko[5] and P. Pacher[2]

[1]IMTTS, Hannover Medical School, Hannover, Germany, [2]NIAAA, NIH, Bethesda, MD, USA, [3]Department of Intensive Care Medicine, University Hospital, Lausanne, Switzerland, [4]Department of Psychological and Brain Sciences, Indiana University, Bloomington, IN, USA and [5]Department of Surgery, University of Medicine and Dentistry of New Jersey, Newark, NJ, USA

Diabetic cardiomyopathy is characterized by left ventricular hypertrophy, early diastolic dysfunction and/or systolic dysfunction that leads to heart failure in diabetic paients. The endocannabinoid system has a recognized role in the development of various cardiac diseases due to involvement in cardiac dysfunction, inflammation, fibrosis and cell death.
In this study, the role of cardiac CB1 receptor signaling was explored in a stertozotocin-induced type 1 diabetic mouse model. The animals with chronically increased blood glucose levels developed characteristic diabetic cardiomyopathy assessed by intraventricular pressure-volume catheter system. At the tissue level, the hearts after 12 weeks of diabetes showed increased myocardial oxidative/nitrative stress, p38/Jun kinase (JNK) and mitogen-activated protein kinases (MAPKs) activation, enhanced inflammation and fibrosis, accumulation of advanced glycation end product (AGE), increased AGE and angiotensin II type 1 (AT1R) receptors, decreased expression of sarcoplasmic/endoplasmic reticulum Ca2+-ATPase (SERCA2a). Overactivation of the endocannabinoid system due to the diabetes was evident by increased cardiac endocannabinoid anandamide levels and cannabinoid 1 (CB1) receptor expression. Pharmacological inhibition or genetic deletion of the CB1 receptors attenuated the diabetes-induced cellular alterations and improved cardiac dysfunction. Most importantly, pharmacological inhibition of CB1 receptors may preserve its beneficial effects on contractile dysfunction even if administered after the development of established cardiomyopathy.
Overactivation of cardiac CB1 receptors by endocannabinoids may play an important role in the pathogenesis of diabetic cardiomyopathy by facilitating various intracellular signaling

(MAPK activation, AT1R expression/signaling, AGE accumulation, oxidative/nitrative stress), inflammation, and fibrosis. Conversely, pharmacological inhibition of cardiac CB1 receptor may be beneficial in the treatment of diabetic cardiovascular complications.

Where applicable, the authors confirm that the experiments described here conform with The Physiological Society ethical requirements.

PCA088

A new index for evaluating the strength of left ventricular vortex: in silico study

E. Shim[1], C. Leem[2] and Y. Earm[3]

[1]Kangwon National University, Chuncheon, Republic of Korea, [2]University of Ulsan, Seoul, Republic of Korea and [3]Seoul National University, Seoul, Republic of Korea

Left ventricular vortex plays a critical role in blood ejection from left ventricle (LV) to aorta. In spite of several parameters for evaluating LV vortex, there still remain fundamental questions to categorize LV vortex. Here, we propose the Reynolds number (Re), based on mitral valvular velocity and diameter, as an evaluation index for LV vortex strength and verify this by using a computational method. For this purpose, we implement an integrative model of heart and blood flow simulating sequential events of heart from cellular electric excitation-contraction to 3D tissue contraction, and eventually blood hemodynamics in LV. Simulation of fluid structure interation (FSI) in this study couples cardiac electromechanical model presented in our previous study [1] with the code of computational fluid dyanamics [2]. Remeshing algorithm is used to account for the mesh vairtion according to vave and ventricular wall motions. First, we verify the present method by comparing computed results with clinical observations. Then, we investigate the effect of Re variation on the strength LV vortex. Simulated results show that the strength LV vortex can be classified by Re, indicating Re is a useful index for diagonizing hemodynamic dysfunction of LV.

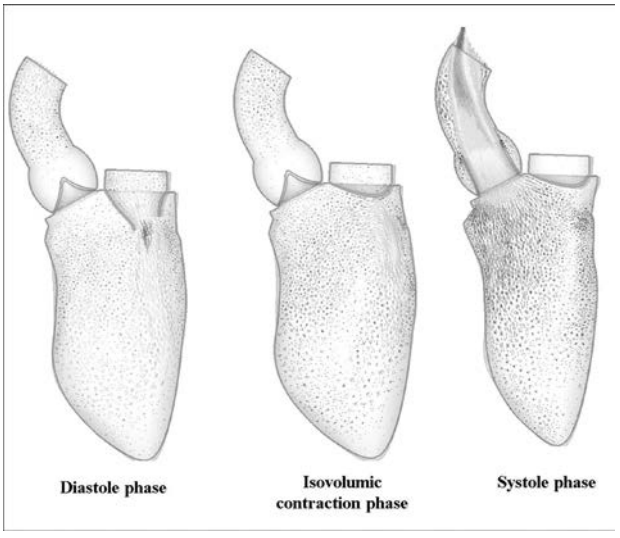

Computed results of left ventricular hemodynamics

Lim KM et al. (2012). J Physiol Sci 62, 11-19.

Shim EB & Chang KS (1997). J Biomech Eng 119, 45-51

Where applicable, the authors confirm that the experiments described here conform with The Physiological Society ethical requirements.

PCA090

Gestational intermittent hypoxia induces sex-differential DNA methylation of corticotropin-releasing hormone receptor 1 associated with anxiety-like behavior in rat offspring

X. Wang[1], F. Meng[1], Z. Liu[2], J. Fan[1], K. Hao[1], X. Chen[1,2] and J. Du[1,3]

[1]Neurobiology and Physiology, Zhejiang University, Hangzhou, China, [2]Key Laboratory of Medical Neurobiology of the Ministry of Health, Hangzhou, 310058, China and [3]Zhejiang Province Key Laboratory for Neurobiology, Hangzhou, 310058, China

Early life stress in gestation may result in an increased vulnerability to disease and behavior alteration in offspring. The fetus may often experience intermittent intrauterine hypoxia stress under a variety of conditions, such as pregnancy at high altitude, pregnancy with anemia, cord compression, hypertension, obstructive sleep apnea and preeclampsia. The mechanism regarding the fetal antecedents contributing to disease development remains limited. Here we reported that maternal gestational intermittent hypoxia (GIH) induced by hypobaric high-altitude hypoxia of 5km (equivalent to ~10.8% O2 at sea level), 4 hour / day for 21 days caused a sex-dependent anxiety-like behavior in 90-day-old (P90) male offspring but not female offspring analyzed by open-field test, light-dark box test and elevated plus maze test (n=10, $p<0.05$). The *CRHR1* mRNA expression in PVN and central amygdala (CeA) of P90 (n=8) and in hypothalamus of embryonic day 19 (E19) (n=7) were tested by quantitative real-time PCR. We found that there was a significant increase of *CRHR1* mRNA expression in male's PVN ($p<0.05$) but not in female's at the age of P90. No difference of *CRHR1* mRNA expression was found in CeA of P90 offspring. GIH also induced an increased *CRHR1* mRNA in the hypothalamus at the E19 ($p<0.05$). There were two CpG (island-1 and -2) within the *Crhr1* gene promoter by the software analysis, and we demonstrated the island-1 between -607 and -502 bp functioned as the major regulatory domain of *Crhr1* transcription activity, and found that the demethylation at the CpG sites of *Crhr1* promoter enhanced *CRHR1* mRNA expression *in vitro* (n=3, $p<0.001$). Furthermore, *in vivo*, the increase of *CRHR1* mRNA expression might be modulated by the decreased methylation at -535 CpG sites within the island-1 occurred in male E19 embryo (n=7, $p<0.05$) and the other in CpG three sites, such as -587 ($p<0.01$), -547 ($p<0.05$) and -544 ($p<0.01$) in the PVN of P90 male offspring (n=10), which might come from a decreased expression of DNMT3b in male offspring after GIH (n=7, $p<0.05$). In conclusion, GIH induces anxiety-like behavior in male adult offspring, which associated with the sex-dependent expression of *CRHR1* mRNA in the PVN but not in the CeA in offspring. GIH can alter *Crhr1* gene methylation, principally via DNMT3b, and *Crhr1* demethylation is associated with high-expressed *CRHR1* mRNA, suggesting a sex-biased mechanism for *Crhr1* gene expression associated with the anxiety-like behavior in GIH adult offspring. Our findings suggest that the vulnerability to hypoxia-induced anxiety in offspring occurs through the sexually differential epigenetic modification of *Crhr1* genomic regions. We address a novel hypothesis, that GIH-induced male-sexdependent demethylation at CpG sites of *Crhr1* DNA in promoter triggers elevation of *CRHR1* mRNA in PVN and anxiety-like behavior in adult offspring.

Where applicable, the authors confirm that the experiments described here conform with The Physiological Society ethical requirements.

PCA091

Codon 104 variation of p53 gene is necessary for enhancing cellular survival strategy in mammals of the Tibet plateau

Y. Zhao[1,2], M. Wang[1,2], X. Chen[2,3] and J. Du[1,2]

[1]Neurobiology and Physiology, Zhejiang University, Hangzhou, China, [2]Key Laboratory of Medical Neurobiology of the Ministry of Health, Hangzhou, China and [3]Key Laboratory of Neuroscience of Zhejiang Province, Hangzhou, 310058, China

While p53 levels and mutations correlate well with tumorigenesis, relatively little is known about the role of p53 variations in environmental adaptation. *Myospalax baileyi* and *Microtus oeconomus*, are native rodents living at the Qinghai-Tibet plateau and well acclimatized to hypoxia, cold, and/or high CO2 environments. The CDS of p53 from *M. baileyi* and *M. oeconomus* were cloned and sequenced. Evolutionary analysis distinguished the codon 104 variation from other sites as an important mutation correlated with the adaptation of these two rodents to plateau environments. The S104N of *M. baileyi* p53 is different from two of its close species *Myospalax cansus* and *Spalax judaei* living at lowland. The S104E of *M. oeconomus* p53 shared with only four fishes and squid, most of which were reported to be hypoxia-tolerant. To address the functional characteristics of their p53, the p53-null human non-small lung cancer cells NCI-H1299 (ATCC CRL-5803) were transfected with expression plasmids of *M. baileyi*, *M. oeconomus* and human p53. As determined by dual-luciferase assays, while the S104N of *M. baileyi* p53 induced stronger transactivation of pro-apoptotic target genes IGFBP3 and Apaf1 (1.9 and 1.5 folds, respectively; $p < 0.001$), the S104E of *M. oeconomus* p53 was responsible for the deficient transactivation of IGFBP3, Apaf1 and bax (0.3, 0.4 and 0.5 folds, respectively; $p < 0.001$). Values are means ± SD, compared by one-way ANOVA (n = 3). Using site-directed mutagenesis and dual-luciferase assays, we demonstrated that the codon 104 variation contributes to its sensitivity to cold and acidic stresses. While *M. baileyi* wt p53 induced IGFBP3 transactivation at 37 °C is 1.5 folds higher than that at 30 °C ($p < 0.001$), both N104S and N104E mutants had similar transactivation to IGFBP3 between 30 °C and 37 °C ($p > 0.05$). At pH 6.0, IGFBP3 induced by *M. baileyi* wt p53 decreased by 40% compared with at pH 7.4 ($p < 0.01$), whereas IGFBP3 induced by N104E mutant only decreased by 10% ($p < 0.05$). We propose that these p53 codon 104 variations are an outcome of environmental adaptation and evolutionary selection that enhances cellular survival strategies befitting the hypoxic, cold, and high CO2 (for *M. baileyi*) environments at the Qinghai-Tibet plateau.

Where applicable, the authors confirm that the experiments described here conform with The Physiological Society ethical requirements.

PCA092

Cellular Localisation and Functions of the ACE2 Metabolite of (Pyr^1)apelin-13

P. Yang, R.E. Kuc, J.J. Maguire, A.L. Brame, N.W. Morrell and A.P. Davenport

Department of Medicine, University of Cambridge, Cambridge, UK

Introduction: Apelin is the endogenous ligand of the G protein-coupled receptor APJ. In human cardiovascular tissues apelin produces endothelium-dependent vasodilatation and positive inotropy *in vitro*, and (Pyr^1)apelin-13 is the predominant isoform of mature apelin in the heart[(1)]. Beneficial roles for both apelin and ACE2, that converts angiotensin-II to angiotensin(1-7), have been reported in pulmonary arterial hypertension (PAH)[(2,3,4)]. Intriguingly, ACE2 also removes the C terminal phenylalanine from (Pyr^1)apelin-13, generating (Pyr^1)apelin-13$_{(1\text{-}12)}$[(5)].

Aims and Hypotheses: Our aim was to investigate whether (Pyr^1)apelin-13$_{(1\text{-}12)}$ is present endogenously in normal and PAH rat and human cardiopulmonary tissues, and to test our hypothesis that this metabolite retains significant biological activity.

Methods: Specific (Pyr^1)apelin-13$_{(1\text{-}12)}$ and ACE2 antibodies were used in peroxidase-anti-peroxidase and dual-labelling fluorescent immunocytochemistry experiments. 30μm sections of cardiopulmonary tissues were from normal and PAH human heart and lung (n=4 for each) and from healthy male Sprague-Dawley rats and rats treated with monocrotaline (60mg/kg s.c.), as a model of PAH (n=4 for each). Biological activity of (Pyr^1)apelin-13$_{(1\text{-}12)}$ was determined in β-arrestin recruitment and receptor internalisation assays, and compared to (Pyr^1)apelin-13 (10^{-11}-10^{-6}M ; n=3-12). Values of pD_2 (negative log10 of the concentration producing 50% of maximum response) and maximum responses were determined using GraphPad Prism.

Results: In both rat and human tissues, (Pyr^1)apelin-13$_{(1\text{-}12)}$-like immunoreactivity(-LI) was present in the endothelium of normal heart and lung and PAH heart and co-localized with ACE2-LI, but was reduced or absent in PAH lung from both species. Furthermore, (Pyr^1)apelin-13$_{(1\text{-}12)}$ exhibited full agonist activity with 5-10 fold lower potency in β-arrestin recruitment (pD_2= 7.84±0.07) and receptor internalisation assays (pD_2= 8.39±0.01) compared to (Pyr^1)apelin-13 (pD_2= 8.76±0.09, pD_2= 8.82±0.01, respectively).

Conclusions: This study demonstrates for the first time that (Pyr^1)apelin-13$_{(1\text{-}12)}$ can be detected in rat and human cardiopulmonary tissues and is present in cells that also express ACE2. Our functional data suggest that ACE2 does not inactivate (Pyr^1)apelin-13, rather the metabolite retains a biological activity comparable to the parent peptide. If the apelin system is beneficial in PAH, it is possible that the observed reduction in (Pyr^1)apelin-13$_{(1\text{-}12)}$ expression in PAH lung may contribute to the pathogenesis of the disease, and generation of (Pyr^1)apelin-13$_{(1\text{-}12)}$ may therefore also contribute to the positive actions of ACE2 therapies.

(1) Maguire JJ *et al.* (2009). *Hypertension* **54**(3): 598-604

(2) Andersen CU *et al.* (2011). *Pulm Circ* **1**(3): 334-346

(3) Kim J *et al.* (2013). *Nat Med* **19**(1): 74-82

(4) Shenoy V *et al.* (2011). *Curr Opin Pharmacol* **11**(2): 150-155

(5) Vickers C *et al.* (2002). *J Biol Chem* **277**(17): 14838 14843

Where applicable, the authors confirm that the experiments described here conform with The Physiological Society ethical requirements.

PCA093

Delivery of Oct4 and SirT1 genes into aged retinal pigment epithelium by cationinc PEI-polyurethanes

J. Cherng

Biochemistry & Chemistry, National Chung Cheng University, Chia-Yi, Taiwan

SirT1, a NAD-dependent histone deacetylase, is an essential mediator of cellular longevity. Oct4, a POU-domain transcription factor, is highly expressed in maintaining pluri-potency and cellular reprogramming process in stem cells. Both Oct4 and SirT1 (Oct4/SirT1) expression was decreased in an age-dependent manner in retina and retinal pigment epithelium cells (RPEs). Cationic polyurethane, a biodegradable non-viral vector, protects DNA from nuclease degradation and helps to deliver genes efficiently. In this study, polyurethane-short branch polyethylenimine (PU-PEI) was used to deliver Oct4/SirT1 into aged RPEs (aRPEs) or light-injured rat retinas. Rats were anesthetized with intramuscular injections of an equal-volume mixture of 2% lidocaine (0.15 mL/kg) and ketamine (50 mg/mL). The light-injured retinas were confirmed with H&E staining and quantified with the changes in the outer nuclear layer (ONL) thickness. The results showed that Oct4/SirT1 overexpression increased the expression of several progenitor-related genes and the self-renewal ability of aRPEs. Moreover, Oct4/SirT1 overexpression resulted in the demethylation of the Oct4 promoter and enhanced the expression of antioxidant enzymes, which was accompanied by a decrease in intracellular ROS production and hydrogen peroxide-induced oxidative stress. Importantly, PU-PEI-mediated Oct4/SirT1 gene transfer rescued retinal cell loss and improved electroretinographic responses in light-injured rat retinas. These data suggest that PU-PEI-mediated delivery of Oct4/SirT1 reprograms aRPEs into a more primitive state and results in cytoprotection by regulating the antioxidative capabilities of these retinal cells.
(Note: all experiments were performed in compliance with the Animal Care and Use Committee guidelines and in accordance with the ARVO Statement for the Use of Animals in Ophthalmic and Vision Research)

Where applicable, the authors confirm that the experiments described here conform with The Physiological Society ethical requirements.

PCA094

Curcumin protects nigral dopaminergic neurons by iron-chelation in the 6-hydroxydopamine rat model of Parkinson's disease

H. Xu

Qingdao University, Qingdao, China

Curcumin is a plant polyphenolic compound and a major component of spice turmeric (Curcuma longa). It has been reported to possess free radical-scavenging, iron-chelating, and anti-inflammatory properties in different tissues. Our previous study showed that curcumin protects MES23.5 dopaminergic cells from 6-hydroxydopamine (6-OHDA)-induced neurotoxicity in vitro. The present study aimed to explore this neuroprotective effect in the 6-OHDA lesioned rat model of Parkinson's disease in vivo. Wistar rats weighing 200–220 g were given intragastric curcumin for 24 days. 6-OHDA lesioning was conducted on day 4 of curcumin treatment. Dopamine content was assessed by high-performance liquid chromatography with electrochemical detection, tyrosine hydroxylase (TH)-containing neurons by immunohistochemistry, and iron-containing cells by Perls' iron staining. Results showed the dopamine content in the striatum and the number of TH-immunoreactive neurons decreased after 6-OHDA treatment. Curcumin pretreatment reversed these changes. Further studies demonstrated that 6-OHDA treatment increased the number of iron-staining cells, which was dramatically decreased by curcumin pretreatment. This indicates that the protective effects of curcumin against 6-OHDA may be attributable to the iron chelating activity of curcumin to suppress the iron-induced degeneration of nigral dopaminergic neurons.

This work was supported by grants from the National Basic Research Development Program of the Ministry of Science and Technology of China (2011CB504102) and the National Natural Science Foundation of China (30930036, 81100955).

Where applicable, the authors confirm that the experiments described here conform with The Physiological Society ethical requirements.

PCA095

A novel antibody against Aβ sequence 31-35 efficiently neutralizes Aβ1-42-induced impairments in spatial memory and synaptic plasticity in rats

L. Cheng, X. Li, Y. Pan, X. Chen and J. Qi

Physiology, Shanxi Medical University, Taiyuan, Shanxi, China

Although the immunotherapy for Alzheimer's disease (AD) has achieved some exciting results, current immunization strategies with amyloid β-protein (Aβ) and its antibodies are causing serious side effects in AD patients, which is partly due to the damage of physiological amyloid precursor protein. Our previous studies indicated that the sequence 31-35 in Aβ is a shorter active center responsible for the neurotoxicity of Aβ, suggesting a more specific target for AD treatment. The present study, on the basis of making a specific antibody against the sequence 31-35 of Aβ, observed the effects of the anti-Aβ31-35 antibody on the Aβ1-42-induced impairments of spatial learning and memory in rats and investigated its electrophysiological and cellular mechanisms using Morris water maze (MWM), primary neuronal culture and hippocampal field potential recording. Under the anesthesia with 1% carbrital (50 mg/kg, i.p.), a stainless steel cannula was implanted into the right lateral ventricle of Wistar rats (200-300g) for intracerebroventricular (i.c.v.) injection of drug/vehicle. MWM tests consisted of acquisition phase and probe trial. The hippocampal long term potentiation (LTP) was examined by recording field excitatory postsynaptic potentials (fEPSPs) in the CA1 region of rats under anesthesia with ethyl carbamate (1.5 g/kg, i. p.). In primary culture experiments, cell viability, LDH release and cell survival rate were checked. All data were presented as means ± standard error of the mean. The statistical significance was defined as $p<0.05$. The results showed that i.c.v. injection of anti-Aβ31-35 antibody alone did not change the spatial memory ($p>0.05$, n=8), the basal synaptic transmission and hippocampal LTP ($p>0.05$, n=7) of rats. However, pretreatment with the anti-Aβ31-35 antibody dose-

dependently (0.05-5 nmol) decreased the escape latencies in underwater platform test ($p<0.05$ in 0.5 and 5 nmol group, n=8) and increased the swim time and distance elapsed in the target quadrant in probe trial ($p<0.05$, n=8); 5 nmol Anti-Aβ31-35 antibody almost completely reversed the Aβ1-42-induced suppression of in vivo hippocampal LTP ($p<0.01$, n=6); Aβ1-42-induced cytotoxicity in cultured cortical neurons was also inhibited by the antibody ($p<0.05$ or $p<0.01$), with a nearly normal cell viability and a reduced LDH release. These results suggest that 31-35 sequence of Aβ may be a new therapeutic target for AD, and the anti-Aβ31-35 antibody will be probably useful in AD immunotherapy as a novel anti-Aβ antibody candidate.

This work was supported by the National Science Foundation of China (No. 31271201); the Special Foundation for High Schools Doctoral Program of Ministry of Education, China (No. 20101417110001); the Natural Science Foundation of Shanxi Province of China (No. 2010011049-3.

Where applicable, the authors confirm that the experiments described here conform with The Physiological Society ethical requirements.

PCA096

Apolipoprotein E4 disrupts the induction, not the maintenance of hippocampal late-phase long-term potentiation in rats

F. Qiao, X. Gao and J. Qi

Shanxi Medical University, Taiyuan, China

Alzheimer's disease (AD) is a progressive and irreversible neurodegenerative disorder associated with memory loss, cognitive deterioration and weakness of intellectual capacity. Inheritance of the ε4 allele of the apolipoprotein E gene (ApoE4) is a major risk factor for the development of AD. Although the association between ApoE4 and AD is well documented, the effects of ApoE4 on hippocampal synaptic plasticity which related to long-term memory is unknown. In the present study, we recorded in vivo late-phase long-term potentiation (L-LTP) of field excitatory postsynaptic potentials (fEPSPs) in hippocampal CA1 region of rats, and investigated the possible electrophysiological mechanism of ApoE4 in the induction and maintenance of L-LTP. 60 male SD rats (250-350 g) were used. Under anesthesia with urethane (1.5 g/kg i.p.), the L-LTP was induced by three groups of high frequency stimulation (HFS); ApoE4 solution (0.2 μg, n=24; 2 μg, n=12) was injected into the hippocampus 30 min before HFS (pre-HFS injection) or 1 min after HFS (post-HFS injection). Control rats (n=24) received only saline. The paired pulse facilitation (PPF) in the CA1 region was also recorded. All values were presented as means±S.E.M. and ANOVA or t-tests was used for statistical analysis. The results showed that: (1) three groups of HFS successfully induced hippocampal L-LTP in control group, with average fEPSP amplitudes of 211.0±7.2%, 170.4±4.5% and 161.2±3.3% immediately, 60 min and 180 min post-HFSs, respectively; (2) in pre-HFS injection group, 0.2μg apoE4 did not change the base line synaptic transmission but significantly ($p<0.01$) inhibited the L-LTP induction, the fEPSPs being 178.3±5.8%, 149.7±5.0% and 142.2±5.0% at the same time points as control group; (3) in post-HFS injection groups, the same concentration (0.2μg) of apoE4 produced a slight, but not significant decrease in the average fEPSP amplitude ($p>0.05$); further, injection of high dose (2μg) ApoE4 after HFS did not enhance the suppression of L-LTP, the fEPSPs still being 152.2±6.6% and 150.7±4.2% at the same time points ($p>0.05$); (4) ApoE4 injection did not affect the PPF, the values before HFS being 164.8±3.4% and 163.2±3.0% in control and ApoE4 (0.2μg) groups, respectively ($p>0.05$); the values after HFS being 132.1±2.4%, 132.9±2.0% and 127.7±3.7% in control, 0.2μg ApoE4 and 2μg ApoE4 groups, respectively ($p>0.05$). These results indicate that ApoE4 injection before HFS, not after HFS, impaired hippocampal L-LTP, suggesting that neurotoxicity of ApoE4 is mainly involved in the suppression of L-LTP induction, but not the maintenance. In addition, the unaffected PPF suggests that the inhibition of L-LTP induction by ApoE4 may be not mediated by presynaptic neurotransmitter release, but postsynaptic signaling.

Where applicable, the authors confirm that the experiments described here conform with The Physiological Society ethical requirements.

PCA097

Neuroprotective effects of Lycium barbarum L on senescence-accelerated mouse

Z. Miao and Y. Wang

Ningxia Medical University, Yinchuan, China

Lycium barbarum L. also called wolfberry, is a Chinese medicine herb which has been used for thousands of years for the purpose of healthy aging. The content of polysaccharide(LBP) in Lycium barbarum L is more than 40%. While neuroprotective effects of the LBP in neuronal cultures have been demonstrated, it is doubtful whether the LBP can cross through blood–brain barrier to elicit neuroprotection. Therefore, experiments in animal model of senescence-accelerated mouse (SAMP8) were performed to investigate its neuroprotective effects. Early Alzheimer's disease (AD) is with decreased nicotinic acetylcholinereceptor (nAChR) density from the cortex and hippocampus. α7 nAChRs expressed on cholinergic projection neurons and target regions have been implicated in neuroprotection against β-amyloid (Aβ) toxicity and maintenance of the septohippocampal phenotype. And some studies have determined that oxidative stress is also a decisive factor in AD. For experiments, adult male SAMP8 (5 months with weights 21–24 g) were housed in temperature-controlled animal room subjected to a 12-h light/12-h dark cycle and provided with sufficient food and water supply.The LBP was dissolved in phosphate-buffered saline (PBS). Animals were fed daily with 0.5 ml of either PBS or different dosages of LBP, including 50 and 100mg/kg, for a total of 8 week. We arbitrary chose 1 week for the experiment as Chinese usually drinks the soup containing Lycium barbarum L. for several days.The results suggest that LBP could prevent the appearance of aging sign and symptoms.From Morris Water Maze experiment, we found that taking different dosages of LBP could improve the learning and memory of SAMP8. Under electron and light microscope, we observed that the injuries of the brain was obviously meliorated after taking LBP and the possible mechanism might be related to upregulation of α7nAChRs level and improvement of antioxidant ability.LBP may have potential therapeutic applications to various neurodegenerative disorders.

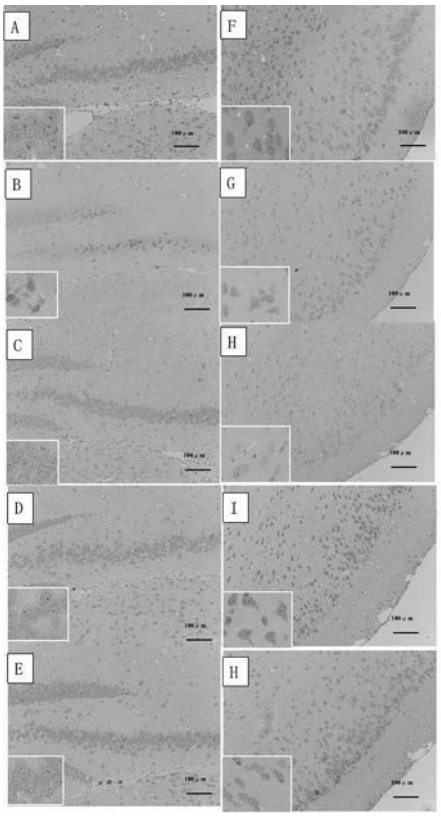

Figure 1
Immunolabeling by α 7 Antibodies in Mouse Brain
A-E:The α7 nAchRCerebral Hippocampus
F-J: The α7 nAchR Cerebral Cortex
A:R1 Con
B:P8 Con
C:P8 PBS
D:P8 LBP 100mg/kg
E:P8 LBP 50mg/kg
F: R1 Con
G:P8 Con
H:P8 PBS
I:P8 LBP 100mg/kg
J:P8 LBP 50mg/kg

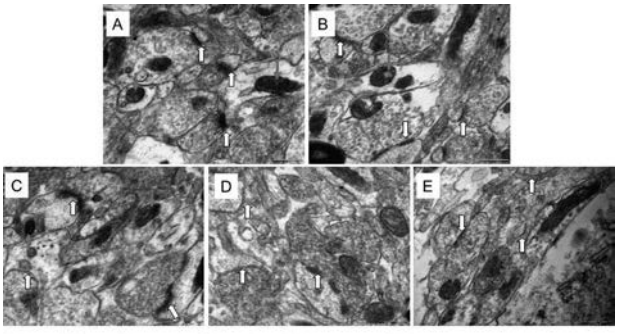

Figure 2 Electron Microscopic Observation of Hippocampus Cell
⇧ synapse ↟ mitochondria
A:R1 Con;B:P8 Con;C:P8 PBS;D:P8 LBP 100mg/kg;E:P8 LBP 50mg/kg

Wang Y, Zhao H, Sheng X, et al. Protective effect of Fructus Lycii polysaccharides against time and hyperthermia-induced damage in cultured seminiferous epithelium. J Ethnopharmacol. 2002 Oct; 82(2-3):169-75.

Ho YS, Yu MS, Lai CS, et al. Characterizing the neuroprotective effects of alkaline extract of Lycium barbarum on beta-amyloid peptide neurotoxicity. Brain Res.2007 Jul 16; 1158:123-34.

Chan HC, Chang RC, Koon-Ching Ip A, et al. Neuroprotective effects of Lycium barbarum Lynn on protecting retinal ganglion cells in an ocular hypertension model of glaucoma. Exp Neurol.2007 Jan; 203 (1):269-73.

Where applicable, the authors confirm that the experiments described here conform with The Physiological Society ethical requirements.

PCA098

14-3-3 regulates hippocampal long-term petentiation in mice

H. Qiao[2,1], M. Foote[2], Y. Wu[2] and Y. Zhou[2]

[1]China Academy of Chinese Medical Sciences Institute of Acupuncture and Moxibustion, Beijing, China and [2]Florida state University College of Medicine, Tallahassee, FL, USA

14-3-3 proteins are implicated in the regulation of synaptic functions based on a Drosophila mutant model and mammalian neuronal cultures. To study the role of 14-3-3 proteins in vivo, we have successfully created lines of transgenic mice which were considered a functional knockout through expressing a YFP fused peptide. Our behavioral studies show that one of the founder lines (132) that has broad hippocampal transgene expression displays impaired spatial learning and memory. Here we examined the hippocampal synaptic plasticity of this founder line using electrophysiological methods. We found that the long-term potentiation (LTP) in the CA3-CA1 connection was dramatically reduced in the 132 line compared to their wildtype littermates. To further investigate the underlying mechanism, we recorded from another founder line (142) that only has CA3 transgene expression and found that LTP was not significantly altered. Interestingly, the 142 line does not exhibit a deficit in hippocampal-dependent learning and memory tasks. These findings suggest that 14-3-3 proteins play an important role in regulating synaptic plasticity, likely through a postsynaptic mechanism.

This work was supported by NIH grant NS50355 (to Y.Z.).

Where applicable, the authors confirm that the experiments described here conform with The Physiological Society ethical requirements.

PCA099

Aging and peri-infarct depolarizations during and after ischemia in rat

A. Institoris[1], D. Clark[2], G. Kozák[1], E. Farkas[2] and F. Bari[2]

[1]Department of Physiology, University of Szeged, Szeged, Hungary and [2]Department of Medical Physics and Medical Informatics, University of Szeged, Szeged, Hungary

Spreading depolarizations (SD) are waves of transient neuronal and glial depolarization that propagate across the cortical surface in response to certain stimuli or injury. During ischemia, SD-like peri-infarct depolarizations (PIDs) occur which can impair tissue by increasing disparity between CBF and metabolism. Despite the largest predictor of stroke in patients being advanced age, there are few studies examining PIDs in aged animals. In the current study we describe electrophysiological and hemodynamic changes in young (1-2 months), middle-aged (9 months) and old (24 months) male Wistar rats exposed to mild focal ischemia. A multi-modal imaging strategy allowed for the study of synchronous changes in: membrane potential, cerebral blood volume, local blood oxygen saturation, and cerebral blood flow (CBF). Multi-modal imaging of the rat cerebral cortex was achieved via closed cranial window mounted over the right parietal bone. Images were captured of the cortex illuminated with light-emitting diodes at wavelengths either preferentially absorbed by deoxygenated hemoglobin or isobestic for deoxygenated and oxygenated hemoglobin (rep-

resenting total hemoglobin). Laser speckle contrast images and florescence images of a voltage sensitive dye (RH-1838) were also captured. The rats were continuously kept under halothane anesthesia and euthanized at the end of the experiments. A similar decrease in CBF was observed immediately following middle cerebral artery occlusion (MCAO) in young (53.8±8.1%), middle-aged (52.2±10.9%) and old rats (51.6±6.4%). Age significantly altered the total number of PIDs during and after MCAO and both middle-aged and old rats had significantly fewer PIDs than young ($p<0.05$). Depolarizations were categorized as follows: PIDs associated with membrane potential recovery (SD-like PIDs) and those without prompt recovery (terminal PIDs). Young animals had more frequent SD-like PIDs than middle-aged or old rats ($p<0.05$). Old animals experienced significantly fewer SD-like PIDs but more terminal PIDs than either middle-aged or young ($p<0.05$). Terminal PIDs were associated with a sustained reduction in local CBF (inverse hemodynamic response) but SD-like PIDs were associated with variable responses in CBF and hyperemia was associated with SD-like PIDs more frequently in young (85%) compared to old rats (58%). Age significantly altered the number, shape and hemodynamic responses of PIDs during mild stroke. Young animals had frequent PIDs, mostly associated with membrane repolarization and increased CBF. Old rats displayed frequent terminal depolarizations coupled with a lasting decrease in local blood flow. The occurrence of such depolarization events likely compromises the cortical tissue of aged animals exposed to even a short duration of focal ischemia.

This work was supported by grants from NFM, NNF 78902, OTKA K81266, OTKA 109626K. DC was supported by Canadian Heart and Stroke Fellowship.

Where applicable, the authors confirm that the experiments described here conform with The Physiological Society ethical requirements.

PCA100

Altered neurophysiological reactivity to hypocapnia and oxidative stress in elderly healthy carriers of the common Alzheimer's risk genetic variants

N. Ponomareva[1], T. Andreeva[2], M. Protasova[2], L. Shagam[2], D. Malina[1], A. Goltsov[2] and E. Rogaev[2,3]

[1]Brain Research, Research Center of Neurology RAMS, Moscow, Russian Federation, [2]Institute of General Genetics, RAS, Moscow, Russian Federation and [3]University of Massachusetts Medical School, Worcester, MA, USA

GWAS studies have provided evidence that in addition to apolipoprotein E (ApoE) gene, CLU and PICALM polymorphisms are associated with risk of Alzheimer's disease (AD) (Harold et al., 2009; Lambert et al., 2009; Golenkina et al., 2010). Cerebrovascular dysfunction may precede cognitive decline in AD. EEG reactivity to hyperventilation (HV), which depends on hypocapnia-induced cerebral vasoconstriction, is significantly reduced in elderly carriers of AD risk variant ApoE ε4 because of the alterations of neuronal and cerebral reactivity to hypocapnia (Ponomareva et al., 2012).
This study was aimed at determining whether the changes of EEG reactivity to HV in normal aging depend on CLU and PICALM polymorphisms.
We examined EEG in resting and under HV in 102 healthy volunteers (age range 28-75 years), stratified by CLU (rs11136000) and PICALM (rs3851179) genotypes. The effectiveness of HV was verified by measuring the end-tidal CO2. The effect of ApoE genotype on EEG was controlled. Informed written consent was obtained from all participants. The experimental protocol of this study was approved by the local Ethics Committee. The presence of AD risk variant CLU CC was associated with the reduction of EEG reactivity to HV during aging. In the CLU CC carriers EEG reactivity to HV decreased with age, while in the CLU CT&TT carriers the changes in EEG reactivity were smaller. The relative theta power under HV showed a negative correlation with age in CLU CC but not in CLU CT&TT subjects. The older CLU CC carriers under HV had lower delta and higher alpha relative powers as compared to the older CLU CT&TT carriers. Similar alterations were associated with PICALM polymorphism. In the elderly carriers of AD risk variant PICALM GG, HV-induced changes of EEG were reduced as compared to the noncarriers. The effect of PICALM on EEG was not attributable to the interaction with CLU or APOE genotypes.
Our observations suggest altered neuronal and cerebrovascular reactivity to hypocapnia in the elderly carriers of CLU and PICALM AD risk variants. In the CLU CC, as well as in the ApoE ε4 carriers, the EEG alterations may be due to the endothelial dysfunction as a consequence of cerebral amyloid angiopathy and atherosclerosis (Miwa et al., 2005). PICALM is involved in clathrin-mediated endocytosis and regulation of Aβ generation (Xiao et al., 2012). PICALM is predominately present in endothelial cells and may participate in Aβ transport across blood-brain barrier (Baig et al., 2011). These processes may be related to the abnormal cerebrovascular regulation in the older carriers of PICALM risk variant for AD. Impaired cerebrovascular reactivity may irreversibly damage the vulnerable areas of the brains through long-term hypoxemia. The results suggest the involvement of vascular factors in AD pathogenesis.

Supported by grants from NIA, RFBR, Ministry of Education and Science Programs, FP7-HEALTH-2009 (ADAMS project).

Where applicable, the authors confirm that the experiments described here conform with The Physiological Society ethical requirements.

PCA101

Melatonin treatment could regulate the levels of pro/anti-inflammatory cytokines in brain of senescence accelerated mouse

G. Yoldi[1], R. Kireev[1], E. Vara[2] and J. Tresguerres[1]

[1]Physiology, Complutense University of Madrid, Madrid, Spain and [2]Biochemistry and Molecular Biology, University Complutense of Madrid, Madrid, Spain

Neuro-inflammation has been proposed as a causative factor of neurological diseases and disorders during the ageing process. The senescence-accelerated mouse (SAM) is known to be a good murine model for accelerated aging.
The aim of this research was to investigate the effect of aging on inflammation in brains obtained from SAMP8 and SAMR1 male mice and the influence of chronic exogenous administration of melatonin.
Animals of 2 (young) and 10-11 months of age (old) were used. The influence of the administration of melatonin in the drinking water for one month at two different dosages (1 and 10 mg/kg/day) on brains of old mice was studied. The levels of pro/anti- inflammatory cytokines were studied by ELISA.
During ageing the level of IL 2 was increased in brain of both mice strains as compared to young animals. However, the level of this cytokine was higher in old SAMP8 as compared with SAMR1 of the same age. The levels of TNF-α and IL 6 were

also increased significantly in brains of SAMP8 and SAMR1 old male mice as compared to young animals. Melatonin treatments in both doses were able to decrease levels of IL2, TNF-α and IL 6 in both strains of mice.
The levels of anti-inflammatory cytokines (IL 4 and IL 10) were decreased in the brain of old SAMP8 male as compared with young mice. Interestingly, the levels of these cytokines did not show differences between young and old SAMR1 male animals. Differences between strains were observed with higher levels of anti-inflammatory cytokines in old SAMR1 as compared with SAMP8 animals of the same age. After chronic treatment with melatonin a significant increase in levels of IL 4 and IL 10 were detected in group of old SAMP8, but not in the case of SAMR1 male mice.
We have demonstrated that in brain of old SAMP8 mice the levels of pro-inflammatory cytokines were increased, but the anti-inflammatory were decreased as compared with SAMR1. Increases in pro-inflammatory cytokines in the brain may be involved in the age-related neural dysfunction and/or learning deficiency in SAMP8 mice. Melatonin treatment was able to improve the dysbalace of neuro-inflammation in brain.

Where applicable, the authors confirm that the experiments described here conform with The Physiological Society ethical requirements.

PCA102

Estrogen and melatonin treatments improved neuroinflammation processes in dentate gyrus of ovariectomized female rats

R. Kireev[1], G. Yoldi[1], E. Vara[2] and J. Tresguerres[1]

[1]Physiology, Complutense University of Madrid, Madrid, Spain and [2]Biochemistry and Molecular Biology, University Complutense of Madrid, Madrid, Spain

The aim of the present study was to investigate the effect of aging and ovariectomy on neuro- inflammation in dentate gyrus of the hippocampus obtained from old female rats and the influence of chronic exogenous administration of estrogens (Eos) and melatonin (Mel) on these.
Thirty-six female Wistar rats of 22 months of age were used. Twelve of them remained intact, and the other 24 were ovariectomized at 12 months of age. Ovariectomized animals were divided into 3 groups and treated for 10 weeks with Eos, Mel or saline. All rats were killed by decapitation at 24 months of age and dentate gyri were collected. A group of 2 month old intact female rats was used as young control. The levels of TNFα, IL1β and IL6 were analysed by ELISA. The expression of TNFα, IL1β, GFAP, nNOS, iNOS, HO-1 and NFkB genes were detected by RT-PCR.
The levels of IL1β and IL6 were significantly elevated in the dentate gyrus of old rats as compared to young ones, and this effect was more evident in ovariectomized animals. The mRNA expression of IL1β was also increase in old intact and ovariectomized females as compared to young. No statistically significant differences were observed between TNFα levels of intact and castrated old female rats. However, a significant increase in mRNA expression of TNFα of ovariectomized versus the old intact group was observed. Administration of Eos and Mel to the ovariectomized females significantly decreased both levels and gene expression of pro-inflammatory cytokines.
Aging significantly increased mRNA expression of iNOS, HO-1 and NFkB and these changes were more marked in ovariectomized animals. The expressions of these genes were significantly attenuated after Eos and Mel replacement in the group of castrated females.
The dentate gyrus of aged rats showed a highly significant increase in mRNA expression of GFAP and ovariectomized rats showed an additional increase. Administration of Eos to the ovariectomized females significantly decreased this parameter, but this was not the case in those treated with Mel.
The results revealed that chronic administrations of Eos and Mel were able to prevent the ovariectomy-induced increase in the levels of pro-inflammatory cytokines and also in the up-regulation of GFAP and NFkB in the dentate gyrus as observed in intact rats.

Where applicable, the authors confirm that the experiments described here conform with The Physiological Society ethical requirements.

PCA103

Haematological, biochemical and physical changes during blood storage in three different blood bags

R.O. Nneli[1,3], J.O. Chukwu[2,3] and M.O. Okhiai[1,3]

[1]Physiology, Federal University of Ndufu Alike Ikwo, Ndufu Alike Ikwo, Ebonyi, Nigeria, [2]Physiology, Ebonyi State University, Abakaliki, Ebonyi, Nigeria and [3]Physiology, Abia State University, Uturu, Abia, Nigeria

Whole blood stored in blood bags with anticoagulants in the blood banks and the condition of the blood determines its viability for transfusion (Duta, 2006). The loss of essential components of blood during storage is still a major problem in our environment. Commonly used anticoagulants are known to have effects on the quality of blood (Bailey and Dove, 1975; Kyou, 1990). We investigated the haematological, biochemical and physical changes during blood storage using the three different blood bags namely: ACD, CPD and CPDA1 bags. Venous blood obtained from 15 apparently healthy male volunteers (18 – 50 years old) divided into 3 groups of 5 males were placed into ACD, CPD and CPDA1 blood bags respectively. The haematological, biochemical and physical profile of the stored blood were determined using standard procedures at weekly intervals for 35 days. The results showed that the red cell indices (Hb concentration, red cell mass, haematocrit, MCV, MCH, MCHC) as well as biochemical parameters declined gradually in ACD while blood showed physical deterioration. In the CPD bags, the profiles showed better integrity while in the CPDA1 bags, no change occurred as the integrity of the parameters were well maintained through out the period of study ($p<0.05$). It is concluded that blood stored in CPDA1 bags had a greater viability, initial survival, long life of red blood cells, preservation and net loss of intracellular potassium ions was less. The specific gravity and the integrity of 2, 3 DPG were maintained. No physical deterioration was observed in the Blood stored in CPDA1 bags as compared with the ACD and CPD bags. CPDA1 anticoagulant bags should be recommended as the bag of choice.

Duta, AB (2006) Textbook of blood banking and transfusion

Bailey, DN; Bove, JR (1975) Transfusion, 15: 2441

Kyou, S (1990) K.J.C.P Volume 10.

We wish to thank specially Mr. Tony Nwovu, Head, Laboratory unit, and staff of chemical, haematological and blood transfusion section, Federal Medical Centre, Abakaliki and staff of Mater Misericoardiae hospital, Afikpo, Ebonyi State Nigeria for their assistance to usduring this study.

Where applicable, the authors confirm that the experiments described here conform with The Physiological Society ethical requirements.

PCA104

Potential ameliorative role of honey supplementation against the adverse effects of exposure to gasoline on red cell indices and bone marrow megakaryocytes in Sprague-Dawley male rats

M.B. Abubakar[1,2], W.Z. Abdullah[3], S.A. Sulaiman[4] and A.B. Suen[2]

[1]Physiology, Usmanu Dan Fodiyo University, Sokoto, Nigeria, [2]Physiology, Universiti Sains Malaysia, Kota Bharu, Kelantan, Malaysia, [3]Haematology, Universiti Sains Malaysia, Kota Bharu, Kelantan, Malaysia and [4]Pharmacology, Universiti Sains Malaysia, Kota Bharu, Kelantan, Malaysia

Gasoline (petrol) is primarily used as fuel for internal combustion engines. Different health risks including haematotoxicity and oxidative stress have been reported for gasoline [1, 2]. Although Malaysia has in the recent years adopted the European fuel quality standards in order to help improve the air quality in the environment, gasoline with Research Octane number 95 (believed to contain benzene and other toxic substances) is still widely in use [3]. Supplementation with antioxidants such as vitamins A, C, and E has been shown to ameliorate the toxicity effects of gasoline vapours exposure [4]. Honey contains vitamins, and polyphenols that possess good antioxidant properties [5].The potential role of honey in preventing gasoline-induced adverse effect on red cell indices and bone marrow megakaryocytes was investigated. Thirty two male rats weighing 170-230g were randomly assigned in to 4 groups (n=8) namely, control (C; given 0.5ml distilled water + exposure to ambient air daily); gasoline exposed (G; exposed to gasoline vapours 11.13±1.1cm3/h, 6h daily, 6 days/week + 0.5ml water daily); honey treated (H; given honey 1.2g/kg body weight daily) and gasoline exposed + honey treated (GH; exposed to gasoline vapours as above and concurrently treated with honey 1.2g/kg body weight daily) At the end of 11 weeks, rats were sedated with itraperitoneal pentobarbitone (100mg/kg body weight) and blood samples for full blood count (FBC) and differential count (DC) were collected by cardiac puncture. Rats were sacrificed (over dosage of pentobarbital) and bone marrow was collected for smear which was stained and examined under the light microscope. Both normal and abnormal megakaryocytes (with disintegrated and/or detached nuclei) were counted and the percentage of abnormal ones was determined for each rat. Data were analyzed using Kruskal-Walis test followed by Mann-Whitney U test. Results are expressed as median (interquartile range). The mean corpuscular haemoglobin concentration (MCHC) was found to be significantly ($p<0.05$) reduced in G [31.0 (2.0)] compared with C [(33.5 (3.0)] and H [33.0 (4.0)], it was however not significantly different compared with GH [32.0 (0)]. The percentage of abnormal megakaryocytes was significantly ($p<0.05$) higher in G [18.1 (15.9)] compared with C [2.7 (4.4)], H [4.5 (4.0)] and GH [4 (3.7)]. This suggests that gasoline vapours inhalation was associated with adverse alterations in MCHC and bone marrow megakaryocytes of rats and administration of honey has the potential to improve such changes in rat model.

Rekhadevi, P.V., et al., Genotoxicity in filling station attendants exposed to petroleum hydrocarbons. Annals of Occupational Hygiene, 2010. 54(8): p. 944-954.

Uboh, F., et al., Effect of vitamin A on weight loss and haematotoxicity associated with gasoline vapors exposure in Wistar rats. Int. J. Pharmacol, 2008. 4(1): p. 40-45

Tan, P. Analyzing fuel quality in Malaysia – 3 out of 6 already Euro II compliant for petrol! 2007 18/02/2013]; Available from: http://www.paultan.org/2007/02/25/analyzing-fuel-quality-in-malaysia-3-out-of-6-already-euro-ii-compliant-for-petrol/.

Uboh, F., et al., Vitamins A and E reverse gasoline vapors-induced hematotoxicity and weight loss in female rats. Toxicology and Industrial Health, 2010. 26(9): p. 559-566.

Kishore, R.K., et al., Tualang honey has higher phenolic content and greater radical scavenging activity compared with other honey sources. Nutrition Research, 2011. 31(4): p. 322-325.

This work was supported by grant No. 304/PPSP/61312005 from Universiti Sains Malaysia (USM), Malaysia. We also express our appreciation to Federal Agricultural Marketing Authority (FAMA), Kedah, Malaysia for supplying the Tualang honey.

Where applicable, the authors confirm that the experiments described here conform with The Physiological Society ethical requirements.

PCA105

Detailing peripheral nerve activities by oligofiber recordings: a resolution of sympathetic nerve discharge

C. Su[1], C. Chiang[1,2], Y. Fan[1] and C. Ho[2]

[1]Institute of Biomedical Sciences, Academia Sinica, Taipei, Taiwan and [2]Department of Anesthesiology, Taipei Veterans General Hospital and National Yang-Ming University, Taipei, Taiwan

Whole-bundle nerve recording is an easy technique to gauge peripheral nerve activities. However, this conventional technique fails to detail individual fiber activities. Aiming for a signal resolution at the single-fiber level, we established a relatively novel experimental model so-called 'oligofiber recordings'. In vitro splanchnic sympathetic nerve–thoracic spinal cord preparations were obtained from Sprague-Dawley neonatal rats. Whole-bundle splanchnic nerves were incubated in a glass micropipette containing 0.5% collagenase for 90 min. The dissociated nerve fascicles were then brought into a small caliber micropipette for electrical signal recordings. Oligofiber activities that displayed several distinct spike potential waveforms were often achieved. Automation of spike sorting was based on spike waveform features using a series of custom-made LabVIEW programs incorporated with MATLAB scripts. Spike data were automatically grouped by k-means clustering algorithms followed by verification of their waveform homogeneity by principal component analysis (PCA). Dissimilar waveforms with exceeding Hotelling's T2 distances from the cluster centroids were retrieved by a subtraction algorithm (SA), which partially resolved overlapped spikes. Both T2-selected and SA-retrieved spikes were combined as unit activities. To evaluate if unit activities truly originated from single fibers, we examined the probability distribution of interspike intervals (ISIs) and determined if a change of waveform features was a function of their preceding ISIs. Using the oligofiber recording techniques, we could simultaneously examine, on average, ~3 single fiber activities per experiment. With some modifications, these techniques should be applicable to any peripheral nerve recordings.

Where applicable, the authors confirm that the experiments described here conform with The Physiological Society ethical requirements.

PCA106

Deregulation of adrenomedullin system in cerebellar vermis of hypertensive rats

A. Stern Israel and L. Figueira

Lab of Neuropeptides, School of Pharmacy, Universidad Central de Venezuela, Caracas, Distrito Capital, Venezuela, Bolivarian Republic of

Adrenomedullin (AM) is a 52-amino acid peptide with important functions in cardiovascular regulation. AM has two specific receptors formed by the calcitonin-receptor-like receptor (CRLR) and receptor activity-modifying proteins (RAMP2, RAMP3), known as AM1 and AM2 receptors, respectively. In addition, AM has affinity for the calcitonin-gene-1 related peptide receptor (CGRP1), composed of CRLR+RAMP1. In brain, AM and their receptors are found in localized areas, including cerebellum. We found by quantitative autoradiography an increase in cerebellar AM density binding sites during hypertension, suggesting a role for cerebellar AM-system in blood pressure regulation. Thus, we assessed whether there is an altered expression of AM and its receptor components in the cerebellar vermis of male adult spontaneously hypertensive rats (SHR) and normotensive control Wistar Kyoto rats (WKY), of 8 and 16 weeks old. Animals were euthanized by decapitation; the cerebellar vermis was dissected, placed in lysis buffer, homogenized and centrifuged. The expression of AM, RAMP1, RAMP2, RAMP3 and CRLR was performed by Western blotting. The experiments were conducted according to good practice for the management of laboratory animals of the Bolivarian Republic of Venezuela and the approval of Animal Ethical Committee of the School of Pharmacy. Values are expressed normalized to β-actin expression as means ± S.E.M., compared by ANOVA. Our findings demonstrate a higher expression of CRLR (8 weeks vs. 16 weeks: WKY= 1.0±0.09 vs. 4.1±0.2 and SHR= 1.0±0.08 vs. 5.1±0.2), RAMP1 (8 weeks vs. 16 weeks: WKY= 1.0±0.03 vs. 4.1±0.1 and SHR= 1.0±0.09 vs. 5.1±0.2) and RAMP3 (8 weeks vs. 16 weeks: WKY= 1.0±0.03 vs. 4.1±0.2 and SHR= 1.0±0.09 vs. 5.1±0.1) in cerebellum of 16 weeks old compared to 8 weeks old rats, both in WKY and SHR rats. While, AM and RAMP2 expression was not altered with rat age. In addition, we found a higher CRLR, RAMP1 and RAMP3 expression and a reduced expression of AM and RAMP2 in the cerebellar vermis of SHR rats when compared with WKY rats, both in 8 and 16 week old rats (AM, 8 weeks old= WKY vs. SHR: 1.0±0.08 vs. 0.6±0.02; 16 weeks old: 1.0±0.09 vs. 0.55±0.03) (RAMP2, 8 weeks old= WKY vs. SHR: 1.0±0.09 vs. 0.55±0.02; 16 weeks old: 1.0±0.09 vs. 0.7± 0.02) (RAMP1, 8 weeks old= WKY vs. SHR: 1.0±0.07 vs. 1.45±0.08; 16 weeks old: 1.0±0.08 vs. 1.55±0.07) (RAMP3, 8 weeks old= WKY vs. SHR: 1.0±0.01 vs. 2.45±0.12; 16 weeks old: 1.0±0.08 vs. 1.55±0.05) (CRLR, 8 weeks old= WKY vs. SHR: 1.0±0.07 vs. 1.53±0.09; 16 weeks old: 1.0±0.07 vs. 1.45±0.08). Our findings demonstrate an age dependent expression of cerebellar AM system which is deregulated during hypertension, suggesting a novel functional role of cerebellar AM in the regulation of blood pressure.

McLatchie L, Fraser N, Main M, Wise A, Brown J, Thompson N, Solari R, Lee M, Foord S. RAMPs regulate the transport and ligand specificity of the calcitonin-receptor-like receptor. Nature. 1998; 393 (6683): 333-339.

Li X, Li L, Shen L, Qian Y, Cao Y, Zhu D. Changes of adrenomedullin and its receptor components mRNAs expression in the brain stem and hypothalamus- pitutitary – adrenal axis of stress - induced hypertensive rats. Acta Physiol Sin 2004; 56 (6): 723 – 729.

Pastorello M, Díaz E, Csibi A, Garrido M, Chabot J, Quirion R, Israel A. Papel de la adrenomedulina cerebelosa en la hipertensión arterial. Archivos Venezolanos de Farmacología y Terapéutica 2007; 26 (2): 98 – 104.

Serrano J, Uttenthal O, Martínez A, Fernández P, Martínez J, Alonso D, Bentura M, Santacana M, Gallardo J, Martínez R, Cutitta F, Rodrigo J. Distribution of adrenomedullin – like inmunoreactivity in the rat central nervous system by light and electron microscopy. Brain Res 2000; 853: 245 – 268.

Ministerio Popular de Ciencia Tecnología e Industrias, Proyecto Misión Ciencia, Sub-proyecto 7, ECCV No. 2007001585.

Where applicable, the authors confirm that the experiments described here conform with The Physiological Society ethical requirements.

PCA108

Orexin-neuromodulated cerebellar folium-p-parabrachial microcomplex adaptively controls redistribution of arterial blood flow for defense behavior

N. Nisimaru[1,2], A. Arata[3,1], T. Hashikawa[1], S. Nagao[1] and M. Ito[1]

[1]RIKEN Brain Science Institute, Wako, Saitama, Japan, [2]Physiology, Oita University, Faculty of Medicine, Yufu, Oita Prefecture, Japan and [3]Physiology, Hyogo College of Medicine, Nishinomiya, Hyogo, Japan

We so far reported that Purkinje cells in a small area (folium-p, fp) of rabbit cerebellar flocculus receive excitatory modulation via diffuse axons of hypothalamic orexinergic neurons (1). Rabbits were preferred because their flocculus has discernible regular folial divisions; this is not the case in rats or mice. We used albino rabbits weighing 1.0-3.1 kg. In the study to be reported, we used axonal transport of DiI and biotinylated dextran amine and found that these Purkinje cells project to the ventrolateral edge of the ipsilateral parabrachial nucleus (PBN), thus forming the fp-PBN microcomplex. Because stimulation of the classic defense area that activates hypothalamic orexinergic neurons induced, as part of defense reactions, redistribution of arterial blood flow between active muscles and visceral organs/resting muscles, we hypothesized that fp-PBN microcomplex adaptively controls the redistribution of arteriasl blood flow, which is primarily controlled by somatosympathetic reflexes (SSRs) and their supraspinal pathways. To support this hypothesis, we previously showed that climbing fiber signals to fp Purkinje cells were elicited by high arterial blood pressure or a high potassium concentration in muscles, both implying errors in redistribution of arterial blood flow (2). In the present study, we evoked defense reactions by applying electric foot shock stimuli to a conscious freely moving rabbit in a cage. The stimuli were 2-4mA, lasting 1-30 s in each trial and repeated once every 10 min 4-7 times in one session. These stimuli evoked quick turning around of the rabbit within the cage. Probes were chronically implanted to measure blood flow in femoral and celiac arteries under α–chloralose (60 mg/kg) and urethane (600 mg/kg) anesthesia. Another probe was implanted to measure blood pressure in femoral artery. Foot shock stimuli induced an increase in arterial blood flow in femoral muscles (FAF) and a reciprocal decrease in visceral organs (VAF). Both the increase and decrease were attenuated after systemic administration of orexin antagonists. After fp lesioning (with local kainate injection), FS-induced FAF increases became significantly larger, whereas FS-induced VAF decreases became significantly smaller and shorter- lasting. Apparently, under orexin neuromodulation, fp functions for effective balance of arterial blood

flow in magnitude and time course between active muscles and visceral organs/resting muscles. Based on these collected data, we conclude that folium-p and PBN jointly form a unique microcomplex that is activated by orexin neuromodulation in defense behavior, and that the so activated microcomplex adaptively controls redistribution of arterial blood flow conforming to the high demand of arterial blood supply to active muscles in defense behavior.

1. Nisimaru N et al. (2006) Abstract, SfN meeting, Atlanta

2. Nisimaru N et al. ((2010) Abstract, Japan Neuroscience Society meeting, Kobe, 2010

Where applicable, the authors confirm that the experiments described here conform with The Physiological Society ethical requirements.

PCA109

Contribution of spinal μ-opioid receptors to inhibition of heat-induced heart rate response by touch in anesthetized rats

N. Watanabe, P. Mathieu and H. Hotta

Department of Autonomic Neuroscience, Tokyo Metropolitan Institute of Gerontology, Tokyo, Japan

It is common experience that pain subsides by touching the skin near the painful site although the mechanism has not been fully elucidated yet. We previously reported that touch (gentle mechanical cutaneous stimulation) inhibited the somatocardiac sympathetic C-reflex evoked by excitation of unmyelinated C-afferent fibers in anesthetized rats (1-2). Such an inhibitory effect was greater when touch was applied to ipsilateral and closer spinal segment to C-afferent input, and was significantly reduced by i.v. injection of non-specific opioid receptor antagonist, naloxone (1). Thus, the present study examined whether the effect of touch is mediated via spinal opioid receptors. Also, we attempted to clarify the subtype of opioid receptors contributing to this effect. For these purposes, we employed tonic noxious heat stimulation in deeply-anesthetized rats.

Experiments were performed on male Wistar rats (5-6 months), that were under urethane anesthesia (1.4 g/kg s.c.). The trachea was cannulated for artificial ventilation. A common carotid artery and jugular vein were catheterized for recording blood pressure and heart rate (HR) and supplying anesthetics and other substances, respectively. A catheter was implanted in the spinal subarachnoid space at the lumbar enlargement level (3) for intrathecal injection of saline or opioid receptor antagonists (5 rats in each group). Heat stimulation (at 46-48°C for 45-43 seconds, respectively) was applied to the lower back using a Peltier thermode at fixed intervals. The same temperature and duration of heat stimulation was used throughout the experiment. Touch was applied to the right inner thigh for 10 minutes using a soft elastomer brush (1-2). Statistical analyses were performed using the one-way factorial or repeated measures ANOVA followed by Bonferroni's multiple comparisons test and statistical significant level was set at $p < 0.05$. Data were expressed as mean ± SEM.

Heat stimulation altered HR by 11.2 ± 0.62 beat per minutes. Evoked HR responses were significantly inhibited by touch in the saline group. The inhibition occurred during touch (by 27.9 ± 7.1 % of pre-touch response) and continued at 10-15 minutes after touch (by 31.8 ± 7.2 %). In the naloxone and CTOP (μ-opioid receptor antagonist) groups, the inhibitory effect of touch was not observed. In the naltrindole (δ-opioid receptor antagonist) group, heat-induced HR responses were inhibited during touch (by 36.7 ± 6.8 %). Prior to touch, the magnitude of heat-induced HR responses and basal HR did not differ between groups. Basal HR over the experimental period was stable in all groups.

The present study results suggest that touch inhibits nociceptive transmission into autonomic reflex pathways predominantly via μ-opioid receptors in the spinal cord.

Hotta H et al. (2010). Eur J Pain 14,806-813.

Watanabe N et al. (2011). J Physiol Sci 61,287-291.

Sato A et al. (1995). Exp Brain Res 105,1-6.

This work was supported by Grant-in-Aid for Young Scientists (B) (No. 23792575).

Where applicable, the authors confirm that the experiments described here conform with The Physiological Society ethical requirements.

PCA110

Provocative motion elicits hypothermia and tail vasodilation in rats and shrews: A new index of nausea in pre-clinical studies?

S. Ngampramuan[1], M. Cerri[2], F.D. Vecchio[2], A. Kamphee[1], J. Rudd[3] and E. Nalivaiko[4]

[1]Research Center for Neuroscience Molecular Biosciences, Mahidol University, Nakhon Pathom, Thailand, [2]Biomedical and Motor Sciences, University of Bologna, Bologna, Italy, [3]School of Biomedical Sciences, Chinese University of Hong Kong, Hong Kong, Hong Kong and [4]School of Biomedical Sciences and Pharmacy, University of Newcastle, Newcastle, NSW, Australia

Nausea elicited by chemo- and radiotherapy, surgical intervention with anaesthesia, motion, and during pregnancy, is a major clinical problem as it is often resistant to anti-emetic drugs1. In contrast to the well-defined pathways mediating vomiting, the neural circuitry responsible for nausea is poorly understood, largely due to the lack of adequate indices of nausea in preclinical studies. Most mechanistic studies on nausea in humans come from perturbing vestibular or visual stimulation. The resulting cardinal symptoms of motion sickness are cold sweating, nausea and vomiting, and facial pallor; a few studies also report motion sickness-related hypothermia2 from cutaneous vasodilation in the limbs3. The aim of the present studies, therefore, was to investigate if similar motion-induced responses are present in rats and in house musk shrews (Suncus murinus – an insectivore possessing vomiting reflex).

Under isoflurane anesthesia (2% in O2), adult male Wistar rats were implanted with telemetric transmitters to record core body temperature. One week later, the animals were administered 5-HT3 receptor antagonist ondansetron (0.5 mg/kg s.c.) or vehicle, and 30 min later were subjected to provocative motion (rotation 0.5 Hz, 40 min) in their home cages; the experiment was repeated one week later using a crossover design (n=7). The rotational stimulus provoked mild hypothermia (from 37.4±0.1 to 35.6±0.2°C, $p<0.001$) that was attenuated by ondansetron by 28% ($P<0.05$). In another groups of rats (un-instrumented, n=6) we used infrared thermography and found that rotation induced a transient increase of tail temperature (from 22.9±0.6 to 25.1±0.6°C $p<0.05$) indicative of vasodilation; this rise appeared to precede the fall in the core body temperature seen in the telemetered studies. Infrared thermography was also used to investigate skin temperature changes induced by motion (linear shaker, 1 Hz, 15

min) in S. murinus (n=6). All animals exhibited episodes of retching and/or vomiting (latency = 205±38 s) that was preceded by a transient increase in tail temperature (from 24.0±1.5 to 27.0±2.2°C, p<0.05). A fall of interscapular temperature (from 38.4±0.5 to 36.6±0.4°C, p<0.001) was also seen during motion testing.

In conclusion, provocative motion appears to induce hypothermia via mechanisms presumably involving dilatation of the vascular bed of the tail. The tail vasodilation that precedes retching/vomiting in S. murinus, and the tail vasodilation in rats could form the basis of a potential index of nausea in experimental animals. The poor effect of ondansetron was predicted since it does not prevent motion sickness-induced nausea in man.

Foubert J, Vaessen G. Nausea: the neglected symptom? Eur J Oncol Nurs. 2005, 9: 21–32.

Mekjavic IB, Tipton MJ, Gennser M, Eiken O. Motion sickness potentiates core cooling during immersion in humans. J Physiol 2001, 535.2; 619-23.

Cheung B, Hofer K. Coriolis-induced cutaneous blood flow increase in the forearm and calf. Brain Res Bull.2001, 54:609-18.

Where applicable, the authors confirm that the experiments described here conform with The Physiological Society ethical requirements.

PCA111

The drive to breathe is tuned via multi-path modulation of inhibitory tonic expiratory neurons in the ventral respiratory column (VRC) network

B. Lindsey[1], L.S. Segers[1], S.C. Nuding[1], M.M. Ott[1], J.B. Dean[1], D.C. Bolser[2], R. O'Connor[1] and K.F. Morris[1]

[1]Molecular Pharmacology and Physiology, USF Morsani College of Medicine, Tampa, FL, USA and [2]Physiological Sciences, University of Florida, Gainesville, FL, USA

Models of the medullary VRC include rostral inspiratory (I) neurons that excite more caudal I neurons, including premotor populations, as well as inhibitory I neurons that act via recurrent and feed-forward connections upon other excitatory and inhibitory I and expiratory (E) neuron populations (1). Our prior work supported the hypotheses that tonic E (t-E) neuron inhibition of premotor I neurons contributes to baroreceptor-evoked reductions in I drive (2), and that central chemoreceptor stimulation enhances drive, in part via reduced I-phase t-E neuron activity and the resulting disinhibition of premotor neurons (3). Aims of the present work were to identify further the functional connections of t-E neurons and test the hypothesis that carotid peripheral chemoreceptors also modulate drive by I-phase inhibition of t-E neurons. Spike trains were acquired by multi-electrode arrays along with signals from phrenic and vagus nerves (10 Hz–10 kHz) from 22 adult cats. Animals were anesthetized with isoflurane mixed with air (induction: 5% ; maintenance: 0.5–3.0%) until decerebration, neuromuscularly blocked (pancuronium bromide; initial bolus 0.1 mg kg–1 followed by 0.2 mg kg–1 hr–1, iv;) and monitored (4), vagotomized, and artificially ventilated. Arterial blood pressure, end-tidal CO2, tracheal pressure, and arterial PO2, PCO2, and pH were monitored. In 6 recordings from 5 animals, yielding data from 219 neurons (4,374 distinct cell pairs), carotid chemoreceptors were stimulated (5 trials) by close 30-s injections of 1.0 mL of a CO2 –saturated 0.9% saline solution. Responses were identified using a bootstrap-based statistical method; p-value threshold was set with a false discovery rate of 0.05 (4). Cross-correlogram features were identified using cycle-shifted surrogates (3) or a Monte-Carlo test with surrogate spike trains (5) generated with a gamma distribution shape parameter; false discovery rate < 0.05. Features in spike-triggered averages of full-wave rectified phrenic signals were identified (3) using a two-sided Wilcoxon signed-rank test (Bonferroni correction; p < 0.05). Overall, from 171 peri-columnar t-E neurons we identified 42 of 599 pairs with cross-correlogram central peaks (detectability index (di) = 13.0 ± 11.8 SD; half-width (hw) = 18.5 ms ± 25.7). Results from the stimulation experiments included assemblies with 8 correlogram troughs indicative of t-E neuron inhibition of I neurons (di = 7.9 ± 2.9; hw = 10.8 ms ± 9.6) and disinhibitory enhancement of I drive. When considered with results from simulations of a computational neuromechanical model for cough (1) and associated in vivo data, we conclude that multiple afferent systems and behaviors exert a "push-pull" control of I drive through modulation of a coordinated network of t-E neurons.

O'Connor R, Segers LS, Morris KF, Nuding SC, Pitts T, Bolser DC, Davenport PW, Lindsey BG. A joint computational respiratory neural network-biomechanical model for breathing and airway defensive behaviors. Front Physio, doi: 10.3389/fphys.2012.00264, 2012.

Lindsey BG, Arata A, Morris KF, Hernandez YM, Shannon R. Medullary raphé neurones and baroreceptor modulation of the respiratory motor pattern in the cat. J Physiol (London) 512: 863-882, 1998.

Ott MM, Nuding SC, Segers LS, O'Connor R, Morris KF, Lindsey BG. Central chemoreceptor modulation of breathing via multipath tuning in medullary ventrolateral respiratory column circuits. J Neurophysiol 107: 603-617, 2012.

Nuding SC, Segers LS, Shannon R, O'Connor R, Morris KF, Lindsey BG. Central and peripheral chemoreceptors evoke distinct responses in simultaneously recorded neurons of the raphé-pontomedullary network. Philos Trans R Soc Lond B Biol Sci. 364: 2501-2516, 2009.

Pauluis Q & Baker S. An accurate measure of the instantaneous discharge probability, with application to unitary joint-event analysis. Neural Comp 12: 647-666, 2000.

Supported by NIH grant NS19814

Where applicable, the authors confirm that the experiments described here conform with The Physiological Society ethical requirements.

PCA112

The Basic Rest-Activity Cycle (BRAC) is present in transgenic rats with ataxin3-mediated destruction of orexin neurons, but amplitudes of the BRAC-associated brown adipose tissue and body temperature change are reduced

B. Blessing[1], M. Mohammed[1], Y. Ootsuka[1] and M. Yanagisawa[2]

[1]Human Physiology, Flinders University, Adelaide, SA, Australia and [2]Department of Molecular Genetics, University of Texas Southwestern Medical Centre, Dallas, TX, USA

In undisturbed Sprague-Dawley rats, with ad libitum access to food and water, body and brain temperatures increase, in association with blood pressure, heart rate, behavioural activity and food intake, approximately every 1-2 hours, and brown adipose tissue (BAT) thermogenesis contributes to the temperature increases (Blessing et al., 2012). Hypothalamic orexin-containing neurons (de Lecea et al., 1998; Sakurai et al., 1998) influence appetite, the sleep-wake cycle, locomotor activity and other physiological variables (Kuwaki, 2011). We have now assessed BRAC-related parameters in conscious unrestrained transgenic (TG) Sprague Dawley rats with ataxin3-mediated destruction of orexin neurons (Beuckmann et al., 2004) in comparison with their wildtype littermates (WT). Under inhaled

isoflurane (2% in oxygen) anaesthesia, TG (n=11) and WT (n=9) male rats (300-450 g) were instrumented with chronically implanted thermistors to measure BAT and body temperature (Blessing et al., 2012). All surgical procedures were performed in accord with the Animal Welfare Ethics Committee of Flinders University. Thermistor cables were passed subcutaneously and connected to a headpiece fixed to the skull with dental cement. After one-week recovery the unrestrained TG or WT rats were housed singly in a quiet closed temperature controlled (24-26°C) cage, with ad libitum access to food and water, and with 12 hour dark/light cycling. Behavioural activity was measured with an infrared grid system. Group results (mean ± SEM) were analysed with factorial ANOVA. There was no difference in the timing of the dark active period BRAC-related episodic BAT temperature peaks between TG and WG rats (106±3 min in TG and 111±3 min in WT, $p>0.05$). However the amplitude of the behavioural activity (7±1 units in TG versus 11±1 units in WT rats, $p<0.05$) and the increases in BRAC-related BAT temperature (1.22±0.02°C in TG and 1.42±0.03°C in WT, $p<0.001$) and body temperature (0.80±0.01°C in TG versus 0.90±0.02 in WT, $p<0.001$) were reduced in the transgenic animals. The difference between BAT and body temperatures was also reduced in the transgenic animals versus the wild type animals (+0.44±0.02°C in TG and +0.55±0.03 °C in WT, $p<0.001$) suggesting that reduced BAT thermogenesis contributes to the reduced BRAC-related increase in body temperature in transgenic animals. Thus the BRAC organization of daily life does not depend on the function of the orexin-containing neurons, but activity of these neurons contributes to the amplitude of BRAC episodes. Our results suggest that orexin-containing neurons increase the intensity with which rats periodically engage with the external environment.

Beuckmann CT, Sinton CM, Williams SC, Richardson JA, Hammer RE, Sakurai T, Yanagisawa M. Expression of a poly-glutamine-ataxin-3 transgene in orexin neurons induces narcolepsy-cataplexy in the rat. J Neurosci. 2004 May 5;24(18):4469-77.

Blessing W, Mohammed M, Ootsuka Y. Heating and eating: brown adipose tissue thermogenesis precedes food ingestion as part of the ultradian basic rest-activity cycle in rats. Physiol Behav. 2012 Feb 28;105(4):966-74.

de Lecea L, Kilduff TS, Peyron C, Gao X, Foye PE, Danielson PE, Fukuhara C, Battenberg EL, Gautvik VT, Bartlett FS 2nd, Frankel WN, van den Pol AN, Bloom FE, Gautvik KM, Sutcliffe JG. The hypocretins: hypothalamus-specific peptides with neuroexcitatory activity.Proc Natl Acad Sci U S A. 1998 Jan 6;95(1):322-7.

Kuwaki T. Orexin links emotional stress to autonomic functions. Auton Neurosci 2011 Apr 26;161(1-2):207-7.

Sakurai T, Amemiya A, Ishii M, Matsuzaki I, Chemelli RM, Tanaka H, Williams SC, Richardson JA, Kozlowski GP, Wilson S, Arch JR, Buckingham RE, Haynes AC, Carr SA, Annan RS, McNulty DE, Liu WS, Terrett JA, Elshourbagy NA, Bergsma DJ, Yanagisawa M. Orexins and orexin receptors: a family of hypothalamic neuropeptides and G protein-coupled receptors that regulate feeding behavior. Cell. 1998 Feb 20;92(4):573-85.

Authors thank Mrs Jessi Moore and Robyn Flook for their technical assistance.

Where applicable, the authors confirm that the experiments described here conform with The Physiological Society ethical requirements.

PCA113

Sudden access to live cochroaches increases brown adipose tissue (BAT) thermogenesis in conscious unrestrained rats

B. Blessing, M. Mohammed and Y. Ootsuka

Human Physiology, Flinders University, Adelaide, SA, Australia

Body and brain temperatures increase when Sprague-Dawley rats explore the external environment, and brown adipose tissue (BAT) thermogenesis contributes to the temperature increases (Ootsuka et al., 2009, Blessing et al., 2012). We have now assessed whether a salient novel environmental event activates BAT thermogenesis. Under inhaled isoflurane (2% in oxygen) anaesthesia, 5 male Sprague-Dawley rats (300-450 g) were instrumented with chronically implanted thermistors to measure BAT and body temperature (Blessing et al., 2012). All surgical procedures were performed in accord with the Animal Welfare Ethics Committee of Flinders University. Thermistor cables were passed subcutaneously and connected to a headpiece fixed to the skull with dental cement. After one-week recovery the unrestrained rats (n=9) were housed singly in a quiet closed temperature controlled (24-26°C) cage. A stocking-mesh bag containing 4 live cockroaches (Periplaneta australasiae) was suddenly introduced into the rat's cage. We recorded BAT and body temperatures for 30 min and then removed the cockroach bag. The rat approached the bag of cockroaches and attempted to bite or rip the stocking-mesh bag. Maximum increases in BAT and body temperatures (mean ± SEM) were recorded and analysed with repeated measures ANOVA. The increase in BAT temperature (1.1±0.16°C) was significantly greater ($P<0.05$) than the simultaneously measured increase in body temperature (0.76±0.11°C), suggesting that BAT thermogenesis contributes to the increase in body temperature. Our results suggest that brain regulated sympathetically-controlled BAT thermogenesis contributes to the increase in body temperature occurring when the rat is confronted with a novel salient stimulus.

Blessing W, Mohammed M, Ootsuka Y. Heating and eating: brown adipose tissue thermogenesis precedes food ingestion as part of the ultradian basic rest-activity cycle in rats. Physiol Behav. 2012;105:966-974.

Ootsuka Y, de Menezes RC, Zaretsky DV, Alimoradian A, Hunt J, Stefanidis A, Oldfield BJ, Blessing WW. Brown adipose tissue thermogenesis heats brain and body as part of the brain-coordinated ultradian basic rest-activity cycle. Neuroscience 2009;164:849-861.

Authors thank Mrs Jessi Moore and Robyn Flook for their technical assistance.

Where applicable, the authors confirm that the experiments described here conform with The Physiological Society ethical requirements.

PCA114

Withdrawal of oestrogen elicits changes in the expression of GABA receptors and markers of GABA transmission in the nucleus of the solitary tract

E. Spary, M.J. Drinkhill, S. Crossland, A. Maqbool and T.F. Batten

Cardiovascular and Diabetes Research, University of Leeds, Leeds, UK

Oestrogen is a known to act centrally as a modulator of autonomic function. Our previous study showed changes in oestrogen receptor (ER) subtype expression in the nucleus of the solitary tract (NTS), an area of the brainstem regulating autonomic

reflexes, are associated with fluctuating plasma oestrogen levels during the oestrous cycle and after ovariectomy (OVX)[1]. GABA transmission in the NTS is critical for baroreflex control of blood pressure (BP) and as the promoter sequences for several receptors, receptor associated proteins, enzymes and transporters involved in GABA transmission include potential oestrogen response element consensus sites we analysed mRNA expression levels for these markers in the NTS of normal cycling and OVX female rats. Female Wistar rats (approx. 150g, n=6) fed a phytoestrogen free diet were subjected to OVX or sham-OVX under anaesthesia (isofluorane, 5% in O_2). Radiotelemetry probes (DSI) were implanted to record from the left carotid artery. BP, heart rate and activity levels were recorded for 3 or 6 weeks post surgery, at which point rats were killed under the same anaesthetic conditions. Micropunches of NTS tissue were taken for reverse transcription of mRNA and analysis by real-time PCR. Percentage body weight gain after 6 weeks in OVX rats (45.48 ± 1.1%; mean ± SE) was significantly greater than in sham-OVX rats (28.68 ± 1.7%, p=0.01), although food intake between the two groups was consistent (approx 110-115g/animal/week). After 3 weeks increases in systolic (+3.4%) and mean (+5.3%) BP were evident in OVX rats compared to starting values. These increases continued to 6 weeks, becoming significantly different (+10.3%, p=0.05; +12.55%, p=0.05). No significant changes in BP were observed in control rats over 3 or 6 weeks. Real-time PCR for the GABA-A subunit mRNAs revealed significantly decreased expression for 4 of the 14 tested (alpha1; alpha 5; gamma3, delta) in OVX rats at both 3 and 6 weeks. Additionally, at 3 weeks a reduction in beta1 was seen, with a reduction in beta3 at 6 weeks. In contrast, mRNA for the epsilon subunit appeared up-regulated. Expression levels for the GABA-B receptor subtypes BR1 and BR2 showed significant reductions ($p<0.05$) in OVX after 6 weeks, as was the case for the GABA transporter GAT1 and the GABA receptor-associated protein GABARAP. In contrast the GABA synthesising enzyme GAD67 and the GABA receptor-associated protein like 1 GABARAPL1 were increased ($p<0.05$) in OVX after 3 weeks. The data are consistent with the hypothesis that circulating oestrogen acts on ERs in the NTS to modulate inhibitory GABAergic influences on autonomic reflexes controlling BP through affecting both GABA synthesis/release mechanisms and GABA receptor composition.

Spary EJ, Maqbool A, Batten TFC. (2010). Changes in oestrogen receptor α expression in the nucleus of the solitary tract of the rat over the oestrus cycle and following ovariectomy. J.Neuroendocrinol. 22:492-502.

Supported by British Heart Foundation Project Grant 10/85/28619

Where applicable, the authors confirm that the experiments described here conform with The Physiological Society ethical requirements.

PCA115

Intrinsic pacemaker activity of pre-sympathetic neurons of adult rats is not altered by chronic intermittent hypoxia (CIH)

C.L. Almado, R.X. Leão and B.H. Machado

Physiology, University of São Paulo, Ribeirão Preto, São Paulo, Brazil

The pre-sympathetic neurons in the rostral ventrolateral medulla (RVLM) are the source of the sympathetic activity and there is evidence that these cells present intrinsic pacemaker activity. However, there are few electrophysiological studies in the literature involving these neurons in neonatal rats and no studies on these neurons in the brainstem slices from adult rats. Herein we studied slices from adult rats (5-6 weeks old) presenting viable RVLM pre-sympathetic neurons for patch-clamp recordings, previously labeled by injection of fluorescent microbeads into the intermediolateral column of spinal cord (T3-T6). Our data show that after application of antagonists of ionotropic glutamate, GABA and glycine receptors in the bath perfusion, these neurons present spontaneous firing action potentials in a regular pattern [frequency: 9.4±1.0 Hz; CV of the inter-spike interval: 0.12±0.01 (n=19)]. In comparison, RVLM respiratory neurons projecting to phrenic nucleus in spinal cord (C3-C5) fired spontaneous action potentials more irregularly and with a lower frequency when compared to pre-sympathetic neurons [frequency: 4.4±0.8 Hz; CV of inter-spike interval: 0.38 ± 0.11 (n=15); P=0.001]. Considering that CIH in rats induces hypertension due to sympathetic overexcitation, we hypothetized that the pre-sympathetic neurons in these animals should present changes in their intrinsic membrane properties and an increase in their frequency discharge. However, our data clearly indicate that the intrinsic membrane properties and the frequency discharge of the pre-sympathetic neurons in rats submitted to 10 days of CIH were not changed: resting membrane potential [Con: -63.9±0.8 mV, (n=21) vs. CIH: -64.8±0.7 mV, (n=23); P=0.41]; input resistance [Con: 341±21 MOhm, (n=18) vs. CIH: 392±34 MOhm, (n=20); P=0,21] and intrinsic frequency discharge [Con: 9.4±1,0 Hz, (n=19) vs. CIH: 9.9±1.2 Hz, (n=21); P=0.74]. The present study shows that: a) it is feasible to record the electrophysiological properties of RVLM pre-sympathetic neurons in brainstem slices from adult rats, b) these neurons present characteristics of pacemakers, and c) their passive and active intrinsic properties were not altered in rats submitted to CIH.

Financial support: FAPESP and CNPQ

Where applicable, the authors confirm that the experiments described here conform with The Physiological Society ethical requirements.

PCA116

Voluntary wheel-running improves neuro-cardiovascular regulation and prevents hyperalgesia in a mouse model of chronic widespread pain

R. Sabharwal[1], L. Rasmussen[2], K.A. Sluka[2] and M.W. Chapleau[1,3]

[1]Internal Medicine, University of Iowa, Iowa City, IA, USA, [2]Physical Therapy, University of Iowa, Iowa City, IA, USA and [3]Veterans Affairs Medical Center, Iowa City, IA, USA

Chronic widespread pain (CWP) as occurs in fibromyalgia is common and debilitating. Fibromyalgia is also associated with orthostatic intolerance, sleep disruption and fatigue. Autonomic nervous system dysfunction has been implicated in the etiology of this disease. Parasympathetic-mediated heart rate variability (HRV) is decreased in people with fibromyalgia with reports of increased sympathetic activity that could contribute to pain by sensitizing nociceptors. Exercise training has been shown to reduce pain in fibromyalgia. The aims of this study were to characterize autonomic dysregulation in an established mouse model of CWP [1], and determine if short duration (5-day) voluntary wheel-running influences neuro-cardiovascular regulation in either healthy or CWP mice. Blood pressure (BP)

and heart rate (HR) were measured by telemetry in conscious, young (10-12 wks) C57BL6 mice. CWP was induced by two intramuscular injections of acidic saline into the left gastrocnemius muscle (100 μl of sterile saline at pH 5, 5 days apart) under 2-5% isoflurane, combined with 2 hours of fatiguing exercise. CWP mice eat, drink, and groom normally, have normal gait patterns, and continue to gain weight similar to mice injected with pH 7.2 as a control (no hyperalgesia), or naïve animals [2]. CWP (hyperalgesia) was assessed by measuring the threshold for hindlimb withdrawal during application of a series of von Frey filaments to the paw. Data (mean±SEM) were analyzed using t-tests and repeated measures ANOVA as applicable, with significance taken at P<0.05 (see Table). Mice were killed with an overdose of pentobarbital at the end of the experiment. Induction of CWP decreased parasympathetic-mediated HRV (RMSSD) without affecting mean BP or sympathetic vasomotor tone measured by the depressor response to the ganglionic blocker chlorisondamine (Table, *P<0.05, CWP vs. Control, n=4-6). Five days of voluntary wheel-running decreased HR, BP and sympathetic tone measured at rest in healthy mice (*P<0.05, Exerc vs. Control) and mice subjected to induction of CWP (†P<0.05), and prevented both the decrease in HRV and secondary mechanical hyperalgesia in the ipsilateral paw (n=8) in CWP mice (†P<0.05, Exerc+CWP vs. CWP, n=4-8). We conclude: 1) This mouse model of CWP exhibits selective impairment of parasympathetic modulation of HR with preserved sympathetic vasomotor tone; and 2) Voluntary wheel-running decreases sympathetic tone, HR and BP in both healthy and CWP mice; and prevents hyperalgesia and decreased HRV in CWP mice. Future studies will explore the mechanisms underlying the beneficial effects of short-duration voluntary exercise.

	Control	Exerc	CWP	Exerc+CWP
Mean BP (mmHg)	124±1	107±2*	121±1	103±2 *†
Mean HR (bpm)	682±21	538±19*	654±12	495±5 *†
HRV-RMSSD (ms)	9±1	14±2*	6±1*	11±3 †
Symp Tone (ΔmmHg)	-62±1	-31±4*	-64±2	-30±3 *†

Yokoyama T, Lisi TL, Moore SA, and Sluka KA (2007). J Pain 8(5):422-429.

The research was funded by grants from the National Institutes of Health, USA (HL14388 and AR061371).

Where applicable, the authors confirm that the experiments described here conform with The Physiological Society ethical requirements.

PCA117

Sustained hypoxia increases excitatory transmission in the nucleus tractus solitarius neurons of juvenile rats

D. Accorsi-Mendonça, C.L. Almado and B.H. Machado

Physiology, University of São Paulo, Ribeirão Preto, São Paulo, Brazil

In previous studies we verified that the synaptic transmission in the nucleus tractus solitarius (NTS) neurons is affected by chronic intermittent hypoxia. Here we evaluated the effect of short-term sustained hypoxia (SH, 24 hours - 10% O2) on the intrinsic properties and synaptic transmission of NTS neurons in the brainstem slices from young rats (3 weeks old) using whole cell patch clamp technique. SH produced no change in resting membrane potential [control: -78.7 ± 2.4 mV (n=15), SH: -72.3 ± 3.7 mV, (n=15)], input resistance [control: 1.4 ± 0.4 GOhm (n=8), SH: 1.4 ± 0.4 GOhm, (n=9)] and capacitance of NTS neurons [control: 14.2 ± 0.9 pF (n=17), SH: 12.4 ± 0.8 pF (n=15)]. However, SH increased the frequency of spontaneous excitatory post-synaptic currents [(sEPSCs) control: 3.6 ± 0.4 Hz (n=18), SH: 7 ± 1.5 pF, (n=15), p<0.05] and the amplitude of evoked excitatory post-synaptic currents [(eEPSCs) control: -289 ± 51 pA (n=15), SH: -472 ± 64 pA (n=15), p<0.05]. Moreover, SH also increased the depression of evoked excitatory post-synaptic currents after five stimuli on afferent fibers in the tractus solitarius [amplitude of 5 evoked currents of control group: 100%, 44%, 34%, 32% and 28% (n=15), amplitude of 5 evoked currents of SH group: 100%, 40%, 28%, 22% and 17% (n=15) *p<0,001 - Two way ANOVA]. These findings suggest that SH affect the excitatory transmission in NTS neurons increasing the release probability in the pre-synaptic terminal. We conclude that 24 hours of SH enhances spontaneous and evoked excitatory synaptic transmission on NTS neurons but does not change their intrinsic properties. These alterations in the synaptic transmission in the NTS neurons induced by SH may play a critical role in the cardiovascular and respiratory problems observed in high altitude.

Financial support: FAPESP and CNPq.

Where applicable, the authors confirm that the experiments described here conform with The Physiological Society ethical requirements.

PCA118

Catecholamines in the medial prefrontal cortex and nucleus accumbens alter cardiorespiratory and metabolic functions

A. Goodchild[1], S.F. Hassan[1] and J.L. Cornish[2]

[1]The Australian School of Advanced Medicine, Macquarie University, Sydney, NSW, Australia and [2]Dept Psychology, Macquarie University, Sydney, NSW, Australia

Purpose: Methamphetamine (METH) blocks and reverses monoamine transporters and its administration evokes behavioural changes associated with frontal brain regions. METH also evokes autonomic effects. We have shown that disinhibition of the medial prefrontal cortex (mPFC) changes cardiorespiratory and metabolic function. We sought to determine whether alterations in monoamine concentrations in the mPFC and nucleus accumbens (NAc) mediate changes in cardiorespiratory and metabolic function. Methods: Electrophysiological experiments were performed in urethane-anaesthetised, artificially ventilated, vagotomised, male Sprague-Dawley rats. Microinjections of METH (35, 105, 335 nmol), dopamine hydrochloride (DA 10, 50,150, 475 nmol) or L-norepinephrine (NA 10, 50, 150 nmol) were made into the infralimbic cortex of the mPFC and NAc. Changes were recorded in iBAT, heart rate (HR), expired CO2, phrenic nerve amplitude and frequency (PNamp and PNf), mean arterial pressure (MAP), splanchnic and lumbar sympathetic nerve activity. Results: METH in PFC evoked respiratory depression at low doses but increased all parameters at high doses. DA evoked increases in thermogenic and metabolic outflows (iBAT;2.2±0.3 deg C, HR;21±4bpm and expired CO2;0.67±0.11% (n=5)) and in respiratory function (PNf;11±1bpm, and, PNamp;137±15% (n=5)) with little change in other parameters only at the highest dose with only respiratory depression evoked at low doses. In contrast in the PFC NA evoked dose dependent increases in MAP (18±2mmHg, 10ug/kg, n=5), iBAT (0.8±0.15 degC), HR (16±2bpm) and expired CO2 (0.35±0.07%) and respiratory function. Conclusions: In PFC respiratory depressant effects were evoked by low doses of METH and these were mimicked by low doses of DA. The increased cardiovascular, respiratory

and metabolic function evoked by METH in PFC was mimicked by NA, although DA may also contribute. Alteration in monoamine levels in frontal brain regions alters cardiorespiratory and metabolic function.

Funding supporting this work:NHMRC 457068, 1028183, Heart Foundation G09S4340, ARC DP120100920

Where applicable, the authors confirm that the experiments described here conform with The Physiological Society ethical requirements.

PCA119

The inflammatory response in the spontaneously hypertensive rat: Effects of anti-hypertensive interventions

P.J. Marvar, F.D. McBryde and J.F. Paton

Physiology and Pharmacology, University of Bristol, Bristol, UK

Previous studies have found inflammation, in particular T lymphocytes, to be a contributing factor in the genesis of various forms experimental hypertension (1,2). Currently, clinical interventions such as renal denervation (RD) and carotid body denervation (CBD) are aimed at targeting the autonomic nervous system to treat hypertension (3). However, the effects of these blood pressure lowering strategies on the immune system are unknown. In the current study, RD and CBD was performed in the spontaneously hypertensive rat (SHR) and flow cytometry used to examine tissue infiltration of T lymphocytes (CD3+) in the aorta and brainstem.

All procedures conformed to the UK Home Office guidelines on animals (Scientific Procedures) Act 1986 and were approved by the University of Bristol's Animal Ethic Committee. Rats were anaesthetised with ketamine (60 mg kg–1; i.m.) and medetomidine (250 μg kg–1, i.m.) and aseptic techniques used. Bilateral RD was achieved via a retroperitoneal incision to exposure of the renal artery. The nerves and adventitia were stripped from the renal artery and renal plexus, which were then painted with a dilute (10%) phenol solution. For CBD, the CB was visualised and branches of the carotid sinus nerve sectioned. Surgical sham-operated SHR (SS) rats underwent the same surgical procedures to expose the kidney and CB but the nerves were left intact. Compared to the SS group, arterial pressure and renal sympathetic nerve activity in the SHR was significantly lowered following both RD and CBD (see abstract by W. Pijacka et al). The percentage of infiltrating CD3+ T lymphocytes in the brainstem (9.6 ± 0.7 vs 6.4 ± 0.8%; $t(9) = 2.79$, $p < 0.05$) as well as the aorta (14.5 ± 1.6 vs 10.0 ± 1.1%; $t(16) = 2.18$, $p < 0.05$) were significantly reduced following RD. Following CBD, there was a trend toward reduced percentage of CD3+ cells in the aorta ($t(13) = 1.36$, $p = 0.19$) but unlike RD, there was no change in CD3+ cells in the brainstem. These data suggest that there is significant systemic CD3+ cell infiltration in the SHR and that some, but not all, procedures targeting the autonomic nervous system may have benefits in lowering tissue inflammation associated with hypertension. We strive to determine the causal relationship between reduced vascular inflammation and the anti-hypertensive effect of RD.

Harrison, D. G. et al. Inflammation, Immunity, and Hypertension. Hypertension 57, 132–140 (2011).

Waki, H. et al. Excessive leukotriene B4 in nucleus tractus solitarii is prohypertensive in spontaneously hypertensive rats. Hypertension 61, 194–201 (2013).

Schlaich, M. P., Hering, D., Sobotka, P. A., Krum, H. & Esler, M. D. Renal denervation in human hypertension: mechanisms, current findings, and future prospects. Curr Hypertens Rep 14, 247–253 (2012).

PJM is supported by a Marie Curie Fellowship and British Heart Foundation and National Institutes of Health funded research.

Where applicable, the authors confirm that the experiments described here conform with The Physiological Society ethical requirements.

PCA120

The role of glucocorticoid receptors within the Basolateral Amygdala on the alteration in morphine-induced conditioned place preference following swim stress

G. Attarzadeh Yazdi[1], S. Yazdi-Ravandi[2], S. Karimi[2] and A. Haghparast[2]

[1]Physiology, Hormozgan University of Medical Sciences, Bandar abbas, Islamic Republic of Iran and [2]Neuroscience Research Center, Shahid Beheshti University of Medical Sciences, Tehran, Islamic Republic of Iran

Stress represents a wide range of physical responses and plays an important role in modulating different stages of memory including reconsolidation. Relapse to drug taking induced by exposure to stimuli or cues associated with drugs of abuse is a main challenge to the treatment of morphine addiction. It has been shown that drug seeking can be inhibited by disrupting the reconsolidation of a drug-related memory, but, the effect of glucocorticoid receptors in Basolateral Amygdala on the alteration in morphine-induced conditioned place preference following swim stress has not been fully studied. We examined the effects of forced swim stress (FFS) and corticosterone on reconsolidation of a drug-related memory using a conditioned place preference (CPP) procedure.

Male adult rats received FSS as a physical stress or corticosterone (10 mg/kg; ip) as a dominant stress hormone in rodents, 10 min before injection of morphine (5 mg/kg; sc), during 3 conditioning days (acquisition) or just prior to CPP test in the post-conditioning day (expression). In FSS procedure, animals were forced to swim for 6 min in cylinder filled with water (24-27 ^{o}C).

All animals underwent extinction sessions until the CPP was extinguished; rats were confined to the previous morphine- or saline-paired compartment for 30 min a day for 8 days. The next day following the last extinction session, morphine CPP reinstatement was induced by FSS as stress-induced reinstatement.

The results showed that animals acquired morphine CPP after conditioning, and that this CPP was inhibited by stress given immediately after re-exposure to morphine. Corticosterone injection which leads to immediate and sudden increase in the level of glucocorticoids fails to reinstate the terminated CPP in rats. Studies on FSS-induced reinstatement show that this behavior is blocked by administration of corticotropin-releasing hormone (CRH) antagonists. Overall, these results suggest that corticosterone plays an important role in relapse to drug seeking behavior induced by stress.

Where applicable, the authors confirm that the experiments described here conform with The Physiological Society ethical requirements.

PCA121

ATP-mediated signalling in the pre-sympathetic area of the brainstem is critical for the development of hypertension in spontaneously hypertensive rats

R. Ang[1], N. Marina[1], S. Kasparov[2] and A.V. Gourine[1]

[1]University College London, London, UK and [2]Bristol University, Bristol, UK

Introduction
Increased sympathetic drive is associated with the development and progression of essential hypertension. Pharmacological studies have shown a direct stimulatory effect of ATP on bulbospinal sympathoexcitatory (pre-sympathetic) neurones of the rostral ventrolateral medulla oblongata (RVLM), leading to marked increases in sympathetic nerve activity and arterial blood pressure (1). Astroglial cells of the RVLM contribute to a significant ATP tone in this area of the brain (2). The aim of this study was to determine whether ATP actions within the RVLM contribute to the control of arterial blood pressure in normotensive and hypertensive rats.
Methods
We developed a lentiviral vector (LVV) to drive the expression of a potent membrane-bound ectonucleotidase – transmembrane prostatic acid phosphatase (TMPAP) for facilitated breakdown of extracellular ATP. LVV-TMPAP or control LVV-GFP were injected stereotaxically into the RVLM of pre-hypertensive (8-weeks-old) spontaneously hypertensive rats (SHRs) and age-matched Wistar rats anaesthetised with a mixture of ketamine (60mg/kg, im) and medetomidine (250μg/kg, im). Anaesthesia was reversed with atipamezole (1mg/kg, im). Blood pressure measurements were commenced 1 week after the injections and repeated weekly for 4 weeks by occlusive tail cuff method in conscious rats. Data is expressed as mean ± SEM and one-way ANOVA was used to assess statistical significance.
Results
Expression of TMPAP in the RVLM of SHRs resulted in a significant reduction in arterial blood pressure. Three weeks after the injections, SHRs transduced to express TMPAP in the RVLM had mean arterial blood pressure of 115.6±8.8 mmHg (n=7), which was significantly (p=0.009) lower than that in SHRs transduced to express GFP (152.9±8.4 mmHg, n=9). In comparison, TMPAP expression in the RVLM had no significant effect on the mean arterial blood pressure of control Wistar rats (91.4±4.5 vs 92.6±3.5 mmHg, p=0.836, n=8 in both groups).
Conclusion
Increased breakdown of extracellular ATP in the brainstem area where the key sympathoexcitatory neurones reside reduces the degree of hypertension in the SHR. These data suggest that ATP-mediated signalling has a significant impact on brain pre-sympathetic circuits and appears to be critical for the development of essential hypertension.

Sun MK et al. (1992). Europ J Pharmacol 224,93–96.

Kasymov V et al. (2013). J Neurosci 33, 435-441.

Where applicable, the authors confirm that the experiments described here conform with The Physiological Society ethical requirements.

PCA122

Evaluation of hypothalamic neuropeptides and inflammatory factors correlated to blood pressure changes in high fat diet-induced obesity in mice

L.J. Chaar, I.M. Ribeiro, N.M. Silva, W.T. Festuccia and V.R. Antunes

Department of Physiology and Biophysics, Institute of Biomedical Sciences, University of Sao Paulo, Sao Paulo, SP, Brazil

Obesity is a worldwide epidemic and a risk factor for cardiovascular diseases, and it is associated with a sympathetic overactivation to different organs that could be involved in obesity-associated hypertension. Moreover, it has been shown that the hypothalamic inflammation induced by high fat diet can alter the neurotransmission of autonomic centers leading to increases in the blood pressure. Here we screened the hypothalamus of diet-induced obesity in mice for neuropeptides and inflammatory factors that could be involved in the changes in mean arterial pressure (MAP) associated with obesity. Male mice C57BL6 submitted to high fat (HF; 60%kcal lipids) or control (C) diet for 8 weeks were evaluated for body weight gain, glucose tolerance, adiposity and plasma levels of leptin, insulin, triglycerides and free fatty acids. Femoral catheterization was performed under anesthesia with isoflurane (5% in O2-air inspired) and MAP was recorded in conscious freely moving mice. Hypothalamic mRNA of inflammation mediators and neuropeptides were quantified by qPCR. Values are expressed as mean±S.E.M., compared by ANOVA or t-Test; $p<0.05$. HF mice developed obesity as evidenced by the increased body weight gain (31%) and adiposity (epididymal, retroperitoneal and inguinal fat depots) in comparison to C group. Furthermore, HF diet increased fasting plasma levels of glucose (C: 177±8 vs HF: 200±6 mg/dL); leptin (C: 8±3 vs HF: 17±5 ug/ml), insulin (C: 43±7 vs HF: 672±127 pmol/L), triglycerides (C: 1.0±0.4 vs HF: 2.2±0.6 mmol/L), free fatty acids (C: 0.2±0.1 vs HF: 0.7±0.2 nmol/L), and induced severe glucose intolerance (C: 24106 vs HF: 35170 u.a., $p<0,0001$). The HF-diet led to two different hemodynamic phenotypes: obese hypertensive (OH: 123±2 mmHg, n=2) and obese resistant hypertension (OR: 102±5 mmHg, n=3) when compared with group C (107±1 mmHg, n=3). The MAP showed strong correlation with the glucose intolerance (r2 = 1.0, n=3). In addition, the HF-diet elicited an increase of the hypothalamic mRNA levels of cocaine- and amphetamine-regulated transcript (CART, +69%, n=5), decreased agouti gene-related peptide (AgRP, -52%, n=5) and interleukin-6 (IL-6, -40%, n=5) when compared to the C group. Our data have shown that high fat diet affected MAP and others obesity-related metabolic changes, such as glucose intolerance, hyperinsulinemia, dyslipidemia, hyperleptinemia, insulin resistance and altered mRNA levels of neuropeptides involved in the regulation of energy balance (CART and AgRP) and cytokines (IL-6) at the hypothalamus level. In fact, there is a great correlation between increasing in MAP and glucose tolerance, that could be also has a causality relationship with changes in neuropeptides and inflammatory factors in the autonomic nucleus of the hypothalamus that control blood pressure.

Supported by FAPESP and CNPq.

Where applicable, the authors confirm that the experiments described here conform with The Physiological Society ethical requirements.

PCA123

Transgenic Sprague Dawley rats with ataxin3-mediated destruction of orexin neurons display reduced tail artery Sympathetic Cutaneous Vasomotor Alerting Responses (SCVARs)

M. Mohammed[1], Y. Ootsuka[1], M. Yanagisawa[2] and B. Blessing[1]

[1]Human Physiology, Flinders University, Adelaide, SA, Australia and [2]Department of Molecular Genetics, University of Texas Southwestern Medical Centre, Dallas, TX, USA

Orexin neurons, located in perifornical hypothalamus (de lecea et al., 1998; Sakurai et al., 1998), influence appetite, the sleep-wake cycle, locomotor activity as well as a number of physiological variables. Transgenic mice with ataxin3-mediated destruction of orexin neurons have attenuated thermogenic and other autonomic responses to arousing environmental stimuli (Zhang et al., 2010), but constriction of the tail artery in response to alerting stimuli has not been assessed in animals in which orexin-containing neurons have been selectively destroyed. We have now assessed sympathetic cutaneous vasomotor alerting responses (SCVARs, de Menezes et al., 2009) in the tail artery of conscious unrestrained transgenic Sprague Dawley rats with ataxin3-mediated destruction of orexin neurons (Beuckmann et al., 2004), in comparison with wildtype control animals. Under inhaled isoflurane (2% in oxygen) anaesthesia, transgenic (n=10) and wildtype (n=8) male rats (300-450 g) were instrumented with ultrasound Doppler flow probes (Iowa Inc, USA) chronically implanted around base of the tail artery. All surgical procedures were performed in accord with the Animal Welfare Ethics Committee of Flinders University. Tail probe cables were passed subcutaneously and connected to a headpiece fixed to the skull with dental cement. After one-week recovery unrestrained rats were placed in a quiet closed wooden box at 24-26°C. The tail artery blood flow signal (40 Hz sampling rate) was recorded, via a swivel device, with PowerLab (ADInstruments). We administered standardized alerting stimuli (salient but not stressful) and assessed the acute effect on blood flow in the tail artery, calculated as the percentage change in flow induced by the stimulus (SCVAR index). Group SCVAR results (mean ± SEM) were analysed with factorial ANOVA. The SCVAR index in transgenic rats was 69 ±2%, significantly less than 84±2% ($p<0.001$), the corresponding wildtype value. Immunohistochemical examination of the perifornical area of the hypothalamus documented complete absence or substantial loss of orexin-containing neurons in the transgenic rats. Our findings support the view that the orexin-containing neurons function to increase the physiological response to the animal's perception of salient, potentially threatening environmental events.

Beuckmann CT, Sinton CM, Williams SC, Richardson JA, Hammer RE, Sakurai T, Yanagisawa M. Expression of a poly-glutamine-ataxin-3 transgene in orexin neurons induces narcolepsy-cataplexy in the rat.J Neurosci. 2004 May 5;24(18):4469-77.

de Lecea L, Kilduff TS, Peyron C, Gao X, Foye PE, Danielson PE, Fukuhara C, Battenberg EL, Gautvik VT, Bartlett FS 2nd, Frankel WN, van den Pol AN, Bloom FE, Gautvik KM, Sutcliffe JG. The hypcretins: hypothalamus-specific peptides with neuroexcitatory activity.Proc Natl Acad Sci U S A. 1998 Jan 6;95(1):322-7.

De Menezes RC, Ootsuka Y, Blessing WW. Sympathetic cutaneous vasomotor alerting responses (SCVARs) are associated with hippocampal theta rhythm in non-moving conscious rats. Brain Res. 2009 Nov 17;1298:123-30.

Sakurai T, Amemiya A, Ishii M, Matsuzaki I, Chemelli RM, Tanaka H, Williams SC, Richardson JA, Kozlowski GP, Wilson S, Arch JR, Buckingham RE, Haynes AC, Carr SA, Annan RS, McNulty DE, Liu WS, Terrett JA, Elshourbagy NA, Bergsma DJ, Yanagisawa M. Orexins and orexin receptors: a family of hypothalamic neuropeptides and G protein-coupled receptors that regulate feeding behavior. Cell. 1998 Feb 20;92(4):573-85.

Zhang W, Sunanaga J, Takahashi Y, Mori T, Sakurai T, Kanmura Y, Kuwaki T. J Physiol. Orexin neurons are indispensible for stress-induced thermogenesis in mice.2010 Nov 1;588(Pt 21):4117-29.

Authors thank Mrs Jessi Moore and Robyn Flook for their technical assistance in this work.

Where applicable, the authors confirm that the experiments described here conform with The Physiological Society ethical requirements.

PCA124

Co-localisation of the neurotransmitter synthesising enzymes GAD67 and choline acetyltransferase in the mouse nucleus tractus solitarius

J. Gotts, I.J. Edwards, S.A. Deuchars and J. Deuchars

University of Leeds, Leeds, UK

The nucleus of tractus solitarius (NTS) is the main integration site for autonomic control. It receives afferent information from arterial baroreceptors, chemoreceptors, cardiac receptors, gastrointestinal receptors and respiratory receptors (1). Details on the neurochemical properties of NTS neurones have been established by many researchers. However information on the co-localisation of choline acetyltransferase (ChAT) and glutamic acid decarboxylase (GAD) immunoreactivity within the NTS has not been reported. This study examined the distribution of ChAT immunoreactivity and co-localisation with green fluorescent protein (GFP) in the NTS of transgenic mice (n=4) expressing GFP under control of the GAD67 promoter (GAD67-GFP mice) (2) using fluorescence immunohistochemistry (3).

Four GAD67-GFP adult mice (mixed sexes) were injected intraperitoneally with 1 % Fluorogold. After 24-48 hours the mice were anaesthetised with 60 mg/kg sodium pentobarbitone and when the withdrawal reflex was absent, they were perfused transcardially with 4 % paraformaldehyde. The brainstems were postfixed with 4 % paraformaldehyde for 24 hours. Brainstems were sectioned (at 50 μm and 30 μm for double and triple labelling respectively). Serial sections were processed utilising fluorescent immunohistochemistry (IHC). One wild type adult mouse was also prepared in the same way as the GAD67-GFP mice. Sections were processed using diaminobenzidine IHC for ChAT to provide a permanent reaction product. ChAT immunoreactive (ChAT-IR) and GAD67-GFP immunoreactive (GAD67-GFP-IR) neurones were found in all NTS subnuclei. Moreover, co-localisation was observed in some NTS subnuclei; predominantly in the intermediate subnucleus (co-localised neurones per section were 6.83 ± 1.89 (mean ± SEM) for the right and 6.67 ± 2.19 for the left NTS column, n = 6 sections) and the central subnucleus (1.00 ± 0.68 (right NTS) and 2.17 ± 1.42 (left NTS)). Nitric oxide synthase immunoreactive (nNOS-IR) neurones in the central subnucleus are reported to be involved in oesophageal regulation (4). In our study, although nNOS-IR neurones were prominent in the central subnucleus, they did not exhibit co-localisation with either ChAT or GAD67-GFP. Although the absence of co-labelling in the central subnucleus with nNOS does not support a role for ChAT/GAD-IR neurones in oesophageal control, this possible

function cannot be excluded at this time. Examination of other brainstem areas revealed co-localisation of ChAT and GAD67-GFP immunoreactivity, including the area postrema, the reticular formation and the lateral paragigantocellular nucleus. Since there is limited information of co-localisation for ChAT and GAD immunoreactivity in the brainstem, it is worth studying further to investigate its roles in these neurones.

Loewy, A.D. and Spyer, K.M. (1990) (eds) New York: Oxford University Press.

Tamamaki et al. (2003) Journal of Comparative Neurology 467(1): 60-79.

Okada et al. (2008) Journal of Chemical Neuroanatomy 35(3): 275-284.

Wiedner et al.(1995) Gastroenterology 108(2): 367-375.

Where applicable, the authors confirm that the experiments described here conform with The Physiological Society ethical requirements.

PCA125

The properties and synaptic inputs of cholinergic interneurones

V.K. Lall, I. Edwards, J. Deuchars and S. Deuchars

School of Biomedical Sciences, University of Leeds, Leeds, UK

The central autonomic area (CAA) contains interneurones which directly influence sympathetic preganglionic neurones (Deuchars et al., 2005). Sensory afferent terminals are located around lamina X and form close appositions with interneurones (Hofstetter et al., 2005). CAA neurones have been identified as being premotor to somatic motor neurones (Stepien et al., 2010). This suggests that these interneurones may coordinate autonomic and motor outflow from the spinal cord and therefore, may receive inputs from primary afferents. This study aims to address how these interneurones fit into circuits involved in autonomic control. To investigate whether interneurones in CAA received direct inputs from myelinated primary afferents, immunohistochemistry for vesicular glutamate transporter 1 (VGLUT1) was conducted in GAD67-GFP mice anaesthetised with pentobarbital (60mg/kg; i.p) and transcardially perfused with 4% paraformaldehyde. Close appositions were observed between VGLUT1 primary afferent terminals and interneurones immunoreactive for GFP (GABAergic) or Choline Acetyltransferase. To determine how interneurones responded to stimulation at the dorsal root entry zone, 7-12 day old mice and 12-21 day old rats, of either sex, were anaesthetised by urethane (2g/kg; i.p). Transcardiac perfusion was followed by decapitation and 300μm transverse slices of lumbar and thoracic spinal cord were cut. Viable interneurones in laminae VII and X were identified and whole cell patch clamp recordings performed. A stimulating electrode was placed at the dorsal root entry zone to deliver stimuli (5-100 Hz) of 1 ms duration. The evoked excitatory postsynaptic potential (EPSP) amplitude was recorded and the latency to onset of the EPSP measured. The standard deviation (SD) of latency gave an indication of variability in latency (jitter). Values are means ± S.E.M, compared by 2 sample t-test. Mouse thoracic interneurones had an action potential threshold of -35.06 ± 1.99 mV, action potential amplitude of 49.52 ± 2.64 mV and afterhyperpolarisation amplitude of -19.45 ± 1.08 mv (n= 15). EPSP jitter was 2.31± 0.01 μs (n= 7). EPSPs followed high frequency tetanic stimulation, without failures indicating that they are likely elicited by monosynaptic primary afferents, and were significantly antagonised by 20 μM NBQX (an excitatory amino acid receptor antagonist) (7.68 ± 0.64 mV in control (n= 7) to 3.28 ± 0.45 mV (n= 7) in NBQX; p< 0.001). In rats, EPSP jitter was 4.23 ± 0.51 μs (n= 16) and EPSP amplitude was significantly reduced with NBQX (6.43 ± 0.04 mV (n= 16) in control to 0.42 ± 0.24 mV (n= 9) in 20 μM NBQX; p< 0.001). Post hoc analysis revealed extensive axon ramifications in both the dorsal and ventral horn. The direct action of primary afferents onto interneurones in the CAA may provide a avenue for the co-ordination of autonomic and motor activity.

Deuchars SA, Milligan CJ, Stornetta RL, Deuchars J (2005) GABAergic neurons in the central region of the spinal cord: a novel substrate for sympathetic inhibition. J Neurosci 25:1063-1070.

Hofstetter CP, Card JP, Olson L (2005) A spinal cord pathway connecting primary afferents to the segmental sympathetic outflow system. Exp Neurol 194:128-138.

Stepien AE, Tripodi M, Arber S (2010) Monosynaptic rabies virus reveals premotor network organization and synaptic specificity of cholinergic partition cells. Neuron 68:456-472.

I would like to thank the Wellcome Trust for funding.

Where applicable, the authors confirm that the experiments described here conform with The Physiological Society ethical requirements.

PCA126

Redox-sensitive endoplasmic reticulum stress and autophagy at rostral ventrolateral medulla contribute to hypertension in SHR

Y. Chao[1,2] and J. Chan[2]

[1]Institute of Basic Medical Sciences, National Cheng Kung University, Tainan, Taiwan and [2]Center for Translational Research in Biomedical Sciences, Chang Gung Memorial Hospital-Kaohsiung Medical Center, Kaohsiung, Taiwan

Perturbations of proper functions of the endoplasmic reticulum (ER) cause accumulation of misfolded or unfolded proteins in the cell, creating a condition known as ER stress. Prolonged ER stress has been implicated in hypertension. Oxidative stress in the rostral ventrolateral medulla (RVLM), where sympathetic premotor neurons for the maintenance of vasomotor tone reside, plays a pivotal role in neurogenic hypertension. This study aimed to evaluate the contribution of ER stress in RVLM to oxidative stress-associated hypertension, and delineated the underlying molecular mechanisms. The expression of glucose-regulated protein 78 kDa (GRP78) and phosphorylation of protein kinase RNA-like ER kinase-translation initiation factor α (p-eIF2α), two major protein markers of ER stress, were augmented in RVLM and preceded the development of hypertensive phenotype in spontaneously hypertensive rats (SHR). In RVLM of SHR, stabilizing ER stress by salubrinal promoted antihypertension, and scavenging the reactive oxygen species by tempol reduced the augmented ER stress. Furthermore, induction of oxidative stress by angiotensin II induced ER stress in RVLM, and induction of ER stress by tunicamycin in RVLM induced pressor response in normotensive Wistar-Kyoto rats. Autophagy, as reflected by the expression of lysosome-associated membrane protein-2 and microtubule-associated protein 1 light chain 3-II (LC3-II), was significantly increased in RVLM of SHR, and was abrogated by salubrinal. In addition, inhibition of autophagy or silencing LC3-II gene in RVLM resulted in antihypertension in SHR. These results suggest that redox-sensitive induction of ER stress and activation of autophagy in RVLM contribute to oxidative stress-associated neurogenic hypertension.

Where applicable, the authors confirm that the experiments described here conform with The Physiological Society ethical requirements.

PCA127

Low extracellular pH leads to free radical formation and mitochondria depolarization in rat brain synaptosomes

S.V. Fedorovich, T. Pekun, V. Lemeshchenko and T. Waseem

Institute of Biophysics and Cell Engineering, Minsk, Belarus

Brain ischemia is accompanied by lowering of intra- and extracellular pH down to 6.5 in the case of hyperglycemia, even down to pH 5.3. It has been shown that stroke often leads to irreversible damage of synaptic transmission. The mechanism of this phenomenon is still not clear. We investigated an influence of lowering of intra- and extracellular pH on free radical formation in synaptosomes, isolated neuronal presynaptic endings. We have used three model of acidosis. 1) Strong extracellular acidification down to pHo 6.0 corresponding to pHi decrease from 7.15 down to 6.04. 2) Moderate extracellular acidification down to pHo 7.0 corresponding to the lowering of pHi down to 6.92. 3) Intracellular acidification induced by addition of 1 mM amiloride corresponding to pHi decrease down to 6.65. We have shown that both types of extracellular acidification, but not intracellular acidification, increase DCFDA fluorescence that reflects reactive oxygen species formation. These three treatments induce the rise of the dihydroethidium fluorescence that reports synthesis of superoxide anion in synaptosomes. However, the impact of intracellular acidification on superoxide anion synthesis was less than that induced by moderate extracellular acidification, although 1 mM amiloride decreases the internal pH more strongly than lowering of extracellular pHo down to 7.0. Mitochondrial uncoupler CCCP (10 μM) and NADPH oxidase inhibitor DPI (30 μM) did not inhibit an increase of fluorescence of both dyes at pHo 6.0. In contrast, superoxide anion synthesis at pHo 7.0 was almost completely eliminated by CCCP, hence not affecting an increase of DCFDA fluorescence. Furthermore, using fluorescent dyes JC-1 and rhodamine-123, we confirmed that extracellular pH lowering, including pHo 7.0, but not intracellular acidification led to depolarization of intrasynaptosomal mitochondria. Assumingly, for moderate extracellular acidification the following chain of events is thought to be probable: proton binding to non-identified receptors, localized on the plasma membrane of neuronal terminals triggers transduction of the signal to the mitochondria where the superoxide anion radical is synthesized and then initiates the development of the oxidative stress. Action of strong extracellular acidification seems to be mediated by an inhibition of antioxidant enzymes and release of iron from proteins.
We have shown that pHo lowering led to oxidative stress in neuronal presynaptic endings that might underlie the long term irreversible changing in synaptic transmission.

Where applicable, the authors confirm that the experiments described here conform with The Physiological Society ethical requirements.

PCA128

Electrophysiological characteristics of newborn cells in the adult mouse midbrain

A. Dey and T. Aumann

Neurodegeneration, Florey Institute for Neuroscience & Mental Health, Melbourne, VIC, Australia

Background: Parkinson's Disease (PD) is the second most common neurodegenerative disorder in the aging population. Cardinal motor symptoms include slowness of movement, muscle rigidity, tremor and postural instability; caused by death of dopamine cells in the substantia nigra pars compacta (SNpc) of the midbrain. Traditional treatment regimes include administration of levodopa, or dopamine receptor agonists. However these produce side-effects and eventually fail in most patients within 5-10 years [1]. Advances in cell transplantation therapies have shown promising results in alleviation of motor symptoms [2] by providing targeted dopamine delivery. However, several problems need to be overcome for more effective outcomes to be achieved, including; acquisition and maintenance of the dopamine phenotype and integration into the adult midbrain. This is best overcome by learning how new dopamine neurons are normally generated in the adult midbrain.
Purpose and Methods: Characterise the electrophysiology of newborn cells in the NesCreERT2/GtROSA+\+ mouse as they proliferate, migrate and differentiate into dopamine neurons; using whole-cell patch clamping techniques.
Results: Recordings were made from regions of the adult midbrain including; lining of the cerebroventricular aqueduct, periaqueduct grey (PAG), ventral midline, ventral tegmental area (VTA) and SNpc. Cells displayed a variety of electrophysiological profiles from relatively immature to fully mature neuronal phenotypes. Cells lining the aqueduct exhibited a relatively negative resting membrane potential (n=15,-76.7±1.2mV), small capacitance (6.0±1pF), no action potentials or synaptic activity. In addition they had no apparent voltage-sensitive conductances, typical of an astrocyte like phenotype. YFP+ cells in the PAG (n=8) exhibited a slightly more mature neuronal phenotype with some evidence of voltage-sensitive conductances and larger capacitance values (12.9±4.3pF). They exhibited spontaneous post-synaptic currents (sPSC) in 25% of cells, indicating receipt of synaptic input from other neurons, although only exhibited action potentials in 50% of cells, in contrast to cells in the midline, VTA and SNpc which had actions potentials in all cells. YFP+ cells in the ventral midline through to the SNpc had larger amplitude (midline: 53.4±4.3mV (n=15), VTA: 57.3±3.7mV (n=7), SNpc: 50.2±4.1 (n=9)) and shorter duration (midline: 1.3±0.3ms (n=15), VTA: 1.1±0.2ms (n=7), SNpc: 1.3±0.3ms (n=9)) action potentials, than the aqueduct or PAG region. Finally, YFP+ cells along this gradient also displayed sPSCs in 47% of cells in the ventral midline and 25% of cells in the VTA and 33% in the SNpc.
Conclusion: Electrophysiology indicate cells appear to be transitioning from precursors to neurons from the cerebral aqueduct to the SNpc, possibly indicating integration of these new born cells into the dopamine system.

[1] Poewe, W., et al., Levodopa in the treatment of Parkinsons Disease: An old drug still going strong, Clinical Interventions in Aging 2010. 5 p229–238

[2] O. Lindvall., et al., Evidence for long-term survival and function of dopaminergic grafts in progressive Parkinson's disease, Ann. Neurol. 35 (1994) 172–180.

Where applicable, the authors confirm that the experiments described here conform with The Physiological Society ethical requirements.

PCA129

Fructose increases ATP-and ROS-dependent neurotransmitter release

K. Wu, S.H. Chan and J.Y. Chan

Center for Translational Research in Biomedical Sciences, Chang Gung Memorial Hosptial, Kaohsiung, Taiwan

High fructose consumption induces increases in sympathetic nerve activity, although the underlying cellular mechanism is not fully understood. ATP is essential for neuronal activity. We verified in the present study the hypothesis that fructose directly increases ATP production in catecholamine-containing neuron to cause the release of neurotransmitter. Application of different concentrations of fructose (12.5, 25, 50 or 100 μmole/L) to the mouse neuroblastama N2A cells for 3 days resulted in a dose-related increase in ATP production in the cell. In addition, reactive oxygen species (ROS) production was also significantly increased in a dose-dependent manner. Oxygen consumption rate and proton production of mitochondria were significantly increased under high fructose status. Dopamine level in the medium was increased in N2A cells exposed to fructose. The expression of tyrosine hydroxylase and surface expression of dopamine transporter were also significantly increased. Moreover, expression of glutamate transporter 2 (GLUT2), a fructose transport, was significantly increased in response to fructose treatment. Down-regulation of GLUT2 by transfection of Glut2 siRNA effectively suppressed the induced GLUT2 expression and attenuated fructose-promoted ATP and ROS production, and dopamine secretion from the N2A cells. The fructose-induced dopamine secretion was also blunted by scavenging ROS with mitoTEMPO. Together our data indicated that fructose may directly increases neuronal activity through increase in ATP and ROS production via activation of GLUT2.

This study was supported in part by research grants CMRPG8A0801to KLHW, Taiwan, Republic of China.

Where applicable, the authors confirm that the experiments described here conform with The Physiological Society ethical requirements.

PCA130

Neuroprotective anti-oxidant effect of a Nitric Oxide synthase inhibitor in cerebral injury induced by transient focal ischemia/ reperfusion in rats

A.M. Saeed[1], H.A. Awooda[2] and G. Sharara[3]

[1]Physiology, University of Khartoum, Khartoum, Khartoum, Sudan, [2]Physiology, Alneelain University, Khartoum, Sudan and [3]Biochemistry, Alexandria University, Alexandria, Egypt

Background: Reports assessing the neuroprotective role of nonselective NO synthase (NOS) inhibitors following cerebral ischemia/reperfusion are contradictory (1-2). Aims: To examine the potential benefits of N-nitro-L-arginine-methylester (L-NAME) on rats subjected to transient focal cerebral ischemia/reperfusion. Materials and methods: The study involved three groups of males adult Wister rat each consist of 10: a control group operated at the neck region without occlusion of left common carotid artery (CCA), a placebo group infused with 0.9% normal saline intraperitoneally 15 minutes prior to left cerebral ischemia/reperfusion induced by transient (30 minutes) left CCA occlusion and a test group infused with L-NAME intraperitoneally 15 minutes prior left cerebral ischemia/reperfusion (3). Anesthesia was induced by ether inhalation and maintained by thiopental sodium (2.5mg/kg). Malondialdehyde (MDA), NO metabolites and total antioxidant capacity (TAC) in serum and the affected cerebral hemisphere were measured. Neurobehavioral deficits were evaluated. Results: The neurological deficit of both placebo and test groups were significantly lower compared to the control group. The test group showed a significant improvement in neurological deficit compared to the placebo group (P <0.001).The placebo group demonstrated a significant increase in the serum levels of both MDA and NO (14.88±1.14 nmol/mL, 42.03±4.56 μmol/L respectively) compared to the control group (5.43±0.44 nmol/mL, 17.84±0.7 μmol/L respectively, P <0.001). Values are means ± S.E.M., compared by ANOVA. Alternatively, the test group showed significant decrease in serum level of MDA and NO (7.18±0.13, 18.44±0.51μmol/L respectively, P <0.001) compared to the placebo group. The serum level of TAC in the placebo group (1.21±0.17 mM/L) was significantly lower compared to the control group (2.52±0.06 mM/L, P <0.001) but not the test group (2.53±0.067mM/L). L-NAME pretreatment resulted in significant higher serum level of TAC compare to placebo group (P <0.001).The brain tissue levels of MDA and NO of the placebo group (8.56±0.7, 8.88±0.57 nmol/mg protein) was significantly higher than the control group (3.24±0.22, 3.48±0.22 nmol/mg protein, P <0.001). The test group showed a significant decrease in tissue level of MDA and NO (3.18±0.1, 4.47±0.4 nmol/mg protein, P <0.001) compared to the placebo group. Administration of L-NAME prior to ischemia result in significant increase of brain TAC level compare to placebo (0.07±0.009 vs 0.02±0.004 mmol/mg protein P < 0.001). Conclusions: L-NAME pretreatment for rats undergoing cerebral ischemia/reperfusion significantly improve neurological deficit through reducing oxidative stress biomarkers in the affected cerebral hemisphere.

1. Willmot M, Gibson C, Gray L, Murphy S, Bath P. Nitric oxide synthase inhibitors in experimental ischemic stroke and their effects on infarct size and cerebral blood flow: a systematic review. Free Radic Biol Med. 2005 Aug 1; 39:325-412.

2.Ding-Zhou L, Marchand-Verrecchia C, Croci N, Plotkine M, Margaill I. L-NAME reduces infarction, neurological deficit and blood-brain barrier disruption following cerebral ischemia in mice. Eur J Pharmacol. 2002 Dec 20;457(2-3):137-46.

3. Kuluz JW, Prado RJ, Dietrich WD, Schleien CL, Watson BD. The effect of nitric oxide synthase inhibition on infarct volume after reversible focal cerebral ischemia in conscious rats. Stroke. 1993 Dec;24(12):2023-9.

Where applicable, the authors confirm that the experiments described here conform with The Physiological Society ethical requirements.

PCA131

Neuroprotective effects of Lycium barbarum polysaccharides in lipopolysaccharide-induced BV2 microglia cells

Y. Wang[1], Y. Li[1], P. Teng[1], X. Hou[2], L. Wang[2], Q. Qi[1], L. Zhou[3], Y. Shen[3], Y. Zhang[1] and Z. Miao[1]

[1]Ningxia Medical University, Yinchuan, China, [2]General Hospital of Ningxia Medical University, Yinchuan, China and [3]Zhejiang University, Hangzhou, China

Polysaccharides, extracted from Lycium barbarum (LBPs), display a wide variety of biological activities. However, the neuroprotective effects of LBPs remain poorly understood. The present study aimed to investigate the inhibitory effects of LBPs on production of lipopolysaccharide (LPS)–induced pro-inflammatory mediators in BV2 microglia. Our data showed that LPS induced the activation of NFκB and its upstream caspase 3 and upregulated the expression of another apoptosis-inducing factor, HSP60 in BV2 microglia cells and increased the release of TNF-α and HSP60 in culture media. After LBPs treatment, activated NFκB and caspase 3 were significantly suppressed. The enhanced expression of HSP60 was reduced and LPS induced release of TNF-α and HSP60 were inhibited. These results suggest that LBPs may offer substantial therapeutic potential for treatment of neurodegenerative diseases that are accompanied by microglia activation.

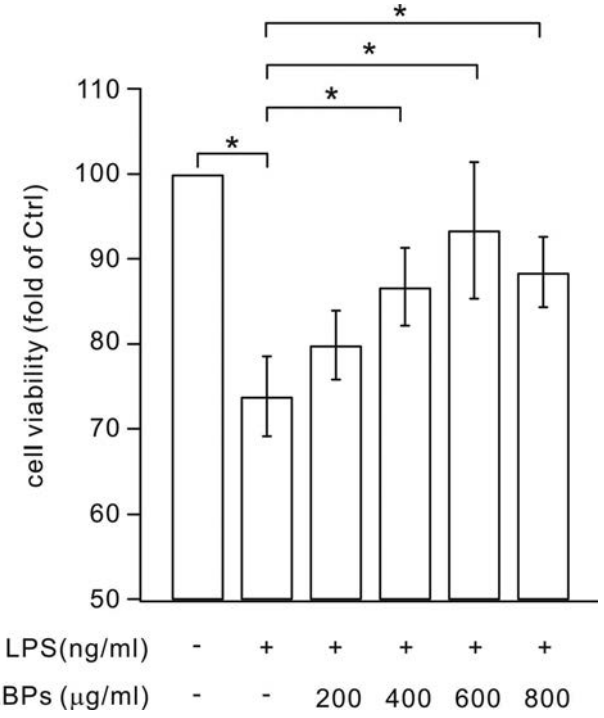

Figure 1. LBPs increase the cell viability of BV2 microglia. BV2 cells were treated with LPS (200 ng/ml) for 1 h and then treated with various concentrations of LBPs (0, 200, 400, 600, or 800 μg/ml) for 24 h. The viability of LPS and LBPs-untreated cells was set to 100. The viability of LPS and LBPs-treated cells was expressed as the percentage of the untreated cells. Results were obtained from 3 independent experiments. *, P <0.05.

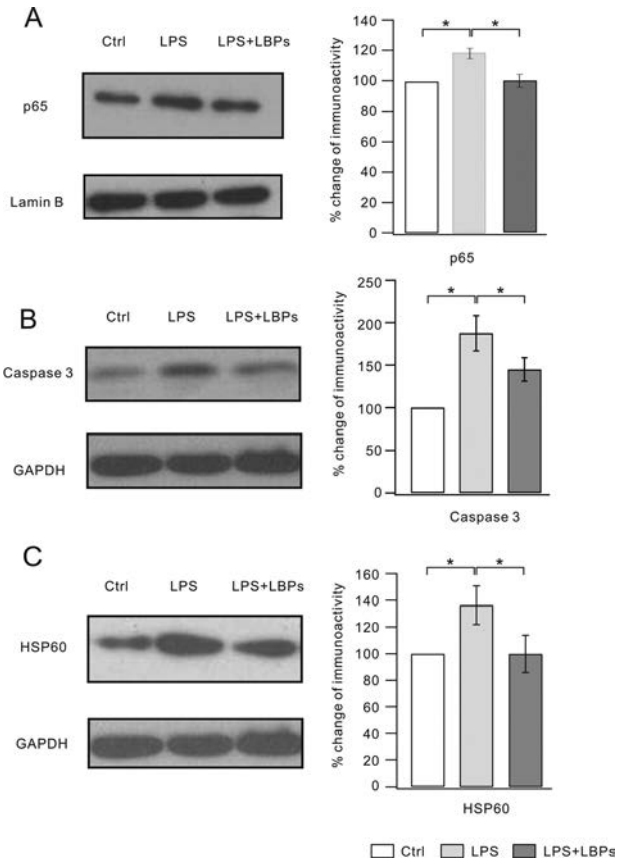

Figure 2. LBPs inhibit the increased expression of NFκB, caspase-3 and HSP60 in LPS-stimulated BV2 microglia. Cells were pre-treated with LPS for 1 h and then incubated with 600 μg/ml LBPs for 24 h. (A) The lysates were probed by immunoblotting with antibodies to p65 and lamin B. The right panel shows ratios of signal intensity of p65/lamin B (Ctrl: 100%; LPS: 119.3±7%; LPS+LBP: 107.3±9%). (B) The lysates were probed by immunoblotting with antibodies to caspase-3 and GAPDH. The right panel shows ratios of signal intensity of caspase-3/ GAPDH (Ctrl: 100%; LPS: 187.4±20.8%; LPS+LBP: 144.9±13.7%). (C) The lysates were probed by immunoblotting with antibodies to HSP60 and GAPDH. The right panel shows ratios of signal intensity of HSP60/GAPDH (Ctrl: 100%; LPS: 136.5±14.4%; LPS+LBP:100±18%). Each experiment was derived from 10 independent cultures. *, P <0.05.

Block M L, Zecca L and Hong J S: Microglia-mediated neurotoxicity: uncovering the molecular mechanisms. Nature Rev. Neurosci 8: 57–69, 2007.

Hanisch Uk and Kettenmann H: Microglia: active sensor and versatile effector cells in the normal and pathologic brain. Nat. Neurosci 10: 1387–1394, 2007.

Li YH, Teng P, Wang Y, Zhang YM, Ma CJ:Expression and regulation of HSP60 in activated microglia cells. J Ningxia Med Univ 8:712-714,2011.

Wang Y, Chen L, Hagiwara N and Knowlton AA: Regulation of heat shock protein 60 and 72 expression in the failing heart. J Mol Cell Cardiol 48:360-366, 2010.

Lin L, Kim SC, Wang Y, Gupta S, Davis B, Simon S, et al. HSP60 in heart failure:abnormal distribution and role in cardiac myocyte apoptosis. Am J Physiol 293:H2238–2247, 2007.

This work was supported by grants from National Natural Science Foundation of China (30960108, 31060140, 31070945, 31100780 and 31260243), The Project-sponsored by SRF for ROCS, SEM for Yin Wang and Special Talent Project of Ningxia Medical University (XT200910).

Where applicable, the authors confirm that the experiments described here conform with The Physiological Society ethical requirements.

PCA133

Peptide hormone ghrelin enhances neuronal excitability by inhibition of Kv7/KCNQ channels

L. Shi[1], X. Bian[2], Z. Qu[1], Z. Ma[1], Y. Zhou[1], K. Wang[2], H. Jiang[1] and J. Xie[1]

[1]Department of Physiology, Shandong Provincial Key Laboratory of Pathogenesis and Prevention of Neurological Disorders and State Key Disciplines: Physiology, Medical College of Qingdao University, Qingdao, China and [2]Department of Molecular and Cellular Pharmacology, State Key Laboratory of Natural and Biomimetic Drugs, Peking University School of Pharmaceutical Sciences, Beijing, China

The gut-derived orexigenic peptide hormone ghrelin enhances neuronal firing in the substantia nigra pars compacta (SNc), where dopaminergic neurons modulate the function of the nigrostriatal system for motor coordination. However, how ghrelin regulates the excitability of dopaminergic neurons remains unknown. Here we describe a novel mechanism by which ghrelin enhances firing of nigral dopaminergic neurons by inhibiting voltage-gated potassium Kv7/KCNQ/M-channels through its receptor GHS-R1a-activated PLC-PKC pathway. Brain slices of the SNc were prepared from SD rats of postnatal 10 days. Nystatin-perforated patch clamp recordings of SNc neurons reveal that ghrelin inhibits native Kv7/KCNQ/M-currents from 25.4 ± 3 pA to 12.1 ± 2.1 pA (n=8, $p<0.01$, Values are means ± S.E.M., compared by Paired t-test.). This effect is abolished by selective inhibitors of GHS-R1a, PLC and PKC. Transgenic suppression of native Kv7/KCNQ/M-channels in mice (6-7-week old rQ2-G279S transgenic mice with background of TB6D2F1/Crl * C57/B6) or channel blockade with XE991 abolishes ghrelin-induced hyperexcitability. In vivo, adult female Wistar rats weighing 200-250 g were anesthetized with chloral hydrate (400 mg/kg, i.p.). Intracerebroventricular ghrelin administration (100 nM or 1000 nM, 5 μl) causes increased dopamine release from 1.3 ± 0.2 μM to 3.9 ± 0.5 μM (n=6, $p<0.05$, Values are means ± S.E.M.) and turnover (n=6, $p<0.05$) in the striatum. Microinjection of ghrelin (1000 nM, 0.5 μl) or XE991 (1 μM, 0.5 μl) into SNc results in contralateral dystonic posturing, and attenuation of catalepsy elicited by systemic administration of the D2 receptor antagonist haloperidol. Taken together, our findings reveal that ghrelin exerts its function by inhibiting voltage-gated Kv7/KCNQ/M-channel, resulting in enhanced excitability of nigral dopaminergic neurons for improvement of motor impairment. The ghrelin/KCNQ signaling is likely a common pathway utilized by the nervous system.

This work was supported by the grants from 973 program to Junxia Xie (2011CB504100) and Hong Jiang (2012CB526703), the grants from the National Natural Science Foundation of China to Junxia Xie (30930036); to Hong Jiang (81170207); to KeWei Wang (30970919); to Xiling Bian (81000552) and to Limin Shi (31200819), and the Bureau of Science and Technology of Qingdao (12-1-4-2-(19)-jch).

Where applicable, the authors confirm that the experiments described here conform with The Physiological Society ethical requirements.

PCA134

Neurorescue effect of rosmarinic acid on 6-hydroxydopamine-lesioned nigral dopamine neurons in rat model of Parkinson's disease

J. Wang[2], H. Xu[1], H. Jiang[1], X. Du[1], P. Sun[2] and J. Xie[1]

[1]Department of Physiology, Shandong Provincial Key Laboratory of Pathogenesis and Prevention of Neurological Disorders and State Key Disciplines: Physiology, Medical College of Qingdao University, Qingdao, China and [2]Department of Neurosurgery, the Affiliated Hospital of Medical College, Qingdao University, Qingdao, China

Rosmarinic acid (RA) is a naturally occurring polyphenolic compound. It has been reported that RA possessed antioxidant and anti-inflammatory properties. Our previous study showed that RA could protect MES23.5 dopaminergic cells against 6-hydroxydopamine (6-OHDA)-induced neurotoxicity in vitro. The purpose of this study was to explore the neuroreparative (neurorescue) effect of RA on 6-OHDA-lesioned rat model of Parkinson's disease (PD) in vivo. In this study, female Wistar rats weighing 200–220 g were given 20 mg/kg RA by intragastric administration from day 1 after 6-OHDA lesioning and continued till the 21st day. Results showed that the dopamine content in the striatum decreased (n=6, $p<0.05$) and the numbers of tyrosine hydroxylase-immunoreactive neurons reduced after 6-OHDA treatment (n=6, $p<0.01$). RA treatment after 6-OHDA administration could restore these changes. Further studies demonstrated that 6-OHDA treatment increased the iron-staining positive cells, which were markedly decreased by RA treatment (n=6, $p<0.01$). Moreover, RA suppressed the increased ratio of Bax/Bcl-2 at gene level induced by 6-OHDA (n=6, $p<0.01$). This indicates that the neurorescue effects of RA against 6-OHDA-induced degeneration of the nigrostriatal dopaminergic system were achieved by decreasing nigral iron levels and regulating the ratio of Bcl-2/Bax gene expression.

This work was supported by grants from the National Program of Basic Research sponsored by the Ministry of Science and Technology of China (2011CB504102), the National Foundation of Natural Science of China (30930036), and the Natural Science Foundation of Shandong Province (Z2008C01, Z2008C06).

Where applicable, the authors confirm that the experiments described here conform with The Physiological Society ethical requirements.

PCA135

6-Hydroxydopamine upregulates iron regulatory protein 1 by activating certain protein kinase C isoforms in the dopaminergic MES23.5 cell line

W. Wang, N. Song, H. Zhang, J. Xie and J. Wang

Department of Physiology, Shandong Provincial Key Laboratory of Pathogenesis and Prevention of Neurological Disorders and State Key Disciplines: Physiology, Medical College of Qingdao University, Qingdao, China

Iron-induced oxidative stress is thought to play a crucial role in the pathogenesis of Parkinson's disease. Our previous studies demonstrated that decreased expression of ferroportin 1 contributes to 6-hydroxydopamine induced intracellular iron

accumulation and that decreased ferroportin 1 expression is caused by increased expression of iron regulatory protein 1. Iron regulatory protein 1 is a central regulator of iron homeostasis and is a likely target of extracellular agents to program changes in cellular iron metabolism. Therefore, the mechanism of iron regulatory protein 1 upregulation induced by 6-hydroxydopamine has become a significant focus of research. Iron regulatory protein 1 is regulated by protein kinase C, although this regulation is tissue specific. Therefore, in the present study, we aimed to determine whether alteration of protein kinase C activity modified iron regulatory protein 1 expression in the dopaminergic MES23.5 cell line. Furthermore, we investigated whether 6-hydroxydopamine induced iron regulatory protein 1 upregulation is mediated by protein kinase C, thus achieving regulation of cellular iron levels. The results showed that iron regulatory protein 1 was upregulated by phorbol 12-myristate-13-acetate, the PKC activator in dopaminergic MES23.5 cells, and ferroportin 1 expression and iron efflux were decreased as a result of iron regulatory protein 1 upregulation. The protein kinase C inhibitor bisindolylmaleimide I hydrochloride abolished the effect of phorbol 12-myristate-13-acetate. Protein kinase C-δ and protein kinase C-ζ, but not protein kinase C-ε were activated by 6-hydroxydopamine. The protein kinase C-δ inhibitor rottlerin inhibited protein kinase C-δ phosphorylation and abolished iron regulatory protein 1 upregulation induced by 6-hydroxydopamine. The protein kinase C-ζ pseudo-substrate inhibitor inhibited protein kinase C-ζ phosphorylation and abolished iron regulatory protein 1 upregulation induced by 6-hydroxydopamine. These data indicate that iron regulatory protein 1 is regulated by protein kinase C in dopaminergic MES23.5 cells and that protein kinase C activated by 6-hydroxydopamine regulates iron regulatory protein 1 expression, thus achieving regulation of cellular iron levels.

We thank Dr. Wei-Dong Le for providing us the MES23.5 cell line. This work was supported by grants from the National Basic Research Program of China (2011CB504102), the National

Natural Science Foundation of China (30930036 and 31171031), the Department of Science &Technology of Shandong Province (ZR2010HM003), the Shandong Provincial Education Department (G09LC09) and Qingdao Municipal Science & Technology Commission (10-3-4-3-16-jch).

Where applicable, the authors confirm that the experiments described here conform with The Physiological Society ethical requirements.

PCA136

HO-1 participates differentially in astroglia and neurons vulnerability

X. Yu, N. Song, H. Jiang and J. Xie

Department of Physiology, Shandong Provincial Key Laboratory of Pathogenesis and Prevention of Neurological Disorders and State Key Disciplines: Physiology, Medical College of Qingdao University, Qingdao, China

Over expression of heme oxygenase-1 (HO-1) was observed in both astroglia and neurons in the substantia nigra pars compacta of patients with Parkinson's disease (PD). However, the role of HO-1 in PD pathogenesis remains unknown. To determine whether and how HO-1 participates differentially in astroglia and neurons vulnerability, we first analyzed time-dependent HO-1 expression induced by 1-methyl-4-phenyl-pyridinium (MPP+) and alpha-synuclein in primary cultured mesencephalic astroglia and neurons. The results showed that both toxins induced a time-dependent HO-1 up-regulation in these cells, however, neuronal HO-1 up-regulation appeared much later than glial. We further demonstrated that HO-1 inhibitor zinc protoporphyrin aggravated MPP+ induced oxidative damage in both astrocytes and neurons, indicating this HO-1 response was cyto-protective. Overexpression of HO-1 induced by activator cobalt protoporphyrin (copp) showed protective effects on neurons in the time of inadequate HO-1 up-regulation, however, aggragates MPP+ induced oxidative damage at the peak of HO-1 response. For astroglia, copp always showed dose-dependent protective effects. These results indicate that between astrogila and neurons, HO-1 was differentially modulated in a time-dependent manner and over-expressed HO-1 might play different roles in cellular antioxidation.

This work was supported by grants from the National Program of Basic Research sponsored by the Ministry of Science and Technology of China (2011CB504102, 2012CB526703), National Nature Science Foundation of China (30930036).

Where applicable, the authors confirm that the experiments described here conform with The Physiological Society ethical requirements.

PCA139

Presynaptic glutamine transport sustains glutamatergic transmission at a mammalian central synapse

B. Billups, M. Marx and D. Billups

Department of Pharmacology, University of Cambridge, Cambridge, UK

Glutamate is the main excitatory neurotransmitter in the mammalian CNS. It has been proposed that presynaptic terminals sequester glutamine from the extracellular fluid to replenish synaptically released glutamate. Using direct electrophysiological recordings from the calyx of Held presynaptic terminal, we investigated the nature of the presynaptic glutamine transport mechanism and assessed its role in maintaining glutamatergic synaptic transmission.

Brainstem sections containing the medial nucleus of the trapezoid body (MNTB) were obtained from P10-15 Wistar rats. Presynaptic terminals were whole-cell voltage-clamped and glutamine transporter currents were elicited by 5 s puff-application of 10 mM glutamine from an adjacent pipette. Values are means ± S.E.M., compared by ANOVA.

In quiescent presynaptic terminals the glutamine induced current (I_{gln}) was almost absent (-0.7 ± 0.4 pA; n=17). However, activation of Ca^{2+} currents in the presynaptic terminal by depolarisation (-80 to 0 mV for 2 ms, repeated at 100 Hz for 2 s) consistently resulted in the rapid establishment of a robust I_{gln} (-12.9 ± 1.6 pA; n=24). The induction of I_{gln} was blocked by the removal of external Ca^{2+} (by 93 ± 3 %; n=3; $p<0.001$) and was inhibited by inclusion of botulinum neurotoxin C in the patch-pipette (by 57 ± 2 %; n=3; $p<0.05$), indicating the involvement of vesicle fusion. Cessation of presynaptic stimulation resulted in down-regulation of I_{gln} with a half-time of <30 s. Furthermore, I_{gln} was eliminated by the removal of external Na^+ (by 99 ± 1%; n=3; $p<0.001$) and by the specific system A neutral amino acid transport inhibitor α-methyl-aminoisobutyric acid (MeAIB; reduced by 94 ± 3 %; n=3; $p<0.001$). At depolarised potentials I_{gln} did not reverse, consistent with activation of a transporter. Additionally, puff application of 200 μM glutamate did not induce a significant membrane current (0.0 ± 0.5 pA;

n=3; p<0.05), indicating a lack of direct presynaptic glutamate uptake.
Miniature EPSCs recorded from the postsynaptic MNTB principal neurons (-38.8 ± 3.5 pA) were inhibited by MeAIB (-28.6 ± 3.4 pA; n=5; p<0.01) following stimulation at 200 Hz to promote turnover of the presynaptic glutamate pool. Single EPSCs in the absence of high frequency stimulation were unaffected by MeAIB (-4.5 ± 0.5 nA in control and -4.3 ± 0.4 nA in MeAIB; n=3 p=0.4), indicating that MeAIB does not have a direct effect on postsynaptic AMPA receptors and is acting to reduce vesicular glutamate content.
These data indicate that system A mediated glutamine transport occurs in glutamatergic nerve terminals and that its functional expression in the presynaptic plasma membrane is dynamically controlled by synaptic activity. They also indicate that system A is important in maintaining the supply of glutamate for excitatory neurotransmission during periods of high frequency stimulation.

Where applicable, the authors confirm that the experiments described here conform with The Physiological Society ethical requirements.

PCA140

Infraslow (<0.5 Hz) brain potentials reflect different neurophysiologic mechanisms of sensory information neuroprocessing in the human brain

I.V. Filippov, A.A. Krebs and K.S. Pugachev

Physiology and Biophysics & Pathophysiology, Yaroslavl State Medical Academy, Yaroslavl, Russian Federation

OBJECTIVE: Our previous studies indicated that infraslow brain potential oscillations (ISO) in sensory cortical areas of rodents were involved in neuroprocessing of sensory information. The aim of this study was to analyze brain ISO over the projections of visual, auditory, and gustatory cortices in volunteers during application of corresponding sensory stimuli.
METHODOLOGY: This work was conducted in adherence with the World Medical Association's Declaration of Helsinki. Fifteen volunteers with the age of 24-41 (n=30 experiments) were included in this study. Surface Ag/AgCl electrodes were placed in the positions Fp1, T3, and O1 in accordance with 10-20 EEG scheme. ISO were recorded using computer EEG data acquisition/stimulation system. ISO were recorded over projections of visual cortex under condition of darkness (0 lx) and during rhythmic photic stimulation (0-1500 lx, 5 Hz, flash duration 40 ms); over projections of auditory cortex under condition of silence and during rhythmic acoustic stimulation (clicks, 40 dB SPL, 1000 Hz tone); over projections of frontal cortex under application of distilled water, 0.55 M glucose and 0.155 M NaCl solutions. Power spectral analysis was used to evaluate ISO dynamics, for statistics we used one-way ANOVA, and an alpha level of P<0.01 was adopted for all significance tests.
RESULTS: There were found complex ISO dynamics in Fp1, T3, and O1 in all recordings, this consisted of: waves in the domain of seconds (0.1-0.25 Hz), multisecond oscillations (0.0167-0.035 Hz), fluctuations in the range of minutes (<0.004 Hz) and millivolt scale potential (+/-20 mV). Statistically significant spectral alterations (as increase of powers of waves in the domain of seconds) were detected in O1 and T3 recordings under rhythmical photic and acoustic stimulations, respectively (compared to ISO dynamics under the condition of darkness and silence there). Stimulus-dependent taste ISO responses were identified in Fp1 recordings again in the range of seconds. There were present clear multisecond oscillation changes (however, different and opposite in their directions in O1, T3, and Fp1 recordings) under exposure of visual, acoustic and gustatory stimuli, although we have not found any statistically significant changes of fluctuations in the domain of minutes and millivolt scale potential under all experimental conditions.
CONCLUSIONS: Obtained data are strikingly similar to what was documented by us in rodents. Altogether, these allow us to conclude that infraslow brain potentials of different frequency domains reflect various neurophysiologic mechanisms of sensory information neuroprocessing in the human brain. Possible clinical implications of these results and this methodology should be strongly considered.

This work was supported by grants from Ministry of Education and Science of Russia.

Where applicable, the authors confirm that the experiments described here conform with The Physiological Society ethical requirements.

PCA141

Characterization of hypoxia inducible factor pathway in neuroprotection and neurorestoration following cerebral ischaemia

R. Chen[1], S. Nagel[2], M. Papadakis[3], C. Schofield[4], P. Ratcliffe[5], C. Pugh[5] and A. Buchan[3]

[1]School of Pharmacy, Keele University, Newcastle under lyme, UK, [2]Department of Neurology, University of Heidelberg, Heidelberg, Germany, [3]Radcliffe Department of Medicine, University of Oxford, Oxford, UK, [4]Department of Chemistry, University of Oxford, Oxford, UK and [5]Wellcome Trust Center for Human Genetics, University of Oxford, Oxford, UK

Activation of the hypoxia inducible factors (HIF) pathway by inhibition of the HIF prolyl-4-hydroxylase enzymes (PHD) confers protection against ischemia/reperfusion injury (Sridharan V, et al. 2007). We investigated the precise function of each PHDs (1-3) in ischaemic stroke by using mice with each isoform genetically suppressed and by applying a novel specific PHD inhibitor – FG2216. Middle cerebral artery occlusion (MCAO)(45min ischaemia/24h reperfusion) was performed under anesthesia with 1.5% isoflurane in O2/N2O (1:3) on male, 8-12 week old PHD1-/-, PHD2+/- and PHD3-/- mice and their wild type (WT) littermates, as well as C57/B6 mice treated with FG2216. During the experiments, regional cerebral blood flow (rCBF) was recorded by a laser Doppler flowmetry. Behaviour was assessed at 24h after reperfusion with a common neuroscore. Infarct volumes, blood brain barrier (BBB) disruption, cerebral vascular density, reactive oxygen species (ROS) and apoptosis were then determined using histological and immunohistochemical techniques. When compared to their WT littermates, PHD2+/- mice had significantly more effective restoration of rCBF upon reperfusion, better functional outcomes (Neuroscores: 1.9±0.5 vs 4.3±0.5, p<0.01) and higher activity rates at 24h after MCAO, there were significantly fewer apoptotic cells in the penumbra and less BBB disruption, with a trend towards reduced infarct volume (26.7±6.7% vs 40±5.5%, p=0.15) but no difference in ROS formation; PHD3-/- mice had impaired rCBF upon early reperfusion but comparable functional outcomes; PHD1-/- mice did not show any significant changes following MCAO. When receiving FG2216 one day before the MCAO, C57/B6 mice had better neuroscores and smaller infarct volumes than those receiving the vehicle (Neuroscores: 2.0±0.6 vs 4.5±0.3; Infarct volumes: 27.0±8.1%

vs 47.4±5.3%, both p<0.05). No significant difference was seen in mice if receiving FG2216 immediately before the MCAO. Genetic inhibition of PHD enzymes produces different effects on outcome after transient cerebral ischemia. Notably, partially knock-out PHD2 confers neuroprotection for cerebral ischaemia. These effects are seen following lifelong PHD deficiency and thus reflect a composite of developmental changes, affecting features such as vessel density and overall sympathetic tone. While Fg2216 induces acute HIF activation amplifying the hypoxic stimuli inherent in this ischaemic/reperfusion model which could contribute to the observed protection. HIF activation upon ischaemic injury is swift, but the HIF transcription is delayed (Sharp FR, et al. 2004). Our study needs to be considered in optimizing therapeutic effects of PHD inhibitors, particularly when isoform specific inhibitors become available.

Sharp FR, et al. 2004, NeuroRx. 1(1): 26–35.

Sridharan V, et al. 2007, Am J Physiol Cell Physiol 292 (2): C719-C728.

We thanks Dunhill Medical Trust and MRC for generous financial support.

Where applicable, the authors confirm that the experiments described here conform with The Physiological Society ethical requirements.

PCA142

Role of Rac1/NADPH oxidase in staurosporine-induced neurite outgrowth in PC12 cells

D. Kim, J. An, J. Kang and J. Seo

Yonsei University College of Dentistry, Seoul, Republic of Korea

Neurite outgrowth, which is the most distinct process during neuronal differentiation and regeneration, is an essential aspect of neuronal plasticity. PC12 cells have provided a number of clues about the signaling pathways involved in neurite outgrowth. PC12 cells differentiate into neuron-like cells in response to various stimuli, such as nerve growth factor (NGF) and staurosporine. The ERK signaling pathways play important roles in NGF-induced differentiation of PC12 cells. In contrast to NGF, however, the mechanism for staurosporine-induced neurite outgrowth is still unknown. In the present study, therefore, we examined the mechanisms by which staurosporine triggers neurite outgrowth. Images of living cells were obtained using a CCD camera and morphometric analysis was performed using Image-Pro Plus software. To assess direct modulation of Rac1 activity by staurosporine, the amount of cellular GTP-bound Rac1 was measured using the GST-PAK-CRIB binding assay. NADPH oxidase activity was measured by lucigenin chemiluminescence-based assay and the level of intracellular reactive oxygen species (ROS) was measured in cells loaded with DCF-DA using a confocal microscope. The statistical significance of differences between experimental groups was determined using an unpaired Student's t-test or one-way ANOVA and Bonferroni's test as appropriate. The results are expressed as means ± standard error of the mean (S.E.M.).

Staurosporine caused rapid neurite outgrowth independently of ERK signaling pathways. In contrast, neurite outgrowth in response to 100 nM staurosporine was accompanied by a 227.9 ± 23.9 % increase in Rac1 activity (p<0.05, n = 3), and the Rac1 inhibitor NSC23766 attenuated the staurosporine-induced neurite outgrowth in a concentration-dependent manner. In addition, suppression of Rac1 activity by expression of the dominant negative mutant Rac1N17 also blocked the staurosporine-induced neurite outgrowth of PC12 cells. Staurosporine caused a 75.4 ± 11.9 % increase in NADPH oxidase activity (p<0.05, n = 5) and increased the ROS production approximately by 150 ± 50 % (p<0.05, n = 5), which was prevented by NSC23766 and diphenyleneiodonium (DPI), an NADPH oxidase inhibitor. Pretreatment of cells with DPI attenuated the staurosporine-induced neurite outgrowth by 66.8 ± 4.2 % (p<0.05, n = 5) and exogenous addition of 100 μM H2O2 accelerated the 10 nM staurosporine-triggered neurite outgrowth by 92.3 ± 9.8 % (p<0.05, n = 7). These results indicate that activation of Rac1/NADPH oxidase, which leads to ROS generation, is required for neurite outgrowth induced by staurosporine in PC12 cells.

This work was supported by the Basic Science Research Program through the National Research Foundation of Korea (NRF) funded by the Ministry of Education, Science, and Technology (2011-0012294).

Where applicable, the authors confirm that the experiments described here conform with The Physiological Society ethical requirements.

PCA143

Lidocaine unmasks L-type Ca^{2+} current-mediated action potentials in rat thalamocortical neurons

I. Putrenko[1,2] and S.K. Schwarz[2]

[1]Cellular and Physiological Sciences, The University of British Columbia, Vancouver, BC, Canada and [2]Anesthesiology, Pharmacology and Therapeutics, The University of British Columbia, Vancouver, BC, Canada

The mechanisms underlying the systemic central nervous system (CNS) toxicity of lidocaine are still largely obscure and not solely explained by its classic action on Na^+ channels. Here, we examined the hypothesis that Na^+ channel-independent actions of lidocaine in the thalamus, a brain area previously implicated as a site for lidocaine's systemic effects, contribute to its CNS toxicity. We investigated the effects of lidocaine at clinically CNS-toxic concentrations (100–600 μM) on firing properties of rat thalamocortical neurons in brain slices (250 μm) *in vitro*, using whole cell patch-clamp recording techniques. Brain slice preparations containing ventrobasal thalamic neurons were obtained from Wistar rats at postnatal days 13–16. Results are expressed as mean ± SEM and compared to control values by one-sample *t* tests, unless mentioned otherwise. Bath application of 100 μM lidocaine abolished typical tonic firing elicited in neurons current-clamped at –58 mV and evoked a distinct regular firing characterized by a more depolarized (higher) activation threshold (mean ± SD, –20.5 ± 8.4 mV vs. –44.3 ± 3 mV; $n = 12$; paired Student's t test, $P < 0.001$) and a different spike configuration. The high-threshold (HT) potentials disappeared completely when superfusing medium was either deprived of Ca^{2+} or contained the high voltage-activated Ca^{2+} channel blocker Cd^{2+} (50 μM). The specific L-type Ca^{2+} channel blocker, nifedipine, at 5 μM, but not at 1 μM, completely blocked the HT potentials, whereas the N-type Ca^{2+} channel blocker, ω-conotoxin GVIA (1 μM) had little effect on them. Neurons pretreated with tetrodotoxin (TTX, 600 nM), a tonic blocker of voltage-gated Na^+ channels, also exhibited regular firing of HT potentials. Their firing rate after reaching a maximum decreased in response to an increase in the magnitude of injected current due to the activation of a slowly recovering after-hyperpolarization (AHP) of the holding membrane potential. Application of lidocaine abolished the

AHP and caused neurons to respond to an increase in the magnitude of injected current with increased rate of HT firing. Furthermore, lidocaine, at 600 μM, increased input resistance in TTX-pretreated neurons by 86 ± 9% (n = 4; P < 0.001) and reduced the magnitude of current pulses required to trigger HT potentials by 24 ± 7% (n = 4; P < 0.05).

We conclude that lidocaine at clinically CNS-toxic concentrations unmasks Ca^{2+}-dependent HT action potentials mediated by L-type Cav1.2 channels. Inhibition by lidocaine of the hyperpolarization-activated mixed cationic current, I_h, and K^+ conductance(s) mediating slow AHPs[1], likely underlies its stronger unmasking effects compared to TTX. Overall, our findings support the notion that impaired Ca^{2+} homeostasis contributes to the complex and multifaceted mechanisms of supraspinal CNS toxicity of systemic lidocaine *in vivo*.

Putrenko I & Schwarz SK (2011). *Anesthesiology* **115**, 822-835.

Where applicable, the authors confirm that the experiments described here conform with The Physiological Society ethical requirements.

PCA144

Developmental changes of TRPV1 expression in C57BL/6 mice brain

W. Huang[1], F. Yu[2], X. He[1] and B. Peng[1]

[1]Physiolgoy, Wuhan University,Basic Medical Sciences, Wuhan, China and [2]Wuhan University, Zhongnan Hospital, Wuhan, Hubei, China

TRPV1 is a polymodel non-selective cation channel that can be activated by capsaicin, pH, heat and other noxious stimuli. In the last few years, expression of trpv1 has been certified in variety tissue and apparented different with species. However, distribution of trpv1 in the CNS is still a controversial question.Increasing evidences has demonstrated important role of TRPV1 in central system diseases, however the functions of TRPV1 in the brain are still an open question. Tom Schilling revealed that TRPV1 cation channels may provide potential therapeutic targets to reduce microglia-induced oxidative stress in Alzheimer's disease (AD). Clinical data showed that TRPV1 mRNA and protein were up-regulated in the mesial temporal lobe epilepsy patients. Our research aims to detect the expression of TRPV1 in hippocampus and cortex on developmental brain in C57BL/6 mice and explore the potential drug therapeutic targets in the age-dependent diseases. Mice model was using differential development C57BL/6 mice: 2-week old (n=12), 4-week old (n=12), 8-week old (n=12) and 16-week old (n=12) mice, respectively corresponded to infancy, adolescence, adult stage and gerontic in human. Detecting the expression of TRPV1 mRNA and protein were respectively by qRT-PCR, western blotting and immunohistochemistry. Values are means ± S.E.M., compared by nonparametric tests. Our findings revealed that trpv1 channel express in both two brain regions in C57B/6 mouse showing age-dependent. Comparing to 2-week old mouse in hippocampus, the mRNA level of 4,8,16 weeks old mice are increased, the relative expression in those groups are enhanced separately by 1.93 fold,11.43 fold and 1.8 fold ($^*p<0.05$). In cortex, the difference multiple of 4,8,16 weeks old mice were about 2.66 fold, 3.02 fold and 2.21 fold compared to 2 weeks old mice, respectively. In addition, protein level of 4,8,16 weeks old mice in hippocampus and cortex from western blotting and immunohitochemistry both increased comparing to 2 weeks old mouse, in keeping with mRNA level both in hippocampus and cortex. These results indicated that TRPV1 expression in developing brain showed an age-dependence pattern, thus raised the possibility that TRPV1 may play a key role related to age and developing brain diseases. Our study provides a basis for further studies of TRPV1 as a possible newly pharmacology target for age-dependent diseases such as Alzheimer's disease, parkinson's disease, age-dependent epileptic encephalopathy and febrile seizures.

Corresponding author Peng Biwen is the recipient of the travel awards for young physiologists from the Chinese Association for Physiological Sciences (CAPS).

This work were supported by National Natural Sciences Foundation of China No. 81100970, 81171127; Natural Science Foundation of Hubei Province of China (2011CDB465, 2010CDA045)

Where applicable, the authors confirm that the experiments described here conform with The Physiological Society ethical requirements.

PCA145

Glucagon-like peptide-1 and exendin-4 change neuronal excitability by modulating currents through $GABA_A$ channels

S. Korol, Z. Jin and B. Birnir

Department of Neuroscience, Uppsala University, Uppsala, Sweden

GABA signaling plays an important role in the regulation of neuronal activity in the mammalian brain. The hippocampus has a high density of receptors for metabolic hormones (Lathe, 2001) which may affect neuronal excitability. It has been shown that insulin influences GABA signaling in the hippocampus (Wan et al., 1997, Jin et al., 2011). Glucagon-like peptide-1 (GLP-1) is another metabolic hormone, secreted by intestinal L-cells, that affects brain function (During et al., 2003, Acuna-Goycolea and van den Pol, 2004). We have examined whether GLP-1 and its analog exendin-4 (Ex-4) can modulate GABA-evoked responses and neuronal excitability in CA3 pyramidal neurons of the rat hippocampus. We used the whole-cell patch-clamp technique in voltage-clamp or current-clamp mode to record GABA-activated currents or change in the membrane potential and action potential (AP) frequency in hippocampal slices from 16–20 days old Wistar rats. Administration of GLP-1 (10 pM–10 nM) or Ex-4 (10–100 nM) evoke tonic GABA-activated currents and increased the frequency of synaptic GABA-activated currents as compared to control. Values are means ± S.E.M., compared by ANOVA. In control conditions tonic currents were 3.3 ± 4.4 pA (n = 5) and were about ten times larger after application of 100 nM Ex-4 (33.8 ± 5.6 pA; n = 5; P < 0.001). The frequency of synaptic GABA-induced currents increased by 96 ± 35 % when neurons were exposed to 10 nM Ex-4 (n = 5; P < 0.05). AP firing frequency decreased and neuronal membrane potential hyperpolarized upon GLP-1 application. When GLP-1 has been washed away membrane potential depolarized back to the initial value (Fig. 1). Our results demonstrate that GLP-1 and Ex-4 enhance GABA signaling that leads to decreased neuronal excitability in rat hippocampal CA3 pyramidal neurons.

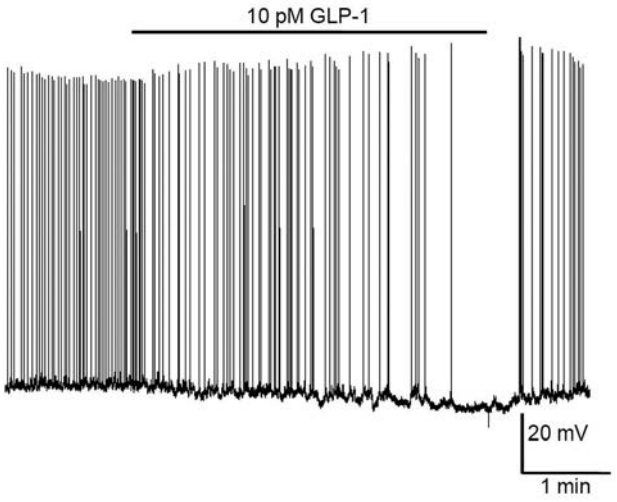

Figure 1. GLP-1 hyperpolarizes the membrane potential and decreases action potential frequency in CA3 pyramidal neurons of the rat hippocampus.

ACUNA-GOYCOLEA, C. & VAN DEN POL, A. 2004. Glucagon-like peptide 1 excites hypocretin/orexin neurons by direct and indirect mechanisms: implications for viscera-mediated arousal. J Neurosci, 24, 8141-52.

DURING, M. J., CAO, L., ZUZGA, D. S., FRANCIS, J. S., FITZSIMONS, H. L., JIAO, X., BLAND, R. J., KLUGMANN, M., BANKS, W. A., DRUCKER, D. J. & HAILE, C. N. 2003. Glucagon-like peptide-1 receptor is involved in learning and neuroprotection. Nat Med, 9, 1173-9.

JIN, Z., JIN, Y., KUMAR-MENDU, S., DEGERMAN, E., GROOP, L. & BIRNIR, B. 2011. Insulin reduces neuronal excitability by turning on GABA(A) channels that generate tonic current. PLoS One, 6, e16188.

LATHE, R. 2001. Hormones and the hippocampus. J Endocrinol, 169, 205-31.

WAN, Q., XIONG, Z. G., MAN, H. Y., ACKERLEY, C. A., BRAUNTON, J., LU, W. Y., BECKER, L. E., MACDONALD, J. F. & WANG, Y. T. 1997. Recruitment of functional GABA(A) receptors to postsynaptic domains by insulin. Nature, 388, 686-90.

Where applicable, the authors confirm that the experiments described here conform with The Physiological Society ethical requirements.

PCA146

Long-term potentiation of excitatory synaptic transmission from primary afferents or descending inputs to neonatal rat spinal cord motoneurons in vitro

M. Wang, Y. Su, X. Jiang, J. Jin, H. Zhang, H. Luo and Y. Zhang

Cell Electrophysiology Laboratory, Wannan Medical College, Wuhu, Anhui Province, China

In an in vitro spinal cord preparation, our previous study and other reports have identified excitatory postsynaptic potentials (EPSPs) in motoneurons (MNs) evoked by ipsilateral dorsal root (iDR)[1], ipsilateral ventrolateral funiculus (iVLF)[2,3], and contralateral VLF (cVLF)[4] stimulation, i.e. iDR-EPSPs, iVLF-EPSPs and cVLF-EPSPs, respectively. But the long-term synaptic plasticity in these synaptic transmissions has been little studied yet. In the present study, the intracellular recordings were performed from MNs in neonatal rat (8-14 days old) spinal cord slices prepared by the previously described procedures under anaesthetized state with ether [5], and membrane electrical parameters were observed. By monitoring the multi-parameter changes of EPSPs after tetanic stimulation on iDR, iVLF or cVLF, efficiency of the excitatory synaptic transmission to MNs were estimated. The increase in EPSP amplitude to more than 120% of control level and at least for 30 min could be referred to as long-term potentiation (LTP). After tetanic stimulation on iDR in 26 MNs, LTP of iDR-EPSPs (i.e. iDR-LTP) was observed in 17 cells, without increase in amplitude of iVLF-EPSPs recorded simultaneously in the same MNs (n=15). Moreover, some relevant changes such as the increase of area under curve, the prolonging of duration and the shortening of latency of iDR-EPSPs but not of iVLF-EPSPs in 15 tested MNs were comparably noted during the iDR-LTP. Similarly, the tetanic stimulation on iVLF and cVLF induced LTP of iVLF-EPSP (iVLF-LTP) in 11 cells of 33 tested MNs, and of cVLF-EPSP (cVLF-LTP) in 2 MNs, respectively. It was also noted that in one MN with cVLF-LTP, the simultaneously recorded iDR-EPSPs were potentiated to reach the criteria for LTP either, suggesting a heterosynaptic LTP. Among 9 tested MNs with iVLF-LTP, the paired-pulse facilitation ratios of amplitude of iVLF-EPSPs elicited by paired-pulse stimulation were different from the baseline in 7 MNs. Considered as a whole, there were no significant changes in the membrane electrical parameters of the tested MNs following induction of LTP. These preliminary data suggest that there may be some forms of LTP in excitatory synaptic transmission from peripheral afferents and descending fibers to MNs in the spinal cord, and it could be considered as a candidate of neural basis underlying the ability of motor learning.

Jiang ZG, Shen E, Dun NJ. Excitatory and inhibitory transmission from dorsal root afferents to neonate rat motoneurons in vitro. Brain Res 1990; 535:110-118.

Wang MY. Responses of motoneurons to ventrolateral funiculus stimulation in neonate rat spinal cord slices. Acta Physiol Sin 1994; 46: 148-153.

Pinco M, Lev-Tov A. Synaptic transmission between ventrolateral funiculus axons and lumbar motoneurons in the isolated spinal cord of the neonatal rat. J Neurophysiol 1994; 72: 2406-2419.

Zhang Y, Jiang X, Wang MY. Synaptic responses of motoneurons evoked by contralateral ventrolateral funiculus stimulation in neonatal rat spinal cord slices. J Wannan Med Univ 2008; 27: 316-323.

Wang MY, Dun NJ. 5-Hydroxytryptamine responses in neonate rat motoneurones in vitro. J Physiol 1990; 430: 87-103.

Project is supported by NSF of China (31271155, WMY).

Where applicable, the authors confirm that the experiments described here conform with The Physiological Society ethical requirements.

PCA147

The Angelman syndrome protein Ube3a regulates synapse development by ubiquitinating Tkv in *Drosophila*

A. Yao, W. Li, H. Zhi, Y. Zhang and K. Kaur

The Institute of Genetics and Developmental Biology of the Chinese Academy of Sciences, Beijing, China

Angelman syndrome (AS) is a neurodevelopmental disorder characterized by severe mental retardation, motor dysfunction, lack of speech, ataxia and developmental delay. It is caused by the absence of ubiquitin ligase Ube3a which is involved in protein degradation through the ubiquitin-associated proteasome-mediated pathway. Ube3a was also associated with autism spectrum disorder. However, little is known about how the loss-of-function of ube3a results in the pathogenesis of AS. Drosophila has a unique homolog of Ube3a, encoded by ube3a. We found that the number of both total boutons and satellite boutons in ube3a mutants was significantly increased compared with wild type. FM1-43 dye-load-

ing assay showed that ube3a mutants had an endocytosis defect in the NMJ synapses. Furthermore, electrophysiological analysis under high-frequency stimulation showed compromised neurotransmission in ube3a mutant synapses, confirming an insufficient replenishment of synaptic vesicles. These data suggest that ube3a regulates synapse morphology and function. Genetic interaction showed that heterozygous mutants of tkv, encoding the BMP receptor thickveins, rescued the synapse phenotype of ube3a mutants. Immunochemical analysis showed Tkv expression level was increased in ube3a mutants. Co-IP experiments showed that Tkv and Ube3a are present in a complex. Tkv can be ubiquitinated by Ube3a in S2 cells. Interestingly, overexpression of Ube3a also led to an increased number of total boutons and satellite boutons and increased Tkv protein level, suggesting that proper level of Ube3a is critically important for the normal synapse development. Our results suggested that Ube3a regulates BMP signaling pathway to control synapse development. These may partialy accounted for the pathological mechanism of Angelman syndrome.

Where applicable, the authors confirm that the experiments described here conform with The Physiological Society ethical requirements.

PCA149

A TRPV channel controls presynaptic Ca^{2+} concentration to regulate presynaptic growth and synaptic vesicle release probability

C. Wong[1], Y. Lin[2], K. Chen[2], G.T. Broadhead[1], L. Duraine[2], A. Ganguly[1], F. Cabral[1], H.J. Bellen[2] and K. Venkatachalam[1]

[1]Department of Integrative Biology and Pharmacology, University of Texas School of Medicine, Houston, TX, USA and [2]Departments of Molecular and Human Genetics and Neuroscience, Baylor College of Medicine, Houston, TX, USA

Presynaptic Ca^{2+} regulates many processes related to neurotransmission including synaptic vesicle (SV) release and endocytosis. However, the role of Ca^{2+} in other aspects of presynaptic function is incompletely understood. Furthermore, the repertoire of Ca^{2+} channels functioning at the synapse remains unknown. In a screen evaluating the roles of TRP channels in *Drosophila* larval neuromuscular junction function and development, we found that the TRPV channel, Inactive (Iav), functions presynaptically to regulate both synaptic growth and SV release probability. We found that the Iav-deficient (*mut*) synapses have a reduced number of presynaptic boutons (number of boutons, *mut* = 33.8±2.4, wild-type (*wt*) = 67.7±4.1, $p<0.05$, all data presented as mean ±SEM and analyzed by ANOVA hereafter) and a concomitant increase in bouton size (bouton volume, *mut* = 320.6 ±74.9 μm^3, *wt* = 142.2±31.5, $p<0.05$). Biochemical and high-resolution imaging experiments revealed that the mutant boutons were characterized by diminished microtubule polymerization (polymerized microtubule percentage, *mut* = 6.6±0.02%, *wt* = 20±0.02, $p<0.05$). Furthermore, we found that calcineurin A1 (CanA1) deficient synapses displayed similar phenotypes. More importantly, expression of constitutively active CanA1 in Iav-deficient motor neurons suppressed the growth defects (bouton number, *mut* expressing CanA1 = 61.2±1.9, *mut* control = 42.9±1.6, $p<0.05$). These data indicate that CanA1 stabilizes microtubules downstream of Iav. Remarkably, expressing human TRPV1 in the Iav-deficient motor neurons rescued the synaptic growth phenotypes (bouton number, *mut* expressing TRPV1 = 67.7±3.2, *mut* controls = 43.3±2.5, $p<0.05$). Examination of the subcellular distribution of Iav and TRPV1 in the motor neurons revealed that both proteins were localized to ER. Furthermore, we found that Iav regulates resting Ca^{2+} levels in motor axon terminals, and the loss of Iav results in a decrease in the amplitudes of evoked excitatory junction potentials (EJP) (*mut* = 12.4±1.1 mV, *wt* = 25.8±2.7, $p<0.05$). Further studies revealed that the SV release probability was markedly diminished in the absence of Iav, and this decrease in release probability underlies the decreased EJP amplitude. Indeed, elevating extracellular Ca^{2+} levels to increase SV release probability suppressed the EJP defect. Interestingly, overexpression of Iav increased SV release probability and EJP amplitudes. Thus, Iav is both necessary and sufficient to determine SV release and function, indicative of the vital role of the protein in neurotransmission. In summary, by releasing ER Ca^{2+}, Iav serves two physiologically distinct and separable functions. First, it regulates synaptic architecture and growth by promoting microtubule polymerization. Second, it determines SV release probability and the strength of synaptic transmission.

Where applicable, the authors confirm that the experiments described here conform with The Physiological Society ethical requirements.

PCA151

The over-expression of TNF-α differentially modulates the synaptic connection in hippocampus and in spinal dorsal horn following peripheral nerve injury

X. Liu, W. Ren, Y. Liu, J. Wang and L. Zhou

Department of Physiology, Zhongshan Medical School of Sun Yat-Sen University, Guangzhou, China

Around 2/3 chronic pain patients suffer from memory deficits and underlying mechanisms are unclear. We have shown that over-expression of TNF-αproduced by spared nerve injury (SNI) leads to both neuropathic pain and impairment of short-term memory (Ren, et al., 2011). In the present work with whole-cell patch-clamp electrophysiology and a single-neuron staining by an intracellular injection of biocytin for morphological analysis, we found that SNI reduced the synaptic connection and NMDA receptor current in hippocampal CA1 pyramidal neurons but increased them in NK-1-positive projection neurons in superficial spinal dorsal horn, and the effect was prevented by genetic deletion of TNFR1. TNF-α mimicked the effect of SNI in cultured hippocampal and spinal cord slices. Mechanistically, brain derived neurotrophic factor (BDNF), which is critical for synaptic formation and plasticity, was down-regulated in hippocampus but up-regulated in spinal dorsal horn following SNI. TNF-α also has the similar effect on BDNF expression in cultured hippocampal and spinal cord slices. Thus, the differential change in synaptic structure and function in hippocampus and in spinal dorsal horn may underlie chronic pain and the memory deficits following peripheral nerve injury. The opposite regulation of BDNF by TNF-αmay be critical for pathological process.

Ren WJ, Liu Y, Zhou LJ, Li W, Zhong Y, Pang RP, Xin WJ, Wei XH, Wang J, Zhu HQ, Wu CY, Qin ZH, Liu G, Liu XG. Peripheral nerve injury leads to working memory deficits and dysfunction of the hippocampus by upregulation of TNF-alpha in rodents. Neuropsychopharmacology 2011; 36:979-992.

Mutso AA, Radzicki D, Baliki MN, Huang L, Banisadr G, Centeno MV, Radulovic J, Martina M, Miller RJ, Apkarian AV. Abnormalities in hippocampal functioning with persistent pain. J Neurosci 2012; 32:5747-5756.

Funding/Support: This work was supported by grants from the National Natural Science Foundation of China (No. U1201223, 30970957 and 31000489) and a grand from the bureau of science and technology of Guangzhou city (No. 50000-4205009).

Li-Jun Zhou is a recipient of the travel awards for young physiologists from the Chinese Association for Physiological Sciences (CAPS).

Where applicable, the authors confirm that the experiments described here conform with The Physiological Society ethical requirements.

PCA152

Serotonin-induced presynaptic inhibition of GABAergic transmission onto cholinergic neurons in the rat basal forebrain

T. Momiyama[1] and T. Nishijo[1,2]

[1]Department of Pharmacology, Jikei University School of Medicine, Tokyo, Japan and [2]Department of Pharmacology, Keio University School of Pharmacy, Tokyo, Japan

A Whole-cell patch-clamp study was carried out to elucidate modulatory roles of serotonin (5-HT) in GABAergic transmission onto basal forebrain cholinergic neurons, using brain slice preparations obtained from P12-19 rat under deep anesthesia with halothane. Animal handling and all experimental procedures were done according to the Guiding Principles for the care and Use of Animals in the Field of Physiological Sciences of the Physiological Society of Japan (2009), the UK Animals (Scientific Procedures) Act 1986, and the guidelines of Jikei University School of Medicine. GABAA receptor-mediated inhibitory postsynaptic currents (IPSCs) were evoked by focal electrical stimulation in the presence of CNQX, D-AP5 and strychnine to block non-NMDA-, NMDA- and glycine receptor-mediated currents components, respectively. Bath application of 5-HT reduced the amplitude of the evoked GABAergic IPSCs in a concentration-dependent manner between 0.1-100 μM The inhibition of IPSCs by 0.1, 1, 10 and 100 μM 5-HT was 21.1 ± 9.17 % (n=6), 35.2 ± 5.52 % (n=5), 58.5 ± 2.36 % (n=41) and 64.1 ± 5.46 % (n=4), respectively. A 5-HT1B receptor agonist, CP93129 (10 μM) also suppressed the IPSCs by 59.8 ± 9.25 % (n=5), whereas a 5-HT1A receptor agonist, 8-OH-DPAT, had no effect. NAS-181, a 5-HT1B receptor antagonist antagonized the 5-HT-induced suppression of IPSCs, whereas NAN-190, a 5-HT1A receptor antagonist did not. 5-HT (1 μM) reduced the frequency of spontaneous miniature IPSCs (mIPSCs) by 52.0 ± 9.85 % (n=6) without changing their amplitude distribution. This effect remained unchanged when extracellular Ca2+ was replaced by Mg2+ (5 mM). In the presence of ω-Aga-TK, ω-CgTX, or SNX-482, an N-, P/Q- or R-type calcium channel blocker, respectively, 5-HT could still inhibit the IPSCs. These findings suggest that activation of presynaptic 5-HT1B receptors on the terminals of GABAergic afferents to basal forebrain cholinergic neurons inhibits GABA release in Ca2+-independent manner.

This work was supported by a Grant-in-Aid for Scientific Research from the Ministry of Education, Culture, Sports, Science and Technology of Japan (no. 24500464) and The Jikei University Graduate Research Fund to TM.

Where applicable, the authors confirm that the experiments described here conform with The Physiological Society ethical requirements.

PCA153

A role for whirlin in proprioceptor mechanotransduction

J. de Nooij[1], A. Simon[2], S. Doobar[1], K.P. Steel[3], T. Jessell[1], R.W. Banks[4] and G.S. Bewick[2]

[1]Department of Biochemistry & Molecular Biophysics, Columbia University, New York, NY, USA, [2]School of Medical Sciences, University of Aberdeen, Aberdeen, UK, [3]Wolfson Centre for Age-Related Diseases, King's College London, London, UK and [4]School of Biological & Biomedical Sciences, University of Durham, Durham, UK

Information on muscle length and tension are essential for the central nervous system to determine the position of body and limbs in space. This is a necessary prerequisite for co-ordinated motor behaviour. This proprioceptive sense is mediated by specialised mechanoreceptors located within the muscle: the muscle spindle (responsive to changes in muscle length) and Golgi tendon organs (responsive to changes in muscle tension). Anatomical and physiological analysis have provided many insights into the properties of the proprioceptor muscle afferents that innervate these mechanoreceptors but the molecular mechanisms that underlie the mechanotransduction process remains largely unknown. Here we show that the PDZ – scaffold protein Whirlin is expressed in proprioceptor neurones in dorsal root ganglia and localises to their peripheral sensory endings. Whirlin mutations have previously been implicated in abnormalities of hair cell and photoreceptor sensory transduction, particularly Usher syndrome (1), raising the possibility that Whirlin also functions in the proprioceptive mechanotransduction process. Recording afferent nerve discharge from an *in vitro* mouse soleus muscle/nerve preparation, we find that the activation of spindle afferents by mechanical stretch is greatly diminished in *whirlin* (*wi*) mutant mice (2) compared to their wild-type (*wt*) littermates (33.6 ± 10.4 Hz, *10* v 106.2 ± 28.2 Hz, *6*; mean ± SE, *n*; $P<0.01$, paired t-test). Application of exogenous glutamate (1 μM) restores afferent excitability in response to stretch (111.1 ± 43.0 Hz, NS v *wt*). Amiloride (10 μM, an inhibitor of DEG/ENaC channels) and PCCG – 13 (1 μM, blocking atypical metabotropic glutamate receptors in mechanosensory endings (3)) reduced the glutamate-mediated enhancement in *wt* animals (from 205.1 ± 74.2 Hz to 95.4 ± 38.0 Hz, *4* (amil) & from 268.7 ± 37.9 Hz to 207.5 ± 43.8 Hz, *6* (PCCG); both $P<0.05$) but have comparatively less effect on the stretch – evoked spike frequency in *wi* mutants (to 99.8 ± 27.4 Hz, *6* & 93.2 ± 29.5 Hz, *8*; both NS v 1 μM glutamate). Together, these data indicate that essential components of proprioceptor mechanotransduction machinery are present but operate inefficiently in the absence of Whirlin function. Whirlin may serve to recruit and/or ensure the proper localisation of transduction molecules in proprioceptor sensory terminals.

van Wijk E *et al.* (2006). *Hum Mol Genet* **15**, 751-765.

Mogensen MM, Rzadzinska A, Steel KP (2007). *Cell Motil Cytoskeleton* **64**, 496-508.

Bewick GS, Reid B, Richardson C, Banks RW (2005). *J Physiol*. **562**, 381-394.

Where applicable, the authors confirm that the experiments described here conform with The Physiological Society ethical requirements.

PCA154

Clathrin and its role in fast endocytosis in retinal bipolar cells and hippocampal neurons

M. Pasche[1], I. Pelassa[2], C. Zhao[3], B. Odermatt[4] and L. Lagnado[1]

[1]Neurobiology, MRC - LMB, Cambridge, UK, [2]Neuroscience Department, Universita' di Torino, Turin, Italy, [3]Southwest Eye Hospital - Lab of Neurobiology, Third Military Medical University, Chong Qing, China and [4]Neuroanatomie, Rheinische Friedrich-Wilhelms-Universität, Bonn, Germany

The classical mode of clathrin-mediated endocytosis in non-neuronal cells occurs on the time-scale of a minute while retrieval of synaptic vesicles usually occurs 1-10 s after fusion. To investigate the molecular dynamics of fast endocytosis, we applied dual-colour total internal reflection fluorescence and confocal microscopy to ribbon synapses of retinal bipolar cells. These cells were derived from transgenic zebrafish expressing either combination of two of the following fluorescently labelled proteins: the fusion reporter sypHy, clathrin-eGFP/mCherry and/or the synaptic ribbon marker ribeye-mCherry.

In bipolar cells we made three striking observations. 1) Calcium-triggered fusion events happen mainly at the rim of synaptic ribbons – highly specialized release sites – and are correlated in time with an increase in the clathrin signal. 2) Individual clathrin events occur significantly further away from ribbons. 3) Two different kinds of clathrin events could be recorded. The first was a sudden decrease in the clathrin signal, signifying movement of clathrin-coated structures away from the plasma membrane. The second signal was an immediate recruitment of clathrin to the membrane colocalized with sites of vesicle fusion.

Findings obtained by fluorescence correlation spectroscopy in both bipolar cell terminals and hippocampal neurons showed that the synaptic vesicle marker synaptophysin was associated with clathrin on the same relatively slowly diffusing structures. Only about 25% of the total clathrin was diffusing freely in the cytosol. These results were also verified by fluorescence recovery after photobleaching.

Taken together our results from ribbon and hippocampal synapses indicate that clathrin is associated with synaptic vesicles even before a fusion event. This may provide a mechanism for priming vesicles of the readily releasable pool for the fast mode of endocytosis, making them readily retrievable.

Where applicable, the authors confirm that the experiments described here conform with The Physiological Society ethical requirements.

PCA156

A novel technique that combines single cell electroporation with extracellular recordings *in vitro* and *in vivo*

B.R. Dempsey, L. Bou Farah, A.J. Turner and S. McMullan

Australian School of Advanced Medicine, Macquarie University, Sydney, NSW, Australia

Single cell electroporation (SCE) is an electrophysiological technique that uses trains of voltage pulses to disrupt the cell membrane and simultaneously drive macromolecules such as fluorescent dyes or DNA into a target cell. SCE has emerged as an important step in developing 'connectomic' technology that can resolve the architecture of neuronal networks in single cell resolution [1]. However, two key limitations restrict the applicability of SCE. Firstly, SCE requires direct visualisation of target neurons, limiting its use *in vivo* to regions of the brain that can be resolved optically. Secondly, SCE is incompatible with standard electrophysiological recording techniques, meaning that data from electroporated cells cannot be interpreted in light of their functional properties. In the current study we validate a novel technique that combines single cell electroporation with extracellular recording, permitting functional identification of neurons prior to electroporation with fluorescent dextrans or plasmids encoding a variety of genes.

Methods: *In vitro* experiments were conducted on acute or cultured brain slices obtained from neonatal (P5-10) rat pups. Rats were deeply anaesthetised with isoflurane and killed by decapitation. *In vivo* experiments were conducted on urethane anaesthetised (acute experiments: dextran) or isoflurane anaesthetised (recovery experiments: plasmid) adult rats (300 – 500 g). Borosilicate pipettes filled with either fluorescent dextran or plasmid solutions were used to obtain extracellular recordings from single neurons. Once physical contact between pipette and cell was established the recording amplifier was programmed to deliver a train of current pulses through the pipette, using pipette resistance to calculate the current required to generate the desired voltage (7.5 V: dextran, -12 V: plasmid).

Results: Dextran labelling was achieved in >95% of cells (N>40) recorded *in vitro*, provided the pipette was within 6 μm of the target cell. *In vivo* successful electroporation was obtained in 48/105 spontaneously active brainstem neurons recorded up to 9 mm deep . Preliminary experiments using plasmid DNA in the recording solution indicate that the same principle is compatible with single cell gene delivery: fluorescent proteins are transcribed within 18 hours of electroporation in cultured neurons and *in vivo*, although further refinements are required to improve the reliability of this approach.

Conclusion: We have developed a technique that combines SCE with extracellular recording, negating the need for optical guidance and permitting functional identification of target neurons prior to electroporation. This technique will permit the application of novel genetic techniques to physiologically characterised neurons.

Marshel, J.H., et al., Targeting Single Neuronal Networks for Gene Expression and Cell Labeling In Vivo. Neuron, 2010. 67(4): p. 562-574.

This work is supported by the Australian Research Council and Macquarie University.

Where applicable, the authors confirm that the experiments described here conform with The Physiological Society ethical requirements.

PCA157

Neuregulin-2 regulates synaptogenesis in hippocampal newborn granule cells

K. Lee[1], H. Lee[1], C. Yang[1], C. Park[2], W. Ho[1] and S. Lee[1]

[1]Physiology, Seoul Nat'l Univ. College of Medicine, Seoul, Republic of Korea and [2]Hanyang Biomedical Research Institute, Hanyang University, Seoul, Republic of Korea

Neuregulin-2 (NRG2) has been identified as a member of the family of growth factor that contains an EGF-like domain with its domain structure similar to NRG1. NRG1 and NRG2 are expressed in distinct cell populations in the brain. Unlike the expression of NRG-1 which is sporadic but widespread over

the brain, NRG2 is expressed in a few restricted regions in the brain including the hippocampal dentate granule cell (GC) layer. NRG2 has been implicated in proliferation of neural stem cells in the subventricular zone, but it is little understood whether NRG2 plays a role in synaptogenesis, which is essential for newborn neurons to be integrated into a preexisting neural circuit. Using retrovirus encoding GFP and RNAi against NRG2, we studied the role of NRG2 in development of GFP-labeled newborn GCs in rat organotypic hippocampal culture. To study the role of NRG2 in synpatogenesis, we infected the organotypic cultured hippocampal slice with retrovirus encoding NRG2-targeting miRNA cloned downstream of tetracycline-response element (TetOn-miNRG-2). Newborn GCs infected with such retrovirus displayed significantly lower expression of NRG2 after treatment with doxycycline (dox) than non-treated newborn GCs as a control. To assess the synaptic development in newborn GCs, we recorded GABAergic or glutamatergic postsynaptic current (GPSC or EPSC) induced by stimulation of the perforant pathway. Under the control conditions, the amplitude of GPSC started to increase from 7th day post-infection (7dpi) and reached a plateau level at 10dpi. Treatment of doxycycline from 4dpi abolished such a steep increase in the GPSC amplitude. Accordingly, immunohistochemistry using anti-VGAT revealed that the number of GABAergic presynaptic terminals on the soma of newborn GCs was lower in the dox-treated hippocampal slice than the control slice. In contrast, dox-treatment from 7dpi or 10dpi displayed no significant effect on GPSC, suggesting NRG2 plays essential role in GABAergic synapse formation at 4~7dpi but not in its maintenance after 7dpi. The amplitude of AMPA and NMDA receptor-mediated excitatory postsynaptic currents (AMPA-EPSC and NMDA-EPSC, respectively) started to steeply increase from 13dpi. We studied the role of NRG2 in glutamatergic synapse formation by treating the culture with dox from 7dpi, which had a limited effect on GPSC. The amplitudes of AMPA- and NMDA-EPSCs were significantly lower in dox-treated newborn GCs compared with control GCs. Furthermore, the ratio of AMPA- to NMDA-EPSC was reduced by dox-treatment from 7dpi, implying that NRG2 contributes to the maturation of excitatory synapses. These results indicate that the NRG2 expression in newborn GCs is essential for both GABAergic and glutamatergic synaptogenesis.

This work was supported by the NRF of Korea (20120004904).

Where applicable, the authors confirm that the experiments described here conform with The Physiological Society ethical requirements.

PCA158

The Cu/Zn superoxide dismutase inhibitor diethyldithiocarbamate inhibits axonal transport in cultured mouse dorsal root ganglion neurons

R. Isonaka[1], T. Kusakabe[2], T. Katakura[1], T. Takenaka[1] and T. Kawakami[1]

[1]Physiology, Kitasato University School of Medicine, Sagamihara, Japan and [2]Sport and Medical Science, Kokushikan University, Tama, Japan

Axonal transport is a fundamental neuronal cell function, which supplies neuron materials and conveys information. Thus, any increase or decrease in axonal transport expresses the state of neurons, and impairment of axonal transport is a cause of neuronal degeneration. Excessive reactive oxygen species (ROS) have been implicated in damage to neurons, therefore oxidative stress is known to be a major cause of neurodegenerative diseases. Cu/Zn superoxide dismutase (SOD1) is an enzyme, which protects cells against ROS. In this study, we investigated the effects of the SOD1 inhibitor diethyldithiocarbamate (DDC) on axonal transport in cultured dorsal root ganglion neurons.

Adult male C57BL/6 mice (n=5) were euthanized by intraperitoneal injection of pentobarbital sodium (60 mg/kg of body weight), and dorsal root ganglia were removed. Cells were enzymatically and mechanically isolated and cultured for 48 h in Ham's F-12 medium containing 10% fetal bovine serum at 37°C under humidified condition in 5% CO2. Movement of organelles in neurites was observed in real-time by using video-enhanced microscopy, and the number of organelles transported in anterograde and retrograde directions was counted manually before and during the addition of DDC (the number of experiments=48).

DDC significantly reduced the number of transported organelles in a time-dependent manner, compared with PSS. The percentage of transported organelles after 40-min treatment with DDC was 50% of the baseline (before application with DDC, in the control PSS medium) at 100 nM, 43% at 1 μM, 25% at 10 μM, 9% at 100 μM. We further examined whether the anti-oxidant α-tocopherol can prevent DDC-induced inhibition of axonal transport. The inhibitory effects of DDC on axonal transport was partially blocked by pretreatment with α-tocopherol, the value after 40-min treatment with DDC at 100 nM-100 μM was significantly higher than administration of DDC alone.

These results suggested that endogenous oxidative stress increased with DDC treatment and that it inhibited axonal transport. The DDC-induced inhibition of axonal transport was blocked by α-tocopherol. Based on these things, α-tocopherol might be of help in rescuing impairment of axonal transport in response to oxidative stress.

Where applicable, the authors confirm that the experiments described here conform with The Physiological Society ethical requirements.

PCA159

Enhanced inhibitory synaptic transmission underlies the input-specific suppression of long-term depression by serotonin in the rat visual cortex

H. Jang[1,2], Y. Jo[1] and D. Rhie[1,2]

[1]Department of Physiology, Catholic University of Korea, Seoul, Republic of Korea and [2]Catholic Neuroscience Institute, Catholic University of Korea, Seoul, Republic of Korea

Serotonin [5-hydroxytryptamine (5-HT)] plays many important roles as a neuromodulator in the central nervous system. In our previous studies, 5-HT inhibited the induction of long-term potentiation (LTP) and depression (LTD) of layer 2/3 field potentials evoked by stimulation of layer 4 in rat visual cortical slices. To study the underlying mechanisms, we investigated the effect of 5-HT on the synaptic transmission mediated by the three major neurotransmitter receptors: AMPA receptors, NMDA receptors, and $GABA_A$ receptors. Whole-cell patch-clamp recording was made on the pyramidal neurons of layer 2/3. AMPA and NMDA receptors currents were measured with K-gluconate-based internal solution. $GABA_A$ receptor current was measured with CsCl-based internal solution. AMPA receptor current was measured with a NMDA receptor blocker at -70 mV of holding potential. NMDA receptor current was meas-

ured with AMPA and $GABA_A$ receptor blockers at 0 mV of holding potential. $GABA_A$ receptor current was measured with AMPA and NMDA receptors blockers at -75 mV of holding potential. To study the effect of 5-HT on long-term synaptic plasticity, LTD of excitatory synaptic potential was induced with low frequency stimulation (1 Hz, 900 stimulation) of the paired pulse stimuli (40-ms interval). Stimulation was applied to either layer 1 (L1-LTD) or layer 4 (L4-LTD). In both stimulation pathways, LTD was well induced. The induction of L1-LTD depended on both metabotropic glutamate and NMDA receptors. However, only NMDA receptor was involved in L4-LTD. Application of 5-HT inhibited L4-LTD but not L1-LTD. The most significant effect of 5-HT on synaptic transmission was ~20% increase in the $GABA_A$ receptor current evoked by layer 4 stimulation only. To test the importance of this increase on the suppression of LTD, we investigated the effect of $GABA_A$ receptor modulators with concentration at which $GABA_A$ receptor current increase or decrease by ~20%. The 20% increase in $GABA_A$ receptor current was sufficient to block the NMDA receptor-dependent L4-LTD but could not block L1-LTD. The 20% decrease in $GABA_A$ receptor current was sufficient to reverse the inhibitory effect of 5-HT on L4-LTD. These results suggest that inhibitory role of 5-HT on NMDA receptor-dependent LTD might be mediated by the enhancement of $GABA_A$ receptor current which could suppress the activation of NMDA receptors. The enhancing effect of 5-HT on $GABA_A$ receptor current was input-specific and the specific input depended heavily on NMDA receptors for the induction of LTD.

Supported by: NRF grant (2012-046621).

Where applicable, the authors confirm that the experiments described here conform with The Physiological Society ethical requirements.

PCA160

Exploring undergraduate medical students' self-directed learning readiness

R.R. Abraham[1], M. Fisher[2], A. Kamath[3], T. Izzati[4], S. Nabila[4] and N. Atikah[4]

[1]Physiology, Melaka Manipal Medical College, Manipal Campus, Manipal University, India, Manipal, Karnataka, India, [2]Sydney Nursing School, University of Sydney, Sydney, SA, Australia, [3]Comunity Medicine, Kasturba Medical College, Manipal University, Manipal, Karnataka, India and [4]Undergraduate medical students, Melaka Manipal Medical College (MMMC), Manipal Campus, Manipal University,, Manipal, Karnataka, India

Background: Medical students are expected to possess self-directed learning skills in order to pursue life long learning (1) . Melaka Manipal Medical College (MMMC), Manipal Campus, Manipal University, India offers a Bachelor of Medicine and Bachelor of Surgery (MBBS) twinning program which is of five years duration. The curriculum adopted at MMMC incorporates strategies which require students to spend considerable amount of time in self-directed learning.
Aims: In the present study, we explored the self-directed learning readiness of first year MBBS students (n=130) using Self-directed Learning Readiness Scale (SDLRS) (2) and also determined the correlation between SDLRS scores of high achievers, medium achievers and low achievers with their academic performance in physiology examinations.
Methods: Based on academic performance in three teaching units, students were categorized into three groups; high achievers (>75%; n=10), medium achievers (64 to 74%; n=41) and low achievers (<64%; n=79). Students were requested to respond to each item of SDLRS on a Likert scale. The median scores of three scales of SDLRS (self-management, desire for learning, self-control) were compared across the three groups of students using Kruskall Wallis test. The SDLRS scores of three groups of students were correlated with their marks in theory paper of first, second and third block-end examinations using Spearmann's correlation coefficient.
Results: The total score was found to be 141.7 (out of 200). The total mean score for self- management, desire for Learning and self-control were found to be 126.16, 134.32 and 164.72 respectively. The mean score for self- control was found to be higher followed by desire for learning and self-management. Data analyses showed significantly high ($p < 0.03$) median scores for self-control for high performers compared to medium and low performer groups. Between the groups, high performers had a higher score for all three scales of SDLRS, followed by low performers and medium performers. Nevertheless, SDLRS scores and academic performance of three groups of students were found to exhibit a weak correlation.
Conclusions: Total scores for each subscale reflected a positive attitude towards readiness for self directed learning. The study threw light upon the fact that inspite of having a high desire for learning and ability of self-control, students need to be supported in their self-management skills.

Wiley K 1983. Effects of a self-directed learning project and preference for structure on self-directed learning readiness. Nursing Research 32 (3): 181-185.

Fisher M, King J, Tague G 2001. Development of a self-directed learning readiness scale for nursing education. Nurse Educ Today 21: 516-525.

The author wish to thank all the students who participated in the study.

Where applicable, the authors confirm that the experiments described here conform with The Physiological Society ethical requirements.

PCA161

Does practical demonstration class help medical students to develop their skill domain?

N. Upadhayay[1], B.H. Paudel[1], A. Kopila[1] and N. Baral[1,2]

[1]Basic and Clinical Physiology, BP Koirala Institute of health Sciences, Dharan, —, Nepal and [2]Biochemistry, BP Koirala Institute of Health Sciences, Dharan, Nepal

Practical demonstration by teachers has been practiced in a medical institute. It is quite difficult to handle and to involve hundred students in the laboratory exercise (Labex) at a particular time. So, practical demonstration class has been practiced in basic medical science discipline (BMSD) to tackle and minimize time and number of students in a labex. But, do practical demonstration class help medical students to develop their skill domain have been questioned by many students and teachers in the institute. So, we aimed to evaluate the importance and efficiency of practical demonstration classes in the institute.
It was a cross sectional descriptive study. Pretested structured questionnaire having both open and close ended questions were administered to MBBS students (n=63) and basic medical science (BMS) teachers (n=24) and their perception were assessed. Data were expressed in frequencies. On the present scenario, both teachers (24/24) and students (57/63) believed that practical demonstrations were very helpful to student for

developing their practical skills. Although most of the students (57/63) and all the teachers (24/24) were satisfied with the lab exercise (Labex) but both gave mixed response on the practical class. Most of the students (53/63) and teachers (17/24) felt and suggested that practical should be demonstration by teachers' followed by practical work by the students, and some of them (students= 8/63 and teachers= 3/24) suggested practical work (Labex) should be briefed and done by the students followed by a feedback.
Almost all the teachers (21/24) responded that they clarify queries raised by the students in the Labex. However, students mention that queries were clarified in few practical classes of BMS disciplines like in anatomy (63/63), biochemistry (61/63) and microbiology (60/63) but in physiology (22/63), pathology (28/63) and pharmacology (37/63) disciplines the clarification of queries perceived by the students was less.
Regarding training on the questions and exam pattern, overwhelming majority of teachers (20/24) agreed to provide training and majority of students (51/63) want to receive the training.
Thus, for the effective students' skill development, practical classes (Labexes) should not be limited to only demonstration by teachers but it should also be done by the students. Moreover, for skill improvement, queries raised during labex should be solved on the spot by the teachers, and it will be more understandable when students involves in practical work, so that students knows how to troubleshoot the problem when they encounter the problems.

Where applicable, the authors confirm that the experiments described here conform with The Physiological Society ethical requirements.

PCA163

New challenge of Physiological Society of Japan – Reform of annual meeting and establishment of Physiology Educator

N. Koibuchi[1,2], A. Nakashima[2], M. Ishimatsu[2], S. Okumura[2], T. Okumura[2], Y. Kawai[2], M. Kuno[2], A. Koizumi[2], M. Shiibashi[2], A. Suzuki[2], T. Matsuda[2], H. Morita[2], T. Yamashita[2] and A. Yamanaka[2]

[1]Department of Integrative Physiology, Gunma University Graduate School of Medicine, Maebashi, Gunma, Japan and [2]Education Committee, Physiological Society of Japan, Tokyo, Japan

The major aim of Physiological Society of Japan (PSJ) is to promote research in the physiological sciences by providing free communications to members and by actively committing itself to the national and international scientific communities. Research field of physiological science deals with a wide variety of areas, from cell physiology to system physiology of various organs. Because of development of modern science, sessions of PSJ annual meeting are finely divided and thus researchers who are outside of the area cannot understand the presentation. As a consequence, many researchers tend to attend other meeting that deals with their own area of interest, such as Society for Neuroscience. On the other hand, to obtain a tenure-track position in academic area such as Medical School, ability to teach a wide area of physiology is strongly required. Until recently, however, PSJ has provided little opportunity to learn teaching skill during annual meeting. Furthermore, to promote globalization of PSJ annual meeting, it has been required that all scientific sessions are presented in English since 2006. This reform was effective in developing an international collaboration by increasing the number of non-Japanese attendees. However, many physiology teachers, who mainly do teaching rather than research, have stopped attending the annual meeting. Such teachers may not be able to obtain up-to-date knowledge of physiology. Thus, quality of teaching may be declining. To provide an opportunity to learn a wide range of knowledge that is required for physiology teaching, Education Committee of PSJ has started a lecture course of physiological science together with model lectures that are designed mainly for undergraduates. These lectures are given in Japanese. To obtain Physiology Educator license, applicants must attend sufficient number of lectures. In addition to lecture attendance, there are additional several conditions that fulfill license application. We hope that these systems may improve physiology teachers' quality of teaching, help to promote postdocs to obtain academic positions, and to increase attendees of the annual PSJ meeting.

Where applicable, the authors confirm that the experiments described here conform with The Physiological Society ethical requirements.

PCA164

Performance 2012: Engaging the public with the physiology and pharmacology of sporting success

D.I. Lewis and C. Haigh

School of Biomedical Sciences, University of Leeds, Leeds, UK

There is considerable public interest in sport, with a significant upsurge following any major international competition. The 2012 Olympic Games therefore provided an ideal opportunity to explore, with the public, biomedical aspects of sport. Funding was obtained from the Wellcome Trust for a programme of three public engagement events entitled "The physiology and pharmacology of performance enhancement in sport"[1]. The aim was to provide the public with knowledge and understanding of exercise physiology and pharmacology, and promote debate on the ethical issues which arise when this knowledge is utilised to enhance sporting performance.
The first event, targeted at young people, gave them the opportunity to act as scientists in a mock drug testing laboratory. They then discussed their results and debated the use of gene doping to enhance sporting performance. The second event was targeted at individuals who provide sporting opportunities for young people and comprised of a facilitated debate in which their roles and responsibilities as coaches was explored. Video case studies of social drug use by athletes and the phenomenon of "pushy parents" were created and utilised to promote discussion. The final event, "The science behind sporting success" was a two-day interactive exhibition, the aim of which was to introduce the general public to the physiology and pharmacology of performance enhancement in sport, and give them opportunity to reflect on any ethical issues which may arise. The exhibition combined "have a go" sporting activities such as wheelchair basketball or racing a friend on a Wii rowing game whilst measuring cardio-respiratory changes, with those which focused more on the science of performance enhancement e.g. how do you measure lactate threshold, or an interactive mind-map where the public could contribute their ideas on the harms and benefits of gene doping in sport for different sections of the community. Individual activities were run by undergraduate student interns. The exhibition attracted more than 900 visitors over its two days
Feedback from all three events was excellent. 95% of school pupils would come to a similar event in the future, it made them think about their views on the use of drugs in sport (Lik-

ert 1-4 scale, mean score = 3.18/4) and increased their understanding of the ethics of gene doping (3.73/4). Coaches similarly enjoyed their debate (3.3/4), with it being of benefit to them in their role as a coach (3.06/4) whilst 82 % of the public found the exhibition interesting.
Performance 2012 has successfully engaged the public with the physiology and pharmacology of performance enhancement in sport. To promote sustainability of the project, all resources will be made available as open educational resources via the project website[1].
www.fbs.leeds.ac.uk/performance2012/index.php

The financial support of the Wellcome Trust is gratefully acknowledged.

Where applicable, the authors confirm that the experiments described here conform with The Physiological Society ethical requirements.

PCA165

Enhancing feedback provision and use through *in situ* audio commenting

K.L. Colthorpe[1], K. Zimbardi[1], A. Dekker[2], P. Hay[3], C. Engstrom[3], A. Bugarcic[1], P. Long[4], L. Lluka[1], P. Chunduri[1], P. Worthy[1] and J. Marrington[2]

[1]Biomedical Sciences, The University of Queensland, Brisbane, QLD, Australia, [2]Information Technology & Electrical Engineering, The University of Queensland, Brisbane, QLD, Australia, [3]Human Movement Studies, The University of Queensland, Brisbane, QLD, Australia and [4]Centre for Educational Innovation & Technology, The University of Queensland, Brisbane, QLD, Australia

Assessment reforms in higher education recognize the need for effective feedback that is timely, informative, and encourages positive attitudes towards future learning amongst students[1]. Although it is well established that feedback to students is one of the educational practices with large positive impacts on student learning[2], evaluating the actual extent to which students engage with and utilize feedback is difficult. Studies show that when students do receive feedback it is often too brief, too broadly stated, and is often misinterpreted by students[3]. Recent studies have suggested that students find audio feedback more engaging and informative than traditional written feedback[4], and prefer either audio or a combination of text and audio[5] to text alone.
During this study, we have developed a 'rich media' marking system, to help markers provide students with timely, detailed and situated feedback, and to investigate the potential of technology to facilitate new methods of feedback provision, such as *in situ* audio comments. The system can support large cohorts of students, large teams of markers, moderation of markers, and provides learning analytics during the feedback process. It consists of three components: 1) *Administration interface* that processes submissions for marking and moderation, 2) *iPad application* that allows markers to provide feedback as audio, handwritten and typed annotations, and to grade using criteria rubrics, and 3) *Feedback viewer* allowing students to view their feedback on any web browser. In addition, the in-built learning analytics allows for extensive evaluation of the provision and use of feedback, providing empirical evidence of both marker and student behaviors. To date, the system has been trialled on 852 student assignments in two separate trials, the first based on a final student laboratory report, and the second on a draft of a scientific literature review.
Preliminary analysis of the learning analytics data indicates extensive provision of feedback by markers and use of the *in-situ* feedback by students. However, it also revealed differences in the ways in which markers use the annotation modalities, with almost half avoiding use of audio annotations whilst the remainder used audio annotations extensively. Differences were also found in student use of feedback, with students in the second trial viewing their feedback for considerably longer time periods than the first, suggesting there was an effect of timeliness of feedback provision. For audio feedback specifically, students reported in interviews that they (i) favoured audio feedback for its greater detail and personalized nature; (ii) valued contextualized, *in-situ* feedback; and (iii) were concerned if audio comments were too long or lacked meaning. These findings are currently being used to target professional development for markers and to enhance the provision of quality feedback.

Boud, D. and Associates (2010) Assessment 2020: Seven propositions for assessment reform in higher education. Sydney: Australian Learning and Teaching Council.

Hattie, J. & Timperley, H. (2007) The power of feedback. Review of Educational Research 77 (1): 81–112.

Nicol, D. J. & Macfarlane-Dick, D. (2006) Formative assessment and self-regulated learning: A model and seven principles of good feedback practice. Studies in Higher Education 31(2): 199-218.

Lunt, T. & Curran, J. (2010). 'Are you listening please?' The advantages of electronic audio feedback compared to written feedback. Assessment and Evaluation in Higher Education, 35 (7), 759-769.

Lees, D. & Carpenter, V. (2012). A qualitative assessment of providing quality electronically mediated feedback for students in higher education. International Journal of Learning Technology, 7(1), 95-110.

Where applicable, the authors confirm that the experiments described here conform with The Physiological Society ethical requirements.

PCA166

Development of a wiki of education and training resources in in-vivo sciences

D.I. Lewis

School of Biomedical Sciences, University of Leeds, Leeds, UK

There is a global shortage of individuals with the knowledge, skills and expertise necessary to undertake in-vivo or whole animal research. To address this skills shortage, many countries, including the UK and the US, have committed significant funds towards training the next generation of in-vivo scientists within their respective countries. There is also a need to provide for continued professional development (CPD). Indeed, the new European Union animal welfare directive 2010/63/EU makes such training mandatory. This training and CPD would be best facilitated with short open educational resources (OERs) or learning objects (LO) and therefore the aim of this project was to collate, evaluate and disseminate OERs and LOs that could be used in educational and training in in-vivo sciences.
Open educational resource repositories and websites of professional and other organisations were searched for suitable OERs and LOs (eg video podcasts, guidance notes, statistical packages). A call was also made to colleagues in relevant professional bodies. Individual resources were evaluated and a brief description of each written. These were then collated into an education and training resources in in-vivo sciences (ETRIS) wiki, subdivided into topics across the entire spectrum of resources required by practicing in-vivo scientists including

surgical procedures, animal welfare and husbandry, ethics and the 3Rs, experimental design and analysis. This wiki is now being made freely available to colleagues.
ETRIS will be of significant benefit and a valuable tool for colleagues engaged in education, training or research in in-vivo sciences. It is envisaged that it will be a living wiki, that will grow as colleagues either contribute or provide links to new OERs and LOs.

This project was funded through the award of a University of Leeds teaching fellowship to DIL

Where applicable, the authors confirm that the experiments described here conform with The Physiological Society ethical requirements.

PCA167

Optimisation of certainty-based assessment scores

A.R. Gardner-Medwin

Physiology (NPP), UCL, London, UK

Certainty-Based Marking (CBM) rewards students for identifying which of their answers are uncertain and which reliable. Confident answers incur negative marking if wrong, while uncertain answers receive lower credit but no penalty. The scheme at UCL is shown in Table 1 (1,2). In self-tests this encourages reflection and deeper learning, because the student gains from evaluating both doubts and justifications. CBM gives a sound measure of knowledge (1) and enhances the statistical reliability of assessments (3,4). Problems arise, however, with student perception of CBM final scores, because average marks as a fraction of the maximum are lower than the percentage of correct answers ('accuracy'). For example, students with 80% accuracy typically get only 50% of the CBM maximum (Fig.1).
A new strategy is analysed here using data from 17 medical exams with CBM at UCL (250-300 true/false Qs, 320-360 students). In this, a CB bonus (+ or -) is added to conventional accuracy to reflect how well or badly the student has distinguished uncertain from reliable answers. This bonus is a fraction of the difference between average CB mark and the average that would have resulted with a uniform certainty level, appropriate to the student's overall accuracy. The multiplying 'Bonus Factor' (BF) is shown here to be optimally ca. 0.1 to give maximum statistical reliability for the resultant 'CB Accuracy' (accuracy + bonus). Reliability was calculated as the rank correlation (r) between scores on subsets (odd and even questions) in each exam. This increased from a mean of 0.80 with BF=0 (i.e. conventional accuracy) to 0.86 with BF=0.1 (increase = 0.060 ±0.0039), almost as high as for the CBM average (0.87). This reflects an increase of 57% in predictive power (Fig. 2a), equivalent to adding 57% more questions without CBM. The power to predict conventional accuracy was increased by 16% (Fig. 2b), showing greater validity for CBM scores even with accuracy as the standard.
The CB bonuses added to accuracy in exam data are typically 2-5%, though students doing online self-tests while studying often get negative bonuses due to misconceptions (confident errors). Bonuses and CB accuracy scores are implemented online using BF=0.1 in LAPT at UCL (2), available for use by other institutions. CBM is also available in Moodle, though additional code (5) is required to implement the enhanced scoring and feedback to students.

Degree of Certainty:	C=1 (low)	C=2 (mid)	C=3 (high)	No Reply
Mark if Correct:	1	2	3	0
Penalty if wrong:	0	-2	-6	0
Probability correct:	<67%	67-80%	>80%	-

Table 1

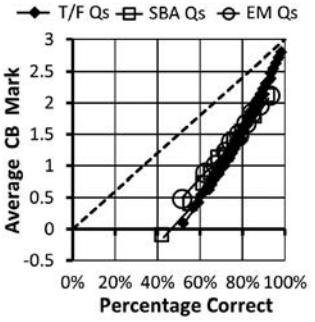

Fig. 1

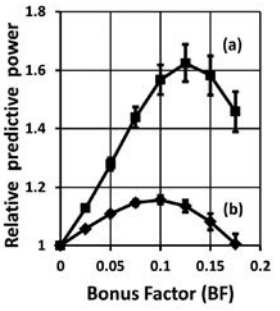

Fig. 2

Fig.1 Data from 9,000 online LAPT self-test sessions with >20 answers, showing mean CBM averages plotted against accuracy, for centiles (True/False Qs) or deciles (Single Best Answer, 4-5 options and Extended Matching Questions, 10 options) ranked by accuracy.

Fig.2 Predictive power *(=r/(1-r))* of 'CB Accuracy' scores as a function of bonus factor, calculated from *r* = Pearson rank correlation comparing (a) CB scores vs CB scores and (b) CB scores vs accuracy, for interleaved question subsets. Mean ± sem for 17 exams.

Gardner-Medwin AR (1995). *ALT-J* **3**, 80-85

London Agreed Protocol for Teaching (LAPT), http://www.ucl.ac.uk/lapt

Ebel RL (1965) *J Educ. Measurement*. **2**, 49-57

Gardner-Medwin AR & Gahan M (2003) *Proc. 7th CAA Conf. July 2003*, 147-155

Gardner-Medwin AR (2012). *CBM and Moodle*, http://www.tmedwin.net/cbm/moodle

Thanks to D.Bender for providing access to past exam data.

Where applicable, the authors confirm that the experiments described here conform with The Physiological Society ethical requirements.

PCA168

Self-tests with certainty-based-marking in early years of medical course

N. Curtin[1] and A.R. Gardner-Medwin[2]

[1]Molec Med, NHLI, Imperial College London, London, UK and [2]University College London, London, UK

Although our Medical class intake are bright and highly motivated students, they need and seek help in adapting to the differences between teaching and learning in the medical course and what they experienced at school. Even the best-achievers quickly discover that in the medical course they will not be able to learn everything presented to them, as they felt they could do with their school curriculum. Consequently, new students commonly want more (and more) guidance about the level and breadth of knowledge expected of them. To help fill this need within the 6-Yr medical Course at Imperial College London, we have developed Self-tests using the LAPT system (www.ucl.ac.uk/LAPT, Gardner-Medwin (1995)). Self-tests are a set of exercises, each on a specific course or topic within Yr1 and 2 of our 6-yr Medicine program. An important fea-

ture of the LAPT system is use of Certainty Based Marking (CBM) in which the student's answer is marked so as to reward not only correctness, but also identification of whether they think their knowledge is secure. The mark scheme ensures honest reporting of uncertainty. See Table 1. The students easily grasp the rationale: "knowledge is knowing what I know, and what I don't know". It is particularly important in medicine: "As a doctor, I must recognize when I am sure enough to act, and when I need more information or help. Guessing can be a disaster for my patients."

Features for students include:

*Links via BlackBoard Learn for use on personal computers or tablets,

*Approximately 2,100 questions in 58 exercises that map onto the Imperial course,

*Can do any number of repeat attempts,

*Instant marking of each answer as it is entered,

*Instant explanations of answers,

*Student comments are shared, anonymous, and linked to each exercise,

*Personalized spread-sheets of performance, including certainty.

Features for staff include:

*Many questions types can be used (SBA, EMQ, ARQ, T/F, etc.)

*Summary spread-sheets of student performance,

*Analysis of correctness and certainty for each question,

*Editing facilities (which also can be available to students on a wiki basis),

*Comments emailed to designated staff for each Self-test.

Most of the Self-tests were written by students (a 'grass-roots' project), then checked by an academic expert. Self-tests are popular with students. Performance comparisons show that the students who do the Self-tests have better exam results than students who do not do the Self-tests.

Marking Matrix

Certainty level:	C=1	C=2	C=3	no reply
Mark if correct	1	2	3	0
Penalty if incorrect	0	-2	-6	0

Gardner-Medwin AR (1995). *ALT-J (Association for Learning Technology Journal)* **3**, 80-85.

Where applicable, the authors confirm that the experiments described here conform with The Physiological Society ethical requirements.

PCA169

Engaging the gen Y students with STD - Speed Triage Dating

L.B. Tee

School of Pharmacy, Curtin University, Perth, WA, Australia

Speed dating "speed networking" was integrated as a tool for interpersonal development (1). Academic sector recognised its potential and adopted speed dating as an educational tool to help students to know each other and share knowledge (2, 3). The main challenge for the pharmacology teaching team is to transform the students' perception of pharmacology as difficult, with a great amount to "know and remember," to an essential and interesting subject which enhances their competency in clinical pharmacology and medication prescription. The aim of this research is to investigate whether the inclusion of the innovative Speed Triage Dating learning method within the Pharmacology modules in the Bachelor of Pharmacy Course at Curtin University enhnaces deep learning in subjects traditionally reliant on memorisation. In this project a modification of speed dating, Speed Traige Dating (STD) is used in tutorial workshop in Pharmacology. Instead of the one-on-one dating, to foster collaborative learning and peer coaching, each "dating" session will involve three students or a triage. Information was relayed from students to students. Before class students undertook a test to assess their prior drug knowledge. At the end of the STD session students undertook another test to assess their improved drug knowledge. For each dating the students were instructed to address different issues pertinent to their individual task with increasing level of thinking progressing from describing the task to critically evaluating and integrating information learned during the process. Students were provided with a drug in which they have to research to develop a comprehensive drug monograph. During the STD session, in Round 1 of the STD, they were instructed to describe their drug. In the subsequent rounds they may be ask to integrate, evaluate and compare and contrast the drugs in various aspects of Pharmacology. There was an increasing spiral of information with increasing rounds of STD with students teaching as well as learning the increasing number drugs. Most importantly students were actively engaging in intergration and communication of knowldege learned. Qualitative data were gathered from eVALUate data of students' feedback on their perception of resources and teaching activities available in the Pharmacology Module including the use of STD during tutorials. Students have valued the STD method and commented positively on STD indicatig that it is engaging, fun and improves their ability to understand the more complex content of pharmacology and foster internalisation of knowledge allowing long term memory to occur more effortlessly.

Finkel EJ, Eastwick PW, Matthews J. Speed-dating as an invaluable tool for studying romantic attraction: A methodological primer. Personal Relationships. 2007;14(1):149-66.

Muurlink O, Poyatos Matas C. From romance to rocket science: speed dating in higher education. Higher Education Research & Development. 2011 2011/12/01;30(6):751-64.

Murphy B. Need to Get Your Students Talking? Try Speed Dating! Teaching Professor. 2005;19(7):1-4

Where applicable, the authors confirm that the experiments described here conform with The Physiological Society ethical requirements.

PCA170

More than semantics: Moving physiology instruction to learner competencies from learning objectives

R.G. Carroll

Physiology, East Carolina University, Greenville, NC, USA

Preclinical medical education is adopting the 'competency' framework that has been successfully used in the postgraduate medical education community. While learning objectives focus on specific content to be mastered, competencies focus on the learner. In 2002, the American Physiological Society and Association of Chairs of Departments of Physiology CDP published Medical Physiology Learning Objectives, which outlined the physiology content that medical students should master during their preclinical training. In contrast, in 2003 these same groups published the List of Professional Skills for Physiologists and Trainees, which took a competency approach, focusing on the skills and attributed of professional physiologists.

The following is proposed as a set of knowledge-based competencies for medical physiology instruction as a compliment to the more specific Learning Objectives
Medical Knowledge: 1. Identify the range of normal physiological values, i.e., plasma electrolytes (Na+, K+, and Cl-) ; arterial and mixed venous blood gasses, blood pressure in the cardiac chambers, the systemic and pulmonary arteries, capillaries, and veins, and key values in assessing cardiovascular, pulmonary and renal function. 2. Use normal values to interpret clinical data in order to identify the direction and degree of variation from normal. 3. Given an alteration in a physiological parameter, identify potential causes for the alteration and the physiological mechanisms which when effective would correct the alteration. 4. Contrast the regulation of a physiological parameter (i.e., blood pressure, plasma glucose, pH or body temperature) by negative feedback, positive feedback and feed forward control mechanisms. 5. For a physiological variable controlled by multiple redundant systems (i.e., plasma glucose or blood pressure), rank the control systems based on time to effect and overall effectiveness.
Professional Development: 1. Demonstrates a positive attitude and regard for education by demonstrating responsibility and preparedness, 2. Demonstrates maturity in soliciting, accepting, and acting on feedback.
Interpersonal and Communication: 1. Effectively leads group discussions, 2. Creates a supportive environment for conversation, 3. Demonstrates collegiality and respect for group members.
In the shift to competencies, instructors must move from the exclusive focus on knowledge and take responsibility for the development of professionalism in all of their students.

Where applicable, the authors confirm that the experiments described here conform with The Physiological Society ethical requirements.

PCA172

Undergraduate-led practical physiology activities can enhance learning for both university students and A-level school pupils

P. Lillie, A.C. Reid and J.R. Harris

University of Bristol, Bristol, UK

The Undergraduate Ambassador Scheme (UAS; http://www.uas.ac.uk/) enables university students to undertake a final year research project in association with a local school. At the University of Bristol we run UAS projects in which pairs of BSc students (a) design, deliver and evaluate biology lessons in the partner school and (b) design, implement and evaluate a complementary research project that includes collecting and analysing biometric data generated with/from the pupils.
We describe a UAS research project designed to illustrate and extend the respiratory and cardiovascular components of the Salter-Nuffield Advanced Biology A-level curriculum. The impact of pupils' height, weight and breathing pattern on the cardio-respiratory variables of vital capacity, breath-hold breaking point and resting heart rate (RHR) was compared to impact on these variables of regular exercise.
One week before visiting our undergraduate physiology teaching lab, 65 A-level pupils took a test to evaluate their cardio-respiratory physiology knowledge and completed a modified Brunel lifestyle questionnaire[1] quantifying their level of regular physical activity. They were then given worksheets explaining the experiments they would do in the lab and preparatory exercises to work through. In the lab, pupils rotated in small groups through three stations: (a) measuring vital capacity with a Benedict spirometer; (b) using ECG recording to measure RHR; (c) measuring their breath-hold (BH) breaking time at rest and after a period of voluntary hyperventilation while monitoring arterial oxygen saturation (SaO_2) with a finger pulse oximeter. At the end of the lab session they completed the same theory test as before.
Little correlation was found between the physiological variables and the subjects' physical activity scores. However, there was strong correlation between height and vital capacity ($r = 0.72$; $P < 0.001$; $n = 19$). BH breaking time was increased from 39 s (SEM 2.6) to 65 s (SEM 5.1) after voluntary hyperventilation for 15 s ($P < 0.001$, Student's t-test; $n = 22$) but SaO_2 did not change. The results were discussed in the lab session and used to illustrate subsequent school lessons on cardio-respiratory anatomy and physiology delivered by the undergraduates. The average marks (out of a total of 11) for the pre- and post-lab physiology tests increased from 3.6 (SEM 0.36) to 6.8 (SEM 0.40); ($P < 0.001$, Wilcoxon signed-rank test; $n = 60$). The accompanying teachers gave very positive feedback on the benefits of the lab session for the pupils' learning and engagement.
We conclude that this type of BSc research project has significant benefits for the school pupils concerned; involves undergraduates in interesting and novel physiology research that also develops their communication skills; and fosters valuable links between universities and schools.

Karageorghis CI, Vencato MM, Chatzisarantis NLD and Carron AV (2005) Development and initial validation of the Brunel lifestyle physical activity questionnaire. Br J Sports Med 39: e23 doi:10.1136/bjsm.2004.014258

Where applicable, the authors confirm that the experiments described here conform with The Physiological Society ethical requirements.

PCA173

Developing students' advanced scientific thinking skills through effective inquiry-based physiology practical classes

K. Zimbardi[1,2], K. Colthorpe[1], J. Kibedi[1] and P. Long[2]

[1]School of Biomedical Science, University of Queensland, St Lucia, QLD, Australia and [2]Centre for Educational Innovation and Technology, University of Queensland, St Lucia, QLD, Australia

Over the last 30 years there has been a wide-spread implementation of inquiry based classes in science education (1), and in tertiary physiology curricula in particular (2), because these pedagogies have been shown to improve student learning of content (3, 4) and important scientific thinking skills such as experimental design and data interpretation (5). However, a multitude of obstacles face instructors aiming to implement inquiry-based practical curricula (6) where poor implementation (7), and both too much and too little guidance (8) have negative effects on student learning. It is therefore important to understand which specific aspects of inquiry-based curricula engage students in effectively developing scientific thinking skills, and when and why the development of these skills goes awry. We have developed a vertically-integrated set of inquiry-based practical curricula for large cohorts (500-900 students) of first and second year physiology students (9) which facilitate the development of students' skills in scientific thinking (10, 11). Video recordings of students engaged in inquiry in class were analysed using the Australian national academic standards for scientific thinking (12) and the theo-

retical framework for critical thinking developed by Bailin (13). Results from this study showed that students used and developed their critical scientific thinking skills when they needed to make scientific decisions. In our physiology practical classes, these decisions typically involved which hypothesis to test and how, and how to analyse and interpret experimental data. Students employed a range of strategies to make these decisions, from uncritical guesses, to using their prior anecdotal experience and instructions from manuals or teaching assistants, through to more scientifically rigorous strategies that included using evidence from their own experiments and scientific literature. Evidence from video tapes of classes has revealed key factors that impact on the degree of scientific rigour students employ when making their decisions. For example, students must be required to 1) demonstrate feasibility of their experimental proposals with pilot data and primary literature, and 2) to critically compare experimental contexts and specific data values when interpreting their experimental findings. This study provides evidence-based strategies for producing curricula that are effective in helping large cohorts of early stage undergraduate physiology students to develop advanced scientific thinking skills.

1. Dunbar K, Fugelsang J. Scientific Thinking and Reasoning. In: Morrison Ha, editor. The Cambridge handbook of thinking and reasoning. New York, NY: Cambridge University Press; 2005. p. 705-25.

2. Michael J. Where's the evidence that active learning works? Advances in Physiology Education. 2006;30(4):159-67.

3. Luckie DB, Maleszewski JJ, Loznak SD, Krha M. Infusion of collaborative inquiry throughout a biology curriculum increases student learning: a four-year study of "Teams and Streams". Advances in Physiology Education. 2004;28(4):199-209.

4. Kolkhorst FW, Mason CL, DiPasquale DM, Patterson P, Buono MJ. An inquiry-based learning model for an exercise physiology laboratory course. Advances in Physiology Education. 2001;25(2):45-50.

5. Myers MJ, Burgess AB. Inquiry-based laboratory course improves students' ability to design experiments and interpret data. Advances in Physiology Education. 2003;27(1):26-33.

6. Silverthorn DU, Thorn PM, Svinicki MD. It's difficult to change the way we teach: lessons from the Integrative Themes in Physiology curriculum module project. Advances in Physiology Education. 2006;30(4):204-14.

7. Kuhn D. Education for Thinking. Cambridge: Harvard University Press; 2005. 218 p.

8. Kirschner PA, Sweller J, Clark RE. Why minimal guidance during instruction does not work: an analysis of the failure of constructivist, discovery, problem-based, experiential, and inquiry-based teaching. Educational Psychologist. 2006;41(2):75-86.

9. Farrand K, Kibedi J, Colthorpe K, Good J, Lluka L, editors. Creating physiology graduates who think and sound like scientists. Third National Attributes Graduate Project Symposia; 2009; Griffith University, Queensland, Australia.

10. Farrand-Zimbardi K, Colthorpe K, Good J, Lluka L, editors. Becoming a scientist: the development of students' skills in scientific investigation and communication through a vertically integrated model of inquiry-based practical curricula. International Society for the Scholarship of Teaching and Learning (ISSOTL) annual conference; 2010; Liverpool, UK.

11. Zimbardi K, Bugarcic A, Colthorpe K, Good JP, Lluka LJ. A set of vertically-integrated inquiry-based practical curricula that develop scientific thinking skills for large cohorts of undergraduate students. Advances in Physiology Education. under review.

12. Jones S, Yates B, Kelder J. Learning and Teaching Academic Standards (LTAS) Project Final Report for the Second-Intake Discipline Groups of: Architecture Building and Construction, Education and Science: Australian Learning and Teaching Council; 2011.

13. Bailin S. Critical thinking and science education. Science and Education. 2002;11:361–75.

This project was supported by a University of Queensland Teaching Fellowship, in residence at the Centre for Educational Innovation and Technology, The University of Queensland.

Where applicable, the authors confirm that the experiments described here conform with The Physiological Society ethical requirements.

PCA174

A practical class to teach masticatory efficiency for dental students

M.A. Rocha, M. Ferreira, D. Gaspar and W. Mestriner-Júnior

Dental School of Ribeirão Preto, University of São Paulo, Ribeirão Preto, São Paulo, Brazil

The aim was to set up a practical class to teach the students about the several factors that can affect masticatory efficiency. Before starting the test we asked the student volunteers to report to the colleagues whether or not they have any masticatory problem and to masticate a piece of parafilm or a sugar-free chewing gum for 20 seconds to remove any resting muscular memory. Subsequently, they are instructed to masticate the way they usually do a Me Mastig® capsule made of polyvinyl acetate filled with beads containing a calcium chlorid fuchsin dye. After 20 seconds, the beads (fragmented or not) are collected and the content is dissolved in 5 ml of water and agitated for 30 seconds. The solution is then filtered through gaze and the fuchsin dye quantified by spectrophotometry. The masticatory force of each volunteer is then calculated by regression analysis of the extracted fuchsin concentration against a standard curve generated from a force-controlled masticatory apparatus. As future dentists, the students are instructed to discuss the problems that the volunteer students reported and discuss the possible factors affecting the respective masticatory efficiency.

Dental School of Ribeirao Preto, USP

Where applicable, the authors confirm that the experiments described here conform with The Physiological Society ethical requirements.

PCA175

Quality of essay plans in finals papers correlates with the mark awarded to the essay by independent examiners

P.D. Langton, R. Helyer and F. MacMillan

Physiology and Pharmacology, Univ Bristol, Bristol, UK

Increasingly, students' written work is word processed. Concerns about students' ability to compose written work seem unfounded for essays composed using a word processor (Goldberg, Russell et al. 2003). However, essays written in end of year examinations are traditionally hand written. We were interested to know if the practice of essay planning, that has been suggested to positively contribute to essay quality (Hounsell 1984), correlated with the mark awarded to the essay.
This was investigated by a post-hoc examination of a complete set of recent final examination scripts for the three Units of the Physiological Sciences programme that are examined by a finals paper. Ignoring the mark sheet, so as to remain blind to the mark awarded, each essay booklet was examined to establish if there was an essay plan. Plans were graded according to a four point criteria with a maximum total of 10 marks:

Title present = 0 to 1 mark
Structure evident = 0 to 2 marks
Scope of the plan = 0 to 4 marks
Reference works listed = 0 to 3 marks
Only after the overall mark for the plan was recorded was the mark awarded for each essay determined from the official records of the examination. The essays written for each unit that were not associated with a plan (unit 2, n=12; unit 3, n=10; unit 4, n=8) were excluded from the correlation analysis. Students who choose not to construct a plan are likely to fall into two groups, 1) those who have attempted to question spot and have done their planning before the exam and, 2) those who simply choose not to construct a plan. For this reason it seems sensible to separate these candidates from the correlation analysis.
Each unit had more than 30 students (unit 2, n=31; unit 3, n=33; unit 4, n=34) who had made a plan. In each case the distribution of marks for the plan and the essay mark were normally distributed and the existence of an association between the mark given for the essay and the plan was determined by a Pearson correlation analysis.
For each unit a statistically significant correlation was found to exist ($p=0.0026$; $p=0.0004$; $p<0.0001$ for units 2,3 & 4, respectively). The Pearson correlation coefficient (r2), which indicates the degree of correlation, ranged from 0.27 to 0.44. In summary, there is a statistically robust correlation between the mark awarded to the essay plan and the mark previously awarded to the essay. In each case the mark awarded to the plan and the mark awarded to the essay (moderated mark) were safely normally distributed. Moreover, the r2 values in each case was greater than 0.25 and so the correlation is reasonably strong. Our current interpretation of these finding supports the assertion that students who have thought more about the structure of their essay achieve higher marks.

Goldberg, A., M. Russell, et al. (2003). The effect of computers on student writing: A meta-analysis of studies from 1992 to 2002. The Journal of Technology, Learning and Assessment 2(1).

Hounsell, D. (1984). Essay planning and essay writing. Higher Education Research AND Development 3(1): 13-31.

I am grateful to Dr P. Brennan and A. James, Prof J. Harris, Prof M. Headley

Where applicable, the authors confirm that the experiments described here conform with The Physiological Society ethical requirements.

PCA176

South East Asian medical students perceive and accept PBL as useful learning process: report from an upcoming medical school in Malaysia

S. Ghosh

Physiology, MAHSA University College, Kuala Lumpur, Selangor, Malaysia

Problem based learning [PBL] has been widely used globally in undergraduate medical education and other professional training programs. Asian students are often found to have aversive reaction to the Problem Based Learning process being introduced in their first year of medical school. The basic apprehension remains that without being told what to learn they will not be able to learn (1). The present study reports that with a proper briefing on the process of PBL first year students appreciate the importance of PBL and accept it as an important teaching learning tool. One week before the real session, a briefing session was conducted for two hours with interactive lecture and video clips to sensitize the first year students of batch 2011 to the process of PBL. A case of an inherited disorder was used for actual training session of the students. 12-14 students were allotted to one facilitator and the case had four triggers. Three sessions of 2 hours each with one week gap were conducted based on the accepted steps of PBL. The second session comprised of presentation and discussion after the students were introduced to the case in the first session. The third session comprised of a mini test, concept map and feedback by the facilitator. After the sessions were over, students were required to give their feedback on a structured questionnaire. Their performance scores in the mini test were correlated with those of the facilitator's during the session.
Students enjoyed this active form of learning alongwith good scores in the minitest. However, the facilitator's scores of their performance did not correlate with the scores of the mini test for some groups. 80% students were aware of the process and accepted it as a good teaching learning activity. 20% students were still unsure of the process and felt lost in studying what they do not know.With proper briefing sessions, most Asian students can be sensitized to the process of PBL and they accept it as a good active learning strategy. The minitest and concept map are good to assess them in PBL objectively.Students are acceptable to newer TLAs which are more active in nature. They can be motivated to undertake such activities with proper briefing and visuals and also feedback being given to make them perform better in subsequent PBL sessions.

Khoo Hoon Eng. Can Asians do PBL,CTDL Brief Newsletter, (2000);Aug, Vol 3 No 3 available at http://www.cdtl.nus.edu.sg/brief/v3n3/sec2.htm

Faculty of Medicine, MAHSA University College,

Students of batch 2011/16

All facilitators who conducted the small group sessions

Prof Dr.Md. Azhar, Deputy Dean & Head of MERDeQA, MAHSA University College

Where applicable, the authors confirm that the experiments described here conform with The Physiological Society ethical requirements.

PCA177

Perception of basic medical science teachers and medical students on objective structured practical examination (OSPE) and viva in a medical institute

N. Upadhayay[1], B.H. Paudel[1], N. Baral[2] and K. Agrawal[1]

[1]Basic and Clinical Physiology, BP Koirala Institute of Health Sciences, Dharan, —, Nepal and [2]Biochemistry, BP Koirala Institute of Health Sciences, Dharan, Nepal

OSPE has been practiced in our all under graduate curricula. However, its utility has been questioned by many teachers and students. This study was undertaken to assess the students and teachers perception on OSPE and viva in basic medical science (BMS) disciplines. We administered pre-designed and pretested structured questionnaire on OSPE and viva to MBBS students (n=63) and BMS teachers (n=24). Majority of students (38/63) considered OSPE as a satisfactory practical evaluation tool whereas almost all the teachers (22/24) believed it as a fairly good tool. More than 50% (34/63) of students and 70.83% (17/24) of teachers believed 5-min to each OSPE station is sufficient enough; however, 42.86% (27/63) of students responded that it was not sufficient for stations having calcu-

lation and additional tail questions. Almost all students (58/63) preferred a gap between practical exams and 100% of them preferred having a rest station between OSPE stations in an exam day. Majority of students preferred a gap between practical exams for proper sleep, coping and minimizing their stress and anxiety, and revising contents. However, teachers (11/24) were against giving the students a gap between practical exams, neither they (14/24) favored rest station among many OSPE stations. Students gave almost equal preference to OSPE stations only (46.03%) as well as combined OSPE plus some procedures (47.62%) during practical exams. Majority of teachers (21/24) opined that students must perform some procedures during practical exams, which has declined over the years. Regarding viva as a station, many students (36/63) and teachers (11/24) supported the ongoing structured of fixed number of questions to evaluate all students. Teachers gave major suggestions: careful questions framing directly linking with the practical, having some liberty for examiners with alternative reserve questions so that bias across the examiners is minimized, question uniformity should be maintained and students' opinion has to be taken to explore the issue further. However, majority of teachers (17/24 or 70.83%) and some students (21/63 or 31.74%) preferred open number of questions with respective weight-age, they believed that it tests the students' knowledge in depth, facilitates and motivates them to study meticulously and helps to evaluate them properly in exams. Thus in BMS, well-framed OSPE directly linking with the practical exercises can be a best tool to assess students' skill, but it should include some working stations (procedures) too. During practical exams students should be provided gap between exams to minimize their stress and for revision. Viva questions should be framed carefully by directly linking with the practical, and having some liberty for examiners with alternative reserve questions to minimize examiner bias.

Johnson G & Reynard K (1994). Journal of Accident and Emergency Medicine 11, 223-226.

Abraham RR, Raghavendra R, Surekha K et al. (2009). Adv Physiol Educ 33, 21-23.

Awaisu A, Mohamed MHN and Mohammad Al- Efan QA (2007). American Journal of Pharmaceutical Education 71, 118.

Where applicable, the authors confirm that the experiments described here conform with The Physiological Society ethical requirements.

PCA178

Doctors' perception about clinical relevance of physiology to practice in the houseman ship in Sudan. Comparison between graduates from Problem based learning and conventional curricula

L.A. Kaddam[1], H. Awooda[1], M. Elnimeiri[2], A. Saeed[3] and R. Badi[3]

[1]Physiology, Alneelain University Faculty of Medicine and Health sciences, Khartoum, Khartoum, Sudan, [2]Community Medicine, Alneelain University Faculty of Medicine and health sciences, Khartoum, Sudan and [3]Physiology, University of Khartoum Faculty of Medicine, Khartoum, Sudan

Physiology is s considered as an essential subject in any medical curriculum. There is an increase in studies that showed poor retention of basic sciences in clinical years and students' perceptions of some parts of physiology as "irrelevant". This mandated rethinking about physiology teaching methods to improve students' competence to apply knowledge in clinical practice.Problem Based learning (PBL) is considered as an ideal curriculum where students are able to integrate their knowledge into clinical application and problem solving. However some studies showed no convincing evidence of improved learning using the PBL curriculum. Other studies showed PBL curriculum resulted in significant gaps in students' understanding of basic physiological concepts. In this study we investigated difference in physiology perception between graduated from faculties adopting PBL curriculum and those graduated from faculties adopting conventional curriculum. We focused on their experience in learning physiology and their self-assessed competence to translate knowledge into practice in their clinical work. 400 self administered questionnaires were distributed among doctors who finish houseman ship residency and sat for a license examination to be registered in Sudan Medical Counsel. As they represented all medical schools across the country. Results: 229 questionnaires were returned for analysis (response rate 57%). Differences between the two groups of graduates was determined using chi-square and two-tailed t-tests for categorical and continuous variables, respectively.BPL based curriculum (n=100) and conventional curriculum (n=129). PBL graduates studied physiology for longer time than conventional one (p=0.02). No difference in self evaluation for time spent in studying physiology. 52.8 % declared they were satisfied by the time spent in learning physiology (55.8% conventional PBL 49%). 91% agreed that learning physiology is essential for medical practice.While 80% stated they applied physiological concepts during medical practice (83.6% conventional 76% PBL). 51% stated they recalled the information from their undergraduate study (56%conventional PBL. p=0.2). 44% Graduates from both curricula agreed lectures are useful method to study physiology 91% (90% conventional, 91% PBL) . Regarding case study 70% declared it is useful tool to learn physiology (57% conventional 86% PBL p=0.00). So, here in Sudan we concluded that no significant difference was found between graduates from conventional curriculum and Problem based study in perception of physiology clinical relevance, satisfaction about time spent in learning physiology and application of physiological concepts in clinical practice

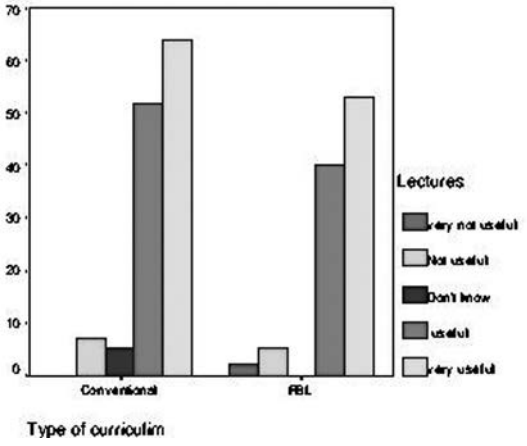

Doctors perception about usefulness of different teaching methods utilized in learning physiology

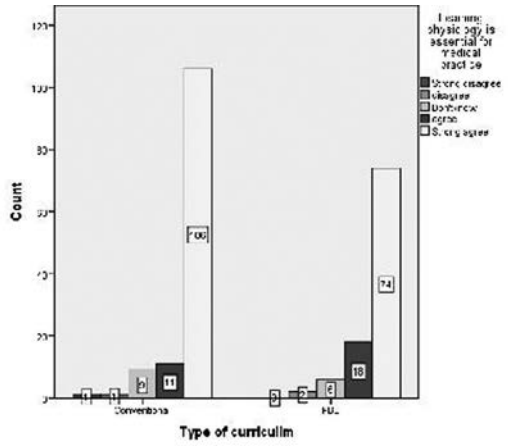

Doctors perception about physiology relevance to clinical practice

Jacobs EA, Kalet A. Defining medical basic science: general internists' special role in the reformation of medical school education. J Gen Intern Med 2009 Nov;24(11):1261-2

Brass EP. Basic biomedical sciences and the future of medical education: implications for internal medicine. J Gen Intern Med 2009 Nov;24(11):1251-4

Custers EJ, Ten Cate OT. Medical clerks' attitudes towards the basic sciences: a longitudinal and a cross-sectional comparison between students in a conventional and an innovative curriculum. Med Teach 2007 Oct;29(8):772-7.

Custers EJ, Ten Cate OT. Medical clerks' attitudes towards the basic sciences: a longitudinal and a cross-sectional comparison between students in a conventional and an innovative curriculum. Med Teach 2007 Oct;29(8):772-7.

Custers EJ. Long-term retention of basic science knowledge: a review study. Adv Health Sci Educ Theory Pract 2010 Mar;15(1):109-28.

To administrators and doctors in the Sudan Medical Council.

Where applicable, the authors confirm that the experiments described here conform with The Physiological Society ethical requirements.

PCA179

Merits and demerits of 'Frequent Discussion Embedded Interactive Lecture (FDEIL)' in learning physiology: a students' opinion

M.U. Khan

Physiology, Noakhali Medical College, Noakhlai, Bangladesh

Background: Lecture is a method of teaching where teacher gives information and the students receive it. Students get less scope to make a point clear (1). Researchers demonstrated that students need to be taught by interactive lectures(2). Frequent discussion interrupted lecture has been preferred as a good method of lecturing in a recent research(3). Interactive lectures are avoided due to time constraints and fear of losing of control over students(4). Objective: To assess the students' opinion about merits and demerits of 'Frequent Discussion Embedded Interactive Lecture (FDEIL)' in learning physiology. Method: This cross-sectional descriptive study was conducted in the Department of Physiology, Noakhali Medical College during March-June'12. By convenient sampling 107 students who attended FDEIL lecture in physiology were enrolled in the study. In FDEIL teachers delivered lecture on a topic for 15-20 minutes and gave a 5-10 minute's discussion-break among students and teacher. A one-hour lecture was divided into 2-3 lecture-discussion cycles. A questionnaire with statements on merit and demerit of FDEIL was distributed to the participants to response. Permission of the authority and consent of the participants were taken. Data was analyzed by a calculator. Result: The number of students chose the statements as follows; 'students get opportunity to understand the topic clearly' 101 (94.4%), 'students can discuss among them about the topic' 92 (86%), 'students can ask question to the teacher before forgotten the critical part, 97 (90.7%), and 'students do not feel tired' 58 (54.2%). The number of students who chose the demerits was as follows; 'students engage in gossiping and chatting' 59 (55.1%), 'teacher may lose attention and time' 34 (31.8%), 'it kills time' 21(19.6%), and 'students attention towards teacher is interrupted' 18 (16.8%), students. 99(92.5%) students thought FDEIL a good learning system. Conclusion: FDEIL was supported as a good lecturing system for large group teaching in Physiology.

Table-I: Summary of response in favor of merits and demerits of FDEIL

Statements in favor of merits of FDEIL system	Frequency (%)
Students get opportunity to understand the topic clearly	101 (94.39)
Students can discuss among them about the topic	92 (85.98)
Students can ask question to the teacher before forgotten the critical part	97 (90.65)
Students do not feel tired	58 (54.21)
Statements in favor of demerits of FDEIL system	Frequency (%)
Students engage in gossiping and chatting	59 (55.14)
Teacher may lose attention and time	34 (31.78)
It kills time	21 (19.63)
Students attention towards teacher become interrupted	18 (16.82)
Comment on FDEIL: it is good for learning Physiology	99 (92.52)

FDEIL; Frequent Discussion Embedded Interactive Lecture

Byrne PS, Harris CM, Long BEL. Teaching the teachers. Med Educ 1976; 10: 189-192.

Maloney M, Lally B. The relationship between attendance at university lectures and examination performance. Irish J Educ 1998 29: 52-62.

Khan UA, Amin R, Begum F, Begum M. Frequent discussion interrupted lecture vs lecture followed by discussion in Physiology: A telephonic survey of students' perception. The Journal of Physiological Sciences. Proceedings of the XXXVI International Congress of Physiological Sciences (IUPS 2009), Function of life: Element and Integration, July, 27-August 1, 2009 in Kyoto, Japan, p-447(Abstract: P4AM-29-10).

Bonwell CC, Eison JA. Active Learning: Creating Excitement in the Classroom. Washington DC: George Washington Univ Press. 1991: 60-62.

I am thankful to the principal of Noakhali Medical College and students of the same Medical college who participated in the study

Where applicable, the authors confirm that the experiments described here conform with The Physiological Society ethical requirements.

PCA180

Cooperative learning, a tool to teach physiology in nursing education

M.A. Kanpurwala[1], S. Saleem[2] and A. Faisal[3]

[1]Physiology, University of Karachi, Karachi, Sindh, Pakistan, [2]Nursing, Baqai University, Karachi, Pakistan and [3]Health Management, Institute of Business Management, Karachi, Pakistan

Nurse educators struggle on how to prepare competitive nurses who can provide best possible quality care to their patients in the increasingly complex healthcare environment of the twenty-first century [1]. Different strategies like lecture, discussion, tutorials, cooperate learning etc are used to convey knowledge to the students so that they will be able to work collaboratively, think critically, draw reasoned conclusions, and make complex decisions in their profession more effectively

[2]. Cooperative learning plays a pivotal role to prepare them to face the contemporary challenges and thus can be helpful in improving overall quality in healthcare [3,4]. The tool could also be beneficial to teach physiology which is the backbone of medical sciences. The objectives of this study are to identify the knowledge about cooperative learning strategy among nursing educators and to assess their attitude and practices about integration of these strategies and the barriers they usually faced in implementing them.

It is a Cross-Sectional Survey in which 100 nursing educators were selected from different institutes of Karachi, Pakistan through Convenient Sampling and a self administered questionnaire was used to achieve the research objectives. Consent was taken from each participants and Data was analyzed through SPSS software.

It has been found that nursing educators have knowledge regarding cooperative learning. 72% of the participants have knowledge about cooperative learning. Besides this they also have positive attitude towards it and approximately 43% of the participants always use cooperative learning structures in their practice but they are facing certain barriers in implementing these strategies. Few of the major barriers are workload, lack of motivation and management support. Hence it can be concluded that nursing educators have knowledge and competencies regarding cooperative learning with respect to teaching physiology. But more emphasis should need to be given on training in relation to cooperative learning as it will not only help in professional development of educators and effective teaching but may also results in the production of efficient competitive nurses who have more self reliance and improved interest in physiology.

Dawood A .Preservice teacher attitude toward and knowledge about cooperative learning in kuwait: a quasi experimental study. [PHD Thesis]. University of North Texas, 2001 Vaunette P. Selz N and Johnson J. Active Learning in Nursing Education

Elaine Simpson RN, Mary Courtney RN. Critical thinking in nursing education: literature review. International journal of nursing practice. 2002;8:89-98.

Slavin RE. Research on cooperative learning: Consensus and controversy. Educational Leadership. 1990;47(4):52-4

Baumberger-Henry M. Cooperative learning and case study: does the combination improve students perception of problem-solving and decision making skills? Nurse education today. 2005;25(3):238-46

Where applicable, the authors confirm that the experiments described here conform with The Physiological Society ethical requirements.

PCA183

Teaching acid-base physiology to medical students: A comparison of group work and peer instruction for interpreting arterial blood gases

M.W. Petersen[1,2], L.N. Toksvang[1], R.R. Plovsing[2] and R.G. Berg[1,3]

[1]Centre of Inflammation and Metabolism, Department of Infectious Diseases M7641, University Hospital Rigshospitalet, Copenhagen Ø, Denmark, [2]Intensive Care Unit 4131, University Hospital Rigshospitalet, Copenhagen Ø, Denmark and [3]Renal and Vascular Research Section, Department of Biomedical Sciences, Faculty of Health Sciences, University of Copenhagen, Copenhagen N, Denmark

Background:

Collaborative teaching strategies are associated with enhanced student performance in quizzes when conveying complex physiological phenomena, (Giuliodori *et al*, 2006), and Mazur's peer instruction may enhance transfer and retention of learning in a time-efficient fashion. This may be of particular relevance when conveying complex physiological phenomena, such as acid-base physiology. In the present study, we hypothesized that peer instruction was superior to conventional group work for teaching medical students to diagnose acid-base disorders by means of arterial blood gas analysis.

Methods:

A total of 41 second-year medical students were included during a respiratory physiology course. They were randomised to (A) conventional group work (n=22) or (B) peer instruction (n=19), and were tested by an identical pre- and post-test, which encompassed four arterial blood gases (see Table). Each correctly diagnosed acid-base disorder was awarded with one point (both tests). During the class, students were presented with eight additional arterial blood gasses that were either solved in groups of two (A; 2 minutes for each case) or by using a peer instruction-based approach (B; individual assessment for 1 minute followed by an assessment in groups of two for 1 minute). The percentage of correct answers and the subjective confidence level (0-100 % certainty of the correct diagnosis) in the pre- and post-tests were determined, and data are reported as median with corresponding interquartile range (IQR).

Results:

Pre-test scores were identical in both groups (median, 2; IQR, 1-2), and a significant increase was observed in both the conventional and the peer instruction study group following intervention (median, 4; 3-4 and 3; 3-4, respectively, both $p < 0.0001$), and scores did not differ between the two groups ($p=0.31$). Confidence levels increased in both groups and they evaluated the class similarly (data not shown).

Conclusion:

Collaborative teaching strategies were efficient for teaching students to diagnose acid-base disorders by means of arterial blood gas analysis. In the present time-restricted setup, we found no evidence that peer instruction is superior to conventional group work. However, a larger study is required before any definitive conclusion on this matter can be surmised.

Acid-base disorder	Group A (n = 22)		Group B (n = 19)	
	Pre-test (%)	Post-test (%)	Pre-test (%)	Post-test (%)
Normal	36	100*	79	95*
Respiratory alkalosis with partial metabolic compensation	55	82*	42	79*
Metabolic acidosis with partial respiratory compensation	27	91*	26	89*
Combined metabolic and respiratory acidosis	23	77*	5	58*

Correct answers. *Difference between pre- and post-test within groups ($p<0.0001$). Within group differences were assessed by Wilcoxon rank sum test, and between group differences by Mann-Whitney U-test.

Giuliodori MJ *et al* (2006). *Adv Physiol Educ* **30**, 168-73.

Where applicable, the authors confirm that the experiments described here conform with The Physiological Society ethical requirements.

PCA184

Using a classic paper by Robin Fåhraeus and Torsten Lindqvist to teach basic hemorheology

L. Toksvang and R.M. Berg

Department of Infectious Diseases, Centre of Inflammation and Metabolism, Copenhagen Ø, Denmark

"The viscosity of the blood in narrow capillary tubes" by Robin Fåhraeus and Torsten Lindqvist (Am J Physiol 96: 562-568,

1931) can be a valuable opportunity for teaching basic hemorheological principles in undergraduate cardiovascular physiology. This classic paper reports that a progressive decline in apparent viscosity occurs when blood flows though glass capillary tubes of diminishing radius, which has later been designated the 'Fåhraeus-Lindqvist effect'. Subsequent studies have shown that apparent viscosity continues to decline at diameters that correspond to the arteriolar segments of the systemic vascular tree, where the majority of the total peripheral resistance resides and is actively regulated in vivo. Here we present how the paper by Fåhraeus and Lindqvist can be used as a teaching tool and a platform for a plenary discussion of these concepts with undergraduate students, as well as of the relationship between hematocrit, vessel diameter, red blood cell deformability, resistance to blood flow, and how these factors may affect the work of the heart.

Where applicable, the authors confirm that the experiments described here conform with The Physiological Society ethical requirements.

PCA185

The contribution of Adolf Beck to Physiology (to 150-anniversary from his birth)

O. Zayachkivska[1], M. Gzhegotsky[1] and A. Coenen[2]

[1]Physiology, Lviv National Medical University, Lviv, Ukraine and [2]Biological Psychology, Donders Centre for Cognition, Radboud University, Nijmegen, Netherlands

Professor Adolf Beck (1863-1942), the founder of Physiology Department of the Lviv National Medical University who stood at the cradle of studies of the manifestation of the electrical brain activity, fought political discrimination and racism (anti-Semitism) on his way to becoming one of the XX century's leading but still unknowing in XXI century to a wide audience, scientist.

A. Beck was a pioneer in neurophysiological and psychophysiological methods to investigate cerebral cortex. Beck's fate was closely tied to the turbulent political and war history of Galicia, a region of the Austrian-Hungarian empire, He performed his influential electrophysiological work at the Jagiellonian University in Cracow and was invited to organize Physiology Department at the Medical Faculty in Lviv, where nominated as professor at the University of Jan Casmir in 1895. This Department in nowadays is in Lviv As professor in Physiology he produced 180 publications and was nominated for the Nobel Prize in Physiology. Dr. Beck's initial interest was the electrophysiology of the nervous system. In 1890 his article about the spontaneous and evoked electrical activity in the brain was published in the 'Centralblatt für Physiologie', a leading European Physiology magazine. Beck accurately localised sensory modalities of the cerebral cortex, by electrical and sensory stimulation during recording of electrical activities. In doing this, Beck also found the spontaneous oscillations of the brain potentials, just as Caton (1875) did, and showed that these fluctuations were not related to heart and breathing rhythms, but had to be regarded as genuine electrical brain activities. After Hans Berger's work on human brain waves (1929), these electrical activities were indicated as the EEG. In the 1890s Beck studied parts of the cerebral cortex that reacted upon stimulation with electro-negativity, first recorded 'evoked potentials'. Moreover, Beck discovered a new element: a decrease in the amplitude of the potentials upon sensory stimulation. Thus, he was the first to describe the phenomenon, which is now known as the desynchronization of the EEG. It is important to note that the research of Beck was not limited to neurophysiology, but he also worked in the field of general Physiology, such as visceral, sensory, and laboratory medicine. However, Beck's groundbreaking work and ideas were uknown to wide scientific community due to the diverse factors, including wars, political, ideological grounds and restricted international contacts between different scientific groups. After the WWII Adolf Beck was mainly disregarded, until M.A.B. Brazier (1904–1995), neuroscientist, expert in the history of neuroscience, translated Beck's dissertation into English (1973). The historical lessons of life story and work Adolf Beck on modern science should be widely explored for educational and scientific purpose.

Where applicable, the authors confirm that the experiments described here conform with The Physiological Society ethical requirements.

PCA188

Natsudaidain isolated from *Citrus* plants inhibits activation of mast cells in the late phase of immediate allergy

T. Matsui[1], H. Shiono[1], C. Ito[2], M. Itoigawa[3] and T. Okada[1]

[1]Physiology, Aichi Medical University, School of Medicine, Nagakute, Japan, [2]Meijo University, Nagoya, Japan and [3]Tokai Gakuen University, Nagoya, Japan

Mast cells play a central role in the immediate allergic reaction and in chronic inflammation associated with fibrosis. Mast cells also express several genetically encoded pattern recognition receptors including Toll-like receptors, which function in innate immunity. Thus, the roles of mast cells are complex, as they function in both immunity and inflammation. This discrepancy may be due to the fact that numerous bioactive chemical mediators including histamine, prostaglandins, and pro-inflammatory cytokines are released following the discrete reactions of mast cells against various stimuli. To understand the physiological roles of mast cells, studies have focused on the mechanisms of mast cell activation, as well as on the molecules that inhibit mast cell activation. Flavonoids, such as quercetin, are found in many plants and inhibit the activity of chemical mediators released from mast cells. Extracts of *Citrus* plants, which contain many flavonoids, exhibit anti-inflammatory, anti-allergy, and anti-cancer effects. We isolated and identified two polymethoxyflavonoids––natsudaidain and nobiletin––from *Citrus* plants. Although nobiletin has an anti-inflammatory effect, the biological activity of natsudaidain, which closely resembles nobiletin, is not fully understood. Here we examined the inhibitory effect of natsudaidain on histamine release, tumour necrosis factor-α (TNF-α) production, and cyclooxygenase-2 (COX-2) expression in Ca ionophore-stimulated rat basophilic leukemia cells (A23187-stimulated RBL-2H3 cells) using spectrofluorometric, ELISA, and immunoblotting methods. The percent of histamine release from A23187-stimulated RBL-2H3 cells pretreated with natsudaidain at 5, 25, or 50 μM was not altered compared with non-treated A23187-stimulated cells. Pretreatment with 100 or 200 μM natsudaidain resulted in slightly reduced levels of histamine release (89.8 ± 3.5% and 71.5 ± 5.6% histamine release at 100 and 200 μM, respectively). Thus, natsudaidain has little effect on histamine release from RBL-2H3 cells, except at high concentrations. On the other hand, natsudaidain inhibited TNF-α protein and mRNA levels in A23187-stimulated RBL-2H3 cells dose-dependently; a concentration of 6.8 μM was required for a 50% reduction. In addition, all levels of this compound tested also inhibited COX-2 protein expression. The mRNA levels of COX-2 in

A23187-stimulated RBL-2H3 cells treated with natsudaidain were also markedly reduced. The phosphorylated-p38 MAPK protein levels in A23187-stimulated RBL-2H3 cells were lower in natsudaidain-treated cells than in non-treated cells. These findings suggest that natsudaidain inhibits TNF-α and COX-2 production by suppressing p38 MAPK phosphorylation; thus, natsudaidain may alleviate inflammatory diseases.

Where applicable, the authors confirm that the experiments described here conform with The Physiological Society ethical requirements.

PCA189

Mer receptor tyrosine kinase promotes resolution of acute sterile inflammation through upregulation of liver X receptor expression and activation

J. Choi[1,2], Y. Yoon[1,2], J.Y. Seo[1,2] and J.L. Kang[1,2]

[1]Physiology, Ewha Womans University, Seoul, Republic of Korea and [2]Tissue Injury Defense Research Center, Ewha Womans University, Seoul, Republic of Korea

Mer signal plays the central roles in the intrinsic inhibition of the inflammatory response to pathogens by macrophages and dendritic cells. Liver X receptors (LXRα and LXRβ) also have a role for the maintenance of immune tolerance. However, physiological relevance of endogenous activation and transrepression pathways has remained unclear. In the present study, we aimed to understand the impact of endogenous Mer signal on TLR-dependent generalized inflammatory responses and LXR activation in zymosan-treated mice, using anti-Mer neutralizing antibody. Treatment with anti-Mer antibody significantly reduced phosphorylation of Mer and Akt, Mer downstream molecule in peritoneal macrophages and/or spleen and lung at hours 6, 24, and 72 after zymosan treatment. Anti-Mer antibody inhibited apoptotic cell clearance by peritoneal macrophages in vivo and ex vivo, but further enhanced neutrophil number and the levels of protein in peritoneal cavity. Moreover, anti-Mer antibody enhanced zymosan-induced pro-inflammatory mediators, including TNF-α, IL-1β, MIP-2 and MMP-9, but reduced anti-inflammatory mediators, such as TGF-β and HGF in peritoneal fluid. Similar findings with anti-Mer antibody and zymosan were shown at the levels of genes of TNF-α and MIP-2, as well as TGF-β and HGF in spleen and lung tissue. After zymosan injection, LXRα expression in spleen and lung reduced at 6 hours and reached the control level at 24hours and increased at 72 h. The level of LXRβ expression dropped at 6 hours, reached to the control level at 24 h, and remained at 72 h. The levels of LXRα/β at these time points after injection of zymosan were reduced by treatment with anti-Mer antibody. The levels of genes and proteins of LXRα/β target molecules, such as ABCA1 and ApoE, were in parallel reduced by treatment with anti-Mer antibody. Importantly, co-administration of T0901317 with anti-Mer antibody enhanced LXRs expression and activation and reversed the increases in these pro-inflammatory mediators, neutrophil numbers, and the levels of protein in peritoneal fluid at 6 and 24 h after zymosan injection. These findings suggest that Mer signaling contributes for the resolution of generalized inflammation through upregulation of LXR induction and activation.

Joseph SB et al. (2004) Cell 119, 299-309

Rothlin CV et al. (2007) Cell 131, 1124-1136

Lee YJ et al. (2012) J Leukoc Biol 91, 921-932

This work was supported by National Research Foundation (NRF) grant funded by the Korean government (MEST) (2012-0009844).

Where applicable, the authors confirm that the experiments described here conform with The Physiological Society ethical requirements.

PCA190

Heterogeneity of commercially available human serum albumin products: thiol oxidation and protein carbonylation

S. Era, T. Terada, T. Minami, T. Takahashi and H. Arikawa

Department of Physiology and Biophysics, Gifu University Graduate School of Medicine, Gifu, Japan

Albumin has been widely served as nutrients for tissue cultures in laboratory field and as plasma expander for blood transfusion in clinical field. Recently, human serum albumin (HSA) is sometime used as supporting materials in medium for human ES and iPS cell culture. In respect of thiol group of the protein, HSA has one highly reactive thiol group at position 34 (Cys-34). When it is a free state, it is called human mercaptalbumin (HMA, reduced form). On the other hand, when the thiol group is modified by oxidation, it is called human non-mercaptalbumin (HNA, oxidized form). HNA is further classified into two forms; HNA-1, mixed disulfide with cysteine; HNA-2, more higher oxidation products. Therefore, HSA in the exracellular fluids (ECF) is a mixture of HMA and HNA, i.e., a protein redox couple in ECF. As a commercially available HSA product is manufactured from large-scale pooled blood, the serum-derived albumin may have a different degree on thiol-redox state and protein carbonylation. By using a convenient HPLC system for the clear separation from HSA to HMA, HNA-1 and HNA-2, we examined the redox state of HSA products from various sources. Protein carbonylation is analyzed by Protein Carbonyl Assay Kit (Cayman Chem. Co.). All HSA products were obtained from Sigma Co. (product No. A1653 (5 lots), A3782 (5 lots) and A9731 (2 lots)). The A1653 is a product corresponding to Cohn Fraction V from serum-derived albumin, which is a starting material from pooled sera. The A3782 is a final product, which is prepared from A1653 through lyophilized and defatted processes. On the other hand, the A9731 is a recombinant HSA product expressed in rice (Cellastim®). Mean HMA values for A1653, A3782 and A9731 were 29.3. 28.2 and 33.1%, respectively. Mean values for carbonyl content of those products were 10.5, 18.7 and 31.4 nmol/mg protein, respectively. In order to evaluate the possible role of HSA as growth-promoting potential for cell culture in vitro, A1653 (lot 030M7034V), A3782 (lot 090M7001V) and A9731 (lot 061M1563) were used for U937 cells. For cell growth response, the ability of A9731 (recombinant albumin) was stronger than those of A1653 and A3782 (serum-derived albumin). These results suggest that the heterogeneity of thiol-redox state and protein carbonylation of various kinds of commercial HSA products appears to occur during manufacturing process of HSA from large-scale pooled blood. However, a recombinant albumin may have a different manner from that of a serum-derived albumin. This is especially important in studies where these products are used to interact with other biological materials in both laboratory and clinical fields.

Where applicable, the authors confirm that the experiments described here conform with The Physiological Society ethical requirements.

PCA191

A fragment of recombinant habutobin inhibited collagen-induced platelet aggregation

M. Nakamura[1], M. Sunagawa[1] and T. Kosugi[2]

[1]Molecular and Cellular Physiology, University of the Ryukyus, Okinawa, Japan and [2]Nursing, Faculty of Human Health, Meio University, Okinawa, Japan

Habutobin is a thrombin-like enzyme isolated from the crude venom of *Trimeresurus Flavoviridis* (the habu snake). We have clarified physicochemical and biological characteristics of habutobin. Habutobin was found to have pleiotropic biological activities such as clotting activity of rabbit fibrinogen, inhibitory activity of platelet aggregation, and stimulatory activity of urokinase release from vascular endothelial cells. In the previous study, recombinat-habutobin (r-habutobin) was produced by the baculoviral expression system from habutobin cDNA. r-habutobin has biological activities such as fibrin forming activity and inhibition of collagen-induced platelet aggregation as native habutobin. It has not been clarified how the structure of habutobin relates to its pleiotropic biological activities, which enable us to develop a reliable antithrombotic drug. We produced four fragments of r-habutobin (F1, F2, F3 and F4) by the truncation of habutobin cDNA in order to identify the functional domain which is responsible for the antiplatelet action of habutobin. We examined whether the r-habutobin fragments prevent platelet aggregation. The effect of two fragments of r-habutobins (F2 and F3) were tested on the aggregation of washed rabbit platelets. Platelet aggregation and ATP release were measured with a light transmission aggregometer using the method of Luciferin-Luciferase reaction. Upon collagen-stimulation of washed platelets, the effect on conformational change of glycoprotein (GP) IIb/IIIa and on the expression of P-selectin were tested by Flow cytometer (FCM) with PAC-1 (which only binds to activated platelets) and P-selectin antibody. The aggregation of washed platelet by collagen was inhibited by F3 r-habutobin. The percent inhibition by F3 r-habutobin was 22.6 ± 5.99 % (n = 7), and that by F2 r-habutobin was 14.75 ± 13.93 (n = 4). F3 r-habutobin also prolonged the lag time of collagen-induced platelet aggregation and slightly inhibited the collagen-induced ATP release from washed platelet. The expression of PAC-1 and P-selectin was decreased by F3 r-habutobin. FCM analysis revealed that F3 r-habutobin decreased FSC/SSC and that platelet membrane expressions of GP IIb/IIIa and P-selectin were decreased by F3 r-habutobin. These results suggested that the reduction of ATP release, decrease of GP IIb/IIIa and P-selectin expression on washed platelets may lead to inhibit the shape change of cytoskeleton in the presence of F3 r-habutobin. The key structure for the inhibition of the expression of P-selectin and the activation of GP IIb/IIIa might be present in F3 r-habutobin.

Where applicable, the authors confirm that the experiments described here conform with The Physiological Society ethical requirements.

PCA192

The effect on anticoagulation by siRNA-mediated tissue factor knockdown in pig aortic endothelial cells in vitro

M. Ji[1] and S.N. Yi[2]

[1]Physiology, Basic medical science school, Central South University, Changsha, Hunan, China and [2]Centre for Transplantation and Renal Research, Westmead Hospital, Sydney, NSW, Australia

Aims: The coagulation disorders leading to the loss of both whole organ xenografts have increasingly been recognized as a critical barrier to successful transplantation. Coagulation is initiated by damage to blood vessel endothelium and the expression of tissue factor (TF). The aim of this study is to determine the effect of TF gene knockdown on pig aortic endothelial cells (SVAP) in coagulation disorders in vitro.
Methods: SVAP were transfected with siRNA specific for TF or a nonspecific control siRNA using lipofectamine 2000. Transfected SVAP were then analyzed for TF gene and protein expression by real-time PCR and FACS respectively. The effect of TF knockdown in SVAP on anti-coagulation was evaluated by incubation with human blood for 60 min. Clots were collected and measured. Platelets, leukocytes and neutrophils were counted by using Beckman Coulter ACT.
Results: TF knockdown resulted in substantially reduced production of TF by SVAP. TF gene level of siRNA transfected SVAP was 22± 4% (n = 4) of naïve SVAP which was determined by real-time PCR. FACS results proved TF protein level of siRNA transfected SVAP had been reduced by 70%(57.1± 5.4% vs13.3±2.4 %, n = 4, $p < 0.01$). Nonspecific
siRNA had no effect (53.6±4.5%, n = 4). When TF siRNA transfected SVAP were
incubated with human blood there was no obvious reduced clot weight (0.42±0.04g vs
0.32±0.05g, n=5, p>0.05) and reduced consumption of platelets (4.1±1.2x10^9/L
vs 6.5±1.3x10^9/L n=5, p>0.05), leukocytes (2.3±0.3x10^9/L vs 2.8±0.5x10^9/L, n=5, p>0.05) and neutrophils (0.94±0.06x10^9/L vs 1.22±0.06x10^9/L, n=5, p>0.05) when compared to that detecte in the well with non-transfected SVAP.
Conclusion: The expression of TF on endothelial cells is involved incoagulation reaction but not the major coagulation factor in xenotransplantation.
Key words: Tissue factor, pig aortic endothelial cells, Anticoagulation, Xenotransplantation
The study was approved by the Sydney West Area Health Service Human and Animal Research Ethics Committees.

van der Windt DJ et al (2009). Am J Transplant 9, 2716-2726.

Biedermann BC et al (2002). Lancet 359 (9323): 2078-2083.

Lin CC et al (2008). Transplantation 86 (5):702-709.

Friedl J et al (2002). Blood 100(4): 1334-1339.

Chih Che Lin et al (2009). Transplant Immunology 21(2): 75-80.

Where applicable, the authors confirm that the experiments described here conform with The Physiological Society ethical requirements.

PCA193

In-vitro reversal of human sickled erythrocytes by high K+ -isotonic solutions

O.I. Ajayi[1], A. Sekumade[2] and P.C. Ogbechie[1]

[1]Physiology, University of Benin, Benin city, Edo, Nigeria and [2]MEDICAL LABORATORY SCIENCE, ACHIEVERS UNIVERSITY, OWO, ONDO, Nigeria

Red cell sickling and adhesion are favoured by cellular dehydration, which increases the rate of hemoglobin polymerization and cell sickling. Potassium chloride co-transport and calcium-activated potassium channel (Gardos channel) mediate erythrocyte dehydration in sickle cell disease and β-thalassemia, but their role in vaso-modulation is less defined. We investigated the in-vitro effect of various concentration of K+ ions in physiological solutions (PSS) as well as in cocos nucifera water which is a natural drink known for its natural high potassium content and health benefits. We obtained blood samples of ten (10) sickle cell disease patients (SCD) confirmed by hemoglobin electrophoresis in the Hematology Laboratory of University of Benin Teaching Hospital, Benin city for this study. One part was treated with sodium metabisulphite (Na2S5O7) solution to induce maximum sickling as controls while the other parts were subjected to different high concentrations of K+ in PSS as well as cocos nucifera water (40mM, 80mM and cocos nucifera water -240m/M) respectively. A thin blood smear was made to ascertain the percentage sickled erythrocytes count before and after the treatment. A mean sickle cell count was obtained after a manual count of three different smears. We observed a maximum percentage count of sickled cells after the addition of Na2S5O7 (45%) which decreased significantly ($P<0.05$ respectively) to about 2% with Cocos nucifera and 10% with80mM K+ PSS. The decrease count in 40mM K+PSS was not statistically significant. We conclude that high potassium ion solutions can activate the rehydration of sickled erythrocytes by probably activating the Gardos channel to increase the mean corpuscular haemoglobin concentration(MCHC) and thereby restoring the normal red cell shape. A probable pharmacological value of the cocos nucifera water and high potassium isotonic solutions in SCD management may be indicated.

Brugnara C.(2000). j.Bio.chem 259, 6472-6480

The Medical Scientists in Hematology Laboratory of UBTH

Where applicable, the authors confirm that the experiments described here conform with The Physiological Society ethical requirements.

PCA194

The roles of Macrophage MHC receptor (MMR)1 in allorecognition: Isolation of a cDNA encoding a novel MHC receptor for HLA-B44, human MMR1

J. Yamaji, T. Shimizu, E. Daikoku, M. Saito, Y. Shiraiwa, R. Yoshida and T. Kubota

Osaka Medical College, Takatsuki, Japan

Previously, we reported that macrophage (H-2D^{b}K^b)-mediated cytotoxicity of allografts [e.g., BALB/c skin (H-2D^{d}K^d)] in the rejection site and that we isolated two cDNAs encoding novel receptors on mouse macrophages or monocytes for H-2D^d and H-2K^d (mouse MHCs) and named them MMR1 and 2. Recently, we identified human homologs of mouse MMR1 and 2 by a search of sequence homology (BLAST) and also isolated two cDNAs encoding human MMR1 and 2 from human PBMCs cDNA library by RT-PCR method. In this meeting, we present the identification and characterization of human MMR1. The predicted amino acid sequence of human MMR1 cDNA (approximately 1.5 kb) encoded a putative single transmembrane protein, and the homology showed 64% identity to the entire mouse MMR1 protein and 96%, 96%, and 98% identity to its respective intracellular, transmembrane, and MHC binding regions. RT-PCR analyses demonstrated that human MMR1 expressed on monocytes in PBMCs. To examine the binding toward HLAs (human MHCs), HEK293T cells expressing human MMR1 were incubated with the beads conjugating 80 kinds of HLA class I or fluorescein-labeled soluble HLA molecules and then were analyzed by flow cytometer. Flow cytometric analyses showed that the mean fluorescence intensity of human MMR1 protein toward HLA-B44 was significantly high and that HEK293T cells expressing human MMR 1 bound specifically to HLA-B44 with a dissociation constant of 3.0×10^{-9} M. These results suggest that human MMR 1 on monocytes or macrophages might be novel receptors for HLA-B44.

Where applicable, the authors confirm that the experiments described here conform with The Physiological Society ethical requirements.

PCA195

When platelets start to function – insight into primary hemostasis in developing murine fetuses using a new in-vivo microscopy model

A. Margraf[1], C. Nussbaum[1,2], S. Schmidt[1], S. Dietzel[1], E. Quackenbush[3], U.H. von Andrian[4] and M. Sperandio[1]

[1]Walter-Brendel-Centre of Experimental Medicine, Ludwig-Maximilians-University, Munich, Germany, [2]Dr. von Hauner Children's Hospital, Ludwig-Maximilians-University, Munich, Germany, [3]Agennix Inc., Munich, Germany and [4]Department of Microbiology and Immunobiology, Harvard Medical School, Boston, MA, USA

Introduction:
Blood loss resulting from vessel injury is prevented in the mammalian organism through well regulated steps in the process of hemostasis. While a fully functional primary hemostatic system can be found in healthy adults, newborns and especially preterm newborns are at an increased risk for bleeding complications including intraventricular hemorrhage. Recent studies in humans reported decreased platelet reactivity in preterm newborns, opposed to data showing shortened bleeding times in term neonates. However, up to today there is no model to examine the development of the hemostatic system and the impact of maturation on primary hemostasis.
Methods:
To examine platelet function and thrombus formation in yolk-sac blood vessels of developing murine fetuses, pregnant C57/Bl6 mice were anesthetized (5mg/ml ketamine, 1 mg/ml xylazine in 10 ml/kg of normal saline; intraperitoneal injection), the abdominal cavity opened, the uterus prepared and one viable fetus inside the yolk-sac exteriorized. Manual microinjection allowed administration of phototoxic FITC-dextran into fetal yolk-sac vessels, as subsequent excitation with high intensity light was applied to induce thrombus formation. Injection of fluorescent microbeads allowed determination of blood flow characteristics in fetal yolk-sac blood vessels. Time course and steps of thrombus formation were deter-

mined in fetuses of ages E13.5 to E17.5. Multiphoton-microscopy was applied to study distribution patterns of the phototoxic dye within the fetal vasculature. FACS-analysis allowed acquisition of platelet counts as well as further investigation of activation patterns of fetal platelets.
Results:
Rate of onset and firm vessel occluding thrombus formation in murine yolk-sac vessels was significantly lower in youngest fetuses compared to older ones (p<0,05). Additionally, reflow after primary thrombus formation appeared more frequent in youngest fetuses. Time until platelet adhesion and stable thrombus formation was prolonged in E13.5 fetuses compared to older fetuses. FACS-analysis revealed significantly decreased platelet counts in fetal blood samples compared to adult levels. Furthermore, changed platelet activation properties on thrombin stimulation could be noted in fetuses compared to adult values.
Conclusion:
This is the first reported in-vivo observation of platelet function and thrombus formation in the developing murine fetus using a newly established intravital microscopy model. We find that during early fetal development, decreased thrombus formation as well as reduced thrombus stability are present, while a gradual normalization of primary hemostasis can be noted towards more mature gestational ages. Therefore, our results are the first to show a developmental regulation of primary hemostasis in the living fetal mammalian organism.

Where applicable, the authors confirm that the experiments described here conform with The Physiological Society ethical requirements.

PCA196

How carnosine affects cardiovascular parameters in remnant kidney model

H. Yapislar[1] and E. Taskin[2]

[1]Physiology, Istanbul Bilim University, Istanbul, Sisli, Turkey and [2]Pediatric Cardiology Department, New York University School of Medicine, New York, NY, USA

Purpose : Chronic kidney disease (CKD) is a major public health concern affecting millions of people .Oxidative stress is a mediator of systemic complications of chronic renal failure (CRF) and involved in the pathogenesis of hypertension, endothel dysfunction, shortened erythrocyte lifespan and deformability(1). One of the main effects of oxidative stress is the decrease in the biological activity of nitric oxide (NO). Endothelial dysfunction is characterized by a reduced synthesis of bioavailability of NO (2). The remnant kidney (RK) model is widely considered to be the classic model of progressive renal disease and it is known that inhibition of NO synthesis has been known to worsens renal disease is the RK model by hemodynamic changes (3). As we know L-carnosine is an antioxidant known to possess free radical scavenging functions (4). In this study, our aim is to induce renal failure in rats with subtotal nephrectomy (RK model) and observe the effect of carnosine on both hemorheologic parameters and blood pressure levels of nephrectomyzed rats and compare the results with their sham operated control group rats.
Material and Methods: 4 months old Male Sprague-Dawley rats were used in the study. The Animals were divided into 4 groups consisted of 6 rats each. 3 days after the subtotal nephrectomy and sham operations, the surviving rats were divided into the four groups; 1 - Sham (S), 2 - Sham + Carnosine (S-C), 3 - Subtotal nephrectomy (N), 4 - Subtotal nephrectomy + Carnosine (N-C). Carnosine was injected i.p. (50 mg/kg in each injection every day for 15 days). The control group received the same volume of physiological saline.RBC dformability indexes, arterial blood pressure and heart rate, MDA and NO levels were measured.
Results:In N group MDA level was statistically increased compared to sham group as we expected (p<0.05). MDA level was significantly decreased in N-C group compared to N group (p<0.05).NO level of N group was found to significantly decrease compared to S group NO levels(p<0.05). There was significantly decreased in N group EI level than in S group level (p<0.05). N-C group EI level was found to significantly increase compared to N group EI level (p<0.05). EI values demonstrates to us that carnosine shows this effect in all shear stress values.In all systolic blood pressure (SBP), diastolic blood pressure (DBP) and mean blood pressure (MBP) measurements, there was no any significant difference between S and N groups (p>0.05).
S-C group heart rate level was significantly increased compared to S group heart rate level (p<0.05). There is no important difference between other groups in terms of heart rate levels.
Conclusion:As a result, we see that carnosine has important effect o RBC deformability indexes, lipid peroxidation and NO levels but it doesn't affect blood pressure and heart rate levels in RK model in rats.

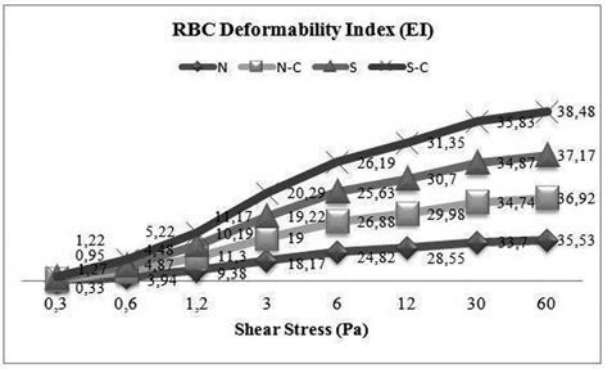

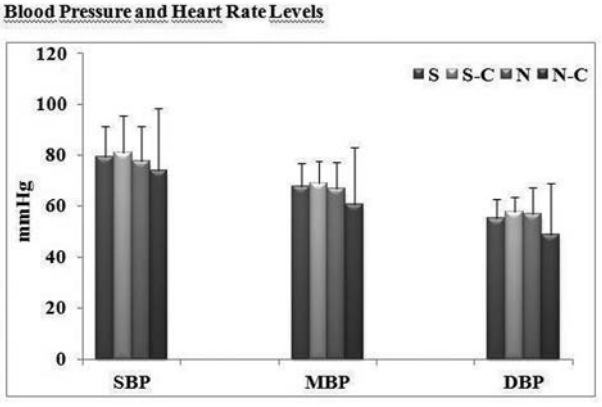

1) Himmelfarb J, Stevinkel P, Ikizler TA, Hakim RM. The elephant in uremia: oxidative stress as a unifying concept of cardiovascular disease in uremia. Kidney Int 2002;62:1524-1538.

2) Vaziri ND, Ni Z, Oveisi F, Liang K. Enhanced nitric oxide inactivation and protein nitration by reactive oxygen species in chronic renal insufficiency. Hypertension 2001;39:135-141.

3) Kang DH, Nakagawa T, Feng L, Johnson R. Nitric oxide modulates vascular disease in the remnant kidney model. American Journal of Pathology 2001;161(1):239-248.

4) Hartman PE, Hartman Z, Ault KT.Scavenging of singlet molecular oxygen by imidazole compounds: high and sustained activities of carboxy terminal histidine dipeptides and exceptional activity of imidazole 4-acetic acid. Photochem Photobiol 1990;51 (1):59-66.

5) Martinez M,Veya A,SarverR,Santaolaria M. Erythrocyte elongation index measured on a Rheodyn SSD laser diffractometer, influence of the hematocrit.Clin Hemorheol Microcirc 1998; 19:255-257.

Where applicable, the authors confirm that the experiments described here conform with The Physiological Society ethical requirements.

PCA197

Lethal and adaptive macroautophagy as typical cellular responses to hypoxia/reoxygenation

A. Kabakov, V. Mosina and K. Budagova

Medical Radiology Research Center, Obninsk, Russian Federation

We investigated consequences of ischemia/reperfusion stress on in vitro models with various types of mammalian cells undergoing hypoxia/reoxygenation. Cultured rat cardiomyocytes (H9c2 line), murine fibroblasts, human vascular endothelium and human kidney epithelium (293 line) were here used for the experiments with prolonged hypoxia (N2 atmosphere, <1% O2, for 18-20 h) followed by reoxygenation under normoxic conditions (21% O2). We found that, independently on cell type, some percentage (8-35%) of the reoxygenated cells dies via mitochondria-dependent apoptosis. Besides, macroautophagic events were clearly observed in all the reoxygenated cells what was manifested in formation of autophagosomes entrapping stress-damaged mitochondria and subsequent formation of large autolysosomes digesting the entrapped mitochondria. Some fraction (5-20%) of those cells underwent autophagic death (i.e. lethal autolysis) afterwards, whereas the other cells survived and even became more resistant to the repeated hypoxia/reoxygenation stress. When we performed stressful preconditioning by means of mild hyperthermia (43 C for 60 min) or shorter (8-10 h) hypoxia, such pretreated cells acquired the enhanced resistance to subsequent (severe) hypoxia/reoxygenation stress: the percentage of apoptotic and autophagic death considerably decreased, although the post-stress macroautophagic processes were not impaired in the preconditioned cells. Furthermore, upon post-hypoxic reoxygenation in the preconditioned (resistant) cells, uptake of mitochondria by autophagosomes began earlier and more intensely as compared with non-preconditioned control; this discrepancy correlated with the decrease in apoptosis and improved survival of the preconditioned cells. In the case of pretreatment with rapamycin, a known inhibitor of macroautophagy, the reoxygenated cells did not exhibit macroautophagic events but, instead, massively died via apoptosis and necrosis. Moreover, rapamycin prevented the acquisition of resistance to the hypoxia/reoxygenation stress after the preconditioning. We suggest that macroautophagy is the characteristic cellular reaction to hypoxia/reoxygenation; this reaction is aimed at compartmentalization of stress-damaged mitochondria into autophagosome followed by their digestion by autolysosomes. Such responses allow some post-hypoxic cells to escape apoptosis resulting from the mitochondrial damage. In some cases, macroautophagy appears to kill the reoxygenated cells if their mitochondrial damage is too severe. According to our observations, the stressful preconditioning may switch the post-hypoxic macroautophagy from its lethal mechanism to the adaptive one. It seems likely that the stress-inducible heat shock proteins are involved in this cytoprotective switching.

Where applicable, the authors confirm that the experiments described here conform with The Physiological Society ethical requirements.

PCA198

MicroRNA let-7i can control TLR4 expression and affect IFN-γ secretion in T cells from patients with ankylosing spondylitis

H. Yu[1,2], W. Liu[1], N. Lai[2,3], H. Chen[4], C. Yu[5], M. Lu[2,3] and H. Huang[1]

[1]Department of Life Science and Institute of Molecular Biology, National Chung Cheng University, Chia-Yi, Taiwan, [2]Division of Allergy, Immunology and Rheumatology, Buddhist Dalin Tzu Chi General Hospital, Chia-Yi, Taiwan, [3]School of Medicine, Tzu Chi University, Hualien, Taiwan, [4]Department of Biomedical Sciences, Chang Gung University, Tao-Yuan, Taiwan and [5]Department of Internal Medicine, National Taiwan University Hospital and National Taiwan University College of Medicine, Taipei, Taiwan

Ankylosing spondylitis (AS) is a chronic inflammatory disorder characterized by dysregulated T cells. We hypothesized that the aberrant expression of microRNAs (miRNAs) in T cells might involve in the pathogenesis of AS. The expression profile of 270 miRNAs in T cells from five AS patients and five healthy controls were analyzed by real-time PCR. After initial analysis, thirteen miRNAs were found potential differentially expression. After validation using 22 AS patients and 18 healthy controls, we confirmed that miR-16, miR-221 and let-7i were overexpressed in AS T cells and their expression levels were positively correlated with the Bath Ankylosing Spondylitis Radiology Index of lumbar spine in AS patients. In addition, the protein molecules regulated by miR-16, miR-221 and let-7i were measured by Western blotting. We found that the protein levels of Toll-like receptor 4 (TLR4), a target of let-7i, in T cells from AS patients were decreased. Lipopolysaccharide (LPS), a TLR4 agonist, inhibited interferon gamma (IFN-γ) secretion by anti-CD3+ anti-CD28 antibodies-stimulated T cells from healthy controls but not AS patients. After transfection of let-7i into normal T cells, LPS promoted IFN-γ production after stimulated by anti-CD3+anti-CD28 antibodies, but the transfection of let-7i does not have effects on IFN-γ production in AS T cells. In summary, we found that miR-16, miR-221, and let-7i were overexpressed in AS T cells and their expression levels were associated with radiographic change. In the functional study, the increased let-7i expression facilitated the Th1 (IFN-γ) immune response in AS T cells.

Chen C *et al*. (2005). *Nucleic Acids Res* **33**,e179.

Braun J & Sieper J. (2007). *Lancet* **369**,1379-90.

Nahid MA *et al*.(2011). *Cell Mol Immunol* **8**,388-403.

Colbert RA *et al*. (2010). *Immunol Rev* **233**,181-202.

This work was supported by the grant from the Buddhist Dalin Tzu-Chi General Hospital (Thematic studies 98-2-1), Taiwan.

Where applicable, the authors confirm that the experiments described here conform with The Physiological Society ethical requirements.

PCA199

ANGII-AT1 receptor antagonizes bone resorption through TLR-4 signaling in an animal model of LPS-induced periodontitis in rat

M. Garrido[1], M. Matos[1], A. Israel[1], L. Perdomo[2] and M. Alvarez[2]

[1]Laboratory of Neuropeptides, Universidad Central de Venezuela, Caracas, Venezuela, Bolivarian Republic of and [2]Instituto Anatómico José Izquierdo, Universidad Central de Venezuela, Caracas, Venezuela, Bolivarian Republic of

Periodontitis is an osteolytic disease characterized by destruction of the tooth-supporting tissues determined by cytokines induced by T-cells activation by oral bacteria products. Receptor activator of NF-kB Ligand (RANKL) stimulates bone resorption, while its soluble decoy receptor osteoprotegerin (OPG) blocks its action. RANKL activates its receptor (RANK) on monocytic precursors, triggering their differentiation into osteoclasts. Evidence indicates that Toll-like receptor (TLR) signaling regulates bone metabolism. TLRs are expressed in periodontal tissues and triggers a variety of downstream signal transduction pathways, including p-38 MAPK and NF-kB, which controls genes expression linked to inflammation and bone remodeling. Angiotensin II (ANG II) is now considered a pro-inflammatory cytokine since AT1 receptor (AT1R) blockade decreases the progression of inflammatory pathologies. The role of ANGII/AT1R in the periodontal disease is not known. We assessed the effect of valsartan (VAL), an AT1R blocker, on osteoclasts number, RANK/RANKL/OPG system expression, AT1 and TLR-4, and phosphorylation of p38-MAPK and NF-kB, in an experimental model of periodontitis induced by lipopolysaccharide (LPS) in rat. Experiments were conducted according to good practice for the management of laboratory animals of the Bolivarian Republic of Venezuela and the approval of Animal Ethical Committee of the School of Pharmacy. Male SD rats (280-300g) were divided into 4 groups: Control, LPS, VAL, LPS+VAL. LPS interdaily injections (10ul) and VAL (20 mg/kg, p.o.)/7 days were applied. Rats were anesthetized with 10% ketamine (60 mg/kg) and euthanized by decapitation, the maxilla dissected and the connective tissue collected. Immunofluorescent staining was used. Immunostaining was visualized with a confocal microscope. Intensity was quantified with NIH Image J software in 3 representative sections. Values are means ± SEM compared by ANOVA. LPS induced the formation of TRAP-positive multinucleated cells, increased tissue AT1R expression (C=3648±209; LPS=6081±150; L+V=4054±300) and TLR-4 (C=5487±66; LPS=7276±293; L+V=6097±62), RANK/RANKL system (C=5067±34; LPS=6161±48; L+V=5387±48/C=5570±130; LPA=7341±122; L+V=6177±189) and diminished OPG expression (C=5451±181; LPS=1007±42; L+V=5638±108). Also, LPS increased p-p38/p38 (C=1; LPS=1.52; L+V=1.19) and p-NF-kB/NF-kB (C=1; LPS=1.72; L+V=1.1). Conversely, VAL blunted all LPS-induce effects. Our results suggest that LPS, through TLR-4 stimulates MAPK and NF-kB-depentent pathways to induce bone resorption. Our data demonstrate a novel role for ANG II and AT1R in the pathogenesis of periodontal disease.

Brasier A. (2010).The nuclear factor-kappaB-interleukin-6 signalling pathway mediating vascular inflammation. Cardiovasc Res. 1;86(2):211-8.

Suzuki Y, Ruiz-Ortega M, Lorenzo O, Ruperez M, Esteban V, Egido J (2003b). Inflammation and angiotensin II. Int J Biochem Cell Biol. 35(6):881-900.

Garcia de Aquino S, Manzolli Leite F, Stach-Machado D, da Silva J, Spolidorio L, Rossa C Jr. (2009). Signaling pathways associated with the expression of inflammatory mediators activated during the course of two models of experimental periodontitis. Life Sci. 84(21-22):745-754.

Andreakos E, Sacre S, Foxwell B, Feldmann M. (2005). The toll-like receptor-nuclear factor kappaB pathway in rheumatoid arthritis. Front Biosci. 10:2478–2488.

Misión Ciencia, Proyecto ECCV No. 2007001585; CDCH PI-06-7638-2008/1

Where applicable, the authors confirm that the experiments described here conform with The Physiological Society ethical requirements.

PCA200

The effect of asthma related allergens in human gingival epithelial cells

A. Son[1,3], S. Lee[1], S. Lee[1], W. Park[2] and D. Shin[1]

[1]Department of Oral biology, Colleage of Dentistry, Yonsei University, Seoul, Republic of Korea, [2]Department of Advanced General Dentistry, College of Dentistry Yonsei University, Seoul, Republic of Korea and [3]Department of Dental Hygiene, Beakseok University, Cheonan, Republic of Korea

Asthma is a chronic inflammatory disease of the airway characterized by variable airflow obstruction and bronchial hyperresponsiveness. In addition, patients with asthma have been reported that high prevalence of dental caries and gingivitis, which are induced by low salivation due to the medication for asthma. However, it is not known that asthma related allergens such as house dust mite (HDM) and German cockroach extract (GCE) have direct effects on the generation of gingival inflammation. HDM and GCE proteases are potent inducers proinflammatory cytokines through protease-activated receptor (PAR). Toll like receptor (TLR) family as the major receptor for endotoxin from GCE and HDM. Furthermore, the NLR family, pyridine domain-containing 3 (NLRP3) inflammasome is activated by a wide rage of danger signals. In the present study, we investigated the level of NLRP3 inflammasone, interlukin-8 (IL-8), IL-6 and IL-1β mRNA expression and the characteristics of Ca^{2+}signal by GCE and HDM in the human gingival epithelial cells. HDM and GCE induced increases in NLRP3 and proinflammatory cytokines mRNA expression level and intracellular concentration of Ca^{2+} ($[Ca^{2+}]_i$), respectively. Endotoxin-free GCE activated PAR2, but endotoxin-free HDM did not activate any PARs. In human gingival epithelial cells, whereas lipopolisacaride, a Gram-negative endotoxin, did not induce Ca^{2+} signal, HDM and GCE containing endotoxins induced Ca^{2+} signal from thapsigargin (Tg), an inhibitor of sarco/endoplasmic reticulum Ca^{2+} ATPase, -sensitive Ca^{2+} stores via phospholipase C (PLC)/inositol 1, 4, 5-trisphosphate (IP_3) pathway. These results suggest that asthma related allergens induce Ca^{2+} signaling and cytokine release in human gingival epithelial cells.

Where applicable, the authors confirm that the experiments described here conform with The Physiological Society ethical requirements.

PCA201

Hypo-osmotic stress regulates RANKL mRNA expression through TRPM3 and TRPV4 in primary cultured human PDL cells

G. Son, S. Lee, Y. Yang, S. Lee and D. Shin

Department of Oral Biology, Yonsei University College of Dentistry, Seoul, Republic of Korea

The periodontal ligament (PDL) is specialized connective tissue fibers for attaching a tooth to the alveolar bone and for supporting the tooth to withstand the mechanical stress occurred during chewing and continuous orthodontic tooth movement. These mechanical stresses induce physiological processes such as inflammatory response, periodontal tissue and bone remodeling. However, the mechanism of hypo-osmotic stress-induced cellular response in PDL cells remains poorly understood. We hypothesized that receptor activator of nuclear factor-kappaB (NF-κB) ligand (RANKL) and osteoprotegerin (OPG) released from PDL cells under hypo-osmotic stress regulate bone remodeling, and investigated the mechanisms of RANKL and OPG expression by primary cultured human PDL cells in response to hypo-osmotic stress. Hypo-osmotic stress increased the mRNA expression of RANKL but not OPG as well as intracellular calcium concentration ($[Ca^{2+}]_i$). This increases in $[Ca^{2+}]_i$ was completely inhibited by gadolinium and lanthanum, non-specific plasma membrane Ca^{2+} channel blockers. We found TRPM3 and TRPV4 expressed in primary cultured human PDL cells and activities of these channels of TRPM3 and TRPV4 were confirmed by a whole-cell patch-clamp technique. Finally, aminoethoxydiphenyl borate and ruthenium red, each blockers of TRPM3 and TRPV4, reduced hypo-osmotic stress-induced increases in $[Ca^{2+}]_i$ and RANKL mRNA expression. These results suggest that hypo-osmotic stress induces increases in $[Ca^{2+}]_i$ through TRPM3 and TRPV4 to regulate RANKL mRNA expression in primary cultured human PDL cells.

Where applicable, the authors confirm that the experiments described here conform with The Physiological Society ethical requirements.

PCA202

Decreased calcium mobility and the lack of secretion in equine sweat gland cells

J. Robertson and D.L. Bovell

Glasgow Caledonian University, Glasgow, UK

Sweat secretion helps maintain the skin surface ecosystem and provides thermoregulation in humans and the Equidae. Mediators of sweat secretion act by activating receptors coupled to phospholipase-C, which results in the breakdown of phosphatidylinositol 4,5-bisphoshate to create inositol 1,4,5-trisphosphate (IP3) which stimulates a Ca2+ signaling process that is biphasic {Putney, 1981; Berridge, 1984}. This biphasic response involves the release of Ca2+ ions from an intracellular organelle, the endoplasmic reticulum (ER), followed by the entry of calcium ions across the plasma membrane. Much is known about the first phase of intracellular calcium release from an intracellular organelle, an effect mediated by IP3 acting on the IP3 receptor {Berridge, 1987}. The resultant rise in calcium is maintained by calcium influx and it is this sustained elevation of calcium which activates the secretory mechanism.

The mechanisms regulating the Ca2+ entry process in sweat glands are not well understood. It is commonly accepted that the degree of emptying of the intracellular Ca2+-stores, generated by IP3 pathway, initiates a signaling process that regulates the rate of Ca2+ entry across the plasma membrane. This process is known as capacitative Ca2+ entry or store–operated Ca2+ entry (SOCE) {Putney, 2005; Parekh, 2005}. Despite the signaling processes underpinning SOCE having been researched over the last two decades, it is only fairly recently that the key molecular components been identified.

We investigated the role of SOCE in horse sweat gland cells from control animals and those that had developed anhidrosis, an inability to produce sweat. The cells used in this study were previously grown from horses destroyed for humane reasons (Wilson et al., 1993) and the methods used to initiate cultures of equine sweat glands are based on protocols elsewhere for human glands (Lee et al., 1986). Western blotting and PCR techniques confirmed the presence of STIM 1 and 2, Orai 1, 2 and 3 and TRPC1 proteins in cell lines derived from control and anhidrotic animals. However, the results indicated a reduction in STIM1 mRNA and protein expression, as well as a decrease in the localisation of STIM1 in the ER of anhidrotic cells compared to control cells. The functionality of the SOCE pathway in both cell lines, in response to agonist stimulation was investigated using FURA-2AM calcium-imaging techniques. Increases in [Ca2+]i could be abolished in the presence pharmacological blockers of SOCE and that anhidrotic cells showed a significant decrease in the [Ca2+]i FURA-2 ratio in response to agonists when compared to control cells. The results suggest that a reduction of STIM1 expression in the SOCE pathway may play a role in anhidrosis in horses.

Putney, J.W., Jr. and Weiss, S.J. (1981). Relationship between receptors, calcium channels, and responses in exocrine gland cells. Methods Cell Biol 23, 503-11.

Berridge, M.J. and Irvine, R.F. (1984). Inositol trisphosphate, a novel second messenger in cellular signal transduction. Nature 312, 315-21.

Berridge, M.J. (1987). Inositol trisphosphate and diacylglycerol: two interacting second messengers. Annu Rev Biochem 56, 159-93.

Putney, J.W., Jr. (2005). Capacitative calcium entry: sensing the calcium stores. J Cell Biol 169, 381-2.

Parekh, A.B. and Putney, J.W., Jr. (2005). Store-operated calcium channels. Physiol Rev 85, 757-810.

Where applicable, the authors confirm that the experiments described here conform with The Physiological Society ethical requirements.

PCA203

A protein arginine methyltransferase isoform controls the HIF-1-mediated adaptation to hypoxia by reducing de novo synthesis of HIF-1α protein

U. Ju[1], H. Park[1], J. Park[1,2] and Y. Chun[1,3]

[1]Department of Biomedical Sciences, Seoul, Republic of Korea, [2]Ischemic/Hypoxic Disease Institute, Seoul, Republic of Korea and [3]Department of Physiology, Seoul National University College of Medicine, Seoul, Republic of Korea

Hypoxia-inducible factor 1α (HIF-1α), which is regulated oxygen-dependently, transactivates numerous genes essential for cellular adaptation to hypoxia. HIF-1α expression is regulated at multiple steps from transcription to protein degradation. Moreover, the stability of HIF-1α protein has been known to be determined by posttranslational modifications such as ubiquitination, sumoylation, neddylation, and acetylation, but the

HIF-1α regulation by methylation has not been reported. Protein methylation at arginine residues is an essential process to regulate gene expressions and signal transductions, and is catalyzed by PRMT enzymes. While testing which PRMT isoforms participate in the HIF-1 signaling pathway, we found that one of PRMTs modulates HIF-1α expression under hypoxia. When the PRMT was knocked-down in glioblastoma cells, HIF-1α was expressed even under normoxia and further induced under hypoxia. The transcriptional activity of HIF-1 was evaluated in reporter systems using EPO enhancer-luciferase or VEGF promoter-luciferase vector, and the HIF-1-driven gene expressions were checked by RT-qPCR. These assays demonstrated that functional HIF-1 was induced by PRMT knockdown. We next studied the mechanism of the HIF-1α induction, and found that HIF-1α was induced at the translational level through activated PI3K/Akt/mTOR signaling. Based on these findings, we propose that the PRMT negatively controls de novo synthesis of HIF-1α protein regardless of oxygen level. Given many literatures supporting the cancer promoting action of HIF-1α, the PRMT could be a potential target for cancer therapy.

ATR controls cellular adaptation to hypoxia through positive

regulation of hypoxia-inducible factor 1 (HIF-1) expression

F Fallone1,2, S Britton1,2, L Nieto 1,2, B Salles1,2,3 and C Muller1,2

1CNRS, IPBS (Institut de Pharmacologie et de Biologie Structurale), Toulouse, France and 2Universite de Toulouse, UPS, IPBS, Toulouse, France. Correspondence: Professor

C Muller, Biology of Cancer, IPBS, CNRS UMR5089, 205 route de Narbonne, BP 6418231077 Toulouse Cedex, France.

E-mail: muller@ipbs.fr

3Current address: TOXALIM, INRA, 180 chemin de Tournefeuille, 31027 Toulouse, France.

GSK-3 regulates cell growth, migration, and angiogenesis via Fbw7 and

USP28-dependent degradation of HIF-1

Daniela Flu gel,1 Agnes Go rlach,2 and Thomas Kietzmann1

1Department of Biochemistry and Biocenter Oulu, University of Oulu, Oulu, Finland; and 2Experimental and Molecular Pediatric Cardiology, German Heart

Center Munich at the Technical University, Munich, Germany

Where applicable, the authors confirm that the experiments described here conform with The Physiological Society ethical requirements.

PCA204

CD73 suppression induces apoptosis and cell-cycle arrest in human breast cancer cells

X. Zhi, M. Xiang, X. Li, L. Yin and P. Zhou

Department of Physiology and Pathophysiology,, Fudan University, Shanghai, China

Ecto-5′-nucleotidase (CD73) is a 70 kDa glycosylated protein that is bound to the outer surface of the plasma membrane by a glycosyl phosphatidyl inositol anchor and co-localized with detergent-resistant and glycolipid-rich membrane sub-domains called lipid rafts. CD73 hydrolyzes extracellular AMP into adenosine and phosphate. Adenosine, a proliferative factor, acting through G-protein coupled receptors, produces a spectrum of physiological functions. In addition, it causes tumor growth, angiogenesis and immune suppression. CD73 upregulation is associated with a highly invasive cancer phenotype, drug resistance and tumor-promoting functions.To date, our knowledge on the mechanisms of CD73 on tumor growth is still limited. The present studies examine the effect of RNAi-mediated CD73 suppression and CD73 overexpression on tumorigenicity in vivo and in vitro on cell growth, and further explore its underlying regulatory mechanisms.

In this study, we tested the hypothesis that increased CD73 may promote tumor progression by examining the effect of CD73 suppression via RNA interference and CD73 overexpression on tumor growth in vivo and in vitro. Using digitized whole-body images, plate clone forming assay and TUNEL assay in frozen tissue sections, we found that the cell growth rate was significantly lowerin vivo and in vitro after CD73 suppression ($n = 3$; $P < 0.05$)and late apoptosis was much higher in xenograft tumors developed from the CD73-siRNA transfected MB-MDA-231 clone (P1) ($n = 10$; $P < 0.01$). By flow cytometry, the P1 cell cycle was arrested in the G0/G1 phase($n = 3$; $^*P < 0.05$). Moreover, Bcl-2 was downregulated, while Bax and caspase-3 were upregulated with CD73 suppression($n = 3$; $P < 0.05$). CD73 inhibitor α,β-methylene adenosine-5′-diphosphate (APCP) functioned similarly with RNAi-mediated CD73 suppression($n = 3$; $P < 0.05$). In addition, in transfected MCF-7 cells, we found that CD73 overexpression increased cell viability and promoted cell cycle progression($n = 3$; $P < 0.05$), depending on its enzyme activity. More intriguingly, CD73 overexpression in MCF-7 breast cancer cells produces a tumorigenic phenotype. We conclude that CD73 plays an important role in breast cancer growth by affecting cell cycle progression and apoptosis.

Key words: CD73; breast cancer; RNA interfere; apoptosis, cell cycle

This article is funded by National Natural Science Foundations, project codes: 81172507,81001170 and 30971163.

Where applicable, the authors confirm that the experiments described here conform with The Physiological Society ethical requirements.

PCA205

8,9-epoxyeicosatrienoic acid inhibits antibody production of B lymphocytes in mice

J. Feng[1], Y. Gao[1], Y. Zhu[1], Q. Xu[2] and X. Wang[1]

[1]Peking University Health Science Center, Beijing, China and [2]Cardiovascular Division, Kings College London BHF Centre, London, UK

Epoxyeicosatrienoic acids (EETs), synthesized from arachidonic acid by cytochrome P450 epoxygenases, are converted to dihydroxyeicosatrienoic acids by soluble epoxide hydrolase. EETs exert anti-inflammatory effects. However, the effect of EETs on humoral immunity is poorly understood. The present study is to investigate the potential role of EETs on B cell function and mechanisms. Firstly, we examined the role of EETs on antibody production of splenic B cells from C57BL/6 (male, 8-week-old, n=8) and ApoE-/- mice (male, 8-week-old, n=8) by means of ELISA. Of the 4 EET regioisomers, 8,9-EET (1 uM) significantly decreased the production of IgM (4.2 ± 0.9 vs. 8.0 ± 0.7 ug/ml) and IgG (35.6 ± 1.8 vs. 57.4 ± 1.0 ng/ml). By use of carboxyfluorescein succinimidyl ester (CFSE) dilution assay, we found that the proportion of dividing cells was lower with 8,9-EET (1 uM) (33.2 ± 0.9% vs. 49.3% ± 1.7%). We next examined the effect of 8,9-EET on B-cell survival stimulated with LPS. And the data showed that the percentage of live cells was substantially lower with 8,9-EET (10.2% ± 3.0% vs. 29.9% ± 2.6%). On the other hand, the generation of CD138+ cells was

markedly inhibited by 8,9-EET (28.1% ± 4.5% vs. 39.5% ± 0.5%). Furthermore, we found that 8,9-EET decreased sIgG1+ cell production (3.9% ± 0.3% vs. 7.8% ± 0.3%), which indicated that 8,9-EET inhibits the class-switch recombination of B cells. Molecular events involved in class-switch recombination were significantly inhibited by 8,9-EET. Additionally, nuclear p65 NF-kB level was increased within 5 min after LPS stimulation and was inhibited by pretreatment with 8,9-EET. To determine whether 8,9-EET regulates B-cell function in vivo, sEH-/- mice treated with 8,9-EET were intraperitoneally injected with 4-hydroxy-3-nitrophenyl acetyl-OVA (NP-OVA). The spleen size of mice with 8,9-EET infusion (15 ng/h) was smaller at day 6 pos-timmunization. The colocalization of CD19 and PNA from immunofluorescence analysis of spleens revealed fewer germinal centers and smaller structures. In summary, 8,9-EET may inhibit B-cell function in vitro and in vivo, which suggests a new therapeutic strategy for diseases with excess B cell activation.

This work was supported by the National Basic Research Program of China [2010CB912504; 2011CB503904], the National Natural Science Foundation of China [81121061; 81000115], and the Fund of the Chinese Ministry of Education [20100001120049].The author is the recipient of the travel awards for young physiologists from the Chinese Association for Physiological Sciences (CAPS).

Where applicable, the authors confirm that the experiments described here conform with The Physiological Society ethical requirements.

PCA207

A simulation study of the effects of GLP-1 on membrane excitability in pancreatic β-cells

Y. Takeda and A. Noma

Ritsumeikan University, Kusatsu, Shiga-ken, Japan

Upon elevation of plasma glucose concentration, pancreatic β-cells generate bursts of action potentials to induce cyclic changes in [Ca2+]i and regulate pulsatile insulin release. This glucose-dependent insulin secretion is synergistically enhanced by an incretin hormone, gucagon-like peptide-1 (GLP-1). To date, it has been well established that GLP-1 activates adenylate cyclase through binding to its G-protein-coupled receptor and increases [cAMP], the key signal underlying the insulinotropic effects. The increase in [cAMP] subsequently activates protein kinase A (PKA) and cAMP-regulated guanine nucleotide exchange factor (cAMP-GEF or Epac), modulating the activities of ion channels at the plasma membrane and ER, which in turn modify the pattern of burst as well as Ca2+ transients. However, because of complex interactions between multiple cellular factors and ion channels or transporters involved in the GLP-1 effects, quantitative aspects of the molecular mechanisms have not yet been determined. In order to overcome this difficulty, we adopted a strategy of modeling analysis; simulation study and mathematical analysis. First, our β-cells model [1] was updated and GLP-1 receptor signal transduction model [2] was incorporated. The modulatory effects of PKA and Epac on ion channels, voltage-gated Ca2+ channels (VGCC), delayed rectifying K+ channels (KDR), ATP-sensitive K+ channel (KATP) and non-selective cation channels (NSCC), were then reconstructed based on experimental observations in electrophysiological and pharmacological studies. Finally, lead potential (VL) analysis [1] were applied to quantitatively determine the functional role of each ion channel in GLP-1 induced increase in membrane excitability (Fig. 1). The analysis revealed that activation of NSCC strongly contributes to shorten burst interval, whereas deactivation of KATP causes insufficient contribution to hyperpolarization during plateau leading to prolongation of burst duration during GLP-1 stimulation. Simulation studies by constructing a comprehensive model based on experimental records and mathematical analyses of the model behavior provide a deeper and more objective insight into cellular functions.

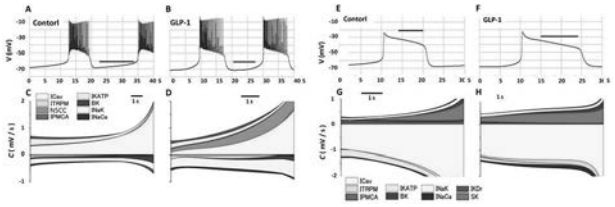

Fig 1. Contribution of ion channel to the interburst and plateau period at 10 mM [Glucose] with and without GLP-1 stimulation. A, B, E, F; Time-dependent changes in Vm trace is overlapped by VL. In order to resolve the change in slow components, action potentials was eliminated by calculating Vm with steady-state solution for gating variables (E,F). C, D, G, H; Time-dependent changes in the contribution (c) of individual currents indicated with different colors. A positive c indicates that the time-dependent change in the corresponding current contributes to depolarization, whereas channels with negative c contributes to hyperpolarization.

1] Cha CY, Nakamura Y, Himeno Y, Wang J, Fujimoto S, Inagaki N, Earm YE and Noma A. (2011). J Gen Physiol 138: 21-37

[2] Takeda Y, Amano A, Noma A, Nakamura Y, Fujimoto S and Inagaki N. (2011) Am J Physiol Cell Physiol 301:C792-C803

Grants-in-Aid for Scientific Research (B)

Where applicable, the authors confirm that the experiments described here conform with The Physiological Society ethical requirements.

PCA209

Transient receptor potential vanilloid 4-dependent calcium influx and ATP release in mouse esophageal keratinocytes

A. Boudaka[1,2], H. Mihara[1,3], T. Sugiyama[3], Y. Moriyama[4] and M. Tominaga[1]

[1]Division of Cell Signaling, Okazaki Institute for Integrative Bioscience (National Institute for Physiological Sciences), National Institutes of Natural Sciences, Okazaki, Aichi-ken, Japan, [2]Department of Physiology, College of Medicine and Health Sciences, Sultan Qaboos University, Muscat, Oman, [3]Department of Gastroenterology, Graduate School of Medicine and Pharmaceutical Sciences, University of Toyama, Toyama, Japan and [4]Department of Membrane Biochemistry, Okayama University Graduate School of Medicine, Dentistry, and Pharmaceutical Sciences, Okayama, Japan

Gastro-oesophageal reflux disease (GERD) is a multi-factorial disease that may involve
oesophageal hypersensitivity to mechanical or heat stimulus as well as acids. Intraganglionic
laminar endings (IGLEs) are the most prominent terminal structures of oesophageal vagal
mechanosensitive afferents and may modulate mechanotransduction via purinergic receptors.
Transient receptor potential channel vanilloid 4 (TRPV4) can detect various stimuli such as warm temperature, stretch and some chemicals, including 4α-phorbol 12,13-didecanoate (4α-PDD) and GSK1016790A. TRPV4 is expressed in many tissues, including renal epithelium, skin keratinocytes and urinary blad-

der epithelium, but its expression and function in the oesophagus is poorly understood. Here, we show anatomical and functional TRPV4 expression in mouse oesophagus and its involvement in ATP release. Methods: Expression studies were performed on mouse esophagus by RT-PCR and immunostaining. TRPV4 channel activities were examined by Ca^{2+}-imaging and Patch-Clamp experiments with primary esophageal keratinocytes isolated from WT and TRPV4KO mice. ATP release from keratinocytes was measured by Luciferin-Luciferase assay. Results: TRPV4 mRNA and protein were detected in esophageal keratinocytes. Several TRPV4 activators such as chemicals, heat and stretch stimulus have increased cytosolic Ca^{2+} concentrations in primary WT keratinocytes, but not in TRPV4KO keratinocytes. GSK and heat stimulus evoked TRPV4-like current responses in WT cells, but not in TRPV4KO cells. The mRNA of a newly identified ATP transporter, VNUT and its protein were also detected in esophageal WT keratinocytes. TRPV4 activators (GSK and heat stimulus) increased ATP release from WT cells, but not from TRPV4KO cells. This release was inhibited by a vesicle-trafficking inhibitor brefeldin A. Conclusion: TRPV4 contributes to ATP release via exocytosis, responding to heat, chemical and possibly mechanical stimuli. TRPV4 could be involved in esophageal mechano- and heat-hypersensitivity and be related to the pathophysiology of GERD.

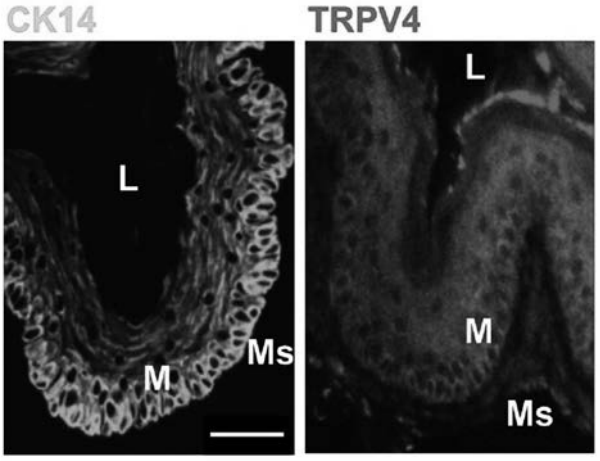

TRPV4 immunoreactivity in WT mouse esophagus. Bars indicate 50 μm. CK14: keratinocyte marker; L: lumen; M: mucosa; Ms: muscle.

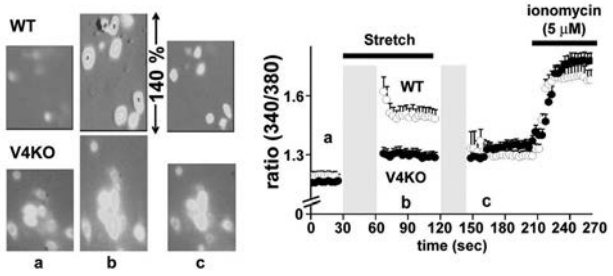

TRPV4-mediated cytosolic Ca^{2+} increase in primary esophageal keratinocytes. Representative pseudocolor images and traces for $[Ca^{2+}]_i$ changes in response to mechanical stimuli (140 %) in WT and TRPV4KO keratinocytes cultured on silicon chambers (mean ± SEM). Images were obtained at points a, b and c indicated on the traces. Mechanical stimulus was applied between the blue boxes (a black bar).

Where applicable, the authors confirm that the experiments described here conform with The Physiological Society ethical requirements.

PCA211

Development of new molecular tools to monitor various inositol compounds in stimulated human HEK-293 fibroblasts

J.T. Tóth, G. Gulyás, D.J. Tóth, L. Hunyady and P. Várnai

Department of Physiology, Semmelweis University, Budapest, Hungary

In recent years it became clear that phosphoinositides (PI) are not only structural lipids in membranes, but they also have important roles in several cellular functions ranging from mediating signalling cascades in the cell by binding to effector proteins, through regulation of ion channels to cell movements. Reversible phosphorylation of the inositol ring at positions 3, 4 and 5 results in the synthesis of seven different PIs. Their levels in the plasma membrane, endomembranes and in the cytoplasm can influence these processes, thus measuring the level of these lipids in living cells can help us to better understand their distinct functions.

Our aim was to develop a highly sensitive method which enables us to follow the dynamic change of these lipids in living cells. For this we performed bioluminescence resonance energy transfer (BRET) measurements between various luciferase-labeled PI-binding domains and a plasma membrane-targeted Venus (yellow fluorescent protein) in HEK-293T cells. To monitor the inositol lipid pools the following domains were used: the PH domain of PLCδ1 for PIP2, the 2xPH domain of OSH2 for PI4P and the PH domain of BTK for PIP3. To measure cytoplasmic IP3 level a recently developed intramolecular BRET sensor, based on the ligand binding domain of the type-1 IP3 receptor, was used.

As expected, stimulation of the cells expressing type-1 angiotensin receptor with 100 nM angiotensin II resulted in a transient response including the decrease of the plasma membrane PI4P and PIP2 level, and increase of the cytoplasmic IP3 concentration, but no change of the PIP3 level. In contrast, more robust, sustained responses could be recorded if 100μM carbachol was applied to stimulate cells expressing M3 muscarinic acethylcholine receptors indicating that cells are able to synthetize huge amount of PI4P and PIP2 upon agonist stimulation. Stimulation of the cells expressing EGF receptor with 100 ng/ml EGF resulted in a sustained increase of the PIP3 and a slowly developing IP3 signal. Both PI4P and PIP2 levels were decreased, but in contrast with Gq-activating hormones, decrease of the PI4P pool was continuous and significantly higher compared to the transient decrease of the PIP2 level.

Our results indicate that this approach is highly sensitive and capable of quantitative and dynamic characterization of inositol lipid changes upon stimulation of the cells with various compounds. Selective measurements of the various lipid pools may result in the discovery of differences between stimuli and therefore the role of inositol lipid pools and inositol modifying enzymes during the activation process.

Support: OTKA K105006

Where applicable, the authors confirm that the experiments described here conform with The Physiological Society ethical requirements.

PCA212

Cholinergic pathways in human chronic myeloid leukemia cell proliferation

B. Aydin[1], M. Goren[2] and H. Cabadak[1]

[1]Biophysics, Marmara University, Istanbul, Turkey and [2]Medical Pharmacology, Marmara University, Istanbul, Turkey

A role may be attributed to cholinergic system in the development of hematological diseases. Recent studies demonstrated a significant increase in AChE activity together with muscarinic receptor expression in normal human peripheral blood lymphocytes as an early response to various stimuli (Battisti et al 2009). K562 cell line was established from a patient with chronic myeloid leukemia (CML) in terminal blast crisis. We have previously demonstrated the presence of muscarinic receptor subtypes namely M2, M3 and M4 in K562 line (Cabadak et al., 2010). We hypothesized that cholinergic agonist ACh is involved in cell proliferation in CML through muscarinic receptors.
In this present study, we aimed to demonstrate the mechanisms of ACh and carbachol (CCh) in cell proliferation. In order to track the roles of ACh we used hemicholinium, a choline uptake inhibitor, eserine hemisulfate, an acetylcholine esterase inhibitor and vesamicol a vesicular choline uptake inhibitor. We also made experiments with atropine the non-specific muscarinic antagonist to show the contribution of muscarinic receptors. K562 cell counts were performed in response to CCh stimulation where proliferation and cell viability were evaluated by the trypan blue exclusion test and BrDU labeling. AChE activity was determined by QuantiChrom TM Acethylcholine Assay kit. Choline acetyl transferase (ChAT) and AChE levels were quantified by using Western Blotting.
In our experiments we detected an inhibition of K562 cell count after 48 hr incubation in response to CCh at a concentration of 1 uM. Non-specific receptor antagonist atropine failed to reverse the inhibitory roles of CCh and ACh. Eserine also acted similarly on K562 cells and inhibited cell proliferation and atropine could not affect this inhibition (Table 1). Neither hemicholium nor vesamicol affected the cell counts. The effects observed with eserine is specifically dependent on ACh since we demonstrated a dose-dependent decrease in AChE activity concurrently. The experiments performed with vesamicole and hemicholinium imply that ACh secreted form other cells decrease proliferation of K562 cells. In conclusion, all these results may imply that extrinsic ACh activity affects cell proliferation in CML through nicotinic mechanisms, but ACh syhthesized within the cell elicits muscarinic receptor mediated effects.

Proliferation Assay Results

Groups	Optic Density at 405 nm (Mean ± SEM)
Control	0.223 ± 0.005
0.1 uM Eserine	0.186 ± 0.003
100 uM Eserine	0.155 ± 0.016
0.1 uM Eserine + Atropin	0.198 ± 0.017
100 uM Eserine+Atropine	0.178 ± 0.015

Battisti V, Schetinger MR, Maders LD, Santos KF, Bagatini MD, Correa MC, Spanevello RM, do Carmo Araújo M, Morsch VM. Changes in acetylcholinesterase (AChE) activity in lymphocytes and whole blood in acute lymphoblastic leukemia patients. Clin. Chim. Acta 402 (1-2), 114-118, 2009.

Cabadak H, Aydin B, Kan B. Regulation of M2, M3 and M4 Muscarinic Receptor Expression in K562 Chronic Myelogenous Leukemic Cells by Carbachol. Journal of Receptors and Signal Transduction, 31(1):26-32, 2010.

Maslinski W. Cholinergic receptors of lymphocytes. Brain Behavior and Immunity, issue, 1-14, 1989.

This research was supported by grants supplied fromTUBITAK (111S312) and Marmara U.(SAG-A-200611-0192).

Where applicable, the authors confirm that the experiments described here conform with The Physiological Society ethical requirements.

PCA213

Differential beta-arrestin2 requirements for constitutive and agonist-induced internalization of CB1 cannabinoid receptor

P. Gyombolai[1,2], E. Boros[1], L. Hunyady[1,2] and G. Turu[1,2]

[1]Department of Physiology, Semmmelweis University, Budapest, Hungary and [2]Laboratory of Molecular Physiology, MTA-SE, Budapest, Hungary

Background: Desensitization and internalization are key procedures in the regulation of hormone receptors, and beta-arrestins play an important role in these processes. Currently, little is known about the role of beta-arrestins in the regulation of the CB1 cannabinoid receptor (CB1R). Therefore, the interaction between beta-arrestins and CB1R, and its role in receptor internalization were investigated.
Materials and methods: The beta-arrestin binding of CB1R was studied by confocal microscopy and bioluminescence resonance energy transfer (BRET) in HeLa and Neuro-2a cells. To follow CB1R internalization, plasma membrane CB1 receptors were selectively stained using Halo-labeling technique. Internalization of the receptors was also monitored by a BRET assay through measuring non-specific BRET between CB1R and ICAM as a plasma membrane marker.
Results: We found that upon activation CB1R binds beta-arrestin2 (beta-arr2), but not beta-arrestin1, and this binding is transient. We also found that internalization following stimulation with CB1R agonists could be impaired either by a dominant negative beta-arrestin2 (beta-arr2-V54D) or by siRNA-mediated knock-down of beta-arr2. Similar inhibitory effects on agonist-induced internalization were detected with BRET measurements. In contrast, neither beta-arr2-V54D nor beta-arr2-siRNA had a significant effect on the constitutive (i.e. spontaneous) internalization of CB1R.
Conclusions: We conclude that upon activation, CB1R binds beta-arr2 in a transient manner (class A GPCR), and this binding is required for the agonist-induced internalization of the receptor. In contrast, constitutive CB1R internalization is independent of the beta-arr2 binding of the receptor, suggesting that the molecular mechanisms underlying these two processes are different.

Supported by Hungarian National Grant OTKA NK-100883.

Where applicable, the authors confirm that the experiments described here conform with The Physiological Society ethical requirements.

PCA214

The role of store operated calcium entry in endocytic vacuole formation in pancreatic acinar cells

D. Collier[1,2], R. Sutton[2,3], A. Tepikin[1,2] and S. Voronina[1,2]

[1]Department of Cellular and Molecular Physiology, University of Liverpool, Liverpool, UK, [2]NIHR Liverpool Pancreas Biomedical Research Unit, University of Liverpool, Liverpool, UK and [3]Department of Molecular and Clinical Cancer Medicine, University of Liverpool, Liverpool, UK

The intracellular activation of trypsinogen in pancreatic acinar cells is an early and probably initiating event in the development of acute pancreatitis (a frequent and life-threatening inflammatory disease). Endocytic vacuoles are the site of trypsinogen activation in pancreatic acinar cells (Sherwood et al 2007).

All inducers of acute pancreatitis trigger prolonged Ca^{2+} responses, involving release of Ca^{2+} from intracellular stores and induction of store-operated Ca^{2+} entry (SOCE). The formation of endocytic vacuoles is a Ca^{2+} dependent process.

The current study examined the specific role of SOCE in the formation of endocytic vacuoles. Fluorescence microscopy and Ca^{2+} sensitive probes (fluo-4 and fura-2) were utilised to test the response of murine pancreatic acinar cells to supramaximal doses of the secretagogue cholecystokinin (CCK), thapsigargin and the bile acid taurolithocholic acid 3 sulphate (TLC-S). All three compounds (known to deplete intracellular Ca^{2+} stores) induced sustained increase in cytosolic Ca^{2+} concentration and endocytic vacuole formation. We observed that pharmacological inhibition of SOCE (verified using fura-2 measurements) resulted in significant (more than 40%) inhibition of endocytic vacuole formation. Inhibition of vacuole formation was observed in experiments utilising supramaximal doses of CCK, TLC-S and thapsigargin, suggesting that SOCE plays an important role in vacuole formation in all three of these models of cellular Ca^{2+} toxicity. It is therefore likely that SOCE is an important component of Ca^{2+} toxicity, responsible for pancreatic acinar cell damage in the early stages of acute pancreatitis, and is a potentially useful pharmacological target in the development of treatment against this disease.

Sherwood MW, Prior IA, Voronina SG, Barrow SL, Woodsmith JD, Gerasimenko OV, Petersen OH and Tepikin AV. (2007). Activation of trypsinogen in large endocytic vacuoles of pancreatic acinar cells. PNAS, 27, 5674-5679.

GlaxoSmithKline

Where applicable, the authors confirm that the experiments described here conform with The Physiological Society ethical requirements.

PCA215

BRET titration experiments to study G protein coupled receptor dimerization: New insights into an old tool

B. Szalai[1], P. Hoffmann[2], P. Várnai[2,1] and L. Hunyady[2,1]

[1]MTA-SE Laboratory of Molecular Physilogy, Budapest, Hungary and [2]Institute of Physiology, Semmelweis University, Budapest, Hungary

G Protein Coupled Receptors (GPCRs) can form dimeric or higher ordered oligomeric complexes, which can remarkably influence the signalling of these receptors.

Bioluminsecent Resonance Energy Transfer (BRET) titration experiments are the gold standards to prove the physical interaction between the protomers of a presumed dimer. In this method the energy transfer (BRET signal) is measured between a luminescent (energy donor) and a fluorescent (energy acceptor) labelled receptor. BRET signal can increase not only due to a specific interaction (dimerization) but due to the random, non-specific interactions between donor and acceptor. To distinguish between the specific and non-specific interaction, BRET signal is measured using fixed amount of donor and varying amount of acceptor labelled receptors, and BRET signal values are plotted as a function of acceptor/donor ratio. In the case of specific interaction this plot shows a saturation curve, while in the case of non-specific interactions it shows a lineal relationship.

Maintaining constant amount of donor labelled receptors is strictly required to the correct interpretation of BRET titration experiments, but it is very hard to achieve in a transient transfection system. In our work, we analysed the effects of changing donor levels on BRET titration curves, and set up a system, where it is possible to distinguish between specific and non-specific interaction even in the case of changing donor amount.

To analyse the effects of changing donor levels on BRET titration curves, we performed Monte Carlo simulations. The results showed, that in the case of non-specific interaction, the BRET signal is only dependent on the amount of acceptor, while in the case of specific interaction it depends on the acceptor/donor ratio. Our simulations also showed, that in the case of changing donor levels, even non-specific interaction can lead to saturation BRET titration curves, which can lead to false interpretation of experimental results.

We tested our simulation results in an inducible dimerization system, where the non-specific interaction between FKBP labelled donor and FRB labelled acceptor molecules could artificial changed with the addition of rapamycin into a specific interaction. Our experimental results verified our simulations. With these new analysis methods, we examined the dimerization between various GPCRs (type I and II angiotensin receptor, V2 vasopressin receptor, β2 adrenergic receptor, calcium sensing receptor, CB1 cannabinoid receptor).

Our research was supported by OTKA NK 100883 of Hungarian National Academy of Sciences

Where applicable, the authors confirm that the experiments described here conform with The Physiological Society ethical requirements.

PCA216

Assessment of gap junction communication between human umbilical endothelial cells and monocytes in response to tumour necrosis factor (TNF-α)

A.H. Qasem, C.H. Fry and R.I. Jabr

Biochemistry and Physiology, University of Surrey, Surrey, UK

Atherosclerosis is a chronic inflammatory disease characterised by accumulation of monocytic cells and lipids within the subendothelial space. This is facilitated by monocyte (MO) transendothelial (EC) migration early in atherosclerosis development and requires direct MO-to-EC contact. This is enhanced by adhesion molecules in the presence of pro-inflammatory stimuli such as tumour necrosis factor-α (TNF-α). Both cell types express connexin (Cx) 43 isoforms that permit formation of gap junctions (GJ); channels permeable to small molecules

(<1KDa). We hypothesised that MOs and ECs communicate through formation of Cx43 GJs, which is enhanced by TNFα. Human umbilical vein endothelial cell (HUVEC) monolayers were maintained in endothelial growth medium whose functional integrity was assessed by measuring trans-endothelial electrical resistance (43.94±3.32Ω.cm^2;n=6). A dye transfer assay examined functional GJ formation between MOs and ECs. HUVEC monolayers were loaded with 5mM calcein-AM dye: free calcein is membrane impermeable and only permeates through GJs. Suspensions of freshly isolated MOs from peripheral blood were added to HUVEC monolayers. Calcein transfer to MOs was measured by flow cytometry and normalised to positive control values obtained from MOs directly loaded with calcein. A negative control used a Cx43 deficient MO cell-line, THP-1 monocytes. Experiments were carried out in endothelial basal medium (EBM) in the absence and presence of 2ng/ml TNF-α. The efficiency of dye transfer to MOs through GJs was measured in: 1) the presence of GJ inhibitor, 2mM heptanol; 2) THP-1 monocytes; 3) HUVECs transfected with Cx43-siRNA. Data are means ± SEM, compared by ANOVA, the null hypothesis was rejected at p<0.05.

Dye transfer to MOs, after incubation with calcein-loaded HUVECs monolayers for 30 minutes in EBM was recorded in 66.3±2.1% (n=3) of cells. This fraction was attenuated by heptanol (9.9±4.5%;n=3;P<0.001) and was comparable to the fraction of loaded THP-1 cells (8.33±4.66;n=3). For HUVECs transfected with CX43-siRNA, the fraction of calcein-loaded MOs also decreased compared to control,11.3±4.5% vs 74.1±2.1%, respectively (n=3;P<0.05). TNF-α enhanced the fraction of calcein-loaded MOs to 89.6±2.5% (n=3;P<0.001) in control monolayer. Such an effect was prevented in monolayer transfected with Cx43-siRNA (13.70±2.45%;n=3; P<0.001).

These results show that calcein-dye transfer through GJs formed between ECs and MOs. Dye transfer was attenuated by lack of Cx43 in MO, knock down of Cx43 in HUVECS with Cx43-siRNA or application of GJ blockers. TNF-α increased calcein transfer to MOs and had no effects in HUVECs with Cx43-siRNA. In this study we confirm the important role of GJ communication between MOs and ECs as an underlying mechanism for early stages of atherosclerosis development.

Where applicable, the authors confirm that the experiments described here conform with The Physiological Society ethical requirements.

PCA217

Measurement of inositol-1,4,5-trisphosphate in living cells using newly developed resonance energy transfer-based biosensors

G. Gulyás[1], J.T. Tóth[1], D.J. Tóth[1], L. Hunyady[1], T. Balla[2] and P. Várnai[1]

[1]Department of Physiology, Semmelweis University, Budapest, Hungary and [2]Section on Molecular Signal Transduction, Program for Developmental Neuroscience, National Institute of Child Health and Human Development, National Institutes of Health, Bethesda, MD, USA

Inositol-1,4,5-trisphosphate (IP3) plays a central role in calcium signalling. Its production is catalyzed by phospholipase C enzymes, which can be activated through receptor stimulation. When investigating these signalling pathways, calcium measurement is not the most appropriate method to detect receptor activation, because several parallel processes can alter intracellular calcium concentrations. To solve this problem, we designed an IP3 probe, which is able to directly reflect the level of this compound, and thus allows a more accurate characterization of these signalling pathways.

To construct this sensor, we used the human type-1 IP3 receptor, in which amino acids 224-605 are responsible for ligand binding. According to crystal-structure data, IP3 binding may lead to a conformational change of this protein domain. Based on this conformational change, we were aiming to construct a resonance energy transfer-based biosensor. In literature, similar probes can be found, but all of them have limitations. In particular, measurement of decreasing IP3 levels is uncertain, due to the high ligand affinity of these sensors. To eliminate this effect, we engineered two lower affinity mutants by impairing the binding site of the protein domain. The arginine in either position 265 or 269 was substituted to lysine (R265K and R269K, respectively). Finally, two appropriate luminescent chromophores were fused to the two ends of the protein domain to enable the monitoring of IP3 concentrations by fluorescence or bioluminescence resonance energy transfer.

To compare our sensors, we needed an experimental system, in which an increase or decrease in IP3 concentration could be equally established. We created a modified HEK-293T cell line, which stably expressed a rapamycin-inducible phosphatidylinositol 4,5-bisphosphate (PIP2) depletion system. To achieve a stochiometric expression of its proteins, the components of this depletion system were cloned into a self-cleaving 2A-peptide containing vector. In addition, type-1 angiotensin receptor was transiently transfected to these cells, so IP3 concentration increased upon angiotensin II stimulus, while a decrease was seen after rapamycin treatment and consequent PIP2 degradation.

Under these conditions both the wild type and the mutant sensors were able to show the increase in IP3 levels, but only the mutants were capable of detecting the decrease of IP3 concentration. Our data suggest that these sensors are suitable to investigate IP3 signalling more accurately by single cell imaging as well as in cell population measurements.

Support: OTKA K105006

Where applicable, the authors confirm that the experiments described here conform with The Physiological Society ethical requirements.

PCA218

A truncated splice variant of LRP1

M. Kolb[1], S. Trettner[1], S. Büttner[1], K. Engel[1], T. Seiboth[2], K. Huse[2] and G. Birkenmeier[1]

[1]Medical Faculty University Leipzig, Institute of Biochemistry, Leipzig, Germany and [2]Leibnitz Institute for Age Research, Fritz-Lipmann-Institute e.V., Jena, Germany

The low-density lipoprotein receptor-related protein-1 (LRP1), identical to the Alpha2-macroglobulin receptor (A2MR), is a member of the LDL receptor superfamily. The ubiquitously expressed LRP1 in particular is a scavenger receptor that mediates clearance of over 50 ligands from the extracellular matrix and the bloodstream among others A2M, proteases, and distinct components involved in modulation of cancer cell dissemination. Moreover, LRP1 is implicated in coordinating cell-matrix interactions, cell migration, as well as tumour promotion. So far, LRP1 was associated with both anti-tumour and recently with pro-invasive functions, thus indicating a more complex functionality. Beyond that LRP1 is involved in regulation of signalling pathways and physiologic processes such

as regulation of lipid metabolism and the proliferation of vascular smooth muscle cells.
NCBI data bank research revealed the expression of a truncated splice variant of LRP1 mRNA (shLRP1). Using standard PCR and Western Blot both its mRNA transcript and protein expression was analysed in human tissues and cancer samples as well as cancer cell lines. In order to localise the shLRP1 protein in cells, shLRP1 protein was over-expressed in cancer cell lines using pcDNA3.1 vector and Lipofectamine and analysed using immune fluorescence microscopy. The gene LRP1 comprising 84.86 kb is localised on chromosome 12q13.3 and is organised in 89 exons coding for a mature mRNA transcript of 14886 nucleotides. Compared to LRP1, the shLRP1 comprises exon 1 – 6 of LRP1 followed by an alternative exon containing a polyadenylation signal. As a result, the respective transcript shLRP1 can escape nonsense-mediated decay. Hence, the shLRP1 mRNA code for a truncated protein of only 296 aa exhibiting a unique C-terminus in contrast to LRP1 comprising 4544 aa. The shLRP1 mRNA was detected to be exclusively present in several solid tumours. Beyond that it was also present in tumours of brain, breast, colon, lung, muscle, and prostate as well as in corresponding tumour cell lines, such as U87-MG, 1321N1 (astrocytoma), MDA-MB-231, HT-29 (colon), A549 (lung), and PC3 (prostate). In contrast, no expression was detected in tumour cells derived from blood cells as well as normal human tissue. Western blot analysis of protein extracts of several cancer cell lines among others 1321N1, PC3, HT-29, and A549 verified translation of shLRP1 mRNA into protein. Consequently, shLRP1, over-expressed in transfected cancer cell lines, was detected in the cytoplasm and the perinuclear region, but not - as the LRP1 - in the cell membrane.
Summarising, these preliminary data offer the possibility to exploit the shLRP1 for tumour diagnosis, and tumour therapy on the one hand. On the other hand, the limited expression of shLRP1 in cancer cells raises the question regarding its involvement in physiological signalling pathways that have to be further investigated.

Where applicable, the authors confirm that the experiments described here conform with The Physiological Society ethical requirements.

PCA220

Effect of the nicotinic acid adenine dinucleotide phosphate antagonist Ned-19 on pancreatic acinar cell calcium signalling

M.R. Charlesworth, O.H. Petersen, J.V. Gerasimenko and O.V. Gerasimenko

Pathophysiology and Repair, Cardiff University, Cardiff, S.Glamorgan, UK

Regulation of the concentration of cytosolic calcium (Ca2+) is vital for the physiological function of many cell types. Three secondary messengers; inositol 1,4,5 trisphosphate (IP3), nicotinic acid adenine dinucleotide phosphate (NAADP) and cyclic adenosine diphosphate ribose (cADPR); have been identified as being able to induce Ca2+ release from organelle Ca2+ stores. Together these messengers allow for temporal and special coordination of Ca2+ signalling.
Acute pancreatitis (AP) is inflammation of the pancreatitis and the surrounding tissue, caused by the improper activation of the digestive enzymes within the acinar cells. This pathological enzymatic activation has been linked to atypical Ca2+ signalling, with mass release from stores; resulting in mitochondrial overload and induction of necrosis. Both the neurotransmitter acetylcholine (ACh) and the hormone cholecystokinin (CCK) induce in release of Ca2+ from stores in pancreatic acinar cells (PAC). ACh has been shown to induce Ca2+ release via generation of IP3, while CCK has been suggested to mobilise Ca2+ via synthesis of NAADP.
NAADP is unique from other secondary messengers as it induces calcium release from a thapsigargin resistant (non-endo/sarcoplasmic) store, shown to be composed of acidic organelles. PAC have a large pool of acidic organelles, mainly composed of zygomorphic granules, creating a significant store of NAADP sensitive Ca2+. Targeting this NAADP sensitive Ca2+ store by manipulating NAADP signalling should allow for an increased understanding of the role of Ca2+ in both the physiological and pathological function of PAC.
Ned-19 is a NAADP antagonist discovered in a screen of the ZINC chemical library using NAADP's 3D electrostatic structure. Its ability to inhibit NAADP induced Ca2+ release has been observed in several different mammalian tissue types and Ned-19 has been used to isolate NAADP's role from that of that the other secondary Ca2+ signalling molecules.
Initial experiments into the effect of Ned-19 on physiological Ca2+ signalling in PAC match the pattern expected by the secondary messengers implicated in the function of the stimulants used. With no changes in ACh induced Ca2+ release observed in the presence of Ned-19, but full to partial inhibition of CCK's ability to increase cytosolic Ca2+ levels.
One of the pathological causes of AP is reflux of bile acid in to the pancreases via the common bile duct. The bile acid taurolithocholic-acid-3-sulfate (TLC-S) has been shown to induces large Ca2+ release via a NAADP depend mechanism; however Ned-19 shows only the ability to delay this release and not inhibit it. Further study into Ned-19's effect on other models of AP and its ability to affect cell fate will provide vital information as to its potential as a treatment for AP.

Baumgartner HK, Gerasimenko JV, Thorne C, Ferdek P (2009) JBC:284(31):20796-803

Churchill G.C. et al. (2002) Cell:111:703-8

Naylor E, Arredouani A, Vasudevan SR et al. (2009) Nature Chem Biol:5(4):220-6

Deliu E, Tica AA et al. (2011) Am J Physiol Cell Physiol:301(3):559-65

Gerasimenko JV, et al. (2006) JBC:281(52):40154-63

Where applicable, the authors confirm that the experiments described here conform with The Physiological Society ethical requirements.

PCA221

Modulation of calcium entry and extrusion mechanisms in relation to the development of acute pancreatitis

E. Stapleton, J.V. Gerasimenko, O.H. Petersen and O.V. Gerasimenko

Biosciences, Cardiff University, Cardiff, S.Glamorgan, UK

Acute pancreatitis (AP) is a human disease characterised by inflammation and necrosis of pancreatic tissue. The most common causes of AP are excessive alcohol intake, gallstones and a fatty diet. The hallmark of AP is premature intracellular activation of digestive, resulting in the digestion of pancreatic tissues[1,2]. The premature activation of enzymes has been shown to be the result of elevated cytosolic Ca^{2+} concentration[1,2].
Pathophysiological Ca^{2+} signals are typically global, sustained increases in cytosolic Ca^{2+} and deplete Ca^{2+} stores. This sustained elevation of cytosolic results in intracellular activation of enzymes[1,2]. Pathological stimulation depletes the ER of Ca^{2+},

this depletion is determined by a Ca^{2+} sensor located in the ER membrane, STIM1[2]. STIM1 is activated by the depletion of ER Ca^{2+}, it is coupled to Orai-1 located in the plasma membrane (PM). Orai-1 is a store-operated Ca^{2+} (SOC) channel activated via depletion of the ER, resulting in Ca^{2+} influx[2]. Store-operated Ca^{2+} entry (SOCE) serves to refill the depleted ER with Ca^{2+} in non-excitable cells. However, during pathological stimulation additional Ca^{2+} entering the cell will serve to further exacerbate already elevated cytosolic Ca^{2+} concentrations. SOCE, as such, is ideal to target in order to reduce cytosolic Ca^{2+}.

C57BL/6 mice were killed humanely in accordance with the UK Schedule 1 of the Animals (Scientific Procedures) Act, 1986. Pancreatic acinar cells were isolated as described previously[3]. Cytosolic Ca^{2+} measurements were made using intact cells loaded with the Ca^{2+}-sensitive dye Fura-2 in AM form.

Preliminary data, using inhibitory compounds of SOC channels, indicate a significant reduction in Ca^{2+} overload and therefore partial protection of necrosis in acinar cells treated with reported pancreatitis-inducing agents[3,4].

In addition to focusing on SOCE, there are other mechanisms that could serve to decrease Ca^{2+} overload, such as potentiation of the plasma membrane Ca^{2+}-ATPase (PMCA) driving Ca^{2+} extrusion from the cell[4] as well as reducing calcium release through the calmodulin regulation[5]. We have measured the rates of Ca^{2+} entry and extrusion under control and pathological conditions, and compared the potential benefits of interfering with different calcium signalling pathways.

Targeting SOC channels and PMCA in order to reduce cytosolic Ca^{2+} overload could be an attractive strategy to reduce necrosis of pancreatic tissue.

Petersen OH & Sutton R (2006). *Trends Pharmacol Sci* **27**, 113-120.

Petersen OH *et al.* (2011). *F1000 Med Rep* **3**, 15.

Ferdek PE *et al.* (2012). *Curr Biol* **22**, 1241-1246.

Gerasimenko OV & Gerasimenko JV (2012). *Pflugers Arch* **464**, 89-99.

Gerasimenko JV *et al.* (2011). *Proc Natl Acad Sci U S A* **108**, 5873-5878.

Where applicable, the authors confirm that the experiments described here conform with The Physiological Society ethical requirements.

PCA224

Cytological remodeling of the periodontal ligament tissues due to mechanical stress

T. Kawakami[1], M. Tomida[2], R. Muraoka[3], T. Nakamura[2] and K. Nakano[1]

[1]Hard Tissue Pathology Unit, Matsumoto Dental University Graduate School of Oral Medicine, Shiojiri, Nagano, Japan, [2]Department of Oral Physiology, Matsumoto Dental University School of Dentistry, Shiojiri, Nagano, Japan and [3]Department of Orthodontics, Matsumoto Dental University School of Dentistry, Shiojiri, Nagano, Japan

[Aim] We examined the transplanted bone marrow-derived cell migration into the periodont ligament tissues. Mesenchymal cells in the bone marrow have abilities of cell migration and differentiation into periodontal cells. We examined the cytological remodeling dynamism of the periodontal ligament tissue due to orthodontic mechanical stress, using mouse experimental model.

[Methods] After the approving by Animal Experimental Control Committee of the University, Bone marrow cells from GFP transgenic mice were transplanted into 8 week-old female C57BL/6 mice, which had undergone 10 Gly of lethal whole-body irradiation for the purpose of inactive all bone marrow/white cells of in the recipient mice. After successful transplantation, the mice received orthodontic mechanical stress using the Waldo method; and the mice were compared as control without receiving orthodontic mechanical stress. Paraffin-sections were immunohistochemically (IHC), fluorescence IHC and TRAP staining techniques and analyzed using a primary anti-GFP-polyclonal rabbit antibody. Semi-quantitative evaluation of IHC staining was prepared and pixel density was counted for each image. Then typical IHC positive staining part was defined as positive area. The pixel number of positive area in the periodontal tissue was compared with the previously calculated total pixel number of the periodontal tissue and the ratio was obtained. The examination results were analysed using Mann-Whitney U test.

[Results and Discussion] We examined the transplanted bone marrow-derived cell migration into periodontal tissues. The IHC revealed that GFP-positive cells were detected in the periodontal tissues, both in the experimental and control specimens. The GFP-positive cells histopathologically differentiated into some cell types. The fluorescence IHC and TRAP staining techniques demonstrated these cells were detected as osteoclasts and macrophages. Furthermore, GFP-positive cells gathered adjacent blood vessels. The data suggest that GFP-positive bone marrow-derived cell migration into periodontal ligament tissues and differentiate periodontal tissues component-cells. The GFP-positive cells histopathologically differentiated into some cell types. The fluorescence IHC and TRAP staining techniques demonstrated these cells were detected as osteoclasts and macrophages. Furthermore, GFP-positive cells gathered adjacent blood vessels. The data suggest that GFP-positive bone marrow-derived cell migrate into periodontal tissues and differentiate periodontal component-cells. As a results of the examination group specimens and control group, the ratio of pixel number of GFP-positive cells in the examination group showed 5.77 ± 3.24 % (mean ± SD); and that in the control group, 0.71±0.45 % (mean ± SD). The examination group was greater than that of control group ($p<0.001$).

[Conclusions] These results suggest that orthodontic mechanical stress induces bone marrow cell migration and differentiation into periodontal ligament tissue component cells.

Where applicable, the authors confirm that the experiments described here conform with The Physiological Society ethical requirements.

PCA225

Assessment of blood perfusion as possible tool in differentiating between human benign skin naevi and malignant melanomas

M. Rossi[1], A. Stefanovska[2], G. Vezzoni[1], M. Pesce[1], B. Loggini[3], F. Ghiara[1], G. Rossi[4], F. Pingitore[3] and P. Barachini[1]

[1]Department of Clinical and Experimental Medicine, University of Pisa, Pisa, Italy, [2]Physics Department, University of Lancaster, Lancaster, UK, [3]Department of Translational Research and New Technologies in Medicine, University of Pisa, Pisa, Italy and [4]Unit of Epidemiology and Biostatistics, Institute of Clinical Physiology, CNR of Pisa, Pisa, Italy

Malignant melanomas (MM) are characterized by hypervascularisation which may affect MM blood flow and its oscillatory dynamic. The hypothesis of this study was that the blood flow assessment at the level of skin melanocytic lesions may aid in differentiating between benign skin naevi and MM. Fifty

one subjects with clinically and dermatoscopically atypical naevi and 23 subjects with clinically and dermatoscopically typical benign naevi underwent blood flow (BF) measurement at the level of the lesion of interest (central and margin lesion site) and at the level of a clinically healthy skin site, contra lateral to the lesion of interest, using a single point laser-Doppler fluxmetry (LDF). After LDF, atypical naevi were excised and underwent histological examination and immuno-histo-chemistry microvessel count. At the histological examination, MM was demonstrated in 9 lesions, atypical benign naevus in 31 lesions and typical benign naevus in 11 lesions. No significant difference in BF was found between clinically benign naevi, histologically benign naevi and histologically atypical naevi (Wilcoxon test), which were then included in a single control group (CG) of 65 naevi. Compared to CG naevi, MM showed a significantly higher BF (at the level of both central and margin lesion site) and a significantly higher ratio in BF between lesion margin site and contra lateral skin site (LMS/CLS ratio), as well as between central lesion site and contra lateral skin site (Wilcoxon test). A LMS/CLS ratio > 1 was observed in 100% of MM and in 60% of CG naevi, with a sensitivity of 100 (95% C.I.: 65.5- 100), a specificity of 40 (95% C.I.: 28.8-52.9) and a ROC area of 0.70 (95% C.I.: 0.64 – 0.76). The results of this study show that MM have a significantly greater BF compared to benign naevi (both typical and atypical) and suggest that a > 1 LMS/CLS BF ratio could be a suitable cut-off for selecting naevi to be examined by histology in order to exclude MM. This last result should be confirmed in a larger group of MM patients.

Results of laser-Doppler blood flow assessment in melanomas and control naevi.

	Melanomas (9)	Control naevi (65)	p
Lesion central site blood flow (PU)	112.0 (39.9-181.6)	15.6 (10.1-29.0)	0.0003
Lesion margin site blood flow (PU)	78.7 (27.6-125.8)	16.8 (10.9-29.3)	0.0004
Contra lateral skin blood flow (PU)	15.9 (13.0-23.0)	12.6 (10.3-16.8)	0.051
LMS/CLS blood flow ratio	3.7 (1.6-6.6)	1.3 (0.8-2.4)	0.006

Data are as median and inter-quartile range. LMS/CLS = margin lesion site/contra lateral skin.

PU= perfusion unit

Häfner HM et al. (2005). J Vascul Res42, 38-46.

Mahabeleshwar G & Byzova T (2007). Semin Oncol34, 555-565.

The authors thank Tuscany Region for the financial support to this study

Where applicable, the authors confirm that the experiments described here conform with The Physiological Society ethical requirements.

PCA226

The effect of SDF1- 3'A and CXCR4 gene polymorphisms on the susceptibility and clinicopathological characteristics of prostate cancer

S. Seckin[2,1], C. Kucukgergin[1,2], F. Isman[1,3], D. Selcuk[1,4], . Bedia[1,5] and O. Sanli[1,6]

[1]Department of Biochemistry, Istanbul Faculty of Medicine, Istanbul University, Istanbul, Turkey, [2]Department of Biochemistry, Istanbul Faculty of Medicine, Istanbul University, Istanbul, Turkey, [3]Clinical Biochemistry Laboratory, Goztepe Teaching and Research Hospital, Istanbul, Turkey, [4]Department of Molecular Medicine, Institute for Experimental Medicine Research,Istanbul University, Istanbul, Turkey, [5]Department of Molecular Medicine, Institute for Experimental Medicine Research, Istanbul University,, Istanbul, Turkey and [6]Department of Urology, Istanbul Faculty of Medicine, Istanbul University, Istanbul, Turkey

Chemokines and their receptors may contribute to pathologic processes such as cell proliferation, angiogenesis, invasion and metastasis of different types of cancers. In the present study, we aimed to investigate the association between SDF1-3A' and CXCR4 gene polymorphisms and the susceptibility and clinicopathological development of prostate cancer.

Consecutive patients with histologically confirmed prostate cancer (n= 152) and healthy controls (n= 149) with normal serum total PSA (< 4 ng/ml) and DRE were prospectively enrolled in this study between 2007 and 2011. SDF1-3'A and CXCR4 gene polymorphisms were assessed by polymerase chain reaction restriction fragment length polymorphism (PCR-RFLP) in all subjects. For the statistical analyses Pearsons's Chi-Squared (χ2), Mann-Whitney U and multiple logistic regression model tests were used where appropriate.

The mean age and smoking status were similar in prostate cancer patients and controls. Total PSA levels were significantly increased in the prostate cancer patients compared with controls. There were no significant differences in the distributions of SDF-1 and CXCR4 genotypes between controls and prostate cancer patients. However, the patients with prostate cancer with AA genotype of SDF1-3'A gene had an increasing risk of 2.02 fold (aOR= 2.02; 95% CI= 1.05-3.90; p= 0.035) to develop high pathological T stage when compared with prostate cancer patients with GG homozygotes of SDF1-3'A gene after being adjusted for age, BMI and smoking status. In addition, the distribution of AA genotype of SDF1-3'A gene polymorphism was found significantly increased in the patients with bone metastasis in comparison to those without bone metastasis (aOR=2.94; 95% CI=1.26-6.82; p=0.012). On the other hand, CXCR4 gene polymorphism was not associated with the clinicopathological characteristics of prostate cancer.

Our results suggest that SDF1-3'A gene polymorphism may be associated with the progression and bone metastasis of prostate cancer.

Where applicable, the authors confirm that the experiments described here conform with The Physiological Society ethical requirements.

PCA227

The role of MCP-1 A2518G and CCR2A V64I gene polymorphisms on the susceptibility and clinicopathological characteristics of bladder cancer

C. Kucukgergin[1,5], F. Isman[2,1], S. Dasdemir[3,1], B. Cakmakoglu[4,1], O. Sanli[5,1] and S. Seckin[6,1]

[1]Department of Biochemistry, Istanbul faculty of medicine, Istanbul, Turkey, [2]Clinical Biochemistry Laboratory, Goztepe Teaching and Research Hospital, Istanbul, Turkey, [3]Department of Molecular Medicine, Institute for Experimental Medicine Research, Istanbul, Turkey, [4]Department of Molecular Medicine, Institute for Experimental Medicine Research, Istanbul, Turkey, [5]Department of Urology, Istanbul faculty of medicine, Istanbul, Turkey and [6]Department of Biochemistry, Istanbul faculty of medicine, Istanbul, Turkey

The gene variants of the chemokine and chemokine receptor genes associated with inflammation may be involved in cancer initiation and progression. The aim of this study was to explore the possible association of monocyte chemoattractant protein-1 (MCP-1) A2518G and chemokine receptor CCR2A V64I gene polymorphisms with the risk and clinicopathological characteristics of bladder cancer (BC) in a Turkish population.

In the present study, 142 individuals diagnosed with histologically confirmed BC between 2008-2011 at the Department of Urology, Istanbul Faculty of Medicine were enrolled as a patient group. The control group (n=197) consisted of urology patients who were treated at our outpatient clinic for various urological complaints but had no evidence of any malignancy based on a detailed evaluation. MCP-1 A2518G and CCR2A V64I gene polymorphisms were assessed by polymerase chain reaction restriction fragment length polymorphism (PCR-RFLP) in all subjects. For the statistical analyses Pearsons's Chi-Squared (χ2), Mann-Whitney U and multiple logistic regression model tests were used where appropriate. There were no significant differences in the distributions of MCP-1 A2518G genotypes between controls and BC patients. However, the carriers with AA genotype or at least one A allele of CCR2 had an increased risk of developing BC (aOR=2.39, 95%CI=1.13-5.03; p=0.022; aOR=1.37, 95%CI=1.04-1.81; p=0.022 respectively). In addition BC patients with AA genotype or at least one A allele of CCR2 had an increased risk of high grade and stage tumors as compared to those with GG genotype (aOR=3.09, 95%CI=1.02-9.34; p=0.045; aOR=1.58, 95%CI=1.07-2.32; p=0.020 respectively). On the other hand, MCP-1 A2518G gene polymorphism was not associated with the clinicopathological characteristics of BC.

Our results suggest that the genetic variants of CCR2A V64I gene polymorphism may modify the BC risk. Furthermore, CCR2A V64I gene polymorphism may contribute to the muscle invasive BC in a Turkish population.

Where applicable, the authors confirm that the experiments described here conform with The Physiological Society ethical requirements.

PCA228

Manganese superoxide dismutase ILE-58THR, catalase C-262T and myeloperoxidase G-463A gene polymorphisms in prostate cancer patients: Relation to advanced and metastatic disease

C. Kucukgergin[1,2], T. Tefik[1,2], O. Sanli[1,2], T. Oktar[1,2], C. Ozsoy[1,2] and S. Seckin[1,2]

[1]Department of Biochemistry, Istanbul Faculty of Medicine, Istanbul University, Istanbul, Turkey and [2]Department of Urology, Istanbul Faculty of Medicine, Istanbul University, Istanbul, Turkey

Known as a multifactorial disease, prostate cancer (PCa) is considered one of the most frequently diagnosed tumors and second leading cause of cancer related deaths among men. We aimed to evaluate the relationship between manganese superoxide dismutase (MnSOD) Ile-58Thr, catalase (CAT) C-262T and myeloperoxidase (MPO) G-463A gene polymorphisms and the susceptibility and clinicopathological characteristics of PCa.

One hundred and fifty five patients diagnosed with PCa and 195 controls with negative digital rectal examination and PSA<4ng/dl were enrolled in this study. MnSOD, CAT and MPO gene polymorphisms were performed by polymerase chain reaction restriction-fragment length polymorphism (PCR-RFLP) methods. For the statistical analyses Pearsons's Chi-Squared (χ2), Mann-Whitney U and multiple logistic regression model tests were used where appropriate.

No statistically significance regarding demographic data and smoking status was observed between groups. As expected, total PSA levels were significantly elevated in the PCa patients compared with controls. No relationship was found between MnSOD Ile-58Thr gene polymorphism and PCa risk. However, there were significant differences in the genotype distributions of CAT C-262T and MPO G-463A gene polymorphisms between PCa patients and controls (aOR:1.57; 95%CI: 1.11-2.21; p=0.010; aOR:1.78; 95%CI: 1.15-2.76; p=0.009, respectively). MnSOD Ile-58Thr and MPO G-463A gene polymorphisms were not found to be associated with clinicopathological characteristics including pathological grade, T stage and metastasis among PCa patients. However, CAT C-262T gene polymorphism was found to be associated with clinicopathological characteristics including T stage and metastasis among PCa patients. The patients with PCa carrying TT genotype had a significantly increased risk of high pathological T stage disease and metastasis compared to patients carrying CC genotype (aOR:1.94; 95%CI: 1.14-3.23; p=0.014; aOR:3.83; 95%CI: 1.75-6.59; p=0.000, respectively).

It seems that there is no association of PCa and MnSOD Ile58Thr polymorphism, whereas TT genotype in CAT C-262T polymorphism and GG genotype in MPO G-463A polymorphism may be associated with increased PCa risk. The TT genotype in CAT C-262T polymorphism may also play as a risk factor in tumor progression and metastasis among Turkish men.

Where applicable, the authors confirm that the experiments described here conform with The Physiological Society ethical requirements.

PCA229

Antioxidant enzymes in prostate cancer

N. Salmayenli[1,2], C. Kucukgergin[2,1], T. Tefik[3,2], O. Sanli[3,2] and S. Seckin[2,1]

[1]Clinical Biochemistry, Istanbul University Medical Faculty, Istanbul, Turkey, [2]Department of Biochemistry, Istanbul Faculty of Medicine, Istanbul University, Istanbul, Turkey and [3]Department of Urology, Istanbul Faculty of Medicine, Istanbul University, Istanbul, Turkey

Prostate cancer is the most important malignancy in men with advanced age. Oxidative stress contributes to the etiology and pathogenesis of the prostate cancer. The aim of this study was to determine the relation of antioxidant enzymes with the prostate cancer and to evaluate whether the activities of these enzymes were correlated with different stages and states with or without metastasis of disease. Moreover, we investigated oxidant-antioxidant state in prostate tissue with and without tumor. We also determined MnSOD expression by Western Blot analysis in the tissue protein extracts.

One hundred sixty five men diagnosed with histologically confirmed prostate cancer were included in the study. The control group also consisted of 168 male subjects who were enrolled to Department of Urology for reasons other than lower urinary tract symptoms. Prostate cancer patients were histologically classified into two groups as low and high stage disease according to 2002 TNM classification. Moreover, tumors with Gleason score >7 were classified as poorly differentiated whereas those with Gleason score <7 were classified as well-differentiated tumors. The presence or absence of bone metastasis was determined by bone scanning of prostate cancer patients with serum PSA level> 10 ng/ml. Twenty one prostate cancer and adjacent non- tumorous specimens were resected with transurethral resection of prostate (TURP). Serum and prostate tissue malondialdehyde (MDA), total thiol (-SH) levels and SOD, GPx, CAT activities were determined spectrophotometrically. Western Blot analysis was performed for evaluating MnSOD protein expression. For the statistical analyses, Mann-Whitney U and Kruskal-Wallis tests were used where appropriate. Serum MDA levels, GPX and SOD activities were significantly higher and total –SH levels were significantly lower in patients with prostate cancer compared to those of the controls. Serum MDA levels were significantly increased in prostate cancer patients with high stage. Moreover, serum MDA levels were significantly elevated in bone metastasis group. However, serum total –SH levels and GPX activities were lower in bone metastasis group. We observed that total MDA levels and SOD activities were also higher in prostate tissues with tumor. GPX, CAT activities and total –SH levels were significantly lower in prostate tissues with tumor. Meanwhile, tumors had higher levels of MnSOD protein when the MnSOD protein expression was evaluated by Western analysis.

In conclusion, we suggest that tissue GPX and CAT activities were decreased due to oxidative injuries in patients with prostate cancer and also increased MnSOD expression in cancerous tissue was to be an indicator for progression and stage of the disease.

Where applicable, the authors confirm that the experiments described here conform with The Physiological Society ethical requirements.

PCA230

SIRT1 expression enhanced antitumor effect of Cisplatin decreased by chronic hypoxia in human non-small cell lung cancer

D. Shin

Pharmacology, College of Medicine, Seoul National University, Seoul, Republic of Korea

Hypoxia induced drug resistance is a major obstacle in the development of effective cancer therapy. Hypoxia is also associated with human non-small cell lung cancer (NSCLC), which is highly resistant to chemotherapy. However, the exact mechanisms driving hypoxia induced chemoresistance of NSCLC remain elusive. We first found that NSCLC cell lines showed hypoxia-induced chemoresistance from human several solid tumors treated with Cisplatin. Especially, IC50 values to NSCLC cell lines, H1299 and A549 are significantly more increased under hypoxic condition than these of normoxic condition. To evaluate why IC50 values are significantly increased in NSCLC cell lines, we measured the expression levels of SIRT1 and pAMPK alpha after normoxic and hypoxic condition 48 h with 21 solid tumors by using Western blot analysis. Surprisingly, the levels of SIRT1 and pAMPK alpha in NSCLC cell lines were highly underestimated in hypoxic condition. Cell viabilities, colony numbers, and IC50 values were diminished by SIRT1 overexpression and SIRT1 activator (SRT1720), which was recovered by AMPK alpha knock-down and AMPK alpha inhibitor (Compound C), and also these were increased by SIRT1 knock-down, SIRT1 mutant (H363Y) expression, and SIRT1 inhibitor (EX527), which was re-decreased by AMPK alpha expression and AMPK alpha activator (A769662). These results suggest that hypoxia-induced chemoresistance is correlation with SIRT1-AMPK alpha axis. To elucidate how SIRT1 can overcome hypoxia-induced chemoresistance, we measured mitochondria activity by using mitochondria morphology change, MitoTracker, and ATP/ADP ratio. SIRT1 expression increased the Area, number, perimeter, ferret's meter, ATP/ADP ration of mitochondria, and promoted cytochrome C release from mitochondria, which was diminished by siAMPK alpha. Moreover, our new combination therapy SIRT1 activator and Cisplatin can overcome resistance to hypoxia-induced chemoresistance through activation of mitochondria activity. Actually, these regime synergistically decreased tumor volume and weight in H1299 xenograft model and significantly increased survival rate in H1299 lung orthotopic model in compared with either each single or non-treatment. Our results showed that SIRT1-AMPK alpha axis by chronic hypoxia makes chemoresistance via the inactivation of mitochondria. However, ectopically increased SIRT1 expression or activity in hypoxia can overcome hypoxia-induced chemoresistance via activated mitochondria. It suggests that SIRT1 is an efficient target for reducing chemoresistance in NSCLC.

Key words: SIRT1, AMPK alpha, hypoxia, chemoresistance, mitochondria activity, Cisplatin

Jemal A, Bray F, Center MM, Ferlay J, Ward E, Forman D. Global cancer statistics.

CA Cancer J Clin 2011; 61: 69—90.

Ramalingam SS, Owonikoko TK, Khuri FR. Lung cancer: new biological insights

and recent therapeutic advances. CA Cancer J Clin 2011; 61: 91—112.

Molina JR, Adjei AA, Jett JR. Advances in chemotherapy of non-small cell lung

cancer. Chest 2006; 13: 1211—1219.

Evolution of cisplatin-based chemotherapy in non-small cell lung

cancer. Chest 2000; 117: 133s—137s.

Nemunaitis J, Swisher SG, Timmons T, Connors D, Mack M, Doerksen L et al.

Adenovirus-mediated p53 gene transfer in sequence with cisplatin to tumors of

patients with non-small-cell lung cancer. J Clin Oncol 2000; 18: 609—622.

This research was supported by Basic Research Program through the National Research Foundation of Korea(NRF) funded by the Ministry of Education, Science and Technology(2010-0029948)

Where applicable, the authors confirm that the experiments described here conform with The Physiological Society ethical requirements.

PCA231

Jia-Wey Shiau-Uau San (JWSYS) is the most commonly Chinese medicine prescribed in Taiwan for disorders of menstruation in female and for sleep disturbances in males

J. Yu[1], C. Ho[2] and C. Chang[3]

[1]Department of Chinese Medicine, Chi Mei Medical Center, Tainan, Taiwan, [2]Department of Medical Research, Chi Mei Medical Center, Tainan, Taiwan and [3]Department of Biotechnology, Southern Taiwan University of Science and Technology, Tainan, Taiwan

Jia-Wey Shiau-Yau San (JWSYS), one of the traditional Chinese herbal formulas, is a famous herbal remedy used for the treatment of various menopause-related symptoms and stress-related neuropsychiatric disorders in Korea, Japan and China. Despite the wide use in clinical applications, the scientific literature on efficacy and safety of JWSYS is not available. The present study is a clinical research to evaluate the drug-use patterns of Chinese herbal medicine JWSYS in Taiwan during 2009.The National Health Insurance Research Database (NHIRD) was applied in this study. The Traditional Chinese Medical (TCM) database, a subset database of NHIRD, is the first national population TCM database, including of TCM ambulatory care expenditures by visits and details of TCM ambulatory care orders. The principal diagnosis was based on the International Classification of Diseases, Ninth Revision, Clinical Modification (ICD-9CM) code. Patients took Jia-Wei-Xiao-Yao powder in 2009 was selected for the study subjects. In a 2009 statistics, it is revealed that a total of 899,712 persons had took JWSYS, and the total prescription number is 2,479,09 times. The age distribution of the 889,712 patients showed that most (30.44%) were between 36 and 50 years of age, and 27.63% were between 21 and 35. In addition, in gender the number of females who take JWSYS is greater than that of males, the ratio is about 4:1 (80.50%:19.50%). As for the top 10 major diseases treated by JWSYS, according to the statistics classified by the Institute with ICD-9 codes, they are different for males and females. The disease treated most with JWSYS for males is disorders of menstruation and other abnormal bleeding from female genital tract (ICD-9:626.9), while for males is sleep disturbances (ICD-9: 780.5). Within the top ten diseases of males and females, five major diseases are the same, including the sleep disorders, contact dermatitis, allergic rhinitis, migraine, and endocrine disorders, and the other remaining five major diseases are not the same. Although our survey tends tio indicate that JWSYS is the most commonly Chinese medicine prescribed in Taiwan of menstruation in female and for sleep disturbances in males, the efficacy and the therapeutic mechanisms of JWSYS in treating disorders of menstruation and sleep disturbances warrant further exploration in future studies.

Where applicable, the authors confirm that the experiments described here conform with The Physiological Society ethical requirements.

PCA233

Photocytotoxicity and excited-state properties of glycoconjugated C60 derivatives

S. Yano[1,2], M. Naemura[2], A. Toshimitsu[2], M. Akiyama[1], A. Ikeda[1], J. Kikuchi[1], A. Narumi[3], K. Ohkubo[4], S. Fukuzumi[4], M. Gottschaldt[5] and U. Schubert[5]

[1]Graduate School of Material Science, Nara Institute of Science and Technology, Ikoma, Japan, [2]Office of Society-Academia Collaboration for Innovation, Kyoto University, Kyoto, Japan, [3]Department of Polymer Science and Engineering, Yamagata University, Yonezawa, Japan, [4]Department of Material and Life Science, Osaka University, Osaka, Japan and [5]Laboratory for Organic and Macromolecular Chemistry, Friedrich-Schiller-University Jena, Jena, Germany

The photodynamic action is initiated by the absorption of a photon followed by many competing radiative and nonradiative reactions which ultimately result in the oxidation and degradation of vital biomolecules (1). Molecular oxygen plays a key role in propagation the initial molecular damage, resulting in vascular collapse, tissue destruction, cell death. The photodynamic therapy (PDT) induces tumor cell necrosis and/or apoptosis by producing reactive oxygen species through activated photosensitizer that accumulates specifically to the tumor. Thus, PDT has much attracted as less invasive method for treating cancer. The potential applications for fullerenes and their derivatives have increased in recent years, particularly in the fields of biology and medicine, where they can be used as DNA photo-cleaving agents, anti-HIV protease inhibitors, antibacterial agents and photosensitizers for photodynamic therapy. Fullerenes are suitable for application as photosensitizer because they are efficient visible-light triplet-sensitizers and their ability to photoproduce singlet oxygen ($^1O_2$) is considerable. Although carbohydrates play essential roles in biological systems, their usage in fullerene-based PDT has remained virtually unexplored; this is essentially true of fullerene in which an intact carbohydrate moiety is connected to fullerene through an appropriate linker. We previously reported that sugar-pendant C60 derivatives prepared from carbohydrate linked azides, having $^1O_2$ producing ability in DMSO under laser irradiation (355 nm) proved by the direct observation of $^1O_2$ emission at 1270 nm (2). The cytotoxicity of PDT was studied in several cancer cell lines cultured with D-glucose residue pendant fullerene and a maltohexaose residue pendant fullerene (3). These glycoconjugated fullerenes induced significant cytotoxicity against cancer cells. In contrast, PDT with these compunds exhibited no significant cytotoxicity against normal fibroblasts, indicating that PDT with these compounds targeted cancer cells. Ideally, PDT-induced tumour destruction should occur without damage to adjacent normal organs. Therefore, it can be expected to design high functional glycoconjugated fullerene. Here, we wish to report on the synthesis of a novel D-glucose pendant C60 compounds derived from D-glucose linked amine, photocytotoxicity against HeLa cells and unprecedented photo-

physical processes together with previously prepared D-glucose pendant azafulleroids (2).

S. Yano, S. Hirohara, M. Obata, Y. Hagiya, S. Ogura, A. Ikeda, H. Kataoka, M. Tanaka, T. Joh, Current states and future views in photodynamic therapy, J. Photochem. Photobiol., C, 12 (2011), 42-67.

Y. Mikata, S. Takagi, M. Tanahashi, S. Ishii, M. Obata, Y. Miyamoto. K. Wakita, T. Nishisaka, T. Hirano, T. Ito, M. Hoshino, C. Ohtsuki, M. Tanihara, and S. Yano, Detection of 1270 nm Emission from Singlet Oxygen and Photocytotoxic Property of Sugar-Pendant Fullerenes, Bioorg. Med. Chem. Lett., 13, 3289-3292 (2003).

E. Otake, S. Sakuma, K. Torii, A. Maeda, H. Ohi, S. Yano, A. Morita, Effect and Mechanism

of a New Photodynamic Therapy with Glycoconjugated Fullerene, Photchem. Photobiol,

2010,86; 1356-1363.

Where applicable, the authors confirm that the experiments described here conform with The Physiological Society ethical requirements.

PCA234

Hyperbaric oxygen treatment ameliorates the course of DSS-induced colitis in BALB/c mice and reduces the Foxp3+ regulatory T cell expansion

M. Mihalj[1], D. Pojatic[1], E. Ugor[2], Z. Kellermayer[2], S. Novak[1], M. Zulj[1], A. Vcev[3], T. Berki[2] and I. Drenjancevic[1]

[1]Department of Physiology and Immunology, Faculty of Medicine University Josip Juraj Strossmayer of Osijek, Osijek, Croatia, [2]Department of Immunology and Biotechnology, Faculty of Medicine University of Pecs, Pecs, Hungary and [3]Department of Internal Medicine, Faculty of Medicine University Josip Juraj Strossmayer of Osijek, Osijek, Croatia

Several studies in both animals and men showed beneficial effects of hyperbaric oxygenation (HBO2) on the course of experimentally induced colitis and inflammatory bowel disease. However, underling mechanisms of its action remain elusive. It was found that adoptive transfer or induction of CD4+CD25+FoxP3+ regulatory T cells (Treg) can prevent disease and reverse the course of established colitis (1). In addition, recent findings suggest that the mesenteric lymph nodes (mLN) are an important site of Treg induction (2). In the present study, we have assessed the effects of HBO2 on the frequencies of Treg in mLN of mice with DSS-induced colitis.

BALB/c mice at the age of 10-12 weeks were randomized into 4 groups (n=9 mice): control mice, control mice undergoing HBO2, mice receiving dextran sodium sulphate (DSS) and DSS treated mice undergoing HBO2. Mice were fed 5% w/v of DSS (Mr 36.000-50.000, MPBomedicals, France) in drinking water ad libidum for 7 consecutive days. HBO2 was initiated at day 1 and was administered until the end of experiment, twice a day 100% O2 for 60 minutes at 2.3 bars with addition of 15 minutes for gradual compression and decompression. Disease activity (DAI) was assessed by daily recording of animal body weight, stool consistency and the presence of occult or gross blood per rectum. On the day 9 mice were scarified by cervical dislocation and their mLN collected and further processed for flow cytometric assessment of Treg. The data are presented as mean±SEM, and were compared by student t test and one-way ANOVA. The study was approved by the Ethical Committee of Faculty of Medicine Osijek.

Mice treated with DSS exhibited severe symptoms of colitis, including diarrhea and gross rectal bleeding starting from day 6. DSS treated mice that underwent HBO2 presented with occult bleeding at day 8 and only a loose stool starting at day 7. DSS treated mice have lost 14.8±1.9% of body weight, whereas the mice which additionally underwent HBO2 lost 5.9±3.4% body weight. There was a significant difference in disease severity between those two groups, as evidenced by DAI on days 6-8 ($p<0.001$, Figure 1). Frequency of Treg in mLN increased significantly in DSS treated mice ($p=0.026$), and was reduced to control values after HBO2 ($p=0.03$, Figure 2).

DSS induced inflammation of the colon resulted in increased frequencies of Treg cells in the mLN. Consistent to previous studies HBO2 significantly reduced symptoms of disease and severity of colitis, which resulted in reversed frequencies of Treg cells, at comparable levels with those found in control mice. Thus our results suggest that the improved course of DSS-induced colitis in BALB/c mice does not involve Treg expansion.

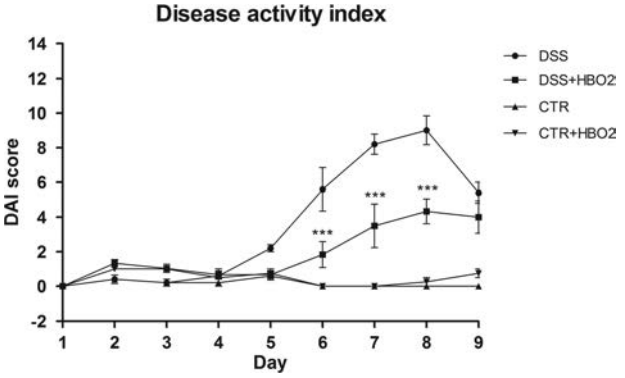

Figure 1. Disease activity index (DAI) was determined by daily assessment of body weight (0-4 depending on % of body weight reduction), stool consistency (0 – normal, 2 – loose stool, 3 – diarrhea) and bleeding (0 – normal, 2 – occult bleeding, 3 – gross bleeding).

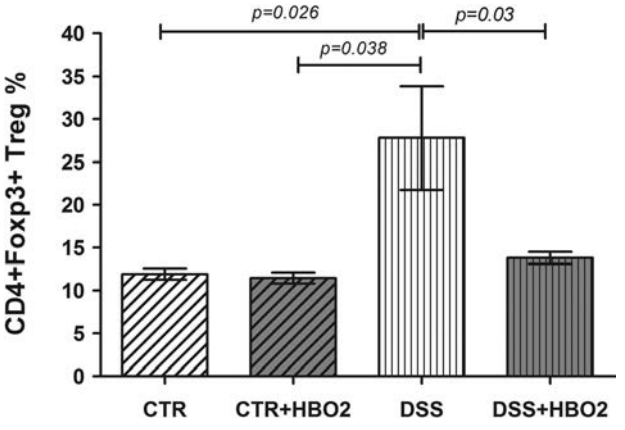

Figure 2. Frequency of Foxp3+ regulatory T cells in mesenteric lymph nodes

Uhlig HH, Coombes J, Mottet C, Izcue A, Thompson C, Fanger A, Tannapfel A, Fontenot JD, Ramsdell F, Powrie F. Characterization of Foxp3+CD4+CD25+ and IL-10-secreting CD4+CD25+ T cells during cure of colitis. J Immunol. 2006 Nov 1;177(9):5852-60.

Pabst O. Trafficking of regulatory T cells in the intestinal immune system. Int Immunol. 2013 Mar;25(3):139-43. doi: 10.1093/intimm/dxs113. Epub 2012 Dec 20.

This project was supported by IPA Hungary – Croatia Cross-border Co-operation Programme, HEALTH IMPULSE project (HUHR/1001/2.1.3/0006)

Where applicable, the authors confirm that the experiments described here conform with The Physiological Society ethical requirements.

PCA235

Treatment of polycystic kidney disease with PPARγ agonists: Effects of sub-pharmacological doses in rodent models

B.L. Blazer-Yost[1,2], S. Flaig[1], A. Carr[2] and V. Gattone[2,1]

[1]Biology, Indiana University Purdue University Indianapolis, Indianapolis, IN, USA and [2]Anatomy and Cell Biology, Indiana University School of Medicine, Indianapolis, IN, USA

The autosomal dominant form of polycystic kidney disease (ADPKD) is the most common renal genetic disease in humans with an estimated incidence of 1:400-1000. Cyst expansion progresses slowly, and renal function is typically not compromised until the fifth decade but then the decline to renal failure is precipitous usually occurring in 5-10 years in 50% of patients. There are currently no drugs approved for the treatment of ADPKD. Based on our previous observations that PPARγ agonists inhibit CFTR synthesis and that pioglitazone feeding ameliorates PKD progression in the PCK rat model, we have hypothesized that the PPARγ agonists, pioglitazone (pio) and rosiglitazone (rosi), could be used to treat ADPKD. CFTR is the Cl^- channel in the epithelial cells lining the cysts that is responsible for Cl^- driven fluid secretion into the cyst lumen causing cyst expansion. Both pio and rosi are insulin sensitizing agents which have been used to treat diabetic patients for many years, albeit with some dose related side effects. We have fed the PCK rat (a slowly progressing PKD model) with super-pharmacological (4.0 mg/kg BW; high dose) and sub-pharmacological (0.04 mg/kg BW; low dose) rosi from week 4 to 28. An alternative, rapidly progressing model of renal cystic disease, the WPK/WPK rats, were fed with high (20.0 mg/kg BW) and low (0.2 mg/kg BW) doses of pio from day 5 to 18. At the end of the appropriate time period, the animals were euthanized with an overdose (i.p.) of sodium pentobarbital. The kidneys were weighed and then prepared for histological sections which were used to determine various parameters including cyst volume. In the PCK rats both super- and sub-pharmacological concentrations of rosi resulted in statistically significant (ANOVA one way, P less than 0.05) decreases in kidney weight and renal cyst volume. The average (±- S.E.M.) kidney weights of the 12 animals on control diet were 4.33 ± 0.18 gr compared to 3.56 ± 0.26 for high dose (n=3) and 3.68 ± 0.14 for low dose (n=8). The average renal cyst volume of the control diet animals was 0.53 ± 0.06 ml compared to 0.27 ± 0.05 for high dose and 0.33 ± 0.09 for low dose. In the Wpk/Wpk animals, the kidney weights and renal cyst volumes of the animals on the high dose were not statistically different from the control diet animals while the animals fed the low dose were significantly different. Kidney weights of control versus low dose = 4.51 ± 0.48 ml (n =11) versus 3.53 ± 0.17 (n =10); renal cyst volume = 3.34 ± 0.36 versus 2.57 ± 0.14. Thus concentrations of PPARγ agonists that are below the doses used to treat diabetic patients are effective in slowing cyst growth in two models of PKD. At these low doses, the drugs are less likely to exert adverse side effects. We suggest that low dose PPARγ agonists may be effective life-long therapy for PKD patients.

Where applicable, the authors confirm that the experiments described here conform with The Physiological Society ethical requirements.

PCA237

Plasmin in urine - a new biomarker and target for renal protection in diabetes

H. Andersen[1,2], U. Friis[1], P. Hansen[1], J. Henriksen[2] and B. Jensen[1]

[1]Cardiovascular and Renal Research, University of Southern Denmark, Odense C, Denmark and [2]Department of Endocrinology, University of Southern Denmark, Odense C, Denmark

Diabetes is often accompanied by hypertension, microalbuminuria and decline in kidney function until renal failure. Diabetic nephropathy is the leading cause of chronic kidney disease. In nephrotic syndrome, aberrant filtration of plasminogen from plasma to preurine with subsequent activation to plasmin may proteolytically activate the epithelial Na^+ channel (ENaC). We hypothesized that plasmin is lost to preurine in diabetic nephropathy and that plasmin in urine may activate ENaC current. This cross-sectional study included patients with type 1 diabetes mellitus with diabetic nephropathy (n=19) and without nephropathy (control, n=20). Patients were matched on age, gender and diabetes duration. Plasma, spot urine samples, 24 h urine collections and 24 h blood pressure recordings were obtained. 24 h urinary protein excretion was 1.8±0.5 (nephropathy, n=17) and 0.07±0.03 g/day (control, n=18, p=0.0007). Urinary plasmin(ogen)/creatinine ratio as assessed by ELISA was significantly higher in nephropathy than control group ($172\pm1.86\times10^{-3}$, n=19, vs. 3.48×10^{-1} $\pm1.32\times10^{-3}$ μg/g, n=18, p<0.0001) and correlated with urine albumin concentration (p<0.0001). Plasma plasmin(ogen) concentration did not differ between nephropathy and control (140±7, n=18, vs. 152±9 μg/ml, n=19). Western immunoblotting supported the presence of urinary plasmin(ogen) in nephropathy, but not in control group. Preliminary data indicated that urine from nephropathy patients (n=3) increased ENaC current more than control group (n=5) as evaluated by whole-cell patch clamp on murine collecting duct cells (67.8±12.8 % vs. 16.5±3.9 %). Mean 24 h systolic, but not diastolic, blood pressure was significantly higher in nephropathy (144/79 mmHg, 95 % confidence interval (CI): 136.0–151.9/74.9-83.2) than control group (132/75 mmHg, 95 % CI: 126.2-137.4/71.8-77.8, p=0.0117) despite being treated with 3.0±0.4 (nephropathy) vs. 1.4±0.3 (control) antihypertensive drugs including diuretics. There was a significant correlation between mean 24 h blood pressure and urine plasmin(ogen) concentration (r^2=0.18, p=0.0102). Furthermore, nephropathy patients dipped significantly less in systolic (7.4±1.8 % vs. 13.3±2.0 %, p=0.04) and diastolic blood pressure (9.1±1.6 vs. 16.1±1.9 %, p=0.008) at night than did the control group.

It is concluded that aberrant presence of plasmin activity in urine in diabetic nephropathy is capable of activating ENaC and may contribute to insufficient hypertension control.

Susanne Hansen and Kenneth Andersen are thanked for excellent technical assistance.

Where applicable, the authors confirm that the experiments described here conform with The Physiological Society ethical requirements.

PCA238

Recruitment mechanisms and anti-inflammatory effects of haematopoietic stem cells in the injured kidney

R.L. White, G. Nash, D. Kavanagh, C. Savage and N. Kalia

Clinical and Experimental Medicine, University of Birmingham, Birmingham, UK

Introduction: Haematopoietic stem cells (HSCs) can migrate to injured kidney and aid in tissue repair. However, clinical success remains poor and can be attributed to limited HSC recruitment. Understanding adhesive mechanisms governing HSC recruitment may allow the development of strategies that enhance their homing, thus improving the efficacy of HSC-based therapies. This study therefore determined the adhesive mechanisms critical for renal HSC recruitment, whether pre-treating HSCs with chemokines enhanced recruitment and the mechanisms by which this occurred and what vasculoprotective effects were being conferred by recruited HSCs.
Methods: Numbers of HSCs, neutrophils and platelet microthrombi in renal peritubular capillaries of sham and ischemia-reperfusion (IR) injured mice (ketamine/xylazine; i.p.) were visualised using dyes that fluoresce different colours. Some HSCs were pre-treated with function-blocking antibodies to surface adhesion molecules (CD49d, CD44, CD18) or chemokines (SDF-1α, KC). Changes in surface expression and clustering of HSC adhesion molecules was determined using flow cytometry and confocally. HSC adhesion to endothelial counterligands (VCAM-1, hyaluronan) was determined using static adhesion assays in vitro.
Results: HSC adhesion was significantly ($p<0.001$) increased in IR kidney when compared to sham controls. This resulted in a significant ($p<0.01$) reduction in adherent neutrophils and platelet microthrombi at 6 hours post-reperfusion when compared to mice receiving no HSCs. Recruitment was dependent on CD49d and CD44, but not CD18. Both SDF-1α and KC pre-treatments significantly ($p<0.01$) enhanced HSC adhesion within IR kidney. Neither pre-treatment strategy increased adhesion molecule expression. However, SDF-1α ($p<0.01$) and KC ($p<0.05$) did increase numbers of CD49d and CD44 surface clusters on HSCs respectively. This likely explained their increased adhesion to VCAM-1 ($p<0.05$) and hyaluronan ($p<0.001$). SDF-1α also significantly ($p<0.01$) increased HSC deformability as demonstrated using a micropipette aspiration method. This resulted in increased ($p<0.01$) numbers of free-flowing HSCs being continuously observed in the renal microcirculation.
Conclusion: Chemokine pre-treatment increased HSC adhesion within injured renal microvessels. Interestingly, it also increased the pool of circulating transplanted HSCs available for renal recruitment. This was possibly due to the increased deformability preventing their entrapment within non-injured tissue (eg. lungs). Our data also demonstrates for the first time that HSCs exhibit marked anti-inflammatory and anti-platelet effects. Ongoing studies will determine whether enhancing their local presence with chemokine pre-treatment confers faster and more efficient vasculoprotective effects.

Supported by MRC

Where applicable, the authors confirm that the experiments described here conform with The Physiological Society ethical requirements.

PCA240

Simulation of the anti-arrhythmic properties of herbal remedies

P. Noble[2], K. Tasaki[2], D. Gavaghan[1], G. Mirams[1] and D. Noble[2,1]

[1]Computing Science, University of Oxford, Oxford, UK and [2]MAviaSB Project, Physiology, Anatomy & Genetics, University of Oxford, Oxford, UK

Computer models of cardiac cells can identify combinations of actions on ion channels that may avoid arrhythmic side effects (1), thus providing a new, more predictive, biomarker, now used in the pharmaceutical industry.
Herbal remedies are naturally multi-action. In some cases, therapeutic effects have been validated by double-blind clinical trial (2), the chemical composition is known, and the action profiles on multiple targets have also been characterised. The data can therefore be used in the same models as for single compound drugs.
The Figure shows that the profile of action of Shen-song yang-xin (SSYX) (2, 4) accounts for the shortening of the cardiac action potential. When early-after depolarizations (5) are induced in the model the actions of SSYX fully reverse the effect on repolarization (right hand panel). We believe this is the first time that simulation has been used to demonstrate the anti-arrhythmic mechanism of a herbal remedy.

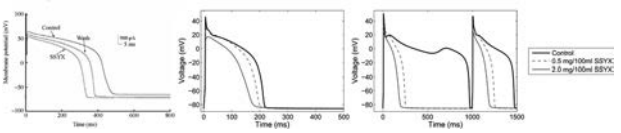

Figure 1. Left: experimental recordings of action potentials of guinea-pig myocytes before, during and after application of SSYX. Middle: simulation of two dose levels using Shannon ventricular cell model (3). SSYX acts on the following six channel proteins with IC50s based on the published data: I_Na: 0.62 g/100ml, I_CaL: 0.83 g/100ml, I_to: 0.49 g/100ml, I_K(mostly s): 1.12 g/100ml, I_K1: 1.01 g/100ml, I_f : 1.02 g/100ml. Right: simulation using the same data on model modified to generate EADs.

Mirams, G. R., Cui, Y., Sher, A., Fink, M., Cooper, J., Heath, B. M., McMahon, N. C., Gavaghan, D. J., and Noble, D. (2011) Simulation of multiple ion channel block provides improved early prediction of compound's clinical torsadogenic risk, Cardiovascular Research 91, 53-61.

Hao, H., Hai-Qin, T., Jie-Hua, L., Lin-Lin, Y., Wen-Juan, T., and Zhong-Ran, Z. e0331 Effects of Shen Song Yang xin capsule for treatment of cardiac arrhythmia: a systematic review, Heart 96, A103-A103.

Shannon, T., Wang, F., Puglisi, J., Weber, C., and Bers, D. (2004) A mathematical treatment of integrated Ca dynamics within the ventricular myocyte., Biophys. J. 87, 3351-3371.

Li, N., Ma, K., Wu, X., Sun, Q., Zhang, Y., and Pu, J. (2007) Effects of Chinese herbs on multiple ion channels in isolated ventricular myocytes, Chinese Medical Journal-Beijing-English Edition- 120, 1068.

Noble, P. J., and Noble, D. (2000) Reconstruction of the cellular mechanisms of cardiac arrhythmias triggered by early after-depolarizations, Japanese Journal of Electrocardiology 20 (Suppl 3), 15-19.

This research was done under the Multiple Actions via Systems Biology Project

Where applicable, the authors confirm that the experiments described here conform with The Physiological Society ethical requirements.

PCA241

Multitargeted therapy of chemotherapy-induced oral mucositis by hangeshashinto, a traditional Japanese herbal medicine

T. Kono[1,2], A. Kaneko[3], R. Nozaki[2], C. Matsumoto[3], C. Miyagi[3], K. Ohbuchi[3], Y. Omiya[3], Y. Mizuhara[3], K. Miyano[4] and Y. Uezono[4]

[1]Faculty of Pharmaceutical Sciences, Hokkaido University, Sapporo, Japan, [2]Advanced Surgery Center, Higashi-Tokushukai Hospital, Sapporo, Japan, [3]Tsumura Research Laboratories, Tsumura & Co, Ibaraki, Japan and [4]Division of Cancer Pathophysiology, National Cancer Center Research Institute, Tokyo, Japan

Chemotherapy-induced oral mucositis (COM) is a common disorder but optimal treatment has not yet been established. COM is characterized by painful inflammation and ulceration involving PGE2. Hangeshashinto (TJ-14), a traditional Japanese herbal medicine (Kampo), has been prescribed for oral mucositis in Japan. Recently, a TJ-14 rinse solution (2.5 g/50 mL) was found to significantly reduce ulcer healing time in patients with grade 2 or worse COM in a randomized controlled trial. However, little is known regarding the anti-COM mechanism of TJ-14. The aim of this study was to identify the multiple actions of TJ-14 on the PGE2 system and cell migration by characterizing the action profiles of its main active ingredients, [6]-shogaol (6SG), wogonin (WGN), and berberine (BBR). COM was induced in hamsters by a combination of 5-fluorouracil (5-FU) administration and mild abrasion of the buccal mucosa. Hamsters were fed either a diet containing 2% (wt/wt) TJ-14 or a control diet throughout the experiments. Although buccal lesions were markedly aggravated by 5-FU, TJ-14 fed hamsters had significantly smaller lesions than animals on control diet and the ulcer healing time was also significantly reduced by half to a level comparable to that observed in humans. The amount of prostanoid synthesized by human oral keratinocytes (HOK) after stimulation with IL-1β for 6 h in the presence or absence of a test sample was measured by EIA. RT-PCR, phospho-MAPK, and COX-enzyme assays were performed to determine the mechanism of action. Levels of inducible PGE2 and PGF2α, metabolites of COX pathways, were reduced by TJ-14 (10–300 μg/mL) without inducing cytotoxicity, while LTB4 production was not affected by either IL-1β or TJ-14 addition. Gene expressions of COX-2, phospholipase A2, and PGE synthase were all down-regulated by TJ-14 exposure. Screening of the active ingredients in TJ-14 revealed that 6SG, WGN, and BBR significantly reduced PGE2 production. WGN and BBR inhibited induction of COX-2 mRNA probably through the blockage of c-Jun N-terminal kinase (JNK) and p38 phosphorylation. 6SG inhibited the enzymatic activity in PGE2 synthesis but did not decrease COX-2 mRNA expression, suggesting that 6SG might regulate PGE2 synthesis at the post-transcriptional level. Migration was evaluated after scratch wounding using sterile pipette tips. HOK migration was increased by TJ-14 (30–100 μg/mL) in a concentration-dependent manner. Pretreatment of HOK with IL-1β, which was highly expressed in inflamed sites of COM, resulted in decreased migratory activity. TJ-14 and BBR improved IL-1β-induced down-regulation of HOK migration. These data suggest that TJ-14 exhibits multiple actions against COM via PGE2 inhibition and promotion of wound healing. The main active ingredients, 6SG, WGN, and BBR, appear to exert different mechanistic actions.

Where applicable, the authors confirm that the experiments described here conform with The Physiological Society ethical requirements.

PCA242

Multitargeted treatment of experimental colitis by daikenchuto, a traditional Japanese herbal medicine

N. Ueno[1], M. Musch[2], T. Hasebe[1,2], T. Kono[3,4], Y. Wang[2], A. Kaneko[5], Y. Omiya[5], M. Yamamoto[5], M. Fujiya[1], Y. Uezono[6], Y. Kohgo[1] and E. Chang[2]

[1]of Gastroenterology and Hematology/Oncology, Department of Medicine, Asahikawa Medical University, Asahikawa, Japan, [2]Department of Medicine, Inflammatory Bowel Disease Center, Knapp Center for Biomedical Discovery, The University of Chicago, Chicago, IL, USA, [3]Faculty of Pharmaceutical Sciences, Hokkaido University, Sapporo, Japan, [4]Advanced Surgery Center, Higashi-Tokushukai Hospital, Sapporo, Japan, [5]Tsumura Research Laboratories, Tsumura & Co, Ibaraki, Japan and [6]Division of Cancer Pathophysiology, National Cancer Center Research Institute, Ibaraki, Japan

Intestinal ischemia, alterations in enteric flora, and pro-inflammatory cytokines (TNF-α and IFN-γ) have been shown to play key roles in the pathogenesis and recurrence of Crohn's disease (CD) (1). Daikenchuto (TU-100), a traditional Japanese medicine (Kampo) composed of processed ginger, ginseng radix, and Japanese pepper, is a pharmaceutical grade multiherbal medicine that is widely prescribed in Japan to improve gastrointestinal disorders such as CD (2). A randomized controlled trial on TU-100 in patients with CD is currently underway in the United States. Basic studies have demonstrated that TU-100 suppresses TNF-α and IFN-γ production in the intestinal mucosa of CD by inducing endogenous adrenomedullin (ADM) release, a potent vasodilatory peptide with anti-inflammatory activity (3,4). We have demonstrated that TU-100 contains transient receptor potential ankyrin 1 (TRPA1) channel ligands, [6]-shogaol and hydroxyl-α-sanshool, which increase intestinal blood flow via enhancing ADM release from the intestinal epithelial cells (5). This shows that TRPA1 present in the intestinal epithelial cells controls intestinal blood flow via ADM release. ADM has also been found to have an antimicrobial effect comparable to that of human β-defensin in the intestinal lumen, suggesting its potential influence on enteric flora. However, little is known regarding the effect of TU-100 on enteric microbiota, which may alter the dynamic relationship between host and microbes to ameliorate colitis. In this study, C57Bl/6 female mice (n=6, 6 weeks old) were housed together to minimize generational and environmental variables that might possibly confound the microbiota analysis. All mice were fed a defined diet (AIN-76A) supplemented with or without 15 g of TU-100 extract/kg diet (1.5% wt/wt) and studied over a 28-day period. Stool samples were analyzed for 16S rRNA gene profiles using terminal restriction fragment length polymorphism (T-RFLP) and 454 pyrosequencing. TU-100 significantly altered the T-RFLP profile of stool microbiota, but only after 28 days of TU-100 treatment. Both taxonomic assignment and operational taxanomic unit (OTU) analysis revealed an expansion of Actinobacteria and Firmicutes at the phylum level and Lactococcus sp. and Clostridium sp. at the genus level. A 28-day supplementation with TU-100 was also investigated in the dextran sulfate sodium (DSS)-induced colitis murine model. TU-100 inhibited weight loss, colon shortening and colonic histological injury, and improved disease activity index in DSS-treated mice, while inducing cytoprotective heat shock pro-

tein expression and suppressing pro-inflammatory cytokine expression, particularly TNF-α. These data address the possibility that TU-100 ameliorates DSS-induced colitis by reshaping the intestinal microbiome, paving the way for a novel therapeutic strategy for CD patients.

1. Devkota S, Wang Y, Musch MW, Leone V, Fehlner-Peach H, Nadimpalli A, Antonopoulos DA, Jabri B, Chang EB. Dietary-fat-induced taurocholic acid promotes pathobiont expansion and colitis in Il10-/- mice. Nature 487:104-8, 2012.

2. Kono T, Kanematsu T, and Kitajima M. Exodus of Kampo, traditional Japanese medicine, from the complementary and alternative medicines: is it time yet? Surgery 146: 837-840, 2009.

3. Kono T, Kaneko A, Hira Y, Suzuki T, Chisato N, Ohtake N, Miura N, and Watanabe T. Anti-colitis and -adhesion effects of daikenchuto via endogenous adrenomedullin enhancement in Crohn's disease mouse model. J Crohns Colitis 4:161-170, 2010.

4. Kono T, Omiya Y, Hira Y, Kaneko A, Chiba S, Suzuki T, Noguchi M, and Watanabe T. Daikenchuto (TU-100) ameliorates colon microvascular dysfunction via endogenous adrenomedullin in Crohn's disease rat model. J Gastroenterol 46:187-1196, 2011.

5. Kono T, Kaneko A, Omiya Y, Ohbuchi K, Ohno N, Yamamoto M. Epithelial transient receptor potential ankyrin 1 (TRPA1)-dependent adrenomedullin upregulates blood flow in rat small intestine. Am J Physiol Gastrointest Liver Physiol 304:428-36, 2013.

Where applicable, the authors confirm that the experiments described here conform with The Physiological Society ethical requirements.

PCA243

Multiple actions via systems biology – ten principles of systems biology and biological relativity

D. Noble, T.W. Tasaki, Y. Mohri, P. Liu, Y. Yang and K.M. Tasaki

Physiology, Anatomy and Genetics, University of Oxford, Oxford, Select State, UK

Systems Biology is the ideal approach for determining the mechanisms of Multiple Actions on biological targets (1) since it is concerned with the interactions following intervention on more than one target (2) and it deals with circular causality in complex systems (3). Computer models can be used to sweep through large parameter spaces, and sensitivity analysis can be used to fine-tune the optimum ratios of the components. The approach is based on the ideas that systems biology is necessarily integrative and multi-scale, or multi-level (4); that "there is no privileged level or scale of causality" (the principle of biological relativity (5); and the idea that causality can be circular (3).

Systems Biology helps illuminate circular processes identified in Multiple Actions, while the systems concept of attractors in complex systems is also important in analysing dynamic balance in the body processes that traditional medicine (sometimes called scholarly medical traditions) is concerned with. Ways of nudging disordered processes towards good attractors can lead to the development of new ways not only of curing disease but also of its prevention, including cost-effective remedies.

This poster discusses the concept of circular causality in Biological Relativity in Ten Principles of Systems Biology (5). It also discusses the relationship between Ten Principles and Multiple Action remedies (1). It shows how the interactions between these ideas and the concepts underlying Multiple Action medicine help to explain why diseases with complex aetiology, which are more prevalent in aging populations, can be treated with multi-component remedies. It also points a way towards new and broader approaches to health and longevity.

1. Tasaki, K. M., Tasaki, T. W., and Noble, D., 2012. Principles of Systems Biology

Relation to Traditional Medicine in East Asia. Register of Chinese Herbal Medicine Journal 9, 5-13.

2. Kohl, P., Crampin, E., Quinn, T. A., and Noble, D., 2010. Systems Biology: an Approach, Clinical Pharmacology and Therapeutics 88, 25-33.

3. Tasaki, K. M., 2012. Circular causality in integrative multi-scale systems biology and its interaction with traditional medicine. Progress in Biophysics and Molecular Biology http://dx.doi.org/10.1016/j.pbiomolbio.2012.09.005

4. Boyd, C.A.R., Noble, D., 1993. The Logic of Life. Oxford: Oxford University Press.

5. Noble, 2012. A theory of biological relativity: no privileged level of causation. Interface Focus 2, 56e64

Where applicable, the authors confirm that the experiments described here conform with The Physiological Society ethical requirements.

PCA244

A reassessment of the linear relationship between VO2max and peak power with age

R.D. Pollock, N.R. Lazarus and S. Harridge

Centre of Human and Aerospace Physiological Sciences, King's College London, London, UK

The majority of research on the effect of age on physiological processes is carried out on subjects that are not physically active. A deficiency with this is that the negative effects of inactivity are implicitly ignored 1 resulting in sub-optimal values being obtained. In order to eliminate this deficiency the use of master athletes, who are less likely to show these negative effects, has been suggested1 as a more objective model of inherent human ageing. Furthermore, as a result of the methods traditionally used to depict physiological changes with age and the use of cross-sectional study designs, it is widely assumed that physiological function shows a linear decline with age. This study set out to test this assumed linear relationship between two aspects of functionality and age on a cohort of endurance trained (but not elite) master cyclists.

57 male subjects (55-79 years) were recruited from an amateur long distance cycling club where the objective of each rider is to complete events in a specified time, irrespective of age. Subjects performed an incremental exercise test to exhaustion on a cycle ergometer, with breath by breath recording of oxygen uptake performed throughout the test (OxyconPro, Jaeger, Netherlands). VO2max was determined as the highest VO2 recorded over a 20s period. Peak (explosive) power output during sprint cycling was also determined using an inertial testing system 2. Both VO2max and peak power were normalised to fat free mass obtained from DXA scans.

When analysed using regression analysis, a modest linear relationship was found between VO2max, power and age (Fig 1 A and C, $r = -.463$ and $-.401$ respectively; $P < 0.003$ in both cases). Thus even in a cohort of individuals performing similar amounts of exercise, where the effects of inactivity are negligible only 21% (VO2max) and 16% (power) of the variability is associated with age. Fig 1 B and D show the same data, but now depicted where each variable is categorised into bandwidths of equivalent function1. Here it can be clearly seen that a wide range of ages (covering up to 2 decades) is present in

the majority of bandwidths. Depiction of the data in this way highlights the spread of data in a manner which suggests functionality and age are not linear processes.
These findings emphasise that even in highly active ageing populations with similar activity patterns, that the relationship between physiological function and age as depicted in cross-sectional studies is not clear and unlikely to be linear. This observation is exemplified when the data are viewed in domains of equivalent function irrespective of age. These data bring in to question the commonly held belief that physiological function linearly declines with age. Longitudinal studies using appropriate models of human ageing are needed to clarify the relationship between age and physiological function.

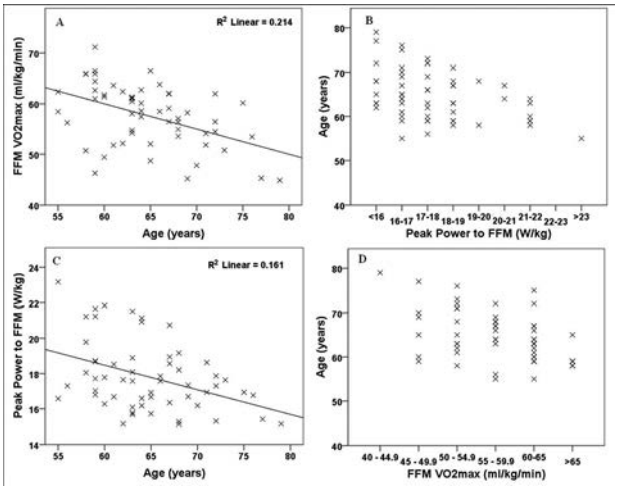

A and C show the relationship between VO2max and Power displayed in the standard format with regression lines shown. B and C show the relationship displayed in the method described by Lazarus and Harridge1.

Lazarus & Harridge (2010). J Gerontol A Biol Sci Med Sci. 65A(8), 854-857.

Pearson et al. (2004). Eur J Appl Physiol. 92(1-2):176-81.

BUPA Foundation

Where applicable, the authors confirm that the experiments described here conform with The Physiological Society ethical requirements.

PCA245

Selective depletion of high abundance extracellular matrix proteins from the secretome of articular cartilage explant cultures does not facilitate identification of lower abundance proteins

A. Williams[1], J.R. Smith[2], D. Allaway[3], P. Harris[3], S. Liddell[1] and A. Mobasheri[1]

[1]The University of Nottingham, Sutton Bonington, UK, [2]Bruker UK, Coventry, UK and [3]WALTHAM® Centre for Pet Nutrition, Waltham-on-the-Wolds, UK

Age-related changes in articular cartilage lead to extracellular matrix (ECM) degeneration and potentially the development of inflammatory osteoarthritis (OA). OA is characterised by increased expression and activity of pro-inflammatory cytokines, chemokines, catabolic mediators and ECM degrading enzymes. During LC-MS/MS analysis, high abundance of proteins of the ECM in the secretome prevented identification of differentially released low abundance protein with potential involvement in cartilage inflammation and ECM degradation. Here we describe the use of two methods, (cetylpyridinium chloride (CPC) precipitation and conacanavalin A (Con A) chromatography), to bind and deplete negatively-charged glycosylated side chains of high abundance ECM proteins and proteoglycans with the objective of uncovering and identifying lower abundance proteins, which would subsequently be quantified by western blotting.
Articular cartilage explant cultures were established from equine metacarpophalangeal joints (tissues derived from animals euthanased for reasons other than research) and incubated (37°C, 5% CO_2) with the pro-inflammatory cytokine IL-1β (10 ng/ml) for 6 days. CPC (5%) was added (3 mg CPC/mg PG), samples were incubated (RT, 30 minutes), and centrifuged (13,000 rpm, 10 minutes). Con A was added (0.5 ml slurry per 200 μl sample) and centrifuged in spin columns (3,300 rpm, 4 minutes). An amaZon speed ETD (Bruker) was used for nanoLC-MS/MS to analyse the principle protein components of each sample. For protein identifications the NCBInr database was searched using Mascot, only peptides with individual ions scores with a $P<0.05$ or greater were accepted.
Silver stained SDS-PAGE protein profiles confirmed that depletion techniques removed many high abundance proteins, leaving a simplified secretome profile. Sixty proteins were identified in undepleted IL-1β treated samples. After Con A depletion 39 proteins were identified. One ECM constituent, HPLP-1, was enriched by Con A depletion with a mascot score of 796. CPC precipitation identified 34 proteins. Both CPC precipitation and Con A chromatography reduced mascot scores for many proteins, especially small proteoglycans including decorin and fibromodulin. Four additional intracellular proteins were reliably identified after depletion steps, including ferritin heavy chain 1 (score 250) and manganese superoxide dismutase (score 260).
In conclusion, whilst depletion methods removed many abundant ECM proteins they were ineffective in identifying a greater range of inflammatory related proteins and few additional low abundance proteins were detected. Such proteins may have been co-extracted through binding with selectively-removed ECM components, or interacted with CPC/Con A.

Where applicable, the authors confirm that the experiments described here conform with The Physiological Society ethical requirements.

PCA246

Ageing differentially affects the short and medium latency motor responses evoked by stochastic vestibular stimulation

C.J. Osler, M. Bancroft, H. Southall and R.F. Reynolds

School of Sport and Exercise Sciences, University of Birmingham, Birmingham, UK

Falls are a major problem for older people, but the underlying mechanisms are not well understood. When a balance disturbance is sensed by the vestibular system, a counteractive whole-body motor response is generated. This demonstrates that this system is a key sensory input for maintaining upright posture. Since age-related changes to the peripheral and central vestibular system have been reported (1, 2), the higher incidence of falls in older people may be partially attributable to a vestibular mechanism. We examined balance reflexes evoked by stochastic vestibular stimulation (SVS) in three groups of human subjects; young (n=9, 28±7years), middle-aged (n=9, 55±6years) and older adults (n=14, 77±4years) (mean±SD). A randomly varying current (filtered white noise, 0-20Hz; RMS amplitude, 0.6mA) was passed between the mas-

toids of subjects stood with feet together and eyes closed. Medio-lateral ground reaction shear force (Fx) was measured for the duration of each trial (6 x 30sec). The relationship between the stimulating waveform and the evoked motor response was then calculated using the cumulant density function (3). As shown in Figure 1A, the resulting SVS-Fx relationship clearly shows that SVS precedes an initial negative peak (average magnitude=0.05±0.02) followed by a larger positive peak in Fx (average magnitude=0.17±0.05). These two components are termed the short latency (SL) and medium latency (ML) responses, respectively. We found the magnitude of these components to be differentially affected by ageing (mixed design ANOVA, age group x component; $F_{2,29}$=10.4, p<0.001, n=32). As shown in Figure 1B, the SL response tended to decrease in older adults, though this effect was not significant. In contrast, the ML response was substantially and significantly increased in middle-aged and older adults (pairwise comparisons, both p<0.04). Although the origin of the SL motor response is unclear (4), the ML response has been attributed to a virtual semicircular canal signal of head roll, and its direction is congruent with the resulting body sway. Our results therefore demonstrate that the functional balance response evoked by electrical activation of semicircular canal afferents is increased in older people. Since the site of electrical activation bypasses the end organ mechanics, this finding may reflect an increased afferent or central sensitivity in order to compensate for an age-related loss of peripheral vestibular hair cells (1).

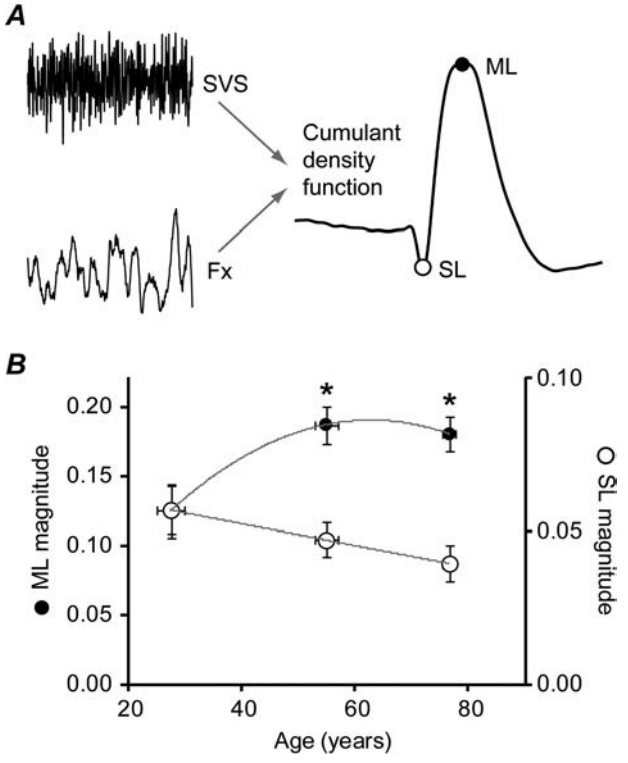

A, The relationship between the stimulating current (SVS) and motor response (Fx) was calculated using the cumulant density function. The short latency (SL) and medium latency (ML) components of the SVS-evoked response are indicated by open and filled markers, respectively. B, SL response magnitude tended to be reduced in older adults. In contrast, the ML response was significantly increased. * indicates a significant difference when compared to the young age group (p<0.04). Grey lines indicate 2nd order polynomial fits.

1. Jahn K et al. (2003). Brain 126, 1579-1589

2. Welgampola MS & Colebatch JG (2002). Clin Neurophysiol 113, 528-534

3. Mian OS & Day BL (2009). J Physiol 587.12, 2869-2873

4. Mian OS et al. (2010). J Physiol 588.22, 4441-4451

CJO is funded by the BBSRC

Where applicable, the authors confirm that the experiments described here conform with The Physiological Society ethical requirements.

PCA247

The impact of age on upper airway morphology: a risk factor for obstructive sleep apnoea?

E. Carthy[1,2], T. Carlisle[2], M. Glasser[1,2], P. Drivas[3], A. McMillan[1,2], N. Ward[1,2], A.K. Simonds[1,2] and M.J. Morrell[1,2]

[1]Academic unit of sleep and breathing, National Heart and Lung Institute, Imperial College London, London, UK, [2]NIHR Respiratory Biomedical Research Unit, Royal Brompton and Harefield Foundation Trust, London, UK and [3]NIHR Cardiovascular Biomedical Research Unit, Royal Brompton and Harefield Foundation Trust, London, UK

Obstructive sleep apnoea (OSA) is a common disorder, affecting 2-4% of middle-aged adults and rising to >25% in older people. Reduced upper airway calibre and greater pharyngeal length are both associated with an increased risk of OSA; however, the effect of age on upper airway morphology in people with and without OSA is unclear. The aim of this study was to investigate the impact of age on upper airway morphology in healthy older and younger people. **Methods:** Upper airway morphology was assessed using magnetic resonance (MR) imaging in healthy older (>60 years) and younger (<40 years) people who were screened to exclude OSA, and matched for body mass index (BMI) plus neck circumference (NC). MR scans of the upper airway were performed using a 1.5 Tesla MR scanner (Siemens Avanto; T1 weighted, 2D Axial and Sagittal spin echo sequences). Selected upper airway parameters were analysed using ImageJ software (version 1.46r, National Institutes of Health, USA) to determine any group differences; group mean differences were tested using Man Whitney U tests (SPSS, IBM Statistics 19, SPSS Inc., USA). **Results:** Fourteen younger (median (quartile 1-quartile 3): age 27.5 (26.3-31.8)years, BMI 25.9 (23.9-27)kg.m-2; NC 38.5 (37.5-41.0)cm) and 11 older (age 65.0 (63.0-68.5)years, BMI 26.6 (25.2-28.8)kg.m-2; NC 39.6 (38.9-40.4)cm) healthy males were studied with ethical approval. Older subjects had significantly longer pharyngeal airways (older: 8.8 (7.8-9.0)cm, younger: 7.7 (7.0-8.3)cm; p=0.025) and greater soft palate cross-sectional area (older: 43.1 (36.0-48.8)cm2, younger: 35.2 (30.5-40.5)cm2; p=0.003) compared to younger subjects. Moreover, there was a significant increase in parapharyngeal fat-pad thickness and fat-pad cross sectional area in the older group despite controlling for BMI and NC (thickness, older: 1.7 (1.4-2.2)cm, younger: 1.2 (1.0-1.8)cm; p=0.029. Cross sectional area, older: 13.8 (9.1-17.1)cm2, younger: 7.4 (5.9-13.0)cm2; p=0.018). **Conclusion:** Ageing was associated with soft tissue enlargement and lengthening of the pharyngeal airway. We speculate that these changes in upper airway morphology result in a greater propensity to airway collapse during sleep, predisposing older people to an increased risk of OSA.

This project was supported by the NIHR Respiratory and cardiovascular Biomedical Research Units at the Royal Brompton and Harefield NHS Foundation Trust and Imperial College London. TC is a National Heart and Lung Institute Foundation PhD Student.

Where applicable, the authors confirm that the experiments described here conform with The Physiological Society ethical requirements.

PCA248

Evidence for refractoriness in a whole-body human balance task

C. van de Kamp[1], P. Gawthrop[2], H. Gollee[2] and I. Loram[1]

[1]HSRI, Manchester Metropolitan University, Manchester, UK and [2]School of Engineering, University of Glasgow, Glasgow, UK

In a sustained movement task, such as human balance, continuous peripheral and serial ballistic intermittent control mechanisms might be integrated [1]. This implies that feedback mechanisms might not act continuously "closed loop" but can be intermittently "open". Intermittent control limits the frequency bandwidth of the human operator and makes it refractory in nature.
Classic experiments by Craik [2] revealed refractoriness in tracking responses to unpredicted, discrete step stimuli closely spaced in time. Recently, we employed a new method of analysis [3] and successfully identified refractoriness in the sustained visuo-manual control of unstable second-order systems [4]. It is, however, unclear whether the observation of refractoriness would generalize to a whole-body movement task like human balance.
In the current study we designed an experimental setup (Fig 1 A) in which participants, standing on both feet, were strapped to a rigid structure that pivots at the ankle joint. This inverted pendulum model of human balance was actuated by a linear motor as a marginally stabilized second order system that run on a computer in real time. Participants controlled the system's position through a myoelectric force signal derived from the combined EMG activity measurements of the tibialis anterior and the gastrocnemius medialis muscles. Visual feedback information about their human-attached-to-structure position was fed back to the participants by means of a sphere displayed on a large TV screen in front of them. The position of the pursuit tracking target was represented by a second sphere on the display (see Fig 1B for the step sequence).
Our method of analysis showed that the goodness of fit of an appropriate order, zero delay ARMA model relating the control signal to the series of paired stimuli step disturbances could be improved by sequentially and individually adjusting the instant of each second step disturbance. This procedure resulted in a distribution of first- and second response times. Results show that the mean (n= 14) response time was significantly higher for the second than for the first stimulus (RT2: 311 ± 145 ms, RT1: 245 ± 145 ms, $F(1, 13) = 15.9$, $p < .005$). The interaction between Stimulus Number and Inter Step Interval, ($F(7, 91) = 9.4$, $p < .0001$) indicates that reducing the ISI had different effects on RT1 compared to RT2 (the two separate post-hoc tests both showed a significant ISI effect). Post-hoc test at each ISI level revealed that first and second response times were significantly different for ISIs up to 500 ms.
These findings suggest that also for this whole-body balance task, the stimulus-response mechanism is refractory in nature; findings that might be better explained by an intermittent- than by a continuous control model.

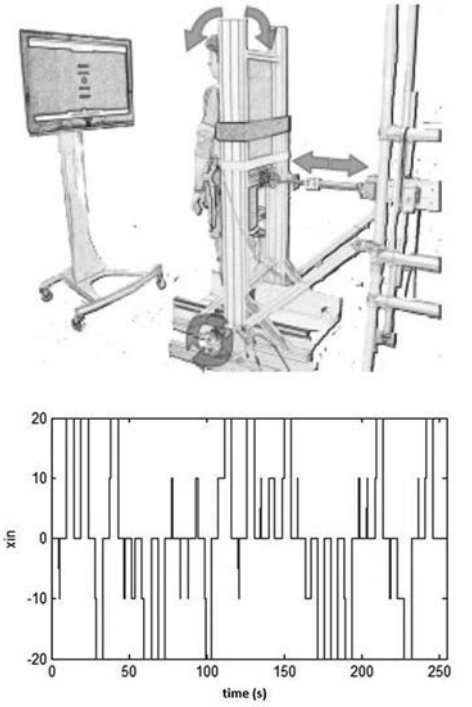

A)experimental setup and B)pursuit tracking sequence

Loram ID, Lakie M. Human balancing of an inverted pendulum: position control by small, ballistic-like, throw and catch movements. J Physiol 540, 1111–1124, 2002

Craik KJW. Theory of the human operator in control systems. I. The operator as an engineering system. Brit J Psychol Gen Sect 38, 56–61, 1947

Loram ID, van de Kamp C, Gollee H, Gawthrop PJ. Identification of intermittent control in man and machine. J R Soc Interface 9, 2070-2084, 2012

van de Kamp C, Gawthrop PJ, Gollee H, Loram ID. Refractoriness in sustained visuo-manual control: is the refractory duration intrinsic or does it depend on external system properties? PLoS CompBiol 9(1), 2013

Where applicable, the authors confirm that the experiments described here conform with The Physiological Society ethical requirements.

PCA249

Position played affects cervical spine range of motion of elite female rugby union players

B.B. Zietsman and P.W. McCarthy

Health, science and Sport, University of Glamorgan, Pontypridd, Wales, UK

Elite male rugby union players have a decreased active cervical range of motion the severity of which correlates to years of playing and position played (Lark and McCarthy; 2007, 2010). Although the female game has yet to attain full professional status, the players are still generally subjected to the same game related activities and therefore might be expected to also accumulate degenerative changes in vertebral joints. This study was therefore designed to determine if playing a contact sport such as rugby union decreases cervical (neck) active flexion/extension in the elite female game.
Methodology
The protocol used in this study is the same as that described previously (Lark and McCarthy, 2007). Female Welsh interna-

tional Rugby Union players in the 2011 pre-season training camp squad were invited to participate (age 24 ±4yrs) volunteered. Exclusion criteria included: current neck pain or trauma, previous surgery or serious pathology/trauma to the cervical spine. A cervical range of motion device (CROM device; Performance Attainment Associates, Minnesota, USA: Capuano-Pucci et al, 1991; Youdas et al,1991) was used to measure active cervical range of motion (ACROM) following a warm up procedure. From the neutral point full flexion and full extension were measured in no set order, (to reduce potential order effects). Ethical approval was granted by The Faculty of Health Science and Sport's Ethics Committee, University of Glamorgan, written informed consent was obtained.

Statistical Analysis

The data was normally distributed (Shapiro-Wilkes), therefore, unpaired T-tests and Cohen's d coefficient of effect size were used to compare Forwards and Backs: see Table 1, all data presented as mean ±1 standard deviation (SD).

Results

Of 35 volunteers, 29 were included. Exclusions: 4 pain on extension, 2 recent severe trauma (whiplash). The 15 Backs (age 24±5 yrs: 3.7±3.9 yrs playing elite) were compared to the 14 Forwards (age 24±4 yrs; 3.8±3 yrs playing elite); see Table 1.

Discussion

These findings confirm that playing in the forward position in elite rugby union is especially associated with a decrease in ACROM regardless of sex. Neck girth is unlikely to be responsible for the difference (Reynolds et al, 2009). This suggests that female elite rugby union players have a similar risk of accelerated degeneration of the vertebral joints as their male counterparts. Further research is needed to determine cause.

Anthropomorphic and ACROM data for position of play

Table 1	Mass(Kg)	Height(m)	Neck(cm)	Age(yrs)	Flexion (degrees)	Extension(degrees)	Total ACROM (degrees)
Forwards (n=14)	78.0±8.3	1.7±0.1	35.7±1.4	24.2±4.2	46.7±16.7	57.3±8.8	104.0±16.6
Backs (n=15)	65.0±8.4**	1.7±0.1	33.8±1.3**	24.1±5.0	56.0±17.5	66.1±17.2*	122.1±19.9**

Data presented as mean ±1SD: * indicates $p<0.05$ and ** $p<0.01$ (t-test; 2-tailed). Effect size (Cohen's d): extension ACROM 0.65 and total ACROM 0.99.

Capuano-Pucci, D., Rheault, W., Aukai, J., Bracke, M., Day, R., & Pastrick, M. (1991). Intratester and intertester reliability of the cervical range of motion device. Archives of Physical Medicine and Rehabilitation, 72, 338–340

Lark S., McCarthy P.W. (2007): Cervical Range of Motion and Proprioception in Rugby Players versus Non-Rugby Players, Journal of Sports Science 25(8):887-94.

Lark SD, McCarthy PW (2010) The effects of a rugby playing season on cervical range of motion. Journal of Sports Science 28(6):649-55

Reynolds, J., Marsh, D., Koller, H., Zenenr, J., Bannister, G., (2009) Cervical range of motion in relation to neck dimension. European Spine Journal. 18: 863-868

Youdas, J. W., Carey, J. R., & Garrett, T. R. (1991). Reliability of measurements of cervical spine range of motion – comparison of three methods. Physical Therapy. 71: 98–106.

The authors would like to thank the Womens WRU for allowing access to the players.

Where applicable, the authors confirm that the experiments described here conform with The Physiological Society ethical requirements.

PCA250

Physics-based soft-tissue modelling and simulation

M.A. Warburton and S.C. Maddock

Computer Science, The University of Sheffield, Sheffield, South Yorkshire, UK

Introduction

Physics-based techniques enable more accurate simulations to be produced [1]. We present an approach for easy automatic model creation and efficient GPU-based finite element (FE) simulation of gross and fine-scale soft-tissue behaviour, including skin wrinkles. Focussing on the forehead region of the face, we simulate both large areas of soft tissue, and detail such as skin layers (necessary to produce wrinkles [2]), unlike current approaches [3]. Our approach could be used in a variety of fields, from animation to surgical simulation, and it can be used to simulate any multi-layered soft body.

Simulation Approach

Our simulation approach involves three stages: creating the multi-surface mesh, creating a suitable simulation model, and simulating the model over time. Any surface mesh can be used. The model creation system then automatically constructs simulation-ready non-conforming (voxel-based) hexahedral FE simulation models with bound surface meshes [4]. This includes automatic computation of skin layers and material properties, muscle properties (such as fibre directions) from NURBS volumes, and boundary conditions.

Our GPU-based non-linear total Lagrangian explicit dynamic (TLED) FE system includes procedures for muscle contraction, and to enable the non-conforming elements to slide along a surface, such as the skull or deep tissue boundary (a phenomenon often neglected [5]), facilitated using a GPU-based semi-brute-force broad-phase collision detection algorithm. The solver has also been optimised for use with our non-conforming models [4]. Figures 1 and 2 show some example models and simulations.

Conclusions

Examples have demonstrated the complexity of models that our approach can generate, and their ability to simulate gross and fine-scale soft-tissue behaviour. Improvements could be made, for example, by using shell elements to better model the thickness of the epidermis. Future work will focus on simulating different-aged skin, and using different material models.

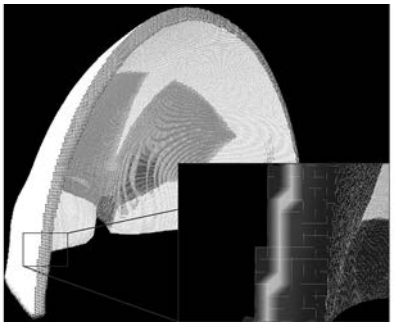

Rear view of a forehead model. Dark spheres represent rigid (fixed) nodes, light spheres represent sliding nodes, and coloured elements overlap a muscle. The material stiffness of the skin layers is visualised in the inset.

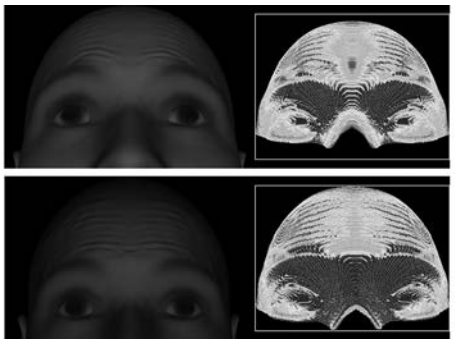

Simulation examples of forehead models with different muscle structures under contraction of the frontalis. Insets visualise the stresses.

Zachow S, Hege HC, Deuflhard P. Computer-Assisted Planning in Cranio-Maxillofacial Surgery. J Comp Inf Technol. 2006;14(1):53-64.

Flynn C, McCormack BAO. Finite element modelling of forearm skin wrinkling. Skin Res Technol. 2008;14(3):261-269.

Hung APL, Wu T, Hunter P, Mithraratne K. Simulating Facial Expressions using Anatomically Accurate Biomechanical Model. In: SIGGRAPH Asia 2011 Posters. Hong Kong, China: ACM; 2011. p. 29:1-29:1.

Warburton M, Maddock S. Creating Animatable Non-Conforming Hexahedral Finite Element Facial Soft-Tissue Models for GPU Simulation. In: Proc. WSCG 2012. Pilsen, Czech Republic: Union Agency; 2012. p. 317-325.

Barbarino G, Jabareen M, Trzewik J, Mazza E. Physically Based Finite Element Model of the Face. In: Proc. ISBMS 2008. London, UK: Springer-Verlag; 2008. p. 1-10.

Where applicable, the authors confirm that the experiments described here conform with The Physiological Society ethical requirements.

PCA251

Pointing at and tracking falling targets: Directional aspects of an internal model of gravity

J.C. Flavell, I.D. Loram and D.E. Marple-Horvat

School of Healthcare Science - IRM, Manchester Metropolitan University, Manchester, Greater Manchester, UK

Gravity acts vertically downwards in the real world. By internalising that reality as an internal model we should perform better when relating to objects 'falling' naturally downwards rather than in some other direction. Several studies have shown that expectation of gravity's effect on vertically descending or ascending targets can over-rule visual information to the contrary (1-3), but this has not been explored for other 'unnatural' directions. We sought evidence for an internal model of gravity by comparing visually guided tracking of objects accelerating at *g* (9.81m/s^2) in straight lines vertically downwards, upwards and horizontally. If a model exists, differences should exist between tracking natural versus unnatural trajectories.

For each direction, 17 subjects executed 3 tracks of a 15cm diameter realistic visual target 'falling' from stationary for 2.475m. The target was back-projected onto a screen 3m ahead of subjects. Tracking was by extending the dominant hand's index finger and pointing at the moving target. Tracking intercept (indicated position on the screen) was determined using a vector from the dominant eye past the fingertip to the screen. Vicon tracked movements. The instantaneous error (tracking position minus target position) was summed in 10ms steps over the time taken for the target to traverse 2.475m (730ms) as a measure of performance. Tracking ahead produced negative error values, and tracking behind positive values.

Direction significantly affected error (one-way ANOVA: F=31.57, p<.001). Post hoc tests revealed all errors were significantly different from one another (p<.001): descending M=-8.405m SD=2.342; ascending M=18.426m, SD=10.022, horizontal: M=7.755m SD=6.965). Tracking, the output of the manual tracking controller, was below the target: leading descending targets and lagging behind ascending targets. Starting errors were also below the target in all conditions. To judge one's tracking position, one is required to keep both finger-tip and target in sight. Due to the physical presence of the arm/hand/finger one must ensure that the target is above the tracked location to prevent total or partial target occlusion. Error when tracking a target accelerating upwards was more than double that for a target accelerating naturally downwards, and tracking fell behind for a horizontally accelerating target. These different errors for different directions suggest that subjects expected non-descending (rising or horizontally moving) targets would not accelerate in the same way as a free-falling target.

This pattern of results suggests subjects used an internal model of gravity to predict the future position of 'free-falling' targets and that the model is directionally tuned. Also, such tuning is evidence that subjects did not use either feedback or direct perception when tracking.

McIntyre J et al. (2001). Nature Neuroscience, **4**(7), 693-4.

Senot P et al. (2005). J Neurophysiology, **94**(6), 4471-80.

Zago M et al. (2004). J Neurophysiology, **91**(4), 1620-34.

Where applicable, the authors confirm that the experiments described here conform with The Physiological Society ethical requirements.

PCA252

Effects of diabetic peripheral neuropathy on muscular activations during stair descent

J.C. Handsaker[1], A.J. Boulton[2], F.L. Bowling[2], S.J. Brown[1], G. Cooper[1], C.N. Maganaris[3,1] and N.D. Reeves[1]

[1]IRM, Manchester Metropolitan University, Manchester, UK, [2]University of Manchester, Manchester, UK and [3]Liverpool John Moores University, Liverpool, UK

Introduction

People with diabetic peripheral neuropathy (DPN) are more likely to fall than age-matched controls, and are particularly at risk during the physically demanding task of stair descent. The timing of lower limb muscle activations is fundamental to controlling joint movement and enabling a safe descent, but such timings may be adversely affected by diabetes and DPN. The aim of this study was to investigate the effect of DPN and diabetes on muscular activations during stair descent.

Methods

12 DPN patients, 12 diabetic patients without neuropathy (D) and 10 age and BMI-matched controls (C), descended a 7 step staircase. Electromyographic (EMG) activity was recorded from the vastus lateralis (VL) and biceps femoris (BF), medial gastrocnemius (MG) and tibialis anterior (TA) muscles, from which onset, cessation, and duration timings relative to footstep contact (FSC) were obtained (Figs. 1 & 2). A one-way ANOVA was used to analyse between group differences (significance p<0.05).

Results

The MG muscle was activated significantly earlier relative to FSC by the DPN group compared to controls, but the D group displayed similar activation timings to controls (Fig. 1). Both the DPN and D groups activated the TA muscle significantly closer to FSC than the C group. The DPN group activated the MG and TA muscles for significantly longer than the C group (Fig. 1).

There were no significant differences between groups for the onset of VL or BF muscle activation (Fig. 2). DPN and D patients activated the VL muscle for a similar duration to the C group, but the DPN group activated the BF muscle for a significantly longer duration compared to the C group (Fig. 2).

Discussion

Differences in muscle activation strategy were observed primarily at the ankle joint, with the DPN group activating MG and TA muscles significantly earlier and later, respectively, than the C group. This modified activation strategy may indicate increased dependence on the plantar flexors to control ankle dorsiflexion upon FSC during stair descent. The DPN group also activated the MG and TA muscles for longer compared to controls, which is likely a mechanism to improve ankle stabilisation. The D group displayed alterations to muscle activation in the same pattern to that of the DPN group, but to a lesser extent, highlighting the progressive nature of diabetes.

The DPN group activated the BF muscle for a longer duration than the C group, but no other differences in muscle activation were observed between groups at the knee joint, further highlighting the predominantly distal adaptation of the stair descent strategy adopted by patients with DPN.

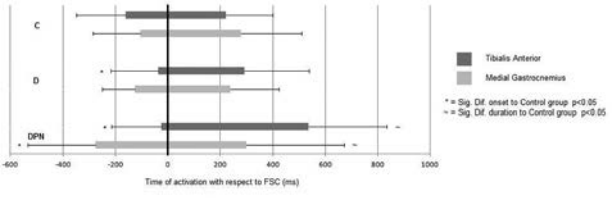

Figure 1. Periods of activation for the tibialis anterior and medial gastrocnemius muscles

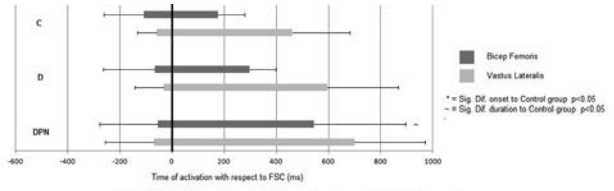

Figure 2. Periods of activation for the biceps femoris and vastus lateralis muscles

Supported by funding from the European Foundation for the Study of Diabetes (EFSD) and the Diabetes Research & Wellness Foundation.

Where applicable, the authors confirm that the experiments described here conform with The Physiological Society ethical requirements.

PCA254

Low-dose L- arginine supplementation improved total antioxidant activity and erythrocyte integrity in sickle cell anaemia subjects

S.I. Ogungbemi[1], C.N. Anigbogu[1], M.O. Kehinde[2] and S.I. Jaja[1]

[1]Department of Physiology, University of Lagos, Lagos, Nigeria and [2]Medicine, university of Lagos, Lagos, Nigeria

Low L- arginine concentration ([R]) has been reported in sickle cell anaemia (SCA). L- Arginine supplementation may be a cheaper alternative to the very expensive inhalation of nitric oxide in the management of SCA in Nigeria. The study investigated the effect of low-dose (1 g/day), oral L- arginine (Mason Vitamins, INC. USA) supplementation on plasma [R], lipid peroxidation (LPx), total antioxidant activity (TAA), red cell osmotic fragility and irreversibly sickled cell (ISC) count. 33 male and female non-sickle cell anemia subjects (NSCAS) and 28 sickle cell anaemia subjects (SCAS) were studied. A written ethical approval was granted for the study (Medical Research Grant and Experimentation Ethics Committee, College of Medicine University of Lagos, Nigeria). Each subject gave informed consent. 5 mL of venous blood was withdrawn from an ante-cubital vein of each subject for the measurements of plasma [R] (Li et al., 2008), malondialdehyde ([MDA] for LPx), TAA (Koracevic et al., 2001), osmotic fragility and ISC count. L- Arginine was then taken orally (1 g/day/6 weeks, Tanimura, 1967) by each subject. Measurements were made before and after L-arginine supplementation. Before supplementation, TAA (1.0±0.1 vs 1.5±0.2 mM/L, P<0.05) and [R] (8.3±0.7 vs 12.4±0.5 mg/dL, P<0.001) were low in SCAS compared to NSCAS while [MDA] (41.4±0.4 vs 33.0±2.0 mM/mg prot, P<0.001), initial lysis (IL: 0.86±0.01 vs 0.63±0.02 g%, P<0.001) and mean corpuscular fragility (MCF: 0.40±0.01 vs 0.45±0.01 g%, P<0.05) were high in SCAS compared to NSCAS. L- Arginine increased TAA (1.0±0.1 vs 1.6±0.2 mM/L in SCAS and 1.5±0.2 vs 2.0±0.1 mM/L in NSCAS, P<0.05) and [R] (8.3±0.7 vs 15.2±0.4 mg/dL in SCAS and 12.4±0.5 vs 18.8±0.6 mg/dL in NSCAS, P<0.001). However, [MDA] (41.4±0.4 vs 14.9±1.1 mM/mg prot in SCAS and 33.0±2.0 vs 14.2±0.7 mM/mg prot in NSCAS, P<0.001), IL (0.86±0.01 vs 0.57±0.02 g% in SCAS and 0.63±0.02 vs 0.49±0.02 g% in NSCAS, P<0.001), MCF (0.40±0.02 vs 0.23±0.01 g% in SCAS and 0.45±0.01 vs 0.22±0.02 g% in NSCAS, P<0.001), complete lysis (0.21±0.02 vs 0.11±0.02 g% in SCAS and 0.22±0.02 vs 0.01±0.01 g% in NSCAS, P<0.001), (and ISC count: 7.9±1.2 vs 2.0±0.3 %, P<0.001 in SCAS only) were reduced after supplementation. L- Arginine caused a greater percent increase in TAA (60.0±10 vs 33.0±6.7 %, P<0.05) and [R] (83.1±3.6 vs 51.6±0.8 %, P<0.001) while reduction in IL was greater (0.29±0.01 vs 0.14±0.01 g%, P<0.001) in SCAS than in NSCAS. Δ[R] correlated with ΔTAA (r=+0.8), Δ[MDA] (r=-0.7) and ΔISC (r=-0.6) in SCAS. Δ[R] correlated with ΔTAA (r=+0.6) and Δ[MDA] (r=-0.5) in NSCAS. Low-dose, oral L- Arginine improved TAA, red cell resistance to osmotic haemolysis and [R] but suppressed LPx in both groups of subjects and reduced ISC count in SCAS. L- Arginine may have beneficial implications in cost effective therapy in the management of SCA.

Dasgupta T, Hebbel RP and Kaul DK (2006). Free Radic Biol Med 41: 1771 – 1780.

Koracevic D, Koracevic G, Djordjevic V, Andrejevic S and Cosic V (2001). J Clin Pathol; 54: 356-361.

Li H, Liang X, Feng L, Liu Y and Wang H (2008). Journal of Food and Drug Analysis, Vol 16 (3); 53-58.

Romero J. Suzuka S. Nagel R and Fabry M (2002). Blood 99: 1103 - 1108.

Tanimura, J (1967). Bull Osaka Medical School; 13: 84-89.

Where applicable, the authors confirm that the experiments described here conform with The Physiological Society ethical requirements.

PCA255

The change in diastolic blood pressure during autonomic blockade is associated with T50 and error signal in young and older women

A.B. Peinado[1,2], E.C. Hart[3], N. Charkoudian[4], M.J. Joyner[2] and J.N. Barnes[2]

[1]Department of Health and Human Performance, Technical University of Madrid, Madrid, Spain, [2]Department of Anesthesiology, Mayo Clinic, Rochester, MN, USA, [3]Department of Physiology and Pharmacology, University of Bristol, Bristol, UK and [4]Thermal and Mountain Division, U.S. Army Research Institute of Environmental Medicine, Natick, MA, USA

Background: Understanding age-related changes in blood pressure regulation is key to preventing and treating hypertension. The blood pressure error signal represents the difference between resting diastolic blood pressure (DBP) and the T50 value, the DBP at which 50% of cardiac cycles are associated with bursts of muscle sympathetic nerve activity (MSNA). We have previously shown that both the T50 and the error signal are different between young men and women, suggesting that sex hormones may have an important influence. The purpose of the present study was to evaluate whether T50 and the error signal relate to the extent of change in blood pressure during autonomic blockade (AB) in young and postmenopausal women. Methods: In 12 young women (YW; 25 ± 1 yrs) and 12 postmenopausal women (PM; 61 ± 2 yrs), we measured MSNA using microneurography, and intra-arterial brachial blood pressure before and during complete AB with trimethaphan camsylate. Relationships between MSNA, T50, error signal (T50-DBP) and ΔDBP with AB were measured using linear regression analysis and Pearson's correlation coefficient. For mean data comparison between YW and PM an unpaired t test was used. Results: ΔDBP was associated with baseline T50 (r=-0.739, p<0.001), indicating that a greater reduction in DBP during AB was associated with higher T50 values in PM women (74.4±7.6 mmHg; r=-0.725, p=0.008) but not in young women (65.7±5.1 mmHg; r=-0.337, p=0.285). There was also an inverse relationship between ΔDBP and the error signal, but only when all women are grouped together (r=-0.715, p<0.001). This means that women who operate at a higher BP than their T50 (i.e. a negative error signal) have a smaller change in DBP when autonomic tone is removed. Women with the most negative error signal (DBP much higher than T50) had the lowest average MSNA (r=0.910, p<0.001) in both groups (YW: r=0.886, p<0.001; PM: r=0.870, p<0.001). Young women had more negative error signals than PM women (-7.6±5.2 versus 2.1±4.6 mmHg, p<0.001; respectively), and lower average MSNA (15.5±4.9 versus 32.9±10.2 bursts/min, p<0.001; respectively). Conclusions: Using T50 and error signal analysis, we have identified important differences in control of MSNA between young and PM women. Postmenopausal women had higher T50 values, more positive error signals, and greater drops in DBP during autonomic blockade. These data are consistent with recent reports from our laboratory regarding greater autonomic support of blood pressure in PM women, and provide further evidence of the importance of reproductive hormone influences on sympathetic mechanisms controlling blood pressure in women.

Where applicable, the authors confirm that the experiments described here conform with The Physiological Society ethical requirements.

PCA256

Stimulation of the otolith organs by ultrasonic bone stimulation of the mastoid increases muscle sympathetic nerve activity in humans

C.A. Ray and C.L. Sauder

Medicine, Penn State College of Medicine, Hershey, PA, USA

Muscle sympathetic nerve activity (MSNA) is altered by stimulation of the vestibular system. Studies indicate that the otolith organs mediate increases in MSNA when engaged by head-down rotation (HDR). These findings are important with regards to postural blood pressure regulation on earth and post-spaceflight orthostatic intolerance. It is currently unknown if nongravitational activation of the otolith organs can mediate increases in MSNA. One method believed to stimulate the otolith organs is ultrasonic bone stimulation (UBS) of the mastoid. To test the hypothesis that UBS can augment MSNA we measured leg MSNA, heart rate, and arterial blood pressure during gravitational stimulation of the otolith organs by HDR and during stimulation of the mastoid via UBS in 14 healthy subjects (4 men and 10 women; age: 25 ± 4 yr; BMI: 24 ± 4 kg/m2). UBS of the mastoid elicited a significant increase in leg MSNA (3 ± 1 bursts/min, 31 ± 10% total activity; P < 0.05). This increase in MSNA via UBS was comparable to HDR (4 ± 1 bursts/min, 35 ± 8% total activity; P < 0.05). UBS of the clavicle (n=10), which served as a control, did not increase MSNA. In all studies, HDR and UBS did not change heart rate or mean arterial blood pressure. These results indicate that UBS stimulation can elicit sympathetic outflow and may assist in maintaining peripheral resistance and arterial blood pressure during orthostatic challenges.

Supported by NIH (HL109952).

Where applicable, the authors confirm that the experiments described here conform with The Physiological Society ethical requirements.

PCA258

Evidence for beat-to-beat myogenic responses in the regulation of resting limb blood flow in man

P.J. Fadel[1], S.T. Fairfax[1], M. Takahashi[2], M.J. Davis[1] and J. Padilla[1]

[1]Medical Pharmacology & Physiology, University of Missouri, Columbia, MO, USA and [2]Institute of Biomedical & Health Sciences, Hiroshima University, Hiroshima, Japan

Previous work assessing the presence of myogenic responses in humans has primarily used experimental manipulations to evoke robust changes in transmural pressure. Although providing evidence for a myogenic response, such manipulations do not provide information about potential contributions of myogenic responses to beat-to-beat limb blood flow control during unprovoked resting conditions. Therefore, we explored spontaneous beat-to-beat relationships between arterial blood pressure (Finapres) and limb blood flow (duplex Doppler ultrasound in brachial and popliteal arteries) during 10 min of quiet supine rest in 15 young men. In addition, considering previous work demonstrating the presence of a myogenic response in the cutaneous circulation, measurements in the brachial artery were repeated with a wrist cuff inflated to 220 mmHg to occlude the hand circulation and thus, eliminate a major portion of skin blood flow. Cross correlations between mean

arterial pressure (MAP) and blood flow were determined using Pearson correlations in which MAP values were systematically offset by ±10 cardiac cycles relative to its real time associated blood flow. Repeated measures ANOVA was used for comparisons and data are presented as means ± standard errors. For both the brachial and popliteal artery, limb blood flow was negatively influenced by MAP such that higher pressures were associated with lower blood flows and vice versa. Indeed, significant negative correlations between MAP and blood flow were observed in both arteries (Figure 1A). Furthermore, the strongest negative relationship was observed when MAP was offset by 2 preceding heartbeats suggesting a consistent time-lag was present. Interestingly, the negative relationship between MAP and brachial artery blood flow was significantly attenuated by wrist occlusion (Figure 1B). These preliminary findings suggest that myogenic responses are detectable on a beat-to-beat basis in human limbs and contribute to the regulation of resting limb blood flow. Furthermore, it appears that the cutaneous circulation is necessary to fully observe the influence of the myogenic response in the forearm. However; partitioning the contributions of cutaneous and skeletal muscle circulations to the observed myogenic responses requires further investigation.

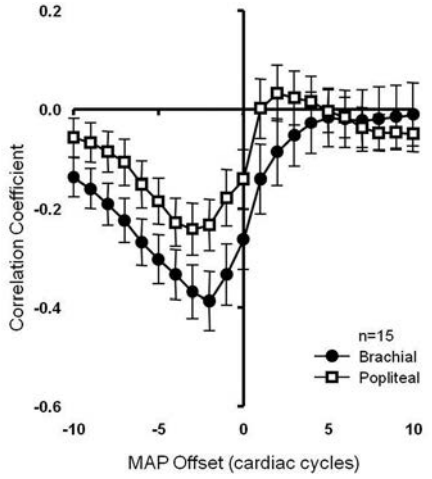

Figure 1A: Correlation coefficients relating MAP and blood flow in the politeal and brachial artery as MAP is offset by ±10 cardiac cycles relative to its real time associated blood flow (0 on x-axis).

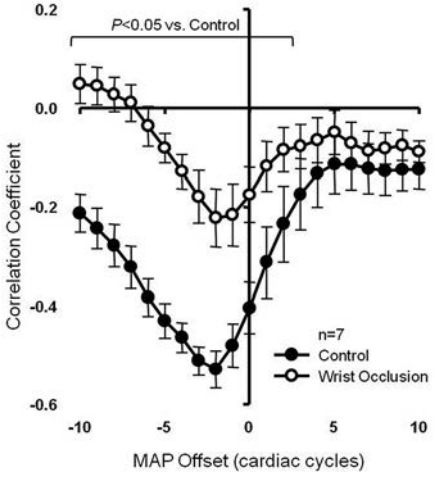

Figure 1B: Correlation coefficients relating MAP and blood flow in the brachial artery before (control) and during wrist cuff occlusion.

Supported by RO1 HL093167

Where applicable, the authors confirm that the experiments described here conform with The Physiological Society ethical requirements.

PCA259

Cardiovascular response to aerobic exercise training is attenuated in middle-aged adults with polymorphism of eNOS gene at position intron 4 a/b: A double-blind study

A. Zanesco, C.H. Sponton, R. Esposti, C.M. Rodovalho, M.J. Ferreira, A.P. Jarrete, C.P. Anaruma and M. Bacci

UNESP, Rio Claro, Sao Paulo, Brazil

We have demonstrated that postmenopausal women with endothelial nitric oxide synthase (eNOS) gene polymorphism at position -786T>C are less responsive in lowering blood pressure after exercise training than those who are not polymorphic (TT genotype),[1]. This response was accompanied by lower nitric oxide (NO) production, measured by plasma nitrite/nitrate. Interestingly, variable number of tandem repeat Intron 4b/a of the eNOS gene has also been associated with reduction in plasma NO levels, decreased eNOS expression or reduced enzyme activity[2]. However, no studies exist evaluating the influence of Intron 4b/a of the eNOS gene in the cardiovascular responses and oxidative stress biomarkers in response to aerobic exercise training (ET) in adults. Therefore, we investigated the relationship between eNOS polymorphism at position Intron 4 a/b and the effect of ET on the blood pressure (BP), nitrate/nitrite levels (NOx-) and oxidative stress biomarkers (superoxide dismutase - SOD, catalase - CAT and malondialdehyde - MDA) in middle-aged adults. Eighty-one subjects (51.1±0.6 yrs) were trained in treadmill, 3 days/week, for 30-40 min/session at moderate intensity, during 24 sessions. A comparison between sphygmomanometer-based and ambulatory BP monitoring (ABPM) was carried out before and after ET. Genotype analysis was performed using sequencing method (ABI3500–Applied Biosystems). All the data acquisition and analysis were performed in a double-blind manner. The volunteers were divided into non-polymorphic (Intron 4bb, n=55) and polymorphic (Intron 4ba+aa, n=26). ET were effective in lowering BP measured by sphygmomanometer-based for both systolic (-4.6mmHg) and diastolic BP (-2.6 mmHg) whereas in ABPM measurements only systolic BP values were significantly reduced (-2.4mmHg) in non-polymorphic group (genotype bb). These beneficial effects were accompanied by increased SOD (+11.7 U/ml) and CAT (+7.9 nmol/ml/min) enzymes activity. In contrast, adults who carry eNOS gene polymorphism for intron 4 a/b (genotype 4ba+aa) showed no changes in BP for both methods, acute and measurement during 24 hr. Interestingly, an increase in SOD (+12.1 U/ml) and CAT (+10.2 nmol/ml/min) enzymes activity were found in polymorphic group. No changes were observed in plasma NOx- and MDA concentrations in response of ET for both genotypes (intron 4bb and 4ba+aa). Our findings show that the polymorphism of eNOS gene at intron 4b/a position attenuated the benefits of the exercise training in lowering blood pressure, but did not affect the antioxidant enzymes activity.

Sponton CH, Rezende TM, Mallagrino PA, Franco-Penteado CF, Bezerra MA, Zanesco

A. Women with TT genotype for eNOS gene are more responsive in lowering blood

pressure in response to exercise. Eur J Cardiovasc Prev Rehabil. 2010; 17(6):676-81.

Zhang M, Ou H, Shen YH, Wang J, Wang J, Coselli J, and Wang XL. Regulation of endothelial nitric oxide synthase by small RNA. PNAS 2005; 102 (47): 16967–72.

São Paulo Research Foundation – FAPESP

Where applicable, the authors confirm that the experiments described here conform with The Physiological Society ethical requirements.

PCA260

Young adult asian males have a lower baro-reflex gain compared to matched caucasians, as measured by heart rate variability analysis

D.A. Saint, L. Casey and A. Elliott

University of Adelaide, Adelaide, SA, Australia

INTRODUCTION: Racial and ethnic differences in risk for cardiovascular morbidity and mortality are well documented. The relative role of genetic vs environmental influences is unclear. A non-invasive measure of autonomic balance, Heart Rate Variability (HRV) has been shown to be correlated with cardiovascular risk in some populations. Whether there are underlying differences in HRV between racial and/or ethnic groups, and whether this might therefore affect cardiovascular risk, is largely unknown.
HYPOTHESIS: Young Asian males will have a higher HRV than matched Caucasians and will show a lower response to postural changes.
METHODS: Subjects were in two groups; 1) Caucasian males aged 18 to 25 living all their life in Australia (n=20) and 2) age and BMI matched Asian males ("Asian" being defined as south east Asia, excluding the Indian sub-continent) resident in Australia (n=30).
Subjects abstained from exercise, consuming alcohol, caffeine or guarana for 2 hours prior to the experiment. After 2 min acclimatisation, either standing or supine, the subject's ECG was recorded for 15 min and HRV analysis conducted with AD Instruments (Australia) Chart 5/HRV module. The time domain measure used was SDdeltaNN, Frequency domain analysis used power spectral analysis to derive LF:HF ratio.
RESULTS: There were no significant differences in age, BMI, hip:waist ratio or heart rate between the groups. There were no differences in blood pressure, except standing systolic blood pressure (137.2 ± 5.2 mm.Hg in Caucasian vs. 123.8 ± 2.8 mm.Hg in Asians; P<0.05).
For both groups there was a significant decrease in SDdeltaNN and an increase in LF:HF ratio when standing compared to supine. Each of these changes was significantly larger for Caucasians compared to Asians for both measures (table 1).
CONCLUSIONS: When moving from supine to standing, Asian subjects showed a lesser fall in HRV by both time domain and frequency domain measures compared to Caucasians. This appears to be because they have a larger reduction in vagal tone during this postural change. This may indicate a genetic difference between groups, and provide insight to the racial differences in risk for cardiovascular mortality and morbidity.

Table 1

SD delta NN	supine		standing		change	
	mean	SD	mean	SD	mean	SD
Asian	46.10	3.85	26.76	6.09	-19.35	5.29
Caucasian	72.47	8.07	24.88	1.96	-47.59	7.44
p	**		ns		**	
LF:HF ratio	supine		standing		change	
Asian	1.43	0.77	4.76	2.55	3.32	2.23
Caucasian	1.17	0.72	6.31	3.33	5.14	2.93
p	ns		ns		*	

Where applicable, the authors confirm that the experiments described here conform with The Physiological Society ethical requirements.

PCA262

Capsaicin-based analgesic balm attenuates the skeletal muscle metaboreflex in humans

L.C. Vianna, I. Fernandes, T. Barbosa and A. Nóbrega

Physiology and Pharmacology, Fluminense Federal University, Niterói, Rio de Janeiro, Brazil

While it is well established that the exercise pressor reflex (EPR) is one of the principal mediators of the cardiovascular response to exercise, the receptors activating the group III and IV fibres that are important to EPR function remains unclear. Recent animal studies have reported that either capsaicin balm or infusion of capsazepine attenuates the pressor response to muscle contraction, indicating the transient receptor potential vanilloid1 (TRPv1) receptor (localized on the group IV afferent neuron) as an important mediator of the EPR via its metabolic component (named muscle metaboreflex). Whether these findings can be extended to human remains to be determined. To begin to address this question, blood pressure (BP, Finometer), muscle sympathetic nerve activity (MSNA, peroneal microneurography) and femoral blood flow (FBF, Doppler Ultrasound) were measured in five male subjects (24±2 yrs) at rest, during static handgrip exercise at 40% maximal voluntary contraction, and during post-exercise muscle ischemia (PEMI) to isolate the metabolic component of EPR. Trials were performed before (T0) and at 30 (T30) and 60 min (T60) after application of a commercially available analgesic balm, containing capsaicin as the active ingredient (0.1%, CAPZASIN-HP), on the volar forearm of the subject's non-dominant arm in a similar manner to that described in the manufacturer's directions. Statistical comparisons of all physiological variables were made utilizing paired t-tests and data are presented as means ± SE. Static exercise evoked increases in mean BP (+32±4 mmHg, P<0.05), MSNA (+26±5 bursts/min, P<0.05; +19±5 bursts/100 heart beats, P<0.05). The BP and MSNA responses to forearm static contraction were not affected by the application of capsaicin balm. During PEMI at T0, BP (+31±4 mmHg, P<0.05), MSNA (+27±5 bursts/min, P<0.05; +36±5 bursts/100hb, P<0.05) remained elevated compared with rest. Additionally, femoral vascular conductance (the ratio of FBF to BP) was slightly but significantly attenuated from rest during PEMI (-0.72±0.2 mL/min/mmHg, P=0.05), indicating reflex vasoconstriction. After application of capsaicin balm, the BP (+25±4 mmHg at T30; +25±2 mmHg at T60, P<0.05 vs. T0) and MSNA (+17±4 bursts/min and +21±5 bursts/100hb at T30; +15±2 bursts/min and +21±4 bursts/100 hb at T60; P<0.05 vs. T0) responses to PEMI were all significantly less than those observed at T0. Capsaicin balm also attenuated vasoconstrictory responses to PEMI (+0.27±0.18 mL/min/mmHg at T30; -0.24±0.18 mL/min/mmHg at T60, P<0.05 vs. T0). In conclusion, capsaicin-based analgesic balm effectively attenuated BP, sympathetic and vasconstrictory responses evoked by metabolically sensitive skeletal muscle afferents in humans. These data are consistent with the concept that TRPv1 receptors contribute to the EPR in humans, via its metabolic component.

Supported by CAPES, CNPq, FAPERJ and FINEP.

Where applicable, the authors confirm that the experiments described here conform with The Physiological Society ethical requirements.

PCA263

Enhanced cardiovascular responses is associated with increased orthostatic tolerance in young men following oral glucose and Vitamin C ingestion

T. Usman, V.A. Olatunji, A.O. Adah and L.A. Olatunji

Physiology, University of Ilorin, Ilorin, Nigeria

Background — Recent studies have shown that ingestion of glucose or vitamin C lowers blood pressure in patients with autonomic dysfunction, and modestly reduce blood pressure in normal subjects. Whether oral glucose loading with vitamin C ingestion affects cardiovascular responses during orthostatic stress in normal young subjects is yet to be determined. We therefore hypothesized that co-administration of glucose and vitamin C will reduce orthostatic tolerance in normal young male volunteers. Methods: In a randomized controlled cross-over fashion, nine non-obese (19.3 ± 0.6 kg/m2), young (21.9 ± 0.6 yr) men ingested nothing (control), glucose (75g) alone and with Vitamin C (1g) 10 min before standing on three separate days of appointment. We measured supine and standing blood pressure, heart rate, haematocrit and blood glucose levels. Orthostatic tolerance was evaluated as the time to presyncope during motionless standing or until presyncopal symptoms were observed. Results: During the first 60 min of standing, 89%, 78% and 0% of subjects experienced presyncopal symptoms when ingested nothing, glucose alone and glucose+vitamin C, respectively. Ingesting glucose alone did not affect orthostatic tolerance (61.4 ± 1.4 vs 63.0 ± 1.7min; $p < 0.05$) while ingesting glucose with vitamin C significantly improved orthostatic tolerance (86.6 ± 2.2 vs 63.0 ± 1.7 min; $p< 0.001$). Increases in systolic blood pressure and heart rate induced by standing were significantly enhanced when glucose+vitamin C was ingested, while changes in diastolic blood pressure were not significantly affected. Ingestion of glucose alone or with vitamin C led to a comparable significant increase in blood glucose levels after standing. However, significant increase in haematocrit level was observed after standing when glucose+vitamin C but not when glucose alone was ingested. Conclusion: The results of the present study demonstrate that oral glucose loading with vitamin C ingestion improves orthostatic tolerance, and the improvement is associated with enhanced systolic blood pressure, heart rate and haematocrit level.

Keywords: Blood pressure, glucose load, haematocrit, orthostatic tolerance, vitamin C

Ting HH, Timimi FK, Boles KS, Creager SJ, Ganz P, Creager MA. (1996). Vitamin C improves endothelium-dependent vasodilation in patients with noninsulin-dependent diabetes mellitus. J Clin Invest; 97: 22–8.

Brown CM, Hainsworth R. (2000). Forearm vascular responses during orthostatic stress in normal subjects and patients with posturally-related syncope. Clin Auton Res; 10: 53 – 55.

Olatunji LA, Soladoye AO, Jaja SI. (2007). Effects of chronic administration of vitamin C on haemodynamic responses to postural stress or cutaneous cold stimulation in healthy young men. The Tropical Journal of Health Sciences 14: 42–46.

Where applicable, the authors confirm that the experiments described here conform with The Physiological Society ethical requirements.

PCA264

Yogic practices can increase estrogen and progesterone levels and heart rate variability in peri-menopausal women

R. Khadka[1], B.H. Paudel[1], S. Majhi[2], N. Shrestha[3], M.C. Regmi[4], S. Chhetri[4], A. Das[1], D. Sharma[1], V. Gautam[1] and P. Karki[3]

[1]Basic and Clinical Physiology, BP Koirala Institute of Health Sciences, Dharan, Nepal, [2]Department of Biochemistry, BP Koirala Institute of Health Sciences, Dharan, Nepal, [3]Department of Internal Medicine, BP Koirala Institute of Health Sciences, Dharan, Nepal and [4]Department of Obstetrics and Gynecology, BP Koirala Institute of Health Sciences, Dharan, Nepal

Higher death rate has been reported in postmenopausal or perimenopausal women with cardiovascular events than in men. Reduced estrogen production from ovaries has been suggested as one of its factors. Studies with estrogen therapy have shown cardio-protective effects. However, estrogen has proliferative effect on breast and its long-term use may be carcinogenic. One of the alternative therapies, yoga has been found to reduce the levels of testosterone and luteinizing hormone in hirsutism. Therefore, we aimed to study the effect of yoga on female sex hormone level and heart rate variability in perimenopausal women. Consenting twenty perimenopausal women were randomized into yoga (n=10, age 44±2.64 years) and control (n=10, age 46±5.09 years) groups. Subjects suffering from any diseases or on medication were excluded from the study. Yoga group practiced meditation, pranayama (breathing exercise) and few easy asnas (postures) for 30 min/day for a month. Control group did not do any yoga/relaxation or any active relaxation procedures. Short-term heart rate variability was recorded in all subjects at zero and one month. Institutional ethical committee approved the work. Both groups were comparable in term of their age, height, weight, BMI, systolic BP, diastolic BP, heart rate, and respiratory rate. Time domain measures of HRV, which are primarily markers of cardiac parasympathetic activity [SDNN: 23.93(18.5-35.4) vs 43.2(34.4-50.1) ms, p=0.014; rMSSD: 17.3(12.45-21.85) vs 30.6(25.15-38.05) ms, p=0.022; NN50: 1(0.25-8.5) vs 34(11-60.5) count, p=0.022] were found increased in yoga group as compared to control group after yoga. High frequency power, which is also one of the markers of parasympathetic activity, increased in yoga group as compared to control group. Both serum estrogen [11.95(5.05-41.32) vs 24.47(12.54-64.90) pg/ml, p=0.036] and progesterone [0.24(0.10-1.02) vs 2.0(0.25-9.73) ng/ml, p=0.012] levels were found increased in yoga group after yogic intervention. In conclusion, parasympathetic activity, estrogen and progesterone levels increased in perimenopausal women after a month of yoga practice. Increased parasympathetic activity and female sex hormone levels indicate that yoga can be a cardioprotective alternative therapeutic measure in perimenopausal women.

(The work is part of a project supported by Nepal India Corpus fund.)

Where applicable, the authors confirm that the experiments described here conform with The Physiological Society ethical requirements.

PCA265

Cerebrovascular reactivity is associated with central pulse wave characteristics in healthy adults

J.N. Barnes[1,2], J.L. Taylor[1] and M.J. Joyner[1]

[1]Anesthesiology, Mayo Clinic, Rochester, MN, USA and [2]Physiology and Biomedical Engineering, Mayo Clinic, Rochester, MN, USA

Cerebrovascular reactivity determines the responsiveness of the cerebral vessels to vasoactive stimuli. However, acute changes in blood pressure may augment the calculated cerebrovascular reactivity. If autoregulatory mechanisms within the brain are intact, fluctuations in blood pressure will not alter cerebral blood flow. Because aging and hypertension may reduce autoregulation, cerebrovascular reactivity is often calculated using conductance to account for changes in mean arterial pressure (MAP). Yet, MAP may underestimate the influence of central hemodynamics on cerebral blood flow. In this context, we investigated whether central pulse wave characteristics were associated with cerebrovascular reactivity in healthy humans. Hypercapnia was used to determine cerebrovascular reactivity of the middle cerebral artery (MCA) in 28 adults (14 men and 14 women) using transcranial Doppler. MAP was measured using finger photoplethysmography and central pulse wave characteristics (i.e. aortic blood pressure, augmented pressure, augmentation index) were determined using arterial tonometry. Baseline MCA velocity was 48.6 ± 3.9 cm/s and cerebrovascular reactivity was 0.79 ± 0.08 AU. Aortic systolic (110 ± 2 mmHg) and diastolic (72 ± 1 mmHg) blood pressure were not associated with cerebrovascular reactivity. However, cerebrovascular reactivity was inversely associated with augmented pressure (8.3 ± 1.0 mmHg; r = -0.43; p<0.05), augmentation index (21.1 ± 2.3 %; r = -0.52; p<0.01), and augmentation index corrected for heart rate (12.1 ± 2.6%; r= -0.50; p<0.01). In conclusion, higher augmentation of the central pulse wave is associated with lower cerebrovascular reactivity in healthy adults. Our results suggest that cerebral blood flow regulation may be affected by central pulse wave characteristics.

Funded by NIH RR-024150, AR-056950, AG-038067, and AG-16574-11PP2

Where applicable, the authors confirm that the experiments described here conform with The Physiological Society ethical requirements.

PCA266

Heart rate variability: the impact of hypoxia and gender

D. Hodson, C.J. Marley, L. Fall, K. Evans, D. Whitcombe, J.V. Brugniaux, K.J. New and D.M. Bailey

University of Glamorgan, Pontypridd, UK

Introduction:
Non-invasive measurements of heart rate variability (HRV) are used to assess cardiovascular autonomic regulation. HRV can be measured using time and frequency domain indexes; changes in these indexes are considered to reflect changes in the parasympathetic and sympathetic modulation (1). A reduction in HRV, with an increase in low frequency (LF) component and LF/HF (high frequency) ratio are common findings when at high altitude, highlighting a shift towards sympathetic modulation and a decline in the vagal activity (2), Little is known regarding the impact of gender on HRV. And existing literature is inconclusive suggesting that females exhibit either an increase (3) or a decrease (4) in HRV measurements when compared to males in normoxia. Therefore, the present aim was to investigate the effect of acute hypoxia and gender on the cardiovascular autonomic function.
Methods:
Sixteen healthy physical activity subjects (6 males, 10 females) aged 26 ± 7 years, 29 ± 6 years (respectively) underwent a 5-minute supine HRV measurement in normoxia (21% O2) and following 4 hour exposure to normobaric hypoxia (12% O2). The following parameters of HRV were calculated: Time domain indexes: standard deviation of RR intervals (SDNN), root-mean-square of successive normal RR interval differences (RMSSD); Frequency domain indexes: Total power (TP, 0.0 – 0.40Hz), LF/HF ratio, HF normalised power (HFnu) calculated as the HFnu =(absolute HF power/TP)x100 and LF normalised power (LFnu) calculated as LFnu = (absolute LF power/TP)x100. Following confirmation of distribution normality using Shapiro-Wilks W tests, data were analysed using a 2-way repeated measures analysis of variance. Significance was established at a level of P<0.05 and data were expressed as mean ± SD.
Results:
Hypoxia induced a reduction in all the time domain indexes (P<0.05) as well as in HFnu, TP, but an increase in LFnu and a significant increase in LF/HF (P<0.05) in all groups. There was no gender difference in any measured HRV index (P>0.05).
Conclusion:
The findings are consistent with the concept that hypoxia induces modifications of the cardiac autonomous nervous system (5). However, the effect of gender remains undetermined in the current study both in normoxia and hypoxia, hence warranting further assessment.

Table 1: Heart Rate Variability indexes in Normoxia and Hypoxia for both male and female.

	Male		Female	
	Normoxia	Hypoxia	Normoxia	Hypoxia
Time Domain Indexes				
SDNN (ms)	82 ±42	59 ±24	91 ± 39	45 ±20
RMSSD (ms)	70 ±49	36 ±22	83 ±52	31 ±19
Frequency Domain Indexes				
HFnu (%)	40 ± 17.7	27.6 ± 20.5	41.9 ± 14.7	25.4 ± 11.9
LFnu (%)	60 ± 17.7	72.4 ± 20.5	58.1 ± 14.7	74.6 ± 11.9
LF/HF	1.89 ± 1.07	4.6 ±3.4	1.68 ±0.94	3.7 ± 2.1
TP (ms2)	5869 ±4713	2936 ±2700	8236 ± 8019	1960 ±1716

Mean ± SD

1. Akselrod S, Gordon D, Ubel FA, Shannon DC, Berger AC, Cohen RJ. Power spectrum analysis of heart rate fluctuation: a quantitative probe of beat-to-beat cardiovascular control. Science. 1981;213(4504):220-2. Epub 1981/07/10.

2. Cornolo J, Mollard P, Brugniaux JV, Robach P, Richalet JP. Autonomic control of the cardiovascular system during acclimatization to high altitude: effects of sildenafil. J Appl Physiol. 2004;97(3):935-40. Epub 2004/05/18.

3. Ryan SM, Goldberger AL, Pincus SM, Mietus J, Lipsitz LA. Gender- and age-related differences in heart rate dynamics: are women more complex than men? Journal of the American College of Cardiology. 1994;24(7):1700-7. Epub 1994/12/01.

4. Jensen-Urstad K, Storck N, Bouvier F, Ericson M, Lindblad LE, Jensen-Urstad M. Heart rate variability in healthy subjects is related to age and gender. Acta physiologica Scandinavica. 1997;160(3):235-41. Epub 1997/07/01.

5. Mairer K, Wille M, Grander W, Burtscher M. Effects of Exercise and Hypoxia on Heart Rate Variability and Acute Mountain Sickness. International journal of sports medicine. 2013. Epub 2013/02/07.

Where applicable, the authors confirm that the experiments described here conform with The Physiological Society ethical requirements.

PCA267

Cardiovascular responsiveness to sympathoexcitatory stress in mild-hypertensive and normotensive participants

E. Carthy[1,2], L. White[1], F.D. Russell[1], M.A. Holmes[1], A.S. Leicht[3], P.R. Brooks[1], D. Hitchen-Holmes[1] and C.D. Askew[1,4]

[1]Faculty of Science, Health, Education & Engineering, University of the Sunshine Coast, Sippy Downs, QLD, Australia, [2]School of Medicine, Imperial College London, London, UK, [3]Institute of Sport and Exercise Science, James Cook University, Townsville, QLD, Australia and [4]Institute of Health and Biomedical Innovation, Queensland University of Technology, Brisbane, QLD, Australia

Autonomic dysfunction is implicated in cardiovascular disease, with studies reporting an exaggerated blood pressure response to sympathoexcitatory stress in individuals with resting hypertension (1-3). It is not clear whether this response is associated with changes in cardiac autonomic modulation or altered peripheral cardiovascular dynamics. The aim of this study was to compare blood pressure (BP), heart rate variability (HRV) and limb blood flow between normotensive (N: mean±SD; BP 116.9±1.4/73.4±0.9mmHg; age 49.4±10.4years, BMI 26.4±4.5kg.m-2; n=49) and mildly hypertensive participants (H: BP 141.3±2.0/88.8±2.2mmHg; age 51.7±11.4years, BMI 30.5±5.0kg.m-2; n=17) at rest and in response to sympathoexcitatory stress. Participants performed a cold pressor test (CPT) and an ischaemic handgrip test (IHGT) and were assessed for BP, forearm blood flow and HRV at rest and in response to the tests. Data are expressed as mean±SD and comparisons were made using ANOVA (SPSS Version 19, IBM Statistics, SPSS Inc., USA). The CPT evoked greater increases in systolic blood pressure (SBP; H: 18.13±13.01mmHg; N: 8.84±12.38mmHg; p=0.011) and mean arterial pressure (MAP; H: 10.13±9.55mmHg; N 4.65±8.16mmHg; p=0.026) in hypertensive compared with normotensive participants. The IHGT evoked greater increases in diastolic (DBP; H: 6.88±5.48mmHg; N: 0.32±7.20mmHg; p=0.001) and MAP (H: 9.24±4.85mmHg, N: 3.26±6.24mmHg; p=0.001) in hypertensive compared with normotensive participants. Hypertensive participants had significantly lower levels of resting cardiac parasympathetic modulations measured as the high frequency power of HRV (H: 31.7±4.1nu; N: 42.1±2.2nu; p=0.026). There were no significant differences in the HRV or blood flow responses to the CPT or IHGT between hypertensive and normotensive participants. This study demonstrated that sympathoexcitatory stress triggered an augmented blood pressure response in hypertensive participants, in line with previous studies (1-3). However, we found no evidence to support stress-activated hyper-reactivity in HRV or forearm blood flow in hypertensive participants. These findings lend support to the notion that sympathetic dominance contributes to the pathogenesis of hypertension. From the findings, we propose that more direct markers of autonomic function be investigated to better understand the role of the autonomic nervous system on the stress induced blood pressure response.

Davis JT *et al.* (2012). Autonomic and Hemodynamic Origins of Pre-Hypertension Central Role of Heredity. *JACC* **59**(24), 2206-16.

Carrol D *et al.* (2012). Systolic blood pressure reactions to acute stress are associated with future hypertension status in the Dutch Famine Birth Cohort Study. *Int J Psychophysiology* **85**, 270-273.

Farah R *et al.* (2009). High blood pressure response to stress ergometry could predict future hypertension. *Eur J Intern Med* **20**(4), 366-368.

This project was funded through a University of the Sunshine Coast research development grant.

Where applicable, the authors confirm that the experiments described here conform with The Physiological Society ethical requirements.

PCA268

A novel integrated tilt table-lower body negative pressure box to investigate differential arterial baroreflex responses with tilt in humans

M. Tymko, N. Ingram-Cotton, M. Howatt, R.J. Skow and T.A. Day

Mount Royal University, Calgary, AB, Canada

The arterial baroreflex responds to acute reductions in mean arterial pressure (MAP) by eliciting a heart rate response, maintaining MAP at normal levels. In the case of traumatic blood loss, Trendelenburg position (i.e., head-down tilt) is often used clinically to help compensate for reductions in MAP through gravity-dependent shifts in blood volume distribution toward the central cavity, but its use is controversial. A lower-body negative pressure (LBNP) box can be used to study baroreflexes by eliciting acute reductions in MAP through shifts in blood volume distribution toward the lower extremities, reducing venous return. We developed a novel integrated tilt table-LBNP box to investigate the cardiovascular and cerebrovascular effects of head-up and head-down tilt (HUT, HDT) on LBNP-induced hypotension. We hypothesized that 45° HUT would elicit a larger arterial baroreflex heart rate response to acute -50 mm Hg LBNP than supine or 45° HDT. Additionally, we hypothesized that there would be differential cerebral autoregulation (CA) between the middle cerebral artery (MCA) and posterior cerebral artery (PCA) during acute LBNP. 13 male volunteers (BMI 26.4±3 kg/m2; 24.2±4.8 yrs) were recruited. Following familiarization and consent, subjects were instrumented for measurement of instantaneous heart rate (IHR; ECG), MAP (mm Hg; finometer), end-tidal (PET)CO2 (Torr) and MCA and PCA cerebral blood velocity (CBV; cm/s; transcranial Doppler ultrasound). Subjects were placed in the tilt-table-LBNP box in supine position, underwent a 10-min baseline period, and exposed to -50 mmHg of acute LBNP for a maximum of ten minutes. The protocol was then repeated in 45° HUT and HDT in randomized order. Subjects were coached to maintain PETCO2 to resting values (±2 Torr). LBNP was terminated if systolic blood pressure was reduced 30% from resting values (pre-syncope; PS). We found that the arterial baroreflex-mediated IHR responses were linear and tilt-dependent. The slopes of the IHR responses were largest in 45° HUT, but less effective at protecting MAP than in supine and 45° HDT during acute LBNP. 10/13 subjects in 45° HUT reached PS in 427.7s, 3/13 subjects in supine position reached PS in 450.3s and no subjects reached PS in 45° HDT. PETCO2 was unchanged during LBNP in all three positions with coached breathing, eliminating the confounding effects of cerebrovascular CO2 reactivity on CBV. Although MAP was unchanged during LBNP prior to PS in all positions, there were differences between baseline and LBNP MCA in 45° HDT and 45° HUT, but there were no differences in the PCA between baseline and LBNP in any body position. Our findings suggest (a) Trendelenburg may be a useful application to prevent hypovolemic shock, and (b) CA may be different between anterior and posterior cerebral arterial circuits during acute LBNP.

Where applicable, the authors confirm that the experiments described here conform with The Physiological Society ethical requirements.

PCA269

Implications of enhanced kynurenic acid and extracellular tryptophan during fatigue

T. Yamamoto

Psychology, Tezukayama University, Nara, Japan

Serotonin, a neurotransmitter synthesized from tryptophan(TRP), has been proposed to play a key role in central fatigue. Here, we examined whether TRP itself and/or its two metabolites, kynurenic acid (KYNA) and quinolinic acid (QUIN), are involved in central fatigue. Experiments were conducted using Sprague-Dawley rats (SDR, 200–250 g, n = 21) and Nagase analbuminemic rats (NAR, 210–255 g, n = 3). Central fatigue was assessed by treadmill running and a Morris water-maze test. First, a microdialysis guide cannula (CMA/12) was inserted into the left striatum under anesthesia with sodium pentobarbital (25 mg/kg i.p.; Abbott Laboratories, USA), and microdialysis (Yamamoto et al, 2012) was used to collect samples for measurement of extracellular concentrations of TRP, serotonin, and 5-hydroxyindoleacetic acid (5-HIAA) in real time as rats (SDR and NAR) ran to exhaustion on the treadmill. Rats (SDR) were first treated with either saline or Branched-chain amino acids (BCAA, valine:leucine:isoleucine, 5:3:2, 250 mg/kg i.p.) 30 min before the exhaustion test. Second, the rats (another group of SDR) were trained in four daily sessions for 10 consecutive days on a Morris water-maze (a circular water tank 147 cm in diameter fitted with a refuge platform 250 mm in height). Rats were tested 6–7 days after injection with 180 nmol QUIN or QUIN plus 20 nmol KYNA into the hippocampus CA3-region through a guide cannula (CMA/12). All animal procedures were conducted in accordance with guidelines of the Japanese Neuroscience Society for animal experiments, and sanctioned by the animal-research ethics committee of Tezukayama University. The concentration of TRP secreted into the extracellular space of the striatum was higher during fatigue, and quickly returned to basal (free moving) levels with recovery from fatigue. Intracerebral TRP levels were directly associated with the time-to-exhaustion and were shown to be easily reduced with BCAA treatment. Compared with the saline group (133 ± 6.3 min), time-to-exhaustion for the BCAA group was clearly prolonged via the dramatic reduction in extracellular TRP caused by BCAA treatment (187 ± 21.5 min) ($t = 2.404$, d.f. = 7, $p < 0.05$). Moreover, return to basal TRP levels was associated with recovery from exhaustion, with real-time release of TRP in extracellular fluid showing that this response was sensitive and specific. Time-to-exhaustion was shorter in NAR, which maintain a higher extracellular level of striatal TRP than do SDR. Impaired memory performance in a water maze task after TRP treatment was attributable to high levels of KYNA and QUIN in the hippocampus acting synergistically on N-methyl-D-aspartic acid receptors. Our findings demonstrate that the increase in fatigue that occurs because of elevated brain TRP can be further amplified with synthetic KYNA and QUIN.

Yamamoto T, Azechi H, Board M. Essential role of exessive tryptophan and its neurometabolites in fatigue. Can J Neurol Sci 2012; 39:40-47.

This work was supported by Tezukayama Gakuen.

Where applicable, the authors confirm that the experiments described here conform with The Physiological Society ethical requirements.

PCA270

PKC-dependent regulation of mTOR activity is mediated through TSC2/Rheb signaling in C2C12 myoblasts

M. Miyazaki

School of Rehabilitation Sciences, Department of Physical Therapy, Health Sciences University of Hokkaido, Ishikari-gun, Hokkaido, Japan

The enhanced rates of protein synthesis overcoming to the protein degradation resulted in a net increase in cellular protein accumulation that leads to skeletal muscle growth and hypertrophy. It has been well documented that mammalian target of rapamycin (mTOR) plays an essential role for the regulation of protein synthesis and subsequent hypertrophy in skeletal muscle. The protein kinase C (PKC)-dependent regulation of mTOR activity and subsequent protein synthesis/cell growth has been suggested, however, the exact molecular mechanisms underlying this regulation are poorly defined in skeletal muscle. The purpose of this study was to determine the regulatory mechanism in PKC-dependent pathway leading to mTOR activation in skeletal muscle cells. C2C12 murine myoblasts were treated with serum/antibiotics free media for 120 min and then stimulated with PKC activator phorbol 12-myristate 13-acetate (PMA) for 20 min (100 nM in serum/antibiotics free media), co-incubated with/without mTOR-specific inhibitor rapamycin (50 nM) and PKC-specific inhibitor bisindolylmaleimide I (BIM-I) (10 μM). Phosphorylation of the p70 ribosomal S6 kinase 1 (S6K1) at both Thr389 and Ser421/Thr424 sites, which show the functional activity of mTOR signaling, were markedly increased (6.21 ± 0.44 fold increase in Thr389 and 12.53 ± 0.59 fold increase in Ser421/Thr424 compared to the control, $p > 0.01$) in response to the PMA treatment. Conversely, inhibition of PKC-dependent pathway by BIM-I treatment completely blocked PMA-induced activation of mTOR signaling. Phosphorylation of tuberous sclerosis complex 2 (TSC2) at S664 site (ERK-specific residue), an upstream regulator of mTOR, was also prevented by PKC inhibition. Overexpression of Ras homolog enriched in brain (Rheb), a downstream target of TSC2 and an mTORC1 activator, was sufficient to activate mTOR signaling. We also identified that, in the absence of Rheb with using siRNA gene knock down, PMA-induced activation of mTOR signaling was significantly prevented (67% decrease in S6K1-Thr389 phosphorylation and complete inhibition of rpS6-Ser240/244 phosphorylation compared to the negative control). These observations demonstrated that, in C2C12 myoblasts, the PKC-dependent activation of mTOR signaling is mediated through TSC2 phosphorylation and its downstream target Rheb. It was also confirmed that Rheb is essential regulator of mTOR activation and enhanced protein synthesis in skeletal muscle cells.

Mitsunori Miyazaki, John J McCarthy, Mark J Fedele and Karyn A Esser, Early activation of mTORC1 signalling in response to mechanical overload is independent of phosphoinositide 3-kinase/Akt signalling, The Journal of Physiology, 2011 Apr;1(589 Pt 7):1831-46.

Mitsunori Miyazaki, John J McCarthy and Karyn A Esser, IGF-1-induced phosphorylation and altered distribution of TSC1/TSC2 in C2C12 myotubes, the FEBS Journal, 2010 May;277(9):2180-91.

Mitsunori Miyazaki and Karyn A Esser, Cellular mechanisms regulating protein synthesis and skeletal muscle hypertrophy in animals, Journal of Applied Physiology, 2009 Apr;106(4):1367-73.

This study was supported by the grant provided from the Japan Society for the Promotion of Science (KAKENHI Grant Number 24800056) and research grant provided from The Uehara Memorial Foundation to MM.

Where applicable, the authors confirm that the experiments described here conform with The Physiological Society ethical requirements.

PCA271

Skeletal muscle damage from eccentric exercise: protective effect of nitric oxide II

Y. Lomonosova[1], B. Shenkman[1] and T. Nemirovskaya[2]

[1]Institute for bio-medical problems, Moscow, Russian Federation and [2]Faculty of basic medicine, Moscow State University, Moscow, Russian Federation

It was shown that eccentric contraction is associated with skeletal muscle damage including cytoskeletal proteins degradation. Moreover, muscle pain and weakness are present that is probably the reason of decrement in muscle performance. We suggested that NO level decreases during eccentric contraction which leads to cytoskeletal proteins degradation in skeletal muscle. Our study was aimed to determine if NO level increase during muscle eccentric contraction can prevent proteolysis and improve work capacity after the contraction. Male Wistar rats were divided into 5 groups: control group (C group, 260-302g, n=8), control group treated with L-arginine, NO precursor (500 mg/kg body wt. per os for 2 days; CA group, 270-305g, n=8), downhill motor-driven treadmill running group (40 min of treadmill running downhill at 16°, 20 m/min; R group, 280-310g, n=10), groups of treadmill running rats with L-arginine (500 mg/kg body wt. per os for 2 days before the running; RA group, 270-298g, n=10) or L-NAME, nNOS inhibitor, administration (90 mg/kg body wt. per os for 2 days before the running; RN group, 265-289g, n=10). The experiment was conducted according to the rules of biomedical ethics (protocol No. 264 of March 5, 2009 was approved by the Russian Academy of Sciences Committee on Bioethics). The rats were sacrificed by nembutal overdose (75 mg/kg body wt.) next day after the running, the m. soleus was immediately frozen in liquid nitrogen. EPR spectroscopy revealed that NO level in CA group was significantly greater than that in C group ($p<0,05$). When tested work capacity it was considerably greater in C and RA groups as compared to R and RN groups ($p<0,05$). Contents of cytoskeletal proteins dystrophin and desmin were tested by immunohistochemistry and western blotting respectively. Degradation of the proteins was significantly greater in both R and RN groups. L-arginine administration in RA group prevented the proteolysis after eccentric contraction. We determined by means of real-time RT-PCR that contents of μ-calpains mRNA in R and RN were significantly greater in comparison with C group. L-arginine administration in RA group considerably decreased μ-calpains mRNA expression as compared to R group ($p<0,05$). Having analysed E3-ligases, MAFbx and MuRF-1, we showed that its mRNA expressions in RA group didn't differ from that in control group, but it was significantly lower in R and RN groups than that in C and RA groups ($p<0,05$). nNOS mRNA expression was greatly higher in R and RN groups as compared to C group ($p<0,05$). It is concluded that NO precursor administration in time of eccentric contraction increases work capacity and prevents proteolysis of cytoskeletal proteins, dystrophin and desmin. However nNOS inhibition at the eccentric contraction lead to dystrophin and desmin degradation and the capacity decrease.

The work was supported by grant RFBR 08-04-01599a

Friden J. et al. (2001). Acta Physiol. Scand. 171(3), 321-326.

Lynch G.S. et al. (1997). Cell Calcium. 22(5), 373-383

Komulainen J. et al. (1999). Acta Physiol. Scand. 165(1), 57-63

Lovering RM. et al. (2004). Am.J. Physiol. Cell Physiol. 286(2), 230-238

Where applicable, the authors confirm that the experiments described here conform with The Physiological Society ethical requirements.

PCA272

Activity of anabolic and catabolic signaling pathways in rat soleus during recovery following gravitational unloading

T. Mirzoev, O. Turtikova, E. Kachaeva and B. Shenkman

State Scientific Center of Russian Federation - Institute of Biomedical Problems of Russian Academy of Sciencies, Moscow, Russian Federation

Nowadays the problem of muscle recovery from disuse atrophy (caused by gravitational unloading or hypokinesia) is urgent for rehabilitation and space medicine. Therefore the aim of the study was to analyse intracellular signaling pathways which are responsible for protein synthesis (anabolic markers – ribosomal kinases p-p70s6K and p-p90RSK) and protein breakdown (markers of proteolysis – E3 ubiquitin ligases MuRF-1 and MAFbx/atrogin-1) in rat soleus muscle.

The experiment was carried out in accordance with the rules of biomedical ethics certified by the Russian Academy of Sciences Committee on Bioethics. Thirty-five male Wistar rats weighing 190-210 g were randomly assigned to the 5 groups (n=7 for each group): ground control (C), hindlimb suspension for 14 days (14HS), hindlimb suspension for 14 days followed by 3-day recovery (14HS+3R), 7-day recovery (14HS+7R) and 14-day recovery (14HS+14R). Gravitational unloading was simulated by hindlimb suspension of rats (Morey-Holton, Globus, 2002). Animals were anaesthetised with 10% avertin (8ml/kg). Ribosomal kinases content was established by gel electrophoreses with immunoblotting. Expression of mRNA of E3 ligases was assessed by RT PCR. Values were expressed as means ± S.E., compared by 2-way ANOVA.

The unloading resulted in 30% decrease of p-p70s6K content but increase of expression of E3 ligases ($p<0.05$) vs. (C). At the same time content of p-p90RSK was 50% higher compared to (C). Content of E3 ligases mRNA was increased after 3 days of recovery ($p<0.05$). The content of p-p90RSK and p-p70s6K was reduced by the 7-th day of recovery vs. 14HS group. Expression of MuRF-1 and MAFbx/atrogin-1 returned to control level after 7 days of recovery. By the 14-th day of recovery period content of both ribosomal kinases retuned to control levels.

Thus, activity of anabolic signaling pathways demonstrated irregular dynamics during recovery period following gravitational unloading. At the same time increased activity of the ubiquitin-proteaosome pathway contributes to degradation of structural and functional proteins in rat soleus. These data can explain low rates of protein restoration in soleus muscle at early stages of recovery from disuse atrophy.

Morey-Holton E & Globus RK (2002). *J Appl Physiol***92**, 1367-1377.

The work was supported by the Program of the Presidium of Russian Academy of Sciences.

Where applicable, the authors confirm that the experiments described here conform with The Physiological Society ethical requirements.

PCA273

Responses of elongation factor 2 and its kinase to short- and long-term hindlimb unloading in rat skeletal muscle

Y. Lomonosova, A. Krasnuy, E. Lysenko and B. Shenkman

Institute of bio-medical problems, Moscow, Russian Federation

Loss of skeletal muscle mass happens under catabolic conditions of gravitational unloading because of combination proteolysis increase and synthesis decrease processes. Increase of proteolytic enzymes expression namely calpains and E3-ligases, MuRF-1 and MAFbx, was shown in soleus at short-time hindlimb unloading of rats. The aim of our study was analysis of protein synthesis elongation mechanism in rat soleus in conditions of different periods of hindlimb unloading. Male Wistar rats were divided into 4 groups: control group (C group, 221-225 g, n=10), hindlimb unloaded group during 3 days (3HS group, 226-240g, n=8), 7 days (7HS group, 223-232g, n=8) and 14 days (14HS group, 227-242g, n=8). Hindlimb unloading was carried out according to Ilyin-Novikov's design with Morey-Holton's modification. The experiment was conducted according to the rules of biomedical ethics (protocol No. 180 of April 6, 2011 was approved by the Russian Academy of Sciences Committee on Bioethics). The rats were sacrificed by nembutal overdose (75 mg/kg body wt), each soleus was weighted, immediately frozen in liquid nitrogen and stored at -80°C until analysis. Atrophy of soleus was found in all hindlimb unloaded groups, the most profound loss (by 40% vs. C group, $p<0,05$) of soleus mass was revealed after 14 days unloading. eEF2 is one of the important member of eEF family catalyzing simultaneous translocation tRNA and mRNA on a 80S ribosome. It's known that eEF2 phosphorylation by its specific eEF2-kinase leads to prevention of elongation translation. We observed two-fold increase of eEF2k mRNA expression in rat soleus as early as 3 days unloading and it's remained high till 14 days unloading as compared to control group ($p<0,01$). Moreover, eEF2k protein content was significantly greater than that in control ($p<0,05$) after unloading lasting 7 and 14 days. P-eEF2 level was also increased since 3 days unloading in comparison with the control group and remained so till 14 days unloading ($p<0,05$). It was shown significant decrease of eEF2 protein content after 7 and 14 days unloading relative to the control ($p<0,05$). However, it wasn't found any changes in eEF2 mRNA level during all periods of unloading. Hereby, inhibition of eEF2 elongation factor function is a result of post-translational regulation by its eEF2-kinase which takes part in decrease of protein synthesis in soleus of rat after short- and long-term hindlimb unloading. The work was supported by grant RFBR 11-04-01769-a

Novikov V. et al. (1989). Aviat. Space Environ. Med. 52(9), 551-553.

Diggle T. et al. (2001). Biochem. J. 353(3), 621-626.

Hornberger T. et al. (2006). J. Cell Biochem. 97(6), 1207-1216.

Where applicable, the authors confirm that the experiments described here conform with The Physiological Society ethical requirements.

PCA274

Evaluation of serum and salivary immunoglobulin classes A, G and M in patients with orofacial squamous cell carcinoma

T.J. Lasisi[1], O.A. Lasisi[2], B.K. Kolude[3] and E.E. Akang[4]

[1]Physiology, University of Ibadan, Ibadan, Oyo, Nigeria, [2]Otorhinolaryngology, University of Ibadan/University College Hospital, Ibadan, Oyo, Nigeria, [3]Oral Pathology, University of Ibadan/University College Hospital, Ibadan, Oyo, Nigeria and [4]Pathology, University of Ibadan/University College Hospital, Ibadan, Oyo, Nigeria

Background: Changes in the humoral immune system of patients with orofacial squamous cell carcinoma are considered important factors in the pathophysiology, prognosis and management of the disease in these individuals[1].
Method: This is a cross sectional human study[2], undertaken to evaluate serum and salivary immunoglobulin levels in patients with histologically diagnosed orofacial squamous cell carcinoma (OSCC) attending the University College Hospital, Ibadan, Nigeria (Ethical approval number: UI/UCH/EC/09/014). Seventy subjects comprising 22 cases of untreated OSCC, 18 cases of OSCC receiving treatment and 30 healthy individuals were included. Levels of IgA, IgG and IgM in serum and saliva samples from subjects were determined using ELISA technique[3].
Results: Values are means ± SD compared by ANOVA and Dunnet's tests. Subjects receiving treatment showed a significant reduction in the mean values of serum IgA, IgG and IgM compared with healthy controls ($p= 0.03$, 0.001 and 0.01 respectively). However, the mean values of serum IgA, IgG and IgM in untreated OSCC subjects were not significantly different from those of treated carcinoma subjects and healthy controls. Mean value of salivary IgG was significantly higher ($p = 0.001$) in untreated OSCC subjects compared with treated OSCC subjects and healthy controls. There was no significant difference in the mean values of salivary IgA and IgM among the groups. Correlation (Pearson's correlation test) between serum and salivary immunoglobulins (IgA, IgG and IgM) showed no significant relationship.
Conclusion: These findings may suggest that elevated salivary IgG probably plays a role in the pathophysiology of orofacial squamous cell carcinoma and hence, may be a reliable marker. In addition, serum IgA, IgG and IgM may be useful in the monitoring of patients undergoing treatment.
Key words: saliva, serum, immunoglobulin, orofacial, squamous cell carcinoma

Table 1: Salivary IgA, IgG and IgM levels* among subjects

Subjects	N	IgG (mg/dl)	IgA (mg/dl)	IgM (mg/dl)
Untreated OSCC	22	1.82 ± 0.58(a)	2.02 ± 0.47	1.13 ± 0.51
Treated OSCC	18	0.87 ± 0.25(b)	1.9 ± 0.43	0.7 ± 0.2
Healthy Control	30	0.67 ± 0.24(c)	2.0 ± 0.56	1.04 ± 0.48
P value		0.001**	0.73	0.06

* mean logrithm values, ** significant (ANOVA), applies to a versus b versus c (Dunnet's test)

Table 2: Serum IgG, IgA and IgM levels among subjects

Subjects	N	IgG (mg/dl)	IgA (mg/dl)	IgM (mg/dl)
Untreated OSCC	22	2102.5 ± 866.4	368.7 ± 89.2	348.6 ± 120.2
Treated OSCC	18	1397.4 ± 1137.3(a)	328.3 ± 90.9(a)	256.7 ± 146.3(a)
Healthy control	30	2353.1 ± 558.9(b)	390.5 ± 52(b)	360.5 ± 85.2(b)
P value		0.001*	0.03*	0.01*

* significant (ANOVA), applies to a versus b (Dunnet's test)

Shpitzer T, Bahar G, Feinmesser R, Nagler RM (2007). A comprehensive salivary analysis for oral cancer diagnosis. *J Cancer Res Clin Oncol* **133**, 613-617.

Krasteva AE, Aleksiev A, Ivanova I *et al*. (2008). Salivary components of treated cancer patients and patients with precancerous lesions. *J IMAB Annual proceeding* **2**, 41-43.

Kan PL, Versperget HW, Peria AS (1993). ELISA assay for quantitative measurement of human immunoglobulins (IgA, IgG and IgM) in nanograms. *J Immunol Methods* **57**, 51-57.

The authors appreciate Professor O.G. Arinola, Mr. Omoruyi and Mrs. Ebele of the Department of Immunology, University of Ibadan, Ibadan, Nigeria for their laboratory assistance.

Where applicable, the authors confirm that the experiments described here conform with The Physiological Society ethical requirements.

PCA275

Ethnic differences in heat adaptation and autonomic tone during intensive exercise in elite athletes

J. Dalzell[2] and A. Datta[1]

[1]Medicine, Hull York Medical School, York, UK and [2]formerly Portsmouth FC, Portsmouth, UK

INTRODUCTION: Athletic performance may be compromised in extreme heat; this was relevant for the Athens and Beijing Olympics and may be for the 2014 (Brazil) and 2022 (Qatar) FIFA World cups; under those conditions prior determination of required fluid intake is vital for athlete safety. Thompson (1954) described lower sweating rates in Bantus compared with Caucasians.

AIMS

1.To determine the English Football Premiership ethnic mix.

2.To establish fluid intake, sweat production and sweat evaporation during exercise in extreme heat and their ethnic differences.

3.To establish cardiorespiratory and other physiological factors contributing to any putative ethnic differences

METHODS: Using Scout 7 software, the English Football Premiership was analysed for ethnic background in 2012. 34% players were of African origin(**AO**) and 66% of European origin(**EO**). On two successive years, studies were performed in Dubai after four days acclimation, during 80 minutes training at 40 ± 2°C ambient temperature; 25 ± 8% relative humidity on 29 professional Premiership footballers from a single team with Ethics clearance. 15 were **AO** and14 **EO**. Players could drink ad libitum. RESULTS: There was no difference between **AO** and **EO** in height, weight, body surface area, skin fold thickness, resting or average heart rate during exercise, QT interval, cardiac chamber dimensions, left ventricular ejection fraction or maximum VO2. During exercise, fluid intake in **AO** ranged from 1.1- 3.0l (1.6 ± 0.63l, median + SD) and in **EO** ranged from 0.5-2.4 l (1.35 ± 0.50; p=0.40; unpaired t-test). Sweat production in **AO** ranged from 1.8 – 3.9 l (2.3 ± 0.54 l) higher than 1.3 – 2.7 l in **EO** (2.00 ± 0.43 l; p = 0.03; Figs. 1&2). Mean ± SD of Peak Heart Rate (Polar Electro) during training in the heat was 186 ± 7 bpm (range 170-197 bpm) in **AO** footballers, significantly higher than **EO** players (178 ± 7 bpm, range 165-188 bpm ; p=0.007). Heart rate variability (HRV; Akselrod, 1981) was calculated from a five minute collection of resting ECG using bespoke frequency domain analysis software using American Heart Association guidelines (Omega Wave; Oregon USA). (Mean ±SD) LF/HF ratio, an index of sympatho-vagal tone balance was 1.07 ± 0.48 in **AO** and significantly higher in **EO** 2.0± 1.27 (p= 0.03).

CONCLUSIONS

1. A large proportion of the English Premiership footballers are **AO**

2. Sweat production during exercise in extreme heat may be up to 3.25 L/hr, and fluid intake 2L/hr. This can lead to significant dehydration of up to 2.4% naked body mass.

3. There is greater sweat production in **AO** players, despite a similar fluid intake to **EO** players; this may confer a performance advantage to exercise in the heat.

4. Increased sweat production in **AO** players appears to be associated with an increased sympathetic tone, which has also been related to an increased risk of cardiac events (Tsuji et al, 1996)

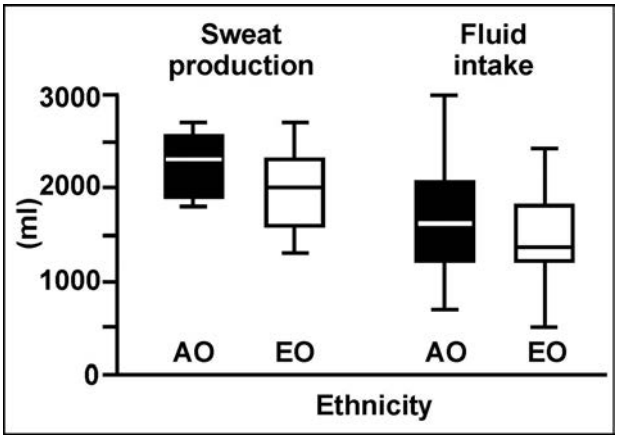

Fig. 1 Sweat production and fluid intake during exercise in the heat for AO (n=15, filled boxes) and EO (n=14, open boxes). Box represents interquartile range, horizontal line represents median vertical line shows range.

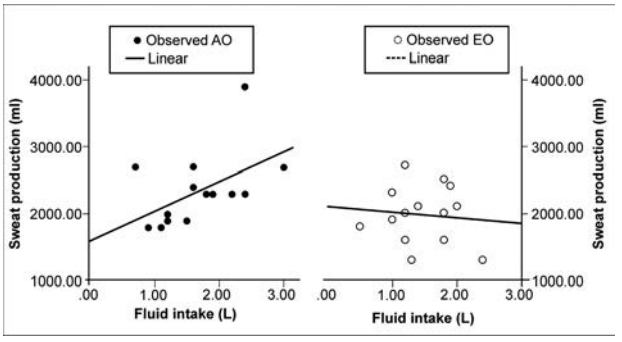

Fig. 2 Sweat production (ordinate) and fluid intake (abscissa) for 15 AO players (Left hand panel, shaded symbols) and 14 EO players (Right hand panel, open symbols) during exercise in the heat. Lines depict linear regression.

Thompson, M.L. (1954) A comparison between the number and distribution of functioning eccrine sweat glands in Europeans and Africans. J. Physiol., 123; 225-233

Tsuji H, Larson M G, Venditti F J, Manders E S, Evans J C, Feldman, C L and Levy D (1996) Impact of Reduced Heart Rate Variability on Risk for Cardiac Events. The Framingham Heart Study. Circulation, 94:2850-2855

Akselrod S, Gordon D, Ubel FA, Shannon DC, Barger AC, Cohen RJ. (1981) Power spectrum analysis of heart rate fluctuation: a quantitative probe of beat-to-beat cardiovascular control. Science. 213:220-222

Where applicable, the authors confirm that the experiments described here conform with The Physiological Society ethical requirements.

PCA276

Exercise training activates behavioral thermoregulation in mice

K. Nagashima[1,2] and C. Lin[3]

[1]Human Sciences, Waseda University, Tokorozawa, Japan, [2]Institute of Applied Brain Sciences, Waseda University, Tokorozawa, Japan and [3]Sport Sciences for the Promotion of Active Life, Waseda University, Tokorozawa, Japan

Aims Dehydration, factors of hypvolemia and plasma hyperosmolality, attenuates heat tolerance in humans and mice. Themoregulation are achieved by autonomic and behavioral responses. However, we know a little about if and how the behavioral responses in heat, such as heat escape behavior or seeking cooler environment are activated by the exercise training. We evaluates the role of behavioral thermoregulation in heat tolerance. Methods All experimental procedures were conducted under the guidelines of the Japanese Physiological Society and Waseda University in Japan. Male ICR mice (6 w age) were housed with/without a running-wheel for 8 wks (WR and NWR groups, n=40 each). In the 5th week, under inhalation anesthesia with 1% isoflurane, they were placed a datalogger with temperature sensor for the measurement of body temperature (Tb) in the abdominal cavity. Mice were got familiarized with being in an experiment box (50 x 10 x 15 cm; made of Plexiglas with 5 temperature-controllable Peltier boards at the bottom), and learned either of following settings: 1) board temperature of 28˚C or 39˚C; 2) operant-behavior setting; each board was set at 39˚C, and the right-end board was changed at 20˚C within 60 sec only when a mice moved on the left two board; and 3) thermal mosaic setting; each board was set at either 15˚C, 22˚C, 28˚C, 35˚C, or 39˚C with a 6-min interval. After the 8-wk training period, a mouse had subcutaneous injection of isotonic- or hypertonic-saline with 0.1 ml 0.5% lidocaine (1 ml/100 g of body wt; 154 or 2,500 mM, IS or HS subgroup), and was exposed to either of the setting for 2 h after 1.5 h baseline (Experiments 1 – 3). Results In Experiment 1, after the 39˚C board exposure, Tb in both subgroups of the WR group was higher than that in the NWR group without any significant differences. In Experiment 2, the NWR group showed smaller operant counts in the HS subgroup than the IS subgroup; however, the WR group did not. In Experiment 3, the WR group had lower temperature of thermal preference than the NWR group without any differences between the subgroups (e.g. 33.4 ± 0.3˚C and 34.7 ± 0.1˚C in the IS subgroups of the WR and NWR groups, respectively). Conclusions Hyperosmotic condition was a stimulus decreasing heat tolerance in heat. However, exercise training in mice may have resulted in 1) lower thermal preference, and 2) greater activation of behavioral thermoregulatory response. Therefore, the training contributes to increase in the heat tolerance.

Horowitz M and Meiri U. Thermoregulatory activity in the rat: effects of hypohydration, hypovolemia and hypertonicity and their interaction with short-term heat acclimation. Comp.Biochem.Physiol.A.Comp.Physiol. 82: 3: 577-582, 1985.

Kanosue K, Crawshaw LI, Nagashima K and Yoda T. Concepts to utilize in describing thermoregulation and neurophysiological evidence for how the system works. Eur.J.Appl.Physiol. 109: 1: 5-11, 2010.

Konishi M, Kanosue K, Kano M, Kobayashi A and Nagashima K. The median preoptic nucleus is involved in the facilitation of heat-escape/cold-seeking behavior during systemic salt loading in rats. Am.J.Physiol.Regul.Integr.Comp.Physiol. 292: 1: R150-9, 2007.

Konishi M, Nagashima K and Kanosue K. Systemic salt loading decreases body temperature and increases heat-escape/cold-seeking behaviour via the central AT1 and V1 receptors in rats. J.Physiol. 545: Pt 1: 289-296, 2002.

Lin CH, Tokizawa K, Nakamura M, Uchida Y, Mori H and Nagashima K. Hyperosmolality in the plasma modulates behavioral thermoregulation in mice: the quantitative and multilateral assessment using a new experimental system. Physiol.Behav. 105: 2: 536-543, 2012.

The present study was partly supported by KAKENHI No. 20390066 from the Japan Society for the Promotion of Science and Sport Sciences for the Promotion of Active Life, Waseda University Global COE Program, and MEXT KIBANKEISEI (2010).

Where applicable, the authors confirm that the experiments described here conform with The Physiological Society ethical requirements.

PCA277

The changes of the cardiovascular function and its hormones regulation of the 28th chinese inland expeditioners at antarctic dome-A environment of hypoxia and extreme cold

Y. Xiong[1], L. Lin[2], H. Gong[1], X. Chen[1], N. Chen[1] and C. Xu[1]

[1]Institute of Basic Medical Sciences, Chinese Academy of Medical Sciences (CAMS); School of Basic Medicine, Peking Union Medical College, Beijing, China and [2]Hua Dong Hospital Affiliated to Fu Dan University, Shanghai, China

Antarctic Dome-A(80°22′02″S, 77°22′23″E) is a place of extreme cold and hypoxia, with average altitude of 4000m and average temperature -58.4 degree Centigrade. We investigated the effect of Dome-A environment on the cardiovascular function and its hormones regulation of the 28th Chinese Antarctic Inland expedition, so as to providing scientific data for making measures of prevention and cure of mountain sick. This study was approved by Institutional Review Boards of the Peking Union Medical College, Informed consent was obtained from each participant after the study objectives and data collection procedures had been fully explained. Using Cardiodynamics monitor to detect cardiovascular function of the 25 members (male, average age 33.9±6.7yr) of the expedition at departure from Shanghai, stayed 2 weeks at Kunlun Station and returned to Shanghai (2012/3/30), synchronously collecting blood sample. Plasma erythropoietin (EPO), angiotensin II (ANG II), brain natriuretic peptide(BNP), atrial natriuretic peptide (ANP) and endothelin (ET-1) were measured by ELISA. Compared with departure, the heart rate(HR), systolic pressure(SBP), diastolic pressure(DBP), mean arterial pressure(MAP), systemic vascular resistance(SVR) and resistance index(SVRI) significantly increased, the stroke volume(SV), stroke index(SI), cardiac output(CO), cardiac index(CI), velocity index(VI), acceleration index(ACI), left ventricular ejection time(LVET) significantly decreased at Dome-A. Two weeks exposure to the hypoxia and extreme cold environment at Dome-A induced significant decrease in cardiac function. HR and left ventricular work (LCW) increased so as to offset the reduction in SV and arterial oxygen saturation. However, this may further increase the oxygen consumption of cardiomyocyte and increase the risk of ischemic cardiovascular diseases. Although obvious changes in cardiac function were observed in expeditioners, no significant change in plasma ANP, BNP, ANGII, BNP and EPO was observed during residence at Dome A. It might be that the exposure time of Chinese expeditioners to Dome A is too short to induce obvious changes in vasoac-

tive peptide. Upon their return to Shanghai, DBP, MAP, CO, CI, SV, SI, VI and ACI remain at lower levels; SVR, SVRI remain at higher levels comparing with departure. Our data suggested that cardiac function significantly decreased after 2 weeks exposure to Dome A. Moreover, cardiac deadaptation process existed 1 month after return to Shanghai. Thus, further monitoring of cardiac function in inland expeditioners is needed after evacuation from Dome A environment .

This work was supported by Chinese Polar Environment Comprehensive Investigation & Assessment Programs (CHINARE2012-02-01) and the State Key Development Program for Basic Research of China(2012CB518204).

Where applicable, the authors confirm that the experiments described here conform with The Physiological Society ethical requirements.

PCA279

Exercise stimulates lactate disposal and monocarboxylate transporter expression in rainbow trout

T. Omlin, L. Teulier and J. Weber

University of Ottawa, Ottawa, ON, Canada

In mammals, exercise is known to stimulate glycolysis, lactate production and lactate disposal. Monocarboxylate transporters (MCTs) mediate inter-tissue lactate trafficking and orchestrate recovery. By contrast, the effects of swimming on lactate kinetics and the existence of MCTs have never been characterized for rainbow trout (Oncorhynchus mykiss), an essential animal model in ectotherm physiology. Therefore, our goals were: (1) to determine the rates of lactate appearance (Ra) and disposal (Rd) during steady-state swimming at 1.7 body lengths/s (BL/s) and graded swimming at 0.5-2.8 BL/s by in vivo continuous infusion of [U-14C] lactate as described in (Omlin and Weber, 2010); (2) to clone trout MCTs, and to determine their tissue distribution and the effects of exhausting exercise on their level of mRNA expression. We reasoned that such measurements would prove important to understand the mechanisms underlying the classic "lactate retention" of trout white muscle after maximal exercise. Results show that steady-state exercise increased Ra and Rd lactate in parallel from resting values of 23 μmol kg-1 min-1 to maximal levels of 29 μmol kg-1 min-1, maintaining plasma lactate concentration below 1.5 mM. For graded exercise, lactate fluxes stayed at baseline below 2.2 BL/s, but both Ra and Rd lactate were stimulated at higher speeds, reaching maximal values of 40 and 35 μmol kg-1 min-1, respectively. Plasma lactate reached 5 mM at high swimming speeds because the increase in lactate use was insufficient to match the increase in lactate production. We also show for the first time that rainbow trout possess MCTs by cloning MCT1a, MCT1b, and MCT2. These lactate transporters are present ubiquitously, but their expression varies greatly between tissues and isoforms. Exhausting exercise increased the expression of MCT1a (+90%) and MCT1b (+50%) in the heart, as well as the expression of MCT2 in the brain (+260%). Other tissues showed no changes after exercise, and we could not clone MCT4, the isoform mainly dedicated to lactate efflux from glycolytic muscles in mammals. The stimulation of MCT expression in heart and brain is consistent with an accelerated use of lactate by these oxidative tissues, and with the observed increase in Rd lactate. Results also provide a possible functional explanation for lactate retention because: (1) white muscle shows the lowest MCT expression of all trout tissues, (2) white muscle MCTs are not stimulated by exercise, and (3) rainbow trout may not express MCT4. All procedures were approved by the Animal Care Committee of the University of Ottawa. This research was supported by an NSERC discovery grant.

Omlin, T. and Weber, J.-M. (2010). J Exp Biol 213, 3802-3809.

Where applicable, the authors confirm that the experiments described here conform with The Physiological Society ethical requirements.

PCA280

Maternal diet influences circadian cardiovascular function in the offspring

C. Gray[1], S.M. Gardiner[2] and D.S. Gardner[1]

[1]School of Veterinary Medicine and Science, University of Nottingham, Loughborough, UK and [2]School of Biomedical Sciences, University of Nottingham, Nottingham, UK

Background: Contemporary diets are typically high in salt and fructose and such a refined diet has been proposed to contribute significantly to the overall burden of non-communicable disease in the population. Exposure to salt diet throughout fetal and neonatal development via maternal diet induces hypertension in the adult offspring. No study has explored potential interactions between maternal intake of salt and/or fructose and characterised offspring cardiovascular response through the circadian cycle.
Methods: Pregnant rats were fed purified food (±4% salt) with freely available water (±10% fructose) before (4 weeks), during (21 days) and after gestation to weaning (21 days). Offspring (n=5/6 males/females from n=5/6 dams per treatment; 4 treatment groups) were weaned onto standard chow diet and from 10 weeks of age acute and chronic cardiovascular responses to anxiety (becoming singly-housed i.e. removal of paired rat from cage), salt-loading (5 days 4% salt in the diet), fructose loading (5 days 10% fructose in drinking water) nitric oxide blockade (with L-NAME) and voluntary physical activity were assessed by in-dwelling telemeters (DSI International).
Results: Prenatal exposure to high salt diet elicited hypertension (142/103 vs. 128/88 ± 3 mm Hg; P=0.003) and an exacerbated baroreflex during an acute episode of anxiety in male, but not female offspring. These effects were unrelated to tonic nitric oxide activity, since chronic blockade with L-NAME elicited similar physiological responses between groups. Prenatal exposure to high fructose diet elicited increased resting heart rate (by 15-20 ±8 beats min-1) and greater pressor responses to fructose intake in both male and female offspring, despite one magnitude greater voluntary physical activity in female vs. male offspring (≈957 vs. 81 m day-1). Furthermore, fructose-exposed offspring displayed a blunted circadian variation (i.e. non-dipping) cardiovascular pattern.
Conclusions: This study has revealed long-term circadian cardiovascular effects of increased maternal salt or fructose intake in the adult offspring, despite little direct exposure themselves. The delayed cardiovascular effects are distinctly sex-specific and thus any anticipated cardiovascular deterioration with age for example with prolonged, rather than short-term, exposure to such refined nutrients is likely to manifest differently in males vs. females.

The authors express their gratitude for the help and support provided by the BioServices Unit on the Sutton Bonington Campus and Julie March for performing the radiotelemetry transmitter implantations. C.G. was supported 50:50 by a BBSRC doctoral training grant and The University of Nottingham (Institute of Clinical Research). Grant support from The Nutricia Research Foundation and The School of Veterinary Medicine and Science is gratefully acknowledged.

Where applicable, the authors confirm that the experiments described here conform with The Physiological Society ethical requirements.

PCA281

Novel protein and mRNA expression of voltage-dependent potassium channels in first trimester human placentae

H.D. Mistry[1], L.O. Kurlak[2], G.S. Whitley[3], J.E. Cartwright[3], F. Broughton Pipkin[2] and R.M. Tribe[1]

[1]Women's Health, King's College London, London, UK, [2]Obstetrics & Gynaecology, University of Nottingham, Nottingham, UK and [3]Biomedical Sciences, St. George's University of London, London, UK

Background: Potassium channel α-subunits encoded by KCNQ1-5 genes (Kv7) form voltage-dependent channels which can be modulated by KCNE1-5 encoded accessory proteins. These channels are known to play a role in regulating the reactivity of blood vessels. We have previously shown that both mRNA and protein data indicates a novel combination of KCNQ3 and KCNE5 expression in placentae from preterm and term pre-eclampsia; the expression of these specific KCNQ and KCNE isoforms in early placental tissue remains to be elucidated.
Objectives: The aims of this study were to determine whether KCNQs and KCNEs mRNA are expressed in first trimester placental tissue and to assess protein expression and localisation of the KCNQ3 and KCNE5 isoforms.
Methods: Placental samples were obtained from women undergoing elective surgical termination of pregnancy (TOP) at ≤10 weeks' (early TOP; n=6) and >10 weeks' (late TOP; n=7) gestations following informed written consent. Expression of mRNA for all KNNQ and KCNE isoforms were measured by qRT-PCR and normalised to three housekeeper genes using geNorm. Protein localisation/expression of KCNQ3 and KCNE5 were assessed by immunohistochemistry.
Results: Expression of mRNA (normalised copy number) of both all KCNQs and KCNEs were observed at all gestations. KCNE5 expression (median [IQR]) was increased in late TOP (239.5 [135, 305]) versus early TOP samples (77.6 [57.5, 111.8], P=0.01). No other significant differences were detected for other KCNQ and KCNE genes (P>0.05).
KCNE5 mRNA expression remained constant between 6 and 10 weeks' (median: 77.6) with a subsequent rise at 11 and 12 weeks' and a larger increase after 13 weeks' (median: 239.5). KCNQ3 mRNA expression was initially lower than KCNE5, but increased at 10 weeks (median: 153.1) and then fell below KCNE5 vales by 12 weeks' (median: 22.3).
Protein expression for both isoforms was localised predominantly to the syncytiotrophoblast with some expression in the mesenchyme.
Conclusion: KCNQ3 and KCNE5 channel isoforms are highly expressed in first trimester human placenta. The changes in mRNA expression mirror temporal changes in the placental tissue oxygen tension which increases between 8-10 weeks'. This precedes the dislocation of the spiral artery plugs, which enables maternal blood to flow freely and continuously into the intervillous spaces. We speculate that mesenchymal protein expression may be related to angiogenesis during this critical window of feto-placental vascular development. We will perform functional studies to determine the potential role of this channel complex in the syncytiotrophoblast. Future work will characterise the complete KCNQ/KCNE profile in first trimester tissue and assess their potential functional roles both in early placentation and in relation to pre-eclampsia.
Funding: Nottingham Hospital Special Trustees (No: 1053904).

Where applicable, the authors confirm that the experiments described here conform with The Physiological Society ethical requirements.

PCA281a

Evaluation of physical fitness of subjects with sickle cell trait: effects of ad libitum fluid intake on thermoregulatory responses in heat environments

A. Samb, M. Diaw, A. Sow, F. Sar, G. Seck, A. Ba and M. Niang

Faculté de Médecine, de Pharmacie et d'Odontologie, UCAD, Laboratoire de Physiologie et d'Explorations Fonctionnelles, Dakar, Senegal

The practice of physical exercises under certain environmental conditions in carriers of sickle cell trait (SCT) may be associated with microvascular injury such as renal vasculary disease (1, 2, 3) . The increase in ambient temperature and high humidity seem to play a significant role in the occurrence of rhabdomyolysis reported post exercise in these individuals (2, 3).
However, adequate fluid intake during exercise would limit the sickling process and therefore reduce the risk of microvascular injury (2).
Our study assessed the effect of hydration ad libitum on thermoregulatory responses during two football matches in carriers of sickle cell trait in tropical climates.
Twenty two students from the Higher National Institute of Popular Education and Sport (INSEPS) of Dakar, male, black, aged 26 ± 2.16 years and weighing 65 ± 5.45 kg, for a size of 1.75 ± 0.08 m, participated to the study.
Eleven (11) subjects were genotype AA (control group) and 11 were of genotype AS (sickle cell trait: SCT). A hemoglobin electrophoresis led to the discovery of the presence of abnormal hemoglobin HbS of SCT carriers.
Subjects were randomized into two teams: A team of 11 players consisting of 6 subjects AA and 5 SCT carriers, and a B team of 11 players, including six SCT and five AA. These teams competed in two football games separated by two weeks in comparable environmental conditions (temperature: 24.5 to 25 ° C, humidity: 65-68%).
In the first game, only players of Team A could drink water freely without restriction during the match (6AA hydrated and 5SCT hydrated), while the players of Team B were not allowed to drink during the match (5AA no hydrated + 6SCT no hydrated). Conditions were reverse in the second match. Rectal temperature of subjects in both groups was taken before and after football matches with a thermometer. Body weight was assessed at rest and recovery in both groups. Our results showed that sickle cell trait is not a limiting factor in thermoregulation and that great hydration during physical exercise can significantly reduce the increase in rectal temperature and weight loss in both groups.
Keywords: Sickle cell trait - Football match - Thermoregulation - Hydration

Baskurt O.K., Meiselman H.J., Bergeron M.F. Re: Point:Counterpoint: Sickle cell trait should/should not be considered asymptomatic and as a benign condition during physical activity. J. Appl. Physiol., 2007, 103 (5): 2142; author reply 2143–2144.

Bergeron M.F., Cannon J.G., Hall E.L., KUTLAR A. Erythrocyte sickling during exercise and thermal stress. Clin. J. Sport Med., 2004, 14 (6): 354-356.

Connes P., Hardy-Dessources M.D., Hue O. Counterpoint: Sickle cell trait should not be considered asymptomatic and as a benign condition during physical activity. J. Appl. Physiol ., 2007, 103 (4): 2138–2140.

Gardner J.W., Kark J.A. Fatal rhabdomyolysis presenting as mild heat illness in military training. Mil. Med., 1994, 159: 160–163.

Where applicable, the authors confirm that the experiments described here conform with The Physiological Society ethical requirements.

PCA282

Changes of AMPK and SirT1 activity in the trophocytes and fat cells of young and old worker honeybees (Apis mellifera)

C. Hsu[1,2] and Y. Chuang[2]

[1]Department of Biomedical Sciences, Chang Gung University, Tao-Yuan, Taiwan and [2]Graduate Institute of Biomedical Sciences, Chang Gung University, Tao-Yuan, Taiwan

Trophocytes and fat cells of honeybees (Apis mellifera) have served as targets for cellular senescence studies; their changes of aging-related molecules and mitochondrial energy utilization with advancing age have been clarified (Hsieh and Hsu, 2011; Chuang and Hsu, 2012). However, the changes of energy-regulated molecues with advancing age in workers are unknown. In this study, young (2-day-old) and old (50-day-old) workers were selected from the same colony in hive on the same days for the experiments. The expression of adenosine monophosphate-activated protein kinase (AMPK), phosphorylated AMPK (pAMPK), silent information regulator 1 (SirT1), and peroxisome proliferator-activated receptor-α (PPAR-α) were evaluated in the trophocytes and fat cells of young and old workers reared in a field hive by Western blotting. The activity of AMPK and SirT1 were evaluated by analytic Kits. The concentration of AMP, ADP, ATP, and AMP/ATP ratio and ADP/ATP ratio were evaluated by ultra performance liquid chromatography. The results showed that (1) AMPK expression increased with advancing age (n = 18, P < 0.01, two-sample t test), whereas pAMPK expression decreased with advancing age (n = 18, P < 0.05, two-sample t test), pAMPK/AMPK ratio decreased with advancing age (n = 18, P < 0.05, two-sample t test), and AMPK activity decreased with advancing age with 0.62 ± 0.11 and 0.14 ± 0.03 450 nm mg-1 protein in young and old workers (n = 48, P < 0.01, two-sample t test); (2) ATP concentration decreased with advancing age with 44.39 ± 3.50 and 30.51 ± 2.43 nmol mg–1 of protein in young and old workers (n = 10, P < 0.01, two-sample t test) and ADP concentration decreased with advancing age with 4.60 ± 0.39 and 2.78 ± 0.26 nmol mg–1 of protein in young and old workers (n = 10, P < 0.005, two-sample t test), whereas AMP concentration was not different with 1.45 ± 0.16 and 1.61 ± 0.28 nmol mg–1 of protein in young and old workers (n = 10, P > 0.01, two-sample t test). ADP/ATP ratio was not different with advancing age (n = 10, P > 0.05, two-sample t test), whereas AMP/ATP ratio increased with advancing age (n = 10, P < 0.005, two-sample t test); (4) SirT1 expression increased with advancing age (n = 21, P < 0.05, two-sample t test), whereas their activity decreased with advancing age with 73.2 ± 0.9 and 59.7 ± 3.7 fluorescence μg–1 of protein in the trophocytes and fat cells of young and old workers (n = 30, P < 0.01, two-sample t test); and (5) PPAR-α expression decreased with advancing age (n = 18, P < 0.01, two-sample t test). These results show that young workers express higher AMPK and SirT1 activity than old workers and that aging results in a decline in AMPK and SirT1 activity in worker honeybees.

Hsieh YS, Hsu CY (2011) Honeybee trophocytes and fat cells as target cells for cellular senescence studies. Exp. Gerontol. 46, 233–240.

Chuang YL, Hsu CY (2012) Changes in mitochondrial energy utilization in young and old worker honeybees (Apis mellifera). Age doi : 10.1007/s11357–012–9490–y

This work was supported by a CMRPD 1A0492 grant from the Chang Gung Memorial Hospital, Linkou, Taiwan

Where applicable, the authors confirm that the experiments described here conform with The Physiological Society ethical requirements.

PCA283

Long-lived and obesity resistant mice exhibit 24 h locomotor circadian rhythms at young and old age

R. Gutman[1,2] and O. Froy[3]

[1]Departments of Nutritional Sciences and Zootechnology, Tel-Hai College, Kiryat Shmona, Israel, [2]2. Unit of Integrative Physiology (LIP), Laboratory of Human Health and Nutrition Sciences., MIGAL - Galilee Research Institute, Kiryat Shmona, Israel and [3]3. Institute of Biochemistry, Food Science and Nutrition, The Robert H. Smith Faculty of Agriculture, Food and Environment, The Hebrew University of Jerusalem, Rehovot, Israel

Ageing is associated with disruption of circadian homeostasis, including reduced entraiment to light-dark cycles, reduced amplitude and desynchronization of circadian physiological rhythms, and shortening or lengthening of the endogenous circadian period length (tau). αMUPA mice carry a transgene encoding the urokinase-type plasminogen activator, an extracellular protease implicated in fibrinolysis, tissue remodeling, and brain plasticity. Female αMUPA mice spontaneously eat ~25% less, live ~20% longer, and show high-amplitude circadian rhythms in food intake, body temperature, and in hepatic clock gene expression levels, compared with WT mice. Herein we examined the tau of locomotor activity of mature (8-month old) and aged (18-month old) female αMUPA and WT mice under total darkness. We show that tau changed in WT mice from a period <24 h at 8 months to a period >24 h at 18 months. However, tau of αMUPA mice was ~24 h at both ages. Deviation of tau from 24 h has shown to be inversely related to life span of rodents and non-human primates. Hence, our results suggest that the sustainable endogenous period of ~24 h in αMUPA mice may contribute to their longevity. These results support the hypothesis that although a non-24-h tau has an adaptive significance in allowing a better response to natural daylight changes, such a lack of resonance between tau and external period length entails a life-shortening metabolic cost.

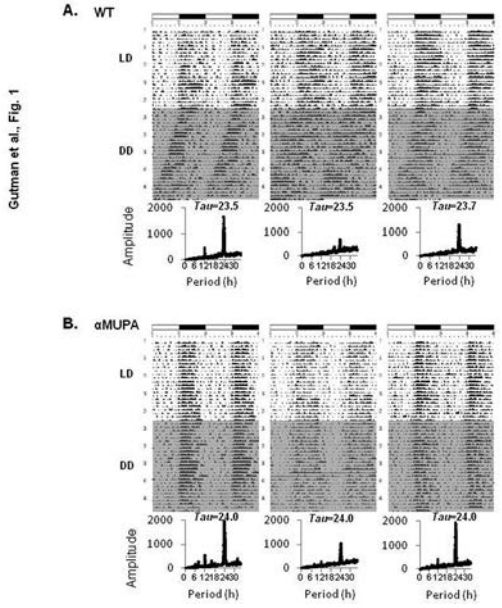

Locomotor activity of representative 8-month-old αMUPA (n=12) and WT mice (n=12) under 12:12 light-dark (LD) regime followed by constant darkness (DD, gray background). Representative double-plotted actograms presenting locomotor activity of FVB/N WT mice (A), αMUPA mice (B) during LD (light area) and DD (dark area). Individual chi-square distribution of activity period length during 28 days in DD is presented below each actogram. White and black bars at the top of each actogram represent the light and dark cycles. Double plotted actograms were generated using Actogram software. Period length of circadian activity rhythms in DD (tau) were calculated individually by Chi-square analyses using Tau software. Actogram and Tau softwares kindly provided by Refinetti R., University of South Carolina.

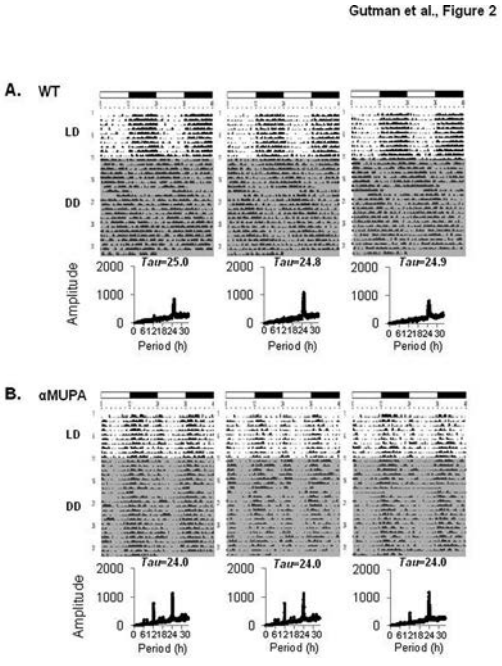

Locomotor activity of representative 18-month-old αMUPA (n=10) and WT (n = 9) mice under 12:12 light-dark regime (LD) followed by constant darkness (DD, gray background). Representative double-plotted actograms presenting locomotor activity of WT mice (A) and αMUPA mice (B) during 10 days under LD (light area) followed by 28 days under DD (dark area). Individual chi-square distribution of activity period length during the corresponding days in DD is presented below each actogram. White and black bars at the top of each actogram represent the light and dark cycles.

Where applicable, the authors confirm that the experiments described here conform with The Physiological Society ethical requirements.

PCA284

Oxidant-antioxidant balance and homocysteine in postmenopausal women: the role of hormone replacement therapy

C. Gokkusu[1,2], S. Seckin[1,2] and S. Tamer[2,1]

[1]Biochemistry, Istanbul Medical Faculty, Istanbul, Turkey and [2]Physiology, Istanbul Medical Faculty, Istanbul, Turkey

The plasma homocysteine (Hcy) concentration is an independent risk factor for cardiovascular disease (CAD). The increase of plasma Hcy levels at menopause suggests a close relationship between Hcy metabolism and estrogen status and proposes one of the mechanisms through which menopause unfavorably affects CAD risk in women. It has been suggested that hyperhomocysteinemia may promote the production of hydroxyl radicals, through Hcy autooxidation and thiolactone formation. Some investigators have suggested that Hcy may cause atherosclerosis by damaging the endothelium either directly or by altering oxidative status during aging. In this study, the effects of hormone replacement therapy (HRT) on plasma levels of endogenous malondialdehyde (MDA) formation, Hcy and total thiol (t-SH) were investigated in healthy postmenopausal women who received HRT for 1 year. We also determined the enzymatic antioxidant activities, such as superoxide dismutase (SOD) and glutathione-S transferase (GST). We hypothesized that HRT would relate positively with antioxidant status.

A number of 80 unrelated healthy postmenopausal women (aged 45–56 years), and 40 unrelated healthy control subjects (aged 30–45 years) were included in the study. Postmenopausal women were selected from the outpoint clinic of the Department of Obstetrics and Gynecology. All participants underwent clinical, biochemical and hormonal screening procedures including gynecologic and physical breast examination. Postmenopausal women were divided into two groups. HRT group involved 45 healthy postmenopausal women who were receiving hormone replacement therapy for 1 year: oral estradiol valerate 2 mg/day plus continuous cyproterone acetate 1 mg/day. NHRT group included 35 healthy postmenopausal women who received orally placebo but not received HRT. In the samples, levels of MDA, t-SH and activities of GST and SOD were measured before and after treatment.

There was no significant change in plasma Hcy levels between HRT and NHRT groups. However, Hcy concentration is significantly elevated in both NHRT and HRT groups as compared to control. MDA and t-SH correlated significantly with Hcy (p=0.388 and p= 0.478, respectively) content and there was a significant negative correlation between E2 level and GST activity (p= -0.425) in HRT group. SOD and HDL-C correlated significantly with t-SH level (p=0.339 and p= 0.336, respectively) in plasma after HRT in women.

Our data have supported the hypothesis that elevated Hcy levels stimulate production of hydroxyl radicals. In addition, our findings are important as it indicates that HRT may reduce oxidative stress in postmenopausal women.

Where applicable, the authors confirm that the experiments described here conform with The Physiological Society ethical requirements.

PCA285

Tissue specific modification of clock methylation in aging mice

Y. Cai, L. Zhang, Q. Lin and L. Li

Xuanwu Hospital, Beijing, China

Circadian rhythms in humans, rodents and other animals tend to change as they age. The molecular mechanisms underlying these age-related changes in circadian rhythms are yet to be elucidated. DNA methylation is a chemical modification of DNA structure and an important epigenetic regulator of gene expression. In addition, DNA methylation differences have been observed to be acquired in multiple tissues with age [1]. To investigate whether DNA methylation of clock genes changed with age, and contributed to circadian dysfunction in aged animals, we examined the methylation of eight clock promoters (Per1, Per2, Cry1, Cry2, Clock, Npas2, Bmal1 and Bmal2) in the stomach, kidney, striatum and spleen using a methylation-specific PCR assay (MSP) [2]. Young (3-months-old, n = 14) and old (24-months-old, n = 14), male C57BL/6 mice were housed at an animal facility on a 12-h light–dark cycle (lights on at 08:00; lights off at 20:00) and allowed to feed ad libitum. Animal treatment was in accordance with the National Institutes of Health (NIH) guidelines for animal experimentation. All mice were sacrificed at 09:00 and samples of stomach, kidney, striatum and spleen were collected for DNA extraction. Methylation frequencies of clock genes in different age groups were compared and analyzed using Pearson Chi-square tests. We compared eight clock genes, using Bonferroni correction for multiple comparisons. Significance levels were established at a P-value less than 0.00625. Partial methylation was present at the Cry1 promoter in all tissues examined, at the Per1 and Bmal1 promoters in the stomach, and at the Bmal2 and Npas2 promoters in the spleen. Regarding age related changes, methylation frequency decreased significantly in the old mice at the stomach Per1 promoter ($p = 0.006$), but was significantly increased in old mice at the Cry1, Bmal2 and Npas2 promoters of the spleen ($p = 0.001$; $p = 0.006$; $p = 0.002$, respectively). Actually, no methylation was detected in the spleen of young mice, while 11/14 old mice demonstrated methylation in at least one locus, suggesting the spleen may be particularly prone to age-related circadian dysfunction. Indeed, circadian rhythms of cell proliferation in the spleen are reduced in aged rats [3]. These results indicated that methylation of some clock promoters were affected with age at least in the spleen and stomach; in turn this may lead to dysregulation of clock expression and changes in circadian rhythms [4]. In conclusion, our data supports the hypothesis that DNA methylation plays a role in age-related circadian dysfunction.

Akintola AD et al. (2008) Am J Physiol Renal Physiol, 294, F170-6.

Lin Q et al. (2012) Biol. Rhythm Res. 43, 341-350.

Cardinali DP et al. (1998) Brain Res. 789, 283-292.

Taniguchi H et al. (2009) Cancer Res. 699, 8447–8454.

This work was supported by National Natural Science Foundation of China (No. 81274120, 81071011), the Program for New Century Excellent Talents in University (NCET-10-0013).

Where applicable, the authors confirm that the experiments described here conform with The Physiological Society ethical requirements.

PCA286

Steroids hormone and nitrite/nitrate levels are unchanged in normotensive and hypertensive postmenopausal women after aerobic exercise training

I. Novais, G. Puga, H. Araújo, R. Esposti, A. Jarrete, C. Sponton, M. Delbin and A. Zanesco

Biosciences Institute, São Paulo State University Júlio de Mesquita Filho, Rio Claro, São Paulo, Brazil

Evidences have shown that the incidence of cardiovascular disease (CVD) increases in women after menopause compared with men of similar age. Estrogen deficiency was ascribed as the main cause of increased rate of CVD in postmenopausal women, but data are not conclusive since clinical trial failed to show beneficial effect of hormonal replacement therapy in the incidence of CVD in this population. Additionally, evidences show a positive relationship between testosterone levels and increased abdominal adiposity as well as arterial hypertension in women after menopause. Although, it is well known that physical exercise promotes beneficial effects in the cardiovascular system with increased nitric oxide (NO) production and/or up-regulation of antioxidant enzymes, no studies evaluated the effect of exercise training (ET) on the steroids hormone levels associated with nitrite/nitrate and redox status in postmenopausal women. Therefore, the aim of this work was to investigate the effects of ET on the cardiovascular biomarkers and steroids hormone in normotensive (NT; n=29) and hypertensive (HT; n=21) women. Women were undergone to twenty-four sessions of ET on a treadmill at moderate intensity. Total testosterone, cortisol, cyclic GMP (cGMP), nitrite/nitrate (NOx-) and malondialdehyde (MDA) levels were measured before and after ET. Superoxide dismutase (SOD) and catalase enzymes activity was also evaluated. Blood pressure was significantly reduced after ET (approximately 5%) for NT and HT. In contrast, no changes were observed in the cardiovascular biomarkers, NOx- (basal: 28.5±4.0, ET: 28.6±3 μM for NT; basal: 38.9±8.0, ET: 55.4±10.4 μM for HT) and cGMP (basal: 5.0±0.5, ET: 6.3±0.7 pmol/mL for NT; basal: 5.5±0.7, ET: 6.4±1.0 pmol/mL for HT). Similarly, serum concentrations of cortisol (basal: 16.6±4.8, ET: 17.5±5.1 μg/dL for NT; basal: 15.7±5.4, ET: 16.4±4.5 μg/dL for HT) and testosterone (basal: 22.7±3.2, ET: 23.6±3.3 ng/dL for NT; basal: 25.2±3.0, ET: 23.4±2.7 ng/dL for HT) were not different in both groups. MDA levels were not different in both groups (basal: 13.8±1.6, ET: 12.2±1.2 μM for NT; basal: 14.2±1.3, ET: 13.3±1.1 μM for HT) as well as catalase activity (basal: 40.2±3.5, ET: 36.5±3.3 nmol/min/mL for NT; basal: 36.5±3.0, ET: 39.1±3.5 nmol/min/mL for HT). In contrast, a marked increase in SOD activity was found in both NT (basal: 12.5±1.4; ET: 24.8±2.3 U/mL) and HT groups (basal: 12.5±1.7; ET: 29.5±1.8 U/mL) after 24 sessions of ET. Our findings show that ET was effective in lowering blood pressure in postmenopausal women that was associated with up-regulation in SOD activity even though we failed to show any changes in NO/cGMP levels. Steroids hormone levels were similar between NT and HT postmenopausal women at baseline and after ET.

Yanes LL & Reckelhoff JF. Postmenopausal Hypertension. Am J Hypertens. Jul;24(7):740-9, 2011.

Zanesco A & Antunes E. Effects of exercise training on the cardiovascular system:

pharmacological approaches. Pharmacol Ther. Jun;114(3):307-17, 2007.

Financial Support: Fapesp

Where applicable, the authors confirm that the experiments described here conform with The Physiological Society ethical requirements.

PCA287

Adding arginine to an essential amino acid (EAA) feed reverses age-related impairments in vascular responsiveness but does not offset age-related anabolic blunting

W. Mitchell[1,2], J.P. Williams[1,2], B. Phillips[1], D. Rankin[1], J.N. Lund[1,2], K. Smith[1] and P.J. Atherton[1]

[1]School of Graduate Entry Medicine, University of Nottingham, Derby, UK and [2]Royal Derby Hospital, Derby, UK

Impaired vascular function in older age compromises the positive effects of nutrition on limb blood flow, perhaps impacting on maintenance of healthy muscle mass. Herein, we explored: (i) the effect of age upon macro and micro-vascular limb blood flow responses to nutrition, and (ii) the potential for arginine, a substrate of nitric oxide synthase, to improve nutrient-mediate vascular responsiveness in older people. Using contrast enhanced ultrasound (CEUS) with Sonovue™ SF_6 microbubbles, along with phase shift Doppler, we measured: changes in leg blood flow (LBF), muscle microvascular blood volume (MBV), microvascular flow velocity (MFV) and their product microvascular blood flow (MBF), in response to a 15g oral mixed EAA feed in 8 young (~20y) and 8 older (~70y) men. An additional 8 older men (~70y) had the same 15g mixed EAA feed, supplemented with 3g L-arginine. Using $^{13}C_6$-phenylalanine tracer, muscle protein synthesis (MPS) was also measured. Measurements were made 2hr before and 4hr after feeding. Young men showed marked vascular responses to EAA feeding with an early increase in MBV (45±13%, P<0.001) due to capillary recruitment. This was achieved by 45 min post feed, preceding changes in LBF, MFV and MBF, which were observed 120-180 min post feed. LBF increased 44±11% (P<0.001), MFV increased 78±31% (P<0.01) and MBF increased 130±52% (P<0.001) from fasting. In contrast, older men fed 15g EAA had no significant changes in LBF or any index of muscle microvascular flow. Older men receiving 15g EAA with 3g arginine displayed increases in LBF (25±5%, P<0.05), MFV (88±48%, P<0.001) and MBF (110±70%, P<0.05, all mean±SEM, 2-way RM ANOVA) though MBV remained unchanged from fasted. Fasting MPS rates were similar in young (0.054%/hr) and older men (0.052%/hr). Young men demonstrated a total synthetic response of 0.27% in 4hrs after 15g EAA feeding. Older men had a blunted anabolic response of 0.22% (P<0.05 vs. young) in the same period, which was not augmented by 3g arginine (0.20%, P<0.05 vs. young, 1-way ANOVA). Oral EAA feeding achieves early recruitment of muscle capillaries (increasing MBV) with little change in flow; this is consistent with dilatation of terminal arterioles and would promote nutrient delivery by increasing exchange surface area and decreasing capillary-to-fiber distance. The later increase in LBF, MFV and MBF is consistent with a proximal shift in the level of regulating vessels. That arginine restores late, but not early, microvascular responses to feeding suggest different underlying mechanisms. Arginine's failure to augment MPS responses to feeding despite restoring LBF and MBF calls into question the physiological significance of the late circulatory response to feeding and promotes interest in early MBV changes.

This work was supported by Ajinomoto Corp.

Where applicable, the authors confirm that the experiments described here conform with The Physiological Society ethical requirements.

PCA288

The effects of bolus versus pulse feeding strategies on muscle anabolism in older men

W. Mitchell[1,2], J.P. Williams[1,2], B. Phillips[1], D. Rankin[1], J.N. Lund[1,2], K. Smith[1] and P.J. Atherton[1]

[1]School of Graduate Entry Medicine, University of Nottingham, Derby, UK and [2]Royal Derby Hospital, Derby, UK

A topical advancement in understanding the control of muscle protein synthesis (MPS) was the discovery of a "Muscle-Full" phenomenon, whereby feeding stimulates only transient increases in MPS, which return to postabsorptive values despite sustained availability of plasma and muscle essential amino acids (EAA) including leucine.

We have explored this phenomenon in relation to aging by measuring MPS using a $^{13}C_6$-phenylalanine stable isotope tracer method. Measurements were made over a 6hr period (2hr fasted and 4hr during / after feeding), using two distinct feeding regimens: 16 older men received either a single 15g mixed EAA feed (N=8, 70±2 y; 'BOLUS') or the same dose in 4 x 3.75g fractions at 45 min intervals (N=8, 70±3 y; 'PULSE').

While MPS was unchanged from fasting in either group 0-90 min after EAA ingestion, it was elevated 90-180 min, irrespective of feeding strategy (BOLUS: 0.051 to 0.084 vs. PULSE: 0.047 to 0.073%/hr). In contrast, while MPS returned to baseline rates in BOLUS between 181-240 min (to 0.052%/hr) this was not the case in PULSE (0.070%/hr, P<0.05 vs. fasting, 2-way RM ANOVA). Despite these temporal differences, equal total MPS responses to feeding regimens were revealed by area under the curve analysis (0.22% vs. 0.23% in 4 h, P>0.05 1-way ANOVA).

While equal total MPS between regimens suggests a dose, rather than time-dependent mechanism regulates the muscle-full state in older men, these data point towards sustainment of the anabolic response over longer durations with PULSE feeding regimens.

This work was supported by the Ajinomoto Corporation.

Where applicable, the authors confirm that the experiments described here conform with The Physiological Society ethical requirements.

PCA289

Optimization and extraction of antioxidants from *Aloe vera* using response surface methodology

S. Kim, A.D. Assefa and S. Park

Biotechnology, Dept. of Molecular Biotechnology College of Life & Environmental Sciences, Konkuk University, 1, Hwayang-dong, Gwangjin-gu, Seoul 143-701 Korea., Seoul, Seoul, Republic of Korea

Antioxidants obtained from the plants are very popular trend in the world and has been utilised for development of functional foods. The natural antioxidant like phenolics and flavonoids help to prevent diseases like diabetes, cardiovascular diseases, arthritis and cancer etc. The main objective of this work is to search for natural antioxidants and optimization of process for *Aloe vera* extract as an antioxidant by using RSM (Response Surface Methodology). The independent vari-

ables were the extraction time (X1) varying within a 1-4 h range, the ethanol percentage X2 of water-ethanol extracting solvent (0-100 % v/v), temperature X3 X3 (25-60 °C), and the liquid-to-solid ratio X4 (30-60 mL/g). The response variables like extraction yield, concentrations of aloins A and B, aloesin, total polysaccharides, total phenolics and their antioxidant activities (FRAP and CUPRAC) were evaluated. The experimental value for yield, aloin A, aloin B, aloesin, total polysaccharide, total phenol and antioxidant activity (FRAP, CUPRAC) of *Aloe vera* extract were varied from 7.711 to 83.486%, 0.098-0.397mg/g extracted solid, 0.288-0.99mg/g extracted solid, 0.047-0.905mg/g extracted solid, 47.296-350.497mg D-mannose equivalent/g extracted solid, 0.477-3.604mg gallic acid equivalent/g extracted solid, 1.617-14.783mg trolox equivalent/g extracted solid, 11.422-104.532μM trolox equivalent/g extracted solid, respectively. Depending on this data in this study we observed that the optimum conditions for extraction of antioxidants from *Aloe vera* with different parameters are, the required time was 1hour, ethanol concentration were 34.34% v/v, extraction temperature were 60 °C, and the liquid-to-solid ratio was 45.75ml/g. The experimental values agreed with those predicted by RSM models, thus indicating suitability of the model employed and the success of RSM in optimizing the extraction conditions for *Aloe vera* antioxidants.

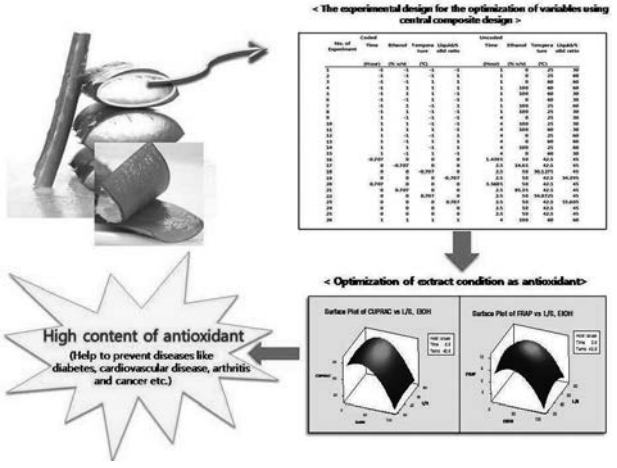

Barinderjit Singh et al. (2012). J. Food Sci. Technol. 41, 294-308

Mohanmmed Moniruzzaman et al. (2012). Molecules 17,12851-12867

Bushra Sultana et al. (2009). Molecules 14, 2167-2180

Liu Chun-Hui et al. (2007). Process Biochem. 42, 961-970

Park MK et al. (1998). Phytochem. Anal. 9, 186-191

This research was supported by Technology Development Program for Bio-industry, Ministry for Food, Agriculture, Forestry and Fisheries, Republic of Korea.

Where applicable, the authors confirm that the experiments described here conform with The Physiological Society ethical requirements.

PCA290

Studying molecular physiology of DNA cruciforms with a coarse-grained computational model

C. Matek[1], T.E. Ouldridge[1], J.P. Doye[2] and A.A. Louis[1]

[1]Rudolf Peierls Centre for Theoretical Physics, Oxford University, Oxford, UK and [2]Physical and Theoretical Chemistry Laboratory, Oxford University, Oxford, UK

Cruciform structures of DNA occur in sequences exhibiting an inverted repeat (IR) structure. They are known to play a role in several regulatory processes of cellular physiology, and have been linked to the development of diseases such as Werner's syndrome and certain types of cancer (1).

Magnetic tweezer assays have enabled the study of these non-canonical DNA structures on a single-molecule scale (2).However, a detailed understanding of structural and kinetic properties of DNA cruciforms is still lacking.

We used a coarse-grained computational model of DNA (3) to study thermodynamic stability and formation kinetics of cruciform structures in a superhelically stressed DNA strand at physiological temperatures.

Thermal quantities of the structures in the DNA model were obtained using a cluster-move Monte Carlo (MC) method. Free-energy landscapes governing the cruciform formation process in a 34bp IR sequence were calculated using umbrella sampling. Kinetic properties of cruciform formation were studied in direct, unbiased MC simulations for 34bp and 64 bp IR sequences.

In the simulations of the cruciform structures we find an asynchronous, but cooperative extrusion mechanism (4). First, a bubble has to diffuse to the centre position of the IR sequence. Then, a size fluctuation of the bubble must be large enough to allow for rearrangement of its single strands, leading to formation of a first hairpin. Upon formation of the first cruciform arm, the second arm rapidly grows to a similar size. This initial asynchronous formation is followed by a synchronous growth mechanism of both cruciform arms, which resolves the remaining superhelical stress. The asynchronous formation mechanism is reflected in the free energy landscapes of the system, which we calculated as a function of the number of base pairs in the system. For all parameters studied, the free energy barrier lies at 8-9k_BT. At a temperature of 39.4°C, we observe that the fully extruded cruciform structure is thermodynamically more stable than the corresponding bubble state of the DNA strand. This result consistent with the *in vivo* genetic instability observed for perfect IR sequences (2).

We have used numerical simulations of a coarse-grained model of DNA to study thermodynamic and structural properties of DNA cruciforms at a length and time resolution presently inaccessible to experimental setups. Our results show a complex asynchronous extrusion behaviour driven by DNA supercoiling and ambient temperature. The genetic instability of perfect IR sequences may be due to the high thermodynamic stability of cruciform structures under physiological conditions of temperature and supercoiling. This highlights the importance of physical properties of the DNA heteropolymer in physiological processes on a molecular scale, such as cruciform extrusion.

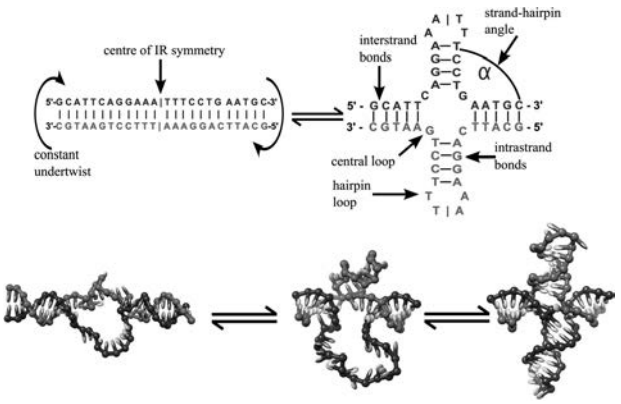

Cruciform extrusion was observed to follow a correlated, but asynchronous cooperative mechanism.

Brázda, V.; Laister, R. C.; Jagelská, E. B.; Arrowsmith, C. BMC Mol Biol 2011, 12, 33.

Ramreddy, T.; Sachidanandam, R.; Strick, T. R. Nucleic Acids Res 2011, 39, 4275–4283.

Ouldridge, T. E.; Louis, A. A.; Doye, J. P. K. J Chem Phys 2011, 134, 085101.

Matek, C.; Ouldridge T.E.; Levy A.; Doye J.P.K.; Louis A.A. J. Phys. Chem. B, 2012, 116, 11616–11625

Where applicable, the authors confirm that the experiments described here conform with The Physiological Society ethical requirements.

PCA293

Pattern of immunogenicity in a representative group of canines following anti-rabies immunization

M. Gunatilake[1], R.M. Pimburage[2], O. Wimalaratne[3], A. Balasuriya[4] and D. Perera[5]

[1]Physiology, Faculty of Medicine, University of Colombo, Colombo, Western, Sri Lanka, [2]Public Health Veterinary Services, Ministry of Health, Public Health Veterinary Services, Ministry of Health, Colombo, Western, Sri Lanka, [3]Department of Rabies Research and Vaccine Quality control, Medical Research Institute, Colombo 08, Colombo, Western, Sri Lanka, [4]Community Medicine, Faculty of Medicine, General Sir John Kotelawala Defense University, Ratmalana, Western, Sri Lanka and [5]Department of Rabies Research and Vaccine Quality control, Medical Research Institute, Colombo 08, Colombo, Western, Sri Lanka

Immunization of dogs against rabies plays a very vital role in reducing mortality due to rabies in humans as well as in animals. In this context, it is important to know whether a representative group of canines; specially Sri Lankan local breed/mongrel breed have antibody titres above the protective level recommended by the WHO following anti-rabies immunization and also whether the antibody titres are maintained above the protective level until the time of annual booster. Healthy domestic, stray dogs and puppies (N = 510) in Kalutara district, Sri Lanka were recruited initially and allocated into 8 groups based on pre-established criteria. A monavalent (inactivated) vaccine recommended by the Government Rabies Control Programme was used to immunize all recruited canines. On the day of vaccination 3-5 ml of venous blood (D0) was collected from each animal and post immunization blood samples were collected on days 30, 180, 360 (D30, D180 and D360). Rapid Fluorescent Focus Inhibition Test (RFFIT) was used to determine the virus neutralizing antibody titres in serum samples, at the Department of Rabies Research and Vaccine Quality Control, Medical Research Institute (MRI), Colombo 08. Total number of blood samples analyzed was 1520 collected from 380 canines that were available until D360 after immunization. The Ethics approval for the study was obtained from the Ethics Review Committees of the Faculty of Medicine, Colombo and MRI. The number (and percentage) of canines in Groups A to H that had antibody titres below the protective level of 0.5 IU/ml on D0, D30, D180 and D360 are indicated in table 1 (Mean antibody titres are not shown here). This is the first descriptive and comparative study involving a representative group of canines done in Sri Lanka. This indicates that a single dose of anti-rabies immunization fails to generate a protective level of immunity which lasts until 1 year in 40.42% of stray dogs in Group A and 57.14% of domestic dogs in Group D. The pattern of antibody titre development in adult domestic dogs in Groups E and F seems to be closely similar irrespective of regularity in immunization. Almost all puppies in Groups G and H need more than one immunization until the time of annual booster. It is evident that maternal antibodies do not protect puppies against rabies until the first anti-rabies immunization.

Table 1

Group	D0	D30	D180	D360
A (n=47) - Stray dogs without previous immunization history against rabies	44 (93.6)	06 (12.76)	06 (12.76)	19 (40.42)
B (n=47) - Stray dogs with previous immunization history against rabies	14 (29.79)	0 (0)	0 (0)	08(17.02)
C (n=47) - Young domestic dogs with previous immunization history	10 (21.28)	02 (4.26)	03 (6.38)	10 (21.28)
D (n=63) - Young domestic dogs without previous immunization history	01 (1.59)	04 (6.35)	04 (6.35)	36 (57.14)
E (n=51) - Adult domestic dogs with regular annual immunization history	12 (23.53)	02 (4)	06 (12)	11 (22)
F (n=48) - Adult domestic dogs without regular annual immunization history	11 (22.92)	0 (0)	02 (4.16)	08 (16.67)
G(n=40) - Puppies of previously immunized domestic bitches	40 (100)	01 (2.5)	07 (17.5)	37 (92.5)
H (n=37) - Puppies of unimmunized domestic bitches	37 (100)	02 (5.41)	08 (21.62)	33 (89.19)

Smith J S, Yager P A, Baer G M. A rapid fluorescent focus inhibition test (RFFIT) for determining rabies virus-neutralizing antibody. In: Meslin F X, Kaplan M M, Koprowski H. Laboratory Techniques in Rabies – 4th Edition, World Health Organization, Geneva. 1996; 181-192.

WHO Expert consultation on rabies. First report. Geneva, World Health Organization, WHO Technical Report Series No. 931, 2004.

National Science Foundation of Sri Lanka for Financial Assistance

Where applicable, the authors confirm that the experiments described here conform with The Physiological Society ethical requirements.

PCA294

Gabexate mesilate mitigates coagulopathy and organ dysfunction in rats with endotoxemia

C. Tsao[1,3], H. Tsai[2], W. Liaw[3] and C. Wu[4]

[1]Anesthesiology, Taipei Veterans General Hospital and National Yang-Ming University, Taipei, Taiwan, [2]Department of Anesthesiology, Mackay Memorial Hospital, Taipei, Taiwan, [3]Department of Anesthesiology, Tri-Service General Hospital, National Defense Medical Center, Taipei, Taiwan and [4]Department of Pharmacology, National Defense Medical Center, Taipei, Taiwan

Sepsis and its complications, including multiple organ failure are associated with high mortality in patients in intensive care unit. Coagulation abnormalities, such as thrombocytopenia, prolonged clotting time and consumption coagulopathy, occurred in nearly all patients with severe sepsis. Gabexate mesilate (GM), a synthetic serine protease inhibitor, is known to be an anticoagulant by competitively inhibiting activities of

thrombin and factor Xa as well as plasmin and plasma kallikrein. Several studies report that GM has protective effects against tissue injury in models of endotoxemia. The aim of this study was to examine whether GM could attenuate organ dysfunction and improve survival rate in an animal model of lipopolysaccharide (LPS)-induced endotoxemia (Tsai et al, 2012). LPS (30 mg/kg over a 4-h intravenous infusion) was administered to male adult Wistar rats (250-300 g). Bacterial LPS (E. coli serotype 0127:B8, L3127) was used in this study. Some of rats received a continuous infusion of GM (10 mg/kg/h for 8.5 h) at 30 min prior to the infusion of LPS as the treatment group. Variables of hemodynamic and biochemistry were measured during the subsequent 6 h after the start of LPS infusion. Parameters of thrombelastography, hemostasis and inflammatory response were also measured, and survival rate was monitored every 30 min during the 8-h experiment. The administration of LPS rats with GM (i) alleviated hypotension, (ii) attenuated the LPS-induced liver and kidney dysfunction, (iii) minimized consumptive coagulopathy displayed by thrombelastography, (iv) attenuated the rises in serum tumor necrosis factor-α, interleukin-6, and plasma thrombin-antithrombin complex as well as plasminogen activator inhibitor-1, (v) reduced neutrophils infiltration score in lung, liver and kidney, and (vi) significantly increased the 8-h survival rate (58.3%), when compared to the LPS group (25.7%, $p<0.05$). These results suggest that the pre-treatment of LPS rats with GM not only reduces organ injury but also improves survival rate. These protective effects of GM may be attributed to its anti-inflammation and anti-coagulation properties.

Kinasewitz GT et al. (2004) Crit Care 8, R82.

Ohno H et al. (1980) Thromb Res 19,579.

Harada N et al. (1999) Crit Care Med 27,1958.

Murakami K et al. (1996) Crit Care Med 24,1047.

Tsai HJ et al. (2012) Blood Coagul Fibrinolysis 23,118.

This work was supported by the grant NSC 101-2320-B-016-014 from the National Science Council, R.O.C., Taiwan.

Where applicable, the authors confirm that the experiments described here conform with The Physiological Society ethical requirements.

PCA295

Erythrocyte osmotic fragility and lipid peroxidation in experimental hyperthyroidism

N. Dariyerli, R. Yucel, S. Ozdemir, S. Toplan, M. Akyolcu and G. Yigit

Istanbul University Cerrahpasa Medical Faculty, Istanbul, Turkey

Erythrocyte osmotic fragility and lipid peroxidation in experimental hyperthyroidism
Thyroid hormones have multifaceted effects on humans. Among others, they influence the basal metabolic rate; the overproduction of thyroid gland hormones results in an increased rate of metabolism and oxygen consumption by cells. Increased thyroid hormone concentrations affect the oxidant/antioxidant equilibrium and may cause harm to the cell. Thyroid hormones, while leading to increase in free radicals also activate the antioxidant enzymes. The purpose of this study is to determine the structural integrity of red blood cells in experimental hyperthyroidism by assessing the osmotic fragility of erythrocytes in primary hyperthyroidism and its relation between lipid peroxidation. In this study, twenty-two Spraque-Dawley-type female rats weighing between 160 and 200 g were divided into two, as control (n=10) and experimental (n=12), groups. The experimental group animals have received tap water and L-Tiroksin (0.4 mg/100 g fodder) added standard fodder for 30 days to induce hyperthyroidism. Control group animals were fed tap water and standard fodder for the same period. At the end of the experimental period, blood samples were drawn from the abdominal aorta of the rats under light ether anesthesia. Triiodothyronine (T3), thyroxine (T4), and thyroid stimulant hormone (TSH) levels, osmotic fragility, malondialdehyde (MDA), glutathione (GSH) levels and superoxide dismutase (SOD) activity were measured. Statistical analysis was done by Mann-Whitney U test. Data were expressed as means ± SD. Differences between groups were considered significant at the ($p<0.05$) level. The statistically significant increase in T3, T4 and the significant decrease in TSH) of experimental group is the evidence of induced primary hyperthyroidism. There was a statistically significant increase found in erythrocyte MDA($p<0.001$) levels, and SOD activity ($p<0.001$), but statistically a significant decrease was detected in GSH ($p<0.05$) levels in hyperthyroid group when compared to controls. In the controls, the osmotic fragility levels were found to be maximum at 0.32 % NaCl and minimum at 0.56 % NaCl, whereas in experimental group reached a maximum at 0.40 % NaCl and minimum at 0.64 %. When statistical evaluations were compared, statistically important increases were detected in maximum and minimum osmotic fragility limits between both the groups ($p<0.001$). This finding, which shows maximum hemolysis ratio, is the evidence of increased osmotic fragility of the erythrocytes in hyperthyroidism. As a result of our study, it may be concluded that hyperthyroidism may led to an increase in osmotic fragility of erythrocytes and this situation may possibly originate from the increased lipid peroxidation in hyperthyroidism.

Where applicable, the authors confirm that the experiments described here conform with The Physiological Society ethical requirements.

PCA296

The effects of experimental hypothyroidism on hemorheology and plasma fibrinogen concentration

S. Toplan, N. Dariyerli, S. Ozdemir, M. Akyolcu, H. Hatemi and G. Yigit

Istanbul University, Cerrahpasa Medical Faculty, Istanbul, Turkey

The effects of experimental hypothyroidism on hemorheology and plasma fibrinogen concentration
Thyroid hormones are responsible for arrangement of general body metabolism. In their deficiency pathological findings arise related to various physiological systems. In hypothroid cases it has been observed that blood rheology alters. Hematological changes, especially anemia, are common and well characterized in hypothyroidism. This study has been planned with the purpose to determine the effects of experimental hypothyroidsm on hemorheological parameters and fibrinogen concentration. In this study, twenty Spraque-Dawley type albino female rats weighing 160-200g were used in both control and experimental group animals. Both control (n=10) and experimental group (n=10) animals were kept in same physical conditions during experimental period and were fed with standard fodder and tap water. To induce hypothyroidism, methimazole (75-mg/100g fodder) was given to experimental group rats for 20 days. At the end of the experimental period, blood samples were drawn from the abdominal aorta of the rats under the light ether anesthesia. Thyroid stimu-

lant hormone (TSH), triiodothyronine (T3), thyroxine (T4) hormone levels, hematocrit (% Hct), hemoglobin (Hb), blood viscosity, erythrocyte rigidity index, plasma viscosity and plasma fibrinogen concentration values of both control and experimental group animals were determined and evaluated. Statistical analysis was done by the Mann-Whitney U test. Data were expressed as means ± SD. Differences between groups were considered significant at the $p<0.05$ level. According to results of our study when values of control group and experimental groups were compared: While T3 and T4 levels of experimental group were found lower ($p<0.001$) but TSH level higher ($p<0.001$) than that of the control group. Statistically significant decreased T3, T4 and increased TSH values in experimental group were taken as the indicator of the primary hypothyroidism. Plasma viscosity and fibrinogen concentration of hypothyroid group were found significantly higher than controls ($p<0.01$). Hematocrit and hemoglobin values were also found lower in experimental group than the control group animals ($p<0.01$). However, there was no significant difference found in blood viscosity at the original Hct value but there was a significant increase at standart Hct value ($p<0.01$). There was also no change in erythrocyte rigidity index between control and experimental groups. According to results of our study it may be concluded that in the early phase of hypothyroidism, changes in hemorheology are only seen as an increase in plasma viscosity. Such an increase may be dependent on increased fibrinogen concentration.

Where applicable, the authors confirm that the experiments described here conform with The Physiological Society ethical requirements.

PCA297

Reference haemoglobin value in apparently healthy Sudanese children in Khartoum state, Sudan

I.M. Hamad[1] and O.A. Musa[2]

[1]physiology, Bahri university, Khartoum, Khartoum, Sudan and [2]physiology, Ribat university, Khartoum, Khartoum, Sudan

The WHO in 1997(5) stated that 12 gm/dl is the borderline for normal Hb level for adult and 15 as a normal mean (16 and 14 gm./dl for male and female respectively) .Dacie & Lewis stated Hb value of 13.0+1.5 gm./d for children 10-12 yl,(4).Few researchers in Sudan worked in reference Hb value, among them Abdella et al in 1987 (1) found the mean of Hb reference value of 12.00gm/dl for children between 6 to 12 y. with no sex difference. Atig in 1995 (3) stated Hb reference value of 11.63+ 0.89gm/dl for Sudanese children between 5 to 12 y. in Khartoum state. Agabeldour (2) in 1997 worked out Hb reference value of 13.18+ 1.46gm/dl for adult males and a value of 11.17 + 2.03 gm/dl for adult females in Sudan
Objective:- The objective of this study is to estimate the reference Haemoglobin value in apparently healthy Sudanese children in Khartoum state, Sudan. To achieve this objective, using stratified random sampling, 1000, capillary blood samples were collected from apparently healthy Sudanese children in Khartoum state within the age group 12 – 14 years, 550 females and 450 males. The subjects were interviewed according to a designed questionnaire, clarifying tribe, nutritional and socioeconomic status as main variables, Haemoglobin (Hb) value was determined for each, using Hb-cyanide method. The mean reference Haemoglobin value for both sexes was 11.69g/dl+ 2.13 while in males and females was 11.67g/dl+ 2.13, and 11.70g/dl+ 2.13 respectively. About 50% of the children reported value less than 12g/dl, while 6.3% showed a value of 9.4g/dl or less, without any symptoms of anemia. Gender and income has no Significant effect on Haemoglobin value in this study, while nutrition and ethnic background affect Hb value, Southerners have the lowest Hb value, while Kordofan tribes have the highest.
Conclusion :- the mean reference Haemoglobin value for both sexes within the age group 12 – 14 years in Sudan is considerably lower than the standard ones stated in books and, differ according to tribes

Tribes, their individual numbers, %, and mean Hb of different Sudanese

tribe	NO.	%	mean Hb in g/l
North	668	66.8%	12
South	107	10.7%	10.68
Noba	45	4.5%	11.41
Darfour	101	10.1%	11.84
Kordufan	79	7.9%	12.05
Total	1000	100%	

1-Abdulla F. D. et al (1987) haematology levels and white blood cell counts in school children in Khartoum city Sud Med.J. Vol. 29 (1-3)1991, 38-45.

2- Agabeldour A.A. (1997) reference value for selected haematological parameters in apparently healthy Sudanese adults in Khartoum state, degree of medical doctorate in clinical pathology, faculty of medicine U.K

3- .Atig, Is (1995)selected anti thrombomtrtic measurement and selected biochemical and haematological parameters in apparently healthy Sudanese children in Khartoum state, MSC thesis, faculty of medicine U.K.

4- Daci,V &Lewis,M (1991)practical haematology, seventh edition

5- WHO, 1997 normal haematology levels computer search

I am thankful to the Sudanese children and their parents who signed the agreements to conduct this research, and to all those who helped me in to do this work and declare that the whole research investigations were entirely my sole work and effort

Where applicable, the authors confirm that the experiments described here conform with The Physiological Society ethical requirements.

PCA298

Determination of hematological and biochemical blood parameters in kitten and adult Angora cats

S. Arikan[1], M. Cinar[2] and O. Simsek[1]

[1]Department of Physiology, Faculty of Veterinary Medicine, Kirikkale University, Kirikkale, Turkey and [2]Department of Biochemistry, Faculty of Veterinary Medicine, Kirikkale University, Kirikkale, Turkey

The purpose of this study was to investigate the reference values of haematological and biochemical blood parameters on kitten and adult Angora cats. In this study, blood samples were taken from a total of 24 Angora cats, 16 adults (1 to 3 year old) and 8 kittens (1.5, 3, 4.5, 6, 7.5, 9 ve 10.5). In the serum, alanin amino transferase (ALT), alkanine phosphotase (ALP), gama- glutamil transpeptidase (GGT), creatine kinase (CK), cholesterol, total protein, calcium (Ca), magnesium (Mg), phosphor (Pi) levels were measured, and from the blood, erythrocyte (RBC), leukocyte (WBC), monocyte (MON), lymphocyte (LYM), hemoglobin (HGB) and hematocrit (HCT) values were determined. Data were analyzed using general linear model in SAS. Fisher's least significant difference (LSD) test was used for mean comparisons. All values are presented as the mean ± S.E.M. The animal care and use protocol was approved by Local Ethical Committee of Kirikkale University.

Monocyte level was found to be high in adult cats, ALP, CK activities were lower in adult cats compared to the kittens. Total protein, RBC, HGB and HCT in kittens (1.5-3 months old) were lower, GGT activity and WBC value in kittens (1.5-3 months old) were higher than other kittens. Concentration of cholesterol, Ca, Pi and Mg was higher in kittens (1.5-3 months old) than in adult cats. As a result of this study, it is the first time these reference values of haematological and biochemical blood parameters in kitten and adult Angora cats were determined. The results of present study will be helpful and an excellent reference document for clinicians.

Table 1

	Kitten Cats			Adult Cats	
Parameters	**1.5-3 months**	**4.5-6 months**	**7.5-10.5 months**	**1-3 years**	**P**
RBC ($x10^6$/µL)	6.16 ± 0.17c	7.47 ± 0.28d	8.74 ± 0.29a	8.33 ± 0.31ab	P<0.05
WBC ($x10^3$/µL)	17.23 ± 1.53a	13.71 ± 1.25b	11.49 ± 0.70b	12.00 ± 0.47b	P<0.05
LYM ($x10^3$/µL)	4.42 ± 0.44	3.89 ± 0.30	4.12 ± 0.32	4.08 ± 0.20	P>0.05
MON ($x10^3$/µL)	0.33 ± 0.04b	0.44 ± 0.06b	0.32 ± 0.01b	0.64 ± 0.06a	P<0.05
HCT (%)	27.37 ± 1.05c	34.7 ± 2.15b	42.87 ± 1.83a	35.19 ± 1.29b	P<0.01
HGB (g/dl)	7.66 ± 0.20b	11.19 ± 0.46a	11.78 ± 0.40a	11.97 ± 0.47a	P<0.001

a,b,c: Different letters in the same line mean signaficantly different (n=16).

Table 2

	Kitten Cats			Adult Cats	
Parameters	**1.5-3 months**	**4.5-6 months**	**7.5-10.5 months**	**1-3 years**	**P**
ALT (U/L)	25.79 ± 1.64	26.17 ± 3.12	31.12 ± 2.56	33.39 ± 5.75	P>0.05
ALP (U/L)	115.41 ± 17.27a	92.22 ± 14.96a	81.69 ± 10.21a	40.00 ± 5.36b	P<0.05
GGT (U/L)	16.09 ± 2.46a	7.61 ± 1.22b	9.42 ± 1.11b	4.33 ± 0.29a	P<0.01
CK (U/L)	218.04 ± 22.55a	173.71±16.86ab	196.78 ± 16.58a	133.27 ± 10.17b	P<0.05
Cholesterol (mg/dl)	158.78 ± 4.08a	142.03 ± 7.50ab	128.39 ± 6.34b	132.54 ± 7.10b	P<0.01
Total Protein (g/dl)	5.92 ± 0.21b	6.92 ± 0.16a	6.68 ± 0.22a	6.77 ± 0.14a	P<0.05
Ca (mg/dl)	11.23 ± 0.19a	9.99 ± 0.23b	10.62 ± 0.18ab	10.52 ± 0.28b	P<0.05
Pi (mg/dl)	8.61 ± 0.23a	7.62 ± 0.24b	8.09 ± 0.39ab	6.51 ± 0.42c	P<0.05
Mg (mg/dl)	2.59 ± 0.08a	2.40 ± 0.08ab	2.25 ± 0.06b	2.36 ± 0.07b	P<0.05

a,b,c: Different letters in the same line mean signaficantly different (n=16).

Financial support for present project was provided by Kirikkale University Research Funds (BAP). Project No: BAP-2008/42.

Where applicable, the authors confirm that the experiments described here conform with The Physiological Society ethical requirements.

PCA299

Dose dependent effects of fish oil on oxidative stress

M.A. Martins[1], M.B. Moss[1], I.K. Mendes[1], C.O. Chamma[1], W.V. Mury[1], M.B. Águila[2], T.M. Brunini[1] and A. Mendes-Ribeiro[1]

[1]Department of Pharmacology and Psychobiology, State University of Rio de Janeiro, Rio de Janeiro, Rio de Janeiro, Brazil and [2]Department of Anatomy, State University of Rio de Janeiro, Rio de Janeiro, Rio de Janeiro, Brazil

Introduction: Despite the cardiovascular benefits provided by polyunsaturated fatty acids (PUFA), there has been concern that these fatty acids exhibit the highest sensitiveness to peroxidation, which in turn could enhance production of reactive oxygen species. Here, we investigated the effects of different amounts of fish oil on oxidative status in red blood cells (RBC) from mice fed a high fat diet.
Methods: C57BL/6 male mice were divided into six groups based on the diet offered; the control group was fed with a standard diet (10% lipids) and the others groups were fed with isoenergetic high fat diets (50% lipids) containing 0%, 10%, 20%, 30%, or 40% of fish oil. The high fat diets were composed of a mixture of lard and fish oil, with a gradual replacement of lard by fish oil. At the end of the experimental period (12 weeks), the animals were anaesthetized with intraperitoneal sodium pentobarbital (0.42 mg/g). Blood samples obtained by cardiac puncture were collected into a tube containing heparin and RBC were isolated by centrifugation. Oxidative damage in RBC was evaluated by determination of carbonyl groups and by the concentration of malondialdehyde (MDA). The activity of catalase (CAT), glutathione peroxidase (GPx) and superoxide dismutase (SOD) enzymes was analysed to evaluate the antioxidant status. The experimental protocols were approved by the local Ethics Committee (CEUA/033/2011). Comparisons among groups were done by one-way ANOVA followed by a Holm-Sidak post-hoc test. Significance level was set at 5%.
Results: Table 1 shows the results of the oxidative stress parameters. Diets absent (F0) or with high concentrations of fish oil (F20, F30, F40) induced an increased RBC lipid peroxidation than standard chow diet. F0 mice also showed an increased protein oxidative damage, assessed by the quantification of carbonyl groups, compared to control, F20, F30, and F40 mice. No significant difference in protein oxidation was observed among none of the fish-oil fed mice. The antioxidant enzyme analysis showed that SOD activity in RBC from F0 and F10 groups was decreased compared to control group. The activity of the other antioxidant enzymes, CAT and GPx, did not differ among groups, except for a reduction in GPx levels from the F40 group compared to the F20 group.
Conclusion: Lipid peroxidation of RBC rises linearly with increasing amounts of fish oil in the diet, however this increased susceptibility was not reflected in protein damage. The use of antioxidant products during dietary fish oil supplementation could be an alternative to ensure that their consumption does not result in detrimental secondary effects.

	Control	F0	F10	F20	F30	F40
MDA (nmol/g Hb)*	0.023 ± 0.003	0.040 ± 0.004[a]	0.030 ± 0.002	0.040 ± 0.002[a]	0.044 ± 0.005[a]	0.049 ± 0.005[a,c]
Carbonyl derivates (nmol/mg protein)	21.8 ± 6.6	77.3 ± 9.9[a]	46.7 ± 18.9	18.7 ± 4.2[b]	16.7 ± 6.7[b]	28.4 ± 8.8[b]
Superoxide dismutase (U/g Hb)	731 ± 80	174 ± 110[a]	112 ± 73[a]	567 ± 56	548 ± 42	577 ± 61
Catalase (U/g Hb)	0.058 ± 0.009	0.060 ± 0.007	0.050 ± 0.006	0.075 ± 0.007	0.069 ± 0.009	0.097 ± 0.017
Glutathione peroxidase (U/g Hb)	3.6 ± 0.6	3.5 ± 0.5	4.8 ± 0.7	6.1 ± 0.8	3.6 ± 0.8	2.9 ± 0.4[a]

*MDA, malondialdehyde. Data desviermean ± S.E.M. [a]p ≤ 0.05 vs control, [b] p ≤ 0.05 vs F0, [c] p ≤ 0.05 vs F10, [d] p ≤ 0.05 vs F20, n=7-9

Table 1. Oxidative stress parameters.

Where applicable, the authors confirm that the experiments described here conform with The Physiological Society ethical requirements.

PCA300

Beneficial effect of Cinnamomum burmannii in streptozotocin-induced type 1 diabetic rats

M.L. Silva[1,2], P. Pereira[1], A. Bernardo[1], M. Moncada[1], J. Singh[2] and F. Mesquita[1]

[1]BioquiLab - Centro de Investigação Interdisciplinar Egas Moniz (CiiEM), Instituto Superior de Ciências da Saúde Egas Moniz, Almada, Portugal and [2]School of Forensic and Investigative Sciences and School of Pharmacy and Biomedical Sciences, University of Central Lancashire, Preston, UK

Cinnamon is a traditional plant which is used as a spice, tea, for flavour and for the taste of food preparation. This spice possesses therapeutic properties to treat diabetes mellitus (DM), acting both as an anti-antioxidant and an anti-inflammatory mediator. There are different spices of cinnamon which can induce hypoglycaemic, protective and beneficial effects in DM, regulating blood glucose and lipid profiles. However, not much work has been done on the species, Cinnamomum burmannii. This study investigated the effect of aqueous C. burmannii extract on streptozotocin (STZ)-induced type 1 diabetic (T1DM) rats.

Aqueous cinnamon extract (CE) of cinnamomum burmannii was adapted from Shen et al method (Biosci. Biotechnol. Biochem. 74(12), 2010). T1DM was induced by a single ip injection of STZ (60 mg/Kg body weight) to young adult male rats (125-149g) and maintained with 12 h:12 h light/dark cycle, at temperature and humidity controlled room. Two weeks following STZ-induction both diabetic and age-matched control rats were administrated daily with 150 mg/Kg bw of CE by gavage method during 11 weeks. Control groups (STZ and control) received the same volume of water. The study had ethical clearance of UCLAN and Veterinary Medicine Faculty of Portugal. Blood glucose level (BGL), body weight and food consumption were measured on a weekly basis. At the end of the experimental protocol, the biochemical parameters and the antioxidant status were determined in each rat. The results show that diabetic rats treated with CE showed no significant decrease ($p>0.05$) in BGL and food consumption compared with control group. However, body weight was significantly (ANOVA; $p<0,05$) increased in diabetic rats treated with CE (363.91±17,80 g) compared with control (257,68±18,08) group. The results also show that C. burmannii had no significant effect on either blood lipid profiles or on HbA1c in STZ-induced diabetic rats compared to control. However, the antioxidant status of C. burmannii was markedly improved in diabetic rats compared to control group, but this was not significant. The results suggest that aqueous C. burmannii extract possesses beneficial effects on T1DM rats through improvement in body weight and via its antioxidant properties. Nevertheless, the mechanism via which cinnamon exerts its antidiabetic effect has to be clarified.

Where applicable, the authors confirm that the experiments described here conform with The Physiological Society ethical requirements.

PCA301

Hypertrophic cardiomyopathy and impairment mitochondrial function in insulin-resistant obese mice

A.S. Santos, C.S. Costa, A.C. Santana, E. Cortez, V.M. Soares, E.P. Garcia-Souza, A.S. Moura and C.A. Nascimento-Saba

Physiological Sciences, State University of Rio de Janeiro, Rio de Janeiro, Brazil

Obesity involves co-morbidities as dyslipidemia, cardiovascular disease, insulin resistance and type 2 diabetes. One characteristic of obesity is the propensity for increased circulating fatty acids. However, a loss of synchronization between fatty acid availability and oxidation would result in accumulation of fatty acid derivatives in non specific tissue such the cardiomyocyte, inducing lipotoxicity that is associated with contractile dysfunction and heart failure. It is also observed mitochondrial dysfunction playing key role in cardiac hypertrophy and failure, that can indicate defects at specific sites in electron transport chain (1, 2, 3, 4). The aim of the study was to investigate how lipid and glucose metabolic alterations affect the ventricular contractile function in mice fed high fat diet, through mitochondrial bioenergetics. After weaning, mouse C57Bl/6 received diet containing 7% (C) or 19% (HF) of soybean oil, until 135 days old. Food intake and body mass were monitored, and glucose tolerance test was realized. At 135 days, body composition was evaluated by Dual-energy X-ray Absorptiometry (DEXA) and after, animals were sacrificed by exsanguination. Lipid profile, leptin, insulin, HOMA-IR and the adiposity index were evaluated. The heart, the pancreas and intraabdominal adipose tissue were collected, weighted and processed to morphological analysis. Left ventricular myocardial fibers were used to analyze mitochondrial respiration by technique of high resolution respirometry. Cardiac hemodynamic was evaluated by Langendorff technique of isolated heart perfusion and proteins related to cardiomyocytes bioenergetics (CPT1, UCP2, GLUT1, GLUT4, AMPK and pAMPK) were analyzed by Western blotting. The group HF presented differences in adiposity (130%) with adipocyte hypertrophy (200%),, glucose intolerance, hyperinsulinemia (80%), insulin resistance and pancreatic islet hypertrophy (200%); hyperleptinemia (22%), increase of triglycerides (49%), LDL (29%) and VLDL (51%), without difference in food intake. The hypertrophic cardiomyopathy observed reflected in hemodinamic alterations as increased contractility (78%), higher ventricular pressure (63%) and impaired diastolic function (-36%). Oxidation of carbohydrates (-47%) and fatty acids (-60%) was decreased in cardiomyocytes, however, the expression of proteins co-related to cardiomyocytes bioenergetics did not differ between the groups. Obesity induced metabolic disorders in series, leading to dyslipidemia, type 2 diabetes mellitus, besides impairment of mitochondrial oxidative capacity and cardiac hypertrophy, causing hemodynamic dysfunction. However, these alterations are dissociated of energetic cardiac sensor.

1- Kenchaiah et al. Obesity and the risk of heart failure. N Engl J Med. 2002 Aug 1;347(5):305-13.

Jeckel et al. The role of dietary fatty acids in predicting myocardial structure in fat-fed rats. Lipids Health Dis. 2011 Jun 7;10:92.

Benderdour et al. Cardiac mitochondrial NADP+-isocitrate dehydrogenase is inactivated through 4-hydroxynonenal adduct formation: an event that precedes hypertrophy development.

J Biol Chem. 2003 Nov 14;278(46):45154-9.

Rosca et al. Cardiac mitochondria in heart failure: decrease in respirasomes and oxidative phosphorylation. Cardiovasc Res. 2008 Oct 1;80(1):30-9.

Our gratitude to the Nutrition Institute of UERJ for the use of DEXA, Mr Nelcir Rodrigues and Ms Andrea Bertoldo for technical care and FAPERJ/Brazil for the finnancial support.

Where applicable, the authors confirm that the experiments described here conform with The Physiological Society ethical requirements.

PCA303

Hypothalamic AMP-activated protein kinase is implicated in leptin-induced sympathetic nerve activation

M. Tanida[1], T. Shibamoto[1] and K. Rahmouni[2]

[1]Department of Physiology II, Kanazawa Medical University, Uchinada, Japan and [2]Departments of Pharmacology and Internal Medicine, University of Iowa Carver, College of Medicine, Iowa city, IA, USA

[Introduction] In mammals, leptin released from the white adipose tissue acts on the central nervous system to control feeding behavior, cardiovascular function, and energy metabolism. Central leptin activates sympathetic nerves that innervate the kidney, adipose tissue, and some abdominal organs in rats [1,2]. AMP-activated protein kinase (AMPK) is essential in the intracellular signaling pathway involving the activation of leptin receptors (ObRb) [3]. We investigated the potential of AMPKα2 in the sympathetic effects of leptin
[Method] We used in vivo siRNA injection to knockdown AMPKα2 in rats, and produced reduced hypothalamic AMPKα2 expression. Under urethane anesthesia (1.2g/kg), effects of

leptin (10μg) injection into the ventricle on sympathetic nerve activities were investigated by electro-physiological recording. Effects of leptin on feeding behavior and blood papameters were examined in conscious rats.
[Result] Leptin effects on body weight, food intake, and blood FFA levels were eliminated in AMPKα2 siRNA-treated rats. Leptin-evoked enhancements of the sympathetic nerve outflows to the kidney, brown and white adipose tissues were attenuated in AMPKα2 siRNA-treated rats. To check whether AMPKα2 was specific to sympathetic changes induced by leptin, we examined the effects of injecting MT-II (600pmol), a melanocortin-3 and -4 receptor agonist, on the sympathetic nerve outflows to the kidney and adipose tissue. MT-II-induced sympatho-excitation in the kidney was unchanged in AMPKα2 siRNA-treated rats. However, responses of neural activities involving adipose tissue to MT-II were attenuated in AMPKα2 siRNA-treated rats.
[Conclution] These results suggest that hypothalamic AMPKα2 is involved not only in appetite and body weight regulation but also in the regulation of sympathetic nerve discharges to the kidney and adipose tissue. Thus, AMPK might function not only as an energy sensor, but as a key molecule in the cardiovascular, thermogenic, and lipolytic effects of leptin through the sympathetic nervous system.

Rahmouni K et al, (2009). Diabetes 58, 536-542.

Niijima A, (1999). Neurosci Lett 262, 125-128.

Long YC & Zierath JR, (2006). J Clin Invest 116, 1776-1783.

Where applicable, the authors confirm that the experiments described here conform with The Physiological Society ethical requirements.

PCA305

Improvement of structural and functional microvascular abnormalities after central sympathetic nervous system modulation in a rat model of metabolic syndrome

A. Nascimento[1,2], M. Lessa[1], M. Machado[1], B. Antunes[1], I. Bonomo[1], P. Bousquet[2] and E. Tibiriçá[1]

[1]FIOCRUZ, Rio de Janeiro, RJ, Brazil and [2]University of Strasbourg, Strasbourg, France

Motivation: We investigated the effects of a chronic anti-hypertensive treatment using centrally-acting sympatho-inhibitory drugs on microvascular parameters in a rat model of metabolic syndrome (MS) induced by long-term high-fat diet with salt supplementation.
Methods: Fifty male adult Wistar rats were used in conformity with the guidelines of the Animals Care and Use Comitee of the Oswaldo Cruz Foundation, Brazil (Autorization P 31-11). They were maintained under normal (CON, n = 10) or high-fat diet (HFD, n = 40) during 20 weeks. Thereafter, the HFD group received oral clonidine (HFD-CLO, 0.1 mg/kg), rilmenidine (HFD-RIL, 1 mg/kg), LNP 599 (HFD-LNP, 10 mg/kg) or vehicle (HFD-CON). Functional capillary density (FCD) was evaluated in the gracilis muscle and skin of the ear using intravital videomicroscopy and structural capillary density (SCD) was studied in the skeletal muscle and left ventricle using histochemical analysis. Systolic blood pressure was evaluated by photo-plethysmography and plasma catecholamines by HPLC determination. Plasma glucose, triglycerides and cholesterol were determined by enzymatic assays.
Results: There was an increase in systolic blood pressure (178±2 vs. 138±3 mmHg, P<0.05) and heart rate (412±8 vs. 336±5 bpm, P<0.05) in the HFD-CON compared to the CON group. The HFD-CON group also presented a decrease in FCD and SCD in the gracilis muscle, compared to CON group (153±8 vs. 253±16 capillaries/mm2 and 1.5±0.08 vs. 1.8±0.04 capillaries/fiber, P<0.05, respectively). However, there were no alterations in FCD in the skin. The SCD was reduced in the left ventricle of the HFD-CON group when compared to the CON group (0.18±0.01 vs. 0.33±0.01 Vv[cap]/Vv[fib], P<0.05). The groups of animals submitted to HFD and treated with clonidine, rilmenidine and LNP 599 presented a similar reduction in systolic blood pressure (155±4, 161±4 and 156±4 mmHg, respectively, P<0.05) when compared to the HFD-CON group (178±2 mmHg) and in adrenaline levels (68±7 and 64±8 and 64±8 pg/mL, respectively, P<0.05) when compared to the HFD-CON group (89±4 pg/mL). These reductions in systemic catecholamines were accompanied by an increase in the FCD and SCD in the skeletal muscle when compared to the HFD-CON group. Moreover, there was an increase in the SCD in the left ventricle in the HFD-RIL group when compared to the HFD-CON group.
Conclusions: The modulation of sympathetic activity using chronic anti-hypertensive treatment with centrally-acting drugs results in a simultaneous reduction of arterial pressure and plasma catecholamines accompanied by an improvement of capillary rarefaction in the skeletal muscle and left ventricle in an experimental model of MS in rats.

Where applicable, the authors confirm that the experiments described here conform with The Physiological Society ethical requirements.

PCA306

Resveratrol induces central hypotensive effect via AMPK-mediated signaling to eliminate fructose induces NADPH oxidase overexpression

P. Cheng[1], C. Tseng[1,2] and L. Ger[1]

[1]Medical Education and Research, Kaohsiung Veterans General Hospital, Kaohsiung, Taiwan and [2]Biomedical Sciences, National Sun Yat-sen University, Kaohsiung, Taiwan

Reactive oxygen species (ROS) in the brain are thought to contribute to the neuropathogenesis of hypertension by enhancing sympathetic nervous system activity. The nicotinamide-adenine dinucleotide phosphate (NADPH) oxidase and its regulatory subunit Rac1 (a small GTPase) play important roles in ROS production in the brain. Resent evidences reported that resveratrol activates AMP-activated protein kinase (AMPK) to suppress oxidative stress. Therefore, we examined whether promotion of AMPK in the brain decreases Rac1-derived ROS generation, thereby reducing blood pressure in fructose-induced hypertensive rats (F rats). In this study we elucidated the ROS level in the nucleus tractus solitarii (NTS) and rostral ventrolateral medulla (RVLM) were greater in F rats than in Wistar-Kyoto rats (WKY). Inhibitions of ROS, oral resveratrol for one week decrease blood pressure and increase NO production in F rats but not in WKY. Diminutions of Rac1 through resveratrol also reduce NADPH oxidase subunit expression (p22-phox and p67-phox) and induce SOD2 production. In addition, inhibition of AMPK by an AMPK inhibitor (compound C) abolished resveratrol-induced decreases in Rac1 and NADPH oxidase activities and resveratrol-induced increases in SOD2 expression, suggesting that AMPK is an important mediator of the resveratrol-induced regulation of these enzymes. Interestingly, abolish Rac1 by overexpression of AMPK that decrease blood pressure through reduced extracellular signal-regulated kinases 1/2 (ERK1/2), ribosomal protein S6 kinase (RSK), and

nNOS phosphorylation in in F rats. These results indicate that the activation of Rac1 in the brain generates ROS via induced NADPH oxidase, which cause dysfunction of ERK1/2-RSK-nNOS signal pathway in F rats, and this mechanism might be important for the neuropathogenesis of hypertension in fructose-induced hypertension.

Where applicable, the authors confirm that the experiments described here conform with The Physiological Society ethical requirements.

PCA307

Neuronal nitric oxide synthase activation is involved in midkine-mediated cardiovascular effect in the nucleus tractus solitarii

H. Chen[1] and C. Tseng[1,2]

[1]Institute of Clinical Medicine, National Yang-Ming University, Taipei, Taiwan and [2]Department of Medical Education and Research, Kaohsiung Veterans General Hospital, Kaohsiung, Taiwan

The renin-angiotensin system (RAS) plays a central role in the regulation of blood pressure. Neuronal nitric oxide synthases (nNOS) is distributed throughout the central nervous system (CNS) and has been proposed to modulate neuronal activity in the nucleus tractus solitarii (NTS). Previous studies demonstrated that Ang II may modulate central blood pressure effects via (Reactive oxygen species) ROS to downregulate ERK1/2, RSK and nNOS in the NTS. Recent evidence has suggested that midkine is produced in the lung and in turn upregulates angiotensin-converting enzyme (ACE) expression. However, the signalling mechanisms involved in midkine-mediated depressor effects in the NTS remained uncertain. Hence, the aim of this study was to investigate these signalling mechanisms. Male Wistar-Kyoto rats (WKY) were anesthetized with urethane, and blood pressure was monitored intra-arterially. Microinjection of midkine into the NTS produced a dose-dependent decrease in BP and HR, and increased nitrate levels in anesthetized WKY. Midkine was unilaterally microinjected into the NTS, and the cardiovascular effects were evaluated before and after microinjection of the N(5)-(1-imino-3-butenyl)-L-ornithine (vinyl-L-NIO), nNOS-specific inhibitors. This depressor effect of midkine was attenuated after pretreatment with an ACE antagonist. Immunoblotting and immunohistochemical analysis further showed that microinjection of midkine significantly increased the expression of ERK1/2 and also increased nNOS phosphorylation. In contrast, L-NIO, eNOS-specific inhibitor, did not diminish these midkine-mediated effects. However, midkine did affect the nNOS phosphorylation level or nNOS upstream ERK1/2 phosphorylation levels. Furthermore, microinjection of nNOS-specific inhibitor did attenuate midkine-induced depressor effects in the NTS. Taken together, these results suggest that the ERK1/2- nNOS signaling pathway may play a significant role in midkine–mediated central blood pressure regulation.

Where applicable, the authors confirm that the experiments described here conform with The Physiological Society ethical requirements.

PCA308

Cross-talk between Wnt and insulin signaling in central blood pressure regulation

W. Cheng[1,2] and C. Tseng[1,2]

[1]Institute of Clinical Medicine, National Yang-Ming University, Taipei, Taiwan and [2]Department of Medical Education & Research, Kaohsiung Veterans General Hospital, Kaohsiung, Taiwan

The Wnt signaling pathway has implicated in numerous physiological and pathophysiological activities. In addition, recent clinical and in vitro studies reveal that aberrant Wnt signaling is thought to play an important role in the onset of diabetes. Our previous studies also mentioned that insulin plays a role in central blood pressure regulation in the nucleus tractus solitarii (NTS), located at the dorsal part of the brainstem. Nevertheless, the relationship between Wnt signaling and insulin pathway and related modulation of blood pressure in the central nervous system has not been established. In the present study, we postulated that Wnt signaling pathway may improve neuronal insulin resistance and that neuronal insulin resistance is a core mechanism involved in triggering hypertension. Intracerebroventricular administration of Wnt3a (0.9 pmol/per day) produced depressor in both spontaneously hypertensive rats (SHRs) and fructose-fed rats (FFRs). Pretreatment with a low density lipoprotein receptor-related protein (LRP) antagonist, Dickkopf-1 (DKK-1) (1 μg/per day) significantly attenuated the depressor effect and nitric oxide (NO) production evoked by Wnt3a. Additionally, immunoblotting and pharmacological studies further showed that inhibition of LRP6 activity by DKK-1 significantly abolished Wnt3a-induced glycogen synthase kinase 3beta (GSK-3beta)S9, extracellular signal-regulated kinases 1/2 (ERK1/2)T202/Y204, ribosomal protein S6 kinase (RSK)T359/S363, AktS473, insulin receptor substrate (IRS)Y612 phosphorylation and increased IRS1S332 phosphorylation. GSK-3beta was also found to direct bind to IRS1 and induced Ser332 phosphorylation in the NTS. Likewise, administration of GSK-3beta inhibitor (TWS119, 0.173 μg/per day) into the brain decreased blood pressure of SHRs and FFRs through enhancing IRS1 activity. Taken together, these results suggest that the Wnt-LRP6-GSK3beta signaling may as a key regulator of insulin pathway and a potential therapeutic target for essential hypertension.

Where applicable, the authors confirm that the experiments described here conform with The Physiological Society ethical requirements.

PCA309

Neuroprotective effects of acetyl-L-carnitine against ischemia-reperfusion injury: a spin resonance study

O. Tokumaru[1], M. Shimada[2,1], Y. Mizutani[2,1], K. Ogata[1], T. Kitano[3] and I. Yokoi[1,3]

[1]Neurophysiology, Oita University Faculty of Medicine, Yufu, Oita Pref., Japan, [2]Medical Student, Oita University Faculty of Medicine, Yufu, Oita Pref., Japan and [3]Medical Education Center, Oita University Faculty of Medicine, Yufu, Oita Pref., Japan

Acetyl-L-carnitine (ALCAR), a guanidino compound, is reported to be neuroprotective against ischemia-reperfusion injury (IRI).[1,2] Energetically, ALCAR provides acetyl-CoA to TCA cycle to maintain aerobic energetic metabolism in electron-transport system. In addition, it is speculated that ALCAR inhibits

peroxidation of tissue as an antioxidant. The mechanism of neuroprotective effects of ALCAR was investigated by spin resonance analyses; phosphorous NMR (^{31}P-NMR)[3,4] and electron spin resonance spectroscopy (ESR). [4]

Wistar rats (male, 6-wks, 200g, n=5 per group) were used. In each experiment, a rat was deeply anaesthetised with diethyl ether and then decapitated. 400-μm-thick brain slices were loaded into a NMR sample tube and superfused with well oxygenated ACSF with ALCAR (0, 0.1, 1 mM) at 27.5°C. High-energy phosphates in brain slices, phosphocreatine (PCr) and ATP, were non-destructively measured by ^{31}P-NMR (DRX300wb, Bruker, Germany). Brain slices were exposed to IRI by halting the perfusion for 1 hr, followed by the reperfusion for 3 hrs. The ESR measurement of the radical scavenging activity of ALCAR was based on the competitive reaction with spin trapping agent DMPO or *g*-CYPMPO.[5] Antioxidant activity of ALCAR on peroxidation in brain homogenate was also evaluated by thiobarbituric acid reactive substances (TBARS) assay. All experiments were repeated 3-5 times. Values are means ± SEM, compared by ANOVA.

^{31}P-NMR demonstrated significantly better recovery of PCr in brain slices superfused with 0.1 mM ALCAR (72±5%) than control (59±1%; $p<0.05$). But no better recovery was observed with 1 mM ALCAR (59±3%). In ESR study, ALCAR exhibited direct radical scavenging activity for ascorbate free radicals (EC_{50} 0.34 mM), DPPH radicals and methyl radicals in dose-dependent manners ($p<0.05$). On the other hand, ALCAR at mM-order concentrations increased amounts of superoxide anion ($O_2^{\bullet-}$) and hydroxyl radicals (•OH) than control. TBARS assay demonstrated that ALCAR inhibited peroxidation by carbon-centered radicals at concentrations between 0.1 μM and 1 mM ($p<0.05$), whereas peroxidation was doubled at 10 mM. ALCAR did not inhibit peroxidation by •OH. In conclusion, it is speculated that ALCAR might be neuroprotective against IRI in a limited range of concentration (*i.e.* μM-order) through its antioxidant activity attributable to its free radical scavenging activity. Interestingly, ALCAR increased amounts of $O_2^{\bullet-}$ and •OH at concentrations in mM-order which might support the findings by NMR and TBARS assay that ALCAR might not be neuroprotective at mM-order concentration.

Supported by JSPS KAKENHI to OT (#24592304), TK (#23592259 and IY (#23592099).

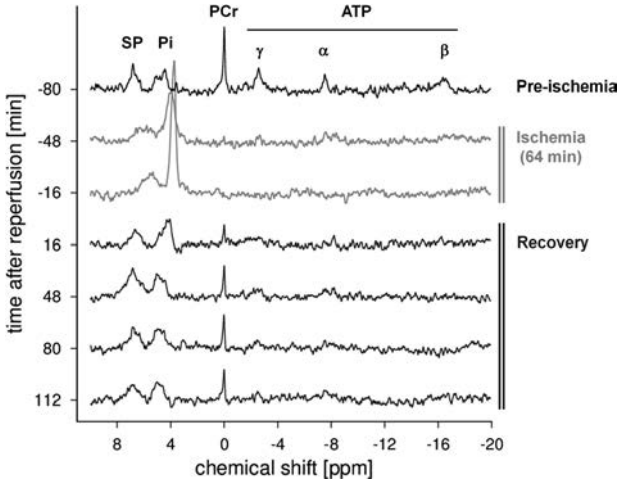

Figure 1. ^{31}P-NMR spectra of rat brain slices. The peaks correspond to, from left to right, sugar phosphate (SP), inorganic phosphate (Pi), phosphocreatine (PCr), γ-, α- and β-phosphate of ATP. During the ischemia, high-energy phosphate substrates, PCr and ATP, were decreased to undetectable levels. After the reperfusion, the peak amplitudes of PCr and ATP recovered to about 60% of the pre-ischemic levels.

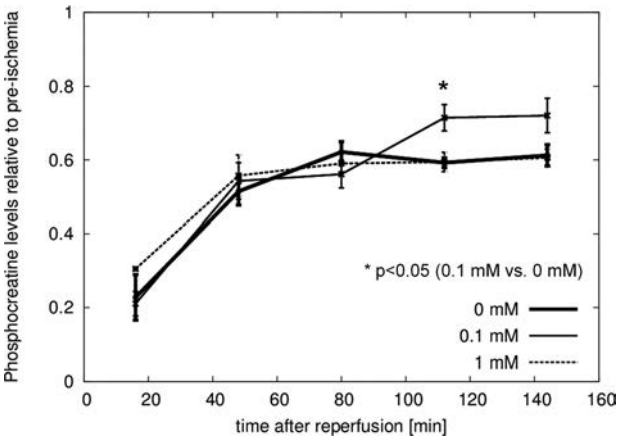

Figure 2. Recovery of phosphocreatine levels after ischemia-reperfusion injury. Values are given relative to pre-ischemic level. PCr had a significantly better recovery when superfused with ACSF with 0.1 mM ALCAR than control ($p<0.05$).

Zanelli SA et al. (2005). *Ann N Y Acad Sci* **1053**,153-161

Elinos-Calderon D et al. (2009). *Exp Brain Res* **197**, 287-296

Tokumaru O et al. (2006). *J Neurosurg* **105(Suppl)** , 202–207

Tokumaru O et al. (2009). *Neurochem Res* **34**, 775-785

Kamibayashi M et al. (2006). *Free Radic Res* **40**, 1166-1172

The authors sincerely thank Dr. M. Kamibayashi for supplying *g*-CYPMPO.

Where applicable, the authors confirm that the experiments described here conform with The Physiological Society ethical requirements.

PCA310

BACE1 overexpression shifts glucose metabolism toward aerobic glycolysis in SH-SY5Y cells

J. Findlay, D. Hamilton, P. Meakin and M. Ashford

Medical Research Institute, University of Dundee, Dundee, Angus, UK

Alzheimer's Disease (AD) is the most common cause of dementia and currently there is no cure or means to slow disease progression. This represents a clear, unmet medical need in light of the ageing population worldwide. While much of the current AD research focuses on the hallmark pathologies (amyloid plaques and neurofibrillary tangles), their appearance is extremely end stage and therapeutic interventions aimed at alleviating them have failed to halt symptom progression. It may therefore be beneficial to look at earlier events, with reduced glucose metabolism and a regional switch to aerobic glycolysis among the earliest changes reported in the AD brain (1, 2). Glucose is a required substrate for neuronal function and important for the induction of long-term potentiation (3) and the consolidation of short to long-term memories. Evidence suggests the aspartyl protease β-site Amyloid precursor protein Cleaving Enzyme 1 (BACE1) as a key enzyme in the aetiology of AD. Previous work from our laboratory has also suggested a role in metabolism, with BACE1 knock out mice displaying enhanced whole-body glucose disposal and insulin sensitivity (4). We have also previously shown that BACE1 overexpression impairs glucose metabolism in neuronal cells (5). This study aimed to further investigate the role of BACE1 in neuronal glucose metabolism. We utilised the human SH-SY5Y neuronal cell line stably overexpressing BACE1. Pyru-

vate dehydrogenase (PDH) activity was determined by activity assay (Mitosciences). A Seahorse extracellular flux analyser was used to determine cellular respiration in real-time. All data are expressed as mean ± standard error of the mean, and statistical significance determined by Student's t-test. Chronic elevation in BACE1 resulted in impaired functioning of a key fuel-partitioning enzyme, PDH (activity reduced to 69 ± 8 per cent, $p < 0.05$, n=6). This reduced substrate delivery to the mitochondria and increased reliance upon aerobic glycolysis for ATP generation (oxygen consumption rate (OCR) reduced to 65 ± 9%, $p < 0.01$, n=7 and extracellular acidification rate (ECAR) increased to 165 ± 16%, $p < 0.01$, n=7). These deficits were significantly attenuated by treatment with the PDH kinase inhibitor dicholoracetate (DCA, 10μM). Thus BACE1 overexpression impairs neuronal glucose oxidation resulting in an increased reliance upon aerobic glycolysis for ATP generation. Therefore this BACE1-dependent change in metabolism may account for some of the earliest clinical observations in people who later develop AD.

Craft S et al. (1992) J Clin Exp Neuropsychol 14, 253-267

Vlassenko AG et al. (2010) PNAS 107, 17763-17767

Yousef FF et al. (2009) West Indian Med J. 58, 410-416

Meakin PJ et al. (2012) Biochem J 441, 285-296

Findlay JA et al. Physiology 2012

Where applicable, the authors confirm that the experiments described here conform with The Physiological Society ethical requirements.

PCA311

Recurrent low glucose exposure attenuates α1AMPK activity and reduces basal metabolism in GT1-7 neurons

E.A. Haythorne, D. Hamilton, C. Beall, J. Findlay, M. Ashford and R. McCrimmon

Medical Research Institute, University of Dundee, Dundee, Angus, UK

The major limiting factor in the successful management of type 1 diabetes is Recurrent Hypoglycaemia (RH), resulting from supraphysiological insulin supplementation, which attenuates the Counterregulatory Response (CRR) to future hypoglycaemic episodes. It is now widely accepted that the hypothalamus contributes to hypoglycaemia detection and activation of the CRR (1). Within the hypothalamus, glucose-sensing (GS) neurons exist which are thought to contain the same glucose sensing cellular machinery as pancreatic β-cells, such as ATP-sensitive K+ channels (K_{ATP}), glucokinase, glucose transporter proteins and AMPK (2). Therefore, we hypothesise that disruption of normal function in these specialised neurons may occur following RH. We have previously shown that mouse hypothalamic GT1-7 cells are GS neurons (3) and display impaired electrical activity to low glucose following RH, independent of changes in glucose uptake/oxidation (4). Here we have investigated AMPK activity and mitochondrial function as possible mediators of altered electrical activity following RH.

GT1-7 cells were exposed to 3 hours of low (0.1 mM) glucose for 3 days to model RH, with cells being assayed on day 4. AMPK activity was measured by radiolabelled kinase activity assay. Cellular Oxygen Consumption Rate (OCR) was measured under euglycaemic conditions using an XF24 extracellular flux analyser (Seahorse Bioscience, Inc.). All data sets are expressed as means ± standard error of the mean. Statistical analysis was performed using either Student's t-test or ANOVA.

Following RH of GT1-7 cells, the normal increment in α1AMPK activity to 0.1 mM glucose stimulus was significantly attenuated after 15 minute (RH = 0.97 fold ± 0.31 vs. Cont = 1.48 fold ± 0.09, $p<0.01$; n = 7) and 3 hour incubations (RH = 1.07 fold ± 0.20 vs. Cont = 3.98 fold ± 0.67, $p<0.001$; n=7). α2AMPK activity was not significantly perturbed and no change in AMPK subunit expression was observed following RH. Additionally there were no significant changes in total or phosphorylated protein levels of the upstream AMPK activating kinases, TAK1 or LKB1. Examination of mitochondrial function following RH showed no change in spare respiratory capacity or the proportion of OCR contributing to ATP synthesis. However, RH significantly reduced basal OCR of GT1-7 cells (RH = 4.85 ± 0.87 vs. Cont = 8.10 ± 0.60 pmoles O_2/min/μg, $p<0.05$; n=5).

We conclude that blunted α1AMPK activation to low glucose following RH reduces substrate flux through the oxidative phosphorylation pathway in association with defective GS of hypothalamic neurons.

Borg WP *et al*. (1994) J Clin Invest. **93**:1677-82

Levin BE *et al*. (2004) Diabetes. **53**:2521-8

Beall C *et al*. (2012) Diabetologia **55**:2432-2444

Haythorne EA *et al*. Physiology 2012

Where applicable, the authors confirm that the experiments described here conform with The Physiological Society ethical requirements.

PCA312

A novel role for IL-6 in the suppression of hypothalamic glucose sensing

G.T. Denwood, K.R. Watterson, A.H. Gardiner, K.L. Ward, E.A. Haythorne, L. Hamilton, K.A. Wright, F.B. Ashford, M.L. Ashford and R.J. McCrimmon

Medical Research Institute, University of Dundee, Dundee, UK

Repeated exposure to hypoglycemia leads to suppression of normal counter-regulatory responses (CRR) to hypoglycemia; increasing severe hypoglycemia risk. The mechanism underlying this is unknown, but believed to result primarily from defective glucose-sensing within the ventromedial hypothalamus (VMH). Hypoglycemia evokes a significant systemic and local stress response with an increase in inflammatory mediators such as interleukin-6 (IL-6). In this study, we sought to determine if IL-6 affected hypothalamic glucose-sensing by examining its action on hypoglycemia-induced changes in membrane potential and AMPK activity in a mouse hypothalamic glucose-sensing cell line (GT1-7) and mouse hypothalamic *ex vivo* slices.

Perforated-patch electrophysiological recordings of GT1-7 cells investigated the acute and chronic effects of IL-6 (5ng/ml and 20ng/ml) on acute hypoglycemia (0.5mM glucose)-induced membrane hyperpolarization. Acute exposure of GT1-7 cells to 5ng/ml and 20ng/ml IL-6 had no significant hyperpolarizing effect during hypoglycemia (0.5mM). Contrastingly, antecedent 3 hour exposure to 5ng/ml IL-6 followed by a 24 hour recovery period significantly attenuated the response of GT1-7 cells to 0.5mM ($\Delta V_{Control}$ = 13.4 ± 1.3mV vs ΔV_{IL6} = 8.6 ± 2.0mV, $p<0.05$; n=10-13). Additionally, IL-6 was found to significantly increase acute AMPK activity in mouse VMH *ex vivo* slices and GT1-7 cells, as demonstrated by increased AMPK phosphorylation, increased phosphorylation of ACC and direct AMPK activity assay compared to controls. Moreover,

antecedent 3 hour exposure of GT1-7 cells to 5ng/ml IL-6 attenuated subsequent hypoglycemia-induced AMPK phosphorylation.
Thus, prior exposure of hypothalamic GT1-7 cells and VMH *ex vivo* slices to IL-6 reduced their responsiveness to a subsequent hypoglycemia challenge. We conclude that rises in systemic or local IL-6 may contribute, at least in part, to hypoglycemia-induced suppression of hypothalamic glucose-sensing.

Where applicable, the authors confirm that the experiments described here conform with The Physiological Society ethical requirements.

PCA313

Role of (Pro)renin receptor in cell proliferation

K. Ohba[1], K. Kaneko[1], H. Nishiyama[1], T. Hirose[2], K. Totsune[3] and K. Takahashi[1]

[1]Department of Endocrinology and Applied Medical Science, Tohoku University Graduate School of Medicine, Sendai, Japan, [2]Department of Planning for Drug Development and Clinical Evaluation, Tohoku University Graduate School of Pharmaceutical Sciences and Medicine, Sendai, Japan and [3]Department of Social Welfare, Tohoku Fukushi University, Sendai, Japan

(Pro)renin receptor ((P)RR) is a specific receptor for renin and prorenin, and is a new component of the renin angiotensin system (RAS) (1, 2). When bound to prorenin, (P)RR activates the angiotensin I-generating activity of prorenin in the absence of cleavage of the prosegment. Moreover, binding of (pro)renin to (P)RR directly activates MAPK ERK1/2 independently of the RAS. The gene encoding for PRR is named ATP6ap2 (ATPase 6 accessory protein 2), and (P)RR was initially found as a truncated form co-purifying with V-ATPase (vacuolar H^+-ATPase). The association of (P)RR and V-ATPase has been shown to be functional and essential for the survival of certain cells. Furthermore, (P)RR is involved in the Wnt/β-catenin pathway. It is therefore likely that (P)RR has an important role in the physiology and pathophysiology of cell proliferation. The aim of the present study is therefore to clarify the role of (P)RR in cell proliferation. Cultured human breast carcinoma cell lines were used in the present study. Western blot analysis (3) showed expression of (P)RR protein in all 4 breast carcinoma cell lines examined; MCF-7, T47D, SK-BR-3 and MDA-MB-231. Transfection of (P)RR specific small interference RNA decreased cell proliferations in breast carcinoma cell lines. Treatment with angiotensin II did not stimulate cell proliferation or phosphorylation of ERK1/2 in cultured breast carcinoma cells, suggesting that the stimulatory effect of (P)RR on cell proliferation occurred independently of the RAS. By contrast, treatment with prorenin increased phosphorylation of ERK1/2 in these cells. Treatment of bafilomycin A_1, an inhibitor of V-ATPase, greatly inhibited cell proliferation of human breast carcinoma cells. These findings suggest that (P)RR stimulates cell proliferation independently of the RAS, possibly via the stimulation of ERK1/2 and/or the function of V-ATPase. The present study has raised the possibility that (P)RR is a novel target for the development of the new therapies, not only in cardiovascular, renal diseases including diabetic nephropathy (4), but also in proliferative diseases including cancers.

Nguyen G *et al.* (2002) *J Clin Invest* **109**, 1417-1427.

Nguyen G (2011) *Clin Sci (Lond)* **120**, 169-178.

Hirose T *et al.* (2009) *Peptides* **30**, 2316-2322.

Takahashi K *et al.* (2010) *Peptides* **31**, 1405-1408.

Where applicable, the authors confirm that the experiments described here conform with The Physiological Society ethical requirements.

PCA314

A central role of E3 ubiquitin ligase MG53 in insulin resistance and metabolic disorders

Y. Zhang[1], R. Song[1], W. Peng[1], F. Lv[1], C. Cao[1] and R. Xiao[1,2]

[1]Institute of Molecular Medicine, State Key Laboratory of Biomembrane and Membrane Biotechnology, Peking University, Beijing, China and [2]Center for Life Sciences, Peking University, Beijing, China

Insulin resistance is a fundamental pathogenic factor shared by various metabolic disorders[1]. While skeletal muscle accounts for 70-90% of insulin-stimulated glucose disposal, the mechanism underlying muscle insulin resistance is poorly understood. MG53, also named TRIM72, is expressed in striated muscle and implicated in cell membrane repair and cardiac ischemic pre- and post-conditioning[2-4]. Here we show that MG53 acts as an E3 ligase targeting insulin receptor (IR) and insulin receptor substrate 1 (IRS1) for ubiquitin-dependent degradation, and when upregulated, causes metabolic disorders.
MG53 is markedly elevated in the skeletal muscle of insulin resistance models. After 35 weeks on high fat diet (HFD), wild type (wt) mice developed metabolic syndrome featuring obesity, hypertension, hyperglycemia and hyperinsulinemia. In contrast, MG53-difficient (mg53-/-) mice were resistant to HFD-induced metabolic disorders. Concomitantly, 35-week HFD induced significant glucose intolerance and insulin resistance in wt, but not in mg53-/-, mice. Furthermore, MG53 transgenic (mg53 TG) mice on regular chow diet developed metabolic syndrome characterized by obesity, hypertensive, hyperinsulinemia, along with severe glucose intolerance and insulin resistance at 38 weeks of age. These results indicate that upregulation of MG53 is both necessary and sufficient to cause systemic insulin resistance and metabolic syndrome.
Insulin signaling involves tyrosine phosphorylation of IR and IRS1, and subsequent activation of PI3K-Akt signaling pathway[5]. Mechanistically, MG53 acts as an E3 ligase which targets IR and IRS1 for ubiquitin-dependent degradation, constituting a central mechanism controlling insulin signal strength in skeletal muscle. Specifically, in skeletal muscle from mg53 TG mice or wt mice on HFD, insulin-stimulated activation of IR, IRS1 and Akt was profoundly impaired. The suppressed insulin signaling is associated with posttranscriptional downregulation of IR and IRS1 via ubiquitin-dependent degradation. Importantly, in mg53-/- mice, HFD had no significant effect on IR and IRS1 protein abundance or insulin signaling efficiency. Taken together, we have shown, for the first time, that elevated MG53 expression is sufficient and necessary for HFD-mediated downregulation of IR and IRS1 and subsequent suppression of insulin signaling in skeletal muscle. These findings define MG53 as a novel therapeutic target for treating metabolic disorders and associated cardiovascular complications.

Eckel RH, Grundy SM, and Zimmet PZ The metabolic syndrome. Lancet, 2005,365:1415-1428.

Cai C, Masumiya H, Weisleder N, Matsuda N, Nishi M, Hwang M, Ko JK, Lin P, Thornton A, Zhao X, Pan Z, Komazaki S, Brotto M, Takeshima H, and Ma J MG53 nucleates assembly of cell membrane repair machinery. Nat Cell Biol, 2009,11:56-64.

Cao CM, Zhang Y, Weisleder N, Ferrante C, Wang X, Lv F, Zhang Y, Song R, Hwang M, Jin L, Guo J, Peng W, Li G, Nishi M, Takeshima H, Ma J, and Xiao RP MG53 constitutes a primary determinant of cardiac ischemic preconditioning. Circulation, 2010,121:2565-2574.

Zhang Y, Lv F, Jin L, Peng W, Song R, Ma J, Cao CM, and Xiao RP MG53 participates in ischaemic postconditioning through the RISK signalling pathway. Cardiovasc Res, 2011,91:108-115.

Saltiel AR and Kahn CR Insulin signalling and the regulation of glucose and lipid metabolism. Nature, 2001,414:799-806.

This work was supported by the National Basic Research Program of China (2012CB518000, 2013CB531200, 2012CB944501), the National Natural Science Foundation of China (81070674, 81070116, 81130073 and 81170100).

Yan Zhang is the recipient of the travel awards for young physiologists from the Chinese Association for Physiological Sciences (CAPS).

Where applicable, the authors confirm that the experiments described here conform with The Physiological Society ethical requirements.

PCA315

Connexin 36 signalling during intercellular communication within pancreatic islets

D. Penko[1,2], H.S. Peiris[3,4], P.H. Coates[1,2], C.S. Bonder[1,5] and C.F. Jessup[3,4]

[1]School of Medicine, University of Adelaide, Adelaide, SA, Australia, [2]Central Northern Adelaide Renal and Transplantation Service, Royal Adelaide Hospital, Adelaide, SA, Australia, [3]Department of Human Physiology, Flinders University of SA, Bedford Park, SA, Australia, [4]Centre for Neuroscience, Flinders University of SA, Bedford Park, SA, Australia and [5]Centre for Cancer Biology, SA Pathology, Adelaide, SA, Australia

Type 2 diabetes mellitus remains an enormous health burden – there are over 300 million sufferers worldwide (1) and 20% of the US healthcare budget is spent on caring for people with diabetes (2). Pancreatic islet dysfunction underlies the development of diabetes. While it is recognised that communication between cells within the islet is essential for proper function, the mechanism responsible is unknown. Connexin 36 is expressed on insulin-producing beta cells, is important for coordinated pulsatile insulin release and may be involved in intercellular communication within pancreatic islets (3). The interaction between pancreatic islets and endothelial cells was investigated *in vitro*. Pancreatic islets were isolated from male C57B6 mice by infusion of collagenase into the pancreatic duct *in situ* followed by digestion at 37°C and density purification. Endothelial cells were grown from C57B6 bone marrow by culture on fibronectin in defined media for one week and confirmed to express endothelial markers (CD31 and E-selectin), bind lectin and uptake acetylated low-density lipoprotein by flow cytometry. To investigate soluble mechanisms, islets were cultured (10 islets per well) with endothelial cell-conditioned medium for 3 days and tested for glucose-stimulated insulin release. Secreted insulin was detected by high-sensitivity ELISA and corrected for total protein and stimulation indices were calculated as insulin secretion at high glucose (20 mM) divided by basal insulin secretion (at 3 mM glucose). Values are means±SEM compared by unpaired t-tests. Endothelial cell-conditioned islets had an increased level of basal insulin release (0.7±0.22 ng/min/mg total protein; n=7) compared to controls (0.2±0.04 ng/min/mg total protein; n=6; p=0.05). However, they had a reduced ability to upregulate insulin release in response to high glucose (stimulation index = 1.3±0.5 compared to 4.2±0.9 for controls; p=0.01). Effects on gene expression were analysed by real-time PCR using Taqman primers (normalizing to the house-keeping gene *B2m*) following 3 day non-contact co-cultures where islets (25 islets per well) were cultured in transwells (0.4 μm pores) above endothelial monolayers. Co-cultured islets significantly down-regulated the expression of connexin 36 (0.4±0.05 fold relative to control islets; n=18; p=0.04). There was no difference in expression of the Insulin gene between groups. These data suggest that connexin 36 expression is modulated during intercellular communication between beta cells and endothelial cells, resulting in dysregulated insulin *release*. We suggest this represents a 'survival' islet phenotype, where baseline insulin secretion is maintained during vascular remodelling. This mechanism may have relevance for islet physiology, where the function and survival of beta cells is critically dependent on the presence of intra-islet vascular endothelium.

World Health Organisation. Diabetes Fact Sheet No 312. Sept 2012.

Herman WH. The economics of diabetes prevention. Med Clin North Am. 2011 Mar;95(2):373-84.

Head WS, Orseth ML, Nunemaker CS, Satin LS, Piston DW, Benninger RK. Connexin-36 gap junctions regulate in vivo first- and second-phase insulin secretion dynamics and glucose tolerance in the conscious mouse. Diabetes. 2012 Jul;61(7):1700-7.

Where applicable, the authors confirm that the experiments described here conform with The Physiological Society ethical requirements.

PCA316

Estrogenic effects of ginsenoside Rg1 in endometrial Ishikawa cells and neuroblastoma SK-N-SH cells were not observed in preosteoblast MC3T3-E1 cells

W. Chen and Q. Gao

Physiology, Qingdao University, Qingdao, China

Ginseng has been used as a medicine for over two thousand years. Studies have showed that ginseng could relieve menopausal symptoms, bleeding disorders, sleeping disorders, depression, anxiety etc. Ginsenoside Rg1 is the major pharmacologically active compound of ginseng. Our previous studies clearly demonstrated the estrogenic activities of Rg1 in human breast cancer MCF-7 cells. However, it is unclear if Rg1 exert selective estrogenic effects in other cell types in vitro. The present study was designed to determine the selective estrogenic effects of ginsenoside Rg1 by using endometrial, neuroblastoma and preosteoblast cell lines. The endometrial Ishikawa cells, neuroblastoma SK-N-SH cells and preosteoblast MC3T3-E1 cells were cultured in phenol-red free DMEM supplemented with 5% sFBS and were treated with different dosage of Rg1(0.0001-1μM, n=3) and 17β-estradiol (0.01μ M, n=3). MTT method was used to detect the cell viability. The western blot was used to detect the protein expressions of mitogen-activated protein kinase kinase (MEK) and estrogen receptor α (ERα). The activity of estrogen responsive element (ERE) promoter was detected by Dual Luciferase Assay. Treatment of three kinds of cells with various concentrations of Rg1 (0.0001-1μM) had no stimulatory effect on cell number. Rg1 significantly increased estrogen receptor-dependent alkaline phosphatase activity in Ishikawa cells (0.0001μM: 1.34±0.081, 0.01μM: 1.28±0.049, 1μM: 1.22±0.023 vs control 1.00±0.018, P<0.01) but not in MC3T3-E1 cells. Similar to estrogen, Rg1 treatment induced the phosphorylation of MEK

(0.0001μM: 1.42±0.075, 0.01μM: 1.42±0.103, 1μM: 1.65±0.117 vs control 1.00±0.030, P<0.05) and ERα (0.0001μM: 1.47±0.049, 0.01μM: 1.72±0.035, 1μM: 2.02±0.100 vs control 1.00±0.029, P<0.05) in a dose-dependent manner in Ishikawa cells. Similar effects were obtained in neuroblastoma SK-N-SH cells. Cells transfected with the ERE-luciferase reporter construct exhibited significantly increased ERE-luciferase activity in the Rg1 presence in Ishikawa cells (0.0001μM: 1.69±0.094, 0.01μM: 1.79±0.108, 1μM: 2.03±0.194 vs control 1.00±0.134, P<0.05) and neuroblastoma SK-N-SH cells (0.01μM: 2.70±0.235 vs control 1.00±0.231, P<0.01), suggesting that the estrogenic effects of Rg1 were mediated through the endogenous ERs. In contrast, Rg1 did not induce any estrogenic responses in preosteoblast MC3T3-E1 cells. Our results suggest that the estrogenic effects of Rg1 are distinct from those of estradiol and are cell type selective. Further study is needed to characterize the action by which Rg1 exerts tissue-selective estrogenic effects in vivo.

Christensen LP. Ginsenoside chemistry, biosynthesis, analysis, and potential effects. Adv Food Nutr Res 2009; 55:1-99.

Geller SE, Studee L. Botanical and dietary supplements for mood and anxiety in menopausal women. Menopause 2007;14:541-549.

Lau WS, Chen WF, Chan RY, Guo DA, Wong MS. Mitogen-activated protein kinase (MAPK) pathway mediates the oestrogen-like activities of ginsenoside Rg1 in human breast cancer (MCF-7) cells. Br J Pharmacol 2009; 156:1136-1146.

This work was supported by National Natural Science Foundation of China (31271150) and Qingdao Municipal Science and Technology Bureau [11-2-4-2-(23)-jch]

Where applicable, the authors confirm that the experiments described here conform with The Physiological Society ethical requirements.

PCA317

Effect of secretory products of colon cancer cells on the cancer-associated fibroblasts: The reverse Warburg effect

Y. Kim[1], H. Shin[1,3], Y. Chun[1,2], C. Cho[1,3] and J. Park[1,3]

[1]pharmacology, Seoul National University College of medicine, Seoul, Republic of Korea, [2]physiology, Seoul National University college of medicine, Seoul, Republic of Korea and [3]Ischmic/hypoxic disease institute, Seoul National University college of medicine, Seoul, Republic of Korea

Tumor microenvironment is composed of malignant epithelial cells and stromal components including fibroblasts, endothelial cells, and inflammatory cells. Especially, cancer-associated fibroblasts (CAFs) are known to play a key role in tumor progression, metastasis as well as drug resistance. Cancer cells utilize the high-energy metabolites from aerobic glycolysis in fibroblast cells for tumor growth and metastasis, which was called as the reverse Warburg effect. To confirm whether the secretory products from cancer cells induce the reverse Warburg phenomenon in CAFs, we incubated mouse embryonic fibroblasts (MEFs) and human colon fibroblast cells (CCD-18CO) with the HCT116 colon cancer cell conditioned media. Then we observed that cancer conditioned media indeed induced the autophagy and/or mitophagy in fibroblast cells. After treated with the cancer conditioned media, the induction of LC3, a marker of autophagy, in fibroblasts were confirmed. The autophagophores as well as autophagosomes were visualized by GFP-LC3 system and Transmission electron microscopy (TEM). Also, we found that the conditioned media from normoxic HCT116 cells could lead to the autophagy in fibroblasts, but that from hypoxic HCT116 cells could not, which means that hypoxic microenvironmental milieu also may influence the tumor-fibroblasts interactions. Interestingly, both HIF-1/2αs were upregulated in normoxic MEFs when they were treated with the conditioned media from normoxic status of cancer cells. But the conditioned media from hypoxic cancer cells increased the HIF-1/2αs much less than that from normoxic ones. In addition, the cancer conditioned media increased the migration potential of fibroblsts, which was observed by F-actin staining. In summary, the secretory products from epithelial cancer cells may induce the autophagy of fibroblasts including mitochondrial degradation and dysfunction. The illumination of key factors in cancer secretome could help to understand the cancer-fibroblasts interaction as well as acquire the novel therapeutic targets in oncologic fields.

Sotgia F et al .(2012) Cell Cycle. 11:7, 1445-1454

Guido C et al.(2012) Oncotarget. 3:8, 798-810.

Where applicable, the authors confirm that the experiments described here conform with The Physiological Society ethical requirements.

PCA318

SIRT1 differentially regulates HIF-1a and HIF-2a activities under hypoxia

H. Yoon and J. Park

pharmacollogy, the college of medicine, seoul national univercity, Seoul, seoul, Republic of Korea

Cancer cells should accommodate to oxygen- and energy-deficient microenvironment to keep growing. The transcription factors HIF-1a and HIF-2a sense the oxygen state, and express hypoxia-induced genes. The deacetylase SIRT1 senses the energy or redox state, and modulates activities of transcription factors that express metabolic genes. Previously, two studies demonstrated that SIRT1 deacetylates HIF-1a at K674 or HIF-2a at K741 and that SIRT1 inactivates HIF-1a but activates HIF-2a. Yet, how SIRT1 differentially regulates HIF- as is uncertain so far. We here tried to clarify the roles of SIRT1 in HIF-1a and HIF-2a regulations. In the present study, we established two assay systems to separately evaluate SIRT1's actions on two HIF-a s; that is, immnoblotting with specific antibodies to acetylated HIF-1a_K674 or acetylated HIF-2a_K741 and reporter assay using Gal4(DBD)-HIF-1a(TAD) or Gal4(DBD)-HIF-2a(TAD), both of which contain the SIRT1 target sites. Consequently, PCAF acetylated the two lysine residues of HIF- as, which was reversed by SIRT1. Also, we confirmed the opposing actions of SIRT1 on HIF-1 and HIF-2 driven transcriptions, namely, it negatively and positively regulated HIF-1 and HIF-2, respectively. RT-PCR analyses showed that SIRT1 reduced mRNA levels of HIF-1 target genes but enhanced those of HIF-2 target genes. These results further support the differential roles of SIRT1 in HIF-1 and HIF-2 signaling under hypoxia. As one of two HIF- as tends to be chosen as a major adaptive factor during tumor evolution, the selective modulation of HIF-1 and HIF-2 signaling can be a promising strategy for cancer therapy. In this aspect, SIRT1 could be a candidate target to develop tailor-made cancer therapy for patients.

Key words: SIRT1, HIF-1a, HIF-2a, hypoxia, cancer

Science. 2009 Jun 5;324(5932):1289-93. doi: 10.1126/science.1169956.

Regulation of hypoxia-inducible factor 2alpha signaling by the stress-responsive deacetylase sirtuin 1.

Dioum EM, Chen R, Alexander MS, Zhang Q, Hogg RT, Gerard RD, Garcia JA.

Mol Cell. 2010 Jun 25;38(6):864-78. doi: 10.1016/j.molcel.2010.05.023.

Sirtuin 1 modulates cellular responses to hypoxia by deacetylating hypoxia-inducible factor 1alpha.

Lim JH, Lee YM, Chun YS, Chen J, Kim JE, Park JW.

J Biol Chem. 2009 Jul 31;284(31):20917-26. doi: 10.1074/jbc.M109.020073. Epub 2009 Jun 2.

Sirtuin 1 functionally and physically interacts with disruptor of telomeric silencing-1 to regulate alpha-ENaC transcription in collecting duct.

Zhang D, Li S, Cruz P, Kone BC.

Nat Rev Cancer. 2011 Dec 15;12(1):9-22. doi: 10.1038/nrc3183.

HIF1α and HIF2α: sibling rivalry in hypoxic tumour growth and progression.

Keith B, Johnson RS, Simon MC.

Where applicable, the authors confirm that the experiments described here conform with The Physiological Society ethical requirements.

PCA319

Green tea (GMB4 clone) catechins influences the retinoid-related orphan receptor α (ROR-α) and CCAAT/enhancer binding protein-α (C/EBP-α) expression in primary cultured of preadipocyte

R. Ratnawati[1], F.K. Hasniy[1], D. Lyrawati[2] and C. Ciptati[3]

[1]Physiology, Brawijaya University, Malang, Jawa Timur, Indonesia, [2]Clinical Pharmacy, Brawijaya University, Malang, Jawa Timur, Indonesia and [3]Chemistry Devision, Institute Technology Bandung, Bandung, Jawa Barat, Indonesia

Background: Obesity is a major risk factor for the development of chronic diseases and mortality. At the cellular level, increasing number and size of adipocytes diferentiated from preadipocytes characterized the obesity. Excess intake of sugars and lipids causes obesity, but certain food components have been reported to reduce the risk of obesity. Catechins, the active constituent of green tea has been regarded beneficial as an anti-obesity. Our previous study has showed that catechins from green tea GMB4 clone inhibited differentiation of preadipocytes, reduced PPARy and increased the adiponectinn level in preadipocytes culture (Ratnawati et al, 2011) and EGCG also decreased C/EBPα and leptin (Ratnawati et al, 2012). Therefore in this study, we investigated the effect of catechins on the positive and negative regulators of lipogenesis and adipogenesis; ROR-α and C/EBP-α.
Method: This study is done in primary cultured of preadipocyte with 4 groups of treatment : (1) control, (2) treated with catechins 5 μM, (3) treated with catechins 10 μM and (4) treated with catechins 30 μM. 2 days post confluence, cell were induce to differentiate into adipocyte with IBMX, DEX and insulin. On days 3 during differentiation, cells were treated with catechins for 24 hour. Cells then harvested and measurement of ROR-α and C/EBP-α were done by ELISA and Immunocytochemistry.
Results: In this study we found that catechins significantly reduced the expression of C/EBP-α by 20%, 24% dan 26,43%. . We found that ROR-α expression increased, but not reach statistical significance.
Conclusion: This results suggested that catechins at least in part inhibit adipogenesis through C/EBP-α. Studies are needed to see whether higher doses of catechins will exert further increase on ROR- expression and/or its activity.

Ratnawati et al, 2011, Proceeding 7th Congress FAOPS

Ratnawati et al 2012, MIFI, in press

Where applicable, the authors confirm that the experiments described here conform with The Physiological Society ethical requirements.

PCA320

The use of bioinformatics to prioritise palmitoylation enzyme isoforms as novel research targets

B. Adeyileka, L. Davies, A. Dempsey, S. Falconer and N. Donohoe

Pharmacy and Life Sciences, Robert Gordon University, Aberdeen, UK

Post-translation lipid modification has been shown to alter the trafficking, targeting and function of a wide range of membrane proteins. Palmitoylation, one type of lipid modification, involves the thioester linkage of palmitate molecules to specific cysteine residues. Palmitoylation is undertaken by a group of 23 palmitoyl-acyl-tranferase (PAT) enzymes which contain a ZDHHC (zinc-finger and aspartate-histidine-histidine-cysteine) motif(1). The potential role of PAT enzymes in physiological control mechanisms, in the causation of disease and as therapeutic targets is the focus of considerable research (2,3,4). This study uses a bioinformatics approach to screen the genomic and proteomic data available for human PATs in order to identify and prioritise isoforms for future laboratory and clinical investigation.
Genomic and proteomic information from the National Centre for Biotechnology Information (NCBI), GeneCards and Uniprot databases was collated and analysed to identify: (a) the number of non-synonymous single-nucleotide polymorphisms (nsSNPs) in PAT genes; (b) their location; and (c) PAT splice variants. The potential of nsSNP to produce damage was analysed using the pre-formulated prediction software systems SNAP, SIFT, Panther, PolyPhen and MutPred as well as damage-prediction scoring system that assigns a damaging score based upon the nature of resulting amino acid (AA) substitutions and their location on functionally important motifs on proteins. An initial screen identified 21,291 nsSNPs, with ~1% displaying high scores (> 50% threshold or equivalent) on the damage–prediction scoring system. Further analysis lead to the prioritisation of six nsSNP candidates; rs111416789 (zDHHC8), rs137852214 (zDHHC9), rs138835172, rs11552044, rs149584176 and rs147199543 (zDHHC24). These nsSNPs are of particular interest due to the nature of the resulting AA substitutions, the close proximity of the substitutions to the enzyme active site and areas involved in post-translational modification, such as palmitoylation and phosphorylation sites.
Prioritised nsSNPs will be examined to determine the functional impact of the resulting amino acid changes in the PAT proteins in laboratory based expression systems and assays; those found to alter PAT function will be investigated with respect to their distribution and incidence within appropriate populations and disease groups.

Fukata M, et al. Methods, 2006; 40(2), p177–182

Berchtold LA, et al. PNAS, 2011; 108(37), pE681-E688

Young FB, et al. Prog. Neurobiol., 2012 May; 97(2), p220-238

EBI. European Bioinformatics Institute Gene and Protein. Cambridge, UK: European Bioinformatics

Dr I. Rowe and Dr S. Cruickshank

The Robert Gordon University

The Institute for Health and Welfare Research

Where applicable, the authors confirm that the experiments described here conform with The Physiological Society ethical requirements.

PCA321

The metabolic profile of pregnant mice fed a diet high in sugar and fat

B. Musial[1,2], S.E. Ozanne[2], A.L. Fowden[1] and A.N. Sferruzzi-Perri[1]

[1]Physiology, Development and Neuroscience, University of Cambridge, Cambridge, UK and [2]Institute of Metabolic Sciences, University of Cambridge, Cambridge, UK

Background: Diets high in sugar and fat (HSHF) are commonly eaten by women of reproductive age and contribute to the increasing prevalence of obesity during pregnancy. In animals, obesogenic diets fed during pregnancy alter the metabolic phenotype of the adult offspring (1) but little is known about the mechanisms involved prenatally. Preliminary work has shown that feeding a HSHF diet throughout mouse pregnancy increased maternal adiposity, glucose and insulin levels, but reduced insulin like growth factor (IGF-I) and fetal growth (2). This project examined the effect of a HSHF diet on the fat content and expression of proteins involved in insulin/IGF-I signalling and lipid metabolism in the maternal liver, muscle and white adipose tissue (WAT) in late pregnancy.

Methods: C57BL6 mice were fed a control diet (energy from fat 11%, sugar 3%) or a HSHF diet (energy; fat 30%, sugar 36%) from day (D)1 of pregnancy (term D20). On D16 and D19, dams were killed and maternal liver, biceps femoralis and retroperitoneal WAT and were dissected and snap frozen for Western blotting. The content of hepatic and muscle fat was measured by the modified Folch method (3). Dietary differences were assessed using ttest and considered significant when, $P<0.05$.

Results: Relative to the control diet, HSHF feeding increased hepatic abundance of specific proteins involved in insulin/IGF signalling in the dam on D16 and D19 (Fig1, $P<0.05$). In contrast HSHF feeding reduced expression of several proteins involved in this signalling pathway in skeletal muscle (Fig2, $P<0.05$) and WAT (IGF1R, PI3K p110α/β and p85α, total Akt and pAkt, $P<0.03$), at both ages. Hepatic lipid metabolic markers were unaffected by HSHF feeding on D16, but PPARα was reduced and LPL, PPARγ, and FAS were increased by D19 (Fig1, $P<0.04$). In maternal skeletal muscle, a HSHF diet increased expression of FAS on D16, and decreased FATP on both D16 and D19 (Fig2, $P<0.05$). HSHF diet reduced FATP, PPARα and FAS on D16 and PPARα and FAS on D19 in maternal WAT ($P<0.04$). The content of fat in maternal liver and muscle was increased by a HSHF diet at D19 ($P<0.001$) but not day 16.

Conclusion: The current study shows that HSHF feeding during mouse pregnancy induces tissue-specific changes in the expression of proteins involved in insulin/IGF signalling and lipid metabolism, consistent with the hyperinsulinaemia and indicative of muscle insulin resistance. These dietary-induced changes in maternal metabolic profile may influence the partitioning of nutrients to fetal growth and thereby explain the intrauterine programming of adult metabolic phenotype.

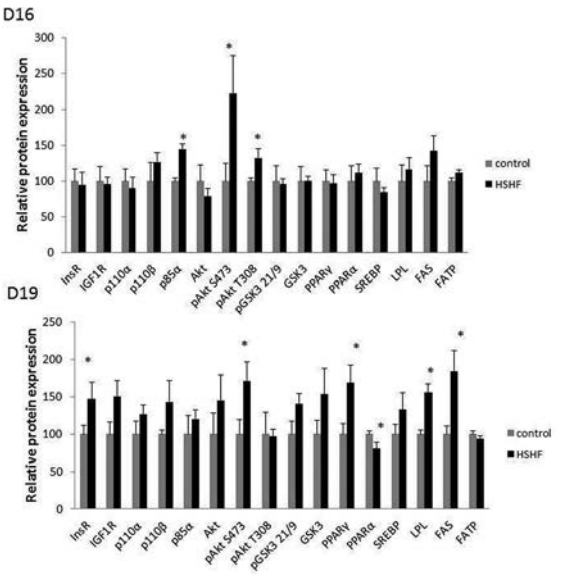

Figure 1. The effect of HSHF feeding on hepatic expression of insulin/IGF signalling pathway and markers of lipid metabolism at D16 and D19 of pregnancy. Data are expressed as mean +/-SEM (control, n=5; HSHF, n=5). The protein expression is relative to the control group.

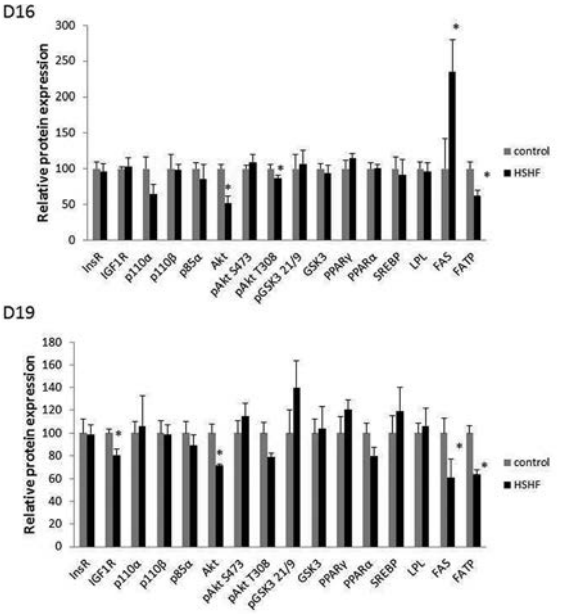

Figure 2. The effect of HSHF feeding on muscle expression of insulin/IGF signalling pathway and markers of lipid metabolism at D16 and D19 of pregnancy. Data are expressed as mean +/-SEM (control, n=5; HSHF, n=5). The protein expression is relative to the control group.

Samuelsson A., et al. (2008) Diet induced obesity in female mice leads to offspring hyperphagia, adiposity, hypertension and insulin resistance. Hypertension 51:383 392

Sferruzzi-Perri A., et al. (2010) High sugar and fat diets alter maternal body composition and feto-placental development in mice. Reprod Sci 17, 231A

Folch J., et al (1957) A simple method for the isolation and purification if total lipids from animal tissues. J Biol Chem, 482 509

Where applicable, the authors confirm that the experiments described here conform with The Physiological Society ethical requirements.

PCA322

Asymmetric dimethylarginine causes adipocyte hypertrophy through NO-independent upregulation of the mTOR lipid biosynthesis pathway

L.B. Dowsett, O. Boruc and J.M. Leiper

MRC Clinical Sciences Centre, Imperial College London, London, UK

Metabolic syndrome is a major healthcare and economic burden. Cardiovascular disease and obesity are major symptoms of metabolic syndrome. Asymmetric dimethylarginine (ADMA) is an endogenously produced inhibitor of nitric oxide synthesis that is an established biomarker of cardiovascular disease. Increased plasma concentrations of ADMA have been reported in obese individuals in whom it is thought to contribute to cardiovascular dysfunction. However, at present little is known about the direct effects of ADMA on adipocytes and obesity. In the present study we examined the effects of ADMA on 3T3-L1 cells *in vitro* and on adipose tissue *in vivo*.
Mouse 3T3-L1 cells were fully differentiated to adipocytes and treated with exogenous ADMA (10μM) after which intracellular neutral lipid was stained with oil red O and adipocyte area quantified by microscopy. To specifically elevate ADMA concentrations in adipocytes in vivo we deleted the enzyme dimethylarginine dimethylaminohydrolase 1 (DDAH1, the predominant enzyme responsible for intracellular ADMA metabolism) in adipocytes using adiponectin driven Cre expression[1]. In vitro treatment with ADMA caused adipocyte hypertrophy (control area 27.65μM^2 ± 1.41, 10μM ADMA area 33.85μM^2 ± 1.62, p>0.01, n=6, all results ±SEM and student T test) which was independent of NO blockade as the nitric oxide synthase inhibitors L-NAME (1mM) and PB-ITU (20μM) had no effect on lipid accumulation (28.02μM^2 ± 1.52 and 25.73μM^2 ± 1.27 respectively). ADMA treatment of 3T3-L1 cells (10μM, 48h) resulted in increased expression of mTOR RNA and protein (2.4X ±0.47, and 1.73X ±0.22 respectively, p>0.05, n=3). Downstream of mTOR the targets of the transcription factor SREBP1c including ACC and FASN were upregulated (4.6±0.8 and 1.4±0.16 fold respectively, p>0.05, n=6) suggesting that ADMA increases adipocyte size through the upregulation of lipid biosynthesis in an NO independent manner. Adipocytes isolated from AdCre-DDAH1$^{-/-}$ mice were found to have increased intracellular ADMA (control 72.1 ±22.36 nmol/mg, KO 85.24 ±11.90 nmol/mg) which caused a corresponding decrease in intracellular NO concentration (control 30.66μM/mg ± 4.9, KO 18.22μM/mg ± 3.86, p>0.05, n=4). Immunohistochemistry revealed that adipocytes within the epididymal depot were larger in AdCre-DDAH1$^{-/-}$ mice than wildtype littermates (18.05±1.01μM^2 and 14.47±0.52μM^2 respectively, p>0.05, n=4). The physiological consequence of this adipocyte hypertrophy was increased macrophage infiltration (control 17.9±0.9, KO 22.2±1.2 cells per frame, p<0.05, n=4). These data suggest that ADMA is a novel regulator of lipid biosynthesis within adipocytes independent to its actions as a nitric oxide synthase inhibitor. Adipocyte hypertrophy causes increased inflammation and is likely to contribute to insulin resistance.

Eguchi J *et al*. (2011). *Cell Metab***13**, 249-259

Where applicable, the authors confirm that the experiments described here conform with The Physiological Society ethical requirements.

PCA323

Interleukin-induced calcium channel current modulation in osteoblasts

H. Kobayashi[2], T. Endoh[1], M. Tazaki[1] and K. Sueishi[2]

[1]Dept of Physiol, Tokyo Dental College, Chiba, Japan and [2]Department of Orthodontics, Tokyo Dental College, Chiba, Japan

Interleukin-1β (IL-1β) and -6 (IL-6) are inflammatory cytokines that are involved in bone resorption under pathological conditions. The cytokines are also involved in bone remodeling under physiological conditions. Voltage sensitive Ca2+ channels (VSCCs) serve as crucial mediators of membrane excitability and many Ca2+-dependent functions such as growth of bone, regulate proliferation, differentiation, enzyme activity and gene expression. The effects of IL-1β and -6 on VSCCs in osteoblast cell line (MC3T3-E1) were investigated using patch-clamp recording. Our results showed that application of 50 pM-50 nM IL-1β facilitated VSCCs current (ICa) carried by Ba2+ (IBa). Application of 50 pM-5 nM IL-6 facilitated IBa. In contrast, 50 nM IL-6 inhibited IBa in MC3T3-E1 cells.

Where applicable, the authors confirm that the experiments described here conform with The Physiological Society ethical requirements.

PCA324

Birth weight is a strong independent determinant of white-to-white corneal diameter of newborns

V.A. Olatunji[1], D.S. Ademola-Popoola[1,2], G.F. Adepoju[1,2] and L.A. Olatunji[3]

[1]Department of Ophthalmology, University of Ilorin Teaching Hospital, Ilorin, Kwara, Nigeria, [2]Department of Ophthalmology, College of Health Sciences, University of Ilorin, Kwara, Nigeria and [3]Department of Physiology, College of Health Sciences, University of Ilorin, Kwara, Nigeria

Measurement of corneal diameter (CD) in children is pertinent in the diagnosis and monitoring of some ocular diseases, especially anterior segment anomalies and congenital glaucoma (1-3). Nonetheless, normal values of CD in African children are not well documented. The present study therefore sought to establish normative values of CD in full-term newborns and to assess relationship with some birth parameters. Horizontal and vertical CD were evaluated with Castroviejo mm caliper in 1000 eyes of 500 normal full-term babies within the first week of life, in a cross-sectional hospital-based study in the North Central zone of Nigeria. The relationship between CD and perinatal variables were assessed by using univariate and multiple linear regression models. A total of 254 (50.8%) male and 246 (49.2%) female babies were involved in the study. The mean value (mean ± SD) of horizontal CD in the right eyes was 9.87±0.40mm (ranged from 9.00-10.50mm) while it was 9.86±0.40mm in the left eyes (range of 9.00-10.75mm). Mean values of vertical CD was 9.59±0.38mm in the right eyes (range 8.75-10.50mm) and 9.62±0.41mm in the left eyes (range 8.75-10.75mm). There were no significant differences between those of the right and left eyes. The horizontal and vertical CD in males were not significantly different from those in females. The study showed a significant association between birth weight and CD irrespective of baby sex, maternal age, birth length, head circumference and postnatal age. The study also indicated that an increase of 0.36 mm for each kg increase

in the birth weight. The results from the present study demonstrate that birth weight is an important independent determinant of CD in newborns. These results would provide useful references for the eye care of newborns in Africa, particularly in Nigeria. Furthermore, the CD values in this study are not consistent with some data from studies in children in other parts of the world. It is therefore plausible to put into account geographical difference when utilizing or interpreting CD values at least in newborns.

Wallace DK, Plager DA. J Pediatr Ophthalmol Strabismus 1996; 33: 230–234

Baumeister M, et al. J Cataract Refract Surg. 2004;30:374–380.

Wei RH et al. Ophthalmology. 2006;113:177–183.

The authors wish to acknowledge the cooperation of the parent of the children used in this study and the assistance of Dr. (Mrs.) O.O. Adesuyi (Consultant Pediatrician)

Where applicable, the authors confirm that the experiments described here conform with The Physiological Society ethical requirements.

PCA325

Alterations in intrauterine electrical impedance in mice measured by four-electrode methods

M. Yamamoto[1], T. Hosono[1], C. Igi[1], M. Arakawa[1], M. Nakamoto[1], K. Akasaka[1], H. Nakamura[2] and T. Kimura[2]

[1]Graduate School of Bimedical Engineering, Osaka Electro-Communication University, Shijonawate, Osaka, Japan and [2]Graduate School of Medicine, Osaka University, Suita, Osaka, Japan

Introduction. Recently, biological electrical impedance (EI) has been widely used as a method to assess body constituents. There are two methods for EI measurement: two-electrode (TEM) and four-electrode (FEM) methods. The apparatus for the TEM is generally simple and inexpensive comparing with the FEM, but the accuracy of measurement in the TEM is lower than in the FEM. The FEM involves two pairs of electrodes, an outer pair and an inner pair. Electrical current passes between the outer pair (current electrode), and the voltage between the inner pair (voltage electrode) is measured. The uterine endometrium (UE) changes its conditions chemically and histologically in each menstrual phase. Since EI varies depending on tissue conditions, EI of UE (UEI) may also vary according to menstrual phases. However, to the best of our knowledge, UEI has been rarely reported. The aim of this study was to clarify the characteristics of UEI using mice. Methods. Animals. Twenty 10-week-old Slc:ddy female mice were used in this study. We checked the estrus cycle of mice by cytological evaluations of vaginal smears using Giemsa staining. The cycle of the mice used consisted of proestrus (PES, n=4), estrous (ES, n=7), metestrus (MES, n=5), and diestrus (DES, n=4). Equipment. We used an impedance checker using the FEM (MLT-50, Toray Medical, Japan). The MLT-50 measures impedances at 140 points between 2.5 and 350 kHz automatically and calculates characteristic parameters such as the impedance at 0 Hz (R0) and infinity Hz (Ri), critical frequency (fc), and resistance (Rfc) and reactance (Ifc) at fc. The intrauterine probe (IUP) was composed of two electrodes and a core of tungsten wire of 0.3 mm in diameter. We rolled platinum wire on the core wire as voltage electrodes at two sites: 2.5 - 5.0 and 7.5 - 10.0 mm from the tip end. We pricked two thin needles into the skins of the fore- and hind-feet and used them as current electrodes. Procedure. Under anesthesia with continuously inspired isoflurane, we performed laparotomy in a supine position, and exposed the uterus. We inserted the IUP into the vagina and advanced its tip into the uterine cavity, and then measured UEI. Results. Our preliminary experiments revealed that there was little difference in values of UEI at the points where the tip of the IUP was located 15, 30, and 45 mm from the external uterine os. UEI at 1 kHz at ES (3.5 ± 0.3 kΩ, mean ± SEM) was significantly larger ($p<0.05$, Kruskal-Wallis test) than those at PES (1.6 ± 0.2 kΩ), MES (0.6 ± 0.1 kΩ), and DES (0.9 ± 0.1 kΩ). There were no significant differences in R0, Ri, fc, Rfc, and Ifc regardless of menstrual stages. Discussion and Conclusion. We measured UEI at various estrous stages using the FEM successfully. The UEI parameters measured by the FEM might be new parameters for evaluating UE conditions.

Where applicable, the authors confirm that the experiments described here conform with The Physiological Society ethical requirements.

PCA326

An increase in intellectual activity during menstruation by abdominal warming using a heat- and steam-generating sheet

C. Igi, T. Hosono, M. Yamamoto, M. Nakamoto, M. Arakawa and K. Akasaka

Graduate School of Biomedical Engineering, Osaka Electro-Communication University, Shijonawate, Osaka, Japan

Introduction. About 80% female school students suffer dysmenorrhea and sometimes experience a decrease in academic performance due to dysmenorrheal pain. Warming the abdomen has been widely used for pain relief as a non-pharmacological method. The heat- and steam-generating (HSG) sheet, which keeps the attached skin area around 40°C for 5 - 8 hours, relieves dysmenorrheal pain with comfort (Hosono, 2010). The comfort may promote the intellectual ability and thus prevent such a decrease in academic performance. The aim of this study was to clarify the effects of abdominal warming using the HSG sheet on the intellectual ability during simple calculations. The protocol of this study was approved by the local ethics committee. Methods. Ten female university students (age 21.5 ± 0.4, mean ± SEM) were included in this study. During menstruation periods, a subject sat in a room of 25°C and attached an HSG sheet (HSGS group) or a non-warming sheet (NWS group, control), as large as the HSG sheet, to the lower abdomen. Measurement was performed only once during a subject's menstruation. When a subject participated in HSGS at the first measurement, the subject participated in NWS in the next menstruation. For the evaluation of the intellectual ability, we used a randomly generated simple single-digit addition similar to the Kraepelin psychodiagnostic test. The subject performed the test just before and 1 hr after attaching the HSG sheet. The subject solved as many questions as possible for 15 min. We counted the number of correct answers (A) per total number of answered questions (B), and obtained the solution rate (SR) as A/B x 100. We also measured the thumb temperature (Tt) for evaluating sympathetic nerve activities (SNS). The subject also recorded her dysmenorrheal pain level using a integral score of zero (no pain) to three (severe pain). Results. The SR in the HSG group (32 ± 25%) significantly increased ($p<0.05$, Wilcoxon signed-rank test) compared to the control (-3 ± 9%). The increase rate of SR in the HSGS was significantly higher than in the NWS. The rate

of subjects with pain scores of more than two after 1-hr HSG sheet application was also significantly lower (Fisher's exact test, $p<0.05$) in the HSG group (50%) than in the control group (71%). The Tt in the HSGS (33.9 ± 1.3°C) was higher than in the NWS (25.6 ± 3.6°C), indicating a decrease in SNS. Discussion and Conclusion. Lower abdominal warming using the HSG sheet was effective for increasing intellectual activities. Interestingly, although three of the subjects did not feel dysmenorrheal pain during the measurements, all of them also experienced an increase in SR. Thus, the increased intellectual activities may not be completely due to only relief from dysmenorrheal pain. The increase in intellectual activities might be related to SNS decrease.

Hosono T (2010). JOGR 36, 818-24.

Where applicable, the authors confirm that the experiments described here conform with The Physiological Society ethical requirements.

PCA327

Phenolic compounds content, antioxidant and antibacterial activities of green / black tea decoction as affected by cooking treatment

K. Dhaouadi[2], H. Jlassi[1], S. Fattouch[2] and M.H. Hamdaoui[1]

[1]Research Unit, high School of Health Sciences and Technical, Tunis, Tunisia and [2]Food Biochemistry Laboratory, INSAT, Tunis, Tunisia

Green or black tea decoction is a popular beverage in Tunisia, Libya and Algeria. It is prepared by cooking the dried tea leaves for a relatively long period of time, which is different from the infusion. The aim of our study was to evaluate the phenolic compounds content and the antioxidant and antibacterial activities of tea extracts after different cooking times, in comparison to tea infusion. Green or black tea leaves (40 g per L of water) were cooked for three times (15, 30 and 60 min) with two different methods (continuously and discontinuously). Tea decoctions obtained were extracted by acetone/water (v/v) according to the method described by Dhaouadi et al. (2011). Phenolic compounds were quantified by Folin –Ciocalteu method and their identifications were obtained by RP-HPLC/LC-MS technique. The antioxidant activities were evaluated by ABTS, DPPH and FRAP methods using Trolox as standard. The analysis of antibacterial activities of the tea preparations were assessed by using collection of microorganisms strains, commercially available as references. Values are means ± S.E.M., compared by ANOVA. Our results showed that the green tea cooked for 15 min contained the higher quantity of phenolic compounds (1388 ± 52 mg / gallic acid equivalent (GAE)/100mL of tea decoction). For the black tea, the higher phenolic compounds content were obtained 30 min after continuously cooking (953 ± 40mg /GAE /100 ml of tea decoction). Detailing of phenolic compounds peaks from different tea decoction extracts was described in the poster. The stronger antioxidant properties corresponded to those obtained from green tea cooked for 15 min (4975 mmol/ equivalent Trolox /100 mL of decoction). The antibacterial potential of tea extract showed that staphylococcus aureus and staphylococcus epidermidis were the most sensitive studied strains. Phenolic compounds of tea extracts from green tea cooked for 15 min are more powerful on the antioxidant and antibacterial activities, followed by black tea decoction obtained 30 min after continuously cooking, than tea infusion or decoctions of other cooking times.

Dhaouadi K et al. (2011). Agric Food Chem 59, 402-406.

Authors would like to thank the Ministry of High Education and Research in Tunisia for its financial support

Where applicable, the authors confirm that the experiments described here conform with The Physiological Society ethical requirements.

PCA328

Oxidative Stress and antioxidant response in rats exposed to permethrin, a pyrethroid insecticide, and ameliorating effect of vitamin C

F.M. El-Demerdash[1], H.M. Nasr[2] and A.B. Jebur[3]

[1]Environmental Studies, Institute of Graduate Studies and Research, Alexandria University, Alexandria, Egypt, [2]Pest Control and Environmental Protection, Faculty of Agriculture, Damanhour, Egypt and [3]Environmental Studies, Institute of Graduate Studies and Research, Aleexandria, Egypt

Pyrethroids are important insecticides used largely because of their high activity as an insecticide and their low mammalian toxicity. The present study was designed to investigate the propensity of permethrin to induce oxidative stress and biochemical perturbations in rat liver and the role of vitamin C in alleviating its toxic effects. Male Wister Albino rats were randomly divided into four groups of 7 each, group I served as control; group II treated with vitamin C (200 mg/kg BW), group III received permethrin (150 mg/kg BW) and group IV treated with permethrin plus vitamin C. Rats were orally administered their respective doses daily for 28 days. The local committee approved the design of the experiments, and the protocol conforms to the guidelines of the National Institutes of Health (NIH). The administration of permthrin significantly caused elevation in lipid peroxidation (LPO) and reduction in the activities of antioxidant enzymes including catalase (CAT), superoxide dismutase (SOD), glutathione S-transferase (GST), glutathione peroxidase (GSH-Px) and glutathione reductase (GSH-Rx). A significant decrease in glutathione (GSH) content was also observed. Liver aminotransferases (AST and ALT) and alkaline phosphatase (AlP) were significantly decreased while lactate dehydrogenase (LDH) was increased. Vitamin C treatment to permethrin intoxicated rat decreased LPO level and normalized CAT, SOD, GST, GPx and GR activities, while GSH content was increased. Also, liver AST, ALT, AlP and LDH were maintained near normal level due to vitamin C treatment. In conclusion, vitamin C has beneficial effects and could be able to antagonize permethrin toxicity.

Fatma M. El-Demerdash, 2007. Lambda-cyhalothrin-induced changes in oxidative stress biomarkers in rabbit erythrocytes and alleviation effect of some antioxidants. Toxicology in Vitro, Volume 21, 392-397

Mokhtar I. Yousef, M.I., Awad, T.I., Edriss H. Mohamed,E. H., 2006. Deltamethrin-induced oxidative damage and biochemical alterations in rat and its attenuation by vitamin E. Toxicology, Volume 227, 240-247

Sadowska-Woda, I., Wójcik, N., Karowicz-bilinska, A., Bieszczad-bedrejczuk, E. 2010. Effect of selected antioxidants in β-cyfluthrin-induced oxidative stress in human erythrocytes in vitro. Toxicology in Vitro, Volume 24, 879-884

Falcioni, M.L., Nasuti, C., Bergamini, C., Fato, R., Lenaz, G., Gabbianelli, R., 2010.The primary role of glutathione against nuclear DNA damage of striatum induced by permethrin in rats.

Neuroscience, Volume 168, 2-10.

Nasuti, C., Cantalamessa, F., Falcioni, G., Gabbianelli, R, 2003. Different effects of Type I and Type II pyrethroids on erythrocyte plasma membrane properties and enzymatic activity in rats. Toxicology, Volume 191, 2003, 233-244.

Where applicable, the authors confirm that the experiments described here conform with The Physiological Society ethical requirements.

PCA329

Protective effect of vitamins C and E on abamectin-induced oxidative stress in rats

H.M. Nasr[1] and F.M. El-Demerdash[2]

[1]Pest Control and Environmental Protection, Faculty of Agriculture, Damanhour University, Damanhour, Egypt and [2]Environmental Studies, Institute of Graduate Studies and Research, Alexandria University, Alexandria, Egypt

The present study was designed to investigate the impact of abamectin to induce oxidative stress and biochemical perturbations in male albino rat (Rattus norvegicus) serum and the role of vitamin C and vitamin E in ameliorating its toxic effects. Rats were randomly divided into 6 groups of 10 each, group I served as control; group II treated with vitamin C (VC; 20 mg/kg BW), group III treated with vitamin E (VE; 200 mg/kg BW/day), group IV received single dose of abamectin (2.175 mg/kg BW/day, 1/4 LD50), group V treated with abamectin plus vitamin C and group VI treated with abamectin plus vit E. Rats were orally administered their respective doses of VC and VE daily for 10 days. The local committee approved the design of the experiments, and the protocol conforms to the guidelines of the National Institutes of Health (NIH). After 10 days of treatment, serum aspartate amino transferase (AST), alanine amino transferase (ALT), gamma-glutamyl transferase (GGT) alkaline (AlP) and acid phosphatase (AcP) as well as malondiadehyde (MDA), glutathione (GSH), glutathione-S-transferease (GST), catalase (CAT) and superoxide dismutase (SOD) were measured. The results revealed significant increase in serum AST, ALT, AlP and AcP activities in abamectin group as compared to the control. Also, the level of MDA was significantly increased in abamectin treated rats. On the other hand, abamectin induced a significant inhibition of GST, CAT SOD and GSH contents as compared with the control group. Supplementation of vitamin C and vitamin E to abamectin - treated rats reduced the toxic effect of abamectin on the above measured parameters and lipid peroxidation in serum. In Conclusion, the findings data suggested that administration of vitamins C and E ameliorated the abamectin -induced oxidative stress in albino rats and the effect of vitamin E in preventing abamectin - induced toxicity was superior to that of vitamin C.

El- Shafey, A. A. M.; Seliem, M. M. E.; El-Mahrouky, F.; Gabr, W. M. and Kandil, R. A., 2011. Some Physiological and Biochemical Effects of Oshar Extract and Abamectin Biocide on Male Albino Rats. Journal of American Science, 7(12), 254-261.

Uchendu, C., Suleiman F. Ambali, S. F., Ayo, J. O., 2012. The organophosphate, chlorpyrifos, oxidative stress and the role of some antioxidants: A review. African Journal of Agricultural Research, 7(18), 2720-2728.

Ali, U. H.; Daniel, E.E.; Lawal, A.; Sherif, I. A.; Malgwi, I., S., 2012. Endosulfan-Induced Changes in Sperm Count, Testicular Weight and Some Erythrocyte Indices in Male Guinea Pigs. British Journal of Pharmacology and Toxicology, 3(4), 151-155.

Soliman, H.A.; Ahmed, M.B.; El-Kashorey. A.A.; Moawad, E.B., 2009. Effect of abamectin on liver function and lipid peroxidation. Egyptian Journal of Natural Toxins, 6(2), 89-99.

Where applicable, the authors confirm that the experiments described here conform with The Physiological Society ethical requirements.

PCA330

The role of adrenergic receptors in nicotine-induced hyperglycemia in the common african toad (*Bufo regularis*)

G.O. Isehunwa, G.O. Adewunmi and A.A. Alada

Physiology, University of Ibadan, Ibadan, Oyo, Nigeria

The role of adrenergic receptors in nicotine-induced hyperglycaemia has not been well studied in amphibians. Thus, this study investigated the effects of alpha and beta adrenergic receptor blockers in nicotine-induced hyperglycaemia in the common African toad *Bufo regularis*. Each toad was fasted for 24hr and anaesthetized with sodium pentobarbitone (3mg/100g i.p). The animals received intravenous (i.v) injection (abdominal vein cannula) of 0.7% amphibian saline, or nicotine (50μg/kg) and thereafter, blood samples were collected for estimation of blood glucose level. In the treated groups, the toads were pretreated with prazosin (0.2mg/kg i.v), propranolol (0.5mg/kg i.v) or prazosin (0.2mg/kg i.v) combined with propranolol (0.5mg/kg, i.v) 30 minutes before i.v. injection of nicotine (50μg/kg i.v). Thereafter, blood samples were also collected from truncus arteriosus for estimation of blood glucose level using the modified glucose oxidase method.

Nicotine caused significant increase ($P<0.01$) in the levels of blood glucose in the common African toad. Pre-treatment of the toads with prazosin (0.2mg/kg i.v) or propranolol (0.5mg/kg, i.v) significantly ($p < 0.01$) reduced the hyperglycaemia induced by nicotine (50μg/kg i.v). However, the combination of prazosin (0.2mg/kg i.v) and propranolol (0.5mg/kg, i.v) abolished the hyperglycaemic effect of nicotine (50μg/kg i.v). The results of this study suggest that both alpha and beta adrenoceptors are involved in nicotine-induced hyperglycaemia in common African toad *Bufo regularis*.

Milton A.S (1966). Effect of nicotine on glucose levels and plasma non-esterified fatty acids levels in the intact and adrenalectomised cat. *Brit.J.Pharmacol* **26**, 256-263.

Tsuijimoto A, Tanimo S, Kurogochi Y (1965). Effect of nicotine on serum potassium and glucose. *Japan .J.Pharmacol* **15**,416-422.

Grayson J and Oyebola DDO (1985). Effect of nicotine on blood flow, oxygen consumption and glucose uptake in canine small intestine. *Brit.J. Pharmacol* **85**, 797-804.

Oyebola DDO and Alada ARA (1993). Effect of adrenergic receptor blockers on adrenaline and nicotine-induced hyperglycaemia in the rat. *Afr.J. Med.Sci* **22**, 13-18.

DDO Oyebola, GO Idolor, EO Taiwo, ARA Alada, OO Owoeye and GO Isehunwa (2009). Effect of nicotine on glucose uptake in the rabbit small intestine. *Afr.J. Med. Med. Sci* **38**, 119-130.

Where applicable, the authors confirm that the experiments described here conform with The Physiological Society ethical requirements.

PCA331

Thyroid hormones in high altitude natives

O. Nepal and B.R. Pokhrel

Physiology, Kathmandu University Medical School, Dhulikhel, Nepal

The endocrine changes related to altitude adaptation in human have attracted physiologists around the globe for long. A number of high altitude studies to detect the physiological changes have been performed now and then. But, the study to see the hormonal changes to compare populations residing at different high altitudes is a scarce. Hence, we have performed a study in native populations of different high altitude comparing changes in thyroid hormones in western Nepal. The Jharkot population included in this study is at altitude of 3760m and Jomsom population at 2800m height from sea bed.
To compare thyroid status between high altitude natives at two different altitudes a cross sectional study is performed by random sampling method. The blood sample was collected in a vacutainer from fifty eight individuals after obtaining the informed consent of participants. The blood collected from antecubital vein was centrifuged in an hour and the plasma obtained was used for biochemical analysis of free triiodothyronine, free thyroxine and thyroid stimulating hormone. ELISA technique was used for bioanalysis of the serum samples collected in this study. Mean free thyroxine (fT4) of Jharkot population is significantly larger ($p = 0.001 < 0.05$) than Jomsom population. Mean thyroid stimulating hormone (TSH) with $p = 0.597 > 0.05$ does not indicate the difference between this two population. There is no significant difference between mean free triiodothyronine (fT3) of Jharkot and Jomsom population ($p = 0.345 > 0.05$). The rise in free thyroid hormone at high altitude is not dependent on the thyroid stimulating hormone released from anterior pituitary. The rise in free thyroxine may be the cause for the rise in free triiodothyronine at higher altitude and low plasma fT3 is not found in population studied at high altitudes.

Comparison of fT3, fT4 & TSH

	Jomsom	Jharkot
fT3		
N	33	25
Mean	2.3721	2.5624
Std Deviation	.84301	.61456
Std Error Mean	.14675	.12291
fT4		
N	33	25
Mean	1.3191	1.5476
Std Deviation	.24002	.26932
Std Error Mean	.04178	.05386
TSH		
N	32	25
Mean	2.8656	2.4672
Std Error Mean	.51635	.53192

Barnholt KE et al. (2006). Am J Physiol 290, 1078–1088

Benso A et al. (2007). Eur J Endocrinol 157, 733–740

Sawhney RC & Malhotra AS (1991). Horm Metab Res 23, 81-84

Richalet JP et al. Am J Physiol 299, 1685-92

Ramirez G et al. Clin Endo 43, 11-18

We gratefully acknowledge the help extended by the Department of Clinical Biochemistry of Dhulikhel Hospital for the biochemical analysis of thyroid hormones in the midst of busy schedule.

Where applicable, the authors confirm that the experiments described here conform with The Physiological Society ethical requirements.

PCA332

Effects of exposure to Bisphenol A on Expression of obesity-related genes in zebrafish

T.Y. Kostrominova

Anatomy and Cell Biology, Indiana University School of Medicine-Northwest, Gary, IN, USA

In recent years, environmental pollutants/endocrine disrupting chemicals (EDCs) have received special attention as metabolic disruptors that produce adverse developmental, reproductive, neurological, cardiovascular, metabolic and immune effects, including predisposition to metabolic syndrome, obesity and type 2 diabetes. Many EDCs are found in everyday products, such as plastic bottles, metal food cans, pesticides, detergents, toys, cosmetics, etc. The knowledge on cellular mechanisms behind the biological effect of EDCs exposure on the development of obesity and type2 diabetes is very limited.
Bisphenol A (BPA) is one of the most abundant EDCs present in the environment. BPA is present in the tested samples of human serum and urine worldwide and is considered to be an “obesogene” that interferes with lipid and glucose metabolism (reviewed in Umar et al., 2013). We focused our study on the effects produced by the exposure to BPA on the expression of obesity-related genes using zebrafish as an experimental model. We have chosen the zebrafish model based on several criteria: 1) recent studies have used zebrafish as a model for studies of the effects of EDCs (Chow et al., 2012); 2) a review by Holtta-Vuori at al. (2010) described zebrafish as an excellent model organism for lipid research; 3) studies of diet-induced obesity show that zebrafish and mammals share common pathophysiological pathways (Oka et al., 2010).
Our experiments showed that exposure of 7dpf zebrafish larvae to 5mg/L of BPA for 24 hours significantly decreased adiponectin and ghrelin mRNA expression (by 29±7% and 26±6 %, respectively, N=5, t-test $p<0.05$) assessed by quantitative RT-PCR using RPLO mRNA expression for the normalization. In the same experiments vitellogenin mRNA expression was increased (by 96±11%, N=5, t-test $p<0.05$) and there were no changes in the mRNA expression of PDK4, perilipin and UCP3. Exposure of 7dpf zebrafish larvae to 5mg/L of BPA for 72 hours decreased adiponectin and ghrelin mRNA expression by 56±4% and 38±5 %, respectively (N=5, t-test $p<0.05$). The data presented here are the first to show that exposure of zebrafish to BPA decreases adiponectin and ghrelin expression. Adiponectin increases fatty acid oxidation and glucose metabolism in muscle, reduces glucose output and enhances insulin sensitivity in liver, and exposure of mammalian adipocytes to BPA inhibits adiponectin release (reviewed in Ben-Jonathan et al., 2009). Ghrelin is involved in regulation of feeding and has potent growth hormone stimulation activity in zebrafish. Our data on increased vitellogenin mRNA expression correlate well with previously reported data on the zebrafish response to BPA (Chow et al., 2012). Overall our data suggest that exposure of zebrafish to BPA displays similarities with obesity-promoting effects of BPA previously documented in mammalian models.

Ben-Jonathan N, Hugo ER, Brandebourg TD (2009) Effects of bisphenol A on adipokine release from human adipose tissue: Implications for the metabolic syndrome. Mol Cell Endocrinol 304: 49-54.

Chow WS, Chan WK, Chan KM (2012) Toxicity assessment and vitellogenin expression in zebrafish (Danio rerio) embryos and larvae acutely exposed to bisphenol A, endosulfan, heptachlor, methoxychlor and tetrabromobisphenol A. J Appl Toxicol,Epub ahead of print

Holtta-Vuori M, Salo VT, Nyberg L, Brackmann C, Enejder A, Panula P, Ikonen E (2010) Zebrafish: gaining popularity in lipid research, Biochem J, 429: 235-242.

Oka T, Nishimura Y, Zang L, Hirano M, Shimada Y, Wang Z, Umemoto N, Kuroyanagi J, Nishimura N, Tanaka T (2010) Diet-induced obesity in zebrafish shares common pathophysiological pathways with mammalian obesity. BMC Physiol 10: 21.

Umar M, Roddick F, Fan L, Aziz HA (2013) Application of ozone for the removal of bisphenol A from water and wastewater-A review. Chemosphere 90: 2197-2207.

Support: IUSM-Northwest.

Where applicable, the authors confirm that the experiments described here conform with The Physiological Society ethical requirements.

PCA334

Changes in hsp mRNA dynamics are involved in HSP72 level regulation during one month of heat acclimation decline

A. Abbas and M. Horowitz

The Hebrew University of Jerusalem, Jerusalem, Israel

We have previously shown in rats (Rattus norvegicus, Sabra strain) that during heat stress (at 41°C), upon heat- acclimation decline, HSP72 maintained heat-acclimatory protein levels despite of the transition to normothermic ambient temperature (at 24 °C). Both basal and heat stress hsp transcripts were profoundly higher than those measured during heat acclimation (continuous exposure at 34 °C, Tetievsky et al., 2008). Increased hsp mRNA/HSP72 protein ratio promoted the hypothesis that dynamic changes in mRNA are responsible for HSP72 proteo-stasis. To test this hypothesis, given that Eif2α is associated with initiation of translation, we measured during 15d and 30d of acclimation decline vs. acclimation: (i) the levels of Eif2α and its phosphorylated form, (ii) the effect of Eif2α dephosphorylation inhibition (using Sal 003, TOCRIS Cat No. 3657) on hsp 72 and 27 transcripts and the encoded HSPs. Our data demonstrated that heat acclimation induced increased Eif2α protein level with decreased phosphorylation. With acclimation decline, Eif2α-phosphorylation gradually increased. Basal and heat-stressed hsp 72 transcripts were elevated whereas HSPs levels were stable, suggesting HSPs proteo-stasis. Daily SAL administration (IP 0.1mg/kg b wgt) during acclimation decline elevated profoundly (vs. non SAL administered groups) hsp 72 transcripts and the mRNA/protein ratio under both basal and heat stress conditions, thus confirming our hypothesis on the importance of mRNA dynamics in HSPs adjustment during heat acclimation decline.

Where applicable, the authors confirm that the experiments described here conform with The Physiological Society ethical requirements.

PCA335

High-performance thermogenesis of brown adipose tissue under hypothermic condition during hibernation in Syrian hamsters

M. Hashimoto[1], H. Ohinata[1] and N. Kitao[2]

[1]Department of Physical Therapy, Teikyo University of Science, Faculty of Medical Sciences, Tokyo, Japan and [2]Public Health Center, Sakai, Japan

Hibernation under extreme cold environment needs a preparation period of some length in which most physiological functions are thought to be remodelled in wide range to adapt to hibernation. Brown adipose tissue (BAT) is an indispensable organ to complete the hibernation behavior, particularly in arousing from hibernation of hypothermia. Taking into consideration the restraint of most physiological functions by low body temperature, remodelling before hibernation occurs possibly in BAT function too. A concrete mechanism of the 'preparation' is still unclear, but the molecular-level remodelling of BAT must be performed during the preparation period of hibernation, because most gene expression stops during deep hibernation. The dominant pathway of BAT thermogenesis occurs through the β3-adrenergic receptor. We investigated the role of the β3-adrenergic system in BAT thermogenesis during arousal from hibernation both in vivo and in vitro. Necessary surgical procedures were carried out under isoflurane anesthesia. Stimulation of BAT by CL316,243 significantly facilitated arousal from hibernation and it also induced arousal in deep hibernating animals, while the β3-antagonist SR59230A inhibited arousal from hibernation. Syrian hamsters in the hibernation group (H) contained BAT that was significantly greater in overall mass, total protein, and thermogenic uncoupling protein-1 than BAT from the warm-acclimated group (WA). Although the ability of the β3-agonist CL316,243 to induce BAT thermogenesis at 36°C was no different between H and WA, its maximum ratio over the basal value at 12°C in H was significantly larger than that in WA. Forskolin, adenylyl cyclase activator, stimulation at 12°C produced equivalent BAT responses in these two groups. These results suggest that BAT in hibernating animals has potent thermogenic activity with a highly effective β3-receptor mechanism at lower temperatures. Hence we hypothesized that the high effectiveness of the receptor mechanism may be due to an increase in number of the receptor that possibly occurs during the preparation period. To investigate the hypothesis, we measured β3-receptor mRNA of BAT removed from animals in 4 stages of activity, WA, CA (cold-acclimated), H and IBA (inter-bout arousal, awake phase during hibernation) by using RT-PCR method. Gene expression of the β3-receptor in BAT of hibernating hamster was significantly smaller by about 40% and 60% than that of WA and CA respectively, but was not different from that of IBA. Results showed that the facilitation of BAT function in hibernating animals may be due to remodelling of the messenger pathway between two molecules, β3-receptor and adenylyl cyclase.

The study was funded in part by JSPS Grant-in-Aid for Scientific Research (B)18390068 and (C) 23500623 to MH.

Where applicable, the authors confirm that the experiments described here conform with The Physiological Society ethical requirements.

PCA337

Endothelial SHIP2 confers age-dependent contrasting affects on whole body glucose homeostasis and vascular function

M. Gage[1], S. Wheatcroft[1], A. Abbas[1], H. Imrie[1], H. Viswambharan[1], S. Galloway[1], P. Sukumar[1], R. Cubbon[1], J. Smith[1], S. Schurmans[2], M. Jacoby[2], E. Dubois[2] and M. Kearney[1]

[1]DCDR, Leeds University, Leeds, UK and [2]IRIBHM, Université Libre de Bruxelles, Brussels, Belgium

Aging is an important risk factor for diabetes and cardiovascular disease (1). Although the vascular implications of endothelial insulin resistance are well understood (2) the effect of enhanced endothelial insulin signaling on glucose regulation and vascular function remain poorly characterized. To investigate this we generated mice with endothelial-specific downregulation of the lipid phosphatase SHIP2 (3). We deleted exons 18-19 of the ship2 gene using Cre-Lox technology under control of the Tie2 promoter generating an inactivate protein. Male heterozygotes (EC-SHIP2+/-) were compared to sex-matched littermate controls. At 8 weeks of age EC-SHIP2+/- mice displayed increased glucose tolerance after glucose challenge (P=0.03) and improved insulin sensitivity (P=0.02) after insulin challenge (glucose/insulin administration via intra-peritoneal injection, blood sampling from tail vein). By 40 weeks of age this phenotype was reversed; EC-SHIP2+/- mice revealed significant insulin resistance 60 min after insulin challenge (P=<0.05). This phenotype was confirmed by euglycemic hyperinsulinemic clamping. In young mice ex vivo aortic vasomotor studies in both controls and EC-SHIP+/- revealed similar contractile responses to phenylephrine and displayed decreased contraction after insulin incubation (Emax 0.88 ± 0.05g vs 0.62 ± 0.05g P=0.002 and 0.83 ± 0.05g vs 0.69 ± 0.05g P=0.025 respectively). Both groups displayed increased contraction after NO synthase inhibitor LNMMA incubation (Emax 0.88 ± 0.05g vs 1.31 ± 0.11g P=0.01 and 0.83 ± 0.05g vs 1.28 ± 0.02g P=<0.0001 respectively). However, at 40 weeks old in EC-SHIP2+/- mice the vasodilatory aortic ring response to insulin was abolished (Emax controls 0.59 ± 0.04g vs 0.47 ± 0.03g P=0.04, EC-SHIP2+/- 0.64 ± 0.04g vs 0.63 ± 0.06g P=0.9) and EC-SHIP2+/- displayed no increase in contraction to LNMMA incubation (Emax controls 0.59 ± 0.04g vs 0.82 ± 0.08g P=0.02, EC-SHIP2+/- 0.64 ± 0.04g vs 0.69 ± 0.07g P=0.5) indicating insulin resistance and lower basal nitric oxide production (NO), suggesting changes in glucose homeostasis may be mediated by NO bioavailability. In conclusion; endothelial functional downregulation of SHIP2 augments whole body glucose disposal in young mice but attenuates whole body glucose disposal in older mice. Our data suggest a previously unrecognised age dependent role for the vascular endothelium in whole body glucose regulation and a novel spatial and temporal specific affect of the lipid phosphatase SHIP2.

Caestelli (1984) *Am J Med* **76**

Imrie H *et al* (2010) *Biochimica et biophysica acta* **1801**

Clément S *et al* (2001) *Nature* **409**

Matthew C. Gage (1), Stephen Wheatcroft (1), Afroze Abbas (1), Helen Imrie (1), Hema Viswambharan (1), Stacey Galloway (1), Piruthivi Sukumar (1), Richard Cubbon (1), Jessica Smith (1), Stephane Schurmans (2), Monique Jacoby (2), Eléonore Dubois (2), Mark Kearney (1).

(1) Division of Cardiovascular & Diabetes Research, LIGHT Laboratories, University of Leeds, UK; and (2) Institut de Recherche Interdisciplinaire (IRIBHM), Université Libre de Bruxelles, Belgium

Where applicable, the authors confirm that the experiments described here conform with The Physiological Society ethical requirements.

PCA338

The impact of advanced maternal age on the initiation and progress of parturition in a pregnant mouse model

R. Patel

Division of Women's Health, Women's Health Academic Centre, King's College London, London, UK

Rima Patel1, Lucilla Poston1 and Rachel M Tribe1. 1Women's Health Academic Centre, King's College London. London SE1 7EH, UK.

Background: Advanced maternal age (defined as ≥35 years at delivery) is associated with adverse obstetric risks including operative delivery, stillbirth, and post-term labour induction. The physiological causes for such complications remain to be ascertained, although myometrial function has been implicated (Smith GC et al., 2011; Arrowsmith et al., 2012). To address the hypothesis that maternal age directly influences successful parturition, we assessed timing of birth and fetal outcome in a pregnant mouse model. The function of myometrium and cervix ex-vivo was also examined.

Methods: Gestation length (days) and parturition duration (hours) in young (3 months old, n=8) and old (8 months old, n=8) nulliparous pregnant C57/BL6 mice were monitored using infrared cameras. The number of viable pups delivered per mouse was recorded. Isolated myometrial tissues from pregnant (day 18) C57/BL6 mice (3 months and 8 months; n=10 each group) were used for isometric tension recording [spontaneous contractility; mean integral tension (g) and contractile frequency (Hz)]. Oxytocin induced contractility (n=5 for both groups) was also measured [mean integral tension(g)]. Maximal cervical distensibilty (mm) was recorded in cervices from pregnant (day 18) C57/BL6 mice (3 months and 8 months, n=5 per group).

Results: Older pregnant mice compared to 3 month old mice had a longer mean (±SEM) gestation (20.08 ±0.49 days vs. 19.05 ±0.25; p<0.001) and significantly longer labours (3.68 ±0.83 hours vs. 1.01 ±0.41; p<0.001). The 3 month old mice gave birth to a greater number of viable pups compared to older mice (7.5 ±0.53 vs. 4.8 ±2.2, p<0.01); 50% of older mice had at least one stillborn pup. The contractile frequency of myometrium ex-vivo was faster in older pregnant mice (0.05 ±0.0098 vs. 0.02 ±0.0046 Hz, p<0.05); however mean integral tension was similar. The 8 month group appeared to exhibit a greater sensitivity to oxytocin (n=5, 10-10 - 10-9 M), but this did not reach significance. Cervical distensibility was significantly greater in older pregnant mice (19.4 ±0.60 vs. 16.6 ±0.75 mm, p<0.05).

Conclusions: Gestation length, labour duration and stillbirth risk were increased in older pregnant mice suggesting that there is an intrinsic problem with parturition processes in older mice. This is unlikely to be due to delayed cervical ripening as evidenced by enhanced distensibility in older mice. However, the increased contraction frequency seen in older mice ex-vivo could potentially result in poorly coordinated myometrial contractions in-vivo.

Funding: BBSRC PhD studentship and Tommy's Charity (Reg No: 1060508)

Where applicable, the authors confirm that the experiments described here conform with The Physiological Society ethical requirements.

PCA339

Phosphodiesterase-5 activity exerts a coronary vasoconstrictor influence in awake swine that is partly mediated via an increase in endothelin production

Z. Zhou[1], V.J. de Beer[1], S.B. Bender[2], H. Laughlin[2], D. Merkus[1] and D.J. Duncker[1]

[1]Cardiology, Erasmus MC, University Medical Center Rotterdam, Rotterdam, Netherlands and [2]Biomedical Sciences, University of Missouri, Columbia, MO, USA

Nitric oxide (NO)-induced coronary vasodilation is mediated through production of cyclic guanosine monophosphate (cGMP), and through inhibition of the endothelin (ET) system. We previously demonstrated that both phosphodiesterase-5 (PDE5) mediated cGMP breakdown and ET each exert a vasoconstrictor influence on coronary resistance vessels. However, little is known about the integrated control of vascular tone of these two vasoconstrictor mechanisms. In the present study, we investigated the contribution of PDE5 and ET to the regulation of coronary resistance vessel tone in swine at rest and during graded treadmill exercise. ET-A/ET-B receptor blockade with tezosentan (3 mg/kg iv) and PDE5 inhibition with EMD360527 (300 μg/min/kg iv) each produced coronary vasodilation at rest that waned with incremental levels of exercise. Interestingly, however, tezosentan failed to produce further coronary vasodilation in the presence of EMD360527. Similarly, tezosentan and EMD360527 each produced concentration-dependent vasodilation in preconstricted porcine coronary small arteries in vitro, while tezosentan again failed to produce additional vasodilation in the presence of EMD360527. Importantly, EMD360527 (3×10-6 M) significantly attenuated BigET-induced, but not ET-induced coronary contraction. In conclusion, PDE5 activity exerts a vasoconstrictor influence on coronary resistance vessels that is in part mediated via an increase in ET production.

This study was supported by The Netherlands Heart Foundation (2000T042 to DM and VJB), The China Scholarship Council (2009624027 to ZZ) and The NIH (T32-AR048523 to SBB).

Where applicable, the authors confirm that the experiments described here conform with The Physiological Society ethical requirements.

PCA340

A toxicity profile of the aqueous calyx extract of Hibiscus sabdariffa in Sprague Dawley rats

F.B. Mojiminiyi

Physiology, Usman Danfodio University, Sokoto, Nigeria

The aqueous calyx extract of Hibiscus sabdariffa (HS) doubles as a beverage and an agent for treating hypertension in Traditional Medicine in Nigeria and other places (Hopkins et al., 2013). Its antihypertensive effect has been scientifically validated (Mojiminiyi et al., 2007) and may be due to its antioxidant properties (Frank et al., 2012). It contains organic acids such as citric acid, anthocyanins, polyphenols and hibiscus acid (Hopkins et al., 2013). However more toxicological studies are needed before the emergence of a drug(s) from it. This study was designed to carry out a toxicological study of HS. 10g of the dry calyces was boiled in 1 litre of water at 100oC for two hours and the cold decoction filtered. The filtrate was evaporated to dryness and the powder was used to prepare the HS solutions. Thirty six inbred Sprague Dawley (SD) rats of either sex weighing 112-140g were randomly divided into three groups (n=12 each): control, HSLD (HS Low dose) and HSHD (HS High dose). All groups received the rat chow while the control drank tap water and HSLD and HSHD drank 1750mg/kg and 3500mg/Kg HS respectively for twelve weeks. Rat Chow, water and HS solutions were available ad libitum. The rats were then anaesthetized individually by means of chloroform inhalation in a jar. Each was removed and blood was obtained rapidly by cardiac puncture into EDTA or plain bottles. In some cases additional chloroform in cotton wool encased in a cone-shaped filter paper was applied to the nose to maintain anaesthesia during the procedure. Blood in EDTA was used for estimation of haematological parameters (packed cell volume: PCV, white blood cell count: WBC, red blood cell count: RBC and Haemoglobin: Hb) in the QBC machine while serum was extracted from the rest and used for cation (Na+and K+) and biochemical (alkaline phosphatase:ALP, aspartate amino transferase: AST, alanine amino transferase: ALT, albumin, total protein and urea) analyses. Results are expressed as mean±SEM and statistical analyses were done by means of one way ANOVA and a post hoc Tukey Kramer multiple comparison test. $P<0.05$ was considered statistically significant.

Haematological and biochemical parameters and serum cation levels remained similar in the HS groups compared to control except WBC count and urea. These rose significantly in the HSHD group (14.03±1.9 x103/ml and 7.63±0.50 mmol/dl; $P<0.001$ and $P<0.05$ respectively) compared to control (7.25±0.76 x103/ml and 5.10±0.96mmol/dl) but remained similar in HSLD group (10.2±0.16 x103/ml and 5.92±0.44mmol/dl). These results suggest that chronic consumption of HS at low doses may be safe. Higher doses may be associated with reactive leucocytosis and renal injury which may be secondary to subtle inflammatory processes in the body following its consumption.

Hopkins AL et al. (2013) Fitoterapia 85, 84–94.

Mojiminiyi FBO et al. (2007) Fitoterapia 78, 292–297.

Frank T et al. (2012) J Sci Food Agric 92, 2207-2218.

A travel grant from the Physiological Society, London is gratefully acknowledged

Where applicable, the authors confirm that the experiments described here conform with The Physiological Society ethical requirements.

PCA341

Endothelial relaxation mechanisms dysfunction are reversed by atorvastatin or metformin in animals with estrogen deficiency state

I.F. Caliman, P.W. Oliveira, A.Z. Lamas, S.G. Figueiredo, P.L. Dalpiaz, G.J. Sousa and N.S. Bissoli

Physiological Sciences, Federal University of Espirito Santo, Vitória, Espirito Santo, Brazil

Deleterious effects in cardiovascular system (CVS) have been reported in females with estrogen deficiency. However, stud-

ies with hormone replacement therapy (HRT) are not concise. Thus, estrogen receptor independent therapies, such as atorvastatin (ATO) and metformin (MET), could be new strategies to substitute HRT. These drugs have been showed pleiotropic effects, but there are limited data comparing ATO and MET with estrogen on the CVS. This study was performed to evaluate the effects of ATO and MET on mesenteric vascular bed (MVB) reactivity from ovariectomized (OVX) female rats. All procedures were approved by Ethics Committee in Animal Experimentation of the Federal University of Espirito Santo (069/2011). All the surgical experiments were carried out under anesthesia (Ketamine 70 mg/kg + xylazine 10 mg/kg, i.p). Female Wistar rats (180-200g) were divided into five groups (n=6): control (SHAM); ovariectomized (OVX), OVX treated with 17βestradiol (EST, 0.5μg/Kg/day), ATO (ATO, 20mg/Kg/day) or MET (MET, 300mg/Kg/day), 21 days after bilateral ovariectomy. On day 35, the MVB was isolated, perfused and constricted with noradrenaline. Dose–response curves of ACh (10-12 to 10-3 M) were obtained in absence or presence of L-NAME (NOS inhibitor) and L-NAME plus Indometacin (COX inhibitor). Inducible NOS (iNOS), endothelial NOS (eNOS) and NADP(H) oxidase type 2 (NOX 2) protein expression were analyzed by western blot (n=6). The data are reported as means ± SEM, compared by ANOVA. OVX showed decreases in vasodilator response to ACh, and all treatments improves this response (Emax - %relaxation SHAM: 80 ± 3; OVX: 54 ± 4*; EST: 82 ± 3; ATO: 88 ± 5; MET: 68 ± 4; *P<0.05 vs SHAM). L-NAME reduce the relaxation to ACh in all groups (Emax - %relaxation SHAM: 32 ± 8; OVX: 24 ± 7; EST: 34 ± 4; ATO: 35 ± 5; MET: 25 ± 4). L-NAME and Indometacin blockade failed to further reduce ACh-induced relaxation (Emax - %relaxation SHAM: 47 ± 10; OVX: 43 ± 7; EST: 40 ± 7; ATO: 36 ± 7; MET: 25 ± 3). OVX showed elevated levels of iNOS and NOX2 protein expression (iNOS: SHAM: 0.84 ± 0.05; OVX: 0.99 ± 0.04* and NOX2: SHAM: 0.76 ± 0.10; OVX: 1.12 ± 0.13*, *p<0.05), and reduced levels of eNOS (SHAM: 1.07 ± 0.10; OVX: 0.71 ± 0.10**, **p<0.01). All Treatments were able to restore the protein expression values (iNOS: EST: 0.81 ± 0.05; ATO: 0.84 ± 0.03; MET: 0.73 ± 0.04; NOX2: EST: 0.80 ± 0.05; ATO: 0.96 ± 0.09; MET: 0.44 ± 0.07; eNOS: EST: 1.13 ± 0.08; ATO: 1.13 ± 0.09; MET: 0.93 ± 0.05). The relaxation dysfunction caused by estrogen deficiency were improved by ATO and MET treatments, through mechanisms related to nitric oxide pathway, by increase eNOS and decrease iNOS levels and by reduction in NOX2/oxidative stress, providing evidence that non-estrogen therapies could be used to improvement the CVS in estrogen deficient state, such as menopause.

Where applicable, the authors confirm that the experiments described here conform with The Physiological Society ethical requirements.

PCA342

Kv7 channels are major determinants of basal coronary flow and active response to ischemia

S. Khanamiri[1], E. Soltysinska[1], T.A. Jepps[2], B.H. Bentzen[1], P.S. Chadha[2], N. Schmitt[1], I.A. Greenwood[2] and S. Olesen[1]

[1]Danish National Research Foundation Centre for Cardiac Arrhythmia and Dept. of Biomedical Sciences, Copenhagen University, Copenhagen, Denmark and [2]Division of Biomedical Sciences, St. George's University of London, Pharmacology & Cell Physiology Research Group, London, UK

The small coronary arteries constitute the primary site for regulation of vascular resistance in cardiac muscle and mediate the increased blood flow by metabolic substrates such as adenosine. The goal of the present study was to determine the role of KCNQ-encoded KV channels (KV7 channels) in the passive and active regulation of coronary blood flow in normotensive and hypertensive rats. In normotensive rats different KV7 activators and inhibitors caused dilatation or constriction of left anterior descending coronary arteries, which were not observed in hypertensive rats. In isolated, perfused heart preparations, coronary flow rate increased in response to the KV7 activator (S)-1, and was significantly diminished in the presence of a KV7 inhibitor. The expression levels of KCNQ1-5 and their known accessory KCNE1-5 subunits in coronary arteries were similar in normotensive and hypertensive rats as measured by quantitative PCR. However, KV7.4 protein expression was reduced in hypertensive rats. Application of adenosine or the protein kinase A mediated A2A receptor agonist CGS21680 produced concentration-dependent relaxations of coronary arteries from normotensive rats. However, the effects of adenosine, A2A receptor and CGS21680 were abolished in presence of KV7 inhibitors. KV7 blockers also attenuated the ischemia-induced increase in coronary perfusion in Langendorff studies. Overall, these data suggest that KV7 channels are crucial regulators of coronary blood flow and utilised by adenosine receptor activation to contribute to metabolic hyperemia.

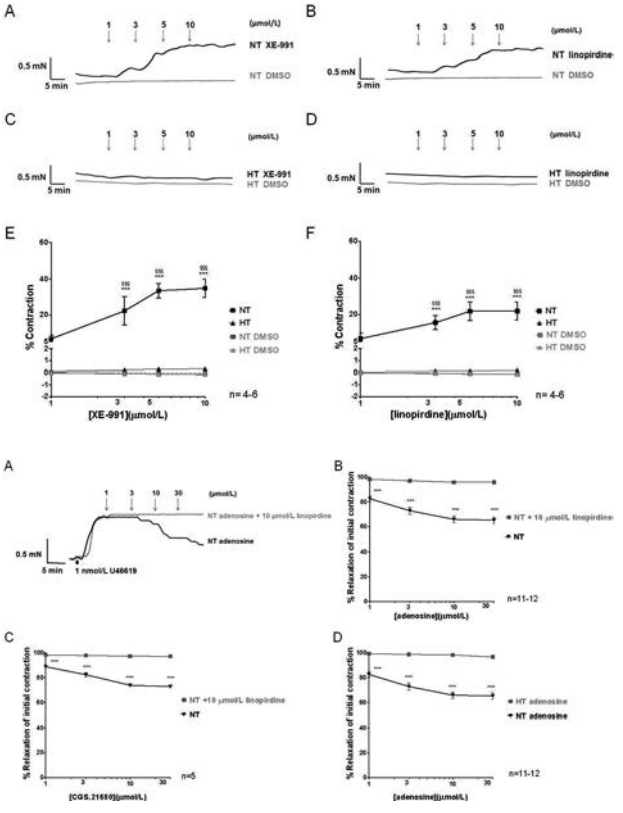

Where applicable, the authors confirm that the experiments described here conform with The Physiological Society ethical requirements.

PCA343

Cardioprotection from cold stress and subsequent fatty diet is mediated by Epac-1 in the isolated mouse heart

F. Edland

Dept of Biomedicine, University of Bergen, Bergen, Hordaland, Norway

Background
Cold stress and subsequent fatty diet reduce infarct size (IS) in the isolated mouse heart when subjected to ischemia and reperfusion. We assessed the hypothesis that Exchange protein directly activated by cyclic adenosine monophosphate 1 (Epac-1) is necessary for cold- and fat stress induced cardioprotection.
Methods
Epac-1 knock-out mice (-/-) (Epac-1 KO) and wild type littermates (WT) were subjected to cold stress (week 5-9) and a fatty diet (week 10-termination) or control environment with room temperature and normal diet. At age 42-43 weeks the mice were sacrificed and the hearts were excised and mounted on a Langendorff perfusion system. The hearts were subjected to 30 min of global ischemia and 1 h of reperfusion, before IS was measured. Hemodynamic parameters were measured at regular intervals.
Results
IS is reported as necrotic tissue/left ventricle ± S.E.M. (%). All groups were n≥6, and group differences were tested by one-way ANOVA combined with Fischer's post-hoc test. WT animals were cardioprotected from cold/fat (WT cold/fat 42±3,5% vs. WT controls 61±6,9%, $p<0.05$, while Epac-1 KO were not (Epac-1 KO cold/fat 65±9,8% vs. Epac-1 KO ctrl 56±5,5%, ns.). Hemodynamic parameters, such as left ventricle developed pressure (LVDP), also suggests a better recovery of the WT cold/fat group, compared to the other groups. LVDP recovery in % of baseline at 30 min of reperfusion, baseline set at 20 min of stabilization: WT cold/fat 94,8±7,4%, WT ctrl 69,9±8,1%, Epac-1 KO cold/fat 59,8±9,1%, Epac-1 KO ctrl 64,8±6,3% ($p<0,05$).
Conclusion
Epac-1 seems to be necessary for the cardioprotective effect of cold stress and fatty diet.

Where applicable, the authors confirm that the experiments described here conform with The Physiological Society ethical requirements.

PCA345

Flow-mediated outward remodeling and NO-dependent dilation of resistance arteries are both determined by sex and age with a key role of timing in estradiol replacement therapy

K. Tarhouni[1], A. Guihot[1], L. Grimaud[1], B. Toutain[1], L. Loufrani[1], F. Lenfant[2], J. Arnal[2] and D. Henrion[1]

[1]BNMI, INSERM, Angers, France and [2]I2MC, INSERM, Toulouse, France

Flow (shear stress)-mediated outward remodeling of resistance arteries is a key adaptative process [1], which declines with age [2]. We recently demonstrated the essential role of 17beta-estradiol in flow-mediated remodeling of resistance arteries in vivo [3]. We now sought to assess the impact of age and timing of estrogen treatment after ovariectomy for better efficacy on this process.
Rats of various ages (3 to 18 months) were submitted to surgery in order to increase locally blood flow in one mesenteric artery in vivo [4, 5], and the arteries, were collected 2 weeks later.
Arterial diameter increased by 27% in high flow arteries of 3-months old male and female rats compared to normal flow vessels. In 12-month old rats, flow-mediated remodeling was absent in males, while it still reached 21% in females. Ovariectomy (3 weeks of estrogen deprivation) of 3, 9 and 12 month-old rats abolished flow-mediated remodeling, that was restored by immediate 17beta-estradiol replacement. Nevertheless, this permissive effect of E2 was attenuated or even abrogated if 17beta-estradiol replacement was delayed by 3 to 9 months respectively. This absence of remodeling was associated with reduction in both estrogen receptor alpha and endothelial nitric oxide (NO) synthase expression levels, associated with reduced NO-dependent dilation in high-flow mesenteric resistance arteries.
Thus, long deprivation of 17beta-estradiol leads to a rapid decline in FMR, that can be prevented by early exogenous 17beta-estradiol supplementation, while delayed substitution of 9 months impairs 17beta-estradiol action. These data underline the importance of "timing" of 17beta-estradiol effect on this vascular process.

Henrion, D., Pressure and flow-dependent tone in resistance arteries. Role of myogenic tone. Arch Mal Coeur Vaiss, 2005. 98(9): p. 913-21.

Dumont, O., et al., Alteration in flow (shear stress)-induced remodelling in rat resistance arteries with aging: improvement by a treatment with hydralazine. Cardiovasc Res, 2008. 77(3): p. 600-8.

Tarhouni, K., et al., Key Role of Estrogens and Endothelial Estrogen Receptor alpha in Blood Flow-Mediated Remodeling of Resistance Arteries. Arterioscler Thromb Vasc Biol, 2013. 33(3): p. 605-11.

Cousin, M., et al., Role of angiotensin II in the remodeling induced by a chronic increase in flow in rat mesenteric resistance arteries. Hypertension, 2010. 55(1): p. 109-15.

Freidja, M.L., et al., The AGE-breaker ALT-711 restores high blood flow-dependent remodeling in mesenteric resistance arteries in a rat model of type 2 diabetes. Diabetes, 2012. 61(6): p. 1562-72.

This work was supported by the National Institut for Health and Medical Research (INSERM, France).

Where applicable, the authors confirm that the experiments described here conform with The Physiological Society ethical requirements.

PCA346

Optimal ROS level is essential for induced pluripotent stem cell adhesion, transendothelial migration, and trafficking in mice

D. Meng[1], Y. Wu[1,2], R. Wang[1,2], N. Li[1], W. Yuan[2] and S. Chen[1]

[1]Department of Physiology and Pathophysiology, Fudan University, Shanghai, China and [2]Department of Physiology, Ningxia Medical College, Shanghai, China

Cell trafficking is essential for cell-based therapy. Reactive oxygen species (ROS) regulate cell proliferation, differentiation, and survival. However, it is not yet known how ROS affects induced pluripotent stem cell (iPSC) trafficking. We found that ROS inhibitor N-acetylcysteine decreased iPSC adhesion, transendothelial migration, and proliferation, and down-regulated major adhesion and migration-related molecules. Exogenous ROS inhibited iPSC adhesion and induced cell apoptosis

and senescence.Male C57BL/6J mice were subjected to operative unilateral hind limb ischemia-reperfusion injury under anesthesia with sodium pentobarbital (50 mg/kg i.p.). The left femoral artery and vein were isolated and clamped for 5 h. After clamp removal, mice were immediately assigned to the following experimental groups (n=9): the MEF (mouse embryonic fibroblasts) group, the iPSC group, the iPSC-NAC group (iPSCs pretreatment with 10 mM NAC for 24 h), the iPSC-H_2O_2 group (iPSCs pretreatment with 50 μM H_2O_2 for 24 h) or the vehicle group (PBS). In each animal, 2.5x10^6 cells/kg body weight (200 μl) or medium was administered through the tail vein 0 h and 24 h after the operation. We found that intravenously administered iPSCs selectively homed to the ischemic tissue and improved blood perfusion and limb function while NAC- or H_2O_2-pretreated iPSCs did not. Our results showed either increased or decreased ROS levels damaged iPSC function. ROS-facilitated IPSC trafficking is essential for their therapeutic effect.

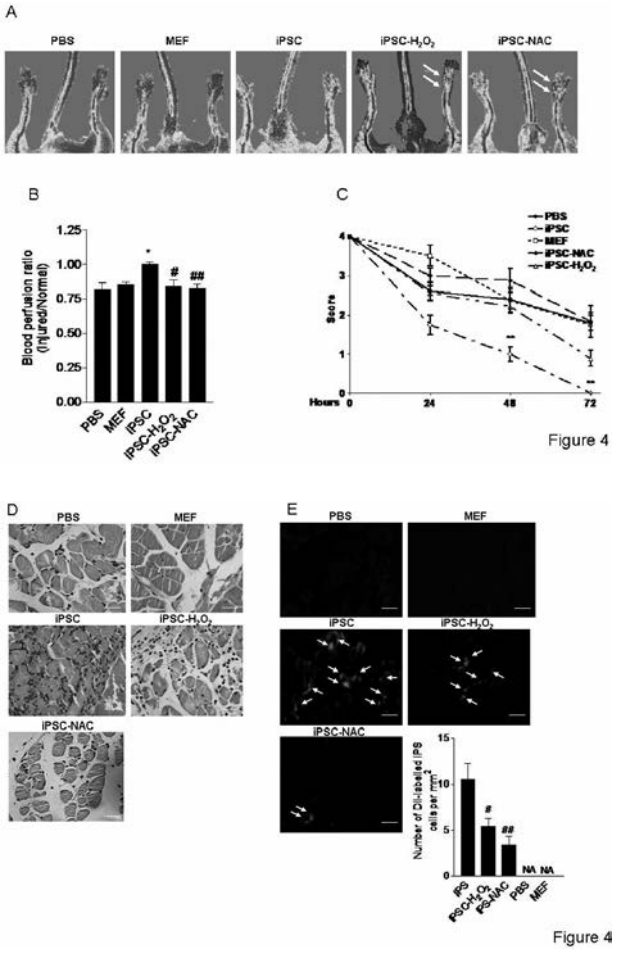

Figure 4

Chavakis E, Urbich C, Dimmeler S. Homing and engraftment of progenitor cells: a prerequisite for cell therapy. J Mol Cell Cardiol. 2008; 45(4):514-522.

Guo YL, Chakraborty S, Rajan SS, Wang R, Huang F. Effects of oxidative stress on mouse embryonic stem cell proliferation, apoptosis, senescence, and self-renewal. Stem Cells Dev. 2010; 19(9):1321-1331.

Le Belle JE, Orozco NM, Paucar AA, Saxe JP, Mottahedeh J, Pyle AD, Wu H, Kornblum HI. Proliferative neural stem cells have high endogenous ROS levels that regulate self-renewal and neurogenesis in a PI3K/Akt-dependant manner. Cell Stem Cell. 2011; 8(1):59-71.

Song H, Cha MJ, Song BW, Kim IK, Chang W, Lim S, Choi EJ, Ham O, Lee SY, Chung N, Jang Y, Hwang KC. Reactive oxygen species inhibit adhesion of mesenchymal stem cells implanted into ischemic myocardium via interference of focal adhesion complex. Stem Cells. 2010; 28(3):555-563.

Armstrong L, Tilgner K, Saretzki G, Atkinson SP, Stojkovic M, Moreno R, Przyborski S, Lako M. Human induced pluripotent stem cell lines show stress defense mechanisms and mitochondrial regulation similar to those of human embryonic stem cells. Stem Cells. 2010; 28(4):661-673.

This work was supported by Key Programs (30830050 and 812101086 to S. Chen, and 81130004 to A.F. Chen), International Cooperation and Exchanges (81220108002 to S. Chen), and General Program (30771003 to S. Chen, and 81170298 and 81270410 to D. Meng) of the National Natural Science Foundation of China, the National Basic Research Program of China to S. Chen (2009CB521900), the Shanghai Municipal Health Bureau Grant of China to D. Meng (c106629), NIH R01 GM077352 and the American Diabetes Association Research Award 7-08-RA-23 to A.F. Chen.

Where applicable, the authors confirm that the experiments described here conform with The Physiological Society ethical requirements.

PCA347

The effect of l-arginine on microvascular reactivity in normotensive subjects with family history of hypertension

Z. Melik, P. Zaletel, T. Virtic and K. Cankar

Institute of Physiology, University of Ljubljana, Faculty of Medicine, Ljubljana, Slovenia

Introduction: Arterial hypertension is the leading risk factor for mortality worldwide. The increasing number of studies support the hypothesis that endothelial dysfunction due to reduced availability of nitric oxide plays a key role in initiation, development and progression of essential hypertension. The aim of our study was to determine whether the ingestion of the food supplement L-arginine actually improves endothelial function, which could be beneficial in the treatment of essential hypertension.

Methods: 30 normotensive healthy men, aged 20-30 years, were divided into two groups according to the family history of hypertension (FN - healthy, not genetically predisposed, FH - normotensive subjects with family history of hypertension). We measured ECG, heart rate, systolic and diastolic blood pressure, cardiac output, stroke volume, total peripheral resistance (Task Force Monitor) and laser Doppler (LD) flux in the microvessels of the skin of the forearm, at rest before and after administration of 0.9 g L-arginine. Endothelium-dependent vasodilation was assessed by iontophoresis of acetylcholine and endothelium-independent vasodilation by iontophoresis of sodium nitroprusside. Values are expressed as mean ± SEM. The study was approved by the National Medical Ethics Committee; written informed consent was obtained from each subject.

Results: After the ingestion of L-arginine the heart rate (FN 67.7 ± 4.3 vs. 62.7 ± 3.3; FH 63.2 ± 2.2 vs. 60.3 ± 2.0 beats/min) and the cardiac output (FN 7.07 ± 0.5 vs. 6.53 ± 0.4; FH 7.19 ± 0.3 vs. 6.38 ± 0.2 L/min) statistically significantly decreased in both groups (paired t-test, $p<0.05$), while arterial blood pressure did not change significantly. In contrast, stroke volume decreased (116.0 ± 6.5 vs. 108.2 ± 5.9 mL) and total peripheral resistance increased (868.9 ± 96 vs. 1114.4 ± 48 MPa s/m3) only in the group of subjets with family history of hypertension (paired t-test, $p<0.05$). We demonstrated that the ingestion of L-arginine in genetically predisposed normotensive subjects acutely improved endothelium-dependent vasodilation (68.8 ± 4.4 vs. 95.4 ± 9.3 PU) (Dunnett's test, $p < 0.05$), which

is consistent with the assumption that endothelial dysfunction is already present in these subjects.
Conclusions: In genetically predisposed normotensive subjects in comparison to healthy subjects without predisposition, L-arginine increased nitric oxide production and improved endothelial function. That justifies L-arginine as a potential therapeutic agent for treatment of arterial hypertension.

Where applicable, the authors confirm that the experiments described here conform with The Physiological Society ethical requirements.

PCA348

Improvement of blood-retinal barrier breakdown in type 2 diabetic rats by alpha-mangostin

C. Areebambud[1], C. Mekseepralard[2] and A. Jariyapongskul[1]

[1]Physiology, Faculty of Medicine, Srinakharinwirot University, Bangkok, Thailand, Bangkok, Thailand and [2]Microbiology, Faculty of Medicine, Srinakharinwirot University, Bangkok, Thailand, Bangkok, Thailand

The blood-retinal barrier (BRB) breakdown is a common feature of diabetic retinopathy. In this present study, effects of long-term supplementation of alpha-mangostin (α-MG), a xanthone isolated from mangosteen fruit, on the ocular blood flow and blood-retinal barrier were investigated in type 2 diabetic rats. Type 2 diabetes was induced in male Sprague-Dawley rats by feeding with high-fat (HF) diet for two weeks followed by intravenous injection of low dose streptozotocin (STZ; 35 mg/kg body weight). The rats were divided into three groups: control group (CON; n=7), type 2 diabetic (HF-STZ; n=7) group and type 2 diabetic rats supplemented with α-MG (HF-STZ-MG; n=7). The use of animals was approved by Faculty of Medicine, Srinakharinwirot University Animal Ethic Committee. Alpha-mangostin was prepared by dissolving in corn oil in the volume of 1 mL per rat. The daily gavage feeding of α-MG 200 mg/kg body weight/day was performed for 40 weeks. At the start of experiment, the rat was anesthetized with pentobarbital sodium (60 mg/kg BW, i.p.) and a tracheotomy was performed to allow for mechanical ventilation with both room air and supplemented oxygen. A catheter was inserted into the femoral vein to inject Evans blue (EB) dye and a femoral artery was cannulated for measurement of arterial blood pressure. After cannulation was performed, ocular blood flow (OBF) was monitored using Laser Doppler flowmeter. The blood-retinal barrier (BRB) leakage was quantified using Evans blue (EB) dye technique. The effect of α-MG on glycemia was assessed by evaluating glycated hemoglobin (HbA1c). The blood sample for HbA1c assessment was obtained from femoral vein. Values were mean ± S.E.M., compared by ANOVA. In type 2 diabetic rats, HbA1c and MAP were increased significantly, whereas OBF was decreased markedly as compared with control group ($p < 0.01$). All of these abnormal parameters were improved by α-MG supplementation (HbA1c = 7.31±0.16 mg/dL for HF-STZ vs 4.31±3.33 mg/dL for HF-STZ-MG, $p < 0.01$; MAP = 132±2.1 mmHg for HF-STZ vs 107.28±3.33 mmHg for HF-STZ-MG, $p < 0.01$; OBF (arbitary unit) = 173.67±5.0 for HF-STZ vs 230.50±1.68 for HF-STZ-MG, $p < 0.01$). Additionally, the leakage of EB dye from retinas was significantly decreased in type 2 diabetes supplemented with α-MG as compared with type 2 diabetes (BRB leakage = 47.84±4.67 μg/mg of retina for HF-STZ vs 30.56±1.75 μg/mg of retina for HF-STZ-MG, $p < 0.01$). These results demonstrated that alpha-mangostin supplementation improved glycemic state, mean arterial pressure and exerted beneficial effects on the ocular blood flow and blood-retinal barrier integrity in type 2 diabetes.

This study was supported by research funds from The Thailand Research Fund (TRF; DBG5480008).

Where applicable, the authors confirm that the experiments described here conform with The Physiological Society ethical requirements.

PCA350

Neuropilin-1 regulates endothelial focal adhesion turnover via p130Cas phosphorylation

I. Evans, W. Pickworth, G. Schey, P. Frankel and I.C. Zachary

Medicine, University College London, London, UK

Neuropilin-1 (NRP1) is a non-tyrosine kinase receptor for vascular endothelial growth factor (VEGF) and a co-receptor for VEGF receptor 2 (VEGFR2) signalling in the endothelium. There is increasing evidence that NRP-1 plays a pivotal role in endothelial migration and angiogenesis, but the mechanisms involved are unclear. Recently, we have shown that NRP-1 is required for VEGF-mediated phosphorylation of the adaptor protein, p130Cas, a critical signalling hub in the regulation of cell motility, and this novel NRP-1-p130Cas pathway is important for endothelial cell migration (Evans et al 2011). Here we show that knockdown of either p130Cas or NRP-1 inhibits the VEGF-induced decrease in endothelial adhesion to fibronectin. Furthermore, NRP-1 and p130Cas are required for VEGF-induced focal adhesion kinase (FAK) phosphorylation, and NRP-1/p130Cas knockdown reduces immunofluorescent staining of focal adhesions by an anti-paxillin antibody. These findings indicate a key role for a NRP-1/p130Cas pathway in VEGF-induced focal adhesion turnover. NRP-1 modulation of focal adhesion turnover is likely to be an important mechanism mediating its role in endothelial migration and angiogenesis.
Evans IM et al (2011). Mol Cell Biol 31, 1174-1185

This work was funded by the British Heart Foundation (Grant RG/11/11/29050)

Where applicable, the authors confirm that the experiments described here conform with The Physiological Society ethical requirements.

PCA351

The role of Na+/H+ exchanger-1 during ischemia-induced cerebrovascular dysfunction

Y. Jung

Ajou University, Suwon, Republic of Korea

The present study has investigated the role of Na+/H+ exchanger-1 (NHE-1) during cerebrovascular endothelial dysfunction during ischemia in a rat cerebral ischemia model in vivo and in mouse brain microvascular endothelial cells (bEnd.3 cells) in vitro. This study shows that specific inhibition of NHE-1 by sabiporide, a well-known NHE-1inhibitor, ameliorates brain edema in vivo, and attenuates cerebrovascular endothelial hyperpermeability induced by ischemia in vivo and in vitro. Occludin and Zonular Occludens-1 (ZO-1) were found to be damaged in the ischemic rat brain, but the inhibition of NHE-1 reversed these damages. Furthermore, during aglycemic hypoxia in bEnd.3 cells, the subcellular distributions of occludin

and ZO-1 were found to be altered, but these changes were also reversed by NHE-1 inhibition. Sabiporide also inhibited aglycemic hypoxia-induced increases in intracellular Ca2+ levels. These findings suggest that NHE-1 plays a critical role during ischemia-induced cerebrovascular hyperpermeability and TJs alteration, and that NHE-1 inhibition can be therapeutic target to protect against cerebrovascular dysfunction during brain ischemia.

Figure. 1

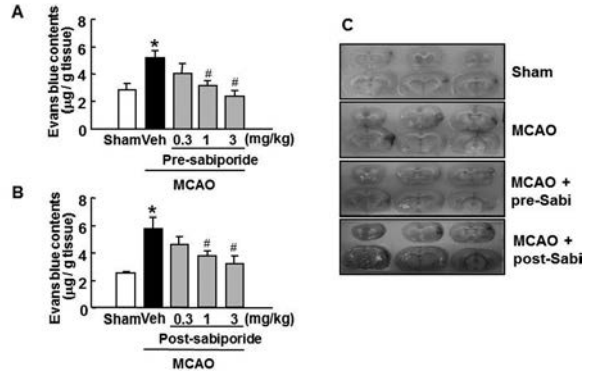

Figure. 1 Effects of sabiporide on ischemia-induced Evans blue extravasation in vivo

Quantitative analysis of Evans blue contents in brain tissues. Evans blue contents were measured 24 h after MCAO in ischemic hemispheres after i.v. pre-treatment (A) or post-treatment (B) with saline (Veh) or sabiporide (0.3, 1, or 3 mg/kg). Data shown are mean ± SEM. (n=5). *p<0.05 vs. the sham control (sham), #p<0.05 vs. vehicle-treated MCAO (Veh). (C) Representative photographs of the sequential cross sections of the brain.

Figure. 2

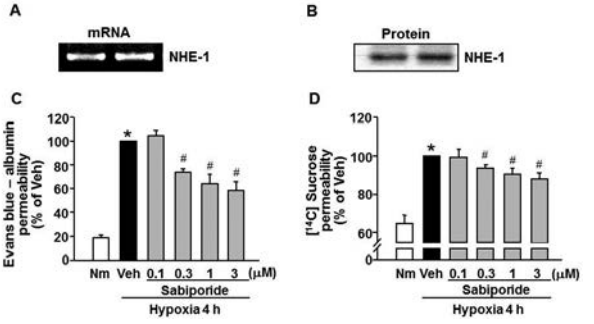

Figure. 2 Effects of sabiporide on aglycemic hypoxia-induced BBB permeability in vitro

(A) RT-PCR for NHE-1 mRNA in bEnd3 cells. PCR for NHE-1 mRNA was performed in normoxic bEnd.3 cells. (B) Western blotting for NHE-1 protein in bEnd3 cells. Western blotting for NHE-1 protein was performed in normoxic bEnd.3 cells. Quantitative analysis of Evans blue–albumin (C) and [14C] sucrose (D) permeability. Data shown are mean ± SEM (n=5). *p < 0.05 vs. normoxia (Nm), #p < 0.05 vs. vehicle-treated aglycemic hypoxia (Veh).

Murakami T etal. (2012). Diabetes 61, 1573-83.

Luo J etal. (2005). J Neurosci 25, 11256 -68.

Sandoval etal. (2008). Neurobiol Dis 32, 200-19.

This work has been supported by a Grant from “Technology Development Program for Bio-industry (2013), Ministry for Food, Agriculture, Forestry and Fisheries”, and a Grant from “the Next-Generation BioGreen 21 Program (2013), Rural Development Administration, Republic of Korea”.

Where applicable, the authors confirm that the experiments described here conform with The Physiological Society ethical requirements.

PCA352

Assessment of arterial distensibility in patients with sarcoidosis

H. Balci[1], S. Sipahi Demirkok[2], M. Yildiz[3], G. Metin[3], M. Hacibekiroglu[1] and G. Simsek[3]

[1]Fikret Biyal Central Research Laboratory, Istanbul, Turkey, [2]Internal Medicine, Istanbul University, Cerrahpasa Faculty of Medicine, Istanbul, Turkey and [3]Physiology, Istanbul University, Cerrahpasa Faculty of Medicine, Istanbul, Turkey

Oxidative stress plays an important role in the pathophysiology of cardiovascular disease. Studies show that sarcoidosis increases oxidative stress. High oxidative stress favors oxidative modification of low density lipoprotein (LDL) . The oxidation of LDL in the artery wall is belived to be primary event leading to the initiation and progression of atherosclerosis. Noninvasive ultrasound techniques are used to evaluate vascular system and cardiovascular condition. One such technique, pulse wave velocity (PWV) is defined as arterial pulse’s velocity of moving along the vessel wall, as an indicator of arterial elasticity. Oxidized LDL may impair arterial function and lead to an increase in arterial PWV. This study aims to investigate arterial distensibility using carotid-femoral (aortic) PWV measurements in patient with sarcoidosis. We recruited 19 patients (12 women, 7 men) with sarcoidosis, and 19 sex-matched healthy controls. In all groups carotid-femoral PWV was measured. PWV was determined by using an automatic device, the Complior Colson which allowed on-line pulse wave recording and automatic calculation of PWV. Triglyseride, total cholesterol, low density lipoprotein (LDL) cholesterol, very low density lipoprotein (VLDL) cholesterol, high density lipoprotein (HDL) cholesterol, oxidized LDL, homocysteine, high-sensitivity C-reactive protein (hs-CRP) levels determined. The association with carotid-femoral PWV and current biochemical parameters had been searched. All the values were expressed as means ± S.D. The obtained results were assesed by independent samples test. Correlations were calculated with the Pearson test. Carotid-femoral PWV, LDL cholesterol and hs-CRP were higher in patient with sarcoidosis than in control subjects (p=0.04, p=0.02, p=0.04 respectively) . There was no significantly change in triglyceride, total, VLDL, HDL cholesterol, oxidized LDL and homocysteine levels. There was a significant correlation between PWV and both total cholesterol (p=0.002, r=0.47) and LDL cholesterol (P=0.001, r=0.51). PWV is influenced by total cholesterol, LDL cholesterol. Patient with sarcoidosis must be followed closely for arterial stiffness.

Where applicable, the authors confirm that the experiments described here conform with The Physiological Society ethical requirements.

PCA353

Increased permeability of pulmonary arterioles after cardiopulmonary bypass

T. Beleznai[1], L. Walker[2], R. Ascione[2] and K.A. Dora[1]

[1]Pharmacology, University of Oxford, Oxford, UK and [2]Bristol Heart Institue, University of Bristol, Bristol, UK

Pulmonary injury is a common complication after cardiopulmonary bypass (CPB) in patients undergoing cardiac surgery. The major causes of tissue damage arise from systemic inflammatory responses, and/or factors released by the ischaemic collapsed lungs. To date, there is no evidence to demonstrate whether this CPB-related pulmonary injury can influence both the permeability and function of the pulmonary arterioles.
We developed a method to isolate, cannulate and pressurize porcine pulmonary arterioles to study their vasomotor function, the leak of fluorescent dyes through the arterial wall, and the expression of key proteins. All arterioles were imaged using linescan confocal microscopy. The fluorescent indicators carboxyfluorescein (CF, 0.1 μM, mw 376.3) or FITC-dextran (1 μM, mw 59,000 – 77,000) were perfused into the lumen of arterioles, and increases in fluorescence immediately outside the arteriolar wall (permeability) measured. Tight junction (Zo-1) and caspase 3 staining was performed on the same arterioles, and imaged while still cannulated, to assess the continuity of cell-cell connections and the onset of apoptosis. Arterioles were studied from pigs which had undergone CPB or sham surgery under anaesthesia and categorized into 4 groups: control (lungs collapsed to air with no ventilation during CPB, equivalent to the current method in patients); IPP-ILFV (intermittent pulmonary perfusion with intermittent low frequency ventilation during CPB); IPP-CLFV (intermittent pulmonary perfusion with continuous low frequency ventilation during CPB); and sham (chest opened only). From each group two samples were obtained, one soon after median sternotomy (baseline) and one at 1 hour of recovery after surgery (reperfusion). All baseline and sham pulmonary arterioles had low permeability to CF and FITC-dextran. When studying reperfused arterioles, the arterioles studied following IPP-ILFV and IPP-CLFV were less permeable to CF when compared to control arterioles. The permeability to FITC-dextran was not increased in any group studied, although a TRPV4 agonist did increase permeability to dextran. Furthermore, tight junction staining showed continuous, uniform cell-cell connections in the endothelium of all baseline arterioles. Interestingly, and consistent with the CF leak data, reperfused lung arterioles from the control group did appear to have gaps in tight junction staining and some caspase 3 staining was evident.
These data suggest that cardiopulmonary bypass and concomitant lung collapse leads to increased permeability of pulmonary arterioles due to damaged cell-cell adhesions, which can be prevented by intermittent pulmonary perfusion with low frequency ventilation of the lungs during CPB.

Where applicable, the authors confirm that the experiments described here conform with The Physiological Society ethical requirements.

PCA354

Peripheral circulatory changes during Valsalva maneuver using DC component of Photoplethysmographic signal

D.S. Chandran, A.J. Kattoor, A.K. Jaryal and K.K. Deepak

Physiology, All India Institute of Medical Sciences, New Delhi, Delhi, India

Introduction: Circulatory changes during Valsalva Maneuver (VM) include venous congestion in the extra-thoracic regions with an associated rise in peripheral venous pressures (1). There is a scarcity of techniques available for non-invasively monitoring the circulatory changes in peripheral veins during VM. The magnitude of the DC component of Photoplethysmographic (PPG) signal which is dependent on the average blood volume in tissues (2) has been shown to correlate with the peripheral venous pressure measured invasively (3). We measured the shift in DC component of PPG at different expiratory pressures of VM with the hypothesis that increasing venous congestion associated with the graded increase in Valsalva pressure would produce a proportional shift in PPG DC component.
Methods: Eleven healthy male volunteers (age range; 17 – 30 years) participated in the study. PPG signal was acquired from right middle finger using a reflection mode transducer at a sampling rate of 1 KHz along with air way pressure while the subject performed VM sequentially at different airway expiratory pressures of 10, 20, 30 and 40 mm Hg. DC component of PPG was extracted from the raw signal using a low pass filter of 0.5 Hz (3). The shift in the DC component was calculated as the difference between maximum signal level during VM at each pressure and the average signal level during the preceding baseline period corresponding to the duration of one respiratory cycle. Repeated measures ANOVA with post hoc Bonferroni's test and Pearson univariate correlation analysis was done to statistically analyze the data.
Results: A proportional rise was obtained in the PPG DC component shift with increase in Valsalva pressure (0.085 ± 0.063 Volts (V), 0.177 ± 0.112 V, 0.264 ± 0.139 V and 0.323 ± 0.152 V for VM conducted at 10, 20, 30 and 40 mm Hg pressure respectively). There was a statistically significant ($p<0.05$) increase in DC component shift with the increase in expiratory pressure from 10 to 20 and 20 to 30 mm Hg but not for the increment from 30 to 40 mm Hg. There was a significant positive correlation between the shifts in DC component and the corresponding Valsalva pressures ($r = 0.99$; $p = 0.004$).
Conclusion: The results indicate that shift in PPG DC component during VM may be utilized as a tool to monitor the peripheral circulatory changes during VM. It may also be utilized as a parameter to check the correct performance of the maneuver by the subject as peripheral venous congestion would only accompany a properly conducted VM. The flattening of the response at higher pressures (30 to 40 mm Hg) probably indicates venous congestion approaching the capacitance limit of vessels.

Porth CJ, Bamrah VS, Tristani FE, Smith JJ. The Valsalva maneuver: mechanisms and clinical implications. Heart Lung. 1984 Sep;13(5):507–18.

Allen J. Photoplethysmography and its application in clinical physiological measurement. Physiol Meas. 2007 Mar;28(3):R1–39.

Nilsson L, Johansson A, Kalman S. Respiratory variations in the reflection mode photoplethysmographic signal. Relationships to peripheral venous pressure. Med Biol Eng Comput. 2003 May;41(3):249–54.

Where applicable, the authors confirm that the experiments described here conform with The Physiological Society ethical requirements.

PCA355

Aliskiren associate with L-Arginine improves vascular reactivity of renovascular hypertension rats

C. Santuzzi, R.V. Tiraddentes, V. Mengal, H. Mauad, P. Matos, S.A. Gouvea, M.H. Cunha and G.R. Abreu

Ciencias Fisiologicas, UFES, Vitoria, ES, Brazil

The antihypertensive therapy with blocked of renin isolated or associate to others drugs is still underexplored in two-kidney one-clip hypertension (2K1C). We investigate the aorta vascular reactivity with aliskiren and its association with L-arginine. Seven days after renal artery clipped, male rats (140-160g, n=8) was divided: 2K1C, 2K1C treated with aliskiren (ALSK) (50 mg/kg /day for 21 days) and 2K1C treated with aliskiren+ L-arginine (L-arg+ALSK). After treatments, rats were anesthetized with pentobarbital (35 mg/kg,i.p.) and killed by exsanguination. The vascular reactivity was analyzed by concentration-response curves to phenylephrine (phen,1 nM-100 μM) and acetylcholine (ach,0.1 nM-300 μM). Were performed blocks (N (G)-nitro-L-argininemethy Ester - L-NAME (100 μM), losartan (10 μM),enalapril (10 μM), incubation with superoxide dismutase(SOD,150 U/ml) and apocynin (0.3 μM). Systolic blood pressure (SBP) was measure before and after treatments by plethysmography and was weighing the left ventricle (LV). In addition, we evaluated the expression of endothelial nitric oxide synthase (eNOS) by the method of Western blotting. Values are means ± S.E.M., compared by ANOVA. (CEUA: 04/2010).The treatments had the following effects: SBP reduced only in the group ALSK + L-Arg (138 ± 4.3 mmHg, P<0.05) compared 2K1C and ALSK groups (204 ± 12.7 and 202 ± 17.7 mmHg, respectively). Was demonstrated that treatment L-arg + ALSK was able to reduce ventricular hypertrophy promoted by hypertension (2K1C:3.32±0.17 mg/g ALSK:2.74±0.14 mg/g ALSK+L- arg:2.58±0.26 mg, P<0.05). 2K1C showed an increase in the concentration response curve to phen and in ALSK and ALSK+L- arg groups this response was reduce. The vasodilator response to ach showed a loss in 2K1C group compared to group ALSK+L-arg. The endothelium removal or incubation with L-NAME increased the vasoconstrictor response to phen in all groups. Apocynin was able to reduce the constrictor response to phen in 2K1C and ALSK+L-arg, however showed no differences in group ALSK. Incubation with SOD showed a decrease in the contractile response to phen in the 2K1C, but no difference in the treated groups. Losartan decrease in contraction to phen in 2K1C and ALSK + L-arg, but not in ALSK group and Enalapril reduce the contractile response only in 2K1C group. In aortic tissue the 2K1C group showed an increase in eNOS protein expression when compared to treatments. The 2K1C showed increase in vascular reactivity to phen, impaired relaxation to acetylcholine and increased expression of eNOS, which seems to be a compensatory mechanism. The ALSK decreased the hyperactivity to phen and expression of eNOS. ALSK+L-arg reduced SBP, vascular reactivity, LV hypertrophy and eNOS expression.These data suggest an important modulation of the renin-angiotensin system and reactive oxygen species in aorta of renovascular hypertension.

Where applicable, the authors confirm that the experiments described here conform with The Physiological Society ethical requirements.

PCA356

Pharmacological analysis of sympathetically-mediated constriction in wild type and α_1-AR knock out mouse tail artery

C. Stevenson[1], C. Daly[1], E. McLachlan[2] and I. McGrath[1]

[1]University of Glasgow, Glasgow, UK and [2]Neuroscience Research Australia, Randwick, NSW, Australia

We have developed transgenic mice lacking the three α1-adrenoceptor (AR) subtypes. Here we report a pharmacological analysis of neurovascular transmission in segments of proximal and distal tail artery of C57/Bl (Wild type), α1AD-AR knock out (ADKO) and α1ABD-AR knock out (ABDKO) mice. In rat proximal tail artery, perivascular stimulation evokes depolarisations mediated by ATP and noradrenaline (1) but contraction is mediated largely by α1- and α2-ARs (2). α2-AR-mediated effects predominate distally (3). The ADKO enables isolation of the α1B-AR which is believed to play a minor role in the vasculature (4) whereas the ABDKO allows study of the remaining receptors to determine the compensatory mechanisms.

Male Wild Type (WT), ADKO and ABDKO mice (4-6 months) were killed by CO2 asphyxiation. Ring segments (2mm) of the tail artery were prepared from proximal (2cm) and distal (5cm) sites. Vessels were mounted on wire myographs under 200mg tension. Contractions were evoked by supramaximal perivascular stimuli (20 V; 0.3 ms pulse width; 20 pulses at 0.5– 8 Hz). Tension was recorded using 'Chart'. The effects of 100nM rauwolscine (α2-AR antagonist), 1mM suramin (P2X receptor antagonist) and 100nM prazosin (α1-AR antagonist) were tested. Data are expressed as mean ± S.E.M. Un-paired t-tests were carried out, with P<0.05 taken as significant.

Proximally, at 0.5 and 8 Hz, the response to nerve stimulation was lower in KO animals compared to WT (P<0.05; WT–n=41; ADKO–n=8; ABDKO–n=14). Distally, the response to nerve stimulation was similar across the strains; except at 8 Hz where the ABDKO response was smaller than the WT response (P<0.05; WT–n=41; ADKO–n=10; ABDKO–n=11). The inhibition of response following rauwolscine incubation at 0.5 Hz was similar in each strain and location (70 % ± 10). However, proximally, at 8 Hz, the reduction was greater in the ABDKO strain compared with the WT and ADKO strain (P<0.05; WT–n=14; ADKO–n=6; ABDKO–n=6). Distally, the reduction was greater in both KO strains compared with the WT response at 8 Hz (P<0.05; WT–n=7; ADKO–n=7; ABDKO–n=6). At both locations following rauwolscine and suramin incubations, a response was detected in the WT and ADKO strains. This response was removed following further incubation with prazosin.

The removal of all α1-ARs or isolation of the α1B-AR has a greater effect proximally. In the WT vessels at 0.5 Hz, the receptor mainly responsible for producing the nerve-mediated response appears to be the α2-AR and this role switches to the α1-ARs at 8 Hz. The residual response following incubation with α2-AR and P2X receptor antagonists in the ADKO indicates a role for the α1B-AR. Even with loss of all of the α1-AR subtypes, the α2-ARs and P2X receptors can support the contraction at both frequencies.

Sneddon P & Burnstock G (1984). *Eur J Pharmacol* **106 (1)**, 149-152.

Yeoh M et al. (2004). *J Physiol* **561**, 583-596.

Medgett IC (1985). *Eur J Physiol* **108**, 281-287.

Daly C et al. (2002). *Physiol Genomics* **9**, 85-91.

This work was funded by a PhD studentship Grant from the British Heart Foundation.

Where applicable, the authors confirm that the experiments described here conform with The Physiological Society ethical requirements.

PCA357

Mathematical modelling of capillary O_2 supply capacity in cardiac and skeletal muscle

A.A. Al-Shammari[1], E.A. Gaffney[1] and S. Egginton[2,3]

[1]Centre for Mathematical Biology, University of Oxford, Oxford, UK, [2]Centre for Cardiovascular Sciences, University of Birmingham, Birmingham, UK and [3]School of Biomedical Sciences, University of Leeds, Leeds, UK

The ability to quantify capillary supply plays a key role in developing effective therapeutic interventions for numerous pathological conditions, e.g. chronic ischaemia in striated muscle, but is fraught with difficulties. Averaged measures – such as mean capillary density (CD) or mean intercapillary distance (ICD) – may characterise global tissue ischaemia [1], but cannot account for local dysfunction associated with the underlying capillary distribution. Detailed tissue geometry including muscle fibre size has been incorporated into indices of capillary supply, e.g. local capillary-to-fibre ratio (LCFR) and local capillary density (LCD), by considering the distribution of *capillary domains*. By identifying vessel locations in a plane perpendicular to muscle fibre orientation, each capillary domain represents the area of supply of its enclosed capillary [2]. Although such geometrical constructs have proven useful in describing oxygenation for homogeneous muscle tissue such as the myocardium [3], it is unclear how well they may capture capillary supply areas in the presence of structural and metabolic heterogeneities.

Using a mathematical framework to assess the maximal capacity of capillary supply in uniform and mixed muscles [4], we theoretically demonstrate that under normal physiological conditions capillary domains can provide an accurate representation of the tissue region supplied by each capillary, or trapping region, based on oxygen flux lines. In contrast, reduced accuracy is found with increasing levels of pathological heterogeneities such as (a) local capillary rarefaction, (b) pathological variations in PO_2 of neighbouring capillaries, and (c) substantial differences in O_2 extraction capacities among different fibre types. For aerobic muscle, the correlation between capillary domain and diffusive supply areas suggests a sensitive local control of angiogenesis on the length scale of fibre diameter.

In contrast, the effect of capillary loss becomes insignificant when localised to glycolytic fibres, suggesting that such rarefaction may be mitigated by reducing the oxygen extraction capacity per fibre volume. Moreover, in the presence of hypoxia, the decay and desaturation of mitochondrial oxygen extraction and myoglobin-O_2 complex, respectively, is predicted to significantly improve the utility of capillary domains. Given that capillary domains are based solely on the spatial distribution of capillaries, this suggests that in chronically hypoxic tissues the oxygen supply of each capillary is predicted to be essentially determined by, and most sensitive to, the distribution of capillaries rather than fibre oxygen demand.

Egginton S (1990) In: Boutilier RG (ed) Vertebrate Gas Exchange from Environment to Cell. Adv. Comp. Environ. Physiol. 6: 73-141

Egginton S, Ross HF (1992) Oxygen Transport in Biological Systems: Modelling of Pathways from Environment to Cell. Cambridge University Press, 298pp

Egginton S, Gaffney EA (2010) Exp. Physiol. 95(10): 971-979.

Al-Shammari A A, Gaffney EA, Egginton S (2012) Bull. Math. Biol. 74 (9): 2204-2231

A. Al-Shammari acknowledges support by a generous studentship awarded by Kuwait University.

Where applicable, the authors confirm that the experiments described here conform with The Physiological Society ethical requirements.

PCA358

The effects of Insulin-like Growth Factor Binding Protein-1 on endothelial repair in the insulin resistant setting

A. Aziz, N. Yuldasheva, J. Smith, N. Haywood, P. Cordell, R. Cubbon, K.E. Porter, M.T. Kearney and S.B. Wheatcroft

University of Leeds, Leeds, UK

Introduction: Insulin resistance predisposes to cardiovascular disease by inducing endothelial dysfunction. Our laboratory has shown that insulin resistance impairs endothelial repair.[1] Additionally, we have discovered that a circulating protein, insulin-like growth factor binding protein-1 (IGFBP-1), is potentially protective in the vasculature by stimulating nitric oxide production and enhancing insulin sensitivity.[2] In cross-sectional studies, low IGFBP-1 levels are associated with diabetes and cardiovascular disease. In this project, we investigated whether IGFBP-1 can enhance vascular endothelial repair in insulin resistant mice in vivo and examined potential mechanisms in human endothelial cells and endothelial progenitor cells in vitro.

Methods: To assess endothelial regeneration, insulin receptor (IR)+/- mice with or without transgenic over-expression of IGFBP-1 (IGFBP1tg) underwent femoral artery endothelial denuding wire-injury. under anaesthesia. Mice were anaesthetised with isoflurane 2-3% before an incision was made. After the operation, the mouse was then placed in an incubator with thermal support until they fully recovered. Mice received post-operative analgesia (buprenorphine 0.25mg/kg s.c.) and were monitored for signs of distress. After five days, the area of regenerated endothelium was quantified in en face sections of injured artery. Endothelial regeneration was also assessed ex-vivo in human tissues by seeding segments of endothelium-denuded human saphenous vein with a sub-confluent density of human coronary artery endothelial cells, which were pre-incubated with or without IGFBP-1. Adherent cells were quantified using con-focal microscopy. The effects of IGFBP-1 on the functional properties of endothelial cells in vitro were examined using cell migration assays.

Results: Endothelial regeneration following wire injury was blunted in IR+/- mice, however regeneration was significantly improved in this model of insulin resistance by IGFBP-1 overexpression (n=5-10 per group). In human umbilical vein endothelial cells (HUVEC), insulin resistance was mimicked by the pro-inflammatory cytokine tumour necrosis factor-alpha, which significantly inhibited migration in a scratch wound assay (n=9). Co-incubation with IGFBP-1 restored the migratory capacity of HUVEC to control levels. There was a trend to enhanced migration of Human Coronary Artery Endothelial Cells (HCAEC) in response to IGFBP-1 in a Boyden chamber assay (P=0.07). IGFBP-1 significantly enhanced

endothelial cell adhesion on a human saphenous vein matrix (n=5, p<0.001).
Conclusions: IGFBP-1 over-expression enhances endothelial repair in the insulin resistant setting. In endothelial cells, IGFBP-1 restores cell migration in a pro-inflammatory setting and improves cell adhesion. Ongoing studies are in progress to examine the underlying mechanisms. Collectively, these data raise the possibility that manipulating IGFBP-1 could be a strategy to enhance endothelial repair in patients with insulin resistance.

Kahn MB et al (2011) Diabetes 60(4):1295-303

Rajwani A et al (2012) Diabetes 61(4):915-24

British Heart Foundation

University of Leeds

Where applicable, the authors confirm that the experiments described here conform with The Physiological Society ethical requirements.

PCA359

Tissue- and agonist-specific isolated murine arterial responses to ageing

C. Nicholson, M. Sweeney, S.C. Robson and M.J. Taggart

Newcastle University, Newcastle Upon-Tyne, UK

Cardiovascular diseases (CVDs) account for almost 191,000 deaths per year in the UK – one in three of all deaths [1]. Age-related functional and structural changes in the resistance vasculature, with consequent alterations in arterial tone, contribute to the overall risk of CVD. There appears to be a marked difference in the prevalence of CVD in men and women, with the risk being smaller in women than men aged 30-50. After the menopause, however, the incidence of CVD increases in women and approaches the incidence rate of men [2] indicating a potential beneficial effect of oestrogen although this has resisted absolute confirmation. Therefore, a clearer understanding of vascular functional changes with ageing, and the influence of oestrogens therein, would be informative for assessing effective cardio-protective treatment options in older women. The aims of this study were to investigate the effects of relaxing agents, including 17-β oestradiol (17-β) and oestrogen receptor (ER)-specific agonists, on small arteries from young (3 month) and aged (24 month) female C57BL mice.
Uterine, mesenteric and tail arteries (<250μm) were dissected and mounted on a wire myograph for isometric force measurement. Endothelium-dependent relaxations were assessed in each by the addition of increasing concentrations of acetylcholine (Ach) (0.1nm - 10μM) to maximally constricted arteries. In addition, arteries were maximally pre-constricted with the thromboxane agonist U46619 (1μM) then exposed to increasing concentrations of one of two ER specific agonists, PPT (ER-α) and DPN (ER-β) or 17-β. Changes in tension were measured and responses between groups were compared using 2-way ANOVA (p<0.05 was significant).
Ach-induced relaxations were significantly reduced in all artery types (maximal relaxations (%): UA Young: 57.2±4.0, UA Aged: 43.0±2.6, TA Young: 61.8±5.1, TA Aged: 43.6±2.2, MA Young: 34.1±1.9, MA Aged: 14.6±2.0). In arteries of young and aged mice, concentration-dependent relaxations of all three artery types were induced by 17-β and PPT. For example, maximal relaxations (%) for UA (n=7), TA (n=9) and MA (n=9), to 17-β from young mice were 54.4±3.5, 52.0±5.4, and 63.3±5.1 and from old mice were 58.8±4.9, 36.6±5.1, and 72.0±7.3. However, in contrast, DPN significantly relaxed arteries of young mice (maximal relaxations for UA, TA and MA, respectively: 38.1±2.5, 21.6±1.5, and 42.2±4.6) but failed to do so in UA or TA from old mice.
In summary, age-dependent alterations in endothelial-dependent function are shared across several arteries from distinct vascular beds. In contrast, tissue-specific effects of ageing are evident in arterial vasodilation by the putative ERβ-specific agonist DPN. The data alerts one to the need to consider tissue-specific responses when exploring age-related changes in vascular function.

Heart Disease Statistics, BHF, 2008.

Dubey RK., et al. (2004). Hypertension. 44(6): p. 789-95.

Funded by Newcastle University and NHS Hospitals Trust BRC and FSF.

Where applicable, the authors confirm that the experiments described here conform with The Physiological Society ethical requirements.

PCA360

Curcumin could ameliorate diabetic vascular inflammation by decreasing ROS overproduction, leukocyte-endothelium interaction, and NOX2 expression

N. Wongeakin[1], P. Bhattarakosol[2] and S. Patumraj[1]

[1]Department of Physiology, Center of Excellence for Microcirculation, Faculty of Medicine, Chulalongkorn university, Bangkok, 10330, Thailand and [2]Department of Microbiology, Faculty of Medicine, Chulalongkorn university, Bangkok, 10330, Thailand

The number of patients with diabetes is expected to increase more than three-hundred million within ten years. Moreover, in chronic diabetes the overproduction of reactive oxygen species (ROS) involves and mediates many cells damaged. Recently, thioredoxin-interacting protein (Txnip) expression and the activated NADPH oxidase enzyme (NOX2) are reported for developing ROS overproduction and causing vascular inflammation in diabetes. The study aimed to investigate the effects of curcumin, a potent antioxidant with anti-inflammatory property, on preventing diabetes-induced vascular inflammation in association with its actions on Txnip expressions and NOX2 enzyme. Male Wistar rats were divided into three groups: control (CON, n=5), diabetic (DM; streptozotocin (STZ), i.v. 55 mg/kg BW, n=5), and diabetes-treated with curcumin (DMCUR; curcumin 300mg/kgBW in corn oil, n=5). The guideline for experiment animals was suggested by the National Research Council of Thailand. The supplementation of curcumin was started at 10 days after STZ-injection. 12th week after STZ injection, iris blood perfusion and leukocyte adhesion of each rat was measured by using laser Doppler and intravital fluorescent microscopy, respectively. Plasma glucose (BG) and HbA1c were determined using enzymatic and turbidimetric immunoinhibition methods, respectively. Txnip expression, P47phox expression (marker of NOX2), and malondialdehyde (MDA) level at eye fundus were determined by Western Blot analysis and TBAR assay, respectively. Values are means±S.E.M., compared by ANOVA. The body weight and iris blood perfusion of DM (271.67±13.22 g, 246±26.99 AU) and DMCUR (258.00±17.64 g, 311.28±31.13 AU) were decreased significantly as compared to CON (424.00±28.28 g, 870.27±39.61 AU) (P < 0.001). BG and HbA1c of DM (410.33±16.77 dL, 9.47±0.47 %) and DMCUR (390.33±11.59 dL, 9.30±0.21 %) were increased significantly as compared to

CON (172.83±11.08 dL, 4.00±0.06 %, P < 0.001). Interestingly, the leukocyte adhesion, p47phox expression, and MDA level in DM (33.71±0.68 cells/frame, 0.87±0.14, and 11.69±0.22 nmole/protein100μg) were increased significantly when compared to CON (3.64±0.68 cells/frame, 0.39±0.03, and 5.17±1.05 nmole/protein100μg, P < 0.05), and DMCUR (14.94±3.85 cells/frame, 0.51±0.05, and 8.36±0.63 nmole/protein100μg, P < 0.05). Txnip expression in DM (0.83±0.14) and DMCUR (0.71±0.1) were significantly higher than CON (0.45±0.06, P < 0.05). It suggested that curcumin could ameliorate diabetic vascular inflammation by decreasing ROS overproduction, reducing leukocyte-endothelium interaction, and also inhibiting NOX2 activation. Moreover the results also showed a linear correlation between the inhibitory effects of curcumin on leukocyte-endothelium interaction and NOX2 inhibition (y=0.0143x+0.3666, r=0.952, P < 0.05).

Where applicable, the authors confirm that the experiments described here conform with The Physiological Society ethical requirements.

PCA361

Apocynin prevents vascular effects caused by chronic exposition to low concentrations of mercury

J.T. Dini, D. Rizzetti, F. Maciel Peçanha, D. Valentim Vassalo and G. Wiggers

Universidade Federal do Pampa, Uruguaiana, Rio Grande do Sul, Brazil

Mercury increases the risk of cardiovascular disease, oxidative stress and alters vascular reactivity. This metal elicits endothelial dysfunction as a result of the decreased NO bioavailability by increased oxidative stress and contractile prostanoids production. NADPH oxidase is the major source of reactive oxygen species (ROS) in the vasculature. Our aim was to investigate whether treatment with apocynin, a NADPH oxidase inhibitor, prevents the vascular effects caused by chronic intoxication by low concentrations of mercury. Three-month-old male Wistar rats were treated for 30 days with: a) intramuscular injections - i.m. - of saline; b) HgCl2 (i.m. 1st dose 4.6 μg/kg, subsequent doses 0.07 μg/kg/day); c) Apocynin (1.5 mM in drink water plus saline i.m.); d) Apocynin plus HgCl2. Mercury treatment: 1) increased aortic vasoconstrictor response to phenylephrine and reduced endothelium-dependent responses to acetylcholine; 2) increased the involvement of ROS and vasoconstrictor prostanoids in phenylephrine response whereas reduced the endothelial NO modulation of such responses, 3) reduced aortic activity of superoxide dismutase (SOD) and glutathione peroxidase (GPx) and increased plasma malondialdehyde (MDA) levels. Treatment with apocynin partially prevented the increased phenylephrine responses and reduced the endothelial dysfunction elicited by mercury treatment. In addition, apocynin treatment increased NO modulation of vasoconstrictor responses and aortic SOD activity and reduced plasma MDA levels, without affecting the increased participation of vasoconstrictor prostanoids observed in aortic segment from mercury treated rats. Conclusions: Mercury increases the vasoconstrictor response to phenylephrine by reducing NO bioavailability and increasing the involvement of ROS and constrictor prostanoids. Apocynin protects the vessel from the deleterious effects caused by NADPH oxidase, but not from those caused by prostanoids, demonstrating a two-way action.

Clarkson TW. (1997) The toxicology of mercury. Crit Rev Clin Lab Sci 34:369–403.

Pecanha FM, Wiggers GA, Briones AM, Perez-Giron JV, Miguel M, et al. (2010). J Physiol Pharmacol 61: 29-36.

Wiggers GA, Pecanha FM, Briones AM, Perez-Giron JV, Miguel M, et al. (2008). Am J Physiol Heart Circ Physiol 295:H1033-H1043.

Where applicable, the authors confirm that the experiments described here conform with The Physiological Society ethical requirements.

PCA362

Sulforaphane pre-treatment reduces Nrf2 content in core and peri-infarct brain regions in rats subjected to ischaemia-reperfusion injury

S. Srivastava, A. Alfieri, R.C. Siow, P.A. Fraser and G.E. Mann

BHF Center of Research Excellence, Cardiovascular Division, King's College London, London, UK

Cerebral stroke is one of the leading causes of adult morbidity within the UK. Oxidative stress is a major consequence of reperfusion injury, resulting in disruption of the blood-brain barrier and neuronal cell death. Activation of the redox-sensitive transcription factor NF-E2 related factor 2 (Nrf2) affords increased protection against stroke via the upregulation of antioxidant defence enzymes such as heme oxygenase-1 (HO-1) and NADPH:quinone oxidoreductase 1 (NQO1). Quantitative immunohistochemistry was employed to examine temporal and spatial distribution of Nrf2 content in contralateral and stroke-affected regions in ex vivo brain sections from male Sprague-Dawley rats (250–300g) subjected to 70 min middle cerebral artery occlusion (MCAo) and reperfusion injury (4, 24 and 72h). Rats were also pre-treated with the Nrf2 inducer sulforaphane (SFN, 5mg/kg i.p.) 1h prior to MCAo followed by 24h reperfusion injury. Coronal brain sections (10μm) were obtained from perfusion-fixed brains and incubated with an anti-Nrf2 primary and horseradish peroxidase conjugated secondary antibody. Core and peri-infarct regions were identified based on glial fibrillary acidic protein (GFAP) expression. Sections were reacted with 3,3'-diaminobenzedine (DAB) and H2O2, and initial rates of DAB polymer formation ((sx103)-1, mean ± S.E.M., n=3-5 animals per group) were measured as an index of Nrf2 concentration. Image processing was used to determine Nrf2 content in nuclear and cytoplasmic compartments. Moreover, murine bEnd.3 brain endothelial cells were treated with SFN (2.5μM) and time dependent expression of HO-1 and NQO1 assessed by immunoblotting. Nrf2 content was greater in cytoplasm compared to nucleus after 4h reperfusion, but was increased in nuclear compartments following 24h reperfusion injury. After 72h, nuclear levels of Nrf2 returned to levels observed at 4h. Total cellular Nrf2 content was greater after 24h reperfusion, with increased levels noted in peri-infarct (1.35±0.016) compared to stroke core (0.72±0.016, P<0.001) regions. Cellular Nrf2 content was also elevated in contralateral regions (0.38±0.005) of stroke versus naïve (0.27±0.004, P<0.001) animals. After 72h, cellular Nrf2 content decreased in stroke-affected regions, but remained elevated in peri-infarct cells. Notably, SFN pre-treatment significantly reduced cellular Nrf2 content in contralateral regions (0.18±0.002) and in peri-infarct (0.049±0.008) and core (0.23±0.005) regions of the stroke hemisphere after 24h reperfusion compared to untreated animals subjected to reperfusion injury (P<0.001). Furthermore, SFN induced a time dependent increase in HO-1 and NQO1 expression in bEnd.3 cells. We conclude that SFN pre-treatment activates the Nrf2

defence pathway, affording protection of the brain against oxidative injury in stroke.

BHF and Henry Smith Charity

Where applicable, the authors confirm that the experiments described here conform with The Physiological Society ethical requirements.

PCA363

Interaction of Sequestosome1/p62 with voltage-activated potassium channels in arterial smooth muscle cells in injury-induced arterial remodeling

T. Ishii[1], E. Warabi[1], R.C. Siow[2] and G.E. Mann[2]

[1]School of Medicine, University of Tsukuba, Tsukuba, Ibaraki Prefecture, Japan and [2]School of Medicine, King's College London, London, UK

Sequestosome1/p62/A170 (SQSTM1) is a multifunctional regulator of cell signaling and metabolism with an ability to modulate targeted degradation of proteins through autophagy. SQSTM1 implements its functions through physical interactions with different types of proteins including atypical PKCs, non-receptor type tyrosine kinase p56Lck (Lck), polyubiquitin and autophagosomal factor LC3. One of the notable physiological functions of SQSTM1 is the regulation of redox sensitive voltage-gated potassium (Kv) channels which modulate membrane potential, signal integration and neurotransmitter release. Kv channels are composed of α and β subunits, (Kvα)4 and (Kvβ)4. Previous studies have established that SQSTM1 scaffolds PKCζ, enhancing phosphorylation of Kvβ. Both PKCζ and SQSTM1 play key roles in acute hypoxia-induced Kv channel inactivation in pulmonary artery.

SQSTM1 is an oxidative stress inducible protein regulated by transcription factor Nrf2, a master regulator of antioxidant system (1). The expression levels of SQSTM1 in vascular cells are up-regulated by atherogenic stimuli, such as oxidized low density lipoprotein and 4-hydroxynonenal, suggesting SQSTM1 has a protective role against oxidative stress (2). We have examined the role of SQSTM1 in neointimal hyperplasia and vascular remodeling in vivo following carotid artery ligation. Neointimal hyperplasia was markedly enhanced near the ligation sites after 3 weeks in SQSTM1-/- compared with wild-type (SQSTM1+/+) mice. The intimal area and stenotic ratio were, respectively, 2.1- and 1.7-fold higher in SQSTM1-/- mice, indicating enhanced proliferation of vascular smooth muscle cells (SMCs). We found that migration of aortic SQSTM1-/- SMCs was enhanced compared to wild type SMCs and that they proliferated more rapidly in response to fetal calf serum and attained 2-3-fold higher cell densities compared to wild type SMCs. The enhanced proliferation of SQSTM1-/- aortic SMCs in vitro highlights a novel role for SQSTM1 in suppressing smooth muscle migration and proliferation following vascular injury (3).

Recent studies have revealed the role of Kv1.3 channels in enhancing migration and proliferation of arterial SMCs (4). As Kv1.3 channels provide a signaling platform and may thereby modulate the migration and proliferation of arterial SMCs and are recognized as a therapeutic target for treatment of restenosis. Based on these studies, we highlight the molecular mechanisms by which SQSTM1 suppresses proliferation of arterial smooth muscle cells and neointimal hyperplasia following carotid artery ligation.

Ishii T. et al. (2000) J Biol Chem 275, 16023-16029.

Ishii T. et al. (2004) Circ Res 94, 609-616.

Sugimoto R. et al. (2010) J Mol Med 14(6B), 1546-1554.

Cidad P. et al. (2012) Arterioscler Thromb Vasc Biol 32, 1299-1307.

Where applicable, the authors confirm that the experiments described here conform with The Physiological Society ethical requirements.

PCA364

Inhibitory Effects of Sprouty4 on proliferation and migration of vascular smooth muscle cells involving in suppression of MAPK and Akt double signal pathways

H. Li[1,2], X. Yang[2], R. Liaw[2], Y. Shi[3], S. Ma[4] and B. Friesel[2]

[11]1Department of Physiology, College of Basic Medicine, Lanzhou University, Lanzhou, Gansu, China, [2]The Center for Molecular Medicine, Maine Medical Center Research Institute, Scarborough, ME, USA, [3]Guangzhou Baiyunshan Pharmaceutical Factory, Guangzhou, China and [4]Northwest Normal University, Lanzhou, China

Sproutys (Sprys) are novel negative modulators of mitogen-activated protein kinase (MAPK) involving in growth factor-mediated tyrosine kinase receptor signaling, and have been suggested to be an anti-oncogene as reduced expressions of Sprys have been shown in several cancers. Among four of Spry orthologs the expression of Spry1, 2, and 4 is widespread in embryos and adults, while that of Spry3 is believed to be more restricted, and most of researches are focused on Spry1, 2. Spry4 can inhibit angiogenesis, however, molecular mechanism of the suppression has not yet been clarified completely, and so far no evidences have been reported in vascular smooth muscle cells (SMCs). In the present study, primary cultured aortic SMCs from Spry4 transgenic mice (produced in the Maine Medical Center Research Institute (MMCRI)) or from wild-type mice were plated in 6-well plates at subconfluent density, and transduced with LacZ (Control), Cre or Myc-tagged mouse Spry4 adenoviruses (provided by MMCRI) at a concentration of 400 virus particles per cell. After overnight incubation with virus, medium was replaced with fresh SmGM-2 and cells were incubated for an additional 24 to 48 hr, then the over-expression of Spry4 in mouse SMCs was determined by RT-PCR and immunoblotting. Cultured mouse SMCs were used from passage 4 to 6 for all experiments. Over-expression of Spry4 could obviously inhibit the resting and ET-1 or PDGF-BB activated Raf-ERK ½ and p38 MAPK signal, down-regulate phosphorylated ERK ½ and p38 levels, decrease phosphorylated CyclinD1 expression and MMP13 mRNA level in primary cultured SMCs. Further, we showed that PI3K/Akt signaling and its down-stream target Foxo1/Foxo3 proteins were negatively regulated by Spry4 over-expression. A scratch wound assay to monitor SMC migration showed that the percent closure of wounds in Spry4 conditional over-expression group was obvious lower than control group after wounding 24 (22.25±4.40% vs. 36.18±5.16%, $p<0.05$) or 48hr (38.44±5.53% vs. 57.83±9.72%, $p<0.05$). For proliferation studies, SMCs were incubated with 5-bromo-2-deoxyuridine (BrdU) for 24hr, and then were immunostained with a monoclonal anti-BrdU antibody and counterstained with DAPI to label all nucleated cells, and significantly more BrdU positive stained cells were observed in fields of Spry4 conditional over-expression SMCs than control group, and the data clearly showed a lower proliferation rate for Spry4 conditional over-expression SMCs (23.43±3.9%) than for control group (38.03±5.8%) ($p<0.05$). The above results demonstrate that Spry4 can inhibit MAPK and Akt double signal transduction pathways and suppress

proliferation and migration of SMCs, which probably contribute to modulate angiogenesis and vascular remodeling, and are also very important mechanisms in prevention of oncogenesis.

Where applicable, the authors confirm that the experiments described here conform with The Physiological Society ethical requirements.

PCA365

TRPV1 and autocrine serotonin signalling elicit Ca^{2+} release from the acidic organelles of ADP-stimulated human platelets

S. Sage[1] and A. Harper[2]

[1]Department of Physiology, Development and Neuroscience, University of Cambridge, Cambridge, UK and [2]Institute for Science and Technology in Medicine, Keele University, Stoke-on-Trent, UK

Introduction: We have previously reported that TRPV1 activation is required for a secondary plateau phase of adenosine diphosphate (ADP)-evoked Ca^{2+} release in human platelets, through its ability to control serotonin release from these cells[1]. Here we have further examined the link between TRPV1 activation and serotonin secretion in ADP-stimulated platelets.
Methods: Platelets were isolated from blood obtained by venepuncture of healthy volunteers under informed consent and with local ethical committee approval in accordance with the Declaration of Helsinki. Changes in cytosolic pH (pH_{cyt}), cytosolic Ca^{2+} concentration ($[Ca^{2+}]_{cyt}$), intracellular Ca^{2+} store concentration ($[Ca^{2+}]_{st}$) and acidic organelle pH (pH_{ao}) were measured in BCECF-, Fura-2-, Fluo-5N- and lysosensor green-loaded human platelets respectively. Platelets were stimulated with either 100 μM capsaicin or 50 μM ADP in the absence of extracellular Ca^{2+} at 37°C. Data are presented as mean ± S.E.M. of the number of samples (n) indicated. Statistical significance was tested by Student's t-test.
Results: Stimulation of platelets with capsaicin in the absence of extracellular Ca^{2+} elicited a small rise in $[Ca^{2+}]_{cyt}$, as we have previously reported[1]. Under the same conditions capsaicin also elicited an acidification of the cytosol, an alkalinisation of the acidic organelles and a small decrease in $[Ca^{2+}]_{st}$ (n=3). Stimulation of platelets with ADP elicited the same effects, which could be partially prevented by treatment of platelets with the TRPV1 inhibitor, 5'-Iodo-resiniferatoxin (20 μM, n= 7-14; $p<0.05$). Conversely, concurrent stimulation of platelets with ADP and capsaicin potentiated the changes in $[Ca^{2+}]_{cyt}$ (131.2 ± 8.7 % of control; n = 6; $p < 0.05$), $[Ca^{2+}]_{st}$ (175.0 ± 19.1% of control; n = 6; $p < 0.05$), pH_{ao} (296.4 ± 75.3% of control; n = 6; $p < 0.05$) and pH_{cyt} (291.3 ± 52.5 % of control; n = 6; $p < 0.05$). Previously we have demonstrated that pretreatment of platelets with ketanserin (a 5-HT_{2A} receptor antagonist that inhibits autocrine serotonin signalling) significantly inhibited ADP-evoked rises in $[Ca^{2+}]_{cyt}$[1]. We therefore investigated whether this might be due to an effect on the ADP-evoked alkalinsation of the acidic organelles. Pretreatment for 2 minutes at 37°C with 25 μM ketanserin inhibited the ADP-evoked changes in $[Ca^{2+}]_{st}$ (31.1 ± 6.2% of control; n = 5; $p < 0.05$), pH_{ao} (56.9 ± 14.3% of control; n = 7; $p < 0.05$) and pH_{cyt} (59.4 ± 7.3% of control; n = 6; $p < 0.05$).
Conclusions: These data suggest that TRPV1 regulates ADP-evoked serotonin secretion from human platelets. Autocrine serotonin signalling then elicits Ca^{2+} release from the acidic organelles, potentiating the initial ADP-evoked Ca^{2+} signal.
Harper AGS *et al.*, (2009). *J Thromb Haemost* **7**:330-338.

This work was supported by The British Heart Foundation.

Where applicable, the authors confirm that the experiments described here conform with The Physiological Society ethical requirements.

PCA366

Exchange protein activated by cAMP (Epac) induces vascular relaxation by activating Ca^{2+}-sensitive K^+ channels in rat mesenteric artery

O. Roberts[1], T. Kamishima[2], R. Barrett-Jolley[3], J.M. Quayle[2] and C. Dart[1]

[1]Institute of Integrative Biology, University of Liverpool, Liverpool, UK, [2]Institute of Translational Medicine, University of Liverpool, Liverpool, UK and [3]Institute of Aging and Chronic Disease, University of Liverpool, Liverpool, UK

Vasodilator-induced elevation of intracellular cyclic AMP (cAMP) is a central mechanism governing arterial relaxation [1]. The vasculature expresses three distinct cAMP effectors: cAMP-dependent protein kinase (PKA), cyclic nucleotide-gated ion channels and the more recently discovered exchange protein directly activated by cAMP (Epac) [2]. The mechanisms by which cAMP induces vasorelaxation are thus likely to be complex and diverse. Here we investigate the role of Epac in mediating vasorelaxation in rat mesenteric arteries.
In myography experiments, the Epac-selective cAMP analogue 8-pCPT-2'-*O*-Me-cAMP-AM (5μM, subsequently referred to as 8-pCPT-AM) elicited a 77.6 ± 7.1% relaxation of phenylephrine-contracted arteries over a 5 minute period (mean ± SEM; n=6). 8-pCPT-AM induced only a 16.7 ± 2.4% relaxation in arteries pre-contracted with high extracellular K^+ over the same time period (n=10), suggesting that Epac's relaxant effect relies upon vascular cell hyperpolarization. This involves Ca^{2+}-sensitive, large-conductance K^+ (BK_{Ca}) channel opening since iberiotoxin (100nM) significantly reduced the ability of 8-pCPT-AM to reverse phenylephrine-induced contraction (arteries relaxed by only 35.0 ± 8.5% over a 5 minute exposure to 8-pCPT-AM, n=5; $p<0.05$ Student's t-test). 8-pCPT-AM increased Ca^{2+} spark frequency in Fluo-4-AM-loaded mesenteric myocytes from 0.045 ± 0.008 to 0.103 ± 0.022 sparks/s/μm ($p<0.05$) and reversibly increased both the frequency (0.94 ± 0.25 to 2.30 ± 0.72s^{-1}) and amplitude (23.9 ± 3.3 to 35.8 ± 7.7pA) of spontaneous transient outward currents (STOCs) recorded in isolated mesenteric myocytes (n=7; $p<0.05$). 8-pCPT-AM-activated STOCs were sensitive to iberiotoxin (100nM) and to ryanodine (30μM). Current clamp recordings of isolated myocytes showed a 7.4 ± 0.9mV (n=4) hyperpolarization in response to 8-pCPT-AM.
Endothelial disruption suppressed 8-pCPT-AM-mediated relaxation in phenylephrine-contracted arteries (24.8 ± 4.9% relaxation after 5 minutes exposure, n=5; $p<0.05$), as did apamin and TRAM-34, blockers of Ca^{2+}-sensitive, small- and intermediate-conductance K^+ (SK_{Ca} and IK_{Ca}) channels, respectively, and N^G-nitro-L-arginine methyl ester (L-NAME), an inhibitor of nitric oxide synthase (NOS). In Fluo-4-AM-loaded mesenteric endothelial cells, 8-pCPT-AM induced a sustained increase in cytosolic Ca^{2+} in 22 out of 47 cells.
Our data suggest that Epac hyperpolarizes smooth muscle by 1) increasing localized Ca^{2+} release from ryanodine receptors (Ca^{2+} sparks) to activate BK_{Ca} channels, and 2) endothelial-dependent mechanisms involving the activation of SK_{Ca}/IK_{Ca} channels and NOS. Epac-mediated smooth muscle hyperpolarization will limit Ca^{2+} entry via voltage-sensitive Ca^{2+} channels and represents a novel mechanism of arterial relaxation.

Morgado M *et al* (2012) *Cell. Mol. Life Sci*. **69**:247
Bos JL (2006) *Trends in Biol. Sci.* **31**:680-686

We thank the British Heart Foundation for their support

Where applicable, the authors confirm that the experiments described here conform with The Physiological Society ethical requirements.

PCA367

Role of Nitric Oxide in the control of the SR Ca^{2+} release in myocytes of arteriolar networks *in situ*

L. Borysova[1], S. Wray[1], D.A. Eisner[2] and T. Burdyga[1]

[1]Department of Cellular and Molecular Physiology, University of Liverpool, Liverpool, UK and [2]Unit of Cardiac Physiology, University of Manchester, Manchester, UK

NO/cGMP signalling pathway represents one of the possible cross-talk mechanisms between myocytes and endothelial cells in macro- and microvessels. Recent data suggest that NO plays a key role in control of Ca^{2+} release from ryanodine- and IP_3-sensitive Ca^{2+} stores. The functional link between Ca^{2+} release and IP_3R phosphorylation has been established. These data suggest that Ca^{2+} oscillations mediated by IP_3 and/or RyR channels could be potential targets of NO/cGMP pathway. In our recent work we have established that in myocytes of arcade arterioles there are two independent Ca^{2+} stores: one is sensitive to caffeine/ryanodine and the other to agonist/2-APB. In the present work we used 2-and 3-dimensional live confocal imaging of ureteric microvascular networks *in situ* to investigate interaction between endothelium Ca^{2+} signalling and Ca^{2+} signalling in myocytes induced by [Arg^8]-Vasopressin (AVP, 5nM) and caffeine (0.5-2mM) of all sections of arteriolar networks. Caffeine induced irregular Ca^{2+} oscillations exclusively in myocytes of arcade arterioles, which appeared as propagating Ca^{2+} waves with variable spatial spread, selectively blocked by ryanodine (50μM). AVP induced Ca^{2+} oscillations in all sections of arteriolar network, which appeared as fully propagating recurrent Ca^{2+} waves. Ryanodine had no effect on AVP-induced Ca^{2+} oscillations in myocytes of all sections of arteriolar network, selectively inhibited by 2-APB (50 μM). Activation of endothelial Ca^{2+} signalling by 1μM CCh produced complete termination of the AVP-induced Ca^{2+} oscillations in myocytes of all sections of arteriolar network but had no effects on Ca^{2+} sparks and caffeine-induced Ca^{2+} oscillations in myocytes of arcade arterioles. L-NAME but not indomethacin prevented the inhibitory effect of endothelial Ca^{2+} signalling on AVP-induced Ca^{2+} oscillations in myocytes, suggesting that NO was involved. NO donor SNAP (20 μM) or SNP (20μM) produced quick and reversible inhibition of AVP-induced Ca^{2+} oscillations in myocytes of all sections of arteriolar network but had no effect on Ca^{2+} sparks and caffeine-induced Ca^{2+} oscillations in myocytes of arcade arterioles. The data obtained suggest that L-Arginine/NO pathway controls agonist induced Ca^{2+} oscillations in myocytes of arteriolar networks by selective inhibition of Ca^{2+} release via IP_3R channels.

We thank the British Heart Foundation for support (PG/12/62/29823).

Where applicable, the authors confirm that the experiments described here conform with The Physiological Society ethical requirements.

PCA368

Asthmatic cytokines IL-13 and TGFβ alter TRPC6 expression and calcium handling via SMAD2/3 in human airway smooth muscle

Y. Shaifta, D.B. Wright, V. Snetkov and J.P. Ward

Asthma, Allergy and Lung Biology, King's College London, London, UK

Asthma associated cytokines IL-13 and TGF-β affect expression of calcium handling proteins in human airway smooth muscle (hASM) cells. We have previously shown an increase in TRPC6 expression and have now investigated the pathways involved and any change in calcium influx using Flufenamic acid (FFA).
The hASM cells were derived from endobronchial biopsies of healthy volunteers, as approved by the local ethical committee and with informed consent. These were grown and then serum starved for 72h before treatment with cytokines. Sequence specific SMAD2 and SMAD3 siRNAs were cloned and transfected using the AmaxaTM nucleofector device (Lonza). Protein expression was measured via western blots. Intracellular calcium was measured as a ratio of 340/380nm excitation after loading with Fura3-PE/AM.
Stimulating hASM cells with TGF-β alone and in combination with IL-13 caused a significant increase in TRPC6 protein (n=9 $p<0.001$ and n=17 $p<0.001$). TRPC6 splice variants were non-uniformly affected by the combination of IL-13 and TGF-β at one week; 75kDa variant increased by 720 ± 196 % compared to control ($p=0.02$) whereas the ≈100kDa variants increased by 185 ± 20 % ($p=0.003$). SMAD2/3 regulates this increase (see figure 1). The increase in TRPC6 expression by TGFβ is not altered by a scramble siRNA, but both SMAD2 and SMAD3 siRNAs, alone and in combination, inhibit this affect. It has also been found that the combination of IL-13 and TGF-β and TGF-β alone also reduced SMAD3 protein expression significantly ($p<0.001$, n =7).
Flufenamic acid (FFA) has been shown to act as a TRPC6 agonist (Foster et al., 2009). Stimulating hASM cells treated with IL-13 and TGF-β with FFA decreased the peak calcium response at 72 hours ($p=0.02$, n=7-8) and 1 week ($p=0.002$, n=4-5). This decrease in peak calcium may be due to the high increase in expression of the 75kDa TRPC6 variant, which could be displacing the functional ≈100kDa variants.
TGF-β but not IL-13 results in a non-uniform increase in TRPC6 splice variants in hASM cells which is regulated partly by SMAD2 and significantly by SMAD3. An alteration in the calcium handling properties of the hASM results, which as previously described in the literature, could play a key role in the pathophysiology of asthma.

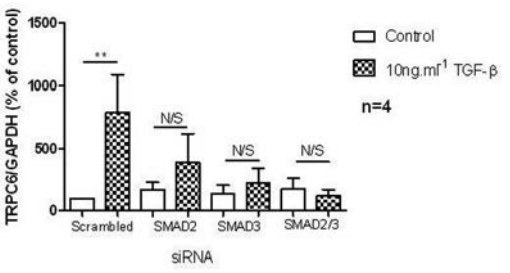

Figure1 SMAD2 and SMAD3 siRNAs inhibit increased expression of TRPC6 in ASM cells by TGFβ.

Foster RR, Zadeh MA, Welsh GI, Satchell SC, Ye Y, Mathieson PW, Bates DO, Saleem MA (2009). Flufenamic acid is a tool for investigating TRPC6-mediated calcium signalling in human conditionally immortalised podocytes and HEK293 cells. Cell Calcium 45(4):384-90

Where applicable, the authors confirm that the experiments described here conform with The Physiological Society ethical requirements.

PCA369

Mechanisms regulating localized and global calcium responses in vascular cells

N. Tsoukias, A. Kapela and J. Parikh

Biomedical Engineering, Florida International University, Miami, FL, USA

The multiplicity of mechanisms involved in regulation calcium (Ca2+) dynamics, the non-homogenous spatial distribution of cellular components and the presence of microdomains in vascular cells (smooth muscle (SMC) and endothelial cells (EC)) result in both intra- and intercellular heterogeneities in Ca2+ levels inside the cells. Experimentation has revealed variety of these intricate intra- and inter-cellular Ca2+ spatiotemporal patterns. The mechanisms behind them remain unresolved. Different variants of deterministic and stochastic models have been proposed to explain global events like Ca2+ oscillations, waves and local events such as Ca2+ sparks and puffs. However, these models are rarely tissue specific and have not been integrated with other important intra- and inter-cellular signaling pathways. Here, we describe the development of detailed computational models that investigate vascular signaling and microcirculatory function. We have previously developed and validated "well-mixed" models of Ca2+ and plasma membrane Vm dynamics in EC and SMC from rat mesenteric arterioles. Models are integrated into multicellular arrangements and adapted to incorporate intra-cellular spatial heterogeneities of cellular components and microdomains like myoendothelial projections. Localized EC Ca2+ mobilization is induced in EC during SM stimulation in the presence of myoendothelial projections which enables an endothelial feedback response that moderates SMC constriction. Myoendotheial IP3 ¬ diffusion is more likely than Ca2+ to mediate this response. Spatial distribution of store or membrane receptor distribution was essential for reproducing intracellular Ca2+ waves in both EC and SMC. Ca2+ diffusion synchronized localized oscillators to form an oscillatory Ca2+ wave. Voltage operated Ca2+ channels modulate Vm oscillations and regulate Ca2+ wave velocity and transition to whole cell oscillations. Electrical current through gap junctions (carried predominantly by K+ ions) is the primary signal that enables conducted responses. Intercellular Ca2+ and IP3 fluxes are small and thus, their passive diffusion is predicted to have a limited effect on Ca2+ mobilization at distant cells. These weak fluxes may be adequate, however, to amplify local current in conducted responses and to promote synchronization of whole cell oscillations of neighboring SMCs in vasomotion. Mathematical models of Ca2+ and Vm dynamics in endothelial and smooth muscle cells allow a more comprehensive investigation of intra and inter-cellular Ca2+ signaling and the elucidation of mechanisms behind localized and global Ca2+ events in the vascular cells.

Kapela A., Parikh J. and N.M. Tsoukias. A unifying theory of cell synchronization in vasomotion. Biophysical Journal (2012). 102(2), 211-20.

Nagarja.S., A. Kapela and N. M. Tsoukias. Intercellular communication in the vascular wall: A modeling perspective. Microcirculation (2012). 19(5):391-402.

Kapela A. and N.M. Tsoukias. A mathematical model of vasoreactivity in rat mesenteric arterioles: II Conducted vasoreactivity. American Journal of Physiology (2010). 298(1):H52-65.

Kapela A., A. Bezerianos and N.M. Tsoukias. A mathematical model of vasoreactivity in rat mesenteric arterioles: I Myoendothelial communication. Microcirculation (2009). 16(8):694-713.

Where applicable, the authors confirm that the experiments described here conform with The Physiological Society ethical requirements.

PCA370

Is platelet mediated leukocyte recruitment a potential therapeutic target in atherosclerosis?

M. Harrison, G.B. Nash, S.P. Watson and E. Rainger

Clinical and Experimental Medicine, University of Birmingham, Birmingham, Other, UK

The role of platelets in the formation of arterial thrombus on atherosclerotic plaque are well documented. However in early disease, platelets also appear to play a role in promoting the recruitment of inflammatory leukocytes. We have recently described a paradigm in which the recruitment of monocytes to TGF-β1 stimulated endothelial cells (EC) is mediated by platelet bridges. TGF-β1 promotes the expression of a matrix of Von Willebrand factor (VWF) on the EC surface which recruits platelets from flowing blood. Upon platelet activation at the EC surface by ADP, monocytes are in turn recruited by platelet P-selectin. The Src family kinases (SFKs) play an important role in platelet activation during haemostasis and we propose that these signalling molecules could represent targets for intervention in platelet mediated monocyte recruitment during atherogenesis. Dasatinib, a broad spectrum SFK inhibitor, ablated ADP dependent aggregation of both human and murine platelets and inhibited the activation of platelets and the secondary recruitment of monocytes on substrates of immobilised VWF or on TGF-β1 stimulated EC. In addition, platelets from the Lyn-/- but not the Fgr-/- mouse, showed deficiencies in aggregation in response to ADP. These data strongly imply that targeting specific SFK members could inhibit platelet dependent recruitment of monocytes in atherogenesis, and these may represent drugable targets for intervening in the chronic inflammatory processes that support atheroma formation.

British Heart Foundation

Where applicable, the authors confirm that the experiments described here conform with The Physiological Society ethical requirements.

PCA371

The role of Na^+/Ca^{2+} exchange and ER Ca^{2+} buffering in the regulation of oxytocin-induced $[Ca^{2+}]_i$ oscillations

B. Hamilton[1], Y. Timofeeva[2] and A. Shmygol[3]

[1]Warwick Systems Biology Centre, University of Warwick, Coventry, UK, [2]Department of Computer Science, University of Warwick, Coventry, UK and [3]Warwick Medical School, University of Warwick, Coventry, UK

Oxytocin (OT) is involved in all aspects of human reproduction. It often triggers an oscillatory $[Ca^{2+}]_i$ response which depends on Ca^{2+} release from the endoplasmic reticulum (ER) and Ca^{2+} entry from extracellular space. The latter process is vital for replenishment of the ER Ca^{2+} store necessary for maintaining $[Ca^{2+}]_i$ oscillations over time. Both, store-operated and receptor-operated Ca^{2+} entry pathways have been implicated in the OT-induced $[Ca^{2+}]_i$ oscillations [1]. The contribution of the Na^+/Ca^{2+} exchange and the role of intraluminal ER Ca^{2+} buffering in OT-induced $[Ca^{2+}]_i$ oscillations have not been described. We used experimental and theoretical approaches to investigate the role of the above two processes in OT-induced $[Ca^{2+}]_i$ oscillations. **Methods:** Mathematical modelling of the OT oscillator was performed using a modified luminal calcium-sensitive DeYoung-Keiser IP3-receptor model implemented in Matlab and XPPAUT. The experiments were performed on Chinese Hamster Ovary cells stably transfected with human oxytocin receptor (CHO-OT1) using Fluo-4 and wide-field fluorescence microscopy. The following experimental manoeuvres were designed to affect the filling state of the ER: (i) manipulation of $[Ca^{2+}]_i$ removal on the Na^+/Ca^{2+} exchanger by removing and re-introducing extracellular Na^+ (isosmotic substitution with sucrose), (ii) manipulation of ER Ca2+ level using membrane permeable low-affinity Ca^{2+} buffer TPEN, (iii) low dose of reversible SERCA pump inhibitor cyclopiazonic acid to slow down the rate of ER Ca^{2+} uptake. **Results:** Application of 1nM OT induced sustained $[Ca^{2+}]_i$ oscillations in the majority of cells. Na+ removal from the extracellular space caused moderate increase in basal $[Ca^{2+}]_i$ and substantially potentiated OT-induced oscillations (typical trace illustrated in Fig.1A). Activation of Na^+/Ca^{2+} exchange by re-introducing the sodium ions into extracellular medium markedly decreased the amplitude and frequency of the OT induced $[Ca^{2+}]_i$ oscillations (Fig1B). TPEN (50 μM) substantially reduced the frequency and amplitude of oscillations (Fig 1C). Higher concentrations of TPEN abolished the oscillations. Application of 100nM CPA did not change basal $[Ca^{2+}]_i$ but dramatically increased the time delay between initial peak and the onset of oscillations. The frequency of subsequent peaks was not different from that in control (Fig. 1D). Higher concentrations of CPA (0.5 – 10 μM) abolished the oscillations and substantially increased base-line $[Ca^{2+}]_i$. Mathematical model captured these observations when sensitivity of the IP3 receptor to intraluminal Ca^{2+} and variable Ca^{2+} flux from outside the cell were introduced. **Conclusion:** The Na^+/Ca^{2+} exchanger plays important role in establishing the sustained $[Ca^{2+}]_i$ oscillations in response to OT. Parameters of these oscillations are extremely sensitive to Ca^{2+} buffering in the ER.

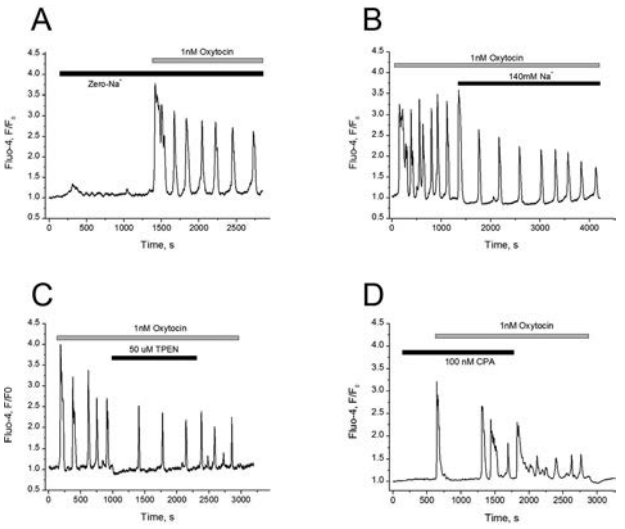

Effects of CPA, TPEN and Na^+ manipulation on the OT-induced $[Ca^{2+}]_i$ oscillations.

D. A. Murtazina et al. (2011) Biology of Reproduction, 85 (2) 315-326.

Where applicable, the authors confirm that the experiments described here conform with The Physiological Society ethical requirements.

PCA372

Restoring Akt1 activity in endothelial progenitors from insulin resistant humans rescues vascular reparative capacity

R. Cubbon, N. Yuldasheva, H. Viswambharan, B. Mercer, V. Baliga, S. Stephen, J. Askham, P. Sukumar, A. Skromna, R. Mughal, H. Imrie, M. Gage, M. Rakobowchuk, J. Li, K. Porter, S. Ponnambalam, S. Wheatcroft, D. Beech and M. Kearney

Multidisciplinary Cardiovascular Research Centre, The University of Leeds, Leeds, UK

Background: Late-outgrowth endothelial progenitor cells (LEPC) are a potential autologous cell source for cardiovascular therapeutics; however, progenitor function is impaired in potential target groups. We aimed to assess if LEPC dysfunction can be reversed by normalising molecular differences relevant to angiogenesis.
Methods: Analysis of in vitro LEPC function (migration, angiogenesis) was performed in 12 South Asian (SA) men and 12 matched white European (WE) controls. Western blotting was used to assess Akt and eNOS abundance. LEPC were transfused into CD1 immunodeficient mice subsequent to angioplasty wire induced femoral artery luminal injury, or femoral artery ligation induced limb ischaemia, to assess in vivo reparative function. In vitro and in vivo studies were repeated after lentiviral gene delivery of constitutively active Akt1 (E17K) or control (EGFP) to SA LEPC. Data are expressed as mean [standard error of mean]; $p<0.05$ by t-test is denoted by *.
Results: Age and cardiovascular risk factors were comparable in the 2 groups, although the SA group was relatively insulin resistant (HOMA-IR 1.2[0.2] vs. 0.5[0.1] au*). SA LEPC exhibited impaired VEGF induced migration (5[0.7] vs. 10[1.7] LEPC/microscope field*) and in vitro angiogenesis (1.9[0.6] vs. 3.8[0.5] tubular structures/microscope field*), associated with decreased abundance of the phosphorylated forms of S473-Akt1 (0.14[0.05] vs. 0.81[0.2] au*) and S1177-eNOS (0.05[0.02] vs. 0.15[0.01] au*). Transfusion of WE LEPC into

immunodeficient mice after femoral artery injury augmented re-endothelialisation; however, neither SA LEPC, nor vehicle, augmented re-endothelialisation (WE: 54.2 [6.4], SA: 36.9 [3.4], vehicle: 31.1 [2.4] % re-endothelialised [absent Evans blue stain]; WE vs. SA*). Whilst control LEPC promoted perfusion recovery after induction of hind limb ischemia, neither SA LEPC nor vehicle did (WE: 66.4 [4.7], SA: 49.3 [5.6], vehicle: 50.6 [2.8] % ischaemic/non-ischaemic limb flux [Laser Doppler]; WE vs. SA*). Lentiviral gene delivery of E17KAkt, but not EGFP control, to SA LEPC was associated with augmented Akt1 activity. Expression of E17KAkt in SA LEPC rescued in vivo re-endothelialisation capacity (E17K: 55.2 [4.4] vs. EGFP 24.1 [1.3] % re-endothelialised; E17K vs. EGFP*; E17K vs. WE non-transduced cells p=0.9). Furthermore, E17KAkt expressing SA LEPC exhibited markedly augmented limb perfusion after femoral artery ligation, in contrast with EGFP control (E17K: 63.4 [2.4] vs. EGFP 48.0 [1.6] % ischaemic/non-ischaemic limb flux; E17K vs. EGFP*; E17K vs. WE non-transduced cells p=0.9). **Conclusions:** These data provide proof of principle for human LEPC based vascular repair therapy, and provide a mechanism by which function of LEPC from insulin resistant humans can be restored.

Where applicable, the authors confirm that the experiments described here conform with The Physiological Society ethical requirements.

PCA373

The effect of IL-6 -174 G/C polymorphism on adiponectin and IL-6 Levels in peripheral vascular disease

N. Salmayenli[2,3], E. Özkök[1,2] and Y. Basar[3,2]

[1]Clinical Biochemistry, Istanbul University Medical Faculty, Istanbul, Turkey, [2]Clinical Biochemistry, Istanbul University Medical Faculty, Istanbul, Turkey and [3]Department of general Surgery, Istanbul University, Istanbul Faculty of Medicine, Istanbul, Turkey

Peripheral vascular disease (PVD) is a chronic disease and is also an atherosclerotic process. It causes occlusion and stenosis of the lower extremity arteries. Inflammation plays a role in pathogenesis and complications of atherosclerosis. It is known that elevated levels of high sensitivity C-reactive protein (hs-CRP) is related with systemic inflammation. hs-CRP is an acute phase reactant and is stimulated by cytokines. It is known that the elevated levels of hs-CRP are correlated with myocardial infarction (MI), stroke and PVD. Interleukin-6 (IL-6) is one of the proinflammatory cytokines which plays an important role in the pathogenesis of coronary artery disease. A polymorphic variant of IL-6 has also a role in inflammation. It has been shown that IL-6 gene polymorphism is related to atherosclerosis of carotid, coronary and peripheral arteries. Adiponectin is an adipocytokine released from adipose tissue. Adiponectin has protective effects on cardiovascular system through its antiinflammatory properties. It has been suggested that decreased of adiponectin levels is an early cardiovascular risk factor. In the light of these knowledges, we aimed to research the relationship among genetic variant of IL-6 -174 G/C and serum levels of IL-6, hs-CRP and, adiponectin in patients with PAD.

The study consisted of 106 patients with PVD. The control group consisted of 65 healthy adults matched for age and gender with patients. Blood samples were collected in vacuum tubes containing disodium EDTA. Genomic DNA was isolated from these samples by using salting –out method. DNA was amplified using designed primers with polymerase chain reaction (PCR) for IL-6 174 G/C genotyping. For the statistical analyses Pearsons's Chi-Squared ($\chi 2$), Kruskal-Wallis tests were used where appropriate.

The levels of IL-6 and hs-CRP were significantly higher in patients with PVD compared to those of the controls ($p<0.001$). However, adiponectin levels were found significantly lower in patients with PVD than healthy controls ($p<0.001$). They were seen that the distributions of IL-6 -174 G/C genotype were not statistically significant between groups ($p>0.05$). The high levels of IL-6 and hs-CRP were statistically significant among carriers of each three genotypes of IL-6 -174 G/C and in patient with PVD compared to controls. Moreover, it was also found the relation between the decreased levels of adiponectin and IL-6 -174 genotypes between the same groups ($p<0.001$) .

In conclusion, we may suggest that there was an important relationship among genotype distributions of IL-6 -174 variants and hs-CRP, IL-6 and, adiponectin levels in patients with PVD and healthy control groups although there were not statistically significancy in the distrubition of IL-6 -174 G/C genotype between groups

Where applicable, the authors confirm that the experiments described here conform with The Physiological Society ethical requirements.

PCA374

Applications of pulse-driven magnetoimpedance sensors to biological magnetic fields

S. Nakayama[1], S. Atsuta[3], M. Kondo[1] and T. Uchiyama[2]

[1]Department of Cell Physiology, Nagoya University Graduate School of Medicine, Nagoya, Japan, [2]Department of Electronics, Nagoya University of, Nagoya, Japan and [3]Division of Technology Development, Fujidenolo, Komaki, Japan

Any living systems that are electrically excitable simultaneously induce a magnetic field. The superconducting quantum interference device (SQUID), has so far been employed to detect biomagnetic activity. However, this sensor system is too large and expensive for personal and single laboratory use.

In order to enable to measure biomagnetic fields in many research labs and clinics, we have improved the sensitivity of a pulse-driven magnetoimpedance (PMI) sensor toward toward a pico-Tesla (pT) level. Since the sensor head is a product of only small electromagnetic parts such as a pickup coil with a small CoFeSiB amorphous wire, it is operated at body temperature and is made as a small electric chip, which can be mounted in a mobile phone and used as a motion sensor of the operation handle in computer games. The excitation pulse (5V, 50-100 ns) is applied to the magnetic amorphous wire at ~1-2 μs intervals. Thus, this sensor enables quasi real time measurements.

Here, we show examples of applications of PMI sensors to physiological and medical studies. All animal experiments were carried out in accordance with the Animal Experimental Guides of Nagoya University. Animals (guinea-pigs) were sacrificed by cervical dislocation after anaesthetising with diethyl ether. Also, in human study, procedures were approved by the Institutional Ethics Committee. Written informed consent was obtained from all participants. This study complies with the Declaration of Helsinki. First, we applied this magnetic sensor to measure biomagnetic fields in small tissues isolated from the stomach, taenia caeci, portal vein, and urinary bladder of guinea-pigs. Spontaneous electric activities were recorded by the sensor head mounted ~1 mm below the samples across a cover glass. In gastric musculatures, spontaneous magnetic activity was simultaneously measured with extracellular elec-

tric activity, indicating that the biomagnetic field measurements reflected pacemaker electric activity. In addition, spike-like magnetic activities were observed in the presence of K+ channels blockers. Next, we measured magnetic fields on the surface of human chest. Spontaneous magnetic activity was simultaneously measured with electric cardiogram. The magnetic activity was maximal in the 4th intercostals near the center of the sterna. Furthermore, averaging the magnetic activity demonstrated magnetic waves mimicking the P wave and QRS complex. Lastly, we introduce new pulse-driven MI systems. Instead of a sample-hold circuit, fast AD/DA converters were used to sample the whole induction decay in the detector coil. Thus, this system can be used as a DC amplifier of magnetic sensor. Possible numerous applications are suggested.

Nakayama S *et al* (2011). *Biosens Bioelectron* **27**, 34-39.

Nakayama S *et al* (2011). *PLoS ONE* **6**(10), e25834

Uchiyama T *et al* (2011). *IEEE Trans Magn* **47**, 3070-3073.

Where applicable, the authors confirm that the experiments described here conform with The Physiological Society ethical requirements.

PCA375

Renal transplantation improves baroreflex sensitivity and arterial stiffness in end stage renal disease patients

M. Kaur[1], D.S. Chandran[1], C. Lal[2], D. Bhowmik[2], A.K. Jaryal[1], K.K. Deepak[1] and S.K. Agarwal[2]

[1]Physiology, All India Institute of Medical Sciences, New Delhi, Delhi, India and [2]Nephrology, All India Institute of Medical Sciences, New Delhi, Delhi, India

Introduction. Cardiovascular events are a major cause of mortality and morbidity in end stage renal disease (ESRD) patients. This could be attributed to the impaired baroreflex function observed in them (1). The effect of renal transplantation on the baroreflex sensitivity (BRS) in ESRD patients has been poorly addressed. Therefore, we investigated BRS and its relation to arterial stiffness indices and cardiovascular variability parameters (heart rate and blood pressure variability – HRV and BPV) in ESRD patients before and after transplantation.
Methods. We studied 23 ESRD patients (mean age; 35.9 ± 9.3 yrs) prospectively before and at 3 and 6 months after renal transplantation. BRS was determined by spontaneous method [sequence and spectral] (2). Short term HRV and BPV were assessed using frequency domain analysis of RR intervals and systolic blood pressure values recorded beat to beat over a duration of 5 minutes (3, 4). Arterial stiffness indices were measured by carotid femoral pulse wave velocity (PWV), augmentation index (AI) and central pulse pressure (5) using Sphygmocor Vx device (Atcor medical, Australia). Data which followed normal distribution are expressed as mean± SD and analysed using Repeated measures ANOVA with Tukey's post hoc multiple comparison test. Data with non-normal distribution are expressed as median with inter-quartile range (1st quartile – 3rd quartile) and analysed using Kruskal Wallis test with Dunns post hoc multiple comparison test.
Results. Renal transplantation was associated with the normalisation of BRS [11.4±7.9 ms/mmHg at 6 months vs. 6.7±3.1 ms/mmHg at baseline; $p<0.05$] only by 6 months. Arterial stiffness indices - AI [27.7±11.3 % vs. 17.1±9.0 %; $p<0.05$] and central pulse pressure [41.7±13.9 mmHg vs. 33.0±11.1 mmHg; $p<0.05$] showed a significant reduction as early as 3 months after renal transplantation. PWV and frequency domain measures of heart rate variability after renal transplantation did not show statistically significant changes except LF/HF ratio which had significant increase only at 6 months as compared to baseline. Systolic BPV total power [134.0 (118.7–149.5) mmHg2 /Hz vs. 100.4 (78.6–127.1) mmHg2 /Hz] showed a significant reduction as early as 3 months after renal transplantation and showed similar reduction in comparison to baseline at 6 months also.
Conclusions. Our data suggests that renal transplantation normalises BRS in end stage renal disease patients by 6 months which follows the improvement in the arterial stiffness indices observed as early as 3 months post renal transplantation. This improvement in BRS at 6 months reduces the blood pressure variability in renal transplant patients.

Johansson M, Gao SA, Friberg P et al. Baroreflex effectiveness index and baroreflex sensitivity predict all-cause mortality and sudden death in hypertensive patients with chronic renal failure. J Hypertens 2007;25:163–168

Parati G, Di Rienzo M, Mancia G. How to measure baroreflex sensitivity: from the cardiovascular laboratory to daily life. J Hypertens 2000; 18:7–19.

Heart rate variability: standards of measurement, physiological interpretation and clinical use. Task Force of the European Society of Cardiology and the North American Society of Pacing and Electrophysiology. Circulation 1996; 93:1043–65.

Parati G, Saul JP, Di Rienzo M et al. Spectral analysis of blood pressure and heart rate variability in evaluating cardiovascular regulation. A critical appraisal. Hypertension 1995; 25:1276–86.

Laurent S, Cockcroft J, Van Bortel L et al. Expert consensus document on arterial stiffness: methodological issues and clinical applications. Eur Heart J 2006; 27:2588–2605

Where applicable, the authors confirm that the experiments described here conform with The Physiological Society ethical requirements.

PCA376

Sympathetic Vascular reactivity to cold pressor test in Parkinson's disease and Parkinsonian variant of Multiple System Atrophy with orthostatic hypotension

S. Roy[1], A.K. Jaryal[1], A.K. Srivastava[2] and K.K. Deepak[1]

[1]Physiology, All India Institute of Medical Sciences, New Delhi, New Delhi, India and [2]Neurology, All India Institute of Medical Sciences, New Delhi, New Delhi, India

Objective:
The two neurodegenerative disorders namely Parkinson's disease (PD) and Multiple System Atrophy of the Parkinsonian type (MSA-P) tend to show similar clinical features of Parkinsonism. These disorders also present with autonomic dysfunctions, frequently manifesting as orthostatic hypotension (OH), (42-58% in PD [1] and 80% in MSA-P show OH [2]). The mechanism of OH in PD is proposed to be due to baroreflex failure (central or peripheral lesions) while in MSA-P it is only due to central lesions [3]. We hypothesized that the baroreflex independent vascular reactivity may also be different in them. To evaluate this we assessed sympathetic vascular reactivity to standard cold pressor test in these patients.
Methods:
The diagnosis of PD was done according to the UK Parkinson's disease Society Brain Bank Clinical Diagnostic Criteria and MSA-P was based on the Second Consensus Statement for diagnosis of MSA-P. Data was recorded in 8 patients of PD and 9 patients of MSA-P, both with documented OH. ECG and PPG (photoplethysmography) signals were continuously acquired during a baseline period (1 min) and during 10 degree C cold

exposure (1 min) of the contralateral hand. The vascular response was evaluated by measuring the pulse transit time and amplitude of the finger-photoplethysmography (PPG) waveform [4]. Analysis was done by an unpaired t test.
Results:
The Pulse Transit Time (PTT) decreased in patients of both PD (192.7±3.225 ms vs 199.4±1.639 ms, p = 0.09) and MSA-P (195.23±6.4ms vs. 198.00±6.08 ms, p = 0.7). The patients of PD showed significantly larger decrease in PTT as compared to MSA-P (-7.78±2.06 ms vs -2.81±0.98, p=0.03). During the cold pressor test the amplitude of PPG decreased in both patient groups but the percentage decrease was greater in patients of PD than in MSA-P (51% vs. 46% respectively).
Conclusion:
The vascular reactivity to cold pressor test in patients of MSA-P is lesser than that of PD. The increase in vascular tone (decrease in PTT) during CPT is preserved in PD but significantly lost in MSA-P. Thus the preliminary study shows that baroreflex independent vascular reactivity is significantly different in the patients of PD and MSA-P with documented OH.

Allcock LM et al. (2004). J Neurol Neurosurg Psychiatry 75, 1470-1471

Ha AD et al. (2011). Parkinsonism Relat Disord 17, 625-628

Iodice et al (2011). J Neurol Sci. 10, 1016

Jaryal AK et al (2009). J Clin Monit Comput 10, 1007

Where applicable, the authors confirm that the experiments described here conform with The Physiological Society ethical requirements.

PCA378

Pericytes derived from the human foetal kidney are progenitors for renin-producing cells

A. Stefanska[1], J. Mullins[1] and B. Péault[1,2]

[1]University/BHF Centre for Cardiovascular Science, Edinburgh, UK and [2]MRC Centre for Regenerative Medicine, Edinburgh, UK

Renin is a proteolytic enzyme released by the kidneys in response to a decrease in blood pressure or extracellular volume. The lineage identity, origin and possible turnover of renin-producing cells remains poorly understood. Recent reports suggest that renin-producing cells are precursors for multiple cell types in the kidney (1). We hypothesized that renin cells are related to pericytes, progenitor cells embedded in the microvascular wall (2). Since renal diseases are often associated with microvascular complications, studies of renal pericytes may identify a new potential target for therapeutic treatment of kidney disease. We have shown that during normal human development pericyte surface markers CD146 and NG2 label multiple kidney cells including interstitial capillaries, afferent arterioles, mesangial cells. We demonstrated that renin producing cells co-express pericyte markers in the juxtaglomerular region and along renal arterioles between 8-20 weeks of gestation. For the first time we have obtained primary cultures of renal pericytes from the developing human kidney. CD146+CD34-CD45-CD56- pericyte populations were isolated from the foetal human kidney via fluorescence-activated cell sorting (FACS). Cells maintained the selected phenotype through culture; they remained positive for pericyte markers and negative for haematopoietic and endothelial cell markers. Primary cultures of foetal renal pericytes showed tri-lineage mesodermal differentiation. Renin expression was induced by cAMP pathway stimulation (10 μm forskolin and 100 μm 3-isobutyl-1-methylxanthine [IBMX] 24h treatment) on the gene and protein level. In conclusion, a subset of pericytes co-express renin suggesting that renin cells have a perivascular origin. Renal pericytes are a widespread and abundant population in the human foetal kidney that can be isolated and propagated in vitro. Primary cultures of renal pericytes can be a model for renin cell recruitment. Future studies will investigate the mechanism through which pericytes switch into renin-producing cells and possible ways of manipulating the renin-angiotensin system by targeting pericytes.

Sequeira Lopez ML et al. (2004) Developmental Cell 6, 719-728

Crisan M et al (2008) Cell Stem Cell 3:301–13

We acknowledge support from the British Heart Foundation Centre for Research Excellence Award. A.S. was the recipient of a BHF 4-year PhD studentship.

Where applicable, the authors confirm that the experiments described here conform with The Physiological Society ethical requirements.

PCA379

Intravital investigations of lymphocyte and platelet recruitment to murine liver following ischemia-reperfusion injury

J. Robinson, D.H. Adams and N. Kalia

College of Medical and Dental Sciences, University of BIrmingham, Birmingham, UK

Introduction: Although a contributory role for neutrophils is well established, recent evidence suggests lymphocytes, in particular T-cells, can also directly mediate IR injury. We have previously demonstrated in vitro that lymphocyte adhesion can be increased following incubation with activated platelets. This study further investigated lymphocyte and platelet recruitment in vivo in a model of mouse hepatic IR injury using intravital microscopy (IVM). Most intravital studies visualise trafficking of ex vivo labelled donor cells. Since this may underestimate actual numbers of cells recruited, we compared adhesion of exogenously injected platelets and lymphocytes with a 'novel' method of labelling these cells endogenously.
Methods: Experiments were conducted in anaesthetised mice undergoing hepatic IR injury or sham surgery. To monitor exogenous cells, donor spleen derived T- and B-cells were labelled with CFSE and cell tracker orange respectively and injected via the carotid artery into mice undergoing IVM. To quantitate donor platelet adhesion, CFSE-labelled whole blood platelets were injected in separate mice. To investigate endogenous cell recruitment, T-cells, B-cells and platelets were fluorescently labelled in vivo with anti-CD3/Alexa 647, anti-CD19/Alexa 488 and anti-CD41/Alexa 555 conjugated antibodies respectively.
Results: Adhesion of ex vivo labelled T-cells, but not B-cells, was significantly ($p<0.001$) increased in IR mice compared to shams, albeit numbers were small (1-2 cells/ 20x field). Although donor platelet numbers were similar in IR and sham mice, they were surprisingly high. A significant ($p<0.001$) decrease in free flowing platelets was observed indicative of poor hepatic blood flow in IR mice. Endogenous T-cell adhesion also significantly ($p<0.001$) increased in IR mice but no difference in B-cell or platelet adhesion was observed. However, we found that the fluorescent intravital images of endogenously labelled cells did not differ from those obtained when fluorescently conjugated IgG antibodies were injected. This could be due to hepatic 'trapping' of the antibodies.
Conclusions: Monitoring donor cells labelled ex vivo with cytoplasmic dyes, rather than conjugated antibody labelled endoge-

nous cells, was a more reliable method for quantitating hepatic cell trafficking. This method demonstrated increased recruitment of T-cells, but not B-cells, following IR injury. Adherent T-cell numbers were small, possibly due to their immediate uptake by the spleen post-infusion. We are currently comparing carotid artery cell infusion to intraportal infusion. Since numerous adherent platelets were observed in the liver, further in vivo studies will be conducted in thrombocytopenic mice to determine whether they mediate T-cell recruitment.

Supported by Bardhan Research & Education Trust

Where applicable, the authors confirm that the experiments described here conform with The Physiological Society ethical requirements.

PCA380

The effect of L-arginine on the function of the microvascular endothelium in healthy trained and sedentary subjects

K. Cankar, T. Virtic, P. Zaletel and Z. Melik

Institute of Physiology, University of Ljubljana, Faculty of medicine, Ljubljana, Slovenia

BACKGROUND Endothelial dysfunction plays a key role in the aging process and in the development of cardiovascular diseases. Endothelial function is associated with the availability of nitric oxide, produced in endothelial cells from L-arginine. We aimed to study the effect of L-arginine on the function of the cardiovascular system, and to determine whether its use can improve endothelial function, which could be beneficial in preventing the formation and development of cardiovascular diseases in trained and sedentary subjects.
METHODS Measurement were performed in healthy normotensive men, divided into four groups, according to age and physical activity: 12 young sedentary (YS), mean age 23,5 ± 2,4) and age matched trained (YT) (N=18); 11 elder sedentary (ES) (mean age 45,7 ± 7,5) and age matched trained subjects (ET) (N=12). Cardiovascular parameters were measured at rest with the Task Force Monitor device. Laser Doppler (LD) fluxmetry was used to measure skin LD flux on the forearm, before and after administration of 0.9 g L-arginine. Endothelium-dependent vasodilation was assessed by ACh iontophoresis and endothelium-independent vasodilatation with NaNP iontophoresis.
RESULTS After ingestion of L-arginine the heart rate in all four groups statistically significantly decreased (YS 70.4 ± 4.2 vs. 66.3 ± 3.3; YT 62.1 ± 2.7 vs. 58.3 ± 2.0; ES 69.6 ± 3.2 vs. 62.7 ± 2.7; ET 58.0 ± 1.8 vs. 53.6 ± 1.2 beats/min) (paired t-test, $p<0.05$). The cardiac output decreased in three groups except in YS subjects (YT 7.04 ± 0.4 vs. 6.32 ± 0.3; ES 6.95 ± 0.5 vs. 5.9 ± 0.4; ET 7.08 ± 0.6 vs. 6.58 ± 0.4 L/min (paired t-test, $p<0.05$). The systolic (126.3 ± 4.1 vs. 120.0 ± 3.2 mmHg) and diastolic pressure (77.6 ± 2.5 vs. 74.3 ± 1.9mmHg) (paired t-test, $p<0.05$) decreased and LD flux at rest (9.3 ± 2.5 vs. 12.5 ± 1.3 PU) (paired t-test, $p<0.05$) increased in the ES group. After ingestion of L-arginine the endothelium-dependent vasodilation (73.4 ± 4.2 vs. 96.0 ± 9.5 PU) (Dunnett's, $p<0.05$) improved only in the group of YT subjects. Endothelium-independent vasodilation was not altered in any of the groups.
CONCLUSIONS The systemic effect of L-arginine was observed. In contrast, the expected improvement of endothelium-dependent vasodilation in elderly subjects was not found. Improved endothelium-dependent vasodilation in response to L-arginine in young trained subjects could justify the use of dietary L-arginine supplementation in athletes. Unresponsive endothelium-independent vasodilation in all groups confirms that the normal function of endothelial cells is necessary for the synthesis of nitric oxide from L-arginine. Additional studies are required for the final assessment of the impact of L-arginine on the formation and development of cardiovascular diseases.

Where applicable, the authors confirm that the experiments described here conform with The Physiological Society ethical requirements.

PCA381

Molecular and functional changes of Cav1.2 channels in vascular smooth muscles after hypoxia

P. Liao

National Institute of Singapore, Singapore, Singapore

Calcium channel blockers are widely used to treat hypertension by reducing vascular contraction. However, numerous animal experiments and clinical trials failed to demonstrate a beneficial effect on outcome of using calcium channel blockers to treat stroke (1,2). Severe side effect of systemic hypotension often occurred during treatment. Voltage-gated Cav1.2 channels are expressed in cardiovascular system and are the main targets for calcium blocker, dihydropyridine. The aim of the study was to investigate the molecular and functional changes of Cav1.2 channels in cerebral vascular smooth muscle cells under hypoxia conditions. Both primary cultured cerebral vascular smooth muscle cells from Wistar rats and A7r5 cell line were used for the study. After chronic hypoxia and glucose deprivation treatment for one day or three days, Cav1.2 channel expression was reduced gradually in both types of cells. Increase of intracelluar calcium concentration in response to membrane depolarization by application of 145 mM K+ into the bath solution was reduced in hypoxic cells as compared with normoxic cells. Interestingly, hypoxic cells also exhibited enhanced sensitivity to calcium channel blocker isradipine (10nM in A7r5 cells and 5nM in primary cultured cells). After scanning the transcript of Cav1.2 channels, we identified the expression of two alternatively spliced exons were altered both in A7r5 cells and primary cultured cells. More Exon 33 was deleted and exon 9* included after chronic hypoxia treatment. Such changes could lead to more dihydropiridine sensitivity and a similar trend was identified in rat hearts of myocardial infarction with altered electrophysiological properties in our previous reports (3,4). We thus postulate that the splicing profile changes of Cav1.2 channels could contribute at least partially to the altered dihydrapiridine sensitivities after hypoxia. These isoforms of Cav1.2 channels are a novel target for designing therapeutic drugs targeting cerebral blood vessels after stroke with minimal side effect on systemic blood vessels.
1) Horn J, de Haan RJ, Vermeulen M, Luiten PG, Limburg M. Nimodipine in animal model experiments of focal cerebral ischemia: a systematic review. Stroke. 2001, 32(10):2433-8.
2) Infeld B, Davis SM, Donnan GA, Yasaka M, Lichtenstein M, Mitchell PJ, Fitt GJ.
Nimodipine and perfusion changes after stroke. Stroke. 1999, 30(7):1417-23
3) Liao P, Li G, Yu de J, Yong TF, Wang JJ, Wang J, Soong TW. Molecular alteration of Ca(v)1.2 calcium channel in chronic myocardial infarction. Pflugers Arch. 2009, 458(4):701-11.
4) Liao P, Yu D, Li G, Yong TF, Soon JL, Chua YL, Soong TW. A smooth muscle Cav1.2 calcium channel splice variant underlies hyperpolarized window current and enhanced state-

dependent inhibition by nifedipine. J Biol Chem. 2007, 30;282(48):35133-42.

Where applicable, the authors confirm that the experiments described here conform with The Physiological Society ethical requirements.

PCA382

Bilobalide enhances coronary artery endothelial potassium currents

W.B. Watanapa, T. Wongsatan and K. Ruamyod

Department of Physiology, Faculty of Medicine Siriraj Hospital, Mahidol University, Bangkok, Thailand

A hallmark of coronary heart disease (CHD) is impaired coronary vasodilation. Bilobalide, a main constituent of the terpenoids found in *Ginkgo biloba* leaves, has been found to induce vasorelaxation in some vascular beds. However, little information exists about bilobalide effects on endothelial cells and the involved mechanisms, and there has been no bilobalide study on human coronary artery endothelial cells (HCAECs). To better understand the electrophysiological profile of bilobalide effects in human coronary artery, we aimed to elucidate the effects of bilobalide on K^+ currents in HCAECs.

Standard whole-cell voltage-clamp technique was employed to record HCAEC ionic currents elicited from a holding potential of -40 mV to voltage steps (-100 to +80 mV; 20 mV increments) for 600 ms. Bilobalide powder was dissolved in DMSO (maximum 0.33 %, v/v) which did not alter HCACE currents. Currents in 1 to 100 μM bilobalide were compared to control. Values are mean ± SEM. Bilobalide, at 10, 30 and 100 μM, dose-dependently and reversibly increased HCAEC currents; mean current density at +60 mV was enhanced by 33.2 ± 7.5% (n=6), 42.4 ± 5.0% (n=6) and 47.3 ± 6.7% (n=5), respectively, when compared with controls ($p<0.01$; ANOVA with post hoc Dunnett's test). The EC_{50} and maximum increase, obtained from a non-linear fit of the data to the dose-response equation, were 6.71 ± 1.28 μM and 45.5 ± 4.4 %.

The effect of bilobalide on small-, intermediate- and large-conductance calcium-activated potassium channels (SK_{Ca}, IK_{Ca} and BK_{Ca} channel, respectively), were investigated using specific blockers: 0.5 μM apamin, 10 μM clotrimazole and 1 mM TEA, respectively. Bilobalide-induced HCAEC currents were significantly reduced when exposed to apamin and TEA by 23.3 ± 2.2 % (n=6) and 18.7 ± 4.6 % (n=6, $p<0.01$; *t*-test), but no significant alteration was observed in clotrimazole, suggesting that bilobalide may increase HCAEC currents via SK_{Ca} and BK_{Ca}, but not IK_{Ca} channels. In addition, exposure of bilobalide-induced HCAEC currents to 10 μM La^{3+}, a specific blocker of nonselective cation (NSC) channel, yielded no statistical difference from control currents. Evidently, NSC channel may not be involved in bilobalide-enhanced HCAEC current.

Bilobalide increases HCAEC currents dose-dependently through SK_{Ca} and BK_{Ca} channels. These finding may provide a basis for the mechanism of bilobalide-induced vasodilator release, involving endothelial ion channels, and suggest that bilobalide may be therapeutically effective in cardiovascular disease.

Where applicable, the authors confirm that the experiments described here conform with The Physiological Society ethical requirements.

PCA383

Bronchoconstrictor signal transduction involves protein kinase C-mediated phosphorylation of Kv7.5 potassium channels in human airway smooth muscle cells

J.M. Haick, L.I. Brueggemann, J.R. Prochot, D.S. Randhawa, C. Wigfield and K.L. Byron

Loyola University Chicago, Maywood, IL, USA

In the bronchioles of the asthmatic lung, hypersensitivity of airway smooth muscle cells (ASMCs) to bronchoconstrictor agonists contributes to airway obstruction, though the mechanisms underlying this pathology remain obscure. Our laboratory recently found that Kv7 potassium channels are expressed in ASMCs. These channels maintain an outward flux of potassium ions (K+) to promote a negative resting membrane voltage in smooth muscle cells, thereby opposing their electrical excitability. In the bronchioles, electrical excitation (membrane depolarization) of ASMCs results in activation of voltage sensitive calcium channels, an increase in cytosolic calcium concentration, ASMC contraction, and bronchoconstriction. We previously found that the selective Kv7 channel blocker, XE991, induced robust bronchiolar constriction in human precision cut lung slices (PCLS). Bronchoconstrictor agonists histamine (Hist) and methacholine (MeCh) were found to inhibit Kv7 K+ currents in guinea pig bronchiolar ASMCs, but the mechanisms by which these agonists regulate Kv7 channels in ASMCs are unknown. In preliminary studies, we found that knocking down Kv7.5 in rat ASMCs resulted in elimination of Hist-sensitive Kv7 currents. In the present study, we tested the hypothesis that protein kinase C (PKC), a downstream effector in Hist and MeCh signaling, phosphorylates and consequently inhibits Kv7.5 channels. To detect phosphorylation of Kv7.5 channels, FLAG-tagged human Kv7.5 (FLAG-hKv7.5) channels were overexpressed in primary cultured human ASMCs derived from trachealis muscle (hASMCs). Following treatment with Hist (1 μM, 10 minutes) or the PKC activator phorbol 12-myristate 13-acetate (PMA) (1 nM, 30 min), channel phosphorylation was monitored using immunoprecipitation with anti-FLAG (n=6) or anti-phosphoserine PKC substrate (n=7) antibodies followed by western blot analyses. Both treatments induced an increase in Kv7.5 phosphorylation. Similar results were obtained using fresh human trachealis strips, in which native Kv7.5 channels were increased in anti-phosphoserine immunoprecipitates following MeCh, Hist or PMA treatment. Hist-induced phosphorylation of FLAG-hKv7.5 was blocked by the PKC inhibitor Ro 31-8220 (1 μM, 1 hour, n=3). hASMCs infected with FLAG-hKv7.5 were also subjected to patch-clamp electrophysiology to monitor the Kv7.5 K+ currents. Treatment with either Hist (1 μM, n=4/6) or PMA (1 nM, n=2) inhibited Kv7.5 currents. Hist-induced inhibition was attenuated upon pretreatment with the PKC inhibitor Calphostin C (250nM, 30 min). PMA (100 nM) also induced profound bronchoconstriction in human PCLS (n=2). These findings suggest that PKC induces phosphorylation of Kv7.5 potassium channels in ASM, resulting in channel inhibition and contributing to agonist induced bronchoconstriction.

Where applicable, the authors confirm that the experiments described here conform with The Physiological Society ethical requirements.

PCA384

Heteromultimerization with TRPC1 affects TRPC5 channel function by regulating its plasma membrane residence and cholesterol-triggered retraction

S. Tumova[1,2], B. Hou[1,2], M.S. Amer[1,3], L. McKeown[1,2], N.K. Moss[1,2], Y.M. Bahnasi[1,4], J. Li[1,2], K.E. Porter[2,3], A. Sivaprasadarao[1,2] and D.J. Beech[1,2]

[1]Faculty of Biological Sciences, University of Leeds, Leeds, UK, [2]Multidisciplinary Cardiovascular Research Centre, University of Leeds, Leeds, UK, [3]Clinical Physiology Department, Menoufiya University, Menoufiya, Egypt and [4]Faculty of Medicine and Health, University of Leeds, Leeds, UK

The channels from the Transient Receptor Potential Canonical (TRPC) family are highly relevant in physiological or pathophysiological calcium signalling, especially in cardiovascular, neural or adipose tissue. TRPC5 channel is one of the family members which can function as a homotetramer or in a heteromultimeric assembly with other TRPC channels including TRPC1 (Sukumar et al, 2012). We studied the channels in human vascular smooth muscle cells obtained with ethical approval and in human embryonic kidney cell line exogeneously expressing TRPC5 alone or in combination with TRPC1. We find that cholesterol causes TRPC5 homomer internalization via caveolin-1-dependent retraction, as evidenced by immunostaining, cell surface TRPC5 quantification and calcium influx measurement. On the other hand, lipid raft analysis and GM1 co-localization indicate that heteromultimerization with TRPC1 changes TRPC5 localization in plasma membrane microdomains and this prevents the cholesterol-triggered retraction. Thus, besides affecting the selectivity or gating mechanism of the channel assembly, introduction of TRPC1 has additional functional impact by modifying the membrane localization of the channel. Our study suggests this would be especially pronounced in the face of increased, pathophysiological cholesterol levels.

Sukumar P, Sedo A, Li J, Wilson LA, O'Regan D, Lippiat JD, et al. Constitutively active TRPC channels of adipocytes confer a mechanism for sensing dietary fatty acids and regulating adiponectin. Circ Res 2012; 111: 191–200.

The work was supported by the Wellcome Trust and the British Heart Foundation.

Where applicable, the authors confirm that the experiments described here conform with The Physiological Society ethical requirements.

PCA385

Overload of cholesterol inhibits L-type Ca2+ channel current and augments its voltage-dependent inactivation in A7r5 cells

R. Ochi, S. Chettimada and S.A. Gupte

Biochemistry and Molecular Biology, University of South Alabama, Mobile, AL, USA

Cholesterol (Chol) localizes predominantly in the lipid rafts and caveolae in the membrane and regulates functions of ion channels. In the aortic smooth muscle cells, Ca2+ influx to initiate contraction is supplied mainly by window ICa,L that is determined by the steady-state activation and inactivation of the channel. We clarified the effect of overload and depletion of Chol on both the activation and the inactivation of ICa,L. Previous studies have reported that the overload of Chol utilizing methyl-β-cyclodextrin (CD): cholesterol complex or Chol dissolved by ethanol induces strong inhibition of ICa,L. We applied water-soluble PEG600: cholesterol (PC) to overload Chol and used CD to deplete Chol. Cultured A7r5, a cell line from fetal rat aorta, cells were dissociated and incubated with normal Tyrode solution containing PC or CD in micro-tubes for longer than 90 min at room temperature. In some experiments CD was added after the pretreatment by PC to examine its reversibility. ICa,L was recorded as whole-cell current with 10 mM Ba2+ as the charge carriers and small T-type Ca2+ channel currents were inactivated by 50 ms pre-pulse to -40 mV. The maximal ICa,L density (ICa,L,max) was obtained at 0 mV and was 6.8±0.8 pA/pF (mean±s.e.m., n=18) in the time-matched control. The pretreatment with PC inhibited ICa,L in a dose-dependent manner without any voltage-shift of the I-V relationship. The ICa,L,max after the incubation with PC was: 0.1 mM, 4.9±0.7 (n=10, $p<0.05$ compared with control), 1 mM, 3.1±0.6 (11, $p<0.001$) and 10 mM, 2.8±0.2 pA/pF (14, $p<0.001$). It was significantly increased by the pretreatment with CD: 10 mM, 8.7±1.2 (n=14, $p<0.05$) and 30 mM, 9.5±1.2 pA/pF (n=13, $p<0.001$). We found that loading of Chol by PC augments the voltage-dependent inactivation of ICa,L. V0.5 for the steady-state inactivation (f-V) curve was: control, -30.1±0.5 mV (n=24); 0.1 mM-PC, -32.6±0.5 mV (n=10); 1 mM, -38.0±0.3 mV (n=15); 10 mM, -42.1±0.3 mV (n=14). On the other hand, the depletion of Chol by CD shifted V0.5 to a depolarizing direction: 10 mM, -26.0±0.6 mV (n=19) and 30 mM, -21.7±0.8 mV (n=20). The addition of 30 mM CD to 1 mM PC-pretreated cells in the tube hardly reversed the PC-induced leftward shift of f-V relationship: V0.5, -35.6±0.4 mV (n=11). It implicates that PC could not be removed by CD from the membrane. However, the addition of 30 mM CD after the overload of Chol by 1 mM-PC augmented ICa,L,max to -12.7±1.6 pA/pF (n=11, $p<0.001$ compared with 30 mM CD alone at -10 mV) and shifted the I-V curve to the left. We conclude that Chol is involved in the regulation of basal window ICa,L by decreasing the current density and by augmenting the voltage-dependent inactivation. Chol may be also involved in the regulation of cellular signaling to modulate ICa,L.

Where applicable, the authors confirm that the experiments described here conform with The Physiological Society ethical requirements.

PCA386

PDGF maintains stored calcium through a non-clustering Orai1 mechanism but evokes clustering if the ER is stressed by store depletion

L. McKeown[1,2], N.K. Moss[1,2], P. Turner[1,3], J. Li[1,2], N. Heath[1], D. Burke[3], O. David[3], M.S. Gilthorpe[4], P.E. Karen[1,2] and D.J. Beech[1,2]

[1]School of Biomedical Sciences, University of Leeds, Leeds, UK, [2]Multidisciplinary Cardiovascular Research Centre, University of Leeds, Leeds, UK, [3]Leeds Teaching Hospitals, Leeds General Infirmary, Leeds, UK and [4]Faculty of Medicine & Health, University of Leeds, Leeds, UK

Rationale: Calcium entry through Orai1 channels drives vascular smooth muscle cell migration and neointimal hyperplasia. The channels are activated by the important growth factor PDGF. Channel activation is suggested to depend on store-depletion which redistributes and clusters STIM1 which then co-clusters and activates Orai1.

Objective: To determine the relevance of STIM1 and Orai1 redistribution in PDGF responses.
Methods and Results: Vascular smooth muscle cells were cultured from human saphenous vein. STIM1 and Orai1 were tagged with green and red fluorescent proteins to track them in live cells. Under basal conditions the proteins were mobile but mostly independent of each other. Inhibition of sarco-endoplasmic reticulum calcium ATPase led to store-depletion and dramatic redistribution of STIM1 and Orai1 into co-clusters. PDGF did not evoke redistribution, even though it caused calcium-release and Orai1-mediated calcium entry in the same time period. After chemical blockade of Orai1-mediated calcium entry, however, PDGF caused redistribution. Similarly, mutagenic disruption of calcium flux through Orai1 caused PDGF to evoke redistribution, showing that calcium flux through the wild-type channels had been filling the stores. Acidification of the extracellular medium to pH 6.4 caused inhibition of Orai1-mediated calcium entry and conferred capability for PDGF to evoke complete redistribution and coclustering.
Conclusions: The data suggest that PDGF has a non-clustering mechanism to activate Orai1 channels and maintain calcium stores replete. Redistribution and clustering become important, however, when the ER stress signal of store-depletion arises, for example when acidosis inhibits Orai1 channels.

Wellcome Trust

Where applicable, the authors confirm that the experiments described here conform with The Physiological Society ethical requirements.

PCA387

Kv1.3 channel modulates human vascular smooth muscle cells proliferation acting on ERK1/2 signaling pathway

T. Perez-Garcia[1,2], P. Cidad[1,2], E. Miguel-Velado[1,2], C. Ruiz-McDavitt[1,2], E. Alonso[1,2], J. Lopez[3], M. Fernández[3], Y. Marroquín[4] and J.R. López-López[1,2]

[1]Biochemistry and Physiology, University of Valladolid, Valladolid, Spain, [2]Instituto de Biología y Genética Molecular, IBGM, Consejo Superior de Investigaciones Científicas, Valladolid, Spain, [3]Servicio de Cardiología, Hospital Clinico Universitario, Valladolid, Spain and [4]Servicio de Nefrología, Hospital Clinico Universitario, Valladolid, Spain

The cellular responses to vascular injury lead to clinical events such as atherosclerosis, hypertension and restenosis. One common feature of these lesions is the proliferation of vascular smooth muscle cells (VSMCs), that undergo a dedifferentiation process (phenotypic switch). The gold standard treatment of this unwanted vascular remodelling is represented by mTOR inhibitors such as rapamycin and everolimus. However, their numerous side effects had advanced the search for novel, more specific targets.
We have previously found that functional expression of Kv1.3 channels contributes to the phenotypic switch of VSMCs, as selective Kv1.3 blockers inhibit VSMCs migration and proliferation. Moreover, proliferation of mouse VSMCs from several vascular beds associates with a Kv1.5 to Kv1.3 channel switch, so that Kv1.3/Kv1.5 ratio can be considered as a landmark of the phenotype. Here, we determined whether this Kv1.5 to Kv1.3 switch is conserved in VSMCs from human vessels, and we investigated the mechanisms involved in this pro-proliferative role of Kv1.3 channels.
Human uterine, renal and coronary arteries and saphenous veins were obtained from donors at the Clinic Hospitals of Barcelona and Valladolid, with protocols approved by their respective Human Investigation Ethics Committees. Either freshly dissociated, (contractile) VSMCs or cultured (proliferating) VSMCs obtained from explants were used for expression experiments (to quantify mRNA and protein) and for functional studies (electrophysiology of K+ currents and proliferation experiments).
We found that changes in Kv1.3:Kv1.5 mRNA ratio represent an early step during the phenotypic switch of VSMCs. This change is due to the decrease of Kv1.5 expression, as Kv1.3 expression was independent of proliferating stimuli. Functional expression of Kv1.3 and Kv1.5 proteins in contractile and proliferating VSMCs shows a good correlation with mRNA expression data.
Selective blockade of Kv1.3 inhibits VSMCs proliferation in all vascular beds. The anti-proliferative effect of PAP-1 (a selective Kv1.3 blocker), was occluded in the presence of ERK1/2 blockers, and PAP-1 treatment decreased PDGF-induced pERK expression in VSMCs. However, PAP-1 effect on proliferation was additive with those of mTOR inhibitors.
Altogether, our data indicate that Kv1.3 channels could represent a novel therapeutical target to prevent human VSMCs proliferation. Additionally the specific blockade of Kv1.3 could be used to potentiate the therapeutic effect of the currently used drugs in the treatment of restenosis as they inhibit VSMCs proliferation acting on different mechanisms.
Cidad et al., (2012) ATVB 32: 1299-307

Supported by grants from ISCIII (R006/009, Red Heracles), MICIN (BFU2010-15898), JCyL (VA094A11-2) and Generalitat of Catalunya (CIDEM- VALTEC09-1-0042).

Where applicable, the authors confirm that the experiments described here conform with The Physiological Society ethical requirements.

PCA388

Study on mRNA and protein expression levels of small conductance calcium-activated potassium channel in human mesenteric artery from patients with hypertension

L. Mao, T. Li, H. Lan, W. Huang, R. Zhou, C. Li, P. Li, Y. Yang and X. Zeng

Institute of Cardiovascular Research, Luzhou medical college, Luzhou, Sichuan, China

Small conductance calcium-activated potassium channel (SKCa) is the key factor in the regulation of endothelium-dependent vasodilatation. The aim of this study was to measure the expression levels of SK2 mRNA and protein in hypertension (HT) and normotensive (NT) patients. Mesenteric arterial tissues were collected from the removed tissues by abdominal operations in Han Chinese normotensive and primary hypertensive patients. The human tissue collection protocol was approved by the Ethics Committee of Luzhou medical College. In the present study, informed consent was obtained from the patients for the use of vascular tissue (which is usually discarded). Hypertension was defined as systolic blood pressure ≥140 mm Hg and diastolic pressure ≥90 mm Hg according to the Chinese and international diagnostic criteria of hypertension guidelines. mRNA and protein of mesentery artery were obtained from 8 NT and 8 HT patients. The expression of mRNA was detected using quantitative Real-time PCR and analyzed with 2(-ΔΔCT) method. The artery protein

extractions were detected using western blot with SK2 antibody. The statistical analysis was done using independent-samples T test by SPSS 17.0. The average age of HT was 59.2500±1.2256, while the age of NT was 56.6250±8.7331. Real-time PCR and western blot experiments of each sample were repeated for 3 times and the average of the data was for analysis. The expression level of SK2 mRNA in HT was reduced by 38.3%, compared with normal arterial pressure patients. The relative expression of SK2 protein in HT was 1.0387±0.4535, while it was 1.7269±0.5825 in NT, P<0.05. There was significant difference in these two groups. Expression levels of SK2 mRNA and protein were significant down-regulation in essential hypertension patients. It may be another important factor in regulating SKCa channel activity. That may lead to the abnormal of vascular smooth muscle hyperpolarization and the occurrence of hypertension.

This work was supported by National Natural Science Foundation of China (No: 81173661 and No: 30870903) and Youth Science Foundation of Sichuan Education Committee (No: 11ZB224).

Where applicable, the authors confirm that the experiments described here conform with The Physiological Society ethical requirements.

PCA389

Changes in the expression, the composition and the function of vascular L-type Ca2+ channels in a mouse model of essential hypertension

J.R. Lopez-Lopez[1,2], S. Tajada[1,2], P. Cidad[1,2], O. Colinas[1,2], E. Alonso[1,2], R. de Pedro[1,2], L.F. Santana[3] and T. Perez-Garcia[1,2]

[1]Physiology, University of Valladolid, Valladolid, Spain, [2]Instituto de Biología y Genética Molecular (IBGM), CSIC, Valladolid, Spain and [3]Physiology and Biophysics, University of Washington, Seatle, WA, USA

The contraction of vascular smooth muscle cells (VSMCs) is critically dependent on the intracellular calcium concentration [Ca2+]i. Relevant mechanisms contributing to tight control of [Ca2+]i include L-type calcium channels (LTCCs), ryanodine receptor channels (RyR), resting membrane potential (Em) and large-conductance Ca2+-activated K+ channels (BK). The increased vascular tone that defines essential hypertension associates to depolarisation of VSMCs. In hypertensive rat models, it has been postulated that depolarization-induced increased expression of α1C subunit of LTCCs leads to elevated basal [Ca2+]i. However, it is unclear whether this mechanism contributes to the genesis and maintenance of essential hypertension, as these models show blood pressure values closed to hypertensive crisis. We have use a genetic mouse model of essential hypertension with moderate blood pressure increase (BPH mice) and its normotensive controls (BPN) to study the functional expression of LTCCs in mesenteric arteries VSMCs. Animal protocols were approved by the Institutional Care and Use Committee of our Institution. Mice were killed by decapitation after isofluorane anaesthesia (5% at 2.5 l min-1 O2), and mesenteric VSMCs were obtained by enzymatic dissociation. Expression and function of LTCCs in VSMCs form BPN and BPH VSMCs were explored with real-time PCR, electrophysiological recordings and observation of calcium influx "sparklets" with total internal reflection fluorescence (TIRF) microscopy . qPCR showed a decreased expression of α1C and β2 mRNA and a significant increase in the $\alpha 2\delta$ subunit in BPH VSMCs. Moreover, LTCCs currents recorded in BPH had a significantly reduced density. Also LTCCs from BPH cells were more sensitive to 5μM BayK 8644 and were differentially modulated by 100 μM gabapentin (GBP), a ligand of $\alpha 2\delta$ subunits, suggesting a different molecular composition of LTCCs. To test this hypothesis, the effect of GBP was explored in HEK cells transfected with different LTCCs subunits. GBP dose-response relationship indicated similarities between α1C+$\alpha 2\delta$+β2 transfected HEK and BPH and between α1C+$\alpha 2\delta$ and BPN. Organization of the LTCCs was studied by TIRF. LTCCs clusters operating in the high open probability mode were significant larger in BPH mice, and sparklets amplitude histograms indicates that LTCCs clusters in BPH are composed of a larger number of channels. In conclusion, we found a decreased mRNA expression and a lower LTCCs current density in BPH. However, LTCCs cluster from BPH were larger and showed higher activity at rest. We postulated that changes in the subunit composition of LTCCs in BPH VSMCs could account for these differences.

Supported by grants from ISCIII (R006/009, Red Heracles), MICIN (BFU2010-15898), JCyL (VA094A11-2) and GenCat (CIDEM- VALTEC09-1-0042).

Where applicable, the authors confirm that the experiments described here conform with The Physiological Society ethical requirements.

PCA390

Myristoylated alanine-rich C kinase substrate (MARCKS) mediates activation of canonical transient receptor potential 1 (TRPC1) channels in vascular myocytes

J. Shi[1], L. Birnbaumer[2], W. Large[1] and A. Albert[1]

[1]St. George's, University of London, London, UK and [2]National Institute of Environmental Health Sciences, North Carolina, NC, USA

TRPC1 Ca2+-permeable cation channels regulate contraction and remodelling of vascular myocytes; phenotypes associated with cardiovascular disease (CVD, Abramowitz & Birnbaumer, 2009). It is apparent that phosphatidylinositol 4,5-bisphosphate (PIP2) and protein kinase C (PKC) are obligatory for TRPC1 channel activation in vascular myocytes (Albert, 2011). Moreover, calmodulin (CaM) is also important for activation of TRPC1 channels (Albert et al, 2006). The present work investigates how interactions between PIP2, PKC and CaM induce TRPC1 channel opening, and reveals a novel role for MARCKS, a membrane-associated phospholipid-binding protein (McLaughlin et al, 2005).
Rabbits were sacrificed using i.v. sodium pentobarbitone (120 mgkg-1), and wild-type (WT) or TRPC1-/- mice were killed by cervical dislocation; both protocols carried out in accordance with the UK Animals Scientific Procedures Act, 1986. Portal vein myocytes were enzymatically dispersed for immunocytochemical staining and patch clamp recording, and tissue lysates were used for immunoprecipiation, Western blot and dot-blot analysis (n=at least 3 replicates or n=at least 6 patches per test condition). Mean data were ± S.E.M, and statistical significance was determined using Students t-test (p<0.05).
MARCKS protein was expressed, and predominantly distributed at the plasma membrane of portal vein myocytes. In rabbit and WT murine portal vein myocytes, a MARCKS inhibitory peptide (MANS) activated whole-cell and single cation channel activities; these channel activities were absence in TRPC1-/- myocytes. MANS-activated TRPC1 channel activity was prevented by lowering PIP2 levels and PKC inhibitors but was

unaffected by CaM inhibitors. These results suggest that constitutive MARCKS activity prevents TRPC1 channel opening, and that TRPC1 channel activation by PIP2/PKC and CaM occur downstream and upstream of MARCKS respectively.
In un-stimulated tissue lysates, TRPC1 associated with MARCKS, and PIP2 primarily interacted with MARCKS. Following stimulation with noradrenaline or MANS, TRPC1 dissociated from MARCKS, and PIP2 was released from MARCKS and interacted with TRPC1. Importantly, noradrenaline stimulated PKC-dependent phosphorylation of TRPC1 but not MARCKS.
We propose that noradrenaline induces TRPC1 channel activity through PKC-dependent phosphorylation of channel proteins, which increases binding of PIP2 to TRPC1 subunits that opens the channels; these levels of PIP2 are provided by MARCKS, which acts as a PIP2 buffer. It is likely that CaM activates TRPC1 by causing MARCKS to release PIP2.
Our conclusions raise the idea that MARCKS is a novel Ca2+ signalling molecule, through modulating TRPC1 and possibly other ion channels, and is a potential therapeutic target for CVD.

Abramowitz J & Birnbaumer L (2009). FASEB J 23, 297-328.

Albert AP et al (2006). Br J Pharmacol 148, 1001-1011.

Albert AP et al (2011). Adv Exp Med Biol 304, 391-411.

McLaughlin S et al (2005). Biochem Soc Sym 72, 189-198.

The work was funded by the BBSRC.

Where applicable, the authors confirm that the experiments described here conform with The Physiological Society ethical requirements.

PCA391

GoSlo-SR-5-69: a novel, potent, efficacious BK channel activator

S. Roy[2], T. Webb[2], A. Akande[1], A. Kshatri[1], R. Large[2], K. Thornbury[1,2], N. McHale[1,2], G. Sergeant[1,2] and M.A. Hollywood[1,2]

[1]Smooth Muscle Research Centre, Dundalk Institute of Technology, Dundalk, Louth, Ireland and [2]Ion Channel Biotechnology Centre, Dundalk Institute of Technology, Dundalk, Louth, Ireland

We previously synthesized a novel library of anilinoanthraquinone derivatives termed the GoSlo-SR family, that shifted the half maximal activation voltage (V1/2) of BK channels by ~ –100 mV with an EC50 of ~ 2 μM (Roy et al., 2012). In the current study we hypothesised that the replacement of the phenylamino ring of the anthraquinone moiety by hydrophobic naphthylamino could enhance their potency and efficacy on BK channels.
All experiments were approved by DKIT Animal Care and Use Committee. Rabbits were humanely killed with pentobarbitone (I.V.), their bladders removed and smooth muscle strips cut into 1 mm 3 pieces. Rabbit Bladder SMC (RBSMC) were isolated by enzymatic digestion and plated in 35 mm Petri dishes. Experiments were performed at 37oC using excised inside/out patch configuration with symmetrical K+ solutions (pH 7.2) containing 140 mM KCl, 10 mM Glucose, 10 mM HEPES and either 1 mM EGTA (for [Ca2+] 100 nM) or 1 mM HEDTA (for [Ca2+] > 300 nM).
Excised patches of RBSMC were held at –60 mV and BK channel currents were evoked using voltage ramps (100 mV sec-1). The single channels had a large conductance (~330 pS), reversed at the K+ equilibrium potential (0 mV), were blocked in the presence of penitrem A (100 nM, n=6) and were sensitive to [Ca2+] such that a 10 fold increase in [Ca2+] to 1 μM shifted the activation V1/2 from 142±4 mV to 13±3 mV (ΔV1/2 = –129±5 mV, n=18). The compounds shown in Figure 1 were synthesized by microwave irradiation using copper catalyzed Ullmann coupling reaction (Baqi & Müller, 2007). Their structures were assigned by 1H NMR and HRMS and purity was determined by HPLC.
The addition of naphthylamino or tetrahydro-naphthylamino rings to anthraquinone moiety (Fig. 1) produced variable effects. For example,10 μM GoSlo-SR-5-103 (Fig. 1B) was significantly less effective than GoSlo-SR-5-6 and only shifted the the ΔV1/2 by –44±4 mV (n=18). Application of 10 μM GoSlo-SR-5-65 (Fig. 1C) produced effects very similar to those of GoSlo-SR-5-6 and the ΔV1/2 was –116±10 mV (n=6). We then synthesized the compounds shown in Figures 1D & 1E to examine if the addition of 2-naphthylamino or tetrahydro-2-naphthylamino ring altered the potency. We found the application of 1 μM GoSlo-SR-5-95 (Fig. 1E) produced a ΔV1/2 of –94±9 mV (n=6), suggesting that it was more efficacious than GoSlo-SR-5-6 at this concentration. Similarly, application of 1 μM GoSlo-SR-5-69 (Fig. 1D) produced a ΔV1/2 of –113±10 mV (n=10) and the mean EC50 was 189 nM (confidence intervals 65 nM to 546 nM, n=3-8 patches).
In conclusion, the results of this study suggest that the addition of a tetrahydro-2-naphthylamino ring to the anthraquinone moiety significantly enhances its ability to activate the BK channels in the rabbit bladder.

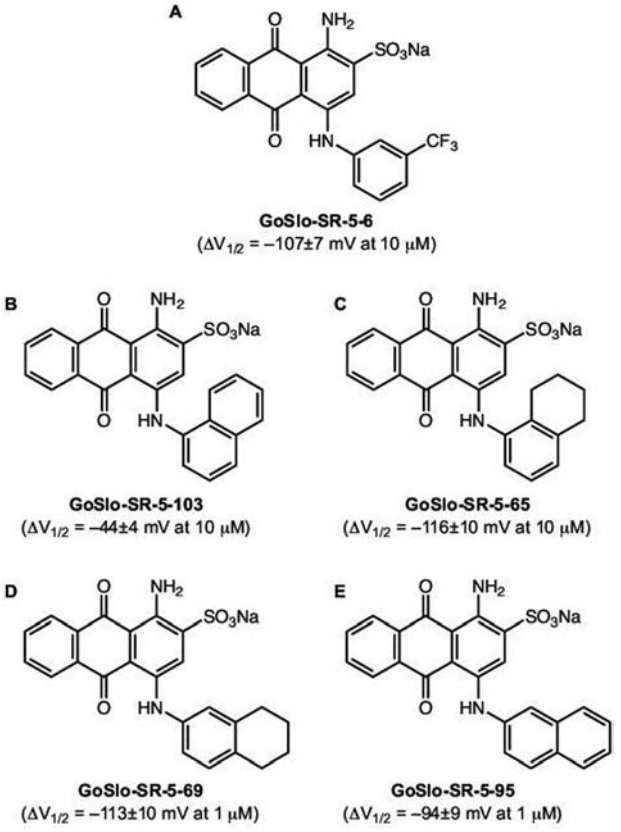

Figure 1. 2-Naphthylamino anthraquinones are potent BK channel openers.

Roy S, Akande AM, Large RJ, Webb TI, Camarasu C, Sergeant GP, McHale NG, Thornbury KT & Hollywood MA (2012). ChemMedChem, 7(10): 1763-1769.

Baqi Y & Müller CE. (2007) Org Lett, 9: 1271-1274.

This work was supported by Enterprise Ireland's Applied Research Enhancement Programme. A. Akande was supported by a Council of Directors Strand1 award.

Where applicable, the authors confirm that the experiments described here conform with The Physiological Society ethical requirements.

PCA392

Using BK channel chimaeras to identify the molecular site of action of the BK channel opener GoSlo-SR-5-6

T. Webb[2], R. Large[2], A. Kshatri[1], S. Roy[2], A. Akande[1], G. Sergeant[1,2], N. McHale[1,2], K. Thornbury[1,2] and M.A. Hollywood[1,2]

[1]Smooth Muscle Research Centre, Dundalk Institute of Technology, Dundalk, Louth, Ireland and [2]Ion Channel Biotechnology Centre, Dundalk Institute of Technology, Dundalk, Ireland

GoSlo-SR-5-6 is a novel, potent BK channel activator [1] that does not require functional Ca2+ sensors to mediate its effect [2]. A recent study [3] has shown that the BK channel opener Cym04 was less effective in the Slo1_9a splice variant, which is expressed in the brain. The purpose of this study was to examine if the effects of GoSlo-SR-5-6 were reduced in the Slo1_9a variant.

All experiments were carried out on BK channel α subunits cloned from rabbit bladder or human brain and expressed in human embryonic kidney cells (HEK293). Site-directed mutagenesis on the resulting cDNA was carried out [4]) and confirmed by sequencing. HEK cells were grown in DMEM medium supplemented with 10% FCS, penicillin and streptomycin. HEK cells were dissociated with trypsin (1%), plated onto 35 mm Petri dishes and maintained in culture at 37oC in 5% CO2 prior to use. All experiments were performed at 37oC using the excised inside/out patch configuration with symmetrical 140 K+ solutions containing either 1mM EGTA or 1 mM HEDTA. Excised patches were held at –60 mV and BK channel currents were evoked using voltage steps from -100 mV up to 200 mV before repolarising back to -80 mV. Peak currents were measured during the voltage steps, corrected for driving force and activation curves constructed.

In cells expressing the BKα subunit and exposed to 100 nM Ca2+ at the cytosolic face of the patch, the half maximal activation voltage (V1/2) was 171±2 mV and this was shifted to 57±3 mV (n=12) in the presence of 1 μM Ca2+. Application of GoSlo-SR-5-6 (10 μM) shifted the mean activation voltage (ΔV1/2) by -121±3 mV (n=12). When we examined the effect of GoSlo-SR-5-6 on the Slo1_9a splice variant we found that although a tenfold increase in Ca2+ (from 100 nM to 1 μM) shifted V1/2 from 158±2 mV to 63±3 mV, GoSlo-SR-5-6 application (10 μM) only changed ΔV1/2 by -38 ± 8 mV compared to normal BK channel, ($p<0.001$ unpaired t test, n=10). To assess the contribution of the proximal linker, we generated a 9A9 chimaera, which contained the alternative proximal linker and found that GoSlo-SR-5-6 shifted the V1/2 by -106 ± 5 mV (n=5). The ΔV1/2 of the 9AA chimaera was -88 ± 7 mV (n=6), but this was not significantly different from the 9A9 chimaera, suggesting that the distal linker contributed little to the response. When we investigated the contribution of the S6 segment using the A99 chimaera, the ΔV1/2 was -53 ± 11 mV (n=6, $p<0.05$), but was not further reduced in the A9A chimaera, (-51 ± 9 mV, n=7).

These data suggest the effect of GoSlo SR5-6 is reduced in the Slo1_9a variant and that the majority of this effect appears to be mediated via differences in the S6 segment of this channel.

Roy, S, Akande AM, Large RJ, Webb TI, Camarasu C, Sergeant GP, McHale NG, Thornbury KT & Hollywood MA (2012). Structure-activity relationships of a novel group of large-conductance Ca2+-activated K+ (BK) channel modulators: The GoSlo-SR family. ChemMedChem, 7(10). 1763-1769.

Large R, Webb TI, Akande A, Roy S, Sergeant GP, Thornbury KD, McHale NG, Hollywood MA. (2012) Functional Ca2+ sensors do not contribute to the effect of the novel BK channel agonist GoSlo-SR5-6. Proc Physiol Soc 27 PC169.

Gessner G, Cui YM, Otani Y, Ohwada T, Soom M, Hoshi T, Heinemann SH. (2012) Molecular mechanism of pharmacological activation of BK channels. Proc Natl Acad Sci. 109(9) :3552-7.

Sawano A & Miyawaki A.(2000) Directed evolution of green fluorescent protein by a new versatile PCR strategy for site-directed and semi-random mutagenesis. Nucleic Acids Res. 28(16):E78.

We would like to acknowledge Prof S. Heinemann for the kind gift of the Slo1_9a clone. This work was supported by Science Foundation Ireland RFP and Enterprise Ireland ARE Scheme.

Where applicable, the authors confirm that the experiments described here conform with The Physiological Society ethical requirements.

PCA393

A mathematical model of pacemaking activity in interstitial cells of Cajal

J. Youm[1,2], H. Kim[2], H. Heo[2], N. Kim[1,2], B. Kim[4], C. Leem[3] and J. Han[1,2]

[1]Department of Physiology, Inje University, Busan, Republic of Korea, [2]Cardiovascular and Metabolic Disease Center, Inje University, Busan, Republic of Korea, [3]Department of Physiology, University of Ulsan College of Medicine, Seoul, Republic of Korea and [4]Division of Longevity and Biofunctional Medicine, Pusan National University School of Korean Medicine, Yangsan, Republic of Korea

It is widely accepted that interstitial cells of Cajal generate pacemaker potentials to propagate slow waves along the whole gastrointestinal tract. Previously, we constructed a biophysically based model of interstitial cells of Cajal in mouse small intestine to explain pacemaking mechanism [1]. Since a significant amount of valuable data characterizing ion channels related with pacemaker activity were then accumulated, we tried to improve our mathematical model by including those ion channels and updating pre-existing components. We incorporated 5 more ion channels in the model. They are voltage-gated Na^+ channel (Nav 1.5), Ca^{2+}-activated Cl^- channel, ERG K^+ channel, Ca^{2+}-activated K^+ (BK) channels, and Na^+-leak channel (NALCN). Most of modeling of ion channels were carried out by data fitting to curves for time course of each current, steady-state activation or inactivation, and voltage-dependence of time constants. The IP_3-mediated Ca^{2+} release is a key event to drive the cycle of pacemaker potential and was updated to reproduce its stochastic behavior. The stochastic currents were reproduced by simulating the random openings and closing of an individual ion channel. The updated model was able to reproduce stochastic feature of pacemaker potentials in interstitial cells of Cajal. Pacemaker potential was not uniform in the size, duration, and frequency. The resting and overshoot potential were -72.42±0.51 (mean±S.D., n=10) and -3.45±0.27 (n=10), respectively.The frequency was about 32 min^{-1} and the duration at 50% repolarization was 614.3±40.6 (n=10). The model suggests that the Na^+-leak channel contributes to depolarization about 10 mV in resting membrane potential. The model also suggests that Ca^{2+}-activated Cl^- chan-

nel is more likely to stabilize membrane potential rather than to excite under the physiological condition. We conclude that this improved mathematical model could explain a stochastic nature of pacemaker activity of interstitial cells of Cajal.

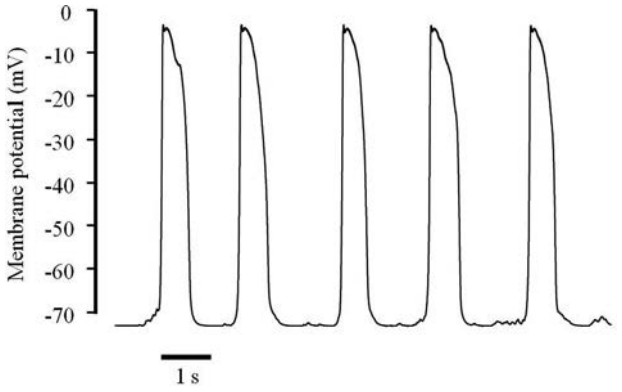

Simulated pacemaker potentials of interstitial cells of Cajal in mouse small intestine

Youm JB et al. (2006). *Philos Transact A Math Phys Eng Sci* **364**, 1135-1154.

This research was supported by Basic Science Research Program through the National Research Foundation of Korea(NRF) funded by the Ministry of Education, Science and Technology(2012R1A1A2008990).

Where applicable, the authors confirm that the experiments described here conform with The Physiological Society ethical requirements.

PCA394

Theregulatorymechanismunderlyingthe enhanced expression of large conductance Ca2+ activated K+channelbytestosterone

R. Azizieh[1], A. Ohno[1], S. Ohya[1,2], Y. Suzuki[1], H. Yamamura[1] and Y. Imaizumi[1]

[1]Nagoya city university, Nagoya, Japan and [2]Department of Pharmacology, Division of Pathological Sciences, Kyoto Pharmaceutical University, Kyoto, Japan

The regulatory mechanisms in ion channel expression by sexual hormones are urgent issues in the understandings of cardiovascular diseases after menopause, gender difference in occurrence of psychiatric diseases, side effects of hormonal therapy of genital organ cancers.
Large conductance Ca2+-activated K+ (BK) channels are activated by changes in membrane potential and/or by increases in concentration of intracellular calcium ion (Ca2+) and substantially contribute to outward K+ currents, modulation of action potential duration and theCa2+-dependent regulation of electrical behaviour in many types of cells including central nervous system and smooth muscles.
The activity and/or expression of BK channels can be modulated by steroid hormones as both long-term genomic and acutenon-genomic effects. Female sexual hormones, progesterone and estrogen, regulate BK channel expression andtheir membrane surface clustering in uterine smooth muscles, particularly during pregnancy.We have shown that the expression of BK channels in the amygdala complex is higher in adult (8-10 week old) male rats than in female. Castration at 4-6 weeks old significantly reduces BK channels expression inthe amygdala to a similar level observed in female.
Effects of testosterone on the BK channel expression and their functional significance were then investigated in vas deferens smooth muscles (VDSM) of male rats.Western blot analysis showed that castration caused the marked decrease in the expression of BK channel α (BK-α) and β1 (BK-β1) subunits in VDSMC membrane proteins. In contrast, castration did not significantly change expression levels for BK-a and BK-b1 transcripts in VDSMs.
We hypothesized that the up-regulation of BK channels expressionin VDSM may be due to the inhibitionof ubiquitin-mediated protein degradation by activation of Androgen Receptors (AR). According to this, we speculated that the down-regulation of BK channel expression, observed in castrated rats, is due the AMPK-activated Ubiquitination of these channels secondary to a decrease of AR activation by testosterone. Therefore we tested the ability of BK channel subunits to bind ubiquitin by co-immunoprecipitation, as well as its ability to bind different Ubiquitin ligase such as Nedd 4, Nedd 4-2 and Cullin 1. Our data suggest that BK-α is indeed able to bind Ubiquitin as well as Nedd 4.
In conclusion, AR activation by testosterone critically up-regulates the functional expression of BK channels in VDSMCs, presumably due to inhibition of proteolysis, and thereby substantially modualtes membrane excitability in VDSMs in male rats.

Where applicable, the authors confirm that the experiments described here conform with The Physiological Society ethical requirements.

PCA395

Identification of functional P2X receptors in rat middle cerebral arteries

O. Povstyan, C. Nichols and M. Harhun

Division of Biomedical Sciences, St George's University of London, London, UK

During sympathetic nerve activity ATP is co-released with noradrenaline leading to constriction in muscular arteries. Current views support the notion that physiological contractile responses to ATP are mainly mediated through activation of homomeric P2X1 receptors of the membrane of vascular smooth muscle cells (VSMCs), while the role of other P2X receptors (P2XRs) remains unclear. In this work we studied P2XRs in rat middle cerebral arteries (RMCA). RT-PCR gene expression analysis was performed using preparations from isolated VSMCs. The expression of proteins was confirmed by immunocytochemistry. Agonist-induced $[Ca^{2+}]_i$ changes were monitored using *x-y* confocal imaging in fluo-3 loaded VSMCs. Electrical recordings were performed using patch-clamp technique. Isometric tension recordings were performed using wire myograph. Our results show that RMCA VSMCs express genes encoding only P2X1 and P2X4 receptor subunits and corresponding proteins in their plasma membrane. Both ATP and a potent P2XR agonist, α,β-meATP, evoked dose-dependent increase in $[Ca^{2+}]_i$ of similar amplitude for each concentration with an EC_{50}=0.38±0.29 μmol/l (n=7-17) and EC_{50}=0.59±0.24 μmol/l (n=7-12) for ATP and α,β-meATP respectively. Sub-maximal concentration of noradrenaline (100 μmol/l) produced less than 10% of amplitude of $[Ca^{2+}]_i$ increase evoked by 100 μmol/l ATP in RMCA VSMCs. Under current-clamp recordings 10 μmol/l ATP evoked either fast transient depolarisation or transient response followed by a sustained depolarisation or only sustained depolarisation of the membrane of different

VSMCs. Similarly, under voltage-clamp both10 μmol/l ATP and 10 μmol/l α,β-meATP evoked either transient rapidly desensitising current (I_{fp2x}) or biphasic current consisting of transient and sustained component or only slowly desensitising current (I_{sp2x}) in different VSMCs. I_{fp2x} rapidly desensitised within 3 s of α,β-meATP application, and completely recovered within 8 min after first application of the agonist. Selective P2XR blocker NF279 inhibited I_{fp2x} in dose dependent manner with an IC_{50}=17±2 nmol/l (n=5-6) and complete inhibited the current at 10 μmol/l. NF279 inhibited I_{sp2x} in dose dependent manner with IC_{50}=25±6 μmol/l (n=4-5). These data suggest that monomeric P2X1R predominantly contribute to I_{fp2x} while heteromeric P2X1/4R predominantly contribute to I_{sp2x}. Isometric tension recordings showed that both 10 μmol/l ATP and 10 μmol/l α,β-meATP produced biphasic contractions of RMCA preparations. Incubation of arterial segments with 10 μmol/l NF279 inhibited α,β-meATP (10 μmol/l) evoked contraction by 75±3% (n=6). 100 μmol/l noradrenaline produced only 8±2% (n=7) of contraction evoked by 10 μmol/l α,β-meATP. Our data suggest that in RMCA ATP may play role of the predominant neurotransmitter and that both homomeric P2X1R and heteromeric P2X1/4R contribute to ATP evoked constriction of these blood vessels.

Where applicable, the authors confirm that the experiments described here conform with The Physiological Society ethical requirements.

PCA396

Hydrogen sulfide inhibits recombinant T-type Ca2+ channels

J. Elies[1], M.L. Dallas[2], J.L. Scragg[1], J.P. Boyle[1] and C. Peers[1]

[1]University of Leeds, Leeds, UK and [2]School of Pharmacy, University of Reading, Reading, UK

Awareness of H2S as an important, widespread signalling molecule is growing rapidly. It is known to influence, for example, proliferation of vascular smooth muscle cells and pain sensation (1). Interestingly, both of these processes involve T-type Ca2+ channel activity (2;3). We have therefore investigated whether H2S modulates T-type Ca2+ channels, using whole-cell patch clamp recordings from HEK293 cells over-expressing, separately, T-type Ca2+ channels Cav3.1, 3.2 and 3.3 (4). Bath application of NaHS, which produces H2S in solution, caused a concentration-dependent inhibition of currents in Cav3.2-expressing cells. Inhibition was observed at all activating test potentials, and all subsequent values are of currents recorded at a test potential of -20mV (holding potential -80mV). Maximal inhibition of 35.3±2.2%, n=6, P<0.0001, student's paired t-test) was observed at the NaHS concentration of 1mM. By contrast, current carried by Cav3.1 channels were unaffected over the same concentration range, and those carried by Cav3.3 were only modestly inhibited (13.2±3.6%, n=5, P=0.022) by 1mM NaHS. Thus, H2S appeared to inhibit Cav3.2 channels selectively. Inhibition of Cav3.2 was only poorly reversible, but could be reversed by dithiothreitol (2mM; n=7), suggesting H2S acts via channel redox modulation. Given the high selectivity of H2S for Cav3.2, we examined its effects in H191Q mutant Cav3.2-expressing cells, since this extracellular histidine residue is known to be essential for redox-sensitive binding of divalent metals (3). These mutant channels were insensitive to H2S (1mM NaHS, n=6). In agreement with previous studies (e.g. (5)), the zinc chelator TPEN (10μM) augmented Cav3.2 currents, by 150±9.0% (n=6), and in its presence NaHS was without significant effect on currents carried by Cav3.2 channels.

Our data indicate that H2S selectively inhibits Cav3.2 T-type Ca2+ channels heterologously expressed in HEK293 cells. Inhibition requires the extracellular histidine residue H191. Our results do not, however, support the previous suggestion that H2S might augment T-type Ca2+ channel activity by acting as a zinc chelator (reviewed in (3)).

Wang,R. (2012) Physiol Rev. 92, 791-896

Cribbs,L.L. (2006) Cell Calcium 40, 221-230

Todorovic,S.M., and Jevtovic-Todorovic,V. (2011) Br. J Pharmacol. 163, 484-495

Fearon,I.M. et al (2000) 441, 181-188

Nelson,M.T. et al (2007) J. Neurosci. 27, 8250-8260

Supported by The British Heart Foundation

Where applicable, the authors confirm that the experiments described here conform with The Physiological Society ethical requirements.

PCA397

Deletion of the ion channel TRPV4 increases detrusor contractility in the mouse

A.C. Ramos-Filho[2], F. Johnson[1], E. Antunes[2] and A. Grant[1]

[1]Wolfson Centre for Age-Related Diseases, King's College London, King's College London, UK and [2]Dept. of Pharmacology, University of Campinas, Campinas, Brazil

The mechanosensitive Ca^{2+} permeable cation channel TRPV4 is expressed in the urothelium and detrusor smooth muscle (DSM) of rodent bladders (Thorneloe *et al*., 2008). Urothelial stretch during bladder filling activates TRPV4 and produces a Ca^{2+}-dependent release of ATP (Mochizuki *et al*., 2009). This ATP release activates $P2X_3$ receptors on sensory nerves to produce a sensation of bladder filling (Vlaskovska *et al*., 2001). Activation of TRPV4 in the DSM by the selective agonist GSK1016790A (10-100nM) produces a slow and sustained contraction, which can be inhibited by nifedipine (Thorneloe *et al*., 2008). We hypothesised that deletion of the TRPV4 channel would reduce the contractility of isolated DSM strips by reducing the intracellular [Ca^{2+}].

Male C57BL/6 wild type (+/+) and TRPV4 knockout (-/-) mice (22-30g) were used in this study. Bladders were collected, sectioned above the level of the ureters, then cut into 2 longitudinal strips. These were suspended under 0.5g tension in a 10ml organ bath containing Krebs' solution (pH7.4) at 37C and bubbled with a mixture of 95% O_2 and 5% CO_2. Changes in isometric force were recorded using a Power Lab v.4 system (AD Instruments, UK). Concentration-response curves to the muscarinic agonist carbachol (cumulative) and the P2X receptor agonist α,β-methylene ATP (non-cumulative) were constructed. Following pre-contraction of the tissue strips with 80mM KCl, a concentration-response curve was obtained for relaxation to the β-adrenergic agonist isoprenaline. Frequency-response curves to electrical field stimulation (EFS: 10s; 80V; pulse width 1ms) were also obtained. Emax and pEC_{50} values (stated as mean±S.E.M) were compared by unpaired t-tests.

Maximal contractions to carbachol were significantly increased in TRPV4 -/- strips (1nM-30μM; +/+ = 0.029±0.004 vs -/- = 0.077±0.011g/mg, p<0.05, n=5) with no effect on pEC_{50} values. Contractions to EFS (4,8,16,32Hz) were also increased in TRPV4 -/- strips compared to +/+ strips. Contractions to α,β-methylene ATP (1-10μM, n=4) were unaltered by loss of TRPV4. Maximal relaxation to isoprenaline was significantly decreased in TRPV4 -/- strips (1nM-30μM; +/+ = 61.6±8.3 vs -/- = 41.8±3.8

% of KCl contraction, p<0.05, n=5) with no effect on pEC_{50} values. Pretreatment with the P2 receptor antagonist suramin (100μM) had no effect on the maximal contraction to carbachol or the pEC_{50} of the response.
These data suggest that muscarinic and β-adrenergic receptors activate a TRPV4-dependent mechanism, probably via urothelial TRPV4, that inhibits DSM contraction. This inhibitory mechanism is not P2 receptor dependent. Activation of P2X receptors is sufficient to cause DSM contraction without the contribution of TRPV4.

Mochizuki, T. *et al*. (2009) *J. Biol. Chem.* **284(32)**, 21257-64.

Thorneloe, K.S. *et al*. (2008) *J Pharmacol Exp Ther*. **326(2)**, 432-42.

Vlaskovka, M. *et al*. (2001) *J. Neurosci*. **21(15)**, 5670-7

Supported by FAPESP project #2010/10553-9 and a Capacity Building Award in Integrative Mammalian Biology funded by the BBSRC, BPS, HEFCE, KTN and MRC

Where applicable, the authors confirm that the experiments described here conform with The Physiological Society ethical requirements.

PCA398

Rapid androgen effects on potassium channels in human coronary artery endothelial cells

K. Ruamyod[1], W.B. Watanapa[1] and C. Shayakul[2]

[1]Department of Physiology, Faculty of Medicine Siriraj Hospital, Mahidol University, Bangkok, Thailand and [2]Department of Medicine, Faculty of Medicine Siriraj Hospital, Mahidol University, Bangkok, Thailand

The mechanisms of testosterone(T)-induced, endothelium-dependent vasodilation are not fully understood. Studies showed that endothelial NO partly mediated this effect (1, 2). The production of endothelial vasodilators, e.g. NO and prostacyclin, are modulated by endothelial ion channels which influence the resting membrane potential, Ca^{2+} electrochemical driving force, the magnitude of Ca^{2+} influx and ultimately $[Ca^{2+}]_i$ (3, 4). This study investigated the effect of T on ion channels of human coronary endothelial cells (HCAECs) and its molecular mechanism using whole-cell patch clamp technique. Values are mean ± SEM (no.) of %increase from control currents. T at 100-1000nM induced a rapid (2-5 minutes), dose-dependent increase in total current [100nM T: 31.9±8.6% (18), 200nM T: 38.8±10.9% (8), 300nM T: 59.7±15.8% (18), and 1μM T: 58.7±7.1% (37)]. The EC_{50} of T, obtained by curve-fitting to the Hill equation was 83.7±1.9nM. 1μMT, after pretreatment with DIDS and La^{3+} (to block Cl^- and transient receptor potential channels, respectively) increased the residual currents (primarily carried by K^+) by 45.2±9.0% (n=13, p<0.05, *t*-test). In contrast, 1μMT did not change currents after pretreatment with K^+ channel blockers TEA + $BaCl_2$ and DIDS or La^{3+} (15.8±8.7% and -0.1±14.1%, n=7 and 7, respectively, n.s., *t*-test). Non-permeant form of T, bovine serum albumin-conjugated T (T-BSA, 1μM), increased HCAEC currents by 93.1±10.2% (n=17, p<0.05; *t*-test). Pretreating with an androgen receptor antagonist flutamide reduced T effect, from 84.8±22.9% (n=7) without to 1.7±4.3% (n=8) with flutamide pretreatment, respectively (p<0.05; *t*-test). The effect of T-BSA was also inhibited by flutamide. However, pretreating with estrogen receptor blocker fulvestrant did not prevent T effects; 101.5±22.0% (n=3) in T vs. 75.2±11.7% (n=8) in T + fulvestrant pretreatment (n.s.; *t*-test). Dihydrotestosterone (DHT), a nonaromatizable androgen, also stimulated HCAEC currents, which was attenuated by flutamide pretreatment; 195.7±45.1% (n=7) without vs. 2.6±19.5% (n=4) with flutamide pretreatment (p<0.05; *t*-test). Incubating HCAECs with pertussis toxin (PTX) partly inhibited the HCAEC current increase by T; 63.1±16.2% (n=6) in T *vs.* 15.2±7.5% (n=6) in PTX pretreatment + T (p<0.05, *t*-test), while pre-incubation with a PLC inhibitor U-73122 did not significantly prevent the T effect. These data suggested that androgens may non-genomicly increase HCAEC K^+ currents via surface androgen receptors. This effect may be partly mediated by $G_{o/i}$-protein but not PLC.

Goglia L *et al* (2010). *Mol Hum Reprod* **16**, 761-9.

Yu J *et al* (2010). *Endocrinology* **151**,1822-8.

Kohler R & Hoyer J (2007). *Kidney Int* **72**, 145-50.

Garland CJ *et al* (2011). *Br J Pharmacol* **164**, 839-52.

Where applicable, the authors confirm that the experiments described here conform with The Physiological Society ethical requirements.

PCA399

Endogenously-generated lipid peroxidation products dilate rat cerebral arteries by activating transient receptor potential channel ankyrin 1 in the endothelium

M.N. Sullivan, A. Bruhl and S. Earley

Vascular Physiology Research Group, Biomedical Science, Colorado State University, Fort Collins, CO, USA

The sole member of the ankyrin (A) subfamily of transient receptor potential (TRP) channels, TRPA1, is Ca^{2+}-permeable and present in the cerebral vascular endothelium.[1, 2] TRPA1 is localized to sites of endothelial cell-smooth muscle communication called myoendothelial junctions.[2] Upon activation with exogenous electrophilic compounds, TRPA1 evokes endothelium-dependent vasodilation,[2] but endogenous agonists of the channel in this tissue remain elusive. TRPA1 channels have been shown to be activated by lipid peroxidation products (LPP)[3, 4] formed from the oxidative degradation of membrane lipids by reactive oxygen species (ROS). Rat cerebral artery immunolabeling revealed the presence of NADPH oxidase isoform 2 (NOX2), a ROS-generating enzyme, in the endothelium within myoendothelial junctions (n = 3). In addition, a proximity ligation assay demonstrated localization of TRPA1 within 40 nm of NOX2, but not NOX4, in intact cerebral arteries (n = 5). We therefore tested the hypothesis that TRPA1 is activated by endogenous LPP generated from local production of ROS by NOX in cerebral arteries. To examine the effect of NOX activation on TRPA1 activity, unitary TRPA1 Ca^{2+} influx events (TRPA1 Ca^{2+} sparklets) were recorded from primary cerebral artery endothelial cells loaded with Ca^{2+} indicator Fluo-4 AM using total internal reflection fluorescence (TIRF) microscopy. TIRF recordings of cells were analyzed using custom software, LC_Pro, where TRPA1 Ca^{2+} sparklets were autodetected, and parameters such as whole-cell frequency (Ca^{2+} sparklets/cell/s) were calculated. Addition of NADPH, a substrate of NOX, to the extracellular solution increased TRPA1 Ca^{2+} sparklet frequency in endothelial cells (0.04 ± 0.02 Hz before vs. 0.28 ± 0.08 Hz after, n = 20-30). This increase in TRPA1 Ca^{2+} sparklet frequency was attenuated by pretreatment with the selective TRPA1 antagonist HC-030031 (HC) (0.03 ± 0.02 Hz, n = 14), indicating that activation of NOX stimulates TRPA1 Ca^{2+} influx in endothelial cells. We then examined the effect of NOX activation in isolated, pressurized (80 mmHg) rat cerebral arteries. Superfusion of NADPH in the bathing solution induced vasodilation in a concentration-

dependent manner (EC_{50} = 1.2 μM). This response was diminished by pre-treatment with HC (61.3 ± 21.6% dilation (NADPH) vs. 8.7 ± 16.2% dilation (HC + NADPH), n = 3). The LPP 4-hydroxy-nonenal (4-HNE) also caused cerebral artery dilation (EC_{50} = 8.4 μM) that was abolished by pre-treatment with HC (51.4 ± 7.8% dilation (4-HNE) vs. 0.0 ± 11.6 % (HC + 4-HNE), n = 5). Together, our findings suggest that NOX-derived LPP generation dilates cerebral arteries through TRPA1 activation. All data are mean ± SE; values of n refer to the number of cells/vessels used per each experiment.

Karashima Y *et al.* (2010) *Biophys J* **98(5)**, 773-83.

Earley S *et al.* (2009) *Circ Res* **104(8)**, 987-94.

Uchida K (2003) *Prog Lipid Res* **42(4)**, 318-43.

Andersson DA *et al.* (2008) *J Neurosci* **28(10)**, 2485-94.

Supported by HL091905 (S. Earley).

Where applicable, the authors confirm that the experiments described here conform with The Physiological Society ethical requirements.

PCA400

NO stimulates BKCa channels in smooth muscle cells of human mesenteric artery

Y. Yang, J. Cheng, J. Wen, P. Li, C. Li, Z. Liu and X. Zeng**

Department of Electrophysiology, Institute of cardiovasology,Luzhou Medical College, Luzhou, Sichuan, China

Nitric Oxide (NO) is an endothelium-independent relaxant agent and its effect is attributed to its direct action on the vascular smooth muscle cells (VSMCs). However, the role of NO in the electrophysiology of human artery SMCs is rarely studied. The aim of this study was to characterize the role of NO on BKCa channels in SMCs freshly isolated from human mesenteric arteries. The use of sodium nitroprusside (SNP) as NO donor in solutions was utilized. The freshly isolated SMCs were used to record BKCa currents using the whole-cell, amphotericin-perforated configuration of patch-clamp technique. Our data show that BKCa currents are often recorded as current spikes (STOCs) and macroscopic currents (MC) under whole-cell voltage clamp conditions. Human mesentery artery SMCs have an average current density of 2.92±0.355 pF/pA (at 0 mV), 16.02±1.15 (at +60 mV) (n=90). In human mesentery artery SMCs, STOCs existed random nature and varied widely from cell to cell and with time, as well as membrane potential. At -30 mV membrane potential, the amplitude was 6-60 pA and frequency 0.03-8 Hz, and at 0 mV, the amplitude (10-120 pA) and frequency (0.5-13 Hz). Extracellular application of SNP enhanced both MC and STOCs. 50 μM SNP increased MC by (8.3±2.3)% (at 0 mV), (29.5% ±16.8)% (at +60mV) (n=3). 100 μM SNP increased MC by (34.6±30.)% (at 0 mV), (41.7±21.1)% (at +60 mV) (n=9), and 200 μM increased MC by (30.9±26.7)% (at 0 mV), (45.5±16.0)% (at +60mV) (n=5). At -30 mV membrane potential, 100 μM SNP increased the frequency of STOCs from 3.32±0.85 (Hz) to 5.43 ±0.75 (Hz) (n=6, $p<0.05$) and amplitude of STOCs from 16.84±1.84 to 18.40±2.61 (pA) (n=6). 200 μM NO induced the frequency to 4.70±1.03 (Hz) (n=4) and amplitude to 16.81±3.15 (pA) (n=4). NO existed short-term effect on BKCa and its action often lasted no more than 10 min after each administration of SNP. The reversibility of NO on BKCa channels was investigated and was determined. Our results suggested that NO could stimulate BKCa channels of human mesenteric artery SMCs in a time dependent and reversible manner.

This work was supported by the National Natural Science Foundation of China (No: 30670763 and No.81173661)

Where applicable, the authors confirm that the experiments described here conform with The Physiological Society ethical requirements.

PCA401

Voltage dependent potassium channels remodeled in hypertrophic intestinal smooth muscle cells induced by partial obstruction in murine

D. Liu, X. Huang, X. Guo, X. Meng, Y. Wu, H. Lu, C. Zhang and W. Xu

School of Medicine, Shanghai Jiaotong University, Shanghai, China

Background: Partial obstruction of the small intestine causes obviously hypertrophy of smooth muscle cells which is a physiological response to the increased pressure in the lumen accompanied by motility disorder.
Aims: To identify electric remodeling of hypertrophic smooth muscle cells in partial obstructed small intestine of mice.
Methods: Partial intestinal obstruction was induced by surgically placing a ring of silicon tube on the distal portion of the ileum in male imprinting control region (ICR) mice. Patch-clamp and intracellular microelectrode recordings methods were used to identify the possible electric remodeling in hypertrophic smooth muscle. Alterations of channel protein expression and phosphorylation level were examined by westernblot, immunofluorescence and immunoprecipitation methods.
Results: Partial obstruction induced smooth muscle hypertrophy in the proximally located intestine after obstruction 14 days and slow waves of intestinal smooth muscles in the dilated region were significantly suppressed, for example, their amplitude and frequency were reduced, whilst the resting membrane potentials were depolarized compared with normal and sham animals. The current density of voltage dependent potassium channel (Kv) was significantly decreased in the hypertrophic smooth muscle cells and changed voltage sensitivity of Kv activation. The sensitivity of Kv currents (IKv) to 4-AP, a Kv blocker, increased significantly but not to TEA, a nonselective potassium channel blocker. However, the Kv4.3 and Kv2.2 expressions were up-regulated in the hypertrophic cell membrane as well as serine and threonine phosphorylation levels of Kv4.3 and Kv2.2 were significantly increased in the hypertrophic smooth muscle cells.
Conclusions: Partial intestinal obstruction-induced smooth muscle hypertrophy accompanyed electric remodeling. The enhanced phosphorylations of serine and threonine in Kv4.3 and Kv2.2 may contribute to membrane potential depolarization of hypertrophic smooth muscle cells.
Key words
Voltage dependent potassium channel; small intestine; partial obstruction; smooth muscle hypertrophy; resting membrane potential.

Where applicable, the authors confirm that the experiments described here conform with The Physiological Society ethical requirements.

PCA402

TRPM2 mediated zinc redistribution mediates H2O2 induced endothelial cell death

N.K. Abuarab, M. Ludlow, J. Ayub, L. Jiang and A. Sivaprasadarao

Multidisciplinary Cardiovascular Research Centre, School of Biomedical Sciences, University of Leeds, Leeds, UK

Oxidative stress plays a central role in the pathogenesis of atherosclerosis. By increasing the production of reactive oxygen species, such as H2O2, oxidative stress causes apoptosis of endothelial cells. Mechanisms by which H2O2 leads to apoptosis, however, are controversial. One study reported that Zn2+ released from H2O2 oxidation of metallothioneins is the cause of cell death [1], while the other suggests that H2O2 activates the TRPM2 channel, resulting in Ca2+ influx and cell death [2].

To address the controversy, we have examined the effect of H2O2 (1 mM, 6h) on human umbilical vascular endothelial cells using live cell imaging. We monitored changes in the intracellular distribution of free Ca2+ and Zn2+ using Fluo-4 and FluoZin-3 respectively. We stained lysosomes and mitochondria with LysoTracker and MitoTracker respectively, and dead cells with propidium iodide. Data recorded from N number of cells and n number of independent experiments are expressed as mean±SEM. P value of <0.05 (Student's t-test) was considered statistically significant.

We found that both Ca2+ and Zn2+ are highly enriched in lysosomes. Mitochondria showed little stain for either ion. H2O2 treatment increased the cytosolic levels of both ions in most cells. In some cells, however, we found striking redistribution of Zn2+ from lysosomes to mitochondria: There was a decrease in the number of lysosomes with Zn2+ (untreated: 61±6%, n/N=3/75; H2O2 treated: 21±1%, n/N=3/49; P<0.01), with a concomitant rise in mitochondria with Zn2+ (untreated: 11±1%, n/N=3/49; H2O2 treated: 41±4%, n/N=3/34; P<0.01). These effects were found in the absence of extracellular Zn2+, indicating redistribution of intracellular Zn2+.

Inhibition of TRPM2 with PJ34 and 2-aminoethoxydiphenyl borate (2-APB) reduced the H2O2 induced release of Zn2+ into the cytoplasm (PJ34: 45±2%, n/N=3/43, P<0.01; 2-APB: 76±1 %, n/N=3/38, P<0.05), as well as its translocation from lysosomes to mitochondria (PJ34: 11±3%, n/N=3/46, P<0.05; 2-APB: 13±2%, n/N=3/35, P<0.05). Transfected HA-tagged TRPM2 channels showed co-localisation with the lysosomal markers, LysoTracker and CD63, suggesting TRPM2 mediates release of Zn2+ from lysosomes.

We next determined the relevance of TRPM2 and Zn2+ redistribution to H2O2-induced endothelial cell death. Blockers of TRPM2 (PJ34 and 2-APB), as well as chelation of Zn2+ with TPEN (N,N,N',N'-tetrakis(2-pyridinylmethyl)-1,2-ethanediamine), completely inhibited H2O2-induced cell death, indicating TRPM2 mediated changes in the redistribution of Zn2+ contribute to endothelial cell death.

In conclusion, we discovered a novel mechanism where H2O2 activation of TRPM2 causes a redistribution of Zn2+ from lysosomes to mitochondria and cytoplasm, resulting in endothelial cell death.

Wiseman, D.A., et al., Alterations in zinc homeostasis underlie endothelial cell death induced by oxidative stress from acute exposure to hydrogen peroxide. American Journal of Physiology-Lung Cellular and Molecular Physiology, 2007. 292(1).

Sun, L., et al., Role of TRPM2 in H2O2-Induced Cell Apoptosis in Endothelial Cells. Plos One, 2012. 7(8).

Where applicable, the authors confirm that the experiments described here conform with The Physiological Society ethical requirements.

PCA403

Mutation of R317 in the BK channel splice variant Slo1_9a partially restores the effect of the GoSlo-SR-5-6

A. Kshatri[1], T. Webb[2], R. Large[2], S. Roy[2], G. Sergeant[1,2], N. McHale[1,2], K. Thornbury[1,2] and M.A. Hollywood[1,2]

[1]Smooth Muscle Research Centre, Dundalk Institute of Technology, Dundalk, Louth, Ireland and [2]Ion Channel Biotechnology Centre, Dundalk Institute of Technology, Dundalk, Louth, Ireland

The BK channel opener GoSlo-SR-5-6 shifts the half maximal activation voltage (V1/2) of BKα subunits by >100 mV at 10 μM[1]. To investigate how it activates BK channels, we examined if its effects were altered in the Slo1_9a splice variant[3]. Experiments were carried out on either BK Slo1_9a α subunits cloned from the human brain or BK α subunits cloned from the rabbit bladder and transiently expressed in human embryonic kidney cells (HEK293). Site-directed mutagenesis on the resulting cDNA was carried out as previously described[2] and confirmed by sequencing. HEK cells were grown in DMEM medium supplemented with 10% FCS, penicillin and streptomycin. HEK cells were dissociated with trypsin (1%), plated onto 35 mm Petri dishes and maintained in culture at 37oC in 5% CO2 prior to use. All experiments were performed at 37oC using excised inside/out patch configuration with symmetrical 140 mM K+ solutions containing either 1mM EGTA or 1 mM HEDTA. Excised patches were held at –60mV and BK channel currents were evoked using voltage steps from -100mV to 200mV before repolarising back to -80 mV. Peak currents were measured during the voltage steps, corrected for driving force and activation curves constructed.

Slo1_9a is expressed exclusively in the brain and differs from the normal BK channel in 13 residues between the end of the S6 domain and the RCK1 linker. Application of GoSlo-SR-5-6 to A99 chimaera (which contains the Slo1_9a S6 sequence but normal BK channel proximal and distal linkers) shifted V1/2 by only -53±11 mV (n=6). We hypothesised that the majority of the reduction in the response to GoSlo-SR-5-6 was mediated by the amino acids in the S6 domain of Slo1_9a and used a combination of mutagenesis and electrophysiology to test this. The V1/2 of Slo1_9a currents in 100 nM Ca2+ was 158 ± 2 mV and was shifted to 63±3mV (n=10) in 1 μM Ca2+. Application of GoSlo-SR-5-6 (10 μM) changed activation voltage (ΔV1/2) by -38± 8mV in the Slo1_9a variant compared to -121±4 mV (n=12) in the normal BK channels. When A323I was mutated in Slo1_9a, application of GoSlo-SR-5-6 (10 μM) significantly changed ΔV1/2 to –61±4 mV compared to the Slo1_9a variant (n=6, p<0.05, unpaired t-test). When we mutated R317S in Slo1_9a, application of GoSlo-SR-5-6 to the this mutant increased ΔV1/2 to -90±6 mV (n=7, p<0.001). GoSlo-SR-5-6 also significantly increased ΔV1/2 in the R317I mutant to -69±9 mV. The effect of GoSlo-SR-5-6 was significantly reduced in the when the S317R mutation was performed, with a ΔV1/2 of -80±8 mV compared to -121±4 mV (p<0.001) in normal BK channels. These results suggest that R317 contributes significantly to the reduced response to GoSlo-SR-5-6 in the BK Slo1_9a variant.

Roy, S, Akande AM, Large RJ, Webb TI, Camarasu C, Sergeant GP, McHale NG, Thornbury KT & Hollywood MA (2012). Structure-activity relationships of a novel group of large-conductance Ca2+-activated K+ (BK) channel modulators: The GoSlo-SR family. ChemMedChem, 7(10). 1763-1769.

Sawano A & Miyawaki A.(2000) Directed evolution of green fluorescent protein by a new versatile PCR strategy for site-directed and semi-random mutagenesis. Nucleic Acids Res. 28(16):E78.

Gessner G, Cui YM, Otani Y, Ohwada T, Soom M, Hoshi T, Heinemann SH. (2012) Molecular mechanism of pharmacological activation of BK channels. Proc Natl Acad Sci. 109(9) :3552-7.

We thank Prof S. Heinemann for the gift of the Slo1_9a clone. Work supported by Science Foundation Ireland RFP and Enterprise Ireland Applied Research Enhancement Scheme.

Where applicable, the authors confirm that the experiments described here conform with The Physiological Society ethical requirements.

PCA404

Identification and characterization of the functional role of calcium-activated chloride channel anoctamin-1 (ANO1) in rat urinary bladder

D.A. Bijos[2,3], M.J. Drake[2,3] and B. Vahabi[1,2]

[1]Applied Sciences, University of the West of England, Bristol, UK, [2]Bristol Urological Institute, Bristol, UK and [3]School of Clinical Sciences, University of Bristol, Bristol, UK

Interstitial cells (ICs), analogous to the interstitial cells of Cajal in the gut, may generate phasic activity (PA) in smooth muscle tissues including the bladder (1). An established marker of the ICs is c-kit. However, recent studies have shown that anoctamin-1 (ANO1, encoded by Tmem16a), a calcium-activated chloride channel (CaCC), has a fundamental role in generation of pacemaker activity in the ICs of the gut and therefore could be used as a novel marker for these cells (2). CaCC blocking drugs such as niflumic acid (NFA) and 5-nitro-2-(3-phenylpropylamino)-benzoic acid (NPPB) were able to alter the pacemaker activity of the ICs in the gut (3) and thus may be important modulators of these cells in other tissues. Thus, the aim of this study was to investigate whether ANO1 is expressed in the rat urinary bladder and to explore the role of NFA and NPPB in modulating the PA of the bladder tissue.

Male Wistar rats (p19-p23) were killed according to UK Home Office regulations using schedule 1. PCR was carried out on the c-DNA synthesized from total RNA isolated from the whole bladder. Primers were designed for the *Rattus norvegicus* ANO1 mRNA (Accession number: NM_001107564.1). PCR products were separated by electrophoresis and sequenced. Longitudinal strips (5-8mm) of intact detrusor were mounted in perspex microbaths, superfused with Krebs' solution and maintained at 37°C. Isometric tension was measured via UF1 force transducers connected to a Powerlab system using LabChart software. After 90 min of equilibration, the effect of 10μM NFA or NPPB (30min exposure) or the drug vehicle (DMSO) on basal PA was investigated by measuring the amplitude and frequency of PA. Percentage change in the amplitude and frequency of PA was calculated in presence of CaCC blockers relative to that in the absence of the blockers. All data are expressed as the mean±SEM. Statistical analysis was carried out using Student's paired *t*-test.

ANO1 mRNA expression was found in the mucosa of the rat urinary bladder. NFA (n=12) significantly ($p<0.001$) reduced the amplitude and the frequency of basal PA by 68.4±8.8% and 78.8±8.9% respectively. Although NPPB (n=6) significantly reduced the amplitude of PA by 45.4±5.5% ($p<0.001$), it did not have a significant effect on the frequency of PA.

We confirm for the first time that ANO1 is expressed in mucosal layer of the rat urinary bladder. CaCC channel blockers were able to modulate the basal PA of rat bladder strips which may suggest a role of ANO1 channels in mediating the PA of ICs found in rat urinary bladder. However, the exact location and function of these channels in rat bladder requires further investigation.

McCloskey et al, J Urol 2002 Aug;168(2):832-6.

Gomez-Pinilla et al,Am J Physiol Gastrointest Liver Physiol. 2009 Jun;296(6):G1370-81.

Sanders et al, Exp Physiol. 2012 Feb;97(2):200-6.

Where applicable, the authors confirm that the experiments described here conform with The Physiological Society ethical requirements.

PCA405

Cholesterol depletion reveals an inhibitory role of PIP_2 on Ca^{2+}-activated Cl^- Channel activity in rat pulmonary arteries

H.T. Pritchard, A.A. Albert and I.A. Greenwood

BMS, St Georges, University Of London, London, UK

Background: Ca^{2+}-activated Cl^- channels (CaCCs) are thought to be encoded for by the gene TMEM16A, and are functionally present in vascular and non-vascular smooth muscle cells (Davis *et al*., 2010, Davis *et al.*, 2013). Our lab recently showed that the amplitude and pharmacology of CaCC currents (I_{CaCC}) in portal vein myocytes was influenced by cholesterol depletion (Sones *et al.*, 2010). The aim of this study was to investigate the mechanism by which CaCCs were regulated by cholesterol depletion and the possible role of phosphatidylinositol 4, 5-bisphosphate (PIP_2) levels.

Methods and Results: Whole-cell configuration of the patch clamp technique was used to measure I_{CaCC} currents in myocytes dispersed from first and secondary-order branches of pulmonary arteries (PA), from male Wistar rats (200-225g), killed by cervical dislocation in accordance with Schedule 1 of the United Kingdom Animals Act (1986). The pipette solution contained a known amount of free Ca^{2+} (500 nM) which immediately induced an I_{CaCC} upon rupture of the cell membrane, which displayed the distinct voltage-dependent kinetics shown in previous studies. Upon stabilisation of the I_{CaCC}, current voltage (IV) relationships were constructed by stepping from a holding potential (-50mV) to test potentials between -100 mV and 100 mV for 1s. I_{CaCC} was augmented rapidly by the cholesterol depleting agent methyl-β-cyclodextrin (mβcd) (3mg/ml), which was prevented by the application of the TMEM16A inhibitor $T16A_{inh}$-A01. Cells pre-treated with the phosphatidylinositol 4-kinase inhibitor wortmannin (20 μM), thereby inhibiting PIP_2 synthesis, augmented I_{CaCC} and subsequently showed an attenuated response to mβcd application. As wortmannin is also a myosin light chain kinase (MLCK) inhibitor we tested ML-9 (10 μM) to establish if MLCK played a role in CaCC activity, but this had no effect on the current. Enrichment of the pipette solution with diC-8 PIP_2 (1 μM) attenuated I_{CaCC}, and attenuated the stimulatory effect of mβcd.

Conclusions: This study suggests that cholesterol depletion of the cell membrane increases TMEM16A activity, partly through the removal on the inhibitory effect of PIP_2.

Davis *et al.*, 2010 Am J Physiol Cell Physiol 299 (5) C948-C959

Davis *et al.*, 2013 BJP 168(3):773-84

Sones *et al.*, 2010 Cardiovascular Research 87 (3): 476-484

Where applicable, the authors confirm that the experiments described here conform with The Physiological Society ethical requirements.

PCA406

Segregated calcium stores are important for stretch-induced calcium signaling in smooth muscle cells: implication in pulmonary hypertension

G. Guillaume, T. Ducret, R. Marthan, J. Savineau and J. Quignard

Université Bordeaux Segalen, INSERM U1045, Bordeaux Cedex, France

Introduction: In pulmonary hypertension (PH) the increased pulmonary blood pressure exerts a stretching force on pulmonary arterial wall that leads to contraction of pulmonary arterial smooth muscle cells (PASMC), a mechanism called myogenic tone. PASMC can transduce the mechanical stretch signal into a biological response by increasing the intracellular calcium concentration via membrane stretch-activated channels (SAC). Here, we investigate how the subcellular organization of calcium stores in PASMC (sarcoplasmic reticulum (SR), lysosomes and mitochondria) is important for the calcium response to stretch during PH.
Methods: PASMC were freshly isolated from normoxic rats (Nx rats) and rats with a pulmonary hypertension induced by an injection of monocrotaline (MCT rats). Inward currents from SAC were recorded after a negative pressure applied by a patch-clamp pipette and calcium variations were recorded with the fluorescent probe indo-1, simultaneously. Cytosolic calcium was also measured with the fluo-4 probe and mitochondrial calcium with the rhod-2 probe by a confocal microscope after an osmotic shock. A pharmacological approach coupled with different coimmunolabelings of ryanodine receptors (RyR) and SERCA2 pumps was used to investigate which RyR subtype is involved in calcium response to stretch. The cellular distribution of lysosomes, mitochondria and sarcoplasmic reticulum was investigated with live cellular probes.
Results: PASMC exhibit different segregated calcium stores: a subplasmalemnal SR store with RyR1 and SERCA2b, associated to mitochondria and a perinuclear SR store with RyR3 and SERCA2a. We showed that a stretch of PASMC induces an inward calcium influx through SAC that is amplified by a calcium release by RyR1. This calcium rise is then buffered by mitochondria. In MCT rats, the subcellular organization of RyR subtypes is modified: RyR3 and SERCA2a are not only expressed in a perinuclear area but also in a subplasmalemnal level. This is correlated with a different organization of mitochondria. In MCT rats, this new organisation leads to a greater amplification by all RyR subtypes and to a higher calcium increase induced by stretch. Furthermore, the calcium response to stretch is enhanced by a mechanism independent on extracellular calcium, involving caveolae.
Conclusion: This study highlights how the spatial organization of calcium stores in PASMC is important for calcium signaling to stretch and that a modification of this segregation leads to PH in rats. Such a study is relevant for a better understanding of cellular mechanisms underlying PH.

Where applicable, the authors confirm that the experiments described here conform with The Physiological Society ethical requirements.

PCA407

Molecular identification of P2X receptors in human arteries

C. Nichols[1], O.V. Povstyan[1], O. Khan[2], G. Vasilikostas[2], T.K. Khong[1], A. Wan[2], M. Reddy[2] and M.I. Harhun[1]

[1]Division of Biomedical Sciences, St George's, University of London, London, UK and [2]Department of Surgery, St. George's Hospital, London, UK

In blood vessels vascular tone is controlled by sympathetic nervous activity, during which noradrenaline and ATP are released from perivascular nerves and contribute to sympathetically regulated vasoconstriction. In muscular arteries the contractile physiological responses to ATP are mediated through activation of P2X receptors, which are non-selective ligand-gated cation channels in the plasma membrane of vascular smooth muscle cells (VSMCs). Data about functional P2X receptors in human blood vessels are very limited; therefore the role of P2X receptors in VSMCs from human omental arteries (HOA) was studied in this work. This study conforms to the principles outlined in the Declaration of Helsinki and was approved by the local Research Ethics Committee (09/H0803/103) for retrieval of human tissue. Prior to surgery consent was obtained from patients undergoing elective abdominal surgery (n=7, 4 females, 3 females). Isolated VSMCs were obtained by enzymatic dispersion of small HOA blood vessels. The agonist-induced responses in $[Ca^{2+}]_i$ were investigated in fluo-3 loaded HOA VSMCs using x-y laser scanning confocal imaging. The genes encoding P2X receptor subunits were identified in preparations obtained from manually collected isolated HOA VSMCs using RT-PCR analysis and the expression of corresponding proteins was confirmed by immunocytochemical and Western blot techniques. Application of 10 μmol/l ATP evoked a robust increase in $[Ca^{2+}]_i$ in fluo-3 loaded VSMCs. 10 μmol/l of selective P2X receptor agonist α,βme-ATP evoked increase in $[Ca^{2+}]_i$ with similar amplitude and kinetic of the fluorescent signal (101.7±4.8% of ATP response, n=7, $p>0.05$) suggesting that stimulatory action of ATP on $[Ca^{2+}]_i$ is most likely mediated via activation of P2X receptors of the VSMC membrane. The exposure to 1 μmol/l selective P2X receptor antagonist NF279 significantly (by 32.3±5.5% of the control response, n=6, $p<0.05$) reduced the amplitude of $[Ca^{2+}]_i$ increase evoked by 10 μmol/l α,βme-ATP. The RT-PCR analysis revealed that HOA VSMCs express genes for P2X1 and P2X4 receptor subunits. The expression of corresponding proteins was confirmed by fluorescent immunocytochemical visualisation of VSMCs labelled with antibody detecting P2X1 and P2X4 receptors. These experiments revealed the presence of P2X1 and P2X4 receptors subunit proteins in the plasma membrane but not in the deeper cytoplasm of VSMCs. The Western blot analysis of the fragments of the HOA showed the presence of monomeric and dimeric byproducts of P2X1 (60 and 120 kDA) and P2X4 (43 and 100 kDa) receptor subunits. These data suggest that VSMCs from HOA express P2X1 and P2X4 receptors subunits with homomeric P2X1 channel receptors serving as a predominant functional target for stimulatory action of extracellular ATP in these blood vessels.

Where applicable, the authors confirm that the experiments described here conform with The Physiological Society ethical requirements.

PCA408

Methanol extract of Poncirus fructus modulates pacemaker activity in interstitial cells of Cajal from the murine small intestine

B. Kim[1], H. Kim[1], S. Choi[2], J. Jun[2], I. So[3] and S. Kim[4]

[1]School of Korean Medicine, Pusan National University, Yangsan, Gyeongsangnamdo, Republic of Korea, [2]College of Medicine, Chosun University, Gwangju, Republic of Korea, [3]College of Medicine, Seoul National University University, Seoul, Republic of Korea and [4]Center for Bio-Artificial Muscle and Department of Biomedical Engineering, Hanyang University University, Seoul, Republic of Korea

Poncirus fructus (PF) has been widely used as a traditional medicine in Eastern Asia, especially to ameliorate the symptoms of gastrointestinal (GI) disorders related to abnormal GI motility. Poncirus fructus (PF), also known as Poncirus trifoliata (L.) Raf. (Rutaceae), is widely used as a traditional medicine in Eastern Asia mainly to ameliorate the symptoms of gastrointestinal (GI) disorders related to abnormal GI motility. In a previous study, a methanol extract of PF was found to have particularly potent gastroprokinetic effects. Interstitial cells of Cajal (ICCs) are pacemaker cells in the gastrointestinal tract, but the action mechanisms of PF extract in mouse small intestinal ICCs have not been investigated. Therefore, in the present study, we investigated the effects of a methanol extract of PF (MPF) in mouse small intestinal ICCs. In addition, we sought to identify the receptors involved. Enzymatic digestions were used to dissociate ICCs from small intestines. The whole-cell patch-clamp configuration was used to record potentials (current clamp) from cultured ICCs. In addition, we analyzed intracellular Ca2+ concentrations ([Ca2+]i). MPF decreased the amplitudes of pacemaker potentials in ICCs, and depolarized resting membrane potentials in a concentration dependent manner. Y25130 (a 5-HT3 receptor antagonist) and RS39604 (a 5-HT4 receptor antagonist) blocked MPF-induced membrane depolarizations, whereas SB269970 (a 5-HT7 receptor antagonist) did not. Pretreatment with Na+ or Ca2+-free solution or thapsigargin (a Ca2+-ATPase inhibitor in endoplasmic reticulum) abolished the generation of pacemaker potentials and suppressed MPF-induced activity. [Ca2+]i analysis showed that MPF increased [Ca2+]i. Furthermore, treatments with PD 98059, SB203580, or JNK II inhibitor blocked MPF-induced membrane depolarizations in ICCs. These results suggest that MPF modulates pacemaker potentials through 5-HT3 and 5-HT4 receptor-mediated pathways via external Na+ and Ca2+ influx, and via Ca2+ release from internal stores in a mitogen-activated protein kinase dependent manner. The study shows MPF is a good candidate for the development of a gastroprokinetic agent. In view of the effects of MPF on ICCs, further research is required, particularly to identify the active compound(s) involved and to determine their action mechanisms.

Where applicable, the authors confirm that the experiments described here conform with The Physiological Society ethical requirements.

PCA409

Different regulatory effects of H2S and NO on gastric motility in mice

X. Huang, X. Meng, D. Liu, Y. Wu, X. Guo, H. Lu and W. Xu

School of Medicine, Shanghai Jiaotong University, Shanghai, China

Background NO and H2S are gaseous signaling molecules that modulate smooth muscle motility. NO has been proved to be an important non-adrenergic non-cholinergic (NANC) inhibitory neurotransmitter which is released in response to nerve stimulation and relaxes smooth muscles. And our previous studies showed smooth muscle tonic contraction to be increased significantly by low-concentration NaHS in the gastric antrum. But few studies have been performed in the GI tract to demonstrate the interaction between NO and H2S. We aimed to identify expressions of enzymes that catalyze H2S and NO generation in mouse gastric smooth muscle, and determine relationships between endogenous H2S and NO in regulating smooth muscle motility. Methods Adult male ICR mice were used in the present study. Western blotting and immunohistochemistry methods were used to track expressions of neuronal nitric oxide synthase (nNOS), endothelial nitric oxide synthase (eNOS), cystathionine β-synthase (CBS) and cystathionine γ-lyase (CSE) in gastric smooth muscle. Smooth muscle motility was recorded by isometric force transducers; cGMP production was measured by a specific radioimmunoassay. Key Results CBS, CSE, eNOS, and nNOS were all expressed in mice gastric antrial smooth muscle tissues, but only CBS and eNOS were detected in gastric antrial smooth muscle cells. Aminooxyacetic acid (AOAA), a blocker of CBS, significantly inhibited smooth muscle contractions in the gastric antrum, which was significantly recovered by NaHS, while DL-propargylglycine (PAG), a blocker of CSE, had no significant effect; Nω-nitro-L-arginine methyl ester (L-NAME), a non-selective inhibitor of NOS, enhanced contractions. NaHS at low concentrations increased basal tension but decreased it at high concentrations; SNP significantly inhibited the contractions, which could be significantly recovered by NaHS both in the absence and presence of CuSO4. 1H-[1, 2, 4]Oxadiazolo[4, 3-α]quinoxalin-1-one (ODQ), an inhibitor of soluble guanylate cyclase, did not block NaHS-induced excitatory effect; 3-Isobutyl-1-methylxanthine (IBMX), a non-selective phosphodiesterase inhibitor, partially blocked this effect; cGMP production in smooth muscle was significantly increased by SNP but not affected by NaHS. Conclusion & inferences Endogenous H2S and NO appear to play opposite roles in regulating gastric motility; their effects may be via separate signal pathways. Intracellular H2S/NO levels may be maintained in a state of balance to warrant normal smooth muscle motility.

Keywords: endogenous H2S, endogenous NO, gastric antrial smooth muscle, motility

Where applicable, the authors confirm that the experiments described here conform with The Physiological Society ethical requirements.

PCA410

Effect of ethanol exposure on slow wave activity and smooth muscle contraction in the small intestine

W. Lammers[1], S.B. Subramanya[2], B. Stephen[1] and H. Schäfer[3]

[1]Physiology, United Arab Emirates University, Al Ain, United Arab Emirates, [2]Dept of Physiology, RAK Medical & Health Sciences University, Ras Al Khaima, United Arab Emirates and [3]University of Applied Sciences, Kaiserlautern, Germany

Background: Ethanol ingestion causes a variety of gastrointestinal disturbances including motility disturbances. Slow waves coordinate gastrointestinal motility and abnormal slow-wave activity is thought to contribute to motility disorders. To date however, little is known about the effect of acute ethanol on motility disturbances associated with slow wave activity.
Method: 7-10 cm duodenum, jejunum and ileal loops from adult male Wistar rats were isolated and mounted in a 300-ml organ bath superfused with a Tyrode solution (100ml/min). The intestinal loops were connected to an inlet and an outlet and intra-luminally perfused with Tyrode (0.5ml/min). Soot markers were applied onto the serosal surface of the segments. After a 15 min equilibration period, the loops were superfused with 1, 3 and 5% ethanol. Motility recordings were performed with a digital video camera and electrical activities were recorded using a single longitudinal row of 32 extracellular unipolar silver electrodes.
Results: In all duodenal, jejunal and ileal segments (n=7), ethanol inhibits motility fully at 3% and 5%. The slow wave activity was also were altered at all the concentration in terms of velocity, frequency and amplitude ethanol. All effects were reversible upon superfusing with normal Tyrode.
Summary: Acute application of ethanol caused widespread but reversible inhibition of slow wave propagation with concurrent inhibition of small intestinal motility.

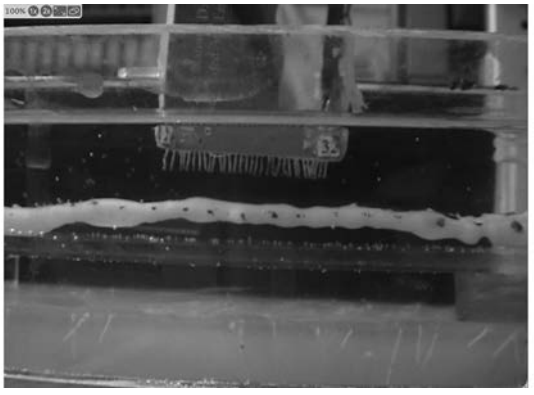

Video shot of a preparation (ileum of a rat) with soot markers applied and a 32-electrode row approaching the preparation for recording the electrical activities.

Where applicable, the authors confirm that the experiments described here conform with The Physiological Society ethical requirements.

PCA411

Electrical propagation in the guinea pig urinary bladder

W. Lammers[1], J.F. Morrison[1], L. Lubbad[2], B. Stephen[1] and F.T. Hammad[2]

[1]Physiology, United Arab Emirates University, Al Ain, United Arab Emirates and [2]Surgery, United Arab Emirates University, Al Ain, United Arab Emirates

Aim: There is not much knowledge about the patterns of macroscopic electrical propagations in the wall of the urinary bladder. Recording from a large number of extracellular electrodes simultaneously is one technology that could be used to study the patterns of electrical propagations.
Method: The urinary bladders from 6 guinea-pigs were isolated and placed in a Tyrode filled organ bath. A 16x4 electrode array was positioned at various sites on the serosal bladder surface and recordings were performed at different intravesical volumes. At the end of 4 experiments, carbachol (CCH; 10-6 M) was added to the superfusing fluid and electrical activities recorded. After the experiments, the extracellular signals were analysed and propagation maps constructed.
Results: Propagation of electrical waves was detected in all experiments and at all sites on the bladder surface. Waves could originate from any site and propagate for a finite distance before terminating spontaneously. The vast majority of waves propagated preferentially in the axial direction and only a few propagated transversely. Increase in vesical volume decreased significantly conduction velocity (from 4.9±1.5 to 2.7±0.7 cm/sec; $p < 0.05$) whereas CCH did not have any major effect on patterns and speed of propagation
Conclusions: Large electrical waves do propagate across the bladder wall, both in the dome, across the peritoneal reflection and in the base. The preferential propagation in the axial direction may have practical implications during surgical interventions. The electrical waves could form the basis for local spontaneous contractions in the bladder.

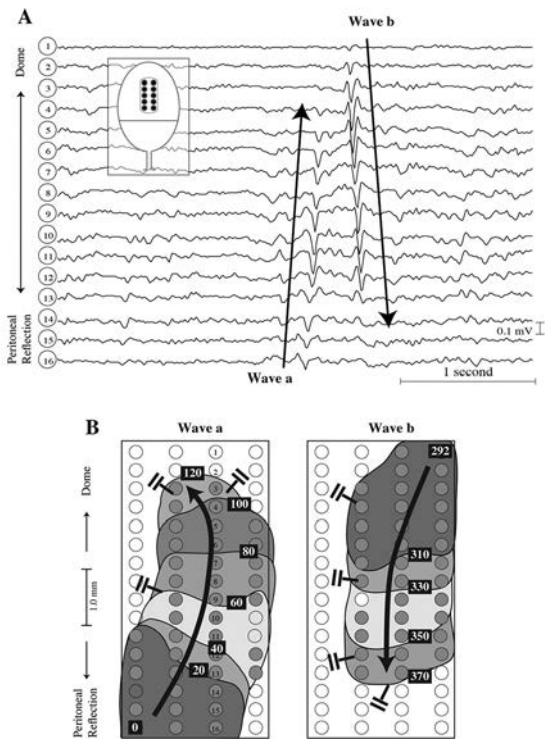

Recording from the dome (location of the electrodes indicated in the inset) showing two waves propagating in opposite directions (bladder volume 4 ml). Both waves originated from outside but stopped within the mapped area. Note the block symbols indicating where the propagating waves had stopped spontaneously.

Where applicable, the authors confirm that the experiments described here conform with The Physiological Society ethical requirements.

PCA413

Inhibition of duodenal movement in vitro of rat by Bisphenol A through nitric oxide mediated guanylyl cyclase and α-adrenergic pathways

K. Sarkar, P. Tarafder, M. Ghosh, A. Ghati and G. Paul

Department of Physiology, University of Kalyani, Kalyani, West Bengal, India

Bisphenol A (BPA), an endocrine disrupting compound, has received much attention for its other probable health effects. It is a monomer of polycarbonate plastics, epoxy and polystyrene resins that are extensively used in the interior coating of cans in the food packaging industry and in dentistry. Human exposure to BPA occurs mainly through the ingestion of food and water from such containers and dental materials that leach BPA. Even though BPA is reported to produce reproductive and behavioural toxicity in experimental animals in various doses, the effect of BPA on the intestinal motility is not known till to date. The present study was designed to examine the effect of BPA on the movement of duodenum in vitro of rat. In this study, the movement of isolated duodenum of adult Sprague-Dawley rats (120-150gm, n=7) were recorded by isotonic transducer coupled to a RMS Polyrite-D machine (RMS Pvt. Ltd., India). The concentration-response of BPA on duodenal contraction was obtained in absence and presence of agonists and antagonists. Values are means±S.E.M. compared by Student's t-test, $p<0.05$ vs. control and the treated preparations were expressed as percent change of the basal (or control) values. It was observed that BPA (10, 20, 40, 80, 160, 320μM) decreases the frequency (90.80±9.2, 84.80±4.9, 76.80±3.3, 55.20±2.2, 20.80±1, 2.4±0.4) and amplitude (66.66±3.2, 41.05±1.5, 39.3± 2.3, 35.84±2.2, 20.12±1.2, 9.3±1.3) of duodenal contraction in a dose-dependent manner. At last two doses (160μM and 320μM) the movement of duodenum were fully inhibited. Besides, BPA induced changes in duodenal movement was not blocked by atropine, the muscarinic receptor blocker. Further, BPA potentiated the inhibitory effect of the duodenal movement pre-treated with sodium nitroprusside (SNP, nitric oxide donor, 3.3 μM and 6.6μM). But the BPA induced inhibition of duodenal movement was blocked when the segment was pre-treated with L-NAME (nitric oxide synthase inhibitor, 90μM and 180μM) or methylene blue (MB, guanylyl cyclase inhibitor, 100 μM and 200 μM) (figure 1), and the blocking action of BPA was found to be fully reversed after 25,20,20 and 15 minutes respectively. It was also observed that phentolamine (3μM and 6μM), an α-adrenergic blocker, blocks the action of BPA upto the dose of 80μM (figure 2). But the BPA induced changes in the movement was not reversed by the propranolol, a β-adrenergic blocker. In other sets of experiments, equivalent doses of DMSO (solvent used for BPA) did not produce any change in the movement of isolated duodenum. From the results, it may be concluded that BPA inhibits the duodenal movement presumably by inducing nitric oxide mediated guanylyl cyclase and α-adrenergic signal pathways in duodenal smooth muscle cells.

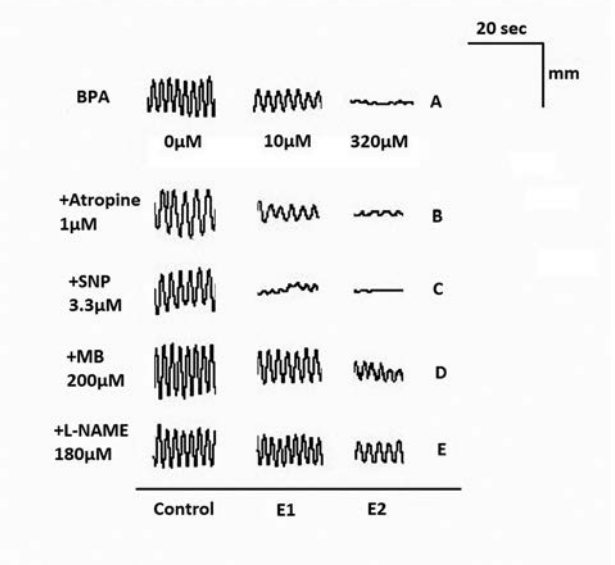

Figure 1: Recordings of the effects of two representative doses of BPA on the movement of isolated duodenal segment pre-treated with atropine (panel B), SNP (panel C), MB (panel D) and L-NAME (panel E). Panel A shows the recordings of effects of representative doses of BPA on the movement of duodenum. E1= Drug+10 μM BPA, E2=Drug+ 320μM BPA.

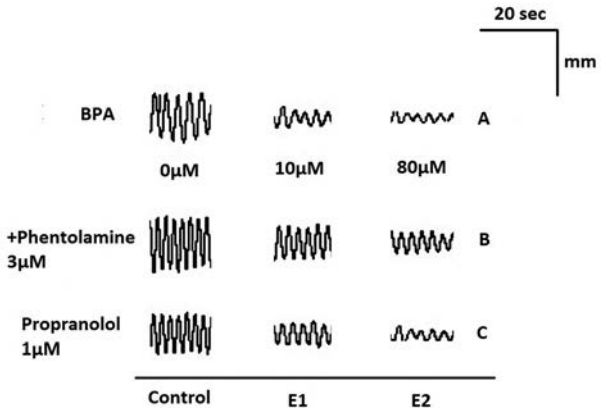

Figure 2: Recordings of the effects of two representative doses of BPA on the movement of isolated duodenal segment pre-treated with phentolamine (panel B) and propranolol (panel C). Panel A shows the recordings of effects of the representative doses of BPA on the movement of duodenum. E1= Drug+10 μM BPA, E2=Drug+ 80μM BPA.

Where applicable, the authors confirm that the experiments described here conform with The Physiological Society ethical requirements.

PCA414

Gender differences in the response to salt stress in uninephrectomised Sprague-Dawley rats

A.K. Oloyo, O.V. Oyeniyi, Y.A. Oduneye, O. Salau and O.A. Sofola

Physiology, University of Lagos, Surulere, Lagos, Nigeria

From puberty onwards, blood pressure (BP) is consistently higher in males when compared with females. The kidney plays a central role in the regulation of BP by regulating salt excretion. High salt diet (HSD) is implicated in the onset of hypertension. Generation of reactive oxygen species (ROS) is one of the mechanisms by which a HSD induces hypertension1, as HSD has been shown to drive production of ROS in the renal tissues2. Both oxidative stress3 and BP elevating effect of a HSD4 have been shown to exhibit sexual differences. Therefore, experiments were designed to assess the effect of gender on oxidative stress in uninephrectomised rats fed a HSD. Weanling Sprague-Dawley rats (90 – 100g) of both sexes were divided into 4 groups (n = 6) each. They were either sham operated or uninepherectomised under (90mg/kg bodyweight ketamine and 10mg/kg bodyweight xylazine i.p) anaesthesia and fed a normal 0.3% or high 4% NaCl salt diet for 10 weeks. Renal weight index and fluid balance were determined. BP was measured via carotid artery canulation under 25% Urethane and 1% alpha chloralose (5ml/kg bodyweight i.p) anaesthesia. Plasma concentration of nitrates was measured, lipid peroxidation (LP) and superoxide dismutase (SOD) activity was determined in the kidney homogenate. H&E histological staining of the kidney was also carried out. HSD increased fluid retention (ml) in sham male (16.83±2.07vs.11.34±1.91) and female (20.5±2.35vs.10.57±2.04) as well as in uninephrectomised male (22.17± 2.39vs.12.43± 1.84) and female (24.17±2.36vs.11.90±1.50) rats. However, gender has no effect on fluid balance. HSD elevated BP (mmHg) in sham male (121±2vs.101±4) and female (117±3vs.95±3) and also in uninephrectomised male (141±5vs.105±3) and female (131±5vs.104±3) rats. BP elevating effect of a HSD and uninephrectomy was higher in the males when compared with females (141±5vs.131±5). Reduction in the weight index of the remnant kidney was more in high salt fed males (0.27±0.015vs.0.30±0.013) and female (0.23±0.023vs.0.30±0.023) as well as in the females when compared with males (0.23±0.023vs.0.27±0.015). Plasma concentration of nitrates was reduced in uninephrectomised plus high salt diet groups: male (0.32±0.08vs.1.24±0.14) and female (0.75±0.07vs.1.60±0.23), and this reduction is more in the male (0.32±0.08vs.0.75±0.07). HSD increased LP (0.11±0.017vs.0.05±0.008) but reduced the SOD activity (2.04±0.26vs.4.02±0.24) in the kidney and this effect was higher in the males: LP (0.11±0.017vs.0.03±0.005). HSD aggravated to a greater extent Bowman's capsule vacuolation and tubular atrophy observed in uninepherectomised groups in male when compared with female rats. Thus reduced NO production, increased oxidative stress and distortion of renal cytoarchitecture can contribute to the gender differences in the response to a HSD in uninephrectomised Sprague-Dawley rats.

1.Tian, N et al. (2007). American Journal of Physiology. 293: H3388 – H3395.

2.de Wardner, H.E and Mc Gregor, G.A (2002). Journal of Human hypertension. 16(4): 213-23.

3.Venegas-Pont, M. et al. (2010). American Journal of Hypertension. 231: 92-96.

4.Hinojosa-Laborde, C. et al., (2004). Hypertension. 44: 405 – 409.

Where applicable, the authors confirm that the experiments described here conform with The Physiological Society ethical requirements.

PCA415

Quantification of urinary exosomes by nanoparticle tracking analysis

W. Oosthuyzen, E. Turtle, J.M. Street, J. Pound, D.J. Webb, C.D. Gregory, M.A. Bailey and J.W. Dear

University of Edinburgh, Edinburgh, Edinburgh, City of, UK

Exosomes are cell-derived vesicles that are released from the kidney into urine. They contain protein and RNA from the glomerulus and all sections of the nephron and represent a non-invasive reservoir for biomarker discovery. Current methods for identifying and quantifying human urinary exosomes are time-consuming and only semi-quantitative. Nanoparticle tracking analysis (NTA) is a technology that can size and count nanoparticles, such as those released from cultured cells and in human plasma. NTA is based on the principle that at any particular temperature, the rate of Brownian motion of nanoparticles in solution is determined solely by their size. Published studies demonstrate that NTA can count and size specific subgroups of particles using fluorescent antibodies against surface proteins, but this has not yet been applied to urine.
In the current study we applied NTA to human urine (n=5) and identified a range of nanoparticles, including exosomes. Using antibodies against the exosomal marker proteins CD24 and aquaporin 2 (AQP2), conjugated to a fluorophore, we could identify a sub-population of CD24 and AQP2 positive particles of characteristic exosomal size (figure 1). Extensive pre-NTA processing of urine was not necessary; however, the intra-assay variability in the measurement of exosome concentration was significantly reduced when an ultra-centrifugation step preceded NTA. Building upon previous work in our group in investigating exosomal signalling between cells, we were also able to track exosomal AQP2 upregulation induced by desmopressin stimulation of murine collecting duct cells by using

NTA. Finally, when urine was stored at room temperature, 4C or frozen, nanoparticle concentration was reduced; freezing at -80C produced the least reduction. This reduction was substantially reduced by addition of protease inhibitors to urine before storage (figure 2). In conclusion, with appropriate sample storage, NTA has potential as a tool for rapidly characterising and quantifying exosome concentration in human urine and for further understanding the mechanism of intra-cellular signalling mediated by exosomes.

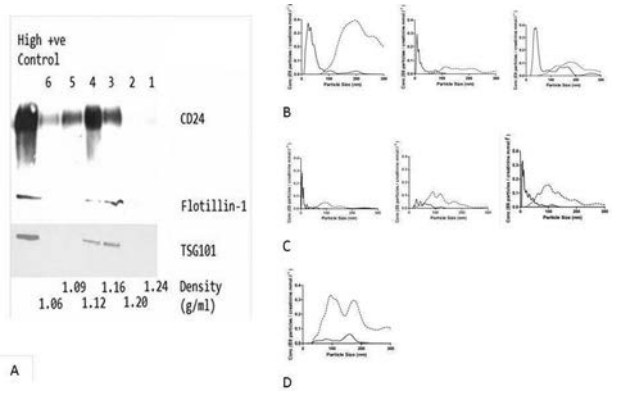

Figure 1. Exosome marker specific fluorescent labelling. A) CD24, flotillin 1 and TSG101 on a sucrose density gradient. B) Human urine samples labelled with CD24-Qdots in light scatter mode (dashed line – all particles) and fluorescent filter in place (solid line – CD24 labelled particles). (n=3). C) Human urine samples labelled with AQP2-Qdots in light scatter mode (dashed line – all particles) and fluorescent filter in place (solid line – AQP2 labelled particles). (n=3). D) Human urine labelled with mouse IgG conjugated to Qdot as isotope control in light scatter mode (dashed line) and with the fluorescent filter in place (solid line).

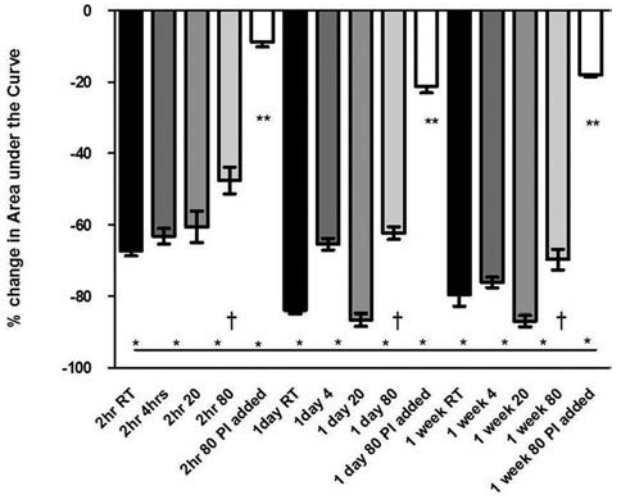

Figure 2. Different storage protocols and urine particle concentration. NTA was used to measure the particle concentration between 20 – 100 nm in diameter (AUC20-100).

Dear JW et al. (2013). Urinary exosomes: A reservoir for biomarker discovery and potential mediators of intrarenal signalling. PROT: n/a–n/a.

Soo CY et al. (2012) Nanoparticle tracking analysis monitors microvesicle and exosome secretion from immune cells. Immun; 136: 192–197

Lässer C et al. (2011) Human saliva, plasma and breast milk exosomes contain RNA: uptake by macrophages. J of Trans Med; 9: 9

Dragovic RA et al. (2011) Sizing and phenotyping of cellular vesicles using Nanoparticle Tracking Analysis. Nanomedicine: Nanotechnology, Biol and Med; 7: 780–788.

Street JM et al. (2011) Exosomal transmission of functional aquaporin 2 in kidney cortical collecting duct cells. J. Physiol. (Lond.); 589: 6119–6127

Co-workers and colleagues of the Centre for Cardiovascular Science and Centre for Inflammation Research at the University of Edinburgh.

Where applicable, the authors confirm that the experiments described here conform with The Physiological Society ethical requirements.

PCA416

Comparison of the phasic activity of upper, middle and lower segments of pig ureter

M.M. ElMahdy[1], M. Drake[1,2] and B. Vahabi[1,2]

[1]Urology, Bristol Urological Institute, Bristol, UK and [2]University of the West of England, Bristol, UK

The propagation of urine from the kidney is initiated by the pacemaker activity in the renal pelvis (1-2). The density of cholinergic nerve fibers in the ureter increases from renal pelvis to the bladder with the ureterovesical junction being the most densely innervated region. The difference in contractile behavior between the upper, middle & lower ureteric segments is not well understood in response to cholinergic modulators. This study investigates the contractile behavior of the different ureteric segments of the pig and the effect of cholinergic-receptor modulators.

Ureters were isolated from freshly slaughtered pigs (6 to 8 months old). Three centimeter longitudinal strips of upper (UU), middle (MU) and lower ureter (LU) were suspended in 25 ML organ baths containing Krebs bicarbonate solution, maintained at 37°C & gassed with 95% O2 & 5% CO2. Tissue tension was measured using isometric force transducers connected to a PowerLab data acquisition system using 'Chart' software. Tissue segments were equilibrated under 2g of tension for 60 min and assessed for basal spontaneous activity (BSA). Tissues without BSA were discarded. Amplitude and frequency of BSA were compared between different ureteric segments. The effect of cholinergic-receptor modulators, carbachol (CCh, 10 μM) and atropine (AT) (1μM) (10-15 min exposure to each drug), on BSA of UU, MU & LU was then investigated. All data is expressed as the mean ± SEM. Statistical analysis was performed using one-way ANOVA and Student's paired t-tests.

Results

100% of UU (n=23), 65% of MU (n=24) & 65% of LU (n=24) segments demonstrated BSA. The amplitude of BSA in the LU (0.028±0.003 g tension/mg tissue) was significantly ($p<0.001$) higher than MU (0.015±0.002 g tension/mg tissue) & UU (0.009±0.002 g tension/mg tissue). However, the frequency of BSA was significantly ($p<0.001$) higher in UU (25.09±2.07 events in 5min) vs. MU (3.08±0.68 events in 5 min) and LU (3.63±0.78 events in 5min) segments. 10μM CCh significantly ($p<0.01$-0.001) enhanced the amplitude and the frequency of BSA in MU (n=13) & LU (n=17) segments, however it did not affect the BSA of UU (n=16). 1μM AT reduced the amplitude of BSA in MU (n=13) & LU (n=14), (although not statistically significant), with no effect on the UU (n=12) segments.

The pattern of BSA was significantly different in UU, LU and MU segments. The frequency of BSA was significantly higher in UU compared to LU and MU strips. In contrast, the amplitude of BSA was significantly higher in the LU compared to MU and UU segments, demonstrating that each segment plays a different role in mediating the peristaltic movement of the ureter. The differences in the sensitivity of different ureteric segments to cholinergic-receptor manipulation can provide a better understanding of ureteric pharmacology and aid devel-

opment of a targeted approach in the management of ureteric conditions.

1- Constantinou CE. Renal pelvic pacemaker control of ureteral peristaltic rate.Am J Physiol 226: 1413–1419, 1974. 7

2- Michael A. Pezzone, Simon C. Watkins, Sean M. Alber, William E. King, William C. deGroat, Michael B. Chancellor and Matthew O. Fraser. Identification of c-kit-positive cells in the mouse ureter: the interstitial cells of Cajal of the urinary tractAm J Physiol Renal Physiol 284:F925-F929, 2003.

Where applicable, the authors confirm that the experiments described here conform with The Physiological Society ethical requirements.

PCA417

The effects of cannabinoid receptor 1 on capsaicin/bradykinin-induced activity of afferent nerve in an ex vivo rat ectopic endometrium preparation

G. Zhang, B. Sun and W. Rong

Physiology, Shanghai Jiaotong University School of Medicine, Shanghai, China

Endometriosis (ENDO) is a disease common in women that is defined by abnormal extra uteral growths of uterine endometrial tissue and associated with severe pain. Recent studies in a rat model and women showed that sensory and sympathetic nerve fibers sprout branches to innervate the abnormal growths. Furthermore, the endocannabinoid system is involved in both endometriosis and its associated pain. It is not clear whether cannabinoid receptor 1 (CB1R) is involved in the sensitivity of afferent nerve innervating ectopic endometrium to capsaicin (Cap)/bradykinin (BK) Herein, using an ex vivo ectopic endometrium preparation from rat model of endometriosis, we examined the sensitivity of afferent nerve innervating ectopic endometium to Cap/BK, and the effects of CB1R agonist ACPA on Cap/BK-evoked activity of afferent nerve. ENDO model: female Sprague-Dawley rats (200-225g, n=9) in diestrus were anesthetized with sodium pentobarbital (50 mg/Kg, i.p.), four pieces of uterine horn (2×2 mm) were sewn around alternate cascade mesenteric arteries starting from the caecum, which will form ectopic uterine cysts. Recording of afferent nerve innervating ectopic cyst was performed in an ex vivo preparation 10 weeks after ENDO. The preparation was superfused continuously at a rate of approximately 15 ml/min with oxygenated (95%O2/5%CO2) Krebs solution at 37 °C. ACPA (300 nM) diluted in Krebs superfused the preparation 10 min before either Cap (300 nM) or BK (300 nM) superfusion. Spike 2 software was used to calculate the change of afferent activity. Values are means ± S.E.M., compared by ANOVA. The response of afferent nerve innervating ectopic cyst either to Cap or BK was changed compared to that in ex vivo naïve ileum preparation. The peak increase of afferent activity was occurred at 90 sec after Cap in ex vivo either ectopic cyst or naïve ileum preparation, while the Cap-induced afferent activity was decreased followed by increase in ex vivo ectopic cyst preparation. The BK-induced increase in afferent activity was occurred at 90 sec and 3 min after BK in ex vivo naïve ileum and ectopic cyst preparations, respectively. The peak increase in afferent activity induced by either Cap or BK was inhibited by ACPA (8.33 ± 0.89 vs. 4.35 ± 0.36 imp/30s, Cap alone vs. Cap + ACPA, $p < 0.05$; 12.37 ± 0.85 vs. 7.33 ± 0.34 imp/30s, BK alone vs. BK + ACPA, $p < 0.05$). However, ACPA did not affect the response of afferent nerve to either Cap or BK in ex vivo naïve ileum preparation. These findings indicate that peripheral CB1R affects the sensitivity of afferent nerve innervating ectopic endometrium to capsaicin or bradykinin.

This study was supported by grants from National Natural Science Foundation of China to Guohua Zhang (no. 81070891 and no. 81271245)

Where applicable, the authors confirm that the experiments described here conform with The Physiological Society ethical requirements.

PCA418

Combined endothelial progenitor cells (EPCs) and mesenchymal stem cells (MSCs) can enhance wound healing in diabetic mice model associated with increased VEGF and decreased neutrophil infiltration

S. Sukpat[1], N. Israsena[3] and S. Patumraj[2]

[1]Physiology, Chulalongkorn university, Bangkok, Thailand, [2]Pharmacology, Chulalongkorn University, Bangkok, Thailand and [3]Physiology, Chulalongkorn University, Bangkok, Thailand

Non-healing diabetic ulcer causes the patient at much higher risk for lower extremity amputation. Several studies showed that both MSCs and EPCs can promote wound healing, increase angiogenesis and release of proangiogenic factors into the wound. Therefore, the objective of this study is to investigate whether the combination of EPCs and MSCs can enhance angiogenesis and wound healing in diabetic mice. Balb/c nude mice were divided into five groups. Group 1 was control group (Con; n=6). Group 2 was diabetic group treated with fibrin gel (DM; n=6). Group 3 was diabetic group injected with 1X106 cells MSCs (DM+MSCs; n=6). Group 4 was diabetic group injected with 1X106 cells EPCs (DM+EPCs; n=6). Group 5 was diabetic group injected with combined 0.5X106 cells MSCs and 0.5X106 cells EPCs (DM+MSCs+EPCs; n=6). Diabetic groups were induced by injection of streptozotocin (45 mg/kg i.p. daily for 5 days). At 7 weeks after, mice were anesthetized with sodium pentobarbital (55 mg/kg i.p.) and created bilateral full-thickness excisional skin wounds on the dorso-rostral back (0.6x0.6 cm2). On day 7 and 14 post-wound, the percentage of wound closure (%WC), the percentage of capillary vascularity (%CV), the neutrophil infiltrations and tissue vascular endothelial growth factor (VEGF) level were determined by using image analysis software, intravital fluorescence microscopy, H&E staining and ELISA, respectively. Values are means ± S.E.M., compared by ANOVA. The %WC in DM+EPCs, DM+MSCs, DM+MSCs+EPCs and Con increased significantly than DM group at day 7 (78.66 ± 2.29, 78.28 ± 4.16, 72.04 ± 4.12, 72.47 ± 4.52 vs. 55.65± 3.92; $p<0.05$) and day 14 (89.65 ± 1.07, 85.43 ± 1.58, 85.42 ± 0.64, 86.36 ± 0.84 vs. 80.42 ± 1.37; $p<0.05$). On day 7, the %CV in DM+EPCs, DM+MSCs, DM+MSCs+EPCs and Con were significantly increased than DM (22.86 ± 1.20, 21.42 ± 0.61, 27.44 ± 1.07, 19.95 ± 0.82 vs. 14.72 ± 1.49; $p<0.05$). The %CV of DM+EPCs+MSCs was increased significantly than DM+MSCs and DM+EPCs ($p<0.05$). On day 14, the %CV of DM+EPCs+MSCs was significantly higher than DM (24.92 ± 1.81 vs. 16.72 ± 1.39; $p<0.05$). Number of neutrophil infiltration in DM+EPCs, DM+MSCs, DM+MSCs+EPCs and Con increased significantly than DM at day 14 (12.40 ± 2.40, 11.60 ± 3.14, 14.60 ± 1.63, 13.00 ± 2.16 cells/field vs. 34.25 ± 4.59 cells/field; $p<0.05$). The VEGF levels in DM+EPCs, DM+MSCs, DM+MSCs+EPCs and Con were significantly higher than DM on day 7 (188.43 ± 28.09, 218.84 ± 27.50, 216.45 ± 53.01, 232.30 ± 44.09 pg/mg protein vs. 44.06 ± 10.70 pg/mg protein; $p<0.05$). In conclusion, the present study has demon-

strated that the combined EPCs and MSCs can increase VEGF level and increased angiogenesis which lead to reduce number of neutrophil infiltration and enhanced wound healing in diabetic mice model.

Where applicable, the authors confirm that the experiments described here conform with The Physiological Society ethical requirements.

PCB001

Inhibition of the ventricular function of rat by Bisphenol A

P. Tarafder, K. Sarkar and G. Paul

Department of Physiology, University of Kalyani, Kalyani, West Bengal, India

Bisphenol A (BPA) is a controversial chemical. The possible toxic effect of BPA on the function of the heart has not been studied in detail till to date. So, the aim of the present study was to examine the effect of BPA on the ventricular function of heart at the molecular physiological level in rat. Studies were performed on adult male rats of Sprague- Dawley strain (150-200gm, n=7). BPA was administered at a dose of 50mg/kg body weight/day for 20 and 30 days by oral gavage. The rats were sacrificed by cervical dislocation on the 24th hour after the last treatment. Paraffin embedded ventricular tissue sections were stained with hematoxylin and eosin (H&E); and Von-Kossa's technique after Bancroft et al, 2008. The activities of superoxide dismutase (SOD)(Marklund and Marklund,1974), catalase (CAT)(Sinha,1972), glutathione reductase (GR)(Staal et al,1969), glutathione peroxidase (GPX)(Rotruck et al, 1973) were determined and the amount of malondialdehyde (MDA)(Devasagayam and Tarachand,1987) was estimated in microsomal fraction of ventricular myocytes (VMs). Acetylcholinesterase (AChE) activity was measured after Ellman et al,1961. Values are means±S.E.M., compared by Student's t-test. We found significant changes in the size and shape of the nucleus of VMs in H&E stained tissue sections of test rats in a duration dependent manner. Moreover, many lacunae were seen in the matrix of the VMs. We also observed significant deposition of Ca2+-salt at all durations in Von-Kossa's stained ventricular tissue section. These findings suggest that BPA damages the VMs and hampers calcium homeostasis by causing Ca2+-salt deposition in VMs. The activities of antioxidant enzymes were seen to be decreased in both 20 and 30 days durations compared to the control groups [(SOD-6.51±0.2 vs. 7.08±0.3 and 6.47±0.2 vs. 6.58±0.3 U/mg protein)(CAT-25.18±0.4 vs. 27.06±0.5 and 24.42±0.5 vs. 26.59±0.6 U/mg protein, p<0.05)(GPX-3.61±0.3 vs. 4.78±0.3 and 3.77±0.2 vs. 4.87±0.4 nmoleGSH/mg protein, p<0.05)(GR-16.23±0.6 vs. 24.28±0.9 and 11.48±0.5 vs. 23.94±0.8 nmoleNADPH oxidized/min/mg protein, p<0.001) respectively]. While, the MDA production was increased in test groups than control groups in both durations [(16.66±0.5 vs. 14.96±0.5 and 19.74±0.2 vs. 13.98±0.7 nmole MDA/mg protein-p<0.001) respectively]. These results suggest that BPA induces oxidative stress in rat VMs by depleting antioxidant defense system and increasing lipid peroxidation. Further, the activity of AChE was decreased significantly in treated rats in both durations [(4.43±0.4 vs. 10.19±0.6 and 3.91±0.3 vs. 10.19±0.6 μmole/min/mg protein, p<0.001) respectively]. This suggests that BPA inhibits ventricular functions by inhibiting AChE at the ventricular synapse. In conclusion, BPA inhibits ventricular function in rat presumably by hampering Ca2+-homeostasis and causing oxidative stress in VMs; and inhibiting AChE activity in ventricular synapse.

Marklund S & Marklund G (1974). European J Biochem 47, 469-474.

Sinha KA (1972). Anal Biochem 47, 389-394.

Staal GEJ, Visser J & Veeger C (1969). Biochem Biophys Acta 185, 39-48.

Rotruck JT, Pope AL, Ganther HE & Swanson AB (1973). Science 179, 588-590.

Devasagayam TPA & Tarachand U (1987). Biochem Biophys Res Commun 56, 836-842.

Where applicable, the authors confirm that the experiments described here conform with The Physiological Society ethical requirements.

PCB002

Relationship between chronic kidney disease and left ventricular mass independent of haemodynamic factors in an African community sample

F. Maunganidze, N.R. Gavin and A.J. Woodiwiss

Physiology, University of The Witwatersrand, Johannesburg, South Africa

Chronic kidney disease (CKD) preceding the development of renal failure, is independently associated with cardiovascular outcomes as explained by a number of mechanisms including haemodynamic and non-haemodynamic factors.[1-3] Our aim was to evaluate whether the relationship between CKD and left ventricular mass (LVM) occurs in a community sample and the extent to which this relationship depends on haemodynamic factors. In 418 randomly selected, non-diabetic participants from a community sample, 236 of whom were normotensive (NT), glomerular filtration rate was estimated (eGFR), [3] LVM and dimensions determined using echocardiography, and aortic BP assessed from applanation tonometry and SphygmoCor software.[4] Unadjusted means and proportions were compared by the large-sample z test and the χ2-statistic, respectively. Relationships were determined using multivariate regression analysis with adjustments for clinic BP (or alternative haemodynamic factors), age, sex, waist circumference, HbA1c, regular tobacco intake, regular alcohol intake, pulse rate and treatment for hypertension in the models. Aortic pulse wave velocity and high quality 24-hour BP values were available from 362 and 304 participants respectively. With adjustments for confounders (including clinic systolic BP), eGFR was associated with LVM index (LVMI) and LVM in excess of that predicted from stroke work (inappropriate LVM, LVMinappr) in the whole sample (LVMI: partial r = - 0.24, p<0.005; LVMinappr: partial r = - 0.33, p<0.0001) and in NT only (LVMI: partial r = - 0.30, p<0.01; LVMinappr: partial r = - 0.37, p<0.0001). Differences in LVMI and LVMinappr were noted in the eGFR range above 105 mls/min/1.73 m2) (p<0.0001 for differences in LVMinappr between upper two quartiles of eGFR). When replacing clinic BP with either aortic systolic BP, 24-hour BP, PWV, stroke work (for LVMI), LV end diastolic volume, or circumferential wall stress in the regression models, eGFR retained the strong association with LVMI (p<0.05 to <0.0005) and LVMinappr (p<0.0001 for all) and these effects were replicated in NT only. Therefore, strong relationships between early renal dysfunction and LVM occur at a community level irrespective of the presence of hypertension and independent of 24-hour and aortic BP, PWV, LV end diastolic volume, stroke work and wall stress. Non-haemodynamic factors appear to explain a considerable proportion of the relationship between early CKD and LV hypertrophy.[5]

	All (n=418)	Normotensives (n=236)
Sex (% female)	65.3	66.9
Age (years)	42.1±17.9	33.0±13.9
Body mass index (kg/m^2)	28.8±7.6	27.1±7.1
Waist circumference (cm)	88.4±15.5	83.9±14.3
% Overweight/obese	24.6/38.8	24.2/30.5
Regular tobacco intake (%)	15.1	14.4
Regular alcohol intake (%)	21.0	21.6
Pulse rate (beats/min)	68±10	68±11
Conventional SBP/DBP (mm Hg)	129±23/84±13	116±11/77±8
Aortic SBP/DBP (mm Hg)	121±23/84±13	108±12/78±8
24 hour SBP/DBP (mm Hg) (n)	118±14/73±10 (304)	112±10/69±7 (166)
Aortic pulse wave velocity (m/sec) (n)	6.37±2.61 (362)	5.30±1.48 (209)
Aortic augmentation index (%)	27.3±13.7	22.6±14.0
Stroke work (g-m)	120±38	107±31
LV systolic wall stress (g/cm^2)	106±27	100±20
% Increased serum creatinine	4.6	2.1
eGFR (ml/s/min/1.73 m^2)	110±29	117±30
Left ventricular mass (LVM) (g)	156±50	146±46
LVM index (g/m$^{2.7}$)	42.9±13.6	39.7±11.7
Inappropriate LVM (LVM_{Inappr}) (%)	123±29	123±27
LV mean wall thickness (mm)	0.95±0.17	0.91±0.14
LV end diastolic diameter (mm)	4.65±0.54	4.63±0.53
% LV hypertrophy	21.8	14.0
% increased LVM_{Inappr}	13.2	10.6

BP, blood pressure; SBP, systolic BP; DBP, diastolic BP; eGFR, estimated glomerular filtration rate.

Table 1. Characteristics of non-diabetic participants from the community sample.

Culleton BF, Larson MG, Wilson PW, Evans JC, Parfrey PS, Levy D. Cardiovascular disease and mortality in a community-based cohort with mild renal insufficiency. Kidney Int 1999;56:853-906.

Mann JF, Gerstein HC, Pogue J, Bosch J, Yusuf S. Renal insufficiency as a predictor of cardiovascular outcomes and the impact of ramipril: The HOPE randomized trial. Ann Int Med 2001;134:629-636.

Cirillo M, Lanti MP, Menotti A, Lorenzi M, Mancini M, Zanchetti A, De Santo NG. Definition of kidney disease as a cardiovascular risk factor: use of albumin excretion and estimated glomerular filtration rate. Arch Int Med 2008;168:617-624.

Norton GR, Majane OH, Maseko MJ, Libhaber C, Redelinghuys M, Kruger D, Veller M, Sareli P, Woodiwiss AJ. Brachial blood pressure-independent relations between radial late systolic shoulder-derived aortic pressures and target organ changes. Hypertension 2012;59:885-892.

Fabian Maunganidze, Gavin R Norton, Muzi J Maseko, Carlos D Libhaber, Olebogeng HI Majane, Pinhas Sareli, Angela J Woodiwiss. Relationship Between Chronic Kidney Disease and Left Ventricular Mass Independent of Haemodynamic Factors in a Community Sample. Journal of Hypertension [In Press]

This study was supported by the Medical Research Council of South Africa, the University Research Council of the University of the Witwatersrand, the National Research Foundation (Women in Research and the Thuthuka Program), the Circulatory Disorders Research Trust, and the Carnegie Programme.

Where applicable, the authors confirm that the experiments described here conform with The Physiological Society ethical requirements.

PCB003

Signal Transducer and Activator of Transcription 3 (STAT3) and heart failure with age: A position-dependent gene knock out model in mice

A. Imamdin[1], J. McCarthy[1,2], S. Lecour[1], K. Sliwa-Hanle[1] and N. Davies[3]

[1]Medicine, Hatter Institute for Cardiovascular Research in Africa, University of Cape Town, Cape Town, South Africa, [2]Chemical Pathology, Division of Lipidology, University of Cape Town / Groote Schuur Hospital, Cape Town, South Africa and [3]Cardiovascular Research Unit, Chris Barnard Division of Cardiothoracic Surgery, University of Cape Town, Cape Town, South Africa

Introduction: Heart failure (HF) is the inability of the left ventricle to fill with or eject blood. It often occurs as a side-effect of cardiovascular complications such as ischemia. At the molecular level, Signal Transducer and Activator of Transcription 3 (STAT3) is linked to HF, as STAT3 deficient (STAT3 KO) mouse models have shown development of HF with age.
Hypothesis: In a mouse model, induction of heart failure consecutive to a deletion in the STAT3 gene depends on the locus of the splice-site in the gene.
Material and methods: STAT3 KO and wildtype (WT) mice were aged to provoke heart failure. Mice were anesthetised for all aspects of this experiment by intraperitoneal injection of Sodium Pentobarbitone (50mg/kg body weight) . A sufficient degree of anaesthesia was considered to be obtained in the absence of the pedal reflex, after which the chest cavity was opened, and hearts were excised. Mitochondrial respiration was measured in aged hearts using permeabilized heart fibres and an oxygen-sensing Clarke-type electrode, with fatty acids (FA) as a substrate (n=4 per group). Inability to respire with FA is a typical metabolic state of a failing heart. Histology staining (picrosirius stain) was also performed on these aged mouse hearts to quantify fibrosis, a marker for heart failure (n=6 KO, n=4 WT).
Results: No significant differences detected in mitochondrial respiration using a FA substrate, indicating similar metabolic profiles in both groups (see Figure 1, $p>0.05$). Failing hearts exposed to FA should have shown impaired mitochondrial respiration. Histology staining for fibrosis in the aged STAT3 KO hearts showed minimal fibrosis, similar to WT hearts (KO 0.83±0.203% and WT 0.57±0.104%, $p> 0.05$), demonstrating no overt heart failure. All data was expressed as mean ± SEM. An unpaired student's t-test was used for all statistical analysis.
Conclusion: The STAT3 KO mouse model in our laboratory presents a different phenotype with aging compared to other published STAT 3 KO mouse models. This may be due to the location of the splicing in the STAT3 gene and the possibility of aberrant STAT3 proteins which contribute to HF in certain models, but not in others. It would therefore appear that the tendency to heart failure in STAT3 KO mice is dependent on the position of the deletion or the duration of aging.

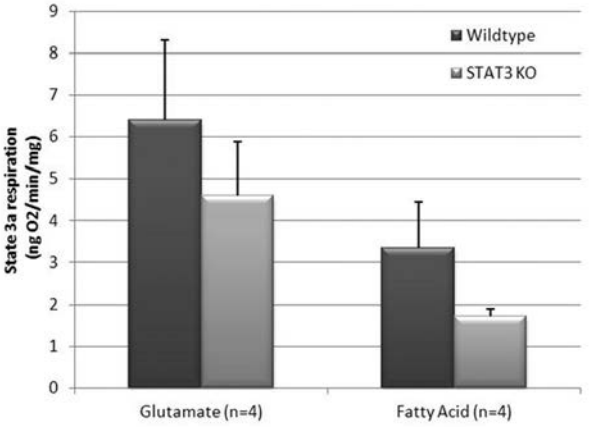

Figure 1: Measurement of state3a respiration (indicating the ability of mitochondria to convert ADP to ATP) is shown in the graph. Glutamate serves as a control substrate to which to compare fatty acid oxidation. There was no significant difference in respiration between wildtype and KO hearts within or between treatment groups (p>0.05).

Jacoby, J. J. et al. Cardiomyocyte-restricted knockout of STAT3 results in higher sensitivity to inflammation, cardiac fibrosis, and heart failure—with advanced age. Proc Natl Acad Sci U S A. 2003. 100; p12929–12934

Hilfiker-Kleiner, D. et al. A Cathepsin D-Cleaved 16 kDa Form of Prolactin Mediates Postpartum Cardiomyopathy. Cell. 2007. 128 (3), p. 589-600

Protein structure: Becker, S., Groner, B. and Müller, C. W. Three-dimensional structure of the Stat3β homodimer bound to DNA. Nature. 1998. 349: p145-151

Cohn, J. N.. The Management of Chronic Heart Failure. N Engl J Med. 1996. 335: p490-498

Smith RM, Suleman N, Lacerda L, Opie LH, Akira S, Chien KR, et al. Genetic depletion of cardiac myocyte STAT3 abolishes classical preconditioning. Cardiovasc Res 2004. 63: 611-616.

National Research Foundation (NRF), Hatter Institute for Cardiovascular Research in Africa

Where applicable, the authors confirm that the experiments described here conform with The Physiological Society ethical requirements.

PCB004

Novel interventions to ameliorate hyperglycemia-induced cardiac dysfunction following ischemia-reperfusion

R.F. Mapanga and M.F. Essop

Physiological Sciences, Stellenbosch University, Stellenbosch, Western Cape, South Africa

Stress-induced, acute hyperglycemia co-presenting with myocardial infarctions is associated with poor prognosis. Hyperglycemia-induced oxidative stress result in DNA damage and subsequent activation of poly-ADP-ribose polymerase (PARP) as a restorative mechanism. However, PARP attenuates glyceraldehyde–3-phosphate dehydrogenase (GAPDH) activity, thereby diverting upstream glycolytic metabolites into damaging non-oxidative glucose pathways (NOGP). For example, hyperglycemia-induced stimulation of four NOGP, i.e. the polyol pathway, hexosamine biosynthetic pathway (HBP), advanced glycation end products (AGE), and PKC activation elicit cardiovascular complications. We therefore hypothesized that NOGP inhibition blunts hyperglycemia-induced oxidative stress and cardiac contractile dysfunction following ischemia-reperfusion. We employed several experimental systems: 1) Isolated rat hearts were perfused ex vivo with Krebs-Henseleit buffer containing 33 mM glucose vs. controls (11 mM glucose) for 90 min, followed by 30 min global ischemia and 60 min reperfusion ± respective NOGP inhibitors added during the first 20 min of reperfusion. The following inhibitors were individually employed: AGE pathway (100 μM aminoguanidine); PKC (5 μM chelerythrine chloride); HBP (40 μM 6-diazo-5-oxo-L-norleucine); and polyol pathway (1 μM zopolrestat); 2) Infarct size determination as in #1) but with 30 min regional ischemia and 120 min reperfusion ± similar treatments. Our data shows that acute administration of each inhibitor attenuated superoxide levels and concomitantly increased superoxide dismutase activity. In parallel, we found that it decreased PARP and enhanced GAPDH activities while diminishing myocardial apoptosis. Each inhibitor employed blunted activation of the other three pathways here examined. Hearts treated with NOGP inhibitors also displayed improved functional recovery and smaller infarct sizes following ischemia-reperfusion. Interestingly, NOGP inhibitors resulted in the same degree of change (for all above-mentioned parameters evaluated) when compared to each other. The current study demonstrates that acute NOGP inhibition initiated after ischemia offers significant potential as therapeutic agent(s) for myocardial infarction under acute hyperglycemia. Moreover, our findings establish for the first time that there is a convergence of downstream NOGP effects in our model, i.e. increased myocardial oxidative stress, further pathway activation, apoptosis, and impaired contractile function. Thus a vicious metabolic cycle is established whereby hyperglycemia-induced NOGP further fuels its own activation by generating even more oxidative stress, thereby exacerbating damaging effects on the heart under these conditions.

Capes SE, Hunt D, Malmberg K, Gerstein HC (2000). Lancet 355: 773–8.

Brownlee M (2001). Nature 414: 813–820

Rajamani U, Essop MF (2010). Am J Physiol Cell Physiol 299: C139–47

Mapanga et al (2012). PLoS One. 2012;7(10):e47322

This work was supported by the South African National Research Foundation and Stellenbosch University (to MFE).

Where applicable, the authors confirm that the experiments described here conform with The Physiological Society ethical requirements.

PCB005

Effect of oral administration of levonogestrel with or without ethinyl estradiol on glucose tolerance and plasma lipid parameters in female Wistar rats

O.S. Michael and L.A. Olatunji

Deparment of Physiology, University of Ilorin, Ilorin, Kwara, Nigeria

Combined oral contraceptives (COCs) have become the most common or popularly used method of reversible contraception worldwide (1). The impact of oral contraceptives (OC) on cardiovascular health remains an important issue due to the popularity of this contraceptive choice combined with the knowledge that OC usage has been linked to adverse cardiometabolic effects (2). Estrogen is believed to have cardiometabolic protection effect; but its beneficial effects have recently been queried. The aim of the present study was to determine whether or not the altered glucose tolerance and plasma lipid profile was associated with OC and due to the estrogenic or progestogenic-component in 120-180g female rats. Rats (8 per group) were divided into control, combined

ethinyl estradiol-levonogestrel OC-treated (LEE) (receiving 0.75μg ethinyl estradiol/7.5μg levonorgestrel, p.o.), and low dose levonogestrel only OC-treated (LOC) (receiving 3.75 μg levonorgestrel, p.o.) groups. Rats were given distilled water (0.3ml, p.o), LEE and LOC daily for 6 weeks. Values are means± S.E.M. Glucose challenge test was performed 48- hours prior to the end of the experiment. The animals had 12-hour overnight fast and glucose tolerance was expressed as a function of the area under the tolerance curve (3,4).The results showed that treatment with a combination of levonogestrel and ethinyl estradiol led to significant decrease in glucose tolerance (370.6±14.9 vs. 280.6±10.1mmol/l) and increase in plasma triglyceride (TG) levels (105.6±9.2 vs. 63.2±1.2mg/dl) while treatment with levonogestrel only did not lead to any alteration in glucose tolerance and TG levels when compared with the control. However, treatment with a combined levonogestrel and ethinyl estradiol or levonogestrel only did not cause significant changes in total cholesterol (TC), high-density lipoprotein-cholesterol (HDL-C), low-density lipoprotein-cholesterol (LDL-C), total cholesterol/high-density lipoprotein-cholesterol (TC/HDL-C) ratio, and fasting blood glucose. In conclusion, the present study demonstrated that the use of OC containing levonogestrel in combination with ethinyl estradiol but not levonogestrel-only OC use caused impaired of glucose tolerance associated with increased triglyceride. This indicates that estrogenic but not progestogenic component of OC may be responsible for the altered glucose tolerance and lipid metabolism in this animal model.

Ågren UM, Anttila M, Mäenpää-Liukko K, Rantala M, Rautiainen H,Sommer WF and Mommers E (2011) Eur J Contracept Reprod Health Care 16: 444–457

Torgrimson BN, Meendering JR, Kaplan PF, Minson CT(2007) Am J Physiol Heart Circ Physiol 292: H2874–H2880

Arnold TS and Thye FW (1977) Am J Clin Nutr 30: 381–387.

Olatunji LA, Oyeyipo IP, Micheal OS, and Soladoye AO (2008) Afr J Med Sci 37:135–139.

Where applicable, the authors confirm that the experiments described here conform with The Physiological Society ethical requirements.

PCB006

Benfotiamine: a novel therapeutic agent for the treatment of hyperglycemia-mediated cardiac contractile dysfunction

R.F. Mapanga, B. Adams and M.F. Essop

Physiological Sciences, Stellenbosch University, Stellenbosch, Western Cape, South Africa

Acute hyperglycemia co-presenting with myocardial infarctions is associated with poor prognosis. Higher oxidative stress and subsequent activation of non-oxidative glucose utilizing pathways (NOGP), i.e. hexosamine biosynthetic pathway (HBP), polyol pathway, advanced glycation end products (AGEs) and PKC have been implicated as potential mediators of this process. Hyperglycemia-induced oxidative stress can also result in dysregulation of the ubiquitin-proteasome system (UPS) that removes misfolded proteins. There are conflicting data whether increased/decreased UPS is detrimental with hyperglycemia and/or in response to ischemia-reperfusion. For example, we found cardioprotection with attenuated UPS activation following ischemia-reperfusion under hyperglycemic conditions, suggesting that increased UPS activity elicits damaging effects on the heart. We recently established that benfotiamine (BFT)-vitamin B1 analog- improved cardiac function under similar experimental conditions by shunting flux away from the NOGP and lowering myocardial oxidative stress. In light of this, we hypothesized that BFT acts as a novel cardioprotective agent by diminishing myocardial oxidative stress and UPS activity in response to ischemia-reperfusion under acute hyperglycemic conditions. Hearts were excised from male Wistar rats and perfused ex vivo with Krebs-Henseleit buffer containing 33 mM glucose vs. controls (11 mM glucose) for 60 min, followed by 20 min global ischemia and 60 min reperfusion ± 100 μM BFT or 5 μM/L lactacystin (a specific UPS inhibitor) added during the first 20 min of the 60 min of reperfusion. In parallel experiments with similar treatments, we determined infarct sizes following 20 min regional ischemia and 120 min reperfusion. The data reveal that BFT enhanced functional recovery of LVDP at baseline (11 mM glucose) and hyperglycemia (33 mM) conditions with the highest dose (100 μM) triggering a robust effect early during the reperfusion period, reaching ~71.1 ± 5.9% ($p<0.01$ vs. respective control) under hyperglycemic perfusion conditions. BFT also reduced infarct sizes to 39.0 ± 2.5% and 49.7 ± 7.4% versus 52.3 ± 2.8% and 74.5 ± 4.9% at baseline and hyperglycemic perfusions, respectively. Likewise, lactacystin administration improved LVDP recovery and decreased infarct sizes following ischemia-reperfusion under hyperglycemic perfusion conditions. BFT treatment also attenuated myocardial oxidative stress and protein carbonylation, and blunted UPS activity. This study demonstrates that BFT may exert its cardioprotective effects by diminishing myocardial oxidative stress and UPS activity following ischemia-reperfusion under acute hyperglycemic conditions. Our findings suggest that the UPS may be a unique therapeutic target to treat ischemic heart disease in individuals that present with stress-induced, acute hyperglycemia.

Ceriello A (2000). Metabolism 49: 27–29

Du X et al (2003). J Clin Invest 112: 1049–1057

Mapanga R et al (2012). PloS one 7(10):e47322.

Where applicable, the authors confirm that the experiments described here conform with The Physiological Society ethical requirements.

PCB007

Congenital Heart Diseases (CHD) and role of NKx 2.5 in Pakistani population

A. Arif, S. Qamarunissa, S. Zehra and A. Azhar

Biomedical Division, Karachi Institute of Biotechnology and Genetic Engineering (KIBGE), Karachi, Sindh, Pakistan

Congenital heart disease (CHD) is worldwide a major threat for children below the age of five, it has high mortality and morbidity ratio. The number is increasing 5% every year in USA, where figures are scanty in our population.

Introduction:

In Pakistan, the adult population with congenital heart diseases is increasing and consanguineous marriages, a custom in region in also playing a role in increasing CHDs. In our study we look social and genetic aspects for these diseases. Nkx 2.5, a transcription factor and first progenitor in cardiac formation. (Olson E. and Srivastava D., 1996) to date, no data is available about the mutations in this gene responsible for CHD in Pakistani population. Nkx 2.5 gene encodes 324 aa. contains a homeodomain (142-200aa) which is highly conserved among vertebrates.

Materials and Methods:

A cohort of 225, CHD patients who were registered at National Institute of Cardiovascular Diseases (NICVD) from 2005-2008 were included in the study; these are non syndromic and sporadic cases. Informed consents and detail family history was obtained. The cohort contains Atrial Septal Defect (ASD), Ventricular Septal Defects (VSD), Tetralogy of Fallot (TOF), Patent Ductus Arteriosus (PDA) and Dextro transposition of Great Arteries (DTGA). Control group (n= 120) is healthy unrelated individuals with mean age 4± 2.0. DNA was extracted and NKx 2.5 gene was amplified and sequenced to check mutations. (McElhinney, D. B., 2003)

Results:

CHD patients (n=225, 57% male and 43% female). Age ranges 0.001-17 yrs. mean age is 4.45 ± 3.5. More than 40 mutations are reported till date (Liu XY., et al, 2011). Our findings were five SNPs in our population. Out of these two are missense, two are in 5'UTR region and one is inframe deletion. These mutations are potent in damaging protein structure predicted by SIFT, mutation taster and polyphen.

Discussion:

CHD is a major cause of child death in the first year of life. Our study concludes a few aspects and will broaden it to other genes as it is a need to find aetiology of these diseases and to combat it with the modern genetic therapeutics.

Liu XY., Wang J, Yang YQ, Zhang YY., Chen XZ, Zhang W, Wang XZ, Zheng JH, Chen YH., (2011) Novel NKX2-5 mutations in patients with Familial Atrial Septal Defects, Pediatric Cardiology; Vol 32 : 193-201

Srivastava D. and Olson EN., (2000) A genetic blueprint for cardiac development, Nature; Vol 407: 221-226

McElhinney, D. B., Geiger, E., Blinder, J., Benson, D. W., Goldmuntz, E.(2003) NKX2.5 mutations in patients with congenital heart disease, Journal of American College of Cardiology; 42: 1650-1655

Wang J, Liu XY and Yang YQ.,(2011) Novel NKX2-5 mutations responsible for congenital heart disease, Genetics and Molecular Research; Vol 10 (4): 2905-2915

We are very thankful to National Institute of Cardiovascular Disease for sample collection and support.

Where applicable, the authors confirm that the experiments described here conform with The Physiological Society ethical requirements.

PCB008

Comparative effect of ciprofloxacin and levofloxacin on systolic, diastolic and mean arterial blood pressure values of dogs

O. Omobowale, O.A. Oridupa, B.O. Fabiyi, J.O. Abiola, T.O. Ajibade and T.E. Adeyeoluwa

University of Ibadan, Ibadan, Nigeria

Antibacterials are among the most commonly used drugs in veterinary medical practice. Among this class of therapeutic agents are the fluoroquinolones which have been widely employed both in veterinary and medical practices because of their excellent antibacterial activities and wide antibacterial spectrum. Despite these known beneficial effects of the fluoroquinolones, adverse reactions affecting several systems including the cardiovascular system have been reported. This study was designed to investigate the possible effect of two commonly used fluoroquinolone drugs, Ciprofloxacin and Levofloxacin on cardiac function in dogs using arterial blood pressure as clinical index

Eight apparently healthy male dogs were equally and randomly divided into 2 groups. Ciprofloxacin and Levofloxacin were orally administered respectively to each group at the dosage of 25mg/kg twice daily for 14 days.Noninvasive blood pressure measurements were taken 30 minutes before administration and thereafter on days 2, 5, 7, 10 and 14 of treatment. Data were analysed using ANOVA at a confidence level of 95%. Following the administration of ciprofloxacin, there was a drop in pre-treatment mean systolic blood pressure from 149.8±20.7 mm Hg to 132.0±8.2 mmHg on day two and further to 122.0±20.9 mmHg on day five. After day five, a gradual increase in the mean systolic blood pressure was observed on days 7 and 10 to 129.3±14.7 mmHg and 133.0±19.5 mmHg respectively. A further decrease in the mean systolic blood pressure was recorded on day 14 to 123.5±12.4mmHg. In the Levofloxacin group, a similar pattern was observed in dogs treated with an initial reduction of the pre-administration mean systolic blood pressure from 133.8±8.7 mmHg to 123.8±24.2 mmHg by day two of treatment and a rise to a peak of 145.8±10.0mmHg by day five of treatment. For these two treatment groups however, there were no statistically significant ($p>0.05$) differences between pre-administration and post-administration values recorded.

Mean diastolic blood pressure decreased in the ciprofloxacin group from 82.5±8.5 mmHg to 62.5±10.7 mmHg by day two of treatment but increased to 77.8±12.1 mmHg and 83.8±10.2 mmHg by days 5 and 7 respectively. Levofloxacin also caused a decrease in the mean diastolic blood pressure from 81.3±12.1 mmHg to79.8±9.3 mmHg on day 2 of treatment. These values increased to 98.5±11.3 mmHg by day five of treatment. There were no statistically significant ($p>0.05$) differences between pre-administration and post-administration Mean Arterial Pressure values for both groups.

From this study ciprofloxacin and levofloxacin did not appear to have any adverse effects on arterial blood pressure values in dogs at the dosage administered. Further work is however required to evaluate the possible effect of longer periods of treatment and higher dosages on blood pressure.

Where applicable, the authors confirm that the experiments described here conform with The Physiological Society ethical requirements.

PCB009

Improvement of the anabolic-to-androgenic ratio of nandrolone decanoate by 5α-reductase inhibition worsen its cardiac effects

G.A. Brasil[1], E.F. Mata[1], A.M. Nascimento[1,3], E.M. Lima[1,3], I.C. Kalil[1], D.C. Endringer[1], G.A. Boechat[1], N.S. Bissoli[3] and T.U. Andrade[1,2]

[1]Pharmacy, UVV, Vila Velha, Espirito Santo, Brazil, [2]Pharmaceutical Sciences, Federal Uniersity of Espírito Santo, Vitoria, Espírito Santo, Brazil and [3]Physiological Sciences, Federal Uniersity of Espírito Santo, Vitoria, Espírito Santo, Brazil

Androgens can act directly on its receptors or via its dehydro metabolite. Its well determined that dehydrotestosterone is more potent than testosterone. Androgenic Anabolic Steroids (AAS) were developed to obtain a drug with its anabolic effect potentialized. Nandrolone decanoate (ND) is one of the most used AAS worldwide, mainly as drug of abuse to improve exercise performance and for aesthetic purposes. Dehydronandrolone (DHN) is less potent in acting on androgen receptor than ND itself. AAS has been implicated in cardiac side effects, such as cardiac hypertrophy, cytokine imbalance, and sudden cardiac death. But if ND or DHN are implicated remain to be evaluated. We investigated if the increase of the anabolic-to-

androgenic ratio of the ND by the inhibition of the 5α-reductase improves the cardiac side effects of ND on heart, especially on cardiac hypertrophy and cytokine imbalance. Male Wistar rats were divided into 3 experimental groups: control animals receiving the vehicle (CONT; n=8; peanut oil, I.M., wekly; 0.9% saline; i.p., daily), animals receiving ND (DECA; n=8; 10 mg.Kg-1, twice a week, I.M.; 0.9% saline; i.p., daily), and animals receiving ND (DECAF; n=8; DN 10 mg.Kg-1, twice a week, I.M.) plus finasteride (100 μg.kg-1, i.p., daily), for four weeks. Surgical procedures were performed under sodium pentobarbital anesthesia (50mg.kg-1, intra-peritoneal, Crystal, Brazil). The experiments were performed in accordance with the ethical principles for animal experimentation by the Brazilian College of Animal Experimentation and were approved by our Institutional Ethics, Bioethics and Animal Welfare Committee (Protocol 68/2009). After the treatment period, animals were euthanized, the hearts were removed for morphometric analyzes, and determination of the cardiac pro- (TNF-α) and anti-inflammatory (IL-10) cytokines. Values are expressed as the mean ± S.E.M, compared with ANOVA using Tukey s post hoc test. Figure 1 shows that animals from DECA group present myocyte hypertrophy. Increasing the anabolic-to-androgenic ratio by finastride action, worsen all the morphometric parameters. Figure 2 presents the results of the cardiac cytokine evaluation. ND treatment increase TNF-α level while reduce the cardiac IL-10 content, indicating that ND determines cytokine embalance. Finasteride co-treatment with ND worsens the imbalance on cardiac cytokine elevating the pro-inflammatory cytokine and reducing the level of IL-10, when compared with the isolated ND treatment. In conclusion, increasing the anabolic-to-androgenic ratio of ND, by 5-α-reductase inhibitions worsen the side effects of ND on cardiac myocyte and cytokine balance, indicating that ND itself, not the DHN, is more important to determine these effects.

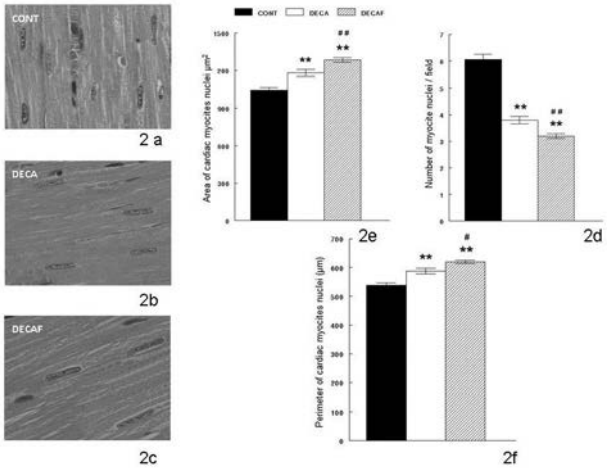

Figure 1: Hystological and morphometric analysis of hearts of CONT (2A), DECA (2B) and DECAF (2C) groups. The samples were stained with hematoxylin and eosin (H&E): 40x. 2D: number myocyte nuclei / high resolution field. 2E: myocytes nuclei area. 2F: myocyte nuclei perimeter. The values are expressed as the mean ± S.E.M, compared with ANOVA using Tukey s post hoc test. **p<0.01 compared with CONT group. #p<0.05 and ##p<0.01 compared with DECA group.

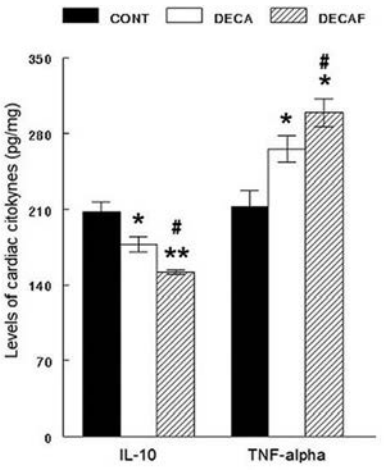

Figure 2: Effect of Nandrolone Decanoate plus Finasteride Treatment on cardiac inflammatory citokynes. There is an increase in pro-inflammatory (TNF-α) and reduced levels of anti-inflammatory (IL-10) cytokine on DECAF group compared with DECA and CONT. The values are expressed as the mean ± S.E.M, compared with ANOVA using Tukey s post hoc test. **p<0.01; *p<0.05 compared with CONT group. #p<0.05 compared with DECA group.

This study was supported by FAPES, CAPES and FUNADESP.

Where applicable, the authors confirm that the experiments described here conform with The Physiological Society ethical requirements.

PCB010

Testosterone in anabolic concentration induces apoptosis of cardiomyocytes in vitro with involvement of tumor necrosis factor alpha and renin angiotensin system

A.M. Nascimento[1,3], E.M. Lima[1,3], D. Lenz[1], D.C. Endringer[1], G.A. Boechat[1] and T.U. Andrade[1,2]

[1]Pharmacy, University Vila velha - UVV, Vila Velha, ES, Brazil, [2]Pharmaceutical Sciences, Federal University of Espírito Santo, Vitória, Espírtio Santo, UK and [3]Physiological Sciences, Federal University of Espírito Santo, Vitória, Espírtio Santo, UK

Anabolic androgenic steroids (AAS) lead to cardiac complications, and relationship among AAS, tumor necrosis factor alpha (TNF-α), and renin-angiotensin system (RAS) has been reported. Apoptosis is implicated in the shifting of the hypertrophic heart to the heart failure. The testosterone (T) in anabolic concentration induces apoptosis in cardiac myocytes. However, little is known about the relationship among testosterone, TNF-α, and RAS in this process. We investigated whether the apoptosis and the caspase-3 activity induced by testosterone in anabolic concentration involves the participation of the angiotensin converting enzyme (ACE) and TNF-α in cardiac myocyte cell culture (H9c2, ATCC). Cardiomyocytes were treated with testosterone (100 μM), doxorubicin (DOX; 5 μg/mL), T + etanercept (Eta; 100 μg/mL), T+losartan (Los; 10-7 M), and T+ Ac-DEVD-CHO (200 μM). The treatment time with testosterone alone or in combination in culture wells was 72 h. Cell viability was evaluated by the MTT assay in different concentrations of T (0,5-200 μM). Apoptosis was determined by flow cytometry, proteolytic activity of caspase-3, TNF-α quantification and ACE activity by ELISA method. Values are expressed as the mean ± S.E.M, compared by ANOVA, followed by the post-hoc Tukey test. T elicit a concentration-dependent decrease in cell viability (0.5 μM: 12.49±1.54%, 5 μM: 21.36±0.94%, 50 μM: 30.06±1.38%, 100 μM: 64.74±1.16%,

200 μM: 74.85±1.97%), and co-treatments with Eta (5.3±1.7%), Los (6.4±1.8%) or Ac-DEVD-CHO (12.9±3.5), reduced the effect of T in anabolic concentration (100 μM; 64.7±1.2%). T also induces apoptosis (concentration-dependent)(Figure 1) and increase in the proteolytic activity of caspase-3, which were reduced by the co-treatments (Figure 2). TNF-α and ACE activity were elevated by T treatment, and co-treatment with Los and Eta were able to reduce these effects (Figure 2). It is concluded that there is an interaction between testosterone, Ang II and TNF-α in inducting apoptosis and caspase-3 activity in cultured cardiac myocytes, which contributes to reducing the viability of these cells (cytotoxic effect) induced by testosterone in anabolic concentration.

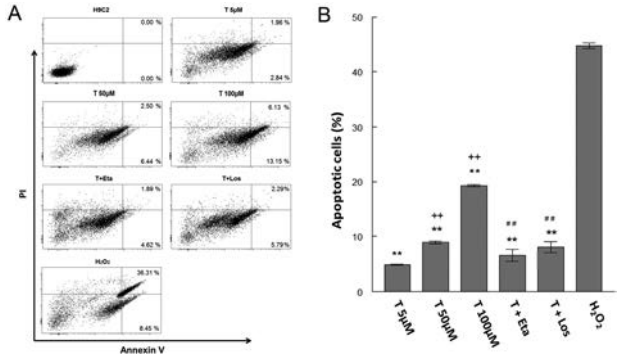

Fig. 1. Concentration-dependent apoptosis (5, 50, 100 μM) induced by testosterone (T) in H9c2 cells. After the treatment period of 72 h cells were stained with Annexin V-FITC and propidium iodide (PI) followed by analysis in the flow cytometer. Cells in the initial stage of apoptosis were defined as annexin-V(+)/PI(-), while late apoptotic cells were defined as double positive. Co-treatment with etanercept H9c2 cells (Eta, 100 μg/mL) or losartan (Los, 10-7M) reduced apoptosis induced by T. A, Data representative of three independent experiments. B, Percentage of apoptotic cells (sum of Annexin-V (+)/ PI(-) and double positive). Eta: etanercept; Los: losartan. Values are expressed as the mean ± S.E.M, compared by ANOVA, followed by the post-hoc Tukey test.; **p<0.01 compared to positive control (H2O2); ++p < 0.01 relative concentrations previous T; ##p < 0.01 compared to T 100 μM.

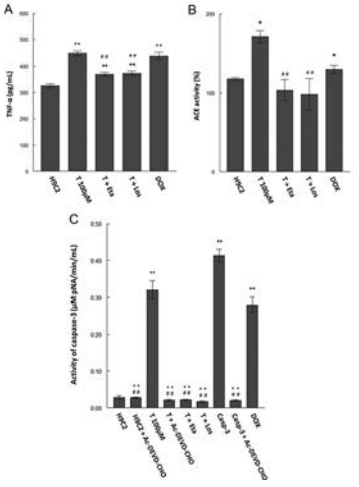

Fig. 2. Testosterone induces increased TNF-α, activity of ACE and caspase-3 activity in cardiomyocytes cells. Cells (H9c2) were treated with Testosterone (T) 100μM with or without co-treatment with etanercept (Eta, 100μg/mL) or losartan (Los, 10-7M); and Doxorubicin (DOX, 5μg/mL) or Ac-DEVD-CHO (200μM) for 72 h. A, Quantification of TNF-α. B, Evaluation of ACE activity. C, Evaluation of caspase-3 activity. Values are expressed as the mean ± S.E.M, compared by ANOVA, followed by the post-hoc Tukey test; *p<0.05 or **p<0.01 compared to control (H9c2). ++p<0.01 and +p<0.05 relative to caspase-3 (casp-3). # #p<0.01 compared to T 100 μM.

This study was supported by "Fundação de Amparo à Pesquisa do Espírito Santo (FAPES)" and "Fundação para o Desenvolvimento do Ensino Superior Privado (FUNADESP)".

Where applicable, the authors confirm that the experiments described here conform with The Physiological Society ethical requirements.

PCB011

Enrichment of metabolic substrates diminish nitric oxide synthase-mediated anti-adrenergic effect of insulin in LV myocytes from normal and hypertensive rats

Z. Zhao, C. Jin, S. Kim and Y. Zhang

Physiology, Seoul National University College of Medicine, Seoul, Republic of Korea

Background & Aim: Metabolic syndrome (MetS) triggers abnormal insulin signaling and insulin resistance, which is associated with impaired nitric oxide (NO) availability. Endothelial NO synthase (eNOS) has been link to insulin signaling but the role of neuronal NOS (nNOS) remains unknown. Recently, nNOS is shown to be up-regulated in hypertensive left ventricular (LV) myocardium (HP). Here, we tested whether enriching metabolic substrates in vitro affects insulin regulation of LV myocyte contraction and the functional contribution of nNOS in normal and in HP rat LV myocytes.

Materials & Methods: LV myocytes were isolated using enzymatic dispersion technique from normal and angiotension II-induced hypertensive rats (*via* osmotic minipump, 125 ng/min/kg, 10-12 weeks, males). Myocyte contraction was assessed by using a video-sarcomere detection system (IonOptix Corp, field stimulation at 2 Hz, 36 ± 1˚C). Metabolic substrates (oleic acid 200 μM, palmitic acid 100μM, linolic acid 100μM, lactate 1mM, pyruvate 100μM and carnitine 50μM) were supplemented (termed nutrition full, NF solution) to the normal tyrode (NT) solution. Insulin (1-10 nM), isoprenaline (ISO, 10-50 nM), S-methyl-L-thiocitrulline (SMTC, 100 nM), L-NG-nitroarginine methyl ester (L-NAME, 1 mM) and n-acetyl cysteine (NAC, 1 mM) were used in the study.

Results: Our results demonstrated that sarcomere shortenings were greater with NF in both normal and HP under basal conditions (P<0.0001, n=19 in normal and P<0.0001, n=8 in HP) and after ISO treatment (P=0.0003, n=14, n=24 in normal and P<0.0001 n=15, n=8 in HP). NAC did not affect NF increases in myocyte contraction in normal (P=0.003, n=6) and in HP (P=0.02, n=5). In normal rats, insulin pre-treatment abolished ISO-stimulation of LV myocyte contraction with NT (P=0.8, n=27) but not with NF (P<0.001, n=20), suggesting impaired insulin response in NF. L-NAME, but not SMTC, prevented the anti-adrenergic effect of insulin in these rats (L-NAME: P=0.004, n=6; SMTC: P=0.16, n=9). In contrast, ISO failed to increase LV myocyte contraction with NT in HP (P=0.1, n=15); SMTC restored the positive inotropic effect of ISO (P=0.004, n=6). The inotropic response of ISO in HP was not affected by insulin (P=0.3, n=11 in NT; P<0.0001, n=11 in NF). SMTC or L-NAME did not affect myocyte contraction the effect of ISO with NF in HP (P=0.8, n=11, n=7 with SMTC; P=0.3, n=11, n=5 with L-NAME).

Conclusion: Our results show that eNOS mediates anti-adrenergic effect of insulin in normal rat LV myocytes and nNOS exerts such an effect in HP. *In vitro* enrichment of metabolic substrates diminished insulin responsiveness in LV myocytes by attenuating the role of NOS. Downstream mechanisms mediating impaired insulin signaling in cardiac myocytes in metabolic syndrome and in HP warrant further study.

Where applicable, the authors confirm that the experiments described here conform with The Physiological Society ethical requirements.

PCB012

Coronary perfuse pressure is associated with angiotensin-converting enzyme (ACE) in female and with ACE2 activity in male SHR

N. Bissoli[1], P.L. Dalpiaz[1], S.G. Figueiredo[1], A. Lamas[1], I.F. Caliman[1], A. Medeiros[2], T. Andrade[3], M. Alves[4], A.K. Carmona[4], W. Gonçalves[5] and M. Moysés[1]

[1]UFES, Vitória, Brazil, [2]Federal Institute of Espirito Santo, Vila Velha, Brazil, [3]Department of Pharmacy, University Vila Velha, Vila Velha, Brazil, [4]Department of Biophysics, Escola Paulista de Medicina, Federal University of São Paulo, São Paulo, Brazil and [5]UNESC, Colatina, Brazil

The renin-angiotensin system (RAS) plays an important role in the pathophysiology of cardiovascular disease (CVD). ACE (angiotensin-converting enzyme) 2 degrades Ang (angiotensin) II, the main effector of the classic RAS, and generates Ang-(1-7). Thus, ACE2 plays a crucial role in the RAS because it opposes the actions of Ang II. However, the activity of ACE and ACE2 and the relationship between theses enzymes with coronary perfusion pressure (CPP) in male and female spontaneously hypertensive rats (SHR) remain unclear and were our objectives. The procedures were approved by the Ethical Committee of the Federal University of Espírito Santo (023/2009). Female and male SHR rats were divided into 4 experimental groups: sham and castrated. After 51 days of the castration, the rats were anesthetized with ketamine (70 mg/kg i.p.) and xylazine (10 mg/kg i.p.) and their hearts were immediately excised. Studies on the coronary vascular bed were performed on whole hearts using a Langendorff preparation for perfused isolated hearts and were perfused with modified Krebs solution, equilibrated with 95% oxygen and 5% carbon dioxide at a controlled pressure of 100 mmHg to give a pH of 7.4. Langendorff preparations were perfused at a rate of 10 mL/min with a peristaltic pump. After the CPP were measured, the coronary were isolated and the ACE and ACE2 activity were evaluated by fluorimetry. Female rats exhibited a higher CPP (125±5 mmHg, $p<0.05$), ACE (110±15 AFU, $p<0.05$) and ACE2 (0.1±0.02 AFU, $p<0.05$) activity than the male rats (CPP: 85±3 mmHg; ACE 60±3 AFU and ACE2 0.06±0.002 AFU). Castration reduced the ACE (32±3 AFU) and CPP (90±5 mmHg) in the female rats but did not affect ACE2 (0.09±0.002), while in the male rats the CPP (145±6 mmHg) and ACE2 (0.03±0.001 AFU) were increased and ACE (46±5 AFU) activity was reduced. One of the main findings of this study was the observation of sex dimorphisms among CPP, ACE and ACE2 activity and the different relationship of RAS on CPP in SHR, dependent of the sex. In female SHR the CPP is associated with ACE, while in male rats is with ACE2 activity. The present results may contribute to understand the sex differences in the regulation of cardiovascular system and the incidence of cardiovascular disease in women.

Grant Casadinho/Procad: 552623/2011-3, FAPES: 012/2011-Universal 54688175/2011.

Where applicable, the authors confirm that the experiments described here conform with The Physiological Society ethical requirements.

PCB013

Elevated myocardial oxygen consumption during cutaneous cold stress in young adult overweight and obese Africans

T.A. Olaniyan[1,2] and L.A. Olatunji[1]

[1]Physiology, University of Ilorin, Ilorin, Nigeria and [2]Public Health, The University of Northampton, Northampton, UK

Increased adiposity has been associated with high risk of developing hypertension and cardiovascular disease (1,2). Exaggerated sympathetic-mediated cardiovascular responses to stressful stimuli (such as exposure to cold) has been linked to the development of hypertension and cardiovascular disease (3,4), which in turn has been demonstrated to predict the development of future hypertension (5). The rate-pressure product (RPP) is considered as the best indirect method to evaluate myocardial oxygen consumption (MVO_2) as well as an indicator of myocardial stress. The aim of the present study was to test the hypothesis that enhanced change in RPP to cutaneous cold stress may be one potential mechanism that predisposes overweight/obese individuals to developing hypertension. We determined heart rate (HR), blood pressure (BP), and RPP in 40 normotensive young individuals aged between 18 – 25 years at baseline and during sympathetic activation elicited by cutaneous cold stimulation (CCS). Following CCS, a change in RPP was also estimated. The median body weight of 59.50kg of the study population was used for classification. This was further standardized by also classifying the participants based on their body mass indices (BMI). There was no significant differences in the baseline RPP between the groups classified by body weight ($P=0.629$) or among the groups classified by BMI ($P=0.415$). However, following CCS, there was a significant enhanced RPP change in overweight individuals ($P=0.019$). Furthermore, multivariate regression analysis showed that BMI, but not body weight had a significant influence on RPP variation following CCS. Thus, it can be concluded that normotensive overweight or obese individuals have an exaggerated RPP response to the CCS. However, exposure to cold may augment sympathetic reactivity in overweight/obese individuals, which may contribute to increased risk of developing myocardial dysfunction, even in young normotensive individuals. Furthermore, RPP changes to CCS could be a useful simple measure for early detection of cardiac complications, particularly in low/middle income countries.

Yan LL, Daviglus ML, Liu K, Stamler J, Wang R, Pirzada A, Garside DB, Dyer AR, Van Horn L, Liao Y, Fries JF, Greenland P. Midlife body mass index and hospitalization and mortality in older age. JAMA 2006; 295:190–198.

Garrison RJ, Kannel WB, Stokes J 3rd, Castelli WP. Incidence and precursors of hypertension in young adults: the Framingham Offspring Study. Prev Med 1987; 16:235–251.

Calhoun DA, Mutinga ML. Race, family history of hypertension, and sympathetic response to cold pressor testing. Blood Press 1997; 6:209–213.

Matthews KA, Salomon K, Brady SS, Allen MT. Cardiovascular reactivity to stress predicts future blood pressure in adolescence. Psychosom Med 2003; 65:410–415.

Treiber FA, Kamarck T, Schneiderman N, Sheffield D, Kapuku G, Taylor T. Cardiovascular reactivity and development of preclinical and clinical disease states. Psychosom Med 2003; 65:46–62.

Toyib Olaniyan,[1,2] Lawrence A. Olatunji[1]

[1]Cardiovascular and Membrane Physiology Unit, Department of Physiology, University of Ilorin, Ilorin, Nigeria.[2]Department of Public Health, The University of Northampton, Northampton, UK.

Where applicable, the authors confirm that the experiments described here conform with The Physiological Society ethical requirements.

PCB014

Diurnal variation in sympathetic control of excitation-contraction coupling: the role of β3 adrenoceptors and nitric oxide

H.E. Crumbie, G.C. Rodrigo and I. Squire

Department of Cardiovascular Sciences, University of Leicester, Leicester, UK

We have previously shown a time-of-day variation in the response of systolic $[Ca^{2+}]_i$ to the non-specific β-adrenergic (β-ADR) agonist isoproterenol (ISO), linked to a variation in Nitric Oxide (NO) signalling [1]. This may reflect stimulation of β3-ADRs, which induces a NO-dependent negative inotropic response [2]. As the action potential duration (APD) regulates systolic $[Ca^{2+}]_i$, and a time-of-day variation exists in the cardiac action potential [3], we set out to investigate the effect of β3-ADR stimulation and NO-signalling on the APD and systolic $[Ca^{2+}]_i$.

Ventricular myocytes were isolated by enzymatic digestion at time points corresponding to 3 hours into the male Wistar rats rest (ZT3) and active-period (ZT15). Measurement of systolic $[Ca^{2+}]_i$ was made in myocytes loaded with Fura-2 and APD using the whole-cell patch clamp technique.

A significant time-of-day variation was found in systolic $[Ca^{2+}]_i$ following stimulation with ISO (10nM), a non-specific β-ADR agonist, which was higher in ZT3 (1040.0 ± 116.9nM) compared to ZT15 myocytes (428.0 ± 63.1nM) (n=3, S.E.M., 2-way ANOVA, $P<0.001$). The difference in systolic $[Ca^{2+}]_i$ during ISO stimulation was abolished following inhibition of NOS with L-NNA (500μM) (2-way ANOVA, *ns*). To determine whether this time-of-day variation in response to ISO can be explained by a variation in AP configuration in response to β-ADR stimulation, APD at 30% (APD_{30}) and 50% (APD_{50}) were recorded. ISO stimulation increased APD_{30} and APD_{50} significantly more in ZT15 than ZT3 myocytes, with % increase in APD_{30} of 120.3 ± 14.9% in ZT15 compared to 10.6 ± 8.2% in ZT3 myocytes (n=3, S.E.M., students t-test, $P<0.001$), and APD_{50} of 95.9 ± 13.2% in ZT15 compared to 11.6 ± 7.4% in ZT3 myocytes (n=3, S.EM., students t-test, $P<0.001$). We also investigated systolic $[Ca^{2+}]_i$ and APD in ZT3 and ZT15 myocytes in response to the specific β3-ADR agonist BRL37344 (200nM), to determine if time-of-day variation in systolic $[Ca^{2+}]_i$ following ISO-stimulation could be explained by variation in β3-ADR signalling. A significant reduction in systolic $[Ca^{2+}]_i$ in ZT3 myocytes was found following BRL37344 stimulation, from 458.5 ± 41.2nM to 361.2 ± 18.0nM (n=4, 2-way ANOVA, $P<0.001$) but no effect on ZT15 myocytes. BRL37344 also significantly reduced APD_{30}, (18.3 ± 2.2ms to 14.4 ± 1.6ms) (n=5, 2-way ANOVA, $P<0.001$), and APD_{50} (32.9 ± 4.3ms to 26.5 ± 3.1ms) (n=5, 2-way ANOVA, $P<0.001$) in ZT3 myocytes with no significant change in ZT15 myocytes.

Our data shows a reduction in systolic $[Ca^{2+}]_i$ in rest-period myocytes (ZT3) in response to β3-ADR stimulation, which may reflect the reduction in APD. This suggests that the reduced response of systolic $[Ca^{2+}]_i$ to ISO-stimulation in active-period myocytes (ZT15) is not due to a strong negative inotropic action of β3-ADR activation during the active period.

Collins, H.E. and G.C. Rodrigo, Inotropic response of cardiac ventricular myocytes to beta-adrenergic stimulation with isoproterenol exhibits diurnal variation: involvement of nitric oxide. Circ Res, 2010. 106(7): p. 1244-52.

Jeyaraj, D., et al., Circadian rhythms govern cardiac repolarization and arrhythmogenesis. Nature, 2012. 483(7387): p. 96-9.

Gauthier, C., et al., The negative inotropic action of catecholamines: role of beta3-adrenoceptors. Can J Physiol Pharmacol, 2000. 78(9): p. 681-90.

Where applicable, the authors confirm that the experiments described here conform with The Physiological Society ethical requirements.

PCB015

Acute pre- or –post, ischaemic treatment with elevated extracellular glucose imparts a cardioprotection to isolated cardiomyocytes

C.E. Poile, I.B. Squire and R.D. Rainbow

Cardiovascular Sciences, University of Leicester, Leicester, UK

Reperfusion of the myocardium after an ischaemic insult can cause marked and irreversible damage. Minimizing infarct size is important for improving prognosis after a prolonged ischaemia. A number of cardioprotective interventions have been demonstrated to improve the outcome after myocardial infarction, including ischaemic pre-and post-conditioning and pharmacological pre-treatment (1, 2, and 3). Here we present data demonstrating that perfusing isolated cardiomyocytes for a short period of time with elevated extracellular glucose prior to, or following, the ischaemic insult, gives a marked cardioprotection. Adult male Wistar rats were culled humanely in accordance with Home Office guidelines and cardiomyocytes were enzymatically isolated. Contractile function of the isolated cardiomyocytes was assessed using a simulated ischaemia/reperfusion injury protocol, where cardiomyocytes were stimulated to contract at 1Hz by electrical field stimulation and perfused with Normal Tyrode (NT) solution at 32±2°C. Ischaemia was simulated using a metabolic inhibition (MI) solution of Substrate-Free Tyrode solution containing cyanide (2mM) and iodoacetic acid (1mM) for 7 minutes, followed by 10 minutes of 'reperfusion' with NT. Our data shows that supplying cardiomyocytes with a 5 minute pre-treatment of an elevated extracellular glucose concentration (20mM) prior to simulated ischaemia significantly increases the percentage of cardiomyocytes able to regain contractile function from 29.5±2.4% (control) to 61.8±2.4%*** (Results presented as mean ±S.E.M; N= 6 experiments, ≥116 cardiomyocytes for each experiment, ***P<0.001 Bonferroni's post-hoc test). Additionally, supplying 20mM glucose for only the first 5 minutes of the 10 minute reperfusion stage significantly increases contractile recovery to 62.8±4.8%*** (Results presented as mean ±S.E.M; N= 6 experiments, ≥115 cardiomyocytes for each experiment, ***P<0.001 Bonferroni's post-hoc test). These data show that both pre- and post-treatment of isolated cardiomyocytes with an acute elevated glucose concentration imparts a degree of cardioprotection. We hypothesise that there is increased glycolytic substrate availability during ischaemia after pre-treatment with 20mM glucose. For cardiomyocytes treated with elevated glucose on reperfusion it is hypothesised to give a more gradual ATP delivery therefore reducing reperfusion injury.

Murry C.E et al. (1986). Preconditioning with ischemia: a delay of lethal cell injury in ischemic myocardium. Circulation. 74, 1124-1136.

Zhao Z.Q et al (2003). Inhibition of myocardial injury by ischemic postconditioning during reperfusion: comparison with ischemic preconditioning. American Journal of Physiology. Heart and Circulatory Physiology. 285, H579-88.

Granfeldt A et al. (2009). Protective ischaemia in patients: preconditioning and postconditioning. Cardiovascular Research. 83, 234-246.

Where applicable, the authors confirm that the experiments described here conform with The Physiological Society ethical requirements.

PCB016

Induced automaticity in the ventricular myocytes of transgenic mouse overexpressing HCN2

K. Oshita[1,2], S. Igata[1], Y. Kuwabara[3], K. Kuwahara[3], K. Ushijima[2] and M. Takano[1]

[1]Department of Physiology, Kurume University School of Medicine, Kurume, Japan, [2]Department of Anesthesiology, Kurume University School of Medicine, Kurume, Japan and [3]Department of Medicine and Clinical Science, Kyoto University Graduate School of Medicine, Kyoto, Japan

Hyperpolarization-activated cyclic nucleotide-gated channels (HCNs) are expressed in the ventricle of fetal hearts, and are silenced during the development. These channels are up-regulated in the hypertrophied heart, and have been suggested to underlie arrhythmogenesis. To test this hypothesis, we generated a transgenic mice overexpressing HCN2 in the heart (HCN2-Tg) using alpha-MHC promoter, and analyzed the electrophysiological properties of ventricular myocytes.
Mice (8-12 weeks old) were deeply anesthetized with 3% sevoflurane. Ventricular myocytes were isolated with collagenase digestion. Action potential and membrane currents were recorded with ruptured whole-cell patch clamp method using standard high K^+ pipette solution. Values are means ± S.D. Statistical analysis was carried out using Student`s T-test. We first confirmed that amounts of mRNA and protein of HCN2 were significantly higher in HCN2-Tg than wild type (WT). However, contrary to our expectation, HCN2-Tg was not vulnerable to arrhythmia. In physiological bathing solution, the resting potential (RMP) of ventricular myocyte was not significantly different between WT (-81.5±1.0 mV) and HCN2-Tg (-81.6±1.6 mV, n=8, p=0.42). No spontaneous action potential (SAP) was recorded in HCN2-Tg myocytes, although robust HCN current (I_h) was recorded in the presence of 1 mM Ba2+. However, application of 0.3 μM isoproterenol (iso) to HCN2-Tg myocytes depolarized their RMP and subsequently induced SAP in 71%, coincident with the shifting of voltage-dependent activation curve of I_h; the voltage for the half maximal activation was -118.5±2.9 mV (control), and -90.2±1.5 mV (iso), respectively (n=4, p <0.01). In HCN2-Tg myocytes without SAP, RMP was significantly more depolarized (-77.2±2.1 mV) than that of WT (-82.1±1.0 mV, n=8, P<0.01). 3 μM ivabradine (iva), a specific HCN channel blocker, reversed iso-induced depolarization to the control level. We further compared the AP waveform elicited by electrical stimulation in WT and HCN2-Tg myocytes without SAP. In HCN2-Tg, action potential duration (APD) at -60 mV was significantly prolonged, and the rates of repolarization at -60 mV were significantly slower, both in the presence and absence of 0.3 μM iso. On the other hand, APD at 0 mV was significantly shorter in HCN2-Tg, most probably due to the outward tail current of I_h. When the myocytes were perfused with 3 mM K^+ bathing solution, RMP was -95.6±1.5 mV in WT, and -91.2±3.3 mV in HCN2-Tg (n=6, p<0.01). Under this condition, SAP was induced in 57% of HCN2-Tg myocytes. Application of 3 μM iva hyperpolarized RMP in HCN2-Tg.
These findings suggested overexpression of HCN2 potentially increased the vulnerability to arrhythmia, particularly in pathological conditions such as excessive β adrenergic stimulation or hypokalemia.

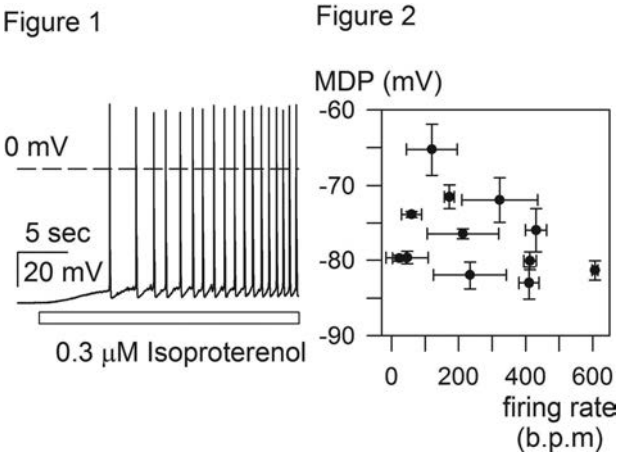

Figure1. Induced automaticity of HCN2-Tg ventricular myocytes. The white bar indicates the application of 0.3 μM iso. Depolarization of RMP is followed by SAP. Figure 2. The scatter plot of maximal diastolic potential (MDP) and firing rate of iso-induced SAP in HCN2-Tg myocytes.

Where applicable, the authors confirm that the experiments described here conform with The Physiological Society ethical requirements.

PCB017

Arrhythmogenic profile of the atrium and atrioventricular node in pulmonary arterial hypertension

I.P. Temple[1], G.M. Quigley[1], O. Monfredi[1], T.T. Yamanushi[2], M. Zi[1], E.J. Cartwright[1], V.S. Mahadevan[1], M.R. Boyett[1] and G. Hart[1]

[1]Medicine, University of Manchester, Manchester, greater manchester, UK and [2]Kagawa Prefectural College of Health Sciences, Kagawa, Japan

Introduction:
Arrhythmias are common in pulmonary arterial hypertension (PAH) causing severe symptoms and sudden death. Current treatments are often ineffective and have considerable side effects and therefore new therapies are required.
Methods:
Male Wistar rats (200 g) were injected with either monocrotaline (MCT) (60 mg/kg) or saline (control). They were sacrificed if they showed clinical deterioration or on day 28. *In vivo* echocardiography and ECG were performed under isofluorane anaesthesia. For whole heart experiments, the heart was excised and mounted on a Langendorff perfusion column at 37°C. For right atrial (RA)/atrioventricular (AV) node experiments, a tissue preparation was superfused at 37°C. Baseline ECG and atrio-His (AH) interval were recorded. Stimulation protocols were used to measure conduction velocity (CV) along the crista terminalis, AV effective refractory period (AVERP) and AV functional refractory period (AVFRP). Optical mapping was used to record the activation sequence across the right atrium.
Results:

Echocardiography demonstrated PAH (decrease in pulmonary artery acceleration time and increase in pulmonary artery deceleration) and right ventricular (RV) hypertrophy (increase in RV wall thickness) in the MCT rats. The whole heart experiments demonstrated an increase in AVERP and AVFRP in the MCT rats. The isolated RA/AV node preparation demonstrated a reduction in CV along the crista terminalis and a high incidence of complete heart block in the MCT rats (Table 1). The decrease in CV was supported by the optical activation sequences.

Conclusions:

Our data demonstrate slow atrial conduction and impaired AV node function in PAH which may serve as a basis for supraventricular arrhythmias. Reversing these changes is a potential theraputic target.

Table 1. Echo and AV node function parameters in control and MCT treated rats.

	Control rats (mean±SEM) n=9-16	MCT treated rats (mean±SEM) n=6-16
Echocardiographic measurements		
PAAT (ms)	34±3	16±2 **
PAD (ms-2)	15±2	32±4 **
RV chamber size (systole) (cm)	0.09±0.01	0.14±0.0 **
RV chamber size (diastole) (cm)	0.30±0.03	0.35±0.04
RV wall thickness (systole) (cm)	0.13±0.01	0.16±0.01 *
RV wall thickness (diastole) (cm)	0.13±0.02	0.22±0.04 *
In vivo and whole heart experiments		
In vivo PR interval (ms)	45±1	47±1
Langendorff PR interval (ms)	43±1	44±1
Wenckebach cycle length (ms)	112±2	116±3
AVERP (ms)	87±1	94±2 *
AVFRP (ms)	115±2	122±2 *
Right Atrial/AV node prep experiments		
AH interval (ms)	38.2±5	53.0±6 (p=0.09)
Incidence of CHB	0%	50% *
CV across crista terminalis (m/s)	0.49±0.04	0.37±0.03 *

* p<0.05, ** p<0.005.

Koskenvuo et al. (2010) *Int J Cardiovasc Imaging* **26**,509-518.

Where applicable, the authors confirm that the experiments described here conform with The Physiological Society ethical requirements.

PCB018

The effects of gastric afferent autonomic activity on cardiac efferent autonomic balance in healthy human volunteers

L.C. Kazadi, J. Fletcher and P. Barrow

Biomedical Science and Physiology, University of Wolverhampton, Wolverhampton, UK

Cardiovascular responses induced by drinking water are blood hypo-osmolality dependent, mediated by TRPV4 receptors in the periphery and osmoreceptors in the CNS acting through sympathetic autonomic efferents1,2, rather than being related to either blood volume loading, or gastric distension1. We investigated the effects of the temperature and hypoosmolality of ingested drinks on cardiovascular parameters in healthy human volunteers who ingested 300ml of either isotonic saline solution or water at either 37 or 6 0C (n=9, aged 24±3 years). Written informed consent was obtained, and the studies were approved by the University of Wolverhampton Life Science Ethics Committee. Factors known to alter autonomic balance were controlled. Following an acclimatisation period (≥20 min.), heart rate (HR) and blood pressure (BP) were continuously monitored using a Finapres device (Ohmeda Ltd). Lead 2 of 3-lead ECG and pneumotrace respiratory strap were used to record ECG and respiratory movements. Subjects' ventilation was paced at 0.2 Hz, to standardise ventilatory function. Recordings lasted for 2 hours and were separated by at least one week. Five minutes of baseline recording were made prior to drink ingestion, followed by 5 minute recordings as various intervals. Cardiac vagal and sympathetic tone were assessed offline using time and frequency domain analysis of R-R interval variability and analysis of corrected QT interval (QTc).Cold saline decreased HR for 110 minutes (mean 2.035±0.26 beats/min reduction, p<0.01, paired t-test), with an increase in parasympathetic tone (mean 14.68±3.67 msec increase in RMSSD, p<0.01, paired t-test), with a concomitant reduction in systolic BP up to 20 minutes after ingestion (mean 11.5423±3.53 mmHg reduction in SBP, p<0.1, paired t-test). Conversely the combined hypo-osmolarity and cold effects of drinking cold water decreased HR for only 40 minutes (mean 3.15±0.86 beats/min reduction, p<0.01, paired t-test), with an increase in parasympathetic tone (mean 25.68±3.63 msec increase in RMSSD, p<0.05, paired t-test) and a fall in systolic BP up to 20 minutes after the drink (mean 5.8±0.45 mmHg reduction in SBP, p<0.1, paired t-test). Analysis of QTc following cold water ingestion indicated a shortening of QTc up to 80 minutes (mean 9.71±0.94 msec reduction in Qtc, p<0.01, paired t-test)3 after which it lengthened (mean 1.38±0.67 msec increase in Qtc, p>0.05, paired t-test) indicating a possible cardiac sympathetic withdrawal in the short term, but sympathetic reintroduction over the longer term. We conclude that the ingestion of the cold saline drink caused an increase in cardiac parasympathetic autonomic tone up to 110 minutes, but this was truncated with cold water drinking due to sympathetically mediated hypo-osmolarity effects leading to CVS parameters returning to near-resting levels.

Brown, C.M., Barberini, A.G., Dulloo, A.G. and Montani, J-P. (2005) Cardiovascular responses to water drinking: does osmolality play a role? American Journal of Physiology. 289 1687-1692

Brierly, S. M., Page, A. J., Hughes, P. A., Adam, B., Liebregts, T., Cooper, N. J., Holtman, G., Liedtke, W. and Blackshaw, L. A. (2008) Selective role for TRPV4 ion channels in visceral sensory pathways. Gastroenterology 134 2059-2069

Magnano, A. R., Holleran, S., Ramakrishnan, R., Reiffel, J. A., Bloomfield, D. M. (2002) Autonomic Nervous System Influences on QT Interval in Normal Subjects. Journal of the American College of Cardiology 39 1820-6.

Where applicable, the authors confirm that the experiments described here conform with The Physiological Society ethical requirements.

PCB019

The transmembrane proteoglycan syndecan-4 regulates cardiac myofibroblast differentiation in response to pressure overload, affecting extracellular matrix composition and myocardial stiffness

K.M. Herum[1,2], I.G. Lunde[1,2], B. Skrbic[1,3], W.E. Louch[1,2], A. Hasic[1,2], I. Sjaastad[1,2], A. Unger[4], W.A. Linke[4], M.F. Gomez[5] and G. Christensen[1,2]

[1]Institute for Experimental Medical Research, Oslo University Hospital and University of Oslo, Oslo, Norway, [2]KG Jebsen Cardiac Research Centre and Center for Heart Failure Research, University of Oslo, Oslo, Norway, [3]Department of Cardiothoracic Surgery, Oslo University Hospital Ullevål, Oslo, Norway, [4]Department of Cardiovascular Physiology, Ruhr University Bochum, Bochum, Germany and [5]Department of Clinical Sciences, Lund University, Malmö, Sweden

Pressure overload of the heart leads to remodeling of the left ventricle involving hypertrophic remodeling of cardiomyocytes and excessive production of extracellular matrix by activated cardiac fibroblasts that differentiate into contractile myofibroblasts. This compromises heart function by increasing the myocardial stiffness. The molecular mechanisms underlying stress-induced myofibroblast differentiation and the role of this process in regulating cardiac stiffness are poorly defined. We recently identified the focal adhesion proteoglycan syndecan-4 as important for myofibroblast differentiation in response to mechanical stress. Here we investigate the role of syndecan-4 in regulating myocardial stiffness and left ventricular remodeling of the extracellular matrix in response to pressure overload.

Aortic banding, performed under anaesthesia, caused a ~6-fold increase in collagen I and III mRNA in the left ventricle of wild-type (WT) mice. Remarkably, this response was completely absent in mice lacking syndecan-4. mRNA levels of the collagen cross-linking enzyme lysyl oxidase (LOX) were also dramatically increased in WT left ventricles, whereas this response was blunted in syndecan-4 knock-out (KO) mice, suggesting a potentially impaired collagen cross-linking following mechanical stress in mice lacking syndecan-4. Supporting these findings, cardiac fibroblasts from syndecan-4 KO mice had lower expression of collagen I and III and LOX when plated on fibronectin in vitro, a model previously shown to induce myofibroblast differentiation. To assess the effect of syndecan-4 deletion on mechanical properties, we measured passive tension of muscle fiber bundles from left ventricular tissue of syndecan-4 KO mice. Passive tension was reduced in cardiac tissue from syndecan-4 KO mice compared to WT and increased in both genotypes following aortic banding, albeit to a lower degree in mice lacking syndecan-4. Salt extraction of myosin and actin filaments was performed to eliminate the effect of titin, a cardiomyocyte protein which is central in determining passive tension. Passive tension after salt extraction was affected equally in muscle fiber bundles from WT and syndecan-4 KO mice, indicating that the reduced passive tension in mice lacking syndecan-4 was due to alterations in the extracellular matrix and not changes in cardiomyocyte titin. Supporting this, no isoform shift of titin was detected in left ventricles of WT and syndecan-4 KO mice.

In conclusion, we demonstrate reduced passive tension in hearts of mice lacking syndecan-4, possibly due to inhibited differentiation of fibroblasts into myofibroblasts, reduced extracellular matrix production and attenuated collagen cross-linking.

Where applicable, the authors confirm that the experiments described here conform with The Physiological Society ethical requirements.

PCB020

AmphiphysinII controls t-tubule formation in cardiac muscle

J.L. Caldwell, D.A. Eisner, K.M. Dibb and A.W. Trafford

University of Manchester, Manchester, UK

Regular invaginations in the surface membrane of ventricular myocytes, known as transverse tubules (t-tubules), enable synchronous intracellular Ca release, facilitating contraction. Evidence shows t-tubules are remodelled in several models of heart failure (HF), leading to delayed asynchronous Ca release. It remains unclear how t-tubule structure and function change during cardiac disease. Previous data indicates a role for Amphiphysin (AMPII) where KO models of AMPII lead to t-tubule disruption, similar to observed in HF (1). We aim to investigate if a) t-tubules and AMPII are reduced in a sheep model of HF; b) t-tubule biogenesis depends on the presence of AMPII; c) loss of AMPII leads to asynchronous Ca release.

Under isoflurane anaesthesia (2-4% v/v oxygen) sheep were instrumented with a pacemaker and pacing lead. Post-operative analgesia (meloxicam 0.5mg/kg) and antibiosis (enrofloxacin 2.5mg/kg) were provided for 24hrs. HF was induced by right ventricular tachypacing at 210bpm for 4-5wks (2). Upon sacrifice, left ventricular (LV) and atrial (LA) myocytes were isolated and tissue samples were snap frozen. T-tubule density was assessed using di4ANEPPS and confocal microscopy (3). Data presented as mean±SEM statistical significance $p<0.05$ (t-test). The distance at which 50% of pixels in sheep HF cells are from a membrane compared with control increases (18±3.3% $p<0.05$ n=7). Western blotting on samples obtained from LV and LA showed a reduction in AMPII protein in HF (LV 24±7.5%, LA 35±12.3% n=7 $p<0.05$). Western blotting shows a reduction in AMPII in atria compared to ventricle in; rat, 58±6.7%, ferret, 55±9.8%, sheep, 27±9.6%, n=7.

Transfecting rat ventricular myocytes with siRNA against AMPII causes t-tubule loss. The distance at which 50% of pixels in target cells are from a membrane compared with scrambled cells increases 50±6.6% $p<0.05$ n=20. Western blotting on transfected cells shows AMPII reduces 14±3.2% $p<0.05$ n=18 in target cells, compared with scrambled. Pearson's coefficient performed on paired data shows the distance at which 50% pixels in target cells are from a membrane increases as AMPII decreases $p<0.05$ n=18. Immunocytochemistry was used to confirm loss of AMPII in transfected cells. Transfected cells, loaded with Fluo-3 AM and field stimulated, showed asynchronous Ca release. The STDEV of time to reach 50% peak fluorescence for each pixel of the line scan increases 159±43.8% $p<0.05$ n=9 in cells transfected with AMPII siRNA compared with cells transfected with scrambled siRNA.

AMPII protein expression is reduced in a sheep model of tachypacing induced HF in both atria and ventricle and in the atria of species that lack t-tubules. There is also a loss of t-tubules in cells transfected with siRNA against AMPII, suggesting AMPII plays a role in the maintenance of t-tubules. This reduction results in asynchrous Ca release, likely to cause reduced contractility and HF.

Reference 1) Muller AJ, Baker JF, DuHadaway JB, Ge K, Farmer G, Donover PS, Meade R, Reid C, Grzanna R, Roach AH, Shah N, Soler AP, Prendergast GC (2003). Targeted disruption of the murine Bin1/Amphiphysin II gene does not disable endocytosis but results in embryonic cardiomyopathy with aberrant myofibril formation. J Mol Cell Biol 23, 4295-306

Reference 2) Briston SJ, Caldwell JL, Horn MA, Clarke JD, Richards MA, Greensmith DJ, Graham HK, Hall MC, Eisner DA, Dibb KM & Trafford AW (2011). Impaired {beta}-adrenergic responsiveness accentuates dysfunctional excitation contraction coupling in an ovine model of tachypacing induced heart failure. J Physiol 589, 1367-1382.

Reference 3) Dibb KM, Clarke JD, Horn MA, Richards MA, Graham HK, Eisner DA, Trafford AW (2009). Characterization of an extensive transverse tubular network in sheep atrial myocytes and its depletion in heart failure. Circ Heart Fail 2, 482-9

Where applicable, the authors confirm that the experiments described here conform with The Physiological Society ethical requirements.

PCB021

Does the crista terminalis possess a key role in the elevated risk of arrhythmogenic episodes in the elderly population?

F.S. Hatch[1], M.K. Lancaster[2] and S.A. Jones[1]

[1]University of Hull, Hull, UK and [2]University of Leeds, Leeds, UK

We have previously reported changes in intracellular calcium handling and associated protein expression within the sinoatrial node (SAN) during ageing (Hatch et al, 2012; Jones et al, 2007). It is however unknown whether other parts of the conduction pathway within the atria, specifically the crista terminalis (CT) and right atrial (RA) muscle itself undergo similar changes. Implicated in atrial arrhythmia generation, changes in the properties of the CT may predispose to ectopic activity and arrhythmias such as atrial fibrillation. Therefore, our study examined the expression of calcium handling proteins across the right atria including the SAN and CT.
Male Wistar rats at the ages of 6 months (young) and 24 months (old) (n=5) were sacrificed by intraperitoneal anaesthetic overdose of pentobarbital. The right atrium was removed and dissected to isolate the CT, SAN and RA muscle. Western blot and immunocytochemistry were used to examine the protein expression of sarcoendoplasmic reticulum Ca2+ ATPase pump (SERCA2a), phospholamban (PLB), ryanodine receptors (RYR2), L-type calcium channels (Cav1.2) and the sodium-calcium exchanger (NCX1). Data are presented as mean±SEM, assessed by t-test or two-way ANOVA as appropriate. Ethical approval was given by the University of Hull.
When compared with the RA in the young animal; the CT consistently exhibited reduced expression of all calcium-regulatory proteins studied, whilst the SAN possessed reduced protein levels of RYR2 and NCX1. Ageing significantly decreased Cav1.2 protein expression by 40.3±2.6% in the SAN from old animals (p=0.009), but conversely in the CT ageing increased of Cav1.2 expression (64.4±3.9%; p=0.011). Similarly with age RYR2 protein levels fell by 32.0±0.2% within the SAN (p=0.03), but rose by 63.8±5.0% (p<0.001) in the CT from old animals. By contrast NCX1 expression remained the same for both ages in the CT, but was up-regulated by 72±13.5% in the aged SAN (p=0.009). SERCA2a regulation was assessed by the ratio of SERCA2a to monomeric PLB. In young animals there was no significant difference in the ratio across the SAN, CT or RA. Ageing evoked a significant decline in the ratio, 29±8.5% within the SAN and a larger reduction of 40±8.5% in the CT (p<0.001). In contrast, there was a non-significant drop of 12±4.5% in the RA.
In conclusion ageing had heterogeneous effects on the expression of calcium regulatory proteins across the right atria. The loss of calcium influx and release channels in the SAN is likely to lead to a reduction in the ability of the pacemaker to operate, despite a potential counter-effect of increasing NCX. In contrast the changes in the CT may increase the likelihood to form an ectopic pacemaker, destabilising the atria and increasing susceptibility to arrhythmias in old age.

Hatch F, Lancaster MK & Jones SA. Age-associated alterations in intracellular calcium handling within the sinoatrial node. Proc Physiol Soc 2012:28;C04&PC04

Jones SA, *et al.* (2007). Circulation **115**, 1183-90

Where applicable, the authors confirm that the experiments described here conform with The Physiological Society ethical requirements.

PCB022

Ageing further increases the diversification between the atria in the expression of cellular calcium regulators: a substrate for increased arrhythmia risk?

F.S. Hatch[1], J.S. Waby[1], M.K. Lancaster[2] and S.A. Jones[1]

[1]University of Hull, Hull, UK and [2]University of Leeds, Leeds, UK

At present ~20% of the Western population are over 65 years of age, and by 2050 this is predicted to increase to 25% [Cracknell, 2010]. The risk of atrial arrhythmias progressively increases in an age-dependent manner presumably due to structural and functional remodelling however the full details of this remains unknown. Our study has examined the effect of age on the protein expression of key calcium regulators and their mRNA expression across the atria.
Male Wistar rats at the age of 6 months (young) and 24 months (old) (n=5) were sacrificed by an intraperitoneal anaesthetic overdose of pentobarbital. The right atrium (RA) and left atrium (LA) of each heart were assessed for changes in sarcoendoplasmic reticulum Ca^{2+} ATPase pump (SERCA2a), phospholamban (PLB), ryanodine receptors (RYR2), L-type calcium channels (Cav1.2) and sodium-calcium exchanger (NCX1). Western blot and immunocytochemistry were used to identify changes in protein expression and quantitative PCR changes in mRNA levels. Data are presented as mean±SEM, assessed by t-test or two-way ANOVA as appropriate (p<0.05). Ethical approval was given by the University of Hull.
A comparison of atria in the young rat identified in the LA significantly higher protein levels of SERCA2a by 65.7±7.89% (p<0.001) and RYR2 60.7±8.09% (p<0.001), which correlated with elevated levels of mRNA in the LA for SERCA2a (92.2±7.8%; p=0.001) and RYR2 (27.5±4.8%; P=0.007). Ageing instigated a significant decline in all the investigated proteins within the RA; Cav1.2 fell by 46.4±6.2% (p=0.005), RYR2 by 25.7±4.11% (p=0.012), SERCA2a by 51.2±10.7% (p=0.009) and NCX1 by 57.1±3.63% (p=0.001), however there were no significant changes in their mRNA levels. In contrast the LA exhibited an increase of protein levels for Cav1.2 (52.5±2.5%, p=0.022) and NCX1 (27.5±2.9%, p=0.034), but in terms of mRNA levels only NCX1 significantly increased by 33.5±5.3% (p=0.005) with age. Data from immunocytochemistry reflected the data from western blot analysis. Comparing atria from the young animals, the ratio of SERCA2a to PLB monomer was significantly greater in the RA by 35.5±0.7% (p<0.001). Conversely considering each atrium and the effect of increased age, the ratio increased in the LA by 46±1.2% (p=0.001), but declined in the RA by 22±4.4% (p=0.01).
In conclusion, existing inter-atrial heterogeneity of cellular calcium regulation increases in old age. The fall in RA proteins might be expected to reduce potential systolic function in old age whilst the LA changes, which have some parallels with changes seen in heart failure, may predispose to arrhythmias

and calcium dysregulation. Combined these changes are a possible substrate for atrial fibrillation.

Richard Cracknell. The ageing population. Key issues for the new parliament 2010. In. Value for money in public services. House of Commons library Research, U.K. 2010, p. 45-46.

Where applicable, the authors confirm that the experiments described here conform with The Physiological Society ethical requirements.

PCB023

Characterization of small-conductance Ca2+-activated K+ channels in patients with chronic atrial fibrillation

M. Li, T. Li, H. Lan, L. Mao, X. Ou, C. Li, Y. Yang and X. Zeng

Key laboratory of medical electrophysiology, LuZhou, China

In 2003, Small-Conductance of Ca2+-activated K+ channels(SK) are first reported to present in Cardiac myocytes, which is expressed more abundant in the atria compared with the ventricles. Genetic knockout of the SK channels results in the delay in cardiac repolarization and showed inducible atrial fibrillation(AF). The purpose of this study was to confirm whether SK channels are involved in electrical remodeling of human chronic atrial fibrillation (CAF).The ionic currents were recorded using whole-cell Conventional patch clamp techniques(35 appendages from patients with SR and 18 appendages from patients with CAF). SK2 channel protein expressions were assayed by western blot technique(12 appendages from patients with SR and 24 preparations from patients with CAF). Our result indicate that SK channels present in patients atrial with SR Group and CAF Group,identified it with SK channel blocker apamin (100nmol/L) . SK channels are voltage-independent and inwardly rectifying . The SK channel current densities were significantly increased in CAF(n=24,[Ca2+]i=500nmol/L,p<0.05) compare to SR (n=49, [Ca2+]i=500nmol/L). The increased proportion of SK channel current densities in CAF(n=8,[Ca2+]i=1000nmol/L,p<0.05) were larger than in SR (n=10,[Ca2+]i=1000nmol/L). it manifested that SK is more sensitive to intracellular Ca2+ in CAF than in SR.Western bloting result demonstrated that SK2 protein level is significant decrease in CAF than in SR.Our results showed SK channels present in patients atrial with SR and CAF ;SK channel density in CAF were significantly increase than in SR.In patients with CAF, the SK channels are more sensitive to [Ca2+]i. Compared with SR,the protein level of SK2 was down-regulation in Patients atrial with CAF.these results indicated the increase densities of SK channel in CAF maybe depend on the more sensitive to [Ca2+]i and higher intracellular Calcium level,which lead to increase channels activity,not by the numbers of channels.It might be one of the treatment targets of patients with Atrial Fibrillation,involving in human atrial electric remodeling in CAF.

Where applicable, the authors confirm that the experiments described here conform with The Physiological Society ethical requirements.

PCB024

Investigation of the interaction between flecainide and hERG potassium channels, through the use of flecainide analogues

D. Melgari[1], A. El Harchi[1], C.E. Dempsey[2] and J.C. Hancox[1]

[1]School of Physiology and Pharmacology and Cardiovascular Research Laboratories, University of Bristol, Bristol, UK and [2]School of Biochemistry, University of Bristol, Bristol, UK

Flecainide is a Class Ic (Na+ channel blocking) antiarrhythmic drug widely use in clinical treatment of atrial fibrillation that has been associated with an increased risk of arrhythmic events in post-myocardial infarction patients (Echt et al., 1991). In addition to its Na+ channel blocking activity, flecainide can inhibit hERG K+ channels at clinically relevant concentrations (Paul et al., 2002; Du et al., 2011; Breindahl et al., 2000). Flecainide's potency against hERG is reduced both by extracellular acidosis (as occurs in myocardial ischaemia) and when the drug is applied directly from the intracellular side of the membrane (Du et al., 2011). This study was conducted to gain greater insight into the interaction between flecainide and hERG, by using charged and uncharged flecainide analogues (Liu et al., 2003). Neutral (NU-Flec; pKa 6.3) and fully charged (QX-Flec) flecainide analogues (ASCENTTM Scientific) were tested in whole cell patch-clamp experiments performed at 37oC on HEK293 cells stably expressing hERG. hERG current (IhERG) tails were measured at -40mV after a 2 sec depolarizing step from -80mV to +20mV (N≥5 at each concentration). Normal flecainide produced concentration-dependent inhibition of IhERG with an IC50 value of 1.69μM (CI:1.44-1.99) and a corresponding Hill coefficient of 0.82 (CI:0.70-0.94). When applied extracellularly both analogues showed a slowed, less extensive blocking action compared with flecainide: 6 minutes of continuous superfusion with 100μM NU-Flec inhibited IhERG by only 49.9±4.3% (n=10); while 100μM QX-Flec produced an IhERG inhibition of 45.5±3.5% (n=10). Differences between the two analogues were observed when they were applied to the cell interior via the patch pipette. 100μM of pipette- applied NU-Flec produced little effect on IhERG density (p>0.5, t-test, unpaired comparison); while 10μM or 100μM of internally applied QX-Flec produced a fast and extensive current density reduction of ~80% and ~97% respectively. One interpretation of these findings is that both charged and uncharged flecainide can cross the membrane, but that the charged form seems to be mainly involved in the physical interaction and block of hERG channels from the cytosolic side of the cell membrane.

Breindahl T (2000). J Chromatog B Biomed Sci Appl 746(2):249-54

Du CY et al. (2011). J Cardiovascular Electrophysiol 22(10):1163-70.

Echt DS et al. (1991). N E J M 324(12):781-8.

Liu H et al. (2003). J Gen Physiol 121(3):199-214.

Paul AA et al. (2002). Br J Pharmacol 136:717-29.

Where applicable, the authors confirm that the experiments described here conform with The Physiological Society ethical requirements.

PCB025

Fat tissue remodelling in persistent atrial fibrillation – 3D quantitative analysis using high-resolution magnetic resonance imaging

C.M. Afonso[1,2], B. Maesen[3,4], R.B. Burton[5], S. Zeemering[4], D.J. Stuckey[5], D.J. Tyler[5], U. Schotten[4], P. Kohl[2,6] and V. Grau[1]

[1]Oxford e-Research Centre and Institute of Biomedical Engineering, University of Oxford, Oxford, UK, [2]The Heart Science Centre, National Heart and Lung Institute, Imperial College London, Harefield, UK, [3]Department of Cardiothoracic Surgery, Maastricht University Hospital, Maastricht, Netherlands, [4]Department of Physiology, Maastricht University, Maastricht, Netherlands, [5]Department of Physiology, Anatomy and Genetics, University of Oxford, Oxford, UK and [6]Department of Computer Science, University of Oxford, Oxford, UK

MOTIVATION: Atrial fibrillation (AF) is a cardiac arrhythmia characterized by a fast and irregular electrical activity in the atria. Highly prevalent (1–5%) and associated with a doubling of mortality and substantial morbidity, AF represents a high socio-economic burden [1]. The unsatisfactory efficiency of AF treatments demands a better understanding of the disease. AF is a complex disease, usually resulting from the interplay of several factors. One of the main factors is structural remodelling, which contributes to the accommodation and progress (paroxysmal to persistent to permanent) of AF itself [2]. One of the less studied structural changes is the increase in fat tissue. Available studies have only analysed the epicardium at relatively low resolution [3]. In this study, we analyse the accumulation of fat tissue in persistent AF, in the 3D structure of the goat left atrial wall (epicardium to endocardium) at unprecedented resolution. METHODS Tissue samples: In open chest experiments, left atrial wall tissue samples were excised maintaining tissue-pretension using rigid clip-on frames from two goat groups: persistent AF (5 goats) and control (6 goats). Persistent AF goats had been under AF for a period of 7 to 12 months. The collected tissue was stored in Karnovky's fixative solution (2% paraformaldehyde, 2.5% glutaraldehyde in 0.1M sodium cacodylate buffer). Magnetic resonance imaging (MRI): Fixed tissue samples were preconditioned in gadolinium-containing (2mM) cacodylate buffer and then stabilised in an MRI tube using low melting 1% agar (Cambrex, Busieve GTG agarose). MRI scans were performed using a vertical-bore, 11.7 Tesla MR system with a Bruker console, a 40mm quadrature-driven birdcage coil (Rapid Biomedical, Würzburg, Germany), and a 3D fast gradient echo sequence: TE/TR 1.8/15ms, 15° pulse, field of view 40mm×40mm×40mm, matrix size 512×512×512, voxel size 78μm×78μm×78μm, and 10 averages. Image processing: MRI images were aligned in an epi- to endocardium view using a 3D rigid transformation. Thresholding and morphological operations were used to first correct the MRI background inhomogeneities, then segment tissue from the background, and finally segment fat from other tissue types. Validation of the fat segmentation was done using whole-mount pictures of tissue samples after excision and trichrome-stained histological slices (for details of histology see [4]). RESULTS and CONCLUSIONS We developed a method to successfully segment fat tissue in MRI data of atrial tissue samples. We are currently quantifying and comparing the accumulation of fat tissue in persistent AF versus control. Preliminary results suggest a larger volume of fat in AF then in control; and its preferential accumulation in near-epicardial layers. We will present the final analysis at the IUPS 2013 congress.

[1] V. Fuster et al; 2011 ACCF/AHA/HRS focused updates incorporated into the ACC/AHA/ESC 2006 guidelines for the management of patients with atrial fibrillation: a report of the American College of Cardiology Foundation/American Heart Association Task Force on practice guidelines; Circulation 123 (10), e269-367, (15 Mar 2011).

[2] U. Schotten et al; Pathophysiological mechanisms of atrial fibrillation: a translational appraisal; Physiol. Rev. 2011;91:265–325.

[3] O. Batal et al; Left atrial epicardial adiposity and atrial fibrillation; Circ. Arrhythm. Electrophysiol. 2010 Jun;3(3):230-6. Epub 2010 May 26.

[4] R. A. B. Burton et al; Three-Dimensional Models of Individual Cardiac Histoanatomy: Tools and Challenges; Ann. N.Y. Acad. Sci. 1080: 301–319 (2006).

Where applicable, the authors confirm that the experiments described here conform with The Physiological Society ethical requirements.

PCB028

The β3 agonist BRL37344 mediates a negative inotropic effect in rat atrial cells

C.L. Sam[1,2], T.B. Bolton[2], I.T. Piper[1], M. Al-Jobarah[1] and N.S. Freestone[1]

[1]Faculty of Science, Engineering and Computing, Kingston University, Surrey, UK and [2]Biomedical Division, St George's, University of London, London, UK

A third cardiac β-adrenoceptor (AR) has been reported in ventricular cells from a number of species including humans (Gauthier *et al.*, 1998). This receptor has been shown to mediate negative inotropic effects unlike the other β-ARs of the heart. BRL37344 is a β3 agonist and upon its stimulation of the β3-AR, the Gi sub-unit is activated which leads to production of nitric oxide (NO) by endothelial nitric oxide synthase (eNOS). The production of NO activates guanylate cyclase (GC) which catalyses the production of cGMP. An increase in cGMP levels activates protein kinase G (PKG) and calcium (Ca^{2+}) entry via the L-type Ca^{2+} channel is inhibited hence causing the cardioinhibitory effects. Due to the negative inotropic effect of BRL37344, investigations of its expression during heart failure have been carried out. It has been shown that these receptors are up-regulated in such circumstances to protect the heart from excess catecholamines (Moniotte *et al.*, 2001). In this study we have used BRL37344 in quiescent WKY rat atrial cells to investigate its effect on Ca^{2+} spark frequency. Atrial cells from WKY rats were loaded with fluo-4AM (5μM) and whole cell and line scan mode images of Ca^{2+} events within these cells were obtained every 3ms using an LSM 510M confocal microscope. Cardiomyocytes were perfused with BRL37344 (300nM) in the presence and absence of a β-blocker, propranolol (200nM). It was discovered that the frequency of Ca^{2+}sparks decreased significantly in the presence of BRL37344 (and propranolol) compared to propranolol on its own (15.4 ± 3.3 sparks s^{-1} compared to 29.3 ± 6.4 sparks s^{-1} respectively ($n = 6$, $p = 0.05$). No larger Ca^{2+} events such as non-propagating wavelets or whole cell waves were observed. Furthermore, when the quiescent atrial cells were perfused with only BRL37344 the mean frequency of Ca^{2+} sparks tended to decrease compared to basal conditions (14.5 ± 2.4 spark s^{-1} to 22.0 ± 3.0 sparks s^{-1} respectively ($n = 5$, $p = ns$). Furthermore, atrial cells under basal conditions expressed on average 1.07 ± 0.24 wavelets s^{-1}. The reduction observed in intracellular Ca^{2+} release events with BRL37344 was due to β3-ARs stimulation, mediated by a PKG-dependent pathway. The neg-

ative inotropic effect of BRL37344 observed in rat atrial cells is associated with fewer spontaneous Ca^{2+} release events.

Gauthier C., Leblais V., Kobzik L., Trochu J.N., Khandoudi N., et al., The negative inotropic effect of β3-adrenoceptor stimulation is mediated by activation of a nitric oxide synthase pathway in human ventricle. *Journal of Clinical Investigation* 1998 ; **102** (7) : 1377-1384.

Moniotte S., Kobzik L., Feron O., Trochu J-N., Gauthier C and Ballingand J-L., Upregulation of β-adrenoceptors and altered contractile response to inotropic amines in human failing myocardium. *Circulation* 2001 ; **103** : 1649-1655.

Dr Oleksandr Povstyan for his assistance on the confocal microscope

Where applicable, the authors confirm that the experiments described here conform with The Physiological Society ethical requirements.

PCB029

Differences in intracellular calcium handling in rabbit atrial and ventricular myocytes

H.C. Gadeberg, C.H. Kong, M.B. Cannell and A.F. James

University of Bristol, Bristol, UK

Atrial myocytes differ from ventricular myocytes in ultrastructure and calcium handling proteins and consequently show subtle differences in calcium signalling. However there is little quantitative information characterising atrial calcium signalling. This study compares atrial and ventricular calcium transport focussing on the removal of calcium from the cytosol by sarcoplasmic Ca-ATPase (SERCA).

All procedures were approved by the University of Bristol ethics committee and conformed to the Animals (Scientific Procedures) Act, 1986. Rabbit atrial and ventricular myocytes were isolated by enzymatic digestion. Isolated cells were loaded with fluo-4, electrically stimulated at 1 Hz and line-scan images acquired using a Zeiss Pascal LSM5 laser-scanning confocal microscope. Rates of decay were obtained by fitting the recovery phase of calcium transients with a single exponential decay. Electrical stimulation of atrial and ventricular cells resulted in calcium transients, which were homogenous across the cell in ventricular myocytes, but were consistent with preferential coupling between calcium entry and release at the edge in atrial cells. However, there was no significant difference in the rate of recovery (k_{twitch}) of the spatially averaged calcium transients in atrial (1.8 ± 1.1 s^{-1}, n=18) and ventricular myocytes (1.5 ± 1.1 s^{-1}, n=11, P=0.21 un-paired t-test). Application of 10 mM caffeine, to release calcium from the sarcoplasmic reticulum and prevent its subsequent re-uptake, significantly slowed the rate of recovery (k_{caff}) in both cell-types. However, whereas k_{caff} was 50.0 ± 5.7% (n=11) of k_{twitch} in ventricular cells, k_{caff} was 14.4 ± 1.2% (n=19) of k_{twitch} in atrial myocytes, indicating that SERCA plays a greater role in the removal of calcium in atrial cells than in ventricular cells. When 10 mM Ni was applied in the presence of caffeine to block Na/Ca exchanger, further slowing of the rate of recovery (k_{Ni}) was observed in both cell types, although to a much larger extent in atrial cells. That k_{Ni} was faster in ventricular cells suggests that other slow pathways contribute more to calcium extrusion in these cells. To confirm the greater role of SERCA in atrial cells, the SERCA inhibitor thapsigargin (TG) was applied during electrically-stimulated calcium transients. Rate constants in the presence of 5 μM TG were significantly reduced in both atrial and ventricular cells, representing 16.8 ± 3.1% of k_{twitch} (n=6) in atrial compared with 49.7 ± 7.2% (n=8) in ventricular cells, consistent with the caffeine data. In summary, the data presented here indicate a greater contribution of SERCA to calcium extrusion in atrial cells compared to ventricular cells and highlights important differences in atrial and ventricular calcium signalling.

Where applicable, the authors confirm that the experiments described here conform with The Physiological Society ethical requirements.

PCB030

Alterations to secreted levels of extracellular matrix moderators in young and aged ovine cardiac fibroblasts

M.A. Horn and A.W. Trafford

Unit of Cardiac Physiology, University of Manchester, Manchester, UK

Heart failure is characterised by an increase in circulating catecholamine levels and alterations to the cardiac extracellular matrix (ECM) – the latter of which we have found to be strongly influenced by age (1). Despite this association little is known regarding how β-adrenergic signalling modulates cardiac fibroblast (CF) – dependent remodelling of the ECM. The aims of this study were; i) determine if β-adrenergic stimulation of CFs alters production of matrix metalloproteinases (MMPs) and the tissue inhibitors of MMPs (TIMPs) and, ii) determine whether these secreted levels change with age.

Female Welsh Mountain ewes aged either 18 months (young) or >8 years (aged) were killed by intravenous administration of 200 mg.kg-1 pentobarbitone sodium following 10,000 U of heparin. CFs were isolated from LV samples (~0.5g) by incubation with 1,000 U/ml collagenase type II (Worthington) for 90mins. Primary cultures were maintained at 37oC, 5% CO2. CF proliferation was measured at passage 3 using a CyQUANT Direct Cell Proliferation Assay kit (Life Technologies). Confirmation that isolated cells were CFs and that they expressed the β2-adrenoreceptor (β2-AR) was carried out by immunostaining. At passage 4, 2x10e6 cells were seeded in 225cm2 culture flasks, serum-starved for 24h, and then media replaced with that containing either PBS (control), 0.1, 1 or 10μM isoprenaline (ISO) for 48h. After which, conditioned-media was collected, concentrated with centrifugal filters (Millipore) and assessed for MMP activity (gelatin zymography) and TIMP proteins (immunoblotting). In these experiments, each sample was run in triplicate and data expressed as a mean change ± standard error of the mean and normalised to vimentin protein level in cell pellet extracts. All statistical comparisons were made using a 2-way repeated measures analysis of variance, apart from the proliferation assay where a t-test was performed.

All cells isolated were positive for the fibroblast marker vimentin. CFs also expressed the β2AR. Proliferation was increased in aged CFs compared to young (P<0.05, n=9 young & 6 aged). Overall, MMP-2 activity in the CF conditioned media was less after treatment with 1μM compared to 0.1μM ISO (P<0.01, n=4 young & 4 aged). Although TIMP-1 protein levels were unchanged with either ISO or ageing, TIMP-2 protein was diminished after treatment with both 1 and 10μM ISO in both the young and the aged CFs (all P<0.01, n=4 young & 4 aged).

These initial experiments suggest that β-adrenergic signalling may play a role in ECM remodelling by altering levels of key players in matrix remodelling, but ageing has little effect on these changes.

All procedures accord to The UK Animals (Scientific Procedures) Act, 1986.

Horn MA, Graham HK, Richards MA, Clarke JD, Greensmith DJ, Briston SJ, Hall MCS, Dibb KM & Trafford AW. Age-related divergent remodeling of the cardiac extracellular matrix in heart failure: Collagen accumulation in the young and loss in the aged, J Mol Cell Cardiol (2012), 53: 82-90.

This work was supported by the British Heart Foundation.

Where applicable, the authors confirm that the experiments described here conform with The Physiological Society ethical requirements.

PCB031

The influence of estrogen on circadian rhythms of body temperature and heart rates in female rats

S. Marui, M. Matsuda and K. Nagashima

Human Sciences, Waseda University, Saitama, Japan

Purpose We aimed to assess influence of estrogen on circadian rhythms of body temperature, heart rates and physical activity, in addition to expression of β-adrenoceptor of the heart. ***Methods*** Under general anesthesia with isoflurane, female Wistar rats (7 wk of age, n = 14) were bilaterally ovariectomized, and implanted a telemetry device for measurements of body temperature (Tb), physical activity (Act), and electrocardiogram (ECG) in the abdominal cavity. Two silicon tubes (o.d., 1.57; and length 30 mm) containing 17β-estradiol were subcutaneously placed for one group (n=7, E2(+)), empty tubes for the other (n=7, E2(-)). The tubes were removed 10 days after the surgery. On Days 7 and 21 after the removal, the heart was excised, and the cell membrane of the atrium and ventricle of the heart was prepared for the determination ofβ-adrenoceptor (Western blotting). Tb, Act, and ECG were continuously monitored during the period. ***Results*** Before the tube removal, Tb was lower (P<0.05) in the E2 (-) group than that in E2 (+) group, but only at 0:30-1:00 am (37.4 ± 0.1°C and 38.0 ± 0.3°C, respectively), which was not seen on Day 15. Before the tube removal, heart rates (HR) in the E2 (-) group were greater (P<0.05) than those in the E2(+) group (387 ± 14 and 336 ± 13 beats/min (bpm) in the light phase, and 450 ± 11 and 389 ± 11 bpm in the dark phase, respectively). HR in E2(+) group increased (349 ± 11, 375 ± 13, and 377 ± 13 bpm in the light phase; and 422 ± 13, 436 ± 13, and 425 ± 16 bpm in the dark phase on Days 1, 7, and 15, respectively). Difference in HR became unclear on Day 15. The expression of β-adrenoceptor of the heart was changed with plasma estrogen level. ***Conclusion*** Estrogen level may affect circadian rhythms of body temperature and heart rates, in which independent mechanism seems to be involved. Moreover, estrogen may influence expression ofβ-adrenoceptor of the heart and HR change after ovariectomy.

Where applicable, the authors confirm that the experiments described here conform with The Physiological Society ethical requirements.

PCB032

Prevention of β-adrenergic myocardial damage by α-linolenic acid enriched diet

A. Folino[2], A.E. Sprio[2], G.N. Berta[2], G. Losano[1] and R. Rastaldo[2]

[1]Dpt. Neuroscience, University of Turin, Torino, Italy and [2]Dpt. Clinical and Biological Sciences, University of Turin, Orbassano, TO, Italy

An increased sympathetic discharge affects the heart since the early stage of a failure. If initially it compensates the reduced cardiac output, its long term effect results in myocardial fibrosis and hypertrophy with worsening of the failure. The damage can be prevented by ω-3 fatty acids. such as docosahexaenoic (DHA), eicosapenaenoic (EPA) and α-linolenic acid (ALA) (1,2). While DHA and EPA are found in fishes, ALA is present in various vegetables included flaxseeds. A flaxseed enriched diet is reported to prevent the appearance of myocardial fibrosis in δ-sarcoglycan-null cardiomyopatic hamsters (2). We studied whether this diet can prevent myocardial fibrosis and hypertrophy in rats treated with isoproterenol (ISO). Wistar rats were divided in 3 groups: Control group (CTR; n=7) after 7 days of acclimatization rats underwent a daily subcutaneous injection of saline (0.5 ml) for 5 days and were fed with a standard pellet chow; ISO group (n=7+7) rats received 100 mg/kg of ISO instead of saline and were fed as CTR; ISO+ALA group (n=7) rats received ISO, but were fed with an ALA enriched diet before, during and after ISO. For all groups the observation lasted 60 days after the end of ISO treatment. Then surviving rats were anaesthetized with peritoneal injection of ketamine (100 mg/kg) and xylazine (5 mg/kg), heparinised (200 IU) and decapitated. The hearts were excised and weighted. Data are expressed as means±SD. One-way ANOVA was used. Seven rats of ISO group died during treatment. Thus 7 additional rats were added to have the same number of hearts to examine in all groups. ALA enriched diet prevented the ISO-induced death. Heart/body weight ratio was 0.32±0.2% in CTR. It increased in ISO group to 0.41±0.15% (p<0.01), while it was unchanged in ISO+ALA. In ISO group, histology (n=4 each group in triplicate) revealed a remarkable production and deposition of collagen, with an increase in the cross sectional area of myocytes from 199±3 μm^2 in the CTR to 250±10 μm^2 (p<0.001). NO change was observed in ISO+ALA.

Western blot analysis (n= 3 each group in triplicate) showed the following changes in ISO group with respect to CTR: 4 time increase (p<0.001) of Transforming Growth Factor-β (TGF-β) expression; reduction by about 25% (p<0.05) of Tissue inhibitor of metalloproteinase 1 (TIMP1) expression; increase by more than 3 times of β-myosin concentration (p<0.001). The changes were not observed in ISO+ALA. Zymography revealed that the activity of both latent and active forms of Metalloproteinase2 (MMP2) increased by about 50% (p<0.05 and p<0.001 respectively) in ISO group. In conclusion, ALA prevents cardiac fibrosis by abolishing the changes in TGF-β, TIMP1 and MMP2 expression induced by β-adrenergic hyperactivity. Moreover, since hypertrophy is related to the increase of TGF-β, it is likely that its prevention by ALA takes place by limiting the expression of this cytokine.

Duda MK et al (2009). Cardiovasc Res 1, 33-41.

Fiaccavento R et al (2006). Am J Pathol 169, 1913-1924.

Where applicable, the authors confirm that the experiments described here conform with The Physiological Society ethical requirements.

PCB033

Cardiac remodeling in obese and non-obese insulin resistant rat models

J. Huang and L. Hung

Chang Gung University, Tao-Yuan, Taiwan

Currently, increasing attention has been paid to insulin resistance as a distinct cause of cardiac dysfunction, cardiomyopathy and heart failure (HF) in diabetic individuals. Therefore, the present study aims to explore the pathogenesis and reciprocal causal relationships between insulin resistance and cardiomyopathy/HF in two obese and non-obese insulin resistant animal models (SD rat). Here, we have created obesogenic diet (45% calorie from fat) induced obese, and atherogenic diet (4% cholesterol) with 10% fructose in drinking water induced non-obese animal models. Both obese and non-obese animals have developed insulin resistance syndrome compared to age-matched controls. Euglycemic-Hyperinsulinemic Clamp technique indicated that the obese animal exhibited insulin resistance (IR). In addition, obese rats accompany with hyperinsulinemia, activation of neurohumoral systems, concentric hypertrophy with slightly impairment of cardiac mechanical performance (Pressure-Volume catheter), fewer changes in both plasma and myocardial metabolites profiling (LC-MS metabolites analysis) compared to non-obese IR rats. In contrast, less insulin resistance, hypoinsulinemia, hyperactivity of neurohumoral systems, eccentric hypertrophy with worse mechanical performance, robust changes in both plasma and myocardial metabolites profiling have been found in non-obese IR rats. In our animal models demonstrate that obese IR heart switched on the physiological adaptation and remodeling in the face of obese and insulin resistant stimuli. Whereas non-obese IR heart seems switched on the pathological adaptation and remodeling, and this adaptive eccentric hypertrophy was consequent detrimental to cardiac function. Our study indicated that insulin resistance but not obesity plays a pivotal role in development of cardiomyopathy. Insulin resistance disturbs systemic metabolic homeostasis may precipitate cardiac maladaptation and remodeling which may consequently lead to evolution of cardiomyopathy.

Where applicable, the authors confirm that the experiments described here conform with The Physiological Society ethical requirements.

PCB034

Unaltered mitochondrial organization and compartmentation in creatine deficient GAMT-/- mouse cardiomyocyte

J. Branovets[1], M. Sepp[1], S. Kotlyarova[1], N. Jepihhina[1], N. Sokolova[1], D. Aksentijevic[2], C.A. Lygate[2], S. Neubauer[2], M. Vendelin[1] and R. Birkedal[1]

[1]Laboratory of Systems Biology, Institute of Cybernetics, Tallinn University of Technology, Tallinn, Estonia and [2]Department of Cardiovascular Medicine, Wellcome Trust Centre for Human Genetics, University of Oxford, Oxford, UK

Creatine kinase (CK) is considered an important spatial and temporal energy buffer in the heart. It catalyzes the transfer of a phosphoryl group between creatine and ATP. Previous studies suggest that mice lacking cytosolic and mitochondrial CK exhibit cytoarchitectural modifications and changes in regulation of mitochondrial respiration in the heart. The aim of this study was to asses whether similar changes occurred in creatine-deficient mice lacking the creatine synthesizing enzyme guanidinoacetate methyltransferase (GAMT). More specifically, we wanted to characterize the modifications in cardiomyocyte mitochondrial organization, regulation of respiration and intracellular compartmentation associated with inhibition of the CK system by GAMT-deficiency. Mice received an i.p. injection of 250U heparin, and were anesthetized with ketamine/dexmedetomidine mixture (150 mg/kg and 0.5mg/kg, i.p.respectively). Cardiomyocytes were successfully isolated from 8 GAMT-/- (4 females and 4 males) and 9 WT mice (5 females and 4 males) of similar age (females WT 46.9 ± 4.9 weeks and GAMT-/- 45 ± 4.3 weeks; males WT 45.6 ± 1.5 weeks and GAMT-/- 45.9 ± 1.4 weeks). Three-dimensional mitochondrial organization at whole cell level was assessed by confocal microscopy.Kinetic measurements on permeabilized mouse cardiomyocytes included ADP and ATP-kinetics of respiration, the competition between mitochondria and pyruvate kinase for ADP produced by ATPases, ADP-kinetics of endogenous pyruvate kinase and ATP-kinetics of ATPases. Using fluorescence microscopy, ADP-kinetics of respiration was confirmed on single permeabilized cardiomyocytes by recording autofluorescence response to changes in ADP. The experimental results were analyzed by mathematical models to estimate intracellular compartmentation. Quantitative analysis of the morphologic and kinetic data, as well as derived model fits showed no difference between GAMT-deficient and wildtype littermates. Thus, we conclude that inhibition of the CK-system by GAMT-deficiency does not alter mitochondrial organization, regulation of respiration and intracellular compartmentation in relaxed cardiomyocytes. This raises questions on the importance of the CK system as a spatial energy buffer facilitating the communication between mitochondria and ATPases in cardiomyocytes.

We wish to acknowledge Prof. Dirk Isbrandt (University of Hamburg, Germany) for generating the strain of GAMT-deficient mice. This research was funded by The Wellcome Trust (Fellowship no. WT081755MA), European Union through the European Regional Development Fund, the Estonian Science Foundation (grant no. ETF8041), and by British Heart Foundation grant RG/10/002/28187.

Where applicable, the authors confirm that the experiments described here conform with The Physiological Society ethical requirements.

PCB035

Ivabradine reverses the extracellular matrix changes and affects fibroblast number and phenotype in heart failure

P. Dias, M. Navaratnarajah, P. Sarathchandra, S. Alayoubi, J.E. Cartledge, N. Latif, M.H. Yacoub and C.M. Terracciano

National Heart and Lung Institute, Imperial College London, London, UK

In the failing heart, the extracellular matrix (ECM) undergoes structural remodelling with changes in the accumulation and organisation of ECM proteins. Ivabradine (IVA) an inhibitor of the pacemaker (If) current has been shown to have beneficial effects in the structure and function of the failing heart including the reversal of myocardial fibrosis. However, whether IVA alters the expression of specific ECM proteins during the progression of heart failure (HF) is unknown. In addition, changes in the fibroblast number and phenotype before and after IVA

treatment have not been studied. HF was induced by permanent coronary artery ligation in rats anaesthetized with Isoflurane. Sham-operated animals (S) were used as controls. After 12 weeks, HF (HF-12) animals (ejection fraction<40%) were treated either with oral IVA (HF-IVA) (10mg/kg/day) or saline (HF-S) for a further 4 weeks. Values are presented as means±S.E.M. and compared by an ANOVA. Using immunofluorescence and confocal microscopy, sections were studied for specific ECM proteins and the percentage area fraction was quantified on 8-10 fields per section (3-4 hearts per group) using ImageJ software. IVA significantly reduced the levels of collagen I (S: 0.76±0.07%, n=69; HF-12: 1.12±0.08%, n=57; HF-S: 1.59±0.12%, n=70; HF-IVA: 0.68±0.06%, n=52; $p<0.05$), collagen III (S: 0.88±0.06%, n=78; HF-12: 1.26±0.09%, n=90; HF-S: 1.91±0.13%, n=74; HF-IVA: 0.75±0.65%, n=60; $p<0.05$) and elastin (S: 0.62±0.06%, n=52; HF-12: 1.16±0.06%, n=85; HF-S: 1.93±0.22%, n=68; HF-IVA: 0.52±0.09%, n=29; $p<0.05$) compared with HF-12. Vimentin, a marker for cardiac fibroblasts was measured using western blotting. IVA reduced the vimentin expression observed in HF-S to sham levels (in arbitrary units, S: 0.33±0.04, n=5; HF-S: 0.59±0.05, n=6; HF-IVA: 0.37±0.02, n=5; $p<0.05$). Since vimentin is also expressed in endothelial cells, von Willebrand factor (vWf) was measured. No change in vWf was observed suggesting that endothelial cell number was not affected. α-smooth muscle actin, a marker used to identify myofibroblasts but also present in smooth muscle cells, was also measured. IVA normalised the levels of α-smooth muscle actin to sham levels (S: 0.50±0.13, n=5; HF-S: 1.00±0.13, n=6; HF-IVA: 0.44±0.08, n=4; $p<0.05$). Expression of the hyperpolarisation-activated cyclic nucleotide-gated channel isoform 4 which encodes the If channels was up-regulated during HF but IVA down-regulated this overexpression (S: 0.31±0.05, n=5; HF-S: 0.57±0.05, n=6; HF-IVA: 0.38±0.05, n=5; $p<0.05$). Our results demonstrate that IVA reverses the accumulation of several components of the ECM and reduce fibroblast number and phenotype which may explain the changes observed in the ECM. Thus IVA appears to play a beneficial role in the structural integrity of the ECM which can be important in the reparative process of the failing heart.

Where applicable, the authors confirm that the experiments described here conform with The Physiological Society ethical requirements.

PCB036

Electrophysiological remodelling in response to chronic mechanical load variations: A multicellular study

S. AlAyoubi[1,2], M. Ibrahim[1], J. Cartledge[1], M.H. Yacoub[1], C.M. Terracciano[1] and P. Camelliti[1]

[1]National Heart & Lung Institute, Imperial College, London, UK and [2]King Fahad Cardiac Center, King Saud University, Riyadh, Saudi Arabia

Chronic variations in load are clinically relevant as mechanical overload can result in heart failure and unloading with left ventricular assist devices is used in the management of patients with heart failure. Previous studies have investigated the effect of chronic load variation on the electrophysiological properties of the left ventricle using isolated cardiomyocytes and whole hearts. Here, we study the load-dependent remodeling using myocardial slices, an intact multicellular preparation that allows the investigation of functional and structural regional heterogeneities.

Lewis rats were anaesthetized with isoflurane and pressure overload was induced by transverse aortic constriction (TAC) for 10 and 20 weeks. Sham-operated animals (S) served as control. Mechanical unloading (MU) was obtained by heterotopic abdominal heart-lung transplantation for 8 weeks. The recipient's native heart acted as control. Vibratome-cut myocardial slices (350μm thick) were prepared from the left ventricle, tangentially to the epicardial surface. Slices were electrically stimulated and studied using a multi-electrode array (MEA) system. Extracellular field potentials, recorded from 60 MEA microelectrodes, were analysed to measure field potential duration (FPD) - an index of action potential duration. Conduction velocity (CV) was also measured. Values are mean ± S.E.M., compared by t-test.

The measurement of heart weight/body weight ratio confirmed the presence of hypertrophy in the TAC group (10 weeks: 4.9±0.2, n=5; S: 3.8±0.1, n=5; $p<0.01$, 20 weeks: 4.1±0.2; n=4; S: 3.1±0.1 n=5; $p<0.05$) and atrophy in the unloading group (MU: 1.4±0.1, n=3; control: 3.5±0.1, n=3; $p<0.05$). Myocardial slices prepared from the TAC group showed significantly faster CV compared with the SHAM group at 10 weeks (TAC: 49±4 cm/s, n=25 slices; S: 35±4 cm/s, n=17 slices; $p<0.05$) but no significant change at 20 weeks (TAC: 67±10 cm/s, n=17 slices; S: 56±6 cm/s, n=22 slices; $p>0.05$). FPD did not change at 10 weeks TAC (TAC: 124±3 ms, n=16 slices; S: 122±2 ms; n=13 slices; $p>0.05$), but was significantly prolonged at 20 weeks (TAC: 122±2 ms, n=18 slices; S: 114±3 ms, n=20 slices; $p<0.05$). Slices obtained from the MU group showed significantly prolonged FPD (MU: 116±2 ms, n=11 slices; control: 108±2 ms, n=13 slices; $p<0.05$), but unchanged CV (MU: 30±3 cm/s, n=10 slices; control: 32±5cm/s, n=13 slices; $p>0.05$). Our data show that chronic mechanical overloading temporarily increases CV with delayed repolarisation. The latter is also observed during unloading without effects on CV. Delayed repolarisation may represent a compensatory response to variations in mechanical load and underlie possible arrhythmogenic effects. Future studies will employ myocardial slices to determine the structural alterations responsible for the observed electrophysiological remodeling.

Where applicable, the authors confirm that the experiments described here conform with The Physiological Society ethical requirements.

PCB037

Sarcoplasmic reticulum content is reduced by the RyR2^{R4496C} mutation at a range of frequencies in mouse cardiac myocytes

C. Circelli, L.A. Venetucci, A.W. Trafford and D.A. Eisner

Unit of Cardiac Physiology, University of Manchester, Manchester, UK

Motivation: Patients with catecholaminergic polymorphic ventricular tachycardia (CPVT) have RyR2 mutations and are prone to delayed after depolarisations (DAD), triggered by Ca^{2+} waves during β- adrenergic stimulation. These arrhythmias are often seen during periods where the heart rate increases; therefore, our objective was to study the effects of various stimulation frequencies in the RyR2^{R4496C} knock-in mouse model of CPVT.
Methods: Ventricular cardiac myocytes were isolated from either control or RyR2^{R4496C} knock-in mutant mouse hearts by enzymatic digestion and loaded with Fluo-5F. Cells were then voltage clamped at -50 mV and depolarised to 0 mV using a 50 ms pulse. Cells were paced at frequencies of 1, 3, and 5 Hz in the presence of 1 μM isoproterenol. SR Ca^{2+} content was measured using the application of 5 mM caffeine and 20 mM 2,3-butane-dione-monoxime, with integration of the Na^{+}-Ca^{2+}

exchange current. All animal experimentation was compliant with the 1986 Scientific Procedures Act (UK). **Results:** Our data show that SR Ca^{2+} content is reduced by the $RyR2^{R4496C}$ mutation at 1, 3 and 5 Hz ($P<0.05$). Furthermore, SR Ca^{2+} content also increases with rate in control cells (1 Hz vs. 3 and 5 Hz $P<0.05$). However, this relationship appears to be impaired in $RyR2^{R4496C}$ mutant cells, with only 1 Hz vs. 5 Hz showing an increase in SR Ca^{2+} content. Our work also shows that increasing the stimulation frequency reduces both the L-type Ca^{2+} current and systolic Ca^{2+} transient amplitude. In addition, the $RyR2^{R4496C}$ mutation does not alter other Ca^{2+} cycling parameters, such as, the rate constant of decay for the systolic Ca^{2+} transient. **Conclusion:** These experiments demonstrate the $RyR2^{R4496C}$ mutation lowers SR Ca^{2+} content at all frequencies of stimulation, and modifies the relationship between frequency of stimulation and SR Ca^{2+} content. These observations suggest that the mutated $RyR2^{R4496C}$ responds differently to increases in the pacing frequency. This abnormal response to high frequencies of stimulation could explain why spontaneous Ca^{2+} release occurs at high frequencies of stimulation. This work offers mechanistic insights into the function of RyR2 in health and disease, aiding the development of future therapeutics.

Where applicable, the authors confirm that the experiments described here conform with The Physiological Society ethical requirements.

PCB038

Regulation of the cardiac sodium/calcium exchanger by protein palmitoylation

L. Reilly, M. Ashford and W. Fuller

Division of Cardiovascular and Diabetes Medicine, University of Dundee, Dundee, UK

The cardiac sodium/calcium exchanger (NCX1) plays a vital role in the regulation of intracellular Ca in cardiac muscle, removing Ca that enters the cell during systole. Inappropriate NCX1 function contributes to cardiac contraction abnormalities and heart failure: reduced NCX1 activity reduces Ca removal and therefore impairs relaxation, whereas overactive NCX1 unloads the intracellular Ca stores and impairs systolic function. Although the structure-function relationship of NCX1 is well characterised, the dynamic regulation of NCX1 function is controversial. The reversible attachment of the 16-carbon fatty acid palmitate to cysteine residues in proteins (palmitoylation) is an important and common post-translational modification in a variety of tissues. However, the cardiac palmitoyl proteome remains largely uncharacterised. In general, palmitoylation targets proteins to the lipid bilayer as addition of palmitate increases the hydrophobicity of proteins. With respect to ion transporters, palmitoylation controls cell surface expression, spatial organisation, and voltage-sensitivity as well as cross talk with other signalling pathways (Linder & Deschenes 2007). Given that multiple ion channels and transporters are palmitoylated, palmitoylation of cardiac calcium handling proteins may be as important as phosphorylation in the regulation of excitation-contraction coupling and thus cardiac output. We investigated the palmitoylation of NCX1 from ventricular myocytes (VM) isolated from adult male Wistar rats by retrograde perfusion of collagenase. Using site-specific resin assisted capture (Acyl Rac), palmitoylated proteins were purified from isolated adult rat VM. Data is presented as mean±SEM, with differences analysed by t-test. NCX1 is substoichiometrically palmitoylated in VM (proportion of NCX1 purified by Acyl Rac: 73±5%, n=6) compared to the constitutively palmitoylated protein, caveolin-3. We expressed NCX1 in HEK-293 cells by transient transfection and measured palmitoylation by Acyl Rac, and cell surface localization using membrane impermeable biotinylation reagents. The global palmitoylation inhibitor 2-bromopalmitate (100μM, 18 hours), significantly reduced NCX1 palmitoylation (by 89±4%% compared to untreated cells, n=4, $p<0.001$), and significantly decreased cell surface expression of NCX1 (by 49±11% compared to untreated cells, n=3, $p<0.05$). NCX1 is regulated via a large intracellular loop between transmembrane domains 5 and 6, in which a number of cysteine residues are located. Site-directed mutagenesis of cysteines 383, 387, 485 or 557 did not reduce NCX1 palmitoylation in transiently transfected HEK-293 cells. In conclusion, palmitoylation of NCX1 influences its turnover at the plasma membrane and/or processing in the secretory pathway. The effect of palmitoylation on NCX1 activity is currently under investigation.

Linder, M.E. & Deschenes, R.J., 2007. Palmitoylation: policing protein stability and traffic. Nature Reviews Molecular Cell Biology, 8(1), pp.74–84.

Where applicable, the authors confirm that the experiments described here conform with The Physiological Society ethical requirements.

PCB039

Pacemaker phenotype is the basis of tachyarrhythmias originating in the atrioventricular rings and the right ventricular outflow tract

S.R. Logantha, H. Schneider, A.J. Atkinson, G. Hao, M.R. Boyett and H. Dobrzynski

Institute of Cardiovascular Sciences, University of Manchester, Manchester, UK

The atrioventricular (AV) ring tissue (surrounding the atrial orifices of tricuspid and mitral valves) and the right ventricular outflow tract (RVOT) are major sources of ectopic electrical activity causing arrhythmias (1, 2). The aim of this study was to characterise these tissues in structurally normal hearts, identify whether they are predisposed to generate arrhythmias and investigate the mechanisms underlying arrhythmogenicity.
Male Wistar rats (275-375 g) were killed in accordance with the United Kingdom Animals (Scientific Procedures) Act, 1986. Isolated tissue preparations were superfused at 37°C and extracellular electrograms were recorded with a multi-electrode array and intracellular action potentials (APs) were recorded using microelectrodes. Ion channel expression was characterised using qPCR and immunohistochemistry. Data are presented as means±SEMs and 'n' denotes number of animals.
In right atrial preparations, multi-electrode array recordings showed the leading pacemaker site at the level of the sinus node; AV ring APs were atrial-like (n=2), showing a maximum diastolic potential (MDP) of -82±1 mV, a fast upstroke velocity (dV/dt_{max}, 205±17 V/s), a large amplitude (102±2 mV) and the time to 50% (T_{50}) and 90% (T_{90}) repolarization of 22±1 ms and 80±1 ms, respectively. Upon detaching the sinus node, spontaneous activity originated in the AV ring and propagated towards the terminal crest. Intracellular APs recorded at the leading pacemaker site in the AV ring were sinus node-like. Spontaneous APs occurred at a frequency of 2.1±0.3 Hz (n=4) and were characterised by a MDP of -50±3 mV, a slow upstroke (dV/dt_{max}, 7±1 V/s), a small amplitude (49±3 mV) and slow diastolic depolarization. The T_{50} and T_{90} were 46±5 ms and 87±8 ms, respectively. Pacemaking in the AV ring was accel-

erated by treatment with the β-adrenergic agonist isoproterenol (0.05 μM) and could be inhibited by either blocking the pacemaker current I_f with 2 mM Cs^+ or disrupting Ca^{2+} release from the sarcoplasmic reticulum with ryanodine (2 μM).
In RVOT preparations, spontaneous electrical activity was observed in 2 out of 7 cases. The leading pacemaker site was located immediately inferior to the pulmonary valve and again showed sinus node-like APs (MDP, -41±2 mV; dV/dt_{max}, 25±7 V/s; amplitude, 44±12 mV; n=2) with prominent diastolic depolarization. Curiously, both the right AV ring and the RVOT showed bursting activity. Consistent with these observations, qPCR and immunolabelling showed an expression pattern of ion channels, Ca^{2+}-handling proteins and receptors in the right AV ring and RVOT similar to that in the sinus node.
The AV rings and the RVOT of the normal heart are capable of pacemaker activity and this is the likely basis of arrhythmias originating in these tissues.

Kistler PM et al. (2006). J Am Coll Cardiol 48, 1010-1017.

Kamakura S et al. (1998). Circulation 98, 1525-1533.

This research was funded by the British Heart Foundation.

Where applicable, the authors confirm that the experiments described here conform with The Physiological Society ethical requirements.

PCB040

Increased sarcoplasmic reticulum diastolic calcium leak can produce biphasic decay of the cardiac systolic calcium transient

R. Sankaranarayanan, Y. Li, D. Greensmith, A.W. Trafford, D.A. Eisner and L.A. Venetucci

Cardiac Physiology, University of Manchester, Manchester, UK

Introduction: Cardiac contraction results from a brief increase in cytosolic calcium (Ca) concentration (systolic Ca transient). The majority of this increase is due to release of Ca from the sarcoplasmic reticulum (SR) through the ryanodine receptor (RyR). For relaxation to occur, the RyRs close and Ca is removed from the cytoplasm, largely by pumping Ca back into the SR via the sarco-endoplasmic reticulum Ca ATPase (SERCA). If the RyR becomes leaky then the resulting extra efflux of Ca from the SR will reduce the effects of SERCA-mediated Ca uptake and decrease SR Ca content and thence the amplitude of the Ca transient. Previous work has also shown that increasing RyR leak slows the rate of decay of the Ca transient and this may contribute to impaired relaxation in heart failure [1]. The aim of this study was to characterize the precise details of this slowing of decay of the Ca transient.
Methods: Single rat ventricular myocytes were voltage clamped using the perforated patch clamp technique. 100 ms duration pulses from -40 to 0 mV were applied at 0.5 Hz. Cytosolic Ca concentration was measured using Fluo-4 AM. SR Ca leak was induced using 1 mM caffeine. Statistical analysis was performed using the t-test.
Results: Application of caffeine decreased the amplitude of the Ca transient (to 45% of control) and its rate constant of decay (to 75%). In 3 out of 11 cells the decay of the Ca transient was clearly biphasic with an initial rapid phase of decay followed by a slower one. This biphasic decay was seen much more frequently (12 out of 15 cells) if caffeine was applied in the presence of isoprenaline (1 μM) as shown in Fig. 1 (A-raw trace and B- normalised). In isoprenaline the Ca transient decays as a single exponential with a rate constant of decay of 18.1±1.8 s^{-1}. The addition of caffeine results in bi-exponential decay with the rate constant of the fast phase (16.5±2.4 s^{-1}) being the same (p=0.61) as in the absence of caffeine. Thus, in the normalized traces (B), the initial fast phase superimposes on that in isoprenaline alone. The slow phase has a rate constant of 1.3±0.3 s^{-1}. We hypothesise that the initial rapid phase of decay is a consequence of the SR Ca content and therefore leak being reduced following systolic release. Only when SR Ca content begins to increase does the leak become sufficient to significantly oppose SERCA. In 6 cells showing biphasic decay in caffeine plus isoprenaline we investigated the effect of partial inhibition of SERCA and found that thapsigargin reduced the amplitude and rate constant of decay of the fast component .
Conclusions: We conclude that Ca leak from the SR can lead to biphasic decay of the Ca transient because the effect of leak is greater at later times when the SR Ca content is increased. These results will be relevant to relaxation in heart failure.

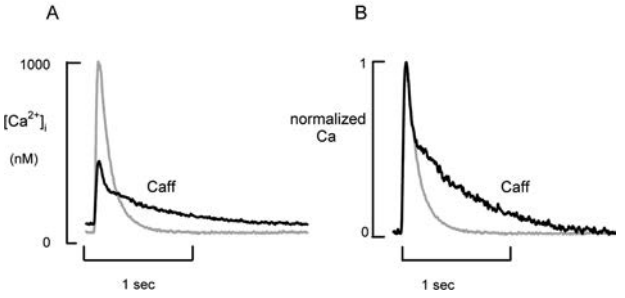

Fig. 1 Averaged (n=10) Ca transients recorded in: Isoprenaline (1 μM), grey; Isoprenaline (1 μM) + Caffeine (1 mM), black. A. Raw traces. B. Normalized traces.

1. Belevych A et al (2007). *Biophys J*:**93(11):**4083-92

Where applicable, the authors confirm that the experiments described here conform with The Physiological Society ethical requirements.

PCB041

The modulation of mitochondrial Ca^{2+}-uptake by inorganic phosphate, pH, adenosine phosphates and Mg^{2+} in single permeabilized ventricular myocytes of rat

J. Lee[1], J. Ha[1], J. Youm[2] and C. Leem[1]

[1]Physiology, University of Ulsan College ofMedicine, Seoul, Republic of Korea and [2]Physiology, Inje University, Busan, Republic of Korea

Mitochondrial Ca^{2+} regulation is closely related to cellular function including energy production and cell viability. Intramitochondrial Ca^{2+} overload is eventually destined to cellular death, therefore, the modulation of the mitochondrial Ca^{2+} uptake is important to regulate cellular function. In this study, we would like to see the effect of inorganic phosphate (Pi), pH, adenosine phosphates and Mg^{2+} on mitochondrial Ca^{2+} uptake kinetics with newly developed quantitative method. We enzymatically isolated single ventricular myocytes of rat. All procedures were accorded with national legislation. Buthanedione monoxime was present to prevent contracture. We measured NADH, mitochondrial Ca^{2+} with Fura-2FF and mitochondrial membrane potential (ψm) with tetramethylrhodamine ethyl ester, simultaneously. To maintain mitochondrial membrane potential, 5 mM of pyruvate and malate were present at all times. The Ca^{2+} uptake rate was increased as extramitochon-

drial Ca^{2+} was increased in a dose dependent manner. As intramitochondrial Ca^{2+} increased, NADH and mitochondrial membrane potential was decreased. The half-activating Ca^{2+} concentration (Kh) was about 0.33 μM. In the presence of Pi,Ca^{2+} uptake was not occurred properly and mitochondrial membrane potential was rapidly depolarized. These phenomena were prevented by ATP and the Kh was 1.79 μM in the presence of ATP and Pi. The Kh was shifted to the right, compared to the control Kh. ADP did not shift the Kh. Mg^{2+} markedly shifted the Ca^{2+} sensitivity to the right and the Kh value was about 1.83 μM. In addition, the maximal uptake rate also decreased. Cytosolic acidification to pH 6.0 also shifted Kh to the right and the Kh was about 1.56 μM. From the above results, ATP, Mg^{2+} and acidic pH decreased the cytosolic Ca^{2+} sensitivity of mitochondrial Ca^{2+} influx and those modulations must be important in diverse pathologic conditions.

This research was supported by Basic Science Research Program through the National Research Foundation of Korea(NRF) funded by the Ministry of Education, Science and Technology(2011-0010965, 2012-0001553)

Where applicable, the authors confirm that the experiments described here conform with The Physiological Society ethical requirements.

PCB043

Pak1 deficiency in cardiomyocytes increases in susceptibility to ventricular arrhythmogenesis in mice

H. Tsui[1], Y. Wang[1], W. Liu[1,2], Y. Shi[3], R. Wang[3], Y. Zhang[1], R. Solaro[4], Y. Ke[4], H. Zhang[5], D. Terrar[6], E. Cartwright[1], X. Wang[2] and M. Lei[1]

[1]Medicine & Human Sciences, University of Manchester, Manchester, UK, [2]Faculty of Life Sciences, University of Manchester, Manchester, UK, [3]Department of Cardiovascular Medicine, Union Hospital, Wuhan, China, [4]Department of Physiology and Biophysics and Centre for Cardiovascular Research, University of Illinois at Chicago, Chicago, IL, USA, [5]School of Physics and Astronomy, University of Manchester, Manchester, UK and [6]Department of Pharmacology, University of Oxford, Oxford, UK

50% of mortalities attributable to cardiac causes are accounted for by ventricular tachyarrhythmias occurring either independently or as a result of other underlying heart diseases. Yet, despite the enormity of this problem, the identification of pathophysiological mechanisms contributing to ventricular tachyarrhythmias as well as the development of safe and effective antiarrhythmic agents remain elusive[1,2]. The aim of the present study is to determine the role and underlying mechanisms for P^{21} activated kinase 1(Pak1) in ventricular arrhythmogenesis under stress conditions in mice carrying a ventricular cardiomyocytes specific deletion of Pak1 mice ($Pak1^{cko}$) and control mice ($Pak1^{f/f}$).

10-12 week old mice were subjected to either acute treatment of isoprenaline (ISO, 5-50nM) or chronic treatment with ISO at concentration 10mg/kg/day for 14-days delivered by mini-osmotic pump. The *in vivo*, *ex vivo* electrocardiography (ECG) and monophasic action potential (MAP) were recorded by Chart5 program. At both *in vivo*, *ex vivo* conditions, $Pak1^{cko}$ mice, but not control $PAK1^{f/f}$ mice, showed high occurrences (4/12 and 8/12 respectively) of ventricular arrhythmias induced by programmed electrical stimulation (PES) protocols, particularly at high stimulation frequencies. At cellular level, action potential (AP) alternans, delayed after-depolarization typed APs and spontaneous APs were frequently observed from $PAK1^{cko}$ myocytes, but not from control $Pak1^{f/f}$ myocytes. The involvement of Pak1 in Ca^{2+} handling was further investigated at cellular level. Dysfunctional Ca^{2+} handling was observed in $Pak1^{cko}$ myocytes in contrast to control $Pak1^{f/f}$ myocytes, in particular, under ISO stress conditions, these include alterations of SR content, the kinetics of NCX, SERCA, SR refilling and the diastolic cytosolic Ca^{2+}. Molecular characterisation demonstrated that SERCA2 protein and mRNA levels were increased in $Pak1^{f/f}$ hearts under ISO stress condition, however, such effect was abrogated in $Pak1^{cko}$ hearts. Further *in vitro* experiments on primary neonatal cardiomyocytes demonstrated that SERCA2 expression is regulated by Pak1 through activation of serum response factor, a transcription factor that has previously been linked to cardiac hypertrophy and development[3].

In conclusion, Pak1 plays a crucial role in regulating cardiac electrical function and Ca^{2+} handling in preventing stress associated ventricular arrhythmogenesis.

Pogwizd, S.M. & Bers, D.M., Trends in Cardiovascular Medicine, 2004; 14: 61-66.

Liu, W. et al., Circulation, 2011; 124: 2702-2715

Balza et al. (2005) JBC 10, 6498-6510

The research was supported by BHF, MRC and Chinese National Nature Science Foundation.

Where applicable, the authors confirm that the experiments described here conform with The Physiological Society ethical requirements.

PCB044

Remodelling of the caveolar domain in right ventricular failure in rats

R. Norman, M. Hardy, E. Fowler, E. White and S. Calaghan

University of Leeds, Leeds, UK

Heart failure (HF) is a major health problem affecting nearly 1 million people in the UK today. The mechanisms which underlie its progression are not fully understood. A hallmark of remodelling in the failing heart is a desensitisation of the β-adrenoceptor (AR) signalling pathway, associated with aberrant spatial control of cAMP. Caveolae, flask-shaped lipid rafts, are key controllers of β-AR signalling [1]. Many of the proteins involved in the β-AR cascade are present in caveolar domains or interact with caveolin. Here we determine whether caveolar remodelling occurs in a model of right ventricular (RV) HF caused by pulmonary hypertension.

Male Wistar rats (190-230g) received an i.p. injection of 60 mg/kg monocrotaline (MCT) or saline (CON). MCT induces RV hypertrophy which progresses to RV HF by 21-28 days post-injection. When clinical symptoms of HF were apparent, the heart was quickly excised and the coronary circulation cleared of blood on a Langendorff apparatus. The RV was homogenised in detergent-free buffer (500mM Na_2CO_3 with protease inhibitor cocktail) then sonicated. Samples were mixed with Laemmli sample buffer for Western blotting to assess total protein expression, or separated on a discontinuous sucrose gradient [1] to assess protein distribution. Proteins of interest include caveolar proteins caveolin (Cav) 1, Cav3 and cavin 1 which are crucial for caveolar formation, and components of the β-AR cascade (β1-AR, β2-AR and adenyly cyclase (AC) 5/6).

As shown in Fig. 1A, expression of all caveolar proteins and both β1 and β2-ARs was decreased in MCT rats compared with

CON (P<0.01, t-test). AC 5/6 expression was not affected by HF. Cav3 is the major caveolar protein in the cardiac myocyte. Following sucrose density gradient fractionation, caveolae-containing membranes (indexed by enrichment in Cav3) are typically found in fraction 5 and 6 which we designate the buoyant fractions (BF). Fig. 1B shows that the distribution of Cav3 in the membrane is perturbed by RV failure. The ratio of Cav3 in BF to heavy fractions (HFr;9-12) was significantly reduced in MCT rats compared with CON (P<0.05, t-test).
Together the finding of decreased expression of caveolar proteins along with a translocation of Cav3 from caveolar fractions is consistent with a disruption of the caveolar microdomain. These changes are likely to impact on both the basal function and AR responses of the myocyte. We consider that a better understanding of the changes which occur in the caveolar domain could lead to identification of possible pharmacological targets for reverse remodelling of the βAR pathway in HF.

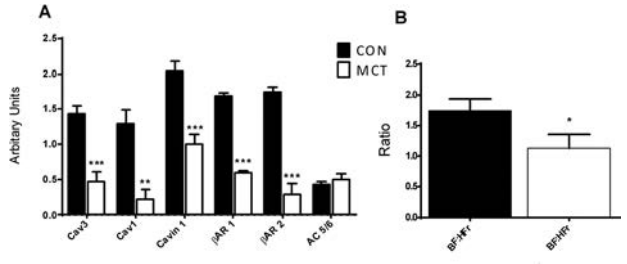

Figure 1. A. Effect of RV failure on caveolar and β-AR cascade protein expression. All values are normalised to β-adaptin. B. Ratio of Cav 3 expression in buoyant fractions (BF;5,6) to heavy fractions (HFr;9-12). All data are mean + S.E.M (n=5-6; *P<0.05; **P<0.01; ***P<0.001).

MacDougall DA et al. (2012) J Mol Cell Cardiol 52:388-40

Where applicable, the authors confirm that the experiments described here conform with The Physiological Society ethical requirements.

PCB046

Regional differences in inflammation and fibrosis in right- and left-sided heart failure

G.M. Quigley[1], I.P. Temple[1], M. Zi[1], E. Cartwright[1], T.T. Yamanushi[2], X. Cai[1], J.F. Yanni[1], H. Dobrzynski[1], G. Hart[1] and M.R. Boyett[1]

[1]Institute for Cardiovascular Research, Univeristy of Manchester, Manchester, UK and [2]Kagawa Prefectural University of Health Sciences, Takamatsu, Japan

Introduction
Left-sided heart failure (HF) is mainly the result of hypertension and coronary disease, whereas isolated right-sided HF results from a different set of conditions, including pulmonary arterial hypertension (PAH) and congenital heart disease. However, pump failure and arrhythmias are common in both types of HF. The aim of this study is to determine if inflammation, fibrosis and apoptosis are involved.
Methods
To induce PAH, monocrotaline (MCT, 60 mg/ml/kg) was injected subcutaneously into 200 g male Wistar rats. Weight-matched saline injected rats were used as controls. The rats were sacrificed ≤ 28 days later. To induce left-sided HF, rabbits underwent two surgical steps. First, volume overload was caused by aortic valve destruction, followed 3 weeks later by pressure overload by partial constriction of the abdominal aorta. Heart samples were frozen for qPCR analysis, histology and immunohistochemistry.
Results
qPCR analysis revealed a significant increase in mRNA levels of inflammatory cytokines, IL1β and TGFβ1, in the sinoatrial node (SAN), right atrium (RA), right ventricle (RV) and right Purkinje fibres (RPF) of the MCT-injected rats. There was an increase in mRNA levels of fibrosis markers, collagen1, elastin, fibronectin, CTGF and TIMP1, in the same tissues. There was an increase in collagen3 mRNA in the RA, RV and RPF. Vimentin mRNA increased in the SAN, RA and RV. In contrast, only modest changes were seen in the left side of the heart and a significant reduction in mRNA levels of collagens1 and 3, elastin, fibronectin and CTGF in the left ventricle (LV). Histology demonstrated proliferation of non-myocyte nuclei in the RV, but not the LV, in the MCT-injected rats. Immunohistochemisty revealed that these cells express vimentin and CD68, demonstrating they are macrophages and possibly fibroblasts. In the rabbit model, the RA demonstrated significant increases in mRNA levels of IL1β, TNF, NFκB and angiotensin II receptor 1 (AT1R). There was an increase in levels of the fibrosis markers MMP2 and TIMPs 1 and 2. The SAN demonstrated a significant increase in collagen3 and fibronectin, and a reduction in AT1R and TIMP3. There was an increase in fibronectin and TIMP1 in the RV, with no change in the LV. Fibronectin mRNA increased in the RPF, while AT1R and TIMP4 were reduced in the left Purkinje fibres (LPF).
Conclusion
In the rat model of right-sided HF, there was increased expression of inflammatory and fibrosis genes in the right side of the heart, including the SAN. This could contribute to dysfunction and predispose to arrhythmias in PAH. Unexpectedly, few changes were found in the LV and LPF in the rabbit left-sided HF model, the majority of changes occuring in the RA. The thin walled chambers of the heart, namely the RA and RV, could possibly be more susceptible to stretch as they mount an inflammatory response to HF triggers.

Where applicable, the authors confirm that the experiments described here conform with The Physiological Society ethical requirements.

PCB047

Ultrastructural evidence of cardiomyocyte apoptosis in acute myocardial infarction and chronic aneurism wall

Y. Kyyak, O. Barnett, H. Kyyak and O. Leshchuk

Lviv National Medical University named by Danylo Halitskyy, Lviv, Ukraine

Acute myocardial infarction (AMI) is characterized by myocardial cell necrosis,inflammatory response and scar formation. The aim was to reveal whether cardiomyocyte (CMC) apoptosis is present in the infarction zone of the left ventricle compared with postinfarction chronic aneurizm wall.
Subject and methods: Myocardial express necropsies from 24 patients (age range 39-71) who suffered mainly from hypertension (HT) and died from STEMI complicated with Heart Failure (HF) or Cardiogenic Shock were examined. Biopsies from postinfarction aneurism wall from five patients (38-61 y.o), suffering from HT and HF were obtained and their ultrastructure was compared with changes in necropcies from infarction zone.
Results. According to electron microscopic investigation in infarction zones of the left ventricle exept necrotic, hibernated and apoptotic myocytes, as well as apoptotic endothelial and

plasmatic cells,macrophages and fibroblasts, with features of pycnosis, nuclear chromatin condensation and cytoplasma vacualization where detected. As the result of prominent interstitial fibrosis, very poor vascularization and moderate matrix edema,CMC usually were dissociated and myocardium loses its synthityal organization. Separately located CMC were hibernated finally resulting in apoptosis. Numerous hibernated and apoptotic CMC were destroyed via secondary necrosis predominantly during short time (three months) after AMI. In aneurism wall 14 years after AMI onset, hibernating and some viable CMC were still present as the result of myocardium neovascularization.
Conclusions: CMC necrosis is the main mechanism of cell death in acute aneurism wall, while apoptosis develops predominantly in subacute periods of AMI. In chronic aneurism wall viable CMC are present, but hibernating and apoptotic CMC prevalent.

Where applicable, the authors confirm that the experiments described here conform with The Physiological Society ethical requirements.

PCB048

Rate-dependency of effective electrical size in healthy and border-zone remodelled myocardium in small mammalian and human ventricular models: implications for modelling scar-related arrhythmias

Y. Hill[1], A. Pavithran[1], G. Plank[2], N. Smith[1] and M. Bishop[1]

[1]Biomedical Engineering, King's College London, London, UK and [2]Institute of Biophysics, Medical University of Graz, Graz, Austria

Sudden cardiac death resulting from cardiac arrhythmia is a significant cause of mortality in Western Society. Effective electrical size (ratio of ventricular size to electrical activation wavelength) plays a significant role in governing reentrant arrhythmia dynamics. Due to similarities in effective size, the rabbit is suggested to be the most useful model for clinical investigations of fibrillatory arrhythmias(1,2). However, how well effective size of the rabbit, or other small mammalians, correlates to the human at slower pacing rates, as commonly seen during scar-related arrhythmias, and how it varies with frequency, is not well understood. In addition, electrophysiological changes in infarct-scar border-zone (BZ) cells(3,4) may cause crucial differences in effective electrical size and restitution between species which may be important in governing reentrant dynamics during infarction. Computational ionic ventricular cell models of human, rabbit, guinea pig and rat were used to investigate interspecies differences in action potential duration (APD), conduction velocity (CV) and wavelength restitution under S1S2 and dynamic restitution protocols. Effective size was calculated to observe how restitution effects combine to induce rate-dependent variations in effective size. Ionic changes were also implemented in rabbit and human models to simulate BZ remodelling and restitution protocols repeated. The human model displayed the steepest restitution curves for all metrics. The rat model displayed negative APD restitution, at single cell and tissue levels due to known limitations with this model. The rabbit model produced the most similar effective electrical size to the human across a range of activation rates (Fig 1), although differences in effective size became more apparent at higher frequencies due to the steeper APD and CV restitution properties of the human model. Similar results were observed between S1S2 and dynamic protocols. Incorporating electrophysiological changes to represent infarct BZ cells demonstrated further differences between rabbit and human models; the human showing more pronounced changes to restitution dynamics than the rabbit in BZ tissue relative to healthy myocardium, although less of an increase in absolute APD. Failure of the rabbit model to produce similar rate-dependent effects in effective size to the human in healthy or BZ tissue suggests potentially important interspecies differences in the initiation and anchoring of reentrant waves around structures, which are currently being investigated in preliminary simulations of reentry in 3D human and rabbit infarct models. This research highlights the need for further investigation into the utility of such models for informing the study of clinical scar-related arrhythmias.

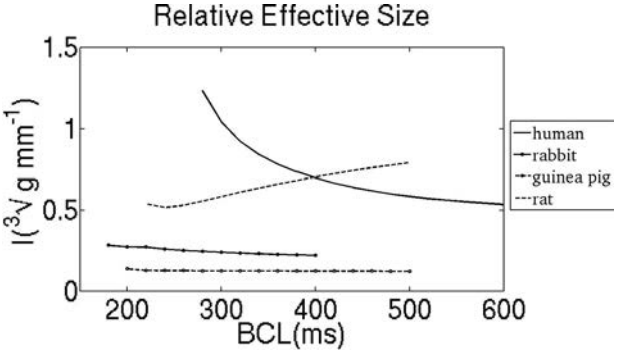

Figure 1. Rate-dependent effective electrical size of the heart in different species. BCL - basic cycle length, I - effective electrical size.

Panfilov A. Is heart size a factor in ventricular fibrillation? Or how close are rabbit and human hearts? *Heart Rhythm* 2006;3(7):862-864.

TenTusscher KH, Mourad A, Nash MP, Clayton RH, Bradley CP, Paterson DJ, Hren R, Hayward M, Panfilov AV, Taggart P. Organization of ventricular fibrillation in the human heart: experiments and models. *Experimental Physiology* 2009;94(5):553-562.

Decker K, Rudy R. Ionic mechanisms of electrophysiological heterogeneity and conduction block in the infarct border zone. *Am J Physiol Heart Circ Physiol* 2010;299(5):H1588-H1597.

Nattel S, Maguy A, Le Bouter S, Yeh YH. Arrhythmogenic Ion-Channel Remodeling in the Heart: Heart Failure, Myocardial Infarction, and Atrial Fibrillation. *Physiological Reviews* 2007;87(2):425-456.

Where applicable, the authors confirm that the experiments described here conform with The Physiological Society ethical requirements.

PCB049

Computational modelling of stress (Takotsubo) cardiomyopathy

S. Land[1], S. Niederer[1], D. Stuckey[2], M. Sikkel[2], S. Harding[2] and N. Smith[1]

[1]Department of Biomedical Engineering, King's College London, London, UK and [2]Faculty of Medicine, Imperial College London, London, UK

Stress cardiomyopathy is a clinical syndrome characterized by acute apical dysfunction, where the shape of the left ventricle resembles the Japanese fisherman's octopus pot (tako tsubo) during systole. Results from a recent animal study have uncovered adrenaline-induced stunning of the myocardium as a potential mechanism (1,2). Exposing cardiac cells with human β_2 receptors to high concentrations of epinephrine cause a decrease in force generated by these cells (3). However, both the quantitative gradients in tension generated by the myocardium, as well as the biophysical mechanisms underpinning this phenomenon remain poorly understood.

In our work we have used biophysically based computational models of the left ventricle to investigate these potential mechanisms. Our first model assumes cellular calcium transients vary from apex to base due to differences in adrenergic stimulation.The properties of this gradient were varied in this model study in combination with the calcium sensitivity of the myofilaments.
Selected results are shown in Figure 1. These show that combination of a gradient in adrenergic effects on the calcium transient, combined with a homogeneous decrease in calcium sensitivity, are potentially sufficient to reproduce apical ballooning at mid-systole. However, by end-systole, apical ballooning is significantly decreased. We hypothesised this to be due to compensation produced by the Frank-Starling mechanism. Further model results confirm that a weakened length-dependent response of cardiac muscle increases apical ballooning at both mid- and end systole. Incorporating this mechanism resulted in a deformation of the ventricle with significant reduction in stroke volume, consistent with reported clinical cases where significant end-systolic ballooning was observed (1).
In conclusion, changes in calcium regulation through adrenergic mechanisms are sufficient to reproduce the magnitude of apical ballooning seen in Takotsubo cardiomyopathy. Significant apical ballooning at end systole may indicate a failure of the Frank-Starling mechanism.

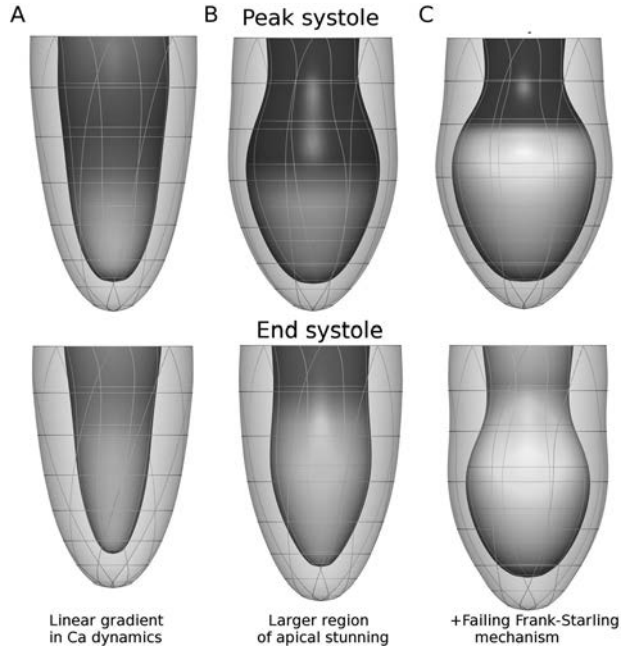

Results of left-ventricular simulations. Darker colours on the endocardium indicate higher active tension.

(A) A linear gradient in calcium transient magnitude from apex to base does not result in significant ballooning at peak systole.

(B) A larger region of apical stunning does show the typical `Takotsubo' shape, though by end-systole this is reduced.

(C) A failure of length-dependent activation increased ballooning during peak systole and end-systole, and decreases stroke volume significantly.

AR Lyon, PSC Rees, S Prasad, PA Poole-Wilson, SE Harding. Stress (Takotsubo) cardiomyopathy - A novel pathophysiological hypothesis to explain catecholamine-induced acute myocardial stunning. Nature clinical practice, 2008

H Paur, PT Wright, MB Sikkel MB, MH Tranter, C Mansfield, P O'Gara, DJ Stuckey, VO Nikolaev, I Diakonov, L Pannell, H Gong, H Sun, NS Peters, M Petrou, Z Zheng, J Gorelik, AR Lyon, SE Harding.

High levels of circulating epinephrine trigger apical cardiodepression in a β_2 -adrenoceptor/G_i-dependent manner: A new model of Takotsubo cardiomyopathy. Circulation, 2012

JH Heubach, U Ravens, AJ Kaumann. Epinephrine activates both G_s and G_i pathways, but norepinephrine activates only the G_s pathway through human β_2 -adrenoceptors overexpressed in mouse heart. Molecular Pharmacology, 2004

Where applicable, the authors confirm that the experiments described here conform with The Physiological Society ethical requirements.

PCB050

Regional action potential heterogeneity in the sheep left ventricle- changes in heart failure and isolated dyssynchrony

G. Kirkwood, M. Richards and A.W. Trafford

Cardiac Physiology, University of Manchester, Manchester, UK

Background
Recent studies have identified that dyssynchronous ventricular activation can have detrimental effects including hypertrophy, dilatation and ultimately heart failure. The mechanisms are incompletely understood but appear to involve regional heterogeneities in ventricular workload. We investigated cellular remodelling in a model of dyssynchrony induced by right ventricular pacing, with regards to regional heterogeneity and how this relates to an existing model of heart failure.
Methods
Experiments were performed in female Welsh Mountain sheep, with isofluorane anaesthesia (1-4%) used for all surgical procedures. For the dyssynchrony model, transvenous pacemaker leads were implanted at the right ventricular apex and right atrial appendage. These were attached to a dual chamber pacemaker, programmed in VDD mode with a 40ms atrioventricular delay. For the heart failure model, the heart was paced at a rate of 210 bpm via a single lead implanted at the right ventricular apex. Pacing continued for 6-8 weeks in the heart failure model and 3 months in the dyssynchrony model. The animals were then euthanased with Pentobarbitone (200mg/kg IV) and the hearts excised. Ventricular myocytes were isolated by enzymatic digestion from the mid layer of the intraventricular septum (IVS) and left ventricular free wall (FW). After loading with Fura-2, these were studied at 37°C using the perforated patch current clamp technique. Action potentials were recorded at a stimulation frequency of 0.5Hz in normal Tyrode's solution, and the time to 70% repolarisation (APD70) was measured. The magnitude of the calcium transient (Ca-Tran) was calculated, along with its exponential decay rate constant (Ca-RC). Statistical comparison was performed using 2 way ANOVA with significance accepted at $p<0.05$.
Results
Results are shown as mean ± standard deviation. APD70 was longer in the septum than the free wall and in both regions was shortened in heart failure. This was associated with a reduction in the magnitude and rate of decay of the calcium transient. Dyssynchrony was associated with a trend towards APD70 shortening, and no apparent effect on the calcium transient.
Discussion
These preliminary data suggest that this model of dyssynchrony may display similar action potential changes to the heart failure model. Further experiments will explore the underlying mechanisms, and whether dyssynchrony might be considered an intermediate stage in the remodelling seen in heart failure.

Measurements for LV Free Wall (FW) and Intraventricular Septum (IVS)

Measurement	APD70 (FW)	APD70 (IVS)	Ca-tran (FW) (Peak:Baseline ratio)	Ca-tran (IVS)	Ca-RC (FW)	Ca-RC (IVS)
Control (n= 55/16)	369.6 ± 109 ms	448.5 ± 82.4 ms	1.5 ± 0.4	1.5 ± 0.4	3.0 ± 1.1 ms^{-1}	2.9 ± 0.9 ms^{-1}
Failure (n= 23/10)	302.4 ± 69 ms	399.2 ± 94.7 ms	1.2 ± 0.1	1.2 ± 0.	1.8 ± 0.4 ms^{-1}	1.7 ± 0.1 ms^{-1}
Dyssynchrony (n = 9/3)	257.8 ± 45.2 ms	368.6 ± 93.1 ms	1.5 ± 0.1	1.8 ± 0.1	2.4 ± 0.4 ms^{-1}	3.2 ± 1.1 ms^{-1}
P (Mid vs Sep)	< 0.005		n.s.		n.s.	
P (Model vs Control)	Failure < 0.05. Dyssynchrony = 0.06 n.s.		Failure < 0.05. Dyssynchrony = n.s.		Failure < 0.05. Dyssynchrony = n.s.	

Where applicable, the authors confirm that the experiments described here conform with The Physiological Society ethical requirements.

PCB051

Freshly isolated adult fibroblasts from normal and overloaded hearts affect viability, cell volume and calcium cycling of cardiac myocytes in co-culture by paracrine TGF-β signalling

J. Cartledge, P. Dias, M. Ibrahim, S. Alayoubi, M.H. Yacoub, P. Camelliti and C.M. Terracciano

Imperial College London, London, UK

The interaction of cardiac fibroblasts (FBs) and myocytes (CMs) is gaining considerable interest due to growing evidence that fibroblasts can affect myocyte structure and function. This interaction can occur through direct cell contact or paracrine communication. Very limited data exists regarding paracrine communication, particularly between adult cells. We examined the effect of fibroblasts from normal and overloaded hearts on adult myocytes. TGF-β is a potential paracrine mediator and was investigated.

Adult Lewis rat CMs were co-cultured with FBs from pressure overloaded (10 week thoracic aortic constriction (TAC)) (T+CM) or sham operated hearts (S+CM) at 1:2 CM/FB ratio in a co-culture system that allows paracrine communication but prevents direct cell contact. CMs co-cultured with CMs (CM+CM) served as control. After 24 hours co-culture, CM viability was measured as the % rod shaped cells. CM volume was measured using di-8-ANEPPS membrane staining. Ca2+ transients were recorded using the Ca2+ sensitive dye Fluo-4. 10 μM SB431542 (SB) was used to block TGF-β type 1 receptors. Data is shown as mean±SEM (n number) and analysed by 1 way ANOVA with Tukeys post hoc analysis.

Co-culture with sham or TAC FBs reduced the viability of co-cultured CMs but this was blocked by SB (in %: CM+CM 70±1.1 (5); CM+CM+SB 72±1.7 (5); S+CM 61±2.3 (6); S+CM+SB 74±2.4 (6); T+CM 52±2.2 (6); T+CM+SB 66±2.8 (6). $p<0.05$: S+CM vs CM+CM, T+CM vs CM+CM, S+CM+SB vs S+CM, T+CM+SB vs T+CM). Both sham and TAC FBs induced CM hypertrophy which was also prevented by SB (in x103μm3: CM+CM 48±1.2 (60); CM+CM+SB 49±1.7 (43); S+CM 53±1.3 (48); S+CM+SB 48±1.4 (47); T+CM 56±1.7 (44); T+CM+SB 50±1.8 (42). $p<0.05$: S+CM vs CM+CM, T+CM vs CM+CM, S+CM+SB vs S+CM, T+CM+SB vs T+CM). Ca2+ transient amplitude was increased after co-culture with sham FBs but reduced after co-culture with TAC FBs. These effects were also prevented by SB (in F/F0: CM+CM 3.4±0.1 (42); CM+CM+SB 3.2±0.1 (33); S+CM 4.6±0.2 (50); S+CM+SB 3.3±0.1 (60); T+CM 2.8±0.1 (36); T+CM+SB 3.3±0.2 (45). $p<0.05$: S+CM vs CM+CM, T+CM vs CM+CM, S+CM+SB vs S+CM, T+CM+SB vs T+CM). Time to 90% decay of the Ca2+ transient was reduced after co-culture with sham or TAC FBs but unaffected by SB (in ms: CM+CM 359±8.5 (42); CM+CM+SB 390±17.2 (33); S+CM 322±6.2 (50); S+CM+SB 339±7.0 (60); T+CM 295±13.5 (36); T+CM+SB 317±9.3 (45). $p<0.05$: S+CM vs CM+CM, T+CM vs CM+CM). Time to peak and time to 50% decay were unaffected.

These results show that FBs affect viability and Ca2+ cycling of CMs by paracrine TGF-β signalling. FBs from overloaded hearts alter Ca2+ cycling of CMs differently from normally loaded FBs, suggesting that this paracrine interaction is sensitive to chronic variations in load and may play a role in the pathophysiology of cardiac disease.

Where applicable, the authors confirm that the experiments described here conform with The Physiological Society ethical requirements.

PCB052

A chromanol-sensitive outward potassium current contributes to the repolarization of action potential in mouse sino-auricular node cells

M. Gonotkov and V. Golovko

Institute of Physiology, Komi Science Centre, the Ural's Division RAS, Syktyvkar, Russian Federation

The aim of the present study was to verify the hypothesis about the contribution of the slow component of delayed rectified K-current (IKs) in the mouse sino-auricular node (SA) pacemaker cells. Methods. Experiments were performed on albino male mice (30±5 g) two months of age (n=13). Using microelectrode technique we examined the effects of 4-chromanol on spontaneously beating strips of sino-auricular region. Results. Application of 4-chromanol (30 μm) slowed the final phase of repolarization from 0.59±0.09 V/sec to 0.43±0.09 V/sec (- 27%, n=5; $p \leq 0.05$) in the true pacemaker cells (dV/dt max ≤ 5V/sec). The velocity of the diastolic depolarization decreased from 146 mV/sec to 113 mV/sec. The frequency of action potential (AP) generation in strips decreased from 308±34 beats per min to 260±29 beats per min compared with the control. The 4-chromanol (30 μm) did not change the other parameters of AP (for example, the amplitude, dV/dtmax). This made it possible to consider this drug as a specific blocker of the slow component of delayed rectified K-current (IKs). The frequency of AP generation was 286±30 beats per min in the latent pacemaker cells (dV/dt max ≥10 V/sec) (n strips = 10). Application of IKs inhibitor 4-chromanol (30 μm) slowed the phase of the "plateau" from 0.43 V/sec to 0.25 V/sec (n=6; $p \leq 0.05$). The phase of final repolarization velocity was decrease from 0.75±0.13 V/sec to 0.37±0.1 V/sec (- 51%). The velocity of the diastolic depolarization was reduced by 52%. As a result, the frequency of AP generation decreased by an average of 31% compared with the control. Interestingly, that 4-chromanol (30 μm) decreased V0max of AP in four times compared with the control and in twice times compared with 10 μm in latent pacemaker cells.

Conclusion. The data have indicated that the contribution of the current sensitive to 4-chromanol (presumably current IKs) to repolarization and diastolic depolarization phase cells SA node mouse cells is 20-30%.

This work was supported by the Ural Branch of the Russian Academy of Sciences (project 12-P-4-1054, 12-U-4-1022) and Russian Foundation for Basic Research (project 12-04-32288 (M.G.).

Where applicable, the authors confirm that the experiments described here conform with The Physiological Society ethical requirements.

PCB053

Can we automatically identify parameters from experiments? Modeling calcium dynamics in the rat cardiac myocytes

S. Gattoni, S. Niederer and N. Smith

Biomedical Engineering, King's College London, London, UK

As part of the NIH funded Virtual Physiological Rat project (VPR) [1], we aim to simulate the integrated cardiovascular function of the rat, with the potential of providing new validated computer models that account for genetic variation across rat strains. Within the cardiovascular system we focus in particular on the heart, and the cardiac cell models of the ventricular myocyte. While there is a long history of significant advances in this field, in many cases the existing electrophysiology models have been derived combining different frameworks, resulting in the majority of currently applied models being parametrized from heterogeneous experimental sources. Thus, what is now required to further develop the field and increase the applicability of models to understanding wet lab contexts, is the development of species and temperature consistent models obtained by directly fitting parameters to experimental data. To address this issue we have implemented a rat electromechanical model by combining the electrophysiological framework of the Pandit 2001 [2] model with the Hinch 2004 [3] model of Ca^{2+} dynamics. To customize the coupled Pandit-Hinch model and automatically identify the parameters, we have implemented a linear regression parameter estimation method, following the approach of Sobie 2009 [4]. Synthetic data have been preliminarily used to generate simulated experimental data, physiological phenotypes have been quantified and a reverse regression has been performed to identify the parameter values specifying the previously generated simulations. The accuracy of the predictions is shown in (Fig. 1) in terms of R^2 values for all the parameters used in the Hinch model using this approach. We were able to identify the majority of the parameters involved in the formulation of the sarcoplasmic reticulum Ca^{2+}-ATPase (SERCA), the RyR channel and the L-type channel within tight ranges; predictions of parameters on the Na^+/Ca^{2+} exchanger were less accurate. This approach will be applied to experimental data as part of the VPR project, with the potential of determing the choice of new experimental protocols according to parameterisation needs.

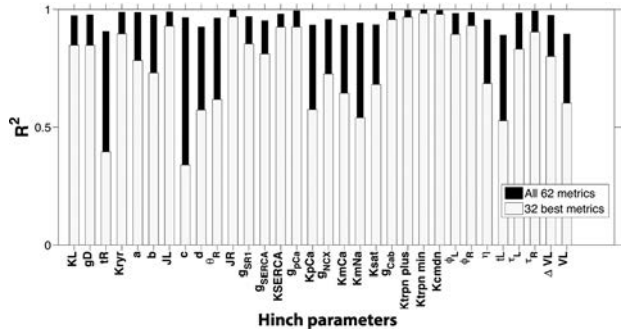

R^2 values showing the level of prediction for 32 parameters in the Hinch [3] model; 100 sets of randomly varied parameters have been collected in an input matrix X. Physiological phenotypes have been quantified from simulations and stored in an output matrix Y for each parameter set. A "reverse regression" has been implemented using 62 phenotypes (black) and the 32 most predictive phenotypes (white) to obtain the displayed regression coefficients.

Daniel A. Beard, Maxwell L. Neal, N. Tabesh-Saleki, C.T. Thompson,J.B. Bassingtwaighte, M. Shimoyama, and B.E. Carlson. "Multiscale Modeling and Data Integration in the Virtual Physiological Rat Project ",Annals of Biomedical Engineering, Vol. 40, No. 11, November 2012 pp. 2365–2378.

Sandeep V.Pandit, Robert B.Clark, Wayne R.Giles, and Samahat S.Demir. "A Mathematical Model of Action potential Heterogeneity in Adult Rat Left Ventricular Myocyte", Biophysical Journal, Vol.81 Dec 2001 pp.3029-3051.

R.Hinch, J.L.Greenstein, A.J. Tanskanen, L.Xu, and R.L. Winslow. "A Simplified Local Control Model of Calcium-Induced Calcium Release in Cardiac Ventricular Myocytes", Biophysical Journal, Vol.87 Dec 2004 pp.3723-3736.

Eric A.Sobie. "Parameter Sensitivity Analysis in Electrophysiological Models Using Multivariable Regression", Biophysical Journal, Vol. 96 Feb 2009 pp. 1264-1274.

This research was supported by the National Institute for Health Research (NIHR) Biomedical Research Centre at Guy's and St Thomas' NHS Foundation Trust and King's College London. The views expressed are those of the author and not necessarily those of the NHS, the NIHR or the Department of Health.

Where applicable, the authors confirm that the experiments described here conform with The Physiological Society ethical requirements.

PCB054

The direct anti-fibrillatory action of vagus nerve stimulation is mediated by nitric oxide release from neuronal nitric oxide synthase

J. Winter, S.H. Chin, K.E. Brack and G. Ng

Department of Cardiovascular Sciences, University of Leicester, Leicester, UK

Introduction

We have previously shown that vagus nerve stimulation (VNS) flattens electrical restitution (RT) slope and increases ventricular fibrillation threshold (VFT) via a nitric oxide (NO) dependent mechanism [1] that is independent on acetycholine [2]. The aim of this study was to elucidate whether NO release from neuronal nitric oxide synthase (nNOS) mediates this anti-fibrillatory effect.

Methods

Adult New Zealand White rabbits (n=5, 3.0-3.5Kg) were presedated with an i.m mixture of ketamine (10mg/kg), medetomidine hydrochloride (0.2mg/kg) and butorphanol (0.05mg/kg). Following sedation, animals were heparinised (1000IU, i.v.), anaesthetised (propofol, 5mg as required, i.v.) and their hearts isolated with intact autonomic innervation. Animals were humanely killed with an overdose of sodium pentobarbitone (160mg/kg, i.v.). The preparations were perfused in constant flow Langendorff mode and instrumented for the measurement of left ventricular pressure (LVP) and epicardial monophasic action potentials. RT slope and effective refractory period (ERP) was measured using single extrastimulus protocol (300ms cycle length). VFT was the minimum current needed to induce sustained VF with burst pacing (30x30ms). The effects of VNS on baseline (BL) parameters were measured in control conditions, during perfusion of the selective nNOS inhibitor (TRIM,200μM) and following drug washout. Data are mean±SEM. 2-way ANOVA with Bonferroni or paired t-test, *P<0.05 vs. BL, **P<0.01 vs. BL, ***P<0.001 vs. BL.

Results

VNS flattened the maximum RT slope (Fig 1A), prolonged ERP (Fig 1B) and increased VFT (Fig 1C). Perfusion of TRIM abol-

ished the effects of VNS on RT slope and VFT but had no effect on the VNS increase in ERP (Fig 1). TRIM exerted a negative inotropic effect reducing peak LVP (33±3 [TRIM] vs. 41±3 [Control] mmHg, P<0.05) with no effect on baseline heart rate (135 ±5 [TRIM] vs. 135±5 [Control] bpm) or coronary perfusion pressure (30±2 [TRIM] vs. 30±1 [Control] mmHg). The degree of heart rate reduction during VNS was reduced by TRIM perfusion (change in heart rate, -45±6 [TRIM] vs. -63±5 [Control] bpm, P<0.05). All effects of TRIM were reversed on drug washout.

Conclusion

NO release from nNOS mediates the direct anti-fibrillatory action of VNS. Further experimental work is required to investigate the mechanism by which NO exerts this protective effects.

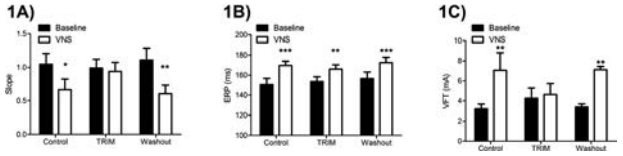

Brack KE, Patel VH, Coote JH, Ng GA. Nitric oxide mediates the vagal protective effect on ventricular fibrillation via effects on action potential duration restitution in the isolated rabbit heart. J Physiol 2007;583(Pt 2):695-704.

Brack KE, Coote JH, Ng GA. The protective effect of vagus nerve stimulation against ventricular fibrillation is independent of muscarinic receptor blockade. Cardiovasc Res 2011;91(3):437-446.

KEB is supported by a British Heart Foundation Intermediate Basic Science Fellowship. SHC is supported by a British Heart Foundation Clinical Training Fellowship.

Where applicable, the authors confirm that the experiments described here conform with The Physiological Society ethical requirements.

PCB055

Independent roles for isoforms 1 and 4 of the plasma membrane calcium ATPase in the development of left ventricular hypertrophy and failure

N. Stafford, M. Zi, M. Shaheen, S. Cook, T. Mohamed, L. Neyses and E.J. Cartwright

Institute of Cardiovascular Sciences, University of Manchester, Manchester, UK

Abnormal calcium handling is known to be instrumental in the development of cardiac hypertrophy and failure. Both isoforms 1 and 4 of the diastolic calcium extrusion pump plasma membrane calcium ATPase (PMCA) are downregulated in failing human and rodent hearts, yet their role in the disease process has not been studied.

Methods: We generated cardiomyocyte-specific knockout mice for PMCA1 (PMCA1-/-), PMCA4 (PMCA4-/-) and the two pumps combined (PMCA1:4-/-), closely modelling the situation in human heart failure. Cardiac phenotype and calcium handling in isolated ventricular myocytes were studied in each mouse line under basal conditions, and in response to pressure overload following two weeks transverse aortic constriction (TAC).

Results: Cardiac structure and function was not altered by the absence of PMCA1 or 4, nor their dual deletion under basal conditions. The PMCA contribution to global calcium extrusion was found to be 2%, and for the first time solely dependent upon PMCA1. When challenged with TAC, PMCA1-/- hearts rapidly progressed into decompensated hypertrophy displaying signs of impaired inotropy, lusitropy and heart failure as evidenced by decreased fractional shortening (20.6±1.6 v 32.4±3.3 %), increased relaxation time constant (8.8±0.8 v 6.6±0.3 ms) and greater normalised lung weight (11.5±1.1 v 7.8±0.8 mg/g) compared to controls. This was accompanied by increased apoptosis and extensive interstitial fibrosis. Analysis of intracellular calcium handling prior to the onset of failure (1 week post surgery) revealed impaired extrusion of the systolic transient in PMCA1-/- TAC cells compared to both wild type TAC and sham PMCA1-/- controls. In stark contrast, the deletion of PMCA4 attenuated the hypertrophic response to pressure overload with an 86% reduction in normalised heart weight compared to wild type TAC controls, whilst systolic and diastolic function were preserved. We hypothesised the deletion of PMCA4 may rescue the failing phenotype in PMCA1-/- mice, so PMCA1:4-/- mice also underwent TAC. Hearts displayed reduced heart weight/tibia length compared to wild type controls (7.0±0.4 v 9.2±0.6 mg/mm), accompanied by preserved function and reduced fibrosis.

Conclusions: These results provide novel evidence of isoform-specific roles for PMCA1 and 4 in cardiac muscle, both capable of influencing the pathological progression of cardiac hypertrophy. PMCA1 may be critical in adapting to the increased demands placed on the heart during pressure overload, whilst the inhibition of PMCA4 may negate the need to adapt altogether and could be a potential target for future anti-hypertrophic therapies.

Where applicable, the authors confirm that the experiments described here conform with The Physiological Society ethical requirements.

PCB056

Prolonged arsenic trioxide treatment increased action potential duration and increased sensitivity to HERG channel blockade in induced pluripotent stem cells cardiomyocytes

M.P. Hortigon-Vinagre[1], I.A. Ghouri[1], F.L. Burton[1], B.D. Anson[3], R. Wallis[2], M. Craig[2] and G. Smith[1]

[1]Cardiovascular and Medical Sciences, University of Glasgow, Glasgow, UK, [2]Clyde Biosciences, Glasgow, UK and [3]Cellular Dynamics Inc., Madison, WI, USA

Long QT syndrome (LQTS) is a heart rhythm disorder that increases the risk of fatal cardiac arrhythmia known as Torsade de Pointes (TdP). One common cause of LQTS (type 2) is a mutation in HERG gene, which encodes the rapidly activating delayed rectifier potassium channel (IKr) and reduces channel activity by causing defective channel trafficking to the surface membrane. Previous studies in animals have shown that arsenic trioxide (As2O3) treatment can disrupt HERG channel trafficking and induce LQTS. In this study we report the ability of As2O3 to induce a LQT phenotype in commercially available human induced pluripotent stem cells (iPSC) cardiomyocytes.

iPSC (obtained from Cellular Dynamics Incorporated), were maintained in culture for 10 days before exposing to 10 μM As2O3 in serum free medium for 1 or 24 hrs. The cells were then washed in serum free medium and exposed transiently to 3 μM Di-4-ANEPPS and left for 60-90mins before electrical recordings were made. The multi-well plate was placed on a stage incubator of an inverted microscope and the spontaneous electrical activity was recorded from the Di-4-ANEPPS fluorescence signal from areas of iPSCs in individual wells visualized using a 40x (NA0.6) objective. Fluoresence signals were

digitized at 10kHz and the digital records subsequently analysed off-line.
Under basal conditions, the spontaneous activity occurred every 1.98±0.54s (n=14) and the mean action potential duration at 75% repolarization (APD75) was 539±18ms. Treatment with As2O3 for 1 hr had no effect on the action potential duration (control vs. As2O3; 433±51 vs. 425±37), exposure for 22-24hrs prolonged APD75 significantly (P<0.05) to 601±21 ms (n=12) without any change in the rate of spontaneous activity (1.93±0.50s). Addition of the HERG channel inhibitor E4031 (30nM) increased APD75 in both groups (control: 1162±181ms and As2O3:1591±129ms). Early afterdepolarizations (EADs) occurred more frequently in the As2O3 group after treatment with E4031 (3 and 10nM) than in the corresponding control group.
In conclusion, As2O3 treatment pronged APD in iPSCs. Treatment with a HERG channel blocker causes a further prolongation of APD and increased the incidence of arrhythmic events when compared to the control group. Thus As2O3 treatment was able to recapitulate the prolonged action potential duration and increased pro-arrhythmic sensitivity to HERG channel blockade associated with LQTS in human hearts.

This work was financially supported by Clyde Biosciences (Glasgow UK), M.P.H.-V. is recipient of a postdoctoral fellowship from Fundacion Alfonso Martin Escudero (Spain).

Where applicable, the authors confirm that the experiments described here conform with The Physiological Society ethical requirements.

PCB057

Reduced expression of creatine kinase and diastolic dysfunction in failing rat ventricular myocytes

E. Fowler, R. Stones, D.S. Steele and E. White

School of Biomedical Sciences, University of Leeds, Leeds, UK

Creatine kinase (CK) catalyses the exchange of inorganic phosphate from phosphocreatine (PCr) to ADP in the myofilament lattice in cardiac myocytes and is essential for normal heart function. CK activity is decreased in heart failure (HF) causing [ADP] to rise, impairing relaxation. We have investigated the role of CK in the diastolic dysfunction of rats with right ventricular (RV) failure.
Male Wistar rats (200 g) were injected with 60 mg.kg^{-1} monocrotaline to induce pulmonary hypertension and RV failure (FAIL; N=14) or an equivalent volume of saline (CON; N=11); FAIL rats were sacrificed upon showing symptoms of HF, CON rats were sacrificed on equivalent days. Homogenates of ventricular tissue were used for Western blotting analysis. Isolated cardiac myocytes were obtained by enzymatic dissociation. Single cell experiments were conducted at 21 or 37 °C. Resting sarcomere length (SL) was measured online by fast Fourier transform of the cell's video image. Data are presented as mean±SEM; 1 or 2-way ANOVA was used to identify differences and p<0.05 was considered significant.
Resting SL was significantly shorter in RV FAIL compared to CON cells (FAIL 1.79±0.01 μm, CON 1.89±0.01 μm; p<0.05, n=79-139). Expression of muscle-isoform CK (normalised to GAPDH) was decreased by 50% in RV FAIL (N=6) compared to RV CON (N=6, p<0.05), there was no difference in CK expression between LV CON and FAIL (N=3) (Fig.1). Compared to Tyrode alone, the CK inhibitor FDNB in Tyrode (20 μM, for 10 min) significantly shortened resting SL in both CON (FDNB 1.78±0.03 μm, Tyrode 1.89±0.01 μm; p<0.05, n=10) and FAIL cells (FDNB 1.67±0.01 μm, Tyrode 1.80±0.01 μm; p<0.05, n=24).
CK binds to the myofilaments of skinned muscle fibres. Saponin-skinned cells were incubated (30 min) in solutions containing or lacking bovine CK (4.4 mg.ml^{-1}) and 10 mM PCr; in their absence the resting SL of FAIL RV was significantly shorter than CON RV (CON 1.95±0.01 μm, FAIL 1.83±0.02 μm, p<0.05, n=24) but not in their presence (CON 1.94±0.01μm, FAIL 1.90±0.01μm; p>0.05, n=24).
The results suggest that in RV failure the shorter SL is caused by reduced CK expression. Reduced CK expression may reduce resting SL by allowing local [ADP] to increase, with consequent effects on cross-bridge cycling. We are currently investigating the functional consequences of this.

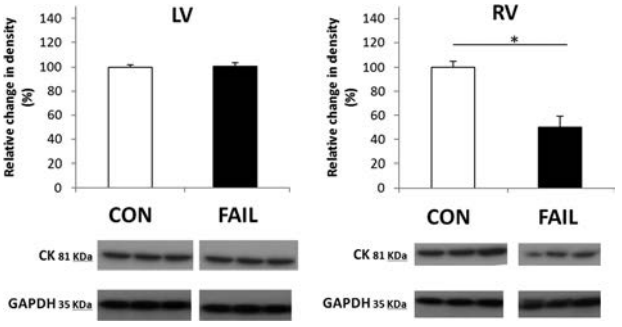

Figure 1. CK expression decreased only in the RV of rats with right heart failure

This work was supported by the MRC and a University of Leeds PhD scholarship to EF.

Where applicable, the authors confirm that the experiments described here conform with The Physiological Society ethical requirements.

PCB058

Differential regulation of the slow and rapid delayed rectifier potassium currents by cGMP dependent nitric oxide signalling pathways in isolated adult guinea pig ventricular myocytes

R.E. Caves[1], K. Brack[2], A. Ng[2] and J. Mitcheson[1]

[1]Cell Physiology and Pharmacology, University of Leicester, Leicester, UK and [2]Cardiovascular Sciences, University of Leicester, Leicester, UK

Recently, nitric oxide (NO) signalling pathways have been linked with abnormalities in cardiac repolarisation and cardiac arrhythmias. Studies from isolated heart preparations have demonstrated an antifibrillatory effect following vagus nerve stimulation, which is NO dependent. The cellular and molecular basis for this protective effect is unknown. In this study, cGMP dependent regulation of repolarisation was investigated using BAY 60-2770, a novel NO and haem independent soluble guanylyl cyclase (sGC) activator. Action potentials (APs) and ionic currents were recorded from isolated guinea pig ventricular myocytes at 37ºC using the perforated patch clamp technique. APs were stimulated at 2 Hz and the slow and rapid delayed rectifier potassium currents, I_{Ks} and I_{Kr} were measured as tail currents elicited by a voltage step from +40 mV to -50 mV. Cellular cGMP was quantified by radioimmunoassay and expressed as a fold change relative to basal levels. Values are presented as means ± S.E.M. compared by paired t test. 1 μM BAY 60-2770 increased cellular cGMP by 2.2 ± 0.3 fold (n=8) and by 7.1 ± 0.8 fold (n=7) in the presence of 100 μM IBMX (3-

Isobutyl-1-methylxanthine), a non-selective phosphodiesterase (PDE) inhibitor. In vitro assays on purified sGC have shown that ODQ (1H-[1,2,4]Oxadiazolo[4,3-a]quinoxalin-1-one) potentiates the action of BAY 60-2770. This was corroborated in our experiments, BAY 60-2770 + 10 μM ODQ increased cGMP by 27.9 ± 9.6 fold (n=4). Despite substantial increases in cellular cGMP, changes in times to 90% repolarisation of action potentials (APD_{90}) were modest. BAY 60-2770 modestly, but significantly ($p<0.001$, n=8) shortened APD_{90} by 11.3 ms, subsequent addition of ODQ in the presence of BAY 60-2770 caused no significant further APD_{90} shortening. In contrast, in the presence of IBMX, BAY 60-2770 significantly ($p<0.05$, n=7) lengthened APD_{90} by 15.7 ms, suggesting PDE inhibition permits repolarising currents to be inhibited by cGMP dependent signalling pathways. Further experiments showed that I_{Ks}, but not I_{Kr}, was inhibited by BAY 60-2770, in the presence of IBMX. IBMX enhanced I_{Ks} by 77 ± 9 % ($p<0.001$, n=8). Subsequent addition of BAY 60-2770 reduced the IBMX dependent enhancement of I_{Ks} by 68 ± 2 % ($p<0.001$, n=8). BAY 60-2770 had no significant effect on I_{Kr}, either on its own or in the presence of IBMX. Overall, these findings demonstrate the complex interplay between cGMP and cAMP mediated effects on the ion channels regulating cardiac repolarisation. The modest effect of BAY 60-2770 + ODQ on APD_{90}, despite a substantial increase in cellular cGMP, highlights that PDEs limit cGMP accumulation close to ion channels in the sarcolemma, thus compartmentalising cGMP signalling.

Where applicable, the authors confirm that the experiments described here conform with The Physiological Society ethical requirements.

PCB059

Regulation of Kv1.5 presence at the sarcolemma in atrial haemodynamic overload

C. Barbier[1], C. Eichel[1], N. Mougenot[3], A. Jacquet[3], C. Rucker-Martin[2], F. Louault[1], A. Coulombe[1], S. Hatem[1] and E. Balse[1]

[1]INSERM U956, Paris, France, [2]INSERM U999, Paris, France and [3]PECMV, Paris, France

The mechanisms responsible for atrial fibrillation (AF) are complex. At the tissue and cellular level, Ca2+ currents are downregulated whereas repolarizing K+ currents are maintained, leading to action potential shortening. At the protein level however, Kv1.5 channels, the molecular expression of IKur, the main repolarizing current in human atria, is significantly decreased.

We used a rat model of atrial remodeling induced by myocardial infarction (dilated atria) which reproduces the substrate of AF to investigate the mechanisms responsible for Kv1.5 channel internalization. Kv1.5 protein was decreased by 30% in dilated atria. However, the whole-cell current as measured by patch-clamp was maintained in dilated myocytes. The discrepancy between reduced protein level and maintained current density suggest that in dilated myocytes more Kv1.5 functional channels are inserted into the sarcolemma. We thus studied the internalization of Kv1.5 channels in control and diseased atria.

Firstly, we investigated the endocytosis pathway for Kv1.5 channels in the atria. High resolution 3-Dimensionnal microscopy revealed that Kv1.5 channels are associated with clathrin vesicles in atrial myocytes but not with caveolin. Electron microscopy (EM) showed that vesicles are found both at the lateral sarcolemma and at the intercalated disc. Blockade of the clathrin pathway using hypertonic media or SiRNA induced an increase in IKur, an accumulation of Kv1.5 channels at the sarcolemma as shown by biotinylation assays and an increased fluorescence recovery after photobleaching (FRAP), supporting the idea that Kv1.5 channels are internalized via the clathrin pathway.

Secondly, we studied the internalization activity in the dilated atria. In dilated atria, Western blot experiments showed a 35% reduction in clathrin levels. High resolution 3-Dimensionnal microscopy showed reduced association between Kv1.5 channels and clathrin vesicles in dilated myocytes. However, EM showed no significant difference in the internalization activity between sham and dilated atria.

Therefore, the reduced clathrin protein synthesis observed in dilated atria is not likely to be responsible for the accumulation of Kv1.5 channels at the sarcolemma. Other mechanisms such as increased recycling and/or membrane stabilization must be investigated to understand how IKur is maintained in dilated atria and during chronic AF.

Where applicable, the authors confirm that the experiments described here conform with The Physiological Society ethical requirements.

PCB060

The effect of stimulation frequency on post-rest potentiation and calcium handling in sheep atrial myocytes

D.K. Wrigley, A.W. Trafford and K.M. Dibb

University of Manchester, Manchester, UK

The atria are the site of the most common arrhythmia observed in clinical practice, atrial fibrillation (AF). It is hypothesized that abnormal calcium (Ca) handling in the atrial myocardium is involved in the pathogenesis of AF. As AF is strongly characterised by abnormalities in rate and rhythm, changes in these are frequently used as experimental manoeuvres to evaluate the behaviour, or to disclose abnormalities of Ca kinetics on excitation-contraction-coupling (1). Accordingly, post-rest-potentiation (PRP) allows indirect evaluation of sarcoplasmic reticulum (SR) function (2,3). PRP is a result of Ca accumulation in the SR during a pause, and an increased fractional release (FR) upon resumption of stimulation (3,4). Previous data focus on the length of the rest period, and how this affects PRP. In this study I aim to investigate the role stimulation frequency plays on PRP in sheep atrial myocytes.

Atrial myocytes were isolated from the left auricle of healthy adult sheep, which were killed by an intravenously administered overdose of pentobarbitone (200mg/kg). Experimental protocols were carried out under perforated patch, voltage clamp conditions, at 37°C. Intracellular Ca was measured using fluo-5F at stimulation frequencies of 1, 3, and 5Hz. PRP measurements were taken after rest periods of 5 seconds. Ca changes are expressed as pseudo ratio (F/F0) measurements. An increase in stimulation frequency resulted in a rise in amplitude for the first Ca transient following a period of rest (2.77±0.41, 3.86±0.70, 3.96±0.38 at 1, 3, and 5Hz respectively, $p<0.01$, n=25). This indicates a positive relationship between PRP and stimulation frequency. Conversely at steady state an effect is observed, where Ca transient amplitude decreases with a rise in stimulation frequency (1.56±0.14, 1.14±0.07, 0.86±0.07, at 1, 3, and 5Hz respectively, $p<0.01$, n=39). There were no differences in peak L-type Ca current for the first PRP following rest, with changes in stimulation frequency.

A rise in stimulation frequency results in an increase in the amplitude of the first Ca transient following a period of rest. In contrast, a negative Ca transient amplitude to frequency

relationship is observed during periods of steady state. As there is no difference in peak L-type Ca current within the first transient post rest between each frequency, a greater amount of Ca released from the SR, as a result of increased SR Ca content may play a role, which could impact on the force generation upon the first activation following rest. However, as I have not directly measure SR Ca content after periods of rest further investigation is required. This positive relationship between PRP and stimulation frequency may play an important role in contraction under arrhythmic conditions.

Endoh M (2004). Force frequency relationship in intact mammalian ventricular myocardium: Physiological and pathophysiological relevance. Eur J Pharmacol 500(1-3), 73-86.

Ravens U, Link S, Gath J, Noble M (1995). Post rest potentiation and its decay after inotropic interventions in isolated rat heart muscle. Pharmacol Toxicol 76(1), 9-16.

Bers DM (2008). Calcium cycling and signalling in cardiac myocytes. Annu Rev Physiol 70, 23-49.

Rossoni LV, Xavier FE, Moreira CM, Falcochio D, Amanso AM, Tanoue CU (2006). Ouabain-induced hypertension enhances left ventricular contractility in rats. Life Sci 79(16), 1537-45

Where applicable, the authors confirm that the experiments described here conform with The Physiological Society ethical requirements.

PCB061

Spontaneously contracting 3D in vitro heart model established from fish for the use in pharmacology

B. Grunow[1], L. Mohamet[2] and H. Shiels[1]

[1]Faculty of Life Science, University of Manchester, Manchester, UK and [2]School of Dentistry, University of Manchester, Manchester, UK

Cellular models are an important tool for studying human heart disease. To date, many research groups focus on mouse models, but murine cardiac physiology is different from human cardiac physiology. Interestingly, recent data suggests the electrophysiology of fish cardiomyocytes largely resembles that of humans (Brette et al. 2008), opening up the possibility of the fish to become a good model system to study heart disease. Recently, a fast and cost-effective in vitro heart model system has been developed (Grunow et al. 2010, 2011, 2012). The model is a 3D cell cluster which beats spontaneously and is generated from fish larvae. Morphological and molecular characterisation of the 3D in vitro heart model revealed high similarities to human heart in terms of beat rate, drug responses and structural morphology (Grunow et al. 2011).The present work uses electrophysiological techniques to characterize underlying ion currents in myocytes acutely isolated from the 3D in vitro heart model. Our results suggest that the 3D in vitro heart model has high potential

Brette F., Luxan G., Cros C., Dixey H., Wilson C., Shiels H.A. (2008). Characterization of isolated ventricular myocytes from adult zebrafish (Danio rerio). Biochemical and biophysical research communications, 374, 143-146

Grunow B., Ciba P., Rakers S., Klinger M., Anders E., Kruse C. (2010): In vitro expansion of autonomously contracting, cardiomyogenic structures from rainbow trout, Oncorhynchus mykiss. Journal of fish biology 76: 427-434

Grunow B., Wenzel J., Terlau H., Langner S., Gebert M., Kruse C. (2011): In vitro developed spontaneously contracting cardiomyocytes from rainbow trout as a model system for human heart research. Cellular Physiology and Biochemistry 27: 01-12

Grunow B., Schmidt M., Klinger M., Kruse C. (2012): Development of an in vitro cultivated spontaneously long-term contracting 3D heart model system as a robust read-out system. Cell Science and Therapy 3:116. Doi:10.4172/2157-7013.1000116

Where applicable, the authors confirm that the experiments described here conform with The Physiological Society ethical requirements.

PCB062

The absence of interference sounds present the phase shifting and signal missing on the heart sound spectral

N. Finahari[1,3], S.P. Sakti[2], R. Ratnawaty[3] and M. Indra[3]

[1]Mechanical Engineering, Widyagama University of Malang of Indonesia, Malang, East Java, Indonesia, [2]FMIPA, Brawijaya University, Malang, East Java, Indonesia and [3]Medical Faculty, Brawijaya University, Malang, East Java, Indonesia

Introduction: The interactions between heart and lungs activities are the manifestation of cardioresipratory synchronization. The harmonization between heart pulse and respiratory rate is a true synchronization phenomenon eventhough not the main variable of cardiorespiratory interaction [1]. From the mechanical physic point of view, the neighboring position of heart and lungs, raising the possibility for the interference sound waves to be occure, so that can be considered as the form of cardiorespiratory synchronization too. So far, the interference sounds just considered as noise that must be minimized or removed [2-4]. This research try to give different ways to understand the interference sounds. In this context, will be proved that the interference sounds bring a unique characteristics to the heart sounds.

Method: The research was done by analyzing the heart sounds spectral obtained from the hold and free breathing condition. These data were recorded simultaneously with the electrocardiograph (ECG) signal and the respiratory rates, from the healthy male/female in sitting position. The free breathing condition was done for 40 seconds, meanwhile the hold breathing was recorded for 15 seconds. All raw data were obtained from Amit et al. [5].

Result: The spectral analysis for the hold breathing heart sounds shows the phenomenon of phase shifting and the signal missing (Fig. 1). The results of correlation analysis prove that the phase shifting correlate with respiratory cycles, meanwhile the signal missing correlate with the ECG signal. These findings seems to be associate to the hold breathing condition that similar with the maximum inspiration condition. It means that the left ventricular filling volume flows constantly so that the heart sounds on the left area just influence by the variation of constraction-relaxation triggered by the heart electricity. The hold breathing condition is seems like permanent inspiration too because of the subject have filled the lungs as much as possible before holding the breathing. This condition makes the minimum filling volume to trigger the heart valve opening to be delayed. It means that the heart sounds generation become delayed also.

Conclusion: The present of phase shifting and signal missing in the recorded heart sounds for the hold breathing condition prove that the interference sounds between heart and lungs do have significant influences to the heart sounds dinamics. Separating the lungs sounds from the heart sounds in the auscultation process will decrease the accuracy of the analysis results.

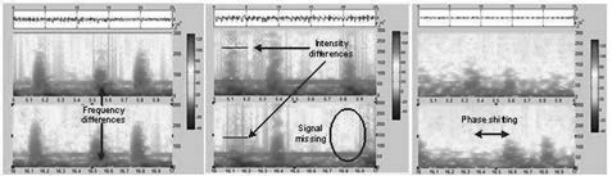

The results of spectral analysis for free (upper) and hold (lower) breathing condition. The colour represent the magnitude of frequency, the horizontal axis represent time (phase), and the vertical axis represent the sound intensity

[1]. Toledo E, Akselrod S, Pinhas I, Aravot D, 2002, Does synchronization refect a true interaction in the cardiorespiratory system? (abstract), Med Eng Phys, 24:45-52

[2]. Ghaderi F., Mohseni HR., Sanei S., 2011, Localizing heart sounds in respiratory signals using singular spectrum analysis, IEEE Transactions On Biomedical Engineering, 58 (12): 3360-67

[3]. Jin F, Sattar F, Goh DY, 2009, A filter bank-based source extraction algorith for heart sound removal in respiratory sounds, Comput Biol Med, 39 (9): 768-77

[4]. Falk TH, Chan WY, 2008, Modulation filtering for heart and lung sound separation from breath sound recordings, Conf Proc IEEE Eng Med Biol Soc 2008, pp. 1859-62.

[7]. Amit G, Shukha K, Gavriely N, Intrator N, 2009, Respiratory modulation of heart sound morphology, Am J Physiol Heart Circ Physiol, 296:H796-H805

Where applicable, the authors confirm that the experiments described here conform with The Physiological Society ethical requirements.

PCB063

Bupranolol blocks the cardiostimulatory effect of CGP12177 in rat atrial myocytes mediated via the low affinity β1-adrenoceptor

C.L. Sam[1,2], T.B. Bolton[2], I.T. Piper[1] and N.S. Freestone[1]

[1]Faculty of Science, Engineering and Computing, Kingston University, Surrey, UK and [2]Biomedical Division, St George's, University of London, London, UK

A number of β-adrenoceptor blockers (eg. pindolol and CGP12177) cause cardiostimulation at high concentrations and have been contraindicated in the treatment of ischemic heart disease due to sympathomimetic effects (Podrid and Lown, 1982). Previously Freestone *et al.* (1999) showed that a non-conventional partial agonist, CGP12177 is pro-arrhythmic in paced mouse ventricular cells. Recently, it has been shown that CGP12177, in quiescent rat atrial cells, provokes an increase in spontaneous calcium (Ca^{2+}) release events from the sarcoplasmic reticulum (SR) even in the presence of propranolol (Sam *et al.,* 2012). These propranolol-insensitive effects have led to the designation of a new receptor subtype - the $\beta1_L$-adrenoceptor (low affinity) distinct from the classical β1-adrenoceptor now called the $\beta1_H$-adrenoceptor (high affinity). A non-selective β-blocker, bupranolol, blocks the $\beta1_L$-adrenoceptor with moderate potency (Kaumann *et al.,* 1998) and thus may inhibit pro-arrhythmic effects caused by CGP12177. In this study we have used bupranolol in quiescent rat atrial cells to investigate its effect on SR Ca^{2+} release stimulated by CGP12177. Atrial cells were isolated from WKY rats (Freestone *et al.,* 2000) and were loaded with the Ca^{2+} fluorescent dye, fluo 4-AM (5μM). Ca^{2+} events within quiescent cells were imaged in whole cell and line scanning mode of the LSM510 M confocal microscope. Cells were perfused with propranolol (200nM) alone, CGP12177 (1μM) in the presence of propranolol (200nM) and CGP12177 (1μM) in the presence and absence of bupranolol (1μM) and the frequency of calcium events recorded. Propranolol produced 0.4 ± 0.1 large but localised Ca^{2+} release events (wavelets) s^{-1}. Co-administration of CGP12177 with propranolol significantly increased the incidence of wavelets to 0.86 ± 0.17 s^{-1} (n=12, $p < 0.005$). Perfusion with bupranolol alone and bupranolol with CGP12177 produced no wavelets. In terms of Ca^{2+} sparks, bupranolol produced an average of 27.4 ± 8.6 sparks s^{-1}. Co-administration of bupranolol with CGP12177, elicited 47.6 ± 12.8 sparks s^{-1} but this difference was not statistically significant. In cells not exhibiting waves or wavelets, CGP12177 increased Ca^{2+} spark frequency (compared to propranolol perfusion alone) from 42 ± 5.3 s^{-1} to 62 ± 6.1 s^{-1} (n=6, $p < 0.01$). As shown previously, CGP12177 (working through $\beta1_L$) isassociated with more potent arrhythmogenic effects in cardiomyocytes than for example, ISO (working through $\beta1_H$). It can also be concluded that bupranolol inhibits spontaneous Ca^{2+} release activity mediated via $\beta1_L$.

Podrid P.J., Lown B., Pindolol for ventricular arrhythmia. *American Heart Journal* 1982 ; **104** (2) : 491-496.

Freestone N.S., Heubach J.F., Wettwer E., Ravens U., Brown D., Kaumann AJ., Putative β4-adrenoceptors are more effective than β1-adrenoceptors in mediating arrhythmic Ca^{2+} transients in mouse ventricular myocytes. *Naunyn-Schmiedebergs Archive Pharmacology* 1999 ; **360** : 445-456.

Sam C.L.S., Bolton T.B., Piper I.T., Freestone N.S., A novel mechanism for the genesis of arrhythmias? The role of the low affinity β1-adrenergic receptor and CGP12177 in spontaneous calcium release in rat atrial myocytes. *Proceedings (P717) of the 6th European Congress of Pharmacology* 2012; Medimond International Proceedings.

Kaumann A.J., Preitner F., Sarsero D., Molenaar P., Revelli J-P., Giacobino J.P., (-)-CGP 12177 causes cardiostimulation and binds to cardiac putative β4-adrenoceptors in both wild-type and β3-adrenoceptor knockout mice. *Molecular Pharmacology* 1998 ; **53** : 670-675.

Freestone N.S., Ribaric S., Scheuermann M., Mauser U., Paul M., Vetter R., Differential lusitropic responsiveness to β-adrenergic stimulation in rat atrial and ventricular myocytes. *Pflügers Archiv : European Journal of Physiology* 2000 ; **441** (1) :78-87.

Dr Oleksandr Povstyan for his assistance using the confocal microscope.

Where applicable, the authors confirm that the experiments described here conform with The Physiological Society ethical requirements.

PCB064

Isoprenaline induced changes of action potential configuration, the role of Ca^{2+} and K^+ currents of canine ventricular cells

K. Kistamás, N. Szentandrássy, L. Bárándi, B. Hegyi, F. Ruzsnavszky, K. Váczi, T. Bányász, J. Magyar and P.P. Nánási

Department of Physiology, University of Debrecen, Medical and Health Science Centre, Debrecen, Hungary

It is well known, that a non-selective β-adrenergic receptor agonist, the isoprenaline (ISO) activates several ionic currents in mammalian myocardium, however their relative contribution to the ISO-induced changes in action potential morphology is not well explored. Therefore, our aim was to describe the effects of ISO on action potential configuration, L-type Ca^{2+} current ($I_{Ca,L}$), slow delayed rectifier K^+ current (I_{Ks}) and fast delayed rectifier K^+ current (I_{Kr}) in canine left ventricular myocytes.

Adult beagle dogs (n=39) were anaesthetized with the mixture of ketamine hydrochloride (10 mg/kg) and xylazine hydrochloride (1 mg/kg, both I.M.) according to a protocol approved by the local ethical committee, which conformed to the principles outlined in the Declaration of Helsinki. Single myocytes were obtained by enzymatic dispersion using the segment perfusion technique. Action potentials were recorded with conventional sharp glass microelectrodes, ionic currents were measured using conventional and action potential voltage clamp techniques on isolated ventricular cardiomyocytes (n=157) from dog hearts. Values are expressed as mean ± S.E.M., compared by ANOVA.
ISO (10-100 nM) caused significant and reversible shortening of action potential duration accompanied by elevation of the plateau potential. Similar results were observed when ISO was applied after pretreatment with an IKr blocker (1 μM E-4031). In the presence of an IKs blocker (1 μM HMR1556) action potentials were significantly lengthened by ISO in spite of the pronounced plateau elevation. Both ISO-induced changes were prevented by pretreatment with nisoldipine ($I_{Ca,L}$ blocker, 5 μM). Action potential voltage clamp experiments revealed a prominent slowly inactivating $I_{Ca,L}$ followed by a rise in I_{Ks}. Similar ISO-induced responses were seen in the presence of 1 μM E-4031, while the ISO-induced activation of I_{Ks} was abolished by 1 μM HMR1556. Conventional voltage clamp experiments revealed that ISO increased I_{Ks}, I_{Kr} and $I_{Ca,L}$ to 420±4 (n=5, p<0.05), 133±1 (n=8, p<0.05) and 340±13 % (n=8, p<0.05) of their baseline values, respectively, with the concomitant EC_{50} values of 14.5±1.1, 13.7±2.5 and 15.3±3.5 nM (n=5, n=8, n=8, respectively).
Our results suggest that the ISO-induced activation of I_{Ks} - but not I_{Kr} - may be responsible for the observed shortening of action potentials in the canine myocytes. The similar EC_{50} values estimated for I_{Ks}, I_{Kr} and $I_{Ca,L}$ may indicate a common mechanism responsible for the ISO-induced activation of these currents.

Keywords: β-adrenergic activation, action potential morphology, calcium current, potassium current, ventricular repolarization, canine myocytes

Where applicable, the authors confirm that the experiments described here conform with The Physiological Society ethical requirements.

PCB065

PDE5 inhibition reduces ICa-L and systolic calcium transient in the failing sheep ventricle

M. Lawless, D.A. Eisner and A.W. Trafford

University of Manchester, Manchester, UK

Heart failure (HF) is a major cause of premature mortality and increased morbidity. One of the hallmarks of HF is a decrease in responsiveness to beta-adrenergic (β-AR) stimulation. As HF patients have elevated levels of circulating catecholamines, it is possible that changes to β-AR signalling are caused by desensitisation of the β-adrenoreceptors. The second messengers cAMP and cGMP enable correct β-AR signalling by facilitating phosphorylation of a number of excitation contraction-coupling (ECC) targets. It is believed that remodelling of the cAMP pathway in HF may lead to β-AR desensitisation. In a similar vein to beta-blocker therapy, inhibitory cGMP pathway activation may improve contractility in HF patients through modulation of the remodelled cAMP pathway. Thus, we sought to investigate the effects on ECC parameters in the presence of a selective inhibitor of the main cGMP-hydrolysing phosphodiesterase isoform, PDE5.
Heart failure was induced in sheep using tachypacing. Animals were anaesthetised for pacemaker implantation (isoflurane, 1-3% in oxygen) and perioperative analgesia provided (meloxicam, 0.5 mg/kg). After 7 days recovery, right ventricular pacing (210-220 bpm) was applied until clinical symptoms of HF were evident. Animals were sacrificed by I.V. injection of pentobarbitone (200mg/kg) and collagenase digestion was used to isolate mid-myocardial left ventricular myocytes for whole cell voltage clamp studies. In the presence of the selective PDE5 inhibitor sildenafil (1 μM), systolic transient amplitude and L-type calcium current (ICa-L) were significantly reduced in both control (n=6, P<0.005) and HF (n=5, P<0.05) myocytes. When co-stimulated with the non-selective β-AR agonist isoprenaline (100 nM), PDE5 inhibition attenuated increases in ICa-L (n=5, P<0.05) with no effect on calcium transient amplitude in control myocytes. No effects of PDE5 inhibition were observed on the responses to β-AR stimulation in HF myocytes. In HF sheep chronically treated (~4 weeks) with the selective PDE5 inhibitor tadalafil (20 mg/kg) preliminary analysis of the ICa-L current properties, in comparison to control myocytes, showed a significant rightward shift of current inactivation and decreased window current. Significance assessed using one way repeated measures ANOVA and student's t-test.
The present data shows that PDE5 inhibition, possibly through increased PKG activity, can reduce baseline ICa-L and systolic calcium transient amplitude in ventricular myocytes from both normal and HF sheep. However, under stimulation of an already impaired β-AR pathway in HF myocytes, the suppressive effects of PDE5 inhibition are not observed. This may suggest a role for remodelling of the signalling pathways governing interaction of cAMP and cGMP.
Experiments were carried out in accordance with the UK Home Office Animals (Scientific Procedures) Act 1986.

Where applicable, the authors confirm that the experiments described here conform with The Physiological Society ethical requirements.

PCB066

Chamber-specific expression of sarcoplasmic reticulum Ca^{2+}-ATPase in healthy and diseased rat hearts

C.L. Sam[1,2], T.B. Bolton[2], A. Feldheiser[3], I.T. Piper[1] and N.S. Freestone[1]

[1]Faculty of Science, Engineering and Computing, Kingston University, Surrey, UK, [2]Biomedical Division, St George's, University of London, London, UK and [3]Department of Anaesthesiology and Intensive Care Medicine, Charité-Universitätsmedizin Berlin, Berlin, Germany

Depolarisation of cardiac cells causes calcium (Ca^{2+}) release from an intracellular store known as the sarcoplasmic reticulum (SR). The transient elevation in intracellular Ca^{2+} concentration that results causes cardiac contraction. SERCA2a enables cardiac relaxation when it pumps Ca^{2+} back into the SR hence refilling the Ca^{2+} store for the next contraction. The abundances of SERCA2a differ in atria and ventricles of various species so that relaxation times are shorter in atria under normal conditions (Freestone *et al.*, 1999). We show that SERCA2a has a tendency to be differently expressed in different chambers from healthy and diseased rat hearts. Left and right atria and ventricles from rats experimentally-induced to manifest heart failure (aorto-caval shunt causing volume overload) and sham-operated Wistar rats, as well as spontaneously

hypertensive rats (SHR) and their normotensive controls were snap frozen and homogenised. Western blotting was carried out and the protein abundance was quantitatively determined by densitometry. Sham-operated and normotensive animals had a tendency to have a higher abundance of SERCA2a than animals with heart failure and hypertension in both atrial and ventricular tissues as shown in Table 1. The ventricular tissue expresses less SERCA2a compared to the atria in both normal and hypertensive animal populations. A trend arises where there is a tendency for less SERCA2a protein in the disease state compared to the normal state. SERCA2a has a tendency to be less expressed in heart failure tissues (especially for left ventricular and left atrial shunt and sham-operated tissues, p = 0.1). SERCA2a also has a tendency to be expressed more in WKY compared to SHR for all four heart chambers, which may relate to less Ca^{2+} release in the SHR animals and consequently less forceful contractions of the hypertrophied heart (Li *et al.,* 2005). SERCA2a is therefore expressed in a chamber-specific manner in the cardiac tissue samples of both healthy and diseased heart.

	WKY	SHR	Sham	Shunt
LV	1.26±0.05	1.00±0.05	1.24±0.02	1.08±0.08
RV	1.04±0.03	1.00±0.01	0.96±0.10	0.87±0.08
LA	1.27±0.14	1.18±0.06	1.32±0.18	0.73±0.04
RA	1.20±0.12	0.81±0.02	1.12±0.16	0.98±0.09

Table 1. SERCA2a abundances in left and right atrial and ventricular tissues under normal conditions and diseased states.

(LV, RV, LA and RA depicts left ventricular, right ventricular, left atrial and right atrial tissues respectively).

Freestone N.S., Heubach J.F., Wettwer E., Ravens U., Brown D., Kaumann AJ., Putative β4-adrenoceptors are more effective than β1-adrenoceptors in mediating arrhythmic Ca^{2+} transients in mouse ventricular myocytes. *Naunyn-Schmiedebergs Archive Pharmacology* 1999 ; **360** : 445-456.

Li S-Y., Golden K-L., Jiang Y., Wang G.J., Privratsky J.R., et al., Inhibition of sarco(endo)plasmic reticulum Ca^{2+}-ATPase differentially regulates contractile function in cardiac myocytes from normotensive and spontaneously hypertensive rats. *Cell Biochemistry and Biophysics* 2005 ; **42** : 1-12.

Dr Andrew Snabaitis for advice in Western blotting experiments

Where applicable, the authors confirm that the experiments described here conform with The Physiological Society ethical requirements.

PCB067

Dietary fat does not alter mechanical efficiency of the rat heart: an isolated working heart study

S. Goo[1], J. Han[2], A. Taberner[2,3], P. Nielsen[2,3], I. LeGrice[1,2] and D. Loiselle[1,2]

[1]Physiology, University of Auckland, Auckland, New Zealand, [2]Auckland Bioengineering Institute, Auckland, New Zealand and [3]Engineering, University of Auckland, Auckland, New Zealand

It has been previously reported [1] that a two-fold increase in mechanical efficiency of the heart can be achieved following dietary supplementation of fish oil, namely DHA and EPA. In the same study, saturated fat-rich diet caused a significant decrease of efficiency. The objective of our study was to re-examine these two findings. Male Wistar rats, at the age of 6 weeks, were divided into three diet groups: reference (REF, n=15), fish oil-rich (FO, n=14) and saturated fatty acid-rich (SAT, n=16). The REF diet contained 6% fat (by weight), whereas both the high-fat groups (FO and SAT) contained 16% fat. Rats were fed the specified diet for 6-8 weeks, reaching weights of 400-500 g. At the end of this period, they were deeply anaesthetised with 5% isoflurane in oxygen and, after cervical-spinal dislocation, their hearts excised. Isolated working heart experiments were performed, as originally described by Neely et al. (1967) [2], at both 37 °C and 32 °C. The perfusate was a modified Tyrode's solution, gased with 100% O2. Hearts were paced at 5 Hz and 4 Hz at 37 °C and 32 °C, respectively, and subjected to a range of preloads and afterloads. Pressure-volume work of the left ventricle, global myocardial oxygen consumption and mechanical efficiency were calculated. Analysis of Variance revealed no statistically significant effect of temperature on any energetic variable. More importantly, there was no difference (p = 0.96) of mechanical efficiency among the diet groups (9.6 ± 0.3, 7.3 ± 0.3 & 7.9 ± 0.2% at 37 °C and 8.7 ± 0.4, 10.6 ± 0.4 & 10.7 ± 0.2% at 32 °C, mean ± S.E.M., for REF, FO and SAT groups, respectively). We conclude that dietary supplementation with neither Omega-3-enriched fish oils nor saturated fat alters the mechanical efficiency of the myocardium.

Pepe, S. and P.L. McLennan, Cardiac membrane fatty acid composition modulates myocardial oxygen consumption and postischemic recovery of contractile function. Circulation, 2002. 105: p. 2303-2308.

Neely, J.R., et al., Effect of pressure development on oxygen consumption by isolated rat heart. The American journal of physiology, 1967. 212(4): p. 804-14.

This study was funded by the National Heart Foundation, New Zealand (Grant No 1428)

Where applicable, the authors confirm that the experiments described here conform with The Physiological Society ethical requirements.

PCB068

Sensitivity of optical action potentials recorded in cardiomyocytes derived from human induced pluripotent stem cells to a range of drugs

I.A. Ghouri[1], M.P. Hortigon-Vinagre[1], R. Wallis[3], F.L. Burton[1], J. Cooper[2], M. Craig[3], B.D. Anson[4] and G. Smith[1,3]

[1]Cardiovascular and Medical Sciences, University of Glasgow, Glasgow, UK, [2]Electrical Engineering, University of Glasgow, Glasgow, UK, [3]Clyde Biosciences, Glasgow, UK and [4]Cellular Dynamics Inc, Madison, WI, USA

The effect of drugs on cardiac electrophysiology is important in commercial screening for human drug development. Isolated tissue from animal models and non-muscle expression-systems are currently used to screen for potential pro-arrhythmic effects. Recently, human cardiomyocytes derived from induced pluri-potent stem cells (iPSCs) with an electrophysiological phenotype similar to the ventricular myocardium have become available commercially. This study investigated the sensitivity of these cells to a series of standard drugs, and compared responses to published effective therapeutic concentrations in humans.

iPSC (obtained from Cellular Dynamics Inc, Madison WI), were maintained in culture for 10 days in a plastic 48 well plate. The cells were washed in serum-free medium and exposed transiently to 3 μM Di-4-ANEPPS. The plate was placed was placed in a stage incubator on an inverted microscope and the spontaneous electrical activity was recorded as the Di-4-ANEPPS fluorescence signal from areas of iPSCs in individual wells using a 40x (NA 0.6) objective. Fluoresence signals were digitized at 10kHz and the records subsequently analyzed off-line. Cells

were exposed to cumulative increases in drug concentrations allowing 30 mins incubation at each concentration. The procedure was repeated up to 9 times and parallel measurements were done on cells with equivalent concentrations of vehicle. Incrementing the drug concentration by 0.5 log units, a threshold was established as the first concentration at which detectable differences between the drug and control group were observed. Action potential parameters were measured, including 10%-90% rise time (Trise) action potential duration at 75% duration (APD75). Drugs used in this study were: E4031, Mexiletine, Nifedipine. Data are expressed as % change from baseline for the drug and vehicle groups.
Significant effects on APD75 were detected at 30nM E4031 vs. the control (40.0% vs. 3.2%, P<0.01 n=9). Mexiletine at 3μM significantly increased Trise (343.5% vs 134.8%, P<0.01 n=9, P<0.01 n=9). Nifedipine decreased APD75 (39.1% vs. 75.5%, P<0.05 n=4 P<0.05 n=4) at 300nM.
The detection threshold for these drug effects co-incides with published values of effective therapeutic plasma levels: (E4031, 3nM, Fujiki et al (1994); Mexiletine 2-4μM, Harner et al (2011); Nifedipine, 4-8nM, Redfern et al (2003). In conclusion, iPS derived cardiomyocytes appear to show drug sensitivities that would make them an appropriate for an invitro screen for electrophysiological effects of compounds invivo.

Fujiki A, Tani M, Mizumaki K, et al. (1994) Electrophysiologic effects of intravenous E-4031, a novel class III antiarrhythmic agent, in patients with supraventricular tachyarrhythmias. J Cardiovasc Pharmacol 23 (3): 374–8.

Harmer AR, Valentin JP, Pollard CE. (19940 On the relationship between block of the cardiac Na channel and drug-induced prolongation of the QRS complex. British Journal of Pharmacology (2011) 164 260–273.

Redfern W.S., Carlsson L., Davis A.S., Lynch W.G., MacKenzie I., Palethorpe S., Sieglf P.K.S., Stranga I., Sullivang A.T., Wallish R., Cammi A.J., Hammond T.G.(2003) Relationships between preclinical cardiac electrophysiology, clinical QT interval prolongation and torsade de pointes for a broad range of drugs: evidence for a provisional safety margin in drug development. Cardiovascular Research 58 32-45.

This work was supported by the BBSRC, Clyde Biosciences M.P.H.-V. is recipient of a postdoctoral fellowship from Fundacion Alfonso Martin Escudero (Spain).

Where applicable, the authors confirm that the experiments described here conform with The Physiological Society ethical requirements.

PCB069

Long non-coding RNAs are differentially expressed in heart failure

E.L. Robinson[1], S. Haider[2], H. Hei[3], G.M. Formovsky[3], L. Roderick[1] and R. Foo[4]

[1]Epigenetics, Babraham Institute, Cambridge, UK, [2]Bart's Cancer Institute, London, UK, [3]Partners Research Facility, Cambridge, MA, USA and [4]Genome Institute Singapore, Genome, Singapore

Heart failure is the gradual inefficacy of the heart to pump blood around the body and contributes at least 10% of the mortality rate in the UK. Hypertrophic cardiomyopathy (HCM) and dilated cardiomyopathy (DCM) are the two main pathophysiological states, the former often progressing into the latter as the condition increases in severity. Although clinically distinct conditions, changes in myocardium gene expression are similar and it is believed there are common underlying biochemical mechanisms.
The revolution in high throughput sequencing technology has enabled unbiased de novo whole transcriptome profiling. It is now known that at least 70% of the genome is transcribed to RNA, with just around 2% of this made up by the known protein-coding genes. The majority of the mammalian genome is transcribed into long non-coding RNAs (lncRNAs), defined as polyribonucleotides of ≥200 nucleotides.
Mechanically stretching neonatal mouse cardiac myocytes with equibiaxial stretch apparatus mimics pathological hypertrophy in the heart and well established alterations in gene expression in cardiac hypertrophy were confirmed by RT-qPCR. My project aims to discover whether the myocardial transcriptome array of lncRNAs changes in our mouse model of HCM.
Paired end RNA-seq from a 300-400bp library of stretched and non-stretched neonatal mouse cardiomyocyte total RNA was carried to generate 30-40 million 76-mer sequence reads per sample.
Stretching resulted in an upregulation of two lncRNAs, MIAT and MALAT-1. RT-qPCR anlaysis also detected upregulation of MALAT-1 and MIAT in the transverse aortic constriction (TAC) mouse model of pressure-overload induced heart failure, validating our findings in the stretched myocyte model. MIAT and MALAT-1 have previously been associated with increased risk of myocardial infarction and metastatic cancers respectively, but never before with cardiomyopathy. Mice undergoing surgery were anesthetized with an initial concentration of 3% isoflurane carried by medical oxygen, delivered via a nose cone. Mice were followed weekly with echocardiography. Compensated hypertrophy and cardiac dilatation were confirmed by weeks four and eight respectively.
Two additional novel unannotated transcripts were identified that showed differential expression in stretched cardiomyocytes. These are regions of the genome that are currently unannotated and potentially transcribe novel lncRNA and differential expression was validated by RT-qPCR.
LncRNA are increasingly recognised as playing a major role in genomic regulation. We therefore hypothesise that changes in expression of target genes which contribute to the deterioration of the failing heart could be due to the actions of these lncRNAs.
Subsequent in vitro and in vivo experiments will seek to understand the role of these lncRNAs in cardiac biology and how they could contribute to the progression of this complex disease.

Where applicable, the authors confirm that the experiments described here conform with The Physiological Society ethical requirements.

PCB072

L-arginine and asymmetric dimethyl arginine (ADMA) levels in human pericardial fluid in patients with open cardiac surgery

Z. Nemeth[1], A. Cziraki[3], S. Keki[2], B. Biri[2], S. Szabados[3], I. Horvath[3], A. Parniczky[1], I. Seffer[1], A. Miseta[4] and A. Koller[1]

[1]University of Pécs Medical School, Pécs, Hungary, [2]University of Debrecen, Faculty of Science, Department of Applied Chemistry, Debrecen, Hungary, [3]University of Pécs, Medical School, Heart Institute, Pécs, Hungary and [4]University of Pécs, Medical School, Department of Laboratory Medicine, Pécs, Hungary

Background - Recent studies provide evidence that vasoactive active substances are present in the pericardial fluid (PF), which levels may change in cardiovascular diseases. Increasing evidence suggests that methylated L-arginine derivative, asymmetric dimethylarginine (ADMA) is a risk factor of most cardiovascular diseases. Furthermore, it has been shown that

ADMA inhibits endothelium-dependent vasodilation by interfering with endothelial nitric oxide (eNOS) activity and/or eliciting oxidative stress, both of which interfere with the bioavailability of endothelium derived nitric oxide (NO). We hypothesized that ADMA levels in the PF reflects/contributes the pathological processes in the heart. Methods and patients - Patients were classified into two groups according to the type of surgery: coronary artery bypass graft (CABG, n = 28) and valve replacement (VR, n = 16). Blood and PF were collected during CABG and VR surgery. Levels of L-arginine and ADMA were determined in plasma and PF (with fluorescent detection after liquid chromatographic separation) of patients underwent CABG and VR surgery, compared them and an indicator of eNOS substrate availability, L-arginine/ADMA ratios were calculated. Values are expressed as means ± S.E.M. Comparisons between groups were performed using paired Student's t-test. Results - We found that in CABG group, the L-arginine levels were similar in plasma and PF (75.7±4.6 micromol/L vs. 76.9±4.4 micromol/L). In VR group, the L-arginine levels were significantly ($p<0.05$) lower in plasma compared to the PF (57.7±5.9 micromol/L vs. 71.5±5.7 micromol/L). In CABG group, the ADMA levels were the same in plasma and PF (0.7±0.0 micromol/L vs. 0.7±0.1 micromol/L). In VR group, the ADMA levels were similar in plasma and PF (0.8±0.1 micromol/L vs. 0.9±0.1micromol/L). In CABG group, the L-arginine/ADMA ratios were significantly higher compared to the VR group in both plasma (125.4±10.7 vs. 74.9±8.3) and PF (110.4±7.2 vs. 79.5±5.8). Conclusion – Based on these findings we propose that the lower L-arginine/ADMA ratios suggest increased methylation of L-arginine and limited substrate availability for eNOS and thus impaired nitric oxide signaling and vascular function in patients with heart valve disease. Keywords: pericardial fluid, vasoactive active substances, coronary heart disease, L-arginine, asymmetric dimethyl arginine, nitric oxide.

Where applicable, the authors confirm that the experiments described here conform with The Physiological Society ethical requirements.

PCB073

Cardioprotection from insulin is dependent on ROS signalling at reperfusion and is abrogated when combined with ischemic postconditioning

E. Helgeland, L. Breivik and A.K. Jonassen

Institute of Biomedicine, University of Bergen, Faculty of Medicine and Dentistry, Bergen, Norway

Reactive Oxygen Species (ROS) generated during ischemic and pharmacological pre- and postconditioning are important triggers of cardioprotection.[1,2] We have previously shown that insulin is cardioprotective both as a continuous infusion (Ins 15' rep)[3] and when given in short bursts of 3x30s at the immediate onset of reperfusion (InsPost, unpublished data), and that this protection is mediated via PI3K-Akt-p70s6K. But whether ROS is involved in insulin mediated cardioprotection is largely unknown. In addition, there has been variable success in combining cardioprotective treatments to give additional cardioprotection.[4,5] Our study therefore explores **(1)** the effect of ROS-scavenging on insulin cardioprotection, and **(2)** the effect of combining IPost with insulin therapy.

We used Langendorff-perfused rat hearts subjected to 20 min stabilization, 30 min of regional ischemia and 120 min of reperfusion. The hearts were randomized to either control (Ctr), IPost, InsPost, Ins 15' rep or Ins 15' rep + IPost, with or without the presence of the ROS scavenger N-mercaptopropionylglycine (MPG, 1 mM or 10 mM). Infarct size was determined by tetrazolium staining, and expressed as percent of area at risk. Values are expressed as means ± S.E.M. compared by one-way ANOVA and Fischer's post hoc test. Significance level was set to 0.05 and all groups were n≥6.

Our results show that both IPost and insulin treatment is dependent on ROS signalling (IPost 34.9±3.1 vs. IPost+MPG 57.0±3.7, InsPost 33.1±7.8 vs. InsPost+MPG 56.0±6.8, and Ins 15' rep 36.0±5.9 vs. Ins 15' rep+MPG 63.4±6.2, all $p<0.05$). MPG had no effect on infarct size alone (Ctr 51.8±5.5 vs. MPG 59.7±3.3 ns.). Combining insulin treatment with IPost did not afford any additional cardioprotection but abrogated it instead (IPost+Ins 1' Rep 41.6±7.5, IPost+Ins 5' Rep 57.0±3.6 and IPost+Ins 15' Rep 60.8±3.8 vs. Ctr 51.8±5.5 ns.) Scavenging free radical formation with MPG did not affect the infarct size regardless of dose (Ctr 51.8±5.5, MPG 1mM 59.7±3.3 and MPG 10 mM 66.4±5.2 vs. IPost+Ins 15' Rep + MPG 1 mM 49.7±7.1 and IPost + Ins 15' Rep + MPG 10 mM 52.3±5.3 ns.)

In conclusion, our data suggest that cardioprotection from insulin is dependent on ROS-signalling. Surprisingly, combining IPost and Ins 15' rep did not afford any additional cardioprotection, but abrogated it via blunted Akt-phosphorylation. The protection was not regained by ROS scavenging with MPG regardless of dose.

1. Tsutsumi YM, Yokoyama T, Horikawa Y, Roth DM, Patel HH. Reactive oxygen species trigger ischemic and pharmacological postconditioning: in vivo and in vitro characterization. Life sciences. Sep 22 2007;81(15):1223-1227.

Eaton M, Hernandez LA, Schaefer S. Ischemic preconditioning and diazoxide limit mitochondrial Ca overload during ischemia/reperfusion: Role of reactive oxygen species. Experimental and clinical cardiology. Summer 2005;10(2):96-103.

Jonassen AK, Sack MN, Mjos OD, Yellon DM. Myocardial protection by insulin at reperfusion requires early administration and is mediated via Akt and p70s6 kinase cell-survival signaling. Circ Res. Dec 7 2001;89(12):1191-1198.

Hale SL, Kloner RA. Combination therapy for maximal myocardial infarct size reduction. Heart disease. Nov-Dec 2001;3(6):351-356.

Chen Z, Li T, Zhang B. Morphine postconditioning protects against reperfusion injury in the isolated rat hearts. The Journal of surgical research. Apr 2008;145(2):287-294.

Where applicable, the authors confirm that the experiments described here conform with The Physiological Society ethical requirements.

PCB074

Estrogen reduced the occurrence of Takotsubo cardiomyopathy via balancing Gs /Gi protein signal pathway

D. Sun, C. Zhou, L. Zhang, X. Cao, L. Fu, L. Sang, J. Chong, S. Kang, Y. Liu and H. Sun

Physiology, Xuzhou Medical College, Xuzhou, China

Some studies show that a high concentration of catecholamines is the triggering factor of Takotsubo cardiomyopathy (TCM), particularly epinephrine (Epi) [1,2]. A high concentration of Epi switches G protein from Gs to Gi protein signal pathway, increasing negative inotropic effect [3,4]. The patients of TCM have a clear gender predilection, most of whom are primarily post-menopausal women [5]. It is unknown whether low estrogen level following menopause is associated with G protein or not in TCM.

Female Sprague–Dawley rats were ovariectomized (OVX). Six weeks later, ventricular cardiomyocytes were isolated. We

found that the shortening amplitude of cardiomyocytes increased in the OVX group, compared with the Sham group (Sham vs. OVX, p<0.05). The decrease of shortening amplitude in cardiomyocytes of Sham group was eliminated by estrogen antagonist (Sham+ ICI182 vs. OVX, p>0.05).
Further, we isolated Sham and OVX rat ventricular cardiomyocytes and subjected to Epi for making TCM model in vitro to explore the relationship between estrogen and G protein in TCM. We found that the percentage of rod-shaped cells and shortening amplitudes of the above cardiomyocytes were all decreased, compared without Epi group (Sham vs. Sham + Epi, OVX vs. OVX + Epi, p<0.05), more seriously in cardiomyocytes from OVX group (Sham + Epi vs. OVX + Epi, P<0.05). But, pertussis toxin, the antagonist of Gi protein, abolished all the differences of the above groups. We also measured the concentration of cAMP, a substance of GS downstream signaling. We found that the concentration of cAMP was increased in the Sham group and decreased in the OVX group, if the cardiomyocytes were pretreated with Epi (Sham vs. Sham + Epi, OVX vs. OVX + Epi, p<0.05). And the concentration of cAMP in Sham group was lower than that in OVX group without Epi state (Sham vs. OVX, p<0.05).
Our results indicated that the estrogen activated Gi protein signal pathway, producing negative inotropic effect at physiological state. And the estrogen activated Gs protein signal pathway rapidly when the concentration of Epi in plasma increased sharply, which limited the negative inotropic effect of Gi protein. Our results suggested that estrogen reduced the occurrence of TCM via balancing Gs /Gi protein signal pathway. In low estrogen levels, such as postmenopausal women, high concentration of Epi doesn't activate the Gs protein signal pathway effectively and the Gi protein signal pathway is strengthened. This may be the reason why TCM usually occurs in postmenopausal women.

[1] Zeb M, Sambu N, Scott P, Curzen N. Takotsubo cardiomyopathy: a diagnostic challenge. Postgrad Med J. 2011;87(1023):51-99.

[2] Gogas BD, Antoniadis AG, Zacharoulis AA, Kolokathis F, Lekakis J, Kremastinos DT. Recurrent apical ballooning syndrome"The masquerading acute cardiac syndrome." Int J Cardiol. 2009;150(1):e17-19.

[3] Paur H, Wright PT, Sikkel MB, Tranter MH, Mansfield C, O'Gara P, et al. High levels of circulating epinephrine trigger apical cardiodepression in a β2-adrenergic receptor/Gi-dependent manner: a new model of Takotsubo cardiomyopathy. Circulation. 2012;126(6):697-706.

[4]Lyon AR, Rees PS, Prasad S, Poole-Wilson PA, Harding SE. Stress (Takotsubo) cardiomyopathy—a novel pathophysiological hypothesis to explain catecholamine-induced acute myocardial stunning. Nat Clin Pract Cardiovasc Med. 2008;5(1):22-29.

[5] Akashi YJ, Goldstein DS, Barbaro G, et al. Takotsubo cardiomyopathy: a new form of acute, reversible heart failure. Circulation 2008; 118:2754-62.

We gratefully acknowledge the excellent technical assistance of Youjian Qi.

Where applicable, the authors confirm that the experiments described here conform with The Physiological Society ethical requirements.

PCB075

The role of nitric oxide and Ca^{2+}-regulation in cardioprotection from remote ischaemic preconditioning

C. Thaitirarot, H.E. Crumbie and G.C. Rodrigo

Cardiovascular Science Department, University of Leicester, Leicester, UK

We have previously shown that ischaemic preconditioning (IPC) of the whole heart protects the isolated ventricular myocytes against Ca^{2+}-overload injury during simulated ischaemia [1]. Nitric oxide (NO) signalling is known to modulate Ca^{2+}-regulation in cardiac myocytes [2] and plays a central role in IPC [3]. We have compared the involvement NO-signalling in cardioprotection in IPC versus remote ischaemic preconditioning (rIPC).
We used an isolated ventricular myocyte model of IPC of whole hearts [1] and compared this to rIPC myocytes, where naïve cardiomyocytes are "remotely conditioned" with the superfusate from preconditioned hearts. Two models of ischaemia-reperfusion (I/R) injury were used to determine protection. 1) Ischaemia was simulated in myocytes centrifuged to a dense pellet and layered with mineral oil to prevent gaseous diffusion (37°C, 30 min), and reperfusion by dispersing the myocyte pellet into oxygenated 2mM Ca^{2+} Tyrode [1] and cell death was assessed by Calcein and Propidium Iodide staining. 2) $[Ca^{2+}]_i$ was recorded from field-stimulated myocytes loaded with Fura-2 and subjected to metabolic inhibition (2 mM NaCN and 1 mM Iodoacetic acid) for 8 min followed by re-energization with 2mM Ca^{2+} Tyrode for 12 min. Cell injury was determined as the inability to maintain low diastolic $[Ca^{2+}]_i$ and to contract in response to electrical stimulation. Data are mean ± S.E.M (n = number of experiments, hearts; one-way ANOVA followed by Tukey's multiple comparison post-hoc test).
IPC and rIPC both significantly reduced the degree of necrotic injury compared to control myocytes [IPC 29.7 $\pm$ 2.1% (n = 32, 6; *P*<0.001); rIPC 30.9 $\pm$ 3.7% (n = 17, 12; *P*<0.001); control 55.1 $\pm$ 2.9% (n = 18, 13)]. The protective effect of rIPC was abolished by the non-specific NOS inhibitor L-NAME (100 μM) at 56.5 $\pm$ 3.8% (n = 13, 10; *P*<0.001), when present during the rIPC stimulus and the I/R protocol. Both IPC and rIPC increased the percentage of myocytes that recovered contractile function on re-energization following metabolic inhibition, from 39.8 $\pm$ 3.7% of control myocytes (n = 30, 12), to 63.8 $\pm$ 2.3% (n = 24, 7; *P*<0.001) and 55.7 $\pm$ 3.2% (n = 24, 9; *P*<0.01) respectively. This increased recovery of contractile function was not blocked by L-NAME present during the rIPC stimulus. However, only IPC increased the percentage of cells able to maintain a low diastolic $[Ca^{2+}]_i$ (fura-2 ratio<1) following re-energization, from 19.4 $\pm$ 3.2% of control myocytes (n = 30, 14) to 48.3 $\pm$ 3.8% of IPC myocytes (n = 24, 7; *P*<0.001) and 24.9 $\pm$ 4.5% of rIPC myocytes (n = 23, 9; ns).
Our data show that the protection against necrotic cell death of rIPC involves NOS-signalling, whereas, the improved recovery of contractile function was NOS-independent. Further, rIPC was not associated with maintained Ca^{2+}-regulation, as seen in true IPC.

Rodrigo, G.C. and N.J. Samani, Ischemic preconditioning of the whole heart confers protection on subsequently isolated ventricular myocytes. Am J Physiol Heart Circ Physiol, 2008. 294(1): p. H524-31.

Hare, J.M., Nitric oxide and excitation-contraction coupling. J Mol Cell Cardiol, 2003. 35(7): p. 719-29.

Cohen, M.V., X.M. Yang, and J.M. Downey, Nitric oxide is a preconditioning mimetic and cardioprotectant and is the basis of many available infarct-sparing strategies. Cardiovasc Res, 2006. 70(2): p. 231-9.

CT is an intercalated BSc student.

Where applicable, the authors confirm that the experiments described here conform with The Physiological Society ethical requirements.

PCB076

Oxidation of DHA is responsible for its anti-arrhythmic effects on mouse ventricular myocytes

J. Roy[1], O. Touzet-Mercier[1], J. Roussel[1], C. Oger[2], J. Galano[2], E. Pinot[2], T. Durand[2] and J. Leguennec[1]

[1]Inserm U1046, Physiologie et médecine expérimentale du cœur et des muscles, Montpellier, France and [2]UMR CNRS 5247, Institut des Biomolécules Max Mousseron, Universités Montpellier-1 et Montpellier-2, ENSCM, Montpellier, France

Since forty years, it is known that long-chain polyunsaturated fatty acids of the series n-3 (PUFAs) have cardioprotective effects by preventing cardiac arrhythmias1. The main n-3 PUFAs are eicosapentaenoic acid (C20:5 n-3, EPA) and docosahexaenoic acid (C22:6 n-3, DHA) that are highly peroxidable due to the presence of the skipped dienes2. The effects of n-3 PUFA on cardiac function are still debated, notably because of the lack of information on the mechanisms involved3. For example, it is not really known which the active lipid is: the PUFA or one of its oxygenated metabolites. A diet enriched in n-3 PUFAs (mainly fish-based), leads to enrichment in these fatty acids of cardiac cell membranes. Our hypothesis is that, during an infarct, the oxidative stress and the generation of reactive oxygen species might be responsible for an oxidation of membrane-bound PUFAs and the oxygenated metabolites generated might modulate the activity of ionic channels to exert anti-arrhythmic effects4. We thus decided to investigate the influence of the peroxidation of DHA on its potentially anti-arrhythmic properties. In this study, we applied DHA free acid or DHA methyl ester (OMe) on freshly isolated mouse ventricular myocytes without or with α-tocopherol (Vitamin E, to prevent oxidation) or hydrogen peroxide (to enhance oxidation). We investigated, using a photometric system, calcium transients (using the ratiometric calcium fluorescent dye Indo-1) and cell shortening of electrically stimulated myocytes. By stimulating β-adrenergic pathways with 10 nM isoproterenol, it is possible to observe the occurence of arrhythmic events. We observed that DHA free acid reduced the percentage of arrhythmic cells but do not DHA-OMe. The effects of DHA are correlated with the peroxidation of the fatty acid since α-tocopherol prevented the anti-arrhythmic effects while hydrogen peroxide enhanced them. In resting cells, single RyR channels spontaneously open with a very low frequency. An increased frequency of these events can cause propagating calcium waves that can lead to arrhythmias. The spontaneous calcium released events named sparks, can be observed by confocal microscopy. Here again, we observed that the frequency of calcium sparks is negatively correlated with the oxidative status of the DHA solution. These results suggest thus that rather than DHA itself, it is one or more non-enzymatic oxygenated metabolites derived from DHA that are potentially anti-arrhythmic such as neuroprostanes and/or neurofuranes4.

1 Bang H., Dyerberg J. & Nielsen A. (1971) Plasma lipid and lipoprotein pattern in Greenlandic west-coat eskimos. Lancet. 1: 1143-1145.

2 Jahn, U., Galano, J-M., Durand, T. (2008). Beyond prostaglandins chemistry and biology of cyclic oxygenated metabolites formed by free-radical pathways from polyunsaturated fatty. Angew Chem Int Ed Eng 47, 5894-5955

3 Saravanan P., Davidson N., Schmidt E. & Calder P. (2010). Cardiovascular effects of marine omega-3 fatty acids. Lancet 376, 540-550

4 Judé, S. Bedut, S., Roger, S., Pinault, M., Champeroux, P., White, E., Le Guennec, JY. (2003). Peroxidation of docosahexaenoic acid is responsible for its effects on ITO and ISS in rat ventricular myocytes. Br. J. Pharmacol. 139, 816-822.

Jérôme Roy*, Olivia Touzet-Mercier*, Julien Roussel*, Camille Oger+, Jean-Marie Galano+, Edith Pinot +, Thierry Durand+, Jean-Yves Le Guennec*.

* Inserm U1046, Physiologie et médecine expérimentale du cœur et des muscles, Universités Montpellier-1 et Montpellier-2. + UMR CNRS 5247, Institut des Biomolécules Max Mousseron, Universités Montpellier-1 et Montpellier-2, ENSCM.

Where applicable, the authors confirm that the experiments described here conform with The Physiological Society ethical requirements.

PCB077

Regulation of calcium homeostasis by palmitoyl-carnitine in ventricular cardiomyocyte: Role of mitochondria

J. Roussel[1], J. Thireau[1], V. Scheuermann[1], C. Brenner[2], A. Lacampagne[1], J. Le-Guennec[1] and J. Fauconnier[1]

[1]U1046, INSERM, Montpellier, France and [2]U769-LabEx LERMIT, INSERM, Châtenay Malabry, France

In physiological conditions, the energy required for cardiac contraction is provided by the β-oxidation of long chain free fatty acids (i.e. palmitate) in the mitochondrial matrix. To diffuse through the mitochondrial membrane, palmitate formed a complex with carnitine called palmitoyl-carnitine (PC). In order to reach the contractile demand, the rate of ATP synthesis is dynamically regulated through a mechanism called excitation-metabolism coupling (EMC). The EMC depends on the Ca2+ movement between the mitochondria and the sarcoplasmic reticulum (SR). In obesity and type 2 diabetes, patients develops a diabetic cardiomyopathy (DC), characterized by a ventricular dysfunction, with contractile and Ca2+ signaling disturbances, associated with a mitochondrial dysfunction. In the DC, the increase of fatty acid oxidation is associated with a decrease of ATP/Oxygen ratio, indicating a mitochondrial uncoupling. Although long chain fatty acid also alter Ca2+ handling, the cross regulation between mitochondria uncoupling and Ca2+ handling are not fully understood. In this work we aimed to study the effect of an acute application of PC on Ca2+ signaling and mitochondrial function on left ventricles of control C57/BL6 mice. The application of 10μM of PC on isolated mitochondria decreases the Adenine Nucleotide Transporter (ANT) activity and induced a depolarization of mitochondrial membrane. This depolarization is also observed in freshly isolated cardiomyocytes and is associated with a massive increase of mitochondrial ROS production. This PC-induced ROS production increases diastolic SR Ca2+ leak through the oxidation of SR Ca2+ release channels (the ryanodine receptor 2 (RyR2)). This disturbance of Ca2+ handling is associated to an increase of arrhythmia episodic. Inhibition of ANT using bongrekic acid prevents the mitochondrial defects, the RyR2 oxidation, altered Ca2+ handling and arrhythmia leading by an acute application of PC. Altogether, these results suggest that an acute elevation of long chain fatty acids disturbed ANT activity which affects Ca2+ handling. Disturbance of ANT activity and increase ROS production may thus contributes to development of DC.

Where applicable, the authors confirm that the experiments described here conform with The Physiological Society ethical requirements.

PCB079

Regulation of a specific population of Nav1.5 channels by CASK

C.A. Eichel[1], F. Louault[1], G. Dilanian[1], M. Essers[2], H. Abriel[2], A. Coulombe[1], S. Hatem[1] and E. Balse[1]

[1]U956, Inserm, Paris, France and [2]Clinical Research, University of Bern, Bern, Switzerland

MAGUK proteins are a superfamily of proteins implicated in the anchoring and scaffolding of macromolecular complexes at the plasma membrane. The MAGUK protein CASK differs from other MAGUKs as it possesses an N-terminal calcium/calmodulin-dependant protein kinase domain, a single PDZ domain and has the capacity to translocate to the nucleus, where it acts as a co-activator to induce the transcription of T-element containing genes. However, apart from the fact that it is expressed in the heart, little else is known about its function in this organ. We found that CASK was expressed at the protein level in rat and human myocardia. Immunostainings of myocardial cryosections revealed that CASK was located at the lateral membrane of myocytes in sharp-contrast with the other cardiac MAGUKs, SAP97 and ZO1, which are found at the intercalated disc. CASK belongs to the costamere complex at the lateral membrane as it colocalized with syntrophin/dystrophin. Co-immunoprecipitation experiments performed on heart lysates showed that CASK and dystrophin interact. Moreover, in MDX mice which lack dystrophin, CASK was no longer present at the lateral membrane of myocytes, confirming that CASK participates in the syntrophin/dystrophin costameric complex. We have previously demonstrated that cardiomyocytes express two distinct pools of Nav1.5 channels: one at the intercalated discs interacting with SAP97 and a second at the lateral membrane interacting with the syntrophin/dystrophin complex. Due to its particular location, we hypothesized that CASK was involved in the targeting of the subpopulation of Nav1.5 channels to the lateral membrane. GST pull down experiments performed on heart lysates showed that CASK interacts with Nav1.5. In addition, immunostainings revealed that CASK and Nav1.5 colocalize in freshly isolated myocytes. Furthermore, in a HEK293 cell line stably expressing Nav1.5 channels, whole-cell patch clamp recordings showed that CASK silencing enhanced the sodium current (INa) (at -30mV, -95.1 ± 10.9 pA/pF, n=12 vs control -51.4 ± 5.7 pA/pF, n=13; mean ± SEM, p<0.01) while CASK overexpression decreased INa (at -30mV, -58.6 ± 10.2 pA/pF, n=8 vs control 88.6 ± 10.6 pA/pF, n=6; mean ± SEM, p<0.05). Finally, in cultured rat atrial myocytes where CASK was silenced, INa was also enhanced. In conclusion, CASK is a new cardiac MAGUK protein which shows unique cell localization. Our results indicate that CASK is present at the costamere level where it interacts with dystrophin. Interestingly, CASK is able to regulate the Nav1.5-mediated current suggesting that it is a new partner of the Nav1.5 macromolecular complex specifically at the lateral membrane. These results characterize a previously unreported ion channel partner and provide new insight into the regulation and organization of cardiac ion channels.

Where applicable, the authors confirm that the experiments described here conform with The Physiological Society ethical requirements.

PCB080

Osmotic activation of Na^+/H^+ exchanger and Na^+/HCO_3^- cotransporter in isolated rat ventricular myocytes

L. Sottmann, P. Swietach and R.D. Vaughan-Jones

Department of Physiology, Anatomy and Genetics, University of Oxford, Oxford, UK

Na^+/H^+ exchanger 1 (NHE1) is a ubiquitous membrane transporter that regulates pH_i, $[Na^+]_i$ and cell volume. In the heart, stretch-activation of NHE1 has been claimed to be a key element of the slow force response to stretch[1]. By raising pH_i and $[Na^+]_i$, NHE1 activation may initiate hypertrophy[2]. We examined osmotic activation of NHE1 and the related Na^+/HCO_3^- cotransporter (NBC) in rat isolated ventricular myocytes.

Adult rat ventricular myocytes were enzymatically isolated. pH_i was imaged using cSNARF-1. 160 mM sucrose was added to increase osmolarity. Data are mean ± SEM, compared with unpaired Student's t-test.

Intrinsic buffering capacity (β_{int}) was measured by ammonium removal. Hyperosmotic shrinkage increased β_{int} 1.6-fold (26.3±1.6mM (n=17) vs. 16.1±1.9mM (n=6) at pH 7.3, P<0.01). pH_i was increased using an ammonium prepulse and the slope of pH_i recovery was used to calculate acid-efflux ($J=dpH/dt^* \beta$). NHE-mediated acid-efflux was greatly increased in hyperosmotic medium (11.0±0.5mM/min (n=25) vs. 2.7±0.3mM/min (n=8) at pH 7.0, P<0.001), producing an alkaline shift of 0.25 pH units in the pH_i-flux relationship.

Upon addition of 160 mM sucrose, myocytes showed gradual NHE-mediated alkalinization of 0.3 pH units over 8 min (n=5). This was abolished by the NHE-inhibitor DMA (5-(N,N-dimethyl)amiloride, 30μM, n=7).

To elucidate the osmotic regulation of NBC, bicarbonate-buffered solutions were used (NHE inhibited with 30μM DMA). NBC-mediated acid-efflux was 1.8-fold increased in hyperosmotic solution (6.3±0.7mM/min (n=17) vs. 3.4±0.3mM/min (n=25) at pH 7.0, P<0.001).

Testing a possible role of carbonic anhydrase (CA) in the osmotic activation of NHE1 and NBC, we found that acid-efflux was not altered by addition of ETZ (100μM) in isosmotic or hyperosmotic bicarbonate-buffered media (isosmotic: 10.5±0.9mM/min (n=21) vs. ETZ 14.1±1.6mM/min (n=6) at pH 6.6, P=0.065; hyperosmotic: 25.9±1.7mM/min (n=15) vs. ETZ 26.7±1.8mM/min (n=5) at pH 6.7, P>0.8). This rules out the necessity of CA activity for the combined osmotic effect on NHE and NBC.

Given the strong osmotic effect on NHE, we examined its role in myocyte volume regulation. Both video-imaging and z-stack techniques[3] showed a rapid shrinkage in hyperosmotic solution within the first minute without subsequent regulatory volume increase (z-stack data as normalized volume: after 1 min, 81.8±0.7%; 5 min, 81.1±1.0%; 10 min, 79.5±1.3%, n=7). The contribution of NHE to cellular volume maintenance during hyperosmotic shock was found to be negligible (30μM DMA added, compared to above data: after 1 min, 86.6±1.2%, P<0.01; 5 min, 83.9±0.7%, P>0.065; 10 min, 81.2±1.0%, P>0.36, n=5).

We conclude that strong activation by hyperosmotic stimuli is a common characteristic of the cardiac acid-extruders NHE1 and NBC, but does not directly involve activation of catalytic activity from native carbonic anhydrase.

[1] Cingolani HE *et al.* (2003). *Cardiovasc Res* **57**:953-960.

[2] Nakamura TY *et al.* (2008). *Circ Res* **103**:891-899.

[3] Satoh H *et al.* (1996). *Biophys J* **70**:1494-1504.

This work was supported by the Boehringer Ingelheim Fonds (LS) and the British Heart Foundation (RDVJ).

Where applicable, the authors confirm that the experiments described here conform with The Physiological Society ethical requirements.

PCB081

Histones induce rat ventricular myocyte arrhythmia and cell necrosis

A. Bleakley, C. Evers, A. Duke, Z. Yang, D. Steele and S.M. Harrison

School of Biomedical Sciences, University of Leeds, Leeds, UK

RATIONALE: Ischaemic heart disease is the leading cause of mortality in the western world. In ischaemic heart disease, the myocardium may be at risk of injury from the products of cell necrosis, such as histones. Histones, which are released into extracellular circulation from the nuclei of necrotic cells, are cytotoxic (Xu et al., 2009). Histone-induced toxicity is mediated through direct cellular membrane interaction and resultant cation influx. The aim of this study was to investigate the effects of histones on Ca^{2+} regulation, contractility and viability in rat ventricular myocytes.
METHODS: Ventricular myocytes were isolated from healthy male adults Wistar rats (200-250 g) that had been killed humanely using an ethically approved Schedule 1 procedure. First, electrically stimulated myocytes (1Hz), loaded with fura-2 AM, were superfused at 30°C with a normal Tyrode solution in the absence and presence of H3 (3.0 μg/ml) or Hmix (H1-H2A-H2B-H3-H4-H5; 3.0 μg/ml) for a maximum of 10 min. Second, this was repeated in the absence or presence of the membrane stabilizing agent pluronic F-68 or foetal calf serum (FCS). Third, quiescent myocytes were incubated at room temp with normal Tyrode solution (with and without FCS) in the absence or presence of H3. Cell viability was measured after 5 and 60 min.
RESULTS: In 33 out of 34 electrically stimulated myocytes, exposure to H3 induced Ca^{2+} overload and spontaneous contractions within 8 min. In 13 out of 22 stimulated myocytes, exposure to Hmix also induced arrhythmogenesis. Pluronic F-68 (100 mg/100 ml) offered no protection on exposure to H3 as 18 out of 18 myocytes were arrhythmic, whereas 5% FCS protected 10 out of 11 myocytes from arrhythmogenesis. For populations of quiescent myocytes, incubation with H3 led to a significant 27% reduction in cell viability ($P<0.05$) from 5 to 60 min, however the presence of 5% FCS protected against necrosis.
CONCLUSION: H3 induced Ca^{2+} overload, arrhythmogenesis and cell death in ventricular myocytes. Pluronic F-68 failed to protect myocytes while FCS protected against cell necrosis, suggesting plasma proteins are potential cytoprotective agents against acute histone-induced cytotoxicity.

Xu J *et al.* (2009). Nature Medicine **15**, 1318-1322

Where applicable, the authors confirm that the experiments described here conform with The Physiological Society ethical requirements.

PCB082

Phosphodiesterase type 4 inhibition increases delayed afterdepolarizations upon β-adrenergic stimulation in cardiac myocytes: Role of protein kinase A and Ca^{2+}/calmodulin kinase II

P. Bobin, R. Fischmeister, G. Vandecasteele and J. Leroy

Signaling and Cardiac Physiopathology, INSERM UMR-S 769 LabEx LERMIT University Paris-Sud, Châtenay-Malabry, France

β-adrenergic receptor (β-AR) stimulation increases cardiac function by increasing cAMP levels and activating protein kinase A (PKA). PKA enhances Ca^{2+}-induced Ca^{2+}-release by phosphorylating L-type Ca^{2+} channels, ryanodine receptors and phospholamban which are also targets of the Ca^{2+}/calmodulin kinase II (CaMKII). Any disregulation in the β-adrenergic pathway can lead to cardiac arrhythmias. Multiple cyclic nucleotide phosphodiesterases (PDEs) regulate local concentrations of cAMP, among which the PDE4 family plays an important role. The aim of this study is to investigate the proarrythmic effects of PDE4 inhibition and evaluate the relative contribution of PKA and CaMKII in this mechanism. Action potentials (AP) were recorded at a frequency of 1 Hz in isolated adult Wistar rat ventricular myocytes using the patch clamp technique. Application of the non selective β-AR agonist Isoprenaline (Iso 1 nM) induced delayed afterdepolarizations (DADs) recorded during 10 s after the cessation of electrical stimulation which were potentiated by the selective PDE4 inhibitor Ro20-1724 (1.5±0.3 DADs/10s, n=18 with Iso alone, $p<0.01$ versus control; and 2.9±0.5 DADs/10s with Iso+10 μM Ro20-1724, $p<0.01$ versus Iso alone, values are means±S.E.M. compared by one-way ANOVA with Tukey *post hoc* test). These DADs correlated with spontaneous calcium release events (SCRs) recorded with an IonOptix® system in myocytes loaded with Fura-2AM (5 μM). The SCRs appeared upon Iso application (1 nM) and their incidence increased from 1.6±0.4 SCRs/10s (n=21) in Iso alone to 4.3±0.5 SCRs/10s (n=25; $p<0.001$) when PDE4 was concomitantly inhibited. The SCRs observed in the presence of Iso+Ro were abolished in cells preincubated with the PKA inhibitor H-89 (10 μM) (n=6; $p<0.001$) and their occurrence diminished by 40% when CaMKII was inhibited by 10 μM KN-93 (n=23; $p<0.05$). The inactive KN92 (10 μM) compound had no effect on SCRs (n=13). These results show that upon β-AR stimulation, PDE4 inhibition promotes DADs due to SCRs through both PKA and CaMKII activation.

Where applicable, the authors confirm that the experiments described here conform with The Physiological Society ethical requirements.

PCB083

Contribution of active and passive stiffness to diastolic dysfunction in rats following aortic banding

.T. Røe[1,2], J. Aronsen[1,2], M. Frisk[1,2], O.M. Sejersted[1,2], I. Sjaastad[1,2] and W.E. Louch[1,2]

[1]Institute for Experimental Medical Research, Oslo University Hospital and University of Oslo, Oslo, Norway and [2]KG Jebsen Cardiac Research Center and Center for Heart Failure Research, University of Oslo, Oslo, Norway

In approximately half of heart failure patients, systolic function is near normal while diastolic function is impaired. This condition is therefore referred to as diastolic heart failure (DHF)

or heart failure with preserved ejection fraction (HFpEF). The mechanisms underlying the diastolic dysfunction are still unclear, but may be attributed to stiffening of the myocardium. Alterations in the extracellular matrix and cytoskeleton have been reported to contribute to greater passive stiffness in this condition (1). However, the contribution of altered Ca2+ handling to the active process of cardiomyocyte relaxation remains largely uninvestigated. Hypertrophy due to aortic stenosis is one of several etiologies associated with DHF, and with aortic banding (AB) we similarly induced hypertrophy and diastolic dysfunction in Wistar rats. All procedures were performed during inhalation anesthesia (65% N2O, 32% O2, 2.5% isoflurane). Experiments were performed 6 weeks after aortic banding. Rats with detectable systolic heart failure (reduced left ventricular shortening) were excluded. Compared to sham-operated controls, echocardiography revealed hypertrophy and diastolic dysfunction in AB. This was indicated by increased posterior wall thickness and decreased peak early diastolic tissue velocity. The in vivo diastolic dysfunction was confirmed by isometric force measurements in myocardial strips. We observed longer time to peak force and slower relaxation in AB across a range of stimulation frequencies (0.5-6 Hz). Surprisingly, isolated cardiomyocytes exhibited the opposite features. Single cell contractions, measured by edge detection, revealed significantly faster time to peak contraction and faster relaxation in AB. At high frequencies, AB cardiomyocytes also showed less diastolic contracture than sham cells. The mechanism underlying the improved single cell relaxation appeared to be faster cytoplasmic Ca2+ removal, evident as more rapid decay of Ca2+ transients (whole-cell fluorescence, fluo 4-AM) in AB across a range of frequencies. Furthermore, with increasing pacing rate AB cardiomyocytes exhibited a less pronounced increase in diastolic [Ca2+] than sham, and elevated SR Ca2+ content. These observations were consistent with a measured increase in the rates of both sarcoplasmic reticulum Ca2+ reuptake and Ca2+ extrusion in AB. Confocal imaging of cells stained with di-8-ANEPPs indicated maintained t-tubule organization, consistent with an unaltered time to peak of Ca2+ transients. Our results consequently indicate that despite improved Ca2+ handling, AB induces diastolic dysfunction in vivo as well as in intact myocardium ex vivo. We therefore suggest that increased passive stiffness is the major contributor to the impaired diastolic function in this condition.

Borlaug BA & Paulus WJ (2011). Eur Heart J 32, 670-679

Where applicable, the authors confirm that the experiments described here conform with The Physiological Society ethical requirements.

PCB085

Smooth Muscle in Turtle Atrial Myocardium: Functional and Histological Evidence

S.N. Saxton[1], J. Stecyk[2], B. Gannon[3], T. Farrell[4] and H. Shiels[5]

[1]Faculty of Life Sciences, University of Manchester, Manchester, UK, [2]Department of Biological Sciences, University of Alaska, Anchorage, AK, USA, [3]Department of Anatomy and Histology, Flinders University, Adelaide, SA, Australia, [4]Faculty of Land and Food Systems and Department of Zoology, University of British Columbia, Vancouver, BC, Canada and [5]Faculty of Life Sciences, University of Manchester, Manchester, UK

In 1887 some unusual characteristics were noted in the contractile properties of tortoise atria that became known as "oscillations of tonus". The oscillations were later found to be present in the turtle atria, and believe to be caused by a layer of endocardial smooth muscle. Since 1925, there has been no further published interest in these oscillations. In this study, histological and immunohistochemical staining techniques were used to confirm the presence of endocardial smooth muscle, and contractile studies were used to further characterise its properties. Atrial tissue was isolated from the red eared slider turtle (Trachemys scripta), and contractile responses to adrenaline, acetylcholine and wortmannin were recorded. Tissue was also embedded in paraffin and stained using haematoxylin & eosin stain, or was labelled using smooth muscle α-actin monoclonal antibodies. Results from these studies will be considered in relation to earlier findings and the significance of the smooth muscle layer in the reptile myocardium will be discussed.

Where applicable, the authors confirm that the experiments described here conform with The Physiological Society ethical requirements.

PCB086

5-HT2 receptor activation maintains phrenic motor output following chronic cervical spinal cord injury

K. Lee[1], B.J. Dougherty[2], M.S. Sandhu[2] and D.D. Fuller[2]

[1]Biological Sciences, National Sun Yat-sen University, Kaohsiung, Taiwan and [2]Department of Physical Therapy, University of Florida, Gainesville, FL, USA

C2 spinal hemisection (C2Hx) results in inactivation of ipsilateral phrenic bursting due to interruption of bulbospinal respiratory pathways. Plasticity in the spinal phrenic circuitry results in partial recovery of phrenic output over weeks to months and the recovery correlates with time-dependent return of spinal serotonin (5-HT) immunoreactivity. Both the 5-HT type 2A and 2C receptor subtypes are present on phrenic motoneurons, and the 5-HT2A subtype is upregulated after C2Hx compared to spinal-intact tissues. We explored the functional role of these receptors by testing the hypothesis that pharmacologic blockade would attenuate phrenic motor output in rats with chronic (8-10 weeks) C2Hx. In initial experiments, bilateral phrenic activity was recorded in anesthetized, vagotomized and mechanically ventilated rats. The 5-HT2A/C receptor antagonist ketanserin (1 mg/kg, i.v.) had no impact on respiratory burst frequency, but triggered a persistent, bilateral reduction in phrenic burst amplitude in C2Hx but not spinal-intact rats. The relative reduction of phrenic bursting was considerably greater in the nerve ipsilateral to the lesion. In additional experiments, tidal volume and diaphragm EMG activity were measured during spontaneous breathing in vagally-intact anesthetized rats before and after i.v. ketanserin. The ipsilateral diaphragm EMG signal was significantly attenuated following ketanserin in C2Hx but not spinal-intact rats. The ketanserin-triggered reduction of ipsilateral diaphragm EMG was accompanied by a small increase in inspiratory tidal volume. We speculate that the increased tidal volume reflects robust compensatory recruitment of accessory inspiratory muscles. We conclude that activation of 5-HT2A/C receptors facilitates phrenic motoneuron bursting following chronic C2Hx, and that these receptors are likely located in the spinal cord.

Support for this work was provided by grants from the National Science Council (NSC, NSC100-2320-B-110-003-MY2)(KZL), National Institutes of Health (NIH 1R01NS080180-01A1)(DDF) and Craig H. Neilsen Foundation #220521 (MSS).

Where applicable, the authors confirm that the experiments described here conform with The Physiological Society ethical requirements.

PCB089

Effect of moderate aerobic exercise on cardiovascular autonomic function in type 2 diabetes mellitus

R.K. Goit[1], R. Khadka[2], L. Thapa[3] and B.H. Paudel[2]

[1]Physiology, Nepalgunj Medical College, Banke, Nepal, [2]Physiology, BP Koirala Institute of Health Sciences, Dharan, Nepal and [3]Internal Medicine, College of Medical Sciences, Bharatpur, Nepal

Several studies have reported that regular physical activity is an important component of a healthy lifestyle and low levels of physical fitness are closely related to several chronic diseases, including type 2 diabetes mellitus (T2DM). Many studies have also suggested beneficial effects of regular exercise in preventing sudden cardiac death in healthy individuals and in patients with cardiovascular disease. Despite this, there is widespread tendency to ignore exercise testing in clinical management of patients with diabetes mellitus even when evidence abound showing that exercise improves health status in patients with diabetes mellitus (George & Russell, 2007). A very serious and common complication of T2DM is diabetic autonomic neuropathy (DAN). Cardiac autonomic neuropathy is the most clinical important and well-studied form of DAN, due to its association with a wide spectrum of adverse cardiovascular outcomes (Vinik et al, 2003). It is commonly perceived that a regular heart beat is a sigh of healthy heart. However, the rhythm of a healthy heart is characterized by significant beat to beat variability. This heart rate variability (HRV) has been used as a simple, non-invasive technique to examine cardiovascular autonomic function. HRV of 15 individuals with T2DM were assessed. Resting electrocardiogram (ECG) at spontaneous respiration was recorded for 5 min in supine position. Recording was performed before and after a six month, supervised, progressive, aerobic training program, three times weekly. The data were expressed as median (interquartile range). The p value <0.05 was considered statistically significant. In the time domain variable square root of the mean of the squared R-R intervals (RMSSD) [29.7 (26 - 34.5) vs. 46.4 (29.8 - 52.2) ms, p=0.02] and number of R-R intervals that differ by more than 50 ms (NN50) [35 (18 - 47) vs. 98 (20-114)] count, p=0.03) were significantly increased after exercise. In the frequency domain variables low frequency (LF) [62.4 (59.1 - 79.2) vs. 37 (31.3-43.3) nu, p=0.03) and LF/HF [1.67 (1.44 – 3.8) vs. 0.58 (0.46 - 0.59) p=0.009] were significantly decreased while high frequency (HF) [95 (67-149) vs. 229 (98-427) power, p=0.006] and HF [37.6 (20.8-40.9) vs. 63 (56.7-68.7) nu, p=0.003) were significantly increased after exercise. In Poincare plot standard deviation (SD) 1 [21.3 (18.5-24.8) – 33.1 (21.5 – 37.2), p=0.027] was significantly increased after exercise. These data suggest that three times weekly, six month, moderate aerobic exercise program is associated with significant improvements in cardiovascular autonomic function in person with T2DM by increasing vagal tone and decreasing sympathetic activity.

George DH & Russell DW (2007). Exercise stress testing in patients with type 2 diabetes: When are asymptomatic patients screened? Clin Diabetes 25:126-130.

Vinik AI, Maser RE, Mitchell BD & Freeman R (2003). Diabetic autonomic neuropathy. Diabetes Care 26: 1553-1579.

Where applicable, the authors confirm that the experiments described here conform with The Physiological Society ethical requirements.

PCB090

Comparison of the functional regenerative activity of Human Umbilical Cord Blood MNCs and CD34+ cells in acute myocardial infarction rat model

N.M. Abogresha[1], M.I. Mohamed[1], M.K. Tawfik[2], M.M. Habba[3] and Y.M. El-Wazir[1]

[1]Physiology, Faculty of Medicine, Suez Canal University, Ismaillia, Egypt, [2]Pharmacology, Faculty of Medicine, Suez Canal University, Ismaillia, Egypt and [3]Radiology Department, Faculty of Medicine, Suez Canal University, Ismaillia, Egypt

Myocardial infarction is a leading cause of morbidity and mortality worldwide. Recently, studies have been focused on myocardial regeneration and neovascularization through stem cell therapy. The aim of this study is to compare between the roles of human umbilical cord blood mononuclear cells (MNCs) and CD34+ stem cells in improving functional changes resulting from induced acute myocardial infarction (AMI) in rats. Methods: Forty albino Wistar rats divided into 5 groups were included; group 1 is control untreated group; group 2 received subcutaneous injection of 0.2 ml saline; group 3 is AMI group; group 4 is MNCs treated group and group 5 is CD34+ treated group. AMI was induced in groups 3, 4 and 5 by isoprenaline hydrochloride. One day after AMI induction cardiac enzymes were assessed to ensure occurrence of AMI. After one week groups 3 and 4 were treated by IV injection in the tail vein with a dose of 107 MNCs/rat and 106 CD34+ cells/rat respectively. After 4 weeks, rats were anesthetized by intraperitoneal injection of urethane in a dose of 1.25 mg/Kg (Iwamoto etal., 1987) and subjected to ECG monitoring and Echocardiography, then animals were sacrificed and hearts were removed for assessment of vascular endothelial growth factor (VEGF) mRNA expression. Results: One day after AMI induction, cardiac enzymes were significantly higher in groups 3, 4 and 5 compared to other groups verifying occurrence of AMI induction. ECG showed marked elevation of ST segment and presence of pathological Q wave in G3 compared to the control group. There was significant reduction in ST segment in rats treated with MNCs or CD34+ cells associated with the disappearance of pathological Q wave compared to rats with AMI. Ejection fraction (EF) was statistically lower in G3 when compared to G1, G4 and G5 indicating that the treatment with CD34+ cells and MNCs improve EF. There was no difference between the two treated groups in both ECG and EF indicating that the treatment with MNCs or CD34+ has the same therapeutic effect. VEGF mRNA gene expression in group 3 was slightly higher than control group and its expression increased significantly in both treated groups compared to control and AMI groups; indicating the formation of new vessels. However, there was no significant difference in both treated groups; indicating that both kinds of treatment have the same effect on the gene expression. Conclusion: Treatment with human umbilical cord blood MNCs and CD34+ cells can improve the chemical, electrical and functional alterations in the heart after AMI induction in a rat model. This improvement could be attributed to enhanced new vessel formation. Keywords: AMI, Human Umbilical cord blood, CD34+ cells, MNCs & VEGF.

Iwamoto K. Et al., (1987). J.pharmacol.Bio.Dyn:10(6):280

Suez Canal University

Where applicable, the authors confirm that the experiments described here conform with The Physiological Society ethical requirements.

PCB091

Ghrelin - Is it cardioprotective in type 2 diabetics?

S. Abd El-Fattah[1], G. Nasr[2], D. Abd-Elhalim[1] and Y.M. El-Wazir[1]

[1]Physiology, Suez Canal University, Ismailia, Egypt and [2]Cardiology, Suez Canal University, Ismailia, Egypt

Diabetes is commonly associated with changes in cardiac structure and function, even in the absence of epicardial atherosclerotic disease. The exact cause of these non-atheroscelrotic cardiac changes is not exactly known (1). In view of the recently reported favorable metabolic effects of ghrelin in type 2 diabetes (2), and also the reports of its beneficial effects in several cardiovascular disorders (3), we assessed fasting serum ghrelin concentrations in 26 diabetics of type 2 with asymptomatic left ventricular structural and functional changes (study group) and 26 age and sex matched subjects having type 2 diabetes without left ventricular structural and functional changes (control group). Both groups were assessed for clinical characteristics, metabolic (lipid profile and fasting blood glucose (FBG) and hormonal parameters (serum leptin, ghrelin and insulin levels), ECG was performed and QTc dispersion (QTcd) was calculated for detection of cardiac autonomic neuropathy and the following LV structural and functional parameters were assessed by two-dimensional echocardiography: left ventricular end-systolic diameter (LVESD), left ventricular end-diastolic diameter (LVEDD), left ventricular posterior wall thickness, (PWT), interventricular septal thickness at end-diastole (IVST), left ventricular mass index in gm/m2 (LVMI, E/A ratio, ejection fraction, Comparing the related parameters in the 2 groups was done by t-test.. Results showed that no significant difference was found as regarding clinical and lipid profile parameters. Study group was found to have significantly higher levels of FBG, leptin and insulin, while fasting serum ghrelin levels were significantly lower in this group of patients. Statistically significant correlations were found between both leptin and ghrelin, with FBG, insulin, QTcd, and all echocardiographic LV structural and functional parameters. In conclusion, left ventricular structural and functional changes among type 2 diabetics are associated with decreased serum levels of ghrelin, and higher levels of serum glucose, insulin and leptin. These data infer that ghrelin might have a cardioprotective effect in patients with diabetes type.

Echocardiographic, metabolic and hormonal parameters in the 2 groups

	Study group (n=26)	Study group (n=26)	p-value
LVMI (g/m2)	107.8 + 36.9	69.1 + 7.1	0.001
EF (%)	62.2 + 3.2	71.8 + 4.01	0.001
E/A ratio	0.8 + 0.1	1.3 + 0.1	0.001
QTc dispersion (msec.)	61.9 + 5.2	47.9 + 4.08	0.001
Fasting blood glucose (mg/dl)	269.5 + 36.8	156.4 + 43.9	0.001
Leptin (ng/ml)	25.5 + 11.1	7.2 + 3.4	0.001
Ghrelin (fmol/ml)	2.2 + 0.4	4.3 + 2.4	0.001
Fasting serum insulin (μU/ml)	18.6 + 13.2	5.7 + 1.6	0.001

Pattoneri P, Sozzi FB, Catellani E, Piazza A, Iotti R, Michelini M, Goldoni M, Borghetti A, Cappellini MD, Manicardi V: Myocardial involvement during the early course of type 2 diabetes mellitus: usefulness of myocardial performance index. Cardiovasc Ultrasound. 2008 Jun 5; 6:27.

Verhulst PJ, Depoortere I.: Ghrelin's second life: from appetite stimulator to glucose regulator. World J Gastroenterol. 2012 Jul 7;18(25):3183-95.

Kishimoto I, Tokudome T, Hosoda H, Miyazato M, Kangawa K.: Ghrelin and cardiovascular diseases. J Cardiol. 2012 Jan;59(1):8-13.

The authors wish to thank Zaki Bahussein, graduate student in the Physiology department for his great help in the practical work

Where applicable, the authors confirm that the experiments described here conform with The Physiological Society ethical requirements.

PCB092

Assessment of autonomic nerve function in patients with irritable bowel syndrome

M. Nayem, N. Begum and S. Ferdousi

Physiology, Bangabandhu Sheikh Mujib Medical university, Dhaka, Bangladesh

Background: Autonomic nerve function impairment is related to development of Irritable Bowel Syndrome (IBS). Heart rate variability (HRV) is a useful tool to measure autonomic nerve function activity and also sympatho-vagal balance.Objective: To assess autonomic nerve function activity by heart rate variability analysis in patients with Irritable Bowel Syndrome. Methods: This cross sectional study was conducted in the Department of Physiology, Bangabandhu Sheikh Mujib Medical University (BSMMU), Dhaka from 1st July 2010 to 30th June 2011. Ninety patients aged 20-50 years of both sexes with Irritable bowel syndrome were included in the study group. They were enrolled from the OPD of Gastroenterology in BSMMU. For comparison age and sex matched 30 apparently healthy subjects were also studied as control. The power spectral HRV parameters were recorded by a digital Polyrite. For statistical analysis ANOVA, independent sample t-test and Pearson's correlation coefficient test were performed. Results: Mean resting pulse rate, mean HR, SBP, DBP, LF, LF norm and LF/HF were significantly higher and total power, HF, HF norm were significantly lower in IBS group compared to those of control. Again total power, HF, HF (nu) were negatively correlated and LF power, LF (nu), LF/HF were positively correlated with duration of disease .But the correlation of total power was statistically significant. Conclusion: The results suggest markedly lower parasympathetic with concomitant higher sympathetic activity and shifting of sympathovagal balance towards sympathetic predominance in patients of IBS. In addition, decreased vagal modulation may be inversely related to the duration of IBS.

Where applicable, the authors confirm that the experiments described here conform with The Physiological Society ethical requirements.

PCB093

Orchidectomy attenuates cardiopulmonary reflex-mediated bradycardia and hypotension in conscious rats

T.U. Andrade[1,2], A.M. Nascimento[1,2], O.A. Heringer[1], K.O. Cassaro[1], P.L. Cunha[1], I.C. Kalil[1] and N.S. Bissoli[2]

[1]Pharmacy, University of Vila Velha - UVV, Vila Velha, Espírito Santo, Brazil and [2]Pharmaceutical Sciences, Fedral University of Espírito Santo - UFES, Vila Velha, Espírito Santo, Brazil

The influence of male hormones in the reflex control of the cardiovascular system has been investigated lately. Testosterone has been shown to improve the baroreflex-madiated bradycardia, but high doses of anabolic-androgenic steroids (AAS) have the opposite effect. Cardiopulmonary reflex is

blunted under AAS influence, but surprisingly, no study has already investigated the physiological role of testosterone on this reflex (the Bezold-Jarisch Refelx-BJR). We investigated the effect of castration, in different periods after orchidectomy (OVX), in the BJR control of diastolic arterial pressure (DAP) and HR. Male Wistar rats were divided into six experimental groups, as stated in Table 1. OVX was performed under sodium pentobarbital anesthesia (50mg.kg-1, intra-peritoneal, Crystal, Brazil). The experiments were performed in accordance with the ethical principles for animal experimentation by the Brazilian College of Animal Experimentation and were approved by our Institutional Ethics, Bioethics and Animal Welfare Committee (Protocol 118/2010). BJR was analyzed by measuring the bradycardia and hypotension responses elicited by phenyldiguanide administration (1.5–24 μg/kg). Mean arterial pressure (MAP) was assessed and myocyte hypertrophy was determined by morphometric analysis. Testosterone and 17β-estradiol were measured in blood samples. Table 1 shows that the reduction of BJR control of DAP starts after 72h of OVX and after 7 days in the control of HR. After 21 days of castration the BJR reach its lowest capacity to control DAP and HR. The levels of testosterone were reduced in orchidectomized groups (OVX24h:0.26±0.02; OVX72h:0.18±0.01; OVX7D:0.12±0.01; OVX14D:0.08±0.01; OVX21D:0.01±0.00 ng/mL; p<0.01) in comparison with SHAM (0.47±0.12 ng/mL). Blood 17β-estradiol (SHAM:0.022±0.003; OVX24h:0.023±0.002; OVX72h:0.028±0.003; OVX7D:0.025±0.003; OVX14D:0.023±0.001; OVX21D:0.026±0.002 ng/mL), MAP (SHAM:104±3; OVX24h:101±5; OVX72h:108±4; OVX7D:110±4; OVX14D:107±5; OVX21D:105±4 mmHg), and myocyte hypertrophy (SHAM:5.3±0.4; OVX24h:4.9±0.3; OVX72h:4.8±0.3; OVX7D:5.6±0.5; OVX14D:5.1±0.4; OVX21D:5.3±0.4 myocyte nuclei/high power filed) did not change among the experimental groups. We conclude that castration of male animals caused decrease in testosterone levels and reduced sensitivity of BJR, indicating a positive physiological role of testosterone on functioning of this reflex.

Groups	Fenyldiguanide (μg. kg^{-1})									
	DAP					HR				
	1,5	3,0	6,0	12	24	1,5	3,0	6,0	12	24
SHAM	47±8	58±8	77±7	89±2	92±5	56±5	75±2	79±2	83±2	87±2
OVX24h	39±11	48±10	63±10	81±5	88±2	58±5	67±4	76±2	80±2	85±2
OVX72h	38±6	49±10	55±6**	69±6**	86±6	40±11	65±9	73±4	80±3	84±3
OVX7D	33±6	45±5**	54±4**	68±5**	83±2*	18±8**	61±5*	78±1	82±1	86±1
OVX14D	18±6**##	33±3**#	45±5**	56±3**	67±3**	20±5**	58±5**	73±5	70±4*	80±5
OVX21D	12±4**##	29±3**#	35±2**##+	42±4**##+	55±4**#+	16±4**	42±5**+	58±3**++	62±3**++	71±2**+

Table 1 Fenyldiguanide induced-decrease in heart rate (HR) and diastolic blood pressure (DAP) in control (SHAM; n=6) and OVX rats after 24h (OVX24h; n=6), 72h (OVX72h; n=6), 7 days (OVX7D; n=6), 14 days (OVX14D; n=6), and 21 days (OVX21D; n=6) of OVX. Values are expressed as the mean ± S.E.M, compared by ANOVA, followed by the post-hoc Tukey test. *p<0.05 and **p<0.01in comparison with SHAM. #p<0.05 and ##p<0.01in comparison with OVX7D; +p<0.05 and ++p<0.01in comparison with OVX14D.

This study was supported by "Fundação de Amparo à Pesquisa do Espírito Santo (FAPES)", "Conselho Nacional de Desenvolvimento Científico e Tecnológico (CNPq)" and "Comissão de Aperfeiçoamento de Pessoal de Nível Superior (CAPES)".

Where applicable, the authors confirm that the experiments described here conform with The Physiological Society ethical requirements.

PCB095

Combined assessment of capillary microcirculation and arterial stiffness to identify cardiovascular risk in human hypertension

M. Dinkel[1,2], M. Saedon[1,2], J. Lismore[2], P. Ray[2], C.H. Imray[2,1] and D.R. Singer[1,2]

[1]Warwick Medical School, Warwick, UK and [2]UHCW NHS Trust, Coventry, UK

Introduction: Both arterial stiffness (AS) and capillary rarefaction are biomarkers of cardiovascular risk. We assessed whether capillary videomicroscopy may complement measurement of arterial stiffness in clinical assessment of cardiovascular risk.
Subjects & Methods: We studied 94 out-patients with treated hypertension (age 63.9±1.5(SE)yrs, blood pressure (Omron) 147/87+2/1mmHg, 27F; hypercholesterolaemia 59, diabetes mellitus 23, chronic kidney disease 28, ischaemic heart disease 27, stroke syndromes 16, peripheral vascular disease 31). AS was estimated from aortic pulse wave velocity (PWV: Arteriograph, Unimedic); basal (BCD) and maximum skin capillary density (MCD) by videomicroscopy (KK Technology): abnormal AS PWV≥10 m/s, BCD ≤59 per 0.6mm^2 field, MCD <66/field. Written informed consent was obtained for the studies, which were approved by the local research ethics committee.
Results: Results were obtained both for PWV (11.1+0.2m/sec) and capillary density (BCD 53.4+1.5/ field; MCD 62.1+1.7/ field) in 70 patients (74%: 95%CI 65-83); for PWV alone (10.5+0.8 m/sec) in 8 patients (8%: 95% CI 3-13%); for capillary density alone (BCD 47.6+2.6/field; MCD 59.9+3.4/ field) in 10 patients (11%: 95% CI 5-17); and neither measurement in 6 patients (6%: 95%CI 1-11). Both PWV and capillary density were abnormal in 29 patients (41%: 95%CI 29-53). Capillary density was low but PWV normal in 22 (31%: 95%CI 20-42). PWV was raised but capillary density normal in 14 patients (20%: 95%CI 11-30); both readings were normal in 5 patients (7% 95%CI 1-13). PWV correlated positively with systolic (r_s=0.457, p<0.001) and diastolic blood pressure (r_s=0.265, P=0.021). Aortic augmentation index (Aix: 31.9+1.8%) also correlated significantly with systolic (r_s=0.459, p<0.001) and diastolic blood pressure (r_s=0.325, P=0.004). Basal capillary density correlated highly with maximum capillary density (r_s=0.831, p<0.001). There was no significant correlation between PWV and BCD or MCD, before or after adjustment for history of ischaemic heart disease. Waist hip ratio was inversely related to MCD in patients without known ischaemic heart disease (n=57: r_s -0.264, P=0.047).
Conclusions: Large and small vessel readings were only concordant in 2 out of 5 patients in indicating increased cardiovascular risk. Capillary imaging identified a third of patients at increased cardiovascular risk not detected by PWV alone. Our findings support use of diagnostic tests for both micro- and macrocirculation when assessing clinical cardiovascular risk in patients with hypertension with or without cardiovascular co-morbidity.

Where applicable, the authors confirm that the experiments described here conform with The Physiological Society ethical requirements.

PCB096

Characterisation of rebound depolarisation in mice deep dorsal horn neurons i*n vitro*

I. Rivera-Arconada and J.A. Lopez-Garcia

Physiology, University of Alcala, Alcala de Henares, Madrid, Spain

The differential array of ionic conductances expressed by a single neuron determines its intrinsic excitability and how it integrates synaptic inputs to generate adequate responses in accordance with its role. Dorsal horn neurons constitute the first relay of somatosensory information participating in sensory and motor processing. Here we show the presence of rebound depolarisation due to the presence of H and T-like currents in these neurons. Rebound behaviour has been related to neuronal plasticity and coding properties of several neuronal types. Spinal cords were removed from 7-12 day-old c57/CBA mice under urethane anaesthesia (2 g/kg; i.p.), hemisected, transferred to a recording chamber and superfused with oxygenated artificial cerebrospinal fluid (ACSF). Whole cell voltage and current-clamp recordings of deep dorsal horn neurons were performed with 5-9 MΩ pipettes. Tetrodotoxin, CsCl, mibefradil, NiCl and NNC 55-0396 were employed to unravel the nature of the ionic currents responsible of rebound behaviour.
Rebound behaviour was observed in 78% of neurons studied (122 out of 156). In 60 neurons rebound presented fast kinetics and high amplitude and was usually accompanied by spike firing. When more than 1 action potential occurred instantaneous firing frequency was very high (79 ± 4 Hz, range 20-128 Hz, n=43). In these neurons the presence of a low threshold, transient inward current was documented. This current and its related rebound were partially sensitive to blockade with mibefradil, NNC 55-0396 and low concentrations of NiCl. Calcium-free ACSF and higher concentrations of NiCl completely abolished the current and the rebound. Pharmacologic and kinetics analysis suggest that the T-type calcium current underlies this fast rebound.
The rebound observed in the remaining 62 neurons was slow and of low amplitude and was rarely associated with spike firing (35%). When more than 1 action potential was fired, instantaneous frequency was low (8 ± 1 Hz, range 5-15 Hz, n=11). In this subset of neurons T-like currents were absent but presented hyperpolarization activated current (IH). This slow rebound and the IH were fully blocked by 4 mM CsCl.
We conclude that the existence of T- and/or H-like currents in deep dorsal horn neurons determines the presence of rebound behaviour at end of hyperpolarization pulses. T-type calcium currents were associated to a strong and fast rebound with high frequency firing. H currents were associated to small rebound, normally without spiking. Rebound depolarization and firing may constitute a mechanism to integrate somatosensory information in the spinal cord.

Supported by the Spanish Government (BFU 2012-37905)

Where applicable, the authors confirm that the experiments described here conform with The Physiological Society ethical requirements.

PCB097

Prion protein mediates synaptic vesicle formation

S.W. Robinson, M.L. Nugent, D. Dinsdale and J.R. Steinert

MRC Toxicology Unit, University of Leicester, Leicester, UK

The cellular prion protein (PrP) plays important roles in many neuronal processes including memory, circadian rhythm, neuroprotection and neurotoxicity[1]. Although physiological roles of PrP remain elusive, its neurotoxic signalling has been investigated more thoroughly. As a consequence of PrP misfolding, several mammalian species develop neurodegenerative conditions known as scrapie, bovine spongiform encephalopathy or Creutzfeldt-Jacob and Gerstmann-Sträussler-Scheinker syndrom (GSS) in human.
The current study investigated synaptic effects of expressing mouse PrP and a mutated form of PrP (PrP^{P101L}, resembling a GSS-like disease in mice) in *Drosophila* to elucidate synaptic functions of PrP. The UAS/Gal4 bipartite expression system was used to drive pan-neuronal expression with the *elav-GAL4* driver[2].
Two-electrode voltage clamp experiments were conducted to record miniature and evoked excitatory junctional currents (m/eEJCs). Intracellular recordings from larval muscle 6 were performed (Milticlamp 900A, pClamp 10, Axon Instruments) in haemolymph-like solution 3 at 25ºC. Data are expressed as mean±SEM (n). Statistical analyses were carried out using ordinary ANOVA and Kolmogorov–Smirnov (K-S) tests, * indicates $p<0.05$.
PrP expression induced an increase in mean mEJC from 0.77±0.03nA (31) in wild type (WT) to 1.17±0.12nA* (4). This augmentation was also observed following expression of PrP^{P101L} (0.92±0.04nA* (17)) although to a lesser extent. The increase in mEJCs is due to a shift in the distribution of single mEJC amplitudes. Relative cumulative frequency histograms for mEJC amplitudes showed an increased probability of larger amplitudes and hence a right shift in mEJC distributions in PrP expressing larvae (K-S test: PrP: D=0.28, $p<0.0001$, PrP^{P101L}: D=0.24, $p<0.0001$) relative to WT. mEJC decay (τ) values did not differ between genotypes (τ_{WT}=10.0±0.4ms; τ_{PrP}=12.1±1.3ms; $\tau_{PrP^{P101L}}$=10.8±0.4ms) nor did τ distributions, indicating that postsynaptic receptor composition was not affected. The frequency of mEJCs was not different between the genotypes (f_{WT}=1.6±0.2s^{-1}; f_{PrP}=1.6±0.4s^{-1}; $f_{PrP^{P101L}}$=1.3±0.2s^{-1}). In agreement with electrophysiological data, electron microscopy revealed that PrP and PrP^{P101L} (but to a smaller degree compared to PrP) expression caused an increase in vesicle diameters (1s boutons: WT: 43.4±0.7nm (6); PrP: 55.4±2.3nm* (3); PrP^{P101L}: 47.5±0.4nm* (4)) suggesting that larger vesicles are responsible for the augmented mEJC amplitudes. Further, PrP expression caused an increase in foraging behaviour as detected in greater crawling distances per 30min (WT: 1.2±0.1m (23); PrP: 1.9±0.1m* (23); PrP^{P101}: 1.8±0.1m* (13)).
This data indicate that PrP mediates some of its physiological effects via formation of synaptic vesicles and that mutated PrP (PrP^{P101L}) as present in prion disease loses this ability thereby contributing to disease progression on the synaptic level.

Linden, R. et al. Physiology of the prion protein. Physiological Reviews 88, 673-728, (2008).

Steinert, J. R. et al. Rab11 rescues synaptic dysfunction and behavioural deficits in a Drosophila model of Huntington's disease. Human Molecular Genetics 21, 2912-22, (2012).

Where applicable, the authors confirm that the experiments described here conform with The Physiological Society ethical requirements.

PCB098

The role of orexin in morphine tolerance and its effect on neural activity of Lateral Paragigantocellularis nucleus

M. Ghaemi Jandabi, Y. Ranjbar-Slamloo, H. Azizi and S. Semnanian

Physiology, Tarbiat Modares University, Tehran, Islamic Republic of Iran

Repetitive administration of opioid agonists rapidly develops tolerance to the effects of these substances and limits their application. Orexin is involved in morphine tolerance and withdrawal. The Lateral Paragigantocellularis (LPGi) is a key brain region implicated in the tolerance and dependence to opiates. In the current study, the effect of OXR1 blockade on tolerance to antinociceptive effect of morphine and also on the neural activity of LPGi during the development of morphine tolerance was studied.

Male Wistar rats weighing 250-300g were used in these studies. To incite tolerance, morphine sulfate was injected intraperitonealy (10mg/kg, i.p.) once a day for 7 days. Tail flick test was used to survey morphine analgesic tolerance. A selective orexin type 1 receptor antagonist (SB-334867) was microinjected into the right cerebral ventricle (10μg/10μl, i.c.v.) immediately before morphine injection. To evaluate tolerance at the cellular level, On day 7 the effect of morphine (10mg/kg, i.p.) on neural activity of LPGi was investigated using in vivo extracellular single unit recording.

In the behavioral studies, daily injections of morphine in a 7-day period caused morphine analgesic tolerance in rats. There was a significant difference of %MPE between saline and morphine treated rats until day 6 but not on day 7 (Data was presented as mean±SEM. $^{*}P < 0.05$, $^{**}P < 0.01$ and $^{***}P < 0.001$ vs. saline group, n = 6 for both groups; one-way ANOVA followed by Tukey's post test). The analgesic effects of morphine (%MPEs) were significantly higher in SB-334867 plus morphine treated rats (n=9) than SB vehicle plus morphine treated (n=11) ones on days 4-7 (Data was presented as mean±SEM. $^{*}P < 0.05$, $^{**}P < 0.01$ and $^{***}P < 0.001$ vehicle plus morphine, one-way ANOVA followed by Tukey's post test). In the electrophysiological studies, 6 days injection of morphine caused significant tolerance in LPGi neurons as a decreased responsiveness of neurons to morphine (10 mg/kg, i.p.) during single unit recording. In a way that on day 7 morphine has not created any significant change in the firing rate of LPGi nucleus. (Data was presented as mean±SEM, n=10; Student's paired t-test). In SB plus morphine treated group (n=17), Microinjection of SB before each morphine injection inhibited the development of tolerance to morphine in comparison to the morphine treated group (Data was presented as mean±SEM, Student's paired t-test).

These studies have shown that central blockade of orexin type 1 receptor inhibits the development of morphine tolerance in both studies. The impediment of tolerance to analgesic effect of morphine by ICV administration of orexin type 1 receptor antagonist may be mediated in part via LPGi neurons. Further studies are required to determine molecular and anatomical mediators which are thought to be involved in this phenomenon.

Aston-Jones G et al. (2010) Brain Res 1314, 74–90.

Georgescu D et al. (2003) J Neurosci 23, 3106–11.

Aston-Jones G et al. (1986) Science 234(4777), 734-7.

Ciriello J et al. (2003) Brain Res 991(1-2), 84-95.

Zhu H et al. (2010) Eur J Pharmacol 636(1-3), 65-72.

Where applicable, the authors confirm that the experiments described here conform with The Physiological Society ethical requirements.

PCB099

Opotogenetic investigation in astrocyte-neurone signalling in locus coeruleus

F. Tang, S. Lane, M. Figueiredo, A.G. Teschemacher and S. Kasparov

School of Physiology and Pharmacology, University of Bristol, Bristol, UK

According to astrocyte-neurone lactate shuttle hypothesis, lactate released from astrocytes, is used by neurones as preferred metabolic substrate (Pellerin and Magistretti, 1994). Here, we used optogenetics to investigate signalling between astrocytes and noradrenergic neurones of the locus coeruleus (LC). In organotypic slice cultures of Wistar rat pups containing LC astrocytes were transduced with an AVV (Adenoviral vectors) to express a mutant version of the light sensitive channel rhodopsin 2 (ChR2-H134R33) fused with a far- red shifted fluorescent protein mKate and NAergic neurons were targeted to express DsRed2 with AVV-PRS8-Dsred (Gourine et al., 2010). Patch clamp recordings were made from DsRed2-positive neurones in LC. Activation of astrocytes with blue light evoked long lasting depolarisations of adjacent LC neurones (depolarisation + 3.08 ± 0.33 mV, n=14). This depolarisation could be blocked by an inhibitor of glycogen breakdown, 1,4-dideoxy-1,4-imino-D-arabinitol (DAB; 500 μM, pre-incubation 1h, depolarisation + 0.96 ± 0.15 mV, n=5, $p<0.001$) or D-lactate (2mM; +1.27± 0.38 mV, n=5, $p<0.01$) but not with the inhibitor of monocarboxylate transporters 4-CIN (100 μM, +2.9± 0.46mV,n=4, $p>0.05$). In the other set of experiments we applied fast scan cyclic voltammetry (FCV) to measure noradrenalin (NA) release from LC neurones in organotypic slices. To selectively stimulate Gs-protein-mediated signalling cascade in astrocytes, we used AVV to express rhodopsin chimera with β2 adrenergic receptors (optoβ2AR; Airan et al., 2009). Light activation of optoβ2AR-expressing astrocytes resulted in a clear increase in noradrenalin release (83.23 ± 10.6 mM*Sec, n=32), which again was abolished by DAB (500 μM, 0.75 ± 7.35 mM*Sec, n=6, $p<0.001$) and D-lactate (400 μM, -0.59±1.107mM*Sec, n=8, $p<0.001$). This was interpreted as evidence for the involvement of L-lactate in this effect. To confirm that optoβ2AR can trigger L-lactate production in astrocytes, we measured pH with SNARF-5AM in primary dissociated glial cultures and found that light simulation resulted in the emission ratio shift, indicative of acidification (144.4% ± 2.206%, n=58) which could be blocked by pre-incubation with DAB (101.3±0.6872%, n=32, $p<0.001$). These experiments imply that activation of astrocytes excites LC neurons and potentiates NA release via release of L-lactate. The mechanism by which L-lactate modulates neuronal activity is currently under investigation.

Airan RD, Thompson KR, Fenno LE, Bernstein H, Deisseroth K (2009) Temporally precise in vivo control of intracellular signalling. Nature 458:1025-1029.

Gourine AV, Kasymov V, Marina N, Tang F, Figueiredo MF, Lane S, Teschemacher AG, Spyer KM, Deisseroth K, Kasparov S (2010) Astrocytes control breathing through pH-dependent release of ATP. Science 329:571-575.

Pellerin L, Magistretti PJ (1994) Glutamate uptake into astrocytes stimulates aerobic glycolysis: a mechanism coupling neuronal activity to glucose utilization. Proc Natl Acad Sci U S A 91:10625-10629.

Where applicable, the authors confirm that the experiments described here conform with The Physiological Society ethical requirements.

PCB100

Characteristics of dorsal root ganglia neurons sensitive to substance P

E.R. Moraes, C. Kushmerick and L.A. Naves

Fisiologia e Biofísica, Universidade Federal de Minas Gerais, Belo Horizonte, Minas Gerais, Brazil

Some nociceptors produce and release Substance P (SP), a peptide cotransmitter with well-described effects on second-order sensory neurons. However, the effects of SP on primary sensory neurons are less clear. We tested the hypothesis that, among primary sensory neurons, SP targets mainly nociceptors. We therefore examined the biophysical and pharmacological profile of rat DRG sensorial neurons that are sensitive to SP. Whole-cell patch clamp was used to measure the response of 92-94 cells to brief applications of pH 7 (26 positive cells), pH 6 (38 positive cells), capsaicin (25 positive cells), and ATP (13 P2X3-type current positive cells). Sensitivity to SP was determined in 87 cells by its effect on cell excitability during stimulation at 1-4 times threshold. The number of action potentials at the threshold, and the slope of the stimulus-response curve were compared before and after SP application. We found that in 14 of the 87 cells examined, SP increased the slope of the stimulus-response curve, and in 12 cells SP increased the number of action potentials at the threshold. In total, 17 out of 87 cells tested (19%) increased excitability measured by one parameter or the other. There was also a decrease in excitability in 11 out of 87 cells. Among the cells responding to SP, the frequencies of sensitivity to pH 7 (61%) and pH 6 (78%) were statistically (Chi-squared test) higher than the frequencies of the non-responding cells (18% and 29% to pH 7 or 6, respectively). The frequencies of sensitivity to capsaicin had a tendency to be higher in the SP responding cells (20% versus 46%). P2X3-type ATP currents were present in 16% of cells that did not respond to SP, while one of the 17 (6%) substance P positive cells presented this current. Also, substance P responsive neurons had the largest diameters, and had broader action potentials with more pronounced after hyperpolarizations. We conclude that the majority of SP sensitive neurons exhibit a profile typical of nociceptors, although P2X3 currents were almost absent in these cells.

Supported by CNPq and FAPEMIG, Brasil

Where applicable, the authors confirm that the experiments described here conform with The Physiological Society ethical requirements.

PCB101

Synaptic vesicles expressing adaptor protein 3 contribute primarily to asynchronous release and regulate the fidelity of neurotransmission at hippocampal mossy fibre terminals

A. Evstratova[1], V. Faundez[2] and K. Toth[1]

[1]Universite Laval, Quebec City, QC, Canada and [2]Emory Univresity, Atlanta, GA, USA

Endocytosis is an important step in the synaptic vesicle recycling; it helps to maintain reliable neurotransmitter release. Two major pathways of endocytosis co-exist in the same presynaptic terminal: clathrin-dependent endocytosis of single vesicles utilizing adaptor protein AP-2 and bulk endocytosis leading to the formation of endosomes and dependent on adaptor protein AP-3. Vesicles derived in these two pathways differ in their molecular content and represent distinct vesicular pools. We used AP-3 knockout mice (Ap3b2-/-) lacking endosomal vesicle formation to explore physiological role of vesicular pool formed via this pathway in synapses between mossy fiber boutons and hippocampal CA3 pyramidal cell. Spontaneous and evoked EPSCs had similar amplitude and kinetic properties, moreover quantal parameters (p, Q and N), ready releasable pool size and its recovery speed were comparable between WT and KO mice. However, in KOs decay time constant of release was significantly faster (3.7 ± 0.4 ms vs 5 ±0.4 ms) and was accompanied with reduced asynchronous release (3.8 vs 7.4 Hz). In addition, stimulation with natural spike trains revealed significantly reduced probability of postsynaptic APs and increased variability of responses, especially prominent at ~100 Hz increase of stimulation frequency. Our data suggest that vesicles generated via bulk endocytosis contribute primarily to asynchronous release. The lack of asynchronous release renders information transfer from granule cells to hippocampal pyramidal cells less reliable, and therefore it could influence spatial memory.

Where applicable, the authors confirm that the experiments described here conform with The Physiological Society ethical requirements.

PCB102

Contribution of endogenous VIP VPAC1 receptor activation during hypoxia and interictal-like activity induced in vitro by 0-Mg2+ to subsequent changes in LTP expression in the rat hippocampus

D. Cunha-Reis

Laboratório de Função Autonómica Cardiovascular, Unidade de Fisiologia Clínica e Translacional,, Instituto de Medicina Molecular, Universidade de Lisboa, Portugal, Lisboa, Portugal

VIP, a modulator of synaptic transmission present in hippocampal interneurones, was shown to inhibit long-term potentiation in the CA1 area of the rat hippocampus through activation of VPAC1 receptors (1). VIP release is triggered by electrical activity, VIP receptors are enhanced in TLE patients (2) and VIP promotes neuronal survival in the absence of electrical activity (3), a situation observed during hypoxic depression. In this work we investigated if VPAC1 receptor activation during brief hypoxia and in vitro interictal-like activity could influence the subsequent expression of LTP in the CA1 area of the hippocampus.

Male wistar rats (6-7 week-old) were decapitated under fluothane anaesthesia. Extracellular electrophysiological recordings of field-excitatory post-synaptic potentials (fEPSPs) evoked by electrical stimulation in hippocampal slices were used to access synaptic transmission. Hypoxia was induced by 3 min superfusion with 95% N2–5% CO2 (normoxia: 95% O2–5% CO2). In vitro interictal-like activity was induced by 30 min superfusion with aCSF containing no 0mM MgCl2 and 6mM KCl (normal comp.: 1mM MgCl2 and 3mM KCl). LTP was induced by θ-burst stimulation (five 100Hz bursts, 4 stimuli, separated by 200 ms) and potentiation of fEPSP slope evaluated 50-60 min after LTP induction. The selective VPAC1 antagonist PG 97-269 was used to block endogenous VPAC1 receptor activation during both insults. Student's t test was used to evaluate the statistical differences between control and test groups.

Θ-burst stimulation in control conditions induced a long-lasting enhancement of fEPSP slope (29.0±2.9%, n=7, 50-60 min after stimulation). Hypoxia caused a brief but marked decrease in fEPSP slope that recovered to basal values 30 min after hypoxia in control conditions but was not complete (89.0±1.8%) after hypoxia in the presence of 100nM PG 97-269. Θ-burst-induced LTP was enhanced to 44.9±1.3% (n=4) and 43.8±1.3% (n=4) when θ-burst stimulation was delivered 30 min and 60 min after hypoxia, respectively. This enhancement was not observed in slices subjected to hypoxia in the presence of PG 97-269 (100nM). Following interictal-like activity induced by 0Mg2+ aCSF, θ-burst-induced LTP was impaired to 17.9±2.3% (n=3) and 24.8±1.5% (n=3) when evoked 30 min and 60 min after interictal-like activity, respectively. When interictal-like activity was induced in the presence of PG 97-269 (100nM), this impairment was not observed (n=3).

These results suggest that activation of VPAC1 receptors by endogenous VIP during brief hypoxia contributes to a subsequent facilitation of LTP induction. In contrast, activation of VPAC1 receptors during interictal-like seizures may contribute to the inhibition of LTP that follows this insult.

1 – Cunha-Reis, D et al., J Mol Neurosci, 2010. 42: 278.

2 – de Lanerolle NC et al., Br Res, 1995. 686: 182-93.

3 – Brenneman et al., Proc Natl Acad Sci U S A. 1986 83: 1159-62.

Supported by FCT.

Where applicable, the authors confirm that the experiments described here conform with The Physiological Society ethical requirements.

PCB103

The maturation of AMPA receptors in human pluripotent stem cell-derived cortical excitatory neurones

M. Livesey[1], B. Bilican[2], G. Haghi[2], G.E. Hardingham[1], S. Chandran[2] and D.J. Wyllie[1]

[1]Centre for Integrative Physiology, University of Edinburgh, Edinburgh, UK and [2]Euan MacDonald Centre and MRC Centre for Regenerative Medicine, University or Edinburgh, Edinburgh, UK

The ability to generate regionally defined neuronal populations from human pluripotent stem cells (hPSCs) provides an important new experimental resource for the investigation of human neuronal physiology. We have developed a protocol in which H9 hPSCs are neuralised in suspension using chemically defined medium. Such an approach is based upon the default model of neurogenesis that minimizes extrinsic and intrinsic signals that lead to alternative cell fates. Analysis of the resulting neural stem cells (NSCs) reveals a forebrain identity as assessed by FOXG1 and OTX2 expression. Subsequently NSCs are plated as a monolayer to generate PAX6-positive precursors that terminally differentiate into an enriched VGLUT1 positive population of cortical neurones that express the cortical layer specific markers CTIP2, SAT2B or Reelin. Importantly, glia and inhibitory interneurones are only nominally present (<10% of total population). In the present study we have used this population of human cortical excitatory neurones (hCENs) to assess the developmental expression and biophysical properties of 2-amino-3-hydroxy-5-methyl-isoxazol-4-yl propanoic acid receptors (AMPARs).

The responsiveness of the cells to AMPA (50 μM) was assessed weekly for 5 weeks following differentiation and significant increases in current densities from week 1 (0.12 ± 0.08 pA/pF, n = 22) to week 5 (1.14 ± 0.2 pA/pF, n = 35) were observed. As would be anticipated AMPAR-mediated currents were blocked by 6-cyano-7-nitroquinoxaline-2,3-dione (CNQX; 5 μM). Non-stationary noise analysis indicated that the mean weighted single-channel conductance of AMPARs expressed by hCENs decreased from 11.1 ± 1.2 pS (week 2; n = 8) to 4.5 ± 0.4 pS (week 5; n = 12). In addition AMPAR-mediated currents at week 5 were insensitive to intracellular block by the polyamine, spermine (100 μM; n = 5). Similar experiments with neurones derived from the 31D1 induced pluripotent stem cell line also indicated the presence of low-conductance AMPARs at week 5 (4.1 ± 1.2 pS; n = 3).

Our data are consistent with the notion that at week 5 hCENs express AMPARs that contain the edited form of the GluA2 subunit. Furthermore, the developmental switch from an AMPAR population possessing higher unitary conductances to one expressing lower unitary conductances is tetrodotoxin insensitive (i.e. action potential independent). In addition this switch is not blocked when neurones are cultured in presence of antagonists of ionotropic glutamate receptors.

Acknowledgements: This work is supported by The Wellcome Trust and the MRC.

Where applicable, the authors confirm that the experiments described here conform with The Physiological Society ethical requirements.

PCB104

Deafness related to hyperbilirubinaemia is associated with transmission failure at central auditory synapses

E. Schiavon, H. Parker and I.D. Forsythe

cell physiology and Pharmacology, University of Leicester, Leicester, UK

Acute and chronic bilirubin encephalopathy (ABE and kernicterus) are serious neurological conditions associated with Jaundice. When plasma free bilirubin is high, it crosses the blood-brain-barrier and causes neuronal damage in the CNS. This investigation focuses on the damage in the brainstem auditory pathway, using the calyx of Held giant glutamatergic synapse, which forms between the anterior ventral cochlear nucleus and the neurons of the medial nucleus of the trapezoid body (MNTB). Hyperbilirubinaemia was induced in CBA/Ca mice (11-20 days old) by a single intraperitoneal injection of bilirubin (0.5 mg/g) and sulfadimethoxine (0.3mg/g). Auditory function was monitored in vivo by auditory brainstem responses (ABR) using click stimulation under anesthesia (Hypnorm/Midazolam/water, ratio 1/1/2: 0.1μl/g intraperitoneally). Electron microscopy (EM) and immunohistochemistry (IHC)

for the presynaptic marker VGLUT2 (vesicular glutamate transporter 2) were performed and patch clamp recording in MNTB neurons were made under voltage clamp in order to record miniature excitatory postsynaptic currents (mEPSCs). Evoked responses were recorded, stimulating the presynaptic trapezoid body fibers at the midline, and clamping the MNTB membrane potential at -65mV or +80mV to investigate AMPAR or NMDAR currents, respectively. ABRs were largely abolished at 4h, but they recovered 24h and 5 days after bilirubin injection. IHC showed reduced staining for VGLUT2 in the calyx of Held at both 4h and 24h after injection. An EM study 4 h after bilirubin injection showed two changes at the calyx of Held synapse: first, the terminals were packed with vesicles and second, the presynaptic terminals were detached from the postsynaptic membrane. 24h after bilirubin injection, the presynaptic terminals had rejoined with the postsynaptic membranes, but the calyx of Held synapses were still abnormally overfilled with vesicles. Whole cell experiments validate the damage of the Calyx of Held synapses showing a significant decrease in the amplitude (62.3±3.5 pA n=7 vs control 83.4±7.3 pA n= 6) and in the frequency of spontaneous mEPSCs, (2.5±0.4 Hz n=7 vs control 7.2±1.1 Hz, n=6) that had recovered after 24h (84.4±8.2, vs control 62.3±3.5 pA, frequency 5.4±0.9 Hz vs control 7.2±1.1 Hz, n=4 and 6 respectively). Evoked AMPAR and NMDAR EPSCs showed a decreased amplitude in 4h injected animals (-4.6±0.3nA and 3.5±0.3nA, respectively vs control -6.9 ±1.2 nA and 4.8 ±0.7nA). We conclude that the acute injection of bilirubin causes short-term damage to the auditory system, involving the calyx of Held and provides a good model for further understanding the mechanisms of bilirubin toxicity in disease.

This research was funded by Action On Hearing Loss UK

Where applicable, the authors confirm that the experiments described here conform with The Physiological Society ethical requirements.

PCB105

Non-genomic effects of estradiol on the excitability of Locus Coeruleus neurons in neonatal rats

A.J. Silva[1,2] and C. Kushmerick[1,2]

[1]Physiology and Biophysics, Universidade Federal de Minas Gerais, Belo Horizonte, Minas Gerais, Brazil and [2]Graduate Program in Physiology and Pharmacology, UFMG, Belo Horizonte, Minas Gerais, Brazil

17β-estradiol (E2) is a sex hormone that regulates gene expression in the reproductive system. In addition to these genomic effects that take place over a relatively long time scale, a growing body of evidence points to rapid effects of E2 mediated by a plasma membrane receptor. In the present study, we examined the acute effects of E2 on the electrical excitability of neurons from the Locus Coerulus. Brain slices containing the Locus Coerulus were obtained from neonatal Wistar rats of post-natal day p5-7, and membrane potentials were recorded using standard intracellular techniques with sharp glass microelectrodes. Resting membrane potentials were -65±6 mV (N=27). Locus Coerulus neurons presented spontaneous action potentials or subthreshold oscillations. Spontaneous action potentials (N=3) or sub-threshold oscillations (N=8) were reversibly abolished within minutes of application of E2 encapsulated in hydroxypropyl-β-cyclodextrin (HBCD; 200 nM). In addition, application of E2 caused a membrane hyperpolarization of 4.9±2.5 mV (N=8). Effects of E2 were completely reversible upon washout, and could be repeated multiple times in the same cell (up to 8 applications over 6 hours) with similar results. Application of the encapsulation vehicle HBCD alone caused no effect (N=4). To determine if the receptor activated by E2 was on the cell surface or intracellular, we tested E2 conjugated to Bovine Serum Albumin (E2-BSA) on LC activity. Similar to encapsulated E2, E2-BSA inhibited spontaneous activity and hyperpolarized the membrane (N=4). We conclude that E2 can inhibit the spontaneous activity of Locus Coerulus neurons by interaction with a plasma membrane receptor.

Funded by CNPq, CAPES, FAPEMIG, PG-FisFar-UFMG

Where applicable, the authors confirm that the experiments described here conform with The Physiological Society ethical requirements.

PCB107

Pharmacological investigation of triheteromeric NMDA receptors in rat substantia nigra dopaminergic neurones

R. Ammari[1], S.J. Scott[2], S. Jones[3] and A. Gibb[1]

[1]Neuroscience, Physiology and Pharmacology, University College London, London, UK, [2]Biomedical Sciences, University of Queensland, Brisbane, QLD, Australia and [3]Physiology, Development and Neuroscience, University of Cambridge, Cambridge, UK

The dopaminergic neurons of the substantia nigra pars compacta (SNc) are important in the circuitry of the basal ganglia, and their degeneration underlies the development of motor symptoms in Parkinson's disease. Several mechanisms may contribute to this degeneration, one of which could be excessive activation of N-methyl-D-aspartate (NMDA) receptors. NMDA receptors are tetrameric assemblies of GluN1 and at least one type of GluN2 (A,B,C and D) subunit which confer distinct and unique characteristics to these receptors. Dopaminergic neurones of the substantia nigra pars compacta (SNc) express a combination of GluN2B and also GluN2D subunits and here we investigated the hypothesis that these receptors are expressed as 'triheteromeric' GluN1/GluN2B/GluN2D receptors. Using patch-clamp whole-cell recordings from SNc neurones in coronal brain slices from 3 week old rats (humanely killed by decapitation under deep isofluorane anaesthesia), we investigated how these unusual NMDA receptors are regulated by the subunit selective allosteric inhibitors, ifenprodil (GluN2B) and DQP-1105 (GluN2C/D) during repeated activation (15s durations at 100s intervals, of 100μM NMDA over a 10 minute time scale). NMDA-evoked currents displayed a maximal inhibition of 58 ± 11% by ifenprodil (10μM, n = 10) with an estimated IC50 = 0.21 μM while DQP-1105 (10μM, n = 9) inhibited currents by 64 ± 7.9%. These results suggest that a proportion of NMDA receptors on dopaminergic neurons of the substantia nigra are triheteromeric GluN1/GluN2B/GluN2D receptors.

Supported by the Wellcome Trust. SJS was supported by a University of Queensland advantage grant from the University of Queensland Office of Undergraduate Education.

Where applicable, the authors confirm that the experiments described here conform with The Physiological Society ethical requirements.

PCB108

Cilostazol does not inhibits KCl and capcaicin induced increase in intracellular calcium signaling in rat sensory neurons

S. Kutlu[1], E. Kacar[2], O. Burma[3] and A. Uysal[3]

[1]Department of Physiology, NE University Faculty of Medicine, Konya, Turkey, [2]Department of Physiology, Firat University Faculty of Medicine, Elazig, Turkey and [3]Department of Cardiovascular Surgery, Firat University Faculty of Medicine, Elazig, Turkey

Cilostazol, a specific cAMP phosphodiesterase III inhibitor, is used for medical treatment of intermittent claudication in peripheral artery disease to prevent leg pain during physical activity. Dorsal root ganglion (DRG) neurons are eligible experimental model for pain investigations. Aim of this study was to figure out the effect of cilostazol on intracellular calcium ([Ca2+]i) signaling in cultured rat DRG neurons. DRG neurones were grown in primary culture following enzymatic and mechanical dissociation of ganglia from 2-day-old Wistar rats. DRG neuronal cultures were loaded with 1μmol Fura-2AM and [Ca2+]i responses to stimulation were assessed by using fluorescent ratiometry. Cultured cells were excited at 340 and 380nm, and emission was recorded at 510nm. Responses were determined by the change in 340/380 ratio (basal-peak) for individual neurons. After basal recordings, KCl (30mM) and capcaicin (1μM) applied to medium for induction of [Ca2+]i . Cilostazol treated alone or co-administered with KCl and capcaicin for determining the possible changes in calcium signaling. Data were analyzed by using one-way analysis of variance followed by a post-hoc Tukey HSD test, with a 2-tailed P level of <0.05 defining statistical significance.
Firstly exposure to cilostazol failed to cause any significant change in basal [Ca2+]i response (basal=100.0±0.0 and cilostazol =99.8±0.2 %). KCl and capcaicin had significant increase in [Ca2+]i responses to 164.71±4.1 % and 191.55±6.4 % (respectively, p< 0.001). But co-application of cilostazol with KCl and capcaicin didnot alter the KCl and capcaicin induced elevation in [Ca2+]i (166.14±3.7 % and 188.26±4.7 %, respectively). In conclusion, the results of present study suggest that cilostazol has no effect on [Ca2+]i signaling in rat sensory neurons in vitro. It seems cilostazol may activate other mechanism(s) at cellular level rather than modulating calcium signaling in DRG neurons.

Where applicable, the authors confirm that the experiments described here conform with The Physiological Society ethical requirements.

PCB109

Detecting purines, catecholamines and glutamate with a mutant α-haemolysin pore one molecule at a time: a synthetic mutant sniffer patch

K.L. Brain[1], A. Boersma[2], P. Sidaway[1] and H. Bayley[2]

[1]Clinical and Experimental Medicine, University of Birmingham, Birmingham, West Midlands, UK and [2]Department of Chemistry, University of Oxford, Oxford, Oxfordshire, UK

We have recently developed a genetically and chemically-modified α-haemolysin pore for the simultaneous measurement of a range of neurotransmitters, including purines, catecholamines and glutamate (Boersma *et al*., 2012). Building upon a previous purine-sensitive pore (Cheley *et al*., 2002), a catecholamine binding side that incorporated Cu^{2+} allowed several catecholamines, including noradrenaline, adrenaline and dopamine, to bind. These measurements were made in a Cl^--free, HCO_3^--free physiological saline containing (mM): 118 NaCl, 10 MOPS, 4.7 KCl, 1.8 $CaCl_2$, 1.8 $MgCl_2$, 11.1 D-glucose; pH 7.4. When such pores are incorporated into an artificial bilipid membrane, and then voltage-clamped, single molecules of these neurotransmitters can be detected as they block the α-haemolysin pore. The identity of each molecule can be determined my measuring both the amplitude of the conductance block and the dwell time of the molecule on the pore. We have demonstrated the ability of this technique to distinguish separate molecules in a cocktail of ATP (5 μM), ADP (5 μM) and noradrenaline (1μM), and describe a technique for calculating the concentration of each component of the mixture. Glutamate (<5 μM) is also detectable with the same pore. Altering the clamp voltage modifies the relative sensitivity of the pore, which provides an additional method for identifying binding molecules. Such a need might arise if very similar species need to be distinguished. We have tested this probe on the spontaneous and epibatidine-evoked release of transmitters from PC12 cells, and in pilot experiments can simultaneously identify ADP, ATP and noradrenaline, as well as a small set of other binding events for which the chemical species responsible have not yet been identified.
The stable nature of α-haemolysin implies that this approach may be developed to produce a relatively simple-to-use method for single-molecule detection of neurotransmitter release in small sample volumes, although several technical challenges remain including the optimization of suitable bilipid membranes (or other methods of supporting the channel), reducing the binding site affinity (to increase the off rate and hence increase the sampling frequency, particularly for catecholamines) and the identification of all biologically relevant binding molecules.

Boersma AJ, Brain KL & Bayley H (2012). *ACS Nano* **6**, 5304-5308

Cheley S, Gu LQ & Bayley H (2002). *Chem Biol* **9**, 829-838

Where applicable, the authors confirm that the experiments described here conform with The Physiological Society ethical requirements.

PCB111

TR(i)P to automation

I. Rinke, C. Haarmann, N. Becker, A. Obergrussberger, S. Stölzle, A. Brüggemann, M. George and N. Fertig

Nanion Technologies, Munich, Germany

Transient receptor potential (TRP) channels are an important class of receptors widely distributed in the mammalian central and peripheral nervous systems. TRP receptors have been shown to be activated and regulated by a variety of stimuli including temperature, mechano-stimulation, divalent cations, pH and different kinds of molecules, which mediate the sensation of taste. Dysfunction of TRP channels can cause various pathological conditions, including an inherited pain syndrome, multiple kidney diseases and skeletal disorders. Hence, TRP channels become potential targets for the treatment of such disorders. Currently within drug development, much attention is paid to the TRP ankyrin 1 (TRPA1) channel. Preclinical data and data from a recent human genetic study[1] highlight TRPA1 antagonists as a promising new approach for the treatment of acute and chronic pain.

Patch clamp electrophysiology remains the gold standard for studying ion channels. We have employed planar patch clamp instrumentation for medium and high-throughput screening (Patchliner and SyncroPatch 96 platforms) to study the TRPA1 channel stably expressed in HEK cells.

TRPA1 is activated by a range of environmental irritants, pungent compounds found in foods, as well as metabolites produced during oxidative stress. Here, we demonstrate the activation of TRPA1 by mustard and cinnamon. Induced currents could be reversibly blocked by the potent antagonist HC030031.

The most challenging characteristics of TRPA1 within screening are the channels` mechano-sensitivity, fast desensitization and its regulation by intracellular calcium. Using a combination of excellent fluidics, allowing for fast solution exchange whilst brief compound application, and the usage of calcium buffered external solution, we have achieved recording of high quality data with a high success rate for obtaining stable giga-seals (typically 60 to 80%), and reliable pharmacology.

Kremeyer, B. et al. A gain of function mutation in TRPA1 causes familial episodic pain syndrome. Neuron 66, 671–680 (2010).

Cells were kindly provided by Millipore

Where applicable, the authors confirm that the experiments described here conform with The Physiological Society ethical requirements.

PCB112

Neuroprotective potential of N-nitro-L-arginine-methylester in transient cerebral ischemia and reperfusion in rats

H.A. Awooda[1], G.M. Sharara[2] and A.M. Saeed[3]

[1]Department of Physiology, Al Neelain UIniversity, Khartoum, Sudan, [2]Department of Biochemistry, Alexandria University, Alexandria, Egypt and [3]Department of Physiology, University of Khartoum, Khartoum, Sudan

Stroke is the second leading cause of death and permanent disability worldwide. The role of nitric oxide (NO) inhibition in cerebral ischemia/reperfusion (I/R) remains controversial (1). Rho-kinases (ROCK) are serine–threonine kinases that play a vital role in cell migration and survival, interaction between NO and ROCK isn't clear (2). Nuclear factor kappa β (NF-kβ) is a transcription factor that contributes to infarction in experimental stroke and its inhibition associated with neuroprotective effects (3). This study investigated the potential neuroprotective effect of nonselective nitric oxide synthase inhibitor (L-NAME) in rat's transient cerebral I/R. 30 adult male Wistar rats (150-250g) were divided into three groups 10 rats in each: first group was sham-operated and served as a control, I/R group of rats infused with 0.9% normal saline intraperitoneally 15 minutes prior to 30 minutes of left common carotid artery occlusion, followed by 24-hour of reperfusion, anesthesia was induced by ether inhalation and maintained by thiopental sodium (2.5mg/kg) (4). A test group infused with L-NAME (15 mg/kg per weight) intraperitoneally 15 minutes prior to same I/R period. Neurobehavioral assessments were evaluated (5), NF-κβ via western blotting and ROCK using enzyme-linked immunosorbent assay were estimated in the left cerebral hemisphere. NO metabolites (nitrite and nitrate) were measured colorimetrically in plasma and brain tissue. Values are means ± S.E.M., compared by ANOVA. The L-NAME group showed a significant improvement in neurological deficit (15.07±0.584) compared to both I/R and control groups (12.798±0.689, 17.50±0.707, respectively P <0.001). In I/R group; NF-κβ was significantly increased (129.2±1.7 RGB unit/mg protein) compared to the control group (53±1.03RGB unit/mg protein, P <0.001) and L-NAME pretreatment resulted in significant decrease in NF-κβ (44.4±1.3RGB unit/mg protein, P <0.001) compared to I/R rats. In I/R group brain tissue levels of ROCK and NO significantly increased (0.022±0.0054 ng/mg protein, 8.88±0.572 nmol/mg protein) compared to the control group (0.013±0.003 ng/mg protein, 3.48±0.228 nmol/mg protein, P <0.001). The L-NAME group showed a significant decrease in tissue level of ROCK and NO (0.005±0.0006 ng/mg protein, 4.47±0.392 nmol/mg protein, P <0.001) compared to the I/R group. Serum level NO was significantly increased in I/R group (42.03±4.558 μmol/L) compared to the control group (17.84±0.701 μmol/L, P <0.001), while L-NAME administration resulted in significant decrease in serum NO (18.44±0.513μmol/L, P <0.001) compared to the I/R group. Thus, L-NAME significantly improved neurological deficit and inflammation evidence by decrease NF-κβ and ROCK in the affected cerebral hemisphere following cerebral ischemic injury.

Fig I: Brain NF-κβ RGB /mg protein in different experimental groups:

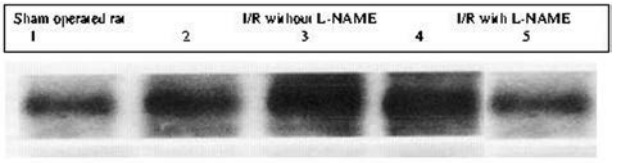

Western blotting of NF-κβ (RGB /mg protein) in affected cerebral hemisphere.

R:red, G:green and B: blue

Fig 2:

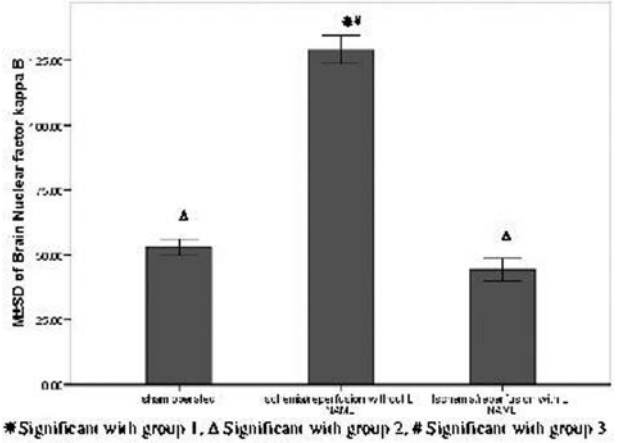

Fig 2: Comparison between the different experimental groups according to Brain NF-κβ (RGB /mg protein)

Mohammadi MT, Shid-Moosavi SM, Dehghani GA. Contribution of nitric oxide synthase in blood-brain barrier disruption during acute focal cerebral ischemia in normal rat. Pathophysiology. 2011;19(1):13-20

Kataoka C, Egashira K, Inoue S, et al. Important role of Rho-kinase in the pathogenesis of cardiovascular inflammation and remodeling induced by long-term blockade of nitric oxide synthesis in rats. Hypertension 2002;39:245–50

Desai A, Singh N, Raghubir R. Neuroprotective potential of the NF-kappaB inhibitor peptide IKK-NBD in cerebral ischemia-reperfusion injury. Neurochem Int. 2010;57(8):876-83

Keefer LK, Garland WA, Oldfield NF, et al. Inhibition of N-nitrosodimethylamine metabolism in rats by ether anesthesia. Cancer Res.1985;45(11 Pt 1):5457-60

Garcia JH, Wagner S, Liu KF, et al. Neurological deficit and extent of neuronal necrosis attributable to middle cerebral artery occlusion in rats. Statistical validation. Stroke.1995;26(4):627-34

To my colleages in Alexandria university, Egypt and AL Neelain university, Sudan

Where applicable, the authors confirm that the experiments described here conform with The Physiological Society ethical requirements.

PCB113

Endocannabinoid modulates developmental plasticity of central vestibular synapses and the expression of vestibular behaviors in rats

W. Shi[1], H. Hu[1], D. Shum[1,2] and Y. Chan[1]

[1]Physiology, The University of Hong Kong, Hong Kong, Hong Kong and [2]Biochemistry, The University of Hong Kong, Hong Kong, Hong Kong

Endocannabinoid (eCB) has been found to mediate retrograde signaling and long-term depression of inhibitory responses (iLTD) in neurons of the amygdala, hippocampus and visual cortex. It remains unexplored whether eCB regulates long-term synaptic plasticity in the vestibular nucleus and behavioral expression of vestibular functions. Whole-cell patch-clamp experiments were performed on brainstem slice of postnatal rats. Theta-burst stimulation delivered to vestibular afferents could induce iLTD of GABAA receptor-mediated evoked-IPSCs in medial vestibular neurons. Such iLTD was induced in 70% of the neurons tested in P5-7 rats but was reduced to 30% in P8-10 rats. In P5-7 rats, the proportion of these neurons was reduced to 30% with bath application of AM251 (antagonist of type 1 cannabinoid receptor). Similar results were obtained in P5-7 rats that had been implanted at P1 with a slice of AM251-loaded Elvax that allowed controlled release of the drug into the underlying vestibular nucleus. In normal P8-10 rats, the proportion was increased to 60% with bath application of WIN55 (agonist of type 1 cannabinoid receptor). Similar results were obtained in P8-10 rats implanted at P1 with WIN55-loaded Elvax slice. To attest the effects of eCB in the expression of vestibular behavior, the Elvax-implanted rats were tested with negative geotaxis, a behavioral indicator of gravity-detection. When compared with normal controls which acquired the re-orienting behavior by P7, emergence of this reflex was accelerated to P5 in AM251-treated rats but was delayed to P11 in WIN55-treated rats. Notably, similar accelerated and delayed emergence of negative geotaxis was observed in rats pre-treated with muscimol (a GABAA receptor agonist) and bicuculline (a GABAA receptor antagonist) respectively. Our results therefore indicate that eCB plays an age-dependent role in modulating the efficacy of GABAergic synapses in the vestibular nucleus, thereby regulating activities of neural network responsible for the expression of gravity-detection behavior.

The development changes of iLTD by eCB

	P5-7	P8-10	P11-14
Normal	70-80% iLTD	20-30% iLTD	20% iLTD
CB1 agonist	70-80% iLTD	50-60% iLTD	30 iLTD
CB1 antagonist	30-40% iLTD	20-30% iLTD	20 iLTD

eCB, endocannabinoid;iLTD, inhibitory long-term depression; CB1, Cannabinoid Receptor

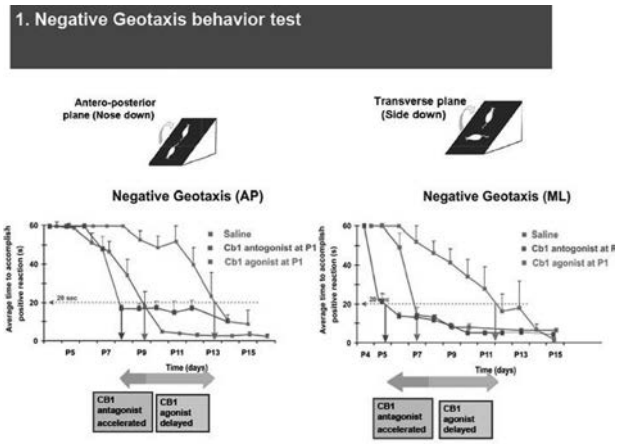

Chevaleyre V and Castillo PE (2003) Heterosynaptic LTD of hippocampal GABAergic synapses: a novel role of endocannabinoids in regulating excitability. Neuron 38: 461-472.

Jiang B, Huang S, de Pasquale R, Millman D, Song L, Lee H, Tsumoto T, Kirkwood A. 2010. The maturation of GABAergic transmission in visual cortex requires endocannabinoid-mediated LTD of inhibitory inputs during a critical period. Neuron 66:248-259.

3. Marsicano G, Wotjak CT, Azad SC, Bisogno T, Rammes G, Cascio MG, Hermann H, Tang J, Hofmann C, Ziegigansberger W et al (2002) The endogenous cannabinoid system controls extinction of aversive memories. Nature 418: 530-534.

RGC761812M

Where applicable, the authors confirm that the experiments described here conform with The Physiological Society ethical requirements.

PCB115

Glutamine transport by System N and System A in astrocytes adjacent to the calyx of Held glutamatergic synapse

M. Marx and B. Billups

Department of Pharmacology, University of Cambridge, Cambridge, UK

Glutamine is thought to play an integral role in the recycling pathway of glutamate. The glutamate-glutamine cycle proposes that perisynaptic astrocytes release glutamine which is then taken up by the presynaptic neuron as a glutamate precursor. Using fluorescent pH_i measurement and whole-cell patch-clamp, we have investigated the transport mechanisms that may mediate this release of glutamine from astrocytes *in situ*. Brainstem slices containing the medial nucleus of the trapezoid body were obtained from P10-15 Wistar rats and perfused with aCSF containing glutamate, GABA and glycine receptor inhibitors. Astrocytes were whole-cell patch-clamped. Transporter substrates were dissolved in external solution and either applied via perfusate or by pressurised ejection from a puffer pipette. For imaging pH_i, 0.5 mM 8-hydroxypyrene-1,3,6-trisulfonic acid (HPTS) was included in the patch pipette and the fluorescence emission ratio measured following illumination at 465 and 405 nm. Values are means ± S.E.M., compared by ANOVA. System A (SA) transporter function was probed using the substrate inhibitors α-methyl-aminoisobutyric acid (MeAIB), alanine and serine, while system N (SN) function was isolated using its unique ability to transport Li^+ in place of Na^+. Histidine was used as a substrate inhibitor of both SA and SN. Puff application of glutamine (5 s) generated a membrane current (-20.0 ± 2.4 pA, n=21) which was blocked by bath applied

alanine (10 mM; 1.6 ± 2.1 pA, p<0.05, n=8) and MeAIB (20 mM; -6.2 ± 2.1 pA, p<0.05, n=6). Substitution of external Na^+ with Li^+ abolished the glutamine current (0.4 ± 1.0 pA, p<0.05, n=6). MeAIB also blocked glutamine-induced currents after membrane conductance was reduced by substituting internal K^+ with Cs^+ (from -25.6 ± 7.3 pA to -1.9 ± 1.0 pA, p<0.05, n=6). Fluorescent pH_i measurement revealed an alkalinisation during puff application of glutamine ($\Delta F/F0 = 0.27 \pm 0.02$, n=34). While bath application of histidine (20 mM) abolished the pH change (p<0.05, n=3), MeAIB only attenuated this change by 50 ± 5% (n=3; p<0.05) and serine (20 mM) blocked the pH change to a comparable extent (41 ± 8%; n=5; p<0.05). In addition, a substantial proportion of the pH change (63 ± 11%; n=7) was insensitive to the substitution of Na^+ with Li^+ (p<0.05).
Together, these data identify two distinct glutamine transport systems within astrocytes. Properties of the glutamine-induced membrane currents indicate expression of SA while pH imaging reveals a second non-electrogenic glutamine transport system with properties identifying it as SN. Furthermore, the lack of effect of serine on SN transport suggests that the SN1 not the SN2 isoform predominates. SN is known to be readily reversible under physiological conditions and we propose that this mediates the astrocytic glutamine release mechanism within the glutamate-glutamine cycle.

Where applicable, the authors confirm that the experiments described here conform with The Physiological Society ethical requirements.

PCB117

Infraslow brain potential oscillations are implicated in multisensory mechanisms of information processing: evidence from intracortical field potential recordings

K.S. Pugachev, I.V. Filippov and A.A. Krebs

Physiology and Biophysics, Yaroslavl State Medical Academy, Yaroslavl, n/a, Russian Federation

INTRODUCTION AND AIM: Multisensory information processing in the brain (e.g. visual in the auditory cortex and auditory in the visual cortex, etc.) is an important direction of current sensory neurophysiology. Although our previous experiments have shown the implication of infraslow brain potential oscillations (ISO) in mono-modal sensory information processing in the brain, the role of ISO (frequencies <0.5 Hz) in multisensory neuroprocessing remains unknown. The aim of this study was to identify the role of ISO dynamical shifts (if any) in multisensory processing of visual, auditory and gustatory information in the primary sensory cortical areas of the brain.
METHODS: Experimental procedures were done in accordance with European Parliament and Council Directive (2010/63/EU) on the protection of animals used for scientific purposes. Experiments were performed on urethane anesthetized (1mg/kg, i.p.) 30 male adult albino rats (n=720 repeated sessions) with stereotaxic electrodes implanted in primary visual (V1), auditory (A1) and gustatory (G1) cortical areas. ISO were rerecorded from V1 during animal exposure to the auditory and gustatory sensory stimuli; ISO from A1 were recorded under application of visual and gustatory stimuli; ISO from G1 were recorded during auditory and visual sensory stimulation. We analyzed ISO dynamics by means of mathematical (power spectral analysis) and statistical (one-way ANOVA) procedures.
RESULTS: In V1, A1 and G1 cortical areas we found various domains of infraslow brain potentials, these were: ISO in the domain of seconds (0.1-0.5 Hz), multisecond ISO (0.0167-0.05 Hz) and ISO in the range of minutes (<0,0055 Hz). Statistically significant shifts (P<0.05) of ISO (mainly in the range of seconds) were observed: in V1 during application of auditory and gustatory stimuli, in A1 during animal exposure to visual and gustatory stimuli, and in G1 under visual and auditory sensory stimulation (e.g. modality-specific and stimulus-specific patterns of ISO arose in V1 in response to the presentation of not only visual stimuli but to auditory and gustatory, in A1 in response to the presentation of not only auditory but to visual and gustatory stimulation, in G1 in response to the presentation of not only gustatory but to visual and acoustic stimuli). In some cases we also documented implication of multisecond ISO dynamical changes in multisensory information processing, but not the ISO in the domain of minutes.
CONCLUSIONS: Based on these results, we suggest that ISO in the domain of seconds and multisecond oscillations are specifically involved in multisensory processing/analysis of afferent sensory information of different modalities in primary sensory cortical areas of the brain.

This work was supported by grants from Ministry of Education and Science of Russia.

Where applicable, the authors confirm that the experiments described here conform with The Physiological Society ethical requirements.

PCB118

Infraslow brain potentials (<0.5 Hz) in primary sensory cortical areas of the rat brain: effects of brain neurotransmission centers electrical stimulation

A.A. Krebs, I.V. Filippov and K.S. Pugachev

Physiology and Biophysics, Yaroslavl State Medical Academy, Yaroslavl, Russian Federation

OBJECTIVE: It was shown in our previous works the presence infraslow brain potential oscillations (ISO) in primary visual (V1), auditory (A1) and gustatory (G1) cortical areas, as also we demonstrated ISO implication in CNS mechanisms of sensory information processing. However, the processes of cortical ISO modulation are little known. The aim of this study was to find how the dynamics of ISO is modulated in V1, A1, and G1 by the influences of locus coeruleus (LC), dorsal raphe nucleus (DRN), and nucleus basalis magnocellularis (NBM), that send noradrenergic, serotoninergic and cholinergic projections, respectively, to neocortex.
METHODS: Experiments were guided by European Parliament and Council Directive (2010/63/EU) on the protection of animals used for scientific purposes. All experiments were performed on 30 (n=75 experiments) adult albino rats anesthetized by urethane (0.7 g/kg, i.p.) with stereotaxic electrodes implanted to V1, A1, G1; LC, DRN, and NBM. The recordings of ISO from these structures were obtained before and after successive electrical stimulation of aforementioned brain nuclei. The positions of electrodes were verified morphologically. ISO recordings were analyzed by means of power spectral analysis and statistical significances of differences were evaluated using one-way ANOVA (an alpha level of 0.05 was adopted for all significance tests).
RESULTS: It was detected that before electrostimulation of LC, DRN, and NBM, multisecond ISO were correlated between these nuclei and aforementioned cortical sites (0.44<r<0.66). We found that electrical stimulation of LC, DRN and NBM induced statistically significant alterations of ISO in V1, A1 and G1, these changes were manifested as specific power patters

of ISO in the domain of seconds (0.1-0.3 Hz) and multisecond waves (0.0167-0.043 Hz) without any alterations of dynamics of fluctuations in the range of minutes (<0.0167 Hz). Each cortical site (e.g. V1, A1, G1) responded to the activation of LC, DRN, NBM by specific power spectral pattern configuration in the range of seconds and dozens of seconds, as also each neurotransmitter center (e.g. LC, DRN, NBM) influenced on ISO neurodynamics of different cortical sites in a highly specific way.

CONCLUSIONS: Based on obtained results, it is possible to conclude that activation of noradrenergic (LC), serotoninergic (DRN) and cholinergic (NBM) systems of the brain have different but specific and powerful effects on neuromodulation of ISO dynamics in the primary sensory cortical areas. We assume that such pre-tuning of ISO in the primary cortical sensory areas by different neurotransmission systems plays an important role for further optimal sensory information processing background.

This work was supported by grants from Ministry of Education and Science of Russia.

Where applicable, the authors confirm that the experiments described here conform with The Physiological Society ethical requirements.

PCB119

HCN channels regulate spontaneous firing rate of olfactory receptor neurons for glomerular formation

N. Nakashima, T.M. Ishii and H. Ohmori

Physiology, Kyoto University, Kyoto, Japan

Genetic instruction is one of the principal aspects of a body plan including the neural network formation. In the olfactory receptor neurons (ORNs) as well, odorant receptor genes are a key determinant of the axonal targeting to the glomeruli in the olfactory bulb to form the network called the olfactory map. Interestingly, ORNs periodically regenerate and also utilize spontaneous firing activity for establishing and maintaining this olfactory neural map. However, (1) the generation mechanism of spontaneous activity and (2) the its role as a guidance cue in the olfactory bulb are not established. Here we addressed these two questions by investigating the nature of the spontaneous ORN firing activity in the acute slice preparations of mouse olfactory epithelium.

We detected the predominant immunoreactivities of hyperpolarization-activated cyclic nucleotide-gated (HCN) channel subtypes 2 and 4 in soma of ORNs. By applying extracellular recording, we found that HCN channels depolarized the membrane of ORNs and boosted the spontaneous firing activity by sensing the cAMP levels that was largely maintained by the basal activation of Gs-coupled beta2-adrenergic receptor; the basal activity of beta2-adrenergic receptor was inhibited by ICI 118,551 (IC50 = 4 μM). We also demonstrated by a whole-cell voltage-clamp configuration that the activation of the olfactory HCN channels (control: V1/2 = –115.7 ± 3.5 mV) was positive-shifted by 1 μM intracellular PIP2 (V1/2 = –98.2 ± 4.6 mV) and further by 1 mM 8-Br-cAMP (V1/2 = –86.0 ± 1.5 mV). The results indicate that HCN channels can be operational at the resting membrane potentials of ORNs (about –70 to –90 mV). Furthermore, we generated mice with HCN4 channel over-expressed by Tet-system, in which the spontaneous ORN firing rate was much higher than that in non-transgenic littermates. Strikingly, the histological architecture of the olfactory map was severely deteriorated; the olfactory bulb became much smaller and the size and number of the olfactory glomeruli were drastically reduced especially in the dorsal region (the maximum numbers of glomeruli was 42.5 ± 1.8 glomeruli in control mice and 23.1 ± 0.5 glomeruli in HCN4 over-expressing mice). Finally, we confirmed that the knockdown of the over-expressed HCN4 by tetracycline derivative successfully recovered these structural changes.

Thus we conclude the rate of the spontaneous electrical activity is a unique guidance cue intrinsically regulated within an optimal range to maximize the diversity and integrity of the olfactory map (Nakashima et al., 2013).

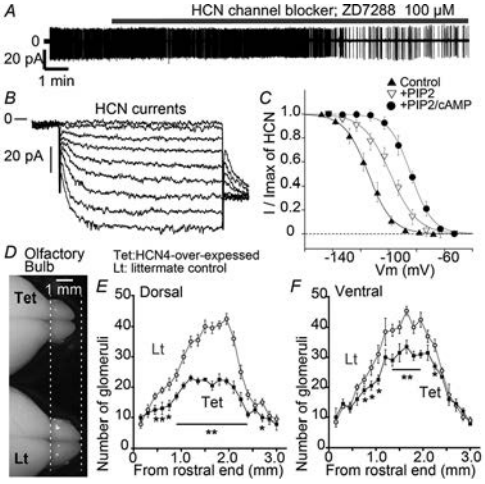

Figure 1. A, the representative trace of the spontaneous ORN firing; it was suppressed by HCN channel blocker, ZD 7288. B, the representative traces of HCN currents recorded in ORNs. C, the activation curves of the olfactory HCN currents; positively shifted by PIP2 and 8-Br-cAMP. D, the dorsal view of the olfactory bulbs in HCN4- over-expressing mice (Tet) and their littermates (Lt). E and F, the numbers of olfactory glomeruli in the dorsal region (E) and the ventral region (F) of the olfactory bulb.

Yu CR et al. (2004) Neuron 42, 553-566.

Imai T et al. (2006). Science 314, 657-661.

Takeuchi H & Kurahashi T (2008). J Neurosci 28, 766-775.

Nakashima N et al. (2013). J Physiol Jan 14. [Epub ahead of print]

Where applicable, the authors confirm that the experiments described here conform with The Physiological Society ethical requirements.

PCB120

Expression of purinergic P2Y12 receptors in rat trigeminal ganglion neurons

A. Kawaguchi[1,2], Y. Shibukawa[1,3], H. Kuroda[1,2], M. Soya[1,2], M. Satou[1], M. Tazaki[3] and T. Ichinohe[2]

[1]Oral Health Science Center hrc8, Tokyo dental college, Chiba, Japan, [2]Dental Anesthesiology, Tokyo Dental College, Chiba, Japan and [3]Physiology, Tokyo dental college, Chiba, Japan

Nerve injury in trigeminal ganglion (TG) neurons occasionally induces neuropathic pain in maxillofacial region. As a part of developmental mechanisms in neuropathic pain, ATP receptors play key roles in pain signaling. These ATP receptors are exists on cell membrane and classified into ionotropic P2X (subdivided into P2X1-7) and G-protein-coupled P2Y (subdivided into P2Y1, 2, 4, 6, 11-14) receptors. Sufficient evidence shows expression of P2X3, and P2X2/3 on sensory neurons, and that of P2X4, P2X7 and P2Y12 on glial cells. Activation of Gαi following P2Y12 receptors activation inhibits adenylate cyclase in cells at brain (in particular glial cells), spinal cord and

platelets. The P2Y12 receptors interact with some molecules (e.g. P2X4 receptors, chemokine receptors, toll-like receptors, mitogenactivatedprotein kinase, Src-family kinase and cathepsin S) in activated micro or satellite glial cells and induces neuropathic pain. P2Y12 receptors are also expressed in satellite glial cells in injured TG neurons, and its activation enhances neuronal activity. Thus, expression and neuro-pathological role of P2Y12 receptors has been well described in the glial cells, however, their expression and physiological roles of P2Y12 receptor in the TG neurons remain to be clarified. In the present study, we investigated expression, localization, physiological and pharmacological properties of P2Y12 receptors by mmunofluorescence analysis, and measurement of intracellular free Ca2+ concentration ([Ca2+]i) with fura-2 fluorescence in the primary cultured rat TG neurons. We observed intense immunoreactions for P2Y12 receptors on soma, dendrites and axons in TG neurons, which co-localized with Pan-neuronal marker, neurofilament 200, isolectin B4, and substance P. In the presence or absence of extracellular Ca2+, application of P2Y1,12,13 agonist (2-MeS-ADP) increased [Ca2+]i transiently with dose-dependent manner. These increase in [Ca2+]i was not observed in the presence of sarcoplasmic reticulum Ca2+-ATPase inhibitor (cyclopiazonic acid) with or without extracellular Ca2+. Moreover, these 2-MeS-ADP-induced increase in [Ca2+]i were significantly inhibited by selective P2Y12 receptor antagonists (AR-C66096 and PSB0739) in the presence of extracellular Ca2+ . These results showed that P2Y12 receptor distribute A-, non-peptidergic C- and peptidergic C-neurons; and indicate that activation of P2Y12 receptors induced release of Ca2+ from the intracellular Ca2+ stores. Further study is needed how an activation of P2Y12 receptors in TG neurons contribute to pain signaling in oral and maxillofacial region.

Where applicable, the authors confirm that the experiments described here conform with The Physiological Society ethical requirements.

PCB121

Ischemic preconditioning as induction of ischemic tolerance after transient cerebral ischemia and reperfusion in rats

H.A. Awooda

physiology, Al Neelain university, Khartoum, Sudan

Ischemic preconditioning (IPC) is a brief episode of ischemia/reperfusion (I/R) that protects the brain from the damage induced by subsequent prolonged ischemia. It confers both early and delayed tolerance over a period of a few minutes to days (1). Rho-kinases (ROCK) are serine–threonine kinases that critical in cell migration and survival, activation of ROCK pathway was observed in cerebral ischemia (2). The aim of the present work was to study the neuroprotective potential of IPC. 24 adult male Wistar rats (150-250g) were divided into three groups 8 rats in each; first group was sham-operated and served as a control, I/R group of rats subjected to 30 minutes of left common carotid artery occlusion followed by 24-hour of reperfusion, anesthesia was induced by ether inhalation and maintained by thiopental sodium (2.5mg/kg) (3). IPC group were treated with three episodes of 5-minutes of ischemia with 10 minutes of reperfusion in between, followed by 30 minutes of ischemia and then allowed for reperfusion for 24-hours. Neurobehavioral assessments were evaluated (4); ROCK using enzyme-linked immunosorbent assay was measured in affected cerebral hemisphere. Values are means ± S.E.M, compared by ANOVA. The IPC group showed a significant improvement in neurological deficit (16.9±0.50) compared to both I/R and control groups (12.798±0.689, 17.50±0.707, respectively P <0.001). In I/R group ROCK was significantly increased (1.13±0.17 ng/mg protein, P <0.001) as compared to IPC group, but not to control group (p=0.198). Rats subjected to IPC demonstrated a significant decrease in ROCK level (0.39±0.19 ng/mg protein, P <0.001) to both control (1.3±0.30 ng/mg protein) and I/R group. So IPC affords protection against a subsequent I/R challenge. We established an Ischemic preconditioning model in which rats showed improvement in neurological deficits and decreased ROCK level following transient focal cerebral ischemia reperfusion in rats.

Dirnagl U, Simon RP, Hallenbeck JM. Ischemic tolerance and endogenous neuroprotection. Trends Neurosci 2003;26:248-54

Satoh S, Hitomi A, Ikegaki I, et al. Amelioration of endothelial damage/dysfunction is a possible mechanism for the neuroprotective effects of Rho-kinase inhibitors against ischemic brain damage. Brain Res Bull. 2010 Jan 15;81(1):191-5.

Keefer LK, Garland WA, Oldfield NF, et al. Inhibition of N-nitrosodimethylamine metabolism in rats by ether anesthesia. Cancer Res.1985;45(11 Pt 1):5457-60

Garcia JH, Wagner S, Liu KF, et al. Neurological deficit and extent of neuronal necrosis attributable to middle cerebral artery occlusion in rats. Statistical validation. Stroke.1995;26(4):627-34

To my supportive family and my husband Dr. Ali Kobil.

We have collaborated with many colleagues in Alexandria University - Egypt,

for whom I have great regard.

To my colleagues in Al Neelain University- Sudan.

Where applicable, the authors confirm that the experiments described here conform with The Physiological Society ethical requirements.

PCB122

Bio-inspired peptide modulators of calcium dependent inactivation revealed the role of $Ca_V1.3$ channels in neuronal development

M. Liu[1] and X. Liu[1,2]

[1]Biomedical Engineering, School of Medicine, Tsinghua University, Beijing, China and [2]School of Life Sciences, Tsinghua University, Beijing, China

Ca^{2+} signaling via voltage-gated Ca^{2+} channels has been suggested to play prominent roles in the development and degeneration of neurons. To elucidate the specific role of L-type $Ca_V1.3$ channels, we designed and tested a series of peptides, derived from the competitive mechanism between calmodulin (CaM) and distal carboxyl tail (DCT) of L-type Ca_V channels, with the capability to enhance or inhibit calcium dependent inactivation (CDI), a negative-feedback mechanism regulating actual Ca^{2+} flux through the channel. Under whole-cell patch-clamp, CDI of rat/human $Ca_V1.3$ was strongly attenuated for co-transfections of $Ca_V1.3$ with derivative peptides from DCT of $Ca_V1.4$. Such inhibitory peptides, termed as iCaMp (inhibitors of CaM pre-association), exerted significant inhibitions on the number and averaged length of dendrites if expressed in cultured cortical neurons, supposedly as the downstream consequence of $Ca_V1.3$ / Ca^{2+} dysregulations. Moreover, peptide $ICDI_{V41A}$, with single point mutation on iCaMp, completely lost its effects on dendritic growth of cortical neurons, in consistence with its loss of CDI effects on

recombinant $Ca_V1.3$ channels. On the other hand, peptide modulators of eCaMp (enhancers of CaM pre-association) opposite to iCaMp have also been sought after. The prototype of eCaMp significantly enhanced CDI of $Ca_V1.3$ from the intermediate level up to the extreme level, at which apparent DCT effects diminish. Taken together, our peptides provide an innovative way to perturb Ca^{2+} signaling specific to L-type $Ca_V1.3$ channels, shedding light on physiological roles of neuronal $Ca_V1.3$ channels as well as its potential relevance with neural degenerative diseases such as Alzheimer's.

Where applicable, the authors confirm that the experiments described here conform with The Physiological Society ethical requirements.

PCB123

Patterning neurons and informing neurite geometry on photolithographically defined parylene-C coated SiO_2

M.A. Hughes[1], A.S. Bunting[2], K. Cameron[2], A.F. Murray[2] and M.J. Shipston[1]

[1]Centre for Integrative Physiology, University of Edinburgh, Edinburgh, UK and [2]School of Engineering, University of Edinburgh, Edinburgh, UK

Interfacing neurons with silicon semiconductors is a challenge being tackled through varied bioengineering approaches. The resulting constructs inform our understanding of neuronal coding and learning, and ultimately guide us towards creating intelligent neuroprostheses and brain-machine interfaces. A fundamental pre-requisite is to dictate the spatial organization of neuronal cells on silicon. We fabricated photolithographically defined designs of parylene-C on SiO_2 wafers. These chips are activated with fetal calf serum, resulting in a culture environment that is differentially cell-adhesive (parylene) or repulsive (SiO_2). LUHMES (Lund human mesencephalic) neurons cultured in isolation find the entire chip cell-repulsive. Applying another cell type (HEK 293 cells) enables LUHMES neurons to secondarily adhere. Over 3-4 days, patterned neurons extend neurites and form networks. Seeking to gain better control of neurite behaviour, we created different geometric arrays of parylene. The basic pattern was a circular node of parylene with four 'spokes' at 0°, 90°,180°, and 270°. Three different versions were trialed (node dia. 50μm, spoke length 125μm; node dia. 100μm, spoke 100 μm; node dia. 250μm, spoke 100 μm). Nodes were arranged orthogonally with respect to one another, with a 100μm interval separating adjacent node/spoke complexes. To quantify the impact of the parylene/SiO_2 construct on neurite orientation, neurites were traced from start point (centred on a parylene node) to end point (defined either as branching point, termination, or encountering another cell body). Traced segments were divided into 100μm sub-segments. A tangent was taken to each sub-segment and the angle, θ, of each segment measured and categorized into 11.25° intervals. This process was conducted for areas encompassing each of the three different node geometries, and for differentiated LUHMES cultured randomly on a polystyrene surface treated to promote homogenous cell adhesion. Entries 180° apart were summed. 12 independent chip experiments enabled acquisition and measurement of 200 neurite sub-segments (each of 100μm length). A radial plot (figure 1) illustrates the orientation of neurite segments. Neurite directionality differed significantly according to parylene geometry (Kolmogorov-Smirnov tests: unpatterned substrate vs 250μm diameter nodes D=0.200, P=0.001; 250μm vs 100μm nodes D=0.204, P=0.001; 100μm vs 50μm nodes D=0.147, P=0.028). There is a trend towards increasingly orthogonal growth as parylene configuration changes from 250μm to 100μm to 50μm diameter nodes. For the generation of patterned neuronal networks capable of meaningful interrogation, there must be control over neurite growth direction and connectivity. We have developed a method of generating orthogonally arranged neuronal networks.

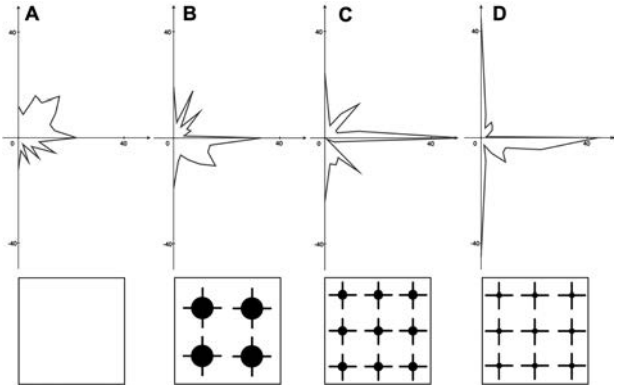

Figure 1: Directionality of neurite growth illustrated in radial plots. (A) LUHMES on plain polystyrene, (B) co-culture on 250μm diameter parylene nodes, (C) co-culture on 100μm diameter nodes, (D) co-culture on 50μm diameter nodes.

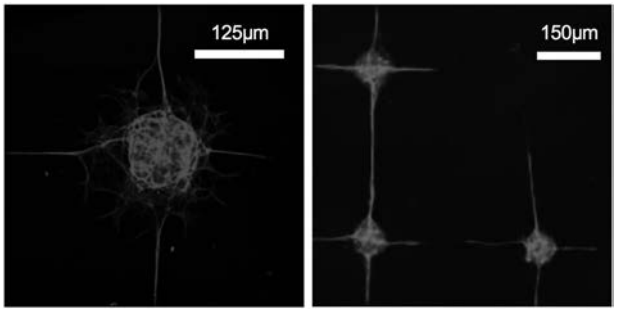

Figure 2: Neuron-specific β-III tubulin stained co-culture of pre-differentiated LUHMES in co-culture with HEK 293 cells. Fixed after 5DIV

Hughes MA, Bunting AS, Cameron K, Murray AF, Shipston MJ. Modulating patterned adhesion and repulsion of HEK 293 cells on micro-engineered parylene-C/SiO2 substrates. JBMR-A 2013; 101(2): 349-57.

Scholz D, Pöltl D, Genewsky A, Weng M, et al. Rapid, complete and large-scale generation of post-mitotic neurons from the human LUHMES cell line. J Neurochem 2011;119(5):957-951.

Funded by a Wellcome Trust Clinical PhD (ECAT)

Where applicable, the authors confirm that the experiments described here conform with The Physiological Society ethical requirements.

PCB124

Orexin-A differentially modulates AMPA responses of ganglion cells and amacrine cells in rat retina

C. Zheng[1,2], M. Wang[2], X. Yang[1] and Y. Zhong[1]

[1]Unit of Retina Research, Institute of Neurobiology, Institutes of Brain Science and State Key Laboratory of Medical Neurobiology, Fudan University, Shanghai, China and [2]Cell Electrophysiology Laboratory, Wannan Medical College, Wuhu, Anhui, China

Two novel neuropeptides, orexin-A and orexin-B, are identified as endogenous ligands of two orphan G-protein-coupled recep-

tors: orexin 1 and orexin 2 receptors (OX1R and OX2R). Orexins are implicated in regulating a variety of physiological processes, such as wake/sleep states, feeding behaviors etc. A previous work (Liu et al, 2011) in this laboratory revealed the expression of orexin-A and orexin-B in rat retinal neurons. In the present work we investigated how orexin-A modulated current responses mediated by AMPA receptor (AMPAR) of ganglion cells (GCs) and amacrine cells (ACs) in rat retina. Animal treatments in this work coincide with the NIH guidelines for animal experimentation and the guidelines of Fudan University on the ethical use of animals. Male Sprague-Dawley rats (P15-20 d) were anaesthetized by intraperitoneal injection with 25% urethane (0.4 ml/100 g) and killed by decollation. By immunofluorescence double labeling, we first showed that OX1R was mainly expressed in GCs, whereas OX2R was present in both ACs and GCs. Using whole-cell patch clamp techniques, we further examined effects of orexin-A on AMPAR-mediated currents recorded from isolated GCs and ACs and explored mechanisms underlying these effects. Administration of orexin-A suppressed AMPAR-mediated currents in GCs, and the effect was abolished by co-application of SB334867, a selective OX1R antagonist, but not by TCSOX229, a selective OX2R blocker. In contrast, orexin-A increased AMPA responses of ACs, which could be reversed by TCSOX229, but not by SB334867. As expected, either preincubation with the Gi/o inhibitor pertussis toxin or intracellular dialysis of the Gi/o activator mastoparan eliminated both the orexin-A effects on GCs and ACs. Signaling pathways mediating the two effects were further explored. Firstly, the two effects involved activation of PKC, as evidenced by the elimination of those by PKC antagonists. Secondly, U73122, a phosphatidylinositol (PI)-phospholipase C (PLC) inhibitor, and D609, a phosphatidylcholine (PC)-PLC inhibitor, abolished the effects on AMPA currents of GCs and ACs respectively. Thirdly, the two effects were different in utilizing intracellular Ca2+. Whilst the effect on GCs may be mediated by the release of intracellular Ca2+ through the IP3-sensitive pathway, that on ACs was independent of intracellular Ca2+. Furthermore, neither cAMP-PKA nor cGMP-PKG pathway was involved in both the effects. In consequence, a distinct PI-PLC/IP3/Ca2+/PKC signaling pathway, following the activation of OX1R, is most likely responsible for the orexin-A-induced suppression of AMPA currents of rat GCs, whereas a PC-PLC/PKC signaling pathway, following the activation of OX2R, mediates the orexin-A-induced potentiation of AMPA currents of ACs.

Liu F, Xu GZ, Wang L, Jiang SX, Yang XL, Zhong YM (2011) Gene expression and protein distribution of orexins and orexin receptors in rat retina. Neuroscience 189: 146-155.

Where applicable, the authors confirm that the experiments described here conform with The Physiological Society ethical requirements.

PCB125

Optogenetically-evoked Ca^{2+} release from intracellular store in the calyx-type presynaptic terminal of the embryonic chick ciliary ganglion

R. Egawa[1,3], S. Hososhima[1,3], H. Katow[1,2], T. Ishizuka[1,2] and H. Yawo[1,2]

[1]Dept Dev Biol and Neurosci, Tohoku Univ, Sendai, Japan, [2]JST, CREST,, Tokyo, Japan and [3]JSPS, Tokyo, Japan

Optogenetics has become a powerful tool in neuroscience either as sensors to survey the function at the cellular level or as actuators to regulate the neuronal activity. The calyx-type presynaptic terminal of embryonic chick ciliary ganglion (CG) is relatively large and therefore accessible to physiological recording methods such as the patch clamp. As it innervates the postsynaptic ciliary neuron in a one-to-one manner at embryonic day 14 (E14), its physiology corresponds to the morphology and electrophysiological responses of its postsynaptic cell. Further progress can be expected if the presynaptic mechanisms of these large terminals can be studied using optogenetics. Here, we carried out simultaneous optogenetic probing and manipulation of this presynaptic terminal and evaluated optogenetics for the presynaptic research. We transfected the plasmid vectors containing one of chimeric variants of channelrhodopsins, channelrhodopsin-fast receiver (ChRFR), and a red-shifted fluorescent Ca^{2+}-sensor, R-GECO1, into the midbrain preganglionic neurons at E2 using *in ovo* electroporation technique (Odani et al., 2008). At E14, the presynaptic terminals in the ciliary ganglion were used for the physiological experiments under high-speed confocal microscopy. The presynaptic Ca^{2+} elevation was triggered by a direct photostimulation of the presynaptic terminal via optical fiber. Although this optically-evoked Ca^{2+} elevation was mostly dependent on the action potential, a significant component remained even in the presence of TTX and N-type voltage-dependent channel inhibitor, ω-conotoxin GVIA, or in the absence of extracellular Ca^{2+}. The remaining component was depleted by repetitive stimulations with sarco/endoplasmic reticulum Ca^{2+}-ATPase (SERCA) inhibitor, thapsigargin. These results suggest that the photo-activation of ChRFR facilitated the Ca^{2+} release from endoplasmic reticulum Ca^{2+} stores directly or indirectly. Therefore, it is necessary to keep in mind that such background Ca^{2+} elevation could modify the biochemical milieu regulating the transmitter release.

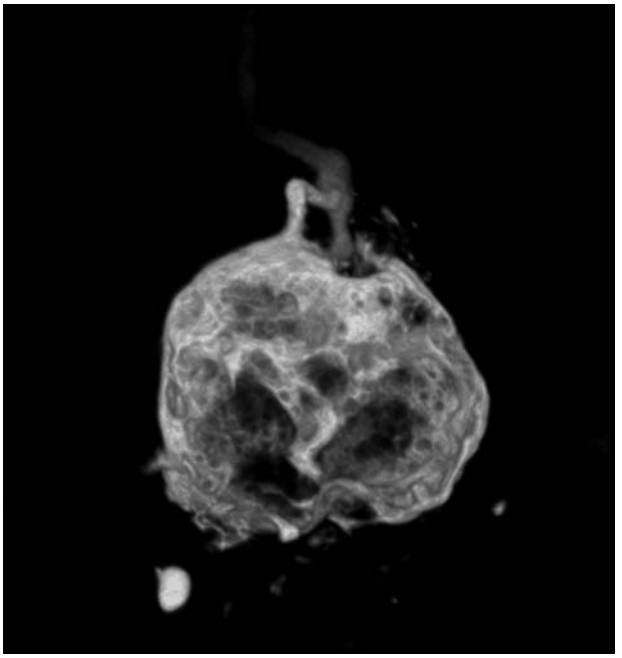

Egawa R, Hososhima S, Hou X, Katow H, Ishizuka T, Nakamura H, Yawo H. (2013) Optogenetic probing and manipulation of the calyx-type presynaptic terminal in the embryonic chick ciliary ganglion. PloS one (in press)

Odani N, Ito K, Nakamura H (2008) Electroporation as an efficient method of gene transfer. Dev Growth Differ 50: 443-448.

Where applicable, the authors confirm that the experiments described here conform with The Physiological Society ethical requirements.

PCB126

Electrophysiological characterisation of neuronal excitability of l-LNv neurons and their role in controlling circadian rhythm

M.L. Nugent[1,2], J. Steinert[2], I. Forsythe[3] and E. Rosato[1]

[1]Genetics, University of Leicester, Leicester, UK, [2]MRC Toxicology Unit, Leicester, UK and [3]Cell Physiology and Pharmacology, University of Leicester, Leicester, UK

A conserved circadian clock provides the temporal framework for rhythmic behaviour and metabolism across the phylla, and is regulated or entrained by environmental factors such as light and temperature, known as zeitgebers (ZT). In flies, entrainment to light is mediated by the blue-light sensitive protein CRYPTOCHROME (CRY). When activated it is able to interact with core clock components to ensure the molecular clock is optimised to the light-dark cycle, as well as many other proteins involved in various physiological processes such as magnetoception, courtship behaviour and metabolism.

This project investigates the role of CRY in the regulation of neuronal excitability in a specific subset of neurons of the Drosophila CNS called the large ventral lateral neurons (l-LNvs). Overexpression of a constitutively active form of CRY (CRYΔ) is used to study the role of CRY within the circuitry involved in circadian clock regulation.

Whole cell patch clamp recordings of l-LNvs in whole brain preparations of adult Drosophila were performed (Multiclamp 700B, pClamp 10, Axon Instruments). Female flies w1118 /UAS cryΔ72.3; tim-GAL4/ UAS GFP co-expressed CRYΔ and GFP in clock cells, including the l-LNvs. w1118 /+; tim-GAL4/ UAS GFP females were used as controls. Recordings were conducted during ZT10-12 to eliminate any changes in the activity seen in the l-LNvs due to a circadian effect. Larval foraging activities were measured as crawling distance in 10min (ANYmaze) using female larvae that were w1118; elav_GAL4/+; UAS-cryΔ4.1/+ and compared to w1118; elav_GAL4/+; +/+ for control. Data are expressed as mean ±SEM (n). Statistical analyses were carried out using standard unpaired t-test, * indicates $p<0.05$.

Electrophysiological recordings revealed that overexpression of CRYΔ in l-LNvs induces increased outward currents at 0mV from 167 ±8pA (3) to 234 ±20pA* (3) and at -10mV from 79 ±4pA (3) to 124 ±17pA* (3). Investigations of the spontaneous action potential (AP) firing frequencies were also conducted but have thus far not shown a significant difference, although there is a trend of increased AP firing rates in response to current injection.

Larval foraging assays to investigate the motor effects of CRYΔ overexpression at the larval neuromuscular junction (NMJ) have shown an increase in the distance travelled by CRYΔ expressing larvae from 0.5 m (14) to 0.67 ±0.04 m* (17).

This data indicates that CRYΔ expression is able to mediate changes in activity at the NMJ as well as in CNS clock cells. Further CNS recordings are needed to allow firm conclusions from the electrophysiological data collected so far.

BBSRC for funding this PhD studentship.

Where applicable, the authors confirm that the experiments described here conform with The Physiological Society ethical requirements.

PCB128

Short term synaptic plasticity defines neuronal groups firing together in cultures of cortical cells

V.G. Lopez-Huerta[1], L. Carrillo-Reid[2], M. Garcia-Munoz[1] and G.W. Arbuthnott[1]

[1]Brain mechanisms for behavior unit, Okinawa Institute of Science and Technology, Onna-son, Okinawa, Japan and [2]Physiology, Feinberg School of Medicine, Northwestern University, Chicago, IL, USA

Synchronized and sequential activity patterns in neural networks have been proposed as a mechanism underlying many complex behaviors, such as procedural memories and decision-making. Hebb (1949) suggested that neuronal assemblies were formed by the strengthening of synaptic connections between cells that often fire together. However, the role of short-term synaptic dynamics in network activity patterns and sequence formation has not been widely studied in living neural networks. We used optical and electrophysiological recordings to describe synaptic properties that accompany co-operative firing and sequential activity patterns of groups of neurons in cultures of mouse cortical cells (>15DIV). Spontaneous activity and connectivity was studied in whole cell patch clamp recordings from a total of 42 neuronal pairs. Oscillatory firing activity was recorded in 26 cells and connectivity rate was 52% (22/42 pairs). Some of the pairs had nearly synchronous up states (starting within <10ms) whereas others were more out of phase. When short term plasticity was tested in these pairs, cells firing together mainly displayed short-term synaptic depression (n=5, i.e., high release probability), whereas cells firing in sequence, mostly displayed short-term synaptic facilitation (n=6, i.e., low release probability). To further investigate the impact of short-term synaptic dynamics in cell assembly behavior we performed calcium imaging with single cell resolution in groups of several hundred cells. The release probability was modified by changing the extracellular calcium concentration. At low extracellular calcium concentrations (1mM) synaptic connections were mainly facilitating (n= 5/7 pairs) and the transitions of activity among groups of neurons were increased showed by calcium imaging (n=6 dishes). On the contrary, at a higher extracellular calcium concentration (4mM) we observed short-term depression in all the connections (n=7 pairs) and a reduced variability of cell assemblies (n=6 dishes). These results suggest a direct relationship between neuronal groups firing together and short-term synaptic plasticity in living neural networks, and suggest that a given microcircuit might be reprogrammed by the targeted modification of the excitatory synaptic dynamics due to the presence of neuromodulators.

Hebb DO (1949) The Organization of Behavior: A Neuropsychological Theory. New York, NY: Wiley.

Where applicable, the authors confirm that the experiments described here conform with The Physiological Society ethical requirements.

PCB129

Mechanism of nitric oxide dependent LTP revealed by kinetic analysis of AMPAR trafficking in rat cerebellar Purkinje cell

K. Yamaguchi

BSI, RIKEN, Wako, Saitama, Japan

Nitric oxide (NO), produced by repetitive activation of the cerebellar parallel fiber (PF), induces long-term potentiation (LTP) of synaptic transmission between PF- Purkinje cell (PC) synapse. Underlying mechanism of this LTP is known to be increase in density of surface expressed AMPA type glutamate receptors (AMPA-Rs), mediated by receptor exocytosis (1). NO directly S-nitrosylates N-Ethylmaleimide Sensitive Factor (NSF) and this S-nytrosylated NSF increase its affinity to GluA2 carboxy-terminus (CT) region, and interaction of NSF – GluA2-CT enhances insertion of AMPA-Rs into the synaptic membrane (2). However, whether actually NO enhanced AMPA-Rs exocytosis or suppress endocytic elimination from the synaptic membrane remained elusive. Here, we quantitatively analyzed interaction between constitutive endocytosis and NO-induced LTP with an aid of data-driven kinetic model of AMPA-R trafficking.
Slice of cerebellar cortex was prepared from rat (P19-23) cerebellum ectomized after decapitation during deep anesthesia with ethyl ether. EPSC evoked by electrical stimulation of the molecular layer was recorded from PC by means of a whole-cell recording method. In basal condition, NO-donor (NOR3 30microM) itself enhanced PF-PC EPSC amplitude to 170% of the basal amplitude (LTP) in rat cerebellar slice. When constitutive endocytosis was blocked by dynamin inhibitor, similar amount of increase in EPSC-amplitude through a constitutive exocytosis of AMPA-R was observed. Because LTP occluded with the constitutive exocytosis of AMPA-Rs, both pathways had to share common mechanism. When EPSC amplitude was reduced to the minimum steady state level by tetanus toxin (TeTx) infusion through a whole-cell patch-pipette (3), NOR3 had no effect on EPSC amplitude. However, when NOR3 was applied early phase of TeTx-action, NO intermitted constitutive endocytic reduction of EPSC amplitude with a slight rebound. By using our kinetic model of AMPA-R trafficking, I successfully reconstituted this time course including a slight rebound of EPSC amplitude by assuming that AMPA-R endocytosis was blocked, but not that exocytosis was enhanced, by NO. Because NSF and AP-2, an adaptor protein required for clathrin dependent endocytosis, compete binding to the overlapping NSF/AP-2 domain at GluA2-CT, S-nitrosylated NSF would competitively inhibit binding of AP-2 to this domain, and consequently suppress endocytosis of GluA2. We conclude that NO induces LTP by blocking GluA2 endocytosis at PF-PC synapse.

1. Kakegawa W and Yuzaki M (2005) PNAS 102: 17846-17851

2. Huang Y et al., (2005) Neuron 46: 533-540

3. Tatsukawa T et al., (2006) J.Nerosci. 26: 4820-4825

This work was partly supported by grant from JSPS KAKENHI Grant Number 23500472.

Where applicable, the authors confirm that the experiments described here conform with The Physiological Society ethical requirements.

PCB130

Expression and function of Kir7.1 in neurons and glia of the mouse CNS

M. Papanikolaou, J. Hallett, A. Lewis and A.M. Butt

Pharmacy and Biomedical Science, University of Portsmouth, Portsmouth, Hants, UK

The inward rectifying potassium channel subtype Kir7.1 has been studied in a variety of potassium transporting epithelia in the retina, thyroid, intestine and kidney. The expression and function of Kir7.1 in the CNS is unresolved, although expression of these channels has been reported in cerebellar Purkinje neurons, hippocampal pyramidal neurons and neural stem cells. Here, we have assessed the expression and function of Kir7.1 in neurons and glia of the mouse CNS. Mice were euthanized humanely in accordance with the UK Animals Act (1986) and tissue was used for RT-PCR, Western blot, immunohistochemistry, tissue culture or isolated intact optic nerves for oxygen and glucose deprivation (OGD). Expression of Kir7.1 in adult brain and optic nerve was demonstrated by rtPCR and western blot. Immunolabelling with the Alomone aKir7.1 antibody confirmed previous reports of Kir7.1 expression in cerebellar Purkinje and hippocampal pyramidal neurons, and demonstrated immunolabelling in astrocytes and oligodendrocytes, the myelinating cells of the CNS. Glial and neuronal expression of Kir7.1 was confirmed in cultures of cells from the neonatal cortex and optic nerve. Like neurons, glial cells are susceptible to hypoxic/ischaemic injury, such as those that occur during stroke. A key factor in hypoxic/ischaemic episodes is that they cause depolarization of the resting membrane potential, resulting in cell dysfunction and death. Kir7.1 are highly sensitive to pH and are suppressed by extracellular acidification, such as occurs in ischemia. We therefore examined whether Kir7.1 may play a role in the susceptibility of glia to ischemia, in isolated intact optic nerves from mice aged postnatal day (P)10 mice subjected to oxygen and glucose deprivation (OGD). Incubation of optic nerves with the Kir7.1 channel blocker VU590 significantly increased cell death of optic nerve glia, measured using propidium iodide (PI) labelling (measured in a constant field of view (FOV), 6 FOV per nerve, n=4 nerves per group; 80 + 30 PI+ cells in controls and 189 + 49 PI+ cells in VU590; $p<0.001$, Anova). Our results demonstrate widespread expression of Kir7.1 in CNS neurons and glia, and indicate a functional importance in protecting glial cells from ischemic damage. Further studies are required to determine the biophysical properties of Kir7.1 and their pathophysiological function in neurons and glia.

Nakamura N, Suzuki Y, Sakuta H, Ookata K, Kawahara K, Hirose S. Inwardly rectifying K+ channel Kir7.1 is highly expressed in thyroid follicular cells, intestinal epithelial cells and choroid plexus epithelial cells: implication for a functional coupling with Na+/K+-ATPase. Biochem J. 1999 Sep 1;342 (Pt 2):329-36.

Derst C, Hirsch JR, Preisig-Müller R, Wischmeyer E, Karschin A, Döring F, Thomzig A, Veh RW, Schlatter E, Kummer W, Daut J. Cellular localization of the potassium channel Kir7.1 in guinea pig and human kidney. Kidney Int. 2001 Jun;59(6):2197-205.

Prüss H, Dewes M, Derst C, Fernández-Klett F, Veh RW, Priller J. Potassium channel expression in adult murine neural progenitor cells. Neuroscience. 2011 Apr 28;180:19-29. doi: 10.1016/j.neuroscience.2011.02.021. Epub 2011 Feb 15.

Hughes BA, Swaminathan A. Modulation of the Kir7.1 potassium channel by extracellular and intracellular pH. Am J Physiol Cell Physiol. 2008 Feb;294(2):C423-31. Epub 2007 Dec 19.

Lewis LM, Bhave G, Chauder BA, Banerjee S, Lornsen KA, Redha R, Fallen K, Lindsley CW, Weaver CD, Denton JS. High-throughput screening reveals a small-molecule inhibitor of the renal outer medullary potassium channel and Kir7.1. Mol Pharmacol. 2009 Nov;76(5):1094-103. doi: 10.1124/mol.109.059840. Epub 2009 Aug 25.

Supported by the MRC, BBSRC and IBBS

Where applicable, the authors confirm that the experiments described here conform with The Physiological Society ethical requirements.

PCB132

Decreased excitability of neurons in the ventral nucleus of the trapezoid body may contribute to medial olivocochlear system dysfunction in the C57BL/6

J. Sinclair[1], M. Barnes-Davies[2] and I.D. Forsythe[1]

[1]Cell Physiology & Pharmacology, The University of Leicester, Leicester, Leicestershire, UK and [2]Medical Education, The University of Leicester, Leicester, UK

Hearing loss is the most prevalent sensory disorder effecting humanity and dysfunction in the medial olivocochlear (MOC) system is thought to be involved. The MOC regulates and protects auditory sensitivity by modifying the activity of the outer hair cells in the cochlea. The majority of MOC neurons in mice are present in the ventral nucleus of the trapezoid body (VNTB) in the brainstem. The C57BL/6 (C57) inbred strain of mouse has early-onset hearing loss, preceded by a failure in the efficacy of its MOC system (Zhu et al., 2007). We examined the neurons of the VNTB in the C57 and compared them with those of a strain which retains auditory sensitivity into old age: the CBA/Ca (CBA). We aimed to determine if differences in excitability in VNTB neurons exist between the strains which could influence MOC function. Mice were decapitated in accordance with the UK Animals (Scientific Procedures) Act 1986 and brainstem slices prepared (Barnes-Davies & Forsythe, 1995). Whole cell recordings were taken from visually identified VNTB cells in pre-hearing onset (P8) and post hearing onset (P16) CBA and C57 mice (Fujino et al., 1997). Prehearing onset, CBA and C57 VNTB cells have similar in current-voltage relationships and action potential (AP) thresholds. Under voltage clamp, cells of both strains display outward currents around -30mV which inactivate rapidly. During a 200ms pulse to -30mV, currents in both strains drop from around 2nA (CBA: 1.77±0.35nA (n=10), C57: 2.36±0.36nA (n=12) to 0.6nA (CBA: 0.75±0.09nA, C57: 0.52±0.08nA). Current clamp recordings indicate that AP thresholds are around -38mV for both strains (CBA:-38.4±2.5mV (n=7), C57:-38.2±1.7mV (n=7). Both strains produce few APs during 200ms current injection of +50pA (CBA: 0.6±0.4, C57: 1.0±1.2). Post-hearing onset, the CBA VNTB neurons develop greater sustained currents at hyperpolarised potentials than in the C57. During a 200ms pulse to -30mV, currents of CBA VNTB cells demonstrate little inactivation (1.73±0.36nA to1.57±0.45nA over 200ms (n=8)). C57 VNTB neurons retain inactivation of low voltage activated currents similar to those present in P8 mice (1.91±0.31nA dropping to 0.49±0.61nA after 200ms(n=7)). Post-hearing onset CBA VNTB neurons also demonstrate greater excitability under current clamp conditions, generating more APs than age matched C57 (CBA: 6.2±1.4 (n=6), C57: 1.5±0.75 (n=4), (P =0.02)) despite having similar thresholds (CBA: -43.6±2.2, C57: 39.5±3.1). These experiments indicate lower excitability of neurons of the VNTB in the C57: a strain of mouse with MOC functional deficits. Decreased activity of MOC neurons in the VNTB would impede efferent control of the sensitivity of the ear and could contribute to the C57 strain's vulnerability to hearing loss. Data ± SEM. Means compared using unpaired t-tests. P : post natal day.

Barnes-Davies M & Forsythe ID (1995). Pre- and postsynaptic glutamate receptors at a giant excitatory synapse in rat auditory brainstem slices. J Physiol 488, 387–406.

Fujino K, Koyano K & Ohmori H (1997). Lateral and medial olivocochlear neurons have distinct electrophysiological properties in the rat brain slice. J Neurophysiol 77, 2788-2804.

Zhu X,, Vasilyeva ON, Kim S, Jacobson M, Romney J, Waterman MS, Tuttle D & Frisina RD (2007). Auditory efferent feedback system deficits precede age-related hearing loss: contralateral suppression of otoacoustic emissions in mice. J Comp Neurol, 503, 593-604.

We would like to thank AgeUK and Action On Hearing Loss for funding this project

Where applicable, the authors confirm that the experiments described here conform with The Physiological Society ethical requirements.

PCB134

Regulation of excitatory synaptic function by estrogen: implications for health and disease

A. Ibrahim and J. Harvey

University of Dundee, Dundee, UK

It is well established that activity dependent changes in the efficacy of hippocampal synaptic transmission is a cellular correlate of learning and memory. Trafficking of AMPA-receptors to and from synapses is an important mechanism underlying hippocampal synaptic plasticity. Increasing evidence implicates hormonal systems in the influence of AMPA-receptor trafficking, and thus synaptic plasticity. Estrogen, primarily known for its reproductive effects, has long been implicated in influencing cognitive processes. Estrogen receptors (ERs), classically found in the nucleus, act as ligand-activated transcription factors in mediating genomic responses. ERs can also mediate rapid non-genomic responses via membrane-associated ERs. Two well characterised ERs, ERα and ERβ, are widely expressed in the hippocampus. However, little is known about how these ER subtypes influence cognitive processes. Moreover, the novel G-protein-coupled receptor, GPR30, has been identified as an estrogen target, and recent studies suggest possible cross-talk between ERα and GPR30.[1] In pilot studies, we have found that the broad-spectrum agonist, 17β-estradiol, induces bidirectional changes in AMPA-receptor trafficking. In addition, recent studies have implicated ERβ-activation in improving performance in hippocampal-dependent memory tasks and increasing key synaptic proteins such as the AMPA-receptor subunit GluR1. In this study, we have examined how estrogen influences AMPA-receptor trafficking by utilising ERα-, ERβ-, and GPR30-selective agonists in an immunocytochemical approach. We show that activation of ERα and GPR30 results in a decrease in GluR1 surface expression likely to be mediated by an exocytosis-dependent mechanism, and that activation of ERβ results in an increase in GluR1 surface expression likely to be mediated by an endocytosis-dependent mechanism. In addition, we demonstrate that the effects of GPR30-activation on GluR1 surface expression are unlikely to be due to ERα-activation. These findings have important implications for the role of estrogen in cognitive decline and neurodegenerative disorders.

Noel SD, et al. (2009). Mol. Endocrinol 23(3):349-59.

Dayne Beccano-Kelly, Amy Alexander, and Wolfson Foundation

Where applicable, the authors confirm that the experiments described here conform with The Physiological Society ethical requirements.

PCB135

Cocaine preferentially potentiates fast releasable vesicle pool in mouse dopaminergic striatum in vivo

P. Zuo[1], L. Zhou[1], X. Kang[1], H. Xu[1], B. Zhang[1], H. Dou[1], F. Zhu[1], L. Liu[1], S. Guo[1], C. Wang[1], Q. Li[1], S. Wang[1], W. Yao[1], H. Gu[2] and Z. Zhou[1]

[1]Peking University, Beijing, China and [2]Ohio State University, Columbus, DC, USA

Cocaine, an addictive drug, increases extracellular dopamine (DA) concentration in basal ganglion. This effect has been commonly assumed mainly through the inhibition of the uptake activity of DA transporters (DAT). Whether cocaine may also potentiate DA release under physiological conditions remains unclear. To investigated cocaine's effect on DA release in striatum in vivo, C57 and DAT-CI mice (male, 25 g) anaesthetized with urethane (0.15 g/100 g, i.p.) were used. The use and care of animals was approved and directed by the Institutional Animal Care and Use Committee of Peking University. We found that two kinetically distinct DA releasable vesicle pools, a fast releasable pool (FRP) and a prolonged releasable pool (PRP), existed following physiological field stimulations at medial forebrain bundle (MFB) in mouse striatum in vivo. Surprisingly, cocaine selectively enhanced the DA release and replenishment from the FRP. Using a cocaine-insensitive-DAT (DAT-CI) mouse model, we found that cocaine-facilitated FRP release is mediated by DAT. In contrast, PRP release is selectively sensitive to D2 receptor (D2R). Finally, FRP and PRP have distinct impacts on locomotor behaviours. Our findings indicate that in addition to blocking DA reuptake, cocaine increases DA release by selectively activating DAT, increasing FRP size, and accelerating FRP replenishment in mouse striatum in vivo.

This study was supported by grants from NSFC, MOST and DOE 2011-program

Where applicable, the authors confirm that the experiments described here conform with The Physiological Society ethical requirements.

PCB136

Investigating neuronal morphology and physiology in the rat lateral reticular nucleus

R. Jordan, S.A. Edgley and S. Jones

Department of Physiology, Development and Neuroscience, University of Cambridge, Cambridge, UK

The lateral reticular nucleus (LRN) in the medullary reticular formation is a major source of mossy fibre afferents to the cerebellum. We have previously shown that many LRN neurones fire extremely regularly and respond to peripheral sensory stimulation with an initial brief pause in firing followed by a resumption of spiking with 'reset' timing (Xu et al., 2012). Here we have investigated the morphology and physiology of rat LRN neurones. Whole-cell patch-clamp recordings were made from 18 LRN neurones in brain slices prepared from rats aged postnatal day (P) 5 to P15 (decapitated under isoflurane anaesthesia), using a K+-based intracellular solution with biocytin. Neuronal morphology was deduced from 9 of these LRN neurones in which biocytin labelling was recovered. Of these, 8 had a morphology consistent with 'triangular' cells (Kapogianis et al., 1982). These triangular neurones showed spontaneous firing (mean frequency, 3.1 ± 0.5 Hz; CV of inter-spike intervals, 0.17 ± 0.04) and a hyperpolarisation-activated Isag (mean amplitude, 63.7 ± 55.6 pA). In 6 of the 8 triangular cells, glycine was applied via a picospritzer (1 mM, 0.1-1 s, 10 p.s.i) and evoked currents that reversed at -38.5 ± 17.5 mV. These triangular neurones in the LRN may be the source of spontaneously firing mossy fibre inputs to the cerebellum.

W. Xu, S. Jones & S.A. Edgley (2012) Journal of Physiology 24 December EPub

E.M. Kapogianis, B.A. Flumerfelt, and A.W. Hrycyshyn (1982) Anat Embryol 164:229-242

Where applicable, the authors confirm that the experiments described here conform with The Physiological Society ethical requirements.

PCB137

Investigating synaptic regulation of neurones in the rat lateral reticular nucleus

J.R. Heckenast, S.A. Edgley and S. Jones

Department of Physiology, Development and Neuroscience, University of Cambridge, Cambridge, UK

The lateral reticular nucleus (LRN) in the medullary reticular formation is a major source of mossy fibre afferents to the cerebellum. We have previously shown that many LRN neurones fire extremely regularly and respond to peripheral sensory stimulation with an initial brief pause in firing followed by a resumption of spiking with 'reset' timing (Xu et al., 2012). Here we have investigated synaptic inputs to rat LRN neurones that might elicit the pause-reset in firing. Whole-cell patch-clamp recordings were made from brain slices containing the LRN, prepared from rats aged postnatal day (P) 5 to P15 (decapitated under isoflurane anaesthesia), using a CsCl-based intracellular solution (E_{Cl} = 0 mV). Synaptic currents were evoked by local electrical stimulation. The glutamate receptor antagonist, kynurenic acid (1 mM) caused 25 ± 11 % inhibition of synaptic currents recorded at -60 mV (n = 4), while the glycine receptor antagonist, strychnine (3 μM) caused 55.6 ± 7.6% inhibition of the kynurenic acid-insensitive synaptic current (n = 6). A combination of strychnine and the $GABA_A$ receptor antagonist, picrotoxin (50 μM) caused 75.8 ± 8.4% inhibition (n = 4). In recordings from anaesthetised rats, iontophoretic application of strychnine reduced, and in some cases abolished, the pause in LRN neuronal firing evoked by peripheral sensory stimulation. These data suggest that glycinergic inhibition contributes to the pause-reset response in LRN neurones.

W. Xu, S. Jones & S.A. Edgley (2012) Journal of Physiology 24 December EPub

Where applicable, the authors confirm that the experiments described here conform with The Physiological Society ethical requirements.

PCB139

Reproduction of transducin timecourse of rod and cone cells under various light intensities

Y. Hosoki[1], C. Koike[2], Y. Takeda[1] and A. Amano[1]

[1]Life Sciences, Ritsumeikan University, Kusatsu, Shiga, Japan and [2]Pharmaceutical Sciences, Ritsumeikan University, Kusatsu, Shiga, Japan

The rod and cone cells have a common phototransduction mechanism. First, the visual pigments are stimulated by absorbing light and activate a G-protein called transducin. This transducin subsequently activates phosphodiesterase, which in turn decreases the cGMP concentration. Subsequently, the cGMP sensitive current reduces, leading to depolarization. In this process, the activated visual pigments are phosphorylated several times by rhodopsin kinases. Although the phototransduction mechanisms are common with rod and cone cells, the response speed and the light sensitivity are considerably different. The phosphorylation rate of the activated visual pigments by the rhodopsin kinases and the transducin activation rate by the stimulated visual pigments are reported in detail for both rod and cone cells by Tachibanaki, Kawamura et al. [1]. In their report, the relation between the phosphorylation rate per activated visual pigment and light intensity shows strong negative exponential characteristics. Also, the relation between the activated transducin per activated visual pigments and the light intensity are not monotonous. A strong light activates less transducin compared to a moderate light. For the quantitative understanding and analysis of the phototransduction mechanism, a detailed model is proposed by Hamer et al. [2]. This includes the transducin activation process by activated visual pigments and the phosphorylation process of the visual pigments by rhodopsin kinase. However, the transducin time course reported by Tachibanaki et al. could not be reproduced by the model. Thus, we propose a modified phototransduction model. In our model, we made two modifications to the Hamer model: First, the calculation of the free rhodopsin kinase was refined. Second, the transducin activation by the activated visual pigment was modified such that it is dependent on the ratio of the activated visual pigments to the total visual pigments. With these modifications, the transducin production and the phosphorylation of the visual pigments under various light intensities were successfully reproduced.

The analysis of the simulation results showed that the amount of the free rhodopsin kinase decreases with the increase in light intensity since the complex of the visual pigment and the rhodopsin kinase increase. This mechanism leads to the nonlinear relation between the phosphorylation rate of the activated visual pigments and light intensity. However, this modification could not reproduce the non-monotonous relation between the transducin activation and light intensity. Although the mechanism is not clear, by introducing the the nonlinear relation between the transducin activation and the visual pigment activation ratio, we could successfully reproduce the non-monotonous relation of the transducin activation.

Tachibanaki S, Tsushima S, Kawamura S., Low amplification and fast visual pigment phosphorylation as mechanisms characterizing cone photoresponses, Proc Natl Acad Sci U S A. 2001 Nov 20;98(24):14044-9.

Hamer RD, Nicholas SC, Tranchina D, Liebman PA, Lamb TD., Multiple steps of phosphorylation of activated rhodopsin can account for the reproducibility of vertebrate rod single-photon responses, J Gen Physiol. 2003 Oct;122(4):419-44.

Where applicable, the authors confirm that the experiments described here conform with The Physiological Society ethical requirements.

PCB141

Methylphenidate enhances NMDA-receptor response in the rat medial prefrontal cortex via sigma-1 receptor: a novel mechanism for methylphenidate action

C. Zhang[1], Z. Feng[1], Y. Liu[1], X. Ji[1], J. Peng[1], X. Zhang[1], X. Zhen[3] and B. Li[1,2]

[1]Institute of Neurobiology and State Key laboratory of Medical Neurobiology, Institutes of Brain Science, Fudan University, Shanghai, China, [2]Center for Neuropsychiatric Disorders, Institute of Life Science, Nanchang University, Nanchang, China and [3]Neuropharmacological Laboratory, State Key Laboratory of Drug Research, Shanghai Institute of Materia Medica, Chinese Academy of Sciences, Shanghai, China

Methylphenidate (MPH), commercially called Ritalin or Concerta, has been widely used as a drug for Attention Deficit Hyperactivity Disorder (ADHD). Noteworthily, growing numbers of young people using prescribed MPH improperly for pleasurable enhancement, take high risk of addiction. Thus, understanding the mechanism underlying high level of MPH action in the brain becomes an important goal nowadays. As a blocker of catecholamine transporters, its therapeutic effect is explained as being due to proper modulation of D1 and α2A receptor. Here we show that higher dose of MPH facilitates NMDA-receptor mediated synaptic transmission via a catecholamine-independent mechanism, in layer V-VI pyramidal cells of the rat medial prefrontal cortex, using in vitro whole-cell patch-clamp recording technique. To indicate its postsynaptic action, we next found that MPH facilitates NMDA-induced current and such facilitation could be blocked by sigma-1 but not D1/5 and α2 receptor antagonists. And this MPH enhancement of NMDA-receptor activity involves PLC, PKC and IP3 mediated intracellular Ca2+ increase, but does not require PKA and extracellular Ca2+ influx. Our additional pharmacological studies including western blot analysis and receptor binding assays, confirmed that higher dose of MPH increases locomotor activity via interacting with sigma-1 receptor. Together, the present study demonstrates for the first time that MPH facilitates NMDA-receptor mediated synaptic transmission via sigma-1 receptor, and such facilitation requires PLC/IP3/PKC signaling pathway. This novel mechanism possibly explains MPH-induced addictive potential and other psychiatric side effects.

Where applicable, the authors confirm that the experiments described here conform with The Physiological Society ethical requirements.

PCB142

Natriuretic peptides decrease calcium transients and neurotransmission in cardiac sympathetic nerves

D. Li, H. Wright, E. Vergari, C. Lu, N. Herring and D.J. Paterson

University of Oxford, Oxford, UK

Natriuretic peptides (NPs) are a family of peptide hormones known to be potent regulators of the cardiovascular system. They play a pivotal role in the regulation of intravascular volume by modulating blood vessel tone and renal function. How-

ever, their effects on sympathetic neurons remain poorly understood considering that NP receptors are present on neurons. We aimed to elucidate the effects of brain natriuretic peptide (BNP) on calcium transients in sympathetic neurons, and on neurotransmission in isolated atria tissue. Four week old SD rats were humanely killed by an approved Home Office schedule 1 method, and the stellate ganglia enzymatically isolated. Immunofluorescent staining and RT-PCR were used to determine NP receptor expression. Intracellular free Ca2+ concentration ([Ca2+]i) was measured by ratiometric fluorescence imaging using fura-2/AM in neurons. The evoked [Ca2+]i transient was evaluated following 30 sec exposure to 50 mM KCl in the Tyrode solution. Fura-2/AM was excited alternately at 350 nm and 380 nm and the emitted fluorescence measured at 510 nm. Natriuretic peptide receptor (NPR) type A and B were expressed in sympathetic neurons. BNP significantly reduced the depolarization evoked [Ca2+]i transient (100 nM BNP: -21.15 ± 4.90 %, n=18, P<0.01; 250 nM BNP: -23.89 ± 6.42 %, n=12, P<0.05). The action of BNP was significantly reduced by the PKG inhibitor (5 μM RP-8-Br-PET-cGMP, n=11, P<0.05) and NPR-A inhibitor (10 μM Isatin, n=15, P<0.01). BNP (250 nM) decreased [3H]-noradrenaline release from isolated spontaneously beating atrial in response to 5Hz field stimulation (n=6), and also significantly reduced the heart rate (HR) responses to sympathetic nerve stimulation (1-7Hz) in- vitro compared to control (n=10). We conclude that BNP reduces cardiac sympathetic neurotransmission by decreasing [Ca2+]i and subsequent noradrenaline release via a pGC-cGMP-PKG coupled pathway downstream from the NPR.

Chan NY, Seyedi N, Takano K, Levi R. An unsuspected property of natriuretic peptides: Promotion of calcium-dependent catecholamine release via protein kinase G-mediated phosphodiesterase type 3 inhibition. Circulation. 2012;125:298-307

Li D, Wang L, Lee CW, Dawson TA, Paterson DJ. Noradrenergic cell specific gene transfer with neuronal nitric oxide synthase reduces cardiac sympathetic neurotransmission in hypertensive rats. Hypertension. 2007;50:69-74.

Li D, Lee CW, Buckler K, Parekh A, Herring N, Paterson DJ. Abnormal intracellular calcium homeostasis in sympathetic neurons from young prehypertensive rats. Hypertension. 2012;59:642-649

This work was supported by BHF Centre of Research Excellence.

Where applicable, the authors confirm that the experiments described here conform with The Physiological Society ethical requirements.

PCB143

Ionotropic purine receptors P2X in frog and turtle retina: an immunocytochemical study

L. Vitanova and P.N. Kupenova

Physiology, Medical University, Sofia, Bulgaria

Purinergic signaling is represented in both peripheral and central nervous system (CNS), and in retina in particular which may be regarded as a part of CNS. Two types of purinergic P2 receptors, which mediate effects of cyclic nucleotides, exist: ionotropic (P2X) and metabotropic (P2Y) ones. While relatively well studied in mammalian retinae, little is known about these receptors in lower vertebrate retinae. That's why the aim of present study was to investigate the distribution of the ionotropic P2X receptors in frog and turtle retinae which possess mixed and predominantly cone type of retina respectively. All procedures with a frog and a turtle were in accordance with the Bulgarian law for scientific experiments. The animals were deeply anesthetized with halothane and decapitated. The eyes were dissected, and the posterior eyecups with retinae were immediately immersed in 4% (w/v) paraformaldehyde in 0.1 M phosphate buffer for 15–30 min. After fixation, the retinae were dissected from the eyecups and cryoprotected in graded sucrose solutions (10%, 20%, and 30% w/v). Cryostat sections were cut at 14 μm and stored at –20 °C. More than 10 primary antibodies directed to all seven P2X1-7 receptors, in addition to an anti-Vimentin antibody, a marker of Müller glial cells, were applied. The indirect immunocytochemical method was used.

The results showed wide-spread expression of all seven purinoreceptors P2X1-7 in both frog and turtle retinae. They were predominantly expressed in Müller cells, the principal glial cells in the retina. All structures typical of Müller cells: the outer and the inner limiting membranes, the cells bodies in the inner nuclear layer, the radial processes in the inner plexiform layer (IPL), and the so called endfeet (frog) or the orthogonal arrays of particles (turtle) in the ganglion cells layer were stained. The colocalizations between P2X1-7 and Vimentin proved that the immunostaining was in the Müller cells. In addition to the glial staining, a neuronal staining was also evident expressed by fine puncta in the inner and outer plexiform layers. Some cell bodies of horizontal and ganglion cells were stained as well.

In order to elucidate how the different purinergic subunits combine to form the ion channels, double labeling studies with different couples of P2X antibodies were performed (when it was possible). The results obtained allow us to suggest that the purinergic P2X receptors contribute significantly to neuron-glia signaling in both mixed-type and cone-type retinae of the lower vertebrates.

This project is supported by the Medical Science Council at the Medical University in Sofia, Bulgaria (grant 38/2012)

Where applicable, the authors confirm that the experiments described here conform with The Physiological Society ethical requirements.

PCB144

Neuroprotective effects and the underlying mechanisms of Paeoniflorin

L. Feng

Dept. of Neuropharmacology, Shanghai Institute of Materia Medica, CAS, Shanghai, China

Paeoniflorin (PF) is a compound isolated from Paeoniae Radix. PF ameliorated brain ischemia on middle cerebral artery occlusion (MCAO) model in rats which was probably mediated by activating adenosine A1 receptor (A1R) to exert its neuroprotective effect. The aim of this study was to investigate the molecular mechanism underlying the neuroprotective effect of PF pretreatment on primary cultured cortical neurons exposed to oxygen-glucose deprivation and reoxygenation (OGD/R). Primary cultured cortical neurons of rats were subjected to OGD/R injury and treated with PF and the survivability of neurons was determined by MTT assay. Phosphorylation of the proteins in the signaling pathways involved in the PF effects was evaluated by Western Blot or immunoprecipitation (IP). Receptor interactions were identified by co-IP and immunofluorescence staining. PF, with concentrations ranging from 10nM to 1μM, was applied to promote the survival of cortical neurons suffered from OGD/R injury. PF phosphorylated Akt and ERK1/2 that contributed to improve the neu-

rons viability. On HEK293 cells stably transfected with A1R (HEK293/A1R), PF induced Akt and ERK1/2 phosphorylation mediated by A1R transactivation of EGFR. Furthermore, both Matrix Metalloprotease (MMP) and Src kinase were involved in signaling pathways regulated by PF. Our results showed that PF promoted neurons survival and relied on Akt and ERK1/2 phosphorylation which was mediated by A1R transactivation of EGFR.

Where applicable, the authors confirm that the experiments described here conform with The Physiological Society ethical requirements.

PCB145

Imaging the motility of inositol trisphosphate receptors in intact mammalian cells using single particle tracking photoactivated localization microscopy (sptPALM)

I. Smith[1], D. Swaminathan[1] and I. Parker[1,2]

[1]Neurobiology and Behavior, University of California, Irvine, Irvine, CA, USA and [2]Physiology and Biophysics, University of California, Irvine, Irvine, CA, USA

Inositol trisphosphate receptors (IP_3Rs) are Ca^{2+}-permeable channels in the membrane of the endoplasmic reticulum (ER) that liberate Ca^{2+} sequestered in ER stores to generate cytosolic Ca^{2+} signals that control diverse cellular functions including gene expression, secretion and synaptic plasticity (Berridge et al., 2000). The spatial distribution of these channels is crucial in determining the patterning of intracellular Ca^{2+} signals. The mechanisms underlying the aggregation and maintenance of IP_3Rs in clusters are controversial. Local Ca^{2+} signals arise at just a few, fixed locations within a cell, suggesting clusters are stable entities; and Ca^{2+} blips generated by 'lone' IP_3Rs are also immotile (Smith et al., 2009). In contrast, GFP-tagged or immunostained IP_3Rs show a dense distribution throughout a cell. Moreover, the majority IP_3Rs can diffuse freely within the ER membrane, and aggregate into clusters following sustained (minutes) activation of IP_3 signaling and/or cytosolic Ca^{2+} elevation, or even undergo clustering in response to IP_3 within just a few seconds (Taufiq Ur et al., 2009).
These apparently different behaviors may be explained because Ca^{2+} imaging studies detect only functional IP_3Rs, whereas imaging studies utilizing immunostaining or GFP-tagged IP_3Rs report on the entire population of IP_3R proteins. We therefore hypothesize that a majority of IP_3Rs are motile, but functionally unresponsive. Local Ca^{2+} signals arise, instead, from a small subset of IP_3Rs that are anchored, individually or in clusters, by association with static cytoskeletal structures and possibly as a consequence of this anchoring, display high sensitivity to IP_3 to Ca^{2+} signals.
To test this hypothesis we have created a fusion protein of the IP_3R tagged with the photoactivatable genetically encoded protein mEos2 to track the motility of thousands of single IP_3Rs with nanoscale spatial and millisecond temporal resolution following transfection in cells (single-particle tracking photoactivated localization microscopy: sptPALM (Manley et al., 2008)). By tracking the movement of single IP_3Rs using sptPALM we show that two populations of molecules exist with differing motilities. A larger (70%) of fast moving molecules ($0.093 \pm 0.009\ \mu m^2\ s^{-1}$) and a smaller (30%) population of IP_3Rs that are essentially immotile ($0.0074 \pm 0.0006\ \mu m^2\ s^{-1}$, $n > 25{,}000$ tracks, 5 cells). Further, we find that these apparently immotile IP_3Rs are preferentially grouped within tight clusters and may correspond to the static Ca^{2+} release sites responsible for generating local Ca^{2+} signals.

Berridge M *et al*. (2000). Nat Rev Mol Cell Biol. 1:11-21.

Manley S *et al*. (2008). Nat Methods. 5:155-157.

Smith IF*et al*. (2009). Sci Signal. 2:ra77.

Taufiq Ur, R *et al*. (2009). Nature. 458:655-659.

Where applicable, the authors confirm that the experiments described here conform with The Physiological Society ethical requirements.

PCB147

Opiorphin inhibits calcium signaling response in capsaicin sensitive rat sensory neurons

M. Ozcan[1], A. Ayar[2], E. Kacar[3] and H. Kelestimur[3]

[1]Biophysics, Firat University Faculty of Medicine, Elazig, Turkey, [2]Physiology, Karadeniz Technic University Faculty of Medicine, Trabzon, Turkey and [3]Physiology, Firat University Faculty of Medicine, Elazig, Turkey

Opiorphin is an endogenous human peptide mediator constituent of human saliva. Initial research with mice shows opiorphin has highly effective analgesic activity than morphine. Effect of opiorphin on capsaicin sensitive sensory neurons was investigated by using in-vitro calcium imaging technique in this study.
Dorsal root ganglions (DRGs) were removed from 1-2 day old (any gender) Wistar neonatal rats after decapitation and DRG neurons were grown in primary culture following enzymatic and mechanical dissociation and cultured in a tissue culture containing nerve growth factor for a short time. Neurons were loaded with 1μmol Fura-2 AM. After loading, the cells were washed 3-4 times for 20min with standard recording medium to remove the extracellular fura-2 AM. [Ca2+]i responses were quantified by the changes in 340/380 ratio by using fluorescence imaging system. Based on the size of cell trunk, DRG neurons were divided into three categories: small, medium and large. Responses to capsaicin (1μM) (small and medium size) was studied by monitoring changes in [Ca2+]i with a microscobic digital image analysis system in fura-2 loaded single neurons. We tested the effects of different concentration of opiorphin treatment after recording of basal [Ca2+]i.
The application of 10μM,100μM and 1000μM opiorphin had significant decrease on capsaicin evoked [Ca2+]i to 99.4±2.0% (n = 48), 51.2±5.8% (n=38, P<0.001) and 2.5±1.2% (n=24, respectively, P<0.0001) in small size neurons. Same doses of opiorphin had significant decrease on capsaicin evoked [Ca2+]i to 99.1±2.3% (n=36), 53.4±5.8% (n=15, P<0.001) and 7.6±1.9% (n=15, respectively, P<0.0001) in medium size cells.
Data from this study revealed that opiorphin inhibits intracellular calcium signaling in cultured rat DRG neurons in a dose dependent manner. Further studies are needed to find out the efficency of opiorphin on pain modulation.

Where applicable, the authors confirm that the experiments described here conform with The Physiological Society ethical requirements.

PCB148

TRPA1 and TRPV4 activation in human odontoblast-like cells stimulates ATP release

O. Egbuniwe[3], S. Grover[1], M. Yazdi[2], T. Renton[2], L. Di Silvio[3] and A. Grant[1]

[1]Wolfson Centre for Age-Related Diseases, King's College London, London, UK, [2]Dept of Oral Surgery, Dental Institute, King's College London, London, UK and [3]Biomaterials, Biomimetics and Biophotonics, Dental Institute, King's College London, London, UK

Brännstrom's hydrodynamic theory postulated that dental pain results from the activation of dental sensory neurons in response to dentinal fluid movement under thermal expansion and contraction. It is not clear whether this is a direct mechanotransduction by neurons or whether other dental structures contribute to the mechanosensation. Immunohistochemical and functional studies suggest the expression of thermosensitive and mechanosensitive Transient Receptor Potential (TRP) A1, M8 and V1 Ca^{2+} permeable cation channels in human and rat odontoblasts. However, a mechanism by which odontoblasts could modulate neuronal activity has not been demonstrated. In this study we investigated functional TRP channel expression in human odontoblast-like cells (OBs) and aimed to identify chemical transmitter release in response to TRP channel activity. Human immortalized dental pulp cells were driven towards an odontoblast-like phenotype by culture in media conditioned with ascorbic acid, β-glycerophosphate and dexamethasone (Egbuniwe *et al*., 2011). Functional expression of TRP channels was determined using RT-PCR and ratiometric calcium imaging with Fura-2. ATP release was measured using a luciferin-luciferase assay. Expression of mRNA for TRPA1, TRPV1 and TRPV4 but not TRPM8 was detected in OBs by RT-PCR. Exposure to the TRPA1 agonists allyl isothiocyanate (AITC) and cinnamaldehyde (1μM–500μM) or the TRPV4 agonist GSK1016790A (1nM–1μM) caused a concentration-dependent increase in intracellular Ca^{2+} concentration that was inhibited by the selective antagonists HC030031 (TRPA1) and HC067047 (TRPV4) (n=5-7 independent triplicate measurements). In contrast, exposure to the TRPV1 agonist capsaicin (1nM–1μM) or the TRPM8 agonist icilin (1nM–1μM) had no effect on intracellular Ca^{2+} concentration (n=3). Treatment for 15 min with AITC (500μM; 28.2±5.1 vs. 10.4±4.5 nM), cinnamaldehyde (500μM; 29.9±8.6 vs. 9.0±2.3 nM) or GSK1016790A (1μM; 15.9±3.5 vs. 6.5±1.2 nM) caused an increase in ATP concentration in culture medium, compared to vehicle treatments (mean±S.E.M; $p<0.05$; t-test with Welch's correction; n=9-10). These data demonstrate that activation of the mechanosensitive TRPA1 and TRPV4 channels in human odontoblast-like cells can stimulate ATP release, which may modulate the activity of adjacent dental sensory neurons *in situ* via purinergic receptors. We were unable to confirm the presence of thermosensitive TRPV1 and TRPM8 that has previously been reported in odontoblasts.

Egbuniwe O, Idowu BD, Funes JM, Grant AD, Renton T, Di Silvio L. (2011) *Cell Cycle* **10(22)**, 3912-9

Supported by a Biomedical Research Centre award to Guy's & St Thomas' NHS Foundation Trust in partnership with King's College London, by the Royal College of Surgeons Faculty of Dental Surgery and by a Capacity Building Award in Integrative Mammalian Biology funded by the BBSRC, BPS, HEFCE, KTN and MRC

Where applicable, the authors confirm that the experiments described here conform with The Physiological Society ethical requirements.

PCB149

Effect of materials based on gold and silver nanoparticles and natural compounds on carrageenan-induced rat paw edema

A. Filip[1], D. Daicoviciu[2], P. Bolfa[3], S. Clichici[4], A. Muresan[5], L. David[6] and L. Olenic[7]

[1]Physiology, Iuliu Hatieganu University of Medicine and Pharmacy, Cluj Napoca, Cluj, Romania, [2]Physiology, Iuliu Hatieganu University of Medicine and Pharmacy, Cluj Napoca, Cluj, Romania, [3]Morphopathology, University of Agricultural Sciences and Veterinary Medicine, Cluj Napoca, Cluj, Romania, [4]Physiology, Iuliu Hatieganu University of Medicine and Pharmacy, Cluj Napoca, Cluj, Romania, [5]Physiology, Iuliu Hatieganu University of Medicine and Pharmacy, Cluj Napoca, Cluj, Romania, [6]Faculty of Chemistry and Chemical Engineering, Babes-Bolyai –University, Cluj Napoca, Romania and [7]National Institute for Research and Development of Isotopic and Molecular Technologies, Cluj Napoca, Cluj, Romania

Inflammation is a complex biological response involved in pathogenesis of a variety of diseases. Although steroids and NSAIDs are the main therapeutic agents in inflammation they cause serious side effects. Therefore, the development of new materials with comparable results and no side effects is needed. The purpose of our study is to investigate the biological activity of materials based on gold (Au-VO) and silver (Ag-VO) nanoparticles and natural compounds extracted from European cranberry bush - Viburnum opulus L. (VO) on acute inflammation model in Wistar rats. The inflammation was induced by intraplantar injection of 100 μl 1% carrageenan and the response was compared to indomethacin (5 mg/kgc) as positive control and saline solution as negative control. The VO extracts (15 and 30 mg/kg b.w.) and the materials based on gold and silver nanoparticles functionalized with VO extract (0.3 mg/kg b.w.) were administrated orally during 4 days before injection of carageenan. At 2h, 24h and 48h after carageenan injection the paw edema were measured and plantar tissue were taken for histopathological and immunohistochemical investigations (iNOS and COX-2) and to evaluate malondialdehyde (MDA), glutathione reduced/glutathione oxidized (GSH/GSSG), IL-1 and IL-6 levels. In addition, catalase and glutathione peroxidase activities were assessed from plantar tissue and erythrocyte lysates. Values are means ± S.E.M., compared by ANOVA and Tukey posttest. Low dose of VO significantly inhibited edema formation (44.54% vs. control group treated with vehicle; $p<0.05$), particularly at 2h, and increased GSH levels, both at 2h (2.98±1.63 nmoles/mg protein; $p<0.01$) as well as at 48h (21.66±14.36 vs. 7.01±1.34 nmoles/mg protein in control group; $p<0.0001$). The inhibition was higher to those produced by indomethacin (22.52%) and Ag-VO (22,52%) and was maintained at 24 h and 48 h, but at lower levels. In parallel, IL-1 and IL-6 levels and iNOS expression decreased ($p<0.01$). Ag-VO and Au-VO remarkably inhibited generation of MDA (0.13±0.09 respectively 0.11±0.04 vs. 0.29±0.12 nmoles/mg protein; $p<0.05$) and GSSG (1.79±0.75 respectively 1.85±0.46 vs 3.52±2.09 nmoles/mg protein in control group; $p<0.001$) in the plantar tissue, decreased IL-1 and IL-6 levels and increased GPx activity in paw tissue (89.25±10.90 respectively 86.25±17.06 vs 38.00±12.11 U/g protein in control group). This findings suggested that the nanoparticles func-

tionalised with natural compounds may be useful in the treatement of inflammatory disease.

This work was elaborated in the frame project no 147/2012, through the program "Partenerships in priority areas-PN II", developed with the support of ANCS, CNDI-UEFISCDI.

Where applicable, the authors confirm that the experiments described here conform with The Physiological Society ethical requirements.

PCB150

Adaptive sampling of visual information by photoreceptor ultrastructure and stochastic reactions

Z. Song[1], M. Postma[2], S. Billings[1], D. Coca[1], R. Hardie[3] and M. Juusola[1]

[1]University of Sheffield, Sheffield, UK, [2]University of Amsterdam, Amsterdam, Netherlands and [3]University of Cambridge, Cambridge, UK

The physical world is vast, noisy and dynamic. Nonetheless, sensory perception of it is reliable, allowing accurate judgments and actions. This conjunction of the variable world and trustworthy perception of it, suggests that sensory neurons are under selective pressure to exploit environmental regularities, such as contrast or colour in natural scenes, generating structural and functional adaptations, which improve sensory information estimates [1]. However, little is understood how the sensory structures and their neural information processing evolved together.

Here we show that by sequestering "unreliable" biochemical reactions into semi-autonomous transduction units, insect phototransduction evolved to generate reliable neural representations of natural light changes, from single photon regimes to full sunlight [2]. To better understand the mechanistic basis of this performance, we synthesized a virtual Drosophila photoreceptor from its biophysical parts. By combining stochastic simulations with intracellular experiments in Drosophila photoreceptors, we show how discrete sampling by phototransduction units (~30,000 microvilli), each producing variable quantum bumps to captured photons, governs macroscopic responses to light changes. Feedbacks and stochasticity in these reactions oppose saturation, dynamically adjusting availability of microvilli, whilst intracellular calcium and voltage adapt their sample size (bump waveform), generating reproducible responses. We further demonstrate how these rules for adaptive sampling predict information processing across a range of species with different visual ecologies. Our results clarify why fly photoreceptors are structured the way they are and function as they do, linking sensory information to sensory evolution and highlighting the benefits of stochasticity for neural information processing [3].

[1]. van Hateren, J.H. (1997). Processing of natural time series of intensities

by the visual system of the blowfly. Vision Res. 37, 3407–3416.

[2]. Hardie, R.C., and Postma, M. (2008). Phototransduction in microvillar

photoreceptors of Drosophila and other invertebrates. In The Senses:

A Comprehensive Reference. Vision, Volume 1, A.I. Basbaum, A.

Kaneko, G.M. Shepherd, and G. Westheimer, eds. (San Diego:

Academic Press), pp. 77–130.

[3]. Zhuoyi Song, Marten Postma, S.A. Billings, Daniel Coca, Roger C. Hardie & Mikko Juusola, (2012). Stochastic Adaptive Sampling of Information in Fly photoreceptors. Curr Biol. 22, 1371–1380

We thank Gonzalo de Polavieja for discussions and Paloma Gonzalez-

Bellido and Trevor Wardill for supplying Coenosia. This work was supported

by the BBSRC grants BB/F012071/1 and BB/D001900/1 (M.J.), BB/

G006865/1 and BB/D007585/1 (R.C.H.), and BB/H013849/1 (D.C., M.J.,

and S.A.B.); the open research fund of the State Key Laboratory of Cognitive

Neuroscience and Learning (M.J.); EPSRC grant EP/H00453X/1 (S.A.B. and

D.C.); and ERC Advanced Investigator Grant 226037 NSYS (S.A.B.).

Where applicable, the authors confirm that the experiments described here conform with The Physiological Society ethical requirements.

PCB151

ATP signals in supporting cells of the organ of Corti in the adult mouse

P. Sirko[1,2], J. Gale[2] and J. Ashmore[2]

[1]MRC Laboratory for Molecular and Cellular Biology UCL, London, UK and [2]UCL Ear Institute, London, UK

It has been suggested that extracellular ATP signalling is implicated in protecting the auditory epithelium of the inner ear from noise-induced damage (Housley et al., 2009). Although ATP receptors have been found on several types of cells in the organ of Corti, these studies have focussed on either dissociated or a limited class of cells (Lagostena et al., 2001). Supporting cells show parallels with glia (Rio et al., 2002), however it is unclear if and how such cells, positioned near the first auditory synapse, might act in a protective manner. Multiple types of supporting cells are present and it is unknown whether ATP affects them similarly or activates different processes in them (Gale et al., 2004). To address these issues we have studied features of ATP-dependent signalling in the adult organ of Corti in an in situ system.

The temporal bone of adult mice (ages P30-P90) was removed after killing the animals by cervical dislocation and the organ of Corti was exposed through a small opening at the apical end of the cochlea. For immunochemistry, antibodies against P2X2 (Alomone Labs) were used on 4% PFA fixed tissue. For calcium imaging, opened cochlear bones were incubated for 40 min in buffer containing 20 μM OGB1-AM, washed and then fluorescent signals were collected by widefield epifluorescence microscopy. Whole cell tight seal patch clamp recordings were made from inner sulcus and phalangeal cells identified visually. In some cases cells were decoupled with the gap junction blocker flufenamic acid (100 μM) to improve voltage clamp.

There was extensive P2X2 immunoreactivity in the supporting cells of the organ of Corti. Comparatively, outer hair cells showed a limited degree of P2X2 on their apical surface. Consistent with these observations, 100 μM ATP puff applied to the organ of Corti produced a rise in intracellular (Cai) in supporting cells measured by OGB1. There was no detectable increase in Cai levels in the inner hair cells.

ATP (100μM) applied to the inner sulcus and phalangeal cells surrounding the inner hair cells produced inward currents in

both types of cells. The ATP gated currents showed inward rectification in both types of cells consistent with the properties of recombinant P2X channels. The ATP dependent currents in inner sulcus cells desensitized ($\tau 1/2$ = 1.6s) whereas little or no desensitization to prolonged application (15s) was observed in recorded phalangeal cells. We suggest that these results indicate differential expression of P2X receptor subunits and could reflect different roles for extracellular ATP signalling in these two cell types.

Gale, J.E., V. Piazza, C.D. Ciubotaru, and F. Mammano. 2004. A mechanism for sensing noise damage in the inner ear. Curr Biol. 14:526-529.

Housley, G.D., A. Bringmann, and A. Reichenbach. 2009. Purinergic signaling in special senses. Trends Neurosci. 32:128-141.

Lagostena, L., J.F. Ashmore, B. Kachar, and F. Mammano. 2001. Purinergic control of intercellular communication between Hensen's cells of the guinea-pig cochlea. J Physiol. 531:693-706.

Rio, C., P. Dikkes, M.C. Liberman, and G. Corfas. 2002. Glial fibrillary acidic protein expression and promoter activity in the inner ear of developing and adult mice. J Comp Neurol. 442:156-162.

Where applicable, the authors confirm that the experiments described here conform with The Physiological Society ethical requirements.

PCB152

Neuronal damage and tau pathology in a murine model of cerebral ischemia

S. Khan, N. Yuldasheva, T.F. Batten and S. Saha

Division of Cardiovascular & Diabetes Research, Leeds Institute of Genetics, Health & Therapeutics, Leeds, UK

Cerebral ischemia is a major cause of death and the later development of neurodegenerative diseases (de la Torre, 2004), which are characterized by neuronal damage and accumulation of phosphorylated tau protein (Alonso et al., 1997). However, cerebral ischemia induced cellular damage that initiates neurodegerative disease remain poorly understood and does not receive proper attention for developing new drug treatment strategies. This is primarily due to lack of clinically relevant models that are highly reproducible as the pathophysiology of cerebral ischemia in animal models is modulated by numerous factors including the species, type of blood vessels occluded, occlusion period and reperfusion time (Hossmann, 1998). The present study aims to optimise a murine model of cerebral ischemia and examine neuronal degeneration and tau pathology in this model. Experiments were performed on 10-12-week-old (26–30 g) C57BL/6 mice (Harlan-Olac, Bicester, UK) under appropriate UK Home Office licence and adhered to regulations as specified in the Animals Scientific Procedures Act (1986). Cerebral ischemia was induced by transient bilateral occlusion of the common carotid arteries using arterial clips under anaesthesia (4% isoflurane saturated with oxygen). Following 5- 20 minutes occlusion the clips were removed and skin wound closed. Sham-operated mice underwent the same procedure except that the carotid arteries were not occluded. Following 1-7 days reperfusion time the mice were re-anesthetised and perfused with 4% paraformaldehyde in phosphate buffered saline (pH 7.0-7.2). Brain sections (50 um) cut on a vibratome were either stained with cresyl violet to assess neuronal damage or processed for immunohistochemistry using specific antibodies to neuronal specific nuclear protein, myelin associated protein, glial fibrillary acidic protein, glutamine synthetase and hyper- phosphory-lated Tau protein to examine the extent of neuronal, glial cell and myelin sheath damage and tau pathology. Antigen-antibody reaction sites were detected either by standard avidin-biotin complex and diaminobenzidine reaction or by using species specific anti-rabbit immu-noglobulin G conjugated to Cy3/ Alexa488. Sections were analysed using an AxioImager Z.1 epifluorescence microscope (Carl Zeiss, Welwyn Garden City, UK). The results showed consistent neuronal and white matter damage and tau pathology in the cortex, striatum and the hippocampus following 15 minutes occlusion and 3-7 days reperfusion. This murine model of cerebral ischemia may be an ideal model to study ischemia induced neurodegen-eration and to develop therapeutic strategies for prevention and treatment of these diseases.

Supported by the Alzheimer's Research-UK, Yorkshire Brach

Alonso et al. (1997) 94:298-303

de la Torre JC. (2004) Lancet Neurol. 3:184-90.

Hossmann K. (1998) Cardiovascular Research 39:106–120

We acknowledge Dr. Zaineb Henderson for providing us with antibodies to phosphorylated Tau protein.

Where applicable, the authors confirm that the experiments described here conform with The Physiological Society ethical requirements.

PCB154

Visual evoked potentials in primary open angle glaucoma

M.K. Jha

Physiology, Kathmandu University School of Medical Sciences, Dhulikhel, Nepal

Jha MK, Paudel BH, Badhu BP*, Limbu N, Thakur D. Department of Basic and Clinical Physiology and *Department of Ophthalmology, BPKIHS, Dharan, Nepal.

Background: Visual evoked potentials (VEPs) assess the integrity of the visual pathways from the optic nerve to the occipital cortex. Primary open angle glaucoma is bilateral condition with optic atrophy and visual field defect. Optic disc cupping and visual field loss have been associated with prolongation of latency of VEP. Therefore, we studied the ocular glaucomatous damage and VEP abnormalities.

Objectives: To study VEPs and ophthalmic variables in primary open angle glaucoma (POAG).

Methods: Pattern reversal and flash VEP tests were done in consenting 20 primary open angle glaucoma eyes and 40 normal control eyes in Electrodiagnosis Lab II at BPKIHS. Statistical tests (paired t-test and Mann-Whitney test) were applied depending on distribution of observations.

Results: In POAG cases the refractive error [3.51±1.88 vs. 1.88±1.11, D, p=0.001], cup disc ratio in percent [66.00±16.98 vs. 28.50±5.80, p=0.000], intraocular pressure [19.55±2.08 vs. 11.65±1.64, mmHg, p=0.000] and automated visual field pattern standard deviation [4.13±6.96 vs. 1.64±0.45, dB, p=0.000] were significantly more than in control. The visual acuity [0.41±0.29 vs. 1.00±0.00, p=0.000], foveal visual sensitivity [25.92±6.88 vs. 33.48±1.75, dB, p=0.000] and automated visual field mean deviation [-9.63±10.58 vs. 0.07±1.54, dB, p=0.000] were significantly less in cases than in control. Among VEP variables pattern reversal latency N145 [149.00±15.75 vs. 137.52±15.20, ms, p=0.011], flash amplitude N75 [2.18±.57 vs. 1.47±.38, μV, p=0.000] and flash amplitude N145 [1.99±.39 vs. 1.43±.38, μV, p=0.000] were increased in cases. The pattern reversal amplitude N75 [1.97±.35 vs. 2.47±.58, μV, p=0.001], amplitude P100 [3.09±.46 vs.

6.07±1.44, μV, p=0.000] and amplitude N145 [2.21±.58 vs. 4.45±1.99, μV, p=0.000] were decreased in cases.
Conclusion: POAG caused deterioration in all the ophthalmic variables measured with increase in latency of N145. The amplitude is different between pattern reversal and flash methods.

Aminoff MJ. Electrodiagnosis in clinical neurology, 4th ed., Churchill-Livingstone 1999:421-49.

Odom JV, Bach M, Barber C, Brigell M, Marmor MF, Tormene AP, Holder GE, Vaegan Visual evoked potentials standard Documentaopthalmologia 2004 (108):115-123.

McCulloch DL, Skarf B, Development of the human visual system: monocular and binocular pattern VEP latency. Investigative Opthalmology and Visual Science. 1991 (32):2372-2381.

Tandon OP, Sharma KN. Visual evoked potential in young adults: a normative study. Indian J. PhysiolPharmacol. 1989 Oct.-Dec.; 33(4):247-9.

Davis ET, Schnider CM, Sherman J. Normative data and control studies of flash VEP's for comparision to a clinical population. Am. J. Optom-Physiol Opt. 1987 Aug;64(8):579-92.

I acknowledge to Professor Bishnu Hari Paudel, HOD, Department of Basic and Clinical Physiology, BPKIHS, Dharan, Nepal, and my guide for his pain staking immense support and showing me the path of research. Similarly i'll be always grateful to my Co-guides Dr. Nirmal Limbu and Dr. Dilip Thakur, Associate Professors, Department of Basic and Clinical Physiology, BPKIHS, Nepal and Professor Badri Prasad Badhu, HOD, Department of Ophthalmology, BPKIHS, Nepal for their expert advice and great involvement in my research.

Where applicable, the authors confirm that the experiments described here conform with The Physiological Society ethical requirements.

PCB155

Effect of transcutaneous auricular vagus nerve stimulation on refractory epilepsy

P. Rong[1], H. Ben[1], L. Li[1], X. Li[1,2] and B. Zhu[1]

[1]Institute of Acu.-Mox., Beijing, China and [2]Beijing University of Chinese Medicine, Beijing, China

Objective:To examine whether transcutaneous auricular vagus nerve stimulation (ta-VNS) is an effective approach for patients with refractory epilepsy.
Patients and Methods:This study was conducted on 191 epilepsy patients who were randomly assigned to the ta-VNS group (n=124), and the transcutaneous non-auricular vagus nerve stimulation (tn-VNS) control group (n=67) from December 2010 to June 2012. The seizure frequency were assessed in week 8, 16 and 24 of the treatment according to the percentage of seizure frequency reduction.
Results:For 124 patients in the ta-VNS group, after 8 week's treatment, 10 were seizure free and 31 had a 50-99% reduction in seizure frequency; after 16 week's treatment, 14 were seizure free, 40 had a 50-99% reduction in seizure frequency; after 24 week's treatment, 17 were seizure free, 46 had a 50-99% reduction in seizure frequency. For 67 patients in the tn-VNS control group, 3 were seizure free, and 11 had a 50% reduction in seizure frequency after the first 8 weeks' treatment. After 16-week treatment of ta-VNS, of the 46 patients, 5 were seizure free, 17 had a 50-99% reduction in seizure frequency. The differences in seizure frequency reduction among groups were significant (P < 0.05).
Conclusion:Our result indicated that ta-VNS can significant suppress epileptic seizures. As a safe, effective, simple, economic therapeutic method with mild side-effect, it may have great potential in treatment of epilepsy.

Henry TR. Therapeutic mechanisms of vagus nerve stimulation. Neurology. 2002;59:S3-14

Yang AC, Zhang JG, Rong PJ, Liu HG, Chen N, Zhu B. A new choice for the treatment of epilepsy: Electrical auricula-vagus-stimulation Med Hypotheses. 2011;77:244-5.

He W, Rong PJ, Li L, Ben H, Zhu B, Litscher G. Auricular Acupuncture May Suppress Epileptic Seizures via Activating the Parasympathetic Nervous System: A Hypothesis Based on Innovative Methods. Evid Based Complement Alternat Med. 2012;2012:615476

Stefan H, Kreiselmeyer G, Kerling F, Kurzbuch K, Rauch C, Heers M, et al. Transcutaneous vagus nerve stimulation (t-VNS) in pharmacoresistant epilepsies: a proof of concept trial. Epilepsia. 2012;53:e115-8.

Shahwan A, Bailey C, Maxiner W, Harvey AS. Vagus nerve stimulation for refractory epilepsy in children: More to VNS than seizure frequency reduction. Epilepsia. 2009;50:1220-8.

1.The Special Program of Chinese Medicine of the National Basic Research Program of China (973 Programs, 2011CB505200,2012CB518503).

2.National Twelfth Five-year Science and Technology Program (2012BAF14B10).

3.China National Nature Scientific Foundation Society (30973798)

Where applicable, the authors confirm that the experiments described here conform with The Physiological Society ethical requirements.

PCB156

Cyclooxygenase-2 mediates striatum activation in the mouse 6-Hydroxydopamine model of Parkinson's disease

D. Oliveira-Tavares[2,3], C.A. Da-Silva[1,2], F.E. Padovan-Neto[2,3] and E. Del Bel[1,3]

[1]Physiology, FORP-University of Sao Paulo, Ribeirão Preto, Sao Paulo, Brazil, [2]Neurology/Neurosciences, FMRP-University of Sao Paulo, Ribeirao Preto, Sao Paulo, Brazil and [3]-, Núcleo Apoio à Pesquisa em Neurociência Aplicada (NAPNA), Ribeirao Preto, Sao Paulo, Brazil

BACKGROUND: Recent studies described inflammation play a role in the abnormal involuntary movements that occur as a consequence of the chronic therapy for Parkinson's disease through the dopamine precursor 3,4-dihydroxyphenyl-L-alanine (L-DOPA). Exogenously administered corticosterone, which inhibit cyclooxygenase (COX) activity, decrease L-DOPA-induced dyskinesia in unilateral dopamine-depleted rats. Between many inflammatory factors found in the Parkinson's disease brain, the inducible isoform COX-2 is a critical enzyme in the mechanism of central nervous system inflammation. In this study we examined the effects of chronic L-DOPA treatment on the appearance of the COX-2 in the striatum of C57BL/6Jmice brain.
METHODS: Dyskinetic symptoms were triggered by repetitive administration of a constant dose of L-DOPA (25 mg/kg, twice a day, for 25 days) in unilaterally 6-hydroxydopamine (6-OHDA) lesioned (striatum) adult male mice (25-30gr, n=6-8/group). Lesioned or sham animals were treated chronically (25 days) with either saline or L-DOPA (25mg/kg, i.p. +benseraside). The animals were anaesthetised with a mixture of ketamine (100mg kg-1) and xilazine (14mg kg-1, both i.m.). After perfusion and fixation, the brains were cut, immuno- stained for tyrosine hydroxylase (TH) immunoreactivity (ir) Cyclooxige-

nase-2 (COX-2)-ir in the striatum and substantia nigra. Comparisons were made between controls (saline microinjected) lesioned (6-OHDA microinjected) and dyskinetic (6-OHDA lesioned, L-DOPA-treated) and non-dyskinetic (6-OHDA lesioned, saline-treated) mice .
RESULTS: Dyskinetic symptoms appear toward the end of the first week of treatment. TH-ir and COX-2-ir were found in neurons in the striatum after dopamine depletion. Dyskinesia was associated with L-DOPA-induced changes in the TH-ir and COX-2-ir in the neurons. Elevated COX-2 expression occurs within completely lesioned regions of the striatum, displaying an inverse correlation with remaining dopaminergic terminals.
CONCLUSIONS: Our results suggest that the presence of COX-2-ir neurons in the striatum may underlie the long-duration response to L-DOPA in Parkinsonian mice. Promotion of these striatal COX-2-ir neurons might be involved in the development of aberrant striatal circuits and the appearance of L-DOPA induced dyskinesia

Financial support: FAPESP, CNPq, CAPES.

Where applicable, the authors confirm that the experiments described here conform with The Physiological Society ethical requirements.

PCB157

Effects of duration of hyperthermic hypoxia on neonatal rats assessed after growth by behavior

T. Hosono[1], M. Yamamoto[1], C. Igi[1], K. Akasaka[1], M. Arakawa[1], M. Nakamoto[1] and K. Minato[2]

[1]Graduate School of Biomedical Engineering, Osaka Electro-Communication University, Shijonawate, Osaka, Japan and [2]Graduate School of Medicine, Osaka University, Suita, Osaka, Japan

Introduction. Neonatal hypoxic-ischemic (HI) encephalopathy (HIE) is often related to long-term neurological impairment, and HI insult with hyperthermia worsens the neonatal prognosis more than with normothermia. Although neonatal rat model of HIE has been generally developed by unilateral carotid artery (CA) ligation followed by 8% oxygen exposure at an ambient temperature (Ta) of 37°C for 1 – 2 hrs, we produced brain insults after 8% oxygen exposure only for 15 min at hyperthermic Ta of 40°C successfully (Hosono, 2010). However, the effects depending on the duration of hyperthermic hypoxia are still unknown. The aim of this study was to clarify the effects of the duration on brain impairment after growth using behavioral study and histology. Methods. Seven-day-old neonatal Wistar rats (n=30) were anesthetized by inspired isoflurane, and the left CA was surgically ligated (n=17, HIE-G). Sham-operated rats (n=13, S-G) without arterial ligation were also established. The pups were returned to their dams for 1 hr. All the rats in the HIE-G were divided into four groups, and placed in a chamber at Ta of 40°C with humidified 8.0% oxygen for 30 (n=4, HG30), 20 (n=4, HG20), 10 (n=4, HG10), and 5 min (n=5, HG5). Then all the pups were returned to the dams and raised. Rotarod test (RT). A 21-day-old rat was placed on the rotating rod, and the interval until falling to the floor was measured for five consecutive days with a rotational frequency of 5, 5, 7, 9, and 11 rpm on the 1st to 5th days, respectively. Step-down passive avoidance test (SPAT). On the first day of measurement, a 60-day-old rat was placed on a round rubber platform with a diameter of 10 cm in 30 cm cube box with a metal grid floor. When the rat went down to the floor, we administrated a mild electrical shock till it remained on the rubber. During the following 2nd to 6th days, the rat was placed on the rubber once a day, and the duration until it went down to the grid was recorded. After all measurements, rat brains were removed under deep isoflurane anesthesia. We prepared 4-μm brain slices, performed MAP-2 staining, and counted numbers of neurons per unit area. Results. RT revealed that the mean length of stay on the rod on the 5th day for HG30 (29 ± 13 sec, mean ± SE) was significantly ($p<0.05$, Kruskal-Wallis test) shorter than for HG20 (77 ± 38 sec), HG10 (161 ± 80 sec), and HG5 (198 ± 28 sec). SPAT revealed that staying times of HG30 (38 ± 28 sec) and HG20 (73 ± 52 sec) were significantly shorter than that of HG5 (194 ± 112 sec). The number of neurons in HIE-G was significantly lower than in SG. Discussion and Conclusion. RT and SPAT revealed reduced motor activity in HG and memory deterioration in HG30 and HG20, respectively. Histology revealed decrease of neuron numbers in HG. Hyperthermic hypoxia for more 10 min may cause brain impairment in the rat HIE model.

Hosono (2010). EJAP 109, 35-9.

Where applicable, the authors confirm that the experiments described here conform with The Physiological Society ethical requirements.

PCB158

Transcutaneous auricular vagus nerve stimulation for the treatment of pediatric epilepsy

W. He, X. Jing, X. Wang, H. Shi, H. Shang, P. Rong, L. Li and B. Zhu

institute of Acupuncutre and Moxibustion, China Academy of Chinese Medical Sciences, Beijing, China

Background
Vagus nerve stimulation (VNS), an alternative method to manage patients with medically intractable epilepsy, has shown favorable results in reducing seizure frequency and improvements in quality of life [1]. As the only peripheral branch of the vagus nerve, the auricular branch of vagus nerve (ABVN) innervates the auricular concha in the surface of the body. It is suggested to treat epilepsy via stimulating the ABVN [2].
Objective
The present study is to investigate the safety and efficacy of transcutaneous auricular vagus nerve stimulation (ta-VNS) on pediatric patients with epilepsy.
Methods
Patients were enrolled from the Xuanwu Hospital and Tiantan hospital affiliated to the Capital Medical University. The ta-VNS was performed at the left auricular concha by using of a ta-VNS instrument. Patients or their caregiver were required to keep a detailed seizure diary. Classification of epileptic syndrome, seizure patterns, age of onset, seizure frequency and adverse effects were recorded. The baseline seizure frequency and the seizure frequency after 8 weeks, 16 weeks and 24 weeks of ta-VNS treatment were counted according to patient's seizure diary. All procedures accorded with the principles of the World Medical Association's Declaration of Helsinki.
Results
One patient aborted the study for ineffective reason after 8 weeks treatment. The remained thirteen patients completed the study for the whole 24 weeks without any changes in medication. After 8 weeks ta-VNS treatment, three patients had seizure free (classified as I), one patient has a seizure frequency reduction of more than 90% (classified as III), 10 patients had seizure frequency reductions of less than 50% (classified as IV).

After 16 weeks ta-VNS treatment, four patients had seizure free (classified as I), one patient has a seizure frequency reduction of more than 90% (classified as II), two patients has seizure frequency reductions of more than 50% (classified as III), six patients had seizure frequency reductions of less than 50% (classified as IV). After 24 weeks ta-VNS treatment, four patients had seizure free (classified as I), one patient has a seizure frequency reduction of more than 90% (classified as II), two patients has seizure frequency reductions of more than 50% (classified as III), six patients had seizure frequency reductions of less than 50% (classified as IV).

Conclusion

Our results suggest that ta-VNS is a safe and effective alternative method for pediatric patients.

Cersosimo RO, Bartuluchi M, Fortini S, Soraru A, Pomata H, Caraballo RH. Vagus nerve stimulation: effectiveness and tolerability in 64 paediatric patients with refractory epilepsies. Epileptic Disord 2011;13: 382-8.

Stefan H, Kreiselmeyer G, Kerling F, Kurzbuch K, Rauch C, Heers M, Kasper BS, Hammen T, Rzonsa M, Pauli E, Ellrich J, Graf W, Hopfengartner R. Transcutaneous vagus nerve stimulation (t-VNS) in pharmacoresistant epilepsies: a proof of concept trial. Epilepsia 2012;53: e115-8.

This work was supported by National Natural Science Foundation of China Research Grants (N0. 81273829, 30901931), Beijing Natural Science Foundation (N0. 7102120)

Where applicable, the authors confirm that the experiments described here conform with The Physiological Society ethical requirements.

PCB159

Production of Tumor Necrosis Factor- alpha by Microglia in Rat Brain After Traumatic Brain Injury

C. Wang[1,2], C. Yang[3], C. Chang[4], M. Chang[5], B. Cheng[1,4], B. Chio[6] and J. Yu[6]

[1]Department of Surgery, Chi Mei Medical Center, Tainan, Taiwan, [2]Department of Recreation and Health-Care Management, Chia-Nan University of Pharmacy and Science, Tainan, Taiwan, [3]The Program for Cancer Biology and Drug Discovery (CBDD), Taipei Medical University, Taipei, Taiwan, [4]Department of Biotechnology, Southern Taiwan University of Science and Technology, Tainan, Taiwan, [5]Department of Electrical Engineering, Southern Taiwan University of Science and Technology, Tainan, Taiwan and [6]Department of Chinese Medicine, Chi Mei Medical Center, Tainan, Taiwan

Tumor necrosis factor-alpha (TNF-α) is elevated early in injured brain after traumatic brain injury (TBI), in humans and in animals. However, it is not known whether etanercept (a TNF-α antagonist) improves outcomes of TBI by attenuating microglia-associated, astrocytes-associated, and/or neurons-associated TNF-α expression in ischemic brain. A well clinically relevant rat model, where a lateral fluid percussion is combined with systemic administration of etanercept (50mg/kg, i.p.) after TBI, was used. To examine the neuronal and glial production of TNF-α, we performed Immunofluorescence staining to identify neurons-TNF-α, astrocytes-TNF-α, and microglia-TNF-α double positive cells in the injured brain of the cortex, white matter, hippocampus, and hypothalamus in TBI animals treated with or without etanercept. The rats were anesthetized with sodium pentobarbital (25 mg/kg, i.p.) and a mixture containing ketamine (4.4 mg/ kg, i.m.), atropine (0.02633 mg/kg,i.m.), and xylazine (6.77 mg/kg, i.m.), and received a 4.8-mm craniotomy to anchor the modified plastic syringe hub over the exposed dura of the right parietal cortex. A moderate FPI (2.2 atm) was produced by rapidly injecting a small volume of saline into the closed cranial cavity with a fluid percussion device (VCU Biochemical Engineering, Richmond, VA, USA). Behavior on an inclined plane was used to assess changes in limb strength. In addition to inducing brain contusion as well as motor deficits, TBI caused significantly higher numbers of microglia-TNF-α double positive cells, but not neurons-TNF-α or astrocytes-TNF-α double positive cells in the injured brain areas than did the sham operated controls, when evaluated 3 days after TBI. The TBI-induced cerebral contusion, motor deficits, and increased numbers of microglia-TNF-α double positive cells in the injured brain were all significantly attenuated by etanercept therapy. Early microglia overproduction of TNF-α in the injured brain region after TBI contributes to cerebral contusion and motor deficits, which can be attenuated by etanercept therapy.

Where applicable, the authors confirm that the experiments described here conform with The Physiological Society ethical requirements.

PCB160

Protective effect of melanin derived from White Silky Fowl on rat model of Parkinson's disease induced by 6-Hydroxydopa

Y. He, F. Zhang and X. Wang

Physiology, China Capital Medical University, Beijing, China

The Protective effect of melanin from White Silky Fowl on on rat model of Parkinson's disease (PD) induced by 6-Hydroxydop (6-OH DA) were studied. PD model were induced by unilateral intrastriatal injection of 6-OH DA to destroy the nigrostriatal dopamine system in the rat (all the operation were performed on anaesthetised rats). The apomorphine-induced rotation test was applied to screen out parkinsonism rats after 5 weeks operation. The melanin (6 or 20mg/Kg) were used on Parkinsonism rats by intragastric administered per day for 4 weeks, normal saline administration as control group. After the 3 and 4weeks drug administration, the rats were detected by rotation test and open-field Test. The results were as shows: In rotation test, 6mg/Kg melanin administration could reduce the rotation movement at 4 weeks significantly and 20mg/Kg melanin administration reduced the rotation at 3 and 4 weeks. In open-field Test, 20mg/Kg melanin administration could increase the loco motor distance of Parkinsonism rats at 4 weeks significantly. Therefore, melanin in White Silky Fowl could be a novel drug candidate for treatment of PD.

Key words: melanin from white silky fowl; Parkinson's disease ; 6-Hydroxydopa

Grant sponsor: National Natural Science Foundation of China; Grant number:81100951;

Grant sponsor: Science explore Foundation of China Capital Medical University; Grant number: 2011ZR01;

recipient of the travel awards for young physiologists from the Chinese Association for Physiological Sciences (CAPS)

Where applicable, the authors confirm that the experiments described here conform with The Physiological Society ethical requirements.

PCB161

Perioperative buprenorphine infusion influences recovery following experimental stroke

D. Corbett[1,2], K.D. Langdon[2], M. Jeffers[1], S. Smith[2] and S. Granter-Button[2]

[1]Cellular & Molecular Medicine, University of Ottawa, Ottawa, ON, Canada and [2]Division of BioMedical Sciences, Memorial University, St. John's, NF, Canada

Buprenorphine administration is recommended following certain surgical procedures in laboratory animals. Although this opioid analog is thought to reduce post-operative discomfort, little research has been undertaken to assess the effects that buprenorphine may have on neuronal and behavioural function, especially in stroke research. This study assessed the effects of buprenorphine administration on survival, histological and functional outcome after cortical stroke. Sprague-Dawley rats (n=73) underwent endothelin-1 (ET-1) forelimb motor cortex stroke under 2% isoflurane anesthesia and were pseudorandomized into one of three experimental conditions that received either 3 (Bupe-3), or 1 (Bupe-1) injection(s) of buprenorphine (0.04 μg/kg, s.c.) or vehicle (Saline). Lidociane injections (2%) and Xylocaine gel (1%) were applied prior to incisions and at wound closure in all animals. Buprenorphine significantly increased core temperature (~0.5o C) for 3 hours immediately post-stroke, but only in the Bupe-1 animals. An overall wellness score consisting of post-operative weight gain, sensory reactivity, respiration rate, etc. revealed that Saline treated animals recovered more quickly than Bupe-3 animals ($p<0.025$). Buprenorphine resulted in a decrease in skilled reaching in the Montoya staircase test (~10%) and increased infarct volume (~20%) and neuroinflammation (~45%), although neither of these results attained statistical significance. Further, buprenorphine significantly increased the mortality rate compared to the Saline group. Based on these results it may be difficult to compare studies where investigators use different drugs and dosing regimens to control pain and discomfort, thereby posing a challenge to successful translation of preclinical research findings.

Research support was provided by the Canadian Institutes of Health Research (CIHR) awarded to DC.

Where applicable, the authors confirm that the experiments described here conform with The Physiological Society ethical requirements.

PCB162

Effect of slow frequency repeated transcranial magnetic stimulation on pain modulation status of female fibromyalgia patients: An electrophysiological study

A.H. Ansari[1,2], S. Jain[1], R. Mathur[1] and M. Bhattacharjee[3]

[1]Physiology, All India Institute of Medical Sciences, New Delhi, Delhi, India, [2]Physiology, Nepalgunj Medical College, Chisapani, Banke, Nepal and [3]Physiology, Vardhman Mahavir Medical College, New Delhi Safdarjung, Delhi, India

Fibromyalgia (FM) is a chronic pain disorder characterized by widespread musculoskeletal pain, tender points and fatigue, secondary to altered pain perception and modulation system. Most of the patients also report muscle stiffness, sleep disorder, irritable bowel syndrome, and mood disorder. There is a lack of appropriate management of pain and associated emotional component. We report the beneficial effect of non-invasive, non-pharmacological and inexpensive management of pain and associated anxiety in FM by transcranial magnetic stimulation (TMS).Female FM patients (n=90) were recruited from our Rheumatology Clinic. Patients received TMS (0.5 Hz, 80% of motor threshold) at right dorso-lateral prefrontal cortex, in 8 sessions of 5 min at 5 min interval /day. The TMS sessions were repeated every day for 5d/week x 4 (TMS group), while controls (sham group) received only sham stimulation. Pre and post TMS at wk 0, 4 and 6, pain was assessed objectively by nociceptive flexion reflex (RIII reflex) from left biceps femoris muscle; the emotional component of pain by Beck Depression Inventory second edition (BDI-II) and the negative strategies for coping with pain by Coping Strategy Questionnaire (CSQ), while pain modulation by diffuse noxious inhibitory control. We also analyzed the potential role of single nucleotide polymorphisms (SNPs) in catechol-O-methyltransferase (COMT) (rs4680) and 5-hydroxytryptamine (serotonin) 2A (5-HT2A) receptor (rs6313) genes on susceptibility to fibromyalgia. Polymerase chain reaction-restriction fragment length polymorphism (PCR-RFLP) method was used for the genotyping analyses. Genotype and allele frequencies were calculated and Chi square test was done for statistical analysis. Post-TMS (wk4), RIII threshold increased ($p<0.01$) in FM patients from 27.4±5.5V to 36.7±5.87V indicating analgesia, while it did not ($p<0.62$) change (28.6 ±6.04V to 29.1±5.5V) in sham group. The latency of RIII also increased ($p<0.045$) from 108.29 ±34.34 ms to 123.56±28.41 ms, post-TMS but not post-sham (112.37±28.65 to 109.78 ±30.21, $p<0.84$), while BDI-II score (12.46±3.21) at wk 0 which reduced ($p<0.03$) post-TMS to 7.45±1.87.The beneficial effect persisted till wk 6. : There were no significant differences in the frequencies of alleles and genotypes between patients and controls for the COMT and the 5-HT2A receptor gene polymorphisms ($P > 0.05$) in present case control study.

Genetic polymorphisms T102C of 5HT2A gene and val158met of COMT gene have no association with fibromyalgia susceptibility. The study showed that repeated TMS in FM patients relieved pain, associated anxiety and depression as indicated by RIII reflex and BDI-II, respectively. We suggest that it may be a valuable and safe new therapeutic option for FM patients.

Willer J.C. Comparative study of perceived pain and Nociceptive Flexion Reflex in Man. Pain 3: 69-80, 1977

Bhattacharjee M, Bhatia R, Gupta N Mathur R. Endogenous opioid system: A novel method to assess healthy volunteers. In Mathur R (Ed), Pain Updated: Mechanisms and Effects. Anamaya Publishers, Delhi. Pg. 11-21, 2006

Sampson SM, Rome JD, Rummans TA. Slow-frequency rTMS reduces fibromyalgia pain. Pain Med. 2006: 7 (2):115-8

Wolfe F, Smythe HA, Yunus MB et al. The American College of Rheumatology 1990 criteria for the classification of fibromyalgia: Report of the multicenter criteria committee. Arthritis Rheuma 1990; 33: 160-172

Julien N, Goffaux P, Arsenault P, Marchand S. Widespread pain in fibromyalgia is related to a deficit of endogenous pain inhibition. Pain. 2005 Mar; 114(1-2):295-302

Thanks to Dr Rima Dada for helping genetic analysis

Where applicable, the authors confirm that the experiments described here conform with The Physiological Society ethical requirements.

PCB163

Altered nerve structure and electrophysiological responses to mechanical stress in the *Trembler-J* mouse model of Charcot-Marie-Tooth disease

B.J. Power, M. Pickering and J.F. Jones

School of Medicine and Medical Science, University College Dublin, Dublin, Ireland

Charcot-Marie-Tooth (CMT) disease is the most common hereditary peripheral neuropathy encompassing a group of heterogeneous disorders characterised by distal limb areflexia and muscle atrophy, high-arched feet (known clinically as *pes cavus*), and decreased axonal conduction velocities. At present, there is no effective drug therapy for CMT despite intensive investigation of the molecular genetics of the condition. Our laboratory has recently found that normal nerve striations (the "bands of Fontana") appear to be absent on the surface of *Trembler-J* mouse nerves, an animal model of CMT type 1A, suggesting structural abnormalities in the underlying undulating course of component nerve fibres in an unstretched specimen. Previous studies have identified a correlation between peripheral nerve injury and the loss of observable striations on whole nerve fascicles (Zachary *et al.*, 1993). In light of these findings, the current study investigated the hypothesis that the chronic progressive peripheral neuropathy of CMT1A is a result of disordered nerve biomechanics and increased susceptibility to stretch-induced axonal injury. *Trembler-J* (*PMP22*$^{Tr\text{-}J}$/+; 21-27g; n=8) and wild-type C57BL/6 (*PMP22*+/+; 20-27g; n=8) mice were killed humanely by stunning and cervical dislocation in accordance with institutional guidelines. Sciatic nerves were isolated and examined using a sealed humidity chamber and stimulated electrically with simultaneous application of uniaxial tensile stresses. Young's modulus of elasticity was derived from the slope of the stress-strain curve and used as a measure of the biomechanical properties of each nerve. Electrophysiological responses to nerve deformation were also recorded as a measure of the capacity of nerves to propagate electrical potentials. Results are presented as mean ± S.E.M. with a criterion for statistical significance set at $p<0.05$. Upon application of tensile force, a significant difference was observed between the change in compound action potential (CAP) peak amplitude per unit of change in percentage (%) strain in both groups; with control mice showing an average decline in CAP of -0.07 ± 0.03mV per unit % strain, while *Trembler-J* nerves showed an average increase of 0.02 ± 0.02mV ($p=0.028$, two-tailed Student's *t*-test) despite no significant difference in Young's moduli ($p=0.5$, Mann-Whitney *U* test). The findings lead to rejection of the original hypothesis and indicate that the peripheral nerves of *Trembler-J* mice are not more prone to stretch-induced failure of impulse conduction.

Zachary, L.S., Dellon, E.S., Nicholas, E.M., Dellon, A.L. (1993) 'The structural basis of Felice Fontana's spiral bands and their relationship to nerve injury.' *Journal of Reconstructive Microsurgery*, 9(2): 131-138.

Ms Power was in receipt of an Undergraduate Vacation Studentship from the Physiological Society (UK and Ireland).

Where applicable, the authors confirm that the experiments described here conform with The Physiological Society ethical requirements.

PCB164

Glucocorticoid negative feedback alters electrical excitability of murine anterior pituitary corticotroph cells

P.J. Duncan and M.J. Shipston

Centre for Intefgrative Physiology, The University of Edinburgh, Edinburgh, UK

Anterior pituitary corticotroph cells are an integral component of the hypothalamic-pituitary-adrenal (HPA) axis which governs the physiological stress response. In response to a stressor, corticotrophin-releasing hormone (CRH) and arginine vasopressin (AVP) from the hypothalamus stimulate adrenocorticotrophic hormone (ACTH) release from corticotrophs. ACTH, in turn, releases glucocorticoids from the adrenal gland which negatively feedback to inhibit ACTH secretion. Corticotroph cells are electrically excitable and fire single-spike action potentials as well as showing complex bursting patterns. The aim of this project was to establish whether glucocorticoid negative feedback changes the electrical properties of murine corticotroph cells.

Corticotrophs were acutely isolated from male mice (aged 2-5 months) constitutively expressing green fluorescent protein (GFP) under control of the POMC promoter (POMC-GFP). Electrophysiological recordings were obtained using the perforated patch clamp technique in the current clamp configuration. Under basal conditions, cells had a resting membrane potential of -53.7 ±1.5mV (n = 7, Data are Means ± SEM) and showed low frequency spontaneous action potentials (0.34 ±0.14Hz). Stimulation with physiological concentrations of CRH and AVP (0.2nM and 2nM respectively) results in an increase in firing frequency and a transition from single spikes to bursting-like behaviour.

Cells pre-treated for 1.5 hours with corticosterone (100nM) were significantly ($p < 0.01$) hyperpolarised compared with controls (-62.9 ±2.2mV) under basal conditions (n = 8). Although CRH and AVP could depolarise resting membrane potential in corticosterone treated cells, this was still significantly ($p < 0.05$) hyperpolarised (-55.7 ±2.6mV) compared with controls treated with CRH and AVP. Basal firing rate was lower in cells treated for 1.5 hours (0.12 ±0.1Hz) and although CRH/AVP was still able to increase firing frequency (0.49 ±0.13Hz), it was significantly ($p < 0.05$) reduced compared with control cells exposed to CRH and AVP. Furthermore, in corticosterone pre-treated cells, CRH and AVP failed to induce a significant transition from single spikes to bursting behaviour.

To summarise, treatment of corticotrophs with corticosterone causes an overall suppression of both spontaneous and CRH/AVP-evoked firing frequency. Interestingly, corticosterone treated cells fail to transition from single spike to complex bursting patterns. This highlights a potential mechanism for corticosterone negative feedback although molecular targets remain to be defined.

Where applicable, the authors confirm that the experiments described here conform with The Physiological Society ethical requirements.

PCB165

Chronic exposure to intermittent hypoxia in lead intoxicated growing rats impairs bone biology

M.I. Conti, A.R. Terrizzi, C.M. Lee, P.M. Mandalunis, C. Bozzini and M.P. Martinez

Physiology, University of Buenos Aires. School of Dentistry, Buenos Aires, Argentina

High-altitude is a physiological stress which induces hypertrophy of the erythropoietic marrow leading to deterioration of bone biomechanical competition (1). Lead (Pb) is a persistent air pollutant implicated in bone disorders (2). The increase in mining activities at high altitude frequently results in populations chronically intoxicated with Pb under hypoxic conditions. We reported growth retardation and damages on femoral bone that predispose to fractures in a rat model performed intoxicating the animals with Pb and exposing them to intermittent hypobaric hypoxia (IHH) (3). These findings aimed us to investigate the deleterious effect of Pb under IHH on bone biology, evaluating the intrinsic stiffness and the efficiency of spatial distribution of bone material to resist deformation, bone mass in terms of histomorphometry and some stress indicators. Sixty female Wistar growing rats were divided into: C (control); Pb (1000 ppm of lead acetate in drinking water for 90 d); IHH (exposed to 506 mbar, 18 h/d during 90 d in a simulated high altitude chamber) and PbIHH (both treatments together). After euthanasia, blood samples were collected to evaluate tumoral necrosis factor-alpha (TNFα); adrenal glands were resected and hemimandibles, femurs and tibiae were dissected to assess cortical mechanical properties (Instron 4442) and histomorphometric studies in decalcified sections stained with H&E. Values are means ± SD, compared by ANOVA and Student-Newman-Keuls. TNFα plasmatic concentration was greater in Pb and IHH animals (53.71±9.65 and 184.11±28.18 vs 2.91±0.78, $p<0.01$). Adrenal gland weight from Pb and IHH groups rose to similar levels (10.78±1.08 and 10.77±0.90 g/100g BW vs 7.99±1.00 for control rats, $p<0.01$) being the increase even greater for the PbIHH group. Stress, a bone material quality indicator, was reduced either by Pb or IHH in both kinds of bones (femur: Pb 90.36±8.91; IHH 59.95±4.89 and PbIHH 80.61±5.03 vs C 102.08±13.84 Nmm-2 and hemimandible: Pb 22.96±5.96; IHH 26.39±4.68 and PbIHH 24.69±3.92 vs C 39.25±8.50 Nmm-2, $p<0.01$). Treatments reduced only the hemimandible cross sectional geometry (Pb 3.78±0.67; IHH 4.13±0.51 and PbIHH 4.23±0.13 vs C 5.02±0.49 mm4, $p<0.01$) and the intrinsic stiffness (Pb 565.32±46.31; IHH 555.39±49.31 and PbIHH 526.31±45.31 vs C 796.32±59.36 Nmm-2, $p<0.01$). Combined treatments reduced tibia and hemimandible bone volume (-45 % and -40% respectively, $p<0.01$) and growth plate cartilage thickness (-19%). These results show a previously unreported effect of heavy metals under intermittent hypoxia on bone. Longer studies should be necessary to evaluate if an adaptation of the architecture to maintain structural properties may occur and if an association between the impairment of bone material quality and the degree of oxidative stress exists. UBACyT 20020090200013.

Bozzini C, Olivera MI, Huygens P, Alippi RM, Bozzini CE (2009). Long-term exposure to hypobaric hypoxia in rat affects femur cross-sectional geometry and bone tissue material properties. Ann Anat 191:212–217.

Campbell JR, Rosier RN, Novotny L, Puzas JE (2004) The association between environmental lead exposure and bone density in children. Environ Health Perspect 112(11):1200–1203.

Conti MI, Terrizzi AR, Lee CM, Mandalunis PM, Bozzini C, Piñeiro AE, Martinez MP (2012) Effects of lead exposure on growth and bone biology in growing rats exposed to simulated high altitude. Bull Environ Contam Toxicol 88(6):1033-1037.

Where applicable, the authors confirm that the experiments described here conform with The Physiological Society ethical requirements.

PCB166

Impact of lead intoxication under intermittent hypoxia on oral health of growing rats

M.P. Martinez, A.R. Terrizzi, C.M. Lee, J. Fernandez Solari, J.C. Elverdin and M.I. Conti

Physiology, University of Buenos Aires. School of Dentistry, Buenos Aires, Argentina

Objective: We recently reported in growing rats chronically intoxicated with lead (Pb) and exposed to the stress of intermittent hypobaric hypoxia (IHH) deleterious effects on periodontal and dental tissues that could be due to a greater vulnerability of them to inflammatory processes (1). Periodontitis is characterized by inflammation of the supporting tissues of the teeth and periodontal pocket formation that result in alveolar bone resorption and soft tissue attachment loss. It has been suggested that the submandibular gland functions are a key regulatory organ in the oral neuroimmunoregulatory network (2). The aim of the present study was to establish in the same rat model, the macroscopic, biochemical and histological parameters consistent with a periodontal disease. Methods: Sixty female Wistar growing rats were randomly divided into 4 groups: C (control); Pb (intoxicated with 1000 ppm of lead acetate in drinking water for 90 d); IHH (exposed to 506 mbar, 18 h/d during 90 d in a simulated high altitude chamber) and Pb-IHH (both treatments together). At the end of the experimental period the submandibular glands (SMG) were extracted to measure TBA-RS, as a marker of cellular oxidative stress and prostaglandin E2 (PGE2) known to be increased under oral inflammatory conditions (3). Hemimandibles were resected to assess bone loss by measuring the distance between the cemento-enamel junction and the alveolar bone crest of the first molars roots and to perform histomorphometric studies in decalcified sections stained with H&E. Values are means ± SD, compared by ANOVA followed by Student-Newman-Keuls tests. Results: Hypoxia enhanced TBA-RS content in SMG being the increase even greater in PbIHH group (C: 11.11±0.73; Pb: 11.59±0.46; IHH: 13.89±0.88 and PbIHH: 15.49±0.70 nmol/mg SMG wet weight, $p<0.01$). Both treatments enhanced PGE2 content in the SMG, showing an additive effect in the PbIHH group (C: 332.69±123.99; Pb: 476.19±135.02; IHH: 546.24±122.42 and PbIHH: 1165.09±204.51, $p<0.01$). IHH showed significantly higher buccal alveolar bone loss vs their control but surprisingly it was lower in the PbIHH group. Conclusion: Treatments enhanced some systemic and oral tissues inflammatory parameters, which could lead to a periodontal disease in individuals living in lead contaminated high altitude areas. UBACyT 20020090200013.

Conti MI, Terrizzi AR, Lee CM, Mandalunis PM, Bozzini C, Piñeiro AE, Martinez MP (2012) Effects of lead exposure on growth and bone biology in growing rats exposed to simulated high altitude. Bull Environ Contam Toxicol 88(6):1033-1037.

Amer M, Elverdin JC, Fernández-Solari J, Medina VA, Chiarenza AP, Vacas MI (2011) Reduced methacholine-induced submandibular salivary secretion in rats with experimental periodontitis. Arch Oral Biol 56(5):421-427.

Offenbacher S, Heasman PA, Collins JG (1993) Modulation of host PGE2 secretion as a determinant of periodontal disease expression. J Periodontol 64:432–444.

Where applicable, the authors confirm that the experiments described here conform with The Physiological Society ethical requirements.

PCB167

Interstitial calcium modulates cholinergic-induced eccrine sweating

K. Metzler-Wilson[1,2] and T.E. Wilson[1,3]

[1]Ohio Musculoskeletal and Neurological Institute, Ohio University, Athens, OH, USA, [2]Department of Physical Therapy, Lebanon Valley College, Annville, PA, USA and [3]Deapartment of Biomedical Sciences, Ohio University Heritage College of Osteopathic Medicine, Athens, OH, USA

Ca^{2+} is an important second messenger in eccrine sweating, with both internal and external sources identified in isolated rhesus monkey palm sweat glands[1]. It is unclear if these isolated gland studies can be translated to *in vivo* interstitial Ca^{2+} level modulation and if this *in vivo* modulation has the capacity to modulate sweat rate (SR) and skin blood flow (SkBF) in intact human forearm skin, which unlike palm skin, is vital to thermoregulation. We hypothesized that lowering interstitial Ca^{2+} levels or attenuating its influx would cause a rightward shift in the SR to acetylcholine (ACh) dose-response relation. 1) To identify that our methods had the capacity to modulate Ca^{2+} concentrations, osmolality was measured during Ca^{2+} or Ca^{2+} chelator (43 mM EDTA) perfusion through a microdialysis membrane into 2 ml distilled water with no Ca^{2+}, 200 mM Ca^{2+}, or EDTA. EDTA decreased perfusate and bath osmolality. To quantify Ca^{2+} in physiologic concentrations, EDTA in distilled water or lactated Ringers (2 mM Ca^{2+}) was perfused through a bath containing the opposite solution. EDTA decreased perfusate and bath Ca^{2+} concentrations via microbore ion chromatography with conductivity detection. 2) 9 healthy human subjects received 6 ACh doses ($1x10^{-5}$ - $1x10^{0}$ M, 10-fold increments) with and without EDTA via forearm intradermal microdialysis. Capacitance hygrometry SR measures were completed directly over microdialysis membranes. SR to ACh dose-response modeling via nonlinear regression curve fitting (mean R^2 0.97±0.05 with, 0.95±0.03 without EDTA) identified maximal responsiveness (E_{max}) and ED_{50} (ACh dose causing 50% E_{max}). EDTA right shifted the ED_{50} (1.5±0.1 -logM) compared to ACh alone (1.0±0.1 -logM; p=0.01). E_{max} was not different between groups (0.60±0.078 and 0.58±0.34 mg/cm^2/min, respectively; p=0.85). 3) The EDTA microdialysis protocol was repeated in 5 subjects, measuring SkBF via laser-Doppler flowmetry to control for the potential of SkBF affecting SR independently. Neither E_{max} nor ED_{50} was significantly different between groups. 3) 10 healthy human subjects received the same 6 ACh doses with and without L-type Ca^{2+} channel blocker (1 mM verapamil) via forearm intradermal microdialysis. SR to ACh dose-response curve fitting (mean R^2 0.96±0.01 with, 0.97±0.01 without verapamil) identified a right shifted ED_{50} (0.9±0.1 -logM) compared to ACh alone (1.6±0.2 -logM; p<0.01). E_{max} was not different between groups (0.45±0.08 and 0.35±0.06 mg/cm^2/min, respectively; p=0.07). Thus, local in vivo Ca^{2+} chelation has the capacity to decrease interstitial Ca^{2+} concentration and to attenuate eccrine sweat gland cholinergic sensitivity. L-type Ca^{2+} channel antagonism also attenuates eccrine sweat gland cholinergic sensitivity. These data suggest that interstitial Ca^{2+} and its influx play a SkBF-independent role in human cholinergic-induced eccrine sweating that is important in thermoregulation.

Sato K & Sato F (1981). Role of calcium in cholinergic and adrenergic mechanisms of eccrine sweat secretion. Am J Physiol 241, C113-120.

Where applicable, the authors confirm that the experiments described here conform with The Physiological Society ethical requirements.

PCB169

Effects of non-lethal cold stress on the mitochondrion-rich cells in gills of the euryhaline milkfish (*Chanos chanos*) acclimated to seawater and fresh water

C. Kang, Y. Chen and T. Lee

Life Sciences, National Chung-Hsing University, Taichung, Taiwan

Milkfish (*Chanos chanos*) is an aquaculture species which could be cultivated in the rearing ponds with different salinities. In the Southern Taiwan, large numbers of milkfish died in the cold current of the winter leading to economic loss of the fisherman. Being an ectothermal species, low temperature seriously influences the homeostasis of the milkfish. In the teleosts, the gills exposed to the external environment are the major osmoregulatory organ. Mitochondrion-rich (MR) cells conduct ion excretion and uptake by ion transporters in gills of seawater (SW) and fresh water (FW) fish, respectively. The present study focused on the remodeling of cellular morphologies and modulation of ion transporters in the gill MR cells of SW and FW milkfish raised in the non-lethal cold stress (18°C) for 1 week compared to the control temperature (28°C) group. The juvenile milkfish (15-20 g, n=12) were fed a daily diet of commercial pellets. Following the experiment, the fish were not fed for 1 day and anaesthetized with Tricaine mesylate (MS-222, 100-200 mg/l) before collecting blood and excising the gill tissues. The facilities and protocols for experimental animals were approved by the Institutional Animal Care and Utility Committee of the National Chung-Hsing University (Approval No. IACUC 96-48 to THL). Values were mean ± SEM, compare by Students' t-test. The plasma osmolality (28°C vs. 18°C: 403.4±4.2 vs. 377.0±3.1 mOsmo/kg, p<0.05) and Na+ concentrations (28°C vs. 18°C: 141.1±3.6 vs. 128.3±3.4 mM, p<0.05) were decreased in SW milkfish exposed to 18°C, while the Cl- concentrations (28°C vs. 18°C: 108.6±6.4 vs. 175.6±5.9 mM, p<0.05) were increased in the FW fish at 18°C. No effect of nonlethal cold was found on the protein abundance of Na^+, K^+-ATPase (NKA) α-subunit and cell size and density of NKA-immunoreactive (IR)/MR cells in gills of the milkfish. In gills of the SW milkfish exposed to 18°C, constant NKA activity and the low percentage of cystic fibrosis transmembrane conductance (CFTR)-IR/NKA-IR cells (28°C vs. 18°C: 43.8±5.5 vs. 14.6±1.6 %, p<0.05) were found. On the other hand, our results revealed that the NKA activity decreased (28°C vs. 18°C: 36.8±6.4 vs. 18.7±4.2 μmol Pi/mg protein/hr, p<0.05) and the apical openings with Na^+, Cl^- cotransporter (NCC) of MR cells reduced (28°C vs. 18°C: 18.5±1.6 vs. 9.7±1.3 %, p<0.05) in gills of the FW milkfish at 18°C. This study was the first to figure out different responses of MR cells with hypo- and hyperosmoregulation in gills of the milkfish when exposed to non-lethal cold stress. The functional morphologies of gill MR cells

played an important role in cold resistance of the euryhaline milkfish.

Where applicable, the authors confirm that the experiments described here conform with The Physiological Society ethical requirements.

PCB170

L-arginine-nitric oxide pathway in neutrophils from chronic renal failure patients under haemodialysis

D.C. Abrantes[1], T.M. Brunini[1], M.B. Oliveira[1], N.O. Pinto[3], C.L. Correa[1], C.S. MAchado[1], S.F. Santos[2] and A. Mendes-Ribeiro[1,3]

[1]Pharmacology, State University of Rio de Janeiro, Rio de Janeiro, Rio de Janeiro, Brazil, [2]Medical Clinic, Discipline of Nephrology, State University of Rio de Janeiro, Rio de Janeiro, Rio de Janeiro, Brazil and [3]Physiological Sciences, Federal University of the State of Rio de Janeiro, Rio de Janeiro, Rio de Janeiro, Brazil

Chronic renal failure (CRF) promotes endothelial cells and neutrophils damage in the severe stages of disease [1]. Disturbances in nitric oxide (NO) bioavailability are involved in the pathogenesis of CRF. [2]. NO is a potent vasodilator, inhibitor of platelet activation and aggregation. Recent studies have demonstrated that activated neutrophils promotes an inhibitory effect on platelet aggregation, contributing to vascular homeostasis [3] . The aim of this study was to evaluate the transport of L-arginine, the activity of the enzyme nitric oxide synthase (NOS) and the platelet-neutrophil relationship in CRF. Six CRF patients under haemodialysis and six healthy controls matched for sex and age were included in this study. The Pedro Ernesto Hospital Ethical Committee approved this study (451– CEP/HUPE), and informed consent was obtained from each participant. Basal NOS activity was measured by the conversion of L-[3H]-arginine into L-[3H]-citrulline. L-arginine transport into neutrophils was analysed in these patients. Saturable influx of L-arginine into neutrophils was mediated by systems y+ and y+L. Platelet aggregation was induced by ADP 5 μM, incubated by neutrophils at different times (5 and 30 minutes) and monitored for 8 min in a four-channel aggregometer. Student's t and Mann Whitney tests were used for statistical analysis and values were considered significant when $p<0.05$. Values were expressed as means ± SEM. Results: Total L-[3H]-arginine transport (controls: 1.56 ± 0.46 vs. CRF: 0.50 ± 0.12 pmol/106cells/min), transport by y+ system (controls: 0.5 ± 0.18 vs. CRF: 0.25 ± 0.05 pmol/106cells/min) and transport by y+L system (controls: 1.06 ± 0.4 vs. CRF: 0.24 ± 0.08 pmol/106cells/min) were reduced in CRF patients. There was a significant decrease in NOS activity (pmol/106 cells/min) in neutrophils from CRF patients (0.18 ± 0.03) compared to controls (0.62 ± 0.02).There was no change in platelet aggregation induced by ADP in CRF patients compared to controls. In the presence of neutrophils, there was a reduction-time dependent in platelet aggregation in both groups with no difference between them.

Conclusion: This study demonstrated a lower L-[3H]-arginine influx associated with a reduction in NOS activity in neutrophils from CRF patients compared with controls. These data suggest alterations in the L-arginine-NO pathway that may lead to a decrease in NO bioavailability in patients under haemodialysis.

Financial Support: FAPERJ, CNPq, CAPES.

1. Siqueira, M.A., et al., Increased nitric oxide production in platelets from severe chronic renal failure patients. Can J Physiol Pharmacol. 89(2): p. 97-102.

2. Mendes Ribeiro, A.C., et al., Abnormalities in L-arginine transport and nitric oxide biosynthesis in chronic renal and heart failure. Cardiovasc Res, 2001. 49(4): p. 697-712.

3. Dong, H.P., et al., Lipopolysaccharide-stimulated leukocytes contribute to platelet aggregative dysfunction, which is attenuated by catalase in rats. Kaohsiung J Med Sci. 26(11): p. 584-92.

Financial Support: FAPERJ, CNPq, CAPES.

Where applicable, the authors confirm that the experiments described here conform with The Physiological Society ethical requirements.

PCB171

Identification of ARAP3 function as a novel modulator of lymphatic vessel morphogenesis

J. Kartopawiro[1], E. Frampton[1], T. Karnezis[2], K. Koltowska[1], N. Bower[1], S. Schulte-Mercker[3], M. Achen[2], J. Kazenwadel[4], N. Harvey[4], B. Hogan[1] and M. Francois[1]

[1]Institute for Molecular Bioscience, The University of Queensland, Brisbane, QLD, Australia, [2]Peter McCallum Cancer Institute, Melbourne, VIC, Australia, [3]Huebrecht Institute, Huebrecht, Netherlands and [4]Center for Cancer Biology, Adelaide, SA, Australia

The process of lymphatic vascular development also known as lymphangiogenesis occurs in the embryo from a sub-population of venous endothelial cells that acquire a lymphatic endothelial cell fate. The main molecular switch responsible to drive the transition from venous to lymphatic identity is the transcription factor SOX18.

We took advantage of Sox18 mutant mice to perform a microarray analysis of purified lymphatic endothelial cells from the skin of both wild type and Sox18 heterozygous mutant mice and identified a subset of Sox18-regulated genes with no previously implicated function in lymphangiogenesis.

To validate on a large scale top gene candidates (>100) from the micro-array, an expression pattern and morpholino knockdown screen was performed in zebrafish and identified the arap3a gene (ArfGAP with RhoGAP domain, ankyrin repeat and PH domain 3) as enriched in zebrafish vasculature throughout embryogenesis. At 56 hours post fertilization (hpf) in zebrafish, we observed that arap3a knock down generates a severe decrease in lymphatic precursor cells and block thoracic duct formation. By contrast, arterial and venous differentiation and sprouting of venous derived intersegmental vessels remained unaffected, demonstrating the specific lymphatic function of arap3a in this model system.

In mice, Arap3 is expressed in a polarized fashion in lymphatic endothelial cell precursors in the cardinal vein suggesting a conserved role in lymphangiogenesis. Conditional loss of Arap3 function in endothelial cells triggered severe subcutaneous edema at 14.5 days post coitum (dpc) and skin lymphatic vessels display severe mis-patterning defects whereas the blood vasculature remained unaffected. Finally, we found in fish and in cultured LECs that ARAP3 acts downstream of vascular endothelial growth factor-c (Vegfc) and may be considered an effector of Vegfc/Vegfr3 signaling to modulate lymphatic endothelial cell migration.

Our work reveals a major regulator of lymphatic vessel morphogenesis and network assembly downstream of the VEGF-C pathway and provides the molecular basis to further target VEGF-C signaling with the view to blocking lymphatic remodeling during solid tumour metastasis.

Where applicable, the authors confirm that the experiments described here conform with The Physiological Society ethical requirements.

PCB172

Interleukin-1β-induced decrease of NHE3 interacting protein PDZK1, as well as sh-RNA-mediated PDZK1 knockdown, is associated with NHE3 dysfunction in the colonic epithelial cell line Caco-2bbe

G. Chodisetti[1], M. Luo[1], A. Klöpper[1], B. Riederer[1], P. He[2], C.C. Yun[2], S. Yeruva[1] and U. Seidler[1]

[1]Dept.of Gastroenterology, Hepatology and endocrinology, Hannover medical school, Hannover, Germany and [2]Div. Of Gastroenterology, Dept. Of Medicine, Emory University, Atlanta, GA, USA

Background: Inflammatory bowel disease (IBD) is a major gastrointestinal disease with diarrhea being a leading symptom. The pathophysiology of inflammatory diarrhea is multifactorial and still ill understood. We have previously reported a dysfunction of the major intestinal sodium absorptive transporter, the Na+/H+ exchanger NHE3, in inflamed colonocytes of ulcerative colitis patients and mouse models of colitis as well as a downregulation of the NHE3-interacting PDZ-protein PDZK1 (NHERF-3) in chronically inflamed murine colonic mucosa.
Aim: The present study investigates whether the inflammation induced reduction of PDZK1 expression is causally related to the defective function of its binding partner, NHE3.
Methods: We used cytokine-treated Caco-2bbe cells as an in vitro model of intestinal inflammation. Real-time PCR and western blots were done to measure PDZK1 and NHE3 mRNA and protein expression. pH-fluorometry using the pH sensitive dye, 2',7'-bis-(2-carboxyethyl)-5-(and-6)-carboxyfluorescein (BCECF), was performed to measure acid activated NHE3 activity. Confocal microscopy was done to analyze NHE3 localization in interleukin-1β (IL-1β) treated Caco-2bbe cells stably expressing human NHE3 (C2N3cells).
Results: Treatment of Caco-2bbe cells with Th1 pro-inflammatory cytokines revealed, IL-1β as the main cytokine with a significant inhibitory effect on PDZK1 expression (50% of decrease in both mRNA and protein compared to control). Treatment of C2N3 cells with IL-1β lead to a significant decrease in PDZK1 protein to approx. 50% of control value, but no change in NHE3 protein expression and membrane localization. However, acid activated NHE3 transport rates were significantly decreased after IL-1β treatment in these cells (22% less than control). When PDZK1 expression was decreased by lentiviral shRNA knockdown in NHE3-transfected Caco2bbe cells to approx 80% of control value, and NHE3 transport activity assessed, an even stronger decrease in acid-activated NHE3 activity (49% less than control) was observed than in IL-1β treated cells. This demonstrates a causal relationship of PDZK1 downregulation and NHE3 dysfunction, independent of inflammation.
Conclusion: A marked decrease in the PDZ-adaptor protein, PDZK1, was observed in the IL-1β treated Caco-2bbe cells. This corresponded to a decrease in NHE3 transport function but no change in NHE3 expression and membrane localization. We therefore conclude that during intestinal inflammation, cytokine mediated PDZK1 down regulation is likely an important causative factor for inflammation-associated NHE3 dysfunction and diarrhea.

Where applicable, the authors confirm that the experiments described here conform with The Physiological Society ethical requirements.

PCB174

Lubiprostone activates CFTR in human bronchial epithelial cells via a protein kinase A independent dependent process

J. Przeworek[1], H. Samvelyan[1], A. Hassouni[1], R. Muimo[2], C. Taylor[3] and L. Robson[1]

[1]Biomedical Science, University of Sheffield, Sheffield, UK, [2]Department of Infection and Immunity - Medical School, University of Sheffield, Sheffield, South Yorkshire, UK and [3]Paediatric Gastroenterology, Sheffield Children's Hospital, Sheffield, South Yorkshire, UK

In human bronchial epithelial cells the cAMP-activated Cl^- channel CFTR, plays a critical role in mediating Cl^- secretion. This important role is highlighted in cystic fibrosis, where CFTR mutations impact significantly leading to defective muco-ciliary clearance and an increased risk of infection. Previous work has suggested that the fatty acid lubiprostone (Lp) activates CFTR in ovine airway [1]. In the current study the impact of Lp on human bronchial cells (16HBE14o–) was tested.
Cells were grown on permeable supports until confluent and a transepithelial resistance of at least 200 Ωcm^2 was achieved. Inserts were mounted in an Ussing chamber with standard Krebs (basolateral side) and low Cl^- Krebs (apical side). Solutions were bubbled (5% CO_2), and all potential and resistance measurements corrected. 10 μA of current was injected to calculate the equivalent short circuit current (I_{SC}). Control measurements were taken for 5 minutes and then 1 μM Lp added apically. At steady-state 10 μM $CFTR_{inh172}$ was then added to provide an indication of CFTR function. This was repeated in unpaired inserts in the presence of inhibitors for either protein kinase A (protein kinase inhibitor - PKI), adenylate cyclase (SQ22,536) or tyrosine phosphatase (phenylarsine oxide - PAO). Statistical significance was tested using ANOVAs or Student's t test as appropriate and assumed at the 5% level.
Addition of Lp increased I_{SC}. Under control conditions I_{SC} was 10.1 ± 1.74 μA/cm^2 and increased to 26.2 ± 2.63 μA/cm^2 with Lp (n=23, mean increase 17.7 ± 2.40 μA/cm^2). Addition of $CFTR_{inh172}$ reversed this increase, a fall of 20.2 ± 2.29 μA/cm^2. Pre-incubation with PKI or SQ22,536 prior to the addition of Lp was without effect. The change in I_{SC} with Lp in the presence of both compounds was not significantly different to control: 20.3 ± 2.05 μA/cm^2 (n=11) and 18.8 ± 4.77 μA/cm^2 (n=8), with PKI and SQ22,536, respectively. The $CFTR_{inh172}$-sensitive I_{SC} was also unaffected: 14.0 ± 1.10 μA/cm^2 (PKI, n=11) and 21.0 ± 4.74 μA/cm^2 (SQ22,536n=8). Conversely, pre-incubation with PAO inhibited the response to Lp. The shift in I_{SC} with Lp was 8.58 ± 1.95 μA/cm^2 (n=10) approximately half of the observed control response. The $CFTR_{inh172}$-sensitive I_{SC} was also reduced at 8.86 ± 2.17 μA/cm^2 (n=10), again approximately half of the control response.
These data indicate that Lp has the ability to activate CFTR in human airway epithelial cells. The action of Lp appears to be independent of cAMP and PKA, the typical CFTR activation pathway, but, given the effect of PAO, appears to involve activation of a tyrosine phosphatase.

1. Cuthbert, A.W., Lubiprostone targets prostanoid EP4 receptors in ovine airways. British Journal of Pharmacology, 2011. 162(2): p. 508-520.

This work was supported by the Sheffield Children's NHS Foundation Trust.

Where applicable, the authors confirm that the experiments described here conform with The Physiological Society ethical requirements.

PCB175

Lubiprostone activates CFTR in human bronchial epithelial cells via a prostanoid receptor dependent process

J. Przeworek[1], H. Samvelyan[1], A. Hassouni[1], C. Taylor[2] and L. Robson[1]

[1]Biomedical Science, University of Sheffield, Sheffield, UK and [2]Paediatric Gastroenterology, Sheffield Children's Hospital, Sheffield, UK

In human bronchial epithelial cells the cAMP-activated Cl^- channel CFTR mediates Cl^- secretion. This critical role is highlighted in cystic fibrosis, where CFTR mutations impact significantly leading to defective muco-cilliary clearance and an increased risk of infection. Previous work has suggested that the fatty acid lubiprostone (Lp) activates CFTR in ovine airway via a prostanoid receptor-dependent process [1]. In the current study the mechanism of action of Lp in human bronchial cells (16HBE14o–) was investigated.

Cells were grown on permeable supports until confluent (transepithelial resistance of at least 200 Ωcm^2). Inserts were mounted in an Ussing chamber with standard Krebs (basolateral side) and low Cl^- Krebs (apical side). Solutions were bubbled (5% CO_2), and all potential and resistance measurements corrected. 10 μA of current was injected to calculate the equivalent short circuit current (I_{SC}). Control measurements were taken for 5 minutes and then 1 μM Lp added apically. At steady-state 10 μM $CFTR_{inh172}$ was then added to provide an indication of CFTR function. This was repeated in unpaired inserts in the presence of inhibitors for EP4 receptors (GW627368X or L161,982). Statistical significance was tested using ANOVAs and assumed at the 5% level.

Addition of Lp increased I_{SC} from 10.1 ± 1.74 μA/cm^2 to 26.2 ± 2.63 μA/cm^2 (n=23), a mean increase of 16.1 ± 2.21 μA/cm^2. In the presence of GW627368X or L161,982 the response to Lp was blunted, with mean increases of 6.26 ± 1.21 μA/cm^2 (n=14) and 7.64 ± 1.98 μA/cm^2 (n=9), respectively. Under control conditions $CFTR_{inh172}$ reversed the increase observed with Lp, a fall of 20.2 ± 2.29 μA/cm^2 (n=23). This effect of $CFTR_{inh172}$ post Lp was reduced by around 50% on pre-incubation with GW627368X or L161,982. The $CFTR_{inh172}$–sensitive I_{SC} was 10.7 ± 1.79 μA/cm^2 (n=14) and 9.55 ± 1.99 μA/cm^2 (n=9), respectively.

These data suggest that Lp activates CFTR in human airway via an EP4 receptor dependent process. Further work is needed to elucidate the downstream pathway involved and determine if any other EP receptors play a role in the response to Lp.

1. Cuthbert, A.W., Lubiprostone targets prostanoid EP4 receptors in ovine airways. British Journal of Pharmacology, 2011. 162(2): p. 508-520.

This work was supported by the Sheffield Children's Hospital Trust and the University of Sheffield SURE Scheme

Where applicable, the authors confirm that the experiments described here conform with The Physiological Society ethical requirements.

PCB176

Carbonic anhydrase II enhances activity of endogenous Na-H exchangers and not the Na/HCO_3 cotransporter, NBCe1, when expressed in *Xenopus* oocytes

F.J. Moss and W.F. Boron

Physiology & Biophysics, Case Western Reserve University, Cleveland, OH, USA

The carbonic anhydrase II (CAII) metabolon hypothesis predicts that CAII binds to electrogenic Na/HCO_3 co-transporters (NBCe1), enhancing their transport of HCO_3-related species. Using a short current-voltage (I-V) protocol (60 ms steps from the reversal potential, E_{rev}), the Boron Lab (BL) showed in 2006 that neither CAII injected into *Xenopus* oocytes expressing NBCe1 nor CAII fused to the NBCe1 C-terminus changed NBCe1 slope conductance (G), the proper measure of NBCe1 activity. Yet in 2007, using 10 s I-V steps and a holding potential (V_h) +100 mV from E_{rev}, Becker & Deitmer (BD) concluded the opposite. We hypothesized that the BD protocol accentuated CAII-mediated dissipation of long-distance HCO_3 and intracellular pH (pH_i) gradients in the cytoplasm, enhancing NBCe1 activity. However, we find that G is unchanged when V_h steps are increased to as long as 30 s. Even when NBCe1 carries large currents (approaching 2.5 μA; V_h= 0 mV), CAII does not enhance recovery rates of pH_i from CO_2-induced acidification, the magnitude of the peak NBCe1 current (ΔI), or G. NBCe1 functional expression levels were typically 3-fold greater in BL vs. BD experiments. However, CAII does not enhance ΔI, G, or the rate of sodium influx ($d[Na]_i/dt$) in oocytes expressing NBCe1 at BD-equivalent levels. These experiments used an N-terminally GFP-tagged NBCe1 construct, EGFP-e1 and purified recombinant human CAII. To replicate the entire BD protocol, we expressed non-EGFP-tagged NBCe1 and injected bovine CAII purified from blood, observing a small but significant CAII-mediated change in ΔI but not G (paired t-test $p<0.05$). However, EGFP-e1 expressing oocytes demonstrate no CAII-dependent changes in ΔI or G. Notably, both recombinant human and purified bovine sourced-CAII enhance, in a concentration-dependent manner, $d[Na]_i/dt$ in control oocytes not expressing NBCe1. The increase is 69% inhibited by 10 μM EZA and is completely and reversibly blocked by 50 μM EIPA. Repeating the BD protocol with oocytes expressing non-EGFP-tagged NBCe1 under constant 50 μM EIPA superfusion abolishes the CAII-mediated increase in ΔI. These data indicate that the catalytic activity of CAII enhances endogenous *Xenopus*-oocyte Na-H exchange, and not the activity of heterologously expressed NBCe1.

Lu J *et al*. (2006). J Biol Chem **281**, 19241–19250.

Becker HM & Deitmer JW (2007). J Biol Chem **282**, 13508-13521.

Funding: NIH DK30344 and DK007470

Where applicable, the authors confirm that the experiments described here conform with The Physiological Society ethical requirements.

PCB177

Confocal microscope observation on paracellular fluid transport in the vascularly perfused submandibular gland

M. Murakami[1], F. Wei[1], T. Narita[2], M. Fukushima[3], S. Hashimoto[4], Y. Shibukawa[4] and M. Sato[4]

[1]National Institute for Physiological Sciences, Okazaki, Japan, [2]Nihon University College of Bioresource Sciences, Fujisawa, Japan, [3]Nihon University School of Dentistry, Matsudo, Japan and [4]Tokyo Dental College, Chiba, Japan

Primary saliva is a mixture of fluid secreted through paracellular route and transcellular route. By quantification of luminal dye-dilution in the isolated acini with confocal microscopy, the transcellular fluid secretion was estimated as 25 μl/g-min. By subtraction of the transcellular fluid secretion from the whole fluid secretion, a paracellular fluid secretion was estimated to be 60 μl/g-min (1). By measurement of the 3H-labeled dextran in saliva, the two different sized paracellular routes were proposed; one is smaller than 5 Å in radius and the other is larger than 5Å (2). In addition the paracellular fluid secretion could include a pressure-dependent and a pressure-independent components; 20 and 40 μl/g-min, respectively (3). In the present study, to assess whether the pressure-dependent paracellular transport corresponds to the wider paracellular route, the submandibular salivary gland was surgically isolated from the rat (Wistar male) under anesthesia with pentobarbitone sodium (50 mg/kg body weight, i.p.). The isolated gland was perfused arterially on the stage of confocal microscope. Using sulfo-rhodamine B in the perfusate, we observed the appearance of the fluorescent dye in the intercellular canaliculi, which can pass through the larger route. The system allowed us to obtain 30 sliced images every 2 s and gave 3D reconstructed image every 2 s (5 Live, Zeiss). When the fluid secretion was induced by alpha1-adrenergic stimulation with phenylephrine, the fluorescence of intercellular canaliculi increased dose-dependently. Combined stimulation with phenylephrine and xamoterol (beta1 agonist) increased the fluorescence more than only phenylephrine. Single stimulation with isoproterenol (1 μM) decreased the fluorescence intensity in the canaliculi, suggesting lowering fluid secretion through pressure-dependent paracellular route. The present findings lead the conclusion that we could observe entry of fluorescent dye from intercellular space to luminal space by pressure-dependent paracellular route by solvent-drag, and that the fluid secretion through pressure-independent route is still open for further studies.

Segawa A et al. (2002) Eur J Morphol 40, 241-246

Murakami M et al. (2001) J Physiol 537, 899-906

Murakami M & Wei F (2010) Int Symp Morphol Scis 20, 50p

This work was supported by JSPS KAKENHI Grant Number 23590271 and Tokyo Dental College HRC8.

Where applicable, the authors confirm that the experiments described here conform with The Physiological Society ethical requirements.

PCB178

Organic cation transporter subtypes of isolated mouse proximal tubules are differently regulated by protein kinases

E. Schlatter, S.K. Holle, D. Guckel, P. Klassen, V. Massmann and G. Ciarimboli

Medzinische Klinik D, University of Münster, Münster, Germany

This study characterizes the complex acute regulation of organic cation transporters (OCT) expressed in the basolateral membrane of isolated mouse proximal tubules (PT). A profound understanding of OCT transport regulation in mouse kidney is required especially as transgenic mouse models play a preeminent role in several pharmacological and physiological studies and in translational medicine and these transporters are involved in renal excretion of many drugs and organic substances used in experimental settings. The main OCT subtype in mouse PT is OCT1, and to a lesser extent (30%) OCT2, while OCT3 is only weakly expressed (1%). The fluorescent substrate ASP, 4-(-4-(dimethylamino) styryl-N-methylpyridinium, was used to quantify OCT transport across the basolateral membrane of isolated mouse proximal tubules (S2 and S3 segments) using a microtiter plate based fluorescence reader (excitation at 450 nm, emission at 590 nm). Tubules were mechanically isolated and transferred into a well of a 384 well microtiter plate. In PT (S2/S3 segments) of wildtype mice (WT) inhibition of phosphatidylinositol-3-kinase (PI3K) by wortmannin, of p56 tyrosine kinase (p56lck) by aminogenistein, stimulation of PKC by dioctanoyl glycerol and inhibition of PKA by KT5720 reduced ASP-uptake. Angiotensin II increased ASP-uptake via stimulation of Ca^{2+}/calmodulin (CaM). In PT isolated from OCT2-deficient mice, which express mostly OCT1, the regulation pattern was identical. In PT from OCT1/2 double knockout mice, expressing only OCT3, ASP uptake was grossly reduced and only the p56lck inhibition altered transport. In HEK293 cells, stably expressing OCT1, 2 or 3 identical findings were observed as in wildtype or OCT2-ko mice. In cells expressing OCT2 only inhibition of CaM activated transport while in cells expressing OCT3 again only the p56lck pathway altered transport. Analysing ASP-kinetics in PT of WT mice revealed that the PI3K, the p56lck, PKC or PKA pathways altered Vmax of the transport, suggesting a modification of transporter trafficking, while activation of CaM resulted in a decrease in Km suggesting an increase in substrate affinity.

In conclusion, acute regulation of mouse OCT in proximal tubules involves similar regulation of the main subtypes OCT1 and OCT2 by various pathways, while the OCT3, which shows only very low expression, is only regulated by p56lck. These effects mostly involve transporter trafficking and only in the case of CaM a modification of substrate affinity. This is the first report unveiling the complex pattern of short-term regulation of OC-transport in freshly isolated mouse PTs.

Supported by German Research Councel CI 107/4-2 and IZKF, University Münster, Cia2/013/13

Where applicable, the authors confirm that the experiments described here conform with The Physiological Society ethical requirements.

PCB179

Adenosine regulates Cl^- channels in human adenocarcinoma cell monolayer

M. Hayashi[1], A. Inagaki[2] and H. Matsuda[1]

[1]Department of Physiology, Kansai Medical University, Hirakata, Japan and [2]Department of Physiology, University of Tokushima, Tokushima, Japan

Introduction: Pancreatic acini secrete ATP and nucleotide-modifying enzymes that include CD39 and CD73. Adenosine, the end product of ATP, elicited Cl^- efflux in pancreatic duct cells that express adenosine receptors (Novak *et al.* 2008). However, effect of adenosine receptors on anion secretion has not been extensively investigated. **Objectives:** The present study aimed to determine whether adenosine receptors regulate anion channels in pancreatic duct cells. **Methods:** Pancreas was obtained from male Wistar rats. Protocols involving handling of animals were approved by the Animal Experimentation Committee, Kansai Medical University. Animals were killed by cervical dislocation. The molecular basis of adenosine receptors was revealed by RT-PCR analysis and immunostaining. We measured equivalent short-circuit current (I_{sc}) in human adenocarcinoma cell line (Capan-1) monolayer. Statistical significance was evaluated using ANOVA. **Results:** Pancreas expressed adenosine A_{2A} receptor (*Adora2a*), confirming findings in previous study. Adenosine A_{2A} receptors localized in luminal membrane of rat ducts and Capan-1 monolayer. The luminal addition of adenosine (100 μM) significantly increased I_{sc} in Capan-1 monolayer (n = 25). The effect was consistent with Cl^- secretion in epithelia. This increase was inhibited by 5-nitro-2-(3-phenylpropylamino) benzoic acid, niflumic acid, or CFTRinh-172 (n = 5). **Conclusion:** These results indicated that the adenosine A_{2A} receptors regulate both Ca^{2+}-activated Cl^- channels and cystic fibrosis transmembrane conductance regulator in Capan-1 cells. Furthermore, the adenosine A_{2A} receptors may be involved in anion transport in pancreatic ducts.

Novak I *et al.* (2008). *Pflügers Arch* **456,** 437–447.

This work was supported by Pancreas Research Foundation of Japan and by JSPS KAKENHI Grant Number 24790226.

Where applicable, the authors confirm that the experiments described here conform with The Physiological Society ethical requirements.

PCB180

Changes in Na+ metabolism and their effects on nutrient absorption in claudin 15 knockout mice

H. Hayashi, Y. Komatsu, M. Watanabe and Y. Suzuki

University of Shizuoka, Shizuoka, Japan

It is known that the claudin family of tight junction proteins is critical in determining paracellular ionic permeability and selectivity. We have shown that loss of claudin 15 results in decreased luminal Na+ concentration and glucose malabsorption in the small intestine. To gain further insight into the relationship between intestinal Na+ metabolism and changes in nutrient absorption induced by the loss of claudin 15, we investigated the site of absorption of electrolytes and nutrients in claudin 15 knockout (cldn15KO) mice and compared this with wild-type mice under in vivo conditions. Mice were fed a powdered diet supplemented with 14C-polyethylene glycol (PEG) 4000 as a non-absorbable marker and 3H-Gly-Sar (non-hydrolyzable dipeptide) or glucose. Three hours after feeding, the small intestine was isolated and divided into six segments, the luminal contents collected for analysis of Na+, K+, and Cl- concentrations and the level of 14C-PEG4000. Na+, K+, and Cl- concentrations were determined using ion-selective electrodes. Glucose concentration was determined by colorimetry. Gastric emptying time, assessed by measuring 14C-PEG4000, was decreased in cldn15KO compared to wild-type mice. Total luminal contents in the small intestine were increased in cldn15KO mice and the retention time of digesta in the upper jejunum was increased approximately 3-fold compared with wild-type mice. Robust Na+ secretion and rate of absorption were observed in the upper jejunum in wild-type mice and this was attenuated in cldn15KO mice. The rate of K+ absorption was increased in cldn15KO mice in the lower ileum. Total luminal glucose and Gly-Sar were increased, while absorption rates of glucose and Gly-Sar were decreased, in the upper jejunum of cldn15KO mice. These results suggest that the sites of absorption and secretion of electrolytes and nutrients are changed by adaptation to the loss of claudin 15.

Where applicable, the authors confirm that the experiments described here conform with The Physiological Society ethical requirements.

PCB181

Erythrocyte Na+-K+ ATPase activity in normotensive underweight, overweight and obese women

A.O. Soladoye, O.E. Ayoola and L.A. Olatunji

Cardiovascular and Membrane Physiology Unit, Department of Physiology, University of Ilorin, Ilorin, Nigeria

Altered activity of transmembrane cation transport has been linked to non-communicable diseases (NCDs) related to obesity. The present study therefore sought to determine the activity of Na+-K+-ATPase in erythrocytes of underweight, normal weight, overweight and obese women. A total of 36 normotensive non-smoker Nigerian women categorized as underweight, normal weight, overweight and obese were enrolled to participate in the study. Membranes of their erythrocytes were harvested and processed for Na+-K+ ATPase activity. Written consent was obtained from the participants for the study. The result showed that Na+-K+ ATPase activity of underweight as well as those of the overweight and obese women were significantly reduced when compared with that of the normal weight women. Impairment of the activity of Na+-K+ ATPase in obese women was significantly greater than those observed in overweight and underweight individuals. Multivariate regression analysis indicated that age is the strongest independent determinant of the activity of Na+-K+ ATPase in underweight women. However, body weight was indicated as the strongest independent determinant of the activity of Na+-K+ ATPase in overweight and obese women. The findings in the present study demonstrate that overweight and obesity as well as underweight are associated with impaired erythrocyte Na+-K+ ATPase activity in women. Furthermore, advanced age may seem to explain the reduced activity of the erythrocyte Na+-K+ ATPase activity in underweight while increase body weight may explain the activity in overweight and obese women.

Where applicable, the authors confirm that the experiments described here conform with The Physiological Society ethical requirements.

PCB182

Mathematical modeling of bicarbonate versus carbonate transport by the electrogenic Na^+/HCO_3^- cotransporter

R. Occhipinti, S. Lee and W.F. Boron

Physiology and Biophysics, Case Western Reserve University, Cleveland, OH, USA

The electrogenic Na^+/HCO_3 cotransporter (NBCe1) regulates acid/base movements in many epithelia (e.g., renal proximal tubule, pancreatic duct) and regulates intracellular pH in numerous cell types (e.g. neurons, glia). In glia, NBCe1 plays an important role during neuronal activity. As neurons fire action potentials, they release K^+ into the extracellular microenvironment, depolarizing glia and causing NBCe1 to import HCO_3^-, thus acidifying the extracellular microenvironment. In 1994, Grichtchenko and Chesler observed that this depolarization-induced extracellular acidification is accentuated by inhibition of extracellular carbonic anhydrase (CA), and suggested that NBCe1 carries one carbonate (CO_3^{2-}) rather than two HCO_3^-. The theory that NBCe1 transports CO_3^{2-} is supported by the results of experiments performed by Lee and Boron in our own laboratory in which acetazolamide (ACZ), a CA blocker, accentuates surface pH (pH_S) changes in oocytes co-expressing NBCe1 and CAIV.
Here we use a three-dimensional mathematical model of a *Xenopus* oocyte to investigate the consequences on pH_S of the influx of two bicarbonate ions (HCO_3^- model) versus the influx of one carbonate ion (CO_3^{2-} model) when CAIV is active or not. The CO_3^{2-} model predicts a change in pH_S that is markedly enhanced by ACZ, in agreement with the experimental data. Thus, we conclude that NBCe1 cannot be a pure bicarbonate transporter. We performed additional simulations in which we implemented simultaneous transmembrane fluxes of carbonate and bicarbonate, with different carbonate/bicarbonate molar ratios but assuming the same total net flux. These simulations lead us to conclude that carbonate is the dominant substrate of NBCe1.

Where applicable, the authors confirm that the experiments described here conform with The Physiological Society ethical requirements.

PCB183

Expression of human heteromeric amino acid transporters in the yeast Pichia pastoris

A. Rosell[1,3], M. Costa-Torres[1,3], E. Álvarez-Marimon[1,3], A. Zorzano[1,3], D. Fotiadis[2,4] and M. Palacín[1,3]

[1]Institute for Research in Biomedicine, Barcelona, Spain, [2]Institute of Biochemistry and Molecular Medicine, Bern, Switzerland, [3]University of Barcelona, Barcelona, Spain and [4]University of Bern, Bern, Switzerland

Human heteromeric amino acid transporters (HATs) play key roles in renal and intestinal re-absorption, cell redox balance and tumor growth. These transporters are composed of a heavy and a light subunit, which are connected by a disulphide bridge. Heavy subunits are the two type II membrane N-glycoproteins rBAT and 4F2hc, while L-type amino acid transporters (LATs) are the light and catalytic subunits of HATs. We tested the expression of human 4F2hc and rBAT as well as seven light subunits in the methylotrophic yeast Pichia pastoris. 4F2hc and the light subunit LAT2 showed the highest expression levels and yields after detergent solubilization. Co-transformation of both subunits in Pichia cells resulted in overexpression of the disulphide bridge-linked 4F2hc/LAT2 heterodimer. Two sequential affinity chromatography steps were applied to purify detergent-solubilized heterodimers yielding ~1 milligram of HAT from 2 liters of cell culture. Our results indicate that Pichia pastoris is a convenient system for the expression and purification of human 4F2hc/LAT2 for structural studies.

Where applicable, the authors confirm that the experiments described here conform with The Physiological Society ethical requirements.

PCB185

Carbonic anhydrase II enhances transport activity of monocarboxylate transporters via direct interaction

H.M. Becker[1], H. Heidtmann[1,2], S. Noor[1], S. Dietz[1], M.H. Stridh[2], M. Klier[2], C.D. Boone[3], R. McKenna[3] and J.W. Deitmer[2]

[1]Division of Zoology / Membrane Transport, Department of Biology, University of Kaiserslautern, Kaiserslautern, Germany, [2]Division of General Zoology, Department of Biology, University of Kaiserslautern, Kaiserslautern, Germany and [3]Department of Biochemistry and Molecular Biology, University of Florida, Gainesville, FL, USA

The proton-linked monocarboxylate transporters MCT1-4 play a crucial role in the shuttling of lactate between glycolytic and oxidative cell types in different tissues like muscle and brain. Using heterologous protein expression in *Xenopus* oocytes, we have recently reported that carbonic anhydrase isoform II (CAII), a ubiquitous enzyme catalyzing the equilibration of carbon dioxide, protons and bicarbonate enhances transport activity of MCT1 and MCT4, while leaving transport activity of MCT2 unaffected. This interaction is independent of CAII catalytic activity, but is mediated by an intramolecular H^+-shuttle within the enzyme (1-4). In a further study we could demonstrate that endogenous CAII co-localizes with MCT1 in mouse astrocytes in which it enhances lactate flux by a non-catalytic mechanism (5).
Comparison of the protein sequence of MCT1, 2 and 4 revealed potential binding sites for CAII in the C-terminal of MCT1 and 4, but not in MCT2. For identification of the binding sites, truncation and single site mutations were placed in the C-terminal tail of MCT1 and MCT4. The transporters were heterologously expressed in *Xenopus* oocytes with and without CAII and transport activity was determined with pH-sensitive microelectrodes. Oocytes were surgically removed under sterile conditions from *Xenopus laevis* females anaesthetized with 1 g/l of 3-amino-benzoic acid ethylester (MS-222) in their bath. The experiments revealed that the acidic amino acid clusters $E^{489}EE$ in MCT1 and $E^{431}EE$ in MCT4 are crucial for the functional interaction with CAII. Direct binding of CAII to MCT1 and MCT4, respectively, via these acidic clusters was confirmed by protein biochemical analysis. To confirm that the inability of CAII to enhance transport activity of MCT2 is due to the absence of an appropriate binding site within the transporters C-terminal, we exchanged the last seven amino acids of the MCT2 C-terminal with the corresponding amino acids of the MCT1 C-terminal (R^{483}DKESSI to P^{483}AEEESP), creating a putative CAII

binding site. Expression of the mutant in *Xenopus* oocytes showed that the insertion of this binding site indeed enabled CAII to enhance transport activity of MCT2.
Our results suggest that the modulation of MCT1/4 transport activity by CAII requires direct interaction between transporter and enzyme, which is mediated by a glutamic acid cluster within the C-terminal tail of the MCTs.

Becker HM & Deitmer JW (2008). Nonenzymatic proton handling by carbonic anhydrase II during H^+-lactate cotransport via monocarboxylate transporter 1. *J Biol Chem* 283, 21655-21667.

Becker HM, Klier M & Deitmer JW (2010). Nonenzymatic augmentation of lactate transport via monocarboxylate transporter isoform 4 by carbonic anhydrase II. *J Membr Biol* 234, 125-135.

Klier M, Schüler C, Halestrap AP, Sly WS, Deitmer JW & Becker HM (2011). Transport activity of the high-affinity monocarboxylate transporter MCT2 is enhanced by extracellular carbonic anhydrase IV but not by intracellular carbonic anhydrase II. *J Biol Chem* 286, 27781-27791.

Becker HM, Klier M, Schüler C, McKenna R & Deitmer JW (2011). Intramolecular proton shuttle supports not only catalytic but also non-catalytic function of carbonic anhydrase II. *Proc Natl Acad Sci U S A* 108, 3071-3076.

Stridh MH, Alt MD, Wittmann S, Heidtmann H, Aggarwal M, Riederer B, Seidler U, Wennemuth G, McKenna R, Deitmer JW & Becker HM (2012) Lactate flux in astrocytes is enhanced by a non-catalytic action of carbonic anhydrase II. *J Physiol* 590, 2333–51.

This work was supported by the "Research Initiative Membrane Biology" and the "Stiftung Rheinland-Pfalz für Innovation".

Where applicable, the authors confirm that the experiments described here conform with The Physiological Society ethical requirements.

PCB186

y^+LAT1 conditional KO mice as the first animal model for LPI

S. Bodoy[1], M. Espino[2], R. Artuch[3] and M. Palacín[1,4]

[1]Institute for Research in Biomedicine, Barcelona, Spain, [2]Medical and Molecular Genetics Center, IDIBELL, L'Hospitalet de Llobregat, Spain, [3]Hospital Sant Joan de Déu, Esplugues de Llobregat, Spain and [4]Universitat de Barcelona, Barcelona, Spain

Lysinuric protein intolerance (LPI, MIM 222700) is an inherited aminoaciduria caused by defective cationic amino acid (CAA) transport at the basolateral membrane of epithelial cells in kidney, and also intestine. As a consequence, intestinal absorption and renal reabsorption of CAA are impaired. LPI is caused by mutations in the SLC7A7 gene, which encodes y^+LAT1 transporter [1]. Typically, symptoms begin after weaning with refusal of feeding, vomiting, diarrhea, and consequent failure to thrive. Hepatosplenomegaly, osteoporosis, hematological anomalies, neurological involvement, including hyperammonemic coma are recurrent clinical features [2]. Major complications are immune-like disorders, such as: pulmonary alveolar proteinosis and chronic renal disease, which are increasingly observed in LPI patients [3] without a known pathogenetic mechanism. Because null Slc7a7 mice is lethal [4], we recently generated the ubiquitous and tamoxifen-inducible ablation of Slc7a7 in mouse (*Slc7a7* $^{-/-}$). LPI patients treatment, low-protein diet and citrulline supplementation [5], is needed to maintain *Slc7a7*$^{-/-}$ mice alive. Under these circumstances (8% of protein in the diet) *Slc7a7*$^{-/-}$ mice showed hyperglutaminemia and orotic acid urine excretion suggesting urea cycle dysfunction. As in humans, low arginine and ornithine plasma concentration may be at the basis of the urea cycle dysfunction of LPI mice. *Slc7a7* $^{-/-}$ mice, like LPI patients, hyperexcrete cationic (lysine, arginine and ornithine) and some neutral amino acids (*e.g.* glutamine, alanine). Renal clearance of CAA is increased and also % of tubular reabsorption of Arg, Orn, Lys and some neutral amino acids is reduced.
In summary, we have generated the first LPI animal model that allows us to study the mechanisms of pathophysiology of LPI.

Torrents D, Mykkanen J, Pineda M, Feliubadalo L, Estevez R, de Cid R, Sanjurjo P,

Zorzano A, Nunes V, Huoponen K, Reinikainen A, Simell O, Savontaus ML, Aula P,

Palacin M. Identification of SLC7A7, encoding y+LAT-1, as the lysinuric protein

intolerance gene. Nat Genet 21: 293–296, 1999.

Simell, O., The Metalolic and molecular bases of inherited diseases. 8th ed, ed. e.a.

Scriver CR. Vol. Lysinuric protein intolerance and other cationic aminoacidurias: McGraw-

Hill.

Ogier de Baulny H, Schiff M, Dionisi-Vici C.Lysinuric protein intolerance (LPI): a multi organ disease by far more complex than a classic urea cycle disorder.Mol Genet Metab. 2012 May;106(1):12-7

Sperandeo, M.P., et al., Slc7a7 disruption causes fetal growth retardation by

downregulating Igf1 in the mouse model of lysinuric protein intolerance. Am J Physiol

Cell Physiol, 2007. 293(1): p. C191-8.

Rajantie J, Simell O, Rapola J, Perheentupa J. Lysinuric protein intolerance: a twoyear

trial of dietary supplementation therapy with citrulline and lysine. J Pediatr.

1980;97:927–32

Financial support is gratefully acknowledged from the Spanish Ministry of Science and Innovation Grant SAF2009-12606-C02-0, the Generalitat de Catalunya SGR2009-1355 (M.P.), CIBERER and Fundación Ramón Areces.

Where applicable, the authors confirm that the experiments described here conform with The Physiological Society ethical requirements.

PCB187

Cesium inhibited HeLa cells proliferation

D. Kobayashi, K. Kakinouchi, K. Matsumura and A. Hazama

Fukushima Medical University, Fukushima, Japan

Cesium (Cs), as well as potassium (K), is a member of alkaline metal elements. In the study of transporter, Cs has been used as a K channel blocker on cells. Doses of CsCl by the intraperitoneal route in mice indicated that a rapid transfer of Cs from blood to tissue compartments (Pinsky and Bose, 1984). Distribution of Cs in the whole bodies had been investigated. However, it is not clear that how the Cs is transported through which kinds of way at the molecular levels, and that the effect of Cs on the cell metabolisms. We examined the proliferation of HeLa cells cultured by Dulbecco's modified Eagle medium supplemented with 10% fatal bovine serum and 10 mM of different types of alkali metals such as Li, Na, K, Rb, and Cs at 37 degree C, 5% CO2. Among them, only Cs inhibited the proliferation of the cells. The proliferation decrease is dependent on Cs concentration. Microscopic examination of the Cs-treated

cells, cell membrane was not smoothly. Two different methods of live and dead assay were performed (i.e., lactose dehydrogenase-release assay and cytometry of Calcein-propidium iodide stained cells). In the Cs concentration that showed inhibition of cell proliferation, the HeLa cell membrane was not damaged by Cs. To confirm extracellular Cs uptake into the cell, intracellular cations were analyzed by capillary electrophoresis (P/ACETM MDQ). The intracellular cation content was analyzed as magnesium-based intracellular cation ratio. The intracellular Cs was detected in Cs-treated cells but not in control cell. The intracellular pH was measured by use of the pH-sensitive dye indicator BCECF. Alkalization of intracellular pH was occurred in the cells cultured with CsCl, but not in the cells cultured with the other alkali metals. Generally, intracellular pH of tumor cells was lower than normal cells. It is considered that Cs added to extracellular media uptake into the cells, and inhibition of cell proliferation possibly due to intracellular alkalization induced by Cs administration.

Where applicable, the authors confirm that the experiments described here conform with The Physiological Society ethical requirements.

PCB188

Human pancreatic duct cells express functional gastric and non-gastric H^+/K^+ ATPases and are sensitive to proton pump inhibitors

I. Novak and J. Wang

Department of Biology, University of Copenhagen, Copenhagen, Denmark

The mechanism by which pancreatic ducts secrete high HCO_3^- has not been fully resolved. This alkaline secretion can be achieved by transporting HCO_3^- from serosa to mucosa or by moving H^+ in the opposite direction. Earlier studies have been focusing on HCO_3^- transport. In the accepted secretion model, basolateral Na^+/H^+ exchangers (NHE) and/or Na^+-HCO_3^- cotransporters (NBC) contribute to cellular HCO_3^- accumulation, while luminal Cl^-/HCO_3^- anion exchangers (AE) release HCO_3^- to lumen. Recently, we have considered the active H^+ transporters, i.e. H^+/K^+ ATPases, and found them expressed and functional in rat pancreatic ducts (1). The aim of the present study was to determine whether also human pancreatic ducts express functional H^+/K^+ ATPases. The expression of H^+/K^+ ATPases was analyzed in human pancreatic duct cell lines (CAPAN-1, CFPAC-1 and PANC-1) by RT-PCR, western blot and immunostaining. Function of H^+/K^+ ATPases was estimated by intracellular pH (pHi) measurements in CAPAN-1 cells. Values are given as mean ± S.E.M., compared by paired student t-test. Both gastric and non-gastric alpha subunits of H^+/K^+ ATPases were found in CAPAN-1, CFPAC-1 and PANC-1 cells on both mRNA and protein levels (n=3 in each series). Also gastric beta-subunit of the pump was detected in duct cell lines (n=3). Localization of H^+/K^+ ATPase subunits in CAPAN-1 monolayers was confirmed by immunohistochemistry and confocal microscopy (n>10 preparations). In order to verify the function of pumps, we used Na^+ and HCO_3^- free solutions to eliminate the contribution of NHE, NBC and AE on pHi. In ducts stimulated with secretin (1 nM), Na^+ independent pHi recovery from acidosis was reduced by 75% in the presence of gastric H^+/K^+ ATPase inhibitor omeprazole (10 μM, n=6, $p < 0.05$); SCH28080 inhibited the recovery by 52% (10 μM, n=5, $p < 0.05$). We demonstrated both types of H^+/K^+ ATPases in human pancreatic duct cell lines, and their sensitivity to H^+/K^+ ATPase inhibitors indicates their potential role in the acid-base transport in human pancreas. We propose that the evidence for expression of H^+/K^+ ATPases in pancreas calls for revision of the model for HCO_3^-/H^+ transport as well as for the use of proton pump inhibitors.

Novak I et al. (2011) J Biol Chem 286, 280-289

Funded: the Lundbeck Foundation; The Danish Council for Independent Research | Natural Sciences

Where applicable, the authors confirm that the experiments described here conform with The Physiological Society ethical requirements.

PCB189

Chimeric constructs endow human CFTR with the sub-conductance state of murine CFTR

Z. Cai[1], I. Callebaut[2], D. Lea-Smith[3], B.J. Stevenson[3], A. Doherty[3], H. Davidson[3], D.J. Porteous[3], J. Mornon[2], P. Lehn[4], A. Boyd[3] and D.N. Sheppard[1]

[1]School of Physiology and Pharmacology, University of Bristol, Bristol, UK, [2]UMR7590, CNRS, Université Pierre et Marie Curie-Paris 6, Paris, France, [3]Medical Genetics Section, Molecular Medicine Centre, Institute of Genetics and Molecular Medicine, University of Edinburgh, Edinburgh, UK and [4]INSERM U1078, Université de Bretagne Occidentale, Brest, France

Cystic fibrosis transmembrane conductance regulator (CFTR) is an anion channel with complex regulation. To explore CFTR structure and function, we exploited functional differences between human and murine CFTR. When compared with human CFTR, murine CFTR has a reduced single-channel conductance (human, 8.29 ± 0.18 pS; murine, 5.76 ± 0.16 pS; [1]) and a distinct pattern of channel gating, characterised by prolonged residence in a sub-conductance state [2]; transitions to sub-conductance states are rare for human CFTR. In previous work, we demonstrated that transfer of both NBDs of murine CFTR endowed human CFTR with dramatically prolonged channel openings similar to those of the sub-conductance state of murine CFTR [3]. However, transfer of both NBDs failed to endow human CFTR with a sub-conductance state like that of murine CFTR [3]. To investigate whether the membrane-spanning domains (MSDs) define the sub-conductance state of murine CFTR, we constructed the human-murine CFTR (hmCFTR) chimeras hmTM1-6, hmTM7-12 and hmTM1-6:TM7-12 containing MSD1, MSD2 and MSD1+2 of murine CFTR and studied their single-channel behaviour in excised inside-out membrane patches. All hmCFTR chimeras exhibited a hybrid gating pattern intermediate between that of human and murine CFTR. Reminiscent of murine CFTR, channel openings were very flickery with open probability decreasing in the rank order: human CFTR > hmTM7-12 > hmTM1-6 > hmTM1-6:TM7-12. The single-channel current amplitude of the full open state of hmCFTR chimeras was smaller than that of human CFTR, decreasing in the rank order: human CFTR > hmTM7-12 > hmTM1-6 ≥ hmTM1-6:TM7-12. Like human CFTR, hmTM7-12 opened predominantly to the full open state; transitions to sub-conductance states were unusual. However, hmTM1-6 resided in multiple sub-conductance states, which were visualised in heavily filtered single-channel recordings and current amplitude histograms. Of note, like murine CFTR, hmTM1-6:TM7-12 resided in a tiny sub-conductance state and only sojourned infrequently to the full open-state. Consistent with hmTM1-6:TM7-12 possessing human NBDs, this construct resided in the sub-conductance state for much shorter periods than murine CFTR. Taken together, our data suggest that amino acid sequences from both MSDs specify the sub-con-

ductance state of murine CFTR and determine intraburst gating.

Lansdell KA, Delaney SJ, Lunn DP, Thomson SA, Sheppard DN, Wainwright BJ. J Physiol. 1998; 508:379-92.

Lansdell KA, Kidd JF, Delaney SJ, Wainwright BJ, Sheppard DN. J Physiol. 1998; 512:751-64.

Scott-Ward TS, Cai Z, Dawson ES, Doherty A, Da Paula AC, Davidson H, Porteous DJ, Wainwright BJ, Amaral MD, Sheppard DN, Boyd AC. Proc Natl Acad Sci U S A. 2007;104:16365-70.

Supported by the BBSRC, CF Trust and Vaincre La Mucoviscidose.

Where applicable, the authors confirm that the experiments described here conform with The Physiological Society ethical requirements.

PCB190

Impact of urate on prostate cancer development

E. Rodrigues and A. Bahn

Department of Physiology, University of Otago, School of Medical Sciences, Dunedin, New Zealand

Prostate cancer is among the four most diagnosed cancers worldwide and it is the most common cause of death in men above the age of 60 in New Zealand. Zinc levels play an important role in normal prostate cells and possibly prostate cancer development due to the fact that the metabolism of prostate glands is mainly based on zinc. It also is a co-factor for many proteins, of which the most prominent one is transcription factor p53. Zinc therefore has an important role in other cell processes. Recently, studies have indicated that patients diagnosed with prostate cancer have elevated levels of urate. This study is attempting to understand the implications of these elevated urate levels on prostate cancer development and to identify the urate transporter involved in these processes. Based on our gene array analysis we examined the regulation of two zinc transporters by urate, namely ZIP1 and ZIP3, in the normal prostate cell line PNT1A and in three prostate cancer cell lines LNCaP, DU145 and PC-3. ZIP1 mRNA and protein expression increased in PNT1A and PC-3 cells upon urate treatment, while they decreased in LNCaP cells and didn't change in DU145 cells. ZIP3 mRNA and protein expression was elevated in PNT1A cells in the presence of 500 μM of urate, but only protein levels were significantly reduced in DU145 and PC-3 cells. Similar to ZIP1 mRNA levels of ZIP3 were down-regulated in LNCaP cells after urate treatment. These results indicate that hyperuricemia has a significant impact on ZIP1 and ZIP3 expression in different stages of prostate cancer and especially in the non-aggressive stages, suggesting that urate may be involved in initial stages of cancer development. Using array analysis and real-time PCR, we were able to delineate the impact of urate on several miRNAs, especially miR-34a, which we have identified as a possible regulator for ZIP3. Exposure to high urate concentrations has significantly down-regulated miR-34a in all prostate cancer cell lines indicating that regulation of miR-34a may be the key mechanism to induce the transition from a normal prostate epithelial cell to a malignant proliferating and metastasising cell. We have identified other miRNAs such as miR-21, miR-106, miR-125 and miR-331, which are vital for the cell cycle and which are up-regulated by high urate plasma levels as well as miR-126 that is down-regulated by hyperuricemic conditions. Two of these, miR-21 and miR-126, are putative regulators of drug and zinc transporters. Further analysis of transporters facilitating the urate effect on prostate cancer cells identified GLUT9, which is known as the major renal urate transporter, as the main candidate. Investigations on primary prostate epithelial cells are underway to prove that high plasma urate levels contribute to the development of prostate cancer by regulating the p53/miR-34a pathway as well as zinc homeostasis, which are or are becoming the hallmarks of cancer.

Where applicable, the authors confirm that the experiments described here conform with The Physiological Society ethical requirements.

PCB191

Investigation of UT-B urea transporter isoforms in the human Ileum

C. Walpole[1], S. Edwards[1], D. Winter[2], A. Baird[3] and G. Stewart[1]

[1]School of Biology and Environmental Science, University College Dublin, Dublin, Ireland, [2]Institute for Clinical Outcomes Research and Education, St. Vincent's University Hospital, Dublin, Ireland and [3]Conway Institute of Biomedical and Biomolecular Science, University College Dublin, Dublin, Ireland

The entry of urea into the lumen of the gastrointestinal tract is facilitated by the urea transporter protein UT-B1. This stage is crucial to our intestinal wellbeing as it is the first step in the urea nitrogen salvaging mechanism which is necessary for healthy gut bacteria. In a previous study a 35kDa glycosylated signal of UT-B1 was strongly expressed in the ascending colon whereas it was almost absent in the descending colon. Our aim was to investigate the expression of UT-B in the whole gastrointestinal tract.

To investigate whether there are multiple UT-B isoforms in the GI tract, a number of primer sets were designed from the human UT-B gene. UT-B1 has been identified as the major, if not sole UT-B urea transporter at the RNA level. Using an antibody raised against bovine UT-B1 we found that the small intestine had the strongest 35kDa signal. Surprisingly the ileum had the highest percentage glycosylation, which deglycosylated to 30kDa as expected. There was a significant decrease in the amount of glycosylated UT-B1 from the ileum to the left colon. This may show importance of UT-B further up the GI tract than previously thought.

In the rat we found that UT-B was solely expressed in the large intestine. According to our results, unlike the rat, UT-B1 is expressed throughout the human GI tract. It is highly glycosylated in the ileum, which suggests it is functionally active here. Further investigation is needed to establish the physiological significance of these findings.

Collins et al. (2010). Am J Physiol Gastro 298: G345 – G351

Collins et al. (2011). J Membr Biol 239(3): 123-30

This research was funded by grant 092524/Z/10/2 from the Wellcome Trust and 11/RFP.1/BMT/3088 from the Science Foundation of Ireland. Human tissue samples were obtained at surgical resection for carcinoma, performed at St.Vincent's University Hospital with

Institutional Review Board approval and informed patient consent

Where applicable, the authors confirm that the experiments described here conform with The Physiological Society ethical requirements.

PCB192

F508del and A561E: cystic fibrosis mutations that disrupt the trafficking, thermostability and gating of CFTR have differential sensitivity to small-molecule CFTR modulators

Y. Wang, J. Liu, C.V. Gorard, J.N. Povey, D.N. Sheppard and H. Li

Physiology & Pharmacology, University of Bristol, Bristol, UK

Cystic fibrosis (CF) is caused by mutations in the cystic fibrosis transmembrane conductance regulator (CFTR) Cl^- channel. In search of transformational drug therapies for CF patients, small-molecules have been identified that target defects in the expression and function of the commonest CF mutation F508del. However, relatively little is known about the mechanism of dysfunction of other CF mutations and their responses to small-molecules. Here, we investigate A561E, the second most common CF mutation in Portugal. CF patients homozygous for A561E have a clinical phenotype similar to that of F508del homozygotes (1, 2). Like F508del-CFTR, A561E-CFTR is a temperature-sensitive folding defect located in the first nucleotide-binding domain (1). To learn whether A561E perturbs CFTR thermostability and function, we investigated the single-channel activity of A561E-CFTR in excised membrane patches from BHK cells at 37 °C following rescue of its cell surface expression by low temperature incubation. Wild-type CFTR had robust channel activity that was stable over time. By contrast, A561E-CFTR exhibited paltry channel activity characterised by brief openings separated by prolonged closures that deactivated rapidly at 37 °C; like F508del-CFTR, A561E-CFTR rundown was complete within 8 minutes and irreversible. To learn whether small-molecules restore expression and function to A561E-CFTR, we studied the CFTR corrector VX-809 and the CFTR potentiators genistein, P2, P3, P4, P5 and P9 (all from Cystic Fibrosis Foundation Therapeutics (CFFT) except VX-809 (Selleck) and genistein (LC Laboratories)) using the iodide efflux technique. Incubation of BHK cells with VX-809 (3 μM) for 24-48 h at 37 °C restored some cell surface expression to F508del-CFTR, but little or none to A561E-CFTR. However, following low temperature incubation, all CFTR potentiators (genistein (50 μM), test potentiators (10 μM)) restored partial function to A561E- and F508del-CFTR. For wild-type CFTR, the rank order of potentiation was genistein ≥ P2 ≥ P9 ≥ P5 ≥ P4 > P3; for F508del-CFTR, it was genistein >> P2 ≥ P5 ≥ P4 ≥ P3 ≥ P9 and for A561E-CFTR, it was genistein > P4 > P9 ≥ P2 > P5 ≥ P3. We conclude that A561E perturbs CFTR thermostability and gating. Thus, the consequences of the A561E mutation are similar to those of F508del, despite the different impacts of the mutations on CFTR structure (3, 4). We further conclude that CFTR potentiators restore, albeit incompletely, function to A561E-CFTR, whereas the corrector tested had little or no effect. Therefore, transformational drug therapy for F508del- and A561E-CFTR will likely require different combinations of CFTR correctors and potentiators.

Mendes F et al. Biochem Biophys Res Commun. 2003; 311:665-71

Hirtz S et al. Gastroenterology. 2004; 127:1085-95

Mornon JP et al. Cell Mol Life Sci. 2008; 65:2594-612.

Roxo-Rosa M et al. Proc Natl Acad Sci U S A. 2006; 103:17891-6.

Supported by the CF Trust. We thank MD Amaral and CFFT for cells and small-molecules, respectively.

Where applicable, the authors confirm that the experiments described here conform with The Physiological Society ethical requirements.

PCB193

Na,K-ATPase studies in Mel-290 uveal melanoma cells that display unusual sodium and potassium concentrations

N. Delamere, E. de Turco and M. Shahidullah

Department of Physiology, University of Arizona, Tucson, AZ, USA

Among tumors of the eye, uveal melanoma is the most common. When metastases occur, mortality approaches 90 %. In studies on a particular uveal melanoma cell line, Mel-290, we discovered what appear to be abnormal steady state cellular levels of sodium and potassium. Measured by atomic absorption spectrometry, the ratio of sodium concentration to potassium concentration in Mel-290 cells was 0.57 compared to 0.1 in a different melanoma cell, OCM-3, and 0.15 in pig ciliary epithelium. Assuming the sum of Na + K concentration totals ~140 mM, Mel-290 cells have resting sodium concentration of approx. 50 mM which is considerably higher than the concentration expected in normal cells. Western blot studies were conducted to examine the Na,K-ATPase alpha 1 which is the most common isoform of Na,K-ATPase in human cells. Mel-290 displayed a lower abundance of Na,K-ATPase alpha 1 subunit protein compared to OCM-3. Differences in Na,K-ATPase alpha subunit phosphorylation also were observed. In contrast to Na,K-ATPase alpha 1, H/K-ATPase beta subunit and H-ATPase (v-ATPase) beta subunit were found by Western blot to be higher in Mel-290 compared to OCM-3. A high sodium:potassium ratio was detected in two other melanoma cell types, suggesting the possible existence of a high sodium sub-group of melanomas. More studies are required to determine whether the high-sodium phenotype is linked to a particular pattern of ATPase expression or regulation. It is noteworthy that high cytoplasmic sodium has been reported in certain liver, breast and brain tumors.

Where applicable, the authors confirm that the experiments described here conform with The Physiological Society ethical requirements.

PCB194

Extracellular cysteine residues form a disulphide bridge in the amino acid transporter PAT2 (slc36a2)

N. Edwards and D.T. Thwaites

Institute for Cell & Molecular Biosciences, Newcastle University, Newcastle upon Tyne, UK

The proton-coupled amino acid transporters PAT1 (slc36a1) and PAT2 (slc36a2) are members of the SLC36 family of mammalian solute carriers (Thwaites & Anderson, 2011). PAT1 is expressed at the brush-border membrane of the small intestine whereas PAT2 is found at the luminal surface of the proximal convoluted tubule (Anderson *et al*. 2004, Bröer *et al*. 2008). Although both carriers transport a broad range of dipolar amino acids and derivatives, there are clear differences in substrate selectivity and affinity suggesting differences in substrate recognition and translocation. Using an *in silico* modelling approach, a high degree of structural homology (>97%) for PAT2 was detected against crystal structures for a number of apparently unrelated prokaryotic transporters. Homology modelling against the LeuT template (Yamashita *et al*. 2005) identified that the cysteine residues in PAT2 in extracellular loops 2 (C185) and 4 (C334) are likely in close spatial proximity. These cysteine residues are conserved in human, rat and mouse PAT1 and PAT2. In human PAT1, these residues form a disulphide bond that is essential for function (Dorn *et al*. 2009). The purpose of this investigation was to determine whether a similar disulphide bond was found in PAT2 and what role it might play in transporter function. Site-directed mutagenesis of rat PAT2 was performed and [^{3}H]amino acid uptake measured in *Xenopus laevis* oocytes in the presence or absence of the reducing agent DTT. The results were compared with those in mouse PAT1 and the *D. melanogaster* ortholog CG1139 (which does not possess cysteine residues at equivalent positions). [^{3}H]Proline uptake (mean ± SEM, n=17-20) in the presence of 30mM DTT showed a 90% reduction in PAT1 (3.42±0.34 pmol.oocyte^{-1} to 0.37±0.06 pmol.oocyte^{-1}), 50% reduction in PAT2 (4.67±0.41pmol.oocyte^{-1} to 2.37±0.25 pmol.oocyte^{-1}) but no change in CG1139 (8.42±0.99 pmol.oocyte^{-1} and 8.09±1.11 pmol.oocyte^{-1}). In PAT1, replacement of either C179 or C328 with serine or alanine reduced amino acid uptake by 70-80% whereas only a 55-60% reduction was observed in the equivalent PAT2 C185 and C334 mutants. Confocal microscopy revealed no apparent differences in membrane localisation. The double PAT1 mutant C179A/C328A was inactive whereas the double PAT2 mutant C185A/C334A retained ~50% activity. The PAT2 double mutant was insensitive to 30mM DTT. These observations demonstrate that conserved extracellular cysteine residues in PAT1 and PAT2 form disulphide bonds that appear to be essential for PAT1 and important in PAT2 for optimal function. The role of the disulphide bridge is not known but is likely important in optimisation of substrate binding and translocation. The relative dependence of PAT1 and PAT2 on the disulphide bond may partly account for differences observed in transporter function.

Anderson CMH *et al*. (2004) Gastroenterology 127, 1410-1422

Bröer S *et al*. (2008) J Clin Invest 118, 3881-3892

Dorn M *et al*. (2009) J Biol Chem 284, 22123-22132

Thwaites DT & Anderson CMH (2011) Br J Pharmacol 164, 1802-1816

Yamashita A *et al*. (2005) Nature 437, 215-223

NE was supported by a BBSRC postgraduate studentship.

Where applicable, the authors confirm that the experiments described here conform with The Physiological Society ethical requirements.

PCB195

Plasmonic gold nanoparticles as a possible potassium channel opener in vascular smooth muscle cells

A. Soloviev[1], I. Ivanova[1], T. Novokhatska[1], S. Zelensky[1], A. Raevska[2], A. Stroyuk[2], V. Ephanov[2] and I. Parneta[2]

[1]Institute of Pharmacology and Toxicology, Kiev, Ukraine and [2]NanoMedTech LLC, Kiev, Ukraine

Potent perspectives of noble nanoparticles (NPs) for biomedical applications are well known but fundamental studies of their molecular interaction with target cell remain largely unexplored. Potassium channels play an important role in the membrane potential regulation in vascular smooth muscle (SM) cells and closely involved in vascular tone regulation. Voltage-gated ionic channels are expected to be modulated by plasmon resonance occurred on surface of gold nanoparticles (AuNPs) leading to alterations in their functionality but the amplitude and directionality of this effect need to be investigated.

Colloidal AuNPs, having plasmon resonance of 525 nm, were synthesized by modified Turkevich method (2006) via reduc-

tion of sodium tetrachloroaurate by sodium ascorbate in aqueous solutions at room temperature. A dynamic light scattering study showed that AuNPs have average hydrodynamic size ~ of 5 nm core size and Zeta-potential of - 35 mV. Experimental design of the study comprised SM contractile recording combined with simultaneous fluorescent intracellular calcium concentration ([Ca2+]i) measurement in isolated rat aortic rings and ionic currents measuring in enzymatically isolated from rat aorta a single cells using patch clamp technique in whole-cell modification.

When externally applied to the organ bath solution, AuNPs (10-6–10-4 M) decreased amplitude of norepinephrine-induced contractions in dose-dependent and endothelium-dependent manner but endothelium disruption did not abolished AuNPs-induced relaxation completely. AuNPs relaxed SM in the absence of decrease in [Ca2+]i. while [Ca2+]i in endothelial cells had increased. All cells demonstrated clearly expressed tail currents suggesting that the currents measured were mainly due to activation of outward potassium channels. Being added to the bath solution in doses close to EC50, AuNPs significantly increased whole cell peak K+ current density (IK) at + 70 mV from 33± 2pA/pF to 57±5 pA/pF (n=14, P < 0.05). Outward current oscillation associated probably with a MaxiK+ channels opening and correlated with [Ca2+]i were seen under AuNPs treatment. When irradiated by 5 mW/532 nm green laser to facilitate plasmon resonance, AuNPs significantly increased both the amplitude of maximal AuNPs-induced relaxation from 46.4±4.7% to 61.3±5.3% (n=10, P<0.05) and sensitivity of SM to AuNPs. Mean value of pD2 were 4.5±0.002 and 4.4±0.04, respectively (n=10, P<0.05). External irradiation increased AuNps-induced increment in IK from 57±5 pA/pF to 98±6 pA/pF (n=10, P < 0.05).

In summary, plasmonic AuNPs are able to open K+- channels and relax SM in both endothelium-dependent and independent manner. One plausible explanation for AuNPs action is the interaction of the channel voltage sensors with local electric field on AuNPs surface. In case of laser irradiation this local electrical field enhanced due to local plasmon resonance which, in turn, increases IK and SM relaxation. In the absence of external irradiation such plasmon may be excited by natural tissue chemoluminescence in the presence of nonlinear effects on AuNPs surface. Of course, further research of AuNPs toxicity and functionality are necessary to create a safe and effective tool for pharmacological intervention which would be able to modulate IK but the data obtained clearly indicate that AuNPs possess the ability to initiate or facilitate K+ channel opening in vascular SM.

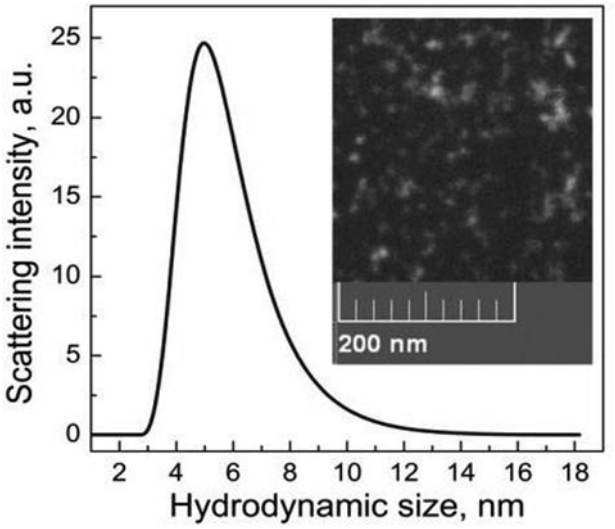

Distribution of colloidal ascorbate-stabilized gold nanocrystals by the hydrodynamic size. Inset: a fragment of SEM microphotograph of Au nanoparticles

Where applicable, the authors confirm that the experiments described here conform with The Physiological Society ethical requirements.

PCB196

Time-resolved spectroscopy and imaging of mitochondrial metabolic state in living cells

J. Horilova[1,2], D. Chorvat[1], A. Mateasik[1] and A. Chorvatova[1]

[1]International Laser Centre, Bratislava, Slovakia and [2]Faculty of Science, Pavol Jozef Safarik University, Kosice, Slovakia

Monitoring processes underlying mitochondrial homeostasis is crucial for understanding of the cell energetics. Nevertheless, we still lack appropriate non-invasive methods capable to evaluate these processes directly in living systems. In the last decades, time-resolved spectroscopy of endogenous fluorescence has been shown a perspective approach for non-invasive investigation of metabolic changes. Combination of time-resolved fluorescence measurement and imaging, known as Fluorescence Lifetime Imaging (FLIM), provides a deeper insight into natural mitochondrial metabolism and has thus been proven as an advanced diagnostic and imaging tool. We studied cell autofluorescence, derived from endogenous fluorophores present in living cells naturally, without need of fluorescent dyes or probes. To evaluate fluorescence lifetimes in combination with fluorescence spectra and/or images, we have applied Time-correlated Single Photon Counting (TCSPC), after excitation with pulsed picosecond lasers. We focused at fluorescence derived from NAD(P)H (excitation 375nm) and flavins (excitation 450-477nm) to characterize changes in the mitochondrial metabolic state in living cells. Activators and inhibitors of the respiratory chain were applied to quantify recorded metabolic changes. Different cell types were compared, ranging from cardiac cells to cancer cell lines. Separation of individual components from complex fluorescence signals is crucial for correct analysis of measured data. Spectral characteristics, unique for each fluorophore, are one way of fluorophore identification in complex biological samples. However, spectra of endogenous fluorophores are often overlapping, which is complicating data analysis. Time-resolved fluorescence decay patterns are additional effective means of

separation of distinct fluorophores. We demonstrate application of advanced analytical approaches for the the extraction of individual fluorescence components from the recorded time-resolved spectroscopy datasets, including the spectral linear unmixing, principal component analysis and blind source separation. Presented study of the time-resolved spectroscopy and imaging of mitochondrial metabolic state in living cells has great potential to improve several biomedical applications, including early diagnostics and treatment of complex diseases, which are often linked with modifications in cellular energetics.

Authors acknowledge support from LASERLAB-EUROPE III (grant agreement n°284464), VEGA No 1/0296/11, VEGA No 2/0094/12 and APVV-0242-11.

Authors acknowledge support from Integrated Initiative of European Laser Infrastructures LASERLAB-EUROPE III (grant agreement n°284464, EC's Seventh Framework Programme) and the Research grant agency of the Ministry of Education, Science, Research and Sport of the Slovak Republic VEGA No 1/0296/11, VEGA No 2/0094/12 and APVV-0242-11.

Where applicable, the authors confirm that the experiments described here conform with The Physiological Society ethical requirements.

PCB197

Hepatoprotective role of ashwagandha (withania somnifera) root extract against gentamicin induced liver damage in rats

N. Sultana

Physiology, Sir Salimullah Medical College, Dhaka, Dhaka, Bangladesh

Liver damage can be occurred due to prolong use of some drugs, exposure to some chemicals or infectious agents1. But liver protective drugs are not available. Many hepatoprotective herbal medicines are often used in the treatment of liver damage. Ashwagandha belongs to the family of solanaceae, is the traditional ayurvedic medicine2, has free radical scavenging activity3 and can be used for the prevention of liver damage4. So, the study was undertaken to observe the hepatoprotective role of ashwagandha root extract against gentamicin induced liver damage in rats. This study was conducted from January to December' 2011 in the Department of Physiology, Sir Salimullah Medical College (SSMC), Mitford, Dhaka, Bangladesh. Total 35 apparently healthy Wistar albino male rats, weighing between 150 to 200 grams, age from 90 to 120 days were used. The animals were purchased from animal house of Bangladesh Council of Scientific and Industrial Research (BCSIR), Dhaka. Ethical permission was taken from the Institutional Ethics Committee (IEC) of SSMC, Mitford, Dhaka and also from the Bangladesh Society of Physiologists (BSP). Prior conducting the study, the animals were acclimatized for 14 days at 23±2degree centigrade room temperature under 12 hour dark- light cycle. During this period, they had free access to food and water ad libitum. After 14 days of acclimatization, body weights were measured, again final body weights of rats before anaesthetized on 23rd day were taken. The rats were divided into control (Group A) and experimental (Group B) groups. Control group was again subdivided into baseline control, (Group A1, consisted of 10 rats) and gentamicin treated control group (Group A2, consisted of 10 rats). Again, experimental group (gentamicin treated group after ashwagandha treatment) consisted of 15 rats. All groups of animals received basal diet for 22 consecutive days. In addition to this, gentamicin treated control group also received gentamicin subcutaneously (100mg/kg body weight/day) for the last eight days. Again, experimental group received ashwagandha root extract (500mg/kg body weight/day, orally) for 22 consecutive days and gentamicin subcutaneously (100mg/kg body weight /day) for last eight days. Then all animals were anaesthetized with the help of chloroform and sacrificed on 23rd day. Their blood samples were collected and liver was removed and was washed in ice cold saline. Then it was wiped in tissue paper, weighed by electric balance analyzer. Blood was centrifuged at the rate of 4000 rpm for 5 minutes and supernatant serum was collected. Out of 35 serum samples, four were hemolyzed. So, 31 samples were estimated. Liver function was assessed by estimating serum levels of aspartate amino transferase (AST), alanine amino transferase (ALT) and bilirubin. However, histological findings of liver tissue were observed under microscope to assess their changes. Values were expressed as mean+SD. Statistical analysis were done by one way ANOVA and Bonferroni test as applicable. Mean serum levels of AST and ALT were significantly higher in gentamicin treated control (90.89+4.53 and 99.11+ 5.26 IU/L respectively, $p<0.001$) and gentamicin treated group after ashwagandha treatment (50.62+2.14 and 54.69+2.93 IU/L respectively, $p<0.05$) in comparison to those of baseline control group (47.33+3.74 and 50.11+2.47 IU/L respectively). Again, these levels of gentamicin treated group after ashwagandha treatment (50.62+2.14 and 54.69+2.93 IU/L respectively) were significantly ($p<0.001$) lower than those of gentamicin treated control group. Serum level of bilirubin was significantly higher in gentamicin treated control group (2.40+1.03 mg/dl, $p<0.001$) and gentamicin treated group after ashwagandha treatment (1.45+0.49 mg/dl, $p<0.01$) in comparison to that of baseline control (0.64+0.12 mg/dl). Again, this level of gentamicin treated group after ashwagandha treatment was significantly ($p<0.01$) lower than that of gentamicin treated control group. Histological examination of liver revealed abnormal findings in 100% of rats in gentamicin treated rats. Again, 84.62% of rats in gentamicin treated group after ashwagandha treatment showed almost normal structure in liver. This data suggests that higher doses of gentamicin produce hepatocellular damage, which can be prevented by taking ashwagandha, due to its antioxidant property5. Some active components of aswagandha have anti-inflammatory property6 thus may be responsible for this hapetoprotectine role 7.

Sakr SA, Samai HAA, Soliman ME. Exploring hepatotoxicity of benomyl:histological and histochemical study on albino rats.J Med Sci 2004; 4(1):77-83.

Mishra LC. Scientific Basis for the therapeutic use of Withania somnifera (Ashwagandha): A Review. Altern Med Rev 2000; 5(4): 334-346.

Das K, Samanta TT, Samanta P, Nandi DK. Effect of extract of Withania somnifera on dehydration –induced oxidative stress- related uremia in male rats. Saudi J of Kidney Dis Transpl 2010; 21(1): 75-80.

Elberry AA, Harraz FM, Ghareib SA, Nagy AA, Gabr SA, Suliaman MI, and Abdel-Sattar E. Antihepatotoxic effect of Marrubium vulgare and Withania somnifera extracts on carbon Tetrachloride-induced hepatotoxicity in rats. JBCP 2010; 1(4): 247-254.

Singh G, Sharma PK, Singh S. Biological activities of Withania somnifera. Annals of Biological Research 2010;1(3): 56-63.

6. Borde AU, Qureshi MI, Patil MK, Mendhe MS, Athawale AM. Protective effect of Withania Somnifera on cadmium chloride induced hematological and biochemical changes in male rats. J Res Educ Indian Med 2008; 15(2): 15-20.

7. Harikrishnan B, Subramanian P, Subash S. Effect of Withania somnifera root powder on the levels of circulatory lipid peroxidation and liver marker enzymes in chronic Hyperammonemia. E-Journal of Chemistry [Internet]. 2008 Oct [cited 2011 Jun 9]; 5(4): 872-877.

Available from: http://www.e-journal.net

I must be thankful to the "Research Grant" of Directorate General of Health Services (DGHS) of Bangladesh for providing the partial financial support for completing the research work. I would also like to express my special thanks to the authority of the Department of Pharmacy, University of Dhaka and BCSIR for their kind cooperation.

Where applicable, the authors confirm that the experiments described here conform with The Physiological Society ethical requirements.

PCB198

The roles of hepcidin and ferroportin in autocrine regulation of iron levels

S. Lakhal-Littleton, D. Biggs, R. Diaz, A. Santos, C. Peerce, B. Davies and P. Robbins

DPAG, University of Oxford, Oxford, UK

Liver-derived hepcidin Hamp regulates iron homeostasis by downregulating ferroportin Fpn expression at the sites of iron absorption (duodenal enterocytes), recycling (reticuloendothelial macrophages) and storage (liver). However, Fpn and Hamp are also expressed in tissues not associated with systemic iron handling, such as the heart, skeletal muscle, lung and brain, raising the possibility of autocrine iron regulation in these tissues. Current mouse models of ubiquitous gene deletion do not enable us to address this hypothesis due to the confounding effects of ubiquitous loss of Hamp and Fpn on systemic iron levels. To overcome this limitation, we have used the LoxP Cre technology to enable tissue-specific manipulation of Hamp and Fpn expression in the mouse. Here we describe, for the first time, the generation and biochemical validation of three mouse models: 1) tissue-specific Hamp knockout, 2) tissue-specific Fpn knockout and 3) tissue-specific Fpn C326Y knock-in (hamp-resistant). Our animal models are valuable tools for micro-dissecting iron regulation at a single-tissue level in health and in disease. They will help achieve the mechanistic understanding necessary for the development of evidence-based iron manipulation therapies for diseases where iron dysregulation contributes to pathogenesis

Funding by Vifor Pharma and The British Heart Foundation

Where applicable, the authors confirm that the experiments described here conform with The Physiological Society ethical requirements.

PCB202

The antioxidant effect of water melon on paracetamol induced liver toxicity

M. Pipedi-Tshekiso, P. Chaturvedi and A. Kefentse Tumedi

Department of Biological Sciences, Faculty of Science, University of Botswana, University of Botswana, Botswana

Vegetables and fruits are well known for their protective effects against oxidative stress because of their antioxidant properties. In the present studies locally available watermelon has been evaluated for its protective effects against paracetamol induced oxidative stress in albino rats. Three doses of fresh water melon extract (2.5ml, 5.0 ml and 7.5 ml per Kg body weight) along with paracetamol (125mg/Kg body weight) have been administred orally to three groups (5 each) of experimental rats for 30 days. Paracetamol control group was administered only paracetamol (125mg/Kg body weight) and normal control group was given equal volume of distilled water.. Rats were killed on day 31 after ether anaesthesia and blood was collected from brachial artery in heparin coated centrifugation tubes. Blood was centrifuged and plasma was separated to measure thiobarbituric acid reactive substances, serum glutamate oxaloacetate transaminase, serum glutamate aspartate transaminase, reduced glutathione, tocopherol, glutathione per oxidase and super oxide dismutase. Results indicate that fresh watermelon extract inhibits lipid peroxidation, boosts the levels of glutathione and tocopherol. It also enhances the activity of super oxide dismutase and glutathione peroxidase. Carotenoid contents of watermelon might be the cause of its protective effects which are absorbed readily from the intestine after its intake.

Key words Carotenoids, thiobarbituric acid reactive substance, glutathione, super oxide dismutase, glutathione peroxidase.

Where applicable, the authors confirm that the experiments described here conform with The Physiological Society ethical requirements.

PCB203

Expression and function of Slc26a9 member of the Slc26 anion transporter family in the gastrointestinal tract

X. Liu[1,2], T. Li[1,3], B. Riederer[1], A. Singh[1], W. Xia[1,4], Q. Yu[1,5], P. Song[4], B. Tuo[2], D. Tian[5], M. Soleimani[6] and U. Seidler[1]

[1]Clinic for Gastroenterology, Hepatology and Endocrinology, Hannover medical school, Hannover, Germany, [2]Department of Gastroenterology, Affiliated Hospital of Zunyi Medical College, Zunyi, China, [3]Department of Gastrointestinal Surgery, Affiliated Hospital of Zunyi Medical College, Zunyi, China, [4]Key Lab of Combined Multiorgan Transplantation, The First Affiliated Hospital, School of Medicine, Zhejiang University, Hangzhou, China, [5]Department of Gastroenterology, Tongji Hospital, Huazhong University of Science & Technology, Wuhan, China and [6]Center on Genetics of Transport and Epithelial Biology, University of Cincinnati, Cincinnati, OH, USA

Background: We recently identified Slc26a9 as an anion conductance that is upregulated in airway inflammation and prevents bronchial mucus obstruction (Anagnostopoulou et al. JCI 2012). Slc26a9 variants were recently found associated with meconium ileus in cystic fibrosis infants (Sun et al. Nature 2012). Aim: The association with meconium ileus raises the question where Slc26a9 is expressed in the gastrointestinal tract and what is its function. Methods: Acid, HCO_3^-,short circuit current (Isc) measurements were performed in isolated mucosa and acid, HCO_3^- and fluid absorptive and secretory rates were measured by single pass perfusion and back titration in anesthetized Slc26a9 KO and WT mice by inhalation of 2.0% isoflurane. Slc26a9 cellular expression was studied by laser dissection and qPCR, and quantitative morphometry was performed in the different segments of the murine gastrointestinal tract. Results: Slc26a9 was found highly expressed in the mucosae of the upper gastrointestinal tract, with abrupt decrease of expression levels to virtually undectable levels beyond the duodenum. As previously reported, Slc26a9 KO mice had completely lost the ability to secrete acid in adulthood. However, Slc26a9 was found highly expressed along the whole gastric gland, even in areas without H^+,K^+- ATPase expression. Proximal duodenal bicarbonate and fluid secretory rates, which are higher in the proximal than the distal duode-

num in WT mice, as well as the ability to stimulate these rates with forskolin, were reduced in the absence of Slc26a9 expression. The gastric antrum, as well as the fundus (after omeprazole treatment to rule out any residual acid secretory capacity) was studied to test whether Slc26a9 transports HCO_3^- itself. Gastric antrum, while expressing high Slc26a9 levels in WT mice, had lower basal and forskolin-stimulated HCO_3^- rate as well as lower Isc response in WT than KO mice, arguing against a role of Slc26a9 as a HCO_3^- transporter. Morphometry revealed strongly elongated fundic as well as antral glands, and slightly elongated proximal duodenal villi as well as crypts. Conclusions: Slc26a9 expression is necessary for normal gastric acid and proximal duodenal bicarbonate secretion, but it is not expressed in more distal parts of the gastrointestinal mucosa. The increased risk for meconium ileus may be due to loss of digestive function of the stomach and proximal duodenum.

Anagnostopoulou et al.(2012). J Clin Invest 122(10):3629–3634.

Sun et al.(2012).Nat Genet 44(5): 562–569.

Xu et al.(2008). PNAS 105(46):17955–17960

Where applicable, the authors confirm that the experiments described here conform with The Physiological Society ethical requirements.

PCB204

Slc26a6 (PAT-1) mediates dipeptide and CO2/HCO3- induced stimulation of jejunal fluid and HCO3- absorption in murine small intestine

Q. Yu[1,2], W. Xia[1,4], A. Singh[1], B. Riederer[1], R. Engelhardt[1], P. Song[4], D. Tian[2], M. Soleimani[3] and U. Seidler[1]

[1]Dep Gastroenterology, Hannover Medical School, Hannover, Germany, [2]Dep Gastroenterology, Tongji Hospital, Tongji Medical College, Huazhong University of Science & Technology, Wuhan city, China, [3]Center on Genetics of Transport and Epithelial Biology, University of Cincinnati, Cincinnati, OH, USA and [4]Key Lab of Combined Multiorgan Transplantation, The First Affiliated Hospital, School of Medicine, Zhejiang University, Hangzhou, China

Background and aim: The jejunum is known to be capable of absorbing large amounts of fluid and HCO3-, but the molecular mechanisms are not clear. We speculated that the large amounts of luminal CO2 and HCO3- generated in the upper jejunum by mixture of HCO3—rich pancreatic juice and H+-rich gastric juice, as well as the jejunal enterocyte proton load generated by H+-coupled dipeptide and aminoacid absorption, are major stimulants of jejunal fluid and Na+HCO3- absorption, and that both the apical Na+/H+ exchanger NHE3 and the multi anion transporter Slc26a6 (PAT-1) may be involved in dipeptide- and CO2/HCO3- induced jejunal fluid and Na+HCO3- absorption. Methods: Two photon fluorometry was applied to measure intracellular pH (pHi) in SNARF1-loaded villous enterocytes of exteriorized jejunum in anesthetized C57BL6 background mice. Jejunal fluid absorption was assessed by single pass perfusion of jejunal segments in anesthetized acid/base-status controlled mice with prewarmed, isotonic solutions of different ionic compositions but constant pH of 7.4; volume and pH of the inflowing and outflowing solution was measured. Results: WT jejunum absorbed fluid and acidified the lumen. Slc26a3 (DRA)-deficient jejunum absorbed less fluid than WT, and acidified the lumen more strongly, consistent with the action of DRA as a Cl-/HCO3- exchanger. Slc26a6 (PAT-1)-deficient jejunum also absorbed less fluid, but resulted in less luminal acidification. NHE3-deficient jejunum also absorbed less fluid, and markedly alkalinized the lumen. Switching the luminal perfusate from isotonic NaCl/O2 gassed to isotonic NaCl/HCO3-, 5%CO2/95%O2 gassed solution, pH 7.4, resulted in stable decrease of villous enterocyte pHi by approx. 0.2 pH units, and a marked stimulation fluid absorption in a PAT-1 - and NHE3- but not DRA-dependent fashion. Switching the solution from CO2/HCO3- buffered Mannitol-containing saline to an isotonic solution where the mannitol was preplaced by 20 mM of the dipeptide GlySar further acidified enterocyte pH and resulted in a further increase of fluid absorption that was dependent on PAT-1 as well as NHE3. Conclusions: The results suggest that luminal CO2/HCO3-, as well as luminal dipeptides, strongly stimulates of jejunal fluid absorption, which occurs to a large part percentage secondary to Na+HCO3- absorption. NHE3 and Slc26a6 (PAT-1) are required for this CO2/HCO3— and dipeptide-augmented Na+HCO3- absorption, and Slc26a6 (PAT-1) may operate in a 2 HCO3-/1 Cl- mode under those circumstances. The results demonstrate an important role of Slc26a6 (PAT-1) in jejunal fluid and HCO3- absorption.

Where applicable, the authors confirm that the experiments described here conform with The Physiological Society ethical requirements.

PCB205

The development of an *in-vitro* mouse proximal tubule cell model as a platform for drug transporter and drug-drug interaction studies

S.F. Billington, G. Chung and C. Brown

Institute of Cell and Molecular Bioscience, Newcastle University, Newcastle Upon Tyne, UK

Accurate prediction of human drug toxicity is a major challenge in drug development. It is estimated that 50% of pre-clinical *in-vivo* screening of novel drug molecules in rodents fails to predict subsequent human toxicity. Regulatory authorities have recognised the poor performance of current *in-vivo* screening and have called for the development of *in-vitro* based screening assays to reduce current animal testing in pre-clinical screening. To address this, we are developing predictive *in-vitro* primary renal cell models, to replace poorly predictive *in-vivo* screening studies.

Aim: To develop an *in-vitro* primary renal proximal tubule model from male CD1 mouse kidney. The initial focus was to optimise the isolation protocol, to generate viable cell monolayers of differentiated renal tubule cells and demonstrate the retention of expression and function of ATP-binding cassette (ABC) transport proteins within primary mouse proximal tubule cells.

Proximal tubule cells were isolated using a collagenase digest protocol followed by isopycnic centrifugation on a Percoll density gradient. A range of collagenase concentrations were tested to determine the optimum digestion protocol. After 7 days of cell culture, relative mRNA expression levels of ABC transporters were determined using a quantitative RT-PCR array (SABiosciences). To demonstrate functional expression of these transporters, cell monolayers were loaded with either Hoechst 33342 or 5-Chloromethylfluorescein Diacetate (CMFDA) fluorescent dyes in the presence and absence of transporter inhibitors.

The highest viable cell yields were found at 0.16 collagenase units per milligram tissue (n=3, $P<0.001$, t-test). The relative mRNA expression levels of the ABC transporters multidrug resistance protein 1 (ABCC1) and multidrug resistance protein

4 (ABCC4) were higher ($2^{-avg\Delta CT}$ values of 6.06 & 11.87 respectively) than multidrug resistance protein 3 (ABCC3) (0.70) or multidrug resistance protein 5 (ABCC5) (1.03). We found no expression of multidrug resistance protein 2 (ABCC2) (0.03). Breast cancer resistance protein (ABCG2) and multidrug resistance protein 1b (ABCB1b) expression levels were 0.39 and 0.21 respectively, giving a rank order of ABCC4>ABCC1>>ABCC3>ABCC4>>ABCB1b>ABCG2. Inhibition of Hoechst 33342 efflux from the cell by cyclosporin A (n=3, IC_{50} 3.60±0.10μM, mean ± SEM) and Ko-143 (n=3, IC_{50} 0.52±0.01μM, mean ± SEM) demonstrated expression of multidrug resistance protein 1 (ABCB1) and breast cancer resistance protein (ABCG2) transporters. Inhibition of CMFDA dye efflux by MK-571 (n=3, IC_{50} 2.60±0.06μM, mean ± SEM) demonstrated expression of multidrug resistance protein (ABCC) transporters.
This data provides the first steps in the characterisation of a primary renal proximal tubule model from mouse kidney.

Sarah Billington is funded by an NC3Rs PhD studentship.

Where applicable, the authors confirm that the experiments described here conform with The Physiological Society ethical requirements.

PCB206

Estrogen increases Na^+ absorption and ENaC channel expression in kidney collecting duct cells

M.Y. Yusef Robles, W. Thomas and B.J. Harvey

Molecular Medicine, Royal College of Surgeons in Ireland, Dublin, Ireland

The active estrogen, 17β-estradiol (E2), exerts a gender-specific anti-secretory effect in distal colon (1). This could provide an explanation for the fluid retention observed in females during periods of high circulating plasma E2. However, an effect of E2 on ion transport in other organs contributing to electrolyte and fluid homeostasis is unknown. The aim of this study was to determine whether E2 has a chronic effect on Na^+ absorption in the renal cortical collecting duct using the M1 kidney cortical collecting duct cell line and to reveal the molecular mechanisms underlying effects of E2 on the amiloride-sensitive epithelial Na^+ channel ENaC.
Electrophysiological experiments using the Ussing chamber technique, demonstrated that treatment with E2 (25 nM) for 24 hrs increased the amiloride-sensitive short-circuit current (I_{SC}) in M1 cells (Control 1.4±0.2 μA/cm^2, E2 3.1±0.6 μA/cm^2; n=7). This increase in Na^+ current was not attributable to changes in the ouabain-sensitive Na^+/K^+-ATPase pump current (Control 11.3±1.6 μA/cm^2, E2 8.9±1.5 μA/cm^2; n=4). Moreover, there were no changes in the abundance of the α- or β-Na^+/K^+ -ATPase subunits.
The increase in the amplitude of the Na^+ current could be explained by changes in the expression of the Na^+ channel ENaC subunits. To test this hypothesis, we looked at changes in the abundance of α-, β-, and γ-ENaC subunits using Western-blotting. We found that the treatment with E2 for 24 hrs did not produce any detectable change in the abundance of the α- or β-ENaC subunits. However, E2 induced a 2-fold increase in the abundance of the γ-ENaC subunit (2.0±0.1, n=4). In conclusion, E2 chronically increases the ENaC mediated absorption of Na^+ in CCD cells. The results suggest that the pro-absorptive effect of E2 could be explained by an up-regulation of the γ-ENaC subunit expression in the apical cell membrane.

1. F. O'Mahony, R. Alzamora, V. Betts, F. LaPaix, D. Carter, M. Irnaten, and BJ. Harvey. 2007. Female gender-specific inhibition of KCNQ1 channels and chloride secretion by 17beta-estradiol in rat distal colonic crypts. J. Biol Chem; 282 (34):24563-73.

Funded by the Higher Education Authority of Ireland (PRTLI Cycle 4) through the National Biophotonics and Imaging Platform Ireland.

Where applicable, the authors confirm that the experiments described here conform with The Physiological Society ethical requirements.

PCB208

Hypercapnia reduces cAMP-dependent HCO_3^- transport across human airway epithelial cells

M.J. Turner[1], M.J. Cann[2] and M.A. Gray[1]

[1]Institute for Cell and Molecular Biosciences, Newcastle University, Newcastle Upon Tyne, UK and [2]School of Biological and Biomedical Sciences, Durham University, Durham, UK

Hypercapnia is a symptom of chronic lung disease and is caused by inefficient gas exchange at the alveoli. We have recently shown that CO_2 modulates cAMP/PKA signalling through changes in G-protein responsive transmembrane adenylyl cyclase (tmAC) activity (1). Since, cAMP signalling plays a vital role in regulating the volume and composition of the airway surface liquid (ASL) we have investigated whether changes in pCO_2 impacts upon cAMP-regulated ion and fluid transport in polarised cultures of human submucosal gland derived airway epithelial cells (Calu-3). Using a radiolabelled cAMP assay, raising pCO_2 from 5% to 10% for 20 mins reduced forskolin-stimulated cAMP levels by 36 ± 8.6% (n=6; p<0.05). Under normocapnic conditions, cAMP agonists produce a drop in intracellular pH of Calu-3 cells due to stimulation of CFTR-dependent HCO_3^- secretion (2). Acute exposure to 10% CO_2 increased both the rate and magnitude of this intracellular acidification by the cAMP agonists adenosine or forskolin approximately 3 fold (n=6; p<0.05). This CO_2 augmentation was independent of changes in either external or internal pH (n=3) and was prevented by either tmAC or PKA inhibition (n=4) suggesting that CO_2 alters the activity of cAMP-dependent HCO_3^- transporters in Calu-3 cells. Pre-loading cells with the Ca^{2+} buffer, BAPTA-AM, and the phospholipase C inhibitor U77312 blocked the effect of 10% CO_2, while carbachol, in normocapnia, mimicked the effect of hypercapnia, indicating that raising CO_2 also changes cytosolic Ca^{2+} levels via the G_q receptor/phospholipase C pathway. Because inhibition of basolateral HCO_3^- transporters abolished the effect of CO_2 whilst CFTR-dependent apical Cl^-/HCO_3^- anion exchange (2) was unaffected, strongly suggests that a change in the activity of a basolateral HCO_3^- transporter underlies the effect of 10% CO_2. Surprisingly, the cAMP-dependent HCO_3^- co-transporter, NBCe1, was unaffected by hypercapnia implying another, as yet unknown, basolateral HCO_3^- transporter is involved. Finally, exposing Calu-3 cells to chronic hypercapnia reduced forskolin-stimulated fluid secretion by 37 ± 6.1% (n=3; p<0.05). Together, these results indicate that raised CO_2 decreases airway anion and fluid secretion by reducing tmAC-derived cAMP levels, and the activity of an unidentified basolateral HCO_3^- importer, through a process that involves crosstalk with Ca^{2+} signalling mechanisms. Since both the quantity and pH of the fluid bathing the airways determines the efficiency of the innate defence mechanisms of the lung, our results suggest that raised CO_2

could have deleterious effects on lung function and contribute to the pathophysiology of chronic airway disease.

Townsend et al. (2009). *J Biol Chem***284**, 784-791

Garnett et al. (2011). *J Biol Chem***286**, 41069-41082

Work supported by an MRC Studentship to MT

Where applicable, the authors confirm that the experiments described here conform with The Physiological Society ethical requirements.

PCB209

Bile acid modulation of Cl^- secretion in Calu-3 airway epithelial cells

S. Hendrick, C.M. Greene, S.J. Keely and B.J. Harvey

Royal College of Surgeons in Ireland, Dublin, Ireland

Bile acids are often present in the lower airways of people with cystic fibrosis, probably resulting from the aspiration of gastroesophageal refluxate, but the effects of bile acids on airway epithelium have not yet been investigated (1,2). In the colon, bile acids have been reported to acutely stimulate or chronically inhibit epithelial Cl^- secretion (3).

We investigated the effects of the conjugated secondary bile acid taurodeoxycholic acid (TDCA, 25 μM) on basal transport and carbachol (100 μM) or forskolin (10 μM)-induced ion transport in Calu-3 airway epithelial cells grown in an air-liquid interface and mounted in Ussing chambers. Electrogenic transpeithelial ion transport was measured as short-circuit current (I_{sc}). Data given as Mean ± S.E.M. Statistics were generated using the Student's paired t-test or one-way Anova analysis, where $p \leq 0.05$ is considered significant.

We found that acute (5 min) basolateral TDCA treatment of Calu-3 cells stimulated basal I_{sc} by 39 ± 7% ($p = 0.0001$, $n = 13$) but had no effect on the I_{sc} responses induced by carbachol or forskolin treatment. The I_{sc} responses to TDCA were abolished in Cl^- -free Krebs solution ($n = 4$) indicating that TDCA modulates Cl^- secretion in Calu-3. Prolonged (24hr) TDCA treatment of Calu-3 had no effect on I_{sc} responses to carbachol or forskolin. In Ussing chambers where CFTR I_{sc} was measured, we found that acute treatment with TDCA produced a 32 ± 9% increase in I_{sc} that was abolished by pre-treatment with $CFTR_{inh172}$ ($p = 0.043$, $n = 5$). We also found that TDCA increases Cl^- secretion through calcium-activated chloride (CaCC) channels in the apical membrane by 18 ± 7 % ($p = 0.01$, $n = 4$). In addition, when Na^+/K^+ATPase generated currents were measured, acute treatment with TDCA increased Na^+/K^+pump activity by 13 ± 3%, while pre-treatment with ouabain eliminated this effect ($p = 0.0005$, $n = 9$). This further supports TDCA stimulation of secretion in Calu-3 cells.

Calcium imaging of Calu-3 cells, grown on glass, revealed that acute treatment with TDCA resulted in a rapid 88 ± 12% increase in calcium mobilization ($p = 0.0002$, $n = 8$). The Ca^{2+} mobilization response to TDCA was abolished in Ca^{2+} -free buffer indicating that TDCA induced Ca^{2+} influx into the cell.

This study shows for the first time that TDCA modulates Cl^- secretion in Calu-3 cells, a model of airway epithelium. Effects of TDCA are dependant upon both the duration and sidedness of exposure to the bile acid. TDCA stimulates Cl^- secretion in Calu-3 cells through CFTR and apical CaCC channels. The activation of basolateral Na^+/K^+ ATPase can indirectly sustain this secretory response. Activation of Cl^- secretion in Calu-3 cells could possibly be initiated through intracellular Ca^{2+} mobilization. This study provides leads for further investigation of the signalling pathways involved in TDCA modulation of airway Cl^- secretion.

Pauwels A, et al. Bile acids in sputum and increased airway inflammation in patients with Cystic Fibrosis. Chest 2011 Dec 1, [Epub ahead of print]

Aseeri, A, et al. "Bile acids are present in the lower airways of people with cystic fibrosis." Am J Respir Crit Care Med 185(4): 463.

Keating, N, et al. Physiological concentrations of bile acids down-regulate agonist induced secretion in colonic epithelial cells." J Cell Mol Med 2009; 13(8B): 2293-303

Where applicable, the authors confirm that the experiments described here conform with The Physiological Society ethical requirements.

PCB210

Development and characterisation of rat primary proximal tubule cells

G. Chung[1], S. Billington[1], N. Soomro[2] and C. Brown[1]

[1]ICAMB, Newcastle University, Newcastle Upon Tyne, UK and [2]Urology, Freeman Hospital, Newcastle Upon Tyne, UK

The kidney is a key organ in the elimination of drug molecules from the body. Renal drug elimination is mediated by a series of membrane transporters expressed in proximal tubular cells that form effective secretory pathways for drug molecules. Transporter-mediated drug-drug interactions leading to nephrotoxicity is common. Current animal models of renal drug transport are not predictive of human exposure. In parallel to our established human proximal tubule cell model, we have developed primary cultures of rat proximal tubule cells which may allow the comparison of the renal handling of drug molecules in both species. Here we report the characterisation of rat primary proximal tubule cells as a model for drug transporter studies.

Tubular cells were isolated from the kidneys from male Sprague-Dawley rats via collagenase digest protocol followed by Percoll gradient centrifugation to purify the proximal tubule cell (PTC). A PCR Transporter array of 86 key transport proteins was used to screen the total cell RNA isolated from cultured rat PTC and native kidney cortical tissue. The results showed Abcc2, Abcc3, Abcc4, Abcc6 and Abcg2 had apparent lower level of expression levels in rat PTC cultured on flasks compared to isolated cells from native tissue. In contrast, Abcb1b expression level was 2-fold higher in cultured cells. The SLC–family members: Slc22a1, Slc22a2, Slc22a6, Slc22a7, Slc16a1 and Slc16a2 were also down-regulated.

To measure the functional expression of key efflux transporters, H33342 and CMFDA cellular retention assays were performed. Rat PTC were loaded with H33342 or CMFDA in the presence or absence of CsA, Ko143 and MK-571, inhibitors of Abcb1b, Abcg2 and Abcc1-6 respectively. In the presence of CsA (5μM), cellular retention of H33342 was significantly higher ($P<0.001$) compared to controls. CsA resulted in a significant reduction in the concentration of H33342 that produced half maximal fluorescence (Km) from 3.44±1.10μM to 0.14±0.03μM, a result consistent with inhibition of transporter-mediated dye efflux. The presence of Ko143 (1μM) also increased cellular retention of H33342 ($P<0.01$) with a significant change in Km for dye loading from 3.44±1.10μM to 0.22±0.08μM. Similarly, retention of CMFDA metabolite GSMF in the presence of Mrp inhibitor MK-571 (10μM) was significantly higher than control. To recapitulate monolayer formation, rat PTC were grown on Transwell filter supports and the transepithelial electrical resistance (TEER) measured. The TEER of the cells after 2 days of

growth increased by 2-fold compared to baseline (P<0.05) and by day 4, TEER peaked at 4.5 times the base resistance (P<0.001). These data suggest that rat cells form confluent cell monolayers on permeable filter supports.
In summary, these results show rat PTC have the potential to be used as an important in vitro model for drug transporter and drug-drug interaction studies.

Where applicable, the authors confirm that the experiments described here conform with The Physiological Society ethical requirements.

PCB211

N-acetylcysteine stimulates glutamate efflux in Xenopus oocytes expressing xCT/4F2hc

E.M. Lofthouse, S.E. Brooks, J.K. Cleal, M.A. Hanson, K.R. Poore, I.M. O'Kelly and R.M. Lewis

University of Southampton, Southampton, UK

Background: The amino acid transporter xCT (SLC7A11) is a sodium independent, chloride dependent exchanger which must form a heterodimer with 4F2hc (SLC3A2) in order to function. xCT mediates the exchange of glutamate and cystine. Cystine is essential for the synthesis of the antioxidant glutathione and it has been suggested that xCT activity is a rate limiting factor for glutathione synthesis [1]. N-acetylcysteine (NAC) is reported to be a substrate for xCT and due to its higher solubility has been used in place of cystine for physiological studies. However it is not clear how it was demonstrated that NAC is a substrate for xCT. Therefore the aim of this investigation was to investigate whether or not NAC is a substrate for human xCT expressed in Xenopus oocytes.
Methods: Xenopus laevis oocytes were detached and defolliculated in oocyte Ringer's 2 buffer, transferred to ND91 buffer and incubated at 18° C overnight before being microinjected with xCT-GFP and 4F2hc cRNA and incubated for a further 48 hours. To determine relative ^{14}c-glutamate uptake rates injected and non-injected oocytes were incubated with 20 μM ^{14}c-glutamate for 5 min before uptake was stopped with 1 ml ice cold ND91 and washed twice. Uptake of ^{14}c-glutamate into oocytes was determined by liquid scintillation counting. To demonstrate efflux by exchange batches of ten injected oocytes (3 batches/condition/experiment) were incubated with 20 μM ^{14}c-glutamate for 30 min at room temperature to preload the oocytes. Oocytes were then washed twice in ND91 buffer and incubated with ND91 buffer alone or 10 mM glutamate, 10 mM NAC, a saturated solution of cystine or 10 mM glycine for five min. The media was removed and efflux of ^{14}c-glutamate determined in a liquid scintillation counter. Parallel experiments were carried out in non-injected oocytes. Data are median fold change from stated control groups (range).
Results: ^{14}c-glutamate uptake into injected oocytes was 1.9 (±0.29) fold higher compared to non-injected controls (n=3). Compared to oocytes incubated with ND91 alone, the efflux of ^{14}c-glutamate into the media was 5.1 (3.3-8.8) fold higher for NAC (n=3 ovaries), 3.4 (1.8-4.4) fold higher for glutamate (n=2) and 4.1 fold higher for cystine (n=1) while glycine (n=2) did not appear to stimulate efflux with a fold change of 1.0 (1.01-1.02). In non-injected oocytes NAC, glutamate, cystine or glycine did not stimulate efflux of ^{14}c-glutamate.
Conclusions: xCT/4F2hc injected oocytes showed increased uptake of ^{14}c-glutamate and efflux of ^{14}c-glutamate was observed in response to NAC, glutamate and cystine but not to glycine which is not an xCT substrate. This study demonstrates that NAC is a substrate for xCT.

Shih AY, Erb H, Sun X, Toda S, Kalivas PW, & Murphy TH (2006). Cystine/glutamate exchange modulates glutathione supply for neuroprotection from oxidative stress and cell proliferation. J Neurosci 26, 10514-10523.

We would like to thank the Gerald Kerkut Charitable Trust for their funding.

Where applicable, the authors confirm that the experiments described here conform with The Physiological Society ethical requirements.

PCB212

Cystathionine is a physiological substrate of cystine/glutamate transporter, System x_c^-

S. Kobayashi[1,2], T. Kasakoshi[1], T. Tsutsui[1], S. Azumi[1], T. Okada[1], T. Soga[3], K. Igarashi[1], S. Bannai[1] and H. Sato[1,2]

[1]Dept. of Food and Applied Life Sciences, Yamagata University, Tsuruoka, Yamagata, Japan, [2]United Graduate School of Agricultural Sciences, Iwate University, Morioka, Iwate, Japan and [3]Inst. of Advanced Biosciences, Keio University, Tsuruoka, Yamagata, Japan

System x_c^- is one of amino acid transporters expressed in the plasma membrane of mammalian cells and specifically exchanges anionic forms of cystine and glutamate. This transporter plays an important role in maintaining intracellular glutathione levels and extracellular redox balance. The substrate-specific component of System x_c^-, xCT, is strongly induced by various stimuli, including oxidative stress. Constitutive expression of xCT is observed only in specific regions of the brain and immune tissues such as thymus and spleen. We generated xCT deficient mice and performed metabolite analysis of various tissues using capillary electrophoresis time-of -fight mass spectrometry, and found that no cystathionine was detected in thymus and spleen of xCT-deficient mice, although a significant amount of cystathionine was detected in these tissues in wild-type mice. These results suggest that cystathionine may be a physiological substrate of System x_c^-. Embryonic fibroblasts derived from wild-type mice did not survive more than 24 h in cystine-free medium, due to a marked decrease in intracellular glutathione levels. However, these cells survived and proliferated when incubated in cystine-free medium containing 0.1 mM cystathionine. In contrast, cells derived from xCT-deficient mice did not survive in the cystine-free medium, even when 0.1 mM cystathionine was added to the medium. Cystine uptake in the wild-type cells was significantly inhibited by cystathionine. When wild-type cells were incubated in the 0.1 mM cystathionine-containing buffer, release of intracellular glutamate was enhanced, and cystathionine concomitantly accumulated in the cells. To induce experimental hypercystathionemia, xCT-deficient and wild-type male mice (8-9 weeks) were injected with propargylglycine, a cystathionine γ-lyase inactivator, diluted in saline (ip, 50 mg/kg) daily for 3 days, and cystathionine in plasma, liver and thymus were measured. In plasma and liver of both xCT-deficient and wild-type mice, cystathionine was significantly increased. In the thymus of wild-type mice, cystathionine was substantially increased while no cystathionine was detected in the thymus of xCT-deficient mice. From these results, we have demonstrated that cystathionine functions as a physiological substrate of System x_c^- and is exclusively transported via System x_c^- in an exchange for glutamate in thymus.

This work was supported by Japan Society for the Promotion of Science.

Where applicable, the authors confirm that the experiments described here conform with The Physiological Society ethical requirements.

PCB213

The single-channel behaviour of F508del-CFTR rescued by the CFTR corrector VX-809

Y. Wang, Z. Cai and D. Sheppard

School of Physiology and Pharmacology, University of Bristol, Bristol, UK

Mutations in the cystic fibrosis transmembrane conductance regulator (CFTR) Cl^- channel cause the genetic disease cystic fibrosis (CF). The commonest CF mutation, F508del-CFTR causes a temperature-sensitive folding defect leading to three fundamental insults: (1) aberrant protein processing and trafficking; (2) defective channel gating and (3) thermal instability[1]. To restore CFTR function to CF patients, CFTR correctors have been developed to rescue the cell surface expression of F508del-CFTR. Here, we investigate the single-channel properties and thermostability of F508del-CFTR delivered to the cell surface by VX-809, the first CFTR corrector to be tested in the clinic[2,3]. In comparison, we studied F508del-CFTR rescued by low temperature-incubation. We incubated BHK cells expressing F508del-CFTR with VX-809 (3 μM) for 24 h at 37 °C prior to single-channel recording at temperatures between 23 - 37 °C using excised inside-out membrane patches. Alternatively, BHK cells were incubated at 27 °C for 24 h and studied as a control.

The channel activity of F508del-CFTR rescued by either low temperature or VX-809 was much reduced compared to that of wild-type CFTR. Instead of the exponential increase in open probability (P_o) observed with wild-type CFTR between 23 and 37 °C, the temperature-dependence of P_o for F508del-CFTR rescued by either low temperature or VX-809 was bell-shaped with a maximum around 30 °C. For F508del-CFTR rescued by VX-809, a subtle increase of the maximal P_o was observed compared to low temperature, although no statistical significance was achieved. (Control, 0.081 ± 0.016; VX-809, 0.098 ± 0.016, means ± S.E.M, n = 7 - 10, P > 0.05, student t-test). Over the temperature range 23 - 37 °C, no difference was observed between the single-channel current amplitude of wild-type CFTR and F508del-CFTR rescued by the two methods. However, at high temperatures, F508del-CFTR rescued by either low temperature or VX-809 frequently opened to sub-conductance states, which were very rarely observed with wild-type CFTR. Like low temperature-rescued F508del-CFTR, VX-809-rescued F508del-CFTR channels were unstable and ran down at 37 °C.

We conclude that VX-809 restores similar temperature-dependent channel behaviour to F508del-CFTR as rescue by low temperature-incubation. This suggests that VX-809 and low temperature might share a common mechanism of rescuing the F508del-CFTR folding defect. Our observation that VX-809 delivers F508del-CFTR to the cell surface without improving its gating defect and thermal instability suggests that CF patients with the F508del-CFTR mutation will likely require combination drug therapy.

Lukacs GL & Verkman AS. (2011). *Trends Mol Med* **18**: 81-91

Van Goor F *et al*. (2011). *Proc Natl Acad Sci U S A* **108**: 18843-8

Clancy JP *et al*. (2012). *Thorax* **67**: 12-8

Supported by CF Trust.

Where applicable, the authors confirm that the experiments described here conform with The Physiological Society ethical requirements.

PCB214

Relationship between temperature and substrate affinity in GAT1, KAAT1 and PepT1

A. Vollero, A. Peres, E. Margheritis and E. Bossi

Dept. of Biotechnology and Life Sciences, University of Insubria, Varese, Italy

The effects of temperature on the functional properties of some members of two solute carrier families were investigated using heterologous expression in Xenopus laevis oocytes and electrophysiology. The kinetic parameters were determined in a range of temperatures from 20 to 30°C. The rat GABA transporter GAT1, three different orthologs of the intestinal oligopeptide transporter PepT1 and the Manduca sexta neutral amino acid transporter KAAT1, have been considered in this studies. These transporters are derived from organisms with different thermal behaviour: GAT1 from the neurons of a homeotherm mammal, KAAT1 from the intestine of a poikilotherm invertebrate, PepT1 from epithelial tissues of two poikilotherm (seabass and zebrafish) and one homeotherm (rabbit) organism. Raising the temperature from 20° to 30°C causes changes in the electrophysiological behaviour. Transport-associated currents, presteady-state currents and substrate affinity were determined for each transporter at 20-25-30°C. In all cases higher temperatures increase Imax and cause a reduction in substrate affinity. On the contrary, the transport efficiency is differently affected : it is increased with temperature in PepT1, decreased in KAAT1, and unaltered in GAT1. The Q10 of the transport-associated currents, is in the order of 3 to 8 in GAT1, 3 to 4 in KAAT1 and 2 to 4 for PepT1, according to the membrane voltage. The transient currents from rabbit PepT1 and from GAT1 show a progressively faster decline as the temperature is increased from 20 to 30 °C, and they become similar to those of KAAT1 and fish PepT1s at room temperature. The amount of charged moved, plotted in the Q/V relationship, is shifted to negative potentials by higher temperatures. The substrate affinity varies differently in the rGAT1, msKAAT1 and rbPepT1, in relation to voltages and temperature, but the effects can be generalized in an increase in the K0.5 from 20° to 30°C. Comparison of the amino acidic sequence between the mammalian and fish orthologs of PepT1 highlights the residues that may be involved in temperature sensitivity. Preliminary results on the Q10 of transport currents show an increase of this parameter when the two charged residues present in fish are introduced in the rabbit transporter (Q188E and A196K, rabbit numbering).

The results presented in this work underline the functional adaptation of transporters to temperature and suggest the presence of specific residues that establish the protein activity in relation to the thermal life condition of the organism.

Where applicable, the authors confirm that the experiments described here conform with The Physiological Society ethical requirements.

PCB215

A novel variant of the Na^+/HCO_3^- cotransporter 4 (NBC4) may regulate the cerebrospinal fluid production via the cAMP signaling axis

H. Fukuda[1,2], K. Kawahara[1], M. Chang[3], M.F. Romero[3] and S. Hirose[2]

[1]Department of Physiology, Kitasato University School of Medicine, Sagamihara, Kanagawa, Japan, [2]Department of Biological Sciences, Tokyo Institute of Technology, Yokohama, Kanagawa, Japan and [3]Department of Physiology & Biomedical Engineering, Mayo Clinic College of Medicine, Rochester, MN, USA

Secretion of HCO_3^- at the apical side of the epithelial cells in the choroid plexus is an essential step in the formation of cerebrospinal fluid. Recently, Na^+/HCO_3^- cotransporter 4 (NBC4), an electrogenic member of the NBC family, was identified in mouse and rat choroid plexus. The stoichiometry of NBC4 has been determined as 3 HCO_3^- : 1 Na^+, which is favorable for the efflux of HCO_3^- and Na^+ from the cell into CSF at the apical side (Millar and Brown, 2008). Very recently, we reported that a novel NBC4 isoform (NBC4g: truncated form of general isoform of NBC4c) expressed highly in rat choroid plexus and represented a DIDS-sensitive HCO_3^- transport activity (Fukuda *et al*., 2013). In the present study, we further demonstrate that (1) RT-PCR analysis using specific primers of NBC4g and NBC4c indicated that NBC4g isoform was clearly expressed, but NBC4c isoform was not detected in the rat choroid plexus. (2) Immunostaining and electron microscopy studies revealed the apical localization of NBC4g in the choroid epithelial cells. (3) Electrophysiological studies using *Xenopus* oocytes injected with NBC4g cRNA showed a forskolin, an activator of membrane adenylyl cyclase (mAC),-dependent outward current in the presence of 5% CO_2/33 mM HCO_3^- in the bathing medium. These results support the hypothesis that NBC4g activity may be regulated by cAMP-dependent protein kinase (PKA) phosphorylation at one or more of the three PKA predicted sites. In conclusion, NBC4g, densely localized to the apical surface of the choroid epithelial cells, may contribute to the production of CSF and regulate its volume and ionic composition in a cAMP-dependent manner.

Millar ID and Brown PD. (2008) *Biochem Biophys Res Commun* **373**, 550-554.

Fukuda H *et al.* (2013) *Biochem J* **450(1)** 179-187.

Where applicable, the authors confirm that the experiments described here conform with The Physiological Society ethical requirements.

PCB216

Regulation of the basolateral Cl^--HCO_3^- anion exchanger by cAMP and the actin cytoskeleton in human airway epithelial cells

S.H. Ibrahim, A. Haigh, C. Comer, M.J. Turner and M.A. Gray

Institute for Cell and Molecular Biosciences, Newcastle University Medical School, Newcastle upon Tyne, UK

We have recently shown that polarised cultures of human airway epithelial cells (Calu-3) express a DIDS-sensitive basolateral Cl^--HCO_3^- anion exchanger (BlAE), which is inhibited via a cAMP-dependent, but PKA-independent, mechanism (1). The aim of this study was to investigate the downstream targets of cAMP responsible for BlAE regulation. The activity of the exchanger was assessed by measuring Cl^--dependent changes in intracellular pH using BCECF-loaded Calu-3 cells grown on Transwell supports. In the absence of cAMP agonists, exposing Calu-3 cells to a Cl^--free solution ($0Cl^-$) in the basolateral perfusate produced an alkalinisation of 0.27 ± 0.03 pH units (mean ± SEM.; $P<0.05$ n=10). Restoring Cl^- caused pH to recover at a rate of 0.62 ± 0.07 pH units min^{-1}. The response to $0Cl^-$ was completely abolished if cells were pre-treated with the adenylyl cyclase (tmAC) activators, forskolin or adenosine, the membrane-permeable cAMP analogue, dibutyryl cAMP or the phosphodiesterase inhibitor, IBMX (n=3-10), clearly implicating a rise in cAMP as a key event in the inhibition of the BlAE. The guanine-nucleotide exchange protein directly activated by cAMP (Epac) is another cAMP target. However, incubating Calu-3 cells with the Epac agonist, 8CPT-2Me-cAMP-AM, had no effect on BlAE activity, nor did it prevent forskolin inhibiting the exchanger (n=4). To investigate if a rise in cAMP was linked to a change in cytosolic Ca^{2+}, Calu-3 cells were acutely exposed to carbachol (n=7) or thapsigargin (n=3), but neither agent affected resting BlAE activity, nor the subsequent inhibition by forskolin. However, pre-loading cells with the Ca^{2+} buffer, BAPTA-AM, did reduce BlAE activity by 63.3±5.8% suggesting some dependence of exchanger function on cytosolic Ca^{2+} levels. To investigate if the actin cytoskeleton was important in cAMP-regulation of BlAE, Calu-3 cells were pretreated with cytochalasin D or lantruculin B for 60 mins. Both agents reduced transepithelial resistance (TER) by ~ 40 % after 20 mins but TER remained stable thereafter (n=3). In cytochalasin D treated cells, resting BlAE activity was similar to untreated cells but there was a marked reduction in the ability of adenosine to inhibit the BlAE (n=4, $P<0.05$). Interestingly, this was not observed for forskolin (n=4), suggesting that actin disruption specifically reduced the ability of adenosine receptors to couple to cAMP production via tmAC, thereby leading to higher BlAE activity. In contrast, lantruculin B reduced resting BlAE activity, but did not prevent cAMP inhibition. In conclusion, our results provide clear evidence that a rise in cAMP inhibits BlAE activity, through a downstream mechanism that does not involve Epac, nor a rise in cytosolic calcium, but does appear to require an intact actin cytoskeleton.

Work supported by an Iraqi Government Studentship to SI

Garnett, J.P., *et al*. (2011). *J Biol Chem*|**286**, 41069-82.

Where applicable, the authors confirm that the experiments described here conform with The Physiological Society ethical requirements.

PCB217

The putative gating residues Y163 and F272 are critical for PAT2 (slc36a2) mediated amino acid transport

N.J. Conlon, N. Edwards, T.R. Cheek, C.M. Anderson and D.T. Thwaites

Institute for Cell & Molecular Biosciences, Newcastle University, Newcastle upon Tyne, UK

Until recently, insights into how mammalian secondary active ion-coupled solute transporters function at a molecular level have been limited. However, a number of prokaryotic transporter structures have been resolved and used to predict key functional characteristics in their mammalian counterparts [e.g. LeuT and the SLC6 family (Yamashita *et al.* 2005)]. The proton-coupled amino acid transporter PAT2 (slc36a2) is a member of the SLC36 family of transporters within the Amino Acid Auxin Permease superfamily (Thwaites & Anderson, 2011).

PAT2 is expressed in the renal proximal tubule and defects in PAT2 contribute to iminoglycinuria (Bröer *et al.* 2008). To identify key functional elements within PAT2, an *in silico* homology modelling strategy was performed using crystal structures in the Protein Data Bank. HHPRED predicted a high degree of structural homology (>97%) for PAT2 and several prokaryotic transporter crystal structures, despite limited primary sequence identity (<20%), and differences in ion/substrate specificity and mode of action. Homology modelling of PAT2 against the LeuT template allowed prediction of functionally relevant amino acid residues. Site-directed mutagenesis of rat PAT2 was performed and transport function measured in *Xenopus laevis* oocytes. A key characteristic of secondary active transport is that during the transport cycle the substrate-bound pocket must be closed momentarily from both sides to prevent transmembrane leak. In LeuT, Y108 and F253 not only contribute to the substrate binding pocket but also form a molecular hatch that occludes bound substrate from the extracellular environment (Yamashita *et al.* 2005). In PAT2, homology modelling identified that Y163 and F272 occupy similar positions to those in LeuT. Mutation of either Y163 or F272 led to a decrease in PAT2 function. Concentration-dependent [^{3}H]proline uptake (PAT2, K_m 136 ± 27 μM, V_{max} 329 ± 14 pmol/oocyte/40min, mean ± SEM N=3) showed reductions in both affinity and capacity for Y163F (K_m 446 ± 115 μM, V_{max} 93 ± 6 pmol/oocyte/40min) and F272Y (K_m 253 ± 63 μM, V_{max} 186 ± 11 pmol/oocyte/40min). Similar observations were made when function was measured as proline-induced inward current by TEVC. Confocal imaging revealed similar membrane localisation of FLAG-tagged PAT2, Y163F and F272Y suggesting that any change in activity was not due to decreased membrane expression. The conservation of tyrosine and phenylalanine residues in these two positions in many prokaryotic and eukaryotic transporters, combined with the changes in affinity (change in the binding pocket) and capacity (reduced ability to form an occluded bound-state), support the hypothesis that these residues play a gating role in PAT2, as observed previously in LeuT (Yamashita *et al.* 2005; Piscatelli *et al.* 2010).

Bröer S *et al.* (2008) *J Clin Invest* **118**, 3881-3892

Piscatelli CL *et al.* (2010) *Nature* **468**, 1129-1132

Thwaites DT & Anderson CMH (2011) *Br J Pharmacol* **164**, 1802-1816

Yamashita A *et al.* (2005) *Nature* **437**, 215-223

Supported by postgraduate studentships from the MRC (to NJC) and BBSRC (to NE).

Where applicable, the authors confirm that the experiments described here conform with The Physiological Society ethical requirements.

PCB218

Roles of NHE1 activity and pH_i regulation in ATM mediated DNA-damage response

G. Lauritzen[1], B. Webb[2], S. Christensen[1], D.L. Barber[2] and S.F. Pedersen[1]

[1]Biology, University of Copenhagen, Copenhagen, Denmark and [2]Department of Cell and Tissue Biology, University of Sanfrancisco, San Francisco, CA, USA

The activation of DNA-damage checkpoints enforces growth arrest of damaged cells to allow DNA-repair mechanisms to repair the damaged DNA. Altered pH regulation and Na^+/H^+ exchanger 1 (NHE1, SLC9A1) activity are characteristic for cell division and cell death [1,2]. Checkpoint recovery constitutes a specialized form of mitotic entry and several lines of evidence suggest that this may be pH-dependent. Further, a global profile of proteins phosphorylated by Ataxia telangiectasia mutated (ATM) after UV-induced DNA damage includes NHE1 [3]. However, the possible link between pH-regulation in DNA damage response is incompletely understood.

By bioinformatic screening, we found that the distal C-terminus of NHE1 (NHE1dCT) contains a consensus motif [$_{784}$DSPSSQR$_{790}$, human sequence] for phosphorylation by ATM.

Here we investigate: *(i)* whether NHE1 is a substrate for ATM *in vitro*, using human (h)NHE1 constructs, and *(ii)* the roles of NHE1 activity and pH regulation in DNA-damage response and cell death in fibroblasts expressing wild type (WT) rat (r)NHE1 (PS120 cells) and rat NHE1-S793A (corresponding to S788 in hNHE1) (PS120-S793A cells).

By using an *in vitro* kinase assay we found, that the hNHE1-637-815 distal C-terminal tail (dCT) is phosphorylated by ATM *in vitro* in a manner fully dependent on Ser788 *(n=3)*. We further tested the influence of the specific ATM phosphorylation site on NHE1 activity and pH regulation. To induce a DNA-damage response and activation of ATM, the cells were treated with (10 μM) of the topoisomerase II inhibitor etoposide for 24 h *(n=6)* or the antibiotic zeocin for 6 h *(n=7)*. Both conditions induced a significant increase in the rate of intracellular pH (pH_i) recovery after an NH_4Cl-prepulse-induced acid load in PS120 cells expressing wild type WT rNHE1. In contrast, no increase in pH_i recovery rate was seen in cells expressing rNHE1-S793A that cannot be phosphorylationed by ATM. Additionally, inhibiting NHE1 with amiloride analogs 5-(N-ethyl-N-isopropyl) (EIPA) (10 μM) sensitized PS120-S793A cells to etoposide-induced loss of cell viability as assessed by MTT assay, whereas it enhanced viability after etoposide treatment in PS120 cells *(n=3)*.

In conclusion, we identified a specific ATM phosphorylation site at Ser788 at the distal C-terminus of hNHE1 and showed that NHE1 activity is increased during DNA damage. Analyses to address the significance of NHE1 regulation by ATM in the DNA damage response and checkpoints are ongoing.

1) Putney and Barber. (2003) J Biol Chem 278, 44645-44645-9

2) Lauritzen et al. (2010). Exp Cell Res 316, 2538-2553

3) Matsuoka et al. (2007). Science 316, 1160-1166

Where applicable, the authors confirm that the experiments described here conform with The Physiological Society ethical requirements.

PCB219

Cooperation of basolateral epithelial amino acid transporters TAT1 and LAT2 investigated in a double knock out mouse model

E.B. Boiadjieva[1,3], C. Vilches[2], S. Bodoy[2], A. Guetg[1,3], F. Verrey[1,3] and M. Palacin[2]

[1]Institute of Physiology, University of Zurich, Zurich, Switzerland, [2]Institute for Research in Biomedicine (IRB), Barcelona, Spain and [3]Zurich Center for Integrative Human Physiology, Zurich, Switzerland

Transcellular transport of amino acids by epithelial tissues includes their import across apical membranes and sequential export through basolateral membranes. In the cell, the basolateral efflux step is driven by the amino acid concentration gradient and is strictly regulated by the cooperative action of various transporter proteins. The basolateral transporter

LAT2-4F2hc (SLC7A8-SLC3A2) is an obligatory exchanger of neutral amino acids and does therefore not directly contribute to the net amino acid transport. Another basolaterally located protein, TAT1 (SLC16A10), transports aromatic amino acids by facilitated diffusion and we have previously shown in X. laevis oocytes that it can complement the vectorial transport of LAT2-4F2hc by recycling exchange substrates[1]. Our hypothesis proposes that the interplay between exchangers and uniporters controls both the vectorial transport of amino acids and the cellular amino acid concentration. We aim at testing the cooperation of these two amino acid transporters (LAT2-4F2hc and TAT1) in a double knock out mouse model and in primary cell culture made from their proximal tubule cells. We are currently characterizing the newly generated LAT2$^{-/-}$TAT1$^{-/-}$ double knock outs and comparing different metabolic parameters with those of the LAT2$^{-/-}$ and TAT1$^{-/-}$ single knock outs, and their wild type littermates[2,3]. Preliminary results show that double knock out mice under high protein diet excrete aromatic amino acids in the urine at a much higher level compared to LAT2$^{-/-}$ and even TAT1$^{-/-}$ mice. Moreover, other neutral amino acids that are substrates of LAT2 but not of TAT1 are hyperexcreted by the LAT2$^{-/-}$TAT1$^{-/-}$ to a much higher extent than in both the single knock out models. This latter observation supports the hypothesis that the basolateral efflux of LAT2 substrates depends on the recycling activity of aromatic amino acids via TAT1.

1. Ramadan T, Camargo SM, Herzog B, Bordin M, Pos KM, Verrey F. Recycling of aromatic amino acids via TAT1 allows efflux of neutral amino acids via LAT2-4F2hc exchanger. Pflugers Arch. 454:507-516, 2007

2. Braun D, Wirth EK, Wohlgemuth F, Reix N, Klein MO, Grüters A, Köhrle J, Schweizer U. Aminoaciduria, but normal thyroid hormone levels and signalling, in mice lacking the amino acid and thyroid hormone transporter Slc7a8. Biochem J. 15:249-255, 2011

3. Mariotta L, Ramadan T, Singer D, Guetg A, Herzog B, Stoeger C, Palacín M, Lahoutte T, Camargo SM, Verrey F. T-type amino acid transporter TAT1 (Slc16a10) is essential for extracellular aromatic amino acid homeostasis control. J Physiol. 15:6413-6424, 2012

Where applicable, the authors confirm that the experiments described here conform with The Physiological Society ethical requirements.

PCB220

Analysis of the human cationic amino acid transporter hCAT-1 in human T lymphocytes

A. Werner[1,2], V. Schnitzius[1,2], A. Habermeier[1], J. Boissel[1], C. Luckner-Minden[2], M. Munder[2] and E.I. Closs[1]

[1]Department of Pharmacology, University Medical Center of the Johannes Gutenberg University, Mainz, Germany and [2]Third Department of Medicine, University Medical Center of the Johannes Gutenberg University, Mainz, Germany

The cationic amino acid L-arginine is essential for the efficient function of human T cells. The absence of L-arginine, a condition found in tumor microenvironment and inflamed tissues, leads to hyporesponsiveness of human T lymphocytes. This manifests in decreased cytokine secretion and a down-regulation of their proliferation, resulting in the arrest in the G0-G1 phase of the cell cycle. Given the importance of L-arginine for T cell function, the transporter responsible for the transmembrane transport of this amino acid must play a crucial role in T cell function. We thus wondered which arginine transporters are expressed in primary human T cells and if they are regulated upon stimulation.

For that reason we examined the expression of all known human L-arginine transporter in stimulated and unstimulated T cells. In addition we studied the influence of arginine availability on the transporter expression. Reverse transcription and subsequent quantitative real time PCR experiments revealed a notable expression of y+LAT-2 and cationic amino acid transporter (CAT) 3, but only a weak hCAT-1 mRNA expression in resting T cells. Upon stimulation with anti-CD3/CD28 coupled beads a distinct hCAT-1 expression occurred, which surpassed the expression of the other transporters. In addition, the observed hCAT-1 mRNA level was even higher in arginine-depleted conditions. We also monitored a strong increase in hCAT-1 protein upon T cell stimulation, which peaked after 48 hours of stimulation.

These results lead us to assume, that hCAT-1 is primarily responsible for influx of L-arginine in activated T cells.

To investigate the subcellular localization of hCAT-1 under different conditions, cell surface expression of hCAT-1 was analyzed in biotinylation experiments. The assays revealed that the upregulated hCAT-1 protein in the absence of L-arginine resulted also in a higher abundance of the transporter in the plasma membrane. Interestingly, the proportion of hCAT-1 detected in the plasma membrane was comparable in cells stimulated in the absence or the presence of L-arginine.

hCAT-1 activity was analyzed by the uptake of [3H]-L-arginine (100 μM) into unstimulated and for 48 h stimulated T cells in either arginine-containing or –deficient medium. The experiments revealed a strong induction of L-arginine transport in stimulated compared to unstimulated T cells in both, cells stimulated for 48 hours in the presence and absence of L-arginine. Additionally, transport was completely inhibited by the irreversible CAT-inhibitor N-ethylmaleimide (200 μM).

In summary our results indicates, that hCAT-1 plays a crucial role in L-arginine transport in stimulated human T cells. This enlarges our current knowledge of T cell function, the adaptive immune system and tumor-associated immune escape.

Where applicable, the authors confirm that the experiments described here conform with The Physiological Society ethical requirements.

PCB221

Modulation of the intestinal epithelial tight junction barrier in response to infection

E. Blakesley[1], S. Carding[1], A. Watson[2] and A. Jones[3]

[1]Gut Health and Food Safety, Institute of Food Research, Norwich, UK, [2]Norwich Medical School, University of East Anglia, Norwich, UK and [3]The Sainsbury Laboratory, Norwich, UK

The intestinal barrier is dependent on three junctional complexes, the tight junction (TJ), the adherens junction and desmosomes. Of these, TJ complexes separate the external lumen from the underlying mucosa. Apical TJs consisting of integral transmembrane proteins including occludin, tricellulin and claudins form a dynamic multimolecular complex that selectively regulates the paracellular flux of ions and molecules through the small intestinal epithelium. The TJ complex also constitutes a highly resistant barrier to the entry of luminal pathogens and toxins, preventing infection of the underlying tissues. How the assembly and function of the TJ complex remains unclear. Evidence suggests TJ complex formation may be regulated by cycles of phosphorylation and dephosphorylation of occludin. Occludin seals the paracellular space between neighboring cells in epithelial and endothelial cell layers and targeted phosphorylation by cellular kinases affects

occludin localisation and interaction with components of the TJ complex. Occludin comprises two extracellular loops, four transmembrane domains and two intracellular N- and C-terminus domains. The aim of my project is to investigate the role of occludin phosphorylation in TJ barrier formation in response to pathogen infection. To address this I have used the major protozoan parasite *Toxoplasma gondii* to assess TJ barrier integrity in the small intestinal epithelial cells (IEC-6). Recombinant protein fragments of occludin domains were used to assess invasion of the intestinal epithelium by *Toxoplasma gondii*. We established *Toxoplasma gondii* tachyzoites bind to the extracellular loops of occludin as a mechanism of invasion and transmigration of the small intestinal epithelium without disrupting TJ barrier function. Our results indicate that *Toxoplasma gondii* can associate with the occludin C-terminus to modulate occludin phosphorylation and assembly at the TJ. We have provided also evidence for targeted phosphorylation of occludin in response to *Toxoplasma gondii* infection using an *in vitro* kinase assay to identify IEC-6 kinases that target occludin. These findings represent a step towards understanding the pathogenesis of intestinal diseases associated with a disrupted TJ permeability barrier.

Where applicable, the authors confirm that the experiments described here conform with The Physiological Society ethical requirements.

PCB222

Reducing noradrenergic stimulation of the epithelial sodium channel (ENaC) may contribute to the blood pressure lowering effect of renal sympathetic denervation

M.K. Mansley, M. Bertog and C. Korbmacher

Institut für Zelluläre und Molekulare Physiologie, Universität Erlangen-Nürnberg, Erlangen, Germany

The discovery that bilateral renal sympathetic denervation significantly lowers blood pressure in patients suffering from resistant hypertension[1] has refocused attention to the renal nerves in the development of hypertension. Little is known regarding the influence of the renal nerves upon salt absorption in the aldosterone-sensitive distal nephron (ASDN), a segment characterised by the presence of the epithelial sodium channel (ENaC). Previously, we reported[2, 3] that the adrenergic transmitter norepinephrine (NE) stimulates ENaC-mediated Na^+ transport in $mCCD_{cl1}$ cells, a model of principal cells of the collecting duct. In the present study we further investigated the effects of NE on ENaC-mediated Na^+ transport. $mCCD_{cl1}$ cells were grown on permeable supports and ENaC-mediated Na^+ transport was assessed by recording equivalent short circuit currents (I_{SC}) across cell monolayers mounted in Ussing chambers. Data are given as mean ± SEM, analysed by ANOVA. NE produces a complex response consisting of an amiloride-resistant peak, followed by a brief inhibition of I_{SC} over 15min and a sustained stimulation of I_{SC} over 2.5h, both of which are amiloride-sensitive. These responses are concentration-dependent, with 100nM causing a significant inhibition of basal I_{SC} from 6.1 ± 0.8 μA cm^{-2} to 4.8 ± 0.9 μA cm^{-2} (n=10, p<0.001). Higher concentrations did not inhibit I_{SC} further. A 10-fold higher concentration (1μM) was required to elicit a stimulation of I_{SC} above baseline from 6.1 ± 0.9 μA cm^{-2} to 8.7 ± 1.0 μA cm^{-2} (n=9, p<0.01). Increasing concentrations augment this stimulatory effect. Application of the β-adrenoceptor antagonist propranolol (1μM) did not alter the response to NE (n = 4), but the α-adrenoceptor antagonist phentolamine (20μM) reduced both the inhibitory response by 88.2 ± 0.1 % and the sustained stimulation by 69.8 ± 0.1 % (n=11). Addition of the specific α_2-adrenoceptor antagonist yohimbine (100nM) did not alter the amiloride-sensitive inhibitory component or the stimulatory response (n=9). Additionally we confirmed that aldosterone (3nM) stimulates I_{SC} in $mCCD_{cl1}$ cells. Interestingly, in cells treated with aldosterone, NE failed to increase I_{SC} above the level reached with aldosterone stimulation alone. This indicates that the stimulatory effects of aldosterone and NE are not additive. We conclude that in $mCCD_{cl1}$ cells the sustained stimulatory effect of NE on ENaC is mediated by basolateral α_1-adrenoceptors. ENaC stimulation by locally elevated NE may contribute to the hypertensive effect of increased renal sympathetic activity in particular in patients with low plasma aldosterone levels, i.e. in patients on a high salt diet. Reduced noradrenergic stimulation of ENaC may contribute to the blood pressure lowering effect of renal sympathetic denervation.

Krum H *et al.* (2009). Lancet **373**, 1275-1281.

Mansley MK *et al.* (2011). Proc Physiol Soc **23**, PC318.

Mansley MK *et al.* (2012). Acta Physiologica **204**, Suppl. 689, P092

Where applicable, the authors confirm that the experiments described here conform with The Physiological Society ethical requirements.

PCB223

Increased apical Na+ permeability in cystic fibrosis is supported by a quantitative model of epithelial ion transport

D.L. O'Donoghue[1], V. Dua[3], G.W. Moss[1,2] and P. Vergani[2]

[1]Centre for Mathematics and Physics in the Life Sciences and Experimental Biology, University College London, London, UK, UK, [2]Department of Neuroscience, Physiology and Pharmacology, University College London, London, UK, UK and [3]Department of Chemical Engineering, University College London, London, UK, UK

We address the question of whether human airway epithelia have increased Na+ permeability in cystic fibrosis (CF) disease. CF is the most common lethal genetic disease among Caucasians. It is known that loss-of-function mutations in the CFTR gene, encoding an anion channel, cause reduced Cl- permeability in CF airway epithelia, however whether increased epithelial Na+ channel (ENaC) activity also arises in the disease state is an open question. We have focused on elucidating the quantitative relationships between individual transport protein activities (e.g. CFTR and ENaC) and the trans-epithelial potential difference (PD). Our study finds that the observed bioelectric properties of CF human nasal epithelial (HNE) cells can only be explained quantitatively if the loss of Cl- permeability is accompanied by a corresponding increase in apical Na+ permeability.

We arrive at this conclusion after developing a biophysically motivated mathematical model which describes the electrical, chemical and osmotic state of the HNE cell during measurement of trans-epithelial PD. Our analysis consists of three stages, first we estimate ionic permeabilities in CF and non-CF HNE cells, by directly fitting model predictions to time series of membrane potentials and intracellular concentrations recorded in primary HNE cell cultures. Then, we investigate the extent to which individual variation in the measured electrophysiological data maps to distributions of ionic permeability values in the normal and disease state. To this end we randomly permute 106 different transport parameter config-

urations, simulate trans-epithelial recordings in silico and determine which configurations allow acceptable CF and non-CF behaviour. Finally, given the distribution of acceptable parameter sets and predicted electrophysiological data, we perform a multivariate sensitivity analysis, to determine which transport parameters have most influence on the recorded properties of interest, such as the trans-epithelial PD and the amiloride sensitive PD.
With these approaches we find that a relative increase in Na+ permeability is necessary to produce the observed differences in bioelectric properties between non-CF and CF airway epithelia, and we find this conclusion holds despite the large variation observed in these electrophysiological properties. The results of our sensitivity analysis show that trans-epithelial PD is relatively insensitive to CFTR permeability, and very sensitive to changes in ENaC permeability, and this gives us the insight into why the apical Na+ permeability must differ in CF, as a loss of Cl- permeability is simply not sufficient to hyperpolarize the trans-epithelial PD to the extent seen in CF.

Where applicable, the authors confirm that the experiments described here conform with The Physiological Society ethical requirements.

PCB224

Molecular cloning and kinetic characterization of fish amino acid transporter B^0AT1 (SLC6A19)

E. Margheritis, R. Cinquetti, G. Terova, A. Cardillo, A. Peres and E. Bossi

Dept. of Biotechnology and Life Sciences, University of Insubria, Varese, Italy

In kidney and intestine, epithelial resorption of various amino acids, across the luminal brush border membrane, is mediated by different cotransporters. Neutral amino acids are thought to be transported by system B^0, in particular an important player is the cotransporter (symporter) B^0AT1 (SLC6A19) that belongs to a cluster of orphan transporters within the family of Na^+- and Cl^--dependent neurotransmitters and amino acid transporters (SLC6).
B^0AT1 is a Na^+ – dependent, nutrient transporter that accepts a wide variety of neutral amino acids. The first fish ortholog of this transporter, sea bass B^0AT1 (*Dicentrarchus labrax*) was cloned and electrophysiologically characterized by heterologous expression in *Xenopus laevis* oocytes. The substrate selectivity was estimated by recording the transport associated currents generated in the presence of different amino acids by the classical two-electrode voltage-clamp technique. The apparent affinity for Na^+ and substrates was determined and our data were compared with those reported for the mouse and human orthologs displaying high similarities. The results showed that the most transported substrate was Leucine and despite the fact that B^0AT1 could transport a broad range of neutral amino acids, this transporter, was also able to transport, with high efficiency, the charged Histidine. pH and ion-dependence was also analyzed; sbB^0AT1 presented a weak pH-dependence and the substitution of Na^+ with Li^+ gave rise only to a small current like the mammalian orthologs. The characterization of this transporter in fish has a nutritional importance, in particular in cultured species, for its ability to transport EAA (essential amino acids).

Where applicable, the authors confirm that the experiments described here conform with The Physiological Society ethical requirements.

PCB225

Interaction of murine and human organic cation transporters with tyrosine kinase inhibitors and platin derivatives

D. Zeeh[1], S. Harrach[1,2], M. Fischer[1], E. Schlatter[1], J. Bertrand[2] and G. Ciarimboli[1]

[11]Experimentelle Nephrologie, Med. D, University Hospital, Münster, Germany and [22]Experimentelle Muskuloskelettale Medizin, University Hospital, Münster, Germany

Transporters are important mediators of specific cellular uptake and thus for effects, but also side effects, metabolism and excretion of many drugs. In particular, cellular uptake of the tyrosine kinase inhibitor (TKI) imatinib and the cytostatic cisplatin seems to be critically mediated by organic cation transporters (OCT). Three subtypes of OCT exist (OCT1, OCT2 and OCT3) with specific organ and species dependent expression. In this work, we have compared the interaction of several TKIs and of platin derivatives with OCT from humans and, to add translational relevance, from mice cloned into human embryonic kidney (HEK) cells. The interaction of these drugs with OCT was examined fluorimetrically with the cation 4-(4-(dimethyl-amino)styril)-methylpyridinium iodide (ASP, 1 μM) as substrate.
All TKI tested and cisplatin interacted with the ASP uptake by OCT. The IC50 differed both between the paralogs within a species and also between human and murine orthologs. Oxaliplatin did not interact with ASP uptake in any OCT. For this reason, we compared the toxicity of oxaliplatin in cells expressing or not hOCT2 by a colorimetric cell viability assay using 3-[4,5-dimethylthiazol-2-yl]-2,5-diphenyltetrazolium bromide (MTT). Incubation of hOCT2 expressing cells with oxaliplatin resulted in a higher cell toxicity than in cells without the transporter. In conclusion, our data show that TKI and cisplatin interact with OCT with different apparent affinities depending on the OCT subtype. Moreover, the interaction strength can be different between mouse and human OCT, indicating that translational studies should be interpreted with caution. As evident in the case of oxaliplatin, a drug can be unable to interact with the ASP transport mediated by OCT, but the transporters seem to be of critical importance for the development of drug-associated toxicities, suggesting that OCT have a broad binding site with different interaction domains for diverse substances.

Table I. IC50-values (μM) for the inhibition of ASP uptake by the tested drugs

Substance/Transporter	mOCT1	mOCT2	mOCT3	hOCT1	hOCT2	hOCT3
Imatinib	0.8 [a,c]	3 [a]	58 [a,c]	5 [c]	3	53 [a,c]
Saracatinib	0.7 [a,c]	2 [a,c]	284 [a,c]	60 [c]	0.8 [a,c]	94 [c]
Tofacitinib	35 [b,c]	69 [c]	135 [c]	158 [a,c]	13 [a,c]	29 [a,c]
Cisplatin	31 [a,c]	360 [a,c]	1398 [a,c]	717 [c]	84 [a,c]	512 [c]

[a] = significantly different from the paralogs ($p<0.05$); [b] = significantly different from mOCT3 (both ANOVA tests); [c] = significantly different from the corresponding ortholog (unpaired t-test)

Supported by IZKF of Münster Medical Faculty (Cia2/013/13).

Where applicable, the authors confirm that the experiments described here conform with The Physiological Society ethical requirements.

PCB226

Exploring with the anticancer gold-based compound-Auphen the mechanism(s) by which Aquaporin-3 participates in cell proliferation

A. Galán-Cobo[1], A. Serna[1], I. Sánchez-Gomar[1], J. Toledo-Aral[1], A. Casini[2], G. Soveral[3] and M. Echevarría[1,4]

[1]Physiology and Biophysics, Instituto de Biomedicina de Sevilla (IBiS), Hospital Universitario Virgen del Rocío/CSIC/Universidad de Sevilla, Seville, Spain, [2]Pharmacokinetics, Toxicology and Targeting, Research Institute of Pharmacy, University of Groningen, Groningen, Netherlands, [3]Research Institute for Medicines and Pharmaceutical Sciences (iMed.UL), Faculty of Pharmacy, University of Lisbon, Lisbon, Portugal and [4]Centro de Investigación Biomédica en Red sobre Enfermedades Respiratorias (CIBERES), Madrid, Spain

The increment in the uptake of glycerol across the cell membrane by Aquaporin-3 has been associated with large ATP content and intracellular phosphorylation status, conditions associated with a larger proliferation capacity (1,2). Recently, the gold (III) complex Auphen has been described as a very selective and potent inhibitor of AQP3 glycerol permeability (3). Then, we decided to further explore the effect that this selective inhibitor produces on the cell proliferation of cell lines that considerable express AQP3 in a natural way (A431) or cells which are stably or transiently transfected for expression of this protein (PC12 or HEK293T), and compare it with cells with low/or none AQP3 expression (NIH-3T3 and PC12-wt). Proliferation rate was evaluated by two methods: first, by counting the number of viable cells that exclude the trypan blue colorant, after 24 and 48h of culture in the presence or not of 5μM Auphen, using a Neubauer haemocytometer; and second, calculating by immunofluorescence staining, the percentage of cells that incorporate BrdU after 2, 4, 6, 8 and 24h of treatment, in the presence or not of Auphen. Lack of cytotoxic effect of Auphen was previously confirmed by cell counting and using a colorimetric assay that evaluates cellular mitochondrial dehydrogenases activity as readout of number of viable cells. Treatment with Auphen strongly reduced the proliferation process of cells that express AQP3. Conversely, Auphen did not reduce the proliferation of cells with low/ or none expression of AQP3. Flow cytometric analysis of the cell cycle phases performed in PC12 over expressing AQP3 showed that the percentage of cells in the G2/M phase, the most proliferative phase, was higher, and lower the percentage of cells in G0/G1 phase, compare to PC12-wt. Additionally, lower percentage of cells in subG0/G1 phase during cell cycle analysis, as well as lower Annexin V specific staining performed in the presence of Nocodazole (5μM), a potent apoptotic inducer, indicates higher resistance to apoptosis in the over expressing AQP3 cells. Finally we analyzed the possible effect that Auphen may have over the cell cycle pattern that could explain the cell proliferation arrest indicated previously. Overall our results demonstrate a significant role of AQP3 in the cell proliferation process and may indicate a potential therapeutic effect of Auphen over tumorogenis. In tissues with large expression of AQP3 as the skin, epidermoid carcinomas and other skin cancer types could benefit from Auphen treatment due to its capacity of interfere in the cell proliferation associated with AQP3, but more studies are necessary to dig inside the molecular basis that underline to this mechanism(s).

M. Hara-Chikuma, A.S. Verkman, Prevention of skin tumorigenesis and impairment of epidermal cell proliferation by targeted aquaporin-3 gene disruption, Mol. Cell. Biol. 28 (2008) 326-332.

M. Hara-Chikuma, A.S. Verkman, Aquaporin-3 facilitates epidermal cell migration and proliferation during wound healing, J. Mol. Med. 86 (2008) 221-231.

A.P. Martins, A. Marrone, A. Ciancetta, A. Galán Cobo, M. Echevarría, T.F. Moura, N. Re, A. Casini, G. Soveral, Targeting Aquaporin Function: Potent Inhibition of Aquaglyceroporin-3 by a Gold-based Compound, PLoS ONE 7 (2012) e37435.

Thanks to "Instituto de Salud Carlos III" (Exp. PS09/00605), and to "Junta de Andalucía" (P08-CTS-03574), Spain.

Where applicable, the authors confirm that the experiments described here conform with The Physiological Society ethical requirements.

PCB227

Bile acids regulate proinflammatory cytokine secretion from human airway epithelial cells

A. Ghatak[1], J. Ward[2], S. Keely[2] and E. Caraher[1]

[1]Centre for Microbial Host Interactions (CMHI) and Centre of Applied Science for Health (CASH), Institute of Technology Tallaght Dublin, Dublin, Ireland and [2]Molecular Medicine Laboratories, RCSI Education and Research Centre, Smurfit Building, Beaumont Hospital, Dublin, Ireland

Bile acids, produced by liver and classically known for their roles in facilitating digestion, are also known to have important roles in regulating several aspects of intestinal physiology, such as epithelial barrier and transport function and mucosal immune responses Although, levels of bile acids can also be elevated in the airways in several diseases, such as gastro-oesophageal reflux disease and cystic fibrosis, little is known about their effects on lung physiology and pathophysiology. The aim of this study was to investigate the effects of bile acids on cytokine secretion from human airway epithelial cells. Calu-3 lung epithelial cells were cultured on permeable supports and transepithelial electrical resistance (Rte) was recorded as a measure of barrier integrity. Cytokine secretion into the bathing medium was measured by sandwich ELISA and stimulated with Poly (I:C) and TNF-α, specific agonists for TLR3 and TNFR1, respectively. Lactate dehydrogenase (LDH) release was used as a measure of cell viability. Statistical analysis was performed by One-way ANOVA with the Tukey-Kramer post-test. p values < 0.05 were considered statistically significant.
The lipophillic bile acid, DCA (200 μM), increased secretion of the proinflammatory cytokines IL-8, IL-6 and TNF-α to 220.1 + 23.5% (n = 10, p < 0.05), 572.6 + 185.5 % (n = 9, p < 0.05), and 431.6 + 223.2 % (n=4), compared to unstimulated Calu-3 cells. In contrast, the more hydrophillic bile acid, UDCA (200 μM), was without effect, as were the taurine-conjugated derivatives of DCA and UDCA. Furthermore, DCA (200 μM) significantly enhanced IL-8 and IL-6 release from Calu-3 cells in response to both the TLR3 and TNFR1 agonists, Poly (I:C) (25 μg/ml) and TNF-α (100 ng/ml), respectively. In contrast, UDCA (500 μM) enhanced TNF-α-induced IL-8 release but did not alter either IL-6 or IL-8 release in response to Poly (I:C). Intriguingly, we found that at lower concentrations, both DCA and UDCA specifically inhibited TLR3-induced TNF-α release. Poly (I:C)-stimulated TNF-α release from Calu-3 cells was reduced from 13.4 + 2.1 pg/ml in control cells to 4.5 + 1.0 pg/ml in DCA (50 μM)-treated cells (n = 7, p < 0.05), whereas UDCA (1 μM) also attenuated Poly (I:C)-stimulated TNF-α release to 5.4 + 1.6 pg/ml (n = 7, p < 0.05). Taken together, these data indicate that bile acids play a complex role in regulating cytokine secretion from Calu-3 cells. Whether they exert anti-inflammatory or proin-

flammatory actions depends on the hydrophobicity of the particular bile acid in question and the concentration present. These findings are important to developing our understanding of the role that bile acids may play in the pathogenesis of lung inflammation.

PRTLI Cycle 5 and co-funded by ERDF

Where applicable, the authors confirm that the experiments described here conform with The Physiological Society ethical requirements.

PCB228

Different expression patterns of FXYD11 and Na+/K+-ATPase in gills of the brackish medaka (Oryzias dancena) when acclimated to hypo- or hyper-osmotic environments

C. Chang, W. Yang and T. Lee

Life Science, Chung Hsing university, Taichung, Taiwan

Upon hyperosmotic or hypoosmotic challenge, Na+/K+-ATPase (NKA) in gills of the teleosts supplied driving force for ion-secreting or ion-absorbing mechanisms, respectively. Meanwhile, FXYD11 plays important roles in modulating (NKA) activity in gills of the teleosts. Little is known, however, about the details of interaction between FXYD11 and NKA upon acute salinity challenges. The brackish medaka is a euryhaline teleost and a useful experimental animal model, which are able to tolerate a broad range of environmental salinities with efficient osmoregulatory mechanisms to maintain homeostasis. Time-course alterations in branchial FXYD11 and NKA expression (mRNA/protein), as well as NKA activity after exposure to salinity changes were first examined in this study to realize the short-term effects of different salinity stresses on FXYD11 regulated NKA activity in gills of the brackish medaka. The brackish medaka were acclimated to brackish water (BW, 15‰) for at least four weeks, and then the BW-acclimated medaka were transferred directly to fresh water (FW) or seawater (SW, 35‰). Upon hyperosmotic and hypoosmotic challenge, the NKA activity significantly increased at 1 hr (7.09 ± 0.80 vs. 5.50 ± 0.96 umol of ADP / mg protein / hr, $p<0.05$) and 12 (7.92 ± 1.05 vs. 5.50 ± 0.96 umol of ADP / mg protein / hr, $p<0.05$) hrs, respectively, while no significant difference of NKA protein abundance was found compared with the control group. Moreover, there was no significant difference found in the levels of FXYD11 mRNA in the salinity stresses. When the medaka were transferred from BW to FW, the FXYD11 protein abundance significantly increased since 12 hrs. Meanwhile, no significant difference was found in the FXYD protein abundance when transferred from BW to SW. Therefore, at 12 hrs upon hyperosmotic challenge, the branchial NKA activity and FYXD11 protein amounts were up-regulated, but NKA protein amounts did not change significantly. On the other hand, at 1 hr upon hypoosmotic challenge, the NKA activity was up-regulated, but NKA and FXYD11 protein amounts were not significantly different. The co-immunoprecipitation results further illustrated that the interaction between NKA and FYXD11 was up-regulated at 12 hrs upon hyperosmotic challenge, but not significantly different at 1 hr upon hypoosmotic challenge. The present study suggested that the brackish medaka used different mechanisms to modulate NKA activity when acclimated to hypoosmotic or hyperosmotic environments. FXYD11 might regulate NKA activity efficiently upon hyperosmotic challenge.

Where applicable, the authors confirm that the experiments described here conform with The Physiological Society ethical requirements.

PCB229

Physiological and pathophysiological effects of various agents on ATP release in pancreatic ducts

J.M. Kowal, K.A. Haanes, N.M. Christensen and I. Novak

Department of Biology, University of Copenhagen, Copenhagen, Denmark

ATP is a signaling molecule that initiates various cellular responses after binding to P2X and P2Y receptors. These two classes of receptors are expressed in the pancreatic duct cells where they regulate ion and fluid transport (1). Our previous studies have shown that ATP is secreted from acinar zymogen granules into duct lumen (2). The aim of the present studies was to establish whether ATP is also released locally by pancreatic ducts and to determine which physiological and pathophysiological stimuli have such effects, and possible involvement of VNUT (Vesicular Nucleotide Transporter). Luciferase/luciferin bioluminescence assay was used to determine concentrations of ATP released from human pancreatic duct cells (e.g. Capan-1) in response to various stimulants and Fluo4-AM was used for detecting calcium changes. Results are given as mean changes from basal values ± S.E.M; $p<0.05$ accepted as significant. We also applied PCR and Western blot to investigate VNUT expression. We observed fast and continuous ATP release in Capan-1 cells in response to hypotonic and mechanical stimuli of 2.0±1.4 nM/10^6 cells/ml (n=6) and 0.9±0.5 μM/10^6 cells/ml (n=7). Ionomycin (5 μM) also induced similar ATP release 1.6 ± 0.9 nM/10^6 cells/ml (n=6). Ethanol (10-100 mM) had no effect on extracellular ATP (n=5). Interestingly, agents that act via receptors induced significant ATP release. For example, addition of UTP (1-10 μM) caused ATP release of 3.2 ± 0.7 nM/10^6 cells/ml (n=7). The bile acid chenodeoxycholate (CDC) induced dose-dependent (0.1-1 mM), fast and maximal ATP release of 1.0±0.3 μM/10^6 cells/ml (n=5). Concomitantly, CDC induced increase in cellular Ca^{2+} and a decrease in intracellular ATP, as detected by fluorescent markers (Fluo-4; Mg-Green) and confocal microscopy (n=4). Fluorescent ATP store markers (quinacrine, MANT-ATP), use of agents that interfere with secretory pathways (n=4) and molecular evidence for VNUT (n=5), indicated that ducts cells contain vesicular ATP stores. Together, our data show that there are various stimuli causing ATP release with different kinetics and this may indicate different releasing mechanisms, including vesicular release. In pancreatic ducts, ATP release might be an important co-stimulatory and protective mechanism for mechanical stimuli, as well as for substances that can enter lumen of pancreatic ducts, e.g. CDC and UTP. In low concentrations ATP can stimulate opening of Cl^- and K^+ channels and fluid secretion (3). However, overstimulation depletes the cells of ATP, partially via ATP release, and can therefore be involved in pathological changes in pancreas.

Novak I (2008) Purinergic Signal. 4(3):237-53

Haanes KA & Novak I (2010) Biochem J. 429(2):303-11

Wang J et al (2012) Am J Physiol Cell In press epub 12

Funding: Lundbeck Foundation, The Danish Research Council | Natural Science

Where applicable, the authors confirm that the experiments described here conform with The Physiological Society ethical requirements.

PCB231

Roles of ezrin, radixin, merlin, and the Na^+/H^+ exchanger NHE1 in regulation of growth and motility of human breast cancer cells

G. Roest, K.F. Mark and S.F. Pedersen

Department of Biology, University of Copenhagen, Copenhagen, Denmark

Invadopodia are actin-rich membrane protrusions which play essential roles in cancer cell invasiveness [1]. Ezrin and radixin, closely related F-actin-plasma membrane linkers of the ERM protein family, have both been implicated in metastasis, while the more distantly related protein merlin functions as a tumor suppressor [2, 3]. The Na^+/H^+ exchanger NHE1 localizes to invadopodia and is implicated in regulation of cancer cell motility [4, 5]. NHE1 interacts directly with ERM proteins, however, the possible link between NHE1 and ERM proteins in regulation of invasiveness and invadopodia function, and the possible functional relation between NHE1 and merlin are both unelucidated.

The aim of this project was to characterize the roles and interactions of NHE1, ezrin, radixin and merlin in regulation of invasiveness and growth in MCF-7 breast cancer cells. Experiments were carried out in the absence and presence of constitutively active, N-terminally truncated ErbB2 (ΔNErbB2), which we and others have shown increases motility and invasiveness of these cells [5]. Expression of ezrin, but not of radixin or merlin was upregulated in ΔNErbB2 expressing MCF-7 cells. Ezrin and radixin colocalized strongly with NHE1 in invadopodial rosettes both in the absence and presence of ΔNErbB2, while merlin did not localize to these structures. siRNA-mediated knockdown of NHE1 increased the average number of invadopodia per cell from 0.23 ± 0.040 to 0.30 ± 0.020 in vector cells (n=3), yet had no effect in ΔNErbB2 cells. Overexpression of wild-type, constitutively active or dominant negative ezrin significantly decreased the average number of invadopodia per cell from 0.30 ± 0.042 to 0.21 ± 0.047, 0.12 ± 0.020 or 0.10 ± 0.017 in vector cells respectively (n=3), whereas it again had no effect in ΔNErbB2 cells. The size of the invadopodia was unaffected by knockdown of NHE1 or knockdown or overexpression of ezrin. Ongoing Boyden chamber- and zymography experiments are evaluating the impact of merlin and NHE1 and/or ezrin knockdown on MCF-7 cell invasiveness. In accordance with its known role as a tumor suppressor, siRNA-mediated knockdown of merlin significantly increased the growth rate of MCF-7 cells, in a manner more pronounced in vector- than in ΔNErbB2-expressing cells. We speculate that this may reflect the dual roles of these proteins in control of invasiveness and proliferation, however, further studies are ongoing to determine the mechanisms involved.

In conclusion, NHE1, ezrin, and radixin colocalized strongly in MCF-7 invadopodial rosettes whereas merlin was not found in these structures. Surprisingly, knockdown of not only merlin, but also of either NHE1, ezrin, or radixin, stimulated cell growth, in a manner most pronounced in the absence of ΔNErbB2 signaling.

Yamaguchi H (2012) *Eur J Cell Biol* ***91****(11-12), 902-7.*

Kobel M et al (2006) Int J Gynecol Pathol **25**(2), 121-30.

Rong R et al. (2004) *Proc Natl Acad Sci U S A* ***101****(52), 18200-5.*

Busco G et al (2010) FASEB J **24**(10), 3903-15.

Lauritzen G et al (2012) *Cancer Lett* ***317****(2), 172-83.*

Funding: Danish Cancer Society, Danish National Research Council.

Where applicable, the authors confirm that the experiments described here conform with The Physiological Society ethical requirements.

PCB232

MicroRNA miR-222 is elevated in human placenta from teenagers with low maternal folate status

B.C. Baker, K. Forbes, S. Lean, F.L. Mackie, C.E. Taylor, A.J. Garrod, S.L. Greenwood and R.L. Jones

Maternal and Fetal Health Research Centre, University of Manchester, Manchester, UK

Low folate in pregnancy leads to adverse outcomes, especially delivery of babies that are smaller than normal for gestational age (SGA), although the mechanism is as yet undefined (Tamura and Picciano 2006). A particularly vulnerable population, who have low folate status and an increased risk of delivering a SGA infant, are pregnant teenagers (Baker et al. 2009). Recent studies have shown impaired placental cell turnover and reduced nutrient transport in placentas from folate deficient teenagers. There is emerging evidence that microRNAs (miRs) regulate these processes in normal pregnancy and are altered in SGA placentas. We hypothesise that placental dysfunction associated with folate deficiency in teenagers is associated with altered miR expression. Expression of a panel of miRs including miR-143, miR-145, miR-22 and miR-222 was examined in placentas obtained from teenagers. Two groups were compared: teenagers with low folate (red blood cell folate 426nM, 324-500nM median + range, n=11)) and adequate folate status (red blood cell folate 927nM, 580-1178nM median + range, n=12; P< 0.001, Fishers exact test). Total RNA was isolated from villous tissue and expression of miRs assessed by quantitative RT-PCR using miR specific primers. Expression of the analysed miRs was normalised to 5s rRNA expression to correct for non-biological intersample variation. Of the miRs investigated, miR-143, miR-145, miR-22 and miR-222 were all expressed in the human placenta. Comparison of expression levels between teenagers with low and adequate folate status revealed that there was no significant difference in expression of miR-143, miR-145 or miR-22 in placental villous tissue. In contrast, miR-222 expression was significantly higher (30%) in placentas from teenagers with low folate status (relative expression 0.37, 0.28-0.71 median + range) compared to those with adequate folate status (relative expression 0.29, 0.15-0.54 median + range; Mann Whitney; P<0.05). Furthermore, miR-222 expression was negatively correlated with maternal folate status (Spearman rank: P<0.05, r = -0.3745). This study demonstrates that expression of miR-222 is elevated in placental tissue in teenage mothers with low folate status. Data from non-placental tissues suggest that miR-222 regulates components of cell cycle, proliferation and apoptotic signalling pathways. Ongoing studies are investigating the targets and functional role of miR-222 in the human placenta.

Baker, PN, Wheeler, SJ, Sanders, TA, Thomas, JE, Hutchinson, CJ, Clarke, K, Berry, JL, Jones, RL, Seed, PT and Poston, L (2009). A prospective study of micronutrient status in adolescent pregnancy. *Am J Clin Nutr* **89**(4): 1114-1124.

Tamura, T and Picciano, MF (2006). Folate and human reproduction. *American Journal of Clinical Nutrition* **83**(5): 993-1016.

Where applicable, the authors confirm that the experiments described here conform with The Physiological Society ethical requirements.

PCB233

Butyrate: a potential anti-angiogenic therapy for breast cancer?

J. Longster, H. Lemar, A. Farmaki, B. Corfe and C. Staton

Oncology, University of Sheffield, Sheffield, UK

New cancer therapies are being sought that target both the tumour cells and the surrounding microenvironment. Butyrate is thought to be an HDAC inhibitor and has been shown to cause cell cycle arrest and apoptosis in colon cancer. More recently studies have suggested that butyrate can also down-regulate the pro-angiogenic factor VEGF in colon cancer. Therefore this study aimed to test the hypothesis that butyrate will stimulate breast cancer cell apoptosis and concomitantly inhibit angiogenic factor expression.
Treatment of MCF-7 and MDA-MB-231 breast cancer cells with increasing concentrations of butyrate (0-20mM) resulted in a significant decrease in breast cancer cell proliferation ($P<0.005$) as measured by MTS assay (EC50 3mM), cell cycle arrest in G1 ($P<0.04$), and a significant increase in apoptosis as measured by BAK expression using high content analysis ($P<0.001$). Protein array analysis following 48 hours of treatment with 5mM butyrate demonstrated a significant ($P<0.05$) decrease in the anti-apoptotic proteins survivin, XIAP, CIAP-1 and CIAP-2 and an increase in the pro-apoptotic p21 and p27 proteins. Analysis of angiogenesis related proteins revealed that the pro-angiogenic factors HIF1-a, VEGF, PDGF-AA and PDGF-AB/BB were consistently down-regulated, there was little change in the angiopoietins and that angiogenin was up-regulated. Further analysis revealed that both VEGF mRNA and protein were significantly ($p<0.02$) down-regulated in MDA-MB-231 cells in a dose dependent manner following butyrate treatment.
These data suggest that butyrate will have dual effects as a treatment for breast cancer; causing apoptosis of the breast cancer cells and indirectly inhibiting angiogenesis. Work is currently underway to establish whether butyrate will also be efficacious under hypoxic conditions.

Where applicable, the authors confirm that the experiments described here conform with The Physiological Society ethical requirements.

PCB234

Corticospinal excitability map in less than 2 minutes

M.L. van de Ruit and M.J. Grey

School of Sport and Exercise Sciences, University of Birmingham, Birmingham, UK

Introduction: Corticospinal excitability maps obtained with transcranial magnetic stimulation (TMS) are used to assess plasticity of the central nervous system in motor learning and rehabilitation. With conventional methods, a single map usually takes 15-20 min to acquire (1-3). Due to this poor temporal resolution this method is not feasible in a clinical research setting. This study aimed to optimise the method in order to reduce the acquisition time. In addition, we investigated the effect of inter-stimulus interval and stimulation intensity on the map. Methods: TMS was used to elicit motor evoked potentials (MEPs) in first dosal interosseous. Frameless stereotaxy (BrainSight 2, Rogue Research) was used to record the 3D position and orientation of 100 stimuli within a 6 x 6 cm2 area over the hand area of the primary motor cortex. The stimulation positions and EMG records were combined and projected on a 2D plane using an off-line custom written Matlab script. The effect of two parameters on the map were studied: inter stimulus interval (ISI; 1, 1.5, 2, 3 and 4 s) and stimulation intensity (SI; 110%, 120% and 130% of resting motor threshold (rMT)). Maps were characterised by centre of gravity (COG), area (A) and volume (VOL). A repeated measures ANOVA with planned comparisons was used to compare ISIs at 1, 1.5, 2 and 3 s with the control ISI of 4 s. Finally, the minimum number of stimuli was determined by randomly removing stimuli and recalculating the correlation coefficient relative to a full map. The minimum number of stimuli required for a map was determined when the correlation coefficient dropped below 0.9. Results: *ISI:* No effect for ISI was found with area ($p=0.738$), volume ($p=0.981$) or COGx ($p=0.648$). A significant main effect was found for COGy ($p<0.001$). However, planned comparisons failed to show any difference for any parameter between 1 s and 4 s ($p=0.737$), suggesting stimuli could be delivered at 1 s or greater without affecting the map. *SI:* The map scaled with SI (A: $p<0.001$; VOL: $p< 0.001$). A Bonferroni post hoc comparison revealed all pairs being different.
The minimum number of stimuli to create a reliable map was 51 ± 19. Conclusion: We have shown that maps may be produced an ISI of 1 s, however some operators reported difficulty at the speed, therefore we suggest 1.5 s may be better. At 1.5 s and 120% rMT, a reproducible map may be created with 70 stimuli (mean + 1 SD), i.e. less than 2 min. Maps were less reproducible at 110% rMT due to greater MEP variability. With this significant reduction in acquisition time the method becomes feasible to be used in the clinic and in motor learning studies where greater temporal resolution is required.

(1) Mortifee P et al. (1994). Electroencephalogr Clin Neurophysiol **93(2)**, 131-137.

(2) Wassermann EM et al. (1992). Electroencephalogr Clin Neurophysiol **85(1)**, 1-8.

(3) Wilson SA et al. (1993). J Neurol Sci **118(2)**, 134-144.

Where applicable, the authors confirm that the experiments described here conform with The Physiological Society ethical requirements.

PCB235

Autonomic nervous response and subjective evaluation about sleep quality for sleep in menstrual cycle

M. Tanaka[1], M. Nagasaka[2], C. Egami[1], M. Kondo[1] and Y. Sakakibara[3]

[1]Nursing, Fukuoka prefectural Univ., Tagawa, Fukuoka, Japan, [2]Nursing, Miyazaki prefectural nursing Univ., Miyazaki, Miyazaki, Japan and [3]Kanazawa Institute of Technology, Kanazawa, Ishikawa, Japan

This study is to investigate the change of sleep in daily life during the follicular and luteal phases of the menstrual cycle. The seven healthy women, subjects aged 19-47 years participated in this study for two days during sleep. The protocol was approved by the institutional ethics review committee. All participants gave their consent to this study. We examined the RR interval variability for two and a half hours from the onset of sleep. After the night experimental, Subjects answered the following questionnaire such as sleep onset latency, awaked

time during sleep, subjective evaluation of the sleep by using visual analog scale. Autonomic function was estimated by the Lorenz plot and time domain for RR interval.
The hours of sleep and sleep onset latency in the follicular and luteal phases was 359.1±80.5 min and 357.0±43.1 min, 25.4±10.3 min and 20.0±11.5 min, respectively. The RR interval during sleep was increased in the beginning, and decreased, and then increased again in both phases. The ultradian rhythm in the sleep cycle of RR interval in both the follicular and the luteal phase was 76.5±11.5 min and 72.8±8.0 min, and there was no significant difference during 2 hours and a half from the onset of sleep between both phases. The correlation between the subjective sleeping quality and hours of sleep was statistically significant (R=0.580, R2=0.336) in the luteal phase, but not in the follicular phase (R=0.208, R2=0.043).
We concluded that although autonomic nervous activities during sleep, the subjective quality of sleep and hours of sleep did not show individually significant differences between the follicular and the luteal phases, the sensation score on sleep quality might be correlated with not only the hours of sleep but also the other thing, especially in the follicular phase.

The correlation between the quality of sleep and the hours of sleep

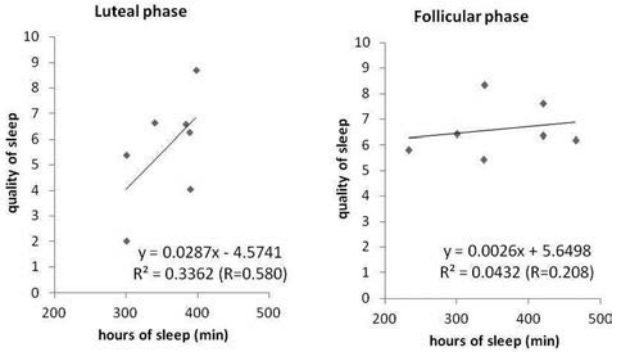

Where applicable, the authors confirm that the experiments described here conform with The Physiological Society ethical requirements.

PCB236

Renal vasoconstriction occurs during isometric calf exercise in humans: role of the muscle mechanoreflex

R.C. Drew[1], M.D. Muller[1], R. Cui[2], C.A. Blaha[1], J.L. Mast[1], M.D. Herr[1] and L.I. Sinoway[1]

[1]Penn State Hershey Heart and Vascular Institute, Penn State University College of Medicine, Hershey, PA, USA and [2]Penn State University, State College, PA, USA

Cardiovascular control during exercise is regulated in part by reflex feedback from muscle afferent nerve fibres (McCloskey and Mitchell, 1972). Handgrip exercise causes renal vasoconstriction in humans (Middlekauff et al., 1997) and muscle mechanoreflex and metaboreflex activation can each cause renal vasoconstriction (Momen et al., 2003). However, it is unknown whether renal vasoconstriction occurs during calf exercise or the extent to which muscle mechanoreflex and metaboreflex activation contribute to this reflex. Therefore, this study examined renal vascular responses during isometric calf exercise, muscle mechanoreflex and/or metaboreflex activation in humans. Nine subjects (4 men, mean ± standard error of the mean 27 ± 1 y, 71 ± 3 kg, 1.72 ± 0.03 m) performed 1.5-min one-legged, isometric calf exercise at 70% maximal voluntary contraction (MVC), 3.5-min post-exercise circulatory occlusion (PECO) of the exercised leg and 3-min passive calf muscle stretch with continued occlusion. A 0% MVC (rest) control trial was also performed. Mean arterial blood pressure (MAP; Finometer), heart rate (HR; ECG) and renal blood flow velocity (RBFV; Doppler ultrasound) were measured. Renal vascular resistance (RVR), an index of renal vasoconstriction, was calculated as MAP / RBFV. Statistical analysis involved repeated measures ANOVA and paired samples *t*-tests. Baseline MAP, HR and RVR were similar between trials (84 ± 3 vs. 84 ± 3 mmHg, 62 ± 2 vs. 64 ± 2 b.min^{-1} and 1.48 ± 0.13 vs. 1.43 ± 0.09 arbitrary units for 0% and 70%, respectively). 70% exercise significantly increased MAP, HR and RVR above baseline and 0% (p<0.05; Table 1). After exercise, these values fell but PECO caused MAP and HR to remain significantly elevated from baseline (p<0.05), whereas RVR returned to resting levels. Stretch significantly increased MAP, HR and RVR from baseline in both 70% and 0% (p<0.05). In conclusion, these findings suggest that renal vasoconstriction occurs during isometric calf exercise in humans. Additionally, muscle mechanoreflex activation via calf stretch increased RVR, both in the presence and absence of local metabolite accumulation. Therefore, muscle mechanoreflex activation may contribute towards renal vasoconstriction occurring during calf exercise.

Table 1 – Relative mean arterial blood pressure (MAP), relative heart rate (HR) and percentage renal vascular resistance (RVR) changes from baseline during the 0% and 70% MVC trials.

	0% MVC trial			70% MVC trial		
	Rest/Exercise	Occlusion/PECO	Stretch	Rest/Exercise	Occlusion/PECO	Stretch
MAP (mmHg)	0±1	2±1	3±1*	9±2*#	4±2*	5±1*
HR (b.min^{-1})	0±1	2±1	5±1*	16±3*#	5±1*#	6±1*
RVR (%)	0±2	-1±2	7±2*	12±4*#	2±2	7±3*

* = significantly different to baseline (p<0.05). # = significantly different to 0% (p<0.05).

McCloskey DI and Mitchell JH (1972). *J Physiol* **224**, 173-186.

Middlekauff HR, Nitzsche EU, Nguyen AH, Hoh CK and Gibbs GG (1997). *Circ Res* **80**, 62-68.

Momen A, Leuenberger UA, Ray CA, Cha S, Handly B, and Sinoway LI (2003). *Am J Physiol Heart Circ Physiol* **285**, H1247-H1253.

Supported by P01 HL096570 (LIS); UL1 RR033184 (LIS).

Where applicable, the authors confirm that the experiments described here conform with The Physiological Society ethical requirements.

PCB237

Effect of a controlled respiratory rate on oxygen uptake kinetics during cycling exercise

T. Saitoh, H. Kobayashi, J. Yanai, R. Nomura, H. Tsutsui, H. Takana and K. Niizeki

Bio-Systems Engineering, Yamagata University, Yonezawa, Japan

Although previous studies have investigated the effect of hyperventilation induced respiratory alkalosis on oxygen uptake kinetics during exercise for the transition on oxygen uptake, the mechanism is still unclear. This study aimed to investigate the effect of a controlled respiratory rate on oxygen uptake kinetics during cycling exercise. Five healthy men participated in this study. The subjects performed baseline cycling exercise for 4 min at 10 W, followed by primary cycling exercise for 6 min at anaerobic threshold (AT), AT minus 40% of the difference between AT and the peak pulmonary oxygen uptake (AT – Δ40%), or AT + Δ40% intensities. Throughout the experiment, respiratory rate of each subject was maintained at 20,

30, or 60 breaths/min (bpm). The pulmonary gas exchange was measured breath by breath, the heart rate was measured using a cardiogram, and the oxy- and deoxyhemoglobin concentrations of the vastus lateralis muscles were estimated using near-infrared spectroscopy at 1 Hz. The kinetics analysis was conducted by using the oxygen uptake response curves and deoxyhemoglobin concentrations during transition to primary exercise. A one-way analysis of variance was used for comparing kinetic values among respiratory rates or workloads. When a significant difference was detected, the post-hoc Scheffe's test was used to identify significant differences. As the respiratory rate was high, the end-tidal partial pressure of CO_2 was lower (20 bpm: 32.7 ± 3.2 mmHg, 30 bpm: 31.1 ± 1.8 mmHg, 60 bpm: 21.7 ± 2.1 mmHg) during baseline exercise. Similarly, as the respiratory rate was high in the analysis of oxygen uptake kinetics, the time delay significantly increased (20 bpm: 12.8 ± 2.4 s, 30 bpm: 15.4 ± 2.1 s, 60 bpm: 18.9 ± 4.2 s in AT + Δ40%; $P < 0.05$) and time constant significantly decreased (20 bpm: 52.2 ± 10.4 s, 30 bpm: 36.2 ± 8.4 s, 60 bpm: 27.9 ± 8.9 s in AT + Δ40%; $P < 0.05$). The time delay and time constant did not differ significantly according to the workload. Similarly, active muscle deoxygenation did not differ significantly according to the respiratory rate and workload. Increase in the time delay at higher respiratory rates suggest that the ATP was mainly supplied by anaerobic metabolism, because the oxyhemoglobin dissociation curve shifted to the left owing to respiratory alkalosis. Decrease in the time constant after an increase in the time delay at higher respiratory rates suggest that the oxyhemoglobin dissociation curve shifted to the right owing to acidification; this occurred because compensation of respiratory alkalosis caused a decrease in the [HCO_3^-] and anaerobic metabolism increased the lactic acid concentration.

Where applicable, the authors confirm that the experiments described here conform with The Physiological Society ethical requirements.

PCB238

A metabolomic approach to investigate metabolic changes induced by acute sprint running before and after long sprint training

C. Enea[1], F. Seguin[1], O. Bernard[1], D. Bon[1], C. Hanon[2] and B. Dugue[1]

[1]University of Poitiers, Poitiers, France and [2]INSEP, Paris, France

Objectives: Metabolomics is has become as an established strategy in the exploration of various stimuli effects. We have recently shown that intense physical exercise can extensively modify the urinary metabolome in human subjects (Ref 1). We have now investigated whether physical training could induce changes at the resting level and after a physical test.
Methods: Fourteen men performed 2 sets of sprint tests separated by a long sprint training program (6 sessions performed in two weeks). Urine specimens were collected at rest and 30 minutes after both sprint tests. Samples were analysed by 1H NMR spectroscopy and multivariate statistical technique (i.e. Principal Component Analysis and Partial Least Square Discriminant Analysis).
Results: Preliminary results show clear separation of the urine profiles obtained from specimens collected before vs. 30 min after the tests and from specimens collected at rest, before and after the training program.
Discussion: Our results shown that metabolomics could provide information on the changes that physical training could induce and seems to be a promising tool to make a deep insight into physiologic states of athletes. We now need to further explore the spectrum profiles of the metabolome in order to indentify the molecules involved.

Enea C. et al.,. 1H-NMR-based metabolomics approach for exploring urinary metabolome modifications after acute and chronic physical exercise. Anal Bioanal Chem 2010; 396:1167–1176.

Where applicable, the authors confirm that the experiments described here conform with The Physiological Society ethical requirements.

PCB240

Acidosis-induced ATP release from skeletal muscle involves activation of CFTR through the cAMP/PKA pathway

J. Tu[1], L. Lu[2] and H.J. Ballard[2]

[1]Shenzhen Key Laboratory for Neuropsychiatric Modulation, Shenzhen Institutes of Advanced Technology, Chinese Academy of Sciences, Shenzhen, China and [2]Department of Physiology, Institute of Cardiovascular Science and Medicine, The University of Hong Kong, Hong Kong, Hong Kong

The cystic fibrosis transmembrane conductance regulator (CFTR) is involved in the acidosis-induced ATP release from skeletal muscle. In many cells, CFTR is activated through the cAMP/protein kinase a (PKA) pathway. We investigated whether this pathway was responsible for CFTR activation in muscle at low pH, and how the signalling pathway was initiated.
Rats were anaesthetised with sodium pentobarbital (70 mg/kg i.p.); the hindquarters were perfused at 1.5 ml/min with modified Krebs Henseleit buffer (pH 7.4) and EDL muscle interstitial fluid was sampled using microdialysis. Addition of lactic acid to the perfusion medium dose-dependently elevated interstitial ATP of buffer-perfused muscle from 38 ± 8 nM in the absence to 67 ± 11 nM in the presence of 10 mM lactic acid: this increase in ATP release was abolished by the specific CFTR inhibitor, CFTRinh-172 or by the PKA inhibitor, KT5720. Forskolin increased the intersitial ATP from 99 ± 20 to 142 ± 21 nM.
Addition of 10 mM lactic acid to the bathing medium of L6 skeletal myocytes increased the intracellular cAMP from 3.2 ± 0.3 to 7.1 ± 1.0 nM, the phosphor-cAMP response element-binding protein (pCREB): β-actin ratio from 0.30 ± 0.02 to 0.71 ± 0.07 and the extracellular ATP from 0.7 ± 0.1 to 1.4 ± 0.2 nM. Addition of the phosphodiesterase inhibitor, IBMX increased extracellular ATP to 3.4 ± 0.7 nM in the absence, or 5.9 ± 1.1 nM in the presence of lactic acid. Addition of 20 μM forskolin the the bathing medium increased extracellular ATP from 0.5 ± 0.02 to 1.3 ± 0.05 nM; CFTR phosphorylation was increased by the addition of forskolin alone, and further increased by the addition of forskolin plus dibutyryl-cAMP and IBMX, but the forskolin-induced increase in CFTR phosphorylation was inhibited by KT5720.
Addition of the Na+/H+-exchanger (NHE) inhibitor, amiloride abolished the lactic-acid-induced increases in both the intracellular cAMP (4.2 ± 0.4 nM in the absence or 3.8 ± 0.4 nM in the presence of lactic acid) and extracellular ATP (0.8 ± 0.2 nM in the absence or 0.9 ± 0.1 nM in the presence of lactic acid). Similarly, the Na+/Ca2+-exchanger (NCX) inhibitor, SN6 abolished the lactic-acid-induced increases in both intracellular cAMP and ATP release from the myocytes.
These data suggest that skeletal muscle CFTR is activated through the cAMP/PKA pathway at low pH; NHE and NCX may

be involved in the signal transduction pathway linking the decreased pH to the initiation of this mechanism.

Jie Tu, Lin Lu, Weisong Cai, Heather J. Ballard. cAMP/protein kinase A activates cystic fibrosis transmembrane conductance regulator for ATP release transmembrane conductance regulator for ATP release from rat skeletal muscle during low pH or contractions. Plos One, 2012; 7(11): e50157.

This work was supported by the Hong Kong Research Grants Council Direct Allocation grant numbers 10207994-14464-21400-323-01, 10400678-14464-21400-323-01, 10401287-14464-21400-323-01, the Li Ka Shing Foundation, grant number 2046-14464-21400-N01-01, the University of Hong Kong, grant number 21372567-14464-21400-N01-01 and the National Natural Science Foundation of China (NSFC), grant number30900594.

Where applicable, the authors confirm that the experiments described here conform with The Physiological Society ethical requirements.

PCB241

Involvement of connexin hemichannels in acidosis- and exercise-induced ATP release from skeletal muscle

H.J. Ballard[1,2], L. Lu[1,2] and W. Cai[1,2]

[1]Department of Physiology, The University of Hong Kong, Pokfulam, Hong Kong and [2]Institute of Cardiovascular Science & Medicine, The University of Hong Kong, Pokfulam, Hong Kong

ATP is an important extracellular signalling molecule which contributes to exercise vasodilation. Both acidosis and muscle contraction stimulate ATP release from skeletal muscle cells through a cystic fibrosis transmembrane conductance regulator (CFTR)-dependent mechanism [1,2]. However, it is unclear whether ATP is released through CFTR itself or whether CFTR regulates a separate ATP-release channel. We investigated whether connexin (Cx) hemichannels were involved in acidosis- or exercise-induced ATP release from rat skeletal muscle.

RT-PCR indicated that cultured rat L6 skeletal myocytes expressed mRNA for both Cx40 and Cx43, but Cx40 was expressed only weakly in western blot, whereas Cx43 was strongly expressed (n=3). CFTR was isolated from a homogenate of L6 cells using an antibody bound to magnetic dynabeads. The immunoprecipitate was shown to contain both CFTR and Cx43 using western blot (n=4).

In rats anaesthetised with sodium pentobarbital (70 mg/kg i.p.), gastrocnemius muscle contractions were induced by sciatic nerve stimulation, and interstitial fluid was sampled using microdialysis. In the absence of drugs, the muscle contracted with an initial force of 0.60 ± 0.05 N (mean ± SEM, n=5) and the interstitial ATP increased from 3.7 ± 0.8 to 119.6 ± 24.5 nM (P<0.02, ANOVA): both of these values were reproducible in repeated contractions. The specific CFTR inhibitor, $CFTR_{inh}$-172 (20 μM) abolished the contraction-induced increase in interstitial ATP without changing the contractile force. The Cx inhibitor, gadolinium (100 μM) abolished the contraction-induced increase in interstitial ATP, but the force was also reduced from 0.68 ± 0.04 to 0.47 ± 0.04 N (n=5). However, another Cx inhibitor, carbenoxolone (100 μM) also abolished the contraction-induced increase in interstitial ATP, and did not significantly alter the contractile force, suggesting that Cx hemichannels may be involved in the contraction-induced ATP release.

A Cx43 over-expression model was created by transfecting the L6 myocytes with a Cx43 plasmid using the Qiagen HiPerFect transfection medium: Cx43 over-expression was confirmed using western blot. In control myocytes, reducing the medium pH from 7.4 to 6.8 increased the extracellular ATP from 0.7 ± 0.07 to 1.2 ± 0.09 nM (n=6; P<0.001, t-test). Cx43 over-expressing myocytes released significantly more ATP than control myocytes at pH 7.4, and reducing the pH from 7.4 to 6.8 increased the extracellular ATP from 1.3 ± 0.1 to 2.1 ± 0.2 nM, suggesting that Cx43 may be involved in acidosis-induced ATP release.

These data suggest that Cx43 co-localises with CFTR in the skeletal muscle cell membrane, and that a connexin may be involved in the release of ATP from skeletal muscle cells during acidosis or muscle contractions; further investigation is required to determine whether and how CFTR interacts with a Cx to induce ATP release.

TU, J., LE, G.Y. & BALLARD, H.J. (2010) Involvement of the cystic fibrosis transmembrane conductance regulator in the lactic-acid-induced increase in interstitial ATP in rat soleus muscle. **Journal of Physiology** 588: 4563-4578.

TU J, LU L, CAI W, BALLARD HJ. (2012) cAMP/Protein Kinase A activates Cystic Fibrosis Transmembrane Conductance Regulator for ATP release from rat skeletal muscle during low pH or contractions in vivo. **PLoS One**: http://dx.plos.org/10.1371/journal.pone.0050157

Where applicable, the authors confirm that the experiments described here conform with The Physiological Society ethical requirements.

PCB242

Amino-terminal propeptide of C-type natriuretic peptide (NT-ProCNP) levels are altered following anaerobic exercise in physically active young men

H. Akseki[1], S.A. Vardar[1,2], M. Demir[3], O. Palabiyik[4], A. Karaca[1], Z. Guksu[1], A. Ortanca[5] and N. Sut[6]

[1]Physiology, Trakya University Medical Faculty, Edirne, Turkey, [2]Department of Sport Physiology, Trakya University Medical Faculty, Edirme, Turkey, [3]Department of Hemotology, Trakya University Medical Faculty, Edirne, Turkey, [4]Department of Biophysics, Trakya University Medical Faculty, Edirne, Turkey, [5]Trakya University Medical Faculty, Edirne, Turkey and [6]Department of Statistics, Trakya University Medical Faculty, Edirne, Turkey

It has been known that plasma level of atrial natriuretic peptide increases following exercise in healthy subjects (Vogelsang et al, 2006). However, no alteration has been found in level of urine C-type natriuretic peptide following exercise in healthy subjects (Bentzen et al, 2004). Amino-terminal propeptide of C-type natriuretic peptide (NT-proCNP) is known as an equimolar product of CNP synthesis. In this study, plasma levels of NT-proCNP were compared in young men who are physically active or sedentary before and after exercise.

Healthy young men (aged between 18 and 25 years) who defined the exercise duration more than 2.5 hours per week at least one year were accepted as physically active (n=10) and those lower than 1.5 hours per week were accepted as sedentary (n=10). Daily energy expenditure of the subjects was recorded by an accelerometer during seven days. Level of maximal oxygen consumption was determined by Astrand test on the first day of the study. Wingate test was applied for anaerobic exercise on the following day. Plasma NT-proCNP levels were measured before anaerobic exercise and one, five and thirty minutes after the exercise. Values were shown as means±SD. Two groups comparisons were made by Mann-

Whitney U test and comparison of continuous variables were made by Wilcoxon Signed Ranks test.
Basal NT-proCNP levels, body mass index and body fat of the groups were similar. Exercise duration of physically active group was reported as 11.3±5.0 hours per week. Daily energy expenditure was found higher in physically active group than the sedentary group (1488.8±169.6 kcal, n=3 vs. 741.8± 299.2 kcal, n=8, respectively, p<0.05). NT-proCNP levels in the fifth minute (0.93±0.23 pmol; p<0.05) and in the thirty minute (0.77±0.21 pmol p<0.05) after exercise were higher than the basal measurements (0.64±0.29 pmol) in physically active group. However, the serial comparison of NT-proCNP levels did not differ in the subjects who are sedentary. The plasma levels of NT-proCNP after fifth minute of exercise were higher in physically active group (0.93±0.23 pmol) than the sedentary group (0.74±0.16 pmol, p<0.05).
The present study demonstrated that plasma levels of NT-proCNP increases following the short term anaerobic exercise in healthy subjects who are physically active but not in sedentary subjects. Physical activity may be a factor affecting the alteration of the secretion of NT-proCNP following exercise.
This work was supported by a grand from Trakya University Research Fund (TUBAP/2011-72).

Where applicable, the authors confirm that the experiments described here conform with The Physiological Society ethical requirements.

PCB243

Bathing with artificial high concentration CO_2-water affected quiet standing posture control

N. Yamamoto[1] and M. Hashimoto[2]

[1]Department of Health Science, Japanese Red Cross Hokkaido College of Nursing, Kitami, Japan and [2]Laboratory of Physiology, Department of Physiotherapy, Teikyo University of Science, Tokyo, Japan

Clinical observations of CO_2-hot spring (CO_2 ≥1000 ppm) immersion revealed the effects, an immersed part reddening, skin blood flow improvements, heart rate reduction[3)] , etc. The previous study was indicated that CO_2-water immersion activates parasympathetic nerve activity in humans[2)]. It is well known that not only systemic nervous system but also autonomous one are involved in posture control in quiet-standing position. CO_2-water immersion may also influence the posture control through the autonomic nervous system activities. This study aimed to reveal the effect of CO_2-water immersion on postural sway during quietly standing in healthy young adults. The healthy male college students (n=5) participated in this study. Body sway was evaluated by recording horizontal ground reaction force for 1 min continuously with a force platform equipped with a data processor. The recording was performed at pre-water immersion and post-water immersion under eyes open condition (EO) and then eyes closed condition (EC). Spectrum analysis by fast Fourier transform (FFT) method of body sway in the medio-lateral and antero-posterior axes was performed. Power spectra of body sway were evaluated by comparing powers in tow frequency bands: 0.02–1.0 (BAND 1), 1.0–10.0 Hz (BAND 2). Each subject was immersed up to the nipples for 15 min in tap and CO_2-water (35°C), respectively. Cutaneous blood flow (BF) was measured on the upper chest and on abdomen by laser-Doppler flowmetry. Statistical evaluation of the data was done by repeated-measures two-way ANOVA, using Turkey test for post hoc multiple comparisons at the 0.05 level of significance. BF was significantly larger in CO_2-water immersion throughout the recording period compared to tap-water immersion. Tap-water immersion changed neither path length of nor area of COP trace measured both under EO and EC conditions. However, the path length of COP was significantly decreased at post CO_2-water immersion in EO (66.1±11.8 vs 55.5±15.7 cm, p<0.05) and EC (88.9±21.8 vs 76.9±17.7 cm, p<0.05). Body sway of BAND 1 was significantly decreased at post CO_2-water immersion in the medio-lateral axes of EO (1.41±0.15 vs 1.13±0.26 cm^2, p<0.05) and the antero-posterior axes of EC (1.72±0.19 vs 1.49±0.33 cm^2, p<0.05), while that of BAND2 was not affected. It is known that body sway of BAND 1 is predominantly stabilized by visual input and vestibular input from the otoliths, and body sway of BAND 2 is stabilized by somatosensory input from the ankles and feet[1)]. Present results indicate that CO_2-water immersion can stabilize standing posture in human. Considering a decrease in BAND1 component, this may indicate a facilitation of visual input or vestibular input by CO_2-water immersion.

Mori S. Discharge patterns of soleus motor units with associated changes in force exerted by foot during quiet standing in man. J Neurophysiol 36:458–471, 1973

Sato M, et al Effects of immersion in water containing high concentrations of CO_2 (CO_2-water) at thermoneutral on thermoregulation and heart rate variability in humans. Int J Biometeorol, 53:25-30, 2009.

Yamamoto N, Hashimoto M Spinal cord transection inhibits HR reduction in anesthetized rats immersed in an artificial CO_2-hot spring bath. Int J Biometeorol, 51 (3):201-208, 2007.

This study was funded in part by a Japan Society for Promotion of Science Grant-in-Aid for Scientific Research (C) #20500556.

Where applicable, the authors confirm that the experiments described here conform with The Physiological Society ethical requirements.

PCB244

Are motor units with different activation thresholds spatially distributed in human *gastrocnemius medialis*?

E. Hodson-Tole[1], I.D. Loram[1], M.A. Minetto[2,3], A. Botter[2] and T.M. Vieira[2,4]

[1]Institute of Biomedical Research into Human Movement and Health, Manchester Metropolitan University, Manchester, UK, [2]Laboratory for Engineering of the Neuromuscular System (LISiN), Politecnico di Torino, Turin, Italy, [3]Division of Endocrinology, Diabetology and Metabolism, Department of Internal Medicine, University of Turin, Turin, Italy and [4]Escola de Educação Física e Desportos, Departamento de Arte Corporal, Universidade Federal do Rio de Janeiro, Rio de Janeiro, Brazil

It has recently been shown that, in human medial gastrocnemius [MG], the fibres of motor units activated during standing occupy localised territories in the longitudinal plane (1). Coupled with the muscle's pennate fascicle architecture there is potential for units with similar intrinsic properties to be concentrated at different points along its length. Aponeurosis material properties and fascicle geometries tend to vary along the length of MG (2-3). Fibres may therefore be arranged within the muscle to occupy a local environment which optimizes their intrinsic properties. Recent evidence indicates that fibres of units activated during standing are more highly represented in the distal portion of MG (4), suggesting low threshold units are preferentially represented in this muscle region. We further investigate this observation by testing whether fibres of

motor units with different activation thresholds have different spatial distributions along the proximal-distal axis of MG. Twelve participants completed the study which was approved by the Local Ethics Committee. Surface EMGs were recorded using 128 electrodes placed over MG. Electrically evoked twitches were elicited by stimulating the tibial nerve branch. Pulses were delivered for 50s with current pulse amplitude increased every 10 stimuli to elicit an increase in muscle activation. Representative ankle torques were calculated from recorded force plate data. The degree of MG stimulation was determined from M-wave root mean square [RMS] values. The location of the highest M-waves along the length of the electrode grid was calculated using barycentre coordinates from the spatial distributions of the incremental M-wave values computed for each stimulation level.

There was a positive linear relationship between mean ankle plantar flexion torque and M-wave amplitude [$p<0.01$, $R^2=0.98$]. Increasing stimulation amplitude therefore increased the number of activated motor units. In eight participants the highest M-wave amplitudes occurred in proximal electrode channels for low amplitude stimulation and in more distal channels at higher amplitudes. As M-wave amplitude is spatially associated to the distribution of activated muscle fibres, the shifts in RMS distribution suggest that, in these participants, there was regional organization along the proximal-distal muscle axis of muscle units according to their activation threshold. In three participants larger M-waves moved to proximal electrode channels with increasing stimulation amplitude. In one participant no spatial shifts in M-wave distribution occurred. Such variability between participants warrants further investigation to establish whether it is the result of the experimental methodology or represents variation across the general population.

1. Vieira TMM Loram ID Muceli S Merletti R & Farina D. (2011). Postural activation of the human medial gastrocnemius muscle: Are the muscle units spatially localised? *J. Physiol.* **589**, 431-443.

2. Kubo K, Kawakami Y, Kanehisa H & Fukunaga T. (2002). Measurement of viscoelastic properties of tendon structures in vivo. *Scandinavian Journal of Medicine & Science in Sports* **12**, 3-8.

3. Shin DD, Hodgson JA, Edgerton VR & Sinha S. (2009). In vivo intramuscular fascicle-aponeuroses dynamics of the human medial gastrocnemius during plantarflexion and dorsiflexion of the foot. *J Appl. Physiol.* **107**, 1276-1284.

4. Hodson-Tole EF, Loram ID & Vieira TMM. (2013). Myoelectric activity along human gastrocnemius medialis: Different spatial distributions of postural and electrically elicited surface potentials. *J. Electromyogr. Kinesiol.* **23**, 43-50.

The Wellcome Trust, FAPERJ (INST-110.842/2012), Compagnia di San Paolo and Fondazione CRT, Italy

Where applicable, the authors confirm that the experiments described here conform with The Physiological Society ethical requirements.

PCB245

24 hours chronomics of blood pressure/heart rate in rotating night shift workers and its relation with 6- sulfatoxy melatonin

N. Verma, B. Anjum, S. Tewari, R. Singh and A. Mahdi

Physiology, KG Medical University, Lucknow, Uttar Pradesh, India

Night shift work is associated with a disruption of circadian rhythms, where a person's internal body clock is in conflict with the rotating shift schedule. The circadian rhythm of the human body is characterized with an alternating cycle of sleep and awake.[1] Among healthy subjects, sleep tends to occur during a particular phase of circadian cycle.[2] It is possible that the circadian sleep propensity rhythm and hormonal rhythm are under influence of circadian pacemaker as well as sleep habit.[3] Most rhythms are driven by an internal biological clock located in the hypothalamic suprachiasmatic nucleus and can be synchronized by external signals such as light-dark cycles.[4, 5,]

In the present prospective study, we examined the 24 hours chronomics of BP/HR in night shift workers and to find out the possible correlation with 6-sulfatoxy melatonin. 62 healthy nursing professionals, aged 20-40 year, performing day and night shift duties were recruited from the Trauma Center, KGMU. Ambulatory blood pressure and heart rate were recorded at every 30 min intervals while awake and each hour in night time synchronically with circadian pattern of urinary melatonin during night and day shift duties. Highly Significant difference was found in double amplitude (2DA) of blood pressure between night and day shift ($p<0.001$). Circadian patterns of systolic double amplitude (Night shift: 24.50 ± 15.07 vs Day shift: 35.07 ± 16.01) ($p<0.001$) was higher in day shift as compare to night shift, diastolic double amplitude (Night shift: 18.96 ± 10.96 vs Day shift : 24.85 ± 11.70) ($p<0.001$) was also increased in day shift than night shift. A circadian pattern of systolic and diastolic 2DA was higher in day shift as compare to night shift. Acrophase of systolic, diastolic blood pressure and heart rate were altered (reversed) during night shift. During night shift, hyperbaric index (HBI) of mean systolic blood pressure was found to be increased at 00-03 am (midnight) while during day shift, peak was found at 06-09 am. It exhibits the desynchronization during night shift and entrainment of circadian rhythm in day shift. Peak melatonin was to be found in early morning as compared to mid night in night and day shift. Altered melatonin at night and in the morning time was related with the symptoms of sleep deprivation.

Shneerson J M, Ohayon M M, Carscadon M A. Circadian rhythm, Rapid eye movement (REM) sleep; Armenian medical network.2007.

Aschoff J. Exogenous and endogenous components in circadian rhythms.,Cold spring Harbor Symp. Ouant Biol.1960; 25:11-28.

Kudo Y, Uchivama M, Okawa M, Shibui K, Kamei Y, Hayakawa T, Kim K, Ishibashi K. Correlation between the circadian sleep propensity rhythm and hormonal rhythm under ultra short sleep wake cycle. Psychiatry Clin Neurosci.1999;53:253-255.

Santhi N, Jeanne F Duffy, Todd S Horowitz, Charles A, Czeiser. Scheduling of sleep/darkness affects the circadian phase of night shift workers. Neuroscience letters. 2005;384: 316-320.

Nagai K, Nagai N, Sugahara K, Niijima A, Nakagawa H. Circadian rhythms and energy metabolism and special reference to the suprachiasmatic nucleus. Neurosci Biobehav Rev. 1994; 18:579-584.

The financial support provided by Council of Science & Technology, UP Government is highly appreciated.

Where applicable, the authors confirm that the experiments described here conform with The Physiological Society ethical requirements.

PCB246

Mitochondrial adaptations to intense exercise training and detraining

D. Bishop[1], C. Granata[1], E. Brentnall[1], K. Renner[2] and R. da Silva Fermino de Oliveira[1]

[1]Institute of Sport, Exercise and Active Living (ISEAL), Victoria University, Melbourne, VIC, Australia and [2]Department of Hematology and Oncology, University Hospital Regensburg, Regensburg, Germany

Mitochondria are essential for life, and maintaining mitochondrial function is important to prevent the progression of many age-related diseases. We have shown that physical activity can increase mitochondrial respiration (1) and many of the proteins associated with mitochondrial biogenesis (2, 3). However, little is known about the effects of intensified training on mitochondrial function (ie mitochondrial respiration) and proteins associated with mitochondrial biogenesis. Furthermore, the effects of detraining on these exercise-induced mitochondrial adaptations are unknown. Ten active men (Peak VO2=47.0 mL/kg/min) took part in an interval training program (IT) 3x/wk for 4 wk, an intensified cycling training program (INT), in which they performed interval training 2x/day for 20 consecutive days, and a 2-wk detraining period (DT) consisting of 6 training sessions. Resting muscle biopsies were taken from the vastus lateralis muscle before the study and after the IT, INT and DT phases. Sub-maximal (0.25 mM) and maximal (5 mM) ADP-stimulated mitochondrial respiration was determined on permeabilised muscle fibers. The relative abundance of the five complexes of the electron transport system (ETS), and proteins associated with mitochondrial biogenesis, was analysed in duplicate via Western blotting. One-way ANOVA, with repeated measures for time, were used to test for the effects of training and detraining on all variables; the level of statistical significance was set at $P < 0.05$. There were no changes in mitochondrial respiration following IT. However, maximal ADP-stimulated and non-coupled mitochondrial respiration increased significantly, by 47% and 48% respectively, during the INT phase, and decreased significantly during the DT phase (17% and 22% respectively); sub-maximal ADP-stimulated mitochondrial respiration showed no significant change during any phase. Following IT, the protein content of the five complexes of the ETS did not change significantly, although there was a trend for all to increase. The protein content of all five complexes was significantly elevated from baseline at the end of INT, with Complex II increasing by ~40%, Complex I and IV increasing by ~20% and Complex V and III increasing by ~10%. Following DT all complexes returned to baseline, except for complex V. There were significant increases in most proteins associated with mitochondrial biogenesis following INT (eg PGC-1α, p53, NRF1, NRF2, TFAM), with some then decreasing towards baseline values following DT (eg p53 and TFAM). Our study demonstrates that three weeks of INT is sufficient to significantly increase mitochondrial respiration, as well as the relative abundance of ETS proteins, and proteins associated with mitochondrial biogenesis. A large proportion of these adaptations are reversed following 2 weeks of detraining, highlighting the remarkable plasticity of skeletal muscle mitochondria.

Bishop DJ, Thomas C, Moore-Morris T, Tonkonogi M, Sahlin K, and Mercier J. Sodium bicarbonate ingestion prior to training improves mitochondrial adaptations in rats. Am J Physiol Endocrinol Metab 299: E225-233, 2010.

Little JP, Safdar A, Bishop D, Tarnopolsky MA, and Gibala MJ. An acute bout of high-intensity interval training increases the nuclear abundance of PGC-1alpha and activates mitochondrial biogenesis in human skeletal muscle. Am J Physiol Regul Integr Comp Physiol 300: R1303-1310, 2011.

Serpiello FR, McKenna MJ, Bishop DJ, Aughey RJ, Caldow MK, Cameron-Smith D, and Stepto NK. Repeated sprints alter signaling related to mitochondrial biogenesis in humans. Med Sci Sports Exerc 44: 827-834, 2012.

Where applicable, the authors confirm that the experiments described here conform with The Physiological Society ethical requirements.

PCB248

Erythropoiesis as an antioxidant response to the oxidative stress of hypoxia; focus on the inhibition of hydroxyl radical formation *in-vivo*

D.M. Bailey[1,2], C. Lundby[3], P. Rasmussen[3], S. Taudorf[4], R.M. Berg[4], B.K. Pedersen[4], M. Gutowski[1], J. Sullivan[5], J. McEneny[6], I.S. Young[6], M. Gassmann[7], E.R. Swenson[8], H. Rahmouni[2], K. Moller[4], M. Culcasi[2] and S. Pietri[2]

[1]Faculty of Health, Science and Sport, University of Glamorgan, South Wales, UK, [2]Institut de Chimie Radicalaire, Aix-Marseille Université, Marseille, France, [3]Institute of Physiology, University of Zurich, Zurich, Switzerland, [4]Department of Infectious Diseases, University of Copenhagen, Copenhagen, Denmark, [5]Burnett College of Biomedical Sciences, University of Central Florida, Orlando, FL, USA, [6]Centre for Clinical and Population Sciences, Queen's University Belfast, Belfast, Ireland, [7]Institute of Veterinary Physiology, University of Zurich, Zurich, Switzerland and [8]Department of Medicine, Division of Pulmonary and Critical Care Medicine, University of Washington, Seattle, WA, USA

Background and Aims: Erythropoietin (EPO) is the key regulator of erythropoiesis, promoting the survival, proliferation and differentiation of erythrocytic progenitors to increase red blood cell mass for the maintenance of systemic O_2 homeostasis (Jelkmann, 2011). However, its action is not merely constrained to that of an endocrine hormone and broader interest in EPO as a cytoprotective molecule has evolved over recent years (Brines and Cerami, 2012). Emerging evidence suggests that the recombinant form of human erythropoietin (rHuEPO) may function directly as an antioxidant though the underlying mechanisms remain unclear (Katavetin et al., 2007). The present study employed an integrated approach to determine if EPO does indeed have the molecular potential to act as a biological antioxidant with a specific focus on its ability to suppress hydroxyl radical (HO•) formation.

Methods: In-vivo study: Radial arterial blood was obtained from 11 healthy males aged 27 ± 4 y old in normoxia (21% O_2) and following 12 h passive exposure to hypoxia (~13% O_2). Blood was assayed for EPO using high-sensitivity ELISA. Electron paramagnetic resonance spectroscopy was employed for the direct detection of ascorbate ($A^{\bullet-}$) and spin–trapped (*N*-tert-butyl-α-phenylnitrone) lipid-derived oxygen-centred alkoxyl (PBN-OR) radicals as an index of free radical-mediated lipid peroxidation (Bailey et al., 2011). In-vitro study: The second-order rate constant for the reaction of rHuEPO with HO• (*k*rHuEPO) generated by Fenton chemistry was determined via the deoxyribose (DR) method (Halliwell et al., 1987). Following confirmation of distribution normality using Shapiro-Wilk *W* tests, data were analysed using paired samples t-tests and relationships determined with Pearson Product Moment Cor-

relations. All data are expressed as mean ± standard deviation (SD).

Results: *In-vivo study:* Hypoxia was associated with an increase in EPO (6.2 ± 2.0 to 22.1 ± 6.3 mU.mL^{-1}, $P < 0.05$) that correlated against the elevation in $A^{\bullet -}$ [2,384 ± 166 to 3,087 ± 276 arbitrary units (AU), $P < 0.05$] and PBN-OR (16,321 ± 2,488 to 19,076 ± 2,122 AU, $P < 0.05$) as illustrated in Figure 1 A-B. *In-vitro study:* *k*rHuEPO was shown to be diffusion-controlled at 1.66×10^{11} M^{-1}.s^{-1} (Figure 2). The site-specific plot suggests that rHuEPO was able to inhibit iron ion-dependant DR degradation and thus capable of binding ions into chelates with poor ability to form HO•.

Conclusions: Collectively, these findings suggest that the cytoprotective benefits of rHuEPO may be due to its exceptional ability to suppress HO• formation subsequent to catalytic iron chelation. In addition to its traditionally accepted haematopoietic role, the systemic rise in EPO during hypoxia may also serve to counter oxidative stress.

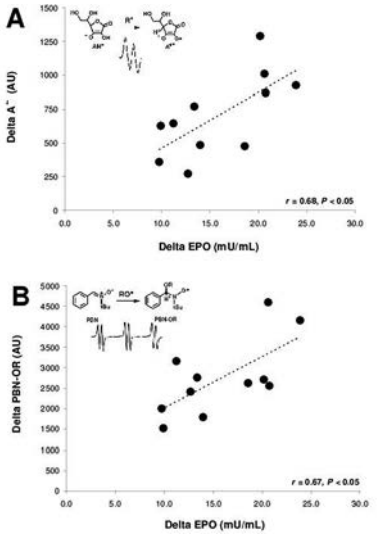

Figure 1. Relationships between the increase (delta: hypoxia minus normoxia) in the arterial concentration of erythropoietin (EPO) and systemic rate of free radical-mediated lipid peroxidation in the form of (A) ascorbate ($A^{\bullet -}$) and (B) *N*-tert-butyl-α-phenylnitrone spin-trapped alkoxyl (PBN-OR) radicals generated in-vivo. Chemical reactions and typical EPR spectra also illustrated.

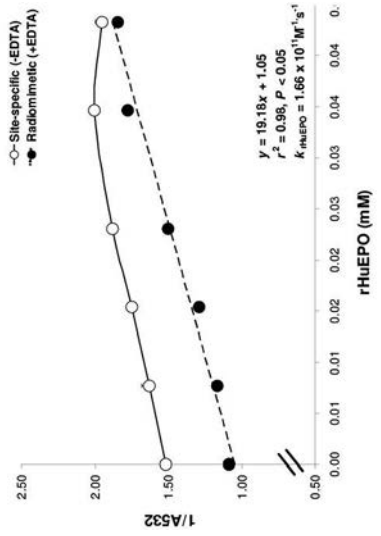

Figure 2. Competition plot of hydroxyl radical scavenging by recombinant human erythropoietin (rHuEPO). Hydroxyl radicals generated by Fenton chemistry (deoxyribose method) in the presence (+) or absence (-) of ethylene diamine pentaacetic acid (EDTA). Corresponding rate constant (*k*rHuEPO) is shown.

Jelkmann W. (2011). *J Physiol*; **589**: 1251-1258

Brines M and Cerami A. (2012). *Mol Med*; **18**: 486-496

Katavetin P, et al. (2007). *Kidney Int Suppl*; **107**: S10-S15

Bailey DM et al. (2011) *Exp Physiol*; **96**: 1196-1207

Halliwell B, et al. (1987) *Anal Biochem*; **165**: 215-219

Funded by Laboratoire Chimie Provence (UMR CNRS #6264 to DMB).

Where applicable, the authors confirm that the experiments described here conform with The Physiological Society ethical requirements.

PCB249

Intracellular DNA damage following isolated muscle contractions: a preliminary investigation into P53 gene expression

G. Davison[1], G. De Vito[2], C. Hughes[1], G. Burke[1], J. McEneny[3], C. McClean[1] and M. Fogarty[4]

[1]University of Ulster, Belfast, UK, [2]University College Dublin, Dublin, Ireland, [3]Queens University Belfast, Belfast, UK and [4]University of Hull, Hull, UK

P53 is an important gene in the regulation of aerobic metabolism and may play a central role in energy production during exercise. In response to intracellular DNA damage, P53 can initiate a series of cell responses and may even fail to function properly. This preliminary investigation was designed to test the hypothesis that high intensity single leg exercise can cause extensive cell DNA damage, which subsequently may affect the expression of the P53 gene. Six (n=6) apparently healthy male participants (age 27 + 7years, stature 174 + 12cm, body mass 79 + 4kg and BMI 24 + 4kg/m2) completed 100 isolated and continuous maximal concentric contractions (minimum force = 200 N, speed of contraction = 60°/sec) of the rectus femoris muscle. Using a spring-loaded and reusable Magnum biopsy gun with a 16-gauge core disposable biopsy needle, human skeletal muscle micro biopsy tissue samples were extracted at rest and following exercise. mRNA gene expression was determined via two-step quantitative real-time PCR using GAPDH as a reference gene. The average muscle force production was 379 + 179 N. High intensity exercise increased mitochondrial 8-OHdG concentration ($P < 0.05$ vs. rest, n=6) with a concomitant decrease in total antioxidant capacity ($P < 0.05$ vs. rest, n=6). Exercise also increased protein oxidation as quantified by protein carbonyl concentration ($P < 0.05$ vs. rest, n=6). P53 expression increased following exercise, however, due to low subject numbers this change was not significant ($P > 0.05$, n=2) These preliminary findings tentatively suggest that maximal concentric muscle contractions can cause intracellular DNA damage with no apparent disruption to P53 gene expression. However, a large-scale study incorporating a greater subject number is warranted to fully elucidate this relationship.

Where applicable, the authors confirm that the experiments described here conform with The Physiological Society ethical requirements.

PCB250

The effect of exertional heat stress induced hypohydration on human physiology and biochemistry

M. Kapoor and L.P. Singh

Heat Physiology, Defence Institute of Physiology and Allied Sciences,Defence Research and Development Organization, Timarpur, India

Hypohydration or dehydration is the condition in which body water level falls below normal.The effects of hypohydration on thermoregulatory, cardiovascular and central nervous function become increasingly detrimental with degree of severity. Soldiers, athletes and commercial kitchen workers etc. are at a greater risk. Physical activity can result in 1-8% body mass loss.Dehydration level of 2% body mass is a threshold above which measurable changes in various physiological parameters are observed. Previous studies on hypohydration have focused on a very few and isolated parameters. The current study has a broader scope and gives and intergrated picture of the effect of 4% body mass loss due to exertional heat stress induced hypohydration in humans.

The study was approved from Institutional human ethical committee. Six healthy military personnel (age:25±4 years, height:172±4cm, weight:66±3 Kg) volunteered to participate in the study. They were informed about the purpose of the study and possible risks and signed a consent form.Volunteers were made to drink appropriate amount of water to attain euhydrated state one hour before the experiment. They were made to perform free hand exercise at 45C and 30% RH in human climatic chamber, till 4% body weight reduction was observed. Various parameters such as Heart Rate Variability, cardiac output and stroke volume, exhaled Nitric Oxide, Bio Impedance, core body and skin mean temperature were measured before and after the heat exposure. Blood samples were drawn and plasma was obtained and stored at -80C for biochemical analysis.

A significant increase in the level of hormones such as cortisol (1.9± .02nMol/L vs 2.2±.02 nMol/L, $p<0.001$), angiotensin II (0.123±0.02ng/L vs .317±0.06 ng/L, $p<0.01$), Antidieuretic hormone(56.5±12.9ng/L vs 123.3±24.4ng/L, $p<0.01$) was observed using paired T-test in plasma samples collected post 4% hypohydration compared to control. Also, a significant increase was observed in core body temperature (36.6 ± 0.1C vs 37.5 ± 0.1C, $p<0.001$), skin mean temperature (35.1±0.1C vs 36.01 ±0.1C, $p<0.001$), total body water (48.99 ± 3L vs 44.83 ± 3L, $p<0.001$), extracellular water (20.90 ±2L vs 19.64 ± 2L, $p<0.001$), the LF:HF ratio(6.20 ± 3 vs 9.04± 4, $p<0.001$) post 4% hypohydration as compared to control using paired T-test. No significant change was observed in the intracellular water volume, exhaled nitric oxide, cardiac output and stroke volume post 4% hypohydration as compared to control.

This is a comprehensive, multi-parametric study, with an aim to analyze the linkage between physiological and biochemical responses generated upon exertional heat stress induced hypohydration. Further in-depth studies are required to attain this goal. We plan to carry out experiments using Rat as model system to elucidate the exact mechanisms and pertinent pathways, which underlie hypohydration.

Where applicable, the authors confirm that the experiments described here conform with The Physiological Society ethical requirements.

PCB251

Red blood cell oxidative stress during prolonged and strenuous exercise

D.M. Lima[1], A. Mendes-Ribeiro[1,3], C.O. Chamma[1], D.C. Abrantes[1], M.A. Martins[1], L. Cameron[2], T.C. Brunini[1] and C. Matsuura[1]

[1]Department of Pharmacology and Psycobiology, State University of Rio de Janeiro, Rio de Janeiro, Rio de Janeiro, Brazil, [2]Department of Genetics and Molecular Biology, UNIRIO, Rio de Janeiro, Rio de Janeiro, Brazil and [3]Physiological Sciences, UNIRIO, Rio de Janeiro, Rio de Janeiro, Brazil

Background. Red blood cells (RBCs) are crucial for tissue oxygen delivery during exercise. Strenuous exercise can affect RBC membrane structure, probably due to mechanical and chemical stress, which ultimately may reduce tissue oxygen supply, and impair exercise performance. The objective of this study was to investigate oxidative stress biomarkers in RBCs during modern pentathlon.

Methods. Six athletes from the Brazilian Modern Pentathlon national team (4 men, 27 ± 4 yr, 1.8 ± 0.1 m, 70.5 ± 8.7 kg) participated in a simulated competition of modern pentathlon, which lasted about 8h. Blood samples were collected at 9 different times: T1, rest; T2, post-fencing; T3/T4, pre/post-200 m swimming; T5/T6, pre/post-horse riding; T7/T8, pre/post-combined event (3 km run interspersed by shooting); T9, after 2 h-recovery. RBCs were isolated by centrifugation for the following experiments: osmotic fragility test; oxidative damage (lipid peroxidation and protein carbonylation); antioxidant enzymes (catalase and glutathione peroxidase, GPx) activities. The procedures conformed to the Declaration of Helsinki and written informed consent was obtained form all subjects. Data were compared against resting values with a paired t-test. Significance level was set at 5%.

Results. All results are shown in Table 1. Osmotic fragility was significantly reduced after swimming (T4) and horse riding (T6) compared to rest (T1). A massive increase in lipid oxidative damage was observed after horse riding, which remained altered up to 2 hours after the end of competition. Protein oxidative damage was observed after horse riding (T6), and returned to basal levels thereafter. After horse riding (T6), a reduction in GPx activity was also observed, which remained depressed until recovery (T9). There were no significant variations in catalase activity throughout the competition, only a slight reduction before horse riding (T5).

Conclusion. Modern pentathlon induces damage to RBC lipid structures, especially after horse riding. This may result from a depletion of the antioxidant enzyme GPx, whose main biochemical function is to reduce lipid hydroperoxides to their corresponding alcohols. Future studies should investigate whether the observed damage is capable of inducing changes in RBC membrane structure, resulting in increased rigidity and impairment in tissue oxygen supply.

Table 1. Oxidative stress biomarkers [mean(SD)].

	T1	T2	T3	T4	T5	T6	T7	T8	T9
OF (%NaCl)	0.66 (0.05)	0.56 (0.03)	NA	0.52 (0.02)*	NA	0.53 (0.01)*	NA	0.60 (0.02)	0.48 (0.03)
CAT (U/gHb)	0.24 (0.01)	0.24 (0.02)	0.23 (0.02)	0.26 (0.01)	0.19 (0.01)*	0.22 (0.03)	0.28 (0.02)	0.25 (0.01)	0.25 (0.02)
GPx (U/gHb)	0.4 (0.02)	0.36 (0.02)	0.49 (0.08)	0.60 (0.01)*	0.58 (0.08)	0.21 (0.01)*	0.22 (0.04)*	0.22 (0.01)*	0.18 (0.01)*
PO (nmol/gHb)	0.016 (0.002)	0.015 (0.002)	0.016 (0.001)	0.011 (0.002)	0.034 (0.012)	0.104 (0.028)*	0.007 (0.004)	0.002 (0.001)*	0.007 (0.005)
MDA (nmol/gHb)	3.9 (0.2)	3.5 (0.9)	8.9 (1.5)*	6.4 (1.5)	76.4 (34.2)	122.6 (16.3)*	98.9 (13.2)*	81.3 (12.8)*	45.8 (4.1)*

NA, not available; OF, osmotic fragility; CAT, catalase; GPx, glutathione peroxidase; PO, protein oxidation; MDA, malondialdehyde; T1, rest; T2, post-fencing; T3, pre-swimming; T4, post-swimming; T5, pre-horse riding; T6, post-horse riding; T7, pre-combined event; T8, post-combined event; T9, 2-h recovery. * P ≤ 0.05 vs. rest.

Where applicable, the authors confirm that the experiments described here conform with The Physiological Society ethical requirements.

PCB252

Effect of go/no-go signal on pulse volume amplitude during motor task performance

K.K. Deepak[1], C. Kharya[2], M. Pal[2], G. Jain[1], A. Jaryal[1], H. Singh[3] and S. Anand[2]

[1]Physiology, All India Institute of Medical Sciences, New Delhi, Delhi, India, [2]Biomedical Engineering, All India Institute of Medical sciences, New Delhi, Delhi, India and [3]CCRH, New Delhi, Delhi, India

Introduction: Anticipation of voluntary motor activity leads to feed-forward activation of sympathetic nervous system. No-go signal serves as an experimental paradigm for studying anticipation of voluntary motor activity, where the intended motor task needs to be suspended. It is hypothesized that no-go signal may induce sympathetic activation required for subject's preparedness for discontinuation of motor command. The present study was designed to evaluate the effect of no-go signal on sympathetic vasomotor function in a motor task performing situation.
Methods: Fifteen healthy subjects were asked to respond to either "YES" (go) or "NO" (no-go) commands. Subjects either had to press the hand grip dynamometer with maximum contraction or ignore in accordance to command structure. These were labeled as Actual Contraction (AC) and no contraction (NC) respectively for go and no-go commands.
The surface EMG was recorded from ipsilateral forearm and photo-plethysmogrpah (PPG) signal was recorded from the middle finger of the contra-lateral hand in sitting posture. The PPG amplitude (pulse volume amplitude, PVA) was used as a measure of sympathetic vasomotor function. The decrease in PVA of the PPG wave was taken as the measure of sympathetic activation.
The baseline EMG and PPG were recorded for 2 min. Average of 2 min PPG amplitudes at rest was considered as baseline amplitude. The PPG and EMG recordings were acquired for 30 sec following both the commands (go/no-go). For AC it was ensured that subjects maintained contraction for 30 sec. Both the go and no-go commands were given three times in random fashion to each subject. The 30 sec PPG records during both AC and NC were further analyzed for PPG amplitudes averaged in 10 sec bin. The amplitude value of three records was averaged for the purpose of analysis. The data was analyzed using paired t test and results are expressed as mean ± SD.
Results: The averages of 10 sec PVAs decreased significantly during AC (280.7 mv ± 103.6 to 122.7 mv ± 65.56; p<0.001; decrease of 56.3 %). The PVAs of initial 10 sec of NC were found to be significantly decreased (280.7 mv ± 103.6 to 191.4 mv ± 110.6; p ≤ 0.001; decrease of 31.81 %). The % decrease of PVA was significantly less during NC compared to AC (p<0.001). However even during no-go signal subjects showed 31.8 % of residual activity. The no-go signal alone showed a sympathetic activation of 56.5 % {(31.8/ 56.3)X100} when compared to AC.
Conclusion: In the present study no-go signal for voluntary motor activity initiated sympathetic drive to vasculature in a situation where motor task was not performed. This reflects that nearly 50 % of sympathetic activation occurs due to readiness, even before the initiation of motor activity. Therefore even to execute no-go command a substantial sympathetic activation is required. This appears to operate through feed forward mechanism.

Where applicable, the authors confirm that the experiments described here conform with The Physiological Society ethical requirements.

PCB253

The influence of voluntary hyperventilation on a standing balance of athletes

M. Malakhov[1], E. Makarenkova[2] and A. Mel'nikov[2]

[1]Yaroslavl State Medical Acadamy, Yaroslavl, Russian Federation and [2]Yaroslavl State Pedagogical University, Yaroslavl, Russian Federation

Introduction. It is known that hyperventilation causes impairment of standing balance, since fast and deep respiratory movements perturb vertical steadiness [1]. Its common knowledge, that athletes integrate sensory information much better than untrained people, so standing balance of athletes is more perfect [2]. Thus, it can be assumed that the influences of hyperventilation on their postural stability will be less. The aim of our work was to study the influence of voluntary hyperventilation on a standing balance of athletes.
Methods. The subjects were divided into two groups: "Athletes" and "Control". The "Athletes" group included 38 participants (19 females) aged 19.8±1.0 The control group consisted of 28 healthy volunteers aged 22.4±4.6 (18 females). At first the subjects stood quietly on the force platform ("Quiet breath"), than they breathed as deep and fast, as possible ("Hyperventilation"), duration of both trials was 20 seconds. The stabilographic parameters (the mean velocity (V, mm/s) and variance of the center of pressure displacement in mediolateral (Qml, mm) and antero-posterior (Qap, mm) directions) were measured with a force platform "Stabilan" ("Ritm", Russia). The ventilation was estimated indirectly by mean of a strain gauge [3], the ventilation index (Vent) was calculated as product of the respiratory amplitude and rate.
Results. We found that Vent significantly increased in both groups during the "Hyperventilation" trial (8.4±4.5 vs. 102.5±41.8, p<0.001 in the "Control" group, 6.12±3.48 vs. 136.49±50.3, p<0.001 in the "Athletes" group). According to the ANOVA results elevation of Vent was more pronounced in the "Athletes" group (p=0.003), so the athletes breathed more deep and fast compared to the control subjects. Thus, obviously the perturbing effect of hyperventilation on the postural stability of the athletes was stronger. All stabilometric indices were also greater at the "Hyperventilation" trial in both groups (2,31±0,67 vs. 4,02±1,33 mm, p<0.001 2,11±0,81 vs. 3,98±1,35 mm p<0.001 for Qml; 3,02±1,09 vs. 6,17±2,00 mm, p<0.001, 2,7±0,82 vs. 6,55±2,40 mm p<0.001 for Qap;

8,51±2,28 vs. 25,45±11,12 mm/s group, 7,06±1,68 vs. 37,76±29,00 mm/s for V in the "Control" and "Athletes" groups respectively), hence hyperventilation leads to impairment of standing balance in all subjects. The ANOVA results showed that only an increase of V was more pronounced in athletes versus control subjects (p=0.02), other indices changed in the same way. So the steadiness in athletes was the same as in untrained subjects despite of more strong influence of the hyperventilation, but the strain of the postural control system was stronger in athletes [2].
Conclusions. The postural control system of the athletes compensated the exposure of hyperventilation more effectively, but through greater efforts.

Hodges PW et al. (2002). Exp Brain Res 144, 293-302.

Asseman F et al. (2005). Inter J of Sports Med 26, 116-119

Kubo HD & Hill BC (1996). Phys Med Biol 1996, 41, 83-91.

Where applicable, the authors confirm that the experiments described here conform with The Physiological Society ethical requirements.

PCB254

Gender-based EEG before and after acute exercise

N. Limbu[1], R. Sihna[2], M. Sihna[2] and B. Paudel[1]

[1]Basic & Clinical Physiology, B.P.Koirala Institute of Health Sciences, Dharan, Nepal and [2]physiology, All India Institute of Medical Sciences, Raipur, Raipur, India

Exercise is associated with changes in brain activity. Studies have examined few EEG frequency bands using few electrodes. There are few reports on EEG activity in response to acute exercise between male and female. We investigated how EEG frequency bands change in females in response to acute exercise compared to males. Consenting healthy adult females (n=15) & males (n=15) bicycled an automated ergometer at 50% HRmax for 20 min. A 16-channel EEG was recorded using international standards from mid-frontal (F4 & F3), central (C4 & C3), parietal (P4 & P3), temporal (T4 & T3) & occipital (O2 & O1). Exercise-induced EEG changes were compared between two sexes by Mann Whitney test. EEG power (μV2) is presented as median & interquartile range. The study was approved by institute ethical committee. In female, as compared to male, resting right side delta, alpha, beta & gamma activities were more in almost all recorded sites [delta: F4=49.82(44.23-63.56) vs. 35.5(32.70-44.44), p<0.001; C4=48.79(38.34-58.64) vs.37.6(26.72-43.80), p<0.01; P4=48.6(43.41-53.12) vs. 35.08(29.48-38.98), p<0.001; O2=58.88(52.65-59.52) vs.34.6(28.16-47.80), p<0.001; T4=17.78(15.77-20.95) vs.14.13(11.74-17.34), p<0.05], [alpha F4: 127.62(112.89-149.03) vs. 49.36(46.37-52.98), p<0.001; C4: 124.95(111.95-147.25) vs.57.07(51 – 59.29), p<0.001; P4=177.42(111.03-196.64) vs.89.91(66.58-98.86), p<0.001; etc], [beta F4=18.96(15.83-25.38) vs.14.77(10.34-17.55), p<0.05; C4=21.16(18.4-25.9) vs.15.48(9.66-19.40), p<0.01; P4=22.88(18.97-32.84) vs.18.7(12.32-24.09), p<0.05; etc], [gamma F4=0.58(0.44-0.87) vs. 0.24(0.20-0.42), p<0.001; C4=0.52(0.36-0.7) vs. 0.22(0.20-0.40), p<0.01; P4=0.54(0.45-0.67) vs. 0.24(0.21-0.40), p<0.001; etc]. Similarly, female resting right theta activity was more in Parietal [P4=33.04(25.1-42.41) vs.22.3 (18.36-34.33), p<0.05] & occipital [O2=50.81(30.64-66.8) vs.26.85 (22.18-34.42), p<0.001] regions than in male. They had similar picture on the left side also. The delta values (difference between post exercise and resting) of right alpha power was less in female in frontal [F4=-11.61(-45.24 -3.64) vs.9.48(1.05-16.58), p<0.01] and central [C4= -72(-32.98-9.48) vs.22.69(13.03-33.05), p<0.01] regions compared to males but they had less left central alpha [C3= -8.32(-32.65-6.1) vs.16.5(0.36-36.36), p<0.01] and temporal beta [T3= -6.29(-10.09- -1.49) vs.1.24(-0.84- 2.8), p<0.001] power compared to male. At rest, female group had more power of all the EEG frequency bands than the male. After acute exercise the female had decreased alpha in right frontocentral region whereas left alpha activity was reduced in central region and beta activity in temporal region. Although at rest females may have high EEG powers in different bands, the actual change in response to exercise, they respond in reverse way as compared to males. They seem less relaxed than the males immediately after moderate intensity of exercise.

Where applicable, the authors confirm that the experiments described here conform with The Physiological Society ethical requirements.

PCB255

Impact of exercise training on cardiopulmonary fitness in obese Thai women

W.S. Khrisanapant, O. Pasurivong, T. Suthitum and J. Namarmarth

Physiology, Khon Kaen University, Khon Kaen, Khon Kaen, Thailand

It is well known that obesity can negatively affect health and function which may be partly restored by several aerobic exercise programmes. We quantitatively investigated the effect of aerobic exercise on the cardiopulmonary fitness in obese Thai women (BMI 29.41 ± 2.9 kg/m2, aged 45 ± 5.34 yrs). The aerobic exercise training (AET) consisted of 12 weeks of leg cycling on an electronically controlled cycle ergometer at or near anaerobic threshold (AT) (30 min/session, 3 sessions/week, 12 weeks). Peak oxygen uptake (VO2peak) and 6 minute walk test (^MWT) were used as a measure of cardiopulmonary fitness. Values are means ± SD. The AET resulted in significant reductions in body mass 2.5 kg (p<0.01), BMI 1.0 kg/m2 (p<0.01), waist circumference 4.1 cm (p<0.05), hip circumference 3.2 cm (p<0.05), % body fat 2.98% (p<0.001), FM 2.95 kg, (p<0.001), SBP 10.9 mmHg (p<0.01), DBP 8.8 mmHg (p<0.01) and MAP 9.5 mmHg (p<0.01) but not FFM. Additionally, it increased VO2peak by 21.6% (p<0.01), work load at anaerobic threshold by 14.3% (p<0.01), maximal work load by 10.7% (p<0.01) and 6MWT by 14.3% (p<0.01) compared to pre- exercise. These data suggest that a 12-week exercise training programme increased cardiopulmonary fitness, aerobic capacity and physical performance but reduced body weight, body composition, SBP, DBP and MAP in obese women.

This study was supported by the Invitation Research Grant from the Faculty of Medicine, Khon Kaen University, Thailand.

Where applicable, the authors confirm that the experiments described here conform with The Physiological Society ethical requirements.

PCB257

Development of a four-day rapid acclimation schedule for military personnel

L.P. Singh and M. Kapoor

Heat Physiology, Defence Institute of Physiology and Allied Sciences,Defence Research and Development Organization, Timarpur, India

During Military operations, the soldiers are often deployed to hot regions. It is very important to acclimatize them in advance to heat stress to reduce the risk of heat illnesses. The existing heat acclimation protocols require eight to fifteen days. We have attempted to develop a rapid acclimatization schedule with duration of four days.

The study was approved from Institutional human ethical committee. Eighteen healthy Military personnel (n=18), age: 25±4 years, height: 172±4cm, weight: 66±3 Kg volunteered to participate in the study. They were informed about the purpose of the study and possible risks and signed a consent form. They were divided into three groups with six volunteers in each group. The volunteers in group I were subjected to a previously standardized acclimation protocol, as per which they were made to perform free hand exercise in human climatic chamber at 45°C and 30% relative humidity for one hour/day for eight days. The volunteers in group II were made to perform free hand exercise in human climatic chamber at 45°C and 30% relative humidity for one hour/day for four days.

The volunteers in group III were made to perform free hand exercise in human climatic chamber at 45°C and 30% relative humidity for two hour/day for four days. One hour exercise was performed in the forenoon followed by one hour rest, after which one hour exercise was performed again. For all the three groups of volunteers, the Core Body Temperature (CBT), Mean Skin Temperature (MST) and Mean Body Temperature (MBT) were noted before and after exercise. For individuals of group I, a significant difference was observed in post exercise CBT (37.14 ±0.14 vs 36.82 ±0.14, $p<0.05$), MST (35.90 ±0.30 vs 35.25 ± 0.23, $p<0.05$), MBT (36.77 ±0.19 vs 36.35 ±0.17, $p<0.01$) at eighth day compared to the first day. For individuals of group II, a significant difference was observed in post exercise CBT (37.16 ±0.04 vs 36.64 ±0.06, $p<0.01$), MST (36.09 ±0.05 vs 35.61 ± 0.11, $p<0.05$), MBT (36.84 ±0.04 vs 36.21 ±0.11, $p<0.05$) at fourth day compared to the first day. For individuals of group III, a significant difference was observed in post exercise MBT (36.98 ±0.02 vs 37.06 ±0.02, $p<0.05$), MST (35.58 ±0.06 vs 35.53 ± 0.10, $p<0.05$), MBT (36.56 ±0.03 vs 36.46 ±0.02, $p<0.05$) at fourth day compared to the first day. There was no significant difference between post exercise CBT, MST and MBT of group I at eighth day and group III at fourth day. A significant difference was observed post exercise in CBT (36.82 ±0.14 vs 36.64 ±0.06, $p<0.01$) MST (35.25 ± 0.23 vs 35.61 ±0.11, $p<0.05$) MBT (36.35 ±0.17 vs 36.21 ± 0.11, $p<0.05$) of eighth day of group I and fourth day of group II. We have successfully shortened the duration of acclimation schedule as can be concluded from the data. It will help to minimize the time and manpower losses suffered by Military for acclimation of personnel.

Where applicable, the authors confirm that the experiments described here conform with The Physiological Society ethical requirements.

PCB258

Whole-body cooling modulates skeletal muscle oxygenation during aerobic exercise

D.D. Gagnon[1], H. Kyröläinen[1], S.S. Gagnon[2], K. Herzig[3,4] and H. Rintamäki[5]

[1]Biology of Physical Activity, University of Jyväskylä, Jyväskylä, Finland, [2]Health and Rehabiliation Sciences, University of Western Ontario, London, ON, Canada, [3]Physiology and Biocenter of Oulu, University of Oulu, Oulu, Finland, [4]Psychiatry, Kuopio University Hospital, Kuopio, Finland and [5]Finnish Institute of Occupational Health, Oulu, Finland

Dynamic exercise results in increased muscle, and decreased skin blood flow in addition to a progressive decrease in tissue oxygenation with increased workload (Peltonen et al. 2012). Cooling of skin and skeletal muscle also reduces tissue oxygenation, in part due to an increase in peripheral vasoconstriction and a decrease in blood volume (Yanagisawa et al. 2007). It is currently unclear whether tissue oxygenation decreases further during aerobic exercise when combined with cold exposure. Using near-infrared spectroscopy (NIRS) technology, we examined the effects of whole-body cooling on muscle tissue oxygenation during aerobic exercise. Healthy male subjects (N = 11), dressed in shorts and t-shirt, completed 6 exercise trials on separate days. They exercised at 50% (walking) or 70% (running) of maximal oxygen consumption (VO2max), for 60 min on a treadmill in a climatic chamber set at 22°C (Neutral, NT), 0°C (Cold, CO), or at 0°C following a precooling period inducing deep tissue cooling (Cold with deep tissue cooling, CD). NIRS optodes were positioned on the muscle belly of the vastus lateralis (VL) and the gastrocnemius (GM) muscles to determine changes in skeletal muscle oxygenated (O2Hb) and deoxygenated (HHb) myo/hemoglobin levels ($\Delta\mu$M.L-1). Core and skin temperatures were also measured. Measurements were collected at baseline, 10, 30 and 60 min of exercise and analyzed by ANOVA (Mean ± SE). Skin temperature decreased by 10.0 ± 0.6 and 11.1 ± 0.5°C in CO and CD, respectively, and remained low during 60 min. Core temperature decreased in CD up to 30 min only (0.65°C ± 0.08) ($p < 0.001$). A clear reduction in muscle oxygenation was observed in GM and VL (70% VO2max only) during exercise ($p < 0.001$), which was greater at 70% vs. 50% VO2max ($p \leq 0.006$). The decrease in O2Hb was greater in CO (22.26 ± 1.27 μM.L-1) and NT (23.75 ± 1.43 μM.L-1) compared to CD (17.70 ± 1.57 μM.L-1) within the GM ($p = 0.023$) at 10 min of exercise only. In VL, however, the decrease was greater in CD compared to other conditions ($p = 0.021$). The increase in HHb was lower in CD (8.77 ± 3.07 μM.L-1) compared to CO (18.92 ± 6.70 μM.L-1) and NT (18.90 ± 2.84 μM.L-1) at 10 min in GM ($p = 0.019$). This was not observed in VL ($p \geq 0.972$). Tissue oxygenation responses differed between GM and VL. Interestingly, no differences in muscle oxygenation were observed between exercise in a neutral and a cold environment without whole-body deep tissue cooling. During the early stages of aerobic exercise, tissue deoxygenation was delayed in GM with deep tissue cooling whereas a greater decrease in O2Hb and unchanged HHb was seen in VL. These results may likely be due to a change in walking and running gait mechanics to perform the same workload relying on a larger muscle mass as muscle cooling is known to reduce mechanical efficiency, thereby modulating oxygen availability and transport.

Peltonen J, et al. (2012) Resp Physiol Neurobi 169, 24-35

Yanagisawa O, et al. (2007) Eur J Appl Physiol 100, 737-745

Where applicable, the authors confirm that the experiments described here conform with The Physiological Society ethical requirements.

PCB259

The use of antioxidant vitamin-E supplement: a study of female athletes

P. Chatterjee

Department of Physiology, University of Calcutta, Kolkata, West Bengal, India

Sports science is one of the newly exploring areas of Physiology that is very important to improve the athletic performance in scientific way. One of such a component that has a great probability to improve the athletic performance is the Antioxidant. More recently, Vitamin E as an antioxidant has come into the picture of muscular activity. Vit. E plays a critical role in protecting the cell from reactive oxygen species (ROS)-induced oxidative stress. There is an abundance of evidence that tissue content of Vit. E is decreased as a result of exercise, narrowing its protective margin against ROS. Because, human cannot synthesize this antioxidant Vit. E, they are dependent exclusively on dietary intake. So, oral supplementation of Vit. E may be a factor that influences physical performances. Total sedentary females were divided into two groups at random. Placebo sedentary group (n=15, given placebo supplementation for one week). Vitamin E-sedentary group (n=15, given 400 mg of Vit. E capsule supplementation for one week). Total female athletes were divided into two groups at random. Placebo athletes group (n=15, given placebo supplementation for one week). Vitamin E - athletes group (n=15, given 400 mg of Vit. E capsule supplementation for one week). Endurance performance has been carried out by Magnetic brake bicycle Ergometer on separate days. The room temperature was between 30-32 degree Celsius and the relative humidity was about 72%. The present study was to find out whether any physiological changes occur after Vit. E supplementation in female athletic and non athletic females.
They are:
1. a. To investigate protective effect of Vit. E on lipid peroxidation as marker of oxidative damage during exercise.
b. To evaluate the effect of endurance exercise and Vit. E supplementation on antioxidant enzyme systems in female athletes and sedentary females.
2. To study, at what extent an additional Vit. E intake can improve the cardio-respiratory parameters of athletes and non athlete females.
On analyzing the data, it was observed that Vit. E, the fat soluble natural antioxidant, plays a critical role in protecting the cell from exercise induced free radical mediated oxidative stress. So,Vit. E supplementation (400mg) can be recommended to female athletes performing regular training and also to individual subjected to strenuous work. This study supports the idea of antioxidant effect of Vit. E which might be useful in the biological preparation of endurance athletes for improving their athletic performance.

Where applicable, the authors confirm that the experiments described here conform with The Physiological Society ethical requirements.

PCB260

Effects of acute ingestion of cashew apple juice on oxidative stress and white blood cells count

N. Leelayuwat, P. Prasertsri, T. Thong-un, S. Muchimapura and J. Wattanathorn

Physiology, Khon Kaen University, Muang, Khon Kaen, Thailand

Oxidative stress could be increased with high-intensity exercise. It is a significant causal factor to dysfunctional immune response. Thus, high-intensity exercise is a risk of immunosuppression. Cashew apple which is a waste product of cashew nut comprises efficient antioxidants such as vitamin C and anacardic acids. Thus, supplementation of juice produced from cashew apple (CAJ) may reduce suppression of immune function. This may prevent post-exercise infection in sport players. The present study aimed to investigate effects of acute ingestion of CAJ on oxidative stress and white blood cells (WBCs) count in healthy trained subjects. This study was randomized crossover design. Ten healthy trained men aged between 16 and 29 years old were enrolled. They randomly ingested either CAJ or placebo (PLA) by 3.5 ml/kg body mass before cycling at 85% of maximal oxygen consumption for 20 min. Blood samples were obtained at rest, 20 min after the ingestion, immediately after the exercise and at 30 min of recovery period to determine oxidative stress and WBCs count. One week later, they received the other research drink and performed similarly to the previous visit. Oxidative stress was determined by plasma vitamin C, malondialdehyde (MDA) and nitric oxide concentrations. WBCs counts were determined by total WBCs, neutrophil, monocyte and lymphocyte counts. Data are expressed as mean ± SD. The differences of variables within and between groups were analyzed by repeated measures ANOVA and Bonferonni. The results show that there were significantly lower plasma MDA concentrations immediately after the exercise (0.83 ± 0.52 vs 1.08 ± 0.65 μmol/L, $p<0.05$) and during recovery period (0.73 ± 0.18 vs 0.95 ± 0.61 μmol/L, $p<0.05$) in the CAJ group compared to the PLA group. There was significantly higher plasma vitamin C concentration at 20 min after the ingestion (0.27 ± 0.11 vs 0.16 ± 0.12 μg/mL, $p<0.05$) in the CAJ group compared to the PLA group. Plasma nitric oxide concentration was not different between PLA and CAJ groups at any time-point. WBCs, neutrophil, monocyte and lymphocyte counts were not changed at any time-point in both PLA and CAJ groups without any difference between groups. In conclusion, acute ingestion of CAJ can decrease oxidative stress by increasing plasma vitamin C and decreasing plasma MDA. However, white blood cells counts were not affected.

Baj Z, Kantorski J, Majewska E, Zeman K, Pokoca L, Fornalczyk E, et al. Immunological status of competitive cyclists before and after the training season. Int J Sports Med 1994; 15: 319-324.

Lusa Cadore E, Lhullier FL, Arias Brentano M, Marczwski Da Silva E, Bueno Ambrosini M, Spinelli R, et al. Salivary hormonal responses to resistance exercise in trained and untrained middle-aged men. J Sports Med Phys Fitness 2009; 49: 301-7.

Hack V, Strobel G, Weiss M, Weicker H. PMN cell counts and phagocytic activity of highly trained athletes depend on training period. J Appl Physiol 1994; 77: 1731-1735.

Kubo I, Masuoka N, Ha T, Tsujimoto K. Antioxidant activity of anacardic acids. Food Chemistry 2006; 99: 555-562.

Peters EM, Anderson R, Nieman DC, Fickl H, Jogessar V. Vitamin C supplementation attenuates the increases in circulating cortisol, adrenaline and anti-inflammatory polypeptides following ultramarathon running. Int J Sports Med 2001; 22: 537-543.

This study was supported by Graduate School Research Grant, Exercise and Sport Sciences Development and Research Group and Faculty of Medicine Invitation Research Grant, Khon Kaen University, Thailand. Many thanks go to Srisupphaluck Orchid, Phuket for kindly supporting the research drink. In addition, we wish to thank all the participants for their enthusiastic cooperation

Where applicable, the authors confirm that the experiments described here conform with The Physiological Society ethical requirements.

PCB261

Relationships between resting metabolism and maximum muscle force

J. Yamauchi

TMU, Tokyo, Japan and FIfSS, Tokyo, Japan

[Introduction]
It is known that basal/resting metabolism is associated with muscle mass and that the maximum force production is related to muscle mass, so that basal/resting metabolism should be associated with the maximum force production. Accordingly, a deterioration of skeletal muscle function is one of the consequences of increase in adipose tissue or a risk of metabolic syndrome, due to a lowering of basal metabolism. However, there is no information available whether a resting metabolism is related to maximum force generation.
[Purpose]
The present study investigated the relations between resting metabolism and maximum force generation of hand and leg in young men and women.
[Methods]
Thirty-six healthy young individuals (age, 20.6±0.8 yr; height, 162.3±7.6 cm; body mass, 55.5±7.7 kg, mean±S.D.) participated in this study. The resting metabolism was measured with the metabolic analyzer. Also, maximum isometric knee extension force of the right leg was measured with the knee extension dynamometer, maximum isometric handgrip force of the right and left hand was measured with a handgrip dynamometer and maximum leg power was measured with a distance of horizontal squat jump performance. All measurements were repeated 3 times, and the mean value of the nearest two measurements was used for further analysis. Data are presented as mean±SD.
[Results]
Lean body mass (LBM) was significantly correlated with hand grip force, leg power, knee extensor force and resting metabolism ($r=0.887$; $p<0.001$, 0.762; $p<0.001$, 0.687; $p<0.001$ and 0.514; $p<0.01$, respectively). Also, a resting metabolism was significantly correlated with hand grip force, leg power and knee extensor force ($r=0.493$; $p<0.01$, 0.579; $p<0.001$ and 0.39; $p<0.05$, respectively). Although there were significant relationships between a resting metabolism and maximum force generation, it was shown that resting metabolism was differently related to force generating capacity in upper and lower body and different type of muscle actions (dynamic vs. static, single joint vs. multi-joint movements).
[Conclusion]
This suggests that resting metabolism is not only related to muscle mass, but also to muscle force. Measurement of maximum muscle force can be useful for a simple evaluation of resting metabolism.

Where applicable, the authors confirm that the experiments described here conform with The Physiological Society ethical requirements.

PCB262

The impact of Pilates on power, speed and endurance parameters of teenage swimmers

F. Ozyener[1], F. Coskun[2], S. Koparan[3], A. Dogan[3] and D. Ediger[2]

[1]Physiology, Uludag University Medical Faculty, Bursa, Turkey, [2]Chest Diseases, Uludag University MedicalFaculty, Bursa, Turkey and [3]Physical Education and Sports, Uludag University, Bursa, Turkey

Centring, coordination and breathing are amongst the leading principles of Pilates exercise (Latey P, 2002), which are also important respiratory functions to consider during swimming. We hypothesized, therefore, that training for swimming along with Pilates could be synergistic to improve overall physical capability, and aimed to observe whether there was any effect of Pilates on the development of motor functions and respiratory capacity of young swimmers. Following approval from the Institutional Ethics Committee, 16 competitive swimmers (CS) (who are in training for the last 5 years for 2 hours/ 4 days/wk) and 12 habitual swimmers (HS) were recruited as volunteers. They were divided into 4 groups: CS who did Pilates training, (CSpil, n=9, 16,7±2.9 years); CS controls, no Pilates (CScon, n=7, 15,7± 1,5 years); HSpil, (n=6; 19,2± 1,8 years; and HScon, (n=6, 21,2±1,7 years). The training was for 8 weeks, as reported by Muscolino and Cipriani (2004). Before Pilates training (bPT), the volunteers were asked to perform incremental exercise test (15-25 W/min) to the tolerable limit for estimation of lactate-threshold (θL) and determination of peak pulmoner oxygen uptake (VO2peak) using Vmax Encore system (VIASYS, USA). The CS group also performed at 25, 50, 100, 200 and 400m freestyle swimming, whereas HS group only at 25 and 50m. The values of hand grip and back power (Takei Kiki Kogyo dynamometers, Japan) as well as vertical jump heights (countermovement jump test) were also determined. All measurements were repeated after PT. Values are median (minimum-maximum) and analysed by Mann-Whitney U and Wilcoxon matched pairs signed-ranks tests. The level of significance is $p \leq 0.05$. CSpil group presented significant improvement at VO2peak which was bPT: 28,5 (16,8-32,3) and aPT: 43,4 (34,7-57,5) ml/kg/min ($p<0.05$), and θL was bPT 14,4 (8,02-20.5); aPT, 21,73 (14,5-34,5) ml/kg/min ($p<0.05$). There was no difference at the power variables except for HSpil group back power values which were: bPT 69,4 (49,70-101,9) and 105,9 (80,1-146,5) kg ($p<0.05$). Swimming performance in seconds did not change significantly except for 200m in CSpil group. There was no difference for flexibility, body mass index, maximum heart rate and maximum load values amongst groups. Since Pilates is relatively easy and less stressful to perform as an exercise, there is a trend to recommend it in many areas. Regarding our study, three sessions of weekly Pilates for 2 months seems to positively affecting the improvement of peak VO2 in young CS. However, the contribution from that type of exercise into the speed and power variables seems less noteworthy. Before recommending Pilates as a "supplement" to the actual exercise during training, further work needs to be done.

Latey P. (2002). J Bodyw Mov Ther, 6(2), 94–101.

Muscolino J, Cipriani S. J. (2004). Bodyw Mov Ther, 8, 15–24.

Where applicable, the authors confirm that the experiments described here conform with The Physiological Society ethical requirements.

PCB263

Does preceding human posture predict the priority of force minimisation over position control?

I. Loram

IRM/Healthcare Science Research Institute, Manchester Metropolitan University, Manchester, UK

A fundamental physiological idea is that the current configuration, sets or reflects parameters within the neurophysiological feedback loops that translate task intentions into muscular activity (3, 4). Human standing requires maintenance of unstable equilibrium with minimal muscular cost while controlling configuration. Whether the postural system prioritises maintenance of joint angles at the expense of muscular costs or prioritises minimisation of joint moments while allowing joint angles to change is uncertain (1, 2). Using gentle perturbations at the knee and observation of the transition into standing from walking, recent evidence (1) shows a common tendency to stiffen the leg joints in a generalised and prevailing manner. This stiffening may result from prior settings within the postural system. This hypothesis is tested by applying an internal perturbation which requires changing joint angles to minimise active joint moments. Hypothesis: perturbation related change in active joint moments can be predicted from the preceding posture.

Twelve participants stood on a force-plate holding a 5 kg bar in both hands. The bar was slowly raised to shoulder level, then slowly moved horizontally forwards to the maximum extent, then held in the forward position. Acceleration was minimal. If joint resistance were low, then during forward movement of the bar, the body should move backwards leaving the combined center of mass of body and bar in the initial position. If leg and trunk position remain constant the combined center of mass would move forwards. Summarising participants over three repetitions, in response to moving the bar anteriorly, the center of gravity moved anteriorly 26±17 mm and the absolute joint moment summed over the ankle, knee and hip increased 32±39 Nm. Both quantities showed substantial difference between participants and no change in repetition (Two-way ANOVA, α=0.05), so repetitions were averaged.

Using forwards, stepwise multiple regression, the increase in summed absolute joint moment normalised by summed absolute joint rotation is predicted by the preceding knee joint extension and hip joint to gravitation vector separation ($F(4,7)=14$, adjusted $R2=0.71$, $p=0.0016$). The fullest model prediction ($F(4,7)=40$, adjusted $R2=0.93$, $p=0.00007$), confirmed trunk angle as most important. The same process applied to normalised EMG activity summed over fourteen leg muscles, also confirmed trunk angle as most important. In this task preceding posture predicts the prioritisation of force minimisation over position control. Control of trunk alignment may be hierarchically and temporally prior to the control of generalised leg stiffness.

1. Di Giulio I. BIOMECHANICAL AND CONTROL MECHANISMS FOR SUSTAINING THE HUMAN POSTURAL ATTITUDE. In: Institute for Biomedical Research into Human Movement and Health (IRM), School of Healthcare Science. Manchester: Manchester Metropolitan University 2011.

2. Kiemel T, Zhang Y, and Jeka JJ. Identification of Neural Feedback for Upright Stance in Humans: Stabilization Rather Than Sway Minimization. Journal of Neuroscience 31: 15144-15153, 2011.

3. Pruszynski JA, and Scott SH. Optimal feedback control and the long-latency stretch response. Exp Brain Res 218: 341-359, 2012.

4. Sherrington CS. The Integrative action of the nervous system. LaVergne, USA: Nabu Public Domain Reprints, 2010.

Thanks are offered to Irene Di Giulio, Linda Tersteeg and Brian Bate for their support during preliminary work and data collection, and to the participants who willingly gave their time.

Where applicable, the authors confirm that the experiments described here conform with The Physiological Society ethical requirements.

PCB264

Effect of acute hypoxia on C_2C_{12} myoblast proliferation

C. Gallagher[1], J. Sharkey[2], N. Martin[2], D. Player[2], S. Myers[1] and M. Lewis[2]

[1]Sport and Exercise Sciences, University of Chichester, Chichester, UK and [2]School of Sport, Exercise and Health Sciences, Loughborough University, Leicestershire, UK

Oxygen (O_2) is an essential component in maintaining physiological homeostasis within mammalian cells and survival is classically viewed as being dependent upon the counterbalance of O_2 supply and O_2 demand (Arthur et al., 2000). Oxygen deprivation (hypoxia), such as that experienced at altitude, provides an important challenge to the organism which may severely compromise body metabolism, promoting reversible or irreversible loss of tissue and cell homeostasis leading to organic and functional decay (Magalhães & Ascensão, 2008). Loss in skeletal muscle mass in chronic hypoxia has been demonstrated during *in vivo* studies by a reduction of muscle (10-15%) and cross sectional area, including a decrease in muscle fibre size (20-25%) above 3000 m (Green et al., 1989; Hoppeler et al., 1990). *In vitro* studies support these findings demonstrating that chronic hypoxia (> 24 hours) leads to a decrease in cell proliferation and differentiation (Chakravarthy et al., 2001). However, the acute response is substantially understudied and could be important in understanding the effects of hypoxia on skeletal muscle during brief exposures such as those observed within intermittent hypoxic training programmes. The purpose of this work was to examine the role of acute hypoxia (24 h) on C_2C_{12} proliferation and relevant gene expression in 2D culture. 15 x 103 C_2C_{12} myoblasts were seeded into six well plates. The cells were maintained in DMEM with 20% FCS. C_2C_{12} myoblasts were either exposed to 21% or 5% O_2 (Figure 1).

At 24, 48, 72 and 96 hours RNA was extracted using the Trizol® method and mRNA expression of myogenic regulatory factors, myoD, myf5 and myogenin were detected using the 2-ΔΔCT method. Cell counts and cell viability were also quantified. Results were analysed using a 2 x 2 ANOVA. MyoD, myf5 and myogenin relative mRNA expression was not significantly different ($P > 0.05$) between the two conditions. Cell counts and cell viability also showed no change in hypoxia compared with normoxia. The data demonstrate that C_2C_{12} myoblasts can be cultured in hypoxia for 24 hours with no significant effect on proliferation. Thus, exposing individuals to 24 hours of hypoxia which results in an intramyocellular O_2 pressure of 5% appears safe for use within hypoxic research studies.

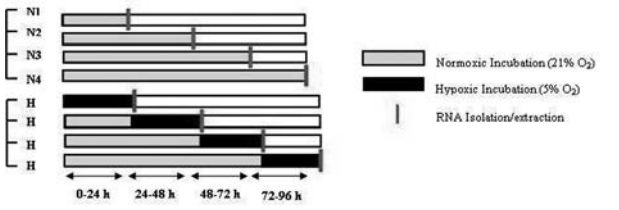

Figure 1. Schematic diagram of study design (N; Normoxic exposure, H; Normoxic exposure with 24 h hypoxic exposure).

Arthur, P.G., Giles, J.J. & Wakeford, C.M. (2000). Protein synthesis during oxygen conformance and severe hypoxia in the mouse muscle cell line C2C12. Biochemica et Biophysica Acta, 1475(1), 83-89.

Chakravarthy, M.V., Spangenburg, E.E. & Booth, F.W. (2001). Culture in low levels of oxygen enhances in vitro proliferation potential of satellite cells from old skeletal muscles. Cellular and Molecular Life Sciences, 58(8), 1150-1158.

Green, H.J., Sutton, J.R., Cymerman, A., Young, P.M. & Houston, C.S. (1989). Operation Everest II: adaptations in human skeletal muscle. Journal of Applied Physiology, 66(5), 2454-2461.

Hoppeler, H., Kleinert, E., Schlegel, C., Claassen, H., Howald, H., Kayar, S.R. & Cerretelli, P. (1990). Morphological adaptations of human skeletal muscle to chronic hypoxia. International Journal of Sports Medicine, 11(Suppl 1), S3-S9.

Magalhães, J. & Ascensão, A. (2008). High-altitude hypoxia. A challenging strain targeting cellular redox homeostasis. Portuguese Journal of Sport Sciences, 8(3), 459-469.

Where applicable, the authors confirm that the experiments described here conform with The Physiological Society ethical requirements.

PCB265

Appetite hormone response and body composition changes after 8 weeks exercise training with low and high intensities in overweight/obese females

H. Kubis, M. Jackson, F. Fatahi, D. King and A. Turner

School of Sport, Health and Exercise Sciences, Bangor University, Bangor, UK

Obesity is developing to pandemic proportions world-wide. One of the common obesity treatments is the prescription of regular exercise for weight reduction. Unfortunately, outcomes of training studies for weight loss show high variability, while responsible mechanisms which limit the effect of exercise for weight loss are not clear. We hypothesised that exercise training of obese female would lead to alterations in appetite hormone levels which would induce compensatory energy intake and no weight loss. To avoid confounding factors like motivation to lose weight and knowledge about study aims, we conducted a randomised single blind study. With ethical approval, healthy female subjects (n=43; BMI 30±3; Age 24±5) were recruited deceiving them about aims and measures, as well as excluding subjects who wanted to take part for weight loss. After random assignment into two groups, subjects trained with high (HI –group = 80-90%VO2peak) or low (LI –group = 50-60VO2peak) intensities three times (~1hour) a week for 8 weeks while the energy expenditure of the groups were matched via heart rate (telemetry). Pre and post measurements included body composition measurements (DXA), venous fasting and postprandial blood samples 1 hour after a test meal, VO2peak, resting metabolic rate, and diet diaries throughout the intervention. Appetite hormones measured via ELISA were insulin, amylin, leptin, ghrelin, and PYY3-36. 22 subjects (11 subjects per group) finished the study attending about 80% of the training sessions. Both groups (HI and LI) showed no alterations in weight (LI: pre 79.9±11.9, post 80.3±11.2; HI: pre 86.2±13.0, post 86.7±13.0 (kg)), fat (LI: pre 38.8±5.0, post 39.2±5.2; HI: pre 39.2±5.1, post 39.0±5.0 (%)) or lean mass after 8 weeks training. Moreover, VO2peak and resting metabolic rate were unchanged in both groups. Appetite hormone levels revealed a significant ($p<0.05$) reduction of fasting amylin (HI: pre 14.74±3.10, post 11.57±1.66; LI: pre 16.29±2.97, post 13.05±2.90 (pM)) and postprandial amylin (HI: pre 18.00±2.22, post 16.21±2.03; LI: pre 22.15±3.08, post 16.10±2.69 (pM)) levels in both training groups. Neither fasting nor postprandial levels of insulin, leptin, ghrelin and PYY3-36 were influenced by training in both groups. Analysis of diet diaries did not reveal any alterations in macronutrient composition over the training period. Amylin is known to influence food intake and gastric emptying; administration of amylin antagonist AC187 increased energy intake and accelerated gastric emptying. We suggest, considering the lack of changes in other measured appetite hormones, that amylin, via reduction in response to chronic exercise training, might enable a long term compensation of energy expenditure for improved body weight control.

Where applicable, the authors confirm that the experiments described here conform with The Physiological Society ethical requirements.

PCB266

Magnetic Resonance Elastography measurement of human skeletal muscle stiffness shows a decline in older adults compared with young

P. Kennedy[2], S. Semple[2], C. Gray[2], E. Barnhill[2], E. van Beek[2], N. Roberts[2] and C. Greig[1]

[1]School of Sport and Exercise Sciences, The University of Birmingham, Birmingham, B15 2TT, UK and [2]Clinical Research Imaging Centre, The University of Edinburgh, Edinburgh, EH16 4TJ, UK

Magnetic Resonance Elastography (MRE) is an emerging imaging technology that measures skeletal muscle stiffness via the study of externally induced sound waves propagating through the muscle. Evidence from mainly animal studies suggests that skeletal muscle connective tissue stiffness increases with advancing age, contributing to muscle weakness. However two recent human MRE studies measuring stiffness (shear modulus) in the relaxed state showed no statistically significant association between stiffness and age in 50-70 y old women1, and no significant differences when young and middle-aged adults were compared2. There are no MRE reports in the literature of stiffness in adults >70 y. We hypothesised that muscle stiffness measured using MRE would be higher in very elderly adults compared with young.

We studied the quadriceps group of n=18 healthy men and women (n=8 older median age 81 y range 69-87 y, BMI mean (SD) 23.8 (3.3); n=10 young median age 24 y range 21-35 y; BMI 25.6 (2.3)) using a 3 tesla MRI scanner (MAGNETOM Trio, Siemens AG, Erlangen, Germany). We used a modified single-shot EPI sequence sensitized to motion by the motion encoding gradient, aligned perpendicular to the image plane. Imaging parameters were TE=56ms, TR=1600ms, FOV=235mm, Matrix=128×128, slice thickness=10mm, scan duration=1min 6s Mechanical excitation was supplied to the muscle via a ring shaped plastic cuff positioned at mid-thigh level and which was affixed to the vibration source via a carbon fibre piston. The data were imported into MATLAB then temporally Fourier transformed, filtered, inverted and averaged as previously

reported3. The data were interpreted over three regions of interest, the whole axial slice, the extensor muscles, and the vastus lateralis. Comparison between groups was by 1-way ANOVA.
We found a significant reduction in stiffness in older muscle compared with young across all regions of interest. Mean (SD) shear modulus for young vs old were 2053.4 (115.9) vs 1783.6 (87.2), p<0.001; 2067.7 (157.2) vs 1801.9 (98.0), p = 0.003; 1929.9 (212.2) vs 1664.5 (146.5), p = 0.02 for the whole slice, extensor muscles and VL alone respectively.
Contrary to our hypothesis, these preliminary data suggest that skeletal muscle stiffness may actually decline with advancing age although this may still adversely affect force transmission. Further research on larger groups, controlling for prior physical activity, muscle length and load, are needed. MRE is non-invasive and does not entail strenuous activity. It is therefore suitable for studies with older adults and may represent a non-invasive, functional biomarker of ageing muscle function.

1. Domire ZJ, McCullough MB, Chen Q, An KN. Feasibility of using magnetic resonance elastography to study the effect of aging on shear modulus of skeletal muscle. J Appl Biomech 2009; 25(1):93-7.

2. Debernard L, Robert L, Charleux F, Bensamoun SF. Analysis of thigh muscle stiffness from childhood to adulthood using magnetic resonance elastography (MRE) technique. Clin Biomech 2011; 26(8):836-40.

3. Klatt D, Papazoglou S, Braun J, Sack I. Viscoelasticity-based MR elastography of skeletal muscle. Phys. Med. Biol. 2010; 55, 6445–6459.

We acknowledge the support of The University of Edinburgh Moray Endowment and Small Project Grant funds, the Scottish Imaging Network (SINAPSE) and the Mentholatum Company.

Where applicable, the authors confirm that the experiments described here conform with The Physiological Society ethical requirements.

PCB268

Chaperone protein binding in human muscle fibres during recovery from unaccustomed exercise

R. Billeter[1], K. Miller[1], D. Thomas[1], Z. Kwan[1], K. Marimuthu[1], P. Greenhaff[1] and H. Hoppeler[2]

[1]School of Biomedical Sciences, University of Nottingham, Nottingham, UK and [2]Institute of Anatomy, University of Bern, Bern, Bern, Switzerland

αB crystallin and Hsp27 are small chaperone proteins that bind to unfolded proteins in order to block potential aggregation sites. Both are abundant cytoplasmic proteins in skeletal muscle fibres. Hsp70 is also a muscle chaperone protein, thought to be involved in folding of nascent and/or unfolded proteins. We hypothesised that unaccustomed exercise would lead to unfolding of proteins, which would be bound by these chaperones.
P70S6kinase phosphorylation at thr 421/ser 424 is increased in type II fibres following resistance exercise, which is thought to reflect increased muscle protein synthesis[1]. Given that unfolded proteins are potentially associated with sites of repair, we hypothesised that fibres with increased chaperone binding would also show enhanced p70S6K phosphorylation.
Biopsy samples were obtained from vastus lateralis muscle of healthy volunteers (n=8, age 21-35), unaccustomed to physical activity, before and after 3, 30 and 180 min of recovery following 30 min of treadmill running at a workload that elicited a steady-state plasma lactate concentration of 4 mM. Immunohistochemistry was subsequently performed on muscle cryostat sections, using classic double fluorescence, as well as in situ proximity ligation to demonstrate co-localisation.
αB crystallin bound tightly and stably to insoluble structures, likely to be myofibrils and/or the cytoskeleton. To compare the extent of αB crystallin binding over the course of recovery, an arbitrary threshold was set just above the staining background of stitched micrographs covering whole sections and the fluorescence of the supra-threshold pixels expressed per muscle fibre area.
Figure 1 shows that peak αB crystallin binding occurred after 3 min of recovery, and then declined to a value close to baseline after 3 hours. Staining was partially diffuse but also punctate, with strongly staining dots. Hsp27 also bound to the αB crystallin dots, in addition to intermediate filaments. In these dots, in situ proximity ligation co-localised the two small chaperones to within 20-40 nm, thus they are likely part of the same complex. The larger, strongest dots stained positive for Hsp70, where it also co-localised with αB crystallin.
Given their established function, we interpret the co-localisation of three different chaperone proteins to the same site to indicate the presence of unfolded proteins. In fibres with numerous αB crystallin dots we found enhanced signals for p70S6K phosphorylation, resulting in a significant correlation between p70S6K phosphorylation and αB crystallin binding (p<0.05, r =0.57, Spearman). We believe this possibly reflects increased muscle protein synthesis at sites of protein unfolding.

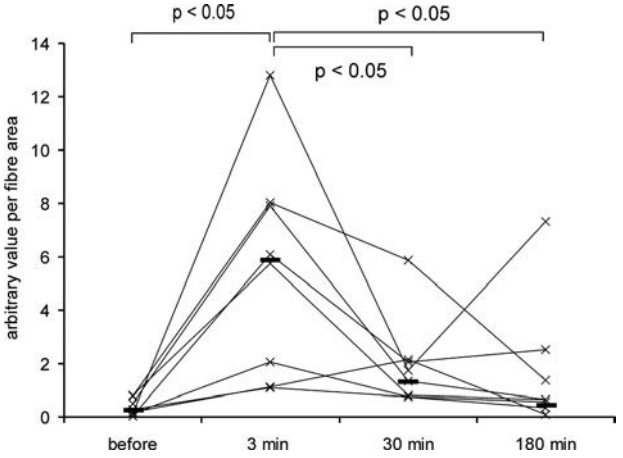

Figure 1: αB crystallin binding to insoluble structures in muscle fibres before and after 30 minutes treadmill running. x indicate bound crystallin per biopsy section, the values of individual subjects are connected. Black bars indicate medians. p values were determined using Wilcoxon's tests.

1. Koopman et al. (2006). Am J Physiol Endocrinol Metab 290(6), E1245-52.

Where applicable, the authors confirm that the experiments described here conform with The Physiological Society ethical requirements.

PCB269

Mechanical hyperventilation enhances static cerebral autoregulation in critically ill patients with severe sepsis

M.W. Petersen[1,2], L.N. Toksvang[1], C.B. Christiansen[1], K. Møller[1,3], R.R. Plovsing[2] and R.G. Berg[1,4]

[1]Centre of Inflammation and Metabolism, Department of Infectious Diseases M7641, University Hospital Rigshospitalet, Copenhagen Ø, Denmark, [2]Intensive Care Unit 4131, University Hospital Rigshospitalet, Copenhagen Ø, Denmark, [3]Neurointensive Care Unit 2093, University Hospital Rigshospitalet, Copenhagen Ø, Denmark and [4]Renal and Vascular Research Section, Department of Biomedical Sciences, Faculty of Health Sciences, University of Copenhagen, Copenhagen N, Denmark

Background:
Hypercapnia may contribute to a functional impairment of static cerebral autoregulation in patients with septic shock (Taccone *et al*, 2010). This may predispose to irreversible brain damage by rendering the brain particularly susceptible to hypo- and hyperperfusion upon decreases and increases in mean arterial blood pressure (MAP), respectively. In the present study we hypothesized that mechanical hyperventilation would enhance static cerebral autoregulation in critically ill patients with sepsis.
Methods:
Six mechanically ventilated patients with severe sepsis were enrolled in the study following ethical approval and informed consent from the next of kin. Invasive MAP and middle cerebral artery blood flow velocity (MCAv) measured by transcranial Doppler ultrasonography were recorded before (baseline) and after mechanical hyperventilation with an intended reduction in $PaCO_2$ of 1 kPa. Steady state testing of autoregulation was achieved by increasing MAP approximately 30 mmHg by means of an intravenous infusion of norepinephrine. Data are reported as median with corresponding interquartile range (IQR).
Results:
Baseline infusion of norepinephrine (from 0.09 (0.02-0.22) to 0.16 (0.11-0.29) $\mu g \times kg^{-1} \times min^{-1}$) increased MAP from 73 (69-79) to 98 (96-107) mmHg ($p<0.05$). The concomitant MCAv values were 38 (36-48) and 47 (43-61) $cm \times sec^{-1}$. Mechanical hyperventilation decreased $PaCO_2$ by 0.7 (0.6-0.8) kPa with a concomitant increase in pH from 7.42 (7.35-7.43) to 7.46 (7.41-7.48) (both $p<0.05$). During hyperventilation, MAP was increased from 78 (74-82) to 105 (97-110) mmHg ($p<0.05$) by increasing the norepinephrine infusion rate from 0.09 (0.02-0.22) to 0.20 (0.14-0.29) $\mu g \times kg^{-1} \times min^{-1}$. The concomitant values of MCAv values were 34 (27-40) and 33 (27-49) $cm \times sec^{-1}$, respectively. The slope of the regression line between MAP and MCAv decreased from 0.19 (0.11-0.42) at baseline to 0.09 (-0.01-0.20) $cm \times sec^{-1} \times mmHg^{-1}$ during mechanical hyperventilation ($p<0.05$).
Conclusion:
Our findings may indicate that mechanical hyperventilation enhances static cerebral autoregulation in patients with severe sepsis, which highlights this intervention as a potential neuroprotective intervention in the critical care setting.

Table 1. Patient characteristics

Patient	Gender	Age (years)	APACHE II	SOFA	Focus of infection	Time from admission (hours)
1	F	74	31	12	Soft tissue	< 24
2	F	67	34	15	CNS	< 24
3	M	58	5	3	Soft tissue	< 72
4	M	43	19	14	Soft tissue	< 48
5	M	63	21	10	Lung	< 24
6	M	69	18	2	Soft tissue	< 72

APACHE II: Acute Physiology and Chronic Health Evaluation II; SOFA: sequential organ assessment score; CNS: central nervous system; F: female; M: male.

Taccone FS *et al* (2010). *Neurocrit Care* **12**, 35-42.

Where applicable, the authors confirm that the experiments described here conform with The Physiological Society ethical requirements.

PCB270

Poor agreement between transcranial doppler and near-infrared spectroscopy-based estimates of cerebral blood flow in patients with sepsis

L.N. Toksvang[1], M.W. Petersen[1,2], R.R. Plovsing[2], K. Møller[1,3] and R.M. Berg[1]

[1]Centre of Inflammation and Metabolism, Department of Infectious Diseases M7641, University Hospital Rigshospitalet, Copenhagen Ø, Denmark, [2]Intensive Care Unit 4131, University Hospital Rigshospitalet, Copenhagen, Denmark and [3]Neurointensive Care Unit 2093, University Hospital Rigshospitalet, Copenhagen, Denmark

Background. Near-infrared spectroscopy (NIRS) has been highlighted as a potentially useful non-invasive clinical tool for continuously monitoring cerebral hemodynamics in critically ill patients with sepsis (Steiner et al, 2009). This is based on the presupposition that changes in cerebral oxygen saturation (ScO2) accurately reflect changes in cerebral blood flow (CBF), but whether this is the case in critically ill patients with sepsis remains to be clarified. In the present study, we therefore compared NIRS- to transcranial Doppler ultrasound (TCD)-derived estimates of vasopressor-associated changes in CBF.
Methods. Eight mechanically ventilated, critically ill patients (mean age 62, SD 11; 2 females) diagnosed with severe sepsis were included following ethical approval and informed consent from the next of kin. In a step-wise manner, the mean arterial blood pressure (MAP) was increased by approximately 30 mmHg over 4–5 steps, remaining 5 minutes at each step, by increasing the norepinephrine infusion rate. The associated changes in CBF were assessed by simultaneous ipsilateral NIRS (ScO2) and TCD (middle cerebral artery blood flow velocity, MCAv) measurements. Data are reported as median with corresponding interquartile range (IQR).
Results. A total of fifteen simultaneous NIRS- and TCD-derived assessments of vasopressors-associated changes in CBF were obtained in the patients. The norepinephrine infusion rate was raised from 0 median (IQR, 0–0 μg/kg/min) to 0.20 μg/kg/min median (IQR, 0.15–0.30 μg/kg/min), which increased MAP from 74 (71–90) to 100 (93–115) mmHg ($p<0.05$). This was associated with an increase in MCAv of 14% (2–22) ($p<0.05$), whereas no changes were observed in ScO2; 1% ([-4]–3) (NS). The Bland-Altman plot (Bland & Altman, 1986), used to compare the two methods, showed a relative bias of 14% with limits of agreement -16 to 44 % change in CBF (Figure).
Conclusion. There was poor agreement between NIRS- and TCD-derived estimates of norepinephrine-induced changes in CBF. This is likely related to contamination of the signal by extracranial tissues, particularly blood flow through the scalp

vessels. Our findings thus question the applicability of NIRS for monitoring cerebral hemodynamics, at least in critically ill patients with sepsis.

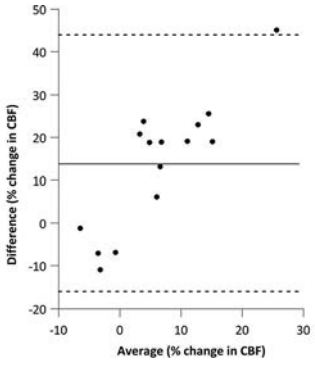

Bland-Altman plot of transcranial Doppler vs. near-infrared spectroscopy based estimates of vasopressor-associated changes in cerebral blood flow (CBF).

Steiner LA et al. (2009). Neurocrit. Care 10, 122-128.

Bland JM & Altman DG (1986). Lancet 1, 307-310.

Where applicable, the authors confirm that the experiments described here conform with The Physiological Society ethical requirements.

PCB271

Correlation between maximal inspiratory pressure and spirometric indices in young rowers

J. Kivastik[1], M. Arend[2] and J. Mäestu[2]

[1]Department of Physiology, University of Tartu, Tartu, Estonia and [2]Institute of Sport Pedagogy and Coaching, University of Tartu, Tartu, Estonia

The pressure differences driving our ventilation are generated by respiratory muscles. Respiratory muscle weakness may sometimes explain dyspnoe and exercise intolerance, training of those muscles has shown to improve exercise performance in both healthy adults and in patients with chronic respiratory illnesses. Such training often asks to perform respiratory efforts against a pressure load equivalent to a certain percent of maximal respiratory pressures. Portable devices are available to measure those maximal pressures, but it can be highly dependent on participant effort. Our aim was to find out whether maximal inspiratory pressure (MIP) correlates with different flow-volume loop parameters in a group of college level rowers and to compare our data from athletes with published reference values.

We studied fourteen 19-33 year-old rowers (two of them female) with mean (range) height 187 (173-202) cm. Flow-volume spirometry was performed according to the international guidelines (1) to determine forced vital capacity (FVC), forced expiratory volume in 1 second (FEV_1), peak expiratory and inspiratory flows (PEF and PIF). In addition we made two forced inhalation maneuvers without previous forced expiration. Measurement of MIP was performed with a hand-held mouth pressure meter, during the forced inhalation from residual volume. The maximum average pressure sustained over a 1 second period was defined as a result, subjects repeated this test 3 times. All measured values were compared with reference data (2, 3) and correlations between MIP, lung function and anthropometric indices were expressed by Pearson correlation coefficients (r). Ethics committee approval was obtained and all participants gave informed consent.

In comparison to reference population our young rowers had values of FVC and FEV_1 mostly above average (97-130% of predicted), whereas PEF ranged from 85 to 120% of predicted. All 3 indices describing forced expiration correlated with height, the strongest correlation was found between FEV_1 and height ($r=0.89$, $p<0.01$). Often only forced expiration is assessed to diagnose airway obstruction, therefore, the measurement and reference values for PIF are less standardized. In 11 subjects the highest PIF value was obtained from the forced inspiration without previous forced expiration. When using MIP reference values depending on age only, we obtained values in a range of 88-212% pred (absolute values 98-234 cm H_2O). MIP correlated significantly only with PIF ($r=0.53$, $p<0.05$).

High lung volumes and flows compared to the reference values from untrained persons indicate an increased functional capacity of respiratory system in studied rowers. We found a wide between-individual variability of MIP in healthy young subjects. MIP values did correlate with neither anthropometric nor spirometric indices (except for PIF).

Miller MR et al. (2005). Eur Respir J **26**, 319-338.

Kuster SP et al. (2008). Eur Respir J **31**, 860-868.

Evans JA & Whitelaw WA (2009). Respir Care **54**, 1348-1359.

Where applicable, the authors confirm that the experiments described here conform with The Physiological Society ethical requirements.

PCB272

Heterogeneity of blood flow and VO2 in exercising normal human muscle assessed by near infrared spectroscopy

P.D. Wagner[1], H. Habazettl[2], I. Vogiatzis[3], Z. Louvaris[3], H.E. Wagner[1] and S. Zakynthinos[3]

[1]Medicine, University of California, San Diego, La Jolla, CA, USA, [2]Institute of Physiology, Charite Campus Benjamin Franklin, Berlin, Germany and [3]Dept of Critical Care Medicine, University of Athens, Athens, Greece

Heterogeneity in the distribution of ventilation and blood flow in the lungs, and its effects on pulmonary gas exchange, are well known, and several methods exist for their quantification. This is not the case in skeletal muscle, where heterogeneity in the distribution of both blood flow and O_2 consumption has not been directly measurable, rendering its effects on muscle function unable to be evaluated. We used near-infrared spectroscopy (NIRS) to measure the regional distribution of VO_2, blood flow (Q), and their ratio (VO_2/Q) in six trained cyclists at rest and during constant load exercise (unloaded pedaling, 20%, 50% and 80% of peak watts) in both normoxia and acute hypoxia (FIO_2=0.12). From each of six optodes on the skin over the upper, middle and lower vastus lateralis, we recorded a) indocyanine green dye (ICG) inflow after IV injection to measure blood flow, and b) oxygenated Hb/Mb (StO_2). Varying both exercise intensity and FIO_2 provided a (directly measured) femoral venous O_2 saturation ($SfvO_2$) range of about 10 to 70%, and a corresponding range in StO_2 of about 35 to 75%. In each subject, a linear relationship was found between mean Q-weighted StO_2 over the 6 optodes and $SfvO_2$. We used this empirical relationship to compute local muscle venous blood O_2 saturation from StO_2 recorded at each optode, from which local VO_2/Q ratios could be calculated by the Fick principle. Multiplying regional VO_2/Q by Q yielded the corresponding local VO_2. Under all conditions, relative dispersion of Q (0.44 ± 0.02) and VO_2 (0.48 ± 0.02) were similar, while that for VO_2/Q was far less (0.14 ± 0.01), indicating in fit young subjects: a)

a strong capacity to regulate Q according to regional metabolic need from rest to heavy exercise in both normoxia and hypoxia, and b) a likely minimal impact of heterogeneity on overall muscle function. Future application of this novel approach, which may require recording from a larger number of optodes, should clarify the extent and importance of heterogeneity in muscle of patients with chronic diseases, and may become useful in the intensive care setting as an indicator of peripheral vascular regulatory integrity.

Where applicable, the authors confirm that the experiments described here conform with The Physiological Society ethical requirements.

PCB274

A single night of fragmented sleep reduces cerebral vascular reactivity and central chemoreceptor CO_2 sensitivity

K. Pugh[1], S. Taheri[2] and G.M. Balanos[1]

[1]School of Sports and Exercise Sciences, University of Birmingham, Birmingham, UK and [2]School of Clinical and Experimental Medicine, University of Birmingham, Birmingham, West Midlands, UK

Purpose: Patients suffering from sleep disordered breathing present with a reduced cerebral vascular reactivity (CVR) [1]. The severity of this reduction is shown to be related to the number of arousals per night [2]. These changes in CVR and the fragmentation of sleep could play a role in the respiratory changes observed in this patient population. Hypotheses: We hypothesized that the change in CVR following a night of artificially fragmented sleep when compared to the CVR change following a normal night. Furthermore, we predicted a decline in respiratory CO_2 sensitivity. Methods: Participants visited the laboratory on two occasions for an overnight stay. One visit included a normal night's sleep (*control*) and the other visit included a night of fragmented sleep (*fragmentation*). During *fragmentation* micro-arousals were elicited during all sleep stages using a 500ms auditory stimulus played every minute. Continuous polysomnography was recorded throughout each night. CVR was assessed before and after each night using transcranial Doppler ultrasound of the middle cerebral artery. During the assessment of CVR participants were exposed to three five-minute steps of hypercapnia: 4, 7 and 10 mmHg above normal end-tidal partial pressures of CO_2($P_{ET}CO_2$). A hypercapnic (10 mmHg>normal $P_{ET}CO_2$) multi-frequency binary sequence test was completed following each night to assess central and peripheral chemosensitivity. A dynamic end-tidal forcing system was used for gas control during each assessment. Results: The mean (±S.E.) change in CVR following *fragmentation* is reduced across all three steps of hypercapnia when compared to the CVR change after the *control* night; -2.23±4.36%, -2.55±2.45% and -9.13±1.89%, respectively. We also observed a reduction in total CO_2 chemosensitivity following *fragmentation*, -41.97±20.25%. Additionally, peripheral chemosensitivity remained unchanged following *fragmentation* -6.20±16.62%. However, central chemosensitivity was markedly reduced -35.77±6.02%. Discussion: These results support our hypothesis of parallel alterations in breathing and cerebral vascular control following a night of disrupted sleep. The poor quality of sleep effecting patients suffering sleep disordered breathing could potentially play a role the respiratory control changes seen in this population, which may ultimately promote the further development of the disease.

1. QURESHI, A.I., W. CHRISTOPHER WINTER, and D.L. BLIWISE, Sleep Fragmentation and Morning Cerebrovasomotor Reactivity to Hypercapnia. American Journal of Respiratory and Critical Care Medicine, 1999. 160(4): p. 1244-1247.

2. Hajak, G.r., et al., Sleep Apnea Syndrome and Cerebral Hemodynamics. CHEST Journal, 1996. 110(3): p. 670-679.

Where applicable, the authors confirm that the experiments described here conform with The Physiological Society ethical requirements.

PCB275

Serum lipids: profile during pregnancy in women in Benin City, Nigeria

M.I. Ebomoyi[1] and C.N. Ekhator[1,2]

[1]Physiology, University of Benin, P.M.B. 1154, Benin City, Edo State, Nigeria and [2]St.Philomena's Catholic Hospital., Benin City, Edo State, Nigeria

Lipid metabolism changes during pregnancy in order to support fetal growth and development .1,2,3 It is believed that this process is under hormonal control.4 There have been reports on serum lipid profile during pregnancy in Caucasians, but very little is known in Africans.5 There has not been a prospective cohort study using the same group of subjects throughout the course of pregnancy in women in this environment, hence this study. The study was therefore to determine serum triglyceride (TG), high density lipoprotein cholesterol (HDL), total cholesterol (TC) and low density lipoprotein cholesterol (LDL) in the three trimesters of pregnancy in the same women, in Benin City, Nigeria. Subjects were 50 pregnant women at the 6th week of pregnancy (first trimester) with no history of midwifery complications or systematic disorders. They were 25-34 yrs, (mean age 28±0.44 yrs). Controls were 50 non-pregnant women of the same age group that met the inclusion criteria. Demographic characteristics and midwifery information were collected by questionnaire. Written informed consent was obtained, and fasting venous blood samples were taken during the 1st, 2nd and 3rd trimesters. Blood pressure was recorded. Mean ± S.E.M. were calculated for all groups. lipid concentrations were measured enzymatically and expressed as mg/dl. Data was analyzed using ANOVA, and $p< 0.05$ was considered statistically significant. TG was lower in the control group than in the 1st, 2nd or 3rd trimester (138.44±0.6 vs 312.3±9.3, 252±3.1 and 247.4±2; $p<0.05$). However, among the pregnant women, TG concentration in the 1st trimester was higher than in the 2nd and 3rd trimester. The 2nd and 3rd trimester TG concentrations were not significantly different. HDL was significantly lower in the 1st trimester than in the control, 2nd or 3rd trimester (48.04±0.3 vs 58.34±0.4, 60.7±1.0, 56.3±0.5). LDL was highest in 1st trimester pregnancy and least in the control group (178.1±1.3 vs 83.04±1.2, 137.7±2.2 and 125.2±0.8; $p<0.05$). TC was higher in pregnant women than in the control (224.7±0.9, 216.8±0.9 and 231.7±2.2 vs 180.44±1.6; $p<0.05$). The significantly raised TG, TC and LDL in the pregnant women compared to the controls, especially during the 1st trimester provides evidence of natural rising in plasma lipids in normal pregnancy due to hormones.4 This rise in TG, TC, and LDL may be due to an increase in hepatic lipase activity and decrease in lipoprotein lipase active, the principle modulator of which is the pregnancy-induced hyperoestrogenaemia. It is concluded that the normal pattern of pregnancy- induced variations in serum lipids is observed in the women studied.

The authors acknowledge all the women that took part in the study.

1. Angel GAL. (2006). Ann Hepatol 5(3), 184-186.

2. Brizzi P, Tonolo G and Esposito F (1999). Am J Obstet Gynaecol 181, 430–434.

3. Sattar N, Greer IA and Louden J (1997). J Clin Endocrinol Metab 82, 2483–2491.

4. Rovinsky JJ and Jaffin H (1966). Am J Obstet Gynecol 95(6), 787–794.

5. Adegoke OA, Iyare EE and Gbenebitse SO (2003). Niger Postgrad Med J 10(1), 32-36.

The authors acknowledge all the women that took part in the study.

Where applicable, the authors confirm that the experiments described here conform with The Physiological Society ethical requirements.

PCB276

RFamide related peptide-1 attenuates gonadotropin-releasing hormone release in immortalized GT1-7 cells without changing intracellular calcium concentration

H. Kelestimur[1], E. Kacar[1], M. Ozcan[2] and S. Kutlu[1]

[1]Physiology, Firat University Medical School, Elazig, Turkey and [2]Biophysics, Firat University Medical School, Elazig, Turkey

Hypothalamic RFamide peptides, gonadotropin-inhibitory hormone (GnIH) and orthologous peptides, which were then discovered in mammals belonging to the RF-amide peptide superfamily (RFRP), seem to be important regulators of hypothalamus-pituitary-gonadal (HPG) reproductive axis. Kisspeptins are reported to be the most potent activators of HPG axis known to date. Kisspeptin increases intracellular calcium concentration ($[Ca^{2+}]_i$) in immortalized GnRH neurons (1). Whether RFamide peptides modulate the effects of kisspeptins on GnRH neurons has not been investigated. The goal of the present study was to examine the effects of RFamide related peptide-1 (RFRP-1), a mammalian orthologous peptide of GnIH, on kisspeptin-stimulated gonadotropin-releasing hormone (GnRH) neurons. In the study the GT1-7 cell line expressing GnRH was used as model to explore the effects of RFRP-1 on kisspeptin-activated GnRH neurons. The effects of RFRP-1 on GnRH release and calcium signaling in GT1-7 cells were investigated. GT1-7 cells were cultured on poly-D-lysine-coated coverslips and maintained in DMEM supplemented with heat-inactivated fetal calf serum, 100 U/ml penicillin and 100 μg/ml streptomycin at 37 oC in 5% CO2. After loading the cells with 1 μM Fura-2 AM, $[Ca^{2+}]_i$ responses were quantified by the changes in 340/380 nm ratio for individual GT1-7 cells. GnRH release to medium was assayed by ELISA. Kisspeptin-10 at 100 nM (n=65) caused a significant increase ($P<0.01$) in GnRH release. Co- treatment with kisspeptin in the presence of 1 μM RFRP-1 (n=43) attenuated ($P<0.05$) kisspeptin-induced GnRH release in GT1-7 cells. Kisspeptin-10 at 100 nM caused a significant increase ($p<0.001$) in $[Ca^{2+}]_i$ compared to basal levels in GT1-7 cells. RFRP-1 did not cause any change in kisspeptin-induced $[Ca^{2+}]_i$ increase in GT1-7 cells. The results suggest that RFRP-1 may have inhibitory effects on kisspeptin-activated GnRH neurons without affecting $[Ca^{2+}]_i$.

Ozcan M. *et al*. (2011). *Neurosci Lett* **492**, 55-58.

We thank Dr. Pamela L. Mellon, Department of Reproductive Medicine, University of California, San Diego, for kindly providing GT1-7 cells. This study was supported by TUBITAK Project # 110S381

Where applicable, the authors confirm that the experiments described here conform with The Physiological Society ethical requirements.

PCB277

Rat supraoptic nucleus neurons respond to glucose increase through closure of ATP dependent potassium channels

Z. Song, W. Stevens and C.D. Sladek

Physiology & Biophysics, University of Colorado School of Medicine, Aurora, CO, USA

Oxytocin (OT) is an anorexic agent. Deficits in OT are associated with human obesity. Glucokinase (GK), a hallmark of glucose-sensing cells, is expressed in the supraoptic nucleus (SON) of the hypothalamus, where OT and vasopressin (VP) are synthesized. Therefore, SON neurons may function as glucose-sensors. It has been shown previously that an increase in glucose induced a rise in intracellular calcium ($[Ca^{++}]_i$) in SON neurons (Song and Sladek, 2011), presumably through GK-driven production of ATP and subsequent closure of ATP dependent potassium channels (K_{ATP}). In our present studies, live-cell calcium imaging was thus used to determine the molecular signaling mechanisms underlying glucose-sensing of SON neurons. Rat hypothalamic explants that include SON were loaded with the calcium sensitive dye, Fura-2AM. Changes in $[Ca^{++}]_i$ were monitored by changes in the 340/380 emission in response to an increase in the glucose concentration from 0.5 to 5 mM in the presence of KCl (13 mM, to increase resting membrane potential). This increment in glucose caused an increase in $[Ca^{++}]_i$ in the majority of SON neurons. The responses still existed in the presence of TTX (3 uM, to block the influence of afferent synaptic inputs) but were abolished when cells were pretreated with either alloxan (4 mM, to inhibit GK activity) or diazoxide (0.4 mM, to open K_{ATP} channels). These findings indicate that SON neurons are capable of sensing glucose increase and respond to it by ATP-driven closure of K_{ATP} channels, which in turn induces an increase in $[Ca^{++}]_i$ and thus will potentially alter OT hormone release. This is the first demonstration that SON neurons monitor extracellular glucose, thus supports a role for OT in maintaining body nutrient homeostasis.

Zhilin Song and Celia D Sladek. Glucokinase and insulin receptor in supraoptic nucleus neurons: Potential role in glucose and metabolic sensing? Experimental Biology 2011, Washington DC.

Supported by NIH R21-HD072428.

Where applicable, the authors confirm that the experiments described here conform with The Physiological Society ethical requirements.

PCB278

Anti-diabetic and antioxidant effects of virgin coconut oil in alloxan-induced diabetic male Sprague Dawley rats

B.O. Iranloye, G.O. Oludare and O.V. Makinde

Physiology, College of Medicine, University of Lagos, Lagos, Lagos, Nigeria

Oxidative stress has been discovered to be involved in the progression of diabetes mellitus (Lenzen, 2008). The antioxidant properties of virgin coconut oil (VCO) among others might have a beneficial effect in ameliorating the disease. This pres-

ent study was aimed at determining the antioxidant property of VCO on alloxan induced diabetic rats.

Twenty-four healthy male Sprague-Dawley rats weighing between 100-150g were divided into four groups of six rats each as follows: Control (C), Diabetes untreated (DUT), Diabetes treated with 7.5ml/kg VCO (DT7.5) and Diabetes treated with 10ml/kg VCO (DT10). An intraperitoneal injection of Alloxan (100mg/kg body weight) was used to induce type 1 diabetes. Virgin coconut oil extracted from the fresh coconut was administered orally once daily. All animals were treated for 4 weeks. The fasting blood glucose level was measured on day 0 (72 hours post alloxan injection) and on the 4th week. Oral glucose tolerance test was conducted on the 4th week. At the end of the experiment, animals were sacrificed by cervical dislocation and Serum samples were and an enzyme linked immunoassay (EIA) system was employed to determine insulin level. The liver was harvested and the reduced glutathione (GSH) content was determined using the method described by Van Dooran et al (1978). Malondialdehyde (MDA) was determined based on its interaction with thiobarbituric acid (TBA).The activity of the superoxide dismutase (SOD) enzyme was determined according to the method described by Sun and Zigman(1978). Values are means ± S.E.M., compared by ANOVA and Tukey's post hoc test.

The results shows that VCO significantly reduced the fasting blood glucose level in DT7.5 rats (132.4 ± 6.911) and DT10 rats (131.6 ± 12.2) compare with DUT rats (320.4 ± 22.99) and improved the oral glucose tolerance. Serum insulin was increased in DT10 rats. GSH activities was significantly increased $P < 0.05$ in DT7.5 (0.04 ± 0.008) and DT10 rats (0.39± 0.022) when compared to DUT rats (0.032 ± 0.004). CAT activities was also significantly increased $P < 0.05$ in DT7.5 (17.63 ± 0.61) and DT10 rats (30.88 ± 0.97) when compared to DUT rats (10.98± 0.6). SOD activities significantly increased $P < 0.05$ in DT7.5 (2.634± 0.04) and DT10 rats (2.258 ± 0.32) when compared to DUT rats (1.366± 0.05) while MDA was significantly reduced $P < 0.05$ in DT7.5 (49.16± 0.5133) and DT10(33.64± 0.4185) rats when compared to DUT rats(99.93± 4.786).

This study revealed that VCO has a hypoglycaemic action enhancing insulin secretion and also ameliorating oxidative stress induced in type I (alloxan-induced diabetic) male rats.

Lenzen (2008). The mechanisms of alloxan- and streptozotocin-induced Diabetes. Diabetologia 51:216–226

Sun, M. and S. Zigmam, (1978). An improved spectrophotomeric assay for superoxide dismutase based on epinephrine autooxidation. Anal. Biochem., 90: 81-89

Van Dooran et al, (1978). Synergistic effects of phorone on the hepatotoxicity of bromobenzene and paracetamol in mice. Toxicol., 11: 225-233

Where applicable, the authors confirm that the experiments described here conform with The Physiological Society ethical requirements.

PCB279

The effect of cyclic monoterpene menthol on blood glucose, water and electrolyte excretion in rats

C. Onwuchekwa[1], K.I. Ghandi[2] and N.D. Ndodo[3]

[1]Department of Physiology, Usmanu Danfodiyo Uniersity, Sokoto, Nigeria, [2]Department of Human Anatomy, Usmanu Danfodiyo Uniersity, Sokoto, Nigeria and [3]Department of Physiology, Usmanu Danfodiyo Uniersity, Sokoto, Nigeria

Rowachol (Rowa Ltd., Bantry, Eire), a proprietary choleretic containing the purified mono- and bicyclic monoterpenes menthol (32% w/v), pinene (17% w/v), menthone (6% w/v), borneol (5% w/v), camphene (5% w/v), and cineole (2% W/V) in olive oil, has been shown to cause dissolution of cholesterol gallstones in man (Doran et al., 1979) and to inhibit hepatic HMG-CoA reductase in rats (Middleton et al., 1979) and man (Ellis et al., 1981) when administered in vivo. The present study was therefore designed to investigate the effect of menthol on water with electrolyte excretion and blood glucose concentration in rats.

Menthol was administered in olive oil by gastric tube in a volume of 2ml/kg. In determining the dose-response relation for menthol, it was given at 1.0, 3.0 and 6.0 mmol/kg of body weight in a volume of 2 ml/kg. Water together with electrolyte excretion and blood glucose concentration were investigated using flame photometric and colorimetric techniques in rats (n= 48). Values are means ± S.E.M. and compared by one –way ANOVA using Graph Pad prism 4.

The treatment of rats with menthol resulted in a decrease in blood glucose concentration (73.0 ± 1.39, 67.5 ±1.41 and 63.9 ±2.06 mg/dl) that was significant ($p< 0.05$) in all the menthol treated animals (1.0, 3.0 and 6.0 mmol/kg) compared to that of the olive oil treated control group (75.4 ± 1.10 mg/dl). There was a significant dose ($p <0.05$) dependent increase in urine Na^+ ion level (420 ± 15.00, 450 ± 8.86, 480 ± 10.52 mmol) and urine output volume (150± 5.67, 200± 9.82, 280± 11.02 ml) in menthol treated animals compared to their control groups 400± 12.82 mmol and 135± 6.55 ml respectively, while urinary K^+ excretion showed no significant change ($p>0.05$) in all the treated animal groups (86± 2.08, 87 ± 2.38, 89±2.09mmol) with respect to the control (81.5 ± 1.75 mmol). The data obtained indicates that menthol increases water intake, urine output and urine Na^+ excretion, and decreases blood glucose concentration.

The ethical guidelines in accordance with NIH Guide for care and use of laboratory animals and with the Organization for Economic Development (OECD) guidelines on good laboratory practice (OECD, 2001) were followed in the handling of the experimental animals during the studies.

Doran, J., Keighley, M.R.B., and Bell, G.D. 1979. Rowachol - a possible treatment for cholesterol gallstones. Gut 20, 312-317

Middleton, A., Middleton, B., White, D.A., and Bell, G.D.1979. The effects of monocyclic terpenes on hepatic S-3-hydroxy-3-methylglutaryl-Coenzyme A reductase in vivo. Biochem. Soc. Trans.7, 407-408.

Ellis, W.R., Bell, G.D., Clegg, R.J., Middleton, B., and White, D.A.1981. Mechanisms for adjuvant cholelitholytic properties of the monoterpene mixture Rowachol.Gastroenterology 80, 1141

Usmanu Danfodiyo University for their financial support

Where applicable, the authors confirm that the experiments described here conform with The Physiological Society ethical requirements.

PCB283

Regulation of 1,25-Dihydroxyvitamin D_3-induced intestinal calcium transport by Fibroblast Growth Factor (FGF)-23 as a part of the bone-kidney-intestinal axis

N. Charoenphandhu[1], J. Teerapornpuntakit[1], P. Khuituan[1], K. Wongdee[2] and N. Krishnamra[1]

[1]Department of Physiology, Faculty of Science, Mahidol University, Bangkok, Thailand and [2]Office of Academic Management, Faculty of Allied Health Sciences, Burapha University, Chonburi, Thailand

1,25-Dihydroxyvitamin D_3 [1,25$(OH)_2D_3$] is widely recognized as a potent stimulator of intestinal calcium absorption, but a hormone that counterbalances its action (negative feedback) has been elusive. A bone-derived hormone, FGF-23, is hypothesized to be a long-awaiting answer of this question since 1,25$(OH)_2D_3$ enhances FGF-23 release from bone whereas FGF-23 reduces the renal synthesis of 1,25$(OH)_2D_3$. In the present study, male mice [Imprinting Control Region (ICR) strain; 7-week-old; n = 6–10 per group] were used and anesthetized by an intraperitoneal injection with 70 mg/kg sodium pentobarbitone. This study has been approved by the Institutional Animal Care and Use Committee of the Faculty of Science, Mahidol University. Here, we found that the mouse duodenal epithelial cells strongly expressed FGF receptor proteins as determined by immunohistochemistry, suggesting that these cells could directly respond to FGF-23. Intravenous administration of recombinant mouse FGF-23 significantly abolished the 1,25$(OH)_2D_3$-induced transcellular and paracellular calcium transport in the mouse duodenum, as determined by Ussing chamber technique and ^{45}Ca radiotracer. However, FGF-23 did not affect the baseline duodenal calcium transport. At the molecular level, FGF-23 antagonized the 1,25$(OH)_2D_3$-induced increases in the mRNA levels of several duodenal calcium transporters, e.g., TRPV5, TRPV6, and calbindin-D_{9k}, but not claudin-2 or -12. Although FGF-23 also reduced the effect of 1,25$(OH)_2D_3$ on the transepithelial water movement (a driving force for the solvent drag-induced calcium transport), it did not alter the paracellular permeability to ^{3}H-mannitol or ^{14}C-polyethylene glycol-4000. It could be concluded that FGF-23 was an efficient negative feedback regulator of the 1,25$(OH)_2D_3$-induced calcium transport in the mouse duodenum. Our findings have thus corroborated the existence of the bone-kidney-intestinal axis of the FGF-23/vitamin D system in the regulation of intestinal calcium absorption.

Khuituan P *et al*. (2012). *Am J Physiol Endocrinol Metab* **302**, E903-E913.

This work was supported by grants from the Mahidol University (to NC), the Thailand Research Fund through the Royal Golden Jubilee Ph.D. Program (to JT), the Strategic Scholarships Fellowships Frontier Research Networks, Office of the Higher Education Commission (to PK), and the Discovery-based Development Grant, National Science and Technology Development Agency (P-10-11281 to NC).

Where applicable, the authors confirm that the experiments described here conform with The Physiological Society ethical requirements.

PCB284

Lipopolysaccharide inhibits the expression of resistin in adipocytes

Y. Li, X. Xiang, W. An, C. Jiang, X. Wang and W. Zhang

Department of Physiology and Pathophysiology, School of Basic Medical Sciences, Peking University, Beijing, China

Inflammation in adipose tissue is intimately linked with the onset and progression of insulin resistance. The link between insulin resistance and obesity is not completely understood. Resistin, an adipocyte-secreted inflammatory molecule, has been implicated as the link between obesity, inflammation and insulin resistance. During bacterial infection, endotoxin/lipopolysaccharide (LPS) elicits immune and inflammatory responses that can result in a fatal shock syndrome and a series of metabolic alterations and impaired insulin action. LPS has been reported to decrease the expression of resistin mRNA and protein in both lean and db/db obese mice, although the underlying mechanism remains unclear. In the present study, several models such as ex vivo culture of adipose tissues, primary rat adipocytes and 3T3-L1 adipocytes were used to further characterize the effect of LPS on the expression of resistin. We found that acute administration at the doses of 1mg/kg body weight or 80 μg/kg body weight significantly improved the glucose tolerance in mice. Similar results were also observed in mice received a daily intraperitoneal injection of LPS at a dose of 80 μg/kg body weight for 7 days. LPS attenuated both the resistin mRNA and protein in a time- and dose-dependent manner. In the presence of actinomycin D, LPS failed to reduce the half-life of resistin mRNA, suggesting a transcriptional mechanism. The lipid A fraction is crucial for the inhibition of resistin expression induced by LPS. Polymyxin B (PMB), which prevents the activation of toll-like receptor 4 (TLR4) by LPS, significantly attenuated the inhibitory effect of LPS on resistin expression in primary adipocytes, 3T3-L1 adipocytes and ex vivo adipose tissues, indicating that LPS activates TLR4 to inhibit the expression of resistin in adipocytes. Pharmacological intervention of c-Jun N-terminal kinase (JNK) reversed the inhibitory effect of LPS. LPS down-regulated CCAAT/enhancer binding protein α (C/EBP-α) and peroxisome proliferators activated receptor γ (PPAR-γ), while activation of C/EBP-α or PPAR-γ by either over-expressing these transcriptional factors or by rosiglitazone, an agonist of PPAR-γ, blocked the inhibitory effect of LPS on resistin. C/EBP homologous protein 10 (CHOP 10) was up-regulated by LPS, while a CHOP 10 antisense oligonucleotide reversed the decrement of resistin protein induced by LPS. Taken together, the present study demonstrates that inflammation induced by LPS can decrease the resistin expression in adipose tissues. LPS inhibits resistin expression through a unique signaling pathway involving TLR4, JNK, CHOP 10, and C/EBP-α/PPAR-γ.

This work was supported by grants from the National Natural Science Foundation of China (81170795 and 30971085), the Program for New Century Excellent Talents in University (NCET-10-0183), and the Beijing Natural Science Foundation (7112080).

Where applicable, the authors confirm that the experiments described here conform with The Physiological Society ethical requirements.

PCB285

Intestinal glucose uptake responses to infusion of glucose, fructose and galactose in dogs

A. Alada, T. Salman and D. Oyebola

Physiology, University of Ibadan, Ibadan, Oyo, Nigeria

Previous studies have shown significant increases in intestinal glucose uptake (IGU) following hyperglycemia of any cause. It is not clear how the intestine would respond to other sugars apart from glucose. The present study therefore was designed to investigate the effects of intravanous (i.v) infusion of fructose, galactose and glucose on canine IGU during postprandial state. Experiments were carried out on fasted, male, anaesthethized adult mongrel dogs divided into four groups with 5 dogs per group. Each of the groups was given i.v infusion of normal saline, fructose (1.1mg/dl/min), galactose (1.1mg/dl/min) and glucose (1.1mg/dl/min) respectively. Through a midline laparatomy, the upper jejunum was secured and cannulated for blood flow measurement. Blood samples were obtained for measurement of glucose content of arterial and venous blood from the upper jejunal sgment.The blood glucose was determined by glucose oxidase method and intestinal glucose uptake was calculated as the product of jejunal blood flow and arterio-venous glucose difference. Values are means ± S.E.M, compared by ANOVA and Student t-test. Fructose, galactose and glucose significantly increased arterial blood glucose from 97.60±1.78 mg/dl to 114.20±1.88mg/dl, 109.80±1.43mg/dl, and 141.20±5.65 mg/dl respectively. Glucose also significantly increased jejunal blood flow from 10.0±0.32ml/min to 14.40±0.93ml/min, however, fructose and galactose did not produce any significant effect on intestinal blood flow. IGU increased by 600%, 350%, and 700% in response to fructose, galactose and glucose respectively. There is no correlation between the increase in blood glucose levels induced by each of the sugars and its corresponding rise in IGU. The data suggest that the intestine responds to fructose and galactose in a similar manner as glucose. However, the mechanism of the responses may not be the same in the three sugars.

Where applicable, the authors confirm that the experiments described here conform with The Physiological Society ethical requirements.

PCB286

Effects of stress hormones on testicular steroidogenesis and role of antioxidants in vitro

M. Aslam

Physiology, Shifa Tameer-e-Millat University, Islamabad, Federal, Pakistan

Hypothesis: Stress is thought to disrupt the balance between prooxidants and antioxidants by generating reactive oxygen species damaging the testicular tissue and steroidogenesis.
Objective: The in vitro model of isolated and cultured Leydig cells of male Sprague Dawley rats was designed to investigate the effects of antioxidants, ascorbic acid and alpha tocopheral separately and combined with stress, hormones [corticosterone and nor epinephrine] at Leydig cell level.
Methods: Four rats were taken per experiment, decapitated and orchitectony was done. After decapsulation and enzymatic dispersion, density gradient Percoll centrifugation method was used and through various steps, we obtained purified Leydig cells with 85,000 cells per culture tube. Purified Leydig cells were incubated with corticosterone [100 nmol/tube], nor epinephrine [10 umol/well], antioxidants ascorbic acid [100 umol/ml] and alpha tocopherol [10 ug/ml] in the presence of LH [50 ul/week]. The testosterone production and extent of lipid peroxidation and superoxide dismutase activity were evaluated by enzyme immunoassay. Data were analyzed by SPSS version 17 and independent sample t test were applied to find difference among control and treated wells.
Results: The data revealed that corticosterone decreased the Leydig cell steroidogenesis through non genomic rapid pathways because we used 3 hours short term cell culture model and genomic pathways need longer duration than this. Whereas, nor epinephrine increased testosterone synthesis at Leydig cell level beyond pregnenolone which we observed after addition of pregnenolone to the culture tubes. Combination of corticosterone and nor epinephrine resulted in decreased [p value< 0.05] testosterone production. The anti-oxidants like ascorbic acid and alpha tocopherol when superadded alone, revealed favourable preventive effects at Leydig cell level and blunted the fall in testosterone and rise in malondialdehyde levels. Combination of antioxidants, ascorbic acid and alpha tocopherol revealed synergistic effect in reducing oxidative stress (p value< 0.001) and prevented stress hormones induced derangements in testicular steroidogenesis.
Conclusion: The antioxidants, ascorbic acid and alpha tocopherol decrease the stress induced lipid peroxidation and prevent the decline in testicular steroidogenesis presumably by stabilizing the membrane of the Leydig cells.

We acknowledge National University of Sciences and Technology and Higher Education Commission for the financial support to carry out this project.

Where applicable, the authors confirm that the experiments described here conform with The Physiological Society ethical requirements.

PCB287

Serum transforming growth factor β concentrations and primary antibodies immunostaining effects on Leydig and Sertoli Cells in streptozotocin-induced and insulin resistant diabetic adult male rat

A.P. Arikawe[1], K.A. Dada[2], A.O. Ogunsola[3], D. Osiagwu[4] and B.O. Iranloye[5]

[1]Department of Physiology, College of Medicine of the University of Lagos, Lagos, Lagos, Nigeria, [2]Department of Physiology, College of Medicine of the University of Lagos, Lagos, Lagos, Nigeria, [3]Department of Physiology, College of Medicine of the University of Lagos, Lagos, Lagos, Nigeria, [4]Department of Anatomic and Molecular Pathology, College of Medicine of the University of Lagos, Lagos, Lagos, Nigeria and [5]Department of Physiology, College of Medicine of the University of Lagos, Lagos, Lagos, Nigeria

The involvement of Transforming Growth Factors in regulation of cellular function in male diabetic rats' testes is less understood.
Adult male Sprague-Dawley rats (120 – 140gm) were divided into 3 groups. Control group (n = 7); fed on normal rat pellets. Streptozotocin diabetic group (n = 7); received a single IP injection of streptozotocin 45 mg/kg BW (Guneli et al., 2008) in Na+ citrate buffer pH 4.5. Insulin resistant group (n = 7); fed

ad libitum on special diet containing 25% fructose W/W for 12 weeks (Arikawe et al., 2006; Arikawe et al., 2012).
Following hyperglycaemia confirmation, blood samples were collected under light anaesthesia (IM ketamine, 10mg/kg) for serum activin and inhibin (Transforming Growth Factor β) Concentrations. Animals were perfused with 4% Paraformaldehyde (PFA). Testes were isolated and fixed in 4% PFA overnight and embedded in paraffin. 5μm thick sections were made and mounted on poly-L-lysine coated slides. Immunohistochemical analysis was assessed using Androgen receptor (C-19) and Sox-9 antibodies (Santa Cruz Biotechnology, USA) through light microscopy.
Serum inhibin was significantly lower ($P < 0.05$) in the insulin resistant group compared to the control and streptozotocin groups. There was no significant difference in serum activin concentrations amongst the three groups. C-19 and Sox-9 indexes were significantly lower ($P < 0.05$) in both experimental groups compared to control group. The results of the study indicate that streptozotocin and insulin resistance affect Leydig and Sertoli cell function.

Guneli E et al. (2008). Eur. Surg. Research Journal, Vol. 40 (4): 354 – 60.

Arikawe AP et al. (2012). Journal of Experimental and Clinical medicine, 29 (3): 209 – 214.

Arikawe AP et al. (2006). African Journal of Reproductive health, Vol. 10 (3): 106 – 113.

Where applicable, the authors confirm that the experiments described here conform with The Physiological Society ethical requirements.

PCB288

CD4+ T cell-derived catecholamines induce a shift of Th1/Th2 balance toward Th2 profile

Y. Qiu, Y. Liu, J. Tang, H. Huang and Y. Peng

Nantong University, Nantong, China

Our previous work has shown that T lymphocytes synthesize and secrete catecholamines (CAs), which regulate T cell function by paracrine/autocrine pathway. CD4+ T cells, a largest class of lymphocyte subsets accounting for 60% of peripheral T lymphocytes, function mainly through T helper (Th) cells. Th1 cells are mainly involved in inflammatory response by secretion of cytokines, such as interleukin (IL)-2, interferon-γ (IFN-γ) and tumor necrosis factor (TNF), while Th2 cells mainly mediate anti-inflammatory response by secretion of IL-4, IL-5 and IL-10. Th1/Th2 balance in differentiation and function is highly important for maintenance of immune homeostasis. Here, we explored the regulation of Th1/Th2 balance by CD4+ T cell-endogenous CAs to extend our knowledge of neuroimmunomodulation. CD4+ T cells were purified from the mesenteric lymph nodes of 4 to 6 week-old ICR mice by using CD4+ T-cell isolation kit. The purified T cells (1.25×106 cells/ml) were incubated for 48 h with concanavalin A (Con A, 5 μg/ml) to induce cell proliferation. To change production of CAs by the cells, we added alpha-methyl-p-tyrosine (α-MT), an inhibitor of tyrosine hydroxylase (TH) that is a rate-limiting enzyme for CA synthesis, or pargyline, an inhibitor of monoamine oxydase that degrades CAs, to the cultures 30 min prior to Con A. Additionally, recombinant TH miRNA expression vector (pcDNA/miR-TH) was transfected into Con A-activated CD4+ T cells using nucleofection technology to silence TH gene in these cells. Expression of TH and cytokines at gene and protein levels in Con A-activated CD4+ T cells was examined by real-time PCR and Western blot, respectively. Concentrations of CAs and cytokines in cultured cells and supernatants were measured by HPLC and flow cytometry, respectively. The exposure to α-MT (10–6 M) reduced contents of CAs including norepinephrine, epinephrine and dopamine both in CD4+ T cells and in supernatants. Simultaneously, α-MT upregulated T-bet, a Th1-specific transcription factor, and IFN-γ expression but downregulated GATA-3, a Th2-specific transcription factor, and IL-4 expression in Con A-activated CD4+ T cells. In contrast, pargyline (10–6 M) increased the three kinds of CAs, downregulated T-bet and IFN-γ, but upregulated GATA-3 and IL-4 in these lymphocytes. In support these findings, CD4+ T cells with TH RNAi expressed less TH mRNA and protein and synthesized less CAs than control cells with mock transfection. Importantly, the silencing of TH gene in Con A-stimulated CD4+ T cells elevated ratio of IFN-γ-producing cells to IL-4-producing cells, increased levels of IL-2, IFN-γ and TNF, but decreased levels of IL-4 and IL-5 in the culture supernatants. These data suggest that CAs synthesized and secreted by CD4+ T cells regulate differentiation and function of Th cells, with an effect facilitating the shift of Th1/Th2 balance toward Th2 polarization.

Where applicable, the authors confirm that the experiments described here conform with The Physiological Society ethical requirements.

PCB289

Diabetes risk factors, interleukin-6 and vitamin d are modified by a short-term yoga-based lifestyle intervention in overweight/obese subjects

R.K. Yadav[1], R. Netam[2], R. Khadgawat[3], K. Sarvottam[4], R. Yadav[5] and D. Magan[6]

[1]Physiology, All India Institute of Medical Sciences, New Delhi, India, [2]Physiology, All India Institute of Medical Sciences, New Delhi, India, [3]Endocrinology and Metabolism, All India Institute of Medical Sciences, New Delhi, India, [4]Physiology, All India Institute of Medical Sciences, New Delhi, India, [5]Physiology, All India Institute of Medical Sciences, New Delhi, India and [6]Physiology, All India Institute of Medical Sciences, New Delhi, India

Introduction: Obesity is a known risk factor for type 2 diabetes mellitus (T2DM), and weight-loss seems prudential in T2DM risk reduction. In the current study, we evaluated the efficacy of a short-term yoga-based lifestyle intervention in weight-loss, and assessed its impact on interleukin (IL)-6, vitamin D, fasting plasma glucose (FPG), insulin resistance, waist/hip ratio, lipid profile, and blood pressure in overweight/obese subjects vs. apparently healthy normal weight control subjects.
Methods: A total of 68 subjects were enrolled in this study, of which 34 were overweight/obese (BMI ≥23 to <35 kg/m^2 per Asian cut-off values) and 34 were apparently healthy normal-weight control subjects. The study was conducted in two phases. In Phase I, all the 68 subjects attended a 10 day directly supervised yoga-based lifestyle intervention program, which was hospital-based. End of Phase I was end-of-study for normal weight subjects while overweight/obese subjects entered Phase II, and continued the intervention while home-based till Day 30. Weight-loss and diabetes risk factors were assessed at Baseline, Day 10 (for both the study groups) and Day 30 (for overweight/obese subjects).
Results: In overweight/obese subjects, there was a significant reduction from Baseline to Day 10 in weight (73.20±10.00 vs. 72.35±9.78 kg, $p=0.0001$), BMI (26.49±3.67 vs. 26.26±3.65

kg/m^2, p=0.004), waist/hip ratio (0.91±0.10 vs. 0.90±0.09, p=0.043), FPG (p=0.005), and a significant improvement in lipid profile (p<0.05). Also in this group, there was a significant reduction in median fasting insulin (8.50 vs. 8.30 μIU/dL, p=0.049), insulin resistance (HOMA-IR; 2.55 vs. 1.53, p=0.018), and levels of IL-6 (1.16 vs. 1.11 pg/mL, p=0.031). At Day 30, weight-loss was sustained, and systolic blood pressure was also decreased (p=0.017). The correlation analysis showed that IL-6 decreased with a decrease in waist/hip ratio. Also, serum 25-OH-vitamin D increased with a decrease in weight, FPG, and increased with increase in HDL. There were no notable changes in the control group.
Conclusions: This short-term lifestyle intervention resulted in a significant weight-loss even in a short duration, as early as 10 days. This reduction in weight resulted in a reduction in diabetes risk factors in overweight/obese subjects.

Authors acknowledge Institute Research Grant provided by All India Institute of Medical Sciences, New Delhi, for financial support for the ELISA kits, and Central Council for Research in Yoga & Naturopathy, Ministry of Health and Family Welfare, Government of India for technical support.

Where applicable, the authors confirm that the experiments described here conform with The Physiological Society ethical requirements.

PCB290

The effects of *Moringa oleifera* Lam. seed oil in ovariectomized rats

P. Kusolrat and S. Kupittayanant

Physiology, Suranaree University of Technology, Muang, Nakhon Ratchasima, Thailand

Estrogen replacement therapy has been the treatment of choice for menopause symptoms, but it can increase risk of breast cancer, heart disease, and stroke. Due to these side effects, a therapy with phytoestrogens (Wuttke et al, 2002); derived xenoestrogens found in plants is currently being challenged. Moringa (*Moringa oleifera* Lam.) seed oil (MSO) has been reported to contain phytoestrogens (Anwar et al, 2007). However, it is not known whether and if it can be a treatment of choice for menopause symptoms. Thus, the aim was therefore to study the effects of MSO in menopause using ovariectomized rats (OVX) as a model. The seeds of Moringa were obtained by cold pressed. The animal cares were followed the guidelines of the Committee on Care and Use of Laboratory Animal Resources, National Research Council of Thailand. The procedure of the experiment was performed with the advice of the Institutional Animal Care and Use Committee, Suranaree University of Technology, Nakhon Ratchasima, Thailand. Adult female virgin rats (200-250 g) were overiectomized and divided into 5 groups of six rats each; sham operated rats (SHAM) received 1% tween 80 (1 ml), OVX received estrogen (0.02 mg/kg BW 17β-estradiol), OVX received 1% tween 80 (1 ml; control group), OVX received MSO (0.5 ml/100 g BW), and OVX received MSO (1 ml/100 g BW) orally/day for 6 weeks. At the end of the treatment the animals were sacrificed. The uterus was removed and weighed. Serum estradiol, total cholesterol, high density lipoprotein (HDL), low density lipoprotein (LDL) and triglyceride concentration were also evaluated. The statistical analysis of differences between groups was performed using one way ANOVA. There was a significant increase in mean relative uterine weight in MSO (1 ml/100 g BW) and estrogen treated-group as compared to the control group ($P < 0.05$). The results showed that serum estradiol (pg/ml) in SHAM, control group, MSO (0.5 ml/100 g BW), MSO (1 ml/100 g BW) and estrogen treated-group was 39.67±2.2, 13.67±1.5, 20.33±3.1, 50.67±8.9 and 82.00±18.0, respectively. There was a significant increase in serum estradiol with estrogen-treated group and MSO (1 ml/100 g BW) as compared to the control group ($P < 0.05$). The concentration of total cholesterol, LDL, and triglyceride was not significantly deferent among groups. However, there was a significant increase in the mean HDL in MSO (1 ml/100 g BW) and estrogen treated-group as compared to the control group ($P < 0.01$). In conclusion, MSO can increase relative uterine weight, serum estradiol, serum HDL in ovariectomized rats. Thus, it may be beneficial for the treatment of menopause symptoms.

Anwar F, Latif S, Ashraf M & Gilani AH (2007). Moringa oleifera: a food plant with multiple medicinal uses. *Phytother Res*21(1), 17-25.

Wuttke W, Jarry H, Westphalen S, Christoffel V & Seidlová-Wuttke D (2002). Phytoestrogens for hormone replacement therapy?. *J Steroid Biochem Mol Biol*83(1-5), 133-147.

We gratefully acknowledge Nakhon Ratchasima Rajabhat University and Suranaree University of Technology for financial support.

Where applicable, the authors confirm that the experiments described here conform with The Physiological Society ethical requirements.

PCB291

Estrogen activities of winged bean seed oil in ovariectomized rats

P. Kupittayanant[1], P. Kusolrat[2], A. Munpanich[2], A. Thaeomor[2] and S. Kupittayanant[2]

[1]Animal Production Technology, Suranaree University of Technology, Muang, Nakhon Ratchasima, Thailand and [2]Physiology, Suranaree University of Technology, Muang, Nakhon Ratchasima, Thailand

Unanticipated increase in risk for breast cancer and cardiovascular disorders among menopausal women taking hormone replacement therapy (HRT) has been reported (Rossouw et al, 2002). Plant extracts with estrogenic properties are of increasing interest as potential alternatives to using HRT (Wylie-Rosett, 2005). One such alternative includes the phytoestrogens, which are plant substances producing estrogenic effects (Lotke, 1998). Winged bean (*Psophocarpus tetragonolobus* L.) is a tropical legume grown in Southeast Asia. The chemical composition of its seeds is very similar to that of soybean, a natural source of phytoestrogens (Benito et al, 1982). However, its estrogenic activities have never been investigated. The aim of the study was to examine estrogenic activities of winged bean seed oil (WBSO) in ovariectomized rats (OVX). WBSO was obtained by cold pressed. The animal cares followed the guidelines of the Committee on Care and Use of Laboratory Animal Resources, National Research Council of Thailand and the experiment procedure was performed with the advice of the Institutional Animal Care and Use Committee. 20 Adult female virgin rats (200-250 g) were subjected to operation. 14 days after operation, the rats were divided into 4 groups (n=5); sham operated rats (SHAM) received 1% tween 80 (1 ml), OVX received 1% tween 80 (1 ml; control), OVX received estrogen (0.02 mg/kg BW 17β-estradiol), and OVX received WBSO (1 ml/100 g BW) orally/day for 6 weeks. Vaginal cornification was determined throughout the experimental period. At the end of the treatment the animals were sacrificed. The uterus was

removed and weighed. Serum estradiol was also evaluated. The statistical analysis of differences between groups was performed using one way ANOVA. The results showed that WBSO induced an opening of vagina on day 8 and cornification of vaginal epithelial cells which occurred 7 days earlier as compared to control. This was observed in all treated animals (100%). The mean relative uterine weight (RU) was significantly different among groups (P<0.05). RU (%) in SHAM, control group, estrogen-treated group, and WBSO was 0.18±0.00, 0.06±0.01, 0.13±0.01, and 0.09±0.01, respectively. Thus, WBSO significantly increased RU when compared to control, but the increase was lesser than those of estrogen. Serum estradiol (pg/ml) in SHAM, control group, estrogen-treated group, and WBSO was 39.29±1.8, 13.78±1.6, 81.93±18.2, and 52.57±3.6, respectively. Thus, there was a significant increase in serum estradiol with estrogen-treated group and WBSO as compared to control (P<0.05). Taken together, WBSO has estrogenic activities as it can induce vaginal cornification, increase relative uterine weight and raise serum estradiol. WBSO may therefore offer the same uses as soybean.

Rossouw JE, Anderson GL, Prentice RL, LaCroix AZ, Kooperberg C, Stefenick ML, Jackson RD, Beresford SA, Howard BV, Jonhson KC, Kotchen JM & Ockene J (2002). Ricks and benefits of estrogen plus progestin in healthy postmenopausal women: principal results from the Women's Health Initiative randomized controlled trial. *JAMA* 288(3), 321-333.

Wylie-Rosett J (2005). Menopause, micronutrients and hormone therapy. *Am J Clin Nutr* 81, 1223-1231.

Lotke PS (1998). Phytoestrogens: a potential role in hormone replacement therapy. *Prim Care*

Update Ob/Gyns 5, 290-295.

Benito O. De Lumen & Seham Fiad (1982). Tocopherols of winged bean (*Psophocarpus tetragonolobus*) oil. *J Agric Food Chem* 30(1), 50-53.

We gratefully acknowledge National Research Council of Thailand and Suranaree University of Technology for financial support.

Where applicable, the authors confirm that the experiments described here conform with The Physiological Society ethical requirements.

PCB292

Exocrine growth hormone?

D. Giterman[1], E. Adeghate[2] and S. Harvey[1]

[1]Physiology, University of Alberta, Edmonton, AB, Canada and [2]Anatomy, United Arab Emirates University, Al Ain, United Arab Emirates

Growth hormone (GH) gene expression is not confined to the somatotrophs of the pituitary gland and occurs in many extrapituitary tissues, including those of the neural, immune and reproductive systems (Harvey, 2010). Its presence in exocrine glands is, however, largely unknown. The possible presence of GH in salivary glands (the submandibular and parotid glands), in the lachrimal gland and in the exocrine pancreas of rats was therefore investigated by confocal immunocytochemistry. Intense GH-immunoreactivity was demonstrated in the parotid and submandibular glands, particularly in the interlobular and intralobular epithelial ducts and in some (but not all) serous and some mucus acinar cells. The presence of GH immunoreactivity inside the salivary ducts indicates the exocrine secretion of GH into saliva. Within the ductal epithelia of the salivary glands, the GH-immunoreactivity was consistently colocalized with immunoreactivity for mucin-1, salivary amylase, renin and nerve growth factor. It was also colocalized with SMR-1 (submandibular rat-1) in some acinar cells. Similar, but weaker, GH staining was also seen in the lachrimal glands. In the pancreas, some acini were GH-negative and some were GH-positive, whereas intense GH-staining was seen in the intermingled alpha (glucagon-immunoreactive) islet cells, but not in the GH-negative (insulin-immunoreactive) beta cells. The GH-immunoreactivity in these tissues was also colocalized with GH-receptor immunoreactivity, suggesting local (non-endocrine) roles for GH in their exocrine activity. In summary, these novel results demonstrate the presence of GH and its receptor in exocrine tissues of the rat, in which GH may have hitherto unsuspected autocrine, paracrine or lumenocrine roles in salivary, lachrimal or pancreatic exocrine function.

Harvey S (2010). *Endocrine* 38, 335-359

Supported by the Natural Sciences and Engineering Research Council of Canada

Where applicable, the authors confirm that the experiments described here conform with The Physiological Society ethical requirements.

PCB294

Differential modulatory activity of leukotrienes on vasopressin secretion in a hypovolemia vs. sepsis condition

L.A. Costa, P.J. Basso and M.A. Rocha

Dental School of Ribeirão Preto, University of São Paulo, Ribeirão Preto, São Paulo, Brazil

Previous work revealed the presence of LTC4 synthase in vasopressinergic neurons suggesting the involvement of leukotrienes in vasopressin secretion (1). While these mediators may activate vasopressin secretion during sepsis, they seem to inhibit during an osmotic stimulus (2, 3). Our aim was to study the effect of an inhibitor of leukotrienes synthesis (MK-886) in the hypovolemia –induced secretion of arginine vasopressin (AVP). Male Wistar rats (250-300 g) were anesthetized with intraperitoneal (i.p.) injection of a mixture of ketamine (45 mg/kg) and xylazine (6 mg/kg) for stereotaxically implanting a stainless steel cannula into the right lateral ventricle 5-7 days before the experiment. They received an intracerebroventricular (i.c.v.) injection of 2 μl of MK-886 at doses of 1, 2 and 4 μg/kg. or vehicle (DMSO 5%) one hour before hypovolemia was induced by a intraperitoneal injection (2 ml/100 g body weight) of polyethylene glycol 4000 (PEG – 200 mg/ml) or PBS (0.01 M) was injected as control. Subsequently they were decapitated 90 minutes after the stimulus. and blood was collected for determination of hematocrit, plasma osmolality, serum sodium and plasma vasopressin levels (n= 6-14 per group). The hypothalamus (n=7-14 per group) was removed and a Western blot for the enzyme LTC4 synthase was performed. In order to assess whether PEG could induce hypovolemia without a decrease in blood pressure, four hypovolemic rats that received i.c.v injection of DMSO 5% had their mean arterial pressure evaluated throughout the experimental period. The results are reported as mean ± S.E.M. Analysis of variance (ANOVA) and a post hoc Student–Newman–Keuls (SNK) test were used to reveal statistical differences. The i.p. injection of polyethylene glycol increased the hematocrit (p>0.05), and the plasma vasopressin concentration (1.26±0.2 pg/ml vs.0.74±0.1pg/ml control) confirming the hypovolemic effect of this protocol. Nonetheless, it did not alter osmolality, serum sodium, and mean arterial pressure in any group. The central administration of MK-886 in any dose did not sub-

stantially affect the hematocrit, osmolality, or serum sodium in any of the groups. However, at higher doses (2 and 4 μg/kg) the drug was able to substantially increase even more the plasma concentration of vasopressin (3.13±0.8 pg/ml vs. 1.26±0.2 pg/ml vehicle) and (3.49±0.8 pg/ml vs.1.26±0.2 pg/ml vehicle) respectively. The groups did not show any statistical differences in hypothalamic LTC4 synthase content.The results lead us to infer that leukotrienes modulate a hypovolemia-induced vasopressin secretion in a different way than they do during sepsis.

Shimada A et al. (2005) Neuroscience, v.131, n.3, p.683-9

Athayde LA et al. (2009) Neuroscience, v 160, p 839-836.

Santos JF et al. (2012) Reg Peptides, v 179, p. 6-9

Financial Support : FAPESP and CNPq

Technical Support: Nadir Martins Fernandes and Milene

Where applicable, the authors confirm that the experiments described here conform with The Physiological Society ethical requirements.

PCB295

Bone marrow adipose tissue as a source of serum adiponectin: The 'adiponectin paradox' explained?

W.P. Cawthorn[1,6], E.L. Scheller[1], B.S. Learman[1], D.T. Broome[1], S.S. Soliman[1], J.L. DelProposto[3], C.N. Lumeng[3], K.A. Gallagher[4], J.D. Miller[5], V. Krishnan[6], P.K. Fazeli[7], A. Klibanski[7], M.C. Horowitz[8], C.J. Rosen[9] and O.A. MacDougald[1,2]

[1]Department of Molecular & Integrative Physiology, University of Michigan Medical School, Ann Arbor, MI, USA, [2]Department of Internal Medicine, University of Michigan Medical School, Ann Arbor, MI, USA, [3]Department of Pediatrics and Communicable Diseases, University of Michigan Medical School, Ann Arbor, MI, USA, [4]Department of Vascular Surgery, University of Michigan Hospital, Ann Arbor, MI, USA, [5]Department of Orthopaedic Surgery, University of Michigan Hospital, Ann Arbor, MI, USA, [6]Musculoskeletal Research, Lilly Research Laboratories, Indianapolis, IN, USA, [7]Neuroendocrine Unit, Massachusetts General Hospital, Boston, MA, USA, [8]Department of Orthopaedics and Rehabilitation, Yale University School of Medicine, New Haven, CT, USA and [9]Maine Medical Center Research Institute, Scarborough, ME, USA

The adipocyte-derived hormone adiponectin promotes insulin sensitivity and anti-atherogenic effects. Serum adiponectin levels are low in obese, insulin-resistant individuals but high in lean states such as caloric restriction (CR) or anorexia nervosa. Indeed, despite being produced exclusively by adipose tissue, serum adiponectin inversely correlates with % body fat. The basis for this so-called 'adiponectin paradox' is yet to be resolved.

The discovery of adiponectin preceded our current understanding of white adipose tissue (WAT) as a major endocrine organ. In contrast, research has largely neglected another adipose depot: bone marrow adipose tissue (MAT). In humans MAT accounts for ≤ 70% of marrow volume and, in contrast to WAT, MAT increases in states of leanness such as CR or anorexia nervosa. Moreover, pharmacological agents such as thiazolidinediones or fibroblast growth factor-21 increase marrow adiposity. Notably, each of these conditions is also associated with increased serum adiponectin.

Based on these observations, we investigated the hypothesis that MAT is a major source of serum adiponectin. To do so, we first isolated WAT and MAT from rabbits, mice and humans. Rabbits were sedated by i.m. injection of ketamine (40 mg/kg) and xylazine (5 mg/kg) before euthanising by i.v. injection of pentobarbital (65 mg/kg); mice were euthanised by CO_2 asphyxiation followed by cervical dislocation; and human tissues were obtained with consent from patients undergoing lower-limb amputation. Immunoblotting of tissue lysates revealed that, in rabbits (n = 9) and mice (n = 6), adiponectin expression is markedly higher in MAT than in WAT. Although this was not consistently observed in human tissues (n = 7), human MAT had increased expression of Ero1-Lα, a protein chaperone that promotes adiponectin secretion. Indeed, adiponectin secretion from cultured MAT explants was far higher than that from WAT explants of rabbits (n = 9) or humans (n = 4), as assessed by immunoblotting. We next investigated if blocking MAT formation affects serum adiponectin levels. To do so we used Ocn-Wnt10b mice, in which the anti-adipogenic effector Wnt10b is transgenically expressed in bone. Expression of adiponectin mRNA in WAT did not differ between Ocn-Wnt10b (1.00 ± 0.21; n = 10) and control mice (0.91 ± 0.11; n = 10); however, Ocn-Wnt10b mice resisted increases in MAT and serum adiponectin with CR. Moreover, we found that, in mice (n = 24), total serum adiponectin negatively correlates with WAT mass (R^2 = 0.441; P = 0.031) but positively correlates with MAT volume (R^2 = 0.524; P = 0.009). In summary, our observations support the hypothesis that MAT expansion is required for increased serum adiponectin with CR, suggesting that MAT may be a major source of serum adiponectin. Thus, adiponectin production from MAT may account, at least in part, for the adiponectin paradox.

Where applicable, the authors confirm that the experiments described here conform with The Physiological Society ethical requirements.

PCB296

Transcriptome responses of the intestinal epithelial cells for the upregulation of gene-related to calcium and nutrient absorption in lactating rats and pituitary-grafted hyperprolactinemic rats

J. Teerapornpuntakit[1], K. Wongdee[2], N. Krishnamra[1], N. Karoonuthaisiri[3] and N. Charoenphandhu[1]

[1]Department of Physiology, Faculty of Science, Mahidol University, Bangkok, Thailand, [2]Office of Academic Management, Faculty of Allied Health Sciences, Burapha University, Chonburi, Thailand and [3]Microarray Laboratory, National Center for Genetic Engineering and Biotechnology (BIOTEC), Pathum Thani, Thailand

Intestinal calcium absorption is markedly enhanced during pregnancy and lactation by prolactin (PRL) from the anterior pituitary. However, its cellular and molecular mechanisms pertaining to the intestinal calcium absorption are not completely understood. The present study aimed to demonstrate the transcriptome responses of intestinal epithelial cells to PRL in hyperprolactinemic animals, i.e., anterior pituitary (AP)-grafted rats and lactating rats, by using robotic spotting cDNA microarray and quantitative real-time PCR. In addition, the effects of PRL on proliferation and differentiation of IEC-6 crypt-like cells were also investigated. This study has been approved by the institutional animal care and use committees of Faculty of Science, Mahidol University. The results showed that several genes related to calcium absorption, e.g., transient receptor potential vanilloid calcium channel (TRPV)-5, TRPV6, calbindin-D_{9k}, and claudin-3, were upregulated in the 4-week AP-grafted rat. Nevertheless, such the PRL action was observed only in the villous cells, but not in the IEC-6 crypt-like cells. PRL did not

increase IEC-6 cell proliferation, suggesting that it did not contribute to the lactation-induced expansion of intestinal surface area. In early lactation, PRL was found to upregulate the expression of TRPV6 and plasma membrane Ca^{2+}-ATPase-1b, which were apical and basolateral calcium transporters, respectively. Further microarray study revealed a number of changes in the expression of genes related to calcium, nutrient, and ion transport (such as TRPM7 and sodium-dependent phosphate transporter (NaPi)-IIb for magnesium and phosphate transport, respectively) in late lactation. In conclusion, PRL increased the intestinal calcium absorption by upregulating the expression of genes related to calcium transport, presumably to provide more calcium for milk production.

Teerapornpuntakit J *et al.* (2012). *Cell Biochem Funct.* **30**, 320–327.

This study was supported by Thailand Research Fund through the Royal Golden Jubilee Ph.D. Program (PHD/0042/2551).

Where applicable, the authors confirm that the experiments described here conform with The Physiological Society ethical requirements.

PCB297

The satiety molecule nesfatin-1 increases body temperature of rat

K. Könczöl[1], D. Zelena[2], O. Pintér[2], J. Varga[2], M. Palkovits[1] and Z.E. Tóth[1]

[1]Dept. of Anatomy, Histology and Embryology, Semmelweis University, Budapest, Hungary and [2]Institute of Experimental Medicine, Hungarian Academy of Sciences, Budapest, Hungary

Nesfatin-1, a fragment of the nucleobindin 2 (NUCB2) protein was described as an agent reducing food intake. However, its wide distribution in the brain suggests additional functions. We assumed that nesfatin-1 may affect also the energy expenditure, therefore we measured duration of food intake, core body temperature, locomotor activity and heart rate of male rats (250-300g) for 48h by telemetry, after icv administration of 25 pmol nesfatin-1 (n=10-12) at the beginning of the dark phase. Body weight, food and water intake were measured daily. One week before the experiment, a cannula was inserted into the lateral ventricle under anesthesia with ketamine (50mg/kg) and xylazine (15mg/kg). At the same time, VitalView biotelemetry emitters were implanted into the abdominal cavity. Telemetric data were collected in every min and calculated as sum ±s.e.m, or mean±s.e.m. Statistics were performed using two way RM-ANOVA. Nesfatin-1 reduced the duration of nocturnal food intake at the beginning of the dark phases (effect of treatment: $F(1,9)=4.63$, $P<0.05$). Food intake had a circadian rhythm (effect of time: $F(11,99)=10.5$, $P<0.01$), but the amplitude was smaller in treated animals (treatment x time interaction: $F(11,99)=3.06$, $P<0.01$). There was a reduction in food and water consumption on the first day and a compensation on the second day (food intake: effect of time: $F(1,21)=4.66$, $P<0.05$, treatment x time interaction: $F(1,21)=6.09$, $P<0.05$, water intake: effect of treatment: $F(1,9)=6.1$, $P<0.05$, effect of time: $F(1,21)=5.2$, $P<0.05$, tendency for treatment x time interaction: $F(1,21)=4.8$, $P<0.056$). Nesfatin-1 treatment elevated core body temperature immediately after injections (effect of treatment: $F(1,9)=7.85$, $P<0.05$). The most marked difference between groups was observed during the light phases of the 48 h observation period, since the circadian curve has been flattened (effect of time: $F(11,99)=10.4$, $P<0.01$). Heart rate and locomotion did not change. To elucidate morphological base of effect of nesfatin-1 on temperature regulation, we tested if cold (4 °C for 2 h) induces neuronal activation (Fos immunoreactivity) in nesfatin-1/NUCB2 (nesfatin)-positive neurons in the brain. Control animals were kept at room temperature. Cold activated nesfatin-positive neurons were present in many thermoregulatory areas of the hypothalamus and the brainstem. In the hypothalamic paraventricular nucleus Fos-nesfatin double labeled neurons colocalised with prepro-thyrotropin-releasing hormone (pTRH). pTRH also colocalised with nesfatin in the nucleus raphe pallidus and obscurus. These nuclei are known to act as sympathetic premotor neurons regulating heat production in brown adipose tissue and vasoconstriction in the skin. In summary, nesfatin has a longer effect than it was known before, and it influences the energy homeostasis not only by reducing food intake, but also by increasing the body temperature.

Nesfatin-1 exerts long-term effect on food intake and body temperature.

Könczöl K, Pintér O, Ferenczi S, Varga J, Kovács K, Palkovits M, Zelena D, Tóth ZE.

Int J Obes (Lond). 2012 Dec;36(12):1514-21.

Where applicable, the authors confirm that the experiments described here conform with The Physiological Society ethical requirements.

PCB298

Neuronal and glial cell changes in a trasngenic mouse model of retinal neovascularisation

L.B. Tee[1], A. Nguyen[1], I.S. Ali Rahman[2] and C.M. Lai[2,3]

[1]School of Pharmacy, Curtin University, Perth, WA, Australia, [2]Centre for Ophthalmology and Visual Science,, The University of Western Australia, Perth, WA, Australia and [3]Molecular Ophthalmology, Lions Eye Institute,, Perth, WA, Australia

Retinal neovascularisation is a major clinical complication of diabetic retinopathy (DR) however, the exact mechanism for the progression of retinal neovascularisation and the role of inflammation in retinal neovascularisation remains to be established. There are two main hypotheses on the pathogenic mechanism underlying DR. The more established theory which has been the focus of many studies is that DR is a disorder affecting the vascular cells in the retina. It is theorised that damage to these cells as a consequence of hyperglycaemia result in the subsequent complications of DR including vision loss. The other theory is that DR causes neuronal and glial cell dysfunction which plays a crucial role in the progression of the subsequent complications. Evidence suggesting neuronal and glial cell dysfunction include; changes in electrophysiological and psychophysical activity, glial cell reactivity, altered glutamate metabolism and apoptosis of retinal cells. The aim of this project is to investigate the neuronal and glial cell changes in the retina in a transgenic mouse model of retinal neovascularisation and to assess the relationship between the vascular abnormalities with the corresponding changes in the neurons and glial cells. The transgenic mouse model, Kimba (Lai et al 2005), was used to examine the neuronal and glial cell changes in retinal neovascularisation. Retinal sections of Kimba and wild type (WT) mice were analysed for vascular neuronal and glial cells changes using immunocytochemistry. Mice aged 2, 8, and 20 weeks were used to look at neuronal and glial changes associated with the progressive stages of neovascularisation.There was an overall decrease in retinal thickness for Kimba mice at all stages with varying patterns of changing

thickness in the outer nuclear layer (ONL) and inner nuclear layer (INL) of the retina. Compared to WT, the retinal blood vessels in Kimba mice transgressed into the outer layers of the retina including the ONL which caused disruption to the normally organised retinal layers. There was a significant (P<0.001) decrease in ganglion cell count in Kimba at all age points. Whilst there was no change in the morphology of astrocytes and Muller cells, there was a significant (P<0.05) decrease in Müller cell count in 8 and 20 weeks Kimba. The study shows changes in both neuronal and glial cells in the retina associated with the different stages of retinal neovascularisation. This study further supports the role of inflammation in the progression of retinal neovascularisation.

Lai et al (2005) British Journal of Ophthalmology 89:911-916.

Where applicable, the authors confirm that the experiments described here conform with The Physiological Society ethical requirements.

PCB299

Targeting BACE1 to improve leptin sensitivity and reverse obesity

P.J. Meakin, S.M. Jalicy, G. Montagut, S.W. Irvine and M.L. Ashford

Division of Cardiovascular & Diabetes Medicine, University of Dundee, Dundee, UK

BACE1 (β-site amyloid precursor protein (APP)-cleaving enzyme 1) is the rate-limiting step in Aβ peptide production. Aβ aggregates and forms amyloid plaques, a major pathological feature of Alzheimer's disease. Mice lacking BACE1 have improved glucose homeostasis and are resistant to diet induced obesity [1], suggesting that BACE1 regulates energy metabolism. Therefore we have investigated whether altered leptin signalling underlies the improved metabolic phenotype of BACE1$^{-/-}$ mice. Wild-type (WT) and BACE1$^{-/-}$ mice (C57Bl/6) were fed regular chow (RC) or high fat (HF; 4% and 45% energy from fat respectively) diet from 8 weeks of age for 20 weeks. For *in vivo* studies mice were injected i.p. twice daily with saline or leptin (2mg/kg) for 3 days and food intake and body weight monitored. For biochemical analysis, mice were starved overnight and injected i.p with saline or leptin (3mg/kg) and hypothalamic arcuate nucleus (ARC) tissue harvested after 3 hours. cDNA expression was measured using Taqman gene analysis. Standard immunohistochemical and immunoblotting techniques were used to measure BACE1 hypothalamic distribution and ARC STAT3 protein levels, respectively. All data expressed as mean ± SEM, and statistical significance determined by Student's t-test.

BACE1 protein was observed in a sub-group of ARC neurons. BACE1 is not co-localised with NPY or AgRP, whereas approximately 30% of POMC neurons display BACE1 immunoreactivity. BACE1$^{-/-}$ mice, on RC diet, exhibit an increased *in vivo* response to leptin displaying a greater reduction in body weight compared to WT mice (KO -7.8±1.0%; WT -5.2±0.4%; $p < 0.05$ n=8-13). This outcome is reflected in a greater increase in ARC STAT3 phosphorylation levels for BACE1$^{-/-}$ mice compared to WT controls (KO 6.7±1.2; WT 3.5±0.6 fold; $p < 0.05$ n=6-8). Following HF diet challenge, BACE1$^{-/-}$ mice retain leptin sensitivity, while WT mice become leptin resistant (body weight change: KO -5.9±0.8%; WT -0.3±0.4%; $p < 0.001$ n=7-9). BACE1$^{-/-}$ mice display increased basal AgRP and NPY gene expression (AgRP 1.6±0.1; NPY 2.3±0.4 fold; $p < 0.05$ n=7), while POMC mRNA levels are unaltered. To investigate the mechanism by which loss of BACE1 enhances leptin sensitivity we examined the expression of negative regulators of leptin signalling. PTP1B and SHIP2 mRNA levels are unaltered in BACE1$^{-/-}$ mice on either diet. Whereas SOCS3 mRNA expression is increased in WT, but not BACE1$^{-/-}$, mice on HF diet (1.8±0.2 and -1.1±0.1 fold respectively; $p < 0.05$, n=7-8), correlating with STAT3 phosphorylation levels.

Taken together these data indicate that BACE1 is a regulator of hypothalamic leptin sensitivity in mice. Consequently, BACE1 inhibition may be a novel therapeutic intervention to recover leptin sensitivity, reduce body weight and improve glucose homeostasis in people with obesity/Type 2 diabetes.

Meakin *et al*. (2012) *Biochem J*. **441**, 285-96

Supported by Diabetes UK, BBSRC, MRC, Astrazeneca and the Wellcome Trust

Where applicable, the authors confirm that the experiments described here conform with The Physiological Society ethical requirements.

PCB300

beta-arrestin1 mediates cholecystokinin functions in pancreatic beta cells

S. Ning[1,3], N. Liang[2,4], J. Su[1], C. Liu[1], J. Dong[1,2], H. Li[1], J. Sun[2,4] and X. Yu[1,3]

[1]Institute of Physiology, Shandong University, School of Medicine, Jinan, Shandong, China, [2]Dept. of Biochemistry and Molecular Biology, Shandong University School of Medicine, Jinan, Shandong, China, [3]Qilu Hospital, Shandong University School of Medicine, Jinan, Shandong, China and [4]Shandong Provincial Hospital, Shandong University School of Medicine, Jinan, Shandong, China

Cholecystokinin (CCK), a gastro-intestinal hormone, is secreted by intestinal I cells after the meal and regulates important digestive and metabolic functions. In pancreatic islets, CCK managed insulin secretion and beta cell mass majorly through CCK A-type receptor (CCKAR), a G protein coupled receptor, while the downstream signaling of CCKAR in pancreatic beta cells were not well defined. Here, we demonstrated that CCK-8s activated CCKAR and induced both IP3 and cAMP accumulation, which coordinately regulated efficient insulin secretion. Apart from activation of G protein signaling, CCK also promotes complex formation of CCKAR and beta-arrestin1. Exploiting RNA interference and beta-arrestin1 knockout (beta-arrestin1-/-) mice, we revealed that beta-arrestin-1 was a key mediator of both CCK promoted insulin secretion and its protective effects against apoptosis in pancreatic β cells. The anti-apoptotic effect of beta-arrestin-1 was through arrestin-mediated cytoplasmic long term ERK activation, which activates the p90RSK-phosphor-BAD antiapoptotic pathway and inhibits the caspase-3 cleavage. Further, we observed that knockdown of beta-arrestin-1 decreased both CCK-8s-induced cAMP and IP3 accumulation statistically, suggesting a crosstalk between beta-arrestin-1 and G protein mediated pathways. The importance of beta-arrestin-1 function downstream of CCKAR in pancreatic beta cells could be appreciated for development of newly anti-diabetic drugs.

Where applicable, the authors confirm that the experiments described here conform with The Physiological Society ethical requirements.

PCB301

Effects of early life leptin intervention on reward-related receptor levels and behaviour

T. South, S. Bae, J. Roberts, A. Mullier, L. Poston, P. Taylor and C. Coen

King's College London, London, UK

Background: Our previous work has shown that the offspring of obese rat dams display an exaggerated and prolonged leptin surge early in life, which may predispose them to the metabolic syndrome in adulthood. It is hypothesized that this surge of leptin influences reward behaviour and the expression of associated receptors (e.g. dopamine D2, cannabinoid CB1 and opioid Mu receptors) in the central nervous system,
Objective: This project investigated the ways in which elevated leptin levels in early life, comparable to those associated with maternal obesity, may alter the neonatal brain and lead to dysfunctional reward-seeking behaviours and obesity later in life.
Methods: Twelve male Sprague Dawley rats were treated ip from post natal day 9-15 day with either leptin (0.3mg/kg, n=6) or vehicle (saline, n=6). At day 30, rats were euthanised and brains were removed for examination of receptor levels via ligand-binding autoradiography. An overnight 'two-bottle sucrose preference test' was also carried out in separate cohorts (n=10/group) at day 30.
Results: Following an overnight sugar preference test, it was found that the leptin-treated rats had a greater preference for sucrose compared to the saline-treated control animals (94.6% vs. 84.7% preference for sucrose, $p<0.05$).Analysis of [3H]-spiperone binding indicated that the leptin treated-rats had a significantly lower D2 level than the control animals in the nucleus accumbens (64.8% lower, $p<0.05$); for CB1 binding, the leptin treatment led to a rise in the nucleus accumbens and decrease in the caudate putamen ($p<0.05$). Opioid mu receptor binding was higher in the nucleus accumbens and thalamus of the leptin-treated rats ($p<0.05$).
Conclusions: Early-life leptin exposure leads to alterations in reward-related receptors and behaviour, which may predispose those individuals to reward-related behavioural disorders later in life, such as obesity or addiction.

Where applicable, the authors confirm that the experiments described here conform with The Physiological Society ethical requirements.

PCB302

Effects of *Curcuma comosa* Roxb. on human osteoblast proliferation and differentiation

D. Tantikanlayaporn[1], L.J. Robinson[2], A. Suksamrarn[3], P. Piyachaturawat[1] and H.C. Blair[2,4]

[1]Physiology, Mahidol University, Rachatewi, Bangkok, Thailand, [2]Pathology, University of Pittsburgh, Pittsburgh, PA, USA, [3]Chemistry, Ramkhamhaeng University, Bangkapi, Bangkok, Thailand and [4]Veteran's Affairs Medical Center, Pittsburgh, PA, USA

Phytoestrogens have recently been receiving more attention as a promising therapeutic agent for the prevention of bone loss in postmenopausal osteoporosis. *Curcuma comosa* Roxb. (*C. comosa*) is a ginger-family plant containing phytoestrogens and has been used extensively as dietary supplement to relieve menopausal symptoms. Diarylheptanoid (3*R*)-1,7-diphenyl-(4*E*,6*E*)-4,6-heptadien-3-ol (DPHD), isolated from *C. comosa*, was identified as the active phytoestrogen. DPHD has previously been found to activate Wnt/β-catenin signaling to increase differentiation in transformed mouse osteoblasts. However, its effect on human bone cells has not been reported. In the present study, we investigated the osteogenic effect and mechanism of action of DPHD in nontransformed human osteoblasts (h-OB). In growth medium, DPHD increased h-OB proliferation, investigated by thymidine incorporation assay and it accelerated osteoblast differentiation in the differentiation medium as indicated by the increases in alkaline phosphatase activity and osteoblast-specific mRNA production at 7-21 days. The effects of DPHD were abolished by estrogen receptor antagonist ICI182780. During the differentiation, DPHD promoted early expression of osteoblast transcription factors; RUNX2 and osterix. Subsequently, DPHD accelerated production of bone structural genes, including collagen type I alpha I (COL1A1) and osteocalcin comparable to 17β-estradiol. Moreover, DPHD increased the osteoprotegerin to RANKL ratio indicated that it could promote osteoblast bone formation. It was supported by the increased bone mineralization of DPHD detected by Von kossa staining. In conclusion, DPHD effectively promotes human osteoblast proliferation, differentiation and mineralization. The stimulating effects of the phytoestrogen from *C. comosa* on human osteoblasts may have clinical relevance for assisting in maintenance of bone mass menopausal women.

Bhukhai K, Suksen K, Bhummaphan N, Janjorn K, Thongon N, Tantikanlayaporn D, et al. A phytoestrogen diarylheptanoid mediates estrogen receptor/Akt/glycogen synthase kinase 3beta protein-dependent activation of the Wnt/beta-catenin signaling pathway. J Biol Chem. 2012 Oct 19;287(43):36168-78.

Suksamrarn A, Ponglikitmongkol M, Wongkrajang K, Chindaduang A, Kittidanairak S, Jankam A, et al. Diarylheptanoids, new phytoestrogens from the rhizomes of Curcuma comosa: Isolation, chemical modification and estrogenic activity evaluation. Bioorg Med Chem. 2008 Jul 15;16(14):6891-902.

This study was supported by Thailand Research Fund (TRF), Royal Golden Jubilee PhD Program grant PHD/0103/2549 (DS and PP); NRU, Faculty of Science, Mahidol University; National Institutes of Health (USA) awards AR053566 (LJR), AR055208 (HCB); Department of Veteran's Affairs (USA) (HCB).

Where applicable, the authors confirm that the experiments described here conform with The Physiological Society ethical requirements.

PCB304

Coupling between electrical and calcium oscillatory activity in beta cell networks in mouse pancreas slices

J. Dolensek[1], M. Skelin Klemen[1], A. Stozer[1,4], E. Miller[2], R. Tsien[2] and M. Slak Rupnik[1,3]

[1]Institute of physiology, Faculty of Medicine, University of Maribor, Maribor, Slovenia, [2]Department of Pharmacology, University of California at San Diego, San Diego, CA, USA, [3]Centre of Excellence for Integrated Approaches in Chemistry and Biology of Proteins, Ljubljana, Slovenia and [4]Centre for Open Innovations and Research, University of Maribor, Maribor, Slovenia

Beta cells secrete insulin in response to glucose stimulation, a process that is cytosolic calcium-dependent. During sustained physiological stimulation, beta cells express oscillatory changes in intracellular calcium concentration that spread over a given islet of Langerhans in a wave-like manner. Electrophysiological records from a single cell inside the beta cell syncytium

show that the single cell electrical activity is well synchronized with the calcium oscillations indicating tight coupling between calcium and electrical changes. However, network properties of beta cells in vivo remain elusive, mostly because of the inherent limitation of electrophysiological recording with the pipette – namely the "one pipette - one cell" rule. To circumvent this limitation and to assess the properties of the tightly electrically coupled network of beta cells at a systems level, simultaneous recording of a large number of cells is needed, a task most suitable for voltage sensitive dyes. Recently, a new generation of voltage sensitive dyes was reported (1) that utilize photo-induced electron transfer as a voltage-sensing mechanism, providing a more robust response to a voltage change than the previous generations of the voltage sensitive dyes. We used VoltageFluor dye VF2.1.Cl to record oscillatory changes in membrane potential in mouse pancreatic slices using confocal fluorescence imaging. With this method, electrical activity of many (>50) cells could be recorded simultaneously. Glucose responding cells showed a stimulus-dependent depolarization that was followed by a sustained oscillatory behavior. Waves of depolarizations were periodically spreading over the plane of an islet. The wave propagation was similar in its speed as the propagation of calcium waves in pancreas tissue slices during the oscillatory phase reported previously (2). In contrast, the repolarizing phase in the electrical activity seems to be at least partially uncoupled with regard to the calcium activity. The repolarization spreading over the plane of an islet showed different spatio-temporal properties than the depolarization waves. Moreover, the pattern of the propagation of repolarization has not been predictable. To directly determine the relationship between the electrical and calcium waves at higher temporal resolution, we recorded both simultaneously, the calcium oscillations from the plane of islet and potential changes in a beta cell from the network. The former was recorded using OGB-1 using a CCD camera and latter with a patch pipette in whole-cell patch-clamp configuration. Electrical activity was best correlated to the calcium oscillation in the nearest group of cells, relative to the patch pipette.

Miller EW, et al. (2012) Optically monitoring voltage in neurons by photo-induced electron transfer through molecular wires. Proc. Natl. Acad. Sci. U. S. A. 109(6):2114-2119.

Stozer A, Dolensek J, & Rupnik MS (2013) Glucose-Stimulated Calcium Dynamics in Islets of Langerhans in Acute Mouse Pancreas Tissue Slices. PLoS ONE 8(1):e54638.

Where applicable, the authors confirm that the experiments described here conform with The Physiological Society ethical requirements.

PCB305

Adverse effects of leptin on sperm count and morphology in Sprague-Dawley rats are reversed between six to eight weeks of recovery

F.A. Almabhouh[1], H. Singh[1], K. Osman[2] and S. Fatimah[2]

[1]Faculty of Medicine, Universiti Teknologi MARA, Kuala Lumpur, Selangor, Malaysia and [2]Faculty of Allied Health Sciences, Universiti Kebangsaan Malaysia, Kuala Lumpur, Selangor, Malaysia

Hyperleptinaemia of obesity is increasingly linked to numerous cardiovascular diseases and infertility. Exogenous leptin administration has been shown to adversely effect sperm count and sperm morphology in normal adult rats (Nizam et al., 2010). It is, however, unknown if these effects are reversible upon discontinuation of leptin treatment. This study therefore examined the effect of 3, 6 and 8-week recovery period on sperm count and morphology in normal adult rats following six weeks of leptin treatment.

Twelve-week old male Sprague-Dawley rats were randomized into four leptin and four saline treated control groups with 6 rats in each group. Intra-peritoneal (i.p.) injections of leptin were given daily at a dose of 60 μg/kg body weight in 0.1 ml 0.9 % saline for 42 days. Controls received 0.1 ml of 0.9% saline. On day 43, one group of leptin treated rats and one group of age-matched saline treated control rats was euthanized for collection of epididymal sperm. The remaining three groups together with their age-matched saline treated controls were allowed to recover further for either 21, 42 or 56 days. Upon completion of the recovery period, animals were euthanized and the epididymis was removed and minced in 2 ml of normal saline. The suspension was then filtered through a nylon mesh and a small drop of the filtrate was placed in the center of the disc area of a Makler counting chamber and covered with a cover slip. The number of total and abnormal sperm in a strip of 10 squares was counted (x10 magnification). This represented the concentration in million per ml. Data were analyzed using ANOVA and presented as mean ± SEM.

* P<0.05; **p<0.01; *** p<0.001 compared to the respective age-matched control

Sperm count was significantly lower and the fraction of abnormal sperm was significantly higher in leptin treated rats on day 1 of recovery i.e. 42 days after leptin treatment. These differences were still evident at days 21 and 42 but not at day 56 of recovery.

It appears the adverse effects of 42 days of leptin treatment on sperm count and morphology are completely reversed within 56 days post-treatment in Sprague-Dawley rats suggesting that the effect of leptin on sperm count and morphology includes effects further upstream in the sperm cycle, which is about 58 days in the rat.

	Total sperm count (Million/ml)	Abnormal sperm (%)
Control Recovery day 1	9.9 ± 0.2	3.6± 0.3
Leptin Recovery day 1	6.1 ± 0.2**	10.9 ± 1.0 ***
Control Recovery day 21	10.1 ± 0.2	3.16 ± 0.29
Leptin Recovery day 21	7.5 ± 0.4***	7.8 ± 0.8***
Control Recovery day 42	10.4 ± 0.3	5.1 ± 0.07
Leptin Recovery day 42	9.6 ± 0.3*	6.4 ± 0.26**
Control Recovery day 56	10.5 ± 0.05	4.95 ± 0.11
Leptin Recovery day 56	10.2 ± 0.1	5.26 ± 0.43

Mohd Nizam Haron, Urban J.A. D'Souza, Hasnan Jaafar, Rahimah Zakaria, Harbindar Jeet Singh. Exogenous leptin administration decreases sperm count and increases the fraction of abnormal sperms in adult rats. Fertility and Sterility 2010; 93(1):322-324

Where applicable, the authors confirm that the experiments described here conform with The Physiological Society ethical requirements.

PCB306

Glucagon-like peptide-1 enhances glucokinase activity in pancreatic β-cells

D. Song, J. Park, J. Bae and S. Im

Physiology, Keimyung University School of Medicine, Daegu, Republic of Korea

Glucokinase (GK), which phosphorylates d-glucose, is a major glucose sensor in β-cells for glucose-stimulated insulin secretion (GSIS) and is a promising new drug target for type 2 diabetes (T2D). In T2D, pancreatic β-cells exhibit defective glucose sensitivity, which leads to impaired GSIS. Although glucagon-like peptide-1-(7–36)-amide (GLP-1) is known to enhance β-cell glucose sensitivity, the effect of GLP-1 on GK activity is still unknown. The present study demonstrated that GLP-1 pretreatment for 30 min significantly enhanced GK activity in a glucose-dependent manner, with a lower Michaelis-Menten constant (Km) but unchanged maximal velocity (Vmax). Thus, GLP-1 acutely enhanced cellular glucose uptake, mitochondrial membrane potential, and cellular ATP levels in response to glucose in rat INS-1 and native β-cells. This effect of GLP-1 occurred via its G protein-coupled receptor pathway in a cAMP-dependent but protein kinase A-independent manner with evidence of exchange protein activated by cAMP (Epac) involvement. Silencing Epac2, interacting molecule of the small G protein Rab3 (Rim2), or Ras-associated protein Rab3A (Rab3A) significantly blocked the effect of GLP-1. These results suggested that GLP-1 can further potentiate GSIS by enhancing GK activity through the signaling of Epac2 to Rim2 and Rab3A, which is the similar pathway for GLP-1 to potentiate Ca^{2+}-dependent insulin granule exocytosis. The present finding may also be an important mechanism of GLP-1 for recovery of GSIS in T2D.

Jörns *et al.* (2002). *Virchows Arch* **440**, 63–69.

Kashima *et al.* (2001). *J Biol Chem* **276**:46046–46053.

Holz GG (2004). *Diabetes* **53**:5–13.

This research was supported by Technology Development Program for Agriculture and Forestry (110135-3), Ministry for Food, Agriculture, Forestry, and Fisheries, Republic of Korea, and by the KRF Grant funded by the Korean Government (MOEHRD) (KRF-2006-00008).

Where applicable, the authors confirm that the experiments described here conform with The Physiological Society ethical requirements.

PCB307

Protein kinase C α downregulation and increased cAMP generation both enhance calcium-sensing receptor-mediated intracellular calcium mobilisation in HEK-293 cells

M. Bin Khayat[1], K.L. Campion[1], A.D. Conigrave[2] and D.T. Ward[1]

[1]Faculty of Life Sciences, University of Manchester, Manchester, UK and [2]University of Sydney, Sydney, NSW, Australia

Extracellular Ca^{2+} homeostasis is maintained by the action of the Ca^{2+}-sensing receptor (CaR) on parathyroid hormone (PTH) secretion and renal Ca^{2+} reabsorption. CaR contains several protein kinase C (PKC) consensus sequences of which one, CaR^{T888}, is the key site responsible for PKC-mediated inhibition of CaR-elicited Ca^{2+}_i mobilisation *in vitro* and PTH secretion *in vivo*. However, we have not yet identified the PKC isotype responsible for CaR^{T888} phosphorylation nor determined whether CaR signalling can be modulated by cAMP given the fundamental regulatory roles of these second messengers in PTH secretion.

Therefore, siRNAs were used to knockdown specific PKC isoforms in turn, in CaR-transfected HEK-293 cells (CaR-HEK) with the effect on Ca^{2+}_i mobilisation then determined in Fura2-loaded cells by epifluorescence microscopy. Experimental buffer contained (mM) 20 HEPES (pH 7.4), 125 NaCl, 4 KCl, 0.5 $CaCl_2$, 0.5 $MgCl_2$ and 5.5 glucose. Following the siRNA-induced knockdown of PKCα, the EC_{50} of the CaR for Ca^{2+}_o was significantly lowered (3.2 ± 0.1 mM PKCα siRNA vs. 3.9 ± 0.2 mM siRNA control transfection; P<0.001, n=9) indicating that PKCα contributes to the inhibition of CaR-induced Ca^{2+}_i mobilisation. In contrast, no significant effect on CaR responsiveness to Ca^{2+}_o was observed following transfection with siRNAs against PKCs β, δ, ε or θ. In addition, PKCα knockdown lowered the threshold for Ca^{2+}_o-induced CaR activation whereby 1.8 mM Ca^{2+}_o elicited Ca^{2+}_i mobilisation in CaR-HEKs transfected with siRNA for PKCα but not with control siRNA (P<0.01; n=6). Intriguingly, this suggests that PKCα may even be active before the CaR elicits detectable Ca^{2+}_i mobilisation. Indeed, a similar effect was seen using the PKC inhibitor GF109203X (1μM) which permitted significant responses to 2mM Ca^{2+}_o that were not observed in the inhibitor's absence (P<0.05, n=7).

Next, following 2.5mM Ca^{2+}_o–induced CaR stimulation, cotreatment with either forskolin (10μM; adenylate cyclase activator), IBMX (75μM; 3-isobutyl-1-methylxanthine, phosphodiesterase inhibitor) or isoprenaline (100nM; β-adrenoceptor agonist) significantly enhanced the resulting Ca^{2+}_i mobilisation. In contrast, the inactive analogue 1,9 dideoxyforskolin (10μM) was without effect. Indeed forskolin (10μM) also reduced the agonist concentration threshold for CaR activation whereby 1.8mM Ca^{2+}_o elicited Ca^{2+}_i mobilisation in the presence of forskolin but not in its absence (P<0.001, n=9).

Together these data demonstrate that in CaR-HEK cells, PKCα inhibits CaR-induced Ca^{2+}_i mobilisation including at sub-threshold agonist concentrations. In contrast, cAMP lowers the threshold for CaR-induced Ca^{2+}_i mobilisation demonstrating the potential of the CaR to provide integration of multiple intracellular signals in Ca^{2+}_o homeostasis.

Where applicable, the authors confirm that the experiments described here conform with The Physiological Society ethical requirements.

PCB308

Litter size manipulation alters hormones plasma concentration and vascular reactivity

A.S. Mecawi[1], P.B. Marangon[1], N.A. Gonzaga[2], P. Passaglia[2], C.R. Tirapelli[2], L.L. Elias[1] and J. Antunes-Rodrigues[1]

[1]Department of Physiology, FMRP-USP, Ribeirão Preto, São Paulo, Brazil and [2]EERP-USP, Ribeirão Preto, São Paulo, Brazil

Litter size manipulation results in body weight gain alterations, such phenotype lingers until the adulthood. Several studies have demonstrated changes in hormonal profile, cardiovascular function and hydromineral homeostasis. Using the model of reduction or enhance of the litter size, the current work aimed to investigate the alterations in plasma angiotensin I and II, atrial natriuretic peptide (ANP), vasopressin and oxyitocin concentration on weaning (21st day) and adulthood (60th day) and vascular reaction of thoracic aorta to phenylephrine,

acetylcholine and sodium nitroprusside on adulthood. The litters were divided into 3 groups: Normal Litter (NL, 10 pups), Small Litter (SL, 3 pups) and Large Litter (LL, 16 pups). The reduction and enhance of the litter size, led to an increase and decrease of the weight gaining in SL (~25%) and LL (~19%) groups, respectively, at the weaning (21st day) till adulthood (60th day). Plasma angiotensin I and II levels were higher in both SL (~40%) and LL (~120%) groups in relation to the NL at the weaning, without differences on adulthood. We also observed a significant rise in the plasma vasopressin (~20%) and oxycitocin (~50%) in LL group on adulthood, without significant differences on weaning. We did not found significant differences on plasma ANP concentration on weaning, but on adulthood we observed an increase in plasma ANP in the SL and decrease in LL group (both ~20%). It was also observed a reduction (~10%) of endothelium-dependent vasodilation induced by acetylcholine in the SL group compared to control. No significant differences were observed in vasomotor responses to phenylephrine and sodium nitropruciato. Our results show that the litter size manipulation can program not only the weight gain, but also plasma hormones related to cardiovascular control and hydromineral balance and endothelium-dependent vascular reactivity.

FAPESP, CNPq, CAPES

Where applicable, the authors confirm that the experiments described here conform with The Physiological Society ethical requirements.

PCB309

Effects of leptin, TNF alpha, IL-1 and insulin on intracellular calcium concentration and pH in human articular chondrocytes from healthy and osteoarthritic cartilage

J.C. Sánchez and D.F. López-Zapata

Faculty of Health Sciences, Universidad Tecnológica de Pereira, Pereira, Risaralda, Colombia

Chondrocytes are the only cells in articular cartilage and are responsible for extracellular matrix metabolism, which confers its characteristic ability to withstand compression and distribute load (1). Osteoarthritis is characterized by an abnormal matrix metabolism which leads to a dysfunction of articular cartilage; this disease is associated with obesity, associated to an increase in leptin, TNF alpha, IL-1 and insulin. Chondrocyte intracellular calcium concentration (ICC) and pH (IpH) regulate matrix metabolism (2). In the present study, the effects of these substances on ICC and IpH, in human articular chondrocytes freshly isolated from healthy and osteoarthritic cartilage, were determined. Cells were isolated from knee or hip load-bearing car-tilage that was obtained from patients undergoing orthopedic surgery. All patients signed an informed consent form. Cells were isolated using a standard method (3).
ICC and IpH were measured by fluorescence employing Fura-2 and BCECF-loaded cells respectively, previous a standard calibration for each dye. The measurements were made in human chondrocytes from healthy cartilage (HCHC) and osteoarthritic cartilage (HCOC). Initial ICC was 88±14 nM in HCHC (n=38) and 79±12 nM in HCOC (n=36), with no significant differences between them. In HCHC, insulin, TNF alpha and IL-1 increased significantly ICC immediately after the application of each agent to 382±34 nM (n=12), 551±32 nM (n=8) and 604±44 nM (n=8) respectively ($p<0.05$ in all cases when compared with control); there were also significant differences between ICC increase induced by TNF alpha and IL-1 when compared with the ICC increase induced by insulin. In HCOC the effects of insulin, TNF alpha and IL-1 on ICC were in the same trend, but they were significantly lower: 211±21 nM (n=9), 243±32 nM (n=9) and 216±24 nM (n=8) respectively, without any significant differences. In both cells, leptin had no significant effect on ICC: 84±21 nM in HCHC (n=10) and 70±26 nM in HCOC (n=10).
On the other hand, initial IpH was 6.94±0.21 in HCHC (n=26) and 6.32±0.12 in HCOC (n=26), with a significant difference between these two data ($p<0.05$); only IL-1 was able to decrease IpH to 6.21±0.16 (n=8) and 6.02±0.09 (n=8) respectively; in both cases the differences were significant ($p<0.05$). Insulin, TNF alpha and leptin had no effect in both groups of cells.
In summary, these findings may help to understand the association between obesity and osteoarthritis because leptin, TNF alpha, IL-1 and insulin are all increased in obesity as a consequence of a metabolic misbalance; the effects of them on chondrocyte calcium and pH homeostasis can affect matrix metabolism and hence cartilage function, which can lead to osteoarthritis.

1. Urban JP. (1994). Br J Rheumatol 33, 901–908.

2. Wilkins et al. (2000). J Membr Biol 177, 95–108.

3. Browning JA et al. (1999). Acta Physiol. Scand.166, 39–45.

We acknowledge to Colciencias (Bogotá, Colombia) for financial support.

Where applicable, the authors confirm that the experiments described here conform with The Physiological Society ethical requirements.

PCB311

Microarray Analysis of the retina in growth hormone transgenic mice

S. Harvey[1], B.T. Martin[1], E.O. List[3], J.J. Kopchick[3] and Y. Sauve[1,2]

[1]Physiology, University of Alberta, Edmonton, AB, Canada, [2]Ophthalmology, University of Alberta, Edmonton, AB, Canada and [3]Edison Biotechnology Institute, Ohio University, Athens, OH, USA

Purpose: Previous work in our lab using the electroretinogram has functionally characterized the bovine growth hormone expressing (bGH) mouse as having depressed oscillatory potentials (OPs) in comparison to wild-type (WT) littermates (1). A microarray analysis of the retina was therefore performed to identify candidate genes contributing to this phenotype.
Methods: Total RNA was extracted from the retinas of 6 WT and 6 bGH mice by BioServe (Beltsville, MD). The expression level of 29,922 gene transcripts was measured using the Phalanx Biotech OneArray (Palo Alto, CA). Hierarchical clustering and functional gene-set analysis was performed on the resulting data to compare the retina of WT and bGH mice.
Results: Gene-sets associated with Angiogenesis revealed 13 member genes in the retinas of bGH mice that had significant alterations ($P<0.05$) in their expression patterns in comparison with WT mice. Similarly, 52 genes associated with Apoptosis were altered, as were 8 genes associated with Diabetes, 12 with Neurotransmission, 10 with Neurotrophins, and 5 with the Janus-kinase (JAK) signaling pathways.
In the Angiogenesis gene set for bGH mice, vascular endothelial growth factor (VEGF) receptor 2 precursor expression was increased to 134% of WT levels, while VEGF-A precursor was increased to 123% of WT levels. Pro-apoptotic transcripts of

death-inducer obliterator 1 were reduced to 71% of WT levels. Transcripts for 6-phosphofructo-2-kinase/fructose- 2,6-biphosphatase 3, an enzyme important for glycolysis with involvement in diabetes, was upregulated to 146% of WT levels. There were significant changes to members of neurotransmission and neurotropic gene sets, including ATP-sensitive inward rectifier potassium channel 12 (118%), somatostatin receptor type 1 (91%), and insulin-like growth factor-binding protein 6 precursor (79%). Lastly, in the JAK pathway, suppressor of cytokine signaling 2 was upregulated to 154% of WT levels.

Conclusion: Mice overexpressing growth hormone show a defect in the ERG analogous to that seen in diabetic retinopathy and retinopathy of prematurity. The results of this study indicate that the defect in these mice may be caused by alterations in vascular function (Vegfa, Kdr), altered cell survival in development (Bnip1, etc.) or changes in several genes linked to diabetes (Mapk8, PFkfb3). The changes in neurotransmission-linked gene expression may be directly responsible for the changes seen in ERG. In particular, genes of the Agxt family are linked to glycine metabolism in retinal amacrine cells, which are likely cellular mediators of the OPs. Changes in the Janus-kinase pathway reflect the heightened GH signaling (Socs2). These changes in gene expression occurred independently of gross morphological changes in the retina, as no significant differences were seen in cell counts or retinal zonation.

Martin BT *et al.* (2011). *Growth Hormone & IGF Res.*21,219-227

Supported by NSERC, Canada

Where applicable, the authors confirm that the experiments described here conform with The Physiological Society ethical requirements.

PCB314

Duodenal I-cells contain CB1 receptor mRNA transcript that is upregulated by energy restriction

A. Sykaras, C. Demenis, R. Case, J. McLaughlin and C.P. Smith

University of Manchester, Manchester, UK

Gut-to-brain signalling has a pivotal role in the regulation of food intake and energy balance. Vagal afferent neurons (VANs) integrate a wide range of signals from the proximal intestine to stimulate or inhibit appetite. Gut hormones and intestinal endocannabinoids (eCBs) are key peptides that act on the vagus nerve and transmit signals to the brain, responding to the food digestion or food deprivation. Enteroendocrine (EE) cells sense nutrients and release gut hormones that regulate food digestion and appetite. I-cells are a subtype of EE cells, primarily localized in duodenum, that secrete the classic satiety hormone cholecystokinin (CCK), mainly in response to fat. Post-prandially, CCK suppresses appetite via vagal CCK-1 receptors and also down-regulates the expression of the orexigenic-signalling associated cannabinoid receptor CB1 in VANs, to inhibit food intake. CB1 receptor is up-regulated during fasting, when CCK levels are low and intestinal eCBs levels are increased, to promote stimulation of appetite. Intestinal eCBs levels can also selectively increase after a fatty meal, a response that is dependent on the orosensory properties of the meal. Elevated eCBs levels further induce fat intake by activating CB1 receptor. Although it is accepted that CB1 receptor is expressed in VANs, it remains unknown if it is expressed in the duodenal epithelium.

The aim of our study was to investigate if CB1 receptor is expressed in the duodenal mucosa and specifically in I-cells. We used the (Cck-EGFP)BJ203 transgenic mouse model to isolate I-cells by using fluorescence activated cell sorting (FACS). 5000-10000 I-cells were isolated by FACS in each experiment. Semi-quantitative RT-PCR analysis of total unamplified RNA prepared from sorted I-cells (eGFP+ cells) and equal number of non I-cells (eGFP- cells) revealed that I-cells are highly enriched in CB1 receptor mRNA transcript in comparison with non I-cells (epithelial cells). RT-PCR analysis was repeated on amplified RNA/cDNA samples from I-cells and non I-cells confirming that CB1 receptor mRNA transcript is specifically expressed in I-cells and cannot be detected in non I-cells. We then examined if the CB1 receptor mRNA levels are regulated by energy intake. We compared CB1 receptor mRNA levels using duodenal mixed cell populations from 3 different groups of mice (fed ad libitum, fasted for 16 hours and fasted for 16 hours/re-fed for 5 hours). Semi-quantitative RT-PCR indicated that CB1 mRNA is upregulated during fasting. Re-feeding of fasted mice down-regulates the expression of CB1 mRNA transcript.

Our results suggest that I-cells contain mRNA transcript encoding CB1 receptor and that its expression is upregulated during energy restriction, similarly with VANs. The presence of CB1 mRNA transcript in I-cells may suggest that eCBs directly inhibit CCK release to promote stimulation of food intake.

Where applicable, the authors confirm that the experiments described here conform with The Physiological Society ethical requirements.

PCB315

Effects of ofloxacin residues on health biomarkers in chicken

M.I. Arshad, S.L. Butt, Z.U. Rahman and F. Asad

Physiology and Pharmacology, University of Agriculture, Faisalabad, Punjab, Pakistan

Now a days quinolones are frequently used antibiotics at poultry farms but their residual effects by oxidative damage to body of chicken have not been addressed. Therefore, we aimed to investigate the effect of antibiotic residues of ofloxacin on total antioxidants, oxidants, paraoxonase, arylesterase and catalase activities. Five weeks old broiler birds were treated with ofloxacin @ 10 mg/kg b.wt/day for 5 consecutive days through drinking water. Six birds were killed for each time interval for the detection of antibiotic residue in muscles and liver by HPLC with fluorescent detection. Experiment was conducted according to the institutional ethics committee. Health biomarkers including paraoxonase, arylesterase and catalase were analyzed by their respective reference methods and concentrations were measured by photometric method from serum, muscles and liver. Ofloxacin did show a residual effect on day 3 which turned into traces in muscles at the end of study. Oxidant status did increase on day 1 after ofloxacin therapy and level remained high throughout experimental period that may lead to deterioration of broiler meat. Ofloxacin did decrease the muscle arylesterase but did not put significant effect on serum arylesterase. Muscle catalase and serum paraoxonase were significantly decreased by ofloxacin at day 1 of the experiment. However, after 4 days of wash out period for drug, the antioxidants status was improved without any significance. In conclusion our results did show that residues of ofloxacin have deteriorative effects on meat quality by increasing the oxidant level in the muscles and serum.

Where applicable, the authors confirm that the experiments described here conform with The Physiological Society ethical requirements.

PCB316

Effect of ciprofloxacin residues on the quality of meat and eggs in layer chicks

Z.U. Rahman, F. Asad and S.L. Butt

Physiology and Pharmacology, University of Agriculture, Faisalabad, Punjab, Pakistan

The extensive use of ciprofloxacin in poultry feed and to treat diseased birds by veterinarians may cause drug residue problems in eggs and meat of chicken. The effect of drug residues on the meat quality and withdrawal period of ciprofloxacin was investigated in experimentally treated birds with ciprofloxacin @ 10 mg/kg b.wt/day for 5 consecutive days. Samples of serum, muscle and eggs were collected, screened and quantified for ciprofloxacin by HPLC with fluorescent detection. Total antioxidant capacity (TAC) and total oxidant status (TOS) was measured and correlated with the presence of residues in meat. Experiment was conducted according to the institutional ethics committee. A significant decrease in antioxidants capacity and increase in oxidant status in muscles was found that may indicate deterioration of chicken meat quality. The mean concentrations of ciprofloxacin were calculated in collected samples from chicken and Analysis of variance and Duncan multiple range test was applied. Significant concentration of ciprofloxacin drug residues was present in serum, muscle, liver and kidney at day 1 of treatment, on different days of experiment and after the slaughter. Serum and muscles antioxidant capacity decreased while total oxidant status increased significantly. As birds were given wash out time after 5 days of treatment, serum TOS was low and little rise in TAC was observed in serum and muscles. Muscle samples positive for ciprofloxacin residues were cooked by two different methods (electric oven and microwave) to see the effect of on residual concentration was measured again. Ciprofloxacin concentration in muscles decreased but did not reach to a significant level after cooking. In conclusion, ciprofloxacin residue did change the TAC and TOS of muscles and indicate the presence of residue in meat, eggs and serum.

Where applicable, the authors confirm that the experiments described here conform with The Physiological Society ethical requirements.

PCB317

Deteriorative effects of norfloxacin residues on quality of broiler meat

S.L. Butt, Z.U. Rahman and F. Asad

Physiology and Pharmacology, University of Agriculture, Faisalabad, Punjab, Pakistan

In current poultry production systems use of antibiotic is going be inevitable for efficient meat production and among the antimicrobial agents quinolones are proved to be efficient in curing various bacterial diseases of poultry. However, the residual effects of norfloxacin (one of the quinolones) in meat of broiler birds have not been largely addressed. Therefore, we aimed to investigate the effect of norfloxacin residues on the quality of broiler meat by measuring the oxidant status and antioxidant capacity. Five weeks old broiler birds were experimentally administered with norfloxacin (10 mg/kg b.wt/day) for 5 consecutive days through drinking water. Six birds were killed for each time interval to detect the norfloxacin residues by HPLC with fluorescent detection as well as oxidant and antioxidant capacity of serum and muscles was measured by photometric method. Animal experimentation was conducted according to the institutional ethics committee. Maximum drug residues were present in serum and muscles on day 1 of norfloxacin treatment. Norfloxacin did decrease the antioxidant capacity in serum and muscles of medicated chicken that may lead to deterioration of broiler meat The reactive oxygen species (ROS) production (oxidative capacity) increased in serum and muscles at day 1 of norfloxacin treatment in broiler birds. However, after 4 days of wash out period for drug, the antioxidants status was improved without any significance.. In conclusion our results did show that residues of norfloxacin have deteriorative effects on meat quality of chicken.

Where applicable, the authors confirm that the experiments described here conform with The Physiological Society ethical requirements.

PCB318

Correlated responses to a multidirectional artificial selection in the bank vole: Changes in organ size

P. Koteja[1], K. Baliga-Klimczyk[1], K.M. Chrzascik[1], G. Dheyongera[1], M. Konczal[1], U. Maiti[1], P. Orlowska[2], A. Rudolf[1], C. Stawski[1] and E.T. Sadowska[1]

[1]Institute of Environmental Sciences, Jagiellonian University, Krakow, Poland and [2]Institute of Zoology, Jagiellonian University, Krakow, Poland

A central question in evolutionary physiology is how complex physiological adaptations evolve in response to natural selection operating on performance traits hypothetically associated with Darwinian fitness. Selection experiments provide a powerful yet underutilized approach to that question [1,2]. We established an artificial selection experiment with lines of bank voles Myodes glareolus selected for high swim-induced aerobic metabolism (A), the ability to maintain body mass on a low-quality herbivorous diet (H), intensity of predatory behaviour towards crickets (P), and unselected control lines (C) (with four replicate lines in each of the categories [3]). In generation 13, voles from the selected lines achieved 48% higher maximum rate of metabolism, lost 38% less mass in the 3-day test with low-quality diet (at the age of 32-35 days), and attacked crickets 5 times more frequently than voles from control lines. Here we report correlated responses in whole body and internal organs mass, measured in 15-18 voles per line (both sexes, mean age 76 days). The animals were euthanized by an overdose of anaesthetic (isoflurane) and dissected. Organs were weighed to the nearest 0.001g. Although the selection was performed on mass-independent traits (residuals from regression), body mass was higher in H than in C lines (Mixed cross-nested linear model, adjusted least square means±SE; C: 22.5±0.57, A: 22.8±0.58, H: 25.9±0.56, P: 20.8±0.58g; effect of selection $p<0.001$). Apparently, selection for the capability to maintain energy balance during a period of undernourishment in juveniles resulted in evolution of increased body size in adults. As expected, mass of heart and gasterocniemus leg muscles were increased in A lines (Heart C: 0.117±0.004, A: 0.143±0.004, H: 0.117±0.004, P: 0.127±0.004g, $p=0.001$; Muscles C: 0.166±0.005, A:0.190±0.005, H:0.159±0.005,

P:0.177±0.005, p=0.003). Because our earlier results showed an increased level of basal metabolism and food consumption in A lines [4,5], we also expected an increased mass of organs related to whole-body metabolism, and the results confirmed the expectation (Liver: C:1.20±0.03, A:1.31±0.03, H:1.19±0.03, P:1.27±0.03g; p=0.02; Kidneys: C: 0.29±0.01, A: 0.34±0.01, H: 0.29±0.01, P: 0.32±0.01g, p=0.003; Small intestine: C: 1.07±0.02, A: 1.18±0.02, H: 1.15±0.02, P: 1.16±0.02g, p=0.030; similar pattern was also found for stomach and caecum). As we expected, brain mass increased in P lines, but surprisingly it was also significantly increased in A lines (Total brain mass C: 0.522±0.006, A: 0.557±0.006, H: 0.531±0.006, P: 0.552±0.006g, p=0.006; similar pattern was found for cerebrum and cerebellum analysed separately). The selected lines of voles will provide a unique model to investigate lower-level histological, biochemical and molecular factors underlining evolution of the organismal performance traits.

Swallow J.G. and Garland T., Jr. 2005. Selection experiments as a tool in evolutionary and comparative physiology: insights into complex traits—an introduction to the symposium. Integr. Comp. Biol.45:387-390.

Swallow, J.G., Hayes, J.P., Koteja, P. and Garland, T., Jr. 2009. Selection experiments and experimental evolution of performance and physiology. Pages 301-351 in: Garland, T., Jr., and Rose, M.R., eds. Experimental evolution: concepts, methods, and applications of selection experiments. University of California Press, Berkeley, California.

Sadowska, E.T., Baliga-Klimczyk, K., Chrzascik, K.M., and Koteja, P. 2008. Laboratory model of adaptive radiation: a selection experiment in the bank vole. Physiol. Biochem. Zool. 81:627-640.

Koteja P., Baliga-Klimczyk K., Chlad A., Chrzascik K.M., Damulewicz M., Dragosz-Kluska D., Morawska-Ploskonka J., and Sadowska E.T. 2009. Correlated responses to a multidirectional artificial selection in the bank vole: activity, metabolism, and food consumption. Journal of Physiological Sciences 59 (Suppl. 1):541.

Koteja, P., Baliga-Klimczyk, K., Chrzascik, K.M., Dheyongera, G., Rudolf, A., Sumicka, S., and Sadowska, E.T. 2011. Experimental evolution of metabolic rates: correlated responses to a multidirectional artificial selection in the bank vole, Myodes glareolus. Journal of Physiology and Pharmacology 62s1:212.

Where applicable, the authors confirm that the experiments described here conform with The Physiological Society ethical requirements.

PCB319

The behavioral satiety sequence in pigeons (*Columba livia*): description and calibration of a test protocol

W.A. Spudeit[1], N.S. Sulzbach[1], M.A. Bittencourt[1], A.C. Andrade[1], A.M. Duarte[1], M.P. Cantarelli[1], G.I. Hunning[1], T.S. dos Santos[1], C. Lino-de-Oliveira[1] and J. Marino-Neto[1,2]

[1]Depto. de Ciências Fisiológicas - CCB, Universidade Federal de Santa Catarina, Florianópolis, Santa Catarina, Brazil and [2]Instituto de Engenharia Biomédica, EEL-CTC, Universidade Federal de Santa Catarina, Florianópolis, Santa Catarina, Brazil

The postprandial thermal and metabolic responses (the specific dynamic action) are physiological traits phylogenetically conserved among vertebrates (refs. 1, 2). Their behavioral counterpart is a sequence of drinking, maintenance and sleep-like behaviors (known as the Behavioral Satiety Sequence, BSS) that have been thoroughly described in rodents, and allowed for refined evaluation of potential appetite suppressants (refs. 3, 4). However, BSS presence and attributes have not been systematically studied in non-mammalian species. Here, we describe the BSS in pigeons (*Columba livia*, adults, 340-400 g bw, N=6,) after 1) a palatable seed mixture (SM) offered to free-feeding (FF-SM) animals; 2) re-feeding after a 24-h food-deprivation (24FD), 3) brief (1-hour) removal of food and water, followed by palatable food presentation (the "seed mixture-induced BSS" or SM-BSS test). Behaviors were examined by continuous recording during 2 h after the meal. A set of graphic representations and indexes related to the temporal structure and the sequential relationships between these behaviors (latency for the 1st occurrence, time-to-peak (TTP) of each behavior, inter-peak interval (IPI) and the first intersection (ItS) between feeding curves and those of other BSS-typical behaviors). These indexes were used to describe changes in the SM-BSS evoked by retesting (3 times, 7-days apart), by gender, by different degrees of food preload (0, 33, 66 or 100 % of their mean intake in 3 preceding tests), by removing water during the test or by changing the palatability of the food offered (Regular chow vs. SM food vs. quinine-adulterated SM. Fasting- and SM-induced feeding were followed by a temporally similar sequence of increased bouts of drinking, then preening and then sleep, which can be integrally observed within 90 min after food presentation. The latency, TTP, IPI and ItS indexes were able to detect, describe and quantitatively assess BSS the temporal and sequential parameters of the BSS. The SM-BSS test indexes were not affected by retesting, by gender or by the absence of water during the test. Despite of significant differences in food intake, the temporal and sequential indexes of the BSS in SM-BSS test, in 24FD animals, after different preloads or foods of varying palatability were similar, suggesting that BSS is triggered by preabsortive signals (all food eaten is still in the crop 90 min after the test start), but its sequential and temporal patterns are not modulated by the meal size. These results diverge from those observed in rodents and primates, indicating that, beyond general behavioral similarities, BSS may be directed by distinct central mechanisms in birds and mammals.

Secor SM (2009) *J Comp Physiol B* **179**,1–56

McCue MD (2006) *Comp Biochem Physiol A*, **144**, 381–394

Halford JC et al. (1998) *Pharmacol Biochem Behav*,**61**, 159-168.

Rodgers R.J. et al., (2010) *Pharmacol Biochem Behav*, **97**, 3–14

Supported by Capes, FAPESC and CNPq grants to J.M.N and C.L.O.

Where applicable, the authors confirm that the experiments described here conform with The Physiological Society ethical requirements.

PCB320

Continuous and intermittent training protocols improve expression of proteins involved in muscle metabolism of induced-obese rats

P.M. Seraphim[1], B.B. Brandao[1], L.M. Souza[1], B.N. Trombetta[1], M.S. Teixeira[3], C.L. Santos[2] and S. Bordin[2]

[1]Physical Therapy, FCT-UNESP - Universidade Estadual Paulista, Presidente Prudente, Sao Paulo/ Presidente Prudente, Brazil, [2]Physiology and Biophysics, ICB- Institute of Biomedical Sciences, Sao Paulo, SP, Brazil and [3]Physics, Chemistry and Biology, FCT - UNESP- Universidade Estadual Paulista, Presidente Prudente, SP, Brazil

Obesity is associated to reduction of glucose transporter 4 (GLUT4) and/or impaired insulin signaling pathway in skeletal muscle(1). Muscle contraction culminates in 5' AMP-activated protein kinase (AMPK) activation and GLUT4 translocation(2). Training stimulates peroxisome proliferator-activated recep-

tor-γ coactivator (PGC1α) transcription in muscle which is involved in GLUT4 regulation(3). We aimed to evaluate the effects of continuous or intermittent training on AMPK (coded by Prkaa2), PGC1α (Ppargc1a gene) and GLUT4 (Slc2a4 gene) expression in muscle of diet-induced obese rats. Sixty male Wistar rats aged 90 days were divided: sedentary control (SC), continuous exercise control (CEC), intermittent exercise control (IEC), sedentary obese (SO), continuous exercise obese (CEO), intermittent exercise obese (IEO). All animals received standard chow and obese also received high fat diet during 16 weeks (wk). Insulin tolerance test and the double effort test were performed after 8 wk of diet and at the end of 8 wk of training using blood collected from the tail distal end. The CEC and CEO groups trained for 30 min at 90% of anaerobic threshold, 3x/wk, 8 wk. The IEC and IEO performed 11 efforts of 2 min, 1 min of interval, 3x/wk, 8 wk, over the delta zero to 120% of the critical load. Rats were anesthetized with Pentobarbital sodium 40mg/kg, ip, for removal of gastrocnemius muscle. RT-PCR and Western blotting were performed for mRNA and protein analysis. The experimental protocol was approved by the Ethics Committee for Animal Research (#74/2009). ANOVA was used for comparison among means with post-hoc (Tukey) if necessary, considering $p<0.05$. Obese presented similar gain of weight after 8 wk of diet (23%,$p<0.05$), which was softened after training (CEC-31%, EIC-28%,$p<0.01$vsSC; CEO-54%, IEO-44%,$p<0.001$vsSO).Obese presented reduced insulin sensitivity (SC=2.3+/-0.23; SO=1.8+/-0.2%/min,$p<0.05$), but both protocols reverted this condition (CEO=2.8+-0.7;IEO=2.4+-0.4%/min,$p<0.05$vsSO). Prkaa2 mRNA was increased with exercise (CEC=70%,EIC=72%,$p<0.01$vsSC;COE=75%, EIO=59%,$p<0.05$vsSO), AMPKα2 protein content was increased in exercised controls (CEC=47%,IEC=51%,$p<0.05$vsSC). pAMPKα2 was reduced in SO (39%,$p<0.05$vsSC), and increased after training (CEO=264%,IEO=299%,$p<0.01$vsSO). Both protocols were efficient to increase Ppargc1a mRNA expression (CEC=62%,IEC=126%,$p<0.05$vsSC; CEO=104%, IEO=152%,$p<0.05$vsSO). Continuous exercise provoked an increase (53%) in Slc2a4 expression in obese ($p<0.05$), Intermittent training improved control (55%,$p<0.05$). Eight weeks of both training protocols were able to soften the gain body mass, improve the insulin sensitivity and increase aerobic capacity, promoting increase of the protein expression involved in muscle metabolism.

Seraphim, P.M. et al. (2001). Braz J Med Biol Res 34, 1353-62.

Hardie, D. G. & Sakamoto K. (2005). Physisology 21, 48-60.

Jornayvaz, F. R. & Shulman, G. I. (2010).Essays Biochem. 47, 69-84.

BB was a recipient of CAPES (Coordination of Developmet Senior Staff) fellowship.

Where applicable, the authors confirm that the experiments described here conform with The Physiological Society ethical requirements.

PCB321

Inflammatory responses to high-intensity intermittent training in diet-induced obese rats

P.M. Seraphim[1], R.J. Moreira[1], A. Panveloski-Costa[1] and M.S. Teixeira[2]

[1]Physical Therapy, FCT-UNESP - Universidade Estadual Paulista, Presidente Prudente, Sao Paulo/ Presidente Prudente, Brazil and [2]Physics, Chemistry and Biology, FCT - UNESP- Universidade Estadual Paulista, Presidente Prudente, Sao Paulo, Brazil

Adipose tissue is a source of inflammatory cytokines, such as TNF-α, characterizing a chronic low-grade inflammatory state (1). Lifestyle behavioral interventions, as physical activity, may have clinically significant benefits for improving inflammation (2). We aimed to investigate inflammatory responses in muscle after intermittent training of high intensity squat jump type in Wistar obese-induced rats. Forty adults male Wistar rats of 2 months-old were divided into: sedentary control (SC), exercise control (EC), sedentary obese (SO), exercise obese (EO). Control groups were fed with standard chow and obese received a cafeteria diet+standard chow ad libitum. The training protocol was performed following the adapted model of force from Tamaki et al. (3). It consisted on 3x a week, interposed by 24h among sessions, 3 series of 12 repetitions of 60s of interval among series with a strength load equivalent to 50% of the body weight (BW) during 6 weeks. An insulin tolerance test (ITT) was performed with venous blood collected from tail distal end for glicemia determinaton after ip injection of regular human insulin (0.5 IU/kg BW). The sacrifice was performed for removal of soleus muscle under anesthesia (Ketamine 80mg/kg,Xylazine 5mg/kg,ip). RT-PCR was performed for evaluation of Tnf and Il10 mRNA levels. ANOVA one-way was used for comparison among means with post-hoc (Tukey) if necessary, considering $p<0.05$. The experimental protocol was approved by the Ethics Committee for Animal Research (#15/2009). Obese (SO=538+/-19.6, EO=494.6+/-14; $p<0.01$vsSC,EC) presented a final weight significantly higher than controls (SC=415+/-18, EC=393+/-14) and significant increase in fat mass (around 49% in SO, $p<0.001$ vs SC; 42% in EO group $p<0.01$vsEC). ITT showed a reduction in insulin sensitivity in obese, however reversed by training (kITT expressed as %/min: SC=5.76+/-0,36;EC=6.63+/-0.45;SO=3.60+/-0.62*#; EO=7.07+/-0.47&;*$p<0.05$vsSC;#$p<0.01$vsEC, &$p<0.001$vsSO). The diet increased fat mass (SC=10.6+/-0.91,SO=20.83+/-0.17x0.001g/g BW, *$p<0.001$), and Tnf RNAm levels in obese group (SC=100.5+/-5.3, OS=133+/-7.9 AU, $p<0.001$). The training caused a 27%-reduction ($p<0.01$vsSO) in fat mass, and 39%-reduction in Tnf mRNA level (EO=80.7+/-6.2, $p<0.05$vsSO). The cafeteria diet positively modulated, while the training reduced Il10 levels mRNA (SC=100.6+/-4.2&, SO=210.4+/-10, EC=42.8+/-9.5&#, EO=153.9+/-13.7*, *$p<0.05$vsOS, &$p<0.001$vsSO, #$p<0.01$vsEO). We can conclude that the cafeteria diet was detrimental to insulin sensitivity in rats, and effective in body weight gain and increase of inflammatory cytokine TNFα levels. On the other hand, high-intensity intermittent training was effective in reversing this situation. Surprisingly, high-intensity intermittent training worsened, but the diet per se increased IL10 gene expression.

Galic S. et al. (2010). Mol Cell Endocrinol 316, 129-39

Nicklas, B.J. et al. (2005). CMAJ 172:1199-209

Tamaki T.et al. (1992). Med Sci Sports Exerc. 24, 881-6.

RJM is recipient of Fapesp fellowship (# 2010/17078-4).

Where applicable, the authors confirm that the experiments described here conform with The Physiological Society ethical requirements.

PCB322

Are FNDC5 gene expression and irisin release regulated by exercise?

S. Pekkala[1], P.K. Wiklund[1], J.J. Hulmi[2], J.P. Ahtiainen[2], M. Horttanainen[1], E. Pöllänen[1], K. Mäkelä[4], H. Kainulainen[2], K. Häkkinen[2], K. Nyman[3], M. Alen[5], K. Herzig[4] and S. Cheng[1]

[1]Department of Biology of Physical Activity, University of Jyväskylä, Jyväskylä, Jyväskylä, Finland, [2]Department of Health Sciences, University of Jyväskylä, Jyväskylä, Jyväskylä, Finland, [3]Jyväskylä Central Hospital, Jyväskylä, Finland, [4]Department of Physiology, Institute of Biomedicine and Biocenter of Oulu, University of Oulu, Oulu, Finland and [5]Department of Medical Rehabilitation, Oulu University Hospital, Oulu, Finland

Irisin, a proteolytic derivative of muscle integral membrane protein FNDC5 is released into the bloodstream after endurance exercise in mice and humans. The gene is regulated by PGC-1α to activate thermogenic programs in white adipose tissue. We wanted to test the hypothesis if FNDC5 and irisin are link to exercise type and duration and if these are age-dependent.

Methods: Middle-aged, non-diabetic and non-athlete men performed a 1-hour low-intensity (50% VOmax) aerobic exercise (AE) with bicycle ergometer (n=17), 21-weeks of endurance exercise (EE, n=9) and a combined endurance and resistance exercise (EE+RE, n=9), and in age matched non-exercised controls (Con, n=2). Vastus lateralis biopsies and blood samples were taken at 3-hours post-exercise. Furthermore, skeletal muscle mRNA fold changes of PGC1α and FNDC5 are investigated after 1-hour and 48-hours of single resistance exercise bout (5 × 10 RM leg press) in (a) young (n=10) and (b) old (n=11) men. FNDC5 mRNA was quantified using Taqman primers by Real-Time quantitative PCR System. PGC1α and GAPDH were quantified using in-house designed primers, iQ SYBR supermix and CFX96 Real-time PCR Detection System. Relative expression levels for FNDC5 and PGC-1α were calculated with the deltaCt method and normalized to the expression of GAPDH. Serum irisin levels were measured from serum samples using a commercial EIA kit.

Results: In non-diabetic and non-athlete middle-aged men no significant changes were observed in skeletal muscle PGC-1α, FNDC5 and serum irisin after 1-hour low-intensity aerobic exercise, 21-week endurance training or 21-week endurance training combined with resistance exercise (RE) training, whereas a single RE bout increased significantly FNDC5 mRNA by 1.4-fold post-RE in young, but not in old previously untrained men. Moreover, while the increase in PGC-1α mRNA at 1-hour post-RE in old men was significant, no significant changes in FNDC5 were detected. Apart from the single RE-bout, large intra and inter-individual variations in PGC-1α, FNDC5 and serum irisin in response to endurance exercise and RE training were observed. Importantly, changes in skeletal muscle PGC-1α gene expression were not consistently accompanied by corresponding changes in FNDC5. Our findings indicate that 1) for the most part, exercise does not increase FNDC5 expression in skeletal muscle; 2) factor(s) other than PGC-1α may be involved in the regulation of FNDC5 expression.

In conclusion, the large intra and inter-individual variation in FNDC5 and irisin in response to different types of exercise indicate that exercise does not seem to increase FNDC5 in skeletal muscle or circulating irisin levels. However, the increase in a subset of young individuals in acute RE warrants further studies to determine whether the effects of exercise on FNDC5 and irisin are collection time, exercise type, protocol, intensity and age-dependent.

Bostrom, P. et al., A PGC1-alpha-dependent myokine that drives brown-fat-like development of white fat and thermogenesis. Nature 481 (7382), 463-468.

Timmons, J.A., Baar, K., Davidsen, P.K., & Atherton, P.J., Is irisin a human exercise gene? Nature 488 (7413), E9-10; discussion E10-11.

Where applicable, the authors confirm that the experiments described here conform with The Physiological Society ethical requirements.

PCB323

Celastrus paninculatus enhances endurance activity by improving angiogenesis, mitochondrial biogenesis, glucose and lactate transport and protect muscle cells against t-BHP induced oxidative and apoptotic damage

H.K. Kandikattu

Biochemistry and Nanosciences, Defence Food Research Laboratory, Mysore, India

Regular exercise and balanced diet are the effective strategies to maintain healthy life style. Moderate exercise improves muscle metabolism, cardiovascular function and mitochondrial biogenesis by fatty acid utilization, enhancing mitochondrial metabolic rate and proliferation. Intense exercise can cause increased free radical production in the skeletal muscle and myocardium and forms muscle fatigue by increasing lactic acid content leading to muscle acidosis. Herbal extract supplementation has been suggested as an alternate therapy to treat fatigue induced stress. In the present study, we evaluated the anti-fatigue activity of Celastrus paniculatus seed extract (CPSE) in swimming endurance model of male BALB/C mice (25±2g). The work is an attempt of obtaining some clues to help elucidate the energy sensing, mitochondrial metabolism, angiogenesis, lactate and glucose transport mechanisms under swimming alone as well as in combination with 50mg/kg body weight CPSE administration by gavage. Here, we observed that CPSE supplementation enhances the swimming endurance by 2.5 folds. In order to understand the molecular mechanisms of exercise endurance activity we measured the exercise responsive skeletal metabolic regulators such as silent information regulator-1 (SIRT-1), peroxisome proliferator-activated receptor gamma coactivator-1α (PGC-1α), AMP-activated protein kinase (AMPK) and lactate transporters monocarboxylic acid transporters-1 (MCT-1) and 4 (MCT-4), glucose transporter-4 (Glut-4), angiogenesis enhancer vascular endothelial growth factor (VEGF) and glycolysis regulator pyruvate dehydrogenase kinase-4 (PDK-4) and oxidative stress biomarkers superoxide dismutase-1 (SOD-1), catalase (CAT) and heat shock protein-70 (HSP-70). CPSE supplementation potentiated the expression of metabolic regulators. Further we used t-butyl hydroperoxide (t-BHP) induced C2C12 mice muscle cell model which mimics the reactive oxygen species (ROS) mediated fatigue stress to illustrate the underlying antioxidant and anti-apoptotic defense mechanism mediated by CPSE. Our observed results demonstrates that pre-treatment of C2C12 muscle cells with CPSE (50μg/ml) for 2h before 24h treatment with t-BHP protects cell damage by regulation of ROS formation by restoring the antioxidant enzyme/proteins SOD, CAT and HSP-70 levels. The extract also prevents t-BHP induced

apoptosis by restoring the mitochondrial membrane potential (MMP) and inhibition of DNA damage. These results demonstrate that CPSE supplementation might be a valuable therapeutic approach in regulation of endurance activity as well as prevention of oxidative and apoptotic damage of cells.

Where applicable, the authors confirm that the experiments described here conform with The Physiological Society ethical requirements.

PCB324

Body mass index impact on in vivo skin's physiology

L. Tavares[1], O.R. Santos[1], L. Palma[1], M.A. Roberto[4], M.J. Bujan[3] and L.M. Rodrigues[1,2]

[1]CBiOS, U Lusofona Fac Health Sc & Technol, Lisboa, Portugal, [2]Pharmacol Sc Departm, U Lisboa Fac Pharmacy, Lisboa, Portugal, [3]UAH, U Alcala Fac Medicine, Madrid, Spain and [4]PRS, St Joseph Hospital -CHLC, Lisboa, Portugal

Changes in skin physiology resulting from overweight appears to be associated to significant modifications in skin hydration, repair mechanisms and biomechanical behavior, but this subject is still poorly documented. The aim of this work is to evaluate the impact of the BMI on normal skin indicators. Our sample involved 89 female volunteers, 20 - 46 (32+7) years old, no relevant pathologies except overweight, obesity and morbid obesity. The study respected the Declaration of Helsinki and subsequent ethical guidelines. Volunteer's weight and height were obtained by anthropometric measurements and the BMI calculated. The sample was divided in four groups according to the WHO classification - Normal (group I), Overweight (group II), Obese(group III) and Morbid (group IV). One single measurement (noninvasive methods, under standard and controlled conditions) was performed, involving measurements on skin hydration, barrier function and biomechanical behavior, in three different anatomical sites: face (zygomatic and forehead), breast and abdomen. Descriptive and comparative statistics were applied (SPSS vs 20.0) and a 95%.significance level adopted. TEWL, Hydration and mechanical descriptors follow a U-shape or a J-shape relationship regarding the BMI as described for other risk biomarkers for cardiovascular disease. An increase in TEWL and a decrease on skin hydration is noted in all anatomic areas when normal subjects are compared with morbid obese. Regarding biomechanical descriptors, significant reductions are detected in all anatomic areas, especially in abdomen, specially involving morbid obesity. Overweight definitely affects skin's function and appearance. These hydration and biomechanical descriptors seems to be interesting biomarkers of the process and eventually correlate with the signs and symptoms that characterize these patient's (most frequent) complaints.

Where applicable, the authors confirm that the experiments described here conform with The Physiological Society ethical requirements.

PCB325

Hydration and biomechanical biomarkers are useful to identify the impact of overweight in skin's physiology

L. Tavares[1], L. Palma[1], O.R. Santos[1], M.A. Roberto[3], M.J. Bujan[4] and L.M. Rodrigues[1,2]

[1]CBiOS, U Lusofona Fac Health Sc & Technol, Lisboa, Portugal, [2]Pharmacol Sc Dep, U Lisboa Fac Pharmacy, Lisboa, Portugal, [3]PRS, St Joseph Hosp - CHLC, Lisboa, Portugal and [4]UAH, U Alcala Fac Medicine, Madrid, Spain

Overweight and obesity have a huge impact on skin pathophysiology. Various related skin disorders seem to involve significant changes in skin hydration and biomechanical characteristics. However related biomarkers are difficult to obtain and to understand, considering skin's intraindividual's variability . This study aims to identify functional biomarkers to describe related changes in skin physiology. The study involved 89 female volunteers, between 19 and 46 (32±7) years old, without any pathologies besides overweight and obesity. All procedures observed the Declaration of Helsinki and subsequent ethical guidelines. Individuals were characterized according with their BMI following the WHO definitions, and cutaneous variables. These, obtained by noninvasive methods, under standard and controlled conditions included skin's epidermal hydration (corneometry), barrier function (TEWL) and several biomechanical descriptors. Z-scores were obtained to designed overall descriptors for hydration and biomechanics respectively. Since some of the indicators were distributed in a reverse scale (the higher the absolute value, the worse the performance of skin) the z-score of these variables became their symmetrical. The global indicators (for each anatomic region) were calculated using the arithmetic mean between these altered partial indicators. Statistical analysis was performed using SPSS version 20.0 and a significance level of 95% adopted.

Data revealed a direct relationship between hydration and biomechanical markers in different anatomical regions. Paradoxally, this is reversed with morbid obesity where an inverse association between skin hydration and biomechanical markers is consistently detected. In any case these relations follow the tendency of isolated descriptors. No matter the tendency, no significant correlation was found in the breast area. This strategy proved to be useful to design global indicators of these functional variables by anatomical area, allowing a fast and clearer view on skin's functional condition.

Where applicable, the authors confirm that the experiments described here conform with The Physiological Society ethical requirements.

PCB326

Central effects of exenatide, a glucagon-like peptide-1 receptor agonist, on human brain activation

S. McKie[1], L. Wasse[2], T. Coulson[3], C. Bryant[2] and J. McLaughlin[2]

[1]Neuroscience and Psychiatry Unit, University of Manchester, Manchester, UK, [2]Gastrointestinal Centre, University of Manchester, Manchester, UK and [3]Salford Royal NHS Foundation Trust, Manchester, UK

Understanding the anorectic effects of native glucagon-like peptide-1 (GLP-1) is challenging because it is rapidly inactivated by the enzyme dipeptidyl peptidase (DPP4) (1). GLP-1

receptors are located throughout the body including the brain and vagal afferent neurones. Exenatide is a long acting GLP-1 receptor agonist which, like GLP-1, reduces food intake, decreases body weight and delays gastric emptying (2), but crucially is resistant to the effects of DPP4. Exenatide may activate central pathways that mediate satiety, however research in humans is lacking. Changes in the blood oxygen level dependent (BOLD) signal measured during functional magnetic resonance imaging (fMRI) can be used as a surrogate correlate of changes in neural activity (3). To examine brain activation in humans after exenatide administration, 15 healthy adult volunteers received a subcutaneous injection of either 5μg exenatide or a placebo in a randomised cross over fashion during 70 minutes of fMRI (3T Philips scanner). For each volunteer, the difference in the mean % BOLD signal change from baseline between exenatide and placebo was extracted from 10 regions of interest covering the brainstem and hypothalamus. The extracted data were analysed in 5 minute blocks using T-tests. Due to excessive movement during scans, 2 volunteers were excluded from analysis. Bilateral increases in BOLD signal in the lower hypothalamus were evident 45 min after exenatide injection ($P<0.05$). The extent and time course of this increase is shown in Figure 1. In the bilateral midbrain there were trends for an increase in BOLD signal after 45 mins ($P<0.075$). This pattern of BOLD signal change was also observed in the right upper hypothalamus and pons. Conversely, BOLD signal was significantly decreased in the left upper hypothalamus 40 mins after exenatide injection ($P<0.05$); a similar trend was evident in the left pons and medulla. The overall pattern is that key appetite regulatory brain regions were progressively activated 45 min after exenatide administration. This suggests the anorectic effects of exenatide in humans may be mediated via activation of central GLP-1 receptors, either directly or via vagal inputs, rather than by a direct effect on delayed gastric emptying of meals since this study was undertaken in a fasting condition.

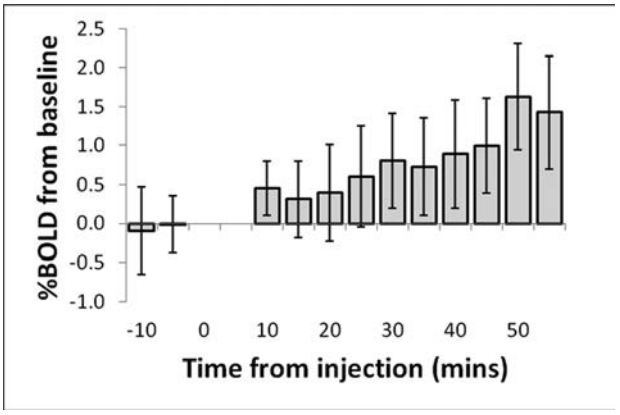

Figure 1. % BOLD signal change in the lower hypothalamus (right) after subcutaneous injection of exenatide

Mentlein R *et al* (1993). *Eur J Biochem* **214**, 829 - 835.

DeFronzo RA *et al* (2008). *Curr Med Res Opin* **24**, 2943 - 2952.

Logothetis NK *et al* (2000). *Nature* **412**, 150-157.

This work was funded by the BBSRC.

Where applicable, the authors confirm that the experiments described here conform with The Physiological Society ethical requirements.

PCB327

Effect of sequential oral and gastrointestinal stimulation on brain BOLD responses to glucose

C. Bryant[1], L. Wasse[1], S. McKie[2] and J. McLaughlin[1]

[1]Gastrointestinal Centre, Institute of Inflammation and Repair, University of Manchester, Manchester, UK and [2]Neuroscience and Psychiatry Unit, Institute of brain behaviour and mental health, University of Manchester, Manchester, UK

Human brainstem and hypothalamic responses to nutritional stimuli have been characterised in vivo using physiological functional magnetic resonance imaging (phys-fMRI)(1,2). This permits detailed comparison of spatiotemporal responses to different nutrient stimuli. One important discrepancy between human studies in this area is the method of nutrient administration used (intragastric versus oral). In reality, oral taste sequentially precedes gastrointestinal chemosensation and it is likely there is an interaction between the two sensory phases, which may occur within the CNS. Therefore, using fMRI, the purpose of the study was twofold: first, to establish the effects of oral and sequential gastrointestinal, "sweetness" on brain activation and second, to investigate whether oral sweet taste affects the gut to brain signal. 15 healthy fasted subjects were scanned in a single blind, randomised control trial involving 4 visits. Brain activation responses were mapped following a test solution of either glucose or artificial saliva (oral control) delivered into the mouth. Subjects were asked to hold the solution in the mouth and swallow on cue. Subjects then received an intragastric (IG) bolus of either glucose or saline (IG control). Data were analysed using Statistical Parametric Mapping (SPM8). First level analysis was performed on each subject for each study condition by splitting the scans into 26 consecutive 1 min time bins (one minute prior to and 25 following the IG infusion) at 5 minutes with Blood Oxygen Level Dependent (BOLD) signal averaged across the bin. The BOLD signal in each time bin was compared with the baseline average. A second level random effects ANOVA was used to investigate the effect that oral taste had on the glucose-induced intragastric BOLD signal. There was a significant ($qFDR<0.05$) interaction between oral taste and gastric infusion in several areas including the hypothalamus, pons and midbrain. Further analysis showed that this interaction was driven by abolition of the glucose-induced BOLD signal after an oral taste of glucose in most brain regions. This abolition was not observed following the artificial saliva condition. A representative time course is shown in figure 1. These findings suggest that pre-stimulation of sweet taste receptors in the mouth abolishes the reduction in BOLD signal previously seen in response to glucose infused directly into the gut lumen. The exact mechanism and physiological significance of this are not known, but sensory inputs transmitted from the oral cavity may directly modulate the gut-to-brain signals activated from the gut lumen by ingested nutrients.

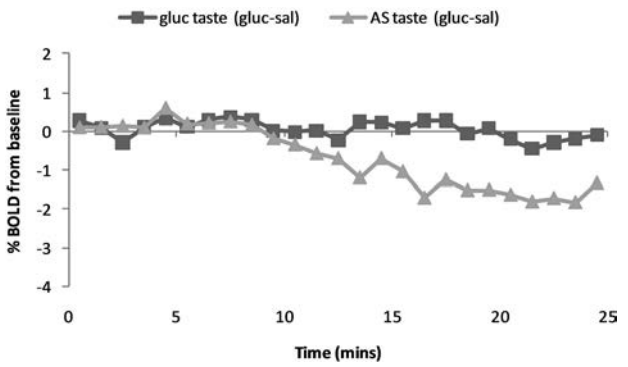

Figure 1. The average cluster time course per minute for oral glucose and artificial saliva during and after an to IG infusion in the hypothalamus region (right).

Lassman DJ, McKie S, et al. 2010, Gastroenterology, 1514-24.

Jones RB, McKie S, et al. 2012, Neurogastroenterology, 1543-1551.

Staff and facilities of the MRIF, Salford Royal Hospital and DRINC BBSRC

Where applicable, the authors confirm that the experiments described here conform with The Physiological Society ethical requirements.

PCB328

Differential effects of intragastric glucose and fructose on human brain activation, a physiological functional magnetic resonance imaging study

L. Wasse[1], C. Bryant[1], S. McKie[2] and J. McLaughlin[1]

[1]Gastrointestinal Centre, University of Manchester, Manchester, UK and [2]Neuroscience and Psychiatry Unit, University of Manchester, Manchester, UK

Using physiological magnetic resonance imaging (physMRI), we previously characterised the spatiotemporal brain responses to intragastric lipid. Significant increases in the blood oxygen level dependent (BOLD) signal were observed in brain areas including the brain stem and hypothalamus (1,2). We recently showed that unlike lipid, intragastric glucose decreases BOLD signal in these brain areas (unpublished data); a finding that persists regardless of administration route, i.e. oral or intravenous. However, the doses of glucose used have been high (1M). The effect of lower, nutritionally relevant doses of intragastric glucose on brain activation remains to be explored. Furthermore it is unknown whether fructose, which is chemically similar to glucose but unlike glucose is not used by the brain as a primary energy source, affects brain activation similarly to glucose. To examine this, 8 healthy human volunteers completed 4 trial visits in randomised order. Participants attended after an overnight fast, had a naso-gastric tube inserted and underwent 30 minutes of physMRI acquisition (3.0T Philips scanner). After a 5 min baseline period, participants received 250 mL of test 'drink' (0.25M glucose, 0.5M glucose, 0.5M fructose or a saline control) into the stomach. Data were analysed using the p-block method with 2 min time-bins. Two one-way repeated measures ANOVAs were used to investigate regions within the brainstem and hypothalamus that showed significant differences at qFDR<0.05 for glucose 0.25M vs glucose 0.5M and for glucose 0.5M vs fructose 0.5M. There was a significant difference between 0.5M glucose and 0.5M fructose observed in the hypothalamus (P<0.05; Figure 1). The BOLD responses were similar until approximately 8 min. They diverged thereafter, with a decrease in BOLD evident with 0.5M glucose but a progressive increase following fructose. In the hypothalamus and pons, BOLD signal was decreased after 0.5M glucose but not after 0.25M glucose. The results demonstrate a dose-response effect to glucose. However, despite glucose and fructose being chemically similar, administration of a 0.5M dose of glucose or fructose elicits a divergent BOLD response in the hypothalamus. The precise mechanism is unknown but neurons within this region may display sugar selectivity and only respond to glucose in this way as the brain's primary fuel. Furthermore, fructose does not elicit the same glycaemic and neuroendocrine responses as glucose, so differential changes in blood glucose and insulin could partly explain the different response seen. Similarly, a lower dose of glucose may be too low to exert any metabolic effect on glucose sensing neurons within the brain compared with 0.5M glucose, and thus explain the absence of a reduction in BOLD signal after a 0.25M glucose dose.

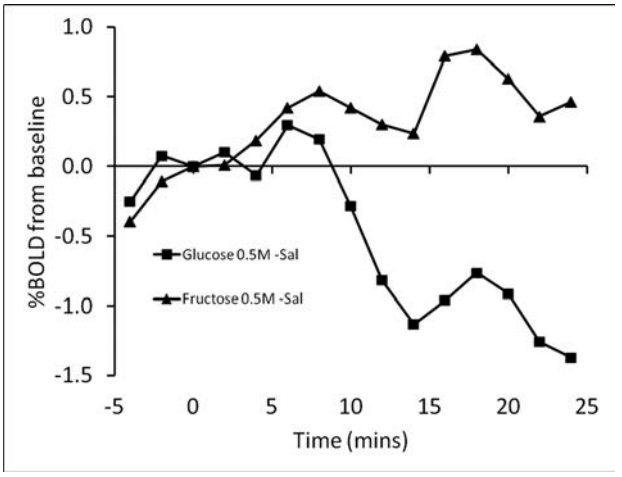

Figure 1. Time course of % BOLD signal change in the hypothalamus after 0.5M glucose and 0.5M fructose

Lassman DJ *et al*. (2010). *Gastroenterology* **138**, 1514 – 1524.

Jones RB *et al*. (2012). *Gut* **61**, 1435 – 1551.

This work was funded by the BBSRC.

Where applicable, the authors confirm that the experiments described here conform with The Physiological Society ethical requirements.

PCB331

Role of the intermediate-conductance Ca^{2+}-activated K^+ channel, $K_{Ca}3.1$ in $CD4^+$ T-lymphocytes of mesenteric lymph node of mice inflammatory bowel disease model

S. Ohya[1,2], Y. Fukuyo[2], M. Matsui[2], H. Yamamura[2], R. Shibaoka[1], H. Niguma[1], M. Fujii[1] and Y. Imaizumi[2]

[1]Pharmacology, Kyoto Pharmaceutical University, Kyoto, Japan and [2]Molecular & Cellular Pharmacology, Nagoya City University, Nagoya, Japan

Dextran sodium sulfate (DSS)-induced rodent colitis models are widely used as a model system for examining IBD (Inflammatory Bowel Disease) pathogenesis including ulcerative colitis and Crohn's disease. Genome expression profile analysis during the development of DSS-induced IBD model showed correlation with IBD patient data. The intermediate-conductance Ca^{2+}-activated K,sup>+ $^{channel, K}_{Ca}$3.1 plays an important role for the modification of Ca^{2+} signaling through the control

of the membrane potential in T-lymphocytes, and $K_{Ca}3.1$ can be a potential target for therapeutic strategies of IBD (Di *et al.*, 2010; Simms *et al.*, 2010). However, pathophysiological impact of $K_{Ca}3.1$ on the immune dysfunction in mucosal lymphoid tissue of IBD model animals remains to be determined. Here, the involvement of $K_{Ca}3.1$ in the enlargement of mesenteric lymph node (MLN) on the pathogenesis of mice IBD model was investigated. Mice IBD model was prepared by exposing male C57BL/6 mice to 5 % dextran sulfate sodium (DSS) for 7 days. All animal experiments were carried out in accordance with the guiding principles for the care and use of laboratory animals in Kyoto Pharmaceutical University and Nagoya City University. Inflammation-induced changes in $K_{Ca}3.1$ activity, the expressions of $K_{Ca}3.1$ and its regulators, and the cell-cycle distribution in MLN $CD4^+$ T-lymphocytes were monitored by real-time PCR, Western blot, voltage-sensitive dye imaging, and flow cytometry analyses. Concomitantly with the up-regulation of $K_{Ca}3.1a$ and nucleoside diphosphate kinase B (NDPK-B), the increase in $K_{Ca}3.1$ activity was observed in MLN $CD4^+$ T-lymphocytes of DSS-induced IBD model. Pharmacological blockade of $K_{Ca}3.1$ produced 1) the significant decrease in disease severities in IBD model, and MLN enlargement, compared with the control mice (n=17), 2) the restoration of the expressions of $K_{Ca}3.1a$, NDPK-B, and Th1 cytokines in MLN $CD4^+$ T-lymphocytes of IBD model (n=4-6), 3) the arrest of both G_1/S and G_2/M transitions during cell-cycle progression in MLN $CD4^+$ T-lymphocytes of IBD model (n=8), and 4) the inhibition of interleukin-6 (IL-6) production in the inflamed tissues (n=4). In addition, tripartite motif containing protein 27 (TRIM27), which suppresses the $K_{Ca}3.1$ activity through the polyubiquitination of PI3K-C2β, was significantly increased in MLN $CD4^+$ T-lymphocytes of IBD model (n=6), suggesting that the up-regulation of TRIM-27 may be a compensatory mechanism in $CD4^+$ T-lymphocyte activation in IBD patients. These suggest that the increase in $K_{Ca}3.1$ activity through the up-regulation of $K_{Ca}3.1a$/NDPK-B complex may be involved in the pathogenesis of IBD via the enhancement of MLN $CD4^+$ T-lymphocyte proliferation. Pharmacological blockade of $K_{Ca}3.1$ may decrease the risk of IBD development.

Di L *et al.* (2010). *Proc Natl Acad Sci U S A* **10**, 1541-1546.

Simms LA *et al.* (2010). *Am J Gastroenterol* **105**, 2209-2217.

Where applicable, the authors confirm that the experiments described here conform with The Physiological Society ethical requirements.

PCB332

Acute effect of dietary and skin TRPM8 ion channel stimulation on human thermoregulation and metabolism

A. Valente[1], A. Jamurtas[2], Y. Koutedakis[2] and A. Flouris[3]

[1]FAME laboratory, University of Thessaly, Trikala, Greece, [2]University of Thessaly, Trikala, Greece and [3]FAME Laboratory, Centre for Research and Technology Hellas, Trikala, Greece

Transient receptor potential melastatin 8 (TRPM8) is the receptor for cold sensation and is located on the cell membrane of brown adipocytes (1) and sensory neurons on the skin (2), and can be activated by both cold and L-menthol (3). Indeed, both skin (4, 5) and dietary (1) L-menthol treatments increase brown adipose tissue activity and metabolism in mice, leading to reduced body weight. However, the effects of these treatments in humans remain incompletely understood. The aim of this study was to examine the effect of dietary and skin TRPM8 stimulation on metabolism and thermoregulation in humans. After obtaining University of Thessaly ethical approval, nine healthy male volunteers were randomly distributed into either L-menthol skin (ST; n=4) and dietary (DT; n=5) treatment groups. Participants in both groups were treated with 10 mg/kg L-menthol (ST: gel; DT: capsule) and placebo (ST: water; DT: lactose capsule) in a random order on two different days. Fasted participants remained seated in a 24-25°C and 40-50% relative humidity environment. Core temperature (Tc), heat storage (S), metabolic rate (M), and mean skin temperature (Tsk) were measured at baseline, immediately following each treatment, and every hour thereafter for 7 hours. Each assessment lasted 15 min. The placebo condition data were subtracted from the L-menthol condition data to eliminate the effect of diurnal variation. Kruskal–Wallis one-way ANOVA was used to assess the effect of each treatment on all variables showing a change across time for both ST and DT (Figure 1; $p<0.05$). Post hoc Mann-Whitney U tests showed that ST reduced Tsk within 2 hours and increased S, M, and Tc within 4 hours ($p<0.05$). A similar, albeit weaker, effect was observed following DT ($p<0.05$). Between-treatments comparisons showed that ST produced a strong vasoconstriction [evident by a greater reduction in Tsk ($p<0.05$)] that resulted in a greater increase in S, M, and Tc ($p<0.05$). It is concluded that TRPM8 stimulation via L-menthol ST and DT result in cutaneous vasoconstriction and increased metabolic heat production. Moreover, the effects produced by ST appear to be stronger, as compared to those of DT.

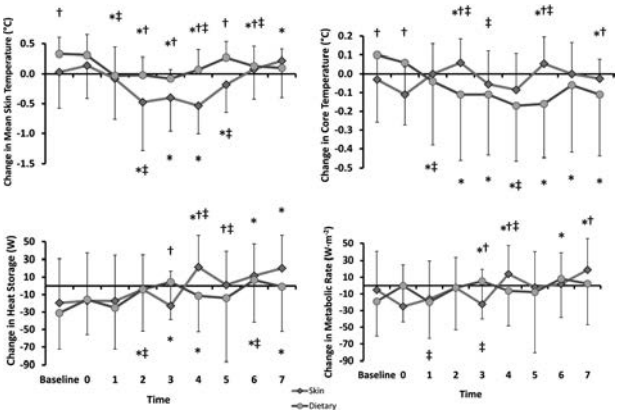

Figure 1. Median±SD change (L-menthol condition minus placebo condition) in mean skin temperature, core temperature, heat storage, and metabolic rate in the skin and dietary treatment groups. Symbols are placed at the respective end of the SD bars: * = difference from baseline for the same treatment; ‡ = difference from the previous time-point for the same treatment; † = difference between treatments for the same time-point.

Ma S, Yu H, Zhao Z, Luo Z, Chen J, Ni Y, et al. Activation of the cold-sensing TRPM8 channel triggers UCP1-dependent thermogenesis and prevents obesity. Journal of molecular cell biology. 2012;4(2):88-96. Epub 2012/01/14.

Tajino K, Hosokawa H, Maegawa S, Matsumura K, Dhaka A, Kobayashi S. Cooling-Sensitive TRPM8 Is Thermostat of Skin Temperature against Cooling. PLOSONE. 2011;6 (3):e17504.

Kozyreva TV, Tkachenko E. [Effect of menthol on human temperature sensitivity]. Fiziol Cheloveka. 2008;34(2):99-103. Epub 2008/05/14.

Bautista DM, Siemens J, Glazer JM, Tsuruda PR, Basbaum AI, Stucky CL, et al. The menthol receptor TRPM8 is the principal detector of environmental cold. Nature 2007;448.

Tajino K, Matsumura K, Kosada K, Shibakusa T, Inoue K, Fushiki T, et al. Application of menthol to the skin of whole trunk in mice induces autonomic and behavioral heat-gain responses. Am J Physiol Regul Integr Comp Physiol. 2007;293(5):R2128-35. Epub 2007/09/01.

This work was supported by funding from the Education and Lifelong Learning Programme of the Greek Ministry of Education, Co-financed by Greece and the European Union (NSRF 2007-2013, IRAKLITOS II, grant no. 162), and the European Union 7th Framework Program (FP7-PEOPLE-IRG-2008 239521; FP7-PEOPLE-2009-IRSES 247631).

Where applicable, the authors confirm that the experiments described here conform with The Physiological Society ethical requirements.

PCB333

Attenuation of unloading-induced rat soleus atrophy with the heat shock protein inducer 17-(Allylamino)-17-Demethoxygeldanamycin

T.L. Nemirovskaya[1] and Y.N. Lomonosova[2]

[1]Faculty of Basic Medicine, Lomonosov Moscow State University, Moscow, Russian Federation and [2]Institute for Bio-Medical Problems RAS, Moscow, Russian Federation

Heat-shock proteins (HSPs) are synthesized in great amounts in skeletal muscle, but HSP90 and HSP70 levels dramatically drop by 70–75% under muscle unloading in parallel with muscle atrophy. Probably, that inability to produce HSPs has an important effect on muscle atrophy during unloading. We assumed that under muscle unloading, HSP90 function, which leads to HSP70 synthesis preclusion, might be changed. We have tested the hypothesis that the HSP90 inducer 17-(allylamino)-17-demethoxygel-danamycin (17-AAG) can prevent HSP70 decrease and attenuate atrophy of unloaded soleus due to modulation of HSP90 function. 17-AAG, which specifically binds to the HSP90 ATP-binding site and disrupts its ATP-dependent function, is known to activate HSP90 nonspecifically by the activation of heat-shock factor, thereby causing the activation of the heat-shock or stress-response pathways. During unloading, we administered HSP90 inducer 17-AAG to disrupt ATP-dependent function and to increase the HSP amounts. The aim of the study was to analyze the involvement of HSP 90 into the anabolic and catabolic signalling alterations under conditions of muscle unloading. Male Wistar rats were divided into control (C, n=7), 3-day hindlimb unloading (HS, n=7), and 3-dayHS with HSP90 inducer administration, 17-AAG (60 mg/kg, HS+17-AAG, n=8). The experiment was carried out in accordance with the rules of biomedical ethics (protocol 264, March 5, 2011) certied by the Russian Academy of Sciences Committee on Bioethics. The HS model was used to employ a tail-traction method of noninvasive tail-casting procedure (without anesthesia), as described previously (Morey, E. R.,1979). The rats were sacrificed by intraperitoneal nembutal overdose (75 mg/kg). The relative weight of soleus muscle to body weight (soleus/BW (mg/g)) in HS group was less than those of the C and HS+17-AAG groups ($p<0,05$). We revealed HSP90, HSP70 mRNA decrease in HS (but not in HS+17-AAG) group vs. C ($p<0,05$). The unloading resulted in significant of μ-calpain and conjugated ubiquitin (Ub) increasing (proteins as well as mRNA levels) vs. C group whereas 17-AAG administration prevented these alterations (studied by SDS-PAGE and rt-PCR). pFOXO3 protein was decreased only in HS group vs. C, but not in HS+17-AAG. Content of E3-lygases (MuRF-1, MAFbx) mRNA was increased in both suspended groups. We found equal amounts of pAkt in control and HS+17-AAG groups (in parallel to pFOXO3 levels), but pAkt levels in the HS group were diminished. Modulation of HSP90 function by 17-AAG treatment lends support to the suggestion that anabolic signaling and phosphorylation of the FOXO3 transcription factor are controlled by Akt. Soleus atrophy attenuation in the HS+17-AAG group was not associated with phosphorylation of p70S6k, because its level was equal in all three groups of rats. In summary, 17-AAG administration (enhancing HSP90 expression) under HS conditions attenuated soleus atrophy and prevented HSPs mRNA drop, maintained p-Akt and p-FOXO 3 content at the control level. Moreover, the prevention of ubiquitination and μ-calpain expression were increased in the HS+17-AAG-treatment group.

Supported by grant RFBR 11-04-00787-a

Where applicable, the authors confirm that the experiments described here conform with The Physiological Society ethical requirements.

PCB334

An explanation of motility dysfunction of gut due to arsenicosis via neurotransmitter pathway regulation and oxidative stress

M. Ghosh and G. Paul

Department of Physiology, University of Kalyani, Kalyani, West Bengal, India

Arsenic contaminated groundwater consumption is the main route of human exposure for arsenicosis. We set out to illustrate the as yet poorly understood cellular mechanisms resulting in altered motility of small gut ensuing severe gastrointestinal dysfunctions related to arsenicosis. The current study was designed in two parts- A. Charles foster rats (male, 100 ± 17g, n=7) were exposed orally to 10 mg/kg body wt/day sodium arsenite for 5, 10 and 20 days and B. in vitro organ-bath studies were conducted on intestine with a combination of different neurotransmitters and arsenite (As+3) applied postmortem. Rats were humanely killed by cervical dislocation following institutional guidelines foregoing anesthesia due to the nature of the experiment. Chronic As+3 treatment resulted in reduced bound calcium deposition (1), consistent with the finding of significantly enhanced contraction of the gut (vide Fig 1), achieved with isotonic transducer (IT-2245) coupled to RMS-Polyrite D. The peak contraction was reached on the 10th day of treatment. Set B results proved, the effect of As+3 on smooth muscle contraction was upstream of calcium release where it acted as a partial antagonist to atropine and exerted synergistic effect with acetylcholine. This was supported by the As+3 induced decrease of acetylcholine esterase activity (2) found under Set A. Set B results further showed that As+3 inhibited the relaxant effect of exogenous nitric oxide and breached the cholinergic blockade completely when coupled with a soluble guanylyl cyclase (sGC) blocker. Evidence under Set A attested to As+3 induced downregulation of nitric oxide synthase leading support to the final conclusion that on the early days of chronic treatment As+3 induced facilitation of intestinal motility by stimulating muscarinic and suppressing sGC receptor. Set A results further showed a decrease in motility increment after 20 days of constant As+3 treatment, supported by histopathological evidence of progressive degeneration and gross architectural damage of the muscle layer of intestine. This was substantiated by studies on oxidative stress indices which showed that As+3 depleted protein thiol levels (3), increased lipid peroxidation (4), and severely depleted reduced glutathione (5) which may explain the decrease of gut motility due to tissue damage after prolonged exposure of 20 days (vide Table 1 for set A results).

Table 1. Effect of chronic arsenite treatment on cell biochemistry

Experiments were performed under set A and the final results are expressed as mean ± SEM, n=7, p< 0.05, *p< 0.05 vs control (T Test) in the table.								
Chronic treatment duration	AChE (acetylcholine esterase)- M /min/g tissue		Protein thiol (Habeeg AFSA, 1972)- mM/mg protein		LPO (lipid peroxidation) - nM MDA/mg protein		GSH (reduced glutathione)- mM/ml 10% homogenate	
	control	treated	control	treated	control	treated	control	treated
5 days	0.033 ± 0.001	0.025* ± 0.0007	119.49 ± 11.3	99.86* ± 6.9	0.89 ± 0.12	1.76* ± 0.09	5.65 ± 0.4	4.41* ± 0.07
10 days	0.033 ± 0.002	0.0225* ± 0.0009	119.49 ± 10	86.96* ± 6.2	0.9 ± 0.1	2.82* ± 0.06	5.65 ± 0.41	3.82* ± 0.09
20 days	0.029 ± 0.002	0.015* ± 0.0007	119.51 ± 11.4	77.42* ± 6.3	0.92 ± 0.1	3.1* ± 0.07	5.64 ± 0.3	3.35* ± 0.11

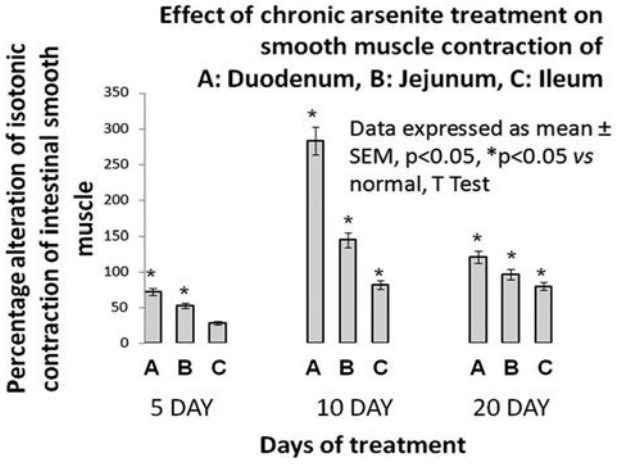

Fig 1. As+3 treated gut motility.

von Kossa J (1901). *Beit Path Anat* **29**, 163-202.

Ellman GL *et al.* (1961). *Biochem Pharmacol* **7**, 88-95.

Habeeb AFSA (1972). *Methods Enzymol* **25**, 457-464.

Buege JKA & Aust SD (1978). *Meth Enzymol* **52**, 302-310.

Moren MS *et al.* (1979). *Biochim Biophys Acta* **582**, 67-78.

We thank DST, SERC, Govt. of India for financial help.

Where applicable, the authors confirm that the experiments described here conform with The Physiological Society ethical requirements.

PCB335

Molecular mechanisms involved in the suppression of atrophy-related genes induced by β2-adrenergic stimulation in denervated mouse skeletal muscles

D. Lustrino[1], W.A. Silveira[1], D.A. Gonçalves[1], N.M. Zanon[1], I.C. Kettelhut[2] and L.C. Navegantes[1]

[1]Physiology, University of São Paulo, Ribeirão Preto, São Paulo, Brazil and [2]Biochemistry and Immunology, University of São Paulo, Ribeirão Preto, São Paulo, Brazil

β-adrenergic signaling pathway represents a novel therapeutic target for skeletal muscle wasting and weakness due to its role in the mechanisms controlling protein metabolism. However, the intracellular pathways that elicit these responses are far from being completely understood. In turn, this study was performed to shed light on the molecular mechanisms induced by chronic treatment with clenbuterol, a selective β2-agonist, in denervated muscles.

For this, C57/BL6 male mice (~30g) were previously anesthetized and submitted to

motor denervation (DEN) by unilateral sciatic nerve section. In the same day, the treatment with saline or clenbuterol (CB, 3mg/kg/day; s.c.) was started (n=5/group). After 3, 7, 14 and 21 days, tibialis anterior (TA) muscles were harvested to examine mRNA levels of atrophy-related genes (MuRF1, Atrogin-1 and cathepsin L) and Sik1, a CREB-target gene, by RT-qPCR, phospho-PKA substrates by western blot, and cAMP levels by ELISA. All experiments were approved by local Ethics Committee (044/2012). Comparisons were made by using Student's t test or two-way ANOVA followed by Bonferroni test ($p<0.05$).

DEN induced loss of muscle mass at 7th day (13%) that was prevented by CB. At 3rd day, CB increased muscle cAMP (857.12 ± 30.68 vs. 709.48 ±22.66 fmol/mg muscle in DEN treated with saline) and reduced the mRNA levels of MuRF1 (151% vs. 553% in DEN treated with saline), Atrogin-1 (-27% vs. 243%) and cathepsin L (129% vs. 208%). A similar profile was obtained to protein content. At 7th day, the expression of Ub-ligases (MuRF1 and Atrogin-1) were normalized in both groups, and DEN by itself increased the content of muscle cAMP (25%), phospho-PKA substrates (~2.2-fold), and Sik1 mRNA expression (~5.2 fold).

The data show that the chronic treatment with CB in vivo suppresses the DEN-induced up-regulation of genes involved in muscle atrophy (atrogin-1, MuRF1, and cathepsin L) and suggest that these effects may be mediated by cAMP/PKA/CREB signaling. Additionally, it seems that this signaling pathway integrates a fine-tuning adaptative mechanism responsible for preventing excessive muscle loss in the progression of DEN.

FAPESP (2012/05697-7)

Where applicable, the authors confirm that the experiments described here conform with The Physiological Society ethical requirements.

PCB338

Using ^{31}P NMR spectroscopy to investigate the effects of iron deficiency on murine skeletal muscle metabolism and function during exercise

M. Curtis[1], L.E. Cochlin[1], M.A. Cole[2], D.P. O'Neill[1], M.S. Dodd[1], D.J. Tyler[1], K. Clarke[1] and P.A. Robbins[1]

[1]Department of Physiology, Anatomy and Genetics, University of Oxford, Oxford, UK and [2]University of Nottingham Medical School, University of Nottingham, Nottingham, UK

Physical work or exercise capacity has been widely reported as being impaired by iron deficiency. Previous, separate, studies using diet-induced iron deficient rats have shown decreased work rate capacity, diminished contractile force generation and an impairment of energetics during exercise, when compared to rats on normal chow. The aim of this project is to develop a technique that allows for the simultaneous assessment of force production, fatigue resistance and metabolic function of murine gastrocnemius muscle during exercise. To address this, a method of *in vivo* gastrocnemius muscle stimulation was established. A bespoke Perspex cradle was designed and manufactured for the hindlimb preparation. In this technique, mice are anaesthetised using 2 % isoflurane in oxygen (2 l/min), the ischiatic nerve is isolated surgically and electrodes are placed distal to the tibial nerve branch. The knee and ankle joints are immobilised, the calcaneal tendon is attached to a force transducer, via a suture thread, before a ^{31}P saddle-shaped coil is placed over the muscle. The cradle is then placed into the 7 Tesla magnet and images of cross-sectional area (CSA) of the gastrocnemius muscle are obtained using the ^{1}H volume coil. The measurement of CSA of the muscle allows the comparison of force produced between muscles of different sizes. A stimulation protocol consisting of a train

of eight pulses of 100 μs at 30 Hz, followed by a rest period of 1.25 seconds, is repeated over a 10 minute period. During this exercise period, and the subsequent 20 minute recovery period, a ^{31}P spectrum is acquired every 100 seconds. Reductions of contractile force in excess of 50 % are exhibited over the 10 minute exercise period, and increases in inorganic phosphate (Pi) and decreases in phosphocreatine (PCr) are acquired by ^{31}P NMR spectroscopy (Figure 1). This technique will facilitate the simultaneous assessment of skeletal muscle function and metabolism, including fatigue resistance, in both diet-induced and genetic mouse models of iron deficiency, in the presence or absence of ferric carboxymaltose.

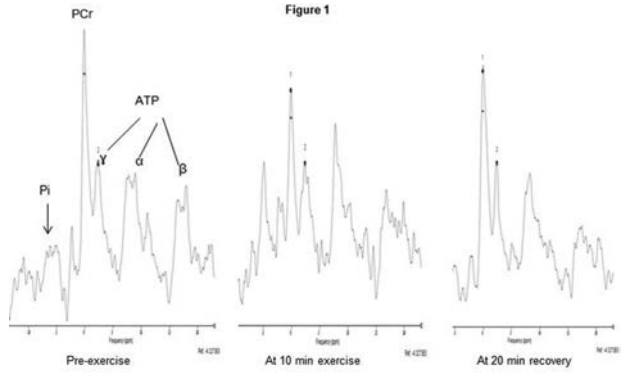

Figure 1: ^{31}P spectra acquired before exercise, after 10 minutes of exercise and at 20 minutes of recovery. The spectra are scaled to the height of the γ-ATP peak and the x-axis shows frequency in parts per million.

This work is funded by Vifor Pharma.

Where applicable, the authors confirm that the experiments described here conform with The Physiological Society ethical requirements.

PCB340

Obesogenic diet alters feto-placental phenotype

A. Sferruzzi-Perri, O.R. Vaughan, M. Haro, B. Musial, M. Constancia and A.L. Fowden

University of Cambridge, Centre for Trophoblast Research, Cambridge, UK

In developed societies, diets high in sugar & fat (HSHF) are commonly eaten by women of reproductive age & contribute to the increasing rates of maternal obesity & excessive weight gain during pregnancy. In mice, offspring of mothers fed an obesogenic HSHF diet during pregnancy develop cardiovascular & metabolic dysfunction as adults, even when their birthweight was normal [1]. However, little is known about the mechanisms operating in utero which might account for the detrimental postnatal effects. This study tested the hypothesis that an obesogenic diet alters growth & function of the placenta, responsible for nutrient transfer to the fetus. We examined the effect of feeding pregnant mice an obesogenic HSHF diet on placental growth & nutrient transport in relation to fetal growth & placental expression of imprinted genes & signalling pathways known to regulate growth & metabolism.
Methods: C57BL6 female mice were fed a control diet (11%fat, 3%sugar) or an obesogenic HSHF diet (30%fat, 36%sugar) during pregnancy. On day (D) 16 or 19, placental transport of 14C-methyl aminoisobutyric acid (MeAIB) & 3H-methyl D-glucose (MeG) was measured in vivo. Placental expression of Slc38a1, Slc38a2, Slc38a4, Slc2a1, Slc2a3, Igf2, H19, Dlk1, Igf2r, Zac1, Snrpn, Grb10, Phlda2, Gtl2, Peg11, Peg3, Cdkn1c genes was quantified by Real Time PCR. Expression of proteins involved in phosphoinositol 3-kinase (PI3K) & mitogen activated protein kinase (MAPK) signalling was determined by Western blotting. Dietary differences were determined by ANOVA & linear mixed model repeated measures as required & significant if $P<0.05$.
Results: HSHF diet reduced fetal weight in parallel with placental weight at D16 ($P<0.001$, Table). By D19, placental weight remained less in HSHF dams ($P<0.001$), whereas the weight of fetuses had normalised (Table). This change in fetal growth trajectory was associated with enhanced placental glucose & amino acid transfer & upregulated Slc2a3 & Slc38a2 nutrient transporter genes on D16 (Fig 1&2, $P<0.03$). In the HSHF placenta there was also increased expression of imprinted genes on D16 (Igf2, Dlk1, Snrpn, Grb10 & H19, $P<0.005$, Fig 2) & PI3K & MAPK signalling proteins on D16 & D19 (PI3K p110α, pAkt, pGsk3 & pMAPK, $P<0.04$).
Conclusion: Placental transport adapts to an obesogenic HSHF diet through local changes in signalling pathways & imprinted genes involved in growth & metabolism. These adaptations help meet the fetal drive for growth even though placental growth is compromised by a HSHF diet. However by altering the provision of specific nutrients, dietary-induced changes in placental phenotype have an important role in tissue programming with implications for the adult health of infants of women eating obesogenic diets

HSHF diet & feto-placental growth

	Control diet (D16)	HSHF diet (D16)	Control diet (D16)	HSHF diet (D19)
Fetal weight (mg)	435±13	395±5*	1195±15	1166±16
Placental weight (mg)	106.0±2.5	94.0±2.4*	88.4±2.1	81.0±2.1*

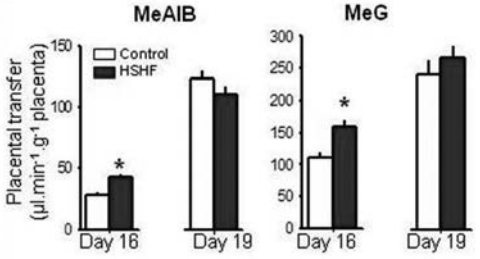

Fig. 1 The effect of a HSHF diet on placental transport

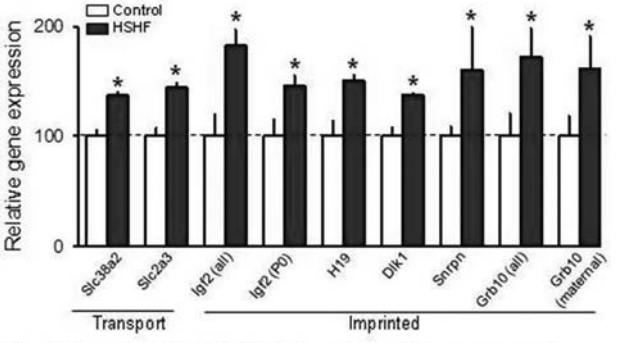

Fig. 2 The effect of a HSHF diet on placental gene expression on day 16. *Igf2(P0)*, the placental specific transcript of *Igf2*.

Samuelsson et al. (2008) Hypertension 51: 383-392.

Where applicable, the authors confirm that the experiments described here conform with The Physiological Society ethical requirements.

PCB342

Signalling from fetus to mother; role of the Delta-like homologue 1

M. Charalambous[1,2], M.A. Cleaton[2] and A.C. Ferguson-Smith[2]

[1]Endocrinology, Queen Mary University of London, London, UK and [2]Physiology, Development and Neuroscience, University of Cambridge, Cambridge, UK

Whilst epidemiological studies robustly support the relationship between compromised maternal energy homeostasis and poor fetal and postnatal outcome, very little is known about the genetic pathways which control maternal energy allocation to the offspring. In turn, how maternal nutrient partitioning influences the growth and proportionality of the organism is not well understood. Furthermore, bi-directional communication between mother and fetus underlie these events and deciphering the molecular signals involved using genetic tools is now feasible and timely.

Late gestation in mammals is accompanied by multiple adaptations of maternal energy homeostasis that are thought to divert maternal resources towards the supply of glucose for the rapidly-growing fetus. These adaptations include peripheral insulin resistance and a reduction in hepatic lipogenesis (1). During pregnancy there is considerable remodelling of the anterior pituitary which causes an increase in somatolactotrophic cells (2). In addition, the syncytiotrophoblast cells of the placenta secrete placental lactogen and a pregnancy-specific version of growth hormone (GH) (2). Since GH and its family members are known to cause insulin resistance and inhibit hepatic lipogenesis (1, 3), increased activity of the pituitary-placental sommatolactotrophic axis may modulate maternal adaptations in late pregnancy.

The product of the imprinted Delta-like homologue 1, DLK1, is an endocrine signalling molecule that reaches a high concentration in maternal serum during late pregnancy (4). We have recently discovered that that the conceptus is the source of this molecule. DLK1 may be a novel endocrine signal from fetus to mother. Our studies with genetically-modified mice show that endocrine DLK1 acts to inhibit hepatic lipogenesis (5 and in preparation).

Our working hypothesis is that DLK1 produced by the conceptus alters the activity of the pituitary-placental somatolactotrophic axis, thus modulating important metabolic changes in maternal resource allocation during pregnancy. Understanding the function of DLK1 in pregnancy has potential clinical value since failures of growth and timely development occur when maternal resource allocation is disrupted. Moreover, maternal serum DLK1 could be a non-invasive biomarker for complications of pregnancy, and/or genetic variation in Dlk1 sequences in mother or fetus may be indicative of poor pregnancy outcome.

Di Cianni, G., et al. Diabetes Metab Res Rev, 2003. 19(4): p. 259-70.

Tulchinsky and Little, Maternal-Fetal Endocrinology 2nd Ed, 1994

Baik M,et. al. Ann N Y Acad Sci. 2011 Jul;1229:29-37

Floridon, C., et al. Differentiation, 2000. 66(1): p. 49-59.

Charalambous M, et. al. Cell Metab. 2012 Feb 8;15(2):209-21.

Where applicable, the authors confirm that the experiments described here conform with The Physiological Society ethical requirements.

PCB343

Periconceptional alcohol exposure impacts on placental structure and gene expression

E.M. Gardebjer, J. Cuffe and K. Moritz

School of biomedical sciences, The university of queensland, Brisbane, QLD, Australia

Perturbations during the periconceptional (PC) period are important determinants of a healthy pregnancy and offspring health. This period however is prior to maternal recognition of pregnancy when alcohol consumption is often a common social practice. Alcohol during pregnancy is known to impair the normal development of many organs and systems including the placenta. It is not known however whether alcohol consumption prior to implantation can impact on post implantation placental outcomes.

This study aimed to examine if there were changes in the late gestation placenta (E20), of fetuses exposed to moderate levels of ethanol (EtOH) prior to implantation.

Sprague-Dawley rats were exposed to a control liquid diet or one containing EtOH (12.5%, n=12/group) during the PC period (from embryonic day (E)-4 to E4). On E20, pregnant dams were deeply anesthetized with ketamine:xylazine (50:50) to ensure blood flow to fetuses and placentas during collection. Placentas from male and female fetuses were either fixed (whole) or frozen (as labyrinth and junctional zone separately). Dry weights of the placental components were derived by oven drying. Cross sectional areas of the labyrinth and junctional zone was determined following haemotoxylin/eosin staining. Relative mRNA expression of glucose transporters (GLUT1, GLUT3) and insulin like growth factors (IGF1 and IGF2) was examined via real-time PCR.

Maternal plasma alcohol concentration reached an average maximum of 0.17%. There was no difference between groups in calorie intake but fetuses were growth restricted ($p<0.05$). Placental dry weight was significantly increased in EtOH-exposed fetuses ($p=0.01$) when normalized to body weight. This was due to an absolute ($p=0.002$) and normalized ($p<0.0001$) increase in weight of the junctional zone only. This was supported by an increase in the cross sectional area of the junctional zone in PC-EtOH exposed placentas ($p=0.03$) whilst the cross sectional area of the labyrinth zone was significantly smaller ($p=0.03$). While gene expression studies for GLUT1 and GLUT3 showed no difference in the labyrinth zone, GLUT3 was expressed at higher levels in the junctional zone of the placenta from PC-EtOH exposed females ($p=0.03$). IGF1 relative gene expression was reduced in the labyrinth of PC-EtOH exposed placentas ($p=0.005$) whereas the expression of IGF2 was unaffected. In contrast, whilst IGF2 expression was upregulated in the junctional zone ($p=0.05$), there was no difference observed for IGF1 expression in this zone.

This study demonstrates that PC-EtOH significantly alters expression of key placental nutrient transporters and growth factors which are important for fetal growth and development. Moreover it also showed that exposure to EtOH prior to implantation alters the structure of the placenta and therefore potentially the future health of the offspring.

Where applicable, the authors confirm that the experiments described here conform with The Physiological Society ethical requirements.

PCB344

Exogenous corticosterone administration increases materno-fetal glucose transport in the mouse in late pregnancy

O.R. Vaughan, H.M. Fisher, A.N. Sferruzzi-Perri and A.L. Fowden

Physiology, Development and Neuroscience, University of Cambridge, Cambridge, UK, UK

Introduction
Fetal glucose supply is a key determinant of growth in utero. Deficient or excess glucose availability is associated with fetal growth restriction and macrosomia, respectively. Glucocorticoid stress hormones influence blood glucose availability by antagonizing the action of insulin, in the non-pregnant animal. Furthermore, they reduce fetal growth and alter placental nutrient transporter expression [1]. This study aimed to determine whether maternal glucocorticoid treatment affects hepatic release and placental transport of glucose in the pregnant mouse in vivo.
Methods
All procedures were conducted in accordance with the Animals (Scientific Procedures) Act 1986. C57BL6/J mice (n=20) were treated with corticosterone (CORT, 76 μg/g/day in drinking water) between day (D) 11 and D16 of pregnancy (term = D21). This procedure is established to raise circulating corticosterone to stressed levels [1]. On D16 or D19, materno-fetal clearance of 3H-methyl-D-glucose (MeG) was measured under anaesthesia (fentanyl-fluanisone:midazolam in water, 1:1:2) [2] then the dam was euthanized and samples of maternal plasma, liver and placenta were collected. Expression of the insulin-insensitive Slc2a1 and Slc2a3 glucose transporter genes was determined in placentae by qPCR. Hepatic glycogen content was determined by enzymatic conversion to glucose using amyloglucosidase. Glucose and plasma insulin concentrations were analysed by automated glucometer and ELISA, respectively. Data were analysed separately at D16 and D19 by Student's t test and significance determined at the level P<0.05. Results are mean±SEM.
Results
Compared to untreated (UT) controls (n=51), CORT reduced placental weight on D16 and fetal weight on both D16 and D19. Maternal plasma insulin concentration was higher in CORT treated than UT dams on D16 (UT, 1.1±0.3 ng/ml, n=7; CORT 40.1±5.3 ng/ml, n=7; P<0.05) but not D19 (UT, 2.6±1.2 ng/ml, n=12; CORT, 2.0±0.7 ng/ml, n=12; P>0.05). However, neither hepatic glycogen content nor blood glucose concentration differed between UT and CORT dams at either gestational age (P>0.05). On D16, CORT increased placental expression of Slc2a1 and Slc2a3 (n=6 per group) but did not affect materno-fetal MeG clearance (UT, n=64 fetuses; CORT, n=25 fetuses) (Figure). Contrastingly, although placental Slc2 expression no longer differed from UT animals at D19, materno-fetal MeG clearance was increased by 26% in CORT treated dams (UT, n=41 fetuses; CORT, n=22 fetuses) (Figure).
Discussion
When maternal glucocorticoid concentrations are raised through stress, illness or exogenous administration, fetal glucose supply may be increased due to changes in placental transport, even if maternal metabolism is unaffected. Ultimately, this may alter fetal growth trajectory and increase neonatal morbidity and metabolic disease risk in the offspring.

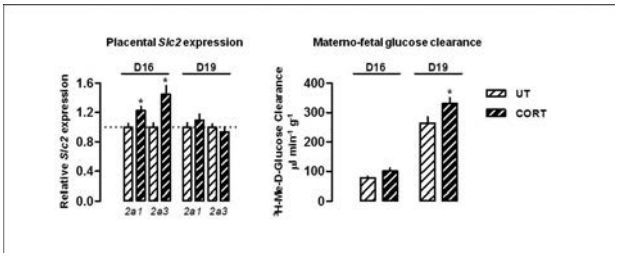

Figure 1. *, P<0.05

Vaughan et al (2012) J Physiol 590 5529

Sibley et al (2004) PNAS 101 8204

Where applicable, the authors confirm that the experiments described here conform with The Physiological Society ethical requirements.

PCB345

Hypoxia, placental phenotype and fetal growth in mice

J.S. Higgins, O.R. Vaughan, A.L. Fowden and A.N. Sferruzzi-Perri

Department of Physiology, Development and Neuroscience, Cambridge University, Cambridge, UK

Introduction: During normal pregnancy, the placenta supplies the fetus with sufficient oxygen (O2) and nutrients to match its demands for growth. The placenta is responsive to environmental cues and is capable of adapting its capacity for substrate transfer to favour fetal growth during adverse conditions, like undernutrition(1). However, relatively little is known about adaptation of placental function to hypoxia; a major cause of fetal growth restriction (FGR)(2,3) and pregnancy complications at high altitude(4,5). Thus, this study aimed to determine the effect of hypoxia on placental transport and fetal growth.
Methods: C57BL/6 female mice were time-mated and exposed to either 13% or 10% atmospheric O2 (13% H and 10% H, respectively) from day (D)14-D19 of pregnancy (term=D20). As exposure to hypoxia reduced maternal food intake, dams in 21% O2 fed ad libitum (ad lib) or pair-fed to the intake of hypoxic mice (13% PF and 10% PF) were used as controls. On D19, placental transport of 14C-methyl aminoisobutyric acid (MeAIB) was assessed in vivo and related to fetal growth. Litter means were analysed using ANOVAs with Bonferroni Post-hoc tests, unless stated otherwise.
Results: Maternal body weight was significantly reduced by 13% and 10% hypoxia compared to ad lib controls (Table 1). Fetuses of 10% H, but not 13% H, mice weighed significantly less than fetuses from ad lib mice (Table 1). Fetuses of 10% PF mice also weighed significantly less than those from ad lib mice but more than 10% H pups (Table 1). Placental weight did not differ significantly between groups although placental efficiency, measured as the ratio of fetal to placental weight, was significantly reduced in 10% H mice compared to all other groups (Table 1). Placental transport of MeAIB tended to be lower in all hypoxic and pair fed groups but was only significantly reduced in 10% H compared to ad lib mice (Figure 1).
Conclusions: In late pregnancy, placental efficiency and fetal growth were maintained in response to 13% O2, despite reduced maternal food intake and body weight. At the more severe insult of 10% O2, placental efficiency and transport were both compromised in association with reduced fetal weight. The data indicate that there is a threshold between 13% and 10% maternal inspired O2, at which the placenta can no longer

support normal fetal growth during hypoxia. They also suggest that, at 10% O2, it is the combined effect of hypoxia and undernutrition which determines maternal nutrient allocation to the fetus, via changes in placenta nutrient transfer capacity. This has implications for the mechanisms of FGR in pregnancies complicated by hypoxaemia.

Table 1: Values are mean ± SEM. On each row, significant differences between values is indicated by a different letter ($p<0.05$ or less). *Ad lib* (n=12), 13% PF (n=8), 13% H (n=9), 10% PF (n=15), 10% H (n=11)

	Ad lib	13% PF	13%H	10% PF	10%H
Maternal D19 weight (g)	35.0 ± 1.2^{a}	31.2 ± 0.9^{ab}	30.0 ± 1.4^{b}	32.3 ± 0.9^{ab}	29.5 ± 0.7^{b}
Fetal weight (mg)	1169.2 ± 11.4^{a}	1167.7 ± 45.4^{ab}	1071.1 ± 19.0^{ab}	1068.3 ± 20.7^{b}	926.8 ± 26.1^{c}
Placental weight (mg)	88.2 ± 2.4	90.9 ± 2.8	89.5 ± 1.9	84.5 ± 2.6	92.2 ± 1.9
Fetus: Placenta	13.4 ± 0.4^{a}	12.9 ± 0.6^{a}	12.0 ± 0.2^{ab}	12.9 ± 0.5^{a}	10.1 ± 0.3^{b}

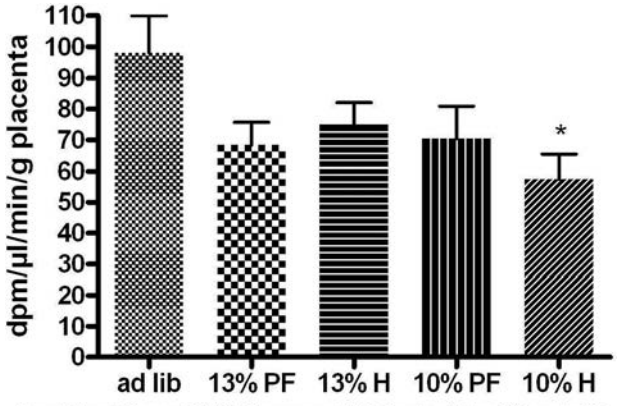

Figure 1: Placental clearance of MeAIB. Values are mean ± SEM. *denotes a significant difference to *ad lib*, as assessed by t-test ($p<0.01$). *Ad lib* (n=9), 13% PF (n=8), 13% H (n=7), 10% PF (n=13), 10% H (n=12).

1. Coan PM, Vaughan OR, Sekita Y, Finn SL, Burton GJ, Constancia M, et al. Adaptations in placental phenotype support fetal growth during undernutrition of pregnant mice. The Journal of physiology. 2010;588(Pt 3):527-38.

2. de Grauw TJ, Myers RE, Scott WJ. Fetal growth retardation in rats from different levels of hypoxia. Biol Neonate. 1986;49(2):85-9.

3. Van Geijn HP, Kaylor WM, Jr., Nicola KR, Zuspan FP. Induction of severe intrauterine growth retardation in the Sprague-Dawley rat. Am J Obstet Gynecol. 1980;137(1):43-7.

4. Keyes LE, Armaza JF, Niermeyer S, Vargas E, Young DA, Moore LG. Intrauterine growth restriction, preeclampsia, and intrauterine mortality at high altitude in Bolivia. Pediatr Res. 2003;54(1):20-5.

5. Krampl E, Lees C, Bland JM, Espinoza Dorado J, Moscoso G, Campbell S. Fetal biometry at 4300 m compared to sea level in Peru. Ultrasound Obstet Gynecol. 2000;16(1):9-18.

Many thanks to both of my lovely supervisors, Amanda and Abby. Also, many thanks to Owen and Nuala Daw who helped me complete this work and to the BBSRC for funding the research.

Where applicable, the authors confirm that the experiments described here conform with The Physiological Society ethical requirements.

PCB346

The role of peroxisome proliferator-activated receptor gamma co-activator 1-alpha in pregnancy

A.C. Delany[1], F.P. McCarthy[3], S.K. Walsh[2] and L.C. Kenny[3]

[1]Physiology, University College Cork, Cork, Ireland, [2]The Robert Gordon University, Aberdeen, Scotland, UK and [3]Obstetrics and Gynaecology, Anu Research Centre, University College Cork, Cork, Ireland

Background: Peroxisome proliferator-activated receptor gamma co-activator 1-alpha (PGC-1α) is a transcriptional co-activator that drives mitochondrial biogenesis and other metabolic programs in many tissues, including the heart. PGC-1α is a powerful regulator of angiogenesis, a process of fundamental importance to the development of a healthy placenta in normal pregnancy. The angiogenic function of PGC-1α has been previously described in the heart where it has been shown to regulate angiogenesis. Its function and expression in the placenta is unknown. It may be the key link between placental development and the imbalance of key angiogenic factors observed in the pregnancy specific condition of pre-eclampsia.

Hypothesis: PGC-1α is expressed in the human placenta and in pathophysiological conditions, such as pre-eclampsia, the expression of PGC-1α is reduced.

Methods: Human placental samples were obtained from normal healthy pregnant women (n=4) for processing and analysed by means of immunohistochemistry using Calbiochem Anti PGC-1α, C-Terminal (777-797) rabbit polyclonal antibody. In addition, protein expression of PGC-1α was examined in placental tissue from normal pregnant rats (n=6) and those with surgically reduced uteroplacental perfusion (reduced uterine perfusion pressure (RUPP) model) (n=4).

Results: Positive staining for PGC-1α was noted in both human and rat placental samples with varying degrees of expression when compared with PBS treated controls. Expression was most prominent in the endothelial cells surrounding the vessels, the trophoblasts, syncytiotrophoblasts and vascular endothelial cells with scattered staining in the maternal decidua and stroma. Furthermore, RUPP placental tissue indicated lower levels of positive staining for PGC-1α when compared with normal and sham rats.

Conclusion: This study indicates that the transcriptional co-activator PGC-1α is expressed in the both human and rat placental tissue and is strongly localised to endothelial cells. Furthermore, our data may implicate PGC-1α in the pathogenesis of complications of pregnancy such as pre-eclampsia, but further investigation is needed to confirm this. Future studies could suggest the use of PGC-1α as a future pharmacological target for the treatment of complicated pregnancies.

This project was funded by the department of Physiology, University College Cork

Where applicable, the authors confirm that the experiments described here conform with The Physiological Society ethical requirements.

PCB347

High fat/high cholesterol diet induces TLRs-associated pulmonary inflammation in C57BL/6J mice

S. Wang[1,2], T. Zhu[2], T. Chen[1,2], L. Zhang[1,2] and X. Lian[1,2]

[1]Center for lipid research, Chongqing Medical University, Chongqing, China and [2]Department of Nutrition and Food Hygiene, Chongqing Medical University, Chongqing, China

Pulmonary inflammation were reported in several lipid metabolism related gene knock out mice. However, the effects of high fat/high cholesterol diet induced dyslipidemia on the homeostasis of wild C57BL/6J mice lung were poorly understood. 6-8 week-old male C57BL/6J mice were randomly divided into two groups and received either regular diet (RD) containing 10%kcal fat or high fat/high cholesterol diet (HCD) with 40%kcal fat, 1.25% cholesterol and 0.5% sodium cholate respectively. After 16 weeks feeding, mice were anaesthetised with pentobarbital (50mg/ kg, i.p.), and then euthanized by exsan-

guination from heart. Measured by autobiochemistry analyzer, Serum lipids results showed that hypercholesterolemia was induced in 16 weeks HCD fed C57BL/6J mice (Serum total cholesterol: 5.14±0.37 vs. 3.74±0.23 mmol/L, p<0.05, n=3; Serum low density lipoprotein: 3.35±0.41 vs. 0.46±0.06 mmol/L, p<0.01, n=3; HCD group vs. RD group). Values are means ± S.E.M, compared by student's t test. Oil red O staining demonstrated that pulmonary lipid accumulation was progressively exacerbated in HCD fed C57BL/6J mice. Hematoxylin and eosin (H&E) and immunohistochemistry studies showed distinctive signs of pulmonary inflammation including macrophage accumulation, lymphocyte infiltration and elevated levels of proinflammatory cytokines like MCP1. (Bronchoalveolar lavage fluid MCP levels HCD group vs. RD group: 110.83±0.79 vs. 81.78±3.69 pg/ml, p<0.01, n=3). Consistently, real-time quantitative PCR and western blotting results showed the mRNA and protein expressions of TLR2 and TLR4 were significantly up-regulated. (mRNA levels of TLR2 and TLR4 in the lungs of HCD group mice were elevated 8.13±0.39 and 3.78±0.23 folds respectively, compared to RD group mice. p<0.05, n=3). Meanwhile, the translocation of NFkappaB into nucleus was activated in high fat/high cholesterol diet fed mice lung. Our findings suggested that high fat/high cholesterol diet could promote lipid accumulation and inflammation in the lung of C57BL/6J mice, which may partly due to the activation of TLRs/NFkappaB pathway triggered by disturbance of lipid metabolism in the lung.

Recipient of the travel awards for young physiologists from the Chinese Association for Physiological Sciences (CAPS)

Grants support: National Natural Science Foundation of China (NSFC 81071907), Natural Science Foundation of Chong Qing (CSTC, 2011BB5128) and the Program for New Century Excellent Talents in University (NCET-10-0997).

Where applicable, the authors confirm that the experiments described here conform with The Physiological Society ethical requirements.

PCB348

Investigating cholesterol homeostasis with a two-compartment mathematical model: Towards tailored prevention and treatment of high cholesterol

O. Hrydziuszko[1,2], K. Kubica[1], A. Wrona[1] and J. Balbus[3]

[1]Institute of Biomedical Engineering and Instrumentation, Wroclaw University of Technology, Wroclaw, Poland, [2]Department of Biosciences and Nutrition, Karolinska Institutet, Huddinge, Sweden and [3]Institute of Mathematics and Computer Science, Wroclaw University of Technology, Wroclaw, Poland

Background:
High blood cholesterol level has been long known as a classic coronary risk factor. It is suspected to cause third of ischaemic heart diseases which adds up to 2.6 millions of deaths each year (World Health Organization). However the underlying mechanisms causing cardiovascular diseases in respect to serum cholesterol levels, uptake of cholesterol from the dietary sources and exercises remain not fully understood, and if anything, rather ambiguous (Gold, Grover et al. 1992; Steinberg 2004).
Aim:
The primary aim of our work is advance our understanding of cholesterol homeostasis, including the transport of cholesterol in the circulatory system. This in turn, could lead to advancing prevention and treatment of high cholesterol, reducing the risk of developing cardiovascular diseases.
Materials & Methods:
The current knowledge on the transport of cholesterol in the circulatory system can be summarized by a set of enzymatic reactions including for instance cholesterol synthesis, cholesterol transport in different types of lipoproteins (chylomicrons, very-low-density intermediate-density, low-density and high density lipoproteins) or the interactions between them cells, tissues and organs. To study the behaviour of cholesterol homeostasis the current knowledge was summarized in the diagram capturing all known (literature reported and validated) cholesterol-related relationships and the diagram was reduced to a two-compartment mathematical model. The model encompasses a set of biochemical enzymatic reactions, with a single equation representing one process (e.g. cholesterol synthesis) and based on the Michaelis-Menten kinetics.
Results & Significance:
Our relative simple model enables modelling the cholesterol homeostasis under normal physiological conditions (serum cholesterol levels within the recommended boundaries) as well as set of pathological states. These, among others, include disorders linked to the disturbances in the creation of LDL and HDL lipoproteins or uptake of LDL lipoproteins by the LDL receptors. The significance of the up and running model of cholesterol homeostasis becomes clearer with the models parameters being adjusted on the individual patient basis and allowing, among others, prediction of the short and long-term impact of the cholesterol lowering drugs or diet modification.

Gold, P., S. Grover, et al. (1992). Cholesterol and Coronary Heart Disease: The Great Debate, Taylor & Francis Ltd.

Steinberg, D. (2004). "Thematic review series: The Pathogenesis of Atherosclerosis. An interpretive history of the cholesterol controversy: part I." Journal of Lipid Research 45(9): 1583-1593.

Where applicable, the authors confirm that the experiments described here conform with The Physiological Society ethical requirements.

PCB349

Pharmacological enhancement of postprandial macro and microvascular blood flow does not enhance the anabolic responses to nutrition in skeletal muscle of young men

B. Phillips[1,2], P. Atherton[1], K. Varadhan[2], M. Limb[1], M. Rennie[1], K. Smith[1] and J. Williams[1,3]

[1]School of Graduate Entry Medicine and Health, University of Nottingham, Derby, UK, [2]School of Biomedical Sciences, University of Nottingham, Nottingham, UK and [3]Anaesthetic Department, Royal Derby Hospital, Derby, UK

Background: Perfusion of the skeletal muscle microvasculature in response to nutrition is thought to be central for muscle mass maintenance (via protein anabolism) and whole-body glucose homeostasis (glucose disposal), both of which can be compromised in a variety of diseases including diabetes, cancer cachexia, COPD and in ageing muscle.
Objective: We set out to define whether enhancing muscle microvascular blood flow (MBF) could influence muscle protein turnover under postabsorptive and postprandial conditions in young men.
Design: We recruited 10 young (23.2±2.1 y) men in whom we measured bulk [femoral arterial] leg blood flow (LBF), muscle microvascular blood flow (MBF) and muscle protein synthesis (MPS) under postabsorptive (12 h fasted) and post-

prandial conditions (I.V glamin (prime: 34 mg.kg^{-1}, constant infusion: 102 mg.kg.hr^{-1}); dextrose to sustain blood glucose between 7-7.5 mmol.l^{-1}). In addition, we infused a pharmacological vasodilator (methacholine) into the artery of one leg to permit bilateral comparison of the effects of nutrition alone or nutrition coupled to pharmacological vasodilation. We measured LBF [femoral artery] by Doppler ultrasound and muscle MBF by contrast-enhanced ultrasound (CEUS) using Definity™ perflutren contrast agent infused at a rate of 1.2 ml.min^{-1} (1.5 ml in 18.5 ml 0.9 % saline). After 9 min to allow attainment of steady state concentrations, Definity™ microbubbles were destroyed by high mechanical index ultrasound and refilling of the microvascular space (MBF) was imaged during 4 consecutive 45 s recordings. Data was analysed using Q-lab quantification software. Rates of MPS and net leucine balance were measured using [1, 2-$^{13}C_2$] leucine tracer coupled to gas-chromatographic/ combustion mass-spectrometric techniques.
Results: We observed increases in LBF (0.51±0.02 vs. 0.57±0.04 l.min^{-1}, P<0.05), MBF (+25±10%, P<0.05), MPS (0.04±0.004 vs. 0.08±0.001 %.h^{-1}, P<0.05) and positive leucine net balance in the postprandial condition (-9.72±4.76 vs. 40.31±12.27 nmol.min.100g lean leg mass^{-1}, P<0.01). However, despite methacholine infusions augmenting nutrition-mediated increases in LBF (0.57±0.04 vs. 1.15±0.08 l.min^{-1}, P<0.05) and MBV (+79±30%, P<0.05) this provided no enhancement of MPS (0.08±0.01 vs. 0.07±0.01 %.h^{-1}) or leucine net balance (40.31±12.27 vs. 57.0±13.66 nmol.min.100g lean leg mass^{-1}).
Conclusion: We conclude that pharmacological enhancement of LBF and MBV above that of nutrition does not further augment muscle protein metabolism. This indicates that muscle nutritive blood flow is not a limiting factor for muscle protein metabolism, at least in young men.

This work was supported by the Dunhill Medical Trust

Where applicable, the authors confirm that the experiments described here conform with The Physiological Society ethical requirements.

PCB350

Reproductive parameters and oxidative status of male Sprague Dawley rats treated with low and high salt diet

B.O. Iranloye, G.O. Oludare, N.A. Esume and L.C. Ekeh

Physiology, College of Medicine, University of Lagos, Lagos, Lagos, Nigeria

Diet and nutrition is a crucial part of reproductive health. Deficiency of minerals and micronutrients has been reported to impair the process of spermatogenesis (1) Salt has been used by women on their husbands to increase their libido (2). The present study was designed to determine the effect of low salt diet and high salt diet on sperm parameters, oxidative status and reproductive hormone levels of male rats. Eighteen healthy Sprague Dawley male rats weighing between 120- 130g were used. The rats were divided into three groups of six rats each. Group I: (control) received 0.3% salt diet, Group II: low salt (received 0.14% salt diet), and group III: high salt (received 8% salt diet). All animals were treated for six (6) weeks after which they were sacrificed by cervical dislocation. Sperm analysis was done on sample derived from the cauda epididymis by conventional methods. Sperm motility was done and expressed as percentage (3). The reduced glutathione (GSH) content of the testis and epididymis homogenate were determined using the method of Van Dooran (4). Malondialdehyde (MDA) was determined based on its interaction with thiobarbituric acid (TBA).The activity of the superoxide dismutase (SOD) enzyme in the testis homogenate was determined according to the method described by Sun and Zigman(5). Serum samples were also collected and an enzyme linked immunoassay (EIA) system was employed to determine testosterone, follicle stimulating hormone (FSH) and luteinizing hormone (LH) levels. Values are means ± S.E.M., compared by ANOVA. This study reports a decreased sperm count in the low salt diet rats (44.06 ± 1.3) and increased sperm count in the high salt diet treated rats (59.6±2.3) Vs control (51.45 ± 2.2). Both low salt and high salt diet treated rats had a significant increase in percentage abnormal sperm cells when compared with control values at P< 0.05 (12.6 ± 1.2, 9.9 ± 1.3 respectively Vs 5.46 ± 0.8) The level of MDA significantly increased while GSH significantly decrease in the epididymis of both low and high salt treated diet (P< 0.05). Also a significant decrease in the activities of SOD and CAT in both the testes and the epididymis were observed in both treated groups. The increased MDA levels in the epididymis and decrease in antioxidant status in both salt diets indicates the presence of oxidative stress thus both low and high salt diet might play a negative role in male rats reproduction/fertility.

Table 1: LH, FSH and Testosterone levels in control, Low and High Salt treated Rats

PARAMETERS	CONTROL	LOW SALT	HIGH SALT
FSH(miu/L)	7.27.2 ± 0.21	7.25 ± 0.22	10.9 ± 0.57*
LH (miu/L)	9.55 ± 0.25	9.35 ± 0.62	6.28 ± 0.38*
Testosterone (nmol/L)	9.9 ± 0.62	12.1 ± 0.45	18.7 ± 2.9 *

Values are expressed as Mean + SEM, n = 6, *P<0.05 compared with control group.

1. Smith OB and Akinbamijo OO. (2000) Anim. Reprod. Sci. : 60-61:549–560.

2. Moiner BM and Drueke TB.(2008). Nephrol Dial Transplant ; 0: 1-8.

3. Zemjanis R. (1977). in Animal Reproduction. William and Wilkins company 1977, Baltimore, USA, p. 242

4.Van Doorn R et al (1978). Toxicology, 11: 225–233.Van Dooran

5. Sun M, Zigman (1978) Anal Biochem 90: 81-89Zigman

Where applicable, the authors confirm that the experiments described here conform with The Physiological Society ethical requirements.

PCB351

Gene polymorhisms of water and glycerol channels aquaporin 7 and 9 in obese and/or diabetic patients

O. Palabiyik[1,2], L. Ozturk[1], T. Sipahi[2] and S. Guldiken[3]

[1]Physiology, Trakya University Faculty of Medicine, Edirne, Turkey, [2]Biophysics, Trakya University Faculty of Medicine, Edirne, Turkey and [3]Endocrinology, Trakya University Faculty of Medicine, Edirne, Turkey

The alterations that may occur during glycerol transport between adipose tissue and liver can play an important role in the development of diabetes or obesity (1,2). In this study, polymorphisms of aquaporin 7 that provides glycerol release from adipose tissue and aquaporin 9 that provides glycerol entry into liver were investigated. After ethical approval, three groups were created by participants who signed the informed consent form. Group 1, the individuals with normal weight and no diabetes (n=49; M/W, 18/31; mean age, 36±10 year), Group 2, the individuals with obesity and no diabetes (n=60; M/W, 29/31; mean age, 47±10 year) and Group 3, the individuals with type 2 diabetes mellitus and obesity (n=89, M/W

venous blood samples. Polymorphisms of aquaporin 7 in 2 locations (V59L "rs: 4008659" and A953G "rs:2989924") and aquaporin 9 in 2 locations (C43T "rs:77284866" and T279A" rs:1867380") were studied. The rate of aquaporin 7 and aquaporin 9 polymorphisms were similar among the study groups. Statistical analysis showed that the levels of insulin and glycerol were significantly different (The mean insulin values 7.21±0.94, 13.71±2.20 and 18.21±2.32; the mean glycerol values 0.68±0.04, 0.79±0.05 and 0.97±0.05 in Group 1, 2 and 3, respectively, $p<0.001$ for both). Considering the polymorphisms of A953G and T276A, plasma glycerol and insulin levels were similar in subjects with different genotypes. These results suggested that polymorphisms of aquaporin 7 and aquaporin 9 were not associated with presence of obesity and/or diabetes.

1. Kuriyama H, Shimomura I, Kishida K, Kondo H, Furuyama N, Nishizawa H, et al. Coordinated Regulation of Fat-Specific and Liver-Specific Glycerol Channels, Aquaporin Adipose and Aquaporin 9.Diabetes 2002;51:2915-21.

2. Miranda M, Ceperuelo-Mallafréa V, Lecubeb A, Hernandez C, Chacona MR, et al. Gene Expression Of Paired Abdominal Adipose Aquaporin 7 And Liver Aquaporin 9 in Patients With Morbid Obesity Relationship With Glucose Abnormalities. Metabolism 2009;1-7.

Where applicable, the authors confirm that the experiments described here conform with The Physiological Society ethical requirements.

PCB351a

The effects of Syzygium aromaticum-derived maslinic acid on blood glucose, blood pressure and kidney function of streptozotocin-induced diabetic rats

B.N. Mkhwanazi[1], F.R. Van Heerden[2] and C.T. Musabayane[1]

[1]Human Physiology, University of KwaZulu-Natal, Durban, KwaZulu-Natal, South Africa and [2]Chemistry, University of KwaZulu-Natal, Durban, KwaZulu-Natal, South Africa

The triterpene, maslinic acid (MA) lowers the blood glucose of adrenaline-induced diabetic mice and partial diabetic mice1. However, the anti-diabetic effects of MA in type 1 diabetes are unclear. Accordingly, we investigated the effects of MA on blood glucose levels streptozotocin (STZ)-induced diabetic rats, an experimental model for type 1 diabetes mellitus along with its influence on renal function and blood pressure; the major complications of diabetes. Oral glucose tolerance tests were conducted in separate groups of non-diabetic and STZ-treated diabetic rats given glucose load (0.86 g.kg-1, p. o.) after 18-h fast, followed by various MA doses (20, 40 and 80 mg kg-1, p.o.). Sub-chronic effects of MA on mean arterial blood pressure (MAP) and renal function were evaluated in conscious diabetic rats administered with MA twice every third day for five weeks. Sub-chronic effects of MA on blood glucose, mean arterial blood pressure (MAP) and renal function were evaluated in rats treated twice every third day for five weeks. Rats treated with deionized water (3 ml/kg, p.o.) and the standard hypoglycaemic drug metformin, 500 mg/ kg, p. o.) acted as untreated and treated positive controls, respectively.The effects of MA on proximal tubular Na+ handling were monitored in non-diabetic rats fed standard rodent chow supplemented with lithium chloride (12 mmol kg-1 dry weight) for 48 h prior to experimentation in order to raise plasma lithium to measurable concentrations without affecting renal Na+ or water excretion2. The animals were anaesthetized and the right jugular vein was cannulated to allow intravenous infusion of 0.077M NaCl. The urinary bladder was also cannulated via an incision in the lower abdomen. After a 3½ h equilibration period, urine samples were taken every 30 min over the 4h post-equilibration period of 1h control, 1h 30 min treatment and 1h 30 min recovery periods; blood samples were taken once per hour for the measurement of electrolyte and clearance marker concentrations. Li+ clearance is widely to assess proximal tubular function of the mammalian kidney3. Glomerular filtration rate (GFR) was assessed by creatinine clearance. Statistical comparison of the differences between the control means and experimental groups was performed with GraphPad InStat Software (version 4.00, GraphPad Software, San Diego, California, USA), using one-way analysis of variance (ANOVA), followed by Tukey-Kramer multiple comparison test. MA induced dose-independent hypoglycaemic responses in STZ-induced diabetic rats. Hepatic glycogen concentrations in STZ-induced diabetic rats were depleted at the end of the 5-week experimental period by comparison with non-diabetic rats. Sub-chronic MA treatment of STZ-induced diabetic rats with MA or metformin restored the hepatic glycogen concentrations to near normalcy. Acute MA infusion increased the fractional excretion of sodium (FENa) and lithium (FELi) in the absence of significant changes in GFR. STZ-induced rats exhibited marked weekly decreases in urinary Na+ excretion and elevated plasma creatinine concentration at the end of 5 weeks with concomitant reduction in GFR. MA treatment attenuated these changes and additionally reduced MAP indicating that maslinic acid might constitute a novel therapeutic strategy which can complement existing modern anti-diabetic medications.

Tang XZ, Guan T, Qian YS et al. Effects of maslinic acid as a novel glycogen phosphorylase inhibitor on blood glucose and hepatic glycogen in mice. Chinese Journal of Natural Medicines 2008; 6: 53-56.

Shalmi M & Thomsen K. Alterations of lithium clearance in rats by different modes of lithium administration. Ren Physiol Biochem 1989; 12: 273-80.

Thomsen K & Shirley DG. The validity of lithium clearance as an index of sodium and water delivery from the proximal tubules. Nephron 1997; 77: 125-38.

This study was partly funded by the NRF South Africa and the University of KwaZulu-Natal, Research Division.

Where applicable, the authors confirm that the experiments described here conform with The Physiological Society ethical requirements.

PCB352

Rab35 regulates pseudopodia extension of breast cancer cells in response to extracellular matrix

Y. Zhu

Nanjing Medical University, Nanjing, China

Pseudopodia extension in directional movement remains poorly defined in breast cancer cells. We showed that the modified Boyden chamber assay could be used for pseudopodia extension and isolation from migrating breast cancer cells in response to ECM (collagen type I). Rab35, enriched in pseudopodia of breast cancer cells, promoted pseudopodia extension in response to ECM. Dominant negative Rab35 mutant or Rab35 shRNA significantly decreased ECM-induced pseudopodia extension. Rab35 was strongly associated with fascin in MDA-MB-231 and MCF-7 cells. Rab35 mRNAs were significantly enriched in pseudopodia of breast cancer cells in response to ECM stimuli. Blocking microtubule assembly by microtubule-depolymerizing agent nocodazole significantly

retarded the asymmetries of Rab35 transcripts in pseudopodia. These findings may shed new light into the mechanism of breast cancer migration.

Zhu, Y., Tian, Y., Du, J., Hu, Z., Yang, L., Liu, J., and Gu, L. (2012). Dvl2-dependent activation of Daam1 and RhoA regulates Wnt5a-induced breast cancer cell migration. PLoS ONE 7, e37823.

Cho, S.Y. and Klemke, R.L. (2002). Purification of pseudopodia from polarized cells reveals redistribution and activation of Rac through assembly of a CAS/Crk scaffold. J. Cell Biol. 156, 725-736.

Mili, S., and Macara, I.G. (2009). RNA localization and polarity: from A(PC) to Z(BP). Trends Cell Biol. 19,156-164.

Mili, S., Moissoglu, K., and Macara, I.G. (2008). Genome-wide screen reveals APC-associated RNAs enriched in cell protrusions. Nature 453, 115-119.

Simt, M., Leng, J., and Klemke, R.L. (2003). Assay for neutite outgrowth quantification. Biotechniques 35, 254-256.

Recipient of the travel awards for young physiologists from the Chinese Association for Physiological Sciences (CAPS). And this word was supported by the grant from the National Natural Science Foundation of China (81101999) to Yichao Zhu.

Where applicable, the authors confirm that the experiments described here conform with The Physiological Society ethical requirements.

PCB353

Role of a jumonji histone demethylase in osteoclast differentiation

S. Kim[1], H. Kim[1], J. Park[1,2] and Y. Chun[1,3]

[1]Department of Biomedical Sciences, Seoul, Republic of Korea, [2]Ischemic/Hypoxic Disease Institute, Seoul, Republic of Korea and [3]Department of Physiology, Seoul National University College of Medicine, Seoul, Republic of Korea

Osteoclasts are bone-resorbing multinucleated cells that differentiate from monocyte/macrophage-lineage precursors. Bone destruction and osteoporosis are attributed to increased and activated osteoclasts. Osteoclast differentiation is a complicated process governed by diverse classes of regulators. In particular, nuclear factor–activated T cells c1 (NFATc1) plays a key role in osteoclast differentiation in response to RANKL. Yet, the regulatory mechanism of the NFATc1 gene has not been uncovered so far. A growing body of evidence has demonstrated that histone methylation and demethylation are responsible for epigenetic regulation during stem cell differentiation. Therefore, we tested the possible involvement of a jumonji histone demethylase in the epigenetic regulation of NFATc1 during osteoclast differentiation. We generated transgenic (TG) mice overexpressing the jumonji demethylase and checked the structures of their long bones using microCT. Consequently, bone volume/tissue volume (BV/TV), trabecular number (Tb.N) and trabecular separation (Tb.Sp) were reduced in 4 month-old TG mice, whereas trabecular thickness (Tb.Th), body weight and tibia/femur length were not. Moreover, we found ex vivo that macrophages from the TG bone marrow have a higher potential for differentiation toward osteoclasts than those of wild type. We also identified that the jumonji histone demethylase associates with NFATc1 in macrophages stimulated by RANKL. These findings suggest that the jumonji histone demethylase potentiates bone resorption by promoting osteoclast differentiation, and imply that the inhibition of this enzyme could be a novel strategy for preventing inflammatory bone destruction or osteoporosis.

Epigenetic gene regulation by plant Jumonji group of histone demethylase

Xiangsong Chen a, Yongfeng Hu b, Dao-Xiu Zhou b,

a National Key Laboratory for Crop genetic Improvement, Huazhong Agricultural University, 430070 Wuhan, China

b Institut de Biologie des Plantes, UMR8618, Université Paris sud 11, CNRS, 91405 Orsay, France

JMJD5, a Jumonji C (JmjC) Domain-containing Protein,

Negatively Regulates Osteoclastogenesis by Facilitating

NFATc1 Protein Degradation

Min-Young Youn‡, Atsushi Yokoyama‡, Sally Fujiyama-Nakamura‡, Fumiaki Ohtake‡, Ken-ichi Minehata§,

Hisataka Yasuda¶, Takeshi Suzuki§, Shigeaki Kato‡1, and Yuuki Imai‡2

From the ‡Institute of Molecular and Cellular Biosciences, The University of Tokyo, Yayoi 1-1-1, Bunkyo-ku, Tokyo 113-0032, Japan,

§Division of Functional Genomics, Molecular and Cellular Targeting Translational Oncology Center, Cancer Research Institute,

Kanazawa University, 13-1 Takaramachi, Kanazawa, Ishikawa 920-0934, Japan, and ¶Bioindustry Division, Oriental Yeast Co., Ltd.,

3-6-10 Azusawa, Itabashi-ku, Tokyo 174-8505, Japan

Where applicable, the authors confirm that the experiments described here conform with The Physiological Society ethical requirements.

PCB355

Coronary vasodilator effect of flavonoid quercetin

A. Monori-Kiss, E. Monos and G.L. Nádasy

Semmelweis University, Institution of Human Physiology and Clinical Experimental Research, Budapest, Hungary

Introduction
Fruits and vegetables contain several types of polyphenols, among them quercetin and its glycosylated products being physiologically important ones. Previous studies have demonstrated their direct vasodilatory capacity on larger arteries. Vasoactive actions on small resistance arteries, however, are still poorly defined.
Methods
Hearts from male Wistar rats (350-400g) were removed in pentobarbital anaesthesia (50 mg/kg, i.p.), and intramural coronary arterioles were prepared. Segments were cannulated at both ends and immersed in normal Krebs-Ringer solution in a glass-bottomed tissue bath of a pressure angiometer. The bath was thermostated and the solution was bubbled with a mixture of 20% O2, 5% CO2 and 75%N2.Inner and outer diameters were measured videomicroscopically at 50 mmHg intraluminal pressure in Krebs-Ringer solution (spontaneous tone) and with 100nM quercetin added. To test the effect of endogenous vasoactive prostanoids indomethacine (10μM) was applied. L-nitro-methil-arginine (100μM) was added to test a potential endothelial effect. Relaxed diameters were measured in calcium-free solution. Smaller arterioles (inner diameter in Krebs-Ringer solution at 50mmHg 103±9μm, n=7) and greater arterioles (201±11μm, n=9) were separately evaluated.
Results
In accordance with previous observations, spontaneous tone of the two groups were substantially different (25.6±3.4 % vs. 13.5±1.7 %, $p<0.05$). Quercetin significantly reduced the tone in both groups (46.7±9.9% and 45.7±9.1%). Indomethacine significantly increased the tone of quercetin treated, relaxed vessels by 44.7±9.9% and 45.3±14.5%. Further, addition of l-nitro-methil-arginine still induced significant relaxation

(18.9±8.4% and 27.8±8.2%, p<0.05). Statistical test was one-way ANOVA.

Conclusion

A physiologically relevant concentration of the flavonoid quercetin significantly decreases the spontaneous tone of intramural coronary arterioles. A substantial part of this vasorelaxation effect is connected to production of vasodilatory endogenous prostanoids while an endothelial NO-mediated mechanism seems to be negligible. These observations suggest the possibility that quercetin appearing in blood plasma from the food induces the operation of a coronary vasodilatory mechanism whose effectiveness is commeasurable with that of the known endothelial actions.

(Supported by OTKA 32019, 42670, the Hungarian Hypertension Society, and the Hungarian Kidney Foundation)

Where applicable, the authors confirm that the experiments described here conform with The Physiological Society ethical requirements.

PCB357

Blood temperature influences erythrocyte ATP release and muscle blood flow in human limbs

K.K. Kalsi, S.T. Chiesa, S.J. Trangmar and J. González-Alonso

Centre for Sports Medicine and Human Performance, Brunel University, London, UK

Human limb muscle and skin perfusion alters with changes in tissue temperature evoked by heating or cooling and these processes may involve temperature sensitive regulatory mechanisms. We have previously shown that passive heating and exercise increase limb tissue blood flow in humans in association with the increases in muscle temperature and plasma adenosine 5'-triphosphate concentration [ATP] (1,2). Reduced haemoglobin O_2 saturation is thought to be the main stimulus for erythrocyte ATP release in the muscle microcirculation (3,4). Recent evidence, however, suggests that temperature is another potent stimulus. Here we tested the hypothesis that the release of the vasodilator mediator ATP from human erythrocytes is sensitive to physiological reductions and increases in blood temperature independently of oxygenation induced ATP release in the human forearm circulation. To accomplish this aim, we measured forearm blood flow (FBF; Doppler ultrasound), deep venous blood temperature (T_b), retrograde venous plasma [ATP], blood gas parameters and calculated forearm vascular conductance (FVC) in the experimental and the control contralateral forearm in 7 males (19 ± 2 years) during 1 hour of passive heating using a water perfused cuff and 1 hour of passive cooling using ice with 1 hour of rest in between. All data are mean ± SEM and were compared with ANOVA and Pearson correlation (SPSS). With heating T_b increased from 34.0 ± 0.5 to 36.8 ± 0.1°C (p<0.05) while with cooling T_b decreased from 34.4 ± 0.4 to 29.1 ± 0.7°C (p<0.05). Plasma [ATP] doubled with heating from 0.21 ± 0.03 to 0.43 ± 0.05 μmol.l^{-1} (p<0.05) but did not change with cooling remaining at 0.23 ± 0.03 μmol.l^{-1} similar to values in the control forearm. FBF progressively and significantly increased with heating from 124 ± 11 to 418 ± 10 ml.min^{-1} (p<0.05) and decreased with cooling from 121 ± 11 to 90 ± 14 ml.min^{-1} (p<0.05). Similar significant responses were observed with FVC, indicating that flow changes with heating and cooling were due to vasodilatation and vasoconstriction, respectively. In contrast, control forearm values for T_b, [ATP], FBF and FVC were unchanged throughout the study. During heating and cooling, FBF and FVC were exponentially correlated to T_b (R^2 = 0.86 and 0.87, respectively; p<0.01) and [ATP] (both R^2= 0.85; p<0.01). Contrary to the reported involvement of the O_2 saturation pathway, plasma [ATP] remained unchanged during cooling despite decreasing O_2 saturation from 62 ± 4 to 35 ± 4% (p<0.05) but increased with heating when O_2 saturation was elevated from 59 ± 6 to 82 ± 4% (p<0.05). These findings suggest that ATP from erythrocytes may be an important mechanism regulating human limb muscle and skin perfusion in conditions that alter blood and tissue temperature. Furthermore, it seems that temperature works through a distinct pathway to that sensitive to blood oxygenation.

Kalsi KK & González-Alonso J. (2012). Temperature-dependent release of ATP from human erythrocytes: mechanism for the control of local tissue perfusion. Exp Physiol, 97, 419-32.

Pearson J, Low DA, Stohr E, Kalsi K, Ali L, Barker H & González-Alonso J. (2011). Hemodynamic responses to heat stress in the resting and exercising human leg: insight into the effect of temperature on skeletal muscle blood flow. Am J Physiol Regul Integr Comp Physiol, 300, R663-73.

Sprague RS, Hanson MS, Achilleus D, Bowles EA, Stephenson AH, Sridharan M,

Adderley S, Procknow J & Ellsworth ML. (2009). Rabbit erythrocytes release ATP and dilate skeletal muscle arterioles in the presence of reduced oxygen tension. Pharmacol Rep, 61, 183-90.

Kirby BS, Crecelius AR, Voyles WF & Dinenno FA. (2012). Impaired skeletal muscle blood flow control with advancing age in humans: attenuated ATP release and local vasodilation during erythrocyte deoxygenation. Circ Res. 111, 220-30.

Where applicable, the authors confirm that the experiments described here conform with The Physiological Society ethical requirements.

PCB358

The NLRP3 inflammasome: link to interleukin-1β production in the human placenta

E. Maneta, D. Hay and R.N. Khan

Academic Division of Obstetrics & Gynaecology, University of Nottingham, Derby, UK

Introduction: Within the last ten years, DAMPs (Damage or Danger Associated Molecular Patterns) have been shown to activate a novel intracellular structure termed the inflammasome (1). Of the four types of inflammasomes that have been discovered, the NLRP3 (cryopyrin) inflammasome is linked to the production of interleukin-1β implicated in the onset of preterm labour. Activation of the NLRP3 inflammasome is complex requiring two 'hits' eventually triggering caspase-1 and release of IL-β, reliant, in part, on the purinergic receptor, P2X7 receptor. The hypothesis tested is that the NLRP3 inflammasome is expressed and functional in leukocytes isolated from the villous tissue of the placenta and cord blood.

Methods: Placentae and blood samples were obtained with ethical approval and informed consent from pregnant women at term. Leukocytes were purified from placentae, cord and peripheral blood using Ficoll-Hypaque isolation. Immunofluorescence was used to detect the presence of the NLRP protein. IL-1β production was measured by ELISA in the presence of antagonists of the P2X7 receptor and caspase-1, a key molecule of the NLRP3 inflammasome complex. IL-1β production ± drugs was compared using one-way ANOVA for n samples.

Results: NLRP3 (cryopyrin) protein was constitutively expressed in peripheral (n=5) and placental (n=8) leukocytes while expression in cord blood leukocytes (n=5) required priming with

lipopolysaccharide. IL-1β release was significantly greater (P <0.05) in villous leukocytes (n=8) compared with cord blood leukocytes (n=8) and enhanced further in placental leukocytes of labouring (P<.05; n=6) compared with nonlabouring women (n=7). Production of IL-1 β was significantly inhibited (P<0.05) following preincubation with the caspase-1 inhibitor, YVAD-CHO (n=6) and a selective P2X7 antagonist (n=6) while progesterone (100 nM) treatment reduced this response (P<0.05; n=6).

Conclusion: The human placental NLRP3 inflammasome is an important intracellular component mediating the release of IL-1β during pregnancy. Increased production of IL-1β and basal expression of NLRP3 in placental and peripheral leukocytes compared with those of cord blood suggest that the maternally-derived signals have a key role in inflammation during pregnancy.

Schroder, K. Tschopp J. (2010). cell 140, 821-832

Where applicable, the authors confirm that the experiments described here conform with The Physiological Society ethical requirements.

PCB359

miRNA-223 regulates platelet function by targeting β1 integrin and factor XIII-A

A. Elgheznawy, V. Randriamboavonjy and I. Fleming

Institute for Vascular Signalling, Frankfurt am Main, Germany

microRNA (miRNA) regulate protein expression levels either by degrading mRNA or repressing translation. Circulating miRNAs have been proposed as biomarkers for different diseases. One particular miRNA i.e. miR-223, is abundant in platelets and markedly downregulated in plasma from patients with diabetes or at a high risk of myocardial infarction. The aim of this study was to determine whether miR-223 is only a biomarker or whether changes in miR-223 also affect platelet function. Two models of miR-223 deletion in platelets were used; miR-223 knockout mice (miR-223 -/-) and platelets from diabetic patients. Values are means ± S.E.M., compared either by ANOVA or the Student t test.Platelets from miR-223-/- mice demonstrated an enhanced platelet aggregation in response to either thrombin (n=8) or collagen (n=22) compared to platelets from wild-type littermates (C57BL/6). Moreover, platelets from miR-223-/- mice developed large aggregates when added to different extracellular matrices such as collagen, fibronectin, and laminin and demonstrated a delayed clot retraction. Platelets from diabetic patients also formed large aggregates (339.8 μm2 ± 60 for diabetic patients vs. 78.46 μm2 ± 40.4 for healthy donors, p<0.05) and showed delayed clot retraction when compared to healthy donors. In miR-223-/- mice, the bleeding time was markedly shorter (419.7 sec ± 67.36 miR-223-/-, vs. 1177 sec ± 101.3 wild-type, p<0.001) and a significantly larger thrombus was developed after FeCl3-induced carotid artery injury than in wild-type mice (p<0.001, n=6). Furthermore, FACS analysis of whole blood showed an enhanced platelet-leukocyte aggregate (0.13 % ± 0.01 miR-223-/-, vs. 0.07% ± 0.008 wild-type, p<0.01) in miR-223-/- mice compared to wild-type. To identify proteins regulated by miR-223 we compared the proteome of miR-223-/- and wild-type platelets using 2D-differential in-gel electrophoresis. Validation of proteins identified by the proteomic analysis confirmed that miR-223-/- platelets expressed higher levels of kindlin-3, β1 integrin, α2 integrin and factor XIII-A (n=13) than wild-type platelets. The same changes in protein expression were also detected in platelets from diabetic patients (n=5). The α2β1 integrin antagonist; rhodocetin (5μg/ml, 5 min), prevented the changes in aggregate formation of platelets from miR-223-/- and diabetic patients. Additionally, factor XIII-A inhibition normalized the clot retraction process. In conclusion, our data indicate that miR-223 plays an important role in the regulation of platelet function through targeting integrin signaling and factor XIII-A expression and activity.

Where applicable, the authors confirm that the experiments described here conform with The Physiological Society ethical requirements.

PCB360

Vasoactive agonists causes changes in vascular smooth muscle cell stiffness and induces stiffness oscillations and remodeling of cytoskeletal architecture

Z. Hong[1], Z. Sun[1], Z. Li[1], J. Trzeciakowski[2] and G.A. Meininger[1,3]

[1]Dalton Cardiovascular Research Center, University of Missouri, Columbia, MO, USA, [2]Department of Systems Biology, Texas A&M University, College Station, TX, USA and [3]Department of Medical Pharmacology and Physiology, University of Missouri, Columbia, MO, USA

We have reported that vasoactive agonists induce coordinated changes in stiffness and integrin-mediated cell adhesion in vascular smooth muscle cells (VSMCs), i.e., vasoconstrictors cause coordinated increases in VSMCs stiffness and adhesion and vasodilators cause opposite results[1]. In these studies a temporal analysis was performed to examine the dynamic effects of vasoactive agonists on VSMCs stiffness and cortical cytoskeletal structure. Atomic force microscopy (AFM) was used to perform real-time measurements of cell stiffness using a nanoindentation protocol (0.1 Hz). Data were analyzed by spectral analysis (Eigen decomposition) and[2]. VSMC stiffness was found to exhibit temporal oscillations with three distinct frequency components at 0.001/1.0, 0.004/0.4, and 0.07/0.3 Hz/kPa frequency/amplitude, respectively. Following treatment with angiotensin II (ANG II, 10^{-6}M), amplitude of the oscillations increased significantly (+100%), whereas adenosine (ADO, 10^{-4}M), a vasodilator, reduced oscillation amplitudes (-30%). To examine whether ANG II and ADO also altered cortical cytoskeletal structure as part of their action, the VSMC membrane topography of the sub-membranous actin cytoskeleton (100-300 nm depth) was acquired by contact mode imaging with AFM. Height and deflection signals from the topographical images were analyzed (Matlab) to compare the cortical actin fiber distribution and orientation before and after treatment with ANG II or ADO (20 min). These data show that ANG II increased the parallel alignment, density and thickness of cortical stress fibers, consistent with a rapid remodeling process involving increased actin polymerization. By comparison, ADO decreased stress fiber alignment, density and thickness of the stress fibers, consistent with disassembly of actin stress fibers. These findings demonstrate that vasoactive agonists dynamically alter temporal behavior and cytoskeletal structure of the VSMCs. These events appear to play an important role in the contractile behavior of VSMCs to vasoactive agonists.

Hong Z, Sun Z, Li Z, Mesquitta WT, Trzeciakowski JP, Meininger GA. Coordination of fibronectin adhesion with contraction and relaxation in microvascular smooth muscle. Cardiovasc Res. 2012;96:73-80.

Zhu Y, Qiu H, Trzeciakowski JP, Sun Z, Li Z, Hong Z, Hill MA, Hunter WC, Vatner DE, Vatner SF, Meininger GA. Temporal analysis of vascular smooth muscle cell elasticity and adhesion reveals oscillation waveforms that differ with aging. Aging Cell. 2012;11:741-50.

This work was supported by NIH P01HL095486 to G.A.M.

Where applicable, the authors confirm that the experiments described here conform with The Physiological Society ethical requirements.

PCB362

Inhibitory effects of menthol and its derivative on intestinal contraction of mice

T. Homma[1], M. Katagiri[1], K. Suzuki[1], M. Itoh[2], N. Yoneda[2], H. Tsuyama[2], M. Fujimoto[2] and Y. Suzuki[3]

[1]Maebashi Institute of Technology, Maebashi, Gunma, Japan, [2]Chiba Institute of Science, Choshi, Chiba, Japan and [3]University of Shizuoka, Shizuoka, Shizuoka, Japan

<Purpose> Efficacy of peppermint or its major component menthol on gut function is generally known. Menthol shows its cooling effect via TRPM8, which can be activated by cold stimulation (lower than 25-28°C). Here, we examined the effect of menthol (M) and synthesized menthol derivative (MD, donated by Takasago International Corporation) on smooth muscle contraction induced by acetylcholine (ACh) using isolated intestine of mice, and action mechanism was investigated with relation to TRP channel activity.
<Methods> Animal experiments were approved by the animal care and use committee at Chiba Institute of Science and Maebashi Institute of Technology. After euthanasia of mice (ddy, male, over 6 weeks ages) by deep anesthesia, intestines were isolated and divided into 5 different positions, that is, jejunum, upper part of ileum, lower part of ileum, colon, and rectum. After intestinal fragment was set in the Magnus tube kept at 37°C, intestinal motility was monitored by tension meter and recorded on chart recorder. M/MD were dissolved in DMSO and applied against the intestine at 100 μM (MD) or 200 μM (M) as a final concentration. Amplitude of contraction by ACh with DMSO was shown as 100% (control), and those with M or MD were relatively shown.
<Results & Discussion> M/MD inhibited ACh-induced intestinal contractions concentration-dependently. MD showed stronger inhibition than M at the same concentration. Inhibitory effects of M/MD were different from intestinal positions, that is, remarkable inhibition could be observed at jejunum and upper part of ileum. At all intestinal positions except jejunum, inhibitory effects of M/MD on ACh-induced contractions became weak at low temperature (23°C). At this temperature, it is thought that TRPM8 has been already activated. So, these results suggested that TRPM8 might involve in inhibitory effects of M/MD and distribution of TRPM8 might be different from intestinal positions. In order to clarify involvement of TRPM8 on inhibitory effects of M/MD, non-specific TRP channel inhibitor 'ruthenium red' or non-specific TRP channel antagonist 'capsazepine' was used. In spite of inhibitory condition of TRP channel (maybe TRPM8 too) by applying these reagents (final concentration was 10 μM), inhibitory effects of M on the ACh-induced contractions could be still observed. As ruthenium red and capsazepine are not specific against TRPM8, these reagents may action to other existed TRP channels in intestinal tissues and action of M may appear indirectly. It was reported TRPM8 was expressed at mucosa but not at muscle on small intestine (1), and the presence of TRPM8 in the gut has not yet been established clearly (2). These results and reports suggest that M may act at other sites in intestine in addition to TRPM8.

L.Zhang *et al.* (2004). *Am J Physiol Gastrointest Liver Physiol*, **286**, G983-G991.

P.Holzer (2011). *Curr Pharm Biotechnol*,**12**, 24–34.

Where applicable, the authors confirm that the experiments described here conform with The Physiological Society ethical requirements.

PCB363

Platelets activate hepatic endothelium and provide P-Selectin as a bridge for leukocyte recruitment

P.F. Lalor, J. Herbert, R. Bicknell and D.H. Adams

Centre for Liver Research, University of Birmingham, Birmingham, West Midlands, UK

Platelets drive liver injury in murine models of viral hepatitis(1) and promote liver regeneration through the release of serotonin(2). Despite their emerging role in inflammatory liver disease little is known about the mechanisms by which platelets bind to the hepatic vasculature. We used human explanted tissue specimens and peripheral blood to investigate the mechanisms and consequences of platelet binding. Human hepatic sinusoidal endothelial cell (HSEC) adhesion receptor expression was determined by analysis of public SAGE expression data. We then used a combination of modified Stamper Woodruff adhesion assays and flow-based endothelial adhesion assays with cultured HSEC and human platelets and leucocyte populations, along with histochemical analysis of human explanted liver specimens and NF-KB activity assays. 1,5353 genes with differentially expressed in HSEC (FDR q-value <=0.05 with posterior probability of >= 0.8) compared to endothelium from kidney, breast, lung and aorta and of these 864 were enriched in HSEC. Expression of sinusoidal endothelial phenotypic indicators(3) CD32b (FCGR2B), LYVE-1, CLEVER-1 (STAB1) and mannose receptor was increased in HSEC, which had reduced expression of VWF, αv integrin and CD31. Exogenous platelets bound avidly to hepatic vessels in normal and chronically injured human liver tissue, and became activated on the diseased tissue. Adhesion was integrin dependent (>60% decrease 100ug/ml RGD peptide, p<0.001, n=3 livers) inhibited by blocking platelet CD41, and supported by binding to immobilised fibrinogen on the tissue endothelium (>50% decrease 100ug/ml Fb-binding peptide, P<0.05, n=3 livers). Flow based adhesion assays confirmed that binding of platelets to HSEC under flow was significantly inhibited by antibody raised against Gp1b (29±18% of control), Fb-peptide(53.5±20%),αIIb integrin(36.7±7.2%) and αv integrin(36.2±4.7%, P<0.05 for all, n=4 HSEC isolates). Binding of platelets resulted in activation of endothelial NF-KB, and a significant increase in secretion of CXCL8 (2600±300pg/ml vs 300±290pg/ml control, n=3 HSEC isolates p<0.001) and CCL2 (900±150pg/ml vs 260±175pg/ml control) by HSEC. Importantly platelet attachment to HSEC increased binding of neutrophils and lymphocytes under flow, and adhesion was inhibited using a P-Selectin inhibitor. In conclusion, we have demonstrated that resting platelets can adhere to human HSEC using the integrins αIIbβ3 and αVβ3 under physiological shear stress. Our findings explain how platelets bind to hepatic vessels and suggest that such interactions promotes immune cell recruitment by triggering chemokine secretion and providing an adhesive substrate for circulating leukocytes.

SITIA G, AIOLFI R, DI LUCIA P, et al. Antiplatelet therapy prevents hepatocellular carcinoma and improves survival in a mouse model of chronic hepatitis B. Proc Natl Acad Sci U S A 2012; 109(32): E2165-72.

Lesurtel M, Graf R, Aleil B, Walther DJ, Tian Y, Jochum W, Gachet C, Bader M, and Clavien PA. Platelet-derived serotonin mediates liver regeneration. Science 312: 104-107, 2006.

Lalor PF, Lai WK, Curbishley SM, Shetty S, and Adams DH. Human hepatic sinusoidal endothelial cells can be distinguished by expression of phenotypic markers related to their specialised functions in vivo. World JGastroenterol 12: 5429-5439, 2006

We are grateful to our patients at QEH for access to their tissue samples. Work in our laboratory is funded by The Medical Research Council and The Wellcome Trust.

Where applicable, the authors confirm that the experiments described here conform with The Physiological Society ethical requirements.

PCB364

Local perfusion conditions influence the epidermal "barrier" function in the lower limb

H. Silva[1,2], H. Ferreira[4], L. Tavares[1], J. Bujan[3] and L.M. Rodrigues[1,2]

[1]CBiOS, U Lusofona Fac Health Sc & Technol, Lisboa, Portugal, [2]Pharmacol Sc Departm, U LIsboa School of Pharmacy, Lisboa, Portugal, [3]U Alcalá School of Medicine, Madrid, Spain and [4]IBEB, U LIsboa Faculty Sciences, Lisboa, Portugal

The study of the relationships between transcutaneous variables, especially microcirculatory flow by Laser Doppler Flowmetry (LDF), transcutaneous gas pressures (tcpO2 and tcpCO2) and transepidermal water loss (TEWL) has provided new directions to better understand local circulatory physiology. The objective is to explore how changes in local perfusion in the lower limb affect the epidermal "barrier" function. A group of fourteen young adult males (24.9 ± 0.6 years old), was selected after informed consent. All procedures complied with the ethical standards for human research by the Declaration of Helsinki and subsequent amendments. Two protocols were designed involving postural change maneuvers (protocol I – elevation of the leg 90° relative to the body axis while sitting; protocol II - supine with elevation of the leg 30°) and one protocol consisting of an occlusion test with application of suprasystolic pressure through a tourniquet-cuff (protocol III). Studied variables in distal locations of the lower limb involved microcirculatory blood flow by LDF (PeriFlux PF5000, PF5010 System, Perimed, Sweden), tcpO2 by transcutaneous gasimetry (Periflux PF5000, PF5040 System, Perimed, Sweden) and TEWL (Tewameter TM300, CK electronics, Germany). All variables were assessed before, during and after these maneuvers. Descriptive and nonparametric statistics were applied and a 95% confidence level was adopted.In Protocol I there was a statistically significant increase in the values of LDF and TEWL and an equally significant decrease in tcpO2 during the elevation of the lower limb. When the lower limb returned to the starting position values returned to baseline. In Protocol II there was a statistically significant decrease of LDF values, TEWL and tcpO2 during the elevation of the lower limb. The values returned to baseline when the lower limb returned to the starting position. In Protocol III there was a statistically significant decrease in the values of LDF and tcpO2 during the occlusion, accompanied by a significant increase of TEWL values, both of which returned to baseline when the tourniquet was removed. The present data confirms previously published results, suggesting that by modifying local perfusion conditions one may influence the epidermal skin "barrier".

Where applicable, the authors confirm that the experiments described here conform with The Physiological Society ethical requirements.

PCB366

Tocolytic Effects of *Talinum Paniculatum* Leaf Extract in Female Virgin Rats

C. Thanamool and S. Kupittayanant

Physiology, Suranaree University of Technology, Muang, Nakhon Ratchasima, Thailand

Talinum paniculatum (*T. paniculatum*) has long been used in Thai herbal recipes because of its various therapeutic properties such as improving vitality or treatment of type-2 diabetes, inflammatory skin problems, gastrointestinal disturbance and general weakness (Shimoda et al, 2001; Pak et al, 2005). *T. paniculatum* is also believed to be beneficial for female reproductive system by inducing lactation and restoring uterine functions after post-partum period (Manuhara et al, 2012). Although, the plant has been reported to influence the female reproductive system, but there is no scientific data regarding to clarify the effects on the uterus to support its therapeutic relevance. Therefore, the purpose of this study was to investigate the effects of *T. paniculatum* leaf extract on uterine contractility and its possible mechanism(s) on adult female virgin rats. In this study, animal cares, environmental conditions, and uses followed the guidelines of Laboratory Animal Resources, National Research Council of Thailand. The procedures of the experiment were approved by the Institutional Animal Care and Use Committee, Suranaree University of Technology, Nakhon Ratchasima, Thailand. The rats (200-250 g) were humanly euthanized by CO_2 asphyxia and uteri were removed. Isometric force was measured in strips of longitudinal myometrium (1-2 mm x 0.5 mm x 10 mm) in organ baths containing physiological Krebs' solution maintained at 37 °C, pH 7.4. The effects of *T. paniculatum* leaf extract at certain concentration level (IC_{50}; 1.67 mg/mL) on spontaneous contraction and agonist-induced contraction such as high KCl (40 mM) solution, Bay K8644 (1 μM), and oxytocin (10 nM) were observed. All values were analyzed by Paired student *t*-test. A probability level less than 5% ($P<0.05$) was considered statistically significant. The results showed that spontaneous uterine contractile activity was found to be dose-dependently inhibited by the extract ($n = 5$). In addition, the extract significantly inhibited the contraction induced by high KCl solution ($P<0.01$) ($n = 5$). In Bay K8644 and oxytocin studies, the extract significantly relaxed the uterus in a time-dependent manner ($P<0.05$) ($n = 5$). Interestingly, the extract could potentially inhibit oxytocin-induced contraction in the absence of external Ca^{2+} ($n = 7$). Taken together, the data implied that *T. paniculatum* produces tocolytic effects on both spontaneous and agonist-induced contractions. The possible mechanisms may be due to the blockade of Ca^{2+} influx via L-type Ca^{2+} channel and Ca^{2+} efflux from internal store.

Manuhara YSW, Yachya A & Kristanti AN (2012). Effect of aeration and inoculum density on biomass and saponin content of *Talinum paniculatum* gaertn. hairy roots in balloon-type bubble. *J Pharm Biomed Sci*2(4), 47-52.

Pak SC, Lim SC, Nah SY, Lee J, Hill JA & Bae CS (2005). Role of Korean red ginseng total saponins in rat infertility induced by polycystic ovaries. *Fertil Steril*84, 1139-1143.

Shimoda H, Nishida N, Ninomiya K, Matsuda H & Yoshikawa M (2001). Javaberine A, new TNF-alpha and nitric oxide production ihibitor, from the roots of *Talinum paniculatum*. Heterocycle*55, 2043-2050.*

We gratefully acknowledge the Office of the Higher Education Commission of Thailand for financial support.

Where applicable, the authors confirm that the experiments described here conform with The Physiological Society ethical requirements.

PCB367

Modulation of urinary bladder muscle contractility and mucosal ATP release by inhibition of intracellular protein phosphatases

J. Clayton, D. Kitney, T. Hague, A. Talstaya, C. Fry and R.I. Jabr

Biochemistry and Physiology, University of surrey, Surrey, UK

Overactive bladder (OAB) is accompanied by abnormal muscle contraction and increased ATP release from the mucosa. An important common factor is an increase of intracellular Ca^{2+}, which in turn activates a central intracellular signalling pathway triggered by the Ca^{2+}-calmodulin-dependent protein phosphatase, calcineurin (Cn). An increase of Cn activity is associated with the development of an overactive bladder phenotype, that may represent a direct action or the secondary activation of other phosphatases such as PP1 and PP2A. The role of these phosphatases may be examined by the use of inhibitors such as cyclosporin (CsA for Cn) or okadaic acid (for PP1/PP2A). To date, the physiological role of Cn-dependent pathways in bladder contractions is unclear. The objectives of this study were: 1) to examine the effects of CsA or okadaic acid on spontaneous and carbachol-evoked, as well as nerve-mediated contractions and 2) the effect of CsA on mucosal-mediated ATP release upon muscle stretch.
Muscle strips were dissected from rabbit urinary bladders, and superfused with normal Tyrode's solution in horizontal organ baths. Isometric contractions were measured from preparations with the mucosa attached or denuded. Contractions were evoked in the absence and presence of CsA by either exposure to the muscarinic receptor agonist, carbachol or electrical field stimulation (20Hz). ATP release from mucosa-intact preparations after a rapid stretch (20% resting length) was measured from superfusate samples using a luciferin–luciferase assay. All data are mean±S.D., differences between data sets were tested with Student's t-test and the null hypothesis rejected at $p<0.05$.
Spontaneous contractions were suppressed by CsA at 1, 5 and 10 μM and also by 0.1 μM okadaic acid (CsA 36.2±12.2 % control; n=6; okadaic acid 40.2±23.1% control; n=4; $p<0.01$). Contractures evoked by 0.1 μM carbachol were unaffected by 1μM CsA but significantly attenuated at 5 and 10 μM (74.8±5.9 and 75.9±4.3% control respectively; n=5; $p<0.05$). Okadaic acid also reduced carbachol contractions (73.6± 11.8 % control; n=4; $p<0.05$). CsA also attenuated contractions from denuded strips evoked by electrical field stimulation, but only to 95±4% control, n=4, $p<0.05$). Finally, CsA reduced stretch-evoked ATP release from mucosa-intact preparations (73.8±4.4 % control; n=10, $p<0.05$).
Inhibition of intracellular phosphatase activity supressed both spontaneous and carbachol-induced contractions, but had a relatively small effect on nerve-mediated contractions: the effect of CsA was more potent on spontaneous activity. CsA also attenuated stretch-induced ATP release, which is a regulator of spontaneous activity. The data suggest that intracellular phosphatases are key regulators of several steps in the pathways that generate contraction in bladder smooth muscle.

Where applicable, the authors confirm that the experiments described here conform with The Physiological Society ethical requirements.

PCB368

Observation and analysis of an ultrafast calcium wave in cultured vascular smooth muscle cells

J.C. Quijano, J. Bény and J. Meister

École Polytechnique Fédérale de Lausanne (EPFL), Lausanne, Switzerland

Communication between vascular smooth muscle cells (SMCs) allows control of arterial contraction and blood flow. The contractile state of the SMCs is regulated by cytosolic Ca2+ concentration and propagates as Ca2+ waves over a significant distance along the vessel. In this work, we studied an intercellular ultrafast Ca2+ wave observed in cultured A7r5 cell line and in primary cultured SMCs (pSMC) from mesenteric arteries obtained from male Wistar rats (250-350g) that were anesthetized with isoflurane (4%) and then decapitated in agreement with the Care of Animals (edited by the Swiss Academy of Medical Sciences and the Helvetic Society of Natural Sciences). Cells were aligned along networks obtained by photolithography technique. Using this microtechnique and a fast acquisition rate (330 Hz) allowed us to analyze fast intracellular Ca2+ fluorescence responses in different parts along the network after mechanical or KCl stimulation in one of the aligned cells. In addition, we have recorded and analyzed membrane potential variations in cells away from the mechanical stimulation site. Values are means ± S.E.M., compared by Student's t-test on paired data. For both types of vascular SMCs, mechanical stimulation evoked an intercellular ultrafast Ca2+ wave with the same velocity (VpSMC=13.9±4.2mm/s, npSMC=10; VA7r5=16.3±3.9mm/s, nA7r5=16; $p<0.01$). Local KCl stimulation also induced an ultrafast Ca2+ wave that had the same magnitude for both SMCs (VpSMC=15.0±2.9mm/s, npSMC=7; VA7r5=14.5±2.7mm/s, nA7r5=9; $p<0.01$). The rate of increasing cytosolic Ca2+ along the network, decreased with distance from the stimulation site for both cases. Experiments performed in the presence of the gap junction uncoupler Palmitoleic acid (PA) (50μM) or in the presence of L-type voltage operated Ca2+ channel (VOCC) inhibitor Nifedipine (Nif)(10μM) suppressed the ultrafast Ca2+ wave propagation in all cases (npSMC,Nif=5; nA7r5,Nif=7; npSMC,PA=3; nA7r5,PA=5), inferring the crucial role of the electrical coupling through gap junctions and the importance of Ca2+ entry through the VOCCs for the ultrafast Ca2+ wave intercellular propagation. On the other hand, mechanical stimulation induced a membrane depolarization that propagated and decayed exponentially with distance. Both types of SMCs present different space constants (λpSMC=0.67mm, λA7r5=0.92mm). Our results suggest that in cultured vascular SMCs, an electrotonic spread of membrane depolarization drives the Ca2+ entry from the external media which can be modeled as an ultrafast Ca2+ wave. This ultrafast Ca2+ wave may triggers the Ca2+ release from intracellular stores that drives observed slower Ca2+ waves.

This work was supported by the Swiss National Science Foundation grant FN 310300-127122.

Where applicable, the authors confirm that the experiments described here conform with The Physiological Society ethical requirements.

PCB369

Lysosome-sarcoplasmic reticulum junctions: A trigger zone for calcium waves in vascular smooth muscle

N. Fameli[1], C. van Breemen[1] and A. Evans[2]

[1]Department of Anesthesiology, Pharmacology & Therapeutics, University of British Columbia, Vancouver, BC, Canada and [2]Centre for Integrative Physiology, University of Edinburgh, Edinburgh, UK

We investigate a hypothesis for the generation of nicotinic acid adenine dinucleotide phosphate (NAADP)-mediated Ca^{2+} waves in the vascular smooth muscle of the pulmonary artery. Agonist-stimulated waves of elevated cytoplasmic calcium concentration regulate blood vessel tone and vasomotion in vascular smooth muscle. In rat pulmonary artery smooth muscle cells, the calcium mobilizing messenger NAADP appears to trigger bursts of Ca^{2+} release from lysosomal Ca^{2+} stores by activating the Two Pore Segment Channel subtype 2 (TPC2). It is suggested that these Ca^{2+} transients initiate a propagating wave by Ca^{2+}-induced Ca^{2+} release from the sarcoplasmic reticulum (SR) via ryanodine receptors (RyRs). Deconvolution and confocal microscopy observations, including immunofluorescence, indicate that lysosome clusters may selectively couple to RyR subtype 3 (RyR3) in regions
where lysosomes and proximal SR are separated by a narrow space possibly < 100 nm and beyond the resolution of light microscopy. These results naturally lead to the hypothesis that lysosome-SR (L-SR) junctions may form a cytoplasmic trigger zone for the observed Ca^{2+} bursts and subsequent cell-wide Ca^{2+} waves. The present study combines prior optical microscopy observations with a thorough ultrastructural characterization of the L-SR junctions in rat pulmonary artery smooth muscle as input data for a quantitative model of the L-SR junction to test the above hypothesis. With this model, we simulate the Ca^{2+} bursts that may be generated in the L-SR junctions
to determine whether or not these bursts give rise to a sufficient increase in junctional [Ca^{2+}] to breach the threshold for RyR3 activation by CICR and thus initiation of a propagating Ca^{2+} wave.

We are grateful to Garnet Martens and the University of British Columbia Bioimaging Facility for their guidance in electron microscopy imaging, to David Walker for his insightful help with ultrastructure identification, to Tom Bartol for his continual assistance with MCell, and to Arash Tehrani for helping with image analysis. This work was supported by Grant No. CIHR MOP-84309 from the Canadian Institute of Health Research and by the British Heart Foundation Project Grants PG/03/065 and PG/10/95/28657.

Where applicable, the authors confirm that the experiments described here conform with The Physiological Society ethical requirements.

PCB370

Microsurgical extrahepatic cholestasis decreases vasoconstrictor response to phenylephrine in rat mesenteric resistance arteries

J. Blanco-Rivero[1,2], L. Caracuel[1,2], E. Sastre[1,2], I. Prieto[2,3], C. Nieto[4], M. Aller[5], J. Arias[5] and G. Balfagón[1,2]

[1]Fisiología, Universidad Autónoma de MAdrid, Madrid, Spain, [2]Instituto de Investigación Sanitaria IdIPAZ, Madrid, Spain, [3]Hospital Universitario La Paz, Madrid, Spain, [4]Servicio de Cirugía General, Complejo Hospitalario de Toledo, Toledo, Spain and [5]Cirugía, Universidad Complutense de Madrid, Madrid, Spain

Introduction: Obstructive cholestasis is clinically characterized clinically by jaundice, discolored urine, pale stools, pruritus, liver cirrhosis and portal hypertension, causing a high rate of morbidity and mortality in human clinical area. Microsurgical extrahepatic cholestasis (MHC) is the most commonly used model to study obstructive cholestasis since it presents with a systemic inflammatory response syndrome, characterized by hyperdynamic circulation, peripheral sympathetic hyperactivity and multiorgan dysfunction. The aim of the present study was to analyse the possible alterations on vascular function produced by microsurgical extrahepatic cholestasis.
Methods: Cholestasis induction was made under anaesthesia (ketamine/xylacine) by a surgical operation based on the ligation of the common bile duct and the 4 bile ducts and then the cut of them. Contraction to phenylephrine (Phe) was measured in MRA from SO (sham-operated) and MHC (maintained for 7-8 weeks) rats. Participation of nitric oxide (NO) and thromboxane A2 (TxA2) in this response was determined, as well as the vasomotor responses to exogenous NO and TXA2.
Results: MHC decreased vasoconstrictor response to Phe in MRA from MHC rats. Preincubation with NO synthesis inhibitor L-NAME increased the Phe-induced contraction in a similar extent in both groups. Preincubation with the COX-1/2 or COX-2 inhibitor (indomethacin and NS-398, respectively), decreased the Phe-induced contraction only in SO animals. TXA2 synthesis inhibitor (furegrelate) also decreased Phe contraction only in SO animals. Vasomotor responses to DEA-NO (NO donor) or U-46619 (TXA2 analog) were not modified by MHC.
Conclusion: MHC decreases Phe-induced vasoconstriction in MRA. This decrease is due to a decrease on contractile prostanoid participation in this response, probably through a decrease on TXA2 release, while the participation of NO on this modification is ruled out.

This study was performed by grants of Ministerio de Ciencia e Innovación (SAF2009-10374, SAF2012-38530) and Fundación Mapfre.

Where applicable, the authors confirm that the experiments described here conform with The Physiological Society ethical requirements.

PCB371

Calcium activated chloride channels have critical functional effects on intracellular calcium and spontaneous contractions in human and rat myometrium

K. Noble and S. Wray

University of Liverpool, Liverpool, UK

The potential for calcium-activated chloride channels (CaCCs) as drug targets has led to the recent development of novel specific small molecule inhibitors of them [1]. These drugs are also enabling a much improved pharmacological dissection of the role of CaCCs within tissues.

Myometrial contractions need to be regulated for successful pregnancy and parturition. Our previous electrophysiological studies showed CaCCs in 30% of isolated myometrial cells in pregnant rats [2]. The aims of this study are thus to use these new inhibitors of CaCCs to determine the functional effects of CaCCs on human and rat myometrium and characterise the effect of CaCCs inhibition on Ca signaling.

Strips of myometrium (4 x 1mm) were dissected from biopsies taken from term, pre-labour elective caesarean sections in women and labouring (LR) or term pregnant (TPR) rats. Contractility was measured on strips under isometric conditions in HEPES buffered physiological salt solution at 37^0C and in some experiments simultaneous measurements of intracellular Ca^{2+} ($[Ca^{2+}]_i$) and force were made on strips previously loaded with Indo -1.

The CaCC inhibitor (CaCCinh-A01) and TMEM16A inhibitor (T16Ainh-A01) were both used at 30μM for 10–20 min based on preliminary dose response experiments. Data are mean ± S.E.M. and changes in baseline $[Ca^{2+}]_i$ are normalised to the amplitude of control phasic transients (100%).

Control spontaneous phasic contractions were established for 30 – 60 min. CaCCinh-A01 completely inhibited spontaneous contractions in all myometrial strips (human, n=5; LR, n=2 and TPR n=3. In contrast T16Ainh-A01 had no effect on spontaneous activity in any preparation.

In rats during control contractions, spontaneous phasic Ca transients (Ca entry through voltage-gated Ca channels; VOCCs) were recorded and basal Ca remained stable. The CaCCinh-A01 induced an immediate and profound decrease in basal $[Ca^{2+}]_i$ before cessation of spontaneous Ca and force transients. After 10 min basal $[Ca^{2+}]_i$ had decreased by 52 ±2%, n=4. CaCC inhibition has been shown to hyperpolarise smooth muscle [3] which might inhibit Ca entry through VOCCs and thus decrease basal Ca. Experiments were therefore repeated in nifedipine (an inhibitor of VOCCs). Nifedipine (1μM) inhibited spontaneous Ca and force transients and decreased basal $[Ca^{2+}]_i$ by 15%. However CaCCinh-A01 further decreased basal $Ca^{2+}]_i$ by 40% (preliminary data, n=2) suggesting that a significant component of CaCC activity on $[Ca^{2+}]_i$ is independent of VOCC entry.

These data suggest that there is a critical and constitutive role for CaCCs, but not the specific TMEM16A channel, in the myometrium in maintaining basal $[Ca^{2+}]_i$ and spontaneous activity. Further work using confocal microscopy will help elucidate the precise role of CaCCs on local and global intracellular calcium.

Namkung W et al. (2011). J Biol Chem 286, 2365-74.

Jones K et al. (2004). Pflugers Arch 448, 36-43.

Dixon RE et al (2012). Biol Reprod 86, 1-7.

Where applicable, the authors confirm that the experiments described here conform with The Physiological Society ethical requirements.

PCB372

Overactive bladder mediated by accelerated Ca^{2+} influx mode of Na^+/Ca^{2+} exchanger in smooth muscle

H. Yamamura[1], W.C. Cole[2], S. Kita[3], S. Hotta[1], H. Murata[1], Y. Suzuki[1], S. Ohya[1,4], T. Iwamoto[3] and Y. Imaizumi[1]

[1]Department of Molecular and Cellular Pharmacology, Graduate School of Pharmaceutical Sciences, Nagoya City University, Nagoya, Japan, [2]Smooth Muscle Research Group, Department of Physiology and Pharmacology, Faculty of Medicine, University of Calgary, Calgary, AB, Canada, [3]Department of Pharmacology, Faculty of Medicine, Fukuoka University, Fukuoka, Japan and [4]Department of Pharmacology, Kyoto Pharmaceutical University, Kyoto, Japan

The Na^+/Ca^{2+} exchangers (NCXs) are expressed in a variety of cell types and participate in the regulation of cytosolic Ca^{2+} mobilization. In mammals, three NCX isoforms (NCX1, NCX2, and NCX3) have been identified as products of the SLC8 gene family. Among alternative splicing variants of NCX1, NCX1.3 and NCX1.7 are the predominant isoforms expressed in smooth muscle tissues. NCX is thought to be a key molecule in the regulation of cytosolic Ca^{2+} dynamics in smooth muscles. The relative importance of the two Ca^{2+} transport modes of NCX activity leading to Ca^{2+} efflux (forward mode) and Ca^{2+} influx (reverse mode) in smooth muscle, however, remain unclear. Unexpectedly, spontaneous contractions of urinary bladder smooth muscle were enhanced in transgenic mice overexpressing NCX1.3 ($NCX1.3^{tg/tg}$ mice) compared to wild-type (WT) mice. For this reason, the present study was undertaken to elucidate the contribution of Ca^{2+} influx via reverse mode NCX activity to the control of membrane electrical excitability, cytosolic Ca^{2+} mobilization in urinary bladder myocytes, urinary bladder smooth muscle contractility, and urinary bladder function. All experiments were approved by the Ethics Committee of the Nagoya City University and were conducted in accordance with the Guide for the Care and Use of Laboratory Animals of the Japanese Pharmacological Society. The enhanced spontaneous contractions of urinary bladder smooth muscle from $NCX1.3^{tg/tg}$ mice were attenuated by KB-R7943 or SN-6. Whole-cell outward NCX current sensitive to KB-R7943 or Ni^{2+} was readily detected in urinary bladder smooth muscle cells from $NCX1.3^{tg/tg}$ mice, but not in WT mice. The half duration of spontaneous transient outward currents (STOCs) in myocytes of $NCX1.3^{tg/tg}$ mice were significantly larger than those of WT mice. Spontaneous Ca^{2+} transients (Ca^{2+} sparks) in myocytes of $NCX1.3^{tg/tg}$ mice were larger and frequently resulted in propagating events and global elevations in cytosolic Ca^{2+} concentration (Ca^{2+} waves). Significantly, $NCX1.3^{tg/tg}$ mice exhibited a pattern of more frequent urination of smaller volumes and this phenotype was reversed by oral administration of KB-R7943. On the other hand, KB-R7943 did not improve it in KB-R7943-insensitive $NCX1.3^{tg/tg}$ ($G833C\text{-}NCX1.3^{tg/tg}$) mice. We conclude that NCX1.3 overexpression is associated with abnormal urination owing to enhanced Ca^{2+} influx via reverse mode NCX leading to prolonged, propagating spontaneous Ca^{2+} release events and a potentiation of spontaneous contraction in urinary bladder smooth muscles. These findings suggest the possibility that NCX is a candidate molecular target for overactive bladder (OAB) therapy.

Supported by Grant-in-Aids from MEXT, JSPS, CIHR, and Nagoya City University (International Research Collaboration).

Where applicable, the authors confirm that the experiments described here conform with The Physiological Society ethical requirements.

PCB373

α1 modulation of spontaneous activity in prostate tissue from men with benign prostatic hyperplasia (BPH) or prostate enlargement

B. Chakrabarty[1], M. Frydenberg[2], N. Lawrentschuk[3], G. Risbridger[2] and B. Exintaris[1]

[1]Drug Discovery Biology, Monash Institute of Pharmaceutical Sciences, Melbourne, VIC, Australia, [2]Anatomy And Developmental Biology, Monash University, Melbourne, VIC, Australia and [3]Department Of Surgery, Austin Health, University of Melbourne, Melbourne, VIC, Australia

Introduction and objective
There are dual reasons for the emergence of BPH: an increase in smooth muscle tone as well as an increase in the size and growth of the prostate gland. Smooth muscle tone is treated using α1 adrenoreceptor antagonists to reduce urethral obstruction by relaxing contractile tissue of the prostate gland and perhaps the urethral muscle as well. However, relatively little is known about smooth muscle function in this organ and the mechanism and effectiveness of α adrenergic drugs and how they directly regulate contractility prostate gland smooth muscle itself, is equivocal. Hence the aim of the current study was to investigate the direct effect of clinically used α1 adrenoreceptor antagonists on prostate contractility in specimens from males with BPH, or prostate enlargement.
Methods
Transition zone tissue (10mm X 15mm) from the prostate gland was obtained from consenting patients undergoing radical prostatectomy. These patients are diagnosed with BPH (volume >70cc and pathology) and have low to moderate grade prostate cancer; they will have had radical prostatectomy to surgically treat both conditions. TZ tissue was placed into ice-cold RPMI medium supplemented with 5% fetal calf serum and antibiotics (penicillin at 300 units/ml, streptomycin at 300 μg/ml and amphotericin at 1 μg/ml). Contractile recordings were made from prostatic preparations (3mm X 10mm) using standard tension recording techniques as we have previously described.
Results
All specimens contracted spontaneously at a frequency of 2.2 +/- 0.4 contractions per minute; the duration of each contraction was >12 seconds (n=18). The basal tension was 4.4 +/- 0.4 mN and the amplitude (normalised for tissue weight) was 0.20 +/- 0.03 N/g. Epidemiological data show that the incidence of BPH is age related and rises in men as they become older. Preliminary data show an age related change in men from 50 to >60 yo such that there is an increase in amplitude (from 0.13 +/- 0.05 N/g to 0.21 +/- 0.03 N/g) and frequency (from 1.4 +/- 0.2 min-1 to 2.5 +/- 0.6 min-1) of the spontaneous smooth muscle contractions with age. Tamsulosin (0.3nM) and prazosin (1.0μM) failed to completely block spontaneous contractility in the TZ of the human prostate gland but appeared to reduce the amplitude of the spontaneous contractions to ~70 % of control (both n=4; p<0.05 Student's paired t test). In addition, there appeared to be variation in the response by individual patients.
Conclusion
The results in human tissues fully substantiate our work with guinea-pig tissues and consistently provide explanation for the aetiology of the increase in smooth muscle tone observed in patients with BPH. The variability in the response to α1 adrenoreceptor antagonists foreshadows the need to consider individual vs group responses to current pharmacotherapy.

Where applicable, the authors confirm that the experiments described here conform with The Physiological Society ethical requirements.

PCB374

Enhanced Ca^{2+}-sensing receptor function in idiopathic pulmonary arterial hypertension

A. Yamamura[1,2], Q. Guo[1], H. Yamamura[1,3], A.M. Zimnicka[1], N.M. Pohl[1], K.A. Smith[1], R.A. Fernandez[1], A. Zeifman[1], A. Makino[1], H. Dong[4] and J.X. Yuan[1]

[1]Department of Medicine, University of Illinois at Chicago, Chicago, IL, USA, [2]Kinjo Gakuin University School of Pharmacy, Nagoya, Japan, [3]Nagoya City University Graduate School of Pharmaceutical Sciences, Nagoya, Japan and [4]Department of Medicine, University of California, San Diego, La Jolla, CA, USA

Idiopathic pulmonary arterial hypertension (IPAH) is a rare, progressive, and fatal disease that predominantly affects women. The pathogenic mechanisms involved in the pulmonary vascular abnormalities (eg, arterial remodeling and sustained vasoconstriction) in IPAH patients remain unclear. A rise in cytosolic Ca^{2+} concentration ($[Ca^{2+}]_{cyt}$) in pulmonary arterial smooth muscle cells (PASMCs) is an important stimulus for pulmonary vasoconstriction and PASMC migration and proliferation (which subsequently cause pulmonary vascular wall thickening leading to the increase in pulmonary vascular resistance). Increased resting $[Ca^{2+}]_{cyt}$ and enhanced Ca^{2+} influx have been implicated in PASMCs from patients with IPAH. We examined whether the extracellular Ca^{2+}-sensing receptor (CaSR), a unique G protein-coupled receptor (GPCR), is involved in the enhanced Ca^{2+} influx and proliferation in IPAH-PASMCs and whether blockade of CaSR inhibits experimental pulmonary hypertension. Approval to use the human lung tissues and cells was granted by the Institutional Review Board of University of Illinois at Chicago and all experiments were approved by the Ethics/Animal Care Committee of University of Illinois at Chicago. In normal PASMCs superfused with Ca^{2+}-free solution, addition of 2.2 mmol/L Ca^{2+} to the perfusate had little effect on $[Ca^{2+}]_{cyt}$. In IPAH-PASMCs, however, restoration of extracellular Ca^{2+} induced a significant increase in $[Ca^{2+}]_{cyt}$. Extracellular application of spermine also markedly raised $[Ca^{2+}]_{cyt}$ in IPAH-PASMCs but not in normal PASMCs. The calcimimetic R568 enhanced, whereas the calcilytic NPS2143 attenuated, the extracellular Ca^{2+}-induced $[Ca^{2+}]_{cyt}$ rise in IPAH-PASMCs. Furthermore, the protein expression level of CaSR in IPAH-PASMCs was greater than in normal PASMCs; knockdown of CaSR in IPAH-PASMCs with siRNA attenuated the extracellular Ca^{2+}-mediated $[Ca^{2+}]_{cyt}$ increase and inhibited IPAH-PASMC proliferation. Using animal models of pulmonary hypertension, our data showed that CaSR expression and function were both enhanced in PASMCs, whereas intraperitoneal injection of the calcilytic NPS2143 prevented the development of pulmonary hypertension and right ventricular hypertrophy in rats injected with monocrotaline and mice exposed to hypoxia. In conclusion, the extracellular Ca^{2+}-induced increase in $[Ca^{2+}]_{cyt}$ due to upregulated CaSR is a novel pathogenic mechanism contributing to the augmented Ca^{2+} influx and excessive PASMC proliferation in patients and animals with pul-

monary arterial hypertension. Targeting CaSR in PASMCs may help develop novel therapeutic approach for pulmonary hypertension.

Yamamura *et al.* (2012). *Circ Res* **111**, 469-481.

This work was supported in part by grants from the National Heart, Lung, and Blood Institute of the National Institutes of Health (HL066012 and HL098053 to J.X.-J.Y.).

Where applicable, the authors confirm that the experiments described here conform with The Physiological Society ethical requirements.

PCB375

TMEM16A currents in urethra smooth muscle

E. Bradley, T. Webb, M.A. Hollywood, K.D. Thornbury, N.G. McHale and G.P. Sergeant

Smooth Muscle Research Centre, Dundalk Institute of Technology, Dundalk, Ireland

Urethral smooth muscle generates spontaneous electrical slow waves that are thought to underpin contraction of this tissue (Hashitani et al., 1996). Several studies suggest that this activity is initiated by activation of Ca^{2+}-activated Cl^- channels (CACCs) in specialised pacemaker cells known as interstitial cells of Cajal (ICC, Sergeant et al., 2000). However, the exact contribution of CACCs to myogenic tone in the urethra has not yet been ascertained, in part, because their molecular identity has not been determined in this tissue. The purpose of the present investigation was to determine if the novel Ca^{2+}-activated Cl^- channel, TMEM16A encoded CACCs in rabbit urethral smooth muscle (RUSM). The patch clamp technique was used to record Ca^{2+}-activated Cl^- currents (I_{ClCa}) in freshly isolated ICC from the rabbit urethra and stably expressed TMEM16A currents in HEK 293 cells. In addition, tension recordings were made from strips of RUSM using a WPI Myobath system. All experiments were approved by the Dundalk Institute of Technology animal care and use committee. Data are presented as mean ± SEM.

Current-voltage relationships were obtained from HEK cells stably expressing human TMEM16A, cloned from the testes. These currents were inhibited by the novel TMEM16A inhibitor, T_{inh}A01 (10 μM) across the voltage range and in 5 cells T_{inh}A01 reduced the mean current evoked by a step to +100 mV from 1.27 ± 0.23 to 0.3 ± 0.06 nA ($p<0.05$, paired t test). Similarly, T_{inh}A01 (30 μM) reduced the peak I_{ClCa} evoked by a step to +50 mV in native ICC from a mean of 797 ± 200 pA to 253 ± 69 pA (n=5, $p<0.05$, paired t test). Urethral ICC develop spontaneous transient inward currents (STICs) when voltage clamped at -60 mV (Sergeant et al., 2000). The amplitude of these events were also inhibited by T_{inh}A01, from a mean of -647 ± 152 pA under control conditions to -30 ± 25 pA in the presence of the drug (n=6, $p<0.05$, paired t test).

Next we investigated the effect of T_{inh}A01 on contractions of RUSM evoked by electrical field stimulation at frequencies of 2, 4 and 8Hz (pulse width 0.3 ms, nominal amplitude 20 V). T_{inh}A01 significantly reduced the peak contraction evoked during 4Hz stimulation from a mean value of 2 ± 0.4 mN under control conditions to 0.4 ± 0.1 mN in its presence (n=9, $p<0.05$). In addition, T_{inh}A01 also decreased spontaneous myogenic tone in strips of RUSM by 0.4 ± 0.07 mN. Finally, contractions of RUSM evoked by exogenous application of phenylephrine (1 μM) were inhibited by T_{inh}A01 from a mean value of 8.9 ± 1.9 to 7 ± 1.4 mN (n=8, $p<0.05$). Taken together these data suggest that TMEM16A channels contribute to I_{ClCa} in urethral ICC and that these channels are crucially involved in the generation and modulation of urethral tone.

Hashitani H, Van Helden DF, Suzuki H. Properties of spontaneous depolarizations in circular smooth muscle cells of rabbit urethra. Br J Pharmacol. 1996 Aug;118(7):1627-32.

Sergeant GP, Hollywood MA, McCloskey KD, Thornbury KD, McHale NG. Specialized pacemaking cells in the rabbit urethra. RAPID REPORT Journal of Physiology. 2000 Jul 15; 526 Pt 2:359-66.

Dr Timothy Webb is supported by Enterprise Ireland's Applied Research Enhancement Programme

Where applicable, the authors confirm that the experiments described here conform with The Physiological Society ethical requirements.

PCB376

Oxytocin reduces the tocolytic effect of magnesium sulphate in human myometrium

S. Arrowsmith[1], H. Wood[1], J. Neilson[2] and S. Wray[1]

[1]Department of Cellular and Molecular Physiology, University of Liverpool, Liverpool, UK and [2]Department of Women's and Children's Health, University of Liverpool, Liverpool, UK

Magnesium sulphate (Mg) *in vitro* directly relaxes smooth muscle including myometrium. It is thought to compete with Ca thus, inhibit L-type Ca channel entry and contractility. Currently, the clinical evidence for using Mg as a tocolytic agent, such as for threatened preterm labour, is questionable: A Cochrane systematic review concluded that Mg for tocolysis *in vivo* is ineffective(1). We investigated whether the presence of the hormone oxytocin, which also effects calcium signalling dynamics, alters the tocolytic capability of Mg on human myometrium *in vitro* and if the effect (if any) could be reversed with the oxytocin antagonist, atosiban.

Methods: Isometric tension recordings were performed on strips of myometrium (1x5x2mm) obtained from 10 pregnant women undergoing pre-labour Caesarean section (with consent and ethical approval). Paired strips from the same woman were superfused with physiological saline and the effect of increasing [Mg] from 1.2mM (control) to 12mM in the presence and absence of oxytocin (0.5nM) was compared by calculating the mean effective concentration causing 50% reduction in force amplitude of contraction (EC50). In a subset of experiments (n=4), the effect of increasing [Mg] in the presence of Atosiban (10^{-7}M) on oxytocin-induced contractions was compared to Mg alone.

Results: Elevated [Mg] produced a significant, dose-dependent inhibition of phasic, spontaneous myometrial contractions: EC50 2mM, complete inhibition achieved at 3.4mM. In contrast, application of oxytocin significantly increased the [Mg] required to affect contractions, such that at 2mM Mg there was little reduction in force amplitude (98.5% of control). The EC50 was 10mM and full abolition of activity in all but 2 cases was achieved at 12mM (i.e.10 times greater than [Mg] in control solution). The addition of Atosiban reduced the [Mg] at which oxytocin-induced contractions were inhibited, from 12mM to 6mM.

Conclusion: *In vitro*, Mg at therapeutic doses (<2.5mM) significantly reduces spontaneous contractility of the myometrium however, the effect of Mg is significantly reduced in the presence of oxytocin; it is only effective at suprapharmacological concentrations. We suggest that the changed hormonal milieu in pregnancy, specifically towards oxytocin, underlies the poor tocolytic ability of Mg *in vivo*. Preliminary data suggest atosi-

ban may reduce the EC50 for Mg and raises the question of whether, clinically, oxytocin antagonists should be used in combination with Mg for uterine tocolysis.

1. Crowther CA, Hiller JE, Doyle LW. Magnesium sulphate for preventing preterm birth in threatened preterm labour. Cochrane Database of Systematic Reviews 2002, Issue 4.

We would like to acknowledge Sparks for funding this research.

Where applicable, the authors confirm that the experiments described here conform with The Physiological Society ethical requirements.

PCB377

Role of BDNF-TrkB signaling in neuromuscular junction remodeling

G. Sieck, L. Ermilov, D. Sieck, W. Zhan and C. Mantilla

Mayo Clinic, Rochester, MN, USA

Our working hypothesis is that synaptic remodeling at the neuromuscular junction is an active process that ensures proper matching between presynaptic activity and postsynaptic response under varying conditions. In this study we specifically hypothesize that this synaptic remodeling requires TrkB signaling at the presynaptic terminal. TrkB signaling requires the presence of the full length receptor (TrkB.FL) and is dependent on phosphorylation and activation of a tyrosine kinase. Using laser capture microdissection coupled with quantitative RT-PCR and protein analyses, we found that TrkB.FL is present only in phrenic motoneurons, but not in diaphragm muscle fibers. Using a specific siRNA we knocked down TrkB expression in phrenic motoneurons and found impairment of neuromuscular transmission that was associated with altered presynaptic remodeling. Using mice expressing knockin alleles that allow selective inhibition (via 1NMPP1 treatment) of Trk kinase activity (TrKBF616A) we also demonstrated impaired neuromuscular transmission and altered presynaptic remodeling. In both cases, the impairment in presynaptic remodeling involved apparent retraction of axon terminals with accumulation of neurofilament. These changes in presynaptic terminals occurred in the absence of any alterations in muscle structure or contractile function. Using a-bungarotoxin to identify postsynaptic cholinergic receptors, there was no apparent change in end-plate area or cholinergic receptor density after 2 weeks. However, previously we did observe changes in postsynaptic ultrastructure including reduced gutter depth and branching complexity which may be attributed to presynaptic effects. Together, these results support the role of endogenous TrkB signaling in neuromuscular junction remodeling.

Where applicable, the authors confirm that the experiments described here conform with The Physiological Society ethical requirements.

PCB378

Effects of 8-Br-cAMP and forskolin on spontaneous activity in isolated rabbit corpus cavernosusm myocytes

C. McCloskey, G.P. Sergeant, M.A. Hollywood, N.G. McHale and K.D. Thornbury

Smooth MuscleResearch Centre, Dundalk Institute of Technology, Dundalk, Co Louth, Ireland

When corpus cavernosum smooth muscle cells (CCSMC) relax, the corporal sinuses fill with blood causing penile erection. Thus knowledge of the mechanisms that cause corpus cavernosum relaxation is essential for understanding and treating erectile dysfunction. Although NO/cGMP is the main inhibitory pathway involved in penile erection, when the NO receptor is knocked out other pathways can compensate (Groneberg et al. 2013). One possibility is that cAMP production, in response to agonist such as adenosine, VIP or PGE1 may mediate relaxation. However, the effects of cAMP on CCSMC have not been adequately characterised. The aim of this study, therefore, was to characterise the effects of cAMP on spontaneous Ca2+-activated Cl- currents, spontaneous depolarisations and Ca2+ events in isolated CCSMC. All of the experiments were approved by DkIT Animal Care Committee. Male New Zealand white rabbits were euthanized with pentobarbitone (iv) and their corpora cavernosum removed. CCSMC were isolated with collagenase and perfused with physiological saline at 37oC. Their electrical events were studied using the patch clamp technique, and their intracellular Ca2+ events were recorded by loading them with Fluo-4AM (500 nM) and imaging with an EMCCD camera attached to a spinning disk confocal microscope.

When CCSMC were voltage clamped at -60 mV, they developed regular spontaneous transient inward currents (STICs), mediated by Cl- channels. 8-Br-cAMP (1 mM) reduced their amplitude from 193± 33pA to 62±39 pA (n=5, P<0.05) and frequency from 20.4 ±6.6/min to 6.4±3.0/min (P<0.05). Forskolin (1 μM) also decreased the frequency from 41.0 ± 13.6 to 14 ± 5.0/min (P<0.05, n=5), but increased amplitude from 323±102 pA to 613±153 pA (P<0.05). When held in current clamp mode, the cells developed regular spontaneous transient depolarisations (STDs). There were reduced in frequency both by 8-Br-cAMP (from 26.4±8.2/min to 11.6±6.1/min, n=5, P<0.05) and forskolin (from 42.4±10.8/min to 12.0±6.1/min, n=5, P<0.05), but both drugs increased the mean duration at half maximum amplitude (8-Br-cAMP from 140±60 ms to 309±136 ms, n=5, P<0.05; forskolin from 340±111 ms to 557±95, n=4, p<0.05).

CCSMC also developed robust global intracellular Ca2+ events that extended along the entire length of the cell. These were also inhibited by 8-Br-cAMP, which reduced their frequency from 15.6±2.9/min to 2.7±1.2/min, (n=5, p<0.05) and reduced basal Ca2+ (F/F0) from 1 to 0.70±0.04 (P<0.05, Wilcoxon). Similarly, forskolin decreased frequency from 19.8±3.4/min to 6.0±1.5/min (n=6, P<0.05) and basal Ca2+ from 1 to 0.66±0.04 (n= 6, P<0.05).

These results suggest that cAMP may reduce tone in CCSMC by inhibiting spontaneous pacemaker activity. This is similar to the action of NO/cGMP described previously (Sergeant et al. 2009).

Groneberg D, Lies B, König P, Jäger R, Friebe A. Preserved fertility despite erectile dysfunction in mice lacking the nitric oxide receptor. J Physiol. 2013, 591:491-502.

Sergeant GP, Craven M, Hollywood MA, McHale NG, Thornbury KD. Spontaneous Ca2+ waves in rabbit corpus cavernosum: modulation by nitric oxide and cGMP. J Sex Med. 2009, 6:958-66.

This work was funded by Science Foundation Ireland (RFP/BIMF377).

Where applicable, the authors confirm that the experiments described here conform with The Physiological Society ethical requirements.

PCB379

Angiotensin 1- 7 inhibits angiotensin II –induced calcium signal in pulmonary arterial smooth muscle cells

O.A. Ogunbayo, H. Yang and M.A. Evans

Centre for Integrative Physiology, University of Edinburgh, UK, Edinburgh, UK

Angiotensin (Ang) II, a vasoactive peptide and one of the main components of the rennin-angiotensin system (RAS), plays a very significant role in regulating blood pressure and may drive in part, the progression of pulmonary arterial hypertension (1). PAH is caused by functional and structural modifications in the pulmonary vasculature, resulting in increased resistance. This remodeling is accompanied by endothelial dysfunction, smooth muscle cell activation and recruitment of circulating progenitor cells (2). PAH contributes to the development of cardiovascular complications and despite advances in antihypertensive drug therapy, uncontrolled hypertension is still prevalent globally (3). Ang 1- 7, an ACE2 (Angiotensin Converting Enzyme 2)-derived metabolite of Ang II exerts cardioprotective effects and is regarded as a potential antagonist of Ang II (1, 4).
Using methods described previously (5), we assessed the mechanism of Ang II–induced Ca2+ signalling in acutely isolated rat pulmonary arterial smooth muscle cells (PASMCs) and the effect of Ang 1-7 on these responses. Extracellular application of 3μM Ang II evoked a robust Ca2+ transient in acutely isolated rat PASMCs, the Fura-2 fluorescence ratio (F340/F380) increasing from 0.44±0.01 to 1.19±0.05 (n=67). Ang II-evoked Ca2+ transients were abolished by the AT1R blocker Losartan (10μM; F340/F380 ratio increasing from 0.68±0.05 to 0.81±0.08 (n=9)), but remained unaffected by the AT2R blocker PD123319 (50μM; F340/F380 ratio increasing from 0.55±0.04 to 1.36± 0.06 (n=9)). Surprisingly, although Ang 1-7 (3μM) had little effect on intracellular calcium in its own right, it significantly attenuated Ang II-evoked Ca2+ transients; Ang II increasing the F340/F380 ratio from 0.46±0.04 to 0.72±0.07 (n=23) in the presence of Ang1-7.
We conclude that Ang II induces Ca2+ signals in rat PASMCs by activating AT1Rs and thus induces voltage-gated Ca2+ influx via L-type Ca2+ channels and SR Ca2+ release via RyRs, and in a manner that is be opposed by Ang 1- 7.

Gomes et al., 2012 International of Hypertension. Vol 2012, Article ID 493129

1. Gomes et al., 2012 International of Hypertension. Vol 2012, Article ID 493129

Morrell et al., 2009 J. Am Coll. Cardio. Vol 54. S20- S31.

Chobanian, 2009 The New England J Med. Vol 361. 878- 887.

Grobe et al., 2007. Amer. J. Physiol. Heart Circ Physiol. Vol 292; 736-742

Kinnear et al., 2004. J Biol Chem Vol 279(52): 54319-26.

Where applicable, the authors confirm that the experiments described here conform with The Physiological Society ethical requirements.

PCB380

Investigation of role of "funny" (If) current in spontaneous and agonist-stimulated contractions in isolated rat myometrium

A. Ayar[1], O. Gedikli[1], A. Kurt[1], R. Sahan[1] and M. Ozcan[2]

[1]Department of Physiogy, Faculty of Medicine, Karadeniz Technical University, Trabzon, Turkey and [2]Department of Biophysics, Faculty of Medicine, Firat University, Elazig, Turkey

Mechanisms underlying generation of spontaneous myometrial contractions are poorly understood. Although morphological evidence indicates existence of interstitial cell of Cajal-like cells in myometrium it remains unclear whether these cells are involved in uterine pacemaking. The "funny" (If) current (or funny channel or pacemaker current), originally described in sinoatrial node and Purkinje fibers, are currently investigated for their potential role(s) in smooth muscles with generation of spontaneous phasic activity. The aim of this study was to obtain pharmacological evidence for the possible role of funny ion channels in spontaneous and agonist - stimulated contractions in isolated rat myometrium using the pharmacological blocker ivabradine. Myometrial strips were removed from nonpregnant rats and placed in an organ bath containing physiological salt solution at 37°C and pH 7.4, constantly bubbled with 95% oxygen-5% carbon dioxide and isometric contractions were recorded. Effects of cumulative concentrations of ivabradine (1, 3 and 10 uM) on amplitude, area-under contractile curve and frequency of spontaneous and oxytocin-and prostaglandin F2 alpha-induced contractions were studied by 10-minutes intervals. Statistical analysis was performed using one –way ANOVA and post-hoc tests were performed with Tukey HSD. Ivabradine (at any cumulative concentration) did not have any significant effect on either contractile parameter (amplitude, AUC or frequency) of spontaneous (n=6) and agonist induced contractions stimulated by oxytocin (n=7) or prostaglandin F2alpha (n=7). Results from this in vitro study involving myometrial strips from nonpregnant rat indicates that, funny currents does not have any significant role(s) in spontaneous contractions and nor they involve in agonist-induced phasic contractions.

Where applicable, the authors confirm that the experiments described here conform with The Physiological Society ethical requirements.

PCB381

Enhanced contractility in the rat diabetic bladder: correlation with cellular remodelling

L. Johnston, K.M. Monaghan, B. McDonnell and K. McCloskey

Queen's University Belfast, Belfast, UK

Diabetes is an increasingly prevalent condition worldwide and is associated with a range of comorbidities including bladder dysfunction (1). The diabetic bladder exhibits an overactive phenotype arising from neurogenic and myogenic mechanisms; moreover, changes in the cellular architecture of the bladder wall occur. The purpose of the present study was to

investigate cellular remodelling in the rat diabetic bladder and correlate with in vitro contractility.
Bladders were removed from Sprague-Dawley female rats – either non-injected controls or diabetics following a single injection of streptozotocin (in accordance with local ethical committee approval and with the UK Animal Procedures Act. Tissue strips were prepared as full thickness or detrusor layers (mucosal layer removed) and studied with in vitro myography. Tissues were also processed for immunohistochemistry. Data are presented as mean±SEM and analysed by ANOVA/Student's t-test.
Diabetic rats (N=8) had significantly lower body mass than non-injected controls (N=6; p<0.042) however; mean bladder /body mass ratio for diabetics (1.96±0.42, N=8) was significantly greater than controls (0.48±0.05, N=6; P=0.01) indicative of smooth muscle hypertrophy. This was confirmed by imaging protocols. Spontaneous activity in full thickness and detrusor strips from diabetic bladder was significantly greater than controls. Control contraction amplitude in full thickness strips was 0.12±0.03g, n=8, N=4) compared with diabetic strips 0.22±0.03g (n=12, N=6, p=0.017). Neurogenic contractions, evoked by electrical field stimulation in the same preparations, were of greater amplitude in diabetic strips across a range of frequencies in both full thickness and detrusor preparations. Contraction amplitude at 16Hz in full thickness control strips was 3.94±0.52g (n=8, N=4), smaller than in diabetic strips 5.96±0.43g (n=12, N=6, P<0.01). Carbachol-evoked contractions (1μM) were significantly greater in diabetic strips whether or not the mucosal layer was present. In full thickness control strips, carbachol-evoked amplitude was 1.49±0.29g (n=10, N=5, p<0.05) compared with 3.01±0.42g (n=12; N=6; p<0.05). Extensive networks of Interstitial Cells (IC), labelled with PDGFRα were distributed in the lamina propria and detrusor layer of control bladders. In diabetic bladders, PDGFRα+-IC were notably disrupted in the detrusor layer but were present in the in the lamina propria.
In conclusion, enhanced contractility in the diabetic bladder; spontaneous activity, neurogenic and agonist-evoked contractions occurs in the presence or absence of the mucosal layer. This altered contractility is correlated with smooth muscle hypertrophy and disruption of detrusor IC.

Kirschner-Hermanns R, Daneshgari F, Vahabi B, Birder L, Oelke M, Chacko S.

Does diabetes mellitus-induced bladder remodeling affect lower urinary tract function? ICI-RS 2011.

Neurourol Urodyn. 2012 Mar;31(3):359-64.

Financial support was received from the European Union, FP7 "INComb" (FP7-HEALTH-2007-B).

BMcD is in receipt of a DEL studentship, Queen's University Belfast.

Where applicable, the authors confirm that the experiments described here conform with The Physiological Society ethical requirements.

PCB382

Retention of caveolae morphology during physiological mechanosensitisation of resistance arteries

M. Sweeney, C. Nicholson and M.J. Taggart

Institute of Cellular Medicine, University of Newcastle, Newcastle upon Tyne, UK

Caveolae are Ω-shaped invaginations of the plasma membrane containing a variety of proteins that have been suggested to participate in the orchestration of many signal transduction events including that of mechanosensitisation. For example, it has recently been reported that cultured HeLa cells respond to hypo-osmotic swelling by rapid (5 mins) disassembly of caveolae and membrane 'flattening' (Sinha et al (2011)). Resistance artery smooth muscle cells have abundant caveolae (Tong et al (2009)) and are highly mechanosensitive. This myogenic reactivity is commonly evinced as an initial dilation to an elevation in intralumenal pressure followed by an active vasoconstrictive response to return the vessel towards its initial diameter. It is physiologically important in maintaining tissue blood flow and minimising pre-capillary blood pressure surges. The purpose of this study was to determine if the morphological appearance of caveolae in vascular smooth muscle cells of resistance arteries, *in situ*, were altered in response to physiological mechanical stress, i.e. an increase in intravascular pressure. Uterine artery segments dissected from 3 month old C57BL mice were mounted in a pressure myograph (physiological salt solution, 5%CO_2-air, 37°C) for continuous monitoring of diameter. Intravascular pressure was initially set at 60mmHg and arteries allowed to equilibrate for 60 mins (diameter=156.2(±15.3)μm, mean(±SEM), n=10) before being exposed to physiological mechanical stress by increasing the intravascular pressure to 120mmHg. This caused vasodilation with a peak of +0.19 (±0.04)-fold change in diameter from 60mmHg. Subsequent myogenic contraction constricted vessel diameters to less than that (-0.13 (±0.05)-fold change c.f. to 60mmHg) previously observed at 60mmHg. Arterial segments in three conditions (i) resting 60mmHg intravascular pressure, (ii) 120mmHg intravascular pressure at peak dilation, (iii) 120mmHg intravascular pressure with myogenic contraction, were fixed within 1-2 seconds and processed for electron microscopic examination of caveolae. In each condition 3-5 segments (two sections of each) were examined. Figure 1 shows one electron micrograph of vascular smooth muscle cells from each of the three conditions. In each, rows of caveolae could be observed along the length of the plasma membrane of the vascular smooth muscle cells. There was no evidence of flattening of the caveolae structure in any sections examined. These results indicate that the integrity of caveolae is retained in vascular smooth muscle cells exposed to an acute, physiological mechanical stress. In addition to data from non-vascular smooth muscle (Gabella and Blundell (1978)), these results suggest that caveolae morphology can be retained during physiological mechanosensitisation.

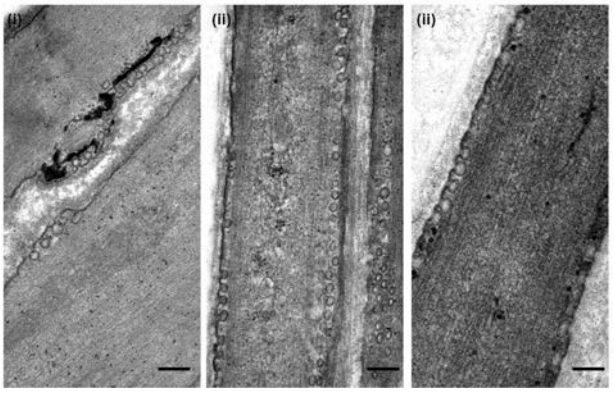

Figure 1. Electron micrographs showing caveolae in vascular smooth muscle cells in each condition. (i) 60mmHg resting, (ii) 120mmHg peak dilation, (iii) 120mmHg myogenic contraction. Black bar = 200nm.

Sinha B *et al.* (2011). *Cell* **144**, 402–413.

Tong WC *et al.* (2009). *J Cell Mol Med* **13**, 995-998.

Gabella and Blundell (1978). *Cell Tiss Res* **190**, 225-271.

Dr. K. White, T. Davey, EM Research Services, Newcastle University

Where applicable, the authors confirm that the experiments described here conform with The Physiological Society ethical requirements.

PCB383

Interrelation between pyeloureteral and peribladder zones pacemaker activity

L. Simonyan and K. Kazaryan

Smooth muscle physiology, L.A.Orbeli Institute of Physiology, Yerevan, Armenia

The ureteral smooth muscle is characterized by a highly autonomous zone, acting as a pacemaker in pyeloureteral anastomosis. Stable slow automaticity promotes the subsequent emergence of spikes along with the ureter, which in turn provides the primary functional significance of the organ is peristaltic activity (1).
The ability of each ureteral individual cell to generate spontaneous electrical waves of excitation can assume about the existence of various rhythmogenic zones (2).
The subsequent identification of automatism also in the bordered area to the bladder pushes the task of studying the mechanisms of interaction between the two rhythmogenic regions in order to ensure functional activity of the whole ureter (3).
All experiments were carried out in situ on white "Albino" rats (300-350g, n=12) anesthetized by Nembutal (50-55mg/kg) intraperitoneally. The ureter was denervated by the section of the splanchnic and pelvic nerves roots. The spike activity was registrated with silver bipolar electrodes, the slow wave activity with silver monopolar ball electrodes by 8-channel EEG. Analysis of the results was carried out using modern packages Lab View software and Origine-8. All experiments were verified by the t-student test.
The histamine was used (Sigma-Aldrich, Germany). The drug was injected into the femoral vein (in 0.2 ml solution) in different concentrations: 10-6, 10-5 and 10-4 Mol/l (n=9).
Morpho-histochemical studies were performed by the orthophosphates detection method. This method allows tracking the smallest functional changes in cellular structures of the organ.
All procedures are performed according to "principles of laboratory animal care" (NIH publication 85-23 revised 1985). The killing was carried out with a lethal dose of anesthetic.
The automatism of perirenal zone is 22±2.05 and peribladder:11±0.67, n=13, $p<0.01$ under normal conditions in rat. The effect of disturbances of propagating spontaneous activity of pyeloureteral anastomosis to the bladder has been studied. The local cooling of the middle portion of ureter showed a small increase (up to 20-22%, n=10) of slow waves genesis of peribladder zone. Conduction disturbance between two ending zones of the rat ureter is also realized by the transection of ureter in its middle part. After a certain period of time in all cases, there was decrease in the frequency of primary pacemaker: 17±1.8 oscillations/min, $p<0.01$ and, respectively, passing the spikes. However, there is some increased frequency of slow waves in the junction of the ureter to the bladder (4). These data show the impact of the primary ureteral rhythmogenesis on the automatism of distal zone: excitatory propagating waves some reduce the genesis of distal autonomous waves.
Of all the variety of physiologically active compounds, changing the excitability of the membrane of ureteral smooth muscle tissue, the histamine causes a certain interest which is able not only to regulate spontaneous activity, but create slow pacemaker oscillations of membrane potential. Such regulation is associated with a high prevalence in the tissues of this organ with one hand H1-histamine receptors, and with another- the presence of mast cells capable of releasing histamine (5).
The subsequent injection of histamine into the femoral vein of the animal at a concentration of 10-4Mol/l leads to a sharp change of certain characteristics of both types of electrogenesis. The increasing rhythm as slow waves as well action potentials has been observed: 24.5±2.6 oscill/min (n=9) increase to 44.3±4.2 oscill/min, n=12, $p<0.01$. It is noted also the improving of conductivity and each spike that occurs on the base of a slow wave, as a rule, reaches the peribladder zone.
The regulatory role of histamine is expressed by activation of ureteral renal zone rhythmogenesis. It is also shown improvement in the conductivity of the propagating wave of excitation to the bladder, and the disturbed coordination of spike activity with slow waves in bordered area with bladder. Morphological analysis of the effect of histamine showed intense staining of cellular elements of the muscular layer in the area of kidney and bladder sections of ureter, which indicates a high functional status of these areas.
Slow-wave activity of peribladder area can be connected to the above-noted leadership role under the suppression of kidney automatism, or transection of the ureter. Lack of coordinated activity between the two ending zones of the ureter may indicate a backup role of peribladder pacemakers in norm. The peribladder area of the ureter, despite the relatively low-frequency of spontaneous activity in comparison with the basic renal pacemaker is characterized by polymodality and may provide a functional role of the ureter.

Lang RJ et al. (2010). Clin Exp Pharmacol Physiol 37, 509-515.

Karen DMcCloskey (2011). In handbook: Handbook of Exper Pharmacology, Urinary Tract, 233-254.

Osman F et al. (2009). Acta Physiologica Hungarica 96,409-26.

Kazaryan K.V. et al. (2010). Jour Evol Biochemistry and Physiology 46, 471-476.(in Russia)

Yilmaz E. et al. (2009). Urology Journ 73, 32-36.

Where applicable, the authors confirm that the experiments described here conform with The Physiological Society ethical requirements.

PCB385

Characterisation of spontaneous activity in the human prostate gland

B. Chakrabarty[1], M. Frydenberg[4], N. Lawrentschuk[3], G. Risbridger[2] and B. Exintaris[1]

[1]Drug Discovery Biology, Monash Institute of Pharmaceutical Sciences, Melbourne, VIC, Australia, [2]Department of Anatomy and Developmental Biology, Monash University, Melbourne, VIC, Australia, [3]Department of Surgery, University of Melbourne, Melbourne, VIC, Australia and [4]Department of Surgery, Monash University, Melbourne, VIC, Australia

Introduction: Changes in spontaneous electrical activity promote an increase in prostatic tone and contractility in the guinea pig prostate gland (Dey et al., 2009). These contractions are likely to be regulating the resting smooth muscle tone of the prostate gland, a major component implicated in Benign Prostatic Hyperplasia (BPH); the most common neoplasm in men. BPH occurs in the transition zone (TZ), as opposed to the peripheral zone (PZ). However, the aetiology of BPH remains poorly understood, and the fundamental reason there is an increase in prostatic smooth muscle tone with age remains unknown. This study focuses on understanding the changes in basic physiology underlying the increase in prostatic tone with age, to ultimately identify a novel therapeutic target that targets the origins and underlying cellular mechanisms of spontaneous activity to potentially treat BPH. Our overall hypothesis is that age-related changes in the mechanisms regulating spontaneous activity of the prostate gland, significantly contribute to the pathogenesis of BPH. In this study, we characterised the spontaneous contractile activity in prostate specimens from 14 men.

Methods: TZ and PZ specimens were obtained from consenting patients undergoing a prostatectomy. Subsequent recordings were made from prostatic preparations (3mmx10mm) using conventional tension recording experiments (Dey et al., 2010).

Results: All specimens from the TZ displayed spontaneous contractions at 1.94±0.19 min^{-1}, with an average amplitude of 0.20±0.03 N g^{-1} (n=14). Spontaneous contractions were abolished in 71% of TZ preparations by an L-type Ca2+ channel blocker, 1μM nifedipine (n=7). Application of neurotransmission blockers, 1μM tetrodotoxin (n=5), 1μM guanethidine (n=4), and 1μM atropine (n=6), had no significant effects on frequency of spontaneous contractions in the TZ (Student's paired t-test, P>0.05). Spontaneous contractions in the PZ were significantly more frequent at 4.64±0.49 min^{-1}, in comparison to the frequency of spontaneous contractions at 2.09±0.41 min^{-1} in the TZ from the same patients (Student's paired t-test, P<0.05, n=5).

Conclusions: This study suggests that spontaneous contractions in the TZ may be myogenic in nature. Furthermore, mechanisms regulating spontaneous contractility may be zone-specific. This study provides novel insight into the basic physiology of the human prostate gland.

DEY, A., KUSLJIC, S., LANG, R. J. & EXINTARIS, B. 2010. Role of connexin 43 in the maintenance of spontaneous activity in the guinea pig prostate gland. Br J Pharmacol, 161, 1692-707.

DEY, A., NGUYEN, D. T., LANG, R. J. & EXINTARIS, B. 2009. Spontaneous electrical waveforms in aging guinea pig prostates. J Urol, 181, 2797-805.

Where applicable, the authors confirm that the experiments described here conform with The Physiological Society ethical requirements.

PCB386

Enhancement of BK channel activity in vascular smooth muscle (VSM) cells by cGMP-dependent protein kinase-induced phosphorylation of identified serine residues

B.D. Kyle, S. Hurst, P.S. Dhaliwal and A.P. Braun

Physiology and Pharmacology, University of Calgary, Calgary, AB, Canada

Background: VSM excitability is regulated by large conductance, calcium-activated K^+ (BK) channels. NO elevates VSM cytosolic cGMP levels, and activates the type I cGMP-dependent protein kinase (cGKI) to phosphorylate the BK channel at key residues. The nature and location of residues phosphorylated remain unresolved, along with their functional importance to the channel enhancement process.

Purpose: To identify key phosphorylatable residues underlying the NO/cGMP/cGKI-mediated BK channel enhancement in VSM and correlate their functional contribution with their phosphorylation status.

Procedures: Proximity ligation assay (PLA) was used to show BKα subunit and cGKI protein co-localization (spatial restriction <40 nm). *In vitro* phosphorylation of immune-purified wild type (WT, GenBank Acc# U09383) BK channel by cGKIα was characterized biochemically using radiolabeled γ^{32}ATP to identify phosphorylated residues using a combination of phosphoamino acid (AA) analysis and peptide mapping. Identified residues were individually replaced and mutant channels were transiently-transfected into A7r5 cells (Lipofectamine method), and studied under cell-attached patch clamp using 1s voltage ramps (-30mV to 200mV, 0mV holding potential).

Results: Freshly isolated rat cerebral VSM cells exhibited PLA fluorescence indicating BKα-cGKI association. Extensive association was also observed in A7r5 cells transiently-expressing BK channels. Non-transfected cells showed no measurable fluorescence.

Biochemical characterization of BK channels phosphorylated by purified cGKI *in vitro* revealed ^{32}P-labeled phosphoserine residues at "Arg/Lys-Arg/Lys/X-X-pSer" locations (where X is any AA). Using these criteria, 9 potential Ser residues were identified within the BKα subunit (see Figure 1). For each location, the critical Ser residue was mutated to Ala and mutant channels were expressed in A7r5 cells for functional analysis. Phosphorylation of WT BK channels by cGKI using γ^{32P}-ATP revealed a major ~120 kDa ^{32}P-labelled band corresponding to the BKα subunit. However, the ^{32}P-labeling intensity was clearly reduced in 3 mutant channels (25%, 50% and 60% reductions at Ser691, Ser873 and Sers1111-1113, respectively), indicating multiple phosphorylation sites.

Recordings from A7r5 cells expressing WT BK channels confirmed current enhancement to NO/cGMP/cGKI pathway stimulation (spermine-nonoate, 5 μM; db-cGMP, 100 μM). However, BK channels containing Ser to Ala substitutions at each of the 3 sites exhibiting low ^{32}P-labeling intensities exhibited no enhancement.

This study uncovers a definitive molecular mechanism explaining the BK channel enhancement following cGMP production *in situ*.

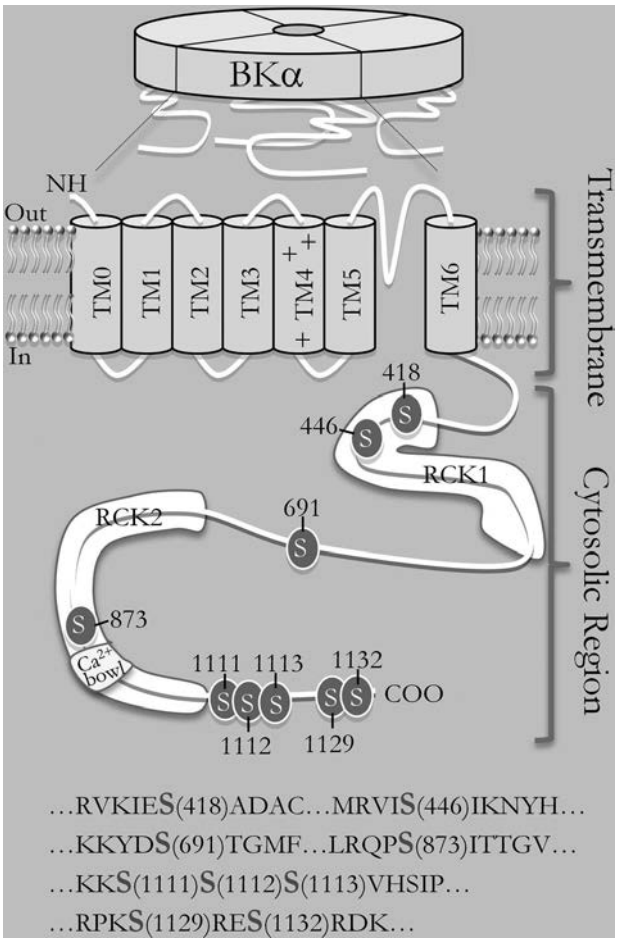

Figure 1 - BKα subunit Ser to Ala mutations; numbering reflects the predicted AA sequence of the BKα subunit cDNA, beginning with the N-terminal sequence MDALI...

This work was funded by research grants to A.P.B. from the CIHR and NSERC. B.D.K. was supported in part by a Kertland Family Fellowship.

Where applicable, the authors confirm that the experiments described here conform with The Physiological Society ethical requirements.

PCB387

Abnormal phosphorylation of myosin light chain phosphatase and myosin downstream of Rho-associated kinase contributes to the dysfunctional cerebral myogenic response of Goto-Kakizaki rats

K.S. Abd-Elrahman[1,2], E.J. Walsh[1,2], M.P. Walsh[1,3] and C.C. William[1,2]

[1]Smooth Muscle Research Group, University of Calgary, Calgary, AB, Canada, [2]Physiology and Pharmacology, University of Calgary, Calgary, AB, Canada and [3]Biochemistry and Molecular Biology, University of Calgary, Calgary, AB, Canada

The myogenic response of cerebral arteries is responsible for intravascular pressure-dependent control of blood flow to the brain1. This mechanism depends on cellular processes intrinsic to vascular smooth muscle cells (VSMCs) including: 1) Ca2+ influx, Ca2+- dependent activation of myosin light chain kinase, and phosphorylation of the 20 kDa regulatory light chains (LC20) of myosin, and 2) Rho-associated kinase (ROK)-dependent phosphorylation of the myosin targeting subunit (MYPT1) of myosin light chain phosphatase and suppression of the phosphatase activity2. Inappropriate regulation of these intrinsic mechanisms leading to dysfunctional control of cerebral arterial diameter may contribute to ischemic and hemorrhagic stroke in type 2 diabetes (T2D)3. Here, we used the Goto-Kakizaki (GK) rat model of T2D to determine if specific alterations in LC20 and MYPT1 phosphorylation contribute to dysfunctional control of cerebral arterial diameter. Rats were killed by halothane inhalation and exsanguination. Endothelium-denuded middle and posterior cerebral arteries of 8-10 and 18-20 week old GK and Wistar (WR) control rats were studied by pressure myography to detect pressure-dependent alterations in diameter (n=8), and by western blotting to quantify changes in LC20 and MYPT1 phosphorylation levels at 10, 60 and 120 mmHg (n=6)4. Values were expressed as mean±SEM and compared by ANOVA. Pressure-dependent increases in phospho-LC20 (from 26±0.5% to 38±1% and 49±1%; $p<0.05$) and phospho-MYPT1-T855 (from 1.0 to 2.0±0.15 and 2.8±0.18 normalized units; $p<0.05$) were detected at 10, 60 and 120 mmHg in vessels of 8-10 and 18-20 wks WR. Vessels of 8-10 wks GK had a compromised myogenic response, with enhanced constriction at low pressure and forced dilation at >100 mmHg, that progressed to a loss of myogenic tone in 18-20 wks GK. Phospho-MYPT1-T855 was elevated at 10 mmHg in 8-10 wks GK compared to WR (1.42±0.04-fold; $p<0.05$), and no increase was detected with pressure elevation to 60 or 120 mmHg (1.54±0.1 and 1.45±0.12). Phospho-LC20 was similarly elevated at 10 mmHg (35±1.8%) in 8-10 wks GK vessels, but no increase was detected on pressure elevation to 60 or 120 mmHg (40±1.9% and 37±2%, respectively). Phospho-LC20 and phospho-MYPT1-T855 levels of 18-20 wks GK and WR were not different at 10 mmHg, but a pressure-dependent increase in phosphorylation was not detected in GK. Inhibition of ROK with H1152 (0.5 μM) abolished the enhanced constriction at low pressure in 8-10 wks GK and suppressed the residual tone of vessels from 18-20 wks GK. Our findings suggest that a progressive dysfunctional control of ROK activity, and consequently inappropriate MYPT1 and LC20 phosphorylation, contribute to the abnormal myogenic response in cerebral resistance arteries of T2D GK rats.

Bayliss W.M. (1902) On the local reactions of the arterial wall to changes of internal Pressure. J Physiol 28: 220-231.

Cole W.C., Welsh D.G. (2011) Role of myosin light chain kinase and myosin light chain phosphatase in the resistance arterial myogenic response to intravascularpressure. Arch Biochem Biophys 510: 160-173.

Goralski K.B., Sinal C.J. (2007) Type 2 diabetes and cardiovascular disease: getting to the fat of the matter. Can J Physiol Pharmacol 85: 113-132.

Johnson R.P., El-Yazbi A.F., Takeya K., Walsh E.J., Walsh M.P., Cole W.C. (2009) Ca2+ sensitization via phosphorylation of myosin phosphatase targeting subunit at threonine-855 by Rho kinase contributes to the arterial myogenic response. J Physiol 587: 2537-2553.

Where applicable, the authors confirm that the experiments described here conform with The Physiological Society ethical requirements.

PCB388

Alterations to spontaneous activity during mild, moderate and severe heating of isolated pig bladder preparations

D. Kitney, R.I. Jabr and C. Fry

Biochemistry and Physiology, University of surrey, Surrey, UK

Detrusor overactivity is a highly prevalent disorder severely affecting patient quality of life and is significantly associated with increased spontaneous activity in isolated bladder wall preparations. Therefore reducing spontaneous activity offers a means to relieve detrusor overactivity. Previously, we have shown that mild heating (42°C) of isolated bladder strips reversibly reduced spontaneous activity without tissue damage and we have tested the hypothesis that greater heating to 46°C (moderate) and 50°C (severe) exerts more profound reduction.

Pig bladders were obtained from a local abattoir and stored in cold Tyrode's solution (95%O_2:5%CO_2,4°C). The ventral wall was opened longitudinally and bladder wall preparations (10x20mm) were dissected and mounted in a horizontal trough superfused with Tyrode's (10ml/min). Isometric contractions were recorded at 37°C or during heating, generated by a heating coil placed directly above the superfusate surrounding the strip. Strips were exposed to either repeated 15 minute 50°C exposures or successive 42, 46 and 50°C with 30 minutes at 37°C between interventions. The amplitude, area under the curve (AUC) and frequency (*f*) of spontaneous contractions were measured for 10 minute periods at the end of control or heating periods. Time controls were done with no heating. Data are mean±S.D., the null hypothesis was rejected at $p<0.05$ using paired Student's *t*-tests.

Repeated exposure of severe heating increased the amplitude and AUC (156.1±95.2% and 148.5±110.9% of control, respectively; n=7). There was no recovery during return to 37°C but subsequent heat exposures further increased the amplitude and AUC. By contrast, mild heating to 42°C reduced both the amplitude and AUC to 41.5±20.7% and 43.2±29.2% of that at 37°C; n=3. Recovery to 37°C was incomplete after 30 minutes. Moderate heating to 46°C had no significant effect on either the amplitude or AUC but there was a significant increase during the recovery phase (119.8±15.5% and 118.9±24.4% of control, respectively; n=3). There was no effect on *f* during heating or upon return to 37°C.

These experiments show that the magnitude to which isolated bladder strips are heated have profoundly different effects on the magnitude of spontaneous contractions. Relatively mild heating to 42°C attenuated the amplitude of contractions, an effect that persisted for at least twice the duration of the heating interval itself. However, high heating (46 and 50°C) increased contraction amplitude, an effect that also persisted following the intervention. This implies that heating influences detrusor contractility by several mechanisms that are currently under investigation. Moreover, the design of heating paradigms to regulate spontaneous activity requires precise temperature ranges to be applied to the bladder.

We acknowledge Boston Scientific

Where applicable, the authors confirm that the experiments described here conform with The Physiological Society ethical requirements.

PCB389

Inhibitory effect of visfatin and leptin on human and rat myometrial contractility

S. Mumtaz[1,2], S. AlSaif[1], S. Wray[1] and K. Noble[1]

[1]Cellular and Molecular Physiology, University of Liverpool, Liverpool, Merseyside, UK and [2]Physiology, Shifa College of Medicine, Islamabad, Federal Capital, Pakistan

Adipokines, active substances secreted from adipocytes influence metabolic functions. Their levels have been shown to alter in pregnancy and it has been suggested that their dysregulation could be associated with complications of pregnancy, including gestational diabetes. Visfatin, is a novel adipokine (originally known as pre-B cell colony-enhancing factor) with multiple functions including insulin mimetic effects, and it has been found to have altered plasma levels in obese women and during gestation. Leptin, one of the best characterised adipokines, has been reported to decrease contractility of the myometrium. We have therefore investigated the effect of visfatin on myometrial contractility and compared them to leptin. Myometrial strips from either term pregnant women having a caesarean section (with informed consent and ethical approval) or humanely killed rats were dissected, superfused with Krebs and the effects of visfatin (500pM- 25nM) or leptin (1nM-1μM) were studied. After establishment of regular contractions the tissue was incubated for control and test response at 37oC for 20mins. In pregnant human myometrium, visfatin at 1nM had little effect on contractility but compared with controls (100%), 10nM produced a significant (unpaired T Test) decrease in the 20 min integral of spontaneous (64±19%, n=13; P=0.02) and oxytocin-induced contractions (55.3± 9%, n=5; P=0.02), mean ± sem. Leptin at this concentration (10 nM) had no effect and at higher concentration of (1μM) produced a smaller inhibitory effect of (~ 80% controls, n=4) on contractions of rat and human myometrium. Preliminary data shows that the inhibitor FK-866 in the presence of visfatin in human myometrium attenuated the inhibitory effect of visfatin by ~ 60% (n=4). These data are the first to show that visfatin can inhibit myometrial contractility and that it may do so more potently than leptin. The visfatin inhibitor FK-866 reduces the inhibition of contraction by visfatin which suggests that visfatin is acting through the NAD-dependent pathway in myometrium. The data suggests that increased output of visfatin and leptin in obese pregnant women may impair uterine contractility resulting in an unplanned Cesarean delivery.

Adali et al, 2009

Fasshauer et al, 2007

Mazaki-Tovi et al, 2009

Vahratian, 2009.

Zhang et al, 2007

Commonwealth Scholarship Commission in The United Kingdom

Where applicable, the authors confirm that the experiments described here conform with The Physiological Society ethical requirements.

PCB391

Prolonged elevation of cAMP enhances spontaneous contractility in human myometrium from pregnant women at term

P.F. Lai[1], R.M. Tribe[2] and M.R. Johnson[1]

[1]Department of Obstetrics & Gynaecology, Imperial College London, London, UK and [2]Women's Health Academic Centre, Kings College London, London, UK

Myometrial contractions in vitro can be inhibited by transient [cAMP] elevation. 48 h exposure to iloprost has been reported to enhance oxytocin-induced contractions in human tissue via increased [cAMP] and PKA activity (1). We have shown cAMP agonists enhance COX-2 expression in human myometrial cells via MAPK signalling cascade (2). The impact of prolonged exposure to cAMP agonists on human myometrial tissue spontaneous contractility has not been demonstrated, despite growing interest in the use of [cAMP]-elevating therapies to prevent preterm labour.

In the present study, human myometrial tissue samples were obtained (informed written consent) from women undergoing caesarean section (37-42 weeks, non-labour, TNL; n=88). Tissue strips were incubated in serum-free DMEM, under tension (5.9-7.9 mN) for 24 and 48 h with rolipram, forskolin, 8-bromo-cAMP, dibutyryl cAMP, 6-Bnz-cAMP and iloprost, plus vehicle controls (DMSO or H2O). Contractile activity was subsequently measured using an isometric organ bath. Mean integral tension (mean ± SEM) and related contraction parameters were analysed. Acute (1 h) exposure of myometrial tissue to cAMP agonists was also assessed. Statistical significance was tested using a Wilcoxon test.

Our experiments showed that pre-treatment (24 h) with 1 mM 8-bromo-cAMP, 1 μM rolipram or 10 μM rolipram resulted in 5.2, 3.4, and 2.8 -fold greater spontaneous contractile activity than vehicle control, respectively ($P<0.05$) (n=6). Pre-treatment (48 h) with 1 mM 8-bromo-cAMP or 1 μM forskolin also resulted in increased spontaneous contractile activity (19.1-fold and 3.7-fold respectively) versus vehicle control ($P<0.05$) (n=6). Oxytocin-induced contractions were enhanced following pre-treatment (24 h) with 1 mM dibutyryl cAMP (1.3-fold versus vehicle control, $P<0.05$) (n=6).

In conclusion, long-term [cAMP] elevation can increase the ability of myometrial tissue to spontaneously contract, as demonstrated with 8-bromo-cAMP and rolipram, without greatly affecting oxytocin-induced contractility. Hence there is a need for caution when considering the use of cAMP agonists as treatments for pre-term labour prevention due to the ability of prolonged [cAMP] elevation in promoting spontaneous contractions.

Fetalvero et al (2008) J. Clin. Invest. 118: 3966-3979

Chen et al (2012) J. Cell. Mol. Med. 16: 1447-1460

The authors would like to thank Action Medical Research for the funding of this project (grant number SP4573)

Where applicable, the authors confirm that the experiments described here conform with The Physiological Society ethical requirements.

PCB392

Intestine of dystrophic mice presents stretch resistance, muscle atrophy and impaired calcium-dependent contractility

G.A. Alves[1], L.R. Silva[1], R.F. Ribeiro[1], E.F. Rosa[4,1], J. Aboulafia[1], E. Freymüller[3], C. Souccar[2] and V.L. Nouailhetas[1]

[1]Biophysics, Escola Paulista de Medicina - Universidade Federal de São Paulo, Sao Paulo, Sao Paulo, Brazil, [2]Pharmacology, Escola Paulista de Medicina - Universidade Federal de São Paulo, Sao Paulo, Sao Paulo, Brazil, [3]Centro de Microscopia Eletrônica, Escola Paulista de Medicina - Universidade Federal de São Paulo, Sao Paulo, Sao Paulo, Brazil and [4]Centro Univesitário São Camilo, Sao Paulo, Sao Paulo, Brazil

The protein dystrophin is a component of the dystrophin-associated protein complex which links the contractile machinery to the plasma membrane to the extracellular matrix. The absence of dystrophin leads to a pathological condition known as the Duchenne muscular dystrophy (DMD), a disease characterized by a progressive skeletal muscle degeneration, disability, and early death. The mdx mice is the most common DMD animal model. Alterations in gastrointestinal tissues from DMD patients and mdx mice are scarcely described, and little understood. Using isolated tissue samples, explanted from mdx and control mice, we thus investigated the possible relationships between possible morphological and contractile properties impairments with alterations in the calcium handling due to the absence of the protein dystrophin in the mdx mice ileum. Absence of dystrophin caused 27% reduction in the longitudinal muscular layer thickness, accompanied by a partial damage to the mucosa layer (Chiu score of 2-4 by dystrophic animal in comparison with 0-2 score in control), and a partial damage to the mitochondria from the longitudinal muscular layer. Functionally, it was shown a higher resistance to basal tissue stretching (as the contractile response under 1 g-basal tension in mdx is maintained the same as under the optimal 0.5 g-basal tension in mdx mice. In control mice, the responses under 1 g-basal tension are already diminished) and impairment in the Emax (maximum effect) of both eletro- (mdx: 2.36 ± 0.09 g and control: 2.77 ± 0.13 g) and pharmacomechanical (mdx: 2.47 ± 0.09 g and control 2.95 ± 0.12 g) signaling associated with altered calcium influx (half-life time of 1.2 min in mdx mice compared to 0.4 in control stimulation with KCl successive stimuli), without any alteration in the sarcoplasmic reticulum calcium storage (maintenance of the caffeine-induced contraction, 1.12 ± 0.07 g in control and 0.98 ± 0.05 g in mdx mice), in the ileum isolated from the dystrophic animal as compared to control animals. It is thus concluded that intestine is sensitive to the dystrophic condition, as the protein dystrophin plays an important role in the preservation of both the micro and ultra structure of mice intestine, while exerting minor roles concerning both the intestinal contractile responsiveness and the SR calcium storage capacity and release in dystrophic mice.

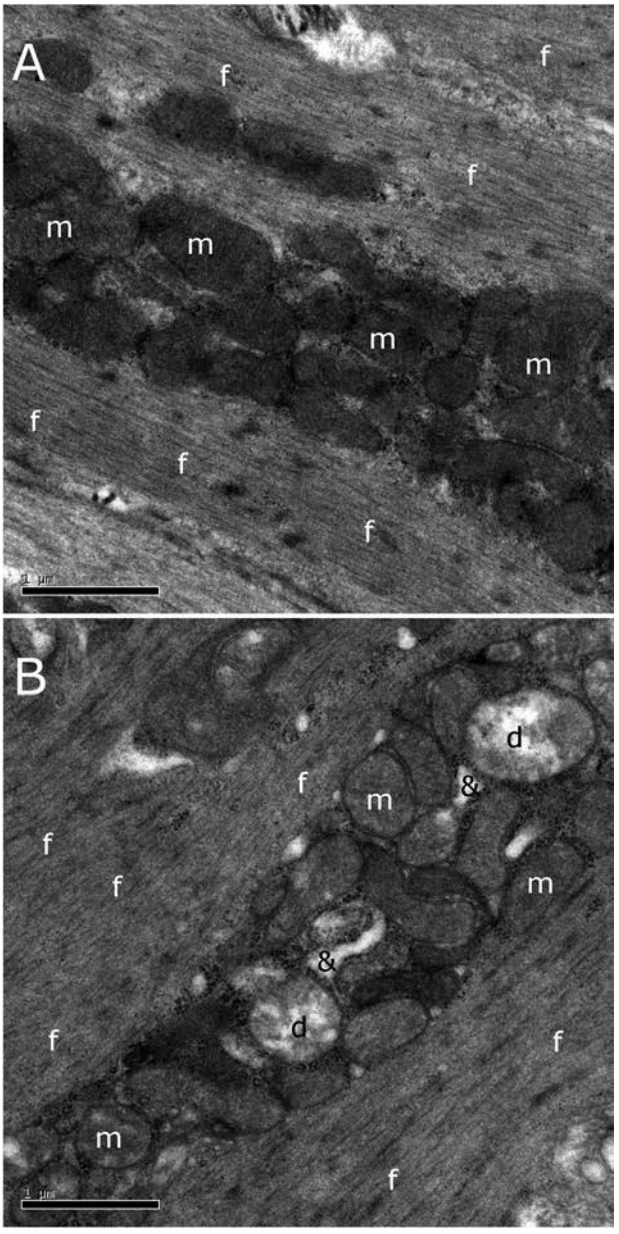

Representative ultramicrographs from smooth muscle cells cytoplasm from ileum isolated from: control (A) and mdx (B) mice. Myofilaments (f), mitochondria (m); disorganized mitochondria (d), loose (thickened) endoplasmic reticulum (&). Scale bar: 1 μm.

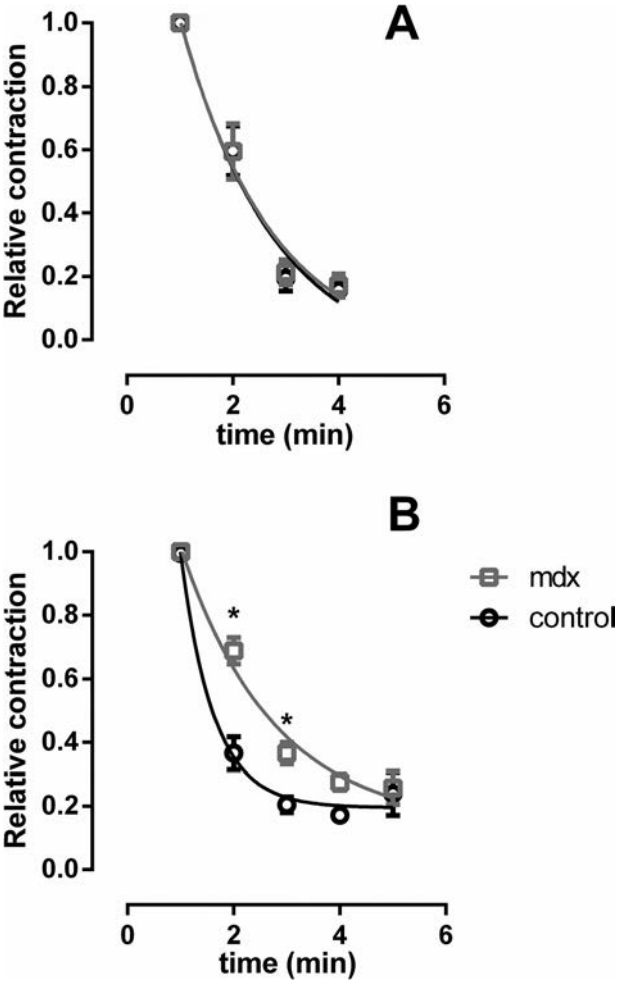

Calcium exit evaluated by measuring contraction in response to repeated stimuli and washes using carbachol 30 μM (A) or KCl 80 mM (B). In (B), t1/2= 0.429 min in control and t1/2= 1.218 min in mdx. *: different from control group (two-way ANOVA, Bonferroni's post-test, P<0.05)

This project was supported by FAPESP (2007 59976-6)

Where applicable, the authors confirm that the experiments described here conform with The Physiological Society ethical requirements.

PCB393

Contrasting effects of gap junction blockers on contractility of rat urinary bladder strips

D.A. Bijos[1,2] and M.J. Drake[1,2]

[1]School of Clinical Sciences, University of Bristol, Bristol, UK and [2]Bristol Urological Institute, NHS North Bristol Trust, Bristol, UK

Gap junctions are present at the coupling of different cell types within the urinary bladder [1]. Detrusor, the smooth muscle of the bladder, displays contractile phasic activity (PA) during urine storage. This PA could be facilitated by cell-to-cell communication e.g. via gap junctions. Increased PA may result in pathologies. Hence, we characterize the effects of known gap junction blockers: isomers 18α- and 18β-glycyrrhetinic acid (18α-,18β-GA) and carbenoxolone (CBX) [2] on intact (including mucosa) and mucosa-denuded detrusor bladder tissue. Bladders were isolated from male Wistar rats (P19-24 days) killed by CO_2 under UK Schedule 1 regulations. Denuded and intact tissue strips (5-8mm long) were placed in superfusion tissue organ baths, maintained in oxygenated Krebs buffer at

37°C and tied to a tension transducer to a resting tension of 1g. In the absence of measureable spontaneous PA in intact strips and in all denuded strips, 1μM carbachol (CCh) was used to induce PA. Changes in the contractile force were measured (ADInstruments) throughout the control period, single dose drug exposure and a washout period, each 30min. 1,10 and 30μM 18β-GA; 30μM 18α-GA and 50μM CBX were used. The effect of a drug or drug vehicle on PA was investigated by measuring the amplitude (g per mg tissue) and frequency of PA (number of contractions during 5 min). Data show mean percentage change ± SEM from at least 7 strips from at least 6 animals (two-tailed paired t-test, $p<0.05$ was considered significant). Amplitude of bladder tissue CCh-induced PA decreased with increasing concentrations of the 18β-GA. In intact tissue 10μM 18β-GA decreased PA amplitude by 15.6 ± 4.7% ($p < 0.05$). Amplitude decreased by 33.3 ± 4.9% ($p < 0.001$) and 32.7 ± 3.4% ($p < 0.01$) with 30μM 18β-GA and 18α-GA, respectively. PA frequency increased by 20.1 ± 5.8% ($p < 0.01$) at 30μM 18β-GA. The effect of 18β-GA was stronger in denuded detrusor strips. 10μM 18β-GA decreased PA amplitude by 36.1 ± 2.0% ($p < 0.001$) and 30μM 18β-GA by 42.6 ± 9.1% ($p < 0.01$). At 30μM 18β-GA PA frequency increased by 51.2 ± 24.0% ($p < 0.05$). In contrast, 50μM CBX showed a trend of increasing PA amplitude in both denuded and intact strips, while simultaneously decreasing PA frequency. The frequency of contractions in intact strips decreased by 26.5 ± 6.1% ($p < 0.01$). Preliminary data on spontaneous, not CCh-induced PA suggest the effects of both drugs are less pronounced in unstimulated tissue. 18β-GA increased frequency and decreased amplitude of CCh-stimulated bladder tissue PA, with a stronger effect in denuded strips. CBX decreased PA frequency - a different observation to 18β-GA – and showed a trend in increasing PA amplitude - opposite to 18β-GA effect. This unexpected difference will be further characterized.

Ikeda Y *et al.* (2007). *Am J Physiol Renal Physiol:* **293**:1018-25

Palani D *et al.* (2007). *Auton Neurosci* **137:** 56-62

Where applicable, the authors confirm that the experiments described here conform with The Physiological Society ethical requirements.

PCB394

Time-dependent structural and functional changes in the spinal cord injured rat bladder

S.M. Gray[1], N. McKerr[1], B. Frias[2], C.D. Cruz[2], F. Cruz[2], G. McMurray[3] and K. McCloskey[1]

[1]Centre for Cancer Research and Cell Biology, Queen's University Belfast, Belfast, UK, [2]Faculty of Medicine of Porto, University of Porto, Porto, Portugal and [3]Neusentis, Pfizer limited, Cambridge, UK

Neurological insults including spinal cord injury (SCI) lead to disturbances in bladder function which include an acute areflexic phase followed by chronic bladder overactivity or underactivity. We previously investigated cellular changes in the SCI rat bladder, 5 weeks after injury and reported altered distribution of interstitial cells (IC), smooth muscle hypertrophy and patchy denervation (1). These changes were correlated with an underactive, hypercompliant phenotype (2). The purpose of the present study was to investigate structural and functional changes in the SCI rat bladder at selected time points after injury.

Female Sprague Dawley rats underwent spinal cord transection at T8/T9 in accordance with the European Commission Directive of 22 September 2010 (2010/63/EU). Animals underwent in vivo cystometry under anaesthesia by subcutaneous injection of urethrane (1.2g/kg) at selected time-points post-SCI before being humanely sacrificed. Bladders were removed and processed for histology, immunofluorescence and confocal imaging. Histological and immunofluorescence studies were carried out on 4 tissue samples from at least 3 animals. Cystometry demonstrated a loss of voiding and non-voiding contractions in acute SCI bladders at 2h (N=5) and 24h (N=4). Overactivity later developed and was characterised by an increased frequency of voiding contractions from 0.43±0.1min-1 (mean±SEM) in spinal-intact animals (N=5) to 1.4±0.64min-1 (N=3; $p<0.05$) at 4wk, and 1.84±0.33min-1 (N=3; $p<0.05$, Anova, post-hoc Dunnett's) at 8wk. Chronic SCI bladders also exhibited urinary retention/incomplete emptying. Initial loss of the urothelial layer in the acute phase was accompanied with inflammation throughout the bladder wall, which was repaired by 2wk. Notable smooth muscle hypertrophy occurred from 1wk. PDGFRα+-IC networks in the lamina propria were disrupted in the acute phase, but recovered in the later stages. PDGFRα+-IC in the detrusor were disrupted as early as 24h with marked loss of cellular morphology. This was correlated with partial denervation. In the chronic phase, the morphology of detrusor IC did not return to normal. Interestingly, α-smooth muscle actin+-myofibroblasts which were not present in controls, were detected in the bladder wall at 1wk and 2 wk post-SCI.

In conclusion, the acute SCI bladder is associated with loss of voiding and non-voiding contractions along with initial disruption of lamina propria PDGFRα+-IC networks. Cellular remodelling throughout the overactive chronic phase appears to restore lamina propria IC but the detrusor layer is typified with persistent hypertrophy, patchy denervation and disrupted IC.

1. Johnston L et al. 2012. Altered distribution of interstitial cells and innervation in the rat urinary bladder following spinal cord injury. J Cell Mol Med. 16(7):1533-43.

2. Young JS et al 2013. The passive and active contractile properties of the neurogenic, underactive bladder.BJU Int. 111(2):355-61.

Financial support was received from the European Union, FP7 "INComb" (FP7-HEALTH-2007-B). SMG is in receipt of a Pfizer-BBSRC CASE Award PhD Scholarship.

Where applicable, the authors confirm that the experiments described here conform with The Physiological Society ethical requirements.

PCB395

In vivo irradiation negatively impacts neurogenic and agonist-evoked contractions in the mouse bladder

B. McDonnell, K. Butterworth, K. Prise and K. McCloskey

Centre for Cancer Research and Cell Biology, Queen's University Belfast, Belfast, UK

Patients undergoing radiotherapy for pelvic malignancies experience adverse effects on bladder function. The cellular basis of radiation-induced bladder dysfunction is incompletely understood and may represent pathologies in several cell types. We previously reported that ex vivo irradiation of guinea-pig bladder tissue attenuated spontaneous and neurogenic contractions (1). The purpose of the present study was to investigate the effect of in vivo pelvic irradiation on mouse bladder neurogenic and agonist-evoked contractions.

C57BL mice underwent pelvic irradiation in accordance with local ethics approval. Animals were sacrificed 1h or 1wk post-irradiation (UK Animal Procedures Act, Schedule 1). Full thickness and detrusor (mucosa removed) tissue strips were studied with in vitro myography and electrical field stimulation (EFS).

Neurogenic contractions, evoked by EFS in full thickness or detrusor strips (0.5Hz–16Hz) one-hour post-irradiation were not significantly different from controls (at 16Hz, 1.18±0.18g vs 1.38±0.15g; both data sets n=10; N=5; p=0.4). However, full-thickness bladder strips from animals one-week post-irradiation had smaller neurogenic contractions at all frequencies tested (n=10, N=5; at 16Hz, 1.18±0.18g in control vs 0.62±0.11g post-irradiation; p=0.012). This effect was not seen in detrusor strips (at 16Hz, 1.03±0.19g control vs 1.2±0.08g, p=0.44). Carbachol-evoked contractions were reduced in irradiated full thickness strips (0.89±0.12g in control vs 0.31±0.06g irradiated, n=10 N=5, p=0.0005) 1 week post-irradiation. Similarly, ATP-responses were reduced 1 week following irradiation (0.37±0.09g vs 0.12±0.02g, n=10; N=5, p=0.014). Interestingly, in detrusor strips, there was no difference in carbachol or ATP responses after irradiation (p=0.42 and p=0.40, respectively). Receptor-independent contractions evoked by high external K+ solution was also reduced in full thickness strips (n=10; N=5) one-week post-irradiation (1.02±0.11g vs 0.64±0.09g, p=0.018); an effect not seen in detrusor strips (n=10, N=5; p=0.78), indicating that the ability of the detrusor smooth muscle to contract was not affected by irradiation.

In summary, in vivo pelvic irradiation reduced neurogenic, agonist, and high external K+-evoked contractions in full thickness bladder strips, one week after irradiation. These differences were not found in detrusor strips, indicating that radiation may impact the cells of the mucosal layer.

McDonnell et al, 2012. Proc Physiol Soc 27

Financial support was received from the European Union, FP7 "INComb" (FP7-HEALTH-2007-B).

BMcD is in receipt of a DEL studentship, Queen's University Belfast.

Where applicable, the authors confirm that the experiments described here conform with The Physiological Society ethical requirements.

PCB396

Simvastatin inhibits human myometrial contractility by mechanisms independent of cholesterol depletion and HMG-CoA reductase inhibition

V. Pang

Obstetrics & Gynaecology, University of Nottingham, Derby, UK

Knowledge of myometrial regulation is essential to understanding preterm labour. Cholesterol depleting agents have been reported to perturb the myometrial membrane microenvironment and therefore key ion channels (1), studies have also demonstrated the pleiotropic effects of such agents (2). Our hypothesis is that simvastatin decreases myometrial contractions via K+channel blockade and inhibition of its pleiotropic effects, including nitric oxide production and isoprenylated proteins. We aim to investigate effects of simvastatin on human myometrium.

Myometrial biopsies were collected with informed written consent from patients undergoing elective caesarean section (>37 weeks). Tissue was mounted for isometric tension recordings and effects of simvastatin (33 nM – 330 μM) on spontaneous contractility, in the absence and presence of SK channel blocker apamin (500 nM), BK channel blocker paxilline (1 μM), broad-acting K+ channel blocker TEA (5 mM), NOS inhibitor L-NAME (1.2 mM) and isoprenoid GGPP (30 μM) assessed. Cholesterol and protein were measured in untreated and treated myocytes, using Amplex red and bicinchoninic acid assays respectively. In all assay-based experiments, 15 mM methyl-β-cyclodextrin (MCD) was used as a comparative cholesterol-depleting agent. Data are presented as means + SEM and compared using ANOVA.

Simvastatin significantly decreased contractions until cessation at 330 μM ($p < 0.0001$, n=6) in contrast to MCD treatment which increased contractions ($p < 0.0001$, n=6). Selective inhibition of both SK ($p<0.05$, n=6), (IC50 = 2.56e-6 vs. 2.10e-7 M), BK ($p<0.01$, n=6), (IC50=4.41e-6 vs. 2.10e-7 M) and addition of both inhibitors ($p<0.001$, n=5), (IC50 = 1.68e-5 vs. 2.10e-7 M) produced a rightward shift of the concentration-response curve. Broad Inhibition of K+ channels with TEA elicited significant partial inhibition of simvastatin relaxation ($p<0.0001$, n=5), (IC50 = 1.84e-4 vs. 2.10e-7 M). Replenishment with GGPP had no effect on simvastatin -induced relaxation ($p>0.05$, n=6), however NOS inhibition was able to significantly inhibit simvastatin relaxation ($p<0.05$, n=4). Finally, only MCD treatment significantly decreased cholesterol concentration ($p<0.001$, n=5) while the total protein concentration was unchanged.

Data demonstrated evidence of K+ channel modulation by simvastatin. Absence of cellular cholesterol modulation and significant inhibition of simvastatin-induced relaxation by L-NAME, suggests an alternative mechanism of statin action, independent of HMG-CoA inhibition of novel cholesterol synthesis. Myometrial relaxation via simvastatin suggests that statins may have implications as tocolytic agents in the treatment of preterm labour, warranting further investigation into their mechanisms and therapeutic potential.

Bergdahl, A., Persson E., Hellstrand P., Sward K. (2003). 'Lovastatin induces relaxation and inhibits L-type Ca2+ current in the rat basilar artery'. Pharmacol Toxicol 93(3): 128-34

Smith, R.D., Babiychuk, E.B,.,Noble, K., Draeger, A., Wray, S. (2005). 'Increased cholesterol decreases uterine activity: functional effects of cholesterol alteration in pregnant rat myometrium', Am J Physiol, cell Physiol 288(5): C982-8

Dr. Raheela Khan, Dr. Cyril Rauch, Mrs. Averil Warren

Where applicable, the authors confirm that the experiments described here conform with The Physiological Society ethical requirements.

PCB397

Rapid dilatation induced by release of muscle compression

M. Turturici and S. Roatta

Neuroscience Dept, University of Turin, Turin, Italy

Several studies have shown that a rapid hyperaemia can be evoked by different stimuli such as short-lasting contractions, muscle compression, arterial occlusion and passive movement (Turturici et al. 2012, Kirby et al. 2007), suggesting that a rapid dilatation could be mediated by mechano-sensitive mechanisms responding to decreases in transmural pressure according to the Bayliss effect (Mohrman & Sparks 1974, Turturici et al. 2012). However the exact nature of the relevant mechanical stimulus is still unclear, given that these stimuli produce both a rapid decrease and rapid return of transmural pressure.

Aim of this study was to investigate the individual effects of these two events by analysing the hemodynamic responses to onset and release of muscle compression.
Hyperaemic responses to the external compression of Masseter muscle (MC) were recorded from the masseteric artery (n=8) of urethane-anaesthetized rabbits (1.2 g/kg, i.v.) (n=4) by means of ultrasound flowmetry.
Mechanical compressions of different duration (1, 10, 20, 50 and 100 s) were exerted by a cylindrical head (1.3 cm^2) pushed by a PC-driven servo-controlled motor (force= 0.9 N) resulting in a locally generated pressure of about 50 mmHg (Turturici et al. 2013).The relative amplitude of the hyperaemic responses was computed as (peak flow – baseline)*100/baseline.
MC did not substantially impair muscle blood flow. On the contrary, two different hyperaemic responses were detected both at the onset and release of MCs (with MC duration >= 10 s) of amplitude Po and Pr, respectively (see Fig. 1). None of these responses depended on MC duration p=(0,94). Po and Pr were not significantly different .Po=240±60% and Pr= 229±80% (averaged over all MC durations 10-100 s).
The 1-s lasting MC evoked a single hyperaemic response whose amplitude (394 ± 124 %) was of significantly higher than both Po and Pr.
In conclusion, rapid release of MC consistently evokes a rapid dilatation. MC does not stop blood flow to the muscle and the hyperaemia does not increase with MC duration, suggesting that metabolic mechanisms are not involved. It is suggested that the rapid dilatation underlying the hyperaemia can be mechanically-activated by both a rapid decrease and a rapid increase in transmural pressure of the musculo-vascular network. This particular manifestation of vascular mechanosensitivity is not explained by the classical myogenic response but is compatible with the dilatory effects reported by Smiesko et al (1971) in the isolated skeletal muscle.

Fig.1

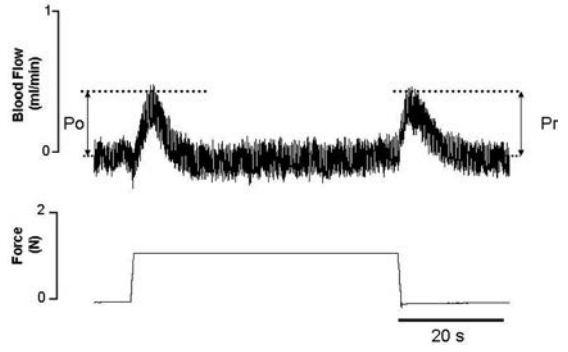

FIG 1: Original record showing hyperaemic responses to masseteric muscle compression on force applied. Po = Peak at onset, Pr = Peak at release.

Kirby BS et al (2007). J Physiol. 583(Pt 3), 861-74.

Mohrman DE & Sparks HV (1974) Am J Physiol. 227(3), 531-5.

Smiesko V (1971) Pflugers Arch. 327(4), 324-36.

Turturici M et al (2012) J Appl Physiol. 113(4). 524-31.

Turturici M et al (2013) Physiol Meas. 34(3). 307-14.

Where applicable, the authors confirm that the experiments described here conform with The Physiological Society ethical requirements.

PCB398

The role of TRPM8 channels in normal rat bladder function

M. King[1], O. Murray[2], S. Gray[2], L. Johnston[2], K. McKloskey[2] and C. Johnson[1]

[1]Biomedical Science Education, Queen's University, Belfast, UK and [2]Cntre for Cancer Research and Cell Biology, Queen's University,, Belfast, UK

Transient receptor potential melastatin 8 (TRPM8) channels are known to be present in rat and human bladder tissue (Stein et al., 2004). Recent studies in our lab (Johnson et al., 2009) have shown that this channel is present and functional in rat vascular smooth muscle. Therefore, this project aimed to examine the functional expression of TRPM8 channels in the bladder of normal rats using isometric contractile studies along with immunohistochemistry.
Bladders were taken from sacrificed male Sprague-Dawley rats (250-350g). Tissues were processed for histology and immunohistochemical staining. Bladder tissues labeled with anti-TRPM8 (N=4) showed positive staining in the urothelium, nerves and in cells with the morphological features of Interstitial Cells (IC) in the lamina propria and detrusor layers. Detrusor smooth muscle was not immunopositive for TRPM8 in contrast to DRGs which were used as positive controls. Isometric contraction studies were conducted in bladder strips pre-tensed to 1g with urothelium in tact or removed. TRPM8 agonist, menthol, (300μM in ethanol) failed to cause any contraction (N=4, n=16 where N=animals, n= preparations). Contraction (1.97±0.15 g; ave.±s.e, N=10, n=18) induced by carbachol (10 μM) was markedly relaxed on addition of menthol (72±5%, N=9, n=18, accounting for relaxation due ethanol alone; P<0.001, ANOVA, Tukey's post hoc test). However, when protocols were repeated in the presence of the L-type calcium channel blocker, nifedipine (10 μM) menthol-induced relaxation was vastly reduced (93 ±4 %, N=9, n=14, not significant). Results for these protocols were unaffected by removal of urothelium. Both WS-12 (10 μM, N=6, n=8) and icilin (10 μM in DMSO, N=3, n=12) failed to have contractile or relaxatory effects with urothelium in tact.
We conclude that in normal rat bladder, TRPM8 channels are not involved in contractile responses. This is consistent with the lack of TRPM8 staining in detrusor smooth muscle. The expression of TRPM8 in urothelium, nerves and IC may be related to sensory mechanisms in the bladder.

Johnson CD. et al., (2009) Am J Physiol. 296, H1868-H1877.

Stein RJ, et al., (2004). J Urol, 172, 1175-1178.

We thank the Centre for Biomedical Science Education and the Centre for Cancer Research and Cell Biology, QUB, for supporting this research.

Where applicable, the authors confirm that the experiments described here conform with The Physiological Society ethical requirements.

PCB399

Effects of chronic administration of virgin coconut oil on the cardiovascular profile in middle aged male rats

N.-. Thongsepee and C. Jansakul

Physiology, Prince of Songkla University, Hat-Yai, Songkhla, Thailand

Coconut oil has been used as a source of fatty acids since ancient times. However, its major chemical components are saturated fatty acids and these are now considered to be a health hazard, especially to the cardiovascular system. In this study we aimed to test for any harmful effects of feeding virgin coconut oil on the cardiovascular system of middle-aged rats. Tests included (1) blood sugar and lipid profiles, (2) basal blood pressure and heart rate, and (3) isolated blood vessel functions. The saturated fatty acid composition (%) of the virgin coconut oil (VCO, Thai pure coconut Co., Thailand) was: C8, 4.7; C10, 6.2; C12 (lauric acid), 51.9; C14, 18.2; C16, 6.9 and C18, 1.9. Middle-aged male rats (14-15 months old) were gavaged with 1 or 3 ml VCO /kg or distilled water (control), once a day for 6 weeks. Basal blood pressure and heart rate were measured from anesthetized rats (sodium pentobarbital, 60 mg/kg, i.p) via the right common carotid artery. Blood sugar and lipids profile were measured by enzymatic methods. The thoracic aorta was isolated from rats decapitated with a guillotine, then placed in oxygenated Krebs Heinseleit solution at 37oC (PSU-Ethic No.10/54) before performing a cumulative concentration response (C-R) curve to phenylephrine (Phe), acetylcholine (ACh) and glyceryl trinitrate (GTN). Data are expressed as a mean ± S.E.M. (6 rats/group/each experiment). Using the Student's paired t-test, a $p \leq 0.05$ between test and control was considered to be statistically significant. After 6 weeks of treatment with 1 or 3 ml of VCO/kg, there were no changes in serum glucose and lipid profiles, mean arterial blood pressure and heart rate when compared to the control group. There were no significant changes in vascular responses to Phe, ACh and GTN for the dosage of 1 ml/kg VCO. At a dosage of VCO of 3 ml/kg, the maximal contractile responses of the endothelium-intact thoracic aortic ring, with or without N-nitro-L-arginine (LNA, 300 μM)), a nitric oxide synthase inhibitor, to Phe was significantly lower than the one obtained from the control group. Also the vasodilatory response to ACh by the endothelium-intact aortic ring preconstricted with Phe (3 μM) was significantly higher than the control group. This effect disappeared when the blood vessels had been incubated with LNA or tetraethylammonium (1 mM) but not by glybenclamide (10 μM). The vasodilatation to GTN was not different from the control for the endothelium-intact thoracic aortic ring treated with LNA. These results indicate that consumption of the virgin coconut oil of 1-3 ml/kg/day had some beneficial effects on the cardiovascular system of the middle-aged male rats by increasing the release of nitric oxide from the vascular endothelium and opening of the Kca channels to cause a higher vasodilatation to ACh and to oppose the vasoconstriction produced Phe.

Where applicable, the authors confirm that the experiments described here conform with The Physiological Society ethical requirements.

PCB400

Inhibitory mechanism of *T*-type Ca^{2+} channel inhibitor, mibefradil on voltage-dependent K^+ channels in coronary arterial smooth muscle cells

S. Na[2], D. Hong[1] and W. Park[1]

[1]Department of Physiology, Kangwon National University School of Medicine, Chuncheon, Gangwon-do, Republic of Korea and [2]Department of Obestetrics and Gynecology, Institute of Medical Sciences, Kangwon National University Hospital, Chuncheon, Gangwon-do, Republic of Korea

We investigated the effects of mibefradil, a *T*-type Ca^{2+} channel inhibitor, on voltage-dependent K^+ channels in smooth muscle cells from rabbit coronary arteries. Mibefradil inhibited the Kv current in a dose-dependent fashion with an apparent K_d of 1.17 ± 0.15 μM (n=5) . It accelerated the decay rate of Kv channel inactivation without altering the kinetics of current activation. The rate constants of association and dissociation for mibefradil were 2.23 ± 0.07 $\mu M^{-1}s^{-1}$ and 2.40 ± 0.42 s^{-1}, respectively (n=5). Mibefradil did not have a significant effect on the steady-state activation (n=5) and inactivation (n=6) curves. The recovery time constant from inactivation was decreased in the presence of mibefradil (n=5, $P<0.05$), and application of train pulses (1 or 2 Hz) caused a progressive increase in the mibefradil blockade (n=4, $P<0.05$), indicating that mibefradil-induced inhibition of Kv current is use-dependent. The inhibitory effect of mibefradil was not affected by extracellular Ca^{2+} free condition (n=5). Moreover, the absence of intracellular ATP did not change the blocking effect of mibefradil (n=4). From these results, we suggest that mibefradil directly inhibited the Kv current, independently of Ca^{2+} channel inhibition. ($P<0.05$ was regarded significant, and data analysis was done with student t-test.)

Hong DA *et al*. (2012). *J Pharmacol Sci* **120**, 196-205.

This study was supported by the 2011 Research Grant from Kangwon National University.

Where applicable, the authors confirm that the experiments described here conform with The Physiological Society ethical requirements.

PCB401

Expression of smooth muscle-specific ion channels in TGF-β1-induced differentiation of human adipose-derived mesenchymal stem cells

Y. Son, D. Hong and W. Park

Department of Physiology, Kangwon National University School of Medicine, Chuncheon, Gangwon-do, Republic of Korea

Human adipose tissue-derived mesenchymal stem cells (hASCs) have the power to differentiate into various cell types including chondrocytes, osteocytes, adipocytes, neurons, cardiomyocytes, and smooth muscle cells. We characterized the functional expression of ion channels after TGF-β1-induced differentiation of hASCs, providing insights into the differentiation of vascular smooth muscle cells. The treatment of hASCs with TGF-β1 dramatically increased the contraction of a collagen-gel lattice and the expression levels of smooth muscle specific genes including α-smooth muscle actin, calponin, SM-MHC, smoothelin-B, myocardin, and h-caldesmon. We observed Ca^{2+} (n=5), big-conductance Ca^{2+}-activated K^+ (BK_{Ca},

n=4), and voltage-dependent K^+ (Kv, n=4) currents in TGF-β1-induced, differentiated hASCs and not in undifferentiated hASCs. The currents share the characteristics of vascular smooth muscle cells (SMCs). RT-PCR and western blotting revealed that the *L*-type (Cav1.2), *T*-type (Cav3.1, 3.2, and 3.3), known to be expressed in vascular SMCs, dramatically increased along with the Cavβ1 and Cavβ3 subtypes in TGF-β1-induced, differentiated hASCs ($P<0.05$, n=4). Although the expression-level changes of the β-subtype BKCa channels varied, the major α-subtype BK_{Ca} channel ($K_{Ca}1.1$) clearly increased in the TGF-β1-induced, differentiated hADSCs($P<0.05$, n=4). Most of the Kv subtypes; also known to be expressed in vascular SMCs, dramatically increased in the TGF-β1-induced, differentiated hASCs ($P<0.05$, n=3). Our results suggest that TGF-β1 induces the increased expression of vascular SMC-like ion channels and the differentiation of hASCs into contractile vascular SMCs. ($P<0.05$ was regarded significant, and data analysis was done with student *t*-test.)

This research was supported by the National Research Foundation of Korea (NRF) funded by the Ministry of Education, Science and Technology (2011-0019422, 2010-0021126).

Where applicable, the authors confirm that the experiments described here conform with The Physiological Society ethical requirements.

PCB402

The effect of PI3 kinase inhibitor LY294002 on voltage-dependent K^+ channels in rabbit coronary arterial smooth muscle cells

D. Hong[1], S. Na[2], Y. Son[1] and W. Park[1]

[1]Department of Physiology, Kangwon National University School of Medicine, Chuncheon, Gangwon-do, Republic of Korea and [2]Department of Obstetrics and Gynecology, Institute of Medical Sciences, Kangwon National University Hospital, Chuncheon, Gangwon-do, Republic of Korea

We examined the effect of LY294002, a phosphatidylinositol 3-kinase (PI3K) inhibitor, on voltage-dependent K^+ (Kv) channels in smooth muscle cells from freshly isolated rabbit coronary arteries using the whole-cell patch clamp technique. The Kv current amplitude was inhibited by LY294002 in a dose-dependent manner, with a K_d value of 1.48 ± 0.20 μM (n=7). Without alteration of the kinetics of activation, LY294002 accelerated the decay rate of Kv channel inactivation. The rate constants of association and dissociation for LY294002 were 1.83 ± 0.01 $\mu M^{-1}s^{-1}$ and 2.59 ± 0.14 s^{-1}, respectively (n=6). Application of LY294002 had no significant impact on the steady-state activation (n=6) or inactivation (n=7) curves. In the presence of LY294002, the recovery time constant from inactivation was increased (n=7, $P<0.05$), and Kv channel inhibition increased under train pulses (1 or 2 Hz, n=6, $P<0.05$). This indicates that LY294002-induced Kv channel inhibition is use-dependent. Furthermore, pretreatment with another PI3K inhibitor, wortmannin (10 μM), did not affect the Kv current, and did not change the inhibitory effect of LY294002 (n=8). Based on these results, we suggest that LY294002 directly blocks Kv current irrespective of PI3K inhibition. ($P<0.05$ was regarded significant, and data analysis was done with student *t*-test.)

This research was supported by the National Research Foundation of Korea (NRF) grant funded by the Korea government (MEST) (2010-0021126, 2011-0028573).

Where applicable, the authors confirm that the experiments described here conform with The Physiological Society ethical requirements.

PCB403

Decreased expression of ATP-sensitive K^+ channel in aortic smooth muscle during isoproterenol-induced left ventricular hypertrophy

Y. Son, D. Hong and W. Park

Department of Physiology, Kangwon National University School of Medicine, Chuncheon, Gangwon-do, Republic of Korea

We investigated the impairment of K_{ATP} channels in aortic smooth muscle cells (ASMCs) from hypertrophied rabbits. The amplitude of KATP channels induced by the K_{ATP} channel opener pinacidil was greater in ASMCs from control than from hypertrophied animals ($P<0.05$, n=6). In phenylephrine pre-constricted aortic rings, pinacidil induced relaxation in a dose-dependent manner. The dose-dependent curve was shifted to the right in the hypertrophied compared with the control model ($P<0.05$, n=4). Although the level of Kir6.2 subtype expression did not differ between ASMCs from the control and hypertrophied models (n=5), those of the Kir6.1 and SUR2B subtypes were decreased in the hypertrophied model ($P<0.05$, n=4). Application of the CGRP and forskolin induced a K_{ATP} current in both control and hypertrophied animals; however, the K_{ATP} current amplitude did not differ between the two groups (n=5). Furthermore, PKA expression was not altered (n=5). These results suggests that the decreased K_{ATP} current amplitude and K_{ATP} channel-induced vasorelaxation in the hypertrophied animals were attributable to the reduction in K_{ATP} channel expression, but not to changes in the intracellular signaling mechanism that activates the K_{ATP} current. ($P<0.05$ was regarded significant, and data analysis was done with student *t*-test.)

Park *et al*. (2012) *Am J Physiol Cell Physiol* **303**, C170-C178.

This research was supported by a National Research Foundation of Korea

(NRF) grant funded by the Ministry of Education, Science and Technology

(R0A-2007-000-20085-0, MEST; 2010-0021126, 2010-0020224).

Where applicable, the authors confirm that the experiments described here conform with The Physiological Society ethical requirements.

PCB404

Physiological dynamics in the reversal of the Fåhraeus effect in the venous microcirculation of the human finger pulp

W.G. Murphy[1,2], S.M. Browne[2], R. Segurado[2], B. Gallagher[3], C. Murphy[3] and E. Tong[4]

[1]Health Service Executive, Dublin, Ireland, [2]University College Dublin, Dublin, Ireland, [3]Irish Blood Transfusion Service, Dublin, Ireland and [4]Department of Surgery, Our Lady's Children's Hospital, Dublin, Ireland

As blood flows from the arterioles into the capillaries the haemoglobin (Hb) concentration falls by approximately 50% to a level of 7 g/dL in the smallest capillaries due to a pro-

gressive increase in the relative amount of plasma in blood flowing through vessels < 300μ in diameter (the Fåhraeus effects). The effects reverse on the venous side of the capillaries - dynamical effects on this reversal process have not been described hitherto. Blood sampled from the human finger pulp comes predominantly from venules and small veins < 300μ and represents the physiological space where the Fåhraeus effects are reversed. The Hb content of blood from the finger pulp has been observed to vary in relation to the Hb content of venous blood in the same individuals with sex and venous Hb levels(1,2,3). We have now studied the relationship between venous and finger pulp Hb levels within individuals over time.

465 blood donors with hereditary haemochromatosis, 360 males and 105 females, underwent repeated 450 ml venesections at a single clinic over a 3 year period. The mean age at first venesection was 50 years (range 24 to 71 years) for men and 52 years (range 21 to 70 years) for women. Men had a mean of 6.3 venesections over the period of the study, range 1 – 26; females a mean of 4.88 venesections, range 1 - 28. The difference between finger pulp and venous Hb levels for each donation was plotted against the finger pulp Hb level for the entire cohort of donors and for each individual donor. For each 1g/dL change in finger pulp Hb level, the mean difference between venous and finger pulp levels changed by -0.694 g/dL (Figure 1a). This relationship is significantly different from zero ($p<0.001$), the value expected for a 1:1 relationship between the Hb levels in the venous and finger pulp vascular spaces. Correcting for donor-specific effects and time-correlation of Hb levels at each donation date, finger pulp Hb levels recovered on average 0.496 mg/dL/day, ($p<0.001$), while venous Hb levels recovered slower: 0.113 mg/dL/day on average ($p=0.019$). The rate of finger pulp Hb recovery between venesections was 4.39 times faster than venous Hb recovery ($t(4798)=2.743$, $p=0.006$). These rates were not affected by sex or season (Figure 1b).

These findings indicate that the Hb level of finger pulp blood affects the reversal of the Fåhraeus effects in blood flowing from smaller to larger vessels on the venous side of the circulation, consistent with vasodilation induced by deoxygenated red cells in the venous microvasculature. A sex difference has been observed before in the relative size of the gap between venous and finger pulp Hb levels per unit Hb level in venous blood (2,3); the net effect of the deoxyHb-associated effect may be to allow red cells in excess of resting requirements to be stored in a low pressure slow moving reserve on the venular side.

Figure 1a

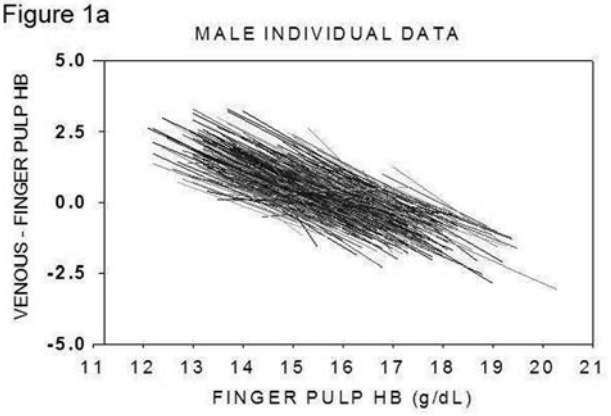

Figure 1b

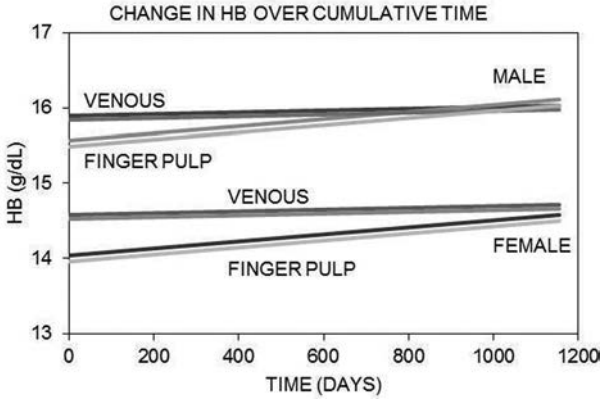

Tong E, Murphy WG, Kinsella A, et al. Capillary and venous haemoglobin levels in blood donors: a 42-month study of 36,258 paired samples. Vox Sang. 2010;98:547-53.

Murphy WG, Tong E, Murphy C. Why do women have similar erythropoietin levels to men but lower hemoglobin levels? Blood. 2010;116:2861-2.

Cable RG, Steele WR, Melmed RS, et al.The difference between fingerstick and venous hemoglobin and hematocrit varies by sex and iron stores. Transfusion. 2012;52:1031-40.

Where applicable, the authors confirm that the experiments described here conform with The Physiological Society ethical requirements.

PCB405

Lercanidipine and labedipinedilol-A play anti-inflammatory role through inhibition of lipopolysaccharide/interferon-γ-induced HMGB1 release and MMP-2, 9 activities in vascular smooth muscle cells

S. Liou, M. Shih and C. Chen

Department of Pharmacy, Chia-Nan University of Pharmacy and Science, Tainan, Taiwan, Tainan, Taiwan

Inflammation is an important molecular basis of atherosclerosis. Several reports have revealed that dihydropyridine calcium channel blockers (CCBs) exert anti-inflammatory effects on various vascular cells. The purpose of the present study was to evaluate anti-inflammatory effects and mechanisms of lercanidipine and labedipinedilol-A, new generation dihydropyridine CCBs, in rat vascular smooth muscle cells (VSMCs) exposed to lipopolysaccharide (LPS) and interferon-γ (IFN-γ). MTT, Griess reagent, RT-PCR, ELISA, gelatin zymography, immunocytochemistry and Western blotting were employed.

We found that lercanidipine and labedipinedilol-A attenuated production of NO, ROS and TNF-α from LPS/IFN-γ-stimulated VSMCs. In addition, they both diminished the LPS/IFN-γ-induced expression of iNOS protein and mRNA, with attenuation of HMGB1 cytosolic translocation and subsequent extracellular release. Furthermore, they down-regulated MMP-2/MMP-9 activities, whereas expression of tissue inhibitor of matrix metalloproteinase-1 (TIMP-1), an inhibitor of MMP-9, was up-regulated. Finally, we found that lercanidipine and labedipinedilol-A inhibited the nuclear translocation of NF-κB and suppressed the phosphorylation of JNK, p38 MAPK and Akt. Lercanidipine and labedipinedilol-A can exert their anti-inflammatory effects through suppression of NO, ROS and TNF-α through down-regulation of iNOS, MMP-2/MMP-9, and HMGB1, with inhibition of signaling transduction of MAPKs, Akt/IkB-α and NF-κB pathways. These findings implicate a valuable role of new generation dihydropyridine CCBs lercanidipine and labedipinedilol-A for the treatment of inflammatory vascular diseases.

Where applicable, the authors confirm that the experiments described here conform with The Physiological Society ethical requirements.

PCB406

Effect of azelastine on cardiac action potential duration and hERG K^+ channel current

M. Park and H. Su

Department of Physiology, School of Medicine, Kangwon National University, Chuncheon, Gangwon-do, Republic of Korea

Azelastine is a second gengeration histamine H_1 receptor antagonist used as an anti-asthmatic and anti-allergic drug that can induce QT prolongation, which may lead to *torsades de pointes*. Since block of cardiac human *ether-a-go-go*-related gene (*hERG*) channels is one of leading causes of acquired long QT syndrome, we investigated the acute effects of azelastine on hERG channels to determine the electrophysiological basis for its proarrhythmic potential. Azelastine increased the action potential duration at 90% of repolarization (APD_{90}) in a concentration-dependent manner, with an IC_{50} of 1.08 μM when action potentials were elicited under current clamp in guinea pig ventricular myocytes. We examined the effects of azelastine on the hERG channels expressed in *Xenopus* oocytes and HEK293 cells using two-microelectrode voltage-clamp and patch-clamp techniques. Azelastine induced a concentration-dependent decrease of the current amplitude at the end of the voltage steps and hERG tail currents. The IC_{50} for the azelastine-induced block of the hERG currents in HEK293 cells at 36 °C was 11.43 μM at +20 mV, while the drug blocked L-type Ca^{2+} channel expressed in HEK293 cells with an IC_{50} of 26.21 μM. The S6 domain mutations, Y652A and F656A partially attenuated (Y652A) or abolished (F656A) the hERG current block. These results suggest that azelastine is a blocker of the hERG channels, providing a molecular mechanism for the arrhythmogenic side effects during the clinical administration of azelastine.

Where applicable, the authors confirm that the experiments described here conform with The Physiological Society ethical requirements.

PCB407

Differential effects of environmental toxicants, PCB 126 and PCB 77, on cardiac electrophysiology

M. Park and S. Jo

Department of Physiology, School of Medicine, Kangwon National University, Chuncheon, Gangwon-do, Republic of Korea

Polychlorinated biphenyls (PCBs) have been known as serious persistent organic pollutants (POPs), causing developmental delays, motor dysfunction. We have investigated the effects of two PCB congeners, 3,3',4,4'-tetrachlorobiphenyl (PCB 77) and 3,3',4,4',5-pentachlorobiphenyl (PCB 126) on ECG, action potential, and the rapidly activating delayed rectifier K+ current (I_{Kr}) of guinea pigs' hearts, and hERG K^+ current expressed in *Xenopus* oocytes. PCB 126 shortened the corrected QT interval (QTc) of ECG and decreased the action potential duration at 90% (APD_{90}), and 50% of repolarization (APD_{50}) ($P < 0.05$) without changing the action potential duration at 20% (APD_{20}). PCB 77 decreased APD_{20} ($P < 0.05$) without affecting QTc, APD_{90}, and APD_{50}. The PCB 126 increased the I_{Kr} in guinea-pig ventricular myocytes held at 36°C and hERG K^+ current amplitude at the end of the voltage steps in voltage-dependent mode ($P < 0.05$), however, PCB 77 did not change the hERG K^+ current amplitude. The PCB 77 increased the diastolic Ca^{2+} and decreased Ca^{2+} transient amplitude ($P < 0.05$), however PCB 126 did not change. The results suggest that PCB 126 shortened the QTc and decreased the APD_{90} possibly by increasing I_{Kr}, while PCB 77 decreased the APD_{20} possibly by other modulation related with intracellular Ca^{2+}. The present data indicate that the environmental toxicants, PCBs, can acutely affect cardiac electrophysiology including ECG, action potential, intracellular Ca^{2+}, and channel activity, resulting in toxic effects on the cardiac function in view of the possible accumulation of the PCBs in human body.

Where applicable, the authors confirm that the experiments described here conform with The Physiological Society ethical requirements.

PCB408

Novel approach to inhibition of neointimal hyperplasia in arteriovenous fistulae

R.W. Corbett[1], N. Demicheli[2], L. Grechy[2], F. Iori[2], J. Crane[1], N. Duncan[1], P. Vincent[2] and C.G. Caro[3]

[1]Imperial College Renal and Transplant Centre, Imperial College Healthcare NHS Trust, London, UK, [2]Department of Aeronautics, Imperial College London, London, UK and [3]Department of Bioengineering, Imperial College London, London, UK

Haemodialysis is a predominant modality for the treatment of end-stage renal failure, but is dependent on high quality access to the circulation to allow effective removal, treatment and return of blood through an extracorporeal circuit. The preferred method is via an established arteriovenous fistula, created surgically by anastomosing a patient's own artery and vein. This technique is, however, hampered by a high failure rate (up to 40% before first use) (1) caused by early neointimal hyperplasia, in the genesis of which haemodynamic factors appear to play an important role (2). Given the seeming importance of the local flow, including its physiological three-dimensionality (3), we have attempted to determine in model studies whether geometric modification at the anastomosis can reduce the burden of neointimal hyperplasia.

Perspex models of a vascular anastomosis were created with planar orientation of the vessels at a range of anastomotic angles. A further, otherwise identical set of models, was created with 'offset' junctions, novel non-planar anastomoses, which mimicked the geometry at the origin of arterial branches. Comparative observations were made under non-pulsatile (but otherwise physiological) flow conditions, using flow visualisation and computational fluid dynamics (CFD).
Similar results were observed in the flow visualisation and CFD work (see Figure). Flow separation occurred in both planar and offset (non-planar) models within both vessels. It is suggested that flow disturbance (including separation, wall shear abnormality and instability) occur in regions associated with neointimal hyperplasia development in humans and animal models.
Flow visualisation and CFD allowed complementary assessment of vascular anastomosis models. Preliminary results suggest that modification of anastomosis configuration can alter the peri-anastomotic and downstream flow fields. Planned observational studies in human patients will increase understanding of how current practice, and resulting flow patterns, correlate with clinical outcomes. Concurrent work, including with animal models, will allow examination of the hypothesis that these changes affect the burden of neointimal hyperplasia, possibly mediated through wall shear stress and/or mass transport mechanisms.

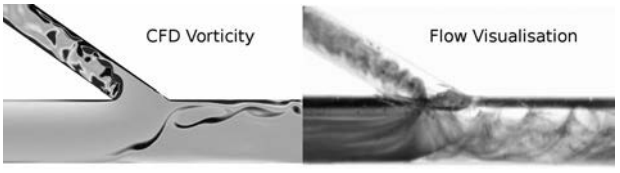

Figure- Flow from left to right with planar anastomosis, flow split 80/20 and Reynolds number 800 in parent tube.

Huijbregts HJ *et al.* (2008) *Clin J Am Soc Nephrol* **3**, 714-719.

Krishnamoorthy MK *et al.* (2012) *Kidney Int* **81**, 745-750.

Coppola G & Caro CG (2009) *J R Soc Interface* **6**, 519-528.

Where applicable, the authors confirm that the experiments described here conform with The Physiological Society ethical requirements.

PCB409

Perivascular adipose tissue inhibits thoracic aorta endothelial function through Cav-1-dependent inhibition of nitric oxide production

S. Chen[1], H. Lee[2], C. Tsao[3] and C. Wu[4]

[1]Nursing, Kang-Ning Junior College of Medical Care and Management, Taipei, Taiwan, [2]Graduate Institute of Life Sciences, National Defence Medical Centre, Taipei, Taiwan, [3]Anaesthesiology, Taipei Veterans General Hospital and National Yang-Ming University, Taipei, Taiwan and [4]Pharmacology, National Defence Medical Centre, Taipei, Taiwan

Perivascular adipose tissue (PVAT) has been proposed as a cause of atherosclerosis, recently. The location of PVAT is in association with the artery wall, which enables diffusion of adipokines (e.g. superoxide anion, angiotensin II, tumor necrosis factor-α, and adiponectin). The adipokines are capable of inducing endothelial dysfunction and enhancing vasoconstriction in rat thoracic aortas. Caveolin-1 (Cav-1), a structure protein of caveolae, is present in most of cells involved in the development of atherosclerosis. Cav-1 inhibits nitric oxide (NO) production by occupying the calcium/calmodulin binding site of endothelial NO synthase. The inhibition of NO production is a characteristic of endothelial dysfunction. In this study, adult male Wistar rats weighing 265 to 305 g were euthanatized by intravenous injection of overdose of sodium pentobarbital. The thoracic aortas were isolated, dissected without the PVAT, divided into endothelium-intact (+E) and endothelium-denuded (-E) groups, and mounted in organ bath containing a Krebs' solution bubbled with 95% O2 and 5% CO2 at 37 C. PVAT was incubated in Krebs' solution for 30 minutes and transferred to organ bath before the isometric tension studies. The remaining aortas were frozen for Western blotting. The dose-response curve of phenylephrine, acetylcholine, and sodium nitroprusside were performed to examine the vascular reactivity and endothelial function, respectively. We found that the unknown factor(s) released from PVAT increased Cav-1 protein expression and induced a vasocontractile effect via inhibition of endothelial NO production in rat thoracic aorta.

Lohn M, Dubrovska G, Lauterbach B, Luft FC, Gollasch M, and Sharma AM. Periadventitial fat releases a vascular relaxing factor. FASEB J 16: 1057-1063, 2002.

Maenhaut N, and Van de Voorde J. Regulation of vascular tone by adipocytes. BMC 9: 25, 2011

Razani B, Woodman SE, and Lisanti MP. Caveolae: from cell biology to animal physiology. Pharmacological Reviews 54: 431-467, 2002.

Wozniak SE, Gee LL, Wachtel MS, and Frezza EE. Adipose tissue: the new endocrine organ? A review article. Digestive Diseases and Sciences 54: 1847-1856, 2009.

Chatterjee TK, Stoll LL, Denning GM, Harrelson A, Blomkalns AL, Idelman G, Rothenberg FG, Neltner B, Romig-Martin SA, Dickson EW, Rudich S, and Weintraub NL. Proinflammatory phenotype of perivascular adipocytes: influence of high-fat feeding. Circulation Research 104: 541-549, 2009.

This work was supported by grants NSC 101-2320-B-016-014 and NSC 101-2320-B-345-001 from the National Science Council, R.O.C., Taiwan.

Where applicable, the authors confirm that the experiments described here conform with The Physiological Society ethical requirements.

PCB410

PKG signalling mediates perivascular adipose tissue function of up- and downstream of secreted adipokines via regulation of the expression and signalling of adiponectin

S. Withers, L. Simpson, M. Werner and A. Heagerty

University of Manchester, Manchester, UK

Objective: Perivascular adipose tissue (PVAT) has an anticontractile effect which is lost in obesity and the metabolic syndrome leading to hypertension associated cardiovascular complications (1). cGMP dependent protein kinase has been implicated in as a key molecule in regulating vascular tone (2), furthermore obesity the intake of a high fat diet is associated with a reduction in PKG expression (3). We investigated the role of cGMP dependent protein kinase (PKG) in PVAT function specifically in modulating adipokine release/signalling and whether activation of PKG is beneficial using an in vitro model of obesity.
Methods: Contractility of mesenteric arteries±PVAT from PKG+/+, PKG-/-, adiponectin-/- knockout and C57/Bl6J mice was investigated by wire myography. All procedures were performed in accord with current UK legislation. Vessels were studied under normoxia +/- DT-2 (PKG1α peptide selective inhibitor)

(125nM), hypoxia (95% N2/ 5%O2)± atrial natriuretic peptide (ANP) (5μM). Contractile responses to noradrenaline (NA) (1x10-5M to 3x10-9M) were calculated as a percentage of KCl (60mM) contraction, and expressed as mean±SEM. Expression of adiponectin was assessed by immunohistochemistry.
Results: Healthy PVAT had an anticontractile effect which was absent in PKG-/- mice and following pharmacological inhibition of PKG signalling (PVAT vs. no PVAT: PKG+/+: P<0.001 n=13; PKG-/-: P=0.052, n=13; DT-2: P=0.071, n=8). Solution transfer studies between preconstricted (3x10-8M NA) PKG+/+ (+PVAT) donor arteries to PKG-/- (-PVAT) recipient arteries and PKG-/- (+PVAT) donor arteries to PKG+/+ (-PVAT) recipient arteries were associated with a significantly impaired relaxation compared with PKG+/+ +PVAT to PKG+/+ -PVAT solution transfer (P=0.023 and P=0.043 respectively, n=13). Experimental hypoxia in PKG+/+ induced a loss of PVAT associated anticontractile effect which was prevented by ANP (PVAT+normoxia vs. PVAT+hypoxia: P=0.0157, n=10; PVAT+hypoxia vs. PVAT+hypoxia+ANP P=0.0093, n=8) No significant effects of hypoxia +/- ANP were observed in PKG-/- animals. Furthermore, the loss of anticontractile effect observed in adiponectin-/- mice was not affected by hypoxia and could not be rescued by ANP (no PVAT vs PVAT: P=0.1486, n=6; PVAT vs. PVAT+hypoxia: P=0.6507, n=6; PVAT+hypoxia vs. PVAT+hypoxia+ANP: P=0.1538, n=6). Immunohistochemical detection of adiponectin demonstrated reduced adiponectin following hypoxia, which was prevented when ANP was present.
Conclusions: Our data implicate PKG signalling in mediating PVAT function both up and down stream of secreted adipose tissue factor(s) through its role in mediating the expression and signalling of adiponectin. Investigations in obesity are necessary to confirm the role of PKG in PVAT dysfunction.

Greenstein AS, Khavandi K, Withers SB, Sonoyama K, Clancy O, Jeziorska M, Laing I, Yates AP, Pemberton PW, Malik RA, and Heagerty AM. Local inflammation and hypoxia abolish the protective anticontractile properties of perivascular fat in obese patients. Circulation 119: 1661-1670, 2009.

Rapoport RM, Draznin MB, and Murad F. Endothelium-dependent relaxation in rat aorta may be mediated through cyclic GMP-dependent protein phosphorylation. Nature 306: 174-176, 1983.

Nikolic DM, Li Y, Liu S, and Wang S. Overexpression of constitutively active PKG-I protects female, but not male mice from diet-induced obesity. Obesity (Silver Spring) 19: 784-791, 2011.

Where applicable, the authors confirm that the experiments described here conform with The Physiological Society ethical requirements.

PCB411

Local cleavage of endothelial cell junctional adhesion molecule (JAM)-C by neutrophil elastase governs development of systemic inflammation

B. Colom[1], J.V. Bodkin[1], M.B. Voisin[1], D.A. Leinster[1], M. Aurrand-Lions[2], T. Chavakis[3], B.A. Imhof[4] and S. Nourshargh[1]

[1]Barts and The London School of Medicine, Queen Mary University of London, London, UK, [2]Institut Paoli-Calmettes, Marseille, France, Centre de Recherche en Cancérologie de Marseille, Marseille, France, [3]Dresden University of Technology, Dresden, Germany and [4]Centre Médical Universitaire, Geneva, Switzerland

JAM-C is a member of the Ig-superfamily that localizes to cell-cell contacts and is specifically enriched at tight junctions. Originally detected on endothelial cells (ECs), JAM-C has since been reported to be expressed on numerous other cell types such as spermatids, epithelial cells, smooth muscle cells, fibroblasts and Schwann cells. As such JAM-C has been associated with numerous biological functions but most notably it has been studied in the context of vascular and inflammatory responses[1]. Despite a growing interest in this complex molecule there remain many unanswered questions with respect to the expression and functions of JAM-C. In the present study we sought to investigate the expression and regulation of expression of EC JAM-C under inflammatory scenarios.
The expression of EC JAM-C was investigated in mouse ear skin and cremaster muscle by immunofluorescent staining and confocal microscopy using whole-mount tissues. With this approach JAM-C was found to be strongly expressed at junctions of ECs in capillaries and venules, but not arterioles. The venular expression of JAM-C was unaltered in ears stimulated with intradermal C5a (1μg), or the chemokines KC and MIP-2 (both at 500ng) but was significantly reduced in LTB4-stimulated tissues (300ng). The latter occurred in a dose and time-dependent manner with reduced expression of JAM-C being noted at 30 mins, peaking at 4 h and returning back to normal levels by 24 h post LTB4 administration. In addressing the mechanism of JAM-C cleavage, studies with neutrophil-depleted mice and neutrophil elastase (NE) KO mice demonstrated a role for neutrophil-derived NE in LTB4-induced loss of EC JAM-C. Local administration of LTB4 induced neutrophil reverse transmigration in mouse cremasteric venules (analysed by confocal intravital microscopy) and this was associated with lung inflammation. These results suggest that loss of local EC JAM-C can lead to disrupted modes of neutrophil transmigration which can in turn contribute to secondary organ inflammation[2].
Collectively, our data indicate that the expression and regulation of expression of EC JAM-C is vessel type and stimuli specific, respectively, and that JAM-C is shed from ECs after LTB4 stimulation in a neutrophil and NE dependent manner, a phenomenon that can contribute to turning a local inflammatory response to a systemic reaction.

Bradfield P.F. et al. ATVB., 2007, 27:2104-12

Woodfin A. et al. Nat. Immunol., 2011, 12:761-9.

This work was funded by The Wellcome Trust

Where applicable, the authors confirm that the experiments described here conform with The Physiological Society ethical requirements.

PCB413

Potentiated vasoconstrictor responses in mesenteric arterioles in elevated extracellular glucose may be due in part to a reduction in receptor desensitisation

R. Jackson[2], N.W. Davies[2] and R.D. Rainbow[1]

[1]Cardiovascular Sciences, University of Leicester, Leicester, UK and [2]Cell Physiology and Pharmacology, University of Leicester, Leicester, UK, UK

Elevated extracellular glucose potentiates vasoconstrictor signalling in vascular smooth muscle. We have previously demonstrated that elevating bathing glucose from 5 to 20mM causes a marked increase in contractile responses, recorded using wire myography, to angiotensin II (ATII), UTP, U46619 in mesenteric(1), and U46619 in coronary arterioles that is PKC-dependent in mechanism(1,2). We hypothesised that 20mM glucose reduced receptor desensitisation in a PKC-dependent manner so providing a mechanism to explain the increased vasocon-

striction in elevated bathing glucose.Rat mesenteric arterioles (200-400μm in diameter) were mounted in a Mulvany-Halpern myograph (Danish Myo Technology, Aarhus, Denmark) and maintained at a constant temperature of 37°C. Arteries were held under a tension equivalent to 90% of the diameter of the vessel at a pressure of 100 mmHg in 1.8 mM Ca2+ recording solution containing 5 or 20mM glucose for 30 minutes prior to experimentation. The myograph chamber was continuously perfused throughout the recording. 60mM potassium was applied to cause a depolarisation-induced contraction and all data was normalised to the peak contraction. 100nM ATII was perfused for 45 seconds followed by 100 (approximate EC50 value), 300 (maximal) and then a second 100μM addition of UTP to measure desensitisation for 5 minutes each, with a 5 minute wash between applications. Finally, 100nM ATII was reapplied at the end of the recording. In 5mM glucose, the second submaximal UTP response was reduced to 54.2±5.3% (n=10) of the first response and was unaffected by inclusion of 20μM L-NAME to inhibit eNOS (61.6±3.9%, n=20). In 20mM glucose this desensitisation was reduced to 76.4±4.2% (82.4±6.5% with L-NAME, P<0.01 compared to 5mM glucose control for both with and without L-NAME, t-test). Similarly, ATII desensitisation was reduced by 20mM glucose (5.1±2.4% vs 34.6±8.6%, 5 and 20mM glucose respectively, 20 vessels in each concentration, P<0.01, t-test). Inhibition of PKCα and β with 300nM Gö6976 in 20mM glucose attenuated the reduction of desensitisation to the same level as in 5 mM glucose control (54.2±5.3%, 76.4±4.2%** to 48.4±3.3%, in 5mM, 20mM glucose and with Gö6976 respectively, **P<0.01, ANOVA with Bonferroni's post-hoc test), and reversed the ATII reduction in desensitisation (5.1±2.4%, 34.6±8.6% to 4.0±2.7% in 5mM, 20mM glucose and with Gö6976 respectively, **P<0.01, ANOVA with Bonferroni's post-hoc test). In this study we demonstrate that receptor desensitisation is markedly reduced by increasing bathing glucose from 5 to 20mM, but that this can be attenuated using conventional PKC inhibition. This data support our hypothesis that glucose-mediated PKC activation reduces receptor desensitisation and enhancing vasoconstrictor responses in elevated glucose.

PKCalpha and beta activation by elevated extracellular glucose cause a marked inhibition of Kv currents in mesenteric arterial smooth muscle

J. L. Brignell, R. I. Norman, R. D. Rainbow

Proc Physiol Soc 27 (2012)

Hyperglycaemia potentiates vasoconstrictor responses in coronary arteries

P. Fielding, M. W. Sims, I. B. Squire, R. D. Rainbow

Proc Physiol Soc 27 (2012)

Where applicable, the authors confirm that the experiments described here conform with The Physiological Society ethical requirements.

PCB415

Outgrowth endothelial cell responses to hypoxia: role for BMP/SMAD signalling?

I. Ali, M. Hookham, T. Schmidt, N. Cantley, M.H. Wilson, A. Mullins, R. Medina, A.W. Stitt and D.P. Brazil

Centre for vision and vascular science, Queens University Belfast, Belfast, select a state, UK

Outgrowth endothelial cells (OECs) can induce de novo blood vessel formation in vivo. The vasculogenic ability of OECs is comprised in diabetes with much lower proliferative potential and reduced ability to respond to proangiogenic cytokines. This results in impaired vascular repair leading to ischaemia which is commonly observed in diabetic complications such as retinopathy due to decreased vascular supply. We replicated the low O2 environment of an ischemic retina by exposing OECs isolated from umbilical cords to 1% O2 and assessed their response at the molecular level. Together with their morphology, high proliferative potential and immunophenotypic expression profile, OEC identity was confirmed in accordance with the phenotype described in the literature. Exposing OECs to 1% O2 induced a state of hypoxia as we were able to detect HIF1α, 2α proteins which accumulate under low O2 conditions. OECs in 1% O2 exhibited an increase in filamentous actin staining, focal adhesion deposition and also enhanced migration indicating that OECs in hypoxia adapt a pro-migratory phenotype. Hypoxia also induced a state of stress-induced premature senescence. We observed a decrease in cell proliferation, changes in morphology and positive staining for β-gal a surrogate marker of cell senescence. There was also a decrease in expression of markers such as CD34, commonly associated with "stemness" after chronic exposure to hypoxia.
Molecular analysis identified that bone morphogenetic protein 4 (BMP4) and several Smad pathway associated genes were up-regulated under hypoxia. We therefore hypothesised that BMP4 and its Smad pathway associated genes are HIF dependent and may play a role in OEC function. We were unable to detect any significant BMP4 activity via ELISA or Western blot either in hypoxic or normoxic conditions. However acute exposure to hypoxia down regulated inhibitory Smad6 protein, which was recovered with MG132 treatment suggesting proteasome dependant degradation. Gremlin, a potent BMP4 inhibitor has been implicated as a proangiogenic cytokine in human umbilical vein endothelial cells. We are now assessing the role of gremlin in OEC function in normoxic and hypoxic conditions. These data taken together should enhance our knowledge of vascular stem cell function in ischaemic diseases.

Michelle B. Hookham, Tina Schmidt, Nathan Cantley, Melanie H. Wilson, Andrea Mullins, Reinhold Medina, Alan W. Stitt and Derek P. Brazil.

Where applicable, the authors confirm that the experiments described here conform with The Physiological Society ethical requirements.

PCB416

Novel inhibitors of serine-rich protein kinase -1 prevent choroidal neovascularization in rodent models - a role for potential topical therapeutics in macular degeneration

M. Gammons[1], A.D. Dick[2], S.J. Harper[1] and D.O. Bates[1]

[1]Physiology and Pharmacology, University of Bristol, Bristol, UK and [2]Cellular and Molecular Medicine, University of Bristol, Bristol, UK

Exudative age related macular degeneration (wet AMD) is a leading cause of vision loss in the western world, and current therapy requires monthly injection into the eye of anti-vascular endothelial growth factor (VEGF) proteins. VEGF is generated as two isoform families by alternative splicing – pro-angiogenic and anti-angiogenic. Retinal pigmented epithelial (RPE) cells require serine-rich protein kinase-1 (SRPK1) to phosphorylate serine/arginine-rich splicing factor-1 (SRSF1) to induce alternative splicing that generates pro-angiogenic isoforms. We tested the hypothesis that SRPK1 selective inhibitors could

be generated that reduce pro-angiogenic isoforms, and that SRPK1 inhibitors could be administered topically to prevent choroidal neovascularisation.
Novel SR Phosphorylation Inhibitors, (SPHINXs) were tested for SRPK inhibition in vitro, pro-angiogenic VEGF production in RPE cells by PCR and ELISA, and for inhibition of choroidal neovascularisation induced by laser photocoagulation in mice and rats.
A novel disubstituted furan inhibitor, SPHINX, was selective for the SRPK family of kinases targeting SRPK1 with an IC50 <1μM (Hills model of regression; log (inhibitor) vs. response – variable slope) and reduced the expression of pro-angiogenic but not anti-angiogenic VEGF isoforms. Choroidal neovascularisation was significantly reduced in vivo by SPHINX (0.039±0.026mm2; n=5) and the known SRPK inhibitor SRPIN340 (0.038±0.008mm2; n=5), compared with vehicle controls (0.11±0.016mm2; p<0.05, One-way ANOVA, Bonferonni post hoc). Topical administration of SPHINX and SRPIN340 significantly inhibited CNV to 38.5±7.4% (n=5) and 53.6±8.5% (n=6) of control respectively (p<0.05, One-way ANOVA, Bonferonni post hoc). These results indicate that novel SRPK1 selective inhibitors could be potential novel topical (eye drop) therapeutics for wet AMD.

This work has been supported by Fight for Sight and the Skin Cancer Research Foundation.

Where applicable, the authors confirm that the experiments described here conform with The Physiological Society ethical requirements.

PCB418

Effect of perivascular adipose tissue and AMPK activation on vascular myocyte BK_{Ca} currents

Y. Dong, G. Edwards and A. Heagerty

Institute of Cardiovascular Sciences, University of Manchester, Manchester, UK

All peripheral arteries are surrounded by perivascular adipose tissue (PVAT) which, in health, releases several factors with vasodilator properties. Recent evidence suggests that one such factor acts by opening voltage-sensitive (Kv7) K^+ channels[1], although our recent experiments suggest that the K^+ channel-opener released is likely to be adiponectin and that it acts by opening large conductance Ca^{2+}-dependent K^+ channels (BK_{Ca})[2]. In many tissues, adiponectin receptors signal via the AMP-dependent protein kinase (AMPK). Opening of BK_{Ca} channels and enhanced activity of AMPK are both linked to smooth muscle relaxation[3,4,5]. The present study investigated the effect of adiponectin and AMPK activation on BK_{Ca} currents in single myocytes which were freshly-isolated (enzymatically) from male Sprague-Dawley rat mesenteric arteries. BK_{Ca} currents were recorded at room temperature using the whole-cell configuration of the patch-clamp technique.
Under the conditions employed (calculated intracellular calcium concentration of 0.2 μM), 500 ms steps from a holding potential of -10 mV to a series of test potentials ranging from -40 to 50 mV generated outward currents with an activation threshold of -20 mV which were inhibited by 0.1 μM iberiotoxin (a selective BK_{Ca} channel blocker). The AMPK activator A-769,662 (10 μM) significantly increased BK_{Ca} currents without modifying the activation threshold of the channel. The current induced by A-769,662 was reversibly inhibited by iberiotoxin (0.1 μM), but was insensitive to the (ATP-competitive) AMPK inhibitor dorsomorphin (2 μM). Furthermore, a less-selective AMPK activator, AICAR (1 mM), did not increase BK_{Ca} currents. Interestingly, the physiological saline solution which had bathed PVAT for 1 h (at 37°C) also increased an iberiotoxin-sensitive outward K^+ current. Neither the background nor the induced current was sensitive to inhibition by either XE-991 (30 μM; a selective blocker of Kv7 channels) or dorsomorphin (2 μM). When myocytes were perfused with adiponectin (0.5 μg/ml), the BK_{Ca} current was also enhanced.
Consistent with our previous findings[2], under the conditions of the present study only BK_{Ca} channels were activated by a PVAT-derived factor and both adiponectin and A-769,662 were able to mimic this effect. The simplest hypothesis is that PVAT releases adiponectin which acts via AMPK to activate BK_{Ca} channels. Nevertheless, we are unable to explain why activation of BK_{Ca} by A-769,662 (which at the concentration employed is considered to be selective for AMPK), was not mimicked by AICAR or inhibited by dorsomorphin, although this might reflect the mechanisms of action of the different drugs and work is currently in progress to investigate this further.

Schleifenbaum, J. et al., 2010. Systemic peripheral artery relaxation by KCNQ channel openers and hydrogen sulfide. J Hypertens, 28, pp.1875–1882.

Lynch, F.M. et al., 2013. Perivascular adipose tissue-derived adiponectin activates BKCa channels to induce anticontractile responses. AJP: Heart and Circulatory Physiology. Epub ahead of print.

Bolotina, V.M. et al., 1994. Nitric oxide directly activates calcium-dependent potassium channels in vascular smooth muscle. Nature, 368, pp.850–853.

Horman, S. et al., 2008. AMP-activated protein kinase phosphorylates and desensitizes smooth muscle myosin light chain kinase. J Biol Chem, 283, pp.18505–18512.

Rossoni, L.V. et al., 2011. Acute simvastatin increases endothelial nitric oxide synthase phosphorylation via AMP-activated protein kinase and reduces contractility of isolated rat mesenteric resistance arteries. Clinical Science, 121, pp.449–458.

We would like to thank the British Heart Foundation for funding this project.

Where applicable, the authors confirm that the experiments described here conform with The Physiological Society ethical requirements.

PCB419

Normotension with enhanced body weight and fat deposition in mice deficient for *CYP17A1*

Z. Aherrahrou[1,4], K. Schmidt[2,4], R. Aherrahrou[1,4], H. Schunkert[3], J. Erdmann[1,4] and C. de Wit[2,4]

[1]Institut für Integrative und Experimentelle Genomik, Universität zu Lübeck, Lübeck, Germany, [2]Institut für Physiologie, Universität zu Lübeck, Lübeck, Germany, [3]Deutsches Herzzentrum München, Technische Universität München, München, Germany and [4]DZHK (German Centre for Cardiovascular Research), Partner site Hamburg/Kiel/Lübeck, Lübeck, Germany

CYP17A1 is an enzyme in metabolism of steroids exhibiting 17alpha hydroxylase and C17-20 lyase activity. It is required for the synthesis of testosterone, estrogens, and cortisol by converting pregnenolone and progesterone to intermediate products. Recently, *CYP17A1* gene was associated with coronary artery disease (CAD) and hypertension in genomewide association studies. A deficiency for this enzyme exists in humans and causes a rare form of congenital adrenal hyperplasia characterized by a dysfunctional sexual development in male patients, glucocorticoid lack, as well as a mineralocorti-

coid excess and according functional consequences (hypokalemia, hypertension). To investigate potential pathomechanisms that contribute to the development of CAD we generated Cyp17a1-deficient mice (Cyp17a1-/-) in the CardioGENE program. Breeding of heterozygous mice yielded offspring according to mendelian ratio. All Cyp17a1-/- littermates exhibited a female phenotype, but genotyping revealed that 55% of the offspring carried a Y-chromosome. Female Cyp17a1-/- mice had a higher body weight and increased subcutaneous as well as visceral fat deposits compared to female wild type littermates. Additionally, blood cholesterol levels were altered. Blood pressure and heart rate was measured in freely moving mice using telemetry. 24h mean arterial pressure (MAP) was similar in Cyp17a1-/- and wild type controls (~111 mmHg), whereas heart rate was slightly reduced in Cyp17a1-/- (591±5 vs. 620±12, *P*<0.05). In female wild type mice MAP was elevated at night (104±1 mmHg vs. 119±4 mmHg, day vs. night, *P*<0.01), as expected during enhanced activity. Similar findings were obtained in genotypic male (111±2 mmHg vs. 117±1 mmHg, *P*<0.05), but not in female Cyp17a1-/- mice (108±2 mmHg vs. 114±2 mmHg, *P*=0.08). Genotypic male Cyp17a1-/- (with female phenotype) had a significantly higher MAP than female wild type controls during day (111±2 vs. 104±1 mmHg, *P*<0.05). Serum potassium concentration was not different between genotypes. In a subgroup of mice voluntary running in a wheel was investigated, in which wild type mice ran up to 6 km/night. Interestingly, Cyp17a1-/- ran less distance (only 25%) but lost approximately 10% of their body weight during this period of 10 d, while weight did not decrease in wild type mice. We conclude that Cyp17a1 has a strong impact on body weight and fat deposition. Its role in blood pressure regulation is less obvious, which is also reflected by the normokalemia suggesting that aldosterone is not produced in excess as observed in humans. It remains to be determined whether the alterations in cholesterol levels enhance atherosclerosis and CAD in these mice or whether obesity itself is the only contributing factor.

Where applicable, the authors confirm that the experiments described here conform with The Physiological Society ethical requirements.

PCB420

Preferential Involvement of PPARβ/δ Versus IP in Mediating PAR-Stimulated Angiogenesis

C.E. Farrar[1], G. Kalindjian[1], J. Mason[3], J. Mitchell[2] and C.P. Wheeler-Jones[1]

[1]Comparative Biomedical Sciences, Royal Veterinary College, London, UK, [2]Cardiothoracic Pharmacology, Imperial College London, London, UK and [3]Imperial Centre for Translational & Experimental Medicine, Imperial College London, London, UK

The enzymatic products of cyclo-oxygenase (COX) activity regulate angiogenesis in vitro and in vivo, implicating altered COX expression and prostaglandin (PG) synthesis in the actions of pro-angiogenic mediators. We have previously shown that inhibition of induced COX-2 activity decreases endothelial cell (EC) tube formation in vitro and that this is rescued by exogenous iloprost (PGI2 analogue), suggesting an autocrine mode of action. PGI2 binds to the cell surface GPCR, IP, and to the ligand-activated nuclear receptor peroxisome proliferator activated receptor (PPAR) β/δ. Here, we have determined the relative contributions of PPARβ/δ and IP to EC function and angiogenesis. Iloprost, cicaprost (binds IP) and selective PPARβ/δ agonists (GW501516; L-165,041) increased neovascularisation in vivo (chick CAM assay; p<0.05 iloprost and cicaprost n=10-13, and p<0.001 PPARβ/δ n=17-26) and EC tubulogenesis on Matrigel in vitro (p<0.05 for all agonists; n=3). The PPARβ/δ antagonist GSK0660 abrogated iloprost- and PPARβ/δ agonist-induced tube formation. The angiogenic responses to thrombin and to protease-activated receptor agonist peptides (PAR2-AP and PAR4-AP) were attenuated by GSK0660 (p<0.01 for all agonists; n=3) and by PPARβ/δ siRNA but not by a specific IP antagonist, CAY10441. Immunoblotting studies showed that thrombin and PAR2-AP, but not PAR4-AP, enhance COX-2 expression and that this is reduced by antagonists of PPARβ/δ but not IP (n=3). EC exposure to thrombin or to PPARβ/δ agonists promoted acute activation of ERK, AMPK and Akt, as well as induction of COX-2 expression, all of which were inhibited by PPARβ/δ blockade (n=3). GSK0660 also reduced phosphorylation of Akt, AMPK and ERK in response to thrombin (n=3). These data implicate PPARβ/δ in the regulation of COX-2 induction by thrombin and PAR2-AP, and in the consequent tubulogenesis, and suggest that PPARβ/δ propagates the angiogenic response through an autocrine feedback loop. The observation that GSK0660 suppressed PAR4-AP-driven tube formation indicates that PPARβ/δ also regulates tubulogenesis through COX-2-independent mechanisms. Together, these studies provide evidence of a key role for PPARβ/δ in mediating agonist-induced angiogenesis.

Where applicable, the authors confirm that the experiments described here conform with The Physiological Society ethical requirements.

PCB421

Patterns of arterial wall permeability to plasma macromolecules change with age –a high-throughput confocal microscopy study

E. Bailey, E. Bazigou, P. Sowinski and P. Weinberg

Bioengineering, Imperial College London, London, UK

Elevated permeability of the arterial wall to circulating macromolecules is implicated in the development of atherosclerotic lesions. Lesions occur near branches, suggesting a role for haemodynamic wall shear stress, and in both human and rabbit aortas their distribution changes with age. To assess the relationship between lesion development and arterial wall permeability, we used a novel high-throughput technique employing tile-scanning confocal microscopy to systematically quantify macromolecule uptake around branch ostia in the rabbit aorta at different ages.

Rhodamine-labelled albumin was administered intravenously via the marginal ear vein to New Zealand white rabbits aged 2, 6 and >12 months (n>4 rabbits/group) and allowed to circulate for 10 minutes. Via the same route an anticoagulant (heparin), followed by an overdose of sodium pentobarbitone (0.8ml/kg) were given. The aorta was fixed post mortem under physiological pressure, excised and scanned en face using confocal microscopy. Tracer concentrations in the inner 10μm of the wall were mapped using MATLAB® and scaled to plasma tracer concentrations. Intensity data were statistically analysed using a nested ANOVA, and mass transfer coefficients were calculated.

In young rabbits, tracer uptake was greater downstream of intercostal branch ostia than upstream. This pattern significantly reversed with increasing age – by 6 months the majority of tracer uptake localised lateral to the branch mouth and by 12 months downstream regions showed the least uptake. (Downstream-upstream)/mean uptake values were signifi-

cantly different between 2 month versus both 6 month and >12 month animals (p<0.001). In young animals, the downstream mass transport coefficient was 1.5 times the upstream value (2.52±0.24x10-8cm/s vs 4.06±0.26x10-8cm/s). Mass transfer coefficients around the branch mouth averaged 3±0.3x10-8cm/s for all ages.
Our results demonstrate changes in permeability patterns that parallel the age-related patterns of lipid deposition seen in rabbit and human aortas, supporting a critical role for permeability in atherogenesis. Our new tile-scanning confocal method can easily image the whole aorta and provide permeability data to compare with shear stress data and lesion maps.

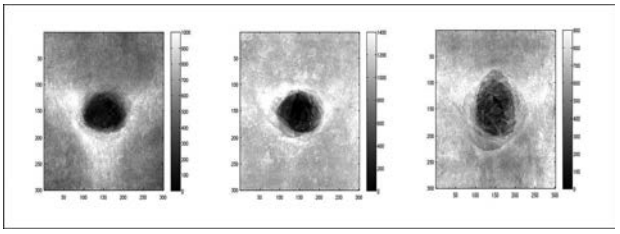

Figure 1. Maps of short-term macromolecule uptake around aortic branch ostia in rabbits of increasing age (left to right: 2 months, 6 months, >12 months). White areas indicate high uptake, Data represents the average of n>12 branches taken from a minimum of n=4 rabbits.

Where applicable, the authors confirm that the experiments described here conform with The Physiological Society ethical requirements.

PCB422

IR emissions from human hands: changes and recovery profiles following a reliable, quantifiable provocation challenge

D. Clegg and P. McCarthy

Clinical Technology and Diagnostic Research Unit (CT-DRU), University of Glamorgan, Pontypridd, UK

INTRODUCTION: Raynaud's disease (RD) is characterised by numb, white and often painful distal extremities[1]. Severity varies and it affects 10-20% of the UK population[2]. Infrared (IR) thermography has previously been used to measure the distal-dorsal difference (DDD) of RD sufferers[3]. The DDD is a parameter for quantifying temperature change between the nail bed and dorsal metacarpophalangeal (MCP) joint of the same digit; a difference of -1ºC or greater in a negative direction is considered clinically relevant[3]. Assessment has typically followed evoking of symptoms by cold water provocation at 0-10ºC from an ambient temperature of 20-24ºC[4,5]. We report here preliminary findings from a less noxious provocation challenge. AIM: The aim of the study was to assess the DDD of hands following a period of warmth provocation using IR thermography in order to determine sensitivity and clinical benefit. METHOD: 6 subjects (4 males, 2 females; age=24±3.6yrs) were recruited for the study. Of the 6 subjects, 2 had a history of primary RD. Following a 15 minute acclimatisation period in a room whose temperature was relatively constant (22ºC ± 1ºC), subjects placed their hands and proximal wrists under a temperature controlled incubator, with an air temperature of 30ºC for 2 minutes. IR images of the dorsal hands were taken at the following intervals: 5, 3 and 1 minute prior to a 2 minute provocation, then immediately following (0), 1, 3 and 5 minutes following the cessation of the provocation. For RD subjects only, additional images were taken at 7 and 9 minutes to allow consideration for any delays in recovery of the circulation which is usual in other forms of testing of RD sufferers[5]. IR images were assessed by measuring the DDD of the 2nd and 4th digits. Images were taken using a LAND FTIM vIR IR camera and analysis software LIPS mini V1.10.02. The DDD and means were calculated using IBM SPSS Statistics V19, figures produced by Microsoft Excel for Windows 2007. Ethical approval was granted by The Faculty of Health Science and Sport's Ethics Committee, University of Glamorgan, written informed consent was obtained.RESULTS Figure 1& 2 show comparisons between recovery profiles. Figure 1 – Recovery profiles for the R 2nd digit normal hands. Both the 2nd and 4th digits of both hands appeared similar in profile. Figure 2 - R 2nd digit recovery profiles for the 2 subjects with RD. CONCLUSIONS Although only a pilot study, results were encouraging as the recovery profiles of the RD sufferers was visibly different to the normals. The large difference in reaction between the 2 RD sufferers suggests that this test might be sensitive to cause of the disease, consistent with DDD assessment following cold provocation[3]. Subjects elicited clinically relevant changes consistent with those elicited following cold provocation.

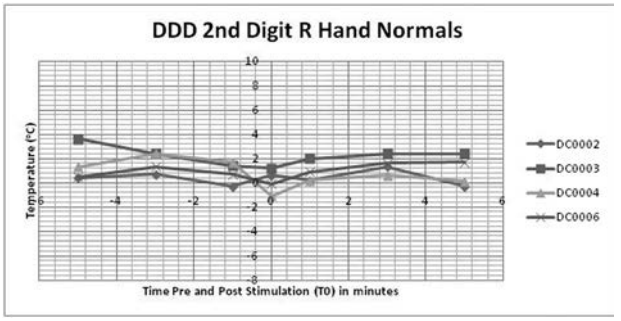

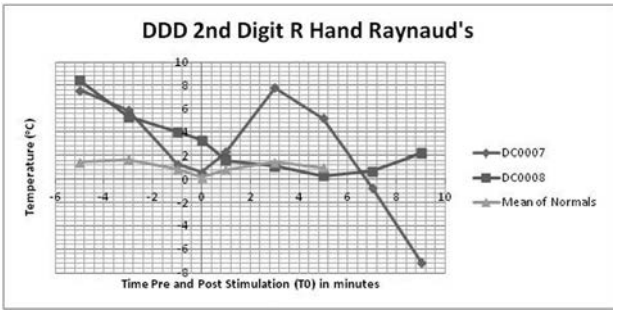

Raynaud, M. (1862). De L'asphyxie Locale et de la Gangrene Symetrique des Extremites. Paris. L. Leclerc, Libraire-Editeur, rue de l'Ecole de Medecine, 14.

Silman, A., Holligan, S., Brennan, P., Maddison, P. (1990). Prevalence of Symptoms of Raynaud's Phenomenon in General Practice. BMJ, 301: 590-592.

Anderson, M.E., Moore, T.L., Lunt, M., Herrick, A.L. (2007). The 'Distal–Dorsal Difference': a Thermographic Parameter by Which to Differentiate between Primary and Secondary Raynaud's Phenomenon. Rheumatology, 46: 533-538.

Thompson, A., House, R., Manno, M. (2007). Assessment of the Hand–arm Vibration

Syndrome: Thermometry, Plethysmography and the Stockholm Workshop Scale. Occupational Medicine, 57: 512-517.

Pelmear, P.L., Roos, J., Leong, D., Wong, L. (1987). Cold Provocation Test Results from a 1985 Survey of Hard-rock Miners in Ontario. Scand J Work Environ Health, 13: 343-347.

Where applicable, the authors confirm that the experiments described here conform with The Physiological Society ethical requirements.

PCB423

Phenotypic characterisation and molecular changes induced by gestational diabetes mellitus on human umbilical endothelial cells: focus on the KDM2B/miR-101/ EZH2 pathway

I. Floris[1], G. Mangialardi[1], A. Posadino[2], G. Capobianco[3], P. Gianfranco[2] and C. Emanueli[1]

[1]Department of Vascular Pathology and Regeneration, Bristol Heart Institute, Bristol, UK, [2]Laboratory of Vascular Biology, Department of Biomedical Science, University of Sassari, Sassari, Italy and [3]Obstetrics and Gynaecology Clinic, University of Sassari, Sassari, Italy

Background and aims: Gestational diabetes mellitus (GDM) is characterised by maternal hyperglycaemia that is first recognised during pregnancy (1). GDM results in chronic foetal hyperglycaemia and hyperinsulinaemia (2), with consequent changes in foetal endothelial gene expression and endothelial cell (EC) function (3). We aim to determine whether exposure to a diabetic intrauterine environment alters human umbilical vein EC (HUVEC) function, with further investigation into microRNA (miR) expression and epigenetic pathways.
Methods: HUVECs were extracted from expecting mothers with and without GDM. We performed functional assays and focused miR and target gene analyses on extracted cell lineages. Finally, we also studied 'healthy' HUVECs that were grown in high glucose conditions.
Results: We observed a reduced capacity of closure on scratch assay, diminished capillary-like tube formation on Matrigel and decreased proliferation in response to foetal bovine serum (FBS), after a period of FBS-starvation, in the GDM-extracted lineages compared with the controls. On microRNA screening we found a tendency towards increased levels of miRs belonging to the miR-15 family. Specifically, miR-101 was significantly upregulated in the GDM-extracted lineages; hence we focused on this miR's molecular mechanisms in our target cell lineages. There was a strong positive correlation between miR-101 levels and apoptosis (Pearson r = 0.9, p value < 0.001). There was a decreased expression of Enhancer of Zester Homolog 2 (EZH2) in the GDM-extracted lineages. Confirming previous reports which have validated EZH2 as a target-gene of miR-101 in HUVECs (4), we found their expression levels were negatively correlated. EZH2 mRNA levels correlated positively with KDM2B and VEGF-A; conversely miR-101 levels correlated negatively with KDM2B. These data are in line with the described KDM2B/EZH2/miR-101/EZH2 axis (5).
Anti-miR-101 treatment in GDM cells resulted in upregulation of EZH2, decreased apoptosis and an improved angiogenic phenotype, restoring the endothelial tube formation to the level seen in control lineages. As expected, in vitro exposure of "healthy" HUVECs to high glucose significantly impaired cellular function. Moreover, we found a concomitant upregulation of miR-101, which is in agreement with high miR-101 levels in GDM HUVECs..
Conclusion: These data identify a signalling pathway that links hyperglycaemia to miR-101 and its target gene EZH2, suggesting new targets in the fields of gestational diabetes and EC dysfunction induced by hyperglycaemia in utero. We characterise a novel mechanism regulating hyperglycaemia-impaired angiogenesis, with the possibility of restoring the angiogenic capacity of GDM cells in vitro by blocking miR-101 and subsequently upregulating its target EZH2.

American Diabetes Association (2011). Diab Care;34(S1):S62-69

Catalano M et al (2011). Am J Obstet Gynaecol;204(6):479-487

Sobrevia L et al (2011). Placenta;25:S159-164

Smith M et al (2011). PLoS ONE;6:e16282

Kottakis F et al (2011). Mol Cell;43:285-298

Where applicable, the authors confirm that the experiments described here conform with The Physiological Society ethical requirements.

PCB424

Modeling of drug kinetics and blood flow response dynamics during transdermal iontophoresis of metacholine and acetylcholine

F. Iredahl[1], J. Hackethal[1], V. Sadda[1], L. Ward[1], E. Tesselaar[1], S. Farnebo[1,2] and F. Sjöberg[1,2]

[1]Department of Clinical and Experimental Medicine, Linköping University, Linköping, Sweden and [2]Department of Hand and Plastic Surgery, County Council of Östergötland, Linköping, Sweden

Transdermal iontophoresis can be used to noninvasively deliver vasoactive drugs into the skin by means of electric current pulses (1). A limitation of iontophoresis is that the delivered drug dose is unknown and the vascular response can only be measured in arbitrary units. Time-response modeling may give better insight in the physiology underlying the vascular drug responses (2).
Acetylcholine (ACh) causes endothelium-dependent vasodilatation after iontophoretic delivery in the skin, and is therefore widely used for measuring endothelial function. ACh is rapidly hydrolyzed by acetylcholinesterase (AChE). Metacholine (MCh) has similar actions as ACh but is hydrolyzed by AChE at a considerably slower rate (3).
In this study, we applied a mechanistic time-response model to the blood flow response to ACh and MCh delivered by iontophoresis in 21 healthy subjects. We measured skin blood flow using laser-Doppler flowmetry. We took into account the physical transport of drugs into the skin and the vascular response to these drugs. The kinetic part of the model consists of one-compartment, with a zero-order influx of drugs, a first order elimination and a lag time constant accounting for the delay between drug delivery and onset of response. The response dynamics are modeled using the Hill equation.
Then, we compared the response to an identical dose (12 mC) of ACh given using a single 10-min current pulse and five 2-minute current pulses with 1-minute intervals.
We found that ACh and MCh caused similar increases in blood flow, whereas the return to baseline perfusion after iontophoresis differed distinctly between drugs (Figure 1). Modeling revealed a mean (95% CI) elimination half-life of 9.0 min (8.0-10.3 min) for ACh and 71 min (41 - 247 min) for MCh. ACh delivered using a single current pulse resulted in stronger vasodilatation than with multiple shorter pulses (38.5 ± 31.7 vs. 30.7 ± 15.5 PU, p < 0.01, Figure 2).
These findings can be explained by the differences in drug kinetics in the skin, as ACh is rapidly hydrolyzed by AChE while MCh is not actively degraded. The sustained vasodilatation after iontophoresis of MCh suggests that washout of these drugs by skin blood flow is slow and that the return to baseline is mainly caused by active degradation.
In conclusion, modeling of drug kinetics and dynamics gives a better understanding for the physiological and pharmacological parameters during iontophoresis of vasoactive drugs and may improve iontophoresis as a non-invasive technique for assessment of vascular function.

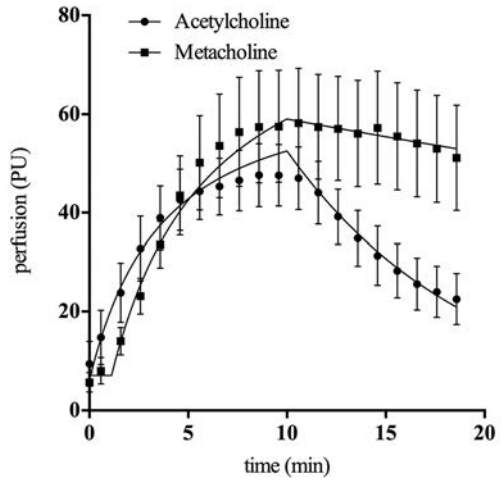

Skin blood flow in response to iontophoresis of acetylcholine and metacholine. Solid lines are the responses predicted by the proposed time-response model.

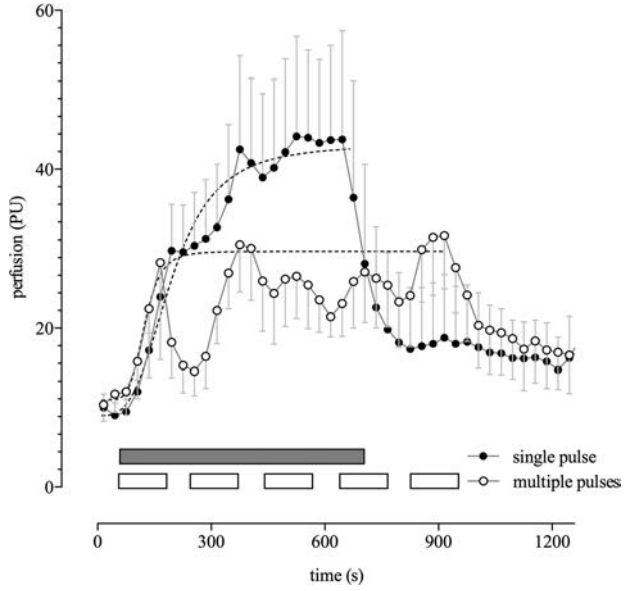

Skin blood flow in response to iontophoresis of acetylcholine, given using a single current pulse or 5 repeated current pulses separated by 1-minute intervals.

Tesselaar E, and Sjoberg F. Transdermal iontophoresis as an in-vivo technique for studying microvascular physiology. Microvasc Res 81: 88-96, 2011.

Tesselaar E, Henricson J, Jonsson S, and Sjoberg F. A time-response model for analysis of drug transport and blood flow response during iontophoresis of acetylcholine and sodium nitroprusside. J Vasc Res 46: 270-277, 2009.

Kimura K, Low DA, Keller DM, Davis SL, Crandall CG. Cutaneous blood flow and sweat rate responses to exogenous administration of acetylcholine and methacholine. J Appl Physiol. 102, 1856-1861, 2007.

Where applicable, the authors confirm that the experiments described here conform with The Physiological Society ethical requirements.

PCB425

Novel mapping of intercellular stresses in endothelial monolayers during contractile responses to hyperpermeability

E. Valent[1], C.C. Hardin[2], R. Krishnan[3], V.W. van Hinsbergh[1] and G.P. van Nieuw Amerongen[1]

[1]Physiology, VU University Medical Center, Amsterdam, Netherlands, [2]Div Pulmonology & Critical Care Med, Massachusetts Gen Hosp, Boston, MA, USA and [3]Center for Vascular Biology Research, Beth Israel Deaconess Medical Center, Boston, MA, USA

Clinical Relevance: The endothelial monolayer is a dynamic, single cell layer which forms a barrier to prevent blood fluids from leaking into the surrounding tissues. During inflammation, endothelial barrier disruption causes vascular leakage which contributes to disease severity in disorders such as sepsis, cancer, diabetes, and atherosclerosis. Despite this tremendous medical threat to the critically ill patients, specific therapy counteracting vascular leakage are lacking up to today.
Rationale: Hyperpermeability of the endothelial barrier is a significant pathogenic phenomenon and is associated with many life-threatening diseases. Previous studies have shown that contractile forces, generated by the endothelium itself, play an important role in the process of barrier dysfunction. With the use of traction force microscopy it is possible to study the developed acto-myosin dependant interaction via the focal adhesions to the cells substrate. However, a measurement of the situation at endothelial cell–cell junctions was not experimentally accessible. Here, we aim for the first time to elucidate the intercellular forces in an endothelial monolayer sheet and observe the developed stresses during thrombin receptor-mediated hyperpermeability.
Methods & Results: Endothial cell monolayer contractions were mapped by the novel described monolayer stress microscopy (1) in combination with previous published traction force microscopy of 4 kPa polyacrylamide gel substrates. (2) Displacements of the caroxylate-modified fluorescent microspheres (Invitrogen, Eugene, OR) incorporated in the gels, were converted into stress components and monolayer traction forces.
Conclusion: Novel intracellular stress mapping in endothelial monolayer was successful and displaced highly diverse stress maps which provides new information about vascular hyperpermeability responses.

Tambe et al., Nature materials, 2011

Krishnan et al. Am J Physiol Cell Physiol, 2011

Supported by Dutch Heart Foundation: 2011T072

Where applicable, the authors confirm that the experiments described here conform with The Physiological Society ethical requirements.

PCC001

Sex differences in the left ventricle ACE activity and ACE inhibition in Spontaneously hypertensive rats

P.L. Dalpiaz[1], A. Lamas[1], I. Caliman[1], L. Gusmão[1], P. Oliveira[1], G. Abreu[1], A. Carmona[1,2], M. Alves[1,2] and N. Bissoli[1]

[1]Physiological Sciences,, Federal University of Espírito Santo, vitoria, espirito santo, Brazil and [2]Biophysics Escola Paulista de Medicina, Unifesp, são paulo, são paulo, Brazil

Studies in humans and hypertension models have demonstrated the role of the RAS in the progression of ventricular dysfunction. The activation of the renin-angiotensin system (RAS) is essential for structural and functional remodeling of the heart. Additionally, it is recognized the role of sex hormones (SH) modulating the RAS. Therefore, we aimed to evaluate the influence of SH on the activity of angiotensin I-converting enzyme (ACE) and angiotensin 2-converting enzyme (ACE2) in male and female rats SHR and the influence of ACE inhibitor in the SRA local and plasma deficiency in HS. Materials and methods: Female (F) and male (M) SHR rats were divided into 8 experimental groups: sham+vehicle (SV), sham+enalapril (SE; 10 mg/kg body weight), castrated+vehicle (CV), and castrated+enalapril (CE). The treatments began 21 days after castration and lasted for 30 days. The ACE and ACE2 activity were measured by fluorimetry. Results: Male rats exhibited a higher values than the female rats in ACE ventricular activity (MSV: 8.47 ± 0.81 AFU, FSV: 5.78 ± 0.79 AFU) and ACE2 (MSV:0.1154 ± 0.017 AFU; FSV: 0.063 ± 0.006 AFU). Regarding ACE activity the castration reduced in males and did not change in female (MCV: 3.72 ± 0.46; FCV: 6.26 ± 0.31). Enalapril treatment both in Sham animals (MSE: 3.99 ± 0.50 and; FSE: 3.91 ± 0.21) as castrated (MCV: 1.94 ± 0.69; FCV: 2.42 ± 0.44) reduced the ACE activity and eliminated the differences between the sexes. In relation to ACE2 activity, in female, none of interventions promoted change in ACE 2 (FSV: 0.063 ± 0.006 AFU; FSE: 0.091 ± 0.010, FCV: 0.095 ± 0.009; FCE: 0.074 ± 0.013). In males the castration promoted reduction in ACE2 (MCV: 0.012 ± 0.003), the enalapril treatment was able to increase ACE2 activity in sham (MSE: 0.167 ± .018) and castrated (MCE: 0.058 ± 0.009) when compared with vehicle values. Conclusion: we observed sexual dimorphism in the plasma and left ventricle ACE activity and in the left ventricle ACE2 activity. Male showed higher activity these enzymes than females. Enalapril treatment reduces the ACE activity regardless of gender and increases ACE2 activity in male, but did not affect in female. The castration, in males, reduced ACE and ACE2, in both plasma and left ventricle depending effects hormones. The effect of enalapril on ACE activity appears to be hormones independent while on ACE2 activity in males appears to dependent on hormones.

Grant Casadinho CNPq/2011

Where applicable, the authors confirm that the experiments described here conform with The Physiological Society ethical requirements.

PCC002

A user-friendly computational model to study Ca^{2+} waves in rat ventricular myocytes

M. Bortolozzi[1,2], K.L. Ford[1] and R.D. Vaughan-Jones[1]

[1]Department of Physiology, Anatomy and Genetics, University of Oxford, Oxford, UK and [2]Department of Physics and Astronomy "G.Galilei", University of Padua, Padua, Italy

Intracellular acidosis is an important modulator of cardiac excitation and contraction, and a potent trigger of electrical arrhythmia, partly through its ability to stimulate acid extruders, which indirectly raises sarcoplasmic reticulum (SR) Ca^{2+}. When this effect is large (a condition known as Ca^{2+}-overload), cardiac myocytes engage in a mode of Ca^{2+} signaling in which Ca^{2+} release from the SR to myoplasm occurs in self-propagating succession along the length of the cell. This event is called a Ca^{2+} wave and is fundamentally a diffusion-reaction phenomenon that is best described with a mathematical model. Wave properties, e.g. frequency, velocity, amplitude and relaxation time are useful parameters to infer how acidic pH affects Ca^{2+}-related components inside the cell, such as the sarco/endoplasmic reticulum Ca^{2+} ATPase (SERCA), myoplasmic Ca^{2+} buffers and the ryanodine receptor (RyR).

We present a new, continuum mathematical model, based on previous work (1), that simulates spontaneous Ca^{2+} waves generated during intracellular acidosis and Ca^{2+}-overload. The model, developed with a user-friendly interface in Matlab, is capable of reproducing Ca^{2+} sparks and wave failure, collision and annihilation. In particular, Ca^{2+} sparks are modeled by a random function that regulates the opening and closing probability of RyRs, which in turn controls the likelihood of wave generation.

Numerical simulations predict that, during Ca^{2+}-overloading conditions, spontaneous Ca^{2+} wave generation significantly helps the cell to control and maintain at a constant level the myoplasmic and luminal Ca^{2+} concentration, as suggested in (2). Increasing Ca^{2+} wave frequency and speed enhances this mechanism, thus giving a simple explanation of what observed experimentally in rat isolated ventricular myocytes, where reducing pH_i increased to 360% (by 60 s) wave frequency, together with increasing wave velocity up to 140%. Inhibiting the sarcolemmal Na^+/H^+ exchanger (NHE) suppressed wave frequency but not the increased velocity. In the model, this behaviour can be reproduced by decreasing K_{ON} of the lumped Ca^{2+} buffers, which is experimentally expected being independent of NHE activity. Wave frequency reduction during NHE inhibition can be explained by a fall in SR Ca^{2+} content mediated by H^+-reduced SERCA activity no longer supported by NHE-driven Ca^{2+} import on NCX. The model shows that reducing SERCA maximum flux instead of its affinity best accounts for the observed experimental change in wave amplitude and relaxation time.

Our model successfully reproduces Ca^{2+} waves using experimentally-derived variables and highlights the importance of SR Ca^{2+} load on wave propagation. At present, we are developing a model to describe a cardiac multicellular system connected by gap junctions, providing Ca^{2+} and H^+ intercellular diffusion.

Swietach P., Spitzer K.W., Vaughan-Jones R.D. (2010) Front Biosci 15:661-680

M. E. Diaz, A. W. Trafford, S. C. O'Neill and D. A. Eisner (1997) Jou Physiol 501.1:3-16

Funded by the British Heart Foundation.

Where applicable, the authors confirm that the experiments described here conform with The Physiological Society ethical requirements.

PCC003

Heart rate variability responses to different intensities of musical auditory stimulation in healthy men

J.A. do Amaral[1], H.L. Guida[2], L. de Abreu[3] and V.E. Valenti[2]

[1]Departamento de Fonoaudiologia, Faculdade de Filosofia e Ciências, UNESP, Marília, Brazil, [2]Departamento de Fisioterapia e Terapia Ocupacional, Faculdade de Filosofia e Ciências de Marília – Universidade Estadual Paulista, UNESP, Marília, Brazil and [3]Departamento de Morfologia e Fisiologia, Faculdade de Medicina do ABC, Santo Andre, Brazil

Introduction: The literature has briefly described the association between auditory stimulation and the cardiovascular system. In this context, it is known that exposure to auditory stimulus of the classic musical for eight weeks improved cardiac autonomic regulation, by analysis of heart rate variability (HRV). Moreover, heavy metal music style is related to stress responses. Thus, it is thought that exposure to this style of music can contribute to the development of cardiovascular disease. Our object is to investigate the association between the intensity of the music and HRV. Method: Eight healthy male subjects aged between 18 and 30 years were analyzed. All procedures were approved by the Ethical Committee in research of our Institution. It was excluded subjects who had disorders of hearing sensitivity, cardiorespiratory, neurological and other impairments known that avoided the subject performing the procedures, treatment with drugs that influence cardiac autonomic control and people involved with music (dancing, singing or musical instruments). We evaluated the linear HRV indices in the time domain and the frequency and low frequency. The subjects were exposed to musical auditory stimulation musical of classical baroque and heavy metal styles. Initially HRV was recorded at rest for 10 minutes. Subsequently the subjects were exposed to auditory stimuli musical equivalence of the following levels: 60-70 dB, 70-80 dB and 80-90 dB. Each exposure lasted five minutes and there was an interval of five minutes between each exposure. Results: In relation to the time-domain index, we did not observe significant changes during exposure to classical and heavy metal musical auditory stimulation. The SDNN index tended to be reduced during heavy metal music style exposure at 80-90 dB (59.6+33 ms) compared to the control condition (73.5+41 ms), however, there was no statistical significance (p=0.4). Similar responses were observed during classical baroque musical auditory stimulation at 80-90 dB (50.6+23 ms) compared to control (60.9+32 ms) (p=0.6) We found no significant changes regarding the RMSSD and pNN50 indices related to the time-domain analysis. With respect to the frequency-domain analysis, we found no significant changes regarding the LF and HF in absolute and normalized units (p>0.05). Conclusion: There was no significant influence of musical auditory stimulation in different equivalent sound levels on the HRV. We believe this is due to the small population evaluated

This study received financial support from FAPESP.

Where applicable, the authors confirm that the experiments described here conform with The Physiological Society ethical requirements.

PCC004

Effect of high glycaemic index diet on heart rate variability in Thai Brugada syndrome survivors

R. Chanavirut[1,2], P. Makarawate[3] and N. Leelayuwat[1,2]

[1]Department of Physiology, Faculty of Medicine, Khon Kaen University, Khon Kaen, Thailand, [2]Exercise and sport sciences development and research group, Khon Kaen University, Khon Kaen, Thailand and [3]Department of Medicine, Faculty of Medicine, Khon Kaen University, Khon Kaen, Thailand

Brugada syndrome is one of the major causes of sudden death among male younger population in Southeast Asian countries including Thailand1. The syndrome manifestation occurs most frequently at night time1. It has been reported that a number of predisposing factors such as exercise, glucose, insulin or meal could modulate the syndrome2-3. In addition, previous studies suggested that an abnormality of autonomic modulation may be related to the syndrome4-5. However, there is no report regarding autonomic response to these factors. Objective of this study was to assess and compare responses of autonomic nervous system to exercise after the ingestion of high glycaemic index (HGI) meal between Thai Brugada syndrome survivors and age-match healthy subjects.

Fifteen patients (age between 40 and 60 years) were randomly assigned to perform exercise on electromagnetic cycle ergometer with and without pre-exercise (an hour) ingestion of 97 g of glutinous rice as a HGI meal. Fifteen age-match healthy subjects also underwent the same protocol. After overnight fasting, an hour before and immediately after the exercise blood samples were collected to analyze glucose and insulin concentrations. Electrocardiogram was recorded and analyzed for heart rate variability (HRV) and heart rate recovery (HRR) throughout the experiment. Data were compared by paired and unpaired-t test and presented in mean ± SE. Our procedure was approved by ethic committee of Khon Kaen University under the Declaration of Helsinki in 1964.

The results revealed that blood glucose (Brugada = 87.67 ± 1.53 and 108.67 ± 5.62 mg/dL and healthy = 93.33 ± 3.70 and 110.93 ± 7.20 mg/dL) and insulin concentration (Brugada = 16.52 ± 3.10 and 25.28 ± 3.00 uIU/ml and healthy = 9.98 ± 1.43 and 24.35 ± 4.46 uIU/ml) significantly increased ($p<0.05$) in both groups with HGI meal. Meanwhile blood parameters were not significantly different between groups without HGI meal.

Having HGI meal did not affect HRR (Brugada with- and without HGI = 22 ± 2, 24 ± 2 beats and healthy = 27 ± 3, 24 ± 3 beats). In addition, both groups did not show any difference in resting HRV. However, Brugada survivor showed a significantly lower sympathetic activity ($p<0.05$) indicated by LF(nu) after exercise without HGI diet. LF(nu) with and without HGI diet during a final stage of exercise testing of Brugada and control were 42.88 ± 6.65, 30.23 ± 5.67 nu and 51.56 ± 3.60, 47.77 ± 3.54 nu, at 1 min of HRR were 47.64 ± 5.83, 34.75 ± 4.32 nu and 44.25 ± 4.01, 49.87 ± 4.40 nu and cool down periods were 43.78 ± 5.92, 32.64 ± 4.59 and 47.24 ± 3.86, 45.51 ± 4.13 nu. Our results suggest that HGI meal stimulated insulin secretion and sympathetic nervous activity in Brugada syndrome survivors whereas without any effect on healthy subjects.

1. Nademanee K. Sudden unexplained death syndrome in Southeast Asia. Am J Cardiol 1997;79:10-11.

2. Nogami A, Nakao M, Kubota S, Sugiyasu A, Doi H, Yokoyama K, et al. Enhancement of J-ST-segment elevation by the glucose and insulin test in Brugada syndrome. PACE 2003;26:332-337.

3. Ikeda T, Abe A, Yusu S, Nakamura K, Ishiguro H, Mera H, Yotsukura M, Yoshino H. The full stomach test as a novel diagnostic technique for identifying patients at risk of Brugada syndrome. J Cardiovasc Electrophysiol 2006;17:602-607.

4. Matsuo K, Kurita T, Inagaki M, Kakishita M, Aihara N, Shimizu W, et al. The circadian pattern of the development of ventricular fibrillation in patients with Brugada syndrome. Eur Heart J 1999;20:465-470.

5. Krittayaphong R, Veerakul G, Nademanee K, Kangkagate C. Heart rate variability in patients with Brugada syndrome in Thailand. Eur Heart J 2003;24:1771-1778.

Where applicable, the authors confirm that the experiments described here conform with The Physiological Society ethical requirements.

PCC005

Redox-sensitive inactivation of the phosphatase and tensin homolog deleted on chromosome 10 contribute to enhanced activation of phosphoinositide 3-kinase/serine/threonine protein kinase signaling in rostral ventrolateral medulla and neurogenic hypertension in spontaneously hypertensive rats

J.Y. Chan and S.H. Chan

Center for Translational Research in Biomedical Sciences, Kaohsiung Chang Gung Memorial Hospital, Kaohsiung, Taiwan

The activity of phosphoinositide 3-kinase (PI3K)/serine/threonine protein kinase (Akt) is enhanced under hypertension. The phosphatase and tensin homolog deleted on chromosome 10 (PTEN) is a negative regulator of PI3K signaling, and its activity is redox-sensitive. In rostral ventrolateral medulla (RVLM), which is responsible for the maintenance of blood pressure, oxidative stress plays a pivotal role in neurogenic hypertension. The present study evaluated the hypothesis that redox-sensitive inactivation of PTEN results in enhanced PI3K/Akt signaling in RVLM, leading to neurogenic hypertension. Compared to age-matched normotensive Wistar Kyoto (WKY) rats, PTEN inactivation in the form of oxidation and phosphorylation were greater in RVLM of spontaneously hypertensive rats (SHR). PTEN inactivation was accompanied by augmented PI3K activity and PI3K/Akt signaling. Intracisternal infusion of tempol or microinjection into the bilateral RVLM of adenovirus encoding superoxide dismutase significantly antagonized the PTEN inactivation and blunted the enhanced PI3K/Akt signaling in the anesthetized SHR. Gene transfer of PTEN to RVLM in the anesthetized SHR also abrogated the enhanced Akt activation and promoted antihypertension. Silencing PTEN expression in RVLM with small interfering RNA, on the other hand, augmented PI3K/Akt signaling and promoted long-term pressor response in normotensive WKY rats. The present study demonstrated for the first time that the redox-sensitive check-and-balance process between PTEN and PI3K/Akt signaling is engaged in the pathogenesis of hypertension, and an aberrant interplay between the redox-sensitive PTEN and PI3k/Akt signaling in RVLM underpins neural mechanism of hypertension.
Wu KLH et al. (2013). Antioxid Redox Signal 18, 36-50.

This work was supported by research grants OMRPG8C0031 (J.Y.C.) and OMRPG8C0021 (S.H.C.) from the Chang Gung Medical Foundation, and NSC100-2320-B-182A-004-MY3 (J.Y.C.) from the National Science Council, Taiwan, Republic of China.

Where applicable, the authors confirm that the experiments described here conform with The Physiological Society ethical requirements.

PCC006

High blood pressure increases brain neuronal nitric oxide synthase activity to buffer salt-sensitive hypertension in Dahl rats

M. Tandai-Hiruma[1], K. Kato[2], T. Kemuriyama[1], H. Ohta[1], A. Tashiro[1], K. Hagisawa[1] and Y. Nishida[1]

[1]Physiology, National Defense Medical College, Tokorozawa, Japan and [2]Psychiatry, Faculty of Medicine, University of Miyazaki, Miyazaki, Japan

We have demonstrated that activity of central neuronal nitric oxide synthase (nNOS) containing neurons and its mediated sympathoinhibition are enhanced in hypertensive Dahl salt-sensitive (DSS) rats (Tandai-Hiruma et al, 2005). However, it is not clear what enhances nNOS activity in these neurons in this rat strain (high salt intake, increased blood pressure or something else) or how these neurons are enhanced in salt-induced hypertension. Are the increases in activity compensatory to buffer the hypertension even though hypertension is not relieved? The aims of the present study were to identify the mechanism underlying enhanced nNOS activity in the brain of hypertensive DSS rats and the consequences of enhanced nNOS activity. Male 8-week-old rats (Dahl/J Seac, n=5 for each group) were fed either a regular (0.4% NaCl) or high-salt (8% NaCl) diet with or without 0.25% nifedipine, for 4 weeks. The effects of nifedipine, which lowers blood pressure peripherally, on central nNOS were determined by measuring nNOS activity, as well as the number of nNOS-positive neurons in the brain stem and diencephalon. The effects of chronic (12 days) intracerebroventricular (i.c.v.) infusion of 7 μg (0.5 μL/h) *S*-methyl-L-thiocitrulline (SMTC, nNOS inhibitor) on mean arterial pressure (MAP) were assessed in conscious freely moving DSS rats using a radiotelemetry system. Rats were anaesthetized with pentobarbital (50 mg/kg, i.p.) and telemetry transmitters installed. Continuous recordings of arterial pressure were made for 20 days (6 days on a regular diet followed by 14 days on a high-salt diet) prior to, and 12 days during, osmotic minipump driven i.c.v. infusion of SMTC. In addition, the number of central nNOS-positive neurons was compared between DSS and salt-insensitive Sprague-Dawley rats (n=5 for each group). Values are means ± S.E.M., compared by ANOVA. Normalization of blood pressure by nifedipine attenuated the increase in nNOS activity in the brain stem of DSS rats. Chronic i.c.v. infusion of SMTC further enhanced hypertension in DSS rats. Differences in average MAP from Day12 to Day 26 were significantly greater ($p<0.05$) in SMTC-infused DSS rats compared with aCSF-infused DSS rats in both the day (31.9 ± 4.7 vs. 17.2 ± 2.1 mmHg) and night (26.1 ± 3.3 vs.12.2 ± 2.2 mmHg) phases (Figure 1). Feeding of a high-salt diet increased nNOS-positive neurons in the lateral parabrachial nucleus, rostral ventrolateral medulla, and nucleus tractus solitarius of DSS compared with Sprague-Dawley rats, whereas nNOS-positive neurons in the paraventricular nucleus remained downregulated in DSS rats. These results suggest that hypertension, rather than a high-salt diet, increases central nNOS activity in hypertensive DSS rats to buffer high blood pressure. However, this compensatory response may be insufficient to relieve salt-induced hypertension.

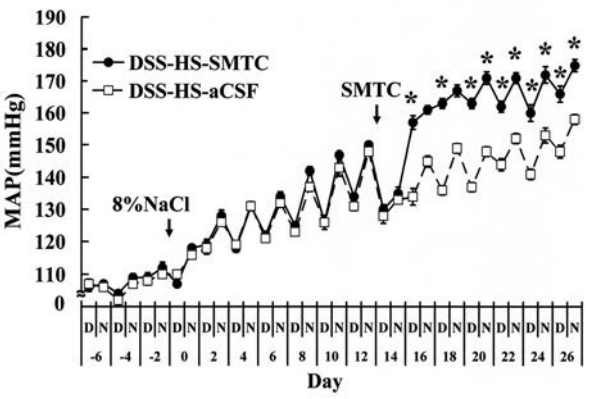

Fig. 1 Changes in mean arterial pressure (MAP) during the day–night (D) and night–day (N) phases in Dahl salt-sensitive (DSS) rats fed a regular diet for 6 days followed by a high-salt diet for 14 days. After 14 days, one group of rats was infused i.c.v. with *S*-methyl-L-thiocitrulline (SMTC; a stereoselective competitive nNOS inhibitor), whereas the other was infused with artificial cerebrospinal fluid (aCSF). Both groups continued on the high-salt diet for a further 12 days. The MAP values in each phase (D or N) of the day are the average of 1440 sampled values obtained by radiotelemetry over 12 h for each group. Data are the mean ± SEM (n = 5 rats per group). $^{*}P<0.05$ compared with average MAP in the corresponding phase on Day 12 in aCSF-infused DSS rats (one-way repeated-measures ANOVA followed by the Tukey–Kramer post hoc test). All night values are significantly larger than the day values, except for the first 4 days of i.c.v. SMTC.

Tandai-Hiruma M *et al.* (2005). *J Hypertens* **23**, 825-34.

Where applicable, the authors confirm that the experiments described here conform with The Physiological Society ethical requirements.

PCC007

Blood pressure responses to L-cysteine injected into the rostral ventrolateral medulla of the anesthetized rat

Y. Takemoto and Y. Matsumoto

Basic Life Sciences, Hiroshima University Institute of Biomedical and Health Sciences, Hiroshima, Japan

The sulfur containing non-essential amino acid L-cysteine known as neurotoxin is suggested to play a physiological role (ref. 1). When injected into the cisterna magna of conscious rats, L-cysteine produces an increase in blood pressure, equivalent to a neurotransmitter of L-glutamate (ref. 2). The present study examined if the rostral ventrolateral medulla (RVLM), which has cardiovascular sympathetic premotor neurons, responds to microinjected L-cysteine in anesthetized rats. The RVLM was directly accessed by the ventral surface of the medulla under urethane anesthesia (1.3 g/kg, i.p.) and catheters were inserted into the terminal aorta for arterial blood pressure measurement and the femoral vein for drug injections (refs. 3-5). The rat was immobilized by i.v. injection of pancuronium bromide (1 mg/kg, additional 0.5 mg/kg) and ventilated by a respirator. An adequacy of anesthesia was assessed by arterial blood pressure stability and/or the absence of a withdrawal response to a firm tow pinch. In the RVLM identified with pressor response to L-glutamate (0.01 M, 46 nl), seven times repeated injections of L-cysteine (0.1 M, 46 nl) produced stable pressor responses without fading (21.4 ± 1.5 mmHg, mean ± SD, for 62.7 ± 3.9 mmHg), suggesting no neurotoxic action for acute repetitive stimulation with L-cysteine less than this dose in the RVLM. Microinjections of L-cysteine increased blood pressure in a dose-dependent manner (0.003 M to 0.1 M), while L-glutamate did from 0.001 M. An equivalent increase of 15 mmHg was obtained with 0.03 M of L-cysteine and 0.01 M of L-glutamate. Preliminary examinations showed that there were no detectable changes in blood pressure for microinjection of each structurally related amino acid: D-cysteine, N-acetyl-L-cysteine, DL-homocysteine with ranging from 0.003 M to 0.03 M, except a pressor response to L-homocysteine at 0.03 M. The pressor response to L-cysteine (0.03 M, 21.3 ± 6.2 mmHg, n=8) was significantly blocked (2.4 ± 3.4 mmHg, $p<0.01$ by t-test) after prior injections of both types of ionotropic excitatory amino acid receptor antagonists MK801 (20 mM, 68 nl) and 6-cyano-7-nitroquinoxaline- 2,3-dione (CNQX, 2 mM, 68 nl), suggesting involvement of NMDA receptors and non-NMDA receptors in the pressor action of L-cysteine in the RVLM of the rat. The findings indicate that 1) neurons in the RVLM of anesthetized rats produce dose-dependently the pressor response to L-cysteine possibly in a molecular structural specific manner, and 2) the pressor response is mediated by ionotropic excitatory amino acids NMDA and non-NMDA receptors.

Janaky R et al. (2000). Neurochem Res 25, 1397-1405.

Takemoto Y (1995). Jpn J Physiol 45, 771-783.

Takemoto Y (2004). Jpn J Physiol 54, 339-345.

Takemoto Y (2005). Auton Neurosci 120, 108-112.

Takemoto Y (2007). Neurosci Lett 425, 12-17.

Where applicable, the authors confirm that the experiments described here conform with The Physiological Society ethical requirements.

PCC008

Changes in cardiovascular function and electrolyte balance following chronic exposure of rats to gasoline fumes

C.N. Anigbogu and S.E. Adewale

Department of Physiology, University of Lagos, Lagos, Lagos, Nigeria

Increased exposure to gasoline and petroleum products is inevitable due to increased use for transport, power generation and even as substance of abuse. The effects of gasoline vapour on various body functions and electrolyte metabolism have not been fully understood. The present study was designed to investigate the effect of gasoline vapour on blood pressure, heart rate and cardiovascular reflexes and to determine plasma Na+ and K+ concentrations in rats. The Sprague Dawley rats used in this experiment were exposed to 27.8±1.7ml of wholly vaporized Premium Motor Spirit (PMS) blend unleaded gasoline (UG) for 6hr/day, 5 days/week, for 4 weeks in glass exposure chambers. The control rats were not exposed to gasoline vapour but were placed in the chambers. All rats were fed with standard rat chow and tap water ad libitum throughout the experimental period. The control and experimental rats were anaesthetized with sodium pentobarbitone (65mg/kg bodyweight) and dissected. The femoral artery was cannulated for blood pressure recording. The carotid arteries were isolated for test of cardiovascular reflexes by bilateral carotid occlusion (BCO) of 30 seconds duration. Heart rate was computed from the blood pressure pulse. Blood samples were thereafter collected by cardiac puncture for measurement of plasma Na+ and K+ concentrations. The results from the experiments revealed that chronic exposure to gasoline vapour induced a significant reduction in systolic pressure (from 131.70±4.6 to 95.40±4.3mmHg)($p< 0.05$), diastolic pressure (from 100.00±6.1 to 62.00±5.1mmHg), mean

arterial pressure (MAP) (from 110.57±5.4 to 73.13±4.7mmHg) and heart rate (from 419.20±14.8 to 363.30±6.4 beats/min). Baroreflex sensitivity tested by carotid occlusion was lower in the treated rats when compared with the control group. The plasma concentration of Na+ ions showed an insignificant increase (from 137.7±1.1 to 140.0±1.7 mmol/L; P>0.05) while K+ ions were significantly higher in treated rats compared with the control rats (from 4.7±0.4 to 6.5±0.3 mmol/L; P<0.05). This may be an indication of interference with membrane functions. These results obtained in this study indicate that exposure to gasoline vapour cause a reduction in cardiovascular functions and increase in plasma Na+ and K+ concentrations which may imply an alteration of metabolic processes.

Where applicable, the authors confirm that the experiments described here conform with The Physiological Society ethical requirements.

PCC009

The influence of nutrition, smoking and alcohol intake on head blood perfusions in the medical students

T. Zaporozhets, L. Korovina and O. Sanyk

Department of Physiology, Ukrainian medical stomatological academy, Poltava, Ukraine

Health state in the young people is a serious problem in Ukraine. Many of them have abundant weight, use fats and take alcohol as well as they have got low physical activities. We have assessed interconnections between nutrition, smoking and alcohol intake on head blood perfusion in the medical students to gain such a goal as feeding and life style correcting. Using rheoencephalography (REG), anthropometric data has been gathered on 97 medical university students with regard to nutrition, smoking and alcohol intake. Average student age was 19,1, ±0,2 years, body mass was 65,8, ±1,4 kg, height was 173,4, ±1,0 cm, Body Mass Index (BMI) was 24,9 ±1,4 kg/m.

REG data showed that blood perfusion in the front part of the head is reduced in 29,9 % of subjects surveyed, is normal in 37,7 %, and is increased in 32,5 % of cases. Rear head blood perfusions are reduced in 45,5%, are normal in 24,7%, and are increased in 29,9 % of those surveyed. The blood perfusion in the front part of the head was correlated inversely with body mass (τ =-0,39, p <0,001), height (τ =-0,42, p <0,001), body surface area (τ =-0,45, p <0,001), BMI (τ =-0,30, p <0,001), and coefficient of hand force (τ =-0,29, p <0,001). Also a negative relationship was observed with the use of lard (τ =-0,21, p <0,05), intensity of smoking (τ =-0,30, p <0,005 and τ =-0,27, p <0,02 accordingly), incidence of alcohol intake (τ =-0,25, p <0,02 and τ =-0,21, p <0,05 accordingly). The blood perfusion level of the back part of the head had a negative correlation with body mass (τ =-0,30, p <0,001), body surface area (τ =-0,27, p <0,001), BMI (τ =-0,31, p <0,001), coefficient of hand force (τ =-0,21, p <0,02) and level of emotional stress during the previous year (τ =-0,23, p <0,05).

A positive correlation of blood perfusion of the front part was observed with the level of consumption of fresh fruit (τ =0,33, p <0,02), vegetables (τ = 0,34, p <0,001), and fish (τ = 0,24, p <0,001). Similarly, the blood perfusion of the back part of the head also had a positive correlation with the level of consumption of fresh fruit (τ = 0,26, p <0,001), vegetables (τ = 0,23, p <0,001), and quantity of fish (τ = 0,37, p <0,001).

The blood perfusion level of the back part of the head had a positive correlation with the training success of the students (τ = 0,27, p <0,005). Thus, the use of fresh fruit, vegetables and fish may increase the level of blood perfusion of the head. Smoking and the frequent use of alcohol may decrease the level of blood perfusion of the head.

Where applicable, the authors confirm that the experiments described here conform with The Physiological Society ethical requirements.

PCC010

Projections from nucleus raphe obscurus to the caudal pressor area in the rat

H.A. Futuro Neto[1,3], J.G. Pires[2,4] and N.F. Silva[1]

[1]Morphology, UFES, Vitoria, E S, Brazil, [2]UNIVIX, Vitoria, E S, Brazil, [3]EMESCAM, Vitoria, E S, Brazil and [4]UNESC, Colatina, E S, Brazil

Previous studies have shown different cardiorespiratory effects induced by stimulation of nucleus raphe obscurus (NRO). The present study demonstrates the existence of c-Fos activation in the caudal pressor area (CPA) after NRO stimulation in barodenervated rats and projections from the NRO to the CPA with HRP. Male Wistar rats (300-350 g, N = 24) were used. The animals in the c-Fos group were barodenervated (chloral hydrate, 0.4 g/kg, ip). One day later the animals were instrumented for cardiorespiratory recordings (urethane 1.2 g/kg, iv, after Fluothane induction). After electrical stimulation of NRO (SNRO, 70μA, for 10s; 11.8 mm caudal to the Bregma and 7.8 mm depth) done every minute for 1 hr, the animals were killed by urethane overdose and the brains were processed for c-Fos. Control rats had the electrode only positioned. The HRP group, under anesthesia (chloral hydrate, 0.4 g/kg, ip), received unilateral HRP microinjection (50 nL, 20% saline) into the CPA (1.0 mm caudal and 1.7 mm lateral to the obex; 2.0 mm depth) and the animals were kept alive for 2-3 days. Following, they were killed by urethane overdose and the brains were processed for HRP. The experimental protocol was approved by CEUA EMESCAM (No. 021/2007). The results are presented as means ± SEM and statistical significance was assessed with t-test. SNRO caused increase in MBP (control 90 ± 5, SNRO: 156.8 ± 6 mmHg, P<0.01), bradycardia (control 416 ± 16, SNRO: 356 ± 16 bpm, P<0.01) and hypopnea (control 26.6 ± 0.9, SNRO: 16.4 ± 0.3 AU, P<0.01). C-Fos-expression was observed into the CPA ~1.0 mm caudal to the calamus scriptorius, ~2.0 mm lateral to the midline, and ~1.7 mm ventral to the medullary surface, respectively. In a total of 6 rats used for the HRP study, 5 showed markings in the NRO. This study provides additional support to the idea that NRO influences upon autonomic functions are partially mediated through projections to the CPA.

UNIVIX/ FAPES

Where applicable, the authors confirm that the experiments described here conform with The Physiological Society ethical requirements.

PCC012

Neurones in the PVN, which project to the intermediolateral cell column, express subunits of the $GABA_A$ and NMDA receptors known to be altered in hypertension and pregnancy

S.C. Cork, P.L. Chazot and S. Pyner

School of Biological and Biomedical Sciences, University of Durham, Durham, UK

Studies suggest that both hypertension and pregnancy are conditions associated with increased activity of the sympathetic nervous system. This increased activity is due, in part, to changes in the neurochemistry of the hypothalamic paraventricular nucleus (PVN).

Work previously presented to the Physiological Society showed that the PVN of both spontaneously hypertensive (SHR) and late-term pregnant rats were associated with a significant decrease in the expression of the α1 and α5 subunits of the $GABA_A$ receptor. In the SHR, α5 expression was 97 ± 2% lower than Wistar controls. Furthermore, the SHR was also associated with a significant increase in expression of the GluN2A subunit of the NMDA receptor. These molecular changes could underpin the sympathoexcitation observed in these two states. We therefore aimed to assess whether these subunits were associated with presympathetic neurones (PSN) targeting the spinal cord.

All experiments were performed in accordance with the Animals (Scientific Procedures) Act, 1986. Female Wistar rats (n=5) were anaesthetised with medetomindine (0.6mg/kg) and ketamine (30mg/kg) and secured into a stereotaxic frame. The T2 region of the spinal cord was exposed and 2μl of 2% Fluorogold (FG) was injected into the IML region. Animals were left to recover for 7 days before being perfused via the descending aorta with 4% paraformaldehyde. Brains were sectioned to 40μm and sections were stained for either the α1 or α5 subunit of the $GABA_A$ receptor or the GluN2A subunit of the NMDA receptor. This was visualised using a fluorescently-conjugating secondary antibody and viewed under epifluorescence.

Quantitative analysis of the number of double labelled neurones show that 55.15 ± 2.5% of PSN express the α1 subunit and 73.29 ± 3.2% express the α5 subunit of the $GABA_A$ receptor. Furthermore, 54.95 ± 2.8% of PSNs express the GluN2A subunit of the NMDA receptor. Of those PSNs which did not express either the α1 or GluN2A subunits, many were found in close apposition to neurones which did express these subunits. Furthermore, a number of neurones were found to be positive for the either of the subunits in the absence of FG expression.

These results suggest that a significant proportion of PSNs emanating from the PVN have the potential to be influenced by the changes in $GABA_A$ and NMDA receptor subunit expression presented previously. The changes observed are likely to significantly increase the level of neuronal activity of these neurones and thus sympathetic activity. Furthermore, it is likely that a number of other neuronal populations within the PVN are also likely to be influenced by these changes.

Where applicable, the authors confirm that the experiments described here conform with The Physiological Society ethical requirements.

PCC013

Superoxide anions in paraventricular nucleus mediate the pressor effects of salusin-β and arginine vasopressin release via PKC signal way in hypertensive rat

H. Sun, L. Zhang, Z. Fan, L. Zhang, X. Xiong, L. Ding, X. Gao and G. Zhu

Department of Physiology, Nanjing Medical University, Nanjing, Jiang Su, China

Salusin-β is a bioactive peptide with peripheral hypotensive, mitogenic, pro-atherosclerotic effects, and stimulates the arginine vasopressin (AVP) release from perifused rat pituitary (Shichiri et al, 2003). Salusin-β was found in paraventricular nucleus (PVN) and posterior pituitary (Suzuki et al, 2007). We recently found that microinjection of salusin-β into the PVN increased blood pressure and sympathetic outflow in renovascular hypertensive rats but not in sham-operated rats, which was mediated by both circulating AVP and AVP in rostral ventrolateral medulla (Chen et al. 2013). However, the downstream pathway in mediating the effects of salusin-β is unkown. The present study was designed to determine whether superoxide anions in the PVN were involved in the effects of salusin-β, and whether the production of superoxide anions was dependent on protein kinase C (PKC) and NAD(P)H oxidase in 2K1C rats. Renovascular hypertension was induced by two-kidney, one-clip (2K1C) in male Sprague–Dawley rats weighing 160-180 g under anaesthesia (pentobarbital sodium, 60 mg/kg, ip). Acute experiments were carried out 4 weeks after the 2K1C or sham operation under urethane (800 mg/kg) and alpha-chloralose (40 mg/kg) anesthesia intraperitoneally. Renal sympathetic nerve activity (RSNA), mean arterial pressure (MAP) and heart rate (HR) were recorded. Superoxide anion levels and NAD(P)H oxidase activity were measured with chemiluminescence method. Plasma AVP levels were determined with commercial Elisa kits. Values were expressed as mean±SE, compared by T-test or ANOVA (n=6 for each group). PVN microinjection of superoxide anion scavenger PEG-SOD (4 IU) almost abolished the RSNA and MAP responses to salusin-β compared with saline (RSNA change: 1.4±1.9 vs. 10.2±2.7 %, $P<0.05$; MAP change: 1.1±1.3 vs. 9.7±2.1 mm Hg, $P<0.05$). Similarly, NAD(P)H oxidase inhibitor apocynin (1 nmol) or PKC inhibitor chelerythrine chloride (CLC, 3 nmol) almostly abolished the effects of salusin-β . Salusin-β in the PVN increased superoxide anion level and NAD(P)H oxidase activity compared with vehicle (26.6±1.6 vs. 13.7±1.5, $P<0.01$, and 20.8±2.9 vs. 8.6±1.9 mean light units/min/mg protein, $P<0.05$, respectively), which was abolished by CLC pretreatment. Pretreatment with either PEG-SOD or CLC abolished the increased plasma AVP levels caused by salusin-β (6.7±0.4 and 7.6±0.2 vs. 12.7±0.9 pg/ml, $P<0.05$ and $P<0.01$, respectively). These results indicate that superoxide anions in the PVN mediate the effects of salusin-β in the PVN on the RSNA, MAP and AVP release, and that the production of superoxide anions in the PVN was dependent on PKC and NAD(P)H oxidase in 2K1C rats.

This work was supported by National Natural Science Foundation of China (31171095 & 31271213).

Where applicable, the authors confirm that the experiments described here conform with The Physiological Society ethical requirements.

PCC014

Further evidence demonstrating the significant role of juxtapulmonary capillary receptors in exertional breathlessness of cardiac disease patients

A. Anand[1], P. Barwad[2], N. Srivastava[1] and S. Ramakrishnan[2]

[1]Exertional Breathlessness Studies Laboratory, Vallabhbhai Patel Chest Institute, Delhi, India and [2]Department of Cardiology, All India Institute of Medical Sciences, New Delhi, India

We established that an increase in dysponea-free duration of exercise in mitral stenosis patients after percutaneous mitral valvulotomy which lowers their raised left atrial pressures and pulmonary congestion, was the reduction of juxtapulmonary capillary (J) receptor stimulus and so of their reflex effects (Anand et. al., 2009) which are to accelerate breathing and limit physical activity (Paintal, 1969). In humans they can be also stimulated chemically by lobeline (Raj,et.al., 1995; Anand et al.,2010). With a view to substantiating this conclusion we studied patients with Eisenmenger syndrome (ES). ES is characterized by both a high pulmonary artery pressure and raised pulmonary vascular resistance index due to a ventricular septal defect which also leads to a fall in arterial oxygen saturation (SaO2). The studies conformed to the Helsinki Declaration and were approved by the ethical committee of All India Institute of Medical Sciences. The protocols involved (i) distance covered in a 6-min walk test (6MWT) (ii) duration of exercise according to a modified Bruce Protocol limited by discomfort or a 20%fall in SaO2 (iii) threshold dose of lobeline for eliciting respiratory sensations. Responses were restudied after 6 weeks of medication with sildenafil (3mg TDS), a phosphodiesterase type-5 inhibitor and a preferential pulmonary vasodilator. After medication the mean (estimated) pulmonary artery systolic pressure fell from 104.5±4.18 to 90.6±2.8 mmHg (P= 0.0001);resting SaO2 which was 89.8± 1.2 mmHg remained unchanged at 89.8± 0.86 mmHg;distance covered in 6MWT increased from 487.5± 44.9 to 551.25±39.0 meters (P=0.0001) and the mean duration of exercise increased from 8.26±0.9 to 10.47±1.06 min (P=0.002), demonstrating a significant improvement in their symptomatic status. Threshold dose of lobeline i.v. gave rise to exercise-related respiratory sensations and decreased significantly from 37.5±3.4 to 20.3±1.8μg/kg (P=0.001).

A fall in lobeline-sensation dose indicates a fall in pulmonary vascular resistance; the latter having been reported with oral tadalafil, also a phosphodiesterase type-5 inhibitor (Mukhopadhyay et al.,2006). Since a reduction in pulmonary vascular resistance with these drugs constitutes a reduction in stimulus to J receptors, their reflexes which are the patients symptoms, will also be attenuated.SaO2 remained unchanged with sildenafil medication for up to 6 weeks and appears to play an insignificant role in the patient's clinical improvement.

Anand et al. (2009). Resp Physiol & Neurobiol. 169, 297-302

Paintal, A.S. (1969). J. Physiol. 203, 511–532.

Raj,et.al.,. (1995). J. Physiol. 482, 235-246.

Anand et al.(2010). Resp. Physiol.& Neurobiol.173, 132-137.

Mukhopadhyay S. et al.(2006). Circulation 114,1807-1810

We thank the Department of Science & Technology (India) and Cardiothorasic Research Centre (AIIMS) for financial support.

Where applicable, the authors confirm that the experiments described here conform with The Physiological Society ethical requirements.

PCC015

The effects of aortic depressor and lingual-trigeminal nerve stimulations on the neurons in the rostral nucleus tractus solitarius

K. Ishizuka and Y. Satoh

Physiology, Nippon Dental University at Niigata, Niigata, Japan

The rostral part of the nucleus tractus solitarius (NTS) is well known as first order gustatory relay center. However, neurons in the rostral NTS also receive afferent inputs from a lot of different structures and respond to various kinds of peripheral stimuli. For example, somatosensory fibers from oral cavity and baroreceptor afferent fibers have shown to project to the rostral NTS. Therefore, we examined the effects of the aortic depressor nerve (AND) and lingual-trigeminal nerve (LTN) stimulations on the activity of the rostral NTS neurons, and also investigated whether these neurons exhibit a pulse-related activity. The experiments were carried out on 7 male SD rats (300-400 g) under urethane-chloralose anesthesia (500 mg/kg and 50 mg/kg, respectively, i.p.). The arterial blood pressure and an ECG were recorded. The right ADN and LTN were dissected and prepared for stimulation. Animals were artificially ventilated with room air containing 20-35% O2 following neuromuscular blockade with pancronium bromide (1 mg/kg, i.v.). The depth of anesthesia was assessed by monitoring the stability of the arterial pressure and heart rate to noxious pinching of the hind paw at regular intervals and if necessary anesthesia was supplemented by injections of urethane-chloralose (50 and 5 mg/kg/h; i.v.). Single unit activity of the rostral NTS neurons were extracellularly recorded using a single microelectrode, and test stimuli (0.1-0.3mA, 1 pulse with 0.2 ms duration at 10Hz for 10 seconds) were applied to the AND and LTN. In the ECG/ABP-triggered correlation histogram, a neuron was classified as having a pulse-related activity if the cardiac coefficient exceeds 2.0. All data are presented as mean ± S.D., and compared using Student's t test. The recording sites were marked and histologically verified. A total of 36 rostral NTS neurons with spontaneous activity were recorded. Among them, 28 neurons (78%) exhibited a pulse-related activity, whereas 8 neurons (22%) did not exhibit it. The ADN stimulation significantly altered ($p<0.05$) their firing rates in 12 (33%) neurons, and did not ($p>0.05$) in 24 (67%) neurons. Out of 12, 11 neurons decreased their firing rate (3.6± 3.5 spikes/sec vs 8.1± 6.1 spikes/sec for pre-stimuli; $p<0.05$), and 1 neuron increased their firing rate (4.7 spikes/sec vs 2.2 spikes/sec for pre-stimuli; $p<0.05$). On the other hand, the LTN stimulation significantly altered ($p<0.05$) their firing rates in 17 (47%) neurons, and did not ($p>0.05$) in 19 (53%) neurons. Out of 17, 11 neurons decreased their firing rate (4.8± 3.6 spikes/sec vs 10.9 ± 6.9 spikes/sec for pre-stimuli; $p<0.05$), and 6 neurons increased their firing rate (11.1 ± 7.1 spikes/sec vs 5.0 ± 3.6 spikes/sec for pre-stimulus, $p<0.05$). We conclude that ADN and LTN stimulations exert inhibitory/excitatory effects on less than half of the rostral NTS neurons, and these neuronal activities may be involved in the reflex cardiovascular responses in part.

Where applicable, the authors confirm that the experiments described here conform with The Physiological Society ethical requirements.

PCC017

Cymbopogon citratus prevents fructose-induced hypertension in rats

A. Thaeomor[1] and S. Roysommuti[2]

[1]School of Physiology, Institute of Science, Suranaree University of Technology, Muang Nakorn Ratchasima, Nakorn Ratchasima, Thailand and [2]Department of Physiology, Faculty of Medicine, Khon Kaen University, Muang Khon Kaen, Khon Kaen, Thailand

In vitro experiments indicate that Cymbopogon citratus possesses cytoprotective, antioxidant and hypotensive activity. This study tests the hypothesis that Cymbopogon citratus prevents fructose-induced hypertension in adult rats. Male Sprague-Dawley rats were fed normal rat chow and drank water alone (C), 10% fructose in water (F), 20% Cymbopogon citratus extract in water (CC) or 10% fructose plus 20% Cymbopogon citratus extract in water (FC) for 8 weeks. At 14 weeks of age, rats were anesthetized with thiopenthal (50 mg/kg body weight, i.p.), and were tracheostomized, and their femoral artery and vein were inserted polyethylene tube (PE-50 fused to PE-10) for the measuring of arterial blood pressure and infusion of phenylephrine and sodium nitroprusside, respectively. All data were expressed means ± S.E.M., compared by ANOVA, body weight, heart rate, baroreflex sensitivity, blood urea nitrogen, plasma creatinine, plasma sodium, plasma potassium and plasma chloride were not significantly different among the four groups. Compared to C group, high fructose intake (F group) significantly increased mean arterial pressure (C, 104±3 mm Hg versus F, 116±4 mm Hg; $p < 0.05$), decreased fasting blood sugar (C, 91±3 mg/dl versus F, 77±5 mg/dl; $p < 0.05$) and displayed glucose intolerance. These fructose effects were all abolished by Cymbopogon citratus extract treatment (FC group). In addition, the Cymbopogon citratus extract treatment alone had no any significant effect on measured parameters. The present data indicate that Cymbopogon citratus extract prevents fructose-induced hypertension in adult rats, likely by increasing insulin sensitivity.

Abdulla MH, Sattar MA, and Johns EJ. The Relation between Fructose-Induced Metabolic Syndrome and Altered Renal Haemodynamic and Excretory Function in the Rat. International journal of nephrology 2011: 934659.

Adeneye AA and Agbaje EO. Hypoglycemic and hypolipidemic effects of fresh leaf aqueous extract of Cymbopogon citratus Stapf. in rats. Journal of ethnopharmacology 112: 440-444, 2007.

Carlini EA, Contar JdDP, Silva-Filho AR, da Silveira-Filho NG, Frochtengarten ML, and Bueno OF. Pharmacology of lemongrass (Cymbopogon citratus Stapf). I. Effects of teas prepared from the leaves on laboratory animals. Journal of ethnopharmacology 17: 37-64, 1986.

Linda T. Tran Violet G. Yuen John H. McNeill. The fructose-fed rat: a review on the mechanisms of fructose-induced insulin resistance and hypertension. Molecular and Cell Biochemistry 332:145–159, 2009

Suranaree University of Technology

Where applicable, the authors confirm that the experiments described here conform with The Physiological Society ethical requirements.

PCC018

Concerted regulation of respiratory activities via central chemoreceptors

Q. Du, N. Song, R. Guan, G. Wu, D. Zhu and L. Shen

Department of Physiology and Pathophysiology, Fudan University, Shanghai, China

There are possibly multiple pH sensitive chemoreceptors in the central nervous system. Recent findings showed that a fall of pH activates a distinct class of cation channels, the acid-sensing ion channels (ASICs) in peripheral and central nervous system (Akaike and Ueno 1994). On the other hand, the two-pore domain weakly inward rectifying K+ channel (TWIK)-related acid-sensitive potassium (TASK) is pH sensitive channel (Talley et al. 2000) too. Respiratory chemosensitivity seems to arise from interactions of multiple mechanisms, rather than a single unique channel, it has been documented that above mentioned pH sensitive channels may express in a single neuron (Chernov et al. 2010). ASIC1 in lateral hypothalamus contributes to breathing control (Song et al, 2012). But little is known about the composed influences of ASICs and TASK on respiratory regulation. This study investigated the cooperation of ASICs and TASK-1 in central respiratory regulation; they are both acid-sensing ion channels, the former for Na+, and the latter for K+. Sprague-Dawley rats (250-350g, n=8) of either sex were performed in the experiment. Rats were anaesthetized by intraperitoneal administration of 20% urethane (7ml/kg). Artificial cerebrospinal fluid (ACSF) with different pH values (pH = 5.5, 6.5, 7.4, 8.0 respectively, 0.1ul), Amiloride (1.0mM, 0.1ul, the blockade of ASICs), and Arachidonylethanolamide (AEA, 0.92g/mL, 0.1ul, the blockade of TASK-1), were respectively or jointly administered into lateral ventricle (LV) to observe the changes of respiratory activities via phrenic nerve discharge (PND) and its integration (PNDI). The respiratory excitability was increased as pH of ACSF decreased, significantly by pH 5.5 ACSF ($P<0.05$, ANOVAs). A convex concentration-effect curve of AEA was achieved within the concentration range from 10% to 100% at pH7.4. The AEA (50%) excited respiration significantly at pH 7.4 ($P<0.05$, ANOVAs), whereas Amiloride (1mM) inhibited it, though insignificantly. In contrast, the AEA didn't significantly excite the activated respiration at pH 5.5, while Amiloride inhibited it significantly ($P<0.05$, ANOVAs). The joint blockings of ASICs and TASK-1 resulted in the effect in-between that of respective blocking of these channels at both pH 7.4 and pH 5.5. The combined effect of Amiloride and AEA suggest that, medications targeted on ASICs and TASK-1 have opposite effects on phrenic nerve output. These two pH sensitive channels play a concerted role in central chemosensitivity during physiological and pathophysiological changes.

NSFC 81070001 and 30670771, STCSM 09JC1402100, Shanghai Leading Academic Discipline Project B112, Shanghai MICCAI Key Laboratory 06DZ22103.

Where applicable, the authors confirm that the experiments described here conform with The Physiological Society ethical requirements.

PCC019

Ionotropic glutamate receptors in paraventricular nucleus mediate adipose afferent reflex in rats

B. Cui, P. Li, H. Sun, L. Ding, Y. Zhou, J. Wang, Y. Han, F. Zhang and G. Zhu

Department of Physiology, Nanjing Medical University, Nanjing, Jiang Su, China

Injection of leptin into white adipose tissue (WAT) increased sympathetic outflow to the epididymal WAT (Niijima, 1998) and kidney (Tanida et al, 2000) in rats. The sensory and efferent sympathetic innervations of WAT were well documented (Bartness & Song, 2007). We recently found that the sympatho-excitatory reflex, adipose afferent reflex (AAR), was caused not only by leptin, but also by capsaicin, bradykinin or adenosine in WAT, and chemical lesion of paraventricular nucleus (PVN) neurons with kainic acid abolished the AAR induced by WAT injection of capsaicin in normal rats (Shi et al, 2012). More recently, we found that the AAR was enhanced in obesity and obesity-related hypertension rats, and the enhanced AAR contributes to sympathetic activation in obesity hypertension (Xiong et al. 2012). It is unknown whether ionotropic glutamate receptors including N-methyl-D-aspartate (NMDA) and non-N-methyl-D-aspartate (non-NMDA) receptors in the PVN are involved in mediating the AAR. Experiments were carried out in male Sprague–Dawley rats weighing between 300 and 400 g. Each rat was anesthetized by intraperitoneal injection of urethane (800 mg/kg) and α-chloralose (40 mg/kg). Renal sympathetic nerve activity (RSNA) and mean arterial pressure (MAP) were recorded. AAR was evaluated by the the RSNA and MAP responses to the injections of capsaicin (1.0 nmol/μl) into four sites of the right inguinal WAT at a rate of 4.0 μl min-1 for 2 min for each site. Values are means ± SE, compared by ANOVA. Compared with the bilateral PVN microinjection of saline, either NMDA receptor (NMADR) antagonist AP5 (1, 3, 9 or 27 nmol) or non-NMDA receptor (non-NMDAR) antagonist CNQX (1, 3, 9 or 27 nmol) attenuated the AAR in a dose-related manner. AP5 plus CNQX completely abolished the AAR Compared with saline treated rats, the RSNA responses to capsaicin in AP5 (9 nmol), CNQX (9 nmol) and AP5 plus CNQX treated rats were 3.6±0.8, 5.9±1.4 and 0.2±1.1 % vs. 17.0±2.5 %, respectively (n=6 for each group, P<0.01); the RSNA responses to capsaicin in NR2A antagonist NVP-AAM077, NR2B antagonist CP-101,606 and NVP-AAM077 plus CP-101,606 treated rats were 10.0±2.2, 11.1±2.1 and 4.2±1.5 % vs. 17.0±2.5, respectively (n=6 for each group, P<0.05). The results indicate that both NMDAR and non-NMDAR in the PVN mediate the AAR. Both NR2A and NR2B subunits of NMDAR in the PVN are involved in the NMDAR-mediated AAR.

This work was supported by National Natural Science Foundation of China (31171095 & 31271213).

Where applicable, the authors confirm that the experiments described here conform with The Physiological Society ethical requirements.

PCC020

Altered expression profile of neurotrophin transcripts and proteins in the NTS of spontaneously hypertensive rats

S. Gouraud[1], H. Waki[1], M. Takagishi[1], A. Kohsaka[1], J.F. Paton[2] and M. Maeda[1]

[1]Physiology, Wakayama Medical University, School of Medicine, Wakayama, Japan and [2]Physiology and Pharmacology, School of medical sciences, University of Bristol, Bristol, UK

Since the nucleus tractus solitarii (NTS) is a pivotal region for regulating the set-point of arterial pressure, we proposed a role for it in the development of neurogenic hypertension. Our previous findings suggest that the NTS of pre-hypertensive and hypertensive rats (SHR) exhibits abnormal inflammatory condition with elevated anti-apoptotic factors, compared to the normotensive rats WKY (1,2). Whether this chronic condition affects the neuronal growth and plasticity in the NTS remains unknown. To unveil the characteristics of the neurodevelopmental environment in the NTS of SHR, we investigated the expression of neurotrophin transcripts and proteins in SHR. Male animals were humanely killed by cervical dislocation and the NTS was dissected out. To screen for differentially expressed neurotrophin transcripts between the NTS of adult SHR and WKY, total RNAs were extracted from the NTS (SHR & WKY, 10 weeks old, n=6) and submitted to the RT2 Profiler PCR Array system targeting rat neurotrophins and their receptors. Genes showing more than 1.5 fold differences in their expression levels between two groups were targeted for further validation using quantitative real-time RT-PCR (SHR & WKY, 3 & 10 weeks old, n=6 each). Their protein expression levels were also assessed in NTS protein extracts from adult animals (SHR & WKY, 10 weeks old, n=12) by using semi-quantitative western-blotting. The data (means ± S.E.M.) were shown as relative fold differences in SHR compared to WKY and unpaired t-test was used. Gene expression of Gfrα3 (Glial cell line-derived neurotrophic factor family receptor alpha-3), which is known to be involved in neuronal survival and migration, was up-regulated (SHR vs WKY: 2.48±0.31 vs 1.08±0.23 p<0.01) in the NTS of adult SHR, while gene expression of Crhbp (Corticotropin releasing hormone binding protein), a potential neurogenesis modulator, was down-regulated (0.131±0.03 vs 1.15±0.27 p<0.001). In parallel, Gfrα3 protein expression was up-regulated (1.36±0.08 vs 1.00±0.08 p<0.01), whereas Crhbp protein expression was down-regulated (0.79±0.04 vs 1.00±0.08 p<0.05) in the NTS of adult SHR. In pre-hypertensive young animals, the Gfrα3 transcript was found increased (1.37±0.08 vs 1.05±0.12 p<0.05) in the NTS of SHR, while Crhbp transcript did not show any differential expression. Together with our previous results showing that the transcript level of Tnfrsf6 (Tumor necrosis factor receptor superfamily, member 6, Fas), known to be involved in neuronal death and branching, was down-regulated in the NTS of both pre-hypertensive and hypertensive SHR (2), these profiles may affect the development of neuronal circuitry regulating cardiovascular autonomic activity and hence result in the development of neurogenic hypertension in the SHR.

Gouraud SS, Waki H, Bhuiyan ME, Takagishi M, Cui H, Kohsaka A, Paton JF, Maeda M. Down-regulation of chemokine Ccl5 gene expression in the NTS of SHR may be pro-hypertensive.J Hypertens. 2011, 29(4):732-40.

Gouraud SS, Waki H, Bhuiyan ME, Takagishi M, Kohsaka A, Maeda M. Increased anti-apoptotic conditions in the nucleus tractus solitarii of spontaneously hypertensive rat. Auton Neurosci. 2011, 162(1-2):15-23.

Supported by KAKENHI (19599022, 1907458, 21300253).

Where applicable, the authors confirm that the experiments described here conform with The Physiological Society ethical requirements.

PCC021

Sympathetic nerve activity during the development of hypertension in Dahl salt-sensitive rats

M. Yoshimoto[1], N. Mineyama[2], M. Shirai[1] and K. Miki[2]

[1]Cardiac Physiology, National Cerebral and Cardiovascular Center Research Institute, Osaka, Japan and [2]Integrative Physiology, Nara Women's University, Nara, Japan

It has been thought that sympathoexcitation is involved in the pathogenesis of salt-sensitive hypertension. However, only a few attempts have been made to directly measure sympathetic nerve activity during the development of salt-induced hypertension. In the present study, we tried to elucidate how sympathetic nerve activity was involved in the development of hypertension in Dahl salt-sensitive (DS) rats, by directly and continuously measuring renal (RSNA) and lumbar sympathetic nerve activity (LSNA) in the same animals during the development of salt-induced hypertension. Instruments were attached to the subject male DS and Dahl salt-resistant (DR) rats in order to record RSNA, LSNA and arterial pressure via telemetry. The experiment consisted of 3 time periods, a 3-day control, a 14-day 8% salt-diet loading, and a 7-day recovery period. Mean arterial pressure (MAP), RSNA, LSNA and heart rate (HR) were measured continuously and simultaneously throughout the experimental period. MAP increased sharply during the first 3 days after the onset of 8% salt loading, from 100 ± 1 mmHg to 126 ± 1 mmHg, then continued to increase gradually from the 4th to the 14th day of salt loading, reaching 141 ± 1 mmHg in the DS rats. RSNA and LSNA decreased slightly, but significantly ($P<0.05$), during the salt loading period, relative to the pre-salt loading level. HR decreased gradually throughout the experimental period. These data suggest that the progressive increases in MAP induced by the 8% salt loading may not be attributed to the changes in the RSNA, LSNA or HR.

After cessation of the 8% salt loading, MAP decreased exponentially over the 7-day recovery period. RSNA increased significantly in a sustained fashion in DS rats after cessation of the salt loading, while it remained unchanged during the corresponding period in the DR rats. No differences were shown in the responses of LSNA and HR to the cessation of the salt loading in DS rats, compared with the DR rats. It is therefore likely that RSNA may sensitively response to the decrease in salt intake, while it is insensitive to the increase in salt intake.

In summary, the present observations suggest that neither RSNA and LSNA may be critically involved in the early phase of hypertension development induced by 8% salt loading in Dahl salt-sensitive rats.

JSPS Grant.

Where applicable, the authors confirm that the experiments described here conform with The Physiological Society ethical requirements.

PCC022

Phenylbiguanide and capsaicin evoke cardio-respiratory reflexes in anesthetized rats involving different vagal afferent pathways

S.B. Deshpande and A. Dutta

Department of Physiology, Institute of Medical Sciences, Banaras Hindu University, Varanasi, Uttar Pradesh, India

The pulmonary artery pressure and pulmonary congestion are regulated by the reflexes originating from the pulmonary C fibre receptors (J receptors) (Paintal 1973; Roberts et al, 1986). Activation of these receptors reflexly diminishes the accumulation of fluid in the pulmonary interstitium (Paintal, 1973). These reflexes can be elicited by phenyldiguanide (PDG), phenylbiguanide (PBG), 5-hydroxytryptamine (5-HT), capsaicin and lobeline in experimental animals. The reflexes evoked manifest as bradycardia, hypotension and apnoea/tachypnoea. These chemicals involve different types of membrane receptors to produce reflex responses. For example, PBG, PDG and 5-HT mediate their actions via 5-HT3 receptors while capsaicin mediates via TRPV1 receptors. Therefore, this study was undertaken to compare the effects of PBG and capsaicin on cardio-respiratory reflexes. In addition, it was aimed to explore the underlying mechanisms. All the experiments were performed after obtaining the approval from the Institute Ethical Committee for conducting animal experiments. Trachea, jugular vein and femoral artery were cannulated in urethane anaesthetized adult rats. Blood pressure, respiratory excursions and ECG were recorded. In some experiments, vagal afferent activity was also recorded. Jugular venous injection of PBG produced concentration-dependent (0.1-100 μg/kg) hypotensive and bradycardiac responses but in case of respiration, there was tachypnoea at lower concentrations (0.1-3 μg/kg) and apnoea at higher concentrations (10-100 μg/kg). After vagotomy, both tachypnoeic and apnoeic responses induced by PBG were abolished along with cardiovascular responses. Ondansetron (5-HT3 receptor antagonist, 10 μg/kg) abolished the PBG-induced reflex responses at all concentrations but capsazepine (TRPV1 receptor antagonist; 3 mg/kg) failed to antagonize the PBG responses. Bolus injection of capsaicin (0.1-10 μg/kg) also produced concentration-dependent apnoea, hypotension and bradycardia but no tachypnoea was observed at any concentrations of capsaicin. Ondansetron failed to block the capsaicin-induced reflex response while bilateral vagotomy abolished the hypotensive and bradycardiac response and attenuated the apnoeic response. In separate series of experiments, PBG produced a burst of activity in afferents along with cardio-respiratory alterations. However, the afferents which evoked activity with PBG failed to evoke any activity with capsaicin even though bradycardia, hypotension and respiratory changes were observed. The present observations indicate that PBG-induced cardio-respiratory responses involve 5-HT3 receptors on vagal afferents where as capsaicin involve different set of afferents.

Paintal AS (1973). Vagal sensory receptors and their reflex effects. Physiol Rev 53, 159-227.

Roberts AM, Bhattacharya J, Schultz HD, Coleridge HM & Coleridge JC (1986). Stimulation of pulmonary vagal afferent C-fibres by lung edema in dogs. Circ Res 58, 512-522.

Supported from the grants from ICMR, New Delhi.

Where applicable, the authors confirm that the experiments described here conform with The Physiological Society ethical requirements.

PCC023

Expression of small conductance Ca^{2+}-activated K^+ channels SK2 and SK4 in venous atrial junctions

F.C. Shenton and S. Pyner

School of Biological & Biomedical Sciences, Durham University, Durham, UK

A characteristic of hypertension and cardiovascular disease is an over-activation of the sympathetic nervous system [1]. The aetiology underlying the development and maintenance of this excitation is still not fully understood. An aspect of the regulatory process that has largely been ignored is the key role played by the sensory input from cardiac mechanoreceptors in sustaining appropriate cardiac output. One component of this input is the atrial volume reflex arc, initiated by receptors at the venous atrial junction of the heart which respond to changes in blood volume.

Although atrial volume receptors have been reported to be primarily within the endocardium [2], details of the receptor location and mode of function have not been previously described. We have shown that Transient Receptor Potential (TRP) channels TRPC1 and TRPV4 are expressed within the endocardial layer of this region [3] and are therefore candidates as the mechanosensitive channel(s) which respond to mechanical deformations of the atrial wall. TRP proteins are nonselective cation channels, most of which allow the passage of Ca^{2+}, the output from other stretch sensitive endings has been shown to be Ca^{2+} dependent [4] and small conductance Ca^{2+}-activated K^+ (SK) channels influence excitability in these endings [5]. We have used immunolabelling to test for the presence of the SK1-4 isoforms in this region.

Three male Hooded Lister rats were killed under Schedule 1 of the Animals (Scientific Procedures) Act 1986. The atria, including entrances of the major vessels, were removed and fixed overnight in 4% formaldehyde. Following cryoprotection in sucrose/PBS, venous atrial regions were dissected out, frozen and 16μm cryosections collected. Double labelling was carried out with anti-SK antibodies together with the sensory nerve ending vesicle marker anti-synaptophysin (SYN). Appropriate secondary antibodies were applied to distinguish between anti-SK reactivity and the anti-SYN marker. Slides were viewed using a Zeiss Fluorescent microscope.

Strong SK2-immunoreactivity (IR) was evident in nerve fibres within the epicardium. SK2-IR did not coincide with SYN-IR in this layer. SK2-IR was occasionally present within the myocardium and endocardium and here it did coincide with SYN-IR. SK4-IR was found in the endocardium giving small patches of diffuse labelling which appeared to be over epithelial cells, but did not coincide with SYN-IR. No evidence of SK1 or SK3 IR was found throughout this region.

Since there was very little SK2 in the endocardium itself, and the SK4 expressed in this layer did not coincide with SYN-IR, these channels are unlikely to directly regulate afferent sensitivity in this instance. Nevertheless, their presence in this general area suggests they could influence responses to atrial stretch by other mechanisms.

Malpas, S.C., Sympathetic nervous system overactivity and its role in the development of cardiovascular disease. Physiol. Rev., 2010. 90: 513-557.

Tranumjensen, J., Ultrastructure of sensory end-organs (baroreceptors) in atrial endocardium of young mini-pigs. J. Anat., 1975. 119: 255-275.

Shenton, F.C., et al., TRPC1 and TRPV4 are expressed in sensory endings found in regions of venoatrial endocardium where atrial volume receptors are located. The FASEB Journal, 2012. 26:1056.5.

Bewick, G.S., et al., Autogenic modulation of mechanoreceptor excitability by glutamate release from synaptic-like vesicles: evidence from the rat muscle spindle primary sensory ending. J. Physiol., 2005. 562: 381-394.

Banks, R. W., et al., P/Q type Ca2+ channels and K-Ca channels regulate afferent discharge frequency in spindle mechanosensory terminals. Society for Neuroscience Annual Meeting, 2009. Chicago, USA

EPSRC/ BSI, Durham University

Where applicable, the authors confirm that the experiments described here conform with The Physiological Society ethical requirements.

PCC024

Anti-oxidant strategies to prevent necrotic, mitochondrial and cardiovascular damage in inflammatory shock

A. Cauwels[1], B. Vandendriessche[1], E. Rogge[1], M. Murphy[2] and P. Brouckaert[1]

[1]Department for Molecular Biomedical Research, Ghent University, Ghent, Belgium and [2]2MRC Mitochondrial Biology Unit, Cambridge, UK

Septic shock is caused by a systemic inflammatory response resulting in hypotension, myocardial depression, multiple organ failure and death. Nitric Oxide (NO) is a potent vasodilator, and inhibition of NO synthases (NOS) increases systemic vascular resistance and blood pressure in shock1. Nevertheless, NO also exerts protective roles, as NOS inhibitors worsen and certain NO donors ameliorate shock.1-3

We study inflammatory shock using I.V. Tumor Necrosis Factor (TNF), lipopolysaccharide (LPS), or other TLR agonists in female C57BL/6 mice. Expression of inducible iNOS, as well as systemic NO accumulation, were not correlated with cardiovascular failure, morbidity or mortality, indicating that inflammation-induced NO is not sufficient to cause shock. In contrast, cardiovascular collapse (hypotension, bradycardia, loss of cardiac contractility) and mortality were completely reversed by tempol, a cell-permeable radical scavenger (100% survival vs. 0%, $p<0.001$, Log-Rank test), indicating a decisive role for ROS rather than NO. Protection by tempol was dose dependent (100-300 mg/kg I.P.) and could be achieved by pre- or post-treatment (-45 to +15 min). For cardiovascular analysis, we used PA-C10 or HD-X11 radio-transmitters (Data Sciences International) implanted under isoflurane anesthesia. Mitochondria may be important sources and targets of ROS. Following TNF or LPS, we found evidence for ROS-mediated damage to mitochondrial complexes. Nevertheless, although the mitochondria-targeted antioxidant mitoQ (5-10 mg/kg, I.P. or I.V.) could partially protect against early morbidity (hypothermia), it did not prevent mitochondrial and necrotic damage (measured via complex I activity in homogenized livers and lactate dehydrogenase activity in plasma, respectively), or cardiovascular failure. Our results thus indicate that ROS radicals are critically involved in the induction and progression of inflammatory cardiovascular collapse, and mitochondrial and necrotic damage. However, using a hyperacute shock model associated with excessive oxidative stress4, we also found evidence for a protective role of certain ROS, presumably H2O2, as catalase treatment both aggravated the hyperacute shock and reduced the long-term protective capacity of tempol.5

In conclusion, our results change the current paradigms on NO and ROS in inflammatory cardiovascular dysfunction. While NO seems predominantly protective, we found evidence for both detrimental and protective ROS effects. Hence, selective antioxidants may be a promising therapy to protect against inflammation-associated cardiovascular, mitochondrial and necrotic damage. Since mitoQ cannot reproduce the protective effects of tempol, we hypothesize that other sources of ROS (e.g. NADPH oxidases) may be involved in the detrimental effects, or that mitochondrial ROS is involved in protective pathways.

1. Lopez, A., et al. Multiple-center, randomized, placebo-controlled, double-blind study of the nitric oxide synthase inhibitor 546C88: effect on survival in patients with septic shock. Crit Care Med 32, 21-30 (2004).

2. Cauwels, A., et al. Nitrite protects against morbidity and mortality associated with TNF- or LPS-induced shock in a soluble guanylate cyclase-dependent manner. J Exp Med 206, 2915-2924 (2009).

3. Cauwels, A. & Brouckaert, P. Nitrite regulation of shock. Cardiovasc Res 89, 553-559 (2011).

4. Cauwels, A., Janssen, B., Waeytens, A., Cuvelier, C. & Brouckaert, P. Caspase inhibition causes hyperacute tumor necrosis factor-induced shock via oxidative stress and phospholipase A2. Nat Immunol 4, 387-393 (2003).

5. Cauwels, A., Rogge, E., Janssen, B. & Brouckaert, P. Reactive oxygen species and small-conductance calcium-dependent potassium channels are key mediators of inflammation-induced hypotension and shock. J Mol Med 88, 921-930 (2010).

Where applicable, the authors confirm that the experiments described here conform with The Physiological Society ethical requirements.

PCC025

BT venom induced vasosensory reflexes involving cardiovascular parameters are mediated through B1-kinin receptor in anaesthetised rats

S.K. Singh and S.B. Deshpande

Department of Physiology, Institute of Medical Sciences, Banaras Hindu University, Varanasi, Uttar Pradesh, India

Intra-arterial (i.a.) injection of Mesobuthus tamulus (BT; 1 mg/kg) venom produces optimal vasosensory reflex responses altering cardiorespiratory parameters in albino rats [1,2]. Since, bradykinin is a constituent of venom therefore, this study was planned to understand the role of kinin receptors in modulating the cardiorespiratory parameters evoked by venom. All the experiments were performed after obtaining the approval from the Institute Ethical Committee for animal experiments. Adult albino rats (200-300g) were anaesthetised with an intraperitoneal injection of urethane (1.5 g/kg). Tracheostomy was performed to keep the airway patent. Femoral artery was cannulated proximally as well as distally to record the blood pressure and to inject the chemicals, respectively. Blood pressure (BP), electrocardiogram (ECG) and respiration (RR) was recorded in presence or absence of antagonists. After i.a. injection of venom there was immediate (within 2 s) increase in RR which reached to 40% within 30 s, followed by a decrease of 40% from initial. Further, there was sustained increase in RR (50%) up to 60 min. The BP began to increase at 40 s, peaking at 5 min (50%) and remained above the initial level up to 60 min. The bradycardiac response started after 5 min which peaked (50%) at 25 min and remained at that level up to 60 min. In des-Arg (B1 receptor antagonist; 10 ng/kg) pre-treated animals, the venom induced respiratory changes were similar to the venom only group but venom induced cardiovascular responses attenuated (20-25% in MAP and HR) significantly ($P < 0.05$, Two way ANOVA). In Hoe-140 (B2 receptor antagonist; 10 ng/kg) pre-treated group, the venom induced respiratory changes were similar to the venom only group but venom induced BP responses attenuated (~25%) from 30-60 min ($P < 0.05$, Two way ANOVA) and HR responses accentuated (25-50%) up to 15 min significantly ($P < 0.05$). Thus, i.a. injection of venom produces immediate hyperventilatory, intermediate hypertensive and delayed bradycardiac responses. BT venom contains serotonin, histamine, bradykinin potentiating factor, peptide toxins, etc which is a potential nociceptive agents [3]. Bradykinin (BK) is an inflammatory mediator and produces the actions involving B1 and B2 receptors [4]. Involvement of kinin and prostaglandin (PG) to noxious stimulation has been shown [5]. In the present study, the B1 antagonist pre-treatment attenuated the venom induced BP and heart rate changes indicating the B1 receptors involvement in producing the responses. These observations are consistent for the B1 receptor involvement in the nociception. However, the involvements of B2 receptor on venom induced cardiorespiratory parameters are less evident in this study.

Singh, S.K., Deshpande, S.B. Intra-arterial injection of Mesobuthus tamulus venom elicits cardiorespiratory reflexes involving perivascular afferents. Toxicon 2005; 46: 820-826.

Singh, S.K., Deshpande, S.B. Nociceptive vascular reflexes evoked by scorpion venom modulates cardiorespiratory parameters involving vanilloid receptor 1. Neuroscience Letters 2009; 451: 194-198.

Wudayagiri, R., Inceoglu, B., Herrmann, R., Derbel, M., Choudary, P.V. and Hemmock, B.D. Isolation and Characterization of a novel lepidopteran-selective toxin from the venom of South Indian red scorpion, Mesobuthus tamulus, BMC Biochemistry, 2001; 2,16-28.

Marceau, F., Hess J.F. and Bacharov, D.R. The B1 receptors for kinins. Pharmacol. Rev., 1998; 50, 357-386.

Matsuzaki, S., hayasi, I., Nara, Y., Kamata, K., Yamanaka, M., Okamoto, H., Hoka, S., and Majima, M. Role of kinin and Prostaglandin in cutaneous thermal nociception. Int. Immunopharmacol 2002 Dec; 2 (13-14): 2005-12.

Where applicable, the authors confirm that the experiments described here conform with The Physiological Society ethical requirements.

PCC026

Mental stress associated changes in heart rate and blood pressure: Relation to body composition, physical fitness and autonomic status

S. Ghosh

Physiology, MAHSA University College, Kuala Lumpur, Selangor, Malaysia

Influence of mental stress on cardiovascular function differs from individual to individual, based on a variety of inherent factors (1). . Some people show characteristically greater cardiovascular reactivity than others to behaviourally stressful situations. Cardiovascular reactivity reflects the functional status of autonomic nervous system (2). The first year medical students are stressed by emotional factors and also have less physical activity The current study was undertaken to establish a basal autonomic status of adolescent south east Asian students and to find out the changes in cardiovascular parameters and their correlation with physical fitness and body composition. 50 healthy medical students of the age group of 17-19 years were recruited for the study. Cardiorespiratory fitness was assessed by Harvard Step Test and Body Mass Index and

body fat% were measured by Body composition analyzer. Basal autonomic status was studied by calculating changes in heart rate under orthostatic stress from electrocardiographic records and measurement of blood pressure by sphygmomanometer (3). All cardiovascular parameters were recorded before and after application of mental stress by means of public speaking in front of peer group. All data were analysed statistically by using SPSS version 19.0. Informed consent was taken from all subjects and permission of the institutional review board was obtained. Results showed that students with low BMI had a 30:15 ratio of 1.2[0.16] while those with high BMI had a ratio of 1.3[0.28]. Upon application of mental stress, the rate of change of heart rate also varied according to the BMI and Body fat%. Rate of change of heart rate was higher [39.5 +/- 1.7; 32.8+/-6.05] in both the high fat group and low fat group as compared to the normal, high fat group showing a bigger change. Rate of change of systolic pressure showed a similar trend while diastolic pressure change was lower in the high fat group. Subjects with low physical fitness had a poor parasympathetic control which may indicate that they are more vulnerable to break down under mental stress. The data suggested that autonomic reactivity to mental stress is correlated with basal physical fitness level of subjects and is also dependent on their body composition. Basal fitness level did not show any relationship with body composition but both low fitness level and high body fat % were found to show poor autonomic regulation of cardiovascular system. In such individuals, mental stress can cause higher alteration of heart rate and systolic blood pressure due to altered autonomic regulation.

Little L, Mental Stress- Associated Blood Pressure Rise Linked to Increase in Creatinine, Medscape Medical News (2005) Available from http//www.medscape.com/viewarticle/505246 accessed on 09/06/2005

Manuck SM, Kasprowicz AL, Muldoon MF, Behaviorally evoked cardiovascular reactivity and hypertension: conceptual issues and potential associations, Ann Behav Med (1990); 12: 17-29.

Kulshreshtha P, Gupta R, Yadav RK, Bijlani RL, Deepak KKClin A comprehensive study of autonomic dysfunction in the fibromyalgia patients. Auton Res. (2012) Jun;22(3):117-22.

The author acknowledges the first year medical students who participated in the study.

Where applicable, the authors confirm that the experiments described here conform with The Physiological Society ethical requirements.

PCC027

Chronic intracerebroventricular infusion of hyperosmotic saline affects arterial baroreflex via brain angiotensin type 1 receptors in Sprague-Dawley rats

T. Zera and A. Nowinski

Dept.Experimental and Clinical Physiology, The Medical University of Warsaw, Warsaw, Poland

Introduction: Increasing evidence points to the key role of neurogenic component in cardiovascular diseases (1). High load of salt in diet contributes to the development of essential hypertension. One of the possible mechanisms linking salt intake with hypertension is an increased concentration of sodium ions in the cerebrospinal fluid (CSF), which rearranges central control of the cardiovascular system (2). Renin-angiotensin-aldosterone system is a key regulator of sodium balance and plays a culprit role in triggering and maintaining elevated arterial pressure (3). In the present study we aimed at finding out if increased CSF sodium ions alter the control of circulatory system and whether it may be mediated by brain angiotensin type 1 receptors (AT1Rs) for angiotenin II in normotensive rats. Methods: The study was performed on adult Sprague-Dawley male rats. The animals were implanted with L-shaped cannulae connected to osmotic mini-pumps for 2-week intracerebroventricular (ICV) infusions of either isoosmotic saline (0.9% NaCl, 5 μl/hr), hyperosmotic saline (5% NaCl, 5 μl/hr) or AT1Rs blocker losartan together with 5% NaCl (12.5 μg/5 μl/hr). After 14 days catheters were inserted into femoral artery and femoral vein for measurement of blood pressure (BP) and heart rate (HR) and for intravenous infusions respectively. All surgical procedures were performed under ketamine (100 mg/kg i.p.) and xylazine (10 mg/kg i.p.) anesthesia. After the implantation of catheters baroreflex was pharmacologically evaluated in conscious freely moving animals by administration of phenylephrine (i.v. from 20 up to 200 μg/kg/min) and sodium nitroprusside (i.v. from 20 up to 200 μg/kg/min) to induce a ramp increase and decrease of BP respectively. Subsequently autonomic ganglia were blocked with hexamethonium i.v. (20 mg/kg) and measurements of BP and HR continued. CSF was collected from cisterna magna before euthanasia of animals. Results: Infusions of 5% NaCl solutions resulted in higher concentration of sodium ions in CSF than in the plasma, while isoosmotic saline did not elevate CSF sodium concentration. The blockade of autonomic ganglia resulted in decrease of BP and increase in HR, which were similar in all groups. Baroreflex was blunted in rats receiving ICV infusion of hyperosmotic saline in comparison to control group. Intracerebroventricular administration of losartan restored sensitivity of baroreflex.

Conclusions: Present results indicate that chronic ICV infusion of hyperosmotic saline desensitizes arterial baroreflex and this is partially mediated by AT1 receptors for angiotensin II.

Szczepanska-Sadowska E, Cudnoch-Jedrzejewska A, Ufnal M, Zera T. Brain and cardiovascular diseases: common neurogenic background of cardiovascular, metabolic and inflammatory diseases. J Physiol Pharmacol. 2010; 61(5):509-21.

Huang BS, Wang H, Leenen FH. Enhanced sympathoexcitatory and pressor responses to central Na+ in Dahl salt-sensitive vs. -resistant rats. Am J Physiol Heart Circ Physiol. 2001; 281(5):H1881-9.

Takahashi H, Yoshika M, Komiyama Y, Nishimura M. The central mechanism underlying hypertension: a review of the roles of sodium ions, epithelial sodium channels, the renin-angiotensin-aldosterone system, oxidative stress and endogenous digitalis in the brain.

Hypertens Res. 2011; 34(11):1147-60.

This study was supported by grant for young researchers from the First Faculty of Medicine, the Medical University of Warsaw, Poland.

Where applicable, the authors confirm that the experiments described here conform with The Physiological Society ethical requirements.

PCC028

Increased expression of angiotensin type 2 receptors in the nucleus of the solitary tract improves baroreflex function and angiotensin converting enzyme 2 levels in renovascular hypertensive rats

G.T. Blanch[1], A.H. Freiria-Oliveira[1], K. Rigatto[2], H. Li[3], E. Colombari[1], C. Sumners[4] and D.S. Colombari[1]

[1]Physiology and Pathology, School of Dentistry - Sao Paulo State University, Araraquara, Sao Paulo, Brazil, [2]Basic Science and Health, UFCSPA, Porto Alegre, Sao Paulo, Brazil, [3]Southern Medical University, Guangzhou, China and [4]Physiology and Functional Genomics, University of Florida, Gainsville, FL, USA

Renovascular hypertensive (2K1C) rats exhibit impaired baroreflexes. Here we studied the effects of increased angiotensin type 2 receptor (AT2R) expression in the nucleus of the solitary tract (NTS) on baroreflex function of 2K1C rats and on selected gene levels at this site. Male Holtzman rats (150-180g) were anaesthetized with a mixture of ketamine (80 mg kg-1) and xylazine (7 mg kg-1, both i.p.) and the left renal artery was partially obstructed with a silver clip (0.2 mm width) or sham surgery. Three weeks later, 2K1C and sham rats were anaesthetized as above and microinjected in the NTS with either AAV2-CBA-AT2R (1.2×10^{12} genomic copies (gc)/ml; n = 6-8/group) or AAV2-CBA-eGFP (1.8×10^{12} gc/ml; n = 4-6/group) to elicit chronic increases in AT2R or GFP (control) expression respectively. Thirty days later, 2K1C and sham rats were anaesthetized as above and femoral artery and vein were cannulated to measure mean arterial pressure (MAP) and heart rate (HR) and perform drug infusions, respectively. The next day, phenylephrine (5 μg/kg, iv) and sodium nitroprusside (30 μg/kg, iv) were used to elicit respective pressor and depressor responses in conscious rats. Reflex HR responses were analyzed to each 10 mmHg change in MAP. Values are means ± S.E.M., compared by ANOVA. Baseline MAP in 2K1C-AT2R rats (173 ± 7 mmHg) was lower than in 2K1C-GFP rats (199 ± 9 mmHg; $p < 0.05$). 2K1C-GFP rats exhibited a significant impairment of the baroreflex (slope: -0.95 ± 0.05, vs. sham-GFP -1.37 ± 0.06, $p<0.05$), which was improved in the 2K1C-AT2R rats (slope: -1.44 ± 0.07). Baroreflex in 2K1C-AT2R was similar to sham-AT2R rats (slope: -1.56 ± 0.06) or sham-GFP. Real time RT-PCR revealed that the lower angiotensin converting enzyme 2 (ACE 2) mRNA levels in 2K1C-GFP rats were normalized in the 2K1C-AT2R rats (sham-GFP: 0.23 ± 0.03; sham-AT2R: 0.18 ± 0.03; 2K1C-GFP: 0.03 ± 0.01; 2K1C-AT2R: 0.31 ± 0.07, $p<0.05$). The results suggest that increased AT2R expression in the NTS of 2K1C rats improves baroreflexes and increases ACE 2 levels and these factors may contribute to the reduction in blood pressure observed in these animals.

PNPD/CAPES, NIH and FAPESP/PRONEX

Where applicable, the authors confirm that the experiments described here conform with The Physiological Society ethical requirements.

PCC029

NF-kB and Nrf2 compete for CREB binding protein in the RVLM of rats with chronic heart failure: the effects of exercise training

K. Haack, A.M. Harlow and I.H. Zucker

Cellular and Integrative Physiology, University of Nebraska Medical Center, Omaha, NE, USA

Chronic Heart Failure (CHF) is a disease characterized by overactivation of the renin-angiotensin system, increased sympathetic outflow, and high oxidative stress. In conditions of high oxidant stress, Nuclear factor erythroid 2 related factor 2 (Nrf2) is dissociated from Kelch-like ECH associated protein 1 (Keap1) to activate antioxidant response element (ARE) genes such as heme oxygenase 1 (HO1) and NQO1 as a compensatory mechanism. p65 nuclear factor kappa B (NF-kB) is one of the primary transcription factors that contributes to the etiology of CHF, recruiting creb binding protein (CBP) to both increase transcription of pro-inflammatory proteins and inhibit transcription of AREs. Exercise training (ExT) has been shown to decrease sympathetic outflow and oxidative stress and improve quality of life in patients with cardiovascular disease, however the mechanism(s) by which ExT is protective remain unclear. The purpose of this study was to investigate the convergence of the Nrf2/Keap1 and NF-kB pathways on CBP in the rostral ventrolateral medulla (RVLM) of the rat brain following CHF and ExT. Animals were anesthetized with isoflourane (0.5-2% in oxygen), intubated and mechanically ventilated. Animals were then infarcted using coronary artery ligation. Following confirmation of CHF by a decrease in ejection fraction using echocardiography, some animals were exercised four weeks post-surgery on a treadmill at a final speed of 25 m/min for 60 minutes, 5 days a week for 6 weeks. Western blot analysis of RVLM micropunches demonstrated that in CHF, there was a significant upregulation in NF-kB and Keap1 proteins compared to sham and a decrease in Nrf2 (n=4-5 per group, $p=0.003$ for Nrf2 and Keap1, $p=0.0016$ for NF-kB by unpaired t-test). ExT significantly increased Nrf2 and Keap1 expression compared to both sham and CHF groups but normalized NF-kB expression in CHF animals (n=4-5 per group). Co-immunoprecipitation experiments were then performed to examine the interaction of NF-kB and Nrf2 with CBP. In CHF, there was an increase in NF-kB/CBP interaction and a decrease in Nrf2/CBP association compared to sham ($p=0.01$ for NF-kB/CBP and Nrf2/CBP by unpaired t-test, n=2). However, during ExT in both sham and CHF groups, there was an increase in Nrf2/CBP interaction and a compensatory decrease in NF-kB/CBP interaction (n=2). Taken together, these data suggest that central Nrf2 is downregulated in CHF and that NF-kB and Nrf2 compete for CBP during CHF and following ExT.

Where applicable, the authors confirm that the experiments described here conform with The Physiological Society ethical requirements.

PCC030

Lack of hormonal regulation of hypercapnia-induced c-Fos expression in norepinephrine neurons of the male rat locus coeruleus

D. de Carvalho[1,4], D. Marques[1,4], R.A. Lopes[3], J.A. Anselmo-Franci[2], K.C. Bícego[1], R.E. Szawka[3] and L.H. Gargaglioni[1]

[1]São Paulo State University, Jaboticabal, SP, Brazil, [2]Dental School of Ribeirão Preto, University of São Paulo, Ribeirão Preto, SP, Brazil, [3]Biological Science Institute, Federal University of Minas Gerais, Belo Horizonte, MG, Brazil and [4]PIPGCF, Federal University of São Carlos, São Carlos, SP, Brazil

Sex hormones have a significant impact on ventilation in mammals. The effects of menstrual cycle, pregnancy, testosterone, estradiol and progesterone on resting ventilation have been well documented. The noradrenergic neurons of locus coeruleus (LC) contain estrogen and androgen receptors and have been reported to regulate the CO2-drive to breathe. We therefore evaluated the role played by sex hormones in the activation of LC noradrenergic neurones in response to CO2 in male rats. We assessed neuronal activity by c-Fos immunoreactivity in gonad-intact (INT) rats and orchidectomized rats treated with oil (ORX), testosterone (ORX+T), or estradiol (ORX + E2). Hypercapnia (7% CO2, 21% O2 and N2 for balance) or normocapnia (control animals) was administered for 2 hrs. The number of c-Fos/tyrosine hydroxylase (TH)-immunoreactive (ir) neurons was counted bilaterally in the LC (c-Fos/TH-ir neurons per section). The results showed that the number of c-Fos/TH-ir neurons in the LC was significantly increased by hypercapnia in INT (9.7 ± 5.7), ORX (7.6 ± 8.9), ORX + E2 (11.3 ± 9.9) and ORX + T (8.1 ± 7.2) male rats compared to normocapnia (3.9 ± 2.4; 2.3 ± 1.4; 2.1 ± 1; 4 ± 4.1, respectively). However, there was no significant effect of hormonal treatments on the response of LC to hypercapnia. These findings suggest that sex hormones seem to play no role in the LC response to hypercapnia in male rats.

Financial support: FAPESP and CNPq, INCT of Comparative Physiology

Where applicable, the authors confirm that the experiments described here conform with The Physiological Society ethical requirements.

PCC031

Computational model of cardiovascular dynamics for assessment of cardiac energetic efficiency

T. Shimayoshi[1], Y. Himeno[2], A. Amano[2], T. Matsuda[1] and A. Noma[2]

[1]Graduate School of Informatics, Kyoto University, Kyoto, Kyoto, Japan and [2]Department of Bioinformatics, Ritsumeikan University, Kusatsu, Shiga, Japan

Cardiac energetic efficiency is a ratio of cardiac workload to cardiac energy consumption, and cardiac workload is subject to vascular system. Although a number of computational circulation models have been developed, most of them represent the left ventricle as a time-varying elastance and so cannot compute cardiac energetic efficiency. In the present study, a cardiovascular dynamics model is introduced to assess cardiac energetic efficiency, by integrating a detailed ventricular cell model into a vasculature closed-loop circuit. The vasculature circuit is based on a vascular system model proposed by Heldt et al. (2004). Left ventricular pressure is converted, according to Laplace's law, from the contractile force of ventricular myocyte which is calculated in a cell model by Kuzumoto et al. (2008). Despite combination of highly nonlinear sub-models, the present model successfully reproduce cardiac properties relating to energetic efficiency; response to variation of cardiac afterload, linearity of end-systolic pressure-volume relationship, and linear relationship between left ventricular oxygen consumption and pressure-volume area, which represents the total mechanical energy generated by ventricular contraction.

T. Heldt, E.B. Shim, R.D. Kamm, and R.G. Mark, "Computational modeling of cardiovascular response to orthostatic stress," Journal of Applied Physiology, vol.92, no.3, pp.1239–1254, March 2002.

M. Kuzumoto, A. Takeuchi, H. Nakai, C. Oka, A. Noma, and S. Matsuoka, "Simulation analysis of intracellular Na+ and Cl– homeostasis during β1- adrenergic stimulation of cardiac myocyte," Progress in Biophysics and Molecular Biology, vol.96, no.1-3, pp.171–186, June 2008.

Where applicable, the authors confirm that the experiments described here conform with The Physiological Society ethical requirements.

PCC032

Subcutaneous reserpine dehydrates Wistar rats and increases nitric oxide production in septic rats

Y. Chan[1,2], G.L. Ackland[1] and M. Singer[1]

[1]Bloomsbury Institute of Intensive Care Medicine, University College London, London, UK and [2]Department of Emergency Medicine, Chang Gung Memorial Hospital, Linkou, Taoyuan, Taiwan

Introduction
Subcutaneous reserpine has been used for chemical sympathectomy. Its effect to deplete catecholamines in rats has been particularly characterized. Here we report some effects of subcutaneous reserpine that have not previously been described, namely to induce dehydration in rats, and to increase in vivo nitric oxide production in septic rats.
Methods
Male Wistar rats (~300g) received three subcutaneous injections of reserpine (4.5 mg/kg body weight dissolved in dimethyl sulfoxide) 48h and 24h prior to and during cannulations of carotid artery and jugular vein under inhalational anesthesia with 2% isoflurane. Fecal peritonitis was induced 24h after instrumentation, and Fluid resuscitation (1:1 solution of 6% hydroxyethyl starch 130/0.4 and 5% glucose) was given 2h later at 10 ml/kg/h via the jugular venous catheter. The body weight, blood pressure, and arterial base excess, plasma lactate and nitrate/nitrite levels at 6h post-peritonitis were compared with non-reserpinized rats.
Results
A total of 22 rats (mean weight, 306 ± 5 g) were pre-treated with reserpine. Of these animals, eight were used as sham-operated controls, and 14 had peritonitis induced. Prior to induction of sepsis, these animals showed marked weight loss (56 ± 2 g; equivalent to 18.3% body weight loss) within 48h. Sham rats presented with metabolic alkalosis and an elevated plasma lactate level, whereas septic rats presented with a more severe metabolic acidosis and higher in vivo nitric oxide production (Table 1). All rats presented with a lower blood pressure at the time of faecal slurry injection. At the 6h timepoint, sham rats responded to fluid resuscitation and their blood pressure was elevated, whereas septic rats remained hypotensive

(Table 1). Reserpinized septic rats had a higher 6h mortality rate (28.6% vs. 6.1%, p <0.01), whereas none of the sham died at this timepoint.

Conclusion

Subcutaneous reserpine induced dehydration in rats within 48h, which resulted in fluid-responsive hypotension and hyperlactatemia. Septic reserpinized rats also developed increased nitric oxide production. Subcutaneous reserpine may as the means of chemical sympathectomy may generate confound results.

Table 1. Differences in mean arterial pressures, arterial base excess, lactate and plasma nitrate/nitrite levels between non-reserpinized and reserpinized Wistar rats.

	Sham				p	Septic				p
	Non-reserpinized		Reserpinized			Non-reserpinized		Reserpinized		
	n	Value	n	Value		n	Value	n	Value	
MAP at 0h (mmHg)	44	111.5 ± 1.9	8	101.6 ± 2.7	<0.05	44	110.4 ± 1.3	11	102.3 ± 4.2	<0.05
MAP at 6h (mmHg)	44	111.5 ± 2.0	8	112.8 ± 3.6	NS	44	131.7 ± 1.4	11	105.2 ± 5.6	<0.01
Arterial BE (mM)	6	0.6 ± 1.0	6	4.1 ± 0.9	<0.05	6	-3.9 ± 1.3	6	-8.6 ± 1.3	<0.05
Lactate (mM)	5	1.3 ± 0.2	5	2.9 ± 0.3	<0.01	5	2.7 ± 0.6	-	-	-
NOx (μM)	15	21.5 ± 2.4	5	18.2 ± 1.2	NS	15	56.7 ± 0.8	5	78.4 ± 13.9	<0.01

- = not measured; BE = base excess; MAP = mean arterial pressure; NOx = nitrate/nitrite; NS = not significant.

Martinez-Olivares R et al. (2006). Auton Neurosci 128, 64-69.

Where applicable, the authors confirm that the experiments described here conform with The Physiological Society ethical requirements.

PCC033

A role of glutamate co-released from orexin neurons in methamphetamine-induced autonomic physiological response

Y. Ikoma[1], K. Miyata[1], T. Kuwaki[1] and Y.Y. Ootsuka[1,2]

[1]Physiology, Kagoshima University, Kagoshima, Kagoshima, Japan and [2]Human Physiology, Flinders University, Bedford Park, SA, Australia

Methamphetamine has a central nervous system stimulant action and causes hyperactivity and elevation of body temperature. Recently, it has been shown that orexin system in the brain plays a key role of stress-related autonomic physiological response such as tachycardia and hyperthermia. In a orexin neuron, various neurotransmitters are co-localized with orexin. Among them, glutamate is focused on since its importance in autonomic physiological response to stress has been suggested. The aim of this study is to explore the role of glutamate as a co-transmitter from orexin neurons in methamphetamine-induced autonomic physiological response. We used a genetically-modified mouse (vGLUT2-KO) in which vGLUT2 is deficient only in orexin neurons and thus glutamate cannot be released from the orexin neurons and a wild type mouse (WT) as a control group. We implanted a telemetry probes to measure heart rate, body temperature and locomotor activity under isoflurance anesthesia (2%, inhalation). After at least one-week recovery period, we examined the effect of methamphetamine (0.5, 2, 5mg/kg, i.p.) on these parameters in conscious free-moving condition. In both groups of vGLUT2-KO and WT mice, methamphetamine caused an increase in body temperature as well as locomotor activity dose-dependently (P<0.05, n=7, Pearson). The amplitude of increases in body temperature as well as activity was significantly greater in vGLUT-KO than in WT mice (by 2.2±0.7 vs by 0.5±0.5 degree Celsius, 0.5mg/kg, n=7, P<0.05, Bonferroni). These results suggest a possible suppressive action of glutamate co-localized in orexin neurons on hyperthermia and hyperactivity induced by methamphetamine.

This research is supported by A Grant from the Kodama Memorial Fund for Medical Research.

Where applicable, the authors confirm that the experiments described here conform with The Physiological Society ethical requirements.

PCC034

Fluoxetine reduces the lung injury induced by infrarenal abdominal aortic ischemia-reperfusion in rats

G. Sahin[1], I. Guner[1], M. Yaman[1], D. Uzun[2], H. Erman[4], N. Yelmen[1], M. Inceli[3], U. Aksu[3], R. Gelisgen[4] and H. Uzun[4]

[1]Istanbul University, Cerrahpasa Faculty of Medicine, Department of Physiology, Istanbul, Turkey, [2]Istanbul University, Istanbul Faculty of Medicine, Istanbul, Turkey, [3]Istanbul University, Science Faculty, Biology, Istanbul, Turkey and [4]Istanbul University, Cerrahpasa Faculty, Department of Biochemistry, Istanbul, Turkey

Lung injury induced by acute aortic occlusion with subsequent aortic ischemia-reperfusion is an important factor in the development of postoperative acute lung injury following abdominal aortic surgery (Gelman,1995). Overproduction and/or insufficient removal of reactive oxygen species during ischemia-reperfusion (IR) result in significant damage to cell structure and organ functions. Fluoxetine, a selective serotonin reuptake inhibitor, has been shown to exert neuroprotective effect against the oxidative stress in animal models but no studies have yet been conducted to test the protective effects of fluoxetine against the lung injury. The present study aimed to examine whether the fluoxetine would be able to prevent the oxidative damage in lung induced by the occlusion and reperfusion of infrarenal abdominal aorta (IAA). Adult male Wistar rats (300-400g, n=24) anaesthetized with pentobarbital sodium (60 mg kg-1,i.p.) were randomized to 3 groups (n=8). Control (Sham), IR, and Fluoxetine+ IR (F+IR) groups. Control group, underwent laparotomy and dissection of IAA without occlusion. The IR group underwent laparotomy and clamping of the IAA for 60 min followed by 120 min of reperfusion. The rats in the F+IR groups received fluoxetine (20 mg kg-1, i.p. Sigma) once daily for 3 days before ischemic surgery. Thirty minutes after the last injection, the same IR procedure was performed. After withdrawn of blood samples, experiment was terminated by deep anesthesia (Pentobarbital sodium; 150 mg kg-1,i.p.). Bronchoalveolar lavage fluid (BALF) and lung tissue specimens were obtained for biochemical evaluations. Lung tissue oxidative stress was investigated by means of lipid hydroperoxide (LHPO), superoxide dismutase (SOD), pro-oxidant antioxidant balance (PAB), ferric reducing/antioxidant power (FRAP) and malondialdehyde (MDA) levels in lung tissue and BALF. Histological evaluation of the rat lung tissues was also performed. Presented values are means + S.E. compared by ANOVA as post-hoc Tukey. Except SOD and FRAP activities, all markers related to lung oxidative stress (PAB, LHPO and MDA) were significantly increased in the lung tissue (p<0.01, p<0.05, p<0.05 vs control; respectively) and likewise BALF samples of IR group (p<0.05vs control). Pretreatment with fluoxetine prevented the increase in PAB, LHPO activities and MDA levels (p>0.05 vs control). SOD and FRAP activities were significantly reduced in the lung tissue and BALF of IR group (p<0.01, p<0.05 vs control), but fluoxetine pretreatment abolished the effect of IR on SOD and FRAP activities (p>0.05 vs control). Fluoxetine also attenuated IR-induced total histo-

logical injury in lung tissue architecture. In conclusion, fluoxetine confers protection against lung IR injury and protective effects seem to be related to the inhibition of oxidative stress and prevention of cellular integrity of lung.

Gelman S (1995) Anesthesiology 82(4),1026-60.

Where applicable, the authors confirm that the experiments described here conform with The Physiological Society ethical requirements.

PCC035

The effects of peripheral NMDA-type glutamate receptors on cardiorespiratory responses in acute hypoxic exposure in rabbits

N. Yelmen, I. Guner, O.M. Yaman and G. Sahin

Physiology, Istanbul University, Cerrahpasa Faculty of Medicine, Istanbul, Turkey

Glutamate is one of the most common excitatory neurotransmitter in the central nerve system. It has been shown that central glutamate N-methyl-D-aspartate (NMDA) receptors are important components of the cardiorespiratory regulation. On the other hand, the presence of NMDA-type glutamate receptors has been demonstrated in many peripheral tissue as lungs, airways and carotid bodies. However the effect of those NMDA receptors on cardiorespiratory parameters is not completely considered. The purpose of this study was to investigate the effect of systemic glutamate NMDA receptors on cardiorespiratory parameters during both normoxia and acute hypoxia in rabbits. In this study 8 adult albino rabbits weighing avarege 2.7 ± 0.4 kg were used. The rabbits were anesthetized with urethane (400mg kg-1, i.v) and alpha-chloralose (40 mg kg-1, i.v). Tracheotomy was performed and the tracheal cannula connected to an inspiratory-expiratory valve was inserted into the trachea. The right femoral arterial catheter was used to collect arterial blood samples. Experiments were terminated by i.v injection of an overdose (500 mg kg-1) of sodyum pentobarbitone. Tidal volume (VT), respiratory frequency (f/min), ventilation minute volume (VE), mean arterial pressure (BP) and heart rate (HR) were recorded during the breathing of the normoxic and hypoxic (8% O2 - 92% N2) gas mixtures, before and after the administration of the i.v MK-801 (glutamate NMDA receptor antagonist) in anaesthetized rabbits. At the end of each experimental phase, PaO2, PaCO2, and pHa were measured. Values are presented as means ±S.E.M., compared by Wilcoxon-Matched Paired t- test. The injection of MK-801 (0.9 mg kg-1, i.v) during normoxia caused a decrease in BP ($p<0.01$), HR ($p<0.001$), VT ($p< 0.01$) and VE ($p<0.01$) values, whereas it caused an increase in f/min ($p<0.001$). After MK-801 administration, when hypoxic gas mixture was breathed to rabbits significant decreases in f/min ($p<0.01$), VE ($p<0.05$) and HR ($p<0.01$) were observed. The elevation response in BP seen during acute hypoxia was completely abolished by MK- 801 administration.

Our findings suggested that glutamate has a excitatory effect on both blood pressure and ventilatory activity via NMDA-type peripheral glutamate receptors during normoxic and acute hypoxic gas breathing. In line, when MK-801 was used to lower blood pressure, its depressor effect on ventilation should be taken into consideration in hypoxic conditions.

Where applicable, the authors confirm that the experiments described here conform with The Physiological Society ethical requirements.

PCC036

Recurrences in cardiovascular dynamics: supine vs. orthostasis

Z. Turianikova[1], M. Javorka[1], K. Javorka[1] and M. Baumert[2]

[1]Department of Physiology, Comenius University, Jessenius Faculty of Medicine, Martin, Slovakia and [2]School of Electrical & Electronic Engineering, The University of Adelaide, Adelaide, SA, Australia

New nonlinear methods are continuously developed to quantify novel aspects of heart rate variability (HRV) and blood pressure variability (BPV) with a potential to reveal subtle changes in the cardiovascular control system. Recurrence is a basic feature of many dynamical systems – it is defined as the repeated occurrence of a given state of the system in time. Recurrence plot (RP) is a graphical representation of such recurrences in a dynamical system. The structures exhibited by RP reveal information on system properties and can be described quantitatively by recurrence quantification analysis (RQA).

The aim of this study was to assess the effect of orthostatic challenge on RQA measures of HRV and BPV in healthy young subjects. The change from supine to standing position is a well-described autonomic stress paradigm that is characterised by an immediate reduction in vagal outflow to the sinus node and an increase in sympathetic nerve activity.

HRV and BPV were assessed in 28 healthy subjects over 15 minutes in the supine and standing positions. Complexity of HRV and BPV was assessed by recurrence quantification analysis from RPs constructed using fixed percentage of recurrences.The magnitude of oscillations was quantified by linear time and frequency domain measures.

We found high sensitivity of RQA measures to the change in autonomic balance accompanying orthostasis. We have also demonstrated the positive properties of RPs with fixed percentage of recurrence points in detection of qualitative change in cardiovascular dynamics. The different behavior of complexity and variability indices was observed: HRV complexity was reduced along with HRV magnitude after changing from supine to standing position; contrary, the BPV magnitude increased and BPV complexity decreased upon standing.

We conclude that RQA of HRV and BPV are sensitive to orthostatic challenge and might therefore be suited to assess changes in autonomic neural outflow to the cardiovascular system. Since analysis of variability and complexity can provide independent information on cardiovascular system control, it is beneficial to use both groups of measures simultaneously in the studies demanding the application of HRV and BPV analysis as a noninvasive tool for the assessment of cardiovascular autonomic nervous system function. We suggest that simultaneous use of both groups of measures can increase the information value and thus improve the sensitivity and reliability of the detection and monitoring of the cardiovascular system dysregulation during various pathological conditions.

The study was supported by project of Centre of Excellence for perinatological research no 26220120036, ESF project ITMS26110230031 and grants VEGA no. 1/0223/12 and 1/0059/13.

Where applicable, the authors confirm that the experiments described here conform with The Physiological Society ethical requirements.

PCC037

Causal baroreflex sensitivity analysis from spontaneous heart rate and blood pressure oscillations in obese children and adolescents

M. Javorka, I. Tonhajzerova, B. Czippelova, Z. Turianikova, L. Chladekova and K. Javorka

Department of Physiology, Comenius University, Jessenius Faculty of Medicine, Martin, Slovakia

Obesity is an important risk factor of arterial hypertension. The impairment of baroreflex – a principal blood pressure control mechanism – could contribute to the development of hypertension in obese patients. Previous studies found a decreased baroreflex sensitivity (BRS) measured by transfer function analysis of spontaneous blood pressure (BP) and heart rate (HR) oscillations in obese subjects. However, this method ignores the causality and directionality of HR and BP oscillations interactions. The novel method for separate analysis of feedback (baroreflex) and feedforward (mechanical) interactions between HR and BP was recently developed. The aim of the study was to analyse BRS in obese normotensive children and adolescents using causal baroreflex analysis method.
Continuous recordings of BP (volume-clamp method) and R-R intervals (ECG) were obtained from 40 obese subjects (aged 10-18 years) and 40 age and gender matched controls. Causal close loop model was used to measure classical (noncausal) BRS and causal feedback interaction from BP to HR (causal BRS).
The noncausal BRS did not show any significant difference between groups. On the other hand, causal BRS was significantly lower in obese group.
In conclusion, the causal BRS analysis is more sensitive in early detection of baroreflex impairment in obese children and adolescents compared to classical BRS method. The results points towards baroreflex as one of the mechanisms involved in future hypertension development in obese patients.

The study was supported by project of CEPV no 26220120036, ESF project ITMS26110230031 and grants VEGA 1/0059/13 and 0223/12.

Where applicable, the authors confirm that the experiments described here conform with The Physiological Society ethical requirements.

PCC038

At matched oxygen delivery (DO_2) chronically hypoxic male Wistar rats have increased skeletal muscle fatigue versus normoxic controls

R.F. Cook, A.M. Coney and C.J. Ray

School of Clinical & Experimental Medicine, University of Birmingham, Birmingham, UK

Patients with chronic heart failure (CHF) and chronic obstructive pulmonary disease (COPD) suffer from exercise intolerance and may also be chronically hypoxic. It is not clear whether this exercise intolerance is due to skeletal muscle dysfunction or changes in oxygen delivery (DO_2). Acclimation to chronic hypoxia involves, increased haematocrit and angiogenesis, which may normalise DO_2, and changes in skeletal muscle. We hypothesised that changes in skeletal muscle that occur with 3 weeks acclimation to chronic hypoxia (CH; 12% O_2) would lead to greater skeletal muscle fatigue. Therefore, the objective of this study was to investigate the effect of changing DO_2 by isovolaemic haemodilution on muscle fatigue, in normoxic (N) and CH male Wistar rats.
CH rats were housed at 12% O_2 in a hypoxic chamber for three weeks before experiments and breathed 12% O_2 throughout the following protocol. In all animals, anaesthesia was induced using isoflurane, 4% in O_2, and maintained with a continuous infusion of Alfaxalone (13.5-18.0 $mg.kg^{-1}.hr^{-1}$ I.V.). Arterial blood pressure, femoral blood flow and tension in the extensor digitorum longus (EDL) muscle were recorded before and during peroneal nerve stimulation (15Hz) to evoke EDL contraction for five 3 minute periods; baselines were allowed to recover between stimulations. In the CH group (n=4) and one group of N animals (NHD; n=5) isovolaemic haemodilution was performed between each period of stimulation to reduced DO_2. A further group of N animals acted as a time control (TC; n=5).
In the TC group the responses to the five 3 minute muscle contractions were consistent (tension time index ~1200$g.s^{-1}$ and fatigue ~40%). CH rats fatigued ~10% more than NHD rats at matched DO_2 achieved by isovolaemic haemodilution. It is therefore possible that skeletal muscle adaptations, evoked by chronic hypoxia, play a greater role in the mechanisms limiting exercise tolerance than reductions in DO_2.

Where applicable, the authors confirm that the experiments described here conform with The Physiological Society ethical requirements.

PCC039

Vascular reactivity and salt sensitivity in normotensive and hypertensive adults

S.O. Elias[1], O.A. Sofola[2] and S.I. Jaja[2]

[1]Physiology, Lagos State University College of Medicine, Lagos, Lagos State, Nigeria and [2]Physiology, College of Medicine of the University of Lagos, Lagos, Lagos State, Nigeria

Vascular Reactivity and Salt Sensitivity in Normotensive and Hypertensive Adults
Exaggerated vascular reactivity is a possible mechanism in the development of hypertension and cardiovascular disease (Stewart and France, 2001). Whereas there has been a lot of attention paid to the relationship of dietary salt intake with the development of hypertension there are not many studies designed to study the relationship between vascular reactivity and salt sensitivity in a black population. Fifty-two hypertensive (HT) (age 44.42±1.28y) and forty-seven age-matched normotensive (NT) subjects (age 41.23±1.40y) took part in the study after informed consent was obtained from them. Ethical clearance was obtained from the College of Medicine, University of Lagos. After control parameters were obtained, vascular hyperreactivity was determined as ΔSBP or ΔDBP ≥ +15mmHg in subjects following exposure to the Cold Pressor Test for 1 minute using cold slurry maintained at 4oC (Flaa et al., 2008). Subjects were then salt-loaded with 200mmol Na+/day for 5 days and salt sensitivty determined as earlier (Elias et al., 2011). Test for vascular reactivity was repeated after the salt load. Values are means±SEM, compared with student t test. Salt-loading led to significant increases in systolic blood pressure among the normotensive subjects from 117.5±1.54 mmHg to 121.1±2.1 mmHg (p = 0.03) and among the hypertensive subjects from 144.9±2.6 mmHg to 1519±3.0 mmHg (p = 0.0001); diastolic blood pressure increased signi-

ficantly only among the hypertensive subjects from 95.73±1.5 mmHg to 100.5± 1.62 mmHg (p = 0.0003). Sytolic and diastolic hyperreactivity were higher among the HT (49% and 39% respectively) compared to NT (44% and 39% respectively) at baseline. However sysstolic hyperreactivity (SHP) increased from 44% to 64% after salt-loading among the NT while diastolic hyperreactivity (DHP) reduced from 39% to 36%. Among the HT, both SHP and DHP reduced from 49% to 33% and from 41% to 31% respectively following salt-loading. Salt sensitivity was higher among HT (56%) compared to NT 34%. Salt sensitivity was positively correlated with systolic reactivity (before salt: r = 0.33; p < 0.05 and after salt: r = 0.25; p > 0.05) but negatively correlated with diastolic reactivity (before salt: r = -0.38; p < 0.05 and after salt: r = -0.40; p < 0.05) among NT. Our results suggest that systolic hyperreactivity may be significant in the development of salt sensitive hypertension among this population.

Stewart JC and France CR (2001). Biol Psychol 58: 105-120

Flaa A, Eide IK, Kjeldsen SE and Rostrup M (2008). Hypertension 52: 336-3

Elias SO, Azinge EC, Umoren GA et al., (2011). Nig Qt J Hosp Med 21, 85-91

Abubakar Muhammed for help in recruiting subjects

Where applicable, the authors confirm that the experiments described here conform with The Physiological Society ethical requirements.

PCC040

Heart valve operations during pregnancy: does cardiopulmonary bypass provide a safe and physiological state?

N. Ergene[1], I.Z. Solak Gormus[2], Y. Dereli[2], O. Tanyeli[2] and N. Gormus[2]

[1]Physiology, Meram Medical School, Konya, Turkey and [2]Cardiovascular Surgery, Meram Medical School, Konya, Turkey

Background: Heart valve operations during pregnancy still have some significant risks for mother and child. Cardiac operations during the third trimester of pregnancy more confident than the first and second trimesters. If a valve treatment needed during the first and second trimesters trans-catheter valve interventions can be preferred. Valve operations can be performed with the use of cardiopulmonary bypass which has a foreign surface that contacts with blood and causes a systemic inflammation. On the other hand patients had a linear flow which provides an arterial tension between 50 to 80 mm Hg during the cardiopulmonary bypass.
Methods: Between 2000 and 2012 6 patients who had mitral valve operation during their pregnancy were evaluated. Out of 2 cases had a mitral valve replacement with a mechanical valve before the pregnancy. They had severe pulmonary edema and stuck valve needing urgent delivery of the child and on-pump cardiac operation. Remaining 4 patients had severe pulmonary edema because of mitral stenosis (3 cases) or mitral regurgitation (1 case). Out of 1 patient had successful transcatheter mitral balloon valvuloplasty, while an other patient had unsuccessful balloon valvuloplasty and needed urgent closed commissurotomy with left thoracotomy.
Results: There were no deaths among the patients. Out of 2 cases had sectio and healthy childs after interventions. Among these cases one of them had a mitral balloon valvuloplasty. The other patient had a 24 week pregnancy, severely calcified mitral stenosis and pulmonary edema needing urgent mitral valve replacement with a mecahnical valve. The operation was performed by using the cardioplumonary bypass with a pulsatile pump flow and continous intrauterin monitoring of the child during and after the operation. The patient and child did well after the operation, 12 weeks later she had a successful sectio and a healthy girl. Out of 4 patients had urgent heart valve operations which can not protected the life of child, even one patient had a closed mitral commissurotomy without using the cardiopulmonary bypass.
Conclusion: The timing of open heart surgery is very significant in pregnancy. Open heart surgery after the delivery of the baby with sectio is the most advised method, if possible. However, urgent surgery may be needed before maturation of fetus, in this situation cardiopulmonary bypass may be used with pulsatile flow in order to protect the life of child during and after the early term of open heart surgery.

Where applicable, the authors confirm that the experiments described here conform with The Physiological Society ethical requirements.

PCC041

Baroreflex modulation of sympathetic nerve activity during deep brain stimulation in humans

Y.B. Sverrisdottir[1,2], A.L. Green[2], F.A. Bahuri[2], S.D. Basanayake[1], T.Z. Aziz[2] and D.J. Paterson[1]

[1]Physiology, Anatomy and Genetics, Oxford University, Oxford, UK and [2]Nuffield Department of Surgical Sciences, John Radcliffe Hospital, Oxford, UK

Modulating the activity of midbrain structures in humans has proven a successful therapy for chronic neuropathic pain and movement disorders. Electrical stimulation of these neurocircuitries is recently shown to change cardiovascular parameters in humans1, indicating that these circuitries may also be of importance in autonomic reflex control of the cardiovascular system.
This study aimed to test the hypothesis that midbrain structures can affect cardiovascular outcome by modulating baroreflex restraint of central sympathetic outflow.
Direct recordings of multiunit efferent postganglionic muscle sympathetic nerve activity (MSNA) was obtained in patients undergoing deep brain stimulation of the periaqueductal gray (PAG) and subthalamic nucleus (STN) for chronic neuropathic pain and Parkinson's disease, respectively. MSNA was expressed as burst frequency, burst incidence and relative median burst amplitude. Blood pressure, heart rate and respiration were monitored during the recording session and spontaneous vasomotor and cardiac baroreflex sensitivity diagrams were assessed. Our results show differentiated changes in sympathetic outflow during on/off stimulation phases of midbrain structures, which are reflected in the hemodynamic response.
Evidence of a differentiated control of probability and amplitude of sympathetic bursts has been reported previously2. While it is not known how the differentiated control of sympathetic bursts is brought about, it has been suggested that the baroreflex modulation of sympathetic outflow occurs at two CNS locations. One site is thought to determine the probability of discharge, and the other site is thought to determine the strength of that discharge3.Our results on the effects of deep brain stimulation on the STN and PAG show differentiated changes in sympathetic outflow during on/off stimulation periods, which are reflected in a differentiated hemodynamic response. As baroreflex modulation of sympathetic

nerve traffic is of vital importance for cardiovascular regulation, our results may shed light on where and how this modulation occurs in the central nervous system.

Thornton JM, Aziz T, Schlugman D, et al. Electrical stimulation of the midbrain increases heart rate and arterial blood pressure in awake humans. The Journal of Physiology. March 1, 2002 2002;539(2):615-621.

McAllen RM, Malpas SC. Sympathetic burst activity: characteristics and significance. Clinical & Experimental Pharmacology & Physiology. 1997;24(11):791-799.

Kienbaum P, Karlssonn T, Sverrisdottir YB, et al. Two sites for modulation of human sympathetic activity by arterial baroreceptors? J Physiol. Mar 15 2001;531(Pt 3):861-869.

Where applicable, the authors confirm that the experiments described here conform with The Physiological Society ethical requirements.

PCC042

Hydrogen peroxide in the medial septal area decreases the activation of vasopressinergic neurons within paraventricular nucleus of the hypothalamus induced by cholinergic activation of the medial septal area

M.D. Melo[2,1], J. Menani[1], D.S. Colombari[1] and E. Colombari[1,2]

[1]Physiology and Pathology, UNESP, Araraquara, Brazil and [2]Physiology, UNIFESP, São Paulo, São Paulo, Brazil

The microinjection of carbachol, a cholinergic agonist, into the medial septal area (MSA) induces anti-diuresis and increase in arterial pressure which is respectively due to vasopressin release and/or increase in sympathetic nerve activity (SNA). MSA projects directly to the paraventricular nucleus of hypothalamus (PVN), an important forebrain area involved in vasopressin release and SNA regulation. In the brain, reactive oxygen species (ROS) may modulate autonomic and behavioral responses. Previously, we have demonstrated that hydrogen peroxide (H2O2) microinjected into the MSA reduced the antidiuresis and the pressor response induced by carbachol into the same area. In the present study we investigate the effects of carbachol combined or not with H2O2 into the MSA on c-FOS expression in vasopressinergic cells of the PVN. Male Holtzman rats (280-320 g) were anesthetized with ketamine (80 mg kg-1) combined with xylazine (7 mg kg-1, both i.p.) and implanted with stainless steel guide-cannulas into the MSA.The Ethics Committee for Animal Care and Use of the Dental School of Araraquara, UNESP, approved the experimental protocols used in the present study (Proc. CEUA 02/2012). Seven days later, rats were randomly assigned for 3 groups (n = 3/group): PBS into ASM + saline into ASM; PBS into ASM + carbachol into MSA and H2O2 into MSA + carbachol into MSA. H2O2 (2.5 μmol/ 0.5 μl) or PBS (0.5 μl) was injected into MSA 1 minute before of the injection of carbachol (4 nmol/0.5 μl) in the MSA. After 90 min, rats were deeply anesthetized with sodium thiopental (50 mg/kg, ip), perfused with 4% paraformaldehyde and sections of PVN underwent double-staining immunohistochemistry for c-FOS and AVP using DAB staining with 1% cobalt chloride and 1% nickel ammonium sulfate to intensify the cell nucleus. Values are means ± S.E.M., compared by ANOVA. Carbachol into the MSA increased c-FOS expression on parvocellular (pPVN) (24.2 ± 4.2, vs. PBS + saline: 0.2 ± 0.1 cells/section, $p < 0.05$) and on magnocellular (mPVN) vasopressinergic cells (98.5 ± 5.9, vs. PBS + saline: 1.1 ± 0.4 cells/section, $p<0.05$). Previous injection of H2O2 reduced the double-labeling on both pPVN (12.7 ± 4.6 cells/section, $p<0.05$ compared to PBS + carbachol) and mPVN (46.4 ± 11.2 cells/section, $p<0.05$ compared to PBS + carbachol). These data show that the pre-treatment with H2O2 into the MSA decreases the activation of PVN vasopressinergic cells induced by carbachol into the same area, which could explain the reduction of the anti-diuresis and in the increase of arterial pressure induced by carbachol into the MSA in H2O2 pre-treated rats.

FAPESP, CNPq, FAPESP/PRONEX

Where applicable, the authors confirm that the experiments described here conform with The Physiological Society ethical requirements.

PCC043

Increased sodium transporter expression induced by sympathetic renal nerve stimulation is dependent of angiotensin II

R.B. Pontes[1], E.B. Oliveira-Sales[2], M.A. Boim[2], G.R. Veiga[1], H.A. Futuro[3], R.R. Campos[1] and C.T. Bergamaschi[1]

[1]Physiology, UNIFESP, Sao Paulo, Brazil, [2]Nephrology, UNIFESP, São Paulo, Brazil and [3]UFES, Vitoria, Espirito Santo, Brazil

It is well known that increase in renal sympathetic nerve activity induces renin release, sodium reabsorption and decrease renal blood flow. However, the exactly mechanism underlying how the sodium reabsorption is processed it is still not well understood. The present study evaluated the effects of renal acute sympathetic nerve electrical stimulation (RSNS) over the gene expression (PCR) of sodium–hydrogen exchanger type 3 (NHE3), epithelial sodium channel (β-ENaC) and water (aquaporin 2 - AQP2) transporters in the kidney in the presence or not of AT1Angiotensin II receptor blockade. Male Wistar rat (250g-300g), were divided in four independent groups: A) Sham (renal sympathetic nerve activity registered for 1h, n=6); B) RSNS for 1h, [15V, 1Hz and 0,5 ms], n=6); C) Sham+Losartan, n=6 (30 mg/kg/day) and D) Losartan+RSNS (n=6). All procedures were performed in anaesthetized animals (sodium tiophental 60mg/Kg, ip). Values are means±SEM compared by ANOVA. Electrical stimulation of renal sympathetic nerve leads to a significant increase in NHE3 (Sham1.0±0.01 vs RSNS 1,6±0,2AU), however, a reduction in β-ENaC (Sham 1,02±,012 vs 0,6±0,1AU) and in AQP2 (Sham 1,06±0,18 vs 0,6±0,1AU) gene expression was found. Animals just treated with Losartan did not present differences at NHE3 expression but a significant reduction of basal renal sympathetic nerve activity was observed (89±4 vs 63±7 pps). Furthermore, a significant reduction in ENAC (0,4±0,1AU) and AQP2 (0,3±0,1UA) expression was induced by losartan when compared to SHAM animals. Treatment with Losartan+RSNS had no effect over the studied transporters. Taken altogether, RSNS produces differential alterations in sodium and water transporters in the renal tubule that can be important for the sodium homeostasis. Apparently, such effects are dependent of AT1 angiotensin II receptor.

Supported by: CAPES, CNPq, FAPESP, FADA

Where applicable, the authors confirm that the experiments described here conform with The Physiological Society ethical requirements.

PCC044

Vagal afferent control of abdominal motor activity during hypercapnia and hypoxia in rats

E. Lemes[2] and D. Zoccal[1,2]

[1]Physiology and Pathology, School of Dentistry of Araraquara, São Paulo State University, Araraquara, SP, Brazil and [2]Physiological Sciences, Center of Biological Sciences, Federal University of Santa Catarina, Florianópolis, SC, Brazil

Stimulation of central and peripheral chemoreceptors increases inspiratory and expiratory motor outputs significantly. With respect to the expiratory component, studies demonstrated that a group of neurons in the parafacial respiratory group (pFRG) are critical for the processing of abdominal expiratory response to these metabolic challenges. Besides, it has been suggested that excitatory and inhibitory mechanisms determine the level of excitation of the pFRG expiratory neurons and then the strength of abdominal muscle contraction. In this regard, we hypothesized that vagal afferent information may modulate the magnitude of expiratory response to hypercapnia and hypoxia. To elucidate this hypothesis, we used anesthetized (urethane, 1.2 g/kg), tracheostomized, spontaneously-breathing male Wistar rats (290-320 g), in which we recorded the electromyographic activity of diaphragm (DIA) and oblique abdominal (ABD) muscles as well as the air flow in response to hypercapnia (5 min 10% CO2) or hypoxia (1 min 7% O2) before and after bilateral vagotomy. Before vagotomy, hypercapnia (n=12) and hypoxia (n=6) produced increases of DIA amplitude contraction (69.1±11.5 and 31.4±9.8 %) combined with a minor increase in ABD activity (4.4±2.2 vs 19.3±5.8 %). After vagotomy, the magnitude of DIA responses to hypercapnia and hypoxia (94.8±20.4 and 50.9±7.8 %) did not differ from those before vagotomy ($P>0.05$). In contrast, we verified a substantial increase in ABD responses to hypercapnia and hypoxia (47.1±7.9 and 63.3±15 %) in relation to the responses observed prior to vagotomy ($P<0.01$). These amplified expiratory responses to hypercapnia and hypoxia after vagotomy were associated with enhanced expiratory air flow ($P<0.01$) and augmented tidal volume responses ($P<0.01$). Our data indicates that, in anesthetized conditions, peripheral afferent inputs, potentially from pulmonary stretch receptors, exerts an inhibitory effect on the processing expiratory motor activity in response hypercapnia and hypoxia, and the removal of this information potentiates the processing of active expiration.

Financial support: FAPESC and CNPQ.

Where applicable, the authors confirm that the experiments described here conform with The Physiological Society ethical requirements.

PCC046

Expression of "pacemaker" channels in the turtle heart: Effects of anoxia and cold-acclimation

J.A. Stecyk[1,2], C.S. Couturier[2] and G.E. Nilsson[2]

[1]Biological Sciences, University of Alaska Anchorage, Anchorage, AK, USA and [2]Molecular Biosciences, University of Oslo, Oslo, Norway

Heart rate of the freshwater turtle (*Trachemys scripta*) is markedly depressed with anoxia exposure and arises in part from a resetting of intrinsic heart rate. Hyperpolarization-activated and cyclic nucleotide-gated (HCN) channels ("pacemaker" channels) constitute an important component in the control of cardiac rhythmicity. HCN channels are tetramers, and four HCN channel subunit isoforms exist, which are encoded for by four genes (HCN1-4). The four isoforms can form homotetramers and heterotetramers, resulting in a number of HCN channels with distinct biophysical properties. Using real-time RT-PCR, we examined the effects of anoxia and subsequent reoxygenation on the expression of HCN1-4 mRNA in the cardiac chambers (sinus venosus, right atrium, left atrium and ventricle) of 21°C- and 5°C-acclimated turtles. With 24 h of anoxia at 21°C, the relative abundance of HCN2 increased in all cardiac chambers, and following 24 h reoxygenation, HCN2 expression returned to control levels. In contrast, at 5°C, few and only minor changes in HCN channel subunit expression occurred with anoxia (14 d) and reoxygenation (13 d). However, compared to 21°C normoxic turtles, cardiac chambers of 5°C normoxic turtles exhibited a pronounced increase in the relative abundance of HCN2. Combined, the findings suggest that modified HCN expression with cold acclimation may prime the turtle cardiac muscle for the approaching anoxic winter, and that cardiac anoxia survival at 21°C may be aided by the circumvention of this priming and through rapid induction of similar changes in HCN expression. The altered HCN expression may serve to facilitate a slowed heart rate during anoxia by fine-tuning the sensitivity of HCN channels to the changing levels of intracellular and extracellular modulators of HCN activity that occurs with anoxia exposure. Indeed, the turtle HCN isoforms show high sequence similarity to their mammalian counterparts, notably at the location of key regulatory motifs.

Supported by the Natural Sciences and Engineering Research Council of Canada, The Research Council of Norway and National Institute of General Medical Sciences of the National Institutes of Health, USA, under Award Number P20GM103395.

Where applicable, the authors confirm that the experiments described here conform with The Physiological Society ethical requirements.

PCC049

Cardio- toxicity induced by inhalation of petroleum products-the role of oxidative stress

O.M. Azeez[2,1], C.N. Anigbogu[1,2], W.A. Saka[1,3] and R.E. Akhigbe[1,4]

[1]Veterinary Physiology and Pharmacology, University of Ilorin, Ilorin, Kwara, Nigeria, [2]Physiology, College of Medicine University of Lagos, Lagos, Lagos, Nigeria, [3]Physiology, Ladoke Akintola University of Technology, Ogbomoso, Oyo, Nigeria and [4]Physiology, Ladoke Akintola University of Technology, Ogbomoso, Oyo, Nigeria

OBJECTIVE: To investigate the effect of inhaling diesel, kerosene and petrol on cardiovascular functions and involvement of oxidative stress in Sprague Dawley rats
METHODOLOGY: Adult male Sprague-Dawley rats were divided into 4 groups with ten in each group. The animals were acclimatized for two weeks, before the commencement of the study. The control was not exposed to any petroleum product. The diesel, kerosene and petrol sub-groups, were exposed to their corresponding contaminants via inhalation. The diesel, kerosene and petrol groups inhaled diesel, kerosene and petrol, respectively for five minutes once a day in fume chamber for

eight weeks. The animals were placed in fume chamber with 1000ml beaker containing 500ml of petroleum products. The difference between the volume before and after the exposure gave the volume consumed. At the end of exposure period, rats were anaesthesized with 1% chloralose and 25% urethane mixture. Blood pressure (BP), heart rate (HR) and Baroreflex response over 30 seconds were measured using blood pressure transducer attached to the polygraph(model 7D); the rate pressure product (RPP) was thereafter calculated. The activities of superoxide dismutase (SOD), catalase (CAT) and concentrations of reduced glutathione (GSH) and Malondialdehyde (MDA) were evaluated in homogenate of lung and heart. The guidelines of the Institution animal ethics Committee was strictly adhered to.
RESULTS: There was significant increase in BP, HR and RPP of all treated groups relative to control. There was also significant increase in baroreflex response in diesel and kerosene, but not in petrol-treated when compared with control. The increase in BP and HR persisted in all the treated groups, one week after withdrawal of exposure. There was significant ($p<0.05$) decrease in the activities of SOD, CAT and GSH and significant ($p<0.05$) increase in MDA concentration in the serum and tissue homogenate of all treated groups relative to control. The cardiac muscle showed varying degrees of degeneration in the myocytes and the fibres. The lung showed degeneration of parenchyma and the alveolar wall.
CONCLUSION: The study showed that oxidative stress induction may have been partly responsible for the cardiotoxicity and alterations of the cardiovascular functions induced by inhalation of petroleum products

Claireaux G, Davoodi F (2010):Effect of exposure to petroleum hydrocarbons upon cardio-respiratory function in the common sole (Soleasolea). Aquatic Toxicology; 98 (2): 113-119

George M. I and Adegoke O. A. (2011): Effect of Vitamin E on Biochemical Parameters in Albino Rats Treated with Gasoline. J. Sci. Res.; 3 (3): 641-649

Mills NL. (2005): Diesel exhaust inhalation causes vascular dysfunction and impaired endogenous fibrinolysis. Circulation.,112:3930–6.

Orisakwe E., NjanA. A., Afonne O. J., Akumka D. D, OrishV. N., Udemezue O. O. (2004): Investigation into the Nephrotoxicity of Nigerian Bonny Light Crude Oil in Albino Rats. Int. J. Environ. Res. Public Health; 1(2):106–110

Uboh F. E., Akpanabiatu M. I., Ndem J. I., AlozieY andEbong P. E. (2009): Comparative nephrotoxic effect associated with exposure to diesel and gasoline vapours in rats. J. Toxicol. Environ. Health Sci.; 1(4): 68-74

The technologists at the Department of Physiology, College of Medicine, University of Lagos, Nigeria.

Where applicable, the authors confirm that the experiments described here conform with The Physiological Society ethical requirements.

PCC050

The effects of different styles of musical auditory stimulation on cardiac autonomic regulation in healthy women

A.L. Roque[1], M.F. Campos[1], H.L. Guida[1], A. Knap[1], L. de Abreu[2], L.M. Vanderlei[3] and V.E. Valenti[1]

[1]Departamento de Fonoaudiologia, Faculdade de Filosofia e Ciências, UNESP, Marília, Brazil, [2]Departamento de Morfologia e Fisiologia, Faculdade de Medicina do ABC, Marília, Brazil and [3]Departamento de Fisioterapia, Faculdade de Ciências e Tecnologia, UNESP, Presidente Prudente, Brazil

Introduction: The literature investigated the effects of chronic classical music auditory stimulation on the cardiovascular system. However, it lacks in the literature the acute effects of different styles of music on cardiac autonomic regulation. We aimed to evaluate the acute effects of classical and heavy metal music on heart rate variability (HRV) in women. Method: The study was performed in 21 healthy women between 18 and 30 years old. All subjects signed a consent letter and all procedures were approved by the Ethic Committee in Research of UNESP. We excluded persons with previous experience with music instrument and those who had affinity with the song styles. We analyzed HRV in the time (SDNN, RMSSD, NN50 and pNN50) and frequency (LF, HF and LF/HF ratio) domains. HRV was recorded at rest for ten minutes. Subsequently they were exposed to classical or heavy metal music for five minutes through an earphone. After the first music exposure they remained at rest for more five minutes and them they were exposed again to classical or heavy metal music. The sequence of songs was randomized for each individual. Results: In relation to the time-domain index, we did not observe significant changes during exposure to classical and heavy metal musical auditory stimulation. The SDNN index tended to be reduced during heavy metal music style exposure (39.1+10 ms) compared to the control condition (47.3+19 ms), however, there was no statistical significance ($p=0.12$). The RMSSD (control: 40.8+23 ms vs. classical music: 38+19 ms vs. heavy metal music: 39.1+20 ms; $p=0.8$) and pNN50 (control: 22.5+22 vs. classical music: 20.6+20 vs. heavy metal music: 22.5+23; $p=0.9$) indices were not changed during musical auditory stimulation with the both styles. The LF index was significantly reduced during heavy metal music auditory stimulation compared to the control condition (control: 685.7+571 ms2 vs. classical music: 595.7+837ms2 vs. heavy metal music: 328.8+143 ms2; $p=0.025$). On the other hand, there was no significant changes with respect to the HF (control: 1059+1191ms2 vs. classical music: 638.2+639ms2 vs. heavy metal music: 695.3+678ms2;$p=0.1$) and LF/HF (control: 2+2 vs. classical music: 1.4+1 vs. heavy metal music: 2+3; $p=0.7$) indices. Conclusion: Acute exposure to heavy metal musical auditory stimulation reduces the sympathetic activity on the heart.

This research received financial support from FAPESP.

Where applicable, the authors confirm that the experiments described here conform with The Physiological Society ethical requirements.

PCC051

Renal denervation leads to a reduction in angiotensin II receptors in central cardiovascular nuclei in renovascular hypertensive rats

E.E. Nishi[1], C.T. Bergamaschi[1], J.C. Perry[2], G.S. Lincevicius[1] and R.R. Campos[1]

[1]Physiology, Universidade Federal de Sao Paulo, Sao Paulo, SP, Brazil and [2]Psychobiology, Universidade Federal de Sao Paulo, Sao Paulo, SP, Brazil

Aim: to investigate whether renal sympathetic nerves play a role in the modulation of Ang II receptors expression in the central nuclei (RVLM, NTS and PVN) in renovascular hypertension.
Methods and results: Denervation of clipped kidney (DnX: visible bundles were dissected + 10% phenol) was performed in ketamine and xylazine (40 and 20 mg/kg, respectively, i.p.)-anaesthetised Wistar male rats (n=5/group) 4-5 weeks after clip implantation (gap width: 0.2mm). Ten days after DnX, mean arterial pressure (MAP) was significantly ($p<0.05$) reduced (15%) in the 2K-1C rats. AT1R was upregulated within the RVLM (76%) and PVN (70%) in the 2K-1C group, DnX normalized these expressions in both nuclei. AT2R expression was increased in the RVLM (57%) and PVN (60%) of 2K-1C group and DnX reduced AT2R in both regions. No change in both Ang II receptors expression was found within the NTS before or after DnX. DnX unchanged plasma renin activity in control and 2K-1C rats. In order to distinguish the effects of DnX from blood pressure reduction 2K-1C rats were treated orally with hydralazine (25 mg/kg/day for 7 consecutive days). Hydralazine significantly reduced MAP (26%) and AT1R within the PVN (30%) in the 2K-1C, however, unchanged AT1R or AT2R within the RVLM and NTS.
Conclusions: the present data show that renal nerves may modulate Ang II receptors within the RVLM independently of blood pressure reduction or plasma renin activity in the 2K-1C model of arterial hypertension.

Financial support: FAPESP and CNPq

Where applicable, the authors confirm that the experiments described here conform with The Physiological Society ethical requirements.

PCC052

Administration of hydrogen sulfide attenuates the oxidative stress in spontaneously hypertensive rats

H.A. Rathore[1], F. ud Din[1], M.A. Sattar[1], A.I. Hussain[1], T.Y. Chia[1], N.A. Abdullah[2] and E.J. Johns[3]

[1]School of Pharmaceutical Sciences, Universiti Sains Malaysia, Pulau Pinang, Malaysia, [2]Faculty of Medicine, Universiti Malaya, Kuala Lumpur, Malaysia and [3]Department of Physiology, University College Cork, Cork, Ireland

Vascular oxidative stress has been demonstrated in spontaneous (genetic) hypertension (1). Hydrogen sulfide (H_2S) has been recognized as a potential antihypertensive agent in various forms of experimental hypertension (2). The present study was aimed to evaluate the antioxidant potential of hydrogen sulfide in SHR. NaHS was used a s a donor of H_2S. For *in vivo* study WKY and SHR rats were divided in 4 groups namely WKY (I), WKY + NaHS (II), SHR (III) and SHR + NaHS. Groups II and IV received NaHS at a dose of 56 μM/kg i.p. daily for 4 weeks. Blood pressure, renal cortical blood perfusion and pulse wave velocity were measured in acute study under pentobarbitone anesthezia (60mg.kg-1).
In vitro , NaHS was found as a free radical scavenger, reductant and inhibitor of lipid peroxidation. *In vivo* study showed NaHS treatment reduced blood pressure, increased renal cortical blood perfusion and increased H_2S and NO plasma levels, and up-regulated the antioxidant defenses in SHR. The findings of this study suggest that the administration of NaHS not only reduces the blood pressure but also attenuates the oxidative stress in spontaneously hypertensive rats.

Systolic blood pressure, diastolic blood pressure, means arterial blood pressure, heart rate, renal cortical blood perfusion, pulse wave velocity and body weight of all the groups.

Parameters	WKY	WKY + NaHS	SHR	SHR + NaHS
SBP (mmHg)	115±4	120±3	161±5 *	143±3 *, **
DBP (mmHg)	81±3	82±4	129±5 *	116v3 *, **
MAP (mmHg)	101±4	106±4	138±4 *	125±4 *, **
HR (bpm)	325±6	320±6	400±7 *	347±5 *, **
RCBP (bpu)	241±6	237±3	178±4 *	229±3 **
PWV (m/s)	5.4±0.1	5±0.1	6.6±0.1 *	5.7±0.1 **
Body Weight (g)	302±3	300±3	297±3	300±3

Notes: SBP= systolic blood pressure, DBP= diastolic blood pressure, MAP= mean arterial blood pressure, HR= heart rate, RCBP= renal cortical blood perfusion, PWV= pulse wave velocity, bpm= beats per minute, bpu= blood perfusion unit, m/s= meter per second. The values are mean ± SEM (n = 6).

Statistical analysis was done by one-way analysis of variance (ANOVA) followed by Bonferroni post hoc test. *p < 0.05 versus WKY control; **p < 0.05 versus SHR control.

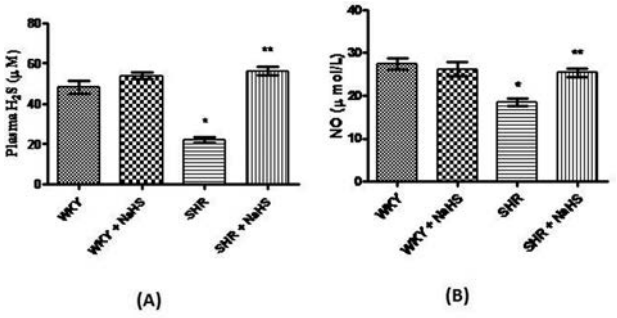

Plasma H2S (A) and plasma NOx (B) of WKY, WKY + NaHS, SHR and SHR + NaHS groups of rats. The values are mean ± SEM (n = 6). Statistical analysis was done by one-way analysis of variance (ANOVA) followed by Bonferroni post hoc test.

Note: *p < 0.05 versus WKY control; **p < 0.05 versus SHR control.

Rodriguez-Iturbe B, Zhan CD, Quiroz Y, Sindhu RK, Vaziri ND. Antioxidant-rich diet relieves hypertension and reduces renal immune infiltration in spontaneously hypertensive rats. Hypertension 2003; 41:341-6.

Ali MY, Ping CY, Mok Y. Regulation of vascular nitric oxide in vitro and in vivo; a new role for endogenous hydrogen sulphide? British Journal of Pharmacology 2006; 149:625-34.

We gratefully acknowledge Ministry of Science, Technology & Innovation (MOSTI), Malaysia for providing a Fundamental Science Research (FRGS) grant to conduct this study.

Where applicable, the authors confirm that the experiments described here conform with The Physiological Society ethical requirements.

PCC054

Isolated use of methyltestosterone in ovariectomized rats improves baroreflex control of cardiovascular system with geno- and cytotoxic safety

E. Lima, D.G. Terra, I.C. Kalil, A.M. Nascimento and T.U. Andrade

Pharmacy, UVV, Vila Velha, ES, Brazil

The addition of testosterone to hormone replacement therapy (HRT) in women has beneficial effects on sexual function, being oral methyltestosterone (MT) indicated for androgen replacement in post-menopause women. There are evidences that MT improves sexual symptoms of menopause, but little is known about its safety and its cardiovascular effects used as isolated androgen therapy. We evaluate the effects of MT in ovariectomized (OVX) rats on the cardiovascular system, especially on the baroreflex sensitivity (BRS). Additionally, general, geno- and cytotoxic safety of the treatment was evaluated. Female Wistar rats were divided into 4 groups (n=6), each): control receiving vehicle (SHAM), control receiving MT (SHAM+MT), OVX receiving vehicle (OVX), and OVX receiving MT (OVX+MT), by gavage. After 21 d of castration treatment with MT (0.04 mg/day) or vehicle (methylcellulose) was performed for 28 days. The surgical procedures were executed under ketamine (100mg/Kg) and xylasine (10mg/Kg) anesthesia. The experiments were performed in accordance with the ethical principles for animal experimentation by the Brazilian College of Animal Experimentation and were approved by our Institutional Ethics, Bioethics and Animal Welfare Committee (Protocol n 118/2010). BJR was analyzed by measuring the bradycardia and hypotension responses elicited by phenyldiguanide administration (1.5–24 μg/kg). BRS was evaluated by phenylephrine (PE: 0.5-8.0μg/Kg) and nitropusside (NP: 1.0-16.0μg/Kg) randomly administration. Mean arterial pressure (MAP) and heart rate (HR) was assessed. Testosterone (T), 17β-estradiol (E2), troponin I, urea, creatinine, ALT, and AST were measured in blood samples, and geno- and cytotoxicity were evaluated by the micronucleus test. Values are expressed as the mean ± S.E.M, compared by ANOVA, followed by the post-hoc Tukey test. There was no change in MAP (SHAM: 106±2; SHAM+MT: 107±3; OVX: 106±7; OVX+MT: 107±3 mmHg), HR (SHAM: 339±13; SHAM+MT: 318±13; OVX: 340±15; OVX+MT: 337±9 bpm), and BJR sensitivity among the experimental groups. As shown in figure 1 BRS was impaired in OVX rats after MT treatment. MT treatment increase the value of T but not change E2 (SHAM 1.43±0.05, 43±3; SHAM+MT 1.38±0.03, 45±2; OVX 1.10±0.03, 15±2; OVX+MT 1.24±0.03ng/mL, 17±5pg/mL) as well as the other biochemical parameters, neither the micronucleus test (Table 1). Rats OVX+MT presented an increase in blood T, with no change in E2. These data suggest that MT as HRT improves BRS, with no lesion on kidney, liver and heart, and with geno- and cytotoxicity safety.

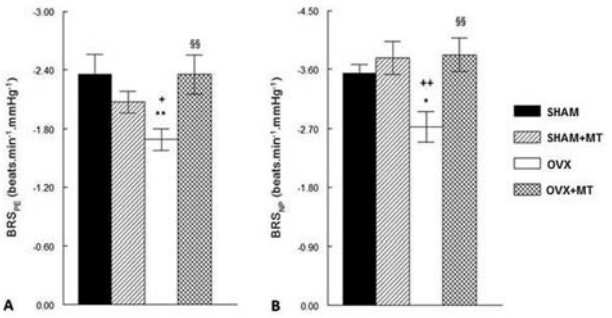

Figure 1: Baroreflex sensitivity (BRS) measured by phenylephrine (Panel A; BRSPE) or nitroprusside (Panel B; BRSNP) in conscious rat. SHAM: sham operated animals; SHAM+MT: sham operated rats plus methyl testosterone treatment; OVX: castrated animals; OVX+MT: castrated animals plus methyl testosterone treatment. Values are expressed as the mean ± S.E.M, compared by ANOVA, followed by the post-hoc Tukey test. **p<0.01 and *p<0.05 compared with SHAM group. ++p<0.01 and +p<0.05 compared with SHAM+MT group. §§p<0.01 compared with OVX group.

Groups	PCE	NCE	MN-PCE	PCE/NCE
NC	112±13	95±11	2.4±1.1	1.17±0.31
CP45	56±5**	146±5**	54.6±4.7**	0.38±0.04**
MT	106±7§§	105±3§§	3.3±1.3§§	1.01±0.09§§

Table 1: Numbers of polychromatic (PCE) and normochromatic (NCE) erythrocytes in 200 cells and micronucleated polychromatic erythrocytes (MN-PCE) in 2000 PCEs, and the PCE/NCE ratio, in the bone marrow of the rats. NC: Negative control; CP40: Positive control (cyclophosphamide 40mg/kg); MT: Group treated with methyl testosterone. Values are expressed as the mean ± S.E., compared by ANOVA, followed by the post-hoc Tukey test. **p<0.01 compared with NC group. §§ p<0.01 compared with CP45 group.

This study was supported by FAPES and FUNADESP

Where applicable, the authors confirm that the experiments described here conform with The Physiological Society ethical requirements.

PCC055

A hypothermic and hypometabolic state produced by A1 adenosine receptor activation in the nucleus of the solitary tract: implication for stroke

D. Tupone, C.J. Madden and S.F. Morrison

Nerurological Surgery, Oregon Health and Science University, Portland, OR, USA

The positive outcome that hypothermia contributes to neuroprotection following brain ischemia has stimulated recent clinical interest in the development of techniques to induce a hypothermic and hypometabolic state. Despite, the increased use of therapeutic hypothermia, the available induction techniques, employing various cold-exposure approaches rather than pharmacological methods, could be of limited utility in reaching an appropriate hypothermic state due to the activation of the central thermoregulatory responses that counteract the fall in temperature by reducing heat loss (cutaneous vasoconstriction) and increasing thermogenesis through brown adipose tissue (BAT) and shivering. Hibernating animals can reduce their energy expenditure by suspending both shivering and non-shivering thermogenesis, even in the face of marked falls in skin and core temperatures. In these species, activation of A1 adenosine receptors in the brain is thought to play a key role in triggering the torpor state. In the current studies, we investigated: 1) the potential for the A1 adenosine receptor agonist, N6-cyclohexyladenosine (CHA), to induce hypothermia in the rat (a non-hibernating species); 2) the pre-

cise thermo-effector mechanisms contributing to the fall in body temperature; 3) the brain circuits involved in the adenosine agonist-induced hypothermia; and 4) the effect of CHA-induced hypothermia on the outcome of ischemic stroke. In inactin-anesthetized (85mg/kg i.v.), Wistar rats, icv administration of CHA (10μl, 1mM) decreased core, skin and BAT temperatures, reduced expired CO2, heart rate (HR), BAT sympathetic nerve activity (SNA) and shivering EMG activity. In awake rats in a 15°C ambient, a similar icv injection of CHA decreased BAT temperature and induced a torpor-like state, in contrast to icv injection of saline vehicle which had no effect on BAT temperature or observed behavioral state. In urethane/chloralose anaesthetized rats, direct nanoinjection of CHA (60nl, 1mM) in the nucleus of the solitary tract (NTS) produced reductions in cold-evoked BAT SNA, BAT temperature, expired CO2 and HR concomitant with an increase of mean arterial pressure. These effects were reversed by local nanoinjection of muscimol (60nl, 1mM) and prevented by pretreatment of the NTS with an A1 adenosine receptor antagonist. We conclude that A1 adenosine receptor stimulation in the NTS produce hypothermia and torpor-like effect in the rat through inhibition of BAT and shivering thermogenesis. This pharmacological approach could provide the basis for induction of a rapid, sustained and controlled hypothermia, improving current methods for inducing hypothermia for neuroprotection following brain ischemia.

Supported by NIH grant NS40987.

Where applicable, the authors confirm that the experiments described here conform with The Physiological Society ethical requirements.

PCC056

Effect of glucose-enriched drink on orthostatic tolerance in young African men

T.M. Abiodun, O.S. Michael, T.O. Usman and L.A. Olatunji

Department of Physiology, University of Ilorin, Ilorin, Kwara, Nigeria

Ingestion of glucose has been confirmed to lowers blood pressure in individuals with autonomic dysfunction (1). Whether glucose drink affects cardiovascular responses during orthostatic stress in young healthy individuals, particularly in Africans is not known. We therefore sought to investigate the hypothesis that glucose drink will reduce orthostatic tolerance in normal young African men. In a randomized controlled cross-over design, eleven men (19.8 ± 0.4 kg/m2; 22.4 ± 0.8yr) ingested nothing, water (250ml) and 30% glucose drink 10min before standing on three separate days. We measured supine and standing systolic blood pressure (SBP), diastolic blood pressure (DBP), heart rate (HR) and blood glucose levels. Orthostatic tolerance was evaluated as the time to presyncope for the period of motionless standing or until presyncopal symptoms were observed (2) and syncope have been found to accounts for 1–3% of admissions to the emergency room (3–4). Throughout the first 60min of upright posture, 81.8%, 23.9% and 45.1% of 11 subjects experienced presyncopal symptoms when ingested nothing, water and 30% glucose drink, respectively. Water ingestion improves tolerance to orthostatic stress significantly while ingesting glucose drink significantly reduced orthostatic tolerance. Increased HR induced by standing was significantly improved, while the increase in SBP was attenuated when 30% glucose water was ingested. Conversely, increased DBP was not significantly affected by glucose drink. Ingestion of glucose drink led to a considerable increase in blood glucose level during orthostatic challenge when compared to when nothing or water was ingested. This study shows that glucose-enriched drink reduces orthostatic tolerance, and this is correlated with enhanced tachycardia and attenuated SBP response. The findings imply that glucose-enriched fluid may not be suitable for individuals predisposed to orthostatic intolerance.

Aksnes A.K., Brundin T., Hjeltnes N., Wahren J. (1994). Glucose-induced thermogenesis in tetraplegic patients with low sympathoadrenal activity. Am J Physiol. 266: E161–E170.

Olatunji L.A., Aaron A.O., Michael O.S. and Oyeyipo I.P. (2011). Water ingestion affects orthostatic challenge-induced blood pressure and heart rate responses in young healthy subjects: gender implications. Nig. J. Physiol. Sci. 26: 011 – 018

Brignole M, Menozzi C, Bartoletti A, Giada F, Lagi A. and Ungar A. (2006). A new management of syncope: prospective systematic guideline-based evaluation of patients referred urgently to general hospitals. Eur Heart J. 27:76–82.

Disertori M, Brignole M, Menozzi C, Raviele A, Rizzon P. and Santini M. (2003). Management of patients with syncope referred urgently to general hospitals. Europace 5:283–91.

Where applicable, the authors confirm that the experiments described here conform with The Physiological Society ethical requirements.

PCC057

3-Mercaptopyruvate sulfurtransferase is expressed in medulla oblongata and can be up-regulated by intrauterine cigarette exposure in neonatal rats

L. Nie[1,2], Y. Hu[1], X. Yan[1], M. Li[1], L. Chen[1], H. An[1], H. Zhou[1] and Y. Zheng[1]

[1]Department of Physiology, West China School of Preclinical and Forensic Medicine, Sichuan University, Chengdu, China and [2]Department of Physiology, School of Basic Medical Sciences, Ningxia Medical University, Yinchuan, China

Noxious substances released from burning cigarettes may cause hypoxia and neurotoxic effects that impede the development of the central nervous system, including brainstem. Our previous studies demonstrated that endogenous hydrogen sulphide (H2S) participate in regulation of respiration (Hu et al. 2008) and play roles in protection of medullary respiratory centres against injury caused by hypoxia (Pan et al. 2010, 2011) in medullary slices of neonatal rats. 3-Mercaptopyruvate sulfurtransferase (3MST) is one of three enzymes found to produce H2S in mammalian. The present study was conducted to investigate whether 3MST exists in the medulla oblongata and its expression can be affected by intrauterine cigarette smoke exposure in the neonatal rats. Sprague-Dawley pregnant rats were randomly divided into 2 groups, control group and cigarette smoke exposure group (n=8 for each). Cigarette smoke exposure rats were exposed to smoke for 60 min (2 cigarettes for 10 min, at an interval of 2 min, repeated 5 times) twice a day (starting at 09:00 and 16:00, respectively) during gds 7-20. The neonatal (P 1) offspring rats were used in the experimental observation. 3MST mRNA and protein expression in the medulla oblongata were analysed by RT-PCR (n=8) and Western blotting (n=8), respectively, and the levels of 3MST expression in the neurons of some medullary nuclei were examined with immunohistochemical technique (n=6). Values are means ± S.E.M., compared with independent-samples t-test. The results of RT-PCR and Western blotting were repeated 2 times, respectively. RT-PCR and Western blotting analyses showed that 3MST mRNA and protein were expressed

in the medulla oblogata in the control group and their expression were promoted in the group of intrauterine cigarette exposure of neonatal rats (1.00 ± 0.13 vs 1.51 ± 0.19 for mRNA, P<0.05; 0.20 ± 0.01 vs 0.43 ± 0.07, P<0.05). Immunohistochemical staining indicated that 3MST existed in the neurons of pre-Bötzinger complex, hypoglossal nucleus, ambiguous nucleus, facial nucleus and nucleus tractus solitarius in the control group and the mean optical densities of 3MST-positive neurons in all the nuclei mentioned above except for the nucleus tractus solitarius were significantly increased in the group of cigarette smoke exposure (values not shown, P<0.05). It can be concluded that 3MST exists in the neurons of medullary nuclei of neonatal rats and its expression can be upregulated by intrauterine cigarette exposure of the animals. These data preliminarily suggest that 3MST-H2S pathway may be involved in response of medullary neurons to injury induced by intrauterine cigarette exposure.

Granted by the National Natural Science Foundation of China (No. 31271233, 30971073) and the Fund of Doctoral Program of Ministry of Education of China (No. 20100181110048) to YZ.

Where applicable, the authors confirm that the experiments described here conform with The Physiological Society ethical requirements.

PCC058

Identification of vagal preganglionic neurones that control ventricular contractility using transoesophageal atrial pacing (TAP) and spinal cord transection

A. Machhada[1,2], N. Marina[1], M.F. Lythgoe[2] and A.V. Gourine[1]

[1]Neuroscience, Physiology and Pharmacology, University College London, London, UK and [2]Medicine, University College London, London, UK

The role of the parasympathetic innervation of the left ventricle remains controversial, although there is evidence that vagus nerve stimulation decreases left ventricular contractility in vivo in the human and pig heart (1). The aim of this study was to identify the anatomical location of vagal preganglionic neurones that control ventricular contractility using an anaesthetised rat model. Male Sprague-Dawley rats (350–400g, n=6) were anaesthetised with pentobarbitone sodium (induction 60 mg/kg i.p.; maintenance 15–20 mg/kg/hr i.v.) and artificially ventilated. The left femoral artery and both femoral veins were cannulated for the measurement of arterial pressure and infusion of fluids and drugs. The right carotid artery was cannulated for left ventricular pressure recording using a Millar pressure probe. Lead II ECG was also monitored. The animal was placed in a stereotaxic frame and the dorsal surface of the brainstem was exposed. To activate vagal preganglionic neurones, an excitatory neurotransmitter glutamate (10mM, 40 nl, pH 7.4) was microinjected into three discrete locations (separated by 0.5 mm) along the rostro-caudal extent of the left and right dorsal motor nuclei of the vagus nerve (DVMN). Responses were measured in a second group (n=3) with transoesophageal atrial pacing (TAP) to abolish chronotropic changes. A third group (n=2) underwent a spinal transection at C1 to remove sympathetic influences followed by gelofusine and vasopressin infusion to maintain mean arterial blood pressure at ~100mmHg. Values are means ± S.E.M., compared by two tailed paired student's t-test. Glutamate microinjections into the most caudal part of the left DVMN caused a significant (p<0.01) decrease in dP/dtmax (-1635 ± 301 mmHg/s), dP/dtmin (1527 ± 322 mmHg/s), mean arterial blood pressure (-27±6 mmHg) and heart rate (-15 ± 4 bpm). Glutamate had no effect on cardiovascular variables after microinjections into the rostral part of the left DVMN or after delivery into the right DVMN. With TAP, Glutamate microinjections into the most caudal part of the left DVMN caused a significant (p<0.05) decrease in dP/dtmax (-1790 ± 279 mmHg/s), dP/dtmin (1270 ± 94 mmHg/s), mean arterial blood pressure (-12±2 mmHg) and end systolic pressure (-16±2 mmHg). Responses elicited following activation of the left caudal DVMN were present after C1 transection, although they were significantly reduced by ~50%. Thus, parasympathetic control of ventricular contractility is provided by a group of vagal preganglionic neurones located in the caudal part of the left DVMN. The role of ventral groups of the brainstem vagal preganglionics (in the nucleus ambiguus) has yet to be determined.

Lewis ME et al. (2001). J Physiol. 534(Pt 2): 547–552.

Where applicable, the authors confirm that the experiments described here conform with The Physiological Society ethical requirements.

PCC059

Acetylcholine analogue mimics the protective effect of cardiac vagal nerve stimulation on ventricular fibrillation threshold

M. Kalla, M. Chotalia, G. Hao, D.J. Paterson and N. Herring

Department of Physiology, Anatomy & Genetics, University of Oxford, Oxford, Oxfordshire, UK

Purpose: Implantable cardiac vagus nerve stimulators are a promising new treatment for heart failure, which may improve both quality of life and ejection fraction[1]. Animal studies also suggest an anti-fibrillatory effect of stimulating the cardiac vagus nerve that may involve a nitric oxide (NO) dependent pathway[2], although the exact site of action in the cardiac-neural axis is still debated. We investigated whether carbamylcholine (CCh), a stable analogue of the neurotransmitter acetylcholine, can mimic the effect of vagus nerve stimulation on ventricular fibrillation threshold (VFT), and whether this mechanism is dependent on muscarinic receptor stimulation and/or generation of NO.

Methods: Experiments conformed to "Principles of laboratory animal care" (NIH Publication No. 85-23, revised 1996) and the Animals (Scientific Procedures) Act 1986 (UK). Hearts were isolated from adult male Sprague Dawley rats (300-350g) and Langendorff perfused with tyrode solution in constant flow mode (11ml/min, baseline perfusion pressure 54.75±7.27mmHg, LV developed pressure 77.5±5.6mmHg, heart rate 282.8±3.4bpm, n=6). VFT was reproducibly determined by pacing at a fixed cycle length (150msec) for 20 beats followed by a 5sec 50Hz burst at increasing current amplitude (mA) until sustained VF was induced. VF was cardioverted to sinus rhythm by perfusion with 1ml of high concentration potassium chloride solution (50mmol/L). VF could be induced on three successive occasions without a significant change in VFT (n=6). All data is presented as mean±SEM.

Results: CCh (200nM, n=9) significantly (p<0.05) reduced baseline heart rate from 292±8 to 224±6bpm). Independent of this heart rate change, CCh also caused a significant increase in VFT in paced hearts similar to vagus nerve stimulation that could be reversed with washout of the drug (control 1.5±0.25 vs. CCh 2.4±0.4 mA vs. wash out 1.14±0.18 mA). The effect of CCh on VFT was completely abolished by atropine (10μM,

n=4) or the non-specific competitive NOS inhibitor N-omega-nitro-L-arginine (L-NA 100μM, n=6). The inhibitory action of L-NA could be reversed by the addition of the NOS substrate L-arginine (5mM). The NO donor sodium nitroprusside (SNP 10μM, n=8) mimicked the effects of CCh and significantly increased VFT (baseline 1.4±0.125 vs, SNP 2.9±0.83 vs. wash out 1.18±0.23 mA).
Conclusions: These data demonstrate that the protective effect of cardiac vagal nerve stimulation on VFT is mimicked by CCh in the rat. Muscarinic receptor stimulation and the generation of NO appear to be involved in mediating this protective effect, presumably via a pre-synpatic and post synaptic coupled pathway.

De Ferrari, G.M., et al., Chronic vagus nerve stimulation: a new and promising therapeutic approach for chronic heart failure. European heart journal, 2011. 32(7): p. 847-55.

Brack, K.E., J.H. Coote, and G.A. Ng, Vagus nerve stimulation protects against ventricular fibrillation independent of muscarinic receptor activation. Cardiovasc Res, 2011. 91(3): p. 437-46.

This research is funded by the British Heart Foundation Centre for Research Excellence, University of Oxford

Where applicable, the authors confirm that the experiments described here conform with The Physiological Society ethical requirements.

PCC060

Site specific impairment of the norepinephrine transporter in the hypertensive rat

J. Shanks, S. Mane, R. Ryan, D. Li and D. Paterson

DPAG, Oxford Univeristy, Oxford, UK

Hypertension is associated with an increase in cardiac sympathetic transmission, although the exact mechanism underlying this is unknown. Enhanced intracellular calcium transients and cardiac norepinephrine (NE) release have been reported in pre-hypertensive and hypertensive spontaneously hypertensive rats (SHR) compared to normotensive controls (WKY: Wistar-Kyoto). This neural phenotype might also result from defective NET-1 transport (uptake-1). The dynamic kinetics of NET were monitored temporally using a novel fluorescent assay (NTUA) of the transporter in cultured postganglionic sympathetic neurons from the cardiac stellate ganglion, the superior cervical ganglion, the celiac ganglia/superior mesenteric ganglia, and the renal sympathetic chain. All NET activity was blocked by desipramine. NET rate was significantly impaired in stellate sympathetic neurons from the pre-hypertensive SHR compared to age matched normotensive WKY (4 week SHR, n=24, WKY, n=21, P<0.05, unpaired t test). A similar response was seen in hypertensive SHR cardiac sympathetic neurons (16 week SHR, n=20, WKY, n=19, P<0.05, unpaired t test). However, no reduction in transporter rate was observed at either age in the other major non-cardiac sympathetic ganglia. NET is modulated by receptor coupled pathways. In particular brain naturitic peptide (BNP) plasma levels are dramatically increased during cardiac stretch, volume overload and left ventricular dysfunction. Interestingly they have also been linked to regulating cardiac sympathetic neurotransmission since BNP reduces intracellular calcium transients and transmitter release. We found BNP significantly reduced the NET transporter in the WKY (S1/S2 ratio control, n=18, BNP 250nM, n=25, P<0.0001, unpaired t test). Taken together this could allow NE to stay at appropriate levels in the synapse. Whether this pathway is dysregulated in the SHR remains to be determined.
Key words: Cardiac, Sympathetic, Hypertension, Spontaneously hypertensive rat, norepinephrine re-uptake transporter.

British Heart Foundation.

Where applicable, the authors confirm that the experiments described here conform with The Physiological Society ethical requirements.

PCC061

Peripheral cardiac sympathetic dysfunction in the pre-hypertensive spontaneously hypertensive rat

J. Shanks, S. Manou-Stathopoulou, C. Lu, D. Li, D. Paterson and N. Herring

DPAG, Oxford Univeristy, Oxford, UK

The adult spontaneously hypertensive rat (SHR) has increased peripheral cardiac sympathetic activity compared to Wistar Kyoto (WKY) controls. Recent studies in 4 week old pre-hypertensive SHRs have also shown increased calcium transients1, and a reduction in NET activity2 in isolated stellate ganglion neurons compared to age matched WKYs. The functional significance of these changes in terms of NE release and change in heart rate during sympathetic stimulation is unknown. We therefore hyposthesised that peripheral sympathetic responsiveness in the SHR at 4 weeks of age would be exaggerated compared to the WKY. Ventricular weight/body weight ratios (WKY: n=7, SHR: n=8) and mean arterial pressure (WKY: n=20, SHR: n=19) measured via the left carotid artery (under 2% isoflurane) demonstrated that SHRs were without left ventricular hypertrophy and were normotensive at this age compared to WKYs. However, a small but significant (p<0.05, unpaired student t-¬test) tachycardia is observed in the young SHR in vivo (WKY: 298±11 bpm, n=20 vs. SHR: 335±8 bpm, n=19) although the heart rate response to vagus nerve stimulation (3Hz and 5Hz, 30sec, 20V, 1msec) is unchanged compared to the WKY (WKY, n=10, SHR, n=12). In an isolated organ bath atrial preparation with intact right stellate ganglion (37±0.5oC) there was a greater heart rate response to stellate stimulation (5 and 7Hz, 30sec, 20V, 1msec) in SHRs compared to WKYs (SHR, n=9, WKY, n=7). There was also a significantly greater release of 3H-NE to field stimulation (5Hz, 20V, 1msec) of right atria (n=7 for both groups) and higher plasma levels of the sympathetic co-transmitter neuropeptide Y sampled from the right atria (measured with ELISA, n=12 for both groups). The difference in 3H-NE release between the young SHR and WKY could be normalized by the NET inhibitor desipramine (1μM, SHR n=10, WKY n=8) but not the α2 receptor antagonist yohimbine (1μM, SHR n=7, WKY n=8). Increased cardiac sympathetic neurotransmission driven by a larger neuronal calcium transient and reduced NE reuptake may therefore represent an early marker in the development of hypertension and contribute to a resting tachycardia in vivo.
Keywords: Spontaneously hypertensive rat, cardiac, autonomic neurotransmission, sympathetic, vagal, hypertension.

Li D, Lee CW, Buckler KJ, Parekh A, Herring N, Paterson DJ. Abnormal intracellular calcium homeostasis in sympathetic neurons from young prehypertensive rats. Hypertension. 2012;59:642-649

Shanks J, Mane S, Ryan R, Paterson DJ. Ganglion-specific impairment of the norepinephrine transporter in the hypertensive rat. Hypertension. 2013;61:187-193

British Heart Foundation

Where applicable, the authors confirm that the experiments described here conform with The Physiological Society ethical requirements.

PCC062

Exercise training improves cardiac autonomic imbalance following physical activity

T. Masters, P. Barrow and J. Fletcher

School of Applied Science, University of Wolverhampton, Wolverhampton, UK

Low levels of cardiac vagal tone have been shown to be a predictor of future cardiac dysfunction and mortality[1]. Post-exercise recovery is significant as strenuous physical activity is associated with an increased risk of cardiac events for a period of around 1 hour[2], thought to be linked to poor return of vagal tone[3].

Delayed parasympathetic return and prolonged sympathetic activity following exercise may have important medical implications. However, improvements in cardiac autonomic control as a result of exercise training may attenuate the delay or imbalance[1]. This study aims to examine how endurance training in middle-aged subjects alters the autonomic recovery following acute exercise.

Baseline ECG was recorded in 15 healthy human subjects (aged 36-49 years, 5 male, 10 female) (ADInstruments Powerlab) during paced breathing (0.25 Hz). Subjects then completed cycle ergometer exercise comprising of a 2 minute warm-up, 10 minutes at 75% age-predicted maximum HR (Karvonen formula), and 1 minute of recovery. Recordings were then taken at 0, 15, 30, 45, and 60 minutes post-exercise. This procedure was then repeated following 12 weeks of endurance exercise training (13 kilocalories/kg/week). Heart rate variability (HRV) and QT measures were assessed offline (Chart, ADInstruments). Changes from baseline were assessed by paired t-test. Values are presented as mean ±SD.

Training improved the rate of recovery of HRV indices of cardiac vagal tone, with the root mean square of successive R-R interval differences (RMSSD) recovering to within baseline values ($P>0.05$) 30 mins post-exercise, whereas pre-training (PRE) time to recovery was 60 mins. High-frequency power took 45 mins to recover PRE, and 30 mins post-training (POST). HR remained elevated above baseline for 45 mins PRE (mean 69 ± 6.3 BPM at baseline, 73.5 ± 8 at 45 mins, $p<0.05$), and 60 mins POST (mean 65.3 ± 11 at baseline, 66.7 ± 11 at 60 mins, $p<0.05$), potentially demonstrating on-going and concomitant sympathetic activity. Markers of this are much more difficult to derive however. The low/high frequency power (LF/HF) ratio remains elevated ($p<0.05$) for 30 mins PRE, and 45 mins POST, suggestive of sympathetic activity. QT interval has been suggested to reflect cardiac sympathetic influences[4]. This remained significantly lower than baseline ($p<0.05$) at all time points PRE and POST, but only at 15 mins PRE and POST when corrected for heart rate using the Bazett formula.

These data suggest that sympathetic activity remains elevated for a considerable period post-exercise, even when parasympathetic markers have recovered. This underlying sympathetic activity along with depressed recovery of vagal tone also may be contributing to the period of increased cardiac risk after exercise. However, neither LF/HF ratio nor QT interval appeared to provide any strong indication of this.

Buch AN, Coote JH, Townend JN. Mortality, cardiac vagal control and physical training – what's the link? Experimental Physiology 2002;87(4): 423-435.

Willich SN, lewis N, Lowel H, Arntz H-R, Schubert F, Schroder R. Physical Exertion as a Trigger of Acute Myocardial Infarction. New England Journal of Medicine 1993;329(23): 1684-1690.

Routledge FS, Campbell TS, McFetridge-Durdle J, Bacon SL. Improvements in heart rate variability with exercise training. Canadian Journal of Cardiology 2010;26(6): 303-312.

Sundaram S, Carnethon M, Polito K, Kadish AH, Goldberger, JJ. Autonomic effects on QT-RR interval dynamics after exercise. American Journal of Physiology – Heart and Circulatory Physiology 2008;294; 490-497.

Where applicable, the authors confirm that the experiments described here conform with The Physiological Society ethical requirements.

PCC063

Tachycardia and increased baroreflex sensitivity in mice with conditional deletion of GalphaO in the pre-sympathetic area of the brainstem

R. Ang[1], L. Birnbaumer[2], A.V. Gourine[1] and A. Tinker[3]

[1]University College London, London, UK, [2]National Institute of Environmental Health Sciences (NIEHS), Research Triangle Park, NC, USA and [3]William Harvey Heart Centre, Queen Mary University of London, London, UK

Introduction

Inhibitory G proteins are known to mediate vagal influences on the heart. However, their role in the central nervous mechanisms of cardiovascular control remains unclear. Previous data have shown mice with global deletion of GalphaO (GαO) exhibit tachycardia, loss of diurnal variation and fairly selective loss of LF component of HRV with preserved total power suggestive of increased sympathetic tone, likely to be of central origin (1). We hence hypothesised that in mice, conditional deletion of GαO in the rostral ventrolateral medulla oblongata (RVLM), which contains sympathoexcitatory (pre-sympathetic) neurones, will have a significant impact on autonomic cardiac reflexes.

Methods

Using the Cre/LoxP approach, GαO was deleted in the RVLM of GαO flx/flx mice aged between 8 to 12 weeks (CKO) by stereotaxic delivery of an adenoviral (AdV) vector to trigger expression of Cre and GFP driven by a CMV promoter. Littermates injected with a GFP-only-expressing AdV served as controls. After 1 week, these mice (under urethane anaesthesia, 1.3 g/kg IP) were given alternating doses of phenylephrine (0.5-2mg/kg, IV) and sodium nitroprusside (0.1-1mg/kg, IV) and the obtained heart rate (HR) and blood pressure (BP) data were used to individually fit sigmoidal baroreflex curves (Figure 1). The animals were then sacrificed and transgene expression was confirmed histologically.

Results

Compared to controls, CKO mice (n=4 in each group) were tachycardic (median minimum HR 608 bpm, IQR 604-639 vs 580 bpm, IQR 576-598) and displayed an increased baroreflex gain (mean BR gain 0.65 bpm/mmHg, 95% CI 0.46-0.83 vs 0.35 bpm/mmHg, 95%CI 0.33-0.37, $p=0.03$ by unpaired t-test).

Conclusion

Mice with conditional deletion of GαO within the sympathoexcitatory circuits of the brainstem display enhanced baroreflex sensitivity consistent with an increased sympathetic tone. This suggests an important role for GαO-mediated signalling in the central nervous inhibitory mechanisms controlling sympathetic outflow.

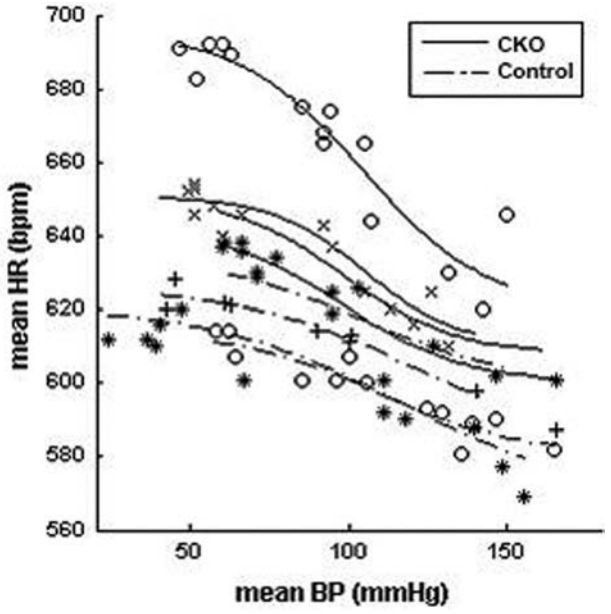

Figure 1: Baroreflex curves. Solid lines represent CKO, interrupted lines represent control, n=4 in each group.

Zuberi Z et al. (2008). Am. J. Physiol. Regul. Integr. Comp. Physiol 295, R1822–R1830.

Where applicable, the authors confirm that the experiments described here conform with The Physiological Society ethical requirements.

PCC064

Construction of asthma susceptivity model by conditional deletion of integrin beta 4 on airway epithelial cell

C. Liu, X. Qin, H. Liu, Y. Xiang, X. Qu and Y. Wang

Central South University, Changsha, China

Integrin β4 was found downregulated on the airway epithelial cell of asthma patients which induce the damaged anti-oxidation ability, inhibited wound repair ability and suppressed Th1 differentiation after OVA stress. These results strongly suggested that decreased expression of integrin β4 may relate to asthma susceptibility. To verify this correlation, in this paper, we construct a model that integrin β4 was conditional knocked out by Tetracycline. Integrin β4 floxed heterozygous mice have been constructed by transgene technology. Cre-CCSP-(otet) double transgenic mice was constructed by double crossing CCSP-rtTA line and (otet)-Cre line. Then floxed integrin β4 Cre-CCSP-(otet) triple transgenic mice was comstructed by crossing Cre-CCSP-(otet) line and integrin β4 floxed mice. By RT-PCR and immunohistochemistry detection, our results showed that integrin β4 expression was deleted successfully after Tetracycline induction in floxed integrin β4 Cre-CCSP-(otet) triple transgenic mice.

Perl AK, Zhang L, Whitsett JA: Conditional expression of genes in the respiratory epithelium in transgenic mice: cautionary notes and toward building a better mouse trap. Am J Respir Cell Mol Biol 2009;40:1-3.

Dave V, Wert SE, Tanner T, Thitoff AR, Loudy DE, Whitsett JA: Conditional deletion of Pten causes bronchiolar hyperplasia. Am J Respir Cell Mol Biol 2008;38:337-345.

Perl AK, Tichelaar JW, Whitsett JA: Conditional gene expression in the respiratory epithelium of the mouse. Transgenic Res 2002;11:21-29.

Liu C, Liu HJ, Xiang Y, Tan YR, Zhu XL, Qin XQ: Wound repair and antioxidative capacity is regulated by ITGB4 in airway epithelial cells. Mol Cell Biochem 2010;341:259-269.

Liu C, Qin X, Liu H, Xiang Y. Downregulation of integrin beta4 decreases the ability of airway epithelial cells to present antigens. PLoS One;7 (4):e32060.

This work was supported by recipient of the travel awards for young physiologists from the Chinese Association for Physiological Sciences (CAPS),National Natural Science Foundation of China; Grant numbers: 30870917, 81170024, 81100016,31100553; Grant sponsor: National Basic Research Program of China (973 Program); Grant numbers: 2009CB522102, 2012CB518104; Grant sponsor: Hunan College Innovation Platform; Grant number: 10K079.

Where applicable, the authors confirm that the experiments described here conform with The Physiological Society ethical requirements.

PCC065

Early changes in sympathetic nervous system activity following coronary artery ligation in the in situ rat

L.M. Passamani[2,1], A. Abdala[1], J. Mill[2], K. Sampaio[3] and J. Paton[1]

[1]Pharmacology and Physiology, University of Bristol, Bristol, Avon, UK, [2]Physiological Sciences, Federal University of Espírito Santo, Vitória, Espírito Santo, Brazil and [3]Pharmacological Sciences, Federal University of Espírito Santo, Vitória, Espírito Santo, Brazil

Aims: Sympathetic nervous system (SNS) over activity post myocardial infarction (MI) has been implicated in morbidity and mortality. The time course and degree of sympathetic activation and loss of cardiac parasympathetic tone post MI remain unclear in rats. Our aim was to investigate the basal sympathetic activity and its reflex regulation immediately following ligation of the left anterior descending coronary artery (LAD) in the rat. Methods and Results: Experiments were performed in an in situ unanaesthetized decerebrated working heart-brainstem preparation (Paton, 1996) of Wistar rats (60-100g). After baseline recordings of phrenic (PNA) and thoracic sympathetic nerve activities (tSNA), heart rate (HR), ECG and perfusion pressure (PP), either occlusion of the LAD was performed or a sham operation. The myocardial area at risk was assessed post-hoc with Evans Blue dye (0.5%) and was 36.3±1.1% of the left ventricle. One hour after LAD there was: (a) a higher level of tSNA and HR in the LAD rats (from 4.1±0.2 to 6.8±0.5μV, from 343±13 to 352±13bpm, n=21, P<0.01) versus a sham group (from 3.7±0.2 to 3.8±0.3μV, from 321±10 to 326±12.bpm, n=19, P>0.05) (paired t-Test). No changes in PP and respiratory rate (RR) were found between the groups; (b) a greater sympathoexcitatory response to peripheral chemoreceptor stimulation (see Table 1; n=7 each group, P<0.01, unpaired t-Test). No differences in peripheral chemoreflex evoked changes in PP, RR and HR were observed;(c) an elevated pressor response to a bolus injection of phenylephrine (30μg, i.a.) and depressed sympathetic (non-cardiac) baroreflex gain (see Table 2; n=6 each group, P<0.01, unpaired t-Test). The baroreflex bradycardia was unaffected; (d) An elevated cardiac sympathetic tone as assessed with atenolol (20μg/ml) showing a greater fall in HR in LAD rats (-108±8bpm, n=7) compared to sham rats (-82±7bpm; n=5, P<0.05, unpaired t-Test). Cardiac vagal tone was unaffected by LAD. Conclusion: The SNS is activated within minutes after myocardial infarction yet cardiac vagal tone appears unaffected. The mechanisms that produce these initial alterations remain to be investigated.

Table 1: Peripheral chemoreceptor reflex response 60 min following LAD

NaCN (0.03%)	Δ Sympatho-excitation (%)		Δ Bradycardic (bpm)		Δ Respiratory rate (%)		Δ Pressor (mmHg)	
	Sham	LAD	Sham	LAD	Sham	LAD	Sham	LAD
25μL	23±3	35±1**	-17±5	-18±10	31±6	40±5	5±1	4±1
50μL	27±2	40±2**	-90±22	-87±24	35±3	34±5	7±2	6±1
75μL	33±2	43±2**	-125±21	-128±32	37±6	40±6	7±2	5±1

**p<0.01 compared to control

Table 2: Baroreceptor reflex response 60 min following LAD

	Δ Pressor (mmHg)	Sympathetic gain (%SI/mmHg)	Δ Bradycardic (bpm)
Sham (n=6)	23.1±1.2	1.9±0.1	-25.6±5.9
LAD (n=6)	31.5±1.4**	1.3±0.1**	-36.8±9.5

**p<0.01 compared to control

Paton (1996). J Neurosci Methods (65)1, 63-8.

Financial support: CAPES, National Institutes of Health and British Heart Foundation.

Where applicable, the authors confirm that the experiments described here conform with The Physiological Society ethical requirements.

PCC066

Investigating changes in calcium homeostasis caused by a cardiotoxic drug

F.E. Mason[1], D.A. Eisner[1], M.J. Morton[2], C.E. Pollard[2] and A.W. Trafford[1]

[1]Institute of Cardiovascular Sciences, University of Manchester, Manchester, UK and [2]AstraZeneca R&D, Macclesfield, UK

Intracellular calcium (Ca) dynamics are finely tuned in the healthy heart. This homeostasis may be interrupted during a response to a cardiotoxic substance, leading to contractile dysfunction and arrhythmogenic activity. Here we aim to investigate the changes in cellular Ca homeostasis occurring upon acute application of the cardiotoxic drug clozapine (atypical anti-psychotic). Clozapine use has previously been associated with cases of myocarditis, arrhythmia and sudden cardiac death. Such in vitro analysis may highlight important new drug-screening targets for the future.

Ventricular myocytes were isolated from male rats (200-250g). Myocytes were perforated-patched and stimulated under voltage clamp control (1mM external Ca), inducing systolic Ca transients. Ca handling parameters were measured both in control conditions and upon acute application of 10μM clozapine. Cytosolic Ca was quantified by Ca-sensitive indicators fluo-3 or fura-2. 10mM caffeine was applied to discharge the sarcoplasmic reticulum (SR) and quantify SR Ca content. Changes in cytosolic Ca extusion (SERCA – sarco-endoplasmic reticulum ATP-ase, NCX – sodium-calcium exchanger) were calculated by comparing the decay rate of Ca transients. The protocol was repeated in cells from a phospholamban knockout mouse model (PLB-KO) in order to assess whether any effects were PLB-dependent. In a protocol to induce spontaneous SR Ca release and waves, external Ca was elevated to 5mM; immediately after a wave 10mM caffeine was applied to discharge the SR. Threshold for spontaneous Ca release was calculated by combining SR content value with the amount of Ca leaving the cell on the wave. Statistical tests used were one way RM ANOVA and student's t-test. Data presented as mean ±SEM. Clozapine reduced mean Ca transient amplitude by 47.7±2.5% ($p<0.001$ n=19) and peak L-type Ca current (ICaL) by 49.7±1.8% ($p<0.001$ n=20). SR content was decreased by 15.5±4.2% ($p=0.004$ n=9), SERCA activity (rate constant) by 33.9±2.6% ($p<0.001$ n=16) and NCX rate constant by 16.6±3.8% ($p=0.005$ n=6). The effect of clozapine on SERCA persisted in PLB-KO indicating that the effect on SERCA is not PLB-dependent. Results suggest that clozapine does not significantly alter the threshold for spontaneous SR Ca release and waves.

Acute application of clozapine to isolated myocytes causes several changes to Ca dynamics, most noticeably a reduction in peak ICaL. It remains unclear if or how the observed effects on Ca handling contribute to the clinical cardiotoxicity of clozapine. One possibility is that the effects on ICaL predispose to refractory heterogeneity across the heart. We also speculate that in the clinical setting there may be accumulation of clozapine in cardiac myocytes over time, supported by our results that the effect of clozapine on systolic Ca transient amplitude is not fully reversible upon wash-out of the drug.

Where applicable, the authors confirm that the experiments described here conform with The Physiological Society ethical requirements.

PCC067

Study on the function of CFTR in Human Bronchial Epithelial Cells under persistent infection by RSV

G. Gao, X. Qin, Y. Xiang, C. Liu and H. Liu

Central South University, Changsha, China

Apical membrane chloride channel critical to the regulation of fluid, chloride and bicarbonate transport in epithelia and other cell types. Build the RSV persistent infection HBECs model. Using whole cell recording method records persistent infection with RSV people bronchial epithelium cells model control group and negative model group cells on the change of CFTR Cl. We through the method of immunofluorescence, WB and realtime-PCR test RSV continued infected cells CFTR protein levels positioning and expression. In the persistent infection with RSV people bronchial epithelium cells model control group cell membrane and negative in the cytoplasm is higher expression on CFTR.tract infection for people bronchial RSV after cells in cells, chloride ion concentrations increasing, and inhibit CFTR Cl current change, at the same time depresses their CFTR expression and function.

Qin XQ, Xiang Y, Liu C, Tan YR, Qu F, Peng LH, et al, The role of bronchial epithelial cells in airway hyperresponsiveness[J]. Sheng Li Xue Bao, 2007, 59(4): 454-464

Hoh PG, Sly PD. Interactions between respiratory tract infections and atopy in the aetiology ofasthma[J]. Eur Respir J, 2002. 19(3): 538-545

Schauer U, Hofjan S, Bittscheidt J, et a1. RSV bronctliolltis and risk of wheeze and allegic sensitisation in the first year of life[J]. Eur Respir J. 2002, 20(5): 1277-1280 1283.

Sigurs N. A cohort of children hospitalized with acute RSV bronchiolitis: impact on later respiratory disease[J]. Paediatr Respir Rev, 2002, 3 (3): 177-183

Sigum N, Bjarnason R, Sigurbergssen F, et a1. Respiratory syncytial virus bronchiolitis in infancy is an important risk factor for asthma and allergy at age 7[J]. Am J Respir Crit Care Med, 2000, 161(5): 1501-1507

This work was supported by National Natural Science Foundation of China; Grant numbers: 30870917, 81170024, 81100016,31100553; Grant sponsor: National Basic Research Program of China (973 Program); Grant numbers: 2009CB522102, 2012CB518104; Grant sponsor: Hunan College Innovation Platform; Grant number: 10K079.

Where applicable, the authors confirm that the experiments described here conform with The Physiological Society ethical requirements.

PCC068

Reduced heart rate in left lateral decubitus position in healthy adults

K. Sasaki, M. Haga, H. Sato, Y. Kimura, E. Kanno and R. Maruyama

Health Sciences, Tohoku University Graduate School of Medicine, Sendai, Japan

Recently, some studies have demonstrated enhanced cardiac vagal nerve activity during the right lateral decubitus position in patients with chronic heart failure and coronary artery disease (Fujita *et al*, 2000 and Yang *et al*, 2008). However, there has been little research on the autonomic nervous system and circulation in the lateral decubitus position for normal healthy volunteers. In the present study, we compared the impact of the left and right lateral decubitus positions and the supine position on heart rate variability (HRV), including circulatory regulation. We performed electrocardiographic measurements in 58 healthy volunteers aged 23.0 ± 3.2 (mean ± SD) years. Further, a skilled cardiologist conducted echocardiographic assessment of the inferior vena cava (IVC) in each posture for 3 of 58 volunteers. A male patient with situs inversus totalis (63 years) also participated in this study. Subjects randomly maintained each lateral position at an angle of over 45° for 10 min after remaining in the supine position. Postural change was performed manually by two trained researchers. The measured data is represented as mean ± SEM. A value of $p < 0.05$ is considered statistically significant. No statistically significant differences were observed either in low frequency (LF) or high frequency (HF) HRV or in their ratio (LF/HF) using multiple comparison among three positions. However, the heart rate (HR) was significantly lower in the left lateral position than in the supine position (61.5 ± 0.9 bpm vs. 64.7 ± 1.1 bpm, respectively, $p < 0.05$, multiple comparison: Dunnet). The shape of the IVC in the supine position appeared oval in echocardiogram, and became more like a plane and a circle while in the left and right lateral decubitus positions, respectively. Both the diameter and area of IVC decreased, and hence, blood flow in IVC became more rapid in the left lateral position compared to the supine position. The echocardiographic evaluation also revealed that the two lateral decubitus positions caused different changes in circulation in the IVC. Unlike the 58 healthy subjects, the patient showed a decrease in HR in the right lateral position compared with the supine position (52.2 ± 0.3 bpm vs. 55.7 ± 1.5 bpm, respectively, $p < 0.05$, paired t-test). The HRV findings suggest that the two recumbent positions have no influence on the autonomic nervous system in healthy volunteers. However, the reduction in HR in the left lateral position may be affected by anatomical changes, especially in the shape of the IVC.

Fujita M *et al*. (2000). The Lancet 356 (25), 1822–1823

Yang JL *et al*. (2008). Circ. J. 72, 902–908

Where applicable, the authors confirm that the experiments described here conform with The Physiological Society ethical requirements.

PCC069

Higher risk of hypertension and autonomic nervous system imbalance in Mongolian young adults with low birth weight compared to Japanese counterparts

S. Bao, W. Gumula, E. Takahashi, M. Dendo, K. Sasaki, E. Kanno and R. Maruyama

Health sciences, Tohoku University Graduate School of Medicine, Sendai, Japan

Objective: Low birth weight (LBW) was confirmed as a risk of high blood pressure in later stages of life (1, 2). Although, a number of studies have shown that Mongolian people have a higher prevalence of hypertension compared to other ethnic groups (3), including the Japanese, the underlying mechanism is still unclear. The purpose of this study was to identify whether there are differences in the relationship of LBW and the risk of hypertension between Japanese and Mongolian.
Method: We performed electrocardiographic measurements in 13 Japanese and 16 Mongolian healthy volunteers aged between 19 and 33 years. We measured blood pressure (BP) and heart rate variability (HRV) at resting condition and postural change for both Japanese as well as Mongolian volunteers with LBW and normal birth weight (NBW) [LBW: 2,065 ± 179.7 g; NBW: 3,044 ± 141.2 g for Japanese vs LBW: 2,500 ± 131 g; NBW: 3,360 ± 67 g for Mongolian], respectively. All the data are expressed as mean ± SE. Student t-test and simple linear regression analysis were performed to compare the two variables. One-way repeated measures ANOVA were also performed to identify the influences of postural change.
Results: In the resting condition, heart rate (HR), BP, high frequency (HF), the ratio of low frequency to high frequency (LF/HF) showed no differences between LBW group and NBW group in the Japanese volunteers. On the other hand, HR, LF/HF were inversely related with birth weight (HR: $r = -0.518$, $p < 0.05$; LF/HF: $r = -0.647$, $p < 0.01$) in Mongolian volunteers. Japanese LBW group showed a significant increase in HR ($p < 0.05$) from supine to sitting position. However, there was no significant increase in HR for Mongolian LBW group. NBW group in both Japanese and Mongolian showed significant decrease in HF after postural change. While the Japanese LBW group showed a significant increase ($p < 0.05$) in LF/HF immediately after sitting position, the Mongolian counterparts did not show any such increase.
Conclusion: Although, there was no relationship between birth weight and BP in the Japanese young adults who participated in the present study, the Mongolians showed an inverse correlation of birth weight with resting HR and sympathetic activity. In Mongolian LBW group, no significant increase in HR, sympathetic activity and decrease in parasympathetic nervous activity were observed after postural change. These results support that LBW is associated with increased sympathetic activity and reduced baroreflex sensitivity in young adults. We conclude that Mongolian young adults have a higher risk of hypertension compared to their Japanese counterparts.

Barker DJ et al, (1990). BMJ. 301(6746): 259-62.

Tamakoshi K et al, (2006). Circ J. 70(3): 262-7.

Li H et al, (2008). Circ J. 72(10): 1666-73.

Where applicable, the authors confirm that the experiments described here conform with The Physiological Society ethical requirements.

PCC070

Effects of estrogen replacement on blood pressure elevation induced by chronic intermittent hypoxia in ovariectomized rats

S. Omoto[1], S. Tazumi[1], R. Yoshida[1], H. Nagai[2], K. Yoshida[2], R. Kudo[3], K. Hatake[3] and K. Morimoto[1]

[1]Department of Environmental Health, Faculty of Life Science and Human Technology, Nara Women's University, Nara, Nara, Japan, [2]Department of Forensic Medicine, Graduate School of Medicine, University of Tokyo, Bunkyo-ku, Tokyo, Japan and [3]Department of Legal Medicine, Nara Medical University, Kashihara, Nara, Japan

Clinical studies suggest that sleep apnea causes systemic hypertension. There is gender specificity in the incidence of sleep apnea. Premenopausal women have a lower occurrence of sleep apnea, whereas in postmenopausal women the incidence of sleep apnea is same as in males. Therefore, female sex hormone, estrogen, may protect women against the sleep apnea-induced hypertension. Intermittent hypoxia (IH) is used to mimic the arterial hypoxemia that occurs during sleep apnea. We examined whether chronic estrogen replacement affects blood pressure (BP) responses to IH in ovariectomized rats. Female Wistar rats aged 9 wk were ovariectomized and implanted with radiotelemetry devices for BP and heart rate measurements. After 4 wk, the rats were assigned either to a placebo-treated (Pla; n=15) group or a group treated with 17β-estradiol (E2; n=15) subcutaneously implanted with either placebo- or 17 β -estradiol (2.5 mg/90-day release) pellets. The atmosphere in IH chamber was controlled by the electronically regulated solenoid switches in a two-channel gas mixer, which gradually lowered oxygen in the chamber over 90 s from 21% to 4% O_2. Chamber ware rapidly flushed with compressed air for the following 90 s to restore O_2 to 21%. Rats were exposed to 20 cycles/h of IH or air-air for 8 h/day during the light phase (9:00-17:00) for 14 days. In the day after the series of IH exposure, mesenteric arteries were dissected from IH-exposed or control rats euthanized by overdoses of pentobarbitone. Using the arteries contracted with 3×10^{-6} M phenylephrine, we test relaxation responses to acetylcholine (Ach, 10^{-8}-10^{-5} M) under inhibitions of endothelium-dependent vasodilators. The expression of endothelial nitric oxide synthase (eNOS) in the mesentery was examined by Western blot analysis. After 7 days, resting mean arterial pressure (MAP) was significantly elevated in IH rats of the Pla and E2 groups similarly during the light phase (IH-phase). On the other hand, during the dark phase (non-IH phase), only the Pla group exhibited the MAP elevation on day 7. However, the MAP in the E2 group was increased to the same level in the Pla group during light or dark phase on day 14. Sensitivity of Ach-induced endothelium-dependent NO (ED_{50}) in mesenteric arteries was higher in the E2 group than that in the Pla group of IH rats. In addition, Western blot analysis showed that eNOS expression in mesentery was increased in the E2 group compared with the Pla group. This study suggests that estrogen replacement delayed the development of IH-induced hypertension in non-IH phase, at least partly, though enhancement in NO sensitivity in mesenteric arteries and overexpressed mesenteric eNOS in ovariectomized rats.

Where applicable, the authors confirm that the experiments described here conform with The Physiological Society ethical requirements.

PCC071

TRPV1 blockade restores the high-pressure baroreflex control of renal sympathetic nerve activity in cisplatin induced renal failure rats

M.H. Abdulla[1], M. Duff[1] and E.J. Johns[1,2]

[1]Physiology, University College Cork, Cork, Ireland and [2]Allianze University, College of Medical Sciences, Penang, Malaysia

Renal failure and injury are associated with inflammatory responses within the kidney which could be mediated through transient receptor potential vanilloid type 1 (TRPV1) receptors. This study investigated whether TRPV1 receptors contribute to the modulation of high-pressure baroreceptor regulation of renal sympathetic nerve activity (RSNA) in cisplatin induced renal failure rats. Wistar rats (300-350g) were divided into a renal failure (RF, n=7) or control (C, n=7) group which received IP either cisplatin (5mg/kg) or saline (0.9% NaCl), respectively, 4 days before the acute study. Rats were anaesthetised with chloralose:urethane mixture (1ml, 16.5:250mg/ml, IP). Cannulae were inserted into the right femoral artery, for mean arterial pressure (MAP) and heart rate (HR) measurement, and vein for saline (3ml/h) infusion. The right kidney was exposed and a small cannula inserted 4.5mm into the rostral pole of the kidney to lie at the corticomedullary border for intrarenal infusion of saline or a TRPV1 blocker capsazepine (CPZ). The left kidney was exposed, a renal sympathetic nerve bundle was dissected and sealed onto recording electrodes. After 2h stabilisation, baroreflex gain curves were generated using IV phenylephrine and sodium nitroprusside (50μg/kg/min). Saline (1ml/h) was infused into the right kidney 20min before, and during the first baroreflex gain curve was generated and then CPZ (5μg/ml) was infused (1ml/h) for 20min before, and during the second baroreflex challenge 2hr after the first baroreflex curve. The animal was euthanized at the end of the experiment and the background noise obtained. Data, mean±SEM were compared using t-test with significance at $P<0.05$. In C, the MAP, HR and RSNA values measured during CPZ infusion were not different from their respective values before CPZ (84±5 vs. 83±5 mmHg, 405±16 vs. 399±16 bpm, 0.68±0.15 vs. 0.65±0.14 μV.s, respectively). Similarly, in RF, the MAP, HR and RSNA were similar to their respective values before CPZ (94±5 vs. 94±5 mmHg, 379±12 vs. 382±10 bpm, 0.82±0.19 vs. 0.75±0.16 μV.s, respectively). In RF, the slope of the baroreflex curve of RSNA following saline infusion was significantly smaller than C (RF vs. C; 0.09±0.01 vs. 0.15±0.02, $P<0.05$). The intrarenal infusion of CPZ in C had no effect on the slope of the baroreflex curve (CPZ vs. Saline; 0.14±0.01 vs. 0.15±0.02). However, in RF, the slope of the baroreflex curve increased significantly following CPZ (CPZ vs. Saline; 0.17±0.02 vs. 0.09±0.01, $P<0.05$). These findings demonstrate that normally TRPV1 receptors have little influence on the baroreflex gain curves. However, in renal failure there is an attenuation of the sensitivity of the baroreflex gain curve which is mediated via TRPV1 receptors as it can be normalised by blockade of TRPV1 receptors.

This work was funded by the Wellcome Trust.

Where applicable, the authors confirm that the experiments described here conform with The Physiological Society ethical requirements.

PCC072

The carotid body is crucial for the full development of renovascular hypertension in rats

W. Pijacka, F.D. McBryde, A.P. Abdala, E.B. Hendy, P. Marvar and J. Paton

Physiology and Pharmacology, University of Bristol, Bristol, UK

We have shown recently that carotid sinus denervation (CSD) reduced arterial pressure (AP) in spontaneously hypertensive rats (SHR) but was without effect in normotensive Wistar rats. It remains unknown whether this anti-hypertensive effect is specific to the SHR. However, since the peripheral chemoreflex is sensitised in the Goldblatt (2 kidney, 1 clip; 2K1C) renovascular hypertensive model, we have tested whether established 2K-1C hypertension can be ameliorated by CSD.
Under ketamine/medetomidine anaesthesia (75mg/kg + 0.5mg/kg, IP), the left renal artery of 6 week old Wistar rats was partially occluded with a silver clip. At 11 weeks of age, rats were instrumented to record AP telemetrically, and after a 7 day baseline recording underwent CSD or Sham surgery. Prior to CSD/Sham surgery, AP rose steadily during baseline at 1.0±0.5 mmHg/day. This continued in Sham (+1.3±1.0 mmHg/day) but not CSD (-0.3±0.9 mmHg/day). Thus, at 14 weeks of age AP was unchanged from baseline in CSD rats (183±16 vs. 182±17 mmHg), but had continued to increase in Sham rats (201±18 vs. 210±21mmHg). Spontaneous baroreflex gain increased in CSD (-1.16±0.16 vs. -1.25±0.15 bpm/mmHg) but not Sham (1.1±0.09 vs. 1.0±0.12 bpm/mmHg). Reductions in low (6.3±0.5 vs. 6.0±0.8 mmHg2) and very low frequency (2.8±0.5 vs. 1.8±0.2 mmHg2) spectral power of systolic AP were seen in CSD but not Sham, suggesting sympathoinhibition. In addition, we have observed a reduction in macrophage infiltration in the brainstem after CSD in 2K1C rats, a response not observed in Sham animals. Using metabolic cages, we are now assessing any alterations of CSD on renal function in 2K1C rats and comparing with a Sham group. Preliminary data indicate that CSD improves glomerular filtration rate. We will present these data in full at the meeting.
In conclusion, CSD appears to stunt the continued increase AP in 2K-1C rat. The mechanisms for this include: sympathoinhibition, improved baroreflex gain and renal function as well as reduced systemic inflammation.

Cibiem & British Heart Foundation funded research.

Where applicable, the authors confirm that the experiments described here conform with The Physiological Society ethical requirements.

PCC073

Chronic inhibition of acetylcholinesterase activity improves the sympathovagal balance during the development of hypertension in spontaneously hypertensive rats (SHR)

R.M. Lataro, C.A. Silva, R. Fazan and H.C. Salgado

Physiology, School of Medicine of Ribeirão Preto, University of São Paulo, Ribeirão Preto, São Paulo, Brazil

The autonomic imbalance in experimental models of hypertension is characterized by an increase in sympathetic and decrease in parasympathetic function. While sympathetic overactivity has received most of the attention, the same appraisal has not been given to the decrease in parasympathetic function. Therefore, it was investigated whether an increase in the availability of acetylcholine will improve the sympathovagal balance during the development of hypertension in SHR. To accomplish this, it was performed the blockade of central acetylcholinesterase with donepezil (DON), a compound that crosses the blood-brain barrier, and also pyridostigmine (PYR), a compound which does not cross the blood-brain barrier, acting particularly in the peripheral synaptic cleft. Thus, it was investigated the chronic effect (16 weeks) of DON or PYR on the following variables: arterial pressure (AP); heart rate (HR); vagal tone; AP and pulse interval (PI) variability in time and frequency domain; plasma norepinephrine (NE) and cardiac function. Acetylcholinesterase blockade started when SHR were 5 weeks old, receiving DON (1.5 mg/kg/day) or PYR (2mg/kg/day) given by osmotic minipump. After 16 weeks, femoral AP was recorded in conscious state and atropine provided the vagal tone, while the combined administration of atropine plus propranolol provided the intrinsic HR (iHR). Cardiac function was assessed under isofluorane anesthesia, with the Millar catheter, 24h after the hemodynamic measurements. Systolic AP (Control: 202±5; DON: 178±8; PYR: 200±7 mmHg) and HR (Control: 354±13; DON: 304±9; PYR: 334±10 bpm) was reduced by DON, but was not affected by PYR. Vagal tone was increased by DON or PYR (Control: 64±5; DON: 105±11; PYR: 132±8 bpm). PYR increased the iHR while DON did not (Control: 340±3; DON: 351±5; PYR: 381±8 bpm). DON decreased the systolic AP variance (Control: 63±5; DON: 39±7) and the power of the low-frequency (LF) band of PI (Control: 32±2; DON: 18±2 nu), while decreased the power of the high-frequency (HF) band (Control: 68±2; DON: 82±2 nu) and the LF/HF ratio (Control: 0.5±0.05; DON: 0.2±0.03) of the PI spectrum. PYR did not promote significant changes in the AP or PI variability. Moreover, DON or PYR did not affect NE concentration (Control: 8.7±0.7; DON: 12±2.2; PYR: 9.6±2 ng/mL) or cardiac function [+dPdt (Control: 9469±574; DON:11461±1156; PYR:9640±1041 mmHg/s), -dPdt (Control: -11665±1085; DON: -11015±570; PYR: -9999±1294 mmHg/s), end diastolic pressure (Control:9±2; DON: 11±3; PYR: 7±1 mmHg)]. In conclusion, despite the increase in cardiac vagal tone elicited by either DON or PYR, the anticholinesterase agent that crosses the blood brain barrier, i.e. DON, was more effective improving the cardiovascular function during the development of hypertension in SHR.

Where applicable, the authors confirm that the experiments described here conform with The Physiological Society ethical requirements.

PCC074

High speed macro imaging of co-cultures

R.B. Burton, S. Bilton, G. Stephens, H.E. Larsen, D. Li, D.J. Paterson and G. Bub

Department of Physiology, Anatomy and Genetics, University of Oxford, Oxford, UK

Introduction: The release of noradrenaline (NA) from the sympathetic nervous system (SNS) exerts powerful chronotropic and inotropic effects (Zaika et al., 2011) and can be pro-arrhythmogenic. Many cardiac arrhythmias have been attributed to formation of macroscopic excitation patterns, but the influence of the SNS on wave dynamics is not well understood. In the current work, we describe new methodologies for dye free mapping of waves in myocyte monocultures and neuron/myocte co-cultures and report the effect of nicotine

and nerve growth factor (NGF) on macroscopic wave dynamics.
Methods: Hearts were isolated from neonatal SD rat pups (P1-P3) and killed by Schedule 1 in accordance to UK Home Office regulations. Briefly, ventricles were isolated, enzymatically digested, and enriched for myocyte content before plating on poly-L-lysine coated petri-dishes. After 24 hours, stellate neurons were isolated from litter mates and plated on top of the myocytes in 1:20 ratio.
We used dye-free imaging techniques to record macroscopic wave patterns and beat rate in myocyte-only and co-culture preparations. Experiments were carried out in an Okolab stage incubator controlled for heat (37°), CO2 (5%) and humidity.
Results: (i) We find that co-culture wave speed is significantly faster than myocyte-only cultures (52%±14%, $p<0.001$, n=7); (ii) Addition of nicotine to co-cultures systems causes an altered behaviour by change in initiation sites of wave patterns, but no significant changes in conduction velocity (n=7); (iii) Application of 10 μM nicotine to co-cultures produced a transient increase in contraction rate of up to 37%, and this was significantly sustained in 3 of 5 experiments; (iv) DAPI-stained images of both myocyte and co-culture plates grown either in the presence or absence of NGF were analysed in terms of a clumping factor (CF), a newly developed statistical measure of cell-cell spacing. CF were significantly higher (indicative of more clumped cells) for cultures grown in the absence of NGF compared to those grown in the presence of NGF (50ng/ml), for both myocyte-only (8.02±0.99, n=6 vs. 5.48±0.51, n=5) and co-culture (9.33±1.17, n=5 vs. 5.99±0.74, n=4) plates (all mean ± S.E.M, comparisons were performed with a t-test, $p<0.05$).
Discussion: Our observations may be relevant to understanding the onset and evolution of complex waves during life threatening cardiac arrhythmias, which can be attributed to large scale spiral waves (Bub et al., 2002; Bub et al., 2005). The finding that NGF modulates the patterning of myocytes raises the question of how NGF and its receptors interact to generate changes in cardiac and synaptic function.

Bub G, Glass L, Publicover NG, Shrier A (2002). PNAS 95, 10283-10287.

Bub G, Shrier A, Glass L (2005). Phys Rev Lett 94, 028105.

Zaika O, Zhang J & Shapiro MS (2011). J Physiol 589, 2559–2568.

This work was supported by the BHF CRE (Oxford), EPSRC, BHF. RABB is an EP Abraham Cephalosporin JRF of Linacre college, Oxford.

Where applicable, the authors confirm that the experiments described here conform with The Physiological Society ethical requirements.

PCC075

Intrinsic electrophysiological properties of late-expiratory and CO2-sensitive neurones in the Retrotrapezoid/parafacial respiratory group of rats

D.J. Moraes, D.B. Zoccal and B.H. Machado

Physiology, School of Medicine of Ribeirao Preto, Ribeirao Preto, Sao Paulo, Brazil

The Retrotrapezoid/parafacial Respiratory Group (RTN/pFRG) contains late-expiratory (late-E) and CO2-sensitive neurones involved with active expiration and central chemoreception, respectively. Here we evaluated whether or not RTN/pFRG late-E and CO2-sensitive neurones present distinct electrophysiological properties and CO2 sensitivity. Using an in situ working heart brainstem preparation of rats (7 weeks old), we performed recordings of abdominal (AbN) and phrenic (PN) nerves activities simultaneously with whole cell path-clamp recordings of late-E or CO2-sensitive neurons in the RTN/pFRG. The data shows that late-E and CO2-sensitive neurones constitute heterogeneous neuronal populations with respect to several electrophysiological properties. During normoxic/normocapnic condition the late-E neurones were silent, while CO2-sensitive displayed continuous frequency discharge (0.83 ± 0.02 Hz; n=8) during the respiratory cycle. The emergence of late-E activity, in late-E neurons, and the coincidently late-E burst in AbN motor activity, both preceding PN bursts, occurred only during hypercapnia (10% CO2; 9.1 ± 0.08 Hz; n=7) or hypoxia (5% O2; 8.5 ± 0.09 Hz; n=7). Input resistance (354 ± 21 vs 235 ± 17 MΩ; $p<0.05$), resting membrane potential (-67 ± 3 vs -54 ± 2mV; $p<0.05$) and rheobase (35 ± 3 vs 58 ± 7 pA; $p<0.05$) were different, suggesting that the expression or properties of some ion channels differ between these neuronal types. Common features of RTN/pFRG late-E and CO2-sensitive neurones included the expression of transient outward potassium current (TOC; at 60 mV: 365 ± 65 vs 380 ± 57 pA/pF), hyperpolarization-activated inward current (at -120 mV: 35 ± 3 vs 47 ± 7 pA/pF) and absence of persistent sodium current. Nevertheless, after synaptic blocked, hypercapnia increased the firing frequency (+1.83 ± 0.05 Hz) and decreased the potassium-mediated leak current (- 3.1 ± 1 nS) of CO2-sensitive neurones, but did not change the late-E neurones activity. This body of electrophysiological evidence indicates that RTN/pFRG late-E and CO2-sensitive neurones from juvenile/adult rats constitute heterogeneous neuronal populations regarding intrinsic electrophysiological properties and CO2 sensitivity, and provide a cellular basis for a better understanding of their involvement in the pathophysiological conditions, such as obstructive sleep apnoea, hypertension and heart failure.

Financial Support: FAPESP, CAPES and CNPQ.

Where applicable, the authors confirm that the experiments described here conform with The Physiological Society ethical requirements.

PCC076

***Mesobuthus tamulus* venom augments the phenylbiguanide and capsaicin-induced cardiorespiratory reflexes involving two disparate mechanisms**

A. Akella, A. Dutta and S.B. Deshpande

Department of Physiology, Institute of Medical Sciences, Banaras Hindu University, Varanasi, U.P, India

Indian red scorpion (*Mesobuthus tamulus*, MBT) venom is known to augment the cardiorespiratory reflexes elicited by phenylbiguanide (PBG) or phenyldiguanide (PDG) [1,2]. These chemicals mediate the action via 5-HT_3 receptors on the vagal C-fibers. Similar to PBG/PDG, capsaicin (a TRPV1 agonist) also produces cardio-respiratory reflexes involving vagal C-fibers [3]. However, the effect of MBT venom on the capsaicin-induced responses is not known. Therefore, the present study was undertaken to ascertain whether MBT venom also augments the capsaicin-induced responses. Further, to delineate the underlying mechanisms.
Animal experiments were performed after obtaining the approval from the Institutional Ethical Clearance Committee. Adult rats of Charles foster strain were used. They were anesthetized with urethane (1.5 g/kg, i.p). The trachea, jugular vein and femoral artery were cannulated. The ECG, respiratory

excursions and blood pressure were recorded. At the end of each experiment, the pulmonary water content was determined by physical method.
Both PBG (10μg/kg) and capsaicin (10μg/kg) produced bradycardia, apnea-bradypnea and hypotension. After exposure to MBT venom (100μg/kg) for 30 minutes, the responses induced by PBG as well as capsaicin were augmented. Pulmonary edema was seen in these animals. The augmentation of PBG-induced responses and pulmonary edema were blocked after pretreatment with prostaglandin synthase inhibitor (indomethacin, 10mg/kg); kinin synthase inhibitor (aprotinin, 6000 KIU) and guanylate cyclase inhibitor (methylene blue, 5mg/kg). The augmentation of capsaicin-induced responses was blocked in indomethacin pretreated animals only but not in aprotinin and methylene blue pretreated animals even though pulmonary edema was not seen in these groups. Elevation of the endogenous cGMP levels by phosphodiesterase-V inhibitor (sildenafil, 100μg/kg) augmented the PBG-induced responses but not the capsaicin-induced responses. Sildenafil pretreated animals exhibited pulmonary edema.
The present results demonstrate that MBT venom also augments the capsaicin-induced responses similar to PBG but involves distinctly different mechanisms. The PBG-induced responses are augmented by pulmonary edema-dependent mechanisms involving prostaglandins, kinins and guanylate cyclase-cGMP pathway whereas the capsaicin-induced responses are independent of pulmonary edema and involve nociceptive action of prostaglandins. The present study substantiates the existence of functionally different types of vagal-afferents. Our results with indomethacin, also implicate the direct and indirect action of prostaglandins in mediating the C-fiber reflexes.

Deshpande SB, Bagchi S, Rai OP, Aryya NC. Pulmonary oedema produced by scorpion venom augments a phenyldiguanide-induced reflex response in anaesthetized rats (1999) J Physiol. 521: 537-44.

Dutta A, Deshpande SB. Indian red scorpion venom-induced augmentation of cardio-respiratory reflexes and pulmonary edema involve the release of histamine (2011) Toxicon. 57:193-8.

Dutta A, Deshpande SB.Cardio-respiratory reflexes evoked by phenylbiguanide in rats involve vagal afferents which are not sensitive to capsaicin (2010) Acta Physiol (Oxf). 200:87-95.

The study was supported by the grants from Indian Council of Medical Research, New Delhi, India.

Where applicable, the authors confirm that the experiments described here conform with The Physiological Society ethical requirements.

PCC077

Non-invasive vagus nerve stimulation enhances parasympathetic influence on autonomic output in healthy humans and heart failure patients

J.A. Clancy, S.A. Deuchars and J. Deuchars

University of Leeds, Leeds, UK

Heart failure (HF) is a debilitating and fatal condition characterised by sympathetic activation and parasympathetic withdrawal. Tackling the underlying autonomic imbalance through parasympathetic stimulation can improve cardiac function and quality of life scores in HF patients[1], however, the current method of cervical vagus nerve stimulation (VNS) is invasive and associated with side effects. This study investigated the autonomic effects of a non-invasive method of VNS - transcutaneous electrical stimulation of the auricular branch of the vagus nerve (tVNS) - in healthy participants (n = 111; 58 female, 53 male; aged 20-66 years) and HF patients (n = 6; 1 female, 5 male; 51-86 years). The study was approved by the University of Leeds Ethics Committee and the National Research Ethics Service and was conducted in accordance with the Declaration of Helsinki. Heart rate (ECG), blood pressure and respiration were recorded continuously. Heart rate variability (HRV) was calculated using spectral analysis of beat-to-beat intervals derived from ECG data. Low frequency (LF; 0.04-0.15Hz) and high frequency (HF; 0.15-0.40Hz) power were calculated. HF power represents parasympathetic/vagal modulation of heart rate and the ratio of low to high frequency power (LF/HF) can be used as an indicator of sympathovagal balance, such that a decrease in LF/HF indicates a shift in autonomic balance towards parasympathetic dominance. Microneurography was also used to record muscle sympathetic nerve activity (MSNA; n = 10). tVNS was applied at either low pulse width and pulse frequency (L-tVNS), high pulse width and pulse frequency (H-tVNS) or sham stimulation. Data were analysed at baseline, during tVNS and during recovery. Repeated measures ANOVAs were used to analyse results (data presented as mean ± S.E.M). L-tVNS (n = 63) and sham tVNS (n = 14) had no significant effect on HRV whereas HRV improved significantly during H-tVNS in healthy participants with a decrease in LF/HF ratio from 1.26 ± 0.15 at baseline to 1.04 ± 0.14 during H-tVNS (n = 34; p = 0.026). There was a significant reduction in single unit MSNA frequency and incidence during H-tVNS (p = 0.001 and p = 0.002 respectively). H-tVNS significantly improved LF/HF ratio in HF patients from 4.78 ± 1.49 to 3.13 ± 1.39 (n = 6; p = 0.028). There was also a significant reduction in LF power during H-tVNS in HF patients (p = 0.028). Based on the results of this study, tVNS can improve HRV in both healthy participants and HF patients. Furthermore, microneurography revealed that the improvement in HRV during H-tVNS is, at least partly, due to a reduction in sympathetic activity in healthy participants. tVNS could be a practical, non-invasive and economical therapy for heart failure patients and warrants further investigation.

De Ferrari et al. (2011). *Eur Heart J* **32**, 847-855.

This study was funded by the University of Leeds.

Where applicable, the authors confirm that the experiments described here conform with The Physiological Society ethical requirements.

PCC078

Anatomical and functional characterisation of pro-opiomelanocortin neurones in the nucleus of the solitary tract of the mouse

S. Cerritelli, N. Balthasar and A.E. Pickering

Physiology & Pharmacology, University of Bristol, Bristol, UK

One of the two main central clusters of pro-opiomelanocortin (POMC) containing neurones is in the nucleus of the solitary tract (NTS), which receives vagal afferent inputs. POMC can be cleaved into the endogenous opioid β-endorphin. Thus, β-endorphin release by POMC neurones may modulate vagal afferent processing within the NTS. To map the anatomical organisation and projection pattern of NTS POMC neurones we used an adeno-associated viral vector (AAV) to drive channelrhodopsin2-mCherry expression in mice selectively expressing cre-recombinase/GFP in POMC neurones (1). We examined the cardiorespiratory effects of NTS POMC neuronal activation in the working heart-brainstem preparation (WHBP, 2). POMC-

Cre mice (n=3) received NTS microinjections of AAV-EF1α-DIO-hChR2-mCherry under anaesthesia (ketamine 70mg.kg-1/medetomidine 0.45mg.kg-1 i.p.). Three weeks later mice were anaesthetised with 5% halothane (until decerebration) for set-up of the WHBP. NTS POMC neurones were activated using a laser and cardiorespiratory responses measured. Naloxone (1-5μM) was used to block opioid receptors and effects compared with responses to DAMGO (2mM), a μ-opioid agonist, microinjection into the NTS and vagal preganglionic cell groups (n=2). Brains were post-fixed and histology performed to determine the location and projection pattern of NTS POMC neurones, based on mCherry fluorescence. Immunohistochemistry was performed for choline acetyltransferase, to label vagal preganglionic neurones, and GFP, to label POMC neurones and imaged using fluorescence microscopy. Immunofor POMC neurones (GFP) and β-endorphin was also performed in the NTS/hypothalamus. GFP positive cells were seen in the hypothalamic arcuate nucleus and NTS (200-300 somata in the caudal NTS). β-endorphin positive POMC neurones were found in the arcuate but not NTS. β-endorphin labelled fibres were found close to NTS POMC neurones. The AAV efficiently and selectively transduced NTS POMC neurones (~180); mCherry was distributed over a 1.4mm rostrocaudal distance. Most mCherry-labelled fibres were seen within the NTS but fibres also projected ventrally and ventrolaterally to the dorsal motor nucleus of the vagus (DMV) and nucleus ambiguus (NA) (n=2). Opto-activation of transduced NTS POMC neurones caused a reproducible, frequency dependent bradycardia, transient apnoea and exaggerated respiratory sinus arrhythmia. These cardiorespiratory responses were reversibly abolished by naloxone (n=1), but not mimicked by DAMGO microinjection into the NTS (n=2). This subgroup of POMC neurones forms an output path from the NTS to other brainstem autonomic centres, including the DMV and NA. Our results suggest that NTS POMC neurones can play a role in modulating vagal afferent processing via opioid release and may mediate cardiorespiratory responses.

Balthasar N *et al.* (2004). *Neuron* **42** : 983-991.

Paton JF (1996). *J Neurosci Methods* **65** : 63-68.

MRC, BPS and Wellcome Trust funded.

Where applicable, the authors confirm that the experiments described here conform with The Physiological Society ethical requirements.

PCC079

Increased baseline arterial pressure and ventilatory responses to hypercapnia in rats fed with high-fat diet

G. Speretta[1], M. Bassi[1], K. Borsari[1], R.C. Vendramini[2], J.V. Menani[1], E. Colombari[1] and D. Colombari[1]

[1]Pathology and Physiology, UNESP, Araraquara, SP, Brazil and [2]Clinic Analyses, UNESP, Araraquara, SP, Brazil

It has been demonstrated that the respiratory responses to hypercapnia are enhanced in obese adult humans. In rats, high-fat diet induces dyslipidemia and hyperglycemia and increases body fat. Thus, the aim of the present study was to evaluate the ventilatory responses to hypercapnia, the mean arterial pressure (MAP) and the angiotensin type 1 receptors (AT1r) expression in the nucleus of the tract solitary (NTS) in rats treated with high-fat diet for 6 weeks. Male Hotzman rats (300-320 g) had ad libitum access for 6 weeks to either the standard rat chow diet (CD) that contained 23 g of protein, 49 g of carbohydrates and 4 g of total fat per 100 g of diet or the high-fat diet (HFD) composed of 20 g of protein, 20 g of total fat and 48 g of carbohydrate per 100 g of diet (n = 8-10/group). Changes in ventilation (VE), respiratory frequency (fR), tidal volume (VT), mean arterial pressure (MAP) and heart rate (HR) to chemoreflex activation by hypercapnia (7% CO2) were measured in conscious rats using pletismography method 6 weeks after starting the access to CD or HFD. Values are means ± S.E.M., compared by ANOVA or Student t test. Rats treated with HFD showed increased body mass (422 ± 6, vs. CD: 409 ± 3 g), glycemia (157 ± 6, vs. CD: 133 ± 5 mg/dl), total plasma cholesterol (72.3 ± 3, vs. CD: 64.5 ± 2 mg/dl), plasma triacylglycerol (56.4 ± 4, vs. CD: 38.6 ± 2 mg/dl), baseline MAP (116 ± 2, vs. CD: 106 ± 2 mmHg) and AT1r in the NTS (0.14 ± 0.03, vs. CD: 0.05 ± 0.02) (all $p < 0.05$), without changes in baseline VE, VT and fR. However, HFD treated rats had increased VE (1250 ± 58, vs. CD: 1021 ± 69 ml/min/kg) and fR (140 ± 7, vs. CD: 122 ± 4 breath/min) without changes in VT (8.9 ± 0.3, vs. 8.3 ± 0.5 ml/kg respectively) during 5 minute exposure to hypercapnia. These results suggest that high-fat diet increases baseline MAP and VE to hypercapnia. Although the mechanisms involved on respiratory changes are not known yet, AT1r overexpression in the NTS may contribute to the hypertension in HFD animals.

Financial Support: CAPES, FAPESP (2011/20040-1), FAPESP/PRONEX (2011/50770-1).

Where applicable, the authors confirm that the experiments described here conform with The Physiological Society ethical requirements.

PCC080

Assessing the upper limit of cerebral autoregulation in anaesthetised rats

E.L. Thompson, A.M. Coney and J.M. Marshall

School of Clinical and Experimental Medicine, University of Birmingham, Birmingham, West Midlands, UK

Cerebral autoregulation allows cerebral blood flow (CBF) to be maintained in the face of changes in systemic arterial blood pressure (ABP): cerebral vasoconstriction occurs when ABP rises and *vice versa*. Ageing is associated with impaired autoregulation, the upper limit being reduced, but the mechanisms are not known. The aim of this study was to develop a protocol to reliably assess the upper limit in rats by using phenylephrine (PE) to increase ABP: PE has limited ability to cross the blood brain barrier and α-adrenoreceptor density on cerebral vessels is low.

In 14 male Wistar rats (333 ± 6g) anaesthetised with Alfaxan (17-20 $mg.kg^{-1}.h^{-1}$ i.v.), PE (0.1–60$\mu g.kg^{-1}.min^{-1}$) was infused i.v. to cause graded increases in ABP. CBF was recorded via a Transonic probe on the right common carotid artery after ligating the external carotid to minimise extra-cranial flow (RCBF). In Group 1, femoral (muscle) BF was also recorded (n=9); in Group 2, left CBF was recorded without ligation (LCBF; n=5). Vascular resistances (CVR, FVR) were computed as ABP/CBF or FBF. Arterial blood gases and pH were monitored at intervals. All procedures were carried out in accordance with UK legislation.

While ABP increased from 125±3 to 141±4 mmHg, RCBF was *not* constant, but fell from 1.3±0.1 to 1.1±0.1$ml.min^{-1}$ due to vasoconstriction: RCVR increased from 106±8 to 134±11 RU ($P<0.05$, unpaired t-test). Thereafter, RCBF achieved a plateau while ABP increased to ~155mmHg and RCVR increased, demonstrating autoregulation. The upper limit of autoregu-

lation, defined as the intersect of two linear regression lines fitted to the 'plateau' and 'rising' portions of mean RCBF was 165mmHg, after which RCBF rose to a maximum of 2.1±0.3ml.min^{-1}. The *changes* induced in LCBF were similar to those in RCBF, but LCBF was 0.98±0.20ml.min^{-1} higher (P<0.05, paired t-test) than RCBF, indicating constant extra-cranial flow. FBF tended to rise (1.7±0.3 to 2.5±0.3ml.min^{-1}) while ABP increased, but fell to 1.8±0.1ml.min^{-1} at the top dose of PE: the trend for FVR to increase did not reach significance (89±15 to 105.6±7.5 RU, P>0.05, one-way ANOVA). P_aCO_2 and pH remained constant, but P_aO_2 fell with increasing doses of PE (to 63±3mmHg), suggesting progressive pulmonary vasoconstriction.

These data indicate that i.v. PE can be used to assess the upper autoregulatory limit in the rat. However, PE induced an initial cerebral vasoconstriction and fall in CBF before the autoregulatory plateau was apparent. This was not an artefact of ligating the external carotid artery. Further, such initial vasoconstriction did not occur in muscle, suggesting it was peculiar to cerebral circulation: it may be that induction of anaesthesia induced cerebral vasodilatation. We are currently investigating the mechanisms contributing to the upper autoregulatory limit that may change with ageing.

British Heart Foundation

Where applicable, the authors confirm that the experiments described here conform with The Physiological Society ethical requirements.

PCC081

A model of sympathetic transmission to smooth muscle cells: the importance of respiratory modulation in understanding neurogenic hypertension

L.J. Briant[1,2], M. Desroches[1], J. Paton[2], A. Champneys[1] and A. Pickering[2]

[1]Engineering Mathematics, University of Bristol, Bristol, UK and [2]Physiology and Pharmacology, University of Bristol, Bristol, UK

Sympathetic nerve activity (SNA) is elevated in hypertension. The question of how the end-organ vasculature responds at a cellular and molecular level to the bursty respiratory component of SNA remains unknown, although this is believed to underlie Traube-Hering waves. Experimental studies have shown that 'irregular' activity generates a larger contractile force in arterial smooth muscle cells (SMCs) than tonic activity of the same average firing frequency [1]. This suggests that the respiratory modulation that SNA exhibits could be a key determinant of blood pressure, and that the change in the respiratory component could cause an increase in blood pressure, as seen in the spontaneously hypertensive rat [2].

To test this hypothesis we have constructed a high-fidelity mathematical model of the pathway of transmission from a sympathetic preganglionic neurone (SPN) to a SMC. A single-cell model of a SPN, previously presented [3], was used to drive the pathway. The presynaptic, intracellular calcium trace was used to drive a model of noradrenaline release. The released transmitter, with a profile fitted to carbon fibre electrode studies [4], activated α1-receptors on the SMC, triggering a G-protein cascade and was modelled with a 6-variable system. The subsequent release of calcium was modelled using a 2-dimensional system describing the calcium fluxes across the sarcoplasmic reticulum. These calcium dynamics were used to drive equations describing binding of myosin to actin and therefore the contractile force generated in the SMC. The resulting 25 dimensional system was run on BlueCrystal at Bristol University, using a commercial software package (MATLAB R2010a).

To mimic the change in the respiratory component of SNA seen in the spontaneously hypertensive rat (SHR) versus the normotensive rat (WKY), the model was stimulated with bursts which had varying within-burst frequencies. The sympathetic inputs had the same average firing frequency of 1Hz. The simulations, shown in the figure, indicate that the respiratory component of SNA is a key determinant of blood pressure, producing a larger change in contractile force than tonic input at the same average firing frequency. Arteries have therefore adapted to the challenge of converting high-frequency output from the sympathetic nervous system, to a lower frequency contraction, and in doing so respond with some specificity to respiratory modulation. These modelling data suggests that alterations to the respiratory component need to be investigated in order to understand hypertension.

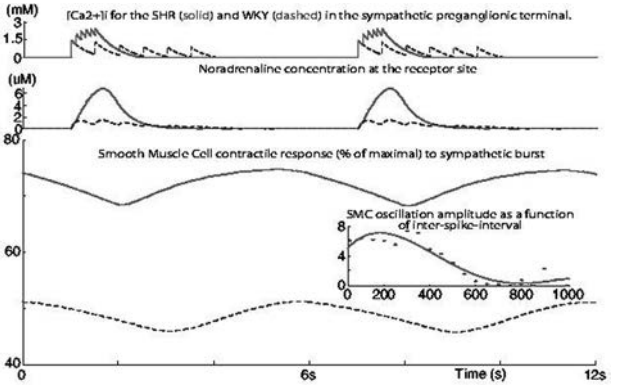

H. Nilsson, B. Ljung, N. Sjöblom and B. G. Wallin. The influence of the sympathetic impulse pattern on contractile responses of rat mesenteric arteries and veins. Acta Physiol Scand. 1985 Mar;123(3):303-9.

Annabel E. Simms, Julian F. R. Paton, Anthony E. Pickering and Andrew M. Allen. Amplified respiratory-sympathetic coupling in the spontaneously hypertensive rat: does it contribute to hypertension? J Physiol 587.3 (2009) pp 597-610.

L. J. B. Briant, M. F. Nolan, M. Desroches, A. R. Champneys, J. F. R. Paton and A. E. Pickering. The A-current as a Low-Pass Filter of Burst Activity in Sympathetic Preganglionic Neurones. Physiology 2012; Edinburgh, UK, 2nd-5th July 2012.

L. Stjärne, J. X. Bao, F. Gonon and M. Msghina. Nerve activity-dependent variations in clearance of released noradrenaline: regulatory roles for sympathetic neuromuscular transmission in rat tail artery. Neuroscience. 1994 Jun; 60(4):1021-38.

Wellcome Trust and BHF

Where applicable, the authors confirm that the experiments described here conform with The Physiological Society ethical requirements.

PCC083

Developing methods for electrophysiological assessment of cell-cell communication between cardiac myocytes and neurons using co-culture model systems

H.E. Larsen, R. Burton, G. Stephens, S. Bilton, A. Sharkey, G. Bub, E. Mann and D.J. Paterson

Dept of Physiology, Anatomy and Genetics, University of Oxford, Oxford, UK

Hypertension is associated with increased activation of the sympathetic nervous system and cardiac beta adrenergic

responsiveness (Anderson et. al., 1989, Li et. al., 2012). However, the exact mechanism remains poorly understood. The physiology and pharmacology of the individual ion channels and signalling molecules on the single neuron and myocyte as isolated systems are well described. However, relatively little is known about the cell-to-cell interaction that takes place. Tao et. al., (2011) have modelled this dual cell coupling using bioinformatics on single cell data to re-assemble the cell network from individual ion channels. Nevertheless the predictive power of this modelling is limited because it has not been experimentally validated against physiologically coupled neurons and myocytes. Here we describe a method of culturing cells as a macroscopic confluent monolayer that will enable detailed in vitro electrophysiological investigations of the communication between the neurons and the myocytes in health and disease. Neonatal ventricular myocytes and stellate ganglia were excised from Spontaneously Hypertensive Rats (SHR), Wistar Kyoto (WKY) and Sprague Dawley (SD) rats in accordance with the Home Office Animals (Scientific Procedures) Act 1986 (UK). The heart and ganglia were enzymatically digested to obtain isolated cells using pancreatin, collagenase and trypsin respectively. Cells were pre-plated for one hour in order to reduce fibroblast contamination before cells were plated on their own, or together to create co-cultures at a ratio of 1:20 neuron:myocyte.

We established a stable co-culture model system (Fig. 1 A-C) and report functional communication between neurons and myocytes by stimulating neurons with 10μM nicotine in which the beat rate increased by 25%, 20% and 33% respectively in three experiments. We have also performed pilot patch clamp studies on control SD cultures and shown how these neurons behave under whole cell current clamp conditions (Fig. 1D). In conclusion, the successful co-culture of ventricular myocytes and stellate ganglion neurons has enabled us to simultaneously investigate different parameters in myocyte-neuron signalling. In particular, the preparation will enable us to establish the electrophysiological profiles of these cell types in cardiac-neural regulation in normal and diseased tissue.

Key words: Hypertension, myocyte, neurons, culture, electrophysiology

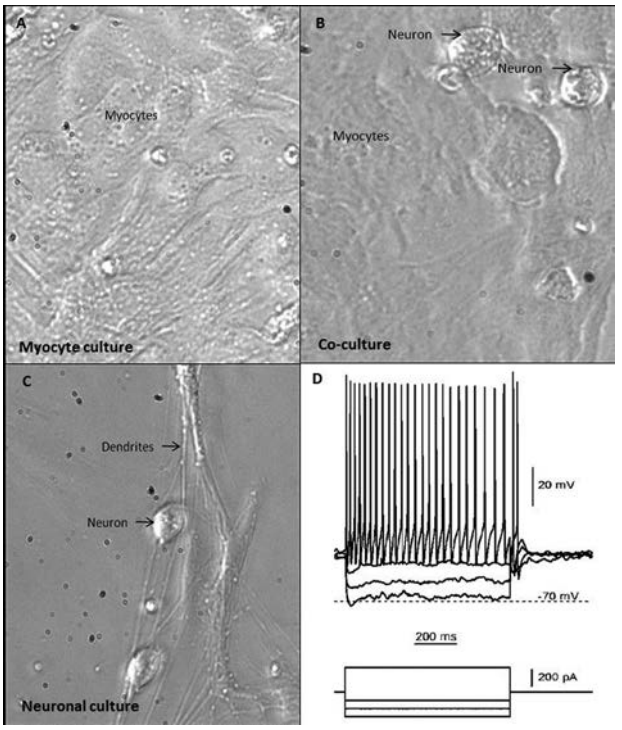

Figure 1. SD neonatal confluent monolayer culture model. A,B and C show phase contrast images of myocyte only, neuronal and co-cultures in confluent monolayers. D shows an example trace of whole cell current clamp of an SD neuron.

Anderson EA, Sinkey CA, Lawton WJ, Mark AL 1989. Hypertension. 14:177-183.

Li D, Lee CW, Buckler KJ, Parekh A, Herring N, Paterson DJ 2012. Hypertension. 59:642-649.

Tao T, Paterson DJ, Smith NP. 2011. Biophys J. 101:594-602.

Acknowledgements: OXION Wellcome Trust Centre, Oxford

Where applicable, the authors confirm that the experiments described here conform with The Physiological Society ethical requirements.

PCC084

The responses induced by obstructive apnea in spontaneously hypertensive rats (SHR) are reduced after inactivation of carotid chemoreceptors

J.M. Angheben, G.H. Schoorlemmer, M.V. Rossi, T.A. Silva and S.L. Cravo

Physiology, Federal University of Sao Paulo, Sao Paulo, Brazil

Introduction: Obstructive sleep apnea is characterized by recurrent episodes of cessation of airflow due to the collapse of the airway during sleep. Patients with sleep apnea tend to have hypertension and increased sympathetic activity. Hypertension and increased sympathetic activity are also observed in spontaneously hypertensive rats. This rat strain also seems to have increased chemoreceptor drive. Objective: We investigated cardiovascular and respiratory responses induced by apnea in SHR, and the role of carotid chemoreceptors in these responses. Method and Results: Rats were anesthetized with ketamine (100 mg/kg i.p.) and xylazine (20 mg/kg i.p.). A balloon was implanted in the trachea that allows the induction of apnea without causing tracheal pain. A thoracic balloon was implanted to measure thoracic pressure, and cannulas were implanted in the femoral vein and artery. Rats received keto-

profen (2 mg /kg s.c.) after surgery. A week later, with the rat awake, 5 apneas, 15 s each, were induced. The effects of apnea were larger in SHR than in WKY. Blood pressure increased by 57±3 mmHg during apnea in SHR, and 28±3 mmHg in WKY (mean ± SEM, $p < 0.05$, n = 8/11). Respiratory effort increased by 53±6 mmHg in SHR, and by 34±5 mmHg in WKY. Heart rate fell by 209±19 bpm in SHR, and by 155±16 bpm in WKY. The carotid chemoreceptors were then inactivated by ligation of the carotid body artery, and apneas were induced two days later. Inactivation of chemoreceptors reduced the responses to apnea, and abolished the difference between SHR and WKY. The apnea-induced hypertension was 11±4 mmHg in SHR, and 8±4 mmHg in WKY. Respiratory effort was 15±2 mmHg in SHR, and 15±2 mmHg in WKY. Heart rate fell 45 ±16 bpm in SHR, and 49±16 bpm in WKY. Similarly, when the chemoreceptors were unloaded by giving 100% oxygen to breath, the responses to apnea were reduced, and the difference between SHR and WKY was small. Blood pressure increased by 24±6 mmHg in SHR, and 13±1 mmHg in WKY. Respiratory effort increased by 18±3 mmHg in SHR, and by 16±3 mmHg in WKY. Heart rate fell 74±17 bpm in SHR, and 93±10 mmHg in WKY. Conclusion: Chemoreceptors contribute to the responses induced by apnea both in normotensive and hypertensive rats, but they are more important in SHR, and account for the exaggerated responses induced by apnea in SHR.

CAPES, FAPESP.

Where applicable, the authors confirm that the experiments described here conform with The Physiological Society ethical requirements.

PCC085

Brain stem areas activated by obstructive apnea in rats with or without carotid chemoreceptors

C.B. Ferreira[1], S.H. Guus[1], A.C. Takakura[2], B.F. Barna[3], T.S. Moreira[3] and S.L. Cravo[1]

[1]Physiology, Federal University of Sao Paulo, Sao Paulo, Brazil, [2]Pharmacology, University of Sao Paulo, Sao Paulo, Brazil and [3]Physiology and Biophysic, University of Sao Paulo, Sao Paulo, Brazil

Several evidences suggest that obstructive sleep apnea may contribute to the development of cardiovascular diseases such as hypertension. However, the mechanisms involved and the role of carotid chemoreceptors are not clear yet. Recently we developed a method to produce obstructive apnea in rats that reproduces the respiratory effort, hypoxia, and hypercapnia observed in sleep apnea patients. In this study, we investigated the brain stem areas activated by apnea in non-anesthetized rats with or without carotid chemoreceptors. Male Wistar rats (300-350 g) were anesthetized i.p. with ketamine (100 mg/kg) and xylazine (20 mg/kg), and tracheal balloon, femoral vein cannula, and subcutaneous EKG electrodes were implanted. One week later, 14 s apneas were induced every 2 min for 1 h in 4 rats. The control group (with tracheal balloon) had no exposition to apnea protocol. Thirty min after the end of apnea rats were perfused. The brain was removed and processed for immunohistochemistry to Fos and tyrosine hydroxylase (TH) (a marker for catecholaminergic neurons). In another group of rats (n=4), the arterial chemoreceptors were inactivated 7 days after implantation of the tracheal balloon by ligation and section of the carotid body arteries. In these rats, carotid chemoreceptor function was abolished (no bradycardia after i.v. injection of 40 μg KCN). Two days after chemoreceptor inactivation, the animals were subjected to the same apnea protocol described previously. In control rats very few or no Fos was detectable. Apnea induced intense Fos expression in commissural and intermediate nucleus of the solitary tract (NTS), and in caudal and rostral ventrolateral medulla (CVLM and RVLM). With respect to the catecholaminergic groups in the brain stem, we observed Fos in 42% of the C1 neurons, 11% in the A1 neurons, 18% in the A2 neurons, and 18% in the C2 neurons. Inactivation of the carotid chemoreceptors reduced apnea-induced Fos expression in the comissural NTS (from 210 ± 5 to 153 ± 3 neurons, mean ± SEM) and intermediate NTS (from 94 ± 13 to 57 ± 7 neurons), but not in CVLM and RVLM. Fos expression in the catecholaminergic cell groups was also reduced (C1: 42% to 23%, A1: 11% to 2%, A2: 18% to 9%, C2: 18% to 4%). We conclude that apnea actives neurons in regions involved with processing the baroreceptors, chemoreceptors, pulmonary stretch receptors, and regions responsible for autonomic and respiratory activity both in the presence and absence of carotid chemoreceptors. Signals from carotid chemoreceptors contribute to activation in NTS region, but apnea induces additional signals that contribute to neuronal activation. This is compatible with the presence of apnea-induced pressor responses, bradycardic, and breathing effort after carotid chemoreceptor activation.

Financial Support: CNPq and FAPESP.

Where applicable, the authors confirm that the experiments described here conform with The Physiological Society ethical requirements.

PCC086

Effect of regular obstructive apnea in rats on sleep structure and the cardiovascular effects of awakening

A.P. Pansani, M.V. Rossi, G.H. Schoorlemmer and S.L. Cravo

Physiology, Federal University of São Paulo, São Paulo, Brazil

Objective: Obstructive sleep apnea (OSA) can provoke cardiovascular impairments. Animal models that mimic OSA can help clarify the roles of changes in sleep architecture and direct effects of apnea on these impairments. This study analyzed the effect of obstructive apneas on sleep structure, and the cardiovascular responses induced by apnea during wakefulness, non-REM sleep, and REM sleep, followed or not by awakening. Methods: Intermittent apneas, 6 s each, once a minute, were made for 8 h in male adult Wistar rats by inflation of a tracheal balloon (Schoorlemmer et al., 2011). Sleep staging was done by analysis of cortical EEG and EMG of the trapezoid muscle as described by Louis et al. (2004). Arterial pressure and ECG were obtained by telemetry. Heart rate and mean pressure were calculated each second, starting 5 s before apnea onset until 10 s after the end of apnea. Results: Apneas did not alter the total time awake (52% with, 44% without apnea), non-REM sleep (39% with, 47% without apnea) and REM sleep (8% with, 10% without apnea (n = 4 rats). Rats awoke in 76% of the apneas made in non-REM sleep, and in 35% of the apneas made in REM sleep. Heart rate and arterial pressure did not change during apnea, independently of the stage of the sleep-wake cycle, and independently of wake-up. Tachycardia was seen after the end of apnea. Heart rate increased by 12 bpm in awake subjects (152 apneas), by 27 bpm when subjects awoke from non-REM sleep (129 apneas), by 3 bpm when subjects failed to wake up from non-REM (28 apneas), by 14 bpm when subjects failed to wake up from REM (19 apneas), and by 29 bpm when subjects woke up from REM (16 apneas). After

the end of apnea, arterial pressure fell by 17 mmHg in subjects that woke up from REM, but did not change in the other conditions. Conclusion: This protocol of apneas did not provoke sleep deprivation, which is suggestive of low stress in rats. Apneas that caused awakening were followed by tachycardia, and if the subject woke up from REM sleep, hypotension. Awakening may exert considerable influence on autonomic changes that occur immediately after apnea.

Louis RP, Lee J, Stephenson R. Design and validation of a computer-based sleep-scoring algorithm. J Neurosci Methods 133: 71–80, 2004

Schoorlemmer GH, Rossi MV, Tufik S, Cravo SL. A new method to produce obstructive sleep apnoea in conscious unrestrained rats. Exp Physiol. 2011; 96(10):1010-8.

FAPESP

Where applicable, the authors confirm that the experiments described here conform with The Physiological Society ethical requirements.

PCC087

Aldosterone contributes for the autonomic changes in renovascular hypertension in Wistar rats

G.S. Lincevicius[1], C.G. Shimoura[1], E.E. Nishi[1], A.A. Ribeiro[2], J.C. Perry[3], D.E. Casarini[2], C.T. Bergamaschi[1] and R.R. Campos[1]

[1]Physiology, UNIFESP, Sao Paulo, Sao Paulo, Brazil, [2]Nefrology, UNIFESP, Sao Paulo, Sao Paulo, Brazil and [3]Psicobiology, UNIFESP, Sao Paulo, Sao Paulo, Brazil

Sympathetic hyperactivity, baroreflex dysfunction and intrarenal alterations are all involved in the renovascular hypertension. It's already known that most of these changes are mediated by high level of circulating angiotensin II (Ang II) which also releases aldosterone. The aim of this study was to evaluate the effects of spironolactone (Spiro) (200mg/Kg/day) treatment, in a renovascular model of hypertension, the 2 kidney-1 clip (2K-1C). We evaluated in conscious rats changes on mean arterial pressure (MAP) and reflex control of renal sympathetic nerve activity (rSNA) in urethane anaesthetized rats (1.2-1.4 g/Kg). The tonic and reflex control of rSNA was evaluated (1 min infusion of phenylephrine 100 μg/mL/min and sodium nitroprusside 200μg/mL/min). Furthermore, the plasma renin activity (PRA) and the intrarenal renin protein expression; renal fibrosis process (expression of α-actin by imunohistochemistry); type 1 Ang II receptor (AT1) and mineralocorticoid receptor (MR) protein expression in renal tissue and central nervous system (CNS) specifically in regions involved with cardiovascular regulation such as the nucleus of tractus solilaty (NTS) and the rostral ventrolateral medulla (RVLM) were investigated. In 2K-1C group Spiro treatment decreased MAP (2K-1C: 198±4,n=9; 2K-1C+Spiro: 170±9 mmHg,n=8; p<0.05 ANOVA -Tukey) and normalized the rSNA (2K-1C: 147±9,n=6; 2K-1C+Spiro: 96±10 spikes/s,n=8; p<0.05 ANOVA-tukey). Spiro treatment increased rSNA baroreceptor reflex sensitivity in both groups (CT: -0,3±0,04, n=6; CT+Spiro: -0,9±0,03, n=5; 2K-1C: -0,2±0,03, n=5; 2K-1C+Spiro: -0,4±0,03 spikes/s/mmHg, n=5; p<0.05 ANOVA-Tukey). Furthermore, the Spiro treatment decreased expression of α-actin in nonclipped kidneys in 2K-1C group (2K-1C: 5±0,6,n=4; 2K-1C+Spiro: 1,1±0,2, %,n=3; p<0.05 ANOVA- Tukey). There was no changes in PRA in 2K-1C, but a decrease in renin protein expression in nonclippped kidney was found (2K-1C: 217±30, n=5; 2K-1C+Spiro: 160±19, %, n=5; p<0.05 Kruskall Wallis-Dunns). In clipped and nonclipped kidneys of 2K-1C, the AT1 and MR receptors protein expression was not modified by treatment, however, Spiro treatment promoted downregulation of AT1 receptors at the CNS in hypertensive group (RVLM= 2K-1C: 129±10, n=10; 2K-1C+Spiro: 84±12, %, n=5; p<0.05 ANOVA -Tukey; NTS= 2K-1C: 148±29,n=5; 2K-1C+Spiro: 68±14, %, n=4; p=0.06 ANOVA -Tukey). Taken altogether, the results suggest that aldosterone has differential effects in kidneys and CNS. Aldosterone is an important mediator in the tonic and reflex control of rSNA as well as contributes for intrarenal fibrosis process in renovascular hypertension.

Supported by: FAPESP and CNPq.

Where applicable, the authors confirm that the experiments described here conform with The Physiological Society ethical requirements.

PCC088

Cardiac arrest produced by ATP in isolated right atrium from normotensive and hypertensive rats

J.Q. Rodrigues, E.D. Silva Junior, H. Camara, G.A. Alves, N.H. Jurkiewicz and A. Jurkiewicz

Pharmacology, UNIFESP, São Paulo, São Paulo, Brazil

Introduction and Aims: The P1 and P2 receptors are expressed in cardiac tissue and activated by purines such as ATP, which are released by sympathetic neurons, endothelial cells and other tissues such as cardiomyocytes (Burnstock, G 2008). However, the role of these receptors in hypertension is still unclear. Therefore, this study proposed to investigate the role of the purinergic receptors and the signaling pathway on cardiac arrest induced by ATP in isolated right atria (RA) from normotensive (NWR) and spontaneously hypertensive rats (SHR). Materials and Methods: RA from NWR and SHR (4-6 months old) were isolated and mounted in isolated organ bath. The RA presented spontaneously beatings and the frequency between 220 and 520 bpm was considered as inclusion criterion. We study the effect of ATP (1 μM to 1 mM) on frequency of RA in the absence and presence of DPCPX (Dipropylcyclopentylxanthine) – a potent and selective antagonist for the adenosine A1 receptor (0.01 to 1 μM / pre-incubated for 20 min), 4-Aminopyridine – a potassium channel blocker (0.1 to 10 mM) and Bay k 8644 – which increases influx of calcium specifically at voltage-gated calcium channels (0.01 to 1μM). The results were analyzed by unpaired t test and one-way ANOVA. All experiments procedures were approved by the Ethics Committee of UNIFESP (n° 0778/11). Results: ATP (1 μM to 30 μM) produced an initial negative chronotropic effect (NCE) which lasted 60-90 s, followed by a negative inotropic effect (NIE) (n = 8). After that, the chronotropism gradually increased, showing a positive chronotropic effect (PCE) lasted 400 s followed by a positive inotropic effect (PIE). ATP 100 μM exerted in 40% of the experiments a biphasic effect. ATP 100 μM and 300 μM induced only a NCE in 60% and 100 % of the experiments, respectively. ATP 1 mM abolished the atrial contraction in SHR and NWR. The DPCPX (1 μM) blocked the NCE produced by ATP (300 μM) in 71.0 ± 1.3% (NWR) and 62.0 ± 1.2% (SHR) of the basal chronotropic effects. The DPCPX (1 μM) blocked the cardiac arrest produced by ATP (1 mM) in SHR and NWR. The 4-amino-pyridine (10 mM) and Bay k 8644 (1μM) blocked the cardiac arrest induced by ATP (1 mM). Conclusion: The results suggest that the cardiac arrest induced by ATP was due to the activation of A1 receptors followed by stimulation of outward K+ currents and blockade of inward Ca2+ currents in RA of NWR and SHR.

Erlinge D, Burnstock G. P2 receptors in cardiovascular regulation and disease. Purinergic Signal. 2008;4:1-20.

Sources of Research Support: CAPES, EPM/UNIFESP, FAPESP.

Where applicable, the authors confirm that the experiments described here conform with The Physiological Society ethical requirements.

PCC089

The lumbar sympathetic nervous system does not contribute to chronic intermittent hypoxia induced hypertension

E.F. Lucking[1], K.D. O'Halloran[2] and J.F. Jones[1]

[1]School of Medicine and Medical Science, University College Dublin, Dublin 4, Ireland and [2]Department of Physiology, School of Medicine, University College Cork, Cork, Ireland

Obstructive sleep apnoea (OSA) is associated with cardiovascular morbidity and recognised as an independent risk factor for hypertension. Sympathetic nervous activity is commonly reported to be increased in OSA patients and animal models exposed to chronic intermittent hypoxia (CIH) and thought to result in increased vasoconstrictor tone. Our previous results indicate that CIH-induced hypertension is not a result of decreased femoral vascular conductance (FVC). We hypothesised that CIH induced systemic hypertension is driven by increased cardiac output and that the lumbar sympathetic chain does not significantly contribute to the hypertensive state. Age-matched adult male Wistar rats (335±4g) were exposed to CIH (n=23) consisting of 90s hypoxia (5% O2 nadir)/210s normoxia cycles, or sham (n=23) treatment (normoxia), for 8h/day for 2 weeks. Under urethane anaesthesia (1.5g/kg, administered via intraperitoneal injection), the cardiac output was determined using transthoracic echocardiography. FVC was determined by placement of a flow probe on the femoral artery. Lumbar sympathetic activity/stimulation was performed using bipolar silver wire electrodes placed at the L3-L4 region. Lumbar sympathetic network density was determined using a glyoxylic acid stain. Data are presented as mean ± S.E.M and were analysed by Student's t-test or two-way ANOVA. CIH exposure significantly increased mean arterial pressure (81.4 ± 2 vs. 91.6 ± 2 mmHg; p= 0.001 n=23) and hematocrit concentration (42.4 ± 0.4 vs. 45 ± 0.4 %; p <0.0001, n=23). In addition, CIH exposure significantly increased cardiac output (25.8 ± 2.6 vs. 19.3 ± 1.7 ml/min/100g; p=0.027, n=8) without any change in FVC or blood volume. Lumbar sympathetic activity was not significantly different, nor was vascular sensitivity to lumbar sympathetic nerve stimulation. Sympathetic hyperinnervation within hindlimb arteries was increased in CIH animals (p=0.012, n=8), however vascular sensitivity to phenylephrine was significantly blunted (p=0.049, n=7). Our findings show that CIH-induced hypertension is a result of increased cardiac output and that the lumbar sympathetic chain does not significantly contribute to the hypertensive state through its influences on FVC. We conclude that hypertension is a compensatory response to CIH exposure whereby the cardiac output is increased, in combination with increased hematocrit, in an attempt to increase oxygen flow to the hypoxic tissues.

Supported by the Irish Research Council and University College Dublin

Where applicable, the authors confirm that the experiments described here conform with The Physiological Society ethical requirements.

PCC090

Diabetes mellitus blunts nociceptive-dependent stem cell liberation following limb ischemia

Z. Dang and P. Madeddu

School of Clinical Sciences, University of Bristol, Bristol Heart Institute, Bristol, UK

Background: Previous work from our group showed that tissue ischemia activates a nociceptive reflex that through the local release of the neuropeptide Substance P (SP) leads to attraction of proangiogenic cells from the bone marrow to the ischemic site thereby supporting revascularization and tissue healing.
Objective: To investigate if diabetes mellitus, a known cardiovascular risk factor, inhibits nociceptive signalling following induction of unilateral limb ischemia.
Methods and Results: CD1 mice were induced diabetes by streptozotocin and studied 17 weeks after first confirmation of overt glycosuria. Age-matched non diabetic mice served as controls. Mice were anesthetized with 2,2,2 tribromo ethanol(0.3gm/kg, i.p.) and Limb ischemia was produced by ligature of the left femoral artery. We found that diabetes reduces the density of SP-positive sensory nerve fibers in bone marrow (H: 368±4.5mm vs T1D: 169±2.5mm in per 20x magnification section, p<0.05. n=5). But the expression of the SP receptor NK1 was not significant modified by diabetes. The responsiveness of total and lineage negative bone marrow cells to SP-induced migration in a Boyden chamber assay was significantly reduced by diabetes (Total BM cells migration, H: 6.51±0.2% vs T1D: 5.11±0.2 %, p<0.05. n=5. lineage negative bone marrow cells migration, H: 9.18±0.3%vs T1D: 7.66±0.2%, p<0.05. n=5)). Likewise lineage negative cKit+Sca+ cells expressing NK1R from bone marrow of diabetic mice were depleted in the migrated fraction by 61% percent (p<0.05. n=5). Furthermore, limb ischemia increases the levels of SP in adductor muscles of nondiabetic mice (SP positive staining: 1939329.4±42 pixel) with this effect being reduced in diabetic mice (SP positive staining: 324262.3±21pixel. p<0.05. n=4). Ischemia increased the peripheral blood levels of NK1R positive progenitor cells in nondiabetic mice with concomitant reduction in bone marrow thus indicating cell mobilization. The NK1R positive progenitor cell mobilization was reduced by 67% and 32% in diabetic mice at 3 and 7 days post-ischemia, respectively. (p<0.05. n=4).
Conclusions: We show for the first time the altered sensory innervation of bone marrow in a murine diabetic model. Furthermore, diabetes inhibits the in vitro and in vivo attractive action of nociceptive mediator SP on proangiogenic bone marrow cells. Depression of pain-induced stem cell mobilization following ischemia might contribute to failed reparative response in patients with diabetes.

Where applicable, the authors confirm that the experiments described here conform with The Physiological Society ethical requirements.

PCC091

Optimal efferent vagus nerve stimulation in large animals and its effect on wall motion during ventricular fibrillation

I. Naggar, K. Nakase, L. Salciccioli, J. Lazar and M. Stewart

SUNY Downstate Medical Center, Brooklyn, NY, USA

The vagus nerve modulates electrical activity of the cardiac ventricles. However, whether the vagus nerve mediates these effects through the conduction system or directly on the myocardium is unknown. Accordingly, we studied vagus nerve stimulation (VNS) during sinus rhythm and during ventricular fibrillation (VF) in porcine and ovine preparations. We sought to determine: 1) what is the most potent frequency with which to stimulate the vagus nerve and 2) whether VNS at that frequency produces any change in cardiac wall motion during ventricular fibrillation. We studied 8 pigs and 10 sheep that were anesthetized with urethane 1 mg/kg intravenously and placed on a ventilator. Platinum vagus nerve electrodes were wrapped around the nerves. Simultaneous electrocardiogram (EKG) and carotid artery blood pressure (BP) recordings were made. VNS was performed in animals with 1-millisecond pulses for 20 seconds at 1, 2, 5, 10, 20, 50, and 100 Hz. This was done on both vagus nerves separately and bilaterally. Potency of the VNS was evaluated by counting the number of beats within the 20 seconds. VF was produced in 4 pigs by opening the thorax and applying direct current to the ventricles. Epicardial echocardiography during VF was performed, and both vagus nerves were stimulated at 50 Hz for 20 seconds. Wall motion data was extracted during VF for three periods—before, during, and after VNS. All data are presented as means with S.E.M. and were compared using repeated measures ANOVA, and p-values are reported. Tukey post-hoc analysis was performed, and statistical significance was taken as p-values < 0.05. In both sheep and pigs, 50 Hz was found to be the optimal frequency required to produce cardiac standstill. Bilateral VNS in pigs at 20, 50, and 100 Hz produced 21 ± 13, 1 ± 1, and 24 ± 14 beats in 20 seconds of stimulation, respectively (p = 0.003, 50 Hz was significantly different from 20 and 100 Hz). Bilateral VNS in sheep at 20, 50, and 100 Hz produced 14 ± 6, 2 ± 2, and 18 ± 7 beats in 20 seconds of stimulation, respectively (p = 0.002, 50 Hz was significantly different from 20 and 100 Hz). Wall motion data during VF showed 0.065 ± 0.005, 0.030 ± 0.008, and 0.057 ± 0.004 centimeters mean displacement before, during, and after VNS, respectively (p = 0.005, wall motion during VNS was significantly smaller than the other groups). We conclude that 50 Hz is the optimal frequency for VNS to exert its optimal cardiac effects. Vagus nerve stimulation affects the ventricles in large animals in both sinus rhythm and VF. These findings suggest VNS may provide an alternative adjunct therapy to treat ventricular arrhythmias.

Where applicable, the authors confirm that the experiments described here conform with The Physiological Society ethical requirements.

PCC092

Carotid body activity is increased in rat hypercaloric models of insulin resistance and hypertension

M.J. Ribeiro[1], J.F. Sacramento[1], C. Gonzalez[2], M.P. Guarino[1] and S.V. Conde[1]

[1]Pharmacology, CEDOC, Faculdade Ciências Médicas, Universidade NOVA, Lisboa, Portugal and [2]Departamento de Bioquímica y Biología Molecular y Fisiología, Universidad de Valladolid, Facultad de Medicina. Instituto de Biología y Genética Molecular, CSIC. Ciber de Enfermedades Respiratorias, CIBERES, Instituto de Salud Carlos III, Valladolid, Spain

The carotid bodies (CB) are peripheral chemoreceptors that classically respond to hypoxia, hypercapnia and acidosis. When activated CB chemoreceptor cells release neurotransmitters that increase chemosensory activity in the carotid sinus nerve (CSN), causing hyperventilation and activation of the sympathoadrenal system (Gonzalez et al. 1994; Marshall et al. 1994). Besides its role in the control of ventilation, the CB has been proposed as a glucose sensor being implicated in the control of energy homeostasis (Pardal and Lopez-Barneo, 2002; Koyama et al. 2000). Since, increased sympathetic activity is a well-known pathophysiological mechanism in IR and hypertension (HT) we hypothesize that overactivation of CB can contribute to the development of IR and HT. Therefore, the objective of this study was to investigate if CB activity is increased in IR and HT animal models.

Experiments were performed in 3 months Wistar rats (200–420 g) of both sexes. anaesthetized with pentobarbitone (60mg/Kg, ip). Two diet-induced IR and HT animal models were used: the rat submitted to a high-fat (HF) diet, a model that combines obesity, IR and HT and the rat submitted to a high-sucrose (HSu) diet, a lean model of combined IR and HT. CB activity was assessed through the evaluation of: in vivo ventilatory responses by measuring spontaneous ventilation and in response to ischemic hypoxia and in vitro by monitoring catecholamines release in basal conditions and in response to acute hypoxia (5%O2) and the expression of tyrosine hydroxylase.

We have observed that spontaneous ventilation as well as ventilation in response to ischemic hypoxia (assessed as the increase in ventilation produced by common carotid artery occlusions for periods of 5, 10 and 15 seconds) were increased in HF and HSu animals, with a more pronounced effect in HF animals. Surgical CSN cut completely abolished the increases in ventilation induced by the diets, showing that these effects are mediated by the CB. Basal release of dopamine was not significantly modified by hypercaloric diets, however the release induced by hypoxia (5%O2) was increased 3.15 and 2.12 fold in HF and HSu rat models, respectively. Also, CBs weight was significantly increased by 36.71% and 27.13% in HF and HSu models, respectively, as well as tyrosine hydroxylase expression, the rating enzyme for catecholamine biosynthesis, that increased by 64.4% in HF ($p<0.01$) and 30.8% in HSu animals ($p=0.12$).

In conclusion, we demonstrated for the first time that CB activity is increased in diet-induced animal models of IR and HT suggesting that CB is involved in the development of IR and HT. Additionally, the more pronounced increases in spontaneous ventilation and in ischemic hypoxia induced-hyperventilation observed in HF animals suggest that these animals hold a higher degree of CB activation.

Gonzalez C, Almaraz L, Obeso A, Rigual R.1994. Carotid body chemoreceptors: from natural stimuli to sensory discharges. Physiol Rev 74: 829-98.

Marshall JM. 1994 Peripheral chemoreceptors and cardiovascular regulation, Physiol Rev 74:543-94

Pardal R, López-Barneo J. 2002 Low glucose-sensing cells in the carotid body. Nat Neurosci 5:197-8

Koyama Y, Coker RH, Stone EE et al.2000. Evidence that carotid bodies play an important role in glucoregulation in vivo. Diabetes 49:1434-42

Supported by PTDC/SAU-ORG/111417/2009

Where applicable, the authors confirm that the experiments described here conform with The Physiological Society ethical requirements.

PCC093

Increase in circulating endocannabinoids worsens the drop in the blood pressure and decreases the tachycardiac response observed during septic shock

F. Alves, D. dos Reis, L. Resstel and F. Corrêa

Pharmacology, University of São Paulo, Ribeirão Preto, Brazil

During sepsis, there are changes in the cardiovascular system that are characterized by a drop in the blood pressure (BP), and increased heart rate (HR). It has been reported that during the septic shock the endocannabinoid system is active, and both anandamide and 2-AG endogenous endocannabinoids could act on CB1 and CB2 receptors. Moreover, the endocannabinoids, acting on CB1 receptors, are potent vasodilators and CB2 receptors modulate the immune response during sepsis. Thus, the increase in the concentration of endocannabinoids may worsen the cardiovascular and immunological response to sepsis. Thereby, we studied the cardiovascular effects of an increase in endocannabinoids by the inhibition of the FAAH (fatty acida mine hydrolase), which is the enzyme responsible by the degradation of endocannabinoids, during the septic shock induced by cecal ligation and puncture (CLP). To that, we utilized male Wistar rats. Animals were anesthetized with 2,2,2-tribromoethanol (250 mg/kg i.p., Sigma-Aldrich, St. Louis, MO, USA) and had a radiotelemetry probe implanted into the descendent aorta, to measure cardiovascular activity. At the same time, tsepsis was induced by cecal ligation and puncture (CLP). The FAAH inhibitor URB597, in the dose of 0,6mgl/kg, was injected intravenous immediately after the end of the surgery, and the cardiovascular parameters were measured during a period of 8h. Institution's Animal Ethics Committee (N-082/2010). The intravenous treatment with URB597, a FAAH inhibitor, did not affect the basal BP (PAM = 97±4 vs 96±3 mmHg; t= 0.6, p>0.05 n=5) and HR, and HR (343±4 vs 345±4 bpm; t=0.2; p>0.05). However, the treatment with URB597 increased the fall in the BP ($F(1,294)= 17$, $p<0.0001$) and decreased the characteristic tachycardia ($F(1,294)=54$, $p<0,0001$) observed during the septic shock caused by CLP.
The present results indicate that endocannabinoids participate in the genesis of the cardiovascular changes observed during septic shock caused by CLP.

FAEPA, FAPESP and CNPQ

Where applicable, the authors confirm that the experiments described here conform with The Physiological Society ethical requirements.

PCC095

Cardiovascular autonomic reflex tests in early detection of background lead exposure in children

S. Tymchenko and H. Evstafyeva

physiology department, Crimea State Medical University Named After S.I.Georgievsky, Simferopol, Ukraine

Cardiovascular autonomic reflex tests based on heart rate variability (HRV) have proven useful for noninvasive detection of autonomic nervous system (ANS) regulation failure in numerous pathological conditions. Although previous studies have suggested that exposure to toxic metals might alter HRV, there were a number of potential limitations in those studies, including the determination of HRV in adults occupationally exposed to heavy metals. The aim of this study was to investigate the relation between lead and HRV in children using cardiovascular reflex tests.
An assessment of cardiac autonomic regulation in children of both genders, aged 10 to 16 years (n=57), who had never been occupationally exposed to lead (Crimea, Ukraine) was carried out using the HRV markers and hair lead concentration determined by X-ray spectophotometry (ElvaX-Med). Five-minute HRV recordings by three-lead electrocardiography (Cardio, Ukraine) were obtained in supine position and during cardiovascular reflex tests (active tilt test, after exercises, during deep breathing, oculocardiac reflex and the psychometric strain test) and standard time and frequency domain HRV parameters were examined. Time-domain indexes included: normal-to-normal intervals (RRNN) between adjacent QRS complexes, the standard deviation of the NN intervals (SDNN), square root of the mean sum of squares of the differences between adjacent NN intervals (rMSSD), and proportion of pairs of adjacent NN intervals differing by more than 50 ms (pNN50). The frequency domain indexes were: high (HF), HF in normalized units (HFn), low (LF), LF in normalized units (LFn), very low (VLF), total power (TP), and the LF/HF ratio.
The results showed no statistically significant correlations between Pb and HRV indices recorded at rest. Statistically significant positive Spearman correlations were found only for lead and SDNN, VLF in oculocardiac reflex ($0.27<r<0.40$; $p<0.05$); lead and SDNN, TP, LF, HF during deep breathing ($0.28<r<0.31$; $p<0.05$); lead and rMSSD, pNN50, HF ($0.26<r<0.29$; $p<0.05$) during active orthostatic test. Most of the correlations were observed between Pb and HRV parameters recorded after exercises: positive with RRNN, SDNN, rMSSD, pNN50, TP, LF, HF, VLF, HFn and negative with LF/HF and LFn ($0.27<r<0.42$; $p<0.05$). Revealed correlations suggest an increased parasympathetic activity in participants with higher lead concentrations during various cardiovascular tests, indicating that lead affects the vagal nerve more than other cardiac nerves. Pb levels were also associated significantly with heart rate during oculocardiac, orthostatic test and after exercises, suggesting negative chronotropic effect of lead ($-0.29<r<-0.36$; $p<0.05$). These findings suggest that recording HRV during simple cardiovascular tests may be more sensitive than recordings during supine rest in low-level lead exposure in children.

Where applicable, the authors confirm that the experiments described here conform with The Physiological Society ethical requirements.

PCC096

Aliskiren and L-arginine reduce the renal sympathetic activity and improves renal function in rats with renovascular hypertension

V. Mengal, R. Tiradentes, H. Futuro Neto, N. Silva, P. Matos, A. Carvalho, S. Gouvea and G.R. Abreu

Physiological Sciences, Federal University of Espirito Santo, Vitoria, Espirito Santo, Brazil

Studies indicate that the renal sympathetic activity plays an important role in progression of renovascular hypertension and tissue damages. The aim of this study is to elucidate the effects of combination Aliskiren (ALK) and L-arginine (L-ARG) on the blood pressure and renal sympathetic activity. Renovascular hypertension (2K1C) was produced in Male Wistar rats (140-160 g). Seven days after the renal artery clipped was performed by plethysmography to measure systolic blood pressure (SBP). The rats were divided in groups:Sham (n=6), 2K1C (n=7), 2K1C treated with aliskiren 50 mg/kg (ALK, n=9), 2K1C treated with L-arg 300 mg/kg (L-ARG, n=9) and 2K1C treated with a combination of ALK and L-arg (ALK + L-ARG, n=10). The treatment was performed for 21 days by gavage. At the end of treatment was made new plethysmography and the urine collection of 24 hours. The animals were anesthetized with urethane (1.2 g/Kg) for direct measurement of SBP and recording of renal nerve activity (RNA). At the end of the protocol, blood samples were taken and analyzed the expression of endothelial nitric oxide synthase (eNOS) in both kidneys by Western blotting. Statistical analysis was determined using 1-way ANOVA and Tukey test. Values are expressed as mean ± SEM and the significance of $P < 0.05$. Only the treatment with the combination of ALK + L-arg was able to normalize SBP (138 ± 4.4 mmHg) compared to groups 2K1C, ALK and L-ARG (204 ± 12.7; 202 ± 17.7 and 176 ± 9 mmHg), since values were similar to SHAM (114 ± 5.2 mmHg). Similarly, the basal RNA in ALK + L-ARG and L-ARG was also normalized (SHAM: 62 ± 6.4; 2K1C: 97 ± 8.4; ALK: 84 ± 2.5; L-ARG: 71 ± 3.1 and ALK + L-ARG: 64 ± 3.4%) and an improvement of sympathetic responsiveness to changes in SBP in ALK + L-ARG group (SHAM: -54 ± 6.1; 2K1C: -25 ± 3.2; ALK: -30 ± 3.8; L-ARG: -34 ± 3.6 and ALK + L-ARG: -55 ± 6.1% Δ ANR with phenylephrine and SHAM: 78 ± 15.6; 2K1C: 13 ± 2.8; ALK: 21 ± 3.67; L-ARG: 38 ± 3.4 and ALK + L-ARG: 49 ± 8.79% Δ ANR with NPS). The animals L-ARG and ALK + L-ARG had natriuretic effect (SHAM: 148 ± 14.13; 2K1C: 48 ± 7.93; ALK: 48 ± 9.25; L-ARG: 121 ± 8.1 and ALK + L-ARG: 129 ± 7.8 mEq/L) and a tendency to present diuretic effect (SHAM: 20 ± 2; 2K1C: 11 ± 0.5; ALK: 9 ± 0.7; L-ARG: 17 ± 2.3 and ALK + L-ARG: 16 ± 2.1 mL/day) and improve urinary flow (SHAM: 0.014 ± 0.001; 2K1C: 0.008 ± 0.001; ALK: 0.006 ± 0.001; L-ARG: 0.011 ± 0.001 and ALK + L-ARG: 0.011 ± 0.001 ml / min), besides improving glomerular filtration rate (ALK + L-ARG: 2.06 ± 0.49; L-ARG: 1.73 ± 0.38; 2K1C: 0.35 ± 0.1; ALK: 0.45 ± 0.1). There was an increased eNOS expression only in the kidney clipped. The combination of ALK and L-ARG was able to reduce the sympathetic hyperactivity, increased diuresis, natriuresis and improved glomerular filtration rate, that contribute to reduce the arterial pressure levels.

Where applicable, the authors confirm that the experiments described here conform with The Physiological Society ethical requirements.

PCC098

Combined acute hyperglycaemia and airway occlusion significantly increases nitrosative stress and poly(ADP) ribose polymerase activation

Z.A. Siddiqui, A.A. Tahrani, P. Kumar and C.J. Ray

School of Clinical and Experimental Medicine, University of Birmingham, Birmingham, UK

Hyperglycaemia in diabetes can cause nitrosative/oxidative stress and subsequent Poly(ADP)Ribose Polymerase (PARP) activation that are implicated in the pathogenesis of microvascular complications. Obstructive sleep apnea (OSA) causes nitrosative/oxidative stress and is common amongst patients with diabetes. We hypothesised that diabetes and OSA together cause greater nitrosative/oxidative stress than either alone and tested this in an acute rat model of hyperglycaemia and airway occlusion.

In 26 male Wistar rats anaesthesia was induced with 3.5% isoflurane in oxygen and was maintained by continuous infusion of Alfaxan ($5mg.ml^{-1}$ at $0.8ml.hr^{-1}$ I.V.). Animals were exposed to one of the following four conditions for six hours: normoglycaemia airway unoccluded (NGAU, n=7), normoglycaemia airway occluded (NGAO, n=6), hyperglycaemia airway unoccluded (HGAU, n=7) and hyperglycaemia airway occluded (HGAO, n=6). In all groups blood glucose was monitored throughout the protocol and in HG groups, glucose was administered via the femoral vein to maintain glucose levels at $12mmol.L^{-1}$. In AO groups, airway occlusions occurred for 15 seconds every minute by mechanical occlusion of a cannula placed in the trachea. Rats were killed by exsanguination followed by cervical dislocation for confirmation and organs were harvested. 3-nitrotyrosine (NT) levels were measured in plasma samples using commercially available ELISA kits (Oxiselect, San Diego) and liver sections were stained for Poly(ADP)Ribose (PAR) using immunohistochemistry. Values are expressed as means ± S.E.M. and significance ($P<0.05$) was determined by one-way ANOVA.

In control NGAU plasma NT was 88±17 nM; 6 hours of hyperglycaemia or airway occlusion alone did not cause a significant increase in plasma NT (114±19 nM and 149±16 nM respectively), however 6 hours combined hyperglycaemia and airway occlusion did significantly increase plasma NT (289±44 nM, $p=0.017$). The same response was seen for PAR staining in the liver with combined HG and AO significantly ($p<0.001$) increasing % PAR stained nuclei (NGAU 19±3 %, HGAU 29±5 %, NGAO 35±3 % and HGAO 49±5 %).

In our model, just 6 hours of combined HG and AO increased levels of NT and downstream effects that influence the progression of microvascular complications than either insult alone. This suggests that OSA in patients with diabetes may exacerbate the development of microvascular complications.

Where applicable, the authors confirm that the experiments described here conform with The Physiological Society ethical requirements.

PCC099

Chronic suppression of paraventricular nucleus of the hypothalamus neuronal activity produces sustained hypotension in spontaneously hypertensive rats

V. Geraldes[1], N. Gonçalves-Rosa[1], R. Laires[1], R. Lopes-Gonçalves[1], J. Paton[2] and I. Rocha[1]

[1]Cardiovascular Autonomic Laboratory, Instituto de Medicina Molecular and Faculty of Medicine, University of Lisbon, Lisbon, Portugal and [2]Bristol Heart Institute, Medical Sciences Building, University of Bristol, Bristol BS8 1TD, Bristol, UK

Several studies suggest that changes in the sympathetic nervous system (SNS) are responsible for the initiation, development and maintenance of hypertension. SNS over activity may result from an inappropriately elevated sympathetic drive from brain centers. One important central sympatho-excitatory region is the paraventricular nucleus of the hypothalamus (PVN), which may become more active in hypertensive conditions, as shown in acute studies.
Objective: Depress chronically the activity of PVN neurons by the over-expression of an inwardly rectifying potassium channel (hKir2.1) in order to evaluate the consequences upon blood pressure regulation in an animal model of hypertension.
In telemetry instrumented spontaneously hypertensive rats (SHRs) lentiviral vectors: LVV-hKir2.1 (LV-TREtight-Kir-cIRES-GFP5 4x10E9: LV-Syn-Eff-G4BS-Syn-Tetoff 6.2x10E9 in a ratio 1:4) were as microinjected bilaterally into PVN stereotaxically. Sham SHRs were bilaterally microinjected with LVV-eGFP (LV-Syn-Eff-G4BS-Syn-Tetoff 6.2x10E9: LV-TREtight-GFP 5.7x10E9 in a ratio 1:4) in the PVN. Blood pressure (BP) and heart rate (HR) were monitored continuously and evaluated using radiotelemetry for 75 days. Baroreflex function was evaluated by measuring HR changes induced by BP variation produced by phenylephrine (25μg/ml, iv) injection. Lobeline (25μg/ml, iv) was used to evaluate peripheral chemoreflex sensitivity. These procedures were performed under anaesthesia.
Heart, kidneys and vessels were collected post-mortem to evaluate, by RT-PCR, the expression of 20 key genes involved in the pathways regulating blood vessel tone.
Results: LVV-hKir2.1 expression by PVN activity in SHRs produced a time-dependent and significant decrease in systolic (158±1 to 134±1mmHg), diastolic (137±1 to 115±1mmHg) and mean BP (144±1 to 121±1mmHg) as well as in HR (314±3 to 295±3bpm) 60 days post-microinjection of LVV-hKir2.1. In SHRs the cBRG significantly increased after LVV-hKir2.1 microinjection (0.51±0.06 and 1.3±0.18bpm/mmHg). The chemoreceptor reflex evoked pressor response and the LF-band decreased in the LVV-hKir2.1-SHR group (0.71±0.3 to 0.42±0.26mmHg2) suggesting reduced sympathetic vasomotor tone. RT-PCR analysis showed a downregulation of angiotensin II receptors together with a decrease on calcium transport.
Conclusion: Our data showed, for the first time, that PVN neuronal excitability plays a major role in the long term control of blood pressure and SNS activity in SHRs. This may be mediated, in part, by improved baroreflex sensitivity and reduced peripheral chemosensitivity and respiratory-sympathetic modulation. Molecular studies showed that the microinjection of LVV-hKir2.1 interfere mainly with the endocrine regulation of BP through angiotensin II. Our results support the PVN as a therapeutic target in the control of blood pressure in neurogenic hypertension.

Where applicable, the authors confirm that the experiments described here conform with The Physiological Society ethical requirements.

PCC100

Depression of rostroventrolateral medulla neurons excitability maintains normotensive values of blood pressure in spontaneously hypertensive rats

N. Gonçalves-Rosa[1], V. Geraldes[1], R. Laires[1], R. Lopes-Gonçalves[1], J. Paton[2] and I. Rocha[1]

[1]Cardiovascular Autonomic Function Lab, Instituto de Medicina Molecular and Faculty of Medicine, University of Lisbon, Lisboa, Portugal and [2]Bristol Heart Institute, Medical Sciences Building, University of Bristol, Bristol BS8 1TD, UK, Bristol, UK

Background: The sympathetic nervous system (SNS) is responsible for the onset, development and maintenance of neurogenic hypertension. It was shown an increased activity of central sympathoexcitatory regions such as the rostroventrolateral medulla (RVLM) in an animal model of hypertension. Changes in autonomic balance can be achieved through spectral analysis of systolic blood pressure and heart rate.
Objective: Depress the activity of RVLM neurons by over-expression of an inwardly rectifying potassium channel (hKir2.1) in order to establish their relative roles in the long-term regulation of blood pressure (BP) in conscious spontaneously hypertensive rats (SHR).
Methods: In telemetry instrumented SHRs (n=7), a lentiviral vector LVV-hKir2.1 (LV-TREtigh-Kir-cIRES-GFP5.4x10E9: LV-Syn-Eff-G4BS-Syn-Tetoff6.2x10E9 in a ratio 1:4) was bilaterally microinjected (0.05μL) into RVLM using stereotaxic coordinates. Sham SHRs (n=4) were bilaterally microinjected with LVV-eGFP (LV-Syn-Eff-G4BS-Syn-Tetoff6.2x10E9: LV-TREtight-GFP5.7x10E9 in a ratio 1:4) in the same region. BP and Heart Rate (HR) were continuously monitored and evaluated using radio-telemetry for 75 days.
Baroreflex gain was calculated by measuring heart rate changes induced by arterial pressure variation produced by phenylephrine (25μg/ml, IV) injection. The chemoreflex activation was evaluated through variations in respiratory rate evoked by the injection of lobeline (25μg/ml, IV). These procedures were performed under anaesthesia.
Heart, kidneys and vessels were collected post-mortem to evaluate, by RT-PCR, the expression of 20 key genes involved in the pathways regulating blood vessel tone.
Results: Depression of RVLM neurons activity in SHRs leads to a significant decrease in of systolic (157±18 to 125±25 mmHg), diastolic (126±11 to 97±25 mmHg), mean (137±12 to 106±25 mmHg) BP and HR (306±35 to 292±29 bpm) 60 days post-injection. In sham rats no significant changes were detected in all parameters.
In SHRs the LF-band decreased after the LVV-hKir2.1 microinjection (0.75±0.46 to 0.53±0.16 mmHg^2). In sham rats there was an increase in LF-band. RT-PCR showed an upper regulation of endothelin a and b receptors together with an expression trend to normality of endothelin 1 and endothelin 2 genes.
Conclusion: These results show that a reduction of RVLM neurons excitability caused a sustained decrease of blood pressure in SHRs. This was probably due to a reduction in sympathetic output, as evidenced by the decrease in the LF and LF/HF bands. This action is supported by changes in endothelial function due to vascular remodeling. By identifying the role of this central area in the long-term control of BP, we expect to

provide realistic targets for therapeutic interventions in hypertension.

Where applicable, the authors confirm that the experiments described here conform with The Physiological Society ethical requirements.

PCC101

Impact of smoking on microcirculation and of its relationships with smoker's clinical characteristics or smoking habit: an observational study

M. Rossi[1], L. Carrozzi[2], F. Pistelli[2], M. Pesce[1], F. Aquilini[2] and G. Santoro[1]

[1]Unit of Sport Medicine, Clinical and Experimental Medicine, University Hospital of Pisa, Pisa, Italy and [2]1st Pulmonary Unit, Cardio-Thoracic and Vascular, University Hospital of Pisa, Pisa, Italy

The impact of smoking on microcirculation has been studied in small groups of subjects, preventing the evaluation of possible influences of smoker's clinical characteristics or smoking habit variables on microcirculation. In order to fill this gap, we measured forearm skin blood flux under basal conditions and in response to ischemia in 100 current smokers (duration of smoking habit: 33.4 + 12.3 years), mean age 51 + 11 years (range: 8 to 86 yrs) consecutively enrolled at the smoking cessation clinic of the University Hospital of Pisa, and in 66 never-smoker controls matched by sex and age, using laser Doppler fluximetry (LDF). Information on smoking exposure and presence of other cardio-vascular risk factors were collected by standardised procedures. Skin post-occlusive reactive hyperaemia (PORH) was expressed as maximal post-ischemic flux (peak-flux) and as post-ischemic percentage change from baseline of the area under the LDF curve (AUC %). The skin LDF tracings were analysed in the frequency domain using an adapted version of Fourier analysis. Using this method we measured: the normalized (%) spectral power within 0.009-1.6 Hz total spectrum of the frequency intervals 0.009–0.02 Hz, related to endothelial-dependent skin vasomotion (SV); 0.021–0.06 Hz, related to sympathetic-dependent SV; 0.061–0.2 Hz, related to myogenic-dependent SV. Basal skin blood flux, peak-flux, AUC % and the sum of the normalized spectral power of endothelial-, sympathetic- and myogenic-dependent SV, were significantly lower (Wilcoxon test) in smokers than in non smokers (table). Smokers with at least one associated cardiovascular risk factor, such as arterial hypertension, diabetes or hypercholesterolemia, showed a significantly ($p = 0.02$) lower AUC %, compared to non-smokers. At the linear regression analysis, an inverse relationship was observed in smokers between AUC% and the smoking habit duration ($r = 0.23$, $p = 0.018$), age ($r = 0.26$, $p = 0.008$) and body mass index ($r = 0.21$, $p = 0.037$) of smokers. This study confirms that smoking is associated with microcirculatory impairment and shows that this impairment is negatively influenced by smoking habit duration, subjects' age, BMI and presence of other cardiovascular risk factors.

Results of skin Laser-Doppler test in smokers and control subjects

	Control subjects	Smokers	p
Basal skin blood flux (PU)	14.6 (10.6 - 6.5)	7.76 (5.74 - 11.79)	0.03
Skin peak-flux (PU)	73.5 (51.9 - 32.4)	39.0 (27.7 - 52.8)	0.004
Skin AUC %	216.8 (190.1 - 156.3)	162.5 (139.3 - 183.0)	0.00016
Normalized skin vasomotion (%)	77.4 (67.9 - 84.6)	71.7 (64.9 - 79.8)	0.017

Data are as median and inter-quartile range.

AUC=area under laser-Doppler curve.

PU=perfusion unit.

Pellaton A et al.(2002). Am Heart J144, 269-274.

Dalla Vecchia L et al. (2004). J Hypertens22, 129-135.

M. Rossi M et al.(2007). Clin Hemorheol Micrcocirc36, 163-171.

Where applicable, the authors confirm that the experiments described here conform with The Physiological Society ethical requirements.

PCC102

The endothelium of pulmonary arterial hypertension patients shows a disturbed adaptation to high levels of shear stress

R. Szulcek[1,3], T.A. Leyen[2], R. Fontijn[2], V.W. van Hinsbergh[3], A.J. Horrevoets[2], A. Vonk-Noordegraaf[1], H.J. Bogaard[1] and G.P. van Nieuw Amerongen[3]

[1]Pulmonology, VU University Medical Center, Institute for Cardiovascular Research (ICaR-VU), Amsterdam, Netherlands, [2]Molecular Cell Biology and Immunology, VU University Medical Center, Institute for Cardiovascular Research (ICaR-VU), Amsterdam, Netherlands and [3]Physiology, VU University Medical Center, Institute for Cardiovascular Research (ICaR-VU), Amsterdam, Netherlands

Rationale We hypothesize that severe pulmonary vascular remodelling in pulmonary arterial hypertension (PAH) is triggered by sustained endothelial injury in pre-capillaries caused by increased shear stress (SS). Therefore we tested whether human pulmonary microvascular endothelial cells (HPMVEC) from PAH patients are capable to adapt to high levels of SS.
Methods and Results HPMVEC were isolated from PAH patients (autopsies and lung transplantations) and controls (rest material from lung tumor surgeries). The study has been approved by the IRB as non-WMO and consent was given. Static controls were compared to cells under physiological low (LSS, 2.3 dyn/cm^2) and pathological high shear stress (HSS, up to 25 dyn/cm^2). Different flow profiles (laminar, bifurcation-like) were applied and electrical resistance of the monolayers was recorded with ECIS (applied biophysics), as a measure for barrier function and cell behavior. Most striking are our findings in structural adaptation to HSS. Control HPMVEC re-aligned in flow direction, whereas HPMVEC from PAH patients failed to align after 72 hrs HSS challenge. Specifically, 65.3%±1.4 of the total number of control HPMVEC elongated, whereas 72.4%±4.4 of those cells re-aligned within an angle of less then 20 degrees relative to the flow direction (n=4, mean±SEM). Opposing only 47.2%±8.5 of PAH cells showed a stretched morphology and alignment randomly in the direction of flow (n=5, mean±SEM). Interestingly, upon HSS stimulation expression of the tested genes, known to play a role in shear sensing and adaptation (e.g. KLF2 and TGF-β), was up-regulated in both PAH and control samples. Under static culture conditions, PAH cells showed an irregular distribution and organization as well as decreased protein expression of the shear sensors VE-cadherin and CD31 (immunostaining and Western blot, n=4). Modeling of the electrical data gave further proof for weakened cell-cell adhesions in PAH cells. On the contrary, PAH and control HPMVEC formed similar endothelial barriers with a baseline resistance of 7767 vs. 8102 ohms. Here the ECIS modeling indicated an increased cell-matrix adhesion as possible cause. Furthermore, application of HSS to PAH HPMVEC caused severe cell loss, when bifurcation-like flow patterns were used. Control HPMVEC on the other hand were able to withstand those flow patterns.

Conclusion and Relevance We showed that HPMVEC from PAH patients have a hampered ability to adapt, but not to sense pathological HSS, which can result in severe endothelial damage at vascular bifurcations. The causes for the failing adaptation are under testing and point towards a misbalance in cell-cell and cell-matrix adhesion. Our findings support the idea for a role of SS in the disease progression of PAH and imply, that new treatment strategies should consider normalization of the pulmonary blood flow to protect endothelial cells from injury and prevent vascular remodelling.

Where applicable, the authors confirm that the experiments described here conform with The Physiological Society ethical requirements.

PCC103

Age dependent changes of carotid intima-media thickness and their possible linkage with activity of sympathetic nervous system in healthy volunteers

V. Fokin, N. Ponomareva and G. Kuncevitch

Brain Research, Research Center of Neurology of Russian Academy of Medical Science, Moscow, Russian Federation

One of the signs of atherosclerosis is the intima-media thickness (IMT) in the common carotid artery (CCA). The development of atherosclerosis is a multifactorial process which besides the age depends on many other factors, including the states of the autonomic nervous systems. In 29 healthy volunteers (12 men and 17 women from 19 to 70 years) IMT of both CCA was measured using ultrasound duplex scanning. Millivolt-scale DC potentials were recorded from 5 sites on head with AG/AgCl electrodes. Scalp electrodes were situated in frontal, central and occipital positions by sagittal line as well as in left and right temporal areas according to 10x20 international scheme (reference electrode on the wrist). Electrode potentials and dermal resistances were controlled (Voipio at al., 2003). IMT correlated with age of volunteers: for the right CCA r =0.60 (p <0.001), for the left CCA r=0.51 (p =0.004). IMT was significantly (p=0.026) thicker in the right than in the left CCA in the volunteers over 45 years. The difference between the right and left IMT=0.10+/-0.04; N=19. DC potential in right temporal area was factor influencing IMT in the right and left CCA: F=5.04 (p=0.033) and F=7.14 (p=0.012) by ANOVA, accordingly. High-amplitude DC potentials in the right temporal area corresponded to high values of IMT in the right and left CCA. Onbas at al. (2007) showed that handedness was a significant factor of IMT asymmetry. In our investigations only right handers women had significant predominance of rightward asymmetry of IMT of the CCA in any age (p<0.05). Right frontotemporal area is representative of cortical afferents of sympathetic nervous system (Craig, 2005) and DC potentials in this area may reflect its activity. This suggestion was confirmed by the investigations of cardiovascular regulation (Fokin et al., 2010).Chronic stress related to the activation of sympathetic nervous system leads to increasing probability of thickening of artery wall (Roepke at al., 2012). The correlation of high sympathetic activity was most pronounced with respect to DC potentials of temporal area of the right hemisphere than of the left hemisphere (Fokin, et al., 2010). Increase of IMT of the CCA was associated with age and a rise of DC potential in right temporal area. The increase of DC potential probably reflected the activation of sympathetic nervous system. Significant rightward asymmetry of IMT of the CCA was found and it was particularly noticeable after 45 years.

1. Fokin VF et al.(2010). Vestnik RAMS. 2010,-6,13-16.
2. Onbas O et al. (2007). Int J Neurosci. 117, 433-441.
3. Roepke SK et al.(2012). Stress.15, 121-129.
4. Voipio J et al. 2003. J Neurophysiol.89, 2208–2214.

Where applicable, the authors confirm that the experiments described here conform with The Physiological Society ethical requirements.

PCC104

Mechanisms of central cardiovascular effects of H2S in SHR rats: the role of reactive oxygen species

H. Yu, D. Cao, H. Xu, R. Wang and N. Lu

Department of Physiology and Pathophysiology,, Fudan University, Shanghai, China

Hydrogen sulfide (H2S) is considered to be a new gaseous molecular alongside with NO and CO. It is produced mainly by cystathionine β-synthase (CBS) in brain. Lots of evidences indicate that H2S performs a wide range of physiological and pathological functions. However, the central cardiovascular effects of H2S are not fully identified. In present study, we tested the hypothesis that H2S in CNS may inhibit NADPH oxidase and decrease the production of reactive oxygen species (ROS), thus mediate central cardiovascular effects. Experiments were completed in Wistar-Kyoto (WKY,250g-300g) rats and spontaneous hypertensive rats (SHR, 250-300g). We used immunohistochemistry method to observe the expression of CBS in rostral ventrolateral medulla (RVLM) of both SHR rats and WKY rats. Artifcial cerebrospinal fluid, NaHS (the H2S donor),or Apocynin (an inhibiter of NADPH oxidase) was given through a cannula implanted into the lateral cerebral ventricle, and mean arterial blood pressure(MAP)and heart rate (HR) were recorded. Lucigenin-enhanced chemiluminescence was used to estimate the level of ROS and the activity of NADPH oxidase in RVLM of rats in each group. One-way ANOVA was used for data stastistics. The following observations were made:1) Expressions of CBS of RVLM were increased in WKY rats compared with SHR rats(P<0.05, n=5). 2) Intracerebroventricular (ICV) infusion NaHS (4nmol/10μl),or Apocynin (100nmol/10μl)significantly decreased MAP and HR in SHR rats.(P<0.05 both, n=6). 3) The level of ROS and the activity of NADPH oxidase in RVLM of SHR control group was higher than the level in WKY control group(P<0.05, n=8), and after infusion with NaHS (4nmol/10μl) or Apocynin (100nmol/ 10μl), the level of ROS and activity of NADPH oxidase was decreased in SHR rats compared with that in SHR controls(P<0.05, n=8). The results of present study suggest that H2S in central nervous system could decrease blood pressure and heart rate in SHR rats by inhibiting the activity of NADPH oxidase in the RVLM in SHR.

Key words: Hydrogen sulfide; ROS; SHR; NADPH oxidase; RVLM

This work supported by the National Natural Science Foundtion of China (No. 81170237)

Where applicable, the authors confirm that the experiments described here conform with The Physiological Society ethical requirements.

PCC105

Modulation of cholinergic and nitric oxide signaling pathways at the local efferent regulation of small intestine of rat by acute exposure of inorganic pentavalent arsenical

G. Paul, M. Ghosh, K. Sarkar and P. Tarafder

Department of Physiology, University of Kalyani, Kalyani, West Bengal, India

Arsenic is a ubiquitous poison that crowns the list of hazardous substances as cataloged by the Agency of Toxic Substances and Disease Registry. Arsenic occurs naturally in over 200 different mineral forms, of which approximately 60% are arsenates. Humans are exposed to pentavalent arsenicals through groundwater and ecological food chains. Absorption of sodium arsenate (As V) through the gastrointestinal tract has been reported to be 94% in humans. However, to date, no basic study has been done on the effect of As V exposure on the response of neurotransmitter pathways and enzymes related to those neurotransmission pathways in the mammalian gastrointestinal system. Intestinal motility is crucial to digestive and absorptive functions of gastrointestinal tract and as such is regulated by a myriad of excitatory and inhibitory neurotransmitters and enzymes catalyzing or synthesizing them. To bridge this knowledge gap we adopted a novel combination of crossover and placebo controlled study (1). The study was designed in two sets. In set A -in vitro organ bath experiments were conducted (following the protocols of crossover methodology) on isolated intestine of Charles foster rats (male, 35±5 day, 100 ± 17g, n=7) with a combination of different neurotransmitters and As V applied postmortem in the tissue chamber. In the first set isolated duodenal segments were first incubated with As V and the neurotransmitter in that order and also in the reversed order. The motility records were obtained by isotonic transducer IT-2245 coupled to RMS-Polyrite D software [RMS (P) Ltd, Chandigarh, India, 2010]. Our study showed that As V induced additive effect to acetylcholine and counteractive effect to nitric oxide. In set B – the test group rats (n=7) were exposed orally to LD50 dose of As V for 24 hours for a placebo controlled study, whereas the control rats were treated with arsenic free distilled water. Rats were humanely killed by cervical dislocation following the institutional guidelines foregoing anesthesia due to the nature of the experiment. In the second set we compared acetylcholinesterase activity (2) and nitric oxide synthase expression profile (3) of male Charles Foster rats (100 ± 17 g) orally exposed to LD50 24h As V to sham-treated animals. The results showed As V treatment inhibited both acetylcholinesterase and nitric oxide synthase in the duodenal smooth muscle of rat. Hence, we may conclude that As V stimulates cholinergic transmission and inhibits nitric oxide mediated neurotransmission in controlling movement of small intestine of rat efferently at the local level.

Tinmouth A & Hebert P (2007). Transfusion 47, 565-567.

Ellman GL, Courtney KD, Andres V & Featherstone RM (1961). Biochem Pharmacol 7(2), 88-90.

Zhou Y, Tan CK & Ling EA (1997). J Anat 190,135-145.

We thank Department of Science and Technology, Science & Engineering Research Council, Government of India for financial help.

Where applicable, the authors confirm that the experiments described here conform with The Physiological Society ethical requirements.

PCC106

Preinduction of HSP-70 by hypobaric hypoxia preconditioning attenuates ischemia, inflammation, oxidative stress and apoptosis in rat brain in heat stroke

C. Chang[1], L. Wang[2], C. Wang[3,4], B. Chio[5], J. Yu[5] and B. Cheng[1,3]

[1]Department of Biotechnology, Southern Taiwan University of Science and Technology, Tainan, Taiwan, [2]Graduate Institute of Clinical Medicine, National Cheng-Kung University Medical School, Tainan, Taiwan, [3]Department of Surgery, Chi Mei Medical Center, Tainan, Taiwan, [4]Department of Recreation and Health-Care Management, Chia-Nan University of Pharmacy and Science, Tainan, Taiwan and [5]Department of Chinese Medicine, Chi Mei Medical Center, Tainan, Taiwan

Despite the indication that the beneficial effects of hypobaric hypoxia preconditioning (HHP) in heatstroke are related to induction of heat shock protein (HSP) 70 in vital organs, there has not been any studies focusing on the relationships among HHP, brain HSP-70, and brain apoptosis, ischemia, inflammation, and oxidative stress in heatstroke. This study was to test whether HHP diminished apoptosis, ischemia, inflammation, and oxidative stress in heatstroke by up-regulating HSP-70. Anesthetized rats were randomly assigned to a) non-heated+non-HHP group, b) heated+non-HHP group, c) heated+HHP rats, and d) heated+HHP+HSP-70 antibodies (Ab) rats. All heated groups were exposed to heat stress (43 °C), 70 minutes) to induce heat stroke. We reported here that HHP induced overexpression of brain HSP-70, which could be ameliorated by HSP-70 antibody treatment in rats. When anesthetized non-HHP (or without brain HSP-70 overexpression) rats, HHP (or with brain HSP-70 overexpression) rats, and HHP+HSP-70 Ab (or without brain HSP-70 overexpression) rats were exposed to heat stress, their survival time values were found to be 89-95 mins, 409-431 mins, and 99-113 mins, respectively. Compared to non-HHP rats or (HHP+HSP-70 antibody) rats, HHP rats displayed higher values of cerebral blood flow and partial pressure of oxygen. In contrast, HHP rats had lower values of apoptotic cells, cellular ischemia and damage markers, pro-inflammatory cytokines, oxidative damage markers, and an indicator for neutrophils accumulation in the brain. The beneficial effects of HHP in improving apoptosis, ischemia, inflammation, and oxidative stress in rat brain in heatstroke could be ameliorated by HSP-70 Ab therapy. These results suggest that HHP improved survival and prevented heat damage to the brain and that the underlying mechanism involved induction of HSP-70 and inhibition of ischemia, inflammation, oxidative stress, and apoptosis.

This work was supported, in part, by the National Science Council [grant numbers NSC 99-2314-B-384-006-MY2, NSC 99-2314-B-384-004-MY3, NSC 98-2314-B-218-MY2, NSC 101-2314-B-218 -001-MY3 and NSC 101-2314-B-384-005] and the Department of Health [grant number of DOH 99-TD-B-111-003] the Center of Excellence for Clinical Trial and Research in Neuroscience of the Republic of China.

Where applicable, the authors confirm that the experiments described here conform with The Physiological Society ethical requirements.

PCC108

Antipyretic effect of Ocimum gratissium on brewer's yeast induced fever in wistar rats

G.I. Grace[1], B.S. Alisa[1], I.U. Vincent[1,2] and S.O. Mercy[1]

[1]physiology, Bingham university, Nasarawa, Nasarawa state, Nigeria and [2]Physiology, University of Sokoto, Sokoto, sokoto, Nigeria

Pyrexia or fever is a disease caused as a result of secondary impact of other diseased states due to the resetting of the hypothalamic set-point. From scientific discovery, antipyretic drugs such as asipirin, NSAIDs, opiods have been developed for use and of which mostly produces side effects including gastrointestinal bleeding,renal,hepatic effect,etc(Cheng et al.,2005,Sharma et al., 2010).Therefore, many herbal plants have been found to be having antipyretic effects.Ocimum gratissimum is a shrub commonly found in Africa and has been used to treat bacterial fevers locally. This study investigates the antipyretic activity of the methanolic extract of Ocimum gratissimumon brewer's yeast induced fever in experimental rats.30 albino rats weighing 150g-200g were used. They were divided in to six groups of five rats each. Group one serve as control(n=5) and was given 1ml of normal saline,group two (n=5)was treated with brewer yeast alone, group three(n=5) was given 100mg/kg of asipirin, while groups four,five and five were treated with 300mg/kg,200mg/kg and 100mg/kg (n=5)of Ocimum gratissimum respectively. A suspension of brewer's yeast was injected subcutaneously to induce fever in all the experimental animals. After 18hrs, the rectal temperature was taken and the animals were administered Ocimum gratissimum(100mg/kg.200mg/kg,300mg/kg) and aspirin (standard group,100mg/kg) orally. The body temperature of the rats was measured rectally over a period of 4hours.Ocimum gratissimum(100mg/kg, 200mg/kg and 300mg/kg) significantly reduced yeast induced pyrexia,36.88±0.39°C, 36.43±0.26°C and 35.83±0.46°C when compared the group two(20ml/kg, brewer's yeast) temperature of 37.80±0.18°C(*p<0.05,respectively). The group three(asipirin,100mg/kg) also show significant reduction 36.55±0.22°C,*p<0.05,compared with group two(20ml/kg,brewer yeast) with temperature 37.80±0.18°C.Thus, this experiment shows that the antipyretic effect of ocimum gratssimum is dose dependent and the effect is as a result of the flavonoid component of the extract.These data therefore suggest that methanolic extract of Ocimum gratissimum leaves possesses significant antipyretic activity and it mechanism could be by inhibition of/release inflammatory mediators.

Keywords:Ocimum gratissimum, brewer's yeast, antipyretics, asipirin,temperature

Table 1:effect of methanolic extract of Ocimun Gratissimum on Brewer's yeast induced pyrexia

groups (n=5)	treatment	Dose(mg/kg)	initial rectal temp. °C	0 hr (°C)	1hr (°C)	2hrs (°C)	3hrs (°C)	4hrs (°C)
I	Control : normal saline	1ml	36.60± 0.35	36.58± 0.34	36.58± 0.34	36.58± 0.33	36.58± 0.31	36.58± 0.33
II	Negative control: brewer's yeast	20ml/kg	36.60± 0.30	37.33± 0.31	38.20± 0.23	37.70± 0.22	37.78± 0.18	37.78± 0.18
III	reference :asipirin	100mg/kg	36.38± 0.20	37.73± 0.51	37.15± 0.41	36.80± 0.29*	36.63± 0.26*	36.55 ± 0.22*
IV	ocimum gratissimum	100mg/kg	36.63± 0.34	37.95± 0.47	37.88± 0.67	37.05± 0.46	36.93± 0.55	36.88±0.39
V	ocimum gratissimum	200mg/kg	35.95± 0.65	37.38 ± 0.58	37.55 ±0.23	36.20± 0.34**	36.10± 0.37**	36.43± 0.26**
VI	ocimum gratissimum	300mg/kg	35.93± 0.38	37.23± 0.15	36.20± 0.38**	35.53± 0.37***	35.75± 0.50**	35.83± 0.41**

all values are expressed as mean ±Sem,(n=5),*p,0.05, **p<0.01,***p<0.001

Cheng L et al.,2005:is COX-2 a pertrator or a protector.Selective Cox-2 inhibitors remain controversial. Acta Pharma Sinica.26:926-933

Sharm U et al.,2010:Screening of Terminilia Bellirica fruits extracts for its analgesic and antipyretic activities. Jordan Journal of Biological Sciences. Volume 3,Number 3.

Where applicable, the authors confirm that the experiments described here conform with The Physiological Society ethical requirements.

PCC109

Acute oral pseudoephedrine administration decreases latency time to central nervous system oxygen toxicity seizures in rats

H.E. Held, R. Pilla and J.B. Dean

Molecular Pharmacology and Physiology, University of South Florida, Tampa, FL, USA

People exposed to high partial pressures of oxygen, such as scuba divers, risk the onset of central nervous system oxygen toxicity (CNSOT). CNSOT presumably results from an accumulation of free radicals such as reactive oxygen species in the brain and produces epilepsy-like grand mal seizures, which may be fatal in an underwater environment. Many divers also use the neuro-excitatory drug pseudoephedrine (PSE) to reduce sinus inflammation. Incident reports from the Divers Alert Network (DAN) suggest a link between PSE use and an increased risk of diving accident or injury. The purpose of this study was to determine whether or not increasing doses of PSE decrease the latency to seizure (LS).

Male and female rats (250 to 350g) were included so that gender-dependent differences could also be elucidated. Rats were surgically implanted under isoflurane anesthesia with radiotelemetry units, which allowed measurement of electroencephalograms without restraint. One week after surgery, each rat received a single 1 mL dose of PSE in saline (0, 40, 80, 100, 120, 160, and 320 mg/kg) via oral gavage. Nine rats were included in each group. Rats breathed 100% oxygen during a dive to 5 atmospheres absolute in a hyperbaric chamber. LS was defined as the duration of time between reaching maximal pressure and onset of seizure (increased electroencephalogram activity coupled with tonic-clonic spasms of forelimbs and head).

Data are presented in Table 1 (mean ± SEM). Males exhibited decreased LS and decreased variability with increased dosage. The decrease in LS was significant at 100 mg/kg and higher. Females exhibited decreased LS following doses of 80 mg/kg, 100 mg/kg, and 320 mg. The decreases at 120 mg/kg and 160 mg/kg did not reach statistical significance, apparently due to increased variability. There were no significant differences between males and females.

We conclude that only high doses of PSE decrease LS. Further testing is underway to determine the effects of menstrual cycle phase, age, and history of pregnancy on LS in female rats.

The first two authors contributed equally.

Table 1

PSE Dose (mg/kg)	0	40	80	100	120	160	320
Male LS (min)	39.4 ± 8.3	50.7 ± 12.7	33.2 ± 11.1	14.8 ± 5.7	9.9 ± 1.7	9.1 ± 1.0	17.7 ± 4.5
Female LS (min)	26.9 ± 4.8	26.7 ± 11.7	14.2 ± 2.3	14.7 ± 3.6	18.2 ± 6.5	22.8 ± 9.9	8.1 ± 1.1

Funded by DAN #0100001072, ONR #N000140710890, ONR #N000141210801

Where applicable, the authors confirm that the experiments described here conform with The Physiological Society ethical requirements.

PCC111

Large-scale correlated wave in the embryonic mouse CNS: Development, origins and pharmacological natures

K. Sato[1,3] and Y. Momose-Sato[2]

[1]Department of Health and Nutrition Sciences, Komazawa Women's University, Faculty of Human Health, Tokyo, Japan, [2]Department of Health and Nutrition, Kanto Gakuin University, College of Human and Environmental Studies, Yokohama, Japan and [3]Opto-Medical Institute, Tokyo, Japan

Spontaneous embryonic movements, called embryonic motility, are produced by correlated spontaneous activity in the cranial and spinal nerves, which is driven by brainstem and spinal networks. Using optical imaging with a voltage-sensitive dye, we have revealed previously that this correlated activity is a widely propagating wave of neural depolarization, which we termed the depolarization wave. We have observed in the chick and rat embryos that the activity spread over an extensive region of the central nervous system, including the spinal cord, hindbrain, cerebellum, midbrain, and forebrain. One important consideration is whether a depolarization wave with similar characteristics occurs in other species, especially in different mammals. Here, we provide evidence for the existence of the depolarization wave in the mouse embryo by showing that the widely propagating wave appeared independently of the localized spontaneous activity detected previously with Ca2+ imaging. Pregnant mice were anesthetized with ether, and the spinal cord was dislocated at the cervical level. Their fetuses were then surgically removed, and the whole brain-spinal cord or brainstem-spinal cord preparation was dissected in an ice-cold solution. We mapped the origin of the depolarization wave and revealed that the wave generator moved from the rostral spinal cord to the caudal cord as development proceeded, and was later replaced with mature rhythmogenerators. Furthermore, we examined the pharmacological nature of the mouse depolarization wave and its developmental changes. We show here that two types of switching in pharmacological characteristics occur during development. One is that the depolarization wave is strongly dependent on nicotinic acetylcholine receptors during the early developmental stage (E11-E12), but is dominated by glutamate at the later stage (E13~). The second is that GABA, which acts as an excitatory mediator of the depolarization wave during the early phase, becomes an inhibitory modulator by E14. These changes seemed to occur earlier in the hindbrain than in the spinal cord. We also show that the second switching causes the loss of synchronization over the network, resulting in the disappearance of the depolarization wave and a segregation of the activity into discrete regions of the medulla and spinal cord. The present study shows that a synchronized wave with common characteristics is expressed in different species, suggesting fundamental roles in neural development.

Where applicable, the authors confirm that the experiments described here conform with The Physiological Society ethical requirements.

PCC112

Could the foetal brain be damaged by molecules released from the placenta?

V. Leinster[1], S. Sanderson[2], J. Henley[3], K. Simon[2] and P. Case[1]

[1]Musculoskeletal Research Unit, University of Bristol, Bristol, UK, [2]BRC Translational Immunology Lab, Experimental Medicine Division,, Oxford University, Oxford, UK and [3]MRC Centre for Synaptic Plasticity, University of Bristol, Oxford, UK

Abnormal blood flow in the placenta, leading to hypoxia or reperfusion is linked to damage to the foetal brain and may occur in a variety of conditions including miscarriage, pre eclampsia and intrauterine growth restriction (1). This may lead to lifelong disability ranging from cerebral palsy to Autism spectrum disorders. Our data shows that hypoxia reperfusion of a cellular model of the placenta induces the release of toxic factors that damage neurons and astrocytes in cortical cultures. In vitro barriers that model the placenta were made from BeWo cells and exposed to various concentrations of oxygen (2%, 2-8%, 2-12%, 2-21%, 21%) and the tissue culture media was collected as conditioned media (CM). Dissociated neurons from rat E18.5 cortical cultures were grown for 12 days before being exposed to CM for 6 days. Hippocampal slices were also taken from P7 rats and grown as organotypic cultures for 14 days before being exposed to CM for 6 days. Cultures/ hippocampal slices were then fixed and fluorescently stained with MAP2 and GFAP to identify the neuronal and astrocyte cell populations. Images were captured using confocal microscopy and cell morphology was analysed using ImageJ. Flow cytometry analysis (LSRII) was also performed on cortical cultures to analyse the effects of the CM on cell death, cell cycle, mitochondrial free radicals and autophagy. Both culture models showed similar results. Control conditions (21% oxygen) showed good neuronal growth and the astrocytes had long process with many branch points and end plates. In cultures that were exposed to hypoxic (2%) CM, there was poor neuronal growth with blebbing. Similarly astrocytes were reduced in number showing a distinct change in morphology with very few processes. Exposure to CM after re-oxygenation (2-8% and 2-21% oxygen) also caused poor neuronal outgrowth. However the astrocytes were increased in number and well branched (2-8% vs 2% and 2-21% vs 2%). These results show that in CM produced in 2% oxygen there are harmful molecules released from trophoblast that damage neurons and astrocytes. Neuronal damage is seen using hypoxic and re-oxygenated CM where as astrocytes appear to be mainly affected by the hypoxic (2% oxygen) CM. Thus, when a hypoxic condition is sustained there is dendritic shortening in neurons and morphological changes in astrocytes. The reduction in process length and cell volume in astrocytes could lead to a reduced contact between neurons and astrocytes. Abnormal signaling between the two cell types results in abnormal neurite outgrowth having an effect on neuronal development, an underlying cause of many neurological diseases. Re-oxygenation does not appear to induce a survival or regenerative affect on the neuronal population in cultures indicating that a therapeutic / pharmacological treatment would be required to overcome any damage from sustained hypoxia.

Mann JR, McDermott S, Bao H, Hardin J, Gregg A. 2010,Pre-eclampsia, birth weight and autism spectrum disorders. .J Autism Dev Disord. 40(5):548-54.

The Waterloo Foundation

Where applicable, the authors confirm that the experiments described here conform with The Physiological Society ethical requirements.

PCC113

PTEN regulates hair cell proliferation, differentiation and innervation in the mammalian inner ear

Y. Dong[1], L. Sui[1], F. Yamaguchi[1], K. Kamitori[1], Y. Hirata[1], A. Hossain[1], A. Suzuki[2] and M. Tokuda[1]

[1]Cell Physiology, Faculty of Medicine, Kagawa University, Kitagun, Kagawa, Japan and [2]Division of Embryonic and Genetic Engineering, Medical Institute of Bioregulation, Kyushu University, Fukuoka, Kagawa, Japan

PTEN (phosphatase and tensin homolog deleted on chromosome 10) is a tumor suppressor gene that regulates various cell processes including proliferation, growth, synaptogenesis and the dynamics of the actin-myosin cytoskeleton. We studied the expression pattern of PTEN in the mouse inner ear during development and explored its function by analysis of PTEN heterozygous null mice. Immunolabeling revealed that PTEN is expressed primarily in differentiating sensory neurons and hair cells, coinciding with the temporal and spatial gradients of hair cell differentiation. In heterozygous null mice the sensory epithelial progenitors withdraw later from the cell cycle than wild type and this is associated with an increase in hair cell number. Disorganization and loss of hair bundles is uniquely associated with the formation of ectopic hair bundles on the inner pillar cells. These results show that PTEN plays an important role in regulating the proliferation, differentiation and innervation of mammalian cochlear hair cells. PTEN signaling pathways provide potential therapeutic targets for the regeneration of mammalian inner ear sensory epithelia.

We thank Mr. Toshitaka Nakagawa for the SEM. The work was supported by a Grant-in-Aid for Scientific Research from the Ministry of Education, Culture, Sports, Science and Technology, Japan and a Grant-in-Aid for Exploratory Research from the Faculty of Medicine, Kagawa University, Japan.

Where applicable, the authors confirm that the experiments described here conform with The Physiological Society ethical requirements.

PCC116

Derivation of oligodendrocyte precursors from bone marrow stromal cells for remyelination therapy

Y. Tsui[1,2], R.S. Li[3], A.C. Lo[3], Y. Chan[2] and D.K. Shum[1]

[1]Department of Biochemistry, The University of Hong Kong, Hong Kong, China, [2]Department of Physiology, The University of Hong Kong, Hong Kong, China and [3]Department of Ophthalmology, The University of Hong Kong, Hong Kong, China

Myelin is crucial for survival of neurons and maintenance of neural network function. Demyelinating disorders are debilitating and are often associated with failure of resident oligodendrocyte precursor cells (OPCs) to differentiate into mature, myelinating oligodendrocytes. Derivation of OPCs from a safe source that evades ethical issues offers a solution to remyelination therapy. We therefore hypothesized that neural progenitor cells harboured at a pre-commitment stage among stromal cells of the adult bone marrow (BMSCs) can be directed to differentiate along the oligodendroglial lineage. We started with adherent cultures of adult rat BMSCs >90% of which were CD90-, CD73- and STRO-1-positive (stromal cell markers) but were CD45-negative (haematopoietic cell marker) and 10% nestin-positive. Tranfer to non-adherent culture fostered expansion of the nestin-positive neural progenitors (NPs) in sphere formation at the expense of stromal cells. The BM-NPs were maintained in adherent culture supplemented with glia-inducing factors, beta-Heregulin, basic fibroblast growth factor and platelet-derived growth factor-AA. Within two weeks, cells positive for OPC markers - NG2, Olig2, PDGFRa and Sox10, were detectable. These cells could be expanded in culture for more than 3 months with no observable decline in marker expression. Co-culture with dorsal root ganglion neurons induced maturation of the BM-OPCs into myelinating oligodendrocytes. We further transplanted BM-OPCs into the retina of adult rats and demonstrated that by 8 weeks, some of the BM-OPC extended, myelin basic protein-positive processes along the otherwise unmyelinated retinal axons. The results not only suppport our hypothesis, but also provide pointers to the adult bone marrow as a safe and accessible source for the derivation of OPCs towards transplantation therapy in demyelinating disorders. [HKU RGC GRF 777810M; HKU S.K. Yee Medical Foundation Grants]

Where applicable, the authors confirm that the experiments described here conform with The Physiological Society ethical requirements.

PCC117

Dark exposure promotes accelerated recovery from monocular deprivation in adult mice

I. Erchova and F. Sengpiel

School of Biosciences, Cardiff University, Cardiff, UK

Dark exposure has been reported to enhance plasticity in the adult visual cortex and to promote recovery from deprivation amblyopia both in rats [1] and in cats [2]. The physiological substrate of this recovery is as yet unknown. We employed optical imaging of intrinsic signals to monitor shifts in ocular dominance (OD) in the primary visual cortex (V1) of mice aged between postnatal day (P) 60 and P90.

C57BL/6J mice were normally reared on a 12-h light/12-h dark cycle. Monocular deprivation (MD) by eyelid suture was carried out under isoflurane anaesthesia (2% in O2, 0.5 L/min). A control group of 7 non-deprived mice was imaged under general anaesthesia (1-2% of isoflurane in O2, 0.5 L/min, supplemented with 25 μg i.m. chlorprothixene as described previously to measure OD [3]. ECG and body temperature were monitored continuously. Animals were stimulated with horizontal white bars on a black background presented in the binocular visual field, drifting periodically across the screen at a rate of 0.125 Hz, with the stimulated eye determined by computer-controlled eye shutters. The magnitude of contra- and ipsilateral eye responses (C, I) was determined for each pixel within the V1 binocular zone by fast Fourier transformation, and an OD index (ODI) was calculated as $(C - I)/(C + I)$.

Compared with the control group, the ODI in 6 mice after 7 days of MD was shifted from 0.18±0.02 (mean ± SEM) to 0.04±0.01 ($p < 0.001$, t-test). We then re-opened the deprived eye under isoflurane anaesthesia and investigated the time course of recovery from MD. In a group of normally reared mice, 5 out of 7 animals (70%) recovered normal ODI values within 72 h (for all 7 mice, ODI=0.15±0.04, p=0.016). In contrast, 72 h of dark exposure immediately after the end of MD did not result in OD recovery; instead a further small OD shift

towards the non-deprived eye was observed (ODI=0.08±0.01, n=7). However, when dark-exposed mice were returned to a normally lit environment, recovery of OD was accelerated. After only 36 h animals showed partial recovery of OD (ODI = 0.09±0.01, n=9, p=0.016), more prominent in the anterior segment of the V1 binocular zone; recovery was complete within 72 h (7 mice; ODI=0.19±0.01). In all groups, both the MD-induced OD shift and subsequent return to baseline were mediated by up- and down-regulation of ipsilateral (non-deprived) eye responses, with little change in deprived eye responses. These data suggest that brief periods of dark exposure, at least in mice, promote recovery from MD on the basis of the existing adult plasticity mechanisms.

He H.Y., Ray B., Dennis K., and Quinlan E.M. (2007). Experience-dependent recovery of vision following chronic deprivation amblyopia. Nat Neurosci 10: 1134-1136.

Duffy K.R. and Mitchell D.E. (2013). Darkness alters maturation of visual cortex and promotes fast recovery from monocular deprivation. Curr Biol, http://dx.doi.org/10.1016/j.cub.2013.01.017.

Kaneko M., Stellwagen D., Malenka R.C., and Stryker M.P. (2008). Tumor Necrosis Factor-α mediates one component of competitive, experience-dependent plasticity in developing visual cortex. Neuron 58: 673-680.

This work was supported by the BBSRC.

Where applicable, the authors confirm that the experiments described here conform with The Physiological Society ethical requirements.

PCC118

Regulatory role of neuronal proheparanase in synaptic plasticity

C. Ma[1,2], Y. Lam[2], W. Cham[2], Y. Chan[1] and D. Shum[2]

[1]Department of Physiology, The University of Hong Kong, Hong Kong, China and [2]Department of Biochemistry, The University of Hong Kong, Hong Kong, China

Perineuronal heparan sulfates (HS) have been implicated in controlling the open-state of AMPA-type glutamate receptors (AMPARs) which govern excitatory synaptic transmission in the hippocampus. We hypothesize that neuronal mechanisms modulate peri-synaptic HS level and as a result regulate synaptic function. Our finding of neuronal heparanase expression in adult rats led us to test if neuronal heparanase is secreted to act on perineuronal HS, thereby contributing to synaptic plasticity. Following phorbol ester stimulation of hippocampal neurons in culture, Western blot analysis of the secreted product revealed proheparanase but not the active heparanase. Synaptosomes prepared from phorbol ester-treated cortex slices were enriched in proheparanase; co-immunoprecipitation studies further showed association of AMPAR subunits (GluA1 and GluA2/3) with both syndecan-3 (transmembrane HS-proteoglycan) and proheparanase, suggesting their clustering as a functional complex. Treatment of hippocampal neuron cultures with recombinant proheparanase triggered internalization of proheparanase, perineuronal HS-proteoglycans and AMPARs. Heparitinase pre-treated hippocampal neuron cultures showed reduced proheparanase-induced internalization of AMPARs, suggesting that proheparanase binds to syndecan-3 via the HS moiety. Consistent with these findings, treatment of hippocampal slices with exogenous proheparanase resulted in declines in both basal synaptic strength and LTP. Proheparanase treatment also prevented glutamate-induced calcium influx of the hippocampal neurons in culture. These results reveal a novel role of neuronal proheparanase in regulating synaptic plasticity by resetting AMPARs and perineuronal HS levels at the synapse. [Supported by HKRGC 774608]

Where applicable, the authors confirm that the experiments described here conform with The Physiological Society ethical requirements.

PCC119

Brain derived neurotrophic factor-mediated GABAergic transmission in the vestibular nucleus modifies developmental acquisition of graviceptive behaviour

F. Botelho, C. Lai and Y. Chan

Physiology, The University of Hong Kong, Hong Kong, China

Brain-derived neurotrophic factor (BDNF) has been implicated in the maturation of GABAergic transmission(1). We demonstrated that neonatal rats implanted with BDNF-loaded Elvax slices over the vestibular nuclei showed an accelerated re-orientation of body against gravity. We hypothesized that this acceleration caused by BDNF is due to changes in the GABAergic transmission. To test this, long-term changes of inhibitory synaptic transmission were studied using whole-cell patch-clamp experiments in medial vestibular (MV) neurons of rats. We found that MV neurons exhibited inhibitory long-term depression (iLTD) and long-term potentiation (iLTP) of GABAA receptor-mediated signal transmission in early and late postnatal stages, respectively. In neonatal neurons, BDNF incubation could induce a slight reduction in GABA-mediated iLTD whereas at late postnatal neurons, iLTD, which is indicative of early developmental stages, could be re-induced with BDNF treatment. These results indicate that developmental acquisition of spatial orientation can be modified by BDNF-mediated refinement of neural networks in the vestibular nucleus.

Huang, Z.J., Kirkwood, A., Pizzorusso, T., Porciatti, V., Morales, B., Bear, M.F., Maffei, L., Tonegawa, S. (1999). BDNF regulates the maturation of inhibition and the critical period plasticity in mouse visual cortex. Cell 98, 739-755.

RGC Grant HKU 761710M

Where applicable, the authors confirm that the experiments described here conform with The Physiological Society ethical requirements.

PCC120

Plasticity of GABAergic synapses in the developing vestibular nucleus governs the expression of spatial navigation in mature rats

W. Chen[1], W. Shi[1], C. Ma[1,2], C. Lai[1], D. Shum[2] and Y. Chan[1]

[1]Physiology, Li Ka Shing Faculty of Medicine, The University of Hong Kong, Hong Kong, China and [2]Beiochemistry, Li Ka Shing Faculty of Medicine, The University of Hong Kong, Hong Kong, China

Vestibular input has been implicated to provide idiothetic cues for spatial navigation. It remains unresolved as to whether GABAergic synapses in the vestibular nucleus (VN) during a postnatal critical period regulates the acquisition of spatial recognition.

To assess the role of GABAergic VN transmission on the acquisition of spatial navigation, we implanted above the VN of postnatal day 1 (P1) rats with a slice of Elvax loaded with GABAA

receptor agonist (muscimol) or antagonist (bicuculline). These pups were allowed to recover and were tested for either activity-dependent plasticity of GABAergic synapses in the developing VN or for navigation test at the adult stage.
First, whole-cell patch clamp recordings were conducted in brainstem slices. In normal animals, theta-burst stimulation delivered to vestibular afferents could induce long-term depression of GABAA receptor-mediated evoked-IPSCs (iLTD) in VN neurons of P7 rats but these responses became hardly inducible by P14. In rats pretreated with muscimol at P1, iLTD observable at P7 was abolished. In rats pretreated with bicuculline at P1, the emergence of iLTD was delayed to P9-14.
To assess the impact of these GABAergic responses on the acquisition of spatial navigation, a path integration task (viz. dead reckoning) that primarily relies on sensory cues from vestibular organ was used. When compared with the sham controls, rats pretreated with muscimol at P1 showed no significant difference in light, dark, and new location probe tests. However, pretreatment with bicuculline at P1 significantly prolonged the training days, searching time, returning time, heading angle, and number of errors in both dark and new location probe tests. Taken together, we have provided evidence that the efficacy of GABAergic synapses in the developing VN constitutes a crucial component required for the expression of spatial navigation behavior in adults.

Supported by RGC 761711M

Where applicable, the authors confirm that the experiments described here conform with The Physiological Society ethical requirements.

PCC121

Impaired synaptic plasticity in the primary motor cortex and motor skill consolidation after dopamine depletion

Q. Li[1,2], Y. Ke[1,2] and W. Yung[1,2]

[1]School of Biomedical Sciences, Faculty of Medicine, the Chinese University of Hong Kong, New Territories, Hong Kong and [2]Shenzhen Research Institute, the Chinese University of Hong Kong, Shen Zhen, Guang Dong, China

The ability to learn and retain new motor skills is important in daily life. After repeated exposure to a specific procedure, motor skill becomes more accurate and automatic. In Parkinson's disease (PD), in spite of the cardinal motor symptoms like akinesia and bradykinesia, patients suffer deficits in motor skill learning. The impaired synaptic plasticity of basal ganglia circuitry has been suggested to be involved. In PD, dopamine innervation originating from the mesocortical pathway is reduced in the primary motor cortex (MI), an area that also contributes to motor learning. However, the impact of dopamine depletion on cortical synaptic plasticity and motor skill learning is not clear. The present study addresses these questions based on in vivo long-term potentiation (LTP) in the MI and motor training on PD rats.

6-hydroxydopamine was bilaterally injected into the MI (AP: +2.5, ML: ±3.0, DV: 1.7mm) of SD rats. After one week's recovery, arm-reaching for food task was conducted (10 trials) to confirm the preferred forelimb being used. A 16-channel microwire recording electrode and a bipolar stimulus electrode (300μm apart) were implanted into contralateral MI forelimb territory, targeting at layer V. In the first set of experiments, intermittent high frequency stimulation (iHFS, 90 trains delivered every 10s; each train consisted of 50 pulses in 250Hz) was delivered to the MI of freely moving rats and evoked local field potential (LFP) was monitored. In the sham-operated group, LTP level was measured as the increment of evoked LFP amplitude 90 mins after the induction protocol (132.8±3.1%, n=4). In contrast, the cortical LTP in the 6-OHDA group was significantly reduced (110.8±3.0%, n=3, $^{**}p<0.01$, compared with sham). In the second set of experiments, arm-reaching task was performed to investigate the correlation between cortical LTP impairment and performance of motor skill. The skillfulness was assessed by the rate of 'single success', namely food pellet obtained on the first reaching attempt. The performance of the PD rats in the initial learning phase was comparable to that of the sham-operated group (1st day: sham, 32.4±1.1%, n=3; 6-OHDA lesion, 30.2±1.8%, n=3; p=0.36). As training continued, PD animals exhibited deficit in consolidating the motor skill, even if they could reach a good success rate in the previous day. After 1 week's training, a significant difference in the 'single success' rate between the two groups was found (sham: 45.1±2.8%, n=3; 6-OHDA lesion: 30.9±4.1%, n=3; $^{*}p<0.05$).

Our study showed that dopamine depletion confined to the MI could lead to impairment in cortical LTP which may preferentially affect the consolidation, but not the acquisition of motor skills.

Li, Q., Y. Ke, et al. (2012). Neuron 76(5), 1030-1041.

Dayan, E. and L. G. Cohen (2011). Neuron 72(3), 443-454.

Suppa, A., L. Marsili, et al. (2011). Exp Neurol 227(2), 296-301

Pendt, L. K., I. Reuter, et al. (2011). PLoS One 6(7), e21669.

This work is supported by the Research Grants Council of Hong Kong (T13-607/12R; HKU6/CRF/11G) and the National 973 Program (2011CB510004).

Where applicable, the authors confirm that the experiments described here conform with The Physiological Society ethical requirements.

PCC123

Haploinsufficiency of SynGAP phenocopies hippocampal deficits reported in the mouse model of fragile X syndrome

S.A. Barnes[1], A.D. Jackson[1], E.M. Osterweil[2], M.F. Bear[2], P.C. Kind[1] and D.J. Wyllie[1]

[1]Centre for Integrative Physiology, University of Edinburgh, Edinburgh, UK and [2]Picower Institute for Learning and Memory, Massachusetts Institute of Technology, Cambridge, MA, USA

The genetic causes of intellectual disability (ID) and autism spectrum disorder (ASD) are frequently associated with mutations in genes that encode synaptic proteins. A recent screen of ID patients has revealed that approximately 4% of individuals carry spontaneous autosomal-dominant *de novo* mutations in the *SYNGAP1* gene some of which result in complete absence of the synaptic GTPase activating protein SynGAP (1). Investigations into the pathological consequences of SynGAP haploinsufficiency ($Syngap^{+/-}$) in mice have reported abnormalities in both behaviour and dendritic spine development. These are analogous to findings from the mouse model of fragile X syndrome (FXS; $Fmr1^{-/y}$), the most common inherited form of ID. One of the prominent phenotypes reported in the $Fmr1^{-/y}$ mouse is that a form of hippocampal long-term depression (LTD) mediated by the activation of Group 1 (Gp1) metabotropic glutamate receptors (mGluRs) is enhanced and independent of new protein synthesis (2). The cause of these deficits in synaptic plasticity, together with other cognitive abnormalities observed in FXS, are thought to arise in part

from an increase in basal protein synthesis, which can be corrected by either inhibiting mGluR5 (3) or reducing Ras and subsequent ERK activity (4). In the present study we examined mGluR-LTD at Schaffer collateral/commissural inputs to CA1 pyramidal neurones in hippocampal slices obtained from *Syngap*$^{+/-}$ mice. Extracellular field recordings reveal that acute application of the Gp1 mGluR agonist dihydroxyphenylglycine (DHPG; 50 μM) induces a form of mGluR-LTD that is greater magnitude in *Syngap*$^{+/-}$ mice relative to wild-type (WT) littermate controls (50 μM: 57 ± 7 %, *Syngap*$^{+/-}$, n = 14 versus 75 ± 3 %, WT, n = 19). Furthermore mGluR-LTD in *Syngap*$^{+/-}$ mice is insensitive to protein synthesis inhibitors (unpaired t-test $P<0.05$, n = 15). In addition, we find basal levels of protein synthesis to be elevated in hippocampal slices from*Syngap*$^{+/-}$ mice relative to their WT counterparts (145 ± 15 %, *Syngap*$^{+/-}$ versus 100 ± 4 %, WT n = 12). The comparable neuropathophysiology we observe between *Syngap*$^{+/-}$ and *Fmr1*$^{-/y}$ mice suggests that SynGAP and fragile x mental retardation protein (FMRP) may converge on similar biochemical pathways raising the intriguing possibility that therapeutic strategies used in the treatment of FXS may also be of benefit in treating individuals with ID caused by mutations in *SYNGAP*.

Hamdan et al., (2011) *Biol Psychiatry* **69**:898-901.

Huber, KM et al., (2002) *Proc Natl Acad Sci USA* **11**:7746-7750.

Osterweil, EM et al., (2010) *J Neurosci* **46**:15616-15627.

Osterweil EM et al., (2012) *Neuron* **77**:243-250.

This work is supported by the BBSRC, MRC and the Patrick Wild Centre

Where applicable, the authors confirm that the experiments described here conform with The Physiological Society ethical requirements.

PCC124

Optogenetic manipulation of presynaptic activity in the ciliary ganglion during embryogenesis of the chick

S. Hososhima[1,3], T. Ishizuka[1,2] and H. Yawo[1,2]

[1]Molecular and Cellular Neuroscience Laboratory, Department of Developmental Biology and Neuroscience, Graduate School of Life Sciences, Tohoku University, Sendai, Japan, [2]CREST, JST, Tokyo, Japan and [3]Research Fellow of Japan Society for the Promotion of Science, Tokyo, Japan

[Introduction] In various nervous systems, a presynaptic neuron once branches extensively and projects its axons to many postsynaptic neurons in early developmental stages. The number of branches is reduced with development and the connections between presynaptic and postsynaptic neurons become refined. The ciliary ganglion of chick embryo has been one of model systems of synaptogenesis. As early as in embryonic day 8 (E8), postsynaptic ciliary neuron is multiply innervated by the presynaptic axons. Before E14 a postsynaptic ciliary neuron receives only one calyx-type presynaptic terminal of a midbrain neuron in the Edinger-Westphal nucleus. It has been hypothesized that the refinement of neuronal connections is dependent on the activity of presynaptic and/or postsynaptic neurons. Here, we invented new system using *in ovo* electroporation and shell-less culture and investigated if the activity of presynaptic neurons is necessary and sufficient for the synapse refinement in the ciliary ganglion using optogenetics.

[Method] CAGGS plasmids containing a tandem construct of chimeric variants of channelrhodopsins (ChRs), such as ChRWR, ChRGR and ChRFR(C167A), and yellow florescence protein (Venus), were introduced in the midbrain of E2 embryo and incorporated in the neuroblasts using *in ovo* electroporation method (Egawa et al., 2013). Some chick embryos that expressed channelrhodopsin were cultured using shell-less culture method. These embryos were LED-flashed between E8 and E14, and examined under confocal microscopy at E14. The unflashed embryos were used as control. The synaptic current was measured from the postsynaptic ciliary neuron at E14 under conventional whole-cell patch clamp.

[Results & Discussion] We found the expression of venus-conjugated ChRs in neurons of the Edinger-Westphal nucleus, axons in the oculomotor nerve and calyx-type presynaptic terminals in the ciliary ganglion of E8-14 embryo. When the ChR-expressing presynaptic terminal was flashed by LED, the light-dependent synaptic currents were evoked in the postsynaptic neuron. Although the ciliary ganglion was somewhat distorted in shape under shell-less culture during E2-14, the calyx-type presynaptic terminals were almost normally developed in appearence. It is suggested that the activity of a presynaptic axon/terminal should be optogenetically manipulated during embryogenesis in the shell-less culture to reveal the relationship between the presynaptic activity and the synapse refinement.

Egawa R, Hososhima S, Hou X, Katow K, Ishizuka T, Nakamura H and Yawo H (2013) Optogenetic probing and manipulation of the calyx-type presynaptic terminal in the embryonic chick ciliary ganglion. PLOS ONE (in press)

Where applicable, the authors confirm that the experiments described here conform with The Physiological Society ethical requirements.

PCC125

Cognitive functions are better during postovulatory phase of menstrual cycle

N. Upadhayay[1] and D. Guragain[2]

[1]Basic and Clinical Physiology, BP Koirala Institute of health Sciences, Dharan, —, Nepal and [2]Pharmacology, Manipal College of Medical Sciences, Pokhara, Nepal

Even though it has been established the neuroprotective effect of estrogen on cognitive functions in postmenopausal women, some discrepancy still exists. Moreover, emerging reports mention that progesterone stimulates reward center and has neuroprotective role on cognitive function, but some contradictory still exists. So this study was aimed to compare cognitive functions between menstruation (low estrogen phase) and postovulatory phase (high progesterone phase) of menstrual cycle (MC) in consenting 34 healthy female volunteers (age 19-37 years).

Menstruation-cognitive functions were assessed in between 2-5 days of start of menses and postovulatory-cognitive functions were assessed in between 23-27 days of the MC. Four aspects of cognitive functions were assessed (viz: attentional, perceptual, executive and working memory). Attentional task as visual reaction time (VRT) and Go/No-Go VRT (pattern), perceptual task as fast counting (FC), executive task as Erisken flanker test (EFT) and Stroop test (ST) i.e. color interference reading and, working memory task as remembering picture 2-back were assessed by using cognitivefun.net program. Data were expressed in median and interquartile range (IQR), compared by using Wilcoxon test.

Postovulatory phase showed better performance in Go/No-Go VRT average time (422.66 ms, IQR: 391.2 to 450 vs. 465.2 ms,

IQR: 425.6 to 504; p=0.003), Go/No-Go VRT combined time (450 ms, IQR: 422 to 457.32 vs. 541.67 ms, IQR: 465.2 to 605; p=0.000), ST percentage accuracy (100% with IQR: 100 to 100 vs. 95.24% with IQR: 90.12 to 100; p=0.000), ST color interference time (1105.3ms, IQR: 1100.3 to 1335.25 vs. 1428ms, IQR: 1346.39 to 1621.25; p=0.001), and FC speed (1081.51 ms, IQR: 902.6 to 1147.18 vs. 1130.6 ms, IQR: 1066.6 to 1209.18; p=0.041) than in menstruation phase. Other cognitive task variables (viz: VRT, EFT, working memory) were comparable between menstruation and postovulatory phase of MC.
Some aspects of cognitive function varied across the MC. But these two phases of MC had no effect on working memory. Thus, it can be concluded that postovulatory phase of menstrual cycle improves attentional (pattern recognition), perceptual, and executive function (as assessed by stroop test) of cognition. Probably progesterone, which is higher during postovulatory phase, is responsible to modulate the neurons action in the brain and enhancing the cognition.

Where applicable, the authors confirm that the experiments described here conform with The Physiological Society ethical requirements.

PCC126

Arginine vasopressin (AVP)-eGFP expression in the hypothalamus after hypovolemia in AVP-eGFP transgenic rats

Y. Ueta, M. Ohno, T. Ishikura, T. Maruyama, H. Hashimoto, T. Matsuura, J. Ohkubo, M. Yoshimura and H. Yamashita

Department of Physiology, School of Medicine, University of Occupational and Environmental Health, Kitakyushu, Japan

Arginine vasopressin (AVP) release is known to be stimulated by hypovolemia as well as osmotic challenge such as dehydration and chronic salt loading. We have generated a transgenic rat that expresses the AVP-eGFP fusion gene in the paraventricular (PVN) and the supraoptic nuclei (SON) of the hypothalamus. Our previous studies revealed that acute and chronic osmotic stimuli up-regulated the expression of the AVP-eGFP fusion gene in the magnocellular neurons of the PVN and the SON. Here, we demonstrated that polyethylene glycol (PEG)-induced hypovolemia was able to cause the up-regulation of the AVP-eGFP gene expression in the PVN and the SON in the transgenic rats. Intraperitoneal (ip) administration of PEG induced isotonic hypovolemia. The intensity of eGFP fluorescence in the PVN and the SON were significantly increased 6 and 24 hours after ip administration of PEG in comparison with controls. Interestingly, the intensity of eGFP fluorescence in the parvocellular division of the PVN was also increased significantly. The present study revealed that PEG-induced hypovolemia caused a significant up-regulation of the AVP-eGFP fusion gene expression in the magnocellular and parvocellular neurons of the PVN and the SON in AVP-eGFP transgenic rats.

Where applicable, the authors confirm that the experiments described here conform with The Physiological Society ethical requirements.

PCC127

Dual effects of nobiletin, a citrus polymethoxy flavone, on catecholamine signaling in cultured bovine adrenal medullary cells

H. Zhang[1], N. Yanagihara[2], Y. Toyohira[2], K. Takahishi[2] and K. Takahashi[3]

[1]Research Center of Traditional Chinese Medicine, Tianjin University of Traditional Chinese Medicine, Tianjin, China, [2]Department of Pharmacology, University of Occupational & Environmental Health, School of Medicine, Kitakyushu, Fukuoka, Japan and [3]Department of Hospital Pharmacy, University of Occupational & Environmental Health, Kitakyushu, Fukuoka, Japan

The peels of citrus fruits are a rich source of flavonoids, which have been shown to exert beneficial properties on human health. Nobiletin (5,6,7,8,3',4'- hexamethoxyflavone) is a major component of polymethoxylated flavones found in the peel of citrus fruits, and is used in a Chinese traditional herbal medicine. Nobiletin exhibits a broad spectrum of pharmacological activities, including anticancer, antioxidative, and anti-inflammatory properties. Furthermore, nobiletin possesses antiatherogenic and cardiovascular protective effects, and neuronal effects such as neurotrophic effects in vitro, and antidementia activities in vivo, although the precise mechanisms underlying these nobiletin's effects remain to be determined. Adrenal medullary cells derived from the embryonic neural crest are functionally homologous to the sympathetic postganglionic cells. In cultured bovine adrenal medullary cells, the Na+ influx induced by acetylcholine (ACh) via nicotinic ACh receptor-ion channels is a prerequisite for Ca2+ influx via the activation of voltage-dependent Ca2+ channels and subsequent catecholamine synthesis and secretion. Stimulation of catecholamine synthesis induced by ACh is associated with an activation of tyrosine hydroxylase, which catalyzes the conversion of tyrosine to L-3,4-dihydroxyphenylalanine (DOPA), the rate-limiting step of catecholamine biosynthesis.
We previously demonstrated that nobiletin enhances catecholamine secretion and Ca2+ influx in cultured bovine adrenal medullary cells (J Neurochem., 114: 1030-1038, 2010). Here we report the effects of nobiletin on catecholamine synthesis in the cells. Nobiletin increased the synthesis of 14C-catecholamines from [14C]tyrosine in a time (20-30 min) and concentration (1.0 -100 microM)-dependent manner. Nobiletin (10-100 microM) also activated tyrosine hydroxylase activity. The stimulatory effect of nobiletin on 14C-catecholamine synthesis was not observed when extracellular Ca2+ was deprived from the incubation medium. Several protein kinase inhibitors such as H-89 and KN-93, inhibitors of cyclic AMP-dependent protein kinase and Ca2+/calmodulin-dependent protein kinase II, respectively, suppressed the stimulatory effects of nobiletin on catecholamine synthesis as well as tyrosine hydroxylase activity. On the other hand, nobiletin (1.0-100 microM) inhibited 14C-catecholamine synthesis induced by acetylcholine. The present findings suggest that nobiletin, by itself, stimulates catecholamine synthesis and tyrosine hydroxylase activity, whereas it inhibits catecholamine synthesis induced by acetylcholine in bovine adrenal medulla.

This research was supported, in part, by Grant-in-Aids (23617035, 23590159, 23617036, and 24890286) for Scientific Research (C) from the Japan Society for the Promotion of Science.

Where applicable, the authors confirm that the experiments described here conform with The Physiological Society ethical requirements.

PCC128

Alterations of CRH mRNA expression levels and neurogenesis in hypothalamic after rats exposure to heat

G. Li[1], X. Zhou[1], H. Tao[1], Y. Luo[1] and O. Shido[2]

[1]Ningxia Medical University, Yinchuan, China and [2]Shimane University Faculdy of Medicine, Izumo, Japan

The hypothalamic-pituitary-adrenal axis (HPA axis) is activated by various stresses. The objective of this study was to observe the acute heat exposure on the expression of hypothalamic corticotrophin-releasing hormone (CRH) mRNA and content of serum adrenocorticotropic hormone (ACTH) and corticosterone (CORT) in rat, and investigate hypothalamic neurons proliferation and differentiate. Male Wistar rats (160-180g) were randomly divided into two groups and exposed to heat at 32 degree (heat exposure, HE) or to a room temperature at 24 degree (control, CN). After 7 days of heat exposure, the body core temperature was measured by telemetry (n=4). The relative weight of the pituitary and adrenal gland were determined (n=4), and the expression of hypothalamic CRH mRNA was detected by using real-time fluorescence quantitative polymerase chain reaction (RT-PCR), and content of serum ACTH and CORT were detected by applying enzyme-linked immunosorbent assay (ELISA) (n=6). Another batch rats (male, 180-200g, n=4) was intraperitoneally injected Bromodeoxyuridine (BrdU) daily (50mg/kg) for 6 consecutive days. After commencing heat exposure, on the 7th day of exposure to heat, rats' brains were removed. Immunohistochemical analysis the numbers of BrdU-positive cells and double-stained by a mature neuron marked cell in the hypothalamus were observed. All rats were anesthetized via intraperitoneal administration of petobarbital sodium (70 mg/kg). Values are means ± S.D., compared by ANOVA. Compared with control group, heat exposure did not obviously affect body core temperature ($p>0.05$) or body weight of the rats ($p>0.05$). Seven days heat exposure increased the relative weight of pituitary and adrenal gland (e.g. CN: 0.026±0.002 vs. 0.17±0.02 mg/g, HE: 0.031±0.001 vs. 0.24±0.02 mg/g, $p<0.05$ respectively), and significantly increased ACTH and CORT contents of serum (e.g. CN: 11.66±1.21 vs. 12.38±3.21 mmol/L, HE: 15.23±2.09 vs. 18.45±2.06 mmol/L, $p<0.05$, $p<0.01$ respectively). The CRH mRNA expression levels increased but had no statistical difference ($p>0.05$). The number of BrdU-positive cells were significantly increased (67.8±11.2 for control rats and 117±12.3 for heat exposure, $p<0.05$), while the number of BrdU-positive cells double-stained by a mature neuron marker no significantly increased after 7 days of heat exposure. Acute heat stress affect hypothalamic pituitary-adrenal (HPA) axis, and may lead to the activation hypothalamic proliferation.

Keywords: heat stress; HPA axis; CRH ; mRNA; hypothalamus

Effect of heat exposure on serum ACTH and CORT contents (mmol/L)

Group	n	ACTH	CORT
CN	6	11.66±1.21	12.38±3.21
HE	6	15.23±2.09*	18.45±2.06**

*p<0.05, **p<0.01

Fig. 1 Effect of heat exposure on body core temperature

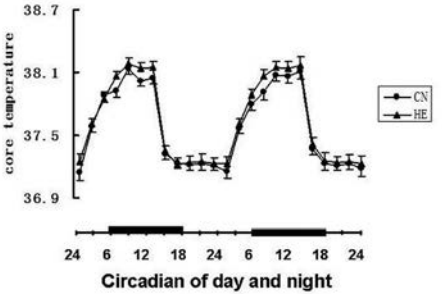

G P Chrousos. The HPA axis and the stress response. Endocrine research, 2000, 26 (4): 513-4

Matsuzaki K, Katakura M, Hara T, et al. Proliferation of neuronal progenitor cells and neuronal differentiation in the hypothalamus are enhanced in heat-acclimated rats. Pflugers Arch. 2009 Aug;458(4):661-73.

Karsten Kluth, Helmut Strasser. Heat acclimation and its relation to resting core temperature and heart rate. Occupational Ergonomics, 2008, 8(4): 185-193

Li GH, Katakura M, Maruyama M et al. Changes of noradrenaline-induced contractility and gene expression in aorta of rats acclimated to heat in two different modes. Eur J Appl Physiol. 2008; 104(1): 29-40.

Eliane Lucassen, Giovanni Cizza. The Hypothalamic-Pituitary-Adrenal Axis, Obesity, and Chronic Stress Exposure: Sleep and the HPA Axis in Obesity. Current Obesity Reports, 2012,1(4): 1223-9

This study was supported by National Natural Science Foundation of China, No. 81060230.

Where applicable, the authors confirm that the experiments described here conform with The Physiological Society ethical requirements.

PCC130

Large conductance calcium- and voltage-gated potassium (BK) channels promote bursting behaviour in murine anterior pituitary corticotroph cells

P.J. Duncan and M.J. Shipston

Centre for Intefgrative Physiology, The University of Edinburgh, Edinburgh, UK

Corticotroph cells from the anterior pituitary are an important component of the hypothalamic-pituitary-adrenal (HPA) axis, which controls the neuroendocrine response to stress. HPA axis dysfunction can have many consequences on health. In response to a stressor, the hypothalamic neuropeptides corticotrophin-releasing hormone (CRH) and AVP act synergistically on corticotrophs to stimulate synthesis and release of adrenocorticotrophic hormone (ACTH). Corticotroph cells are electrically excitable and fire single-spike action potentials as well as showing complex bursting patterns. There is evidence to suggest that large conductance calcium- and voltage-gated potassium (BK) channels promote bursting behaviour in multiple pituitary cell types. The aim of this project was to establish the role of BK channels in corticotroph excitability.

Corticotrophs were cultured from male mice (aged 2-5 months) constitutively expressing green fluorescent protein (GFP) under control of the POMC promoter (POMC-GFP). Electrophysiological recordings were obtained using the perforated patch clamp technique in the current clamp configura-

tion. Under basal conditions, cells had a resting membrane potential of -53.7 ±1.5mV (n = 7, Data are Means ± SEM) and showed low frequency spontaneous action potentials (0.34 ±0.14Hz). CRH and AVP (0.2nM and 2nM respectively) caused a significant ($p < 0.01$, ANOVA) depolarisation of the resting membrane potential to -47.4 ±0.74mV. There was also a significant ($p < 0.01$) increase in firing frequency from 0.34 ±0.14Hz to 0.99 ±0.27Hz. The increase in firing frequency was associated with a transition from a predominantly single-spike firing pattern to a bursting-like behaviour.

To address whether BK channels control bursting activity, experiments were performed on cells treated with BK channel blocker paxilline (1μM). Bursting was quantified by calculating mean event length and mean peaks/event (burst factor, BF). While CRH/AVP significantly increased bursting in control cells, pharmacological inhibition of BK channels greatly reduced, but did not abolish bursting. The role of BK channels in promoting bursting was further investigated using cells isolated from BK knockout mice. These cells also failed to significantly transition from spiking to bursting following CRH/AVP stimulation.

In summary, it can be concluded that the BK channel plays an important role in the generation of bursting behaviour in corticotroph cells. Interestingly, bursting was not completely abolished in paxilline treated or BK knockout cells. This would indicate that although the BK channel is an important component in the generation of bursting behaviour in corticotroph cells, there may be contribution from other ion channels.

Where applicable, the authors confirm that the experiments described here conform with The Physiological Society ethical requirements.

PCC131

Electrophysiological distinction between OT and VP magnocellular neurons does not match their molecular phenotypes

M.P. Silva, R.M. Merino, A.S. Mecawi and W.A. Varanda

Physiology, School of Medicine of Ribeirao Preto - University of Sao Paulo, Ribeirao Preto, SP, Brazil

The phenotypic distinction of magnocellular neurons (MNs) from the supraoptic (SON) nucleus is thought to be relevant to understanding of the effects of specific substances on the electrical activity of these neurons. Although the firing patterns of oxytocin (OT) and vasopressin (VP) neurons differ, they might appear the same both in vivo, and in vitro, making impracticable the phenotypic determination based solely on this feature. The recording of sustained outward rectifying potassium currents (SOR) and inward rectifying hyperpolarization activated currents (IR), presumably present in OT and absent in VP neurons, has been used to determine the phenotype of MCs. Nevertheless, this protocol clearly fails to identify the neurons that produce both peptides in equivalent concentration, i.e., the intermediate phenotype. For this reason, we aimed to analyze the confidence of the electrophysiological protocol by comparing their results with the molecular phenotype of the cells. For this purpose, we used hypothalamic slices containing the SON (200 μm) from Wistar rats (100g). Whole-cell patch-clamp was used to record currents in response to hyperpolarizing voltage steps (from -40 mV to -130 mV). I x V curves were built and the presence or absence of SOR and/or IR was used to distinguish between OT and VP neurons. At the end of the electrophysiological recordings, the cytoplasm of the neuron was sucked into the pipette and used for mRNA reverse transcription, cDNA pre-amplification and qPCR. Our results show that, from a total of 69 neurons, 20 showed a linear IxV relationship typical of vasopressinergic neurons, 48 showed IR and/or SOR current, characterizing oxytocinergic neurons, and one neuron could not be identified by its electrophysiological profile. On the other hand, the molecular analysis showed that 71% (n =49) of the phenotypes did not match the electrophysiological characterization, indicating that vasopressinergic neurons can exhibit both outward and inward rectifying currents. Moreover, 39% of the neurons were identified as intermediate in the qPCR experiments (n=27). Since the amount of cDNA collected from single cells is very small and needed to be amplified prior to the qPCR, a positive control of the pre-amplification was made to check if this process could modify the molecular phenotype of cell. For this purpose, the cDNA was amplified once for a first qPCR followed by a second amplification and another qPCR quantification. We observed that this procedure did not interfere with the molecular phenotype of the cells (n=10). In conclusion, due to the high specificity and reliability offered by RT-qPCR, we suggest that the electrophysiological protocol is not sensitive enough to be used as a single criterion to discriminate the different phenotypes of magnocellular neurons.

CAPES, CNPq, FAPESP and FAEPA

Where applicable, the authors confirm that the experiments described here conform with The Physiological Society ethical requirements.

PCC132

Anti-ulcerogenic and proton pump (H+, K+ ATPase) inhibitory activity of Kolaviron (Garcinia kola biflavonoid) in rats

A.S. Onasanwo[1,2], N. Singh[2], B.S. Olaleye[1] and G. Palit[2]

[1]Physiology, University of Ibadan, Ibadan, Nigeria and [2]Pharmacology, Central Drug Research Institute (C.S.I.R.), Lucknow, India

Kolaviron, isolated from Garcinia kola seed (Family: Guttiferae), is known for numerous medicinal and therapeutic values. The anti-ulcer, anti-inflammatory and antioxidant properties of Garcinia kola seed have been reported. The main mechanisms through which kolaviron exert its anti-secretory with cyto-protective potential has not been elucidated. So, the present research work therefore evaluated anti-secretory and cyto-protective potentials of the anti-ulcer properties of kolaviron using different ulcer models in rats. Cold-restraint (CRU), aspirin (ASP), alcohol (AL), pyloric ligation (PL) induced gastric ulcer models were used to assess its anti-ulcerogenic activity in rats. KV's effects on gastric juice for free and total acidity, peptic activity and mucin secretion were evaluated. The H+,K+-ATPase activity was assayed in gastric microsomes, spectrophotometrically. In CRU model, which is the basic model for screening anti-ulcer agent, KV (100, 150 and 200mg/kg, p.o.) showed percentage protection of 52.1%, 53.5% and 69.0% ($P<0.01$) respectively while omeprazole (10mg/kg, p.o.) showed a protection of 84.6% ($P<0.001$) with reference to the control group. In ASP and PL -induced gastric ulcer model, KV (200mg/kg, p.o.) showed protection index of 68.6% and 67.6% ($P<0.01$) respectively, whereas omeprazole (10mg/kg, p.o.) exhibited 84.3% and 69.0% ($P<0.01$) protection respectively. KV (200mg/kg, p.o.) produced 51.5% ($P<0.01$) protection against gastric mucosal damage, induced by absolute alcohol. Sucralfate (500 mg/kg, p.o.) exhibited 76.3% ($P<0.001$) protection

under the same condition, when compared with the control group. Likewise, KV (200mg/kg, p.o.) reduced free acidity, total acidity and peptic activity by 32.6%, 56.2% and 35.4% (P<0.05) respectively, while omeprazole (10mg/kg, p.o.) significantly reduced free acidity, total acidity and peptic activity by 61.8%, 69.9% and 46.7% (P<0.01) respectively, compared with the control group. The same dose of KV and omeprazole (10mg/kg, p.o.) increased the mucin secretion by 40.1% and 47.9% (P<0.01) respectively, compared with the control. The incubation of KV (60-100μg/ml) with the microsomes, inhibited the inorganic phosphate release from gastric proton pump activity proportionately from 17.2% (288.3μM/hr/mg protein) to 74.3% (89.5μM/hr/mg protein) respectively, with IC50 of 43.8μg/ml. Likewise, omeprazole (10-50μg/ml) inhibited the enzyme from 12.5% (304.5μM/hr/mg protein) to 87.5% (87.0μM/hr/mg protein) respectively, with IC50 = 32.3μg/ml. Kolaviron possesses anti-ulcer activity against experimentally-induced peptic ulcer models and exhibited a proton pump inhibitory activity. So, it has both cyto-protective and anti-secretory potentials. Hence, kolaviron may emanate as a potent anti-ulcer compound.

Post-Doctoral Fellowship by TWAS (Italy) and CSIR (India) is acknowledged.

Where applicable, the authors confirm that the experiments described here conform with The Physiological Society ethical requirements.

PCC134

Disrupted functional connectivity in neural circuit of cardiac vagal baroreflex of mice with neurogenic hypertension

C. Tsai, C. Su and S. Chan

Chang Gung Memorial Hospital, Kaohsiung, Taiwan

A clinical hallmark of hypertension is impairment of the cardiac vagal baroreflex, which maintains stable blood pressure and heart rate under physiological conditions. There is also evidence that oxidative stress in the brain is associated with neurogenic hypertension. However, whether an oxidative stress-induced disruption of the functional connectivity between nucleus tractus solitarii (NTS), the terminal site of baroreceptor afferents, and nucleus ambiguus (NA), the origin of the vagus nerve, underpins the impaired cardiac vagal baroreflex during neurogenic hypertension has not been assessed. the present study tested the hypothesis that an augmented superoxide level in the NTS contributes to the depression of cardiac vagal baroreflex during neurogenic hypertension by disrupting the functional connectivity between the NTS and NA. An experimental model of neurogenic hypertension that employed intracerebroventricular infusion of angiotensin II by osmotic minipump in male adult C57BL/6 mice was used. Based on tractographic evaluations using magnetic resonance imaging/diffusion tensor imaging of the brain stem, we found that the functional connectivity between the NTS and NA was disrupted during neurogenic hypertension, concurrent with depression of the cardiac vagal baroreflex detected by radiotelemetry. We further found that the disrupted NTS-NA functional connectivity was reversible, and was related to oxidative stress induced by augmented levels of NADPH oxidase-generated superoxide in the NTS. We conclude that depression of the cardiac vagal baroreflex induced by oxidative stress in the NTS during neurogenic hypertension may be manifested in the form of dynamic alterations in the functional connectivity between the NTS and NA.

Supported by the National Science Council, Taiwan (NSC98-2923-B-182A-001-MY3) and Chang Gung Medical Foundation, Taiwan (CMRPG871341, CLRPG871342, and OMRPG8C0021).

Where applicable, the authors confirm that the experiments described here conform with The Physiological Society ethical requirements.

PCC135

Identification of sites of sympathetic outflow at rest and during emotional arousal: concurrent recordings of skin sympathetic nerve activity and fMRI in humans

V.G. Macefield[1,2], C. James[1] and L.A. Henderson[3]

[1]School of Medicine, University of Western Sydney, Sydney, NSW, Australia, [2]Neuroscience Research Australia, Sydney, NSW, Australia and [3]Discipline of Anatomy & Histology, University of Sydney, Sydney, NSW, Australia

The sympathetic innervation of the skin primarily subserves thermoregulation, but the system has also been commandeered as a means of expressing emotions. In order to understand the central neural processes involved in emotional processing and the generation of autonomic markers of emotion we recorded skin sympathetic nerve activity (SSNA) concurrently with functional magnetic resonance imaging (fMRI) of the brain at rest in thermoneutral conditions, or while showing subjects neutral or emotionally-charged images from the International Affective Picture System (IAPS). Methods: SSNA was recorded via tungsten microelectrodes inserted into the peroneal nerve in 21 subjects. Gradient echo, echo-planar fMRI was performed using a 3T scanner (Philips Achieva). Two hundred volumes (46 axial slices, TR=8 s, TE=40 ms, flip angle=90 deg, raw voxel size =1.5x1.5x1.5 mm) were collected in a 4s-ON, 4s-OFF protocol. Total sympathetic burst amplitudes were measured during the period between scans. Blood Oxygen Level Dependent (BOLD) changes in signal intensity (SPM5, uncorrected p<0.001) were measured during the subsequent period to account for neurovascular delays. Results: Resting SSNA was positively correlated to signal intensity in the orbitofrontal, frontal and insular cortices on the right side, midcingulate and precuneus, and negatively correlated to signal intensity in the left orbitofrontal and left insula. Positive and negative emotionally-charged images evoked significant increases in total SSNA and signal intensity in the orbital, dorsolateral and ventromedial prefrontal cortices, amygdala, nucleus accumbens and anterior insula. Increases in signal intensity during increases in SSNA occurred in a number of brain regions, including the central and lateral amygdala, dorsolateral pons, thalamus, nucleus accumbens, and cerebellar cortex. Signal intensity decreases during emotionally evoked increases in SSNA occurred in the left orbitofrontal, frontal and right precuneus cortices. Conclusions: We have identified structures in the brain differentially engaged in the generation of sympathetic markers of introspection and emotional arousal.

This work was supported by the National Health & Medical Research Council of Australia.

Where applicable, the authors confirm that the experiments described here conform with The Physiological Society ethical requirements.

PCC136

A new method to quantify the activity of axonal transport of cultured neurons

T. Katakura[1], R. Isonaka[1], T. Takenaka[2] and T. Kawakami[1]

[1]Physiology, Kitasato University School of Medicine, Sagamihara, Kanagawa, Japan and [2]Facuty of Physical Education, Kokushikan University, Tama, Tokyo, Japan

Introduction: Takenaka and co-workers had developed a video-enhanced microscopy technique to visualise axonal transport without staining nerves nor transporting organelles in 1980s. Their method to evaluate axonal transport is very useful but requires a special talent, a keen dynamic vision. We have recently developed another new method to quantify axonal transport with an aid of microcomputer with the open source programme, ImageJ. Method: Preparation of video clips and pretreatment on NIH Image J (1)Enhanced video images were digitized and converted to QuickTime video clips (sampling rate, 10 Hz, duration time,120 seconds). Make video clip every 3 minutes intervals for about an hour. (2) Run ImageJ 1.46, read each video clip and rotate video image 90˜180 degrees if necessary in order to fix the orientation of organelles movement from the left to the right as anterograde axonal transport direction, and the opposite direction as retrograde axonal transport. (3) 128 pixel x 128 pixel area is cropped on ImageJ, in which axonal transport is displayed appropriately. The dimension of the cropped area is fixed and adapted for all the video clips of the same experiment. (4) Subtract adjacent frame (slice) image successively in order to reduce background noise and not moving organelles. Quantification of the activity of axonal transport (Flow analysis) Using KBI plugin, the activity of axonal transport is quantified as the sum of particles which moves more than 3 pixels per second. The velocity of the particle is 0.1 um/s or more. Velocity vectors are calculated (the velocity and the degree of an angle of the moving particle within a fixed area at a given resolution pixels, such as 4, 8, 16, 32 pixels). We can easily distinguish and sum up the number of anterograde transporting particles and retrograde transporting particles by the sign of an angle of velocity vector, where the former has a plus sign and the latter has a minus sign respectively. Results: Parameters of widthXy and stepXy 4 pix and greater value is suitable for the velocity calculation. With 4 pix or 8 pix value, the results from flow analysis are coincided with the results obtained from our traditional quantification method. 16 pix or more value sometimes dismissed moving particles and thus the calculated values are not consistent with our previous results. Concluding Remarks: Using NIH ImageJ with KBI plugin, the progressive movement of particles can be analyzed. Orientation, velocity, and the number of transported organelles within a fixed area are calculated easily from one video clip. (1) We define the activity of axonal transport as the sum of a particle which possesses the moving velocity more than 0.1 um/s within an limited area. (2) We suppose the velocity of particles is directly proportional to the activity of axonal transport.

Where applicable, the authors confirm that the experiments described here conform with The Physiological Society ethical requirements.

PCC137

Visceral nociceptive afference could facilitate the response of subnucleus reticularis dorsalis to Acupoint stimulation

P. Rong, L. Li, L. Yu, X. Gao and B. Zhu

Physiology, Institute of Acup.-Moxi., Beijing, China

Objective: To explore the area and sensitization variance of acupoint when internal organs is under pathological condition. To observe quantity-effect variance of subnucleus reticularis dorsalis to electro-acupuncture under both physiological and pathological condition. To explain medulla oblongata mechanism of acupoint sensitization. Method: Mustard oil (20μl2.5% Sigma-Aldrich, St.Louis, MO) was imported into colon and rectum of male SD rats (anaesthetised with pentobarbital sodium 50-60mg.kg-1) in order to observe its influence to acupoint sensitization. SRD Neuron activities were recorded. Visceral nociceptive stimulus was generated by colorectal distension (CRD with an intensity 40 mmHg). Quantity-effect variance of neuron activity to electroacupuncture to “Zusanli-Shangjuxu” area both before and after CRD was observed. Result: Visceral inflammation could facilitate SRD neuron activity to acupoint stimulation. Visceral nociceptive afference could enhance neuron activity to acupoint acupuncture. WDR neuron activity caused by electro-acupuncture increased when visceral nociception is raised. Conclusion: the area of acupoint could be changed if visceral function changes, also, sensitivity of acupoint would change too.
Key words: Sensitization of acupoints, Neurogenic inflammatory reaction, subnucleus reticularis dorsalis, colorectal distension (CRD)

Zhu B et al. (2004). Brain Res. 1011,228-237.

Chang L et al. (2003). Am J Gastroentero l98,1354-1361.

Miranda A et al. (2004).Gastroenterology.;126,1082-1089.

Peles S et al. (2004).J Physiol. 560, 291-302.

Dugast C, Almeida A and Lima D. (2003). Eur J Neurosci. 18,580-588.

This study was supported by the National Basic Research Program of China (973 Program, 2011CB505200, 2012CB518503) and National Natural Science Foundation of China (C30973798).

Where applicable, the authors confirm that the experiments described here conform with The Physiological Society ethical requirements.

PCC138

Peripheral nerve conduction correlation with body mass index of healthy individuals

D. Thakur[1], B.H. Paudel[1] and C.B. Jha[2]

[1]Basic & Clinical Physiology, B.P.Koirala Institute of Health Sciences, Dharan, Nepal and [2]Anatomy, B. P. Koirala Institute of Health Sciences, Dharan, Nepal

Nerve conduction study (NCS) assesses peripheral nerve functions and its parameters are known to vary with anthropometric measurements. This cross sectional normative study was done in Electro-diagnosis Lab II of department of Basic and Clinical Physiology. It was aimed to study the relation of BMI on NCS variables of the peripheral nerves of upper and lower limbs. The study was done in 34 consenting healthy adults of either sex. The anthropometric factors, compound muscle

action potential (CMAP) and sensory nerve action potential (SNAP) were recorded using standard technique. The relation of BMI with NCS variables were analyzed using Pearson's correlation test. After the adjustment of other anthropometric factors, BMI (21.8±2.11 Kg/m2) showed a negative correlation with the CMAP duration of most of the motor nerves: right median (r= -0.388, p<0.005), left median (r= -0.342, p<0.05), left ulnar (r= -0.375, p<0.005), left tibial and right common peroneal (r= -0.347, p<0.05). The CMAP amplitudes of the right median (r= -0.341, p<0.05), left median (r= -0.456, p<0.01) and right common peroneal (r= -0.361, p<0.05); CMAP latencies of bilateral ulnar, left radial and right common peroneal were also negatively correlated. However, a positive correlation was seen with the SNAP amplitude of the right sural (r= 0.441, p<0.01) and a negative correlation with conduction velocity of left median sensory nerve (r= -0.420, p<0.05). The SNAP duration, latency and CMAP F-waves latency did not show any correlation. BMI showed a significant correlation with the NCS parameters of most of the motor and few sensory nerves. Diagnostic conclusions made from the nerve conduction data without corrections for the BMI may be invalid in patients who are at its extreme. This must be also considered while developing standard/reference normative data for different nerves.

We would like to acknowledge the technical staffs and the participating volunteers for supporting the research.

Where applicable, the authors confirm that the experiments described here conform with The Physiological Society ethical requirements.

PCC139

Autoantibodies and relation to clinical features in Sudanese patients with acquired autoimmune myasthenia gravis: a case control study

R. Badi[1], M. Elzubeir[2], A. Musa[1], L. Jacobson[3], E. Khalil[2], A. Vincent[3] and A.E. Ahmed[1]

[1]Physiology, University of khartoum, Khartoum, Sudan, [2]University of Khartoum, Khartoum, Sudan and [3]Oxford University, Oxford, UK

Prevalence of autoantibodies targeting the neuromuscular junction in autoimmune myasthenia gravis (MG) varies among different populations, probably due to genetic and environmental differences. We present a cross sectional, case-control study carried in the years 2011- 2012. The study aimed to detect the prevalence of AChR-Abs, and MuSK-Abs in Sudanese MG patients, and to relate the autoantibodies status to their clinical presentation. The study was ethically approved. 59 MG cases were recruited from two national MG centers in Khartoum and matched by age and sex to 157 controls. AChR-Abs and MuSK-Abs were measured in plasma, using radioimmunoprecipitation assay (RIPA) (1).Plasma from patients who tested negative for both autoantibodies by the RIPA were further tested for low affinity AChR-Abs by the Cell Based Assay (CBA) (2). AChR-Abs were detected in; 76.3% of all MG patients (median, IQR= 1.6, 0.2- 26 nmol/L), 80 % of generalized MG patients (GMG), 64 % of ocular MG patients, and 3.8% of the controls (median, IQR= 0.1, 0.01– 0.16 nmol/L). MuSK-Abs were detected in; 16.7% of AChR-Ab-ve GMG patients, 1/33 of AChR-Ab+ve GMG patients, and 1/106 of the controls. 20% of MG patients remained seronegative for both autoantibodies. AChR-Ab+ve GMG patients and seronegative GMG patients were not significantly different regarding disease severity. Seronegative GMG patients were all females (7/7) (P<.05, Fisher's Exact test). The prevalence of associated autoimmune diseases (AuID) was 86 %(6/ 7) in seronegative GMG patients and 14% (5/35) in AChR-Ab+ve GMG patients; relative risk 6 (2.5 to 14.27) (P= 0.001, Fisher's Exact test). MuSK-Ab+ve cases were two late onset MG males (onset >40 years), one early onset MG female, and had dominant bulbar symptoms. This study provided the first insight into autoantibody profile of MG patients in an Arabian- African population. The detection rates of AChR-Abs and MuSK-Abs were within the range of detection rates in other series. Some clinical features (sex and AuID) were found to be related to the autoantibody status of MG patients. These findings suggest involvement of factors like sex and genetic susceptibility to autoimmune diseases in determining the pathogenesis and homeostasis of autoantibodies in MG.

Hoch, W., J. McConville, S. Helms, J. Newsom-Davis, A. Melms and A. Vincent (2001). "Auto-antibodies to the receptor tyrosine kinase MuSK in patients with myasthenia gravis without acetylcholine receptor antibodies." Nat Med 7(3): 365-8.

Leite, M. I., S. Jacob, S. Viegas, J. Cossins, L. Clover, B. P. Morgan, D. Beeson, N. Willcox and A. Vincent (2008). "IgG1 antibodies to acetylcholine receptors in 'seronegative' myasthenia gravis." Brain 131(Pt 7): 1940-52.

1st – We would like to acknowledge the following bodies for funding the research:

1-The Ministry of Higher Education and Scientific Research, Khartoum, Sudan

2-The Nuffield Department of Clinical Neurosciences, U of Ox, UK.

2nd - Our sincere gratitude for Professor Angela Vincent for encouraging, supporting and directing the collaboration between the Department of Physiology, U of K and the Nuffield Department of Clinical Neurosciences, U of Ox

Where applicable, the authors confirm that the experiments described here conform with The Physiological Society ethical requirements.

PCC140

Noisy vestibular stimulation modulates neuronal activities of the substantia nigra through vestibulo-thalamo-striatal pathway in Parkinsonian rats

H. Koo[1,2], N. Kim[1,2], M. Kim[1,2] and B. Park[1,2]

[1]Physiology, Wonkwang University School of Medicine, Iksan, Republic of Korea and [2]Brain Research Institute, Wonkwang University, Iksan, Republic of Korea

Galvanic noisy vestibular stimulation (NVS) to Parkinson disease (PD) patients could relieve balance impairments. This study was designed to observe changes of the neuronal activity in the substantia nigra pars reticulata (SNr) of an animal PD model following NVS and its neural pathway. To make an animal model of PD, 6-hydroxydopamine (6-OHDA) was injected to the right medial forebrain bundle of Sprague-Dawley rats. Rats (male, 250~300g, n=35) were anesthetized with isoflurane. Two to three weeks after 6-OHDA lesion, extracellular single-unit activity of the ipsilesional SNr was recorded before and after NVS of the horizontal semicircular canal nerve unilaterally or bilaterally under anesthesia. The baseline neuronal activity was measured during 2 minutes before NVS. NVS continued for 5 minutes and then a recording was resumed for 2 minutes. Extracellular single-unit activity of the parafascicular nucleus (PFN) of the thalamus to stimulation of the vestibu-

lar nerve was recorded. Evoked field potentials with polysynaptic nature were recorded in the contralateral PFN to the stimulation site but not in the ipsilateral PFN. Recording the single-unit activity of the ipsilesional SNr revealed that slow oscillations (<2.5Hz) of SNr spike trains significantly increased following 6-OHDA lesion. These slow oscillations were remarkably reduced and the irregularity of firing pattern was also significantly decreased by unilateral or bilateral NVS. Furthermore, the contralateral or bilateral NVS to hemi-lesioned side tended to decrease the neuronal activity of SNr neurons, while the ipsilateral NVS showed the increase tendency of that, relatively. Theses electrophysiological evidences suggest that the noisy electrical stimulation to the peripheral vestibular apparatus may modulate abnormal neuronal activities of basal ganglia in an animal model of PD through the vestibulo-thalamostriatal pathway.

Pal S et al. (2009). J Vestib Res 19, 201-207.

Pan W et al. (2008). J Neurol 255, 1657-1661.

Shiroyama T et al. (1995). Brain Res 704, 130-134.

Smith Y et al. (2009). Brain Res Bull 78, 60-68.

Lai H et al. (2000). Brain Res, 872, 208-214.

Supported by a grant from the Korea Basic Science Institute.

Where applicable, the authors confirm that the experiments described here conform with The Physiological Society ethical requirements.

PCC141

Modulation of immune function by the cerebellar fastigial nucleus via its GABAergic projections to the hypothalamus

Y. Peng, B. Cao, J. Lu and Y. Qiu

Nantong University, Nantong, China

We have previously reported that cerebellum modulates immune system function. Since there is no direct structural connection between cerebellum and immune system, exploring pathways mediating cerebellar immunomodulation is important to understand the phenomenon. It has been well known that hypothalamus is a crucial immunoregulatory center, which modulates immune cells via sympathetic system and hypothalamic-pituitary-adrenal axis. Moreover, direct bidirectional connections between the cerebellum and hypothalamus that constitute cerebellar-hypothalamic circuits have been found. Based on these findings, we hypothesized that direct cerebellar-hypothalamic projections transmit cerebellar immunoregulatory information to hypothalamus, through which the regulatory information is then conveyed to immune cells. Here, we focused on cerebellar fastigial nucleus (FN), one of three cerebellar nuclei, to investigate its immunoregulatory pathway via hypothalamus. Sprague-Dawley rats (either sex, 220-240 g) were deeply anesthetized with pentobarbital (55 mg/kg, i.p.) before any surgery and generally recovered to normal state 3-4 h after the anesthesia. Texas red dextran amine (TRDA), a neuroanatomical anterograde tracer, was delivered into FN of rats that had been mounted in a stereotaxic frame following deep anesthesia to observe cerebellar-hypothalamic projections. Fluoro-Ruby (FR), a retrograde tracer, was injected into lateral hypothalamic area (LHA) and 8 days later, the cerebellar sections were stained with immunohistochemistry for GABA. To change cerebellar-hypothalamic GABAergic transmission, we microinjected vigabatrin, an inhibitor of GABA-transaminase that degrades GABA, or 3-mercaptopropionic acid (3-MP), an antagonist of glutamic acid decarboxylase that synthesizes GABA, bilaterally into FN. Immune function, including concanavalin A-induced T cell proliferation, anti-sheep red blood cell (SRBC) IgM antibody and natural killer (NK) cell cytotoxicity, was measured by CFSE/CD3 double labeling, ELISA and flow cytometry, respectively, on day 3 after the drug injection. Simultaneously, GABA content in hypothalamus was tested by HPLC. We found that the TRDA-labeled fibers from FN traveled through superior cerebellar peduncle (SCP), crossed in decussation of SCP, and primarily terminated in LHA. The retrograde tracing with FR from LHA to FN confirmed the direct projection route. Many FR-positive neurons in FN were GABA-immunoreactive. Compared with intact or saline-treated rats, the vigabatrin treatment increased both number of GABA-immunoreactive neurons in FN-LHA projections and GABA content in hypothalamus. Simultaneously, vigabatrin led to a decrease in T cell proliferation, in serum anti-SRBC IgM antibody level and in NK cell cytotoxicity. In support of these findings, 3-MP caused changes that were all opposite to those induced by vigabatrin. These results show that cerebellar FN has a direct GABAergic projection to hypothalamus and suggest that this projection mediates cerebellar immunomodulation.

Where applicable, the authors confirm that the experiments described here conform with The Physiological Society ethical requirements.

PCC142

Analysis of parietal EEG following hippocampal injection with kainic acid in rats

A. Issuriya[1], E. Kumarnsit[1], U. Vongvatcharanon[2] and C. Wattanapiromsakul[3]

[1]Physiology, Faculty of science, Prince of Songkla University, Hadyai, Songkhla, Thailand, [2]Anatomy, Faculty of Science, Prince of Songkla University, Hadyai, Songkhla, Thailand and [3]Phamacognosy, Faculty of Phamaceutical Science, Prince of Songkla University, Hadyai, Songkhla, Thailand

Electroencephalogram (EEG) pattern represents the electric activity of brain cells. Its recordings have helped clinicians for decades to diagnose specific diseases of the central nervous system. The present study characterized behaviors and EEG patterns after injection with kainic acid (KA) in rats. Male Wistar rats (300-350g, n=6) were anesthetized with 60 mg/kg Zoletil® 100 (i.m.). Assessment of depth anesthetic was evaluated by gentle toe pinch withdrawal reflex. During the surgery, the depth of anesthetic was also evaluated periodically and additional anesthetic was injected to animal that was found with any reaction of too light anesthesia. Then rats were implanted stainless steel screw electrodes on both sides of the parietal cortices (AP; -4, ML; 4) for EEG recording and a cannula for KA injection into right dorsal hippocampus (AP; -4.2, ML; 3.6, DV; 3.8). Rats were sacrificed by thiopental sodium overdose injection. Results showed that the injection of KA (1 nmol/μl) 1 μl into hippocampus (continuously 7 days) induced hyperactivity of hippocampal neurons via kainate receptor. KA administration did not induce neither increase in explorative behavior nor change in learning and memory behavior, observed in Y-maze test (5min.). EEG signals of individual rats were recorded for 2-h period through connection of recording cables. EEG signals were digitized at 400 Hz by a PowerLab/4SP system (AD Instruments) with 12-bit A/D, and stored in a PC through the Chart program software. The EEG signals were processed through 1.25 – 45 Hz band pass filter. The digitized EEG data were segmented into 1024-point (50%

overlap) and the signals were converted to power spectra by the fast Fourier transform algorithm (Hanning window cosine transform). Intrahippocampal injection of KA induced paroxysmal discharges in the ipsilateral EEG. This abnormality of brain wave of frequent spikes occurred either in isolated or short bursts. Saline injection did not induce any change in EEG patterns. EEG spectral power analysis revealed the ipsilateral increase in power density (μV2/Hz) of slow wave activity (0.125-5 Hz, 18.55%) and decrease in power density of fast wave activity (23-45 Hz, 6.97%) compared to pretreatment levels ($p<0.05$,compared by T-test). The 7th day after injection (last day) rats with KA administration showed only the decrease in theta activity (4-7 Hz, 5.32%). No similar finding was observed contralaterally. This study demonstrated cortical EEG characteristics following activation of hippocampal neurons via glutamate receptor. The data suggest that EEG study is sufficiently accurate to identify brain site and time dependent effects of neurodegenerative induction.

This work was supported by Prince of Songkla Scholarship, Prince of Songkla University, Thailand

Where applicable, the authors confirm that the experiments described here conform with The Physiological Society ethical requirements.

PCC143

Exercise promotes axon regeneration of newborn projection neurons in rats after stroke

Q. Zhang and F. Sun

Dept. Neurobiology, Fudan University, Shanghai, China

Neurogenesis exists in adult brains of mammalian, which can be stimulated by hypoxic/ischemic brain injury. Stroke-induced newborn striatal neurons can develop long axons to project into the substantia nigra and integrate with preexisted neural networks. Rehabilitative training improves striatal neurogenesis in brains after stroke. However, whether it can improve axon-regeneration of new striatonigral projection neurons remains unknown, which is critical anatomical basis for recovering motor function. Therefore, we investigated the effects of exercise on axon-regeneration of newborn projection neurons in rat brains following ischemic stroke. Adult male Sprague–Dawley rats (250-280g, n=25) were divided into stroke (MCAO) and stroke+exercise (MCAO+EX) groups. Rats were anesthetized with 10% chloral hydrate (360 mg/kg, i.p.) and then subjected to a transient middle cerebral artery occlusion (MCAO) to induce ischemic stroke, followed by 30 minutes of exercise training daily for 5 to 28 days after MCAO (MCAO+EX). Motor function was tested using the rotarod test. We used fluorogold (FG) nigral injection to trace striatonigral and corticonigral projection neurons, and GFP-targeting retroviral vectors combined with FG double labeling (FG+-GFP+) to detect newborn projection neurons. The results further showed that such exercise could improve recovery of motor function of rats after MCAO. Under this experimental condition, we observed that FG+-GFP+ cells were detected in ipsilateral cortex and striatum of rats to MCAO, suggesting existence of newborn striatonigral and corticonigral projection neurons in ischemic injured brain, which was consisted with our previous reports (1,2). Interestingly, exercise poststroke could significantly increase the number of FG+-GFP+ neurons in ipsilateral striatum and cortex. The number of GFP+-FG+ cells in MCAO+EX rats increased 2.52-fold and 1.78-fold of MCAO rats in the cortex and striatum, respectively. This data suggested that exercise enhanced the capacity for axon-regeneration of newborn neurons. Moreover, the tyrosine hydroxylase immunostaining results showed that exercise significantly increased dopaminergic neurons in the substantia nigra, a region remote from the ischemic territory, compared with the controls. In summary, present study provides the first evidence that passive exercise poststroke can effectively improve axon-regeneration of newborn projection neurons and accelerate the reestablishment of new neural circuitry within the basal ganglia after ischemic injury, which should provide very important anatomical foundation for the recovery of motor behavioral function. Our results illustrate mechanisms, at cellular level, for passive rehabilitative treatment poststroke in the clinic.

Sun X, Zhang QW, Xu M, et al. New striatal neurons form projections to substantia nigra in adult rat brain after stroke. Neurobiol Dis. 2012;45: 601-609.

Guo JJ, Liu F, Sun X, Huang JJ, Xu M, Sun FY. Bcl-2 enhances the formation of newborn striatal long-projection neurons in adult rat brain after a transient ischemic strok. Neurosci Bull. 2012;28: 669-679.

This work was supported by grants from National Nature Science Foundation of China (81030020 and 30770660).

Where applicable, the authors confirm that the experiments described here conform with The Physiological Society ethical requirements.

PCC144

Multisensory integration in ferret auditory cortex: Effects of inactivating visual cortex

S.M. Town, K.C. Wood and J.K. Bizley

Ear Institute, UCL, London, UK

Neurons in ferret (*Mustela putorius furo*) auditory cortex respond to simple visual stimuli and auditory responses to broadband noise can be modulated by the presence of visual stimuli (Bizley et al., 2007). Visual interactions in auditory cortex may arise from input connections from neurons in visual cortex, parietal cortex and the suprageniculate nucleus of the thalamus (SGN). However the functional relevance of these inputs remains to be demonstrated. Here, we investigated the role of a sub-region of visual cortex – the suprasylvian cortex (SSY) - in multisensory integration. SSY sends dense projections to auditory cortex, particularly regions of anterior auditory cortex and we studied the effects of SSY inactivation on responses of auditory cortical neurons.

Multi-unit neural activity was recorded at 13 sites within the auditory cortex of three ferrets anesthetized through intravenous administration of ketamine (5 mg kg^{-1} hr^{-1}) and medetomidine (0.022 mg kg^{-1} hr^{-1}). Neural activity within auditory cortex was recorded before and during inactivation using cooling loops that reduced the cortical surface temperature of SSY to between 4 and 7°C. Simultaneous recording of neural activity within SSY of two ferrets confirmed the efficacy of inactivation through cooling.

Auditory cortical units were found in which cooling significantly reduced visual but not auditory responses. Furthermore units were found in which visual modulation of auditory responses was selectively reduced by cooling. We also found evidence for the involvement of regions outside of SSY as several units demonstrated visual responses robust to cooling. Units were also discovered for which cooling reduced visual responses but only within a circumscribed period of the response. Additionally in sporadic cases, cooling led to the

emergence of visual responses or the visual modulation of auditory responses within auditory cortex.
Together these preliminary findings support the role of SSY in multisensory integration within auditory cortex, but also indicate the involvement of additional brain regions possibly including other subdivisions of visual cortex, parietal cortex and SGN. Our results also suggest that SSY inputs to auditory cortex may involve both excitatory and inhibitory mechanisms. Future work will focus on elucidating the contributions of regions beyond SSY to visual activity within auditory cortex and their relevance for behaviour.

Bizley JK, Nodal FR, Bajo VM, Nelken I & King AJ (2007) *Cereb Cortex* **17**, 2172-2189.

Funded by the BBSRC (grant no. BB/H016813/1) and a Royal Society Dorothy Hodgkin Research Fellowship to J.K.B.

Where applicable, the authors confirm that the experiments described here conform with The Physiological Society ethical requirements.

PCC145

Magnesium L-threonate prevents and restores memory deficits associated with neuropathic pain by inhibition of TNF-α

J. Wang, L. Zhou and X. Liu

Department of Physiology, Zhongshan Medical School of Sun Yat-Sen University, Guangzhou, China

Clinical studies have shown that about two third of patients with chronic pain suffer from short-term memory (STM) deficits and effective drug for treatment of the neurological disorder is lack at present. We tested whether chronic oral application of magnesium L-threonate (MgT), which has been shown to improve memory in normal and aging animals by elevating Mg2+ in brain, could prevent or restore the STM deficits induced by spared nerve injury (SNI), an animal model of chronic neuropathic pain. The mechanisms underlying the effect of MgT on STM deficits were also investigated. The experiments were conducted in a random and double blind fashion in adult male rats. MgT was administrated via drinking water at a dose of 609 mg/kg/d for 2 weeks, starting either one week before SNI (preventative group) or one week after SNI (therapeutic group), and the water without drug served as control. STM was accessed with a novel object recognition test (NORT), followed by recording of long-term potentiation (LTP) in hippocampus in vivo and the measurement of the expression of tumor necrosis factor-α (TNF-α) with Western Blot or Immunohistochemistrical staining. AMPA and NMDA receptor (NMDAR) currents were recorded with patch clamp in CA1 neurons in acute and cultured hippocampal slices. We found that chronic oral application of MgT was able to prevent and restore the deficits of STM and of LTP at CA3-CA1 synapses in rats under urethane anesthesia induced by SNI. Furthermore, both preventative and therapeutic chronic oral application of MgT blocked the up-regulation of TNF-α in hippocampus, which has been previously shown to be critical for memory deficits. SNI reduced NMDAR current and the effect was dramatically attenuated by elevating extracellular Mg2+. In cultured hippocampal slices, chronic application of recombinant rat TNF-α (rrTNF-α) for 3d reduced NMDAR current in a concentration-dependent manner and the effect was again blocked by elevating extracellular Mg2+. Our data suggested that oral application of MgT was able to prevent and restore the STM deficits in animal model of chronic neuropathic pain by revising the dysfunction of NMDAR produced by over-expression of pro-inflammatory cytokines. Oral application of MgT may be a simple and potent means for handling this form of memory deficits.

Ren WJ, Liu Y, Zhou LJ, Li W, Zhong Y, Pang RP, Xin WJ, Wei XH, Wang J, Zhu HQ, Wu CY, Qin ZH, Liu G, Liu XG. Peripheral nerve injury leads to working memory deficits and dysfunction of the hippocampus by upregulation of TNF-alpha in rodents. Neuropsychopharmacology 2011; 36:979-992.

Funding/Support: This work was supported by grants from the National Natural Science Foundation of China (No. U1201223, 30970957 and 31000489) and a grand from the bureau of science and technology of Guangzhou city (No. 50000-4205009).

Where applicable, the authors confirm that the experiments described here conform with The Physiological Society ethical requirements.

PCC146

An excitatory preoptic pathway for cutaneous vasoconstriction in fever

R. McAllen, M. Tanaka and M.J. McKinley

Florey Institute, Parkville, VIC, Australia

The central neural pathways for thermoregulation and fever are not well understood. It is known, however, that cutaneous vasoconstrictor nerves such as those to the rat's tail are under tonic inhibitory control from the preoptic area [1]. Thermoregulatory and febrile control of those vessels is thought to be brought about by variations in the inhibitory tone from preoptic warm-sensitive neurons, acting on sympathetic premotor neurons in the medullary raphé [2]. Recently, however, we identified an excitatory pathway from the preoptic area to the medullary raphé, and found that this mediated the reflex vasoconstrictor response to cooling the skin [3]. We wondered whether that excitatory pathway could also be responsible for the tail vasoconstrictor response in fever.
Two types of experiment were performed on urethane-anaesthetised rats (1.4 g/kg i.v), which were artificially ventilated but not paralysed. Experimental fever was induced by Prostaglandin E2 (PGE2), given by microinjection either into the rostromedial preoptic area [1] (0.2ng in 60nl) or into the lateral cerebral ventricle (50ng in 1.5μl). Single or few-unit nerve activity was recorded from tail vasoconstrictor fibres [1, 3].
In the first series, preoptic microinjections of PGE2 were followed by microinjections into the same site of either the inhibitory amino acid, glycine (0.5M, 60nl), or vehicle. Preoptic glycine (but not vehicle) injections roughly halved the tail vasoconstrictor fibre response to preoptic PGE2, suggesting that an excitatory output signal from that region had been blocked.
In the second series, the antagonist of ionotropic glutamate receptors, kynurenate (50mM, 120nl), was injected into the medullary raphé. Raphé kynurenate (but not vehicle) injections fully reversed the tail vasoconstrictor fibre response to intra-preoptic or intracerebroventricular injections of PGE2.
These findings suggest that in PGE2-induced fever, an excitatory output signal from the preoptic area contributes to the tail vasoconstrictor response. They also show that this response depends entirely on excitatory (ionotropic glutamatergic) neurotransmission in the medullary raphé. Directly or indirectly, therefore, a descending excitatory pathway from the preop-

tic area mediates rat tail vasoconstrictor responses to experimental fever. These findings alter our understanding of thermoregulatory mechanisms in fever. It remains to be shown whether fever uses the same descending excitatory pathway that mediates tail vasoconstrictor responses to cold skin [3].

Tanaka, M., M.J. McKinley, and R.M. McAllen, Am J Physiol Regul Integr Comp Physiol, 2009. 296(4): p. R1248-57.

Morrison, S.F., J Appl Physiol, 2011. 110(5): p. 1137-49

Tanaka, M., M.J. McKinley, and R.M. McAllen, J Neurosci, 2011. 31(13): p. 5078-88.

This work was supported by the National Health and Medical Research Council

Where applicable, the authors confirm that the experiments described here conform with The Physiological Society ethical requirements.

PCC147

Taste perception of coffee induces similar electroencephalographic response to drinking coffee

E. Kumarnsit[1], N. Samerphob[2] and S. Watanasit[2]

[1]Physiology, Faculty of Science, Prince of Songkla University, Hatyai, Songkhla, Thailand and [2]Biology, Faculty of Science, Prince of Songkla University, Hatyai, Songkhla, Thailand

Refreshing foods and beverages have been used in daily life to improve alertness and mood. Coffee is one of the most common drinks which are related to performance enhancement. However, its effects on brain function have been unclear in terms of coffee ingredient or taste perception impact. This study investigated electroencephalographic (EEG) patterns after receiving taste without swallowing and normal drinking of coffee in both genders of 20 subjects aged between 20 to 30 years old. This project was approved by ethical committee for using human subjects. Electrodes were placed on the scalp over the frontal and parietal cortices. Freeze dried instant coffee (Moccona, Royal gold) was purchased from commercial source. EEG signals from individual subject were recorded for 5 min for baseline levels and 10 min following taste alone or drinking of coffee. Fast Fourier Transform (FFT) algorithm was used to analyze EEG signal in frequency domain. The parietal EEG analysis showed that slow frequency activity (0.8 – 4.5 Hz, delta band) was reduced by both taste and drinking of coffee with similar magnitude. In addition, high frequency activity (18 – 35 Hz, beta2 band) of parietal EEG was increased by both types of trials. No significant change was detected in frontal EEG. These patterns are general characteristics of refreshing beverages. In summary, taste perception was demonstrated to be as effective as drinking of coffee ingredients. These findings suggest that taste perception might induce conditioned response through associative learning. Besides, coffee taste may be alternative choice to prevent relapse during coffee withdrawal period.

Nonlinear dynamical systems effects of homeopathic remedies on multiscale entropy and correlation dimension of slow wave sleep EEG in young adults with histories of coffee-induced insomnia Homeopathy, Volume 101, Issue 3, July 2012, Pages 182-192

Iris R. Bell, Amy Howerter, Nicholas Jackson, Mikel Aickin, Richard R. Bootzin, Audrey J. Brooks

The Acute Physiological and Mood Effects of Tea and Coffee: The Role of Caffeine Level

Pharmacology Biochemistry and Behavior, Volume 66, Issue 1, May 2000, Pages 19-28

Paul T. Quinlan, Joan Lane, Karen L. Moore, Jennifer Aspen, Jane A. Rycroft, Dawn C. O'Brien

Effects of homeopathic medicines on polysomnographic sleep of young adults with histories of coffee-related insomnia Sleep Medicine, Volume 12, Issue 5, May 2011, Pages 505-511

Iris R. Bell, Amy Howerter, Nicholas Jackson, Mikel Aickin, Carol M. Baldwin, Richard R. Bootzin

This research was supported by the department of Physiology, Faculty of Science, Prince of Songkla University, Thailand.

Where applicable, the authors confirm that the experiments described here conform with The Physiological Society ethical requirements.

PCC148

Excitatory interneurons that mediate non-reciprocal excitatory reflex in primate spinal cord: their input-output relations and firing pattern during voluntary wrist movement

G. Kim[1,2], T. Takei[1,2] and K. Seki[1,3]

[1]Dept. Neurophysiol, Nat. Inst. Neurosci., Kodaira, Japan, [2]Dev. Physiol, Nat. Inst. Physiol. Sci, Okazaki, Japan and [3]PREST, Japanese Sci. Tech. Agency, Tokyo, Japan

Reflex circuit in the spinal cord has been extensively studied in the anesthetized animals, and several type of interneuron has been identified as a key neurons that define unique input-output relations for each reflex. However, there are no direct evidence showing their function in the generation and control of muscle activity during voluntary movement. To address this issue, we identified spinal interneurons (INs) mediating segmental reflex from proprioceptors and examined their activities during voluntary movements. Three macaque monkeys were trained to perform a wrist flexion and extension task with an instructed delay period. An oval spinal chamber was implanted to vertebrae (C4-T1) and a glass-coated elgiloy microelectrode was used to record the activity of INs. Electromyographic activities (EMGs) were recorded from wrist flexor and extensor muscles (n=8-12) by chronically implanted wire electrodes. In addition, nerve cuff electrode was implanted to the deep radial (DR) nerve that innervates most of wrist extensor muscles. Surgeries for these implants were performed while the animals were anesthetized with isoflurane (1.0% – 2.0% in 2:1 O2:N2O) or sevoflurane (1.5% – 3.0% in 2:1 O2:N2O) under aseptic conditions. Experiments in this study were performed in accordance with the National Institutes of Health Guidelines for the Care and Use of Laboratory Animals and were approved by the Animal Research Committee at the National Institute for Physiological Sciences, Japan. In the monkeys performing wrist movement, we identified the peripheral input to INs by their responses to the electrical stimulation to the DR nerve. The INs that responded within a segmental latency of 1ms were identified as the cells with direct projection (first-order INs) from DR afferent nerve. Output of these INs to muscles were examined by the spike-triggered averaging of EMGs. In the 81 INs that showed monosynaptic response to the DR stimuli, 32 INs (39%) showed postspike effects to one or more muscles (22 post-spike facilitations (PspF, 69%), 7 post-spike suppressions (PspS, 22%), or 3 PspF & PspS (9%)). Among 22 INs with PspF, 18 INs (82%) showed their PspF exclusively in the extensor muscles, and number of muscle that showed PspF from each INs ("muscle field") was 2.0±1.0. These results suggest that the spinal INs that mediating proprioceptive input from extensor muscles preferen-

tially facilitated the extensor muscles (autogenetic facilitation). Next, we analyzed the modulation of firing rate of the first-order INs as a function of task sequence. First-order INs with PspF to extensor muscles (n=18) showed sustained activity throughout the extension torque. In contrast, the first-order INs without PspF in any tested muscles (n=49) transiently increased their firing during torque onset, but it decreased significantly while monkey sustained extension torque ($p < 0.01$). These results suggest that disynaptic, excitatory reflex pathway that mediating autogenetic facilitation of extensor muscle is involved in the maintenance of static muscle force during voluntary movements. We propose that voluntary muscle activity could be automatically augmented by this reflex system.

This work was supported by MEXT(18020030, 18047027,21700437) and JST-PREST.

Where applicable, the authors confirm that the experiments described here conform with The Physiological Society ethical requirements.

PCC149

Protective effects of Astragaloside IV on oxygen and glucose deprivation-induced ischemic injury in PC12 cells

B. Chiu[1], C. Chang[2], C. Wang[3,4], Y. Hsu[1], J. Yu[1], C. Chen[2], C. Hsu[5], M. Chang[6] and B. Cheng[2,3]

[1]Department of Chinese Medicine, Chi Mei Medical Center, Tainan, Taiwan, [2]Department of Biotechnology, Southern Taiwan University of Science and Technology, Tainan, Taiwan, [3]Department of Surgery, Chi Mei Medical Center, Tainan, Taiwan, [4]Department of Recreation and Health-Care Management, Chia-Nan University of Pharmacy and Science, Tainan, Taiwan, [5]Department of Surgery, School of Medicine, College of Medicine, Taipei Medical University and Division of Cardiovascular Surgery, Department of Surgery, Taipei Medical University, Taipei, Taiwan and [6]Department of Electrical Engineering, Southern Taiwan University of Science and Technology, Tainan, Taiwan

The Chinese medicine Astragali radix has been used to treat stroke sequelae for a long time. A few reports indicate that Astragali Radix extract or its purified components can affect brain function, protect the brain againt ischemia, promote neurogenesis and improve sensorimotor deficits and recovery of learning, memory and cognitive functions following ischemia. In addition, the mechanism of Astragalosides(AST) protection is not completely known. This study will observe the neurological protective effects of AST on ischemia and reperfusion injury model of PC12 cells and investigate what's the molecular mechanisms involved in apoptosis and autophagy. PC12 cells were exposed to oxygen and glucose deprivation(OGD) and restoration(OGD-rep) were used as an in vitro model of ischemia and reperfusion. PC12 cells were divided into three groups: Control, Ischemia-Reperfusion(I/R) and I/R+ AST(AST). The duration of ischemia and reperfusion was separately 5h and 24h. MTS assay and lactate dehydrogenase(LDH) leakage were used to evaluate the survival rate and protective effects of AST. DNA fragmentation were analyzed using DNA gel electrophoresis. Sub G1phase cell cycle arrest had identified by the flow cytometry analysis with PI stain. Caspase-3 protein expression and activities were measured by using assay kits with ELISA reader and Western blotting assay for apoptosis. Beclin-1 and LC3B-II expression, acridine orange staining assay were used to evaluate autophagy. Intrinsic apoptosis pathway were observed from ER stress involving Bip, caspase-12 expression and mitochondrial dysfunction involving mitochondrial membrane potential collapse and caspase-9 activation. Extrinsic apoptosis pathway were observed from caspase-8 expression. We found that, AST concentration-dependently attenuated neuronal damage with characteristics of increasing injured neuronal absorbance of MTS, decreasing cell apoptosis, subG1 phase cell cycle arrest, and caspase-3 activity induced by OGD-Reperfusion(OGD-R). AST treatment also alleviated the mitochondrial transmembrane potential dropped, mitochondria stress(caspase-9 activation), ER stress(Bip and caspase-12 activation) following OGD-R. In addition, OGD-R rapidly induced autophagy(evidenced by increased microtubule- associated protein-1 light chain 3(LC3) levels and punctured distribution of the autophagic vesicle-associated form LC3-II) and necrosis(evidenced by increased lactate dehydrogenase). AST treatment adopted at the start of OGD-R significantly reduced the OGD-R- induced apoptosis, autophagy and necrosis in PC12 cells. The appropriate concentration of AST can effectively protect PC12 against OGD-R injury by reducing apoptosis and autophagy through decreasing the oxidative stress, ER stress and mitochondrial dysfunction.

This work was supported by the National Science Council [NSC 101-2314-B-218 -001-MY3]

Where applicable, the authors confirm that the experiments described here conform with The Physiological Society ethical requirements.

PCC150

High-density EEG recordings from human motor cortices reveal deliberation process preceding a movement decision

D.F. Kutz[1], W. Hürster[3], F.P. Kolb[1] and J. Nida-Rümelin[2]

[1]Institute of Physiology, University of Munich, Munich, Germany, [2]Department of Philosophy IV, University of Munich, Munich, Germany and [3]Research & Consulting, Ulm, Germany

Question: Deliberation is the process of weighing alternatives. The aim of this study was to investigate neuronal correlates of a deliberation process leading to a motor decision.
Methods: In this study 23 young right-handed subjects (age: 18 - 27, 12 female) had to press a key with either the right or left hand, depending on a visual stimulus. The stimulus consisted of a word indicating a colour written either in the corresponding colour (e.g. word "red" written in red : match condition) or written in a different colour (mismatch condition). Subjects had to decide between responding with the right hand in the match condition, or with the left hand in the mismatch condition. High-density multi-channel EEG activity was recorded as well as behavioural data. In addition reaction times of the deliberation tasks were compared with those of a corresponding simple motor task.
Results: The reaction time in the deliberation task was significantly different from that observed during the simple motor task. Moreover, within the deliberation task the reaction times for the mismatch condition are significantly longer than those for the match condition.
The EEG patterns recorded from above the motor cortices during both tasks show clear differences. During the simple motor task a typical pre-motor positivity is observed preceding the key press whereas during the deliberation task a strong negativity approximately 300 ms before movement onset is found. Subtracting the motor task pattern from the EEG pattern of

the deliberation task augments the preceding negativity, presumably implying a required cognitive process.
Conclusions: The deliberation process during movement decision is represented by an increasing negativity in the motor region before movement onset. As both hemispheres show a similar activation it is assumed that competing motor plans are processed simultaneously. This result supports the idea for an involvement of the motor cortices in the deliberation process.

Supported by the Munich-Center for NeuroSciences – Brain and Mind (Nida-Rümelin 2011).

Where applicable, the authors confirm that the experiments described here conform with The Physiological Society ethical requirements.

PCC151

Extracellular hippocampal glutamate and GABA levels during spatial alternation testing in memantine/saline treated rats

G. Beselia[1], M. Sephashvili[2], T. Naneishvili[1], M. Burjanadze[1] and D. Mikeladze[2]

[1]Behavior and Cognitive functions, I.Beritashvili Center of Experimental Biomedicine, Tbilisi, Georgia and [2]Institute of Chemical Biology, Ilia State University, Tbilisi, Georgia

For over a decade intensive research has been dedicated to search for NMDA receptor antagonists as a potential neuroprotective treatment for both acute (e.g., stroke) and chronic neurodegenerative diseases. Although only very few such agents reached late stages of clinical development because of side effects, it was discovered that several compounds currently in clinical use such as memantine, amantadine and others have NMDA blocking properties which likely play a role in their therapeutic efficacy. It is still not clear, however, as to how memantine produces its symptomatological improvement of memory in demented patients. The effects of memantine on in vivo hippocampal glutamate levels has not been examined. The followimg investigation was conducted to determine the effects of chronic memantine treatment on hippocampal Glu and GABA release prior to, during, and after spontaneous alternation test. Also, we have investigated the effects of chronic treatment with memantine on basal and KCl-stimulated release of GLU and GABA in the hippocampus. A total of 18 male Wistar rats (Department of Animal Care, I. Beritashvili Center of Experimental Biomedicine) were used in the present study. All experiments were approved by the Animal Care and Use Committee of the Center and were in accordance with the principles of laboratory animal care. Two groups of rats were treated either with memantine (2,5 mg/kg/day; i.p. Sigma Chemical Co., St. Louis, MO) or with vehicle (saline) for a period of 4 weeks. Memantine-treated rats, relative to saline rats, had a significantly lower level in the number of arms entered during the testing session. However, the groups did not differ in the level of alternation behavior. The results indicate that memantine treatment produced decreased locomotor (exploratory) activity ($p<0,05$) but did not affect spatial working memory in adult rats assessed in spontaneous alternation task ($p>0,05$). Glu release during the 10 min samples taken at the time of the behavioral testing of memantine or saline treated animals increased during behavioral testing but were not significantly different ($p>0,05$) from those seen immediately before and after testing. We found increase in KCl-stimulated glutamate and GABA release in the hippocampus of memantine treated rat compared to the saline treated rat. This difference in KCl response between memantine treated and control rat was statistically significant ($p<0,05$). Our evaluation of memantine reveals that changes in Gluergic neurotransmission after chronic memantine treatment did not affect working memory in adult rats assessed in spontaneous alternation task.

The designated project has been fulfilled by financial support of Presidential Grant for Young Scientists (Grant #PG/55/7-276/12) .

Where applicable, the authors confirm that the experiments described here conform with The Physiological Society ethical requirements.

PCC152

Enriched environment improved anti-stress effects of antidepressants in repeated rat forced swimming test

C. Lino de Oliveira[1,3], F. Possamai[1,3], J. Santos[1], J. Marcon[1] and J. Marino-Neto[1,2]

[1]Ciências Fisiológicas, Universidade Federal de Santa Catarina, Florianópolis, Santa Catarina, Brazil, [2]Instituto de Engenharia Biomédica (IEB-CTC-UFSC), Universidade Federal de Santa Catarina, Florianópolis, Santa Catarina, Brazil and [3]Programa Multicêntrico de Pós-Graduação em Ciências Fisiológicas, Universidade Federal de Santa Catarina, Florianópolis, Santa Catarina, Brazil

Environmental enrichment is able to induce behavioral effects in rats and mice exposed to the forced swimming test as well as in the morphology of the central nervous system. Our aim was to evaluate the effects of environmental enrichment from weaning on behavioral output of control and antidepressants-treated adult rats in the repeated Forced Swimming Test (1). In addition, we investigated cell proliferation in the hippocampal dentate gyrus of these rats. Male Wistar rats (n=80) were housed for 40 days from postnatal day 21 in standard (SE) or enriched (EE) environment. After this period they were exposed to the Pre-test (day 1, 15 min of forced swimming). In the next day (day 2), rats were randomly assigned in one of 4 groups and 1 hour before the Test (i.e. 5 min of forced swimming) they received an intraperitoneal injection with saline (SAL), or imipramine (IMI, 2.5 or 5 mg/kg) or fluoxetine (FLX 2.5 mg/kg). A daily injection of these compounds was performed to the respective group from the day 3 (one day after the Test) until day 7 (the day of the Retest 1, i.e., 5 min of forced swimming) and until day 14 (the day of Retest 2, i.e., 5 min of forced swimming). Pre-test, Test and Retests 1 and 2 were videotaped for posterior analysis of behavior (latency, frequency, duration of immobility, swimming, climbing). Duration of immobility was considered an index of behavioral despair. After retest 2, rats were anesthetized and sacrificed for brain dissection and preparation for Ki-67 (proliferation marker) immunohistochemistry in hippocampal dentate gyrus. Effects of retesting were analyzed using repeated measures Anova. Between groups analysis were performed using One Way Anova. When appropriate post hoc Duncan's test was performed. Housing in EE failed to affect behavior in the Pre-test or Test but attenuated the effects of re exposure on behavior of control rats. Antidepressants decreased the index of behavioral despair after 7 (Retest 1) and 14 (Retest 2) days of treatment as compared to saline in SE groups. The efficacy of FLX, not IMI, in reduce behavioral despair increased with the time (from Test to Retest 2) in SE groups. In EE groups, antidepressants (IMI 5 mg/kg and FLX 2.5 mg/kg) decreased the index

of behavioral despair after 14 days of treatment (Retest 2) when compared to their effects after 1 day of treatment (Test). Surprisingly, these later treatments also decreased the counting of Ki-67 in the dentate gyrus as compared to saline. These data suggest that enriched environment improved the coping with forced swimming stress and improved the effects of chronic treatment with imipramine on behavioral despair in a fashion unrelated to the increased proliferation in dentate gyrus of adult rat hippocampus.

Mezadri T J, et al. J Neurosci Methods. 2011 Feb 15;195 (2):200-5

Financial Support: Alexander von Humboldt Foudation (Germany), Fapesc (Florianópolis, SC, Brazil), Capes (Brazil), CNPq (Brazil).

Where applicable, the authors confirm that the experiments described here conform with The Physiological Society ethical requirements.

PCC153

The effect of erythropoietin pretreatment on S100B and NSE serum levels and brain inflammation in pentylenetetrazole induced generalized seizures; Evaluation of antiseizure effect of erythropoietin

N. Bahcekapili[1], I. Albeniz[2] and G. Uzum[3]

[1]Neurology, Istanbul state hospital, Istanbul, Turkey, [2]Biophysic, Medical Faculty of Istanbul, Istanbul, Turkey and [3]Physiology, Istanbul Medical Faculty, Istanbul, Turkey

Epilepsy is a common neurological disorder often unresponsive to pharmacological treatment. Seizures initiate brain inflammation in glia and promote blood brain barrier (BBB)damage. Erythropoietin(EPO)has been suggested a promising therapeutic and prophylactic for epilepsies based on its neuroprotective, antiapoptotic, and antiinflammatory potency. Exogenously given EPO traverses BBB through EPO receptors.Our previous study showed that pretreatment with recombinant human EPO (rhEPO) suppresses epileptic seizures and prevents BBB damage, but the mechanisms are still unclear. The present study investigated a possible role of EPO pretreatment in reducing inflammatory events, in pentylenetetrazole(PTZ)-induced generalized epilepsy model. Adult male Sprague-Dawley rats were used (seven animal/each group). PTZ (80mg/kg i.p) was given to induce generalized seizures. rhEPO (3000 IU/kg i.p) applied 24 h before PTZ administration. The control group was given saline, the EPO control group was given the same dose of EPO.After injection of PTZ, seizures were observed for two hours and scored as seizure stage, latency. Under general anesthesia(thiopental sodium, 50mg/kg) blood samples were taken from heart and immediately the brain removed. NSE, S100B and imflammation biomarkers were performed with ELISA tests. The serum levels of neuron specific enolase(NSE) and S100B(astrocytic protein) as peripheral markers of neuronal and BBB damage, respectively and levels of proinflammatory cytokines, interleukin-1β (IL-1β), tumor necrosis factor-α (TNF-α),interleukin(IL-6) as indicator of brain inflammation were measured in brain tissue. Data represented as mean±SEM and were compared among groups by using oneway ANOVA. PTZ induced seizures significantly ($p<0.001$) increased proinflammatory cytokines (IL1β:1,584±0.187pg/ml vs 0.434±0.434pg/ml control, TNFα :0.488±0.083 pg/ml vs 0.120±0.015pg/ml control, IL-6:0.610±0.043 pg/ml vs 0.509±0.042 pg/ml control). Likewise, the serum levels of S100B and NSE significantly ($p<0.001$)were increased (S100B: 0.89±pg/ml vs 0.32±0.05pg/ml control, NSE: 0.83± 0.087pg/ml vs 0.051± 0.011pg/ml control). EPO pretreatment significantly($p<0.001$) reduced seizure stage. Serum markers of BBB and neuron damage and all cytokines fell to control levels (IL1β:0.593±0.065pg/ml vs 1.584±0.187pg/ml PTZ group, TNFα: 0.177±0.007pg/ml vs 0.488±0.083 pg/ml PTZ group, IL-6: 0.339±0.017pg/ml vs 0.610±0.043 pg/ml PTZ group). Likewise, S100B and NSE fell to control levels (S100B: 0.33±0.041pg/ml vs 0.89±0.03 pg/ml PTZ group, NSE: 0.2±0.075pg/ml vs 0.83± 0.087pg/ml PTZ group). We suggest that the anticonvulsive effect of EPO is result of BBB protection due to its antiinflammatory activity.

Where applicable, the authors confirm that the experiments described here conform with The Physiological Society ethical requirements.

PCC154

The modulation of the hippocampal function by the cholinergic and noncholinergic cells of the septum

M. Dashniani, T. Naneishvili, M. Burjanadze, N. Chkhikvishvili and E. Abzianidze

Behavior and Cognitive functions, I.Beritashvili Center of Experimental Biomedicine, Tbilisi, Georgia

Although the importance of the septohippocampal projections in learning and memory is generally accepted, the degree to which damage to particular set of septohippocampal projections contributes to deficits within specific cognitive domains is less clear. In the present study, using novelty-preference paradigm, we tested the behavioral effects of electrolytic, neurotoxic (ibotenic acid) or immunotoxic (192 IgG-saporin) lesions of medial septum (MS) to gain insights into the differential roles of septohippocampal cholinergic and noncholinergic projections in exploratory behavior and recognition memory. A total of 39 male Wistar rats (Department of Animal Care, I. Beritashvili Center of Experimental Biomedicine) were used in the present study. All experiments were approved by the Animal Care and Use Committee of the Center and were in accordance with the principles of laboratory animal care. The size and location of the electrolytic and ibotenic acid lesions were determined by microscopic examination of serial coronal sections (25 μm) stained with cresyl violet. The immunotoxic lesions of MS were verified by observing decreased Acetylcholinesterase (AChE) staining of the MS and hippocampal sections. Statistical analysis was performed using ANOVA. The results indicate that the MS lesioned rats did not differ from control rats in the activity level measured by grid crossing. The MS electrolytic lesioned rats were impaired in habituating to the environment in the repeated spatial environment, but rats with immuno- or neurotoxic lesions of the MS did not differ from control ones. The MS electrolytic and ibotenic acid lesioned rats showed an increase in their exploratory activity to the objects and were impaired in habituating to the objects in the repeated spatial environment; rats with immunolesions of the MS did not differ from control rats. The electrolytic lesions of the MS disrupt spatial recognition memory; rats with immuno- or neurotoxic lesions of the MS were normal in detecting spatial novelty; all of the MS-lesioned and control rats clearly reacted to the object novelty by exploring the new object more than familiar ones. In conclusion, our results observed across lesion techniques demonstrates dissociation between the two major components (cholinergic and noncholinergic) of the septohippocampal pathway in exploratory behavior assessed in the open field and indicate that: deficits after nonselective damage of MS are lim-

ited to a subset of cognitive processes dependent on the hippocampus; the selective loss of septohippocampal cholinergic or noncholinergic projections does not disrupt the function of the hippocampus to a sufficient extent to impair spatial recognition memory.

The designated project has been fulfilled by financial support of Shota Rustaveli Georgian National Science Foundation (Grant #13/10).

Where applicable, the authors confirm that the experiments described here conform with The Physiological Society ethical requirements.

PCC155

Fast network oscillations in the lateral septum in vivo

T. Korotkova[1], N.P. Denisova[2] and A. Ponomarenko[1]

[1]Behavioural Neurodynamics Lab, Leibniz Institute for Molecular Pharmacology (FMP) / NeuroCure Cluster of Excellence, Berlin, Germany and [2]Behavioural Neurodynamics Lab, Charité University Clinic, Berlin, Germany

Animal's behavior relies on the processing of environmental cues and signals about bodily state, yet physiology of their coordination remains poorly understood. Hippocampal and cortical information is relayed to hypothalamus and midbrain in rodents and other mammals mainly via the lateral septal nucleus (LS). We used high-density single and dual-site electrophysiological registration of local field potentials and of neuronal discharge in behaving mice to study network synchronization in LS and its coordination with inputs from the medial prefrontal cortex (mPFC) and hippocampus. Local field potentials (LFP) and neuronal discharge in LS displayed intermittent episodes (40-120 ms duration) of synchronization at frequencies between 40 and 90 Hz. These fast oscillations were behavioral state-dependent, coordinated within LS and, strikingly, were coherent with concurrently recorded gamma oscillations in the mPFC and, less prominently, in the hippocampus during slow- and theta-rhythmic epochs, respectively. Neuronal activity in LS was modulated by locally recorded LFP gamma oscillations: the discharge of the vast majority of recorded cells was significantly modulated by the locally recorded rhythm. As a population, LS units fired near troughs of gamma cycles. LFP and the neuronal discharge
recorded simultaneously from LS and mPFC displayed coordinated patterns of activity
between the two regions in the gamma frequency band. Furthermore, our recordings
of LFP and neuronal activity in LS in novel and familiar environments suggest experience-dependence of network synchrony in LS and its potential relevance for shaping behavioral responses to novelty processed by hippocampus and mPFC.

This study is supported by NeuroCure Cluster of Excellence

Where applicable, the authors confirm that the experiments described here conform with The Physiological Society ethical requirements.

PCC156

Erythropoietin pretreatment suppresses pentylenetetrazole induced generalized seizures by inhibiting iNOS and increasing eNOS activity in hippocampus

G. Uzum[1], N. Bahcekapili[2], A. Kapucu[3], A. Kandil[3] and K. AkgünDar[3]

[1]Physiology, Istanbul University Istanbul Medical faculty, Istanbul, Turkey, [2]Neurology, Istanbul state hospital, Istanbul, Turkey and [3]Biology, Istanbul University Science Faculty, Istanbul, Turkey

Erythropoietin (EPO) is an antiapoptotic, neuroprotective and antiinflammatory hormone. EPO antiseizure effect elicits but the molecular mechanism is still not fully understood. Status epilepticus(SE) trigger inflammatory mediators in brain, produces neuronal damage preferential in the hippocampus, the underlying mechanism is still unsettled. Nitricoxide (NO) is synthesized from L-arginine (L-Arg) by three different isoforms of NO synthase (NOS), i.e. the constitutive neuronal and endothelial NOS (nNOS and eNOS) and the inducible NOS (iNOS). NO has been involved in the pathophysiology of epilepsy, but available data are conflicting and the role of NO in epilepsy still remains to be clarified. However, SE increases microglia activity and induces iNOS expression in hippocampal neurons, leading to apoptotic neuronal cell death in the hippocampus. In this study, the possible modulatory effect of recombinant human erythtopoietin (rhEPO) pretreatment on NO synthases (NOS; neuronal, inducible and endothelial) expressionin hippocampus after pentylenetetrazole (PTZ) induced seizures were analyzed. PTZ is a common convulsant agent used in animal models to investigate the mechanisms of seizures. Adult male Sprague-Dawley rats were used (seven animal/each group). PTZ (80mg/kg i.p) was given to induce generalized seizures. rhEPO (3000 IU/kg i.p) applied 24 h before PTZ administration. The control group was given saline, the EPO control group was given the same dose of EPO. After injection of PTZ, seizures were observed for two h and scored as seizure stage, latency. Under general anesthesia (pental sodium, 50 mg/kg) immediately brain removed and hippocampus was removed to examined NOS isoforms using immunohistochemistry. Data are expressed as mean± SD. Behavioral data were analyzed by one-way ANOVA followed by Duncan post host doc test. PTZ induced generalized seizures iNOS immunreactivity increased, eNOS immunreactivity decreased in hippocampus. EPO pretreatment significantly ($p<0.001$) reduced seizures stage (2.7 ±0.01 vs 4.8±0.2 PTZ-group), and did not effect seizure latancy. Besides, it increased markedly eNOS activity, decreased markedly iNOS activity, did not effect nNOS activity. The data suggest that anticonvulsant effect of EPO might be related to the decrease of iNOS and increase of eNOS.

Where applicable, the authors confirm that the experiments described here conform with The Physiological Society ethical requirements.

PCC157

Effects of medial septal electrolytic and immunotoxic lesions on place and response learning of rats in the Morris water maze

L. Kruashvili, D. Manana and G. Beselia

I.Beritashvili Center of Experimental Biomedicine, Tbilisi, Georgia

In this experiment the ability of medial septal electrolytic, selective ACh lesioned (by immunotoxin 192 IgG-saporin) and sham-operated rats, to learn the location of a visible, as well as submerged platform in a water maze was investigated. A total of 36 male Wistar rats were used in the study. Experimental protocol was approved by Animal Studies Committee of I. Beritashvili Center of Experimental Biomedicine and were in accordance with the principles of laboratory animal care. The size and location of the electrolytic lesions were determined by microscopic examination of serial coronal sections (25 μm) stained with cresyl violet. The immunotoxic lesions of MS were verified by observing decreased Acetylcholinesterase (AChE) staining of the MS and hippocampal sections. The rats' responses in the competition test were classified as either cue or place directed, based on the swim path for those trials. Sham-operated rats acquired both the visible and hidden platform versions of the task, but when required to choose between the spatial location they had learned and the visible platform in a new location, majority of them swam first to the old spatial location. The medial septal electrolytic lesioned rats acquired the visible platform version of the water maze task but failed to learn the platform location in space. When the visible platform was moved to a new location they often swam directly to it. The medial septal selective ACh lesioned rats, as well as sham-operated, acquired the platform location in space. Sham-operated and selective ACh lesioned rats identified as place responders, had significantly more accurate searches during hidden platform training, providing additional evidence of their effective use of a place learning strategy rather than medial septal electrolytic lesioned rats. These findings suggest that the septo-hippocampal system is essential for accurate spatial learning and suggest its role in processing information about the spatial environment, but deficits observed after septal electrolytic lesions cannot be accounted solely to the loss of hippocampal ACh and raised the unexpected possibility that hippocampal ACh is not essential for all types of hippocampal-dependent memory.

The designated project has been fulfilled by financial support of Presidential Grant for Young Scientists (Grant #PG/57/7-276/12) .

Where applicable, the authors confirm that the experiments described here conform with The Physiological Society ethical requirements.

PCC158

Effect of toluene chronic exposure on exploratory behavior and recognition memory in adolescent and adult rats

N. Pochkhidze, M. Zhvania, N. Japaridze and L. Chilachava

I.Beritashvili Center of Experimental Biomedicine, Tbilisi, Georgia

Toluene and toluene-containing volatile substances are the most widely abused solvents with demonstrative addictive potential in humans. Several data indicate that as a result of toluene misuse alterations in learning and memory in organisms of different age take place. But because of differences in species, length of exposure, dose or rate of administration, it is not always possible to conclude whether adolescent experience results in changes in learning and memory are comparable to that seen in adults. The present study has been undertaken to determine whether toluene chronic exposure provokes immediate and/or persisting effect on exploratory behavior and recognition memory in open field in adolescent and adult rats. We exposed male Wistar rats at ages P 28-32 (adolescents) and P 70-75 (adults) to 2000 ppm inhaled toluene for 40 days. The immediate and persisting effects of toluene misuse (immediately after the end of toluene chronic inhalation and 90-day after the end of toluene chronic inhalation, correspondingly) were evaluated. Experimental protocol was approved by Animal Studies Committee of I. Beritashvili Center of Experimental Biomedicine. The major findings are: (1) toluene misuse alters exploratory activity and recognition memory in adolescent and adult rats; (2) the level of alterations depends upon the postnatal age of testing animals. In particular: in adolescent rats the most significant behavioral alterations were observed by the day following toluene chronic exposure. These alterations do not progress significantly during abstinence period: some altered parameters were almost the same as observed the day following immediately after toluene misuse and others were very close to observed in control animals. Therefore, in adolescent rats the most expressed was immediate effect of toluene misuse. Contrary to it: in adult rats most alterations significantly progress during 90 d period of abstinence. So, in these animals more substantial was persistent effect of toluene chronic exposure. On the bases of our data it is possible to suggest that adolescent rats may show partial recovery from once the toluene toxic effect no longer persists.

The designated project has been fulfilled by financial support of Presidential Grant for Young Scientists (Grant #PG/54/7-276/12) .

Where applicable, the authors confirm that the experiments described here conform with The Physiological Society ethical requirements.

PCC159

Activation of Epac has epic effects on diabetic sensory axon regeneration

D. Shewan, K. Steel, A. Murray, S.J. Tucker, N.E. Cameron and M.A. Cotter

School of Medical Sciences, University of Aberdeen, Aberdeen, UK

Neuropathy is a common complication of diabetes, reducing neuronal function, including impaired regeneration. Failure of CNS axons to regenerate after injury is at least partly due to intrinsic neuronal factors. Cyclic AMP (cAMP) activation promotes sensory axon regeneration through an Epac-mediated pathway. We therefore explored whether diabetic neurons are defective in cAMP-Epac signalling. We used cultured dissociated dorsal root ganglion (DRG) neurons from terminally-anaesthetised streptozotocin –induced diabetic and age-matched control rats to study their growth and responses to axon guidance cues. Growth of DRG neurons on a laminin substrate was significantly greater in controls compared with diabetic rats after 48 hours (35.9 ± 3.1% control neurons grew processes of at least 3 cell body diameters (3 cbd) vs. 27.4 ±

2.0% diabetic neurons, p<0.05; two-tailed, unpaired Student's t-test was used in all statistical analyses). The cAMP agonist, Sp-cAMPS (20μM), enhanced neurite outgrowth of diabetic and control neurons at both 24 and 48 hours, but a selective Epac agonist, 8 pMeOPT-2'-O-Me-cAMP (2μM), significantly increased neurite outgrowth in control neurons (18.8 ± 1.6%) compared to diabetic neurons (12.6 ± 1.8%, p<0.05) after 24 hours. By 48 hours, the Epac agonist significantly improved the outgrowth of diabetic neurons (39.1 ± 1.5% Epac agonist vs. 27.4 ± 2.0% control, p<0.05), which was similar to the effect of the Epac agonist on age-matched control rat neurons at this time point (33.1 ± 3.2%). Activating cAMP or Epac also reversed the repulsive response of diabetic DRG neuronal growth cones to a gradient of the cAMP-dependent trophic factor, nerve growth factor (NGF). After 48 hours 13 out of 16 control growth cones turned towards the gradient, with a mean turning angle (MTA) of 17.6 ± 6.5°, while 9 out of 11 diabetic growth cones were repelled by a NGF gradient, showing a MTA of -22.5 ± 9.1°(p<0.001). Bath application of 20μM Sp-cAMPS, to elevate cAMP activity in diabetic neurons, converted diabetic growth cone repulsion to attraction at the 48 hour time point (MTA with Sp-cAMPS was 11.9 ± 4.9° vs. -22.5 ± 9.1° without Sp-cAMPS, p<0.001), as did bath application of the Epac agonist (MTA of 5.7 ± 5.9° with agonist vs -22.5 ± 9.1° without agonist, p<0.01). Blocking cAMP with the Rp-cAMPS isomer (20μM), which binds to Epac but does not activate it, abolished both the attraction of control growth cones in a NGF gradient and repulsion of diabetic neurons. An 18.9% decrease (p<0.05) in Epac expression was seen in diabetic neurons by Western blot and a 35% decrease (p<0.05) of Epac expression in growth cones by immunocytochemistry. Together, these results suggest that adult diabetic rat neurons exhibit reduced expression of Epac, resulting in a compromised ability to regenerate neurites and an inability to respond to cAMP-dependent chemoattractive guidance cues.

Where applicable, the authors confirm that the experiments described here conform with The Physiological Society ethical requirements.

PCC160

The excitation of rat primary afferent fibres by p-benzoquinone, a metabolite of paracetamol (acetaminophen APAP)

T.A. Sears, D.A. Andersson, C. Gentry and S. Bevan

Wolfson CARD, King's College London, London, UK

Recently, two metabolites of paracetamol were shown to activate TRPA1, a receptor involved in neurogenic airway inflammation1 and thermal, mechanical and chemical nociception.2 Thus p-benzoquinone (p-BQ) and n-acetyl-p-benzoquinoneimine (NAPQI) increased [Ca2+]i in CHO cells expressing TRPA1;and a subset of cultured DRG neurones displaying such Ca2+ responses was strongly depolarised, suggesting a spinal and presynaptic role in APAP analgesia2; our in-vivo studies address this possibility. In anaesthetised rats (Urethane, i.p.) the spinal cord was exposed, and L1-S1 dorsal roots prepared for recording either orthodromic sensory nerve action potentials or ones arising centrally and conducted antidromically (Fig1, lower trace). These arise in small diameter myelinated and C-fibres in contrast to the larger spikes recorded from the peripheral end of the same cut root in response to tactile or proprioceptive stimulation (not shown).
The upper trace shows the mean spike rate counted in 5.0 sec bins. Within seconds of application to the spinal cord root exit zone 10micro litres of 1.0 microM p-BQ evoked a five-fold increase in net impulse rate persisting for 2 minutes before return to baseline level. The next dose (10μl p-BQ at 10 microM) evoked a prompt sixteen-fold rate increase at its peak with recruitment of new spikes; this activity was sustained for a further 3 minutes after the illustrated trace. This response was elicited on each occasion (35 in 18 rats) with BQ concentrations ranging from 300nM to 600microM ; we attribute this to variations both in the integrity of the pia at the site and dispersion of the applied drug. Although retrograde impulse activity can be directly attributed to the depolarisation of TRPA1 afferent terminals some glutamatergic collaterals may excite internuncial pathways causing presynaptic depolarisation via GABA or glycine receptors. However, this does not seem relevant for APAP analgesia. The P-wave of the cord dorsum potential evoked by sural nerve stimulation, an electrical sign of presynaptic inhibition, was unaffected in 5 rats followed for up to 2 hours after s.c. injection of the same doses (300mg/kg) used in the behavioural studies. These results thus support the hypothesis that paracetamol analgesia is, in part, mediated by its metabolite p-BQ activating TRPA1 receptors leading to depolarisation and consequent presynaptic inhibition of pain pathway(s) mediating antinociception2.

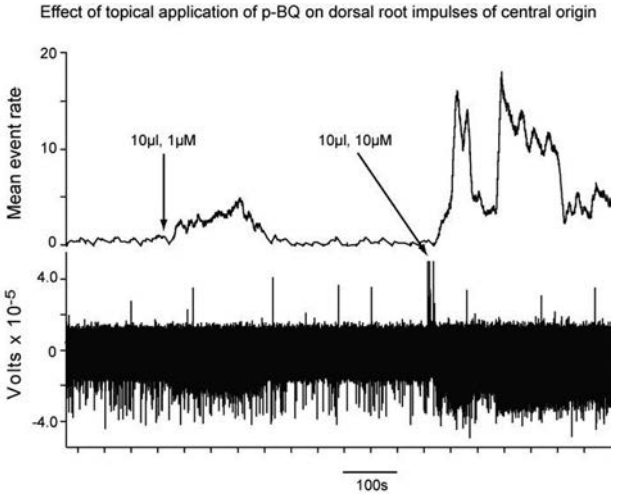

Fig1

1. Nassini,R.,Materazzi,S, Andre,E. et.al. Acetaminophen, via its reactive metabolite N-acetyl-p-benzo-quinoneimine and transient receptor potential ankyrin-1 stimulation, causes neurogenic inflammation in the airways and other tissues in rodents. FASEB J. 24, 4904-4916 (2010)

2. Andersson,D.A., Gentry,C., Alenmyr,L., et al. TRPA1 mediates spinal antinociception induced by acetaminophen and the cannabinoid Δ9-tetrahydrocannabiorcol. Nature Communications 2,551 (2011)

Where applicable, the authors confirm that the experiments described here conform with The Physiological Society ethical requirements.

PCC161

Effects of chronic infusion of kisspeptin and its antagonist on cognitive functions and behavior in female rats

S. Eyuboglu Dinc[1], S. Canpolat[2], H. Akkaya[1], B. Elibol-Can[3], E. Kilic[4] and B. Yilmaz[1]

[1]Department of Physiology, Yeditepe University, Istanbul, Turkey, [2]Department of Physiology, Karadeniz Teknik University, Trabzon, Turkey, [3]Department of Biology, Middle East Technical University, Ankara, Turkey and [4]Department of Physiology, Medipol University, Istanbul, Turkey

Kisspeptin and its membran receptor (GPR54) are expressed in various brain regions, especially in the hypothalamus, hippocampus and cortex. Effects of this neuropeptide on reproductive functions and puberty onset have been investigated. However, functions of kisspeptin/GPR54 system in the hippocampus have not been clarified. Therefore, we have examined effects of kisspeptin and its antagonist on learning, memory, animal activity, depression and anxiety behavior and their underlying mecanisms. Adult female Sprague Dawley rats were devided three groups (n=8/group): Control animals received saline (osmotic minipump, icv) for 28 days. Rats in the second and third groups were administered with osmotic minipump driven infusion of kisspeptin-10 (10 nmol/kg/day, icv) and kisspeptin antagonist (p234; 10 nmol/kg/day, icv), respectively. Alzet miniosmotic pump and icv infusion kits were inserted by using a stereotaxic frame under anaesthetised with a mixture of ketamine (75mg/kg) and Xylazine (5 mg/kg). The experiments were approved by the local ethics committee. Cognitive functions (using Barnes maze), animal activity, anxiety behavior were determined before and after the treatment period. At the end, all animals were decapitated, brains removed and frozen. Coronal brain sections (15 μ) were cut. Number of neurons, changes in ERK1/2 of phosphorilation, NCAM and PSD-95 protein expression in hippocampus were evaluated by cresyl violet staining and western blotting, respectively. The results were statistically analyzed by using One-Way ANOVA. Kisspeptin significantly increased phosphorilation of ERK 2 ($p<0.05$). Cresyl violet stained sections showed no difference in the morphology and number of the neurons in the dentate gyrus, CA1, CA2 and CA3 regions of the hippocampus. Treatment with the kisspeptin antagonist significantly increased the distance and duration to find the target box in the Barnes maze ($p<0.05$) compared to the control group. No significant differences were observed in the other sensorymotor behavioral tests in any of the groups. In conclusion, our findings suggest that chronic inhibition of kisspeptin/GPR54 system in adult animals significantly reduces cognitive functions. Role of exogenous kisspeptin infusion should be studied in a memory deficit animal model.

Where applicable, the authors confirm that the experiments described here conform with The Physiological Society ethical requirements.

PCC162

Induction of brain kinin B1 receptor and its association with stereotypic nocifensive behaviour in diabetic rat

R. Couture, J. Dias, H. de Brito Gariépy and B. Ongali

Physiology, Université de Montréal, Montreal, QC, Canada

While brain kinin B1 receptor (B1R) is virtually absent in control rats, it is induced by the oxidative stress in various peripheral tissues and the spinal cord in type 1 and type 2 diabetic models. In the model of insulin resistance induced by high glucose feeding, B1R is associated with pain neuropathy, insulin resistance and hypertension. This study aims at determining whether B1R is also induced in the brain of glucose-fed rats via the oxidative stress and whether it can affect nocifensive behaviour. Male Sprague-Dawley rats (50-75 g) received either 10% D-glucose in their drinking water or only tap water (controls) and were maintained under a normal chow diet or a diet enriched with alpha-lipoic acid (antioxidant, 1g/kg diet) for 12 weeks. An intracerebroventricular (i.c.v.) guide cannula was implanted into the right lateral brain ventricle in isoflurane anesthetised rat 7 days before initiating experiments. After completion of experiments, rats were anaesthetized with CO2 inhalation and killed to collect the brain, which was frozen in 2-methyl butane cooled at -45°C with liquid nitrogen and kept at -80°C for determining B1R binding sites by autoradiography with [125I]-HPP-des-Arg10-Hoe 140 (150 pM) on brain tissue sections. Behavioural activity to the selective B1R agonist, Sar-[D-Phe8]-des-Arg9-BK (10 μg/1μl, i.c.v.) was measured before and after treatment with receptor antagonists (10 μg/1μl, i.c.v.) for B1 (SSR240612, R-715), substance P NK-1 (RP-67580) and glutamate NMDA (DL-AP5). Other studies included the nitric oxide synthase (NOS) inhibitor L-NNA (10 μg/1μl, i.c.v.). Results showed striking increases in the density of specific B1R binding sites in various areas of the cortex, diencephalon, basal ganglia, mesencephalon and medulla of glucose-fed rats in comparison with age-matched control rats. The latter increases in B1R binding sites were prevented by the antioxidant diet in all studied brain areas. The B1R agonist had no effect in control rats, yet it induced significant behavioural manifestations in glucose-fed rats (face washing, sniffing, head scratching, rearing, teeth chattering, grooming, digging, licking, biting, wet-dog shakes) when compared to aCSF. These responses were prevented by all antagonists and the inhibitor tested. The same pharmacological treatments had no direct effect on behaviour in the absence of B1R agonist. Data suggest that kinin B1R is induced and up-regulated by the oxidative stress in the brain of glucose-fed rats and that its intracerebral activation induces stereotypic nocifensive behaviour involving the release of several central mediators, notably substance P, glutamate and nitric oxide.

Supported by Canadian Institutes of Health Research (CIHR)

Where applicable, the authors confirm that the experiments described here conform with The Physiological Society ethical requirements.

PCC164

An experimental model to evaluate the whole-brain neurovascular coupling during spontaneous cerebral activity

A. Zagrean[1], A. Calin[1], S. Mirica[1], A. Gonzales[1], L. Zagrean[1] and M. Moldovan[2]

[1]Physiology and Neuroscience, Carol Davila University of Medicine and Pharmacy, Bucharest, Romania and [2]Neuroscience and Pharmacology, Panum, University of Copenhagen, Copenhagen, Denmark

A transient increase in cortical neuronal activity is followed by a complex sequence of cellular, metabolic, and vascular processes resulting in a transient increase in cerebral blood flow occurring with a slower time-course. This physiological neurovascular coupling is used to infer neuronal activity in vascular-based modern functional brain imaging techniques. Nevertheless, the process of neurovascular coupling itself can become altered with aging and disease and the consequences of such alterations to interpretation of imaging studies remain poorly understood. It thus becomes increasingly important to develop methods to evaluate the process of neurovascular coupling at the whole brain level.
The current methodological approach is to investigate the mean hemodynamic changes in response to repeating somatosensory stimuli that generate identifiable cortical evoked responses that can be recorded non-invasively by electroencephalography (EEG). Here we proposed a novel approach. During general anesthesia, with increasing anesthetic concentrations the EEG becomes discontinuous consisting of whole-brain bursts of activity on a suppressed background referred to as burst-suppression (BS). We hypothesized that neurovascular coupling could be investigated by burst-triggered averaging of the hemodynamic changes during BS. We investigated the fluctuations in cerebral blood flow during BS induced by chloral hydrate overdose in adult male Wistar rats. The EEG recorded via fronto-occipital epidural electrodes (1-30Hz) was first rectified (rEEG) and then averaged in 200 ms bins. The corresponding binary BS signal, derived by an unsupervised statistical classifier, was then used to identify the bursts onset. The laser Doppler (LD) signal recorded from the frontal cortex was first filtered for cardiac cycle and respiratory fluctuations and then averaged in 200 ms bins. We could then construct a burst-onset triggered average of the change in rEEG and LD from the levels just prior to the burst. We found that following burst onset there was an increase in LD that peaked within 1 second after the rEEG peak, consistent with a neurovascular response. The magnitude of the response was several orders of magnitude smaller than the cardiac LD fluctuation so that averaging of more than 100 bursts was required to construct a reliable response. At a readily controllable burst suppression of 50-75% ratio (the relative time spent in suppression), a 10 minutes recording was typically sufficient. Our study provides proof of concept that whole-brain neurovascular coupling can be evaluated during spontaneous cerebral activity by inducing a safely reversible anesthetic BS state. This should be accounted for in the design of clinical neurovascular coupling studies combining non-invasive methods such as EEG and near-infrared spectroscopy.

Where applicable, the authors confirm that the experiments described here conform with The Physiological Society ethical requirements.

PCC165

Are male cognitive functions better than female postovulatory phase cognitive functions?

S. Guragain[1] and N. Upadhayay[2]

[1]Pharmacology, Manipal College of Medical Sciences, Pokhara, Nepal and [2]Basic and Clinical Physiology, BP Koirala Institute of Health Sciences, Dharan, Nepal

Previous studies have shown gender differences in specific cognitive abilities. Female generally, showing an advantage in verbal fluency, perceptual speed and accuracy and in fine motor skills, while male generally showing an advantage in spatial, working memory and mathematical abilities. Many studies have also shown that estrogen and testosterone accentuate cognitive functions in a similar fashion. However, between male and female who performs better on specific cognitive abilities have contradictory reports. As well as studies with progesterone hormone on cognitive function have contradictory reports, whether it accentuates or attenuates the cognitive abilities.
So, we aimed to study and compare postovulatory phase cognitive functions of female with male cognitive functions. Female cognitive functions were assessed during postovulatory phase of menstrual cycle as it is well-known that blood progesterone level is high during postovulatory phase. The study was conducted in healthy 21 male and 21 female volunteers of age range 19-37 years. Four aspects of cognitive functions were assessed (viz: attentional, perceptual, executive and working memory). Attentional task as visual reaction time (VRT) and Go/No-Go VRT, perceptual task as fast counting (FC), executive task as Erisken flanker test (EFT) and Stroop test (ST) i.e. color interference reading and, working memory task as picture 2-back remembering were assessed by using cognitivefun.net program. Data were expressed in median and interquartile range (IQR), compared by using Mann-Whitney U test.
On comparing cognitive functions between male and female there were no significant differences in all cognitive task variables except in VRT and ST (percentage of color accuracy). Male performed better than female in VRT (331.66 ms, IQR: 286.99 to375.33 vs. 367.8 ms, IQR: 340.66 to 435.66; p=0.05). However, in ST female have higher accuracy in reading color interference than that of male (100%, IQR: 95.12 to 100 vs. 95.24%, IQR: 86.36 to 100; p=0.04). Male showed trend of better performance than female in EFT congruent and incongruent time, working memory accuracy and combined time and in FC speed and accuracy. However, male showed trend of poorer performance than female in Go/No-Go VRT accuracy, average and combined time, ST color reading normal time and interference time and in working-memory average time.
Thus, male performs better in attentional VRT than female postovulatory phase attentional VRT. Female has advantage in postovulatory phase and performs better than male in executive cognitive functions as assessed by ST. Perceptual and working memory in both male and female are comparable to each other. Therefore, in female at postovulatory phase progesterone hormone might be responsible to alter some aspects of cognitive functions.

Where applicable, the authors confirm that the experiments described here conform with The Physiological Society ethical requirements.

PCC166

Glutamate microinjection in the preoptic area increases body temperature in freely moving rats

T. Sengupta, A.K. Jaryal and H. Mallick

Physiology, All India Institute of Medical Sciences, New Delhi, India

Role of preoptic area (POA) in thermoregulation is suggested by many studies. Thermosensitive POA neurons receives and integrates local and afferent thermal information from peripheral thermoreceptors(1). Thermoregulatory responses are exercised by its neural connections with brainstem thermoefferent structures and target tissues. Many endogenous substances affect thermoregulation by altering activity of the POA thermosensitive neurons. Microinjection and microdialysis studies reveal the role of different neurotransmitters in the POA regulating body temperature. Presence of excitatory neurotransmitter, glutamate at the POA is known(2). Its role in many physiological functions has been reported (3,4). However, role of glutamate per se on thermoregulation is not reported in awake rats. The present study was done as per the guidelines of the Institutional Animal Ethics, AIIMS and Committee for the Purpose of Control and Supervision of Experiments on Animals (CPCSEA). Under sodium pentobarbitone anesthesia (40mg/kg BW,i.p), 14 adult male Wistar rats (8 glutamate injected, 6 saline injected) were implanted with a K-type thermocouple at hypothalamus(5) and peritoneal transmitter to record brain and body temperature (Tbr, Tb) respectively. Voveron (0.1mg/kg BW) was given to reduce pain during postoperative recovery. Gentamicin (40 mg/kg BW,i.m) was given as antibiotic for 3days. Effect of intrapreoptic microinjection of glutamate (20ng/200nl) on Tb, Tbr (2h prior and 4h postinjection) was studied after 10 days of post-surgical recovery. Microinjection site was confirmed histologically. Tb and Tbr are expressed as mean±SD. There was a constant rise in Tb ranging from 38.3±0.7°C to 38.8±0.3°C which spanned the total post-injection recording period and the maximum Tb was 39.0±0.5°C. There was also rise in Tbr during the post-injection recording period, ranging from 38.6±0.3°C to 38.9±0.2°C and the maximum Tbr was 39.0±0.1°C. At each time-point (15 min interval), 4 h post-injection data of glutamate and saline was compared with the corresponding time-matched control data using independent sample T-test. It was found that glutamate microinjection led to significant increase in Tb and Tbr at all time-points ($p<0.05$, $p<0.005$, $p<0.001$). During most of the post-injection time of hyperthermia, rats maintained curled up posture with pilorection and immobility. Whereas, maximum rise in Tb and Tbr after saline microinjection was 37.9±0.3°C and 37.7±0.2°C respectively, which was significantly lower than the hyperthermia, observed after glutamate microinjection. Moreover, hyperthermia due to glutamate was decreased by intraperitoneal injection of propranalol, indicating involvement of brown adipose tissue thermogenesis. We propose that glutamate in the POA participate in both heat production and conservation mechanisms.

Nagashima K *et al*. (2000) *Auton Neurosci* 85, 18-25.

Van Den Pol *et al*. (1994) *J of Comp Neurol* 343, 428–444.

Mahesh KK *et al*. (2011) *Behav Brain Res* 217, 240-243.

Dominguez JM *et al*. (2006) *J Neurosci* 26, 1699 –1703.

Srividya *et al* (2004) *Neurosci* 139, 853-864.

The study was supported by Ajinomoto Co. Inc., Japan.

Where applicable, the authors confirm that the experiments described here conform with The Physiological Society ethical requirements.

PCC168

The effect of affective pictures on heart rate variability

S.K. Deo, D. Sharma and R. Khadka

Department of Basic and Clinical Physiology, B.P.Koirala Institute of Health Sciences, Dharan, Nepal

Emotion regulation depends critically on an individual's ability to adjust physiological arousal on a momentary basis. Heart rate variability (HRV) is a measure of the continuous interplay between sympathetic and parasympathetic influences on heart rate that yields information about autonomic flexibility and thereby represents the capacity for regulated emotional responding. Although researches still does not provide theoretical and empirical support for the emergence of Heart rate variability as a marker of emotion regulatory ability. The objective of this study was to assess Heart rate variability in response to negatively and positively valenced pictures. One hundred and two International Affective Picture System (IAPS) photographs were grouped into 3 sets of 34 photographs: neutral, positive and negative. Each picture in a set was displayed for 6 seconds followed by 3 second interval before the next picture. The study was conducted in 24 healthy male students [age= 25(24-26)]. Each student was shown three sets of stimuli and their ECG was recorded simultaneously for 5 minutes. Time and frequency domain variables of HRV were calculated and compared among different sets of stimuli. Statistical significance was tested with Friedman test. P value < 0.05 was considered significant. Sympathetic (LF pr, LFnu, LF/HF) and parasympathetic indices (SDNN, RMSSD, NN50cnt, HFpr, HFnu) of HRV analysis in three different sets of stimuli were insignificant when compared among the sets. These data suggest that the affective pictures from International Affective Picture System (IAPS) shown in our study have no effects on cardiac sympathetic and parasympathetic activity.

Where applicable, the authors confirm that the experiments described here conform with The Physiological Society ethical requirements.

PCC169

Nerve conduction and short-term heart rate variability in football players

D. Sharma, B. Paudel, D. Thakur and R. Khadka

Basic and Clinical Physiology, BP Koirala institute of health sciences, Dharan, Nepal

Regular aerobic exercise causes autonomic/cardiac electrophysiological changes. Repetitive motions, muscle contractions, rapid & coordinated movements, and extreme foot positions in footballers influence somatic nerve electrophysiological properties. These training effects on somatic nerves are less clear. Heart rate variability (HRV) & nerve conduction study (NCS) variables together in athletes have been poorly studied. Thus we hypothesized that chronic exercise causes changes in HRV and NCS variables simultaneously and aimed at studying somatic nerve conduction and heart rate variability in football players. The football players (n=27, age 22.74±2.52 yrs) with excellent or good cardio-res-

piratory fitness, as assessed by simple three-minute step test, and sedentary controls (n=29, age 23.41±2.95 yrs) formed the study population. Their tibial and sural nerve conduction and short term heart rate variability were assessed following standard protocols. The difference between the groups was tested by Mann-Whitney U test. A p-value <0.05 was considered statistically significant. The football players had lower resting heart rate, systolic and diastolic BP than sedentary controls. In nerve conduction study; right tibial proximal compound muscle action potential (CMAP) amplitude [12.30(10-17.70) vs 11.10(8.0-13.50) mV, p=0.035], left tibial proximal [14.0(10.20-17.0) vs 11.20(7.33-14.30) mV, p=0.045] and distal [16.80(13.80-19.50) vs 14.20(10.15-17.80) mV, p=0.049] CMAPs amplitude were higher whereas right tibial proximal [7.50(7.0-8.80) vs 9.0(7.30-10.75) ms, p=0.005] and distal [7.20(6.70-8.10) vs 8.30(7-10.25) ms, p=0.046] CMAPs duration were lower in players compared to controls, similar results were obtained for left tibial CMAPs duration. They also had lower left sural sensory nerve action potential (SNAP) duration [1.80(1.50-1.80) vs 2.00(1.69-2.16) ms, p=0.018]. In HRV, high frequency power, a parasympathetic marker, was higher [1019(582-2127) vs 277(105.50-695.0) ms2, p=0.001] but low frequency in normalized unit [42.30(31.40-50.50) vs 57.80(43.60-70.55), p=0.001] and LF/HF [0.734(.459-1.02) vs 1.372(.775-2.40), p=0.001], the sympathetic markers, were lower in players compared to controls. Higher tibial CMAPs amplitude in football players suggests increase in size / number of muscle fibers / increase in efficiency of neuromuscular transmission. Less tibial CMAPs and sural SNAP duration indicate increase in synchronicity of muscle fibers and sensory nerve fibers discharge respectively. Increase in synchronicity of discharge may be due to narrow range of conduction velocities in motor axons and in sensory axons. Along with somatic nerve changes, football players had higher cardiac parasympathetic and lower sympathetic activity, suggesting synchronized autonomic and somatic adaptation in response to aerobic training.

Where applicable, the authors confirm that the experiments described here conform with The Physiological Society ethical requirements.

PCC170

Nerve conduction study and heart rate variability in obese persons

R.L. Yadav, R. Khadka, D. Thakur, K. Agrawal and B. Paudel

Department of Basic and Clinical Physiology, B.P.Koirala Institute of Health Sciences, Dharan, Nepal

Obesity increased worldwide (35.5% obese & 66% overweight in USA, 2012; 30%- Mexico, 2009) and in other South Asian countries, including Nepal & Bangladesh (from 1.6% - 10% & from 2.7% - 8.9% respectively, 2006). Studies have indicated an increase in all cause mortality (>300,000 deaths/year) with increased obesity, especially death from cardiovascular disease. Hence, obesity is considered as a major public health problem. Though measurement of body fat is too complex, body mass index (BMI, kg/m2) & waist-hip ratio (WHR) are used in daily practice. According to WHO, BMI≥30 kg/m2 is classified as obese & WHR cut-off being 0.9. There are controversial results of different studies regarding effects of obesity on autonomic nervous system and peripheral somatic nerves. Thus, our objective is to study the nerve conduction (NCS) and heart rate variability (HRV) in adult obese persons. The study was conducted on 30 adult obese persons (BMI>30, kg/m2) and 29 healthy normal weight persons (BMI, 18-24, kg/m2). In all subjects, short-term heart rate variability (HRV) and nerve conduction were assessed using standard protocol. The data obtained were analysed between the groups using Mann Whitney U test and presented as median (inter-quartile range). P value < 0.05 were considered as statistically significant. In comparison to normal weight persons, obese had lower compound muscle action potential (CMAP) amplitudes of right median [9.09(7.62-10.20) Vs 10.75(8.71-12.2), mV, p=0.025], and right [8.5(7.04-11.18) Vs 12.1(10.55-15), mV, p=0.000] and left tibial [9.08(6.58-11.65) Vs 13.05(10.2-15.6), mV, p=0.002] nerves. Whereas, obese persons had prolonged CMAP durations of right [10.5(9.62-12) Vs 10(8.4-10.3), mV, p=0.02] and left median 10.85(10-11.88) Vs 10(9-10.57), mV, p=0.019] nerves, and right tibial [10(9-11) 8.5(7.92-10), mV, p=0.032] nerve. Sensory NCS showed similar results. Among HRV variables, SDNN [35.55(26.77-49.25) Vs 46.15(37.22-58.57) ms, p=0.038], RMSSD [28.75(16.72-38.35) Vs 41.55(30.6-56.75), ms, p=0.018], NN50 count [15.5(2-39) Vs 83.5(32.75-116.25), p=0.010], pNN50, HF power and SD1, which reflect cardiac parasympathetic activities were significantly lower whereas, sympathetic marker LF/HF [1.2(0.65-2.20) Vs 0.79(0.5-1.02), p=0.045] was higher in obese persons than in the normal weight persons. Thus, we conclude that obesity affected autonomic modulation with an increase in sympathetic tone coupled with a reduction in vagal tone, indicating poor cardiac rhythm control. However, nerve conduction study showed a tendency of poorer amplitudes and lengthened CMAP and SNAP durations, which might lead to future somatic neuropathy in obese persons. The obesity affected predominantly parasympathetic function and the parasympathetic fibers are usually myelinated. Thus, both the NCS & HRV indicates that obesity might alter the myelination of both somatic & autonomic nerve fibers.

Where applicable, the authors confirm that the experiments described here conform with The Physiological Society ethical requirements.

PCC171

Effects of yoga on surface electromyography (EMG) of upper trapezius muscle and pain score in cervical spondylosis

D.M. Limbu

Basic and clinical physiology, BPKIHS, Dharan, Nepal

Introduction: Cervical spondylosis is a degenerative disorder of intervertebral disk progressing with advancing age. It is characterized by pain in the neck and shoulders, and headache.
Objectives: The study aimed at investigating the effect of yoga on neck muscle EMG in cervical spondylosis and pain associated with it.
Hypothesis: Yoga will provide effective adjuvant therapy in cervical spondylosis patients.
Materials and Methods: EMG of upper trapezius and neck disability index (NDI) were recorded in cervical spondylosis patients (n=10). Pain was evaluated by 0-10 grade visual analogue scale (VAS). Then, the patients did selective yoga techniques (Tadasana, Pranayama and Schandhachakra) for four weeks. All the variables were recorded after four-week yoga. The pre- and post-yoga data were compared by Wilcoxon Sign Ranks test.
Results: Yoga decreased EMG amplitude on both sides of upper trapezius muscle during Tadasana. NDI and VAS were significantly reduced but EMG frequency showed decrement trend.

In addition, the doses of the nonsteroidal anti-inflammatory drugs were reduced by >50%.
Conclusion: It is concluded that four-week prescribed yogic techniques are useful as an adjuvant therapy for cervical spondylosis by reducing muscular tension and spasm possibly by correcting posture leading to better oxygen consumption in damaged tissue and reversal of abnormal bone growth.

Swami Karmananda.Yogic management of common diseases. Yoga publications Trust. Munger, Bihar school of yoga . Ist ed.2001. p151.

Ott MJ . Mindfulness meditation: a path of transformation and healing. J Psychoses Nurs Ment Health Serv 2004 Jul;42(7);22-9.

Kulkarni GS. editor. Text book of Orthopedic and Trauma. Vol III Jaypee 1999.

Paynee EE, Spillane JD. The cervical spine- an anatomicopathological study of 70 specimens with particular reference to the problem of cervical spondylosis. Brain 1951;80:571- 97.

FriedenbergZ B, Hiller WT. Degenerator disk disease of the cervical spine- a comparative study of symptomatic and asymptomatic patients. JBJS 1963;45A: 1171- 8

Limbu DM, Paudel BH, Bhatia SC, Singh GK*, Gulati R Department of Physiology, *Government of India Advisor to BPKIHS

Where applicable, the authors confirm that the experiments described here conform with The Physiological Society ethical requirements.

PCC172

Effects of acupuncture and moxibustion on mechanical and thermal pain threshold in master cell deficiency rats

X. Gao, K. Liu, H. Wang, Q. Qin, L. Qiao, C. Cui, Y. Zhao, L. Li and B. Zhu

China Academy of Chinese Medical Sciences Institute of Acupuncture and Moxibustion, Beijing, China

Objective: Previous study has showed that acupuncture analgesia is closely related to the functional status and degranulation of mast cells, and the analgesic effects of manual acupuncture rely on mast cell and its degranulation more. The present study recruited a c-kit gene knockout rats which mast cells are not expressed to explore the analgesic effects of manual acupuncture, different intensities of electroacupuncture- and moxibustion-like stimulation.
Methods: The present study was performed on WsWs—, a c-kit gene knockout rat which mast cells is not expressed, and homogenous wildtype WsRC++ rats, twenty of both kinds were recruited to be control. The thresholds to noxious thermal and mechanical stimuli were measured with Ugo Basile Tail Flick Unit and electronic Von Frey anesthesiometer respectively. Somatic stimulation as 43 and 46 degree centigrade warm water, electroacupuncture of 1mA, 3mA and manual acupuncture were selected before pain thresholds tested.
Results: For the WsRC++ rats, electroacupuncture, manual acupuncture and moxibustion increased the paw mechanical and thermal withdrawal latency, and high intensity stimulation showed better effect than low intensity stimulation, especially for electroacupuncture with high intensity. Compared in the WsWs—rats, the mechanical threshold increase induced by manual acupuncture in WsRC ++ was not attenuated, whereas the increased mechanical thresholds induced by electroacupuncture with low intensity and moxibustion were lower in knockout animals than those in wildtype, if not, even no increase was observed. Thermal threshold in c-kit knockout rats was not significant different from that of wildtype.
Conclusion: For mechanical threshold, the analgesic effect of electroacupuncture might be closely related to mast cells. Whereas, the analgesic effect of manual acupuncture is not dependant on mast cells. And for the thermal threshold, none of the three stimulations was dependant on mast cells obviously.

The study was supported by National Scientific Foundation of China (No. 81173345). And Xin Yan GAO is a recipient of the travel awards for young physiologists from the Chinese Association for Physiological Sciences (CAPS).

Where applicable, the authors confirm that the experiments described here conform with The Physiological Society ethical requirements.

PCC173

Effect of simvastatin on erythrocyte membrane proteins in endotoxemic rats

H. Yorulmaz[1], G. Ates[3], E. Ozkok[2], I. Albeniz[4] and A. Tamer[3]

[1]School of Nursing, Halic University, Istanbul, Turkey, [2]Neuroscience, The Institute for Experimental Medicine, Istanbul, Turkey, [3]Physiology, Isanbul University, Istanbul, Turkey and [4]Biophysics, Istanbul University, Istanbul, Turkey

Motivation/problem statement: Sepsis, which causes deterioration of the microcirculation homeostasis, biochemical and physiological changes in the blood vessels. Sepsis leads to death of the organism as a result of organ failure. Membran proteins are alpha- and beta-spektrin, ankyrin, actin (band 5) and band-3, protein 4.1 and glycophorin A,B,C have an important roles in the maintaining in structural and functional integrity and the protection of shapement of the red blood cells. Studies shown that sepsis causes increased free radicals and lipid peroxidation of membrane proteins and erythrocyte deformability in literatures. Recent studies in patients with acute systemic inflammation were reported that simvastatin inhibits vascular hyporeactivity and reduced the development of sepsis. In this study, we aimed the effects of simvastatin on membrane proteins in lipopolysaccharide (LPS) treated with Wistar albino rats.
Methods/procedure/approach : Following the approval of the ethical commitee adult rats were divided into 4 groups including control, endotoxemic, simvastatin and simvastatin plus endotoxemic.
Control group; was taken %0.9 NaCl (i.p.)(n=10).
Endotoxemic group; LPS (E.coli: O127:B8;20 mg/kg, i.p.) was given to occuring endotoxemia, after 4 hours, animals were taken experiment (n=10).
Simvastatin group: Simvastatin was given (20 mg/kg, p.o.) for 5 days and end of the 5th days animals were decapitated (n=10).
Simvastatin plus Endotoxemic group: Simvastatin was given for 5 days. At the 5th days, LPS was given and after 4 hours animals were taken experiment (n=10).
At the end of the experiment, blood samples were taken into tube with EDTA and erythrocytes were separated. Erythrocyte membrane proteins were detected with Sodium dodecyl sulphate polyacrylamide gel electrophoresis (SDS-PAGE). All of samples were applicated and run to SDS-PAGE with suitable molecular weight of markers. SDS-PAGE procedures were replicated three times for each samples.
RESULTS: In endotoxemic group, we shown decreased α-(280 kDa) and β-spektrin (MW: 246 kDa), ankyrin(MW: 210 kDa), compared to control group. However we found that there were

disappeared bands; actin (band 5) (MW: 43 kDa) and Band-3 (MW: 100 kDa), protein 4.1(MW: 82 kDa) and glycophorin A,B,C (MW: 30 kDa) in the endotoxemic group.There were same protein bands compositions between control and simvastatin groups.
CONCLUSION/IMPLICATIONS: We found that decreased membrane proteins; alpha-spectrin, beta-spectrin, ankyrin and disappeared Band-3, Actin, Protein 4.1 Glycophorin A,B,C, proteins in the endotoxemic group. We also observed that simvastatin administration in LPS treated animals, distrupted red cell membrane proteins were found to improve in the study. It may represent a compensatory defensive mechanism supporting RBC function for living organism.

BALK RA., Severe sepsis and septic shock, Crit Care Clin, 16,179-92, (2000).

Whitfield CF, Follweiler JB,Lopresti-Morrow L and Miller BA (1991) Deficiency of Alpha –Spectrin Synthesis in Burst –Formimg Units –Erytroid in Lethal Hereditary Spherocytosis . Blood 78: 3043-3051.

Namzek JA, Hugunin K MS,Opp MR (2008) Modelling Sepsis in the laboratory :Merging Sound Science with Animal Well –Being.Comparative Medicine, 58:120-128.

Condon MR, Feketova E, Machiedo GW, Deitch EA, Spolarics Z. Augmented

erythrocyte band-3 phosphorylation in septic mice. Biochim Biophys Acta. 2007

May;1772(5):580-6. Epub 2007.

Garrabou G, Morén C, López S, Tobías E, Cardellach F, Miró O, Casademont J.

The effects of sepsis on mitochondria. J Infect Dis. 2012 Feb 1;205(3):392-400.

doi: 10.1093/infdis/jir 764. Epub 2011.

Where applicable, the authors confirm that the experiments described here conform with The Physiological Society ethical requirements.

PCC174

Bevacizumab: modulation of the bone microenvironment to reduce angiogenesis and metastasis?

S. Lunj, M.W. Reed, K.J. Reeves, C.A. Staton, I. Holen and N.J. Brown

Oncology, University of Sheffield, Sheffield, UK

Introduction: Bone metastasis is a major cause of breast cancer associated morbidity. Currently bisphosphonates are used to treat bone metastasis however no effective preventative measures are available. Vascular Endothelial Growth Factor A (VEGF) and associated receptor expression has been identified in bones from patients with metastatic breast cancer, representing a potential therapeutic target. Bevacizumab (Bz) inhibits VEGF-receptor interactions so may be effective in inhibiting angiogenesis and hence the formation of bone metastasis.
Methodology: 6-week old Balb/c nude female mice were injected intra-cardiac in the left ventricle with $1x10^5$ MDA-MB-231 luciferase labelled breast cancer cells under anaesthesia (isoflurane). Once bioluminescence (IVIS-Lumina2) was detected in bone by *in vivo* imaging, treatment commenced with Bz (0.1 or 0.5mg/kg, intraperitoneal twice-weekly for 6 weeks) or control vehicle (n=6/group). Tumour growth was monitored by twice weekly bioluminescence imaging. At the end of the experiment, hind limbs were harvested and processed for μCT analysis and bone histomorphometry.
Results: Bz (0.1mg/kg) inhibits breast cancer-induced bone metastasis compared to the vehicle control (treatment vs. control; 1000000 vs. 790000 total flux [p/s]) however bone mineral density remains unchanged. Initial analysis of osteoblasts (Ob) and osteoclasts (Oc) not in direct contact with the tumour suggests there is no difference in Oc number present on the trabecular surfaces in Bz-treated or control animals (Osteoclasts: Bz vs control; 0.125 vs. 0 per mm trabecular bone surface). In contrast, there appears to be decreased Ob numbers in similar regions in the Bz treated group (Osteoblasts: Bz vs control; 2.6 Bz vs. 7.5 control).
Conclusions: Preliminary data from this study indicate for the first time, that Bz reduces the bone tumour burden, however further in-depth analysis into the molecular mechanisms by which this is occurring, is being performed (i.e., CD31 vessel analysis, Ob/Oc counts in contact with the tumour).

Funding from the Breast Cancer Campaign is gratefully acknowledged

Where applicable, the authors confirm that the experiments described here conform with The Physiological Society ethical requirements.

PCC175

Cathepsin B is more active at acidic pH and regulates airway surface liquid through the cleavage of γENaC

C. Tan[1], M. Sameni[2], Y. Dang[1], H. He[1], B.F. Sloane[2], J. Stutts[1] and R. Tarran[1]

[1]Cystic Fibrosis/Pulmonary Research and Treatment Center, University of North Carolina at Chapel Hill, Chapel Hill, NC, USA and [2]Department of Pharmacology, Wayne State University School of Medicine, Detroit, MI, USA

BACKGROUND: Na^+ transport via the amiloride-sensitive epithelial Na^+ channel (ENaC) regulates airway surface liquid (ASL) volume and mucus clearance. In cystic fibrosis (CF) airways, increased sodium absorption depletes the ASL resulting in dysfunctional mucocilliary clearance and bacteria colonisation of the lung. Although serine protease such as prostasin is an important regulator of ENaC activity, it is largely inactive at pH seen in the acidic environment of CF airways. Here, we investigate the effect of pH and Cathepsin B (CTSB) activity on the regulation of ENaC. METHODS: The activity and expression of CTSB in polarised primary human bronchial epithelial cultures (HBECs; normal and CF) and ASL lavage were examined using fluorogenic substrates that are specifically cleaved by CTSB (Z-Arg-Arg-MCA, 50 μM) and western blotting respectively. We studied the effects of CTSB on amiloride-sensitive ENaC whole-cell currents (Δ*Iami*) using two voltage clamp and cleavage of ENaC by surface biotinylation in *Xenopus* oocytes. To demonstrate the physiological relevance of CTSB in polarised HBECs, we used confocal microscopy to measure the ASL height in the presence and absence of a cell-impermeable CTSB inhibitor (CA074, 10 μM). RESULTS: The activity of CTSB on the apical membrane surface and ASL lavage harvested from normal and CF polarised HBECs was significantly greater at pH 6 compared to pH 7.5, 7 or 6.5. Western blotting revealed that CTSB was secreted into the ASL in both normal and CF HBECs. Basal Δ*Iami* in oocytes expressing rat αβγENaC and CTSB exposed to pH 6 or pH 7.3 were not significantly different. However, coexpression of ENaC and CTSB stimulated ΔIami by approximately 6-fold from 681.7 ± 61.4 to 4143.3 ± 417.1 nA ($p < 0.0001$, n = 6) at pH 7.3. In the presence of hCTSB, trypsin, but not chymotrypsin, further stimu-

lated the Δ*lami*. Importantly, western blotting indicated a reduction in the molecular weight of surface-expressed γENaC in oocytes expressing ENaC and CTSB. In normal and CF HBECs, exposure to pH 6 Ringer solution significantly affect ASL regulation and reduced height from 13.4 ± 1.1 to 11.4 ± 0.9 μm ($p < 0.05$, n = 5) and 12.1 ± 0.8 to 7.5 ± 0.5 μm ($p < 0.05$, n = 5), respectively. CA074 significantly increased the ASL height in normal (11.4 ± 0.9 to 15.2 ± 1.5 μm, $p < 0.05$, n = 7) and CF (7.5 ± 0.5 to 11.5 ± 0.6 μm, $p < 0.01$, n = 7) HBECs at pH 6 but not pH 7.5. CONCLUSIONS: Taken together, these results indicate that CTSB, is secreted into the ASL, is more active at acidic pH and can regulate ASL height through the cleavage of γENaC. This is the first study to implicate CTSB in the pathphysiology of CF, suggesting that inhibitors of CTSB could potentially be used for the treatment of the disease.

Where applicable, the authors confirm that the experiments described here conform with The Physiological Society ethical requirements.

PCC176

Inositol hexaphosphate modifies the mucin component of the intestinal barrier

E.M. Onyango[1], B.M. Habiyambere[1], C. Madsen[2] and S. Gendler[2]

[1]East Tennessee State University, Johnson City, TN, USA and [2]Mayo Clinic, Scottsdale, AZ, USA

Consumption of increased dietary fiber is generally positively correlated to improved colon cancer prevention (1). Inositol hexaphosphate (IP6 or phytic acid) is an ingredient in plant foods such as legumes and cereals and has variously been shown to have anti-cancer activity (2). Our goal is to understand the influence of IP6 on the intestinal mucosal barrier function that may contribute to its anticancer activity. The objective in this study was to investigate the effect of IP6 on intestinal morphology and on mucosa mucin proteins that are constituent components of the intestinal barrier in mouse. In particular, expressions of specific mucins (Muc2, Muc3 and Muc4) were examined in the study (3, 4). C57BL/6 mice were randomized into 3 groups of 6 mice. Mice were orally dosed with IP6 (0, 1, 2 g/kg body weight) for 5 days and killed on the sixth day. Sections of the intestine were removed, fixed in methacarn, sectioned, stained with Alcian blue-PAS to visualize mucins, and immunostained for the presence of Muc2, Muc3 and Muc4 proteins. Mucosa from the jejunum and colon were removed and total RNA prepared using Trizol®. cDNA was prepared using random hexamers and specific primers were used for quantitative PCR amplification of the message for Muc2, Muc3 and Muc4. The iQ5 software (Bio-Rad, Hercules, CA) was used to calculate the expression of each gene at the different IP6 dose levels. Expressions at 1 or 2 g/kg dose were then calculated as fold changes relative to expression at the 0 g/kg dose. Expression of Muc2 in the jejunum increased 6.9 fold at 1 g/kg dose and 9.2 fold at 2 g/kg dose. In the colon it increased 1.6 fold at 1 g/kg dose but didn't change at 2 g/kg dose in the colon. Expression of Muc3 in the jejunum was unchanged when IP6 was dosed. In the colon, the expression increased 2.1 fold at 1 g/kg dose but decreased 5 fold at 2 g/kg dose. Expression of Muc4 in the jejunum increased 1.5 fold at 1 g/kg dose but didn't change at 2 g/kg dose. In the colon, it increased 1.3 fold at 1 g/kg dose but didn't change at 2 g/kg dose. Immunostaining with specific antibodies confirmed similar expression of these mucin proteins in the respective intestinal sections. The goblet cell count increased in the duodenum but decreased in the jejunum and ileum in IP6-treated animals. Thus, IP6 seems to modulate the goblet cell count and mucin protein component of the intestinal mucosal barrier.

Du W, Li WY, Lu R, Fang JY (2010). Folate and fiber in the prevention of colorectal cancer: between shadows and the light. World J Gastroenterol 16(8):921-926.

Fox, C. H. and M. Eberl (2002). "Phytic acid (IP6), novel broad spectrum anti-neoplastic agent: a systematic review." Complement Ther Med 10(4): 229-34.

Chang SK, Dohrman AF, Basbaum CB, Ho SB, Tsuda T, Toribara NW, Gum JR, Kim YS (1994). Localization of mucin (MUC2 and MUC3) messenger RNA and peptide expression in human normal intestine and colon cancer. Gastroenterology 107(1):28-36.

Weiss AA, Babyatsky MW, Ogata S, Chen A, Itzkowitz SH (1996). Expression of MUC2 and MUC3 mRNA in human normal, malignant, and inflammatory intestinal tissues. J Histochem Cytochem 44(10):1161-1166.

Research was supported by East Tennessee State University and Mayo Clinic.

Where applicable, the authors confirm that the experiments described here conform with The Physiological Society ethical requirements.

PCC177

Significance of crosstalk α-d-mannose- and sialic acid-containing glycoconjugates and inflammation in compromised esophageal mucosal integrity

O. Zayachkivska, N. Hrytsevych, M. Savytska, M. Gzhegotsky, A. Yaschenko and A. Lutsyk

Physiology, Lviv National Medical University, Lviv, Ukraine

Inflammation and endothelial dysfunction are central to esophageal barrier impairment and starting point for abnormal restitutio ad integrum and neoplastic processes [1]. WHO indicated that risk for premalignant Barrett's esophagus increased with chronic esophagitis. Glycoproteins incorporated into plasma membrane are essential for the initiation and regulation of immune responses and effective tool of representing injury-cell-associated immunogenicity in vivo. We hypothesized that α-d-mannose (αdMan) and sialic acid (NEU5AC) containing glycoconjugates interacted at a defence/receptor level in much the same fashion as pro-inflammatory cytokine in esophageal integrity. We therefore evaluated the receptor αdMan and NEU5AC profiles and inflammatory signaling contributed for the esophageal phenotype of integrity and cytoprotection without/with L-tryptophan (L-Try) and melatonin (MT)-pretreatment, which enhancing esophageal barrier functions.

Erosive esophagitis (EES) by perfusion solution of 0,25 N HCl & pepsin and non-erosive esophagitis (NES) by Takagi, 1964 were induced in rats without/with L-Try (200 mg/kg per os) and MT (20 mg/kg/ip) treatment which were anaesthetized with intramuscular administration of ketamine (60 mg kg-1); after 24 h of injury rats were killing and the healing of esophageal lesions and estimation of esophageal mucosa destruction, inflammation and hyperplasia via histological score index (HSI), αdMan, NEU5AC expression by lectinhistochemistry; IL-1β, TNFα by ELISA.

Acidic perfusion induced topical EES and HSI was 2,5-folds time more than with MT treatment; NES was with constantly increased HSI in 150% in compare to MT treated rats showing the same effect as in model of acidic EES. Dynamic changes in

esophageal mucosa glycobiology features with higher intensity NEU5AC labeling in EES vs NES, and highest αdMan labeling was in endothelium of vessels in NES, indicated ion endothelial dysfuction in physiopathogenesis of non-erosive and erosive esophagitis. Basal IL-1β was 24,16±0,30 pg/ml, TNFα - 1,05±0,11 pg/ml. Induction of EES led to increased IL-1β to 55,35 ± 7,88 pg/ml, TNFα - 5,56 ± 0,55 pg/ml (p <0,05). In non-erosive lesions IL-1β increased at 38,7 %, TNFα - 65,6% relatively to control (p <0,05). Potent angiotropic Mel and L-Try effects were estimated on esophageal cytoprotection and repair via decreasing αdMan expression in esophageal vascular walls. Anti-inflammatory effect of L-Try was less then MT that caused decrease of IL-1β to 21,8%, TNFα – 35,1% compared to control.

This study suggests an important role for αdMan and NEU5AC in EES and NES cell survival. Novel findings relating to high αdMan expression in endothelium and NEU5AC in compromised esophageal mucosa integrity might be associated with the development low grade inflammation and metaplasia.

Zayachkivska O. (2012) Front Gastrointest Res 30:148–160.

Where applicable, the authors confirm that the experiments described here conform with The Physiological Society ethical requirements.

PCC178

Ob/Ob mouse jejunum has dysfunctional chloride secretion compared to lean controls

L. Leung, J. Kang, E. Rayyan, A. Bhakta, B. Barrett, D. Wilson, L. Tamura, K. Corbell, T.L. Broderick and L. Al-Nakkash

Physiology, Midwestern.edu, Glendale, AZ, USA

The ob/ob leptin-deficient mouse is hyperglycemic and obese. We used 14-week old ob/ob and lean mice. The goal of this study was to characterize jejunal function in this clinically relevant mouse model. We measured transepithelial short circuit current (Isc), across freshly isolated segments of jejunum. Basal Isc was significantly decreased 2-fold, in the ob/ob mice (50.5±9.5 μA/cm2, n=5) compared to lean mice (95.2±20.3 μA/cm2, n=4, P<0.05). The Isc in response to forskolin (10 μM, bilateral), bumetanide (100 μM, basolateral), and acetazolamide (100 μM, bilateral) was similar for ob/ob and lean mice. Jejunum morphology indicates that crypt depth was similar for both groups, and thus structural changes do not contribute towards the reduced Isc of the ob/ob mice. Villi length was significantly increased (by ~100 μm) in the ob/ob mice, suggesting a greater surface area for absorptive function. Expression of the transporter protein, Glut5 (normalized to GAPDH), was significantly increased in ob/ob mice 0.74±0.06 (n=l4, P<0.05), compared to leans (0.37±0.06, n=l l), whereas, expression of the Glut2 transporter was similar for both groups. These data suggest that basal jejunal Isc in ob/ob mice is ~1/2 that of lean mice, and may reflect slower transit times in the gastrointestinal tract in the ob/ob mice, which may contribute towards increased nutrient absorption (specifically increased fructose uptake via Glut5), increased weight gain, and the associated diabetic phenotype. The contribution of key jejunal epithelial transporters is under investigation.

Layla Al-Nakkash was supported by MWU intramural funds and Soy Health Research Program.

Where applicable, the authors confirm that the experiments described here conform with The Physiological Society ethical requirements.

PCC179

Involvement of TRPC channel in fibrogenic stenosis and inflammation in human colonic myofibroblast

R. Kurahara, M. Sumiyoshi and R. Inoue

Physiology, School of Medicine, Fukuoka University, Fukuoka, Japan

Purpose: Increasing attention has recently been directed to the pivotal role of myofibroblasts in the pathogenesis of fibrogenic stenosis and inflammation. Available evidence suggests that part of myofibroblastic function may reflect altered Ca2+ homeostasis. We thus explored a potential role of canonical transient receptor potential (TRPC) channels expressed therein by using human colonic myofibroblast cell line InMyoFib. Here we show that transforming growth factor (TGF)-β1, the major stimulator of intestinal fibrosis, requires TRPC4 and TRPC6-mediated Ca2+ influx for its effect on myofibroblast differentiation and interleukin synthesis.

Methods: InMyoFib were grown in SmBM medium supplemented with 5%FBS and growth factors (insulin, hFGF-B, hEGF, FBS and gentamicin/ amphotericin-B). Immunobotting and immunoprecipitation were performed to detect the expression and interactions of proteins, and Ca2+ influx through TRP channels was evaluated by digital imaging of Fura-2 fluorescence. The results were compared between control and TGF-β1(5ng/ml in 1%FBS/SmBM)-treated groups of InMyoFib and statistically evaluated by single and multiple comparison tests.

Results: the expressions of fibrosis marker α-smooth muscle actin (α-SMA) and cadherin were detected with TRPC6 and TRPC4, respectively. The expression level of α-SMA and cadherin was augmented by TGF-β1 stimulation, and this was significantly suppressed by treatment with SK&F96365 or transfection of TRPC4- and TRPC6-specific siRNA or their dominant negatives, respectively. Biochemical analysis indicated that the calcineurin-NFAT signaling is involved in the effects.

In realtime-PCR experiments, the production of four interleukins from InMyoFib was found significantly accelerated by siRNA knockdown and dominant negative transfection of TRPC6. Detailed immunoblotting and biochemical analyses suggested that Ca2+ influx through TRPC4 and TRPC6 may prevent the phosphorylation of Smad2, Erk1/2, and p38 MAPK proteins at the downstream of TGF-β receptors.

Conclusion: from these results, it is speculated that TRPC4 and C6 channels may play non-trivial roles in myofibroblast transformation/differentiation via NFAT signaling, thereby promoting fibrogenesis in the colon. It is also suggested that myfibroblast signaling pathways regulating interleukin production, which seem associated with the phosphorylation of Smad2, Erk1/2, and p38 MAPK as well as TRPC6-mediated Ca2+ influx, could be a promising target in treating fibrotic and inflammatory bowel diseases.

Hai L(Kurahara Rin), Kawarabayashi Y, Imai Y, Honda A, Inoue R. / Counteracting effect of TRPC1-asscoiated Ca2+ influx on TNFα-induced COX-2-dependent prostaglandin E2 production in human colonic myofibroblasts. (Am J Physiol Gastrointest Liver Physiol. 2011 301(2): G356-67)

Kawarabayashi Y*, Hai L(Kurahara Rin)*, Honda A, Horiuchi S, Tsujioka H, Ichikawa J, Inoue R. / Critical Role of TRPC1-Mediated Ca2+ Entry in Decidualization of Human Endometrial Stromal Cells. (* contributed equally) (Mol Endocrinol. 2012 May;26(5):846-58)

Davis J. et al./ A TRPC6-dependent pathway for myofibroblast transdifferentiation and wound healing in vivo.(Dev Cell. 2012 Oct 16;23(4):705-15)

MEXT-Supported Grant-in-Aid for Young Scientists (B)22790677; MEXT-Supported Program to supporting research activities of female researchers; Kaibara Morikazu Medical Science Promotino Foundation; Clinical Research Foundation; Central Research Institute of Fukuoka University

Δ130 and 3A TRPC6 was kindly provided by Dr. Nishida M at Kyusyu University

Where applicable, the authors confirm that the experiments described here conform with The Physiological Society ethical requirements.

PCC180

A polygalacturonic acid binding lectin from *Phaseolus vulgaris* induces selective toxicity on human liver carcinoma HepG2 cells

W. Pan, E. Fang and T. Ng

The Chinese University of Hong Kong, Hong Kong, Hong Kong

Lectins and hemagglutinins are proteins/glycoproteins, which have at least one non-catalytic domain that exhibits reversible binding to specific monosaccharides or oligosaccharides. They can bind to the carbohydrate moieties on the surface of erythrocytes and agglutinate the erythrocytes, without altering the properties of the carbohydrates. Being omnipresent in nature, lectins have been found in different kinds of organisms encompassing fungi, viruses, bacteria, plants, animals, and humans. Recently, lectins have been got much attention as therapeutic agents due to their diversity of function including anti-viral, anti-bacteria, anti-fungal anti-insect and anti-tumor activity.

We described here the purification and characterization of a *Phaseolus vulgaris* lectin that exhibits selective toxicity to human hepatoma Hep G2 cells and lacks significant toxicity on normal liver WRL 68 cells. This polygalacturonic acid–specific lectin (termed BTKL) was purified from seeds of *P. vulgaris cv. Blue tiger king* by liquid chromatography techniques. The 60-kDa dimeric lectin showed strong and broad-spectrum hemagglutinating activity toward human, rabbit, rat, and mouse erythrocytes. Bioinformatic analysis unveils substantial N-terminal sequence similarity of BTKL to other *Phaseolus* lectins. Among a number of tumor cells tested, BTKL exhibits potent anti-Hep G2 activity which is associated with (1) induction of DNA fragmentation, (2) production of apoptotic bodies and chromatin condensation, (3) triggering of cell apoptosis and necrosis, and (4) depolarization of mitochondrial membrane. Furthermore, BTKL could induce inducible nitric oxide synthase (iNOS) expression and subsequent nitric oxide production in vitro in mouse macrophages, which may contribute to its antitumor activity. In addition, BTKL could bring about a significant dose-dependent increase in the production of mRNAs of proinflammatory cytokines including interleukin-1 beta, interleukin-2, tumor necrosis factor alpha, and interferon-gamma. Taken together, the antitumor activity and mechanism of BTKL provided here suggest that it has potential therapeutic value for human liver cancer.

Where applicable, the authors confirm that the experiments described here conform with The Physiological Society ethical requirements.

PCC181

Effect of hypothermic perfusion in the isolated perfused rat liver (IPRL) on the proteasome

T. Carbonell[1], S. Sanchez[1], S. Dewey[2], N. Alva[1] and A. Gomes[2]

[1]Physiology and Immunology, University of Barcelona, Barcelona, Spain and [2]Physiology, Neurobiology and Behavior, University of California, Davis, Davis, CA, USA

Recently, much attention has focused on the use of hypothermic perfusion in isolated organs (Hessheimer, 2012). Preservation of livers at hypothermia (20 °C) lead to significant improvements (Vairetti, 2009) but also induces oxidative stress (Alva, 2013). The initial protection against oxidative damage may require the rapid removal of oxidized proteins by the ubiquitin-proteasome system (UPS). Whereas there is some consensus in that proteasomal activity degrades oxidized proteins, it remains controversial whether oxidized proteins are tagged by ubiquitin and then degraded by the 26S proteasome, or whether they are removed independently of ubiquitin (Shang, 2011).

The aim of the present work was to study the production of oxidative stress and the role of the UPS after hypothermic perfusion in isolated liver.

The procedure was approved by the Committee of Animal Care following EC guidelines. Male SD rats (n=6 per group) were anesthetized (sodium pentobarbital, 60 mg/Kg ip) and their livers removed for perfusion (3 mL/min/g) with Krebs-Henseleit buffer. Normothermic livers (NT) were perfused at 37 °C thoroughly the experiment (30 min). Hypothermic livers were perfused 15 min at 37 °C and then were switched to cold at 26 °C (HT26) or 22 °C (HT22) further 15 min. We measured 4-HNE protein adducts and advanced oxidation protein products (AOPP); the expression of ubiquitin conjugates and subunits of the proteasome 26S: the 19S regulator (Rpt1, Rpt6 and phosphoRpt6 proteasomal ATPases) and the 20S core. The 26S β5 proteasome proteolytic activity was also assayed. Data (mean ± SEM) was analyzed by ANOVA.

Our results showed that hypothermic perfusion leads to protein oxidation as demonstrated by increased HNE-protein adducts and AOPP ($p<0.05$). As regards to the UPS, the presence of poly-ubiquitinated proteins was higher in hypothermia ($p<0.001$). No differences were observed in the expression of the 20S. The expression of Rpt1 and Rpt6 did not change. However, we found a significant increase in the ratio phospho-Rpt6/Rpt6 from NT (0.59±0.06) to HT26 (1.06±0.09, $p<0.05$) and HT22 (1.24±0.1, $p<0.01$). Rpt6 S120 phosphorylation has been suggested to cause an enhancement in the 26S proteasome activity. Accordingly, the 26S β5 activity was significantly increased in HT26 (46%) and HT22 (42%) groups ($p<0.01$).

These results suggest that phosphorylation of 19S subunit, Rpt6 at S120, which is part of the 26S proteasome, activates the proteasome during hypothermia. This is likely to be an important mechanism to quickly increase in the activity to the proteasome independent of increasing the amount of the proteasome.

Conclusion: Hypothermic perfusion induces protein oxidation. The UPS is activated to repair this damage, which partly increases its activity due to the Rpt6 subunit phosphorylation.

Alva N, et al; (2013) Experimental Physiology doi:10.1113/expphysiol.2012.071365.

Hessheimer AJ, et al ; (2012) Current Opinion in Organ Trasplantation 17 :143-147.

Shang F, et al; (2011). Free Radical Biology and Medicine 51, 5-16.

Vairetti M, et al; (2009). Liver Transplantation 15, 20-29.

Supported by research grant FIS and ERDF (PI08-1389)

Where applicable, the authors confirm that the experiments described here conform with The Physiological Society ethical requirements.

PCC182

Dietary plasma protein supplements prevent in part changes in colonic mucosal permeability that characterizes the mdr1a-/- mice model of colitis

M. Moretó[1,3], L. Miró[1,3], M. Maijò[1,3], J. Polo[2] and A. Pérez-Bosque[1,3]

[1]Departament de Fisiologia, Universitat de Barcelona, Barcelona, Spain, [2]APC Europe, Granollers, Spain and [3]Institut de Nutrició i Seguretat Alimentària, Universitat de Barcelona, Barcelona, Spain

Dietary supplementation with animal plasma proteins can prevent intestinal inflammation induced by enterotoxin B of S. aureus in rats, and reduce the lung inflammatory response induced by LPS in mice. The mechanism of action involves the modulation of the gut associated and nasal associated lymphoid tissue, respectively. We have also shown that dietary supplementation with plasma proteins can reduce the structural and functional changes observed in the colon during the development of spontaneous colitis. This study examined the effects of these supplements on the expression of mucosal mucins and of a representative tight-junction protein, as they are determinant for the permeability properties of the crypt epitheilium. Wild-type (WT) mice and mice lacking mdr1a gene (KO) were obtained from Taconic (Germantown, NY) and maintained in the Animal Facility Service of the Barcelona Science Park (n = 10-12 mice per group). Mice were grown and maintained in specific pathogen free conditions until week 4 when they were transferred to conventional housing. Animals were supplemented with spray-dried porcine plasma protein (SDP, 8% w / w) or milk proteins (control diet). Diets were fed from day 19 (weaning) until day 56. The index of disease activity (DAI) was recorded throughout the experimental period. The permeability of the mucosa of the colon was analysed ex vivo by confocal microscopy using FITC-dextran 10 kDa as marker; the expression of E-cadherin was measured by Western blot, and the expression of transmembrane mucines MUC1 and MUC4 and secretory mucin MUC2 by RT-PCR. DAI increased progressively from day 39, reaching a value of 2.8 ± 0.5 in KO mice (0.7 ± 0.3 in WT controls, $P < 0.05$) at 56 days and this correlated well with the Histopathological index and the goblet cell depletion index. MUC1 expression was increased 4 times and no effects of diet were observed; MUC4 expression was increased 3-fold and this effect was prevented in part by SDP. The expression of secretory MUC2 followed the profile of goblet cell depletion, as expected. SDP was also effective in reducing the changes in MUC4 and MUC2 observed during colitis consolidation. Increased mucosal permeability in the KO mice was inversely correlated with E-cadherin expression. Both effects were prevented by dietary SDP. We conclude that dietary supplementation with SDP is able to prevent in part the changes in the expression of transmembrane and secretory mucines, and of junctional E-cadherin during the development of spontaneous colitis. The good correlation between DAI and crypt permeability indicates that junctional proteins and mucine production are adequate markers of the colitis syndrome.

Supported by TRACE 2009 0317, Ministerio de Economía y Competitividad, Spain.

Where applicable, the authors confirm that the experiments described here conform with The Physiological Society ethical requirements.

PCC183

Protective effect of hypothermic preconditioning against ischemia/reperfusion in isolated rat liver. Assessment of the oxidative status

N. Alva[1,2], J. Palomeque[1], A. Negre-Salvayre[2] and T. Carbonell[1]

[1]Physiology and Immunology, Faculty of Biology, University of Barcelona, Barcelona, Spain and [2]Inserm U1048-I2MC, Paul Sabatier University, Toulouse, France

Introduction:
Some stressful stimuli are capable of inducing resistance when applied before ischemic events, which are known as preconditioning. The preconditioning by hypothermic perfusion has been validated in the heart perfused at 26 °C (Khaliulin et al. 2007). We have previously shown that perfusion of the liver at 22 °C improves antioxidant/oxidant profile compared with perfusion at 26 °C. Therefore, this study was designed to demonstrate the preconditioning effect of perfusion at 22 °C applied prior to an episode of ischemia in isolated rat liver focusing on oxidative stress indicators.
Material and Methods:
Fifteen male rats (200-250g) were anesthetized (sodium pentobarbital 60 $mg.g^{-1}$ I.P.) and then underwent laparotomy. The livers were perfused with oxygenated Krebs Henseleit buffer (95% O_2/5% CO_2, pH 7.4 at 37 °C) (Vairetti et al. 2006), excised and placed in an isolated perfused rat liver system at a flow rate of 4 $mL.min^{-1}.g^{-1}$. Livers were randomly divided into three experimental groups. The buffer temperature varied as follows: 20 min of normothermic perfusion in Ischemia/reperfusion (IR) group and 10 min of hypothermic perfusion (22 °C) + 10 min of rewarming (37 °C) in preconditioning + ischemia/reperfusion (PC + IR) group. Both groups underwent 40 min of ischemia and 20 min of reperfusion. Sham livers (S) were frozen without treatment. The levels of lipoperoxidation products (TBARS, 4-HNE and MDA), nitric oxide derivates, and protein oxidation indicators (AOPP) were measured in tissue homogenates. Paraffin-embedded liver sections were evaluated after incubation with antibodies anti-4-HNE.
Results and Discussion:
All data were expressed as percentage of Sham values ± S.E.M analysed by two-way ANOVA.TBARS increased after ischemia/reperfusión (IR) treatment but this harmful effect was reverted by preconditioning(from 207.2 ± 22.5 in IR to 95.6 ± 12.6 in PC+IR, $p<0.01$). The protection was also evident in MDA production (decreasing from 147.5 ± 16.9 to 83.1 ± 8.5, $p<0.01$) while was less clear in 4-HNE (from 182.2 ± 7.6 to 140.9 ± 6.0). The PC treatment also tended to diminish the liver content of nitric oxide products (from 216.3 ± 36.6 to 78.5 ± 48.21) and AOPP (from 108.8 ±8.4 to 72.4 ± 10.3). Histological examination of liver sections showed an increase in sinusoidal spaces in IR group that is less evident in the PC + IR group while immunohistochemistry assays showed a cytosolic location of 4-HNE antibodies in IR group.
Conclusion
A 10-min hypothermic perfusion was capable of reducing oxidative damage in the liver when applied just prior to an ischemic episode that shows its value as a preconditioning stimulus.

The tissue damage markers seem to indicate a modulation of the MDA production as main effect of this treatment.

Khaliulin I et al. (2007) *J Physiol* **581**, 1147-1161.

Vairetti MP et al. (2006) *J Hepatology* **44**, 894-901.

This study was supported by research grant PI081389

Where applicable, the authors confirm that the experiments described here conform with The Physiological Society ethical requirements.

PCC185

A PKG inhibitor enhances Ca2+-regulated exocytosis in guinea pig antral mucous cells: cAMP accumulation by inhibition of PDE2A

S. Tanaka[1,2], C. Shimamoto[1], Y. Kohda[1], H. Matsumura[1] and T. Nakahari[2]

[1]Laboratory of Pharmacotherapy, Osaka University of Pharmaceutical Sciences, Takatsuki, Japan and [2]Physiology, Osaka Medical College, Takatsuki, Japan

In antral mucous cells, acetylcholine (ACh, 1μM) activates Ca2+-regulated exocytosis, consisting of an initial peak that declines rapidly (initial phase) followed by a second slower decline (late phase) lasting during ACh stimulation. The initial phase is enhanced by cGMP (1). This enhancement was inhibited by a PKG inhibitor (Rp8BrPETcGMPS, 100 nM). However, Rp8BrPETcGMPS produced a delayed, but transient, increase in the exocytotic frequency during the late phase. On the other hand, cGMP is known to stimulate phosphodiesterase 2 (PDE2) which degrades cAMP (2). The aim of this study is to confirm that the delayed, but transient, increase induced by Rp8BrPETcGMPS was caused by inhibition of PDE2.

Male guinea pigs were anaesthetized by pentobarbital-Na (70 mg/kg, ip.). Antral mucous cells were isolated by a collagenase digestion. The exocytotic events were observed by videomicroscopy. The experiments were performed in accordance with the Guidelines of the Animal Research Committee of Osaka Medical College and the Guiding Principles for the Care and Use of Animals in the Field of Physiological Sciences (Physiological Society of Japan).

ACh alone stimulated cGMP accumulation, which enhances the initial phase in ACh-stimulated antral mucous cells (1).

Rp8BrPETcGMPS induced a delayed, but transient, increase in the frequency of the late phase, while it decreased the frequency of the initial phase. We examined the effects of a PKA inhibitor (PKI-amide) on the delayed and transient increase during the late phase induced by Rp8BrPETcGMPS in ACh-stimulated exocytotic events. A PKI-amide abolished the delayed and transient increase during the late phase induced by Rp8BrPETcGMPS. This suggests that Rp8BrPETcGMPS accumulates cAMP.

Analyses of Western blot and immunohistochemistry demonstrated that PDE2A exists in antral mucous cells. A PDE2 inhibitor (BAY-60-7550) induced a delayed and transient increase in the frequency of the late phase in ACh-stimulated exocytosis similarly to Rp8BrPETcGMPS. The measurement of cAMP content in antral mucosae revealed that BAY-60-7550 accumulates cAMP similarly to Rp8BrPETcGMPS during ACh stimulation. These results suggest that, in antral mucous cells, Rp8BrPETcGMPS decreases the activity of the cGMP-dependent PDE2 by inhibiting PKG, leading to cAMP accumulation.

Rp8BrPETcGMPS inhibited PDE2 in antral mucous cells, leading to cAMP accumulation by inhibiting cAMP degradation. This accumulation of cAMP induced the delayed, but transient, increase in the frequency of the Ca2+-regulated exocytotic events.

Saad AH et al. (2006). *Am J Physiol Gastrointest Liver Physiol* 290, G1138-G1148.

Komine N et al. (2002) *Odontology* 90, 7-12.

Where applicable, the authors confirm that the experiments described here conform with The Physiological Society ethical requirements.

PCC186

PPARα-induced enhancement of Ca^{2+}-regulated exocytosis in antral mucous cells of guinea pig

T. Nakahari[1], S. Tanaka[2], N. Sugiyama[2], C. Shimamoto[2] and H. Matsumura[2]

[1]Physiology, Osaka Medical College, Takatsuki, Osaka, Japan and [2]Pharmacotherapy, Osaka University of pharmaceutical Sciences, Takatsuki, Osaka, Japan

In antral mucous cells, acetylcholine (ACh, 1μM) activates Ca^{2+}-regulated exocytosis, consisting of an initial peak that declines rapidly (initial transient phase) followed by a second slower decline (late phase) lasting during ACh stimulation. We have reported that the initial phase is enhanced by PPARα in antral mucous cells (1). However, at present, it still remains uncertain how PPARα enhances $CaCa^{2+}$-regulated exocytosis in antral mucous cells. The aim of this study is to clarify the mechanism following the PPARα activation in antral mucous cells.

Guinea pigs were anesthetized by pentobarbital-Na (70 mg/kg, ip). Antral mucous cells were isolated by a collagenase digestion. The exocytotic events were observed by videomicroscopy. The procedures and protocols for these experiments were performed in accordance with the Guidelines of the Animal Research Committee of Osaka Medical College and the Guiding Principles for the Care and Use of Animals in the Field of Physiological Sciences (Physiological Society of Japan).

GW7647 (a PPARα agonist) enhanced the frequency of initial phase stimulated by 1 μM ACh. In the presence of GW6471 (a PPARα blocker), GW7647 did not enhance the initial phase, and rather the frequency of the initial phase was reduced to about 65 % of that seen in the absence of GW7647. However, GW6471 produced a delayed, but transient, increase in the frequency of late phase. A PKG inhibitor has been reported to produce a similar delayed, but transient, increase in the late phase, since the inhibition of PKG suppresses PDE2 leading to cAMP accumulation by inhibiting cAMP degradation. We examined the effects of a PKG inhibitor on the $CaCa^{2+}$-regulated exocytosis enhanced by GW7647. In the presence of a PKG inhibitor or a NOS inhibitor, GW7647 did not enhance the initial phase, and rather the frequency of the initial phase was reduced to about 65% of that seen in the absence of GW7647. However, a PKG inhibitor or a NOS inhibitor produced a delayed, but transient, increase in the frequency of the late phase. In the presence of GW6471, 8BrcGMP or NOC12 (an NO donor) still enhanced the Ca2+-regulated exocytosis without any delayed increase in the frequency of the late phase. This suggests that PPARα stimulates NO synthesis leading to cGMP accumulation. Moreover, 1 μM ACh or GW7647 increased NO production and cGMP contents in the antral mucosae. Analyses of Western blotting and immunohistochemistry demonstrated that NOS1 exists in antral mucous cells. Thus, PPARα stimulates NOS1 leading to NO synthesis and then NO accumulates cGMP resulting in the enhancement of Ca^{2+}-regulated exocytosis in antral mucous cells. A novel

autocrine mechanism mediated via PPARα maintains $CaCa^{2+}$-regulated exocytosis.

Sawabe Y et al. (2010) Peroxisome proliferation activation receptor alpha modulation of $CaCa^{2+}$-regulated exocytosis via arachidonic acid in guinea-pig antral mucous cells. Exp Physiol 95: 858-868.

Where applicable, the authors confirm that the experiments described here conform with The Physiological Society ethical requirements.

PCC187

Exercise attenuates ischemia-reperfusion injury of nonalcoholic fatty liver of the OLETF rat

T. Shibamoto, Y. Yamamoto, M. Tanida, Y. Kurata and S. Miyamae

Pysiology II, Kanazawa Medical University, Uchinada, Japan

Purpose: We sought to determine whether obesity prevention by exercise conferred protection against subsequent ischemia-reperfusion injury (IRI) to the fatty liver of the hyperphagic, Otsuka Long-Evans Tokushima Fatty (OLETF) rat after temporary vascular occlusion of 70% of the liver.
Methods: At 19 week of age, male OLETF rats (n= 7–8/group) were randomized to groups of sedentary (OLETF-SED)-IR, running exercise (OLETF-EX)-IR, or OLETF-SED-nonIR. Nonhyperphagic, control strain Long-Evans Tokushima Otsuka (LETO) rats were similarly assigned. Rats in the running exercise groups were subjected to running training on a motorized treadmill for 5 weeks. The rats anesthetized with pentobarbitone were cannulated in the carotid artery and jugular vein. After laparotomy, the bile duct was cannuated for measurement of bile flow rate. A laser Doppler probe was placed on the left lateral lobe to monitor peripheral liver blood flow (LBF). Regional ischemia was induced by applying an atraumatic vascular clip around the entire vascular supply to the median and left lateral lobes, enabling vascular occlusion of 70% of the liver, for 30 minutes. The animals were then monitored for 2 hours of reperfusion. Blood samples for alanine transferase (ALT) estimation (as a measure of parenchymal injury) were drawn immediately prior to ischemia, as well as 60 and 120 minutes after reperfusion. LBF and bile flow rate were measured at 15 min intervals.
Results: Exercise attenuated the increases in body weight and liver weight in the OLETF-SED rats. The ALT levels after reperfusion in the OLETF-SED rats were greater than that in the OLETF-EX rats as well as the LETO-SED rats. Exercise attenuated the reduction in LBF and bile flow rate due to ischemia-reperfusion in the LETO-SED group. In contrast, exercise did not provide significant influences on the LETO-SED rats.
Conclusion: Exercise attenuated the obesity and the ischemia reperfusion-induced disturbances of hepatic microcirculation and parenchymal injury of the hyperphagic, Otsuka Long-Evans Tokushima Fatty rats.

Where applicable, the authors confirm that the experiments described here conform with The Physiological Society ethical requirements.

PCC188

Concanavalin A-induced immune-mediated liver injury is attenuated by depletion of gastrointestinal bacteria

B. Mallard[1,2], A. Mabuchi[2], L. Quinlan[1] and A.M. Wheatley[1,2]

[1]Physiology, National University of Ireland Galway, Galway, Ireland and [2]Physiology, University of Otago, Dunedin, New Zealand

Background: Intravenous administration of Concanavalin (Con) A leads to an immune-mediated hepatitis in mice. Con A hepatitis involves the activation of T cells and Kupffer cells, which produce the cytokines interferon (IFN)-γ and tumour necrosis factor (TNF)-α. The lipopolysaccharide (LPS)/Toll-like receptor (TLR) 4 signalling pathway is involved in several forms of liver injury. Furthermore, several forms of experimental liver injury involve increased gut permeability. Con A-induced hepatitis is attenuated in mice deficient in TLR4. In the current study, the effect of depleting gut bacteria on Con A-induced hepatitis was investigated. The effect of Con A on gut permeability was also examined.
Methods: Groups of mice (C57BL/6) were treated for 5 days with Polymyxin B (150 mg/kg/day) and Neomycin (450/mg/kg/day) via drinking water to deplete Gram-negative bacteria in the gut. Control mice were given normal drinking water. Administration of Con A (20 mg/kg i.v) followed antibiotic treatment. Blood and tissue were harvested 8 or 24 hours later. Liver injury was assessed by measuring plasma ALT and histologically. In a separate group of mice, FITC-dextran was administered by oral gavage prior to Con A administration and its subsequent appearance in plasma was measured to assess gastrointestinal tract permeability. Permeability was further examined using an Ussing chamber to measure transepithelial resistance.
Results: Control mice developed severe liver injury following Con A administration, indicated by elevated plasma ALT and confirmed by histology. However, mice treated with antibiotics prior to Con A administration showed no significant elevation in plasma ALT at either 8 or 24 hours and reduced injury was seen on histological inspection. Mice treated with Con A displayed increased gut permeability, indicated by an increase in plasma FITC-dextran levels compared control (1578 ±370 ng/mL in Con A treated vs. 160 ± 26 ng/mL in control mice). Furthermore, Con A treated mice displayed a 20% reduction in transepithelial resistance compared to control mice, which is consistent with increased permeability.
Discussion: Our results show that Con A causes liver injury in mice with a normal bacterial population resident in the gastrointestinal tract. However, following the depletion of Gram-negative bacteria, Con A-induced injury is attenuated. Con A also increased gut permeability, indicating a disruption in the barrier function of the gastrointestinal tract. Together, these results suggest that the mechanism for Con A-induced liver injury involves increased translocation of LPS from the gastrointestinal tract by an as yet unknown mechanism and that the liver injury is dependent on activation of the LPS/TLR4 pathway.

Where applicable, the authors confirm that the experiments described here conform with The Physiological Society ethical requirements.

PCC189

Physiological roles of ezrin in the regulation of chloride secretion by cholangiocytes

R. Hatano[1], K. Akiyama[1], S. Hosogi[2], Y. Marunaka[2] and S. Asano[1]

[1]Department of Molecular Physiology, College of Pharmaceutical Sciences, Ritsumeikan University, Kusatsu, Shiga, Japan and [2]Dept of Molecular and Cellular Physiology, Graduate School of Medical Science, Kyoto Prefectural University of Medicine, Kyoto, Kyoto, Japan

The secretin dependent biliary secretion of ions and water by transporters and/or channels, which located at apical membrane of cholangiocytes, is essential for the regulation of bile flow. The cystic fibrosis transmembrane conductance regulator (CFTR) plays a critical role in the chloride secretion into the bile. In the cystic fibrosis (CF) patients, totally 5 to 10% of patients develop the progressive biliary fibrosis resembling primary sclerosing cholangitis. The loss of cystic fibrosis transmembrane conductance regulator (CFTR) ion channel function leads to the onset of liver disease in human. The ezrin, radixin and moesin (ERM) proteins are identified as cross-linkers between the plasma membrane proteins and actin cytoskeleton. Ezrin interacts with NHERF1 via its N-terminal binding domain and crosslink it with actin cytoskeleton via its C-terminal binding domain. On the other hand, CFTR interacts with NHERF1 via its c-terminal PDZ binding motif. In the cholangiocyte, ezrin, but not radixin or moesin, is exclusively expressed and colocalizes with CFTR and NHERF1 at apical membrane of cholangiocyte. Here we investigated that physiological role of ezrin in the regulation of biliary chloride secretion by CFTR in vitro. In the normal immortalized cholangiocytes, ezrin colocalized with CFTR and NHERF1 at the apical membrane. The apical surface expression of CFTR was examined by immunofluorescent staining and surface biotinylation. In the normal and wild type ezrin transfected cholangiocytes, CFTR colocalized with NHERF1 and ezrin at apical surface. However, the surface expression of CFTR was significantly reduced in the dominant negative (DN) ezrin transfected cholangiocyte. The dibutyryl cAMP treatment increased the surface expression of CFTR in DN-ezrin expressing cholangiocyte whereas it was still lower than normal and wild type ezrin transfected cells, suggesting that ezrin plays an important role for the apical targeting of CFTR. Consistent with the reduction of surface expression of CFTR, chloride efflux activity was also decreased in the DN-ezrin expressing cholangiocytes. In conclusion, ezrin is required for the correct apical membrane localization of CFTR in the cholangiocyte.

Where applicable, the authors confirm that the experiments described here conform with The Physiological Society ethical requirements.

PCC190

Reversal of delayed gastric emptying in diabetic NOD mice by treatment with interleukin-10 (IL-10) is associated with restoration of network and function of intersitial cells of Cajal (ICC)

S.J. Gibbons, K. Choi, L. Sha, A. Beyder, P. Verhulst, J.E. Mason, T. Ordog, D.R. Linden, J.H. Szurszewski, P.C. Kashyap and G. Farrugia

Enteric Neurosciences Program, Mayo Clinic, Rochester, MN, USA

Delayed gastric emptying (GE) in non-obese diabetic (NOD) mice occurs in a subset of diabetic mice that fail to sustain elevated heme oxygenase-1 (HO1) expression in alternatively activated M2 macrophages (1). We demonstrated that mice with delayed GE and low HO1 expression have increased oxidative stress and loss of interstitial cells of Cajal (ICC). Induction of HO1 by treatment with hemin reverses delayed GE (2,3). Similar results were seen with interleukin-10 (IL-10) treatment. The aim of this study was to examine ICC morphology and function in IL-10 –treated mice. Methods: Mice were included if they developed delayed GE (T½ >118 min) within 10 weeks of start of hyperglycemia (glucose>250mg/dl). GE was measured every week. Mice with delayed GE were treated with vehicle (n = 5) or IL-10 (1 μg ip twice daily, n = 5). Smooth muscle membrane potential and electrical slow waves were recorded from circular muscle of the stomach at 12 regions distributed from the proximal body to distal antrum. After recording, tissues were doubly immunolabeled for HO1 and for Kit to identify ICC. Confocal images were also collected at 12 places distributed across the tissue. ICC and HO1 labeling were scored by 2 independent investigators blinded to the image source. Results: Prior to treatment, mean T½ value were 180±19 min (n = 8, all delayed). While GE remained delayed in mice treated with vehicle (T1/2 = 157±11 min, n = 5), GE returned to normal after 3.1 ± 0.9 weeks in IL-10-treated mice (T1/2 = 106 ± 4 min, n=5). There were significant abnormalities in the electrical slow wave of all vehicle treated mice; abnormalities were not observed in IL-10 treated mice. Slow waves had a higher frequency, the rise time was faster and the events were broader in IL-10 treated mice than in vehicle-treated mice ($p < 0.05$, paired sign test). The parameters in IL-10 treated mice were similar to previously recorded slow waves from mice with normal GE. The most pronounced differences were seen in the distal antrum where slow waves in IL-10 treated mice had a faster frequency (Veh: 0.04±0.01, IL-10: 0.07±0.02 Hz, Mean±SEM, $p<0.05$, ttest) and lower variation in peak amplitude than in vehicle treated mice (Veh: 3.85±0.71, IL-10: 0.58±0.41, Mean±SEM, $p<0.05$ ttest). HO1 expression was significantly higher in tissues from IL-10 treated mice. ICC networks in vehicle-treated mice had patchy damage and were scored as significantly less intact than networks from IL-10 treated mice. Conclusions: Uneven damage to ICC networks likely underlies electrical abnormalities in the stomachs of diabetic mice with delayed GE. Treatment of delayed GE with IL-10 normalizes delayed GE, changes to ICC networks and slow wave abnormalities.

Choi KM et al. (2008). Gastroenterology 6, 2055-64

Choi KM et al. (2010). Gastroenterology. 7, 2399-409

Kashyap PC et al. (2010). Am J Physiol Gastrointest Liver Physiol. 6, G1013-9

This work was supported by NIH grants DK68055 and P30DK084567

Where applicable, the authors confirm that the experiments described here conform with The Physiological Society ethical requirements.

PCC192

Neuropeptide S reduce small intestinal motility in rats and humans

W. Wan Saudi[1], A. Halim[2], D. Webb[2], L. Gillberg[3], T. Rudholm Feldreich[3], M. Sundbom[4], E. Näslund[5], A. Sommansson[1], P.M. Hellström[2] and M. Sjöblom[1]

[1]Department of Neuroscience, Uppsala University, Uppsala, Sweden, [2]Department of Medical Sciences, Uppsala University, Uppsala, Sweden, [3]Department of Medicine, Gastroenterology Unit, Karolinska Institutet, Solna, Sweden, [4]Department of Surgical Sciences, Uppsala University, Uppsala, Sweden and [5]Clinical Sciences, Danderyd Hospital,, Karolinska Institutet, Stockholm, Sweden

Neuropeptide S (NPS) and its receptor are expressed by several cell types within the gastrointestinal (GI) tract, such as the epithelium, smooth muscle cells, submucosal neurons and enteroendocrine cells, in both rat and man. Polymorphisms of the NPS receptor are linked to increased risk of inflammatory bowel disease (IBD) as well as motor and sensory disturbances of the gut, suggesting a role for NPS in GI disorders. The aim of the present study was to elucidate the actions of NPS on duodenal mucosal barrier function and motility.

Male Sprague-Dawley (SD) rats (n=36; 300-350 g) were anaesthetized with thiobutabarbital 120 mg/kg body weight intraperitoneally The surgical and experimental protocol and methodology used have been described previously [1]. A brief summary is given here. A ~30 mm segment of the proximal duodenum was perfused in situ. The effects of intravenous (IV) administration of NPS and NG-nitro-L-arginine methyl ester (L-NAME) were investigated on mucosal paracellular permeability, bicarbonate secretion (DBS), motility and net fluid flux. In addition, studies of migrating motor complexes were carried out in SD rats (n=30; 300-350 g) with electrodes implanted in the small bowel. After baseline recordings with saline infusion, NPS was infused IV for 60 min and effects on myoelectric activity recorded. To relate the findings in rat to the human GI tract, circular muscle strips of human small intestine (n=7) was studied in an organ bath. The human tissue specimens were excised from patients during surgery for stomach or intestinal resection. All patients gave informed consent to enter the study. Tension changes were measured after stimulation with 1.0-20 nM NPS with and without electric field stimulation (EFS). Values are mean ± SEM, compared by 1-way ANOVA or paired t test when appropriate.

NPS (0.5, 5.0 and 50 nmol kg^{-1} h^{-1}) caused dose-dependent decrease in duodenal motility and paracellular permeability (e.g. from 431 ± 66 to 145 ± 51 AUC 10 min^{-1} and from 0.21 ± 0.03 to 0.09 ± 0.02 ml $min^{-1}100g^{-1}$, n=10, P<0.001 respectively). NPS did not induce any changes in DBS or net-fluid-flux. Pre-treating animals with L-NAME (3.0 mg kg^{-1} bolus dose followed by infusion of 1.0 mg kg^{-1} h^{-1}) abolished the effect of NPS on duodenal motility, but did not change that on permeability.

Similarly, NPS at 1.0 nmol $kg^{-1}min^{-1}$ increased irregular spiking, while 4.0 nmol $kg^{-1}min^{-1}$ (each dose n=6) significantly reduced spiking activity and increased the MMC cycle length (P=0.005).

In human smooth muscle strips, NPS (5.0 nM, n=7) dampened small intestine circular muscle contractility with and without EFS. In colonic muscle strips (NPS 5.0 nM) only sporadic dampening without EFS, but more consistent dampening (NPS 1.0 nM, n=5 P=0.04) with EFS, was observed.

In conclusion, these findings reveal evidence that NPS significantly decreases small intestinal motility and contractility in tissue of both human and rat origin. In addition, NPS decreases paracellular permeability. L-NAME abolished the effect of NPS on motility but was without effect on that to permeability. These results suggest important roles of NPS in the regulation of GI barrier functions and motility.

Sommansson A, Nylander O, Sjöblom M. Melatonin decreases duodenal epithelial paracellular permeability via a nicotinic receptor-dependent pathway in rats in vivo. J Pineal Res. 2013 Apr;54(3):282-91.

Where applicable, the authors confirm that the experiments described here conform with The Physiological Society ethical requirements.

PCC194

Acute and long-term administration of melatonin reduce ethanol-induced increases in duodenal mucosal permeability and motility in rat

A. Sommansson and M. Sjöblom

Department of Neuroscience, Uppsala University, Uppsala, Sweden

Melatonin is released from enterochromaffin cells in the intestinal mucosa, but the influence of melatonin on gastrointestinal function is still largely unknown. Recently we found that administration of melatonin decreases basal duodenal mucosal paracellular permeability and increases duodenal bicarbonate secretion (DBS).

The aim of the present study was to elucidate the acute and long-term effects of melatonin administration on ethanol-induced alterations of duodenal mucosal paracellular permeability and motility.

In this study male Sprague-Dawley (SD) rats (n=44; 250-375 g) were used. For evaluation of long-term effects of melatonin administration rats were given melatonin (0.1 mg/ml), or vehicle, in the drinking water for 14 days, while the other rats were given normal tap water.

Rats were anaesthetized with thiobutabarbital sodium (Inactin®) 120 mg/kg body weight intraperitoneally. The surgical and experimental protocol and methodology used have been described previously [1]. A brief summary is given here. A laparatomy was performed and a ~30 mm segment of the proximal duodenum, with an intact blood supply, was perfused in situ with saline for basal recordings followed by 15% ethanol (v/v) for 30 min. Effects on duodenal mucosal permeability [blood-to-lumen clearance of 51Cr-EDTA] and motility were investigated. Values are mean ± SEM, compared by 1-way ANOVA or paired t test when appropriate.

Luminal perfusion with 15% ethanol induced significant ($p<0.05$) increases in mucosal paracellular permeability and duodenal motility from 0.18 ± 0.06 to 1.67 ± 0.29 ml $min^{-1}100g^{-1}$ (n=9) and from 537 ± 46 to 1209 ± 148 AUC 10 min^{-1} (n=9) respectively. Pre-treating animals with an intravenous (IV) injection of melatonin 20 mg kg^{-1} 10 min before ethanol exposure reduced the ethanol-induced increase in 51Cr-EDTA clearance to 0.65 ± 0.23 ml min^{-1} $100g^{-1}$, $p<0.05$, n=6). In animals pretreated with 20 $mgkg^{-1}$ melatonin IV 15% ethanol failed to augment duodenal motility. Hexamethonium (10 $mgkg^{-1}$ IV followed by continuous IV infusion at a rate of 10 mg $kg^{-1}h^{-1}$, n=9) abolished the effects of IV melatonin.

In animals administered melatonin for 14 days 15% ethanol induced significantly ($p<0.05$) less increases in mucosal paracellular permeability compared to their corresponding vehicle (from 0.12 ± 0.02 to 2.30 ± 0.46 $mlmin^{-1}100g^{-1}$ (n=4) compared to 0.18 ± 0.06 to 2.94 ± 0.42 $mlmin^{-1}100g^{-1}$ (n=6) respectively). No increases in duodenal motility in response to 15% ethanol was observed in melatonin treated animals.
Our results show that melatonin reduces ethanol-induced increases in duodenal paracellular permeability partly via enteric neural pathways involving nicotinic receptors. In addition, melatonin inhibits ethanol-induced increases in duodenal motor activity. These results suggest that melatonin may serve important gastrointestinal barrier functions.

Where applicable, the authors confirm that the experiments described here conform with The Physiological Society ethical requirements.

PCC195

P2Y1 receptors are developmentally regulated in mouse pancreatic acinar cells

W.J. Wilkinson, J.V. Gerasimenko, O.V. Gerasimenko and O.H. Petersen

School of Biosciences, Cardiff University, Cardiff, Wales, UK

Purinergic (P2) receptors for extracellular adenosine triphosphate (ATP) are widely distributed throughout the body where they play diverse roles in cell signalling. P2Y receptors are metabotropic receptors that are also able to respond to ADP and uridine nucleotides, mobilising intracellular Ca2+ via the production of inositol 1,4,5-triphosphate. Ionotropic P2X receptors respond to physiological ATP and have varying degrees of Ca2+ permeability. P2Y1 receptors have previously been implicated in exocrine glands where they are thought to play a developmental role in salivary gland.
The potential for purinergic signalling in the pancreas is great since ATP is a ubiquitous neuronal co-transmitter and millimolar concentrations of ATP are found in pancreatic zymogen granules. Purinergic signalling is implicated in exocrine pancreas pathophysiology since P2Y2, P2X7 and the ectonucleotidase CD39 are all upregulated in pancreatitis and pancreatic cancer and CD39 expression levels correlate with long term disease survival. The mouse is frequently used in models of pancreas pathophysiology, but the role of purinergic signalling in the mouse exocrine pancreas is unreported.
Experiments were carried out on acutely isolated pancreatic acinar cells from C57BL6 mice, killed by cervical dislocation in accordance with UK Schedule 1 regulation of the Animal (Scientific Procedures) Act, 1986. Intracellular Ca2+-responses were measured by loading cells with Fura-2.
We observed in adult animals only a minority (34 ± 4 %; N = 17) of pancreatic acinar cells responded to 100 μM ATP, whilst 19 % of cells responded to ADP and 8 % to UTP. In the absence of extracellular Ca2+, ATP responses were maintained. However no cells responded to ATP in the presence of extracellular Ca2+, but not in its absence; suggesting there were no functional P2X receptors at the plasma membrane.
The proportion of cells responding to ATP increased to 90 ± 4 % (N = 7) when acinar cells were isolated from juvenile (6-18 days) mice, suggesting a developmental role for purinergic signalling in exocrine pancreas. In juvenile animals 87 % of cells responded to ADP, and 79 % responded to 100 nM MRS2365 a specific agonist of P2Y1 receptors. This response could be blocked by 100 nM MRS2500 a specific P2Y1 antagonist. Taken together these results suggest the developmental expression of P2Y1 receptors in pancreatic acinar cells. We also found in these cells that P2Y1 receptors were functionally coupled to enzyme secretion via the detection of extracellular amylase activity (with fluorescent BIODIPY-DQ starch dye) following P2Y1 receptor activation.
These results show P2Y1 receptors are developmentally regulated in pancreatic acinar cells and suggests P2Y1 receptors play an important role in exocrine gland maturation.

Novak I et al., (2002) Cell Physiol Biochem 12:83-92

Park MK et al., (1997) Am J Physiol 272:C1388-C1393

Where applicable, the authors confirm that the experiments described here conform with The Physiological Society ethical requirements.

PCC196

L-glutamate secretion in the pancreatic juice involves transport and metabolism of neutral amino acids in exocrine pancreas and is influenced by the content of protein in the diet

S. Araya[1], C. Lutz[1], L. Mariotta[1], B. Herzog[1], F. Verrey[1], T. Reding[2], R. Graf[2] and S.M. Camargo[1]

[1]Institute of Physiology and ZIHP, University of Zurich, Zurich, ZH, Switzerland and [2]Department of Surgery, University Hospital of Zurich, Zurich, ZH, Switzerland

The pancreas efficiently absorbs amino acids for the synthesis of enzymes, but also secrets free amino acids in the pancreatic juice which are re-absorbed by the small intestine. Under free protein diet, the release of amino acids on the pancreatic juice (PJ) may play important role on the homeostasis maintenance of the small intestine. From the 20 proteinogenic amino acids analyzed in the PJ, L-glutamate (Glu) was 4 fold more concentrated in PJ when compared to plasma levels. The concentrative mechanism could be due to an increase in the transport of Glu and the synthesis of Glu in the exocrine pancreas. Since there is a high expression of neutral amino acids and L-glutamine (Gln) transporters in the pancreas and they localize to the basolateral membrane of the acinar cells, we hypothesize Glu is synthesized in acinar cells and secreted to the pancreatic juice. We analyzed at mRNA level the expression of the 2 glutaminase isoforms (gls1 and gls2), glutamine synthase (Glul), alanine aminotransferase 1 and 2 (GPT1, GPT2) and aspartate aminotransferase 1 and 2 (GOT1 and GOT2) in pancreas. Our results showed that the two glutaminase isoforms (Gls1 and Gls2) are expressed in the pancreas, GLS2 is localized in the acinar cells, and that the levels of gls2 and of the cytoplasmatic GPT were elevated in animals receiving diet free of protein. These results suggest Glu may be synthesized in the exocrine pancreas from Gln and L-alanine and that the dietary protein content can modulate the expression of enzymes involved in the synthesis of Glu. The secretory mechanism of Glu to PJ could involve zymogen vesicles and transport via apical membrane. Our experiments showed that Glu and its precursors were not concentrating in zymogen granules vesicles (ZGV) but were found at high concentrations in the cytoplasmic fraction, suggesting the secretory mechanism does not involve exocytosis. Immunofluorescence and western blotting of isolated ZGV suggested that the sodium-dependent Glu transporter EAAT1 (Slc1a3) is present on the zymogen vesicles membrane. Additionally, immunofluorescence of pancreatic tissue showed that EAAT1 localizes proximal to the apical membrane of acinar cells. Our results support the hypothesis that EAAT1 is involved in the secretion of

Glu during vesicular docking to the apical membrane of acinar cells. These preliminary exciting results suggest a new mechanism for Glu concentration and secretion on the pancreatic juice, as well a recycling of neutral amino acids (L-alanine, Gln) and Glu between the pancreas and intestine.

Where applicable, the authors confirm that the experiments described here conform with The Physiological Society ethical requirements.

PCC197

Comparative levels of butyrate transporters in ulcerative colitis, Crohn's disease and normal patients

S. Roux[1], S. Daniell[2,1] and E.S. Fredericks[1]

[1]Biochemistry and Microbiology, NMMU (South Campus), Port Elizabeth, South Africa and [2]Pharmacy, NMMU (South Campus), Port Elizabeth, South Africa

It has long been known that butyrate manages oxidative stress and inflammation in the colon. Butyrate is absorbed in the colon and transported into colonocytes by monocarboxylate transporter isoform 1 (MCT1) and sodium-coupled monocarboxylate transporter (SMCT1). Butyrate is the major energy source for colonocytes and is produced by fermentation of carbohydrates by resident microbiota. Ulcerative colitis (UC) and Crohn's disease (CD) are two forms of idiopathic inflammatory bowel disease (IBD). Their exact etiologies are unknown, but a decrease in butyrate metabolism in colonocytes has been suggested to be a possible contributing factor. A transport deficiency of butyrate can possibly be a major contributing factor for the decreased butyrate metabolism.
AIM: To analyse and compare SMCT1 and MCT1 levels in colon biopsy samples of normal (n=19), ulcerative colitis (n=9) and Crohn's disease (n=8) patients.
METHOD: Colon biopsies were obtained with consent from normal, UC and CD patients. RNA was extracted from these samples and prepared for analyses using RT-qPCR. ALUSq, ALUSx and SF3A1 were used as reference genes.
RESULTS: The results of the RT-qPCR were analysed using one-way ANOVA and a Mann-Whitney test. SMCT1 is less expressed than MCT1 in the colon of all patients. MCT1 is significantly down regulated in colon samples of both UC and CD's patients when compared to normal patients with no colon pathology. MCT1 is also significantly less expressed in UC compared to CD patients.
CONCLUSION: MCT1 is the most important butyrate transporter in the colon. Lower butyrate transport expression can contribute to a less inflammatory inhibition in the colon. The lower expression of MCT1 in UC patients compared to CD patients could explain the higher incidence of developing colorectal cancer in UC patients.

Berno Burger for support in this study.

Where applicable, the authors confirm that the experiments described here conform with The Physiological Society ethical requirements.

PCC198

Potential effects of selenium on liver functions after ischemia reperfusion in old female rats

N.N. Lasheen and A.A. Mohamed

Physiology, Faculty Of Medicine, Cairo, Egypt

Background and aim: Ischemia/reperfusion (I/R) injury of the liver is an important clinical problem encountered in hepatic failure after shock, liver transplantation, or liver surgery, and in diverse situations, including heart failure, liver trauma, and blood occlusion to the liver. Liver functions are decreased in old age and oxygen radicals probably mediate some of the structural and functional alterations associated with ageing and with reperfusion of ischemic liver. This study aimed at investigating the effects of pre-treatment with the antioxidant selenium in an experimental model of hepatic I/R in old female rats.
Materials and Methods: The study was carried out on 40 old female Wistar albino rats(250-300 grams), allocated into 4 groups; I. Sham-operated control group, II. Partial liver I/R group, under anaesthesia with pentobarbital 40 mg/kg B.W. subjected for partial hepatic ischemia for 20 minutes followed by reperfusion for 20 minutes, III. Selenium pretreated group with 20 μg/Kg B.W. i.p. for 2 weeks followed by partial liver I/R, and IV. Selenium treated group for 2 weeks. At the end of experimental procedure, blood samples were collected, and the separated plasma was used for determination of liver enzymes (SGPT, SGOT & γ-GT) and plasma total antioxidant capacity (TAC). Liver malondialdehyde (MDA) was measured and liver tissue was examined histologically.
Results: Values are in Mean ± SEM, compared by ANOVA. Compared to the sham operated control, in partial liver I/R group; significant increase in SGPT (373.8±35.5 vs 40±5.1, IU/L) SGOT(364.9±7.1 vs180.9±18.8, IU/L), γ-GT (11.7±1.9 vs 6.5±0.87, IU/L) and liver malondialdehyde (24.9±1.2 vs 17.2±1.5, μM/gm wet tissue) and a significant decrease in total antioxidant capacity (0.35±0.05 vs 0.66±0.07, mM/L), associated with leukocyte infiltration of liver tissue. Although selenium treatment for 2 weeks had a non-significant improving effect on normal liver functions of old rats (SGPT: 21.1±3.7, SGOT: 173.1±11.2, γ-GT:6.9±1.2, MDA: 18.4±2.8, TAC: 0.68±0.04), selenium pretreatment for 2 weeks before partial liver I/R resulted in amelioration of the I/R hepatic injury, evidenced by the significant decrease in liver enzymes SGPT (286.3±20.9), SGOT (312.1±8.9), γ-GT (5.5±0.54) and liver MDA (19.7±1.1) and a significant increase in plasma TAC (0.72±0.05) associated with decreased leukocyte infiltration of liver tissue when compared to the partial liver I/R group.
Conclusion: Liver I/R in aged rats induces oxidative stress that markedly impairs liver functions and structure. Pretreatment with the dietary antioxidant selenium slightly improves liver functions in old rats, and of much value in protection of the liver of aged rats against I/R injury.

Where applicable, the authors confirm that the experiments described here conform with The Physiological Society ethical requirements.

PCC199

Villous movement of intestine is regulated by mutual interaction of subepithelial fibroblasts and afferent neurons via atp and substance-P

K. Furuya[1], S. Furuya[2] and M. Sokabe[3]

[1]FIRST Res Center Innovative Nanobiodevice, Nagoya University, Nagoya, Japan, [2]Natl Inst Physiol. Sci, Okazaki, Japan and [3]Dept Physiol, Med Sch, Nagoya University, Nagoya, Japan

Intestinal villi are a unique structural and functional unit for the luminal sensing, digestion, absorption, secretion and immune defense in the small intestine. Subepithelial fibroblasts of the intestinal villi, which form a contractile network beneath the epithelium, are in close contact with epithelial cells, neurons, capillaries, smooth muscles and immune cells, and play pivotal roles in the villous functions. Here, we investigate the functional roles of subepithelial fibroblasts physiologically and morphologically using a primary culture and isolated epithelium-free villi of duodenum isolated from rats, which were anesthetized by pentobarbital (0.1ml/100g) and decapitated. Villous subepithelial fibroblasts possess purinergic receptor P2Y1 and tachykinin receptor NK1. ATP and substance-P (SP) induce increase in intracellular Ca2+ and cell contraction in cultured cells and also isolated villi observed using a two-photon laser microscope with indo-1 calcium dye. The localization of NK1R and SP in the villi was examined by light and electron microscopic immunohistochemistry. NK1R-like immunoreactivity was intensely localized on the plasma membrane of villous subepithelial fibroblasts. The villous subepithelial fibroblasts form synapse-like structures with both SP-immunopositive and -immunonegative nerve varicosities, mostly intrinsic afferents nerve terminals. They are highly mechano-sensitive and stretch stimulation of the cells cultured on an elastic (PDMS) chamber, induced ATP release, which observed by real time luciferin-luciferase bioluminescence imaging system using an image intensifier and a high sensitive EM-CCD camera equipped on an upright microscope. Large transient ATP releases (peak concentration over 10 μM) were observed in sparse cells and the released ATP spreads to the surrounding over several hundred μm and keeps enough concentration to activate P2Y1 for several ten seconds, which forms propagating Ca2+ waves and contraction of the cells. From these findings, we propose that the mutual interaction between villous subepithelial fibroblasts and afferent neurons via SP and ATP plays important roles in refined and coordinate villous movement in intestine.

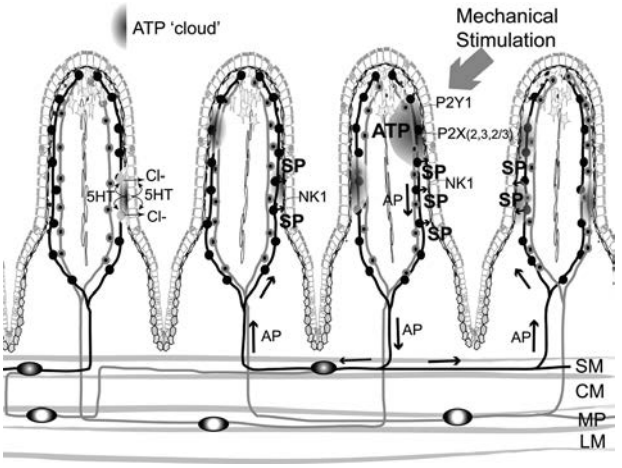

Fig. 1 Plausible contribution of the ATP and SP signaling to the coordinate movement of the intestinal villi.

Mechanically induced signal in a villus may spread to several neighboring villi through a trans-somatic reflex in an IPAN and also through synaptic connections. Activated IPAN may release SP from the varicosities in the surrounding villi, and the subepithelial fibroblasts are activated and contract by the SP via NK1. This inter-villus signaling via ATP and SP may contribute to coordinate movement and elegant mechanical properties of a mass of villi. ATP cloud (or circumstances) may be occurred here and there by mechanical and chemical (SP, ET or hypo-osmotic) stimuli of the subepithelial fibroblasts in the villi and enhance or modulate other signaling such as SP induced contraction of the subepithelial fibroblasts.

Furuya, S., Furuya, K., Shigemoto, R., Sokabe, M., 2010. Localization of NK1 receptors and roles of substance-P in subepithelial fibroblasts of rat intestinal villi. Cell Tissue Res. 342, 243–259

Furuya, S., Furuya, K., 2007. Subepithelial fibroblasts in intestinal villi: roles in intercellular communication. Int. Rev. Cytol. 264, 165–223.

Furuya, K., Sokabe, M., Furuya, S., 2005. Characteristics of subepithelial fibroblasts as a mechano-sensor in the intestine: cell-shape-dependent ATP release and P2Y1 signaling. J. Cell Sci. 118, 3289–304.

Furuya, S., Furuya, K., 2013. Roles of substance-P and ATP in the subepithelial fibroblasts of rat intestinal villi. Int.Rev.Cell Mol. Biol. in press

Where applicable, the authors confirm that the experiments described here conform with The Physiological Society ethical requirements.

PCC200

A physiological dietary regime for the management of gastroesophageal reflux disease - a pilot study

M.A. Randhawa[1], S.M. Mahfouz[2], N.A. Salem[3], T. Yar[4] and A. Gillessen[5]

[1]Pharmacology, College of Medicine, University of Dammam, Dammam, Saudi Arabia, [2]Endoscopy, King Faisal Hospital, Taif, Saudi Arabia, [3]Endoscopy, King Faisal Hospital, Taif, Saudi Arabia, [4]Physiology, College of Medicine, University of Dammam, Dammam, Saudi Arabia and [5]Internal Medicine, Sacred Heart Hospital, Muenster, Germany

The occurrence of gastroesophageal reflux disease (GERD) is increasing (1). Drug treatment is risky, particularly, in long term use, which is required in most cases. Irregular dietary habits possess strongest association with GERD (2). Transient lower esophageal sphincter relaxations (TLESRs) are important cause of GERD. Gastric distention in upper stomach is the strongest stimulus for generation of TLESRs and is aggravated by intake of food in between meals (3). Considering pathophysiology of GERD, it is suggested that increasing interval

between meals will reduce reflux episodes. The present pilot study was conducted on 20 patients, outpatients in Sacred Heart Hospital, Muenster, Germany and King Faisal Hospital, Taif, Saudi Arabia. All had heartburn symptoms and endoscopically proven reflux oesophagitis, Los Angeles grad a, b or c. They were offered to take two meals per day plus only soft drinks in between. On day 14 they were contacted to ensure compliance on study criteria, two meals per day and no medication; and evaluated for pain, heartburn and reflux during last two weeks. Patients, 9 males and 11 females, were aged between 15 and 68 years and continued our suggested meal regimen for two weeks. On day 14th 15 (75%) were free of pain and heartburn, etc, 2 (10%) had partial improvement and 3 (15%) reported no difference. Those who did not respond were advised omeprazole or ranitidine for further treatment. Results revealed that two meals a day and only soft drinks in between, was an effective and physiological dietary regimen for the management of GERD in 75% of cases.

Al-Humayed SM, Mohamed-Elbagir AK, Al-Wabel AA, Argobi YA. The changing pattern of upper gastro-intestinal lesions in southern Saudi Arabia: an endoscopic study. Saudi J Gastroenterol. 2010;16(1):35-37.

Yamamichi N, Mochizuki S, Asada-Hirayama I, Mikami-Matsuda R, Shimamoto T, Konno-Shimizu M, Takahashi Y, Takeuchi C, Niimi K, Ono S, Kodashima S, Minatsuki C, Fujishiro M, Mitsushima T, Koike K. Lifestyle factors affecting gastroesophageal reflux disease symptoms: a cross-sectional study of healthy 19864 adults using FSSG scores. BMC Med. 2012; 10: 45. Published online 2012 May 3. doi: 10.1186/1741-7015-10-45. PMCID: PMC3353848

Hershcovici T, Mashimo H, Fass R. The lower esophageal sphincter. Neurogastroenterol Motil. 2011;23(9):819-30.

Authors gratefully acknowledge the cooperation of the patients and the nursing staff for their help in the study.

Where applicable, the authors confirm that the experiments described here conform with The Physiological Society ethical requirements.

PCC201

Bile acids inhibit secretion of the proinflammatory cytokine, interleukin-8, from U937 monocytes

A.M. O Dwyer, J.B. Ward and S.J. Keely

Molecular Medicine, Royal College of Surgeons, Dublin, Dublin, Ireland

Inflammatory Bowel Disease (IBD) is a group of disorders characterised by chronic intestinal inflammation. The intestines of patients with IBD contain increased numbers of newly recruited monocytes, which augment the level of several inflammatory mediators in the gut. Among these inflammatory mediators is interleukin-8 (IL-8), a proinflammatory cytokine and potent neutrophil attractant that has been implicated in the initiation and perpetuation of IBD. Although bile acids are classically known for their role in lipid digestion they are also capable of activating nuclear and membrane receptors that regulate immune responses in the intestine and the liver. The aim of this study was to investigate the effects of the naturally-occurring bile acids, ursodeoxycholic acid (UDCA) and deoxycholic acid (DCA), on IL-8 secretion from U937 monocytes.

IL-8 release from U937 monocytes was induced with either bacterial lipopolysaccharide (LPS) [1 μg/mL] or the endogenous proinflammatory cytokine, TNFα [5 ng/mL] for 1hr. Cells were co-treated with either UDCA or DCA. Supernatants were then analysed for IL-8 protein by sandwich ELISA. IL-8 mRNA expression was assessed by qPCR. Cytotoxic effects of bile acids were determined by detection of lactate dehydrogenase release. Statistical analysis was performed using one way ANOVA with the Tukey-Kramer post test.

LPS and TNFα induced a 6.4 ± 1.5 and 2.2 ± 0.3 fold increase in IL-8 release from U937 monocytes, respectively ($n = 5$; $p < 0.05$). UDCA, at concentrations of 200 μM and 500 μM, attenuated LPS-induced IL-8 release to 75 ± 7.9% and 34 ± 4.5% of controls, respectively ($n = 5$; $p < 0.05$). DCA, 100 and 150 μM, also exerted a concentration-dependent inhibition of LPS stimulated IL-8 release to 54 ± 12.3% and 44 ± 8.7% of controls ($n = 5$ $p < 0.05$). TNFα-stimulated IL-8 release was inhibited to 39 ± 4.6% of controls by UDCA (500 μM) and to 42 ± 5.5% by DCA (200 μM) ($n = 4$ $p < 0.05$). UDCA (500 μM) and DCA (150 μM) also reduced LPS-induced IL-8 mRNA expression to 24.6 ± 9.7% of control ($n = 4$; $p < 0.05$) and 11.4 ± 7.7% respectively. UDCA and DCA did not exert toxic actions at any of the concentrations tested. The taurine-conjugates of the bile acids, tauroursodeoxycholic acid (TUDCA) and taurodeoxycholic acid (TDCA) did not have any effect on LPS or TNFα-induced cytokine production.

The results of this study demonstrate that the naturally-occurring bile acids, UDCA and DCA, attenuate IL-8 release from monocytes through inhibition of mRNA expression for the cytokine. Such actions suggest that UDCA and DCA may exert anti-inflammatory effects in vivo and that manipulation of the colonic bile acid pool could prove useful as a new therapeutic strategy for IBD.

Where applicable, the authors confirm that the experiments described here conform with The Physiological Society ethical requirements.

PCC202

Bile acids regulate innate barrier functions of colonic epithelial cells

N.K. Lajczak, M.S. Mroz, V. Saint-Criq and S.J. Keely

Molecular Medicine, Royal College of Surgeons in Ireland, Dublin, Dublin, Ireland

Intestinal epithelial cells constitute the first line of defence against the entry of toxins and pathogens from the lumen to the body, with several processes contributing to this innate barrier function. For example, fluid secretion flushes pathogens from the lumen, defensin production protects against bacterial invasion, autophagy aids in clearing bacteria from infected cells, and restitution repairs the epithelium after injury. Although bile acids are known to be involved in the pathogenesis of IBD, the mechanisms by which they regulate epithelial barrier function are not well understood. Therefore, the aim of this study was to investigate the effects of deoxycholic acid (DCA) on epithelial responses that contribute to barrier function.

T_{84}colonic adenocarcinoma cells were grown on permeable supports and were treated with DCA (50 μM -1 mM) for 1 h to 72 h. Protein expression was investigated by western blotting and mRNA expression by qPCR. Epithelial restitution in polarised T_{84} cell monolayers was investigated using a wound healing assay. Muscle stripped sections of human colonic mucosa were mounted in Ussing chambers for measurements of ion transport by monitoring changes in short circuit current (Isc) under voltage-clamped conditions. All experiments involving human tissue had the approval of Beaumont Hospital Ethical Committee.

DCA (150 μM, 48 h) attenuated restitution of mechanically wounded T_{84} cell monolayers by 2.08 ± 0.14 fold compared to untreated controls ($n = 3$; $p < 0.05$). Furthermore,

DCA (200 μM, 24 h) stimulated autophagy in T_{84} cells, as indicated by a 1.8 ± 0.9 fold increase in the expression of the autophagy marker, microtubule-associated protein light chain 3 (LC-3 II), when compared to controls (n = 5; p < 0.001). In contrast, the more hydrophillic bile acid, UDCA (50–500 μM) was without effect on LC-3 II expression. DCA also increased expression of mRNA for the constitutively expressed hβD-1 by 7.0 ± 0.9 fold, compared to untreated cells (n = 5; p < 0.001). Levels of inducible hβD-2 mRNA were also significantly upregulated by 4.3 ±0.4 fold in response to DCA (n = 4; p < 0.01). When added to voltage clamped sections of human colonic tissue, DCA, at concentrations of 200 μM and 500 μM, stimulated Isc responses of 4.0 ± 0.0 μA/cm2 and 24.0 ± 0.0 μA/cm2 (n = 2). Furthermore, DCA pretreatment attenuated Cl- secretory responses to the Ca^{2+} dependent agonist, carbachol (CCh, 100 μM) from 320 ± 274 μA/cm2 to 56 ± 3 μA/cm2, n = 2). At concentrations of > 500 μM, DCA rapidly damaged colonic tissues, as demonstrated by a 5.7 ± 0.9 fold increase in transmucosal conductance (n = 2).

Taken together, these data implicate colonic bile acids, such as DCA, as important regulators of intestinal epithelial barrier function and suggest they might be good targets for the development of new approaches to treat IBD.

Where applicable, the authors confirm that the experiments described here conform with The Physiological Society ethical requirements.

PCC203

High-fat diet increase the firmly adherent mucus layer in rat colon

T.B. Waldén, D. Ahl, A. Jägare, M. Phillipson and L. Holm

Medical Cell Biology, Uppsala University, Uppsala, Sweden

INTRODUCTION: The colon is subjected to a plethora of potentially damaging agents against which its first line of defense is the protective mucus bilayer, consisting of a removable loosely adherent layer and a firmly adherent layer difficult to remove [1]. We have recently shown that the firmly adherent mucus layer acts as a physical barrier to the microbiota. The mucus bilayer also reduces shear stress to the mucosa [2]. The colonic microbiota and mucosal health has been linked to different constituents in the diet [3]. The aim of this study was to investigate if a high-fat diet with or without prebiotic bilberry fibers influence on the thickness and secretion of the colonic mucus bilayers.

METHODS: Male Sprague-Dawley rats (80g) were given a diet consisting of either low-fat diet (LFD), high-fat diet (HFD), LFD with bilberry extract (LFD+BB) or HFD with bilberry extract (HFD+BB), for 8 weeks. On the last day of experiment, rats (n=8/group) were anesthetized (Inactin, 120 mg/kg) and operated on for in vivo measurements of mucus thickness. The distal part of the colon was opened up along the anti-mesenteric border and draped over a truncated cone with the luminal side up. A mucosal chamber with warm saline was placed over the mucosa. To ease visualization through the microscope, saline-suspended charcoal was dropped on the mucus gel. To perform measurements, micropipettes, held by a micromanipulator at an angle of 35-45 degrees to the cell surface, was pushed into the mucus gel. The distance (l) to the epithelial surface was measured with a "digimatic indicator". Mucus thickness (T) was then calculated using the formula: T =l x sin a. Mucus thickness was measured at different intervals, before and after removing the loosely adherent mucus by suction. Distal colon tissue was paraffin-embedded, sectioned and PAS-stained to count the number of goblet cells.

RESULTS: Here we have demonstrated that: (1) 8 weeks of HFD supplementation with or without BB leads to increased thickness of the firmly adherent mucus layer (e.g. the mean firmly adherent mucus thickness rats fed a HFD or a HFD+BB (84.2±1.2 and 82.7±0.7 μm) was significantly higher than the respective LFD and LFD+BB controls (78.7± 0.7 and 78.6±0.9; Students t-test p< 0.0002 and p<0.001); (2) the loosely adherent mucus thickness is only increased by a diet with a combination of bilberry extract and high-fat (e.g. the mean loosely adhesive mucus thickness in the rats fed HFD+BB (40.7±1.5 μm) was significantly higher than in rats fed a HFD only (31.3±3.2 μm; Students t-test p<0.05). (3) a pilot study indicate an increase in the number of goblet cells in rats fed HFD+BB and a decrease in rats fed HFD only.

SUMMARY: High-fat diet, with our without bilberries, increase the protective firmly adherent mucus layer, while only a combination of high-fat diet and bilberries increase the thickness of the loosely adherent mucus layer.

Atuma, C et al. (2001). Am J Physiol Gastrointest Liver Physiol 280, G922-929.

Dicksved, J et al. (2012). PLoS One 7, e46399.

Brownlee, I.A et al. (2003). Proc Nutr Soc 62, 245-249.

Where applicable, the authors confirm that the experiments described here conform with The Physiological Society ethical requirements.

PCC204

Intestinal biotransformation of maslinic acid, a natural triterpenoid from *Olea europaea* L

G. Lozano-Mena[1], M. Sánchez-González[1], A. García-Granados[2], M. Juan[1] and J. Planas[1]

[1]Department of Physiology and INSA-UB, Universitat de Barcelona, Barcelona, Spain and [2]Department of Organic Chemistry, Universidad de Granada, Granada, Spain

Maslinic acid is a bioactive compound found in olives and olive oil to which a myriad of beneficial effects have been attributed, such as antioxidant, antitumor and antidiabetic. Here, we present a high performance liquid chromatography coupled to mass spectrometry (HPLC-MS) method to determine maslinic acid and its metabolites in rat intestinal content after the oral administration. The pentacyclic triterpene was orally administered to three groups of male Sprague-Dawley rats at single daily doses of 5, 2 and 1 mg/kg, respectively. At 24 h after the last administration, the content of the duodenum and jejunum, ileum, caecum and colon was obtained. Analytes were extracted with methanol 80% by homogenization and stirring. Chromatographic separation was carried out using a gradient elution of water and acetonitrile and detection was performed in a single quadrupole mass spectrometer, with an atmospheric pressure chemical ionization (APCI) source. The metabolites were identified by LC-APCI-LTQ-Orbitrap-MS. The analytical method was validated by spiking blank intestinal content samples with maslinic acid at the concentrations of 0.1, 0.5, 1, 5, 10, 20 and 30 μM. The mean coefficient of correlation was 0.994, the mean recovery was 97.87 ± 0.76% and the limit of quantification was 5 nM. The intra- and inter-day precisions were 4.32 ± 1.69% and 6.22 ± 1.05%, respectively. After 24 h of the last administration of maslinic acid, the analysis of the content of the different intestinal segments demon-

strated the presence of maslinic acid ($C_{30}H_{48}O_4$) together with nine metabolites: five monohydroxylated derivatives ($C_{30}H_{48}O_5$) (M1-M5), two monohydroxylated and dehydrogenated metabolites ($C_{30}H_{46}O_5$) (M6-M7) and two dihydroxylated derivatives ($C_{30}H_{48}O_6$) (M8-M9). Metabolites of the same m/z differed by the retention time (t). The percentage that each compound represented over the total amount along the small and large intestine was calculated. Maslinic acid accounted for 18.9 ± 1.2% and the major metabolites were the monohydroxylated M1(t = 6.6 min), representing an average of 55.4 ± 2.3%, followed by M2 (t = 7.3 min), which accounted for 17.0 ± 5.8%. To a lesser extent, the monohydroxylated and dehydrogenated metabolites M6 (t = 6.8 min) and M7 (t = 8.1 min) represented an average of 4.9 ± 2.8% and 2.8 ± 0.7%, respectively, and the rest of the derivatives (M3, M4, M5, M8 and M9) accounted for less than 1%. These results show that 24 h after the oral administration, maslinic acid undergoes extensive phase I metabolism, following the same pattern at three different doses. Two monohydroxylated derivatives are the most abundant, one of them accounting for more than double of the maslinic acid fraction in the whole intestinal content.

Supported by grants AGL2009-12866 from MCT Spain and 2009-SGR-00471 from the Generalitat de Catalunya.

Where applicable, the authors confirm that the experiments described here conform with The Physiological Society ethical requirements.

PCC205

Does DNA methylation play a role in B°AT1 transcriptional regulation along crypt-villus axis?

E. Tumer, T. Juelich and S. Broer

Research School of Biology, Australian National University, Canberra, ACT, Australia

Hartnup disorder is an autosomal recessive disorder caused by mutations in the B°AT1 (Slc6a19) gene encoding the major transport system for neutral amino acids in the intestinal brush-border membrane. B°AT1 protein is expressed at the apical membrane of enterocytes in increasing amounts along the crypt-villus axis.
Previously, we showed that HNF1a and HNF4a bind to the Slc6a19 promoter up-regulating transcription. Sox9, by contrast, suppressed the promoter activity induced by HNF1a and HNF4a. Sox9 is a transcription factor known to be involved in the differentiation of stem cells into mature enterocytes, and is highly expressed in the crypt region, but absent at the villus tip. Thus Sox9 expression could explain the gradient of B°AT1 in the intestine. However, despite HNF1a and HNF4a expression in the liver, B°AT1 is not expressed, while Sox9 is absent. As a result we considered DNA methylation as a mechanism to regulate B°AT1 expression. DNA methylation of a transcription factor binding sites can prevent transcription factor from binding to the DNA.
Kikuchi et al (2010) suggested that HNF1a binding to the B°AT1 promoter could be prevented by methylation in the liver. However, they observed particular methylation in the liver at position -1080, which is 940 bp upstream of the HNF1a binding site.
In this study we investigated the DNA methylation status of the B°AT1 promoter, using bisulfate sequencing. DNA methylation was determined in a 1.2 kb region upstream of the B°AT1 transcriptional start site in liver, kidney and crypt-villus preparations. From each experiment a minimum 10 independent clones were sequenced. Twenty CpG sites were analysed and found to be differentially methylated in the chosen tissues.
We found that CpG dinucleotides around HNF1a, HNF4a and TATA binding sites were hypomethylated in the villus, whilst being hypermethylated in the crypt and in liver tissue.
These results indicate that DNA methylation might play a role together with Sox9 in the repression of B°AT1 expression in the crypt, whereas in the liver cells DNA methylation itself might be sufficient.

Kikuchi, R., S. Yagi, et al. (2010). "Genome-wide analysis of epigenetic signatures for kidney-specific transporters." Kidney international 78(6): 569-577.

Where applicable, the authors confirm that the experiments described here conform with The Physiological Society ethical requirements.

PCC206

Impact of simvastatin on hepatic tissue in lipopolysaccharides treated rats

G. Ates[1], E. Ozkok[3], I. Aydin[2], H. Yorulmaz[4] and A. Tamer[1]

[1]Physiology, Istanbul University, Istanbul, Turkey, [2]Histology and Embyriology, Istanbul University, Istanbul, Turkey, [3]Neuroscience, The Institute for Experimental Medicine, Istanbul, Turkey and [4]School of Nursing, Halic University, Istanbul, Turkey

Motivation/problem statement: Sepsis is defined systemic inflammatory response syndrome (SIRS) after serious microbial infection. The liver is the main organ for bacterial scavenging, bacterial products inactivation, and inflammatory mediator clearance and production. Macrophages in liver can clear the endotoxin and bacteria that initiate the systemic inflammatory response. The hepatic dysfunction can be viewed as a primary dysfunction that occurs in the first hours after sepsis. Simvastatins are a class of drugs used to lower cholesterol levels by inhibiting the enzyme HMG-CoA reductase, also it has anti-inflammatory activities. We aimed to investigate effects of simvastatin on hepatic tissue in rats with Lipopolysaccharides (LPS).
Methods/procedure/approach: Following the approval of the ethical commitee male Wistar albino rats were used in this study. The rats were divided into four groups as control (n=10) LPS(n=10). Simvastatin (n=10), LPS+Simvastatin groups (n=10). Sepsis was induced by administration of LPS (E.coli O127:B8; 20 mg/kg, i.p) in anesthetized rats. After 4 hours, animals were taken experiment. Simvastatin was given (20 mg/kg, p.o.) for 5 days.At the end of the 5th days animals were decapitated. Histopathologic changes in the liver sections stained with hematoxylin and eosin in all groups.
Results: We seen large sinusoidal structure, degenerative lobule and cell membrane, increment of glycogen droplets and collagen in LPS and simvastatin groups in hepatic tissue sections, compared to control. In LPS+Simvastatin groups, tissue histology is as same as control's. Also hepatic tissue has normal sinusoidal and lobule structure, and glycogen droplets.
Conclusion/implications: The changes in the histologic structure of the liver were significantly affected by only treated simvastatin or LPS. Simvastatin administration in LPS treated animals improved to hepatocellular degeneration.

Kantrow SP, Taylor DE, Carraway MS, Piantadosi CA.Arch Biochem Biophys. 1997 Sep 15;345(2):278-88.

Lancaster, J. R., Laster, S. M., and Gooding, L. R. (1989) FEBS Lett. 248, 169–174.;Stadler, J., Bentz, B. G., Harbrecht, B. G., DiSilvio, M., Curran, R. D., Billiar, T. R., Hoffman, R. A., and Simmons, R. L. (1992) Complex V, however, was decreased in samples from Ann. Surg. 216, 539–546.

Taylor, D. E., Ghio, A. J., and Piantadosi, C. A. (1995) Arch. Biochem. Biophys. 316, 70–76.

Rooyackers OE, Kersten AH, Wagenmakers AJM. Mitochondrialprotein content and in vivo synthesis rates in skeletal muscle from critically ill rats. Clin Sci 1996; 91:475–81;.Singer M, Brealey D. Mitochondrial dysfunction in sepsis.Biochem Soc Symp 1999; 66: 149–66.

Singer M. Metabolic failure. Crit CareMed 2005; 33: S539–42.

We thank to Professor Ayhan Bilir from department of Histology and Embyriology,Faculty of Medicine Istanbul University.

Where applicable, the authors confirm that the experiments described here conform with The Physiological Society ethical requirements.

PCC207

Acute sacral nerve stimulation in an animal model has no effect on motor function of the anal canal but elicits a profound potentiation of cortical sensory input from this region

L. Devane, J. Evers, R. O'Connell and J. Jones

University College Dublin, Belfield, Dublin, Ireland

Sacral nerve stimulation (SNS) has an established role in treatment of faecal incontinence, however the mechanism of action remains unknown. Our laboratory has previously shown that acute SNS augments somatosensory cortical potentials evoked by anal canal stimulation in a rat model (Griffin et al., 2011). The aim of this study is to examine the effect of acute SNS on motor function of the anal sphincters in the same animal model.

Eight virgin female Wistar rats were anaesthetised with urethane (1.5g.kg-1 i.p.). The combined force of the internal anal sphincter (IAS) and external anal sphincter (EAS) was measured using a force transducer, by mounting the distal 4-5mm of the anal canal as an isometric ring preparation in situ. A novel method was used to separate the EAS and IAS force recordings by stimulating the inferior rectal nerve (which supplies the EAS) at 1Hz. The frequency and amplitude of the slow waves of the IAS were also measured. Three minute recordings were taken before, during and after SNS at S1 [1ms pulses at 10Hz and at 0.5-1.1 Volts (just above motor threshold)]. A balloon was then inserted into the rectum and inflated with 0.3ml saline for 10 sec to evoke the recto-anal inhibitory (RAIR) and recto-anal excitatory (RAER) reflexes. Cortical evoked potentials were recorded in 8 rats as described previously. The results were analysed with repeated measures ANOVA. The criterion for statistical significance was $p<0.05$.

SNS did not have any significant effect on the IAS force ($p=0.135$), EAS force ($p=0.126$), slow wave frequency ($p=0.239$), slow wave amplitude ($p=0.999$), RAIR ($p=0.202$) or RAER ($p=0.268$). However the amplitude of cortical evoked potentials increased by a mean of 62% (SEM=16) after SNS.

The experiment suggests that SNS does not have a direct motor effect. From our current and previous study of anal canal cortical evoked potentials, it appears that the mechanism of action is through augmentation of sensory feedback to the cortex. These results reflect the clinical use of SNS as the current is delivered at the sensory (sub-motor) threshold.

Griffin KM et al. (2011). Br. J. Surg. 98(8):1160-9.

Research received funding from Medtronic Inc., Minneapolis, Minnesota, U.S.A.

Where applicable, the authors confirm that the experiments described here conform with The Physiological Society ethical requirements.

PCC208

Protective effects of *L. reuteri* on DSS-induced colitis in CX3CR1 deficient mice

D. Ahl[1], M. Qundos[1], S. Roos[2], M. Phillipson[1] and L. Holm[1]

[1]Medical Cell Biology, Uppsala University, Uppsala, Sweden and [2]Microbiology, Swedish University of Agricultural Sciences, Uppsala, Sweden

INTRODUCTION: Preliminary results from our laboratory suggest that two strains of the probiotic bacteria *Lactobacillus reuteri* (rat-derived strain R2LC and human-derived strain ATCC PTA 4659) ameliorate DSS-induced colitis in mice. The underlying mechanisms involved in this protection are not known, but a link to intestinal resident immune cells can be assumed. The chemokine receptor CX3CR1 is expressed by circulating monocytes and by intestinal lamina propria resident cells believed to be macrophages and/or dendritic cells. Mice deficient in CX3CR1 ($CX3CR1^{GFP/GFP}$) develop an aggravated DSS-induced colitis, suggesting a role of CX3CR1 in the maintenance of colonic homeostasis.

AIM: To investigate if the protective mechanism of *L. reuteri* R2LC or ATCC PTA 4659 involve CX3CR1, colitis was induced by DSS in $CX3CR1^{GFP/GFP}$ mice.

METHODS: Colitis was induced by 3% DSS in drinking water, administrated for 8 days to C57Bl/6 (wt) and $CX3CR1^{GFP/GFP}$ mice (C57Bl/6 background). Two groups from each strain were given *L. reuteri* R2LC or ATCC PTA 4659 by gavage once daily for 15 days in addition to DSS for the last 8 days. Disease severity was assessed through scoring of clinical symptoms (DAI, disease activity index) and histology scoring of H&E stained paraffin sections of distal colon. Multi-array measurements of the pro-inflammatory cytokines IL1-β, IL-6, TNF-α and mKC were also performed from colonic tissue samples.

RESULTS: DAI was significantly reduced the last day of DSS treatment in the groups of wt mice treated with either strain of *L. reuteri* (2.9±0.17 for DSS (n = 20), 1.8±0.18 and 1.4±0.30 for DSS+4659 (n = 16) and DSS+R2LC (n = 11) respectively, SEM values). In the $CX3CR1^{GFP/GFP}$ mice DAI increased slightly more by DSS than in the wt, and the *L. reuteri* strains did not significantly reduce DAI. The levels of all proinflammatory cytokines measured in colon tissue were significantly higher in DSS treated $CX3CR1^{GFP/GFP}$ mice than in wt. Treatment with either strain of *L. reuteri* significantly reduced all cytokines in wt and $CX3CR1^{GFP/GFP}$ mice, with the exception of IL1-β in the latter group. Preliminary histology scoring demonstrates reduced inflammation in all *L.reuteri* treated groups.

CONCLUSIONS: These results indicate that the protective role of the two different strains of *L. reuteri* on DSS-induced colitis is slightly reduced in $CX3CR1^{GFP/GFP}$ mice, compared to wt mice. Thus, the mechanism by which *L.reuteri* bacterial strains ameliorate colitis might involve CX3CR1. However, the possibility that the reduced protection by *L. reuteri* in the $CX3CR1^{GFP/GFP}$ mice is due to higher DAI and cytokine levels in these mice can not be excluded.

The authors gratefully acknowledge the technical assistance of Annika Jägare.

Where applicable, the authors confirm that the experiments described here conform with The Physiological Society ethical requirements.

PCC209

Ursodeoxycholic acid inhibits colonic mucosal cytokine release and prevents colitis in a mouse model of disease

J.B. Ward[1], O.B. Kelly[1,4], J. Ní Gabhann[2], S. Smith[2], M.M. Tambuwala[3], C.T. Taylor[3], F.E. Murray[4], C. Jefferies[2] and S.J. Keely[1]

[1]Molecular Medicine Laboratories, Royal College of Surgeons in Ireland, Dublin 9, Ireland, [2]Molecular and Cellular Therapeutics, Royal College of Surgeons in Ireland, Dublin, Ireland, [3]Conway Institute of Biomedical and Biomolecular Research, University College Dublin, Dublin, Ireland and [4]Gastroenterology, Beaumont Hospital, Dublin, Ireland

Toll-like receptors (TLR) promote cytokine release from intestinal epithelia, thereby driving inflammation. Although ursodeoxycholic acid (UDCA) is well known to exert anti-inflammatory effects in the liver, its potential for treating intestinal inflammation has not been well-studied. Here, we investigated UDCA effects on TLR-driven colonic mucosal cytokine release and induction of inflammation in a mouse model of colitis. Resected human colonic mucosa and T84 colonic epithelial cells were treated with specific TLR agonists (TLR3: Polyinosinic-polycytidylic acid, 25 μg/ml; TLR4: lipopolysaccharide (LPS), 100 ng/ml), in the presence or absence of UDCA. Released cytokines were measured by ELISA and luciferase reporter assays were performed in HEK293T cells. Dextran sodium sulphate (DSS) colitis was induced by administering DSS (2.5 %) in the drinking water of male C57BL/6 mice, along with daily intraperitoneal injections of UDCA (30 or 100 mg/kg) or vehicle for 5 days. Colitis severity was recorded as disease activity index (DAI) and by histological inflammation score. Results were analysed by ANOVA using Tukey multiple comparisons test and are expressed as the mean ± standard error of the mean. In T84 cells, UDCA (200 μM) attenuated TLR3-stimulated tumour necrosis factor α (TNFα) release from 32.9 ± 4.1 to 23.8 ± 3.7 pg/ml; interleukin-8 (IL-8) release from 1197.5 ± 110.1 to 923.8 ± 110.3 pg/ml and IL-1β release from 2.0 ± 0.2 to 1.6 ± 0.2 pg/ml ($n = 4$, $p < 0.05$). Apical LPS (6 hours) induced basolateral IL-8 secretion from human colonic mucosa from 435 ± 46 in unstimulated controls to 959 ± 22 pg/ml and caused a 3 fold increase in secretion of Regulated on Activation, Normal T cell Expressed and Secreted (RANTES); increases that were abolished by UDCA (250 μM) ($n = 3$, $p < 0.001$). Using NFκB and P125 luciferase reporter assays we determined that UDCA (200 μM) exerts its anti-inflammatory effects at the level of TANK-binding kinase 1 (TBK1) ($n = 5$, $p < 0.01$). In the DSS model of colitis, UDCA (30 mg/kg and 100 mg/kg) significantly reduced disease severity from a DAI of 10.0 ± 0.3 in mice treated with DSS alone to 7.2 ± 0.7 and 5.8 ± 0.5, respectively ($n = 6 – 12$, $p < 0.001$). Furthermore, histologically the inflammation score was also significantly reduced in UDCA (100 mg/kg)-treated animals to 24.3 ± 4.4, compared to 37.3 ± 0.8 in mice treated with DSS alone ($n = 4 – 6$, $p < 0.05$). In conclusion, our data show that UDCA prevents inflammation in a mouse model of colitis and that the protective effects of UDCA may be due to inhibition of TLR-induced proinflammatory cytokine release. These findings suggest that UDCA represents a good target for developing new therapeutic approaches to treat IBD.

This work was funded by Science Foundation Ireland.

Where applicable, the authors confirm that the experiments described here conform with The Physiological Society ethical requirements.

PCC210

Condenser-free Zernike phase contrast microscopy

K.F. Webb

Institute of Biophysics, Imaging & Optical Science, University of Nottingham, Nottingham, Notts, UK

Background
Biological samples tend to be low in intrinsic contrast to visible transmitted-light microscopy. The development of contrast-enhancing methods such as phase contrast during the 20th century allowed the investigation of highly transparent yet detail-rich specimens by exploiting differences in refractive index and optical path difference to produce interference between two beam paths emerging from the sample plane[1]. Phase contrast microscopy has gone on to become a ubiquitous technique in cell biology and physiology, yet the optical design has remained relatively unchanged over recent decades; consisting of a light source, collimating optics, phase annulus, and condenser producing a hollow cone of illumination which passes through the sample. On the detection side, phase contrast objective lenses introduce a complementary ring of phase-retarding and attenuating material to alter the phase relationship of the undeviated illumination with respect to light deviated by passage through the sample. By recombining these two beams onto the detector contrast is obtained by exploiting constructive and destructive interference on the basis of the phase shift induced in transiting the sample.
Method
Presented here is a modified version of Zernike phase contrast microscopy[1], in which condenser optics are entirely dispensed with yielding a condenser-free yet highly effective method of obtaining phase contrast in visible light microscopy. A ring of light emitting diodes is positioned within the optical light-path such that observation of the back focal plane of the objective places this ring, observed at virtual “infinity” with respect to the objective focal length, in appropriate conjunction with the phase ring to produce phase contrast.
Results
It is demonstrated that true phase contrast is obtained, whose geometry can be arbitrarily manipulated to provide a range of working distances and form factors. LED-ring phase contrast is demonstrated at phase position L, 1, 2, 3 and 4 across a range of magnifications and numerical apertures up to 100x and 1.4NA. LED phase contrast illumination is further implemented in conjunction with scanning ion conductance microscopy (SICM) to image a range of cultured cell lines; including ARPE-19, 3T3 fibroblast, and Caco-2 cells.
Conclusion
Condenser-free phase contrast microscopy using LED rings has significant potential to benefit physiology and cell biology by providing for arbitrary working distances in illuminating optics. By eliminating the need for a condenser assembly a range of concurrent imaging and measurement techniques will be technically facilitated through the provision of extra room to work. In addition the compact, low power, and versatile nature of LED illumination will further lend itself to miniaturisation and

modification of existing phase contrast microscopy schemas in the future.

Zernike F. How I discovered phase contrast. Science. 1955 Mar 11;121(3141):345-9

Where applicable, the authors confirm that the experiments described here conform with The Physiological Society ethical requirements.

PCC211

A morphological assessment of the autophagosomal fusion process using superresolution structured illumination microscopy

B.-. Loos

Physiological Sciences, Stellenbosch University, Stellenbosch, Western Cape, South Africa

Autophagy is a major protein degradation system, which targets primarily long-lived cytoplasmic proteins. A large body of evidence indicates that impaired autophagy is implicated in the onset and progression of human pathologies such as heart disease, neuro-degeneration and cancer. Central to the functional role of autophagy is the successful fusion event of autophagosomes with lysosomes, forming and autophagolysosome. Although substantial progress has been achieved in understanding the molecular machinery of the autophagic pathway and its regulation, a fundamental challenge remains to identify the driving forces that govern the fusion event. This however requires a highly resolved detail that describes the fusion process morphologically. By utilizing superresolution structured illumination microscopy (RS-SIM) techniques, the aim of this study was to characterize the three-dimensional morphology of autophagosomes and lysosomes in single mammalian cells, and to assess the fusion region between these 2 organelles.

Rodent derived cardiac myoblast H9c-2 cells were grown in Dulbecco's Modified Eagle's Medium (DMEM) supplemented with 10% foetal bovine serum (FBS), and incubated under 5% CO2 conditions. The light-chain 3 (LC3) and lysosomal associated membrane protein (LAMP) were utilized as markers for autophagosomes and lysosomes respectively. Cells were transfected with 800 ng of the LC-3-GFP-DSred tandem plasmid, GFP-LC3 as well as LAMP-YFP using GenJuice® Transfection Reagent (Novagen®) according to the manufacturer's protocol. SR-SIM image acquisition and processing was performed on a LSM-780 Elyra system and z-stack image acquisition was utilized to capture both autophagosomes and lysosomes at high resolution in three dimensions. Surface rendering was performed to assess the fluorescence signal distribution.

This study reveals a highly heterogeneous morphological distribution of both autophagosomes and lysosomes, indicating the dynamic membrane turnover process during autophagosome and lysosome formation. Moreover, a morphologically highly complex fusion zone is observed. These data indicate a previously unknown complexity of membrane morphology and dynamics of both organelles. Importantly, this study highlights the strength of SR-SIM in deriving numerical geometrical data that allow the prediction and modelling of the likelihood for a complete or incomplete fusion event to take place. This approach provides insights that may result in novel means to exploit the autophagic machinery for therapeutic purposes.

The authors acknowledge Prof Tamotsu Yoshimori, Osaka University Graduate School of Medicine, Japan, for providing the tf-LC3, the GFP-LC3 as well as the LAMP-YFP plasmids. This work was supported by the National Research Foundation (NRF) and Medical Research Council (MRC), South Africa.

Where applicable, the authors confirm that the experiments described here conform with The Physiological Society ethical requirements.

PCC212

Na^+/H^+ exchangers are differentially involved in cell migration in the gastrointestinal cell lines RGM-1 and Caco2bbe

A. Klöpper[1], F. Busch[1], S. Yeruva[1], B. Riederer[1], G. Chodisetti[1], M. Menon[2], A. Schwab[3] and U. Seidler[1]

[1]Department of Gastroenterology, Hepatology and Endocrinology, Hannover Medical School, Hannover, Germany, [2]Institute of Biochemistry, Hannover Medical School, Hannover, Germany and [3]Institute of Physiology II, University of Münster, Münster, Germany

Background: The Na+/H+ exchanger isoform 1 (NHE1) is believed to be essential for directional cell migration during wound healing and tumour invasiveness. However, in the intestinal epithelium, which displays very rapid cellular restitution of surface wounds, other NHE isoforms (NHE2, NHE3) are expressed far more strongly. **Aim and methods**: We studied the role of NHE isoforms 1, 2 and 3 on wound healing velocity in RGM1 cells, a nontransformed rat gastric surface cell line and in Caco2bbe cells, a well differentiating human colonic tumour cell line. Migration velocity was studied during growth factor-stimulated and low pH-stimulated as well as serum starvation-inhibited wound healing. To assess cell migration speed objectively, a fluorescent dye-based plate reader assay was used [1]. NHE1 and 2 were dose-dependently inhibited by HOE642 [2], whereas NHE1 and 3 were selectively inhibited by S1611 [3]. 5-(N,N-Dimethyl)amiloride (DMA) was used to inhibit Na+/H+ exchangers less specifically [4]. Stable NHE3 overexpression was performed in Caco2bbe cells, while lentiviral transient NHE2 overexpression was achieved in RGM-1 cells. **Results**: In confluent monolayers, RGM1 cells express NHE1 mRNA in far higher levels than other NHEs, whereas NHE2 mRNA expression is higher than NHE1 and NHE3 in Caco2bbe cells. Both cell lines displayed cell migration after experimental wounding even after serum starvation, where migratory speed was independent of NHE activity in either cell line. Fetal calf serum (FCS) significantly stimulated cell migration in a partly NHE1-dependent fashion in RGM-1 cells, but in a NHE-independent fashion in Caco2bbe cells. Preincubation at low pH also stimulated migratory speed in a NHE1-dependent fashion in both RGM-1 and Caco2bbe cells. NHE2 overexpressing RGM-1 cells migrated more slowly in the presence of FCS, and more so after low pH preincubation, which was reversed by pharmacological NHE2 inhibition. NHE3 overexpression as well as inhibition did not result in a change in migratory speed. DMA impaired cell migration more strongly than Na+/H+-exchange inhibition could account for, implying nonspecific effects of the amiloride analogue. **Conclusions**: Wound closure is possible even in the absence of NHE functional activity in gastrointestinal epithelial cells. Dependency of cell migration velocity on NHE1 varies among cell types. Low pH enhances cell migration in a NHE1-dependent fashion, whereas stimulation by growth factors is predominantly NHE1-independent. NHE2 slows cell migration speed. Therapeutic NHE inhibition for gastrointestinal malignancy is therefore likely to

have a highly variable effect on tumour invasiveness depending on the cell type.

Menon MB, Ronkina N, Schwermann J, Kotlyarov A, Gaestel M. Fluorescence-based quantitative scratch wound healing assay demonstrating the role of MAPKAPK-2/3 in fibroblast migration. Cell motility and the cytoskeleton. 2009; 66:1041-7.

Scholz W, Albus U, Counillon L et al. Protective effects of HOE642, a selective sodium-hydrogen exchange subtype 1 inhibitor, on cardiac ischaemia and reperfusion. Cardiovascular Research. 1995; 29:260-268.

Schwark JR, Jansen HW, Lang HJ, Krick W, Burckhardt G, Hropot M. S3226, a novel inhibitor of Na+/H+ exchanger subtype 3 in various cell types. Pflugers Archiv : European journal of physiology. 1998; 436:797-800.

Kleyman TR, Cragoe Jr. EJ. Amiloride and Its Analogs as Tools in the Study of Ion Transport. The Journal of Membrane Biology. 1988; 105:1-21.

Where applicable, the authors confirm that the experiments described here conform with The Physiological Society ethical requirements.

PCC213

Hyperactivation of UNC-105 causes loss of mitochondrial membrane potential and impaired mitochondrial ATP production in *C. elegans*

C.J. Gaffney, D. Constantin-Teodosiu, P.L. Greenhaff and N.J. Szewczyk

MRC/ARUK Centre for Musculoskeletal Ageing Research, University of Nottingham, Nottingham, UK

Background: *C. elegans* is a free-living nematode known for its utility in genomics research. A dominant gain-of-function mutation in *unc-105*, a putative mechano-sensitive ion channel of the ENaC/Degenerin family, causes mitochondrial fragmentation in body-wall muscles (Szewczyk *et al*. unpublished data) and a movement defect (1). These defects are ameliorated in *unc-105; let-2* suppressed mutants (*let-2* encodes a collagen).
Objectives: Mitochondrial membrane potential and maximal rates of ATP production (MRAP) were determined in wild-type (WT) and *unc-105* mutants to quantify disruption, if any, of mitochondrial function. The *unc-105; let-2* mutants were also assessed to quantify any potential rescue of mitochondrial function.
Methods: Mitochondrial membrane potential was quantified *in vivo* using JC-10 and Mitotracker® CMXRos, which reflect potential-dependent accumulation. JC-10 fluorescence was quantified using ImageJ. Membrane potential was also quantified in isolated mitochondria (n=10 assays of mixed-age worms; n≈300 per assay) using JC-1 and flow cytometry (2). MRAP and citrate synthase (CS) activity were also determined in similarly isolated mitochondria. MRAP was determined through incubation with a bioluminescent luciferase-based monitoring reagent, and a combination of respiratory substrates and ADP. All data were analysed using one-way ANOVA.
Results: Mitochondrial accumulation of JC-10 was reduced in *unc-105* versus WT (P <0.001), suggesting the loss of membrane potential in *unc-105* mutants *in vivo*. Similarly, Mitotracker® CMXRos accumulated *in vivo* in WT (P <0.01) and *unc-105; let-2* suppressed mutants (P <0.01), but not in *unc-105* mutants. In keeping with these *in vivo* observations, JC-1 accumulation in isolated mitochondria was 25% lower in *unc-105* than in WT and *unc-105; let-2* (P <0.001). MRAP were reduced in *unc-105* mutants vs. WT and *unc-105; let-2* suppressed mutants (Figure 1). The respiratory substrate combinations were glutamate and succinate (GS), palmitoyl-L-carnitine and malate (PCM), pyruvate and malate (PM), succinate (S) and glutamate and malate (GM). Data were normalised for CS activity to account for mitochondrial content. * P <0.05 vs. WT and † P <0.05 vs. *unc-105*.
Conclusion: *Unc-105* mutants showed evidence of disrupted mitochondrial membrane potential compared to WT, which was accompanied by impaired MRAP. In *unc-105; let-2* suppressed mutants, mitochondrial membrane potential and MRAP were similar to WT. Thus, as in mammalian cells (3), constitutive cationic influx leads to pathological changes in mitochondrial function in *C. elegans* muscle. These results establish that it is possible to use *C. elegans* to understand the genomic control of mitochondrial function.

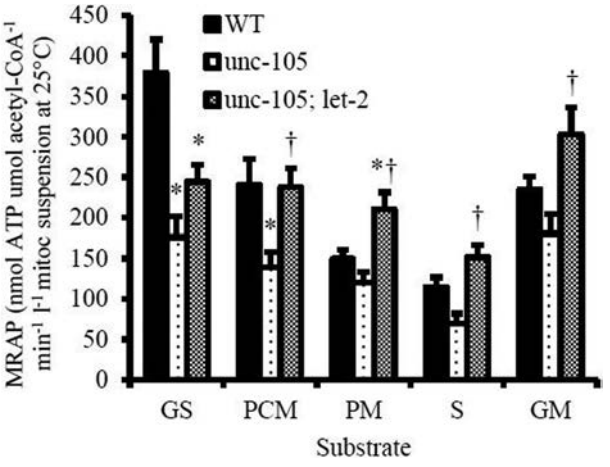

Figure 1: Maximal rates of ATP production (MRAP) are depressed in *unc-105*

Park EC, Horvitz HR. (1996). *Genetics* **113**, 853-867.

Jacotot *et al*. (2001). *J Exp Med* **193**, 509-519.

Iwai *et al*. (2002). *Cardiovasc Res* **55**, 141-149.

Where applicable, the authors confirm that the experiments described here conform with The Physiological Society ethical requirements.

PCC214

Lipid peroxidation and antioxidant status in preeclampsia

R. Begum

Physiology, Enam Medical College, Dhaka, Dhaka, Bangladesh

Preeclampsia is the most common & major medical complication of pregnancy with a high incidence of national health problem & also responsible for high maternal & fetal morbidity & mortality1,2. In preeclampsia there is an abnormally increase in the lipid peroxidation in maternal blood and also in normal pregnancy3.4. But serum antioxidants are significantly decreased that lead to pathogenesis of preeclampsia5,6. For this, the study was undertaken to assess the lipid peroxidation product, serum Malondialdiehyde(MDA) & antioxidant (vitamin-E)levels in women with preeclampsia as well as in normal pregnancy.The study was conducted on 40 pregnant women(Group-B as study group) age ranged from 25 to 35 years in the Department of Biochemistry, Budi Kemuliaan Maternity Hospital(BKMH) in Jakarta in the year of 2006. The study group was further divided into B1-(normal pregnant women) & B2(preeclamptic patient).For comparison age matched 20 apparently healthy non pregnant women (Group-

A as control group)was also included in the study. The study subjects were selected from outpatient department (OPD) of Obstetrics & Gynaecology of BKMH in Jakarta. The ethical permission was taken from Ethical Review Committee of BKMH, Jakarta. Serum MDA (lipid peroxidation product) was measured by Thiobarbituric acid reactive substances assay (TBRAS) method & vit-E was estimated Spectrophotometrically. Data were analyzed statistically by ANOVA test among the groups and unpaired Students "t" test between the groups by using SPSS. The mean serum MDA levels were (1.23+ 0.5, 3.64 + 0.12, 7.28 +1.05 mmol/ml) and vitamin E levels were (7.43 +1 40, 5.75 + 1.24, 2.69 +0.17 micro mole/L) in group A, B1, and B2 respectively. However, MDA levels were significantly ($p<0.001$) higher in preeclampsia than those of normal pregnant women. Again the serum MDA levels were significantly ($p<0.001$) higher in both the study groups than that of non-pregnant control group. But the serum vit-E level were significantly ($p<0.001$) lower in preeclampsia than those of normal pregnant women as well as control group. This results revealed that lipid peroxidation is an important factor in the pathogenesis of preeclampsia. In preeclamptic patients serum antioxidants are excessively utilized to counteract the cellular changes mediated by free radicals7.

Dutta DC. Hypertensive disordesr in pregnancy, In: Test Book of Obstetrics. Ed. Konar HL.5th edition, New Central Book Agency (P) Ltd. 2001; 234-255.

Nelson GH, Zuspan FP, Milligan LT. Defect of lipid metabolism in toxaemia of pregnancy. Am J Obst Gynaecol 1989; 114: 582-8.

Riza Madazli, Ali Benian, Koray Gumata et al. Lipid peroxidation and antioxidants in preeclampsia.Eur J Obstet Gynaecol & Reprod Biol 1999; 85(2):205-208.

Poranen AK, ekblad U,Uotila P, Ahotupa M. Lipid peroxidation and antioxidants in normal and pre-eclamptic pregnancies. Placentas 1996; 17: 401-405.

Simmi Kharb, Sharina BD. Vitamin E and preeclampsia. Euro J Obstet. & Gynaeco Reprod Biol 2000; 93(1) : 37-39.

6. Jain SK, Wise R, Relationship between elevated lipid peroxides, vitamin E deficiency and hypertension in preeclampsia. Mol Cell Biochem 1995 : 151, 33-38.

7. Wang Yand, Walsh SW. Antioxidant activities and mRNA expression of superoxide dismutase, catalase and glutathione peroxidise in normal and preeclamptic placenta. J Soc Gynaecol Investig 1996; 3 : 179-184

Acknowledgement : I would like to express my special thanks to authority of BKMH, Jakarta for their active cooperation in completing this study. I am also grateful to the study subjects, for their full cooperation and active participation

Where applicable, the authors confirm that the experiments described here conform with The Physiological Society ethical requirements.

PCC215

Effects of vitamin E on antispermatogenic activity of alcohol in male albino rats

C.O. Akintayo[1,2] and O.T. Olaniyan[2,1]

[1]Physiology, Bingham University, Karu Nasarawa state, Nigeria, Karu, Nasarawa, Nigeria and [2]Physiology, University of Ibadan, Ibadan, Ibadan, Nigeria

Several factors affect fertility, ranging from environmental factor, nutritional factor, toxins and the way of life. However, Alcohol is often associated with fertility disturbances with low sperm count and impaired sperm motility. The sertoli cell seems to be the first testicular cell injured as a result of alcohol exposure. However, chronic alcohol administration to male animals is often associated with testicular atrophy and gonadal failure. This study was designed to investigate the effect of vitamin E, a known antioxidant, on alcohol induced antispermatogenic action in male rats. Mature wistar rats(200-250g) were divided into: Group I (control) received 0.2ml of 0.9% normal saline, group II (received alcohol 0.003ml/g b.w as 40%v/v orally), group III (received alcohol 0.003ml/g b.w as 20% v/v orally), group IV (received alcohol 0.003ml/g b.w as 40%v/v + Vitamin E 100mg/kg b.w orally), and group V (received alcohol 0.003ml/g b.w as 20%v/v + Vitamin E 100mg/kg b.w orally). All animals were treated for 30 days. At the end of each experimental period, animals were sacrificed via cervical dislocation and organ weights, sperm characteristics, serum testosterone levels, and fertility were assessed. There was a significant reduction ($p<0.05$) in sperm motility, viability and of alcohol treated groups (sperm motility: 69.12±2.6, 57.70±3.07)compared with the control group(89.06±1.07) However, there was a recovery/reversibility of sperm motility in groups treated with alcohol with co-administration of vitamin E showed that vitamin E was able to ameliorate the effect produced by alcohol on sperm characteristics . There was a significant increase in organ weights (testis, heart, kidney and liver) of alcohol treated rats. However, the study showed that Vitamin E (100mg/kg b.w) administration was able to prevent the antispermatogenic action of alcohol.

Keywords: Alcohol, Vitamin E, testosterone, reproductive organs, fertility, sperm parameters, rats

Effect of vitamin E on Spermatozoa indices of alcohol treated rats

Group	control	0.003m/gbw as40%v/v (alcohol)	0.003m/gbw as20%v/v (alcohol)	0.003m/gbw as40%v/v+Vit E (alcohol+vitamin E)	0.003m/gbw as20%v/v + Vit E (alcohol+vitamin E)
Sperm count(x106/ml)	80.00a±1.01	60.40b±2.8	57.70b±3.07	72.70a±2.45	76.90a±3.85
Sperm motility (%)	89.06a±1.07	69.12b±2.6	67.46b±2.00	77.43a±2.17	79.65a±4.36
Sperm morphology(%)	6.90a±0.32	9.53b±0.02	8.37b±0.12	6.57a±0.09	5.17a±0.25
Sperm viability (%)	74.32a±2.77	58.25b±5.21	54.38b±3.69	71.25a±6.45	73.77a±4.59

Means on the same column with different superscripts (a,b,c,) indicate significant difference ($p<0.05$)

Adams, M.L., Little PJ, Bell B and Cicero TJ (1991). Alcohol affects rats testicular interstitial fluid volume and testicular secretion of testosterone and β-endorphin. J. Pharmacol. EXP Ther. 258: 1008-1014

Bouloux P, Warne DW, Loumaye E (2002). FSH study group in men's infertility. Efficacy and safety of recombinant human follicle stimulating hormone men with isolated hypogonadotropic hypogonadism. Fertile Sterile 77(2) 270-273.

Ching, M., Valenmca, M., and Negro-Vitar, A. Acute ethanol treatment lowers hypophyseal portal plasma LHRH and systemic LH levels in rats. Brain research 443:325-328, 1998.

Cicero, T.J., Nock; B., O' Connor, L.; Adams, M.L.; Sewingo, B.N; and Meyer, E.R. Acute alcohol exposure markedly influences male fertility and fetal outcome in the male rats. Life Sciences 55:901-910, 1994.

Emanuele, M.A.; Tentler, J. Hallor, M.M.; Emanuele, N.V; Wallock, L.; and Kelly, M.R. The effect of acute in vivo ethanol exposure on follicle stimulating hormone transcription and translation. Alcoholism: Clinical and Experimental Research 16:776-780, 1992.

I would like to acknowledge my first degree supervisor (Dr Falokun O.P), who showed me how to believe in myself. Who encouraged me to have a world of possibility, though he's late but his memory and good works can never be forgotten.

Where applicable, the authors confirm that the experiments described here conform with The Physiological Society ethical requirements.

PCC216

Trophoblast signalling of DNA damage and cell death to hES cells in response to oxidative stress

A. Rogers and C.P. Case

University of Bristol, Bristol, UK

A variety of toxicants that cause oxidative stress can cause DNA damage across a placental like trophoblast barrier1. This damage at a distance does not occur because the toxicants, including metal ions, pass through the barrier. Instead it is mediated by intercellular signalling, involving ATP release and Ca wave propagation, culminating in the secretion of as yet unidentified molecules, which cause DNA damage in the cells beneath and separate from the barrier2. Here we have examined whether this transbarrier signalling in response to Co and Cr ion exposure above the barrier could cause damage to human embryonic stem cells (hESCs). hESCs (H9 cell line) were exposed to Co and Cr6+ (50:40 ppb Co:Cr) for 24h across a confluent barrier of BeWo cells (a trophoblast cell line). Mass spectrometry analysis confirmed that Co and Cr did not pass through the BeWo barrier. Values are means ± standard deviations, compared by students T test. DNA damage was significantly higher in exposed cells (EC) compared to control cells (CC) when assessed by comet assay (mean tail moment CC 1±0.28 Vs 2.27±0.4, P≤0.05) and staining for γ-H2AX (% cells with ≥4 foci CC 8.76±3.37 Vs 21±2.19 EC, P≤0.05). Cells with >4 γ- H2AX foci appeared in small clusters of neighbouring cells (3-10 cells per cluster) throughout exposed colonies. Addition of connexin mimetic peptide Gap26 to H9 cells prior to exposure partially rescued EC from DNA damage (% cells with ≥4 foci C 9.78±1.70 Vs EC 20.22±1.95, P≤0.01; EC 20.22±1.95 Vs EC + Gap26 15±1.20, P≤0.05) and reduced clustering (% clustered cells CC 5.06±1.38 Vs EC 23±2.07, P≤0.01; EC 23±2.07 Vs EC + Gap26 13.9±1.38, P≤0.01). Cell counts detected a significant decrease in viable, adherent cells following exposure (number of cells recorded in 12 fields of vision at X20 magnification CC 1914.67±190.18 Vs EC 1126.22±264.96, P≤0.001) concomitant to vastly increased TUNEL staining (n=9 control and 9 exposed populations). A similar loss is not seen in cells directly exposed to Co and Cr (DEC), although DEC do have increased DNA damage compared to unexposed control cells (UEC) (comet assay mean tail moment UEC 1±0.29 Vs DEC 5.44±0.13, P≤0.001). This suggests that the loss of EC is not secondary to DNA damage but is caused by the release of a signalling molecule from the barrier in response to Co and Cr exposure. Investigation of barrier conditioned media by ELISA has established TNF α as a potential candidate for cell death effects (absorbance at 450nm CC 0.009±0.008 Vs EC 0.023±0.003, P≤0.05 in one tailed test). This investigation has shown that hESCs may be damaged by exposure to metal ions through a trophoblast barrier. In addition, it has highlighted an important potential biological mechanism, whereby the trophoblast barrier between mother and fetus may secrete an apoptosis inducing signal to the embryo in response to oxidative stress.

1. Sood A, Salih S, Roh D, Lacharme-Lora L, Parry M, Hardiman B, Keehan R, Grummer R, Winterhager E, Gokhale P, Andrews P, Abbott C, Forbes K, Westwood M, Aplin J, Ingham E, Papageorgiou I, Berry M, Liu J, Dick A, Garland R, Williams N, Singh R, Simon A, Lewis M, Ham J, Roger L, Baird D, Crompton L, Caldwell M, Swalwell M, Birch_Machin M, Lopez-Castejon G, Randall A, Lin H, Suleiman M-S, Evans W, Newson R and Case C (2011) Signalling of DNA damage and cytokines across cell barriers to nanoparticles depends on barrier thickness. Nature Nanotechnology 6:824-823

2. Bhabra G, Sood A, Fisher B, Cartwright L, Saunders M, Evans W, Surprenant A, Lopez-Castejon G, Mann S, Davis S, Halis L, Ingham E, Verkade P, Lane J, Heesom K, Newson R and Case C (2009) Nanoparticles can cause DNA damage across a cellular barrier. Nature Nanotechnology 4:876-883

Where applicable, the authors confirm that the experiments described here conform with The Physiological Society ethical requirements.

PCC217

Reduction of human placental taurine transporter activity is associated with compromised syncytiotrophoblast renewal

C. Hirst, S.L. Greenwood and M. Desforges

The Maternal and Fetal Health Research Centre, The University of Manchester, Manchester, UK

Pre-eclampsia (PE) is a serious disease of pregnancy affecting 4 million women/year. The disease etiology is complex but its origin lies in abnormal placental development and function. PE is associated with increased nitrative stress and abnormal renewal of syncytiotrophoblast (STB), the transport epithelium of human placenta. STB is renewed by cytotrophoblast cells (CTB) that proliferate, differentiate, and fuse with the multinucleated STB and this is balanced by apoptosis and shedding of aged nuclei. In non-placental tissues the amino acid taurine regulates proliferation, differentiation, and apoptosis. Taurine is accumulated in STB by the taurine transporter (TauT) and we have shown that TauT activity is significantly lower in PE compared to normal pregnancy[1]. TauT activity can be downregulated by nitrative stress and in PE those placentas with a lower TauT activity also had elevated nitrotyrosine expression, a marker of nitrative stress. Furthermore, generation of STB nitrative stress in vitro with SIN-1 reduced TauT activity by 14%[2].

Here we test the hypothesis that reducing placental TauT activity by nitrative stress alters CTB proliferation and apoptosis.

Placental villous explants from normal pregnancy were cultured for 7 days. On day 5 explants were treated with 1mM SIN-1 for 48hrs to reduce TauT activity. Immunohistochemistry was used to assess proliferation (detected by Ki67) and apoptosis (detected by M30: caspase-cleaved cytokeratin). The apoptotic index was calculated as the area of M30-positive staining expressed as a percent of total villous area using image pro plus software. To quantify proliferation explants were dual stained for ki67 and the CTB marker E-cadherin. Proliferation index was calculated as the number of cells positive for both ki67 and E-cadherin (i.e. proliferating CTB) expressed as a percent of the total number of E-cadherin positive cells (i.e. CTB). For each experiment, 8 fields of view were assessed and a mean calculated.

There was no difference in villous area or number of CTB between control and SIN-1 treated placental explants. SIN-1 treatment significantly reduced CTB proliferative index (Fig1) and significantly increased apoptotic index compared to controls (Fig2). Inspection of stained tissue sections showed morphological integrity was maintained throughout culture and secretion of hCG, an indicator of endocrine viability, was unaffected by SIN-1 treatment.

Nitrative stress reduces placental TauT activity[2], inhibits CTB proliferation and increases apoptosis. Future work will determine whether this abnormal STB renewal is a direct effect of nitrative stress or a result of reduced TauT activity. We propose that in PE placental TauT activity is reduced by nitration,

leading to altered CTB proliferation and apoptosis, resulting in abnormal renewal of the STB.

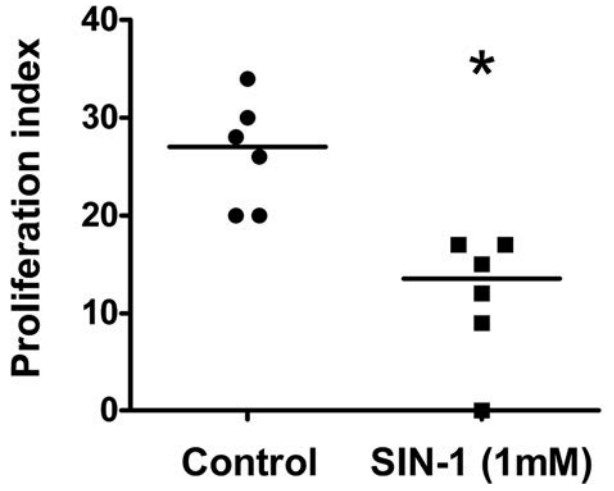

Figure 1: Cytotrophoblast cell proliferation in control and SIN-1 treated placental explants. N=6, line represents the median. *p<0.05, Wilcoxon matched pairs signed rank.

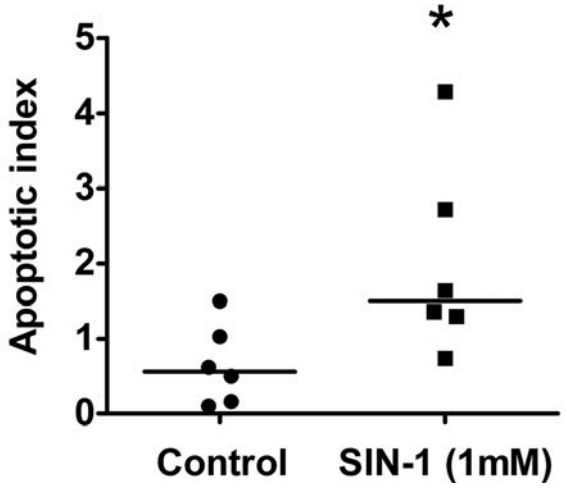

Figure 2: Cytotrophoblast cell apoptosis in control and SIN-1 treated explants. N=6, line represents the median. *p<0.03, Wilcoxon matched pairs signed rank.

Hirst,C. et al (2012) Reproductive Sciences 19:377A.

Hirst,C. et al (2012) Placenta 33:A40.

Supported by The Wellcome Trust.

Where applicable, the authors confirm that the experiments described here conform with The Physiological Society ethical requirements.

PCC218

Mathematically modelling the system L amino acid exchanger in human placenta

K.L. Widdows[1], N. Panitchob[2], I. Crocker[1], S. Brooks[3], C. Please[3], E. Johnstone[1], B. Sengers[2], J. Glazier[1] and R. Lewis[3]

[1]Maternal and Fetal Health Research Centre, University of Manchester, Manchester, UK, [2]Bioengineering Research Group, University of Southampton, Southampton, UK and [3]University of Southampton, Faculty of Medicine, Southampton, UK

System L is a heterodimeric Na+-independent amino acid (aa) membrane transporter that mediates the transport of essential aa's. System L activity has been demonstrated in the microvillous (MVM) and basal (BM) plasma membranes of the human placental epithelial exchange barrier, the syncytiotrophoblast. System L transporters are thought to act as obligatory 1:1 aa exchangers, transporting one aa in exchange for another. However, other modes of carrier-mediated transport are implicated; system L substrates can be transported across MVM and BM under zero-trans conditions, without exchangeable aa. This led to our hypothesis that system L-mediated transport may not occur solely via an obligatory exchange mechanism. To investigate this, we applied an integrated mathematical modelling approach to predict how transport of serine (Ser), a system L substrate, would behave under theoretical models of transport.

Mathematical predictive models of obligatory aa exchangers, along with facilitated transport, were developed based on assumptions of carrier-mediated transport. Exchanger transporters were assumed to bind aa to confer 1:1 transport across the plasma membrane, whilst facilitated transport was assumed to be driven by the transmembrane aa gradient. The model predicted that for an exchanger together with a facilitated (slower rate) transport component, an outwardly directed substrate gradient would lead to an overshoot of substrate accumulation above tracer equilibrium concentration (Fig 1A).To test the models, we measured uptake of 7.5μM ^{14}C-Ser (tracer) into MVM vesicles isolated from normal term placentas, in vesicles preloaded with 250μM (equal to extravesicular Ser concentration) or 1mM Ser (outwardly directed substrate gradient). Uptake of ^{14}C-Ser mediated by system L was taken to be that inhibitable by 20mM 2-amino-2-norbornanecarboxylic acid (BCH), a system L substrate.

In the presence of equal intravesicular and extravesicular Ser (250μM), ^{14}C-Ser accumulated in a time-dependent manner to reach tracer equilibrium concentration (7.5μM; assuming an intravesicular volume of 1 μl/mg protein) by 10min, indicating uptake of ^{14}C-Ser in the absence of a transmembrane substrate gradient. However, an outwardly directed substrate concentration gradient evoked a rapid overshoot of ^{14}C-Ser accumulation above tracer equilibrium concentration, which was abolished by BCH (Fig 1B). These observations suggest trans-stimulation of system L activity showed good correspondence to model predictions with both an exchanger and facilitated transport component, suggesting system L activity in MVM vesicles is mediated by both components, although their molecular identities remain to be determined. This study emphasizes the utility of mathematical modelling in predicting aa modes of transport, providing an improved quantitative understanding of placental aa transporter mechanisms.

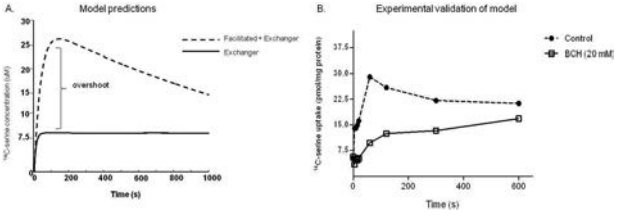

Figure 1. Experimental validation of model predictions for system L activity in MVM. (A) Modelling either exchanger activity (solid line) or exchanger with facilitated transporter (dashed line) predicts tracer accumulation to equilibrium (7.5μM) or overshoot above equilibrium, respectively. (B) Testing this model experimentally in MVM vesicles demonstrated good correspondence to the exchanger plus facilitated model with overshoot (dashed line), which was abolished by BCH (solid line). This suggests the presence of both an exchange plus facilitated transport component mediating serine transport across MVM in the human placenta

Where applicable, the authors confirm that the experiments described here conform with The Physiological Society ethical requirements.

PCC219

The expression of facilitated amino acid transporters in the human choriocarcinoma BeWo cell line

C. Simner[1], N.C. Harvey[2], K.A. Lillycrop[3], R.M. Lewis[1] and J.K. Cleal[1]

[1]Institute of Developmental Sciences, University of Southampton, Southampton, UK, [2]MRC Lifecourse Epidemiology Unit, University of Southampton, Southampton, UK and [3]Centre for Biological Sciences, University of Southampton, Southampton, UK

Amino acids are vital for fetal growth, and must be supplied by the mother via the placenta. Previously we have shown that the facilitated amino acid transporters TAT1 (slc16a10), LAT3 (slc43a1) and LAT4(slc43a2) mediate efflux of specific amino acids from the placenta into the fetal circulation. TAT1 and LAT3 mRNA levels in human placentas are related to measures of fetal growth whereas LAT4 mRNA levels are affected by maternal nutritional status. It is now important to establish how these transporters are regulated. This study aimed to establish whether the human choriocarcinoma, BeWo, cell line is a suitable model for investigating the regulation of facilitated amino acid transporters.

BeWo cells were cultured in 35 mm diameter 6 well plates at 37C (5% CO2) in DMEM/Ham F-12K nutrient mix supplemented with 10% fetal bovine serum and 1% penicillin/streptomycin. At 70-80% confluence cells were harvested for RNA and protein extraction. Total RNA was extracted (Ambion mirVanaTM miRNA isolation kit) and reverse transcribed into cDNA. PCR was carried out on BeWo cDNA (n=3) with specific primers to detect the expression of TAT1, LAT3 and LAT4 transcripts. Western blotting was carried out to detect the protein expression of TAT1 and LAT4 (LAT3 not tested). BeWo preparations (45 μg protein, n=3) were run on SDS-PAGE gels and transferred to PVDF membranes. Blots were incubated with rabbit anti-TAT1 or anti-LAT4 primary antibody then goat anti-rabbit-HRP secondary antibody. Immunoreactive signals were visualized using enhanced chemiluminescence.

The presence of TAT1, LAT3 and LAT4mRNA in BeWo cells was confirmed by PCR. The presence of TAT1 and LAT4 proteins in BeWo cells was confirmed by Western blotting demonstrating antibody specific bands which were not present in the negative control. Immunoblotting for B-actin on each blot indicated similar protein loading in each lane.

BeWo cells are placental in origin and commonly used to study human placental function. BeWo cells express the facilitated amino acid transporters at both the mRNA and protein level as seen in human placental tissue. They may therefore provide a useful model for studying the regulation of the facilitated amino acid transporters TAT1, LAT3 and LAT4 in the placenta.

The Gerald Kerkut Trust

Where applicable, the authors confirm that the experiments described here conform with The Physiological Society ethical requirements.

PCC220

The effect of adenovirus-VEGF gene therapy on placental nutrient transport mechanisms in an ovine model of intrauterine growth restriction

J. Naftel[1], D.J. Carr[2], R.P. Aitken[3], J.S. Milne[3], J.M. Wallace[3], A.L. David[2], L.R. Green[1] and J.K. Cleal[1]

[1]Institute of Developmental Sciences, University of Southampton, Southampton, UK, [2]Institute of Woman's Health, University College London, London, UK and [3]The Rowett Institute of Nutrition and Health, University of Aberdeen, Aberdeen, UK

Intrauterine growth restriction is a major cause of perinatal mortality and morbidity. Injection of an adenovirus (Ad) vector containing the vascular endothelial growth factor-A165 (VEGF-A165) gene into the uterine arteries increased growth velocity and birth weight (trend) in growth restricted fetal sheep (1,2). Ad.VEGF-A165 treatment increased mRNA levels of the VEGF receptor FLT1/KDR in maternal but not fetal placental tissues and placental efficiency near term (trend) (1,2). We measured late gestation placental expression of genes regulating growth (insulin-like growth factor receptor 1, IGF-1R), lipid handling (lipoprotein lipase, LPL) and amino acid transport (TAT1) in normal and growth-restricted pregnancies with and without Ad.VEGF-A165 treatment. Single embryos (from superovulated single sire inseminated donor ewes) were transferred into adolescent recipient ewe uteri under general inhalational anaesthesia (isoflurane in O2/NO). Recipients were fed control (C n=12) or high (H n=45) intake of complete diet from 4-131 days' gestational age (dGA term=145dGA) to induce normal and restricted fetal growth, respectively (3). At 89dGA under general anaesthesia (induction with propofol IV then as above) both uterine arteries were injected with 5x1011 particles of Ad.VEGF-A165 (H-Ad.VEGF, n=18) or control vector Ad.LacZ/control saline (H-Ad.LacZ/saline, n=27; C-saline, n=12). At 131dGA ewes were killed (pentobarbitone overdose IV). RNA was extracted from separated fetal and maternal placental compartments (frozen at -80C) and real-time quantitative PCR was performed to measure mRNA levels of LPL, TAT1 and IGFR-1 (normalised to GAPDH and βactin geometric mean). Data are mean±SEM and were analysed by two-way ANOVA (placental compartment and group [C-saline; H-Ad.VEGF; H-Ad.LacZ/saline]) then Least Squares Difference correction. Regardless of placental side TAT1 and LPL mRNA levels were lower in H-Ad.VEGF compared to H-Ad.LacZ/saline (TAT1, 0.54±0.08 vs. 0.75±0.06, P=0.02; LPL, 0.77±0.09 vs. 0.97±0.07, P=0.06) and compared to C-saline (TAT1, 0.54±0.08 vs. 0.76±0.09, P=0.07; LPL, 0.77±0.09 vs. 1.03±0.10, P=0.06). Regardless of group LPL, IGFR-1 and TAT1 mRNA levels were greater in the fetal compared to maternal placental side (LPL: 1.22±0.07 vs. 0.66±0.07; IGFR-1: 1.19±0.07 vs. 0.99±0.07; TAT1: 1.24±0.07 vs. 0.13±0.06; P <0.05). These data suggest that increased fetal growth velocity following Ad.VEGF-A165 is independent of altered IGFR-1 gene expression. Decreased TAT1 and LPL gene expression following Ad.VEGF-A165 is unexpected but may reflect complex amino acid and lipid transport regulation in these animals which requires further molecular analysis. Higher expression of genes related to nutrient transfer in the fetal-facing placental portion may indicate membrane specific placental nutrient transport mechanisms.

Carr DJ, Aitken RP, Milne JS, Peebles DM, Martin J, Zachary I, Wallace JM, David AL. Maternal Ad.VEGF gene therapy increases fetal growth velocity in growth restricted sheep fetuses. BJOG 2011; 118(8):1009

Carr DJ, Aitken RP, Milne JS, Peebles DM, Martin JF, Zachary IC, David AL, Wallace JM. Prenatal gene therapy increases fetal growth velocity and expression of VEGF receptors in an ovine paradigm of fetal growth restriction. Reproductive Sciences 2012; 19(3):78A

Wallace J, Aitken R, Cheyne M. Nutrient partitioning and fetal growth in rapidly growing adolescent ewes. Journal of Reproduction and Fertility 1996;107: 183-190.

Where applicable, the authors confirm that the experiments described here conform with The Physiological Society ethical requirements.

PCC221

Effects of avian influenza virus (H5N1) on cytokine and chemokine gene expression in human respiratory epithelium

N. Huipao[1], S. Hiranyachattada[1], S. Borwornpinyo[2], A. Thitithanyanont[3], C. Pholpramool[4], D. Cook[5] and A. Dinudom[5]

[1]Physiology, Prince of Songkla University, Hat Yai, Songkhla, Thailand, [2]Biotechnology, Mahidol University, Ratchathewi, Bangkok, Thailand, [3]Microbiology, Mahidol University, Ratchathewi, Bangkok, Thailand, [4]Physiology, Mahidol University, Ratchathewi, Bangkok, Thailand and [5]Physiology, University of Sydney, Camperdown, NSW, Australia

One important feature of influenza A/H5N1 immunopathogenesis is the appearance of hypercytokinemia (cytokine storm) which is characterized by the extreme production and secretion of large numbers and excessive levels of pro-inflammatory cytokines. H5N1 targets specific host cells, i.e., bronchiolar cells, macrophages and type 2 alveolar pneumocytes. These cells, but not those in the tracheal or the upper path of the respiratory tract, express the α2-3 sialic acid receptors, the binding site for H5-hemagglutinin. It has been reported that H5N1 infection induced the production of TNF-α, IP-10, IL-6 and IFN-β in human alveolar and bronchial cells. Recent data, however, suggest that H5N1 can also induce cytokine release via an infection-independent mechanism. This study aimed to investigate the mechanism by which H5N1 triggers expression of cytokines/ chemokines in the respiratory epithelium. Expression of the mRNAs of interest in 16HBE14o cells treated with inactivated-H5N1 was analyzed by quantitative RT-PCR. Our results showed that the inactivated-H5N1 increased mRNA expression of IL-6 and IL-8 but not of TNF-α, RANTES and IP-10. Since cytochalasin D treatment, which disrupts actin cytoskeleton and, hence, inhibits endocytotic uptake of the virus, had no effect on the effect of the inactivated-H5N1 on cytokines mRNA expression, this effect of H5N1 did not require the presence of the virus particles in the cytosol. Cytokines production can, therefore, be initiated by an interaction between H5N1 capsule and surface membrane of the respiratory epithelial cells. The underlying mechanism by which H5N1 generates this infection-independent effect on cytokine production is currently under investigation.

Where applicable, the authors confirm that the experiments described here conform with The Physiological Society ethical requirements.

PCC222

Characterisation of genetically disrupted strains of *Staphylococcus aureus* shows that sugar transport is important for apical growth in an airway-bacterial co-culture model

D. Braun[1], J.P. Garnett[1], A.J. McCarthy[2], J.A. Lindsay[2], E.H. Baker[1] and D.L. Baines[1]

[1]Biomedical Science, St Georges, University of London, London, UK and [2]Clinical Sciences, St Georges, University of London, London, UK

Glucose concentration in the airway surface liquid (ASL) is normally lower than blood (~0.4mM compared to ~5mM). We developed an in vitro model of airway glucose homeostasis and showed that, normally, glucose diffuses from blood/interstitial fluid across the respiratory epithelium into the ASL via paracellular pathways, and this is limited by epithelial permeability, glucose uptake and metabolism. In this model, increasing the diffusion gradient for glucose across the epithelium (e.g. hyperglycaemia) elevated glucose in ASL [1, 2].

Sugars (glucose and fructose) are known to promote the growth of *S. aureus* [3]. The growth of *S. aureus* on the apical surface of an in vitro model of human airway epithelium (H441) was significantly increased by elevating basolateral glucose concentration from 10mM to 20mM or 40 mM (colony forming units; cfu increased by 155±49% or 392±105%, $p<0.05$ and $p<0.001$, respectively, n=9). Furthermore, there were significantly more bacteria post infection in the airways of an in vivo mouse model of diabetes (db/db) (4611±995 bronchoalveolar lavage; BAL cfu) than wild type mice (950±293 BAL cfu, $p<0.001$, n=9).

To confirm that *S. aureus* utilised sugars that diffused across the epithelium into ASL, we obtained several *S. aureus* JE2 derived strains from the Nebraska Transporon Mutant Library which contained genetically disrupted genes associated with sugar transport. We firstly characterised the effect of these mutations on growth in the presence of sugars. Addition of either fructose (10 mM) or glucose (10 mM) significantly increased the growth of the parent strain (JE2) (measured as log10 OD600) at 8 hours ($p<0.001$, n=3, respectively). Glucose (10 mM) promoted the growth of all *S. aureus* strains, although two strains, NE1944 and NE172, with mutations in the glucose specific domain of the phosphoenolpyruvate-dependent sugar phosphotransferase system (PTS), exhibited mildly reduced growth at 8 hours ($p<0.05$, n=3). NE768 a strain in which the fructose specific permease had been disrupted, exhibited significant growth inhibition in the presence of fructose compared to glucose ($p<0.001$, n=3) consistent with an inability to utilise fructose to support its growth. Comparison of sugar induced JE2 and NE678 growth in bacterial epithelial co-culture showed that basolateral fructose increased apical JE2 but not NE678 growth at 7 hours ($p<0.05$, n=5).

These data provide new evidence that fructose in addition to glucose diffuses across the airway epithelium and is utilised by *S. aureus* as a substrate for growth. This provides a proof of concept for *S. aureus* utilisation of glucose in ASL. Our data also indicate that pathways for glucose uptake in *S. aureus* are more complex and may involve multiple mechanisms.

Kalsi KK *et al.* (2009). *Pflugers Arch* **457**,1061-1070.

Garnett JP *et al.* (2012). *Eur Respir J* **40**,1269-76

Brennan AL *et al.* (2007). *J Cyst Fibros* **6**, 101-109.

Supported by the Wellcome Trust

Where applicable, the authors confirm that the experiments described here conform with The Physiological Society ethical requirements.

PCC223

2,6-bis-4-(hydroxyl-3-methoxybenzylidine)-cyclohexanone (BHMC) prevents allergic airway inflammation in ovalbumin-sensitized mice

C. Tham[1], K. Lam[2], N. Md[3], M. Sulaiman[1] and D. Israf Ali[1]

[1]Biomedical Science, Universiti Putra Malaysia, UPM Serdang, Malaysia, [2]Faculty of Pharmacy, Universiti Kebangsaan Malaysia, Kuala Lumpur, Malaysia and [3]Scientific Chairs Unit, Taibah University, Madina, Saudi Arabia

Asthma is affecting approximately 300 million people worldwide with 250,000 annual deaths. The marked increase in the global prevalence of asthma is likely to continue over the next two decades. Over the years, corticosteroids remain the mainstay in the treatment of asthma despite recently raised issues regarding safety and lack of responsiveness in 5-10% of asthmatic individual. Therefore, there is an urgent need in the search of more effective and safer treatment for patients with allergic asthma which is associated with increased pulmonary inflammation and airway hyperresponsiveness. A novel curcuminoid derivative, 2,6-bis-4-(hydroxyl-3-methoxybenzylidine)-cyclohexanone (BHMC) has been designed and synthesized as a non-steroidal anti-inflammatory agent in our previous study. BHMC has been proven to inhibit the synthesis of pro-inflammatory mediators in macrophages, restores endothelium dysfunction and decreases mortality in septic mice through specific disruption on p38 MAPK enzymatic activity. Recent preliminary research findings further demonstrated potential anti-inflammatory effects of BHMC in both acute and chronic models of inflammation in rodents. The present study addressed the effects of BHMC on allergic airway inflammation in an acute murine model. Mice were sensitized with ovalbumin (OVA) and treated with various doses (0.1, 1 and 10 mg/kg) of BHMC intraperitoneally. Respiratory function was measured whereas bronchoalveolar lavage fluid (BALF), blood and lung tissue were collected. Treatment with BHMC significantly attenuated airway hyperresponsiveness, number of inflammatory cells in BALF and infiltration of inflammatory cells into the airways. These observations were further strengthened by the findings that BHMC inhibited production of Th2 cytokines and goblet cells hyperplasia without reducing the level of total IgE in peripheral blood serum. Collectively, the preventive effects of BHMC on acute allergic inflammation open further avenue of research and development of a synthetic non-steroidal small molecule, BHMC, as an additional option of currently available anti-asthma therapies.

Where applicable, the authors confirm that the experiments described here conform with The Physiological Society ethical requirements.

PCC224

Serum levels of antioxidants enzymes glutathione peroxidase (GPx) and cupper zinc superoxide dismutase (Cu Zn SOD) in Sudanese asthmatics and their relationship with the severity of asthma

M.M. Sherief[1], A.H. Yousif[2] and A.M. Saeed[2]

[1]Physiology, International University of Africa Faculty of Medicine and Health Sciences, Khartoum, Khartoum, Sudan and [2]University of Khartoum Faculty of Medicine, Khartoum, Sudan

Asthmatic patients tend to have increased oxidative stress caused by imbalance between oxidants and antioxidants. Changes in the level of antioxidant enzymes, Cu Zn SOD and GPx may play an important role in the development and progression of asthma. It was hypothesized that asthmatic individuals with higher level of oxidative stress may have greater loss of these enzymes, which would be reflected clinically by development of severe asthma. The abnormalities in redox are magnified in asthmatic airways in response to exacerbating factors (1). In this study we aimed to investigate the role of oxidative stress in asthma by determining serum levels of Cu Zn SOD and GPx in patients with asthma compared to healthy individuals. Furthermore, to find out whether the acute attack or severity of asthma would change the serum levels of these enzymes. Serum Cu Zn SOD and serum GPx concentrations were measured in 96 asthmatic adult patients and 55 healthy control subjects matched for age and sex. The patients were recruited from asthma clinics and wards of two tertiary referral hospitals: Al shaab and Omdurman teaching hospitals in Khartoum State. Guided by the GINA classification of asthma, patients were grouped according to asthma severity to mild and severe and according to existence of symptoms to symptomatic and asymptomatic(2). Serum Cu Zn SOD and serum GPx concentrations were measured in these patient groups. Concentrations of serum were measured using ELIZA kits assay according to instructions of manufacturers. Mean serum GPx was found significantly decreased in patients compared with controls (247.24μ/l in patients and 302.42μ/l in controls and P = 0.001). Mean serum Cu Zn SOD was found lower in cases than controls (86.5μg/l in patients and 87.6μg/l in controls). Mean serum Cu/Zn SOD of mild and severe stable cases was 80.64μg/ml and 98.21μg/ml respectively. Mean serum Cu/Zn SOD in symptomatic and asymptomatic was 84.95μg/ml and 102.78μg/ml respectively. Mean serum Gpx of mild and severe was242.14μg/ml and 258.43μg/ml respectively. Mean serum Gpx in symptomatic and asymptomatic was 213.μg/ml and307.73 μg/ml respectively. These findings revealed oxidative stress exists in asthmatic patients showed by deficiency of the antioxidant enzymes compared to controls. Also, their levels decreased during the acute attack compared to the steady state. Control of oxidative stress at the appropriate time with the proper methods is mandatory for effective management of asthma

Fig 2: Mean serum level of Superoxide dismutase (Cu Zn SOD) and Glutathione Peroxidase (Gpx1) in ug/ml in cases and controls

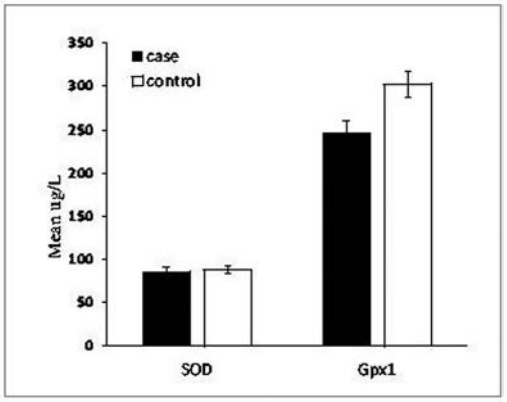

Comhair SA. Redox Control of Asthma. Antioxidant Redox Signal 2010 Jan; 12 (1):93-124

Global Strategy for Asthma Management GINA [updated March, 2010]

This Study was supported by grants from the Departments of Scientific Research University of Khartoum and the Ministry of Higher Education Republic of Sudan.

Where applicable, the authors confirm that the experiments described here conform with The Physiological Society ethical requirements.

PCC225

Elevated glucose flux across cystic fibrosis airway epithelium is an important factor for *Pseudomonas aeruginosa* growth in airway epithelial co-culture

J.P. Garnett[1], R. Tarran[2], M.A. Gray[3], M. Brodlie[3], E.H. Baker[1] and D.L. Baines[1]

[1]Division of Biomedical Sciences, St George's, University of London, London, UK, [2]Department of Cell Biology and Physiology, University of North Carolina, Chapel Hill, NC, USA and [3]Institute for Cell and Molecular Biosciences, Newcastle University, Newcastle, UK

The airway epithelium is covered by a thin layer of surface liquid (ASL), which is vital for maintaining the sterility of the respiratory tract. The glucose concentration of the ASL (~0.4mM) is much lower than that in blood and is tightly regulated by the airway epithelium (1). ASL glucose is elevated in patients with cystic fibrosis (CF; ~2mM) and is associated with increased incidence of respiratory bacterial infection (2). The aim of this study was to compare the effect of *P. aeruginosa* on the mechanisms governing airway glucose homeostasis in polarized monolayers of CF and non-CF primary human bronchial epithelial (HBE) cells. In addition, Calu-3 monolayers were used to evaluate the potential importance of glucose on *P. aeruginosa* growth, in comparison to other hallmarks of the CF ASL, namely mucus hyper-viscosity and reduced bicarbonate content/acidic pH (3).

The addition of *P. aeruginosa* filtrate to HBE monolayers reduced transepithelial resistance and was associated with an increase in paracellular permeability of glucose, as well as enhanced glucose-uptake. The increase in paracellular glucose flux was much greater across CF HBE monolayers (145±28%) compared to non-CF (56±23%, $p<0.05$, n=3) and was associated with elevated *P. aeruginosa* growth. No difference in glucose uptake was observed between non-CF and CF monolayers ($p>0.05$, n=4). Increasing the basolateral glucose concentration from 5 to 15mM resulted in a 54±12% increase in *P. aeruginosa* growth on the apical surface of HBE monolayers ($p<0.05$, n=3) and a 76±16% increase on Calu-3 monolayers ($p<0.01$, n=7), after 6 hours of co-culture. Removal of bicarbonate from the bathing solution (replaced with HEPES) led to elevated bacterial growth (by 109±7%, $p<0.01$, n=3) and the pH of the surface fluid was also more acidic (7.06±0.03 compared to 7.43±0.03 using bicarbonate; $p<0.01$, n=3). *P. aeruginosa* growth was significantly reduced by 57±18% following the addition of the cAMP-agonist forskolin (5μM, $p<0.05$, n=3) and this was associated with an alkalinisation in fluid pH to 7.51±0.01, (in bicarbonate-buffered solution; $p<0.05$). In both cases, elevating basolateral glucose increased apical bacterial growth. The presence of a thick mucus layer across Calu-3 monolayers also increased *P. aeruginosa* numbers by 84±13% ($p<0.05$, n=3). Similarly, under these conditions raising basolateral glucose enhanced the growth of the bacterium by 53±8% ($p<0.05$, n=3).

These results indicate that *P. aeruginosa* induced an elevated glucose leak across the CF epithelium compared to non-CF. In addition, elevating glucose increased *P. aeruginosa* growth over and above the effects of pH/bicarbonate and mucus. Together these studies highlight the potential importance of glucose in promoting *P. aeruginosa* growth and respiratory infection in CF and CF-related diabetes.

Garnett JP *et al.* (2012). *J Immunol* **189**, 373-380

Brennan AL *et al.* (2007). *J Cyst Fibros* **6**, 101-109.

Pezzulo AA *et al.* (2012). *Nature* **487**, 109-113.

Where applicable, the authors confirm that the experiments described here conform with The Physiological Society ethical requirements.

PCC226

Oscillations in airway surface liquid pH and pCO2 enhance antimicrobial activity

D. Kim[1,3], J. Liao[1], N.B. Scales[1], M.L. Palmer[2], R. Robert[1], S.C. Fahrenkrug[2], S.M. O'Grady[2] and J.W. Hanrahan[1,3]

[1]Physiology, Mcgill University, Montreal, QC, Canada, [2]Physiology, Univeristy of Minnesota, St Paul, MN, USA and [3]Groupe d'étude des protéines membranaires, Montreal, QC, Canada

A microscopic layer of secreted fluid covers the airways and provides the first line of defense against inhaled pathogens. Depletion of this airway surface liquid (ASL) in cystic fibrosis (CF) disrupts mucociliary clearance and leads to chronic infections by Pseudomonas aeruginosa and other bacteria. Epithelial bicarbonate secretion is also reduced in CF, resulting in a decrease in pH that may promote infection in CF pig airways, although it remains uncertain whether the measured reduction from pH 7.14 to 6.96 inhibits antimicrobial activity significantly. We found that Pseudomonas is sensitive to alkaline pH in pure solutions when pH is elevated by a decrease in luminal pCO2 or increase in HCO3- concentration. Computer simulations suggested that CO2, which varies between 0.035% during inspiration and 5% during expiration, may equilibrate with ASL. To test this experimentally we studied thin layers of liquid placed on monolayers of fixed Calu-3 cells, a human airway epithelial cell line Calu-3. BCECF-dextran microfluorimetry was used to measure surface liquid pH, a computer-controlled gas mixing pump was used to generate pCO2 oscillations that simulate tidal breathing, and pCO2 was mon-

itored using a fast response CO2 analyzer. Physiological pCO2 oscillations caused the surface pH to vary by ~1.5 units, with pH reaching maximal values of pH 8.7 - 9.2 depending on HCO3- concentration. Similar values were observed under steady-state conditions when secretions were equilibrated with 5% CO2 (7.42± 0.11, mean ± s.d., n=8) or room air (9.2 ± 0.14; n=7). The antimicrobial effect of oscillating pH was assessed by comparing by counting colony forming units on agar plates after exposure to physiological CO2 oscillations or various (constant) pCO2 levels for 1, 3, or 6 hours at 37oC. The number of viable bacteria increased 3-fold after 6h exposure to 5% CO2 but not 2.5% CO2, presumably due to moderate elevation of the pH. Oscillations between 5% and 0.035% were also bacteriostatic when secretions were collected from unstimulated Calu-3 cells. Importantly, 90% killing was observed if fluid was collected from forskolin-stimulated control Calu-3 cells, but not if fluid was collected from CFTR knock-down cells. Similar results were obtained using other HCO3- secretagogues (VIP, cpt-cAMP) and with mucoid and non-mucoid strains of Pseudomonas. We conclude that HCO3- allows rapid, transient alkalinizations during physiological variations in pCO2. Bacteria are sensitive to alkaline pH, and this sensitivity is enhanced by pCO2 oscillations and by stimulated HCO3- secretion. These results provide the first evidence for dynamic alterations in airway surface pH and help clarify the role of CFTR and bicarbonate secretion in airways host defense.

Pezzulo AA et al., (2012) Nature 487, 109-113.

Support: Cystic Fibrosis Canada and the Ministère des Finances et de l'Économie Québec

Where applicable, the authors confirm that the experiments described here conform with The Physiological Society ethical requirements.

PCC227

Computational model of a circulation current that controls electrochemical properties in the mammalian cochlea

F. Nin[1,2], H. Hibino[1], S. Murakami[2] and Y. Kurachi[2]

[1]Molecular physiology, Niigata university, Niigata, Japan and [2]Molecular and cellular pharmacology, Osaka university, Osaka, Japan

Sound-evoked mechanical stimuli permit endolymphatic K^+ to enter sensory hair cells. This transduction is sensitized by an endocochlear potential (EP) of +80 mV in endolymph. After depolarizing the cells, K^+ leaves hair cells in perilymph, and it is then circulated back to endolymph across the lateral cochlear wall. In theory, this process entails a continuous and unidirectional current carried by apical K^+ channels and basolateral K^+ uptake transporters in both the marginal cell and syncytial layers of the lateral wall. The transporters regulate intracellular and extracellular [K^+], allowing the channels to form K^+ diffusion potentials across each of the two layers. These diffusion potentials govern the EP. What remains uncertain is whether these transport mechanisms accumulating across diverse cell layers make up a continuous circulation current in the lateral wall and how this current might affect the characteristics of the endolymph. To address this question,we developed an electrophysiological model that incorporates channels and transporters of the lateral wall and channels of hair cells that derive a circulation current. The simulation replicated normal experimental EP values and reproduced experimentally measured changes in the EP and intra- and extracellular [K^+] in the lateral wall when different transporters and channels were blocked. The model predicts that, under these different conditions, the circulation current's contribution to the EP arises from different sources. Finally, our model also accurately simulated EP loss in a mouse model of a chloride channelopathy associated with deafness.

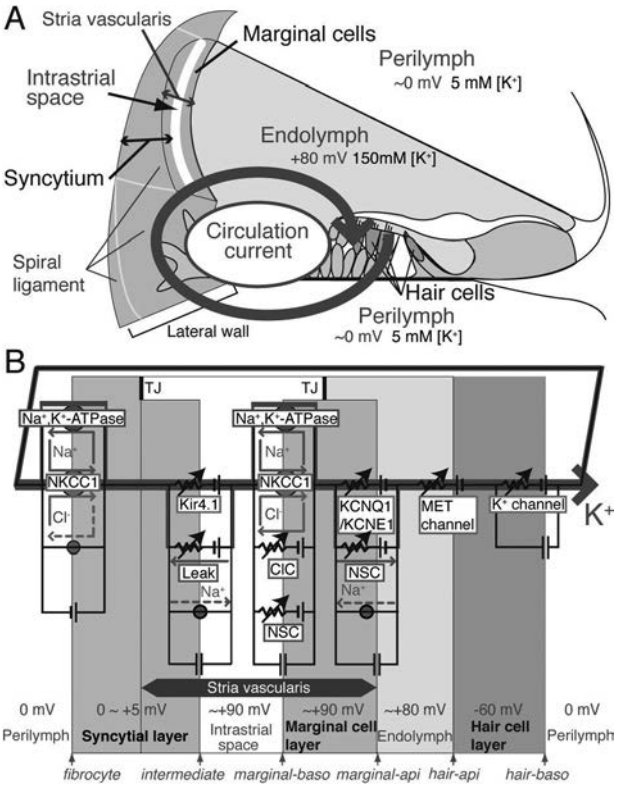

Key elements of the NHK(Nin-Hibino-Kurachi) model. (A) Structure of the cochlea and the concept underlying the circulation current. The circulation current (arrow) unidirectionally flows through a pathway comprising the endolymph, hair cells, perilymph, and lateral cochlear wall, and it flows back to the endolymph. In normal conditions, this flow would be carried by K^+. (B) The electrical circuit and its components used in the modeling. The channels and transporters that are involved in driving the circulation current as well as the potential in each compartment are described. The fibrocytes belong to the spiral ligament (A). The stria vascularis contains three cell types: basal cells, intermediate cells, and marginal cells. Basal cells, which are omitted in this scheme, are apposed to the fibrocytes and intermediate cells.

Nin F *et al*. (2012). *Proc Natl Acad Sci USA* **109**(51), 21076-21080.

This work is supported by the following research grants and funds: the Global Center of Excellence (COE) Program in silico medicine at Osaka University, a grant for Research and Development of Next-Generation Integrated Life Simulation Software, Grant-in-Aid for Scientific Research on Innovative Areas 22136002, and a grant supporting the Center for Hybrid Medical Engineering from the Ministry of Education, Culture, Sport, Science and Technology of Japan.

Where applicable, the authors confirm that the experiments described here conform with The Physiological Society ethical requirements.

PCC228

The role of interleukin-6 in gastrointestinal contractile activity in a mouse model of Duchenne Muscular Dystrophy

J. Manning and D. O'Malley

Physiology, University College Cork, Cork, Ireland

Introduction: Duchenne Muscular Dystrophy (DMD) is characterised by severe progressive wasting of skeletal muscle and a shortened life expectancy of between 20-30 years. Deficiency of the protein dystrophin, results in progressive necrosis, muscle fibre degeneration and a chronic inflammatory response. The pro-inflammatory myokine, interleukin-6 (IL-6), is elevated in patients with DMD. Dystrophin is absent from smooth muscle cells; and a little-reported symptom of DMD is altered gastrointestinal (GI) function. Patients suffer from bloating, constipation and in more severe cases, acute gastric dilation and intestinal pseudo-obstruction.

The aims of this study are to investigate IL-6 and the stress hormone, corticotropin-releasing factor (CRF) in mdx mice to determine if elevation of IL-6 and possible interactions with CRF are associated with changes in (GI) physiology.

Methods: Morphology was investigated in transverse sections (10μm) of colon stained with Haematoxylin & Eosin. Diameter and thickness of the mucosal and muscular layers were scored. Whole colon sections taken from wildtype (WT) and mdx (C57BL/10ScSn-Dmdmdx/J) mice (10 weeks old) were suspended in organ baths to compare contractile activity under basal conditions and following stimulation with IL-6 (200nM) and/or CRF (200nM).

Results: Histological investigations determined that mdx mice exhibit a thickened muscular layer (141±7.918μm, n=4) as compared to WT mice (95.26±7.494μm, n=4, $p<0.001$). The mucosal layer and colonic diameter was unchanged from WT mice.

To assess if the thickening of the muscle translated into changes in contractile activity, excised colon was suspended in organ baths and stimulated to evoke contractile response. Carbachol (500nM, 20 mins) was added to the bath to evoke a maximal response. No significant difference was observed between the strains (n=6). Thus, responses to IL-6 and/or CRF were normalised to the carbachol response. IL-6 stimulated a six-fold greater contractile response in mdx (172.6± 66.48%, n=6, $p<0.05$) as compared to WT (30.39± 6.512%, n=7) mice. Pre-incubation of the tissue with the Na+ channel blocker, tetrodotoxin (TTX, 250nM) attenuated this response in mdx mice (26.14±14.58%, n=5, $p=0.05$) but had no effect in the WT mice (24.68±3.078%, n=4, $p>0.05$). In both strains (n=6, $p>0.05$) the stimulation of contraction by IL-6 and/or CRF was similar. However, the neuronally-mediated effects of IL-6 in mdx mice was borne out by the inhibitory effects of TTX on IL-6 plus CRF in mdx mice only (1.681±0.6920%, n=6, $p<0.01$).

Discussion: These data begin to elucidate the physiological GI changes in the dystrophin-deficient mdx mice which may contribute to altered function. From these studies it appears that neuronally regulated IL-6-induced muscular contraction is important in GI pathophysiology in this strain.

Muscular Dystrophy Ireland

Where applicable, the authors confirm that the experiments described here conform with The Physiological Society ethical requirements.

PCC229

Tear volume and tear stability across the phases of the menstrual cycle

A.D. Ighoroje[2,1] and J.A. Ebeigbe[1,2]

[1]Physiology Department, University of Benin, Benin City, Edo State, Nigeria and [2]Optometry Department, University of Benin, Benin City, Edo State, Nigeria

Dry eye is a very common condition among many women. Women are said to be twice likely to have dry eyes than men. Research suggests that dry eyes may be related to women's monthly cyclical changes in hormone levels, particularly estrogen levels. (Fresina and Campos, 2007). The menstrual cycle has been reported to affect many physiological processes. In addition to the effects of the menstrual cycle on the cardiovascular and nervous systems, it has also been reported to affect such ocular parameters like intraocular pressure, visual acuity, tear volume and tear stability (Tarlipinar et al, 2001). In Nigeria, there is a dearth of literature on effects of the menstrual cycle on tear volume and tear stability. This study was a cross sectional one to investigate the changes in tear volume (TV) and tear stability (TS) during the different phases of the menstrual cycle in Nigerian women. 100 healthy women aged 20 to 35years with regular cycles of 26 to 29 days were recruited for this study after informed consent was obtained from them. They were screened for systemic and ocular diseases. Exclusion criteria included irregular menstrual cycle, use of oral contraceptive pills, history of hypertension, cardiovascular abnormalities, diabetes mellitus and any ocular infections that could affect tear volume or stability. They were examined for changes in tear volume and tear stability during the follicular, ovulation and luteal phases. Ophthalmoscopy was done to rule out any posterior segment disease. Schirmer's test, which measures tear volume and the noninvasive tear break up time (NTBUT) which measures tear stability were carried out. (Schaumberg et al, 2001). Values are in means ± S.E.M, compared by ANOVA and student t test. Tear volume across the phases of menstrual cycle was statistically significant, $p < 0.0001$- Follicular 24.76±1.26, Ovulation 17.54±1.33, Luteal 21.14±1.50 (n=100). Reduction in TV (follicular vs ovulation was significant, $p<0.05$ and increase in TV (ovulation vs luteal was also significant, $p<0.05$.) However the difference in tear volume between the follicular phase and the luteal phase was not significant ($p>0.05$). Increase in tear stability during the menstrual cycle was also statistically significant, $p<0.05$. Follicular 13.70±1.10, Ovulation 16.32±1.42, Luteal 18.44±1.53 (n=100). Hormonal variation during the different phases of the menstrual cycle influence tear volume and tear stability in healthy young women of reproductive age. These changes may be clinically significant particularly in contact lens wearers where fluctuations in ocular parameter may alter the contact lens fit leading to a possible change in comfort and reduced visual acuity.

Keywords: Tears, menstrual cycle, follicular, ovulation, luteal.

Fresina P, Campos E. (2007). Ocular surface changes over the menstrual cycle in women with and without dry eyes. Ophthal Physio. 9; 120-128.

Schaumberg D.A, Buring J.E, Sullivan D.A and Daria M.R. (2001). Hormone Replacement Therapy and dry eye syndrome. J Am Med Assoc. 286; 2114-2119.

Tarlipinar S, Gedik S, Irkee M, Orhan M and Erdener U. (2001). Ocular ferning during the menstrual cycle in healthy women. Eur J. Ophthal. 11(1); 15¬18-1521.

Where applicable, the authors confirm that the experiments described here conform with The Physiological Society ethical requirements.

PCC231

Extrarenal potassium homeostasis after chronic potassium deficiency and after potassium repletion in rats

P. Napradit[1] and P. Piyachaturawat[2]

[1]Department of Physiology, Phramongkutklao College of Medicine, Bangkok, Thailand and [2]Department of Physiology, Faculty of Science, Mahidol University, Bangkok, Thailand

Potassium (K) plays an important role in several cellular homeostasis. K deficiency causes derangements of various tissue and organ functions. In order to study the effect of chronic K deficiency and subsequent to K repletion on extrarenal potassium homeostasis, adult male and female Sprague-Dawley rats were divided into 2 groups. K depletion was induced by feeding with a K-deficient diet and deionized water ad libitum for 120 days. The other group was paired-fed with normal rat chow at the same amount consumed by the former group serving as controls. During K depletion, rats had low food intake and their growths were retarded compared to control period. Polyuria, polydipsia, and a reduction in urinary K+ excretion were observed. Dietary K deprivation for 16-17 weeks resulted in a significant decreased in plasma K+ concentration to 1.5-2 mEq/L whereas plasma Na+ concentration was virtually not changed. In addition, K deficiency caused a metabolic alkalosis, a reduction in K+ but an accumulation in Na+ contents in soleus and extensor digitorum longus muscle. However, 2 weeks repletion of K by feeding normal rat chow resulted in marked increases in body weight, rapid restoration in water intake and urine output. Moreover, changes in plasma and muscles electrolyte and acid-base status were also reversible. To investigate extrarenal potassium homeostasis; K–depleted (n=7), K-supplemented (n=8), diet-restricted (n=11), and normal-untreated rats (n=11), were anesthetized with Inactin i.p.. Functional nephrectomy and adrenalectomy were performed and acute K-loading was challenged by intravenous infusion with KCl at a dose of 2 mEq/kg/hr for 1 hour. This resulted in elevations of plasma K+ concentration and muscle K+ content in all groups. The increment in plasma K+ concentration was significantly lower in K-depleted rats vs. normal rats (1.9±0.3 vs. 3.9±0.1 mEq/L, $p<0.001$), whereas the increases in muscle K+ content was higher than those in other groups. Values are means±S.E.M., compared by ANOVA. Furthermore, following KCl infusion blood pH was significantly decreased ($p<0.05$) and plasma Na+ concentration was increased ($p<0.05$) in K–depleted rat but those in the other groups were virtually not changed. These results were related to a greater K uptake in K–depleted rat indicating an alteration in extrarenal potassium disposal after chronic K deficiency. It is concluded that following KCl infusion the K+ ion may be an appropriate stimulus that leads to a marked activation of the residual Na+-K+ pump in K–depleted rats sufficient to lower plasma K+ concentration than in normal rats. This effect may be mediated by insulin as well as an accumulation of Na+ in muscle, increase in extracellular HCO3- and metabolic alkalosis developed after chronic K deficiency. However, alteration in extrarenal potassium disposal is completed reversed after K repletion.

Where applicable, the authors confirm that the experiments described here conform with The Physiological Society ethical requirements.

PCC232

Interaction between Ang1-7 ('Mas') and AT1 receptors in regulating renal sodium and water excretion

J. O Neill, V. Healy and E.J. Johns

Physiology, University College Cork, Cork, Ireland

Intra- renal (IR) Ang (1-7) has diuretic and natriuretic actions that are proportional to the degree of activation of the Renin Angiotensin System (RAS). The question is why the magnitude of this diuresis and natriuresis is compromised in high sodium fed rats (HNa+)(suppressed) RAS and enhanced in low sodium fed rats (LNa+)(activated RAS)? Could the answer lie with changes in IR AT 1 or 'Mas' receptor expression?

IR Ang (1-7) increased sodium and water excretion in both LNa+ and normal sodium fed rats (NNa+), but the excretory responses were reduced in the presence of the AT1 receptor antagonist (Losartan) and completely blocked by the, 'Mas' receptor antagonist (A-779). These data suggest that both AT1 and 'Mas' receptors need to be functional in order to fully mediate the renal responses to IR Ang (1-7). The aim of this study was to determine whether there is a relationship between changes in the renal expression of AT1 and 'Mas' receptors and the altered responsiveness to IR Ang (1-7) during dietary sodium manipulation.

Male Wistar rats (250-300g)(n=4-5) were fed LNa+ (0.03%), NNa+ (0.3%) or HNa+ (3%) for 2weeks. Rats received 1ml Chloralose-Urethane anaesthetic (16.5 and 250 mg/ml, respectively) via the intraperitoneal (IP) route. The right femoral vein was cannulated to facilitate the administration of both sustaining (0.05ml/30mins) and terminal (1.5ml) anaesthesia. The latter was performed after removal of both kidneys. Kidneys were dissected and homogenized. AT1 and 'Mas' receptor expression in renal cortex tissue was evaluated using Western blotting and densitometry. Data ±SEM were subjected to a Students t-test and significance was set at ($P<0.05$).

AT 1 receptor expression was increased by 5 fold and reduced by 2 fold in renal cortex tissue of LNa+ and HNa+ rats respectively, (both $P<0.05$) when compared with rats fed a NNa+ diet. 'Mas' receptor expression was the same in all 3 groups. The Ang (1-7) levels in the cortex of LNa+ rats were significantly greater than those in the cortex of NNa+ and HNa+ rats ($P<0.05$).

The current data shows that there is a proportional relationship between AT1 receptor expression in the cortex and the magnitude of the renal actions of IR infused Ang (1-7), which is only partially dependent on the level of 'Mas' receptor expression. These data suggest that although the renal tubular responses to IR Ang (1-7), are mediated by the Mas receptor, their magnitude is dependant upon the level of AT1 receptor expression and more specifically Ang II/ AT1 receptor signalling. Thus, in LNa+ rats, IR infused Ang (1-7) acts via the 'Mas' receptor to inhibit Ang II/ AT 1 receptor signalling. In HNa+ fed rats the down regulated AT 1 receptor expression implies a reduction in Ang II/AT1 receptor signalling which renders the counter-regulatory effect s of IR infused Ang (1-7) redundant.

This work is funded by IRCSET

Where applicable, the authors confirm that the experiments described here conform with The Physiological Society ethical requirements.

PCC233

The acute effect of smoking on blood fluidity

T. Kimura[1], S. Taito[2,3], K. Sekikawa[3], M. Takahashi[3] and H. Hamada[3]

[1]Yasuda Women's College, Hiroshima, Japan, [2]Division of Clinical Support, Hiroshima University Hospital, Hiroshima, UK and [3]Department of Health and Sports Medical Sciences, Graduate School of Health Sciences, Hiroshima University, Hiroshima, UK

Introduction: Smoking is well known as a risk factor of arteriosclerotic disease and for effects on blood fluidity. The chronic effects of smoking on hematology are the increase of WBC and hematocrit. Chronic smoking causes a decrease of blood fluidity, but the acute effect of smoking on blood fluidity is not well known. In this study, we examined the changes of blood fluidity before and after smoking to estimate the acute effect of smoking on blood fluidity.
Subject: The subjects were 14 young men (7 controls; age 23.4±2.3 year, 7 smokers; age 23.3±2.2 year,) who don't have internal disease. We obtained informed consent from them.
Method: The blood collections were done before smoking, right after smoking and 5 minutes after smoking. The subjects quit smoking at least six hours before blood collection. The blood was drawn from the elbow nasal venules of retina. We used a microchannel array flow analyzer (MC-FAN). The MC-FAN utilizes 8736 micro channels fabricated in silicon, simulates capillary vessels in vivo and is also an imaging instrument to visualize the state of blood flow. The whole blood passage time of 100 micro liters was measured to evaluate blood fluidity. The platelet rich plasma passage time of 100 micro liters was measured to evaluate platelet function. An automatic cell counter (Beckmancoulter Co., Ltd.) was used to measure red blood cells, white blood cells, hemoglobin, hematocrit, and platelets.
Result: The whole blood passage time and the platelet rich plasma passage time did not show significant differences in the two groups. In the smokers, the whole blood passage time measured "right after smoking" (48.0±5.0 sec) was significantly longer than that of "before smoking" (45.5±4.4 sec) and "5 minutes after smoking" (44.4±3.5sec) almost returned "before smoking". In the smokers, the platelet rich plasma passage time did not show significant differences on the time course.
Discussion: There were no significant differences between smokers and non-smoker on the blood fluidity and blood cell counts. The whole blood passage time of "right after smoking" was significantly longer than that of "before smoking". The blood cell counts of "right after smoking" showed a tendency to increase.

Kikuchi, Y., Sato, K., Mizuguchi, Y. Modified cell-flow micro channels in a single-crystal silicon substrate and flow behavior of blood cells. Microvasc. Res., (1994), 47, 126-139.

Where applicable, the authors confirm that the experiments described here conform with The Physiological Society ethical requirements.

PCC234

Cardiovascular reactivity in response to othostatic challenge in healthy young individuals with family history for increased cardiovascular risk

N.Y. Belova

Physiology, Medical University of Sofia, Sofia, Bulgaria

Cardiovascular (CVS) diseases remain a leading cause for morbidity and mortality worldwide.
The aim of our study was to assess cardiovascular reactivity in healthy young adults with family history related increased CVS risk. 48 individuals aged 20-24 years were studied: 38 with family history for CVS diseases, obesity and/or diabetes type 2 - F+ group; 10 were their age matched controls without family history - F-. All subjects gave informed consent for their study participation. The orthostatic test, which consisted of three 5-minute periods – baseline supine (BAS), active standing (OT) and supine recovery (REC), was applied as a sympathetic challenge. Continuous electrocardiogram, non-invasive blood pressure and brachial-ankle pulse wave velocity (ba-PWV) were recorded using BiopacMP100 and Finapress device. Data were analyzed by means of the Acknowledge and MIS2000 software. Blood pressure variability (BPV) was assessed with fast Fourier analysis (FFT). The spectral α-index of spontaneous baroreflex sensitivity (BRS) was calculated (Pitzalis et al. 1998). Ba-PWV was measured for arterial stiffness evaluation (Sugawara et al. 2005). Results are presented in Table 1 as means ± SEM. Statistical significance was evidenced with the t-test.
CVS response to OT in F+ was more pronounced. Systolic arterial pressure (SAP) was significantly higher during the 3 studied periods; F+ responded to OT with a larger increase in SAP as compared to F-. BPV was considerably higher in F+ although statistical significance could not be shown due to the well known interindividual variance in this parameter. BRS decreased during OT (more markedly in F+). During REC BRS indices were significantly lower in F+ as compared to F-. Pulse pressure (PP) and ba-PWV data were higher in F+. Our data suggest the existence of subtle changes in the autonomic cardiovascular function with a sympathetic predominance in F+, which is in conjunction with our previous studies (Belova et al., 2007). An early and clinically non-manifested autonomic dysregulation might explain the higher CVS reactivity and the less sensitive baroreflex leading to greater BPV in F+. We might speculate that the increased sympathetic outflow to vascular smooth muscle cells causes functional increase of arterial stiffness and underlies the greater pulse pressure as well. We suggest that OT might be used as a screening tool for individuals at higher CVS risk and for primary prevention of CVS diseases.

Table 1

	SAP (mm Hg)	BPV (mmHg^2)	α-LF (ms/mm Hg)	α-HF (ms/mm Hg)	Heart rate (beats/min)	PP (mm Hg)	ba-PWV (m/s)
F+ BAS	130.4 ± 2.9 P<0.01 vs. F-	37.9 ± 8.8	10.9 ± 0.9	16.1 ± 1.4	72.6 ± 2	54 ± 2.5 P<0.01 vs. F-	9.6 ± 0.2 P<0.02 vs. F-
F+ OT	140 ± 3.6 P<0.01 vs. F- P<0.007 vs. F+ BAS (paired t-test)	127.7 ± 41.5 P<0.02 vs. F+ BAS (paired t-test)	6.5 ± 0.5 P<0.0001 vs. F+ BAS (paired t-test)	7.4 ± 1 P<0.0001 vs. F+ BAS (paired t-test)	92.6 ± 2.3 P<0.0001 vs. F+ BAS (paired t-test)	51 ± 2.5 P<0.01 vs. F-	
F+ REC	133.4 ± 3. P<0.01 vs. F-	73.4 ± 24.8	9.8 ± 0.7 P<0.005 vs. F-	16.5 ± 1.8 P<0.005 vs. F-	71.2 ± 1.7	58.1 ± 2.5 P<0.004 vs. F-	10.2 ± 0.3 P<0.05 vs. F-
F- BAS	110.6 ± 3.8	19 ± 3.4	9.3 ± 1.4	22.5 ± 1.1	70.5 ± 5.5	36.9 ± 4.2	8 ± 0.4
F- OT	115.5 ± 5.8	43 ± 3 P<0.02 vs. F- BAS (paired t-test)	6.6 ± 1.1	8.8 ± 1.7 P<0.01 vs. F- BAS (paired t-test)	83 ± 6.7 P<0.001 vs. F- BAS (paired t-test)	35.3 ± 2.8	
F- REC	112.7 ± 4.8	19.3 ± 4.5	16 ± 3.2	26.4 ± 5.2	68 ± 5.2	39.1 ± 3.5	8.8 ± 0.5

Belova NY et al. Autonom Neurosci: Basic and Clin. 2007; 131: 107-122.

Pitzalis MV et al. Circulation. 1998; 97:v1362-1367.

Sugawara J. J Hum Hypertens. 2005; 19: 401-406.

Where applicable, the authors confirm that the experiments described here conform with The Physiological Society ethical requirements.

PCC235

Effects of anaerobic threshold and respiratory compensation point on optimal fat utilisation in sedentary male subjects

S. Ugras[1], B. Yilmaz[2], I. Serhatlioglu[3] and O. Ozcelik[1]

[1]Physiology, Firat University, Medical School, Elazig, Turkey, [2]Physiology, Yeditepe University, Medical School, Istanbul, Turkey and [3]Biophysics, Firat University, Medical School, Elazig, Turkey

Fat and carbohydrates are the main substrates in the human skeletal muscle, both at rest and during exercise. Understanding the regulation of fuel selection in muscle is an important issue that needs to be clarified in clinical and sports sciences. It has been suggested that fat is the major substrate oxidised by muscle during low and moderate intensity exercise and it declines with increased exercise intensity. However, there is no specific exercise region that defines the optimal fat burning zone. During an incremental exercise test, anaerobic threshold (AT) and respiratory compensation point (RCP) reflects two important exercise intensities: onset of aerobic to anaerobic metabolic transition and onset of hyperventilation, respectively. In the present study, we have investigated the effects of exercise intensity corresponding to AT and RCP on fat and also carbohydrate utilisation. After obtaining an informed consent which was approved by the local ethics committee, nine sedentary male subjects (20.2±1.6 yr, 75.5±5.8 kg) performed an incremental exercise test (15 W/min) until the limit of tolerance using a cycle ergometer. During exercise, the ventilatory and pulmonary gas exchange indices were estimated breath-by-breath. V-slope method used to estimate AT (1) and increased VE/VCO2 and decreased PETCO2 used to estimate RCP (2). Then they participated five 30 min (or until exhaustion) stages of exercise at intensities of corresponding to 25% below AT (W1), AT (W2), RCP (W3), 25% above AT (W4) and %100 above AT (W5). The respiratory quotient (RQ) was used to evaluate substrate utilisation. Statistical analysis was done by using paired t test. Maximal exercise capacity (Wmax), AT and RCP were found to be 221±25 W, 134±21 W (60% of Wmax) and 160±24 W, (72% of Wmax) respectively. The RQ at the end of the exercise was found to be 0.925±0.05 for W1 and 0.931±0.04 for W2 (p>0.05), reflecting ~75% CHO and 25% fat utilisation. RQ decreased to 0.904±0.04 in W3 (p<0.05) reflecting ~65% CHO and 35% fat utilisation. The subjects were not able to complete 30 min of exercise duration in W4 and W5. The RQ was systematically higher than 1.00 in W4 (1.060±0.04) and W5 (1.374±0.1). The highest fat oxidation ratio (as seen a marked decrease in RQ) was observed in the work rate corresponding to the RCP. In conclusion, these findings suggest the region between AT and RCP can be used as an optimal fat burning zone. In addition, investigators should consider RCP instead of using low-moderate-high intensity criteria as determined % values of Wmax or maximal O2 uptake.

1. Beaver WL, Wasserman K, Whipp BJ. A new method for detecting anaerobic threshold by gas exchange. J Appl Physiol 1986; 60: 2020-2027.

2. Wasserman K, Hansen JE, Sue DY, W Stringer, BJ Whipp. Principles of Exercise Testing and Interpretation: Including Pathophysiology and Clinical Applications, Lippincott Williams & Wilkins; Fifth edition, 2012.

Where applicable, the authors confirm that the experiments described here conform with The Physiological Society ethical requirements.

PCC236

Medium-intensity rhythmic exercise and high-intensity resistance exercise reduces fasting plasma cholesterol/HDL Ratio

J.R. Wells

University of Gloucestershire, Gloucester, UK

Different modes of exercise have been shown to reduce the health risks associated with elevated plasma Cholesterol (Tjonna, Lee et al. 2008) (Martins, Verissimo et al. 2010). However the results do not agree on the modes of exercise that are beneficial. Some recent research, the STRRIDE clinical study, has shown little Cholesterol reduction (Bateman, Slentz et al. 2011). The mode of high-intensity, short-duration, resistance exercise has not been compared with the Government recommendations of moderate-intensity exercise. PURPOSE: To compare changes in Total Cholesterol and in HDL over 3 months in moderate-intensity rhythmic exercisers and high-intensity resistance exercisers. METHODS: 63 participants in a health club setting gave voluntary informed consent and completed 3 months of supervised exercise, divided between 30-minute bouts of moderate-intensity rhythmic exercise 3 to 5 times a week (MI), 8 minute bouts of high-intensity resistance exercise only 1 to 2 times a week (HI) and a no additional physical activity control group (CON). Venous blood samples (12 hour prior fast) were taken before and after the 3 months. Total Cholesterol and HDL were determined using an automated photometric chemistry analyser. RESULTS: The mean reductions in the Total Cholesterol / HDL ratio (+/- standard error) over the 3 months for the groups were: MI (n=18) 0.11 +/- 0.16, HI (n=23) 0.26 +/- 0.11 and CON (n=22) –0.04 +/- 0.09. However, as can be seen in plots, the MI exercise was more beneficial than this data indicates. Although the Cholesterol/HDL ratios were balanced between the 3 starting groups, uneven attrition has distorted the results. CONCLUSION: These results show that, over a 3-month period, 30-minute bouts of moderate-intensity rhythmic exercise and short bouts of high-intensity resistance exercise both reduce the Cholesterol/HDL ratio. Further research, in which the total work done is controlled, is now required to see if it is the mode or intensity of

the exercise that has the greatest effect. Plus greater participant numbers are required for this reported research to strengthen the statistics.

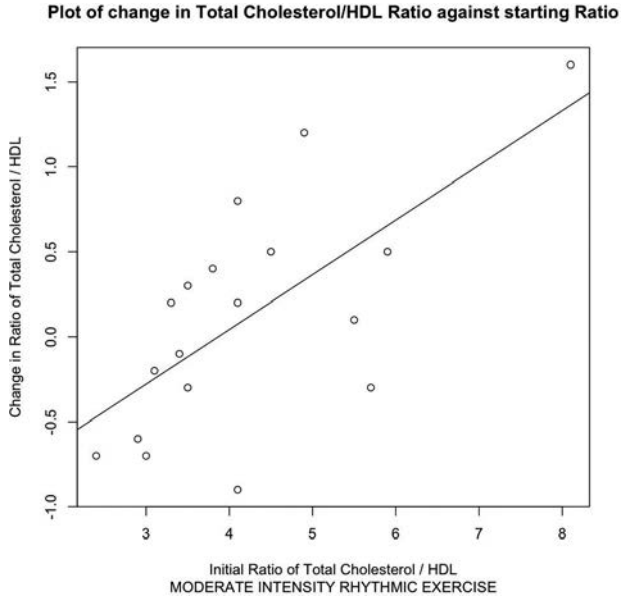

Moderate Intensity

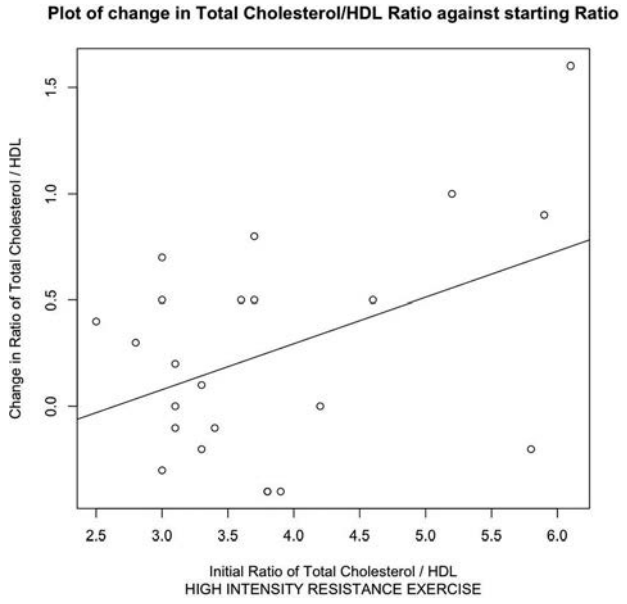

High Intensity

Bateman, L. A., C. A. Slentz, et al. (2011). "Comparison of aerobic versus resistance exercise training effects on metabolic syndrome (from the Studies of a Targeted Risk Reduction Intervention Through Defined Exercise - STRRIDE-AT/RT)." Am J Cardiol 108(6): 838-844.

Martins, R. A., M. T. Verissimo, et al. (2010). "Effects of aerobic and strength-based training on metabolic health indicators in older adults." Lipids Health Dis 9: 76.

Tjonna, A. E., S. J. Lee, et al. (2008). "Aerobic interval training versus continuous moderate exercise as a treatment for the metabolic syndrome: a pilot study." Circulation 118(4): 346-354.

Where applicable, the authors confirm that the experiments described here conform with The Physiological Society ethical requirements.

PCC237

Dietary nitrate supplementation improves cerebral haemodynamic function in males

J.V. Brugniaux, C.J. Marley, D. Hodson, K. Evans and D.M. Bailey

Neurovascular Research Laboratory, University of Glamorgan,, Pontypridd, UK

Background and aims
Beetroot juice (BJ) is a natural source of nitrate, which can be reduced into nitrite and ultimately nitric oxide (NO), leading to an increase in circulating NO (1). Because of its vasodilatory properties, NO can lower blood pressure even in normotensive subjects (2). Amongst other signalling pathways, it has also been suggested to modulate mitochondrial respiration, supporting recent observations of ergogenic effects of dietary nitrate supplementation, such as BJ, on aerobic performance (3). Following the aforementioned vascular pathway, one can speculate that the effects of an increase in NO are not limited to the systemic circulation and could extend to the brain, hence inducing an increase in cerebral perfusion and oxygenation. Therefore, the aim of this study was to determine the impact of dietary nitrate supplementation in the form of BJ on the resting cerebral hemodynamic function.
Methods:
10 healthy males (age: 26±1 years; height: 182±1 cm; weight: 80±2 kg) consented to this double-blind randomized placebo-controlled trial. Middle cerebral artery velocity (MCAv, Transcranial Doppler) and changes in frontal cortical oxygenation (cO2Hb, near-infrared spectroscopy) were recorded continuously during a 5-minute baseline period, followed by a 3-minute hypercapnea (5% CO2 in balanced O2 and N2), before and 3.5 hours after the ingestion of 500ml of either BJ (containing ≈5.2mmol of nitrate; Beet It, James White Drinks, Ipswich, UK) or a low-calorie blackcurrant juice cordial (negligible nitrate content). Trials were separated by a week and the participants' diet was monitored during a 3-day lead-in period. Exhaled NO (ozone-based chemiluminescence) was measured before and 2 hours post-ingestion. Haemodynamic data were averaged over the last 30 seconds of the respective stage. Data were analysed using a 2-way repeated measures ANOVA (time x drug) and paired samples t-tests. Significance was set at $P \leq 0.05$ and data are presented as mean±SD.
Results:
BJ raised the exhaled NO concentration 2h post ingestion (Figure 1A). The increase in cO2Hb in response to the hypercapnic challenge was greater post BJ ($P<0.05$) than placebo (Figure 1B). However, the hypercapnia-induced alteration in MCAv was not different post supplementation (BJ vs. Placebo). The alterations in NO and cO2Hb post-supplementation were positively correlated ($P=0.05$) (Figure 2).
Conclusion:
The present results demonstrate for the first time that dietary nitrate supplementation increases cerebral oxygenation but without altering perfusion during hypercapnea. While the underlying mechanisms remain to be fully unravelled, this observation has clear implications not only from a physical performance point of view, but also for the clinician. Indeed, increased oxygenation can be seen as being a neuroprotective mechanism possibly able to prevent the development of dementia in later life.

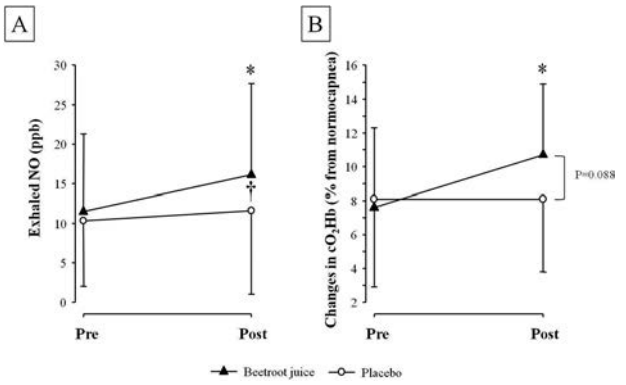

Figure 1: Changes in exhaled nitric oxide (NO, A) and cerebral oxygenation (cO2Hb, B) in response to 3 minutes of hypercapnea (5% CO2) following the ingestion of the nitrate supplement (Beetroot juice) or Placebo (n=10 in each group).

Values are mean + SD; *P<0.05 vs. Placebo; †P < 0.05 vs. Placebo.

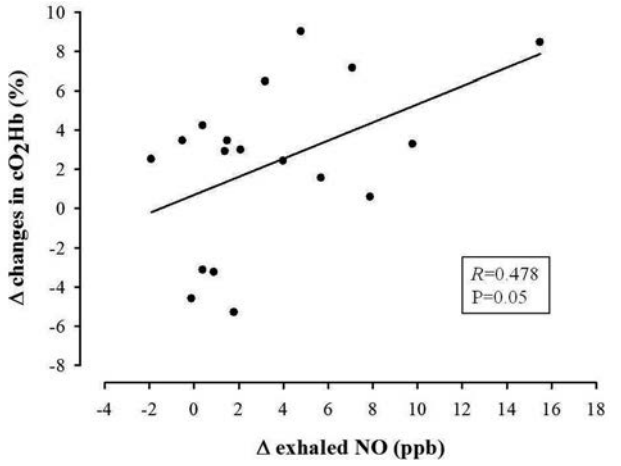

Figure 2: Relationship between the changes in exhaled NO and cO2Hb in response to 3 minutes of hypercapnea (5% CO2).

Lundberg JO, Govoni M. Inorganic nitrate is a possible source for systemic generation of nitric oxide. Free Radic Biol Med. 2004 Aug 1;37(3):395-400.

Kapil V, Milsom AB, Okorie M, Maleki-Toyserkani S, Akram F, Rehman F, et al. Inorganic nitrate supplementation lowers blood pressure in humans: role for nitrite-derived NO. Hypertension. 2010 Aug;56(2):274-81.

Jones AM, Bailey SJ, Vanhatalo A. Dietary nitrate and O(2) consumption during exercise. Med Sport Sci. 2012;59:29-35.

Where applicable, the authors confirm that the experiments described here conform with The Physiological Society ethical requirements.

PCC238

Cutaneous and muscular influences on beer- lambert and spatially-resolved indicators of blood volume in near infrared specroscopy

A. Messere and S. Roatta

University of Turin (Italy), Turin, Italy

Near-infrared spectroscopy (NIRS) is a non-invasive optical technique increasingly used to assess muscle oxygenation during exercise, although the possible interference by cutaneous circulation remains a major limitation of the technique (Davis et al. 2006). Spatially resolved spectroscopy (SRS) was proven to effectively reduce the influence of extracranial blood flow in cerebrovascular assessesments as compared to original Beer-Lambert (BL) NIRS but its potential effectiveness in muscle circulation is currently unexplored.

The aim of this study is to compare BL vs SRS indices of blood volume during selective cutaneous and muscle hyperemia.

To this purpose we performed the NIRS assessment with the NIRO 500 (Hamamatsu) which provides simultaneous BL and SRS indices of blood volume, tHb and THI, respectively. In 10 healthy subjects enrolled in the study NIRS optodes were placed along the belly of the flexor carpi radialis (left arm) and skin blood flow was measured with laser-Doppler flowmetry. Selective cutaneous vasodilatation was obtained by locally warming the left forearm with warm air flow and selective muscle dilatation was obtained by a 10-s lasting maximum voluntary wrist flexion, producing an exercise-hyperemia in the relevant muscles

In the two conditions changes in blood volume were computed as absolute changes for tHb (in uM*cm) and relative changes (%) for THI. In addition a warm/exercise ratio (WER) was computed as the ratio between changes observed during the warm- and exercise-hyperaemia (in %) This index quantifies and allows to compare the dependence on cutaneous circulation of THI and tHb: the higher the WER, the higher the dependence.

Warming (26.6± 0.9 to 33.2±1.3 °C) produced marked changes in cHB in all subjects (19.5±7.4 uM*cm) associated with the increase in skin blood flow while THI was unresponsive to warming in 5 out of 9 subjects and highly responsive in the others (average on all subjects11.8±18.6 %) Consequently, also the warm/exercise ratio exhibited a bimodal distribution for THI: 2.2 ±22.5% (indicating that the response to warming is 2% of exercise hyperemia) in 5 subjects and 531±261 % (n=4). WER for tHb was on average: 333±258 %.

The results confirm that changes in skin blood flow can markedly affect NIRS parameters. As observed for cerebrovascular monitoring (Canova et al. 2011) SRS spectroscopy appears to be less dependent on cutaneous circulation than the classical BL technique. The reason for high WER values in the THI of 4 subject may represent an additional problem for NIRS assesments whose excact nature remains to be ascertained.

Canova D et al. (2011) J Appl Physiol 110(6),1646-1655

Davis SL et al. (2006) J Appl Physiol 100(1), 221-224

Where applicable, the authors confirm that the experiments described here conform with The Physiological Society ethical requirements.

PCC240

Respiratory muscle power (RMP) in normal subjects, asthmatics, trained police officers and healthy obese adults in Sudan

O.A. Musa[1], O.A. Elbadri[2], S.E. Ibrahim[3], A.A. Magzoub[1], K.M. Awad[1], F.G. Abdalla[1] and B.A. Hussein[1]

[1]Physiology, National Ribat Uinversity, Khartoum, Sudan, [2]Physiology, Alshaikh Abdulla University, Barbar, Sudan and [3]Physiology, Gezira University, Madani, Sudan

Respiratory muscle power (RMP) is the main drive for respiration in health and disease. Negative correlation was found between age and RMP for both sexes. Height, obesity and physical training have been shown to increase RMP. The use of RMP in asthma as a tool of investigation and as a predictor of training has not been investigated. Asthma diagnosis when mild or intermittent is a clinical challenge in between attacks, and the

common pulmonary function tests (PFTs) are not very sensitive. An extensive study has been performed on the RMP in normal individuals, in asthmatics as a new diagnostic tool, in trained police officers, and in obesity.
Methods: A total of 653 subjects from Gezira and Khartoum states, Sudan were included. Two hundred and sixty normal adult volunteers both sexes, aged 16-60 years have performed RMP measurement (Maximum Expiratory and Inspiratory Pressures, MEP and MIP) by mouth pressure meter and pulmonary function (FVC, FEV1 & PEFR) by microplus spirometer. RMP and PFTs in 30 young adults aged 16 -23 years were compared with 30 old subjects aged 65-85 years. Respiratory muscle thickness at the end of quiet and maximum inspiration were measured using ultrasound device .Fifty asthmatic and 50 matching controls have performed reversibility test and spontaneous variability by RMP and PFTs. Fifty nine trained policemen and 28 policewomen were compared with 61 matching control. Diaphragmatic thickness and RMP was performed in 10 chronic asthmatics, matched with 10 controls. Obesity and RMP was studied in 52 obese individuals and 43 matching controls.
Results: Both RMP and PFTs in males were significantly higher than in females (mean MIP (cmH2O) and FEV1 (L) were 111±21 and 3.7 ± 0.5 in males compared to 75.8± 16.3 and 2.8 ± 0.3 in females .Both RMP and PFTs values decreased with age in both sexes (mean MIP and FVC (L) in young subjects were 114.3±28.4 and 4.1± 0.5 compared to 78±19 and 2.9±0.5 in old subjects. The sensitivity of MEP and MIP was better than FEV1 and PEFR in asthma diagnosis by reversibility test (49% & 71% for MEP & MIP, and 40% & 31% for FEV1 and PEFR) and in variability test (53% & 61% for MEP & MIP and 40% & 46% for FEV1 and PEFR). MEP and MIP significantly increased in obese subjects (p=0.01 and 0.00 respectively) and insignificant difference (p=0.73) was found in lung function between obese subjects and controls (Mean FVC (L), MEP and MIP (cmH2O) were 3.58 ±0.9, 109±29.8 and 78±17.2 respectively in obese subjects compared to 3.63±0.7, 94.6 ±27.7 and 67.8±18.7 respectively in non-obese controls). The diaphragm muscles thickness was significantly increased in chronic asthmatics compared to healthy controls (diaphragm thickness in quiet inspiration was 4 mm in asthmatics and 3.1 mm in controls). RMP and PFTs were found significantly higher in trainee polices officers compared to controls (mean MIP and FVC in policemen were 106.9 ±28.2 and 3.96 ± 0.5 compared to 88.1 ±31 and 3.58± 0.8 in controls).
In conclusions: RMP differences between males and females and in younger and old adults can explain the differences in their lung function values. RMP reversibility and variability is a new potential diagnostic tool for asthma. Obese and trained subjects have Higher RMP which could explain their lung function values.

To Sudan Ministry of Higher Education for funding this work

Where applicable, the authors confirm that the experiments described here conform with The Physiological Society ethical requirements.

PCC241

Effects of Ginkgo biloba extract 50 on beta-amyloid-induced apoptosis and oxidative stress in hippocampal neurons

Z.Z. Xiong and X.C. Yi

Basic Medical Science College, Shanghai University of Traditional Chinese Medicine, Shanghai, China

Objective To study the effect of Ginkgo biloba Extract 50 (GBE50) on beta-amyloid(Aβ)-induced apoptosis and oxidative stress in hippocampal neurons in vitro. Methods The primary hippocampal neuron was cultured in vitro and reduced to apoptosis and oxidative stress by 20 μM Aβ25-35. The MTT, flow cytometry and fluorescent probes labeling were used to observe the effect of GBE50 with different concentrations on cell viability, apoptosis and generation of intracellular reactive oxygen species (ROS) in neurons. Results (1) 20 μM Aβ25-35 could reduce the cell vitality significantly ($P < 0.05$). There was statistical difference between GBE50 group with different concentrations (10 μg/ml except) and Aβ group ($P < 0.05$). GBE50 could improve cell vitality with certain concentration dependence. (2) The cell apoptosis rate and necrosis rate were obviously increased by 20 μM Aβ25-35 ($P < 0.01$) and higher about 14.5% and 8.6% respectively. However, 50 μg/ml GBE50 could significantly reduce the cell apoptosis and necrosis rate ($P < 0.05$) and lower about 47.7% and 59.5% respectively. (3) The result of intracellular reactive oxygen species generation detected by fluorescent probes DCFH-DA show that the statistical difference was observed between Aβ group and control group ($P < 0.05$), and 20 μM Aβ25-35 could enhance ROS. However, any difference wasn't detected between every concentration of GBE50 group and control group($P > 0.05$). Conclusions The 20 μM Aβ25-35 could induce hippocampal neuron apoptosis and generations of intracellular ROS, which were inhibited by GBE50 with different degrees. Through these effects and improving cell vitality, GBE50 could availably protect hippocampal neurons.
KEYWORDS Ginkgo biloba extract 50; beta-amyloid; hippocampal neuron; apoptosis; oxidative stress

Where applicable, the authors confirm that the experiments described here conform with The Physiological Society ethical requirements.

PCC242

The role of SIRTI in Ginkgo biloba extract 50 delaying telomere shortening in the hippocampus of natural aging rats

Z.Z. Xiong and H. Li

Basic Medical Science College, Shanghai University of Traditional Chinese Medicine, Shanghai, China

Objective To investigate the role of SIRTI in Ginkgo Biloba Extract 50 (GBE50) delaying telomere shortening in the hippocampus of natural aging rats
Method Thirty Sprague-Dawley (SD) rats (male, 21 months, 700-1050g) were randomly divided into GBE50 treated group, Ginkgo biloba extract 761(EGB761) treated group and model group (n=10 each). Eight SD rats (male,1 months, 100-110g,) were control group. GBE50 group and EGB761 group were respectively administered intragastrically with GBE50 (100mg/kg/day) and EGB761 (100mg/kg/day) dissolved in 1% Carboxymethyl-cellulose Sodium (CMC-Na) for 60 days. The

control group and the model group were treated intragastrically with 1% CMC-Na for 60 days. Rats in each group were anaesthetised with 25 urethane(3ml kg-1, both i.p.) and sacrificed after 60 days, and hippocampus were taken out for analysis of RNA, DNA and protein. Telomere length and SIRTl mRNA in the hippocampus were determined by fluorescent quantitative real-time polymerase chain reaction (RT-PCR), Western blot was used to analyze the levels of Sirtl, p53 and p21 respectively. Expressions of p53 and p21 in hippocampal region CA1 were quantified by immunohistochemistry .
Results (1) Significant difference in telomere length was observed between model group and control group (P<0.05). The length of telomere was significantly longer in GBE50 group compared to model group (P<0.05). GBE50 could delay telomere shortening(24.2%). (2) SIRTl mRNA and protein levels were significantly lower in model group relative to control group (P<0.05). GBE50 could increase SIRTl mRNA and protein level compared to model group (P<0.05). (3) The protein level of p21 was increased in model group relative to control group (P<0.05). GBE50 could significantly decrease p21 compared to model samples (P<0.05). However, any difference wasn't detected in the expression of p53 among model group, control group and GBE50 group (P>0.05). (4) GBE50 could inhibit protein expressions of p21 in hippocampal region CA1 (P< 0.05).
Conclusion GBE50 might delay telomere shortening in the hippocampus of natural aging rats through up-regulated the SIRTl expression, and the expression of p21 were down-regulated.

Where applicable, the authors confirm that the experiments described here conform with The Physiological Society ethical requirements.

PCC244

Middle cerebral artery blood velocity in response to dynamic upright resistance exercise: effect of load and repetition

B. Perry[1], Z.J. Schlader[1], M.J. Barnes[1], D.J. Cochrane[1], S.J. Lucas[2] and T. Mündel[1]

[1]School of Sport and Exercise, Massey University, Palmerston North, New Zealand and [2]Depratment of Physiology, University of Otago, Dunedin, New Zealand

Weightlifting is a common mode of exercise because of its positive effects on a host of physiological outcomes. However, the transient and extreme nature of the mean arterial blood pressure (MAP) response during and following resistance exercise, particularly whilst upright, will likely translate into fluctuations in middle cerebral artery blood flow velocity (MCAv). We examined the effect of resistance load and number of repetitions on the dynamic responses of MCAv during and following upright squatting exercise. Healthy resistance trained males (n = 12; mean ± SD: 26 ± 5 y; 94 ± 13 kg) completed 30, 60 and 90% of a predetermined 6 repetition maximum (RM) load, in a randomised order. Participants completed 2 or 6 repetitions of their 6 RM during two separate visits (order randomised between participants). Beat-to-beat MCAv and blood pressure, continuous end-tidal PCO2 and heart rate were measured. Peak MCAv and MAP during exercise, and nadir, recovery and peak following exercise were compared to a pre-exercise standing baseline period (1 min). There was no difference in average peak MCAv during exercise between loads (P = 0.737) or repetitions (P = 0.892). MAP was greater during the 60% compared to the 30% set (P = 0.015), and with 6 repetitions (P = 0.02 vs. 2 repetitions); specifically, 122 ± 9 vs. 135 ± 11 mm Hg for 2 and 6 repetitions at 30%, respectively; and 128 ± 13 vs. 143 ± 14 mm Hg for 2 and 6 repetitions at 60%, respectively. Only 3 participants had a satisfactory blood pressure trace for both 90% sets; MAP at this load peaked at 150 ± 2 and 176 ± 6 mm Hg mm Hg for 2 and 6 repetitions, respectively. Participants only performed a Valsalva manoeuvre during both 90% repetition sets, with an average mouth pressure of 43 ± 6 and 44 ± 10 mm Hg for the 2 and 6 repetition sets, respectively. Post-exercise MCAv reductions occurred via a selective, load-dependent (P < 0.001) decrease in diastolic MCAv. The 90% load produced the lowest MCAv nadir (-19 ± 6 cm/s, P < 0.001) and MAP nadir (-36 ± 10 mm Hg, P < 0.001) following exercise. Greater reductions in MCAv were seen at 30 and 60% loads following 6 repetitions (both P <0.05 vs. 2 repetition sets), but not for MAP (P= 0.59). The MAP nadir occurred later (13.3 ± 7.6 s) than MCAvmean nadir (6.7 ± 5.2 s) for all loads and repetitions (all P ≤ 0.05). Higher loads increased the time to MAP nadir (P = 0.05) but not MCAvmean nadir (P > 0.10). In summary, the combination of heavier loads and the Valsalva manoeuvre challenge cerebral autoregulatory processes and produce a greater reduction in MAP and subsequently MCAv immediately following dynamic upright resistance exercise. However, dynamic cerebral autoregulation begins to restore MCAv within the same time frame regardless of the magnitude of the drop in MCAv, and the magnitude and time course of the reduction in MAP.

Where applicable, the authors confirm that the experiments described here conform with The Physiological Society ethical requirements.

PCC245

Power performance in swimmers- a physiological multiparametric analysis

C. Prabha and S. Prakash

Department of physiology, Meenakshi medical college& research institute enathur kanchipuram tamilnad india, Kanchipuram, Tamil Nadu, India

The athletic status is a composite multi-factorial output. Sprinting success can be pinned purely on nature and nurture. Along with societal factors investment in infrastructure, training system and powerful desire play an important role. The evolutionary advantage in the form of ACTN3, gene for speed, the physiological determinant of the sprinting ability has come into main focus recently. Most studies have demonstrated a relationship between the presence of Alpha actin3 and the ability of muscle to generate force. The aim of our study was to analyse the various physiological factors contributing to the power performance of adolescent swimmers. The study assessed their socio-economic status, anthropometric measurements, pulmonary function tests and ACTN3 genotype. This was a case control study. The cases being 35 in number and age matched controls, 70 in number. Human ethical committee clearance was obtained. The subjects were chosen from different swimming pools in Chennai, Tamilnadu, India. All members were briefed about the intent and conduct of tests. The volunteers were then chosen in strict adherence to the inclusion and exclusion criteria. Informed consent was obtained from the participant and Anthropometric measurements were recorded. After demonstration of proper technique Spirometry was done. ACTN3 gene testing was done from cheek swabs. The results were statistically analysed using Graph Pad Prism-version 5. The mid-arm circumferences of swimmers and con-

trols were compared. Unpaired 't' test was applied. The P value was 0.002. The means were significantly different, P<0.05. Fisher's test was performed and variances compared. The P value was 0.0224. The proportion test of ACTN3 genotype was done. It was inferred that RR type and RX type difference in proportion between cases and controls was not significant but XX type proportion was significant between groups. On analysis of results we concluded that swimmers had better anthropometric measurements. Their Spirometry revealed better values. The ACTN3 genotyping showed R allele was associated with elite swimming performance.

MacArthur DG, Seto JT, Chan S, Quinlan KGR, Raftery JM et al. 2008. An ACTN3 knockout mouse provides mechanistic insights into the association between áactinin-3 deficiency and human athletic performance.Hum.Mol.Genet, 17(8): 1076-1086.

Yang N, MacArthur DG, Gulbin JP, Hahn AG, Beggs AH et al. 2003. ACTN3 genotype is associated with human elite athletic performance. Am J Hum.Genet, 73: 627 – 631.

MacArthur DG, North KN 2004. A gene for speed? The evaluation and function of a -actinin-3. Bio Essays,26: 786 – 795.

Himanshul Goel and Balraj Mittal,ACTN3 athlete gene prevelance in N.India.Current science vol92.no1, 10 jan 2007.

A Study Of Pulmonary Function Of Competitive Swimmers. Pherwani AV, Desai AG, Solepure AB. Indian J Physiol Pharmacol. 1989 Oct-Dec;33(4):228-32

Prof Dr.M.Chandrasekar, HOD, Dept. of Physiology, MMCH & RI.

Dr.Nilesh Kate M.D, Dr.Nitesh Mishra M.D and Dr. Gajalaxmi Ph.D, MMCH & RI.

Mr.S.S.Vanangamudi, Managing Director, Apex laboratories, Chennai.

The team from Super Religare Laboratories.

Management, staff and students of Sethu Bhaskara Higher Secondary School, Ambattur.

Coaches of the various swimming pools in Chennai.

Medical statisticians of MMCH & RI.

My family and friends.

Where applicable, the authors confirm that the experiments described here conform with The Physiological Society ethical requirements.

PCC246

The effect of adiposity on skeletal muscle size and strength in untrained women

D.J. Tomlinson, R.M. Erskine, C. Morse, K. Winwood and G. Pearson

The Institute for Performance Research, Manchester Metroploitan University, Crewe, Cheshire, UK

Background: It is not known how elevated adiposity in obese individuals or abnormally low levels of adiposity in underweight people affects the size and strength of skeletal muscle. Resistance training is known to induce gains in both muscle size and strength (Erskine et al., 2010), while prolonged muscle disuse has been shown to cause a reduction in these variables (de Boer et al., 2007). Moreover, simulated hypergravity for a 3 week period has been shown to increase muscle strength (Bosco et al., 1984), while low-load, high volume resistance exercise has been shown to enhance muscle protein synthesis more than conventional high-intensity resistance exercise (Burd et al., 2010). Therefore, we hypothesised that chronic over-loading of skeletal muscle in obese individuals would lead to greater lower-limb lean mass and higher absolute strength values compared to under-weight and normal-weight individuals.

Method: Fifty untrained healthy women aged 19-49 yrs (mean ± SD: 25.1 ± 8.7 yrs) were recruited to take part in this study. Body fat and lean mass were assessed using dual-emission X-ray absorptiometry. Plantar flexion maximum voluntary isometric contraction (MVC) torque was assessed in the dominant limb using an isokinetic dynamometer at different ankle joint angles (-5 to +10 deg plantar flexion; 0 deg = neutral ankle position). MVC joint torque was corrected for voluntary muscle activation level (assessed using the interpolated twitch technique) and antagonist muscle co-activation (assessed via surface EMG).

Results: Body mass index was 26.0 ± 7.0 kg/m2 (range: 17.0 – 51.9 kg/m2. Body fat percentage was 35.4 ± 8.8% (range: 19.6 – 51.9%). There was a positive relationship between lower-limb lean mass and MVC plantar flexion torque ($r2 = 0.594$; $p<0.005$). Moreover, total body fat mass was positively correlated with lower-limb lean mass ($r2 = 0.500$; $p<0.005$) and MVC plantar flexion torque at optimum joint angle ($r2 = 0.332$; $p<0.005$). A superior positive correlation though existed between total body mass and optimum MVC plantar flexion torque ($r2 = 0.458$; $p<0.005$).

Conclusion: Our findings confirm that total body fat mass is associated with lower-limb fat-free mass and maximum strength in untrained women. This suggests that the anti-gravity muscles of the lower-limb may possibly adapt to chronically low and high levels of adiposity in a similar manner to chronic unloading or overloading of the muscles, as seen following prolonged periods of bed-rest or resistance training.

Bosco, C., Zanon, S., Rusko, H., Dal Monte, A., Bellotti, P., Latteri, F., Candeloro, N., Locatelli, E., Azzaro, E. and Pozzo, R. (1984) The influence of extra load on the mechanical behavior of skeletal muscle. Eur J Appl Physiol Occup Physiol. 53(2):149-54.

Burd, N.A., West, D.W.D., Staples, A.W., Atherton, P.J., Baker, J.M., Moore, D.R., Holwerda, A.M.,Parise, G., Rennie, M.J., Baker, S.K. and Phillips, S.M.(2010). Low-Load High Volume Resistance Exercise Stimulates Muscle Protein Synthesis More Than High-Load Low Volume Resistance Exercise in Young Men. PLoS ONE 5(8): e12033.

de Boer MD, Maganaris CN, Seynnes OR, Rennie MJ, Narici MV. (2007). Time course of muscular, neural and tendinous adaptations to 23 day unilateral lower-limb suspension in young men. J Physiol. 583:1079-91.

Erskine, R.M., Jones, D.A., Williams, A.G., Stewart, C.E. and Degens, H. (2010). Inter-individual variability in the adaptation of human muscle specific tension to progressive resistance training. Eur J Appl Physiol. 110(6).1117-25.

Where applicable, the authors confirm that the experiments described here conform with The Physiological Society ethical requirements.

PCC247

Sweat potassium concentration decreases with increased sweating in perimenopausal women

E. Amabebe[1], S.I. Omorodion[2] and J.O. Ozoene[2]

[1]Physiology, Niger Delta University, Amassoma, Bayelsa, Nigeria and [2]Physiology, University of Benin, Benin, Edo, Nigeria

Sweat rate is higher in perimenopausal women than in premenopausal and postmenopausal women (Minkin et. al., 1997) and excessive sweating during menopause depletes some of

the body's essential nutrients, especially potassium (Balch and Balch, 1999).

In this study, we assessed whether there is an association between sweat rate (SR), sweat volume (SV) and sweat potassium concentration (S[K+]) in premenopausal (preM), perimenopausal (periM) and postmenopausal (postM) women after a moderate exercise.

Thirty (30) healthy women comprising of preM (aged 22.5±0.8yrs, n=10), periM (aged 46.5±1.1yrs, n=10) and postM (aged 52.2±0.9yrs, n=10) participated in the study. Participants were adequately informed of the experimental procedures and they all consented to it. TP was rated using the Visual Analogue Scale, VAS. Sweat was obtained with the sweat suction apparatus from a 120cm2 circular area marked on the skin of the face and neck (Ugwu and Oyebola, 1996), after a moderate exercise (a 15min walk on the treadmill) at a speed of 4.2 km/h at 270C, with the start time noted and SV and [K+] measured. SR was determined using the formula: (volume of sweat collected)/(exercise time) .

The results show that periM women exhibited a significantly higher SR (0.12±0.01 ml/min vs preM - 0.07±0.02 ml/min vs postM - 0.06±0.01 ml/min) ($p<0.05$), but a significantly lower S[K+] (19.98±1.5 mmol/l vs preM – 23.37±1.3 mmol/l vs postM - 24.88±1.8 mmol/l) ($p<0.05$). However, there was no significant difference in the SV (periM – 1.7±0.2 ml vs preM – 1.3±0.4 ml vs postM – 0.9±0.1 ml). The linear regression plot showed a significant ($p<0.05$) inverse relationship (negative correlation) between S[K+] and SR, but the negative relationship between S[K+] and SV was not significant, i.e. increase in SR and/or SV produced a decrease in S[K+].

In conclusion, these data indicate that although excessive sweating can lead to depletion of the body's potassium concentration, the sweat potassium concentration decreases with increasing sweat rate and volume especially in perimenopausal women during moderate exercise.

Balch, JF and Balch, PA (1999). "Prescription for Nutritional Healing" . Lanier, J. eHow.

Minkin, MJ., Carol, MD. and Wright, V. (1997). Yale Univ. Press. 2: 261-269.

Ugwu, AC. and Oyebola, DDO. (1996). J. Med. Lab. Sci. 5: 171-176.

We appreciate the support of Prof Ugwu AC. and Prof Obika LFO, our esteemed subjects, the Departments of Physiology, Niger Delta University and University of Benin as well as the Chemical Pathology Laboratory of University of Benin Teaching Hospital.

Where applicable, the authors confirm that the experiments described here conform with The Physiological Society ethical requirements.

PCC249

Lipopolysaccharide infusion enhances dynamic cerebral autoregulation with no effects of acute isocapnic hypoxia in healthy volunteers

R.M. Berg[1,2], R.R. Plovsing[3], K.A. Evans[4], C.B. Christiansen[1], D.M. Bailey[4], N. Holstein-Rathlou[2] and K. Møller[1,5]

[1]Centre of Inflammation and Metabolism, Department of Infectious Diseases, University Hospital Rigshospitalet, Copenhagen Ø, Denmark, [2]Renal and Vascular Research Section, Department of Biomedical Sciences, Faculty of Health Sciences, University of Copenhagen, Copenhagen N, Denmark, [3]Intensive Care Unit 4131, University Hospital Rigshospitalet, Copenhagen Ø, Denmark, [4]Neurovascular Research Laboratory, Faculty of Health, Science and Sport, University of Glamorgan, Copenhagen Ø, UK and [5]Neurointensive Care Unit 2093, University Hospital Rigshospitalet, Copenhagen Ø, Denmark

Sepsis may be associated with disturbances in cerebral oxygen transport and cerebral haemodynamic function, thus rendering the brain particularly susceptible to hypoxia (Berg et al, 2011). The purpose of the present study was to assess the impact of isocapnic hypoxia on dynamic cerebral autoregulation in a human-experimental model of the systemic inflammatory response during the early stages of sepsis.

A total of ten healthy volunteers were exposed to normoxia (FIO2 = 21%) and acute isocapnic inspiratory hypoxia (FIO2 = 12%) before and after a 4-hour lipopolysaccharide (LPS) infusion (2 ng kg-1). Middle cerebral artery blood follow velocity was assessed using transcranial Doppler ultrasound, and dynamic autoregulation was evaluated by transfer function analysis.

Transfer function analysis revealed an increase in the phase difference between mean arterial blood pressure and middle cerebral artery blood flow velocity in the low frequency range (0.07–0.20 Hz) after LPS (Table). In contrast, there were no effects of isocapnic hypoxia on dynamic autoregulation.

The observed increase in phase suggests that the dynamic cerebral autoregulation is enhanced after LPS infusion and resistant to any effects of acute hypoxia; this may protect the brain from ischemia and/or blood-brain barrier damage during the early stages of sepsis.

Dynamic cerebral autoregulation during normoxia (FIO2 = 21%) and acute isocapnic hypoxia (FIO2 = 12%), before and after lipopolysaccharide (LPS) infusion in healthy volunteers (n=9).

	Baseline		LPS	
	Normoxia	Hypoxia	Normoxia	Hypoxia
MAPsp (mmHg2)	4.5 (3.4-6.3)	9.0 (4.7-13.8)	3.6 (1.9-9.2)	9.0 (2.2-11.0)
MCAvsp (cm2 sec-2)	7.7 (5.5-10.0)	12.6 (7.6-18.7)	5.6 (1.7-14.2)	13.1 (5.7-23.4)
Gain (cm mmHg-1 sec-1)	1.24 (1.04-1.36)	1.27 (1.18-1.34)	1.17 (1.04-1.24)	1.29 (1.17-1.33)
Phase (radians)	0.64 (0.49-0.76)	0.49 (0.45-0.60)	0.80† (0.77-0.83)	0.91† (0.76-1.01)
Coherence (units)	0.87 (0.82-0.88)	0.91 (0.86-0.93)	0.76 (0.70-0.84)	0.88 (0.69-0.94)

Data are presented as median (IQR). Values for the spectral power of mean arterial blood pressure (MAPsp) and middle cerebral artery blood flow velocity (MCAvsp), as well as transfer gain, the MAP-to-MCAv phase difference, and coherence are presented for the low frequency range (0.07–0.20 Hz). Only data for subjects with coherence ≥0.4 are presented. Different from the same intervention (normoxia/ hypoxia) at baseline, † $p < 0.01$.

Berg, R.M.G. Møller, K. and Bailey, D.M. (2011) Neuro-oxidative-nitrosative stress in sepsis. J. Cereb. Blood Flow Metab. 31, 1532–1544

Where applicable, the authors confirm that the experiments described here conform with The Physiological Society ethical requirements.

PCC250

Correlation of serum estradiol, IL-6 and IGF-1 with bone density in menopausal women with and without regular exercise

V. Tarawan[1], I. Akbar[1], A. Purba[1] and F. Tandjung[2]

[1]physiology, school of Medicine universitas Padjadjaran, Bandung, westjava, Indonesia and [2]Orthopedic, Faculty of Medicine Padjadjaran University, Bandung, West Java, Indonesia

Increase of medicine technology and health service will increase quality of life and will be followed with increasing the number of menopausal women. Thus make osteoporosis disease increase which will give impact in increasing morbidity and mortality caused by osteoporosis. This study is done to detect osteoporosis early in menopausal women. The objective of this study is to analyze differentiation, correlation, risk factor between serum estradiol, IL-6, IGF-1 level to bone density in menopausal women with and without regular exercise and to analyze role of regular exercise. The method used was cross sectional that conducted on 56 menopausal women first decade who chosen randomly and divided into two groups, with and without regular exercise. Data were analyzed with T-test for normal and Mann-Whitney test for abnormal data distribution, Pearson correlative test, multiple linier regression test, multiple logistic regression test, and count risk factor used RP (Prevalence Ratio) risk and 95% CI (Confident Interval). The results showed that menopausal women with regular exercise had increased estradiol level significantly (22.94 (6.09) vs 14.23 (3.54)) ($p<0.05$), decreased IL-6 level significantly (1.69 (0.95) vs 3.198 (2.82)) ($p<0.05$) and increased IGF-1 level non significantly (89.36 (39.33) vs 79.57 (32.37)) ($p=0.243$) compare with menopausal women without regular exercise, although non significantly, there was tendency increasing IGF-1. Menopausal women with regular exercise showed higher bone mass density significantly compare with menopausal women without regular exercise ($p<0.001$). Menopausal women with regular exercise had positive correlation between IGF-1 with bone mass density (BMD-T) significantly ($r=0.648$; $p<0.05$). Menopausal women with and without regular exercise had positive correlation between estradiol with IL-6 significantly ($p<0.05$). Base on multiple linier regression test in menopausal women with regular exercise, there was significant correlation ($p<0.001$) between IGF-1 and BMD-T, but there was no correlation between estradiol, IL-6 and BMD-T. Based on ROC curve, estradiol cut off point ≤16.38, IL-6 ≤ 1.661, IGF-1 ≤ 69. If estradiol level ≤16.38, IL-6 > 1.661, IGF-1 ≤ 69 possibility for osteoporosis 28.2% among menopausal women with regular exercise and 64.7% among menopausal women without regular exercise. In conclusion, menopausal women with regular exercise have estradiol level higher, IL-6 level lower, and IGF-1 level higher and bone mass density higher vs. menopausal woman without regular exercise. There are correlation between serum IGF-1 level and bone mass density among menopausal women with regular exercise. The value of serum estradiol, serum IL-6, and serum IGF-1 can become risk factors of osteoporosis and sensitive measurement for the diagnostic test.

Where applicable, the authors confirm that the experiments described here conform with The Physiological Society ethical requirements.

PCC251

The role of local tissue temperature on resting and exercising skeletal muscle haemodynamics in the human leg

S.T. Chiesa, S.J. Trangmar, K.K. Kalsi and J. González-Alonso

Brunel University London, Uxbridge, UK

Introduction: The haemodynamic responses of skeletal muscle to localised changes in tissue temperature are still poorly understood, despite the widespread therapeutic use of heating and cooling. We aimed to systematically identify these responses both at rest and during one-legged exercise over a wide range of physiologically relevant temperatures. Methods: Leg tissue temperatures in 7 males (age 22±1 years) were altered at rest over 1hr through the use of frozen gel packs (cooling) or a water perfused suit (heating). Core, skin and deep muscle (T_m) temperatures were measured throughout. Haemodynamic alterations in 3 major arteries of the leg (common, superficial, and profunda femoral arteries: CFA, SFA, and PFA) were assessed using duplex Doppler ultrasound, with the contralateral leg providing control measures. Systemic haemodynamic responses were measured non-invasively using infrared plethysmography. Following each intervention, CFA flow was measured during incremental single-legged knee extensor exercise in the experimental or control leg (10±1, 16±1, 23±2, and 30±2W). All values are means ± SEM, with T_m and flows analysed using RM-ANOVA and conductance using linear regression. Results: At rest, 1hr of localised cooling (T_m 34.9±0.3°C to 29.5±0.6°C;$p<0.05$) led to small but significant decreases in blood flow to all three vessels (40-60ml.min^{-1} or 15-25%;$p<0.05$), with heating (T_m 34.5±0.5°C to 36.8±0.1°C;$p<0.05$) leading to significant increases (100-360ml.min^{-1} or 63-99%;$p<0.05$). Blood flow through the PFA (the major supply artery of the thigh skeletal muscle and therefore representative of muscle blood flow) showed significant alterations following both interventions (25% decrease and 63% increase respectively;$p<0.05$). PFA vascular conductance showed a strong linear relationship with muscle temperature during both interventions (R^2=0.95 and 0.96;$p<0.01$), with the sensitivity of the response increasing considerably at ~35 °C (i.e. normal resting muscle temperature; 0.11±0.03 to 0.70±0.07ml.min^{-1}.mmHg^{-1}.°C^{-1}). Systemic and control leg values remained unchanged. During exercise, prior cooling of the leg had no effect on CFA flows. In contrast, exercise following heating resulted in significantly higher CFA flows throughout the duration of the protocol (~500ml.min^{-1};$p<0.05$). Conclusions: These findings suggest that local temperature exerts significant effects on skeletal muscle haemodynamics both at rest and during exercise over a wide range of temperatures, but with significantly increased sensitivity observed at temperatures ≥ 35°C. The maintenance of an increased blood flow throughout exercise following heating suggests an independent role for temperature in the hyperaemic exercise response, potentially mediated through the rapid increases in local muscle and blood temperature experienced when undertaking dynamic muscular contractions.

Where applicable, the authors confirm that the experiments described here conform with The Physiological Society ethical requirements.

PCC252

Line dance class with their spouse increase participation on exercise and Improve physical fitness and health status among Palembang's traffic police officers

Y. Fediani, S. Andriyani and M. Irfannuddin

Biomedical Science, University of Sriwijaya, Palembang, South Sumatra, Indonesia

Lack of physical activity and increase risk of degenerative disease have become problems among traffic police officers. Demanding schedule and exposure of air pollutants are daily life cycle trough the years. A delightful line dance class has been organized in traffic police quarter. The officers were asked to join the course with their spouse to increase participation. Most of total 70 traffic police officers in Palembang were interested to join the class, but class only received 40 officers with their spouse due to limited room. Line dance training packet was transpired for 2 months, 3 times a week, and 45 minutes for each session. The class was opened flexible adjusted shift schedule. The couple could choose 1 of 2 time options in each their schedule day in the morning or afternoon. There are 37 officers aged 35-48 years old complete their class properly and participated in physical fitness test before and after the course. In 2 months, line dance training could significantly improve physical fitness capacity among officers. The VO2max increase from 33.6±2.1 to 36.3±2.2 ml/kg/min ($p<0.001$), BMI decrease from 26.7±2.8 to 26.5±2.7 ($p=0.01$), sit and reach flexibility test improve from 42.4±4.7 to 43.5±4.5 cm ($p<0.001$) and relative muscle strength increase from 4.7±0.9 to 4.9±9.8 ($p<0.001$). The training also improves resting mean arterial pressure from 106.2±9.7 to 102±8.8 mmHg ($p<0.001$).
A delightful line dance could improve physical activity and physical fitness among traffic police officers. Training with their spouse could increase their participation.

To Palembang's Traffic Police officers for their participation in this study.

To Palembang's Traffic Police Department for their permission to publish the result of this study

Where applicable, the authors confirm that the experiments described here conform with The Physiological Society ethical requirements.

PCC253

Effects of long-term exercise on norepinephrine transporter gene expression of cardiac sympathetic ganglion in SD rats

X. Li and L. Chen

Graduate Division, ShanDong Institute of Physical Education and Sports, Jinan, ShanDong Province, China

Backgroup: Norepinephrine transporter (NET) is synthesized in sympathetic ganglion and arrived to presynaptic membrane of sympathetic nerve ending by axoplasmic transport. The synaptic norepinephrine concentration is regulated through norepinephrine release and norepinephrine re-uptake by NET, thus maintaining cardiac function. Regular exercise training has been associated with improvement of the sympathetic nervous system in several animal models and in some human studies. Although these data are consistent with the hypothesis that exercise training reduces the incidence of cardiovascular diseases, ameliorates cardiac function and enhances exercise performance via reduced sympathoexcitation, the mechanisms are unknown. Objective: The present study was to observe the effects of long-term exercise on NET gene expression of cardiac sympathetic ganglion in SD rats and to investigate the possible mechanism of exercise-induced improvement of cardiac sympathetic nerve function. Methods: Ten SD rats performed 12-week aerobic treadmill running (exercise group, EG) and the other ten SD rats as control group (CG) maintained resting state. After experiment and coeliac anesthesia with 1% pentobarbital (30mg/kg), exhaust time (ET) was determined during incremental treadmill test; left ventricular end-systolic diameter (LVESD), left ventricular end-diastolic diameter (LVEDD), fractional shortening (FS), left ventricular ejection fraction (LVEF) and heart rate (HR) using echocardiography; myocardial and plasma norepinephrine (NE) by high pressure liquid chromatography-electrochemical detection; cardiac sympathetic ganglion and myocardial NET mRNA level were determined by real-time fluorescent quantitation PCR; cardiac sympathetic ganglion and myocardial NET protein and myocardial tyrosine hydroxylase (TH) protein by Western blot. Results: Compared with CG, ET (42.6±4.2 vs 27.4±3.8 min, $P<0.01$) increased; LVEDD (7.15±0.81 vs 8.82±0.91 mm, $P<0.05$), FS (57.8±4.6 vs 45.0±4.3 mm/s, $P<0.01$) and LVEF (67.6±5.8 vs 52.4±4.7%, $P<0.01$) raised but HR reduced (314±37 vs 395±39 b/min, $P<0.05$); both plasma NE (375.7±47.2 vs 464.6±42.9 pg/ml, $P<0.01$) and myocardial NE (528.2±54.4 vs 664.1±39.8ng/g, $P<0.01$) lowered; NET mRNA (1.75±0.20 vs 1.00±0.07, $P<0.01$) and protein (1.82±0.17 vs 1.00±0.09, $P<0.01$) of sympathetic ganglion elevated; NET mRNA of heart was not detected but NET protein step-up (1.69±0.18 vs 1.00±0.08, $P<0.01$); TH protein was not significantly different (1.15±0.22 vs 1.00±0.12, $P>0.05$). Conclusion: Long-term exercise training improved cardiac construction and sympathetic nerve function, as well as enhancing exercise capacity, the mechanism of which might be related to upregulation of NET gene expression of cardiac sympathetic ganglion.

Schroeder C, Jordan J. Norepinephrine transporter function and human cardiovascular disease[J]. Am J Physiol Heart Circ Physiol, 2012,303(11):H1273-82.

Ikeda N, Yasu T, Tsuboi K, et al. Effects of submaximal exercise on blood rheology and sympathetic nerve activity[J]. Circ J, 2010,74(4):730-4.

Backs J, Haunstetter A, Gerber SH, et al. The neuronal norepinephrine transporter in experimental heart failure: evidence for a post-transcriptional downregulation[J]. J Mol Cell Cardiol, 2001,33(3):461-72.

Li H, Ma XQ, Ye F, et al. Expressions of cardiac sympathetic norepinephrine transporter and beta1-adrenergic receptor decreased in aged rats[J]. J Zhejiang Univ Sci B, 2009,10(3):203-10.

Rapacciuolo A, Esposito G, Caron K, et al. Important role of endogenous norepinephrine and epinephrine in the development of in vivo pressure-overload cardiac hypertrophy[J]. J Am Coll Cardiol, 2001,38(3):876-82.

Thanks to the experimental group and give us support and help of all my colleagues

Where applicable, the authors confirm that the experiments described here conform with The Physiological Society ethical requirements.

PCC254

Dehydration reduces blood flow to the human brain and increases oxygen extraction during prolonged exercise in humans

S.J. Trangmar[1], S.T. Chiesa[1], K.K. Kalsi[1], N.H. Secher[2] and J. González-Alonso[1]

[1]Centre for Sports Medicine and Human Performance, Brunel University, Uxbridge, UK and [2]The Copenhagen Muscle Research Centre, Department of Anaesthesia, Rigshospitalet, Faculty of Health Sciences, University of Copenhagen, Copenhagen, Denmark

Background: Dehydration accrued during prolonged exercise in the heat induces significant cardiovascular strain on the human body characterised by reductions in cardiac output, active muscle and skin blood flow, arterial blood pressure, vascular conductance and an overall impaired exercise capacity (1). However, it is presently unknown whether progressive dehydration during exercise in the heat reduces blood flow to the brain, thereby impairing aerobic metabolism. A hyperthermic-hyperventilation induced lowering of the $PaCO_2$ may reduce blood flow to the brain, assuming that reductions in middle cerebral artery velocity (MCA V_{mean}) reflect reductions in cerebral blood flow (CBF) (2,3,4,5). This study tested the hypothesis that progressive dehydration reduces CBF during prolonged exercise in the heat, in part through mechanisms associated with $PaCO_2$, but without impairing brain VO_2. **Methods:** We assessed blood flow in the internal carotid artery (CBF) using Doppler ultrasonography and middle cerebral artery velocity (MCA V_{mean}) in ten cyclists (VO_{2PEAK}: 59 ± 2 ml/kg/min), who performed two hours of prolonged cycling exercise in a warm environment (182 ± 6 W; 35°C), without fluids to induce moderate dehydration (DEH; 3.1 ± 0.3 % body mass loss). Subjects returned one week later to repeat the protocol, but with regular fluid ingestion to maintain hydration status (Control). Blood samples were obtained from the brachial artery and left internal jugular vein (DEH only) to measure a-vO_2 differences and for the calculation of brain VO_2. All data are mean ± SEM and were compared with ANOVA and Pearson correlation (SPSS). **Results:** During dehydration CBF and MCA V_{mean} increased by 13 ± 3 % from rest to 30 min (p<0.05). Thereafter CBF declined to resting values with flow at 120 min significantly lower than at 30, 60 and 90 min (p<0.001). During control, CBF and MCA V_{mean} increased from rest to 30 min and were subsequently maintained throughout exercise (Increase ≥ 25%, p<0.05). Reductions in CBF and MCA V_{mean} during DEH were accompanied with significant increases (p<0.05) in a-vO_2 diff resulting in an unchanged brain VO_2. $PaCO_2$ declined in accordance with flow and velocity (p<0.05) with changes in flow correlated to changes in $PaCO_2$ (R^2 = 0.75, p<0.001), supporting a role for $PaCO_2$ in cerebral vasoconstriction. **Discussion:** The present findings show that progressive dehydration during prolonged exercise results in a marked reduction in CBF, whereas in control CBF did not decline. Compensatory increases in cerebral oxygen extraction allow for the maintenance of brain VO_2 throughout exhaustive exercise. These findings suggest that a reduction in brain VO_2 is an unlikely mechanism underpinning exercise capacity during prolonged, exhaustive exercise with dehydration.

González-Alonso J, Crandall CG & Johnson JM. (2008). The cardiovascular challenge of exercising in the heat. J Phyisol 586, 45-53.

Serrador JM, Picot PA, Rutt BK, Shoemaker JK & Bondar RL. (2000). Stroke **31,** 1672-1678.

Nybo L & Nielsen B. (2001). Middle cerebral artery blood velocity is reduced with hyperthermia during prolonged exercise in humans. J Physiol **534,** 279-286.

Nybo L, Moller K, Volianitis S, Nielsen B & Secher NH. (2002). Effects of hyperthermia on cerebral blood flow and metabolism during prolonged exercise in humans. J Appl Physiol **93,** 58-64.

Rasmussen P, Nybo L, Volianitis S, Moller K, Secher NH & Gjedde A. (2010). Cerebral oxygenation is reduced during hyperthermic exercise in humans. Acta Physiol **199,** 63-70.

This work was support by the Gatorade Sports Science Institute, PepsiCo, USA.

Where applicable, the authors confirm that the experiments described here conform with The Physiological Society ethical requirements.

PCC255

Reversing potential immobilisation induced deficits in muscle blood flow does not reverse immobilisation induced blunting of forearm glucose uptake in humans

S.L. Skirrow, E.J. Simpson, K. Tsintzas, I.A. Macdonald and P.L. Greenhaff

MRC-ARUK Centre for Musculoskeletal Ageing Research, University of Nottingham, Nottingham, UK

Physical inactivity has been proposed as a major contributor to the age-related loss of muscle mass and strength [1, 2]. Alongside these impairments are several metabolic adaptations, such as the development of insulin resistance [3], which may result from an age-related decline in muscle perfusion [4]. This study investigated the impact of forearm immobilisation on brachial artery blood flow and glucose uptake. We hypothesised that if inactivity induced decrements in muscle blood flow are responsible for blunting forearm glucose uptake, this would be ameliorated by the vasodilatory action of glyceryl trinitrate (GTN).

Sixteen healthy men (20.4 ± 0.4yrs, BMI 22.9 ± 0.6kg.m^{-2}) participated and were randomly assigned to placebo or GTN group. Measurements were made before and after 5wks immobilisation of the non-dominant forearm. Subjects underwent an oral glucose tolerance test (OGTT) and received either 400μg sublingual GTN or placebo mouth spray at t=0 and t=30. Brachial artery blood flow (BF) was measured during the OGTT using Doppler ultrasound, forearm glucose uptake (FGU) was calculated from the arterialised-venous and venous difference in blood glucose concentration, and total FGU over the 3hr OGTT was calculated from the incremental AUC. Forearm muscle volume was quantified with MRI and isometric strength was measured using handgrip dynamometry. The study was approved by the University of Nottingham Ethics Committee. Values represent mean ± SEM. Single measures were compared between groups using Student's t-test. Postprandial responses were analysed using two-way ANOVA with repeated measures. Statistical significance was set at P<0.05.

Before immobilisation, GTN did not affect FGU AUC during the OGTT (GTN 99.9 ± 25.7mmol/l/mm^2 vs. Placebo 74.8 ± 13.6 mmol/l/mm^2, P=0.42). Immobilisation reduced hand grip strength by 27.1 ± 7.3% and 21.0 ± 5.7% from baseline in the placebo and GTN group respectively (P<0.01), but had no effect on muscle volume in either group (placebo change 0.05 ± 1.83% vs. GTN change -0.7 ± 1.33%, P>0.05). Immobilisation reduced FGU AUC by 42.4 ± 14.2% (P<0.05) in the placebo group. GTN increased brachial artery diameter by 15.2 ± 0.7% (P<0.01) throughout the OGTT and increased BF by 17.3 ± 2.9%

during the first hour of the OGTT (P<0.05). However the immobilisation induced decrement in FGU AUC was no different from the placebo response (55.9 ± 21.2%, P=0.64).
Immobilisation reduced FGU in response to an OGTT. The administration of GTN increased brachial artery diameter and blood flow during the OGTT, but did not improve the immobilisation induced deficit in FGU. This suggests that an immobilisation induced deficit in muscle blood flow is not responsible for the decline in glucose disposal, but instead is a muscle centric phenomenon.

Evans, W.J., *What is sarcopenia?* Journals of Gerontology - Series A Biological Sciences and Medical Sciences, 1995. **50**(SPEC. ISSUE): p. 5-8.

Kortebein, P., et al., *Effect of 10 Days of Bed Rest on Skeletal Muscle in Healthy Older Adults.* JAMA: The Journal of the American Medical Association, 2007. **297**(16): p. 1769-1774.

Srikanthan, P., A.L. Hevener, and A.S. Karlamangla, *Sarcopenia Exacerbates Obesity-Associated Insulin Resistance and Dysglycemia: Findings from the National Health and Nutrition Examination Survey III.* PLoS ONE, 2010. **5**(5): p. e10805.

Phillips, B., et al., *Resistance exercise training improves age-related declines in leg vascular conductance and rejuvenates acute leg blood flow responses to feeding and exercise.* Journal of Applied Physiology, 2012. **112**(3): p. 347-353.

Where applicable, the authors confirm that the experiments described here conform with The Physiological Society ethical requirements.

PCC256

Nutritional status, physical activity and food habit of children of a selected government primary school of Bangladesh

M.U. Khan[1], M.M. Abedin[1] and M.A. Salam[2]

[1]Physiology, Noakhali Medical College, Noakhlai, Bangladesh and [2]Pharmacology, Noakhali Medical College, Noakhali, Bangladesh

Background: Increase in childhood overweight and obesity have become a major public health problem in industrialized nation (1). It is also increasing in developing countries (2). Bangladesh is a developing country. School going children of this country is suffering from malnutrition rather than obesity. The national nutrition survey (1995-96) report shows that about 62% of the children aged 6-9 years are malnourished (3). The nutritional status, physical activity and food habit of school going children of Bangladesh is not known. Objectives: To know the nutritional status, physical activity and food habit of children of a selected government-run primary school at a peripheral district town of Bangladesh. Method: We conducted this cross-sectional descriptive study in the Department of Physiology, Noakhali Medical College, Bangladesh during the period of April, 2012 –June, 2012. Two hundred and twenty students of a selected government-run primary school of a district town of Bangladesh were enrolled for the study by using convenient sampling. Data on diet, physical activity, height (cm) and weight (kg) were collected using a structured questionnaire. Permission was taken from concerned authorities consent from participants. BMI <5, 5-85, >85, and >95 percentile were considered under-weight, normal, overweight, and obese respectively. Data were analyzed by using SPSS (version 12) for windows and web-based "Excel BMI calculator". Result: There were 41.4 percent boys. The mean age was 9.3±1.6 years. The main diet was rice or bread made of wheat-flour (85.5%) in breakfast, rice with meat, fish, egg, or vegetables for lunch (95.45%) and same menu for dinner (98.64%). Forty-six percent students drank cow's milk and 22.7% soft drinks. Ninety-nine percent students participated in games for a mean period of 2.81±1.25 hours. The mean±SD period of playing outdoor-game, indoor-game and game-at-school was 1.35±0.58, 1.04±0.45, and 0.76±0.31 hours respectively. Eighty-three percent students did household work for a mean period of 1.03±0.65 hours. The mean±SD height, weight and BMI of the students were 126.6±9.9 cm, 22.01±5.07 kg and 13.56±1.60 respectively. Conclusion: Sixty-five percent students were underweight, 34.55% normal weight and 0.45% obese. The prevalence of under-weight was alarmingly high and that of overweight and obesity was extremely low among the students of a government-run primary school in a peripheral district town of Bangladesh. Ninety-nine percent students participated in physical activity. The menu of diet contained all kinds of food but the quantity of food was not measured.

Ebbeling CB, Pawlak DB, Ludwing DS. Childhood obesity. Public-h ealth crisis, common sense cure. Lancet 2002;360:473-82

Workd Health Organization. Obesity: Preventing and Managing the Global Epidemic. Report of a WHO consultation on obesity. Geneva: WHO 1998.

Jahan, K. and Hossain, M. Nature and Extent of Malnutrition in Bangladesh. Bangladesh National Nutrition Survey,

1995-96, Institute of Nutrition and Food Science, University of Dhaka, July, Part-1,1998;116:134.

We are thankful to teachers of Khademul Islam Primary School, Maijdee, Noakhali, Bangladesh for their support in collecting data.

Where applicable, the authors confirm that the experiments described here conform with The Physiological Society ethical requirements.

PCC257

Effects of age, gender and starting age on muscle and bone side differences in veteran tennis players

A. Ireland[1], T.M. Maden-Wilkinson[1], B. Ganse[2], H. Degens[1] and J. Rittweger[2,1]

[1]IRM, Manchester Metropolitan University, Manchester, UK and [2]Department of Space Physiology, German Aerospace Centre, Cologne, Germany

The effectiveness of regular exercise for bone strength into older age, or when begun after puberty is not fully understood. Comparisons of sedentary individuals and athletes may introduce a self-selection bias, whereas study of tennis players allows the non-racquet arm to act as a control for the exercising racquet arm.
Therefore, peripheral quantitative computed tomography (pQCT) scans were taken at radius, ulna and humerus mid-shaft, and distal radius in both arms of ninety veteran tennis players (mean age 63.7±11.8y). Large side differences in muscle and bone size and strength – in favour of the racquet arm – were found. The most pronounced findings were a 13±10% higher distal radius bone mass and 23±12% larger cortical area in the humerus (both $P < 0.001$). There was no age effect on bone mass (all $P > 0.2$; except humerus where $P = 0.055$ and $R^2 = 0.002$). Proximal radius and ulna strength in bending and torsion were positively associated with increasing age (all $P < 0.05$). Despite no age effect on training volume ($P = 0.201$) many side differences were less pronounced in older players – particularly in the humerus where side differences in bone mass, cortical thickness and stiffness in bending and torsion were 43-47% less in 80- than 40-year olds (all $P < 0.01$). Gender effects on side difference were found for a number of bone

parameters - in all cases differences were more pronounced in men than women. This was most apparent in the humerus where male side differences in most parameters (except cortical BMD and endocortical circumference) were 22-37% greater than in females despite similar training volumes for both genders. Bone strength side differences in players who began playing in adulthood were smaller than those who began during childhood – in particular in total bone CSA, and periosteal circumference at all sites (all $P < 0.05$).
In summary, whilst regular tennis participation in older age is associated with greater racquet arm muscle and bone size and strength these differences are lower at old age and in females. The age-associated decline is likely due – at least in part – to the reduced racquet arm advantage in muscle size and strength at older age. In addition, the effectiveness of exercise for bone when begun in adulthood (i.e. after epiphyseal closure) is less - mainly due to the lack of significant periosteal apposition.

Where applicable, the authors confirm that the experiments described here conform with The Physiological Society ethical requirements.

PCC258

A new equation to estimate oxygen consumption during exercise on the cycle ergometer

F. Formenti[1,2], J. Ives[2], E. Seminati[3], S. Sethi[2], N.J. Somerville[2], A.E. Minetti[3] and F. Borrani[4,2]

[1]Nuffield Division of Anaesthetics, Nuffield Department of Clinical Neurosciences, University of Oxford, Oxford, UK, [2]Department of Sport and Exercise Science, University of Auckland, Auckland, New Zealand, [3]Institute of Human Physiology, University of Milan, Milan, Italy and [4]Department of Physiology, University of Lausanne, Lausanne, Switzerland

Direct measurement of human metabolism is recommended for accuracy in individuals' exercise testing; when direct measurement is not feasible, estimation of metabolism during exercise is acceptable. The American College of Sports Medicine (ACSM) suggests estimating oxygen consumption (VO2) during exercise on a cycle ergometer through a straightforward equation that considers an individual's body mass and work rate (ACSM, 2009). Despite avoiding complex calculations, this equation does not consider the effect of pedalling rate (PR) on VO2. However, when cycling at a given work rate, PR can be a strong determinant of VO2 (Seabury et al., 1977, Zoladz et al., 2000). We hypothesised that, for sub-maximal exercise on the cycle ergometer, including PR in the ACSM equation would allow more accurate VO2 prediction.
Seven healthy male participants (average ± standard deviation: age 26 ± 9 years, height 180 ± 6 cm, weight 76 ± 10 kg) took part in the study, which conformed to the Declaration of Helsinki and had been approved by the local Ethics Committee. Participants' VO2 was recorded during steady-state exercise on the cycle ergometer at four PR (50, 70, 90, 110 revolutions per minute); each PR was studied at four subsequent sub-maximal external work rates (0, 50, 100, 150 W). Participants rested for a period of at least 40 min between tests. Participants' VO2 was also predicted as a function of participant's body mass, work rate and PR (Minetti, 2011):
VO2 = 3.5 + 10.8 * WR/BM + 0.0000076 * PR (Equation 1)
Here, 3.5 is an assumed constant for resting VO2 (ml O2 kg-1 min-1), WR indicates work rate (W), and BM participant's body mass (kg); PR is pedalling rate (revolutions per minute), and represents the metabolic equivalent of the internal work. Participants' VO2 was also predicted through the ACSM equation as a means of comparison. Data were analysed by Student's paired t-test and linear regression analysis.
The recorded VO2 values ranged from 6 to 37 ml O2 kg-1 min-1. Figure 1 shows the VO2 values predicted by Eq. 1 and by the ACSM equation as a function of measured VO2 values. Both sets of predicted VO2 values showed a direct linear relationship with measured VO2 values. When plotted against the measured VO2 values, those predicted by Eq. 1 were closer to the identity line than values predicted by the ACSM equation. We conclude that PR is an important determinant of VO2, and that Eq. 1 improves the accuracy of the ACSM equation for exercise on the cycle ergometer. These preliminary findings need to be confirmed in a larger sample population.

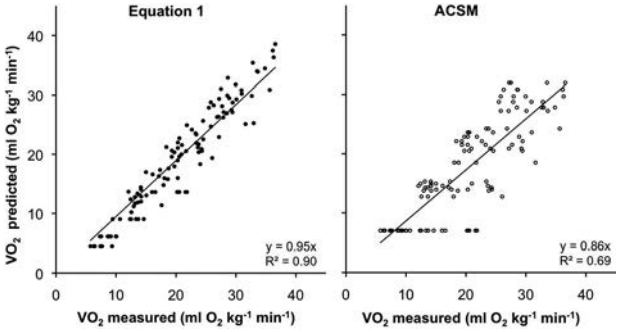

Figure 1. VO2 values predicted by (left) Eq. 1 and by (right) the ACSM equation are shown as a function of measured VO2 values. Each circle shows data recorded at steady state for 2 min in one participant, at a given combination of work rate and PR (n = 112). The straight lines illustrate the respective linear regression lines.

ACSM 2009. ACSM's Guidelines for Exercise Testing and Prescription, Lippincott Williams & Wilkins.

MINETTI, A. E. 2011. Bioenergetics and biomechanics of cycling: the role of 'internal work'. Eur J Appl Physiol, 111, 323-9.

SEABURY, J. J., ADAMS, W. C. & RAMEY, M. R. 1977. Influence of pedalling rate and power output on energy expenditure during bicycle ergometry. Ergonomics, 20, 491-8.

ZOLADZ, J. A., RADEMAKER, A. C. & SARGEANT, A. J. 2000. Human muscle power generating capability during cycling at different pedalling rates. Exp Physiol, 85, 117-24.

Where applicable, the authors confirm that the experiments described here conform with The Physiological Society ethical requirements.

PCC259

Remote ischemic preconditioning increases the time to task failure during rhythmic handgrip exercise in men: underlying hemodynamic mechanisms

T.C. Barbosa[1], A.C. Machado[1], I.D. Braz[1,3], I.A. Fernandes[1], L.C. Vianna[1], A.L. Nobrega[1] and B.M. Silva[1,2]

[1]Department of Physiology and Pharmacology, Fluminense Federal University, Niterói, Brazil, [2]Department of Physiology, São Paulo Federal University, São Paulo, Brazil and [3]School of Sport and Exercise Sciences, University of Birmingham, Birmingham, UK

Ischemic preconditioning (IP) protects both the tissue where it is applied (Local IP) and others (Remote IP) against injury induced by prolonged ischemia. Local IP can increase maximal power output in an exercise test. However, it is not clear whether Remote IP could also increase physical performance and which mechanisms associates IP and physical performance. This study investigated the effects of Remote IP on physical performance during handgrip exercise and possible mech-

anisms associated. Thirteen men underwent randomly Remote IP or Sham intervention in 2 sessions. After that, they performed handgrip exercise until task failure. Time to task failure was measured as well as brachial blood flow and conductance, forearm normalized concentration of deoxygenated hemoglobin and myoglobin (Deoxy-Hb norm.), tissue oxigenation index (TOI norm.), heart rate (HR), stroke volume (SV), mean arterial pressure (MAP) and total peripheral resistance (TPR). Comparisons between conditions were made at equal exercise time (20%, 40%, 60%, 80% and 100% of shorter session exercise time) and at peak exercise of each session. Measurements of maximal voluntary contraction, exercise time and brachial artery diameter were reproducible (intraclass correlation coefficient >0.9) and mean coefficient of variation was between 5.1% to 13.5%. Time to task failure increased by 25.3%, from 191±21 s after Sham intervention to 244±37 s after Remote IP (Student's T test P=0,019). The increment of exercise time between Remote IP and Sham correlated positively to the increment of blood flow, conductance, TOI norm. and SV at 100% of total exercise time, and correlated negatively to the impairment of Deoxy-Hb norm., HR, MAP and TPR at 100% of total exercise time. At peak exercise, Remote IP led to a higher Deoxy-Hb norm. and lower TOI norm. Subjects who were responders to Remote IP (exercise time increment >13.5%; n=6) had lower MAP and TPR and higher VS at 100%, compared to Sham. At peak exercise, Remote IP increased blood flow. However, Deoxy-Hb norm. and TOI norm. were similar between conditions in these subjects. In conclusion, Remote IP increased exercise performance, possibly by improvement of blood flow and vascular conductance response to exercise. This improvement, in turn, could be due to a greater local vasodilation and an attenuation of sympathetic tone.

Murry CE *et al.* (1986). Circulation 74(5): p. 1124-36.

de Groot PC *et al.* (2010). Eur J Appl Physiol 108(1): p. 141-6.

Crisafulli A *et al.* (2011). J Appl Physiol 111(2): p. 530-6.

Jean-St-Michel E *et al.* (2011). Med Sci Sports Exerc 43(7): p. 1280-6.

Bailey TG *et al.* (2012). Med Sci Sports Exerc 44(11): p. 2084-9

Where applicable, the authors confirm that the experiments described here conform with The Physiological Society ethical requirements.

PCC260

Age, but not osteoarthritis is related to a reduction in skeletal muscle Na^+,K^+ -ATPase content in older adults

B. Perry[1], P. Levinger[1,4], F.R. Serpiello[1], M.K. Caldow[2,5], D. Cameron-Smith[3], J.R. Bartlett[6], J.A. Feller[4], N.R. Bergman[6], I. Levinger[1] and M.J. McKenna[1]

[1]Institute of Sport, Exercise and Active Living, Victoria University, Melbourne, VIC, Australia, [2]School of Exercise and Nutrition Sciences, Deakin University, Melbourne, VIC, Australia, [3]Liggins Institute, University of Auckland, Auckland, New Zealand, [4]Musculoskeletal Research Centre, Faculty of Health Sciences, La Trobe University, Melbourne, VIC, Australia, [5]Basic and Clinical Myology Laboratory, Department of Physiology, University of Melbourne, Melbourne, VIC, Australia and [6]Warringal Medical Centre, Melbourne, VIC, Australia

Introduction: Knee osteoarthritis (OA) is a debilitating disorder that is accompanied by loss of muscle mass and strength and is prevalent in older populations (Lawrence *et al.*, 2008). In skeletal muscle the Na^+,K^+ -ATPase (NKA) regulates membrane potential and excitability and thereby directly influences skeletal muscle force generation (McKenna *et al.*, 2008). This study examined the effects of both OA and ageing on muscle NKA content in old participants. *Methods:* Thirty-six older adults participated (range: 55-81 years old); nineteen had OA (69.9 ± 6.5 yr, mean age ± SD) and 17 were asymptomatic age-matched controls (CON; 66.8 ± 6.4 yr). A vastus lateralis muscle biopsy was taken and analysed for NKA content ($[^3H]$ ouabain binding sites), NKA $\alpha_{1\text{-}3}$ and $\beta_{1\text{-}3}$ isoform protein abundance (immunoblotting) and NKA isoform mRNA content (real time RT-PCR). Participants also underwent knee extensor muscle strength testing and completed a physical activity questionnaire. Differences in NKA between OA and CON were assessed using independent t-tests, and association between age and NKA content was investigated using bivariate correlation in both the OA and CON group individually, and in the pooled data. *Results:* OA participants had 40.8% lower strength ($p = 0.005$), but 34% higher NKA α_2 ($p = 0.006$) and 1 fold greater NKA α_3 ($p = 0.016$) abundance compared to CON. OA participants performed more incidental physical activity ($p = 0.035$). No significant differences were found between groups for total NKA content, NKA $\alpha_{1\text{-}3}$ and $\beta_{1\text{-}3}$ isoform mRNA content, and NKA α_1, β_1, β_2, and β_3 isoform abundance. There was an inverse correlation between age and $[^3H]$ ouabain binding sites with both participant groups combined ($r = -0.467$, $p = 0.038$, Figure 1), and in the OA participants ($r = -0.626$, $p = 0.03$). *Conclusions:* NKA content was not decreased in OA compared to asymptomatic controls. We also reported that age is negatively correlated with $[^3H]$ ouabain content independent of disease state which may suggest that age but not knee OA is related to decreased muscle NKA content.

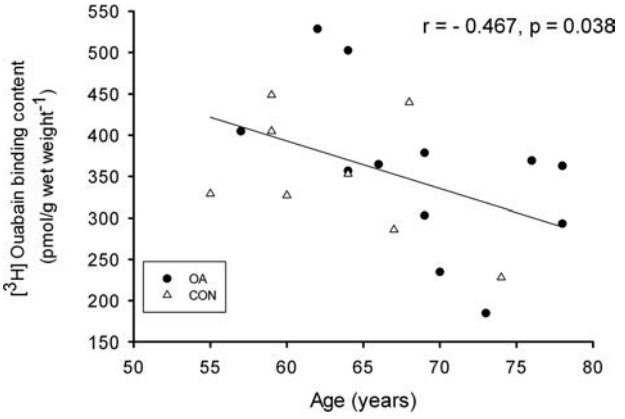

Figure 1: Spearman correlation coefficient: age and ouabain binding site content. Filled circles: OA, unfilled triangles: CON.

Lawrence RC, Felson DT, Helmick CG, Arnold LM, Choi H, Deyo RA, Gabriel S, Hirsch R, Hochberg MC & Hunder GG. (2008). *Arthritis & Rheumatism* **58**, 26-35.

McKenna MJ, Bangsbo J & Renaud JM. (2008). *Journal of Applied Physiology* **104**, 288-295

Where applicable, the authors confirm that the experiments described here conform with The Physiological Society ethical requirements.

PCC261

Fibre type specific differences and adaptability of the Na^+,K^+-ATPase α1-3 and β1-3 isoforms to intermittent training in human single skeletal muscle fibres

V.L. Wyckelsma[1], R.M. Murphy[2], F.R. Serpiello[1], C.R. Lamboley[1] and M.J. McKenna[1]

[1]ISEAL, College of Sport and Exercise Science, Victoria Univerisity, Melbourne, VIC, Australia and [2]Department of Zoology, La Trobe University, Melbourne, VIC, Australia

Introduction The Na^+-K^+-ATPase (NKA) plays a key role in skeletal muscle excitability but little is known on the fibre-specific NKA abundance in human skeletal muscle. Exercise training is a proven modality for upregulating NKA in skeletal muscle and enhancing exercise performance. Repeated-sprint exercise (RSE) training comprises multiple "all-out" efforts interspersed by brief recovery periods and might differentially upregulate NKA isoforms in different fibre types. Therefore we investigated the fibre-specific differences in the abundance of all six NKA isoforms expressed in single human muscle fibres and whether fibre-specific adaptations in NKA occurred in response to intense RSE training.

Methods Eight healthy participants trained three times per week for 4 weeks, each session comprising three sets of five, 4-s maximal sprints. A vastus lateralis biopsy was taken before and after training, single fibres were separated and fibre type (MHC I and IIa) and NKA isoform protein abundance (α1-3, β1-3) were determined by western blotting.

Results All six NKA isoforms were co-expressed in both Type I and IIa fibres. None of the three α isoforms were expressed in a fibre type specific manner; although there was a tendency for α1 protein to be more abundant in type I compared to type IIa fibres (Figure 1). The NKA β1 and β3 isoforms were also not expressed in a fibre type specific manner (Figure 2). The NKA β2 abundance was higher in type I than in Type IIA fibres (1.33±0.18 vs. 0.83±0.07, respectively, P=0.012). RSE training upregulated NKA β1 in both type I (Pre-train 0.91±0.08, vs. Post-Train1.22±0.08, P=0.035); and Type IIa fibres (Pre-train 0.81±0.06 vs. Post-Train 1.17±0.08, P=0.05). There was a tendency for upregulation of other NKA isoforms in MHC IIa fibres post training with moderate effect sizes detected for α1 (ES=0.6), β2 (ES=0.4) and β3 (ES=0.5).

Discussion The first important finding was that all six NKA isoforms were detected at the protein level in each human single muscle fibre; furthermore, these fibres showed homogeneity of NKA isoform expression across the type I and IIa fibre types. The only major exception was the greater abundance in β2 in Type I fibres. These findings contrast sharply with previous studies conducted on rat muscle. Four weeks of RSE training upregulated β1 in both fibre types, which may have implications for increasing NKA activity. However RSE training did not increase the NKA α isoform abundance in either fibre type; this may reflect insufficient physiological stress induced by 4-s sprints with RSE.

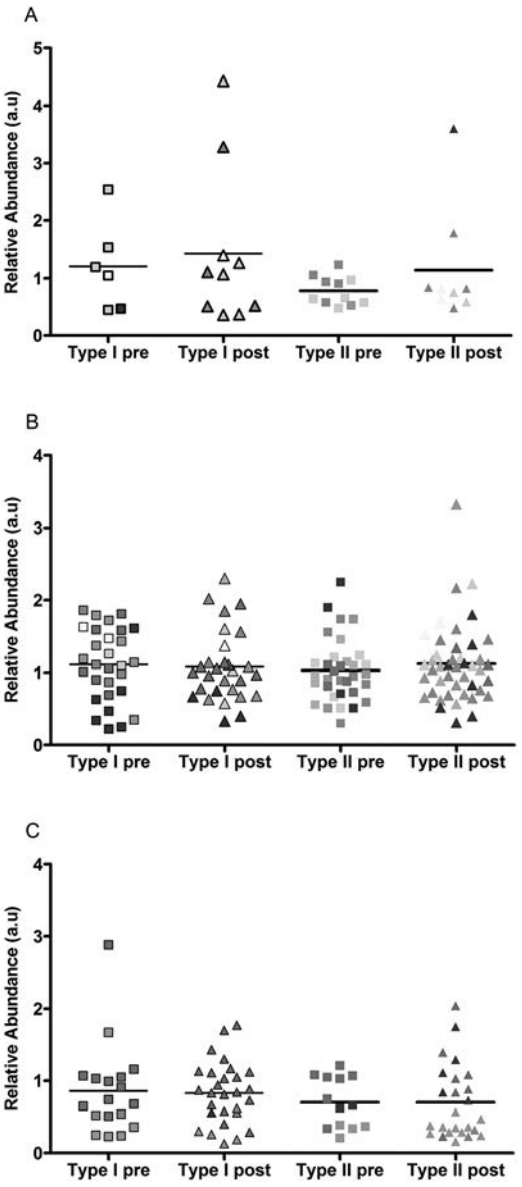

Individual and mean data of fibre type specificity of Na^+, K^+-ATPase α1-3 isoforms in single fibres pre-training and following four weeks of repeat sprint training. Individual fibres colour coded to participants which they belong to. Each isoform is normalised to the average of the type IIa fibres on each gel and expressed as relative abundance (a.u), (A) α1 (B) α2 (c) α3. Training changes measured by independent t-test. Data expressed as mean ± SEM

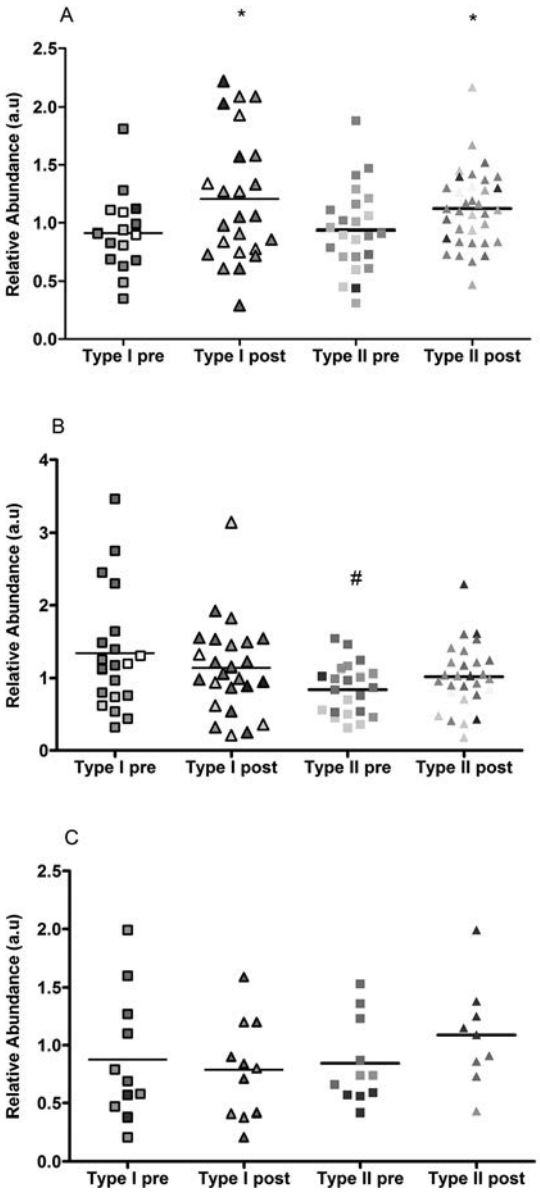

Individual and mean data of fibre type specificity of Na^+, K^+-ATPase β1-3 isoforms in single fibres pre-training and following four weeks of repeat sprint training. Individual fibres colour coded to participants which they belong to. Each isoform is normalised to the average of the type IIa fibres on each gel and expressed as relative abundance (a.u), (A) β1 (B) β2 (c) β3 * P<0.05 from pre-training # P<0.05 from MHC IIa. Data expressed as mean ± SEM

Where applicable, the authors confirm that the experiments described here conform with The Physiological Society ethical requirements.

PCC262

Arterial baroreceptor loading does not alleviated heat-induced hyperventilation

R.A. Lucas[1,2], J. Pearson[1,3], Z.J. Schlader[1] and C.G. Crandall[1]

[1]Institute for Exercise and Environmental Medicine, Texas Health Presbyterian Hospital, Dallas, TX and Department of Internal Medicine, University of Texas Southwestern Medical Center, Dallas, TX, USA, [2]Centre for Global Health Research, Umea University, Umea, Sweden and [3]Cardiff Metropolitan University, Cardiff, UK

Introduction: Hyperthermic hyperventilation has been well documented in humans; however, the mechanisms and the physiological relevance of such a response remains unclear. Reductions in mean arterial pressure (MAP) often coincide with hyperthermia due to heat dissipation mechanisms. Given that reductions in MAP stimulate increases in ventilation this study tested the hypothesis that arterial baroreceptor loading would reverse heat-induced increases in ventilation and accompanying decreases in end-tidal carbon dioxide ($P_{ET}CO_2$).

Methods: Eleven individuals (26 ±5 y; 71 ±15 kg) underwent passive heat stress via a water perfused suit while lying supine with their lower legs resting off the end of the bed, their knees at an angle of ~80° and their feet supported. This was done to aid venous pooling and augment heat-related reductions in MAP. Intestinal temperature (HQ Inc.), mean skin temperature, MAP (Finometer Pro), central venous pressure (central venous catheter, n=4), minute ventilation, tidal volume, respiratory rate (Parvo-Medics) and $P_{ET}CO_2$ (capnograph) were monitored continuously. After intestinal temperature was elevated (P<0.05) 1.8 ±0.5°C, causing a sustained rise in ventilation (by 4.9 ±2.7 $L.min^{-1}$, P<0.01) and reductions in $P_{ET}CO_2$ (by 5 ±2 mm Hg, P<0.01) plus MAP (by 9 ±7 mm Hg, P<0.01), phenylephrine was infused over 5 min to restore MAP to normothermic values.

Results: Phenylephrine infusion increased MAP by 11 ±5 mm Hg (P<0.01), restoring it to normothermic values, but did not change (P>0.05) ventilation or $P_{ET}CO_2$. Intestinal and skin temperatures did not change (P>0.05) with phenylephrine infusion. See Table.

Conclusion: The absence of a reduction in ventilation upon returning arterial baroreceptor loading to pre-heat stress levels indicates that hyperthermic hyperventilation is not caused by arterial baroreceptor unloading coincident with the heat stress.

Table: Thermal, haemodynamic and respiratory measures during normothermia, hyperthermia and phenylephrine infusion.

	Normothermia	Hyperthermia	Phenylephrine infusion
Intestinal temperature (°C)	36.9 ±0.2	38.7 ±0.4 *	38.9 ±0.5 *
Mean skin temperature (°C)	33.9 ±0.5	39.9 ±0.5 *	39.8 ±0.5 *
MAP (mm Hg)	85 ±7	76 ±8 *	87 ±9 #
Ventilation ($L.min^{-1}$)	7.6 ±2.3	12.5 ±2.8 *	11.6 ±4.6 *
$P_{ET}CO_2$ (mm Hg)	41 ±2	36 ±3 *	36 ±3 *
Tidal volume (L)	0.51 ±0.14	1.01 ±0.43 *	0.99 ±0.49 *
Respiratory rate (breaths per min)	14.8 ±2.1	14.5 ±5.9	13.4 ±5.8

$P_{ET}CO_2$, end-tidal carbon dioxide; MAP, mean arterial pressure. * Significantly different from normothermia P<0.05, # Significantly different from hyperthermia P<0.05.

Supported by NIH Grant HL061388

Where applicable, the authors confirm that the experiments described here conform with The Physiological Society ethical requirements.

PCC263

Aged garlic extract improves on metabolic parameters in exercise trained obese rats

D. Seo[1], H. Kwak[2], L. Dizon[1], Y. Baek[3], N. Kim[1], B. Rhee[1], K. Ko[1], S. Lee[1], B. Park[4] and J. Han[1]

[1]Cardiovascular and Metabolic Disease Center, College of Medicine, Inje University, Busan, Republic of Korea, [2]Department of Kinesiology, Inha University, Inchon, Republic of Korea, [3]Department of Physical Education, Pusan National University, Busan, Republic of Korea and [4]Division of Leisure & Sports Science, Dong Seo University, Busan, Republic of Korea

Aged garlic extract (AGE) is known to have a protective effect against immune system, endothelial function, oxidative stress

and inflammation. We examined the effects of exercise with and without aged garlic extract administration on body weight, lipid profiles, inflammatory cytokines, and oxidative stress marker in high-fat diet (HFD)-induced obese rats. Forty-five Sprague-Dawley rats were fed either a HFD (HFD, n = 40) or a normal diet (ND, n = 5) for 6 weeks and thereafter randomized into ND (n = 5), HFD (n = 10), HFD with AGE (n = 10), HFD with Exercise (n = 10), or HFD with Exercise+AGE (n = 10) for 4 weeks. AGE groups were administered at a dose of 2.86 g/kg/body weight, orally. Exercise consisted of running 15-60 min 5 days/week with gradually increasing intensity. AGE ($P < 0.01$), Exercise, and Exercise+AGE ($P < 0.001$) attenuated body weight gain and food efficiency ratio compared to HFD. Visceral fat and liver weight gain were attenuated ($P < 0.05$) with all three interventions with a greater effect on visceral fat in the Exercise+AGE than AGE ($P < 0.001$). In reducing visceral fat ($P < 0.001$), epididymal fat ($P < 0.01$) and liver weight ($P < 0.001$), Exercise+AGE was effective, but exercise showed a stronger suppressive effect than AGE. Exercise+AGE showed further additive effects on reducing visceral fat and liver weight ($P < 0.001$). AGE significantly attenuated the increase in total cholesterol and low-density lipoprotein-cholesterol compared with HFD ($P < 0.05$). Exercise+AGE attenuated the increase in triglycerides compared with HFD ($P < 0.05$). Exercise group significantly decrease in C-reactive protein ($P < 0.001$). These results suggest that AGE supplementation and exercise alone have anti-obesity, cholesterol lowering, and anti-inflammatory effects, but the combined intervention is more effective in reducing weight gain and triglycerides levels than either intervention alone.

Hagan S & Niswender KD (2012). Pediatr Blood Cancer 58, 149-153.

Iyer et al. (2012). Exp Diabetes Res 758614. doi: 10.1155/2012/758614. Epub 2011 Oct 10

Xu et al. (2011). Am J Physiol Regul Integr Comp Physiol 1, 1115-1125.

Li et al. (2010). Lipids Health Dis 9,131.

Petersen AM & Pedersen BK (2005). J Appl Physiol 98, 1154-1162.

This work was supported by Priority Research Centers Program through the National research Foundation of Korea (NRF) funded by the Ministry of Education, Science and Technology (2010-0020224, and R13-2007-023-00000-0)

Where applicable, the authors confirm that the experiments described here conform with The Physiological Society ethical requirements.

PCC264

Changes in body composition and rates of fat oxidation following 12 weeks high intensity exercise

L. Bagley, M. Slevin, N. Al-Shanti, M. Piasecki, G. Morrissey, H. Foulkes, M. Carroll, C. Murgatroyd, D. Liu, W.S. Gilmore and J.S. McPhee

Institute for Biomedical Research into Human Movement and Health, Manchester Metropolitan University, Manchester, England, UK

Intro:
A typical High Intensity Interval Training (HIIT) programme involves only around 4 min exercise per session, yet improves cardiorespiratory function and increases fatty acid oxidation. It remains unclear whether such short duration, high intensity exercise will lead to significant loss of fat mass over time.
Methods:
Men and women (n=42, 57% male, mean (SD) age: 33 (±5) yrs;) from the general Manchester population gave written informed consent to participate. Measurements of body composition by Dual energy X-ray absorptiometry (DXA), maximal oxygen uptake (VO2max) and maximal rates of fat oxidation (FATmax) were taken in the fasted state before and after 12 weeks HIIT. HIIT consisted of 4 x 20 sec sprints on a cycle ergometer at a workload of approximately two-times higher than VO2max; 3 times per week, totalling 4 mins exercise per week.
Results:
VO2max increased by 7%(pre-training: 2.9 ml/min-1(±0.9) vs post-training:3.1ml/min-1 (±0.88) p=0.0003). The maximal rate of fat oxidation during steady-state exercise increased by 19%, from 7.8 mg/kg/min-1 (±3.2) to 9.3 mg/kg/min-1 (±3.9) (p=0.02). There were no significant changes to total body lean mass, lean mass of the legs or of the arms. Total body fat mass decreased by 5.42% (pre-training: 18.25 kg (±6.10) vs post-training 17.24 kg (±5.96) P=0.0002). Trunk fat decreased by 3% (pre-training: 9.1 kg (±3.9) vs post-training 8.8 kg (±3.8) p=0.007) and leg fat decreased by 6% (pre-training: 6.8 kg (±1.1) vs post-training: 6.4 kg (±1.1) p=<0.0005).
Conclusion:
A total of 4 min exercise per week over 12 weeks significantly increased VO2max and fat oxidation. It also decreased total body, trunk and leg fat mass. These adaptations might improve health status and reduce risk of metabolic and cardiovascular disease.

Babraj JA, Vollaard NBJ, Keast C, Guppy FM, Cottrell G, Timmons JA, Extremely short duration high intensity interval training substantially improves insulin action in young healthy males. BMC Endocrine Disorders, 2009. 9(3)

Venables C, Achten J, Jeukendrup AE. Determinants of fat oxidation during exercise in healthy men and women: a cross sectional study. J Appl Physiol, 2005. 98: p160-167

Perry CGR, Heigenhauser GJF, Bonen A, Spriet LL. High-intensity aerobic interval training increases fat and carbohydrate metabolic capacities in human skeletal muscle Applied Physiology, Nutrition and Metabolism, 2008. 33 (6): p. 1112-1123

Where applicable, the authors confirm that the experiments described here conform with The Physiological Society ethical requirements.

PCC266

Caveolin-1 negatively regulates TLR4 to activate MAPK pathway in LPS-challenged mammary epithelial cells

X. Wang[1], Z. Wu[1], H. Huang[1], C. Han[1], W. Zou[1,2] and J. Liu[3]

[1]Liaoning Normal University, Dalian, China, [2]Liaoning Key Laboratories of Biotechnology and Molecular Drug Research and Development, Dalian, China and [3]The First Affiliated Hospital, Dalian Medical University, Dalian, China

Mastitis is an inflammation of the mammary gland commonly caused by bacterial infection. Mammary epithelial cells mount defense against invading pathogens by detecting their respective danger signals or ligands and initiating appropriate immune responses. Caveolaes are a subset of lipid rafts that are rich in glyco-sphingolipids and cholesterol, mediate non-clathrin-dependent endocytosis, and regulate the internalization of particles such as bacteria. Caveolin-1, component of caveolae membranes, has been implicated as a modulator of innate immunity and inflammation. TLRs, Toll-like receptors, play central roles in the regulation of the host immune system and each TLR recognizes specific pathogen-associated molec-

ular patterns. TLR4 is one of the well characterized pathogen recognition receptors that recognizes the LPS of Gram-negative bacteria. To explore the role of caveolin-1 gene silencing on mitogen-activated protein kinase (MAPK) activation in lipopolysaccharide (LPS)-challenged human mammary epithelial cells, we established MCF-10ACE of caveolin-1 gene silencing from human mammary epithelial cell line MCF-10A by iRNA technology. DNA micro-assay was used to detect the expression file of inflammation-associated genes in MCF10ACE. Western blot analysis was used to examine the activation of mitogen-activated protein kinase (MAPK) in lipopolysaccharide (LPS)-challenged MCF-10A and MCF-10ACE. Moreover, immunofluorescence and Western blot analysis were performed to detect the co-localization of caveolin-1 and toll-like receptor 4 (TLR4) in human mammary epithelial cells. We found that MCF-10ACE exhibited significant increases in inflammation-associated genes expression, such as Prostaglandin-endoperoxide synthase 2 (PTGS2), B-cell lymphoma 2 (BCL2), Fas ligand (FAS) and Interleukin 2 receptor alpha (IL2Rα) were increased by >1.5-fold, even Interleukin 6 (IL-6) was increased by 7-fold and Interleukin 6 receptor (IL-6R) was increased by 17-fold.. In addition, LPS-induced p38 MAPK and JNK MAPK activation were significantly increased in MCF-10ACE ($p<0.01$). Furthermore, caveolin-1 colocalized with TLR4 and appeared a negative correlation trend. In conclusion, caveolin-1 gene silencing promotes MAPK activation via TLR4 signaling in human mammary epithelial cells response to LPS.

Aitken SL, Corl CM, Sordillo LM. Immunopathology of mastitis: insights into disease recognition and resolution. J Mammary Gland Biol Neoplasia 2011;16(4):291-304.

Ibeagha-Awemu EM, Lee JW, Ibeagha AE, Bannerman DD, Paape MJ, Zhao X. Bacterial lipopolysaccharide induces increased expression of toll-like receptor (TLR) 4 and downstream TLR signaling molecules in bovine mammary epithelial cells. Vet Res 2008;39(2):11.

Bastiani M, Parton RG.Caveolae at a glance. J Cell Sci 2010;123(Pt 22):3831-6.

Jin Y, Lee SJ, Minshall RD, Choi AM.Caveolin-1: a critical regulator of lung injury.Am J Physiol Lung Cell Mol Physiol. 2011;300(2):L151-60.

Wang XM, Kim HP, Song R, Choi AM. Caveolin-1 confers antiinflammatory effects in murine macrophages via the MKK3/p38 MAPK pathway. Am J Respir Cell Mol Biol. 2006 ;34(4):434-42.

This work was supported by the National Natural Science Foundation of China (No. 30570225; No. 30970353).

Where applicable, the authors confirm that the experiments described here conform with The Physiological Society ethical requirements.

PCC267

The relationship between brain cortical activity and brain oxygenation in the prefrontal cortex during hypergravity exposure

C. Smith[1,2], N. Goswami[2], R. Robinson[3], M. von der Wiesche[4] and S. Schneider[5]

[1]Sport and Exercise Sciences, University of Birmingham, Birmingham, UK, [2]Institute of Physiology, Medical University Graz, Graz, Austria, [3]Centre of Human & Aerospace Physiological Sciences, King's College London, London, UK, [4]Institute of Aerospace Medicine, German Aerospace Center (DLR), Cologne, Germany and [5]Institute of Movement and Neurosciences, German Sport University Cologne, Cologne, Germany

Artificial gravity has been proposed as a method to counteract the physiological de-conditioning of long duration spaceflight, however the effects of hypergravity on the central nervous system has had little study. The study aims to investigate whether there is a relationship between prefrontal cortex brain activity and prefrontal cortex oxygenation during exposure to hypergravity. Twelve healthy participants were selected to undergo hypergravity exposure aboard a Short Arm Human Centrifuge. Participants were exposed to hypergravity in the +Gz axis, starting from 0.6+Gz for females, and 0.8+Gz for males, gradually increasing by 0.1+Gz, until the participant showed signs of syncope. Brain cortical activity was measured using electroencephalography (EEG), and localized to the prefrontal cortex using standard low resolution brain electromagnetic tomography (LORETA). Prefrontal cortex oxygenation was measured using near-infrared spectroscopy (NIRS). Analysis of variance, including Fisher's least significant difference post hoc test were used to determine significant changes in prefrontal cortex cortical activity and oxygenation, and Pearson's test of correlation to determine any relationship between the two. A significant increase in prefrontal cortex activity ($p < 0.05$) was observed during hypergravity exposure compared to baseline. Prefrontal cortex oxygenation was significantly decreased during hypergravity exposure, with a decrease in oxyhemoglobin levels ($p < 0.05$) compared to baseline, and an increase in deoxyhemoglobin levels ($p < 0.05$) with increasing +Gz level. No significant correlation was found between prefrontal cortex activity and oxy/deoxyhemoglobin. It is concluded that the increase in prefrontal cortex activity observed during hypergravity was most likely not the result of increased +Gz values resulting in a decreased oxygenation produced through hypergravity exposure. No significant relationship between prefrontal cortex activity and oxygenation measured by NIRS, concludes brain activity during exposure to hypergravity may be difficult to measure using NIRS. Instead, the increased in prefrontal cortex activity might be attributable to psychological stress, which could pose a problem for the use of a SAHC as a countermeasure.

I would like to thank the team at the Institute of Movement and Neurosciences, German Sports University, who allowed me to partake in this study, providing help throughout, and being extremely generous with their time. I would also like to thank the team at the German Aerospace Center for allowing me to partake in this study and the use of their Short Arm Human Centrifuge.

Where applicable, the authors confirm that the experiments described here conform with The Physiological Society ethical requirements.

PCC268

Diet related water seems to affect in vivo skin hydration and biomechanics

L. Palma[1], L. Tavares[1], C. Monteiro[1], M.J. Bujan[3] and L.M. Rodrigues[1,2]

[1]CBiOS, U Lusofona Fac Health Sc & Technol, Lisboa, Portugal, [2]Pharmacol Sc Departm, U Lisboa School PHarmacy, Lisboa, Portugal and [3]UAH, U Alcala Faculty Medicine, Madrid, Spain

The biomechanical behaviour of human skin has been studied in order to better understand this complex behaviour allowing all types of movements, within the physiological limits, without cracking. Water from diet allegedly affect skin hydration and both seems to play a role in this context. So, the aim of this study is to identify the relationship between ingested water, skin hydration and skin biomechanical properties. Forty

healthy volunteers, female, mean age 24,30±5,53 y.o. participated in the study, after informed written consent. All procedures respected Helsinki principles and respective amendments. Volunteers with different dietary water intakes were asked to drink 2L water/dayly during 1 month. Measurements of skin physiological variables were taken in day 0 (t0) and day 30 (t30) and focused several anatomical regions (zygomatic, forehead, ventral forearm, hand and, external leg). Representative variables were transepidermal water loss (TEWL, measured by Tewameter TM300, CK electronics), epidermal hydration (measured by MoistureMeter SC and MoistureMeter D, Delphin) and biomechanical descriptors (Cutometer CM575, CK electronics).. Statistics included a t-student paired sample, hypothesis testing Shapiro - Wilk, Spearman, and a Pearson and Spearman correlation with a confidence level of 95%
A significant positive correlation between hydration and total extensibility (Uf) and a negative correlation (p<0,05) with total elasticity (Ua/Uf) elasticity (Ur/Ue), visco-elastic index (Ue/Uv) and total deformation recovery at the end of stress-off period (Ua) was noted. Thus, a positive impact on skin physiology seems to result from higher water intakes, in particular in those individuals that regularly consume less water

Where applicable, the authors confirm that the experiments described here conform with The Physiological Society ethical requirements.

PCC269

Adipogenic transdifferentiation of fibroblasts, but not myogenic stem cells, from human skeletal muscle

C.C. Agley, A. Rowlerson, C.P. Velloso, N.R. Lazarus and S.D. Harridge

Centre of Human & Aerospace Physiological Sciences, King's College London, London, UK

Several pathologies of adult skeletal muscle are associated with increased intramuscular adipose tissue, but the cellular source of the adipocytes is disputed. In order to establish which cell types from human skeletal muscle might be responsible we undertook experiments *in vitro* on cells extracted from muscle biopsy samples. These were obtained (following local anesthesia, 2% Lignocaine), from the vastus lateralis of healthy male volunteers aged (25.6±3.5 years). We first optimised an immuno-magnetic method to separate human myogenic stem cells from non-myogenic cells (predominantly fibroblasts). This gave initial purities of 96.9±1.4 and 90.5±3.12 (mean ±SD, n=5 biopsies) for myogenic (CD56+ve/desmin+ve) and fibroblast (CD56-ve/TE-7+ve) populations respectively. We then tested if the purified cell populations could transdifferentiate into adipocytes in response to treatment with fatty acids (600μM palmitic and oleic acid) or Adipocyte Inducing Medium. This experimental approach was combined with quantitative analysis of Oil-Red O staining for lipid acummulation and immunostaining for lineage markers and transcription factors. Both treatments caused the fibroblasts to transdifferentiate into adipocytes, as evidenced by loss of the intracellular connective tissue protein TE-7 (from 94.6±3.6% to 5.0±2.% of cells, P<0.001), significant upregulation of the adipogenic transcription factors PPARγ and C/EBPα (P<0.001), and adoption of the typical Oil-Red O+ve lipid-laden adipocyte morphology. Lipid content per cell (Oil-Red O+ve area μm^2) was significantly greater (P<0.001) in fibroblasts compared to muscle cells both before (muscle cells 13.1±5.5 vs. fibroblasts 80.0±17.6) and after fatty acid treatment (muscle cells 149.5±75.9 vs. fibroblasts 556.0±224.0). Muscle cells did not transdifferentiate under any condition, but significantly upregulated PPARγ and C/EBPα in response to fatty acids (P<0.001). Contrastingly, PPARγ and C/EBPα were slightly, but significantly decreased (P<0.001) in muscle cells cultured in AIM medium, revealing differences in the regulation of these transcription factors between myogenic cells and fibroblasts. After 15 days of AIM treatment muscle cells, all of which were incapable of adipogenesis, contained on average ~500 fold less lipid per cell than the fibroblasts which had transdifferentiated into adipocytes. These data suggest that skeletal muscle fibroblasts and not myogenic cells, are the major cellular source of intramuscular adipose tissue. Our findings have clear implications for therapeutic approaches aimed at regulating adipogenesis in skeletal muscle.

CA is funded by a PhD studentship from King's College London

Where applicable, the authors confirm that the experiments described here conform with The Physiological Society ethical requirements.

PCC270

Evidence for centrally-induced cholinergic vasodilatation in skeletal muscle at the start of voluntary one-legged cycling and during motor imagery in humans

K. Ishii[1], K. Matsukawa[1], N. Liang[1], K. Endo[1], M. Idesako[1], H. Hamada[2], K. Ueno[3] and T. Kataoka[3]

[1]Department of Integrative Physiology, Graduate School of Biomedical and Health Sciences, Hiroshima University, Hiroshima, Japan, [2]Department of Health and Sports Medical Sciences, Graduate School of Biomedical and Health Sciences, Hiroshima University, Hiroshima, Japan and [3]Department of Health Care for Adults, Graduate School of Biomedical and Health Sciences, Hiroshima University, Hiroshima, Japan

We have recently shown that neurogenic vasodilatation in non-contracting and contracting vastus lateralis (VL) muscles is induced by descending signal from higher brain centres (termed central command) at the start of voluntary one-legged cycling and during motor imagery of the exercise (Ishii et al. 2012). The centrally-induced vasodilatation may be mediated by a sympathetic cholinergic mechanism as our laboratory reported previously using voluntary static exercise in conscious cats (Komine et al. 2008). On the other hand, as another possibility, central command may activate sympathetic adrenergic nerve, which in turn causes β-adrenergic vasodilatation in skeletal muscle. We examined which of the two vasodilator mechanisms contributes to the centrally-induced vasodilatation in both non-contracting and contracting VL muscles at the start of voluntary one-legged cycling with the right leg and during motor imagery of the cycling. The blood flow responses in the VL muscles during the two interventions were compared before and after intravenous injection of atropine sulfate (10 μg/kg) or propranolol (0.1 mg/kg). The relative concentrations of oxygenated- and deoxygenated-hemoglobin (Oxy- and Deoxy-Hb) in the bilateral VL muscles were measured with near-infrared spectroscopy as an index of muscle tissue blood flow in nine subjects. The Oxy-Hb increased by 3.5 ± 1.2% (mean ± S.E.M.) in the non-contracting VL muscle and by 3.1 ± 2.0% in the contracting VL muscle at the start of the one-legged cycling, although the Deoxy-Hb was unchanged throughout the cycling. The results suggested the increased in tissue blood flow to both contracting and non-contracting VL muscles. Atropine abolished the initial increases in the Oxy-

Hb of both non-contracting and contracting VL muscles. In contrast, propranolol did not affect the initial hyperaemia in both VL muscles but tended to reduce the Oxy-Hb responses during the later period of one-legged cycling, suggesting that the initial hyperaemia cannot be explained by β-adrenergic vasodilatation. Motor imagery of the right one-legged cycling caused increases in the Oxy-Hb of bilateral VL muscles (right VL: 2.4 ± 0.5%; left VL: 3.1 ± 0.6%) without changing the Deoxy-Hb. The centrally-induced increases in Oxy-Hb were abolished by atropine, but they were not affected by propranolol. Taken together, it is concluded that central command transmits cholinergic, but not β-adrenergic, vasodilator signals to both non-contracting and contracting skeletal muscle at the start of voluntary exercise and during motor imagery.

Ishii et al. (2012). J Appl Physiol 112, 1961-1974

Komine et al. (2008). Am J Physiol Regul Integr Comp Physiol 295, R1251-1262

Where applicable, the authors confirm that the experiments described here conform with The Physiological Society ethical requirements.

PCC271

Team sports are as effective as traditional aerobic exercise training at reducing risk factors associated with the development of type 2 diabetes mellitus

A.E. Mendham[1], R. Duffield[2], A.J. Coutts[2], F. Marino[1] and D.J. Bishop[3]

[1]School of Human Movement, Charles Sturt University, Bathurst, NSW, Australia, [2]Sport and Exercise Discipline Group, University of Technology Sydney, Sydney, NSW, Australia and [3]ISEAL, Victoria University, Melbourne, VIC, Australia

The majority of research on the benefits of physical activity to counter the occurrence of diabetes has employed continuous aerobic exercise, often performed at a low or moderate intensity. Recent research has identified intermittent exercise, as performed during team sports, as a promising alternative for those otherwise not inclined towards conventional aerobic exercise training, particularly given the associated greater enjoyment, motivation and social benefits. However, there is limited evidence for the efficacy of intermittent exercise for improving factors normally associated with the development of diabetes. In the present study, we investigated whether small-sided games (SSG) could be an effective alternative to traditional continuous exercise training. Thirty middle-aged, sedentary, men (48.6±6.6 y) were randomly assigned to a cycle ergometry (n=11), SSG (n=10), or control group (n=9). Participants in both exercise groups trained 3 d/wk for 8 wk, while control participants maintained normal activity and dietary patterns. All participants completed pre- and post-intervention testing, including: dual-energy x-ray absorptiometry scan, incremental exercise test, resting oral glucose tolerance test (OGTT) and a resting muscle biopsy. Plasma glucose and insulin concentrations were measured in a fasted state and throughout the 2 h OGTT. Total content of proteins associated with mitochondrial biogenesis, and glucose and insulin signaling, were analysed via western blotting. Two-way RM ANOVA with post hoc and effect sizes for difference between groups. Paired sample t-tests for within-group significance. Peak oxygen consumption improved by 19% in both exercise groups (P<0.05). In response to the OGTT, the control group exhibited no changes, while both the cycling and SSG groups showed a decline in the area under the curve (AUC) for glucose, and only SSG showed a decline in the AUC for insulin (P<0.05). There was a trend for an increase in PGC-1α (effect size (ES) ± confidence interval: 0.49±0.62), p53 (ES 0.47±0.55) and GLUT4 (ES 0.57±0.65) within the SSG group, and for mitochondrial complex I (P<0.05; ES 1.0±0.67) and IV (P<0.05; ES 1.1±0.77) within the cycling group. Participants in both exercise groups decreased total body fat mass (%) and intra-abdominal fat mass (kg; P<0.05). Collectively, SSG training in sedentary middle-aged populations was as effective as traditional cycle ergometry in reducing clinical risk factors normally associated with the development of diabetes. In addition, SSG training evoked skeletal muscle adaptations involving an increase in p53, PGC-1α and GLUT4 proteins, collectively important for mitochondrial biogenesis and glucose regulation. These changes show the potential relevance of intermittent exercise training via SSG as a chronic disease prevention strategy.

Where applicable, the authors confirm that the experiments described here conform with The Physiological Society ethical requirements.

PCC272

Pattern of skeletal muscle deoxygenation during incremental exercise is associated with cardiorrespiratory fitness in subjects with metabolic syndrome

A.D. Machado[1], A.K. Sales[1], A.F. Campos[1], T.C. Barbosa[1], L.C. Vianna[1], A.L. Nobrega[1] and B.M. Silva[1,2]

[1]Department of Physiology and Pharmacology, Fluminense Federal University, Niterói, RJ, Brazil and [2]Department of Physiology, São Paulo Federal University, São Paulo, SP, Brazil

Motivation. The pattern of skeletal muscle deoxygenated hemoglobin and myoglobin (deoxy [Hb + Mb]) during incremental exercise is typically fitted by a sigmoid model and is a proxy of microvascular fractional O_2 extraction. Given previous studies showing that metabolic syndrome subjects (MetS) have an altered vascular function, which possibly contributes to an imbalance between O_2 supply and O_2 demand during exercise, we tested the hypothesis that their sigmoidal increase in deoxy [Hb + Mb] would show a leftward shift when compared to healthy (H) controls, and that the deoxygenation pattern would be associated with cardiorespiratory fitness. **Methods.** Twenty subjects with MetS (4 women) and 14 H controls (7 women) were recruited. All subjects were submitted to a maximal cardiopulmonary exercise test performed on a cycle ergometer. In addition, a subgroup of twelve subjects with MetS (3 women) and nine H controls (6 women) were submitted to dual energy X-ray absorptiometry (DEXA). Cardiorespiratory fitness was evaluated by the oxygen consumption at the ventilatory threshold (VO_2VT) and the peak pulmonary oxygen consumption (VO_2peak), which were measured by a metabolic analyzer. Deoxy [Hb + Mb] was measured by near-infrared spectroscopy in the Vastus Lateralis muscle. This signal was normalized to the total response amplitude and expressed in relation to power output (PO) by a sigmoid function [$f(x)=f0+A/[1+e^{-(-c+dx)}]$], which generated the variable *c/d* (PO at 50% of deoxy [Hb + Mb] response). **Results.** There was no difference between groups' age (MetS: 37±7 vs. H: 33±9 years, mean±SD, p=0.15), test duration (MetS: 535±90 vs. H: 540±101 s, p=0.88), and absolute VO_2peak (MetS: 2.2±0.6 vs. H: 1.9±0.5 L/min, p=0.24). Within the subgroup, there was no difference in VO_2peak corrected for lean body mass (MetS: 38.3±5.7 vs. H: 42.2±5.6 ml/kg/min, p=0.13). The deoxygenation pattern was adequately fitted by the sigmoid

model (r≥0.95 for all cases). There was no difference for *c/d* between groups (MetS: 109±25 vs. H: 110±32 W, p=0.88), however there was a significant correlation between *c/d* and absolute VO_2VT and absolute VO_2peak in the whole sample (VO_2VT r=0.67, p<0.0001; VO_2peak r=0.69, p<0.0001), and within groups [(MetS VO_2VT r=0.68, p=0.001; VO_2peak r=0.69, p=0.001) (H VO_2VT r=0.74, p=0.002; VO_2peak r=0.76, p=0.001)]. Moreover, within the subgroup submitted to DEXA, we observed a significant correlation between *c/d* and VO_2peak corrected for lean body mass r=0.56, p=0.008 in the whole group, and within groups (MetS: r=0.52, p=0.08; H: r=0.67, p=0.049). **Conclusions.** The pattern of skeletal muscle deoxygenation was similar between groups, probably due to similar cardiorespiratory fitness, as the deoxygenation pattern was significantly associated with cardiorespiratory fitness.

Ghiadoni L *et al.* (2008). Hypertension 51:440-445

Ferreira LF *et al.* (2007). J Appl Physiol 103:1999-2004

Where applicable, the authors confirm that the experiments described here conform with The Physiological Society ethical requirements.

PCC273

Benefits of aerobic fitness on cerebrovascular reactivity to carbon dioxide

C.J. Marley[1], D. Hodson[1], J.V. Brugniaux[1], K.J. New[1], P.N. Ainslie[2], K. Evans[1] and D.M. Bailey[1]

[1]Department of Sport and Exercise, University of Glamorgan, Treforrest, UK and [2]School of Health and Exercise Sciences, University of British Columbia, Kelowna, BC, Canada

Background and aims: Impaired cerebrovascular reactivity to carbon dioxide (CVR_{CO2}) is an established risk factor for stroke (1) and has been linked with cognitive dysfunction (2). Preliminary evidence suggests that CVR_{CO2} may be improved through increases in physical activity (3; 4). However, data are scarce and cross-sectional studies are lacking.
Methods: Ten *untrained* (25 ± 5 years; 86 ± 12 kg; < 150 minutes of aerobic exercise per week; maximal oxygen consumption (VO_{2MAX}), 37 ± 5 $ml.kg^{-1}.min^{-1}$) and 10 *trained* (23 ± 4 years; 79 ± 10 kg; > 150 minutes of aerobic exercise per week; VO_{2MAX}, 57 ± 8 $ml.kg^{-1}.min^{-1}$) healthy males participated in the study. CVR_{CO2} was assessed in response to a 3-minute exposure to hypercapnea (5% CO_2). Blood flow velocity in the middle cerebral artery (transcranial Doppler) and end-tidal CO_2 (capnography) were continuously recorded throughout the procedure as described previously (5). VO_{2MAX} was assessed via an incremental exercise test to volitional exhaustion (semi-recumbent cycle ergometer) and online expiratory gas exchange. Following confirmation of distribution of normality (Shapiro-*W*-Wilk Tests), CVR_{CO2} and VO_{2MAX} data were analysed using independent samples *t*-tests. The relationship between VO_{2MAX} and CVR_{CO2} was examined using a Pearson Product Moment correlation. Significance was established at $P < 0.05$ and data are expressed as mean ± SD.
Results: By design, the *trained* participants recorded a higher VO_{2MAX} ($P < 0.05$). The *trained* were able to elicit a greater CVR_{CO2} compared to their *untrained* counterparts (3.64 ± 1.1 *vs.* 1.87 ± 0.8 %/mmHg; $P < 0.05$) during the hypercapnic challenge (Figure 1). Figure 2 illustrates the positive correlation between VO_{2MAX} and CVR_{CO2} (r = 0.79; $P < 0.05$).
Conclusion: These findings highlight the cerebrovascular benefits of regular physical activity, which may act as a potential preventative mechanism against cerebrovascular diseases in later life.

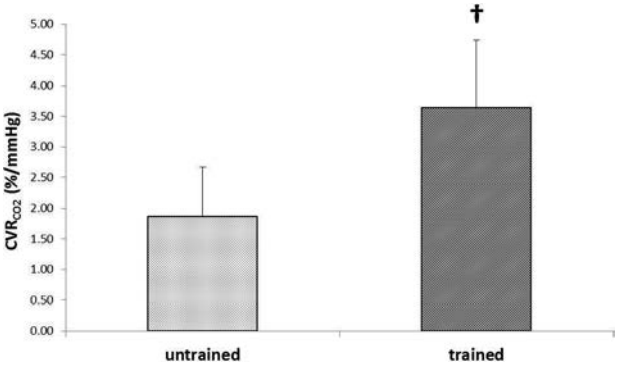

Figure 1: Differences in CVR_{CO2} between cohorts.

Values are mean ± SD; † $P < 0.05$ *vs. untrained*.

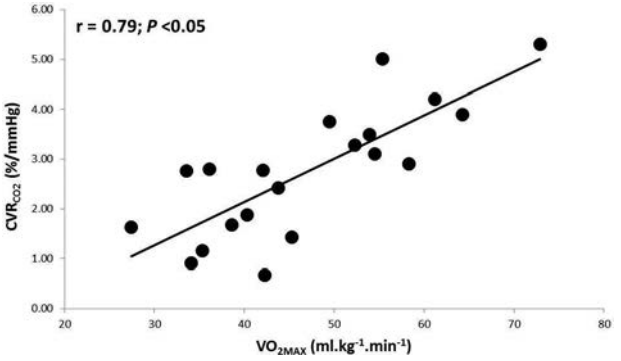

Figure 2: The relationship between aerobic fitness (VO_{2MAX}) and CVR_{CO2}.

(1) Markus and Cullinane (2001) *Brain*; **124**, 457-467.

(2) Novak (2012) *Current Cardiovascular Risk Reports*; **6**, 380-396.

(3) Murrell *et al.* (2012) *Age (Dordr)*.

(4) Ivey *et al.* (2011) *Stroke*; **42**, 1994-2000.

(5) Bailey *et al.* (2013) *Clin Sci (London)*; **124**, 177-189.

The present research was supported by the JPR Williams Trust, in co-ordination with the University of Glamorgan.

Where applicable, the authors confirm that the experiments described here conform with The Physiological Society ethical requirements.

PCC274

Four legs good, two legs bad: Visual and tactile mechanisms underlying interpersonal control of postural sway

R. Reynolds, P. Watts and C.J. Osler

Sport & Exercise Sciences, University of Birmingham, Birmingham, UK

Fingertip contact with another person reduces sway(1). However, this represents a complex control loop, with both persons relying on a moving reference point. Here we attempt to understand this control loop with a combination of experiment and modelling. We also determine whether vision of another person drives sway, and if this interacts with touch. We studied 8 pairs of subjects standing next to each other on separate forceplates. We included 3 conditions of touch (no contact(NC), light touch(LT), shoulder contact (SC)) and 3 visual conditions (both eyes closed, both eyes open, asymmetric). Centre of pressure velocity (COPv) was the measure

of sway. Magnitude and timing of sway coupling was quantified by the COPv-COPv cross-correlation function (XCORR). Data was compared with a Simulink model(2) consisting of a two inverted pendulums and PID controllers coupled together. Physical contact (LT & SC) reduced sway, with a greater effect for shoulder contact (Fig 1A; F=193,21;p<0.01). Vision also reduced sway but less so with increasing tactile contact (p<0.01). When only light touch was available, XCORR's exhibited twin peaks at ~500 and -500ms (Fig 1B). Vision alone produced strikingly similar XCORR's. However, the effect of touch and vision did not summate with both available. During asymmetric vision, XCORR's showed only 1 peak at positive lag. In contrast to light touch, shoulder contact produced XCORR's with a single peak at ~0ms lag irrespective of visual condition. We modelled the interaction in simulink as follows. Firstly, we coupled both sensory feedback loops to each other, such that each (model) person's feedback error was summed with 20% of their partner's. This recreated the XCORR shape and timing observed during both visual and light touch conditions (Fig 1C). Secondly, we coupled the torque output, such that 20% of one person's ankle torque summed with the other (while maintaining the sensory coupling). This recreated the XCORR seen during shoulder contact.

Firstly we conclude that tactile sway coupling is a continuous bidirectional sensorimotor process with a delay in each direction of ~500ms. It is unnecessary to invoke 'switching' mechanisms to explain the interaction, whereby a sway leader and follower periodically swap roles; a continuous control model was sufficient to recreate the XCORR characteristics. Unlike light touch, effects of shoulder contact were explained by mechanical linkage. Secondly, we have shown that vision of another person produces sway coupling near identical to touch. This is despite only peripheral vision of one's partner, and abundant veridical feedback from the laboratory. The observation that the effects of touch and vision did not summate suggest sensory redundancy. Paradoxically, the visual coupling demonstrates that sometimes the partner with eyes closed lead the sighted partner.

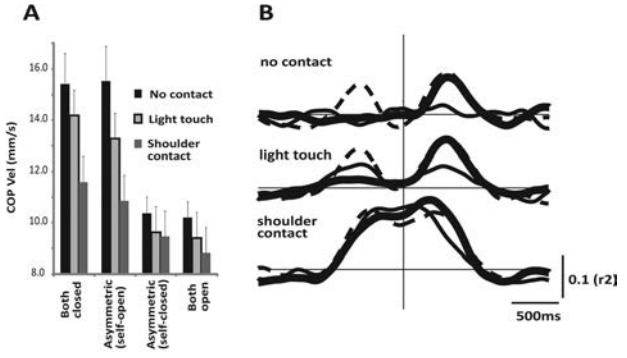

Figure 1 - Interpersonal sway
A shows mean sway; B shows mean XCORRS and C shows model XCORRS

1. Johannsen L, Wing AM, Hatzitaki V Contrasting effects of finger and shoulder interpersonal light touch on standing balance. J Neurophysiol 2012; 107: 216-225

2. Peterka RJ Postural control model interpretation of stabilogram diffusion analysis. Biol Cybern 2000; 82: 335-343

Where applicable, the authors confirm that the experiments described here conform with The Physiological Society ethical requirements.

PCC275

Biochemical changes in patients before and after the different types of premedications

R. Rokyta[1], J. Fricova[2], M. Vejrazka[3] and P. Stopka[4]

[1]Normal, Pathological and Clibical Physiology, Charles University, 3 rd Faculty of Medicine, Prague, Czech Republic, [2]Anesthesiology, Resuscitation and Intensive Care, Pain Management, Charles University, First Faculty of Medicine, General University Hospital, Prague, Czech Republic, [3]Biochemistry and Toxicology, Charles University, First Faculty of Medicine,, Prague, Czech Republic and [4]Inorganic Chemistry, Academy of Scinces of the Czech Republic, Prague, Czech Republic

Introduction

The aim of our study was to assess the changes of free radicals and other biochemical parameters after nociceptive stimulation in patients. We detected whether preemptive analgesia had a positive effect on acute postoperative pain.

Patients and methods:diagnosis: hernia inquinalis,operation:herniotomia,group of patients (n=63), men (n=50), women (n=13),timing of the investigations from blood samples: immediatelly before operation,4 hours after operation,24 hours after operation. Patients were divided into three groups: without premedication, the premedication with pethidin,the premedication with morphine .We measured biochemical parametres: proteins, albumins, prealbumins, apolipoproteins A, B, CRP, glucose, lipids (LDL, HDL, total cholesterol, triacylglycerols) and uric acid.

Results

We found out that nitroxid and hydroxyl free radicals and singlet oxygen increased significantly after nociceptive stimulation. In particular, we measured the free hydroxyl radicals and singlet oxygen by EPR method. Our goal was to find the most effective combination for the effective analgesic treatment of acute postoperative pain. Free radicals increased in individual samples during the postoperative course in pethidine and without premedication. After application of morphine the free radicals were insignificantly reduced,especially in the third sampling. The increase in measured values of free radicals is statistically significant in patients without premedication.Beside finding an optimal preemptive and postoperative analgesia, we tried to understand the mechanisms of postoperative pain and oxidative stress. We were able to objectify the biochemical changes in acute postoperative pain on the basis of postoperative stress. This method is absolutely a priority and has never been used before. Earlier experimental results were partially clinically verified using different types of acute and chronic pain in humans. In all these pain syndromes are different biochemical changes.

Our next goal was to find the most effective combination for the effective analgesic treatment of acute postoperative pain.

Conclusions

We studied postoperative analgesia and the effects of various types of analgetics, including preoperative and postoperative medication and its objective evaluation. We focused on an objective assessment of pain using different biochemical parameters, especially the free radicals that are significantly changed during acute pain. It was shown that morphine is the best indication in preemptive analgesia prior to surgery with an expected moderate pain. Morphine in comparison with Pethidine and the group without premedication only significantly reduced levels of free radicals 24 hours after surgery. We tried to explain the relationship of postoperative pain and oxidative stress.

The abstract was supported by Research Goal MSM0021620816 and PRVOUK P 34

Where applicable, the authors confirm that the experiments described here conform with The Physiological Society ethical requirements.

PCC276

The role played by Nav1.8 channels in the somatic pressor chemoreflex

A.J. Stone, J. Kim and M.P. Kaufman

Heart and Vascular Institute, Penn State University College of Medicine, Hershey, PA, USA

Thin fiber muscle afferents (Aδ and C) are supplied by NaV 1.8 channels, whereas thick fiber afferents (spindles and tendon organs) are not. We determined the role played by NaV 1.8 channels on the thin fiber afferents evoking the reflex pressor response to femoral arterial injections of lactic acid (24mM; ~0.1mL) and capsaicin (0.1ug) in decerebrated Sprague Dawley rats with either patent or ligated femoral arteries. This was done both before and after femoral arterial injection of the A803467 (500μg, 1mg, and 2mg), a NaV 1.8 antagonist. We also recorded the responses of spindle afferents to succinylcholine (200μg) and stretch before and after injecting A803467. Rats were anesthetized with 2% isoflurane and 100% O2 until decerebration. In "freely perfused" rats (n=6), 1 mg of A803467 significantly reduced the pressor responses to lactic acid (16±5 to 4±4ΔmmHg) and capsaicin (47±7 to 26±8ΔmmHg). In "ligated" rats, 1 mg of A803467 significantly reduced the pressor response to lactic acid (32±13 to 3±3ΔmmHg, n=6), whereas 2 mg of A803467 was required to significantly reduce the pressor response to capsaicin (66±11 to 37±17ΔmmHg, n=4). Surprisingly, we found that A803467 (1mg) reduced the responses of 10 spindle afferents to succinylcholine (34±11 to 4±3 Δ imp/s p=0.04) and stretch (83±17 to 0.4±1 Δ imp/s; p<0.01). We conclude that A803467 reduces the chemoreflex response to lactic acid and capsaicin; however, it may be working on channels other than NaV 1.8 such as voltage-gated calcium channels.

Where applicable, the authors confirm that the experiments described here conform with The Physiological Society ethical requirements.

PCC277

Thirst perception and water intake in older males following exercise

V.U. Igbokwe[1] and L.F. Obika[2]

[1]Department of Physiology, Usmanu Danfodiyo University, Sokoto, Nigeria and [2]Department of Physiology, University of Benin, Benin City, EDo State, Nigeria

The oropharyngeal satiety mechanism of thirst in the elderly is a subject not resolved. However, since other oropharyngeal senses such as taste changes with age, it may be that oropharyngeal satiety mechanism of thirst is also diminished with age. This however remains to be proven experimentally. This work therefore investigates thirst perception (TP) and water intake in young males (n = 10, age = 19 – 25 years) and older males (n = 9, age = 44 – 58 years). All the subjects live a normal active life, that is they go about their daily business or work but none of them, was athletically trained as "defined by the absence of a regular exercise programme during the last six months before the experiment" (Kokkinos et al, 1995). Thirst perception (TP) and dryness of mouth (DM) before exercise were obtained using the visual analogue scale (Takamata et al, 1994). Thereafter subjects performed exercise at 30kmh-1 till exhaustion at a workload of 0.5kgm on a bicycle ergometer. After exercise TP, DM and water intake were assessed. Subjects did not drink any water during the exercise but were given clean tap water ad libitum at 16OC to drink at the end of the exercise (Boulze, et al, 1983). The results are presented as mean ± standard error of mean. The paired and unpaired student t-test was used to compare the difference between the means within a group and between the group means respectively. The basal TP and DM in the older males were 1.08 ± 0.40cm and 0.6 ± 0.29cm respectively, and that of the young males were 1.46 ± 0.47cm and 1.63 ± 0.55cm respectively. There was no significant difference in the basal TP and DM between the young and older male subjects. After exercise the changes in TP and DM in the young males (3.75 ± 0.93 and 3.23 ± 0.92) and in the older males (1.26 ± 0.57 and 1.48 ± 0.76) did not show any significant difference. However the time spent on exercise (43.2 ± 3.53mins for young males and 9.6 ± 1.28min for older males) and the water intake after exercise (405 ± 47.29ml and 160 ± 70.0ml for the young and older males respectively) were different (p<0.05).
It is concluded therefore that thirst following dehydration in older males is similar to that of young males. The difference in fluid intake between the young and older males might be due to the time spent on exercise. Thirst perception might not show a decrease with increase in age as does taste.

Boulze, D., Montastruc P., Cabanac M. (1983): Water intake, pleasure and water temperature in humans. Physiological Behaviours 30:97-102

Kokkinos, P.F., Narayan P., Colleran J.A., Pittaras A., Notargiamo A. (1995): Effects of regular exercise on blood pressure and left ventricular hypertrophy in African-American men with severe hypertension. New England Journal of Medicine 333:1462 – 1467

Takamata, A., Mack G.W., Gillen C.M., and Nadel E.R. (1994): Sodium appetite, thirst and body fluid regulation in humans during rehydration without sodium replacement. American Journal of Physiology 266 (35):R1493 – R1502

Will like to acknowledge the Usmanu Danfodiyo University Sokoto for the research grant to carry out this study

Where applicable, the authors confirm that the experiments described here conform with The Physiological Society ethical requirements.

PCC278

Plasma amino acid profile, redox state and nitric oxide synthesis in red blood cells from girls with anorexia nervosa

N.R. Pereira[2], T. Brunini[2], M.A. Siqueira[2], M. Moss[1], C. Assumpção[2] and A. Mendes-Ribeiro[2,1]

[1]Departamento de Ciências Fisiológicas, Universidade Federal do Estado do Rio de Janeiro, Rio de Janeiro, Brazil and [2]Departamento de Farmacologia e Psicobiologia, Universidade do Estado do Rio de Janeiro, Rio de Janeiro, UK

Background: Anorexia nervosa is a debilitating eating disorder with profound biological and psychological consequences. Recent evidence implicates nitric oxide abnormalities in the pathogenesis of anorexia nervosa. Objective: To investigate nitric oxide bioavailability in red blood cells from adolescents with anorexia nervosa and its association with the arginase

pathway, redox state and systemic amino acid profile. Methodology: A case-control study of plasma amino acid levels, nitric oxide synthase and arginase activities, and oxidative stress markers (lipid peroxidation, protein oxidation, reactive oxygen species production and superoxide dismutase activity) in red blood cells from volunteer adolescents with anorexia nervosa (n=10) recruited at the Center for Studies on Adolescent Health - State University of Rio de Janeiro, and healthy controls (n=10), age-matched. The Ethical Committee of the State University of Rio de Janeiro approved this work (CEP -1485), and informed consent was obtained from each of the patients. The student t test was used for statistical analysis and statistic difference was considered when $p<0.05$. Results: Nitric oxide synthase activity was impaired in red blood cells (controls: 8.22 ± 1.45 vs patients: 3.88 ± 0.46 pmol/108 cells/min) in the presence of increased arginase activity in anorexia nervosa (controls: 0.02 ± 0.01 vs patients: 0.09 ± 0.03 pmol urea/mg protein/2h). Asymmetric dimethylarginine, an endogenous inhibitor of nitric oxide synthase, was not affected, whereas L-lysine (controls: 160 ± 10 vs patients: 130 ± 7 μM/L) and L-ornithine (controls: 93 ± 9 vs patients: 64 ± 6 μM/L) were reduced in plasma from patients with anorexia nervosa compared to controls. No oxidative damage or increased reactive oxygen species production was observed in anorexia nervosa. On the other hand, diminished anti-oxidant protection by superoxide dismutase was present in red blood cells from patients with anorexia nervosa (controls: 15260 ± 2803 vs patients: 4791 ± 678.4 U of SOD/g of haemoglobin). Conclusions: Our findings provide the first evidence of reduced nitric oxide synthesis associated with diminished antioxidant defence and arginase activation in red blood cells, which may contribute to impaired vascular nitric oxide bioavailability in anorexia nervosa.

Financial support: FAPERJ and CNPq

Where applicable, the authors confirm that the experiments described here conform with The Physiological Society ethical requirements.

PCC279

The influenses of hand work and stand up on the function of autonomic nervous system during menstrual cycle in healthy female college students

Y. Itoi[1], M. Onozaki[1], T. Shimizu[2] and T. Okada[3]

[1]International University of Health and Welfare, Otawara, Japan, [2]Toin University of Yokohama, Yokohama, Japan and [3]Juntendo University Graduate School of Medicine, Bnkyouku, Japan

Purpose: The purpose of this study was to examine the correlation between functional modulation of the autonomic nervous system and the menstrual cycle.Methods: Subjects were comprised of 11 healthy female college students (19.5±0.5 years old) with regular menstrual cycles. The changes in emotional sweating induced by hand work (beans work and puzzle) and the modulation in autonomic nervous system(electrocardiograph and heartbeat) with active orthostatic load were compared among the follicular, luteal and menstrual phases. The Japanese version of the Profile of Mood State (POMS), healthy life habit (DIHAL.,2,junior high school student~adult) were also examined. Analysis: Effect size of the difference between group or correlation were evaluated. Results:Emotionalsweating(task is beans work) during the menstrual phase was significantly higher than those during follicular and luteal phases and it associated with the high score of "depression dejection" of POMS factors. Group with the highest T score (standardized score) of "depression dejection" emotional sweating was significantly higher during luteal phase. In addition, the group which complained subjective low healthy state, showed higher emotional sweating (beans work) during luteal phase.Fluctuations of heart rate at rest(the size of the activity),during menstrual phase was significantly higher than those during follicular phase, although it was a normal range.The balance of the autonomic nervous activity at rest (balance) was significantly higher during luteal phase compared to menstrual phase, indicating predominance of sympathetic nervous system. Active orthostatic load-induced fluctuations of heart beat(powers of the response)was significantly higher during follicular phase compared to those during menstrual and luteal phase, although it was a normal range. Fluctuations of balance of the active orthostatic load (powers of the change) was significantly higher during menstrual phase than that during follicular phase; the range which need special medical attention. In addition, there found an association between balance and "confusion". Group with the highest T score of "confusion" factors, showed predominant sympathetic nervous system during menstrual phase.Conclusion:These findings suggest that Stresses of beans work may influence the function of the autonomic nervous system to during menstrual phase . In addition, these findings suggest that powers of the change was higher during menstrual phase, the range which need special medical attention. Students with the high T score of "confusion" factors, showed the balance is sympathetic nerve predominance during menstrual phase.

Where applicable, the authors confirm that the experiments described here conform with The Physiological Society ethical requirements.

PCC281

Fixed dose combinations of bromocriptine, glibenclamide and metformin improve insulin resistance in hyperglycaemic rats

A.A. Adeneye[1] and J.A. Olagunju[2]

[1]Department of Pharmacology, Lagos State University College of Medicine, Ikeja, Lagos State, Nigeria and [2]Department of Medical Biochemsitry, Lagos State University College of Medicine, Ikeja, Lagos State, Nigeria

Background: In recent years, attention has been drawn to the therapeutic usefulness of bromocriptine in the effective management of insulin resistance diabetes mellitus. Materials and Methods: The present study evaluates the effects of the oral treatments with 10 mg/kg bromocriptine in fixed combinations with 1 mg/kg glibenclamide, 20 mg/kg metformin and glibenclamide/metformin combination on body weight, blood glucose, lipids and cardiovascular risk profile in dexamethasone-induced hyperglycemic male Wistar rats for 30 days. The effects of these drug combinations on OGTT of the treated rats were also evaluated. Results: Repeated daily dexamethasone injection for 30 days caused significant increases in the average body weight, blood glucose, triglycerides, total cholesterol, LDL-c, VLDL-c and cardiovascular risk indices in the treated male Albino Wistar rats. However, these increases were significantly attenuated in rats orally pretreated with bromocriptine and its various combinations. In addition, bromocriptine and its combinations significantly improved OGTT in the treated rats. Conclusions: Overall, results of this study suggest that the antihyperglycaemic, antihyperlipidaemic and cardio-

protective effects of the fixed-dose drug combinations were possibly mediated via improved glucose tolerance mechanism.

Table 2: Effects of bromocriptine, glibenclamide and metformin combinations on serum lipids and cardiovascular risk indices

Groups	TG (mg/dl)	TC (mg/dl)	HDL-c (mg/dl)	LDL-c (mg/dl)	VLDL-c (mg/dl)	AI	CRI
I	94.83 ± 6.83	86.33 ± 4.56	45.83 ± 3.50	21.53 ± 1.80	18.97 ± 1.37	0.46 ± 0.04	1.89 ± 0.06
II	162.00 ± 16.00b	147.33 ± 15.33b	29.17 ± 6.56f	85.77 ± 6.30b	32.40 ± 3.20b	3.09 ± 0.43b	5.25 ± 0.56b
III	110.17 ± 6.89c	103.33 ± 7.67c	55.00 ± 5.33h	26.30 ± 1.20d	22.03 ± 1.38d	0.48 ± 0.02d	1.89 ± 0.05d
IV	101.00 ± 5.00c	91.17 ± 5.83d	52.50 ± 4.17h	18.47 ± 3.78e	19.70 ± 1.33d	0.36 ± 0.09d	1.73 ± 0.10d
V	86.83 ± 6.78d	80.17 ± 7.22e	49.17 ± 4.50h	13.67 ± 4.49e	17.33 ± 1.38d	0.29 ± 0.1e	1.64 ± 0.12e
VI	73.17 ± 12.17e	64.00 ± 12.00e	42.50 ± 9.17g	6.87 ± 1.87e	14.63 ± 2.43e	0.17 ± 0.05e	1.52 ± 0.08e

a and b represent significant increases at p<0.05 and p<0.001 respectively when compared to Group I values while c, d and e represent significant decreases at p<0.05, p<0.01 and p<0.001 when compared with Group II values. f represents a significant decrease at p<0.001 when compared to Group I values while g and h represent significant increases at p<0.05 and p<0.001 respectively, when compared to Group II values.

Group I: 10 ml/kg of 0.9% normal saline per oral + 1 ml/kg of 0.9% normal saline subc.

Group II: 10 ml/kg of 0.9% normal saline per oral + 10 mg/kg dexamethasone subc.

Group III: 10 mg/kg of bromocriptine per os + 10 mg/kg dexamethasone subc.

Group IV: 1 mg/kg of glibenclamide per os + 10 mg/kg of bromocriptine per os + 10 mg/kg dexamethasone subc.

Group V: 20 mg/kg of metformin per os + 10 mg/kg of bromocriptine per os + 10 mg/kg dexamethasone subc.

Group VI: 1 mg/kg of glibenclamide per os + 20 mg/kg of metformin per os + 10 mg/kg of bromocriptine per os + 10 mg/kg dexamethasone subc.

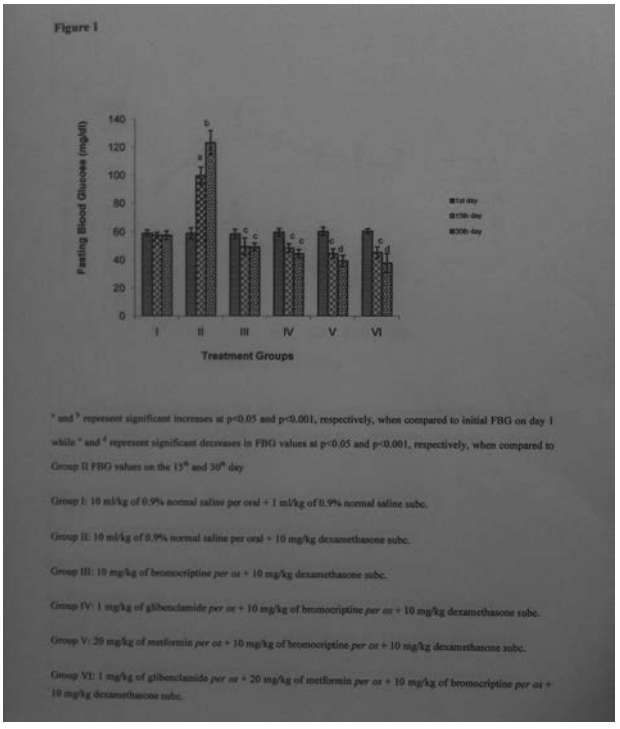

Figure 1: Effects of oral treatments with the fixed dose combinations of bromocriptine, glibenclamide, metformin on the fasting blood glucose levels in dexamethasone-induced insulin resistant rats

Cincotta, A.H., B.C. Schiller and A.H. Meier, 1991. Bromocriptine inhibits the seasonally

occuring obesity, hyperinsulinaemia, insulin resistance, and impaired glucose tolerance in Syrian hamster, Mesocricetus auratus. Metabolism, 40: 639-644.

DeFronzo, R.A., 2011. Bromocriptine: A sympatholytic, D2-dopamine agonist for the treatment of type 2 diabetes. Diabetes Care, 34(4): 789-794.

de Leeuw van Weenen, J.E., E.T. Parlevliet, P. Maechler, L.M. Havekes, J.A. Romijn, D.M. Ouwens, H. Pijl and B. Guigas, 2010. The dopamine receptor D2 agonist bromocriptine inhibits glucose-stimulated insulin secretion by direct activation of the α2-adrenergic receptors in beta cells. Biochemical Pharmacology, 79(12): 1827-1836.

Kerr, L., E.M. Timpe and K.A. Petkewicz, 2010. Bromocriptine mesylate for glycaemic management in type 2 diabetes mellitus. Annals of Pharmacotherapy, 44(11): 1777-1785.

Where applicable, the authors confirm that the experiments described here conform with The Physiological Society ethical requirements.

PCC283

Nicotine alters male reproductive hormones in male albino rats

I.P. Oyeyipo[1,2], Y. Raji[2] and A.F. Bolarinwa[2]

[1]Physiology, Osun State University, Osun, Osun State, Nigeria and [2]Physiology, University of Ibadan, Ibadan, Oyo State, Nigeria

The use of nicotine through smoking remains a serious health problem. It has been associated with reduced fertility (Oyeyipo et al, 2011), although the mechanism responsible is still unclear. The present study was designed to investigate the effects of nicotine administration on male reproductive hormones in male albino rats. Forty male rats weighing between 200-230g (8-10 weeks) were divided equally into five groups and treated orally for thirty days. Group I, which served as the control received 0.2ml / kg normal saline, Group II and III received 0.5mg/kg (low dose) and 1.0mg/kg (High dose) body weight of nicotine respectively. The fourth and fifth groups were gavaged with 0.5mg/kg and 1.0mg/kg body weight of nicotine but were left untreated for another 30 days. These groups served as the recovery groups. At the end of the experimental period, animals were anaesthetized with 1.9% ether and blood was collected through cardiac puncture. Serum was analysed for testosterone, luteinizing hormone (LH), follicle stimulating hormones (FSH) and prolactin using radioimmunoassay. Values were expressed as mean ± S.E.M compared by ANOVA. Results showed that nicotine administration significantly decreased ($p<0.05$) testosterone in the low and high treated groups (3.46 ±0.16 ng /ml; 2.16 ± 0.18 ng /ml) and FSH (0.97 ±0.06 mIU/ml) in the high dose treated group when compared with the control group (4.94 ± 0.18; 2.01 ± 0.14) respectively. There was a significant increase ($p<0.05$) in mean LH (3.49 ± 0.20 mIU/ml) and mean prolactin level (8.10 ±0.32 IU/ml) in the high dose treated group when compared with the control (1.68 ±0.08 mIU/ml; 4.23 ± 0.26 mIU/ml) respectively. However, the values of the recovery groups were comparable with the control. Thus, these findings suggest that nicotine administration is associated with distorted reproductive hormones in male rats although ameliorated by nicotine cessation. It is plausible that the decreased testosterone level is associated with testicular dysfunction rather than a pituitary disorder.

I.P. Oyeyipo, Y. Raji, B.O. Emikpe and Adeyombo F. Bolarinwa (2011): Effect of nicotine on sperm characteristics and fertility profile in adult male rats: a possible role of cessation. J Reprod Infertil. 12(3):201-207

Where applicable, the authors confirm that the experiments described here conform with The Physiological Society ethical requirements.

PCC285

Coffee attenuates induction of insulin resistance by high sucrose-diet in rats

A. Morakinyo, D.A. Adekunbi and O.A. Adegoke

Physiology, University of Lagos, Lagos, Nigeria

Numerous epidemiology reports suggested that consumption of coffee is associated with lower risk of diabetes mellitus (Natella & Scaccini, 2012). These epidemiological observations have not been evaluated experimentally. The present study therefore employs an animal model to examine the relationship between intake of coffee and risk of type 2 diabetes mellitus (in this case, insulin resistance). In the study, high-sucrose feeding (30% w/v) was used to induce insulin resistance (Riberio et al, 2005). Sprague-Dawley rats (male, 120-150g) were maintained for 12 weeks on a normal diet (ND, n=6), normal diet supplemented with coffee (ND+COF, 300 mg/kg BW, n=6), high sucrose-diet (HSD, n=6) and high sucrose-diet supplemented with coffee (HSD+COF, n=6). Glucose tolerance and insulin resistance were measured by performing the oral glucose tolerance test (OGTT) and insulin tolerance test (ITT) respectively; and for both tests, the area under curve (AUC) was determined. The serum insulin was estimated using ELISA while an automatic blood chemical analyzer was employed for the measurement of total cholesterol (TC), triglycerides (TG), high-density lipoprotein (HDL) and low-density lipoprotein (LDL). Malondialdehyde (MDA), glutathione reduced (GSH) and superoxide dismutase (SOD) were measured using previously described standard methods. Data were expressed as mean±SEM, compared by ANOVA. HSD rats showed reduced glucose tolerance (AUC: 2016.8±119.2 vs. 1017.5±59.9, $p<0.05$) and insulin sensitivity (AUC: 535.88±36.41 vs. 414.5±29.08, $p<0.05$) when compared with ND rats but intragastric administration of coffee prevented these metabolic abnormalities in HSD+COF (AUCOGTT: 1132.3±64.5; AUCITT: 388.75±26.27). In addition, insulin concentration was markedly increased in HSD rats compared with ND rats (12.25±0.51 vs. 7.69±0.22, $p<0.05$), but was suppressed in HSD+COF rat treated with coffee (9.21±0.66, $p<0.05$). Whereas compared with the HSD rats, the levels of TG and LDL (0.44±0.06 vs. 1.43±0.32; 0.75±0.03 vs. 0.91±0.06 respectively, $p<0.05$) decreased; HDL (1.10±0.06 vs. 0.69±0.02, $p<0.05$) increased significantly in HSD+COF rats. Additionally, MDA level was reduced (21.4±2.36 vs. 37.4±3.59, $p<0.05$), GSH (0.53±0.03 vs. 0.24±0.01, $p<0.05$) and SOD (4.38±0.47 vs. 1.63±0.01, $p<0.05$) activities were increased in HSD+COF when compared with HSD rats. Collectively, our data indicate that coffee consumption confers protection against the risk of contracting non-insulin dependent diabetes in rats and lends support to the idea that coffee consumption is associated with a lower risk of type 2 diabetes. Understanding some aspect of the relationship between coffee and diabetes is a desirable step in the context of healthy eating habits and disease control.

Natella F & Scaccini C (2012). Nutr Rev 70: 207-217.

Ribeiro RT et al. (2005). Diabetologia 48: 976-983.

Where applicable, the authors confirm that the experiments described here conform with The Physiological Society ethical requirements.

PCC286

Mercury chloride-induced glucose intolerance in rats: role of oxidative stress

A.O. Morakinyo, B.O. Iranloye, G.O. Oludare, J.O. Oyedele and O.O. Ayeni

Physiology, University of Lagos, Lagos, Lagos State, Nigeria

Although mercury is recognized as a hazardous chemical, its commercial importance and applications has led to an increase in occupational and environmental exposures in many parts of the world. This study evaluated the impact of HgCl2 on glucose homeostasis and the possible involvement of oxidative stress. In addition, the potential protective effects of the antioxidant Alpha Lipoic Acid (ALA) were investigated. Thirty Sprague Dawley rats were divided into five equal groups of six animals: Group 1 (control) received 0.5 ml distilled water; Group 2 (ALA) received 100 μg/kg of ALA; Group 3 (LDM) and Group 4 (HDM) received 250 and 500 μg/kg body weight of HgCl2, respectively; and Group 5 (HDM-ALA) received 500 μg/kg of HgCl2 and 100 μg/kg of ALA. Both HgCl2 and ALA were administered orally for 14 days. Fasting blood glucose was measured and all groups were subjected to Oral Glucose Tolerance Test (OGTT) using One-Touch Ultra Easy Glucose Meter, Lifescan, U.K. The activities of reduced glutathione (reaction of Ellman's reagent to the thiol group of GSH), superoxide dismutase (auto oxidation of epinephrine), catalase (measuring the exponential disappearance of H2O2) as well as the level of lipid peroxidation (indexed by MDA as the presence of thiobarbituric acid reactive substances) were estimated. Values are means ± SEM, compared by one way ANOVA. The fasting blood glucose (mmol/L) for Control, ALA, LDM, HDM and HDM-ALA were as follows; 4.02 ± 0.35, 4.6 ± 0.26, 7.23 ± 0.48, 8.03 ± 0.64 and 4.45 ± 0.41 respectively. After thirty minutes of glucose load (2ug/kg body weight) blood glucose levels were 6.62 ± 0.85, 7.22 ± 0.64, 9.43 ± 1.07, 9.43 ± 1.05 and 7.03 ± 0.52 in the Control, ALA, LDM, HDM and HDM-ALA respectively. Subsequent values were obtained every 30 minutes and after 3 hours, the blood glucose values were 2.32 ± 0.43, 4.26 ± 0.23, 7.29 ± 0.29, 8.28 ± 0.33 and 3.97 ± 0.21 in the Control, ALA, LDM, HDM and HDM-ALA respectively. The results on MDA in the Control, ALA, LDM, HDM and HDM-ALA groups are; 0.0318 ± 0.005, 0.0242 ± 0.004, 0.069 ± 0.004, 0.104 ± 0.011 and 0.045 ± 0.006 respectively. Superoxide dismutase activity was; 46.74 ± 4.85, 43.16 ± 3.68, 24.42 ± 3.17, 19.62 ± 2.51, 35.32 ± 3.38. Reduced glutathione values were; 0.31 ± 0.04, 0.32 ± 0.04, 0.15 ± 0.02, 0.13 ± 0.03, 0.21 ± 0.02 and catalase activity were; 224.60 ± 15.03, 230.98 ± 14.98, 155.11 ± 17.63, 139.38 ± 16.44, 162.94 ± 15.62 in the Control, ALA, LDM, HDM and HDM-ALA respectively (values are in units/mg protein). The results showed changes in glucose tolerance and oxidative indices in rats exposed to HgCl2. However, treatment with ALA attenuated all HgCl2 triggered changes. This study shows the induction of glucose intolerance by HgCl2 and suggests the involvement of oxidative stress as an important regulator of glucose homeostasis during HgCl2 exposure.

Barnes and Kircher (2005). Toxicol. Vitro, 19: 207-214.

Järup, L, (2003). Br. Med. Bull., 68: 167-182.

Where applicable, the authors confirm that the experiments described here conform with The Physiological Society ethical requirements.

PCC287

Metabolic disorders and oxidative stress in type 1 diabetes mellitus; role of testosterone

A.O. Morakinyo, D.A. Adekunbi and O.A. Adegoke

Physiology, University of Lagos, Lagos, Nigeria

A bidirectional relationship has been established between testosterone deficiency (TD) and type 2 diabetes mellitus (T2DM). Low testosterone level has been reported to be a predisposing factor to T2DM (Selvin et al., 2007), while recent clinical studies have shown a high prevalence of low testosterone in diabetic individuals (Dhindsa et al., 2004). However, it is not known if any relationship exists between type 1 diabetes mellitus (T1DM) and testosterone level. This study was designed to investigate the effects of TD on T1DM. Sprague-Dawley rats (male, 140-160g) were randomly divided into four groups designated as control, diabetic, orchiectomized and orchiectomized-diabetic. Diabetes was induced with alloxan (100mg/Kg BW i.m.) and orchiectomy was performed under aseptic surgical conditions. Rats were anesthetized with Ketamine (90mg/kg BW) and Xylazine (10mg/kg BW) intramuscularly, for bilateral removal of the testes. After 3 weeks, glucose tolerance was assessed by oral glucosee tolerance test (OGTT) where each rat received an oral glucose of 2g/kg BW and blood sample drawn from tail vein afterwards at intervals of 30, 60, 120 and 180 min for measurement of glucose level. The area under the glucose (AUC glucose) was calculated using the trapezoidal rule. Serum insulin was analysed using ELISA system and lipid parameters were analysed enzymatically with kit obtained from Randox, UK. Oxidative analyses of the liver homogenate were carried out using previously described standard methods (Morakinyo et al., 2011). Values are means ± S.E.M., compared by ANOVA. The results shows that baseline glucose values in the orchiectomized-diabetic group was lower (217.5±18.81mg/dl $P<0.05$) compared to diabetic group (340.75±17.15), although this was higher than the baseline glucose for both control (99.67±3.23) and orchiectomized group (95.5±4.60). The AUC during OGTT showed that the orchiectomized-diabetic group expressed an enhanced ability to metabolize glucose than the diabetic group. (51139.65±1592.52 vs. 77961.00±2806.43, $P<0.05$ respectively). The MDA level in the diabetic group was increased (103.20±5.05, $P<0.05$) compared with control and orchiectomized group (87.12±4.18, 78.08±3.78 μmol/ml respectively). More so, there was a decrease in GSH activity and an increase in SOD activity in the diabetic group compared with control. (GSH: 1.09±0.13 vs. 1.77±0.15, SOD: 2.68 ±0.11 vs. 2.03 ± 0.20, μmol/ml $P<0.05$). Meanwhile, the activities of GSH and CAT were significantly reduced in the orchiectomized as well as orchiectomized-diabetic group (GSH: 0.17±0.03, 0.16±0.03, CAT: 5.39±0.22, 3.75±0.28, $P<0.05$, respectively) when compared with both control and diabetic group (GSH: 1.77±0.15, 1.10±0.12, CAT: 10.85±0.99, 10.95±0.77 respectively). These data indicates that testosterone promotes glucose intolerance and oxidative stress under type 1 diabetic condition.

Dhindsa S, Prabhakar S, Sethi M, Bandyopadhyay A, Chaudhuri A, Dandona P. (2004). J Clin Endocrinol Metab. 89: 5462 –5468.

Morakinyo AO, Iranloye, BO, Daramola, AO, Adegoke, OA. (2011). Adv Med Sci. 56:1-8

Selvin E, Feinleib M, Zhang L, Rohrmann S, Rifai N, Nelson W. (2007). Diab Car. 30: 234 –238.

Where applicable, the authors confirm that the experiments described here conform with The Physiological Society ethical requirements.

PCC288

In vivo and in vitro reproductive toxicity of Quassia amara extract and Quassin: action on sperm capacitation and acrosome reaction in male Wistar rats

O.O. Obembe[1,2] and Y. Raji[2]

[1]Physiology, Osun State University, Osogbo, Osun, Nigeria and [2]Physiology, University of Ibadan, Ibadan, Oyo, Nigeria

Quassia amara is a medicinal plant with several pharmacological properties [1-3]. There are preliminary reports implicating this plant in male reproductive toxicology. Its bioactive principle quassin has been reported as the antifertility agent. However, the mechanism of action remains to be elucidated, but the major site of action appears to be the epididymis. The action of Q. amara and quassin on epidydimal reproductive parameters was therefore investigated. Effect on sperm cells in vitro was also examined.

Q. amara extract (100mg kg-1 p.o.), quassin (0.1 and 2mg kg-1 p.o.) and distilled water (0.5ml p.o.) were administered daily for 6 weeks to male rats (180-200g, n=5), and thereafter sacrificed [4]. Organ weights, sperm, hormonal and biochemical analysis were conducted. Sperm capacitation and acrosome reaction were determined by Coomassie brilliant blue staining technique. Values are Mean ± SEM, compared by ANOVA. In vitro extender studies were conducted on graded doses of the crude extract (50-500 μg/ml).

The respective weight (g) of testes (0.78±0.14; 0.81±0.15; 0.99±0.14 vs 1.18±0.02), caudal epididymis (0.15±0.02; 0.12±0.02; 0.14±0.02 vs 0.30±0.01), seminal vesicle (0.9±0.18; 0.21±0.09; 0.28±0.09 vs 1.6±0.01) and prostate (0.15±0.02; 0.16±0.02; 0.16±0.01 vs 0.29±0.02); %sperm motility (42.0±10.2; 68.0±3.74; 68.0±3.74 vs 93.75±0.97), %viability (88.0±2.55; 88.6±3.39; 94.2±1.8 vs 97.25±0.75), count (58±4.24; 94±7.89; 88.8±5.61 vs 121.2±4.24) and volume (5.15±0.004; 5.14±0.02; 5.16±0.02 vs 5.20±0) were significantly reduced ($p<0.05$) in all treatment groups, except %viability for quassin high dose. No effect was observed on the weight, histology of visceral organs and liver function biomarkers. Lipid profile of the extract treated group were not affected, while quassin significantly reduced HDL (0.3±0.03; 0.2±0.02 vs 0.6±0.08, $p<0.05$) and increased LDL (0.9±0.04; 1±0.09 vs 0.7±0.07; $p<0.05$). Total epididymal protein were significantly reduced (0.67±0.11; 0.60±0.07; 0.70±0.17 vs 1.65±0.32, $p<0.05$). Q. amara extract significantly reduced ($p<0.01$) LH (0.6±0.14 vs 1.5±0.18) and testosterone level (0.03±0.01 vs 0.32±0.09), while quassin reduced FSH level (1.6±0.19; 2.2±0.2, $p<0.05$). In vitro extender study to verify these results showed that the action of the extract on sperm parameters is consistent, as progressive motility declined and abnormal morphology increased with dose. Also, after in vitro induction of sperm capacitation, the percentage of "acrosome reacted capacitated sperm cells" was significantly lower (27.2±1.98; 24.0±2.74; 37.8±10.72 vs 95.2±0.86, $p<0.01$) in all treated groups. Q. amara and quassin may have reproductive specific toxic effect and its deleterious effect on sperm cells affects capacitation and acrosome reaction.

Ajaiyeoba E.O. and H.C. Krebs, 2003. Antibacterial and antifungal activities of Quassia undulata and Quassia amara extracts in vitro. Afr. J Med Med Sci.,32(4): 353-356

Faisal K., S. Parveen, R. Rajendran, R. Girija, V.S. Periasamy, B. Kadalmani, A. Puratchikody, K. Ruckmani, B.M.J. Pereira and M.A. Akbarsha, 2006. Male reproductive toxic effect of Quassia amara: Observations on mouse sperm. JER, 10(1): 66-69

Raji Y and Oloyede G. K., 2012. Antiulcerogenic effects and possible mechanism of action of Quassia amara (L. Simaroubaceae) extract and its bioactive principles in rats. Afr J Tradit Complement Altern Med. 9(1):112-119

World Medical Assossiation, American Physiological Society, 2002. Guiding principles for research involving animals and human beings. Am. J. Physiol. Regul. Integr. Comp. physiol., 283: R281-R283

Where applicable, the authors confirm that the experiments described here conform with The Physiological Society ethical requirements.

PCC289

Overexpression of GLUT2 protein in obesity mices with nonalcoholic steatohetatitis

A.D. Silva[1], R.R. Favaro[2], R.C. Petroni[3], D.T. Furuya[1], P.E. Silva[1], H.S. Freitas[1], A.C. Poletto[1], M.M. Okamoto[1], F. Barrence[2], T.M. Zorn[2] and U.F. Machado[1]

[1]Physiology and Biophysics, Institute of Biomedical Sciences - University of Sao Paulo, Sao Paulo, Sao Paulo, Brazil, [2]Cell biology and development, Institute of Biomedical Sciences - University of Sao Paulo, Sao Paulo, Brazil and [3]Medical Sciences, Medical School - University of Sao Paulo, Sao Paulo, Brazil

Background and aims:
We believe that GLUT2 (Glucose transporter 2) can be involved in the development of nonalcoholic steatohepatitis (NASH). Considering the importance of knowing the glucose flux in liver of obesity animals with nonalcoholic steatohepatitis, we studied the expression of GLUT2 protein.
Materials and methods:
We studied obesity mices (MSG) and control mices (C). The obesity was induced by neonatal subcutaneous dose of monosodium glutamate (2mg/g) during 5 days and a higher dose (4mg/g) at the 7th day of life. After the weanig, the animals were fed with normal fat diet (ND) and high fat diet (HD - 60% of fat) by 12 weeks. We obtain four groups: MSG-ND, MSG-HD, C-ND and C-HD. The obesity it not always related with the high weigh, thus measures of adiposity, Lee index and weigh of periepididymal adipose should be used. The GLUT2 protein was analysed by western blot. Paraffin-embedded liver were stained by regular hematoxylin-eosin (HE) methot for evaluation of liver histology.
Results:
The histological analyses demonstrated that nonalcoholic steatohepatitis is present in MSG-HD mices. In comparison to C-ND ($P<0,05$) and MSG-ND ($P<0,01$) animals, the MSG-HD showed higher weigh. The MSG-HD mices also showed higher Lee index when compared with the other groups ($P<0,01$). The weight of periepididymal adipose was higher in MSG-HD group when compared to C-HD group ($P<0,01$). The histological analyses shows nonalcoholic steatohepatitis in MSG-HD mices. In comparison to C-DN and C-DH animals, MSG-DN and MSG-DH mices showed increased GLUT2 protein content in and liver ($P<0,05$).
Conclusions: We demonstrated a new data in the literature: the treatment of monosodium glutamate associated with high fat diet, leads to NASH. NASH is related to insulin resistance where there is a higher output of fatty acids and glucose to the liver. This glucose can be converted into triglycerides by the de novo lipogenesis, contributing for the hepatic steatosis. Thus, the GLUT2 can collaborate to NASH, by falicilitate the glucose input to hepatocyte

Where applicable, the authors confirm that the experiments described here conform with The Physiological Society ethical requirements.

PCC290

Repeated acute restraint-induced stress: Effects on body weight, cortisol and reproductive hormones in female Wistar rats

S.O. Sulaiman, L.A. Olayaki and M.T. Salman

Physiology, University of Ilorin, Nigeria, Ilorin, Kwara, Nigeria

Stress through its response, be it chronic or acute, produces behavioural and chemical deficits that affect most body functions especially reproduction (Selye, 1936; Khodaei-Motlagh et al., 2011). Although chronic exposure to stress has been reported to affect reproduction in an adverse manner (Krulich et al., 1974; Blake, 1975; Hillier and Tetsuka, 1998), effects of acute exposure to stress on reproduction have been controversial. To study the effects of repeated acute restraint-induced stress on reproductive hormones in female rats, fifteen female Wistar rats were divided into three groups of five rats each. Groups I and II rats were restrained for 10 minutes and 20 minutes respectively for seven days while group III rats served as control. All the rats were weighed everyday before the restraint throughout the duration of the experiment. On the 7th day, immediately after the restraint, the rats were anaesthetized using chloroform and killed, then their blood samples collected into heparinized tubes and centrifuged. The supernatant plasma from each blood sample was then used to analyse reproductive hormones and cortisol. Statistical analysis was done with one-way ANOVA and the results were expressed using mean ± SEM. The results showed that there were increases in weights and hormonal levels of the restrained rats compared to the control. The weight increase was significant only in 10 minute restrained rats when weights of days 1 and 7 were compared (180 ± 9.08g vs. 188 ± 8.60g). In 10 minute restrained rats, levels of oestradiol (240 ± 17.55pg/ml), progesterone (41.25 ± 1.94ng/ml) and FSH (1.33 ± 0.06mIu/ml) significantly increased when compared to their corresponding control values of (174.00 ± 8.28pg/ml), (13.13 ± 1.40ng/ml) and (0.3 ± 0.3mIu/ml) respectively. Levels of cortisol (7.63 ± 0.76μg/ml), LH (4.80 ± 0.49mIu/ml) and prolactin (4.25 ± 0.32ng/ml) also increased in the 10 minute restrained rats compared to their control values of (3.90 ± 1.10μg/ml), (4.42 ± 0.28mIu/ml) and (3.50 ± 0.20ng/ml) respectively but the increases were not significant. Thus, it was concluded that acute stress such as 10-minute and 20-minute restraint used in this study could lead to increases in body weight and reproductive hormones.

Selye H (1936). Syndrome produced by diverse nocuous agents. Nature 138:32.

Khodaei-Motlagh M et al. (2011). Alterations in reproductive hormones during heat stress in dairy cattle. African Journal of Biotechnology 10(29):5552-5558.

Krulich, J et al. (1974). The effects of acute stress on secretion of LH, FSH, prolactin and GH in the normal male rat, with comments on their statistical evaluation. Neuroendocrinology 16: 293-311.

Blake CA (1975). Effects of “stress’ on pulsatile luteinizing hormone release in ovariectomized rats. Proc Soc Exper Biol Med 148:813-815.

Hillier SG & Tetsuka M (1998). An anti-inflammatory role for glucocorticoids in the ovaries? J Reprod Immunol 39:21-27.

I acknowledged Dr. biliaminu of the Department of Chemical Pathology, University of Ilorin Teaching Hospital, Ilorin, Nigeria

Where applicable, the authors confirm that the experiments described here conform with The Physiological Society ethical requirements.

PCC291

Identification and characterisation of progesterone-induced microRNAs in mouse endometrial epithelial cells

D. Yuan, Q. Xu, L. Yu, T. Qu, S. Zhang, Y. Zhao, Y. He, J. Zhang and L. Yue

Department of Physiology, West China School of Preclinical and Forensic Medicine, Sichuan University, Chengdu, Sichuan, China

It is essential for progesterone to inhibit estrogen-induced proliferation of endometrial epithelial cells (EECs) and make endometrial epithelium to convert into the secretory epithelium for the preparation of embryo implatation. But the mechanism of progesterone effect on EECs remains unclear. Recent studies have indicated that some reproductive hormones can regulate the expression of some special genes in post-transcriptional level. MicroRNAs are important post-transcriptional regulators in target mRNA, thus they are involved in many physiological and pathological processes. We speculate that there should be progesterone-induced microRNAs which mediate the physiological effect of progesterone on EECs.

In this study, 20 six-week-old ovariectomized female Kunming mice were randomly divided into 2 groups, 10 mice for each. One group (P4 group) was treated both estrogen (100ng / daily for 2 days) and progenstrone(2 mg). The other one (control group) was treated with only estrogen and sesame oil. All mice were sacrificed and their uteri were collected. The EECs were enzymatically isolated and the total RNA was respectively extracted from each group. Small RNA molecules were purified by PAGE, ligated a pair of Solexa adaptors and amplified by PCR, thus 90 bp of DNA were isolated with agarose gel. The purified DNA was used for cluster generation and sequencing analysis using the Illumina's Solexa Sequencer. Then we evaluated sequencing quality, calculated length distribution of small RNA reads and filtrated impure reads. Finally, clean reads were identified and analyzed based on the known mice miRNA of miRBase database 19.

The miRNA expression of two groups was compared to find out the differentially expressed miRNA. The results showed that there were 149 up-regulated miRNAs of which the differences is more than twice of control group. Afterwards, the target genes of these miRNAs were predicted using the following algorithms: miRanda, PicTar, and TargetScan.

22 miRNAs were selected from the 149 up-regulated miRNAs, of which the target gene proteins are involved in significant biological functions, such as cell adhesion, transmembrane transport, cell cycle and metabolism (table). To data, 9 microRNAs (miR-23a-3p, mmu-miR-26a-5p, mmu-miR-1a-3p, mmu-miR-133a-3p, mmu-miR-195a-5p, mmu-miR-3473b, mmu-miR-204-5p, mmu-miR-145a-5p, mmu-miR-143-3p) have been verified by real time PCR. The results proved that their expression is progesterone-dependent on the EECs.

In our conclusion, progesterone can specifically regulate the expression of some miRNAs in EECs, which possibly mediate the effect of progesterone on the structure and function of endometrial epithelium for preparing for implantation through influencing some functinal proteins. This project will be helpful for further exploring the molecular mechanism of progesterone's effect on EECs.

Table 1: miRNAs differentially expressed induced by progesteron

miRNA	fold-change(log2 P4/control)	P value	prediction of target gene	biological function
mmu-mir-3473e	7.73594959	0	Slc1a1, Slc8a2	Transport
mmu-miR-133b-3p	6.1258222	1.17E-59	aquaporin 1, cyclin D2, Slc6a1	Cell cycle, Transport
mmu-mir-3473b	5.7644203	0	Slc1a1, Slc8a2	Transport
mmu-miR-133a-3p	4.6586954	0	aquaporin 1, cyclin D2, Slc6a1	Cell cycle, Transport
mmu-miR-143-3p	3.87758442	0	oxysterol-binding-protein-related protein,extracellular matrix versican protein, Slc4a8	Cell adhesion, Transport
mmu-miR-1a-3p	3.85008061	0	cyclin D1,CDK6	Cell cycle
mmu-miR-451a	3.13804818	0	drug-transporter protein P-glycoprotein	Metabolism
mmu-miR-145a-5p	3.11601302	0	Friend leukemia integration 1 transcription factor, Kcna4, Slc1a2, cyclin D2	Transport, Metabolism, Cell cycle
mmu-miR-196b-5p	3.07723026	0	Slc9a6	Transport
mmu-miR-195a-5p	2.58527859	1.37E-233	cyclin D1,cyclin E1, Atp1b4	Cell cycle, Transport
mmu-miR-193a-3p	2.45775613	0	Slc39a5,	Transport
mmu-miR-342-3p	2.28018339	0	Slc5a3	Metabolism
mmu-miR-204-5p	2.23891765	6.47E-218	Slc43a1, Cacng2	Transport
mmu-miR-10b-5p	2.23401271	0	Scn3a,	Transport, Cell adhesion
mmu-miR-142-5p	2.13266154	1.54E-301	Slc16a9, Slc18a2	Transport,
mmu-miR-27a-3p	1.84593295	6.74E-193	cyclin E	Cell cycle
mmu-miR-152-3p	1.78353572	0	oxysterol binding protein-like 11, CDK19	Cell cycle, Metabolism
mmu-miR-199b-3p	1.72214173	0	low density lipoprotein receptor-related protein 2	Metabolism
mmu-miR-199a-3p	1.72208762	0	low density lipoprotein receptor-related protein 2	Metabolism
mmu-miR-23a-3p	1.56479773	0	cyclin D1;CDK7;IGFbp 5	Cell cycle
mmu-miR-23b-3p	1.53857472	0	cyclin D1;CDK7	Cell cycle
mmu-miR-26a-5p	1.38397348	0	EZH2	Cell cycle

Where applicable, the authors confirm that the experiments described here conform with The Physiological Society ethical requirements.

PCC293

The inducible nitric oxide synthase and proinflammatory cytokines expression are decreased by thyroid hormone treatment in skeletal muscle of diabetic rats

A.P. Costa, S.S. Teixeira, L.L. Poyares and M. Nunes

Physiology and Biophysics, University of São Paulo, São Paulo, Brazil

In vitro (Bérdad et al., 1997) and in vivo (Carvalho-Filho et al., 2005) studies have shown that cytokines decrease glucose uptake in skeletal muscle in response to insulin by increasing the expression of inducible nitric oxide synthase (iNOS). Thyroid hormone treatment was shown to increase the insulin sensitivity and decrease the glycemic levels in db/db mice (Lin and Sun, 2011). In this context, this study aimed to evaluate whether thyroid hormone treatment could affect insulin sensitivity in diabetic rats by altering TNF-α, IL-6 and/or iNOS expression in oxidative skeletal muscle. Methods: Male Wistar rats were assorted in control (C), diabetic (D) and T3-treated diabetic group

(D T1,5) – 15. 10-3 μg. g-1 b.w.. The diabetes was induced by aloxan injection (150 mg. Kg-1 b.w.) and after 15 days, the glycemia was measured. The animals which presented glycemia levels higher than 250 mg/dL were included in the diabetic groups. A subset of diabetic rats was treated with T3 for a 28 day-period (D T1,5). After this period, the skeletal muscle (soleus) was removed and TNF-α, IL-6 and iNOS content was analyzed through western blotting. Results: T3 treatment decreased the amount of TNF-α, IL-6 and iNOS protein and improved insulin sensitivity in oxidative skeletal muscle tissue (soleus), as shown by the increased Akt kinase phospho-

rilation in response to insulin administration. Conclusion: The present data provide evidence that at least part of the benefits of T3 treatment in insulin sensitivity of diabetic rats occurs by its negative modulation of cytokines and iNOS expression.

Bérdad S et al. (1997) Biochem. J. 325, 487–493.

Carvalho-Filho MA et al. (2005). Diabetes 54, 959-967.

Lin Y & Sun Z (2011). Br J Pharmacol 162, 597-610.

Where applicable, the authors confirm that the experiments described here conform with The Physiological Society ethical requirements.

PCC294

GPR30 mediates the fast effect of estrogen on mouse blastocyst and its role in implantation

L. Yu, T. Qu, S. Zhang, D. Yuan, Q. Xu, J. Zhang, Y. He and L. Yue

Department of Physiology, Sichuan University, Chengdu, Sichuan, China

It was reported that that there was a fast action of estrogen on the target cells. Recent researches on some kinds of cells have suggested that G protein-coupled receptor 30 (GPR30) is involved in the rapid effects of estrogen as its membrane receptor. The aim of this research is to reveal whether GPR30 mediates the fast action of estrogen on mouse blastocyst and its role in embryo implantation.

We firstly used RT-PCR to detect the expression of GPR30 mRNA, immunocytochemistry to detect the expression of GPR30 protein and FITC- E2-BSA to detect the binding sites of estrogen in the mouse blastocyst cells further to be compared with the GPR30's location. We found that the mRNAs and proteins expressed on the mouse blastocyst cells and their location was mostly consistent with the binding sites of estrogen on the plasma membrane (Figure 1).

To study GPR30 mediating the fast action of estrogen on mouse blastocyst, we used Fluo-3/AM (3μmol/L) to label intracellular calcium and confocal laser scanning microscopy to detect the dynamic change of [Ca2+]i in different groups of mouse blastocysts, which were treated respectively with 1μmol/L E2, 1μmol/L E2-BSA, 1μmol/L G1, a GPR30-specific agonist and 1μmol/L G15, a GPR30-specific antagonist, followed by 1μmol/L E2-BSA. The results showed that E2, E2-BSA as well as G1 could induce their rapid increase of Cai2+, while G15 could inhibit the fast effect of E2-BSA (Figure 2).

To study the role of GPR30 mediating the effect of estrogen on mouse blastocyst in implantation, total 53 blastocysts from donor mice were divided into two groups, one is G15 group (n=26) in which blastocysts were pretreated with 1μmol/L G15 for 30 minutes, the other one is for control (n=27) in which blastocysts were pretreated with the same amount of vehicle, and then both groups of blastocysts were separately transplanted into the bilateral uterine horns of five day 4 pseudopregnant recipient mice and the implantation rates on day 10 between two groups were compared. The results indicated that the implantation rate of G15 group was 19.2%, significantly lower than 55.5% of control group ($P<0.05$).

Recent studies have implicated GPR30 as a mediator of the rapid effects of estrogens in some kinds of cells. We provided the first evidence that GPR30 expressed on the mouse blastocysts, and their locations were mostly consistent with the binding sites of estrogen on the blastocyst cells. Furthermore, both estrogen and GPR30-selective agonist could induce the rapid increase of Cai2+ of blastocyst cells, while GPR30-selective antagonist could specifically block the fast effect of estrogen. Moreover, the pretreatment of G15 on blastocysts lead to a lower implantation rate, compared with that of control. Thus, it can be inferred that GPR30 can mediate the fast effect of estrogen on blastocysts and play important role in embryo implantation.

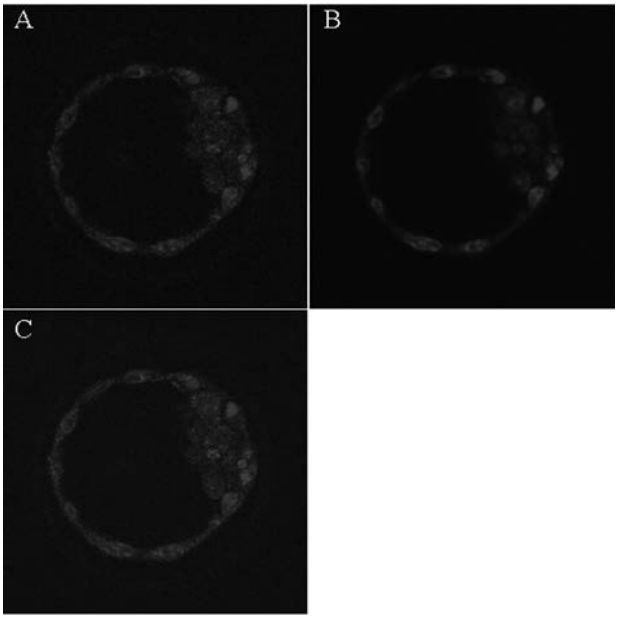

The expression and locations of GPR30 protein on mouse blastocyst cells. A: The green indicates that the binding of E2-BSA-FITC on the plasma membrane B: The red indicates that GPR30 is localized in the mouse blastocyst cells, C: merged image indicates GPR30 proteins were mostly consistent with the binding sites of E2.

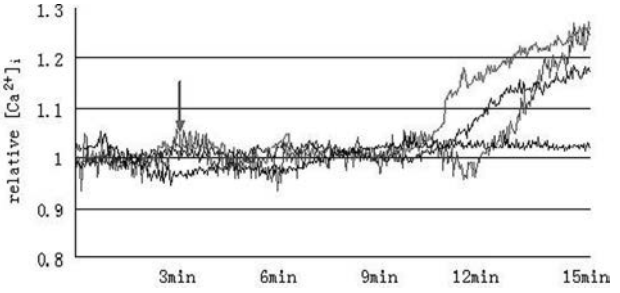

The mobilizations of Cai2+ which induced by different factors in blastocyst cells. Arrow: To add E2/E2-BSA/G1, Red line: E2 group, Blue line: E2-BSA group, Green line: G1 group, Black line: G15+E2-BSA group.

Where applicable, the authors confirm that the experiments described here conform with The Physiological Society ethical requirements.

PCC297

Integrins are involved in GPR30 mediating the fast effect of estrogen on mouse blastocysts in implantation

T. Qu, L. Yu, S. Zhang, D. Yuan, Q. Xu, J. Zhang, Y. He and L. Yue

Department of Physiology, Sichuan University, Chengdu, China

It is necessary for estrogen to rapidly activate mouse blastocysts, so that they may attach to endometrial epithelium in implantation. Our previous and recent work has shown that estrogen induces the fast effect on mouse blastocysts in implantation which is mediated by G protein-coupled receptor 30 (GPR30). There also were evidences that integrins and their ligands are involved in embryo–endometrium interaction. Thus, we infer integrins may be involved in GPR30 medi-

ating the fast effect of estrogen on mouse blastocysts in implantation.

Firstly, blastocysts were collected from day 4 pregnant Kunming mice and divided into 5 groups, 3 embryos for each, which were treated respectively with the same amount of vehicle, 1μmol/L estradiol (E2), 1μmol/L E2 conjugated with bovine serum album (E2-BSA), 1μmol/L G1, a GPR30-specific agonist, and 1μmol/L E2-BSA with pretreatment of 1μmol/L G15, a GPR30-specific antagonist. Immunocytochemistry staining and confocal microscopy were used to examine the expression of integrins. The experiment was repeated three times. The result showed that E2, E2-BSA and G1 could induce their clustering, while G15 may block the clustering induced by E2-BSA (Fig 1).

To explore GPR30 mediating the fast effect of estrogen on the affinity of integrins in mouse blastocysts. The collected some other blastocysts were pretreated as the above experiment, followed by the treatment of 50μg/L fibronectin labled with FITC (FN-120-FITC), one kind of integrin ligands, The fluorescence intensity was examined which represented the affinity of integrins with their ligand. The result indicated that E2, E2-BSA and G1 could increase the FN binding activity of integrins in blastocyst cells, while G15 may block this effect of E2-BSA on it (Fig 2).

In order to study integrins are involved in the effect of estrogen on mouse blastocysts in implantation, blastocysts (n=38) were pretreated with 1μmol/L E2, and then divided into two groups. One group was cultured in M2 medium containing RGD, (Arg-Ala-Asp) peptide (1mmol/L) for 30 minutes, which can specifically block the binding of integrins with their ligands, the other group was cultured in non-specific RGE peptide (1mmol/L) as control. Two groups of blastocysts were separately transplanted into the bilateral uterine horns of recipient mice on the pseudopregnant day 4 and the implantation rate between two groups were compared in 10 days. We found that the implantation rate in RGD group (3/19, 16%) was significantly lower than that in RGE group (13/19, 68%), $P<0.05$.

In conclusion, GPR30 mediating the fast effect of estrogen may induce the clustering of integrins and increase the affinity of integrins with their ligand in mouse blastocysts, which play important roles in the process of implantation.

Funding: This work was supported by the National Natural Science Foundation of China (Grant No.31100844)

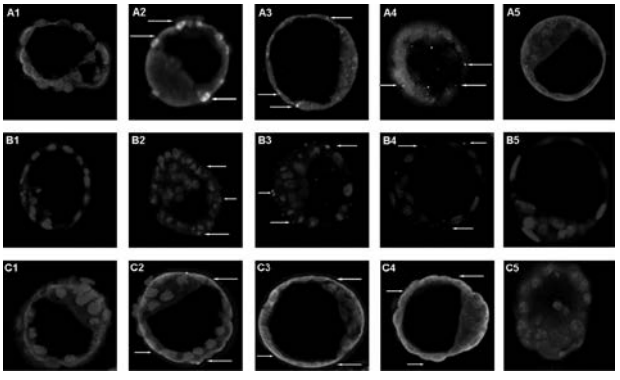

Fig. 1 The localization of integrin αv, β1 and β3 in mouse blastocysts treated with different factors. A.integrin αv, B.integrin β1, C.integrin β3. 1.vehicle, 2.E2, 3.E2-BSA, 4.G1, 5.G15+E2-BSA. The green and red indicate the locations of integrins. The blue indicates the nuclei. The arrows indicate integrin clusters. Each image is representative of three embryos at each group.

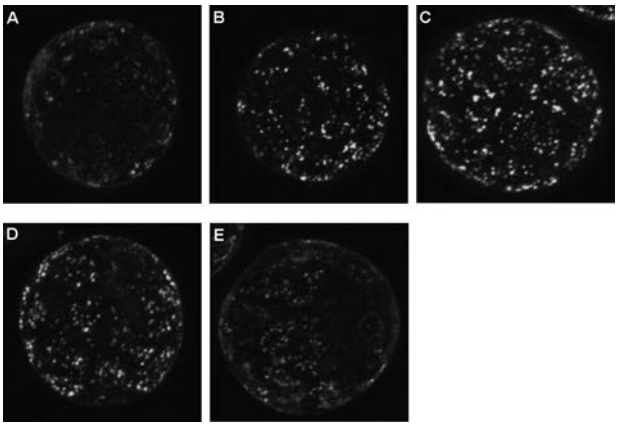

Fig. 2 The binding of FN-120-FITC on mouse blastocyst cells. A:vehicle, B:E2, C:E2-BSA, D:G1, E:G15+E2-BSA.

Where applicable, the authors confirm that the experiments described here conform with The Physiological Society ethical requirements.

PCC300

Acute vs chronic caffeine: Are the effects on insulin sensitivity mediated by altered insulin/AMPK signaling pathway?

J.F. Sacramento, M.J. Ribeiro, M.P. Guarino and S.V. Conde

Pharmacology, CEDOC, Faculdade de Ciências Médicas, Universidade NOVA, Lisboa, Portugal

Caffeine is the most widely behaviorally active substance consumed in the world. We have recently showed that chronic caffeine intake prevents the development of insulin resistance (IR) in diet-induced IR rats (Conde et al. 2012). In contrast, acute caffeine administration decreases insulin sensitivity in a dose dependent manner (Sacramento et al. 2012). However, the mechanism behind the distinct effects of acute and chronic caffeine administration on insulin sensitivity is not clarified. Herein we have investigated if the mechanism that contributes to the differences between acute and chronic caffeine effects on insulin sensitivity is mediated by altered insulin/AMPK signaling pathway in skeletal muscle.

Experiments were performed in 3 months Wistar rats anaesthetized with pentobarbitone (60mg/Kg, ip). Six groups of animals were used to evaluate if the effects of chronic caffeine intake on insulin sensitivity are mediated by altered insulin/AMPK pathway. A control group (fed with a sham diet), an high sucrose (HSu; 35% sucrose in drinking water, 28 days) and an high fat (HF; lipid rich diet with 45% fat, 21days) groups were randomly divided into two subgroups, treated and not treated with 1g/l caffeine during 15 days. Insulin sensitivity was measured by an insulin tolerance test (ITT). Acute caffeine administration effects on insulin/AMPK signaling pathway were evaluated in animals submitted to an i.v. administration of different doses of caffeine (0.001-5 μM) 15 minutes before the ITT. Blood was collected by heart puncture and skeletal muscle was removed for Western-blot detection and quantification of insulin receptor, insulin receptor phosphor-Tyr1322, AMPKα1, AMPKα1 Thr172 and Glut4 transporters.

Glut4 expression decreased by 59.35% in HSu animals, an effect not modified by chronic caffeine. In contrast, acute caffeine administration decreased significantly Glut4 expression at 0.5μM of caffeine ($p<0.01$). HSu and HF diets decreased significantly AMPKα1 expression by 70.45% and 33.93%, respec-

tively. Chronic caffeine intake increased significantly AMPKα1 in HSu animals (42.54%) and in HF group AMPK α1 expression was restored to control levels. AMPK α1 activity decreased significantly in HF animals (44.74%), however chronic caffeine intake did modify those values. In opposite, acute caffeine intake did not alter AMPK α1 expression. Insulin receptor decreased significantly in HF animals (59.43%) but chronic caffeine intake did not alter this value. Acute and chronic caffeine did not altered insulin receptor phosphor-Tyr1322 expression. In conclusion, the effect of chronic caffeine intake on insulin sensitivity is not mediated by altered insulin and/or AMPK signaling pathway. In contrast, the effect of acute caffeine administration on insulin sensitivity seems to involve a decrease in Glut4 transporters.

Conde SV, Nunes da Silva T, Gonzalez C, Mota Carmo M, Monteiro EC, Guarino MP. (2012) Chronic caffeine intake decreases circulating catecholamines and prevents diet-induced insulin resistance and hypertension in rats. Br J Nutr. 107:86-95.

Sacramento JF, Ribeiro MJ, Guarino MP, Conde SV. (2012) The effect of acute caffeine administration on insulin sensitivity is mediated by A1 and A2B adenosine receptors. 6th European Congress of Pharmacology, Granada, Spain.

PTDC/SAU-ORG/111417/2009

Where applicable, the authors confirm that the experiments described here conform with The Physiological Society ethical requirements.

PCC301

Vascular endothelial growth factor (VEGF)-mediated microvascular remodeling in the pituitary gland

J. Castle-Miller[1,2], H. Poole[1], C. Sullivan[1], D. Bates[2] and D. Tortonese[1]

[1]Centre of comparative and clinical anatomy, University of Bristol, Bristol, UK and [2]Microvascular research labatories, University of Bristol, Bristol, UK

The pituitary gland contains a complex portal system that transfers signals from the pars tuberalis (PT) and infundibulum to the pars distalis (PD). Vascular loops arising from the PT, traverse to the infundibulum, an area encompassing glial cells and endothelium in close proximity, before descending towards the PD as long portal vessels. Vascular endothelial growth factor (VEGF), originally isolated from the pituitary gland, has been identified as a key regulator of endothelial function, controlling angiogenesis and vascular permeability, the latter via regulation of fenestrations. We hypothesised that VEGF-mediated remodeling of pituitary microvasculature may therefore play a role in the control of reproductive function by acting to either maintain, remodel or signal through this vasculature. If this was the case, one would expect the functional remodeling of this microvasculature to be under seasonal regulation in photoperiodic species as a key mechanism underlying the control of temporal changes in seasonal fertility. To test this hypothesis, pituitary glands from adult ewes were collected during the breeding season (BS; n=5) and non-breeding season (NBS; n=5). The expression of pro- (VEGFxxx) and anti- (VEGFxxxb) angiogenic isoforms was revealed in PT cells co-expressing the melatonin receptor MT1-R, endothelial cells of the vascular loops, and both glial and endothelial cells of the infundibulum. Seasonal variation in VEGF isoform expression was observed in the PD, with a significantly higher content of the anti-angiogenic VEGFxxxb during the BS ($p<0.01$), and an increase in the expression of angiogenic VEGFxxxa ($p<0.01$) during the NBS. Consistent with these findings, total cell proliferation and endothelial cell proliferation were both significantly increased in the PD during the NBS ($p<0.01$). In contrast, no such seasonal changes of VEGF expression or cell proliferation were detected in the PT ($p>0.05$). The expression of S-100, a marker of folliculo-stellate cells (FSC) known to produce VEGF, was significantly increased during the NBS in the PD ($p<0.01$), where expression of VEGFR2 by lactotrophs, endothelial cells, FSC and other endocrine cells was also observed. Critically, seasonal alterations to the intrinsic morphology of the vascular loops of the infundibulum were also identified. The number and area of these loops were significantly increased during the NBS ($p<0.05$). These findings support a role for VEGF-mediated pituitary vascular remodeling in the mechanisms underlying the pituitary control of temporal changes in fertility.

Where applicable, the authors confirm that the experiments described here conform with The Physiological Society ethical requirements.

PCC302

Antioxidative and anti-immflammatory activity of Croatian propolis preparations in alloxan induced diabetes in mice

S. Novak[1], D. Sirovina[2], I. Ivic[3] and N. Oršolić[2]

[1]Department of Physiology and Immunology, Medical Faculty Osijek, J.J. Strosmayer University Osijek, Osijek, Croatia, [2]Department of Animal Physiology, Faculty of Science, University of Zagreb, Zagreb, Croatia and [3]Department of Pathophysiology and Gerontology, Medical School, University of Pécs, Pécs, Hungary

Introduction: Diabetes mellitus is metabolic disease and its consequences are seen in many different tissues. Hyperglycemia results in developing reactive oxygen species which induce inflammatory process. The antioxidant capacity of propolis could protect organism from oxidative stress, diminished hyperglycemia effect and could reduce inflammation.
Hypothesis: Antioxidant and anti-inflammatory effect of propolis improve life quality and lifespan in alloxan-induced diabetic mice.
Methods: Diabetes was induced in Swiss albino mice with a single intravenous injection of alloxan (75 mg kg-1). Two days after alloxan injection, water soluble derivative of propolis (WSDP) or ethanol extract of propolis (EEP) (50 mg kg-1 per day) were intraperitoneally injected for 7 days in diabetic mice. We have measured in vivo lipid peroxidation of liver, spleen, and brain in mice treated with WSDP or EEP. Functional activity of macrophages was also examined and effect of WSDP or EEP on body weight and survival of alloxan-induced diabetic mice.
Results: The lipid peroxidation in liver tissue was improved in animals treated by EEP and WSDP ($p <0.001$). In addition, WSDP was able to lower the extent of lipid peroxidation of kidney and spleen ($p <0.05$). In our study, we couldn't observe a difference in malondialdehyde (MDA) levels of diabetic and healthy brain, but in WSDP-treated diabetic animals a significant reduction in MDA levels could be noted. The results showed a statistically significant increase in the number of activated macrophages in untreated diabetic mice and in mice treated with WSDP or EEP ($p <0.001$) versus healthy animals. Diabetic animals treated with WSDP showed a significantly increased number of functional activated macrophages as compared to untreated diabetic mice ($p <0.001$). Increased life span was observed in diabetic mice treated with either aqueous or

ethanol propolis preparations for 30.43% (WSDP) and 20.67% (EEP), respectively, in relation to control diabetic mice.
Conclusions: Our results have shown that propolis preparations have a promising role in the protection against oxidative stress damage in diabetic mice, which may be mainly attributed to its antioxidant and anti-inflammatory potential. The mechanism of polyphenol/flavonoid action on mice with diabetes mellitus is yet to be determined.

(Support: This work was supported by the Ministry of Sciences, Education and Sports of the Republic of Croatia project No. 119-0000000-1255.)

Where applicable, the authors confirm that the experiments described here conform with The Physiological Society ethical requirements.

PCC303

Calcium oscillations and waves in beta cells from acute mouse pancreas tissue slices

A. Stozer[1,2], J. Dolenšek[1], M.S. Klemen[1] and M.S. Rupnik[1,2]

[1]Institute of Physiology, University of Maribor, Faculty of Medicine, Maribor, Slovenia and [2]Centre for Open Innovations and Research, University of Maribor, Maribor, Slovenia

In beta cells from Langerhans islets, cell stimulation is coupled to insulin secretion. Upon stimulation with glucose, the concentration of intracellular calcium ions ([Ca2+]i) oscillates in phase with accompanying oscillatory changes in membrane potential and insulin secretion. The calcium oscillations in different cells within a single islet of Langerhans are well synchronized, with phase differences between oscillations in individual cells of up to a few seconds (1, 2). Furthermore, some studies have reported the presence of calcium waves in islets of Langerhans, with a speed of 20-200 μm/s (3).
However, many different types of calcium oscillations have been reported in isolated islets which are the most widely used experimental model. It has been suggested that the duration and conditions of islet culture influence the types of responses and that calcium waves occur only in cultured islets (4-6). Additionally, due to limited diffusion of fluorescent calcium indicators, calcium imaging experiments performed on isolated islets enable insight only into the most peripheral parts of islets, where beta cells are least abundant in mice and where other types of cells are present (7).
To enable access to all cellular layers of an islet and clarify the existing controversy regarding types of oscillations present in islets and the existence of calcium waves, we combined the recently introduced acute pancreas tissue slice method (8) with confocal laser scanning calcium imaging, using the Oregon green® 488 BAPTA-1 fluorescent calcium indicator. The study was conducted in accordance with all national and European recommendations pertaining to work with isolated tissue and our protocol was approved by the Veterinary Administration of the Republic of Slovenia. The tissue slices were prepared from agarose-injected pancreata of 10-20 week old NMRI mice of either sex, upon sacrifice by cervical dislocation as described in detail previously (8). Taking advantage of previous reports that islet cell types can be identified by their characteristic responses to glucose (7), this enabled simultaneous recording of [Ca2+]i in a large number of cells from all layers of an islet. We showed that fast [Ca2+]i oscillations (4-6 /min) superimposed on a sustained increase in [Ca2+]i are the predominant type of response to 12 mM glucose in beta cells in mice. Additionally, we were able to detect other types of responses, characteristic of alpha and delta cells, predominantly at the periphery of islets. The changes in [Ca2+]i were well synchronized exclusively between coupled beta cells (Figure 1).
Finally, employing high speed calcium imaging (20 frames/s) we detected calcium waves spreading in an orderly manner across the beta cell syncitium at a velocity of 80-90 μm/s as the mechanistic substrate of synchronicity between beta cells in uncultured acute pancreas tissue slices (Figure 2).
A detailed quantification of activation and deactivation phases before and after the sustained plateau with superimposed oscillations revealed that large amplitude changes in [Ca2+]i are insufficient to ensure intercellular synchronization during stimulation with glucose and that metabolic activation is necessary to align the activity of a heterogeneous population of beta cells.

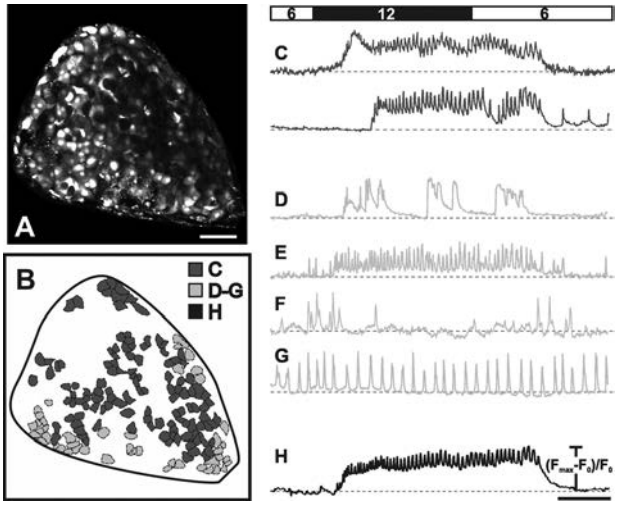

Figure 1. Types of responses. A Oregon green 488 BAPTA-1 labeled most of the cells in the focal plane. Scale bar indicates 50 μm. B A grayscale-coded representation of cells from A, responding to stimulation with 12 mM glucose as represented in C-G (N=177 cells). C A sustained increase with superimposed fast oscillations was the predominant type of response and is characteristic of beta cells (N=124 cells, 70 %). D Slow [Ca2+]i oscillations with superimposed fast oscillations, indicative of poorly coupled or cAMP-depleted beta cells (N=6 cells, 3 %). E Responses characteristic of delta cells (N=30 cells, 17 %). F Responses characteristic of alpha cells (N=5 cells, 3 %). G Some cells displayed [Ca2+]i oscillations not responsive to higher glucose, most probably indicative of already maximally activated delta cells. H The average signal confirming the synchronicity of fast oscillations superimposed on the sustained increase in individual cells. Scale bar indicates 200 s.

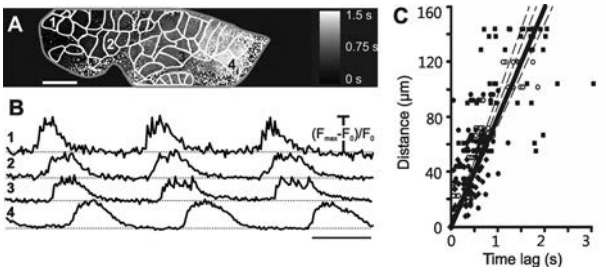

Figure 2. [Ca2+]i waves are the mechanistic substrate of synchronization between individual beta cells. A Cross-correlation determined grayscale-coded time delays for each pixel demonstrating the average direction of spreading of [Ca2+]i waves for 6 subsequent oscillations in 45 cells indicated as regions of interest in white. Scale bar indicates 20 μm. B 3 consecutive [Ca2+]i oscillations in 4 cells indicated in A. Scale bar indicates 2 s. C In 4 different islets, for 6 consecutive oscillations in 10 cells from each islet, the average speed of waves was 80 μm/s (R2 = 0.62, p<0.001), solid line. The respective values obtained in 4 islets were 98 μm/s (R2 = 0.83, p<0.001), 88 μm/s (R2 = 0.34, p<0.001), 80 μm/s (R2=0.40, p<0.001), and μm/s (R2 = 0.46, p<0.001), dashed lines.

Santos RM, et al. (1991) Widespread synchronous Ca oscillations due to bursting electrical activity in single pancreatic islets. Pflügers Archiv European Journal of Physiology 418(4):417-422.

Gilon P, Shepherd RM, & Henquin JC (1993) Oscillations of secretion driven by oscillations of cytoplasmic Ca2+ as evidenced in single pancreatic islets. Journal of Biological Chemistry 268(30):22265-22268.

Aslanidi OV, et al. (2001) Excitation Wave Propagation as a Possible Mechanism for Signal Transmission in Pancreatic Islets of Langerhans. Biophysical journal 80(3):1195-1209.

Gilon P, Jonas J, & Henquin J (1994) Culture duration and conditions affect the oscillations of cytoplasmic calcium concentration induced by glucose in mouse pancreatic islets. Diabetologia 37(10):1007-1014.

Bergsten P (1995) Slow and fast oscillations of cytoplasmic Ca2+ in pancreatic islets correspond to pulsatile insulin release. American Journal of Physiology - Endocrinology And Metabolism 268(2):E282-E287.

Where applicable, the authors confirm that the experiments described here conform with The Physiological Society ethical requirements.

PCC304

Effects of estrogen replacement on high-fat diet-induced insulin resistance in ovariectomized rats

N. Yokota, S. Omoto, S. Tazumi, M. Kawakami and K. Morimoto

Dept. Environm. Health, Facult. Human Life & Environm. Sci., Nara Women's University, Nara, Nara, Japan

Menopause is associated with obesity and insulin resistance. However, the effects of estrogen on insulin sensitivity in ovariectomized rats fed on high-fat diet (HFD) remains unclear. In this study, we examined in vivo effects of estrogen on energy intake, body weight, fat accumulation, insulin sensitivity and insulin signaling in ovariectomized (OVX) rats fed on HFD or standard chow diet (SD). Female Wistar rats aged 9 week were ovariectomized. After 4 week, the rats were assigned either to a placebo-treated (Placebo; n=26) group or a group treated with 17β-estradiol (Estrogen; n=26) subcutaneously implanted with either placebo- or 17β-estradiol (1.5 mg/60-day release) pellets. Simultaneously, rats in either group were divided into two groups and given either SD (13% of calories from fat) or HFD (60% of calories from fat). Four weeks after the replacement and HFD treatment, intravenous glucose tolerance test (IGTT, 1g/kg) was performed for assessment of insulin sensitivity. Blood samples were taken at 0, 5, 10, 30 and 60 min from the catheter implanted into the right jugular vein of rat. Plasma glucose and insulin were measured by the glucose oxidase method using a glucose assay kit and by ELISA assay kit, respectively. Two days after the IGTT, 10^{-5} mol/l insulin was injected into the portal vein in each group of rats, and the liver, hind-limb muscle and mesenteric adipose tissue were dissected for insulin signaling analysis. The Akt and phosphorylated Akt in these organs were assayed by Western blotting. In the Placebo group, HFD increased energy intake compared with SD for 3 weeks after the diet started, while in the Estrogen group it decreased energy intake remarkably for 2 weeks. Four weeks after replacement and HFD, the accumulation of intra-abdominal fats was enhanced in the Placebo group, but was suppressed in either diet group of the estrogen-treated rats. The basal levels of plasma glucose and insulin concentrations were higher in the Placebo group than in the Estrogen group. IGTT revealed that insulin sensitivity was decreased in the Placebo group than that in the Estrogen group of rats fed on SD. Furthermore, HFD reduced insulin sensitivity in the Placebo group, but had little effects on the sensitivity in the Estrogen group. In addition, insulin injection increased Akt phosphorylation in the liver of the Estrogen group, but not in the Placebo group. These results suggest that HFD induces insulin resistance in the OVX rat by impairing insulin-stimulated Akt activations in insulin target organs, which are ameliorated by estrogen replacement.

Where applicable, the authors confirm that the experiments described here conform with The Physiological Society ethical requirements.

PCC305

The interstitial GABA concentration and pharmacology of GABAA channels in human pancreatic islets

Y. Jin, S. Korol, Z. Jin and B. Birnir

Department of Neuroscience, Uppsala University, Uppsala, Sweden

Gamma-aminobutyric acid (GABA) is known as the inhibitory neurotransmitter in the adult mammalian central nervous system (CNS). It is also produced in the islets of Langerhans in pancreas where it serves as an paracrine and autocrine signaling molecule regulating the hormone secretion of pancreatic cells through GABAA channels (1). The GABAA channel is a ligand-gated ion channel permeable to chloride and bicarbonate. When the GABAA channels are activated, they depolarize the β-cells and hyperpolarize the α-cells in the human islets, due to different intracellular chloride concentrations (2). In pancreatic islets, GABA is synthesized in the β-cells, and released by both vesicular and nonvesicular processes (3). We have recently shown GABA modulates hormone release in islets from type 2 diabetic and normoglycaemic individuals. Moreover, both phasic and tonic GABAA channels activation were recorded in intact islet cells (4). Whereas the normal range of interstitial GABA concentration is not known, and information regarding the islets GABAA channel pharmacology is not available either. We, therefore, did whole-cell patch-clamp recordings on cells in intact human islets to further investigate the pharmacological characteristics of the native GABAA channels expressed in the islets. The results show that in 16 out of 23 cells, the GABAA channels conductance in human pancreatic islets are enhanced maximally (82 + 23 pS), when 100 nM or 1 μM GABA is applied, as compared to the channel conductance (39 + 17 pS) activated by the interstitial GABA. Among the 16 cells, channels in 9 cells desensitize in 1 μM GABA. These results support the notion that GABAA channels with very high affinity are present in the islet cells. Furthermore, the endogenous interstitial GABA concentration is in the range between 10 nM and 1 μM in islets when 20 mM glucose is present. We further examined several known GABAA channel modulators: pentobarbital, diazepam, zolpidem and propofol. The results demonstrated that 100 μM pentobarbital (15 cells), 1 μM diazepam (12 cells) and 50 μM propofol (13 cells) consistently potentiated the GABAA channels, whereas 100 nM zolpidem (10 out of 11 cells) did not. The results identify the pancreatic islet cells' GABA channels are high-affinity, high-conducting, extrasynaptic GABAA channels.

1. Rorsman P, Berggren PO, Bokvist K, Ericson H, Möhler H, Ostenson CG, Smith PA: Glucose-inhibition of glucagon secretion involves activation of GABAA-receptor chloride channels. Nature 1989;341:233-236

2. Braun M, Ramracheya R, Bengtsson M, Clark A, Walker JN, Johnson PR, Rorsman P: Gamma-aminobutyric acid (GABA) is an autocrine excitatory transmitter in human pancreatic beta-cells. Diabetes 2010;59:1694-1701

3. Braun M, Wendt A, Karanauskaite J, Galvanovskis J, Clark A, MacDonald PE, Rorsman P: Corelease and differential exit via the fusion pore of GABA, serotonin, and ATP from LDCV in rat pancreatic beta cells. J Gen Physiol 2007;129:221-231

4. J. Taneera, Z. Jin, Y. Jin, S. J. Muhammed, E. Zhang, S. Lang, A. SalehiO, Korsgren, E. Renström, L. Groop, B. Birnir: γ-Aminobutyric acid (GABA) signalling in human pancreatic islets is altered in type 2 diabetes. Diabetologia 2012;

Where applicable, the authors confirm that the experiments described here conform with The Physiological Society ethical requirements.

PCC306

The effects of sodium acetate availability on phosphorylation of hormone sensitive lipase in 3T3-L1 cells

N. Aberdein[1], M. Schweizer[2] and D. Ball[1]

[1]Health and Exercise Research Group, Heriot-Watt University, Edinburgh, UK and [2]Biological Sciences Research Group, Heriot-Watt University, Edinburgh, UK

We recently reported that exposing white adipose cells to 4mM sodium acetate reduces the rate and total release of non-esterified fatty acids (NEFA) [1]. It was unclear from this study whether NEFA release was suppressed or whether acetate inhibited lipolysis. The aim of the current study was to examine whether acetate administration reduces the phosphorylation of hormone sensitive lipase (pHSL) in 3T3-L1 cells that were stimulated with the β-adrenergic receptor agonist, isoproterenol (ISO). The 3T3-L1 cell line was used throughout this study at day 9 post-differentiation. Cells were treated with a combination of the following: ISO (5μM), insulin (1μg/ml) and sodium acetate (4mM) for 3 hours. Under sodium acetate conditions cells were pre-treated (4mM) for 30 minutes. Samples of media were collected every 60 minute for a total duration of 180 minutes and analysed for NEFA and glycerol concentration. Cells for western blot analysis were lysed after 120 minutes. All samples were normalised to total protein content and statistical analysis was by non-parametric Friedman and Mann-Whitney tests. Over the 3 hour period, ISO stimulation of the cells resulted in a >2 fold increase in both NEFA (Fig. 1) and glycerol release and the greatest relative volume of pHSL (Fig. 2) at 120 minutes. Insulin with ISO resulted in a reduction in NEFA release at 120 and 180 minutes (P=0.010; (P=0.016, respectively) (Fig. 1). Incubation with acetate and ISO also reduced NEFA release at 120 and 180 minutes, compared with ISO ((P=0.004; (P=0.004, respectively). Glycerol release was found not to differ between treatment groups (data not shown). Under ISO stimulated lipolysis, the relative quantity of pHSL at serine residue 563 was lower in the presence of acetate, insulin and acetate plus insulin compared with ISO treatment alone (Fig. 2). These data support our previous findings that acetate reduces the appearance of NEFA under ISO stimulated lipolysis. The reduced accumulation of NEFA appears to be due to a down regulation of pHSL and thus lipolysis. The acute metabolic effects of increased acetate availability on lipolysis closely resemble those of insulin however; it is unlikely that the mechanism of reducing pHSL under these two conditions is the same. Future studies to identify the effects of an increase in acetate availability on other lipolytic proteins and secondary messengers upstream of pHSL are warranted.

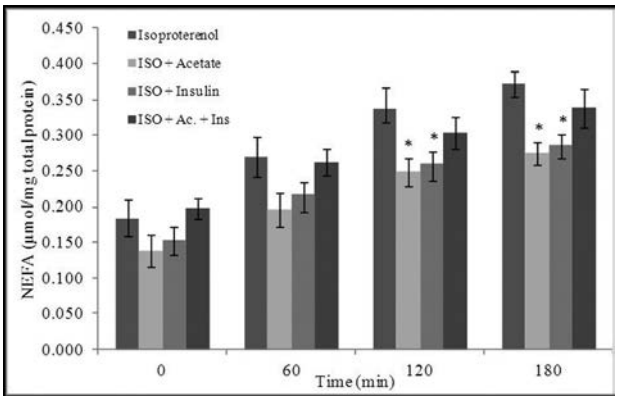

Fig. 1 NEFA release over 180 minutes under conditions of ISO stimulation alone and with insulin, acetate and insulin + acetate. Values are mean±SE (n=3-6) *P<0.05 vs. Isoproterenol.

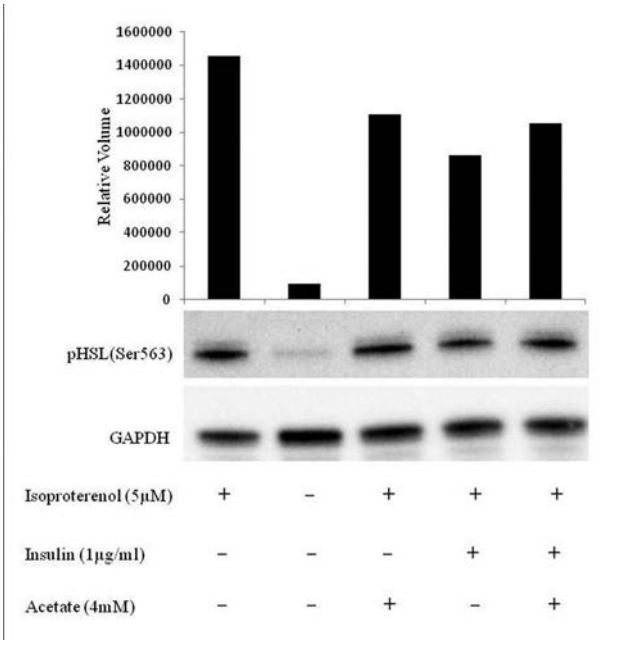

Fig. 2. Sodium acetate, insulin and sodium acetate plus insulin all reduce the phosphorylation of HSL(Ser563) during ISO stimulation. Cell lysates were analysed using western blot with relative volume calculated and normalised to GAPDH. (n=1)

Aberdein, N., Schweizer, M., Ball, D (2012) Acetate reduces NEFA release under basal and isoproterenol stimulated conditions in 3T3-L1 cells. Proc Phys Soc 27:PC330

This work was partly supported by The Gen Foundation.

Where applicable, the authors confirm that the experiments described here conform with The Physiological Society ethical requirements.

PCC308

Hypothalamic Apolipoprotein E Effects on Plasma Lipids in obese rats with metabolic syndrome

M. Bunea[1], C. Scheau[1], R. Moldovan[2], C. Ciornei[1], R. Papacocea[1], S. Tache[2] and A. Badarau[1]

[1]Physiology I, University Of Medicine and Pharmacy "Carol Davila", Bucharest, Bucharest, Romania and [2]Physiology, "Iuliu Hatieganu" University of Medicine and Pharmacy Cluj-Napoca, Cluj-Napoca, Romania

The metabolic syndrome is defined by raised values of plasma cholesterol, raised plasma triglycerides and elevated waist circumference (1), among other parameters. Nevertheless, the role of apolipoprotein E (ApoE) in the on set of obesity in the metabolic syndrome remains unclear, although apolipoprotein E is a key surface component of triglyceride-rich lipoproteins, low density lipoproteins (VLDL) chylomicrons remnants and high density lipoprotein (HDL). Also, traces of it are found in the hypothalamic area of the hunger center (2).
Objective: This study searches for the possible cause for obesity in metabolic syndrome due to a hypothalamic ApoE deficiency, associated with an increased level of combined ApoE in the systemic circulation, using a metabolic syndrome model in rats.
Methods: Wistar rats (male, 179-240 g, n=10), on a high caloric, high fat diet (20 g/day/rat of combined fodder grain + pork lard as fat supplement 2ml/day/rat) for 60 days, had measurements of their plasma levels of triglycerides, cholesterol and glycaemia taken every 30 days. Also weight and arterial pressure were measured. A group (n=10) of male Wistar rats (148g-220 g) on a normal caloric diet (20 g/day/rat ad libidum of combined fodder grain) was used as control. After showing raised blood lipids and obesity, according to the diagnostic criteria (cholesterol level ranging from 158 – 170 mg/dl, triglycerides levels 201- 558 mg/dl) the rats were injected with 8 μl liquid ApoE (Millipore apolipoprotein E, Merck) in the hypothalamic area, following the coordinates of 2.2 mm posterior to bregma and 7.4 mm ventral to dura (3). The procedure was performed under anesthesia with a mixture of ketamine 10% and Xilazine 2%. Blood samples were taken by non traumatic tail incision and arterial pressure was measured using the tail-cuff method.
Results: After the intracerebroventricular administration of apolipoprotein E the two parameters of plasma lipids have fallen to lower values (cholesterol) or even to normal values (triglycerides values ranging between 94-113 mg/dl) and a decrease in the food appetite of the rats was noticed. Daily food intake was noted to fall to 63%. Further measurements of the plasma leptin values, before and after administration of ApoE will take place.
Conclusion: Preliminary data shows that apolipoprotein E has hypothalamic effects that concern metabolic disorders and raised plasma lipid values. Although further study is highly necessary we can conclude that deficient ApoE in the hypothalamic area can lead to a greater food intake and have possible consequences in raised plasma lipid values.

Third report of the National Cholesterol Education Program NCEP Expert Panel on Detection, Evaluation, and Treatment of High Blood Cholesterol in Adults (Adult Treatment Panel III): final report. Circulation 2002, 106: 3143 – 3421

Shen L, Wang DQ, Tso P, Jandacek RJ, Woods SC, Liu M.

Apolipoprotein E reduces food intake via PI3K/Akt signaling pathway in the hypothalamus. Physiol Behav. 2011;105:124-8

Shen L, Tso P, Wang DQ, Woods SC, Davidson W, Sakai R, Liu M.

Up-regulation of apolipoprotein E by leptin in the hypothalamus of mice and rats.

Physiol Behav. 2009 ; 98: 223–228.

ACKNOWLEDGEMENT: This paper is supported by the Sectoral Operational Programme Human Resources Development (SOP HRD) 2007-2013, financed from the European Social Fund and by the Romanian Government under the contract number POSDRU/107/1.5/S/82839

Where applicable, the authors confirm that the experiments described here conform with The Physiological Society ethical requirements.

PCC310

L-cysteine reduces food intake and suppresses plasma ghrelin levels in rats

A.K. McGavigan[1], H.C. Greenwood[1], C. Wong[1], A. Lehmann[2], M.A. Ghatei[1], S.R. Bloom[1] and K.G. Murphy[1]

[1]Section of Investigative Medicine, Imperial College London, London, UK and [2]Research and Development, AstraZeneca, Mölndal, Sweden

Protein is the macronutrient that induces the strongest feeling of satiety. Protein-induced satiety may be mediated by the specific amino acids generated by protein digestion. We have identified L-cysteine as an amino acid with anorexigenic properties.
Food intake was measured in overnight fasted male Wistar rats, following oral gavage of water, 1, 2 or 4mmol/kg L-cysteine and a conditioned taste aversion protocol employed to investigate the possibility of treatment associated consequences. Subsequently, rats received an oral gavage of water or 4mmol/kg L-cysteine and 30 minutes post administration were culled by decapitation and trunk blood collected. Plasma levels of insulin and the anorexigenic hormones glucagon-like peptide-1 (GLP-1) and peptide YY (PYY) were measured by radioimmunoassay, and plasma levels of the orexigenic hormone acyl-ghrelin were measured by an enzyme immunoassay. The effect of repeated administration of L-cysteine on food intake was also investigated. All data are expressed as mean ± sem.
Oral gavage of 2 and 4mmol/kg L-cysteine significantly reduced food intake compared to water control in the 0-1 hour period following administration (water: 6.8 ±0.6g vs. 2mmol/kg L-cysteine: 4.3 ± 0.6g, $p<0.05$; vs. 4mmol/kg L-cysteine: 2.7 ± 0.3g, $p<0.001$, one-way ANOVA, n=7-8). Doses of L-cysteine that reduced food intake did not induce any aversive behaviour suggesting the reduction in food intake was not secondary to unpleasant post-ingestive consequences. L-cysteine significantly reduced plasma acyl-ghrelin levels 30 minutes post administration compared to water control (water: 8.8 ± 1.6pmol/l vs. L-cysteine: 3.6 ± 0.9pmol/l, p=0.019, t-test, n=7-8) and significantly increased plasma insulin levels compared to water control (water: 68.0 ± 7.7pmol/l vs. L-cysteine: 125.7 ± 20.7pmol/l, p=0.020, t-test, n=8). However, there was no effect on plasma GLP-1 or PYY levels. Repeated administration of L-cysteine over 5 days significantly reduced cumulative food intake compared to water and glycine (negative control) treated controls (day 5, water: 144.7 ± 3.5g, glycine: 145.7 ± 3.0g, vs. L-cysteine: 130.1 ± 2.5g, $p<0.001$, two-way ANOVA, n=6-9).
L-cysteine may therefore contribute towards protein induced satiety by suppressing the release of the orexigenic hormone

ghrelin. Altering the amino acid content of foods may represent a possible intervention to manipulate appetite.

Where applicable, the authors confirm that the experiments described here conform with The Physiological Society ethical requirements.

PCC311

Effect of Cassava (Manihot Esculenta) Feed Formulations on Tetra-iodothyronine (T4), Tri-iodothyronine (T3) and Thyroid stimulating hormone (TSH) of Adult Wister Rats

A.O. Oyabambi

Physiology, university of Ilorin, Ilorin, Kwara, Nigeria

Cassava meals are common in many tropical countries and are processed into different forms of human delicacies and animal feeds (Adekunle et al.2011) .It is fast becoming the major ingredient of many diets in Nigeria especially in the bakery, brewery and pharmaceutical industries. . A study was conducted to determine the effect of cassava feed formulations on thyroid functions and their relevance in clinical diagnosis. Thirty wister rats mean weight of 238±25.6g were acclimatized for one week and fed the different cassava feed formulations and water ad libitum. Thereafter, the rats were sorted out into 5 groups of six each. Group 1,2,3,4 and 5(control) were fed on 30g each of garri, cassava flour, tapioca, fresh cassava and grower's mash (local rat diet) respectively. After 4 weeks, each animal was exposed to 5mls of chloroform in cotton wool and anaesthetized by inhalation. Blood samples were collected by cardiac puncture and then assay for tetra-iodothyronine (T4), tri-iodothyronine (T3) and thyroid stimulating hormone (TSH). The data obtained were presented in tables and the significance determined at $p<0.5$ using paired samples t-test. In comparison with the control, group1 shows a significant decrease in T3 and T4 and group 2 shows a significant increase in T4 and TSH $p<0.05$. Group 3 shows a significant decrease in level of TSH $p<0.05$ while in group 4, the increase in T3 and T4 and the decrease in TSH had no statistical significant difference $p>0.05$.It was concluded that garri and cassava flours lower thyroid functions (goitrogens) while Tapioca and fresh cassava increase serum T3 and T4 activities and could worsen cases of hyperthyroidism.

Adekunle A.A., Fatunbi A.O. and Sanni L.O(2011). Commercial Utilization of Cassava in Nigeria, an Illustrated Guide

1. Biliaminu S.A.Department of Chemical Pathology, University of Ilorin, Ilorin.

2. Ajayi O.A.Departments of Physiology, University of Ilorin, Ilorin.

Where applicable, the authors confirm that the experiments described here conform with The Physiological Society ethical requirements.

PCC312

Assessment of correlation of microcirculation parameters and secretion of c-peptide in diabetic patients

O.V. Suchkova(Makeeva)

Scientific clinical center JSC "Russian Railways", Moscow, Russian Federation

The growing incidence of the overweight has an enormous impact on increasing the risk of impaired glycemic control or insulin resistance and peripheral vascular disease. Often the problem of diagnosing errors lies in the development of contrinsular reactions in response to hyperinsulinism. The assessment of this condition is extremely complicated in the laboratory-instrumental level. Due to the rapid hormone destruction in blood serum the definition of insulin secretion is difficult.

Purpose of the study: To assess correlation between microcirculation parameters and secretion of c-peptide in diabetic patients.

Material and methods: A population of 72 diabetic patients was divided into 2 groups: group 1 included 31 normotensive patients with diabetes type 2 (49,7±10,9 years) with normal secretion of c-peptide (697,2±284,4 pmoll), group 2 consisted of 40 patients with diabetes (49,9±9.1 years) and c-peptide hypersecretion (1317,3±502,9 pmoll). In both groups there were the patients with the early stage of arterial hypertension. The level of glycated hemoglobin was similar in both groups: 8,37±1,9% in the 1st one and 8,2±1,7% in the 2nd one. The control group (n=43) consisted of nondiabetic normotensive individuals (50,1±9,9 years).

We performed a non-invasive vital capillaroscopy (Center for Analyses of Substances) to evaluate the density of vascular network, degree of coiled capillaries, diameters of capillary parts, perivascular zone size, average capillary blood velocity (aCBV) and blood aggregation.

Results: In the second diabetic group with C-peptide hypersecretion high value of BMI (Body Mass Index) was revealed, compared to the 1st group that confirmed the relationship of obesity and insulin resistance hypersecretion of c-peptide on the back of metabolic syndrome. Most important difference in microcirculation parameters was a significant expansion of the diameters of all parts of capillaries, especially of arterial one ($p<0,05$) that confirmed the anabolic effect of c-peptide on microcirculation system on the background of the decrease of the aCBV, which was significantly lower ($p<0,03$) in diabetic patients, than in the controls. Coiled capillaries quantity in both groups was significantly lower in comparison with the controls ($p<0,05$). There was no significant difference in the density of vascular network between the diabetic group and the controls.

Conclusion: C-peptide hyper secretion resulted in microcirculation abnormalities more than diabetes with c-peptide normal secretion, especially regarding expansion of diameters of all parts of capillaries. We suppose it is possible to assess abnormal c-peptide secretion with the help of the non-invasive vital capillaroscopy. Microcirculation parameters are already changed in the first weeks of administration of drugs that affect hyperinsulinism.

Makeeva O.V., Gurfinkel Y.I. «The significance of micro and macrocirculation in clinical trials at patients with diabetes type 2», Paris 2011 (in frame of CVCT forum).

Where applicable, the authors confirm that the experiments described here conform with The Physiological Society ethical requirements.

PCC313

Glycemic control behaviors among adults with type 2 diabetes mellitus: preliminary results from the western province of Sri Lanka

T. Amarasekara[4,2], W. Fongkaew[2], C. Chanprasit[3] and S. Wimalasekera[1]

[1]Department of Medical education and Health sciences, Faculty of Medical Sciences, University of Sri Jayewardenepura, Nugegoda, Sri Lanka, [2]Nursing Science, Faculty of Nursing, Chiang Mai University, Chiang Mai, Thailand, [3]Public health Nursing, Faculty of Nursing, Chiang Mai University, Chiang Mai, Thailand and [4]physiology, University of Sri Jayewardenepura, Nugegoda, Sri Lanka

Amarasekara A.A.T.D1, Fongkaew W2, Chanprasit C3, Wimalasekera S. W.4
Institutions: Department of Medical education and Health sciences1, Department of Physiology4, Faculty of Medical Sciences, University of Sri Jayewardenepura, Nugegoda, Sri Lanka; Nursing Science division2, & Department of Public health nursing3, Faculty of Nursing3, Chiang Mai University, Chiang Mai, Thailand

The prevalence of type 2 Diabetes mellitus (T2DM) has increased over the last decade and is expected to continue to increase in Sri Lanka. Most Sri Lankan diabetics are in the working age and debility amongst them adds to the economic burden of the country. Diabetics are advised on appropriate medical therapy, dietary and life style modifications free of charge in health care institutions, but most patients' compliance to the advice is poor. This study attempts to determine these effects using quantitative data from patients. The objective of the study was to determine the glycemic control and behavioral factors influencing glycemic control among adults with T2DM. A descriptive cross sectional study was done on consenting T2DM patients (n=50) attending diabetic clinics. Data were obtained by interviewer administered questionnaire and medical records. The data were analysed using SPSS version 16 statistical software. The mean age of the males and females were similar and the gender ratio was 1:1. The fasting blood glucose (FBS) was normal in only 14.3% subjects. The mean FBS was 172.9 ± 62.2 (SD) and 177.7 ±72.9 mg/dL (SD) respectively for females and males ($p > 0.05$). There was a significant negative correlation between the BMI and the diet control/exercise pattern among the subjects in this study (Pearsons correlation coefficient - 0.286, $p < 0.04$). There was a positive association between FBS and BMI ($p< 0.05$). Diet control behavior ($p > .05$), and duration of diabetes ($p > 0.05$) were not associated with the FBS in this study. HbA1C is not routinely assessed amongst Sri Lankan patients attending free health care facilities in Sri Lanka. 27% patients were engaged in some physical activity. The study reveals that dietary control and regular exercise are aspects poorly addressed by T2DM patients in Sri Lanka. Although glycaemic control is considered a priority most patients were not motivated to actively control their glycaemic levels by dietary control, and regular exercise and compliance to medication.

research grant ASP/06/RE/MED/2012/38 of the University of Sri Jayewardenepura is gratefully acknowledged

Where applicable, the authors confirm that the experiments described here conform with The Physiological Society ethical requirements.

PCC314

The effect of cAMP on cytosolic calcium oscillations in beta cells within mouse pancreatic slices

M. Skelin Klemen[1], J. Dolensek[1], A. Stozer[1,2], S. Seino[4] and M. Slak Rupnik[3,2]

[1]Institute of Physiology, University of Maribor, Faculty of Medicine, Maribor, Slovenia, [2]Centre for Open Innovations and Research, University of Maribor, Maribor, Slovenia, [3]Institute of Physiology/CIPKEBIP, University of Maribor, Maribor, Slovenia and [4]Division of Cellular and Molecular Medicine, Department of Physiology and Cell Biology, Kobe University Graduate School of Medicine, Kobe, Japan

Insulin is secreted from pancreatic beta cells in response to glucose stimulation via regulated exocytosis. The exocytosis of insulin granules is triggered upon increase in cytosolic calcium concentration and can be further amplified by cAMP [1]. How does cAMP amplify glucose-induced insulin secretion? General consensus is that cAMP augments insulin secretion by acting through PKA- and Epac2-dependent pathways, but precise mechanism is not fully understood [2, 3]. It was previously suggested that one of the many roles of cAMP is the enhancement of calcium signals either by voltage-dependent calcium entry or intracellular calcium mobilization [4]. To determine the role of cAMP in calcium dynamics we used forskolin which increases the cytosolic cAMP concentration through the activation of adenylate cyclase. Oregon Green 488 BAPTA-1 AM (OGB-1) calcium dye was used to record oscillatory changes in cytosolic calcium concentration in mouse pancreas tissue slices using confocal laser scanning fluorescence imaging. In the absence of forskolin the sub-stimulatory glucose concentration failed to increase cytosolic calcium concentration in beta cells while the stimulatory glucose concentration caused stable fast calcium oscillations (3-6/min) on a sustained plateau phase. Addition of 10 μM forskolin in the extracellular solution triggered high frequency calcium oscillations (3-6/min) even at otherwise sub-stimulatory glucose concentration. The effect on calcium oscillations was belated, triggered several minutes after the addition of forskolin. When the same concentration of forskolin was added to the extracellular solution together with the stimulatory glucose concentration, the frequency of calcium oscillations almost doubled (6-12/min) compared to glucose stimulus only. Again, the effect of forskolin was observed after several minutes. To determine which of the two cAMP dependent pathways was responsible for augmented calcium oscillations in pancreatic beta cells, we performed the same sets of experiments on the pancreatic slices from mice lacking the Epac2 protein. Most probably Epac2 is not crucial for cAMP-augmented cytosolic calcium oscillations in mouse pancreatic beta cells since forskolin triggered calcium oscillations at sub-stimulatory glucose concentration also in the Epac2 KO mice. Furthermore, at stimulatory glucose concentration the frequency of calcium oscillations was increased after addition of forskolin. These results corroborate previously published data describing that phosphorylation of several targets by PKA is responsible for cAMP augmented calcium oscillations in pancreatic beta cells [5].

Malaisse WJ, Malaisse-Lagae F & Mayhew D. (1967). A possible role for the adenylcyclase system in insulin secretion. The Journal of clinical investigation 46, 1724-1734.

Renström E, Eliasson L & Rorsman P. (1997). Protein kinase A-dependent and -independent stimulation of exocytosis by cAMP in mouse pancreatic B-cells. The Journal of physiology 502, 105-118.

Seino S & Shibasaki T. (2005). PKA-Dependent and PKA-Independent Pathways for cAMP-Regulated Exocytosis. Physiol Rev 85, 1303-1342.

Kang G, Chepurny OG, Rindler MJ, Collis L, Chepurny Z, Li WH, Harbeck M, Roe MW & Holz GG. (2005). A cAMP and Ca2+ coincidence detector in support of Ca2+-induced Ca2+ release in mouse pancreatic beta cells. The Journal of physiology 566, 173-188.

Ammala C, Ashcroft FM & Rorsman P. (1993). Calcium-independent potentiation of insulin release by cyclic AMP in single beta-cells. Nature 363, 356-358.

Where applicable, the authors confirm that the experiments described here conform with The Physiological Society ethical requirements.

PCC315

Vitamin D levels in type 2 diabetic individuals

M.A. Kanpurwala[1] and K. Afzal[2]

[1]Physiology, University of Karachi, Karachi, Sindh, Pakistan and [2]Dow University of Health Sciences, Karachi, Pakistan

Type 2 diabetes Mellitus (T2DM) is a chronic disease which has an increased risk for hip and vertebral fracture. Diabetic bone is showed to be more fragile than non-diabetic bone [1] and is another possible cause of disability in these patients after a trauma or fall [2]. Diabetes may affect the bone in multiple ways including change in bone mass density especially when there is deficiency of vitamin D which worsens the condition. It has been seen that vitamin D and calcium are required for good skeletal health. Adequate vitamin D levels prevent autoimmune diseases, hypertension, and diabetes and there is reduced risk of cancer and falls or fractures [3]. Many studies have shown some association between impaired glucose mediated insulin release and decrease levels of serum vitamin D [4]. Thus, the present study is conducted to assess the serum Vitamin D levels in T2DM patients. Despite good exposure to sunlight in this part of the world, the vitamin D deficiency has become more prevalent and the basis of risk of diabetes and its related falls and fractures.

We conducted a cross sectional study in which 210 T2DM patients who visited the diabetic Out Patient Department of National Institute of Diabetes and Endocrinology were enrolled in the study after an informed consent. Patients with Tuberculosis, Patients with known renal or liver or thyroid diseases were excluded from the study. Demographic profile and anthropometric measurements of these patients were noted and blood sample was collected from each subject to assess glycosylated haemoglobin (HbA1c) levels, serum calcium and Vitamin D levels.

It was observed that majority of patients (n=113; 53.8%) had diabetes for 5-10 years, followed by 25.7% in those with less than 5 years, 16.2% in those with 11-15 years whereas only 4.3% had diabetes for more than 15 years. Though the mean vitamin D of the sample was 10.04 +6.65ng/dl, the levels greatly varied across the sample, minimum being 3.99 and the maximum being 48ng/dl. Mean serum calcium was 8.98 +0.64 mg/dl. The mean HbA1c of sample was 8.47 +3.79gm%. Only 0.5% of the total sample have sufficient Vitamin D levels, while 37.1% of sample have insufficient levels of Vitamin D. Majority of the subjects i.e. 62.4% have vitamin D deficiency.

This study confirms the association between serum vitamin D levels and diabetes mellitus. This uncovers the fact that diabetics individuals in our population are suffering from significant vitamin D deficiency. It is suggested that future studies should be carried out to address the efficacy of vitamin D supplementation in preventing frequency of falls and fractures in diabetic patients.

CATEGORIZATION OF VITAMIN D LEVELS (n=210)

Levels	Frequency (n=210)	Percentages (%)
Deficiency	131	62.4
Insufficiency	78	37.1
Sufficiency	01	0.5

Jehle PM, Jehle DR, Mohan S, Bohm BO. Serum levels of insulin-like growth factor system components and relationship to bone metabolism in type 1 and type 2 diabetes mellitus patients. Journal of endocrinology 1998;159(2):297

Adami S. Bone health in diabetes: considerations for clinical management. Current medical research and opinion 2009;25(5):1057-72.

Pittas AG, Lau J, Hu F, Dawson-Hughes B. The role of vitamin D and calcium in type 2 diabetes. A systematic review and meta-analysis. Journal of Clinical Endocrinology & Metabolism 2007:2017-29.

Khazai N, Judd SE, Tangpricha V. Calcium and vitamin D: skeletal and extraskeletal health. Current rheumatology reports 2008;10(2):110-7

Where applicable, the authors confirm that the experiments described here conform with The Physiological Society ethical requirements.

PCC316

Regulation of insulin and glucagon secretion in a mouse model of neonatal diabetes

M.F. Brereton[1], M. Iberl[1], A. Clark[2], P. Rorsman[2] and F.M. Ashcroft[1]

[1]Department of Physiology, Anatomy and Genetics, University of Oxford, Oxford, UK and [2]Oxford Centre for Diabetes, Endocrinology and Metabolism, University of Oxford, Oxford, UK

Neonatal diabetes, diagnosed as severe hyperglycaemia within the first 6 months of life, is often caused by gain-of-function mutations in the K_{ATP} channel subunit, Kir6.2. Using a conditional transgenic mouse model selectively expressing the Kir6.2-V59M mutation exclusively in pancreatic β-cells (iβ-V59M), we investigated the effect of hyperglycaemia on pancreatic function.

Gene expression was induced at 12 weeks of age and resulted in severe hyperglycaemia within 2 days (control: 6.0±0.1mM vs. iβ-V59M: 23.7±1.0mM). After 4 weeks, blood glucose was 26.2±0.5mM and postprandial serum insulin had decreased (control: 0.6±0.3pM vs. iβ-V59M: 0.1±0.03pM) but no changes in serum glucagon levels were detected (73.5±2.4pM vs. 80.8±21.5pM). Glucose tolerance was impaired and glucagon sensitivity increased in iβ-V59M mice as assessed using an intraperitoneal glucose and glucagon tolerance test, respectively. Four-week exposure to hyperglycaemia resulted in a ~3-fold reduction in total pancreatic islet area from 17.5±2.6μm2x10-5 (controls) to 5.3±0.8μm2x10-5 (iβ-V59M). The remaining islets were predominantly composed of glucagon-positive cells; the percentage of islet area composed of glucagon-positive cells increased from 16.6±0.9% (controls) to 73.5±2.1% (iβ-V59M). This was accompanied by a marked reduction in insulin-positive cells (control 86.5±0.3% vs. iβ-V59M 27.8±1.7%).

iβ-V59M mice were implanted subcutaneously with a high-dose, slow-release pellet (17mg/kg/day) of the sulphonylurea glibenclamide, which closes K_{ATP} channels. Within 2 days of implantation, blood glucose had returned to control levels

(6.1±0.1mM) and remained stable for 4 weeks. Glibenclamide therapy improved glucose tolerance, but did not restore it to that of control mice. However, it prevented the reduction in islet area and changes in insulin/glucagon-positive cell number.
Gain-of function mutations in β-cell Kir6.2 subunits result in hyperglycaemia, hypoinsulinemia and alterations in glucose tolerance, glucagon sensitivity and islet cell morphology. These effects can be prevented, in part, by glibenclamide therapy. Therefore, iβ-V59M provides a good model to study the effects of hyperglycaemia on pancreatic function.

Where applicable, the authors confirm that the experiments described here conform with The Physiological Society ethical requirements.

PCC317

Alterations in metabolic relations and adiposity during and after cigarette smoke exposition, in young female and male mice

R.P. Gaspar-Reis, C.C. Silva, T.S. Magdalena, E.G. Aguiar, K.P. Albuquerque, S.S. Alves, A.S. Santos, Y.A. VIllaça, E.P. Garcia-Souza and C.A. Nascimento-Saba

Physiological Sciences, University of Rio de Janeiro State, Rio de Janeiro, Rio de Janeiro, Brazil

Cigarette smoking is worrisome in adults and also in adolescents. Actually, smoking rates have grown and little is known about the damages caused in these organisms still young and the consequences in adulthood (1, 2). This study aims evaluate the influence of smoking in puberty and the consequences of withdrawal in body composition of female and male mice. At 35 days, Swiss mice reproduced and maintained at the animal house of Phisiological Sciences department were exposed to 3R4F cigarette smoke (Tobacco and Health Research Institute), 8 h/day for 15 days (S, n = 24).Then, half of animals were evaluated and the other half was maintained and evaluated thirty days after stop exposure (30d AS). An unexposed group accompanied the events (NS, n = 24). Body mass, food intake, body composition (by Dual-energy X-ray Absorptiometry, DEXA), serum levels of insulin, lipids and glucose (ipGTT), subcutaneous and intra-abdominal adipose tissue mass were evaluated. During all experimental period food intake was similar in all groups (5.06±0.35g), however, S groups showed lower body mass gain. 30dAS, female S group presented similar body mass (36.39±0.56g) while male S group presented lower body mass (NS: 46.64±1.05g; S: 45.06±1.05g). In females was observed a significant increase in total body (NS: 11.86±0.07g; S: 15.17±0.87g) and trunk fat (NS: 9.17±1.16g; S:13.00±0.68g) during exposure and in lean mass 30dAS (NS: 13.60±1.89g; S:17.25±1.49g), while no alterations were developed in male's body composition. In males none region of fat differs during exposure: retroperitoneal (NS:0.411±0.030; S:0.475±0.079), mesenteric (NS:0.344±0.036; S:0.349±0.051) and subcutaneous (NS: 0.243±0.066; S:0.290±0.062). While in females the retroperitoneal was increased (NS: 0.360±0.039; S:0.575±0.079), the mesenteric decreased (NS:1.077±0.08; S:0.917±0.242) and subcutaneous did not alters (NS: 0.217±0.021; S:0.287±0.026). In regard to serum analyses during exposure, females had higher insulinemia and glycemia at 30min but no alterations were observed in males. On the other hand, withdrawal induced in male high insulinemia and low glycemia but in female, normal insulinemia and low glycemia. The set of results indicates different response to cigarette smoke in young that seem to start in females and lead malefic metabolic alterations in adulthood.

Muller F, Wehbe L, Smoking and smoking cessation in Latin America: a review of the current situation and available treatments. Int J Chron Obstruct Pulmon Dis; 3 (2):285-93, 2008.

Nuorti JP, Butler JC, Farley MM, Harrison LH, McGeer A, Kolczak MS, Breiman RF. Cigarette smoking and invasive pneumococcal disease. Active Bacterial Core Surveillance Team. N Engl J Med. Mar 9;342(10):681-9, 2000.

We express our gratitude to Nutrition Institute of the University of Rio de Janeiro State for the use of DEXA (DXA/Lunar IDXA-GE Healthcare), to Dr Mario José S Pereira for the support on static analysis and the use of video capture system. The research was supported by Fundação Carlos Chagas Filho de Amparo à Pesquisa do Estado do Rio de Janeiro (FAPERJ-Brazil) and Sub-reitoria de Pós-graduação e Pesquisa da Universidade do Estado do Rio de Janeiro (SR2-UERJ).

Where applicable, the authors confirm that the experiments described here conform with The Physiological Society ethical requirements.

PCC318

Altered agonist sensitivity of the N321K mutation of type-2 vasopressin receptor in a patient with nephrogenic diabetes insipidus

L.S. Erdélyi[1], A. Balla[1], M. Tóth[2] and L. Hunyady[1]

[1]Department of Physiology, Semmelweis University, Budapest, Hungary and [2]2nd Department of Internal Medicine, Semmelweis University, Budapest, Hungary

Loss of function mutations of the type-2 vasopressin receptor (V2R) in kidney lead to nephrogenic diabetes insipidus (NDI). The function of misfolded mutant receptors can be rescued using pharmacochaperons, which promote plasma membrane localization of V2Rs. We identified with genetic analysis a previously described, but not characterized, mutation in a NDI patient. In order to determine personalized therapy for the individual, properties of the mutant receptor were characterized. Based on the findings we could propose a therapeutical strategy.
The N321K mutation was identified with sequencing of the PCR product of genomic DNA isolated from peripheral blood. We constructed a highly sensitive Epac based BRET (bioluminescence resonance energy transfer) biosensor to perform real-time cAMP measurments. The β-arrestin binding of the receptors was examined with luciferase-tagged β-arrestin and mVenus-tagged V2Rs using BRET technique. The BRET measurements were performed on transiently transfected HEK293 cells using 96-well plates and Berthold Mithras LB 940 multilabel reader. Cell surface expression was determined with flow cytometry using anti-HA-Alexa488 antibodies. Localization examinations were implemented with fluorescent tagged receptors visualized with Zeiss LSM510 confocal laser-scanning microscope. The effect of agonists on V1R was tested on mouse arteries by wire myography.
Previous studies have identified the pathogenic N321K mutation is in the 7th transmembrane helix of the V2R. Flow cytometry and confocal microscopy revealed that cell surface expression of the mutant receptor is similar to that of the wild type receptor. Determination of the ligand induced cAMP generation of the mutant receptor showed increased EC50 in arginine-vasopressin (AVP) stimulation and lack of signal in desmopressin (DDAVP) stimulation. BRET experiments revealed

decreased β-arrestin binding of N321K-V2R. The mutant receptor also showed different sensitivity for V2R agonists. Valine-desmopressin (DVDAVP) relatively efficiently stimulated N321K-V2R, whereas even high doses of DVDAVP did not have effect on mouse arterioles, which are sensitive to AVP-induced vasoconstriction.
N321K mutant V2R showed cell surface expression, the physiologically essential cAMP generation of the receptor can be activated with elevated dose of AVP, while with clinically used DDAVP was not efficient. Different internalization of the receptor may occur through altered β-arrestin binding. Function of the mutant receptor can be rescued with administration of V2R receptor agonist DVDAVP, which had no detectable side effects on V1R in the effective concentration. Our in vivo experiments suggest that DVDAVP can rescuse the function of the N321K-V2R in a NDI patient with no significant side effect on V1R.
Supported by TÁMOP (4.2.1.B-09/1/KMR-2010-0001), OTKA 100883.

Where applicable, the authors confirm that the experiments described here conform with The Physiological Society ethical requirements.

PCC320

High-fat diet intake suggests changes in reproductive function of young male rats

C.C. Silva, R.P. Gaspar-Reis, E.O. Guedes de Aguiar, A.S. Santos, S.S. Alves, K.P. Albuquerque and C.A. Nascimento-Saba

Physiological Sciences, State University of Rio de Janeiro, Rio de Janeiro, Brazil

Obesity seems affect reproductive function, lowering sex hormones and reducing sperm concentration. Excess of lipids on diet influences metabolism and testis reproductive function. Among physiological determinants of weight and appetite are Leptin and insulin, hormones secreted in proportion to fat mass and glucose levels regulating peripherally the metabolism, moreover in hypothalamus interact with receptors, favoring satiety (1). Obese people may have higher serum concentrations of this hormones and exhibit resistance to its action. The relationship between obesity, reproductive changes and metabolic syndrome is not yet fully clarified (2). Thus, the aim of the study was evaluate the effect of high fat diet, containing soybean oil, on body composition and reproductive system of young male rats.
Wistar rats, at 21days (after weaning) were fed with diet containing 7% (control diet, C) or 19% (high fat diet, HF) of soybean oil, manufactured according to AIN-93 G, until 30 and 60 days of age. At the end of each experimental period, body composition was evaluated by Dual-energy X-ray Absorptiometry (DEXA) and liver, adipose tissue, testis, epididymis and blood were collected. Serum analysis of glucose, lipids, insulin, leptin and testosterone were measured. During all experimental period food intake and body mass were monitored but no difference was observed between groups.
After feeding animals with a high-fat diet for nine days showed a higher testosterone concentration (C:1.36±1.1; HF:24.9±6.4ng/dl), while surprisingly lean mass (C:60.0±3,03; HF: 42,6 ±3,47g) and triglycerides (C:60.0±9.6; HF:32.7±6.9mg/dl) decreased, in spite of the protein content control and the high percentage of soybean oil in the diet. At 60 days, testosterone (C: 0.95±0.26; HF:30.4±3.5ng/dl), epididimal mass (C:0.3±0.01; HF:0.41±0.026g), mesenteric adipose tissue mass (C:2.15±0.18; HF:3.09±0.32g), liver mass (C:8.25±0,2; HF: 10.5±0,55g) and glucose (C:167.5±10.8; HF: 269.8±20.0mg/dl) increased in HF group. The other evaluated parameters, total fat mass (C:24.8±2,0/HF:28.0±2.17g;C:64,0±1,54/HF:59,67±6,108g); leptin (C: 0.98±0.17/ HF:1.34±0,17;C: 1,50±0,08/HF:2,04±0,35 ng/ml) and insulin (C: 21.9±29/HF: 21.4±3.9; C:25.8±4.6/HF:27.8±4.6 ng/ml) did not differ between the groups at 30 and 60 days, respectively.
Since nine days of high-fat diet intake, the excess of lipids reflects negatively on testis function with high levels of testosterone. Moreover, after thirty nine days of high-fat diet intake the effects on adiposity, glycemia and reproductive function are more evidents. It could predict some adult reproductive dysfunction, once the changes started early and were increasing in these young animals.

HALPERN ZSC, RODRIGUES MDB, COSTA RF. Determinantes fisiológicos do controle do peso e apetite. 2004. Rev. psiquiatr. Clin. v.31 n.4 São Paulo.

SANDE-LEE SV, VELLOSO LA. Disfunção hipotalâmica na obesidade. Arq Bras Endocrinol Metab. 2012; 56(6)

Our gratitude to the Nutrition Institute for the use of DEXA, and Mr Ulisses Risso for animals care. The research was supported by CAPES and FAPERJ.

Where applicable, the authors confirm that the experiments described here conform with The Physiological Society ethical requirements.

PCC321

A role for large conductance calcium-voltage activated potassium channels in inflammatory mediator release in murine 3T3-L1 adipocytes

T. Scullion and S. Dolan

School of Life Sciences, Glasgow Caledonian University, Glasgow, UK

Large conductance calcium-voltage activated potassium (BKca) channels are important modulators in an extensive number of cellular functions, including hormone release from endocrine cells. White adipose tissue is increasingly regarded as the largest endocrine organ in the body, and adipocytes as key regulators of inflammation through the synthesis and secretion of a battery of pro- or anti-inflammatory cytokines. This study set out to characterise the expression of BKca channel and a "gain of function" splice variant STREX in adipocytes, and investigate BKca channels as potential modulators of cytokine release from these cells.
Mouse fibroblast 3T3-L1 pre-adipocyte cells were cultured in DMEM with 10% foetal bovine serum (FBS), and differentiated into mature adipocytes by replacing cell growth media with 10% FBS DMEM supplemented with 0.5 mM 3-isobutyl-1-methylated, 0.25 μm dexamethasone and 1 μg/ml insulin and incubated for 48 hours. Thereafter, cells were treated with media with 10% FBS, 1 μg/ml insulin complemented DMEM for up to 10 days. Total RNA was extracted on day 0, 4, 8, 10 and 10+ (n = 5 per group), reverse transcribed and levels of BKca and STREX mRNA, and the pro-inflammatory cytokines tumour necrosis factor (TNF)-α, interleukin (IL)-6 and IL-1β mRNA, and the anti-inflammatory cytokine IL-10 mRNA measured using real-time PCR. The effects of treating mature adipocytes (day 10+) for 24 hours with the BKca channel agonist NS 1619 (20 μg), or channel blocker iberiotoxin (IBX; 10

ng), or drug-vehicle on gene expression were also analysed. Values are means ± S.E.M., compared by ANOVA.
BKca and STREX mRNA and all four cytokines examined were found to be constitutively expressed in both pre- and mature adipocytes. In mature day 10 adipocytes, a 2 fold up-regulation in BKca and 32 fold STREX mRNA expression was observed. TNF-α, IL-6 and IL-1β mRNA were induced in mature day 10 adipocytes (all $P < 0.01$ vs. day 0); IL-10 mRNA levels were unchanged. Following treatment with IBX, futher up-regulation in expression of TNF-α (4 fold), IL-6 (2.7 fold) and IL-1β (6 fold), but not IL-10 mRNA were detected ($P < 0.01$ vs. vehicle and NS 1619 treated cells).
These data show that BKca channel and splice variant STREX are expressed in adipocytes. Furthermore, adipocyte derived pro-inflammatory cytokines were induced by blockade of BKca channel activity. These findings suggest that BKca channels may play a role in regulating the inflammatory response associated with obesity

Poulsen, A. N., H. Wulf, et al. (2009). "Differential expression of BK channel isoforms and beta-subunits in rat neuro-vascular tissues." Biochimica et biophysica acta 1788(2): 380-389

Cui, J., H. Yang, et al. (2009). "Molecular mechanisms of BK channel activation." Cell Mol Life Sci 66(5): 852-875.

Chen, L., L. Tian, et al. (2005). "Functionally diverse complement of large conductance calcium- and voltage-activated potassium channel (BK) alpha-subunits generated from a single site of splicing." The Journal of biological chemistry 280(39): 33599-33609.

Chen, S. R., Y. Q. Cai, et al. (2009). "Plasticity and emerging role of BKCa channels in nociceptive control in neuropathic pain." J Neurochem 110(1): 352-362.

Woolf, C. J., & Salter, M. W. (2000). Neuronal plasticity: increasing the gain in pain. Science, 288(5472), 1765-1769.

Where applicable, the authors confirm that the experiments described here conform with The Physiological Society ethical requirements.

PCC322

Plasma TNF-α in obese type II diabetic patients: Is it a cause or a result of hyperglycemia?

T.H. Merghani and A.O. Alawad

Physiology, Tabuk University, Tabuk, Saudi Arabia

Hyperglycemia is a known cause of inflammation (1,2) followed by increased production of acute phase proteins and pro-inflammatory cytokines, including TNF-α.(1-3) Monocytes taken from diabetic patients produce higher levels of TNF-α in comparison with control monocytes taken from healthy subjects.(4) On the other hand, TNF- α is a known cause of hyperglycemia secondary to insulin resistance. Hypoglycemia was reported as one of the complications of treatment with TNF-α inhibitors.(5) This study was conducted to evaluate plasma TNF-α in obese diabetic patients and to determine its relation to glycemic control. A random sample of 40 obese type II diabetic patients (cases) and 40 obese non-diabetic subjects (controls) were interviewed and examined clinically to exclude presence of acute or chronic medical illness. The two groups were matched according to age, sex, body mass index and area of residence. Hemoglobin A1c was measured for each participant using the "NycoCard Hemoglobin A1c test" (Axis -Shield/ Norway). Fasting blood sugar was measured using one touch® glucometer (LifeScan Canada Ltd). Plasma TNF-α was measured using commercially available ELISA kits from ADIPO Bioscience/ USA. The research conforms to the ethical principles of medical research developed by the World Medical Association Declaration of Helsinki. The chi square test was used to test distribution of categorical variables. The difference in mean between the test and the control groups was assessed with the independent student's t test. The majority of obese diabetic patients had high plasma TNF-α values (≥ 5pg/ml) with "mean ± SEM" = "11.09 ± 3.03" whereas the majority of obese non-diabetic subjects had lower values with "mean ± SEM" = "4.68 ± 2.31"; P= 0.003. More than half (58%) of those with high TNF-α values had abnormal hemoglobin A1c (≥ 6.5%, P= 0.037). The relation between plasma TNF-α and fasting blood sugar in all participants was statistically insignificant (P= 0.515). These data suggest that the higher plasma TNF-α in obese diabetic patients compared to the non-diabetics cannot be explained by obesity alone since both groups were obese. A significant relation was found between high plasma TNF-α and poorly controlled diabetes mellitus, indicating that hyperglycemia might be responsible for the rise in TNF-α. The relation between plasma TNF-α and fasting blood sugar was statistically insignificant. This indicates that TNF-α production is most probably associated with a long term, rather than a short term effect of hyperglycemia.

Plasma TNF-α among obese diabetic and obese non-diabetic subjects in the study group

Group	< 5 pg/ml n (%)	≥ 5 pg/ml n (%)	Total
Obese Diabetic	18 (45%)	22 (55%)	40 (100%)
Obese Non-diabetic	31 (77%)	9 (33%)	40 (100%)
Total	49 (61%)	31 (39%)	80 (100%)

P= 0.003

Plasma TNF-α in relation to hemoglobin A1c among all participants

Hemoglobin A1c	< 5pg/ml n (%)	≥ 5pg/ml n (%)	Total
< 6.5%	33 (67%)	13 (42%)	46 (57%)
≥ 6.5%	16 (33%)	18 (58%)	34 (43%)
Total	49 (100%)	31 (100%)	80 (100%)

P=0.037

Sposito K, Nappo F, Marfella R, Giugliano G, Giugliano F, Ciotola M, Quagliaro L, Ceriello A, Giugliano D: Inflammatory cytokine concentrations are acutely increased by hyperglycemia in humans: role of oxidative stress. Circulation 2002, 106:2067-2072.

Temelkova-Kurktschiev T, Henkel E, Koehler C, Karrei K, Hanefeld M: Subclinical inflammation in newly detected Type II diabetes and impaired glucose tolerance. Diabetologia 2002, 45:151.

Morohoshi M, Fujisawa K, Uchimura I, Numano F: Glucose-dependent interleukin 6 and tumor necrosis factor production by human peripheral blood monocytes in vitro. Diabetes 1996, 45:954-959.

Gacka M, Dobosz T, Szymaniec S, Bednarska-Chabowska D, Adamiec R, Sadakierska-Chudy A: Proinflammatory and atherogenic activity of monocytes in type 2 diabetes. J Diabetes Complications 2010, 24:1-8.

Czajkowska JB, Shutty B, Zito S. Development of Low Blood Glucose Readings in Nine Non-diabetic Patients Treated With Tumor Necrosis Factor-alpha Inhibitors: a case series. J Med Case Reports. 2012; 6(1):5.

We would like to thank the Department of Physiology/ Al-Neelain University- Sudan for allowing us to use departmental equipment. We would like to extend our thanks to the Ministry of Health and to the administration staff of Gabir Abu-Eliz centre in Khartoum for their kind permission and close supervision during the process of data collection. We would like to express our appreciation and special thanks to the participants for their understanding and cooperation.

Where applicable, the authors confirm that the experiments described here conform with The Physiological Society ethical requirements.

PCC323

Measured versus predicted resting metabolic rate in obese diabetic and obese non-diabetic subjects

T.H. Merghani[1,2] and A.O. Alawad[1,3]

[1]Physiology, Tabuk University, Tabuk, Saudi Arabia, [2]Physiology, Khartoum University, Khartoum, Sudan and [3]Physiology, Al-Neelain University, Khartoum, Sudan

In clinical practice, predictive equations provide valuable information about energy expenditure that is used in estimation of metabolic needs for different individuals; however, accuracy of these equations is questioned in the tropical countries. The aim of this study was to determine which predictive equation is similar to indirect calorimetry in estimation of resting metabolic rate in obese diabetic and obese non-diabetic subjects. A random sample of 40 obese diabetic patients (cases) and 40 obese non-diabetic subjects (controls), 35 to 50 years of age, were selected from patients attending Gabir Abu-Eliz centre in Khartoum- Sudan. The PowerLab 8/35 with a gas analyzer (AD Instruments, Castle Hill Australia) was used for measurement of VO2, VCO2 and RER for each participant. Resting metabolic rate was derived from these parameters using Weir's formula.(1,2) Three predictive equations (Harris-Benedict (3), Mifflin (4) and Food and Agriculture Organization/ World Health Organization/ United Nations University (FAO/WHO/UNU) equations (5) were assessed for their accuracy in predicting resting metabolic rate for the two groups. Using Weir's derivation, resting metabolic rate ("mean±SD" kcal/day) was significantly higher among diabetic patients "1480.7 ± 274.2" compared to non-diabetics "1362.4 ± 184.8"; P= 0.027. The three predictive equations showed insignificant difference between the two groups; P>0.05. Resting metabolic rate measured with indirect calorimetry was significantly different from that measured with Harris-Benedict or FAO/WHO/UNU equations, P<0.05; whereas difference from Mifflin equation was statistically insignificant, P= 0.164. Resting metabolic rate, whether calculated or predicted, was significantly higher among males compared to females; P< 0.05. It was concluded that Mifflin equation is more reliable than Harris-Benedict and FAO/WHO/UNU equations in estimating resting metabolic rate in obese diabetic patients. Predictive equations are unlikely to detect difference in resting metabolic rate between obese diabetic and obese non-diabetic subjects.

Comparison in resting energy expenditure between obese diabetic and obese non-diabetic participants

Measurement method	Study group	Resting metabolic rate (mean ± SD) kcal/day	Confidence intervals kcal/day	P value
Indirect calorimetry	Diabetics (n=40)	1480.7 ± 274.2	1393.0-1568.4	0.027
	Non-diabetics (n=40)	1362.4 ± 184.8	1303.3-1421.5	
Harris-Benedict's equation	Diabetics (n=40)	1646.6 ±176.4	1590.1-1703.0	0.308
	Non-diabetics (n=40)	1689.3±195.7	1627.0-1751.9	
Mifflin's equation	Diabetics (n=40)	1547.6 ± 170.3	1493.2-1602.1	0.198
	Non-diabetics (n=40)	1598.1 ± 177.0	1541.5-1654.6	
FAO/WHO/UNU equation	Diabetics (n=40)	1691.6 ± 194.6	1629.3-1753.8	0.528
	Non-diabetics (n=40)	1719.2 ± 195.1	1656.8-1781.6	

Indirect calorimetry versus Mifflin's equation in calculation of resting metabolic rate

	Resting metabolic rate (kcal/day)			
	Diabetic (n= 40)		Non-diabetic (n= 40)	
Parameter	Indirect Calorimetry	Mifflin's equation	Indirect Calorimetry	Mifflin's equation
Range	1155.6-2238.8	1260.3-1941.3	1057.3-1787.3	1354.0-2023.8
Mean ± SD	1480.7 ± 274.2	1547.6±170.3	1362.4± 184.8	1598.1±177.0
Difference (%)	4.5%		17%	
P value	0.164		0.000	

deWeir JB. New Methods for Calculating Metabolic Rate with Special Reference to Protein Metabolism. J Physiol 1949;109: 1-9.

Mansell PI, Macdonald IA. Reappraisal of the Weir's equation for calculation of metabolic rate. AJP - Regu Physiol 1990; 258(6): R1347-R1354.

Harris J, Benedict F. a biometric study of human basal metabolism. Proc Natl Acad Sci 1918; 4 (12): 370–3.

Mifflin, MD; St Jeor, ST; Hill, LA; Scott, BJ; Daugherty, SA; Koh, YO. A new predictive equation for resting energy expenditure in healthy individuals. The American journal of clinical nutrition 1990;51(2): 241–7

FAO/WHO/UNU. Energy and Protein Requirements. Report of a Joint FAO/WHO/UNU Expert Consultation. Technical Report Series No. 724. Geneva: World Health Organization, 1985.

We would like to thank the Department of Physiology/ Al-Neelain University- Sudan for allowing us to use departmental equipment. We would like to extend our thanks to the Ministry of Health and to the administration staff of Gabir Abu-Eliz centre in Khartoum for their kind permission and close supervision during the process of data collection. We would like to express our appreciation and special thanks to the participants for their understanding and cooperation.

Where applicable, the authors confirm that the experiments described here conform with The Physiological Society ethical requirements.

PCC324

Bronchodilator reversibility among patients with non-obstructive spirometric patterns

T.H. Merghani[1,2] and M.E. Alamin[3]

[1]Physiology, Tabuk University, Tabuk, Saudi Arabia, [2]Physiology, Khartoum University, Khartoum, Sudan and [3]Medicine, National Ribat University, Khartoum, Sudan

Reversibility testing is typically positive in asthmatic patients showing obstructive pattern on spirometry; however, few studies evaluated this test among overweight and obese patients presenting with non-obstructive patterns. A sample of 218 overweight and obese adult asthmatic patients who satisfactorily completed spirometry and bronchodilator reversibility testing were selected for analysis. A portable spirometer (All flow, Clement Clarke International, UK) was used for measurement of lung ventilator function for each patient before and after inhalation of four separate doses of 100μg salbutamol given by a metered dose inhaler and using a spacer. Female to male ratio was 1.9:1. BMI (mean (SD)) was 31.6 (4.7). About one third of patients showed positive reversibility testing. Among these, more than one third (38%) had restrictive pattern, one third (33%) had combined pattern, 22% had obstructive pattern and only 7% had normal pattern (P= 0.000). Statistical differences between males and females in both spirometric patterns and reversibility testing were insignificant (P= 0.822 & 0.082 respectively). Reversibility testing was found to be positive in a significant proportion of overweight and obese asthmatic patients presenting with non-obstructive patterns on spirometry. The diagnosis of asthma can be confirmed with positive reversibility testing irrespective of spirometric pattern.

		Normal n (%)	Obstructive n (%)	Restrictive n (%)	Combined n (%)	Total	P value
Gender	Male	13 (18%)	11 (15%)	37 (50%)	13(18%)	074 (100%)	0.822
	Female	27 (19%)	27 (19%)	63 (44%)	27 (19%)	144 (100%)	
	Total	40 (18%)	38 (17%)	100 (46%)	40 (18%)	218 (100%)	
Reversibility	Positive	5 (7%)	17 (22%)	29 (38%)	25 (33%)	076 (100%)	0.000
	Negative	35 (25%)	21 (15%)	71 (50%)	15 (10%)	142 (100%)	
	Total	40 (18%)	38 (17%)	100 (46%)	40 (18%)	218 (100%)	

Parameter		Reversibility Testing			P value
		Positive n (%)	Negative n (%)	Total n (%)	
Gender	Male	20 (27%)	54 (73%)	074 (100%)	0.082
	Female	56 (39%)	88 (61%)	144 (100%)	
Age (years)	< 40	28 (30%)	64 (70%)	92 (100%)	0.362
	40-59	28 (35%)	51 (65%)	79 (100%)	
	≥ 60	20 (43%)	27 (57%)	47 (100%)	
Height (cm)	< 160	62 (38%)	101 (62%)	163 (100%)	0.090
	≥ 160	14 (25%)	41 (75%)	55 (100%)	
BMI	25-29.9	29 (30%)	67 (70%)	96 (100%)	0.201
	≥ 30	47 (39%)	75 (61%)	122 (100%)	

Restrictive pattern is the most dominant spirometric pattern among overweight and obese asthmatic patients. Positive reversibility testing is found in a significant proportion of patients with restrictive pattern.

Reversibility testing is not related to gender, age, height or BMI of patients in the study group (P > 0.05)

We would like to express our appreciation and special thanks to the participants for their understanding and cooperation.

Where applicable, the authors confirm that the experiments described here conform with The Physiological Society ethical requirements.

PCC326

Investigation of hypoglycaemic effect of the methanolic leaf extract of *A.lindleyana* on rats

B. Samanmali[1], M. Gunatilake[2], R.D. Guneratne[1] and T. Perera[3]

[1]Chemistry, University of Colombo, Colombo 3, Western, Sri Lanka, [2]Physiology, University of Colombo, Colombo 8, Western, Sri Lanka and [3]University of Colombo, Colombo 8, Western, Sri Lanka

Diabetes mellitus is considered as a major public health problem and one of the leading causes of deaths in the world today. There are many herbal preparations used in ayurvedic and other traditional systems of medicine which are claimed to have hypoglycaemic potential with fewer side effects. This study investigated the hypoglycaemic effect of tender leaves of the medicinal plant named *Aporusa lindleyana*.[1] The hypoglycaemic effect of the methanolic leaf extract of *A. lindleyana* on fasting blood glucose level, random blood glucose level and the effect on oral glucose load were tested using three oral doses of the extract (100, 400, 800 mg/kg body weight) in normoglycaemic adult male Sprague-Dawley rats weighing 200-250 g (n=6 for each dose, control and reference drug). In determining the effect of fasting and random blood glucose level, glucose concentration was measured prior to the treatment and hourly for four hours.[2] For the evaluation of glucose tolerance, blood was collected prior to the treatment and hourly for four hours after the administration of glucose load.[2] Blood (0.25 ml) was collected from the tail vein of the rats under light ether anesthesia (about 1ml by inhalation route) using aseptic precautions, serum was separated and the glucose concentration was determined spectrophotometrically using Randox glucose oxidase assay kit. Ethics approval was obtained from the Ethics Review Committee of Faculty of Medicine, University of Colombo for animal experimentation. Results were statistically analyzed by ANOVA followed by Dunnett's multiple comparison test and expressed as mean ± S.E.M. using Minitab 15 software. The results exhibit a dose dependent hypoglycaemic effect with lowest blood glucose level observed at 4 h after the treatment. All the three doses significantly reduce the fasting blood glucose level of rats at 4h after the treatment (Control vs. 100 mg/kg: 94.6±0.807 vs. 81.2±2.95 mg/dl, p<0.05; Control vs. 400 mg/kg: 94.6±0.807 vs. 77.8±2.80 mg/dl, p<0.05; Control vs. 800 mg/kg: 94.6±0.807 vs. 69.4±1.53 mg/dl, p< 0.05). Only intermediate and high doses show significant reduction in serum glucose level in normoglycaemic non fasted rats (Control vs. 400mg/kg: 129±3.00 vs. 114±2.63 mg/dl at 4h, p<0.05; Control vs. 800mg/kg: 129±3.00 vs. 113±3.03 mg/dl at 4h, p<0.05) and significant glucose tolerance when tested on oral glucose load (Control vs. 400mg/kg: 98.9±2.79 vs. 87.7±1.76 mg/dl at 4h, p<0.05; Control vs. 800 mg/kg: 98.9±2.79 vs. 85.2±1.18 mg/dl at 4h, p<0.05). According to the above results, it can be concluded that *A.lindleyana* leaves have hypoglycaemic activity since it significantly (p<0.05) reduces the blood glucose level in normoglycaemic rats and significantly (p<0.05) enhances the glucose tolerance.

A Sri Lankan Study of Compendium of Medicinal Plants, volume 4, pp.30-33, Department of Ayurveda, Sri Lanka, 2004.

Jayakody JRAC & Ratnasooriya WD (2008).*phcog. mag* 4, 341-349.

Where applicable, the authors confirm that the experiments described here conform with The Physiological Society ethical requirements.

PCC327

CFTR is an essential component in cAMP-dependent granular priming in human and mouse β-cells insulin secretion

A. Edlund[1], J.L. Esguerra[1], M. Flodstrom-Tulberg[2] and L. Eliasson[1]

[1]Clinical sciences in malmö, Lund University Diabetes Centre, Malmö, Sweden and [2]CIM, Karolinska Institute, Stockholm, Sweden

Aim: Cystic fibrosis transmembrane conductance regulator (CFTR) is an anion channel and regulator of proteins[1]. Mutations in CFTR cause cystic fibrosis (CF) and a major complication of CF is diabetes[2]. It is largely unknown why these patients develop diabetes but there is increasing evidence that CFTR is involved in islet hormone release[3]. The aim of this project is to investigate presence of CFTR in mouse and human pancreatic islets and role of CFTR in mechanisms controlling β-cell insulin release. **Method**: Experiments where performed on islets and single β-cells from human donors and NMRI-mice. Detection of CFTR was investigated using PCR and confocal microscopy. Insulin secretion was measured with RIA. Patch-clamp measurements of currents and exocytosis were performed. Statistical significance was calculated using t-test. **Results**: Human- and mouse islets express CFTR mRNA and CFTR protein was detected in β-cells. The whole-cell configuration of the patch-clamp technique was used and a ramp from -100 mV to +100 mV was applied to single human and mouse β-cells to measure cAMP-activated currents. Forskolin (10 μM) evoked an increase in current that was inhibited by CFTR antagonists, CFTRinh-172 (10 μM) or GlyH-101 (25 μM, GlyH; P<0.001, n_{human}=21, n_{mouse}=17). A major part of the cAMP-activated current was also reduced by the chloride channel blocker DIDS (200 μM), where the remaining part was inhibited by GlyH-101 (P<0.05, n_{human}=6, $_{mouse}$=10). The calculated CFTR conductance was small and we propose that CFTR act as a regulator of the DIDS-sensitive chloride channel Outward Rectifier Chloride Channel (ORCC) as suggested in other cell-types[4]. This was further confirmed by insulin secretion measurements. Glucose- and cAMP-stimulated insulin secretion was reduced by 43±5% (p<0.001, n=11 donors) and 40±12% (p<0.05, n=5) in the presence of GlyH (50 μM) in human and mouse islets, respectively. When DIDS was added, GlyH had no further inhibitory effect on insulin secretion in mouse islets, confirming that CFTR controls ORCC. However, in human islets,

addition of GlyH caused a further reduction ($p<0.05$, n=5 donors), suggesting that CFTR interact with additional proteins. Moreover, cAMP-amplified exocytosis elicited by a train of ten depolarizations from -70 mV to 0 mV and measured as an increase in membrane capacitance in single human and mouse β-cells was significantly reduced by >40% after pre-incubation with CFTR antagonists ($P<0.05$, $n_{human}=5$; $n_{mouse}=7$). The reduction was most prominent during the first two pulses representative of release of primed granules and first phase insulin secretion[5]. **Conclusion**: Based on our results we postulate that CFTR is an essential component in cAMP-dependent insulin secretion and exocytosis in human and mouse β-cells and hypothesize CFTR to be vital for granular priming and first phase insulin secretion.

Schwiebert EM et al. (1999). Physiol rev. 79, S145-166

Moran A et al. (2010). Diabetes care. 33, 2677-2683

Olivier AK et al. (2012). J Clin Invest. 122, 3755-3768

Gabriel SE et al. (1993). Nature 36. 263-268

Eliasson L. et al. (2008). J physiol 586, 3313-3324

Where applicable, the authors confirm that the experiments described here conform with The Physiological Society ethical requirements.

PCC328

C-C chemokine receptor type 5 knockout mice protects against obesity induced inflammation and insulin resistance by high-fat diet in gender difference

D. Li and L. Hung

Biomedical Sciences, Chang Gung University, Tao-Yuan, Taiwan

Obesity is a high risk factor in the development of insulin resistance and type 2 diabetes. Obesity increases macrophage infiltration into adipocyte and overproduction proinflammatory cytokines that leads to development of insulin resistance. T cell also plays an important role link between obesity and insulin resistance. CC-chemokine ligand 5 (RANTES) is a chemokine secret by T cells, eosinophils, and basophils, and plays an active role in recruiting leukocytes thus trigger sever inflammation. The CC-chemokine receptor 5 (CCR5) interactions with RANTES and mediates activation of T lymphocytes and macrophages by chemokines. It has been demonstrated high-fat diet-induced obesity, adipose inflammation, and insulin resistant could be attenuated in CCR5 knockout mice. Since the level of inflammation is also influenced by the difference of gender. Thus, the present study was aimed to investigate whether CCR5 knockout mice protect against high-fat diet (HFD)-induced obesity and insulin resistance has gender difference. C57Bl/6 male and female mice were fed with HFD for 24 weeks to induction of obesity and insulin resistance. The HFD mice developed insulin resistant syndrome characterized by elevated body weight, hyperglycemia, hyperinsulinemia, and hyperlipidemia. In addition, HFD mice exhibited impairment of oral glucose tolerance test (OGTT), increasing of glucose-stimulated insulin secretion, and decreasing of insulin sensitivity during insulin tolerance test (ITT). CCR5-/- attenuated diet induced obesity and glucose stimulate insulin secretion especially in female mice. The insulin sensitivity is improved only on CCR5-/- female mice during insulin tolerance test. Deficiency of CCR5 also attenuated obesity-induced fatty liver. The weights of fat pads were significantly decreased in CCR5-/-male and dramatic reduced in female mice. In addition, our results show that the insulin receptor protein level was reduced in liver of HF mice. CCR5-/- female mice increased protein expression of insulin receptor and Akt threonine phosphorylation. These results indicate that CCR5 deficiency protect against high-fat diet-induced obesity and insulin resistance especially in female mice.

Where applicable, the authors confirm that the experiments described here conform with The Physiological Society ethical requirements.

PCC329

Role of Li-permeable Na/Ca exchangers, NCLX, in the Exocytosis of Pancreatic β Cells

Y. Han, S. Park, S. Lee, S. Ryu and W. Ho

Department of Physiology and Biomembrane Plasticity Research Center, Seoul National University College of Medicine, Seoul, Republic of Korea

The Na+/Ca2+ exchangers are key regulators for Ca2+ homeostasis in pancreatic β cells, but their exact role in insulin secretion is not fully understood. In the present study, we investigated the role of Na+/Ca2+ exchangers on cytosolic Ca2+ dynamics and exocytosis in INS-1 cells. We newly discovered that the Li-permeable Na+/Ca2+ exchangers (NCLX), which are known as mitochondrial Na+/Ca2+ exchangers, contribute to plasma membrane Na+-dependent Ca2+ transport, and confirmed the presence of NCLX in the plasma membrane using immunocytochemistry and cell surface biotinylation experiments. We further investigated the role of NCLX on exocytosis function by measuring depolarization-induced capacitance increase in siNCLX-transfected INS-1 cells. Downregulation of NCLX significantly suppressed the second phase capacitance increase without affecting the first phase, but inhibition of mitochondrial Na+/Ca2+ exchange alone by removing intracellular Na+ did not cause a significant effect. These results suggest that normal surface NCLX activity is required for vesicle recruitment in the second phase. In addition, we discovered that oligomycin inhibited the second phase capacitance increase in the presence of intracellular ATP, suggesting that local metabolic control by mitochondria is critical for this phase. Our data indicate that the activity of surface NCLX may regulate local Ca2+ to optimize mitochondrial local metabolic control and thus contributes to vesicle recruitment for the normal secretory function in pancreatic β cells.

This research was supported by the Converging Research Center Program (2009-0094081) and SRC program (2010-0029394) through the National Research Foundation of Korea (NRF) funded by the Ministry of Education, Science and Technology.

Where applicable, the authors confirm that the experiments described here conform with The Physiological Society ethical requirements.

PCC330

Regulation of inflammatory cytokines by nitric oxide in the kidney

D.S. Majid, P. Singh, R. Stephenson and A. Castillo

Physiology, Tulane University Health Sciences Center, New Orleans, LA, USA

Previous studies performed in our laboratory using dogs, rats and mice have demonstrated that inhibition of nitric oxide (NO) increases superoxide activity in the kidney and this imbalance enhances tubular sodium reabsorption leading to salt retention and the development of salt sensitive hypertension. However, recent findings in our laboratory also show that systemic NO inhibition results in an increase in tumor necrosis factor-alpha (TNF-α; a pro-inflammatory cytokine) and a decrease in interleukin-10 (IL-10; an anti-inflammatory cytokine) levels in plasma and in renal tissue which are associated with marked infiltration of macrophages in the kidneys. As these cytokines are suggested to be involved in the pathophysiology of salt-sensitive hypertension, we examined the hypothesis that high salt (HS) intake in NO deficient condition enhances the production of pro-inflammatory cytokines in the kidney. Using appropriate ELISA kits, the levels of different cytokines (pro-inflammatory, TNF-α, and IL-6 and anti-inflammatory, IL-10) were measured in plasma and renal tissues collected from wild type (WT; C57BL6) and eNOS enzyme knockout (eNOS-KO) mice (~8 wks old) which were fed either normal (NS) or HS (4% NaCl) containing diet for 2 weeks. Mean systemic blood pressure (measured by tail-cuff plethysmography) was significantly increased in eNOS KO (111±4 to 136±8 mmHg) but not in WT (99±5 to107±4 mmHg) due to HS intake. The changes in cytokines levels are summarized in the Table 1. The plasma level of TNF-α remains undetected in both WT & eNOS KO mice during NS intake but showed a slight increased during HS intake. During NS intake, the plasma level of IL-6 was higher and that of IL-10 was lower in eNOS KO mice compared to WT mice. However, compared to the values during NS intake, all the renal levels of cytokines were lower in the kidney during HS intake both in WT as well as eNOS KO mice. These findings indicate that HS intake generally suppresses the levels of both anti- as well as pro-inflammatory cytokines, particularly in the kidney. These data suggest that NO inhibition induced by deficient activity of eNOS enzyme generally responsible for upregulation of inflammatory cytokines in the kidney.

Table 1

Cytokines		WT		eNOS-KO	
		NS (n=6)	HS (n=6)	NS (n=6)	HS (n=6)
TNF-α	Plasma (pg/mL)	UD	202±146	UD	175±68*
	Renal (pg/mg protein)	325±73	114±17 *	624±67#	115±18*
IL-6	Plasma (pg/mL)	13±11	UD	180±44#	UD
	Renal (pg/mg protein)	166±61	81±14*	619±106#	56±7*
IL-10	Plasma (pg/mL)	701±54	344±52*	510±125#	327±67*
	Renal (pg/mg protein)	3929±378	865±130 *	6087±567#	882±141*

UD, undetected; *, P<0.05 vs corresponding NS; #, P<0.05 vs WT-NS

Where applicable, the authors confirm that the experiments described here conform with The Physiological Society ethical requirements.

PCC331

Sex hormones differentially modulate angiotensin-converting enzyme 2 (ACE2) activity in kidney of spontaneously hypertensive rats

P.M. Dalpiaz[1], A.S. de Medeiros Garcia[2], A.Z. Lamas[1], I.F. Caliman[1], G.R. Abreu[1], T.U. Andrade[3], M.F. Alves[4], A.K. Carmona[4], S.G. Figueiredo[1] and N.S. Bissoli[1]

[1]Department of Physiological Sciences, Federal University of Espirito Santo, Vitoria, Espírito Santo, Brazil, [2]Biological and Health Sciences, Federal Institute of Education, Science and Technology, Vila Velha, Espírito Santo, Brazil, [3]Department of Pharmacy, University Vila Velha, São Paulo, Espírito Santo, Brazil and [4]Department of Biophysics, Federal University of São Paulo, São Paulo, São Paulo, Brazil

Male spontaneously hypertensive rats (SHR) had a higher systolic blood pressure than female SHR. Previous studies have shown that castration lowered the blood pressure of male rats and can increase in female SHR. Differences between males and females have been found in components of the renin-angiotensin system (RAS) and these differences can be associate to sexual dimorphism in hypertension development. However, the activity of angiotensin-converting enzyme (ACE) and ACE2 in male and female SHR remain unclear. Therefore, this study was designed to investigate whether: 1) there are sex differences in ACE and ACE2 in the kidney in spontaneous hypertension; 2) sex hormones play a role in these sex differences. The procedures were carried out in compliance with the guidelines for the ethical use of animals in scientific research and were approved by the Ethical Committee of the Federal University of Espírito Santo (023/2009). Female and male SHR rats were divided into 4 experimental groups: sham and castrated. After 51 days of the castration, the rats were anesthetized with ketamine (70 mg/kg i.p.) and xylazine (10 mg/kg i.p.) and their kidneys were immediately excised and the ACE and ACE2 activity were evaluated by fluorimetry. Female rats exhibited a higher ACE (25±1 AFU, $p<0.05$) and ACE2 (0.15±0.002 AFU, $p<0.05$) activity than the male rats (ACE 17±3 AFU and ACE2 0.02±0.002 AFU), but female rats have more favorable ACE2/ACE ratio (0.006±0.001, $p<0.05$) than male (0.001±0.0001) rats. Castration did not affect the ACE activity in both sex (female 23±3 and male 16±2 AFU) but decreased ACE2 in the female rats (0.03±0.002 AFU, $p<0.05$), while increased in the male rats (0.14±0.001 AFU, $p<0.05$). The castration change the ACE2/ACE ratio in both sex, male rats (0.009±0.001, $p<0.05$) replaced by more favorable ratio than female (0.0012±0.0002). In conclusion, this study identified sexual dimorphisms among the ACE and ACE2 activity in SHR; sex hormones differentially modulate ACE2 activity. The higher ratio of the renal RAS (ACE2/ACE) in females observed in the present study may contribute to sex differences in the regulation of arterial pressure in SHR and can affect on the severity and the progression of renal disease, that is more rapid in men compared with women.

Capes/CNPq Casadinho/Procad 552623/2011-3, FAPES 012/2011-Universal 54688175/2011.

Where applicable, the authors confirm that the experiments described here conform with The Physiological Society ethical requirements.

PCC333

Evaluation of serum Cystatin C as an indicator of glomerular filtration rate in pre-eclamptic, in comparison to normal pregnant and non-pregnant Sudanese women

H.M. Beheiry[1,2], D.A. Rayis[3] and A.M. Saeed[4]

[1]Physioigy, International University of Africa, Khartoum, Sudan, [2]Physiology, Ahfad University /School of Medicine, Khartoum, Sudan, [3]Head Department of Obstetrics and Gynaecology, University of Khartoum, Khartoum, Sudan and [4]Physiology, University of Khartoum, Khartoum, Sudan

The glomerular filtration rate (GFR) is the best global indicator of renal function in health and illness. It decreases early in renal disease before onset of renal failure (1). Serum cystatin C has been introduced as a superior and sensitive endogenous marker of GFR. However, there are conflicting reports regarding its use in pregnancy and pre-eclampsia. Sudanese women who develop pre-eclampsia and subsequently eclampsia is still high and a genuine concern. The main target organ is the kidney as glomerular endotheliosis (2). The aim of this study was to assess GFR changes and evaluate the use of serum cystatin C in pre-eclampsia. This is a cross-sectional, case-control and hospital-based study performed in the period from December 2008 to December 2010 in Omdurman Maternity Hospital. The study group was 81 pre-eclamptic compared to100 second half normal pregnant and 65 non-pregnant Sudanese women. A blood sample and a 24-hour urine were collected. Serum cystatin C was determined using latex particle-enhanced immunoturbidimetry with Dako cystatin C PET Kit (3), serum creatinine by Jaffe method and uric acid by Fossati enzymatic reaction at St. Helier Hospital London. Kruskal Wallis test was used for comparisons of means. The mean ± S.E of serum cystatin C for the pre-eclamptic, normal pregnant and non-pregnant were 1.31 mg/L ±0.04, 1.0 mg/L ±0.03 and 0.80 mg/L± 0.01 respectively (P=0.0001). GFR of the pre-eclamptic 66.71 ml/min/1.73 m2 ± 3/09 was significantly lower than that of normal pregnant 89.54 ml/min/1.73 m2 ±2.74 and that of the non-pregnant 86.85 ml/min/1.73 m2 ± 3.31 (P=0.0001). There was no significant correlation of mean GFR of pre-eclamptic cases neither with serum cystatin C (r= -0.16, P=0.25) nor with serum uric acid (r=-0.19, P =0.16), but negatively significant with serum creatinine (r= -0.37, P=0.004) using Spearman's correlation. The correlation of mean GFR of normal pregnant group was negatively significant with serum cystatin C (r= -0.26, P=0.02), serum creatinine (r= -0.31, P=0.003) and serum uric acid (r= -0.35, P=0.001). The correlation of mean GFR of the non-pregnant group did not correlate neither with serum cystatin C (r= -0.19, P=0.17) nor with serum creatinine (r= -0.05, P=0.73) or serum uric acid (r= -0.10, P=0.45). The diagnostic accuracy of serum cystatin C level showed it to be sensitive to detect pre-eclampsia at cut-off value equals 1.0 mg/L and specific for pre-eclampsia at cut-off value above 1.0 mg/L for cystatin C. The diagnostic accuracy of serum cystatin C tested using ROC-plot at different cut-off values of GFR found to be not a reliable test for GFR changes in pre-eclampsia. Serum cystatin C may be a useful indicator of pre-eclampsia but not a reliable marker of GFR changes in pre-eclampsia.

Figure 1: Correlations between Serum Cystatin C, Serum Creatinine, Serum Uric Acid levels and GFR in Non-pregnant ■, Pregnant ■ and Pre-eclamptic ■ Subjects

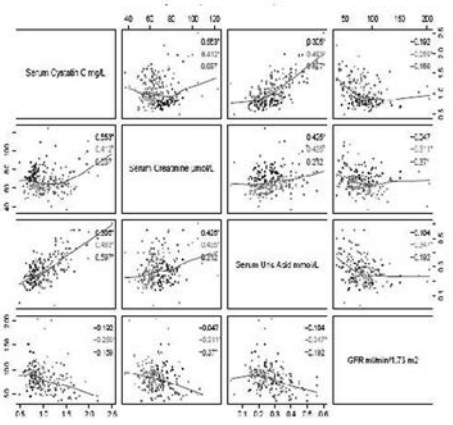

Figure 2: The Diagnostic Values of Serum Cystatin C at Different Cut off Levels for Detection of Pre-eclampsia and at ROC-60 Plot in comparison to serum creatinine and serum uric at cut off GFR (60ml/min/1.73m2) in pre-eclamptic subjects

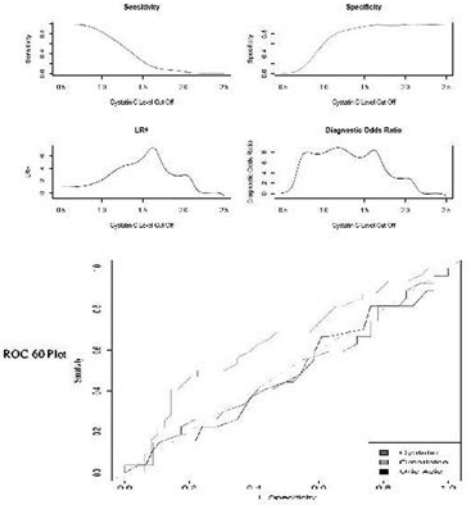

Manjunath G, Sarnak MJ, Levey AS. Estimating the glomerular filtration rate. Dos and don'ts for assessing kidney function. Postgrad Med. 2001 Dec;110(6):55-62; quiz 11

Hladunewich M, Karumanchi SA, Lafayette R. Pathophysiology of the clinical manifestations of preeclampsia. Clin J Am Soc Nephrol. 2007 May;2(3):543-9

Kyhse-Andersen J, Schmidt C, et al. Serum cystatin C, determined by a rapid, automated particle-enhanced turbidimetric method, is a better marker than serum creatinine for glomerular filtration rate. Clin Chem. 1994 Oct;40(10):1921-6.

Dr. Pravin Makwana-St.Helier Hospital

Where applicable, the authors confirm that the experiments described here conform with The Physiological Society ethical requirements.

PCC334

Proteomic analysis of protein expression in lipid droplet of rat RMICs

W. Su, Q. Han, J. Yang and Y. Guan

Department of Physiology and Pathophysiology, Peking University Health Science Center, Peking, China

Basically, renomedullary interstitial cells (RMICs) are full of lipid droplets (LDs), which have been thought to be the source of vasodilators. Previous studies have indicated that the renomedullary interstitial cells of the renal papilla can secrete medullipin, which is a vasodilator that suppresses sympathetic tone, causes diuresis and natriuresis and apparently has a suppressive effect on the central nervous system. However, the chemical characteristic of medullipin is still unknown. Aim of this study was the identification of LD proteins based on purification of rat RMICs' lipid droplet followed by proteomic analysis using 2D-LC-MS/MS technics. To enhance the validity of the data, only proteins with at least two unique peptides were accepted. We found over 300 RMICs' LD associated proteins. Among these proteins, 92 proteins have been reported to be LD proteins in previous studies, 17% were associated with lipid metabolism and 15% were associated with mitochondria, suggesting close interactions of LDs with mitochondria, and that LDs were involved in metabolism of triglycerides, fatty acids, phospholipids, and sterol esters. We also found enzymes involved in arachidonic metabolism including CYP4F5, CYP4F6, CYP2E1 and CYP2A3, previous study report that LDs are specific sites of novo formation of LTC4 and PGE 2 in leukocytes, suggesting LDs in RMICs may also involved in regulating eicosanoid formation. The difference in the morphology and protein profile of LDs in renal medulla of SHR (spontaneously hypertensive rat) and Wistar-Kyoto(WKY) rats were further analyzed. Electron microscopy revealed more LDs in renal medulla of SHR than in that of WKY rats. Proteomic analysis revealed 15 differently expressed proteins in renal medulla of SHR when compared with WKY rats. Western blot further confirmed that the expression of clathrin and CYP4A3 were upregulated, whereas the expression of UBXD8 was downregulated in renal medulla LDs of SHR. In conclusion, these preliminary results have suggested that LDs in RMICs are rich in many enzymes involving lipid metabolism and blood pressure regulation. To further study the biological function of these proteins in LDs will shed light on the understanding of the mechanisms of high blood pressure.

Where applicable, the authors confirm that the experiments described here conform with The Physiological Society ethical requirements.

PCC335

Undernourished children have increased microalbuminuria

V.B. Martins[1], R. Sesso[2], A.P. Neves[1], A.G. Clemente[1] and A.L. Sawaya[1]

[1]Physiology, UNIFESP, Santo André, São Paulo, Brazil and [2]Medicine, UNIFESP, São Paulo, Brazil

Increased cardiovascular and renal disease has been described in humans with intrauterine or early life undernutrition. Microalbuminuria (MA) is a marker of renal and endothelial dysfunction, and a predictor of cardiovascular and renal disease. We hypothesized that undernourished children have increased MA, and after nutritional recovery, the MA concentrations would decrease to normal values. We evaluated the concentration of MA in three groups of children (mean age: 10.75 ± 2.45; range: 5.62 to 15.94): treated in a day-hospital and recovered from previous undernutrition (R group (n=32) height/age (HAZ) (mean±SD) -0.58 ± 0.68, BMI/age (BAZ) -0.46 ± 0.74); undernourished group (U group (n=48); HAZ -1.40 ± 1.10; BAZ -1.76 ± 1.06) and control group (C group (n=50); HAZ -0.37 ± 0.91; BAZ -0.27 ± 0.86). All families of participants signed the Free and Informed Consent form. The study was approved by Research Ethics Committee of the Federal University of São Paulo (number 1302/09).
Children underwent preliminary tests to detect urinary infection, anemia and thyroid axis alterations. Those with positive results were treated and afterwards included in the study; and if not possible, excluded. A morning spot urine sample was collected by the mother after waking up of the child. The mothers were instructed at least in two occasions about the procedure and reminded by phone call the day before the collection. Albuminuria was measured by an immunoturbidimetric assay and the results were expressed as the ratio of urinary albumin/creatinine (mg/g). The U group showed lower anthropometric values than the other two groups (HAZ: U= -1.4 ± 1.1, C= -0.37 ± 0.91 and R= -0.58 ± 0.68; BAZ: U=-1.76 ± 1.06, C=-0.27 ± 0.86 R= -0.46 ± 0.74, both ANOVA $p<0.001$); and greater mean values of MA than the R and the C groups (U= 10.4 ± 16.1 mg/g, C= 6.3 ± 8.2 mg/g and R= 4.6 ± 4.3 mg/g, $p=0.040$, ANOVA). Eight percent of the U group showed MA (defined as > 20 mg/g). None of controls had MA. When evaluating the difference in prevalence between the type of undernutrition (stunting or underweight), 12.5% of children with stunting had MA, while the underweight group had 4.2%, while the R group had a prevalence of 6.3%. Using a MA lower cut-off > 10 mg/g was used to identify children at risk, we found that 16.7% of the R group, 31.2% of the U group and 8.5% of C group showed elevated albuminuria (Pearson chi-square = 0.018). Our results showed the presence of microalbuminuria in undernourished children which may be a marker of higher risk for cardiovascular and renal disease in future life. On the other hand, after treatment for undernutrition, recovered children showed results similar to controls.

Martins VJ et al. (2011). Int J Environ Res Public Health. 8(6):1817-46.

Luyckx VA et al. (2010). J Am Soc Nephrol. 21(6):898-910.

Menne J et al. (2010). J Hypertens. 28(10):1983-94.

Langley SC et al. (1994). Clin Sci (Lond). 86(2):217-22

Dewey KG & Begum K (2011). Matern Child Nutr. 7 Suppl 3:5-18.

The authors wish to thank the Fundação de Apoio a Pesquisa do Estado de São Paulo (FAPESP, grant 2010/51237-2) and CAPES for granting financial support for this study

Where applicable, the authors confirm that the experiments described here conform with The Physiological Society ethical requirements.

PCC336

The renal functional responses to Angiotensin 1-7 in the DOCA salt hypertensive rat

E. Barry and E.J. Johns

Department of Physiology, University College Cork, Cork, Ireland

Angiotensin 1-7 (Ang1-7) has diuretic/natriuretic properties at the kidney. There is evidence that this response is due to a counter-regulation of the anti-diuretic/anti-natriuretic actions

of Angiotensin II and is therefore dependant on the level of activation or suppression of the endogenous renin-angiotensin system (RAS). This study investigated whether the excretory responses to intrarenal Ang1-7 are altered in Deoxycorticosterone Acetate (DOCA) salt hypertensive rats where the RAS is known to be depressed.

Male Wistar rats received two s.c. injections weekly of DOCA(15mg/kg) in arachis oil (2ml/kg) and 9% NaCl/2% KCl drinking water for four weeks, one week following unilateral nephrectomy performed under 5% isoflurane (0.5L/min O_2) induction/2% (0.2L/min O_2) maintenance. Prior to the terminal experiments animals were placed in metabolic cages to determine baseline excretory function. Anaesthesia was induced using 1ml/kg body weight sodium pentobarbital i.p. The femoral artery was cannulated, to monitor mean arterial pressure (MAP), and vein, for infusion of saline at 3ml/h containing inulin. The left ureter was cannulated for urine collection and a small cannula inserted into the cortico-medullary border for the infusion of saline and Ang1-7 ($6x10^{-6}$M) at 1 ml/h. After 1.5h, 20 min clearances were taken, two before and two 50 mins after the start of the Ang1-7 infusion. The rats were killed at the end of the experiment by anaesthetic overdose. Data, means±SEM were subjected to t-tests and significance taken at $P<0.05$.

DOCA treated group (n=6) had a higher GFR than the control group (n=7), at 3.3±0.2 *vs.* 1.1±0.06ml/min/kg respectively, and a higher urine volume (UV), at 131.5±11.1 *vs.* 29.5±3.6μl/min respectively. Sodium excretion values were also higher for the DOCA treated group compared to the control group, with absolute sodium excretion (UVNa) values of 29.0±2.1 *vs.* 1.42±0.09 μmol/min respectively, and fractional sodium excretion values(FENa) of 5.4±0.4 *vs.* 0.9±0.05% respectively. Ang1-7 had no effect on blood pressure, at 111±5 mmHg for control rats and 162±4 mmHg for DOCA rats, or GFR, at 4.4±0.4ml/min/kg and following Ang1-7 infusion 5.2±0.5ml/min/kg for control rats and for DOCA rats 9.1±2.2ml/min/kg and 10.9±2.8ml/min/kg before and after infusion respectively. In control rats, UV significantly increased ($P<0.05$) from 100.9±6.9 to 139.1±4.5 μl/min, UVNa, from 16.0±1.3 to 24.3±1.0 μmol/min and FENa by 2.3±0.5 to 2.9±0.5%. In the DOCA model these responses to Ang1-7 were completely blunted, with UV, 163.5±35.7μl/min, UVNa, 39±11μmol/min and FeNa, 2.4±0.07% and following Ang1-7 infusion UV, 145.4±47.7μl/min, UVNa, 29.4±8.5μmol/min, and FENa, 1.5±0.2%.

These findings suggest that the suppression of the RAS in the DOCA model of hypertension interferes with the diuretic/natriuretic response seen in normal animals to intra renal Ang1-7 infusion.

Where applicable, the authors confirm that the experiments described here conform with The Physiological Society ethical requirements.

PCC337

Preservation of retinal glycocalyx integrity by a slow release hydrogen sulfide (H_2S) donor

J. Whatmore[1], K.I. Wolanska[1], A. Perry[2], M. Wood[2] and M. Whiteman[1]

[1]University of Exeter Medical School, University of Exeter, Exeter, UK and [2]Biosciences, University of Exeter, Exeter, UK

Background: Leukocyte adhesion to the vascular endothelium is mediated by endothelial adhesion molecules binding to their leukocyte ligands. The endothelial adhesion molecules are embedded in the glycocalyx, a dense network of membrane-bound proteoglycans and glycoproteins. In health, the glycocalyx contributes to the anti-inflammatory regulation of the vascular wall, effectively 'hiding' the adhesion molecules from the circulating leukocytes. However, in pathological conditions associated with glycocalyx loss such as diabetes this protective mechanism is lost, possibly contributing to the associated microangiopathies e.g. diabetic retinopathy. Indeed, the early stages of retinopathy are characterised by increased leukocyte adhesion, contributing to inflammation and vessel blockage. Thus, strategies to maintain glycocalyx integrity may be beneficial in the treatment of diabetic retinopathy.

It is possible that diabetes-associated glycocalyx loss is due to reduced bioavailability of H_2S. We have shown that plasma H_2S levels are significantly lower in individuals with type 2 diabetes compared with sex/age/BMI matched controls, and that reduced H_2S levels correlate with microvascular dysfunction. However, the direct effects of H_2S on the glycocalyx are unknown.

Aim: To investigate (a) the effects of the slow release H_2S donor GYY4137 on hyperglycaemia-induced changes to the glycocalyx and leukocyte adhesion and (b) potential mechanisms of action of GYY4137, specifically endothelial K_{ATP} channel activation.

Methods: Bovine retinal endothelial cells (BREC) were exposed to 5.6mM glucose (NG) and 25mM glucose (HG) ± GYY4137 for 24h. A cell based fluorescence assay was used to study glycocalyx changes. Glibenclamide (Glib), gliclazide (Glic) and cromakalim (Crm) were used to test involvement of endothelial K_{ATP} channels. Leukocyte adhesion to BREC was measured at a shear stress of 1dyn/cm^2. Data are presented as mean±SD.

Results: HG-induced glycocalyx degradation was reversed by GYY4137 [HG 93±5% vs HG + GYY 107±8%, $p<0.001$, n=12; control,100%)]. Crm, Glib or Glic had no effect on glycocalyx changes. HG enhanced leukocyte adhesion and this was attenuated by H_2S [HG 348±110% vs HG GYY 124±47%; p=0.028, n=4; NG control,100%]. The H_2S mediated decrease in adhesion was not inhibited by Glib or Glic suggesting no involvement of endothelial K_{ATP} channel activation. H_2S added simultaneously with HG to BREC pre-treated with Crm did not affect leukostasis.

Conclusions: Glycocalyx degradation and increased leukocyte adhesion induced by HG were reversed by GYY4137, highlighting the therapeutic potential for H_2S donors in hyperglycaemic conditions.

Where applicable, the authors confirm that the experiments described here conform with The Physiological Society ethical requirements.

PCC338

Aging reduces the vasodilatory response of mesenteric resistance arteries to calcium channel blockers

S. Albarwani[1], A. Al-Kaabi[1], A. A-Busaidi[1], S. Al-Hadhrami[1], I. Al-Husseini[1], I. Al-Lawatiya[1] and M.O. Tanira[2]

[1]Physiology, Sultan Qaboos Uinversity, Muscat, Oman and [2]Pharmacology, Sultan Qaboos University, Muscat, Oman

Calcium channel blockers are widely used to treat cardiovascular disease (CVD) including hypertension. Aging is an independent risk factor for CVD and the use of these blockers increases with aging. The aim of this study was to evaluate the response of resistance mesenteric arteries to nifedipine, verapamil and diltiazem which are chemically unrelated calcium channel blockers. Male F344 rats, aging 2.5-3 months (young)

and 22-26 months (old) were used. Animals were sacrificed with an overdose of a mixture of ketamine (140 mg kg–1 I.P.) and xylazine (40 mg kg–1 I.M.). Third order mesenteric arteries were mounted on wire myograph and tension was measured in isometric recording in the presence and absence of different blockers. In all experiments, the viability of arteries was assessed by a contractile response to KCl (60 mM) and the integrity of the endothelium was assessed by a dilator response to acetylcholine (1μM). Arteries were sub-maximally pre-contracted with phenylepherine (PE; 4μM) and then relaxed in a cumulative dose-response manner with nifedipine (0.1-10uM), verapamil or diltiazem (0.1-5 μM) or sodium nitroprusside (SNP; 0.1-10 μM). Values (mean ± s.e.m..; statistically significant difference was calculated using unpaired Student t-test; $p < 0.05$). Contractions induced by KCl were 10.8±0.6 vs. 10.7±0.7 mN and PE 13±0.5 vs. 12±0.8 mN (young vs. old) were not significantly different. Concentration-response curves to the three calcium channel blockers were shifted to the right in arteries isolated from old rats with statistically significant IC50s. In arteries isolated from old rats compared to young rats, IC50 increased from 3.6 to 11 nM (nifedipine n= 8), 94 to 187 nM (verapamil n=7) and 250 to 400nM (diltiazem, n=12). To investigate that this response was particularly associated with calcium channel blocking, arteries relaxed with SNP in a cumulative dose response (0.1 nM to10 μM) showed no significant difference between young and old groups (n=8). In conclusion, our results suggest that aging reduces the response of mesenteric arteries to the vasodilatory effect of these calcium channel blockers.

Where applicable, the authors confirm that the experiments described here conform with The Physiological Society ethical requirements.

PCC339

Exercise training could ameliorate age-induced changes in cerebral blood flow and capillary vascularity by up-regulated VEGF and eNOS levels

S. Patumraj and S. Viboolvorakul

Physiology, Faculty of Medicine, Chulalongkorn University, Bangkok, Thailand

Aging has been reported to increase the risk of developing cerebrovascular disease. Exercise training is well known to have beneficial effects to brain health, including promoted blood flow, angiogenesis and enhanced vascularization. The present study aims to investigate effect of exercise training on age-induced brain microvascular alterations in associated with VEGF and eNOS protein levels.
Male Wistar rats were divided into 4 groups: sedentary-young (aged 4-6 months) (SE-Young, n=5), sedentary-aged (aged 23-24 months) (SE-Aged, n= 8), immersed-aged (IM-Aged, n=5) and exercise trained-aged (ET-Aged, n= 8) rats. The study was approved by Ethics Committee on Care and Use of Laboratory Animals, Faculty of Medicine, Chulalongkorn University. ET-Aged rats were individually swum in cylindrical tanks for 60 minutes/day, 5 days/week for 8 weeks. Regional cerebral blood flow (rCBF) was measured by a laser Doppler Flowmeter. Laser-scanning confocal fluorescence microscopy provided high-quality visualization of microvascular network from surface through superficial intraparenchyma. Fluorescent images were recorded and then off-line analyzed for capillary vascularity (CV) by using image analysis software. VEGF and eNOS protein levels in isolated brain microvessels were determined using immunoassay technique.
ET-Aged rat was significantly reduced in MAP compared to the IM-Aged group ($P<0.05$). The rCBF was significantly diminished in SE-Aged (134.99±14.74 PU), IM-Aged (131.09±17.53 PU), and ET-Aged (255.83±13.17 PU) groups when compared to SE-Young group (334.27±35.00 PU). However, the rCBF in the ET-Aged group was significantly higher than that in the IM-Aged group ($P<0.05$). CV was significantly reduced ($P<0.05$) in SE-Aged (15.85±1.25%), IM-Aged (16.46±1.59%) and ET-Aged (29.81±1.64%) groups when compared to SE-Young group (39.25±2.18%). The capillary vascularity of ET-Aged group was significantly greater when compared to that of IM-Aged group ($P<0.05$). The VEGF level was significantly lower ($P<0.05$) in SE-Aged (20.51±1.75 pg/mg protein) and IM-Aged (19.07±1.27 pg/mg protein) groups compared to SE-Young group (32.27±0.93 pg/mg protein). Swimming training could significant increase ($P<0.05$) of VEGF level in ET-Aged (28.35±1.53 pg/mg protein) group when compared to that of IM-Aged group. Both SE-Aged and IM-Aged groups have significantly lower ($P<0.05$) eNOS levels (575.62±70.14 and 459.94±98.02 pg/mg protein, respectively) when compared to SE-Young group (994.39±88.49 pg/mg protein). Regular swimming significantly elevated ($P<0.05$) eNOS level in ET-Aged group (926.75±65.08 pg/mg protein) when compared with that of IM-Aged group.

This study was supported by Ratchadaphiseksompot Endowment Fund and Chulalongkorn University Dutsadiphiphat Grant.

Where applicable, the authors confirm that the experiments described here conform with The Physiological Society ethical requirements.

PCC341

Aging - induced structural changes in arteries. Role of collagen and laminin isoforms

I. Ivic

Pathophysiology and Gerontology, University of Pecs, Pecs, Hungary

Introduction: Aging greatly affects the structure of the blood vessels in order to adapt to - among other things - the changes in the hemodynamic environment. Thus, we investigated rat carotid arteries from young and old rats regarding changes in their structural components.
Hypothesis: That aging induces substantial changes in the morphology and components of the arterial wall.
Methods: Carotid arteries were isolated from young (1 month: 1m), adult (12 months: 12m) and senescent (29 months: 29m) Wistar rats. Cryosections were taken from different age groups and immunofluorescence staining for cellular and extracellular matrix components of the vessel wall was employed to determine the structural characteristics of vessels. Measurements were divided in two groups: biomechanical and morphological measurements (measurements of intensity). All measurements and analyses were performed using the Volocity image analysis program.
Results: Changes in the biomechanical characteristics of carotid arteries from young to old: wall thickness, number of nuclei per section, artery inner volume, and artery wall surface increased significantly with age ($p<0.05$). Changes in the intensity of extracellular matrix components of carotid arteries from young to old: smooth muscle actin, elastin, endothelium marker MECA-32, nuclei, laminin Pan, laminin γ1, laminin α2, laminin α5, laminin β2, collagen I, collagen III, collagen IV,

increased significantly with age (p<0.05). The most substantial change was found in collagen type I and III, laminin γ1 and smooth muscle actin.
Conclusions: The data suggest that aging results in substantial structural changes in the vascular wall. Vessels size increases with age and it is associated with increases in extracellular matrix components, especially the fibrillar collagen content (collagen type III), which is several times higher than that of the laminins which increase evenly with age.
I. Ivic1, L. Yousif2, Z. Vamos1, P. Cseplo1, R. Hallmann2, L. Sorokin2, A. Koller1
1University of Pecs, Medical School, Department of Pathophysiology and Gerontology, Pecs, Hungary
2University of Münster, Institute of Physiological Chemistry and Pathobiochemistry, Münster, Germany

(Support: FP7-Marie Curie-SmART, Hungarian Natl. Sci. Res. Found (OTKA) K71591 and T67984, MHT 2010/2011 SROP-4.2.1/b-10/2/KONV-2010-0012, SROP-4.2.2.A-11/1/KONV-2012-0024).

Where applicable, the authors confirm that the experiments described here conform with The Physiological Society ethical requirements.

PCC342

Fluid shear stress modulates redox signalling in bovine aortic endothelial cells

S.R. Mc Sweeney[1], M. Fowler[2], G.E. Mann[1] and R.C. Siow[1]

[1]BHF Centre of Research Excellence, Cardiovascular Division, King`s College London, London, UK and [2]Unilever Discover - R&D, Unilever, Bedford, UK

Fluid shear stress (FSS) exerted by blood flow on the endothelium is critical for the maintenance of vascular redox homeostasis. Regions in the vasculature where FSS is low (LS), oscillatory (OS) or turbulent tend to be associated with atherosclerotic lesion development and an impaired redox balance[1]. High unidirectional, laminar shear stress (HS) maintains endothelial cells (EC) in an "atheroprotective" phenotype by inducing the expression of cytoprotective antioxidant enzymes, such as heme oxygenase-1 (HO-1), which are regulated by the transcription factor nuclear factor (erythroid-derived 2)-like 2 (Nrf2)[2]. LS and OS are associated with an increase in vascular oxidative stress and expression of "pro-inflammatory" genes[3]. In the current study we have investigated whether FSS alters the expression of Nrf2 and antioxidant defence genes in EC.
Bovine aortic endothelial cells (BAEC) were isolated from unwanted aortas obtained from an abattoir and cultured in DMEM containing 10% fetal calf serum. BAEC were seeded into micro channel slides and after 24 h, a fluidic unit air pump system (Ibidi) was used to expose cell monolayers to HS (15 dynes/cm^2) or OS (±15 dynes/cm^2, 1 Hz) for 2-24 h. Expression of antioxidant proteins Nrf2, HO-1, peroxiredoxin-1 (Prx-1) and glutamate-cysteine ligase catalytic subunit (GCLC) were assessed by western blot analyses and immunofluorescence.
Nuclear translocation of Nrf2 elicited by HS was increased after 2h and 24 h compared to static cultures. Western blot analysis revealed that exposure of BAEC to HS caused a significant two-fold increase in Nrf2 protein expression after 24 h vs. static cultures (p<0.05, n=4). HS and OS (24h) significantly increased HO-1 protein levels >17 fold and Prx-1 levels >2.5fold (p<0.05, n=5). Finally HS and OS significantly increased GCLC levels >1.9 fold in comparison to static cultures (p<0.05, n=5).
We have demonstrated that HS caused a significant induction of Nrf2 protein expression and an increase in Nrf2 nuclear translocation in BAEC. In addition FSS differentially increased the expression of HO-1, Prx-1 and GCLC. These results suggest that high laminar FSS may protect EC through the enhanced expression of endogenous antioxidant genes.

Davies PF. Nat Clin Pract Cardiovasc Med. 2009;**6**:16-26

Warabi E *et al*. Free Radic Biol Med. 2007;**42**:260-269

Takabe W. Antioxidants & Redox Signaling. 2011;**15**(5):1415-26

BBSRC and Unilever

Where applicable, the authors confirm that the experiments described here conform with The Physiological Society ethical requirements.

PCC343

Catechin prevents rat cerebrovascular damage due to hypoperfusion and reperfusion

D. Lapi, T. Mastantuono, D. Sapio, M. Fantozzi and A. Colantuoni

University, Naples, Italy

Catechin is an antioxidant polyphenol abundant in green tea and exhibits biological and pharmacological properties. Several studies have demonstrated the long term consumption of catechin prevents dyslipidemia, improves the cerebral blood flow and reduces the inflammatory response and the neuronal damage during cerebral ischemia.
The aim of the present study was to assess the in vivo dose-dependent effects of catechin on rat pial microcirculation during hypoperfusion and reperfusion injury.
Male Wistar rats were anesthetized with alpha-chloralose (50 mg/Kg b.w. intraperitoneally administered), tracheotomized and intubated.
Pial microcirculation of male Wistar rats was observed by fluorescence microscopy through a closed cranial window. Hypoperfusion was induced by bilateral common carotid artery occlusion (BCCAo) for 30 min; thereafter, pial microcirculation was observed for 60 min.
Arterioles were classified according to Strahler's ordering scheme. Arteriolar diameter was determined by computer assisted-method as well as permeability increase, leukocyte adhesion, perfused capillary length (PCL) and capillary red blood cell velocity (VRBC). Neuronal damage was evaluated by TTC staining.
Catechin (2 – 4 mg/kg b.w.) or L-N5-(1-Iminoethyl) Ornithine Hydrochloride (L-NIO: 15 mg/Kg b.w.) prior to catechin were intravenously administered before BCCAo and at beginning of reperfusion.
In ischemic rats, BCCAo caused decrease in order 2 arteriole diameter, reduced by 13.7 ± 2.0 % of baseline at the end of reperfusion (RE). Microvascular permeability and leukocyte adhesion were marked. PCL and VRBC decreased at RE.
At the end of BCCAo, catechin dose-dependently reverted order 2 arteriolar diameter decrease, causing vasodilation at RE. Microvascular leakage and leukocyte adhesion were prevented as well as the cortex and striatum neuronal loss in both hemispheres at RE. L-NIO prior to catechin abolished the catechin-induced effects. Western blotting showed that endothelial nitric oxide synthase (eNOS) protein concentration significantly increased in rats treated with cathechin at RE.
In conclusion, catechin administration prevents pial microvascular damage induced by hypoperfusion and reperfusion reduc-

ing vasoconstriction, microvascular permeability, leukocyte adhesion, capillary blockade and neuronal loss. It is reasonable to suggest that catechin's effects are mainly due to nitric oxide release and to free radical scavenger activity.

Where applicable, the authors confirm that the experiments described here conform with The Physiological Society ethical requirements.

PCC345

A pilot study investigating whether dipeptidyl peptidase-IV inhibition alters vascular function in obese men

K.M. Gooding, A. Shore, D. Mawson, C. Ball, A. Pitt, K. Aizawa and W. Strain

Diabetes and Vascular Medicine, University of Exeter Medical School, Exeter, Devon, UK

There is increasing interest in whether incretin based medications have favourable vascular actions, including improving endothelial function and reducing ischaemia-reperfusion insult, in humans. Previous research has predominantly used in vitro or animal based models.
Aim: This pilot study examines whether dipeptidyl peptidase-IV (DPP-IV) inhibition, slowing the breakdown of endogenous incretins, alters vascular function in obese men.
Study design: Crossover, randomised double-blind placebo-controlled study.
Method: 15 obese men were recruited (age range:28-72years). Following recruitment participants were randomised to Vildagliptin (100mg/day) or placebo for 12 weeks. At end of the treatment vascular assessments were performed (maximum hyperaemia; endothelial (in)dependent microvascular function; microvascular filtration capacity; capillary density; peak reactive hyperaemia; fovea thickness and applanation tonometry). Following a 4 week washout period the participant received the alternative treatment for 12 weeks. Vascular assessments were repeated within the last 2 weeks of treatment.
Results: 14 participants completed the study. Active treatment resulted in a small but significant reduction in HbA1c (Active mean±standard deviation: 38.1±4.8 vs 39.1±4.1mmol/mol, p=0.003 paired T-test). Capillary density was increased with DPP-IV inhibition (n=7, active median(25th,75th centiles) 126 (118,144)mm2 vs placebo 117 (109,142)mm2, p=0.028 Wilcoxon Signed Rank test). There was no significant change in other vascular assessments or fovea thickness
Discussion: In this pilot study DPP-IV inhibition successfully reduced HbA1c in obese men. Capillary density significantly increased with Vildagliptin. However, as there were no significant changes in parameters associated with capillary density, namely microvascular filtration capacity, this observation needs to be confirmed with further research.

Where applicable, the authors confirm that the experiments described here conform with The Physiological Society ethical requirements.

PCC346

Mechanosensitive TRP channel expression in rat retinal microvessels

M. McGahon, A.V. Zholos, G.J. McGeown and T.M. Curtis

Centre for Vision and Vascular Sciences, Queen's University, Belfast, Northern Ireland, UK

The pressure-induced vasoconstriction or "myogenic response" of small arteries and arterioles is thought to be a primary mechanism contributing to blood flow autoregulation in many vascular beds. In cerebral arteries, activation of TRPC6 (1) and TRPM4 (2) channels has been shown to contribute to pressure-induced smooth muscle cell depolarisation and myogenic vasoconstriction. To date, no studies have addressed the role of TRP channels in mediating arteriolar myogenic responses. In the present study, we have begun to define the molecular and functional expression of mechanosensitive TRP channels in retinal arteriolar smooth muscle cells.
Using mechanical dissociation, arteriolar enriched samples of rat retinae were screened (using RT-PCR) for expression of mRNA encoding a number of known mechanosensitive TRP channels. mRNA transcripts for TRPC1, TRPM7, TRPV1, TRPV2, TRPV4 and TRPP1 channels were detected. In contrast to larger resistance arteries, retinal arterioles do not appear to express TRPC6 or TRPM4 channels. Immunohistochemical staining of whole flat mounts of rat retinae revealed cytosolic and membrane expression of TRPV1, TRPV2, TRPP1 and TRPM7 in arteriolar smooth muscle cells surrounding arterioles, while TRPV1, TRPV2, TRPV4 and TRPM7 were also detected in the endothelial cells lining arterioles, capillaries and venules. These expression patterns were confirmed using multiple antibodies to different epitopes within the respective channels.
Whole-cell patch-clamp recordings were subsequently made from rat retinal arteriolar smooth muscle cells embedded within isolated arteriolar segments, using Cs+ based internal and external solutions containing 10 μM nimodipine, and 2 s voltage ramps from -80 to +80 mV. Application of the TRPV2 agonist, delta-9-tetrahydrocannabinol (Δ9THC; 10 μM), elicited an increase in inward current at negative voltages, from -43.9 ± 16.7 pA/pF at -80 mV in absence of Δ9THC to 61.9 ± 22.9 pA/pF in the presence of Δ9THC (mean ± SEM, n=9, P=0.03, paired Student's t-test) and in the outward current at positive voltages (88.6 ± 40.6 pA/pF in the absence of Δ9THC compared to 125.8 ± 55.5 pA/pF at +80 mV in the presence of Δ9THC; P=0.04). The current activated by Δ9THC was outwardly rectifying and reversed at -9.7 ± 4.0 mV. Both the inward and outward portions of the current elicited by Δ9THC were inhibited by pre-incubation of the vessel with the TRPV2 inhibitor, tranilast (10 μM; n=5). Our results suggest that retinal arteriolar smooth muscle cells express a range of mechanosensitive TRP channels and that TRPV2 channels may be strong molecular candidates underpinning the myogenic response in this vascular bed.

Welsh DG, Morielli AD, Nelson MT, Brayden JE. Transient receptor potential channels regulate myogenic tone of resistance arteries. Circ Res. 2002;90(3):248-250.

Earley S, Waldron BJ, Brayden JE. Critical role for transient receptor potential channel TRPM4 in myogenic constriction of cerebral arteries. Circ Res. 2004;95:922–929.

This work is supported by funding from BBSRC.

Where applicable, the authors confirm that the experiments described here conform with The Physiological Society ethical requirements.

PCC347

L-NAME alters sub-cellular distribution of eNOS and caveolin-1 in the perfused human placental microvascular bed

L. Leach, V. Ghori, A.J. Fox, H. Noori and P. Santidamrongkul

School of Biomedical Sciences, University of Nottingham, Nottingham, UK

Endothelial nitric oxide synthase (eNOS) is expressed in the endothelium of placental vessels and also surprisingly in the syncytiotrophoblast lining of these vessels in the human placenta. eNOS is thought to play an important role in basal nitric oxide release to maintain maximal vasodilatation of fetal capillaries. Caveolin-1 is known to bind eNOS and inhibit it by compartmentalisation within caveolae. The aim of this study was to investigate the effects of L-NAME, the non-selective competitive inhibitor of eNOS, on the spatial localization of eNOS and caveolin-1 in the human placental vascular tree. Using a well-established dual perfusion system, placental lobules of normal term placentae (n=6) were perfused for 30 min with/without 5 mM L-NAME added to the fetal circulation, with continual monitoring of fetal perfusion pressure. Following perfusion fixation, tissue biopsies were frozen, cryosectioned and immunostained for eNOS and caveolin-1. Chorionic villi and vascular profiles within were visualized by fluorescence microscopy and quantitative analysis (blinded) of villous/vascular profiles was performed. In control perfused placenta eNOS was located predominantly in the endothelium of larger stem and intermediate villous vessels at the expense of terminal villous capillaries. A similar differential expression was seen for caveolin-1. Both eNOS and Cavelolin-1 was also localised to the syncytiotrophoblast. In L-NAME perfused placentae there was an altered pattern of eNOS staining in the syncytiotrophoblast: from a mixed punctate (caveolar/vesicular) and diffuse (cytosolic) localization to a predominantly punctate staining pattern ($p \leq 0.05$). An increase in caveolin -1 positive puncta (frequency and intensity) was also seen in the L-NAME group. The induced alteration in expression profiles of both proteins suggest that L-NAME inhibits release of eNOS from the caveolae in the syncytiotrophoblast and this also allows a greater visualisation of caveolin-1. This study also highlights the role of the syncytiotrophoblast in regulating vascular tone of fetal capillaries in the human placenta.

Where applicable, the authors confirm that the experiments described here conform with The Physiological Society ethical requirements.

PCC348

Thromboxane vasoconstrictor response of chorionic vessels from pregnancies complicated with gestational diabetes

A.A. Razak, L. Leach and V. Ralevic

School of Biomedical Sciences, University of Nottingham, Nottingham, UK

In human placenta, lack of autonomic innervation suggests that vascular tone is controlled by humoral factors such as thromboxane. A recent study on vasoconstriction to a thromboxane mimetic, U46619, in chorionic plate arteries from pregnancies with maternal obesity, showed that responses were unaltered[1]. The effect of gestational diabetes (GDM) on the contractile response of chorionic vessels to U46619 is not known. Since functional studies on fresh placental tissue can be challenging because of the unpredictability of placenta availability, responses were investigated in both fresh vessels and after overnight storage. Human placentas from normal (n=7) and GDM (n=3) pregnancies were collected following elective caesarean sections at term. Segments of chorionic arteries and veins were dissected and divided into two: (a) fresh and (b) overnight-stored (physiologic salt solution[2] with 2% Ficoll and 5% CO_2 in air gassing, 4°C). Responses of the vessel segments to U46619 were investigated by isometric tension recording[3]. Cumulative responses to U46619 were expressed as a percentage of the contractile response to KCl (60 mM). Data were analysed using two-way ANOVA. U46619 (1 nM - 30 μM) elicited concentration-dependent contractions in the chorionic arteries and veins. Contractile responses to U46619 were similar between GDM and normal groups in both arteries and veins ($P>0.05$). After overnight storage, contractile responses to U46619 were also similar between GDM and normal groups, in both arteries and veins ($P>0.05$), suggesting a stable agonist response that can be studied after overnight storage. Contractile responses to U46619 are unchanged in chorionic arteries and veins from GDM pregnancies, as in chorionic arteries from pregnancies with maternal obesity.

Hayward CE *et al.* (2013). *Placenta* **34(3)**, 281-287.

Wareing M *et al.* (2006). *Placenta* **27(1)**, 42-48.

Donoso *et al.* (2005). *Am Physiol* **288**, 2439-2449.

AAR is supported by Islamic Development Bank under Merit Scholarship Programme.

Where applicable, the authors confirm that the experiments described here conform with The Physiological Society ethical requirements.

PCC349

Novel Vascular Morphology in Human Glomeruli

C.R. Neal[1], P. Winlove[2], J. Bell[2] and S.J. Harper[1]

[1]School of Physiology and Pharmacology, Bristol University, Bristol, UK and [2]Physics and Astronomy, University of Exeter, Exeter, Devon, UK

Human glomeruli have a larger ratio of perfused volume to afferent arteriole conductance than mice or rats. These differences are likely to influence glomerular haemodynamics and blood pressure this study uses reconstructions of the human vascular tree to build upon previous work which revealed vascular chambers at the human glomerular vascular pole (Betteridge 2011).

Seven human kidneys not required for transplantation were perfused with Soltran solution (Baxter Healthcare, UK), and transported on ice. Fresh tissue wedges were removed for multiphoton microscopy (3 kidneys) and the sample site clamped off from the rest of the kidney. The remaining kidney tissue was perfused (100mmHg pressure) with mammalian HEPES Ringer containing Ficoll 400 (25mmHg colloid osmotic pressure), followed by glutaraldehyde (2.5%) fixative at the same pressures. Tissues were dehydrated, embedded in resin and Toluidine Blue stained 1μm serial sections used to reconstruct 3D images of the glomerular vasculature. In two fresh and two fixed unstained kidneys the vasculature was imaged in 0.5-1mm thick tissue slices using multiphoton microscopy as described previously (Arkill 2010). Fibrous collagen was visualised using second harmonic generation and elastin from its

intrinsic two photon autofluorescence in a multiphoton microscope.
Reconstructed human glomeruli (n=14) from resin sections show both afferent arterioles (22±1μm diam. mean±SEM) and efferent arterioles (16±1μm diam.) leading into ellipsoidal vascular chambers (VCs). Afferent VCs (49±3 x 48±4 x 32±2μm diam.) are larger than efferent VCs (46±9 x 43±4 x 26±1μm diam.) and lead into (on average) 7 unbranched wide vessels (Conduit vessels; 16±1μm diam.) with a paucity of podocytes that convey blood to the peripheral glomerulus. The smaller efferent VCs have (on average) 13 highly branched vessels (10±0.4μm diam.) draining into them. VCs scale with glomerular volume and could be absent from glomeruli smaller than 160μm diameter.
Multiphoton microscopy confirmed this morphology in two fresh and two fixed kidneys but also demonstrated coherent emission in Second Harmonic Generation consistent with Collagen I or III in a position matching the Vascular Chamber wall. Fibrous elastin was not detected, however the entire structure exhibited background autofluorescence.
VCs and Conduit vessels are not apparent in classical biopsy sections but they are revealed by perfusion fixation at in vivo matching pressures reinflating the glomerular vascular tree to in vivo diameters. Collagen III is observed in the mesangium of collagen glomerulopathies but this report is the first to find banded collagen (I or III) in normal glomeruli. VCs and Conduit vessels are likely to be important in the distribution of blood flow among the human glomerular lobes and are implicated in glomerular disease where complications originate at the vascular pole where these structures are located.

Arkill KP, Moger J, Winlove CP (2010) The structure and mechanical properties of collecting lymphatic vessels: an investigation using multimodal nonlinear microscopy. J Anat 216(5): 547–555.

Betteridge KB, Salmon AHJ, Neal CR. (2011) A Novel Vascular Chamber Discovered in the

Human Renal Glomerulus. Microcirculation 18(5):419 PC35

Where applicable, the authors confirm that the experiments described here conform with The Physiological Society ethical requirements.

PCC350

The functional role of acid-sensing channel 3 in the urinary bladder

L. Adjei[1], G. Sui[2], M. Roberts[1], W. Rong[3], J. Li[1] and C. Wu[1]

[1]University of Surrey, Guildford, UK, [2]St Thomas Hospital, London, UK and [3]Shanghai Jiaotong Univeristy, Shanghai, China

Acid-sensing ion channels (ASIC) are a class of ion-channels that are classically expressed in the neurones to sense extracellular acidification and pain. These molecules are also found in a variety of peripheral tissues as a sensory molecule. Recently several subtypes of ASICs have been identified in the urinary bladders, in particular ASIC3 which is preferentially expressed in the urothelium and has been suggested to have important pathological implications(1). However, the functional role of these channels in the bladder is poorly understood, in particular in native tissue. This study used a recently identified ASIC3-specific activator 2-guanidine-4-methylquinazoline (2GMQ) (2;3) to examine the role of ASIC3 channels in urothelium-mediated smooth muscle contraction and ATP release.
Guinea-pigs (male Dunkin-Hartley 450-600g) were sacrificed with schedule-1 procedure and urothelium-intact smooth muscle strips and urothelium sheets were isolated from the urinary bladders. The preparation was superfused in a HEPES-buffered Tyrode's solution and isometric tension was recorded with a tension-transducer via a bridge-amplifier. ATP was measured by sampling the superfusate adjacent to the urothelium and using a luciferin-luciferase assay.
Spontaneous contractions were consistently observed in urothelium-intact smooth muscle strips (μN/mg tissue, median (25%-75% range): 734 (272-1966), n=10) which were absent in urothelium-denuded smooth muscle strips. 2GMQ (100μM-500μM) augmented the peak contractile force in urothelium-attached muscle strips (net increase, μN/mg tissue, median (25%-75% range): 100μM 2GMQ: 707 (414 – 1981), n=5, p<0.05, paired Wilcoxon signed-rank test); 500μM 2GMQ: 320 (91-3601), n=5, p<0.05). ATP release was detected from the urothelium attached muscle strips (pmoles/g tissuse/min, median (25%-75% range): 15 (7-90), n=20) and a greater ATP release was generated from the urothelium sheets (182 (23-286), n=20, p<0.05). Application of 2GMQ (10μM-500μM) enhanced ATP release in the urothelium-intact smooth muscle (% control, median (25%-75% range); 10μM 2GMQ: 173 (116 – 276); n=8, p<0.05); 100μM 2GMQ: 250 (177 – 739); n=7, p<0.05; 500μM 2GMQ: 178 (131-270); n=8, p<0.05). Consistently, 2GMQ also increased ATP release from the urothelium sheets (10μM 2GMQ:163 (116-246), n=8, p<0.05); 100μM 2GMQ: 173 (140-296), n=7, p<0.05); 500μM 2GMQ: 165 (135-294), n=5, p<0.05).
These data provide the first evidence that ASIC3 channels enhance urothelium-mediated smooth muscle contractions and stimulate ATP release in the bladder wall, mainly attributed to a release from the urothelium. The latter may exert an autocrine/paracrine effect on both motor and sensory function in the urinary bladder.

Sanchez-Freire V, Blanchard MG, Burkhard FC, Kessler TM, Kellenberger S, Monastyrskaya K. Acid-sensing channels in human bladder: expression, function and alterations during bladder pain syndrome. J Urol 2011; 186(4):1509-1516.

Alijevic O, Kellenberger S. Subtype-specific modulation of ASIC function by 2-guanidine-4-methylquinazoline. J Biol Chem 2012.

Yu Y, Chen Z, Li WG, Cao H, Feng EG, Yu F et al. A nonproton ligand sensor in the acid-sensing ion channel. Neuron 2010; 68(1):61-72.

We thank BBSRC for financial support

Where applicable, the authors confirm that the experiments described here conform with The Physiological Society ethical requirements.

PCC351

Vascular endothelial growth factor (VEGF)C; a protective glomerular mediator?

S.L. Baker[1], N.R. Buckner[1], C.R. Neal[2], G.I. Welsh[1], D.O. Bates[2], S.C. Satchell[1] and R.R. Foster[1]

[1]Academic Renal Unit, University of Bristol, Bristol, UK and [2]MicroVascular Research Laboratories, University of Bristol, Bristol, UK

Introduction
In diabetic nephropathy, increased VEGFA expression is associated with proteinuria [1], however blocking VEGFA therapeutically also blocks its beneficial effects [2]. Previously we have shown that, in contrast to VEGFA, VEGFC decreases protein passage in human glomerular endothelial cells (GEnC) and tyrosine phosphorylates the same receptor as VEGFA, VEGFR2 [3]. Our aims were to determine how VEGFC induces differential signaling effects to VEGFA in GEnC in culture and in a

transgenic mouse model, and the impacts of this on GEnC health.

Methods

A podocyte-specific, inducible VEGFC overexpressing mouse (podVEGFC) was developed by crossing PodrtTA mice with TetO-VEGFC mice. Mice were either terminally anaesthetised (Dormitor 1.6mg/kg, Narkitan 100mg/kg, H2O (1:1:1) i.m.) or killed by schedule 1. Glomeruli were isolated from podVEGFC mice using dynabeads as previously [4], RNA extracted, reverse transcribed and QPCR performed for VEGFC, VEGFR2, VEGFA and GAPDH. PodVEGFC kidneys were wax embedded, sectioned and stained with Periodic Acid Schiff, or snap frozen and sectioned. Kidneys were also fixed using cardiac perfusion with gluteradehyde, processed and imaged by electron microscopy (EM). VEGFR2/R3 heterodimerisation was analysed in fresh frozen kidney using a proximity ligation assay (PLA). Cultured GEnC were stimulated with vehicle, 1nM VEGFA or 10nM mature VEGFC for varying times and either stained with trypan blue and counted or protein/RNA extracted. Protein was Western blotted and probed for specific phospho-/pan VEGFR2 or phospho-/total Akt antibodies. QPCR was performed for VEGFR2 and GAPDH.

Results

VEGFC treatment did not phosphorylate VEGFR2 at tyrosine residues 1175, 1214 or 951 in GEnC (min. n=7). QPCR demonstrated that glomerular VEGFR2 (0.39±0.155 fold decrease) and VEGFA (0.62± 0.1 fold decrease, $p<0.05$, n=3) expression was decreased in podVEGFC mice and VEGFR2 was also decreased in GEnC stimulated with rhVEGFC (0.19±0.01 fold decrease compared to vehicle). A PLA demonstrated increased VEGFR2/3 heterodimerisation in podVEGFC mouse glomeruli ($p<0.01$, n=3). VEGFC promoted decreased trypan blue positive GEnC over 24h ($p<0.05$, n=5), increased Akt phosphorylation (n=3) and there were no morphological changes by light (min. n= 5) or EM (n=4) in podVEGFC glomeruli.

Conclusions

Although VEGFA and VEGFC both induce VEGFR2 phosphorylation in GEnC, VEGFC affects VEGFR2 and VEGFA expression and activates VEGFR2/R3 heterodimerisation in glomeruli ex vivo. Both VEGFC and VEGFA promote GEnC cell survival, and glomerular VEGFC overexpression has no detrimental effects on glomerular filtration barrier structure or function. Since VEGFC can reduce protein passage through GEnC monolayers, these results indicate potential therapeutic benefits of glomerular VEGFC on proteinuric kidney disease.

Cooper, M.E., et al., Increased renal expression of vascular endothelial growth factor (VEGF) and its receptor VEGFR-2 in experimental diabetes. Diabetes, 1999. 48(11): p. 2229-39.

Eremina, V., et al., VEGF inhibition and renal thrombotic microangiopathy. N Engl J Med, 2008. 358(11): p. 1129-36.

Foster, R.R., et al., Vascular endothelial growth factor-C, a potential paracrine regulator of glomerular permeability, increases glomerular endothelial cell monolayer integrity and intracellular calcium. Am J Pathol, 2008. 173(4): p. 938-48.

Takemoto, M., et al., A new method for large scale isolation of kidney glomeruli from mice. Am J Pathol, 2002. 161(3): p. 799-805.

This work was funded by the British Heart Foundation (FS/10/017/28249).

Where applicable, the authors confirm that the experiments described here conform with The Physiological Society ethical requirements.

PCC352

Guinea pig preterm birth is affected by the lysine deacetylase inhibitor tichostatin A

W. Tong[1], M. Karolczak-Bayatti[1], B.F. Mitchell[2], G.N. Europe-Finner[1] and M.J. Taggart[1]

[1]Institute of Cellular Medicine, Newcastle University, Necastle upon Tyne, UK and [2]Department of Obstetrics & Gynecology, University of Alberta, Edmonton, AB, Canada

There is increasing interest in investigating the roles of protein lysine acetylation in mediating cell function. Recently, evidence was presented for a role of lysine deacetylase inhibitors (KDACi) in regulating human uterine function by epigenetic and non-epigenetic actions that highlighted a possibility of utilising such substances to target pathways involved in preterm labour [1]. The pregnant guinea pig, unlike rat or mouse, has a similar endocrine physiology to that of human and is therefore a useful model of human parturition [2]. We therefore sought to determine whether trichostatin A (TSA), a broad KDACi, could affect the timing, or duration, of parturition in a guinea pig model of experimentally-induced preterm labour [3,4].

All animal experimentation was performed under Home Office License. Preterm birth was induced in time-mated pregnant guinea pigs with RU486 (3 mg/kg body weight) on gestation day d55 and d56 (analogous to ~32 weeks human gestation) and oxytocin (2 U/kg) on d57. Animals in the treatment group received additional daily doses of TSA (1.03 mg/kg) from d54 to d57. All pregnancies were monitored to determine the exact timing of birth. Effects of TSA were quantified by the following assessments: LS, time between last injection to 1st pup's appearance; LE - time between last injection to last pup's appearance; LD - labour duration between 1st and last pups appearance; and litter survival rate (SR). Mean ± SEM data in preterm (PTL) and TSA- treatment groups were compared using two-tailed unpaired t-test with Welsh's correction.

Term delivery occurred at d67.9 ± 0.1 (n=11). LD was 0.37 ± 0.02 hr. Of 37 pups, 30 appeared healthy and 7 were either stillborn or died shortly after birth (SR = 80.5 ± 5.0 %). In PTL group (n=4), delivery occurred in all animals on d57. LS was 2.83 ± 0.18 hr, LE was 5.53 ± 0.63 hr and LD was 2.53 ± 0.63 hr. No pups survived. In the TSA-treated group (n=7), 4 animals progressed to term (completed delivery > d67) and 3 delivered on d57-d58. Remarkably, one animal that had begun delivery on d57 (with one stillborn pup) also delivered two more pups on d69 that appeared normal and healthy. Overall, delivery was completed on d64.7 ± 0.4 ($n=6$, $p<0.05$), LS was 114.63 ± 1.65 hr, LE was 176.43 ± 1.93 hr ($n=6$, $p<0.05$) and LD was 45.43 ± 1.73 hr (n=6). Of the 19 pups, 10 appeared healthy but 9 did not survive (SR = 52.4 ± 10.1 %, $n=6$, $p<0.05$). In conclusion, TSA inhibits the onset of parturition, and/or increases the length of gestation in ~50% of cases of a guinea pig model of preterm birth with improved neonatal survival. KDACi are thus promising tools for elucidating the basis of preterm and term parturition. Further work to establish the mechanism(s) of action and optimise the efficacy of KDACi may also result in the development of new tocolytic agents.

Karolczak-Bayatti M *et al.* (2011). *J Biol Chem*, **15**:94-108.

Taggart & Mitchell. (2009). *Am J Physiol Regul Integr Comp Physiol*, **297**(3):R525-45

Chwalisz K. (1994). *Human Reproduction*, **9**(supp1):131-161

Tong WC *et al* (2012) *Reproductive Sciences*, **19**:190A

Supported by MRC (UK, G0900525, G0902091) & AIHS & WCHRI (Canada).

Where applicable, the authors confirm that the experiments described here conform with The Physiological Society ethical requirements.

PCC353

BK_{Ca} channels are functionally coupled to L-Type Ca^{2+} channels but not IP_3R-mediated Ca^{2+} waves in hamster cremaster arterioles

W.F. Jackson and E.B. Westcott

Pharmacology & Toxicology, Michigan State University, East Lansing, MI, USA

Large conductance, Ca^{2+}-activated K^+ channels (BKCa) appear to be activated by Ca^{2+} influx through L-Type, voltage-gated Ca^{2+} channels (VGCC) in arteriolar smooth muscle cells. In these same cells, Ca^{2+} influx through VGCC also stimulates IP_3R-dependent Ca^{2+} waves. However, the contribution of these IP_3R-dependent events to the regulation of BKCa in arterioles is not known. To test the hypothesis that VGCC-triggered, IP_3R-dependent Ca^{2+} signals contribute to the functional activity of BKCa, we studied isolated, cannulated hamster cremasteric arterioles by pressure myography in the absence and presence of the VGCC-agonist, Bay K 8644 (BayK, 5 nM) and the IP_3R antagonist 2-aminoethoxydiphenyl borate (2-APB, 100 μM). In arterioles pressurized to 20 cm H2O (to obviate pressure-dependent activation of VGCC), the BKCa blocker tetraethylammonium (TEA, 1 mM), had no significant effect on diameter (44 ± 4 vs. 42 ± 2 μm; n = 3, p > 0.05), consistent with low activity of VGCC and BKCa. Exposure to BayK (5 nM), constricted the arterioles from 44 ± 4 to 28 ± 3 μm (p < 0.05), and in the presence of BayK, TEA (1 mM) now produced robust constriction from 28 ± 3 to 18 ± 1 μm (p < 0.05). Identical results were obtained in the presence of 2-APB (100 μM): 2-APB had no effect on resting diameter (44 ± 4 vs. 43 ± 3 μm; p > 0.05) and did not affect the subsequent responses to BayK (29 ± 2 μm; p > 0.05 vs. BayK alone) and TEA (19 ± 2 μm; p > 0.05 vs. BayK + TEA alone). Efficacy of this concentration of 2-APB was verified by complete block of phenylephrine-induced constriction and abolition of Ca^{2+} waves in Fluo-4 loaded preparations. Before 2-APB, phenylephrine (20 nmols) constricted arterioles by 22 ± 4 μm, in the presence of 2-APB phenylephrine-induced constriction = 0.3 ± 0.2 μm (n = 3, p < 0.05). Before 2-APB, Ca^{2+} wave frequency = 0.21 ± 0.06 Hz, after 2-APB Ca^{2+} wave frequency = 0.04 ± 0.02 Hz (n = 6, p < 0.05). These data indicate that BKCa are activated by Ca^{2+} influx through VGCC, and that this occurs independent from IP_3R-dependent Ca^{2+} waves.

Supported by HL-32469, PO1 HL07687 and AHA Fellowship 0815778G.

Where applicable, the authors confirm that the experiments described here conform with The Physiological Society ethical requirements.

PCC354

Optical mapping of action potential spatiotemporal waveforms in isolated guinea pig heart and uterus

W. Tong and M.J. Taggart

Institute of Cellular Medicine, Necastle upon Tyne, UK

Elucidation of the electrophysiological characteristics of uterine smooth muscle is important for understanding the electrical events that regulate parturition at the end of pregnancy [1]. Similarly, this may be informative in developing tocolytic drugs directed against ion channel targets for the treatment of premature labour. Two steps are important in this regard. First, it would be informative to determine the spatiotemporal characteristics of action potential (AP) propagation in the uterus in order to identify how electrical excitation-contraction coupling may be co-ordinated at a tissue and organ level. Second, consideration should be given to possible off-site actions of drugs targeting electrogenic events. In this regard, it is important to also understand the actions of electrogenic modulators on cardiac AP waveforms. The guinea pig is a useful model of human cardiac [2] and uterine [3] function. We, therefore, have undertaken pilot experiments using high frequency optical mapping to examine the spatiotemporal characteristics of AP propagation in hearts and uteri isolated from adult female guinea pigs. Fluorescence was excited by light-emitting diodes (at 488 nm) and the filtered emission images (590 nm long pass) were acquired by a high speed camera (up to 2.5 kHz) with a viewing area of 128x128 pixels, resulting in spatial resolutions of 200 x 200 μm^2. Following well-established methods [4], the optical mapping system was validated by recording epifluorescence images from perfused ex vivo intact hearts loaded with voltage-sensitive dye di-4-ANEPPS and mechanical uncoupler blebbistatin (Fig 1). Uterine tissues were mounted on a silicone support and superfused with MOPS-based Krebs solution at 37 °C. After a period of stabilization, the tissues were loaded with di-4-ANEPPS (5-10 μM), contraction was minimised with wortmannin (17-25 μM) and the fluorescent images were acquired at 0.5 kHz (Fig 2). In summary, our optical mapping procedure enables recordings of up to 0.4 msec and 200 μm resolution in 2.5 x 2.5 cm^2 areas of isolated hearts and uteri from guinea pigs. To our knowledge, these are the first reported visualisations of AP spatiotemporal patterns in uterine smooth muscle and offer much promise to add to our knowledge gathered thus far from spatially distributed surface electrode recordings [5]. In addition, the ability to visualise AP characteristics in both uterine and cardiac tissues will assist with (i) elucidating tissue-specific mechanisms of electrogenesis and (ii) investigating putative tissue-specific actions of ion channel modulators in both tissue types from one animal.

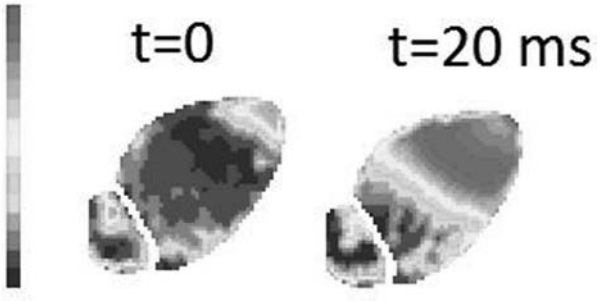

Figure 1. A stimulated excitation wavefront (red) in the left ventricle propagating from apex to base.

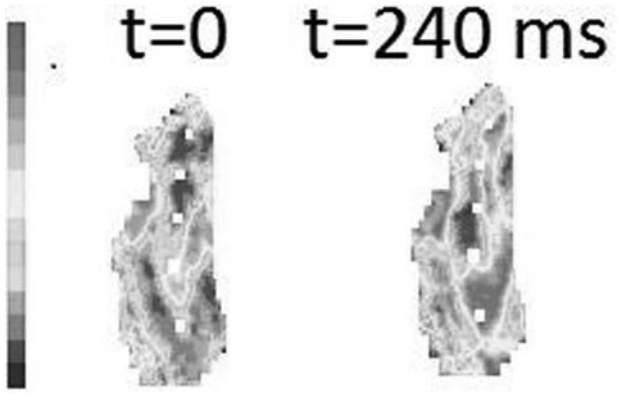

Figure 2. APs (red) propagating across an intact uterus horn.

Tong WC *et al* (2011) *PLoS One<.i>* ***6****(4):e18685.*

James AF et al *(2007)* Prog Biophys Mol Biol ***94****:265-319*

Mitchell BF& Taggart MJ (2009) Am J Physiol ***297****:R525-45*

Matiukas A et al *(2007)* Heart Rhythm ***4****:1441-1451*

Lammers WJ et al *(2008)* Am J Physiol Regul Integr Comp Physiol ***294****(3):R919-28.*

Supported by MRC (UK, G0900525, G0902091). We would also like to thank Dr. O Bernus (Bordeaux University) and Prof. W Lammers (United Arab Emirates University) for their valuable input.

Where applicable, the authors confirm that the experiments described here conform with The Physiological Society ethical requirements.

PCC355

The role of ER stress in vascular calcification

M. Furmanik and C.M. Shanahan

Department of Cardiology, King's College London, London, UK

Vascular calcification is a pathological process of deposition of calcium and phosphate crystals in the form of hydroxyapatite (HAp) in the blood vessel wall. Its presence in the vessel wall causes stiffness and leads to left ventricular hypertrophy and increases cardiovascular morbidity and mortality. It is a serious health problem common in ageing populations and widely prevalent in pathological conditions such as diabetes and chronic kidney disease.

Vascular calcification is a regulated, cell-mediated process, similar to bone formation that involves osteogenic transdifferention of vascular smooth muscle cells (VSMCs) characterized by expression of bone-specific genes in the calcified vessel. However, the exact mechanisms responsible for triggering this process are unknown.

The endoplasmic reticulum (ER) is involved in the production, correct folding and secretion of newly synthesized proteins in cells. ER stress occurs as a result of unfolded protein accumulation or an increased demand for protein secretion. It results in activation of a signalling pathway called the unfolded protein response (UPR), mediated by three main ER stress transducers IRE1, PERK and ATF6. Importantly, ER stress has recently been implicated in bone development. Therefore, we hypothesized that phenotypic conversion and calcification of VSMCs can be regulated by ER stress.

Human primary VSMCs were treated with tunicamycin and thapsigargin and expression of bone markers in response to ER stress was examined by Western blotting and quantitative real-time PCR. ER stress was shown to regulate expression of BMP2, a key bone morphogen and Osterix, an obligate bone specific transcription factor, as well as its downstream targets bone sialoprotein, alkaline phosphatase and osteoprotegerin in VSMCs. However no effects on Runx2 were observed. In addition, the two different ER stress inducers were found to have differential effects on activation of these bone markers. Using siRNA knock-down it was established that two branches of the UPR represented by ATF6 and ATF4 (downstream of PERK) play a role in mediating these effects on bone gene expression. Further analysis of Osterix, the osteogenic transcription factor shown to be regulated by ER stress, demonstrated that it localised predominantly in cytoplasmic foci and was present in matrix vesicles secreted by VSMCs suggesting it may play a novel role in mediating the VSMC response to ER stress.

Where applicable, the authors confirm that the experiments described here conform with The Physiological Society ethical requirements.

PCC356

The protein kinase C alpha and delta isozymes gene silencing restores vascular function in diabetic rats

K. Klymenko[1], T. Novokhatska[1], I. Kizub[1], V. Dosenko[2] and A. Soloviev[1]

[1]Institute of Pharmacology and Toxicology of National Academy of Medical Sciences, Kiev, Ukraine and [2]Bogomoletz Institute of Physiology of National Academy of Sciense, Kiev, Ukraine

Cardiovascular diseases are currently the principal causes of morbidity and mortality in patients with diabetes mellitus and current therapy is still ineffective. Protein kinase C (PKC) is a key enzyme involved in endothelial dysfunction and decrease of vascular tissues potassium (K^+) channels activity. Endothelium and K^+ channels, in turn, are the main factors for maintenance of normal vasodilator potential at different pathological conditions, including diabetes.

The aim of this study was to evaluate the effect of silencing of PKC-α and -δ genes using siRNA on endothelial dysfunction and potassium channelopathy in vascular smooth muscle cells (SMCs) at diabetes.

Experimental design of the study comprised isolated rat aorta contractile recordings and whole-cell patch-clamp technique in isolated aortic SMCs. Dilator responses of vascular rings to acetylcholine (ACh, 10^{-9} - 10^{-5} M) were expressed as a percentage of the maximum contractile response produced by norepinephrine (10^{-6} M).

Diabetes was induced by streptozotocin intraperitoneal injection to male Wistar rats (STZ, 65 mg/kg) and then verified by the presence of hyperglycaemia (glucose level was 30.05±0.51 mM, n=12, P<0.05) in 3d month after STZ injection and at the day of experiment.

Diabetic rats were injected intravenously with siRNA targeted to PKC-α or -δ. Animals were killed on the 7th day by cervical dislocation following ketamine (45 mg/kg, i.p.) and xylazine (10 mg/kg, i.p.) anesthesia.

The concentration-response curve to ACh in diabetic aortas precontracted with norepinephrine (10^{-6} M) was significantly shifted to the right (EC_{50} = 6.93±0.11, n=12, P<0.05 *vs.* 7.59±0.08, n=7 in control). Maximum dilatation to ACh in diabetic tissues was depressed (56.7±4.26%, n=12, P<0.05 *vs.* 96.5±3.05%, n=7 in control)

PKC-α and -δ gene silencing led to significant restoration of ACh-induced dilatation in diabetic aortas with the maximum

of 91± 2.11%, n=17; P>0.05 (EC_{50} = 7.58±0.07) for siRNA PKC-α, and 90.1±1.34 %, n=15, P<0.05 (EC_{50} = 7.9±0.1) for siRNA PKC-δ.

In isolated diabetic aorta SMCs total outward K^+ current was reduced (peak current density was 15.9 ± 0.9 pA/pF (n=13, P<0.05) as compared to control (55.6 ± 5.8 pA/pF, n=8). Aortic SMCs from animals treated with siRNA PKC-α showed significant increase in total K^+ current in comparison to non-treated diabetic rats with peak density 23.5±1.9 pA/pF (n=12, P<0.05). The similar results were obtained in SMCs from animals treated with siRNA PKC-δ (23.9±2.7 pA/pF, n=7, P<0.05).

In conclusion, the silencing of both PKC-α and -δ gene expression using siRNA led to increasing of total K^+ outward current in vascular SMCs and restoring of endothelium-dependent vasodilatation in rats with diabetes mellitus. It is likely that siRNA technique can be a good therapeutic tool to normalize diabetic angiopathies.

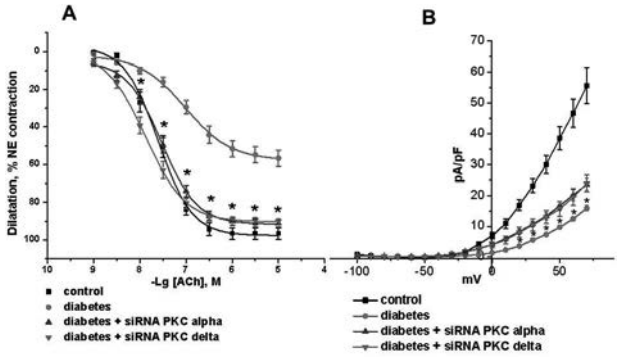

A: Dose-response curve for ACh in isolated rat aortic rings precontracted with norepinephrine (NE, 10^{-6} M) obtained from control (n=7), diabetic animals (n=12) and diabetic animals treated with siRNA PKC-α (n=17) or siRNA PKC-δ (n=15). B: Steady-state current-voltage relationships for whole-cell outward K^+ current density in isolated rat aorta SMC from control (n=8), diabetic animals (n=13), and diabetic animals treated with siRNA PKC-α (n=12) or siRNA PKC-δ (n=7). Data are shown as means + S.E.M. *P < 0.05 versus control.

Where applicable, the authors confirm that the experiments described here conform with The Physiological Society ethical requirements.

PCC357

Serum proteins fetuin-A and albumin alter the cytotoxic effects of calcium phosphate nanocrystals on human vascular smooth muscle cells

Y. Dautova[1], D. Kozlova[2], M. Epple[2], M. Bootman[3,1] and D. Proudfoot[1]

[1]Signalling Laboratory, Babraham Institute, Cambridge, UK, [2]Institute of Inorganic Chemistry and Center for Nanointegration Duisburg-Essen (CeNIDE), University of Duisburg-Essen, Essen, Germany and [3]Department of Life, Health and Chemical Science, The Open University, Milton Keynes, UK

Controlled deposition of calcium phosphate (CaP) in bone matrix is essential for stability and strength of bones and teeth, but such deposits are also found within other tissues in association with several diseases including atherosclerosis. CaP can interact with host proteins *in vivo*, including albumin and fetuin-A, which may modulate crystal interactions with cells (1).

We recently demonstrated that CaP nanoparticles induced rapid rises in intracellular calcium ($(Ca^{2+})_i$) in vascular smooth muscle cells (VSMCs) and subsequent cell death (2). Incubation of CaP crystals with serum prior to addition to VSMCs abolished elevation of $(Ca^{2+})_i$ suggesting that serum may offset the detrimental effects of CaP crystals. Compared to synthetic CaP, crystals isolated from calcified atherosclerotic tissue had little effect on $(Ca^{2+})_i$ and were less potent in inducing cell death, possibly due to their association with endogenous serum proteins such as fetuin-A, which has been previously shown to inhibit VSMC calcification and apoptosis (3).

Due to the important role of VSMC in stabilising atherosclerotic plaques, we determined whether fetuin-A and albumin can prevent CaP-induced VSMC death. In parallel, we also investigated changes in $(Ca^{2+})_i$ in response to CaP crystal stimulation in the presence and absence of a range of physiological and sub-physiological concentrations of fetuin-A and albumin. Cytotoxicity assessment (MTT) revealed that the crystals reduced cell viability in a dose-dependent manner. Pre-incubation with albumin or fetuin-A (10, 3 and 1 μM but not 0.1 μM) in serum-free medium blocked the cytotoxic effects of the CaP crystals (25 μg/ml) (P < 0.0001). Furthermore, functionalised particles (fetuin-A or albumin attached to CaP) were less toxic than naked CaP. CaP-fetuin particles were less potent at evoking cell death compared to CaP-albumin.

The initial $(Ca^{2+})_i$ oscillations appeared after 14.6 ± 1.3 min (n=16) and cells that died exhibited a large, unrecoverable $(Ca^{2+})_i$ peak just prior to cell death which occurred at 31.3 ± 1.76 min (n=17) after CaP addition. Only those cells where $(Ca^{2+})_i$ levels increased to a particular threshold died (peak amplitude (PA) 0.93 ± 0.03; n=17). In surviving cells, the $(Ca^{2+})_i$ oscillations were maintained or dampened over time, and were of much smaller amplitudes (PA 0.58 ± 0.04 (n=8)) compared to cells that died (P < 0.0001). Pre-incubation with 1 μM but not 0.1 μM fetuin-A or albumin silenced $(Ca^{2+})_i$ activity resulting in protection from cell death. The results suggest that CaP-induced cytotoxicity in VSMCs depends on $(Ca^{2+})_i$, and that presence of fetuin-A or albumin can provide protection against CaP-induced cell death. The cellular mechanisms underlying this protection are currently under investigation.

Woolf AD & Dieppe PA (1987). *Br Med Bull* **43**: 429-444.

Ewence AE *et al*. (2008). *Circ Res* **103**: e28–e34.

Reynolds JL *et al*. (2005). *J Am Soc Nephrol* **16**: 2920–2930.

Where applicable, the authors confirm that the experiments described here conform with The Physiological Society ethical requirements.

PCC359

Neuropilins and vascular remodeling

C. Pellet-Many, V. Mehta, I. Evans, J. Ruivo and I. Zachary

Medicine, University College London, London, UK

Aim: Neuropilin 1 (NRP1) and the structurally-related molecule, neuropilin 2 (NRP2), are co-receptors both for class 3 semaphorins, a family of secreted polypeptides with key roles in axonal guidance, and for various members of the VEGF family. Neuropilins were also identified to be key players in other physiological and pathological settings such as the primary immune response and cancer. Our group identified Neuropilins (NRPs) as regulators of vascular smooth muscle cell (VSMC) migration 1. In this study, we explored the role of NRP1 in abnormal VSMC accumulation in vivo in the rat carotid artery model of neointimal hyperplasia following balloon injury, in which VSMC migration and proliferation play important roles.

Methods: Male Sprague-Dawley rats were subjected to balloon angioplasty and left to recover for 7, 14 or 28 days. Quantitative PCR and Western blotting were used to look at endoge-

nous levels of NRPs expression in carotid arteries at the different recovery times. At the time of surgery, we applied 30% pluronic gel containing 10E10 adenoviral (Ad) particles expressing control LacZ, NRP1 Wild-Type (WT) or a truncated form, devoid of intracytoplasmic domain (NRP1ΔC), to the adventitia. Morphometric analysis was used to quantify the intima/media ratios in adenovirus-transduced arteries; Western blot and absolute RT-qPCR were used to detect changes in protein expression and mRNA levels respectively.
Results: Endogenous NRP1 and NRP2 mRNA and protein levels are upregulated after carotid injury with a maximum protein expression 7 days after injury, expression remaining elevated thereafter. Morphometric analysis of the vessels revealed that the over-expression of NRP1-WT did not alter the extent of neotinima formation but the NRP1ΔC mutant decreased the formation of neointimal hyperplasia.
Conclusions: These results strongly suggest a role for NRPs in the development of neointima in the rat carotid artery model of restenosis. Insights into NRP function in the aberrant migration and proliferation of VSMC in this model could be crucial to understand the mechanism of VSMC accumulation occurring in vascular remodeling.

Pellet-Many C, Frankel P, Evans IM, Herzog B, Jünemann-Ramírez M, Zachary IC. (2011) Neuropilin-1 mediates PDGF stimulation of vascular smooth muscle cell migration and signalling via p130Cas. Biochemical Journal. 435(3):609-18.

This work is funded by the BHF project grant PG/08/088/25873.

Where applicable, the authors confirm that the experiments described here conform with The Physiological Society ethical requirements.

PCC361

Spatial and temporal expression of Nrf2-inducible antioxidant defences in the gliovascular complex after stroke

A. Alfieri[1], S. Srivastava[1], R. Siow[1], M. Modo[2], M. Duchen[3], P. Fraser[1] and G. Mann[1]

[1]Cardiovascular Division, King's College London, London, UK, [2]Institute of Psychiatry, King's College London, London, UK and [3]Department of Cell and Developmental Biology, University College London, London, UK

Astrocytes are closely associated with cerebrovascular endothelium, providing functional and metabolic support. The relationship between these two cell-types has been defined as gliovascular complex. Activation of the redox sensitive transcription factor Nrf2 in the brain is a key mechanism underlying endogenous protection against oxidative stress. In the present study, we have investigated expression of Nrf2, constitutive antioxidant enzyme heme-oxygenase-2 (HO-2) and Nrf2-inducible HO-1 in cerebral microvessels after experimental stroke. Male Sprague-Dawley rats (250-300g) were subjected to 70 min right middle cerebral artery occlusion (MCAo) under isoflurane anaesthesia and followed by 4, 24 or 72 h reperfusion. HO-2, HO-1 and Nrf2 were detected by immunofluorescence and immunohistochemistry in brain coronal sections along with brain injury and cell markers. Cerebral ischaemia-reperfusion did not change constitutive HO-2 expression, however levels were significantly higher in perivascular astrocytes than endothelial cells. HO-1 expression was induced in microvessels of the peri-infarct region after 4-72 h, where it was mainly expressed by perivascular astrocytes. Nrf2 expression was significantly increased in microvessels after stroke between 4-24 h, peaking after 4h and remaining elevated after 72 h in perivascular astrocytes. In the endothelium, Nrf2 peaked after 24 h and declined by 72 h. In conclusion, astrocytes play a central role in protecting the gliovascular complex by expressing antioxidant enzymes. As Nrf2 and HO-1 expression are increased in cerebral microvessels following stroke, the Nrf2 defence pathway may be a therapeutic target to protect the brain against stroke.

Alfieri et al. (2011). J Physiol 589, 4125-4136

This work was funded by the Henry Smith Charity and British Heart Foundation

Where applicable, the authors confirm that the experiments described here conform with The Physiological Society ethical requirements.

PCC362

Acute inhibition of hERG K^+ channel by the antipsychotic drug fluphenazine

B. Lee, S. Jo and M. Park

Department of Physiology, School of Medicine, Kangwon National University, Chuncheon, Gangwon-do, Republic of Korea

Fluphenazine is a potent antipsychotic drug that can increase action potential duration and induce QT prolongation in several animal models. Since block of cardiac human *ether-a-go-go*-related gene (hERG) channels is one of leading causes of acquired long QT syndrome, we investigated the acute effects of fluphenazine on hERG channels to determine the electrophysiological basis for its proarrhythmic potential. We examined the effects of fluphenazine on the hERG channels expressed in *Xenopus* oocytes using two-microelectrode voltage-clamp techniques. Fluphenazine induced a concentration-dependent decrease of the current amplitude at the end of the voltage steps and hERG tail currents. The IC_{50} of fluphenazine-dependent hERG block in *Xenopus* oocytes increased progressively relative to the degree of depolarization. Fluphenazine affected the channels in the activated and inactivated states but not in the closed states. The S6 domain mutation Y652A attenuated the hERG current block. The IC_{50} value of fluphenazine-dependent hERG block increased from 13.3 μM to 89.0 μM by the mutation from tyrosine to alanine at 652 amino acid of the channel. These results suggest that the antipsychotic drug, fluphenazine is a blocker of the hERG channels, providing a molecular mechanism for the drug-induced arrhythmogenic side effects.

Where applicable, the authors confirm that the experiments described here conform with The Physiological Society ethical requirements.

PCC365

Reversal of murine plaque hypoxia prevents apoptosis and necrotic core expansion

T. Theelen[1], E. Marsch[1], M. van Gink[1], S. Meex[1], M. Gijbels[1], E. Biessen[1], B. Janssen[1], M. Daemen[2] and J. Sluimer[1]

[1]Maastricht University medical center, Maastricht, Netherlands and [2]Amsterdam medical center, Amsterdam, Netherlands

Murine and human plaque macrophages are hypoxic. We hypothesized that hypoxia stimulates pro-atherogenic processes, including inflammation, and that reversal of plaque

hypoxia by hyperoxic gas breathing will consequently alleviate plaque progression.
To study whether hyperoxic carbogen gas (95% O2, 5% CO2) could increase arterial pO2, blood was samples from canulated femoral arteries of LDLR-/- mice (n=4 males, chow) subjected to a single 30 min exposure of carbogen (5L/min, normobaric). Carbogen significantly increased arterial pO2 from 97±3mmHg at baseline to 498±50mmHg after exposure (p<0.0001). Next, the effect of the carbogen-enhanced arterial pO2 on plaque hypoxia was studied. LDLR-/- mice with advanced, hypoxic plaques (11-wk-old males, n=5/group, 12 weeks of diet) were subjected to a single 90 minute exposure of carbogen or compressed air (21% O2), injected with pimonidazole to detect hypoxia and sacrificed directly after exposure. Single carbogen treatment of advanced plaques led to a dramatic 80% reduction of plaque hypoxia in the aortic arch (p=0.029) compared to control. Therefore, the effect of chronic carbogen exposure on atherogenesis was studied. LDLR-/- mice (20-wk-old males, n=15/group) were placed on a high cholesterol (0.25 %) diet for an initial 4 weeks, followed by 4 weeks of high fat diet and carbogen gas or compressed air (21% oxygen) 5 days/week for 90 min/day. Twenty-four hours after the last exposure, mice were sacrificed and plaque hypoxia and atherogenesis were studied in the aortic arch and root. Even 24 hours after the last exposure, chronic carbogen exposure resulted in a 42% decrease of plaque hypoxia in the aortic root (p=0.028) compared to control. Chronic carbogen exposure did not alter plaque size or macrophage content in aortic root or arch, but reduced necrotic core size by 37% in advanced plaques of the aortic root compared to control (p=0.0003). In parallel, carbogen treatment reduced plaque apoptosis (TUNEL+cells/total cell) (-50%, p=0.03) compared to compressed air, likely due to improved efferocytosis of apoptotic cells by MAC3+ macrophages (+36%, p=0.03). These plaque-stabilizing effects were independent of serum cholesterol, hematological parameters (Hb, Ht, erythrocyte counts), hematopoiesis and systemic inflammation (blood, spleen, lymph nodes, and bone marrow). Mechanistically, hypoxia reduced efferocytosis in vitro in bone marrow-derived macrophages and decreased gene expression of efferocytosis receptors (-52% MerTK, -56% CD36). Also, M2 gene expression was reduced (MRC1 -60%, IL10 -51%), whereas M1 genes were up-regulated (IL6 +250 fold, iNOS +178 fold), suggesting a hypoxia-mediated shift away from M2 pro-phagocytic macrophages.
Thus, we conclude that carbogen exposure successfully enhanced plaque oxygenation and prevented necrotic core expansion, most likely by enhancing efferocytosis.

Where applicable, the authors confirm that the experiments described here conform with The Physiological Society ethical requirements.

PCC366

Crosstalk between mesenchymal stem cells and endothelial cells inhibits inflammatory leukocyte recruitment

N. Luu, H.M. McGettrick, C.D. Buckley, P. Newsome, G. Rainger, J. Frampton and G.B. Nash

University of Birmingham, Birmingham, UK

Mesenchymal stem cells (MSC) have immuno-modulatory capacity, but their effects on endothelial cells (EC) and recruitment of leukocytes are unknown. We cocultured human bone marrow-derived MSC and EC, and found that MSC could down-regulate adhesion of flowing human neutrophils or lymphocytes, and their subsequent transendothelial migration. This applied for EC treated with tumour necrosis factor-alpha (TNF), interleukin-1beta (IL-1) or TNF and interferon-gamma combined. Supernatant from cocultures added to EC also had an inhibitory effect on recruitment. This supernatant had much higher levels of IL-6 than supernatant from cultures of the individual cells, and the individual supernatants had no inhibitory functions. Addition of neutralising antibody against IL-6 removed the bioactivity of the coculture supernatant and also the immunomodulatory effects of coculture. Studies using siRNA to reduce IL-6 production in each cell type showed that it came mainly from the MSC in coculture, and reduction in production in these cells alone was sufficient to lose the inhibitory effects of coculture. Interestingly, studies using siRNA to reduce IL-6-receptor expression also showed that expression in MSC contributed to the effects of coculture. This was explained when we detected soluble IL-6R in supernatants and showed that receptor removal greatly reduced the potency of supernatant. Thus, crosstalk between MSC and EC caused up regulation of production of IL-6 by MSC which in turn down regulated the response of EC to inflammatory cytokines, an effect potentiated by release of soluble IL-6R. These studies establish a novel mechanism by which MSC delivered from the blood might have protective effects against inflammatory pathology and cardiovascular disease.

This work was supported by The British Heart Foundation (grant number RG_10-153).

Where applicable, the authors confirm that the experiments described here conform with The Physiological Society ethical requirements.

PCC367

Sphingosine 1-phosphate inhibits angiogenesis in *ex vivo* human aortic valves

K.S. Mascall, G. Small, G. Gibson and G.F. Nixon

School of Medical Sciences, University of Aberdeen, Aberdeen, UK

Aortic valve stenosis (AVS) is closely associated with increased valve inflammation leading to calcification and ultimately results in cardiac failure if untreated. Currently the only therapeutic option is surgical valve replacement. Recent studies have indicated that increased angiogenesis within the valve may facilitate access of inflammatory cells and this plays an important role in the pathogenesis of AVS. Preventing angiogenesis in aortic valves is therefore a novel therapeutic target in this disease. Sphingosine 1-phosphate (S1P) is a lipid mediator present in plasma and produces intracellular effects via specific S1P receptors. We have previously shown that S1P can inhibit angiogenesis in human arteries (Mascall *et al*, 2012). The aim of the current study was to determine the effect of S1P on angiogenesis in human aortic valves. Valves from patients undergoing valve replacement surgery for AVS (diseased) or aortic regurgitation (non-diseased) were cut 2mm^2 pieces and embedded in Matrigel. Valve pieces were incubated for up to 14 days in growth factor-supplemented medium and angiogenic sprouts were quantified. Sprouts consisting of endothelial cells (confirmed by uptake of acetylated-LDL) increased in number from day 5 until day 14 and this was significantly greater in diseased compared to non-diseased valves (number of sprouts observed at day 14, non-diseased 60 ± 8 versus diseased 110 ± 12, n=4 per group, mean ± s.e.m., ANOVA, p<0.05). Treatment of either diseased or non-diseased valve tissue with 1μM S1P resulted in a significant decrease in

endothelial sprout formation compared to non-treated valves (number of sprouts observed at day 14, non-diseased valves - untreated 71 ± 5 versus S1P-treated 18 ± 3, n=3 per group; diseased valves - untreated 116 ± 9 versus S1P-treated 38 ± 5, n=3 per group, $p<0.05$). To examine this further, we assessed the activity of matrix metalloprotineases (MMPs) which are associated with angiogenesis. Activity of MMP-2 was significantly greater in diseased compared to control valves as assessed by *in vitro* gelatinolytic activity. Incubation with 1μM S1P decreased MMP activity in diseased valves (gelatinolytic activity observed at day 14, 94 ± 11% decrease in untreated valves compared to treated, n=3 per group, $p<0.05$). To determine the potential mechanisms involved we examined expression of the angiostatic protein, soluble fms-like tyrosine kinase-1 (sflt-1). Immunoblotting of valve homogenates demonstrated that sflt-1 expression is significantly decreased in diseased valves compared to control valves. Homogenates from diseased valves incubated with 1μM S1P for 14 days had a significantly increased expression of sflt-1 (n=3 per group). In conclusion, S1P can inhibit angiogenesis in human aortic valves, possibly via increasing expression of the angiostatic protein sflt-1. This mechanism may provide a therapeutic target in AVS.

Mascall KS *et al*. (2012). *J Cell Science* **125**, 2267-2275.

Where applicable, the authors confirm that the experiments described here conform with The Physiological Society ethical requirements.

PCC368

The AMPKα2 subunit is crucial for myeloid cell-mediated post-ischemic revascularization

B. Fisslthaler, R. Abdel Malik, P. Seifert, N. Zippel and I. Fleming

Institute for Vascular Signalling, University Frankfurt, Frankfurt, Germany

Infiltrating immune cells play a key role in regulating angiogenesis through the production and release of a wide range of pro-angiogenic mediators and cytokines. As the AMP-activated protein kinase (AMPK) has been shown to positively regulate angiogenesis, we investigated the effect of deleting the AMPKα2 subunit in myeloid cells (LysM-AMPKα2) on macrophage and neutrophil function as well as on vascular repair.
Wild-type and LysM-AMPKα2 mice were subjected to hindlimb ischemia by femoral artery ligation. The recovery of blood flow (laser Doppler), capillary density (immunohistochemistry) and immune cell infiltration (flow cytometry) were determined. To assess the functional role of AMPKα2 in myeloid cells, bone marrow monocytes were differentiated (in M-CSF) and polarized to M1 (IFN-γ and LPS) or M2 (IL-4 and IL-13) macrophages. Polymorphonuclear cells (PMN) from the murine bone marrow were stimulated with LPS (2 hours). Expression levels of cytokines and growth factors were analyzed using quantitative real time PCR.
Recovery of blood flow after hindlimb ischemia was significantly impaired (80%) in LysM-AMPKα2 versus the wild-type littermates. In addition, LysM-AMPKα2 mice showed significantly reduced capillary density and decreased myeloid cell infiltration into the ischemic limb. The deletion of the AMPKα2 subunit had no significant effect on the mRNA expression levels of the M1 markers (TNF-α, IL-1β and inducible nitric oxide synthase) in macrophages. The M2 markers (FIZZ-1, arginase and YM-1) as well as VEGF were under basal decreased in macrophages from LysM-AMPKα2 mice. In PMNs deletion of the AMPKα2 resulted after stimulation with LPS in a significant increase in inflammatory markers whereas the expression of stromal cell-derived factor-1 and the metalloproteinase-9 was significantly reduced compared to cells from wild-type littermates.
Deletion of the AMPKα2 in the cells of the myeloid lineage almost abolished vascular repair after hindlimb ischemia. These results indicate that the AMPKα2 subunit plays a crucial role in regulating the inflammatory state and angiogenic potential of myeloid cells.

Where applicable, the authors confirm that the experiments described here conform with The Physiological Society ethical requirements.

PCC369

Aortic vasodilatation capacity of the glycosaminoglycan sulodexide is mediated by nitric oxide

Y. Mathison[1,3], G. Vásquez[2], J. Vásquez[1], A. Israel[3] and E. Romero[1]

[1]School of Medicine José María Vargas, Pharmacolgy Department, Universidad Central de Venezuela, Caracas, Venezuela, Bolivarian Republic of, [2]PEEI School of Medicine, Universidad Central de Venezuela, Caracas, Venezuela, Bolivarian Republic of and [3]School of Pharmacy, Laboratory of Neuropeptides, Universidad Central de Venezuela, Caracas, Venezuela, Bolivarian Republic of

Diabetes mellitus (DM) is a chronic metabolic disorder considered to be a major risk factor for cardiovascular diseases. DM-induced endothelial dysfunction is associated with cardiovascular risk. In human and diabetic animals models, decrease levels of glycosaminoglycans (GAGs) have been associated with a generalized vascular dysfunction (Deckert y col. 1989), and recent studies has demonstrated a beneficial effect of sulodexide (SUL) (glycosaminoglycan composed from heparin-like and dermatan fractions) in experimental models of endothelial damage (Kristová et al. 2000; 2008).Since NO plays a key role in vascular function, we assessed the possible endothelium-protective effect of SUL (15mg/kg, s.c) on vascular relaxation and nitric oxide synthase (NOS) activity in aortic rings of diabetic rats. Diabetes type 1 was induced in male Sprague-Dawley rats (200-250, n=8-10/group) by administration of streptozotocin (STZ), 60 mg, i.v. Animals were randomly allocated in four groups: C=control, STZ=diabetic, SUL=control+SUL and STZ+SUL= diabetic+SUL. After three months of treatment, the animals were euthanized in thiopenthal anesthesia (30 mg/Kg i.p.) and the aorta was microdissected. Basal and SUL-stimulated NOS activity was assayed by monitoring the conversion of [3H]-L-arginine to [3H]-L-citruline. Phenilephrine precontracted aortic rings were used to evaluated acetylcholine (ACh: 1x10-7, 3x10-7, 1x10-6, 3x10-6) and nitroprusiate (NPS:10-8,10-7,10-6) relaxation capacity. Values are means ± E.E.M, compared by ANOVA. Basal NOS activity was lower in STZ-diabetic rats than in control group (57.2±4.02 vs. 90.58±4.6 $p< 0.01$), and this activity was restored by SUL treatment (100.83±12). In diabetic rats ACh relaxation was 28.8-35.1% lower than in control rats, but relaxation in SUL y SUL+STZ groups was similar to control. No significative statistical differences were found in endothelium-independent NPS relaxation, between the different groups. Our results demonstrated that pretreatment with SUL prevents loss of the relaxing capacity induced by diabetes in aorta of diabetic rats, by a mechanism involving the production of nitric oxide, and suggest a potential use of this drug to improve endothelial dysfunction in diabetes.

Deckert T, Felt-Rasmussen B, Borch-Johnsen K, Jensen T, Kofoed-Enevoldsen A. Albuminuria reflects widespread vascular damage. The Steno hypothesis. Diabetologia 1989; 32: 219-26.

Kristová V, Kriska M, Babál P, Djibril MN, Slámová J, Kurtanský A: Evaluation of endothelium protective effects of drugs in experimental models of endothelial damage. Physiol Res 49: 123-128, 2000.

Kristová V, Liskova S, Sotnikova R, Vojtko R, Kurtansky A. Sulodexide improves endothelial dysfunction in streptozotosin-induced diabetes in rats. Physiol Rev 2008; 57:491-4

Supported by CDCH PI-09-7287-2088, LOCTI-Facultad de Medicina, Misión Ciencia (FONACIT-Min. PP de Ciencia y Tecnología) N°2007001585

Where applicable, the authors confirm that the experiments described here conform with The Physiological Society ethical requirements.

PCC371

Asiatic acid alleviates metabolic and hemodynamic alterations in high-fat, high-carbohydrate diet-induced metabolic syndrome rats

P. Pakdeechote[1], S. Bunbupha[1], U. Kukongviriyapan[1], P. Prachaney[2], A. Timinkul[1] and V. Kukongviriyapan[3]

[1]Physiology, Faculty of Medicine, Khon Kaen University, Khon Kaen, Thailand, [2]Anatomy, Faculty of Medicine, Khon Kaen University, Khon Kaen, Thailand and [3]Pharmacology, Faculty of Medicine, Khon Kaen University, Khon Kaen, Thailand

Consumption of high-fat, high-carbohydrate diet mainly contributed in the development of metabolic syndrome, which is associated with obesity, insulin resistance, dyslipidemia, and high blood pressure. It is well established that asiatic acid, a natural triterpenoid compound derived from Centella asiatica, exhibited biological effects including, antiinflammation, antioxidant and antihyperglycemia. In the presen study, we examined the metabolic, cardiovascular responses as well as antioxidant properties of asiatic acid in rats with metabolic syndrome (MS) induced by high-fat, high-carbohydrate (HFHC) diet. Male Sprague-Dawley rats (160-180 g) were fed with HFHC diet with 15% fructose in drinking water for 12 weeks to induce MS. Then, MS rats and normal rats received asiatic acid (10 mg/kg) or vehicle for further 3 weeks. Fasting serum insulin, fasting blood glucose (FBG), oral glucose tolerance test (OGTT) and systolic blood pressure (SBP) were measured once a month. At the end of treatment, rats were anaesthetized with peritoneal injection of pentobarbital-sodium (60 mg/kg) and hemodynamic status, lipid profiles and oxidative stress markers were evaluated. All procedures are complied with the standards for the care and use of experimental animals and approved by Animal Ethics Committee of Khon Kaen University, Khon Kaen, Thailand (AEKKU 36/2555). Data are expressed as the mean ± S.E.M., compared by ANOVA. Results showed that rats fed with HFHC diet had an impairment of OGTT, high homeostasis model assessment of insulin (HOMA-IR), high cholesterol, and high SBP, indicating metabolic syndrome (MS) in these rats ($p<0.05$). Moreover, mean arterial blood pressure (MAP) (MS: 114.61 ± 3.7 vs. 90.58 ± 1.7 mmHg control, $p<0.05$), hindlimb vascular resistance (HVR) (MS: 30.64 ± 2.5 vs. 11.46 ± 0.6 mmHg/min/100 g/ml control, $p<0.05$) were significantly increased, relating to the augmentation of vascular superoxide production (MS: 114.9 ± 15.1 vs. 56.9 ± 4.3 counts/min/mg dry weight control, $p<0.05$) and plasma MDA levels (MS: 5.8 ± 0.5 vs. 2.9 ± 0.2 μM control, $p<0.05$) in MS group. Treatment with asiatic acid significantly attenuated dyslipidemia and improved insulin sensitivity as shown by the decreased HOMA-IR ($p<0.05$). We found reductions in MAP (about 11.4%) and HVR (about 36%) in MS rats received asiatic acid ($p<0.05$). Moreover, asiatic acid exhibited antioxidant properties by markedly reducing oxidative stress markers in vascular tissues and plasma in MS rats ($p<0.05$). In conclusion, asiatic acid improved metabolic and hemodynamic changes as well as oxidative stress in HFHC diet induced MS rats.

This work was supported by a grant from the Thailand Research Fund (MRG 5580001).

Where applicable, the authors confirm that the experiments described here conform with The Physiological Society ethical requirements.

PCC373

K^+ and Cl^- channels modulate retinal blood flow *In Vivo*

M.A. Needham, T.A. Gardiner, M.K. McGahon, P. Bankhead, N. Scholfield, T.C. Curtis and G. McGeown

Centre for Vision and Vascular Science, Queen's University Belfast, Belfast, UK

Regulation of tissue blood flow is an important arteriolar function. Membrane potential in vascular smooth muscle regulates vascular tone and resistance, and is modulated by ion channel activity. This study directly tested the roles of K^+ and Cl^- channels in determmining retinal blood flow in vivo, using Hooded Lister (HL) rats (male, 320-450g). Channel blocker specificity was first established *in vitro* using electrophysiological recordings from isolated arterioles(1). Correolide (10μm), a KV1 inhibitor, blocked an A-type current and penitrem A (100nM) blocked a large conductance (BK) Ca^{2+}-activated K^+-current. Inhibition of K^+-currents using Cs^+-pipette solution and 10mM 4-aminopyridine, revealed a Ca^{2+}-activated Cl^- current (I_{ClCa}), which was blocked by 1mM disodium 4,4'-diisothiocyanatostilbene-2,2'-disulfonate (DIDS). This inhibition showed little voltage dependence, and DIDS had no effect on L-type Ca^{2+}-currents, Kv or BK currents(2). The effects of these inhibitors on retinal blood flow were then investigated *in vivo*. Rats were anaesthetised with an intraperitoneal injection of ketamine (130 mg/kg) and xylazine (17.5 mg/kg). Volumetric blood flow was assessed in arterioles in the superior retina using a confocal scanning laser ophthalmoscope (Heidelberg Engineering, Germany). Intraperitoneal injection of acridine orange was used to label leukocyte DNA and the velocity of leukocyte transit through retinal arterioles determined from sequential confocal images (8.8 frames/s). Fluorescein angiography was then used to estimate the diameter of these arterioles, allowing velocity to be converted to flow. Drug effects were assessed from recordings 15 min after intravitreal drug injection (10μl). Data was summarised (mean ± SEM; n=number of animals) and analysed using nonparametric ANOVA (Kruskal Wallis) and Dunn's *post hoc* test. In non-injected eyes, mean flow in single arterioles was 12.3 ± 0.2 nL/s (n=9). This was unchanged following injection of Hanks' solution (12.8 ± 0.3 nL/s, n=9, $P>0.05$). Injection of DIDS (estimated intraocular concentration=10mM) increased volumetric flow (15.7±0.4 nL/s, n=9, $P<0.001$), while penitrem A (1μM) and correolide (40μM), reduced flow rates (11.2±0.4 nL/s, n=11, $P<0.01$; and 11.3±0.3 nL/s, n=10, $P<0.05$, respectively). Et-1 (104nM) induced vasoconstriction and dramatically reduced flow (4.6±0.2 nL/s, n=8, $p<0.001$). This response was not affected by K^+ channel blockers ($p>0.05$ vs Et-1 alone), but was reversed by DIDS (14.71±0.272 nL/s, n=7, $p<0.001$ vs Et-

1). These results suggest that K^+ and Cl^- channels in vascular smooth modulate basal blood flow in the retina and activation of I_{ClCa} appears to be an important mechanism underpinning the vasoconstrictor actions of Et-1.

McGahon MK, Dawicki JM, Arora A, Simpson DA, Gardiner TA, Stitt AW, et al. Kv1.5 is a major component underlying the A-type potassium current in retinal arteriolar smooth muscle. Am J Physiol Heart Circ Physiol. 2007 Feb;292(2):H1001-8.

McGahon MK, Needham MA, Scholfield CN, McGeown JG, Curtis TM. Ca^{2+}-activated Cl^- current in retinal arteriolar smooth muscle. Invest Ophthalmol Vis Sci. 2009 Jan;50(1):364-71.

European Social Fund, JDRF, The Wellcome Trust, BHF.

Where applicable, the authors confirm that the experiments described here conform with The Physiological Society ethical requirements.

PCC375

ANG 1-7 restores no mediated dilation in response to flow in human microvessels from subjects with CAD

A.M. Beyer[1,2] and D.D. Gutterman[1]

[1]Medicine, MCW, Milwaukee, WI, USA and [2]Physiology, MCW, Milwaukee, WI, UK

Reactive oxygen species (ROS) are important modulators of vascular reactivity. Coronary artery disease (CAD) changes the mechanism of human arteriolar flow-mediated dilation (FMD) from NO to hydrogen peroxide (H2O2), a signaling ROS. Evidence suggests that mitochondrial ROS (mtROS) production and the longevity of a cell or organism are inversely related. Nuclear telomerase activity (TA), prevents cellular senescence and tissue aging, and shows a reciprocal relationship with mtROS production. Recently telomerase activity has been identified in the mitochondria where its ability to regulate. mtROS production could increase NO bioavailability, restoring vascular function.

Pro-atherosclerotic factors have been shown to inactivate telomerase [1]. Two antagonistic components of the renin angiotensin system, ANG II (pro) and ANG 1-7 (anti), have long been implicated in atherosclerosis. ANG II down-regulates telomerase activity in the endothelium, through accumulation of ROS [2]. This could explain the elevation in blood pressure seen in telomerase-deficient mice. ANG 1-7, a counter regulator to the actions of ANG II, increases NO bioavailability [3], decreases production of ROS [4], is anti-atherosclerotic and causes vasodilation [5].

Therefore, we hypothesize that ANG 1-7 operates through a mechanism involving stimulation of telomerase activity to reduce mitoROS production and restore the NO-mediated mechanism of dilation to shear in patients with CAD.

Human coronary arterioles (~200 μm) from discarded atrial and visceral adipose tissue were cannulated for videomicroscopy. Dilation to graded degrees of shear was measured in vessels constricted with endothelin-1. Pharmacological inhibition of TA (BIBR 1532; 10 μM 15-20 h) in vessels from healthy individuals shifted the mechanism of FMD from NO to H2O2 (Figure 1). In arterioles from patients with CAD, ANG 1-7 (1 nM 15-20 h) shifted the mechanism of FMD from H2O2 to NO. This effect was prevented by BIBR 1532 (Figure 2).

To evaluate if ANG 1-7 enhances telomerase expression by increasing expression, we used cultured endothelial cells (HUVECs) treated with either vehicle or ANG 1-7 (1 nM). Western blot analysis (Figure 2, right) suggests an increase in telomerase expression after ANG 1-7 treatment.

We conclude that ANG 1-7 increases telomerase activity in the vasculature, which plays a critical and acute role in modulating microvascular function.

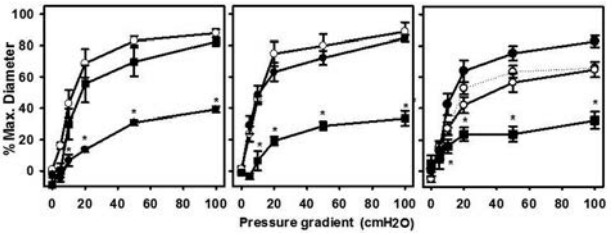

Fig 1. Inhibition of teloemrase in microvessels from healthy human subjects changes the mechanism of FMD from NO to H2O2.

Healthy Adipose Vessels Vehicle treatment (left) Healthy Adipose Vessels BIBR 1532 15-20h (center) Healthy Atrial Vessels BIBR 1532 15-20h (left) Open circles - Vehicle; Closed circles - L-NAME; Closed squares - PEG Catalase. (N≥4;* P < 0.05 one way ANOVA RM)

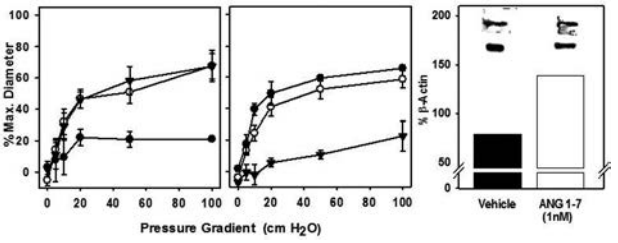

Fig 2. ANG 1-7 restores NO mediated dilation by increasing telomerase. In microvessels from subjects with CAD, ANG 1-7 (1 nM) reverts the mechanism of FMD from H2O2 to NO (left) in a telomerase dependent manner (center) (N=3 . The same dose of ANG 1-7 increased telomerase expression in cultured endothelial cells (HUVECs).functional studies (N=1) top band ANG 1-7 bottom beta-actin.

Breitschopf, K., A.M. Zeiher, and S. Dimmeler, Pro-atherogenic factors induce telomerase inactivation in endothelial cells through an Akt-dependent mechanism. Febs letters, 2001. 493(1): p. 21-25.

Imanishi, T., T. Hano, and I. Nishio, Angiotensin II accelerates endothelial progenitor cell senescence through induction of oxidative stress. Journal of hypertension, 2005. 23(1): p. 97-104.

Pörsti, I., et al., Release of nitric oxide by angiotensin (1–7) from porcine coronary endothelium: implications for a novel angiotensin receptor. British journal of pharmacology, 2012. 111(3): p. 652-654.

Mordwinkin, N., et al., Angiotensin-(1–7) Administration Reduces Oxidative Stress in Diabetic Bone Marrow. Endocrinology, 2012. 153(5): p. 2189-2197.

Raffai, G., M.J. Durand, and J.H. Lombard, Acute and chronic angiotensin-(1–7) restores vasodilation and reduces oxidative stress in mesenteric arteries of salt-fed rats. American Journal of Physiology-Heart and Circulatory Physiology, 2011. 301(4): p. H1341-H1352.

This work was funded by NIH/NHLBI R01

Thanks go to Dr. David Gutterman for great mentor ship.

We like to thank Joe Hochenberry and Dr Matt Durant for experimental and intellectual support.

Where applicable, the authors confirm that the experiments described here conform with The Physiological Society ethical requirements.

PCC376

Beta adrenergic overstimulation modulated vascular contractility via disorganization of actin-cytoskeleton in rabbit cerebral artery

H. Kim, K. Ko, B. Rhee, S. Lee, N. Kim, J. Youm and J. Han

National Research Laboratory for Mitochondrial Signaling, Department of Physiology, College of Medicine, Cardiovascular and Metabolic Disease Center, Inje University, Busan, Republic of Korea

Background and Purpose
Beta adrenergic overstimulation may increase the vascular damage and stroke. However, the underlying mechanisms of beta adrenergic overstimulation in cerebrovascular dysfunctions are not well known. We investigated the possible cerebrovascular dysfunction response to isoproterenol induced beta-adrenergic overstimulation (ISO) in rabbit cerebral arteries (CAs).
Methods
ISO was induced in six weeks aged male New Zealand white rabbit (0.8-1.0 kg) by 7-days isoproterenol injection (300 μg/kg/day). We investigated the alteration of protein expression in ISO treated CAs using 2DE proteomics and western blot analysis. Systemic properties of 2DE proteomics result were analyzed using bioinformatics software. ROS generation and following DNA damage were assessed to evaluate deteriorative effect of ISO on CAs. Intracellular Ca2+ level change and vascular contractile response to vasoactive drug, angiotensin II (Ang II), were assessed to evaluate functional alteration of ISO treated CAs. Ang II-induced ROS generation was assessed to evaluated involvement of ROS generation in CA contractility.
Results
Proteomic analysis revealed remarkably decreased expression of cytoskeleton organizing proteins (e.g. actin related protein 1A and 2, α-actin, capping protein Z beta, and vimentin) and anti-oxidative stress proteins (e.g. heat shock protein 9A and stress-induced-phosphoprotein 1) in ISO-CAs. As a cause of dysregulation of actin-cytoskeleton organization, we found decreased level of RhoA and ROCK1, which are major regulators of actin-cytoskeleton organization. As functional consequences of proteomic alteration, we found the decreased transient Ca2+ efflux and constriction response to angiotensin II and high K+ in ISO-CAs. ISO also increased basal ROS generation and induced oxidative damage in CA; however, it decreased the Ang II-induced ROS generation rate.
These results indicate that ISO disrupted actin cytoskeleton proteome network through down-regulation of RhoA/ROCK1 proteins and increased oxidative damage, which consequently led to contractile dysfunction in CA.

Where applicable, the authors confirm that the experiments described here conform with The Physiological Society ethical requirements.

PCC377

Atherosclerosis differentially affects Ca^{2+} signalling in endothelial cells from aortic arch and thoracic aorta in Apolipoprotein E knockout mice

C. Prendergast, J. Quayle, T. Burdyga and S. Wray

Cellular & Molecular Physiology, University of Liverpool, Liverpool, UK

Apolipoprotein-E knockout ($ApoE^{-/-}$) mice develop hypercholesterolemia and are a good model of atherosclerosis. Changes in Ca^{2+} are vital to the function of endothelial cells within vessels, but understanding of how atherosclerosis changes these signals, especially early in the disease, is limited. We have examined the effect of hypercholesterolemia on carbachol-mediated Ca^{2+} signals in aortic endothelial cells from wild-type (WT) and $ApoE^{-/-}$ mice of different ages; 10 weeks, before overt plaques are present and 24 weeks, where plaques are well established. The extent of plaque development was confirmed using en face staining with Sudan IV. Using confocal microscopy (Fluo-4-AM loading) allowed us to distinguish clearly the Ca^{2+} signals emanating from the endothelial cells alone, with the endothelium:smooth muscle interface intact. In addition, we compared the CCh response in thoracic aorta and in the more plaque-prone aortic arch. Three parameters of the Ca^{2+} responses were measured; the size of the initial Ca^{2+} peak, the size of the secondary plateau phase and area under the curve (AUC). Significance was assessed using the Students t-test.
All aortae from older $ApoE^{-/-}$ mice exhibited clear atherosclerotic plaques (n=9), whereas aortae from 10 week old $ApoE^{-/-}$ mice showed either no plaque or barely visible tiny areas indicating where plaques would later form (n=10). No WT mice exhibited atherosclerotic plaques in the aorta (n=5-10). In all tissues, CCh produced a concentration-dependent increase in all 3 parameters of the intracellular Ca^{2+} response. The aortic arch is more prone to development of atherosclerotic plaques than the thoracic aorta and it is this region in $ApoE^{-/-}$ mice that demonstrated the greatest alteration in CCh-mediated Ca^{2+} signalling. Thus, in aortic arch from 24 week old $ApoE^{-/-}$ mice, a significantly increased Ca^{2+} response was seen to all CCh concentrations (0.3-10μM) compared to WT, measured as peak, plateau or AUC responses (n=4-6 mice). In aortic arch from 10 week olds, the dose-response curves for peak Ca^{2+} were identical in WT and $ApoE^{-/-}$, however for the plateau and AUC responses, again a larger Ca^{2+} response was observed in the $ApoE^{-/-}$ mice, though this time the difference was seen at lower concentrations (1 & 3μM, n=4-5 mice). In thoracic aorta from young and older mice, a significant difference was only seen between WT and $ApoE^{-/-}$ responses at the highest concentrations of CCh, with the $ApoE^{-/-}$ mice showing a greater peak, plateau and AUC response to 10μM CCh. Therefore there was no age-dependent alteration in response in thoracic aorta.
It appears that hypercholesterolemia alone is enough to modify the CCh response in both thoracic and arch sections of $ApoE^{-/-}$ aortae, though the presence of atherosclerotic plaques causes a much more significant change in Ca^{2+} signalling.

Where applicable, the authors confirm that the experiments described here conform with The Physiological Society ethical requirements.

PCC378

GABAergic regulation of arteriolar tone in the rat retina

K. Hinds[1], K.P. Monaghan[1], B. Frølund[2], G. McGeown[1] and T. Curtis[1]

[1]Centre for Vision and Vascular Science, Queen's University of Belfast, Belfast, UK and [2]Department of Medicinal Chemistry, University of Copenhagen, Copenhagen, Denmark

Although the neurophysiological and neurotrophic actions of GABA in the retina are well-recognised, less is known about the role of GABA in the regulation of the retinal microcirculation. In the present study, we have examined the actions of GABA on retinal arterioles of the rat retina using *ex vivo* retinal whole mount preparations and isolated vessel segments. All animal experiments conformed to the UK Animals (Scientific Procedures) Act (1986). We began by examining the effects of GABA on arterioles pre-constricted with Et-1 (10nM) in retinal whole mounts. Application of 100μM GABA evoked vasodilation in 39% of vessels, vasoconstriction in 8%, and no response in the remaining 53% of vessels. When the concentration of GABA was increased to 1mM, a larger percentage of vessels responded, with 59% displaying vasodilation, 18% vasoconstriction and 23% no response. 1mM GABA was found to have no effect on the diameter of isolated vessels pre constricted with 10nM Et-1. In whole-mounts, muscimol (10μM), a $GABA_A$ receptor agonist, caused vasodilation in 6% of vessels, vasoconstriction in 6% and no response in the remaining 88% of vessels. In contrast, arteriolar responses to $GABA_B$ receptor agonists more closely resembled those observed with 1mM GABA. Baclofen (100μM) elicited vasodilation in 50% of vessels, while the remaining 50% exhibited no response. Application of SKF97541 (100μM) induced vasodilation in 39% of vessels, vasoconstriction in 8%, and no response in the remaining 53%. The selective $GABA_C$ receptor agonist, 5-methyl-imidazole-4-acetate (100μM), failed to evoke a vasomotor response in any vessels tested. Following pre-incubation of the whole-mount preparations with the $GABA_A$ receptor inhibitor, bicuculline (100μM), 70% of vessels that had previously exhibited a vasodilator reaction to 1mM GABA displayed a second, similar-sized response. In the presence of the $GABA_B$ receptor antagonist, 2-hydroxysaclofen (100μM), all vessels that had previously been responsive to GABA failed to exhibit a vasodilator response. Bicuculline or 2-hydroxysaclofen was subsequently applied to retinal whole-mount preparations where the arterioles had not been pre-constricted with Et-1. Bicuculline caused vasoconstriction in 1 out 20 arterioles, whilst 2-hydroxysaclofen induced vasoconstriction in 4 out 31 arterioles. Our data demonstrate that GABA can exert a dual effect on arteriolar tone in the rat retina, inducing either vasoconstriction or vasodilation. These reactions are entirely dependent upon the presence of the adjacent retinal neuropile and appear largely dependent upon the activation of $GABA_B$ receptors. Despite these findings, we find little evidence to suggest that endogenous GABA makes a significant contribution to the regulation of basal vascular tone in the rat retina at least under the *ex vivo* conditions used in our experiments.

We thank DEL, NI and Fight for Sight, UK for financial support

Where applicable, the authors confirm that the experiments described here conform with The Physiological Society ethical requirements.

PCC379

3D imaging of renal glycocalyx by scanning electron microscopy with focused ion beam milling

K.P. Arkill[1], C.R. Neal[2], D.O. Bates[2], J.M. Squire[2] and K. Qvortrup[3]

[1]Physics and Astronomy, University of Birmingham, Birmingham, UK, [2]MVRL, Physiology and Pharmacology, University of Bristol, Birmingham, UK and [3]CFIM, Medical Sciences, University of Copenhagen, Copenhagen, Denmark

The glomerulus is the primary filtration unit of the kidney. It is a bundle of capillaries approximately 130μm in the Rat. The filtration barrier is a specialised capillary wall of which it is believed the glycocalyx layer forms a molecular filter for large proteins. The permeability and hydraulic conductivity of the glycocalyx depends on many factors including thickness, fibre spacing, fibre organisation, and completeness of coverage. Robust structural imaging of the glycocalyx has proved non-trivial, in part due to pairing physiological variables with micrographs.

Presented here is the use of Scanning Electron Microscopy paired with Focused Ion Beam Milling (FIB-SEM) to image glomerular and peritubular glycocalyx. The tissue was harvested from a left-ventricle, oncotically balanced, perfusion fixed rat (after an injected lethal dose of 0.7 mL/kg sodium pentobarbitone). In addition to standard fixation, Lanthanum Dysprosium Glycosaminoglycan adhesion (LaDy GAGa), was added to show the endothelial glycocalyx. Sections of tissue were prepared as blocks for standard transmission electron microscopy (TEM). A section was cut from a block and imaged with TEM (Phillips 100) to use as a map. The remaining block was trimmed and coated with gold for FIB-SEM. FIB-SEM imaging was performed with a Quanta 3D (FEI) with a backscatter detector (vC-BS-ED, FEI) using an accelerating voltage of 2kV. Once an area of interest is identified then the block is tilted to 52 degrees and trenches milled with a focued ion beam (Ga) either side, a 1μm layer of Pt is put on along the expected cutting depth. Serial sections were then imaged by SEM after a 10nm layer is removed by the Ga Beam.

The FIB-SEM showed the capillary wall effectively over a 4μm*4μm*3μm sample volume. Estimated imaging resolution was 25nm. The serial sections were aligned and corrected for tilt angle (FIJI,NIH). Within the XYZ volume, slit diaphragms, foot processes and fenestrations were clearly visible. The glycocalyx thickness and location could be measured but not fibre spacing. The glycocalyx appeared similar in the peritubular capillaries and in the glomerulus, though it was not stained in all vessels. The peritubular capillaries had more glycocalyx contrast. The glycocalyx was not evenly stained, there were tufts of taller regions, as well as areas of little or no coverage, including the appearance of gaps, possibly related to the underlying fenestrations.

In conclusion though compared to electron tomography the resolution is not as high, FIB-SEM has a much greater sample volume, giving it a useful niche in the technical armory to investigate physiological understanding of glycocalyx.

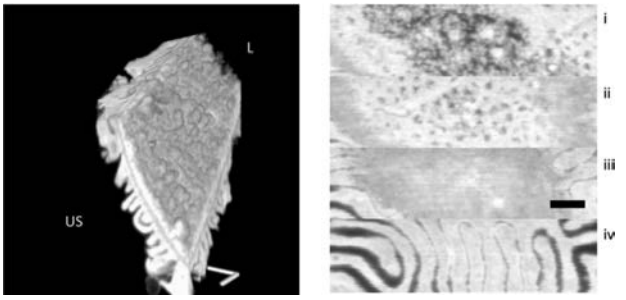

Figure 1: Left: A 3D surface image of the glomerular capillary xyz stack. (US: Urinary space side of capillary wall, L: Luminal side, Scale Bar is 1μm). Right: A set of stills though the glomerular filtration barrier. i) Glycocalyx, ii) fenestrations, iii) glomerular basement membrane, iv)podocyte foot processes (Scale Bar is 500nm).

BBRSC

Richard Bright VEGF research trust

Core Facility for Integrated Microscopy, University of Copenhagen

Where applicable, the authors confirm that the experiments described here conform with The Physiological Society ethical requirements.

PCC380

Analysis of the expression of myosin phosphatase targeting subunit splice variants in human smooth muscles

J. Lartey, M. Sweeney, J. Taggart, S.C. Robson, H. Wessel and M.J. Taggart

Institute of Cellular Medicine, Newcastle University, Newcastle Upon Tyne, UK

Myosin phosphatase is a trimeric protein that regulates vascular tone by inducing dephosphorylation of smooth muscle regulatory myosin light chains. The 110-130 kDa myosin phosphatase targeting subunit (MPYT) is essential for this process. Nitric oxide- mediated arterial relaxation has been suggested to occur partly via PKG interactions with a leucine zipper (LZ) region of MYPT1 that is generated by alternative exon splicing of the 3' end of the gene [1]. The relative expression of MYPT1 LZ+ to LZ- isovariants may thus influence arterial sensitivity to endothelial-mediated vasodilators and/or NO donors. Interestingly, the sensitivity of isolated human myometrial arteries to endothelial-mediated vasodilators is greater than that of placental arteries from pregnant women (2). In addition, non-vascular uterine smooth muscle shows variable responsiveness to NO donors. We propose that tissue-specific differences in human MYPT1LZ+ to LZ- isovariant expression, not previously assessed in human tissues, may offer an explanation for these findings.

Human tissue samples were obtained, following written informed consent, from normal pregnant women undergoing elective Caesarean section at term. Myometrium, myometrial arteries (MA) and placental arteries (PA) were microdissected free of all surrounding tissue. The human MYPT1LZ+ sequence (NM_002480.1) was aligned with chicken (NM_205123) and mouse (NM_027892) MYPT1LZ- sequences to detect a shift in the reading frame that generates the putative human MYPT1LZ- sequence. RNA was isolated (Qiagen RNeasy fibrous kit) and reverse transcribed (Stratagene AffinityScript cDNA synthesis Kit) from the human tissues and qPCR, with isovariant-specific primers and PerfectProbe amplification (Primer Design, UK), used to measure MYPT1LZ+ and MYPT1LZ- isovariant expression. Human smooth muscle RNA (Clonetech, USA) was used as an internal calibrator.

MYPT1LZ+ expression was less in the myometrium (fold-change relative to calibrator RNA of 0.33+0.04) than MA (1.33+0.12) and PA (2.07+0.17; $p<0.01$, n=10, mean+SEM, ANOVA). A similar pattern was seen for MYPT1LZ- expression wherein changes relative to calibrator were 0.06+0.17 (myometrium), 0.45+0.05 (MA) and 0.65+0.07 (PA). This reveals differences in MYPT1LZ+ and MYPT1LZ- expression between human myometrium, MA and PA. Of note, the ratio of MYPT1LZ+ to LZ- expression in MA was not greater than in PA. As the former is more sensitive to endothelial-dependent relaxant agonists, this suggests that a correlation between MYPT1LZ+ expression and physiological sensitivity to PKG and/or NO stimulation in these human tissues may be an over-simplification. Further research is required, however, to determine such a relationship in relevant clinical conditions of heightened smooth muscle tone.

Yuen S, Ogut O, Brozovich F, MYPT1 Protein Isoforms Are Differentially Phosphorylated by Protein Kinase GJ J. Biol Chem. 2011 Oct 28;286(43):37274-9.

Sweeney M, Wareing M, Mills TA, Baker PN, Taggart MJ Characterisation of tone oscillations in placental and myometrial arteries from normal pregnancies and those complicated by pre-eclampsia and growth restriction. Placenta. 2008 Apr;29(4):356-65.

Supported by Wellcome Trust/AMS and Newcastle upon Tyne Hospitals FSF.

Where applicable, the authors confirm that the experiments described here conform with The Physiological Society ethical requirements.

PCC381

Ex-vivo expansion of human endothelial progenitor cells leads to cellular senescence

R. Medina[1], C. O'Neill[1], S. Chambers[1], J. Guduric-Fuchs[1], E. Reid[1], J. Neisen[2], D. Waugh[2], D. Simpson[1] and A. Stitt[1]

[1]Centre for Vision and Vascular Science, Queen's University Belfast, Belfast, UK and [2]Centre for Cancer Research and Cell Biology, Queen's University Belfast, Belfast, UK

Endothelial progenitor cells (EPCs) play a reparative role during vascular regeneration in ischemic pathologies such as myocardial infarction, stroke, peripheral vascular disease, and ischemic retinopathies. For autologous therapy, EPCs need to be expanded in vitro in order to obtain sufficient numbers for therapy. Many EPC sub-classes have been described and this creates confusion surrounding EPC nomenclature. For this study, we have concentrated on the subpopulation known as Outgrowth endothelial cells (OECs) because these EPCs have unequivocal endothelial phenotype and significant proliferative potential. Here, we examined implications that this long term in vitro expansion step has on human OEC biology.

OECs were isolated from human peripheral and umbilical cord blood and expanded in culture until they reached their Hayflick limit. Cellular senescence was characterised by growth curves, cell cycle analysis, senescence-associated beta-galactosidase evaluation and DNA damage quantification. Furthermore, changes in gene/protein expression associated with OEC senescence were assessed by transcriptome, proteome and secretome analysis. OEC function was evaluated in vitro by migration and tubulogenesis assays. The therapeutic potential of

senescent OECs was evaluated in vivo using a mouse model of ischaemic retinopathy.
Proliferation capacity in late passage-OEC diminished significantly, with more than 70% of cells arrested in G0/G1 phase of the cell cycle. These late passage-OECs displayed a significant increase in cytoplasmic volume, increased β-galactosidase activity and accumulated γ-H2AX foci ($p<0.001$). There was also a significant decrease in telomerase activity coupled with telomere shortening. Senescent OECs demonstrated impaired migratory and tubulogenic capacity compared to early-passage OECs ($p<0.001$). Inflammatory signalling pathways were identified as major components of the OEC senescence programme by transcriptome analysis. IL8 was found significantly upregulated on the secretome of senescent OECs. shRNA mediated knock-down of IL8 in OECs significantly extended ex-vivo lifespan, delayed senescence and enhanced cellular function. Using the in-vivo animal model of ischaemic retinopathy, both early and late-passage OECs significantly reduced retinal avascular area compared to vehicle treated eyes ($p<0.001$). However, senescent OECs showed reduced ability to integrate into the retinal vasculature compared to early-passage OECs. Furthermore, only early-passage OECs significantly reduced the area of pathological pre-retinal neovascularisation ($p<0.001$).
Ex-vivo expansion of human OECs ultimately leads to replicative senescence linked to cellular dysfunction in vitro and in vivo. Modulation of OEC senescence is an important strategy to improve reparative potential and usage as an autologous cell therapy.

Fight for Sight. The Sir Jules Thorn Trust.

Where applicable, the authors confirm that the experiments described here conform with The Physiological Society ethical requirements.

PCC382

Endothelial progenitor cell-derived extracellular vesicles as a vehicle for microRNA delivery to endothelial cells

J. Guduric-Fuchs, A. O'Connor, R.J. Medina, C.L. O'Neill, A.W. Stitt and D.A. Simpson

Centre for Vision and Vascular Science, Queen's University Belfast, Belfast, UK

Extracellular vesicles (EVs) released from various cell types can mediate paracrine signalling and control important pathophysiological responses. MicroRNAs transferred within EVs represent one of the main mechanisms by which they influence the recipient cells. Circulating endothelial progenitor cells (EPCs) release EVs that are readily taken up by endothelial cells. We hypothesized that EPC derived EVs can be manipulated to deliver specific microRNAs to endothelial cells and thereby modulate their angiogenic response.
Human EPCs isolated from the umbilical cord blood displayed endothelial imunophenotype, being positive for CD31, CD146 and CD105 and negative for haemathopoetic markers CD45 and CD14. EVs were collected by ultracentrifugation of the EPC conditioned media. To identify microRNAs exported from EPCs, the small RNA contents of EPCs and their EVs were analyzed by deep sequencing. Several miRNAs were highly enriched in EVs compared to their expression levels in EPCs and there was remarkable consistency in miRNA expression in the cultures from different donors. EVs were then isolated from EPCs transfected with several vectors driving the expression of microRNAs, including miR-146a, and miR-451. Enrichment of these microRNAs in EPC EVs was demonstrated by RT-qPCR. Following direct transfection of human microvascular endothelilal cells (HMEC) with plasmid vectors driving the expression of miR-146a, downregulation of specific miR-146a predicted target genes such as CCND2, ELAVL1 and CRIM1, was revealed by microarray. When HMECs were incubated with miR-146a enriched EPC derived EVs, these EVs were taken up by HMECs, resulting in the reduced mRNA expression of the same miR-146a targets.
We show that the content of EPC released EVs can be manipulated to include significant amounts of exogenous miRNAs, which can be taken up by endothelial cells. The ability of EVs to carry anti- or pro-angiogenic microRNAs can be exploited to modulate angiogenesis in various models and may have therapeutic applications in multiple disease conditions associated with abnormal angiogenesis.

This work was funded by BBSRC.

Where applicable, the authors confirm that the experiments described here conform with The Physiological Society ethical requirements.

PCC383

M13 filamentous phage as a potential system for improved wall shear stress measurement

K.P. Arkill[1], R. Pacheco-Gomez[2], F. Gower[2], T.J. Proctor[2], I. Hands-Portman[3], M.R. Hicks[2], S.K. Sandhu[2], M.J. Simmons[4] and T.R. Dafforn[2]

[1]Physics and Astronomy, University of Birmingham, Birmingham, UK, [2]Biosciences, University of Birmingham, Birmingham, UK, [3]Life Sciences, University of Warwick, Coventry, UK and [4]Chemical Engineering, University of Birmingham, Birmingham, UK

Suitable wall shear stress (WSS) measurements are important due to the wall being the point of many chemical interactions. This applies particularly to the vascular system where WSS is known to affect endothelial surface reactions. Measuring the near WSS is particularly difficult in the circulation, even with bulk flow approximations, due to the particulate nature of blood and the 3-dimensional nature of the system.
Here a novel methodology using the M13 filamentous bacteriophage virus (BPV) is presented as a possible solution to this problem. The BPV is a 1μm long cylinder but with a diameter of around 7nm. In this case, the BPVs are cultured by incubation with *E. coli* and separated with polyethylene glycol, then purified using a caesium chloride gradient, has been fluorescently tagged along its length using fluorescein Isothiocyanate (FITC) or tetramethylrhodamine-6-isothiocyanate (TRITC, Invitrogen). The BPV has 2700 possible binding sites for FITC or TRITC and so is trivial to detect in a fluorescent wide-field microscope even with as little as 5% binding efficiently. Free dye was removed with a salt trap (PD10, GE Healthcare) or dialysis. Linear dichroism was used to determine alignment with shear rate in bulk solution.
Additionally anti-collagen IV antibody was attached using a maleimide-cysteine reaction to one end of the BPVs prior to TRITC binding. This would enable the BPV to bind from one end to collagen coated glass flow sides and the other to align along the flow direction. Preliminary analysis and results are presented.
Optical and Electron microscopy were used to observe the additional affect of the TRITC- BPVs to form longer nano-rope,

assemblies more suited to low resolution visualisation techniques (Figure 1).
In conclusion suitably bound fluorescent BPVs has the potential to detect wall shear direction suitable for microfluidic devices and the circulation including 3D capillary beds such as the glomerulus.

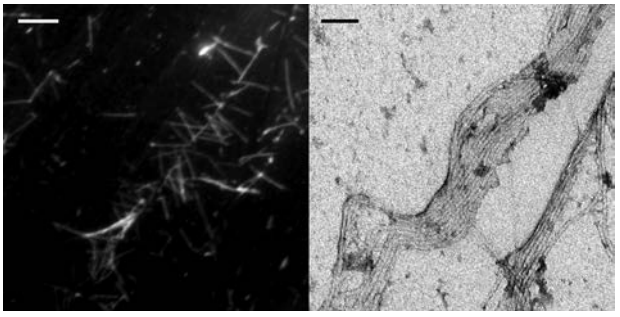

Figure 1: Self assembly of TRITC-Bacteriophage virus into nano-ropes. Left: Light microscopy (scale bar 5μm). Right: Electron Micrscopy (scale bar 100nm).

Science City Research Alliance

EPSRC

BBSRC

Where applicable, the authors confirm that the experiments described here conform with The Physiological Society ethical requirements.

PCC384

The influence of tumour aldehyde dehydrogenase activity on prostate cancer cell metastatic potential and interaction with the bone endothelium *in vivo*

K.J. Reeves[1], G. van der Pluijm[3], M.G. Cecchini[4], C.L. Eaton[2], F.C. Hamdy[5] and N.J. Brown[1]

[1]Oncology, University of Sheffield, Sheffield, UK, [2]Human Metabolism, University of Sheffield, Sheffield, S Yorks, UK, [3]Urology, Leiden University Medical Centre, Leiden, Netherlands, [4]Urology Research Laboratory, University of Bern, Bern, Switzerland and [5]Urology and Oncology, University of Oxford, Oxford, UK

Cancer metastasis to the skeleton is the cause of significant morbity and mortality in prostate cancer patients. Despite its prevalence, the mechanisms involved in the development of bone metastases remain unclear. A metastatic initiating cell (MIC) phenotype CD44+/CD24- has been identified in prostate cancer, but a complementary approach to aid MIC cell recognition, involves detection of aldehyde dehydrogenase (ALDH) activity. This study characterises the proliferative and invasive functional behaviour of prostate cancer (PC-3) cell ALDH subpopulations *in vitro*. We also used a new *in vivo* model developed by our laboratory, to study bone micrometastasis and interaction with the bone marrow endothelial cells.
A metatarsal from a newborn mouse (1-3 day old) was engrafted into a Dorsal Skinfold Chamber (DSC) implanted on a severe combined immunodeficient (SCID) mouse (5-6 weeks old) under systemic ketamine/xylazine anaesthesia. PC3 labelled with red fluorescent protein (RFP) cells were sorted into $ALDH^{high}$ (7%) and $ALDH^{low}$ (20%) cell-subpopulations using the ALDEFLUORkit and flow cytometry. The subpopulations ($1x10^5$ cells) were administered via intra-cardiac injection into groups of animals (n=10). An additional group was used to evaluate the homing response of $ALDH^{high}$ cells treated with weekly zoledronic acid for 4 weeks (zol; intraperitoneal, 25μg/kg/injection; 100μg/kg total). Microscopy recordings of the chamber tissue and bone-graft were made at 48hr intervals for up to 4 weeks. At the end of the study, tissue was harvested and processed for microCT, multi-photon analysis, histology and immunohistochemistry. ALDH subpopulation cell proliferation, migration and invasion were investigated via functional in vitro assays.
$ALDH^{high}$ cells home to bone and interact with the bone microvascular endothelium in significantly higher numbers than $ALDH^{low}$ cells (Day 15: mean ± SEM; $ALDH^{high}$ 12.3±1.8 cells vs. $ALDH^{low}$ 1.9±0.5 cells; $p<0.05$). Treatment with zol does not influence $ALDH^{high}$ PC3 cells homing to bone and intereacting with the microvascular endothelium and bone microenvironment *in vivo*. PC3-$ALDH^{high}$ cells display increased proliferation, migration and invasion ability *in vitro*.
In summary PC3-$ALDH^{high}$ exhibit functional characteristics associated with enhanced metastatic potential i*n vitro*, with increased homing to and interaction with the bone microvasculature and metastatic-niche *in vivo*, which appear resistant to a standard current treatment regime.

Funded by Sixth European Framework Programme (PROMET) and Yorkshire Cancer Research

Where applicable, the authors confirm that the experiments described here conform with The Physiological Society ethical requirements.

PCC386

$VEGF_{165}b$ confers protection in early diabetic nephropathy

Y. Qiu[1], S. Oltean[1], J.K. Ferguson[1], C. Neal[1], K. Harris[1], K.P. Arkill[1], C.F. Symonds[1], A. Russell[1], M. Stevens[1], C. Alsop[1], S.C. Satchell[2], S.J. Harper[1], D.O. Bates[1] and A.H. Salmon[1,2]

[1]MicroVascular Research Laboratories, University of Bristol, Bristol, UK and [2]Academic Renal Unit, University of Bristol, Bristol, UK

Diabetic nephropathy is the UK's leading cause of end-stage renal failure. Levels of Vascular Endothelial Growth Factor (VEGF), produced by podocytes and required for normal glomerular function, are frequently abnormal in diabetic nephropathy. Multiple splice variants of VEGF, including the traditional "$VEGF_{165}$" and opposing "$VEGF_{165}b$" forms, exist in the kidney. $VEGF_{165}$ overexpression accelerates diabetic nephropathy. We therefore investigated whether $VEGF_{165}b$ reduces albuminuria in rodent diabetic nephropathy models and modifies glomerular permeability in human kidneys. C57Bl/6 mice overexpressing human $VEGF_{165}b$ in podocytes (nephrin promoter: *neph*$VEGF_{165}b$), or wild-type littermates (WT), were rendered diabetic with 100mg/kg Streptozocin (STZ) i.p. daily for 3 days. As compared with diabetic-WT mice, diabetic *neph*$VEGF_{165}b$ mice had less albuminuria (68% reduction). Diabetes was also induced in DBA2J mice with 5 days of STZ (50mg/kg i.p.). After 2 weeks of hyperglycemia (>20mmol/L), mice received saline or 1μg $VEGF_{165}b$ injections i.p. bi-weekly for 6 weeks. Albumin-creatinine ratio (ACR) increased to 4.6-fold above baseline at 6 weeks in the sham-treated group, but only to 1.2-fold in the $VEGF_{165}b$-treated group. In db/db mice, bi-weekly intraperitoneal injections of $VEGF_{165}b$ for 8 weeks decreased albuminuria ($p<0.05$, two-way ANOVA), but did not alter GFR ($p>0.05$, one-way ANOVA). In diabetic mice, substantial upregulation of total and phosphorylated forms of VEGF receptor 2 (VEGFR2) (both 5.1-fold increase) was noted in glomeruli in response to systemic injections of $VEGF_{165}b$. To test whether diabetic glomerular func-

tion can be improved through direct modulation of the capillary wall, single glomeruli were isolated from untransplantable kidneys from diabetic and non-diabetic donors and corrected ultrafiltration coefficient (*LpA/Vi*, $min^{-1}.mmHg^{-1}$) was measured. *LpA/Vi* of human glomeruli from diabetic donors {2.3±0.4 (16/3)} was higher than *LpA/Vi* from non-diabetic donors {1.0±0.1 (25/3)} ($p<0.001$, unpaired t-test). Treatment with 1nM $VEGF_{165}b$ (1hr) restored *LpA/Vi* to normal in diabetic human glomeruli {1.0±0.2 (13/3)} ($p<0.001$, one-way ANOVA). $VEGF_{165}b$ appears to modify *LpA/Vi* of diabetic glomeruli via activation of VEGFR2, since the actions of $VEGF_{165}b$ on STZ-diabetic rat glomeruli were prevented by the VEGFR2-blocker ZM323881 (diabetes: 1.4±0.1; diabetes+$VEGF_{165}b$: 0.8±0.1*; diabetes+$VEGF_{165}b$+ZM323881: 1.3±0.2; *$p<0.05$, one-way ANOVA}. We have demonstrated that increasing $VEGF_{165}b$ levels locally (through podocyte-specific overexpression) and systemically (via repeated intraperitoneal injections), in both type 1 and type 2 diabetes, effectively reduces the functional features of early diabetic nephropathy and $VEGF_{165}b$ effect is through activation of VEGFR2. Our study suggests the potential of using $VEGF_{165}b$ as a therapeutic agent to slow the progression of diabetic nephropathy.

Where applicable, the authors confirm that the experiments described here conform with The Physiological Society ethical requirements.

PCC387

Senescence-induced remodelling in large and small arteries of mice: impact of high-fat diet

F. Jiménez-Altayó[1], A.P. Dantas[2], Y. Onetti[1], M.A. Oliveira[3], M.H. Carvalho[3] and E. Vila[1]

[1]Departament de Farmacologia, Terapèutica i Toxicologia, Universitat Autònoma de Barcelona, Bellaterra (Cerdanyola del Vallès), Spain, [2]Institut Clínic del Tòrax, Institut d'Investigacions Biomèdiques August Pi i Sunyer, Barcelona, Spain and [3]Department of Pharmacology, Institute of Biomedical Sciences, University of São Paulo, São Paulo, Brazil

Aging and weight gain are independent cardiovascular risk factors, which have shown to be increasingly associated. We hypothesize that high-fat intake could lead to arterial remodelling similar to that promoted by vascular aging and worsen the remodelling exerted by senescence. For this purpose we analysed structure of large (aorta) and small (mesenteric artery, MA) arteries from senescence accelerated mice (SAM) following a Western-type diet (WD; 21 % fat). Five-month-old SAM prone (SAMP8) and resistant (SAMR1) female mice were fed a WD for 8 weeks. At 7 months of age, aortas and MAs were dissected. In aorta, vascular structure and mature or newly synthesized collagen was analysed by morphometric analysis of haematoxylin and eosin-stained cross sections and picrosirius red, respectively. In MA, vascular structure, collagen I/III protein and mRNA expression, and nuclei distribution was evaluated by pressure myography, immunofluorescence, RT-qPCR and confocal microscopy, respectively. Values are means ± S.E.M. compared by two way ANOVA with Bonferroni's post-test. On normal chow, weight gain, abdominal fat and cholesterol levels were comparable between strains and similarly increased after WD (Jiménez-Altayó *et al.*, 2012). In aorta, wall thickness (WT), but not cross sectional area (CSA), was increased by senescence (SAMR1: 171.3±4.8 μm, n=7; SAMP8: 194.6±6.1 μm, n=8, $p<0.05$). WD only modified aortic structure in SAMR1 (control: 171.3±4.8 μm, n=7; WD: 209.8±10.0 μm, n=7, $p<0.01$) paralleled by an increase in mature (n=11) and newly synthesized (n=9) collagen. In MAs, senescence did not alter the wall/lumen ratio but diminished ($p<0.05$) the CSA and WT in association with reduced number of adventitial (SAMR1: 2339±194, n=6; SAMP8: 1145±81, n=3, $p<0.01$) and smooth muscle (SAMR1: 3535±213, n=6; SAMP8l: 2613±68, n=3, $p<0.05$) cells per mm^3. WD decreased MA CSA ($p<0.01$), WT ($p<0.001$) and wall/lumen ratio ($p<0.05$) in SAMR1 paralleled by diminished adventitial (control: 2339±194, n=6; WD: 1393±269, n=6, $p<0.05$) and smooth muscle (control: 3535±213, n=6; WD: 2314±230, n=6, $p<0.01$) cells per mm^3. Nevertheless, WD intake in SAMP8 did not further modify MA structure. Collagen I/III protein (n=4-6) and mRNA expression (n=4-6) was unaltered by senescence or diet. Therefore, senescence induces qualitatively different remodelling in large and small arteries of mice. High-fat intake promotes remodelling in non-senescent mice consistent with accelerated senescence, whereas the vasculature of senescent mice does not display any further alteration. In both cases, arterial remodelling may exacerbate vascular injury.

Jiménez-Altayó F *et al.* (2012). *Age (Dordr). in press*

Supported by SAF2010-19282, 2009SGR-890 and HBP2011-0054_PC. Y.O. was supported by MEC

Where applicable, the authors confirm that the experiments described here conform with The Physiological Society ethical requirements.

PCC388

Vascular activity and endothelial cell toxicity of metal organic frameworks

C.J. Kelsall[1], L.J. McCormick[3], M.K. Doherty[2], P.D. Whitfield[2], R.E. Morris[3] and I.L. Megson[1]

[1]Diabetes and Cardiovascular Science, University of Highlands & Islands, Inverness, UK, [2]Lipidomics, University of Highlands and Islands, Inverness, UK and [3]School of Chemistry, University of St Andrews, St Andrews, UK

Nitric oxide (NO) donors are agents that release NO by chemical reaction, either spontaneously or under specific biophysical conditions. NO donors have been widely used in a variety of clinical situations, with mixed success [1]. Alternatively, metal organic frameworks (MOFs) have potential to provide targeted, flexible applications in gasotransmitter delivery. Here, we describe bioactive properties of two designs of MOF loaded with NO.

MOFs derived from 2,5-dihydroxyterephthalic acid and nickel (Ni_2(dhtp)) or magnesium (Mg_2(dhtp)) were prepared and pressed into 20 mg discs containing 10wt% Teflon. The discs were dehydrated under vacuum at high temperature, cooled and exposed to an atmosphere of NO. Once loaded, MOF discs were stored individually under argon until use. Unloaded discs were also prepared to act as controls. . Previous studies revealed the gas is rapidly released from the discs upon exposure to an aqueous environment at 37°C [2]. Pig hearts were obtained from an abattoir and in vitro coronary artery endothelial function (relaxation to bradykinin; BK, 0.1 nM – 10 μM) was measured in arteries by myography. Segments lacking reactivity to BK following removal of the endothelium were then exposed for 10 minutes to NO-loaded MOFs Ni_2(dhtp) or Mg_2(dhtp). In separate experiments, human umbilical vein endothelial cells (HUVEC), passage 1 to 3, were exposed for 1, 6, 24 or 72h to medium conditioned for 1h in the presence of unloaded Ni_2(dhtp) and Mg_2(dhtp) MOFs to assess toxicity

by MTT assay. Data are presented as mean ± SEM; statistical analysis was by *t*-test or 2-way ANOVA with *post hoc* analysis, as appropriate.

Endothelium-denuded pig coronary arteries constricted with 0.1 μM U46619, a thromboxane mimetic, showed significantly greater relaxation in the presence of NO-loaded Ni_2(dhtp) compared to Mg_2(dhtp) MOFs (59.1±9.4%, *n*=5 vs 9.5±3.5%, *n*=3; *p* 0.004). Unloaded MOFs induced no vascular reactivity (data not shown). Colourimetric analysis of mitochondrial activity (MTT assay) in HUVECs showed significantly greater toxicity of Ni_2(dhtp) than Mg_2(dhtp) MOF-conditioned medium at all time-points except 1h (fig 1).

The data indicate that capacity for storage and release of NO is much greater in MOFs which use Ni^{2+} as the core metal ion rather than Mg^{2+}, but the greater performance in releasing biologically relevant amounts of NO is, in this case, offset by an increased risk of toxicity to endothelial cells. Use of the Ni_2(dhtp) MOF design for delivery of gasotransmitters in pathophysiological settings should be restricted to procedures which do not involve chronic exposure of endothelium. Other more sensitive bioassays are required to fully assess the potential of Mg_2(dhtp) MOFs.

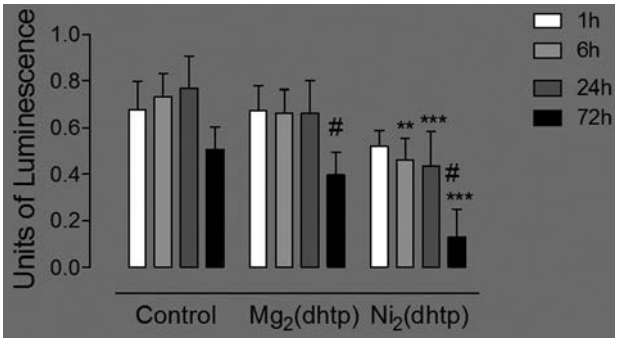

Figure 1: Colourimetry by MTT assay of mitochondrial activity in HUVEC. n=5 per group, ** p <0.01, *** p <0.001 vs time-matched control, # p <0.01 vs treatment-match at 1h.

Miller MR and Megson IL (2007). Br J Pharmacol 151; 305-321.

McKinlay AC et al (2008). J Am Chem Soc 130; 10440-10444.

This work was funded by the British Heart Foundation.

Where applicable, the authors confirm that the experiments described here conform with The Physiological Society ethical requirements.

PCC389

VEGF signalling is required for arteriolarisation resulting from a combination of shear stress and Ang1

O.A. Stone and D.O. Bates

Microvascular Research Laboratories, Univ Bristol, Bristol, UK

The generation of arterioles (arteriolargenesis) from capillaries in response to shear stress requires members of the vascular endothelial growth factor (VEGF) and Angiopoietin (Ang) families of growth factors. While Ang1 is known to be involved in pericyte recruitment and VEGF in endothelial growth, how these two signaling pathways interact during cell recruitment to the vessel wall during flow is not clear. To test the hypothesis that both Ang1 and VEGF are required for functional remodelling (generation of arterioles from capillaries as well as new pericyte covered capillaries), we used adenovirus-mediated over-expression of eNOS, Ang1, and the VEGF inhibitor sFlt1, in the fluothane anaesthetised (3-5% in 75%O2) adult rat mesentery after laparotomy as a model of blood flow dependent vascular remodeling. Blood flow and angiogenesis /arteriolargenesis were assessed by intravital and confocal microscopy respectively. The effects of VEGF inhibition and Ang1 inhibition were investigated using Ad-Flt1 and Ad-sTie2 respectively. Ang1+eNOS increased angiogenesis (vascular area 43±3% of mesenetery, p<0.01) compared with eNOS alone (30±1%), and this was inhibited by sFlt1 (33±2%). However, the Ang1 induced increase in pericyte coverage (50±1% vessel coverage compared with 27±2% without Ang1) was enhanced, not inhibited by sFlt1 (65±2%). This was accompanied by an inhibition of the Ang1 induced smooth msucle cell coverage (from 8.6±1.3% to 0%, p<0.01). Thus, in this setting, inhibition of endogenous VEGF signaling impaired VSMC recruitment, but enhanced pericyte coverage. Thus, while VEGF signaling inhibits pericyte recruitment, it is required for VSMC recruitment.

These results indicate that the de novo formation of a functional, mature vasculature, with VSMC-containing arterioles requires tight control of endogenous VEGF and exogenous Angiopoietin signaling. Therapeutic vascular remodeling paradigms may therefore require treatments that activate endogenous VEGF, in combination with exogenous Ang1, to effectively remodel the vasculature.

Where applicable, the authors confirm that the experiments described here conform with The Physiological Society ethical requirements.

PCC390

The tyrosine phosphatase SHP-2 enhances angiogenic processes during hypoxia by HIF-1α stabilisation

H. Mannell[1], Y. Stampnik[1], J. Pircher[1], K. Zimmermann[2], U. Pohl[1] and F. Krötz[3]

[1]Walter-Brendel Centre of Experimental Medicine, Ludwig-Maximilians-University, Munich, Germany, [2]Institute of Pharmacology and Toxicology, Bonn University, Bonn, Germany and [3]Interventional Cardiology, Starnberg Community Hospital, Munich, Germany

Question: The tyrosine phosphatase SHP-2 plays an important role in growth factor signalling. We previously demonstrated its importance for growth factor dependent angiogenesis. Here we studied whether SHP-2 influences endothelial cell proliferation, vessel sprouting and HIF-1α signalling upon hypoxia.

Methods: Overexpression of wild type (SHP-2 WT), catalytically inactive (SHP-2 CS) or constitutively active (SHP-2 E76A) SHP-2 in human microvascular endothelial cells (HMEC) was achieved by lentiviral transduction. Vessel sprouting was assessed by the aortic ring assay. Cells and isolated aortae were exposed to hypoxia (95 % N_2, 5% CO_2) for 4h or 24h. Proliferation was assessed by MTT reduction. HIF-1α protein levels and ERK activity (Thr/Tyr-phosphorylation) were detected by western blot. HIF-1α mRNA levels were quantified using real-time PCR.

Results: Compared to SHP-2 WT, expression of constitutively active SHP-2 enhanced proliferation during normoxia by 48±8% and hypoxia by 57±10% (both p<0.05, ANOVA, n=8). After hypoxia exposure, vessel sprouting *ex vivo* (p<0.05, ANOVA, n=5) as well as hypoxia inducible factor 1α (HIF-1α) protein levels (p<0.05, ANOVA, n=4), but not mRNA levels (n=3), were enhanced by 5-fold and 1.3-fold respectively in cells expressing constitutively active SHP-2. This was associated with an enhanced activity of the potential HIF-1α regulator MAPK ERK1/2 (n=3).The increased hypoxic proliferation was com-

pletely blocked upon HIF-1α inhibition (Echinomycin 10ng/ml, p<0.05, t-test, n=6) and also upon treatment with a MAPK-pathway inhibitor (GW5074, p<0.05, t-test, n=6).
In contrast, expression of catalytically inactive SHP-2 impaired proliferation during normoxia (p<0.05, ANOVA, n=7) and hypoxia (p<0.05, ANOVA, n=8) as well as *ex vivo* vessel sprouting after hypoxia exposure (p<0.05, n=4) compared to SHP-2 WT. In addition, hypoxic HIF-1α protein accumulation (p<0.05, ANOVA, n=4) and ERK1/2 activity (n=3) were reduced. However, the reduction in HIF-1α protein was rescued by treatment with proteasomal inhibitors (MG132 or Epoximicin, n=3).
Conclusion: In addition to being important for angiogenic processes during normoxia, SHP-2 also affects endothelial cell proliferation and vessel sprouting during hypoxic conditions. During hypoxia endothelial cell proliferation and HIF-1α protein stabilisation is further enhanced when increasing SHP-2 catalytic activity, possibly through ERK activation. Thus, controlled induction of SHP-2 catalytic activity may be therapeutically promising for angiogenesis induction in ischemic conditions.

Where applicable, the authors confirm that the experiments described here conform with The Physiological Society ethical requirements.

PCC393

Pulse arrival time to the capillary bed of the finger tip compared to the carotid-radial pulse transit time during and after aerobic exercise

N. Potocnik[1], A. Danieli[2,3], H. Lenasi[1] and V. Starc[1]

[1]Institute of Physiology, University of Ljubljana, Ljubljana, Slovenia, [2]Department of Neurology, University medical centre Ljubljana, Ljubljana, Slovenia and [3]Barsos Medical Centre, Ljubljana, Slovenia

Physical activity is known to have beneficial effects on prevention of cardiovascular disease and on microcirculation. The aim of our study was to compare the carotid-radial pulse transit time as a measure of small artery compliance being under strong sympathetic control and the pulse arrival time to the capillary bed of the finger tip as a measure of the state of the microvasculature in middle aged healthy subjects before, during and 20 minutes after aerobic exercise.
Experiments were performed on 11 males, 47±6 years old. The study was accordant to the Declaration of Helsinki and approved by the national Ethics Committee. We measured ECG, arterial blood pressure using Finapres Ohmeda with a finger cuff on the middle finger of the right hand, laser Doppler skin blood flow on the finger pulp of the pointer finger of the same hand and carotid or radial pulse with a tonometer (Millar SPT 30). After 5 minutes supine rest subjects mounted the cycloergometer and their right arm was fixed on an armrest. They rested in sitting position for additional 5 minutes, than they started a graded exercise at the workload of 40 W. The workload increased in steps of 50W lasting 3 minutes each until 85% of the estimated maximal heart rate was reached. After ceasing exercising, the parameters were measured for subsequent 25 minutes. Carotid-radial pulse transit time (c-rtT) and pulse arrival time to the capillary bed (PATc) using pulse arrival time to the radial artery on the same hand as a reference were calculated. RR interval duration was determined using ECG.
Our results revealed that c-rtT exhibited no statistically significant differences before and 20 minutes after exercise (100,8 ±3,1ms and 99,3 ±2,0ms), but was significantly decreased at highest workload (84,1±0,2ms). On the other hand PATc was increased 20 minutes after exercise compared to resting values (126,0 ±9,2ms and 116,7 ±5,2ms) and significantly decreased at highest workload (107,8±1,6ms). The heart rate at peak exercise was 150,2±0,9bpm, 20 minutes after exercise it remained significantly higher then at rest (82,4 ±1,5 bpm and 62,8 ±1,3bpm respectively), while arterial blood pressure returned to control values short after the cessation of exercise. A linear correlation between c-rtT and corresponding RR interval duration during exercise was found (p<0.001) but no correlation between PATc and RR.
We conclude that during exercise increased sympathetic tone is the main reason for increasing c-rtT, but other mechanisms should contribute to the regulation of the finger tip skin microcirculation, where termoregulation plays a major role. Further experiments are needed to elucidate exact mechanisms involved in the small artery and microvasculature response to exercise.

Bernjak A et al. (2009). Physiol Meas 30, 245-60

Humeau A et al. (2007). Med Biol Eng.Comp. 45, 412-35

Laurent S et al. (2006). Eur Heart J. 27, 2588-605

Where applicable, the authors confirm that the experiments described here conform with The Physiological Society ethical requirements.

PCC394

Dysregulation of hydrogen sulfide producing enzyme cystathionine γ-lyase contributes to maternal hypertension and placental abnormalities in preeclampsia

K. Wang[1], W. Abu-Alkhier[1,5], S. Ahmad[1], M. Cai[1], J. Rennie[2], T. Fujisawa[2], F. Crispi[3], J. Baily[2], R. Wang[4], E. Gratacós[3], I. Buhimschi[5], C. Buhimschi[5] and A. Ahmed[1]

[1]Vascular Biology Unit, Aston University, Birmingham, UK, [2]Gustav Born Centre for Vascular Biology, University of Edinburgh, Edinburgh, UK, [3]Department of Maternal-Fetal Medicine, University of Barcelona, Barcelona, Spain, [4]Lakehead University, Thunder Bay, ON, Canada and [5]Yale School of Medicine, Yale University, New Haven, CT, USA

The exact aetiology of preeclampsia is unknown, but there is a good association with an imbalance in angiogenic growth factors and abnormal placentation (Ahmad & Ahmed, 2004). Hydrogen sulphide (H2S), a gaseous messenger produced mainly by cystathionine γ-lyase (CSE), is pro-angiogenic vasodilator (Yang et al, 2008; Papapetropoulos et al, 2009). We hypothesized that a reduction in CSE activity may alter the angiogenic balance in pregnancy and induce abnormal placentation and maternal hypertension. Plasma levels of H2S were significantly decreased in preeclamptic women (p<0.01), which was associated with reduced CSE message and protein expression in human placenta as determined by real-time PCR and immunohistochemistry. Inhibition of CSE activity by DL-propargylglycine (PAG) in first trimester (8-12 weeks gestation) human placental explants had reduced placenta growth factor (PlGF) production as assessed by ELISA and inhibited trophoblast invasion in vitro. Endothelial CSE knockdown by siRNA transfection increased the endogenous release of soluble fms-Like tyrosine kinase-1 (sFlt-1) and soluble endoglin, (sEng) from human umbilical vein endothelial cells while adenoviral-mediated CSE overexpression inhibited their release. Administration of PAG to pregnant mice induced hypertension, liver damage, and promoted abnormal labyrinth vascularisation in the placenta and decreased fetal growth. Finally, a slow releas-

ing, H2S-generating compound, GYY4137, inhibited circulating sFlt-1 and sEng levels and restored fetal growth that was compromised by PAG-treatment demonstrating that the effect of CSE inhibitor was due to inhibition of H2S production. These results imply that endogenous H2S is required for healthy placental vasculature and a decrease in of CSE/ H2S activity may contribute to the pathogenesis of preeclampsia.

Ahmad S & Ahmed A (2004). Elevated placental soluble vascular endothelial growth factor receptor-1 inhibits angiogenesis in preeclampsia. Circ Res. 95, 884-891.

Yang G et al (2008). H2S as a physiologic vasorelaxant: hypertension in mice with deletion of cystathionine gamma-lyase. Science. 322, 587-590.

Papapetropoulos A et al (2009). Hydrogen sulfide is an endogenous stimulator of angiogenesis. Proc Natl Acad Sci U S A. 106, 21972-21977.

This work was supported by grants from the British Heart Foundation (PG/06/114) and Medical Research Council (G0601295 and G0700288) and Aston University Strategic Funds.

Where applicable, the authors confirm that the experiments described here conform with The Physiological Society ethical requirements.

PCC395

Blast injury and its effects on the endothelium

A. Spear[1], E. Davies[2,1], E. Kirkman[1], C. Taylor[1], M. Midwinter[2] and S. Watts[1]

[1]Dstl, Salisbury, UK and [2]RCDM, Birmingham, UK

Introduction: It is known that the tolerance for return to normal neuromuscular function in tissue exposed to ischemia with concomitant hemorrhagic shock is significantly reduced compared to ischemia alone (Hancock et al., 2011). With an increased incidence of explosive related injuries in military casualties, the ischemic tolerance following blast injury with or without hemorrhagic shock may also be altered. A possible mechanism of altered tolerance is via damage to the endothelium. Endothelial integrity may influence clinical outcomes locally and systemically.
Aim: This study determined whether blast injury alone caused activation of, or damage to, the endothelium and whether this was correlated with the level of blast load.
Methods: Experiments were performed under the auspices of Animals (Scientific Procedures) Act 1986 and thus had undergone local Ethical Review. Groups of terminally anaesthetised female New Zealand White rabbits were exposed to 4 different levels of blast over the gastrocnemius muscle via a compressed air device. Arterial blood samples were taken pre-injury and 1, 6 and 11hr post-injury to determine levels of circulating endothelial cells (CECs) using CD146-based immunomagnetic separation. 12 hours post injury animals were culled with an overdose of anaesthetic and tissue removed for histological and gene expression analysis. The incidence of haemorrhage, oedema and inflammatory cell infiltration were subjectively scored. mRNA levels of markers associated with the activation of the endothelium were measured using qRT-PCR with multiple reference gene normalisation. Differences in CECs between groups were assessed with 2-way ANOVA ($p<0.05$ and power = 0.8). Histology scores were assessed using a Cuzicks trend test ($p<0.05$). qRT-PCR results were expressed as calibrated normalised relative quantities (CNRQ), transformed and assessed using one-way ANOVA ($p<0.05$).
Results: At 6 hr post-injury, the number of CECs in blood was significantly higher in the high blast group versus no blast group ($p<0.05$). There was a significant trend ($p<0.0001$) in increasing scores for oedema, haemorrhage and cell infiltrate with increased blast load. Expression of a variety of endothelial activation markers were significantly increased in the high blast versus no blast group including E-selectin, TNFα, HIF-1α and Thrombomodulin.
Conclusions: This study demonstrates that blast injury causes activation and damage to the endothelium and surrounding muscle tissue and that this is dependent on blast load. This has the potential to impact on limb salvage strategies and requires further investigation to determine the implications for casualties injured in an explosion. Understanding the mechanism of damage may also identify possible mitigation strategies.

Hancock HM *et al.* et al. (2011) *Journal of Vascular Surgery* **53**, 1052.

Where applicable, the authors confirm that the experiments described here conform with The Physiological Society ethical requirements.

PCC396

Vitamin D preserves endothelial function and blood pressure in inflammatory prone mitogen and stress kinase 1/ 2 knock-out mice *In vivo*

N. Akbar[1], S.J. Arthur[2], J.J. Belch[1] and F. Khan[1]

[1]Vascular and Inflammatory Diseases Research Unit, University of Dundee, Dundee, Angus, UK and [2]The MRC Protein Phosphorylation Unit, University of Dundee, Dundee, Angus, UK

Background: Cardiovascular diseases are united in pathology by atherosclerosis; signal transduction is essential in this process for the expression of cell adhesion molecules early in the disease, capturing, tethering and transmigrating monocytes into the sub-endothelial space. Mitogen and stress activated kinases (MSK) 1/ 2 are critical for the homeostatic control of cytokine expression through interleukin-10 and dual specificity protein-1 (DUSP-1). Macrophages from MSK 1/ 2 knock-out (KO) animals display reduced IL-10, DUSP-1 expression and bare a hyperinflammatory phenotype. Calcitrol, the active form of vitamin D, exerts its anti-inflammatory effects through up regulation of IL-10 and DUSP-1 *in vitro*, with an ability to curb cytokine expression (tumour necrosis factor-α and IL-6); however the effector pathway remains poorly understood with limited *in vivo* studies.
Aim: To elucidate the relationship between Calcitrol and MSK 1/ 2 in endothelial dysfunction.
Method: Skin microcirculation was assessed on the flanks of anesthetised (1.5-2% isoflurane with oxygen) 16 week old C57/Black MSK 1/ 2 KO (n=24) mice. Following baseline measurements animals were fed a proatherogenic diet (2% cholesterol) and subdivided (n=12) to receive vehicle (carboxymethyl cellulose sodium 0.5%) or 200ng Calcitrol twice a week for the study duration (16 weeks). Laser Doppler Imaging (LDI) in combination with iontophoresis of phenylepherine (PE), acetylcholine (ACh), sodium nitroprusside (SNP) and localised skin heating (44^0C) were used to measure vascular function. Results are expressed as group mean, skin perfusion in arbitrary units (AU)±standard error of mean (SEM). Blood pressure was assessed non-invasively using a tail cuff system (mmHg±SEM);

cardiac hypertrophy was calculated by: cardiac mass (mg)/body weight (g).T-test analysis was used for statistical significance (p <0.05).

Results: There were no significant differences at baseline for vascular responses. Vehicle (259±6AU) treated animals displayed reduced ACh responses at 16 weeks when compared to Calcitrol (292±5AU) treated mice (p = 0.0006). There were no significant differences for endothelium-independent responses (SNP) or cardiac mass between the two groups. Calcitrol supplemented animals displayed lower systolic (119±3 mmHg VS. vehicle 129±3 mmHg, p = 0.04) and diastolic (84±3 mmHg VS. vehicle 99±2 mmHg, p = 0.01) blood pressures.

Conclusion:ACh induced vasodilation was significantly reduced in MSK 1/ 2 KO vehicle mice, but was preserved in Calcitrol treated animals. Maximal dilatory capacity was not significantly different between groups, suggesting modulation at the level of the endothelium. For the first time we provide *in vivo* longitudinal data showing the protective effects of vitamin D on endothelial dysfunction, possibly through modulation of inflammation.

Where applicable, the authors confirm that the experiments described here conform with The Physiological Society ethical requirements.

PCC397

Molecular and functional characterisation of TRPV3 and TRPV4 channels in the retinal microvascular endothelium

J. McNaughten, M.K. McGahon, G. McGeown and T. Curtis

Centre for Vision and Vascular Science, Queens Universtiy Belfast, Belfast, UK

Transient receptor potential vanilloid (TRPV) channels are members of a superfamily of non-selective cation channels possessing a vast range of physiological functions. Our aim was to fully characterise the molecular and functional expression of TRPV3 and TRPV4 channels in the retinal microvascular endothelium.

Retinal microvascular endothelial cells (RMECs) were cultured from bovine retina. mRNA transcripts were detected for TRPV3 and V4 using RT-PCR. Protein expression was confirmed by Western blot analysis. Fura-2-based Ca2+ microfluorimetry was used to test for the functional expression of TRPV3 and V4 in RMECs using a selection of appropriate agonists and antagonists. The TRPV3/TRPA1 activator, carvacrol (100uM), evoked consistent [Ca2+]i responses in RMECs (0.2±0.03 R340/380, mean±SEM, n=5), which were reduced, but not abolished in the presence of the TRPA1 inhibitor, HC-030031 (10μM) (0.14±0.01 R340/380, n=6; p<0.05 v carvacrol alone). The functional expression of TRPV4 channels was tested using the selective activator GSKA (100nM). This drug elicited a transient rise in [Ca2+]i (1.88±0.62 R340/380, n=13) that was blocked by pre-incubation with the specific TRPV4 antagonist, HC067047(1uM) (0.06±0.04 R340/380, n=6; p<0.01 v. GSKA alone). The cellular localisation of TRPV3 and TRPV4 channels was subsequently examined in bovine retinal wholemounts and isolated RMECs using immunohistochemistry. TRPV3 was located predominantly in the nuclei of endothelial cells in retinal wholemounts with some punctate staining in the cytoplasm. No differences in localisation were observed in endothelial cells of arteries, capillaries and veins. RMECs also showed predominantly nuclear staining for TRPV3. TRPV4 was found to be located in both the nuclei and cytoplasm of endothelial cells lining the vasculature in retinal wholemounts. Interestingly sparse, punctate TRPV4 staining was noted in endothelial cells on the arterial side of the circulation, while those on the venous side presented with noticeably increased TRPV4 staining in both the nuclei and cytoplasm. In isolated RMECs, TRPV4 was localised to both the nucleus as well as tubular-like structures in the cytoplasm. Localisation patterns for each channel were confirmed using multiple antibodies to different epitopes and the specificity of staining was confirmed using blocking antigens.

This study provides molecular and functional evidence for the expression of TRPV3 and V4 in bovine retinal endothelial cells. Further research is now required to elucidate their physiological significance.

With thanks to DEL, NI and BBSRC

Where applicable, the authors confirm that the experiments described here conform with The Physiological Society ethical requirements.

PCC398

Altered vascular response to acetylcholine and reduced pO2 in isolated carotid arteries in rats fed by chow containing varied zinc and selenium content

I. Ivic[1], S. Novak[2], A. Cosic[2], A. Cavka[2], I. Grizelj[2], Z. Loncaric[3], A. Koller[1] and I. Drenjancevic[2]

[1]Department of Pathophysiology and Gerontology, Medical School University of Pecs, Pesc, Hungary, [2]Department of Physiology and Immunology, Faculty of Medicine Osijek, University of J.J. Strossmayer Osijek, Osijek, Croatia and [3]Desk of Plant Nutrition and Fertilization, Faculty of Agriculture Osijek, University of J.J. Strossmayer Osijek, Osijek, Croatia

Objective: Since zinc (Zn) and selenium (Se) are important components for cell protection against certain oxygen species it has been suggested that Zn and/or Se deficiency impairs the potent antioxidant defense capacity and may be involved in the initiation of endothelial dysfunction (1-5). However, there is a lack of functional studies to address this issue. The aim of this study was to determine if changes in dietary content of Zn and Se affect vascular responses in rat isolated carotid arteries.

Methods: Fifteen male Sprague Dawley rats were fed with 3 types of custom made rat chow (Faculty of Agriculture University of Osijek, Croatia) from weaning for 10 weeks: a) high Zn(70.81mg/kg)-low Se(0.043mg/kg) group (N=5); b) high Se (0.363mg/kg)-low Zn(30.16mg/kg) group (N=5) and c) low Zn(28.56mg/kg)-low Se(0.03mg/kg) group (N=5). Prior to decapitation, rats were anesthetized with 75 mg/kg ketamine+2.5 mg/kg midazolam. Carotid arteries were isolated and their isometric tensions were measured by DMT multi-wire Myograph system. We tested dose responses to ACh (10-9-10-5 M) and response to reduced pO2 (in the bath bubbled with gas mixture containing N2 95%, CO2 5%) after precontraction with noradrenaline (NA) for 5 minutes, in the absence/presence of the NOS inhibitor L-NAME or COX-1,2 inhibitor indomethacin (INDO) in the tissue bath. Viability of rings at the end of the hypoxic relaxation protocol was tested with their ability to contract in bath solution bubbled with 95% O2-5% CO2 gas mixture. To compare differences between groups and treatments One-way ANOVA or t-test was used when appropriate. Statistical significance was set at P<0.05 (SigmaPlot v11.2).

Results: ACh induced relaxation (AchIR) was significantly reduced in low Zn-low Se group and high Se-low Zn group compared to high Zn-low Se (P<0.001 for 10-7-10-4 M Ach con-

centration). L-NAME (P<0.001 for 10-7-10-4 M Ach concentration) and INDO (P<0.001 for 10-6-10-4 M Ach concentration) blocked AChIR in all three groups of rats. Hypoxia induced relaxation (HIR) was significant in all study groups. However, there was no difference in HIR among groups. L-NAME and INDO significantly blocked HIR in high Zn-low Se and high Se-low Zn groups. In low Zn-low Se group HIR was blocked only after INDO administration.

Conclusions: These data suggest: 1) Zn and Se deficiency affected vascular response to ACh and reduced pO2 in rat isolated carotid arteries and 2) it seems that for ACh dependent relaxation Zn level is more important than Se level.

Support: This study was supported by grants of Ministry of Science, Education and Sports, Croatia, #219-2160133-2034, #079-0790462-0450 and FP7-Marie Curie-SmART, Hungarian Natl. Sci. Res. Found (OTKA) K71591; T67984, MHT 2010/2011 SROP-4.2.1/b-10/2/KONV-2010-0012, SROP-4.2.2.A-11/1/KONV-2012-0024.

Brigelius-Flohe R, Banning A, Schnurr K. Selenium-dependent enzymes in endothelial function. Antioxid redox Signal 2003; 5(2):205-15.

Tomat AL, Weisstaub AR, Jauregui A, Pineiro A, Balaszuk AM, Costa MA, Arranz CT. Moderate zinc deficiency influences arterial blood pressure and vascular nitric oxide pathway in growing rats. Pediatr Res. 2005 Oct; 58(4):672-6.

Funk CD, Boubez W, Powell WS. Effects of selenium-deficient diets on the production of prostaglandins and other oxygenated metabolites of arachidonic acid and linoleic acid by rat and rabbit aortae. Biochim Biophys Acta 1987; 921(2):213-20.

Dimitrova AA, Strashimirov DS, Russeva AL, Betova TM, Tzachev KN. Changes in the activity of Cu/Zn superoxide dismutase, lipid profile and aorta morphology of spontaneously hypertensive rats on zinc diet. Folia Med (Plovdiv.) 2007; 49(3-4):52-7.

Oner G, Bilgen I, Edremitlioglu M, Alkan Z, Cirrik S. Dietary zinc modifies the characteristics of endothelial dilation in normozincemic rats. Biol Trace Elem Res 2003; 92(2):123-38.

Where applicable, the authors confirm that the experiments described here conform with The Physiological Society ethical requirements.

PCC399

Alpha calcitonin gene-related peptide (αCGRP) plays a long-lasting protective role in both the onset and sustained models of angiotensin-II induced hypertension and vascular inflammation/remodelling

S. Smillie[1], R. King[1], G. Pozsgai[1], L. Liang[1], E. Fernandes[1], P. De Winter[2], R. Siow[1] and S. Brain[1]

[1]Cardiovascular Division, Kings College London, LONDON, UK and [2]Division of Surgery and Interventional Science, University College London, LONDON, UK

Calcitonin gene-related peptide (CGRP) is a sensory nerve-derived neuropeptide and the most potent microvascular vasodilator known to date. Suggested previously to be protective in a range of models of hypertension1, the aim of this study was to learn the influence of CGRP on vascular mechanisms in an angiotensin-II (Ang II) model of hypertension. Matched C57BL/6 wildtype (WT) and selective αCGRP knockout (KO) mice were anaesthetised and osmotic minipumps with Ang II (1.1 mg/kg/day for 14 days or 0.9mg/kg/day for 21 days) or vehicle (saline) were implanted as described previously2. Blood pressure was recorded by tail-cuff plethysmography until days 14/28 when the experiment was terminated. Vascular hypertrophy was assessed by histology and mRNA expression by RT-qPCR. Data were analysed using ANOVA plus Bonferroni's post test. CGRP deletion did not affect baseline blood pressure regulation under normotensive conditions. Systolic pressure significantly increased after 14 days Ang II in WT (129±3.84) and αCGRP KOs (140±7.23, p<0.001), this being significantly enhanced in the αCGRP KOs (p<0.001). This exacerbated hypertensive response was still apparent at day 28 (204±9.8, p<0.01). αCGRP mRNA expression was upregulated in the aorta and mesentery of hypertensive WTs at both 14 (p<0.01) and 28 (p<0.001) days, indicating the potential for αCGRP to influence in a chronic, in addition to acute manner. Vascular inflammation/remodelling was apparent in hypertensive subjects, characterised by increased collagen expression. This remodelling was exacerbated in Ang II-treated αCGRP KOs at both time-points (p<0.001). This study provides evidence that i) CGRP is upregulated at the vascular level in hypertension and ii) deletion of CGRP is associated with enhanced Ang II-induced hypertension and vascular injury. This suggests a sustained protective role for CGRP in this model.

1Li and Wang (2005) Hypertension, 23, 113-8

2Liang et al. (2009) Hypertension, 54, 1254-61

S-J S is supported by the BHF. Other funders are the BBSRC, and an IMB capacity building grant.

Where applicable, the authors confirm that the experiments described here conform with The Physiological Society ethical requirements.

PCC400

Suppressed Nrf2 mediated redox signalling and decreased DJ1 expression in human foetal endothelial cells from gestational diabetes: prenatal priming of endothelial dysfunction in offspring

X. Cheng[1,2], S. Chapple[1], B. Patel[1], W. Puszyk[1], R.C. Siow[1] and G.E. Mann[1]

[1]Cardiovascular Division, British Heart Foundation Centre of Research Excellence, School of Medicine, King's College London, London, UK and [2]Cardiac Surgery Department, Peking University Third Hospital, Beijing, China

Increased generation of reactive oxygen species is associated with endothelial dysfunction and targeting endogenous antioxidant defences has only recently been considered in the treatment of vascular diseases (Cheng et al., 2011). Offspring from gestational diabetic (GDM) pregnancies are predisposed to endothelial dysfunction in later life (Buchanan & Xiang, 2005), and endothelial cells from GDM umbilical cords exhibit abnormal nitric oxide production and reduced growth rates, indicating phenotypic changes caused by GDM (Sobrevia et al., 1995; Mann et al., 2003). To investigate the underlying mechanisms, we examined redox regulation in human umbilical vein endothelial cells (HUVEC) from GDM (n=40) and normal (n=47) pregnancies cultured in M199 (with 20% or 1% FCS). Mitochondrial superoxide production measured by luminescence in GDM HUVEC was significantly higher than normal controls (210 ± 22 vs 81 ± 6 mean light units, mean ± SEM, n=6, P<0.001) whereas basal DNA fragmentation was comparable between groups. However, GDM HUVEC were more susceptible to the lipid peroxidation (4-hydroxynonenal, 20μmol/L) induced DNA fragmentation (n=5, P<0.05). Basal and HNE stimulated levels of glutathione (GSH), a key intracellular antioxidant, were also lower in GDM HUVEC. Moreover, HNE induced activation of the redox sensitive transcription factor NF-E2 related factor 2 (Nrf2), which mediates adaptive increases in GSH synthesis (Mann et al., 2003), was suppressed in GDM

(n=5, p<0.05). Deficits in Nrf2 mediated redox signalling were further confirmed by abrogated HNE induced mRNA expression of the cystine/glutamate transporter (xCT) and phase II defence enzyme NAD(P)H quinone oxidoreductase 1 (NQO1) (n=6, P<0.05 and P<0.01 respectively). Nrf2 silencing in normal HUVEC partly reproduced the phenotypic changes of GDM HUVEC. To examine whether Nrf2 in GDM cells is epigenetically silenced, methylation of CpG islands in the promoter region of Nrf2 was measured by bisulphate restriction analysis. Although we could not detect differences in methylation between normal and GDM cells, protein expression of DJ-1, a known cytosolic Nrf2 stabilizer, was markedly reduced in GDM HUVEC (n=7, P<0.01). In summary, an altered vascular phenotype in utero may contribute to the increased risk of type 2 diabetes and cardiovascular disease in the offspring of gestational diabetic mothers in later life.

Buchanan, T.A. et al. (2005) J. Clin. Invest. 115:485-491

Cheng, X. et al. (2011). Antiox. Redox Signaling 14: 469-487

Cheng, X. et al. (2011). Antiox. Redox Signaling 14: 469-487

Sobrevia, L. et al. (1995). J. Physiol. 489:183-192

The presented work is supported by British Heart Foundation and China Scholarship Council

Where applicable, the authors confirm that the experiments described here conform with The Physiological Society ethical requirements.

PCC401

A new role for the regulator of G-protein signalling-1 in inflammatory cell function in angiotensin ii-induced aortic aneurysm formation

J. Patel, E. McNeill, G. Douglas, J.P. de Bono, D.R. Greaves and K.M. Channon

Oxford University, Oxford, UK

Chemokine-induced macrophage recruitment into the vascular wall is critical in the progression of atherosclerosis and aortic aneurysm formation. Macrophage activation and chemotaxis can be mediated by chemokine ligation of multiple G-protein coupled receptors. The Regulator of G-Protein Signalling-1 (RGS1) acts to down-regulate the response to sustained chemokine stimulation. Studies in our laboratory have shown it to be up-regulated in ApoE-/- mice in association with atherosclerotic plaque progression and with monocyte-macrophage activation; however an in vivo role for RGS1 in macrophage function has not been investigated.

RGS1 has a non-redundant role in macrophage chemotaxis in vitro. Rgs1-/-ApoE-/-macrophages have significantly enhanced migratory responses to the chemokines CCL2, CCL3 and CCL5 (p<0.05) and have impaired desensitisation to repeated or sustained chemokine signalling, such that they show increased migration to CCL5 re-stimulation (p<0.001). RGS1 has a role in the accumulation of macrophages in lesions in the initial stages of atherosclerosis. In the absence of RGS1, atherosclerosis is attenuated in early lesions in the aortic root and aortas of female ApoE-/- mice (p<0.001). This was accompanied by reduced levels of macrophages in the aortic root.

To investigate aortic leukocyte trafficking, an Angiotensin II model of acute vascular inflammation was used. At 9 weeks of age, Rgs1-/-ApoE-/- mice had significantly less CD45+ leukocytes and CD11b+ myeloid cells in aortas than ApoE-/- mice (p<0.05) after 5 days of Angiotensin II infusion. Notably, during a 2 week infusion, ApoE-/- mice were more susceptible to aortic aneurysm rupture in comparison to Rgs1-/-ApoE-/- mice with 56% survival vs. 94% (p=0.0147). Furthermore, between days 2 and 10, Angiotensin II treatment increased systolic blood pressure more in Rgs1-/-ApoE-/- mice than ApoE-/- mice (ApoE-/-117.4±4.0 mmHg vs. Rgs1-/-ApoE-/- 137.7±3.1 mmHg) suggesting aneurysm formation in these mice is independent of Angiotensin-II induced hypertension. To examine the effects of Rgs1 disruption on vasomotility, myography studies were undertaken using the Gαq-coupled agonists; phenylephrine, angiotensin II and PGF2-α. Preliminary experiments showed only the contraction to phenylephrine was significantly enhanced in ApoE-/- rings compared to Rgs1-/-ApoE-/- (p<0.01) which may indicate a compensatory down regulation of α1-adrenergic receptors in Rgs1-/-ApoE-/- aortas.

These findings identify a new role for RGS1 in inflammatory cell function and support a role for RGS1 in Angiotensin II induced-aneurysm formation. Furthermore, these data suggest a potential interaction between RGS1 and Gαq-coupled receptors that could account for the alterations in vascular contractile function and blood pressure observed in Rgs1-/-ApoE-/- mice.

Where applicable, the authors confirm that the experiments described here conform with The Physiological Society ethical requirements.

PCC402

An *in vitro* model system of hyperoxia-induced retinal endothelial cell death and senescence

O.M. Galvin, K.S. Edgar, T.A. Gardiner and D.M. McDonald

CVVS, Queen's University Belfast, Belfast, UK

Purpose:Hyperoxia is a dominant pathogenic factor in retinopathy of prematurity (ROP) resulting in an arrest of normal retinal vascular development accompanied by vaso-obliteration of pre-established vessels. The increased generation of endothelial cell-derived reactive oxygen species (ROS) and reactive nitrogen species (RNS) are associated with vessel loss during hyperoxia; in particular, dysregulated endothelial nitric oxide synthase (eNOS) is implicated in aberrant generation of such effectors in animal models of ROP. Defining the key pathways involved in vaso-obliteration will aid the discovery of therapeutic targets that protect the retina from hyperoxia-induced vascular damage. Therefore we established a model system to investigate the effect of hyperoxia and eNOS over-expression on retinal microvascular endothelial cells *in vitro*, examining nitrosative stress, cell death via apoptosis and cellular senescence.

Methods:Primary retinal microvascular endothelial cells (RMECs) were exposed to physiologically relevant 6% oxygen, standard cell culture incubator conditions (21% oxygen) and 70% oxygen. Apoptosis was quantified by nuclear morphology, active caspase-3 and TUNEL staining. Mechanisms of cell injury were investigated using inhibitors and scavengers of superoxide and of peroxynitrite and nitrotyrosine quantified by western blotting. Senescence was determined by β-galactosidase staining the co-localisation of γH2AX and 53BP-1 nuclear foci, and the formation of multiple nuclei. eNOS overexpression was achieved by viral infection with an adenovirus encoding eNOS-GFP and compared to control, GFP expressing virus.

Results:24 hour hyperoxia treatment of RMECs increased nitrotyrosine formation and apoptosis. Inhibition of either peroxynitrite or inhibition of superoxide reduced hyperoxia-mediated apoptosis. In addition, hyperoxia induced a significant

increase in the senescence markers β-galactosidase and 53BP-1. eNOS over-expression further increased apoptosis under hyperoxic conditions.
Conclusions:Collectively, our results demonstrate that hyperoxia increases cellular senescence and cell death via apoptosis in RMECs. This apoptosis can be reduced through inhibition of ROS and RNS. eNOS over-expression increased RNS production, leading to a further increase in hyperoxia induced apoptosis.

Where applicable, the authors confirm that the experiments described here conform with The Physiological Society ethical requirements.

PCC403

Antioxidant and vascular protective effect of curcumin on phenylhydrazine-induced hemolytic anemia in rats

K. Sompamit[1], V. Kukongviriyapan[3], W. Donpunha[2], U. Kukongviriyapan[2] and P. Surawattanawan[4]

[1]Preclinic, Mahasarakham University, Muang, Mahasarakham, Thailand, [2]Physiology, Khon Kaen University, Muang, Khon Kaen, Thailand, [3]Pharmacology, Khon Kaen University, Muang, Khon Kaen, Thailand and [4]Government Pharmaceutical Organization, Rajatevee, Bangkok, Thailand

Curcumin, a major active component from turmeric (Curcuma longa), widely grown in tropical regions of Asia. Normally, it was used as a spice to give specific flavor and color of food. Moreover, curcumin is a medicinal plant which possesses neuroprotective, cardioprotective, anti-carciogenic, anti-inflammation, and antioxidant properties. Phenylhydrazine (PHZ) is a strong oxidant agent and has been used in an animal model of hemolytic anemia (1). PHZ oxidation causes free iron release resulting in massive free radicals generation, oxidative stress and vascular dysfunction (2). The aim of this study was to investigate the effect of curcumin on PHZ-induced hemolytic anemia in rats. Male Sprague-Dawley rats were obtained from National Animal Laboratory Center, Thailand, and were housed and treated at North-Eastern Laboratory Animal Center, Khon Kaen University, Thailand. All animal procedures were reviewed and approved by the Institutional Animal Ethics Committee of Khon Kaen University (AE 41/2555). Rats (n= 8/group) were exposed to PHZ (15 mg/kg/day; i.p.) and orally administered with curcumin (30 and 100 mg/kg/day) for 8 days. After 8 days of PHZ administration, rats were anaesthetized with pentobarbital sodium (60 mg/kg; i.p) then arterial blood pressures and hind limb blood flow (HBF) were measured. At the end of experiment, blood samples were collected from abdominal aorta for assays of hematocrit values, non-transferrin bound iron (NTBI), oxidative stress markers including, plasma malondialdehyde (MDA) and protein carbonyl levels. Tissue samples, heart, kidneys, and liver, were also removed to measure MDA and protein carbonyl levels. Subsequently, the thoracic aorta was excised rapidly from the animals and used for measurement of superoxide production. The systolic, diastolic and mean arterial blood pressure of PHZ treated rats were markedly decreased whereas HBF and serum NTBI level were dramatically increased when compared with normal controls. Interestingly, the restoration of hemodynamic disturbance and anemia during PHZ exposure were related to the alleviation of free iron release, superoxide production and oxidative stress status. Results in this study reveal the effects of curcumin that may offer potential advantage of practical use in prevention of vascular dysfunction and oxidative stress in PHZ treated rats.

1. Berger, J., 2007. Phenylhydrazine haematotoxicity. J. Appl. Biomed. 5, 125-130.

2. Luangaram, S., Kukongviriyapan, U., Pakdeechote, P., Kukongviriyapan, V., Pannangpetch. P., 2007. Protective effects of quercetin against phenylhydrazine-induced vascular dysfunction and oxidative stress in rats. Food Chem. Toxicol. 45, 448-455.

This work was supported by Faculty of Medicine, Mahasarakham University, Thailand.

Where applicable, the authors confirm that the experiments described here conform with The Physiological Society ethical requirements.

PCC405

The endothelial glycocalyx surface layer depth, measured directly using confocal microscopy, is altered in the mesenteric microvessels of proteinuric rats

K.B. Betteridge[1], K.P. Arkill[2], C.R. Neal[1] and A.H. Salmon[1]

[1]School of Physiology and Pharmacology, University of Bristol, Bristol, UK and [2]School of Physics and Astronomy, University of Birmingham, Birmingham, UK

The luminal surface of blood vessels is coated with a size limiting, specialised, composite endothelial glycocalyx-surface layer (EG-SL) which has a fundamental role in microvessel permeability. EG-SL disruption occurs in major global diseases (inc. diabetes, atherosclerosis, sepsis, advanced kidney disease). Advancing knowledge about the EG-SL is seriously limited by difficulties in detecting, imaging and accurately quantifying the EG-SL, particularly in functioning vessels in vivo. We have developed a new technique for studying the EG-SL in vivo, and used this system to demonstrate changes in the EG-SL in an animal model of early kidney disease.
Male Sprague Dawley rats were injected with either Puromycin Aminonucleoside to cause Nephrosis (PAN) or PBS (sham controls). Mesenteric microvessels of pentobarbitone-anaesthetised (60 μg per g in weight) rats were exposed, cannulated, and perfused with octadecyl-rhodamine-B chloride (R18: membrane label) and Fluorescein-Isothiocyanate-conjugated Wheat Germ Agglutinin (FITC-WGA lectin: EG-SL label), and imaged using Confocal Microscopy (Nikon D-eclipse C1, CM) with a 60x objective (1.4 NA, Nikon). Vessels of sham injected rats were then perfused with neuraminidase for 20min, an enzyme that cleaves sialic acid residues within the glycocalyx, and re-imaged. EG-SL depth was estimated based on the anatomical distance between peak fluorescence of FITC-WGA and R18 signals (FIJI/IMAGEJ, NIH) at the maximum vessel width.
EG-SL depth in sham rats was 288±24nm (n=5). This value was significantly reduced to 185±32nm following perfusion of the same vessel with neuraminidase ($p<0.01$, paired t-test). EG-SL depth in PAN was 147±23nm (n=5), demonstrating significantly reduced EG-SL depth in these proteinuric rats compared with sham-treated rats ($p<0.01$, unpaired t-test).
We have demonstrated a sensitive technique for measuring changes to EG-SL depth in vivo using CM. EG-SL depth is significantly reduced in proteinuric PAN-treated rats, perhaps a contributing factor to the increased systemic permeability observed in proteinuric patients.

Where applicable, the authors confirm that the experiments described here conform with The Physiological Society ethical requirements.

PCC406

The cellular density of Myeloid Angiogenic Cells alters their secretome profile and determines the angiogenic potential of retinal microvascular endothelium

C.L. O'Neill, R.J. Medina, M.T. O'Doherty, S.E. Chambers, J. Guduric-Fuchs and A.W. Stitt

Centre for Vision and Vascular Sciences, Queens University Belfast, Belfast, UK

Endothelial progenitor cells (EPCs) promote angiogenesis and facilitate vascular repair. Recent clinical trials have demonstrated the feasibility, effectiveness and safety of EPCs for treatment of various ischaemic diseases. However, results from such trials have been inconsistent. This is due to the heterogeneous mix of cells used, as the term EPC has been applied to a broad range of blood derived cells that display endothelial markers and enhance angiogenesis. We have previously characterised two EPC subsets in vitro, Myeloid angiogenic cells (MACs) and Outgrowth endothelial cells (OECs). Although OECs are the EPC subset with progenitor and endothelial characteristics, MACs may still play an important role in angiogenesis indirectly. We have recently shown that cell therapy using MACs significantly enhanced vascular repair in a murine model of retinal ischaemia. This MAC response is mediated by the paracrine release of IL8 since it can be blocked using CXCR receptor inhibitors or a neutralising IL8 antibody. This pro-angiogenic potential of MACs could be harnessed as a novel cellular therapy for the treatment of ischaemic retinopathy but further optimisation of MACs as a cell therapy, including optimisation of the density of cells is required.

A co-culture system of MACs with retinal microvascular endothelial cells (RMECs) was used as an *in vitro* angiogenesis model to determine MACs effects at various densities. An angiogenesis protein array was then used to identify conditioned media components.

An *in vitro* angiogenesis assay demonstrated that MACs significantly increased RMEC tube formation ($p<0.01$) when used at a ratio of 4/1(RMECs/MACs). However, RMECs co-cultured with a higher density of MACs significantly decreased RMEC tube formation ($p<0.01$). Analysis of conditioned media by an angiogenesis protein array highlighted upregulation of specific anti-angiogenic factors (PTX3, PAI1, CXCL16) in the high density group, whilst showing a significant decrease in IL8 levels and an imbalance in the MMP9/TIMP1 ratio. Exposure of RMECs to recombinant PTX3 confirmed the anti-angiogenic role of this protein by showing a significant decrease in tube formation ($p<0.05$) and migration ($P<0.01$). Furthermore, the anti-angiogenic effect of high density MACs was partly rescued by using an antibody targeted against PTX3 ($p<0.01$).

We have shown that MACs are capable of inducing angiogenesis and act as M2 macrophages. However, at high density, MACs significantly inhibit angiogenesis. This effect is due to secretome changes, and release of negative regulators of angiogenesis, such as PTX3. Therefore, MACs density is an important consideration when using them as a cellular therapy for ischaemic retinopathy.

Fight for Sight (FFS)

Sir Jules Thorn Trust

Medical Research Council (MRC)

Where applicable, the authors confirm that the experiments described here conform with The Physiological Society ethical requirements.

PCC407

Aging modulates the anti-contractile effects of perivascular adipose tissue; the role of nitric oxide

H.M. Melrose, A. Heagerty, G. Edwards and C. Austin

FMHS, University of Manchester, Manchester, UK

Introduction: Aging is widely considered the biggest independent risk factor for cardiovascular disease, the leading cause of death worldwide. Advanced age is associated with endothelial dysfunction, hypertension and increased risk of stroke and myocardial infarction; the mechanisms behind these increased risks are little understood. It has long been known that there is an age-related endothelial dysfunction, due to decreased bioavailability of the endogenous vasodilator nitric oxide (NO), synthesised in the vascular endothelium (Barton et al., 1997). Vascular reactivity is further regulated via the perivascular adipose tissue (PVAT), which has a net anti-contractile effect (Greenstein et al., 2009). PVAT is also known to be a source of NO (Gil-Ortega et al., 2010), in addition to secreting locally acting factors that augment endothelial NO production (Gao et al., 2007).

Hypothesis: PVAT dysfunction may occur with aging, and is due at least in part to reduced bioavailability of NO.

Methods and Results: Third order mesenteric arteries were taken from male Wistar rats aged 3 months old (m.o.), 12 m.o., 18 m.o. and 24 m.o. and contractility to increasing concentrations of the thromboxane A2 receptor agonist U46619 (10nM-3μM) assessed via wire-myography in the presence and absence of PVAT and the NO-synthase inhibitor Nω-nitro-L-arginine (L-NNA) (50μM). Results were analysed via two-way ANOVA (Bonferroni post-hoc). PVAT was anti-contractile in 3 m.o. rat arteries (-PVAT max change in tension to U46619 (mN/mm) +1.2±0.52 (n=6), +PVAT +0.55±0.07 (n=3)) and 12 m.o. rat arteries (-PVAT +0.61±0.06 (n=5), +PVAT +0.44±0.13 (n=5), p=0.0280) but that this effect had been lost by 18 months (-PVAT +0.99.±0.11 (n=7), +PVAT 0.96±0.18 (n=5)), and remained absent at 24 m.o. (-PVAT 0.85.±0.11 (n=8), +PVAT 0.88±0.15 (n=8)). Incubation with L-NNA prevented the anti-contractile effect of PVAT at 3 months (+PVAT/+L-NNA +1.09±0.36 (n=4)). At 24 months, incubation with L-NNA had no effect on contractility (+PVAT/+L-NNA +0.64±0.28 (n=7)) in either the presence of absence of PVAT.

Summary: The anti-contractile effect of PVAT is lost with age in rats, due at least in part to a reduced bioavailability of NO. Further studies are currently being undertaken to further investigate the mechanisms involved.

Barton M, Cosentino F, Brandes RP, Moreau P, Shaw S & Lüscher TF. Anatomic Heterogeneity of Vascular Aging: Role of Nitric Oxide and Endothelin. Hypertension 30, 817-824 (1997).

Gao YJ, Lu C, Su LY, Sharma AM & Lee RMKW. Modulation of vascular function by perivascular adipose tissue: the role of endothelium and hydrogen peroxide. British Journal of Pharmacology 151, 323-331 (2007).

Gil-Ortega M, Stucchi P, Guzmán-Ruiz R, Cano V, Arribas S, González MC, Ruiz-Gayo M, Fernández-Alfonso MS & Somoza B. Adaptative Nitric Oxide Overproduction in Perivascular Adipose Tissue during Early Diet-Induced Obesity. Endocrinology 151, 3299-3306 (2010).

Greenstein AS, Khavandi K, Withers SB, Sonoyama K, Clancy O, Jeziorska M, Laing I, Yates AP, Pemberton PW, Malik RA & Heagerty AM. Local inflammation and hypoxia abolish the protective anticontractile properties of perivascular fat in obese patients. Circulation 119, 1661-1670 (2009).

This work is funded by a BHF studentship (FS/10/52/28678)

Where applicable, the authors confirm that the experiments described here conform with The Physiological Society ethical requirements.

PCC408

Correlative 3D estimation of the vascularization in the murine hind limb

L. Schaad, C. Sollberger, R. Hlushchuk, S. Barré and V. Djonov

Institute of Anatomy, Bern 9, Switzerland

Background: According to PubMed, at least 3000 articles are published in the field of "blood vessels in muscle" every year. The skeletal muscles of the rodent hind limb are the most frequently used experimental model. However, most of the studies are based on a single muscle and and usually on solitary cross-sections. Taking into account that capillarization differs dramatically between different muscles and even within the same muscle, we decided to introduce a complex 3D assay of structure of the vasculature in the murine hind limb.
Methods & Results: Although imaging and quantification of bones by μCT is well developed and established, visualization of striated muscle capillaries is a challenging issue, mainly due to lack of satisfactory contrast agents. Therefore, to visualize the 3D structure of the vascular network with a resolution up to the level of capillaries, vascular casting with PU4ii® polymer (vasQtec, Zurich) has been performed. To enhance the contrast, after maceration the casts have been immersed in osmium tetraoxide and freeze-dried thereafter and investigated with a μCT (Skyscan 1172, voxel size below 1μm). Additionally, special a histological approach has been employed. Since cutting of mineralized bone with an ordinary microtome is not feasible, the entire hind limb was decalcified in EDTA for 4 days. Subsequently, the limb was embedded in paraffin and series of 5μm-thick sections of the entire hind limb obtained. After deparaffinization and trypsinization of the tissue sections, the capillaries were stained with BS-1 lectin. This method allows comparative evaluation of the capillary-to-fibre ratio, capillary density, fibre type i) of all 11 muscles on a single cross-section; ii) at different levels in the same muscle, i.e. proximal to distal. Based on this method, we were able to show alterations among the above-mentioned parameters depending on the level examined.
Implications: We present a comparative method to evaluate the vasculature of all skeletal muscles on a cross-section of the whole hind limb simultaneously and at different levels. This method allows a time-efficient, 3D and comparative evaluation of the hind limb vascularization.

Where applicable, the authors confirm that the experiments described here conform with The Physiological Society ethical requirements.

PCC409

Effects of hypoxia & inflammation on vascular reactivity in rats: a model of co-morbidities in chronic obstructive pulmonary disease?

A. Gassama[1], A. Turner[1], S. Egginton[1,2] and P. Kumar[1]

[1]Clinical & Experimental Medicine, University of Birmingham, Birmingham, UK and [2]Biomedical Sciences, University of Leeds, Leeds, UK

Chronic obstructive pulmonary disease (COPD) is characterised by a poorly reversible airflow limitation. It is a complex disease associated with both pulmonary and systemic vascular inflammation, linked to subsequent development of cardiovascular complications including pulmonary hypertension. Inflammatory mediators and hypoxia promote endothelial damage causing an imbalance between vasodilator and vasoconstrictor intermediaries, thus altering vascular tone. These lead to increased smooth muscle cell proliferation and vasoconstriction as well as vascular remodelling and subsequently resulting in an increased pulmonary arterial pressure.[1,2] The pathogenesis of systemic effects of COPD has not yet been fully elucidated.
Pulmonary artery (PA) was dissected from normoxic control (C) and chronically hypoxic (CH – 10% O_2; 1 week) Wistar rats and 2 mm segments of the vessels were mounted on a wire myograph in physiological saline (95% O_2, 5% CO_2, 37°C). U46691 was used to generate a pre-tone and a cumulative dose-response curve for a vasodilator (carbachol -CC or sodium nitroprusside –SNP) was constructed. A pro-inflammatory cytokine (TNF-α, IL-8 or IL-β) was then added for 1 hour before vasodilator responses were re-assessed. Right ventricular (RV) to left ventricular and septum (LV+S) ratio was used to assess RV hypertrophy in control and chronic hypoxic rats. All procedures were in accordance with current UK legislation. Significance was taken as $P<0.05$.
One week hypoxia induced a significant increase in RV hypertrophy in rats (C= 0.27±0.026, CH= 0.40±0.028 n=3 t-test). Our preliminary data on control and CH rats did not show any significant difference in the maximum percentage of the endothelial dependent vasodilation by CC (C= 62±8.1% n=8, control+IL-8= 57±6.5% n=8, CH= 83±16.1% n=3 CH+IL-8= 68±7.6% n=3 ANOVA). CH increased the maximum vasodilatation by endothelial independent vasodilator, SNP by ~25% when compared to the control (CH=36±3.9% n=3, C=45±6.3% n=4) and the addition of IL-8 augmented SNP induced vasodilation in both groups (control+IL-8= 41±5.7% n=6, CH+IL-8= 30±3.1% n=3). However, these differences did not reach significance in both groups.
Our findings suggest that (1) acute cytokine exposure has little effect on vasoreactivity; (2) one-week CH can cause structural changes in RV, even though a functional difference was not observed in PA vasodilatation in the same time. This might represent a difference in the time course for structural changes to be observed in the cardiovascular and pulmonary systems consequent to CH, or that hypoxia and pro-inflammatory cytokine effects are synergistic, and future longitudinal studies are planned.

Peinado VI, Pizarro S, Barberà J. CHEST. 2008;134(4):808-814

Wrobel JP, Thompson BR, Williams TJ. The J of Heart and Lung Transp. 2012;31(6):557–564

Thanks to Andy Coney for his support during this work.

Where applicable, the authors confirm that the experiments described here conform with The Physiological Society ethical requirements.

PCC410

Impact of circulating endothelial progenitor cells and platelet microparticles on platelet activation in hypertension associated with hypercholesterolemia

N. Alexandru, D. Popov, E. Andrei, E. Dragan and A. Georgescu

Pathophysiology and Pharmacology, Institute of Cellular Biology and Pathology 'Nicolae Simionescu', Bucharest, Romania

Aim: The purpose of this project was to evaluate the influence of circulating endothelial progenitor cells (EPCs) and platelet microparticles (PMPs) on blood platelet function in experimental hypertension associated with hypercholesterolemia. Methods: Golden Syrian hamsters were divided in six groups: (i) control, C; (ii) hypertensive-hypercholesterolemic, HH; (iii) 'prevention', HHin-EPCs, HH animals fed a HH diet and treated with EPCs; (iv) 'regression', HHfin-EPCs, HH treated with EPCs after HH feeding; (v) HH treated with PMPs, HH-PMPs, and (vi) HH treated with EPCs and PMPs, HH-EPCs-PMPs. Results: Compared to HH group, the platelets from HHin-EPCs and HHfin-EPCs groups showed a reduction of: (i) activation, reflected by decreased integrin β3, FAK, PI3K, src protein expression; (ii) secreted molecules as: SDF-1, MCP-1, RANTES, VEGF, PF4, PDGF and (iii) expression of pro-inflammatory molecules as: SDF-1, MCP-1, RANTES, IL-6, IL-1β; TFPI secretion was increased. Compared to HH group, platelets of HH-PMPs group showed increased activation, molecules release and proteins expression. Compared to HH-PMPs group the combination EPCs with PMPs treatment induced a decrease of all investigated platelet molecules, however not comparable with that recorded when EPC individual treatment was applied. Conclusion: EPCs have the ability to reduce platelet activation and to modulate their pro-inflammatory and antithrombogenic properties in hypertension associated with hypercholesterolemia. Although, PMPs have several beneficial effects in combination with EPCs, these did not improve the EPC effects. These findings reveal a new biological role of circulating EPCs in platelet function regulation, and may contribute to understand their cross talk, and the mechanisms of atherosclerosis.

This research was financially supported by a grant of the Romanian National Authority for Scientific Research, CNCS – UEFISCDI, project ID PNII-CT-ERC-2012 – 1 (6ERC- like/July 18, 2012) and by Romanian Academy.

Where applicable, the authors confirm that the experiments described here conform with The Physiological Society ethical requirements.

PCC411

Back to physiology: adaptation of human endothelial cells to normoxia alters Nrf2 antioxidant defences and redox homeostasis

S. Chapple[1], D. Mastronicola[2], T. Keeley[1], R. Siow[1] and G. Mann[1]

[1]Cardiovascular Division, King's College London, London, UK and [2]Department of Biochemical Sciences, Sapienza University of Rome, Rome, Italy

Conventional in vitro models classically use cells cultured in ambient air/5% CO2 which are hyperoxic compared to the environmental milieu in vivo. Given the intrinsic role of molecular O2 in determining reactive oxygen species (ROS) production and redox homeostasis, the current study sought to determine whether redox homeostasis is altered in cells adapted to physiological O2 tensions. Experiments were conducted using primary human umbilical vein endothelial cells (HUVEC) cultured under conventional 21% O2 or adapted to physiological 5% O2 for 1-day or 5-days. Using specialised oxygen workstations, we assessed (i) transcriptional DNA binding activity of the key redox-sensitive transcription factor Nrf2 by ELISA, (ii) induction of Nrf2-mediated antioxidant and phase II enzymes, GSH related genes or Nrf2 negative regulatory proteins Keap1 and Bach1 mRNA and protein by qPCR or immunoblotting, (iii) GSH synthesis by OPA fluorescence and (iv) cellular and mitochondrial ROS generation using DHE fluorescence. Whilst Nrf2 nuclear translocation or DNA binding of Nrf2 was not altered under 5% O2 conditions, progressive adaptation of cells to normoxic 5% O2 resulted in a depression of Nrf2-mediated antioxidant heme oxygenase-1 (HO-1) and NAD(P)H:quinone oxidoreductase (NQO1) induction in response to the known electrophilic Nrf2 inducer diethylmaleate. In contrast, GSH synthesis or induction of critical GSH related genes glutamate cysteine ligase catalytic subunit (GCLC) or the cystine glutamate transporter (xCT) were unaltered, whereas induction of the negative Nrf2 regulator Bach1, but not Keap1, was elevated under normoxic conditions. Measurement of cellular ROS generation using DHE or mitochondrial targeted DHE (Mitosox Red), revealed that adaptation of cells to normoxic 5% O2 results in alterations in ROS output with enhanced sensitivity to the mitochondrial complex I inhibitor antimycin A. Collectively these findings suggest that under normoxic 5% O2 conditions human endothelial cells exhibit a dramatically altered redox profile to cells cultured under standard air/5% CO2 conditions. Differential Nrf2 regulation of HO-1, GCLC and Bach1 suggests that undetermined factors modulated by O2 tension influence Nrf2 gene transcription, with significant implications for cellular ROS generation and ultimately cell redox homeostasis.

Supported in part by Heart Research UK. We are grateful to Don Whitley Scientific and Ruskinn-Baker for their support with O2-regulated workstations.

Where applicable, the authors confirm that the experiments described here conform with The Physiological Society ethical requirements.

PCC412

Circulating microparticles and endothelial progenitor cells in atherosclerosis; pharmacological effects of irbesartan

A. Georgescu[1], N. Alexandru[1], E. Andrei[1], I. Titorencu[1], E. Dragan[1], C. Tarziu[2], S. Gheorghe[2], E. Badila[2], D. Bartos[2] and D. Popov[1]

[1]Pathophysiology and Pharmacology, Institute of Cellular Biology and Pathology 'Nicolae Simionescu' of Romanian Academy, Bucharest, Romania, Bucharest, Romania and [2]Emergency Hospital, Bucharest, Romania, Bucharest, Romania

Aims: This study aimed to (a) employ our newly designed model, the hypertensive–hypercholesterolemic hamster (HH) in order to find whether a correlation exist between circulating microparticles (MPs), endothelial progenitor cells (EPCs) and their contribution to vascular dysfunction and (b) to assess the effect of irbesartan treatment on HH animals (HHI). Methods and Results: The results showed that compared to control (C) group, HH displayed: (i) a significantly increase in plasma cholesterol and triglyceride concentration, and an augmentation of systolic and diastolic arterial blood pressure, and of heart rate; (ii) a marked elevation of MPs and a significant decrease in EPCs; (iii) structural modifications of arterial wall correlated with altered protein expression of MMP2, MMP9, MMP12, TIMP1, TIMP2 and collagen type I and III; (iv) a considerably altered reactivity of arterial wall closely correlated with MPs and EPC adherence; (v) an inflammatory process characterised by augmented expression of P-Selectin, E-Selectin, vWF, TF, IL-6, MCP-1, RANTES. Additionally, the experiments showed the potential of irbesartan to correct all altered parameters in HH and to mobilize EPCs by NO, chemokines and adhesion molecules dependent mechanism. Conclusions: Hypertension associated with hypercholesterolemia is accompanied by structural modifications and expression of pro-inflammatory molecules by vessel wall, the alteration of vascular tone, enhanced release of MPs and reduced EPCs; the ratio between the latter two may be considered as a marker of vascular dysfunction. Irbesartan that exhibit a pharmacological control on the levels of MPs and EPCs has the potential to restore homeostasis of the arterial wall.

This work was supported by a grant of the Romanian National Authority for Scientific Research, CNCS – UEFISCDI, project ID PNII-CT-ERC-2012 – 1 (6ERC- like/July 18, 2012) and by Romanian Academy.

Where applicable, the authors confirm that the experiments described here conform with The Physiological Society ethical requirements.

PCC413

Involvement of TRPA1 and reactive oxygen species in cinnamaldehyde-induced vasodilatation in the peripheral vasculature

A.A. Aubdool[1], X. Kodji[1], E.S. Fernandes[1], S. Bevan[2] and S.D. Brain[1]

[1]Cardiovascular Division BHF-Centre of Cardiovascular Excellence and Centre for Integrative Biomedicine, King's College London, London, UK and [2]Wolfson CARD Centre, King's College London, London, UK

The non-selective transient receptor potential ankryrin-1 (TRPA1) channels have been previously reported to be a major chemosensory receptor for reactive oxidants in sensory neurons in both in vivo and in vitro studies, but its importance to the vascular field has yet to be investigated. We have previously shown that cinnamaldehyde can activate TRPA1 and release potent microvascular vasodilators neuropeptide CGRP and nitric oxide (Aubdool et al., 2012) and, causes vasodilatation. We hypothesised that reactive oxygen species (ROS) are involved in the downstream signalling mechanism and this was investigated using the mouse ear model. Using laser Doppler flowmetry, cutaneous blood flow was measured in male CD1 mice (20-25g) under anaesthesia (ketamine-75mg/kg; medetomidine-25mg/kg, i.p.) and following topical application of cinnamaldehyde (10%) and vehicle (10% DMSO in ethanol). Ear samples were collected and hydrogen peroxide (H2O2) levels were assessed using the amplex red assay. All animals were randomly assigned to drug-treated or respective control groups. Results were expressed as mean + S.E.M. in arbitrary flux units and analysed by 2-way ANOVA + Bonferroni's test. A sustained (30 min) increase in vasodilatation was observed after topical application of cinnamaldehyde and this was significantly attenuated by a treatment of ROS scavenger N-acetylcysteine (NAC, 300mg/kg), (379.0 + 40.1 x 1000 flux units for control-treated vs 168.4 + 24.2 x 1000 flux units for NAC-treated, n=5-6, $p<0.001$). No change in H2O2 levels was observed in cinnamaldehyde-treated ears compared to vehicle. There was no significant change in cinnamaldehyde-induced vasodilatation in vehicle or NADPH oxidase inhibitor apocynin (20mg/kg, i.v.) pre-treated wild-type (WT) mice (n=6, $p>0.05$). However, TRPA1-mediated vasodilatation was significantly reduced by a co-treatment of superoxide dismutase (SOD) and catalase (25000U/kg, $p<0.01$, n=6), but not deactivated enzymes, supporting a novel role for ROS generation. This response was also attenuated in WT mice pre-treated with the iron chelator deferoxamine (25mg/kg, $p<0.001$, n=6) or the permeable SOD mimic TEMPOL (30mg/kg, $p<0.001$, n=6), suggesting a potential involvement of hydroxyl radicals and oxidative stress. These studies provide novel evidence that ROS are involved in TRPA1-dependent neurogenic vasodilatation in vivo.

Aubdool AA et al (2012). BPS Focused Meeting on Neuropeptides 028P pA2 Online.

This study was supported by a BBSRC-led IMB capacity building award.

Where applicable, the authors confirm that the experiments described here conform with The Physiological Society ethical requirements.

PCC414

Hydrogen peroxide via thromboxane A_2 receptors mediates myogenic response of small skeletal muscle veins in rats

B. Debreczeni[2,1], E. Gara[2], Z. Veresh[2,3], A. Marki[2], A. Racz[2], R. Matics[4], J. Hamar[4], R. Tamas[1] and A. Koller[2,4]

[1]Department of Plastic Surgery, Military Hospital, Budapest, Hungary, [2]Department of Pathophysiology, Semmelweis University, Budapest, Hungary, [3]First Department of Obstetrics and Gynecology, Semmelweis University, Budapest, Hungary and [4]Department of Physiology and Gerontology and Szentagothai Res Centre, University of Pécs, Pécs, Hungary

We aimed to test two hypotheses: 1) Isolated small veins develop substantial myogenic tone in response to elevation of intraluminal pressure. 2) H_2O_2 contributes to the mediation of myogenic response via activation of arachidonic acid (AA) cascade and release constrictor prostaglandins.
Methods:Small veins were isolated from gracilis muscle of male rats, then cannulated. Changes of diameter to increases in intraluminal pressure, H_2O_2 and arachidonic acid in the presence and absence of various inhibitors were measured by videomicroscope and microangiometer. At the end of experiments the passive diameter were obtained in Ca^{2+} - free PSS solution.
Results: Isolated rat gracilis muscle small veins developed a substantial myogenic tone in response to increases in intraluminal pressure (1 - 12 mmHg). Calculated maximum myogenic tone was 70 ± 5 % at 10 mmHg. Presence of catalase or indomethacin or SQ 29,548 reduced significantly the pressure-induced myogenic response. Also, H_2O_2 (10^{-9} - 10^{-5} M) and arachidonic acid (10^{-7} - 10^{-4} M) elicited concentration dependent constrictions, which were inhibited by the presence of indomethacin or SQ 29,548.
Conclusion:We propose that both myogenic response and pressure-induced release of H_2O_2 play important roles in regulating the vasomotor function of venules both in physiological and pathological conditions.
Key words: small veins, myogenic response, prostaglandins, hydrogen peroxide, indomethacin, SQ 29,548, catalase, arachidonic acid

Where applicable, the authors confirm that the experiments described here conform with The Physiological Society ethical requirements.

PCC415

Angiopoietin-1 increases turnover of endothelial glycocalyx in glomerular endothelial cells

S. Desideri[1,2], B. Foster[2], S. Satchell[2] and A. Salmon[1,2]

[1]School of Physiology & Pharmacology, University of Bristol, Bristol, UK and [2]Academic Renal Unit, University of Bristol, Bristol, UK

Endothelial glycocalyx is a gel-like structure present on the luminal surface of blood vessels [Weinbaum et al, Annu Rev Biomed Eng. 2007, 9:121:67]. Endothelial glycocalyx comprises proteoglycan core proteins, glycosaminoglycans (GAG) chains, sialoglycoproteins and contributes to the selective sieving action of the glomerular capillary wall. The endothelial glycocalyx is a critical determinant of permeability in kidney glomeruli. Disruption of the endothelial glycocalyx is linked with microalbuminuria in diabetes.Angiopoietin-1 is a paracrine growth factor synthesised by glomerular podocytes, that exerts paracrine actions on glomerular endothelail cells. Angiopoietin-1 decreases the ultrafiltration coefficient of single isolated glomeruli. In other capillary beds, parallel actions of angiopoietin-1 on hydraulic conductivity are mediated by increased depth of the endothelial glycocalyx. We have examined release of GAGs from the surface of human conditionally immortalized glomerular endothelial cells (ciGEnC) in vitro, and studied the effect of angiopoietin-1 on this process. Primary GEnCs, previously immortalised in our laboratory [Satchell et al, Kidney Int. 2006, 69 (9): 1633 - 1640] proliferate at 33°C, and differentiate to a non-proliferative quiescent state at 37°C. These ciGEnCs were differentiated and grown to 60–70% confluency, serum-starved for 3 hours, in the presence or absence of angiopoietin-1 (200ng/ml). After harvesting this supernatant, cell monolayers were exposed to either pronase (0.01%) or vehicle for 1 minute and the supernatant again aspirated. Harvested supernatant was added to an Alcian Blue solution, and the linear relation between GAG mass and decreased absorption of 488 nm light by Alcian Blue solution was used to quantify supernatant glycosaminoglycan content, referenced to known concentrations of GAG (chondroitin sulphate) standards. Supernatant GAG concentration was 72.57±39.65 (n=4) μg/ml from vehicle-treated endothelial cells, and significantly higher (150.3±61.81 (n=4) μg/ml) from pronase-treated endothelial cells ($p<0.01$, paired t-test). Supernatant harvested from endothelial cell monolayers exposed to angiopoietin-1 (90.94±21.89 μg/ml, n=3) demonstrated significantly higher GAG concentrations than supernatant from monolyers treated with serum-free media alone (50.35±13.73 μg/ml, n=3) ($p<0.05$, paired t-test). Increased GAG turnover by glomerular endothelial cells in response to angiopoietin-1 matches physiological data and studies in other capillary beds. The glycocalyx of glomerular endothelial cells thus appears modifiable by endogenous, paracrine agents.

We gratefully acknowledge funding from Kidney Research UK.

Where applicable, the authors confirm that the experiments described here conform with The Physiological Society ethical requirements.

PCC416

Nebivolol induces dilation in isolated rat cerebral artery, independent of NO-cGMP pathway

P. CSEPLO[1,2], Z. Vamos[2,3], O. Torok[1], I.Z. Batai[1], J. Hamar[1] and A. Koller[1,4]

[1]Department of Pathophysiology and Gerontology, Univ Pecs, Medical School, Pecs, Hungary, [2]Hungarian National Ambulance Service, South-Danubian Region, Hungary, [3]Department of Anesthesiology and Intensive Therapy, Univ Pecs, Medical School, Pecs, Hungary and [4]Department of Physiology, New York Medical College, Valhalla, NY, USA

Keywords: nebivolol, cerebral artery, vasomotor, basilar artery, isolated artery, NO, cGMP
INTRODUCTION: Experimental and clinical studies have demonstrated that nebivolol has antiarrhythmic, antihypertensive effects and in peripheral arteries elicits dilation, in which mediation for nitric oxide (NO) has been suggested. However, its effect on the diameter of cerebral vessels has not been investigated. We hypothesized that nebivolol increases the diameter of isolated cerebral arteries.
METHODS: Basilar arteries (BA) were isolated from male Wistar rats and were mounted into a pressure-flow myograph chamber and cannulated at both ends. Vessels were incubated until a spontaneous active diameter developed. Diameters (D)

of vessels were measured with video-microscopy. Vasomotor function of vessels was studied in response to nebivolol and the nitric oxide (NO) donor sodium nitroprusside (SNP). NO synthase was inhibited by Nω-nitro-L-arginine methyl ester (L-NAME). Soluble guanylate cyclase was blocked by 1H-[1,2,4]oxadiazolo[4,3-a]quinoxalin-1-one (ODQ). At the end of the experiments the passive diameter of vessels (PD) was determined in Ca2+-free Krebs solution.
RESULTS: The active diameter of BA was ~220 μm (n=9). Nebivolol caused significant vasodilation (10-5M: ΔD = 67±18 μm; p<0,05). Incubation of BA with L-NAME significantly reduced the active diameter (by ΔD = 25±10 μm). In the presence of L-NAME nebivolol caused significant vasodilation, similar to control conditions (10-5 M: ΔD = 47±10 μm). Also, in the presence of ODQ, nebivolol elicited significant vasodilation (10-5 M: ΔD = 87±16 μm), whereas the SNP-induced dilation was significantly decreased (SNP 10-4 M: from ΔD[1] = 126±14 μm to ΔD[2] = 1±17 μm).
CONCLUSION: These findings demonstrate that in isolated cerebral arteries 1) nebivolol elicits significant dilation, 2) NO contribute to the development of basal tone, 3) but NO-cGMP pathway does not contribute significantly to the nebivolol-induced dilation. Elucidating the underlying mechanisms could contribute to a better understanding of the effects of nebivolol on cerebral circulation.

(Supported by: OTKA K71591, K67984, AHA Founders Aff., 0855910D, SROP-4.2.2.A-11/1/KONV-2012-0024.)

Where applicable, the authors confirm that the experiments described here conform with The Physiological Society ethical requirements.

PCC417

Novel role of the Plasma Membrane Calcium ATPase protein as an endogenous inhibitor of VEGF-induced angiogenesis

R.R. Baggott[1], A. Alfranca[2], T.A. Mohamed[3], B.C. Ornés[2], M.D. López-Maderuelo[2], A. Escolano[2], J. Oller[2], F.B. Rowther[1], D. Oceandy[3], J. Brown[4], E.J. Cartwright[3], W. Wang[1], L. Neyses[3], J.M. Redondo[2] and A.L. Armesilla[1]

[1]Research Institute in Healthcare Science, University of Wolverhampton, Wolverhampton, UK, [2]Dept of Vascular Biology and Inflammation, Centro Nacional de Investigaciones Cardiovasculares CNIC, Madrid, Spain, [3]Cardiovascular Research Group, University of Manchester, Manchester, UK and [4]Aston Research Centre for Healthy Ageing, Aston University, Birmingham, UK

A large body of data has demonstrated that aberrant expression of VEGF (Vascular Endothelial Growth Factor) plays a critical role in the abnormal vascularisation associated with several human diseases. Angiogenic responses stimulated by VEGF involve the activation of the calcineurin/NFAT (Nuclear Factor of Activated T-cells) signal transduction pathway. We have previously identified an inhibitory interaction between the Plasma Membrane Calcium ATPase (PMCA) family of proteins and calcineurin in HEK-293 and breast cancer cells. PMCAs are enzymatic low capacity, high-affinity systems involved in the extrusion of Ca^{2+} from the cell. It is thought that PMCA regulates the activity of the calcineurin/NFAT pathway by tethering calcineurin to low Ca^{2+} microdomains created by the Ca^{2+} extrusion activity of the pump. Given the relevance of the calcineurin/NFAT pathway in the progression of angiogenesis, we have investigated whether PMCA plays a significant role as an endogenous inhibitor of VEGF-mediated angiogenesis.
"Gain of function" studies conducted in HUVEC cells overexpressing PMCA4 by infection with Ad-PMCA4 (an adenovirus encoding human PMCA4), resulted in a significant decrease in the VEGF-induced activation of the calcineurin/NFAT pathway (31.92±8.74% reduction compared to the value observed in cells infected with control adenovirus Ad-LacZ, n=5). Similarly, VEGF-induced up-regulation of the NFAT-dependent, angiogenic genes Cox-2 and RCAN-1 was significantly attenuated (55.04±4.12%, n=5, and 48.42±4.72%, n=5, decrease respectively) by infection with Ad-PMCA4. PMCA4 overexpression also reduced the migration (39.8±4.08 reduction, n=6) and in vitro tube formation (42.24±10.92 reduction, n=5) of VEGF-stimulated HUVEC cells infected with Ad-PMCA4b. Moreover, *in vivo* angiogenesis assays performed by subcutaneous inoculation of a mixture of low growth factor-matrigel, VEGF and adenoviral vectors, in mice anesthetized with an intra-peritoneal injection of ketamine (75mg/kg)-xylazine (10mg/kg) showed a reduction of blood vessel formation (41.8±8.55 decrease, n=8) in plugs containing Ad-PMCA4.
Conversely, "loss of function" experiments performed in mouse lung endothelial cells (MLEC) isolated from PMCA4-/- knockout animals showed a significant increase in the activation of the calcineurin/NFAT pathway (4.25±1.08 fold-increment), the expression of the RCAN-1 protein as observed by western blot (n=3) and the migration of cells in wound-healing assays (1.66±0.56 fold-increment) when compared to the corresponding values in wild-type MLEC cells
These results strongly demonstrate that PMCA4 plays a critical role as a negative regulator of VEGF-mediated angiogenesis *via* inhibition of the calcineurin/NFAT pathway. Thus, modulation of endothelial PMCA4 activity might be exploited in clinic to design new anti-angiogenic approaches.

Where applicable, the authors confirm that the experiments described here conform with The Physiological Society ethical requirements.

PCC418

Ferrous ion potentiates ascorbate-dependent iron release from ferritin in vitro

C. Badu-Boateng, R.C. Siow, G.E. Mann and R.J. Naftalin

Cardiovascular Division, BHF Centre of Research Excellence, School of Medicine, King's College London, London, UK

Ferritin is a multimeric protein that stores 30% of human body iron as oxidised crystalline ferric phosphate, mainly in liver and heart muscle and in haemopoetic tissue and endothelium. Ascorbate causes iron release from ferritin by reducing stored iron (Km≈ 2 mM). Raised concentrations of non-protein bound iron catalyse formation extracellular and intracellular reactive oxygen species (1). Since intracellular and extracellular concentrations of ascorbate are generally within the range 40-250μM, this process is considered unlikely to contribute to pathological oxidation reactions. Only when ascorbate is raised > 2mM by i.v. injection is it deemed to be pro-oxidant (2). However, we have observed that ascorbate-dependent ferrous iron loss from horse spleen ferritin 50 nM (Sigma-Aldrich, UK), monitored for 2-3 h using a plate reader at 24°C to detect changes in absorption of ferrozine at 562μm (pH 7.0 buffered with sodium citrate 10 mM; MOPS 50 mM and 75μM ferrozine) is synergized by ferrous iron > 2 μM). Raising Fe(II) from 0 to 10μM decreases the Km of ascorbate-dependent Fe(II) release to 185±10μM (P < 0.001) and increases the Vmax of release 5-fold from 11.4±0.2 to 60±2.0 nmol Fe(II) mg-1ferritin min-1(P < 0.001). In the absence of external iron, hydrogen peroxide

acts as a potent non-competitive inhibitor of Vmax of ascorbate-dependent iron release by promoting two electron Fe(II) oxidation within ferritin(I.C50 111±34 μM). The IC50 of H2O2 on the apparent Km of ascorbate-dependent Fe(II) release is 352±92μM; addition of 10 μM Fe(II) with superoxide dismutase (50 units ml-1) reduces the IC50 to H2O2 30±42μM ($P < 0.01$) without altering the Vmax of Fe(II) release. Thus, H2O2 changes from a non-competitive inhibitor of ascorbate dependent of Fe(II) release in the absence of external Fe(II) to a competitive inhibitor when Fe(II) is present. These results suggest that single electron reactions generated by iron-ascorbate interaction, possibly resulting from ascorbyl and ferryl radical are a potent means of iron reduction and release from ferritin (3,4) and that this release mode differs from that caused by ascorbate alone, which may reduce bound di-Fe(III) at the ferroxidase centre by a bidentate two-electron reduction. Our novel finding that ascorbate and iron synergistically exacerbate iron release from ferritin has many implications relating to inflammatory mechanisms, the most immediate provides a rationale for iron-chelation therapy of arthritis and atherosclerosis, where iron and ascorbate and H2O2 released from necrotic macrophages and endothelium provide essential substrates for Fenton-Haber-Weiss reactions continuously generating superoxide and •OH radicals (5).

Vlachodimitropoulou, E., R.J. Naftalin and P.A. Sharp (2010). Free Radic. Biol. Med. 48: 1366–1369.

Du, J., J.J. Cullen and G.R. Buettner (2012). Biochim. Biophys. Acta 1826: 443–57.

Burkitt, M.J. and B.C. Gilbert. (1990). Free radical research communications. 10: 265–80.

Bou-Abdallah, F., et al. 2008. Journal of the Am. Chem. Soc. 130:17801–11.

Parkes, H. G., et al. (1991). J. Pharmaceut. Biomed. Analysis 9: 29–32 .

We acknowledge support from the School of Biomedical Sciences for a Summer Studentship to CBB.

Where applicable, the authors confirm that the experiments described here conform with The Physiological Society ethical requirements.

PCC419

Signalling pathways involved in 5-HT-induced contraction dependent on connexin 43 and superoxide anion production in rat intrapulmonary arteries

N. Khoyrattee[1], M. Billaud[2], A. Bourdieu[1], G. Cardouat[1], R. Marthan[1], J. Savineau[1] and C. Guibert[1]

[1]Centre de Recherche Cardio-Thoracique de Bordeaux, Bordeaux, France and [2]Robert M. Berne Cardiovascular Researh Center - University of Virginia, Charlottesville, VA, USA

We previously showed that serotonin (5-HT) produces superoxide anion ($O_2^{\bullet-}$) in the intrapulmonary artery (IPA) smooth muscle. Then, $O_2^{\bullet-}$ passes through the myoendothelial junction (connexin (Cx) 43) to decrease the bioavailability of endothelial NO and strengthen IPA vasoreactivity (Billaud et *al.,* 2009). Here, we further addressed the signalling pathways involved in such process.

Male Wistar rats were humanely killed according to national guidelines. IPA were used for immunofluorescence labellings and recording of $O_2^{\bullet-}$ levels by electron paramagnetic resonance (EPR). Mitochondrial Ca^{2+} (Ca^{2+}_m) was assessed in smooth muscle cells with Rhod-2. Isometric contraction was recorded on IPA rings with an organ bath system. Results were expressed as mean ± S.E.M. Significance was considered when $P<0.05$ and tested with Mann-Whitney (unpaired samples) and Student *t*-Test (paired samples). n represents the number of rats for EPR and immunofluorescence, the number of arterial rings for the contractile studies and the number of cells for Ca^{2+}_m recordings.

5-HT (100 μM) significantly increased $O_2^{\bullet-}$ levels in rat IPA (8672.8 ± 752.9 arbitrary units per $mg.ml^{-1}$ of proteins in response to 5-HT vs 5205 ± 589.7 in basal conditions, n=12-13). Endothelin-1 (ET-1) (0.1 μM) and phenylephrine (Phe) (10 μM) had no effect. Ketanserin (1 μM), a blocker of $5\text{-}HT_{2A}$ receptors significantly decreased 5-HT-induced $O_2^{\bullet-}$ production whereas blocking the $5\text{-}HT_{1B}$ receptors and the 5-HT transporter (5-HTT) by GR 127935 (1 μM) or citalopram (1 μM) respectively had no effect (n=11-12). EPR recordings showed that removal of extracellular Ca^{2+} (Ca^{2+}_e) decreased 5-HT-induced $O_2^{\bullet-}$ increase (6310 ± 585.8, p=0.016) whereas depleting intracellular Ca^{2+} stores with thapsigargin (1 μM) had no effect (n=12-13). Blockers of $O_2^{\bullet-}$ sources namely apocynin (30 μM) and rotenone (5 μM) for NADPH oxidase (Nox) and the complex I of the mitochondrial respiratory chain (MRC I) respectively, reduced 5-HT-induced $O_2^{\bullet-}$ increase (n = 10-19). 5-HT enhanced the Ca^{2+}_m level with or without Ca^{2+}_e (n=30-40). Inhibition of PKC_ε significantly reduced $O_2^{\bullet-}$ production to its basal level (n=8-9). Unlike $5\text{-}HT_{1B}$ and ET_B receptors, both $5\text{-}HT_{2A}$ and α_{1D} receptors (Phe receptors) colocalised with Cx 43. $5\text{-}HT_{2A}$ receptors and Cx 43 also colocalised with caveolin-1. Unlike the contraction to ET-1, the contraction to 5-HT and Phe was significantly modified after caveolae removal with methyl-β-cyclodextrin (7 mM) (n=12-26).

Altogether, 5-HT acts on $5\text{-}HT_{2A}$ receptors and induces a calcium influx responsible for Ca^{2+}_m increase and $O_2^{\bullet-}$ production (via MRC I). This process activates PKC_ε which in turn may activate $O_2^{\bullet-}$ production by Nox. Interestingly, $O_2^{\bullet-}$ production in rat IPA seems to be 5-HT specific and would happen in caveolae localised near to Cx43.

Billaud M *et al. (2009). PLos One* **4:**e6432

Where applicable, the authors confirm that the experiments described here conform with The Physiological Society ethical requirements.

PCC420

Tissue plasminogen activator and plasminogen activator inhibitor-1 promote biointegration of porous polyethylene implants

M.E. Hessenauer[1,2], C.A. Reichel[1,2], A. Berghaus[2] and S. Strieth[3]

[1]Walter Brendel Centre of Experimental Medicine, Munich, Germany, [2]Department of Otorhinolaryngology, Head and Neck Surgery, Ludwig-Maximilians-Universität München, Munich, Germany and [3]Department of Otorhinolaryngology, Head and Neck Surgery, Goethe-University, Frankfurt/M., Germany

Background

Rapid fibrovascularization and a moderate inflammatory response are considered as prerequisites for a successful engraftment of porous polyethylene (PPE) implants. Plasmin is the principal effector protease in the fibrinolytic system and has recently been implicated in tissue integration of biomaterials. Tissue plasminogen activator (tPA) is the main plasminogen activating protease, whose activity is tightly controlled by plasminogen-activator inhibitor-1 (PAI-1). So far, the functional relevance of tPA and PAI-1 for the engraftment of biomaterials remains largely unclear.

Materials and Methods
Using *in vivo* fluorescence microscopy, vessel density and leukocyte-endothelial cell interactions were evaluated on days 7, 10, and 14 after implantation of PPE implants in dorsal skinfold chambers in wild-type, tPA-/-, or PAI-1-/- mice. Tissue integration was analyzed on day 14 by measuring the force needed for mechanical removal of the implant out of the host tissue. Collagen deposition within the implant was assessed by second-harmonic imaging microscopy. PPE implants coated with recombinant or modified proteins were analyzed in a separate set of experiments. All surgical procedures were performed under anesthesia with ketamine (75 mg/kg b.w. i.p.) and xylazine (25 mg/kg b.w. i.p.). For statistical analysis, the ANOVA on ranks test followed by the Student-Newman-Keuls test was used.
Results
Vessel density and leukocyte-endothelial cell interactions in the host tissue did not significantly differ among experimental groups. In contrast, vessel density and leukocyte-endothelial cell interactions in the implant on days 7 and 10 after implantation as well as collagen deposition within the implant were significantly diminished in tPA- or PAI-1-deficient animals. Moreover, mechanical integration of the implant material was significantly attenuated in tPA or PAI-1 deficient animals. Conversely, surface coating with recombinant tPA or PAI-1 significantly accelerated implant vascularisation in wild-type mice, while leukocyte-endothelial cell interactions in the implant or the host tissue as well as mechanical integration of the implant were not significantly altered. Surface coating with a tPA mutant lacking its enzymatic activity did not significantly improve implant vascularisation.
Conclusions
Endogenous tPA and PAI-1 promote functional tissue integration of PPE biomaterial through effects on implant fibrovascularisation. In this context, tPA is thought to mediate these effects largely via its proteolytic properties. As a clinical perspective, surface coating with recombinant tPA or PAI-1 might provide a novel strategy for accelerating the vascularisation of PPE implants under unfavorable conditions for implantation.

Where applicable, the authors confirm that the experiments described here conform with The Physiological Society ethical requirements.

PCC421

Semi-automatic analyses of skin capillary density: validation and reproducibility studies

D. Muris[1,2], E. Gronenschild[3], M. Schram[1,2], . Karaca[1,2], C. Stehouwer[1,2] and A. Houben[1,2]

[1]Department of Internal Medicine, Maastricht University, Maastricht, Netherlands, [2]Cardiovascular Research Institute Maastricht (CARIM), Maastricht University, Maastricht, Netherlands and [3]Department of Psychiatry and Neurophychology, Maastricht University, Maastricht, Netherlands

Background: Skin capillaroscopy has been proven to be a valid tool to study microvascular function non-invasively in humans. Unfortunately, the analysis of capillary density from video-clips is very time-consuming, since this is done manually. This impedes the use of this technique in large-scale studies. We aimed to develop a (semi-)automated assessment of skin capillary density.
Methods: CapiAna (Capillary Analysis) is a newly developed semi-automatic image analysis application. The technique involves four steps: 1) movement correction, 2) positioning of the region of interest (ROI) and selection of the frame range, 3) automatic detection of capillaries, and 4) manual correction of detected capillaries. We assessed accuracy, reproducibility, and time-savings of the semi-automatic method as compared to the manual counting procedure. For this, finger skin capillary density was measured in 10 healthy participants (6 women; mean age 55.7 (49 – 68) years). First, to investigate agreement between the semi-automatic method and the manual procedure, we used linear regression and Bland-Altman analysis. Second, intra- and interobserver reproducibility of the semi-automatic method was assessed by calculating coefficients of variation (CV). For this, an experienced investigator semi-automatically counted the number of capillaries twice with a two week interval. In addition, a second experienced investigator semi-automatically counted the number of capillaries in exactly the same ROI. Finally, the difference in analysis-time between the semi-automatic and the manual method was assessed.
Results: Linear regression of the data resulted in a correlation (r) of 0.88 between the semi-automatic method and the manual procedure. The comparison between the semi-automatic method and the manual method by the Bland-Altman analysis, showed a bias of -3.9 capillaries/mm2 (<5%) and limits of agreement (± 2 SD) of +13.6 to -21.4 capillaries/mm2 (approximately 17%). The intra- and interobserver CV of the semi-automatic method were 2.0% and 5.4% respectively. Finally, the mean analysis time for the semi-automatic method was on average 30 minutes versus 90 minutes for the fully manual procedure.
Conclusion: In conclusion, we have developed a semi-automatic image analysis application for the assessment of skin capillary density. The results indicate that the semi-automatic method is in good agreement with the manual procedure, with a good correlation and with a small bias and reasonable limits of agreement. In addition, the semi-automatic method is more reproducible as compared to previous data for the manual procedure. Finally, analysis time with the semi-automatic method was significantly reduced. This new analysis technique offers opportunities for skin capillaroscopy as a tool to estimate microvascular function in large-scale studies.

Where applicable, the authors confirm that the experiments described here conform with The Physiological Society ethical requirements.

PCC422

Targeted lentiviral gene delivery to the vasculature using the magnetic microbubble technology

Y. Stampnik[1], F. Krötz[5], J. Pircher[1], K. Zimmermann[2], D. Eberbeck[6], M. Wörnle[4], M. Anton[3], U. Pohl[1] and H. Mannell[1]

[1]Walter-Brendel Centre of Experimental Medicine, Ludwig-Maximilians-University, Munich, Germany, [2]Institute of Pharmakology and Toxicology, Bonn University, Bonn, Germany, [3]Institute of Experimental Oncology and Therapy Research, Klinikum rechts der Isar, Technical University, Munich, Germany, [4]Nephrology, Medical Policlinic, Ludwig-Maximilians-University, Munich, Germany, [5]Interventional Cardiology, Starnberg Community Hospital, Munich, Germany and [6]Physikalisch-Technische Bundesanstalt, Berlin, Germany

Question: Achievement of site-specificity and potent gene transfer is a great therapeutic challenge. Here we investigated whether intravascular application of lentiviruses (LVs) coupled to magnetic microbubbles (MMBs) could efficiently establish a localised gene transfer *in vivo*. As a technique for tissue spe-

cific targeting the efficiency of a combination of trapping the MMBs by localized magnetic field (MF) application and their subsequent destruction by ultrasound (US) exposure in the mouse dorsal skin fold chamber model was tested.
Methods: Coupling of LVs containing a membrane GFP-fusion protein to MMBs was verified by flow cytometry. Mice (C57BL/6) were anesthetized with intraperitoneal injection of 3mg/kg body weight Midazolam, 0.03mg/kg body weight Fentanyl and 0.3mg/kg body weight Medetomidinhydrochloride in 0.9 % NaCl. *In vivo*, LV-coupled MMBs (1.6x106-1.5x107 infectious particles) were targeted to vessels of the mouse dorsal skin after intra-arterial injection by combined MF (1T) and US exposure (1MHz, 2W/cm2, DC50%, 30sec). Reporter gene expression (GFP) in the dorsal skin and in organs not exposed to MF and US was assessed by real-time PCR in tissue homogenates obtained 48-96h after treatment. Biodistribution of MNPs, to assess time of tissue clearance, was measured in homogenized organs by magnetic particle spectrometry 1h and 96h after injection of MMBs. Residual viral particle amount in blood, urine, stool and saliva 48-96h after treatment was analyzed with p24 ELISA and cell culture.
Results: LVs readily associated with MMB *in vitro* (20-fold increase in fluorescent units, $p<0.05$, ANOVA, n=3). *In vivo*, MMB specifically delivered the coupled genetic material to the dorsal skin after MF and US application. The achieved gene transfer efficiency of LV-associated MMB in the dorsal skin was enhanced 120-fold compared to pDNA-associated MMB, as assessed by reporter gene expression ($p<0.05$, t-test, LV n=4; pDNA n=10). MNP accumulation was detected mainly in the lung and liver (19±4% and 41±9% of administered dose respectively, n=5) 1h after treatment, which was strongly reduced 96h after treatment (0.2±0.07% and 0.3±0.09% of administered dose respectively, n=4). No residual LVs were detected in the collected biological samples 48-72h after LV-MMB application (n=3).
Conclusion: Magnetically-guided microbubbles were successfully applied as carriers for lentiviral gene vectors. Using the combination of magnetic targeting and US induced MB destruction, they allow for highly efficient and site-specific vascular gene transfer. Moreover, our data provides evidence that the coupled magnetic nanoparticles are effectively cleared from the organism indicating the aptitude of our method as a biocompatible therapy approach. In conclusion, the LV-associated MMB technology may represent a valuable tool for vascular gene therapy.

Where applicable, the authors confirm that the experiments described here conform with The Physiological Society ethical requirements.

PCC423

Waist circumference and blood pressure are associated with microvascular vasomotion in a healthy population: the Maastricht Study

D. Muris[1,2], M. Schram[1,2], A. Houben[1,2] and C. Stehouwer[1,2]

[1]Department of Internal Medicine, Maastricht University, Maastricht, Netherlands and [2]Cardiovascular Research Institute Maastricht (CARIM), Maastricht University, Maastricht, Netherlands

Background: Microvascular vasomotion, i.e. rhythmic changes in vascular diameter, is thought to play an important role in ensuring optimal delivery of nutrients and oxygen to tissue. Impaired microvascular vasomotion has been demonstrated in states of obesity and type 2 diabetes mellitus (T2DM) (i.e. decreased vasomotion), and hypertension (i.e. enhanced vasomotion). It is unclear however, which factors influence microvascular vasomotion. Therefore, we investigated associations between traditional risk factors and microvascular vasomotion in a healthy population.
Methods: We measured skin microvascular vasomotion in 241 healthy individuals (mean age 56 ± 8 years, 42% men, mean body mass index (BMI) 25.4 ± 3.6 kg/m2) enrolled in the Maastricht Study. We selected a healthy population without T2DM, hypertension, prior cardiovascular disease, or use of cardiovascular medication. Skin blood flow was measured with a laser Doppler probe at the dorsal side of the left wrist. Fast-Fourier transform analysis was performed to determine the five frequency components to the variability of the laser Doppler signal (i.e., endothelial, 0.01–0.02 Hz; neurogenic, 0.02–0.06 Hz; myogenic, 0.06–0.15 Hz; respiratory, 0.15–0.40 Hz; and heart beat, 0.40–1.60 Hz). The associations of age, sex, waist circumference, total-to-HDL cholesterol, 24-h mean arterial pressure (MAP), fasting plasma glucose, and cigarette smoking with microvascular vasomotion was analyzed by use of multiple linear regression analysis.
Results: Higher waist circumference and 24-h MAP were associated with a lower and higher total microvascular vasomotion, respectively. Per one standard deviation (SD) higher waist circumference total microvascular vasomotion was -0.17 SD (95%CI: -0.32; -0.03) lower. One SD higher 24-h MAP was independently associated with a 0.18 SD (0.04; 0.32) higher total microvascular vasomotion. We found no associations of microvascular vasomotion with age, sex, total-to-HDL cholesterol, fasting plasma glucose, or smoking. Analysis of the five frequency bands revealed that these results were largely attributable to the contributions of the endothelial, neurogenic, and myogenic components. Sub-analysis with exclusion of the obese subjects (BMI>30 kg/m2; n = 23) gave similar results.
Conclusion: In conclusion, in a healthy population waist circumference is inversely associated with microvascular vasomotion. In addition, blood pressure is directly associated with microvascular vasomotion. These data suggest that both elevations in waist circumference and blood pressure may affect microvascular vasomotion, and subsequently optimal nutrients delivery and tissue perfusion.

Where applicable, the authors confirm that the experiments described here conform with The Physiological Society ethical requirements.

PCD001

Cyclic AMP binds to the HCN2 C-terminus with higher affinity than cyclic GMP

S.S. Chow, F. Van Petegem and E. Accili

University of British Columbia, Vancouver, BC, Canada

Pacemaker HCN channels are found in a variety of excitable cells in heart and brain to control membrane potential. Both cAMP and cGMP facilitate HCN2 opening to the same extent, but the former is more potent (1,2). We asked if the greater cAMP potency, based on electrophysiological assay of its effects on channel opening, was due to better binding or to a more sensitive post binding event. Here, we purified the HCN2 C-terminus and measured binding affinity of cAMP and cGMP to the tetrameric form using isothermal titration calorimetry. We show that cGMP binds to the HCN2 C-terminus with negative cooperativity, as does cAMP, but with a lower affinity for single the high affinity site and the three low affinity binding sites. The overall lower affinity of cGMP binding to the

HCN2 channel explains its lower potency as compared to that of cAMP. Nevertheless, high affinity binding of cGMP, K_d < 1M, occurs in a range of concentrations that could be relevant *in vivo*.

DiFrancesco D, Tortora P. Direct activation of cardiac pacemaker channels by intracellular cyclic AMP. Nature 351, 145-7, 1991.

Zagotta WN, Olivier NB, Black KD, Young EC, Olson R, Gouaux E. Structural basis for modulation and agonist specificity of HCN pacemaker channels. Nature 425, 200-5, 2003.

Where applicable, the authors confirm that the experiments described here conform with The Physiological Society ethical requirements.

PCD002

Importance of Caveolin-1 in ouabain-induced Na^+K^+-ATPase signaling and cardiac hypertrophy but not in inotropic effect in mouse hearts

Y. Bai, J. Wu, D. Li and L. Liu

Biochemistry, University of Toledo, Toledo, OH, USA

Cardiac glycoside ouabain, when bound to cardiac Na^+K^+-ATPase (sodium pump), inhibits the pump leading to positive inotropy. It also stimulates sodium pump interacting with other proteins and activates several signaling pathways including phosphatidylinositol 3-kinases (PI3K) /Akt and ERK pathways (1,2). These events originate in the plasma membrane caveolae (3,4). In cardiomyocytes, caveolins 1, 2 and 3 are present. This study aims to examine the role of caveolin-1 in Na^+K^+-ATPase mediated cardiac signaling and cardiac function using wild type (WT) and caveolin-1 knockout (cav-1KO) mice. Ouabain-induced PI3K/Akt and ERK activation and - caused cardiac hypertrophy were reduced markedly in cav-1 KO cardiomyocytes. Additionally, association of the Na^+K^+-ATPase α1 subunit and caveolin-3 was decreased in cav-1 KO cardiomyocytes. Moreover, ouabain-induced interaction of the α1 subunit of Na^+K^+-ATPase and PI3K was also reduced in cav-1 KO cardiomyocytes. Deletion of cav-1 reduced protein content of PI3K/Akt and the β1 subunit of Na^+K^+-ATPase in caveolar fractions in cardiomyocytes. Transient ouabain infusion increased cardiac contractility in WT and KO mice monitored through cardiac catheterization. Surprisingly, the effect of ouabain on cardiac contractilities was not reduced when cav-1 was absent. This was further confirmed with isolated working hearts from WT and cav-1 KO mice. Our data indicate that ouabain-induced cardiac signaling and hypertrophy is mediated by a mechanism through interaction of cav-1 and Na^+K^+-ATPase. However, ouabain exerted caveolin-1-independent cardiac contractility.

Bai Y, Morgan EE, Giovannucci DR, Pierre SV, Philipson KD, Askari A, Liu L.(2012) Different roles of the cardiac Na+/Ca2+ exchanger in ouabain-induced inotropy, cell signaling, and hypertrophy. Am J Physiol Heart Circ Physiol. Nov 30. [Epub ahead of print] PMID: 23203972

Liu, L., Zhao, X., Pierre, S.V., and Askari, A. (2007) Association of PI3K-Akt signaling pathway with digitalis-induced hypertrophy of cardiac myocytes. Am J Physiol Cell Physiol. 293(5):C1489-497. 2007

Liu, L., Mohadmmadi, K., Aynafshar, B., Wang, H., Li, D., Liu, J., Ivanov, A., Xie, Z., and Askari, A. (2003) Role of caveolae in the signal transducing function of Na+/K+-ATPase. Am. J. Physiol. Cell. Physiol. 284:C1550-C1560.

Liu, L. and Askari, A.(2006) The beta-subunit of cardiac Na+/K+-ATPase dictates the concentration of the functional enzyme in caveolae. Am J Physiol Cell Physiol 291: C569-C578.

This work was supported by National Heart, Lung, and Blood Institute Grant HL-36573.

Where applicable, the authors confirm that the experiments described here conform with The Physiological Society ethical requirements.

PCD003

Identification a pool of cardiac phospholemman that does not interact with the sodium pump

K. Wypijewski[1], J. Howie[1], L. Reilly[1], K. Aughton[2], M.J. Shattock[2], S. Calaghan[3] and W. Fuller[1]

[1]Division of Cardiovascular & Diabetes Medicine, College of Medicine Dentistry & Nursing, University of Dundee, Dundee, UK, [2]Cardiovascular Division, King's College London, London, UK and [3]School of Biomedical Sciences, Faculty of Biological Sciences, University of Leeds, Leeds, UK

Phospholemman (PLM), the principal quantitative sarcolemmal substrate for protein kinases A and C in the heart, regulates the cardiac sodium pump. Much like phospholamban, which regulates the sodium pump-related calcium ATPase SERCA, PLM is reported to oligomerise. We investigated subpopulations of PLM in adult rat ventricular myocytes based on phosphorylation status.

Calcium-tolerant ventricular myocytes (ARVM) were isolated from adult male Wistar rats (200-250g) by retrograde perfusion of collagenase in the Langendorff mode. Myocytes were left to recover for 2 hours at 35ºC before experiments.

Coimmunoprecipitation identified two pools of PLM: one not associated with the sodium pump phosphorylated at serine 63 (S63), and one, associated with the pump, both phosphorylated at serine 68 and unphosphorylated. Phosphorylation of PLM at S63 following activation of PKC did not abrogate association of PLM with the pump, so its failure to associate with the pump was not due to phosphorylation at this site. All pools of PLM co-localised to cell surface caveolin-enriched microdomains with sodium pump α subunits, despite the lack of caveolin-binding motif in PLM. Mass spectrometry analysis of phosphospecific immunoprecipitation reactions revealed no unique protein interactions for S63- phosphorylated PLM, and crosslinking reagents also failed to identify any partner proteins for this pool. The sodium pump α subunit co-immunoprecipitated with PP2A from ARVM lysates. Since PLM-S63 is the only phosphorylation site in PLM dephosphorylated by PP2A, this likely explains the lack of S63-phosphorylated PLM associated with the pump.

In lysates from hearts of heterozygous transgenic animals expressing wild type and unphosphorylatable PLM, S63- phosphorylated PLM co-immunoprecipitated unphosphorylatable PLM, therefore confirming the existence of PLM multimers.

Hence we report the existence of a subpopulation of PLM that interacts only with other PLM molecules and not with the Na pump, with a unique phosphorylation status driven by differential proximity of protein phosphatases. Like phospholamban regulation of SERCA, PLM exists as a sodium pump inhibiting monomer and an un-associated oligomer. The distribution of different PLM phosphorylation states to different pools may be explained by their differential proximity to protein phosphatases, rather than a direct effect of phosphorylation on PLM association with the pump.

This work was supported by the grants from the British Heart Foundation, RG/12/4/29426 and PG/10/92/28650

Where applicable, the authors confirm that the experiments described here conform with The Physiological Society ethical requirements.

PCD004

Proteome-wide characterisation of lipid raft proteins in adult rat ventricular myocytes

K. Wypijewski[1], M. Tinti[2], S.C. Calaghan[3] and W. Fuller[1]

[1]Division of Cardiovascular & Diabetes Medicine, College of Medicine Dentistry & Nursing, University of Dundee, Dundee, UK, [2]College of Life Sciences, University of Dundee, Dundee, UK and [3]School of Biomedical Sciences, Faculty of Biological Sciences, University of Leeds, Leeds, UK

The lipid raft concept proposes that membrane environments enriched in cholesterol and sphingolipids cluster certain proteins and form platforms to integrate cell signalling. In cardiac muscle, caveolin-enriched rafts concentrate signalling molecules and ion transporters, and therefore play a vital role in adrenergic regulation of cardiac excitation-contraction coupling. The aim of this project was to define the proteome of cardiac lipid rafts, and to investigate dynamic changes in the protein constituents of rafts following activation of α1, β1 and β2 adrenoceptors (AR).

Calcium-tolerant ventricular myocytes (VM) were isolated from the hearts of adult male Wistar rats by retrograde perfusion of collagenase. Myocytes were left to recover for 2 hours at 35ºC before experiments. VM were treated with methyl-β-cyclodextrin (MβCD) to deplete cholesterol and disrupt lipid rafts. Rafts were prepared from MβCD-treated and control cell lysates using a standard discontinuous sucrose gradient. Buoyant rafts were harvested, pelleted, resolubilised, alkylated, digested and labeled with iTRAQ reagents, and proteins identified by LC-MS/MS on a LTQ Orbitrap Velos Pro. Proteins were defined as lipid raft resident if they were consistently depleted from the raft fraction following MβCD treatment, and as contaminants (principally mitochondrial) if they were not.

We typically identified 600-850 raft proteins per experiment, of which 254 were defined as high-confidence lipid raft residents. Functional annotation clustering indicates that cardiac lipid rafts are enriched in integrin signalling, guanine nucleotide binding, ion transport, and insulin signalling clusters. The presence of selected proteins of each group in the lipid rafts was validated by immunoblotting.

In order to define changes in cardiac lipid rafts during adrenergic signalling, field-stimulated VM were treated with α- (10μM phenylephrine, 10μM atenolol), β1- (100nM isoprenaline, 100nM ICI118,551) and β2- (10μM zinterol, 300nM CGP20712A) AR agonists for 10 min prior to lysis and preparation of lipid rafts. Following iTraq analysis, raft resident proteins showing a change in abundance in a minimum 3 out of 4 experiments were selected. β1 AR activation is associated with a decrease in abundance of PKA RIIα and an increase in abundance of cavin isoforms in cardiac lipid rafts. β2 AR stimulation increases the abundance of G protein and L-type Ca channel subunits in cardiac rafts.

In conclusion, we have identified 254 lipid raft proteins in adult rat cardiac myocytes and shown for the first time that these domains are re-organised on an acute timescale in response to β-AR stimulation. Dynamic changes in certain raft components may be necessary to ensure a rapid and high fidelity response to adrenergic stimulation in cardiac muscle.

This work was supported by a grant from the British Heart Foundation, PG/10/92/28650

Where applicable, the authors confirm that the experiments described here conform with The Physiological Society ethical requirements.

PCD005

Metabolic stress alters the balance between palmitoylation and glutathionylation of the Na pump regulatory protein phospholemman

J. Howie[1], J. Swarbrick[1], M.J. Shattock[2] and W. Fuller[1]

[1]Cardiovascular and Diabetes medicine, University of Dundee, Dundee, UK and [2]Cardiovascular Division, King's College, London, UK

Acute regulation of the cardiac Na pump by extracellular stimuli is crucial in allowing the heart to match its output to systemic requirements. Phospholemman (PLM) regulates the cardiac Na pump. Unphosphorylated PLM inhibits the pump, and PLM phosphorylation causes pump activation. Phospholemman is also palmitoylated at cysteines 40 and 42, which inhibits the pump, and glutathionylated at cysteine 42, which relieves oxidative inhibition of the pump.

Since PLM may be palmitoylated and glutathionylated at the same cysteine, we investigated competition between these post-translational modifications during oxidative and metabolic stress in freshly dispersed adult rat ventricular myocytes (ARVM, isolated from adult male Wistar rats) and FT293 cells stably expressing wild type (WT), C40A and C42A PLM. Palmitoylation was measured by resin-assisted capture of acylated proteins followed by quantitative immunoblotting, and glutathionylation by streptavidin affinity purification after loading cells with biotinylated glutathione ethyl ester. Data are presented as mean±SEM, with differences analysed by t-test.

Acute exposure of ARVM and FT293 cells expressing wild type PLM to hydrogen peroxide (1μM–10mM, 30min at 37˚C) was without effect on PLM palmitoylation. Metabolic stress was induced in FT293 cells expressing WT PLM by 18 hours culture in media supplemented with glucose (HG, 25mM) and / or palmitic acid (HP, 0.4mM). Although HG or HP alone were without effect on PLM palmitoylation, combined HG/HP caused a substantial reduction in PLM palmitoylation (5.7±2.4 fold reduction compared to untreated cells, n=4, $p<0.05$). Glutathionylated PLM was undetectable in untreated FT293 cells expressing WT PLM, but readily detectable following 18 hours HG/HP culture.

In order to identify which palmitoylation site in PLM is susceptible to metabolic stress, FT293 cells expressing palmitoylation site mutants were cultured in HG or HG/HP conditions. HG/HP culture induced a substantial reduction in palmitoylation of C40A PLM (3.0±0.8 fold reduction compared to untreated cells, n=3, $p<0.05$), but was without effect on the palmitoylation of C42A PLM.

In conclusion, metabolic but not acute oxidative stress promotes glutathionylation of PLM cysteine 42 with a concomitant reduction in palmitoylation at this site. Metabolic stress may therefore influence Na pump activity by promoting glutathionylation over palmitoylation of PLM. The cellular outcome of HG/HP stress is mitochondrial free radical production, yet exogenous hydrogen peroxide is without effect on PLM palmitoylation, so the subcellular location at which oxidising species are generated or the duration of an oxidant stress are important determinants of the balance between PLM palmitoylation and glutathionylation.

This work was supported by a grant from the British Heart Foundation (RG/12/4/29426).

Where applicable, the authors confirm that the experiments described here conform with The Physiological Society ethical requirements.

PCD006

Kolaviron, a biflavonoid of Garcinia kola seed offered cardioprotection against ischaemic/reperfusion injury by up-regulation of pro-survival and down-regulation of apoptotic signaling pathways

A.A. Oyagbemi[1,2], E.O. Farombi[2,1], J.D. Bester[2,3] and A.J. Esterhuyse[2,3]

[1]Veterinary Physiology, Biochemsitry and Pharmacology, University of Ibadan, Ibadan, Oyo, Nigeria, [2]Drug Metabolism and Toxicology Unit, Department of Biochemistry, College of Medicine, University of Ibadan, Ibadan, Oyo, Nigeria and [3]Oxidative Stress Research Centre, Department of Biomedical Sciences, Cape Peninsula University of Technology, Bellville, 7535, South Africa, Cape Town, Western Cape, South Africa

Possible cardioprotective effect of Kolaviron (KV) administration and the molecular mechanism (s) involved in ischaemic/reperfusion injury of isolated rat hearts were assessed. Twenty rats were used for this study. They were grouped into ten rats of group of two. Rats in group I received 2ml/kg of corn oil (vehicle) while animals in groups II received 200 mg/kg body weight of Kolaviron (KV) for four weeks respectively. Isolated rat hearts were stabilized for 5 minutes on Langendorff, perfused on working heart model for 10 minutes and subjected to global ischaemia for 15 minutes followed by 25 minutes reperfusion. Antioxidant enzymes, markers of oxidative stress and western blot analyses were carried out on snap-frozen heart tissues. There was significant ($p<0.05$) increase in superoxide dismutase (SOD), catalase (CAT) and glutathione peroxidase (GPx), oxygen radical absorbance capacity (ORAC) and concomitant significant ($p<0.05$) decrease in malondialdehyde (MDA) and intracellular reactive oxygen species (ROS) in isolated rat hearts of animals that received KV compared to the control. Western blot analysis revealed significant up-regulation of Akt/PKB, p- Akt/PKB, HSP27, p-HSP27 and down-regulation of p38 MAPK, Caspase 3, cleaved Caspase 3and cleaved PARP. Taken together, KV offered cardioprotection by enhancing the expression of pro-survival signaling pathway and abrogation of apoptotic pathway in isolated rat hearts subjected to ischaemic/reperfusion injury

Where applicable, the authors confirm that the experiments described here conform with The Physiological Society ethical requirements.

PCD007

Targeting ventricular arrhythmias: MKK7 a remarkable player?

S.K. Chowdhury[1], M. Zi[2], W. Liu[1,2], H. Tsui[2], Y. Wang[2], H. Shiels[1], E.J. Cartwright[2], M. Lei[2] and X. Wang[1]

[1]Faculty of Life Sciences, University of Manchester, Manchester, UK and [2]Cardiovascular Research Group, School of Biomedicine, Faculty of Medical & Human Sciences, University of Manchester, Manchester, UK

Heart failure and cardiac arrhythmias are known consequences of ventricular remodelling. Key signalling pathways responsible for such hypertrophic remodelling include the mitogen-activated protein (MAP) kinase cascade. MAP kinase kinase 7 (MKK7), positioned at a bottleneck of this stress-responsive pathway, is known to be vital for survival under hypertrophic stimulation (1,2).

To assess the role of MKK7 in arrhythmogenesis, ventricular cardiomyocyte specific MKK7 knockout (MKK7CKO) and littermate wild-type mice (male, 8-12 wks old) were subjected to different stress stimuli. Chronic Angiotensin-II (Ang-II, 0.7μgm/kg/min) stimulation for 14-days using subcutaneous mini-osmotic pumps and transverse aortic constriction (TAC) for 3-days (3% Isoflurane or Ketamine-Xylazine anaesthesia, Buprenorphine 0.1mg/kg analgesia) were provided to mimic chronic hypertension and acute pressure overload, respectively. Mean (± S.E.M.) values were appropriately compared by ANOVA or paired T-tests. In both cases, MKK7CKO mice had augmented cardiac hypertrophy under stress, evidenced by increases in heart weight / tibia length ratios (n=9-16/group) and cardiomyocyte cross-sectional areas (n=3-4/group). Transthoracic echocardiography confirmed an associated comparative decrease in left ventricular contractile function (n=8-15/group). Masson's trichrome staining revealed 3-4 folds increases in ventricular fibrosis in the MKK7CKO mice compared to wild-types receiving similar stimuli (n=3-4/group).

A striking finding was the electrical remodelling featuring about 25-30% longer rate-corrected mean QT (Bazett's) intervals in the stressed MKK7CKOs (n=8-12/group) *in-vivo* ECG recorded under terminal anaesthesia (Tribromoethanol, 200mg/kg). Programmed electrical stimulation induced more arrhythmias in MKK7CKOs than controls following stress. Between S1S2 delays of 100-40ms, 78% Ang-II treated MKK7CKOs generated ventricular arrhythmias or premature contractions, compared to 10% similarly treated wild-types and none of the untreated mice (n=8-10/group). Ventricular effective refractory periods increased after TAC, more so in MKK7CKOs, but without any statistical significance (n=8-12/group). Molecular analysis of whole ventricle extracts revealed, MKK7CKOs undergoing TAC had reduced versatile membrane-adapter Ankyrin-B and inward-rectifier potassium channel subunit Kir6.2 transcript (n=6-9/group) and protein levels (n=3-5/group) than similarly-treated wild-type mice.

This study reveals the significant role of MKK7 in preserving the functional integrity and rhythmicity of the heart, as well as indicating novel and therapeutically promising signalling regulation of hearts electrical activities under hypertrophic stress.

Wang X, Destrument A, Tournier C. Physiological roles of MKK4 and MKK7: insights from animal models. Biochimica et biophysica acta. 2007 Aug;1773(8):1349–57

Liu W, Zi M, Chi H, Jin J, Prehar S, Neyses L, et al. Deprivation of MKK7 in cardiomyocytes provokes heart failure in mice when exposed to pressure overload. Journal of molecular and cellular cardiology. Elsevier Ltd.; 2011 Apr;50(4):702–11

The Commonwealth Scholarship Commission, UK.

Where applicable, the authors confirm that the experiments described here conform with The Physiological Society ethical requirements.

PCD008

Cardioprotective adaptation of rats to chronic hypoxia is accompanied by changes in myocardial adenylyl cyclase signaling

K. Hahnova[1], B. Volfova[1], L. Hejnova[1], J. Neckar[2], F. Kolar[2] and J. Novotny[1]

[1]Department of Physiology, Charles University, Faculty of Science, Prague, Czech Republic and [2]Department of Developmental Cardiology, Academy of Sciences, Institute of Physiology, Prague, Czech Republic

It is known that cardiovascular diseases are the leading cause of morbidity and mortality in the western world. Recently it was observed that adaptation of myocardium to chronic hypoxia can contribute to the improvement of ischemic tolerance of myocardium. Chronic hypoxia can induce a wide range of adaptive changes in myocardium, which could be considered as cardioprotective, but exact molecular mechanism of these adaptive changes is still unclear. Adaptation to chronic hypoxia leads to increased activity of the sympathetic nervous system, thus increasing catecholamine levels in the body. The increased level of catecholamines and their effect on β-adrenergic signaling could contribute to the development of cardioprotection. Beta-adrenergic receptors (β-ARs) form an interface between the sympathetic nervous system and cardiovascular system and therefore they act as effective regulators of cardiac activity, which can be modulated by sympathetic transmitters.

The aim of this study was to pursue changes in the β-adrenergic signaling in rat myocardium after adaptation to two different regimens of hypoxic conditions: 1/ intermittent normobaric hypoxia - INH/R (23 h hypoxia, 1 h reoxygenation) and 2/ continuous normobaric hypoxia - CNH (24 h hypoxia). We assessed the effect of adaptation to hypoxia on the total amount of β-ARs, the ratio of β-ARs subtypes (β1-ARs to β2-ARs) and activity of adenylyl cyclase (AC) in the left (LV) and right ventricles (RV). The results determined in the hearts from rats (male, 250-350 g, n=10 in each group) adapted to hypoxia were compared with those obtained in the corresponding normoxic animals.

It was found that adaptation to INH/R and CNH was accompanied by a significant decrease (about 25%) in the total number of β-ARs in the RV. Although the statistical analysis (one-way ANOVA) revealed significant changes (decrease) in the ratio of β1-ARs to β2-ARs only for CNH model in the RV, there was a clear downward trend in the transcription and expression of β1-ARs in the RV from rats adapted to CNH or INH/R. Activity of AC was also affected by the adaptation of rats to INH/R and CNH. Whereas AC activity stimulated by different activators (GTPγS, NaF or forskolin) was increased in the LV, it was decreased in the RV. These results indicate that AC signaling may play an important role in the adaptive process to chronic hypoxia.

Where applicable, the authors confirm that the experiments described here conform with The Physiological Society ethical requirements.

PCD009

Chronic morphine treatment alters the adenylyl cyclase signaling system of the rat heart

J. Skrabalova[1], B. Volfova[1], J. Novotny[1], L. Hejnova[1], J. Neckar[2] and F. Kolar[2]

[1]Department of Physiology, Charles University in Prague, Faculty of Science, Prague, Czech Republic and [2]Department of Developmental Cardiology, Academy of Sciences, Institute of Physiology, Prague, Czech Republic

Morphine is a very potent analgesic which is widely used for treatment of both acute and chronic pain. This drug is highly addictive and its repeated use may cause dependence. Cellular effects of morphine are mediated by opioid receptors (ORs) and their cognate Gi proteins. Since all the basic components of opioid signaling system are present in heart tissue, it is conceivable that morphine may influence function of this organ. Interestingly, it has been observed that morphine can significantly limit tissue damage that occurs during myocardial ischemia (Schultz et al., 1996), but the molecular mechanisms by which morphine acts on the heart are still very poorly understood.

The aim of this study was to investigate the effects of chronic (10- and 27-day) administration of low (1 mg/kg/day, i.m.) and high (10 mg/kg/day, i.m.) doses of morphine to rats (male, 290-370 g, n=10 in each group) on the expression of selected G-protein coupled receptors (GPCRs), G-protein subunits and the expression and activity of adenylyl cyclase (AC) in the heart. Whereas 27-day morphine treatment decreased the expression of κ-ORs by about 18 % (Student t-test), 10-day treatment had no effect. Determination of the expression of β-adrenergic receptors by saturation binding studies showed an appreciable increase by 57 % in the total number of these receptors after 27-day treatment with high doses of the drug. Morphine did not affect the expression of any of the selected G-protein subunits (Gsα, Gi/oα, Gzα, Gq/11α and Gβ), but high doses of the drug significantly (by 50-80 %) elevated the amount of AC isoforms type V/VI. Subsequently, the expression level of AC was reduced in proportion to the time after discontinuation of morphine administration. Low doses of morphine increased by 23 % the expression of AC type V/VI only after 27-day administration. These changes were accompanied by increase in AC activity stimulated by Mn2+ (66 %), NaF (91 %), forskolin (73 %) and isoprenaline (105 %). On the other hand, the ability of OR agonists DADLE and U-50488 to inhibit forskolin-stimulated AC activity was rather decreased.

Our results indicate that chronic morphine treatment does not primarily induce changes in the amount of myocardial κ-ORs and G-proteins, but significantly enhances the expression of AC V/VI. Increased amount of AC may at least partially explain the observed supersensitization of the enzyme. It can be concluded that prolonged morphine exposure may strongly affect myocardial β-adrenergic receptor-mediated AC signaling.

Schultz JE et al. (1996). Circ. Res. 78, 1100-1104.

Where applicable, the authors confirm that the experiments described here conform with The Physiological Society ethical requirements.

PCD010

Effects of exercise training on cardiac myocytes and fibroblasts intercellular coupling

M.M. Alves, P. Kaur, J.B. Moreira, K. Solvang-Garten, H. Morten, R. Rosbjorgen, G. Silva and U. Wisloff

ISB, NTNU, Trondheim, Norway

Cardiac fibroblasts (CF) are emerging as key components of normal cardiac function, as well as the response to stressors and injury, by interacting with cardiomyocytes (CM) via paracrine mechanisms and direct cell–cell interactions (Chilton et al, 2007; Kakkar and Lee, 2010). We have previously shown that in a direct contact cell-to-cell or by the use of cell inserts, CF leads to reduced calcium contractility and prolonged time of calcium decay in sedentary rats. We aimed to test on CF and CM interaction, a program of exercise training (TR), which mimics some therapeutics agents, and has been shown to improve cardiomyocytes (CM) contractility (Wisloff et al, 2001). Adult Female Spague-Dawley rats, n=35, weighting 220-350g, were given inhalational anesthesia with isoflurane (5% for 2-3 min). CM and CF were isolated as previously described with minor modifications for CF centrifugation time (Guatimosim et al, 2002). We used a noncontact protocol by keeping freshly isolated cardiomyocytes in conditioned media from CF of trained (TR) and sedentary (SED) rats, CF were used when they achieved 60-70% of confluence. Epifluorescence measurements (using Fura 2) have shown reduced Ca2+ transient amplitude in cardiomyocytes (n>7 CM for each treatment) (Control: 0,198±0.02, vs SED FB: 0,118±0,007, vs TR FB: 0,095±0,008, fura ratio, $p<0.05$,) and reduced shortening (Control: 6,2±1.1, vs SED FB: 2,23±0.29, vs TR FB: 2.52±0,56, % of shortening, $p<0.05$), but not diastolic calcium removal as measured as time interval to 50% decay of Ca2+ concentration (Control: 0.176±0.01, vs SED FB: 0.222±0.01, vs TR FB: 0.223±0,03, seconds, $p<0.05$) when CM were alone (Control) or together with SED FB or TR FB, for 18h. Values are means ± S.E., compared by ANOVA. Conditioned media did not have altered pH compared to control media (approximately 7.67 and 7.68, pH, respectively). We initially conclude that CF from SED and TR rats have paracrine secretion which leads to reduced CM maximum rate of shortening and reduced Ca2+ transient amplitude and this does not seem to be related to altered media pH.

Chilton, L et al. J Physiol. 2007; 583.1: 225–236.

Wisløff, U et al. Cardiovasc. Res. 2001; Jun; 50:495-508.

Guatimosim, S et al. J. Mol. Cell Cardiol. 2002; Aug; 34(8):941-50. Review.

Kakkar, R and Lee, R. Circulation Res. 2010; 106: 47-57 2010. Review.

K.G. JEBSEN, NTNU

Where applicable, the authors confirm that the experiments described here conform with The Physiological Society ethical requirements.

PCD011

Na+/K+-ATPase activities in normotensive human subjects with and without family history of hypentension in south - Western Nigeria

O.S. Oyekunle[1] and A.O. Soladoye[2]

[1]Physiology, Ladoke Akintola University of Technology,, Ogbomoso, Oyo, Nigeria and [2]Pyhsiology Department, University of Ilorin, Ilorin, Kwara, Nigeria

Hypertension is a global cardiovascular diseases where treatment remains a major financial burden (Lloyd-Jones et al., 2009). Some studies have identified important aetologic factors while others on mechanisms focused on genetic factors and ATPase activities (Manesh et al., 1987) but the findings are inconclusive. Therefore, erythrocyte Na+/ K+ -ATPase activities were measured in 99 normotensive human subjects aged 16-30 years with and without family history of essential hypertension (FH/WF H). Na+/ K+ -ATPase activities were measured using inorganic phosphate (Pi) released from ATP hydrolysis. The level of Pi was determined by the method of Fiske and Subbarow (1925). Only subjects who consented and were medically fit were allowed in the study. Erythrocyte membrane preparation and protein estimation were determined using standard procedure (Hamlyn and Duffy, 1978; Stewart, 1974). Mean values + S.E.M were recorded in this study and statistical analysis was by student's t-test. The results showed that in males with FH, Na+/ K+-ATPase activities were lower (13.46 + 1.242, n=35) than corresponding values WFH males (16.72+ 1.831, n= 64; $p<0.0001$). The Na+/K+-ATPase values in FH females and WFH females were not different. Furthermore, the systolic and diastolic blood pressure (SBP & DBP) values were not significantly different. It is therefore concluded that Na+/K+-AT Pase activities in hypertensive subjects with FH and WFH groups are familial and may underlie membrane cation transport in these subjects.

Fiske, C. H. and Subbarow, Y. (1925). The colometric determination of phosphorus. J. Biol. Chem. 68: 375-400.

Hamlyn, J.M and Duffy, T. (1978): Direct stimulation of human erythrocyte membrane (Na+, K+-), Mg2+-AtPase activity in viro by physiological concentrations of d-aldosterone. Biochem, Biopys. Res. Commun. 84:458-464.

Lloyd-Jones, D, Adams, R, and Carnethon, M. et al. (2009). A report from the American Heart Association Statistics Committee and Stroke Statistics Subcommittee. Circulation. 119: 21-181

Manesh, K. F., Venkataraman, K., Samant, D. R. and Gadgil, U. G. (1987): Effects of diltiazem on cation transport across erythrocyte membranes of hypertensive humans. Hypertension, 9:18-23.

Stewart, D. J. (1974): Sensitive automated methods for phosphate and (Na+ +K+)-ATpase. Analytical Biochemistry 62 (2): 349-364

1.Mr. James Adegboye, Chemical Pathology Scientist, Bowen University Teaching Hospital (Baptist Medical Centre), Ogbomoso. Nigeria.

2. All students of College of Health Sciences, Ladoke Akintola University of Technology, Ogbomoso, who participated in the research.

3. Dr. Olufemi Alamu, Department of Anatomy and Cell Biology, Faculty of Basic Medical Sciences, Ladoke Akintola University of Technology, Ogbomoso.

Where applicable, the authors confirm that the experiments described here conform with The Physiological Society ethical requirements.

PCD012

The soluble guanylate cyclase activator BAY 58-2667 protects against morbidity and mortality in endotoxic shock by recoupling organ systems

B. Vandendriessche[1], E. Rogge[1], V. Goossens[1], P. Vandenabeele[1], J. Stasch[2], P. Brouckaert[1] and A. Cauwels[1]

[1]Department for Molecular Biomedical Research, VIB - Ghent University, Ghent, Belgium and [2]Institute for Cardiovascular Research, Bayer HealthCare, Wuppertal, Germany

Sepsis and septic shock are associated with mortality rates of up to 50-70% and the majority of patients die due to complications of multiple organ failure. The cyclic GMP (cGMP) producing enzyme soluble guanylate cyclase (sGC) is crucially involved in the maintenance of (micro)vascular homeostasis, cardiac function and, consequently, organ function. Reactive oxygen species (ROS) can inactivate sGC by oxidizing the iron in the haem group, the resulting haem-free sGC can be reactivated by BAY 58-2667 (Cinaciguat) (Evgenov et al., 2006). We tested BAY 58-2667 in a murine model of endotoxic shock because of its assumed specificity for tissues that are suffering from (metabolic) hypoxia and oxidative stress. To induce shock, mice were injected i.v. with 190-220 μg E. coli lipopolysaccharide (LPS). We report that post-treatment with BAY 58-2667 can protect against endotoxic shock-induced progressive hypothermia (compared to vehicle controls, repeated measure ANOVA, n = 15) and mortality (66% vs. 0% survival rate for vehicle controls, log-rank test, n = 15), which was associated with reduced cardiomyocyte apoptosis (assessed by TUNEL assay, 77.9 ± 11.73 (mean ± SEM) vs. 47.9 ± 8.9 TUNEL positive cells, normalized over surface area, one-way ANOVA). The sGC stimulator BAY 41-2272 and phosphodiesterase 5 (PDE5) inhibitor Sildenafil did not have a beneficial effect on either LPS-induced morbidity or mortality. Furthermore, we assessed mean arterial pressure (MAP), heart rate (HR) and BP variability (BPV) indices continuously in conscious, freely moving mice. Mice were anaesthetized with isoflurane and PA-C10 radio-transmitters (Data Sciences International) were implanted. MAP and HR were both significantly decreased for 180 min post-treatment compared to vehicle controls (linear mixed model). Linear (normalized low frequency, LF (nu)) and nonlinear (detrended fluctuation analysis, DFA) indices of BPV were calculated in Labchart (ADInstruments) and software from the PhysioNet toolkit (Goldberger et al., 2000). The difference in BPV index trends was examined 40 min pre-treatment vs. 40 min post-treatment. Treatment with BAY 58-2667 increased LF (nu) and DFA scaling factors, compared to vehicle controls (n = 4), indicative for improved communication between the autonomic nervous system and the heart. Our results emphasize the pivotal role of sGC signaling in endotoxic shock. Stabilization of sGC function with BAY 58-2667 can prevent mortality induced by endotoxic shock when given in the correct treatment window, which probably depends on the dynamics of the haem-free sGC pool, in turn influenced by ROS production. We speculate that the effect of BAY 58-2667 on microcirculatory perfusion and (metabolic) hypoxia supports organ function by recoupling inter-organ communication pathways.

A. L. Goldberger et al., PhysioBank, PhysioToolkit, and PhysioNet: components of a new research resource for complex physiologic signals., Circ 101, E215–20 (2000).

O. V Evgenov et al., NO-independent stimulators and activators of soluble guanylate cyclase: discovery and therapeutic potential., Nat Rev Drug Disc 5, 755–68 (2006).

Where applicable, the authors confirm that the experiments described here conform with The Physiological Society ethical requirements.

PCD013

Glucagon-like peptide-1 eluting mesenchymal stem cells reduce apoptosis and improve viability of ischemic human cardiomyocytes in vitro

E.J. Wright[1], C. Wallrapp[2], A.L. Lewis[3], M. Kassem[4], N. Malik[1] and C.M. Holt[1]

[1]Institute of Cardiovascular Science, University of Manchester, Manchester, UK, [2]CellMed AG, Alzenau, Germany, [3]Biocompatibles UK Ltd, Farnham, UK and [4]KMEB, University of Southern Denmark, Odense, Denmark

Aims: Cell therapy is a promising treatment for myocardial infarction. Increasingly, cells are being modified to enhance secretion of cardioprotective factors to improve efficacy in vivo. This study utilized human mesenchymal stem cells (MSCs) that were immortalized and engineered to secrete a fusion protein of Glucagon-like Peptide-1 (GLP-1). We have previously shown a cardioprotective effect of this therapy in vivo (1). To investigate direct paracrine effects on apoptosis, these cells were tested against ischemic adult human cardiomyocytes (hCMs) in vitro.

Methods and Results: hCMs underwent ischemia for 1 hour before incubation with either: MSC conditioned media, MSC+GLP-1 conditioned media, 100nM GLP-1, 100nM Exendin-4 or normal media. Cells were pre-incubated with the inhibitors Exendin-9, Wortmannin or U0126 to investigate pathways involved. After 24 hours, apoptosis was measured using TUNEL staining (n=8). After 48 hours, cell viability was measured using trypan blue to identify live/dead cells (n=4). MSC+GLP-1 conditioned media significantly reduced TUNEL+ cells compared to media alone (media: 6.14±0.48%, GLP-1: 3.96±0.56%; Ex-4: 5.1±1.22%; MSC media: 3.71±0.56%; MSC+GLP-1 media: 2.97±0.4%, P<0.05). All agonists reduced the number of dead cells (trypan blue stained) compared to normal media (media: 19.05±6.80%; GLP-1: 5.05±0.54%; Ex-4: 7.88±0.39%; MSC media: 5.41±0.39%; MSC+GLP-1 media; 2.58±1.65%, P<0.05). All agonists increased cell viability, normalised to media alone (GLP-1: 8.40±5.77%; Ex-4: 25.48±6.85%; MSC: 26.29±14.21%; MSC+GLP-1: 26.95±7.14%, P=NS). All antagonists/inhibitors appeared to partially block the effects on apoptosis and cell viability.

Conclusions: MSC+GLP-1 conditioned media had a significant beneficial effect on both apoptosis and viability of ischemic hCMs in vitro, greater than MSC conditioned media. This effect appeared to be mediated through the GLP-1R and the PI3K and ERK1/2 pathways.

1. Wright EJ, Farrell KA, Malik N, Kassem M, Lewis AL, Wallrapp C, et al. Encapsulated glucagon-like Peptide-1-producing mesenchymal stem cells have a beneficial effect on failing pig hearts. Stem Cells Transl Med 2012;1(10):759-69.

We thank Biocompatibles UK Ltd and MRC UK for funding this project.

Where applicable, the authors confirm that the experiments described here conform with The Physiological Society ethical requirements.

PCD015

Investigating the role of epicardial fat as an imaging biomarker in type-2 diabetes

D.B. Cassidy[1], S.J. Gandy[3,4], S. Duce[1], F. Khan[2], P. Martin[3], R.S. Nicholas[3,4] and J.G. Houston[1,3]

[1]The Institute of Cardiovascular Research, University of Dundee, Dundee, UK, [2]Vascular & Inflammatory Diseases Research Unit, University of Dundee, Dundee, UK, [3]Clinical Radiology, NHS Tayside, Ninewells Hospital, Dundee, UK and [4]Medical Physics, NHS Tayside, Ninewells Hospital, Dundee, UK

Introduction: Visceral obesity is associated with an adverse metabolic and cardiovascular risk profile.[1] Myocardial fat deposited around the heart can be subdivided into epicardial adipose tissue (EAT), enclosed by the visceral pericardial sac, and pericardial layer, anterior to EAT. It has been postulated that the outer pericardial layer remains relatively inert however EAT hosts a metabolic active role [2] MRI has become gold standard for assessing the structure and function of the heart, but quantitative assessment of myocardial fat using MRI may provide additional prognostic information. The purpose of this study was to measure the extent of EAT in a diabetic population (DM) with cardiovascular disease (CV) using MRI, and to correlate these measures with MRI-derived pulse wave velocity (PWV) as an index of arterial stiffness.
Methods: Fifty fully consenting patients were recruited into the following cohorts: (G1) Type 2 DM with CVD, (G2) Type 2 DM without CVD, (G3) no DM with CVD, and (G4) no DM and no CVD. Each patient underwent a cardiovascular MR imaging assessment on a 3T Magnetom Trio MRI scanner (Erlangen, Germany). For derivation of the EAT region, a cardiac-gated 2D CINE segmented TrueFISP sequence was acquired in the four-chamber orientation. Segmentation of the region was manually contoured at end-diastole (ED) and subsequently reviewed by an experienced radiologist. The PWV was acquired from axial oblique cardiac-gated 2D segmented free-breathing CINE phase-contrast MRA (PC-MRA) sequences at slice locations across the aortic arch and the descending aorta above the renal bifurcation. Image processing was performed using Segment v1.9 R1917 (Heiberg, Germany). The PWV was calculated using the transit time method, and the distance between each measurement plane. Results are expressed as mean+/- SD. Comparison of variables was performed by means of a two-tailed t-test.
Results: For EAT, G1 (5.32+/-1.9cm^2), G2 (4.52+/-2.07cm^2) and G3 (4.98+/-1.80cm^2) were found to be highly significant in comparison to G4 (P<0.001) however no significance was between patient groups. PWV values in G1 (DM and CVD) 8.42+/-2.55 m/s and G3 (CVD) 8.98 +/-3.14 m/s compared to control cohort G4: 6.50+/-1.74 m/s was found to be significant (p=0.03, p=0.02). No significance was found with G2 (DM only) and G4 or between the patient groups (G1,2,3).
Conclusion: Recent studies are beginning to highlight EAT playing an active role as a cardiometabolic risk factor.[3] In this study, EAT was found to be associated with CVD and DM. However arterial stiffness, a known marker of CVD and DM,[4] showed an association with CVD and DM but not solely DM.

Despres et al, Crit Pathw Cardiol. 2007 Jun;6(2):51-9

Iacobellis et al, J Clin Endocrinol Metab 2005;90:6300-6302

Manco et al, Atheros. 2013, 225(490) 495

Van der Meer et al, JMRI 2008, 9(4) 645-51

Where applicable, the authors confirm that the experiments described here conform with The Physiological Society ethical requirements.

PCD016

Effect of cigarette smoke and cook smoke on nasal mucociliary clearance

P. Johnson[1], P.K. Muthu[4], P. Paul[3], S. Ramadoss[5], M. Baby[6], P. Ramasamy[1] and K. Balakrishnan[2]

[1]Physiology, Sri Ramachandra University, Chennai, Tamilnadu, India, [2]Environmental Health Engineering, Sri Ramachandra University, Chennai, Tamilnadu, India, [3]Physiology, Tagore Medical College, Chennai, Tamilnadu, India, [4]Physiology, Donor Action Program, National Network of Organ Sharing, Chennai, Tamilnadu, India, [5]Physiology, Sree Balaji Medical College, Chennai, Tamilnadu, India and [6]Endocrinology, Sri Ramachandra University, Chennai, Tamilnadu, India

Background: Globally, the most important risk factor for chronic lung diseases is smoking of tobacco. Cigarette smoke, passive smoking, biomass smoke and infectious organisms may activate alveolar macrophages, bronchial epithelial cells and other cellular elements in the airways of genetically susceptible individuals leading to the development of chronic lung diseases. But, unfortunately, a first diagnosis of such disease is established in smokers and/or exposed to other smoke exposures only at a later stage after being exposed for several decades. However, before reaching this clinical stage, lot of structural and functional changes in the respiratory tract do occur deteriorating respiratory defence mechanisms leading to appearance of symptoms, worsening of quality of life and ultimately death. Early diagnosis of such impairment may have important stimuli to either quit smoking or to participate in smoke intervention programmes. With this background, this study was conducted to evaluate the nasal mucociliary clearance (mirror image of bronchial clearance/biomarker of nasal mucosal function) of subjects exposed to tobacco smoke, cook smoke and to compare with that of the healthy volunteers unexposed to such smoke.
Materials & Methods: NMC was measured in 25 smokers, 25 non smokers,50 biomass fuel users and in 50 clean fuel users of age group ranging from 18 – 45 years who had no medications and no systemic illness. The time elapsing until the first experience of sweet taste at posterior nasopharynx, following the placement of saccharin particle approximately 1cm behind the anterior end of inferior turbinate was recorded as NMC clearance time.
Results: Mean NMC of the smokers (481.2 ± 29.8 secs) was significantly higher than that of non smokers (300.32 ± 17.4 secs), (p<0.01). NMC was found to be increasing as the duration of smoking increased. (NMC in smoking <1 year =492.25 ± 79.93 secs, NMC in smoking for 1 – 5 years = 516.7 ± 34.01 secs, > 5 years = 637.5 ± 28.49 secs). NMC was also significantly (p =0.02) prolonged in biomass fuel users (604.97 ± 220.42 secs) in comparison to clean fuel users (455.12 ± 161.76 secs). Prolonged clearance observed in smokers and biomass fuel users may be due to the toxic effects of the components of smoke.
Conclusion: NMC measurement is a simple, inexpensive, non-invasive, screening test which can be used as an early diagnostic tool for respiratory diseases caused by exposure to air pollutants such as cook smoke and tobacco smoke. Our study impresses upon the important role of NMC in the health of sinonasal cavities and the need for initiating smoking cessa-

tion programs and efforts to promote cleaner fuels, improved stoves, better home ventilation which in turn may promote the lung health of the general population.

Where applicable, the authors confirm that the experiments described here conform with The Physiological Society ethical requirements.

PCD017

Correlates of cigarette use in High Schools in Chatsworth, Durban, South Africa

P. Gathiram[1], T.M. Esterhuizen[2] and S.S. Naidoo[3]

[1]College of Health Sciences, Unievrsity of KwaZulu-Natal, Durban, KwaZulu-Natal, South Africa, [2]College of Health Scineces, University of KwaZulu-Natal, Durban, KwaZulu-Natal, South Africa and [3]School of Health Sciences, Durban University of Technology, Durban, KwaZulu-Natal, South Africa

Introduction: Approximately 1 billion men and 250 million women in the world smoke, accounting for about 35% of men in high-resource countries to about 50% in developing countries [1]. The increasing trend of earlier age of smoking initiation in children and early adolescents leads to greater use in adulthood, especially in the developing world [2]. The aim of this study was to assess the prevalence of regular and frequent smoking in high school learners as well as the factors associated with cigarette use. Early identification of correlates and risk factors for cigarette use will be useful in designing intervention and prevention programmes.

Methods: This cross-sectional study used a validated questionnaire to assess the extent of and factors associated with cigarette use among learners from Chatsworth high schools. Following institutional ethics approval, the study was conducted among a cluster sample of 1612 learners in grades 10 to 12 from 10 of the 18 Chatsworth public high schools. An IBM SPSS (version 20) package was used for data analysis. Crude and adjusted factors associated with regular smoking were assessed using logistic regression analysis. The cluster effect of school was dealt with by controlling for school in the analysis. A p value <0.05 was considered as statistically significant. Results are presented as odds ratios and 95% confidence intervals by gender.

Results: In grades 10, 11 and 12 prevalence of regular smokers in males were 23.8%, 34.8% and 38.6%, respectively, with an overall of 30.7%, and in females 17.7%, 12.1% and 14.2%, respectively, with an overall of 15.2%. The total prevalence was 22.5%. The prevalence of frequent smokers among males by grade was 11.2%, 19.5% and 28% respectively, with an overall of 17.8% and females, 3.6%, 4.9% and 7.8%, respectively and an overall of 5%, whilst the total prevalence was 11.1%. The prevalence was significantly higher in males than females in all grades. After adjusting for school clusters and other confounders, in males there was a significant increase in risk of smoking from grade 10 through grade 12. In both genders, Zulu speaking learners were at lower risk of smoking than English speaking learners, and having a brother, sister and best friend who smokes significantly increased the risk. In females, a significant association existed between regular smoking females and having peers who smoke, as well as with having repeated a grade.

Conclusion: This study showed an increase in the prevalence of cigarette smoking especially among female smokers compared with a similar study in 1993 [3]. The percentage of frequent smokers in the current study was slightly lower than in the USA (13.8%) [4]. These data warrants an urgent intervention programme to be initiated at all levels beginning at home and then at school.

Shafey O, Eriks M, Ross H, Mackay J. The Tobacco Atlas. 3rd ed. Society TAC, editor. Atlanta, GA: The American Cancer Society.; 2009.

Lando H.A., Hipple BJ, Muramoto M, Klein JD, Prokhorov AV, Ossip DJ, et al. Tobacco is a global paediatric concern. 2010 [cited 88]; 2-]. Available from: http://www.who.int/bulletin/volumes/88/1/09-069583/en/index.html.

Naidoo S. An Investigation of Substance use among High School Pupils in Chatsworth [MFamMed Dissertation]. Durban: University of Natal; 1993

Center for Disease Control and Prevention. Trends in Cigarette Smoking Among High School Students —United States, 1991—2001. 2002 [http://www.cdc.gov/mmwr/preview/mmwrhtml/mm5119a1.htm17 May 2002]; Available from: http://www.cdc.gov/mmwr/preview/mmwrhtml/mm5119a1.htm.

The University of KwaZulu-Natal for the travel grant.

Where applicable, the authors confirm that the experiments described here conform with The Physiological Society ethical requirements.

PCD018

Cardiac systolic and diastolic functions in spinal cord injured patients during lower body heating

M. Shibasaki[1], Y. Umemoto[2], T. Kinoshita[2], K. Kouda[2], T. Ito[2], T. Nakamura[2], C.G. Crandall[3,4] and F. Tajima[2]

[1]Nara Women's University, Nara, Japan, [2]Wakayama Medical University, School of Medicine, Wakayama, Japan, [3]Institute for Exercise and Environmental Medicine, Texas Health Presbyterian Hospital, Dallas, TX, USA and [4]University of Texas Southwestern Medical Center, Dallas, TX, USA

Elevations in skin blood flow and sweating during heat stress are driven through an integration of elevated internal and skin temperatures, with internal temperature being the primary controller. Passive heat stress increases cardiac output through elevated heart rate coupled with maintained stroke volume, the latter of which is achieved by improved systolic function and maintained diastolic function in healthy individuals. The contribution of thermal inputs from the skin in mediating these cardiac responses is unknown. This study tested the hypothesis that cardiac responses during heat stress are primarily mediated by internal temperature. To test this hypothesis, eight healthy (AB) and seven spinal cord injured (SCI) volunteers underwent a lower body heat stress; heating applied only to insensate skin in the SCI subjects. Echocardiographic indices of diastolic and systolic function were performed at normothermia and after an increase in internal temperature of approximately ~1.0 °C. Cardiac output (CO_2 rebreathing) increased during heat stress in both groups, but the increase was smaller in SCI (1.7±0.4(SD) l/min) relative to AB (2.3±1.0 l/min; P=0.06). The table shows the effects of heat stress on indices of diastolic and systolic function.

These data suggest that improved ventricular systolic function during heat stress primarily occurs by increases in internal temperature, with little to no influence from skin thermoceptors. Notably, smaller increases in atrial and ventricular systolic function in SCI subjects may contribute to their impaired increase in cardiac output during heat stress.

	Healthy (AB)		Spinal cord injured (SCI)	
	Normothermic	Hyperthermic	Normothermic	Hyperthermic
Indices of diastolic function				
E (cm/s)	69±14	67 ±11	59 ±11	56 ±13
Septal E' (cm/s)	10.7 ±1.2	10.6 ±2.1	9.0 ±1.9	8.7 ±2.0
Lateral E' (cm/s)	12.3 ±2.0	13.5 ±2.5	11.5 ±3.9	12.4 ±3.2
IVRT (ms)	71 ±12	56 ±8*	76 ±26	65 ±17*
Indices of atrial systolic function				
A (cm/s)	49 ±10	66 ±8*	43 ±6	49 ±8†
Septal A' (cm/s)	10.2 ±1.6	11.8 ±1.4*	9.8 ±1.2	9.8 ±1.8†
Lateral A' (cm/s)	9.3 ±1.2	11.8 ±1.7*	8.7 ±1.0	9.1 ±0.6†
[A/(A+E)]*100 (%)	41.6 ±5.0	49.5 ±3.1*	42.2 ±5.9	47.2 ±5.1*
Indices of ventricular systolic function				
Septal S' (cm/s)	9.6 ±1.8	12.3 ±1.2*	8.4 ±0.4	10.0 ±1.4*†
Lateral S' (cm/s)	10.5 ±1.9	14.6 ±1.6*	9.9 ±2.0	11.6 ±1.5*†
Septal IVA (cm/s^2)	121 ±43	169 ±55*	109 ±35	152 ±35*
Lateral IVA (cm/s^2)	96 ±33	145 ±64*	92 ±22	120 ±33*

E, Early diastolic filling velocity; E', Early diastolic annular tissue velocity; IVRT, Isovolumetric relaxation time; A, Atrial filling velocity; A', Late diastolic annular tissue velocity; [A/(A+E)], Atrial contribution to diastolic filling; S', Systolic annular tissue velocity; IVA, Isovolumic acceleration; * Significantly different from normothermic baseline, P <0.05; † Significantly different from AB, P <0.05.

Where applicable, the authors confirm that the experiments described here conform with The Physiological Society ethical requirements.

PCD019

Localizing the intracellular ADP diffusion restrictions in trout cardiomyocytes

N. Sokolova, M. Sepp, M. Vendelin and R. Birkedal

Laboratory of Systems Biology, Institute of Cybernetics, Tallinn University of Technology, Tallinn, Estonia

Permeabilized cardiomyocytes have intracellular structures that restrict the diffusion of ADP from the surrounding medium to the mitochondria. Intracellular diffusion restrictions are also present in rainbow trout (Oncorhynchus mykiss) cardiomyocytes. This was surprising, because trout cardiomyocytes are no more than a few μm thick, lack t-tubules, have a lower sarcoplasmic reticulum density and only a single layer of myofilaments surrounding a central core of mitochondria. However, the extent of diffusion restrictions is smaller than in mammalian cardiomyocytes. The aim of the present study was to locate the diffusion restrictions in permeabilized trout cardiomyocytes. We measured mitochondrial respiration stimulated by ADP and ATP, and evaluated the rate of inhibition of ATP stimulated respiration by an ADP trapping system, consisting of phosphoenolpyruvate (PEP) activating endogenous and exogenous pyruvate kinase (PK), which competes with mitochondria for ADP. We found a high activity of hexokinase, which stimulates mitochondrial respiration when activated by glucose. To study its role in more detail, all experiments were performed in the absence and presence of 2 mM glucose. Additionally, we performed ADP titrations on cells alone, in the presence of glucose, and in the presence of creatine kinase and creatine. Our results showed that in contrast to rat cardiomyocytes, there is no functional coupling between creatine kinase and respiration. Trout cardiomyocytes have a high activity of hexokinase, which is functionally coupled to respiration. This suggests that trout cardiomyocytes have a different ADP-feedback system than mammalian cardiomyocytes. The experimental results were fitted with a mathematical model showing that diffusion is restricted in cytosol as well as by the outer mitochondrial membrane.

This work was supported by Wellcome Trust (Fellowship No. WT081755), Estonian Science Foundation (Grant No. 8041) and European Union through the European Regional Development Fund.

Where applicable, the authors confirm that the experiments described here conform with The Physiological Society ethical requirements.

PCD020

The influenses of hand work and stand up on the function of autonomic nervous system during menstrual cycle in healthy female college students

Y. Itoi[1], M. Onozaki[1], T. Shimizu[2] and T. Okada[3]

[1]International University of Health and Welfare, Otawara, Japan, [2]Toin University of Yokohama, Yokohama, Japan and [3]Juntendo University Graduate School of Medicine, Bunkyouku, Japan

Purpose: The purpose of this study was to examine the correlation between functional modulation of the autonomic nervous system and the menstrual cycle.Methods: Subjects were comprised of 11 healthy female college students (19.5±0.5 years old) with regular menstrual cycles. The changes in emotional sweating induced by hand work (beans work and puzzle) and the modulation in autonomic nervous system(electrocardiograph and heartbeat) with active orthostatic load were compared among the follicular, luteal and menstrual phases. The Japanese version of the Profile of Mood State (POMS), healthy life habit (DIHAL.,2,junior high school student~adult) were also examined. Analysis: Effect size of the difference between group or correlation were evaluated. Results:Emotionalsweating(task is beans work) during the menstrual phase was significantly higher than those during follicular and luteal phases and it associated with the high score of “depression dejection” of POMS factors. Group with the highest T score (standardized score) of “depression dejection” emotional sweating was significantly higher during luteal phase. In addition, the group which complained subjective low healthy state, showed higher emotional sweating (beans work) during luteal phase.Fluctuations of heart rate at rest(the size of the activity),during menstrual phase was significantly higher than those during follicular phase, although it was a normal range.The balance of the autonomic nervous activity at rest (balance) was significantly higher during luteal phase compared to menstrual phase, indicating predominance of sympathetic nervous system. Active orthostatic load-induced fluctuations of heart beat(powers of the response)was significantly higher during follicular phase compared to those during menstrual and luteal phase, although it was a normal range. Fluctuations of balance of the active orthostatic load (powers of the change) was significantly higher during menstrual phase than that during follicular phase; the range which need special medical attention. In addition, there found an association between balance and “confusion”. Group with the highest T score of “confusion” factors, showed predominant sympathetic nervous system during menstrual phase.Conclusion:These findings suggest that Stresses of beans work may influence the function of the autonomic nervous system to during menstrual phase . In addition, these findings suggest that powers of the change was higher during menstrual phase, the range which need special medical attention. Students with the high T score of “confusion” factors, showed the balance is sympathetic nerve predominance during menstrual phase.

Where applicable, the authors confirm that the experiments described here conform with The Physiological Society ethical requirements.

PCD021

The beginning of the calcium transient and contraction in rat embryonic heart

T. Kobayashi, S. Maeda, N. Ichise, T. Sato, T. Miyakawa, Y. Yamada and N. Tohse

Cellular Physiology and Signal Transduction, Sapporo Medical University School of Medicine, Sapporo, Japan

Although many researchers have examined the embryonic heart, the precise relationship between the morphological changes of the heart and heart function, i.e., excitation- contraction coupling, around the period of the beginning of the heartbeat remains obscure. Here, we recorded and evaluated the beginning of the calcium transient and contraction of the Wistar rat heart. The heart primordium, the so-called cardiac crescent, of Wistar rats begins to contract at embryonic day 9.99-10.13. The contracting area is initially small and becomes enlarged with time. Repetitive calcium transients are observed regularly in the whole heart primordium, before the initiation of contraction. Nifedipine, but not ryanodine, abolished the calcium transients. Thapsigargin did not affect the calcium transients. These results indicate that the calcium transients involve exclusively calcium entry through L-type calcium channels, in contrast to the situation in mature hearts. This study reveals the precise relationship between morphological changes in the heart primordium and the beginning of the calcium transient and contraction.

Where applicable, the authors confirm that the experiments described here conform with The Physiological Society ethical requirements.

PCD023

Postnatal change of heart rate and sinoatrial node pacemaker activity in mice

T. Adachi, S. Shibata, Y. Okamoto, S. Sato, S. Fujisawa, T. Ohba and K. Ono

Cell Physiolosy, Akita University Graduate School of Medicine, Akita, Japan

It is well established that heart rate (HR) changes during the course of postnatal development in mammalian species. In general, the HR of large animals, including humans, rabbits, and dogs, decreases with development. The HR of small animals such as mice and rats has been reported to increase after birth. These contrasting HR changes may be related to the size of the body and heart, and may be purposely designed to most effectively propel the blood around the body in various mammalian species. Nevertheless, the physiological significance and mechanisms underlying these postnatal changes in HR remain poorly understood. In the present study, we examined the mechanisms of postnatal change in murine HR using *in vivo* non-invasive measurement of HR and electrophysiological analysis of ion channels in isolated sinoatrial node (SAN) cells. Non-invasive measurement of murine HR was accomplished using a piezoelectric transducer (PZT) sensor. Mice were simply placed on the PZT sensor, and the heart sound signal was extracted and used for calculating HR. In this method, HR was 323 ± 17 bpm at P0, and increased daily during 2 weeks after birth. The HR at P14 was 685 ± 18 bpm. Under pharmacological blockade of the autonomic nervous system, the HR of approximately 300 bpm was largely constant at P0–5, and then increased daily to 500 bpm at P14. In intracellular potential recordings, the spontaneous beating rate of the SAN tissue preparation was traced to similar curve of *in vivo* HR under pharmacological blockade. These findings indicate that the postnatal increase in HR is derived from increased sympathetic influence that becomes apparent immediately after birth, and increased intrinsic activity of SAN cells that emerges 5–6 days after birth. In spontaneous action potential recordings in isolated SAN cells by the whole cell patch clamp method, the beating rate and diastolic depolarization rate of SAN cells was significantly less in neonatal mice than in adult mice. Isolated pacemaker cells possessed similar morphological and electrophysiological characteristics for sinoatrial pacemaker cells. The I_{CaL} was activated at more positive potentials and the current amplitude was smaller in newborn SAN cells than in adult cells, however no significant difference was detected in the I_f and I_{CaT} density and kinetics. Quantitative PCR using the SAN tissue preparations revealed no statistical differences in the expression levels of $Ca_V1.2$, $Ca_V1.3$, $Ca_V3.1$, $Ca_V3.2$, and HCN4 between neonate and adult SAN tissues. We conclude that the postnatal increase in HR is caused by increased sympathetic influence and the intrinsic activity of SAN cells, and that the different conductance and kinetics of I_{CaL} may be involved in the postnatal increase in pacemaker activity.

Where applicable, the authors confirm that the experiments described here conform with The Physiological Society ethical requirements.

PCD024

The role of extracellular Ca2+o and voltage-gated calcium channels in vasculogenesis in the fetal lung

S.C. Brennan[1], B.A. Finney[2,1], D. Al Alam[3], R.L. Townsend[1], M. Lazarou[1], D. Adriaensen[4], E. Jesudason[3,5], D. Warburton[3], P.J. Kemp[1] and D. Riccardi[1]

[1]Cardiff School of Biosciences, Cardiff University, Cardiff, UK, [2]Center for Cardiovascular Sciences, Institute for Biomedical Research, University of Birmingham, Edgbaston, UK, [3]Developmental Biology and Regenerative Medicine Program, Saban Research Institute, Children's Hospital Los Angeles, Los Angeles, CA, USA, [4]Department of Veterinary Sciences, Laboratory of Cell Biology and Histology, University of Antwerp, Antwerp, Belgium and [5]Division of Child Health, University of Liverpool, Liverpool, UK

Postnatal lung function depends on a tightly controlled and complex developmental programme which regulates lung branching morphogenesis, vasculogenesis and fluid secretion. A number of these processes begin during the pseudoglandular stage (weeks 9 – 17 in human, and embryonic day (E)11.5 – 16.5 in the mouse) and occur in a relatively hypercalcemic environment (~1.7 mM v ~1.2 mM for a normocalcemic adult [1]). Previously, our group has demonstrated that this increase in extracellular calcium ([Ca2+o]) is an important extrinsic factor for lung development, suppressing branching and cellular proliferation and enhancing Cl—dependent fluid secretion through activation of the calcium-sensing receptor (CaSR) [2]. To further understand the role of Ca2+o in lung development, we have now examined the effect of fetal hypercalcemic conditions on vasculogenesis using the Flk-1+/LacZ reporter mouse model. Fetal liver kinase (Flk)-1, a receptor for vascular endothelial growth factor-A, is predominately expressed in the early stages of mouse lung development (E9.5 – E13.5), during which vascular endothelial cells have been shown to actively proliferate [3]. E12.5 mouse lung explants cultured for 48 h

in medium containing adult Ca2+ concentrations (1.05 mM) showed Flk-1 expression confined to the mesenchymal spaces between developing branches. However, culturing lung explants in the presence of fetal (1.70 mM) [Ca2+o] induced a marked increase in Flk-1 expression, accompanied by a change in localization with the vasculature criss-crossing over and around the developing branches. The addition of the CaSR activator NPS-568 (30 nM) at 1.05 mM Ca2+o did not affect Flk-1 expression, suggesting that the CaSR is not directly involved in regulation of vasculogenesis. Immunohistochemistry of E12.5 whole mouse embryos and human fetal lungs showed expression of a number of voltage-gated calcium channels – including the L- and R-type calcium channels Cav1.2, Cav1.3 and Cav2.3 – within the epithelium of the developing lung, suggesting an alternate mechanism for [Ca2+o] sensitivity. Functional experiments with the L-type calcium channel blocker nifedipine and the R-type calcium channel blocker SNX-482 at 1.70 mM Ca2+o led to significant increases in lung branching (39.8 ± 4.1% n=11 vs. 70.6 ± 4.5% n=9 p<0.01 and 81.1 ± 11.7 n=6 p<0.001 respectively. Values are mean ± SEM, compared by ANOVA) and further increases in Flk-1 expression over 48h. In summary, functional L-/R-type calcium channels may provide an alternative and complementary mechanism for the [Ca2+o] sensitivity of fetal lung development, including branching morphogenesis and vasculogenesis.

Kovacs, C.S. and H.M. Kronenberg. (1997). Endocr Rev. 18(6): p. 832-72

Finney, B. A., et al. (2008). J Physiol. 586(Pt 24): 6007-6019

Yamamoto, Y., et al. (2007). Anat Rec 290(8): 958-973

This work was supported by the Marie Curie Initial Training Network Multifaceted CaSR (FP7-264663).

Where applicable, the authors confirm that the experiments described here conform with The Physiological Society ethical requirements.

PCD025

Effect of postnatal Leptin on cardiac structure and function

A. Samuelsson[1], J. Clark[2], M.J. Shattock[2], O. Rudyk[2], J. Pombo[1], S. Eun Bae[1], T. South[1], C.W. Coen[1], L. Poston[1] and P.D. Taylor[1]

[1]Division of Women's Health, Women's Health Academic Center, King's College London and King's Health Partners, UK, King's College London, London, UK, London, UK and [2]Cardiovascular Division, King's College London, UK., London, UK

Obesity in pregnancy is associated with cardiovascular dysfunction in adult offspring. We have previously reported an exaggerated leptin surge, in neonatal offspring of obese rats (1) associated with the development of sympathetic mediated hypertension and cardiac hypertrophy (2-3). We have now addressed the hypothesis that the high levels of leptin in early postnatal life may underlie early origin of hypertension and cardiac hypertrophy.

To investigate the role of increased neonatal leptin exposure on the development of sympathetic mediated hypertension and the cardiac hypertrophy in offspring of obese dams.

Pups from lean Sprague-Dawley rats were randomly assigned for intraperitoneal administration of recombinant rat leptin (L-Tx, 3mg/kg) or saline (S-Tx) at postnatal day 9-15. At day 23, juvenile rats were subjected to radiotelemetry surgery under general anaesthesia (2% isofluorane in O_2 at 2 l/ min) using a carotid artery placement of the small animal transmitters (DSI-PhysioTel® PA-C10). Pre and post-operative analgesia (Buprenorphine 0.1 mg/kg, intramuscular) was maintained for 24h. Heart rate and blood pressure were recorded after one-week recovery by schedule sampling for 10 s every 5 min using A.R.T.10 software (Dataquest IV, DSI). Heart structure and function were analysed using *in vivo* micro-echocardiography (2% isofluorane, Vevo 770-ECHO system) and *ex vivo* langerdorf perfusion. The cardiomyocyte number and surface area were determined using hemomtoxylin-eosin and anti-laminin immunoflourescence.

Neonatal leptin treated male and female rats (L-Tx) showed increased night-time (active period) systolic blood pressure (SBP [mmHg] mean±SEM: male L-Tx, 132±1 versus S-Tx, 119±1, n=6, p< 0.05; female L-Tx, 132±2 versus S-Tx, 119±1, n=6, p< 0.01, *RM-ANOVA*), in comparison to S-Tx.

Female L-Tx demonstrated increased heart weight (P<0.05, n=6,*t-test*) with evidence of increased cardiomyocyte number at day 30. The *in vivo* imaging revealed altered left ventricle dimensions and diminished left ventricular systolic function and isolated heart showed evidence of impaired contractile function in the L-Tx versus S-Tx.

This study implicates a central role for neonatal leptin in the origins of sympathetic mediated hypertension and cardiac morphology and function, in offspring of obese rodents. Evidence of cardiac dilatation together with impaired contractility may reflect early stages of heart failure.

Kirk SL *et al*. (2009). *Plos One* **4**:e5870.

Samuelsson AM *et al*. (2010). *Hypertension* **55**. 76-82.

Rajani CK *et al*. (2009). *J DOHAD* **1**:S247.

This study was supported by the British Heart Foundation (FS/10/003/28163) and the BBSRC (BBD5231861). LP is funded by Tommy's Charity (1060508).

Where applicable, the authors confirm that the experiments described here conform with The Physiological Society ethical requirements.

PCD026

Maternal high fat diet during pregnancy and lactation alters mitochondrial electron transport chain activity and gene expression in adult mouse offspring heart

M. Bordbar Amirian, K.L. Hyde, K.D. Bruce, H. Thomas, C.D. Byrne, M.A. Hanson and F.R. Cagampang

Institute of Developmental Sciences, Human Development and Health, University of Southampton Faculty of Medicine, Southampton, UK

Increasing diabetes prevalence and life expectancy are two key factors raising the health care burden from the consequences of cardiovascular disease (CVD). Whereas an obesogenic diet in adulthood is a known risk factor for type 2 diabetes and CVD, there is growing evidence that obesogenic diets during pregnancy increase CVD and diabetes susceptibility in the offspring later in life. While most studies focused on changes in vascular physiology that result from maternal high fat (HF) feeding, the metabolic and molecular changes that occur in the offspring's heart itself remains to be elucidated. The mitochondria play a key role in the normal functioning of the heart, and in the pathogenesis and development of various types of heart disease. We therefore examined whether mitochondrial electron transport chain (ETC) activity and expression of genes with key roles in mitochondrial metabolism were altered in heart tissues of offspring from obese mothers fed a HF diet. Female C57/BL6J mice were maintained

under controlled conditions and fed either a HF diet (HF; 45% kcal fat) or standard chow diet (C; 21% kcal fat) 4-6 weeks prior to and during gestation and lactation. Weaned offspring were fed the HF or C diet, generating the dam-offspring groups: C/C, C/HF, HF/C, HF/HF. Hearts were taken from 15-week old male offspring (n=4-5 per offspring group). The left ventricle (LV) was dissected and processed for the analysis of mitochondrial Complex I and II enzyme activity using spectrophotometric assay, and for qPCR of the mitochondrial sirtuin Sirt3, uncoupling proteins UCP2 and UCP3, the adenine nucleotide translocases ANT1 and ANT2, the transcriptional coactivator PGC1α, and the nuclear respiratory factor NRF1. Complex I and II activity was reduced by 1.5 fold ($p<0.001$, ANOVA) in the HF/HF offspring heart vs C/C. Complex II activity also reduced by 3-fold ($p<0.0001$) in the HF/C group vs C/C. Sirt3 mRNA level was 2.6-fold lower ($p<0.01$) in offspring hearts from HF-fed dams (HF/C and HF/HF groups) vs C/C group. UCP2 and UCP3 mRNA levels were 2.3 and 4-fold higher (both at $p<0.0001$), in HF/HF vs C/C hearts, with UCP2 also increased 5-fold ($p<0.0001$) in the HF/C hearts vs C/C. Furthermore, ANT1 and ANT2 transcript levels were reduced by more than 1.3-fold ($p<0.01$) in HF/HF hearts vs C/C. PGC1α mRNA levels were 1.4-fold lower ($p<0.01$) while NRF1 mRNA levels were 3-fold higher ($p<0.0001$) in HF/HF hearts vs C/C. NRF1 transcript levels were also 2.5-fold ($p<0.0001$) higher in the HF/C tissues vs C/C. The results suggest maternal high fat diet during pregnancy and lactation alters mitochondrial ETC activities and expression of genes involved in mitochondrial function and biogenesis. This priming effect in early life increases offspring risk to cardiac pathologies in later life.

Supported by BBSRC and BHF

Where applicable, the authors confirm that the experiments described here conform with The Physiological Society ethical requirements.

PCD028

Distribution of the pacemaker cardiomyocytes in the vertebrate heart

V.I. Prosheva

Institute of Physiology, Syktyvkar, Russian Federation

It is known that there are large differences in the morphology of the vertebrate heart: from the Cyclostome and fish hearts with its single atrium and single ventricle to the bird and mammalian hearts with two fully separated atria and ventricles. At present it is necessary to revise the data on the topography of the atrial pacemakers in the vertebrate heart. Pacemaker cells have some specific electrophysiological properties that make them different from atrial working myocardium and conducting cells. In this study, we aimed to establish a functional topography of the pacemaker cardiomyocytes in the isolated sinoatrial and atrioventricular areas of the heart in different representatives of vertebrates: lamprey (Lethenteron japonocum), carp (Carassius carassius L.), frog (Rana temporaria L.), lizard (Lacerta vivipara L.), chicken (Gallus gallus domesticus), pigeon (Columba livia L.), mouse (Mus musculus) and cat (Felis catus L.), using microelectrode mapping of action potentials (APs). All experimental procedures conformed to the Guide for the care and use of laboratory animals published by the US National Institutes of Health (NIH publication No. 85-23, revised 1985). It was found that in the lamprey, carp, frog and lizard hearts APs of pacemaker cells were recorded from the base of leaflets of sinoatrial and atrioventricular valves. In the chicken and pigeon hearts sinoatrial pacemaker is localized in the base of the right sinoatrial valve. In the atrioventricular area pacemaker cells are embedded in fibrous tissue and located near the base of the right muscle atrioventricular valve and in the region of the coronary sinus. In the mouse and cat hearts, cells with pacemaker activity are distributed in the region of the mouth of the superior vena cava, in the area adjacent to the coronary sinus and also in the base and in the leaflets of the atrioventricular valves. In the studied animals the maximal depolarization rate of pacemaker APs in the sinoatrial area increases in the anterograde direction, while their APs duration decreases. In the atrioventricular area the reverse regularity of the APs parameters distribution is observed. Thus the areas of the valves are supposed to be specific places of pacemaker cells localization in the Cyclostome, fish, amphibian, reptilian, avian and mammalian hearts. The data obtained indicate the conservatism of the evolution of cardiac pacemakers.

This study was supported by the Russian Foundation for Basic Research (grant # 11-04-01933).

Where applicable, the authors confirm that the experiments described here conform with The Physiological Society ethical requirements.

PCD029

The features of regulation of the heart rate and external respiration observed in Aborigines and Europeans of the Russia's northeast

A. Maximov

Laboratory for Physiology of Extreme States, Scientific-Research Centre "Arktika" FEB RAS, Magadan, Russian Federation

Recently a population of the residents born in the north within their 1st – 3rd generations being Europeans, is forming in Russia's northeast. Besides, an Aboriginal population also resides in the region. It is presented by ethnic Chukchee and Evens. The Aborigines of the north are characterized by having some morphofunctional parameters that are fixed at genetic levels, in contrast to the north-born Europeans whose adaptation changes are mainly determined by a phenotype. To study physiological profiles of the adaptive changes in the north-born Europeans in comparison with the Aborigines, we examined young male people aged 17–21 (n = 350) being residents of Magadan region that is situated within the range of 60–64° NL and 145–162° EL. The average year temperature in the region is 7° C below zero. The examined people underwent general measurements of registering their heart rate R-R intervals at rest and at orthostatic exercise as recommended by the European and North America's Association of Cardiologists. Based on the values of the heart rate variability, its statistical and spectral-wave characteristics were calculated. The results found no reliable difference between the heart rate variability indices of the north-born Europeans and the Aborigines at rest. However, during the orthostatic test that can reveal cardiovascular system's reserves, a reliable difference between the examined populations was observed in the following indices: mode (Mo), variation range (MxDMn), standard deviation (SDNN), stress index (SI), total power of the spectrum of the heart rate frequencies (PT) as well as its low (HF) and very low (VLF) components. Of note that, the heart rate structure difference suggested more pronounced tension of regulatory mechanisms in the Aborigines compared to the Europeans, at the background of activation in the sympathetic vegeta-

tive nervous system and lower functional reserves of cardiohemodynamics. Found that, only two of the 11 values of the external respiration function registered at rest, showed a reliable difference. The Aborigines demonstrated the lung vital capacity and the volume of the expired air per second, respectively, 570 ml and 410 ml less than those of the Europeans. Thus, we can suggest that the north-born Europeans and the Aborigines of Russia's north have no difference in the series of cardiorespiration parameters. This fact enables to say of the forming of a convergent type of adaptation in the modern population of Russia's north. In the meantime, the Aborigines proved to have reliably lower functional reserves in some physiological systems as compared to those of the European north-born residents.

Where applicable, the authors confirm that the experiments described here conform with The Physiological Society ethical requirements.

PCD030

A new noninvasive method to estimate mixed venous oxygen content with a pulse oximeter

K. Uchida

Physical Therapy, Yamagata Prefectural University of Health Sciences, Yamagata, Japan

To assess the gas exchange in a lung mixed venous oxygen content (CvO2) is one of the most important factors connecting cardiac output and oxygen uptake. Unlike the other fundamental factor arterial oxygen content (CaO2), CvO2 cannot be easily measured. Therefore, estimation of CvO2 is in high relevance to clinical medicine as well as to basic research. Oxygen saturation (SpO2) and heart rate (HR) were measured for 13 healthy students (4 males and 9 females ages 20 to 24) of Yamagata Prefectural University of Health Sciences, who joined a study tour in Colorado from Sep. 19 to 27, 2012. The means and standard deviations for their height and body weight were 162.0 ± 9.5 cm and 58.0 ± 7.8 kg. They had no cardio-respiratory diseases. SpO2 and HR were measured using a pulse oximeter (PULSOX-2, KONICA MINOLTA) with their informed consents. They put their fingers into the oximeter in a sitting position to measure SpO2 and HR. Averaged values of SpO2 for 13 students were 98 ± 0.95, 97 ± 1.4, 94 ± 1.9, 93 ± 1.7 and 87 ± 2.8 % at the Narita Airport (altitude 130 m), Denver City (1,609 m), Estes Park (2,499 m), Hidden Valley (2,816 m) and the Alpine Visitor Center (3,595 m), respectively. Averaged HR values simultaneously measured with SpO2 were 75 ±11, 78 ±5.8, 74 ± 7.4, 92 ±11 and 85 ±7.6 beats/min. These values except for those at the Narita Airport were measured within 6 hours on the fourth day for staying in Denver. Despite more than 10 % decrease in SpO2 within 6 hours, no student felt unwell at the height of 3,595 m. Based on the Fick principle, a correlation of SpO2 in % with 1/HR in min/beats was described with a regression line that SpO2 = 2650(1/HR) + 60.6 with a coefficient of determination 0.600. With the standard oxygen content combined to hemoglobin in arterial blood 20.1 vol% by assuming the normal hemoglobin concentrations for each student, CvO2 was estimated from the intercept of the regression line as 12.2 vol%1). The difference between the CaO2 values obtained from SpO2 and the estimated CvO2 (CaO2 – CvO2) at the Narita Airport was obtained as 7.8 vol%, which was consistent with that estimated by a rebreathing method at similar altitude as Narita2). The CaO2 – CvO2 value at 3,595 m was 5.2 vol%, which was higher than that reported by Wolfel et al.3) 4.0 vol% at Pikes Peak 4,300 m. This difference is probably due to the lower CaO2 at the higher altitude. These results suggest that CvO2 can be estimated from the regression line between SpO2 and 1/HR measured at different altitudes. At low altitudes SpO2 in healthy subjects is hardly less than 90 % even with severe exercise, and in this sense the application of our noninvasive method to estimate CvO2 is limited. However, our method can be used by measuring SpO2 and HR with inspired gases at various low O2 concentrations which simulate high altitudes.

1) Uchida K, Mixed venous oxygen content estimated from oxygen saturation and heart rate measured for healthy students during a study tour in Colorado. 2013; 16: Yamagata J Health Sci. (in press).

2) Uchida K, Shibuya I, Mochizuki M. Simultaneous measurement of cardiac output and pulmonary diffusing capacity for CO by a rebreathing method. Jap J Physiol (successor; J Physiol Sci) . 1986; 36: 657-70.

3) Wolfel EE, Selland MA, Cymerman A, Brooks GA, Butterfield GE, Mazzeo RS, Grover RF, Reeves JT. O2 extraction maintains O2 uptake during submaximal exercise with β–adrenergic

blockade at 4,300 m. J Appl Physiol.1998; 85: 1092-1102.

Where applicable, the authors confirm that the experiments described here conform with The Physiological Society ethical requirements.

PCD031

Effects of exercise on the L-arginine nitric oxide pathway and redox state in chronic heart failure patients

L.R. de Meirelles[1,3], A. Salgado[3], C. Matsuura[1], N.R. Pereira[1], P.G. Cascarelli[3], A. Mendes-Ribeiro[1,2] and T.M. Brunini[1]

[1]Pharmacology, State University of Rio de Janeiro, Rio de Janeiro, Rio de Janeiro, Brazil, [2]Physiological Sciences, Federal University of the State of Rio de Janeiro, Rio de Janeiro, RIo de Janeiro, Brazil and [3]Hospital Universitário Pedro Ernesto, State University of Rio de Janeiro, Rio de Janeiro, RIo de Janeiro, Brazil

Background: Chronic heart failure (CHF) is a clinical syndrome with high morbidity and mortality and the full understanding and adequate treatment of this pathology remain a challenge. Nitric oxide (NO), a short half-life gas, plays an important role in the regulation of vascular homeostasis, influencing both endothelium and platelets. NO bioavailability depends not only on its synthesis but also its degradation, mediated by reactive oxygen species (ROS), mainly superoxide anion (O2.-). We have previously demonstrated that CHF patients with sinus rhythm have platelet hyperggregability associated with alterations in NO bioavailability and oxidative stress1. Objective: The aim of this study is to investigate the effect of physical training (PT) on the intraplatelet L-arginine-nitric oxide pathway, oxidative stress and inflammatory markers in CHF without arrhytmias. Methods: Thirty CHF patients with left ventricular ejection fraction (LVEF) of 31±1% were randomized to 24 weeks of supervised exercise training (consisting of 30 minutes of moderate intensity treadmill exercise followed by resistance and stretching exercises, performed three times a week) or to a control group that remained sedentary. Blood was drawn before and after the intervention for platelet and plasma obtainment. The Ethical Committee of the State University of Rio de Janeiro approved this work (CEP-1435), and informed consent was obtained from each of the patients. The student t test was used for statistical analysis and statistic difference was considered when $p<0.05$. Results: Exercise tolerance was significantly increased in CHF patients who were submitted to exercise training. Platelet aggregation induced by ADP and collagen was significantly reduced in CHF patients after 24 weeks

of exercise training. Paradoxically, nitric oxide synthase activity in platelets, assessed by the conversion of L-[3H]-arginine into L-[3H]-citrulline, decreased after exercise training, and no significant difference was observed in intraplatelet cGMP levels among the groups. In relation to oxidative stress markers, systemic and intraplatelet TBARS production and carbonylation were diminished after 24 weeks of training in CHF patients. Moreover, systemic levels of CRP, fibrinogen and TNF-α were also reduced in CHF after training. Conclusion: Our results suggest that chronic exercise has anti-oxidant, anti-inflammatory and anti-aggregant effects, regardless of NO production, showing it be an important non-pharmacological tool in the treatment of CHF.

de Meirelles LR et al. Clin Exp Pharmacol Physiol. 2011 Oct;38(10):705-10

Financial support: FAPERJ and CNPq grants

Where applicable, the authors confirm that the experiments described here conform with The Physiological Society ethical requirements.

PCD032

Angiotensin II serum levels after different exercise intensities in human

S. van Ginkel[1,2], M. Flueck[1], A. de Haan[2] and J. de Koning[2]

[1]IRM Manchester, Manchester, UK and [2]Vrije Universiteit, Amsterdam, Netherlands

High blood pressure (hypertension) indicates the deterioration of the set points of metabolic fitness and is one of the most frequent metabolic risk factors in Western countries. Pharmacological inhibition of angiotensin 2 (ANGII) by ACE inhibition action may have undesirable side effects, particularly, in the situation when one wants to exploit the sympatholytic and angiogenic benefits of physical therapy. Limited studies investigated ANGII levels related to exercise intensity and duration, but it seems to be that there is only an increase above with exercise intensity above the anaerobic threshold. The aim of this research is to detect changes in human ANGII levels after exercises of different intensities at or above the anaerobic threshold. On three separate occasions fit healthy male subjects (n=10, age: 29.6±2.1 year, length: 180.9±7.6 cm, mass: 76.1±5.6 kg) performed a maximal incremental exercise tests, a 12-minutes test at an intensity were they reached their aerobic threshold intensity and a 3-minutes test their ventilator compensation point intensity. Expired air was measured breath-by-breath, blood samples were taken before and 0, 3, 6 and 12 minutes after exercise and subject were screened for the ACE I-allele polymorphism. Blood was measured on lactate concentration and serum on ANGII levels. Values are means ± S.E.M. Direct after the 3-minutes cycling test there was a 1.8-fold increase in ANGII serum levels compared to resting levels (paired T-Test, 3.20±0.83 vs. 5.75±0.81 pg/mL, p=0.001) and after the 12-minutes test there was a 1.2-fold increase (paired T-Test, 4.4±1.47 vs. 5.5±1.30 pg/mL, p=0.24). ANGII levels were not affected after the maximal exercise test. 12 minutes after maximal exercise subjects with the ID/DD genotype had a significant lower ANGII serum level compared to subjects with the II genotype (ANOVA, 1.7±1.0, 9.6±5.5, p<0.05). ANGII levels were not correlated with blood lactate levels. ANGII could be detected after a non-maximal high intensity exercise. The data indicate that variability in the response of the major vasoconstrictor, ANGII, in serum after exercise is related to the ACE genotype dependent but not blood lactate.

This research was funded by the European Commission through MOVE-AGE, an Erasmus Mundus Joint Doctorate programme (2011-0015).

Where applicable, the authors confirm that the experiments described here conform with The Physiological Society ethical requirements.

PCD033

Block-face imaging of wax-embedded tissue as a modality to aid three-dimensional histological reconstruction of the heart

U. Siedlecka[1], R. Casero Canas[2], R. Burton[3], C. Afonso[4], C. Bollensdorff[6,1], V. Grau[4,2] and P. Kohl[1,5]

[1]Cardiac Biophysics and Systems Biology, Imperial College London, Harefield, UK, [2]Oxford e-Research Centre, University of Oxford, Oxford, UK, [3]Department of Physiology, Anatomy and Genetics, University of Oxford, Oxford, UK, [4]Department of Engineering Science, University of Oxford, Oxford, UK, [5]Department of Computer Science, University of Oxford, Oxford, UK and [6]Qatar Cardiovascular Research Center, Doha, Qatar

Introduction: The histo-anatomical structure of the heart is a key determinant of cardiac function. Histological staining of sectioned tissue provides high-resolution identification of cells and sub-cellular structures in two dimensions (2D). However, the sections cannot easily be projected to 3D images, as they do not represent an inherently co-registered stack. In order to develop detailed 3D representations of heart structure, spatial reintegration of serial 2D sections has been guided by additional data, such as magnetic resonance imaging (MRI) [1,2]. However, histology processing involves dehydration and re-embedding, causing significant changes in volume and shape of wax-embedded sample in comparison to the MRI images. This makes the combination of data obtained with both methods challenging. To overcome this, we introduce block-face imaging of black wax-embedded tissue as an intermediate imaging step in the processing pipeline for tissue reconstruction.

Method: Briefly, rat hearts were excised after Schedule 1 killing according to the UK Home Office guidance on the Operation of Animals (Scientific Procedures) Act of 1986, and swiftly perfused via the aorta with normal Tyrode solution (mM: NaCl 140; KCl 5.4; MgCl2 1; HEPES 5; Glucose 10; CaCl2 1.8; pH 7.4). After washing, hearts were arrested using modified Tyrode containing elevated potassium (20mM), and fixed with a fast-acting Karnovsky's fixative. For histological follow-up, hearts were embedded in black wax to improve the contrast between wax and tissue surface. Wax blocks were mounted on Leica SM2400 heavy-duty sledge-type microtome. Sections were cut at 10μm thickness, and an image of wax block surface was taken prior to each section. Images were taken with a remote-controlled Canon EOS 450D camera mounted above the sledge, equipped with a polarisation filter. The LED light was coupled to a beam-splitter in front of the camera. Suitable rotational alignment of the collection filter allowed selection of reflected (polarized) light from the topmost layer of the wax/exposed tissue. This was used to identify the outline of tissue contained in the next section.

Discussion: Detailed reconstruction of extended tissue volumes, such as whole hearts, requires a combination of imaging methodologies, ideally ranging from *in vivo* cine MRI, to *ex vivo* fixed tissue anatomical and diffusion-tensor MRI, through to histology allowing identification of cells. 3D reconstruction of histology stacks, and registration to other modalities,

is aided significantly by an approach providing a set of inherently aligned images of the tissue acquired as it is serially sectioned. Block-face imaging of the wax-embedded tissue provides its consistent 3D volume, which can be used to guide spatial reconstruction of serial histology sections.

Burton RA et al. (2006). Ann NY Acad Sci 1080, 301–319.

Hales PW et al. (2012). Prog Biophys Mol Biol 110, 319–330.

BBSRC; Magdi Yacoub Institute

Where applicable, the authors confirm that the experiments described here conform with The Physiological Society ethical requirements.

PCD034

3D reconstruction of the human cardiac conduction system based on micro-CT and histology

A. Atkinson, T. Nikolaidou, M.R. Boyett and H. Dobrzynski

Institute of Cardiovascular Sciences, University of Manchester, Manchester, UK

Introduction
3D computer models of the heart are important tools for teaching, research and drug discovery. In current human heart models, the heart's wiring system (the cardiac conduction system, CCS) is oversimplified or omitted and the aim of this study is to create a 3D model including the CCS: the sinus node (SN), the paranodal area (transitional pacemaker tissue bordering the sinus node; PN (1)), atrioventricular node (AVN) and His-Purkinje system.
Methods
A whole human heart as well as an isolated human SN preparation (intercaval region of right atrium) were scanned using micro-CT at resolutions of 86 and 31 μm, respectively. The whole heart was then serially sectioned in the coronal plane at 50 μm thickness onto adhesive collection tape using a cryomacrotome and the SN was sectioned parallel to the crista terminalis at 30 μm thickness onto Superfrost Plus slides. Masson's trichrome histology was performed on whole heart sections at 1 mm intervals and SN sections at 500 μm intervals. Immunolabelling of the pacemaker channel HCN4 was carried out on sister sections to help identify the tissues of the CCS.
Results
Many of the major components of the CCS, including SN and AVN, were identified in whole human heart sections. The PN, as well as the SN, were identified in the sections of the isolated human SN preparation. The PN appears as a region of loosely-packed myocytes in close proximity to the SN. However, the PN, whilst being in close proximity to the SN, is at no point in direct contact with it. The SN extends from the superior vena cava along the crista terminalis about a third of the distance to the inferior vena cava. In contrast, the PN is a far more extensive structure than the SN and was traced along much of the length of the crista terminalis extending from the superior to the inferior vena cava. This could be reason why the leading pacemaker site in the human can be at any point from the superior to the inferior vena cava. Avizo software is being used to align histology sections with the micro-CT data and image analysis is being used to segment the SN, PN, AVN and His-Purkinje system. Following segmentation, we will create a 3D reconstruction of the whole human heart incorporating the CCS.
Conclusion
We are using a novel combination of techniques to create a detailed 3D reconstruction of the whole human heart including the CCS. The 3D reconstruction will enable more accurate simulations of cardiac electrophysiology.

Chandler N et al. (2011). *Anat.Rec.(Hoboken)* **294**, 970-979

Human heart samples were provided by Prof. Paul Iaizzo, Visible Heart Laboratory, University of Minnesota, USA; and Prof. Peter Molenaar, Biomedical Sciences, Queensland University of Technology, Australia.

Where applicable, the authors confirm that the experiments described here conform with The Physiological Society ethical requirements.

PCD035

The inter-relationship between the junctional SR and the sarcolemma; a big hug that makes your heart beat

C. Pinali, H. Bennett, B. Davenport, A.W. Trafford and A. Kitmitto

University of Manchester, Manchester, UK

The ultrastructural morphology of the sarcoplasmic reticulum (SR) is not well understood being represented as a sequence of compartmentalised domains limited by the sarcomere [1] or as a continuous network spread across the cell [2]. Since structure is dictated by function it is of primary importance to investigate it. We used serial block face imaging SEM to produce the first 3D reconstruction of the SR within a cardiomyocyte and identified junctional domains at the sarcolemma. We used sheep heart since its size and rate are similar to those of man. Sheep (n=4) were killed with an overdose of pentobarbitone (200mg/kg iv). All procedures were carried out in accordance to the United Kingdom Animals Act of 1986 and the University of Manchester's ethical review process. Small portions of left ventricle were put in 4% PFA and 2.5% GA in 0.1M sodium cacodylate buffer with 50mM CaCl2 to enhance the staining of the SR [3]. After washings, samples were put in 1% OsO4 and 1.5% K4Fe(CN)6, dehydrated and embedded in Taab LV. Resin blocks were trimmed to ~ 0.5 mm3, gold coated and positioned in a FEI Quanta 250 FEG SEM equipped with a Gatan 3View system which takes an image of the block face after a slice has been cut at a specific thickness, with images taken after each slice to generate 3-D data with a resolution of ~15nm in the X and Y directions (block surface) and ~ 50 nm in the Z direction (entering into the block). Images were aligned, analysed, reconstructed and segmented in Fiji [4] or IMOD [5]. The size of the tissue examined means that the SEM images at least 5-8 cells with the removal of each slice, generating volumetric data for each myocyte. Using the staining described the SR is highly contrasted and appears black. 3D reconstruction showed that the SR runs along the mitochondria throughout the cell and is also in close contact to the myofilaments parallel to the mitochondria. It also forms connections perpendicular to the myofilaments mostly located at the Z-line and is a continuous network connecting one end of the cell to the other. We found that junctional portions of the SR (jSR) not only form patches in apposition to the t-tubules but also adopt a similar organisation with the sarcolemma. This novel technique has generated detailed images of entire SR network within a cell at a resolution close to 15 nm. The identification of the jSR patches in close apposition to the sarcolemma is consistent with a functional role for spark generation in myocytes at the surface of the cell. A similar organisation would be relevant to myocytes which do not have a developed t-system like atrial myocytes of small mammals. The SR is also in close contact with the mitochondria which

may underlie a critical role in local Ca2+ transfer between the two organelles.

Page E, Surdyk-Droske M. Distribution, surface density, and membrane area of diadic junctional contacts between plasma membrane and terminal cisterns in mammalian ventricle. Circ Res 1979 Aug; 45(2): 260–7.

Yamasaki Y, Furuya Y, Araki K, Matsuura K, Kobayashi M, Ogata T. Ultra-high-resolution scanning electron microscopy of the sarcoplasmic reticulum of the rat atrial myocardial cells. Anat Rec 1997 May; 248(1): 70–5.

Brochet DX, Yang D, DiMaio A, Lederer WJ, Franzini-Armstrong C, Cheng H. Ca2+ blinks: rapid nanoscopic store calcium signaling. Proc Natl Acad Sci U S A 2005 Feb 22; 102(8): 3099–104.

Schindelin J, Arganda-Carreras I, Frise E, Kaynig V, Longair M, Pietzsch T, Preibisch S, Rueden C, Saalfeld S, Schmid B, Tinevez JY, White DJ, Hartenstein V, Eliceiri K, Tomancak P and Cardona A. Fiji: an open-source platform for biological-image analysis, Nature Methods 2012 Jun 28; 9(7): 676-682.

Kremer JR, Mastronarde DN, McIntosh JR. Computer visualization of three-dimensional image data using IMOD. J. Struct. Biol. 1996 Jan-Feb; 116(1): 71–76.

We acknowledge and thank the British Heart Foundation for funding this work (RG/11/2/28701).

Where applicable, the authors confirm that the experiments described here conform with The Physiological Society ethical requirements.

PCD036

The comparison of the kinetics of of rapid and slow delayed rectifier currents in undiseased human, dog, rabbit and guinea pig ventricular myocytes

C. Corici[1], Z. Kohajda[1], A. Horvath[1], M. Bitay[3], G. Bogats[3], J.G. Papp[1,2], L. Virag[2,1], A. Varro[2,1] and D. Jost[1,2]

[1]Division of Cardiovascular Pharmacology, Hungarian Academy of Sciences, Szeged, Hungary, [2]Department of Pharmacology & Pharmacotherapy, University of Szeged, Szeged, Hungary and [3]2nd Department of Medicine, Division of Cadiac Surgyery, University of Szeged, Szeged, Hungary

To understand the large inter-species variation in the drug effect on repolarization, and to identify the most human like species, the properties of the rapid (IKr) and the slow (IKs) components of the delayed rectifier potassium currents were compared in myocytes isolated from undiseased human donor (HM), and from three commonly used animal model, the dog (DM), rabbit (RM) and guinea pig (GM) ventricles by applying the patch-clamp and conventional microelectrode techniques at 37 °C. The amplitude of the IKr tail current measured at -40 mV after, a 1 s long test pulse to 20 mV, was very similar in HM and DM (0.35±0.07 and 0.38±0.02 pA/pF, respectively, n=12-15) but larger in RM and GM (0.66±0.05 pA/pF and 1.0±0.08 pA/pF, respectively, n=10). The IKs tail current was considerably larger in GM (amplitude at -40 mV, after a 5 s long test pulse to 50 mV was 3.3±0.6 pA/pF, n=10) than in RM (1.22±0.7 pA/pF, n=7) and DM (0.9±0.05 pA/pF, n=24). In HM IKs tail was even smaller than in DM (0.2±0.05 pA/pF, n=14). IKr activated rapidly and monoexponentially in each studied species. The corresponding activation time constants measured at 30 mV were: 36±3 ms in HM, 53±6 ms in DM, 35±3 ms in RM and 30±2 ms in GM, respectively (n=6-26). The deactivation of IKr in HM, DM and RM measured at -40 mV, after a pulse to 30 mV was slow and biexponential (t1=0.6±0.05 s and t2=6.7±0.9 s in HM; t1=0.4±0.02 s and t2=3.3±0.3 s in DM ; t1=0.6±0.03 s and t2=6.5±0.3 in RM, respectively, n=8-26), while in GM the IKr tail current was best fitted triexponentially (t1=0.14±0.01 s, t2=0.8±0.01 s and t3=6.6±.06 s, n=10). IKs measured at 30 mV, activated slowly and had apparently a monoxponential time course in HM, DM and RM (t=0.9±0.2 s in HM, t=1±0.1 s in DM, and t=0.8±0.05 in RM, respectively, n=6-21). In contrast, in GM the activation was clearly biexponential (t1=0.5±0.02 s and t2=3.2±0.01 s, n=10). In HM, DM and RM IKs deactivation measured at -40 mV, was fast and monoexponential (t=0.15±0.02, t=0.14±0.01 s and t=0.16±0.05, respectively, n=6-22), while in GM, in addition to the fast component (t1=0.16±0.01 s, A1=860±98 pA) an another slower component was also revealed (t2=0.6± 0.1 s, A2=670±79 pA, n=10). Selective IKr blockade resulted in substantial and comparable APD lenghthening in all species, while IKs blockade lengthened significantly APD only in GM, but not in HM, DM and RM (Fig 1). These results suggest that IK in HM resembles that measured in DM and RM, and considerably differs from that observed in GM. These findings suggest that the dog and rabbit IKr and IKs currents resemble more human than guinea pig and these species are more appropriate for preclinical evaluation of new potential drugs expected to affect cardiac repolarization.

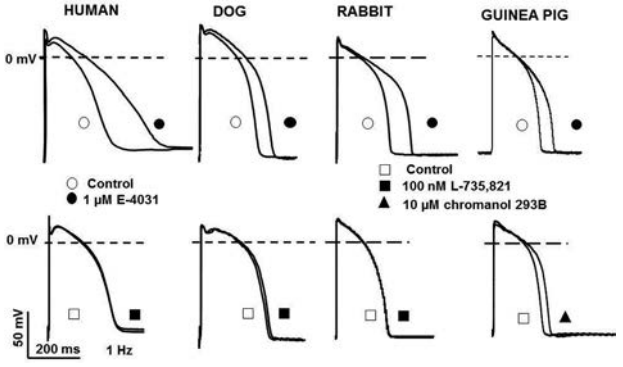

Fig. 1. Effect of selective IKr and IKs blockade on the APD in right venricular HM, DM, RM and GM at the 1 Hz simulation frequency.

Supported by grants from OTKA (K-82079 and NK-104331) and Hungarian Academy of Sciences.

Where applicable, the authors confirm that the experiments described here conform with The Physiological Society ethical requirements.

PCD037

An integrated method to quantify calcium fluxes in cardiac excitation-contraction coupling

M. Laasmaa, M. Vendelin and R. Birkedal

Institute of Cybernetics, Tallinn University of Technology, Tallinn, Estonia

In cardiac excitation-contraction (EC) coupling, calcium enters the cytosol via L-type Ca^{2+}-channels (I_{Ca}), reverse Na^{+}/Ca^{2+}-exchange (NCX_{rev}), or is released from the sarcoplasmic reticulum (SR) by Ca^{2+}-induced Ca^{2+}-release (CICR). The magnitude of calcium influx via the different pathways varies with the state of the cell. For example, in case of heart failure, CICR decreases and influx via NCX_{rev} increases. We have developed a new method to quantify the calcium influxes in EC coupling. We used a combination of perforated patch clamp with fluorescence microscopy and mathematical modeling to study rainbow trout (*Oncorhynchus mykiss*) cardiomyocytes. First, the action potential (AP) of each cell was recorded at a fre-

quency of 1.1 Hz. Second, we used the recorded AP to stimulate the cell in voltage clamp. I_{Ca} or NCX were inhibited to determine their respective currents with or without inhibition of SR. Fluorescence changes induced by Ca^{2+}-transients were recorded by loading the cells with Fluo-4 AM. To estimate the contribution of I_{Ca}, NCX, and CICR, we composed a mathematical model of Ca^{2+}-dynamics, which also takes into account intracellular buffering. For the given buffering constants, using spline approximated fluxes through I_{Ca}, NCX and CICR, and fluorescence gain as parameters, the model estimates the intracellular Ca^{2+} and fluorescence transients. Spline approximation of I_{Ca} and NCX fluxes can be found directly from the current measurements. CICR fluxes and other model parameters were found by least square fitting of the calculated and recorded fluorescence. Recordings of 27 different cells were used for analysis. In the control case, 9 cells were used to measure I_{Ca} and 6 cells to measure NCX current. When SR was inhibited, 6 cells were used to measure both I_{Ca} and NCX currents. Experiments were performed at 23 ºC. Our data and analysis suggest that during in trout cardiomyocytes at the given temperature and frequency, the Ca^{2+}-influxes are: 15-20% via L-type Ca^{2+}-channels, 15-20% via NCX_{rev} and 60-70% via CICR. When the SR was inhibited, we saw ~10% increased influx via L-type Ca^{2+}-channels and ~40% increase via NCX_{rev} compared to respective influxes in control case. The method is applicable to different species – including genetically modifiable mice and zebrafish – to study the cardiac functional phenotype under a range of physiological conditions.

This work was supported by Wellcome Trust International Senior Researcher Fellowship (WT081755), Estonian Science Foundation (Grant No. 8041), and European Union through the European Regional Development Fund.

Where applicable, the authors confirm that the experiments described here conform with The Physiological Society ethical requirements.

PCD038

A novel steady-state K^+ current inhibited by noradrenaline via a pertussis toxin-sensitive β_2 adrenoceptor-mediated pathway in rat atrial myocytes

R. Bond, S.C. Choisy, S.M. Bryant, J.C. Hancox and A.F. James

Physiology and Pharmacology, University of Bristol, Bristol, UK

Steady state outward K^+ currents (I_{Kss}) activate rapidly on depolarisation, show little inactivation and are thought to be important in action potential repolarisation. In ventricular myocytes, I_{Kss} has been suggested to be under adrenergic control (Choisy *et al*. 2004, Ravens *et al*. 1989, Scamps 1996). At present, however, there are no published data describing a noradrenaline (NA) –sensitive I_{Kss} in atrial myocytes. This study was designed to characterise I_{Kss} and investigate its modulation by NA in atrial myocytes. Procedures were approved by the Ethics Committee of the University of Bristol and were conducted in accordance with UK legislation. Male Wistar rats were anaesthetised by sodium pentobarbital (60-100 mg/kg i.p.) and left atrial myocytes isolated from the excised heart as previously described (Choisy *et al*. 2004). Ionic currents were recorded in whole cell voltage clamp mode using an external Tyrode's solution and K^+-based pipette solution. Superfusion of cells with 1 μM NA potentiated the L-type Ca^{2+} current (I_{CaL}) at 0 mV by 205±39.7 % and inhibited I_{Kss} at +50 mV by 44±4.6 % ($p \leq 0.001$, Student's paired t-test, n=6). While the effect of NA on I_{CaL} was abolished by the β_1-antagonist atenolol (10 μM), the inhibition of I_{Kss} was unaffected. The inhibitory action of NA on I_{Kss} was also unaffected by the α_1-antagonist, prazosin (5 μM), or atenolol plus prazosin. However, in the presence of the β_1/β_2-antagonist, propranolol (1 μM), the NA-induced inhibition of I_{Kss} was abolished. Furthermore, the action of NA on I_{Kss} was mimicked by the β_2-agonist, zinterol (1 μM) in the presence of atenolol (10 μM).

The steady state outward current was markedly reduced and the inhibitory effect of NA lost when recordings were made under K^+-free conditions, indicating the involvement of a K^+-selective current. NA reduced the power of the noise of I_{Kss}. Power spectral analysis of the NA-sensitive current indicated a single channel conductance of 27.6±5.1 pS (n=14). The NA-sensitive current was partially inhibited by 4-aminopyridine (3 mM). The action of NA on I_{Kss} in rat atrial myocytes was abolished in pertussis toxin-treated cells. The effect on action potential duration (APD) of I_{Kss} inhibition by NA was examined in the presence of 10 μM atenolol to prevent changes in I_{CaL}. In cells stimulated at 1 Hz, 1 μM NA prolonged APD_{30} by 17±5.4 % ($P \leq 0.05$, Student's paired t-test, n=8) but had no effect on APD_{60} or APD_{90}. In summary, these data demonstrate the existence of a steady state K^+ current that plays a role in modulation of APD by NA via a pertussis toxin-sensitive β_2-adrenoceptor mediated pathway in rat atrial cells.

Choisy SC, Hancox JC, Arberry LA, Reynolds M, Shattock MJ and James AF (2004) Evidence for a novel K^+ channel modulated by α_{1A}-adrenoceptors in cardiac myocytes. *Mol Pharmacol* **66:** 735-748.

Ravens U, Wang X-L and Wettner E (1989) Alpha adrenoceptor stimulation reduces outward currents in rat ventricular myocytes. *J Pharmacol Exp Ther* **250:** 364-370.

Scamps F (1996) Characterization of a β-adrenergically inhibited K^+current in rat cardiac ventricular cells. *J Physiol* **491:** 81-97.

RCB was supported by a BHF CRTF Award (FS/10/68)

Where applicable, the authors confirm that the experiments described here conform with The Physiological Society ethical requirements.

PCD039

Use of chimeras to investigate the molecular basis of differences in agonist and antagonist action between human P2X1 and P2X2 receptors for ATP

R. Allsopp, L.K. Farmer, A.G. Fryatt and R.J. Evans

Department of Cell Physiology and Pharmacology, University of Leicester, Leicester, UK

P2X receptor subtypes can be distinguished by their sensitivity to ATP analogues and selective antagonists. We have used chimeras between human P2X1 and P2X2 receptors to address the contribution of the extracellular loop, transmembrane segments and intracellular termini to the action of partial agonists (higher potency and efficacy of BzATP and AP5A at P2X1 compared to P2X2 receptors) and antagonists (NF449 ~ 1,500 fold more potent at P2X1 compared to P2X2). P2X receptors and chimeras were expressed in Xenopus oocytes and currents recorded with TEVC.

Replacing the extracellular loop of the P2X1 receptor with that from P2X2 (P2X1-2EXT) produced a receptor that had low sensitivity to NF449 equivalent to that at the WT P2X2 receptor. Sensitivity similar to WT P2X1 receptors was recorded in the reciprocal P2X2-1EXT chimera for NF449. These data show that antagonist sensitivity was conferred by the extracellular loop, and indicates that these chimeras do not result in major conformational changes. In contrast the effectiveness of partial

agonists was increased above P2X1 levels for both the loop transfers suggesting interactions with the rest of the receptors played an important role in regulating agonist sensitivity and efficacy.
Swapping TM1 increased the efficacy of AP5A and BzATP at P2X1-2TM1 and P2X2-1TM1 chimeras. Replacement of the TM2 region had reciprocal effects on partial agonist efficacy; P2X1-2TM2 showed partial agonist sensitivity similar to that at P2X2 and P2X2-1TM2 showed partial agonist sensitivity intermediate between P2X1 and P2X2. These results suggest a complex interaction between the TMs and the rest of the receptor in regulating partial agonist efficacy.
Exchanging the intracellular N- terminus had no effect on agonist potency, but increased partial agonist efficacy at P2X2-1N and decreased it at P2X1-2N chimeras. This demonstrates that potency and efficacy can be independently regulated. Further subdivision of the N- terminus showed amino acid residues 1-16 predominate in the control of efficacy. The C-terminal chimera P2X2-1C had no effect of partial agonist sensitivity, whereas the reciprocal chimera (P2X1-2C) had partial agonist efficacy intermediate between P2X1 and P2X2. Chimeras and point mutations also identified residues in the C-terminus that regulated recovery from channel desensitization.
In summary this study shows that interactions between the extracellular, transmembrane and intracellular portions of the P2X receptor regulate channel properties and suggest that transitions to channel opening, the behaviour of the open channel and recovery from the desensitized state can be controlled independently.

Where applicable, the authors confirm that the experiments described here conform with The Physiological Society ethical requirements.

PCD041

PDZ domain-binding motif of the cardiac sodium channel Nav1.5 regulates compartment-specific channel expression and cardiac conduction in cardiomyocytes

D. Shy[1], L. Gillet[1], J. Ogrodnik[1], M. Albesa[1], A.O. Verkerk[2], M.C. Essers[1], R. Wolswinkel[3], N. Syam[1], R.F. Marsman[3], A.M. van Mil[4], S. Rotman[5], C.R. Bezzina[3], C. Remme[3] and H. Abriel[1]

[1]Department of Clinical Research, University of Bern, Bern, Switzerland, [2]Department of Anatomy, Embryology and Physiology, Academic Medical Center, University of Amsterdam, Amsterdam, Netherlands, [3]Department of Clinical and Experimental Cardiology, Academic Medical Center, University of Amsterdam, Amsterdam, Netherlands, [4]Department of Clinical Genetics, Center for Human and Clinical Genetics, Leiden University Medical Center, Leiden, Netherlands and [5]Department of Pathology, University of Lausanne, Lausanne, Switzerland

Regulation of cardiac ion channels is essential for functional expression of ion channels and excitability of cardiac cells. Previous results with dystrophin-deficient (*mdx*) mice showed that disruption of the dystrophin-syntrophin macromolecular complex impairs excitability and impulse propagation by interfering with the interaction between the PDZ domain-binding motif of the cardiac sodium ion channel Nav1.5 and syntrophin at the lateral membrane of cardiomyocytes. In addition, interfering with the association between Nav1.5 and another PDZ domain-containing protein, SAP97 that is located at the intercalated discs, led to reduction of sodium current (I_{Na}).
To study the *in vivo* significance of this PDZ domain-binding motif on Nav1.5 function, we created and characterized a homozygous knock-in mouse strain which removed this motif by truncating the last three amino acids, Ser-Ile-Val (ΔSIV), of the Nav1.5 C-terminus. Western blots detected a 25% decrease in Nav1.5 protein level in ΔSIV hearts, while levels of associating proteins were unaffected. Immunostainings revealed loss of Nav1.5 expression at the lateral cardiomyocyte membrane but not at the intercalated discs. This reduction corresponded to a 36% decrease of whole-cell I_{Na} in ΔSIV cardiomyocytes and a 62% reduction of I_{Na}, specifically at the lateral membrane, in macropatch recordings. A significant slowing of 35% of maximal upstroke velocity of the cardiac action potential was detected. On surface ECGs, ΔSIV mice displayed a pronounced QRS-interval prolongation, indicating impeded ventricular conduction. This was confirmed with optical mapping of ΔSIV hearts showing prolongation of activation time and increased anisotropy due to a preferential decrease in transversal conduction velocity.
We also investigated the effects of a specific mutation within the PDZ domain-binding motif of Nav1.5 (p.V2016M) that was found in a patient with Brugada syndrome. This mutation changes the last amino acid of the PDZ domain-binding motif from valine to methionine (SIV to SIM) at the Nav1.5 C-terminus. HEK293 cell transfections of mutant V2016M channels revealed a 24% decrease in cell surface expression compared to WT in biotinylation experiments. Patch-clamp recordings of V2016M mutant channels revealed a 49% decrease in peak I_{Na}. Pull-down experiments with Nav1.5 WT or mutated C-terminus GST fusion proteins showed a significant decrease in the interaction of Nav1.5 and SAP97. Taken together, these results emphasize the importance of the Nav1.5 PDZ domain-binding motif in correct ion channel expression, protein interaction, and cardiac function.

Where applicable, the authors confirm that the experiments described here conform with The Physiological Society ethical requirements.

PCD043

Altered Ca^{2+}-handling features in TRIC-A channel-deficient and overexpressing vascular smooth muscle cells

D. Yamazaki[1], N. Miyuki[1], J. Ma[2] and H. Takeshima[1]

[1]Graduate School of Pharmaceutical Sciences, Kyoto University, Kyoto, Japan and [2]Davis Heart and Lung Research Institute, Ohio State University, Columbus, OH, USA

Intracellular Ca^{2+} stores are functionally maintained by Ca^{2+} uptake and release processes, both of which are electrogenic events. It has been predicted that counter-ion movements may balance the membrane potential to establish efficient Ca^{2+} release and uptake mechanisms in intracellular stores. However, molecular components mediating counter-ionic currents are unknown. We recently identified TRIC channel subtypes derived from distinct genes, namely TRIC-A and TRIC-B. TRIC channels are distributed to the endo/sarcoplasmic reticulum (ER/SR) and nuclear membranes in various cell types; TRIC-A is preferentially expressed in excitable tissues, while ubiquitous expression is observed for TRIC-B. TRIC channels are composed of ~300 amino acid residues, and contain three putative membrane-spanning segments to form a bullet-shaped homo-trimeric assembly. Both purified native and recombinant TRIC subtypes form functional monovalent cation-selective channels in a lipid bilayer reconstitution system. Based on the electrophysiological data indicating that TRIC channels behave as K^+ channels under intracellular conditions, we have been examining the physiological roles of the TRIC subtypes

using the gene-knockout and transgenic mice. Animal experiments were conducted with approval of the Animal Research Committee according to Kyoto University regulations. All surgical procedures were performed under pentobarbital anesthesia (50 mg/kg, intraperitoneal). Double-knockout mice lacking both TRIC subtypes show embryonic heart failure, and Ca^{2+} release during excitation-contraction coupling is compromised in the mutant cardiomyocytes. *Tric-a*-knockout mice develop hypertension resulting from vascular hypertonicity, and the knockout vascular smooth muscle exhibits depolarized resting potential due to insufficient spontaneous Ca^{2+} sparks for inducing hyperpolarization. In contrast, mutant mice carrying the smooth muscle-specific *Tric-a* transgene develop hypotension. Moreover, *Tric-b*-knockout mice show respiratory failure at birth and Ca^{2+} release essential for surfactant handling is impaired in the mutant alveolar epithelial cells. Therefore, TRIC channels seem to mediate ER/SR counter-K^+ movements in part to facilitate physiological Ca^{2+} release mediated by ryanodine and inositol-trisphosphate receptor channels in various cell types. This poster highlights the *Tric-a*-knockout hypertension and *Tric-a*-transgenic hypotension, and sets out the proposed physiological functions of TRIC channel subtypes in vascular smooth muscle cells.

Supported by the Japan Society for Promotion of Science and the US National Institute of Health.

Where applicable, the authors confirm that the experiments described here conform with The Physiological Society ethical requirements.

PCD044

Class 3 inhibition of hERG K^+ channel by caffeic acid phenethyl ester (CAPE) and curcumin

S. Choi[1], D. Shin[1], K. Kim[1], H. Yoo[1], H. Choe[2], W. Kim[3], Y. Zhang[1] and S. Kim[1]

[1]Physiology, Seoul National University Seoul National University College of Medicine, Seoul, Republic of Korea, [2]Physiology, University of Ulsan, College of Medicine, Seoul, Republic of Korea and [3]Internal Medicine, Dongguk University, Seoul, Republic of Korea

Human *ether-á-go-go* related gene (hERG) K^+ channel current (I_{hERG}) is inhibited by various compounds and genetic mutations, potentially resulting in cardiac arrhythmia. Here we investigated effects of caffeic acid phenethyl ester (CAPE) and curcumin, two natural anti-inflammatory polyphenols, on I_{hERG} in HEK-293 cells overexpressed with hERG. CAPE dose-dependently deceased repolarization tail current of hERG ($I_{hERG,tail}$; IC50, 10.6 ± 0.5 μM). CAPE also shifted half-activation voltage (V1/2) to the left (from –17.5 to –26.5 mV), and accelerated activation and inactivation kinetics. The CAPE inhibition of $I_{hERG,tail}$ was not attenuated in the pore-blocker site mutants of hERG (Y652A and F656A). A point mutation of Cys723 (C723S) mimicked the effects of CAPE; left shift of V1/2 and acceleration of $I_{hERG,tail}$ deactivation. However, $I_{hERG,tail}$ inhibition by CAPE was still observed in C723S. Taken together, CAPE inhibits hERG channel by class 3 mechanism, i.e. modification of gating, not by blocking the pore. Curcumin induced changes of I_{hERG} similar to those of CAPE while additional interaction with pore blocking sites was suggested from attenuated $I_{hERG,tail}$ inhibition in Y652A and F656A. Interestingly, I_{hERG} induced by human action potential voltage clamp was increased by CAPE while decreased by curcumin. Above results revealed intriguing roles of Cys723 in hERG kinetics, and suggested that conventional drug screening by using step pulse protocol for $I_{hERG,tail}$ would overlook the hERG kinetics modulations that could compensate the apparent decrease of $I_{hERG,tail}$.

Where applicable, the authors confirm that the experiments described here conform with The Physiological Society ethical requirements.

PCD045

Functional targeting of the $K_{ir}2.1$ 3′ UTR by multiple microRNAs

J.M. Yarham, L. Ferguson, M. McGahon, D. Simpson and A. Collins

CVVS, Queen's University, Belfast, Antrim, UK

MicroRNAs are increasingly recognised as important downregulators of gene expression. Luciferase-based assays have traditionally been used for identifying microRNA targets but these are limited. Previously we have reported miR-212 targeting of the $K_{ir}2.1$ 3' UTR using a novel functional microRNA targeting assay and here we report targeting by miRs-15b, -132 and -424. These microRNAs have been shown to be upregulated in heart failure, which features downregulation of $K_{ir}2.1$ activity in its pathophysiology. In the assay the 3′ UTR of the inward rectifier K^+ channel $K_{ir}2.1$ was inserted downstream of the mCherry red fluorescent protein sequence in an expression plasmid. MicroRNA, siRNA control or non-targeting control (SCR) sequences were inserted into the pSM30 expression vector, which provides enhanced green fluorescent protein as an indicator of microRNA expression. HEK293 cells were transiently co-transfected with the pSM30- and mCherry-based plasmids and the mean red and green intensity of each cell was measured using Volocity software. The principle of the assay is that functional targeting of the 3′ UTR by the microRNA decreases the cell red/green fluorescence intensity ratio. It was validated with a siRNA targeting the 3′ UTR of $K_{ir}2.1$ and used to investigate targeting of the $K_{ir}2.1$ 3′ UTR by miR-15b, miR-132 and miR-424 as predicted by bioinformatics. Red/green intensity ratio was significantly lower in siRNA-expressing and microRNA-expressing cells vs. SCR-expressing controls ($p<0.001$ for all microRNAs and siRNA by ANOVA; n range 322 to 2935). Similar results were obtained in 3 independent experiments for each microRNA. These results indicate functional targeting of the 3′ UTR of $K_{ir}2.1$ by miR-15b, miR-132 and miR-424, and suggest their involvement in $K_{ir}2.1$ downregulation in heart failure.

British Heart Foundation.

Department for Employment and Learning.

Where applicable, the authors confirm that the experiments described here conform with The Physiological Society ethical requirements.

PCD046

The basis of antagonist binding at cardiovascular P2X receptors for ATP

L. Farmer and R.J. Evans

University of Leicester, Leicester, UK

P2X1 and P2X4 receptors have important roles in the cardiovascular system, including contributions to blood clotting and

blood pressure control. Therefore subtype selective P2X antagonists have therapeutic potential for treatment of cardiovascular disease. The mechanism of antagonist binding at P2X receptors is currently unclear. NF449 is a potent antagonist at the human P2X1 receptor (hP2X1) and has an IC50 of ~1nM. The rat P2X4 (rP2X4) receptor is insensitive to NF449 up to concentrations of 100μM. The difference in antagonist sensitivity between hP2X1 and rP2X4 subtypes can be used to investigate the molecular basis of antagonism.

In this study chimeras have been generated between the two cardiovascular P2X receptors to replace regions of one receptor with corresponding residues from the other. The effects of these mutations on NF449 potency have then been observed. Initially four chimeras were generated, A,B,C and D which split the ligand binding extracellular loop into four sections of approximately equal size. Each of these sections incorporated a section of the residues surrounding the ATP binding pocket, a site at which antagonist binding has been implicated. The chimeras were expressed in Xenopus oocytes and two electrode voltage clamp recordings performed.

Replacing residues 56-133 (chimera A) and 261-324 (chimera D) of the NF449 sensitive hP2X1 receptor with residues of insensitive rP2X4 had no significant effect on NF449 potency. Therefore the variant residues within these sections of the extracellular loop do not account for the difference in NF449 action. When residues 136-181 of hP2X1 were replaced with those of rP2X4 (chimera B), antagonist sensitivity was reduced ~130 fold compared to WT hP2X1. Region 136-181 therefore plays a role in the antagonist sensitivity of the hP2X1 receptor. Within this region four positive charges at positions 136-140 have previously been shown to be involved in NF449 action. Reintroducing these charges to chimera B gave nanomolar NF449 potency, highlighting their importance. Neither making the reciprocal chimera (hP2X1 into rP2X4), nor introducing the four charges alone, gave antagonist sensitivity to the insensitive rP2X4 receptor. Other residues within the receptor must therefore be needed for NF449 to inhibit the current.

Replacing residues 184-261 of hP2X1 with those of the rP2X4 receptor (chimera C) also caused a significant ~130 fold decrease in NF449 potency. Residues within this region are therefore likely to be involved in the inhibition of the hP2X1 receptor by NF449. This fits with a model of NF449 binding to the four positive residues and an area within chimera C. In ongoing work, sub-chimeras are being made within this region to find specific residues/regions that the NF449 molecule may be interacting with.

Where applicable, the authors confirm that the experiments described here conform with The Physiological Society ethical requirements.

PCD047

Regulation of hERG channel function and pharmacology by a KCNE1 variant

C. Du[1], A. El Harchi[1], N. Kerr[2] and J.C. Hancox[1]

[1]School of Pgysiology and Pharmacology, University of bristol, Bristol, UK and [2]School of Clinical Sciences, University of Bristol, Bristol, UK

The rapid delayed rectifier K^+ current (I_{Kr}) plays an important role in ventricular repolarisation in the mammalian heart. The pore-forming subunit of I_{Kr} is considered to be encoded by human *ether-à-go-go-related gene* (hERG)(Sanguinetti and Tristani-Firouzi, 2006). In *vivo*, functional I_{Kr} channels may involve other ancillary subunits (Abbott et al., 2007). KCNE1, a protein which is best known as the β-subunit of the slow delayed rectifier K^+ current (I_{Ks}), has been suggested to modify hERG channel function (McDonald et al., 1997). Diverse clinically-used drugs produce hERG channel blockade and lead to acquired long QT syndrome. There is some evidence that KCNE1 variants may influence hERG current (I_{hERG}; eg.Ohno et al., 2007); however it is not known whether or not such variants may influence susceptibility to drug induced arrhythmias by influencing I_{hERG} pharmacology. We have addressed this issue through experiments on recombinant hERG channels co-expressed with either wild-type (WT) KCNE1 or a variant (A8V) that has previously been reported to influence I_{hERG} magnitude and be associated with a long QT phenotype (Ohno et al., 2007). Whole-cell patch-clamp measurements of I_{hERG} were made at 37°C. Consistent with prior observations (McDonald et al., 1997), we found that expression of WT KCNE1 in hERG expressing cells produced a hyperpolarising shift in the voltage dependence of I_{hERG} activation ($V_{0.5}$ of -16.06 ± 0.97 mV for I_{hERG}, n= 14 cells; and $V_{0.5}$ of -26.94 ± 1.09 mV for $I_{hERG\text{-}KCNE1}$, n= 9 cells). A similar shift was also seen for A8V KCNE1 variant ($V_{0.5}$ of -26.40 ± 1.8 mV for A8V KCNE1, n= 9 cells, p>0.05 versus WT KCNE1). The amplitude of I_{hERG} was smaller for A8V KCNE1 + hERG than for WT KCNE1 + hERG, under both conventional voltage clamp and "action potential" clamp (AP clamp; performed using a physiological ventricular AP waveform). Using paired AP commands, with the second AP waveform applied at varying time-intervals to mimic premature ventricular excitation, the response of I_{hERG} carried by A8V KCNE1 + hERG was reduced in comparison to that of WT KCNE1 + hERG. The I_{hERG} blocking potency of the Class I antiarrhythmic drug quinidine was similar between WT KCNE1 (IC_{50} of 0.54 ± 0.13 μM) and A8V KCNE1 (IC_{50} of 0.47 ± 0.11 μM). On the other hand, the I_{hERG} inhibitory potency of the antibiotic clarithyromycin was reduced for the A8V KCNE1 variant (IC_{50} of 80.26 ± 9.2 μM) compared with WT KCNE1 (IC_{50} of 40.85 ± 4.39 μM). These results demonstrate that, in principle, the A8V KCNE1 variant may alter the protective response of hERG channels to premature excitatory stimuli and the sensitivity of hERG channels to inhibition by drugs linked to acquired long QT syndrome.

ABBOTT, G. W., XU, X. & ROEPKE, T. K. (2007) Impact of ancillary subunits on ventricular repolarization. J Electrocardiol, 40, S42-6.

MCDONALD, T. V., YU, Z., MING, Z., PALMA, E., MEYERS, M. B., WANG, K. W., GOLDSTEIN, S. A. & FISHMAN, G. I. (1997) A minK-HERG complex regulates the cardiac potassium current I(Kr). Nature, 388, 289-92.

OHNO, S., ZANKOV, D. P., YOSHIDA, H., TSUJI, K., MAKIYAMA, T., ITOH, H., AKAO, M., HANCOX, J. C., KITA, T. & HORIE, M. (2007) N- and C-terminal KCNE1 mutations cause distinct phenotypes of long QT syndrome. Heart Rhythm, 4, 332-40.

SANGUINETTI, M. C. & TRISTANI-FIROUZI, M. (2006) hERG potassium channels and cardiac arrhythmia. Nature, 440, 463-9.

This work was supported by Heart Research UK (RG 2594/11/13).

Where applicable, the authors confirm that the experiments described here conform with The Physiological Society ethical requirements.

PCD048

Voltage-dependent stochastic gating of TRIC-B channels derived from TRIC-A knockout mouse skeletal muscle

A. Matyjaszkiewicz[1,2], E. Venturi[1], D. Yamazaki[3], M. Nishi[3], K. Tsaneva-Atanasova[4], H. Takeshima[3] and R. Sitsapesan[1]

[1]School of Physiology & Pharmacology, NSQI and Bristol Heart Institute., University of Bristol, Bristol, UK, [2]Bristol Centre for Complexity Sciences, University of Bristol, Bristol, UK, [3]Graduate School of Pharmaceutical Sciences, Kyoto University, Kyoto, Japan and [4]Department of Engineering Mathemathics, University of Bristol, Bristol, UK

The trimeric intracellular cation channels, of which there are two subtypes (TRIC-A and TRIC-B), are located on endo/sarcoplasmic reticulum (ER/SR) and nuclear membranes where they are thought to provide counter-current for ER/SR Ca^{2+}-release [1, 2]. TRIC-B knockout mice die immediately after birth demonstrating the essential role of this isoform [3]. We aimed to define the key aspects of TRIC-B channel gating and investigate how gating is regulated by voltage. Both TRIC-A and TRIC-B are present in most tissues and therefore to be certain that we record only TRIC-B single-channel events, we incorporated skeletal muscle light SR from TRIC-A knockout mice into artificial membranes under voltage-clamp conditions [2]. Recordings were obtained in symmetrical 210 mM K-PIPES, pH 7.2. Single-channel recordings were idealized using the segmental k-means (SKM) algorithm implemented in QuB software [4]. We developed Markov models of TRIC-B gating, with up to 4 distinct sub-conductance states (S1-S4), using both QuB and our own software. Mean-variance histograms [5] were computed using our own code. There was a high degree of variability in TRIC-B gating behaviour but almost 90% of channels (7 of 8 channels) exhibited voltage-dependent gating where channel activity was higher at positive than at negative holding potentials. At positive potentials, gating was characterised by long closures interspersed with bursts of openings in which the majority of time was spent in the full open state. At negative potentials, channel openings were rare and usually consisted of brief openings to the lower-conductance open states (S3 and S4). Even at positive holding potentials, Po plateaued to relatively low levels (< 0.2) over the voltage range +20 to +60 mV. Transitions to the full open state were typically preceded by brief transitions through a range of sub-conductance states. During an opening burst, TRIC-B often gated rapidly between the full open state and the higher-conductance open states, S1 and S2. Closure of the channel at the end of a burst also usually consisted of a tail of transitions through multiple sub-conductance states. The variable gating of TRIC-B and the frequent, rapid transitions between sub-conductance states prevents the development of reliable gating models using conventional single-channel analysis alone. We have therefore used mean-variance plots to provide additional quantitative and visual information that allows us to describe the key features of TRIC-B gating. Our model of TRIC-B gating provides the basic framework for developing an understanding of how TRIC-B may be regulated in situ and will help us to determine the individual and combined roles of TRIC-A and TRIC-B in supporting intracellular Ca^{2+}-release.

Yazawa M, Ferrante C, Feng J, Mio K, Ogura T, Zhang M, Lin PH, Pan Z, Komazaki S, Kato K, Nishi M, Zhao X, Weisleder N, Sato C, Ma J, Takeshima H (2007) TRIC channels are essential for Ca^{2+} handling in intracellular stores. Nature 448:78-82.

Pitt SJ, Park KH, Nishi M, Urashima T, Aoki S, Yamazaki D, Ma J, Takeshima H, Sitsapesan R (2010) Charade of the SR K^+-channel: two ion-channels, TRIC-A and TRIC-B, masquerade as a single K^+-channel. Biophys J 99 (2):417-426.

Yamazaki D, Komazaki S, Nakanishi H, Mishima A, Nishi M, Yazawa M, Yamazaki T, Taguchi R, Takeshima H (2009) Essential role of the TRIC-B channel in Ca^{2+} handling of alveolar epithelial cells and in perinatal lung maturation. Development 136:2355-2361.

Qin, F. (2004) Restoration of single-channel currents using the segmental k-means method based on hidden Markov modeling. Biophys J 86 (3):1488-1501.

Patlak JB (1993) Measuring kinetics of complex single ion channel data using mean-variance histograms. Biophys J 65:29-42.

Supported by the BHF, EPSRC and Japan Society for Promotion of Science

Where applicable, the authors confirm that the experiments described here conform with The Physiological Society ethical requirements.

PCD049

pH regulates the single-channel gating behaviour of TRIC-B channels derived from TRIC-A knockout tissue

F. O'Brien[1], E. Galfré[1], E. Venturi[1], A. Matyjaszkiewicz[1,2], D. Yamazaki[3], M. Nishi[3], H. Takeshima[3] and R. Sitsapesan[1]

[1]School of Physiology & Pharmacology, NSQI and Bristol Heart Institute., University of Bristol, Bristol, UK, [2]Bristol Centre for Complexity Sciences, University of Bristol, Bristol, UK and [3]Graduate School of Pharmaceutical Sciences, Kyoto University, Kyoto, Japan

TRIC-B is one of two subtypes of trimeric intracellular cation channels found in the endo/sarcoplasmic reticulum (ER/SR) [1, 2]. The TRIC-B knockout mouse dies in respiratory failure following birth and there is evidence that release of intracellular Ca^{2+} in the alveolar type II epithelial cells is severely disrupted [3]. The unique physiological role of TRIC-B and the mechanisms that regulate channel opening are not fully understood. Since monovalent cation flux across ER/SR membranes is known to be influenced by pH changes, we have investigated whether TRIC-B function is sensitive to pH. We incorporated the light SR membrane fraction isolated from skeletal muscle of TRIC-A knockout mice into artificial membranes under voltage-clamp conditions [2]. Recordings were obtained in symmetrical 210 mM K-PIPES at pH 6.2, 7.2 and 9.2. Where multiple channels incorporated, noise analysis was performed because the complex sub-conductance state gating prevented accurate assessment of the probability of dwelling in the various open states. Student's t-test was used to to access significance.We found that the single-channel conductance of the TRIC-B full open state was not affected by changing the pH on the cytosolic side of the channel. The full open state single-channel conductance was 205.8±2.18 pS at pH 6.2, 205.3±1.57 pS at pH 7.2 and 204.9±0.06 pS (SEM; n=3-7) at pH 9.2. As previously observed [2], TRIC-B channels were more open at positive holding potentials and exhibited variable gating behaviour with a wide range of open probabilities. For example, at pH 7.2 and at the holding potential of +30 mV, the single-channel mean current obtained from noise analysis was 1.55±0.58 pA/s (SEM; n=7) but this ranged from 0.03 to 3.36 pA/s for individual experiments. We observed that TRIC-B channels became more open as the cytosolic pH was increased. At +30 mV, as pH was raised from 7.2 to 9.2, we observed a 32.16 fold increase in the single-channel mean current (SD; n=3; p<0.

01) whereas when pH was lowered from pH 7.2 to 6.2, mean current decreased 2.08 fold (n=4).
In summary, we find that in addition to being a voltage-regulated channel, TRIC-B activity is also modulated by cytosolic pH. Such regulation may be particularly relevant for excitation-contraction coupling in skeletal muscle during fatigue or in cardiac muscle under conditions of myocardial ischaemia. Further work is necessary to understand the mechanisms governing TRIC-B activity in a cellular situation and how TRIC-B channel opening is important in supporting ER/SR Ca^{2+}-movements.

Yazawa M, Ferrante C, Feng J, Mio K, Ogura T, Zhang M, Lin PH, Pan Z, Komazaki S, Kato K, Nishi M, Zhao X, Weisleder N, Sato C, Ma J, Takeshima H (2007) TRIC channels are essential for Ca^{2+} handling in intracellular stores. Nature 448:78-82.

Pitt SJ, Park KH, Nishi M, Urashima T, Aoki S, Yamazaki D, Ma J, Takeshima H, Sitsapesan R (2010) Charade of the SR K^{2+}-channel: two ion-channels, TRIC-A and TRIC-B, masquerade as a single K^{+}-channel. Biophys J 99 (2):417-426.

Yamazaki D, Komazaki S, Nakanishi H, Mishima A, Nishi M, Yazawa M, Yamazaki T, Taguchi R, Takeshima H (2009) Essential role of the TRIC-B channel in Ca^{2+} handling of alveolar epithelial cells and in perinatal lung maturation. Development 136:2355-2361.

Supported by the BHF, EPSRC and Japan Society for Promotion of Science

Where applicable, the authors confirm that the experiments described here conform with The Physiological Society ethical requirements.

PCD050

Effects of muscarinic agonists and RGS4 on voltage-dependent responses of cardiac g protein-gated potassium currents

I. Chen, K. Furutani, A. Inanobe and Y. Kurachi

Osaka University, Osaka, Japan

ACh released from vagal nerve terminals opens G protein-gated potassium (KG) channels at nodal cells, thereby leading to bradycardia. One of the characteristics of ACh-induced KG currents in native cardiac myocytes is a time-dependent slow increase in current amplitude during hyperpolarizing voltage steps (1). This feature is referred to as "relaxation". We previously reported that RGS (regulators of G-protein signaling) proteins are responsible for the relaxation behavior (2, 3). RGS proteins are known to accelerate the GTP hydrolysis of G protein α subunits, and sequestrate free G protein $\beta\gamma$ subunits. Thus, the proteins hasten the speed of activation and deactivation of ACh-induced KG current, and cause the slowly developed current response. The voltage-dependent regulation of G protein-signaling underlies the latter response. In the present study, we examined the KG currents elicited by several muscarinic agonists (such as ACh and pilocarpine) in atrial myocytes. For electrophysiological experiments, the myocytes were enzymatically isolated from hearts removed from adult male Wistar rats, which were deeply anesthetized by intraperitoneal injection of a combination anesthetic (0.3 mg/kg of medetomidine, 4.0 mg/kg of midazolam, and 5.0 mg/kg of butorphanol). Unlike the relaxation of ACh-induced KG currents, the pilocarpine-induced KG currents were time-dependent slow decrease in current amplitude during hyperpolarizing voltage steps. In order to clarify the molecular mechanism underlying this voltage-dependent response, we reconstituted the KG channels in Xenopus oocytes by expressing Kir3.1 and Kir3.4. In oocytes that express Kir3.1/Kir3.4 with m2 muscarinic receptor, we recorded the pilocarpine-induced KG current which did not show the deactivation and failed to reproduce the current response of myocytes. However, when co-expressed with RGS4, we succeeded to record the voltage-dependent response resembling to cardiac KG current. By expressing truncation mutants of RGS4, we could reproduce the result of our previous study that only RGS domain itself was needed to reproduce the relaxation of ACh-induced KG current (3). However, we found that both N-terminus and RGS domain of RGS4 were essential to reproduce the voltage-dependent response of pilocarpine-induced KG currents. These data suggest that RGS4 proteins are critical for the voltage-dependent response, and the RGS4-induced modulation of G protein-signaling are varied with muscarinic agonists.

Noma A, Trautwein W. Relaxation of the ACh-induced potassium current in the rabbit sinoatrial node cell. Pflugers Archiv : European journal of physiology. 1978;377(3):193-200. Epub 1978/11/30.

Yamada M, Inanobe A, Kurachi Y. G protein regulation of potassium ion channels. Pharmacological reviews. 1998;50(4):723-60. Epub 1998/12/22.

Inanobe A, Fujita S, Makino Y, Matsushita K, Ishii M, Chachin M, et al. Interaction between the RGS domain of RGS4 with G protein alpha subunits mediates the voltage-dependent relaxation of the G protein-gated potassium channel. The Journal of physiology. 2001;535(Pt 1):133-43. Epub 2001/08/17.

Where applicable, the authors confirm that the experiments described here conform with The Physiological Society ethical requirements.

PCD051

Remodeling of the diaphragm in mice during the development of heart failure

T. Gillis[1], M. Plat[2], A. Arkell[2], A. Foster[2] and J. Simpson[2]

[1]Integrative Biology, University of Guelph, Guelph, ON, Canada and [2]Human Health and Nutritional Sciences, University of Guelph, Guelph, ON, Canada

In this study we examined the contractile function, and protein composition of diaphragm muscle following 18 weeks of transverse aortic constriction (TAC) induced heart failure in mice Diaphragm function was characterized following 2 and 18 weeks of TAC. Hearts after 18 weeks of TAC had multiple indicators of systolic and diastolic dysfunction, demonstrated a reactivation of the fetal gene program and interstitial fibrosis. Contractile function of skinned diaphragm muscle preparations (~2.9 mm x 250 μM) was measured over a range of Ca concentrations at a sarcomere length of 2.3 μM. At each Ca concentration the maximum activated force was measured, as was the rate of force redevelopment following rapid release and re-stretch. The Ca sensitivity of force generation was significantly reduced in the 18 week TAC group compared to the sham mice and the two week TAC group. The Kf½ (Ca concentration at half maximum force generation) for the 18 week TAC group was 2.2 ± 0.17 μM while that for the sham group and 2 week TAC group were 1.86 ± 0.14 and 1.90 ± 0.15 μM respectively. In addition, the maximum Ca activated force was significantly lower for the 18 week TAC mice (22.1 ± 2.4 mN mm-2) compared to those from the sham group and 2 week TAC group, 30.5 ± 2.6 and 25.1 ± 2.2 mN mm-2, respectively. Western blotting indicates a significant increase in the presence of a high molecular weight protein complex containing TnT in diaphragm from the 18 week TAC group. There was also a reduction in the rate of cross-bridge cycling, in the diaphragm from the 2 and 18 week TAC as compared to sham. In the sham

group, as Ca activated force increased there was a parallel increase in the rate of cross-bridge cycling. Comparatively, in the 2 and 18 week TAC groups, as force increased there was an initial increase in cross-bridge cycling but this reached an asymptote and then decreased before maximum force was reached. As a result, the rate of cross-bridge cycling in the diaphragms from the two treatment groups was significantly lower compared to those from the sham group for the latter half of the Ca activation curve. This reduction in cross-bridge cycling rates may be a compensatory mechanism to reduce the metabolic cost of contraction. However, this would reduce the rate of force development and therefore power generation by the muscle. The results of this study indicate that chronic hypertension initiates a series of changes in diaphragm contractility that have the potential to cause dysfunction in heart failure and may play a role in exercise intolerance and dyspnea, the chief complain from patients with heart failure.

This work was funded by support from NSERC (Canada) to TG and JS

Where applicable, the authors confirm that the experiments described here conform with The Physiological Society ethical requirements.

PCD053

Increased glomerular water permeability in streptozotocin-induced diabetes: roles of hyaluronan and chondroitin sulphate

A. Russell and A.H. Salmon

Microvascular Research Laboratories, University of Bristol, Bristol, UK

Changes in glomerular permeability, manifesting as albuminuria, occur early in diabetic nephropathy. The endothelial glycocalyx is an important regulator of glomerular permeability, and is disrupted in diabetic patients with albuminuria (Nieuwdorp et al (2006). Which component of the endothelial glycocalyx contributes to altered glomerular permeability in diabetes is not known. We have examined the roles of hyaluronan and chondroitin sulphate in regulating glomerular water permeability in healthy and diabetic animals.
Male Sprague Dawley rats received sodium citrate (sham) or streptozotocin (45 mg/kg) i.v. to induce diabetes. On day 7, rats were anaesthetised (sodium pentobarbital) and kidneys were perfused via the abdominal aorta with Ringer-Albumin solution. Right renal perfusate also contained Octadecyl-Rhodamine-B Chloride (R18: cell membrane label) and either Chondroitinase ABC (7.25U/kg) or Hyaluronidase (15000U/kg). Successful selective glomerular perfusion was confirmed with confocal microscopy. Following exsanguination and nephrectomy, glomeruli were sieved from the cortex of each kidney, aspirated onto a micropipette and equilibrated in 1% BSA perifusate. Perifusate switch to 8% BSA caused glomeruli to shrink. The initial rate of change in glomerular volume was recorded, calculated off-line, and used to determine volume-corrected glomerular water permeability (LpA/Vi: min-1 mmHg-1), assuming σ=1. One-way ANOVA (Bonferroni correction) was used to compare mean±sem(n) LpA/Vi between groups.
Glomerular LpA/Vi was increased in diabetic rats (sham: 0.85±0.08(58); streptozotocin: 1.23±0.13(39); p<0.0001). Neither chondroitinase nor hyaluronidase significantly altered LpA/Vi in sham- treated animals (chondroitinase: 0.844±0.08(28); hyaluronidase: 0.678±0.06(30); both p>0.05 vs vehicle-sham). In diabetic animals, only hyaluronidase modified LpA/Vi (chondroitinase: 1.22±0.27(19); hyaluronidase: 0.674±0.10(19)*; *p>0.05 vs vehicle-streptozotocin).
Glomerular water permeability (LpA/Vi) is increased in diabetic animals. Hyaluronan appears to be an important contributor to this diabetes-related change in glomerular water permeability.

Nieuwdorp, M et al. (2006). Diabetes 55, 1127-1132).

Where applicable, the authors confirm that the experiments described here conform with The Physiological Society ethical requirements.

PCD054

Respiratory health status of rural Indian women. Does Domestic Cooking fuel really matter?

M. Phatak and N. Sukhsohole

Physiology, Indira Gandhi Govt. Medical college, Nagpur, Maharashtra, India

Whether continued use of biomass fuels along with other fuels in presence of poor domestic cooking conditions is as detrimental to respiratory health as the exclusive use of biomass fuels is unknown. The present study is an attempt to assess the risks associated with indoor air pollution in the context of adverse domestic cooking environmental conditions in rural women of central India. Hence we conducted a community based, cross-sectional study in 760 non-smoking, rural women of central India – 265 used non-biomass fuels (Group A), 243 biomass and other fuels (Group B) while 252 exclusively biomass fuels (Group C). Exposure to domestic smoke was estimated according to the average time per day spent near the fireplace (exposure index). Abnormal pulmonary function of the study subjects was assessed by the measurement of peak expiratory flow rate (PEFR) according to standards recommended by American thoracic society. PEFR less than 80% of the predicted was considered as abnormal pulmonary function. It was observed that robust multivariate analyses which adjusted for height, illiteracy, physical activity, environmental exposure to tobacco smoke (ETS), mud house, overcrowding, inadequate ventilation and respiratory morbidity revealed that illiteracy [Odds ratio (OR) 2.48, 95 % Confidence interval (CI) 1.04-5.87]; physical activity (OR 3.93, 95 % CI 1.52-10.14); inadequate cross ventilation (OR 2.43, 95 % CI 1.23-4.77) and respiratory morbidity (OR 2.65, 95 % CI 1.38-5.08) were significant predictors of low PEFR for group C (P<0.05). Whereas none of the predictors were found to be significantly associated with group B. Since women using partial biomass fuels showed no association of low PEFR with domestic cooking environment and respiratory morbidity even after robustly adjusting for confounding variables, we can conclude that even partial abolition of biomass use may be beneficial in improving the lung function of rural, non-smoking women in spite of having inadequate domestic cooking environment.

Perez-Padilla R, Schilmann A, Riojas-Rodriguez H. Respiratory health effects of indoor air pollution. Int J Tuberc Lung Dis 2010;4(9):1079-86.

World Health Organization. In :Bruce N, Perez-Padilla R, Albalak R, editors. The health effects of indoor air pollution exposure in developing countries. Protection of the Human Environment Geneva 2002. p. 5-10.

Gao X, Yu Q, Gu Q, Chen Y, Ding K, Zhu J,et al. Indoor air pollution from solid biomass fuels combustion in rural agricultural area of Tibet, China. Indoor Air 2009;19(3):198-205.

Reddy TS, Guleria R, Sinha S, Sharma SK, Pandey JN. Domestic cooking fuel and lung function in healthy non smoking women. Indian J Chest dis Allied Sci 2004;46:85-90.

Bruce N, Perez-Padilla R, Albalak R. Indoor air pollution in developing countries: a major environmental and public health challenge. Bulletin of the World Health Organisation 2000;78(9):1078-92.

Where applicable, the authors confirm that the experiments described here conform with The Physiological Society ethical requirements.

PCD055

Characterization of a new mouse model of COPD via conditional over-expression of RAGE by alveolar epithelium

P.R. Reynolds

Physiology and Developmental Biology, Brigham Young University, Provo, UT, USA

Receptors for advanced glycation end-products (RAGE) are multiligand cell-surface receptors detected abundantly in pulmonary tissue. Our previous work revealed increased RAGE expression in cells and lungs exposed to tobacco smoke (1) and that the initiation of RAGE signaling following smoke exposure leads to cytokine expression via pro-inflammatory mechanisms mediated by Ras and NF-kB (2,3). Furthermore, we have discovered important pro-apoptotic embryonic effects when RAGE is genetically upregulated in mice (4,5). RAGE expression is elevated in various pathological states, including chronic obstructive pulmonary disease; however, precise contributions of RAGE to the progression of emphysema and pulmonary inflammation are yet unknown. In the current study we generated a RAGE transgenic mouse (RAGE TG) that conditionally over-expressed RAGE by ATII cells in the respiratory compartment. RAGE was induced from weaning (20 days of age) until sacrifice date at 50, 80, and 110 days (representing 30, 60, and 90 days of RAGE over-expression). H&E staining and mean chord length measurement revealed incremental dilation of alveolar spaces as RAGE over-expression persisted. TUNEL staining and electron microscopy confirmed increased apoptosis and blebbing of alveolar epithelium in lungs from RAGE TG mice when compared to controls. Immunohistochemistry using specific antibodies for matrix metalloproteinase 9 (MMP-9) revealed an overall increase in MMP-9 expression, which correlated with decreased elastin expression in RAGE TG mice. Furthermore, RAGE TG mice manifested significant inflammation measured by elevated bronchoalveolar lavage protein, leukocyte infiltration, and secreted cytokines. These data support the concept that innovative transgenic mice that over-express RAGE may model pulmonary inflammation and alveolar destabilization independent of tobacco smoke. Furthermore, it validates RAGE signaling as a target pathway in the prevention or attenuation of smoke-related inflammatory lung diseases.

Reynolds PR et al. (2008). AJP: Lung Cell Mol Physiol 294(6):L1094-101.

Reynolds PR et al. (2010). Am J Resp Cell Mol Biol 45(2):411-8.

Robinson AB et al., (2012). AJP: Lung Cell Mol Physiol 302(11):L1192-9.

Reynolds PR et al., (2011). Am J Resp Cell Mol Biol 45(6): 1195-202.

Stogsdill JA et al., (2011). Am J Resp Cell Mol Biol. 47(1):60-6.

This work was supported by a grant from the Flight Attendant's Medical Research Institute (FAMRI, P.R.R.) and a BYU Mentoring Environment Grant (P.R.R.).

Where applicable, the authors confirm that the experiments described here conform with The Physiological Society ethical requirements.

PCD057

Characterization of respiration in mice with Rett syndrome mutations T158A and R168X

J.M. Bissonnette[1], S.J. Knopp[1], L.R. Shaevitz[2] and Z. Zhou[3]

[1]Oregon Health & Science University, Portland, OR, USA, [2]Tufts University, Medford, MA, USA and [3]University of Pennsylvania, Philadelphia, PA, USA

The X-linked disorder, Rett syndrome (RTT), is caused by mutations in the gene encoding methyl-CpG-binding protein 2 (MeCP2). A featuring phenotype of RTT is abnormal respiration characterized by frequent apnea and an irregular inter-breath pattern. Mice with a large deletion of Mecp2 show similar breathing abnormalities to RTT. Here we characterize respiration in two mouse models that genetically mimic common RTT mutations, heterozygous females with a missense mutation, T158A (Mecp2T158A/+) or a nonsense mutation R168X (Mecp2R168X/+). Previous studies demonstrated that MeCP2 T158A protein shows impaired binding to methylated DNA and MeCP2 R168X retains the methyl-DNA binding domain but lacks the large C-terminus of the protein including the transcription repression domain. Oregon Health & Science University IACUC approved the protocol that was in agreement with the National Institutes of Health "Guide for the Care and Use of Laboratory Animals". Mice were 7.7 to 12.5 months old when studied, un-anaesthetized, in a body plethysmograph. We found that both mutant strains show abnormal breathing consisting of a slower frequency, frequent apnea and an irregular inter-breath interval, compared to their respective wild type littermates (Mecp2+/+) (Table 1).

The breathing phenotype in Mecp2R168X/+ mice, however, varies significantly among individuals as might be expected in an X-linked disorder. For comparison, we classified Mecp2R168X/+ mice into a mild group and a severe group based on phenotypic severity. Mecp2T158A/+ mice fall between these two groups. Our findings demonstrate that there is considerable inter animal symptom variability in mouse models of RTT, reflecting the fact that RTT is a spectrum disorder. This is likely due to a combination of random X-chromosome inactivation and the different types of mutations on MeCP2. These heterozygous females are well suited for preclinical treatment trials that utilize respiration as an outcome measure, but classification of individual animal respiratory severity is necessary prior to treatment trials. In addition the varied respiratory phenotype in these mutant mice affords an opportunity to further define mechanisms that underlie abnormal breathing in Rett syndrome.

Table 1

Strain	Number	Frequency (bpm)	Apnea (# / hour)	Irregularity score (variance)
Mecp2+/+	8	223±4.7	7.1±2.2	4.9±1.3
Mecp2T158A/+	8	198±7.6*	41.1±5.4**	11.3±1.3*
Mecp2+/+	7	190±6	3.8±1.5	1.99±0.33
Mecp2R168X/+ (mild)	4	169±4.8*	14.4±4.2*	3.5±0.62*
Mecp2R168X/+ (severe)	4	119±9.1***	111±46.7***	13.9±2.6***

Values are mean ±SEM, *p<0.05 **p<0.01 ***p<0.0001 ANOVA

Support: Rett Syndrome Research Trust, NewLife Foundation (UK) (JMB); International Rett Syndrome Foundation (JMB and ZZ); NIH grant NS058391 (ZZ). ZZ is a Pew Scholar in Biomedical Science.

Where applicable, the authors confirm that the experiments described here conform with The Physiological Society ethical requirements.

PCD058

Apoptotic cell instillation promotes antifibrotic feedback loop between COX-2/PGE2 signaling and HGF in the bleomycin-stimulated lung

Y. Yoon[1,2], Y. Choi[1,2] and J.L. Kang[1,2]

[1]Physiology, Ewha Womans University, Seoul, Republic of Korea and [2]Tissue Injury Defense Research Center, Ewha Womans University, Seoul, Republic of Korea

Previous our study reported that instillation of apoptotic cells after bleomycin induces persistent HGF production and protects from fibrosis, but the mechanism underlying this antifibrotic effect remains unclear. In the present study, we investigated immediate and prolonged effects of apoptotic cell instillation on the potent antifibrotic molecules, such as COX-2/PGE2. Furthermore, we characterized the functional interaction between these molecules and HGF upon in vivo exposure to apoptotic cells in the injured lung processing extensive fibrosis, using selective inhibitors of these molecules. Apoptotic cell instillation after bleomycin results in further enhancement of immediate and prolonged expression of COX-2 in lung and alveolar macrophages compared with those of bleomycin only treated mice. Coadministration at the same time with apoptotic cells and sequential administration of the COX-2 selective inhibitor, NS-398, the selective PGE2 receptor EP2 inhibitor, AH6809, reversed the increases in immediate and prolonged mRNA and protein expression of HGF in lung and alveolar macrophages. On the other hand, inhibition of HGF signaling using the c-Met antagonist PHA-665752 reversed the immediate and prolonged increases in COX-2 mRNA and protein expression as well as PGE2 production in lung and alveolar macrophages following apoptotic cell instillation. In functional relevance, these inhibitors, including NS-398, AH6809, and PHA-665752, reversed the reduction of hydroxyproline content, as well as proapoptotic activity of caspase-3 and -9 and MPO activity following apoptotic cell instillation. These findings indicate that interaction with apoptotic cells in vivo induces persistent upregulation of COX-2/PGE2 and HGF in a positive feedback loop. The greater and prolonged production of these molecules may be an important mechanism whereby apoptotic cell instillation exerts the net results of anti-inflammatory, anti-apoptotic and anti-fibrotic action.

Lee YJ et al. (2012). Eur Respir J 40, 424-435

Huynh ML et al. (2002). J Clin Invest 109, 41-50.

This work was supported by the National Research Foundation of Korea (NRF) grant funded by the Korea government (MEST; 2010-0029353)

Where applicable, the authors confirm that the experiments described here conform with The Physiological Society ethical requirements.

PCD059

Effects of asthma, TGF-β treatment and allergen sensitization on expression of p115-RhoGEF and other RhoA-associated proteins in human airway smooth muscle cells and mouse lung

Y. Shaifta, K. O'Brien, D. Wright, N. Irechukwu, J. Ward and G. Knock

Asthma, Allergy& Lung Biology, King's College London, London, UK

The cytokines transforming growth factor-β (TGF-β) and interleukin-13 (IL-13) have been implicated in the patho-physiology of asthma (Vignola et al., 1997; Batra et a., 2004) and may be contributing to the associated altered airway smooth muscle function. We hypothesized that these cytokines may be mediating this altered smooth muscle function through changes in RhoA/Rho-kinase signalling, which has also been implicated in allergen-induced airway hyper-responsiveness (Chiba et al., 2004). Human airway smooth muscle cells (hASMC) were obtained by bronchoscopy from moderate asthmatic or healthy subjects. We examined the protein expression of RhoA, Rho-kinase (ROCK), myosin phosphatase targeting subunit-1 (MYPT-1), myosin light-chain-20 (MLC20), and the Rho-specific guanine nucleotide exchange factor p115-RhoGEF in serum-starved healthy hASMC with or without prior 24 hr incubation with TGF-β (10ng/ml) or IL-13 (10ng/ml) or the two cytokines in combination. We also investigated differences in the protein expression of p115-RhoGEF in serum-starved hASMCs derived from moderate asthmatics compared to gender-matched healthy subjects (all male), and in lung tissue of ovalbumin (OVA) sensitized 1295SVJ/Black Swiss mice, compared to non-sensitized controls. Expression of MLC20, MYPT-1 and p115-RhoGEF in healthy hASMCs were all significantly enhanced by TGF-β and by TGF-β in combination with IL-13, but not by IL-13 alone, whereas expression of RhoA and ROCK were not altered by any of the treatments (Fig. 1; expressed as percentage of control vehicle treated cells; * $P<0.05$, $^{**}P<0.01$, $^{***}P<0.001$; derived from one-way repeated measures ANOVA with Holm-Sidak post-tests for individual comparisons). Expression of p115-RhoGEF was approximately 3-fold greater both in asthmatic hASMC compared to controls and in OVA-sensitized mouse lung compared to controls (Fig. 2, $^{*}P<0.05$ by unpaired t-test, n=3 in all cases, data expressed as a ratio of p115-RhoGEF/GAPDH expression). Our data suggest that TGF-β-induced changes in expression of RhoA-associated proteins may contribute to altered airway smooth muscle function in asthma. In particular, the guanine nucleotide exchange factor p115-RhoGEF, which activates RhoA in response to G-protein coupled receptor activation and integrin engagement (Wells et al., 2001; Dubash et al.,2007), may be important in mediating enhanced RhoA/Rho-kinase activity in asthmatic and allergen-sensitized airways.

Protein	Effects of treatment on protein expression (mean ± SEM)		
	TGF-β	IL-13	TGF-β + IL-13
MLC_{20} (n=6)	253 ± 31***	126 ± 12	268 ± 31***
MYPT-1 (n=6)	199 ± 28**	123 ± 14	199 ± 27**
p115-RhoGEF (n=6)	223 ± 41*	92 ± 6	252 ± 46**
RhoA (n=5)	109 ± 3	113 ± 8	109 ± 6
ROCK (n=5)	111 ± 9	125 ± 15	120 ± 9

Fig. 1. Effects of cytokine treatment (24 hrs, 10ng/ml) on protein expression in hASMCs.

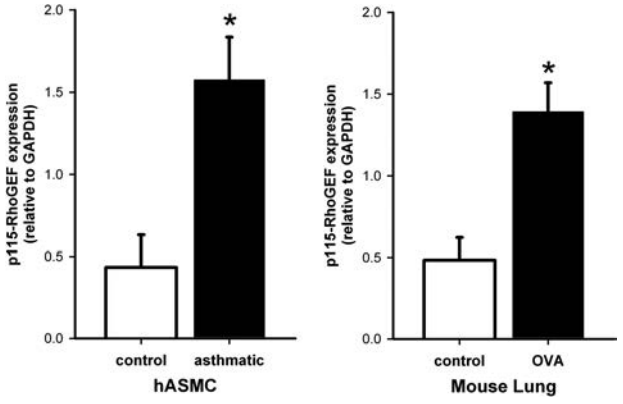

Fig. 2. Enhanced expression of p115-RhoGEF in asthmatic hASMC and after OVA-sensitization in mouse lung compared to controls (*P<0.05 by unpaired t-test, n=3 in all cases)

Batra V, Musani AI, Hastie AT, Khurana S, Carpenter KA, Zangrilli JG, & Peters SP (2004). Bronchoalveolar lavage fluid concentrations of transforming growth factor (TGF)-beta1, TGF-beta2, interleukin (IL)-4 and IL-13 after segmental allergen challenge and their effects on alpha-smooth muscle actin and collagen III synthesis by primary human lung fibroblasts. Clin Exp Allergy 34, 437-444.

Chiba Y & Misawa M (2004). The role of RhoA-mediated Ca2+ sensitization of bronchial smooth muscle contraction in airway hyperresponsiveness. J Smooth Muscle Res 40, 155-167.

Dubash AD, Wennerberg K, Garcia-Mata R, Menold MM, Arthur WT, & Burridge K (2007). A novel role for Lsc/p115 RhoGEF and LARG in regulating RhoA activity downstream of adhesion to fibronectin. J Cell Sci 120, 3989-3998.

Vignola AM, Chanez P, Chiappara G, Merendino A, Pace E, Rizzo A, la Rocca AM, Bellia V, Bonsignore G, & Bousquet J (1997). Transforming growth factor-beta expression in mucosal biopsies in asthma and chronic bronchitis. Am J Respir Crit Care Med 156, 591-599.

Wells CD, Gutowski S, Bollag G, & Sternweis PC (2001). Identification of potential mechanisms for regulation of p115 RhoGEF through analysis of endogenous and mutant forms of the exchange factor. J Biol Chem 276, 28897-28905.

Funded by the Wellcome Trust, MRC, Asthma UK

Where applicable, the authors confirm that the experiments described here conform with The Physiological Society ethical requirements.

PCD060

Nitro-oxidative stress markers with diagnostic and prognostic value in occupational exposure to isocyanates

P. Alina Elena[1], C. Florinela[2], P. Ovidiu[3], T. Marian Aurel[4] and O. Remus[2]

[1]Pathophysiology, Iuliu Hastieganu University of Medicine and Pharmacy, Cluj Napoca, Romania, [2]Physiology, Iuliu Hastieganu University of Medicine and Pharmacy, Cluj Napoca, Romania, [3]Occupational Medicine, Regional Public Health Center, Cluj Napoca, Romania and [4]Pathology, University of Agricultural and Veterinary Sciences, Cluj Napoca, Romania

Experimental and human studies have demonstrated that dermal exposure to isocyanates is a significant risk factor for sensitisation to isocyanates. Recent occupational medicine studies demonstrated the link between exposure to isocyanates, skin sensitization and astma. The aim of the study was to evaluate the nitro-oxidative stress markers in human subjects with occupational exposure to isocyanates and without clinical and functional manifestations of occupational asthma. Workers occupationally exposed daily for two weeks to isocyanates and without asthma (n = 70, M/F =23/47) were compared to a control group of healthy individuals (n=50, M/F=25/25) not exposed to isocyanates or other toxic agents. Nitro-oxidative stress was evaluated by measuring serum nitrotyrosine (3NT), total nitrites and nitrates (NOx), total oxidative status (TOS), total antioxidant reactivity (TAR) and oxidative stress index (OSI). Tissue injury was appreciated by measuring serum MMP-9. Values are means ± S.E.M., compared by ANOVA. In subjects occupationally exposed to isocyanates the systemic levels of NOx (85,11±5,46 vs. control 42,46±6,12μmol/L, p<0.05), 3NT(358,96±52,04 vs. control 161,72±14,48 μmol/l, p<0.05) TOS (13,95± 1,22 vs. control 11,95±0,29 μmol echivalent H2O2/L, p<0.05), OSI (3,71±0,32 vs. control 1,23±0,0005, p<0.05) and MMP-9 (13,55±1,99 vs. control 10,34±1,24 ng/ml, p<0.05) were significantly increased, and TAC (0,37±0,08 vs. control 1,23±0,05 mmol echivalent trolox/L, p<0.05) was lower than in healthy subjects. The nitro-oxidative stress parameters did correlate with serum MMP-9 level. These data suggest that occupational exposure to isocyanates is associated with systemic nitro-oxidative stress before onset of clinical signs of occupational asthma. 2. Serum nitro-oxidative stress tests correlate with MMP-9. 3. These tests may be recommended for early diagnosis in hypersensitivity to isocyanates.

This work was financially supported by the Ministry of Education, Research and Youth, CNCSIS grant PNII-IDEI 1273/2008, and by The Regional Public Health Center, Cluj-Napoca, Romania

Where applicable, the authors confirm that the experiments described here conform with The Physiological Society ethical requirements.

PCD061

Fasudil, but not N–Acetylcystein or Hyperoxia accelerates recovery from pulmonary hypertension induced by exposure to chronic hypoxia

O. Vajnerova[1], K. Plocova[1], H. Maxova[2], M. Vizek[2] and J. Herget[1]

[1]Physiology, 2nd Med Sch, Charles University, Prague, Czech Republic and [2]Pathophysiology, 2nd Med Sch, Charles University, Prague, Czech Republic

Pulmonary hypertension (PH) is frequent complication in patients of advanced heart failure and it is a sign of poor clinical outcome (Ghio et al, 2001). We studied rats recovering in air for two weeks after hypoxic PH induced in isobaric hypoxic chamber (FiO2 = 0.1, 3 wks).
To accelerate the recovery we used antioxidant N-acetylcysteine (NAC) (group H+NAC, n = 9, 20 g / l drinking water, 2 wks), Rho-kinase inhibitor fasudil (group H+F, n = 10, 30mg/kg/day, i. p., 2 wks). Control group recovered in ambient air was treated with saline (n = 9). The third experimental group recovered in hyperoxic environment (FiO2 = 0.3, 2 wks) (group H+HO, n = 7), controls (n=8) recovered in air.
After two weeks of recovery all rats were anesthetized with Thiopental (40 mg/kg, i.p.) and pulmonary arterial mean blood pressure, cardiac output and ratio of the weights of the right and left heart ventricles were determined. Groups H+NAC, H+HO and relevant controls did not differ in any of measured parameters. In rats treated with fasudil the mean pulmonary arterial blood pressure was after two weeks recovery significantly lower (20 ± 4 mmHg, mean ± SEM) than in controls (27 ± 4 mmHg). The ratio of the weights of the right and left heart ventricles, however, did not differ from controls. Cardiac output did not differ between the groups.
Inhibition of Rho kinase pathway but not change in metabolism of oxygen radicals are related to the pattern of recovery of lung circulation after chronic hypoxia.

Ghio S et al (2001). J Am Coll Cardiol 37, 183-188.

Study was supported by Grant IGA NT/13358 and GACR 13-01710S

Where applicable, the authors confirm that the experiments described here conform with The Physiological Society ethical requirements.

PCD062

Onset to hypoxia produces increased matrix metalloproteinase activity in peripheral pulmonary arteries and generation of collagen fragments

J. Novotna[1] and J. Herget[2]

[1]Medical Biochemistry, 2nd Med Sch, Charles University, Prague, Czech Republic and [2]Physiology, 2nd Med Sch, Charles University, Prague, Czech Republic

Chronic ventilatory hypoxia results in remodelling of pulmonary vasculature and hypoxic pulmonary hypertension. Hypoxia increases the turnover of extracellular matrix proteins in peripheral pulmonary blood vessels.
We studied hypoxia – induced changes in collagen isolated from pulmonary peripheral arteries and from systemic mesenteric peripheral arteries. Our hypothesis is that presence of collagen cleavage products in the walls of hypoxic peripheral pulmonary arteries starts the vascular remodelling.
Two groups of rats were exposed to hypoxia (FiO2 = 0,1) for four days (pulmonary arteries - H4, N=7 - and mesenteric arteries - systH4, N=6) and three weeks (pulmonary arteries - H21, N=7 and mesenteric arteries - systH21, N=6). Two relevant control groups were kept in air. Collagen proteins ex¬tracted from arteries by limited pepsin digestion were studied using SDS polyacryl amide electrophoresis and Western blot. Presence of collagenolytic enzyme, matrix metalloproteinase-13 (MMP-13) and inducible NO synthase (iNOS) were also studied using Western blot. In the peripheral pulmonary arteries of rats exposed to hypoxia three weeks we found already described ~75 kDa cleavage fragment (three-fourth fragment of collagen type I molecule) but not its one-fourth (~25 kDa) counterpart. In peripheral pulmonary arteries of rats exposed to 4 days hypoxia, however, both three-fourth and one-fourth fragments of collagen type I and type III were identified. In the control normoxic group no collagen cleavages were detected in lung vessels. Three-fourth and one fourth fragments of collagen type I were found also in mesenteric peripheral arteries of rats exposed four days to hypoxia but theirs relative density was significantly lower than in lung vessels. MMP-13 and iNOS were detected in early phase of pulmonary hypoxic hypertension in peripheral pulmonary arteries but not in arteries of rats exposed to hypoxia three weeks or any systemic vessels. We interpret breakdown of collagen to one-fourth and three-four fragments in an early phase of hypoxia exposure as a result of relative low resistance of poorly cross-linked molecule to proteolysis by specific MMPs. Resulting accumulation of collagen cleavages ("matrikines") stimulates the fibrotization of prealveolar pulmonary vessels.

Study was supported by Grants IGA NT/13358 and GACR 13-01710S.

Where applicable, the authors confirm that the experiments described here conform with The Physiological Society ethical requirements.

PCD063

Switching of lower jaw movements between the inspiratory and expiratory phases generated by chemoreceptor inputs

K. Nakayama[1], M. Yokomatsu[2], A. Mochizuki[1], T. Inoue[1] and I. Yazawa[3]

[1]Department of Oral Physiology, Showa University Shcool of Dentistry, Tokyo, Japan, [2]Department of Pediatric Dentistry, Showa University Shcool of Dentistry, Tokyo, Japan and [3]Department of Anatomy, Showa University Shcool of Medicine, Tokyo, Japan

Using electrophysiological techniques in a decerebrate and arterially perfused *in situ* rat preparation (P9–24 days; n = 28), extracellular recording were recorded to investigate the interplay of neuronal discharge patterns involved in relationships between a respiratory state and lower jaw movements. The perfusate was an oxygenated (95% O_2-5% CO_2) Ringer's solution containing an oncotic agent (Ficoll 70). Body temperature was set at room temperature. Respiratory discharge was recorded from the phrenic and/or the hypoglossal nerve, and neuronal discharge regarding lower jaw movements was obtained from the trigeminal nerve controlling the digastric muscle. The frequencies of neuronal burst discharges from all nerves increased with increases in the perfusion flow rates. When the flow rate was set at about 6× the total blood volume per minute, the phrenic discharge showed "eupneic pat-

tern" and "regular rhythm". As the flow rate further increased, the preparation was exposed to a hyperoxic/normocapnic state and all nerve discharges became clearly organized into episodes of greater frequency and duration, punctuated by periods of quiescence. All neouronal discharges involved in lower jaw movements were synchronous to the phrenic discharge at all flow rates tested. Although the frequencies of all burst discharges became faster when body temperature was set at above 25°C, the same results as mentioned above were obtained in all cases (n = 3). It was indicated that opening movements of mouth were generated in the inspiratory phase.
When the preparation was perfused by Ringer's solution infused with a 92% O_2-8% CO_2 gas mixture at room temperature, the same results mentioned above were obtained in all cases (n = 6) though the amplitude of all neuronal discharges increased. After the preparation was temporarily exposed to anoxia by applying 500 μM sodium cyanide (NaCN), the trigeminal discharge was produced in both the inspiratory and expiratory phases. After the preparation was exposed to an anoxic state by applying 500 μM NaCN for 1 to 2 minutes, the trigeminal discharge was completely produced in the expiratory phase (n = 5). Based on these results, it was indicated that the amount of inputs from the peripheral and central chemoreceptors changed the timing of opening and closing mouth.
From the above, it was suggested that switching of lower jaw movements between the inspiratory and expiratory phases was generated by increasing and decreasing inputs from chemoreceptors.

Where applicable, the authors confirm that the experiments described here conform with The Physiological Society ethical requirements.

PCD066

The importance of the diaphragmatic ligament in maintaining contractile function in the preterm sheep diaphragm

G.J. Pinniger[1], K. Karisnan[1,2], C. Berry[2], P. Noble[1,2], J.J. Pillow[1,2] and A.J. Bakker[1]

[1]School of Anatomy, Physiology and Human Biology, The University of Western Australia, Crawley, WA, Australia and [2]Centre for Neonatal Research and Education, School of Paediatrics and Child Health, The University of Western Australia, Crawley, WA, Australia

The diaphragm is an atypical skeletal muscle in that its length is not determined by changes in joint angle, but rather is influenced by negative intrapleural pressure and movement of the rib cage. In this arrangement, the diaphragm may be susceptible to large changes in sarcomere length thus compromising contractile function and predisposing it to damage. The diaphragmatic ligament may be important in setting muscle length and protecting against muscle damage, particularly during development (1). Therefore, we examined the influence of the diaphragm ligament on contractile function and susceptibility to stretch induced damage in the diaphragm of preterm sheep.
This study was approved by the animal ethics committee of the University of Western Australia. Preterm lambs were delivered via hysterotomy at 121 d gestational age (term = 150 d) and killed immediately with pentobarbitone (150 mg/kg IV). The costal diaphragm was dissected and longitudinal strips of muscle fibres were isolated and mounted in an in vitro test system. An adjacent strip of fibres, from which the diaphragm ligament had been carefully removed, was mounted in a second system for concurrent analysis. Muscles were maintained in mammalian Ringer solution (pH 7.3, 25°C) bubbled with carbogen. Each muscle strip was manually adjusted to optimal muscle length (Lo) at which maximum tetanic force (Po), maximum twitch force (Pt), time to peak twitch force (TTP), half relaxation time (½ RT) and maximum rate of force development (df/dt) were determined. Maximum unloaded shortening velocity was determined using the slack test method and susceptibility to muscle damage evaluated from a series of 5 eccentric contractions in which the fibres were stretched to 110% Lo while stimulated. Muscle mass and Lo were recorded for calculation of CSA and specific force (N.cm2). Differences between ligament (LIG: n = 11) and no ligament (NL: n=11) groups were analysed by student t-tests.

Removal of the diaphragm ligament had no significant effect on Po or Pt. However, the twitch time course was slower in the NL group as reflected by significant increases (~50%) in TTP and ½ RT and significantly lower df/dt (NL 389 ± 41 g/s, LIG 525 ± 44 g/s; $P<0.05$). The maximum unloaded shortening velocity was 14% lower in the NL group compared LIG and the decrease in peak force after 5 eccentric contractions was significantly greater without the ligament (NL 4.2 ± 2.2%; LIG 1.2 ± 0.1%; $P<0.05$). Lo was not significantly different between the groups.
These data indicate the importance of the diaphragmatic ligament in maintaining contractile function in the preterm diaphragm and support previous studies suggesting the diaphragmatic ligament provides a structural framework for diaphragm muscle fibre development (2).

1 Griffiths, RI, Shadwick, RE & Berger, PJ (1992) Functional importance of a highly elastic ligament on the mammalian diaphragm. Proc. R. Soc. Lond. B, 249:199-204.

2 Griffiths, RI & Berger, PJ (1996) Functional development of the sheep diaphragmatic ligament. J Physiol, 492.3:913-9.

This study was supported by NHMRC APP1010665

Where applicable, the authors confirm that the experiments described here conform with The Physiological Society ethical requirements.

PCD067

Effect of active sensitisation to acarian allergen on rat airway function and morphology

B. Mounkaila[3] and E. Roux[1,2]

[1]U1034 Adaptation cardiovasculaire à l'ischémie, Bordeaux Segalen University, Pessac, France, [2]U1034 Adaptation cardiovasculaire à l'ischémie, INSERM, Pessac, France and [3]Faculty of Health Sciences, Abdou-Moumouni University, Niamey, Niger

This study has analysed the occurrence of hyperreactivity and airway remodelling in a model of asthmatic disease in brown Norway rats sensitized to Dermatophagoides pteronyssinus allergen (D pter).
Male brown Norway rats (250-300 g) (n=7) were sensitized by 2 subcutaneous injections of D pter (50 IR/ml) (Stallergenes AS, France) and Al_2O_3 at days 0 (D0) and 3 (D3), followed at D17 by intratracheal instillation of D pter. Control (C) rats (n=5) underwent the same protocol but with saline solution instead of D pter. Witness (W) rats (n=5) were not submitted to any treatment. At D24, enhanced expiratory pause (Penh), used as an index of airway resistance, was measured using a barometric plethysmograph for conscious animals. At D25, rats were killed, a bronchoalveolar lavage (BAL) was performed, and isometric contraction was measured on rings isolated from

trachea (T), extrapulmonary (EPB) and intrapulmonary bronchi (IPB) using an organ bath system. Maximal contraction (Fmax) and LogEC50 were derived from cumulative concentration response curves to -8 to-3 LogM carbachol (CCh). Wall thickness and smooth muscle area of proximal and distal bronchi were measured on Masson's trichrome stained serial paraffin slides of lung. Results are expressed as mean ± SEM. Statistical comparisons were done by non parametric tests using SPSS software. Differences were considered significant when $P < 0.05$.

Allergen challenge increased Penh in S, but not in C and W rats. In vitro stimulation by D pter induced contraction of T, EPB and IPB rings isolated from S, but not C and W rats. In response to metacholine (MCh) challenge, MCh concentration (in LogM) inducing 300 % increase in Penh was significantly lower in S (-4.36 ± 0.44) and C (-3.92 ± 0.54) versus W (-2.86 ± 0.55) rats. Fmax to CCh was significantly higher in IPB from S (1966 ± 232 mg/mg wet weight) versus C (1613 ±189 mg/mg ww) and W rats (1191 ± 113 mg/mg ww), and LogEC50 (in LogM) significantly lower (S: -6.22 ± 0.03; C: -5.64 ± 0.02; W: -5.23 ± 0.02). In BAL fluid, cellular density was significantly higher in S (334 ± 52 cells/μl) versus C (217 ± 18 cells/μl) and versus W (165 ± 52 cells/μl) rats, as was the percentage of eosinophils (S: 8.75 %; C: 1.74 %; W: 0.7 %) and mast cells (S: 0.5 %; C: 0.2 %; W: 0 %). No significant difference was found for bronchial wall thickness and smooth muscle area between S and W rats.

Sensitized rats showed (i) in vivo and ex vivo specific bronchoconstriction to allergen stimulation, (ii) in vivo hyperresponsiveness and ex vivo hyperreactivity and hypersensitivity to cholinergic stimulation, and (iii) increased proportion of eosinophils and mast cells in BAL fluid, indicating that such sensitized rats are a relevant model of asthma. Absence of significant morphometric change indicates that airway hyperresponsiveness associated change occurs prior to airway remodelling.

Where applicable, the authors confirm that the experiments described here conform with The Physiological Society ethical requirements.

PCD069

Simulating bronchoconstriction in a patient specific model of the major airways

R.M. Bordas[1], B. Brook[2], D. Kay[1] and K. Burrowes[1]

[1]Computer Science, University of Oxford, Oxford, UK and [2]Mathematical Sciences, University of Nottingham, Nottingham, UK

The use of computational fluid dynamics (CFD) to simulate ventilation in the major airways of the lung has been shown to demonstrate greater specificity in assessing lung function over spirometry measures and visual analysis of computed tomography (CT) images. Currently, CFD is limited to simulating ventilation in a static airway geometry derived directly from CT. It cannot be used to assess the change in ventilation as a result of acute bronchoconstriction or long term remodelling of the airway wall. We have developed a multiscale biomechanical model of bronchoconstriction in the major airways. The model integrates an active tension produced by airway smooth muscle (ASM) and the passive mechanical properties of airway walls and lung parenchyma to simulate constriction and allow assessment of changes in ventilation.

Initially, a finite element model (FEM) of the mechanics of a single airway embedded in a layer of parenchyma was developed. The model was used to parameterise material laws governing the airway wall mechanics in generations 1-10 and to validate the mechanical behaviour of the model in comparison to experimental data. ASM is embedded circumferentially in the model acting at a given angle to the airway cross section. The model is used to assess the reduction in airflow in response to ASM contraction in both normal and remodelled airway wall cases and the distribution of mechanical stress in the airway wall.

To extend the methodology to a patient specific setting, a CT scan of a healthy adult was segmented to obtain a surface mesh of the airway wall. A volumetric mesh encompassing the airway walls was subsequently generated for use with the FEM model. Wall thickness in the mesh is varied to represent airway wall remodelling.

The single airway model was used to investigate changes in airway resistance in response to remodelling. For example, a 19.5x increase in resistance between a normal and a remodelled generation 3 airway in response to a ASM activation (15 degree fibre angle at 8 cmH2O pleural pressure) was shown. The patient specific model was used to demonstrate the change in airflow and material stress around a number of bifurcations for several prescribed ASM tensions, again demonstrating the change in flow in response to ASM constriction and airway wall thickening.

We have developed a methodology for simulating bronchoconstriction on patient specific geometries. The single airway model is well validated and validation of the patient specific model against clinical data is ongoing. The method reveals the importance of the structure of airway bifurcations in governing total airflow in the major airways. The results suggest that simulating bronchoconstriction on patient specific geometries can provide insight into the reduction in ventilation due to acute ASM contraction and chronic airway wall remodelling.

Where applicable, the authors confirm that the experiments described here conform with The Physiological Society ethical requirements.

PCD070

Simulation of pulmonary function test using a one dimensional airway ventilation model

M. Kim, D. Kay and K.S. Burrowes

Department of Computer Science, University of Oxford, Oxford, UK

Pulmonary function test is the most common diagnostic method to evaluate the integrated mechanical capacity of lung ventilation. This test can help to assess the conditions of airway diseases such as asthma and chronic obstructive pulmonary disease (COPD). The constricted airways in these diseases disturb the normal stream of respiratory flow and cause heterogeneous ventilation leading to ventilation-perfusion mismatch affecting gas exchange.1,2 However, none of the lung ventilation models to-date presented the lung function test in the full conducting airway geometry. The goal of the current study is to simulate the lung function test using one dimensional (1D) ventilation model and to demonstrate the difference between a normal and a constricted lung models.

One dimensional (1D) centerlines of central airways were obtained from patient-specific geometry segmented from CT images. Then, the skeletons of conducting airways down to terminal bronchioles were generated using a volume-filling branching algorithm within the lung surface boundary.3 In addition to the normal case, the bronchoconstricted lung was

modelled by reducing radii of selected airways. To compute the dynamic pressure distribution, a fully coupled mathematical model including acinar tissue deformation and airway network flow was introduced.4 We assumed quiet breathing and minimal airway wall compliance to simplify the model. For the input boundary condition, a wave representing the changes in pleural pressure during the lung function test was imposed on each acinar unit. Flow volume and flow rate during inhalation and exhalation were computed to test the function of the model.

The respiratory flow in the normal lung model showed a physiologically reasonable level of lung capacity. Both peak flow rate and tidal volume decreased in the bronchoconstricted lung model. According to the reduction of the lung capacity, heterogeneity in ventilation was increased in the constricted airway model. Computed parameters of the lung function test such as FEV1, FVC and FEV1/FVC in the normal lung were in the clinically acceptable range for the healthy subjects. But, those values were notably decreased by bronchoconstriction. The inspiratory flow-volume curves showed typical shape of normal and constricted lung curves as reported in clinical measurements.

We simulated pulmonary function tests in normal and bronchoconstricted lungs. The pulmonary function of the lung model weakened as the constriction and ventilation heterogeneity increased. The ventilation model presented in this study could be an effective tool to assess respiratory flow characteristics and increase our understanding of the lung function.

Tzeng YS et al. (2009), J Appl Physiol 106, 813-822

Tgavalekos NT et al. (2005), J Appl Physiol 99, 2388-2397

Tawhai MH et al. (2004), J Appl Physiol 97, 2310-2321

Kim M et al. (2013), Americal Thoracic Society, San Francisco.

This work was funded through the European Commission, FP7 grants: AirPROM (www.airprom.eu) and Synergy-COPD (www.synergy-copd.eu).

Where applicable, the authors confirm that the experiments described here conform with The Physiological Society ethical requirements.

PCD071

Respiratory pattern of newborn male rats (P6) exposed to fluoxetine during prenatal period

V. Biancardi, L.A. Patrone, K.C. Bícego and L.H. Gargaglioni

Animal Physiology and Morphology, FCAV - UNESP, Jaboticabal, Sao Paulo, Brazil

Selective serotonin reuptake inhibitors (SSRIs) as fluoxetine are generally prescribed as antidepressant for depression treatment. Fluoxetine administration during pregnancy might be a risk factor for cardiorespiratory diseases in human fetus, as persistent pulmonary hypertension (Chambers et al., 2006). Serotonin (5-HT) is a neurotransmitter involved in nervous maturational processes even at the fetal stage, being an important modulator of respiratory rhythm. The serotoninergic receptors 5-HT1A and 5-HT2A are found within respiratory neurons and they play a key role in this process, beyond they are related to hypercapnia and hypoxia responses. Therefore, the goal of the present study was to evaluate the possible effects of an exposure to SSRIs during a critical period of the development, prenatal period, on respiratory control system of newborn male rats (P6). To this end, pregnant female rats received via oral gavage vehicle (apyrogenic sterile saline + 0.2% Tween-80) or fluoxetine (10mg/kg) from 15th to the 21st day of gestation and the ventilation of pups was studied. The pups were divided in control group (mother received saline during pregnancy) or SSRI group (mother received fluoxetine during pregnancy). We calculated minute ventilation (VE) of newborn male rats (P6) by using the pressure-plethysmography from the body chamber method which shows the pressure signal that we measured during breathing is directly proportional to tidal volume (VT). These measurements were made during 30 min exposure to room air followed by 30 min exposure to 7% CO2 (hypercapnia) or 30 min exposure to 10% O2 (hypoxia), then the newborns were recovered in normocapnic/normoxic conditions for 45 min and exposed to 10% O2 or 7% CO2 for 30 min. Hypercapnia exposure induced an increase in VE in the control group but did not change ventilation in the SSRI group. There were differences between groups [20 min of hypercapnia: control group: 112.95±1.31 (% of baseline); SSRI group: 104.76±3.61 (% of baseline), $p<0.05$, two-way ANOVA]. Hypoxia induced an increase in VE in both groups, however the ventilatory response to hypoxia was higher in SSRI group [30 min of hypoxia: control group: 128.14±13.76 (% of baseline); SSRI group: 163.91±11.72 (% of baseline), $p<0.05$, two-way ANOVA]. The depressor response to hypoxia in the control group is not observed in SSRI group. These preliminary results suggest that in SSRI group the CO2 chemosensitivity might be reduced whereas the O2 chemosensitivity might be increased.

Chambers CD, Hernandez-Diaz S, Van Marter LJ, Werler MM, Louik C, Jones KL, Mitchell AA. Selective serotonin-reuptake inhibitors and risk of persistent pulmonary hypertension of the newborn. N Engl J Med., v. 354(6), p. 579-587, 2006.

FAPESP, CNPq, INCT - Fisiologia Comparada

Where applicable, the authors confirm that the experiments described here conform with The Physiological Society ethical requirements.

PCD072

The orexin receptor 1 (OX1R) in the Locus Coeruleus contributes to the hypercapnic chemoreflex in unanesthetized rats

M.B. Dias[1], M.C. Vicente[2] and L.H. Gargaglioni[2]

[1]Physiology, UNESP, Botucatu, SP, Brazil and [2]Animal Morphology and Physiology, UNESP, Jaboticabal, SP, Brazil

It has been suggested that orexin is involved in the ventilatory response to CO2. As the Locus coeruleus (LC) is a chemoreceptor site and expresses an extensive population of orexin receptor 1 (OX1R), we tested the hypothesis that OX1R located in the LC is involved in chemoreception. For the surgical procedures, male Wistar rats were subjected to general anesthesia by i.p. ketamine (100 mg/kg) and xylazine (10 mg/kg). One week later, in unanesthetized rats, we injected SB-334867 (OX1R antagonist, 5 mM) unilaterally into the LC. Pulmonary ventilation (VE) was recorded in a whole body plethysmograph, together with body temperature (Tb, dataloggers), mean arterial pressure (MAP) and heart rate (fH) in air followed by hypercapnia (7% CO2). Hypercapnia caused an increase in VE, which resulted from increases in respiratory frequency (fR) and tidal volume (Vt), but did not affect MAP, fH or Tb in all groups. SB-334867 caused a significant attenuation (70% reduction), of the hyperventilation induced by hypercapnia (n=9) compared with its vehicle (n=6; $P< 0.05$). This effect was due to

both decreased Vt and f. Basal ventilation, MAP, fH or Tb, were not affected by OX1R antagonism. These results suggest that projections of orexin-containing neurons to the LC contribute via orexin R1 to the hypercapnic chemoreflex control in unanesthetized rats.

FAPESP, CNPq

Where applicable, the authors confirm that the experiments described here conform with The Physiological Society ethical requirements.

PCD073

Theoretical estimates of pulmonary diffusing capacity

T.K. Roy[1] and T.W. Secomb[2]

[1]Dept of Anesthesiology, Mayo Clinic, Rochester, MN, USA and [2]Dept of Physiology, University of Arizona, Tucson, AZ, USA

The process of pulmonary oxygen uptake is analyzed to obtain quantitative estimates of pulmonary diffusing capacity $D_{LO}2$. An axisymmetric model is used to represent radial diffusion of oxygen from alveoli through the alveolar-capillary membrane, through the plasma, and into the erythrocytes. Analysis of unsteady diffusion due to the passage of the discrete erythrocytes shows that the transport of oxygen through the alveolar-capillary membrane occurs mainly in the regions adjacent to erythrocytes, and that oxygen transport through regions adjacent to plasma gaps can be neglected. Calculations are performed for a range of discharge hematocrit and capillary diameter values. The model developed above is used to calculate values of $D_{LO}2$ as a function of capillary diameter and hematocrit. The values obtained range from 50 to 90 ml O_2 min^{-1} $mmHg^{-1}$, with values at the higher end of the range corresponding to higher hematocrit and lower capillary diameter and therefore a high lineal density of erythrocytes. These values are much lower than the estimates obtained by others using the morphometric method, which considers the total membrane area and the specific uptake rate of erythrocytes. Representing relative resistances in terms of an inverse Sherwood number demonstrates that under normal circumstances, resistances due to intraerythrocyte diffusion, plasma diffusion, and alveolar-capillary membrane are of similar magnitude, and that the transport resistance due to oxygen unloading is negligible. Additional calculations performed for increasing alveolar-capillary membrane thickness demonstrate the expected effect of decreasing lung diffusing capacity. Finally, simulations of pulmonary oxygen uptake based on the new estimates of lung diffusing capacity are consistent with experimental data on oxygen uptake in exercise and hypoxia.

Where applicable, the authors confirm that the experiments described here conform with The Physiological Society ethical requirements.

PCD074

Coal dust in the working environment- Effects on Forced Expiratory Flow 25 – 75 % amongst Sri Lankans

S. Wimalasekera[1], L. Wanigabadu[2], A. Senevirathne[3], S. Paranevitane[4] and V. Palipane[5]

[1]of Physiology, Faculty of Medical Sciences, University of Sri Jayewardenepura, Nugegoda, Sri Lanka, [2]of Community Medicine, Faculty of Medical Sciences, University of Sri Jayewardenepura, Nugegoda, Sri Lanka, [3]Family Medicine, Faculty of Medical Sciences, University of Sri Jayewardenepura, Nugegoda, Sri Lanka, [4]Family Medicine, Ceymed Health care services, Nugegoda, Sri Lanka and [5]Labour, Ministry of Labour, Sri Lanka, Nugegoda, Sri Lanka

Exposure to dust in the work environment is often responsible for respiratory disability. To what extent does this exposure contribute to respiratory dysfunction? This question has led to controversies and research in occupational settings for a long time. Subsequent studies have given controversial results on the level of exposure to dust and its effects on respiratory symptoms and respiratory function. Coal mining is one of the earliest industries known to affect respiratory function in the world. Many studies have assessed the effect of coal dust on the function of the respiratory system on coal miners but the effects of coal dust on workers handling coal are scarce. Many workers are currently involved in the coal power generation industry in Sri Lanka. It is the first coal power operated plant in the country and therefore the workers are not aware of the respiratory and other hazards they may encounter in this industry.

The objectives were to study the respiratory function amongst the workers engaged in the coal power generation industry in Sri Lanka and to determine the association between coal exposure and respiratory function amongst coal handlers and non coal handlers.

A descriptive cross sectional study was done on workers exposed to coal dust in the Norochcholai coal power plant. The workers (n=80) consisted of Coal handlers (CH) (n=51)and non-coal handlers (NCH) (n=29). The respiratory symptoms were determined using an interviewer administered questionnaire and all subjects were clinically examined. Respiratoy function was assessed using a Vitallograph spirometer (Vitallograph Inc. UK). Spirometry data were analysed at uni-variate level using t test and at multi-variate level using Pearson's correlation coefficient.

Measured FEF25 – 75 % was significantly lower amongst Non coal handlers ($p = 0.031$) and ($p = 0.047$) respectively. Measured FEF25 – 75 % was a significant correlate with duration of work (Pearson correlation coefficient 0.242, and $p = 0.031$). Percentage FEF25 – 75 % was a significant correlate with duration of work (Pearson correlation coefficient 0.239, $p = 0.033$).This study highlights the use of FEF25 – 75 % as an important index in detecting early impairment of lung function. Previously undetected early impairment of lung functions was noted among non-coal handlers. Protective appropriate face masks should be worn by all workers to prevent respiratory disability. The study highlights the need for further longitudinal studies to assess the impact of coal exposure on lung function of the workers and the people living in the vicinity of the coal power plant.

workers participating in the study

Electricity board of Sri Lanka for assistance in the study

Where applicable, the authors confirm that the experiments described here conform with The Physiological Society ethical requirements.

PCD077

Heparanase upregulation in the inflammatory airway facilitates syndecan shedding and sustained inflammation

L. Wu[1], S. Chan[1], M. Ip[2] and D. Shum[1]

[1]Biochemistry, The University of Hong Kong, Pokfulam, Hong Kong and [2]Medicine, The University of Hong Kong, Pokfulam, Hong Kong

Unopposed protease activity resulting from anti-elastase resistant supramolecular complexes of neutrophil elastase and shed syndecan-1 in the airway fluids is thought to be the cause of persistent inflammation resulting in airway damage and deteriorating lung function in COPD and bronchiectasis (1, 2). We aim to develop strategies to decrease syndecan-1 shedding for the treatment of COPD and bronchiectasis.

The levels of heparanase, syndecan-1 and MMP-7 activity were measured in sputum samples of local patients. Values are means ± S.E.M., compared by Student's T-test. The sputum from such patients contained elevated levels of heparanase (n=3, normalized pixel densities from Western blot, $p<0.05$) and shed syndecan-1 (200 ± 11 ng/ml in bronchiectasis patients n=13 and 128 ± 7 ng/ml in COPD patients n=20 vs 21 ± 4 ng/ml in induced sputum from healthy individuals n=5, $p<0.05$ respectively) but not elevated levels of matrix metalloproteinase (MMP) activity (3.22 ± 0.14 in COPD n=5 and 17.90 ± 5.06 in bronchiectasis n=5 vs 2.99 ± 1.36 μM/μg/min in induced sputum from healthy individuals n=3, p=0.8 and 0.04 respectively), we propose that the action of the GAG digesting enzyme heparanase on syndecan-1 modifies it such that it becomes more susceptible to shedding by MMP cleavage.

We show in vitro that heparanase induced syndecan-1 shedding in air-liquid interface cultured human epithelial cells (shed syndecan concentration in medium 11.2 ± 0.7ng/ml vs 131.5 ± 1.8 ng/ml after heparanase treatment, $p<0.05$), and that heparanase-treated recombinant syndecan-1 was more readily cleaved by MMP-7 than control treatment of the recombinant syndecan-1(0.21 vs 1.22 ng/ml/h, determined by ELISA). Surface plasmon resonance analysis demonstrated an increase in affinity of syndecan-1 for MMP-7 upon heparanase treatment (affinity constant increase from 6.83 × 105 to 2.31 × 1010 M^{-1}, n=5). Co-immunoprecipitation study targeting syndecan-1 found associated MMP-7 higher in the sputum samples of bronchiectasis and COPD patients than in induced sputum of healthy individuals; normalized pixel density ratios of MMP-7: syndecan-1 of bronchiectasis and COPD patients (7.0 and 5.7 vs 1.8 in induced sputum) reinforced the suggestion of increased affinity of MMP-7 for syndecan-1 that had been exposed to heparanase activity. The results support that heparanase activity in the inflammatory airway environment enhances shedding of syndecan-1 and thus a target for the treatment of bronchiectasis and COPD.

Chan SC et al. (2009). Am J Respir Cell Mol Biol 41, 620-628.

Chan SC et al. (2003). Am J Respir Crit Care Med 168,192-198.

Where applicable, the authors confirm that the experiments described here conform with The Physiological Society ethical requirements.

PCD078

A fast fibre optic sensor with potential to detect rapid arterial PO2 oscillations in Acute Respiratory Distress Syndrome (ARDS)

F. Formenti, R. Chen, H. McPeak, A.D. Farmery and C.W. Hahn

Nuffield Division of Anaesthetics, Nuffield Department of Clinical Neurosciences, University of Oxford, Oxford, UK

In healthy humans arterial PO2 is almost constant, showing virtually no oscillations within the respiratory cycle [1]. In Acute Respiratory Distress Syndrome (ARDS) [2], arterial PO2 is thought to oscillate widely due to breath-by-breath variations in pulmonary shunt as a consequence of atelectasis, when alveoli open and collapse during each respiratory cycle. Commercially-available fibre optic oxygen sensors [3] are not suitable for clinical intravascular use, and may not be sufficiently fast to detect these arterial PO2 oscillations at elevated respiratory rate (RR).

We have developed an in house, fast (response time ~ 50 ms) fibre optic intravascular sensor [4] (which can be placed into standard arterial cannulae) to detect oxygen oscillations at different simulated RR, and compared the performance of our sensor with a commercially-available sensor (response time ~ 470 ms; Foxy-AL300, Ocean Optics, USA).

The sensors were tested in an extracorporeal circuit comprising two standard paediatric oxygenators (Medos-HILITE1000) through which minimally heparinised lambs' blood was circulated at 39° C via two coupled peristaltic pumps [5]. This provided two independent parallel circuits, in which PO2 was 5 or 50 kPa, and PCO2 was 5 kPa; these values were constantly controlled by a precision gas mixing pump, and monitored through samples for gas analysis before each experiment. A computer-controlled electronic switch opened and closed solenoid valves that diverted the circuits exposing the sensor to PO2 values oscillating between 5 and 50 kPa, simulating arterial PO2 oscillations in ARDS, where severe cyclical shunt exists. The simulated RRs studied were 10, 30 and 50 breaths per minute (bpm).

Figure 1 shows results from the PO2 oscillations' tests in blood. The in house and the AL300 sensors performed comparatively well at a simulated RR of 10 bpm, where they recorded the whole PO2 oscillation amplitude from 5 to 50 kPa. In contrast, only the in house sensor was able to detect the full dynamic range of the oxygen oscillation at simulated RRs of 30 and 50 bpm, where the AL300 sensor detected only about 70% of the actual PO2 oscillation amplitude.

Improvements in fibre optic sensing technology and materials may afford the development of an intravascular sensor for real-time detection of rapid oxygen oscillations, and hence cyclical atelectasis, in ARDS. Further studies are needed to validate the use of this fast intravascular technology in vivo and in clinical trials of whether this information can better inform individualised ventilation management in adult and paediatric intensive care units.

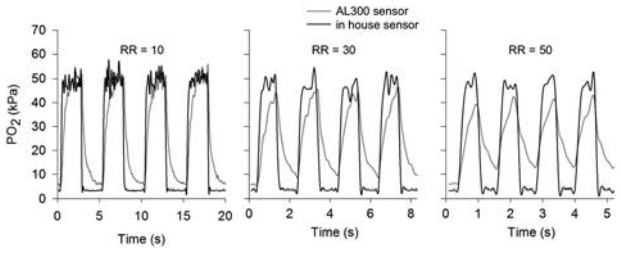

Figure 1. PO2 values recorded by the two sensors are shown as a function of time for simulated respiratory rates of 10 (left), 30 (middle), and 50 (right) breaths per minute. Black and grey lines indicate results from the in house and the AL300 sensor respectively

Lumb, A., Nunn's Applied Respiratory Physiology. Fifth Edition ed. 2000, Oxford: Butterworth-Heinemann

Ashbaugh, D.G., et al., Acute respiratory distress in adults. Lancet, 1967. 2(7511): 319-23

Baumgardner, J.E., et al., Effects of respiratory rate, plateau pressure, and positive end-expiratory pressure on PaO2 oscillations after saline lavage. Am J Respir Crit Care Med, 2002. 166(12 Pt 1): 1556-62

Chen, R.S., et al., A Cylindrical-Core Fiber-Optic Oxygen Sensor Based on Fluorescence Quenching of a Platinum Complex Immobilized in a Polymer Matrix. IEEE Sensors Journal, 2012. 12(1): 71-75

Chen, R., C.E. Hahn, and A.D. Farmery, A flowing liquid test system for assessing the linearity and time-response of rapid fibre optic oxygen partial pressure sensors. Respir Physiol Neurobiol, 2012. 183(2): 100-7

Where applicable, the authors confirm that the experiments described here conform with The Physiological Society ethical requirements.

PCD079

Gender variation in lung function; could it be explained by difference in respiratory muscle power?

A.A. Magzoub[1], O.A. Musa[1], A.A. Bashir[2] and S.E. Ibrahim[3]

[1]Physiology, Faculty of Medicine,National Ribat University, Khartoum, Sudan, [2]Physiology, Faculty of Medicine, El Imam Elmahdi University, Kosti, Sudan and [3]Physiology, Faculty of Medicine, University of Gezira, Madani, Sudan

Gender variation in lung function is more evident in lung volumes and capacities involving forced muscle contraction. Few studies have been done to demonstrate the reason behind gender difference in lung function and none was conclusive. This study aimed to investigate gender difference in respiratory muscle power and its correlation with the lung function test parameters.

The study was performed in two groups of University students 25 males and 25 females matched for age, height and weight at National Ribat University in Khartoum, Sudan during January 2011. The two groups were of the same ethnic class, socioeconomic status and perfect health. Lung Function Tests including Forced Vital Capacity (FVC), Forced Expiratory Volume in the first second (FEV1), and Peak Expiratory Flow (PEF) were performed using a digital spirometer and maximum inspiratory and expiratory pressers (MIP &MEP) as indicators for respiratory muscle power were measured using a Respiratory Pressure Meter (MicroRPM).For MIP test: after fitting the mouth piece the subject was asked to exhale to residual volume then perform a forced inhalation against the MicroRPM with as much effort as possible for as long as possible. For MEP test: the subject was asked to inhale to total lung capacity then perform a forced exhalation against the MicroRPM as maximum and long as possible. To ascertain a best value, each test was repeated 3 times. Data were analyzed using SPSS software and independent t- test was used to compare the mean difference in results.

The mean age (year), height (cm) and weight (Kg) of males group under the study were 20.32 ± 0.80, 167.88 ± 2.99 and 61.36 ± 5.87 respectively while in females group were 20.00 ± 0.64, 165.96 ±4.36, 61.88 ± 7.15 respectively. Mean FVC(L), FEV1(L) and PEF(L/min.) in males group were 4.09 ± 0.51, 3.68 ± 0.45 and 561.60 ± 70.10 respectively, while in females group FVC, FEV1 and PEFR were 2.93 ± 0.45, 2.80 ± 0.36, 389.60 ± 46.68 respectively. Statistically significant sex difference was found in the three lung function test parameters ($p<0.001$).

Mean MEP and MIP (cm/H2O) were 143.48 ± 23.83 and 111.92 ± 15.05 respectively in the males group compared to 87.72 ± 20.02 and 73.08 ± 12.35 respectively in the females group with statistically significant sex difference ($p < 0.001$). A significant positive correlation between respiratory muscle power indicators (MEP or MIP) and lung function parameters (FEV1, FVC and PEF in both sexes ($p < 0.001$).

In conclusion: gender variation in lung function is likely explained by gender difference in the power of the respiratory muscles. MEP and MIP measuring could be applied to study sport variation in lung function and low lung function in conditions affecting muscle power.

Where applicable, the authors confirm that the experiments described here conform with The Physiological Society ethical requirements.

PCD080

Effects of gremlin haploinsufficiency on the pulmonary vascular endothelium in the hypoxic murine lung

S.C. Rowan, E. Cahill and P. McLoughlin

School of Medicine and Medical Sciences, University College Dublin, Dublin 4, Ireland

Chronic exposure to hypoxia such as at high altitude causes pulmonary hypertension (PH). PH is characterised by vasoconstriction, remodelling of the pulmonary vessels and sustained increases in pulmonary vascular resistance. The bone morphogenetic proteins (BMPs) play a vital role in maintaining normal pulmonary vascular homeostasis. Attenuated BMP signaling has been found in many common forms of PH including hypoxic PH. Recent work in our laboratory indicated that lung specific, hypoxia induced, upregulation of expression of the BMP antagonist gremlin1 (Grem1) plays a central role in the pathogenesis of hypoxic PH (1). Grem1 may act as a VEGFR2 agonist leading to VEFR2 dependent angiogenic responses (2). VEGFR2 activation increases eNOS production of NO, which has essential anti-remodelling and pro-angiogenic roles in the lung. However, through its BMP blocking action a hypoxia induced increase in grem1 could lead to a reduction in eNOS expression and activity (3). Given these potentially antagonist roles we examined the effect of heterozygous loss of grem1 on angiogenesis and eNOS expression and activity in the hypoxic mouse. Wild-type (WT) and gremlin heterozygous knockout mice (Grem+/-) were exposed to either normoxia (FIO2=0.21) or hypoxia (FIO2=0.10) for 2 days or 3 weeks. Following exposure they were anaesthetized (sodium pentobarbital 60mg.kg-1, i.p.) and exsanguinated. The lungs were removed and the resistance assessed using an isolated ventilated perfused lung preparation (n=17-20 per group). Separate groups of lungs (n=10-12 per group) were fixed for stereological assessment of the pulmonary vascula-

ture as previously described (4). eNOS expression and NO activity were measured by western blot (n= 8 per group). In agreement with our previous work Grem+/- mice showed an attenuated increase in PVR (2.92±0.08 mmHg.ml.min-1) that was significantly lower (P<0.01, t-test) than that observed in the wild type mice (3.31±0.06 mmHg.ml.min-1). eNOS expression and NO activity were significantly elevated (P<0.01, Mann Whitney U) in 2 day hypoxic Grem+/- mice in comparison to WT controls. Quantitative stereology demonstrated similar significant (P<0.05, t-test) hypoxia induced increases in epithelial and endothelial surface area, consistent with hypoxia-induced angiogenesis, in both hypoxic WT and Grem+/- mouse lungs. These data suggest that the loss of grem1 protects against hypoxic PH, at least in part, by increasing NO expression and activity. The heterozygous loss of grem1 did not lead to a reduction in hypoxia-induced angiogenesis. These finding suggest that gremlin does not have a significant VEGFR agonist activity in the hypoxic lung but primarily acts to antagonise BMP signaling.

Cahill E. et al. (2012). Circulation 125(7):920-30

Mitola S et al. (2010). Blood 116(18):3677-80

Anderson L et al. (2010). Am J Physiol 298(3):R833-42

Howell K et al (2009). Am J Physiol 296(6):L1042-50

This research was generously funded by the Health Research Board and Science Foundation Ireland

Where applicable, the authors confirm that the experiments described here conform with The Physiological Society ethical requirements.

PCD082

The transcription factor CREB1 is required to maintain normal pulmonary vascular resistance

L. Li[1], K. Howell[1], M. Sands[1], M. Banahan[1], S. Frohlich[1,2], S.C. Rowan[1], D. Ryan[2] and P. McLoughlin[1]

[1]School of Medicine and Medical Science, Conway Institute, Dublin, Ireland and [2]Department of Anaesthesia and Critical Care, St Vincent's University Hospital, Dublin, Ireland

Chronic hypoxia causes pulmonary hypertension associated with structural alterations in pulmonary vessels and sustained vasoconstriction. The transcriptional mechanisms responsible for these distinctive changes are unclear. We have previously reported that CREB1 is activated in the lung in response to alveolar hypoxia but not in other organs (1). To directly investigate the role of CREB1 in the regulation of pulmonary vascular resistance we examined the responses of mice in which the α and Δ isoforms of CREB had been inactivated by gene mutation, leaving only the β isoform intact (CREB$^{\alpha\Delta}$ mice) (2). Wild type and CREB$^{\alpha\Delta}$ mice were exposed to hypoxia (10% O2) or normoxia (21% O2) for three weeks following which they were anaesthetized (sodium pentobarbital 60mg.kg-1, i.p) and exsanguinated. The lungs were removed and pulmonary vascular resistance (PVR) assessed using an isolated ventilated perfused preparation (n=5-13). After the baseline of measurements, a potent rho-kinase inhibitor Y-27362 (10-5 M) was added and the inhibitory effect of Y-27362 on PVR was assessed. Separate groups of lungs (n=8-9) were isolated and fixed for stereological assessment of the pulmonary vasculature as previously described (3). Gene expression (n=10-28) was investigated by real-time PCR. Protein expression (n=8) was measured by western blot.

Expressions of CREB regulated genes, brain derived neurotrophic factor (BDNF), follistatin (FST), and tissue plasminogen activator (PLAT), was increased in the CREB$^{\alpha\Delta}$ mice ($p<0.05$, Mann-Whitney U). CREB$^{\alpha\Delta}$ mice had greater pulmonary vascular resistance than wild types, both basally in normoxia and following exposure to hypoxic conditions for 3 weeks ($p<0.01$, 2-way ANOVA). There was no difference in vasoconstrictor activity between CREB$^{\alpha\Delta}$ and wild type mice. Stereological analysis of pulmonary vascular structure showed characteristic wall thickening and lumen reduction in wild-type mice, with similar changes observed in CREB$^{\alpha\Delta}$. CREB$^{\alpha\Delta}$ mice had larger lungs with reduced epithelial surface density ($p<0.01$, 2-way ANOVA) demonstrating increased pulmonary compliance, which caused increased vascular resistance.

These findings show that CREB1 regulates homeostatic gene expression in the lung. Furthermore normal CREB1 activity is essential to maintain low pulmonary vascular resistance in both normoxic and hypoxic conditions and is required to maintain the normal alveolar wall structure and compliance. Interventions that enhance the transcriptional activity of CREB1 warrant further investigation as a potential therapeutic strategy in hypoxic lung diseases.

Leonard MO *et al*. (2008) *Am J Respir Crit Care Med* **178**, 977-983

Hummler E *et al*. (1994) *Proc Natl Acad Sci U S A* **91**, 5647-565.

Howell K *et al*. (2009) *Am J Physiol Lung Cell Mol Physiol* **296**, L1042-1050.

This work was supported by the Health Research Board. S Frohlich was supported by a Health Research Board-Health Service Executive National Academic Fellowship and St Vincent's Anaesthesia Foundation.

Where applicable, the authors confirm that the experiments described here conform with The Physiological Society ethical requirements.

PCD083

Lung microvascular endothelial cells exposed to hypoxia reveals novel microRNAs that may contribute to the pathophysiology of chronic lung disease

N. Ali[1], N. Mah[2], P. McLoughlin[1] and C. Costello[1]

[1]UCD Conway Institute, University College Dublin, Dublin, Ireland and [2]Max Delbrück Center for Molecular Medicine, Berlin, Germany

Pulmonary hypoxia is a common complication of chronic lung diseases leading to the development of pulmonary hypertension. The underlying sustained increase in vascular resistance is a response unique to the lung, suggesting that there are genes whose expression is selectively modulated in the lung in hypoxia. Recent studies suggest an important role for microRNAs (miRNAs) in hypoxia-mediated responses. miRNAs are short RNA sequences that modulate gene expression. The aim of the present study was to elucidate the miRNA profile underlying lung-selective gene expression in hypoxia.

Primary human microvascular endothelial cells from lung (HMVEC-L) and cardiac (HMVEC-C) cells were cultured in normoxia or hypoxia (1% O2) for 3hr, 24hr or 48hrs (n=6 experiments for each time-point). To identify lung-selective miRNAs, total RNA was extracted and hypoxic conditions confirmed by real time PCR using the hypoxic responsive gene VEGF-A. RNA was probed to miRNA microarrays (MRA-1001; 1,719 human miRNAs), and results confirmed by real time PCR analysis. In silico analysis using TargetScan and microRNA.org iden-

tified genes targeted by identified miRNAs. The predicted gene targets were confirmed by real time PCR.
Using a subtractive miRNA strategy, 238 lung-selective hypoxic responsive miRNAs were identified (ANOVA p<0.05) which were differentially regulated in response to hypoxia in the pulmonary (p<0.05), but not the cardiac cells. Confirmatory real time PCR experiments showed that miR-125a-5p and miR-424 were significantly up-regulated in response to hypoxia in vitro. In silico analysis predicted that miR-424 targets aquaporin 11 (AQP11). Aquaporins are water channels that have been documented to transport gases such as the vasodilator Nitric Oxide. Furthermore, miR-424 targets cullin 2 (CUL2), which has previously been shown to stabilize hypoxia-inducible factor-α and promote angiogenesis. In line with miRNA inhibiting expression of their target genes, real time PCR confirmed that both AQP11 and CUL2 were down-regulated in response to hypoxia in HMVEC-L.
We conclude that hypoxia, causes alterations in miRNA expression in the pulmonary endothelium in a manner that is specific to that cell type and is different from the pattern of gene response observed in cardiac endothelial cells. We have identified a number of miRNAs which are potentially important mediators of vascular changes in hypoxic lungs disease. Little has been reported of many of the hypoxic responsive lung-selective miRNAs identified in our microarray, however, based on current knowledge of gene function, miR-424 may play important roles in pulmonary vascular remodelling and angiogenesis.

This work is supported by Science Foundation Ireland (SFI) research grant

Where applicable, the authors confirm that the experiments described here conform with The Physiological Society ethical requirements.

PCD085

In utero inflammation impaired preterm lamb diaphragm function

K. Karisnan[1], G. Pinniger[1], A. Bakker[1], S. Yong[1,2], C. Berry[2], P. Noble[1,2] and J.J. Pillow[1,2]

[1]School of Anatomy, Physiology and Human Biology, The University of Western Australia, Crawley, 6009, WA, Australia and [2]Centre for Neonatal Research and Education, School of Paediatrics and Child Health, The University of Western Australia, Crawley, 6009, WA, Australia

The integrity of the immature diaphragm may critically influence the susceptibility to respiratory failure after preterm birth. We aimed to investigate the effect of LPS administered at single or multiple doses at different time points during gestation on the function of preterm diaphragm. This study was approved by the Animal Ethics Committee of The University of Western Australia. Pregnant Merino ewes received ultrasound guided intra amniotic injections of LPS (10 mg) or saline. LPS exposures consisted of single injections at either 2, 7 or 21 day (d) or multiple injections (7+14+21 ds) before operative delivery (pentobarbitone;150 mg/kg I.V) at 121 d gestational age. Preterm lambs were killed with pentobarbitone (150 mg/kg I.V) and the right hemi-diaphragm was dissected. One diaphragm strip was frozen in liquid nitrogen for skinned fibre force analysis. Another strip was mounted in an *in vitro* muscle test system and contractile parameters and fatigue resistance were assessed (1). For skinned fibre analysis, muscle strips (control and 21 d LPS) were processed as described by Ottenheijm., 2010 (2). Small bundles of fibre were attached to the force transducer and activated in solutions of different pCa and pSr (4.1-8.0). Single 21d and multiple LPS exposures during gestation significantly reduced P_0 by ~40 %, relative to saline control (Table 1). The P_t decreased by ~30 %, and was accompanied by a significant increase in ½ RT and TTP. 21d LPS exposure did not alter either the pCa_{50} or F_{max} compared to controls. The severity of contractile dysfunction was greater when the initial exposure occurred 21 d prior to delivery and multiple LPS exposures did not cause additional impairment in contractile function. The skinned fibre results suggest that the muscle weakness (at 21 day exposure) is mediated by altered calcium handling rather than myofilament dysfunction.

Table 1

		LPS Groups			
	Saline controls n=8	2 d n=6	7d n=6	21 d n=7	7+14+21ds n=5
P_t (N.cm^2)	8.0 ± 0.9	5.7 ± 0.8*	5.5 ± 0.4*	5.3 ± 0.2*	5.3 ± 0.4*
P_0 (N.cm^2)	15.6 ± 1.5	11.2 ± 1.3*	10.5 ± 0.3*	9.3 ± 0.5*	9.6 ± 0.6*
TTP (ms)	160 ± 40	115 ± 6	235 ± 59	358 ± 7*	369 ± 20*
½ RT (ms)	190 ± 31	220 ± 17	259 ± 25	307 ± 21*	330 ± 60*
FI	0.3 ± 0.0	0.3 ± 0.0	0.4 ± 0.0	0.5 ± 0.0*	0.5 ± 0.0*
Skinned fibre data					
	n=4			n=6	
F_{max}	4.2 ± 0.4			3.5 ± 0.4	
pCa_{50}	6.4 ± 0.0			6.4 ± 0.0	

Values are means±SEM compared by ANOVA or student t-test (* P<0.05 compared to controls). P_t, maximum twitch force; P_0, maximum specific force; TTP, time to peak twitch force; ½ RT, half-relaxation time; F_{max}, maximum force; pCa_{50}, pCa producing one-half maximal tension

Lavin T, Song Y, Bakker AJ, McLean CJ, Macdonald WA, Noble PB, Berry CA, Pillow JJ, Pinniger GJ. Developmental changes in diaphragm muscle function in the preterm and postnatal lamb. Pediatr Pulmonol. 2013 Feb [Epub ahead of print]

Ottenheijm, CA, Hooijman, P, Dechene, E, Stienen GJ, Beggs AH, Granzier, H. Altered myofilament function depresses force generation in patients with nebulin-based nemaline myopathy (NEM2). J Struct Biol. 2010 May;170(2):334-43

Where applicable, the authors confirm that the experiments described here conform with The Physiological Society ethical requirements.

PCD086

Respiratory parameters and molecular profile of anti-inflammatory therapy in experimental meconium aspiration syndrome

P. Mikolka[1], D. Mokra[1], J. Kopincova[1], L. Tomcikova[1], J. Hatok[2] and A. Calkovska[1]

[1]Department of Physiology, Jessenius Faculty of Medicine, Comenius University, Martin, Slovakia and [2]Department of Medical Biochemistry, Jessenius Faculty of Medicine, Comenius University, Martin, Slovakia

Aims: Pathophysiology of neonatal meconium aspiration syndrome (MAS) is complex and includes airway obstruction, dysfunction of pulmonary surfactant, and induction of local inflammation followed by formation of lung edema. Standard therapy of MAS is based on ventilatory support and administration of exogenous surfactant, but in serious cases it can be ineffective. The reduced effect of therapy is caused by generation of inflammation, signalling through TLR4/MD-2 CD14 complex, and increasing production of inflammatory markers, reactive oxygen species and proteolytic enzymes which can inactivate and degrade surfactant (Salvesen et al, 2010). Therefore, an agent affecting pro-inflammatory transcription factors, budes-

onide, was used to inhibit expression of inflammatory markers, as we expected that budesonide may improve effectiveness of surfactant therapy in MAS (Mokra et al, 2007).
Methods: In anesthetized and oxygen-ventilated New Zealand rabbits, respiratory failure was induced by intratracheal administration of meconium. Animals were divided into four groups: without therapy (Mec), with surfactant therapy (Surf), with budesonide therapy (Bud), and with combined surfactant and budesonide therapy (Surf+Bud). Saline was given instead of meconium in the control group (Sal). Blood gases, ventilatory pressures, and other respiratory parameters were registered before and after meconium instillation, and 0.5, 1, 2, 3, 4, 5 hours after the therapy. After sacrificing the animals, inflammation markers were determined in lung tissue and plasma. Lung edema expressed as wet/dry weight (W/D) ratio, oxidative damage of lipids (thiobarbituric acid-reactive substances, TBARS) and proteins (3-nitrotyrosine), levels of interleukins (IL)-1b and -8 and TNFα in plasma, and mRNA expression of IL-2, -10, -13, and TNFα were analysed.
Results: Combined Surf+Bud therapy rapidly improved oxygenation and lung function parameters compared with other groups ($p<0.05$) since 30 min of the therapy and this improvement persisted till the end of experiment. Combined therapy reduced both W/D ratio and TBARS ($p<0.05$ vs. Mec group). All kinds of therapy decreased levels of IL-1b and IL-8 ($p<0.5$ vs. Mec) in plasma, but effect of Surf+Bud was superior (IL-1b $p<0.009$, IL-8 $p<0,003$). Similarly, the most potent effect of therapy on mRNA expression of IL-13 and TNFα was observed in the Surf+Bud group.
Conclusions: Combined surfactant and budesonide therapy had positive and long-term effects on lung functions and reduced lung edema, oxidative damage of lipids and proteins, and inflammation expressed by decrease in interleukins on protein and mRNA levels. The results indicate that addition of anti-inflammatory agent to surfactant therapy may reduce surfactant inactivation and enhance effectiveness of the therapy of MAS.

Salvesen B et al. (2010). Mol Immunol 47, 1226-1234.

Mokra D et al. (2007). J Physiol Pharmacol 58 Suppl 5(Pt 1), 389-398

Supported by: APVV-0435-11, VEGA 1/0057/11, VEGA 1/0291/12

Where applicable, the authors confirm that the experiments described here conform with The Physiological Society ethical requirements.

PCD089

A statistical model to predict expected pulmonary function Indices in type 2 diabetes individuals

M.A. Kanpurwala[1,2], Z. Ayoob[2], M.A. Qureshi[2] and Z. Shaikh[3]

[1]Physiology, University of Karachi, Karachi, Sindh, Pakistan, [2]Physiology, Dow University of Health Sciences, Karachi, Pakistan and [3]Diabetes & Endocrinology, Dow University of Health Sciences, Karachi, Pakistan

Type 2 Diabetes Mellitus (T2DM) is a chronic disease with increasing prevalence throughout the world. Almost every system of the body is affected by the disease [1-3]. Pulmonary function impairment has also appeared to be a complication of diabetes [4,5]. The aim of this study is to develop a statistical model as a primary prevention tool which can predict pulmonary function indices in diabetic individuals at an early stage in situations where spirometry is not possible because of any means.

73 Diabetics and 77 age matched Non Diabetics' individuals, who were non smokers and had no apparent pulmonary diseases were recruited. All subjects underwent screening with detailed history, anthropometry, HbA1c and spirometric measurements. There was a significant reduction in the Force vital capacity (FVC) [mean difference (95% CI) 0.495L (0.27, 0.72) $P < 0.001$], Force expiratory volume in first second (FEV1) [mean difference (95% CI) 0.34L (0.15, 0.53) $P < 0.001$] and FEV1/FVC ratio [mean difference (95% CI) -0.018 (-0.036, -0.0003) $P \leq 0.05$] in the diabetic subjects as compared to the healthy individuals. A model was built using multivariable regression analysis to predict FVC with adjusted R2 value of 0.778. The model equation is as follows. FVC = $\beta0 + \beta1(X1) + \beta2(X2) + \beta3(X3) + \beta4(X4) + \beta5(D1) + \beta5(D2)$. Whereas, $\beta0 = -2.78$ (constant), X1=gender, X2=height, X3=age, X4=HbA1c, D¬ = duration of disease >10years.
Female gender taken as reference, Duration of disease: ≤5 years (reference), 6 – 10 years (non significant) & > 10 years
T2DM individuals had subclinical lower FVC and FEV1 as compared to the non diabetics. The effect on the FVC was even more pronounced in diabetics who had inadequate glycemic control and prolonged duration of disease. Therefore, regular assessment of the diabetic patients for the subclinical pulmonary function impairment should be done either through spirometry or from the statistical model derived above so as to prevent the respiratory complications that may follow later.

Pulmonary Function tests in diabetic and non diabetic groups

	Non Diabetic (77) Mean ± SD	Diabetic (73) Mean ± SD	Mean difference (95% CI)	P value
FVC (L)	3.33 ± 0.79	2.84 ± 0.61	0.495 (0.27 - 0.72)	< 0.001
FEV1 (L)	2.69 ± 0.63	2.36 ± 0.53	0.34 (0.15 - 0.53)	< 0.001
FEV1/ FVC ratio	0.81 ± 0.06	0.83 ± 0.05	-0.018 (-0.036 - 0.0003)	≤ 0.05

International Diabetes Federation. IDF Diabetes Atlas, 5th edn. Brussels, Belgium: International Diabetes Federation, 2011. http://www.idf.org/diabetesatlas

Shaw JE, Sicree RA, Zimmet PZ. Global estimates of the prevalence of diabetes for 2010 and 2030. Diabetes Research and Clinical Practice.2009;87(1):4-14.

4. Latest diabetes figures paint grim global picture, Montreal, Canada. 19 October 2009 [cited; Available from: http://www.idf.org/latest-diabetes-figures-paint-grim-global-picture

Davis TME, Knuiman M, Kendall P, Vu H, Davis WA. Reduced pulmonary function and its associations in type 2 diabetes: the Fremantle Diabetes Study. Diabetes Research and Clinical Practice. 2000;50(2):153-9.

8. Yeh HC, Punjabi NM, Wang NY, Pankow JS, Duncan BB, Cox CE, et al. Cross-sectional and prospective study of lung function in adults with type 2 diabetes: the Atherosclerosis Risk in Communities (ARIC) study. Diabetes Care. 2008 Apr;31(4):741-6.

Dow University of Health Sciences, Karachi for funding the research.

Where applicable, the authors confirm that the experiments described here conform with The Physiological Society ethical requirements.

PCD090

Neonatal conditioning of rat upper airway dilator muscle by chronic intermittent hypoxia

F.B. McDonald[1] and K.D. O'Halloran[2]

[1]School of Medicine and Medical Science, University College Dublin, Dublin, Ireland and [2]Department of Physiology, University College Cork, Cork, Ireland

Introduction: Chronic intermittent hypoxia (CIH) is a feature of respiratory diseases such as obstructive sleep apnoea and apnoea of prematurity. There is a relative paucity of information on the effects of CIH on respiratory muscle physiology despite the clinical relevance. We have shown that CIH causes an age- and sex-dependent impairment of upper airway dilator muscle. The intensity, duration and pattern of CIH exposure are all key determinants of the respiratory muscle phenotype. Recently we reported that CIH exposure during early life causes upper airway dilator muscle weakness, an effect that persists for several weeks upon return to normoxia. Aim: We wished to determine 1) if neonatal exposure to CIH (nCIH) persists into adulthood and 2) if nCIH increases sensitivity to CIH exposure during adulthood. Methods: Six Wistar litters (with respective dams) were exposed to alternating bouts of hypoxia (5% O2 at the nadir) and normoxia (21% O2) for 12 cycles per hour, 8h/day for 3 weeks from the first day of life (a paradigm that causes sternohyoid dysfunction in neonatal but not adult animals). Sham experiments (continuous normoxia) were run in parallel. The litters were then returned to normoxia for 10 weeks. At this point, rats were treated with CIH for 3 weeks or normoxia. All groups were studied at 16 weeks. Sternohyoid tissue was harvested for functional assessment. Contractile and endurance properties of the muscle were determined in an in vitro isometric bath preparation in Krebs solution gassed with 95%O2/5%CO2 at 35°C. Results: At 16 weeks, sternohyoid force-frequency relationship in nCIH rats was not significantly different from the sham group (P>0.05; 2-way ANOVA) i.e. muscle weakness had fully recovered. Adult exposure to CIH had no effect on sternohyoid function. However, in nCIH rats re-treated with CIH the sternohyoid muscle was weaker (P=0.016). CIH had no effect on sternohyoid muscle endurance. Conclusion: CIH exposure in early life causes airway dilator muscle weakness that persists for several weeks in normoxia but recovers in adulthood. However, repeat exposure to the same CIH paradigm - that in-of-itself has no effect on adult muscle - is sufficient to cause muscle weakness in nCIH rats highlighting a persistent susceptibility ('deficit memory') to CIH in nCIH muscle. The upper airway dilator muscles play a crucial role in the breath-by-breath control of airway patency. A similar phenotype in human infants exposed to CIH, such as that occurring in apnoea of prematurity, could lead to long-term susceptibility of the upper airway muscles to hypoxia in later life. We speculate that nCIH could increase the propensity for airway collapse in mature adults. Our data may have relevance to the association of apnoea of prematurity in infants with obstructive apnoea in later life.

Where applicable, the authors confirm that the experiments described here conform with The Physiological Society ethical requirements.

PCD091

Effect of petrol vapours on the petrol pump workers lung function indices

M.A. Kanpurwala

Physiology, University of Karachi, Karachi, Sindh, Pakistan

Various studies have indicated that petrol and its vapours affect proper functioning of many organs, and some of the constituents of petrol are considered to be carcinogen. Incidence of lungs, kidneys, liver, pharyngeal, and laryngeal cancers were in higher petrol pump workers as compare to the normal population[1,2]. Studies have shown that petrol pump workers have lower value of Force vital capacity (FVC) and force expiratory volume in first second (FEV1) as compare to the control group [3,4]. Hence, the present study aims to confirm the decline in the respiratory functions in petrol pump workers (filling attendants) who are continuously exposed to petrol/diesel vapours during duty hours. Petrol pump workers in Karachi, Pakistan are working on a 24 hours shift, which is a considerable amount of time of exposure to petrol and its vapours. A comparative cross sectional study was conducted on 60 males working at petrol pump served as study group, while 40 age match healthy individuals were chosen to be control group. Petrol Stations were visited by the research team and after meeting with the manager; consent was taken from him and the subjects (petrol pump workers) who were involved in this study. Subjects were asked about demographic data, and after that were asked to perform the spirometry on vitalograph three times after the explanation about the procedure. The best value out of those was recorded for the analysis. Height and Weight were also measured along with the pulmonary functions. The two groups were compared by using 'independent - t' test and p value of less than 0.01 was considered significant. The mean FVC and FEV1 values of the study group was 3.15 ± 0.45 and 2.85 ± 0.56 compared to control group's which was 3.92 ± 0.62 and 3.27 ± 0.63 respectively. While the FEV1/FVC ration were within the normal range in both of these groups. These results showed that both FVC and FEV1 values were significantly lower i.e. $P < 0.001$ and $P \leq 0.001$ respectively in petrol pump workers as compare to the control group. Due to the nature of the job, petrol pump workers are constantly exposed to petrol vapours and these findings shows that these petrol and diesel vapours are causing considerable damage to the pulmonary functions mainly on lower airways showing restrictive pattern of disease. Therefore efforts are required in this area both at the government as well as at the private level so that we can come up with a solution to negate these effects to ensure healthier environment. Hence cohort studies are needed to analyse these effects in further details.

Comparision of Pulmonary Function Indices of Petrol Pump workers to Control group

Pulmonary Function Indices	Petrol Pump Workers (60)	Healthy Individuals (40)	P value
FVC	3.15 ± 0.45	3.92 ± 0.62	< 0.001
FEV1	2.85 ± 0.56	3.27 ± 0.63	≤ 0.001
FEV1/FVC	90.28 ± 12.6	83.82 ± 10.6	< 0.01

Reed MD, Barrett EG, Campen MJ, Divine KK, Gigliotti AP, McDonald JD, et al. Health effects of subchronic inhalation exposure to gasoline engine exhaust. Inhalation toxicology. 2008 Oct;20(13):1125-43

McDonald JD, Reed MD, Campen MJ, Barrett EG, Seagrave J, Mauderly JL. Health effects of inhaled gasoline engine emissions. Inhalation toxicology. 2007;19 Suppl 1:107-16

Kesavachandran CR, S. K. Anand, M. Mathur, N. Dhawan, A. Lung function abnormalities among petrol-pump workers of Lucknow, North India. CURRENT SCIENCE -BANGALORE-. 2006;VOL 90(NUMB 9):pages 1177-8

Singhal M, Khaliq F, Singhal S, Tandon OP. Pulmonary functions in petrol pump workers: a preliminary study. Indian journal of physiology and pharmacology. 2007 Jul-Sep;51(3):244-8

Where applicable, the authors confirm that the experiments described here conform with The Physiological Society ethical requirements.

PCD095

Amygdala and prefrontal cortex mediate respiratory activation in response to brief and prolonged stressors

E. Bondarenko[1,2], D.M. Hodgson[2] and E. Nalivaiko[1]

[1]School of Biomedical Sciences, University of Newcastle, Callaghan, NSW, Australia and [2]School of Psychology, University of Newcastle, Callaghan, NSW, Australia

Respiratory arousal is one of the most sensitive indices of autonomic activation, but despite close links between emotions and respiration in humans, few studies have assessed these links in animals. We have earlier reported that: a) respiratory activation is much more sensitive to brief alerting stimuli than traditionally used cardiovascular indices (1); b) these respiratory responses are sensitive to anxiolytics (2); and c) they are abolished after pharmacological inhibition of dorsomedial hypothalamus (3), a major neuronal centre of autonomic integration. Our current aim was to investigate potential roles of central amygdala (CAm) and medial prefrontal cortex (mPFC) in mediation of respiratory responses to alerting stimuli and stress.

Outbred Wistar rats were implanted with guide cannulas targeting CAm (n=8) or mPFC (n=6) under isoflurane (2% in O_2) anaesthesia. Respiratory recordings (whole-body plethysmography) were performed after microinjections of either $GABA_A$ agonist muscimol (200 nmol/ 200 nl) or saline to the targeted areas. Subsequently, rats were presented with six acoustic stimuli (40-90 dB, white noise, 0.5 sec) and subjected to restraint stress (15 min).

Values presented are means ± S.E.M. compared by 1-tail paired samples t-tests between saline and muscimol pre-treatment trials. Acoustic stimuli produced brief increases in respiratory rate proportional to stimulus intensity, ranging from 12±9 cpm increase over baseline after 40 dB stimulus to 276±67 cpm increase after 90 dB stimulus. Inhibition of CAm by muscimol significantly decreased amplitudes of responses to 70, 80 and 90 dB stimuli (from 180±49 to 15±8 msec, p=.009; from 219±49 to 59±27 msec, p=.021; and from 276±67 to 103±49 msec, p=.043, respectively), but did not affect latencies of responses. Inhibition of mPFC, on the other hand, did not affect amplitudes, but increased latencies of respiratory responses to 80 and 90 dB stimuli (from 101±31 to 149±20 msec, p=.014, and from 33±4 to 81±16 msec, p=.024, respectively). Restraint stress elevated resting respiratory rate from 98±12 to 155±7 cpm (p<.001). Inhibition of CAm significantly reduced this stress-provoked increase in respiratory rate during the first 5 minutes of restraint from 57±12 to 12±15 cpm (p=.024), while inhibition of mPFC significantly decreased it during the last 5 minutes from 40±10 to 11±4 cpm (p=.02).

Our study is the first where latency of autonomic responses to sensory stimuli was assessed at the timeframe compared to that of initial sensory processing in the brain. Our major novel finding is that PFC provides tonic influences favoring faster processing. Our data also indicate that integrity of amygdala neurons is essential for the expression of respiratory responses to brief arousing stimuli and for generating of initial, but not late-stage, tachypnoeic response to prolonged stressor.

Kabir MM *et al.* (2010). *Physiol Behav* **101**, 22-31.

Nalivaiko E *et al.* (2011). *FASEB J* **25**, 1111.4.

Nalivaiko E *et al.* (2010). *FASEB J* **24**, 1019.16.

Where applicable, the authors confirm that the experiments described here conform with The Physiological Society ethical requirements.

PCD096

Lidocaine prevents lung proinflammatory response secondary to ischemia reperfusion

L. Rancan[1], C. Muñoz[1], C. Garcìa[1], E. Vidaurre[2], I. Garutti[3], C. Simon[2] and E. Vara[1]

[1]Biochemistry and Molecular Biology III, School of Medicine, Complutense University, Madrid, Spain, [2]Thoracic surgery, Universitary Hospital Gregorio Maranon, Madrid, Spain and [3]Anesthesiology, Universitary Hospital Gregorio Maranon, Madrid, Spain

Ischemia reperfusion injury (IRI) is an increasingly important problem in clinical transplantation. Its pathogenesis involves a variety of mechanisms including the increase of proinflammatory mediators. Different prophylactic and therapeutic measures have been investigated to prevent lung injury secondary to IRI. Lidocaine (Lido) is a commonly used local anesthetic agent which has also been found to possess anti-inflammatory activity in several disorders but data available are not enough to demonstrate this fact on lung tissue. This study was designed to investigate a possible protective effect of lidocaine on lung injury secondary to IRI. Two groups (LIDO and control) of six large-white pigs each were submitted to a left lung autotransplant. Both groups received the same anesthetic induction (fentanyl 3 ug/Kg, propofol 3 mg/Kg, atracurium 0,5 mg/Kg). In addition animals of LIDO group received a continuous IV of lidocaine 1,5 mg/kg during surgery. Lung tissue samples were taken in four different moments: 1) pre-pneumonectomy (5 min before pulmonary artery clamp), 2) pre-reperfusion (5 min before reperfusion), 3) 30 min post-reperfusion (PR30) and 4) 60 min post-reperfusion (PR60). mRNA and protein expression of different proinflammatory mediators (interleukin 1 (IL-1), tumor necrosis factor alpha (TNFa), monocyte chemoattractant protein 1 (MCP-1), interleukin 10 (IL10), and endothelial nitric oxide synthase (eNOS)) were measured. Each lung sample was immediately frozen in liquid nitrogen. mRNA expression was measured by means of RT-PCR using the SYBR Green PCR Master Mix and 300 nM concentrations of specific primers. Relative changes in gene expression were calculated using the 2-ddCt method. Western blots were used to measure the protein expression (4 replicates). In addition, plasma NO and CO levels were determined by spectrophotomety. Non-parametric tests were used to find statistical meaning. The Mann-Whitney U-test was applied to establish differences between the analysed groups. In addition, the Wilcoxon test for paired data was used to study the evolution of the intra-group values. Lung ischemia reperfusion (I/R) significantly increased both mRNA and protein expression of TNFa ($p<0.01$), IL-1 ($p<0.05$) and MCP1 ($p<0.05$). This expression was even higher after 60 minutes of reperfusion ($p<0.05$). On the contrary, I/R decreased IL10 expression ($p<0.05$). Lung

I/R decreased eNOS expression ($p<0.05$) and this effect was accompanied by a decrease in plasma NO levels ($p<0,01$). These effects were blocked by lidocaine. No changes were observed in CO levels. These results suggest that lidocaine prevents I/R-induced lung injury through the reduction of proinflammatory cytokines. The administration of lidocaine might be a prospective management for preventing lung injury secondary to I/R.

Where applicable, the authors confirm that the experiments described here conform with The Physiological Society ethical requirements.

PCD097

The role of TRPM8 channels in normal rat trachea function

B. Hicks[1], A. Zholos[2] and C. Johnson[1]

[1]Biomedical Science Education, Queen's University, Belfast, UK and [2]Centre for Vision and Vascular Science, Quen's University, Belfast, UK

Several TRP channel subtypes have been found previously in airway smooth muscle. Several recent studies have found that airways respond to cold and to menthol, both of which may act through the TRPM8 channel, possibly present in epithelial cells and afferent nerve fibres (see Fischer, 2011). Our recent studies have identified that TRPM8 channels contribute to control of vascular smooth muscle tone (Johnson et al, 2009). There have been no studies as to whether this channel is present in airway tissue. Here we examined whether this channel is present in rat trachea by a combination of PCR and functional isometric tension studies.

Tracheas were taken from sacrificed male Sprague-Dawley rats (250-350g). Semi-quantitative PCR was performed for TRPM8 mRNA with 3 different primers. All 3 primers were positive at the appropriate bands, both with the epithelium in tact and removed (N=1, n=3 for each primer). Isometric contraction studies were conducted in tracheal rings pre-tensed to 0.5 g with endothelium in tact. TRPM8 agonists, menthol, (300 or 600μM in ethanol; N=7, n=24), icilin (10 μM; N=3, n =10) failed to cause any contraction (where N=animals, n= preparations). Contraction (0.92 ± 0.03 g (ave.±s.e.), N=7, n=24) induced by KCl (60mM) was markedly relaxed on addition of menthol (66±1%, N=7, n=24; $P<0.001$, Student's paired t-test). Ethanol alone failed to cause any relaxation to the KCL contraction (N=5, n=14). As recent studies have shown that menthol may have non-specific actions on L-type calcium channels (Baylie et al., 2010), protocols were repeated in the presence of the L-type calcium channel blocker, nifedipine (10 μM). Contraction was still present (0.64±0.02g). Menthol-induced relaxation was reduced compared with no nifedipine ($P<0.001$) but still present (88±2 %, N=4, n=7, $P<0.01$). In the presence of the TRPM8 antagonist, AMTB (20 μM), the relaxatory affect of menthol was unaffected. We conclude that menthol has a relaxatory effect in normal rat trachea that is mediated mainly by L-type calcium channels, although some of this relaxation may involve activation of TRPM8 channels.

Baylie RL et al., (2010). J Physiol Pharmacol. 61, 543-50.

Fisher JT (2011). Curr Opin Pharmacol. 11, 218-23.

Johnson CD et al., (2009). Am J Physiol. 296, H1868-H1877.

We thank the Centre for Biomedical Science Education and the Centre for Vision and Vascular Science, QUB, for their support.

Where applicable, the authors confirm that the experiments described here conform with The Physiological Society ethical requirements.

PCD098

Rotating phase advanced shifts of lighting regimen disturb circadian rhythms of heart rate, blood pressure clock genes expression and plasma hormones in rats

M. Zeman, L. Molcan, M. Okuliarova, A. Vesela and I. Herichova

Physiology and Ethology, Comenius University, Bratislava, Slovakia

Disturbances of endogenous circadian rhythms may result in adverse effects on metabolic and cardiovascular processes and participate in a higher incidence of diseases in shift workers. Physiological mechanisms underlying negative effects of chronodisruption are not completely understood and animal studies are needed for identifying key negative factors. In our study, in two independent experiments, we exposed mature male Wistar rats to repeated 8h phase advance shifts (PAS) of light/dark (LD) regimen (3 shifts per week) for12 weeks. In the first experiment blood pressure (BP), heart rate (HR) and locomotor activity (LA) were measured by radiotelemetry (Data Sciences Inc. USA) in 12 rats. Pressure sensor (TA11PA-C40) was implanted into the abdominal aorta under ketamine (75mg kg-1)/xylazine (10mg kg-1, i.p.) anaesthesia. Two weeks after surgery HR, BP and LA were monitored one week under control LD12:12 and then on week 1, 5, 10 and 11 of PAS exposure. Data were recorded continuously in 30s intervals over 24 hours (Dataquest ART 4.1, DSI). In the second experiment, male rats were exposed either to PAS (n=36) or control LD12:12 (n=36) and after 12 weeks they were killed by decapitation under CO2 anaesthesia in regular 4h intervals over 24 hours. Melatonin and corticosterone were measured by radioimmunoassay in plasma and melatonin was measured also in the pineal gland, heart and kidney. Clock gene (Bmal1 and per2) expression was measured by real time PCR in the heart. Data were evaluated with Cosinor analysis and ANOVA. As expected, higher values of BP, HR and LA were observed during the dark than the light phase of the day under control LD conditions. Circadian rhythms of BP, HR and LA were desynchronized in rats after exposure to repeated PAS but we did not find an increase of BP values. A transitory increase of absolute values in BP and HR was recorded only during the first week of phase shifts. Both mesor (1273 vs. 772 pg/gland) and amplitude (1554 vs. 611 pg/gland) of melatonin rhythm were damped in the pineal gland of PAS animals as compared to controls and no rhythmic changes were found in the plasma of PAS rats. The melatonin rhythm in the heart of PAS rats was damped and its acrophase was phase advanced by 4h in comparison with controls. Circadian rhythms of both clock gene expression in the heart were suppressed but in the phase with controls. Plasma corticosterone rhythm was found in controls but was absent in PAS rats in which high levels persisted during the passive phase of the day. We conclude that under repeated and frequent phase advanced shifts the circadian system is damped, animals may lose their ability to predict regular environmental loads with negative consequences on health in stressful environment.

Supported by the grants VEGA 1/0686/12, APVV-0150-11

Where applicable, the authors confirm that the experiments described here conform with The Physiological Society ethical requirements.

PCD099

Chronodisruption alters cardiovascular and behavioural responses to emotional stressors in rats

M. Okuliarova, L. Molcan, A. Vesela and M. Zeman

Animal Physiology and Ethology, Faculty of Natural Sciences, Comenius University, Bratislava, Slovakia

Chronodisruption can be involved in development of several diseases and it is necessary to elucidate possible causal physiological, behavioural and psychosocial mechanisms underlying these adverse effects. In our model of chronic phase shifts in a lightning regimen disturbed rhythms of cardiovascular parameters and activity were found in rats. In the present study, we manipulated either the lightning schedule or both lightning and feeding regimens to analyse an ability of desynchronized rats to cope with emotional stressors. Adult male Wistar rats (n=12) were implanted into the abdominal aorta with radio-telemetric transmitter TA11PA-C40 (DSI, Minnesota, USA) to continuously monitor heart rate (HR) and blood pressure (BP). A mixture of ketamine (75mg kg-1) and xylazine (10mg kg-1, i.p.) was used as anaesthesia. Following synchronisation to the LD regimen of 12:12h, one half of the rats were exposed to phase delay shifted (PDS) schedule (by 8 hours longer dark phase every second day over 5 weeks). In both groups, diet (Fresubin-isocaloric liquid drink, Fresenius Kabi, Germany) was provided only during the passive phase of the day. Cardiovascular response to a novelty (open-field test) was measured before (0w) and 5 weeks (5w) after the treatment. In addition, two groups of non-implanted rats were simultaneously housed under either control LD (n=8) or PDS (n=8) regimens with standard diet ad libitum. After 5 weeks, their behaviour was quantified in the open-field test, the black-white box and the elevated plus maze using video-tracking software Any-maze (Stoelting Co.). Cardiovascular response was analysed as an increase of HR and systolic BP over the basal levels during the 20-minute test. An area under the curve was calculated (means ± S.E. are given) and compared between 0w and 5w within each treatment by paired t-tests. Rats on the control LD regimen with diet in antiphase decreased their cardiovascular response between 0w and 5w (HR: 118694±15596 vs. 48427±18632; BP: 23045±474 vs. 17857±705) while no changes were found in rats on PDS regime with diet in antiphase (HR: 103633±8198 vs. 71717±23414; BP: 22438±2996 vs. 19506±4198). Behaviour of non-implanted rats on control LD and PDS regimens was analysed by independent t-tests. As compared to controls, PDS rats displayed increased locomotion and rearing in both the open-field and black-white box tests. They spent more time in the white compartment of the black-white box and showed increased risk assessment behaviour and decreased grooming in the elevated plus maze. In conclusion, disturbances of two strong Zeitgebers influenced the pattern of stress induced changes in HR and BP as well as spontaneous motor activity and exploration in rats. Results indicate that weakened circadian organization may alter an ability to cope with stressful events.

Supported by the grants VEGA 1/0686/12, APVV-0150-11

Where applicable, the authors confirm that the experiments described here conform with The Physiological Society ethical requirements.

PCD100

Simulation of developmental changes in energy metabolism between fetal and adult ventricular cells

T. Toki[1,2], H.I. Sano[1,3], C. Okubo[1,3], Y. Naito[1,3] and M. Tomita[1,3]

[1]Institute for Advanced Biosciences, Keio University, Tsuruoka, Japan, [2]Department of Policy Management, Keio University, Fujisawa, Japan and [3]Department of Environment and Information Studies, Keio University, Fujisawa, Japan

Ventricular cells in fetal guinea pigs have higher anaerobic glycolytic capacity and lower activities of mitochondrial enzymes. In general, embryonic ventricular cells contain approximately 10 times more glyocogen than adult ventricular cells. Although embryonic ventricular cells consume more energy for growth and differentiation, they also utilize contractile proteins that consume less energy than adult ventricular cells. Also, it has been reported that several glycolytic enzyme activities are different between embryonic and adult ventricular cells. As such, the neonatal ventricular cells can maintain the ATP concentration longer than the adult ventricular cells in hypoxic condition; ATP concentration was decreased by 44% in adult rabbit ventricular tissues and 18% in neonatal rabbit ventricular tissues after perfusion of the heart to hypoxic condition (Jarmakani *et al*., 1978). Although high glycogen content is considered as a cause for the fetal ventricular cells to retain ATP concentration under hypoxic condition, role of the developmental changes in activities of several glycolytic enzymes in ATP production of fetal ventricular cells remain uncertain.

We have previously modeled developmental changes in action potentials of rodent ventricular cells (Itoh *et al*., 2007) on the basis a guinea pig ventricular cell model (Kuzumoto *et al*., 2008). The quantitative changes in individual ionic components on both cellular membrane and sarcoplasmic reticulum were represented as relative current densities, which were computed from current-voltage curves of the specific ionic components in rodent ventricular cells. Here, we further modified the model to represent the developmental changes in energy metabolism of ventricular cells by implementing glycolytic pathway from glycogen to lactate (Lambeth *et al*., 2002), and hexokinase kinetics (Lueck *et al*., 1974), both of which were reported in rodent skeletal muscles. The developmental changes in enzymatic activities were presented as the activities relative to those in the adult ventricular cells, and implemented accordingly to the model to represent specific stages in development. We then simulated effects of hypoxic condition to dynamic changes in contractile force and ATP concentration using the modified model.

As a result, the developmental changes in concentrations of intermediate metabolites in glycolytic pathway were well represented in the simulation. Also, we showed that the fetal ventricular cells maintained ATP for longer periods of time than the adult cells, which is consistent with the reported dynamics of the changes under hypoxic condition. On the basis of the simulation, we showed that developmental changes in enzymatic activities of several glycolytic enzymes play important role in maintenance of intracellular ATP concentration under hypoxic condition.

Itoh, H., Naito, Y., *et al*. (2007) Simulation of developmental changes in action potentials with ventricular cell models, *Systems and Synthetic Biology*, **1**, 11-23.

Jamrmakani, J. M,, Nagatomo, T., *et al*. (1978) Effect of hypoxia on myocardial high-energy phosphates in the neonatal mammalian heart, *The American Physiological Society*, **235**(5):H475-481.

Kuzumoto, M., Takeuchi, A., *et al*. (2008) Simulation analysis of intracellular Na+ and Cl- homeostasis during beta 1-adrenergic stimulation of cardiac myocyte. *Prog Biophys Mol Biol*., **96**(1-3): 171-186.

Lambeth, J. & Kushmerick, J. (2002) A computational model for glycogenolysis in skeletal muscle. *Ann Biomed Eng*., **30**(6): 808-827.

Lueck, J.D. & Fromm, H.J. (1974) Kinetics, mechanism, and regulation of rat skeletal muscle hexokinase. *J. Biol Chem., 10*; **24** (5): 1341-1347.

Where applicable, the authors confirm that the experiments described here conform with The Physiological Society ethical requirements.

PCD101

Simulation of developmental change in structure of transverse tubules and intracellular Ca^{2+} dynamics using cardiac ventricular cell models

R. Aoki[1,2], H.I. Sano[1,2], C. Okubo[1,2], Y. Naito[1,2] and M. Tomita[1,2]

[1]Institute for Advanced Biosciences, Keio University, Yamagata, Japan and [2]Department of Environment and Information Studies, Keio University, Fujisawa, Japan

Transverse tubules (t-tubules) are largely absent in neonatal cells and develop rapidly after birth. In adult ventricular cells, a mobile Ca^{2+} buffer calmodulin exists predominantly near t-tubules in the cell. Ca^{2+} influx via the L-type Ca^{2+} channel (I_{CaL}) triggers Ca^{2+} release from the sarcoplasmic reticulum (SR) via the ryanodine receptor (RyR), and Ca^{2+} flow in a restricted subspace located between the junctional SR and t-tubules. On the other hand, t-tubule network is largely absent, SR is relatively sparse, and I_{CaL} expression is diminished in neonatal ventricular cells; as such, Ca^{2+} transient in neonates occurs predominantly at the periphery of the cell. In addition, the maximal binding capacity of Ca^{2+} buffer is much lower than that of Ca^{2+} buffer in adult ventricular myocytes. Here, we utilized human ventricular cell model (tenTusscher *et al*., 2006) and guinea pig ventricular cell model (Kuzumoto *et al*., 2008) to assess the differences between neonatal and adult ventricular cells in terms of intracellular Ca^{2+} dynamics and structure of t-tubules.

In our previous study (Itoh *et al*., 2007), we showed that a developmental change in action potentials (APs) can be well reproduced with common sets of mathematical equations and by changing relative densities of ion currents on the Kyoto model, a guinea pig ventricular cell model. In this study, we first modified the human ventricular cell model by implementing the relative densities to represent developing ventricular cells at early and late embryonic stages. We then removed t-tubules and accompanying subspaces from the model to represent ventricular cells without t-tubules. As a result, removal of the subspace structure increased the amplitude of Ca^{2+} transient by four-fold and prolonged the basic cycle length by 800ms in early embryonic ventricular cell model. On the other hand, the amplitude of Ca^{2+} transient was decreased by 30 % in late embryonic ventricular cell model without subspace, which indicates that existence of the subspace structures affect the amplitude of Ca^{2+} transient in both early and late embryonic ventricular cell models.

The Kyoto model was then expanded to represent developmental changes in the t-tubule structures by implementing the subspace structure to the model. We also considered predominant localization of the I_{CaL} and I_{NaCa} (sodium-calcium exchange current) on t-tubules and assessed the effect of Ca^{2+} release via the I_{NaCa} to intracellular Ca^{2+} dynamics. We simulated APs and dynamic behaviors of currents with the Kyoto model considering the developmental changes of t-tubules structures in four different stages. As a result, the effects of the developmental changes in t-tubule structures and intracellular subspace at four different stages were simulated in terms of the excitation-contraction coupling.

Itoh, H., Naito, Y., *et al*. (2007) Simulation of developmental changes in action potentials with ventricular cell models. *Syst Synth Biol*., 1(1): 11-23.

Kuzumoto, M., Takeuchi, A., *et al*. (2008) Simulation analysis of intracellular Na^+ and Cl^- homeostasis during beta 1-adrenergic stimulation of cardiac myocyte. *Prog Biophys Mol Biol*., 96(1-3): 171-186.

ten Tusscher, KHWJ. and Panfilov, AV. (2006) Alternans and spatial breakup in a human ventricular tissue model. *Am J physiol Heart Circ Physiol*, 291(10): 1088-1100.

Where applicable, the authors confirm that the experiments described here conform with The Physiological Society ethical requirements.

PCD102

Perlecan heparan sulfate in hypoxia-induced pulmonary vascular remodeling

Y. Chang[1], P. Tannenberg[1], C. Tseng[1], P. Tran[2], U. Hedin[1] and K. Tran-Lundmark[1]

[1]Department of Molecular Medicine and Surgery, Karolinska Institutet, Stockholm, Sweden and [2]Department of Cardiothoracic Surgery, Uppsala University Hospital, Uppsala, Sweden

Motivation:
Chronic hypoxia can induce pulmonary vascular smooth muscle cell (SMC) proliferation, which contributes to blood vessel constriction and lumen narrowing, leading to pulmonary hypertension. Perlecan is the major heparan sulfate proteoglycan in the basement membrane. The heparan sulfate chains of perlecan have been shown to inhibit SMC proliferation in the carotid artery. In this study, we examine if perlecan heparan sulfate can inhibit pulmonary SMC proliferation induced by hypoxia.
Methods:
Mice with heparan sulfate deficient perlecan (*Hspg2*$^{\Delta 3/\Delta 3}$) were compared to wild-type (Wt) controls. 8-11 week-old female mice were subjected to hypoxia (10% O_2) for 7 weeks. Controls were kept in normoxia. This generated 4 groups, *Hspg2*$^{\Delta 3/\Delta 3}$ versus Wt, with or without hypoxic treatment. Hemoglobin levels and the right ventricle/left ventricle+septum weight ratio (RV/(LV+S)) were measured. Serial sections from lung tissue were obtained for immunohistochemical and morphological analysis. Degree of muscularization of intra-acinar vessels was determined by double staining for von Willebrand factor and smooth muscle α-actin, followed by manual counting. Proteins and total RNA were isolated from whole lung homogenate. Genotype and treatment were blinded for all data acquisition.
Results:
To our surprise, at baseline (normoxia) *Hspg2*$^{\Delta 3/\Delta 3}$ mice have a significantly lower proportion of muscularized intra-acinar vessels compared to Wt. After 7 weeks of hypoxia, a significant increase in muscularized vessels was found in both *Hspg2*$^{\Delta 3/\Delta 3}$ (2.8 fold) and Wt mice (1.5 fold). The RV/(LV+S) ratio, as a measurement of right ventricular hypertrophy, is the same in *Hspg2*$^{\Delta 3/\Delta 3}$ and Wt at normoxia, and it increases significantly following hypoxia, with no difference between the genotypes. For Wt mice, RNA expression of FGF-2 and PDGF-B are both upregulated in hypoxia. In *Hspg2*$^{\Delta 3/\Delta 3}$ mice, FGF-2 is upregulated already in normoxia, possibly as a compensation for increased elimination. For PDGF-B the increase

following hypoxia is higher in *Hspg2*$^{\Delta 3/\Delta 3}$ mice compared to Wt.

Conclusions:

The lower proportion of muscularized vessels at baseline in *Hspg2*$^{\Delta 3/\Delta 3}$ mice is interesting and needs to be further investigated. With hypoxia treatment, the relative difference in the increase of muscularization, 2.8-fold in *Hspg2*$^{\Delta 3/\Delta 3}$ versus 1.5-fold in Wt, indicates that *Hspg2*$^{\Delta 3/\Delta 3}$ mice are more reactive in their vessels and therefore may be more vulnerable to hypoxia. The differences in muscularization may be caused by defective sequestration of heparin binding growth factors in the extracellular matrix and thereby also different regulation of those growth factors in response to hypoxia. The results suggest that perlecan heparan sulfate chains are important for the regulation of muscularization of pulmonary vessels during vessel development and during hypoxia.

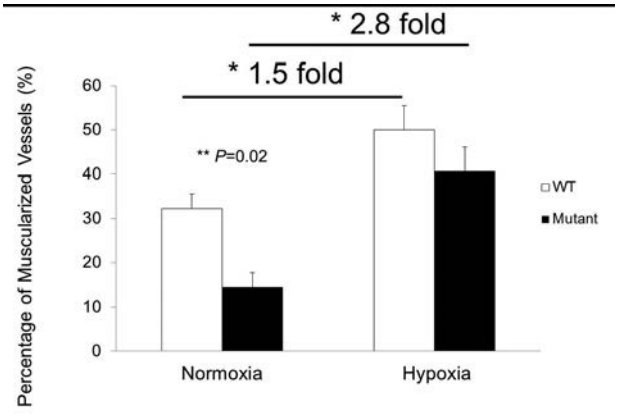

Figure 1. Degree of muscularization of intra-acinar vessels following hypoxia treatment (n = 10 for *Hspg2* $^{\Delta 3/\Delta 3}$, and n = 9 for Wt) as compared to normoxia (n = 6 for *Hspg2* $^{\Delta 3/\Delta 3}$, and n = 6 for Wt). The data shown are averages of four sets of double staining for von Willebrand factor and smooth muscle α-actin. Values are expressed as mean±SEM. (* $p< 0.05$, ** $p=0.02$)

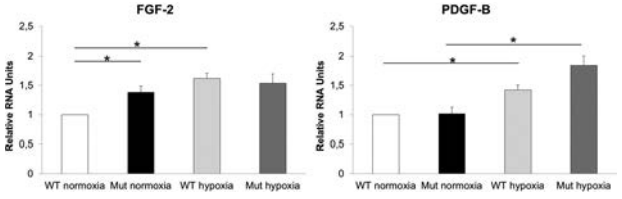

Figure 2. Quantitative PCR on mRNA from whole lung homogenates show different regulation of heparin binding growth factors in *Hspg2* $^{\Delta 3/\Delta 3}$ mice, compared to Wt controls. (n = 4 for *Hspg2* $^{\Delta 3/\Delta 3}$, and n = 3 for Wt, * $p<0.05$)

Tran, P. K., K. Tran-Lundmark, et al. (2004). *Circ Res* **94**(4): 550-558.

Schermuly, R. T., E. Dony, et al. (2005). *J Clin Invest* **115**(10), 2811-2821.

Izikki, M., C. Guignabert, et al. (2009). *J Clin Invest* **119**(3): 512-523.

Where applicable, the authors confirm that the experiments described here conform with The Physiological Society ethical requirements.

PCD103

Comparison of the agonist activities of treprostinil and naxaprostene in systemic blood vessels

N.H. Syed[1,2] and R.L. Jones[1]

[1]SIPBS, University of Strathclyde, Glasgow, Scotland, UK and [2]University College of Pharmacy, University of the punjab, Lahore, Punjab, Pakistan

Treprostinil, a prostacyclin analogue, is used to treat pulmonary hypertension. However, the mechanism of action whereby this drug modifies the pathophysiological status may involve more than prostacyclin (IP) receptors, as Whittle et al (2012) have shown that it activates human recombinant prostanoid DP1, EP2 and IP receptors.

In view of the recent emergence of highly selective EP2 receptor antagonists (e.g. PF-04418948; Forselles et al., 2011), it was decided to determine whether our current armoury of prostanoid antagonists was adequate to elucidate the complex pharmacology of treprostinil. Treprostinil lacks the ether oxygen moiety at C6-9 present in prostacyclin (PGI2) and has a benzene ring inserted in its α-chain. Naxaprostene also has both functionalities and we decided to compare its inhibitory profile with that of treprostinil.

In the current study, we have used isolated preparations of rabbit saphenous vein (rSV) and inferior vena cava (rVC). 5 mm rings were dissected from male rabbits (1.5-2.5 kg) and were mounted under isometric conditions (resting tension of 0.75 – 1.0 g) in 10 ml baths at 37°C. Contractions were elicited by adding histamine and phenylephrine (300-600 nM) respectively. We have used BW-245C, ONO-AE1-259, TCS-2510 and AFP-07 as selective DP1, EP2, EP4 and IP agonists respectively. The corresponding antagonists were BW-A868C and MK-0524, ACA-23 (same series as PF-04418948), GW-627368 and RO-1138452 (Jones et al., 2009).

A simple antagonist reversal protocol showed that both preparations contain inhibitory DP1, EP2, EP4 and IP receptors. In further experiments, preparations were pretreated with 3 of the antagonists (e.g. BW-A868C / ACA-23 / GW-627368), followed by cumulative doses of treprostinil or naxaprostene and finallyfollowed by the fourth antagonist (CAY-10441) in an attempt to reverse the relaxation. In this way we could apportion DP1, EP2 and IP agonism to treprostinil, but only IP agonism to naxaprostene. In some preparations naxaprostene behaved as a partial agonist. The relevance of these findings to the therapeutic use of prostacyclin analogues will be discussed.

af Forselles KJ, Root J, Clarke T, Davey D, Aughton K, Dack K and Pullen N. (2011). Br. J. Pharmacol., 164: 1847-1856.

Jones RL, Giembyez MA and Woodward DF. (2009). Br. J. Pharmacol., 158: 104-145.

Whittle BJ, Silverstein AM, Mottola DM and Clapp LH. (2002). Biochem. Pharmacol., 84: 68-75.

University College of Pharmacy, University of the Punjab, Lahore, Pakistan

Where applicable, the authors confirm that the experiments described here conform with The Physiological Society ethical requirements.

PCD104

Particles, pore size, pulse and pressure - the physico chemistry of osmosis

F. Prior[1,2] and G. Clegg[2,1]

[1]The Laboratory, The Osmosis Unit, Longnidddry, UK and [2]Emergency Medicine, Edinburgh Royal Infirmary Medical School, Edinburgh, UK

The Kedem Katchalski equation has been the standard formula describing fluid balance and exchange in the capillary. The osmotic component in this formula is suggested to be the difference in osmolalities between the plasma and interstitium corrected by a factor c described as the osmotic reflection coefficient.

Our in vitro studies show that the membrane osmotic pressure (MOP) of plasma components are curvelinear with concentration (MOP= ac2 + bc +i where c = concentration) and inversely proportional to membrane pore size. Small increases in membrane pore size can greatly reduce plasma MOP even where there is no change in concentration of plasma.

As the pore size in the capillary is highly dynamic, and as pore size is the major factor controlling plasma osmotic pressure, we suggest a better model of fluid balance and exchange is required to describe fluid balance and exchange.

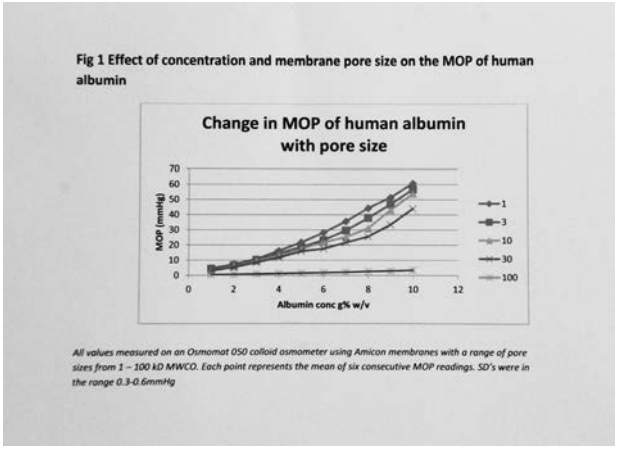

Prior FGR et al (2005). Filtration 1, 113-128

Kargol K (2000). J Memb Sci 174, 43-53

Prior FGR (1999), Care of the Crit Ill, 15, 167-172

Where applicable, the authors confirm that the experiments described here conform with The Physiological Society ethical requirements.

PCD105

Hypertension, oedema and shock - diseases of capillary fluid imbalance?

F. Prior[1,2], G. Clegg[2] and S. Richardson[2]

[1]The Osmosis Unit, Longnidddry, UK and [2]Emergency Medicine Dept, Edinburgh Royal Infirmary, Edinburgh, UK

In order to achieve fluid balance, the mean capillary pressure must be equal and opposite to the membrane osmotic pressure (MOP) across the capillary membrane. Capillary pressure is difficult to measure but mean arterial pressure (MAP) can be used as a surrogate 1,4 . If fluid balance is achieved when MAP = MOP then four imbalance situations can be envisaged; high MAP + low MOP, high MAP +high MOP, low MAP + low MOP and low MAP + high MAP. These correspond to oedema, hypertension and high and low osmotic pressure shock (Fig1).

The MAP's and MOP10K's of 30 healthy volunteers 1,4 fell within the "normal area". The outliers to the right had consumed party volumes of alcohol the night before the study! Thirty five patients with clinical oedema 1,2 had high MAP's and low MOP10K's. The MAP and MOP10K's of 22 hypertension patients fell into the raised MAP and MOP sector 1,2. Our most recent study of 57 patients admitted with shock, 23 had low (<24mmHg), 17 had normal (24-27mmHg) and 13 had high MOP's. These results are shown graphically in Fig 2.

These studies give growing support to the concept that oedema, hypertension and shock are osmotic diseases resulting from imbalances between MAP and MOP10K

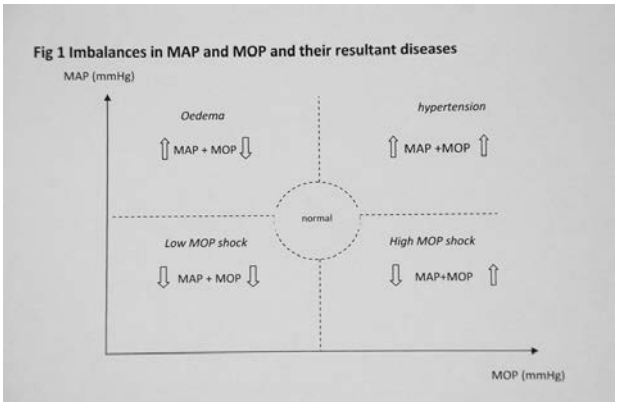

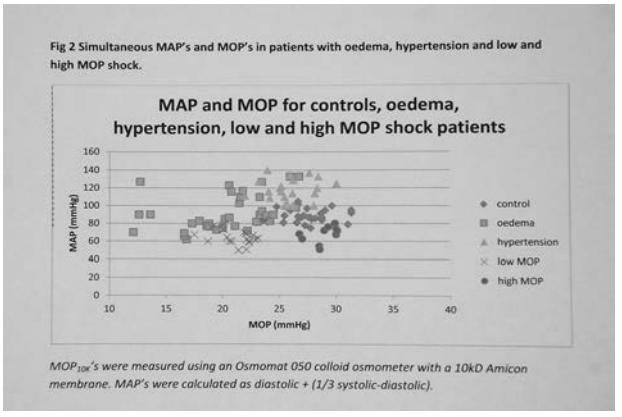

Prior FGR et al (1999). Int J Artif Orgs 22, 138-144

Prior FGR et al (2005) Filtration 1, 113-128

Prior FGR et al (1999) Care of the Crit Ill, 15, 167-172

Prior F.G.R et al (1996) Int J Artif Orgs 19, 487-492.

Prior FGR et al (2013), In preparation

Where applicable, the authors confirm that the experiments described here conform with The Physiological Society ethical requirements.

PCD106

Factors released from the placenta cause changes to glutamate and GABA receptors in cortical neurones

T. Phillips, P. Case, V. Leinster and E. Molnar

University of Bristol, Bristol, UK

Schizophrenia is a severally debilitating conditions affecting approximately 1% of the world's population. While there is no defining sign or symptom of schizophrenia the range of symptoms can be classified as positive (e.g. hallucinations), cognitive (e.g. impaired memory) and negative (e.g. social incompetence). Despite having 0.8 heritability Schizophrenia has no classical Mendelian inheritance patterns or fully penetrant genes. The highly homogenous nature of Schizophrenia has lead to a variety of theories as to its etiology with the current prevailing evidence suggesting a developmental insult leading to hyper levels of glutamate and hypo-function of the NMDA receptors of the glutamatergic system(1).

It has recently been found by our group that the placental tissue when exposed to hypoxic conditions releases an increased concentration of glutamate(2) into the surrounding media. It was hypothesised that this glutamate release might alter the presentation and function of receptors in the developing brain. To investigate this, human first trimester placental explants were exposed to oxygen concentrations of 2-8% and 21% in neurobasal media which was then collected. Cortical neurones from e18 rats were cultured on Poly-L-Lysine coated coverslips for 12 days then exposed to the conditional media for 7 days before fixation. Other neuronal cultures were similarly grown then exposed to varying concentrations of glutamate. Fluorescent immunostaining was performed on permalised and non-permalised cultures using antibodies for NMDA R1, NR3A, GABA A α1 and GABA B1. These targets were chosen to provide information on the functional capacity of the excitatory and inhibitory systems in the cultures.

It was found that increasing the concentration of glutamate leads to a reduction in the detection of NMDA R1 and an increase in the detection of NR3A. This would indicate that the increase in glutamate is causing the neurones to reduce the number and function of NMDA receptors(3). This effect was mirrored when using hypoxia conditioned media where 2-8% conditioned media resulted in increased detection of NR3A and reduced levels of NMDA R1. These finding correspond to those found in post mortem studies of patients with schizophrenia(4). The increased levels of hypoxia and glutamate were shown to cause a reduction in the presentation of GABA A α1 and an increase in the presentation of GABA B1 suggesting a deregulation of the gabaergenic system(5).

This findings suggest that factors, notably glutamate, secreted by the placenta during an hypoxic event cause alterations to the excitatory and inhibitory signalling systems on neurones in a similar manner to that recorded in Schizophrenic patients.

Kristiansen et al NMDA receptors and schizophrenia. Current Opinion in Pharmacology 2007, 7:48–55

Bhabra G, Sood A, Fisher B, Cartwright L, Saunders M, Evans WH, Surprenant A, Lopez-Castejon G, Mann S, Davis SA, Hails LA, Ingham E, Verkade P, Lane J, Heesom K, Newson R, Case CP. Nanoparticles can cause DNA damage across a cellular barrier. Nat Nanotechnol. 2009 Dec;4(12):876-83.

Henson et al. Influence of the NR3A subunit on NMDA receptor functions. Progress in Neurobiology Volume 91, Issue 1, May 2010, Pages 23–37

Mueller HT, Meador-Woodruff JH 2004. NR3A NMDA receptor subunit mRNA expression in schizophrenia, depression and bipolar disorder. Schizophr Res 71:361–370.

Kehrer et al Altered Excitatory-Inhibitory Balance in the NMDA-Hypofunction Model of Schizophrenia Front Mol Neurosci. 2008;1:6. doi: 10.3389/neuro.02.006.2008

Where applicable, the authors confirm that the experiments described here conform with The Physiological Society ethical requirements.

PCD107

Glutamate release from placenta can be blocked to protect foetal neurones from injury

A. Sood and P. Case

Musculoskeletal Research Unit, University of Bristol, Bristol, UK

Disturbances in the prenatal environment have been postulated to play a role in the pathogenesis of conditions such as schizophrenia and autism later in life. For example in preeclampsia and intra-uterine growth restriction, where there is a change in oxygen flow to the foetus, resulting in short term hypoxia, have been linked with a higher incidence in schizophrenia and foetal growth restrictions. The excitatory amino acid glutamate is involved in many cellular and physiological processes. In many neurological disorders, glutamate is implicated as being over expressed, and may be the key molecule that could cause dendrite shortening and simplification of the neurones. For this reason during pregnancy, it is important to regulate the levels of glutamate the foetus is exposed to.

We used first trimester placental tissue and a primary trophoblast cell barrier model to condition media after the effects of 2%, 21% and 2-8% and 2-21% oxygen changes. This media was then applied to E18.5 rat cortical cultures after 12 days in vitro and found to cause reductions in dendrite lengths, as measured via MAP2 staining and GFP transfections, after 6 days of exposures. In addition, the neurones were also simplified in structure and found to contain fewer spines, therefore impacting on their action potentials and their ability communicate with one another.

On analysis of the media, we found a specific and significant increase in glutamate when the tissue was exposed to hypoxia and reoxygenation. We then probed the reason to the mechanism of this release. There are five glutamate transporters within the human body (EAAT1-5), interestingly, 3 of which are only found in the placenta, further highlighting the importance for the regulation of glutamate during pregnancy. We used pharmacological interventions to block these transporters, DL-TBOA, a glutamate transporter antagonist, and DHA, a specific EAAT2 blocker. The results found that DHA being specific to only one transporter was not efficient in blocking the effects on the dendrites. However, DL-TBOA's actions being non-specific, was found to considerably rescue the dendrite lengths.

We hope that our findings and future work could lead to a potential therapy, by inhibiting the effects of glutamate, so that it does not pose a risk to the developing foetus. By understanding the mechanism of release, we aim to pave the way in developing a drug that is able to offer protection to the developing foetus and to reduce the risk of causing the onset of neurological disorders.

Where applicable, the authors confirm that the experiments described here conform with The Physiological Society ethical requirements.

PCD108

Effect of increased corticospinal excitability by quadripulse transcranial magnetic stimulation to the primary motor cortex on the spinal inhibitory circuit

N. Matsuda[1], F. Kaneko[2], E. Shibata[1] and T. Kimura[1]

[1]Graduate School of Health Sciences, Sapporo Medical University, Sapporo, Japan and [2]Second Division of Physical Therapy, Sapporo Medical Univercity, Sapporo, Japan

Ia reciprocal inhibition and presynaptic inhibition are related to motor control. The effect of corticospinal excitability to on the spinal inhibitory circuit is studied by repetitive transcranial magnetic stimulation (rTMS). However, a relationship between corticospinal excitability and spinal inhibitory circuit has not been considered sufficiently. In recent years, quadripulse transcranial magnetic stimulation (QPS) has attracteds attention as a new technique to induce neural plasticity. QPS induce to increases a corticospinal excitability more effectively than does rTMS. The aim of this study was to clarify the relationship between corticospinal excitability and inhibition of the H- reflex. In Experiment 1, control H-reflex of the flexor carpi radialis (FCR) was induced by stimulation of the median nerve, and the test stimulus intensity was modulated so that the H-reflex was 20% of M max. To assess the Ia reciprocal inhibition and presynaptic inhibition, we applied conditioning stimulation to the radial nerve. The intensity of conditioning stimulation was set to 90% intensity of the M-wave threshold. The interstimulus interval (ISI) was set at 0-5,10,12,14,16,18,20,25,or 30 ms. The conditioned H-reflex was normalized to control H-reflex (% control amplitude). ISI-Ia was set to the minimum % control amplitude from ISI of 0 to 5 ms, in the same way ISI-presynapse was determined from ISI of 10-30 ms. In Experiment 2, the motor evoked potential (MEP) amplitude and H-reflex of the FCR were measured. To measure the conditioned H-reflex, we adopted the ISI-Ia and ISI-presynapse. QPS was performed for 30 minutes. QPS intensity was set to 90% of the motor threshold. We measured the H-reflex and MEP amplitudes twice before QPS (pre QPS-1, pre QPS-2) and every 20 minutes after QPS (post QPS-0, post QPS-20, post QPS-40, post QPS-60). The ratio of % control amplitude to pre QPS-1 was calculated (% pre1 amplitude). A one-way repeated measures analysis with time period as a factor was used to determine the effect of QPS on MEP amplitude and % pre1 amplitude ($p<0.05$). Dunnett multiple comparisons were performed as post hoc tests ($p<0.05$). In Experiment 1, The average of ISI-Ia was 4.5 ms and the average of ISI-presynapse was 20 ms. In Experiment 2, the MEP amplitude in post QPS-0 increased significantly compared with that in pre QPS-1 ($p=0.01$). The % pre1 amplitude of ISI-presynapse in post QPS-0 decreased significantly compared with that in pre QPS-2 ($p=0.021$). Although the differences were not statistically significant, the MEP amplitude in post QPS 20 increased and the % pre1 amplitude of ISI-presynapse in post QPS 20 decreased. These experimental results suggested that increased corticospinal excitability and increased presynaptic inhibition at the spinal level occurred in parallel.

Where applicable, the authors confirm that the experiments described here conform with The Physiological Society ethical requirements.

PCD109

Prenatal hypoxia-ischemic affects neurons distribution in ventral tegmental area and nucleus accumbens, modifying memory in rats

I.M. Sab, M.M. Ferraz, C.M. Sequeira, M.R. Ferraz, T.M. Brunini and A. Mendes Ribeiro

Departamento de Farmacologia e Psicobiologia, State University of Rio de Janeiro, Rio de Janeiro, Brazil

Prenatal hypoxia-ischemia (HI) is one of the major causes of mortality and chronic neurological diseases in newborns that can evoke permanent effects such as attention deficit hyperactivity disorder (ADHD), epilepsy and cerebral palsy. These damages are associated with a delay in neural development and death of neurons. Some of the cognitive deficits may be due to impairments in mesolimbic pathway. The ventral tegmental area (VTA) to the nucleus accumbens (NAc) pathway is involved in reward, attention, motivation and learning. Nitric oxide (NO) is a gas with many physiological functions, such as vasodilatation and neurotransmission, and it is produced by the oxidation of L-arginine through NOS, using NADPH-diaphorase (NADPH-d) as the electron donor. The aim of our study was to investigate the effects of prenatal HI on NO production in NAc and VTA by NADPH-d technique, a specific histochemical marker for NOS in the brain, and the effects on the motor and habituation by the open field test (OFT). HI was induced by clamping the uterine arteries of pregnant rats (Wistar) for 45 minutes, anesthetized intraperitoneally with Avertin® (2,2,2-Tribromoethanol, 250-500 mg/kg), on the 18th day of gestation (HI group). In the other group of females the surgery was the same, but without clamping the arteries (SHAM group - SH). Three groups were examined in behavior tests: HI, SHAM and CTRL (nom-manipulated group). The motricity and habituation of the pups in P90 were analyzed by OFT on 2 consecutive days. For NADPH-d histochemistry technique, rats from both groups (HI and SH) were intracardially perfused with saline and paraformaldehyde, and the brain was coronally sectioned. The experimental procedures were approved by the Institutional Animal Care and Use Committee (CEA/051/2009) and were conducted in accordance with the National Institutes of Health Guide for the Care and Use of Laboratory Animals. Data were compared with a one-way ANOVA, expressed by mean± SEM, and significance level was set at 5%. HI animals (n=16) did not show difference in motor behavior from first (37.1 ± 4.9) to second day of the test (37.8 ± 4.0), but a decreased activity was observed in SH (52.6 ± 6.0 on 1st day, 41.5 ± 6.8 on 2nd day, n=15) and CTRL (59.2 ± 5.8 on 1st day, 40.9 ± 5.4 on 2nd day, n=16) groups. There was no difference in motricity between groups. HI animals showed a decreased number of NADPH-d positive neurons (216±66.36 in NAc; 150±16.7 in VTA, n=3) compared to SHAM (358±119.9 in NAc; 274±48.42 in VTA, n=3) group (preliminary data). Our findings showed that HI impairs habituation but not the motor activity, and also affects NADPH-d-positive neurons distribution in NAc and VTA.

Financial support: FAPERJ and CNPq

Where applicable, the authors confirm that the experiments described here conform with The Physiological Society ethical requirements.

PCD110

Altered brain morphology in a mouse model of mental retardation

K.K. Gill, P. Kangesu, J.G. Jefferys and A.D. Powell

Neuronal Networks, University of Birmingham, Birmingham, UK

Altered brain morphology in a mouse model of mental retardation

Mental retardation (MR) affects 2-3% of the population; those due to X-linked mutations are a common cause of moderate to severe MR. *OPHN1* (*Ophn*-1 in mice) is one of the genes implicated in X-linked mental retardation (XLMR), encoding oligophrenin-1, a RhoGAP protein. Loss of function mutations affect Rho GTPase-dependent signalling pathways and alter actin cytoskeleton dynamics which are important for many neuronal functions, including morphogenesis and neuroepithelial development. Structural abnormalities, namely, abnormal cerebral ventricles typically associated with hydrocephalus, have been shown in brains of MR patients with *OPHN1* mutations and *Ophn*-1 null mice. A systematic study has been conducted to explore alterations in brain anatomy in *Ophn*-1 mice. *Ophn*-1 mice (male 15-30g, 6 week old (n=6 for both genotypes) and 3 month old (*Ophn*-$1^{+/y}$ n=8 and *Ophn*-$1^{-/y}$ n=6)) were anaesthetised by I.P. injection of medetomidine (1mg/kg) and ketamine (76mg/kg). Values are expressed as mean ± S.E.M, analysed by ANOVA or Student's t-test. To investigate the impact of loss of oligophrenin-1 on cerebral ventricles, ventricular volumes were analysed. Lateral ventricles were larger in *Ophn*-$1^{-/y}$ mice than *Ophn*-$1^{+/y}$ mice at 6 weeks of age (26.2±10.5 mm^3 and 3.81±0.44 mm^3; respectively; p=0.002) and 3 months of age (7.78±2.54 mm^3 and 3.42±6.99 mm^3; respectively; p=0.02). Lateral ventricle dilatation was associated with a reduction in motor cortex thickness (6 weeks: *Ophn*-$1^{-/y}$ 0.91±0.05 mm and *Ophn*-$1^{+/y}$ 1.09±0.03 mm; p=0.016 and 3 months: *Ophn*-$1^{-/y}$ 0.94±0.03 mm and *Ophn*-$1^{+/y}$ 1.04±0.02 mm; p=0.04) without alteration in somatosensory, auditory and ectorhinal cortices. Hippocampal volume was similar in *Ophn*-$1^{+/y}$ and *Ophn*-$1^{-/y}$ mice (7.38±1.40 mm^3 and 9.29±0.7 mm^3; respectively; p=0.23), neither the thalamus area (15.78±0.91 mm^2 and 13.46±0.69 mm^2; respectively; p=0.07) nor total brain area (51.8±1.6 mm^2 and 46.9±3.05 mm^2 respectively; p=0.18) were affected.

This study demonstrates brain malformation in *Ophn*-$1^{-/y}$ mice, primarily expansion of the lateral ventricles, which may be due to loss of oligophrenin-1 expression in ependymal cells, chorial villi or endothelium. Thus, this could result in impairments in cilia function, ependymal proliferation, abnormal production/absorption of cerebral spinal fluid or obstruction of cerebral aqueduct and/or fourth ventricle. How the ventriculomegaly and reduction in cortical thickness contribute to the cognitive deficits remains to be explored.

Where applicable, the authors confirm that the experiments described here conform with The Physiological Society ethical requirements.

PCD111

NADPH oxidase 4-derived reactive oxygen species mediate the activation of adaptive antioxidant pathways in early diabetic retinas of db/db mice

M. He, H. Pan, C. Xiao and M. Pu

Anatomy, Peking Univ Hlth Science Ctr, Beijing, China

Recent studies suggest that oxidative stress plays a major role on retinal dysfunction in diabetes. The Nrf2/ARE antioxidant pathway has been found to be adaptively activated to counteract increased oxidative stress. However, the activation of Nrf2/ARE pathway has not been studied in the retina of the genetic type 2 diabetic animal model, db/db mice. The present study is to investigate the oxidative status and the activation of Nrf2/ARE antioxidant pathway in retinas of db/db mice. Male db/db C57BLKS/J mice aged at 8, 12, and 20 wks were used in this study. Age-matched male heterozygous db/m littermates were used as control. Animals were enucleated under anesthesia induced with ketamine and xylazine (80 mg/kg+10 mg/kg; intraperitoneally) and isolated retinas were prepared for reactive oxygen species (ROS) detection, immunohistochemistry, and western blotting analysis. All experiments were performed in accordance with Peking University guidelines for animal research and the ARVO Statement for the Use of Animals in Ophthalmic and Vision Research. ROS generation was detected by dihydroethidium (DHE) assay, the expression of NADPH oxdase-4 (Nox4) and heme oxygenase-1 (HO-1) were examined by immunohistochemistry and western blotting.

ROS generation in the retinas of db/db mice increased at 8 wks and continued to progress at 20 wks of ages, compared to age-matched db/m mice (8 wks: dm: 9.67±0.84; db: 22.71±4.74, p<0.01, n=5; 20 wks: dm: 8.11±0.56; db: 21.13±3.71, p<0.01, n=5). However, the increased expression of Nox4 was only observed in the retina of 8 wks (dm: 10.80±1.23; db:17.10±5.37, p<0.01, n=5), but not 20 wks db/db mice compared to age-matched db/m mice. Meanwhile, in comparison with age-matched db/m mice, the expression of HO-1, an Nrf2-mediated antioxidant, was also increased in the retinas of db/db mice aged at 8 wks (dm: 9.68±1.17; db: 17.35±1.13, p<0.001, n=5), but not at 20 wks.

In conclusion,the antioxidant pathway was adaptively activated to counteract hyperglycemia-induced oxidative stress to maintain the redox status in early stages of the diabetic retina (8 wk). As diabetes developed, the antioxidant capacity was damaged by the continuous hyperglycemia and oxidative stress.

Where applicable, the authors confirm that the experiments described here conform with The Physiological Society ethical requirements.

PCD112

Investigating the role of interneurons in epileptic high frequency activity

G. Morris[1], P. Jiruska[2], W. Chang[1], A.D. Powell[1] and J.G. Jefferys[1]

[1]Neuronal Networks, University of Birmingham, Birmingham, UK and [2]Department of Developmental Epileptology, Institute of Physiology, Academy of Sciences of Czech Republic, Prague, Czech Republic

Temporal Lobe Epilepsy is the most common form of epilepsy – a neurological disorder characterised by abnormal excitation and synchronisation of neuronal networks. High frequency

activity (HFA) is defined as network activity with frequency of over 100 Hz and is a biomarker for the epileptic hippocampus. The underlying mechanism is unknown, but it is hypothesised that interneurons, which are capable of firing action potentials (APs) at frequencies in the HFA range, could synchronise local pyramidal cell activity. High frequency interneuronal firing imposes synchronous IPSPs upon on a population of pyramidal cells, creating temporal windows in which they can fire. This could lead to synchronised high frequency population events. Using the VGAT-Venus A strain of rats that selectively express the fluorescent Venus protein in interneurons, we have examined the role of hippocampal interneurons in the genesis of HFA.

Adult VGAT-Venus A rats were anaesthetised with 0.24mg/kg medotomidine and 58.2mg/kg ketamine via I.P. injection before transcardial perfusion with sucrose ACSF, and 300 μm horizontal brain slice preparation. Extracellular recordings were made from stratum pyramidale (SP) in hippocampal region CA3b. Interictal-like discharges (ILDs) were induced by superfusion of the slices with high potassium (9mM). Following induction of ILDs, whole-cell patch clamp recordings were made from interneurons, irrespective of location, which were identified using fluorescence microscopy. Data is given as the mean±SEM.

Superfusion of high potassium generated ILDs (frequency = 0.72±0.04Hz; n=11), on which HFA (190.6±9.8 Hz; n=10) was superimposed. Interneurons were divided into four categories, as defined by their firing pattern. Group 1 neurons fired throughout ILDs and correlated with HFA (mean max. firing frequency = 207.5; n=2), whilst group 2 neurons fired throughout ILDs but were not correlated with HFA (182.50±20.4 Hz; n=4). Group 3 neurons fired a single AP on each ILD (n=2) whereas group 4 neurons fired randomly except for 2-3 APs at the onset of each ILD (120±31.8 Hz; n=3). Those neurons whose activity correlated with HFA were found in SP and stratum oriens and those which fire single APs were found in SP and stratum radiatum. Interneurons which are capable of maintaining HFA frequency firing, but do not correlate with HFA, were found throughout the layers of the hippocampus.

These results show that a sub-population of interneurons correlate with HFA and are candidates for pacing this activity. Pharmacological or electrophysiological manipulation of candidate cells has the potential to affect epileptic field activity by reducing the pathological synchronisation of pyramidal cell activity.

This work was supported by an Epilepsy Research UK to JGRJ, ADP and PJ.

Where applicable, the authors confirm that the experiments described here conform with The Physiological Society ethical requirements.

PCD113

Functional connections between the ventrolateral periaqueductal grey and cerebellum – a role in fear behaviour?

J.J. Crook, S. Koutsikou, E.V. Earl, J. Leith, R. Apps and B.M. Lumb

Physiology and Pharmacology, University of Bristol, Bristol, UK

Activation of neurons in the ventrolateral periaqueductal grey (vlPAG) matter has been shown to be associated with the expression of freezing responses to conditioned fear (1). These responses are reduced following lesions of the vlPAG, indicating that this structure plays an essential role in the freezing response to conditioned fear (2).

Previous anatomical studies have demonstrated pathways from the vlPAG to the cerebellum (3,5). Data are presented here which suggest that such a functional connection, via the inferior olive, plays a role in the expression of conditioned freezing behaviour.

Electrical stimulation of the vlPAG in anesthetised male Wistar rats (Sodium Pentobarbital; 60mg.kg$^{-1}_{ip}$) was found to evoke climbing fibre field potentials in lateral lobule VIII of the cerebellar vermis. The functional significance of this climbing fibre mediated connection was investigated in relation to the finding that chemical stimulation of the vlPAG significantly increases hindlimb-evoked H-reflex amplitude (average increase = 45.2±11%, n=16, P<0.001, Repeated measures ANOVA with Newman-Keuls post-hoc test) in alphaxalone-anesthetised male Wistar rats (Alfaxan; 25mg.kg^{-1}.hr$^{-1}_{iv}$)*.

It was hypothesised that the cerebellum supports this descending effect upon spinal a-motoneurone excitability, which may be linked to the increased muscle tone associated with freezing behaviours. It was found that cerebellectomy (n=4) or neurotoxic lesion (n=4) of the caudal inferior olive abolished the effect of vlPAG stimulation upon H-reflex amplitude.

In another set of rats localised lesions of connections to/from vermal lobule VIII, using the toxic tracer cholera toxin b-subunit-saporin (CTb-Sap) (4), were made under ketamine/medetomidine anaesthesia (Vetalar 50mg.kg$^{-1}_{ip}$ and Domitor 300μg.kg$^{-1}_{ip}$). In these animals (n=12) fear-conditioned freezing was significantly disrupted (P<0.001, Mann-Whitney test) compared to sham controls (n=10), despite appearing otherwise normal in a battery of motor and affective behavioural tasks. The same CTb-Sap treated animals were subsequently alphaxalone-anesthetised (n=6) as previously and the effect of vlPAG stimulation upon H-reflex amplitude found to be abolished. Changes in freezing behaviour as a function of H-reflex facilitation were plotted for individual animals. Consistent with the concept of H-reflex excitability being a proxy measurement for muscle tone underlying freezing behaviour, a positive correlation between the two was found (r^2= 0.75, P < 0.05, Linear regression).

In summary, these data indicate that vermal lobule VIII of the cerebellum plays an important role in the expression of vlPAG mediated freezing behaviour.

(*Preparatory surgery for these experiments was conducted under 1.5-4% halothane anaesthesia.)

Carrive P *et al.* (1997). *Neuroscience*, **78**, 165-177.

De Oca BM *et al.* (1998). *Journal of Neuroscience*, **18**, 3426-3432.

Flavell C (2009). *PhD Thesis*, University of Bristol.

Pijpers A *et al.* (2008).*Journal of Neuroscience*,**28**, 2179-2189.

Swenson RS & Castro AJ (1983). *American Journal of Anatomy*, **166**, 329-341.

Work was funded by the BBSRC.

JJC is an MRC scholar.

Where applicable, the authors confirm that the experiments described here conform with The Physiological Society ethical requirements.

PCD114

Chronic neuropathic pain is alleviated by the highly specific iNOS inhibitor, 1400W

C.A. Staunton, L. Djouhri, R. Barrett-Jolley and S. Thippeswamy

Musculoskeletal Biology, University of Liverpool, Liverpool, UK

Chronic neuropathic pain may result from nerve injury and is refractory to currently available analgesic therapies. It is a debilitating pain condition and one that involves numerous complex underlying mechanisms that are poorly understood.
Following nerve injury, astrocytes and microglial cells become active leading to the synthesis of neurotoxic mediators and prolonged Inducible Nitric Oxide Synthase (iNOS) transcription. Such mediators alongside excessive levels of nitric oxide (NO) have been shown to correlate with an increase in pain severity and provoke ectopic neuronal cell activity. This hypersensitivity leads to the formation of peripheral and central sensitization (1-3).
We used a well established model of neuropathic pain, L5-Spinal Nerve Axotomy (L5-SNA) (4), which was carried out on Wistar rats under deep gaseous anaesthesia (2% isoflurane, 2L/min O2 and NO2). Two dosing regimens of a high selective iNOS inhibitor, N-(3-(Aminomethyl) benzyl) acetamidine dihydrochloride (1400W), or equal volume of vehicle were administered. We examined the effects of iNOS inhibition on two parameters used to characterise pain behaviour in humans; heat hyperalgesia (HH) and mechanical Allodynia (MA). Baseline behaviour was recorded prior to surgery and drug treatments and was continued for 7-14days post L5-SNA. Data are expressed as mean ±SEM. Statistical significance was calculated using either a Mann-Witney U t-test or a 2-way repeated measure ANOVA with Bonferroni's post tests, as appropriate.
Following L5-SNA and prior to drug interventions, both MA (27±0.6g to 18±0.7g, n=16) and HH (17±0.5s to 9±1s, n=16) were markedly reduced indicating a significant increase in pain levels $p<0.0001$).
When 1400W was administered 18hr post surgery, we observed increases in both HH and MA thresholds, indicating a significant decrease in pain levels (n=9; $p<0.05$). The greatest significant increase in MA following 1400W was observed at 74hr post surgery (22.4±0.8g for 1400W, n=9, compared to 15.6±0.9g for vehicle, n=7; $p<0.001$). For HH, 162 hr post surgery, the largest increase caused by 1400W was observed (15.7±0.4s for 1400W, n=9, compared to 7.2±0.7s for vehicle, n=7; $p<0.001$). However, when 1400W was administered 7days post L5-SNA, no effect was observed with 1400W at any time point post-L5 SNA (n=5 per treatment group).
The in vivo behavioral testing results strongly suggest that iNOS plays a key role in the hypersensitivity associated with trauma-induced NP during early stages of nerve injury. The results from this study indicate that 1400W has the ability to affect some analgesia, but became ineffective once chronic pain had fully established. We conclude that iNOS inhibiting drugs may have potential future use in neuroprotection and medical analgesia.

Koch A, Zacharowski K, Boehm O, Stevens M, Lipfert P, von Giesen HJ, et al. Nitric oxide and pro-inflammatory cytokines correlate with pain intensity in chronic pain patients. Inflammation research : official journal of the European Histamine Research Society [et al]. [Research Support, Non-U.S. Gov't]. 2007 Jan;56(1):32-7.

Leung L, Cahill CM. TNF-alpha and neuropathic pain - a review. J Neuroinflamm. 2010 Apr 16;7.

Levy D, Hoke A, Zochodne DW. Local expression of inducible nitric oxide synthase in an animal model of neuropathic pain. Neurosci Lett. 1999 Feb 5;260(3):207-9.

Li YB, Dorsi MJ, Meyer RA, Belzberg AJ. Mechanical hyperalgesia after an L5 spinal nerve lesion in the rat is not dependent on input from injured nerve fibers. Pain. 2000 Apr;85(3):493-502.

Work supported by Pain Relief Foundation

Where applicable, the authors confirm that the experiments described here conform with The Physiological Society ethical requirements.

PCD115

Characterization of recurrent laryngeal nerve function in rats

I. Naggar, N. Mor, K. Nakase, P. Zolkind, J.B. Silverman, K. Sundaram, M. Stewart and R. Kollmar

SUNY Downstate Medical Center, Brooklyn, NY, USA

The recurrent laryngeal nerve (RLN) is a branch of the vagus nerve that controls the movement of the vocal folds and arytenoid cartilages. Since it is damaged in 4-10% of thyroid surgeries, a better characterization of its function may aid in finding ways to repair the consequent vocal fold paralysis after damage. To this end, we developed methods to measure RLN function and vocal fold movement in rats under normal conditions, after nerve crush or cut, and upon RLN stimulation in rats. Rats were anesthetized with urethane 1.5 mg/kg intraperitoneally. Right RLN activity was recorded, along with electrical activity of the posterior crico-arytenoid and thyro-arytenoid muscles. A microsuspension laryngoscope was fashioned to visualize the arytenoid cartilages, and the deviation of the cartilages from the midline on video served as a quantitative measure of vocal fold function. Breathing was assessed by recording changes in resistance over a piece of conductive rubber wrapped around the thorax. Recordings from the above techniques were taken simultaneously during normal vocal fold function and after nerve crush or cut. Average waveforms of a single respiratory cycle during normal function and after nerve injury were calculated for each recording. The RLN was stimulated at 1, 2, 5, 10, 20, and 50 Hz with 1-millisecond pulses under normal and nerve injury conditions. A total of 31 adult rats were used in these experiments. Under normal conditions, we found rhythmic firing in the RLN that correlated in time with electromyogram (EMG) activity, vocal fold movement, and breathing. Cutting or crushing the right RLN resulted in normal breathing, but cessation of RLN and EMG activity, as well as paralysis of the ipsilateral arytenoid near the midline position. Stimulation of the distal RLN under normal and cut conditions caused arytenoid twitches that occurred upon each pulse in the 1-10 Hz range. At 20 or 50 Hz, the arytenoid moved to or stayed at the midline during stimulation. The development of quantitative techniques to study RLN function is an important step towards validating a rat model for RLN lesions. Normal RLN activity causes opening and closing of the arytenoids, but overstimulation of the RLN may overpower the adductor muscles and cause midline paralysis of the vocal folds. Our results have implications for the study of RLN regeneration after injury, as nerve impulses occurring after re-innervation may be similar to indiscriminate RLN stimulation.

Where applicable, the authors confirm that the experiments described here conform with The Physiological Society ethical requirements.

PCD116

Localization of cortical areas activated by visual memory task using functional magnetic resonance imaging

A. Sokolov[1], V. Fokin[1], E. Aleksandr[1] and S. Vorobyev[2]

[1]Radiology, Medical Military Academy, Saint-Petersburg, Russian Federation and [2]Neurology, Medical Military Academy, Saint-Petersburg, Russian Federation

Purpose: To localize cortical areas activated by visual memory tasks by the mean of functional magnetic resonance imaging (fMRI).
Methods: We used 1.5 T MR-scaner and BOLD-method (Blood Oxygenation Level Dependent), based on distinctions of magnetic properties of hemoglobin. We studied 27 healthy volunteers (20-32 year old). All of them passed MMSE, FAB, CES-D, attention and memory tests. There were done anatomical and fMRI fast imaging technique: echo planar imaging (EPI), whole brain scan (36 slices) matrix 64x64, 3.7 second. Fast imaging technique on modern MR-scanners with ≥ 1.5 T provides precise statistical maps of oxygenation increase with high spatial resolution. SPM8 software package was used for fMRI assessment and statistical analysis. For test stimuli we used series of 12 not related images for "baseline" and 12 images with 6 presented before for "active". Stimuli were presented 3 times with reduction of repeated images to 4 and 2.
Results: the investigation showed bilateral activity of anterior cingulate gyrus in 90% cases. In 70% cases activity was evidenced in parahippocampal gyrus (bilateral – 20%, left parahippocampal gyrus – 70%). We also noted activation of superior frontal gyrus (Brodman area 6 – BA6) in 45% cases, BA 21, 37, 38 in 40% cases.
Conclusion: our data are well co-coordinated with neurophysiologic and clinical findings that several brain areas are involved in realization of visual memory tasks. Visual memory is provided by integrative processes in brain cortex. These data will be able to use in clinical practice in patients with cognitive disorders.

Where applicable, the authors confirm that the experiments described here conform with The Physiological Society ethical requirements.

PCD118

Repeated exposure to novel spatial arrangement of objects: impact on hippocampal-dependent learning and synaptic plasticity

. Amaro-Leal, A.J. Carmo, I. Rocha and D. Cunha-Reis

Laboratório de Função Autonómica Cardiovascular, Unidade de Fisiologia Clínica e Translacional, Instituto de Medicina Molecular, Universidade de Lisboa, Lisboa, Portugal

It was recently demonstrated that exposure to novel configurations of objects in familiar environments enhances long-term depression (LTD) in vivo (1). LTD is an important cellular physiological process involved in memory reformulation and memory pathway regeneration. Recently we developed a cognitive training program aiming to impair cognitive decline in pathologies leading to saturation of synaptic function. Rats undergoing this 3-week training were shown to express enhanced LTP evoked by theta-burst stimulation (five or ten 100Hz bursts, 4 stimuli, separated by 200 ms) and depotentiation induced by low frequency stimulation (LFS, 1Hz, 15min) in the CA1 area of hippocampal slices obtained from trained rats.
Male Wistar rats (4 weeks-old at the beginning of training) were exposed for two weeks to three objects always presented in a new spatial configuration. Objects were placed inside wholes at the corners of an 80x80cm square arena (holeboard). Exposure either to objects in a fixed configuration or absence of objects were used as control. Behaviour during the training sessions was evaluated by addressing exploratory activity (nose-pokes, rearings and total distance travelled). In the final day of training all animals were exposed to objects in a new configuration. The impact of this training program in hippocampal-dependent spatial learning was evaluated using the radial-arm maze test. The latency to find each of the three baited arms, number of wrong arm entries and re-entries in previously visited baited arms were determined.
During training, all animals showed increased exploratory activity and decreased general exploration of objects (nose-pokes). In the final day, the animals exposed to this situation for the first time showed increased general exploration of objects (nose-pokes). Animals that were submitted to the training program (n=9) and matched controls experiencing repeated exposure to objects kept in a fixed configuration (n=9) showed decreased latency to find all baited arms in the radial arm maze when compared to animals trained in the absence of objects (n=9). All these groups performed better in the radial arm maze when compared to animals that were never exposed to the holeboard (n=8). When tested one week after the end of radial arm training, trained rats were more efficient ($P<0.05$, One-Way ANOVA) in finding the baited arms (radial arm recall test) suggesting that they have better retention of memories. Altogether, this suggests that training routines based on these aspects of novelty exposure may have a significant impact on cognitive performance in spatial learning tasks. This may be useful in cognitive recovery in neurological diseases involving synaptic pathology such as temporal lobe epilepsy.

1 - Kemp and Manahan-Vaughan, 2004, Proc Natl Acad Sci USA 101:8192.

Supported by FCT

Where applicable, the authors confirm that the experiments described here conform with The Physiological Society ethical requirements.

PCD119

Auxiliary KChIP4a suppresses voltage-gated A-type K+ current through ER retention and promoting closed-state inactivation of Kv4 channels

Y. Tang, J. Zhou, Y. Lu, P. Liang, L. Lei, X. Bian and K. Wang

Peking University, Beijing, China

In the brain and heart, auxiliary KChIPs coassemble with pore-forming Kv4 α- subunits to form a native channel complex and regulate the expression and gating properties of Kv4 currents as well as membrane excitability. Among the KChIP1-4, KChIP4a exhibits a unique N-terminus that is known to suppress Kv4 function, but the underlying mechanism for Kv4 inhibition remains unknown. In this study, using approaches of confocal imaging, biochemistry and electrophysiology, we identified the hydrophobic and aliphatic residues 12-17, LIVIVL within the KChIP4a N-terminus, that function as a novel ER retention motif to reduce surface expression of Kv4-KChIP channel complex. The ability of LIVIVL motif to retain Kv4 proteins is transferable and depends on its flanking location, but not buried

in the middle of protein sequence. Interestingly, adjacent to the ER retention motif, the residues 19-21 (VKL motif) directly interact with Kv4.3 to enhance closed-state inactivation (CSI) and lead to Kv4.3 current inhibition. Because that auxiliary KChIPs can alter biophysical and physiological properties of Kv4 channels by regulating subunit composition of native Kv4 channel complex, we then analyzed the expression profile of two KChIP4 splice variants KChIP4a and KChIP4bl that have opposite effects on Kv4 function in rat dorsal root ganglion (DRG) neurons under pain conditions. Our findings show that KChIP4a mRNA was down-regulated in L4-5 DRG neurons 7 days after spinal nerve ligation in rats that received chloral hydrate (0.3 g/kg, intraperitoneally) before operation. Taken together, our findings reveal two distinct mechanisms by which KChIP4a suppresses Kv4 function through ER retention and promoting CSI. Differential regulation of auxiliary KChIPs expression in DRG neurons are likely involved in development of pathological pain conditions.

An, W. F., Bowlby, M. R., Betty, M., Cao, J., Ling, H. P., Mendoza, G., Hinson, J. W., Mattsson, K. I., Strassle, B. W., Trimmer, J. S., and Rhodes, K. J. (2000) Nature403, 553-556.

Holmqvist, M. H., Cao, J., Hernandez-Pineda, R., Jacobson, M. D., Carroll, K. I., Sung, M. A., Betty, M., Ge, P., Gilbride, K. J., Brown, M. E., Jurman, M. E., Lawson, D., Silos-Santiago, I., Xie, Y., Covarrubias, M., Rhodes, K. J., Distefano, P. S., and An, W. F. (2002) ProcNatlAcadSci U S A99, 1035-1040.

Wang, H., Yan, Y., Liu, Q., Huang, Y., Shen, Y., Chen, L., Chen, Y., Yang, Q., Hao, Q., Wang, K., and Chai, J. (2007) Nat Neurosci10, 32-39.

Liang, P., Wang, H., Chen, H., Cui, Y., Gu, L., Chai, J., and Wang, K. (2009) J BiolChem284, 4960-4967.

Jerng, H. H., and Pfaffinger, P. J. (2008) J BiolChem283, 36046-36059

This work was supported by research grants to KWW from the National Science

Foundation of China, 30970919 and 81221002, the Ministry of Education of China,111 Project China (B07001).

Where applicable, the authors confirm that the experiments described here conform with The Physiological Society ethical requirements.

PCD120

A novel compound targeting Kv7.2/3 channels relieves inflammatory and neuropathic pain

A. Peretz, E. Patrich, P. Kornilov, N. Menaker and B. Attali

Tel Aviv University, Tel Aviv, Israel

M-channels generate sub-threshold, non-inactivating voltage-gated K+ currents that play an important role in controlling neuronal excitability. In our quest to target neuronal M-type K+ channels, encoded by Kv7.2/Kv7.3 subunit assembly, we previously designed novel diphenylamine carboxylates that are powerful Kv7.2 channel openers or blockers. Recently, we designed a Kv7.2 channel opener, NH29, which was found to stabilize the Kv7.2 channel open state by interacting with its voltage sensing domain (VSD). Using the same structural framework, we designed a novel gating-modifier molecule, NH34, to test its activity on neuronal excitability and probe its potency in vivo on inflammatory and neuropathic pain. In transfected CHO cells, NH34 significantly increased Kv7.2 currents, by producing a hyperpolarizing voltage shift of the activation curve and slowing deactivation kinetics (EC50 = 17.5 μM). Interestingly, two S4 mutants, R198A and R207W significantly decreased the opener potency of the drug, suggesting that NH34, like NH29, may interact with the VSD of Kv7.2 channels. Results indicated that NH34 preferentially acts as an opener of Kv7.2 and Kv7.3 homomeric and heteromeric channels. NH34 was ineffective on Kv7.4 and Kv7.5 channels but produced a significant inhibition of TRPV1 cation channels. Patch-clamp intracellular recording of CA1 pyramidal neurons from 2 weeks-old rat hippocampal slices showed that NH34 reduced the spike discharge frequency evoked by injection of depolarizing current. Data from hippocampal slices also revealed that NH34 significantly depressed the slope of field EPSPs and the fiber volley amplitude recorded extracellularly in the CA1 pyramidal region following stimulation of the Schaeffer collaterals. NH34 reduced the frequency of evoked spike discharge in dorsal root ganglion neurons. In vivo, NH34 (3-30 mg/kg p.o) significantly relieved the hyperalgesia evoked by mechanical pressure of the paw in a rat model of inflammatory pain (Complete freund adjuvant). Similarly, NH34 (3-30 mg/kg p.o) was very efficient in alleviating the hyperalgesia evoked by mechanical pressure or cold allodynia in a Seltzer rat model of neuropathic pain. In all, the data suggest that NH34 is a very promising drug template for treating inflammatory and neuropathic pain.

Where applicable, the authors confirm that the experiments described here conform with The Physiological Society ethical requirements.

PCD121

Cyclin-dependent kinase 5 (Cdk5) regulates TRPV1 membrane trafficking through phosphorylating KIF13B

Y. Zhang, B. Xing, Y. Yang, J. Du and Y. Wang

Neuroscience Research Institute, Peking University Health Science Center, Beijing, China

TRPV1 (transient receptor potential vanilloid 1) is a key molecule involved in the development of peripheral sensitization, which is believed to be the peripheral mechanism of pathological pain. Phosphorylation/dephosphorylation regulation plays a critical role in TRPV1 sensitization/desensitization. Multiple protein kinases, such as protein kinase A, protein kinase Cε, CaMKII (calmodulin-dependent kinase II) and Cdk5 (cyclin-dependent kinase 5), contribute to this process. Here, we reported an alternative way of functional regulation of TRPV1 by Cdk5, independent of the direct phosphorylation of TRPV1. The main findings are as follows:
(1) TRPV1 can associate with KIF13B (kinesin-3 family member 13B) FHA domain. Knock down of endogenous KIF13B expression resulted in a significant decrease of the surface expression of TRPV1 in primary cultured DRG (dorsla root ganglion) neurons.
(2) *In vitro* kinase assays showed that Cdk5 phosphorylated the KIF13B-FHA domain at Threonine-506.
(3) Inhibition of Cdk5 activity decreased threonine phosphorylation of the KIF13B-motor FHA domain and the number of TRPV1-KIF13B-motor FHA complexes in CHO cells stably expressing TRPV1 (TRPV1-CHO cells) transfected with GFP-KIF13B motor FHA domain plasmids.
(4) Transmembrane TAT-T506 peptide inhibited TRPV1 surface expression in DRG neurons.
(5) Intrathecal delivery of the TAT-T506 peptide inhibited TRPV1 sensitization after inflammation and alleviated heat hyperalgesia behaviors in CFA-induced inflammatory pain models in rats.
Conclusions:

Regulation of the membrane trafficking of TRPV1 by Cdk5 through phosphorylating KIF13B contributes to inflammatory heat hyperalgesia. TAT-T506 might be a potential candidate for analgesic drug development.

Xing BM*, Yang YR*, Du JX*, Chen HJ, Qi C, Huang ZH, Zhang Y[CA] and Wang Y[CA]. Cyclin-dependent kinase 5 controls TRPV1 membrane trafficking and the heat sensitivity of nociceptors through KIF13B. J Neurosci. 2012 Oct 17;32(42):14709-21

This work was supported by National Natural Science Foundation of China Grants 30830044, 30925015, 30900582 and 81161120497; Beijing Natural Science Foundation Grant 7092061, and Specialized Research Fund for Doctoral Programs of Higher Education Grants 200800011028. Ying Zhang is the recipient of the travel awards for young physiologists from the Chinese Association for Physiological Sciences (CAPS).

Where applicable, the authors confirm that the experiments described here conform with The Physiological Society ethical requirements.

PCD122

Insulin modulates GABAA channels-mediated inhibition in rat hippocampal and amygdala neurons

Z. Jin, Y. Jin, S. Korol and B. Birnir

The Division of Molecular Physiology and Neuroscience, Department of Neuroscience, Uppsala University, Uppsala, Sweden

GABA (gamma-aminobutyric acid) regulates neuronal excitability and network activity by activating GABAA channels that generate phasic and tonic currents. The pancreatic hormone insulin, in addition to its critical role in peripheral glucose regulation, has effects on neuronal excitability and memory functions. Hippocampus and amygdala, both important components of the limbic system participate in the memory formation. We have previously shown that insulin can enhance the GABAA mediated tonic conductance in rat hippocampal CA1 neurons (Jin Z, et al., 2011). The aim of this study is to investigate 1) if insulin receptor is expressed in the rat and human amygdala 2) the effect of insulin on GABAA channels-mediated inhibition in rat hippocampal and amygdala neurons. Quantitative RT-PCR was run on total RNAs isolated from rat and human post-mortem amygdala. Standard whole-cell and single channel recordings were performed on hippocampal and amygdala slices were prepared from postnatal 16-22 days old Wistar rats and incubated with ACSF (artificial cerebrospinal fluid) or low physiological concentration of insulin. The mRNA transcript for insulin receptor was detected in both rat (n=3) and human (n=12) amygdala samples. In the rat amygdala, the insulin receptor was expressed in both the central nucleus and the basolateral nucleus. The incubation of 1nM insulin increased GABAA-mediated tonic currents in rat hippocampal CA1 neurons (n=24) and reduced the action potential firing frequency (n=13). The enhanced tonic current is partially carried by alpha5, gamma2 containing GABAA channels. The insulin-induced GABAA channels have very high-affinity (pM) with novel pharmacological profile. Our results suggest GABAA-mediated tonic conductance regulate basal neuronal excitability when it is prominently expressed.

Jin Z, Jin Y, Mendu SK, Eva D, Leif G and Birnir B. (2011) Insulin reduces neuronal excitability by turning on GABAA channels that generate tonic current. Plos One, 6(1): e16188

Brain tissues were provided by the New South Wales Tissue Resource Center at the University of Sydney supported by the National Health and Medical Research Council of Australia, National Institute of Alcohol Abuse and Alcoholism, and NSW Department of Health.

Where applicable, the authors confirm that the experiments described here conform with The Physiological Society ethical requirements.

PCD123

Brain temperature is a critical determinant of neuronal excitability through TRPV4 activation

K. Shibasaki[1], K. Yamada[2], H. Miwa[1], M. Tominaga[3] and Y. Ishizaki[1]

[1]Gunma University Graduate School of Medicine, Maebashi, Japan, [2]Hirosaki University Graduate School of Medicine, Hirosaki, Japan and [3]National Institute for Physiological Sciences, Okazaki, Japan

Physiological brain temperature is an important determinant of brain functions, and it is well established that changes in brain temperature dynamically influence hippocampal neuronal activity. We previously revealed that the thermo-sensor TRPV4 (activated above 34°C) is activated by physiological brain temperature in hippocampal neurons and thereby controls their excitability in vitro (J. Neurosci. 2007, Shibasaki et al.). Here, we examined whether TRPV4 regulates neuronal excitability through its activation by brain temperature in vivo. We developed an original device to cool local brain temperature to inactivate TRPV4. The cooling treatment clearly demonstrated that constitutive TRPV4 activation was occurred in mouse brain, and we found that hippocampal theta-frequency electroencephalogram (EEG) activities in TRPV4KO mice during wake periods were significantly reduced compared with those in WT mice. Furthermore, slice patch clamp recordings from dentate gyrus of hippocampus revealed that WT neurons further depolarized compared with TRPV4KO neurons. Depending on the differences of the resting membrane potentials, WT neurons had smaller fEPSPs and higher firing than KO neurons at 35°C (above TRPV4 activation), however, the differences were abolished at 30°C (less than TRPV4 activation). Taken together, for the first time we reveal that TRPV4 is an important transducer that converts brain temperature into neuronal electrical excitability in mammals.

Shibasaki, K., Suzuki, M., Mizuno, A. & Tominaga, M. Effects of body temperature on neural activity in the hippocampus: regulation of resting membrane potentials by transient receptor potential vanilloid 4. The Journal of neuroscience : the official journal of the Society for Neuroscience 27, 1566-1575 (2007).

Shibasaki, K., Murayama, N., Ono, K., Ishizaki, Y. & Tominaga, M. TRPV2 enhances axon outgrowth through its activation by membrane stretch in developing sensory and motor neurons. The Journal of neuroscience : the official journal of the Society for Neuroscience 30, 4601-4612 (2010).

This research was supported by Grants-in-Aid for Scientific Research (Project No. 21200012, 20399554, 24111507< Brain Environment> to K.S) from the Ministry of Education, Culture, Sports, Science and Technology, Japan, by a grant from Uehara Memorial Foundation (to K.S.), by a grant from Takeda Science Foundation, Tokyo, Japan (to K.S.), by a grant from the Sumitomo Foundation (to K.S.), by a grant from the Brain Science Foundation (to K.S.), by a grant from Narishige Neuroscience Research Foundation (to K.S.), and by a grant from Salt Science Research Foundation No.12C2 (to K.S.).

Where applicable, the authors confirm that the experiments described here conform with The Physiological Society ethical requirements.

PCD125

Trafficking of AMPA receptors in dorsal horn neurons during persistent pain: the changes in synaptic and extrasynaptic receptor pools

O. Kopach, A. Sotnik, P. Belan and N. Voitenko

Bogomoletz Institute of Physiology, Kiev, Ukraine

AMPA receptors (AMPARs) mediate fast excitatory synaptic transmission and play a critical role in synaptic plasticity in the CNS. In adult neurons, most AMPARs have low Ca2+ permeability due to GluR2 subunit expression. Cumulative evidence indicates that AMPAR subunit composition is not static and subject to change during activity-dependent plasticity. Here, we studied how the trafficking of AMPARs is changed in dorsal horn (DH) neurons of spinal cord during persistent pain produced by peripheral inflammation.

Persistent peripheral inflammation was induced by complete Freund's adjuvant (CFA, 100 μl), injected subcutaneously into the plantar side of one hind paw of the deeply isoflurane-anesthetized rats. The animals were used in accordance with protocols that were approved by the Animal Care and Use Committee at the Bogomoletz Institute of Physiology and were consistent with the ethical guidelines of the National Institutes of Health and the International Association for the Study of Pain. AMPAR functioning was investigated using whole-cell patch-clamp recording combined with Ca2+ imaging.

We found that peripheral inflammation increases the functional expression of Ca2+-permeable AMPARs in both the synaptic and extrasynaptic membranes of DH neurons. Peripheral inflammation promotes internalization of GluR2 subunits from the synapses of DH neurons during the maintenance period of CFA-induced persistent inflammatory pain (Park et al., 2009). At the same time, a dramatic increase in the functional expression of GluR1-containing Ca2+-permeable AMPARs was observed in the extrasynaptic plasma membrane in lamina II DH neurons. This increase occurred only in SG neurons characterized by intrinsic tonic firing properties, but not in those exhibiting a strong adaptation (Kopach et al., 2011).

Altogether, our results demonstrate that persistent inflammation increases the number of Ca2+-permeable AMPARs in both the synaptic and extrasynaptic membranes and their proportion within the entire AMPARs population in DH neurons. That leads to increased Ca2+ influx in the neurons resulting in increased neuron excitability and altered synaptic efficacy during persistent inflammatory pain.

Park et al., J. Neurosci. 2009;29:3206-3219.

Kopach et al. Pain. 2011; 152 (4): 912-923.

Acknowledgements: This work was supported by NASU Biotechnology, DFFD F46.2/001, F47/066 Grants (N.V.), STCU Grant #5510 (P.B.), and NASU Grant for Young Scientists (O.K.).

Where applicable, the authors confirm that the experiments described here conform with The Physiological Society ethical requirements.

PCD126

D-series resolvins suppressed sensory TRP activities resulting in multiple anti-nociception

S. Yoo[1,2], S. Bang[1,2], T. Yang[1,2], J. Lim[1,2] and S. Hwang[1,2]

[1]Department of Medical Science, Korea University, Ansan, Gyeonggi, Republic of Korea and [2]Translational Research Institute for Incurable Diseases, Korea University College of Medicine, Ansan, Gyeonggi, Republic of Korea

Sensory transient receptor potential (TRP) ion channels present in DRG nerve termini and skin keratinocytes serve a crucial role in detection of environmental harmful stimuli. Little is known about endogenous molecules that negatively control these TRP activities. Resolvins are anti-inflammatory and pro-resolving lipid molecules naturally generated during inflammatory processes. We asked whether D-series resolvins (RvDs) modulate the sensory TRP channel activation. We examined the effects of 17(S)-RvD1 and 17(R)-RvD1 on sensory TRPs using calcium imaging and whole cell electrophysiology experiments with a HEK cell heterologous expression system, cultured sensory neurons and HaCaT keratinocytes. Changes in agonist-specific acute nociceptive behaviors (licks, flicks and flinches) and TRP-related mechanical and thermal pain behaviors were also checked with or without inflammation. As a result, 17(S)-RvD1 targeted multiple TRP channels while 17(R)-RvD1 specifically acted on TRPV3. 17(S)-RvD1 inhibited TRPA1, TRPV3 and TRPV4 at nanomolar and micromolar levels. Consistent decreases in acute pain indices by local administration of 17(S)-RvD1 were also detected. Peripheral treatment of 17(S)-RvD1 significantly prevented mechanical and thermal hypersensitivity in inflamed tissues. For 17(R)-RvD1, TRPV3-specific in vitro and in vivo responses were suppressed upon its application. The administration of 17(R)-RvD1 reversed thermal hypersensitivity caused by inflammation. A molecular mechanism of such inhibition appears to be a shift in voltage-dependence of TRP channels. In conclusion, RvDs are potent endogenous sensory TRP channel inhibitors. The result implicates that our body has an internal antinociceptive potential with endogenous TRP-regulating lipids. This finding may also help understand pain mechanisms involving TRP interactions with pro-resolving substances.

This work was supported by the National Research Foundation of Korea Grant (2012000540) and Korea Health technology R&D Project of Ministry of Health & Welfare Grant (A111373), Republic of Korea.

Where applicable, the authors confirm that the experiments described here conform with The Physiological Society ethical requirements.

PCD127

Identifying ligand induced conformational changes of human P2X1 with voltage clamp fluorometry

A.G. Fryatt and R.J. Evans

Department of Cell Physiology and Pharmacology, University of Leicester, Leicester, UK

P2X receptors are a distinct family of ATP-gated trimeric cation channels involved in a wide array of physiological processes. Recent advances have been made to understanding the molecular structure and function of these ion channels, including

the generation of crystal structures of zebrafish P2X4 in both ATP-free and ATP-bound states. However, the structures give snapshots of the conformation of the receptor and do not address the time-course of conformational changes following agonist binding, channel opening, desensitization or agonist unbinding. To address these questions we used voltage clamp fluorometry to study human P2X1 receptors by introducing single cysteine point mutations along the subunit interface at residues around the cysteine rich head region (K138C, E181C), adjacent to the agonist binding site (N284C, K190C) and linking the binding site to the transmembrane portions (D320C, P196C, I62C).

Voltage clamp fluorometry allows the simultaneous measurement of channel current and the fluorescence of labelled mutant cysteine residues to detect changes in receptor conformation. In this study cysteine mutant human P2X1 receptors were expressed in *Xenopus* oocytes and labelled with 2-((5(6)-Tetramethyl-rhodamine)carboxylamino)ethyl Methanethiosulfonate (MTS TAMRA). MTS TAMRA labelled each of the single cysteine point mutants detailed above but did not label the wild type P2X1 receptors. Additionally labelling with MTS TAMRA had no effect on agonist evoked currents, showing that binding of the fluorescent probe did not inhibit channel function. ATP application had little or no effect on fluorescence at D320C, P196C, I62C and E181C mutants however decreases in fluorescence were recorded at K138C, N284C and K190C mutants (approximately 5%, 10% and 15% decrease respectively). These decreases in fluorescence returned to baseline levels following removal of ATP, however the time-course of this recovery appeared dependent on the cysteine mutant. This suggests that there are temporally distinct conformational changes in different parts of the receptor.

Where applicable, the authors confirm that the experiments described here conform with The Physiological Society ethical requirements.

PCD128

A DMD-based multicolor irradiation system for the optogenetic analysis of neural circuits

S. Sakai[1,2], T. Mishima[1,2], T. Ishizuka[1,2] and H. Yawo[1,2]

[1]Graduate School of Life Sciences, Tohoku University, Sendai, Japan and [2]JST, CREST, Tokyo, Japan

The brain consists of many types of neurons which make a complex network. The brain's network performance has been investigated through the analysis of its input–output relationship using electrodes. Recently, optical stimulation methods using a photosensitive ion channel, such as channelrhodopsin-2 (ChR2) from *Chlamydomonas reinhardtii*, has been developed as a powerful tool for the investigation of neural circuits *in vivo* and *in vitro*. Neurons can also be inactivated by light-driven Cl^- or H^+ pumps, such as halorhodopsin (NpHR) and archaerhodopsins (Arch, ArchT).

To manipulate neuronal activity positively or negatively with desired spatiotemporal patterns, the irradiation system has to be optimized. Spatial light modulators based on the digital mirror device (DMD) is an ideal tool for patterned photostimulation because each micro-mirror can be turned on and off at high frequencies up to several kHz (Sakai et al., 2012). Here, we improved the multicolor irradiation system using a DMD-based mercury lamp projector and a multiband-pass optical filter in combination. It is expected that ChR2 is activated by the filtered blue light whereas ArchT is activated by the filtered yellow light. To test this, we recorded the activity of a neuron, which expressed both ChR2 and ArchT, in the hippocampal slice under whole cell patch clamp. The activity was switched up and down simply with the changes of irradiating colors. Our multicolor irradiation system enables one to manipulate neuronal activity with desired spatiotemporal patterns. In the dentate gyrus (DG) of hippocampus, a hilar mossy cell (HMC) receives excitatory inputs convergently from a group of granule cells (GCs) and sends excitatory output divergently to another group of GCs. Based on this anatomical feature HMCs would regulated the dynamic state of hippocampus through positive feedback association with GCs. Here, using optogenetics and the DMD-based irradiation system, we tested whether the magnitude of HMC activity is dependent on the spatiotemporally patterned inputs. Hippocampal slices were prepared from a Thy1.2-ChR2-*Venus* transgenic rat line in which GCs are expressing ChR2 (Ji et al., 2012). Whole cell patch clamp recordings were made from HMCs, which is identified by the electrophysiological characteristics and the morphology. Under current clamp, spontaneous action potentials were observed at low frequency. However, bursts of high-frequency action potentials were often generated in synchronous with rhythmical irradiation of whole DG at 10 Hz. The bursting activity continued for 10-40 s after cessation of irradiation. On the other hand, the activity of HMC was rather inhibited when the granule cell layer was selectively irradiated with the same rhythm. It is suggested that the bursting activity of HMC is dependent on the spatiotemporal pattern of GC inputs.

Sakai et al. (2012) *Neuroscience Research* doi: 10.1016/j.neures.2012.03.009

Ji et al. (2012) *PLoS One* 7, e32699

Where applicable, the authors confirm that the experiments described here conform with The Physiological Society ethical requirements.

PCD129

Selective changes of AMPA, NMDA and Kainate receptor subunit mRNAs in the hippocampus and orbitofrontal cortex but not in prefrontal cortex of human alcoholics

A.K. Bhandage[1], Z. Jin[1], I. Bazov[2], O. Kononenko[2], E.R. Korpi[3], G. Bakalkin[2] and B. Birnir[1]

[1]Neuroscience (Molecular Physiology), Biomedical Center, Uppsala University, Uppsala, Sweden, [2]Pharmaceutical Bioscience (Biological Research on Drug Dependence), Biomedical Center, Uppsala University, Uppsala, Sweden and [3]Pharmacology, Institute of Biomedicine, University of Helsinki, Helsinki, Finland

Glutamate is the main excitatory and γ-aminobutyric acid (GABA) is the main inhibitory transmitter in the human brain. Drugs that affect the glutamatergic or the GABAergic signaling systems will alter the normal balance regulating neuronal excitability. The brain is one of the main targets of alcohol. Ethanol, the active molecule in alcoholic beverages, targets both glutamate and GABA-gated ion channels. We have examined the expression of glutamate channel subunit mRNAs in human post-mortem hippocampal dentate gyrus (HP-DG), orbitofrontal (OFC), and dorsolateral prefrontal cortex (DL-PFC) of individuals suffering from alcohol dependence and have compared the results to brain samples from individuals without alcohol dependence. HP-DC, OFC and DL-PFC samples from 21 controls and 19 individuals with chronic alcohol dependence were included in the study. Total RNA was isolated and assayed using the method of quantitative RT-PCR as described

(Jin et al., 2011). Statistical analysis was carried out using SigmaPlot and SigmaStat analysis software. Shapiro-Wilk normality test was used to examine the normality of data distribution. The differences between the control and alcoholic groups were analysed by one-way ANOVA with Bonferroni post hoc test for normally distributed data and by non-parametric Kruskal-Wallis ANOVA on ranks with Dunn's post hoc test for not normally distributed data. A significant level was set to $p < 0.05$. Out of the 16 glutamate receptor subunits, mRNAs encoding two AMPA (2-amino-3-(3-hydroxy-5-methyl-isoxazol-4-yl)propanoic acid) receptor subunits: GluA2, GluA3; three kainate receptor subunit : GluK1, GluK2, GluK5 and six NMDA (N-Methyl-D-aspartate) receptor subunits: GluN1, GluN2A, GluN2B, GluN2C, GluN2D, GluN3A in the HP-DG region were significantly increased. In the OFC, mRNA encoding the NMDA subunit GluN3A was increased. In the DL-PFC no changes in mRNA levels were detected between controls and alcoholics. Alcohol consumption clearly alters the expression of genes encoding the glutamate channels in a brain area-specific manner. Our laboratory has shown previously that genes encoding GABA-A receptors are altered in the HP-DG and the OFC from alcoholics (Jin et al, 2011). Whether changes in one neurotransmitter system drives changes in the other or if they change independently remains to be resolved.

Zhe Jin et al., Selective Changes of GABAA Channel Subunit mRNAs in the Hippocampus and Orbitofrontal Cortex but not in Prefrontal Cortex of Human Alcoholics, Front Cell Neurosci. 2011; 5: 30.

Brain tissues were provided by the New South Wales Tissue Resource Center at the University of Sydney supported by the National Health and Medical Research Council of Australia, National Institute of Alcohol Abuse and Alcoholism, and NSW Department of Health.

Where applicable, the authors confirm that the experiments described here conform with The Physiological Society ethical requirements.

PCD130

A P2X receptor from the model cnidarian *Hydra*: expression in a unique cell type

S. Hanmer, W. Wilkinson, P. Kemp and W. van der Goes van Naters

School of Biosciences, Cardiff University, Cardiff, N/A, UK

P2X receptors are ATP-gated ion channels with a number of roles in humans and other vertebrates. To understand the full range of physiological functions served by this receptor family, we are investigating P2X receptors in model invertebrates. *Hydra*, a member of the cnidarian phylum, is thought to be a modern proxy for the first organisms to have evolved a defined nervous system. Considering the important physiological and pathophysiological functions of P2X receptors in higher organisms, understanding P2X receptor signaling in non-mammalian phyla may allow us to uncover new functions that the family serves and further understand the evolutionary origins of purinergic signaling.

A P2X receptor from *Hydra vulgaris* was bioinformatically identified and subsequently cloned and sequenced. Following heterologous expression in human embryonic kidney 293 cells of a synthesized construct of the P2X receptor, with codon usage matched to human usage, we have used whole-cell voltage-clamp electrophysiology to study its pharmacology. Extracellular ATP application results in a concentration-dependent increase in inward current with a mean EC_{50} of 123.8 ± 21.8 μM (n = 8 cells; SEM) with a Hill coefficient of 1.3. AMP, ADP, dATP, UTP, α,β-methylene ATP and β,γ-methylene ATP all failed to evoke currents at 1 mM. The broad-spectrum antagonists PPADS and suramin (both at 0.1 mM) had little or no effect on ATP-induced currents, with the compounds Brilliant Blue G and Phenol Red also having no effect. Co-application of the P2X4 receptor modulator ivermectin at 3 μM with 0.1 mM ATP potentiated currents by approx. 40%. Ion substitution experiments reveal that the receptor is permeable to K^+ ions (P_K/P_{Na} = 1.75 ± 0.22, n = 11) and Ca^{2+} (P_{Ca}/P_{Na} = 1.64 ± 0.18, n = 6), but largely impermeable to the inorganic cations $Tris^+$ (0.24 ± 0.03, n = 6) and $NMDG^+$ (0.08 ± 0.02, n = 8). The receptor is Cl^- impermeable (P_{Cl}/P_{Na} = 0.02 ± 0.007, n = 9). From this, the *Hydra* P2X receptor displays a rank order of permeability to ions as follows: $K^+ \geq Ca^{2+} > Na^+ > Tris^+ >> NMDG^+ > Cl^-$, consistent mammalian homologues.

A custom polyclonal antibody was raised against a peptide corresponding to part of the *Hydra* P2X receptor C-terminus. Whole polyp immunohistochemistry using the antibody suggests that the receptor is expressed in the phylum-specific nematocytes. Specifically, the P2X receptor appears to be localised to the nematocyst capsule wall and not to the harpoon-like inner structure used to capture prey, or to the nematocyte cell in which the nematocyst is embedded. The internal pressure within the nematocyst capsule used to expel the internal harpoon is in the MPa range (Nüchter *et al*., 2006) and we hypothesize that the P2X receptor may play a role in the osmotic potential that underlies this. The current focus of the study is to investigate this hypothesis through RNAi mediated knockdown of the receptor.

Nüchter T *et al.* (2006). *Curr. Biol.* **16**, R316-318.

Where applicable, the authors confirm that the experiments described here conform with The Physiological Society ethical requirements.

PCD131

Regulation of TREK1 two pore domain potassium channels by amitriptyline

E. Al-Moubarak, E.L. Veale and A. Mathie

Medway School of Pharmacy, University of Kent, Chatham Maritime, UK

TREK1, two pore domain potassium (K2P) channels are responsible for background currents that regulate neuronal excitability. Deletion of TREK1 has previously been shown to result in a depression-resistant phenotype in mice (Heurteaux et al. 2006). In this study we investigated the effect of the tricyclic antidepressant, amitriptyline, on TREK1 channels. Additionally, amitriptyline is used for relief of neuropathic pain and TREK-1 is also involved in pain perception (Alloui et al. 2006). tsA-201 cells were transiently transfected with wild type and mutated K2P channels. The whole cell patch clamp technique was used to obtain current recordings. Homology models for TREK1 were constructed using Modeller. Amitriptyline was docked to these models using the MOE program.

Amitriptyline (50 μM) significantly inhibited WT TREK1 channel current by 77.4 ± 3.7 % (n=9). While the inhibitory effect of amitriptyline was reversible, on wash, it was often followed by an over-recovery of current to above the baseline level. We have previously investigated the effect of the antidepressant, citalopram, on TREK1, and found that it inhibited the channel. Subsequently we identified a number of amino acids in both the pore region and transmembrane domains M2 and M4 of

TREK1 that were important for its effect (Al-Moubarak et al. 2013). Interestingly, mutations of several amino acids, T142A, L289A and T251A, which reduced the effectiveness of citalopram had no effect on the observed inhibition by amitriptyline. Other mutations, L169A and I167A had no effect on inhibition by either compound. Mutation L174A (in the M2 transmembrane domain of TREK1), however, significantly reduced inhibition by both citalopram (Al-Moubarak et al 2013) and amitriptyline (50 μM, 49.0 ± 3.1 %, n=6, $p < 0.05$). As previously found for citalopram, the E306A gain of function mutation completely prevented inhibition by amitriptyline. Docking of amitriptyline into the TREK1 homology model, guided by the obtained electrophysiology results, predicts a different binding profile for amitriptyline compared to citalopram.

Thus we have shown that amitriptyline is a potent inhibitor of TREK1 potassium channels. This action may contribute to the therapeutic usefulness of this compound in both the treatment of depression and pain.

Alloui et al. (2006). TREK-1, a K+ channel involved in polymodal pain perception. EMBO Journal, 25 2368-237.

Al-Moubarak et al. (2013). Regulation of TREK1 two pore domain potassium channels by citalopram. FASEB Journal, 27 in press.

Heurteaux et al. (2006). Deletion of the background potassium channel TREK-1 results in a depression-resistant phenotype. Nature Neuroscience, 9 1134-1141.

Supported by BBSRC and Pfizer.

Where applicable, the authors confirm that the experiments described here conform with The Physiological Society ethical requirements.

PCD132

TRPV4 and KCa: The model couple?

C.H. Feetham[1], N. Nunn[1,2], R. Lewis[1] and R. Barrett-Jolley[1]

[1]Institute of Ageing and Chronic Disease, University of Liverpool, Liverpool, UK and [2]Institute of Translational Medicine, University of Liverpool, Liverprool, UK

Cardiovascular disease is an increasing problem in the UK, resulting in over 159,000 deaths each year. Cardiovascular disease has been linked to disturbed osmosensing, known to effect sympathetic activity altering blood pressure (BP) and heart rate (HR)[1]. The hypothalamus is responsible for maintaining plasma osmolality within a narrow range (~290-300mOsm)[2]. However, the mechanisms involved have yet to be established. The paraventricular nucleus (PVN) of the hypothalamus is thought to have a role in osmoregulation; hypertonic solutions increase electrical activity of PVN neurones[3]. Recent studies implicate the transient receptor potential vanilloid channel (TRPV4) and calcium activated potassium channels (KCa) as possible candidates for osmosensing [4].

Using a combination of in vivo, in vitro and in silico we have investigated a possible functional coupling of TRPV4 and KCa in PVN cardiovascular control neurone regulation in response to osmotic challenge. Mice were anaesthetized intraperitoneally with urethane-chloralose (1.4-2.2mg/kg-7-11μg/kg). BP was measured by arterial cannulae and compounds applied by intracerebroventricular (ICV) injection. Cellular mechanisms were investigated using the NEURON simulation environment and experimentally by cell-attached patch-clamp recording in mouse PVN hypothalamic brain slices. Results are given as mean±SEM; in vivo and in vitro significances were assessed by two-way ANOVA with post-hoc Tukey comparison and Student's paired t-tests respectively.

ICV injection of hypotonic saline led to a rapid decrease in BP, whereas isotonic saline had no effect (-9±2mmHg vs. -2±1mmHg; n=6; $p<0.01$). These decreases in BP were abolished by the selective TRPV4 inhibitor RN1734 (-1±1mmHg; n=6).

Using action currents to indicate action potential frequency in PVN brain slice experiments, we established that the osmotic effect on action potential frequency is dependent upon both TRPV4 channels (hypotonic: 70±14% reduction vs. hypotonic with RN1734: 45±15%; n=6; $p<0.05$) and small conductance KCa (SK) (hypotonic: 79±10% reduction vs. hypotonic with the SK channel inhibitor UCL-1684: 37±7%; n=5; $p<0.01$), but no significant effects of the intermediate and large conductance KCa channel inhibitors TRAM-34 and iberiotoxin. In order to verify the presence of TRPV4 within the parvocellular PVN, single channel activity was recorded. A population of ion channels was identified with a mean slope unitary conductance of 57±7pS and reversal potential of -5±3mV (n=6); indicative of a non-selective cation channel. This channel activity was seen in 50% of patches (8/16), with a mean open probability (Po) of 0.1±0.0 at -40mV. Po increased by 48±9% (n=4) upon addition of the TRPV4 agonist 4αPDD.

These results strongly suggest that central osmolality changes modulate the cardiovascular system by functional coupling of TRPV4 and small conductance KCa channels in the parvocellular PVN.

Chen, Q.H. and G.M. Toney, AT(1)-receptor blockade in the hypothalamic PVN reduces central hyperosmolality-induced renal sympathoexcitation. Am J Physiol Regul Integr Comp Physiol, 2001. 281(6): p. R1844-53.

Bourque, C.W. and S.H. Oliet, Osmoreceptors in the central nervous system. Annu Rev Physiol, 1997. 59: p. 601-19.

Chu, C.P., H. Kannan, and D.L. Qiu, Effect of hypertonic saline on rat hypothalamic paraventricular nucleus parvocellular neurons in vitro. Neurosci Lett, 2010. 482(2): p. 142-5.

Gao, F. and D.H. Wang, Impairment in function and expression of transient receptor potential vanilloid type 4 in Dahl salt-sensitive rats: significance and mechanism. Hypertension, 2010. 55(4): p. 1018-25.

Work supported by BBSRC.

Where applicable, the authors confirm that the experiments described here conform with The Physiological Society ethical requirements.

PCD133

Recombinant α9α10 nicotinic cholinergic receptors depend on extracellular Ca2+ to reach maximum activation

J.C. Boffi, P. Plazas, M. Lipovsek, E. Katz, B. Elgoyhen and B. Elgoyhen

Instituto de investigaciones en Ingeniería Genética y Biología Molecular "Dr. Héctor N. Torres", Ciudad Autonoma de Buenos Aires, Argentina

The activation of α9α10 nicotinic receptors in cochlear hair cells can ameliorate acoustic trauma. Therefore, maximized α9α10 receptor activation may favor the prevention of noise-induced hearing loss. Hence, understanding the conditions in which α9α10 receptors reach maximum activation could have a potential therapeutic use in noise-induced hearing loss.

In this work we aimed to characterize how extracellular Ca2+ affects the activation of recombinant α9α10 receptors expressed in X. laevis oocytes under two-electrode voltage-clamp. Previous work from our lab suggests that the homomeric α9 receptor reaches maximum activation at trace con-

centrations of extracellular Ca2+ and is blocked by higher concentrations (IC50 = 100±10 μM, n = 3). We now show that the α9α10 receptor, as opposed to homomeric α9, reaches its lowest maximal currents (at saturating acetylcholine) at trace levels of extracellular Ca2+ (50±15% of maximal currents at physiological 1.8 mM Ca2+; n = 4) and its maximal activation at Ca2+ concentrations close to 0.1mM (260±55% of maximal currents at 1.8 mM Ca2+; n = 5). Furthermore, increasing extracellular Ca2+ concentrations reduces the receptor's EC50 dose dependently (trace Ca2+: EC50 = 54±4 μM, n = 7; 1.8 mM Ca2+: EC50 = 13±2 μM, n = 8).

This differential dependency upon extracellular Ca2+ suggests that the α10 subunit provides the structural determinants. In order to delineate these structural determinants, we constructed chimeric α10-α9 subunits. Receptors with chimeric α10 subunits bearing the α9 extracellular and the α10 transmembrane and intracellular domains reached maximal activation at trace levels of extracelular Ca2+ (190±20% of maximal currents at 1.8 mM Ca2+; n = 5). The inclusion of α9 transmembrane regions facing the extracellular domain (the TM2-TM3 loop and extracellular segment of TM1) in the chimeras further boosted the activation at trace extracellular Ca2+ (390±40% of maximal currents at 1.8 mM Ca2+; n = 4). Altogether, our results suggest that extracellular Ca2+ greatly affects α9α10 receptor activation and that the structural determinants of this effect are located at the interphase between extracellular and transmembrane domains of the α10 subunits, a region known to be responsible for channel gating.

Where applicable, the authors confirm that the experiments described here conform with The Physiological Society ethical requirements.

PCD134

GABA-A channel subunit expression in cell lines derived from human glioblastoma

O. Babateen[1], Z. Jin[1], A. Bhandage[1], B. Westermark[2], K. Forsberg-Nilsson[2], L. Uhrbom[2], A. Smits[1] and B. Birnir[1]

[1]Department of Neuroscience, Uppsala University, Uppsala, Sweden and [2]Department of Immunology, Genetics and Pathology, and Science for Life Laboratory, Uppsala University, Uppsala, Sweden

Gliomas are the most common form of primary brain tumors with an overall incidence of about 4 - 5 per 10^5 persons. There is growing evidence for a widespread role of the neurotransmitter γ-aminobutyric acid (GABA) in the growth regulation of many cell types, including neuronal stem cells and perhaps tumor stem cells. Recently we showed that human brain tumors express GABA-A receptors subunits that are generally down-regulated in glioblastomas (Smits et al, 2012). We further showed that there was a correlation between GABA-A channel subunits and patient survival. Whether tumor cells that are equipped with functional GABA-A channels maintain proliferative activity upon in physiological concentrations of GABA may depend on which *subtype* of GABA-A channels are activated. We have now examined 8 glioblastoma derived cell-lines and examined which GABA-A subunits are expressed and then, selected one cell line to study in detail the functional and pharmacological properties of the GABA-A channels expressed. We used the method of RT-PCR for determining the subunits expressed, immunocytochemistry to identify cellular location of subunits and the whole-cell patch-clamp technique to record GABA-activated currents. Our results show that the eight different cell lines all express GABA-A receptor subunits but the type of subunits that are expressed varies. Cell line U3047 expressed α1, α2, α3, α5, β2, β3, δ, γ3 and θ GABA-A receptors subunits mRNAs and was selected for studies of properties of the GABA-A receptors expressed in glial/tumor cells. Immunocytochemistry demonstrated expression of the α3 and β3 proteins. GABA concentrations ranging from 1 to 1000 μM were applied to the cells and gave a half-maximal concentration of current activation (EC50) of 10 μM. The current response to 10 μM GABA was enhanced by 1 μM diazepam and 50 μM propofol, modulators of GABA-A channels. The currents were inhibited by the GABA-A channels antagonists SR-95531 (100 μM) and picrotoxin (100 μM). Our results show that the GABA-A receptors in the glioblastoma cell line U3047 are functional and respond to classical agonists and antagonists of GABA-A receptors. The profile of the subunits expressed is similar to what we reported in glioblastoma tumors from humans (Smits et al., 2012). We propose that the cell line can be used as a model system to study how GABA signaling affects tumor development.

Smits, A, Jin, Z, Elsir, T, Pedder, H, Nistér, M, Alafuzoff, I, Dimberg, A, Edqvist, PH, Pontén, F, Aronica, E, Birnir, B (2012) GABA-A channel subunit expression in human glioma correlates with tumor histology and clinical outcome. *PLos One*, 7(5):e37041

Where applicable, the authors confirm that the experiments described here conform with The Physiological Society ethical requirements.

PCD135

Relation between Ia and motoneuron responses induced by vibratory stretches in a cat

M. Mizote

Teikyo Heisei University, Toshima-ward, Tokyo, Japan

Primary endings were classified into three types by vibration threshold (1976) and a spike of motoneuron was elicited by acceleration sensitive Ia impulses (1993). The reports suggested that motoneuron is activated by Ia on which different types of intrafusal fibers are selectively induced by different vibratory stretch phases. Four cats were anesthetized with an initial intraperitoneal dose of 10% urethane and 1% chloralose (4cc/kg). Subsequent doses, as required, were given intravenously via a catheterized cubital vein. 10cc/kg of 10% urethane was given intravenously at the end of experiment. Left triceps surae muscle of cats were dissected free from surrounding tissues, while blood supply was kept intact. All other nerves in the left hip and leg were cut except nerves of the muscle. A cat was fixed on a frame mounted securely on an animal tablet and the calcaneus was attached firmly by a metal. The dorsal and ventral roots between L6 and S1 were exposed by the conventional 1aminectomy. Thin afferent and efferent filaments were hooked on each pair of electrodes at about 20mm from their entry into the spinal cord and motoneuron activity was recorded by antidromic electric stimulations of motor nerve. An afferent fiber (over 80m/s) was identified as a spindle ending Ia by their behavior during twitch contraction of the muscle elicited by stimulating its nerves. Impulses of single Ia and intracellular neuron activities were recorded simultaneously while tendon of medial or lateral gastrocnemius muscle or soleus muscle was stretched by 100Hz vibration of amplitude 100μm for 0.5 sec every 2 sec and vibration was repeated 5 times. The muscle was contracted by electric single shock stimulations before stretches. Ia impulses were classified into three types corresponding to a sensitive cyclic phase of sinusoidal stretch at which Ia impulses were elicited. Impulse

of acceleration sensitive Ia was discharged at initial phase of vibratory stretch and elicited a motoneuron spike. Velocity sensitive and displacement sensitive Ia impulses were driven while the muscle was stretched in 37 cycles. Latency of velocity sensitive Ia impulses from the vibratory stretches was 4.26±0.05ms and latency of displacement sensitive Ia was 4.92±0.05ms in 37 cycles. All of EPSPs and initial serial 4 spikes of motoneuron were driven by Ia impulses which was induced by 100Hz vibration. But spikes of motoneuron appeared intermittently every 2 or 3 Ia impulses except initial 50ms during 500ms vibration. It is suggested that velocity sensitive Ia impulses elicit motoneuron spikes rapidly in early period when muscle is stretched but motoneuron activity is inhibited gradually by some reflexive inhibitory mechanism as stretches are repeated although physical property of primary endings is not changed during vibration.

Mizote M (1976). Prog in Brain Res 44. 133-140

Mizote M(1993). 32nd Congress IUPS. 322.11/P

Where applicable, the authors confirm that the experiments described here conform with The Physiological Society ethical requirements.

PCD138

Renal denervation decreases alpha 1 adrenergic receptor protein in the renal cortex of rabbits with chronic heart failure

A. Schiller, K.K. Haack, P.L. Curry and I.H. Zucker

University Nebraska Medical Center, Omaha, NE, USA

Chronic heart failure (CHF) is a disease characterized by an overactive sympathetic nervous system. The kidney is especially vulnerable to this adaption and responds with a decrease in mean renal blood flow (MRBF). To assess any possible alpha-1 adrenergic receptor (A1ADR) mediated contributions to this response we instrumented male New Zealand White rabbits with ventricular pacing leads, surgically removed the renal nerves from one kidney and implanted radiotelemetry to record mean arterial pressure (MAP). To perform these surgeries rabbits were anesthetized with a combination of Ketamine (35 mg/kg), Rompun (5.8 mg/kg) and atropine sulfate (0.01 mg/kg) given IM and followed by Forane gas anesthesia (0.5-3.0%). CHF was induced by rapid ventricular pacing at 380 bpm and validated by echocardiography. Values are means ± S.E.M., compared by an unpaired t-test. In rabbits with CHF (n = 5) we found that removing the renal nerves (n =5) significantly increased MRBF (23.3 ± 3.7 vs. 34.1 ± 2.3, $P < .05$) at resting MAP compared to rabbits with CHF and intact renal nerves (n = 5). In order to assess contribution of A1ADR stimulation in MRBF control, 100 mg/kg phenylephrine (A1ADR agonist) was infused IV at 0.25 ml/min. At 100 mmHg MRBF in CHF rabbits remained decreased compared to CHF rabbits without renal nerves (13.1 ± 0.9 vs. 21.9 ± 2.3 intact and denervated, respectively, $P < 0.5$). At the completion of the study the kidneys were removed and native membrane proteins were extracted from cortical tissue. Levels of A1ADR receptor were determined by standard western blot technique. Intact rabbits with CHF expressed significantly higher levels of A1ADR (5.7 ± 1.5; A1ADR/total protein) compared to CHF rabbits without renal nerves (1.8 ± 0.3, $P < .05$). These data suggest that chronic removal of the renal nerves in animals with CHF contributes to increases in MRBF, in part, by down-regulation of AD1ADR in the kidney.

Where applicable, the authors confirm that the experiments described here conform with The Physiological Society ethical requirements.

PCD139

Analgesic and anti-inflammatory effects of honey is modulated by alpha-1 adrenergic antagonist

B.V. Owoyele and K. Ajomole

Department of Physiology, University of Ilorin, Ilorin, Nigeria

Honey is used variously as food, flavour, energy source and medicine. Its medicinal effects continue to be subjects of research. Such investigations include the effects of honey on wound healing, inflammation and pain (1,2). We previously reported its anti-inflammatory and nitric oxide inhibitory effects (2). Therefore, the present study was designed to investigate whether tamsulosin an alpha 1 blocker has effect on the anti-inflammatory and analgesic effects of honey. Rats used for both analgesic and anti-inflammatory studies were divided into five similar groups. These groups comprises of five rats each. Group A and B received saline and indomethacin (5mg/Kg) respectively, while group C received tamsulosin (3μg/kg) only, group D received honey (200 mg/Kg) and tamsulosin, group E received honey (600mg/Kg) and tamsulosin. All drugs were administered orally, pain was accessed chemically using the formalin paw licking model and thermally using the hot plate latency assay. Acute inflammation was accessed using carrageenan induced paw oedema. Values are means ± S.E.M. and statistical analysis was by ANOVA. The results showed that tamsulosin demonstrated analgesic effects in the formalin model by reducing the licking time in the early phase from 96.40±9.27 to 43.40±8.49s ($p<0.05$) and in the late phase from 79.0±8.26 to 46.20 ± 10.78s ($p<0.05$). It also enhanced the analgesic effect of honey in this model especially in the late phase for the 200 mg/Kg (control: 79.0±8.26 vs honey: 13.60± 2.34s, $P<0.05$) . However, both honey and tamsulosin did not produce analgesic effect in the hot plate test. In the anti-inflammatory study, tamsulosin did not produce anti-inflammatory effect but it abolished the anti-inflammatory effect of honey when administered together. The findings from this study show that alpha 1 adrenoceptor has the capacity to enhance the analgesic effect of honey in chemically induced pain but it inhibits its anti-inflammatory effects. On the other hand honey may be promoting its anti-inflammatory effects partly by stimulating alpha 1 adrenoceptor. Therefore, caution should be taken if subjects are receiving alpha-1 adrenergic blockers concurrently with honey administration especially if honey is been administered for the treatment of inflammatory conditions.

1. Alzubier A. A. and Okechukwu P.N.(2011): World Acad. Sci. Engr. Technol. 80: 47 -52.

2. Owoyele, B. V., Adenekan, O. T. and Soladoye, A.O. (2011): J. Chin. Integr. Med. 9: 447- 452.

Where applicable, the authors confirm that the experiments described here conform with The Physiological Society ethical requirements.

PCD141

Electrophysiological study of voltage-gated ion channels in photoreceptors and bipolar cells in the human retina

E. Miyachi[1], F. Kawai[1], M. Ohkuma[1] and M. Horiguchi[2]

[1]Department of Physiology, Fujita Health University School of Medicine, Toyoake, Japan and [2]Department of Ophthalmology, Fujtia Health University School of Medicine, Toyoake, Japan

The photoreceptors and bipolar cells in the vertebrate retina were considered non-spiking neurons. However, we showed that human photoreceptors can generate sodium action potentials in response to membrane depolarization (Kawai *et al*, 2001). In this study, we performed physiological and molecular biological analyses to confirm the presence of the sodium channel in photoreceptors and bipolar cell in the human retina. A small piece of retina was excised from each of 15 adult patients with a fresh retinal detachment during the surgical procedure to reattach the retina. In the standard vitreous surgery to reattach a detached retina, the fluid between the detached retina and the retinal pigment epithelium is removed through an artificial retinal hole that is made during surgery. To make the artificial hole, a small piece of retina (diameter 1 mm) had to be exercised, and this piece was used in our experiment. The estimated time between retinal detachment and surgery was 2 days. In all cases, functional recovery of the retina occurred after surgery, indicating that there was no severe pathology of the retina. All experiments were performed in compliance with the guideline of the Declaration of Helsinki and the ethics committee of Fujita Health University. All patients were informed of the purpose of the surgery and the necessity of removing the retinal tissue, and signed informed consent to allow the use of the tissue for these experiments. The SCN2A, the type II sodium channel ($Na_v1.2$) transcript, was observed in photoreceptors and bipolar cells by single-cell RT-PCR analysis. Under voltage-clamp conditions, depolarizing voltage steps induced fast transient inward currents, which were inactivated within 5 ms and blocked by a voltage-gated sodium channel blocker tetrodotoxin, in several bipolar cells, as well as rods and cones. These results indicate that human photoreceptors and bipolar cells express $Na_v1.2$ voltage-gated sodium channels, and suggest that the sodium channels may serve to amplify the release of the neurotransmitter when membrane potential is depolarized. We also observed the hyperpolarization-activated current, the h current (I_h), in human rods. Dopamine reversibly decreased the amplitude of the I_h induced by hyperpolarizing voltage steps. The D2 dopamine agonist inhibited I_h, but the D1 agonist had no effect. Dopamine-induced reduction of I_h amplitude was blocked by the D2 dopamine antagonist. These results suggest that dopamine reduced I_h through a D2 receptor and that dopamine slows the recovery phase of responses to light stimuli by inhibiting I_h in human rods. We consider that I_h may contribute to preventing visual flickering by inhibiting the generation of spontaneous Na^+ spikes in human photoreceptors.

Kawai F *et al*. (2001). Na^+ action potentials in human photoreceptors. *Neuron* 30, 451–458.

Supported by Grant SENRYAKU 1001034 from the Ministry of Education, Culture, Sports, Science & Technology in Japan.

Where applicable, the authors confirm that the experiments described here conform with The Physiological Society ethical requirements.

PCD142

Salicylate enhances depolarization suppression of excitation in cartwheel neurons from the dorsal cochlear nucleus of the rat

J. Zugaib and R.M. Leao

Physiology, University of São Paulo, Ribeirão Preto, SP, Brazil

Intoxication by sodium salicylate induces tinnitus in both humans and experimental animals. Tinnitus, in most cases, is caused by central mechanisms leading to hyperactivity of some central auditory regions, in special the fusiform neurons of the dorsal cochlear nucleus (DCN) in the brainstem. One hypothesis for the origin of hyperactivity is an unbalance of the inhibitory and excitatory neurotransmission in auditory areas. Salicylate inhibits the enzyme cyclooxygenase 2 which takes part in the oxidative degradation of endocannabinoids. Here we are testing the hypothesis that salycilate interferes with endocannabinoid mediated synaptic plasticity in the DCN. For this we tested the effect of sodium salicylate on the phenomenon of depolarization suppression of excitation (DSE) in parallel fibers (PF) synapses on glutamatergic fusiform and glycinergic cartwheel neurons of the DCN, which is mediated by endocannabinoids. Brain slices were prepared from 18 to 22 days old Wistar rats, and glutamatergic neurotransmission was elicited by stimulating the (PF) with a bipolar electrode, in the presence of picrotoxin and strychnine to block inhibitory neurotransmission. Post-synaptic currents were recorded at -80 mV in whole-cell voltage clamp. DSE was produced by a depolarization to 0 mV with duration of 0.5, 1, 2 and 4 seconds. As reported in mice DSE was stronger in cartwheel than in fusiform neurons (maximum DSE at 4 seconds: cartwheel 41 ± 5%; fusiform 21 ± 5%. N = 19 and 12 respectively. P = 0.0002, 2-way ANOVA). Incubation of the slices with sodium salicylate (NaSal, 1.4 mM) for at least 1 hour before the recording did not affect the PF-evoked EPSC amplitude either in cartwheel (control: -414 ± 60 pA; NaSal: -756 ± 207 pA; n=12 and 18 respectively, p=0.08, t-test) and fusiform neurons (control: -454 ± 104 pA; NaSal: -404 ± 66 pA; n=8 and 10 respectively. p=0.68, t-test). However, salicylate enhanced the DSE in cartwheel neurons significantly ($p<0.05$, 2-way ANOVA; n=9) but not in fusiform neurons. Maximum DSE after 4 seconds depolarization in cartwheel neurons was not affected by salicylate, but was attained earlier after 2 seconds depolarization (control 26 ± 5 %; NaSal: 43 ± 7%; p = 0.05, t-test). Acute applications of salicylate produced similar changes in the DSE profile of cartwheel neurons but again did not affect DSE in fusiform neurons. We conclude that sodium salicylate in concentrations similar to found in the cerebrospinal fluid after tinnitus-inducing salicylate intoxication is able to enhance DSE in DCN's cartwheel neurons. Since cartwheel neurons produces feed forward inhibition onto fusiform neurons, an increased DSE can weakens inhibition during high frequency trains of firing from the PF and can contribute for generating hyperactivity in the fusiform neurons after salicylate intoxication.

Funded by FAPESP, CNPQ

Where applicable, the authors confirm that the experiments described here conform with The Physiological Society ethical requirements.

PCD143

Comparative study on the dopaminergic D_1 and D_2receptor modulation of the electroretinographic responses in the dark-adapted frog retina

E. Popova and P. Kupenova

Physiology, Medical University, Sofia, Bulgaria

Dopamine plays an important role in visual function and retinal sensitivity control. Its actions are mediated through two subfamilies, D_1- and D $_2$-class receptors that are positively and negatively linked to adenylyl cyclase, respectively. However, the data about the specific D_1- and D $_2$-class receptor contribution to retinal responses to light increments and decrements (ON and OFF responses, respectively) are contradictory. A possible explanation might be that many of the results were obtained using non-selective dopamine antagonists and within a limited stimulus intensity (I) range. In this work, the effects of selective blockade of D_1-class receptors by 10 μM SCH 23390 and D $_2$-class receptors by 40 μM sulpiride applied in isolation or in combination on the intensity-response (V - log I) functions of the electroretinographic (ERG) ON (b-wave) and OFF (d-wave) responses were studied. The electroretinograms were obtained from dark-adapted frog eyecup preparations (Rana ridibunda; for details see Popova and Kupenova, 2009). By using a very wide range of stimulus intensities (11 log units, $I_{max} = 6 \times 10^8$ quanta. s^{-1}. μm $^{-2}$), we obtained both rod- and cone-dominated responses. During the isolated D_1-class receptor blockade by SCH 23390, the amplitude of both the b- and d-wave was increased (Two-way ANOVA $p<0.000001$, $n=10$). During the isolated D_2-class receptor blockade by sulpiride, a significant enhancement of the b- and d-wave amplitude was seen in the lower intensity range, where rod-dominated responses were obtained (Two-way ANOVA, $p<0.00003$, $n=11$). The amplitude of the two waves was, however, diminished in the higher intensity range (It > -5), where cone-dominated responses were obtained (Two-way ANOVA, $p<0.0000002$). A similar effect on the b-, but not d-wave amplitude was seen during the combined application of SCH 23390 and sulpiride. The d-wave amplitude was enhanced over the whole except for the highest intensity range (It > -3.5) during the combined D_1 and D_2 receptor blockade ($n=15$). The results obtained indicate that the endogenous dopamine has an overall inhibitory action on the rod-mediated ERG ON and OFF responses, but its action on the cone-mediated responses shows clear ON-OFF asymmetry. It is excitatory upon the ON responses, but inhibitory upon the OFF responses except for those in the highest intensity range. Participation of different types of dopamine receptors (predominantly D_2-class for the ON versus D_1-class for the OFF response) is probably responsible for this difference.

Popova, E., Kupenova, P., 2009. Contribution of proximal retinal neurons to b- and d-wave of frog electroretinogram under different conditions of light adaptation. Vision Res 49, 2001-2010.

This work was supported by grant 14/2012 from the Council for Medical Science, Medical University Sofia.

Where applicable, the authors confirm that the experiments described here conform with The Physiological Society ethical requirements.

PCD144

Comparison of rectangular pulse and triangular pulse on evoking retinal ganglion cell responses in retinal degenerated (*rd1*) mice

Y. Goo[1,2], K. Ahn[1,2], W. Lee[1,2] and J. Kim[1,2]

[1]Physiology, Chungbuk National University School of Medicine, Cheongju, Republic of Korea and [2]Nano Artificial Vision Reserch Center, Seoul, Republic of Korea

Retinal prosthesis has been developed for the patients with retinitis pigmentosa (RP) and age related macular degeneration (AMD), and is regarded as the most feasible method to restore vision [1-2]. Extracting optimal electrical stimulation parameters for the prosthesis is one of the important prerequisites for the success of retinal prosthesis. Previously, we proposed the optimal stimulation parameter range (e.g. amplitude, duration) for evoking retinal ganglion cell (RGC) responses using rectangular pulse shape in wild-type and *rd1* mice [3]. Traditionally, rectangular pulse shape has been the choice for neural stimulation. Not much attention has been paid to alternative pulse shapes. Therefore, we investigated pulse shape effect on evoking RGC responses. The well-known animal model for RP, *rd1* (*Pde6b* ^{rd1}) mice [4] at postnatal 8 weeks and after were used. From the *ex-vivo* retinal preparation, retinal patches were mounted on planar 8x8 microelectrode array (MEA), ganglion cell layer down onto the MEA mimicking the epiretinal prosthesis configuration. While applying current stimulus through one channel of MEA, retinal waveforms were recorded with remaining channels of MEA. Biphasic-charge balanced current pulses in the form of cathodic phase-1st and anodic phase-2nd were applied once per second (1 Hz, x 50). We tested 3 different pulse shapes with same charge; 1) biphasic rectangular pulse (I: intensity, D: duration), 2) biphasic triangular pulse with double intensity (2xI, D), 3) biphasic triangular pulse with double duration (I, 2xD). For intensity modulation, duration of the pulse was fixed to 500 μs and the intensities of the pulses were modulated from 5 to 40 μA. For duration modulation, pulse amplitude was fixed to 30 μA and the pulse durations were modulated from 60 to 500 μs. The electrically-evoked RGC spikes was defined as positive when the number of RGC spikes for 400 ms after stimulus was 1.3 times higher than that for 400 ms before stimulus in post-stimulus time histogram. RGC responses were well modulated both with rectangular and triangular pulse by varying the amplitude and duration of the pulse. Amplitude modulation shows that RGC response is preferentially activated by biphasic triangular pulse with double duration especially with 5 and 10 μA amplitude ($p<0.001$). Duration (D) modulation shows that RGC response is preferentially activated by triangular pulse with double duration especially with 60 and 100 μs ($p<0.001$), while triangular pulse with double amplitude is most efficient at 200 μs pulse duration ($p<0.001$). Now, we are comparing the stimulus threshold among three different pulse shapes in this study.

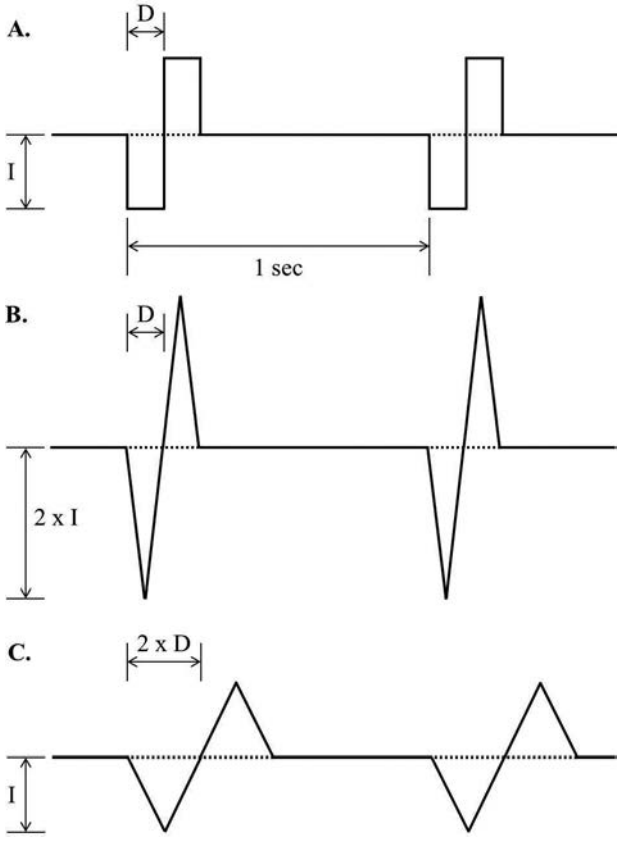

A. Rectangular pulse, B. Triangular pulse with intensity doubled, C. Triangular pulse with duration doubled.

Chader GS et al. (2009). Prog Ret Eye Res 175, 317-332.

Zrenner E et al. (2011). Proc Biol Sci 278, 1489-1497.

Goo YS et al. (2011). J Neural Eng 8(3), 035003.

Farber DB et al. (1994). Prog Ret Eye Res 13, 31-64.

This work was supported by grants of MEST (2010-0020852) in Republic of Korea.

Where applicable, the authors confirm that the experiments described here conform with The Physiological Society ethical requirements.

PCD145

Localization of the chemokine receptor XCR1 in rat spinal and nucleus caudalis (Vc) trigeminal dorsal horn: A novel regulator of nociception?

I. Obara[1,2], C. McDonald Wood[1], M. Singh[1], F.M. Boissonade[3] and A.E. King[1]

[1]School of Biomedical Sciences, University of Leeds, Leeds, UK, [2]School of Medicine, Pharmacy and Health, University of Durham, Durham, UK and [3]Deptartment of Oral and Maxillofacial Medicine and Surgery, University of Sheffield, Sheffield, UK

Chemokines are expressed by immune cells and cause monocyte extravasation at a site of tissue injury. They are divided into 4 families; CC, CXC, C and CX3C. There is evidence for involvement of several chemokines in pain mechanisms, notably CX3CL1, CCL2 and CX3C (Old & Malcangio, 2012). Their role is not fully understood but they are linked to mechanisms of neuron-glia communication and altered excitability of pain pathways following neuropathic or inflammatory injury (Ren & Dubner, 2010). Lymphotactin (XCL1), the only member of group C, is chemotactic for lymphocytes and mediates its effects via its cognate receptor XCR1. The role of lymphotactin and XCR1 in nociception and pain is unknown. We have used immunohistochemistry to characterize expression of XCR1 within nociceptive areas of the adult rat spinal and trigeminal dorsal horn (DH).

All procedures were carried out in accordance with UK Home Office legislation. Under irreversible anaesthesia (pentobarbital, 50 mg/kg i.p.) and after transcardiac perfusion-fixation, the spinal trigeminal nucleus caudalis (Vc) of the caudal brainstem and spinal cords were removed from rats (Wistar, 28 days). Brainstem (caudal to obex) and spinal cord (cervical and lumbar) transverse sections (30 μm) were cut and processed for immunofluorescence visualization of XCR1 either alone or in co-labelling studies with the vesicular glutamate transporters VGLUT 1 or VGLUT2 which mark glutamatergic synaptic terminals. Confocal imaging of spinal cord sections revealed intense labelling for XCR1 within nociceptive DH laminae I and II. Similarly, intense XCR1 labelling was localized to the most superficial layers of Vc and was also within the spinal trigeminal tract (STt). The diffuse pattern of labelling was indicative of an axonal or fibre localization rather than in cell bodies. In double-labelling studies with either VGLUT1 or VGLUT2, labelling for XCR1 in either spinal or Vc DH overlapped extensively with VGLUT2 in superficial layers whereas VGLUT1 staining was distributed to deeper regions with little evidence of overlap. This pattern of staining infers that XCR1 may be expressed on either the terminals of excitatory DH interneurons or small diameter nociceptive primary afferents, putatively A-delta or C-fibre subtypes in these two CNS regions (Todd et al., 2003).

Taken together, these observations reveal, for the first time, the expression of XCR1 within structures that are key areas in the transmission and subsequent modulation of nociceptive signals that give rise to both acute and chronic pain. These data may have important implications for the role of novel chemokines in the pathogenesis of chronic pain, including trigeminal oro-facial pain.

Old, E.A. & Malcangio, M., 2012, Curr. Opinion Pharmacol., 12:67-73

Ren, K. & Dubner, R., 2010, Nature Medicine, 16:1267-1276

Todd, A.J. et al., 2003, Eur. J. Neurosci., 17 :13-27

Research funded by BBSRC as an Industrial Partnership award with Pfizer, UK.

Where applicable, the authors confirm that the experiments described here conform with The Physiological Society ethical requirements.

PCD146

The cooperation of sustained and phasic inhibitions regulates the sensitivity to interaural time difference cue in the nucleus laminaris of birds

R. Yamada[1,2], H. Okuda[2], H. Kuba[1,3], E. Nishino[2], T.M. Ishii[2] and H. Ohmori[2]

[1]Department of Cell Physiology, Nagoya University Graduate School of Medicine, Nagoya, Japan, [2]Department of Physiology and Neurobiology, Kyoto University, Kyoto, Japan and [3]JST PRESTO, Saitama, Japan

Sensing the interaural time difference (ITD) of a sound is crucial in localizing the sound source particularly for low-frequency sounds. However, the range of ITD that animals experience is quite small and inhibitory synapses are proposed to be signi-

ficant in enhancing the ITD sensitivity. In birds, neurons in nucleus laminaris (NL) detect the coincidence of bilateral excitatory inputs from the cochlea nucleus and change their firing rate as a function of the ITD. Sound-intensity-dependent inhibition from superior olivary nucleus (SON) is known to have sustained effects in NL neurons and control the gain of coincidence detection, which makes the ITD sensitivity of NL neurons tolerant to strong-intensity sound. Here, we found a time-dependent phasic inhibition in chicken brain slices that follows the excitatory inputs from ipsilateral cochlea nucleus, sharpens coincidence detection and may enhance ITD sensitivity in low-frequency NL neurons. Coronal brainstem slices were obtained from post-hatch chickens and whole-cell recordings were made from NL neurons. The electrical stimulation to the ipsilateral projection fibers generated a polysynaptic IPSC that followed EPSC with 1~2 ms latency in the low-frequency NL neurons. These IPSCs were elicited even when SON was dissected out. GABA-positive small neurons are distributed in and near the NL and generated IPSCs in NL neurons when photoactivated by a caged glutamate compound. These results suggest that these GABAergic neurons are interneurons that mediate phasic inhibition to the NL neurons. Consistently, these IPSCs have fast decay kinetics that is attributable to the α1 subunit of GABAA receptor, the expression of which dominates in the low-frequency region of the NL. Model simulations demonstrate that phasic IPSCs narrow the time window of coincidence detection and increase the contrast of ITD-tuning during the low-level excitatory input. These effects of phasic inhibition are prominent in the ITD-tuning of low-frequency sound. Furthermore, cooperation of the phasic and sustained inhibitions effectively increases the contrast of ITD-tuning over a wide range of excitatory input levels. We propose that the complementary interaction between phasic and sustained inhibitions is the neural mechanism that regulates ITD sensitivity for low-frequency sound in the NL.

Where applicable, the authors confirm that the experiments described here conform with The Physiological Society ethical requirements.

PCD147

VEGF165b attenuates hyperglycaemia-induced sensitisation of neuronal TRPA1 activation: implications for diabetic neuropathy

R.P. Hulse[1,2], H. Riaz[1], P. Singhal[1], D.O. Bates[1,2] and L.F. Donaldson[1]

[1]Physiology and Pharmacology, University of Bristol, Bristol, UK and [2]Microvascular Research Laboratories, University of Bristol, Bristol, UK

Diabetes is becoming a significant burden on global health care systems due to the onset of associated complications. A large proportion of diabetic patients develop neuropathy leading to chronic pain [1] as a result of glucose toxicity, which directly damages neurons. The transient receptor potential ankyrin 1 (TRPA1) channel has a fundamental role in the development of diabetic neuropathy resulting in pain and sensory neuronal loss in rodents [2]. We have demonstrated that vascular endothelial growth factor (VEGF) 165b has neuroprotective actions, and that systemic treatment of diabetic rats with the VEGF165b prevented development of diabetic neuropathy (enhanced nociception and loss of cutaneous nerve terminals) in vivo [3]. We therefore tested the hypothesis that TRPA1 activity in sensory neurons was altered by hyperglycaemia, and that VEGF165b could modify this.

Immortalised embryonic dorsal root ganglion cells [4] were incubated in neurobasal medium for 48hrs and differentiated by 24hr incubation in 75μM forskolin. Cells were then incubated in experimental media for 24hrs (+ 75 μM forskolin) as follows; normal neurobasal media (control), neurobasal media + additional 30mM glucose (hyperglycaemia); neurobasal media + 30mM glucose + VEGF165b (2.5nM) or neurobasal media + 30mM mannitol (osmotic control). Cells were loaded with fluo4 for 1hr at 37oC, and agonist-induced increases in intracellular calcium measured in response to 100μM allyl isothiocyanate (AITC; TRPA1 agonist).

Hyperglycaemia increased total AITC-induced calcium increase (0.92+0.068 fold change.s n=10; mean+SEM of area under curve) compared to control (0.43+0.20 fold change.s vs glucose n=10 $p<0.01$ one way ANOVA with post Bonferroni). No change was seen in the presence of 30mM mannitol (0.37+0.092 fold change.s). Treatment of cells with VEGF165b under hyperglycaemic conditions attenuated the response to AITC compared to hyperglycaemia alone (hyperglycaemia 0.92+0.068 fold change.s vs. hyperglycaemia + VEGF165b 0.33+0.16 fold change.s, $p<0.05$ n=4 Kruskal Wallis with Dunns multiple comparison).

These data demonstrate that agonist-activation of TRPA1 is enhanced by hyperglycaemia in vitro, and that this can be attenuated by treatment with the growth factor isoform VEGF165b. TRPA1 has been shown to contribute to diabetic neuropathy (neuronal loss and pain). We propose that VEGF165b may attenuate the consequences of diabetic neuropathy including nerve terminal loss and pain, through inhibition of hyperglycaemic sensitisation of TRPA1.

[1] Barrett AM, et al. Pain Med. 2007;8 Suppl 2:S50-62.

[2] Koivisto A, et al. Pharmacol Res. 2012;65(1):149-58.

[3] Hulse et al. Diabetes UK Professional conference presentation 2013

[4] Chen et al. 2007 J Peripher Nerv Syst. 2007;12(2):121-30.

Where applicable, the authors confirm that the experiments described here conform with The Physiological Society ethical requirements.

PCD148

Electrophysiological characteristics of GABAergic neurons and localization of calcitonin receptor-like receptor in the mouse trigeminal subnucleus caudalis

S. Kuwana[1], Y. Hosokawa[2], T. Sugita[3], N. Umezawa[3], A. Matsumoto[3], H. Arisaka[3], K. Yoshida[3] and S. Sakuraba[3]

[1]Department of Physiology, Faculty of Health Sciences, Uekusa Gakuen University, Chiba City, Japan, [2]Department of Anesthsiology, Kitasato University School of Medicine, Sagamihara City, Japan and [3]Division of Anesthesiology, Department of Clinical Care Medicine, Kanagawa Dental College, Yokosuka City, Japan

The trigeminal subnucleus caudalis (SpVc) plays a crucial role in relaying inputs from the primary nociceptive afferents within the orofacial area to higher brain centers. In the SpVc, the central endings of most of primary afferents are located and release excitatory neurotransmitters and neuropeptide such as glutamate, substance P and calcitonin-gene related peptide (CGRP) in response to noxcious stimuli, which can lead excitation in the second-order nociceptive neurons (Sessle et al., 2000). We showed previously that GABAergic neurons densely distributed in the SpVc using the glutamic acid decarboxylase (GAD) 67-green fluorescence protein (GFP) knock-in neonatal mice (Kuwana et al., 2006). In the present study, we investigated the electrophysiological characteristics of GABAergic

and non-GABAergic neurons, and the relationship between localization of CGRP receptors (calcitonin receptor-like receptor, CRLR) and GABAergic neurons in the SpVc of GAD67-GFP knock-in mice. The mouse was deeply anesthetized with diethyl ether and the brainstem was isolated. We recorded activities of GFP-positive (GABAergic, n=20) and GFP-negative (non-GABAergic, n=33) neurons by whole-cell patch clamp technique in the sagittal slice of brainstem attaching the trigeminal nerve rootlet. Electrical stimulations to the trigeminal nerve rootlet evoked excitatory postsynaptic potentials (EPSPs) in most of cells from both groups (20 GFP-positive and in 31 GFP-negative neurons). On the other hand, inhibitory postsynaptic potentials (IPSPs) were not frequently evoked especially in GFP positve neurons (3 in GFP-positive and 13 in GFP-negative neurons). In morphological study, most GFP-positive neurons had multipolar-shaped somata (n=8/10) while GFP-negative neurons had bipolar (n=5/10) or triangular (n=5/10) somata. However, there is no difference in the size of neurons between groups. These data show that GABAergic neurons characterized by multipolar-shaped somata in the SpVc received exclusively excitatory postsynaptic inputs in response to electrical stimulation. Furthermore, we investigated the localization of CRLR by immunohistochemical technique in the SpVc. The CRLR-immunoreactions appeared in about 30% of GFP-positive neurons and some GFP-negative neurons of the SpVc, suggesting that the CRLR-immunoreactive neurons are second-order of nociceptive neurons in the SpVc. Therefore, we conclude that the excitatory synaptic input to GABAergic neuron may be induced by glutamate and CGRP because the primary afferent terminals containing glutamate form synapses with the dendrites of GABA neurons (Iliakis et al., 1996).

Iliakis B, Anderson NL, Irish PS, Henry MA, Westrum LE. Electron microscopy of immunoreactivity patterns for glutamate and gamma-aminobutyric acid in synaptic glomeruli of the feline spinal trigeminal nucleus (Subnucleus Caudalis). J Comp Neurol. 1996;366(3):465-77.

Kuwana S, Tsunekawa N, Yanagawa Y, Okada Y, Kuribayashi J, Obata K. Electrophysiological and morphological characteristics of GABAergic respiratory neurons in the mouse pre-Botzinger complex. Eur J Neuroscience. 2006;23:667-674.

Sessle BJ. Acute and chronic craniofacial pain: brainstem mechanisms of nociceptive transmission and neuroplasticity, and their clinical correlates. Crit Rev Oral Biol Med. 2000;11(1):57-91.

This work was supported by JSPS KAKENHI (23590719).

Where applicable, the authors confirm that the experiments described here conform with The Physiological Society ethical requirements.

PCD149

An illusion of grasping your own finger

S. Gandevia[1,2], L. Walsh[1,2], A. Butler[1,2] and M. Héroux[1,2]

[1]Neuroscience Research Australia, Randwick, NSW, Australia and [2]University of New South Wales, Randwick, NSW, Australia

Accurate movement requires the CNS to use proprioceptive information about the joints of the body, the interrelations between body parts and knowledge of which parts belong to the body. Muscle spindle signals can contribute to determine which parts 'belong' (Walsh et al. J Physiol 2011: 589, 2009). With vision excluded, 20 subjects estimated the perceived vertical distance between the test right index finger and their left index finger when positioned ~12 cm apart. Subjects selected a line from a chart containing multiple vertically oriented lines varying from 0 to 20 cm in length. The subject's left index finger and thumb were located near a realistic artificial finger or were positioned by an experimenter to grasp the artificial finger. Studies were repeated with and without digital nerve blocks.

Perceived vertical spacing was 8.2 [6.0, 10.0] (median [IQR]) cm with no grasp of the artificial finger, and this was significantly less than the absolute distance of 12 cm ($p<0.05$). Perceived spacing diminished markedly during the passive grasp of the artificial finger (4.0 [2.0, 8.0] cm, $p<0.05$). Some subjects reported that they were holding their own right index finger, showing evidence of ownership over the artificial finger. This 'finger grasp' illusion was similar if the test index finger was anaesthetised. However, in separate experiments, the 'finger grasp' illusion was not present when the grasping left index and thumb and the test right index finger were anaesthetised ($p>0.05$), or when the artificial finger was replaced with a piece of wood ($p>0.05$).

In conclusion, passive tactile inputs which are consistent with holding a real finger are able to induce a sense of ownership of an artificial finger. These inputs can change the central representation of the body and the perceived position of the hands.

Where applicable, the authors confirm that the experiments described here conform with The Physiological Society ethical requirements.

PCD150

Spatial- and motion selectivity of population responses in primate area MT

S.C. Chen[1,2], J.W. Morley[3] and S.G. Solomon[4,2]

[1]School of Medical Sciences, University of Sydney, Sydney, NSW, Australia, [2]ARC Centre of Excellence in Vision Science, Sydney, NSW, Australia, [3]School of Medicine, University of Western Sydney, Campbelltown, NSW, Australia and [4]Institute for Behavioural Neuroscience, University College London, London, UK

Neurons in primate visual cortical area MT show precise visuotopic organisation and are known to be highly sensitive to motion direction. It is generally thought that the large receptive fields of these neurons make them incapable of providing precise signals for spatial position. The spatial precision of neuronal populations depends, however, on both receptive field size and the extent of overlap in receptive fields. Here we directly compare spatial- and motion selectivity of area MT by measuring from populations of MT neurons.

Recordings were made in area MT from marmosets (Callithrix jacchus) (n=3). The animals were anaesthetised throughout the duration of the experiment (induction: 12 mg/kg Alfaxan, i.m., maintenance: 6-12 μg/kg/hr sufentanil, i.v.) and artificially ventilated through a tracheostomy. Muscular paralysis was then used to prevent eye movements (0.3 mg/kg/hr pancuronium bromide, i.v.). Level of anaesthesia was established by continuous monitoring of EEG and ECG; anaesthesia was taken as dominance of low frequencies (< 5Hz) in EEG and absence of changes in EEG/ECG during application of noxious stimuli (paw pinch). A craniotomy was made and an electrode array (10x10) implanted in and around area MT in one hemisphere of the animal. The visual stimulus was a white disc moving along each of several possible linear trajectories at 20 °/s. Multi-unit activity at each electrode was counted in 0.05 s bins. Linear support vector machines (SVM) were used to establish whether neural activity in area MT was able to discriminate between pairs of spatial locations up to 8° apart, along trajectories that differed in motion direction by up to 36°. Dis-

criminability depended on a combination of both factors. An elliptical surface fit to the data indicates that for moving objects an average 1.69° (±.04, 95%CI) difference in spatial position was as discriminable as a 30° change in motion direction. Tuning curve width of these neurons was on average 3.2° (±2.0, s.d.) in space and 45.7° (±12.1, s.d.) in motion direction. Receptive fields of neurons in area MT are smaller when close to the fovea, and the performance of the SVM paralleled this. Near the fovea, a separation of 1.48° (±.06, 95%CI) was required, and in the periphery a separation of 2.13° (±.27, 95%CI) was required, to match performance for a 30° change in motion direction.

We conclude that populations of neurons in area MT provide signals for spatial position that are as precise as the signals they provide for motion direction. In addition our analyses show that while neurons show broad tuning for spatial position and motion direction, overlap in these dimensions allows precision in the population response. We speculate that the combination of broad tuning and high overlap is an efficient mechanism for simultaneous encoding of multiple dimensions of visual analysis.

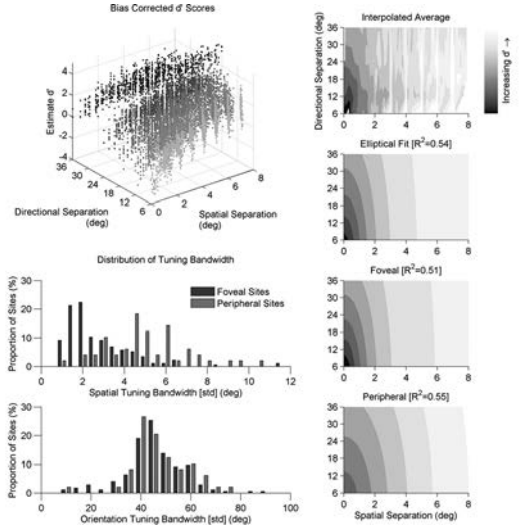

Discrimination (d') depended on a combination of spatial and directional separation. An elliptical fit was used to describe the relationship. The elliptical ratio depended on the eccentricity of the visual space, related to the difference in receptive field sizes.

Where applicable, the authors confirm that the experiments described here conform with The Physiological Society ethical requirements.

PCD151

Visual evoked potential in primary open angle glaucoma patients

B. Paudel[1], M. Jha[2], B. Badhu[3], N. Limbu[4] and D. Thakur[5]

[1]Basic and Clinical Physiology, BP Koirala Institute of Health Sciences, Dharan, Nepal, [2]Physiology, Kathmandu University School of Medical Sciences, Kavre, Nepal, [3]Ophthalmology, BP Koirala Institute of Health Sciences, Dharan, Nepal, [4]Basic and Clinical Physiology, BP Koirala Institute of Health Sciences, Dharan, Nepal and [5]Basic and Clinical Physiology, BP Koirala Institute of Health Sciences, Dharan, Nepal

Visual evoked potential (VEP) is used to assess the functional integrity of the visual pathway. We studied VEP and other ophthalmic variables in clinically diagnosed primary open angle glaucoma (POAG) patients (n=20 eyes) and compared with health controls (n=40 eyes) with an objective of whether POAG causes any neuro-ophthalmic damage. Their age ranged from 38 to 74 years. Pattern reversal (checker board) VEP latency and amplitude; and refractive error, cup disc ratio, intraocular pressure, automated visual field pattern, visual acuity, and foveal visual sensitivity were recorded. The patients were on beta blocker (timolol) for intraocular pressure control. The patients with history of head injury or stroke, on drugs that might affect VEP, secondary glaucoma, diabetes mellitus, media opacity, amblyopia, aphakia, strabismus, high myopia or refractive error, macular degeneration, maculopathy, age-related macular degeneration, non-glaucomatous optic abnormality, & any retinal disorder other than due to glaucoma were excluded from the study. The study was approved by the institute ethical committee. Since some of the variables were not normally distributed Mann-Whitney U test was used to compare the cases and controls. The variables are expressed as mean and standard deviation. Both the groups were comparable in terms of BMI (23.27±1.82 vs. 22.1.47, kg/m sq., p=NS). In POAG cases, the refractive error (3.51±1.88 vs. 1.88±1.11, D, p<0.001), cup disc ratio in percentage (66.00±16.98, vs. 28.50±5.80, p<0.001), intraocular pressure (19.55±2.08 vs. 11.65±1.64, mmHg, p<0.001) and automated visual field pattern standard deviation (4.13±6.96 vs. 1.64±0.45, dB, p<001) were significantly more than in controls. However, the visual acuity (0.41±0.29 vs. 1.00±0.01, p<001), foveal visual sensitivity (25.92±6.88 vs. 33.48±1.75, dB, p<0.001), and automated visual field mean deviation (-9.63±10.59 vs. 0.07±1.54, dB, p<0.001) were significantly less in cases than in controls. Among VEP variables, pattern reversal latency of N145 ((149±15.75 vs. 137.52±15.20, ms, p<0.01) was more in cases than in controls. The amplitudes (microV) of pattern reversal VEP of N45 (1.97±0.35 vs. 2.47±0.58, p<0.001), P100 (3.09±0.46 vs. 6.07±1.44, p<0.001) and of N145 (2.21±0.58 vs. 4.45±1.99, p<0.001) were less in cases as compared to controls. It is concluded that primary open angle glaucoma caused marked deterioration in visual functions including prolongation of VEP latency and reduction in amplitude.

All the patients and the control volunteers of the study.

Where applicable, the authors confirm that the experiments described here conform with The Physiological Society ethical requirements.

PCD152

Coupling between apical inner hair cells of the adult mouse cochlea

A.M. Garcia de Diego[2], P. Sirko[2] and J. Ashmore[1,2]

[1]Neuroscience, Physiology & Pharmacology, UCL, London, UK and [2]UCL Ear Institute, UCL, London, UK

The mammalian cochlea contains a population of sensory cells, inner hair cells (IHCs), which act as the input cells to the auditory system. The IHCs signal to the auditory system through ribbon synapses, each cell having multiple release sites onto single auditory neurites. It is generally thought that the sharp neural tuning seen in single fibres in hearing animals reflects the selectivity of individual IHCs. Using a preparation which allows recording from adult hair cells, rather than immature systems more conventionally used, we have employed a fluorescent probe to investigate calcium signalling at the IHC synapse by using simultaneous multiphoton confocal imaging and cell recording.

Cochlear inner and outer hair cells were visualised in the intact isolated temporal bone from mice aged between P25 and 10 months. Animals were killed by rapid cervical dislocation in accordance with UK legislation and guidelines. The apical cochlea was opened to reveal the 10-15 kHz cochlear region with the cells placed in identifiable positions and orientation. The tectorial membrane was removed to allow recording and the chamber was superfused with (in mM) Na, 140; Ca, 1.3; K, 4; Cl 147, hepes 10, phosphate 0.7 to pH 7.3 at room temperatures. Cells were recorded in the whole cell tight seal mode, the pipette including 0.5, 5 or 10 mM EGTA and 0.25 mM OGB5N. Cs was used to reduce large outward currents to less than 1.5 nA at 0 mV.

These recordings showed distinct calcium entry sites, 'hotspots', when the IHC was depolarized to 0 mV from -60 mV. The kinetics of the Ca rise and fall often slowed with extended recording time over 10 mins. After OGB5N loaded for 3-5 mins it was also often found that a proportion of neighbouring cells appeared to be fluorescently loaded. Up to 9 adjacent cells could be found filled with OGB5N. Recording time constants in such cases exceeded the single cell values and could be modelled on the assumption that the cells were electrically coupled with an intercellular resistance of less than 10 megohms. Calcium responses imaged in such coupled IHCs showed that the kinetics generally differed from that of the recorded cell, suggesting that the coupling did not permit the movement of large Ca buffers between cells.

The present data thus indicate that adult IHCs can be coupled. The extent of the observed coupling would not significantly degrade the frequency selectivity of individual auditory nerves, at least in low frequency fibres, but may increase the signal/noise ratio in the pathways leading from the apical cochlea.

Supported by the Wellcome Trust

Where applicable, the authors confirm that the experiments described here conform with The Physiological Society ethical requirements.

PCD153

Antinociceptive and anti-inflammatory effects of essential oil of Nepeta pogonosperma Jamzad et Assadi in Wister rats

T. Ali[1,2], M. Javan[2], A. Sonboli[3] and S. Semnanian[2]

[1]Physiology, Bangabandhu Sheikh Mujib Medical University, Dhaka, Bangladesh, [2]Physiology, Tarbiat Modares University, Tehran, Islamic Republic of Iran and [3]Biology, Shahid Beheshti University, Tehran, Islamic Republic of Iran

Concerning the variability of effectiveness of essential oils from different species of Nepeta genus on CNS including analgesia, this study was designed to evaluate antinociceptive and anti-inflammatory effects of essential oil of Nepeta pogonosperma Jamzad et Assadi (NP). Air-dried aerial parts of NP were hydrodistillated and GC-MS analysis of obtained essential oil was conducted. Total 24 male Wister rats (225±25gm) were taken care according to international guidelines on use of laboratory animals and studied. Experimental rats received 50, 100 and 200mg/kg of NP essential oil and control rats received equal volume (2ml/kg) of normal saline intraperitoneally (n=6/group). Antinociception was assessed by tail flick test (D'Amour and Smith, 1941) followed by formalin test (50 μl of 2% formalin, subcutaneously) using a modification of original formalin test protocol (Dubisson and Dennis, 1997). Euthanasia was done by di-ethyl ether (99%, 10-12ml) followed by decapitation (Zschenderlein et al. 2011) and anti-inflammation was measured by water plethysmometry (Fereidoni et al. 2000). Data were mean±SEM and analyzed by ANOVA with Tukey's post-hoc test. NP essential oil consisted of 4aα,7α,7aα nepetalactone (14.5%) and 1,8 cineole (31.2%) mainly. In tail flick test, 50mg/kg (10.25±8.06 vs. 11.04±5.9%) did not produce any analgesia, but 100 (26.99±2.79%; p<0.01) and 200 (43.98±7.73%; p<0.001) mg/kg reduced pain significantly. In early phase of formalin test, all doses reduced jerking frequency/5min (50mg/kg=78.66±20.67; 100mg/kg=64.5±15.47; 200mg/kg=30.83±7.16; control=201.33±14.01; p<0.001, in all doses), flexing seconds/5min (50mg/kg=62.5±20.24; 100mg/kg=65.33±18.31; 200mg/kg=50.5±21.14; control=148±21.57; p<0.05, p<0.05, p<0.01, respectively) and licking seconds/5min (50mg/kg=28.83±17.97; 100mg/kg=23.66±7.56; 200mg/kg=4.33±3.94; control=82±8.95; p<0.05, p<0.001, p<0.001, respectively). Again, in late phase of formalin test, all doses reduced jerking frequency/5min (50mg/kg=45.79±7.54; 100mg/kg=34.42±7.75; 200mg/kg=38.48±7.08; control=112.03±10.53; p<0.001, in all doses), flexing seconds/5min (50mg/kg=60.59±21.53; 100mg/kg=76.07±27.69; 200mg/kg=40.94±26.19; control=224.06±20.43; p<0.001, p<0.01, p<0.001, respectively) and licking seconds/5min (50mg/kg=12.83±3.22; 100mg/kg=18.46±4.78; 200mg/kg=5.66±1.66; control=33.03±3.83; p<0.01, p<0.05, p<0.001, respectively). Moreover, all doses reduced paw edema in % of control (50mg/kg=0.21±0.04, nonsignificant; 100mg/kg=0.13±0.02, p<0.01; 200mg/kg=0.2±0.03, p<0.05). This study reveals that NP essential oil may minimize both acute and chronic forms of nociception and may have potent role against inflammation.

D'Amour FE & Smith DL (1941). J Phamacol Exo Ther 72, 74 -79

Dubisson D & Dennis SG (1997). Pain 4, 161 - 174

Zschenderlein C et al. (2011). PLoS One 6(1), e16116.

Fereidoni M et al. (2000). J Pharmacol Toxicol Methods 43, 11 -14

Department of Physiology, Tarbiat Modares University, Tehran, Iran and Iranian Society of Physiology and Pharmacology.

Where applicable, the authors confirm that the experiments described here conform with The Physiological Society ethical requirements.

PCD154

Effect of vitamin B12 on pain and inflammation in Long Evans rats

M. Imtiaz, N. Begum and T. Ali

Physiology, Bangabadhu Sheikh Mujib Medical University, Dhaka, Bangladesh

Concerning the analgesic and anti-inflammatory effects of combination of Vitamin B12 with other B Vitamins or traditional drugs, this study was designed to evaluate the effect of Vitamin B12 alone on nociceptive pain, inflammatory pain and inflammation. Total 24 male Long Evans rats (225±25gm) were taken care according to international guidelines on use of laboratory animals and divided into two groups. Single supplemented rats (n=12) were intraperitonialy treated with a single dose of 15 mg/kg B12 (n=6) or equal volume (15 ml/kg) of normal saline (n=6). Similarly chronic supplemented rats (n=12) were divided into normal saline (n=6) and B12 (n=6) groups with same dose and route of treatment per day for consecutive 7 days. Analgesia was assessed by warm water (±55 degree

Celcius) tail immersion test (Steinmiller and Young 2007) followed by formalin test (50 μl of 2% formalin, subcutaneously) using a modification of the original formalin test protocol (Dubisson and Dennis, 1997). Euthanasia was done by di-ethyl ether (99%, 10-12ml) followed by decapitation (Zschenderlein et al. 2011) and anti-inflammation was measured by water plethysmometry (Fereidoni et al. 2000). The data were expressed as mean±SEM and analyzed by independent sample 't' test. The single supplementation of vitamin reduced the nociceptive pain (%MPE=4.56±1.05 vs. 4.27±1.59; jerking frequency/5min in early phase=89±3.79 vs. 101.5±4.40; flexing+licking duration in seconds/5min in early phase=247.33±10.62 vs. 260.33±6.93) nonsignificantly, inflammatory pain (jerking frequency/5min in late phase=69.28±2.40 vs. 75.44±1.26, p<0.001; flexing+licking duration in seconds/5min in late phase=277.57±2.16 vs. 288.85±2.59, p<0.01) and inflammation (ml of edema volume=0.16±0.02 vs. 0.23±0.02, p<0.01) significantly. Similarly, chronic B12 supplementation reduced the nociceptive pain (%MPE=7.08±1.3 vs. 3.85±1.55; jerking frequency/5min in early phase=86.5±3.42 vs. 87.5±5.75; flexing+licking duration in seconds/5min in early phase=243.5±7.1 vs. 260.17±6.16) nonsignificantly, inflammatory pain (jerking frequency/5min in late phase=64.07±2.07 vs. 84.65±2.45, p<0.001; flexing+licking duration in seconds/5min in late phase=275.89±1.88 vs. 289.91±1.77, p<0.01) and inflammation (ml of edema volume=0.11±0.02 vs. 0.23±0.02, p<0.01) significantly. In addition, in all study variables a better trend of decrement was found in the chronic supplementation. The study reveals that vitamin B12 may possess effective role against nociceptive and inflammatory pain, as well as inflammation, and chronic supplementation may be better useful than the acute one.

Steinmiller CL & Young MA (2008). Psychopharmacology 195, 497-507

Dubisson D & Dennis SG (1997). Pain 4, 161-174

Zschenderlein C et al. (2011). PLoS One 6(1), e16116

Fereidoni M et al. (2000). J Pharmacol Toxicol Method 43, 11-14

Where applicable, the authors confirm that the experiments described here conform with The Physiological Society ethical requirements.

PCD155

Kinesthetic perception based on integration of motor imagery and afferent inputs from antagonistic muscles with tendon vibration

E. Shibata[1,2] and F. Kaneko[3]

[1]Graduate School of Health Sciences, Sapporo Medical University, Sapporo, Japan, [2]Shinoro Orthopedic Hospital, Sapporo, Japan and [3]Second Division of Physical Therapy, Sapporo Medical University, Sapporo, Japan

The perceptual integration of afferent inputs from two antagonistic muscles, or the perceptual integration of afferent input and motor imagery are related to the generation of a kinesthetic sensation. However, it has not been clarified how, or indeed whether, a kinesthetic perception would be generated by motor imagery if tendon vibrations induced afferent inputs from two antagonistic muscles. The purpose of this study was to investigate how a kinesthetic perception would be generated by motor imagery during co-vibration of two antagonistic muscles at the same frequency.

Sixteen healthy subjects participated in this experiment. All subjects provided informed consent for participation in this study. Illusory movements such as wrist flexion or extension were evoked by tendon vibration. The left wrist flexor and extensor muscles were vibrated according to 4 patterns such that there was no difference between the two vibration frequencies (flexor vs. extensor: 40 Hz vs. 40 Hz, 60 Hz vs. 60 Hz, 80 Hz vs. 80 Hz, and 100 Hz vs. 100 Hz). The subjects imaged wrist flexion movement (MI-slow, MI-fast) simultaneously with tendon vibration. After each trial, the perceived movement sensations were quantified on the basis of the velocity and direction of the ipsilateral hand-tracking movements. Two-way ANOVA with a simple main effects test was used to test the effect of the "imagery" factor and "frequency" factor on the average velocities ($p < 0.05$).

When the difference in frequency between the wrist flexor and the extensor was 0 Hz, practically none of the subjects perceived such movement. However, during motor imagery, the velocity of the perceived movement was higher than the velocity without motor imagery. There was a significant main effect of motor imagery and vibration frequency (Imagery: $F = 11.115$, $p < 0.0005$, Frequency: $F = 6.837$, $p = 0.014$). The interaction between the vibration frequency and condition of motor imagery was also significant ($F = 3.818$, $p = 0.040$). A post-hoc test revealed that the velocity was significantly increased during 60Hz-MI-fast compared to 60Hz-MI-none, 80Hz-MI-slow and 80Hz-MI-fast compared to 80Hz-MI-none, and 100Hz-MI-slow and 100Hz-MI-fast compared to 100Hz-MI-none. Furthermore, that velocity was significantly increased during 80Hz-MI-fast and 100Hz-MI-fast compared to 40Hz-MI-fast.

The result of the current research showed that the imagined movement direction was perceived during motor imagery with co-vibration of two antagonistic muscles, even though the subjects experienced no kinesthetic perception by co-vibration of two antagonistic muscles at the same frequency without imagery. Furthermore, the kinesthetic perception resulting from these integrations of vibration and motor imagery differed with the imagined movement velocity and the vibration frequency.

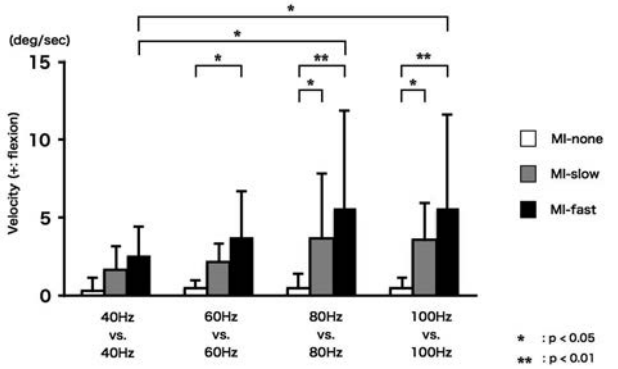

Average (±S.D.) illusory movement velocity with four different frequency during MI-fast, MI-slow, and MI-none.

Where applicable, the authors confirm that the experiments described here conform with The Physiological Society ethical requirements.

PCD156

Interplay between mast cells, 5-HT and TRPA1 in sensory signalling from the GI tract: Influence of ageing

Y. Yu, L. Nocchi, A. Rust, C. Keating, W. Jiang and D. Grundy

Biomedical Science, University of Sheffield, Sheffield, UK

TRPA1 is expressed on sensory neurons supplying the gastrointestinal (GI) tract and contributes to both normal mechanosensitivity and nociception [1, 2]. TRPA1 is also expressed in enterochromaffin (EC) cells leading to the release of serotonin [3], which has the potential to sensitize sensory nerve endings. Mast cell can also contribute to hypersensitivity [4]. We hypothesise therefore that there is a complex interplay between EC cells and mast cells, which serves to amplify TRPA1 signalling. Since sensory signaling from the GI tract diminishes with age [5] we further hypothesise that these modulating interactions are attenuated in aged mice.

All experiments were performed on adult (3 month) or aged (24 month) male C57/BL6 mice in accordance with UK Home Office regulations. Afferent discharge was recorded from mesenteric nerves innervating a 2 cm segment of jejunum. The TRPA1 selective agonist allyl-isothiocyanate (AITC) was bath applied (1mM) at 50-minute interval and resulted in a reproducible afferent response. Treatment with cromolyn sodium (100 μM) or granisetron hydrochloride (30 μM) 15 minutes prior to the second application of AITC was used to determine contribution of mast cells and 5-HT3 receptors to AITC response. Data are expressed as mean afferent discharge frequency ± SEM and analysed using Students t-test. Quantitive RT-PCR was performed (in duplicate) using specific probes for mouse TRPA1 and 5-HT3 receptor on RNA isolated from DRGs and jejunum wall of aged and control mice. Data are expressed as fold change (aged vs. control) with > 2-fold change taken as significant.

The increase in afferent discharge in response to AITC was significantly attenuated by cromolyn (72.5 ± 21.3 vs. 32.7 ± 9.8, $P<0.05$, paired t-test, N=6), suggesting that mast cells mediators amplify TRPA1 signalling. The response to AITC was also significantly inhibited by 30 μM granisetron (72.4 ± 15.4 vs. 21.3 ± 5.4, $P<0.05$, paired t-test, N=5) indicating a role for endogenous 5-HT, possible from EC cells. In aged mice, responses to AITC at a range of concentration were all significantly attenuated (100 μM: 19.9 ± 3.6 vs. 6.8 ± 3.4, $P<0.05$; 300 μM: 47.2 ± 10.2 vs. 15.7 ± 5.9, $P<0.05$; 1mM, 74.9 ± 7.3 vs. 28.8 ± 9.7, $P<0.01$; unpaired t-test, N=5). Expression of TRPA1 in the DRG and jejunum were not significantly different in young and aged mice (DRG, 1.58, N=5; jejunum, -1.42, N≥6), while 5-HT3B was significantly down regulated in jejunum (-2.11, N≥6) but not DRG (-1.06, N=4), which might contribute to the attenuation of TRPA1 signalling with ageing. This data suggests that there is an interplay between mast cells, EC cells and TRPA1 channels that might include both direct effects at the level of the sensory nerve terminal and amplification following the release of 5-HT and other inflammatory mediators. These mechanisms may be attenuated with ageing.

Kwan, K.Y., et al., TRPA1 contributes to cold, mechanical, and chemical nociception but is not essential for hair-cell transduction. Neuron, 2006. 50(2): p. 277-89.

Brierley, S.M., et al., The ion channel TRPA1 is required for normal mechanosensation and is modulated by algesic stimuli. Gastroenterology, 2009. 137(6): p. 2084-2095 e3.

Nozawa, K., et al., TRPA1 regulates gastrointestinal motility through serotonin release from enterochromaffin cells. Proceedings of the National Academy of Sciences, 2009. 106(9): p. 3408-3413.

Schemann, M., et al., Human mast cell mediator cocktail excites neurons in human and guinea-pig enteric nervous system. Neurogastroenterol Motil, 2005. 17(2): p. 281-9.

Wade, P.R. and T. Cowen, Neurodegeneration: a key factor in the ageing gut. Neurogastroenterol Motil, 2004. 16 Suppl 1: p. 19-23.

Where applicable, the authors confirm that the experiments described here conform with The Physiological Society ethical requirements.

PCD157

Study of the effect of excitability change in the primary motor cortex on the sensitivity of kinesthetic perception

M. Okawada[1], F. Kaneko[2], E. Shibata[1], N. Aoki[2] and N. Matsuda[1]

[1]Graduate School of Health Sciences, Sapporo Medical University, Sapporo, Japan and [2]Second Division of Physical Therapy, Sapporo Medical University, Sapporo, Japan

Information from muscle spindles is important for kinesthetic perception. In a previous study, the contralateral primary motor cortex (M1) and primary sensory cortex (S1) were activated when kinesthetic illusion was induced by tendon vibration. Therefore, it appears that a brain neural network (e.g., M1, S1) may contribute to the pathway of the kinesthetic feelings. The purpose of this study was to study the effect of excitability change in M1 on the sensitivity of kinesthetic perception. Two experiments were performed in this study. Nine healthy right-handed male volunteers participated in the experiments, with 7 of 9 subjects taking part in each experiment. Each experiment consisted of two sessions that were at least a week apart. Participants received quadripulse transcranial magnetic stimulation (QPS), in which each train consisted of four magnetic pulses separated by an interstimulus interval of 5 msec (QPS-5), or Sham in each session. In experiment 1, the motor evoked potential (MEP) was recorded to evaluate M1 excitability. In experiment 2, the movement detection threshold was measured to examine the sensitivity of kinesthetic perception. MEP amplitude and movement detection threshold were recorded two times before QPS-5 or Sham (pre-1, pre-2) and at 0, 15, 30, 45, and 60 min after QPS-5 or Sham (post-0, post-15, post-30, post-45, and post-60). The ratio of MEP amplitude and movement detection threshold against pre-1 were calculated. Two-way ANOVA was used to test the effect of the "CONDITION" factor (SEP-5, Sham) and "TIME" factor (pre-2, post-0, post-15, post-30, post-45, post-60) on the MEP amplitude and movement detection threshold. For the factors that yielded significant main effect and interaction, we performed post hoc pair-wise comparisons with Bonferroni correction ($p < 0.05$). In MEP amplitude, there was a significant interaction between CONDITION and TIME factors. Post hoc test results revealed that MEP amplitude increased significantly after QPS-5. On the other hand, there was no effect of Sham on the MEP amplitude. In the movement detection threshold, there was a significant interaction between the CONDITION and TIME factors. Post hoc test results showed that the movement detection threshold decreased significantly after QPS-5.

Where applicable, the authors confirm that the experiments described here conform with The Physiological Society ethical requirements.

PCD158

Ontogenetic plasticity of the metabolic apparatus and electrical properties of *Calliphora vicina* photoreceptors

J. Rudolf, A. Meglič, G. Zupančič and G. Belušič

Department of Biology, Biotechnical Faculty, University of Ljubljana, Ljubljana, Slovenia

The physiology of neural tissue is greatly shaped by information processing efficiency vs. energy cost trade-offs. A good model for studies of energy demands with respect to sensory performance is the insect eye due to its relatively simple repetitive structure and easiness of genetic manipulation (e.g. Niven et al., 2007). In our study we examined the metabolic and electrical properties of *Calliphora vicina* (white-eyed strain chalky) photoreceptors with respect to their ontogenetic plasticity.
We employed *in vivo* spectrophotometric measurements (Zupančič, 2003) to asses the metabolic activity of mitochondria in blowfly photoreceptors. By analyzing the differential absorption spectra recorded from the eyes under normoxic and anoxic conditions we estimated the dynamic range of redox states of electron transport chain components (haems in cytochromes: a, a_3, b and c). We found that the range of redox states increased with post-eclosion age in all studied haems. The largest change was found in the first week. We attributed the change mostly to the changes in cytochromes' (Cyt) concentration, which we confirmed by biochemical analysis of the Cyt c content in isolated retinal mitochondria in flies of different age. The results were in good agreement with our spectrophotometric measurements, showing a 5-fold increase in Cyt c concentration in the first two weeks post eclosion.
Long-term light adaptation profoundly influenced the performance of mitochondria. The changes in haems' dynamic redox range were significantly smaller in dark-bred animals (e.g. 2.9-fold increase for haem c in the first two weeks) compared to animals bred under 12/12h day/night cycle (4.8-fold increase).This implies that lower metabolic load results in smaller ontogenetic changes in the metabolic capacity of the photoreceptors.
The maintenance of ion gradients over the membrane was shown to be the primary energy sink in the insect photoreceptors (Laughlin et al., 1998). Thus, we expected the plasticity of photoreceptors' electrical properties to follow a similar ontogenetic time course as the one observed in the mitochondrial apparatus. We employed single electrode voltage- and current-clamp to compare the electrical parameters (cell resistance and capacitance) of blowfly photoreceptors at different age and rearing conditions. We observed significant differences in resting cell capacitance between age groups with a peak at 2 weeks after eclosion, but small changes in the resting conductance of photoreceptor cells.
Our findings indicate the existence of relevant age related changes in both studied aspects of the photoreceptor's functionality.

Laughlin SB, van Steveninck RRD, Anderson JC. (1998) The metabolic cost of neural information. Nature Neuroscience 1(1):36-41.

Niven JE, Anderson JC, Laughlin SB. (2007) Fly photoreceptors demonstrate energy-information trade-offs in neural coding. Plos Biology 5(4):828-840.

Zupancic G. (2003) A method for dynamic spectrophotometric measurements in vivo using principal component analysis-based spectral deconvolution. Pflugers Archiv-European Journal of Physiology 447(1):109-119.

Where applicable, the authors confirm that the experiments described here conform with The Physiological Society ethical requirements.

PCD159

A comparison of medial prefrontal cortical activity during micturition in the awake and anaesthetised rat

R. Mason[2], G. Fenton[2], C. Spicer[2] and Y. Mbaki[1]

[1]School of Biomedical Sciences, University of Nottingham Malaysia Campus, Selangor Darul Ehsan, Malaysia and [2]School of Biomedical Sciences, University of Nottingham UK Campus, Nottingham, UK

Anatomical and imaging studies have implicated the involvement of the medial prefrontal cortex (mPFC) and thalamus in micturition control. The present in vivo electrophysiological study, investigates (i) the contribution of the mPFC and thalamus in the control of micturition in the anaesthetised female rat, compared with (ii) the role of the mPFC in "executive decision making" in the micturition behaviour of the awake-behaving rat.
(i) Female Sprague-Dawley rats (230-280g; n = 6) were initially anaesthetised with isoflurane (50%N_2O:50%O_2) and then maintained with urethane (1.2 g kg^{-1}, i.v.). Multiple single-unit and local field potentials (LFPs) were recorded simultaneously from the mPFC and thalamus using microelectrode arrays (MEAs). Bladder contractions were monitored and evoked by infusion (0.1 ml min^{-1}) of saline into the bladder. (ii) Awake-behaving studies were conducted on female Sprague Dawley rats (230-280g; n = 2) and male Lister-hooded rats (350-400g; n = 4) receiving MEA implants. Combined electrophysiological and video recordings were undertaken to monitor micturition on a daily basis over a number of weeks; on completion the individuals were anaesthetised and prepared in order to monitor saline-evoked bladder as above. All experiments were performed, in accordance with the Animals (Scientific Procedures) Act 1986 UK.
Multiple single-unit and LFP activity correlated to bladder contractions following saline infusion were identified within the anterior cingulate gyrus of the mPFC and thalamus in the anaesthetized female rat. In the awake-behaving study comparisons were made between pre- and post-void conditions and demonstrated altered LFP activity in power spectral density and partial-directed coherence (PDC) analysis.
This electrophysiological study demonstrates the involvement of the mPFC and thalamus in the control of micturition in the rat, and revealed a disparity in response reflecting anaesthetic state.

Where applicable, the authors confirm that the experiments described here conform with The Physiological Society ethical requirements.

PCD160

ERK/MAPK in the spinal cord is involved in pain hypersensitivity in a mouse model of type 2 diabetes

H. Cao[1], X. Xu[2], H. Chen[2] and L. Xu[2]

[1]Institute of Neurobiology, Fudan University, Shanghai, Shanghai, China and [2]Department of Endocrinology, Wuxi People's Hospital, Nanjing Medical University, Wuxi, Jiangsu, China

Painful diabetic peripheral neuropathy (PDPN) is a common complication of diabetes mellitus [1]. The painful symptom becomes a major factor in decreased quality of life for patients with diabetes, while it is lack of effective treatments. The aim of the present study is to investigate the changes of pain thresholds in the early stage of diabetes in db/db mice, an animal model of type 2 diabetes mellitus [2], and the underlying mechanisms. Diabetic mice (db/db) and non-diabetic littermates (wild type, WT) of C57BLKS strain were used in present study. Body weight, blood glucose and behavioral responses to various stimuli were measured every week in db/db mice and the non-diabetic littermates mice (WT) at 4-12 weeks of age. The mechanical and thermal threshold was measured by probing von Frey hairs (von Frey, Stoelting, USA) and Hargreaves' tests, respectively [3]. Western blot was used to measure the expression of phosphorylated and total ERK1 and ERK2, GAPDH as well. Mice were deeply anesthetized by 25% urethane (1.5g/kg body weight) before tissue collection for Western blot analysis. We found that (1) db/db mice, with a leptin receptor null mutation, are characterized by obese and hyperglycaemic; (2) db/db mice were hypersensitivity to mechanical and thermal stimuli at early stage of diabetes; (3) phosphorylations of ERK1 and pERK2, but not total ERK in the spinal cord from db/db mice are significantly increased as compared with that from wild-type mice; (4) at the age of 8 weeks, db/db mice showed increased pain hypersensitivity in the formalin test. In parallel, the expressions of pERK1 and pERK2 were largely increased in the ipsilateral spinal cord of diabetes after formalin injection. Our results indicated that activation of ERK may be a potential molecular mechanism involving in the pain hypersensitivity in type 2 diabetes.

Keywords:painful diabetic peripheral neuropathy (PDPN); db/db mice, pain hypersensitivity, extracellular signal-regulated kinases (ERK)

McGreevy K, Williams KA. Contemporary Insights into Painful Diabetic Neuropathy and Treatment with Spinal Cord Stimulation. Curr Pain Headache Rep 2012,16:43-49.

Coleman DL. Obese and diabetes: two mutant genes causing diabetes-obesity syndrome in mice. Diabetologia 1978,14:141-148.

Bao F, Chen ML, Zhang YQ, Zhao ZQ. Hypoalgesia in mice lacking aquaporin-4 water channels. Brain Res Bull. 2010, 83: 298-303.

This work was supported by National Natural Science Fund of China (NSFC, 31121061, 30900444 and 31070973). We are grateful to travel support by Chinese Association for Physical Science(APS).

Where applicable, the authors confirm that the experiments described here conform with The Physiological Society ethical requirements.

PCD161

Increased A-nociceptor-evoked Fos expression in a functionally distinct subdivision of midbrain periaqueductal grey in a rat model of inflammatory pain

J. Mendes Gomes, M. Hsieh, L.F. Donaldson and B.M. Lumb

Physiology and Pharmacology, University of Bristol, Bristol, UK

Specific patterns of survival (defence) behaviours that are coordinated by the different functional columns of the midbrain periaqueductal grey (PAG) may be triggered by A- and C-nociceptive inputs that have different behavioural significance, in that they mediate 'first' and 'slow' pain respectively, and have different roles in the initiation and maintenance of chronic pain. It is of considerable importance therefore to determine to the columnar organisation of A- and C-nociceptor inputs in normal animals and in animal models of chronic pain.

Our previous studies[1,2] have shown that, in uninjured animals, inputs arising from these different fibre types target different regions of the PAG: C-fibre inputs target the ventrolateral column of the PAG (VL-PAG) and A-nociceptor inputs, the dorsolateral/lateral column (DL/L-PAG). This current study was designed to determine the activation of different regions of the PAG following either A- or C-nociceptor stimulation in an area of secondary hyperalgesia in a rat model of inflammatory arthritis.

Arthritis was induced by injection of Freund's Complete Adjuvant into the left knee joint under brief isoflurane/O2 anaesthesia (2% in O2). Animals (4-6/group) were re-anaesthetised 7 days later (halothane (2% in O2), alfaxan maintenance (i.v. 25.mg.kg.h-1) and either C- or A-nociceptors preferentially activated respectively, by slow (2.5°C.s-1, 30-55°C) or fast (7.5°C.s-1, 30-57°C) contact heating of the left hindpaw dorsum (area of secondary hyperalgesia). Some inflamed rats did not receive any stimulation (control group). Two hours after stimulation, animals were perfuse fixed and brains processed immunocytochemically for visualisation of Fos-like immunoreactivity (FLI). Fos-positive PAG neurones were counted (Image J, NIH) and their locations assigned to the different functional columns of the PAG throughout its rostrocaudal extent.

FLI was greater in caudal than rostral PAG in stimulated and control animals. Hindpaw A-nociceptor stimulation increased FLI in the caudal right (contralateral) L-PAG but in no other area, in arthritic rats. These results demonstrate that caudal L-PAG activation is greater in response to A-nociceptor input from the area of secondary hyperalgesia than in inflamed unstimulated rats. These data may indicate that processing of 'first' pain in L-PAG is enhanced in secondary inflammatory hyperalgesia.

1. Lumb BM (2002). *Exp Physiol* 87(2), 281-286.

2. Parry DM et al. (2008). *Neuroscience* 152, 1076-1085.

CAPES Foundation – Ministry of Education of Brazil, University of Bristol Centenary Fund and the Medical Research Council.

Where applicable, the authors confirm that the experiments described here conform with The Physiological Society ethical requirements.

PCD162

Intracranial recording of the primary motor and somatosensory activity during kinesthetic perception

F. Kaneko[1] and Y. Kubota[2,3]

[1]Second Division of Physical Therapy, Sapporo Medical University, Sapporo, Japan, [2]Department of Neurosurgery, Asakadai Central General Hospital, Saitama, Japan and [3]Department of Neurosurgery, Tokyo Women's Medical University, Tokyo, Japan

Several studies have demonstrated that the sensorimotor areas were associated with kinesthetic perception. Specific contrasts were shown that the perception of an illusory movement in the right wrist joint was specifically related to activation in the left premotor, sensorimotor, and parietal cortices as well as in bilateral supplementary motor and cingulate motor areas. In previous studies, cerebral activity during kinesthetic perception was demonstrated, but the inhibitory or facilitatory effect of those cerebral activity has not been clarified. In the current study, we had an oppotunity to record the cerebral activity directly in a patient with epilepsy, so this research was done to show the cerebral activity in the sensorimotor areas associated with kinesthetic perception. A 14-year-old male with intractable epilepsy participated in this study. Informed consent for study participation was obtained from the patient and his parents before the experimental procedure was performed, as required by the Helsinki Declaration. The patient underwent intracranial electrodes implantation to identify the epileptogenic zone. The following study was carried out 10 days after the implantation of the electrodes. During the study, no epileptiform discharge was observed by an epileptologist on the electroencephalogram (EEG) recorded from the intracranial electrodes. Cerebral activity was recorded during the performance of 5 kinds of task, including resting. The main task was to apply the tendon vibration to the wrist joint flexors and/or extensors, to induce a kinesthetic illusory feeling. To induce an illusory feeling of moving in the extensional direction, we stimulated the flexors with 50-Hz (F50 condition) or 100-Hz (F100 condition) vibration. We also induced the illusion of flexion by stimulating the flexors with 100-Hz vibration and the extensors with 50-Hz vibration (F100-E50 condition). On the other hand, there was no illusory feeling when the 50-Hz or 100-Hz vibration was applied to both flexors and extensors (Non-50, Non-100). Negative peak values for the channel of the primary motor area depended on the amount of differences in vibration frequency between flexors and extensors. The highest peak value was recorded during the F100 condition (-82.1 μV), and the lowest value was observed under the Non-100 condition (-45.2 μV). Time frequency analysis revealed that signals around 10 Hz increased after the beginning of vibration in the channel of the primary motor cortex, while the signals around 10 Hz were suppressed in the channel of the primary somatosensory cortex. An EEG signal around 10 Hz indicated a different trend between the channels for the motor cortex and the somatosensory cortex. The cerebral activity reported in this study was recorded from only one patient; however, the recordings provided very unusual and noteworthy data.

Where applicable, the authors confirm that the experiments described here conform with The Physiological Society ethical requirements.

PCD163

Movement deficits of patients presenting with cerebellar degeneration during precise auxometric finger movements

D.F. Kutz[1], D. Timmann[2] and F.P. Kolb[1]

[1]Institute of Physiology, University of Munich, Munich, Germany and [2]Department of Neurology, University of Duisburg-Essen, Essen, Germany

Question: In his famous work on patients presenting acute with cerebellar injuries Gordon Holmes demonstrated that some exemplary patients with unilateral damage (N=3) showed a delayed start of auxometric finger movements as well as incomplete force production [1]. The aim of this study was to investigate these results in more detail.
Methods: Patients presenting with cerebellar lesions (N=9, age: 51.6 years) and age and sex matched subjects (N=9, age: 51.3 years) performed a sequence of precise auxometric finger movements with a custom-made dynamometer. The apparatus consists of a hinge (58 mm legs) kept open by a leg spring at an angle of 11°. The spring had a constant of 39.4 Nmm/° resulting in a force range of 8.7 N (initial value) to 16.2 N (maximal value). Subjects had to squeeze the hinge each time a 1 kHz tone (duration: 2 s) was presented. Trial intervals varied randomly between 10 – 15 s. During each trial the tone was presented twice with a constant inter-stimulus interval of 2 s. Mean values for reaction time (RT) and movement time (MT) of both hands were compared statistically. During the procedure electro-myographic activity (EMG) of the thenar muscle (TH) and first dorsal interosseus muscle (FDI) were recorded.
Results: In the patient group (CBL), RT and MT of the two movements in the sequence were significantly increased (both $p < 0.05$) compared with the control group (CTRL), regardless of the hand in use. Interestingly, for the right hand RT and MT of the second movement were clearly reduced (both $p < 0.05$) compared with the first movement (RT: 435 vs. 355 ms, MT: 374 vs. 250 ms, respectively) in CBL, indicating an improvement of movement performance when timing is predictive. The EMG-onsets of FDI were significantly later in CBL than in CTRL. Detailed analysis revealed that the mean EMG-onset asynchronicity between TH and FDI was significantly greater in CBL (right hand 72 ms, left hand 131 ms) than in CTRL (right hand 30 ms, left hand 25 ms), suggesting better co-ordination of the muscles around the thumb joint in CTRL.
Conclusions: Patients presenting with cerebellar degeneration have more difficulties in starting precise auxometric finger movements. This may be, in part, due to a limited co-ordination of co-acting muscles around a joint. Nevertheless, they can improve in performing simple movements when timing remains predictive, because of a fixed interval.

Gordon Holmes. The symptoms of acute cerebellar injuries due to gunshot injuries. Brain, Vol. 40, pp. 461 – 535, 1917.

Supported by the "Else-Kröner-Fresenius Stiftung" (A12/07).

Where applicable, the authors confirm that the experiments described here conform with The Physiological Society ethical requirements.

PCD164

Impact of birth order on child development in a rural community, India

S. Sadat Ali[1], S.S. Goudar[2] and D. Sm[3]

[1]Department of Physiology, Dr. B R Ambedkar Medical College, Bangalore, Karnataka, India, [2]Department of Physiology, Jawaharlal Nehru medical College, KLE University, Belgaum, Karnataka, India and [3]Pediatrics, Jawaharlal Nehru medical College, KLE University, Belgaum, Karnataka, India

Objective: To assess the impact of birth order on child development among preschool children. Design and method: A cross sectional study was conducted through anganwadi schools among 530 children at three years staying in a rural community in a Primary health centre area, to assess the developmental delay using screening tool, Ages and stages questionnaire (ASQ). Then, these children were correlated and analysed for birth order in the family with their global development. The study was approved by Institutional Ethics Committee for Human Subjects Research. Chi-square test was used to compare categorical variables. Differences were considered significant at P<0.05 level. Results and conclusions: The prevalence of global developmental delay assessed by ASQ was 19.8%. [1] A majority of the children (85.8%) were from joint family and majority (81.5%) were of 1st and 2nd birth order. In the present study, ASQ score for personal social skill was low for a child who stayed with fewer number of children at home as against those who stayed with more number of children (P=0.07), though not statistically significant. The gross motor development was better in 1st and 2nd order children compared to higher order and this showed a statistically significant change (P=0.04). The rest of the domains didnot show any significant correlation. The results of the present study showed that there was a trend towards higher ASQ scores from higher birth order to lower birth order.

Ali SS, Balaji PA, Dhaded SM, Goudar SS. Assessment of growth and global developmental delay: a study among young children in a rural community of India, International Multidisciplinary Research Journal 2011; 1(7):31-34.

We acknowledge all the participating children and their mother for their support in the study.

Where applicable, the authors confirm that the experiments described here conform with The Physiological Society ethical requirements.

PCD165

Mechanisms of calcium independent but voltage dependent secretion (ciVDS) and calcium dependent secrtion (CDS) in somata of primary sensory neurons

C. Wang[1,2], X. Zhang[1,2], X. Wu[1,2], Z. Chai[1,2], P. Hou[3], H. Liu[3], Y. Liu[3], T. Liu[1,2], Y. Wang[1,2], B. Liu[1,2], C. Zhang[1,2], W. Guo[1,2], S. Wang[1,2], X. Zhang[1,2], J. Ding[3] and Z. Zhou[1,2]

[1]Peking University, State Key Laboratory of Biomembrane and Membrane Biotechnology and the Center For Life Sciences, Beijing, China, [2]Peking University, Institute of Molecular Medicine, Beijing, China and [3]Huazhong University of Science and Technology, School of Life Sciences, Wuhan, China

The somata of primary sensory neurons, including dorsal root ganglion (DRG) neurons and mesencephalic trigeminal nucleus (MeV) neurons, release neurotransmitters and neuropeptides. In addition to the conventional Ca2+-dependent secretion (CDS), Ca2+-independent but voltage-dependent secretion (ciVDS) also occurs in the somata of isolated DRG neurons (Zhang et al., 2002; Liu et al., 2011) and brain slice MeV neurons (Zhang et al., 2011). Electrical stimulation induces both CDS and ciVDS, which differ in size and are coupled with different types of endocytosis contributed by ciVDS and CDS, respectively. However, it is unclear whether they use a common vesicle pool, so we investigated the relationship between the vesicle pools of CDS and ciVDS. DRG neurons were isolated from Wistar rats (male, ~ 60 g) treated with 0.6 ml/100 g 25% urethane. Membrane capacitance recording and photolysis of a caged-Ca2+ compound showed that, in low external Ca2+ solutions, the depolarization-induced exocytosis contained two (fast and slow) phases, which were contributed by ciVDS and CDS respectively. Depletion of the CDS readily-releasable pool using photolysis did not affect the ciVDS. When the ciVDS and CDS vesicle pools were depleted by electrical stimulation, the pools had different sizes. Their kinetics of exocytosis-coupled endocytosis were also different. Thus, ciVDS and CDS used different vesicle pools in somata of primary sensory neurons.

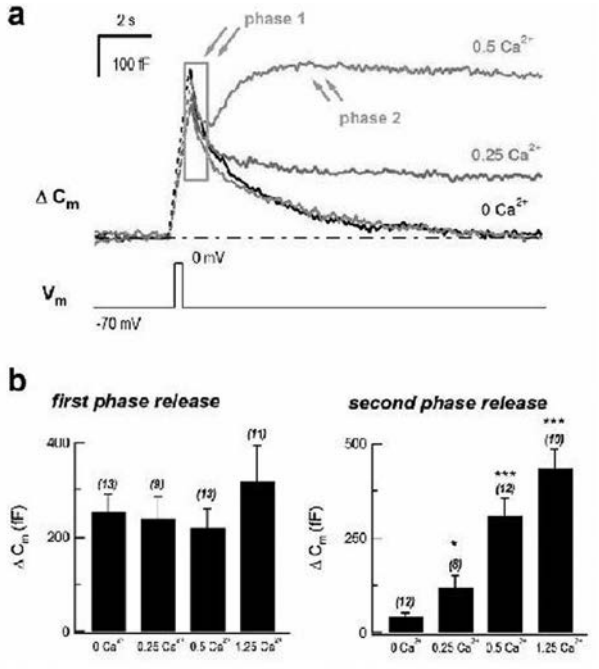

Figure 1. The first phase of exocytosis was CIVDS in low external Ca^{2+} solution. a, Representative traces of depolarization induced C_m response of a DRG neuron in different concentration of external Ca^{2+} solutions. The first phase (phase 1) was indicated in grey blank rectangle, the second phase was indicated by phase 2. **b,** Summary graph of peak of ΔC_m response of first phase and second phase in different external Ca^{2+} solutions. All data represent mean ± s.e.m. *t*-test, **P* <0.05, ****P* <0.001; NS, not significant.

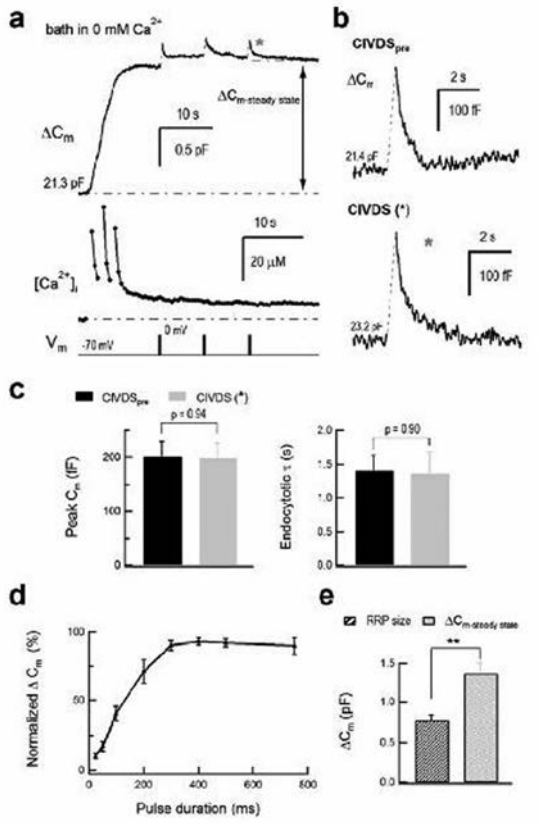

Figure 2. Depletion of CDS RRP didn't affect CIVDS. **a,** Representative traces of C_m recording and intracellular Ca^{2+} measurement in photolysis in 0 Ca^{2+} external solution. $\Delta C_{m\text{-steady state}}$ measures the peak C_m change as shown in the upper trace. **b,** A CIVDS marked as * in (a) (CIVDS(*))was used for comparison with CIVDS recorded before photolysis ($CIVDS_{pre}$) in a same cell. **c,** Peak C_m change and endocytotic time constant (τ) (n = 11) of CIVDS. **d,** Plot of ΔC_m against pulse duration (n = 8). **e,** Comparison of DRG neuron RRP size (ΔC_m induced by a single 400 ms depolarization) and photolysis induced $C_{m\text{-steady state}}$ as shown in (a) (RRP size: n = 8; $DC_{m\text{-steady state}}$, n = 9). All data represent mean ± s.e.m. *t*-test, $^{**}P < 0.01$; NS, not significant.

This study was supported by grants from NSFC, MOST and DOE 2011-program

Where applicable, the authors confirm that the experiments described here conform with The Physiological Society ethical requirements.

PCD166

Modelling mechanotransduction in primary sensory endings

T.J. Suslak[1,2], G.S. Bewick[3], J.D. Armstrong[1] and A.P. Jarman[2]

[1]Doctoral Training Centre in Neuroinformatics and Neural Computation, University of Edinburgh, Edinburgh, UK, [2]Centre for Integrative Physiology, University of Edinburgh, Edinburgh, UK and [3]Institute of Medical Sciences, University of Aberdeen, Aberdeen, UK

Mechanotransduction is a process fundamental to life. It underpins a variety of sensory modalities from hearing to blood pressure regulation. However, the molecular components of the mechanosensory mechanisms in primary sensory endings are poorly understood. Experimental approaches to solving this problem are long and laborious. Therefore, a theoretical approach was proposed as an efficient means to circumventing this process.

A mathematical, biophysical model of mechanosensory endings was implemented, which reproduced existing experimental data of the receptor potential of the mammalian muscle spindle primary ending. This probabilistic model combines mathematical representations of different ion channel types to produce an output which is the predicted receptor potential of the sensory ending, given the presence of specific ion channels. The model outputs the tension-dependent electrical response of the receptor, given a stretch stimulus. The parameters required for this model identify the necessary molecular entities required for this behaviour to occur.

The dbd (dorsal bipolar dendritic) neuron in D. melanogaster larvae fulfils a similar role to the muscle spindle in mammals. Electrophysiological data was obtained from these neurons via whole-cell patching. It was shown that the dbd neuron can respond to both electrical and mechanical stimuli, but that these responses are noticeably distinct. Furthermore the stretch-evoked data obtained from these receptors was equivalent to that predicted by the model, demonstrating a cross-taxa correlation between the behaviour of neurons in this class.

This finding enables simple genetic assays to be carried out in D. melanogaster to ascertain the identity of molecules which are involved in primary mechanotransduction at the sensory terminal. A simple bioinformatics search has yielded a shortlist of candidates which fulfil the criteria of the model predictions. These can now be experimentally tested in a simple and direct approach.

Suslak et al. (2011). Network, 22(1-4), 133-42.

Baines RA & Bate M (1998). J Neurosci, 18(12), 4673-83.

Hunt et al. (1978). J Gen Physiol, 71, 683-98.

This work was funded by the MRC and EPSRC, through the DTC at the University of Edinburgh

Where applicable, the authors confirm that the experiments described here conform with The Physiological Society ethical requirements.

PCD167

Role of the cerebellum in descending control of nociception

N. Weerasinghe, B.M. Lumb, R. Apps and J.C. Murrell

Physiology and Pharmacology, University of Bristol, Bristol, UK

The cerebellum is critically involved in motor control; however there is evidence to indicate that it also has a role in nociceptive processing. Previous studies suggest a dual role, whereby stimulation of the anterior lobe of the cerebellum invokes antinociception (1-3), and posterior lobe stimulation invokes pronociception (4,5). However, these data are difficult to interpret with respect to (i) somatic nociceptive pathways as they investigated visceral nociception and (ii) precise localisation of the origin of descending control as previous studies utilised electrical stimulation of the cerebellum, where current spread to neighbouring structures, activation of fibres of passage and antidromic activation are important confounds. The aim therefore of the present study was to investigate modulation of somatic nociception in rats following activation of the anterior (lobule V) and posterior (lobule VIII) lobes of the cerebellum using DL Homocysteic acid (DLH), an excitatory amino acid that allows cerebellar activation to be restricted to target neurons thereby overcoming some of the limitations of electrical stimulation. Rats were initially anaesthetised with

halothane (2-3% in 0_2) delivered by face mask and maintained with a continuous infusion of alfaxalone (25mg/kg/hour i.v). EMG was recorded from the biceps femoris while pinching the ipsilateral hindpaw. The change in mechanical withdrawal threshold (the force required to elicit an EMG response) and magnitude of EMG activity at threshold was assessed following injection of either DLH (0.1M) or an equivalent volume of saline into lobule VIII (n=8 and n=7 respectively), or lobule V (n=4 and n=5 respectively) of the cerebellar cortex. Values are mean ± SEM compared by paired t test. Pronociception was observed following lobule VIII stimulation, indicated by a statistically significant decrease on average of 23% in mechanical withdrawal threshold following DLH injection (from 56.5 ± 5.0 g/mm^2 to 43.2 ± 4.3 g/mm^2, P=0.0038). There was also a statistically significant facilitation on average of 63% in EMG activity (from 0.007 ± 0.002 v/s to 0.012 ± 0.002 v/s, P= 0.0077). In contrast, there was no statistically significant change in mechanical withdrawal threshold or EMG activity following DLH administration into lobule V or after injection of saline in either lobule VIII or V. These data indicate that stimulation of the anterior and posterior lobe of the cerebellum has a differential effect on nociceptive processing, which may be explained by activation of different cerebellar modules. However, recording EMG responses does not discriminate between effects due to modulation of sensory and/or motor components of the spinal pathways activated by the noxious stimulus. Further experiments will therefore investigate cerebellar modulation of sensory input by making recordings from dorsal horn neurons.

Siegel P, Wepsic JG. Alteration of nociception by stimulation of cerebellar structures in monkey. Physiology & Behavior. 1974 1974;13(2):189-94.

Dey PK, Ray AK. Anterior cerebellum as a site for morphine analgesia and post stimulation analgesia. Indian Journal of Physiology and Pharmacology. 1982 1982;26(1):3-12.

Hagains CE, Senapati AK, Huntington PJ, He J-W, Peng YB. Inhibition of spinal cord dorsal horn neuronal activity by electrical stimulation of the cerebellar cortex. Journal of Neurophysiology. 2011 Nov;106(5):2515-22.

Saab CY, Willis WD. The cerebellum: organization, functions and its role in nociception. Brain Research Reviews. 2003 Apr;42(1):85-95.

Saab CY, Willis WD. Cerebellar stimulation modulates the intensity of a visceral nociceptive reflex in the rat. Experimental Brain Research. 2002 Sep;146(1):117-21.

Funded by an MRC studentship.

Where applicable, the authors confirm that the experiments described here conform with The Physiological Society ethical requirements.

PCD168

Development of fluorescent and biotinylated agonists for a novel glutamate receptor in mechanosensory terminals

S. Watson[1], C. Zanato[1], S. Dall'Angello[1], R.W. Banks[2], I. Greig[1], M. Zanda[1] and G.S. Bewick[1]

[1]School of Medical Sciences, University of Aberdeen, Aberdeen, UK and [2]School of Biological & Biomedical Sciences, University of Durham, Durham, UK

Mechanotransduction by proprioceptive sensory organs, such as muscle spindles, is poorly understood. We recently reported that stretch releases glutamate from synaptic-like vesicles within spindle terminals, and activates a non-canonical mGluR (Bewick et al, 2005) coupled to phospholipase D (PLD), modulating afferent firing. In further investigations into this receptor's pharmacology, ligands selective for classical mGluRs were screened for their ability to alter stretch-evoked spindle firing. We now report on the development of a fluorescent and a biotinylated agonist. These agonists will be in the key in the next stages of the investigation, isolating the receptor using a pull-down/precipitation assays. Nerve-muscle preparations were excised from humanely killed (Schedule 1, ASPA, 1986) adult male Sprague-Dawley rats. Spindle discharges during 1mm stretch-and-hold cycles were compared with and without drug. Differences in mean firing frequencies were evaluated by two-way ANOVA with Bonferroni post test (sig. threshold P=0.05). Four compounds were found to increase afferent firing; kainate (1 μM, n = 7, P = 0.01) quisqualate (1 μM, n = 8, P = 0.05), t-ADA (1 μM, n = 9, P = 0.05) and L-CSA (0.1 μM, n = 7, P = 0.05). NBQX, a kainate and AMPA receptor antagonist, had no effect on afferent firing when applied alone (n= 4) or in combination with kainate (n = 7), adding further evidence that classical kainate or AMPA ionotropic receptors are not responsible for the increase in stretch-induced afferent firing with application of kainate. In addition PCCG-13 was able to attenuate the effect of kainate (n = 4) suggesting kainate is acting on the PLD-coupled mGluR. Kainate was used as the parent compound in the synthesis of click-chemistry amenable (Kolb et al, 2001) analogues; ZCZ49, ZCZ50 and ZCZ90. Only ZCZ90 retained activity in the system, increasing afferent firing at 1 μM (n = 7, P = 0.01). From this fluorescent (ZCZ172) and biotinylated (ZCZ180) versions were synthesised. Both retained activity, increasing afferent firing at 10 μM (n = 8, P = 0.001) and 1 μM (n = 8, P = 0.01) respectively. These data show kainate is a useful base ligand for the development of tools to isolate and further characterise this intriguing receptor.

Bewick, GS, Reid, B, Richardson, C & Banks, RW (2005). Autogenic modulation of mechanoreceptor excitability by glutamate release from synaptic-like vesicles: evidence from the rat muscle spindle primary sensory ending. The Journal of Physiology 562, 381-394.

Kolb, HC, Finn, MG & Sharpless, B (2001). Click Chemistry: Diverse Chemical Function from a Few Good Reactions. Angewandte Chemie International Edition 40, 2004 – 2021.

This work was funded by: SULSA, Eli Lilly, Roemex and KETF (University of Aberdeen)

Where applicable, the authors confirm that the experiments described here conform with The Physiological Society ethical requirements.

PCD169

Spinal mu and delta opiate receptors differentially modulate a-nociceptor processing in primary and secondary inflammatory hyperalgesia in rats

M. Hsieh, L.F. Donaldson and B.M. Lumb

School of Physiology and Pharmacology, University of Bristol, Bristol, UK

Delta and mu receptors (DOR & MOR) are differentially expressed by A- and C-nociceptors, and are hypothesised to differentially modulate mechanical and thermal nociceptive behaviours respectively[1]. A- and C-nociceptors can be preferentially activated by controlled contact heating[2], allowing identification of the nociceptor population driving nociceptive changes, with no confound of different stimulus modalities. Neurons in the superficial dorsal horn (dh) process C-nociceptor inputs from the area of primary hyperalgesia. This is hypoth-

esised to activate lamina I projection neurons, higher centres, and descending control pathways, which contribute to central sensitisation leading to enhanced responses of dh neurons to A-nociceptor input in secondary hyperalgesia. We hypothesised that sensitised responses to specific A- and/or C-nociceptor inputs, rather than to stimulus modalities (mechanical/thermal) are differentially controlled by MOR/DOR in inflammatory hyperalgesia.

1° & 2° inflammatory hyperalgesia were induced by injection of Freund's Complete Adjuvant into dorsal hindpaw and knee joint respectively under brief isofluorane anaesthesia (2-4% in O_2). After 7 days, animals were re-anaesthetised (halothane 2-4% in O_2, alfaxan maintenance (25.mg.kg^{-1} i.v.)) and DAMGO (MOR agonist 12 pmol/20μl) and SNC80 (DOR agonist 120 nmol/20μl) given intrathecally in inflamed or control animals. Withdrawal thresholds were determined in response to preferential activation of C- or A-nociceptors with contact heat stimulation, and to mechanical stimulation of the hindpaw.

MOR and DOR agonists both inhibited A- and C-nociceptor evoked-responses in all groups (control, 1° & 2° hyperalgesia). SNC80 had a significantly greater effect on A-nociceptor-withdrawal thresholds in 2° hyperalgesia compared to controls, and a significantly smaller effect on A-nociceptor-evoked responses on 1º hyperalgesia (control, 8.6±0.4°C.hr; 1°, 5.9±0.6°C.hr; 2°, 13.2±1.4°C.hr; AUC mean±SEM, p<0.01). DAMGO had equivalent effects on preferential A- and C-nociceptor thermal stimulation under all conditions, but significantly increased withdrawal thresholds in response to mechanical stimuli in 2º but not 1º hyperalgesia compared to controls (control, 11.6±4.5°C.hr; 2°, 35.9±9.6°C.hr; p < 0.05). SNC80 had a greater effect on mechanical stimuli than DAMGO in all animals (p<0.05), but effects were equivalent in hyperalgesic and control animals.

These results suggest that both MOR and DOR can modulate both unmyelinated and myelinated nociceptive inputs. DOR may have a greater contribution to the processing of A-nociceptor inputs in thermal 1° and 2° hyperalgesia than MOR, and MOR may be more important in modulation of responses to mechanical stimulation in 2° hyperalgesia.

Scherrer G et al. (2009). Cell 137, 1148-1159

Leith JL et al. (2007). J Neurosci 27, 11296-11305

Acknowledgements: Supported by the University of Bristol Centenary Fund (M-TH)

Where applicable, the authors confirm that the experiments described here conform with The Physiological Society ethical requirements.

PCD170

Sacral neuromodulation facilitates anal canal evoked potentials but not median nerve evoked potentials in the primary somatosensory cortex in a rat model

J. Evers[1], R.P. O'Connell[1,2] and J.F. Jones[1]

[1]School of Medicine and Medical Science, University College Dublin, Dublin, Ireland and [2]Centre for colorectal disease, St. Vincent's Hospital Dublin, Dublin, Ireland

Introduction

Faecal incontinence (FI) may follow pudendal nerve injury sustained during childbirth. Sacral neuromodulation (SNM) is a treatment option for FI, when conservative treatment has failed.

The mechanism of action of SNM is yet unclear. However SNM may augment anal sensation via afferent somatosensory fibres, as small sensory fibres are more susceptible to damage than the larger motor fibres. This study investigates, how fore paw, hind paw and anal canal evoked cortical potentials (EPs) are affected by SNM in an animal model.

Methods

Six female virgin Wistar rats (body mass: 230g–270g) were used. Experiments were carried out in accordance to protocols approved by the UCD Animal Ethics Research Committee and licenced by the Irish Department of Health and Children. Experiments were performed under urethane anaesthesia (1.5g.kg-1, i.p.) and vital signs were stable throughout. A craniotomy was performed over the right primary somatosensory cortex. A 32 channel multi-electrode array, placed extra-durally, recorded EPs created by electrical anal canal stimulation, left tibial nerve stimulation and left median nerve stimulation. SNM was performed utilizing a concentric needle electrode placed in the left first sacral foramen. Stimulation parameters were 10Hz, 15V and 1ms pulse duration for 3min. EPs before and 10 and 40min after SNM were compared for each location. Values are expressed as mean ± sem; the criterion for statistical significance was P<0.05.

Results

EPs consisted of one upward deflection and a small less marked downward deflection (Figure 1). Anal canal EPs had a latency of 11.5ms±0.73ms and amplitude of 18.8μV±3.56μV; tibial nerve EPs 9.0ms±0.42ms and 32.6μV±5.17μV; median nerve EPs 8.4ms±1.1ms and 21.5μV±3.79μV. SNM induced an increase in the maximal amplitude of 50% in anal canal and tibial nerve EPs, but not in median nerve EPs (Figure 2). A two-factor (location and time) repeated measures ANOVA showed that this result was highly significant (location factor: P<0.0001).

Conclusions

S1 neuromodulation causes facilitation of afferent fibre input of the same spinal segmental level but not higher segmental level. This study provides evidence that SNM selectively restores sacral inputs and may improve cortical awareness of the anorectum. The finding that a limb nerve input is also augmented may serve as a surrogate marker of the efficacy of SNM. This fact also suggests that percutaneous posterior tibial nerve stimulation, a novel treatment for FI, may share a similar mechanism to SNM.

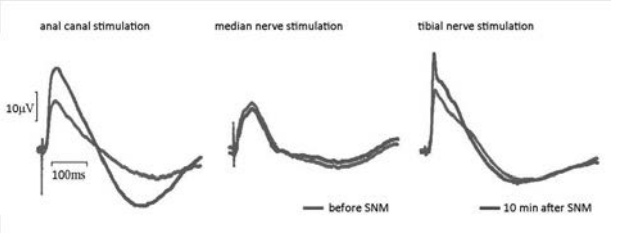

Figure 1 Mean triggered EPS of group data before and 10 min after SNM.

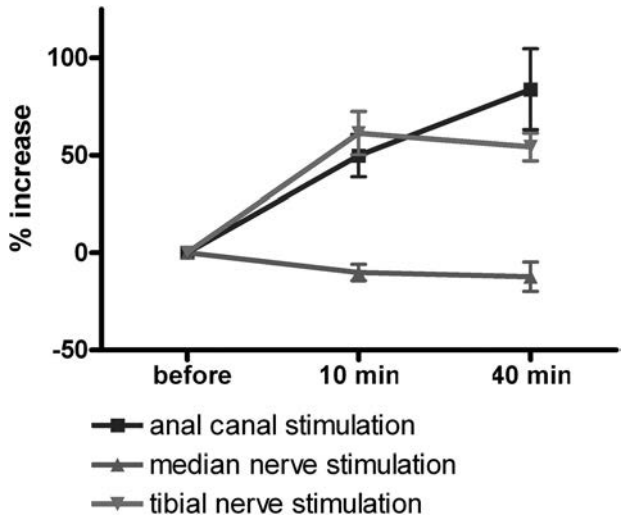

Figure 2 Percent increase of the maximal amplitude 10 and 40min after application of SNM.

The authors wish to acknowledge the support of Science Foundation Ireland.

Where applicable, the authors confirm that the experiments described here conform with The Physiological Society ethical requirements.

PCD171

EP3 receptor activation in the ventrolateral periaqueductal grey facilitates nociceptive spinal reflexes in the normal and arthritic rat

R. Drake, L. Leith, B. Lumb and D. Lucy

University of Bristol, Bristol, UK

Descending controls on spinal nociception, particularly descending facilitatory pathways from the midbrain periaqueductal grey (PAG), play major roles in the initiation and maintenance of chronic pain, and are important determinants of the pain experience. A better understanding of these systems may inform the development of more effective chronic pain treatments. Prostaglandin receptors EP1-4 in the ventrolateral periaqueductal grey (vlPAG)1 contribute to acute inflammatory pain and in nerve injury vlPAG EP1 receptors contribute to tonic descending facilitation in naïve and injured rats2.
Inflammatory arthritis was induced in male rats under brief isoflurane anaesthesia (2% in O2) by left knee intra-articular injection of Freund's complete adjuvant (100μl/1mg.ml-1). Naïve animals were used as controls. After 7 days, rats were re-anesthetised with halothane (3% in O2) and maintained on alfaxan infusion (i.v. 25mg.kg.h 1). Bipolar steel wire electrodes were placed in the bicep femoris of the left hind limb to record electromyographic activity, and a micropipette positioned stereotaxically in the left PAG. A and C nociceptors were preferentially activated by application of fast (7.5°C.s-1) or slow (2.5°C.s-1) rates of contact skin heating applied to the dorsal surface of the left hind-paw3 respectively. Withdrawal thresholds to A- and C-nociceptor stimulation (interstimulus interval 8 min) were determined before and after delivery of drug/vehicle into the PAG by pressure ejection.
There was a prolonged secondary (hindpaw) hyperalgesia 7 days after induction of inflammation, indicated by a reduction in A- but not C-nociceptor withdrawal thresholds (naïve vs. arthritic A-nociceptor thresholds: 57±1oC vs 54±1.2oC . p<0.0001 unpaired t test. n=16 naïve, 18 arthritic). In naïve animals EP3 receptor antagonism (GW671021B 250nM/200nl) in the vlPAG increased C- but not A-nociceptor evoked-reflexes. In contrast in secondary hyperalgesia, EP3 receptor antagonist increased A-nociceptor responses (AUC GW A-nociceptor effect vs AUC Vehicle A-nociceptor effect: 352.1±85.0oC.min vs 116.8±26.10oC.min. p<0.0357 Mann Whitney. n=5 for GW, n=3 for Vehicle.) with minimal effect on C-nociceptor reflexes. Inflammatory knee joint arthritis produces secondary hyperalgesia of the hind paw involving sensitisation of A- but not C-nociceptor-evoked spinal reflexes. Blockade of prostaglandin EP3 receptors in the vlPAG predominantly modulates A-nociceptor withdrawals in the hyperalgesic state but selectively alters C-nociceptor reflexes in the normal rat. In the transition to chronic inflammatory pain, descending EP3 receptor-mediated facilitation from vlPAG switches from C-nociceptor facilitation in naïve rats to A-nociceptor facilitation in inflammatory secondary hyperalgesia.

Oliva et al. Eur J Pharmacol. (2006) 530, 40.

Palazzo et al. Molecular Pain (2011) 7, 82

Leith et al. J Neurosci (2007) 27, 11296.

Where applicable, the authors confirm that the experiments described here conform with The Physiological Society ethical requirements.

PCD172

Mechanically elicited evoked potentials: A physiological approach to assessment of anorectal sensory pathways

E.V. Carrington[1,2], J. Evers[1], M.S. Scott[2], C.H. Knowles[3], R.P. O'Connell[1,4] and J.F. Jones[1]

[1]School of Medicine and Medical Science, University College Dublin, Dublin, Ireland, [2]GI Physiology Unit, The Wingate Institute of Neurogastroenterology, Queen Mary, University of London, London, UK, [3]National Centre for Bowel Research and Surgical Innovation, Queen Mary, University of London, London, UK and [4]Centre for Colorectal Disease, St. Vincent's Hospital Dublin, Dublin, Ireland

Introduction
Normal defaecation is dependent upon activation of anorectal mechanoreceptors, which respond to pressure and stretch. Evoked potentials (EPs) have been used to interrogate these pathways but are typically recorded in response to non-physiological electrical stimuli, known to directly depolarise nerve fibres without receptor activation. However, the use of a mechanical stimulus should provide a more physiological assessment of these pathways. This study compared EPs elicited via mechanical and electrical stimulation of the rat anal canal.
Methods
In fourteen anaesthetised (urethane i.p., 1g/kg) female Wistar rats (body mass 180 - 270g) mechanical and electrical EPs were recorded using a 32 channel multi-electrode array placed over the right primary somatosensory cortex. Stimulations for electrically elicited EPs were applied with a 2mm anal plug electrode (1Hz, 1ms, 10V) and mechanical stimuli via an interdental brush placed on a rotating stepper motor (1Hz, 1ms, 15o rotation). Response latency, response amplitude and activated spatial extent (expressed as an index) were evaluated. A P value of <0.05 was considered to be statistically significant.
Results
Mechanical and electrical EPs were recorded successfully in all animals. Mean maximal response amplitude (electrical 25.9μV (SD 22.2) vs. mechanical 19.3 μV (12.6)) and onset latency

(electrical: 13.8ms (2.6) vs. mechanical: 14.2 ms (2.2)) were similar (Student's t-test P = 0.25 and P = 0.62). Cortical location and waveform profile were also similar. An activated spatial extent index was significantly lower for mechanical stimulation (2.1 (1.4) vs. (4.5 (2.4), Mann-Whitney U-test P = 0.0015). Figure 1 illustrates this in one animal as a colour map encoding the maximal amplitude for each channel.

Conclusions

To the authors' knowledge these are the first mechanically elicited anal EPs recorded in animals. Cortical responses to mechanical stimulation appear to be more focal, a finding which may reflect more selective activation of ascending sensory pathways. Mechanical EPs may prove useful in the further exploration of treatments that modulate the neuronal control of defaecation such as sacral nerve stimulation.

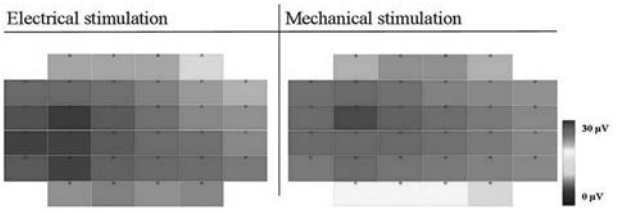

Figure 1 Representative colour maps encoding the maximal amplitude in each channel for electrical and mechanical anal canal stimulation.

The authors wish to acknowledge the generous support of the Bowel Disease Research Foundation (UK) and Science Foundation Ireland.

Where applicable, the authors confirm that the experiments described here conform with The Physiological Society ethical requirements.

PCD173

The descending noradrenergic system spatially restricts and temporally delays the onset of A-fibre mediated heat hypersensitivity in a model of neuropathic pain

S. Hughes, T. Pickering and B. Lumb

University of Bristol, Bristol, UK

Previous work from our laboratory has studied the functional roles of distinct types of nociceptors in acute pain processing [1, 2]. We have demonstrated that descending control can differentially modulate A- vs C-fibre evoked responses and we have shown that thermal nociception is under tonic regulation by descending noradrenergic control [3]. However, the different roles these nociceptors have in the development of heat hyperalgesia during chronic pain states and the changes descending control are poorly understood. Here we have investigated the descending noradrenergic control of A- and C-heat nociceptor evoked responses during the development of neuropathic hyperalgesia. Wistar rats (300-350g) had tibial nerve transection (TNT) under ketamine (50mg/kg) and medetomidine (300μg/kg) recovery anaesthesia [4]. Subsequently heat ramp withdrawal experiments were performed at day 3-5 or day 19-21 post-TNT under alphaxalone (9 - 15mg.kg-1.h-1 i.v.) anaesthesia. Fast (7.5°C/s) or slow (2.5°C/s) rates of skin heating were applied to the dorsal hindpaw to preferentially activate A- or C-heat nociceptors, respectively. EMG withdrawal response thresholds were recorded from the biceps femoris. A 32 gauge intrathecal catheter was inserted at the L5-L6 interspace for administration of yohimbine (α2-AR antagonist, 30μg) or clonidine (α2-AR agonist, 15μg). Changes in dopamine-beta-hydroxyalse (DBH) immunoreactivity were analysed at days 19-21. Data are expressed as mean withdrawal thresholds ± SEM or %DBH immunoreactivity analysed using either t-test or one-way ANOVA with Bonferroni's post tests. Following TNT animals showed substantial A- but not C-fibre evoked ipsilateral hyperalgesia by day 21 (TNT: A-fibre: day 3 55.2±0.7°C vs day 21 47.8±0.9°C P<0.001 n=5) when compared to sham. Intrathecal yohimbine revealed sensitivity of A- but not C-fibre evoked responses at day 3 (control 55.2±0.7°C vs 51.6±0.6°C post yohimbine P<0.001 n=4). Once hyperalgesia had developed (by day 19) yohimbine had no further sensitising effect on A-fibre responses however intrathecal clonidine increased A-fibre thresholds to beyond cut off (>58°C, P<0.01, n=3). Yohimbine was without effect in sham animals (n=3). Interestingly, yohimbine revealed contralateral heat hypersensitivity mediated by A- but not C-fibres at days 19-21 (A-fibre: 54.6±0.8°C to 49.0±0.8°C P<0.01, n=5). By days 19-21 there was a loss of DBH-ir in the ipsilateral L4-L6 spinal cord when compared to sham (n=3).These data demonstrate that descending pontospinal noradrenergic tone preferentially modulates, both temporally and spatially, the development of fast, prickling, heat hypersensitivity mediated by A-fibres following a loss of descending noradrenergic innervation to the lumbar region.

McMullan, S. and B.M. Lumb Pain, 2006. 124(1-2): p. 59-68.

Leith, J.L., et al., J Neurosci, 2007. 27(42): p. 11296-305.

Howorth, P.W., et al.. J Neurosci, 2009. 29(41): p. 12855-64.

Lee, B.H., et al. Neuroreport, 2000. 11(4): p. 657-61.

Research funded by the Medical Research Council and Wellcome Trust

Where applicable, the authors confirm that the experiments described here conform with The Physiological Society ethical requirements.

PCD174

Whisker photostimulation evokes barrel cortical response of ChR2 transgenic rat

T. Honjoh[1], A. Sumiyoshi[2], Y. Yokoyama[1], Z. Ji[1], T. Ishizuka[1], R. Kawashima[2] and H. Yawo[1]

[1]Graduate School of Life Sciences, Tohoku University, Sendai-shi, Japan and [2]Institute of Development, Aging and Cancer, Tohoku University, Sendai-shi, Japan

In one of thy1.2-channelrhodopsin 2 (ChR2)-Venus transgenic rat lines, W-TChR2V4, the ChR2 was expressed in the mechanoreceptive subpopulation of trigeminal ganglion neurons which innervate whisker follicles. It is thus well expected that a whisker-related sensory perception should be induced by the photostimulation of their follicles.

To test this, the barrel cortex responses were examined using electrophysiological recordings and functional magnetic resonance imaging (fMRI). Under anesthesia with urethane (1.3g/kg i.p.), the whiskers were trimmed and connected with optic fibers of which other endings were connected to LEDs. Pulsative irradiation of blue LED light was used as a test and that of red LED light as control.

We found that the blue light irradiation of whisker follicles evoked enhanced unit activities as well as a local field potential in the barrel field of contralateral somatosensory cortex whereas the red light did not. The blue light irradiation also induced blood oxygenation level-dependent (BOLD) and cerebral blood volume (CBV) responses in the barrel field of con-

tralateral somatosensory cortex. It is suggested that the optogenetic whisker stimulation could activate the whisker-barrel cortical pathway of mechanoreceptive signaling. This method would facilitate to study how the spatio-temporal pattern of the whisker mechanoreception would be integrated in the cortex.
All animal procedures were conducted in accordance with the guiding principles of Physiological Society of Japan and NIH.

Where applicable, the authors confirm that the experiments described here conform with The Physiological Society ethical requirements.

PCD175

Effect of tetrahydrobiopterin deficiency on hyperoxia-induced vascular damage in the retina

K.S. Edgar[1], N. Matesanz[1], T.A. Gardiner[1], Z.S. Katusic[2] and D.M. McDonald[1]

[1]Centre for Vision & Vascular Science, Queen's University Belfast, Belfast, N. Ireland, UK and [2]Anesthesiology and Molecular Pharmacology and Experimental Therapeutics, Mayo Clinic, Rochester, MN, USA

Purpose: Neovascularisation is a serious complication of several retinal diseases including diabetic retinopathy and retinopathy of prematurity. In these diseases an oxidative insult damages the endothelium leading to vascular closure, tissue ischaemia and the eventual abnormal neovascular response that characterizes these diseases. Endothelial nitric oxide synthase (eNOS)-derived nitric oxide (NO) plays an important role in maintaining vascular integrity, normal eNOS function, however is dependent upon the cofactor tetrahydrobiopterin (BH4) whose deficiency plays a pivotal role in the reduced NO bioavailability observed in diabetic vascular disease. We have previously shown that eNOS is dysfunctional in hyperoxia-induced vascular damage in a model of oxygen induced retinopathy (OIR). Thus, here our aim was to investigate the effect of hyperoxia-induced vascular closure in BH4 deficient mice (hph-1).
Methods: BH4 levels in retinas, aortas and lung samples were analyzed by HPLC analysis. Normal vascular development was confirmed by lectin staining of retinas from postnatal day 7 (P7) animals. For OIR, animals were exposed to 75% oxygen for 5 days from P7 to P12 and returned to room air. Eyes were collected at various time points between P12 and P17 and vascular preservation and ischaemia-induced growth quantified by B simplicifolia isolectin staining of retinal flat mounts. Avascular, normal vascular and neovascular areas were quantified using image analysis software. NO production was quantified by NOS activity assay in the presence and absence of BH4. In situ superoxide and peroxynitrite were quantified by DHE, DCF and nitrotyrosine immunoreactivity.
Results: BH4 levels in hph-1 retinal samples were significantly lower than wild-type litter mate controls and comparable to levels observed in aorta and lung samples. All BH4 levels were further reduced following in vivo hyperoxia treatment. Surprisingly, despite evidence of reduced retinal BH4 levels, hph-1 animals were partially protected from hyperoxia-induced damage which correlated with reduced reactive oxygen and nitrogen species production. In contrast, in response to ischaemia hph-1 animals displayed a significantly reduced neovascular response.
Conclusions: Our results show that BH4 deficient hph-1 animals are protected from hyperoxia-induced vasodegeneration. However, the attenuated angiogenic drive observed in these animals suggests a reduced ability to respond to ischaemic insult.

Where applicable, the authors confirm that the experiments described here conform with The Physiological Society ethical requirements.

PCD177

Hypothalamic Gαi2 proteins: A central molecular mechanism that counters the development of salt-sensitive hypertension

R.D. Wainford and J.T. Kuwabara

Pharmacology & Experimental Therapeutics, Boston University, Boston, MA, USA

Aim: We have demonstrated up-regulation of hypothalamic paraventricular nucleus (PVN) Gαi2-proteins is required to suppress norepinephrine (NE) mediated sodium retention during high salt intake in the Sprague-Dawley rat (1, 2). In these studies we examined the role(s) of PVN Gαi2 proteins in the pathophysiology of salt-sensitive hypertension in Brown Norway (BN), Dahl salt-resistant (DSR), Dahl salt-sensitive (DSS) and congenic DSSBN8 (3) rat strains.
Methods: BN, DSR, DSS or DSSBN8 rats were maintained on a normal (NS-0.4% NaCl) or high (HS-8% NaCl) diet for 21-days. Additional groups of intact and bilateral renal denervated (RDNX) DSR and DSS rats received a 21-day i.c.v. infusion of a scrambled (S) or a Gαi2 targeted oligodeoxynucleotide during high salt-intake. MAP was continuously recorded by radiotelemetry. 24h sodium balance, plasma NE, Fractional excretion of sodium (FENa) and PVN Gαi2 protein levels were determined after 21-days on a NS or HS diet (N=8/group ± SEM).
Results: HS-intake did not alter MAP, increased FENa and suppressed plasma NE in BN, DSR and S infused DSR rats (Δplasma NE [nmol/L]; BN -32±4, DSR -35±3, DSR S -33±5, $P<0.05$). HS-diet evoked a site-specific increase in PVN Gαi2 protein levels in salt-resistant BN, DSR and S infused DSR rats (4.8, 4.2 and 3.9-fold respectively, $P<0.05$) but not in hypertensive DSS rats. Oligodeoxynucleotide-mediated CNS Gαi2 protein down-regulation evoked hypertension (MAP [mmHg]; DSR S HS 98±4 vs. DSR Gαi2 HS 124±3, $P<0.05$), sodium retention and elevated plasma NE content (plasma NE [nmol/L]; DSR S HS 75±8 vs. DSR Gαi2 HS 108±7, $P<0.05$) in DSR rats and profoundly exacerbated DSS hypertension (MAP [mmHg]; DSS S HS 155±5 vs. DSR Gαi2 HS 178±5, $P<0.05$). RDNX prevented the development of hypertension (MAP [mmHg]; DSR Sham RDNX HS Gαi2 128±4 vs DSR RDNX HS Gαi2 97±4, $P<0.05$), sodium retention and sympathoexcitation in DSR rats and prevented the exacerbation of DSS hypertension. BN chromosome 8 substitution restored salt-induced PVN specific Gαi2 protein up-regulation (3.6-fold, $P<0.05$), attenuated the development of salt-sensitive hypertension (MAP [mmHg]; DSS HS 159±4 vs. DSSBN8 HS 138±3, $P<0.05$) and global sympathoexcitation (plasma NE [nmol/L]; DSS HS 98±6 vs. DSSBN8 HS 65±6, $P<0.05$) in DSSBN8 vs. DSS rats.
Conclusion: Up-regulation of PVN Gαi2 protein-gated pathways represents a conserved central molecular mechanism that suppresses renal nerve-dependent NE mediated sodium reabsorption to maintain a salt-resistant phenotype. We speculate PVN Gαi2 protein-gated regulation of NE secretion influences renal NCC expression (4) to maintain salt-resistance. SNP's in the GNAI2 gene correlate with human hypertension (5) suggesting the translational potential of our mechanistic studies.

Kapusta et al. (2013). Hypertension 61, 368-375.

Kapusta et al. (2012). FASEB J 26, 2776-2787.

Mattson et al. (2008). Am J Physiol 293, F837-842.

Mu et al. (2011). Nat Med 17 573-580.

Menzaghi et al. (2006). J Am Soc Nephrol 17 S115-119.

R01HL107730

Where applicable, the authors confirm that the experiments described here conform with The Physiological Society ethical requirements.

PCD178

Water and sodium intake by hyperosmotic rats treated with moxonidine into the lateral parabrachial nucleus depends on the activation of central cholinergic mechanisms

C.F. Roncari, R.B. David, P.M. De Paula, D.S. Colombari, L.A. De Luca Jr., E. Colombari and J.V. Menani

Department of Physiology and Pathology, Dentistry School, UNESP, Araraquara, Sao Paulo, Brazil

Recently it was demonstrated that plasma hyperosmolarity, a classic dipsogenic stimulus, can also facilitate sodium intake if inhibitory mechanisms are deactivated by the injections of moxonidine (α_2-adrenoceptor/imidazoline receptor agonist) into the lateral parabrachial nucleus (LPBN). It has also been suggested that water intake induced by plasma hyperosmolarity depends on the activation of central cholinergic mechanisms. Therefore, in the present study, we investigated whether central cholinergic mechanisms are important for water and sodium intake by hyperosmotic rats treated with moxonidine into the LPBN. Male Holtzman rats (290-310 g, n = 9) were anesthetized with ketamine (80 mg/kg of body weight) and xylazine (7 mg/kg of body weight) subcutaneously and stainless steel guide-cannulas were implanted into the lateral ventricle (LV) and bilaterally into the LPBN. Five days after the brain surgery, the animals received an intragastric load of 2 M NaCl (2 ml) and an injection of saline or atropine (muscarinic antagonist; 20 nmol/1 μl) in the LV. Forty-five minutes later, the animals received bilateral injections of vehicle or moxonidine (0.5 nmol/0.2 μl) into the LPBN. Water and 0.3 M NaCl intake was measured for 2 h starting 15 min after LPBN injections. Results are reported as mean ± SEM. Two-way ANOVA using treatments and times as factors followed by Newman–Keuls tests was used for comparisons. Bilateral injections of moxonidine into the LPBN of hyperosmotic rats that received saline in the LV significantly increased water (13.0 ± 4.4 ml/2 h, vs. vehicle: 6.9 ± 1.0 ml/2 h, $p < 0.05$) and 0.3 M NaCl intake (18.6 ± 5.2 ml/2 h, vs. vehicle: 0.2 ± 0.1 ml/2 h, $p < 0.05$). The pre-treatment with atropine into the LV abolished water (0.7 ± 0.3 ml/2 h, $p < 0.05$) and 0.3 M NaCl intake (1.3 ± 0.4 ml/2 h, $p < 0.05$) induced by hyperosmolarity combined with moxonidine injected into the LPBN. The results suggest the involvement of central cholinergic muscarinic mechanisms on water and sodium intake by hyperosmotic rats treated with moxonidine injected into the LPBN.

Financial Support: FAPESP, CNPq.

Where applicable, the authors confirm that the experiments described here conform with The Physiological Society ethical requirements.

PCD179

The combined administration of natriuretic peptides (ANP and CNP) in the lateral ventricle modulates the fluid intake in response to sodium depletion and water deprivation

L. Margatho, B. Fortes de Morais, L. Elias and J. Antunes-Rodrigues

School of Medicine of Ribeirao Preto-USP, Ribeirao Preto, Brazil

The physiological actions of the natriuretic peptides are first modulated by interactions with their receptors. The NPR-A receptor recognizes the atrial natriuretic peptide (ANP) and the NPR-B receptor shows specificity for the natriuretic peptide type-C (CNP). In this study we investigated the effects of combined injections of ANP or CNP in the lateral ventricle (LV) on water and 0.3M NaCl intake in rats submitted to 24 h of sodium depletion or water deprivation. Methods and Results: Male Wistar rats (250–300 g, n = 5-8) with sham or stainless steel cannulas implanted into the lateral ventricle (AP= 0.8 mm caudal to bregma; L=1.2 mm lateral to midline and V=4 mm bellow dura mater) were used. All surgical procedures were performed under ketamine (80 mg/kg of body weight) combined with xylazine (7 mg/kg of body weight) anesthesia. Water and 0.3 M NaCl intake was induced by water deprivation (the rats had water bottles removed from the cages with free access to food for 24 h) or sodium depletion [the rats received a subcutaneous injection of the diuretic Furosemide (20 mg/kg,0.2 ml/kg) followed by access to sodium deficient diet and water for 24 h]. ANP (1 μg/5 μl) or CNP (1 μg/5 μl) were injected consecutively in the LV with a range interval of 10 min. Sham rats received only vehicle in the LV. At the end of the injections, two glass burettes with 0.1 ml divisions containing 0.3 M NaCl or water were offered to rats and the intake was measured every 15 min for 1h. Values are means ± S.E.M., compared by ANOVA. Results: Lateral ventricle injection of ANP plus CNP reduced 0.3 M NaCl intake in response to water deprivation (1.4 ± 0.4 ml vs. sham: 5.3 ± 1.5 ml, p = 0,01) and sodium depletion (3.2 ± 1.2 ml vs. sham: 8.0 ± 2.5 ml, $p < 0,05$) without changes on water intake. Also, CNP plus ANP reduced 0.3 M NaCl intake (1.8 ± 0.5 ml) only in response to water deprivation. There were no changes on sodium intake in rats previously treated with CNP plus ANP in the LV and subjected to sodium depletion. This last result shows that the previous injection of CNP was able to inhibit the inhibitory effect of ANP on sodium intake. A decrease in water intake was observed when CNP plus ANP were administered into the LV in response to water deprivation (3.7 ± 1.4 ml vs. sham: 16.8 ± 4.5 ml, $p < 0,05$) and sodium depletion (0.5 ± 0.2 ml vs. sham: 1.6 ± 0.5 ml, $p < 0,05$). Conclusion: In rats subjected to intra- or extracellular thirst, the results are pioneers in demonstrating an inhibitory modulation of the ANPergic pathway on the CNPergic path in rats previously treated with ANP plus CNP in the LV reducing sodium appetite; as well as the previous injection of CNP plus ANP reducing water intake.

The authors thank Maria Valci Silva for her excellent technical assistance.

Financial Support: FAPESP (2011/08572-8 and 2010/50917-0)

Where applicable, the authors confirm that the experiments described here conform with The Physiological Society ethical requirements.

PCD180

Adrenomedullin-induced modulation of calcium channels in osteoblasts

T. Endoh[1], H. Kobayashi[2], M. Tazaki[1] and K. Sueishi[2]

[1]Dept of Physiol, Tokyo Dental College, Chiba, Japan and [2]Dept of Orthodont, Tokyo Dental College, Chiba, Japan

Adrenomedullin (ADM) is a 52-amino-acid peptide originally isolated from a human pheochromocytoma. It is structurally and functionally related to calcitonin gene-related peptide (CGRP) and belongs to the amylin peptide family. Voltage-dependent calcium channels (VDCCs) serve as crucial mediators of membrane excitability and many calcium-dependent functions such as growth of bone, regulation of proliferation, enzyme activity and gene expression. The purpose of this study was to investigate the effects of ADM on VDCCs currents in osteoblasts using a patch-clamp recording method. Murine osteoblastic MC3T3-E1 cells were cultured at 37 C in a 5%(v/v) CO2 atmosphere with alfa-modified minimal essential medium. Fabricated recording pipettes (2-3 M ohm) were filled with the internal solution of the following composition (in mM): 150 CsCl, 5 EGTA, 10 D-glucose, and 10 HEPES. The pH was adjusted to 7.3 with CsOH. Extracellular solution was a solution containing the following (in mM): 115 BaCl2 and 20 HEPES. The pH was adjusted to 7.4 with TEA-OH. Application of 1 micro M ADM rapidly and reversibly facilitated barium current from minus 49 pA to minus 127 pA (159% facilitation). Application of 0.1 micro M ADM rapidly and reversibly facilitated barium current from minus 78 pA to minus 93 pA (19% facilitation).

Where applicable, the authors confirm that the experiments described here conform with The Physiological Society ethical requirements.

PCD181

Apical KCNN4c channel regulated by Epac1 signaling affect epithelial Cl- secretion in diarrhea

I.A. Sheikh[1], R. Sinah[2], D. Nag[2], H. Koley[2], M.K. Chakraborty[1] and M.H. Kazi[1]

[1]Pathophysiology, National Institute of Cholera & Enteric Diseases, Kolkata, West Bengal, India and [2]Microbiology, National Institute of Cholera & Enteric Diseases, Kolkata, India

KCNN4 (IK) is a calcium activated potassium (K) channel. However, its role in diarrhea and regulation by Epac1 in cAMP stimulation is unknown. By RT-PCR and Western blot, we dentified KCNN4 expression in mouse intestine and human intestinal cell line. We hypothesized that apical KCNN4 was involved in diarrhea and regulated by Epac1 associated signaling. Depletion of Epac1 protein and apical addition of TRAM-34, a specific KCNN4 inhibitor significantly abolished cAMP stimulated Cl secretion and apical K conductance IK(ap) in T84 cells. We studied the current-voltage relationships in basolaterally permeabilized monolayers treated with 8-pCPT-2'-O-Me-cAMP in a symmetric K ion concentration. The presence of an inwardly rectified, Ca-activated K channel was evident in T84WT cells, whereas 8-pCPT-2'-O-Me-cAMP was not able to activate this inwardly rectified current in Epac1 knock down (Epac1KDT84) cells. Furthermore, addition of KCNN4 channel specific activator, 1-EBIO to intact wild type (T84WT) cells resulted 44±5 μA/cm2 rise in Isc while in Epac1KDT84 cells and T84WT + TRAM 34, 1-EBIO enhanced Isc was only 5±1 μA/cm2 and 4 ± 3 μA/cm2 respectively. Reconstructed confocal image in the X-Z plane of T84Epac1KD monolayers revealed redistribution of KCNN4c proteins into sub-apical intracellular compartment. We compared the surface amount of KCNN4c in these cells that Epac1 depleted cells have ~83% lower surface membrane expression of KCNN4c compared with T84WT cells. The role of Epac1-Rap1 signaling in endogenous regulation of KCNN4 was further assessed in T84 cells by Rap1 activation assays. FSK and 8-pCPT-2'-O-Me-cAMP induced GTP-loading of Rap1 in T84WT cells. To better understand the specific involvement of Rho-A and Rho-associated kinase ROCK in KCNN4 regulation in intestinal Cl secretion, Isc and IK(ap) was measured in T84WT cells. Finding that both Rho-A and ROCK kinase inhibitors significantly reduced FSK stimulated Isc as well as IK(ap). To explore the therapeutic potential of Epac1 regulated signaling of KCNN4c channels, we tested the effect of Rap1a inhibitor GGTI-298, ROCK inhibitor H1152 or KCNN4c inhibitor TRAM-34, in a closed loop mouse model. Our result demonstrated Epac1-Rap1-Rho-A-ROCK signaling lead to the alleviation of diarrhea by recruiting KCNN4c to the apical membrane which has important therapeutic value in diarrhea

1.Hoque, K. M., Woodward, O. M., van Rossum, D. B., Zachos, N. C., Chen, L., Leung, G. P., Guggino, W. B., Guggino, S. E., and Tse, C. M. (2010) J. Gen. Physiol. 135, 43–58.

2.Warth R, Barhanin J. (2003) J Membr Biol. 193(2):67-78

3.Cook DI, Young JA. (1989)J Membr Biol. 110(2):139-46.

4.Sandle GI, Rajendran VM. (2012) Am J Physiol Cell Physiol. 303(3):C328-33.

5.Basalingappa KM, Rajendran VM, Wonderlin WF. (2011) Am J Physiol Gastrointest Liver Physiol. 301(5):G905-11. Epub 2011 Aug 25.

This work was supported by the Government of India, Ministry of Science & Technology, Department of Biotechnology grant (BT/HRD/35/02/07/2009) to KM Hoque, Scientist & Ramalingaswami Fellow. IA Sheikh is a recipient of Indian Council of Medical Research (ICMR) Junior Research Fellowship. We gratefully acknowledge the help and research facilities provided to us by the Dept. of Molecular Pathophysiology, NICED, Kolkata, India.

Where applicable, the authors confirm that the experiments described here conform with The Physiological Society ethical requirements.

PCD182

Interleukin-1β reduces K^+ channel activity through phosphorylation processes mediated by protein kinase C in human kidney proximal tubule cells

K. Nakamura, Y. Komagiri and M. Kubokawa

Department of Physiology, School of Medicine, Iwate Medical University, Yahaba, Iwate, Japan

It is well known that proinflammatory cytokines, such as interleukin-1β (IL-1β), interferon-γ (IFN-γ), tumor necrosis factor-α, induce cell injury in various organs, including kidney. Some investigators reported that changes in K^+ channel activity contributed to the renal tubular cell injury during ischemia or endotoxemia (1, 2). Thus, it is possible that the proinflammatory cytokines may cause cell injury partly by modulating K^+ channel activity in the kidney. However, little information was available regarding the effects of cytokines on activity of renal K^+ channels. In cultured human kidney proximal tubule cells purchased from Lonza (Walkersville, MD, USA) which isolated these cells under informed consent, an inwardly rectifying K^+ chan-

nel with an inward conductance of 40 pS was most frequently observed under the control condition (3). We have reported that IFN-γ possessed an acute stimulatory effect and a delayed suppressive effect on activity of this 40 pS K^+ channel (4). In this study, we investigated the effect of IL-1β on activity of the 40 pS K^+ channel in cultured human proximal tubule cells, using the patch-clamp technique and Fura-2 Ca^{2+} imaging. Values are means±S.E.M., compared by ANOVA. In cell-attached patches, IL-1β (15 pg/ml) significantly reduced channel activity to 33±9 % of the control (n=10, p<0.01) in a few minutes. This acute suppressive effect was blocked by an IL-1 receptor antagonist (IL-1ra, 20 ng/ml), suggesting that the effect of IL-1β was mediated by its specific receptor. An inhibitor of protein kinase C (PKC), GF109203X (500 nM), also blocked the acute suppressive effect of IL-1β. In inside-out patches, effects of phorbol 12-myristate 13-acetate (PMA) and PKC were examined in the presence of ATP (1 mM) and Ca^{2+} (1 μM). While PMA (500 nM) alone had no appreciable effect, the subsequent addition of PKC (1 U/ml) reduced channel activity to 21±6 % of the control (n=6, p<0.01). Since it has been reported that phospholipase C (PLC) plays important role in activation of PKC by providing diacyl glycerol and inositol 1,4,5-triphosphate which in turn causes Ca^{2+} release from the intracellular store (5), we next examined the effect of a PLC inhibitor, neomycin, on the acute suppressive effect of IL-1β in cell-attached patches. Neomycin (300 μM) completely blocked the suppressive effect of IL-1β. Finally, we examined whether IL-1β would actually increase intracellular Ca^{2+} concentration ($[Ca^{2+}]_i$). The Fura-2 Ca^{2+} imaging revealed that IL-1β transiently caused a 1.5±0.2-fold increase in $[Ca^{2+}]_i$ (n=9, p<0.01). In accordance with the patch-clamp experiments, this increase in $[Ca^{2+}]_i$ was blocked by IL-1ra or neomycin. These results suggested that the acute suppressive effect of IL-1β on activity of the 40 pS K^+ channel in cultured human kidney proximal tubule cells would be dependent, at least in part, on the PKC-mediated phosphorylation processes.

Engbersen R *et al.* (2000). *Br J Pharmacol* **130**, 1678–168

Zager RA *et al.* (2006). *Am J Physiol Renal Physiol* **290**, F1453-F1462

Nakamura K *et al.* (2002). *Am J Physiol Renal Physiol* **283**, F784-F791

Nakamura K *et al.* (2009). *Am J Physiol Renal Physiol* **296**, F46-F53

Berridge MJ *et al.* (1984). *Biochem J* **220**, 345-360

Where applicable, the authors confirm that the experiments described here conform with The Physiological Society ethical requirements.

PCD183

Determination of the oligomeric assembly and intramolecular distances in the TRPV1 ion channel via FRET measurements

L.D. Islas, V. De la Rosa and G. Rangel

Physiology, UNAM, School of Medicine, Mexico City, DF, Mexico

The TRPV1 channel is an important molecular detectors of irritating compounds, elevated temperatures and other stimuli such as extracellular pH and divalent cations. Since these channels are regulated by several other compounds involved in signaling pathways related to pain and inflammation, their study has relevance in the clinical field. In spite of their obvious physiological importance, relatively little is known of their structure and molecular organization. TRP channels have so far been refractory to traditional structural analyses, such as X-ray protein crystallography and NMR. Among the structural approaches to date, there exists a low resolution structure determined by cryo-electron microscopy (Moiseenkova-Bell et al., 2008) and at least to molecular homology models based on the available structures from Kv channels.

As an alternative approach, we have undertaken determinations of the oligomeric state and inter and intra subunit distances of the TRPV1 ion channel, using FRET (Fluorescence Resonance Energy Transfer) measurements.

We have constructed several fluorescently-tagged channels using the pair of fluorescent proteins(FPs) eCFP/eYFP, were the fluorescent proteins have being inserted in the N- and/or C- termini of the protein. By means of co-expressing different combinations of these constructs in HEK 293 cells, we measured apparent FRET efficiencies using a spectral-FRET method (Zheng et al. 2002). We were able to determine that the most likely number of subunits in the functional TRPV1 channel is four. The distances between FPs at the C- termini are shorter than the distances between N- termini. This suggest that the N- termini are located in the periffery of the C-termini. We have also used FRET between a non-fluorescent membrane probe and the YFP constructs to determine the distance between the C and N termini and the plane of the membrane.

These experiments provide us with a glimpse of the possible gross molecular architecture and organization of the TRPV1 channel. The distances are consistent with both N and C termini being intracellular and forming a large mas of the channel. Some of our measurements are summarized in the figure below.

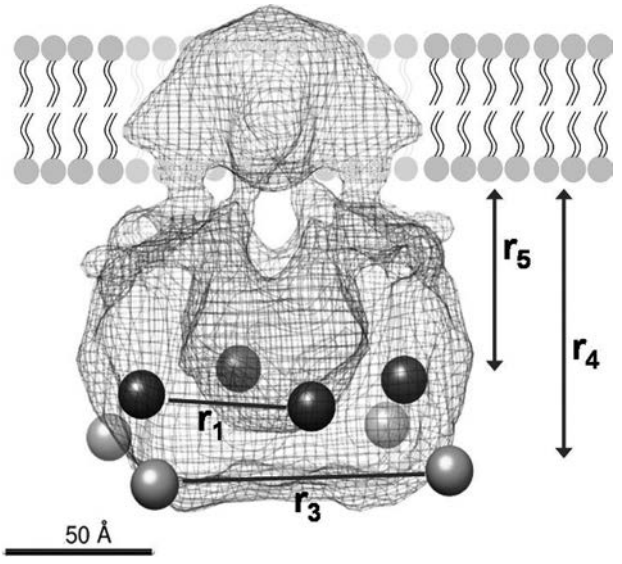

The FRET-determined positions of the N- termini (light spheres) and C-termini (dark spheres) mapped into the available electron density of TRPV1 obtained by (Moiseenkova-Bell et al., 2008).

Moiseenkova-Bell, V. Y., Stanciu, L. A., Serysheva, II, Tobe, B. J., and Wensel, T. G. (2008) Proc Natl Acad Sci U S A 105(21), 7451-7455Zheng, J., Trudeau, M. C., and Zagotta, W. N. (2002) Neuron 36(5), 891-896

Zheng, J., Trudeau, M. C., and Zagotta, W. N. (2002) Neuron 36(5), 891-896

This study was supported by grants from CONACYT No. 151297, DGAPA-PAPIIT IN212612 and ICYT-DF PIFUTP09-262 to L.D.I.

Where applicable, the authors confirm that the experiments described here conform with The Physiological Society ethical requirements.

PCD184

Expression of exogenously transfected ROMK K^+ channel activity favors the polarized apical membrane of cultured M1 collecting duct cells

M. Kubokawa[1], K. Nakamura[1], T. Mayanagi[2] and K. Sobue[2]

[1]Department of Physiology, School of Medicine, Iwate Medical University, Yahaba, Japan and [2]Department of Neuroscience, Institute for Biomedical Science, Iwate Medical University, Yahaba, Japan

Potassium secretion along the renal collecting duct plays a key role in the body fluid potassium homeostasis. ROMK K^+ channels (Kir1.1) cloned from rat kidney by Hebert's group (1) are the major candidate for the route of this secretion. To date, several investigators have demonstrated the regulation of functional expression of transfected ROMK K^+ channels in various cells (2, 3, 4). However, little is known about the affinity of the functional expression of ROMK K^+ channels to the specific cell membrane. Recently, we have cloned ROMK1 (Kir1.1a) K^+ channel and examined the exogenous expression of the cloned ROMK1 fused with EGFP in polarized and non-polarized membranes of cultured mouse collecting duct (M1) cells. We used two types of cellular conditions in culture. One was single M1 cells on conventional glass dishes, and the other was confluent M1 cells on membrane inserts to expose the polarized apical membrane of the cells. Visual expression of ROMK-EGFP in the cells was confirmed with a fluorescent microscope, and the functional expression was examined using the cell-attached and the whole-cell modes of the patch-clamp technique. Values are mean ± S.E.M., compared by ANOVA. Without the exogenous transfection, ROMK-like K^+ channel has not been detected in both single and confluent cells. The lack of intrinsic ROMK in M1 cells was also confirmed by Western blot. The current identical to ROMK1 K^+ channel was observed in the ROMK-EGFP-expressing M1 cells in both single cells on glass and confluent cells on membrane inserts in cell-attached patches. Although no appreciable difference in fluorescence intensity and the localization of ROMK-EGFP was observed between the two conditions, there was a significant difference of the frequency of the ROMK current acquisition. Namely, active ROMK1 K^+ channels were detected in 67.9 % of the confluent cells and in 15.6 % of single cells. Numbers of active ROMK1 K^+ channels in individual patch-membranes of the confluent cells and the single cells were 2.21±0.44 (n=28) and 0.40±0.17 (n=45), respectively, indicating that expression of ROMK1 K^+ channel activity in the confluent cells is significantly higher than that in the single cells in cell-attached patches ($p<0.01$). Moreover, whole-cell current of the single cells with transfected ROMK-EGFP was not affected by K^+ channel blocker, Ba^{2+} (2 mM), but that of the confluent cells with ROMK-EGFP was markedly attenuated by Ba^{2+}. From the above data, it is strongly suggested that the exogenously transfected ROMK1 K^+ channel has a high affinity to the polarized apical membrane to express its activity in cultured M1 cells. The factor for this affinity remains to be investigated.

Ho K *et al*.(1993).*Nature* **362**, 31-8.

Yoo D *et al*.(2003).*J Biol Chem* **278**, 23066-75

O'Connell AD *et al*. (2005). *Proc Natl Acad Sci USA* **102**, 9954-59.

Welling PA & Ho K. (2009). *Am J Physiol Renal Physiol* **297**, F849-63

This work was supported in part by a Grant-in-Aid for Scientific Research from the Japan Society for the Promotion of Science (to M. K., 23590264).

Where applicable, the authors confirm that the experiments described here conform with The Physiological Society ethical requirements.

PCD185

Mathematical modelling of unique subconductnace level states in heteromeric Kir4.1/Kir5.1 channels from Xenopus tropicalis

L. Shang

School of Medical Sciences, University of Bradford, Bradford, UK

Ion channels are proteins which sit in the membrane of every cell in the body and control the flow of positively charged ions such as sodium and potassium into and out of the cell. The traditional view is that an ion channel exists in one of two stochastic states i.e. open or closed. However, this is challenged by the observation of intermediate conductance, or 'subconductance', states in a number of ion channels, including several potassium (K+) channels. It has previously been shown that heteromeric XTKir4.1/XTK5.1 channels are a model system for observing the usually short-lived subconductance levels [1]. These particular channels exhibit long-lived subconductance states and that an ortholog of Kir5.1 from Xenopus tropicalis causes a dramatic change in the frequency and duration of these substates. It is theorised that these sublevels correspond to the movement of the individual subunit which form the channel.

In this study we used the different pieces of available software [2-4] to details the kinetic analysis on this model system, based on my experimental data gathered using single channel recording [Fig1,2].

Figure 1 Single-channel recording of the rat Kir4.1-Kir5.1 channel. The S1 and S2 subconductance states are visible in an expanded trace on the right.

Figure 2 Left Hand Panel: Single channel currents from the X.tropicalis XTKir4.1/XTKir5.1 heteromeric channel showing the extended duration of the S1 sublevel state. Right Hand Panel: This long S1 sublevel duration is also observed with the ratKir4.1 subunit therefore the difference is due to the presence of the XTKir5.1 subunit. In both dimers all four conductance levels are visible.

For the measurement of subconductance states in all type of channels we used the threshold-crossing method, amplitude histograms and HMM (Hidden Markov Model) analysis. Single-channel events were analyzed first by idealizing the recording into closed and open dwells, and then fitting histograms of dwell times with mixtures of exponential functions that reflect the dwells in various states using Clampfit 9.2 and HJCFIT software. To ensure the unambiguous detection of brief sublevel events and comparison of sublevel durations we will use QuB analysis software.

A combination of amplitude histograms and dwell time analysis under different analysis software have been compared and contrasted to build a mathematical model to show how many sublevel states exist is formed and to gain some insight into its mechanism.

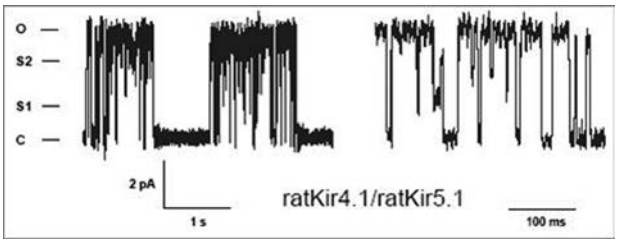

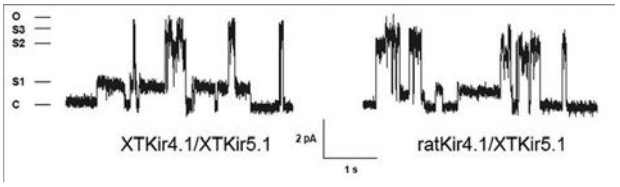

Shang L, et al. (2009) Kir5.1 underlies long-lived subconductance levels in heteromeric Kir4.1/Kir5.1 channels from Xenopus tropicalls. Biochemical and Biophysical Research Communication, 388:501-5

http://www.ucl.ac.uk/Pharmacology/dcpr95.html

Qin F et al. (1997). Maximum likelihood estimation of aggregated Markov processes. Proc Roy Soc B. 264:375-383

Qin F et al (2000). Hidden Markov Modeling for Single Channel Kinetics with Filtering and Correlated Noise, Biophys. J. 79: 1928-1944

Where applicable, the authors confirm that the experiments described here conform with The Physiological Society ethical requirements.

PCD186

TRPC1/C6 and STIM/Orai channels may regulate cell cycle progression of bone marrow stromal cells

J. Ichikawa and R. Inoue

Department of Physiology, Fukuoka University School of Medicine, Fukuoka, Japan

Ca^{2+} influx induces various physiological events such as contraction, exocytosis, gene expression, and cell growth and death. Transient receptor potential (TRP) and store-operated Ca^{2+} (SOC) channels are the representative of non-voltage-gated Ca^{2+} entry channels, and serve as major Ca^{2+} entry routes for non-excitable cells. Many reports indicate that Ca^{2+} influx through these channels is causally associated with cell cycle progression or growth, but the mechanism underlying it seems to vary depending on the cell type.

To question how the proliferative potential and cell cycle progression of adult stem cells are controlled is an attractive theme for regenerative medicine and bioengineering, but the implication of non-voltage-gated Ca^{2+} entry channels therein is poorly elucidated. In this study, we investigated the roles of TRP and STIM/Orai channels on cell cycle progression of bone marrow stromal cells (BMSCs) from adult rat which include mesenchymal stem cells. Cultured BMSCs were synchronized in G_1, S, G_2 or M phases, and the mRNA levels of respective TRPC and STIM/Orai subtypes were assessed by the quantitative real-time PCR. In the S phase, the expression levels of TRPC1, STIM and Orai were significantly enhanced. On the other hand, that of TRPC6 was greatly reduced in the S phase and significantly enhanced in the G_1 phase. In experiments measuring the intracellular Ca^{2+} concentration with Fura 2, SOC-mediated Ca^{2+} influx, which was evoked by thapsigargin or cyclopiazonic acid, was inhibited by 1μM Gd^{3+}. The Ca^{2+} influx was significantly enhanced in the S phase. Gd^{3+} (1μM), SKF96365 or pyrazole compound (Pyr2) suppressed cell proliferation. To seek a role of TRPC6 channels for cell cycle progression, we evaluated the resting membrane potential (RMP) of cells using a voltage-sensitive dye $DiBAC_4(3)$ or by the current-clamp mode of patch clamp technique. siRNA knockdown of TRPC6 expression but not of TRPC1 produced a significant negative shift of RMP. RMP in the S phase was deeper than in the other cell cycle stages. From these observations, we speculate that TRPC6 channels may work as a modulator of RMP thereby controlling the driving force for Ca^{2+} influx in the S phase. Cell cycle analysis by the flow cytometry revealed that siRNA knockdown of TRPC1, TRPC6 or STIM/Orai expression differentially affected the distribution of cell cycle stages. The fraction of cells residing in the G_0/G_1 phase was increased by siRNA of STIM/Orai but decreased by siRNA of TRPC1 or TRPC6. siRNA of TRPC6 significantly increased the fraction of cells in the G_2/M phase. To elucidate these observations more explicitly, the correlation between cell cycle-regulating molecules such as cyclins and the functions of TRPC1/C6 and STIM/Orai will need to be investigated.

Where applicable, the authors confirm that the experiments described here conform with The Physiological Society ethical requirements.

PCD187

Inhibition of TRPM7 by oxidative stress is dependent on intracellular magnesium

H. Inoue[1], T. Murayama[2] and M. Konishi[1]

[1]Physiology, Tokyo Medical University, Tokyo, Japan and [2]Cellular and Molecular Pharmacology, Juntendo University Graduate School of Medicine, Tokyo, Japan

TRPM7 is a non-selective cation channel which permeates Ca^{2+} and Mg^{2+} and plays important roles in fundamental cellular functions, including Mg^{2+} homeostasis, proliferation, migration, and viability. In various cell types, it has been reported that during whole-cell patch-clamp recordings, low $[Mg^{2+}]_i$ conditions induced activation of cationic currents called magnesium inhibited cation (MIC) currents, which is considered to be endogenous TRPM7 currents. We previously demonstrated that MIC currents were activated by lowering $[Mg^{2+}]_i$ under the whole cell recordings and inhibited by hydrogen peroxide in white adipocytes isolated from mice (ref.1). In the present study, we investigated whether or not hetelorogously overexpressed murine TRPM7 is inhibited by oxidative stress as endogenous MIC currents. First, to clarify if the molecular identity of MIC channel was TRPM7, shRNAs for human TRPM7 were introduced to HEK293T cells which express MIC currents similar to that in white adipocytes. Introduction of shRNAs for human TRPM7 reduced both the expression of MIC currents and TRPM7 mRNA to ~30% of control cells. Thus TRPM7 might be responsible for MIC currents. Next murine TRPM7 variants 1 and 2 were cloned from mouse white adipose tissue and then tetracycline-inducible HEK293 cell lines for each variants were established. Under the whole-cell recordings, both veriant 1 or 2 of TRPM7 showed similar properties to endogenous MIC currents in white adipocytes and HEK293T cells; outward rectification in the presence of extracellular divalent cations, liner I-V relationships in the absence of extracellular divalent cations, and inhibition by 2-aminoethoxydiphenil borate (100 or 200μM) and N-methyl maleimide (100 μM). On the other hand, hydrogen peroxide (500 μM) could not inhibit TRPM7 currents when Mg^{2+} was eliminated from intracellular solutions in both of variants of TRPM7. However when $[Mg^{2+}]_i$ was added to the intracellular solution, TRPM7 currents were inhibited by hydro-

gen peroxide concentration dependently. The inhibition was irreversible during whole-cell recordings. From these results, it is suggested that oxidation of TRPM7 or its regulatory proteins by hydrogen peroxide inactivate TRPM7, possibly by sensitizing it to intracellular Mg^{2+}.

Inoue H et al. (2012). *J Physiol Sci* **62**, S77

Where applicable, the authors confirm that the experiments described here conform with The Physiological Society ethical requirements.

PCD188

Serotonin-specific reuptake inhibitor (SSRI) enhances anoctamin 6 (ANO6) calcium activated Cl^- channel activity

H. Kim[1], Y. Kim[1], M. Lee[2] and J. Nam[1]

[1]Physiology, Dongguk University College of Medicine, Gyeongju, Gyeongsangbukdo, Republic of Korea and [2]Pharmacology, Yonsei University College of Medicine, Seoul, Republic of Korea

Ca^{2+}-activated Cl^- channels (CaCCs) control diverse functions in several physiological processes. Recently, anoctamins (ANOs) have been identified as a family of putative Cl^- channels, and ANO1 and ANO2 have been identified as essential components of the CaCCs. (1) However, the role of other members of the ANO family in generating Cl^- currents by increasing the intracellular Ca^{2+} concentration is still a debatable matter. Recently, a study showed that ANO6 generates a small-conductance Ca^{2+}-activated nonselective cation current. (2) In addition, ANO6 has been linked to phosphatidylserine exposure in platelet apoptosis and platelet activation. However, other studies have shown ANO6 as an essential component of the outward-rectifying Cl^- channels or CaCCs. (3,4) It is therefore unclear whether ANO6 belongs to the family of CaCCs or to a family of proteins with heterogeneous functions. Serotonin-specific reuptake inhibitors (SSRIs) are widely used antidepressants that primarily act as selective serotonin reuptake inhibitors, and they inhibit various ion channels, including voltage-activated K^+ channels, two-pore K^+ channels, and CaCCs. In particular, ANO1 is sensitively inhibited by fluoxetine. (1) Using the whole-cell patch-clamp technique, we examined the effects of SSRIs, including fluoxetine, paroxetine, and sertraline, on cloned human ANO6 expressed in HEK293 cells. We identified that ANO6 can produce calcium-activated Cl^- currents that have low sensitivity to calcium ions. (EC_{50}: 29.9 ± 2 μM, n=5) Surprisingly, in contrast to ANO1, SSRI enhances ANO6 currents in a concentration-dependent manner. However, these mechanisms need to be elucidated in the future.

Yang YD *et al*. (2008). *Nature* **455**,1210-1215.

Yang H *et al*. (2012). *Cell* **151**, 111-122

Martins JR *et al*. (2011). *Proc Natl Acad Sci U S A* **108**, 18168-18172

Shimizu T *et al*. (2013). *Am J Physiol Cell Physiol* (in press)

This work was supported by the National Research Foundation of Korea (NRF) grant funded by the Korea government (MEST) (NO 2011-0014404)

Where applicable, the authors confirm that the experiments described here conform with The Physiological Society ethical requirements.

PCD189

Membrane-dependent activation of the bile acid-sensitive ion channel (BASIC), a DEG/ENaC channel expressed in the liver

D. Wiemuth, A. Schmidt and S. Gründer

Physiology, RWTH Aachen, Aachen, Germany

The physiological function of members of the DEG/ENaC family of ion channels ranges from Na^+-reabsorption over pH-sensing and neuronal transmission to mechanosensation and the sensation of taste. As diverse as their physiological functions are their modes of activation. Constitutively active channels like the epithelial Na^+ channel (ENaC) and proton-sensitive channels like the acid-sensing ion channels (ASICs) are found in this ion channel family as well as mechanosensitive channels like MEC-4 and peptide-gated channels like Hydra Na^+ channels (HyNaCs).

The bile acid-sensitive ion channel (BASIC) adds another layer of diversity to the DEG/ENaC family. It is expressed in cholangiocytes, the epithelial cells lining the bile ducts and strongly activated by bile acids. Both, physiological function and the mode of activation are not known so far. Bile acids are negatively charged, amphiphilic derivatives of cholesterol that affect structure, curvature and fluidity of membranes. They could activate BASIC either indirectly by interfering with the membrane or directly in a ligand-like manner by binding to the channel. We addressed this question by employing a pharmacological approach and used molecules, which are known to affect biological membranes. Crenating agents like trinitrophenol (TNP) and cup-forming molecules like chlorpromazine (CPZ) were applied to Xenopus oocytes expressing BASIC or co-applied with bile acids. Interestingly, the anionic TNP had a stimulatory effect when co-applied with bile acids or when applied alone at millimolar concentrations while the cationic CPZ displayed an inhibitory effect when co-applied with bile acids. Other membrane active substances like anionic or cationic tensides also affected the activity of BASIC. These data point towards a mechanism of activation, where the membrane is modulated and BASIC functions as a sensor for this modulation. In addition to the pharmacological approach we are using a chimeric approach with ASIC1a, a related but bile acid-insensitive channel, in order to define the domains of BASIC that are crucial for sensing membrane modulation induced by bile acid. Taken together our data will help to understand the events leading to the activation of the DEG/ENaC channel BASIC.

Where applicable, the authors confirm that the experiments described here conform with The Physiological Society ethical requirements.

PCD190

A gate-coupled expansion of the cytoplasmic pore of mammalian inward rectifier potassium channels

A. Inanobe[1], A. Nakagawa[2] and Y. Kurachi[1]

[1]Department of Pharmacology, Osaka University, Graduate School of Medicine, Suita, Japan and [2]Osaka University, Institute for Protein Research, Suita, Japan

Inward rectifier potassium (Kir) channels comprise transmembrane and cytoplasmic domains. Various cytoplasmic regulators associate with the cytoplasmic domain to control the

gate at the transmembrane domain. Despite increasing knowledge about its structure, it remains unclear how conformational change in the cytoplasmic domain couples to the gate. To approach this question, we focused on 2 spatially adjacent residues, Glu236 and Met313, of G protein-gated Kir channel subunit Kir3.2, whose side chains face the cytoplasmic pore when it is in a closed state. These 2 residues reside on adjacent β-strands which form a β-sheet. Since the cytoplasmic pore appeared to expand its inner diameter during gating, it could be speculated that effect of mutations reflects conformational changes surrounding these residues. We introduced mutations into either of residues, expressed them with m2-muscarinic receptor in Xenopus oocytes and measured the acetylcholine (ACh)-dependent potassium currents. Mutants at Glu236 tended to shift dose-response curves to the rightward direction. On the other hand, mutations at Met313 tended to render the concentration-dependent curve with shallow slope. These results suggest that, even though 2 β-strands lie adjacent in the closed state, both strands shift differently during gating. One of the Glu236 mutants showed the malconduction and the constitutive activity. In crystal structure of the mutant, the residue introduced contacts with main chains of the adjacent subunits. These results strongly suggest that the Kir channels change the inner diameter of the cytoplasmic pore during gating, and the strands differently contribute to pore expansion to control of Kir channel gating.

Where applicable, the authors confirm that the experiments described here conform with The Physiological Society ethical requirements.

PCD191

Contribution of Orai-STIM to histamine-induced store operated Ca^{2+} entry and functional coupling with Ca^{2+}-activated K^+ channels in Chondrocytes

M. Inayama[1], Y. Suzuki[1], H. Yamamura[1], S. Ohya[2] and Y. Imaizumi[1]

[1]Molecular and Cellular Pharmacology, Nagoya City University, Graduate School of Pharmaceutical Sciences, Nagoya, Aichi, Japan and [2]Department of Pharmacology, Kyoto Pharmaceutical University, School of Pharmacy, Kyoto, Kyoto, Japan

In articular cartilage inflammation, histamine release from mast cells enhances cytokine production and matrix synthesis, and also promotes cell proliferation of stimulated chondrocytes. The response to histamine H1 receptor stimulation induces Ca^{2+} release from endoplasmic reticulum (ER) through inositol trisphosphate (IP3) production in chondrocytes. The depletion of Ca^{2+} in the ER may trigger the opening of plasma membrane store operated Ca^{2+} entry (SOCE) channels. Activation of Ca^{2+}- activated K^+ (K_{Ca}) channels due to rise of $[Ca^{2+}]_i$ produces membrane hyperpolarization, which may enhance Ca^{2+} entry through SOCE channels in chondrocyte.
The present study was undertaken to reveal the functional impact of functional coupling between KCa and SOCE channels in the regulation of $[Ca^{2+}]_i$ in chondrocytes in responses to store depletion using OUMS-27 cells, as a model of chondrocytes derived from human chondrosarcoma.
Application of histamine induced a significant $[Ca^{2+}]_i$ rise and synchronized membrane hyperpolarization, and both effects were mediated by H1 receptor activation. The histamine-induced membrane hyperpolarization was attenuated to approximately 50% by large conductance K_{Ca} (BK) channel blockers, and further reduced by intermediate (IK) and small conductance K_{Ca} (SK) channel blockers (Funabashi, et al.). The $[Ca^{2+}]_i$ rise induced by application of 2.2 mM Ca^{2+} after store depletion by thapsigargin in Ca^{2+} free solution (SOCE) was enhanced and inhibited by 2-APB at low (5 μM) and high (30 μM) concentrations, respectively. RT-PCR analysis suggests that the molecular basis of SOCE channel may be Orai-STIM combination (Orai1, Orai2, STIM1 and STIM2). The SOCE was significantly reduced by application of siRNA of Orai1.
The movement of STIM1-YFP following store depletion and subsequent punctual co-localization with Orai1-CFP were visualized using total internal reflection fluorescence microscopy (TIRFM). The expression of mutant (E106Q) Orai1 in OUMS-27significantly decreased histamine-induced $[Ca^{2+}]_i$ rise than in the control. K_{Ca} channel activation by $[Ca^{2+}]_i$ rise contributed to the sustained Ca^{2+} entry through SOCE channels, presumably via the predominant combination of Orai1 and STIM1.
The functional coupling between K_{Ca} channel and SOCE channel plays substantial roles as a positive feedback mechanism for the sustained $[Ca^{2+}]_i$ rise following stimulations. The sustained $[Ca^{2+}]_i$ rise may enhance cytokine production and matrix synthesis, and also promote cell proliferation of stimulated chondrocytes.

Funabashi et al.,(2010) Am J Physiol Cell Physiol 298, C786-C797.

This investigation was supported by a Grant-in-Aid for Scientific Research on Priority Areas (23136512; to Y.I.) from the Ministry of Education, Culture, Sports, Science, and Technology, and a Grant-in-Aid for Scientific Research (B) (23390020; to Y.I.)

Where applicable, the authors confirm that the experiments described here conform with The Physiological Society ethical requirements.

PCD192

Effects of local anaesthetics on ion channels of canine articular chondrocytes

M. Wegg[1], R. Lewis[1], A. Mobasheri[2] and R. Barrett-Jolley[1]

[1]Musculoskeletal Biology, University of Liverpool, Liverpool, UK and [2]University of Nottingham, Nottingham, UK

Local anaesthetics (LAs) are routinely injected into joints at high concentrations during joint surgery [1], although consistent findings show local anaesthetics are chondrotoxic [2,3]. Studies have shown that LAs modulate both potassium and sodium channels, but the mechanism of cell chondrotoxicity is not known. In previous studies, we have shown that both transient receptor potential (TRP) channels and epithelial sodium channels (ENaC) exert a profound effect over chondrocyte cellular volume control and therefore interaction with these channels could potentially also be toxic [4, 5]. In this study we investigate whether any of a range of LAs modulate either ENaC-like channel activity and/or that of a TRP-like non-specific cation (NSC) conductance.
Articular chondrocytes were isolated from canine stifle joints using standard procedures [4] from dogs euthanatized for unrelated veterinary reasons under local Ethical Approval. Standard physiological HEPES buffered saline solutions (150mM NaCl/5mM KCl) were included in both patch pipette and bath solutions. Membrane potentials were corrected for junction potential calculated using JPCalc (University of New South Wales, Auz). Ion channel activity was recorded in cell–attached mode. LAs were added to the patch pipette solution at typical clinical concentrations as follows: 20mM prilocaine, 35mM mepivacaine, 70mM mepivacaine and 15mM bupivacaine. Statistical tests were performed with Minitab (PA, USA).

We first characterised an NSC single channel conductance, g of 43±13pS (n=14), sensitive to gadolinium III (75±9% reduction of open probability with 100μM), with a reversal potential (Vrev) of 1±9mV (n=14) and an ENaC-like ion channel (8.2±2.6pS, n=5) with Vrev 75±9mV (n=5) near to the predicted ENa of 85mV. The NSC channel was seen in 14/20 patches under control conditions, and the ENaC-like channel seen in 5/20 patches. Following exposure of the cells to each of the LAs there were no significant (ANOVA), changes in Vrev or g of the NSC channel (20mM prilocaine:-2±9mV, 45±9pS, n=4; 35mM mepivacaine 5±10mV, 65±16pS, n=9; 70mM mepivacaine 5±2mV, 31±5pS, n=6; 15mM bupivacaine 5±5mV, 67±25pS, n=6). However, this conductance was seen significantly more frequently in the presence of mepivacaine and bupivacaine ($p<0.05$, $p<0.01$ respectively; one sample sign test), but not prilocaine. No ENaC-like channel activity was detected in the presence of any of the local anaesthetic treatments used.

This data shows that at the concentrations used routinely in clinics, local anaesthetics have profound effects on a chondrocyte ion channel activity. Future studies will be directed at establishing whether these acute ion channel effects do mediate decreases in chondrocyte survival.

Guindon, J., Walczak, J. S. and Beaulieu, P. (2007) 'Recent advances in the pharmacological management of pain', Drugs, 67(15), 2121-33.

Chu, C. R., Izzo, N. J., Coyle, C. H., Papas, N. E. and Logar, A. (2008) 'The in vitro effects of bupivacaine on articular chondrocytes', J Bone Joint Surg Br, 90(6), 814-20.

Hennig, G. S., Hosgood, G., Bubenik-Angapen, L. J., Lauer, S. K. and Morgan, T. W. (2010) 'Evaluation of chondrocyte death in canine osteochondral explants exposed to a 0.5% solution of bupivacaine', Am J Vet Res, 71(8), 875-83.

Lewis R, Asplin K, Bruce G, Dart C, Mobasheri A and Barrett-Jolley R. (2011a). The role of the membrane potential in chondrocyte volume regulation. J Cell Physiol 226, 2979-2986.

Lewis, R., Feetham, C.H., Gentles, L., Tohami, W., Mobasheri, A. and Barrett-Jolley, R., (2012) Benzamil-sensitive ion channels contribute to volume regulation in canine chondrocytes. Br J Pharmacol. DOI: 10.1111/j.1476-5381.2012.02185.x

Work supported by Wellcome Trust

Where applicable, the authors confirm that the experiments described here conform with The Physiological Society ethical requirements.

PCD193

Expression of TRP channels in isolated single Merkel cells from hamster oral mucosa

M. Soya[1,2], H. Kuroda[1,2], A. Kawaguchi[1,2], M. Sato[1], U. Sobhan[1], M. Tazaki[3], T. Ichinohe[2] and Y. Shibukawa[1,3]

[1]Oral Health Science Center hrc8, Tokyo Dental College, Chiba, Japan, [2]Department of Dental Anesthesiology, Tokyo Dental College, Chiba, Japan and [3]Department of Physiology, Tokyo Dental College, Chiba, Japan

Sensory receptors throughout the body, including those in the oral epithelium, produce sensation in response to stimulation. Merkel cells (MCs) in the oral mucosa constitute a distinct cell population localized at the border between the epidermis and the dermis, and are believed to form part of an MC-neurite complex with myelinated Aβ-neurons which acts as a mechano-electric transducer. Transient receptor potential (TRP) channels, which constitute a large and functionally versatile family of cation-permeable transmembrane proteins, are mainly considered to be polymodal cell sensors involved in various cellular functions, including thermo/mechano/osmo-sensitivity. In rat footpad, these channels were found to be sensitive to mechanical and osmotic stimulation. The localization and physiological role of TRP channels in oral mucosal MCs, however, remain to be clarified. We isolated quinacrine-positive single MCs from hamster oral mucosa to investigate the expression, localization, and activity of TRP channels by immunohistochemical analysis and measurement of intracellular free Ca2+ concentration ([Ca2+]i) using fura-2 fluorescence. Intense immunoreaction for cytokeratin 20 (CK20), which co-localized with quinacrine fluorescence, was observed in the acutely isolated MCs. Both CK20 and quinacrine are used as specific markers to identify MCs. Intense immunoreactions for TRP vanilloid subfamily members (TRPV)-1, TRPV2, and TRPV4, and TRP ankyrin subfamily member (TRPA)-1 and TRP melastatin subfamily member (TRPM)-8 were observed on quinacrine-positive MCs. Transient increases in [Ca2+]i were osmo-dependently observed by application of hypo-tonic solution (140 to 300 mOsm/L). These [Ca2+]i increases were inhibited by TRPV1, TRPV2, TRPV4, or TRPA1 channel antagonists, but not by TRPM8 channel antagonist. In the presence of extracellular Ca2+, TRPV1, TRPV2, TRPV4, or TRPA1 channel agonists induced an increase in [Ca2+]i in MCs, but not in the absence of extracellular Ca2+. The present results indicate that hypotonic solution-induced membrane stretch activates TRPV1, TRPV2, TRPV4, and TRPA1 channels, and suggest that these channels play a key role as molecular sensors in the sensory transduction process in either MCs or MC-neurite complexes.

This research was supported by Oral Health Science

Center Grant hrc8 from Tokyo Dental College, and by a

Project for Private Universities: matching fund

subsidy from MEXT of Japan, 2010-2012.

Where applicable, the authors confirm that the experiments described here conform with The Physiological Society ethical requirements.

PCD194

Role of membrane cholesterol and lipid rafts in cellular mechanotransduction and actin remodeling

V.I. Chubinskiy-Nadezhdin, Y.A. Negulyaev, S.Y. Khaitlina, T.N. Efremova and E.A. Morachevskaya

Russian Academy of Sciences, Institute of Cytology RAS, St.Petersburg, Russian Federation

Cholesterol is a major lipid component of mammalian cells which regulates dynamical and physical properties of the plasma membrane. Lipid rafts are cholesterol- and sphingolipid-enriched regions of membrane that are implicated in various cellular responses. Considering the major impact of cholesterol in the mechanical properties of lipid bilayer, the role of lipid rafts and their integrity in regulation of cellular mechanotransduction is of peculiar interest.

Cholesterol-depleting treatment of cells with methyl-beta-cyclodextrin (MbCD) significantly suppressed the activation of mechanosensitive (MS) stretch-activated ion channels in human myeloid leukemia K562 cells. Particularly, the open state probability (Po) of MS channels significantly decreased (Po=0.08±0.03 after MbCD treatment vs. 0.28±0.03 in control) whereas the minimal level of stimulus, that was needed for channel activation increased (70 80 mm Hg after MbCD vs. 30 40 mm Hg in control). Atomic force microscopy revealed

the increase of plasma membrane stiffness after cholesterol depletion. The observed alteration of mechanical properties of the membrane and the inhibition of MS channels after MbCD treatment could not be explained by the change of dynamic properties of lipid bilayer after cholesterol sequestration. We hypothesized, that this effect was mediated by actin cytoskeleton rearrangement after lipid raft disruption. The disruption of rafts was confirmed by fluorescent staining of lipid raft marker GM1 ganglioside. Importantly, fluorescent data revealed the formation of F-actin network in K562 after cholesterol depletion. Importantly, the high level of MS channel activity in cholesterol-depleted cells was fully restored after F-actin disruption with cytochalasin D or latrunculin B. Experiments on different cell lines showed that the effect of cholesterol depletion on actin organization is determined by the initial state of microfilament system in the cell. Particularly, in cultured normal BALB/3T3 fibroblasts that characterized with highly developed microfilament system, the cholesterol depletion resulted in actin disassembly and reduction of stress fibers. On the contrary, in transformed 3T3B-SV40 fibroblasts, containing low amount of fibrillar actin, MbCD treatment induced intensive formation of stress fibers and increased cell spreading. Thus, the functional impact of cholesterol depletion and lipid raft disruption on actin cytoskeleton can be determined by an initial balance of fibrillar and globular actin. Cholesterol-regulated actin rearrangement may affect different signaling processes in living cells, including cellular mechanotranduction. Particularly, the assembly of F-actin network in K562 cells after cholesterol depletion increases the stiffness of plasma membrane and thus inhibits MS channel activity.

Where applicable, the authors confirm that the experiments described here conform with The Physiological Society ethical requirements.

PCD195

Altered expression of two-pore domain potassium (K_{2P}) channels in cancer

S. Williams, A. Bateman and I. O'Kelly

Faculty of Medicine, University of Southampton, Southampton, UK

Ion channels have been implicated in both the behaviours of cancer cells and the development of cancer. Potassium channels (KCh) play fundamental roles in cell behaviours linked to cancer progression, including proliferation, migration and apoptosis. One family, the two-pore domain (K_{2P}) KCh are of particular interest since when functionally expressed these channels are constitutively active. Of the 15 K_{2P} family members, 4 channels; K_{2P}2.1, K_{2P}3.1, K_{2P}9.1, K_{2P}5.1, are reported to show expression and functional implications in cancer. Supporting the hypothesis that alterations to K_{2P} channels expression or function may play a role in cancer progression and that targeting these channels may lead to novel therapies.

To determine the expression of the KCNK genes, encoding the K_{2P} channels, in a range of cancer types we used the online cancer microarray database, Oncomine (www.oncomine.org). Each gene was examined across 20 cancer types, comparing mRNA expression in cancer to normal tissue. Searches were performed using threshold criteria (p-value < 0.05, fold change > 2, gene rank percentile < 10%) so that positive analyses for altered expression were above these. mRNA expression of K_{2P} channels were also examined in human cancer cell lines by RT-PCR.

Significantly overexpression of K_{2P} channels was observed in a range of cancers including breast, leukaemia and lung. The data highlights K_{2P} channels with overexpression in a range of cancers; K_{2P}1.1, K_{2P}3.1, K_{2P}12.1. More cancers and channels showed underexpression rather than overexpression, suggesting that underexpression of K_{2P} channels may be important in cancer. Six K_{2P} channels have a wide underexpression pattern across the cancer types examined; K_{2P}1.1, K_{2P}3.1, K_{2P}5.1, K_{2P}6.1, K_{2P}7.1, K_{2P}10.1. There was significant underexpression of K_{2P} channels in a wide range of cancer types; brain, colorectal, gastrointestinal, kidney, lung, melanoma, oesophageal. Three K_{2P} family members; K_{2P}4.1, K_{2P}16.1, K_{2P}18.1 did not show altered expression in cancer.

Using RT-PCR we examined the expression of K_{2P}3.1 mRNA in cancer cell lines and found expression in breast, lung and kidney cell lines. K_{2P}9.1 mRNA was also identified in several cancer cell lines including brain, breast, colorectal, and oesophageal. K_{2P}15.1 mRNA has been detected in all cancer cell lines examined to date.

K_{2P} channels alter cell resting membrane potential therefore altered expression in cancer cells would change this potential and influence the activity of other ion channels causing behavioural consequences. K_{2P} channels also show sensitivity to physiological stimuli including pH, oxygen tension and glucose concentration; physiological parameters which are disrupted in the tumour microenvironment. This information will be instrumental towards understanding the role of K_{2P} channels in cancer progression.

With thanks to The Gerald Kerkut Trust for their funding

Where applicable, the authors confirm that the experiments described here conform with The Physiological Society ethical requirements.

PCD196

Voltage-gated Na^+ channels contribute to depolarised membrane potential in the MDA-MB-231 human breast cancer cell line

M. Yang and W.J. Brackenbury

Biology, University of York, York, UK

Voltage-gated Na^+ channels (VGSCs) initiate and conduct action potentials in excitable cells. Functional VGSCs are also present in cells from a number of cancers. Inhibiting Na^+ current (I_{Na+}) reduces cancer cell migration and invasiveness (Brackenbury, 2012). We previously reported that phenytoin, an antiarrhythmic agent, inhibits I_{Na+} in human MDA-MB-231 breast cancer cells, thus reducing migration and invasion (Yang *et al.*, 2012). Membrane potential (V_m) is finely tuned in cellular activities such as proliferation and differentiation. Cancer cells possess depolarised V_m (Marino *et al.*, 1994), which favours cell cycle progression (Sundelacruz *et al.*, 2009). Here, we used whole-cell current clamp to study the involvement of VGSCs in regulating V_m of MDA-MB-231 cells. Cells were firstly perfused with standard physiological saline solution (PSS) for 60s, followed by a 'test' PSS for 150s, and finally a wash-out step with standard PSS for a further 150s. V_m values (sampled at 100Hz) within the last 5, 15, 30 and 60s in each of the 3 stages were analysed using ANOVA followed by Tukey *post-hoc* tests. Values are mean ± SEM. We firstly replaced extracellular Na^+ with choline in the PSS. Na^+ depletion reversibly hyperpolarised the V_m by ~10mV (Table 1). We next tested if VGSCs are involved in V_m regulation by applying 10 μM phenytoin in the PSS. Phenytoin hyperpolarised the V_m by ~3mV

while the drug carrier 75μM NaOH had no effect (P=0.98). The effect of phenytoin was thus more subtle than Na^+ depletion. Interestingly, after washing out phenytoin, the V_m did not recover (Table 2). We conclude that (1) Na^+ conductance contributes to the depolarised V_m in MDA-MB-231 cells, and (2) phenytoin partially inhibits the Na^+-mediated V_m depolarisation in a non-reversible manner. Given that depolarised V_m is a hallmark of malignancy (Sundelacruz *et al.*, 2009), we propose that Na^+-mediated V_m regulation may play a role in cancer progression.

Table 1. Na^+ depletion reversibly hyperpolarised the V_m

Measurement period	V_m in PSS (mV)	V_m in Na^+-free PSS (mV)	V_m following washout with PSS (mV)
Last 5 s	-10.4 ± 1.0	-20.4 ± 1.9***	-12.9 ± 2.2###
Last 15 s	-10.4 ± 1.0	-19.9 ± 1.9***	-13.0 ± 2.2##
Last 30 s	-10.3 ± 0.9	-19.6 ± 1.8***	-13.0 ± 2.1##
Last 60 s	-10.3 ± 1.0	-18.4 ± 1.8***	-13.0 ±2.1##

***P<0.001 compared to PSS. ##P<0.01 and ###P<0.001 compared to Na^+-free PSS. n=10.

Table 2. Phenytoin non-reversibly hyperpolarised the V_m

Measurement period	V_m in PSS (mV)	V_m in 100 μM Phenytoin (mV)	V_m following washout with PSS (mV)
Last 5 s	-12.5 ± 1.5	-15.7 ± 1.7***	-14.6 ± 1.8
Last 15 s	-12.7 ± 1.4	-15.9 ± 1.8**	-14.8 ± 1.8
Last 30 s	-12.8 ± 1.5	-15.6 ± 1.8**	-14.9 ± 1.8
Last 60 s	-13.0 ± 1.4	-15.4 ± 1.8*	-15.2 ±1.9

*P<0.05, **P<0.01, ***P<0.001 compared to PSS. n=12.

Brackenbury WJ. (2012). Voltage-gated sodium channels and metastatic disease. *Channels (Austin)*, **6**, 352-61.

Marino AA *et al.* (1994). Electrical potential measurements in human breast cancer and benign lesions. *Tumour Biol*, **15**, 147-52.

Sundelacruz S *et al.* (2009). Role of membrane potential in the regulation of cell proliferation and differentiation. *Stem Cell Rev*, **5**, 231-46.

Yang Y *et al.* (2012). Therapeutic potential for phenytoin: targeting $Na_v1.5$ sodium channels to reduce migration and invasion in metastatic breast cancer. *Breast Cancer Res. Treat*. **134**, 603-615.

This work was supported by the Medical Research Council [Fellowship number G1000508(95657)].

Where applicable, the authors confirm that the experiments described here conform with The Physiological Society ethical requirements.

PCD197

Extracellular ATP arrests the adaptive reaction in mouse eggs subjected to hypotonic stress

M. Pogorelova[1,2] and V. Pogorelova[1]

[1]Institute of Theoretical and Experimental Biophysics RAS, Pushchino, Russian Federation and [2]Biological Department, Moscow State University, Moscow, Russian Federation

Cell volume homeostasis is particularly critical for early preimplantation development [1]. The ability to regulate cell size first appears in the oocyte after ovulation is triggered [2]. The nature of the regulatory mechanisms governing the volume changes in the mature oocyte during regulatory volume decrease (RVD) is not clear. Volume-sensitive organic osmolyte-anion channel or VSOAC is known to be involved in RVD in most somatic cells. It was shown that VSOAC-like channel may also participate in egg volume regulation [3]. The most important property of VSOAC is the open-channel block by millimolar concentrations of extracellular ATP [4]. The aim of this study was to investigate the external ATP influence on kinetics of mouse metaphase II (MII) oocyte osmotic response under hypotonic stress.

Eggs (MII oocytes) were obtained from 8-10-week-old SHK female mice. The females were superovulated by an i.p. injection of 10 IU of Folligon (Intervet, Holland) followed by an i.p. injection of 5 IU of human chorionic gonadotropin (hCG, Intervet, Holland) 46-48 hs later. The MII oocytes were flushed from excised oviducts of sacrificed by cervical dislocation animals 14 hs after hCG administration. The hypotonicity was created by replacing 140mM NaCl in Dulbecco`s solution with 70mM NaCl. Eggs were exposed for 90 minutes in the hypotonic conditions. The similar procedure was employed for Dulbecco`s containing 5 mM ATP (Sigma, USA). Osmotic adaptation in single oocyte has been studied employing the direct measurement of cell volume with the quantitative microtomography [5]. Egg volume was determined with laser scanning microscopy followed by three-dimensional reconstruction (3-DR). The keeping of the intact volume of mature mouse oocyte was based on freeze-drying technique. After cryofixation in liquid propane and subsequent low-temperature dehydration the cell was immediately immersed in the Epon medium. The monolayer of freeze-dried embedded oocytes was examined with a laser scanning microscope (Leica DM2500, Germany). Using 532-nm laser a gallery of optical slices of mouse oocyte was collected in Z-direction with deepness step of 1 μm thick. 3-DR was performed in the 3ds max medium. All results are presented as means ± S.D., compared by Student's *t*-test.

Our data indicate that hypoosmotic incubation for 20 minutes resulted in the swelling peak of oocyte volume of 221±15 pl *vs.* initial level of 121±13 pl, p<0.05. After 90 minute exposure the cell volume was recovered to 174±24 pl *vs.* 213±17 pl in hypotonic Dulbecco`s with ATP, p<0.05.

In the given research it was shown that mouse MII oocytes are capable of RVD. The recovery is pronounced but not completed at 90 minutes. RVD in mouse eggs is inhibited by external ATP of 5mM. This finding suggests the involvement of the VSOAC-like mechanism in osmotic response of mature oocyte to hypotonic stress.

Baltz JM & Tartia AP (2010). *Hum Reprod Update* **16**, 166-176.

Tartia AP *et al.* (2009). *Development* **136**, 2247-2254.

Baltz JM & Zhou C (2012). *Mol Reprod Dev* **79**, 821–831.

Jackson PS & Strange K (1995). *J Gen Physiol* **105**, 661-676.

Pogorelov AG & Pogorelova VN (2008). *J Microsc* **232**, 36-43.

Where applicable, the authors confirm that the experiments described here conform with The Physiological Society ethical requirements.

PCD198

STIM and Orai proteins regulate store-operated calcium entry and NADPH oxidase activity in primary human monocytes

S. Saul, B. Pasieka, D. Conrad, G. Schwär, R. Kappl, B. Niemeyer and I. Bogeski

Biophysics, Saarland University, Homburg, Saarland, Germany

In the innate immune defense, professional phagocytes such as neutrophils, monocytes and macrophages play an important role in clearance of pathogenic intruders and in triggering the adaptive immune system. Monocytes invade tissues as a result of chemokine attraction wherein they differentiate into macrophages and dendritic cells and act as first line of host defense.

Store-operated calcium entry (SOCE) through calcium release activated calcium (CRAC) channels composed of Orai1-3 and STIM1 and 2 proteins is implicated in a plethora of cellular functions. While a major role for CRAC channels was revealed especially in T cells and neutrophils, it is presently not known if and what role Orai and STIM proteins play in human monocytes.
For efficient immune response, monocytes need to generate high amounts of oxidants upon encounter with an antigen. Hence, we investigated the role of Orai and STIM isoforms on reactive oxygen species (ROS) production, Ca2+ homeostasis, and the effects of their interplay for monocyte function. Expression analysis using qRT-PCR showed the presence of all CRAC channel components in human monocytes, with comparatively high Orai3 and STIM2 levels. To determine the interplay of SOCE and ROS production, monocytes were activated by internal Ca2+ store depletion using thapsigargin or bacterial products (fMLF). To determine the specific contribution of a particular CRAC channel component in monocyte SOCE we used small interfering RNA gene silencing. Our measurements showed a significant contribution of Orai1 and STIM1 and, in contrast to other phagocytes, also Orai3 and STIM2 proteins. Not unexpectedly, NADPH-oxidase 2 (NOX2) was identified as the main enzymatic source of ROS in monocytes, which showed a clear dependency on not only internal Ca2+ concentration, but also on SOCE. To determine the dependency of NOX2 on Ca2+ and thus Orai and STIM, we analyzed quantitative and temporal parameters of ROS generation using fluorescent dyes and electronic paramagnetic resonance (EPR) spectroscopy. Down-regulation of Orai1, STIM1 and STIM2 expression levels resulted in altered kinetics and a decrease in ROS production. Contrary to these results, lower levels of Orai3 led to enhanced SOCE and consequently increased ROS production.
We demonstrate the existence of a regulatory feedback loop between Orai channels and NOX2 enzymes essential for monocyte function. Based on our preliminary data we are currently investigating the contribution of Orai and STIM proteins in monocyte migration and invasion and phagocytosis.

Where applicable, the authors confirm that the experiments described here conform with The Physiological Society ethical requirements.

PCD199

Synergistic activation of the human bile acid-sensitive ion channel (hBASIC) by chenodeoxycholic and deoxycholic acid

C.M. Lefèvre, S. Gründer and D. Wiemuth

Institute of Physiology, Aachen, Germany

The human bile acid-sensitive ion channel hBASIC is a member of the DEG/ENaC gene family. According to the main site of expression, the intestinal tract, hBASIC was initially named hINaC (human intestinal Na^+ channel), BASIC from mouse and rat were named BLINaC (brain liver intestine Na^+ channel) as they were additionally found in brain and liver. Based on their sensitivity for bile acids, INaC/BLINaC were recently renamed BASIC. Furthermore immunohistochemical data suggest that the channel is strongly expressed in cholangiocytes, the epithelial cells of the bile ducts. Despite the high degree of sequence identity between hBASIC and its orthologs from mouse and rat, the pharmacological and electrophysiological features vary drastically between these channels. While mBASIC is a constitutively open channel, hBASIC and rBASIC are almost completely blocked by physiological concentrations of extracellular Ca^{2+}. Consequently removal of Ca^{2+} opens the channels. rBASIC is strongly activated by the bile acids chenodeoxycholic acid (CDCA) and hyodeoxycholic acid (HDCA), which are both present in murine bile. When co-applied, CDCA and HDCA cause a synergistic activation of the channel. In contrast, hBASIC is strongly activated by CDCA but only weakly by HDCA and co-application caused no synergistic effect. However, only CDCA but not HDCA is present in human bile. Therefore we extended our study to bile acids present in the human bile acid pool and applied the most common human bile acids CDCA, cholic acid (CA) and deoxycholic acid (DCA) individually and in combination. Interestingly DCA activates hBASIC as potently as CDCA and a synergistic activation could be observed when co-applied. Additional removal of extracellular Ca^{2+} during the application of bile acids leads to increased current amplitudes without changing the amplitude relationship. Thus, removal of extracellular Ca^{2+} and bile acids displayed a synergistic effect on hBASIC activity. In summary human and rat BASIC differ in their sensitivity for different bile acids. Furthermore they show a preference for bile acids present in the respective species-specific bile acid pool, supporting the hypothesis that BASICs may have co-evolved to match the bile acid prevalence of different species.

Where applicable, the authors confirm that the experiments described here conform with The Physiological Society ethical requirements.

PCD200

Lipid rafts as regulators of P2X7 receptor and pannexin-1 signalling

L. Robinson and R. Murrell-Lagnado

Department of Pharmacology, University of Cambridge, Cambridge, UK

The ATP-gated P2X7 receptor is a low affinty cation channel which mediates a range of responses, from cell proliferation to cell death, and is a key regulator of the inflammatory response. Emerging evidence supports an important role for lipid rafts in the regulation of P2X7 receptor signalling, but the mechanism of this regulation is not yet understood (Garcia-Marcos et al., 2006; Barth et al., 2007; Gonnord et al., 2009). Lipid rafts are regions of the plasma membrane enriched in cholesterol and sphingolipids which provide specialised platforms for the organisation of signalling pathways, and by dynamic remodelling can directly modulate signal transduction.
We have evidence that disrupting lipid rafts enhances P2X7 receptor-mediated large pore formation, as measured by dye uptake. Dye uptake, measured using confocal microscopy, is predominantly mediated via the P2X7 receptor but following cholesterol depletion, the enhanced kinetics of dye uptake appears to involve the pannexin-1 hemichannel. Inhibitors of pannexin-1 can block this increase and so can the non-specific caspase inhibitor, Z-VAD-FMK. To investigate targeting of the P2X7 receptor and pannexin-1 to lipid rafts we have separated cellular components on a discontinuous sucrose gradient by ultracentrifugation following their heterologous expression in either HEK293 cells or TSA 201 cells. Both proteins appear in the light lipid raft fractions although not exclusively. This targeting can be manipulated by the co-expression of either wild type or a dominant negative mutant of caveolin-1 and by stomatin. Interactions between these proteins are being investigated by co-immunoprecipitation experiments and FRET as are the effects on P2X7 receptor—pannexin-1 signalling.

Garcia-Marcos M, *et al.* (2006), Journal of lipid research **47**, 705.

Barth K, *et al.* (2007), The FEBS journal **274**, 3021.

Gonnord P, *et al.* (2009), The FASEB Journal **23**, 795.

Where applicable, the authors confirm that the experiments described here conform with The Physiological Society ethical requirements.

PCD201

Evaluation of the role of pH in cancer cell proliferation

U. Bose, C. Allegrucci, C. Rauch, C. Tufarelli and R. Khan

University of Nottingham, Derby, UK

Objective: A common feature of tumours is a shift in cellular metabolism generating a high acid load in the tumour microenvironment. In addition, hypoxia contributes to the exacerbation of tumour extracellular acidosis. The potential toxic effects of low extracellular pH (pHe) are counteracted by cellular mechanisms including potassium channels and the H^+/K^+ ATPase proton pump. We hypothesize that regulation of pH of the tumour microenvironment affects cancer cell proliferation through pH sensitive membrane proteins. The present study was aimed at investigating the effect of pH and cellular pH regulating mechanisms on proliferation of the SKOV3 and MG63 cell lines.

Materials and method: Ovarian cancer (SKOV3) and osteosarcoma (MG63) cell lines were cultured media of Extracellular pH (pHe) ranging from 6 to 7.5 . Cells were also maintained at 3% O2 to induce a low pHe and to compare their response to alterations in pHe in normoxia. Cell proliferation and cell viability assays were performed in the presence and absence of drugs known to inhibit the H^+/K^+ATPase proton pump (omeprazole), EAG channel (E-4031) and the pH-sensitive potassium channel, TASK3 (methanandamide) over 24 and 72 hour time-points using MTS cell proliferation assay. Data was compared using one-way ANOVA. All experiments were repeated thrice.

Result: The SKOV3 and MG63 cells showed an increased rate of proliferation after culturing for 72 hours in pH 6.0 compared with pH 7.5 ($p<0.05$). E-4031 and methanandamide at 0.1 μM increased cell death by 35% and 20% respectively in SKOV3 and MG63 cells after 72 hours in pHe 6.0 in comparison to pHe 7.5 ($p<0.05$). Omeprazole at 10 μg/ml significantly decreased cell proliferation of MG63 cells within 24 hours at a pHe of 6.5 in comparison to cells treated with omeprazole at pHe 7.5 ($p<0.05$).

Discussion and Conclusion: Inhibitors of potassium channels and proton pumps elicited a variable response from proliferation experiments with MG63 and SKOV3 cell lines. A change in pHe influenced proliferation, indicating dependence on cellular pH regulating systems and membrane protein. The presence of these pH regulating systems often works in correlation with change in cellular metabolism owing to altered intracellular pH and pHe. Further investigation is required to understand the fundamentals of pH regulatory systems to meet the challenge of targeting tumour metabolism and acidosis as an anti-cancer therapy.

Where applicable, the authors confirm that the experiments described here conform with The Physiological Society ethical requirements.

PCD202

The role of P2X7 receptor C-terminal in trafficking and targeting to the plasma membrane

M. Brunet, L. Robinson, M. Shridar and R. Murrell-Lagnado

Pharmacology, Cambridge University, Cambridge, Cambridgeshire, UK

The P2X7 receptor (P2X7R) is a ligand-gated non-selective cation channel activated by extracellular ATP. With prolonged ATP exposure the receptor pore dilates to accommodate larger cations up to 900Da and this promotes cell death. P2X7 receptors are not always found at the plasma membrane; cell- and species-dependent differences in its trafficking have been reported (1). These differences range from the receptor being predominantly intracellular to predominantly at the cell surface. Determinants of P2X7R trafficking have been identified within its uniquely long cytoplasmic tail, but mechanisms that regulate its trafficking remain poorly understood (2). P2X7 receptors are predominantly expressed in immune and epithelial cells in physiological conditions but are up-regulated in many other cell types in pathophysiological conditions. An example is fibroblasts, where up-regulation of P2X7R contributes to lung, kidney and pancreatic fibrosis (3,4,5). We are interested in the regulation of P2X7R in fibroblasts and the role of caveolin-1 in this regulation. Heterologous expression of P2X7R in fibroblast cell lines was surprisingly toxic compared to other epithelial cell lines. There was a correlation between toxicity and levels of caveolin-1 expression and over-expression of caveolin-1 in HEK293 or HeLa cells increased cell death associated with P2X7R expression. Increased expression of caveolin-1 increased targeting of P2X7R to lipid rafts, as measured by fractionation on a sucrose density gradient. To study the role of the P2X7R C-terminus in trafficking and targeting, we generated chimeras in which the C-terminal tail (Ct) of either rat or human P2X7 was fused downstream of the transmembrane region of CD8 alpha. Human P2X7R shows much greater ER retention than rat P2X7R. Expressed in HeLa cells, immunocytochemistry combined with flow cytometry showed that CD8a is expressed at the plasma membrane (pm) whereas the rat Ct chimera shows pm expression but more endoplasmic reticulum (ER) retention and the human Ct chimera, much greater ER retention. In the REF52 fibroblast cell line a different distribution was observed. The Ct chimeras were much more efficiently trafficked to the pm than in HeLas. This increased trafficking could explain the greater toxicity of P2X7R in these cells. Unlike CD8 a, which is excluded from lipid rafts, the P2X7 Ct chimeras showed targeting to the light raft fractions. There were two molecular mass species of the Ct chimeras consistent with a post-translational modification. Only the higher mass species was targeted to the raft fractions; this targeting was disrupted by coexpression of a dominant negative mutant of caveolin-1.

Mammalian P2X7 receptor pharmacology: comparison of recombinant mouse, rat and human P2X7 receptors. D. L. Donnelly-Roberts, M. T. Namovic, P. Han, and M. F. Jarvis. (2009), Br J Pharmacol.; 157(7): 1203–1214.

C terminus of the P2X7 receptor: treasure hunting. H. M. Costa-Junior, F. Sarmento Vieira, and R. Coutinho-Silva. (2011) Purinergic Signal.; 7(1): 7–19.

ERK pathway mediates P2X7 expression and cell death in renal interstitial fibroblasts exposed to necrotic renal epithelial cells. M. Ponnusamy, N. Liu, R. Gong, H. Yan, and S. Zhuang. (2011) Am J Physiol Renal Physiol.; 301(3):F650-9.

Extracellular ATP is a danger signal activating P2X7 receptor in lung inflammation and fibrosis. Riteau N, Gasse P, Fauconnier L, Gombault A, Couegnat M, et al. (2010) Am J Respir Crit Care Med.; 15;182(6):774-83.

The P2X7 receptor supports both life and death in fibrogenic pancreatic stellate cells. Haanes KA, Schwab A, Novak I. (2012) PLoS One; 7(12):e51164.

Pharmacology Department, Cambridge University

Gates Cambridge Scholarship.

Where applicable, the authors confirm that the experiments described here conform with The Physiological Society ethical requirements.

PCD203

Role of TRPV6 calcium channels in proliferation of human T lymphocytes

V.N. Tomilin, Y.A. Negulyaev and S.B. Semenova

Institute of Cytology RAS, St.Petersburg, Russian Federation

The calcium influx plays a key role in processes of activation, proliferation and cytokine synthesis in human T lymphocytes. Although the calcium currents in blood cells are well studied, the molecular identity of ionic channels involved in such an important process as T-cell activation and normal/pathological cell proliferation remains elusive. Several members of transient receptor potential (TRP) channel family were shown to play a role in changes of [Ca2+]in in blood cells, however the properties and expression profiles of these channels in human lymphocytes are not yet fully determined. In our previous study, using RT-PCR and Western blot analyses we have shown the expression of TRPV6 (transient receptor potential vanilloid type 6) channels in Jurkat T- cells and in normal human blood lymphocytes (HBLs), isolated from the peripheral blood of healthy volunteers. Moreover, it was found that the levels of mRNA and protein expression of TRPV6 were significantly higher in malignant T-cells than in quiescent HBLs. In this study we performed electrophysiological and immunofluorescent experiments to reinforce our hypothesis that TRPV6 channels could be involved in human blood lymphocytes proliferation. We used outside-out patch-clamp recordings to search for TRPV6 channels in quiescent lymphocytes, phytohemagglutinin (PHA)-treated (48h) lymphocytes and Jurkat cells. TRPV6 single channels recording was assessed in divalent free solution at negative membrane potential (-70 mV), and the channels activity was reduced in presence of nonselective inhibitor of TRPV6 channels, Ruthenium Red (IC50=10μM). Overall, single TRPV6 channel activity was obtained in 77% (17 out of 22) of outside-out patches in Jurkat cells; in 83% (5 out of 6) of outside-out patches in PHA-treated HBLs; and in 40% (2 out of 5) of outside-out patches in quiescent HBLs. Next, immunofluorescence method was employed to examine the TRPV6 channel density and subcellular distribution in these cells. Immunofluorescence signal was detected on the plasma membrane of T- cells and HBLs and the intensity of the signal was substantially higher in Jurkat and PHA-treated HBLs than in quiescent HBLs. Thus, both electrophysiological and immunofluorescence data showed that TRPV6 channel activity and TRPV6 channel density are significantly higher in transformed lymphocytes (Jurkat) compared to quiescent lymphocytes. Moreover number of TRPV6 channels increases after activation of HBLs to proliferation. In whole, present findings suggest a potential role of TRPV6 in normal and/or pathological proliferation of human blood lymphocytes. We hope that in the future, TRPV6 can be considered as a potential molecular marker for early diagnosis of T-cells malignancy.

Supported by Russian Foundation for Basic Research (RFBR)

Where applicable, the authors confirm that the experiments described here conform with The Physiological Society ethical requirements.

PCD204

Propylamine activates and blocks ELIC channels

A. Marabelli, R. Lape and L.G. Sivilotti

University College London, London, UK

Prokaryotic channels, such as ELIC and GLIC, give key structural information for the Cys-loop superfamily. ELIC, a cationic channel from Erwinia chrisanthemi, is suitable also for single channel recording because of its high conductance (> 80 pS) (Zimmermann and Dutzler, 2011). Here we report on the kinetic properties of recombinant ELIC channels expressed in HEK293 cells.

Single channel currents elicited by the full agonist propylamine (0.5-50 mM) were recorded from outside-out patches at -60 mV and analysed by maximum likelihood direct global fitting of kinetic schemes to the idealized data (HJCFIT program; Colquhoun et al 2003). Several mechanisms were tested and their adequacy was judged by comparing the predictions of the best fit obtained with the experimental open/shut time distributions and the dose response curve. The fitted model had to account also for the time course of macroscopic propylamine-activated currents, elicited by fast theta-tube applications (50-600 ms, 1-50 mM, -100 mV).

Other Cys-loop channels, such as glycine receptors, activate via a pre-opening intermediate ('flip' model, Burzomato et al., 2004) and, when fully liganded, open with high efficacy to a single open state. In contrast with that, ELIC open time distributions at saturating propylamine showed more than one component. Thus, more than one open state must be accessible to the fully liganded channel. The `primed` model (Mukhtasimova et al., 2009) allows that by including more than one fully liganded intermediate. The best fit of this type of model showed that ELIC maximum open probability (99%) is reached when three molecules of agonist have bound to the channel. The overall efficacy of the fully liganded branch was 130 ± 20 (n = 3 sets; c.f. 20 for $\alpha1\beta$ glycine channels; Burzomato et al., 2004). The microscopic affinity for the agonist was seen to increase as the channel activated, from a resting state value of 6.2 ± 0.6 mM to 0.19 ± 0.11 mM (n = 3 sets) for the partially activated intermediate state.

Macroscopic responses to propylamine had a monoexponential rising phase (time constant of 33 ± 4 ms at 10 mM, n= 16 patches), but a complex off-relaxation. This was notable for the presence of an almost instantaneous rebound current at the end of the application. The amplitude of this rebound current (normalized to the peak of the agonist current itself) increased with increasing propylamine concentration to reach 10% at 50 mM, but was voltage independent. We will present evidence that the rebound current is due to the relief of a low affinity, voltage-independent propylamine block of the open ELIC channel. The decay phase of the agonist currents (from the peak of the rebound current) appeared to be sigmoidal (e.g. two exponential components with amplitudes of opposite sign) and this time-course was well-described by the 'primed' mechanism fitted to the single channel records.

Zimmermann and Dutzler (2011) PLoS Biol 9, e1001101.

Colquhoun et al. (2003) J Physiol 547, 699-728.

Burzomato et al. (2004) J Neurosci 24, 10924-10940.

Mukhtasimova et al. (2009) Nature 459, 451-454.

Where applicable, the authors confirm that the experiments described here conform with The Physiological Society ethical requirements.

PCD205

Dose-dependent effects of Angiotensin-(1–7) on the NHE3 exchanger and the [Ca2+]i in *in vivo* proximal tubule

R.C. Castelo-Branco[1], D. Leite-Dellova[2] and M. Mello-Aires[1]

[1]Department of Physiology and Biophysics, University of São Paulo, São Paulo, São Paulo, Brazil and [2]Department of Basic Sciences, University of São Paulo, São Paulo, São Paulo, Brazil

The acute direct action of Ang-(1-7) on net bicarbonate reabsorption ($JHCO_3^-$) was evaluated by stationary microperfusion of *in vivo* middle proximal tubules of rat kidney, using H ion-sensitive microelectrodes. The mean control value of $JHCO_3^-$ is 2.82 ± 0.078 nmol. cm^{-2}. s^{-1} (50) and Ang-(1-7) (10^{-12} or 10^{-9} M) into luminally perfused tubules causes a significant decrease [to 1.80 ± 0.21 nmol. cm^{-2}. s^{-1} (52) and 1.11 ± 0.119 nmol. cm^{-2}. s^{-1} (78), respectively] but Ang-(1-7) (10^{-6} M) increases it to 5.09 ± 0.46 nmol. cm^{-2}. s^{-1} (70). A779 [10^{-6} M; an Ang-(1-7) receptor Mas antagonist] alone increases the $JHCO_3^-$ to 3.68 ± 0.394 nmol. cm-2. s-1 (64); these data indicate that in the basal situation intratubular Ang-(1-7) inhibits $JHCO_3^-$. However, A779 prevents the inhibitory and the stimulatory effects of Ang-(1-7) in $JHCO_3^-$. S3226 (10^{-6} M; an inhibitor of NHE3 isoform of Na^+/H^+) alone decreases the $JHCO_3^-$ to 1.56 ± 0.168 nmol. cm^{-2}. s^{-1} (53), does not affect the inhibitory effect of Ang-(1-7) and changes its stimulatory effect on an inhibitory effect [1.98 ± 0.358 nmol. cm-2. s-1 (47)]. So, our results indicate that the biphasic dose-dependent effect of Ang-(1-7) on $JHCO_3^-$ is mediated by the Mas receptor and via NHE3. The mean control value of cytosolic free calcium ($[Ca^{2+}]_i$), monitored by FURA-2-AM, is 101 ± 2 nM [6 (n° of tubules; each tubule is the average of 10 areas)] and Ang-(1-7) (10^{-12}, 10^{-9} or 10^{-6} M) causes a transient (3 min) increase of it [to 252 ± 8 nM (5), 203 ± 3 nM (6) or 153 ± 8 nM (5), respectively]. A779 alone increases the $[Ca^{2+}]_i$ to 126 ± 2 nM (5) but impairs the stimulatory effect of Ang-(1-7) all doses. The results are compatible with stimulation of NHE3 by a moderate increase in $[Ca^{2+}]_i$ with Ang-(1-7) (10^{-6} M) and its inhibition by large increase in $[Ca^{2+}]_i$ with Ang-(1-7) (10^{-12} or 10^{-9} M). Our findings are the opposite of those found for the biphasic dose-dependent effect of Ang II on the Na^+/H^+, since several studies indicate the stimulation of the Na^+/H^+ with low doses of Ang II by a small increase in $[Ca^{2+}]_i$ and inhibition of the Na^+/H^+ with high doses of Ang II by a large increase in $[Ca^{2+}]_i$. It is therefore reasonable to assume that, in the intact animal, the interaction of the opposite dose-dependent effects of Ang-(1-7) and Ang II on the Na^+/H^+ and $[Ca^{2+}]_i$ may represent an important physiological regulation in terms of intra- and extracellular volume and/or pH changes.

Where applicable, the authors confirm that the experiments described here conform with The Physiological Society ethical requirements.

PCD206

Regulation of glomerular filtration rate by canonical transient receptor potential 6 in glomerular mesangial cells

R. Ma, Y. Ding, C. Smedley, B. Zhu, Y. Wang, M. Ding and S. Chaudhari

University of North Texas Health Science Center, Fort Worth, TX, USA

Glomerular mesangial cells (MCs) regulate glomerular filtration rate (GFR) by regulating effective filtration surface area. Canonical transient receptor potential (TRPC) 6 is a Ca2+ permeable cation channel and playa an important role in renal physiology and pathophysiology. We have recently demonstrated that TRPC6 was expressed in MCs and modulated MC contractile function. The aim of the present study was to determine whether and how TRPC6 in MCs can regulate GFR. GFR in mice was estimated using a two-compartment clearance model. 5% FITC-inulin (3.74 μl/g body weight) was retroorbitally injected under anesthetized state and blood samples were periodically collected from the tail vein under the conscious state. GFR in rats was evaluated based on the plasma inulin clearance during intravenous infusion of 1% FITC-inulin at a rate of 1 ml/h/100 g BW. Blood samples were collected from the left common carotid artery and urine samples were collected from either the bladder or the urether under the anesthetized state (pentobarbital, 50 mg/kg BW, i.p). In vivo knockdown of TRPC6 in rat kidneys was achieved by injection of shRNA constructs against rat TRPC6 via the left renal artery under anesthetized state. Ca2+ imaging was employed to assess intracellular Ca2+ level. Furthermore, MC contractile response was assessed by measuring a change in the planar surface area of MCs in response to Ang II. We found that GFR in TRPC6 knockout mice (881 ± 238 μl/min, n=6) was remarkably elevated compared to wild type mice (177 ± 61 μl/min, n=7) (P<0.01, Student t-test). In rats, acute infusion of Ang II significantly reduced GFR (1.2 ± 0.1 vs. 0.7 ± 0.1 ml/min/100 g BW, before vs. after Ang II, n=8, P<0.05, paired t-test). However, the Ang II response was abolished by knockdown of TRPC6 in kidneys. Immunohistochemistry showed that MCs were the predominantly transfected glomerular cells. Consistently, the GFR of the transfected kidney significantly decreased by Ang II when transfected with control vectors (0.53 ± 0.21 vs. 0.33 ± 0.21 ml/min/100 g BW, before vs. after Ang II, P<0.05, paired t-test, n=5), but did not have a significant change when transfected with shRNA against TRPC6. There were no significant differences in blood pressure and renal blood flow between TRPC6-knocked down and control rats. Furthermore, Ang II-stimulated Ca2+ entry was significantly inhibited in MCs isolated from TRPC6 knockout mice and in human MCs with TRPC6 knocked down. Moreover, the Ang II-stimulated contraction was significantly suppressed in TRPC6 deficient mouse MCs. These results suggest that TRPC6 channel is an important component regulating GFR by modulating MC Ca2+ signaling and contraction.

This study was supported by National Institutes of Health Grant 5 RO1 DK079968-01 from NIDDK and Grant-in-Aid from American Heart Association South Central Affiliate (11GRNT7560013).

Where applicable, the authors confirm that the experiments described here conform with The Physiological Society ethical requirements.

PCD207

Real-time electrochemical detection of endogenous substance release in freshly isolated perfused kidney

O. Palygin[1], V. Levchenko[1], D.V. Ilatovskaya[1,2], T.S. Pavlov[1], R.P. Ryan[1], A.W. Cowley[1] and A. Staruschenko[1]

[1]Physiology, Medical College of Wisconsin, Milwaukee, WI, USA and [2]Institute of Cytology RAS, St. Petersburg, Russian Federation

The structural and functional heterogeneity of the kidney and fast transient changes in signaling molecules present a tremendous experimental challenge to study variety of functional processes in whole organ. Extracellular nucleotides such as adenosine, 5'-triphosphate (ATP) are essential local signaling molecules in many organs including the kidney. Goal of this study was to develop quantitative approach for detection of hydrogen peroxide (H_2O_2) and ATP in freshly isolated whole organs. We established and described a novel approach to measure acute concentrations changes in endogenous substances in the freshly isolated perfused kidney. This method is based on using enzymatic microelectrode biosensors and utilizes standard amperometry technique. In addition to measurements of basal levels of H_2O_2 and ATP, this technique allows rapid detection of purinergic signaling, and immediately provides observation of changes and fluctuations in ATP concentration in freshly isolated organs during vehicle or drug perfusion. The real time changes in ATP and H_2O_2 concentrations in response to angiotensin II (Ang II), a pluripotent peptide hormone of the renin-angiotensin system, were measured. Freshly isolated kidneys of the Sprague Dawley (SD) or Dahl salt-sensitive (SS) rats were flushed with 1 μM Ang II under constant laminar perfusion. For these experiments rats were anesthetized with isoflurane inhalation and the surgical procedure was performed on a temperature controlled table. The kidneys were perfused through the distal aorta with a HBSS to clear blood from the organs. The flushing was continued for 2-3 min until the kidneys were completely blanched, then the animal was euthanized by pneumothorax. The left kidney was then removed and aorta ligated above the renal artery for the consequent perfusion. After surgery, the flushed kidney with catheterized renal vessels was placed into the bath solution and swathed to the silicone resin to avoid movement during perfusion. Dual simultaneous amperometric recordings were made with the biosensors detecting ATP and H2O2 levels. Biosensors were obtained from Sarissa Biomedical Ltd (Coventry, UK). Ang II perfusion produced a rapid simultaneous release of both ATP and H_2O_2 in the kidney cortex. Substance release rate and total integral release were also estimated. Controls with AT_1 receptor antagonist losartan and catalase revealed specificity of used biosensors. Renal cortex interstitial H_2O_2 concentration was also determined in SS rats fed low or high salt diets by traditional microdialysis and analyzed with Amplex red to compare these two approaches. The data indicate that SS rats have increased levels of H_2O_2 compared to SD rats, especially when fed a high salt diet. Furthermore, Ang II induced ATP and H_2O_2 release, which can stimulate arteriolar vasoconstriction or effect renal tubular transport in the kidney, and this effect is also enhanced in SS rats. In conclusion, current method is a unique powerful approach for substance release detection during pathological or normal conditions in whole organs including the kidney.

Supported by the NHLBI.

Where applicable, the authors confirm that the experiments described here conform with The Physiological Society ethical requirements.

PCD208

Acute effects of angiotensin II on TRPC6 channels in the podocytes of the freshly isolated glomeruli

D. Ilatovskaya[1,2], V. Chubinskiy-Nadezhdin[1], Y. Negulyaev[1] and A. Staruschenko[2]

[1]Institute of Cytology RAS, St. Petersburg, Russian Federation and [2]Medical College of Wisconsin, Milwaukee, WI, USA

Genetic studies have led to the identification of proteins playing a crucial role in glomerular slit-diaphragm signaling and maintenance of podocyte integrity. Particularly, the gene encoding transient receptor potential canonical channel 6 (TRPC6) was identified as the genetic basis for an autosomal dominant form of focal segmental glomerulosclerosis (FSGS). A key role for podocytes in the pathogenesis of proteinuric diseases has been established since the injury of these cells leads to proteinuria and foot process effacement. Interstitial angiotensin II (Ang II) is found to be a key mediator of renal inflammation and fibrosis in chronic nephropathies. It was shown that expression of Ang II and its receptors (ATRs) is increased in patients with progressive glomerulopathies; what is more, Ang II application can increase intracellular calcium, and members of the TRPC-family channels emerged as prime candidates for this raise.

The goal of this research was to define the signaling mechanisms mediating the effect of Ang II on TRPC6 channels in the podocytes and to study the potential capabilities of ATRs inhibitors in the treatment of FSGS. To address this aim we established a new approach allowing to measure ion channels activity and calcium concentration changes in the freshly isolated decapsulated glomeruli. We examined the effects of Ang II on intracellular Ca^{2+} concentrations in intact podocytes of the rat glomeruli. Changes in intracellular Ca^{2+} stimulated by 100 nM and up to 10 μM of Ang II in the presence or absence of thapsigargin or 100 μM TRPC inhibitor 2-APB were measured in Fura-2AM loaded podocytes of the intact glomeruli. Depletion of internal Ca^{2+} stores with thapsigargin did not affect cell activation by Ang II, but 2-APB totally blocked calcium flux. This therefore allows hypothesizing that TRPC channels in the podocytes mediate calcium influx in response to Ang II.

Western blotting and IHC staining revealed that TRPC1, 3 and 6 are expressed in the Sprague Dawley rat glomeruli. Single channel electrophysiological analysis with patch-clamp demonstrated that 100 nM Ang II acutely activates native TRPC-like channels in the podocytes, as well as TRPC6 channels transiently overexpressed in CHO cells together with the ATR1; the detected effect was mediated by changes in the channel open probability.

The ability of podocytes to precisely regulate intracellular Ca^{2+} plays a central role in glomerular diseases, therefore, manipulating Ca^{2+} levels by inhibiting TRPC channels or their activators may be a useful strategy for treating patients with FSGS. In this study we provide evidence of Ang II-dependent activation of TRPC6 channels in podocytes, which might play a significant role in the development of kidney diseases.

This research was supported by the NIH (HL108880) and the Zeiss-OPTEC LLC grant'2012

Where applicable, the authors confirm that the experiments described here conform with The Physiological Society ethical requirements.

PCD209

The mouse calcium sensing receptor of the intercalated cell type B in the collecting duct may contribute to alkali secretion via stimulation of pendrin during dietary calcium loading

Y. Yasuoka[1], Y. Sato[2], H. Nonoguchi[3] and K. Kawahara[1]

[1]Physiology, Kitasato University, School of Medicine, Sagamihara, Japan, [2]Molecular Diagnostics, Kitasato University, School of Allied Health Sciences, Sagamihara, Japan and [3]Internal Medicine, Kitasato University, Medical Center, Kitamoto, Japan

Background: Urinary acidification and polyuria regulated by stimulation of calcium sensing receptor (CaSR) may reduce the risk for urolithiasis caused by hypercalciuria (Renkema KY *et al.* 2009). However, expression level of CaSR, localized at the basolateral membrane of intercalated cell type B (IC-B) in the mouse kidney collecting duct (CD), was unexpectedly decreased during metabolic acidosis caused by NH_4Cl-loading (Yasuoka Y *et al.* 2011). Thus, we further investigated a role of the CaSR for the Ca and pH metabolism in the kidney using a combination of functional and molecular biology technique. Methods: C57BL/6J mice (male, 10 weeks) were subjected to (1) normal (1%) Ca diet (control, n=6), (2) high (2.5%) Ca diet (calcium (CaX) loading, n=6), and (3) NH_4Cl-loading (2.5%) diet (acidosis, n=6). For blood analysis, heparinized blood, collected from the carotid artery of mice anesthetized with 1.5% isoflurane, was analyzed as usual. Values are means ± SE., compared by Student's *t*-test. Results: The level of blood [Ca^{2+}] remained in normal ranges even after administration of CaX and NH_4Cl for 28 and 6 days, respectively. Blood pH of CaX-loading mice was also unchanged (7.37 ± 0.02), whereas that of NH_4Cl-loading mice significantly decreased (7.25 ± 0.02, $P < 0.005$) compared with control (7.38 ± 0.01). Urinary [Ca^{2+}] of CaX- and NH_4Cl-loading mice was significantly increased (6.2 ± 0.1 mg/dl ($P < 0.05$) and 12.1 ± 0.9 mg/dl ($P < 0.005$), respectively), compared with control (5.6 ± 0.4 mg/dl). Urinary pH of CaX- and NH_4Cl-loading mice was significantly lower (6.07 ± 0.07 ($P < 0.005$) and 5.96 ± 0.03 ($P < 0.005$), respectively) than control (6.48 ± 0.04). When mice were kept with NH_4Cl for 6 days, the expression of H-ATPase, carbonic anhydrase (CA) XII and anion exchanger (AE) 1 increased, whereas the levels of the transient receptor potential vanilloid 5 (TRPV5), CaSR, and pendrin expression were decreased. On the other hands, the expression levels of all these molecules were markedly increased by CaX-loading. Interestingly, NH_4Cl-loading increased cell height of IC-A in CDs and CaX-loading increased it at both IC-A and IC-B. All these results suggest that hypercalciuria, reduced reabsorption of Ca^{2+} due to acidosis-induced downregulation of TRPV5 at the distal convoluted tubule (DCT), may stimulate acid secretion of IC-A and alkali secretion of IC-B in parallel, probably due to an activation of CaSR of IC-B through unknown mechanisms. Conclusions: CaSR of IC-B may contribute to alkali secretion to prevent urolithiasis in the mouse kidney collecting duct during dietary surplus Ca loading.

Renkema KY *et al.* (2009). *J Am Soc Nephrol*. 20, 1705-13.

Yasuoka Y *et al.* (2011). *Am Soc Nephrol*, Philadelphia. (abstract)

Where applicable, the authors confirm that the experiments described here conform with The Physiological Society ethical requirements.

PCD210

Identification and characterization of a new promoter regulating expression of Slc4a10 in rat kidney, and localization of Slc4a10 proteins in renal tubules

D. Wang, Y. Liu, Y. Guo, D. Jiang, Z. Xie and L. Chen

Department of Biophysics and Molecular Physiology, Key Laboratory of Molecular Biophysics of Ministry of Education, Huazhong University of Science & Technology School of Life Science & Technology, Wuhan, Hubei Province, China

The electroneutral Na-coupled HCO3– transporter NBCn2, encoded by SLC4A10, plays critical roles in intracellular pH regulation and transepithelial HCO3– movement. In human, dysfunction of SLC4A10 is associated with multiple pathological conditions, including complex epilepsy, mental retardation, autism spectrum disorders, as well as dysmorphic features. We have previously demonstrated that Slc4a10, under the control of two distinct promoters, is capable of expressing two groups of NBCn2 variants differing in the extreme amino termini (Nt), one starting with "MEIK" (the first four residues of the Nt), and the other, "MCDL". In rat, MEIK-NBCn2 is specifically expressed in the central nervous system, whereas MCDL-NBCn2 is predominantly expressed in the kidney.

In the present study, by 5'-rapid amplification of cDNA ends and cDNA cloning, we identified from rat kidney a third new promoter located between the two previous ones in Slc4a10. From this new promoter, two types of Slc4a10 transcripts can be produced, one encoding a protein identical to the previous MCDL-NBCn2. The other lacks exon 3, thus could in theory produce a new type of NBCn2 with a truncation at the Nt. The genomic sequences of the three promoters, including P1 expressing MEIK-NBCn2, the new P2 expressing MCDL- plus the Nt-truncated-NBCn2, and P3 expressing MCDL-NBCn2, were cloned and analyzed by luciferase reporter assay. Among the three promoters, P2 showed the highest activity in human embryonic kidney cells HEK293, while P3 showed just basal activity. Our data are consistent with the notion that MCDL-NBCn2 is expressed under the control of promoter P2 in the kidney. By immunocytochemistry with anti-MCDL-NBCn2, NBCn2 was predominantly localized in the cortex of rat kidney. Surprisingly, a higher magnification view showed that NBCn2 was localized at the apical membrane of epithelial cells in renal tubules, likely the proximal segments. The physiological role of NBCn2 in the kidney remains to be addressed.

Our study is important for the field of acid-base transport. Firstly, disclosing the promoters of Slc4a10 represents a critical step forward towards understanding the mechanism underlying the regulation of tissue-specific expression of Slc4a10. Secondly, the characterization of the promoters could also be important for studying the differential regulation of Slc4a10 expression in response to acid-base stress in different tissues. Finally, our finding about the cellular localization of NBCn2 in the kidney might impact our understanding of the molecular mechanism involved in the acid-base transport in renal tubules.

This work was supported by NSFC grants 30900513 (YL), 31271208 (LMC), and 31000517 (LMC). Dr. Chen was the recipient of the Travel Awards for Young Physiologists from the Chinese Association of Physiological Sciences.

Where applicable, the authors confirm that the experiments described here conform with The Physiological Society ethical requirements.

PCD211

Histological analysis of quercetin effects on cisplatin-induced acute renal failure in rats

S. Hiranyachattada[1], P. Muangnil[1], P. Boonyoung[2] and P. Kirirat[2]

[1]Physiology, Prince of Songkla University, Hatyai, Songkhla, Thailand and [2]Anatomy, Prince of Songkla University, Hatyai, Songkhla, Thailand

The remarkable side effect of cisplatin, a cytotoxic agent in cancer treatment, is acute renal failure which limited its clinical uses. An increase in free radicals has been shown to play an important role in this renal pathogenesis. Our previous studies have shown a significant increase in renal melondialdehyde level on day 3 along with a marked reduction in renal blood flow, glomerular filtration rate and urinary Na+ and K+ excretion on day 3 and day 7 after cisplatin (7.5 mg/kg i.p.) injection in rats. The number of survived animals and the degree of renal damage assessed by clearance technique have been improved with quercetin, a strong antioxidant, co-treatment. In this study, we used histopathological scoring analysis of glomerular and tubular lesions on day 3, 7 and 14 after 7.5 mg/kg cisplatin i.p. injection in rat to strengthen our prior data. The protective effects of oral administration of quercetin, 50 mg/kg, twice 24 hr and 10 min, before cisplatin injection were thoroughly determined. Experiments were performed in male Wistar rats, 200-300 g. The number of rats in each sub-groups were between 5-11. All experimental rats were maintained and handled according to the approval of the Prince of Songkla University Animal Ethics Committee. On the day of experiment, the animals were anesthetized with 60 mg/kg pentobarbitone sodium, i.p., then, the kidneys were retrograde perfused and isolated. Each kidney was longitudinal cut into two pieces and fixed in 10% buffer neutral formalin for 24 hrs before further process. The embedded renal tissues were sectioned at 6 μm thick ribbon and stained with hematoxilin and eosin. Glomerular injury was defined according to the percentage of glomerular atrophy in the renal cortex whereas renal tubular injury grading was defined by the percentage of nuclear swelling, pyknosis and karyorrhexis and tubular dilatation in renal cortical and outer strip of outer medullary area. Intraluminal hyaline cast formation was also randomized graded in both cortex and medulla. Both glomerular and tubular lesions were classified into five grades according to the degree of damage incremently. It is found that the oral co-administration of quercetin with cisplatin injection blunted the progressive lesions of glomerular atrophy, tubular dilatation and intraluminal hyaline cast formation observed on day 7 and 14 but blunted the tubular nuclear damage observed on day 3, 7 and 14. These effects were indicated by the significant reduction in the number of rat with higher lesion grades. It is noticed that one of the mechanisms responsible for the renal protective effect of quercetin in cisplatin- induced acute renal failure rats is via glomerular and tubular structural remodeling.

Where applicable, the authors confirm that the experiments described here conform with The Physiological Society ethical requirements.

PCD212

The citrus flavonoid naringenin inhibits the growth of Dictyostelium and MDCK-derived cysts in a polycystin-2-dependent manner

A. Waheed[1], M. Ludtmann[2], N. Pakes[2], S. Robery[2], A. Kuspa[3], C. Dinh[3], D. Baines[4], R. Williams[2] and M. Carew[1]

[1]School of Pharmacy & Chemistry, Kingston University, Kingston upon Thames, Surrey, UK, [2]School of Biological Sciences, Royal Holloway University of London, Egham, Surrey, UK, [3]Department of Biochemistry and Molecular Biology, Baylor College of Medicine, Houston, TX, USA and [4]Biomedical Sciences, St George's University of London, Tooting, London, UK

Introduction Altered cell proliferation is critical to the progression of neoplastic disorders such as cancer and polycystic diseases. Identifying new potential therapeutic agents to target cell proliferation may therefore provide improved treatments for these disorders. Here, we used the simple, tractable biomedical model *Dictyostelium* to investigate the molecular mechanism of naringenin, a dietary flavonoid with antiproliferative and chemopreventive actions *in vitro* and in animal models of carcinogenesis [1,2]. **Methods and Results** *Dictyostelium discoideum* cells (wild type Ax2) were grown in liquid culture. Naringenin inhibited *Dictyostelium* growth, but not development, after 48-96 hours with an EC50 of 50-100 μM. Screening of a library of random gene knockout mutants identified a mutant (*pkd2-*) lacking the polycystin-2 protein (DDB_G0272999) that was resistant to the effect of naringenin (200 μM, 21 days) on growth and random cell movement. Naringenin (100 μM) reduced cell growth by 37% in wild type cells at 48 and 72 hours, but had no significant effect in the gene knockout mutant *pkd2-*. Polycystin-2 is a divalent cation channel, where mutations in the protein give rise to type 2 autosomal dominant polycystic kidney disease [3]. We therefore translated these results to a mammalian kidney model and grew Madin-Darby Canine Kidney (C7) cells in culture and as cysts in a collagen matrix [4]. Data are expressed as mean ± SEM from 3 independent experiments. Naringenin inhibited MDCK cell growth as measured by neutral red and SRB protein assay with an EC50 of 28 ± 1 μM and inhibited cyst growth with an EC50 of 3-10 μM. Levels of polycystin-2 protein were knocked down to 56 ± 5% after 24 and 48 hours by siRNA in this model. Polycystin-2 knockdown increased the EC50 value for naringenin in MDCK cells to 65 ± 1 μM. Cysts were larger following polycystin-2 knockdown compared to untransfected controls and resistant to the same concentration of naringenin: e.g. 10 μM naringenin: control 0.84 ± 0.03 mm^2; polycystin-2 knockdown 1.44 ± 0.07 mm^2; 30 μM naringenin: control 0.65 ± 0.01 mm^2, polycystin-2 knockdown 1.18 ± 0.06 mm^2. Metformin (10 μM), an activator of AMP-activated kinase and inhibitor of mTOR, reduced the size of both control and transfected cysts equally. **Conclusion** The antiproliferative actions of naringenin in *Dictyostelium* and mammalian kidney cells suggested a conserved effect of naringenin on cell growth mediated by polycystin-2. Further studies will determine if naringenin is a drug candidate for the treatment of ADPKD where polycystin-1 is lost but polycystin-2 is intact [5].

[1] R.S. Williams, K. Boeckeler, R. Gräf, A. Müller-Taubenberger, Z. Li, R.R. Isberg, D. Wessels, D.R. Soll, H. Alexander, S. Alexander, Towards a molecular understanding of human diseases using *Dictyostelium discoideum*, Trends Mol. Med. 12 (2006) 415-424.

[2] E. Meiyanto, A. Hermawan, Anindyajati, Natural products for cancer-targeted therapy: citrus flavonoids as potent chemopreventive agents, Asian Pac. J. Cancer Prev. 13 (2012) 427-436.

[3] S. González-Perrett, K. Kim, C. Ibarra, A.E. Damiano, E. Zotta, M. Batelli, P.C. Harris, I.L. Reisin, M.A. Arnaout, H.F. Cantiello, Polycystin-2, the protein mutated in autosomal dominant polycystic kidney disease (ADPKD), is a Ca^{2+}-permeable nonselective cation channel, Proc. Natl. Acad. Sci. USA. 98 (2001) 1182–1187.

[4] H. Li, I. A. Findlay, D. N. Sheppard, The relationship between cell proliferation, Cl^- secretion, and renal cyst growth: A study using CFTR inhibitors, Kidney Int. 66 (2004) 1926–1938.

[5] V. Takiar, M.J. Caplan, Polycystic kidney disease: pathogenesis and potential therapies, Biochim. Biophysica Acta 1812 (2011) 1337-1343.

This work was funded by a grant awarded jointly to Baines, Carew and Williams from the SouthWest Academic Network (SWAN), a research collaboration between Kingston University, St George's, and Royal Holloway, University of London.

Where applicable, the authors confirm that the experiments described here conform with The Physiological Society ethical requirements.

PCD213

Sialylation of N-glycan stimulated by protein kinase C (PKC) increases urea transporter UT-A1 activity

G. Chen, X. Li and J.M. Sands

Physiology, Emory University, Atlanta, GA, USA

The protein abundance of the UT-A1 urea transporter in kidney inner medulla (IM) is dramatically increased under diabetic conditions, particularly the highly glycosylated 117 kDa form of UT-A1. This change is consistent with the increase in urea permeability in the perfused rat inner medullary collecting duct (IMCD). In diabetes the diacylglycerol (DAG) - protein kinase C (PKC) pathway is activated. It is not known whether and how the elevated DAG and activated PKC pathway contribute to the increased kidney IMCD urea permeability under diabetes conditions. In this study, diabetic animal model was induced in SD rats by tail vein injection of streptozotocin (62.5 mg/kg BW). At 14 day, kidney IM was dissected and cell plasma membrane was isolated by sucrose gradient ultracentrifugation and used for lectin pullown. Diabetes causes significant UT-A1 glycan changes of increased sialic acid as demonstrated by sambucus nigra lectin (SNA) pulldown assay. We then investigated the role of PKC in UT-A1 protein expression. Treatment of 2 μM PDBu, the protein kinase C (PKC) activator, significantly increases UT-A1 protein abundance in UT-A1 MDCK cells. The glycan structure change of UT-A1 was examined using sugar-specific binding lectins. Interestingly, activation of PKC markedly increases UT-A1 glycan sialic acid. Rat kidney IMCD suspensions were prepared and treated with 2 μM PDBu for 4 h. Activation of PKC by PDBu specifically increased UT-A1 sialylation from kidney IMCD. Functionally, increased UT-A1 sialylation has enhanced urea transport activity when the UT-A1 MDCK cells were incubated with 2 mM sialic acid for 24 h. Our study suggests that activation of DAG- PKC pathway may participate in elevated tubular urea reabsorption by increasing UT-A1 sialylation, which plays an important role to prevent the osmotic diuresis caused by glucosuria under diabetic conditions.

Where applicable, the authors confirm that the experiments described here conform with The Physiological Society ethical requirements.

PCD214

The membrane cytoskeletal crosslinker ezrin is essential for the regulation of phosphate and calcium homeostasis

R. Hatano[1], E. Fujii[1], H. Segawa[2], K. Mukaisho[3], M. Matsubara[4], K. Miyamoto[2], T. Hattori[3], H. Sugihara[3] and S. Asano[1]

[1]Molecular Physiology, Ritsumeikan University, Kusatsu, Japan, [2]Molecular Nutrition, University of Tokushima Graduate School, Tokushima, Japan, [3]Pathology, Shiga University of Medical SciencesSchool, Otsu, Japan and [4]Molecular Medicine, Tohoku University School of Medicine, Sendai, Japan

Ezrin is an actin-binding protein that crosslinks between the plasma membrane proteins (adhesion proteins, transporters, channels) and actin cytoskeleton. It is involved in microvilli formation, membrane fusion and protein trafficking. Ezrin is highly expressed in stomachs, small intestines, and kidney. In the kidney, it is mainly localized at brush border membrane (BBM) of proximal tubules, where phosphate (P_i) is reabsorbed by Na^+/P_i cotransporters. There, ezrin is reported to be associated with a major Na^+/P_i cotransporter, Npt2a, through a scaffolding protein, Na^+/H^+ exchanger regulatory factor (NHERF) 1. In the present study, we focused on the physiological role of ezrin in the renal Pi reabsorption and duodenal Ca^{2+} absorption by using ezrin knockdown (*Vil2*$^{kd/kd}$) mice in which expression of ezrin was down-regulated as low as 7% compared with wild-type (WT) mice (Tamura et al. 2005). We found that *Vil2*$^{kd/kd}$ mice exhibited hypophosphatemia and hypocalcemia. The reduced plasma concentration of P_i was attributed to the defective urinary P_i reabsorption. Immunofluorescence staining revealed that cell surface expression of Npt2a and NHERF1 was impaired in the kidney of *Vil2*$^{kd/kd}$ mice. Immunoblotting also revealed that the Npt2a and NHERF1 expressions at the BBM fractions of proximal tubules were markedly reduced in the kidney of *Vil2*$^{kd/kd}$ mice. On the other hand, urinary loss of Ca^{2+} was not observed in *Vil2*$^{kd/kd}$ mice. Plasma concentration of 1,25-dihydroxyvitamin D was elevated following reduced plasma Pi level, and mRNA level of vitamin D-dependent TRPV6 Ca^{2+} channel was increased in the duodenum of *Vil2*$^{kd/kd}$ mice. However, the expression of TRPV6 at apical membrane was disturbed in *Vil2*$^{kd/kd}$ mice due to ezrin knockdown. *Vil2*$^{kd/kd}$ mice also exhibited osteomalacia. Bone mineral density in tibiae was significantly lowered in the adult and young *Vil2*$^{kd/kd}$ mice compared with WT mice. These results strongly suggest that ezrin is required for the regulation of systemic P_i and Ca^{2+} homeostasis in vivo.

Tamura A (2005). J Cell Biol 169, 21-28.

This research was supported by a Grant-in-Aid for Scientific Research (21590082) from the Ministry of Education, Culture, Sports, Science and Technology of Japan.

Where applicable, the authors confirm that the experiments described here conform with The Physiological Society ethical requirements.

PCD215

Mechanoprotection by Polycystins against Apoptosis Is Mediated through the Opening of Stretch-Activated K2P Channels

R. Peyronnet[1], E. Honoré[2] and F. Duprat[2]

[1]Heart Science, National Heart & Lung Institute, Harefield, Middlesex, UK and [2]Institut de Pharmacologie Moléculaire et Cellulaire, UMR CNRS 7275, Université de Nice Sophia Antipolis, Valbonne, France

How renal epithelial cells respond to increased pressure and the link with kidney disease states remain poorly understood. Pkd1 knockout or expression of a PC2 pathogenic mutant, mimicking the autosomal dominant polycystic kidney disease, dramatically enhances mechanical stress-induced tubular apoptotic cell death. We show the presence of a stretch-activated K+ channel dependent on the TREK-2 K2P subunit in mouse proximal convoluted tubule epithelial cells (isolated cells were obtained following the protocol described in Barriere et al. 20031). Our findings further demonstrate both on isolated cells and on the whole kidney in vivo, that polycystins protect renal epithelial cells against apoptosis in response to mechanical stress, and this function is mediated through the opening of stretch-activated K2P channels. Thus, to our knowledge, we establish for the first time, both in vitro and in vivo using mouse model, a functional relationship between mechanotransduction and mechanoprotection. We propose that this mechanism is at play in other important pathologies associated with apoptosis and in which pressure or flow stimulation is altered, including heart failure or atherosclerosis.

Barriere, H., Belfodil, R., Rubera, I., Tauc, M., Lesage, F., Poujeol, C., Guy, N., Barhanin, J., and Poujeol, P. (2003). Role of TASK2 potassium channels regarding volume regulation in primary cultures of mouse proximal tubules. J. Gen. Physiol. 122, 177–190.

Where applicable, the authors confirm that the experiments described here conform with The Physiological Society ethical requirements.

PCD216

Upregulation of NOX4 mediates TGFβ-induced apoptosis in mouse podocyte

R. Das, S. Xu, X. Quan, S. Cha, I. Kong and K. Park

Physiology, Yonsei University Wonju College of Medicine, Wonju, Republic of Korea

Podocytes are terminally differentiated, actin-rich epithelial cells present on the glomerular basement membrane and critical for glomerular filtration process. Podocyte injury leads to onset of chronic renal diseases characterized by proteinuria. Elevated level of TGFβ in pathogenic condition is associated with podocyte damage ultimately resulting in apoptosis and detachment. The underlying mechanism of apoptosis, however, remains not clearly understood in these cells. We investigated pathogenic mediators for proapoptotic effects of TGFβ in cultured immortalized mouse podocytes. TGFβ induced podocyte apoptosis was mediated by elevated level of reactive oxygen species (ROS) which was blocked by N-acetyl-cystein, an antioxidant. Exogenous TGFβ1 selectively increased the expression of only Nox4, excluding other NADPH oxidase (NOX) enzymes. Consistent with Nox4 upregulation, the total NOX activity was higher in TGFβ1-treated podocytes. TGFβ1 enhanced total ROS and elicited apoptosis indicated by the increased number of apoptotic nuclei and elevated level of cleaved caspase-3. These changes by TGFβ1 were blocked by SB431542 and DPI, a potent inhibitor of Type I TGFβ receptor and a selective inhibitor of NADPH oxidases, respectively. Knock-down of Nox4 by siRNA (siNOX4) treatment blocked TGFβ1-induced ROS production and caspase activation. In podocyte, Nox4 was localized to mitochondria as it co-localized with mitochondrial protein Cox1. TGFβ1 elicited mitochondrial membrane depolarization which was recovered by siNOX4 or DPI treatment. In addition, siRNA for smad2 or smad3 reduced Nox4 in transcript and protein level, total ROS generation, and cleaved caspase-3 activation. These results suggest that TGFβ-induced activation of Smad2/3 is responsible for Nox4 up-regulation, and ROS production by NOX4 closely participates in TGFβ-induced apoptosis via mitochondrial dysfunction which might be a crucial mechanism for the development and progression of proteinuric glomerular diseases including diabetic nephropathy.

This study was supported by grant from Korean National Research Foundation (2010-0014617).

Where applicable, the authors confirm that the experiments described here conform with The Physiological Society ethical requirements.

PCD217

Sinaling pathways involved in the rapid biphasic effect of aldosterone on Na+/H+ exchanger in IRPTC cells

D.C. Leite-Dellova[1], G.K. Fonseca[2], M. Oliveira-Souza[3] and M. Mello-Aires[3]

[1]Veterinary Medicine, University of Sao Paulo, Pirassununga, Sao Paulo, Brazil, [2]Basic Sciences, University of Sao Paulo, Pirassununga, Sao Paulo, Brazil and [3]Physiology and Biophysics, University of Sao Paulo, Sao Paulo, Sao Paulo, Brazil

We demonstrated that the rapid nongenomic dose-dependent biphasic effect of aldosterone on Na+/H+ exchanger in proximal tubule is compatible with stimulation of this exchanger by small increases in intracellular calcium concentration ([Ca2+]i) (at 10-12 M aldosterone) and inhibition due high increases in [Ca2+]i (at 10-6 M aldosterone) (Leite-Dellova et al, 2008); however, the signaling pathways involved in these effects are still unknown.The purpose of this study is researching the involvement of the mineralocorticoid receptor (MR), glucocorticoid receptor (GR), extracellular signal-regulated Kinases 1 and 2 (ERK1/2), adenosine 3`,5`-monophosphate (cAMP) and protein kinase C (PKC) in the aldosterone rapid effects on the Na+/H+ exchanger and [Ca2+]i of proximal tubule. The hormonal effects on intracellular pH (pHi) and [Ca2+]I were investigate in immortalized proximal tubule cells of rats (IRPTC), using fluorescence microscopy and the probes BCECF-AM (3 μM) and FURA 2-AM (5 μM), respectively. The values shown are means ± S.E.M. and the comparisons are made by ANOVA ($p < 0.05$). The pHi recovery rate (pHirr), after cellular acidification with a NH4Cl pulse, was 0.24 ± 0.011 pH units/min (N=8). EIPA (20 μM; Na+/H+ exchanger inhibitor) and HOE 694 (5 μM; NHE1 specific inhibitor), but not S3226 (1 μM; NHE3 specific inhibitor), cause a decrease in pHirr (63% and 59%, respectively). The mean baseline [Ca2+]i was 100 ± 4 nM (N=10). Aldosterone (10-12 M; 2 min preincubation) increases the pHirr (50%) and the [Ca2+]i (63%), but aldosterone (10-6 M; 2 min preincubation) decreases the pHirr (46%) and increases the [Ca2+]i (132%). RU 486 (1 μM; GR inhibitor),

PD 98059 (15 μM) and U0126 (15 μM) (ERK1/2 inhibitors), Cheleritrine (1 μM) and Stausporine (10-5 M) (PKC inhibitors) abolish the effects of aldosterone on pHirr and [Ca2+]i. Eplerenone (10-5 M, MR inhibitor) and 8Br cAMP (10-5 M; cAMP analogue) do not alter these parameters. The present results confirm our previous data indicating that the rapid biphasic (stimulatory/inhibitory) effect of aldosterone on NHE1 is associated with the rapid stimulatory dose-dependente effect of aldosterone on the [Ca2+]i. The observed effects of aldosterone on pHirr and [Ca2+]i occur via GR (data consistent with GR detection in IRPTC cells by RT-PCR and Western blot) and are mediated by ERK1/2 and PKC signaling pathways and seem to be independent of MR and cAMP.

Keywords: aldosterone rapid effects, NHE1, pHi, intracellular calcium

Leite-Dellova DCA, Oliveira-Souza M, Malnic G, Mello-Aires M (2008). Genomic and nongenomic effects of aldosterone on Na+/H+ exchanger in proximal S3 segment: role of cytosolic calcium. Am J Physiol Renal Physiol, 295:F1342-F1352.

CNPq and FAPESP

Where applicable, the authors confirm that the experiments described here conform with The Physiological Society ethical requirements.

PCD218

An antatomically-unbiased approach for analysis of renal BOLD magnetic resonance images

R.I. Menzies[1], A. Zammit-Mangion[2], M.A. Jansen[1], D.J. Webb[1], J.J. Mullins[1], J.W. Dear[1], G. Sanguinetti[2] and M. Bailey[1]

[1]Centre for Cardiovascular Sciences, The University of Edinburgh, Edinburgh, UK and [2]The School of Informatics, The University of Edinburgh, Edinburgh, UK

Oxygenation defects may contribute to renal disease but pO_2 is difficult to measure. Microelectrodes offer quantitative but localised measurements and are invasive. A global "map" of pO_2 can be obtained post-mortem by immunohistochemical detection of pimonidazole adducts. This is non-quantitative and insensitive. BOLD MRI provides an alternative for longitudinal measurement of oxygen gradients. However, post-acquisition data analysis often relies on manual selection of region(s) of interest, which excludes from analysis significant quantities of biological information and is subject to selection bias.

We applied k-means clustering as an anatomically unbiased analytical approach, clustering individual voxels on quantitative nearness of the R2* signal. This quantitative similarity does not necessarily imply close anatomical association of voxels or compartmentalization within a given region of the kidney.

Scans were performed on anesthetized (2% Isofluorane) F344 rats (n=6) using a 7T MRI scanner. A birdcage volume coil and a 4-channel phased array surface coil were used for radio frequency transmission and signal reception, respectively. We employed two complementary strategies to affect R2*. Acutely, we administered acetylcholine IV; chronically we infused via osmotic minipump angiotensin II (60ng/min) over a 3-day period, after which rats were rescanned.

Data (mean ± SE) were analysed by RANOVA. In control rats, low R2* clustering was located predominantly within the cortex and higher R2* clustering within the medulla (70.96±1.48 versus 79.00±1.50; 3 scans per rat; n=6; P<0.01) consistent anatomically with a cortico-medullary oxygen gradient. An IV bolus of acetylcholine caused a transient reduction of the R2* signal in both clustered segments (P<0.01), which was nitric oxide dependent. Chronic infusion of angiotensin II disrupted the cortico-medullary gradient, producing less distinctly segmented mean R2* clusters (71.30±2.00; versus 72.48±1.27; n=6; NS). The acetylcholine-induced attenuation of the R2* signal was abolished by chronic angiotensin II infusion, consistent with reduced nitric oxide bioavailability.

In summary, we have developed an anatomically unbiased method for the assessment of renal function by BOLD MRI, employing signal analysis to remove errors inherent in manual ROI selection. This method offers a global insight into intrarenal oxygenation and the dynamic response of R2* to acetylcholine can provide information relating to renal NO bioavailability.

This work was funded by the British Heart Foundation Centre of Research Excellence Award

Where applicable, the authors confirm that the experiments described here conform with The Physiological Society ethical requirements.

PCD219

The effects of Angiotensin 1-7 on renal haemodynamics

W.E. Osman, E.J. Johns and A.F. Ahmeda

Physiology Department, UCC, Cork, Ireland

The renin angiotensin system (RAS) is involved in the regulation of renal function and cardiovascular homeostasis. The actions of the vasoconstrictor and anti-natriuretic factor angiotensin II (Ang II) are well described, however, recently the discovery of a second isoform of angiotensin converting enzyme which generates angiotensin 1-7 (Ang1-7) has generated further interest in this peptide. Studies to date suggest that Ang1-7 opposes the effects of Ang II, that is it is vasodilator and has diuretic properties. This study investigated the effects of Ang 1-7 on regional renal haemodynamics in animals of different dietary sodium intakes to stimulate or suppress the endogenous RAS.

Three groups (n=6), 250-300g, of male Wistar rats fed a normal salt (NS) [0.3% Na+], high salt (HS) to suppress the RAS [3% Na+], or low salt (LS) to stimulate the RAS [0.03% Na+] diet for three weeks, were anaesthetised with 1 ml i.p. chloralose/urethane (16.5/250 mg/ml, respectively).

The right femoral vein and artery were cannulated for infusion of saline (154 mM NaCl) at 3 ml/h, anaesthetic supplementation (0.05 ml every 30 min), and measurement of arterial blood pressure and heart rate.

The left kidney was exposed via a flank incision, placed in a holder and a small cannula was inserted 4.5 mm into the corticomedullary border (CMB) for infusion of saline or Ang1-7 at 1.0 ml/h.

Two Laser-Doppler microprobes were inserted 1.5 and 4.0 mm into the kidney to measure cortical (CP) and medullary (MP) blood perfusion. 90 minutes were allowed for recovery from the surgery followed by baseline recording, and then infusion of the Ang (1-7) at two different doses (low, 15ng/min and high, 50ng/min) into the CMB for 40 min. At the end of experiments the rats were killed with an overdose of anaesthetic.

Data, presented as mean ± SEM, were subjected to the Student's t-test and significance taken at P<0.05.

Baseline recordings for CP and MP in NS were 227±50PU and 98±12PU, in HS were 313±48PU and 132±20PU and in LS were 293±40PU and 123±9PU, respectively.

Infusion of Ang 1-7 at low and high doses increased CP in all groups (15±5% and 7±3% in NS, 9±2% and 18±10% in HS, and 9±2 and 1±3% in LS; P<0.05).
MP increased significantly (P<0.05) only following the infusion of the low dose on both normal and high salt fed rats by 10± 3% and 8±3%, respectively. In LS group, where RAS is activated and Ang II is at a high level, the MP remained unchanged at both doses.
These results indicate that Ang 1-7 caused a vasodilatory effect on the renal microvasculature, expressed as an increase in blood perfusion, which was much more evident in the cortical region but could not be related to the level of dietary sodium intake. Ang 1-7 caused a similar vasodilation in the medullary region except when the RAS was suppressed by the high salt intake when no effect could be demonstrated.

Where applicable, the authors confirm that the experiments described here conform with The Physiological Society ethical requirements.

PCD220

Cell signaling responses in rabbit renal proximal tubules exposed to acute acid-base disturbances

L. Skelton and W.F. Boron

Physiology and Biophysics, Case Western Reserve University, Cleveland, OH, USA

Acute exposure of rabbit proximal tubule suspensions (PTs) to acid-base disturbances alters ErbB1 and ErbB2 tyrosine phosphorylation. Here we examine whether Src (which can transactivate ErbB1/2) or proteins downstream of ErbB1/2 are involved in the CO_2/HCO_3 signaling cascade. New Zealand White rabbits were euthanized under anesthesia using ~10ml intravenous 5% pentobarbital sodium. PTs were purified from rabbit renal cortex using a method similar to Doctor RB *et al.* (1998), modified for rabbit. We exposed purified PTs for 5 or 20 min to: *HEPES* (i.e., HEPES/pH 7.40); *Butyrate* (HEPES/pH 7.10 + 20 mM butyrate);*EGF* ('HEPES' + 10 nM EGF); *Physiological* CO_2/HCO_3 (5% CO_2/22 mM HCO_3/pH 7.40); *respiratory acidosis* (RAc; 10% CO_2/22 mM HCO_3/pH 7.10); *compensated RAc* (10% CO_2/44mM HCO_3/pH 7.40); *metabolic acidosis* (MAc; 5% CO_2/11 mM HCO_3/pH 7.10), *respiratory alkalosis* (RAlk; 2.5% CO_2/22 mM HCO_3/pH 7.70), or *metabolic alkalosis* (MAlk; 5% CO_2/44 mM HCO_3/pH 7.70) +/- PD168393, an ErbB family inhibitor. We probed lysates with phospho-specific (p) antibodies to ErbB1/ErbB2, Src, ERK1/2 (p44 & p42), and PLCγ1. PTs exposed to RAlk for 5 min exhibited a decreased ratio of Src-pY-416 (kinase-activating) to Src-pY-527 (kinase-inactivating). Concurrently ErbB1-pY845 (Src-transactivated) fell. RAlk or MAlk for 5 min reduced pERK1/2 levels compared to the other treatments; PD168393 inhibited only p44 after MAlk. At 5 min, butyrate, RAc, or Compensated RAc reduced PLCγ1-pY-783; at 20 min, pY for butyrate and RAc remained low. In conclusion, rabbit PTs exhibit acid-base–dependent signaling responses in pathways up- and downstream from ErbB1/2, and these signals evolve over time.

Doctor *et al.* (1998). Am J. Physiol. 274 (Renal Physiol. 43):F129-F138

Where applicable, the authors confirm that the experiments described here conform with The Physiological Society ethical requirements.

PCD222

Cleavage of SPAK kinase by kidney-enriched protease(s)

N. Markadieu[1], P.A. Welling[2] and E. Delpire[1]

[1]Anesthesiolgy, Vanderbilt University Medical School, Nashville, TN, USA and [2]Physiology, University of Maryland Medical School, Baltimore, MD, USA

The Ste20 kinases SPAK and OSR1 regulate Na^+ transport in the distal nephron. Western blot analysis of kidney lysates revealed the presence of multiple SPAK fragments in the kidney medulla, which are thought to have inhibitory effects on OSR1 in the thick ascending limb of Henle [1, 2]. The nature of these fragments is still not completely understood. Based on a 49 kDa band size found in multiple tissues, we proposed earlier that translation also starts at an alternative methionine, resulting in a shorter protein sometimes called SPAK2 [3]. Analysis of Expressed Tag Sequences databases also revealed the presence of a shorter SPAK transcript consistent with a 34 kDa protein (KS-SPAK) [2]. Here, we demonstrate using a C-terminal anti-SPAK antibody that mouse kidney lysate cleaves in a dose- and time-dependent manner a fusion protein consisting of GST followed by full-length SPAK. The incubation results in five to seven proteolytic fragments with two of the fragments having sizes compatible with SPAK2 and KS-SPAK. We further confirm that thrombin, which protease site is located at the end of GST, produces only one fragment of a larger molecular size. When we used equal protein amounts from lysates prepared from mouse brain, spleen, liver, and kidney, we only observed the cleavage pattern with kidney, indicating that the protease(s) is/are enriched in this tissue. We demonstrate that the cleavage is resistant to aprotinin (2.5 μM), leupeptin (40 μM), PMSF (3 mM), and EDTA (5 mM), indicating inefficacy of traditional protease inhibitors. The cleavage was also resistant to pepstatin (1-10 μM), and CuSO4 (1 mM) or doxycycline (200 μM), potentially eliminating cathepsins and metalloproteases as possible proteolytic enzymes. We show, however, that the cleavage was sensitive to DTT, as proteolysis was significantly reduced with 1 mM of the reducing agent and completely eliminated at 10 mM. This observation indicates that the protease is stabilized by di-sulfide bridges. The protein cleavage occurred over a wide temperature range (4ºC – 45ºC), but was impaired at 55ºC and eliminated at 65ºC and higher temperatures. Finally, we tested SPAK cleavage over a wide pH range (pH 5.5 – 9.5) and made the following observation: the proteolysis leading to the higher size fragments occurred equally over the entire pH range, whereas the proteolysis leading to the smaller two fragments was significantly inhibited by basic pH and markedly activated by acidic pH. This observation indicates the possible involvement of two distinct proteases. Future work will seek to identify the amino acid sequences in SPAK targeted for proteolytic cleavage and determine the identity of the protease(s) involved.

McCormick *et al.* (2011). *Cell Metabolism*. **14**: 352-364.

Grimm *et al.* (2012). *J. Biol. Chem*. **287**: 37673-37690.

Piechotta and Delpire (2003) *J. Biol. Chem*. **278**: 52848-52856.

This work was supported by NIH grant: DK093501 to E.D. and P.A.W.

Where applicable, the authors confirm that the experiments described here conform with The Physiological Society ethical requirements.

PCD223

Glucocorticoid receptor haploinsufficiency causes salt-sensitivity and dysregulation of the thiazide-sensitive Na-Cl cotransporter

J.R. Ivy[1], L.C. Evans[1], R.V. Richardson[1], P.W. Flatman[2], K.E. Chapman[1], C.J. Kenyon[1] and M.A. Bailey[1]

[1]Molecular Physiology (CVS), University of Edinburgh, Edinburgh, UK and [2]Centre for Integrative Physiology, University of Edinburgh, Edinburgh, UK

The distal convoluted tubule (DCT) plays key roles in blood pressure (BP) homeostasis. Reabsorbing up to 7% of the sodium load, DCT length changes with demand, optimizing sodium delivery into the collecting duct. The Na-Cl co-transporter (NCC) is the predominant route for apical sodium entry. Aldosterone activates NCC but the conventional paradigm of mineralocorticoid protection by 11β-hydroxysteroid dehydrogenase 2 does not apply: the enzyme is not expressed in the DCT and NCC can be regulated by glucocorticoids.
Glucocorticoid receptor (GR) heterozygous mice on a standard (0.25%) sodium diet have elevated BP and increased circulating corticosterone. We found in vivo that NCC reabsorbs ~2% of the filtered sodium load in both wild-type and GR+/- mice. When mice were a fed high salt diet (2.5%), a reduction of thiazide-sensitive transport was seen in wild type mice but not in GR+/-. Heterozygotes entered positive sodium balance ($P<0.01$, n=6, one way ANOVA) and BP increased ($P<0.05$ n=16, one way ANOVA). High sodium diet caused a moderate increase ($P<0.05$) in mRNA abundance for slc12a3, the gene encoding NCC, in GR+/-, but not in controls (n=8, Student's t-test). Surprisingly, the high sodium diet increased total expression of NCC in both genotypes and there was no difference in expression between genotypes under either dietary regimen ($P>0.05$, n=6, Student's t-test).
These data indicate that inappropriate NCC activity contributes to salt sensitive hypertension in GR haploinsufficiency. Sustained NCC activity in vivo does not correlate with protein abundance and may reflect alterations in post-translational modification (e.g. phosphorylation), protein-protein interactions or membrane trafficking.

Where applicable, the authors confirm that the experiments described here conform with The Physiological Society ethical requirements.

PCD224

Systemic iPSs decrease kidney injury dependent on ROS-facilitated engraftment

M. Xiang, N. Li, P. Lu, L. Le, J. Quan, D. Meng, X. Wang, R. Wang, A. Chen and S. Chen

Department of physiology and pathphysiology, Shanghai Medical College,Fudan University, Shanghai, China

Aims: Induced pluripotent stem cells (iPSs) are believed to have great therapeutic potential. Treatment for acute kidney injury is challenging. Therefore, we aimed to demonstrate if iPSs attenuate acute kidney injury and the possible mechnisms.
Methods: In vivo experiments: Male C57BL/6 mice were anesthetized with an intraperitoneal injection of 4% sodium pentobarbital (Nembutal). Kidneys were exposed and subjected to right nephrectomy, followed by left renal ischemia for 50min, then resuscitated with Ringer's lactate. After operation, the mice were injected iPSs with or without 100uM NAC pre-treated. The kidney tissue and serum were collected 24 h, 48h after resuscitation. Creatinine, pathology score, cytokine expression, iPSs quantification and identification in injury kidney were detected. In vitro EC- iPSs experiments: mice glomerular endothelial cells isolated from C57BL/6 were pre-treated with MCP-1 (10 U/ml) 4h, and then added iPSs with or without NAC(100 uM) treated. Following that the adhesion and transendothelial migration of IPS were detected.
Results: In vivo study showed iPSs decreased the scores from 2.5±0.2 at 24h and 3.9±0.1 at 48h in mice receiving PBS to 1.1±0.1 and 0.25±0.1, respectively. The scores of mice receiving NAC-pretreated iPSs were in between. The serum creatinine levels to 248.14±13.66 umol/L at 24h and 280.94±9.89 umol/L at 48h. Intravenous injection of iPSs decreased serum creatinine levels to 99.54±4.65 umol/L at 24h and 93.9±4.58 umol/L at 48h . The serum creatinine level had no significant difference between mice receiving PBS and NAC-pretreated iPSs.Administration abolished the increases in the expressions of IL-6, GRO, and GM-CSF in the kidney. NAC-pretreated iPSs had the same effect as untreated iPSs. The positive cells were found in the kidney that received iPS or NAC-pretreated iPSs, but not in the mice that received PBS by FISH staining.
In vitro study showed the rate of adhesion of iPSs to MCP-1-activated GEC was significantly higher than to untreated GEC. NAC-pretreatment decreased the transendothelial migration of iPSs by 47.2%, adhesion to activated GEC by 57.1%, and adhesion to untreated GEC by 14.4%.
Innovation and conclusion: The novel findings of the present study included isogenic iPSs decreased renal ischemia/reperfusion injury. iPSs selectively homed to injured kidneys and became an integrated part of glomeruli and renal tubules in a ROS-dependent manner. Our results also showed that iPSs can be regulated by modulating either iPSs themselves or the endothelial cells of target tissue.

Robinton, D. A. & Daley, G. Q.(2012) . Nature 481, 295-305,doi: 10.1038 / nature 10761 nature10761 [pii] (2012).

Carvajal-Vergara, X. et al. (2010). Nature 465, 808-812, doi:nature09005 [pii] 10.1038/nature09005.

Han, J. et al. (2010). Nature 463, 1096-1100, doi:nature08735 [pii] 10.1038/nature08735.

Jiang, M. et al. (2011). Mol Cell Biochem 354, 67-75, doi:10.1007/s11010-011 -0806-5.

Bae, Y. S., et al. (2011). Mol Cells 32, 491-509, doi:10.1007/s10059-011-0276-3

This work was supported by Key Programs (30830050 to S. Chen and 81130004 to A.F. Chen), Great International Cooperation Program (81220108002 to S. Chen) and General Program (30771003 to S. Chen, 81170298 to D. Meng and 81100047 to M. Xiang) of the National Natural Science Foundation of China, the National Basic Research Program of China to S. Chen (2009CB521900), NIH R01 GM077352 and the American Diabetes Association Research Award 7-08-RA-23 to A.F. Chen.

Where applicable, the authors confirm that the experiments described here conform with The Physiological Society ethical requirements.

PCD225

Extracellular nucleotides increase albumin permeability of isolated intact wistar rat glomeruli

M. Kasztan[1], A. Piwkowska[2], E. Kreft[1], R. Kowalski[1], M. Szczepanska-Konkel[1] and M. Jankowski[1,2]

[1]Department of Therapy Monitoring and Pharmacogenetics, Medical University of Gdansk, Gdansk, Poland and [2]Laboratory of Molecular and Cellular Nephrology, Mossakowski Medical Research Center Polish Academy of Sciences, Gdansk, Poland

INTRODUCTION: Renal glomeruli consist of endothelial cells, mesangial cells, acellular basement membrane and epithelial cells called podocytes. Interactions between these cells and amorphic membrane affect the glomerular barrier function. Activity of these cells is regulated by extracellular nucleotides via P2-receptors in para-/autocrine manner. These receptors are nucleotides-gated ion-channels receptors (P2X) and G protein-coupled receptors (P2Y). The expression of purinoceptors is up-regulated in some forms of chronic renal injury and inflammatory diseases characterized by increased glomerular permeability leading to development of albuminuria/proteinuria, a sign of kidney disease and independent risk factor for the progression of renal failure and for cardiovascular morbidity and mortality.
AIM: The aim of study was to investigate the effects of P2-receptors activation on glomerular-capillary permeability for albumin.
METHODS: The osmotic pumps (ALZET, model 2001, reservoir volume 200μl, pumping rate 1μl/hr) with specific and non-selective agonists of P2-receptors, 2-MeSATP (10-6M), ATP-γ-S (10-6M) or buffer were implanted subcutaneously into Wistar rats for 7 days. Afterwards pumps were removed and glomeruli were isolated by sieving technique. Isolated, affixed to a dishes coated with poly-L-lysine, glomeruli were incubated with buffer or natural nucleotides (ATP, ADP, AMP, UTP, UDP) or synthetic nucleotides (2-methylothioATP, ATP-γ-S). Glomerular-capillary permeability for albumin (Palb) was measured as a volume response of glomerular capillaries to an oncopressive medium generated by defined concentrations of albumin. Measurements were conducted using video-microscopy (Olympus IX51). Glomerular volume was derived from the area of glomerular image calculated using CellSens Dimension Software (Olympus). The reflection coefficient of albumin (Salb) was calculated as Salb = ΔVexperimental/ΔVcontrol. Palb was calculated as Palb = 1-Salb. Cultured rat podocytes were used for immunofluorescence studies.
RESULTS: Palb in control glomeruli was 0.10±0.03. 2-MeSATP and ATP-γ-S (10-6M, 10 min, 37°C) induced increase in Palb to 0.58±0.04 and 0.37±0.08, respectively. Palb in glomeruli isolated from rats in vivo exposed to 2-MeSATP or ATP-γ-S (released from osmotic pumps) were significantly increased (0.35±0.03 vs. 0.13±0.02. and 0.52±0.02 vs. 0.13±0.02, respectively). Palb in glomeruli incubated with natural agonists of P2-receptors were increased and amounted to 0.24±0.04 (ATP 10-6M, 2min), 0.34±0.04 (ADP 10-6M, 2min), 0.33±0.05 (AMP 10-6M, 2min), 0.35±0.10 (UTP 10-6M, 2min), 0.23±0.05 (UDP 10-6M, 2min), respectively. 2-MeSATP and ATP-γ-S affects cortical actin remodeling in cultured podocytes.
CONCLUSIONS: Our results suggest that activation of P2-receptors increases glomerular-capillary permeability for albumin and may be involved in pathogenesis of renal diseases.

Where applicable, the authors confirm that the experiments described here conform with The Physiological Society ethical requirements.

PCD226

Expression of the extracellular calcium-sensing receptor, CaSR, in rat, human and mouse kidney

J. Graca[1], M. Schepelmann[2], D. Riccardi[2] and S. Price[1]

[1]AstraZeneca, Macclesfield, UK and [2]Cardiff University, Cardiff, UK

The calcium sensing receptor (CaSR) is a GPCR with a key role in the regulation of calcium homeostasis. Although the initial cloning and characterization of the CaSR in kidney was performed in 1995, discrepancy in the expression pattern within this organ and species differences have been reported by different groups. Determining the expression of the CaSR along the nephron is key to understanding the physiological role of the CaSR in the kidney.
We aimed to determine the localisation of the CaSR in rat, human and mouse kidney, using *in situ* hybridisation and immunohistochemistry methods.
In situ hybridization was carried out using a sensitive branched-DNA methodology. CaSR mRNA showed highest expression in the thick ascending limb (TAL), but was also expressed in the distal tubule (DT) and collecting duct (CD), with weaker expression in the proximal tubule (PT). For immunohistochemistry three different antibodies raised against different epitopes of the CaSR were used to determine whether the differences reported previously could be ascribed the different antibodies used. By western blotting, all the three antibodies used produced bands of the expected immunoreactivity and molecular weight for CaSR protein in mouse and rat kidney. Immunolocalisation of the CaSR was similar with the three different antibodies; generally CaSR immunoreactivity was stronger in the medulla and weaker in the cortex. Dual labelling was also carried out using antibodies against specific markers for DT (thiazide-sensitive Na+-Cl- cotransporter, NCC), TAL (Tamm-Horsfall protein) and CD (aquaporin 2), to confirm the exact nephron segments expressing the CaSR. The CaSR co-localized with CD, TAL and DT markers, with the strongest signal in the TAL.
Our data show that the CaSR exhibits the strongest expression in the TAL, and that it is also expressed in other nephron segments including the PT, CD and DT. These findings have clarified the expression pattern of the CaSR in kidney in several species, using different techniques. This work will enable the full physiological role of the CaSR in kidney to be determined.

Where applicable, the authors confirm that the experiments described here conform with The Physiological Society ethical requirements.

PCD227

MO25β has no physiological role in electrolyte homeostasis or systemic blood pressure maintenance

K. Siew[1], P. de los Heros[2], D.R. Alessi[2] and K.M. O'Shaughnessy[1]

[1]Clinical Pharmacology Unit, Department of Medicine, University of Cambridge, Cambridge, UK and [2]MRC Protein Phosphorylation Unit, College of Life Sciences, University of Dundee, Dundee, UK

Introduction: Hypertension (HT) affects 1 in 4 age 25+ years, contributing to ~12.8% of global deaths. Thiazide diuretics are

amongst the most widely used Anti-HT drugs that reduce blood pressure (BP) by inhibition of the Na^+-Cl^- Cotransporter (NCC) in the renal distal convoluted tubule (DCT) causing salt-wasting. Genetic disorders & knockout (KO) mice targeting proteins SPAK, OSR1 or WNKs that form a cascade regulating NCC activity & expression in the DCT have also resulted in BP modulation via parallel changes in NCC function & renal Na^+ excretion. So the WNK/SPAK/OSR1 pathway represents a novel therapeutic HT target (1-3). Recently mouse protein-25 alpha (MO25α/CAB39) was discovered to be the master regulator of SPAK/OSR1; it colocalises with NCC, increases SPAK/OSR1 activity up to 100-fold independent of WNKs, facilitates SPAK/OSR1 monomer interactions & stabilises active conformations, which in turn enhance NCC activity & Na+ reabsorption (3-5). It was hypothesised that MO25 deficiency would result in a hypotensive salt-wasting phenotype, however the embryonic lethality of MO25α-KO mice has limited *in vivo* data & focus to its sister isoform MO25beta (MO25β/CAB39L). MO25β shares 79% sequence identity with MO25α, interacts similarly with substrates such as LBK1 & has high renal expression (4). Thus MO25β-KO mice were utilised to test *in vivo* effects of the MO25α paralog. Methods: Age matched C57Bl/6 MO25β-KO mice & wildtype (WT) littermates between 2-4 months were either fed a normal Na^+ diet (0.25%) or placed on a high Na^+ diet (3%) for 10 days before switching to a low Na^+ diet (0.03%) with urine collected for electrolyte analysis at 0hrs, 3hrs, 6hrs, 24hrs & 4 days post-switch. BP was measured by direct carotid manometry (MLT844, AD Instruments) under terminal anaesthesia (isoflurane 2% at 2L/min O_2). The procedure terminated with blood collection via cardiac puncture for electrolyte analysis & excision of the kidneys. Data are presented as mean ± SEM; means were compared by Student's t-test with $P < 0.05$ considered statistically significant. Results: There were no differences between KO vs. WT mean arterial pressures on normal Na^+ [80.2 ± 2.4 mmHg (n=4) vs. 79.0 ± 2.3 mmHg (n=3)] or low Na^+ diets [80.0 ± 1.2 mmHg (n=11) vs. 80.7 ± 1.1 mmHg (n=11)]. No significant differences were detected for urine or plasma levels of creatinine, Na^+, K^+, Cl^-, Ca^{2+}, Mg^{2+} or PO_4^{3-} on any diet with the one exception of Mg^{2+} on a normal Na^+ diet (see table). We therefore conclude MO25β does not play a significant role in BP or electrolyte homoeostasis *in vivo*.

Baseline Urine Electrolytes (0.25% Na^+ diet)

Genotype	Creatinine (mmol/L)	Na^+	K^+	Cl^-	Ca^{2+}	Mg^{2+}	PO_4^{3-}
WT	5.00 ± 0.39 (n = 10)	8.06 ± 1.18 (n = 10)	13.22 ± 1.23 (n = 10)	17.85 ± 1.12 (n = 10)	0.95 ± 0.15 (n = 7)	22.41 ± 1.46* (n = 7)	4.15 ± 0.97 (n = 7)
KO	4.17 ± 0.24 (n = 10)	10.31 ± 0.68 (n = 10)	15.96 ± 1.43 (n = 10)	21.01 ± 1.68 (n = 10)	1.59 ± 0.26 (n = 8)	28.46 ± 2.15* (n = 8)	1.94 ± 0.63 (n = 8)

Electrolytes were normalised against creatinine (electrolyte conc./creatinine conc.]. * ($P<0.05$).

Rafiqi FH *et al*. (2010). *EMBO Mol Med* **2**, 63-75

Lin SH *et al*. (2011). *Proc Natl Acad Sci USA* **108**,17538-17543

Ponce-Coria J *et al*. (2012). *Am J Physiol Cell Physiol* **303**, 1198-1205

Filippi BM *et al*. (2011). *EMBO J* **30**, 1730-1741

Grimm PR *et al*. (2012). *J Biol Chem* **287**, 37673-37690

Where applicable, the authors confirm that the experiments described here conform with The Physiological Society ethical requirements.

PCD228

Iodinated contrast media induced oxidative stress and tubular necrosis in isolated thick ascending limb of rat

Z. Liu, K. Schmerbach, P. Persson, E. Seeliger, C. Kathleen, A. Patzak and M. Sendeski

Institut fuer Vegetative Physiologie, Charité-Universitätsmedizin Berlin, Berlin, Germany

Introduction: The cases of contrast induced acute kidney injury (CI-AKI) are increasing. A toxic effect of contrast media on the tubular cells is generally accepted as the key feature in CI-AKI(1,2). We investigate the hypothesis that contrast media induce tubular cell death by generating oxidative stress and reducing nitric oxide.

Methods: Male Sprague-Dawley rats were killed using isoflurane and isolated thick ascending limbs (TALs) were perfused with either vehicle solution or iodixanol. Nitric oxide bioavailability and superoxide concentration were quantificated by the fluorescent dyes DAF-FM and dihydroethidium (DHE), respectively. Propidium iodide was used to estimate the cell death rate. The expression of oxidative stress related genes and the activity of superoxide dismutase (SOD) in tubuli were investigated using a microarry and the OxiSelect kit in an ex vivo setup. DHE, DAF-FM and Propidium iodide data were compared using Brunner's test. RNA microarray and the activity of SOD data were compared by the Student's t-test.

Results: Iodixanol increased DHE fluorescence ratio (9.6±1.4%, n=7) compared to the control group (1.7±1.0%, n=8) in 4min, whereas tempol, a superoxide dismutase mimic, inhibited the increase by iodixanol. DAF-FM fluorescence intensity decreased during iodixanol treatment (-0.6±0.6%, n=7) and by nitric oxide synthase inhibitor L-NAME, whilst it increased by 1.6±0.3% in the control group within 12min (n=7). Propidium iodide intensity was significantly enhanced by iodixanol (n=8) compared to the control group (n=6) within 20min. Moreover, during total 4-hour perfusion, iodixanol increased propidium iodide intensity to 17.7±3.1%, while in control group was 7.0±1.0%. Only two of 84 investigated genes related to oxidative stress were differentially expressed in the tubuli. The SOD activity did not differ between iodixanol perfused rats and control animals.

Conclusion: The study shows that contrast media increase superoxide concentration, implying oxidative stress in TALs. Further, an impaired nitric oxide bioavailability happens due to contrast media. TAL cells are damaged by contrast media. This damage is not because of changes in the expression of oxidative stress related genes or SOD activity.

Sendeski MM (2011). CLIN EXP PHARMACOL P 38, 292-299.

Persson PB et al. (2005). Kidney Int 68, 14-22.

This work was supported by grants from the Else Kroener-Fresenius-Stiftung (M. Sendeski, 309 P40/09//A29/09) and the Deutsche Forschungsgemeinschaft (S. Hippenstiel, DFG HI 789/7-1).

Where applicable, the authors confirm that the experiments described here conform with The Physiological Society ethical requirements.

PCD229

Inflammatory cytokines provokes a macrophage phenotype switch by modulation of Ivns 1abp

C. Mastora[1,2], A. Sola[2], M. Ventayol[2], S. Buenestado[2], T. Carbonell[1] and G. Hotter[2]

[1]Physiology, University of Barcelona, Barcelona, Spain and [2]Ischemia and Inflammation, IIBB-CSIC-IDIBABS, Barcelona, Spain

Macrophages are phagocytic cells involved in a number of functions that secrete a large number of cytokines, chemokines and growth factors that can activate different cell types and play a role in inflammation. Macrophages can be classically or alternatively activated, obtaining either the pro-inflammatory phenotype M1 or the anti-inflammatory phenotype M2. Inflammatory cytokines, such as TNF-a and IFN-gamma are known to provoke a M1 phenotype but the mechanism responsible are unknown.

Ivns1abp is a gene coding for a 642 amino acid protein that localizes to both the nucleus and the cytoplasm. Functioning as a homodimer, Ivns1abp associates with F-actin and, via this association, plays an important role in the organization and stabilization of the actin skeleton.

The aim of this work was to study the mechanism involved in cytokine regulation of macrophage phenotype switch. For this purpose, murine BMDMs, obtained by Swiss CD1 mice, sacrificed by an overdose of isoflurane, were cultured in presence of GM-CSF during 7 days to achieve macrophage phenotype. After this period of time macrophage overexpressing ivns1abp and control macrophages in the presence or absence of cytokines and c-myc inhibitors were cultured to evaluate cytokines, ivns1abp and c-myc production.

Results indicated that cytokines provoke a a decrease in Ivns1abp, c-myc expression, M2 cytoskeletal features and anti-inflammatory mediators (IL-10, mannose receptor), showing an increase in M1 cytoskeletal features . C-myc inhibitors provoked the same results indicating that cytokines act on c-myc to down regulate ivns1abp, anti-inflammatory mediators and cytoskeletal M2 features.

Based on these results, we conclude that cytokines trough its inhibitory action on c myc, down regulates ivns1abp expression that in turns provokes a phenotype change trough cytoskeleton stabilization.

Where applicable, the authors confirm that the experiments described here conform with The Physiological Society ethical requirements.

PCD233

T-cell trafficking during inflammation is regulated by a novel PEPtide Inhibitor of Trans-Endothelial Migration, a pathway defective in chronic disease

M. Chimen[1], H.M. McGettrick[2], C.M. Yates[1], A. Martin[3], F. Barone[2], L.S. Walker[2], C.D. Buckley[2], G. Nash[1] and G.E. Rainger[1]

[1]School of Clinical and Experimental Medicine, University of Birmingham, Birmingham, UK, [2]School of Immunity and Infection, University of Birmingham, Birmingham, UK and [3]School of Cancer Sciences, University of Birmingham, Birmingham, UK

T-cells are recruited from the blood into extra-vascular tissues during acute inflammation. However, in chronic inflammatory diseases, an inappropriate accumulation of T-cells in the diseased tissue contributes to pathogenesis. Very little is known about the mechanisms by which T-cell trafficking is regulated during inflammation. Here we describe a unique immune regulatory peptide that imposes a tonic inhibition of T-cell trafficking during inflammation. PEPtide Inhibitor of Trans-Endothelial Migration (PEPITEM) introduces a new paradigm into the pathways that regulate the inflammatory response. We present evidence that this new pathway is compromised in chronic inflammatory diseases. We propose that loss of this regulatory pathway makes the immune system 'leaky', allowing inappropriate access of T-cells to vulnerable tissues. Lymphocyte trafficking was assessed in vitro using videomicroscopy on TNF-α/IFN-γ activated endothelial cells (EC) and lymphocytes isolated from healthy donors or patients with chronic inflammatory diseases. In vivo, lymphocyte recruitment was assessed in a model of zymosan-driven peritoneal inflammation. PEPITEM was identified using mass spectrometry. Our studies began with an interest in adiponectin, an anti-inflammatory adipose tissue-derived cytokine. Using an in vitro migration assay, we observed that the migration of human lymphocytes was dose-dependently blocked by adiponectin with an EC50=37.2nM. Adiponectin achieves its effects on T-cell migration by the induction of a novel mediator released from B-cells. Thus, the effect of adiponectin was lost when B cells are absent, but could be regained by the addition of supernatants from adiponectin stimulated B-cells. Interestingly, the B-cell derived product did not act directly on T-cells; rather, it stimulated EC to release the lipid mediator sphingosine-1-phosphate, which in turn inhibited the migration of T-cells. We used mass spectrometry to isolate a B-cell derived peptide, corresponding uniquely in the human genome to a proteolytic excision product of the 14.3.3$\zeta\delta$ protein. Synthetic PEPITEM could also effectively inhibit T-cell migration with an EC50=18.6pM. In zymosan-induced peritonitis in the mouse, T-cell recruitment was significantly increased in BABL/C mouse strain lacking B cells (Jh-/-) when compared to wild-type animals. This excess of T-cell recruitment was ameliorated by intravenous treatment with PEPITEM. Importantly, lymphocytes isolated from patients with chronic inflammatory disease (type-1-diabetes) were released from the inhibitory effects of adiponectin, but this regulatory pathway could be re-established by the addition of exogenous PEPITEM. We believe that PEPITEM and its associated pathway may have therapeutic efficacy in a number of disease scenarios.

Where applicable, the authors confirm that the experiments described here conform with The Physiological Society ethical requirements.

PCD234

Comparison between automated inflation and manual inflation for forearm blood flow measurements made with venous occlusion plethysmography in humans

R. Junejo, F. Pavliv, C.J. Ray and J.M. Marshall

Clinical & Experimental Medicine, University of Birmingham, Birmingham, UK

Venous occlusion plethysmography has been used for over a century and is still a powerful tool for recording limb blood flow. It has been used to investigate autonomic regulation, vasodilator responses to exercise, ischemia, emotional stress and changes in body temperature, and to follow changes in endothelium-dependent responses in a number of diseases. Comparisons made between the older, air-filled plethysmographs and the more modern mercury/indium-gallium in silas-

tic strain gauges have indicated that the estimates made of limb blood flow are very similar (see Joyner et al, 2001). Recently, automated rapid inflation systems have been introduced to inflate the sphygmomanometer cuffs that are used to occlude the venous drainage, replacing the use of manual inflation. To our knowledge, there have been no direct comparisons between the blood flow measurements made with automated and manual inflation.

In an initial study on 7 male subjects (18-25 years old), forearm blood flow (FBF) was recorded by venous occlusion plethysmography, by using an automated system (E20, Rapid Cuff inflator, Hochansen Inc, USA) that inflated the cuff around the upper arm to 50mmHg. FBF was 8.4±1.1 at rest, 61.2±8.1 ml.min-1.100ml-1 immediately after 3 minutes static contraction at 60% maximum voluntary contraction (MVC) and 53.4±6.1, 45.4±7.9, 35.3±8.2, 29.8±5.4, and 20.9±3.3 ml.min-1.100ml-1 at 30s, 1, 3, 5 and 7 min respectively after contraction: FBF increased at maximum by ~7-fold. By contrast, we previously reported that in a similar group of subjects, FBF increased from 6.8±0.6 ml.min-1.100ml-1at rest, by only ~3.2 fold after static contraction at 60%MVC (Win & Marshall, 2005), suggesting the responses were much larger when recorded with automated inflation. Thus, in a separate study on 5 subjects (3F/2M; 20-30 years old), direct comparisons were made between automatic and manual cuff inflation before and following static contraction at 70% MVC for 1min. With automated inflation, FBF was 7.2±0.6 ml.min-1.100ml-1 at rest and 44.4±6.8 ml.min-1.100ml-1 immediately after, and 32.9±4.7, 26.8±3.4, 21.5±3.4, 16.9±2.9,11.6±3.4 ml.min-1.100ml-1 at 30s, 1, 3, 5 and 7 min respectively after contraction, whereas with manual inflation the corresponding values were 8.2±2.2 at rest and 32.8±5.5, 20.3±1.7, 17.8±2.7, 14.6±2.8,12.4±2.4 and 9.6±2.6 ml.min-1.100ml-1. These values were significantly different from 0-3min after contraction ($P<0.05$, repeated measures ANOVA).

Venous occlusion plethysmography underestimates limb blood flow relative to the thermodilution technique (Joyner et al, 2001). The present results indicate that automated cuff inflation gives a better estimation than manual inflation; this would have tremendous implications for use of the technique in physiological and clinical studies.

Joyner MJ, Dietz NM & Shepherd JT (2001). From Belfast to Mayo and beyond: the use and future of plethysmography to study blood flow in humans. J Appl Physiol 91, 2431-2441.

Win TS & Marshall JM (2005). Contribution of prostaglandins to the dilation that follows isometric forerm contractiobn in human subjects: effects of aspirin and hyperoxia. J Appl Physiol 99, 45-52.

Where applicable, the authors confirm that the experiments described here conform with The Physiological Society ethical requirements.

PCD235

The effect of longer cold water immersion time in the contrast bath on the skin temperature and parasympathetic activity

K. Inoue[1,2], J. Udagawa[1], N. Wakasugi[2] and K. Endo[3]

[1]Shiga University of Medical Science, Otsu, Japan, [2]Hatanaka Orthopedics, Rehabilitation Clinic, Amagasaki, Japan and [3]Institute for Frontier Medical Kyoto Univeriity, Kyoto, Japan

Recent reports suggest the relationship between the decrease in the body temperature and hypotension or the onset of diabetes mellitus, in people whose normal temperature is more than 36.5 degrees. Autonomic nervous system regulates blood flow, thermogenesis, and glucose and adipose metabolisms, therefore, it is important to keep the autonomic function adequately for preventing the circulatory and metabolic diseases. The contrast bath therapy is one of rehabilitation therapies. In usual way, the body part is immersed in warm bath for 4 minutes, then in cold bath for 1 minute, and this procedure is repeated 5 times. This therapy improves local blood circulation through vasodilatation and vasoconstriction. Furthermore, immersion of the body part in cold water activates the parasympathetic function. In this study, we examined whether or not longer immersion time in cold water improves parasympathetic function and prevents the skin temperature from decreasing. Twenty healthy subjects (10 men and 10 women: mean age 22.0±1.8 years old) with no history of any pathological condition were recruited. All subjects signed an informed consent before participating in this study. A hand was immersed for 4 minutes in cold water and for 1 minute in warm water, and this procedure was repeated 5 times in this contrast bath. The contrast bath was performed twice or three times a week and was continued for four weeks. We carried out cold immersion test in which a hand was immersed in 10 degrees of water for 16minutes before starting and after completing a series of the contrast bath. RR interval were monitored by electrocardiograph during cold water immersion test, and a high-frequency (0.30 – 0.40 Hz) RR interval variation was analyzed by FFT to quantify parasympathetic activity. After cold water immersion test, the skin temperature was immediately measured on the proximal nail fold of the index finger. Paired t-test and Scheffe's test were used to analyze the change of skin temperature and electrocardiogram, respectively.

The skin temperature did not decrease by cold water immersion test after 4 weeks of the contrast bath whereas it significantly decreased before starting the contrast bath. Moreover, parasympathetic activity significantly increased 10 minutes after cold water immersion in the test by performing 4 weeks of the contrast bath.

Present results suggest that longer cold water immersion time in the contrast bath stimulates parasympathetic nervous system, increases blood circulation in the periphery, and keeps skin temperature of the finger-tip.

Where applicable, the authors confirm that the experiments described here conform with The Physiological Society ethical requirements.

PCD236

Pre-cooling for endurance exercise performance in the heat: a systematic review

P.R. Jones, C. Barton, D. Morrissey, N. Maffulli and S. Hemmings

Centre for Sports and Exercise Medicine, Queen Mary University of London, London, UK

Background: Endurance exercise capacity diminishes under hot environmental conditions. Time to exhaustion can be increased by lowering body temperature prior to exercise (pre-cooling). This systematic literature review synthesizes the current findings of the effects of pre-cooling on endurance exercise performance, providing guidance for clinical practice and further research.

Methods: The MEDLINE, EMBASE, CINAHL, Web of Science and SPORTDiscus databases were searched in May 2012 for studies evaluating the effectiveness of pre-cooling to enhance endurance exercise performance in hot environmental conditions (≥28°C). Studies involving participants with increased susceptibility to heat strain, cooling during or between bouts

of exercise, and protocols where aerobic endurance was not the principle performance outcome were excluded. Potential publications were assessed by two independent reviewers for inclusion and quality. Means and standard deviations of exercise performance variables were extracted or sought from original authors to enable effect size calculations.
Results: In all, 13 studies were identified. The majority of studies contained low participant numbers and/or absence of sample size calculations. Six studies used cold water immersion, four crushed ice ingestion and three cooling garments. The remaining study utilized mixed methods. Large heterogeneity in methodological design and exercise protocols was identified. Effect size calculations indicated moderate evidence that cold water immersion effectively improved endurance performance, and limited evidence that ice slurry ingestion improved performance. Cooling garments were ineffective. Most studies failed to document or report adverse events. Low participant numbers in each study limited the statistical power of certain reported trends and lack of blinding could potentially have introduced either participant or researcher bias in some studies.
Conclusions: Current evidence indicates cold water immersion may be the most effective method of pre-cooling to improve endurance performance in hot conditions, although practicality must be considered. Ice slurry ingestion appears to be the most promising practical alternative. Interestingly, cooling garments appear of limited efficacy, despite their frequent use. Mechanisms behind effective pre-cooling remain uncertain, and optimal protocols have yet to be established. Future research should focus on standardizing exercise performance protocols, recruiting larger participant numbers to enable direct comparisons of effectiveness and practicality for each method, and ensuring potential adverse events are evaluated.

Where applicable, the authors confirm that the experiments described here conform with The Physiological Society ethical requirements.

PCD237

Using perceived exertion to self-regulate exercise on a wheelchair ergometer in able-bodied novice participants

B.L. Savill[1,2], V. Tolfrey[3] and T. Paulson[3]

[1]Medicine, Cardiff University, Cardiff, UK, [2]Sport & Exercise Science, Loughborough Univerisity, Loughborough, UK and [3]Peter Harrison Centre for Disability Sport, Loughborough University., Loughborough, UK

Spinal cord injuries require rehabilitation programs immediately after injury. Ratings of perceived exertion (RPE) have been demonstrated as a suitable means to regulate exercise intensity for those trained in wheelchair propulsion. The use of RPE with novice wheelchair users has not been validated. Ten able-bodied males with no previous wheelchair experience (mean ± SD, age 22 ± 2 years, height 1.79 ± 0.08 m, mass 76.0 ± 12.1 kg) completed an incremental submaximal test followed by a VO2peak test on a wheelchair ergometer. In a second visit, two 12-min intermittent exercise tests of three 4-min bouts were completed at a moderate (40% VO2peak) and a vigorous intensity (60% VO2peak). On a separate day, participants completed the two 12-min tests at a self-selected intensity corresponding to the RPE noted during the second visit. During the last minute of each 4-min bout measures of VO2, HR and blood lactate concentration [La-] were recorded. Power output (PO) was measured continuously. There were differences in average VO2, %VO2peak, HR, and %HR between the Imposed and RPE-regulated Trial at a moderate ($P<0.05$) but not at a vigorous intensity ($P>0.31$) for these measures, whilst [La-] showed no difference at either intensity. There were no differences in PO between the Imposed and RPE-regulated Trial at a vigorous intensity. PO was however ~13% higher during the RPE-regulated Trial at the moderate intensity ($P \leq 0.01$). These data supports the use of RPE as a method of regulating exercise at a vigorous but not at a moderate intensity during wheelchair propulsion in novice able-bodied males. Research is needed into familiarisation with wheelchair propulsion to improve RPE accuracy at a moderate intensity, since large inter-individual differences were observed when comparing the Imposed and RPE-regulated Trial

Goosey-Tolfrey VL, Lenton JP, Goddard J, Oldfield V, Tolfrey K, Eston R (2010) Regulating intensity using perceived exertion in spinal cord-injured participants. Med Sci Sports Exerc 42:608-613

Lewis JE, Nash MS, Hamm LF, Martins SC, Groah SL (2007) The relationship between perceived exertion and physiologic indicators of stress during graded arm exercise in persons with spinal cord injuries. Arch Phys Med Rehabil 88:1205-

Müller G, Odermatt P, Perret C (2004) A new test to improve the training quality of wheelchair racing athletes. Spinal Cord 42:585-590

Nash MS (2005) Exercise as a health-promoting activity following spinal cord injury. J Neurol Phys Ther 29:87-106

Tucker R, Noakes TD (2009) The physiological regulation of pacing strategy during exercise: a critical review. Br J Sports Med 43:e1

The author would like to thank Dr. Vicky Tolfrey for her guidance and patience, and all subjects who gave up their time to participate. The author is also very grateful for the support, technical guidance and expertise with the laboratory testing of Mr Tom Paulson.

Where applicable, the authors confirm that the experiments described here conform with The Physiological Society ethical requirements.

PCD238

The role of prostaglandin and antioxidant availability on recovery from forearm ischemia-reperfusion injury in humans

S.E. Carter and M. Rakobowchuk

School of Biological Sciences, University of Essex, Colchester, Essex, UK

Endothelial dysfunction, manifesting as attenuated flow mediated dilation (FMD), following ischemia-reperfusion (IR) injury is a clinically important measure of vascular health. Antioxidants may prevent this dysfunction by scavenging reactive oxygen species, however the acute effects of oral antioxidant administration in humans are unknown. Low-flow mediated constriction (L-FMC), a further parameter of endothelial health, is largely unstudied and the mechanisms for this response are unclear. This study assessed interventions that impact FMD and L-FMC throughout an IR injury protocol. Twelve healthy subjects (5 female, 7 male) attended the lab on 3 occasions. The initial test acted as a baseline measure. Prior to subsequent visits subjects ingested either: 1) an antioxidant cocktail (300mg α-lipoic acid, 500mg Vitamin C and 200IU Vitamin E) 2 hours prior and a further cocktail (300mg α-lipoic acid, 500mg Vitamin C and 400IU vitamin E) 1.5 hours prior; or 2) 1200mg of a prostaglandin inhibitor (Ibuprofen) 1 hour prior in a blinded fashion. Endothelial function was assessed by non-invasive ultrasound of the right brachial artery. For each vascular function protocol vessel diameters were determined

throughout 5 min of forearm ischemia and 3 min after. Following a baseline measure (Pre) IR injury was induced by a 20 min upper arm occlusion. Subsequent vascular function protocols were carried out at 15, 30 and 45 min of recovery. Values are means ± SD, analysed by ANOVA. Endothelial dysfunction was evident in all three conditions. FMD was attenuated at 15 min post-IR injury (Control Pre: 5.96±3.41%; Post15: 0.67±3.26%; Antioxidant Pre: 6.90±3.83%; Post15: 0.68±2.87%; Ibuprofen Pre: 5.85±4.81%; Post15: -0.63±4.81%; $p<0.05$) but recovered by 45 min to near basal values. Antioxidant administration did not preserve FMD compared to control ($p>0.05$). The magnitude of L-FMC was augmented at 15 min compared to basal values (Pre: 1.44±0.27%; Post15: 3.75±1.73%; $p<0.05$) and recovered by 45 min. Ibuprofen administration produced the largest constrictive response and a significant time x condition interaction was observed (Ibuprofen Pre: -1.13 ±1.71%; Post15: -5.57 ±3.82%; Control Pre: -1.58 ±2.26%; Post15: -3.58 ±2.65%; interaction: $p<0.05$). Results demonstrate the presence of endothelial dysfunction following IR injury and the inability of acute oral antioxidant supplementation to preserve vascular function. Data also suggests that a lack of shear stress during occlusion combined with prostaglandin blockade magnifies L-FMC; possibly due to augmented expression of endothelin-1. Moreover, when prostaglandins are blocked their habitual role in inhibiting endothelin-1 secretion is abolished, increasing endothelin-1 bioavailability, and leading to a more pronounced L-FMC.

Society for Biology Undergraduate Summer Studentship to Sophie Carter.

Where applicable, the authors confirm that the experiments described here conform with The Physiological Society ethical requirements.

PCD239

Effects of acute strenuous exercise on vascular endothelial cell activation

K. Fukada[1], H. Kushi[2], K. Oki[2], R. Koshizawa[2] and A. Mori[2]

[1]Graduate School of Literature and Social Sciences, Nihon University, Tokyo, Japan and [2]College of Humanities and Sciences, Nihon University, Tokyo, Japan

Introduction: Plasminogen activator inhibitor-1 (PAI-1) is a marker of vascular endothelial cell activation. The aim of this study was to evaluate whether a difference in low-density lipoprotein cholesterol (LDL-C) concentration affects the PAI-1 level during acute strenuous exercise.
Subjects and Methods: Thirteen healthy trained men aged 19 to 23 years participated in this study: 7 of these were categorized in the low LDL-C (LL) group (LDL-C concentration < 100 mg/dL), and 6 in the high LDL-C (HL) group (LDL-C concentration, 100-140 mg/dL). Venous blood samples were collected from the subjects before and after they performed the Cooper 12-min test (running as far as possible within 12 min). LDL-C concentrations were measured by direct methods using samples collected before exercise, and PAI-1 (total amount of active form, latent form, tissue plasminogen activator/PAI-1 complex) level was measured by Latex Photometric Immunoassay using samples collected before and after exercise. LDL-C concentrations in the LL and HL groups were compared using an unpaired t-test. PAI-1 levels were compared using a two-way analysis of variance (group × time) with repeated measures. Statistical significance was set at $P < 0.05$.
Results: The mean (± SE) age, height, and weight of the subjects in the LL group were 21.0 ± 0.5 years, 172.8 ± 1.7 cm, and 64.7 ± 3.0 kg, respectively, and the corresponding values for the subjects in the HL group were 20.6 ± 0.5 years, 171.0 ± 3.5 cm, and 84 ± 7.8 kg, respectively. LDL-C concentration was significantly higher in HL group (121.8 ± 4.4 mg/dL) than in the LL group (87.5 ± 2.8 mg/dL; $P < 0.05$). There was a significant difference in PAI-1 level between the LL and HL groups ($F=0.54$; $P < 0.05$). PAI-1 level before (30.4 ± 6.5 mg/dL) and after (25.2 ± 7.2 mg/dL) exercise did not change significantly in the LL group, whereas it increased significantly in the HL group (40.6 ± 7.0 mg/dL to 58.7 ± 7.8 mg/dL; $P < 0.05$). There were no significant differences in the PAI-1 levels before exercise in the LL and HL groups, whereas the levels after exercise were significantly different ($P < 0.05$).
Conclusions: It was reported that PAI-1 level does not decrease or change significantly after acute strenuous exercise. In this study, the PAI-1 level increased significantly in the HL group. Therefore, we conclude that a difference in LDL-C concentrations affects vascular endothelial cell activation during acute strenuous exercise.

Where applicable, the authors confirm that the experiments described here conform with The Physiological Society ethical requirements.

PCD240

Comparison of Cardiopulmonary Exercise Tests for Patients with COPD and Overlap Syndrome

F. Coskun[1], A. Ertem Cengiz[1], F. Ozyener[2] and A. Ursavas[1]

[1]Chest Disease, Uludag University, Bursa, Turkey and [2]Physiology, Uludag University, Bursa, Turkey

Chronic Obstructive Pulmonary Disease (COPD) is a disease that progresses through inflammation and the main reason for morbidity in COPD is this inflammation. The rate of appearance of OS (Overlap Syndrome) and COPD together is %1 in the general public. Systemic inflammation increases the severity even more when the two diseases appear together. This is why the morbidity and mortality rates are higher with patients diagnosed with OS.
Purpose: The purpose of this study is to find out whether there is a significant difference between the cardiopulmonary exercise test results for patients with the moderate and serious form of COPD.
Method: 18 patients were subjected to Cardiopulmonary Exercise Tests (KPET) within the scope of the study. 12 of the patients were diagnosed with COPD and 6 of them with OS. A symptom-limited incremental KPET was performed using a Vmax Encore, USA device. The study was designed and carried out in accordance with principles of the Declaration of Helsinki and with approval from the Ethics Review Board of Uludag University (15th June 2010, 2010-13/2). Informed consent was obtained from all subjects.
Findings: The results of the KPET revealed that the maximum oxygen consumption (VO2max ml/kg/min) in the group of patients with COPD was 15,5 ±6,4, and 12,4±6 in the group with OS. There was no significant difference in that sense ($P>0,05$). There was also no significant difference in carbon dioxide outturn between the two groups (VCO2 L/min) ($p>0,05$). The maximum work-watt in the group of patients with COPD was 59,2±29, and 45,8±19 in the group with OS. There also was no significant difference between these results ($p>0,05$). The maximum throb of the group of patients diag-

nosed with COPD was 120±21, and 116±18 in the group with OS. The comparison of Oxygen pulse value (ml/Pulse) and maximum throb did not show any significant difference either (p>0,05). The maximum ventilation rate (VEmax-L/min) in the group of patients with COPD was 43±13, and 36,6±9,2 in the group with OS. No significant difference was found between the two groups. (p>0,05). End-tidal CO2 values and end-tidal O2 values did not show any significant difference either. When compared (p >0,05) . The respiratory quotient RQ in the group with COPD was 1,1 ±0,4 whereas in the group with OS the value was 1,1±0,4. No significant difference. The anaerobic tree-shot (AT) values in both groups were similar. No statistically significant difference was found between these two values either. (p>0,05).

Conclusion: Although the KPET values of patients diagnosed with COPD and OSD were below the general population, there were no significant differences between the two diseases.

Keywords: COPD, Overlap Syndrome, KPET

Cooper CB, Storer TW. Exercise testing and interpretation: a practical approach. London: Cambridge University Press; 2001.

American Thoracic Society; American College of Chest Physicians. ATS/ACCP Statement on cardiopulmonary exercise testing. Am J Respir Crit Care Med 2003;167:211-77

Gallagher CG, Younes M. Breathing pattern during and after maximal exercise in patients with chronic obstructive lung disease, interstitial lung disease, and cardiac disease, and in normal subjects. Am Rev Respir Dis 1986;133:581-6.

Belman MJ, Brooks LR, Ross DJ, Mohsenifar Z. Variability of breathlessness measurement in patients with chronic obstructive pulmonary disease. Chest 1991;99: 566–71.

O'Donnell DE, D'Arsigny C, Webb KA. Effects of hyperoxia on ventilatory limitation during exercise in advanced chronic obstructive pulmonary disease. Am J Respir Crit Care Med 2001;163:892-8.

Where applicable, the authors confirm that the experiments described here conform with The Physiological Society ethical requirements.

PCD241

Oxidative stress is not involved in the morphofunctional impairments of non-pregnant murine uterus caused by intense and exhaustive exercise

A.E. Costa[1], M.J. Simões[3], J.L. Silva[2] and V.L. Nouailhetas[1]

[1]Biophysics, Escola Paulista de Medicina/Universidade Federal de São Paulo, São Paulo, São Paulo, Brazil, [2]Universidade Nove de Julho, São Paulo, São Paulo, Brazil and [3]Morphology and Genetics, Escola Paulista de Medicina/Universidade Federal de São Paulo, São Paulo, São Paulo, Brazil

Intense exercise (IE) causes damage to organs and tissues such as in the gastrointestinal tract, urinary, and brain. Even though IE is associated with dysfunctions in the female reproductive system, little is known about the mechanisms underlying its effects mainly on the non-pregnant uterus. We investigated the effects of intense and exhaustive exercise (IEE) program on the isolated uterine morphology, tissue responsiveness, and oxidation markers. Female C57Bl/6 mice (20 g), 3-month old, were acclimated for 5 days, and the oestrous cycle followed by daily vaginal smears. Animals were then allocated into 2 groups: control (CT) and exercised (EX) groups. EX group performed 2-consecutive days of a daily bout of treadmill running at 85% of its maximum running velocity (MV) until animal exhaustion. MV was determined by maximal incremental test (MIT 1) performed by all animals 24-h before the beginning of IEE program. Training responses were evaluated the time each animal took to reach exhaustion (TTE) and the MV, evaluated by the second MIT (MIT 2) performed 24-h after the end of the second exercise session. CT and EX animals were in the oestrous stage at the beginning of the exercise program. Tissue morphology was evaluated by histological analysis of 4-μm HE-stained uterine slices; tissue responsiveness was evaluated through concentration-isometric contractile response curves evoked by either KCl or carbachol (CCh) (de Jalon solution, T° 37°, pH 7.4, and 0.2 g basal tension); and uterus lipid peroxidation and protein oxidation were evaluated by MDA and carbonyl concentration measurements, respectively. IEE decreased animal physical performance as it caused 32 and 29% decreases in TTE and MV, respectively (N = 60), decreased the longitudinal muscular layer (from 79 ± 2 μm to 71.1± 2 μm, N = 6, p<0.05), impaired CCh-evoked contraction (increase in EC50 from 2.8 ± 1.2 to 18 ± 3 μM, and decrease in Emax from 1.7 ± 0.3 (N = 4) to 1.0 ± 0.2 g, (N = 6), p<0.05), but caused only strong trend to impair KCl-evoked contraction (increase in EC50 from 5.7 ± 1.3 to 9 ± 3 mM, and decrease in Emax from 1.4 ± 0.2 to 1.2 ± 0.16 g, N = 4-6, p>0.05), reduced MDA concentration from 400 to 180 nmol/mL.g dry tissue (N = 5-6, p<0.05), without affecting the level of protein carbonyl (4 and 4.3 nmol/ mg protein, in CT and EX, respectively, N = 5-6, p>0.05,). Is concluded that C57BL/6 mice non-pregnant uterus is an important exercise-target, and displays important morpho-functional alterations in response to intense and exhaustive exercise which, nonetheless, are not related to signs of uterus oxidative stress, but may be well related to exercise-induced uterine dysfunction.

FAPESP, CAPES, CNPq

Where applicable, the authors confirm that the experiments described here conform with The Physiological Society ethical requirements.

PCD242

Do the vascular responses to cool water immersion in young Asian males give them greater susceptibility to Non-Freezing Cold-induced Injury (NFCI) than white Caucasians?

W. Blevins[1], C.J. Ray[1], M.J. Tipton[2] and J.M. Marshall[1]

[1]Clinical & Experimental Medicine, University of Birmingham, Birmingham, UK and [2]Institute of Sport & Exercise Science, University of Portsmouth, Portsmouth, UK

Prolonged or repeated exposure to cool, wet conditions is known to induce Non-Freezing Cold-induced Injury (NFCI), sometimes known as trench foot. Susceptibility to NFCI appears to be greater in certain populations. Epidemiological studies show a greater incidence of NFCI in Afro-Caribbean populations than Caucasian populations, while being a Gurkha is protective There is also evidence amongst Indians, that Southern Indians show less pronounced cold-induced vasodilatation than High altitude natives or Gurkhas, raising the question as to whether they are more susceptible to NCFI (Imray et al 2011). Thus, in the present study, we compared the cardiovascular responses evoked by repeated immersion of the right leg in cool water at 15 degrees C between Caucasian and Asian young males (aged 20.1 ± 0.3 years, n=8 in each group). Immersion was repeated 5 times for 2-minute periods separated by 2-minute recovery periods at room temperature. The left leg was supported at near horizontal throughout.

In the Caucasians, cutaneous red cell flux (RCF), measured using laser Doppler fluximetry, fell, for eg from 8.1±1.0 to 7.5±1.3PU in the immersed foot in the 1st immersion and from

17.9±2.2 to 14.4±1.3PU in the contralateral foot and recovered well between immersions. However, in the Asians, RCF in the immersed, right foot fell during immersion from 8.0 ± 0.5 PU at baseline to 6.0 ± 0.5* PU in the 5th immersion (*: p<0.01, repeated measures ANOVA) and did not return to baseline during the recovery periods: 6.3 ± 0.8* PU immediately before the 5th immersion. Further, immersion caused a reduction in RCF in the contralateral, left foot: from 15.2 ± 1.3 PU at baseline to 12.4 ± 0.8* PU. In the Caucasians, left calf blood flow (CBF), measured by venous occlusion plethysmography, did not change significantly throughout the protocol, but in the Asians, CBF fell, reaching significance during the recovery periods from 5.4 ± 0.9 at baseline to 3.8 ± 0.5* ml.min-1.100ml-1 before the 5th immersion. These changes in blood flow in the Asians reflected increases in cutaneous and calf vascular resistance.

These data indicate that the local and reflex vasoconstrictor responses evoked by cool water immersion in cutaneous and muscle circulations of the lower limb are greater and more persistent in young Asian males, than young Caucasian males. The fact that the vasoconstriction was particularly pronounced in the immersed foot suggests an important role for local mechanisms in initiating the vasoconstriction. Exaggerated reductions of limb blood flow in Asians in cold wet conditions might be expected to lead to tissue damage through ischaemia and increase susceptibility to NFCI. Future work will concentrate on the role of locally synthesised prostaglandins in the vascular response to cold.

Imray CH, Richards P, Greeves J & Castellani JW (2011). Non-freezing cold induced injuries. JR Army Med Corps157, 79-84.

Where applicable, the authors confirm that the experiments described here conform with The Physiological Society ethical requirements.

PCD244

Sex difference of the human brain functional connectivity related to the second to fourth digit ratio

T. Donishi[1], M. Terada[2] and Y. Kaneoke[1]

[1]System Neurophysiology, Wakayama Medical University, Wakayama, Wakayama, Japan and [2]Wakayama-Minami Radiology Clinic, Wakayama, Japan

Difference in human behavior is in part related to the prenatal brain exposure to androgen. Thus the brain functional network may vary with the magnitude of the androgen exposure, which can be estimated by the second to fourth digit ratio (2D:4D). Digit length was measured from the basal crease proximal to the palm to the tip of the digit on a photocopy of the right hand. We measured global functional connectivity of the gray matter in the human brain regions ("regional global connectivity," rCG), and examined its correlation with 2D:4D. A 3 Tesla magnetic resonance imaging system (MRI, Philips) with a 32-channel head coil was used to obtain T1-weighted anatomical and resting state functional images of the healthy subjects (103 males and 96 females, mean (SD) age was 21±2 years old for both groups). During the acquisition (a series of three 5-min sessions), subjects were asked to stay awake with their eyes closed. Preprocessing of the blood oxygenation level dependent (BOLD) signal was performed using the analysis tools in SPM8 and in-house software developed on MATLAB, which includes head motion realignment, normalization with the standard template for echo planar imaging, and spatial/temporal smoothing and noise reduction. For each voxel (6x6x6 mm) in the gray matter, cross-correlation coefficients with all other gray matter voxels were calculated and averaged to determine each voxel's rGC. The rGC values had significant relationship with 2D:4D at several regions as revealed by Pearsons's correlation coefficient (t-test, p<0.05, corrected for multi-comparison with Monte Carlo simulation). We found marked sex difference in the hippocampus and adjacent regions (parahippocampus and fusiform gyrus): in male, negative correlation was seen in the bilateral regions, while positive correlation was seen in the left side in female. Further, in female, positive correlation was found at the left supra-parietal cortex, and negative correlation at the anterior and medial cingulate cortex and the superior medial frontal cortex. Hippocampus is known to be involved in various cognitive and emotional functions, as well as memory. Recent studies demonstrate that the hippocampal volume is affected by the prenatal androgen exposure as measured by the second to fourth digit ratio (2D:4D) in female. Thus, it is likely that the hippocampus may be a key region to construct sex-related identity. Our results suggest that, in female, the low hippocampal rGC is related to personality such as dominance and aggression (known to be related to low 2D:4D). In contrast, in male, the high hippocampal rGC may be related to the risk-taking decision making, since 2D:4D is known to be inversely related to the male day traders' ability.

Where applicable, the authors confirm that the experiments described here conform with The Physiological Society ethical requirements.

PCD245

Preliminary methods for automated detection of fasciculations associated with motor neuron disease

P.J. Harding[1], I.D. Loram[1], N. Costen[2], N. Combes[3] and E. Hodson-Tole[1]

[1]Institute of Biomedical Research into Human Movement and Health, School of Healthcare Science, Manchester Metropolitan University, Manchester, UK, [2]School of Computing, Mathematics and Digital Technology, Manchester Metropolitan University, Manchester, UK and [3]Dpt. Clinical Neurophysiology, Royal Preston Hospital, Lancashire Teaching Hospitals NHS Foundation Trust, Preston, UK

Motor neuron disease (MND) is a devastating neurodegenerative disease. Diagnosis requires invasive, often painful, intramuscular myoelectric signal recordings from multiple body regions to identify the occurrence of electrophysiological events such as fasciculations [involuntary firing of a motor unit]. It has recently been shown that fasciculations can be seen by eye in ultrasound images collected at ~75Hz (1) and that assessment of images provides more sensitive detection than myoelectric signals in some muscles, e.g., biceps brachii (2). These studies are however based on manual, visual assessment of images to identify the occurrence of fasciculations. Here an automated, quantitative approach based on computationally tracking movement of features in collected images is assessed to determine the feasibility of using such techniques to automatically identify the occurrence of fasciculations. Development of such non-invasive, quantitative methods could facilitate earlier screening and diagnosis of suspected cases of MND.

Nine human participants completed the study. Three participants, recruited through the MND Care and Research Centre at Royal Preston Hospital [RPH], had previously been diagnosed with MND. The study was approved by authorities at RPH and

the universities local ethics committee. All participants provided informed written consent. In all participants B-mode ultrasound images simultaneously showing medial gastrocnemius [MG] and soleus [SO] were recorded. In those with MND, images were also collected from biceps brachii. The occurrence of fasciculations [localized tissue displacements lasting 0.2-1s (3)] were manually identified by two experienced operators. Features in each image were mathematically identified and tracked between images using methods described in (4). Resulting feature data were used in a mutual information [MI] analysis to provide a statistical classification of movement of tracked features between images.

Correspondence between manually identified fasciculations and spikes in the MI metric was quantified by compiling receiver operating characteristics to identify the true positive rate at which the number of false positives and true negatives were equal [HEE]. For MG/SO image sequences HEE was 87% in healthy participants and 79% for participants with MND. HEE was 81% in sequences recorded from biceps. These strong preliminary results indicate excellent potential for the development of quantitative, automated detection of fasciculations in ultrasound images. The MI metric was not sensitive to the smallest manually identified movements and was influenced by the inherent noise in collected images. Further improvements in accuracy can therefore be expected with the application of more sophisticated analysis approaches.

Pillen S, Nienhuis M, van Dijk JP, Arts IMP, van Alfen N & Zwarts MJ. (2009). Muscles alive: Ultrasound detects fibrillations. *Clinical Neurophysiology.* **120**, 932-936.

Misawa S, Noto Y, Shibuya K, Isose S, Sekiguchi Y, Nasu S & Kuwabara S. (2011). Ultrasonographic detection of fasciculations markedly increases diagnostic sensitivity of ALS. *Neurology.* **77**, 1532-1537.

Scheel AK &Reimers CD. (2004). Detection of fasciculations and other types of muscular hyperkinesias with ultrasound. *Ultraschall. Med.* **25**, 337-341.

Harding PJ, Hodson-Tole EF, Cunningham R, Loram ID & Costen N. (2012) Automated detection of skeletal muscle twitches from B-mode ultrasound images: An application to Motor Neuron Disease. *Proc. of Int. Conf. on Pattern Recognition.* 2630-2633.

Where applicable, the authors confirm that the experiments described here conform with The Physiological Society ethical requirements.

PCD246

Exploration of functional mutations of ryanodine receptor in malignant hyperthermia

T. Yamazawa[1,4], H. Oyamada[2], T. Murayama[3], N. Kurebayashi[3], K. Oguchi[2], T. Sakurai[3], M. Iino[4] and S. Takemori[1]

[1]Department of Molecular Physiology, The Jikei University School of Medicine, Minato-ku, Tokyo, Japan, [2]Department of Pharmacology, School of Medicine, Showa University, Shinagawa-ku, Tokyo, Japan, [3]Department of Pharmacology, Juntendo University Graduate School of Medicine, Bunkyo-ku, Tokyo, Japan and [4]Department of Pharmacology, Graduate School of Medicine, The University of Tokyo, Bunkyo-ku, Tokyo, Japan

Ryanodine receptors, located in the sarcoplasmic/endoplasmic reticulum (SR/ER) membrane, are required for intracellular Ca^{2+} release that is involved in a wide range of cellular functions. Malignant hyperthermia (MH) is a pharmacogenetical complication of general anesthesia resulting from abnormal Ca^{2+}-induced Ca^{2+} release (CICR) via the type 1 ryanodine receptor (RyR1) in skeletal muscles. The typical symptoms include a rapid increase in body temperature and induction of a hypermetabolic state with skeletal muscle rigidity. More than 100 mutations in the RyR1 gene have been reported in MH patients. Most of those mutations have been found in three "hot spots" regions (#1-614, #2129-2458 and #4637-4973 as the amino acid numbers) of RyR1. However, there were only a few experimental results confirming those mutations being responsible for the increment of the CICR sensitivities, since such a long cDNA of RyR1 not only required much complicated procedures for making desired mutations but also caused its low transfection efficiency of the mutant DNAs. We improved the method for making MH mutants in the cDNA of RyR1. We characterized the functional mutations on RyR1 in non-muscle cells, specifically HEK293 cells with tetracycline-regulated RyR1 expression. Rabbit RyR1 channels carrying corresponding Japanese mutations (L13R, Q155K, R163C, D166G, R533H, etc.) were expressed in HEK293 cells for functional assay. HEK293 cells were loaded at room temperature with fura-2 AM in physiological salt solution. Fluorescence images at >420nm were acquired using an inverted microscope equipped with a objective, a cooled CCD camera and a polychromatic illumination system at a rate of one frame every 1 or 2 s. It was found that R163C and Q155K mutations of the RyR1 resulted in enhanced Ca^{2+} release activity, therefore these mutations would be responsible for the MH incidence. These results suggest that exploration of the functional mutations of RyR1 is probably effective in preventive diagnosis of patients associated with MH disease.

Where applicable, the authors confirm that the experiments described here conform with The Physiological Society ethical requirements.

PCD247

ATP release from rat skeletal muscle may involve chloride channels

L. Lu[1], J. Tu[2], W. Cai[1] and H.J. Ballard[1]

[1]Department of Physiology, Institute of Cardiovascular Science and Medicine, The University of Hong Kong, Hong Kong, Hong Kong and [2]Shenzhen Key Laboratory for Neuropsychiatric Modulation, Shenzhen Institutes of Advanced Technology, Chinese Academy of Sciences, Shen Zhen, China

ATP is released from skeletal muscle cells under basal conditions, and at higher rates during acidosis or muscle contractions. The cystic fibrosis transmembrane conductance regulator (CFTR) is involved in the stimulated ATP release, but neither inhibition of CFTR nor silencing of CFTR expression could abolish the basal ATP release. Chloride channels such as the maxi anion channel or voltage-sensitive-outwardly- rectifying (VSOR) channel are known to mediate ATP release in a number of cell types. We investigated whether chloride channels were involved in the release of ATP from rat skeletal muscle.

Using RT-PCR (n=3), rat L6 skeletal myocytes were shown to express CFTR, ClC 2, 3 and 7, and VDAC (Voltage-dependent anion channel); the maxi anion channel and VSOR, whose molecular identities are uncertain, were not tested. Whole cell chloride currents were measured in the myocytes using patch clamp: reducing the pH from 7.4 to 6.8 increased the current from 69.8 ± 8.8 to 98.6 ± 9.6 pA/pF (mean ± SEM, n=9; $P<0.05$, ANOVA) at 70 mV; this increase could be partially inhibited by the specific CFTR inhibitor, $CFTR_{inh}$-172. Addition of DIDS (100 μM) reduced the current to 16.2 ± 3.4 pA/pF at pH 7.4;

lowering the pH to 6.8 in the presence of DIDS increased the current to 25.6 ± 3.8 pA/pF (P<0.05; n=4).
Gastrocnemius muscle contractions were induced in rats anaesthetised with sodium pentobarbital (70 mg/kg i.p.) by stimulation of the sciatic nerve at 1 Hz and supramaximal voltage; the interstitial fluid was sampled using microdialysis. In the absence of drugs, muscle contractions increased the interstitial ATP from 1.4 ± 0.1 to 44.1 ± 12.8 nM (n=5); this increase was reproducible in repeated contractions in the absence of drugs. Injection of DIDS (100 μM) reduced the interstitial ATP to 0.3 ± 0.05 nM at rest and 3.8 ± 2.0 nM during contractions.
During buffer-perfusion of the rat hindquarters, infusion of lactic acid (10 mM) increased the EDL muscle interstitial ATP from 31 ± 5 to 50 ± 7 nM (n=14); addition of SITS (100 μM) to the perfusate abolished the lactic-acid-induced increase in ATP.
The ATP concentration in the medium surrounding the cultured L6 myocytes was increased from 0.6 ± 0.06 to 1.1 ± 0.08 nM (n=57; P<0.001, t-test) by the addition of 10 mM lactic acid to the medium. Addition of the maxi anion channel inhibitors gadolinium (100 μM, n=12) or sodium orthovanadate (100 μM, n=6) to the medium increased the extracellular ATP, but the acidosis-induced increase in ATP was abolished. The VSOR inhibitor, phloretin (100 μM, n=6) also increased extracellular ATP, but failed to inhibit a further increase in ATP when the pH was reduced to 6.8.
These data suggest that lowering of the pH opens both CFTR and another chloride channel, and that a chloride channel, which may be the maxi-anion channel, contributes to ATP release from skeletal muscle.

Where applicable, the authors confirm that the experiments described here conform with The Physiological Society ethical requirements.

PCD248

Alterations in calcium handling in isolated fast fibres from speed gene knockout mice

S.I. Head[1], S.C. Chan[1], P.J. Houweling[2], R.M. Murphy[3], K.G. Quinlan[2] and K.N. North[2]

[1]School of Medical Sciences, University of New South Wales, Sydney, NSW, Australia, [2]Institute for Neuroscience and Muscle Research, The Children's Hospital at Westmead, Sydney, NSW, Australia and [3]Department of Zoology, La Trobe University, Melbourne, VIC, Australia

Background: Absence of the fast-twitch skeletal muscle Z-line protein, α-actinin-3, encoded by the ACTN3 speed gene, is associated with poorer sprinting performance in athletes and a slowing of relaxation in fast-twitch muscles of Actn3 knockout (KO) mice. Around 20% of the world's population are ACTN3 deficient. Fast-twitch muscles from KO mice display longer twitch half-relaxation times than muscles from wild-type (WT) mice. In mechanically skinned fast fibres the sarcoplasmic reticulum (SR) in fibres from KO mice load calcium more slowly than the SR in fibres from WT mice (Chan et al., 2011).
Aim: Our present study investigates the calcium kinetics of fast-twitch fibres from Actn3-KO and WT mice and SERCA pump and parvalbumin protein expression, to see whether any changes in calcium kinetics and associated SR and calcium buffering proteins can account for the previously observed effects of α-actinin-3 deficiency on whole muscle relaxation and SR calcium loading.
Methods: Mice were killed with an overdose of halothane, UNSW animal ethics approval 11/140B. Flexor digitorum brevis (FDB) muscles were dissected out and digested in collagense 1a to yield individual fibres. Fibres were plated onto a chamber placed on a Nikon inverted microscope attached to a Cairn spectrophotometer to monitor calcium transients using a photomultiplier tube (PMT). An intracellular microelectrode was used to ionophorese the free acid form of fura-2 or low affinity fura-ff to give a final concentration 5-50 μm. Fibres were electrically stimulated using a bipolar concentric electrode positioned near the neuromuscular junction. In some cases the fibre was immobilized with BTS (4-methyl-N-(phenylmethyl) benzenesulfonamide)to stop contractions
Results: In FDB fibres of α-actinin-3-deficient KO mice, the calcium transient in response to a single action potential displayed a lower peak, a slower rate of rise and a faster rate of relaxation than the calcium transients from fibres of WT mice (n=15 for KO, n=19 for WT). Interestingly it was found that KO animals have 50% higher density of SERCA protein while the amount of parvalbumin protein is unchanged. The rate of ICE (calcium release cocktail)-induced SR calcium release was higher in KO. However there does not appear to be a difference in releasable calcium. Calcium-frequency curves showed no significant differences between fibres from KO and WT mice.
Conclusions: The faster decay of the calcium transients in fibres of α-actinin-3-deficient KO mice is consistent with data showing an increased density of SERCA pumps in the SR of fibres from KO mice. However, the observations from previous studies that whole fast-twitch muscles from KO mice relax more slowly, and that SR loading is slowed in KO mice, suggest that there may be an increased calcium leakage from the SR of KO mice via the SERCA pump calcium leak pathway.
Chan S, Seto JT, Houweling PJ, Yang N, North KN & Head SI (2011) Muscle and Nerve 43: 37-48.

NHMRC of Australia

Where applicable, the authors confirm that the experiments described here conform with The Physiological Society ethical requirements.

PCD249

Is the replacement of skeletal alpha-actin by cardiac alpha-actin in skeletal muscles beneficial?

J. Ochala[1], H. Iwamoto[2], G. Ravenscroft[3] and K. Nowak[3]

[1]Centre of Human and Aerospace Physiological Sciences, King's College London, London, UK, [2]JASRI, SPring8, Hyogo, Japan and [3]Centre for Medical Research, The University of Western Australia, Perth, WA, Australia

Nemaline myopathy is the most common congenital myopathy and is notably caused by mutations in the ACTA1 gene encoding skeletal alpha-actin. The main features of ACTA1 null mutations (absence of skeletal alpha-actin) are generalized skeletal muscle weakness and premature death. A mouse model mimicking this condition can be rescued by incorporating the ACTC gene into skeletal muscles and hence, by overexpressing cardiac α-actin (ACTCCo/KO). Nevertheless, muscle fibres from ACTCCo/KO animals generate less force than normal cells (-20-25%). To understand the underlying mechanisms, here, we have undertaken a detailed functional study of fibres from ACTCCo/KO. Mechanical and X-ray diffraction pattern analyses of single membrane-permeabilized fibres showed, upon maximal Ca2+ activation and under rigor conditions, lower stiffness but maintained meridional and equatorial reflections in ACTCCo/KO when compared with age-

matched wild-type animals (WT). Overall, these results demonstrate that in ACTCCo/KO, the presence of cardiac alpha-actin instead of skeletal alpha-actin alters the formation of myosin cross-bridges by finely altering the strain of individual actomyosin interaction, thus lowering muscle fibre force production. These findings provide important information that has to be taken into consideration when considering the incorporation of the ACTC gene as a therapy for ACTA1-based nemaline myopathy.

Where applicable, the authors confirm that the experiments described here conform with The Physiological Society ethical requirements.

PCD250

Viscoelastic analysis of myosin adsorbed to gold

T. Ohno[1], M. Wagatsuma[2], M. Ichihashi[2] and A. Itoh[2]

[1]Physiology, Jikei Univ., Tokyo, Japan and [2]Research & Development Division, Ulvac, Inc, Tokyo, Japan

We observed the adsorption process of myosin to the gold surface by QCM (quartz crystal microbalance). Using the AFFINIXQN Pro (Initium, Tokyo), viscoelasticity of the myosin adsorbed to the surface of the gold electrode and its surrounding solution as a whole was estimated by the response of quartz crystal to the resonance frequency and the frequencies in the vicinity.
Samples were measured in both solution and air. The adsorbed protein volume was calculated from the data in the air.
When myosin adsorbed more sparsely than 0.2 ug/cm^2, viscoelastic change accompanied with myosin adsorption was almost the same as to the viscoelasticity of buffer except myosin. The resonance frequency falls as to weight of adsorbed myosin. This implies that myosin adsorbed at low density plays as a solid globular protein. On the other hand, when myosin adsorbed at higher density, large viscoelastic change has been obserbed. Viscoelastic analysis indicate myosin plays as a protein having viscoelasticity.

Where applicable, the authors confirm that the experiments described here conform with The Physiological Society ethical requirements.

PCD251

Monoclonal antibodies to myosin head retard formation of rigor actin-myosin linkages in skinned rabbit psoas muscle fibers

T. Kobayashi[1], T. Abe[1], K. Kimura[1] and H. Sugi[2]

[1]Department of Electronic Engineering, Shibaura Institute of Technology, Tokyo, Japan and [2]Department of Physiology, Teikyo University, Tokyo, Japan

Muscle contraction results from cyclic attachment and detachment between myosin head in the thick filament and actin in the thin filament. According to biochemical studies on the actomyosin ATPase reaction, the myosin head (M), in the form of M • ADP • Pi, first attaches to actin (A), and exerts a power stroke, associated with release of ADP and Pi, so that at the end of power stroke, M forms rigor linkage AM with A. Upon binding with a new ATP, M detaches from A to extert a recovery stroke, associated with the reaction, M • ATP → M • ADP • Pi, and reattaches to actin. The presence of the rigor linkage AM during muscle contraction is, however, not yet proved by X-ray diffraction studies on contracting muscle fibers. To give information about formation of the rigor linkages, we examined development of rigor linkages in single skinned rabbit psoas muscle fibers in response to removal of ATP from the relaxing solution by recording changes in muscle fiber stiffness, measured by applying sinusoidal vibrations (peak-to-peak amplitude, 0.2% of L_0; 2kHz) at 20°C. If 4mM $MgCl_2$ was present in the ATP-free rigor solution, the fibers exhibited a long latent period of 40-60s until starting to develop appreciable stiffness, which then increased slowly to a peak with a half rise time of 20-30s. By the addition of three different monoclonal antibodies (against catalytic, converter and lever arm domains, respectively; Sugi et al. BBRC 405: 651-656, 2011), both the latent period and the half rise time of rigor stiffness development increased by a factor of 1.5-2. When Mg ions in the ATP-free rigor solution was removed by 10mM EDTA, The latend period for rigor stiffness development markedly decreased to 2-3s, and the antibodies had no effect on the latent period, but still increased the half rise time of rigor stiffness development by a factor of 1.5-2. The result that the rigor linkage formation is retarded by the antibodies seem to imply that, in the present experimental conditions, the rigor linkage formation requires some structural changes in the catalytic, converter and lever arm domains, so that binding of antibodies to these domains retards the rigor linkage formation. Meanwhile the antibodies had no effect on the relaxation of rigor force and stiffness when rigor fibers were returned to the relaxing solution containing 4mM ATP.

Where applicable, the authors confirm that the experiments described here conform with The Physiological Society ethical requirements.

PCD252

Physiological finger tremor size mirrors speed of finger movement due to muscle thixotropy

C.A. Vernooij, R.F. Reynolds and M. Lakie

School of Sport and Exercise Sciences, University of Birmingham, Birmingham, UK

Human physiological finger tremor is described as an inevitable small trembling of the finger consisting of two main frequency components; one 8-12 Hz and one over 15 Hz. When the finger is extended, both of these peaks are present in the frequency spectrum, but their relative size is variable. When moving the finger, the low frequency peak is much larger and usually the high frequency peak is no longer identifiable. Our recent studies revealed a main role for mechanical resonance in generating finger tremor. In contradiction to previous beliefs, a specific neural input was not necessary. Both tremor frequencies could be explained based on a changing resonant frequency due to altered muscular stiffness with movement. How the tremor frequencies transform during the transition between posture and movement and the interaction with EMG is described here.
With ethical permission, physiological tremor of 15 healthy subjects (23.7 ± 9.9 yr, 12 male) was measured using a miniature accelerometer taped to the splinted middle finger. A retroflective laser sensor, pointed at the tip of the finger, measured finger position. A pc placed ~2 m in front of the subjects showed finger position and a target with which subjects had to align their finger position. The target started with 10 s at a comfortable static middle position of the finger which progressed into a vertically orientated sinusoidal chirp signal ranging from 0 Hz to 0.05 Hz over 50 s. Over the subsequent 60 s

the target consisted of a mirror image of the first half, ending with a 10 s static middle position (see Fig 1a). The maximum required angular velocity of the finger was 3 deg/s. Each subject was asked to repeat the 120 s trial 10 times, during which surface EMG was recorded from the extensor digitorum communis muscle (m. EDC). We calculated a wavelet transform for acceleration and rectified EMG for each trial which afterwards were averaged across trials and participants. A Pearson's correlation was computed between acceleration size and EMG size and between these measured variables and position and speed of the finger.

Unsurprisingly, EMG correlated strongly with the vertical position of the finger (r^2 = 0.84) (Fig 1, top), because more extension required more EMG. In contrast, acceleration size seemed to correlate best with the speed of the finger (r^2 = 0.72) (Fig 1, bottom), and less strongly with EMG (r^2 = 0.19). We propose that primarily the movement-related (thixotropic) character of the muscles determines the size of physiological finger tremor. With increased speed of finger movement, an increased amount of muscle tissue is moved about and the overall muscle stiffness will progressively drop. This is associated with an increase in the size of the resonance and thus finger tremor. This must cause computational difficulties in finger control when making the transition from posture to movement.

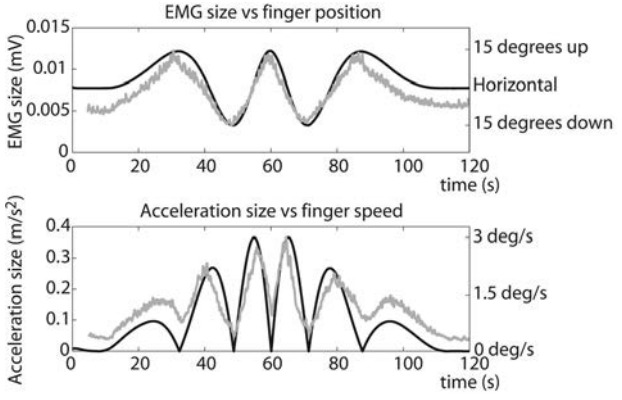

Figure 1.
Top graph: EMG size (grey) is adjusted with finger position (black).
Bottom graph: Acceleration size (grey) is adjusted with finger speed (black).

Where applicable, the authors confirm that the experiments described here conform with The Physiological Society ethical requirements.

PCD253

Mdx mice skeletal muscle differentiation and recovery of neuromuscular junctions after bone marrow stem cells transplantation

A.V. Sokolova[1], V.V. Kravtsova[2], N.A. Timonina[2], I.I. Krivoi[2] and V.V. Mikhailov[1]

[1]Institute of Cytology of the Russian Academy of Sciences, Saint-Petersburg, Russian Federation and [2]Saint-Petersburg State University, Saint- Petersburg, Russian Federation

Mdx mice are a model of Duchenne muscular dystrophy caused by deficiency of dystrophin. Striated muscle fibers (SMFs) of mdx mice are characterized by high level of death. As a result most SMFs of mdx mice have centrally located nuclei. Furthermore, neuromuscular junctions (NMJs) in mdx mouse are altered. Usually acetylcholine receptors (AChRs) of mdx mice are distributed as small islands in contrast to original AChRs branches of C57BL/6 mice NMJs. Our previous results showed that single intramuscular injection of C57BL/6 Lin(-) bone marrow (BM) stem cells ameliorate structure of NMJs of mdx mice SMF. 4 months after BM local transplantation total NMJs area was increased in 1.5 times due to increase of area of AChRs clusters simultaneously with increase of their number. The part of dystrophin-positive SMFs was increased from 0.5±0.1 % up to 1.8±0.4 %. We also changed mutant BM for BM of wild type. Male, 2 month old mdx mice (gift of Prof. T.A. Partridge, UK) were irradiated by X-ray in dose 3 Gy. BM cells were harvested from C57BL/6 mice (Rappolovo animal farm, St. Petersburg) killed by ether narcosis. 24 h after irradiation, mdx mice were anaesthetized with nembutal (40 mg kg-1, i.m.) and injected intravenously by BM cells. The study of m. quadriceps femoris and diaphragm was made at 2, 4, 6 month after transplantation. To localize NMJs we used tetramethylrhodamine-α-bungarotoxin (Biotium, USA) with help of Leica TCS SL confocal microscope. Values are means ± S.E.M. Experiments were performed at the animal care facility of Institute of Cytology of the RAS. We observed the increasing part of dystrophin-positive SMFs in m. quadriceps femoris mdx mice up to 27.6±6.7 % at 6 month after transplantation which was accompanied by decreasing of SMFs death from 2.2±0.6 % to 0.7±0.1 % and by accumulation of SMFs without central nuclei from 10.5±1.0 % up to 22.6±1.9 %. Similar to m. quadriceps femoris the increasing of part of dystrophin-positive SMFs was observed in diaphragm of mdx mice up to 12.0±3.2 % in 4 month after transplantation. The part of muscle SMFs without central nuclei increased from 8.4±0.6 % up to 30.4±1.5 % in diaphragm of mdx mice. The part of diaphragm NMJs with clusters of AChRs distributed as continuous branches was increased from 14±3 % up to 42.6±6 % and part of NMJs with AChRs clusters as islands was decreased from 75.8±3 % up to 53.7±6 %. Recovery of structure of NMJs was accompanied by recovery of the resting potential of the diaphragm end-plate membrane. Replacement of mutant BM stem cells for stem cells of wild type in condition of non-lethal X-ray irradiation is reason of recovery of dystrophin synthesis and of NMJs structure and function. This study was supported by Research Project #1.37.118.2011 of St. Petersburg State University, the Russian Foundation for Basic Research (#13-04-00973a).

Where applicable, the authors confirm that the experiments described here conform with The Physiological Society ethical requirements.

PCD254

Involvement of the lateral reticular nucleus in the suppression induced by stimulation of the red nucleus on the jaw-opening reflex

Y. Satoh[1], E. Yajima[2], K. Ishizuka[1], Y. Nagamine[2] and S. Iwasaki[1]

[1]Physiology, Nippon Dental University, Niigata, Japan and [2]Orthodontics, Nippon Dental University, Niigata, Japan

The jaw-opening reflex (JOR) can be evoked by electrical stimulation of either the low- or high-threshold afferents of the trigeminal nerve. The JOR evoked by high-threshold afferents is thought to be evoked by noxious stimulation (Lund et al., 1984). We have reported that stimulation of the red nucleus (RN) facilitated the low-threshold afferent-evoked JOR and suppressed the high-threshold afferent-evoked JOR. The effect is probably mediated by an indirect pathway, since there is little evidence for direct projections from the RN to the trigeminal motor nucleus. A possible interneuronal link in this pathway could be located within the lateral reticular nucleus (LRN).

This region has been proposed as a site engaged in the mechanisms of analgesia (Hall et al., 1982; Morton et al., 1983) and to receive contralateral projections from the RN (Flumerfelt and Gwyn, 1974). Furthermore, stimulation of the LRN suppressed the JOR evoked by noxious stimulation (Sotgiu, 1986). We therefore decided to examine whether lesion of the LRN affects RN-induced modulation of the JOR. The experiments were performed on 10 male Sprague-Dawley rats weighing 319-364 g. The rats were anesthetized with urethane and α-chloralose (500 m/kg and 50 mg/kg, respectively; i.p.), so as to maintain anesthesia at a level at which no withdrawal reflex was evoked by noxious stimulation of the paw. Arterial blood pressure was monitored to confirm the condition of the rat throughout the experiment. The test stimulation was applied to the inferior alveolar nerve (1 pulse, 0.1 ms in duration, 1 Hz) to evoke the JOR. The stimulus intensity was either 1.2 (low threshold) or 4.0 (high threshold) times the threshold. The electromyograms were recorded from the anterior belly of the digastric muscles. The conditioning stimulation (1pulse, 0.2 ms in duration, 1 Hz, 100 μA) was applied to the RN 10 or 30 ms before the test stimulation. The control JOR responses were recorded as well as the modulation induced by stimulation of the RN. The LRN lesion was made contralateral to the RN by the passage of electric current (20 μA, 2 min). The effect of the RN stimulation on the JOR was tested at the termination of lesion. At the end of each experiment, the stimulating sites were verified histologically. RN-induced facilitation of the JOR was not affected by lesion of the LRN (n=7, Wilcoxon t-test with Bonferroni correction, $P > 0.05$). On the other hand, RN-induced suppression of the JOR is significantly reduced by lesion of the LRN (n=7, Wilcoxon t-test with Bonferroni correction, $P < 0.05$). RN-induced modulation of the JOR was not affected by lesion of the outside of the LRN (n=3, Wilcoxon t-test with Bonferroni correction, $P > 0.05$).These results suggest that the suppressive effect of RN stimulation on the JOR is mediated partly by a relay in the contralateral LRN.

Where applicable, the authors confirm that the experiments described here conform with The Physiological Society ethical requirements.

PCD255

The contractile properties of slow and fast skeletal muscles from Protease Activated Receptor-1 null mice

A. Bakker[1], S. Paran[1], P. Charles[2], M. Eleanor[2] and G. Pinniger[1]

[1]School of Anatomy, Physiology & Human Biology, The University of Western Australia, Perth, WA, Australia and [2]School of Veterinary Science, The University of Melbourne, Melbourne, VIC, Australia

Protease activated receptors (PARs) are unique G-protein-coupled receptors that are activated by proteolytic cleavage. Four PAR isoforms (PAR-1 to 4) have been identified. PARs may play an important role in skeletal muscle development, as they are highly expressed in myoblasts and myotubes in tissue culture (Mackie et al., 2008), and show marked changes in expression in muscle fibres during embryonic development (Chevessier et al., 2001). In order to increase our understanding of the role of PAR-1 receptors in muscle development, we compared the contractile properties of slow and fast skeletal muscles from PAR-1 null (P-1N) and wild type (WT) mice.
Experiments were conducted on 12 week old P-1N null (n=7) and WT littermate mice (n=5). This study was approved by the animal ethics committee of the University of Western Australia. Mice were anaesthetized by intraperitoneal injection of pentobarbitone (40mg/kg). The soleus (mainly slow twitch) and extensor digitorum longus (EDL) (fast twitch) muscles were surgically removed and connected to a force transducer system. The muscles were maintained in Kreb's mammalian Ringer solution bubbled with Carbogen (95% O2 and 5% CO2). Twitch force characteristics, the force frequency relationship and maximum specific force (force normalised to muscle cross sectional area) were determined, and the rate of fatigue and post-fatigue recovery were assessed. Muscle fibre type proportions were determined using immunohistochemistry.
The absence of PAR-1 receptors in soleus muscles resulted in a significantly greater mean peak twitch force (P-1N: 6.2 ± 0.231 N.cm-2, WT: 4.6 ± 0.392 N.cm-2, $p<0.05$) and mean twitch time to peak values (P-1N: 57.0 ± 3.0 ms, WT: 41.0 ± 1.0 ms, $p<0.05$) and produced a significant shift of the force-frequency curve to the left. In addition, the soleus muscles from the P-1N mice fatigued significantly more slowly ($p<0.05$) and exhibited a significantly faster post fatigue recovery ($p<0.05$) than muscles from WT mice. There was no difference in maximum specific force between soleus muscles from P-1N and WT mice. There was a 24% increase in the proportion of type 1fibres, and a 90% decline in the proportion of type IIb fibres in the soleus muscles from PAR-1 null mice compared to soleus controls. In P-1N EDL muscles, no significant differences were found, except for a slower rate of fatigue compared to controls.
The results of this study indicate that the absence of PAR-1 receptors significantly alters the contractile properties of skeletal muscle, especially in the predominately slow twitch soleus. The absence of PAR-1 results in a slower skeletal muscle contractile phenotype, likely due to an increase in type I and a decrease in type IIb fibre numbers. These results suggest that PAR-1 receptors may play a role in setting fibre-type proportions during skeletal muscle development.

Mackie EJ, Loh LH, Sivagurunathan S, Uaesoontrachoon K, Yoo HJ, Wong D, Georgy SR, Pagel CN. Protease-activated receptors in the musculoskeletal system. Int J Biochem Cell Biol 2008;40(6-7):1169-1184.

Chevessier F, Hantai D, Verdiere-Sahuque M. Expression of the thrombin receptor (PAR-1) during rat skeletal muscle differentiation. Journal of cellular physiology 2001;189(2):152-161.

Where applicable, the authors confirm that the experiments described here conform with The Physiological Society ethical requirements.

PCD256

The impact of resveratrol and hydrogen peroxide on C2C12 myoblast regenerative cascade is dose-dependent

A. Bosutti and H. Degens

Institute for Biomedical Research into Human Movement and Health, School of Healthcare Science, Manchester Metropolitan University, Manchester, UK

Myoblast migration represents a key step in muscle regeneration following microdamage after exercise (1). Myosatellite cell fusion with the damaged myofibre and subsequent differentiation pilots muscle remodelling (2). While increased production of Reactive Oxygen Species (ROS) is crucial in exercise-induced muscle damage (3). In line with this, antioxidant supplementation, such as the polyphenol resveratrol, may suppress skeletal muscle damage and improve anti-oxidant capacity (4). However, ROS is also crucial for exercise-mediated adap-

tation and repair (5). The way at which ROS and/or resveratrol modulate myoblast function in muscle repair remains unclear.

Here, we explored the individual and combined effect of different concentrations of resveratrol (RS; 10-20-40-60 μM) and hydrogen peroxide (H_2O_2; 2-1 mM, 800-500-100-50-10μM) on non-differentiated (myoblasts) and differentiated (myotubes) mouse skeletal muscle-derived cells (C2C12). The impact of RS on myoblasts regenerative capacity was tested by assessing cell morphology, proliferation (MTS assay), migration (wound healing), sprouts formation (spheroids assay) and myotube formation and/or shrinking. In myoblasts, we tested the effect of RS plus H_2O_2 on cell migration. In 8-days differentiated myotubes we studied the impact of RS plus H_2O_2 on the oxidative capacity [succinate dehydrogenase (SDH) activity] and myosin ATPase activity and composition (total and type1-myosin). Data analysed by ANOVA in five replicates.

The effect of RS on cell mitosis (24-48h) and proliferation (72h) was dose dependent; RS 10-20μM did not show significant effects, but at higher doses (40-60μM) it impaired both cell processes ($p<0.01$). RS 10-20μM enhanced ($p=0.03$) migration and the formation of myoblast sprouts, but not cell fusion. RS 40-60μM almost blocked myoblast regenerative capacity. In parallel, low doses of H_2O_2(10-500μM) enhanced motility with the highest efficiency at 100μM, while higher doses showed damaging effects. Notably, 24h of RS pre-conditioning (10-20μM) prevented the deleterious effects of H_2O_2(1mM) and further enhanced cell migration induced by $H_2O_2$100μM.

Evidence suggests that RS may increase fibre oxidative metabolism (4). Surprisingly, we did not find any effect of RS on myotube oxidative capacity (SDH), while we found a reduction ($p<0.01$) in myosin type1-ATPase activity and increased total myosin ATPase content. Finally, H_2O_2 (1mM) induced a reduction ($p<0.01$) in total and myosin type1 ATPase activity, that was prevented by RS in a dose-dependent manner.

In conclusion, our data support the notion that low concentrations of ROS enhance myoblast regenerative capacity while it is impaired at high concentrations. High doses of anti-oxidants may also impair regenerative capacity, while low doses may abolish the detrimental impact of high concentrations of ROS on muscle regeneration.

Cermak NM *et.al.* (2013). *Med Sci Sports Exerc* **45**, 230-237.

Anderson JE *et.al.* (1998). *Biochem Cell Biol* **76**,13-26.

Davies KJ *et.al.* (1982). *Biochem Biophys Res Commun* **107**,1198-1205.

Denu JM (2012). *Cell Metab* **15**, 566-567.

Petersen AC *et.al.* (2012). *Acta Physiol (Oxf)* **204**, 382-392.

Where applicable, the authors confirm that the experiments described here conform with The Physiological Society ethical requirements.

PCD257

The adaptive response of capillarisation to disuse is muscle-specific

A. Bosutti[1], M. Salamova[2], J. Rittweger[3] and H. Degens[1]

[1]Institute for Biomedical Research into Human Movement and Health; School of Healthcare Science, Manchester Metropolitan University, Manchester, UK, [2]Vegetative Anatomy, Neuromuscular Group, Charité Universitätsmedizin, Berlin, Germany and [3]Institute of Aerospace Medicine, German Aerospace Center, Cologne, Germany

Human skeletal muscle adapts to microgravity-induced disuse by atrophy and weakness, switch of fibre types (from slow to fast twitch fibres), changes in muscle energy metabolism and metabolic demand (1) and capillarisation (2). We hypothesize that a change in capillarisation precedes muscle fibre atrophy during disuse. Bed rest s a well-accepted model of either inactivity induced by deconditioning or simulated microgravity in healthy humans. There is some evidence that milk-based proteins, such as whey proteins, can act as an effective countermeasure to alleviate or attenuate the atrophy during prolonged bed rest.

Here we explored the changes in capillarisation in response to 21 days of medium-term bed rest with and without countermeasure (Whey protein diet). Muscle biopsies were taken from the soleus (SOL) and vastus lateralis (VL) muscles before (pre) and after bed rest (post) with or without whey protein supplementation (n = 5, each). Fibre types and capillaries were identified by immunohistochemical co-staining of muscle section with anti-myosin type1 and lectin. Analysis was done with the method of capillary domains (3). Statistical analysis was done by repeated measures ANOVA. Ethical approval was obtained from the local Ethics Committee and each participant provided informed consent before enrolment in the study.

Surprisingly, bed rest did neither affect fibre type composition nor fibre size in both SOL and VL muscles. Capillary density was, however, 10% less in the SOL ($p<0.01$), but not in the VL muscle after bed rest. Despite the reduced capillary density in the SOL, the heterogeneity of capillary spacing was not significantly changed in both muscles. Whey protein did not have a major effect on the impact of bed-rest-induced muscle adaptations.

In conclusion, our results show that medium-term bed rest induced a reduction in capillary density in the soleus but not in the vastus lateralis muscle. The absence of significant muscle fibre atrophy suggests that a reduction in capillary supply may precede fibre atrophy in disuse.

Sandonà D et al. (2012). PLoS One. 7, e33232

Egginton S (2010). J Physiol 588, 4607-4608.

Degens H et al. (2006). Microcirc 13, 467-476.

We appreciate the support of the European Space Agency

Where applicable, the authors confirm that the experiments described here conform with The Physiological Society ethical requirements.

PCD259

Temperature and 'fatigue' effects on ATP induced actomyosin dissociation kinetics

C. Karatzaferi[1] and M.A. Geeves[2]

[1]PE & Sports Science, University of Thessaly, Trikala, Greece and [2]School of Biosciences, University of Kent, Canterbury, UK

The functional characteristics of the various types of skeletal muscles, are largely dictated by the expression of class II myosin heavy chains (MyHC) isoforms; especially contraction velocity, a manifestation of the rate of actomyosin (A.M.) interaction and of ATP turnover. Higher levels of expression of a fast MyHC isoform lead to faster contraction velocity, while higher levels of expression of a slow MyHC lead to a slower contraction velocity. It has been observed that in slow myosin isoforms ADP binding to A.M is tighter than with fast isoforms, and one of us has shown that with slow isoforms multiple A.M.ADP complexes are present. The in vivo muscle temperature ranges from 34 to > 40 degrees Celsius (oC) while in extreme fatigue, pH drops and inorganic phosphate (Pi) accumulates. Still, most kinetics characterisations in the past have been done in 'standard' conditions e.g. 20oC, pH 7 and no added phosphate. Recent data by one of us highlighted the importance of investigating possible synergisms between temperature and such 'fatigue' factors which may gain different 'importance' in the different fibre types.

We thus examined the fast kinetics of ATP induced dissociation of A.M. (with and without ADP) of rabbit fast and slow myosin for a range of temperatures (from 5 to 35oC) using stopped flow to examine the effects of pH (7 vs 6.2), and Pi (0, 15 and 30 mM), individually or in combination. We also examined the temperature dependence of these 'fatigue' factors. The experimental protocol was approved by the local Animal Ethics Committee, and all the experimental procedures conformed to the UK Animals (Scientific Procedures) Act, 1986.

Temperature did not have an evident effect on ADP affinity nor did low pH seem to affect ADP affinity for the fast myosin. For slow myosin, ADP affinity weakened at pH 6.2, also at 35oC. Addition of Pi affected the two myosin typess differently, Pi competing with the ADP inhibition in fast but almost abolishing ADP inhibition in slow myosin at the higher Pi concentration. In slow myosin Pi and low pH combined affected ATP induced dissociation of A.M in the lower range of the temperatures studied.

Our results provide further evidence of distinct mechanochemical coupling between the myosin types. Results will be also discussed in relation to the effects of fatigue on velocity of contraction.

This research has been partially cofinanced by the European Union (European Social Fund – ESF) and Greek national funds through the Operational Program "Education and Lifelong Learning" of the National Strategic Reference Framework (NSRF) Research Funding Program: THALES Investing in knowledge society through the European Social Fund (project 4525, MIS 377260).

Where applicable, the authors confirm that the experiments described here conform with The Physiological Society ethical requirements.

PCD260

Endogenous and maximal SR calcium content in human vastus lateralis muscle fibres is decreased with ageing

C. Lamboley[1], R.M. Murphy[2], M.J. McKenna[1] and G.D. Lamb[2]

[1]ISEAL, Victoria University, Melbourne, VIC, Australia and [2]Zoology, La Trobe University, Melbourne, VIC, Australia

A progressive decline in skeletal muscle function is part of the normal ageing process. The observed loss of specific force in aged muscle suggests that a Ca2+ dependent process may be impaired in ageing.

The muscle force production is closely related to the amount of Ca2+ released from the sarcoplasmic reticulum (SR). For this reason, it would be important to have a reliable measurement of total SR Ca2+ content ([CaT]SR) in aged human skeletal muscle fibres under physiological resting conditions. The present study examined for the first time, in individual fibres from human skeletal muscle biopsies, whether endogenous SR Ca2+ content and maximal SR Ca2+ capacity are different between young and aged healthy adults.

A muscle biopsy was taken from the vastus lateralis muscle from eleven and nine healthy young (23±0.8 yo) and old (70±0.7 yo) adults, respectively. After injection of a local anesthetic into the skin and fascia (1% lidocaine (Xylocaine)), a muscle sample was taken using a Bergstrom biopsy needle. Individual fibre segments, obtained from the biopsy, were mechanically skinned under paraffin oil so that they still contained their endogenous Ca2+ content. The total amount of Ca2+ contained in each fibre could be quantified by pre-equilibrating the fibre in a solution with a known concentration of the calcium-buffer BAPTA and then transferring the fibre to an emulsion of 1% Triton X-100 and paraffin oil (TX-oil) in order to lyse all membranous compartments and release any Ca2+ from within the fibre (Fryer & Stephenson, 1996). The total amount of Ca2+ present in the fibre can be calculated from the BAPTA concentration and the magnitude of the force response upon lysis. Furthermore, other fibre segments, prior to the TX-oil lysing, were loaded to their maximal SR Ca2+ capacity. Finally, using Western blotting, each muscle fibre was classified as type I or II according to the myosin heavy chain isoform present.

When fibres with an endogenous Ca2+ content were assayed, the endogenous [CaT]SR obtained (expressed relative to intact fibre volume) was significantly decreased in aged subjects compared to young individuals (0.58±0.01 (n=15) and 0.67±0.03 (n=8) mmol.l^{-1}, respectively, in type I fibres, and 0.62±0.02 (n=10) and 0.77±0.02 (n=15) mmol.l^{-1}, respectively, in type II fibres). By loading the SR of the fibres maximally, the study also revealed that the maximal SR Ca2+ capacity was significantly decreased in fibres of aged subjects compared to young adults (1.22±0.03 (n=12) and 1.36±0.04 (n=14) mmol.l^{-1}, respectively, in type I fibres, and 1.45±0.03 (n=11) and 1.72±0.03 (n=19) mmol.l^{-1}, respectively, in type II fibres).

The present results suggest that the appreciable decrease with ageing of the endogenous and maximal [CaT]SR in both type I and II fibres could be an important factor in muscle weakness in the elderly.

Fryer MW & Stephenson DG (1996) *J Physiol* 493, 357-370.

Where applicable, the authors confirm that the experiments described here conform with The Physiological Society ethical requirements.

PCD261

Effect of ascorbic acid on force frequency relationship of skeletal muscle fibers in long term cold exposed Sprague Dawley rats

A. Shahid[1] and U. Khan[2]

[1]Physiology, Wah medical college, Wah Cantt, Pakistan and [2]Physiology, Al-Nafees Medical College, Islamabad, Pakistan

Background: On exposure to prolonged cold temperature, the body responds for effective heat production, both by shivering and nonshivering thermogenesis.1 Cold exposure increases the production of reactive oxygen species (ROS) which influence the sarcoplasmic reticulum Ca++ release from the skeletal muscles and affect their contractile properties.2 The role of ascorbic acid supplementation on force-frequency relationship of cold exposed skeletal muscles was evaluated in this study. Method: Ninety healthy, male Sprague Dawley rats were tagged and randomly divided into three groups of control (I), cold exposed (II) and cold exposed along with ascorbic acid supplementation (III). Rats of group I were kept at room temperature at 22±3˚C. Group II and III were given cold exposure of 8-14˚C, by keeping their cages in ice-filled tubs for 1hr/day for one month.3 Rats of group III were also given ascorbic acid supplement, as 500mg of L-Ascorbate (MERCK, research grade Cat No. 500074) in powder form mixed per liter of drinking water, for one month.4 After the study period, the rats were ether anesthetized in glass jars and then extensor digitorum longus muscle was dissected out. The muscle was placed on the muscle holder of Power Lab ADInstruments 4/26T [ML856] and force-frequency relationship in the skeletal muscle fibers was analyzed on computerized data acquisition system.5 (Fig. 1) Results: The cold exposed group II showed a significant decline in the contractile properties of skeletal muscle fibers at different frequencies as compared to the control group I (p value <0.05). In group III, however, the force was contraction was better than group II (p value <0.05). Conclusions: Chronic cold exposure delays the contractions in skeletal muscles, while supplementation with ascorbic acid prevents the decrease in force of contraction in muscles exposed to chronic cold.

Key words
Ascorbic acid, cold stress, force of contraction, skeletal muscles

Table 1: Comparison of force frequency relationship between cold exposed group and cold exposed with ascorbic acid supplement group after four weeks

Frequency (Hz)	Cold exposed group (n=30) Force (N)		Cold exposed with ascorbic acid supplement group (n=30) Force (N)		p -value
	Mean	Std. Deviation	Mean	Std. Deviation	
1 Hz	0.016	0.002	0.018	0.002	< 0.05*
5 Hz	0.082	0.007	0.065	0.002	< 0.01**
10 Hz	0.095	0.003	0.102	0.003	< 0.01**
30 Hz	0.110	0.003	0.107	0.002	< 0.05*
50 Hz	0.113	0.002	0.117	0.002	< 0.01**
70 Hz	0.119	0.002	0.126	0.002	< 0.01**
90 Hz	0.113	0.032	0.135	0.003	< 0.05*
110 Hz	0.137	0.005	0.140	0.002	< 0.01**

* p -value < 0.05 is taken as significant

** p -value < 0.01 is taken as highly significant

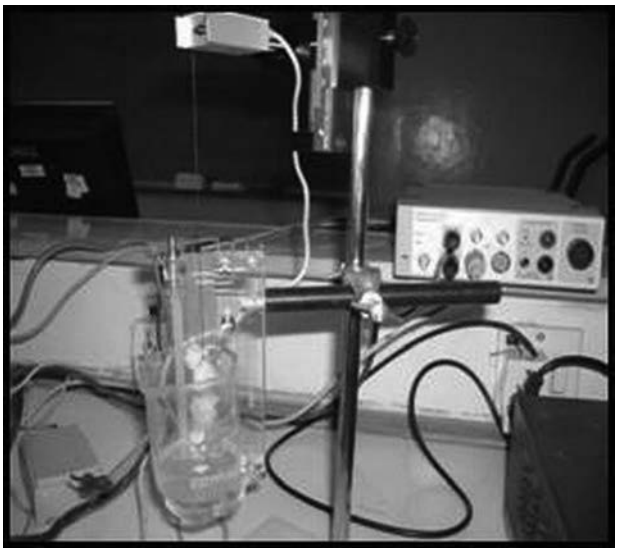

Fig. 1

Muscle set-up in powerLab

Mohamed T, Roman G, Harold S, David J. Interplay between calcium and reactive oxygen/nitrogen species: an essential paradigm for vascular smooth muscle signaling Antioxid Redox Signal 2010; 12: 657-74.

Aydin J, Shabalina IG, Place N, Reiken S, Zhang SJ, Bellinger AM, et al. Nonshivering thermogenesis protects against defective calcium handling in muscle. FASEB J 2008; 22: 3919–24.

Nomura T, Kawano F, Kang MS, Lee JH, Han EY, Kim CK, et al. Effects of long term cold exposure on contractile properties in slow – and fast – twitch muscles of rats. Jap J Physiol 2002; 52: 85 – 93.

Hsu, P.C., Liu, M.Y., Hsu,C.C., Chen, LY, Guo YL. Effect of vitamin E and/or C on reactive oxygen species-related lead toxicity in the rat sperm. Toxicology 1998:128; 169-79.

Warmington SA, Tolan R, McBennett S. Functional and histological characteristics of skeletal muscle and the effects of leptin in the genetically obese (ob/ob) mouse. Int J Obes Relat Metab Disord 2000; 24: 1040-50.

I am greatly thankful to my ex-supervisor Brig Amjad Hameed, Dr. Mustafa Lodhi and all the vetrinary staff that helped me complete this project.

Where applicable, the authors confirm that the experiments described here conform with The Physiological Society ethical requirements.

PCD262

Contributions of lower muscle mass and specific force to muscle weakness in old mice

S. Ballak[1,2], H. Degens[1], A. de Haan[1,2] and R. Jaspers[2]

[1]Institute for Biomedical Research into Human Movement and Health, Manchester Metropolitan University, Manchester, UK and [2]Move Research institute Amsterdam, Faculty of Human Movement Sciences, VU University Amsterdam, Amsterdam, Netherlands

Age-related muscle wasting and weakness (sarcopenia) ultimately lead to a dependent lifestyle. The general thought is that age-related reduction in force is primarily the consequence of a loss of muscle mass, due to both loss of fibres and fibre atrophy, and to a limited extend to a reduction in specific force of the remaining muscle tissue.

To investigate the quantitative contribution of each of these factors to the age-related muscle weakness 9-month- (adult, n=9) and 25-month- (old, n=10) old male C57BL/6j mice were studied. Maximal isometric tetanic force of the m. plantaris was measured *in situ*(1). All mice received a subcutaneous injection of 0.06 ml 1% temgesic as an analgesic and 4% isoflurane, 0.1L*min^{-1} O_2 and 0.2L*min^{-1} normal air for anaesthesia (1.5-2.5% during operation). Wet muscle mass was measured directly after excision. The fibre type composition was determined by immunohistochemical staining of 10-μm sections of the muscle using antibodies, against type I, IIA, IIX and IIB, respectively. An ANOVA was used to determine age-related differences. Data are expressed as mean±SD.

The maximal isometric force of the plantaris muscle of old mice was 13% lower than that of adult mice (968±122 vs. 840±109mN; p<0.05). The m. plantaris, gastrocnemius medialis and soleus muscle masses were 5-8% lower in old than adult mice (24.2±2.3 vs. 22.4±2.4mg, 65.2±5.9 vs. 60.08±5.3, 13.3±1.0 vs. 12.2±1.3; p<0.05, respectively). Fibre number was similar in the m. plantaris of adult and old mice (Adult vs. Old: 1033±195 vs. 1109±174). A shift towards a slower phenotype was observed, reflected by a lower proportion of type IIB fibres (46.5±4.6 vs. 38.4±4.5%; p<0.05) in the older animals. Fewer than 1% type I fibres and similar proportions of type IIA and IIX fibres in adult and old mice were observed (Adult vs. Old: 26.8±4.4 vs. 30.2±5.1% and 25.6±2.9 vs. 29.1±3.4%, respectively). Although the specific force (40.94±3.72 vs. 37.58±4.31N/gr; p=0.108) did not differ significantly between m. plantaris muscles from adult and old mice, linear regression suggested that 60% of the variance of force was explained by specific force (R^2=0.598) and the other 40% by muscle mass (R^2=0.392).

The most important outcome of this study is the reduction in force generating capacity with age, accompanied by a shift towards a slower phenotype. Moreover, age-related reduction in muscle force was explained by reductions in muscle mass (40%) and s

De Haan A, Bien M, Verdijk PW. Stimulation frequency-dependent reductions in skeletal muscle force and speed in creatine kinase-deficient mice. Acta physiologica Scandinavica. 1999;166(3):217-22. Epub 1999/09/01.

The authors wish to express their appreciation to Tinelies Buse for performing all operations. This research was funded by the European Commission through MOVE-AGE, an Erasmus Mundus Joint Doctorate programme (2011-0015).

Where applicable, the authors confirm that the experiments described here conform with The Physiological Society ethical requirements.

PCD263

Acute effects of curcumin on skeletal muscle contractile function

J. Lam, G.J. Pinniger and A.J. Bakker

University of Western Australia, Perth, WA, Australia

Curcumin, a component of the spice turmeric (*Curcuma longa*), has been reported to alleviate the symptoms of muscular dystrophy in *mdx* mice (Pan et al., 2008) and decrease the expression of inflammatory mediators involved in muscle injury (Epstein et al., 2012). Therefore, curcumin could provide an new avenue for the treatment of muscle disorders (Pan et al., 2008; Alamdari et al., 2009; Epstein et al., 2012). However, curcumin has also been reported to impair skeletal muscle Ca^{2+} handling (Bilmen et al., 2001; Logan-Smith et al., 2001), which could result in curcumin-induced muscle weakness. The aim of this study was to investigate the acute effects of curcumin exposure on skeletal muscle contractile function using intact and skinned fibre preparations from isolated extensor digitorum longus (EDL) muscles of the mouse.

ARC(s) mice (male, 6 week old, n=12) were anaesthetized with sodium pentobarbitone (40 mg/kg, I.P.) and intact EDL muscles were surgically removed and attached to a force transducer system. Muscles were maintained in an organ bath containing Kreb's mammalian Ringer solution, bubbled with carbogen (95% O_2 and 5% CO_2) at 25°C. The contractile properties (twitch force parameters, maximum tetanic force, force-stimulation frequency relationship and rate of muscle fatigue) were compared after a 60 minute exposure to curcumin or vehicle (0.01% DMSO). To determine the effect of curcumin on the Ca^{2+} sensitivity of the myofilaments, chemically skinned EDL fibres were exposed to highly buffered Ca^{2+} solutions of different known Ca^{2+} concentrations, in the presence of curcumin or DMSO. All values are expressed as means ± SEM.

Curcumin (15μM) significantly decreased maximum specific force in whole EDL muscles (control: 21.84±0.64 N/cm^2; curcumin: 19.07±0.57 N/cm^2, p<0.05), and shifted the force-frequency relationship to the left, with significantly greater relative forces at stimulation frequencies of 10-80Hz in the curcumin group (p<0.05). Curcumin also significantly increased the time to peak force of the twitch response (control: 17±1 ms; curcumin: 20±1 ms, p<0.05), but had no significant effect on other twitch force parameters. In addition, the rate of muscle fatigue was significantly slower in the curcumin exposed group, compared to controls (p<0.05, n=6). In skinned fibre experiments, curcumin (15μM) produced a small increase in the sensitivity of the myofilaments to Ca^{2+} (pCa_{50}: -6.26±0.05; control pCa_{50}: -6.13±0.09, p<0.05), and a marked decrease maximal force production to 52.8±10.6% of controls (p<0.05). These findings show that, at a bath concentration of 15μM, curcumin significantly decreases maximal force production in skeletal muscle, most likely via a direct effect on the force generating ability of the myofilaments. These findings have important implications for the use of curcumin as a treatment for diseases resulting in skeletal muscle weakness.

Alamdari, N., O'neal, P. & Hasselgren, P.-O. 2009. Curcumin and muscle wasting—a new role for an old drug? Nutrition, 25, 125-129.

Bilmen, J. G., Khan, S. Z., Javed, M.-U.-H. & Michelangeli, F. 2001. Inhibition of the serca ca2+ pumps by curcumin. Eur. J. Biochem., 268, 6318-6327.

Epstein, J., Sanderson, I. R. & Macdonald, T. T. 2012. Curcumin as a therapeutic agent: The evidence from in vitro, animal and human studies. Br. J. Nutr., 103, 1545-1557.

Logan-Smith, M. J., Lockyer, P. J., East, J. M. & Lee, A. G. 2001. Curcumin, a molecule that inhibits the ca2+-atpase of sarcoplasmic reticulum but increases the rate of accumulation of ca2+. J. Biol. Chem., 276, 46905-46911.

Pan, Y., Chen, C., Shen, Y., Zhu, C.-H., Wang, G., Wang, X.-C., Chen, H.-Q. & Zhu, M.-S. 2008. Curcumin alleviates dystrophic muscle pathology in mdx mice. Mol. Cells, 25, 531-537.

Where applicable, the authors confirm that the experiments described here conform with The Physiological Society ethical requirements.

PCD264

Ca^{2+}-calmodulin/calcineurin mediated signaling pathways are essential for upregulation of MHC I mRNA level in C2C12 cells

Y. Mori[1], M. Yamamoto[1], R. Hiroshima[1], T. Nakano[1] and M. Watanabe[1]

[1]Kansai Univ. of Welfare Sciences, Kashiwara, Japan and [2]Osaka Med. Coll., Takatsuki, Japan

Maintenance of skeletal muscle mass is essential for overall health, functionality and quality of life, and it is critical to elucidate the fundamental mechanisms underlying the maintenance. Skeletal muscle has been known to cause disuse atrophy during long-term recumbence and to recover by exercise. Although there are many studies about skeletal muscle regulatory factors, such as IGF-1, FGF, HGF, and IL-6, that are known to affect skeletal muscle mass, mechanism of exercise on muscle cell proliferation is still unclear. Our previous study using rat soleus muscle indicated that myosin heavy chain (MHC) and HSP 70 proteins were significantly increased by the exercise after disuse atrophy. It is well known that the mechanical stress by exercise raises intracellular calcium level in the muscle cell, therefore we examined effects of increase in intracellular Ca^{2+} on MHC I, HSP 70, and IL-6 mRNA expression level using real-time PCR method in C2C12 skeletal myoblasts. The C2C12 cells which were differentiated into myocyte in D-MEM containing 2% FBS was incubated with ionomycin in 6 or 24 hr. First, we measured MHC I mRNA level and it was significantly increased by the 6 hr incubation with ionomycin compared with control. 24 hr incubation with ionomycin significantly upregurated HSP 70 mRNA level, although 6 hr incubation with it did not affect the mRNA level. IL-6 mRNA level was significantly increased by the 6 hr incubation of ionomycin. Second, we examined the effect of IGF-1 on MHC I, HSP 70, and IL-6 mRNA expression levels. IL-6 mRNA level was significantly increased by the 24 hr incubation with IGF-1, although MHC I and HSP 70 mRNA levels were not increased. Third, we examined the effect of IL-6 on MHC I, HSP 70, and IL-6 mRNA expression levels. The mRNA levels of IL-6 and HSP 70 were significantly increased by the 24 hr incubation with IL-6, although MHC I mRNA level was not increased. Thus, it is considered that activation of Ca^{2+}-dependent signaling pathways, such as calcineurin, could act as a major factor upregulating MHC I mRNA levels. Therefore, we confirmed that effect of calcineurin inhibitor on ionomycin induced increase in mRNA level of MHC I. Ionomycin induced upregulation of MHC I mRNA level was significantly attenuated by the application of FK506. These results indicate that activation of Ca^{2+}-calmodulin/calcineurin mediated signaling pathways might have essential roles for upregulation of MHC I mRNA level.

Where applicable, the authors confirm that the experiments described here conform with The Physiological Society ethical requirements.

PCD265

Mutation of the valosin-containing protein (VCP) decreases the fatigue tolerance of fast-twitch skeletal muscle fibres

L. Cully[1], G. Watts[1] and G. Mutungi[2]

[1]Biomedical Research Centre, University of East Anglia, Norwich, UK and [2]Department of Medicine, Norwich Medical School, University of East Anglia, Norwich, UK

Valosin-containing protein (VCP) is a member of the AAA+ (ATPases associated with diverse cellular activities) protein family that is involved in many cellular processes including cell cycle regulation, Golgi biogenesis, and the degradation of misfolded proteins1. Its mutation causes inclusion body myopathy, Paget's disease of bone and frontotemporal dementia (IBMPFD) 2. The IBM is accompanied by muscle fibre degeneration, rimmed vacuole formation and ubiquitin containing sarcoplasmic inclusions. Moreover, muscle fibres of VCPR155H/+ knock-in mice display severely swollen and abnormal mitochondria2; suggesting that they may have impaired energy metabolism. However, no studies have investigated the fatigue resistance of fast and slow muscle fibres isolated from VCP mutant mice. The primary aim of this study was to investigate the fatigue resistance of fast- and slow-twitch muscle fibres isolated from either wild type (WT) or VCP mutant mice.

Experiments were performed at 20°C on small bundles of 10-20 muscle fibres dissected from the extensor digitorum longus (EDL, a mainly fast-twitch muscle) and soleus (a mostly slow-twitch muscle) from both VCP mutant and WT mice (cross sectional diameter 340±110μm; n=14). Mice were killed according to the Animals (Scientific Procedures) Act 1986, UK and all the experiments conformed to the local animal welfare committee guidelines. The fibre bundles were mounted horizontally between two stainless steel hooks in a muscle chamber perfused with Ringer's solution prepared as previously described3. The sarcomere length (SL) was adjusted to 2.5μm and fibre bundle was allowed to equilibrate for ~20 minutes before subjection to the fatigue protocol (FP). During the FP, the fibre bundles were subjected to maximum isometric contractions once every 9 sec (for EDL) or every 4 sec (for soleus). After ~70 contractions, the stimulation rate was reduced to once every 90 sec and the fibre bundles were allowed 15-20min recovery. Only fibre bundles that recovered ≥90% of the force recorded at the start of the FP were included.

Our results show that VCP mutation decreased the fatigue resistance of fast-twitch fibres without affecting that of slow-twitch fibres, or the maximum isometric tension (Po). For example, at contraction 60 of the FP, Po declined by 39.6±16% in the fast twitch fibres isolated from the transgenic mice (n=8) but by only 2±8% in WT mice (n=2). The corresponding values in slow-twitch fibres were 9.7±2% and 10±7.6% in the WT (n=2) and transgenic mice (n=2) respectively. Our findings suggest that the effects of VCP mutation in skeletal muscle fibres may be fibre type dependent.

Badadani, M. et al, 2010. "VCP associated inclusion body myopathy and Paget disease of bone knock-in mouse model exhibits tissue pathology typical of human disease." PLoS One no. 5 (10)

Watts GD. et al, 2004. "Inclusion body myopathy associated with Paget disease of bone and frontotemporal dementia is caused by mutant valosin-containing protein." Nat Genet 36: 377–381

Hamdi, M. and Mutungi, G. (2011) "Dihydrotestosterone stimulates amino acid uptake and the expression of LAT2 in mouse skeletal muscle fibres through an ERK1/2-dependent mechanism." J. Physiol 589 (14) 3623-3640

Where applicable, the authors confirm that the experiments described here conform with The Physiological Society ethical requirements.

PCD266

Intrinsic ankle stiffness is reduced by increasing ankle sway in standing individuals

T.E. Sakanaka, R. Reynolds and M. Lakie

School of Sport and Exercise Sciences, University of Birmingham, London, London, UK

Previous research studies defined the upper and lower bound values of ankle stiffness in quiet standing [1] [2]. While freely standing on footplates, subjects were submitted to a series of small disturbances that simulated the ankle movement common to this task. In this study, for a better understanding of the muscle thixotropy property – one of the short range passive phenomena in quiet standing [4] –, in addition to the sequence of small disturbances, we applied a slow and continuous large sway to reduce muscle thixotropy's influence, and correlating it with static ankle stiffness.
The experiment was approved by the local human ethics committee and conducted in ten participants that gave a written informed consent. A servo tube motor was connected to two footplates and programmed to apply different types of stimulus to the foot, summing up to eight different conditions. Fast, small and randomly positive or negative cosine-wave type disturbances (0.2 and 0.8 deg amplitude, 140ms duration) were followed by inter stimulus intervals of 2-4 seconds of stillness, or added to a randomized continuous slow sway of a higher amplitude (2-3 deg amplitude). Subjects were asked to stand freely on top of the footplates, with eyes open or closed – assuming that without a visual reference they would sway more. Types of conditions were determined by the differences of ankle sway size that each condition would incite. Torque was measured with miniature load cells attached to the footplates. For the ankle and body sway measurements, two laser-reflex sensors were placed at the umbilicus and mid-tibia levels. The accelerometer (attached to the bottom of the left footplate), left and right torque and relative angle data (captured by a potentiometer) were used for the Savitzky-Golay filter analsysis to calculate muscle stiffness.
Despite the natural large disparities between subjects, the data suggests that ankle stiffness is inversely related to the stimulus size and body sway, indicating the decreasing effect that muscle thixotropy has on static ankle stiffness as the body sway increases.

Table 01: Correlation between combined relative stiffness (%, intrinsic ankle stiffness divided by toppling torque) and ankle sway are displayed in the table above. As the sway increases, the ankle stiffness decreases.

	Combined Relative Stiffness (%)	SEM	Ankle sway (°/s)	SEM
0.3° 07Hz: still, eyes open	73.1372	±6.2342	0.9332	±0.0368
0.3° 07Hz: still, eyes closed	68.9216	±4.9471	1.0557	±0.0569
0.3° 07Hz: with sway, eyes open	45.9292	±4.9881	2.2060	±0.1366
0.3° 07Hz: with sway, eyes closed	54.9461	±6.5305	2.4682	±0.1867
0.9° 07Hz: still, eyes open	49.4740	±4.4004	2.8414	±0.0356
0.9° 07Hz: still, eyes closed	50.5986	±3.8307	2.9371	±0.0613
0.9° 07Hz: with sway, eyes open	45.6861	±5.0818	3.4788	±0.1167
0.9° 07Hz: with sway, eyes closed	48.4831	±4.5147	3.5660	±0.1132

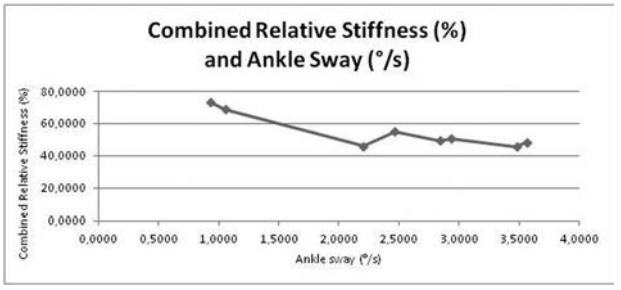

Loram, I.D., Lakie, M. (2002). Direct measurement of human ankle stiffness during quiet standing: the intrinsic mechanical stiffness is insufficient for stability. J. Physiol. 545.3, 1041-1053.

Casadio, M., Morasso, P.G., Sanguineti, V. (2005). Direct measurement of ankle stiffness during quiet standing: implications for control modelling and clinical application. Gait Posture. 21, 410-424.

Loram, I.D., Maganaris, C.N., Lakie, M. (2007). The passive, human calf muscles in relation to standing: the non-linear decrease from short range to long range stiffness. J. Physiol. 584.2, 661-675.

Campbell, K. S. and Lakie, M. (1998) A cross-bridge mechanism can explain the thixo

Where applicable, the authors confirm that the experiments described here conform with The Physiological Society ethical requirements.

PCD267

Skeletal muscle myopathy in zebrafish larvae following knockdown of desmin

M. Li[1], M. Andersson-Lendahl[2], T. Sejersen[3] and A. Arner[1]

[1]Dept. of Physiology and Pharmacology, Karolinska Institutet, Stockholm, Sweden, [2]Dept. of Cell and Molecular Biology, Karolinska Institutet, Stockholm, Sweden and [3]Dept. of Women's and Children's Health, Karolinska Institutet, Stockholm, Sweden

Skeletal muscle was examined in zebrafish larvae, to address questions related to the function of the intermediate filament protein desmin and its role in the pathogenesis of human desminopathy. A novel approach including mechanical and structural studies of skeletal muscles from 4-6 day larvae was applied. Gut motility was studied with confocal imaging. Two desmin genes were identified in the larvae with the experession both in skeletal musclese and gut. Morpholino antisense oligonucleotides were utilized to knock down desmin. Expression was assessed using mRNA and protein analyses. Histology and synchrotron-light based small angle x-ray diffraction were applied. Functional properties were analyzed with in vivo studies of swimming behavior and with in vitro mechanical examinations of muscle. The two desmin genes normally expressed in zebrafish could be knocked down by about 50%. This resulted in a phenotype with disorganized skeletal muscles with altered attachments to the myosepta. The knockdown larvae were smaller and had diminished swimming activity. Active tension was lowered and muscles were less vulnerable to acute stretch-induced injury. X-ray diffraction revealed wider interfilament spacing. In conclusion, desmin intermediate filaments are required for normal active force generation and affect the vulnerability during eccentric work in skeletal muscles. This is related to the role of desmin in anchoring contractile units for optimal force transmission. The results also show that partial lack of desmin, without protein aggregates, is sufficient for causing skeletal muscle pathology resembling that in human desminopathy.

Supported by grants from the Swedish Research Council, the Swedish Heart Lung Foundation and a grant from the Association Française contre les Myopathies. X ray diffraction was performed at the A2 beamline in HASY-Lab, Hamburg Germany, and at the I911-SAXS beamline at Max IV Laboratory, Lund, Sweden.

Where applicable, the authors confirm that the experiments described here conform with The Physiological Society ethical requirements.

PCD268

High cholesterol level and statin treatment affect the calcium homestasis of rat skeletal muscle cells

J. Vincze[1], M. Fuzi[1], A. Jenes[1], B. Dienes[1], P. Szentesi[1], P. Kertai[2], G. Paragh[3] and L. Csernoch[1]

[1]Department of Physiology, University of Debrecen, Debrecen, Hungary, [2]Department of Preventive Medicine, University of Debrecen, Debrecen, Hungary and [3]Department of Internal Medicine, University of Debrecen, Debrecen, Hungary

Statins are the most widely used drugs in the treatment of hyperlipidaemia. Their side-effects on skeletal muscle, however, have been reported with increasing frequency. Although the pathomechanism of the statin associated myopathy has been studied in detail and several theories do exist, there is still no final consensus.

To study of the effects of statin on skeletal muscle rats were fed with a special diet to achieve high blood cholesterol levels and fluvastatin was administered to them orally. Single skeletal muscle fibers were isolated enzymatically from the *extensor digitorum communis* muscles of rats. The surface membrane was permeabilized using a relaxing solution containing saponin. Cells were then loaded with Fluo-4 and imaged using a Zeiss LSM 510 META laser scanning confocal microscope to study localized calcium release events. Images were automatically analysed using the method published by Szabó LZ *et al.* (2010). All data are presented as mean±S.E.M.

Blood cholesterol levels of rats kept on a cholesterol-rich diet rose more than seven fold (from 1.5±0.1 to 10.7±2.0 mmol/L; n=15 and 16) with a dramatic increase in LDL/HDL ratio (from 0.29±0.02 to 1.56±0.17), proving that our model is usable for the study of hypercholesterolaemia. Previously published (Füzi *et al.* (2012)) elevation of the resting calcium level of adult skeletal muscle cells in both hypercholesterolemic and statin-treated rats was also accompanied by changes in the frequency of localized calcium release events (sparks). Muscle cells from statin-treated animals kept on normal cholesterol diet had higher spark frequency than cells from control animals (1.59 vs 0.88 $s^{-1}sarc^{-1}$) and cells from statin-treated animals kept on a high cholesterol diet had higher spark frequency than those from untreated hypercholesterolemic animals (1.48 vs 0.94 $s^{-1}sarc^{-1}$). Full width of half maximum values of sparks were slightly elevated and amplitude values were slightly decreased in all groups compared to the control.

Fluvastatin and rosuvastatin were also applied on rat primary cell cultures to assess their effects on in vitro proliferation an differentiation. Effects on the cytoskeletal structure of muscle cells were visualized using immunofluorescence. Skeletal muscle cell proliferation and differentiation were impaired and a decrese in the level of fibrillar actin was seen in statin-treated cultures.

The effects of statins on the calcium homeostasis, proliferation, differentiation and structure of adult and developing muscle cells may contribute to the explanation of certain adverse effects seen in clinical use.

Szabó LZ *et al.* (2010). *J Theor Biol* **4**, 1279-92.

Füzi M *et al.* (2012). *J Muscle Res Cell Motil* **32**, 391-401.

This work was supported by grants OTKA K-75604, NK-78398, ETT 186/2009 and K-2009-TÁMOP-4.2.2-08/1/2008-0019.

Where applicable, the authors confirm that the experiments described here conform with The Physiological Society ethical requirements.

PCD269

Impact of Kv7 voltage-gated potassium channel modulators on contractile activity of myometrium from pregnant women at term

Y. Mansour[1], L.A. McCallum[1], I.A. Greenwood[2] and R.M. Tribe[1]

[1]Division of Women's Health, King's College London, London, UK and [2]Division of Biomedical Sciences, St George's University of London, London, UK

Background: Voltage gated potassium (Kv) channels play an important role in regulating resting membrane potential, and in smooth muscle are key determinants of contractile frequency. KCNQ-encoded Kv7 channels have been extensively studied in the cardiac and nervous systems due to their importance in normal physiological function. There is now an established role for these channels in smooth muscle and we have recently identified mRNA for these channels (Kv7.1-7.5), and their modulatory subunits (KCNE1-5), in pregnant human myometrium1. The aim of this study was to characterise the functional effects of a range of Kv7 activators and blockers on the contractility of myometrium from pregnant women at term ex vivo.

Methods: Myometrial tissue was obtained, with informed written consent, from pregnant women undergoing elective lower segment Caesarean section at term (> 37 weeks', not in labour) (Ethics approval number EC00/137). Spontaneous contractile activity (mean integral tension, MIT and contraction frequency) was measured in isolated myometrial strips and the effect of Kv7 inhibitors (XE991, 20 μM; Chromanol 293B, 20 μM) and activators (retigabine, 20 μM; maxipost, 20 μM; acrylamide S-1, 20 μM) determined and compared to vehicle controls (DMSO). The effect of the ERG inhibitor (dofetilide, 10 μM) was also assessed.

Results: Retigabine significantly decreased %MIT (35.98% ± 11.28 versus control 83.43% ± 5.4; n=5, $p<0.05$) and acrylamide S-1 appeared to have a more potent relaxant effect than retigabine. The pan Kv7 blocker (7.2-7.5) XE991 increased %MIT and contractile frequency (n=10) whereas the Kv7.1-specific blocker chromanol 293B (n=10) had no significant effect on MIT. Administration of maxipost had no demonstrable effect on MIT.

Conclusions: These data suggest that Kv7.2-7.5, but not Kv7.1, and ERG channels contribute significantly to the regulation of spontaneous myometrial contractions in tissues from pregnant women at term. The relaxation induced by Kv7 activators highlights a potential use of these agents for the treatment of spontaneous preterm birth.

McCallum et al. (2011) J Cell Mol Endo, 15(3) 577-586.

Supported by: MRC/KCL PhD studentship, Action Medical Research with Rosetrees Trust, and Tommy's Charity.

Where applicable, the authors confirm that the experiments described here conform with The Physiological Society ethical requirements.

PCD270

Flow mediated dilation is associated with endothelial cell oxidative stress in humans

A.N. Gurovich[1], J.C. Avery[2] and R.W. Braith[2]

[1]Applied Medicine and Rehabilitation, Indiana State University, Terre Haute, IN, USA and [2]Applied Physiology and Kinesiology, University of Florida, Gainesville, FL, USA

Cardiovascular diseases, including coronary artery disease and stroke, are the leading cause of death in the Western World (Rosamond et al., 2007). According to current medical theory, endothelial dysfunction is the primary cause of atherosclerosis, which is responsible for 90% of acute coronary syndrome and 80% of strokes (Mallika et al., 2007). Multiple factors affect endothelial function, but endothelial oxidative stress and low endothelial shear stress may be the most relevant (Davies, 2009, Thuillez and Richard, 2005). Flow mediated dilation (FMD) is considered a biomarker for endothelial function and brachial FMD is well correlated with coronary artery endothelial function.(Harris et al., 2010) However, the relationship between FMD and endothelial oxidative stress in vivo is still to be determined. Therefore, here we sought to determine if brachial artery FMD is associated with endothelial oxidative stress in humans. Twenty-three apparently healthy young men (25±4 yrs) with different activity background (e.g. sedentary, active recreational) underwent brachial artery FMD testing and venous endothelial cell biopsies on 2 occasions within 6 weeks. Protocol was approved by University of Florida Institutional Review Board. Immuno-fluorescence quantification was used to assess nitrotyrosine (NT), a criterion marker of endothelial oxidative stress. Values for NT expression were reported as a ratio of endothelial cell to human umbilical vein endothelial cell average pixel intensity. As shown on the figure, brachial FMD was inversely correlated with NT ($R=0.273$, $p<0.05$). The inverse relationship observed in the present study supports the hypothesis that FMD is associated with endothelial cell oxidative stress. Larger brachial dilations, relative to baseline vessel diameters, are associated with lower NT expression and vice versa. These results provide additional evidence to support the use of FMD as a non-invasive bio-marker for endothelial dysfunction.

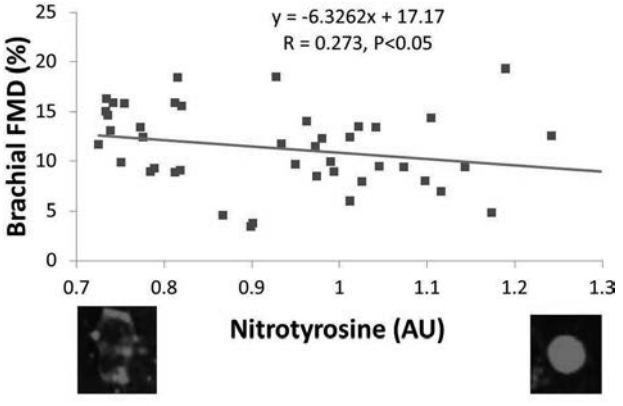

Figure: Correlation between brachial FMD (%) and Nitrotyrosine (AU).

DAVIES, P. F. 2009. Hemodynamic shear stress and the endothelium in cardiovascular pathophysiology. Nat Clin Pract Cardiovasc Med, 6, 16-26.

HARRIS, R. A., NISHIYAMA, S. K., WRAY, D. W. & RICHARDSON, R. S. 2010. Ultrasound Assessment of Flow-Mediated Dilation. Hypertension, 55, 1075-1085.

MALLIKA, V., GOSWAMI, B. & RAJAPPA, M. 2007. Atherosclerosis pathophysiology and the role of novel risk factors: a clinicobiochemical perspective. Angiology, 58, 513-22.

ROSAMOND, W., FLEGAL, K., FRIDAY, G., FURIE, K., GO, A., GREENLUND, K., HAASE, N., HO, M., HOWARD, V., KISSELA, B., KITTNER, S., LLOYD-JONES, D., MCDERMOTT, M., MEIGS, J., MOY, C., NICHOL, G., O'DONNELL, C. J., ROGER, V., RUMSFELD, J., SORLIE, P., STEINBERGER, J., THOM, T., WASSERTHIEL-SMOLLER, S. & HONG, Y. 2007. Heart disease and stroke statistics—2007 update: a report from the American Heart Association Statistics Committee and Stroke Statistics Subcommittee. Circulation, 115, e69-171.

THUILLEZ, C. & RICHARD, V. 2005. Targeting endothelial dysfunction in hypertensive subjects. J Hum Hypertens, 19 Suppl 1, S21-5.

Where applicable, the authors confirm that the experiments described here conform with The Physiological Society ethical requirements.

PCD271

Cerebrovascular reactivity and systemic haemodynamic parameters in response to acute hyperoxia in stroke patients and healthy volunteers

I. Hegedus[2], A. Cosic[1] and I. Drenjancevic[1]

[1]Medical Faculty Osijek, University of J.J. Strossmayer Osijek, Osijek, Croatia and [2]Clinical Hospital Center Osijek, Osijek, Croatia

Background: High pO2 responses in cerebral circulation can be altered in disease(1,2,3,4). This study aimed to determine the effects of acute hyperoxia on cerebrovascular reactivity (CVR), thromboxane B2 (TXB2, a stable metabolit of TXA2) plasma levels and systemic haemodynamic parameters in acute stroke patients(SP) and healthy volunteers(HV).
Methods: The study protocol and procedures were approved by the Ethical Committee of the Faculty of Medicine Osijek, and conformed to the standards set by the latest revision of the Declaration of Helsinki. 52 SP (age 68±6.7 yrs) with acute ischemic stroke (within 72 hours) and 52 HV (64.5±8.3 yrs) were included. Mean blood flow velocity (MBFV) in middle cerebral artery (MCA), pulsality index (IP) and resistance index (IR) were determined by transcranial Doppler before (basal), during 15 minutes (hyperoxia), and 15 minutes after the acute hyperoxia (inhalation of 100% O2 over facial mask). Systolic and diastolic blood pressure (SBP, DBP), heart rate (HR) and pO2 (measured by pulse oxymeter) were assessed at the same time points. Tromboxane B2 (TXB2) levels in venous blood samples were measured by ELISA before and immediately after hyperoxia. Mixed factorial ANOVA with repeated measures and Games-Howell post hoc test were used with logarithmic transformation; $p<0.05$ was considered significant. Data are expressed as mean±SD.
Results: Basal MBFV was significantly lower in SP(53±14) compared to HV(61±17). During hyperoxia MBFV significantly increased in SP(58±15; by 10%), while it decreased in HV(57±16; by 7%) compared to respective basal values. IP (basal=1±0.36; hyperoxia=1± 0.35; after=1± 0,40) and IR (basal=0.67±0.08; hyperoxia=0.67±0.10; after=0.66±0.08) were significantly higher in SP compared to HV (PI: basal=1±0.30; hyperoxia=1±0.35; after= 1±0.28); RI: basal=0.61±0.09; hyperoxia=0.61±0.09; after=0.60±0.08) in all 3 time points. Hyperoxia did not affect IP and IR in both groups, nor HR in SP, while HR decreased in HV (7%, $p<0.01$). SP had significantly higher SBP/DBP (basal=144±18/91±12;

hyperoxia=145±18/92±12; after=142±17/89±11) at all 3 points compared to HV (SBP/DBP: basal=129±17/83±11; hyperoxia=130±15/87±11; after=126±19/82±10). SBP/DPB significantly increased in both groups during hyperoxia compared to basal values. pO2 during hyperoxia increased in SP only (4%, p< 0.001). There was 8% decrease in TXB2 levels in SP and 4% increase in TXB2 in HV in hyperoxia, however, did not reach significance (p>0,05). TXB2 showed weak negative correlation with MBFV in both studied groups.
Conclusion:This study demonstrated paradoxical vasodilation of MCA, with decreased TXB2 in SP, and vasoconstriction with increased TXB2 in HV, suggesting the role of cyclooxygenases' metabolites mediating these changes in both, SP and HV. Hyperoxia affected haemodynamic parameters also.

Liu W, Khatibi N, Sridharan A, Zhang HJ. Application of medical gases in the field of neurobiology. Medical Gases Research 2011, 1:13.

Nishimura N, Iwasaki K, Ogawa Y, Shibata S. Oxygen administration, cerebral blood flow and dinamic cerebral autoregulation. Aviat Space Environ Med. 2007;78:1121-7.

Rousseau A, Bak Z, Janerot- Sjoberg B, Sjoberg F. Acute hyperoxemia – induced effects

on regional blood flow, oxygen consumption and central circulation in man. Acta Physiol Scand. 2005;183:231-240.

Johnston AJ, Steiner LJ, Gupta AK, Menon DK. Cerebral oxygen vasoreactivity and cerebral tissue oxygen reactivity. BJA, 2002;90:774-786.

Where applicable, the authors confirm that the experiments described here conform with The Physiological Society ethical requirements.

PCD272

Comparison of endothelial function using three non-invasive methods: flow-mediated dilation, changes in distension and changes in pulsewave velocity

A. Faulkner[1], S.E. Carter[1] and M. Rakobowchuk[2,1]

[1]School of Biological Science, University of Essex, Colchester, UK and [2]Centre for Sports Medicine & Human Performance, University of Brunel, London, UK

Endothelial function is routinely assessed by non-invasive techniques but is expensive and requires skilled technicians precluding its routine use as a clinical tool to predict cardiovascular disease risk. Commonly assessed in the brachial artery, due to access and calibre similarities to the coronary circulation, dysfunction is defined as an inability of the artery to dilate in response to reactive hyperaemia. Recently changes in carotid-radial pulsewave velocity have been suggested as an alternative method to measure endothelial function. Moreover, changes in arterial distension following reactive hyperaemia should provide similar predictive utility, but has not been evaluated. Eleven participant's (female=4) attended the laboratory on up to 4 occasions and underwent repeated vascular function protocols. Ischaemia-reperfusion injury was induced on each occasion to reduce endothelial function thus providing a range of flow-mediated dilation (FMD) values within each participant. Trials were also preceded by one of four experimental conditions to further provide a range of FMD values. Participants ingested either: 1) water ad libitum, 2) an antioxidant cocktail at 2 and 1.5 hours, 3) 1200mg Ibuprofen 1 hour prior; or 4) a combination of 2 and 3 in a blinded fashion. FMD was determined using an Aloka Alpha6 Doppler ultrasound system. Diameters were acquired at 2MHz before and after a 5-minute forearm occlusion period. The spatial resolution of diameter measurements was 0.05mm acquired using echotracking. The time delay between the R-wave of the ECG and the foot of the diameter waveform were used to calculate pulse transit time (PTT). Maximal relative change in PTT was determined as (PTTmax-PTTmin)/PTTmin x 100%. Brachial artery distension was determined on a beat-by-beat basis throughout the reactive hyperaemia period and maximal relative change was determined as (distension max-distension min)/distension min x 100%. Relationships between the three measurement modalities were determined by correlation analysis using Pearson product-moment correlation coefficient. Significance was assumed if p≤0.05. No relationship was observed between pulsewave velocity and FMD (r=-0.113, p=0.352) or absolute FMD (r=-0.003, p=0.98). Furthermore, no relationship existed between the change in brachial artery distension and FMD or absolute FMD (r=0.03, p=0.80; r=-0.006, p=0.96 respectively). The results of this study suggest that non-invasive measures of vessel stiffness changes induced by reactive hyperaemia do not represent an adequate assessment tool for measures of endothelial function within the brachial artery. Flow-mediated dilation remains the 'gold-standard' for non-invasive measurement for assessment of endothelial function.

Where applicable, the authors confirm that the experiments described here conform with The Physiological Society ethical requirements.

PCD273

Muscular arterial stiffness is not altered by ischemia-reperfusion injury and not influenced by cyclooxygenase inhibition by Ibuprofen

A. Reed[1], S.E. Carter[1] and M. Rakobowchuk[2]

[1]Biological Sciences, University of Essex, Colchester, UK and [2]Centre for Sports Medicine and Human Performance, Brunel University, London, UK

Ischemia-reperfusion injury induces endothelial dysfunction related to oxidative stress and a lack of nitric oxide bioavailability. The non-invasive forearm ischemia-reperfusion model is commonly used to evaluate interventions to attenuate decrements in brachial artery endothelial function. To date, no study has evaluated the impact of an ischemia-reperfusion injury on the mechanics of the brachial artery, which should also be altered by this injury.
10 healthy participants (6 male, 4 female) underwent ischemia-reperfusion injury (IRI) on 2 separate visits to the laboratory. The first visit provided control measurements, in the absence of supplements. One hour prior to the second visit, participants took 1200mg Ibuprofen (cyclooxygenase inhibitor). IRI was induced by a 20 minute upper-arm supra-systolic occlusion. Measures of brachial artery stiffness were made immediately before, and then 15, 30 and 45 minutes post-IRI. Brachial artery stiffness was determined by non-invasive ultrasound assessment of arterial diameter using echo tracking software at 2MHz (Hitachi Aloka Alpha 6). Arterial perfusion pressures were measured by applanation tonometry on the contralateral radial artery. Immediately prior to each measure the tonometer was calibrated to contralateral brachial artery pressures using an oscillometric sphygmomanometer. Values are mean ± SD. Significance was assessed at 95% confidence levels using two-way repeated-measures ANOVA (SPSS v19).
Results show that IRI did not significantly change arterial compliance (Control Pre: 0.06±0.02; Post 15: 0.08±0.02; Post 30: 0.08±0.03; Post 45: 0.07±0.03; and Ibuprofen Pre: 0.07±0.03;

Post 15: 0.07±0.03; Post 30: 0.07±0.03; Post 45: 0.07±0.03 mm^2/kPa) from baseline over time or between conditions (p=0.55, p=0.65, respectively). Similarly, IRI and Ibuprofen intake had no significant effect on change in arterial diameter (p=0.93 and p=0.43, respectively) and pulse pressure (p=0.39 and p=0.97, respectively).
These data demonstrate neither detrimental effect of IRI, nor palliative effect of Ibuprofen before or after IRI, at the brachial artery. It seems that reduced nitric oxide bioavailability as a result of IRI and prostaglandin inhibition by Ibuprofen have no effect on the mechanical properties of a muscular peripheral artery such as the brachial artery in apparently healthy individuals.

Where applicable, the authors confirm that the experiments described here conform with The Physiological Society ethical requirements.

PCD274

Effect of hypoxia during incubation on the metabolic rate and thermal preference of 8–10-day-old chicks

K.C. Bicego[1], P.A. Velasquez[1], M.H. Fernandes[2], C.S. Scarpellini[1], M. Macari[1] and L.H. Gargaglione[1]

[1]Animal Morphology and Physiology, Sao Paulo State University, FCAV Jaboticabal, Jaboticabal, Sao Paulo, Brazil and [2]Animal Science, Sao Paulo State University, FCAV Jaboticabal, Jaboticabal, Sao Paulo, Brazil

It has been reported that thermal and non-thermal stressful stimuli early in the development may influence thermoregulation of juvenile or adult animals (Arjona et al., 1990; Soriano and Branco, 2010). Moreover, it is known that hypoxia can induce decreases in body temperature, metabolic rate and thermal preference of several species (Bicego et al., 2007; Tattersall and Milsom, 2009; Branco et al., 2010). To our knowledge, the effect of hypoxia during incubation in thermoregulation of juvenile chicks has not been investigated until now. Thus, we studied the influence of hypoxia at different phases of incubation on the metabolic rate and thermal preference of 8–10-day-old broiler chicks (Gallus domesticus). To this end, three groups of broiler eggs were distributed in a completely randomized design: normoxia for the entire period of incubation (N; 21% O2 during the 21 days), hypoxia during the first week of incubation (HI; 15% O2) and hypoxia during the last week of incubation (HL; 15% O2). After hatching, all the animals were maintained at thermoneutral zone (TNZ) up to the day of experiments. Measurements of oxygen consumption (VO2) were obtained by open-flow respirometry at (29oC), above (34oC) and below (19 and 24oC) TNZ. Thermal preference was assessed in a thermal gradient chamber. In each experiment, 6-8 animals were used per group. Values are means ± S.E.M., and the data were analyzed as a completely design with repeated measurements using the MIXED procedure of SAS version 9.2. VO2 of chicks at TNZ was lower in the HL (24.47 ± 4.33 mL.min-1.kg-1 STPD) than in HI (37.5 ± 5.03 mL.min-1.kg-1 STPD) and N (40.04 ± 4.28 mL.min-1.kg-1 STPD) groups ($p< 0.05$). Exposure to 19 and 24oC caused increases in VO2 of N and HL, but not HI, animals ($p< 0.05$). In contrast, no significant change in VO2 of all groups was observed at 34oC. In the thermal gradient, N chicks spent most part of the time (frequency of distribution) at ambient temperatures of 29-31oC and HI and HL at 24-26oC (ANOVA, $p< 0.01$). Based on the present results, we can conclude that exposure to hypoxia during the first or the last week of incubation interferes with the metabolic rate and thermal preference of 8–10-day-old chicks.

Arjona, A.A.; Denbow, D.M.; Weaver, W.D. Jr. Neonatally-induced thermotolerance: physiological responses. Comp Biochem. Physiol. A, 95(3): 393-399, 1990.

Soriano RN, Branco LG. Reduced stress fever is accompanied by increased glucocorticoids and reduced PGE2 in adult rats exposed to endotoxin as neonates. J Neuroimmunol., 225(1-2):77-81, 2010.

Bicego K. C., Barros R.C.H., Branco L.G.S. Review Physiology of temperature regulation: Comparative aspects. Comparative Biochemistry and Physiology, Part A 147: 616–639, 2007.

Tattersall, G. J.; Milsom, W. K. Hypoxia reduces the hypothalamic thermogenic threshold and thermosensitivity. The Journal of Physiology, v. 587, p. 5259-5274, 2009.

Branco LG, Bicego KC, Carnio EC, Pittman QJ. Gaseous neurotransmitters and their role in anapyrexia. Front Biosci., 2: 948-60, 2010.

Financial support: FAPESP, CNPq; INCT in Comparative Physiology.

Where applicable, the authors confirm that the experiments described here conform with The Physiological Society ethical requirements.

PCD275

Amelioratory effect of proanthocyanidine on paraquat - induced oxidative stress, biochemical and histopathological changes in rat kidney

A.B. Jebur[1], F.M. El-Demerdash[2] and A.M. Attia[3]

[1]Ministry of Education, Baghdad, Iraq, [2]Environmental Studies, Institute of Graduate Studies and Research, Alexandria University, Alexandria, Egypt and [3]Environmental Studies, Institute of Graduate Studies and Research, Alexandria University, Alexandria, Egypt

Paraquat (PQ) is a highly toxic quaternary nitrogen herbicide capable of increasing superoxide anion production. The present study was carried out to evaluate the oxidative damage induced by PQ in rat kidney and its effect on antioxidant defense system and nephrotoxicity biomarkers in addition to the role of proanthocyanidin in alleviating its toxic effects. Male Wister albino rats were randomly divided into four groups of 10 each, group I served as control; group II treated with proanthocyanidin (25 mg/kg BW), group III received single dose of paraquat (PQ; 10 mg/kg BW; i.p) and group IV treated with both PQ and proanthocyanidin. Rats were orally administered their respective doses of proanthocyanidine daily for 21 days. The local committee approved the design of the experiments, and the protocol conforms to the guidelines of the National Institutes of Health (NIH). The administration of PQ caused significant elevation in lipid peroxidation (LPO) and reduction in the activities of antioxidant enzymes including superoxide dismutase (SOD), catalase (CAT) and glutathione S-transferase (GST). A significant reduction in glutathione (GSH) content was also observed. Serum urea, creatinin and lactate dehydrogenase (LDH) activity were significantly increased. Histopathological manifestations were investigated in tissues from rat kidney. As expected, PQ administration induced marked changes in the morphological structure of the kidney in PQ demonstrated animals since necrotic changes in both glomeruli and renal tubules were observed. Proanthocyanidin treatment to PQ treated rats decreased LPO level and normalized SOD, CAT and GST activities, while GSH content was increased. Also, urea, creatinin and LDH were maintained near normal level due to proanthocyanidine treatment. In addi-

tion, proanthocyanidin attenuated the morphological damages induced by PQ in the kidney tissue of experimental animals. Our results suggest antitoxic and antioxidant effects of proanthocyanidin against paraquat.

Hirai, K.I., Witschi, H., Cote, M.G., 1985. Mitochondrial injury of pulmonary alveolar epithelial cells in acute paraquat intoxication. Exp. Mol. Pathol. 43:242–245.

Bus, J.S., Aust, S.D., Gibson, J.E., 1976. Paraquat toxicity proposed mechanism of action involving lipid peroxidation. Environ. Health Perspect. 16:139–146.

Pasi A., 1978. The toxicology of paraquat, diquat and morphamquat. Bern Switzerland: Hans Huber. pp 230–244.

Bagchi, D., Bagchi, M., Stohs, S.J., Das, D.K., Ray, S.D., Kuszynski, C.A., Joshi, S.S., Preuss, H.G., 2000. Free radicals and grape seed proanthocyanidin extract: importance in human health and disease prevention. Toxicology 148: 187–197.

Natella, F., Belelli, F., Gentili, V., Ursini, F., Scaccini, C., 2002. Grape seed proanthocyanidins prevent postprandial oxidative stress in humans. J. Agric. Food Chem. 50: 7720–7722

Where applicable, the authors confirm that the experiments described here conform with The Physiological Society ethical requirements.

PCD276

Oxidative Stress, biochemical perturbations and environmental safety in Petrochemical Industry

M.A. ElMasry[1], E.M. Salem[2], F.M. El-Demerdash[3] and H.M. Hassan[4]

[1]Environmental Studies, Institute of Graduate Studies and Research, Alexandria, Egypt, [2]Environmental Studies, Alexandria University, Institute of Graduate Studies and Research, Alexandria, Egypt, [3]Environmental Studies, Alexandria University, Institute of Graduate Studies and Research, Alexandria, Egypt and [4]Sidi Kerir Petrochemicals Company, Alexandria, Egypt

The Petrochemical Industry is based upon the production of chemicals from petroleum such as natural gas and crud oil. Hydrocarbons are known to be human carcinogens and are associated with the development of chronic health disorders. The aim of the present study was undertaken to investigate the oxidative stress, antioxidant defense response, liver and kidney function parameters and lipids profile and to assess the environmental safety awareness in Egyptian petrochemical workers (300 workers) who are exposed to hydrocarbon. The study was approved by the committee of ethics in research of the Alexandria University and informed consent was required from all participants, according to the guidelines of the local ethics committee. Fifty workers and thirty control subjects were enrolled in the present study. All subjects were matched for age, sex and socio-economic level. Venous blood samples from all the subjects were collected with the anticoagulant, EDTA. Results showed a significant increase in kidney and liver function parameters in addition to lipid proxidation. On the other hand, a significant decrease in enzymatic (SOD, CAT, GST) and non enzymatic (GSH) antioxidants was observed. Also, perturbations in some hematological parameters and lipids profile were detected. In conclusion, a state of oxidative stress in hydrocarbon exposed workers is produced by the depletion of antioxidant capacity that may play a role in the mechanism of its toxicity. Also, environmental safety requirement is good but need more application and update.

Moro, A. M., Charão, M., Brucker, N, Bulcão, R., Freitas, F., Guerreiro, G., Baierle, M., Nascimento, S., Waechter, F., Hirakata, V., Linden, R., Thiesen, F.V., Garcia, S.C. (2010). Effects of low-level exposure to xenobiotics present in paints on oxidative stress in workers. Science of the Total Environment 408: 4461–4467

Georgieva, T., Michailova, A., Panev, T., Popov, T. (2002). Possibilities to control the health risk of petrochemical workers. Int. Arch. Occup. Environ. Health. 75:S21–S26.

Hayes, J.D., McLellan, L.I. (1999). Glutathione and glutathione-dependent enzymes represent a co-ordinately regulated defence against oxidative stress. Free Radic. Res., 31: 273–300.

Mutti, A., Alinor, R., Bergamaschi, E., Biagini, C., Cavazzini,S., Franchini, I., Lauwerys, R.R., Bernard, A.M., Roels, H.,Gelpi, E.,Rosello, J.,Ramis,I., Price, R.G.,Taylor, S.A., De Broe, M., Nuyts, G.D., Stolte, H.,Fels, L.M. and Herbort, c. (1992). Nephropathies and exposure to precholroethylene in dry – cleaners. Lancet, 340: 189-193.

Boogaard,P.J. and Caubo, M.E.J.(1994). Increased albumin excretion in industrial workers due to shift work rather than to prolonged exposure to low concentrations of chlorinated hydrocarbons. Occupational and Environmental Medicine. 51:638-641.

Where applicable, the authors confirm that the experiments described here conform with The Physiological Society ethical requirements.

PCD277

Heterothermy in free-living vervet monkeys as an index of environmental stress

A. Fuller[1], A. Lubbe[1], R. McFarland[1], D. Mitchell[1], L. Barrett[2,1], P. Henzi[2] and R. Hetem[1]

[1]University of the Witwatersrand, Johannesburg, South Africa and [2]University of Lethbridge, Lethbridge, AB, Canada

Under future climate change scenarios, many species will be faced with natural habitats which progressively fail to meet their niche requirements. For vervet monkeys and other long-lived, slowly reproducing mammals, physiological plasticity is likely to be the first and most robust response to rapidly changing environmental conditions. In order to investigate how physiological plasticity may allow free-living vervet monkeys to respond to environmental change, we implanted miniature data loggers, during surgery (anaesthesia by blowdart with 5 mg/kg ketamine and 0.25 mg/kg midazolam, maintained with 0-2% isoflurane inhaled in oxygen), to measure body temperature and activity continuously in adult animals (3-6 kg) for one year. Data loggers were removed during surgery, with the same anaesthetic protocol, at least one year later, and animals were returned to their natural habitat. Despite black-globe temperatures ranging from below freezing to over 50°C over the year, and a mean 24-h variation in black-globe temperature of 30.0°C, vervet monkeys maintained body temperature around a mean of ~38°C with a 24-h amplitude of the body temperature rhythm of only 2.9 ± 0.1 °C (n=6). The 24-h amplitude of the body temperature rhythm, however, was significantly higher in mid-winter (3.2 ± 0.4°C) than in mid-summer (2.5 ± 0.1°C; paired t-test, t=5.47, P<0.01). In summer, when the primary thermoregulatory challenge was heat dissipation at high environmental temperatures, vervet monkeys had ad libitum access to a natural source of water and long day-lengths that allowed a flexible activity schedule. In winter, short day lengths limited the amount of time available to achieve fundamental activities, with activity also influenced by thermoregulatory requirements at low environmental temperatures and social stress of the coinciding mating season. Heterothermy in winter was associated with low environmental temperatures and low food availability. In free-living mam-

mals, homeothermy appears to be a luxury, evident only in individuals that are well nourished, hydrated and not energetically compromised. Whether the lability of body temperature in vervet monkeys under conditions of environmental stress reflects an inability to maintain homeothermy or a regulated adjustment of the thermoregulatory system to conserve energy remains to be elucidated.

Where applicable, the authors confirm that the experiments described here conform with The Physiological Society ethical requirements.

PCD278

Cheetah do not abandon hunts because they overheat

R.S. Hetem[1], B.A. de Witt[1], A. Fuller[1], L.G. Fick[1], L.C. Meyer[2,1], S.K. Maloney[3,1] and D. Mitchell[1]

[1]Brain Function Research Group, School of Physiology, University of the Witwatersrand, Johannesburg, South Africa, [2]Department of Paraclinical Sciences, University of Pretoria, Pretoria, South Africa and [3]School of Anatomy, Physiology and Human Biology, University of Western Australia, Perth, WA, Australia

Cheetah (*Acinonyx jubatus*) are the fastest mammals, and use "stalk and chase" hunting. Anomalously, they abandon more than half of their chases when prey ought to be in range, and both successful and unsuccessful hunts are followed by periods of inactivity. The entrenched explanation is that cheetah abandon hunts because they overheat. That explanation can be traced to a single study, in which Taylor and Rowntree (1973) ran two hand-reared cheetah on a treadmill, and concluded that cheetah stored metabolic heat to the extent that further exercise soon became impossibly thermally. They predicted that cheetah would not run when body temperature reached 40.5°C. We used biologgers to measure core body temperature (abdominal cavity) and locomotor activity (subcutaneous, hind leg) of four cheetah, living free, and hunting, in a conservancy in Namibia. For implantation, the cheetah were immobilized and anaesthetized with medetomidine (0.023±0.002mg.kg^{-1}, mean±SD) and zoletil (1.5±0.2mg.kg^{-1}) intramuscularly, via capture dart, and intubated; anaesthesia was maintained under spontaneous breathing with 2-4% halothane in oxygen. After recovery, the cheetah were released into the conservancy. We observed both successful (12±3 per cheetah) and unsuccessful (6±2 per cheetah) hunts. We found that the cheetah abandoned many hunts but not because they overheated. Indeed, core body temperature only rarely exceeded 40.5°C, and did not rise significantly during a chase. The abdominal temperature at which unsuccessful hunts were abandoned was 38.3±0.2°C. Abdominal temperature did rise gradually after the chase, for 44±17min after successful hunts. The temperature increase (1.3±0.2°C vs. 0.5±0.1°C, $0.0001<P<0.04$, unpaired t tests on each cheetah) and the area under the temperature increase/time curve (78±19°C.min vs. 9±8°C.min, $0.0004<P<0.04$, unpaired t tests on each cheetah) were significantly higher after successful hunts than after unsuccessful hunts, despite there being no difference in activity between successful and unsuccessful hunts. A similar increase in core body temperature was evident in one cheetah that participated in a feed after a successful hunt by siblings, but was not directly involved in the hunt. We propose that the increased body temperature relates to sympathetic activation, greater following successful than unsuccessful hunts. Why cheetahs abandon a chase when the prey ought to be in range therefore remains unknown.

Taylor C R & Rowntree V J (1973). *Am J Physiol* 224, 848–851.

We thank the AfriCat Foundation and Okonjima Lodge, Namibia. Funded by the South African National Research Foundation and the Carnegie Foundation.

Where applicable, the authors confirm that the experiments described here conform with The Physiological Society ethical requirements.

PCD279

Effects of high-fat feeding during pregnancy and lactation on the morphofunctional development of the hippocampus in rat offspring

G.L. Gonzalez[1], A.S. Santos[1], A.C. Santana[1], R.P. Gaspar-Reis[1], C.A. Nascimento-Saba[1] and P.C. Barradas[2]

[1]Physiological Sciences, State University of Rio de Janeiro, Rio de Janeiro, Brazil and [2]Pharmacology, University of Rio de Janeiro State, Rio de Janeiro, Rio de Janeiro, Brazil

Change in lifestyle, as increased consumption of dietary fats and reduced physical activity in modern society, are causes of obesity that can lead to diabetes melliuts, hypertension and dementia. Maternal obesity has been documented to play a direct role in the transmission of obesogenic and diabetogenic traits to the next generation and has also been shown to influence the nervous system of offspring. A high-fat diet (HFD) disrupts cognition and contributes to neurodegenerative diseases as well as impairing hippocampal synaptic plasticity, neurogenesis and cognitive abilities. The aim of these study was investigate the effects of maternal high-fat intake in the hippocampal formation of offspring at 10 days of age.
Female adult Wistar rats were feeding with a normal diet (ND, 4% soybean oil, n=6) or a high-fat diet (HFD, 19% soybean oil, n=7) during pregnancy and lactation. Mother and offspring body mass and food intake were monitored. Lipid profile was evaluated. Intraabdominal adipose tissue were collected and weighted. For morphology evaluation, the rats were anesthetized and perfused intracardially with 4% paraformaldehyde in 0.1M PBS (pH 7.4). The brains were transferred to a 30% sucrose solution and then cryoprotected and sectioned serially at 20 μm. The imunohistochemistry evaluation used Ki-67, for cellular proliferation associated with identification of Neu-N (Millipore) - a marker for mature neurons or GFAP (Sigma), a marker of astrocytes. In pregnancy the average body mass of the rats was 234.2 ± 10.91 g. However, at the end of the lactation period the rats of HFD group showed 26% of gain in body mass, without significant difference of food consumption. Offspring of mother fed with HFD showed an increase (16%) in body mass and triglycerides, but intra abdominal adipose tissue mass did not differ. Labeling with Neu-N demonstrates that the granular layer appears thicker in both GD as Ammon's horn (CA1 and CA3). The double labelling (Ki-67 /GFAP) suggests an increase of proliferative cells in the dendate gyrus. The staining with anti-GFAP was more intense and presents more radial profiles (radial glia), suggesting an increased proliferation and/or developmental differentiation of astroglia. Thus, it seems that maternal diet can affect metabolic parameters and slow hippocampal development.

We express our gratitude to Mr Nelcir Rodrigues for animals care. The research was supported by Fundação Carlos Chagas Filho de Amparo à Pesquisa do Estado do Rio de Janeiro (FAPERJ-Brazil), by Conselho Nacional de Desenvolvimento Científico e Tecnológico (CNPq-Brazil) and Sub-reitoria de Pós-graduação e Pesquisa da Universidade do Estado do Rio de Janeiro (SR2-UERJ).

Where applicable, the authors confirm that the experiments described here conform with The Physiological Society ethical requirements.

PCD281

The developmental transition of epicardial, pericardial and omental adipose tissue during early life in the sheep

G.R. Davies[1], M. Birtwistle[1], M. Pope[1], V. Perry[2], H. Sacks[3], H. Budge[1] and M. Symonds[1]

[1]Early Life Nutrition Research Unit, Academic Division of Child Health, School of Clinical Sciences, University of Nottingham, Nottingham, UK, [2]School of Veterinary Medicine and Science, University of Nottingham, Nottingham, UK and [3]Endocrinology and Diabetes Division, VA Greater Los Angeles Health Care System, Los Angeles, CA, USA

Brown adipose tissue is essential in the newborn to protect against hypothermia through thermogenesis and has a crucial role in energy balance in later life in some animal models. Epicardial and pericardial fat depots have both been shown to possess uncoupling protein 1 (UCP1) and function as brown fat [1,2]. The development and modification of these depots in early life in comparison to classical white adipose tissue has not previously been studied. This study focused on the comparison of epicardial, pericardial and omental fat during early postnatal life through gene expression analysis. UCP1 was analysed as a marker of brown or beige fat capable of thermogenesis. Expression of the white fat markers leptin and adiponectin were investigated to elucidate white adipocyte characteristics of each depot. Peroxisome proliferator-activated receptor (PPAR) gamma is involved in white and brown fat differentiation and was assessed as an indicator of mature adipocyte development.
Methods: Four triplet-bearing mothers were entered into the study and a randomly selected triplet was euthanased at 1, 7 or 28 days of age for adipose tissue sampling (n=4 per time point) under Home Office Approval, UK. Pericardial adipose tissue was sampled at 1, 7 and 28 days whereas epicardial and omental adipose tissues were only sampled at 7 and 28 days due to a lack of any observable fat in these depots in 1 day old sheep. RNA was extracted and gene expression analysed by qRT-PCR. Relative mRNA expression was calculated using the GeNorm method corrected to the geometric mean of reference genes IPO8 and RPO, and expressed in arbitrary units [3]. Data are presented as mean ± SEM and analysed using one way ANOVA or unpaired t-Test for comparisons with age.
Results: With increasing age, UCP1 expression decreased and the white fat marker leptin increased in all depots studied (see Figure 1). UCP1 was detectable in epicardial and pericardial adipose tissue and, to a lesser extent in omental fat, at 7, but not 28, days of age. Adiponectin also increased up to 28 days which was most pronounced in the pericardial fat depot. PPAR gamma increased significantly in all depots with age.
Conclusion: Our study suggests a brown to white fat transformation in all adipose tissues during the first month of postnatal life, even in those depots which are undetectable immediately after birth. This may be accompanied by a loss of brown adipose tissue and increased adipocyte differentiation.

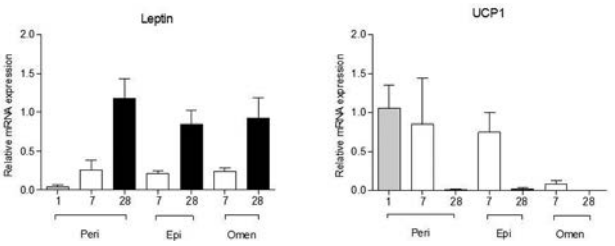

Figure 1 UCP1 and Leptin mRNA expression for pericardial (Peri), epicardial (Epi) and omental (Omen) fat depots with age.

Sacks HS *et al.* (2009) *The Journal of Clinical Endocrinology and Metabolism* , **94**, 3611-5.

Ojha S *et al.* (2013) *Paediatric Research* (In Press).

Vandesompele J *et al.* (2002) *Genome Biology*, **3**, 7.

Where applicable, the authors confirm that the experiments described here conform with The Physiological Society ethical requirements.

PCD282

Maternal obesity results in lower energy expenditure in adult offspring when exposed to an obesogenic diet in adulthood

X. Maragkoudaki, L. Poston and P.D. Taylor

King's College London, London, UK

Background: Converging lines of evidence suggests that maternal obesity is an independent risk factor for childhood obesity and metabolic syndrome. We have developed a murine model of maternal diet-induced obesity, which gives rise to offspring obesity and metabolic syndrome.
Objective: We investigated whether maternal obesity could alter offspring energy balance and whether offspring exposure to an obesogenic diet in adulthood would exacerbate the effect.
Methods: Female mice were fed standard chow or a highly palatable obesogenic diet, for 6 weeks before mating and throughout pregnancy and lactation. Offspring were weaned onto standard chow. At 3-months of age food intake, energy expenditure (EE) and Respiratory Exchange Ratio (RER) were measured continuously by indirect calorimetry, (Labmaster, TSE). The animals were then challenged for 3 weeks with an obesogenic diet before re-estimation of EE, RER and food intake.
Results: At 3-months of age, offspring of obese mothers (OffOb, n=11) had lower RER over 24hrs ($P<0.05$) compared to offspring of control dams (OffCon, n=10). Following the obesogenic diet challenge OffOb females showed increased calorific intake (OffCon: 17.56±1.72 kcals vs OffOb: 27.65±3.24 kcals, $P<0.01$). OffOb showed reduced average EE compared to OffCon (OffCon: 12.12±0.75 kcal/h/kg, n=11; vs OffOb: 10.76 ±0.31 kcal/h/kg, n=10 $P<0.01$). By 4-months males OffOb showed significantly increased bodyweight (OffCon: 43.93±1.16 g vs 48.1± 1.34 g, $P<0.05$).
Conclusions: Maternal obesity results in lower offspring RER. Maternal obesity showed an apparent interaction with the adult obesogenic diet to increase food intake in females and reduce energy expenditure in both males and females, resulting in increased risk of obesity.

Where applicable, the authors confirm that the experiments described here conform with The Physiological Society ethical requirements.

PCD283

Identification and characterisation of human foetal adrenocortical progenitor cells

J. Sampson, D. Wilson and I. O'Kelly

Human Development and Health, Faculty of Medicine, University of Southampton, Southampton, Hampshire, UK

The foetal adrenal gland comprises of two distinct zones; the foetal zone (FZ) and the smaller subcapsular definitive zone (DZ). The FZ produces large amounts of androgens used by the placenta during oestrogen synthesis and expresses cytochrome P450 enzymes, such as CYP21, involved in the synthesis of aldosterone and cortisol. The DZ has been proposed to contain a population of adrenocortical progenitors. These cells are thought to migrate centripetally, perhaps via the distinct columns of cells radiating from the inner layer of the DZ to the outer layers of the FZ, to populate the rest of the gland. This study aims to identify and characterise these cells.
Murine studies have identified Sonic Hedgehog (SHH) pathway in a possible subcapsular non-steroidogenic progenitor population. Activation of this pathway has been implicated in the patterning of other developing endocrine glands however its involvement in the human foetal adrenal gland has yet to be defined. DAX1, dosage-sensitive sex reversal adrenal hypoplasia critical region on chromosome X gene 1, is known to inhibit steroidogenic factor 1 mediated steroidogenesis and murine studies show similar expression profiles to that of SHH. Hence DAX1 expression in the absence of steroidogensis could highlight a progenitor population. We therefore hypothesised that a human adrenal progenitor cell population may be identified using a combination of markers for adrenal DZ and the SHH pathway.
To test this hypothesis a combination of reverse transcription PCR and immunohistochemistry was used to examine the expression of Sonic hedgehog, Smoothened (G protein coupled receptor of the SHH pathway), Gli1 (transcriptional activator of SHH pathway), CD56 (DZ marker), CYP21 and DAX1 mRNA and protein in the human foetal adrenal. Positive transcripts for each of the markers were observed from mRNA extracted from total foetal adrenals (n = ≥1). By immunohistochemistry both SHH and GLI1 showed positive signal at the periphery of the gland, in a similar region to CD56 (n = ≥1). DAX1 expression was also observed to be highest at the periphery of the gland but also localised with CYP21 in the FZ (n = ≥1).
This study has identified a population of GLI1 and DAX1 positive cells which may be representative of an adrenocortical progenitor population. These findings will be advanced by further investigating the involvement of the SHH pathway in the proposed progenitor population. Cyclopamine, an inhibitor of SMO, will be used to assess the importance of the SHH pathway by its effect on the amount of Ki67 and CD56 positive cells in the DZ. Identification and characterisation of the human foetal adrenal progenitors will give a better understanding of gland development.

With thanks to the MRC for funding this research

Where applicable, the authors confirm that the experiments described here conform with The Physiological Society ethical requirements.

PCD284

Impact of increased carbohydrate and fat intake during postnatal and juvenile life on gene expression in the sternal fat of sheep

M. Birtwistle[1], P. Khanal[2], A. Kongsted[2], M. Nielsen[2], H. Budge[1] and M.E. Symonds[1]

[1]Early Life Nutrition Research Unit, School of Clinical Sciences, University of Nottingham, Nottingham, UK and [2]Department of Veterinary Clinical and Animal Sciences, Faculty of Health and Medical Sciences, University of Copenhagen, Copenhagen, Denmark

Background and aims:
It has been established that the early life nutritional environment affects current and later adiposity, and therefore adult health outcomes and phenotypes (1). Using sheep as a model, we examined the effects of excess energy intake during early postnatal life on the subsequent growth and development of sternal adipose tissue. Specifically we looked at the expression of adipose tissue-related genes including leptin, adiponectin, FABP4, HOXC9, PPARγ, RIP140 and CIDEA. We hypothesised that excess energy intake would increase the amount of sternal fat, and that genes involved in excess adiposity would respond accordingly.
Materials and methods:
Weight-matched offspring of 13 twin-bearing ewes were separated from their mothers and randomly allocated to one of two different dietary groups from day 3 postpartum until 6 months of age. Each group was balanced by sex. The control group (C, n=13) was fed milk replacer diet for 8 weeks, with green hay added from 14 days of age. The high-carbohydrate high-fat group (HCHF, n=13) was fed a 1:1 mixture of milk replacer and cream together with maize from 14 days of age. At 6 months animals were humanely euthanased and sternal adipose tissue depots dissected. The relative expression of genes of interest was assessed by qPCR. Expression of genes of interest was normalised to the geometric mean expression of two reference genes that had been tested for stability. Gene expression was determined by the comparative C_T method after corrections for qPCR efficiency. Values shown are the mean ± SEM in arbitrary units. A two-tailed t-test or Mann-Whitney U-test, as appropriate, was used to compare gene expression between the two groups.
Results:
At 6 months of age, animals on the HCHF diet were heavier than those on the control diet (C: 36.05 ± 0.79 kg; HCHF: 42.28 ± 2.63 kg; $p<0.05$) and possessed more sternal fat than controls, both in total (C: 36.5 ± 2.5 g; HCHF: 168.3 ± 14.8 g; $p<0.001$) and per kg body weight (C: 1.02 ± 0.07 g; HCHF: 3.96 ± 0.21 g; $p<0.001$). However, expression of mRNA in adiponectin (C: 1.00 ± 0.05; HCHF: 0.60 ± 0.09; $p<0.001$), PPARγ (C: 1.00 ± 0.03; HCHF: 0.52 ± 0.04; $p<0.001$) and CIDEA (C: 1.00 ± 0.14; HCHF: 0.55 ± 0.15; $p<0.01$) was reduced in animals on the HCHF diet compared to controls. There was no difference in the expression of leptin, FABP4, HOXC9 and RIP140 between the two groups.
Conclusions:
Increased energy intake from a high-fat high-carbohydrate diet in early postnatal and juvenile life promotes adiposity, which in the sternal depot results in endocrine adaptations that would be predicted to prevent metabolic and related dysfunction. Future analysis will examine the other major fat depots to assess whether similar responses are found.

1. Symonds ME, Sebert SP, Hyatt MA, Budge H. Nutritional programming of the metabolic syndrome. Nat Rev Endocrinol. 2009;5(11):604-10

Where applicable, the authors confirm that the experiments described here conform with The Physiological Society ethical requirements.

PCD285

Exposure to maternal obesity or to maternal weight loss around the time of conception in the sheep has long term impact on hepatic fatty acid metabolism in the offspring at four months of age

L.M. Nicholas[1], L. Rattanatray[1,2], S.M. MacLaughlin[1], D.O. Kleemann[3], S.K. Walker[3], J.L. Morrison[1], S. Zhang[1] and I.C. McMillen[1]

[1]Sansom Institute for Health Research, School of Pharmacy and Medical Sciences, University of South Australia, Adelaide, SA, Australia, [2]Discipline of Physiology, School of Molecular and Life Sciences, University of Adelaide, Adelaide, SA, Australia and [3]Turretfield Research Centre, South Australian Research and Development Institute, Rosedale, SA, Australia

The obesity epidemic has resulted in an increase in the number of women entering pregnancy overweight or obese range (1). We have previously shown that exposure to maternal obesity in the periconceptional (PC) alone resulted in increased adiposity in female lambs (2). Maternal obesity both before and throughout pregnancy has been shown to result in alterations in hepatic fatty acid (FA) oxidation and lipogenesis, which are characteristic of non-alcoholic fatty liver disease (3-5). This has led to interest in understanding the type of dietary interventions before and during pregnancy, which may lead to optimal outcomes for the mother and offspring (1). Our aim was to determine the impact of exposure to maternal obesity or weight loss around conception in sheep on programming of molecules involved in hepatic FA oxidation and de novo lipogenesis in male and female lambs at 4 months of age.

Donor ewes were allocated to 1 of 4 groups & fed the following diets in the PC period: 100% metabolisable energy requirements (MER) for ≥ 20wks (CC); 100% MER for ≥ 16wks & then 70% MER for 4wks (CR); ~180% MER for ≥ 20wks (HH); ~180% MER for ≥ 16wks & then 70% MER for 4wks (HR). This continued for 1wk post-conception before single embryos were transferred into recipient ewes of normal weight. At 16wks after birth, liver samples were collected to determine gene expression (qRT-PCR) and protein abundance (Western Blotting) of molecules regulating hepatic FA oxidation and synthesis. The effects of PC nutrition and sex were determined using a two-way ANOVA. A Duncan's post hoc test was used to determine significant differences between groups.

HH lambs had decreased gene expression and protein abundance of PPARα and a parallel decrease in PGC1α abundance ($P<0.05$). These lambs also had increased SIRT1 and decreased GCN5 abundance ($P<0.05$). Hepatic AMPKα1, AMPKα2 and SREBP1 was also increased ($P<0.05$) in these lambs. Exposure to maternal weight loss in obese ewes did not abolish all of the effects of maternal obesity on gene expression and protein abundance of these molecules. Furthermore, there was decreased ($P<0.05$) hepatic PGC1α and GCN5 abundance as well as increased ($P<0.05$) AMPKα2 abundance in CR lambs.

We have shown that exposure to maternal obesity in the PC period programs potentially irreversible changes in hepatic lipid metabolism that persist in later life. We have also shown that dietary restriction in obese ewes in unable to abolish all of the effects of maternal obesity. Exposure of both normal weight and obese ewes to moderate dietary restriction resulted in an additional suite of changes within the liver. This highlights that there is vulnerability in offspring after exposure to periconceptional undernutrition to dysregulated hepatic lipid metabolism.

Zhang S, Rattanatray L, McMillen IC, Suter CM, Morrison JL. Periconceptional nutrition and the early programming of a life of obesity or adversity. Progress in Biophysics and Molecular Biology 2011;106:307-14.

Rattanatray L, MacLaughlin SM, Kleemann DO, Walker SK, Muhlhausler BS, McMillen IC. Impact of maternal periconceptional overnutrition on fat mass and expression of adipogenic and lipogenic genes in visceral and subcutaneous fat depots in the postnatal lamb. Endocrinology 2010;151:5195-205.

Borengasser SJ, Lau F, Kang P, et al. Maternal obesity during gestation impairs fatty acid oxidation and mitochondrial SIRT3 expression in rat offspring at weaning. PLoS ONE 2011;6

McCurdy CE, Bishop JM, Williams SM, et al. Maternal high-fat diet triggers lipotoxicity in the fetal livers of nonhuman primates. Journal of Clinical Investigation 2009;119:323-35.

Oben JA, Mouralidarane A, Samuelsson AM, et al. Maternal obesity during pregnancy and lactation programs the development of offspring non-alcoholic fatty liver disease in mice. Journal of Hepatology 2010;52:913-20.

Where applicable, the authors confirm that the experiments described here conform with The Physiological Society ethical requirements.

PCD287

Central role for melanocortin system in energy balance and blood pressure regulation in offspring of obese dams

A. Samuelsson, A. Mullier, A. Stepien, K. Patel, J. Pombo, C.W. Coen, L. Poston and P.D. Taylor

Division of Women's Health, Women's Health Academic Center, King's College London and King's Health Partners, UK, King's College London, London, UK

Background: Maternal obesity in rat leads to sympathetic mediated hypertension in the juvenile offspring and hyperphagia and increased adiposity in the adult offspring (1-2). We hypothesise that maternal obesity permanently influences the development of the melanocortin system in the offspring.

Objective: To investigate the role of the melanocortin receptor 3 and 4 (MC3/4R) signaling, using a pharmacological intervention, on the development of juvenile sympathetic mediated hypertension, secondary to maternal obesity.

Methods: Offspring of control (OffCon) and diet-induce obese dams (OffOb; at 23 or 172 days of age) were implanted with telemetry transmitter, inserted into the carotid artery in juvenile rats (DSI PhysioTel PA-C10) and abdominal aorta in adult rats (DSI PhysioTel PA-C40) under general anaesthesia (2% isofluorane). Pre and post-operative analgesia (Buprenorphine 0.1 mg/kg, intramuscular) was maintained for 24h. For drug i.c.v infusion, juvenile rats were anesthetized with ketamine (75 mg/kg, i.p) and domitor (0.5 mg/kg, i.p) and then placed in a stereotaxic frame. Cannula placement was made in the lateral ventricle (coordinates AP-0.9 mm, DV-3.5mm from bregma). MC3/4R antagonist (SHU9119, 1 nmol/h) or saline (Alzet osmotic pump; 0.5 ul/h, i.c.v) was chronically administrated for 7 days and body weight (BW), food intake (FI), mean arterial pressure (MAP) and heart rate (HR) recorded. After the experiments were completed, the rats were sacrificed with overdose of sodium pentobarbital, and their brain removed

and sectioned to confirm accurate placement of the i.c.v cannula. At 6 months of age, MC4R agonist, Melanotan II (MTII, 2 mg/kg, i.p) and saline were injected and BW, FI, MAP and HR were recorded.
Results: Juvenile OffOb rats showed an increased MAP prior to obesity. MC3/4R antagonism (SHU-9119) increased the BW and FI in OffOb relative to OffCon and elicited a greater decline in MAP (OffOb -29±4 mmHg versus OffCon, -12±3 mmHg, P<0.001, n=8). HR was lowered to the same extent in both groups. MTII treatment on the other hand increased HR to a greater extent in the OffOb versus OffCon without any significant difference in MAP response between groups. MTII was also more effective in reducing BW in the OffOb despite not having a differential effect on the FI.
Conclusions: CNS melanocortin system contributes to the elevated MAP in OffOb and may play a key role in the early origin of sympathetic mediated hypertension. Increased signaling by the melanocortin receptor (MC3/4R) is also implicated in altered energy balance in this model.

Kirk S *et al*. (2009). *Plos One*. **4**:e5870

Samuelsson AM *et al*. (2010). *Hypertension*. **55**. 76-82.

This study was supported by the British Heart Foundation (FS/10/003/28163) and the BBSRC (BBD5231861). LP is funded by Tommy's Charity (1060508).

Where applicable, the authors confirm that the experiments described here conform with The Physiological Society ethical requirements.

PCD288

Identification of human adipose tissue native progenitor cell subsets in distinct adipogenic states

D. Esteve[1], N. Boulet[1], A. Zakaroff-Girard[1], S. Ledoux[2], P. Decaunes[1], J. Iacovoni[1], C. Heymes[1], A. Bouloumié[1] and J. Galitzky[1]

[1]I2MC, INSERM U1048, Toulouse Cedex4, France and [2]2-Center Support of Obesity, Hopital Louis Mourier, Colombes, France

Adipogenesis plays an important role in adipose tissue (AT) expansion and in adipocyte turnover. This process involving transcriptional activation/repression netwoks is defined by the shift of undifferentiated and non-committed mesenchymal cells to differentiated metabolically active adipocytes, through different states as comitted progenitors or preadipocytes. Human native progenitor cells CD34+/CD31-, contained in stroma vascular fraction (SVF), display adipogenic potential. However different cellular state markers are lacking. While white and brown AT were well studied in mice, a brite adipocyte was recently evinced in mice and human. More metabolically active than white, brite adipocytes exhibit features at the crossroads of brown and white adipocytes and could be a new target to fight against obesity associated pathologies. We propose to characterize heterogeneity of CD34+/CD31- to identify cell subsets in different states and/or with distinct white or brite fates.Heterogeneity of human CD34+/CD31- cells was studied by flow cytometry (n=54). In vitro experiments on native CD34+/CD31- were done to evaluate modifications on cell subsets ratio during adipogenesis (n=13). Cell sorting approaches were developped to isolate the progenitor subsets. Adipogenic potential of selected cell subsets was assessed in vitro (n=6). Cell subsets states and/or fates in terms of white or brite potentials were assessed by gene expression analyses (n=10). In vivo adipogenic potential of human progenitor subsets was assessed by cellular graft in NMRI mice. 6 weeks after graft, adipocyte formation was checked on implantation site (n=3).We identified 3 progenitor subsets in adult human native AT-SVF. The first one (P1) decreases with obesity. P1 is less represented in human visceral AT (VAT) than in subcutaneous AT (SAT). Futhermore this freshly harvested cell subset displays the highest expression of anti-adipogenic genes as KLF2. Finally P1 has the lowest adipogenic potential in vitro and in vivo. Inversly the second one identified (P2) increases with obesity. P2 is less present in VAT than in SAT. Expression of pro adipogenic genes is higher in P2 compared to P1: PPARγ2 (1.5 fold increase, p<0.05), CHREBP (2 fold increase, p<0.01), and PLIN1 (3 fold increase, p<0.01). P2 displays the better adipogenic potential in vitro and in vivo. P2 has a significant higher expression in brite/brown markers than P1 as CIDEA or TMEM26 (n=9, p<0.05). Mitochondria content, assessed using Mitotracker, is higher in P2 (n=6, p<0.01). The last one (P3) has an intermediate phenotype based on gene expression profile and on adipogenic potential in vitro and in vivo. Our data allow to identify 3 human progenitor subsets in CD34+/CD31- population in different states or with distinct fates. P2 appears as the most committed cell subset and probably contains the white and brite preadipocyte.

Where applicable, the authors confirm that the experiments described here conform with The Physiological Society ethical requirements.

PCD289

Effects of Bone Morphogenetic Proteins (BMPs) on human adipose conversion and adipose tissue (AT) development

N. Boulet, D. Esteve, P. Decaunes, A. Bouloumié and J. Galitzky

I2MC, INSERM U1048, Toulouse, France

Adipogenesis corresponds to the commitment and differentiation of AT progenitor cells into adipocytes. Human AT progenitor cells are CD34+/CD31- and have adipogenic potential under pharmacological PPARγ agonist treatment (1). However in human endogenous signals leading to adipogenic commitment are not clearly known. In mice, BMP2/BMP4 and BMP7 induce the commitment in white and brown adipogenesis respectively (2-3). A third type of adipocytes has been described, brite adipocytes which are white adipocytes with some brown characteristics (4). The present study was undertaken to characterize the effects of these BMPs on human native AT progenitor cells white and brown/brite adipogenesis. Human subcutaneous AT cell populations (adipocytes, immune cells, endothelial cells, and progenitor cells) were isolated by immunoselection/depletion approaches. BMPs gene expressions were determined by RT-qPCR analyses in the different AT cell populations (n=6). BMP receptor gene expressions were performed by RT-qPCR on isolated human AT progenitor cells (n=5). AT progenitor cells were treated (or not, control (ctl)) for 48 hours by BMP2, BMP4 or BMP7 (50ng/ml) then cultured in basal adipogenic medium (without PPARγ agonist) for 9 days (n=7). At day 9, adipogenesis was evaluated by lipid accumulation quantification and RT-qPCR analyses on white and brown/brite adipocyte gene markers were performed (n=6). BMP2 gene expression is higher in immune and endothelial cells compared to adipocytes and progenitor cells (1.5 and 5 fold increase respectively, p<0.05), BMP4 and BMP7 gene expressions are higher in progenitor cells than in others (3 and 50 fold increase respectively, p<0.05). Human AT progenitor cells express BMP receptors ALK2, ALK3, ALK6, BMPR2 and ACVR2. Early BMP2, BMP4 or BMP7 treatment on human AT progenitor cells increases lipid accumulation (3 fold increase

vs ctl, p<0.001) and induces the expression of common adipogenic gene markers such as PPARγ, LEPTIN and PERILIPIN 1 after 9 days (3 fold increase vs ctl, p<0.05). However only BMP7 induces the expression of the common brown/brite adipocyte gene marker UCP1 (3.5 fold increase vs ctl, p<0.05). Classical brown adipocyte genes as PRDM16, CIDEA and PGC1α are not significantly induced by BMP7 treatment. Our study shows that human AT progenitor cells express BMP receptors and that early BMPs treatment induces the commitment and/or differentiation of human AT progenitor cells into adipocyte. BMP2 and BMP4 are white adipogenesis inducers whereas BMP7 induces brown-like/brite adipogenesis. These results suggest that human AT progenitor cells might have brown-like/brite potential and represent a target to fight against obesity-associated pathologies. Finally, BMPs could be produced locally by AT cells and could be endogenous adipogenic signals regulating human white and brite adipogenesis and obesity.

Sengenes C et al., (2005) J Cell Physiol 205:114–122

Huang H et al., (2009) PNAS 106:12670-12675

Tseng YH et al., (2008) Nature 454:1000-1004

Petrovic M et al., (2010) J Biol Chem 285:7153-7164

Where applicable, the authors confirm that the experiments described here conform with The Physiological Society ethical requirements.

PCD290

The effects of gravidity, digestion, and exhaustive activity on oxygen consumption in the viviparous checkered garter snake

A.G. Jackson[1], N. Ford[2] and J.W. Hicks[1]

[1]Ecology and Evolutionary Biology, University of California, Irvine, Irvine, CA, USA and [2]Biology, University of Texas at Tyler, Tyler, TX, USA

The oxygen transport capacity of the cardiopulmonary system has evolved to meet the demands of simultaneously interacting elevated metabolic states (1). Consequently, scientists have become increasingly interested in the interaction of elevated metabolic states, namely digestion and activity (2). A third, less thoroughly studied physiological state capable of significantly elevating metabolism is gravidity (3). The goals of this study were to measure oxygen consumption (VO2) of gravidity, and study the interactive effects of exhaustive activity and digestion in a viviparous squamate reptile, the Checkered Garter Snake. We examined the metabolic changes during gravidity in this species by measuring oxygen consumption using flow through respirometry.

We hypothesized that 1) gravidity would increase the resting metabolic rate above the resting values of non-gravid females, and 2) that this species would demonstrate an additive response to simultaneous elevated metabolic demands (both metabolic demands will be met with a sufficient supply of oxygen without affecting the performance of either state). Specifically, females would consume more oxygen during digestion, fasting exhaustive activity, and post-prandial exhaustive activity while gravid than during the non-gravid state.

Current results indicate that females of this species increase resting VO2 during gravidity by a factor of 1.6 compared to the non-gravid resting state. Furthermore, compared to non-gravid females, gravid females consume significantly more oxygen during digestion (scope =1.52), but consume significantly less oxygen during fasting exhaustive activity (scope = .830). However, both gravid and non-gravid females demonstrate partial additivity of the digestive and activity responses by consuming more oxygen during post-prandial exhaustive activity (scope =1.30) than either digestion or fasting exhaustive activity alone.

Current results indicate that our hypothesis for increased oxygen consumption during gravidity is supported. On the other hand, our hypothesis for an additive response to simultaneous elevated metabolic states is more complicated. This species does demonstrate an additive response to gravidity and digestion, but not to gravidity and exhaustive activity. Finally, both gravid and non-gravid females experience an additive response to digestion and exhaustive activity. Therefore, we conclude that this species is capable of demonstrating peak VO2 levels only when exhaustive activity is combined with digestion. Future studies might help explain why gravid females demonstrate higher VO2 levels during digestion, but not during exhaustive activity, by examining cardiopulmonary patterns such as ventilation and blood flow distribution patterns.

Hicks, JW., Bennett, AF. (2004). Eat and run: Prioritization of oxygen delivery during elevated metabolic states. Respiratory Physiology & Neurobiology, 144(2004), 215-224.

Jackson, DC. (1987). Assigning priorities among interacting physiological systems. In New directions in Ecological Physiology (ed. M. E. Feder, A.F. Bennett, W. W. Burggren and R. B. Huey), pp. 310-326. New York: Cambridge University Press.

Robert, KA., Thompson, MB. (2000). Energy consumption by the embryos of a viviparous lizard, Eulamprus tympanum, during development. Comparative Biochemistry and Physiology. 127, 481-486.

Funding for this research was provided by NSF grant IOS 0922756 to JWH.

Where applicable, the authors confirm that the experiments described here conform with The Physiological Society ethical requirements.

PCD291

Comparative effects of the long-term black or green tea decoction consumption on lipid digestibility and adipose abdominal tissue mass in rat fed high-fat diet

C. Snoussi[1], K. Dhaouadi[1,2], H. Abaidi[1], S. Fattouch[2] and M.H. Hamdaoui[1]

[1]Research Unit, high School of Health Sciences and Technical, Tunis, Tunisia and [2]Food Biochemistry Laboratory, National institute of applied sciences and technology, tunis, Tunisia

In previous studies, we observed that green or black tea decoction (GTD, BTD) reduced body weight gains and adipose abdominal tissue mass (AATM) in young rats. However, the role of lipids digestibility in this reduction is not yet clear. In the present study, we compared the long-term effect of GTD or BTD consumed ad-libitum on lipid absorption and evaluate its impact on AATM in rats fed high-fat diet (HFD). Thirty-six male Wistar rats were used during an experimental period conducted over 10 weeks. After the adjustment period, the rats were weighed and randomly assigned into 3 groups (n=12 each)with comparable body weights. After, the rats were given the HFD ad libitum with or without tea decoctions as follows: the group 1 received the HFD+ distilled water (CGr), the group 2 received the HFD + GTD (GTGr) and the group 3 received the HFD+ BTD prepared from 50g/L (BTGr). Food intake was recorded throughout the experimental period and quantified by weighing the amount of food spilled and refused. The volume of tea decoction consumed by each rat was measured daily. Fecal matters were individually collected 2 times per

week, lyophilized and stored for total polyphenols, total lipids, triglycerides and caffeine analysis. At the end of the experience, the rats were weighed, and then killed by decapitation. Fasting blood was drawn and the plasma was removed for analysis of total polyphenolic compounds, caffeine, total lipids, some metabolic variables and leptin concentration. In addition, liver, perirenal and epididymal white adipose tissues from abdominal cavity were removed, weighed and stored at -20°C until lipid analysis. Values are means ± S.E.M., compared by ANOVA. After 10 weeks treatment, GTD and BTD reduced body weight gains (CGr: 114.8 ± 5.5 vs. GTGr: 86.8 ± 6.4 and BTGr: 67.8 ± 7.8 g, $p<0.05$) and AATM (CGr: 5.04 ± 0.16 vs. GTGr: 3.13 ± 0.24 and BTGr: 1.97 ± 0.9 g, $p<0.05$). Additionally, they increased plasma polyphenols (CGr: 31 ± 3.3 vs. GTGr: 101.3 ± 6 and BTGr: 76.6 ± 9.4 μg/mL, $p<0.05$) and plasma caffeine (CGr: 0.625 ± 0.13 vs. GTGr: 4.1± 0.5 and BTGr: 6.5 ± 0.6 μg/mL, $p<0.05$). In contrast, GTD and BTD increased lipids (CGr: 213.9 ± 15 vs. GTGr: 301.2 ± 7.6 and BTGr: 351.6 ± 6.5 mg/g, $p<0.05$) and polyphenols (CGr: 112.5 ± 6.2 vs. GTGr: 644 ± 38.9 and BTGr: 643.1 ± 61.9 μg/g, $p<0.05$) excretion in fecal matter. Results showed that the reduction of AATM may be ascribed to the modulation of lipids digestibility by tea-polyphenol and tea-caffeine in the gastro-intestinal lumen and adipose tissue organ which involved different mechanisms and physiological pathway including sympathetic nervous system regulation.

Authors would like to thank the Ministry of high education and research in Tunisia which had financially supported this study

Where applicable, the authors confirm that the experiments described here conform with The Physiological Society ethical requirements.

PCD292

A new mouse model for obesity and steatosis

H. Weng, Y. Naito, K. Endo and N. Iwai

Department of Genomic Medicine, National Cerebral and Cardiovascular Center, Suita, Osaka, Japan

Obesity and obesity-associated fatty liver disease (FLD) are becoming global health problems (Evans et al. 2004). Hepatic triglyceride (TG) accumulation is considered to be a prerequisite for developing FLD. Peroxisomes are single membrane-bound organelles, which have many important functions in lipid metabolism, including fatty acids β-oxidization. Pex11α is one of Pex11 gene factor was shown to promote peroxisome division (Delille et al. 2010, Koch et al. 2010). The pathogenic link between obesity and FLD and peroxisome biogenesis remains unclear. To understand the molecular and physiological functions of the Pex11α gene, we disrupted this gene in mice. Five-week old Pex11α-/- (KO) mice and matched C57BL/6 (WT) mice were fed a high-fat diet (HFD) for 12 weeks. Body weights in KO mice were significantly higher than those in WT mice fed a normal diet or an HFD. The amount of food intake was similar between KO mice and WT mice. Oxygen consumption was significantly lower in KO mice than WT mice. Weights of Epididymal white adipose tissue (e-WAT) of KO mice were significantly greater than WT mice. Large adipocytes were more prevalent in KO mice. Fatty acid synthase and peroxisome proliferator-activated receptor γ mRNA levels were significantly higher in the brown adipose tissues of KO mice than in WT mice by approximately ten- and two-fold. Hepatic TG concentrations in KO mice were significantly higher than those in WT mice fed a normal diet or an HFD. We also characterized the response to 24-hr fasting. Hepatic TG concentrations in fasted Pex11α-/- mice were significantly higher than in fasted WT mice. Very low density lipoprotein production test showed that plasma TG levels increased at higher rates in WT mice than in KO mice after treatment with 500mg/kg of lipoprotein lipase inhibitor tyloxapol. By both catalase (a peroxisome matrix protein) and PMP70 (a peroxisome membrane protein) immunofluorescence staining, the number of peroxisomes was lower in the livers of KO mice than in those of WT mice. Ultrastructural analysis showed that small and regular spherical peroxisomes were more prevalent in KO mice fed normal chow supplemented without or with 0.015% fenofibrate (w/w) for 2 days. We observed a significantly higher ratio of empty peroxisomes containing only PMP70 but not catalase in KO mice. Immunoblotting results also showed a significantly lower ratio of catalase and PMP70 proteins in the peroxisomes of KO mice after fenofibrate treatment. mRNA expression levels of peroxisomal fatty acid oxidation-related genes (ATP-binding cassette, sub-family D, member 2 and acyl-CoA thioesterase 3) were significantly higher in WT mice than in KO mice. Our results provide the first evidence that Pex11α deficiency impairs peroxisome elongation and abundance and peroxisomal fatty acid oxidation, thus contributing to increased lipid accumulation in the liver and increased de novo lipogenesis in adipose tissue.

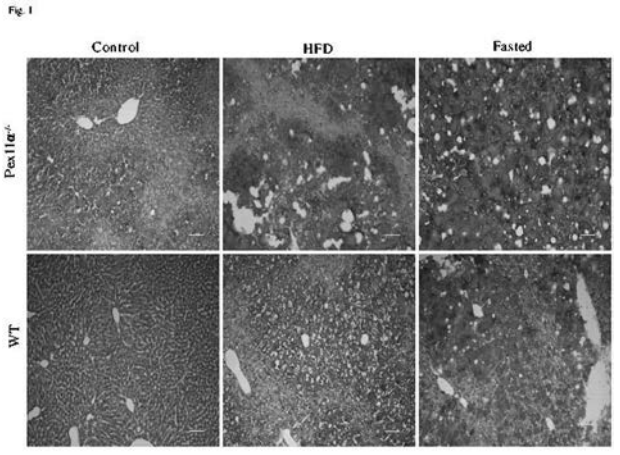

Fig. 1. Pex11α-/- mice develop a fatty liver. WT and Pex11α-/- mice were fed a high fat diet (HFD) for 12 weeks or deprived of food for 24 hr. Oil red O staining of liver sections of mice fed a normal diet (Control), HFD, or fasted for 24 hr. Scale bars = 50 μm.

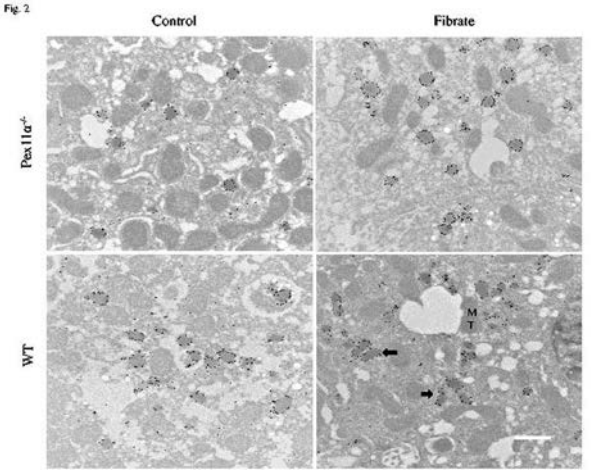

Fig. 2. Electron microscopy indicates that Pex11α deficiency impairs peroxisome elongation and size.Pex11α-/- and WT mice were fed normal chow supplemented without or with 0.015% (w/w) fenofibrate (control and fibrate, respectively) for 2 days.Tubular or elongated peroxisomes are visible (arrows); MT, mitochondria. Scale bar: 1 μm.

Evans RM, Barish GD, Wang YX. PPARs and the complex journey to obesity. Nat Med 2004;10:355-61

Delille HK, Agricola B, Guimaraes SC, Borta H, Luers GH, Fransen M, Schrader M. Pex11pbeta-mediated growth and division of mammalian peroxisomes follows a maturation pathway. J Cell Sci 2010;123:2750-62.

Koch J, Pranjic K, Huber A, Ellinger A, Hartig A, Kragler F, Brocard C. PEX11 family members are membrane elongation factors that coordinate peroxisome proliferation and maintenance. J Cell Sci 2010;123:3389-400.

Where applicable, the authors confirm that the experiments described here conform with The Physiological Society ethical requirements.

PCD293

Hydroxysteroid sulfotransferase SULT2B1b promotes hepatocellular carcinoma cells proliferation in vitro and in vivo

X. Yang, P. Zhou, Y. Ning, X. Zhi, X. Li and L. Yin

Depart of Physiology and Pathophysiology, Fudan University, Shanghai, China

Hydroxysteroid sulfotransferase 2B1b (SULT2B1b) is highly selective for the addition of sulfate groups to 3β-hydroxysteroids. Although previous reports have suggested that SULT2B1b is correlated with cell proliferation of hepatocytes, the relationship between SULT2B1b and the malignant phenotype of hepatocarcinoma cells was not clear. In the present study, we found that SULT2B1b overexpression promoted the growth of the mouse hepatocarcinoma cell line Hepa1-6, while Lentivirus-mediated SULT2B1b interference inhibited growth as assessed by the CCK-8 assay. Likewise, inhibition of SULT2B1b expression induced cell-cycle arrest and apoptosis in Hepa1-6 cells by upregulating the expression of FAS and p-JNK, downregulating the expression of cyclinB1, BCL2 and MYC in vitro and in vivo at both the transcript and protein levels. Knockdown of SULT2B1b expression significantly suppressed tumor growth in nude mouse xenografts. Moreover, proliferation rates and SULT2B1b expression were highly correlated in the human hepatocarcinoma cell lines Huh-7, Hep3B, SMMC-7721 and BEL-7402 cells. Knock-down of SULT2B1b inhibited cell growth and cyclinB1 levels in human hepatocarcinoma cells and suppressed xenograft growth in vivo. In conclusion, SULT2B1b expression promotes proliferation of hepatocellular carcinoma cells in vitro and in vivo, which may contribute to the progression of HCC.

This work was supported by the National Natural Science Foundation of China (NSFC 81270497 and NSFC 81170253).

Where applicable, the authors confirm that the experiments described here conform with The Physiological Society ethical requirements.

PCD294

Effects of a crude *Aloe vera* leaf aqueous extract and fenofibrate on diet induced metabolic dysfunction in growing rats

K.H. Erlwanger[1], Z.P. Gasa[1] and S. Makaula[1,2]

[1]School of Physiology, University of the Witwatersrand, 7 York Road, Parktown 2193, Johannesburg, Gauteng, South Africa and [2]Walter Sisulu University, Mthatha, Nelson Mandela Drive, PBag X1, UNITRA 511, South Africa

Globally, the consumption of unhealthy diets and leading sedentary lifestyles contribute significantly to the high prevalence of metabolic syndrome (MetS). Although the complications of MetS can be managed with conventional medicines, there is a growing use of medicinal plants. Previous studies exploring the metabolic effects of *Aloe vera* have been in adult animals in which metabolic dysfunction was induced pharmacologically.

We evaluated the effects of a crude *Aloe vera* leaf extract and fenofibrate on growth, visceral fat, circulating and stored metabolic substrates, and glucose tolerance of growing rats fed a high carbohydrate diet. Fifty nine male Sprague-Dawley rats (21 days old) were randomly allocated to six groups. Group I was fed normal rat chow (NRC). Group II received a high carbohydrate diet (HCD); Group III received NRC and fenofibrate at 100mg.kg^{-1}; Group IV received a HCD and fenofibrate at 100mg.kg^{-1}; Group V received normal rat chow and *Aloe vera* at 300mg.kg^{-1}; Group VI received a HCD and *Aloe vera* at 300mg.kg^{-1}. The *Aloe vera* crude aqueous leaf preparation and fenofibrate were administered in gelatine cubes. After 20 weeks the rats were fasted over night, an oral glucose tolerance test was performed, the rats were then killed with sodium pentobarbital (200mg.kg^{-1} i.p.) and tissue collected for further analysis.

The rats fed the HCD had a significantly higher body mass than the other groups ($p < 0.05$, ANOVA), however the administration of fenofibrate prevented the HCD-induced increase in body mass whilst *Aloe vera* was not effective. Linear growth as measured by the tibial length was not significantly different between the groups ($p > 0.05$, ANOVA). Fasting concentrations of glucose, triglycerides and free fatty acids were not significantly different between the groups and no significant differences ($p > 0.05$, ANOVA) were observed in the circulating concentrations of insulin and the index of insulin resistance (HOMA-IR). The rats in all groups were able to tolerate an oral glucose load. Feeding the rats a HCD resulted in a significantly increased ($p < 0.05$, ANOVA) visceral fat mass. Fenofibrate administration prevented the HCD-induced visceral fat mass gain whilst *Aloe vera* administration had no effect. Although there was no significant difference in the lipid and glycogen content in the liver, fenofibrate administration resulted in a significantly increased liver mass compared to the other groups.

Thus, weaning rats onto a high carbohydrate diet and feeding them the diet for 20 weeks resulted in the development of visceral obesity without altering their glucose tolerance and concentrations of metabolic substrates. Treatment with fenofibrate prevented the high carbohydrate diet-induced visceral adiposity however the *Aloe vera* leaf preparation was ineffective.

Where applicable, the authors confirm that the experiments described here conform with The Physiological Society ethical requirements.

PCD295

Dietary supplementation with coriander (Coriandrum sativum L) seed: Effect on growth performance, circulating metabolic substrates, and lipid profile of the liver and adipose tissue in healthy female Sprague Dawley rats

T.T. Nyakudya[1], S. Makaula[2,3], N. Mkumla[2] and K. Erlwanger[2]

[1]Human Anatomy and Physiology, University of Johannesburg, Johannesburg, South Africa, [2]School of Physiology, University of the Witwatersrand, Johannesburg, South Africa and [3]Physiology, Walter Sisulu University, Unitra, South Africa

The prevalence of diabetes mellitus and metabolic syndrome has reached epidemic levels globally. The rising incidence of diabetes and metabolic syndrome has been attributed to a sedentary lifestyle and the adoption of high energy diets that are deficient in omega-3 fatty acids, and contain excessive amount of omega-6 fatty acids. Coriander seeds, commonly used for culinary purposes, are rich in essential oils and have established hypoglycaemic and hypolipidaemic effects in the obese and diabetics. We investigated the effects of dietary coriander seeds on growth performance, hepatic and visceral adipose tissue lipid storage and circulating metabolic substrates in healthy growing rats. Female Sprague Dawley rats (150-200 g) were fed either standard rat chow (n = 8) or standard rat chow supplemented with crushed coriander seeds (n = 8; 500 mgkg-1 body mass) suspended in gelatine cubes. After five weeks, there were no significant differences in body mass gain, plasma free fatty acids, blood glucose and triglyceride concentrations of the rats from the two dietary groups ($p > 0.05$; t-test). Blood for the determination of circulating metabolites was collected by cardiac puncture under anaesthesia with sodium pentobarbitone. Whilst dietary supplementation with coriander did not affect the lipid content of the liver, however it significantly increased the amount of monounsaturated (MUFA) (22.62 ± 6.48%) and polyunsaturated (PUFA) (54.89 ± 5.10%) fatty acids in the visceral adipose tissue where it also decreased the saturated fatty acid content ($p < 0.05$; t-test). The physiological significance of the effect of coriander on MUFA and PUFA storage in visceral fat, but not in the liver, needs further investigation. The lower ratio omega 6: omega 3 in the visceral adipose tissue may explain some of the health benefits of coriander. These data suggest that dietary coriander supplementation may have beneficial effects on visceral adipose tissue lipid metabolism in healthy subjects.

Where applicable, the authors confirm that the experiments described here conform with The Physiological Society ethical requirements.

PCD297

Attenuation of acetaminophen-induced hepatotoxicity by short day photoperiod in Wistar rats

L.A. Olayaki, E.O. Mbukanma and A.T. Abdulraheem

Physiology, University of Ilorin, Ilorin, Kwara, Nigeria

Short day photoperiod enhances cellular immunity, cortisol production and melatonin secretion, especially in the laboratory animals (Pandi-Perumal et al., 2006; Bilbo et al., 2002). However, field studies of seasonal changes in immunity typically report reduced immune function during the short photoperiod of winter (Sinclair and Lochmiller, 2000). Acetaminophen (Paracetamol, PCM) is widely used as an over-the-counter analgesic and antipyretic drug. Intake of a large dose of PCM may result in severe hepatic necrosis. Therefore, this present study was carried out to investigate the liver protection effect of short photoperiod against acetaminophen-induced hepatotoxicity. Twenty four adult male rats weighing 160±7g were conditioned to different photoperiod regimens for 6 weeks. Group 1, control group, Normal Photoperiod (NP) (12:12, light on from 07:00hr to 19:00hr). Group 2, NP (12:12, light on from 07:00hr to 19:00hr) treated with acetaminophen. Group 3, Short Photoperiod (SP) (8:16, light on from 09:00hr to 17:00hr) treated with acetaminophen. Group 4, Long Photoperiod (LP) (16:8, light on from 05:00hr to 21:00hr) treated with acetaminophen. At the end of the 6th week, rats in groups 2, 3 and 4 were administered oral 2g/kg of PCM solution, while the rats in the control group were administered saline by way of gastric catheter. 24 hours after PCM administration, the rats were sacrificed by cervical dislocation and blood was collected for liver enzymes estimation and liver tissues were collected and homogenised for estimation of lipid peroxidation. The estimated parameters were aspartate aminotransferase (AST), alanine aminotransferase (ALT), alkaline phosphatase (ALP), gamma glutamate transpeptidase (GGTP) and malondialdehyde (MDA) as an index of lipid peroxidation.

Administration of PCM caused a significant ($P<0.001$) elevation of liver enzymes (AST, ALT, ALP and GGTP) level and lipid peroxidation marker, malondialdehyde (MDA) in all the treated groups (groups 1, 2 and 3) when compared to the control (group 1) (See Table 1). However, there was a significant ($P<0.01$) decrease in the serum levels of the liver enzymes concentration and MDA in the group 4 (SP group) compared to the rats in groups 2 and 3. It was concluded that the short day photoperiod has hepatoprotective effect and this could be due to its inhibitory effect on hepatic tissue lipid peroxidation.

Effect of Acetaminophen-Induced Hepatic Toxicity on Serum Liver Enzymes and Liver Tissue Malondialdehyde in Rats

Group	AST (U/L)	ALT (U/L)	GGT (U/L)	ALP (U/L)	MDA (mmol/mg protein)
Group 1	34.5±2.6	72.3±4.3	22.3±4.3	157.6±6.9	172.3±3.3
Group 2	205.7±8.6**	356.7±12.4**	79.1±5.2**	313.9±14.5**	356.7±4.3**
Group 3	201.6±6.7**	361.6±11.8**	64.4±6.4**	327.2±14.2**	348.5±4.6**
Group 4	136.5±8.4*	277.5±7.4*	37.2±4.8*	267.6±9.5*	291.8±3.7*

Values are means ± S.E.M., compared by ANOVA

*p<0.05, **p<0.001

Bilbo SD et al. (2002). PNAS 99:4067-4072

Pandi-Perumal SR et al. FEBS Journal 273:2813-2838.

Sinclair JA and Lochmiller RL (2000). J Can Zool 78:254-264.

Where applicable, the authors confirm that the experiments described here conform with The Physiological Society ethical requirements.

PCD298

Protective effects of cumin essential oil and a probiotic bacterial strain against cadmium hepatotoxicity in rats

L.S. El Hosseiny[1], F.M. El-Demerdash[2], H.H. Baghdadi[3] and M. El-Shenawy[4]

[1]Environmental Studies, Alexandria University, Institute of Graduate Studies and Research, Alexandria, Egypt, [2]Environmental Studies, Alexandria University, Institute of Graduate Studies and Research, Alexandria, Egypt, [3]Environmental Studies, Alexandria University, Institute of Graduate Studies and Research, Alexandria, Egypt and [4]Environmental Studies, Alexandria University, Institute of Graduate Studies and Research, Alexandria, Egypt

Heavy metals are ranked among the top 10 of the most 275 most hazardous substances in the environment on the current Priority List of Hazardous substances for the Agency for Toxic Substances and Disease Registry (ATSDR). Of all toxic heavy metals, cadmium ranks the highest in terms of damage to human health. Although, there are many studies which have established the toxic effects of cadmium on biological systems, the mechanism of cadmium detoxification and novel detoxifying agents are still under considerable debate and discussion. Accordingly, the present study aimed at investigating the role of a probiotic bacterial strain and cumin essential oil on the hepatotoxic effects induced by cadmium in experimental rats. Seventy male albino rats were used and were handled in accordance with the principles of laboratory animal care as contained in NIH guide for laboratory animal welfare. The rats were assigned into 7 groups of 10 rats each and were orally administered with cadmium chloride (5 mg/Kg BW), cumin essential oil (0.125 mg/Kg BW) and live culture of Lactobacillus bulgaricus (ca 107 cfu) singly or jointly for a period of 30 days. Following the exposure period blood and liver were collected for biochemical and histological analyses. The in vivo exposure of rats to cadmium induced an array of hepatotoxic effects at both the biochemical and histological levels, which ranged from biochemical irregularities in total protein, albumin, globulin and bilirubin levels to structural changes as manifested by elevations in hepatocellular injury biomarkers (aminotransferases, LDH and AlP) and hepatohistological alterations indicative of necrotic and inflammatory lesions. Moreover, an oxidative stress status was evidenced in liver tissue of rats as inferred by escalation in lipid peroxidation and depletion in antioxidant defense parameters including both non-enzymatic and enzymatic antioxidants (GSH content, GST, CAT and SOD). Cumin essential oil and the probiotic bacterial strain alleviated the hepatic dysfunction associating cadmium toxicity as inferred by the restorative effect on hypoproteinemia, hypoglobulinemia, hypoalbuminemia and hyperbilirubinemia. Structurally they restored hepatocellular injury biomarkers to normal or near normal levels and restored their activities both at the tissue and serum levels. Moreover, they preserved the hepatic histological architecture where the hepatic lesions associating cadmium toxicity were alleviated by their single or joint administration. They also combated the oxidative stress status induced by cadmium in liver tissue. Conclusively, both cumin and Lactobacillus exhibited beneficial effects against the physiological threats posed by cadmium and they hold health promoting effects at the biochemical and histological levels.

ATSDR. (2007). Agency for Toxic Substances and Disease Registry."CERCLA Priority List of Hazardous Substances".

John, R., Ahmad, P., Gadgil, K. and Sharma, S. (2008). Effect of cadmium and lead on growth, biochemical parameters and uptake in Lemna polyrrhiza L. Plant Soil Environ., 54: 262–270.

Matović, V., Buha, A., Bulat, Z. and Dukić-Ćosić, D. (2011). Cadmium toxicity revisited: focus on oxidative stress induction and interactions with zinc and magnesium. Arh. Hig. Rada. Toksikol., 62:65-76.

Koyu, A., Gokcimen, A., Ozguner, F., Bayram, D.S. and Kocak, A. (2006). Evaluation of the effects of cadmium on rat liver. Mol. Cell Biochem., 284:81-85.

Liu, J., Qu, W. and Kadiiska, M.B. (2009). Role of oxidative stress in cadmium toxicity and carcinogenesis. Toxicol. Appl. Pharmacol., 238:209-214.

Where applicable, the authors confirm that the experiments described here conform with The Physiological Society ethical requirements.

PCD299

Antioxidative and hepatoprotective effect of beta carotene on acetaminophen induced liver damage in rats

O.T. Oyelowo[1], A. Morakinyo[2], B. Iranloye[3] and J. Nnaji[4]

[1]Physiology, University of Lagos, Lagos, Nigeria, Lagos, Nigeria, [2]Department of Physiology, University of Lagos, Lagos, Nigeria, [3]Department of Physiology, University of Lagos, Lagos, Nigeria and [4]Department of Physiology, University of Lagos, Lagos, Nigeria

Acetaminophen (APAP) or paracetamol is a widely prescribed analgesic and antipyretic drug either as a single compound or in combination with other medications (Kaplowitz 2004). Excessive use of APAP can damage the liver and if not treated, overdose can lead to liver failure (Larson et al 2005). Beta carotene (BC) is an example of carotenoids and is the major precursor of Vitamin A with immune and antioxidant properties. The role of oxidative stress on hepatic damage caused by acetaminophen (APAP) and the possible protective effects of BC supplement against this damage were investigated. Wistar rats were randomly divided into four groups: control, APAP, BC and APAP+ BC. The control group received distilled water while APAP (750 mg/kg body weight), BC (10 mg/kg/day body weight) were administered to the other groups accordingly. Treatments were administered orally via gavage and lasted for seven consecutive days. Twenty four hours after the last drug administra¬tion, the animals were anaesthetized with diethyl ether and blood was collected from each rat and prepared serum samples were thereafter used for biochemical analy¬sis. The liver from each rat was carefully collected and weighed. They were homogenized with phosphate buffer and used for oxidative analysis. SOD activ¬ity was determined (epinephrine in 0.005 N HCl). CAT (determined by measuring the exponential dis¬appearance of H2O2) and GSH (Ellman's reagent) activities were determined. Lipid peroxidation was also analyzed by the forma¬tion of malondialdehyde (MDA).The serum levels of SGPT, SGOT, and SAP were determined using an automatic enzyme analyzer (Beckman, California, USA). Values are mean ± SEM, compared with ANOVA to show significant differences among groups, Tukey's post hoc test was used to determine specific pairs of groups that were statistically different (GraphPad Software, USA).The serum glutamate oxalate transaminase (SGOT) level of the APAP group was significantly increased compared to the control (272.27 ±18.77 vs 197.75 ± 28.20). An increase was also observed in the serum glutamic pyruvate transaminase (SGPT) (82.80±8.91vs 58.40 ±5.76) as well as the serum alkaline phosphatase (SAP) levels of (177.60±19.53 vs 169.80±13.83; $p<0.01$). These increased levels were ameliorated by the administration of β-carotene. The

SOD, GSH and CAT levels of the APAP groups which were significantly decreased (P<0.001) when compared to the control had a boost in the antioxidant level after the application of BC. SOD level was (APAP vs APAP+ BC; 35±1.50 vs 80± 4.05); GSH (APAP vs APAP+ BC; 40±2.75 vs 70± 5.65); CAT levels (APAP vs APAP+ BC; 300±10.50 vs 460± 12.65). The reverse was the case in the MDA activity (APAP vs APAP+ BC; 15±0.5 vs 10± 0.7). The study showed that BC ameliorates the damaging effect of acetaminophen on liver tissues.

Kaplowitz N (2004). Acetaminophen hepatotoxicity: what do we know, what don't we know, and what do we do next? Hepatology, 4(1): 23-26

Larson AM, Polson J, Fontana RJ, Davern TJ, Lalani E, Hynan LS., Reisch JS., SchiØdt FV., Ostapowicz G, Shakil AO, Lee WM., and the Acute Liver Failure Study Group (2005). Acetaminophen-Induced Acute Liver Failure: Results of a United States Multicenter, Prospective Study. Hepatology, 42:1364-1372

Where applicable, the authors confirm that the experiments described here conform with The Physiological Society ethical requirements.

PCD300

Assessment of coal tar creosote toxicity in rat liver: role of rosemary

E.A. Abbady[1], F.M. El-Demerdash[2] and H.H. Baghdadi[3]

[1]Environmental Studies, Institute of Graduate Studies and Research, Alexandria University, Alexandria, Egypt, [2]Environmental Studies, Alexandrria University, Institute of Graduate Studies and Research, Alexandria, Egypt and [3]Environmental Studies, Alexandrria University, Institute of Graduate Studies and Research, Alexandria, Egypt

Coal tar is a significant product generated from coal pyrolysis. Coal tar can be utilized as raw materials for various industries such as synthetic fiber, dyestuff, medication, coating and national defense. It is also a type of raw materials from which phenols, naphthalenes and anthracene can be extracted for the production of washing oil, cementitious agents, antiseptic agents, and catalytic hydrogenated to produce gasoline, diesel oil, etc. Therefore, the present study was designed to investigate the possibility of coal tar creosote to induce oxidative stress and biochemical perturbations in rat liver and the role of rosemary in ameliorating its toxic effects. Male Wister Albino rats were randomly divided into four groups of 10 each, group I served as control; group II treated with rosemary (10 ml of extract/kg BW for 21 days), group III received coal tar creosote (200 mg/4ml olive oil/kg BW for 3 days) and group IV treated with both rosemary and coal tar creosote. The local committee approved the design of the experiments, and the protocol conforms to the guidelines of the National Institutes of Health (NIH). The administration of coal tar creosote significantly caused elevation in lipid peroxidation (LPO) and reduction in the activities of superoxide dismutase (SOD), catalase (CAT) and glutathione S-transferase (GST). A significant decrease in reduced glutathione (GSH) content was also observed. Liver aminotransferases (AST and ALT) and alkaline phosphatase (AlP) were significantly decreased while lactate dehydrogenase (LDH) was increased. Rosemary treatment to coal tar creosote treated rat decreased LPO level and normalized SOD, CAT and GST activities, while GSH content was increased. Also, liver AST, ALT, AlP and LDH were maintained near normal level due to rosemary treatment. In conclusion, Rosemary has beneficial effects and could be able to antagonize coal tar creosote toxicity.

Al-Sereiti, M.R.; Abu-Amer, K. M.; Sen, P. (1999). Pharmacology of rosemary

(Rosmarinus officinalis Linn.) and its therapeutic potentials. Indian Journal Experimental Biology, 37, 124-130.

Bozin, B.; Mimica-Dukic, N.; Samojlik, I.; Jovin, E. (2007). Antimicrobial and

antioxidant properties of rosemary and sage (Rosmarinus officinalis L. and

Salvia officinalis L., Lamiaceae) essential oils. Journal Agriculture and Food

Chemistry, 55, 7879-7885.

Gachkar, L.; Yadegari, D.; Rezaei, M. B.; Taghizadeh, M.; Astaneh, S. A.; Rasooli, I.

(2007). Chemical and biological characteristics of Cuminum cyminum and

Rosmarinus officinalis essential oils. Food Chemistry, 102, 898-904.

Agency for Toxic Substances and Diseases (ATSDR). (2002). Toxicological profile for WOOD CREOSOTE, COAL TAR CREOSOTE, COAL TAR,COAL TAR PITCH, AND COAL TAR PITCH VOLATILES.

Druzhinin, V.G et al. 2000. Cytogenic disorders in workers of coal-tar chemical industry. Medistina Truda i Promyschlennaya Ekologiya 10:22-23.

Where applicable, the authors confirm that the experiments described here conform with The Physiological Society ethical requirements.

PCD301

The role of the anti-inflammatory cholinergic pathway in the pathogenesis of a rat model of acute colitis

M. Kolgazi[1], U. Uslu[2], M. Yuksel[3], A. Velioglu-Ogunc[3], F. Ercan[4] and I. Alican[1]

[1]Department of Physiology, Marmara University School of Medicine, Istanbul, Turkey, [2]Department of Histology and Embryology, Yeditepe University School of Medicine, Istanbul, Turkey, [3]Marmara University Vocational School of Health Related Professions, Istanbul, Turkey and [4]Department of Histology and Embryology, Marmara University School of Medicine, Istanbul, Turkey

Introduction: Intense local immune response, associated with recruitment and activation of lymphocytes and macrophages, and subsequent release of cytokines and other inflammatory mediators all cause tissue damage and contribute to many of the clinical features of colonic inflammation. The cholinergic anti-inflammatory pathway is a neuro-immune mechanism that regulates innate immune function and controls inflammation. The functional activity of this pathway can be modulated through its neuronal and non-neuronal (α7nACh receptors) cholinergic components. Objective: To explore the role of cholinergic anti-inflammatory pathway in acetic acid-induced acute colitis in rats. Materials and Methods: The colonic inflammation was induced in Sprague-Dawley rats (200-250 g; n=8/group) by intrarectal administration of 0.8 ml of 5% (v/v) acetic acid in 0.9% NaCl. The control rats received same volume of isotonic saline by the same route. The treatment groups were treated with either a natural acetylcholinesterase inhibitor huperzine A (HUP; 0.1 mg/kg) or a cholinergic agonist nicotine (NIC; 1 mg/kg) intraperitoneally. Drugs were given 5 min after induction of colitis and continued for 3 consecutive days. On the fourth day all rats were decapitated. The distal colon was scored and stored for the measurement of malondialdehyde (MDA) and glutathione (GSH) levels, and myeloperoxidase (MPO) activity. The presence of NFκB in colon was also

examined. Formation of reactive oxygen species in colons was monitored by chemiluminescence (CL) method. Trunk blood was collected for the assessment of serum tumor necrosis factor (TNF-α) interleukin (IL)-1β and IL-10 levels. Results: The extent of colonic lesions in colitis group was reduced by HUP and NIC macroscopically ($p<0.05$), the microscopic score was only reduced by HUP treatment ($p<0.05$). Increased NFκB content in colitis group was reduced by HUP and NIC. Increase in colonic lipid peroxidation and lucigenin-enhanced CL in rats with colitis were attenuated by HUP ($p<0.01$). Stimulation of MPO activity in colitis group was attenuated by NIC ($p<0.05$). Increased serum TNF-α and IL-1β levels in colitis group were prevented by HUP ($p<0.001$ and $p<0.05$, respectively). Serum IL-10 level of the colitis and control groups was not significantly different but was increased by both NIC and HUP. Tissue GSH content did not differ among groups. Monitorization of body weigths during the course of study demonstrated a significant reduction in colitis rats which was reversed by NIC ($p<0.05$). Conclusion: Inhibition of AChE or treatment with a cholinergic agonist is beneficial on inflammatory parameters in a rat model of acute colitis. This supports the potential role of anti-inflammatory cholinergic pathway in the treatment of colonic inflammation.

The authors are grateful to Bayindir Hospital Group for the financial support of this work.

Where applicable, the authors confirm that the experiments described here conform with The Physiological Society ethical requirements.

PCD302

Treating overweight/obesity using alginate enriched bread

D. Houghton[1], M. Wilcox[1], I. Brownlee[2], C. Seal[3] and J. Pearson[1]

[1]Institure for Cellular and Molecular Bioscience, Newcastle University, Newcastle Upon Tyne, Tyne and Wear, UK, [2]Food and Human Nutrition Department, Nanyang Polytechnic, Ang Mo Kio, Singapore and [3]Human Nutrition Research Centre, Newcastle University, Newcastle Upon Tyne, Tyne and Wear, UK

Background and Objectives. Obesity is a rapidly growing medical issue worldwide, and is fast becoming one of the leading causes of mortality. Data from our laboratory have demonstrated that alginates have the ability to inhibit pancreatic lipase activity in-vitro, and may therefore reduce the fat absorbed in the diet [1-3]. This project has developed a bread vehicle designed by Greggs PLC that incorporates alginate and may be used in foods that people are already consuming in a "health by stealth" manner in the battle against obesity. In an acceptability study with 40 participants there were no adverse side effects with either bread, and participants preferred the alginate bread compared to the control bread. The purpose of the present study was to assess the ability of alginate enriched bread to inhibit fat digestion in-vitro and in-vivo. Method. Control bread (CB) and alginate enriched bread (AB) were used in the current study. In-vivo: data presented is preliminary data from a double blind crossover study conducted using ileostomy patients (n=13). Participants consumed a calorific set meal the night before and were then fasted for 12h. Upon arrival participants consumed either 105g CB or AB as toast which included 20g of butter. Blood samples were taken at baseline, immediately post eating and then every 30 minutes for 5 hours, and placed on ice until analysis. Free glycerol and total triglycerides was measured in plasma to assess fat digestion. In-vitro: three fat substrates (Trioctanoate, Trioleate and Tributyrate) were digested in an open model gut system developed within this laboratory, which replicates digestion in the mouth, stomach and small intestines. 500μl of each substrate was added alone or with 5.2g AB or CB (n=9) at 0 minutes. A 1ml sample was then taken at 180 minutes for each sample. Free glycerol was measured to assess fat digestion. A t-test was used to compare CB and AB with normal substrate digestion in the model gut, and to compare total triglycerides in plasma between CB and AB at various time points in ileostomy patients. Data presented as mean ± standard error of the mean (SEM). Results. Preliminary data from ileostomy plasma samples indicated a reduction in the total triglycerides in the plasma ranging from 9-34% from 0-5h compared with the control bread, with a significant difference at 210 minutes ($p>.05$). In the model gut at 180 minutes there was a significant reduction in fat digestion of 47.7% (1.2), 32.5% (2.4) and 51.1% (1.3) for trioctanoate ($p>.05$), tributyrate ($p>.05$) and trioleate ($p>.05$) respectively. Conclusion. This study has the potential to provide evidence that normal foods supplemented with alginate can be used to treat obesity/overweight and could be utilised by the food industry. Further recruitment is required to acquire a larger group of ileostomy patients and to analyse the ileum effluent fluid to determine levels of undigested fat.

STRUGALA, V., KENNINGTON, E. J., CAMPBELL, R. J., SKJAK-BRAEK, G. & DETTMAR, P. W. 2005. Inhibition of pepsin activity by alginates in vitro and the effect of epimerization. International Journal of Pharmaceutics, 304, 40-50.

SUNDERLAND, A. M., DETTMAR, P. W. & PEARSON, J. P. 2000. Alginates inhibit pepsin activity in vitro; A justification for their use in gastro-oesophageal reflux disease (GORD). Gastroenterology., 118.

WILCOX, M. 2011. Bioactive Alginates. Degree of Doctor of Philosophy, Newcastle University

Where applicable, the authors confirm that the experiments described here conform with The Physiological Society ethical requirements.

PCD303

Intestinal handling of glucose in rats treated with Kolaviron (A biflavonoid of Garcinia Kola seed)

S.B. Olaleye and O.A. Odukanmi

Physiology, University of Ibadan, Ibadan, Nigeria

Kolaviron (KV) a fraction of Garcinia kola has been found to have hypoglycemic effect on glucose metabolism. The mechanism of its hypoglycemic effect was investigated. KV was isolated according to Iwu et al(1990).The study was executed in three phases. Phase I was conducted to investigate the effect of KV on blood glucose concentration in rats (male, 180-200mg), n=,6) fasted for 18 hours while phase II and IIIwere to investigate the route(s) of glucose utilization in KV treated rats via the artero-venous (A-V) and intestinal glucose absorption where 10-20 cm long segments of the jejunum and ileum were used respectively. The rats (male, 180-200mg) were grouped into four groups of six animals each. Group I represented the control(treated with ?saline) while group II, III and IV were treated with 50mg, 100mg and 200mg of KV per kilogrammme body weight respectively via oral administration using a metal feeding canular. The rats were anaestesized in phases II and III with urethane (0.6ml/ 100mg body weight) given subcutaneously prior to laparotomy. Values bare represented as Mean+/- S.E.M., compared by one way analysis of variance and unpaired Student's 't ' test. Results from phase I showed significant decrease in blood glucose concentration from the various treated groups after 4 hours of administra-

tion, (Control= 69.00+/-2.66 mg/dl, KV 50mg/kg= 64.33+/-2.40mg/dl, KV 100mg/kg= 59.83+/-2.48 mg/dl and KV200mg/kg= 54.00+/-2.82mg/dl) . The A-V study revealed a 13.7%, 36. 99% and 47.94% decrease in blood glucose concentration in the KV50, KV 100 and KV 200 mg /kg groups respectively compared to the control group after 3 hours of administration of KV. The jejunum and ileum glucose absorption significantly increased in all the treated groups compared bro the control animals after 40 minutes of infusion, P<0.05. KV possibly exerts its reported profound hypoglycemic effects through the increased glucose extractions by intestinal cells. More work is required to determine the possible role of insulin and counter- regulatory glucose hormones in mediating the hypoglycemic effect reported.

Blood glucose concentration in rats treated with Kolaviron

Treatment	0 hour	1hour	4hour
Control	70.83+/-2.54	70.67+/-2.25	69.00+/-2.66
KV50	69.67+/-3.04	67.50+/-2.91	64.83+/-2.40*
KV100	70.50+/-2.31	65.83+/-2.34	59.83+/-2.48 *
KV200	69.17+/-2.12	64.67+/-1.84	54.00+/-2.46 *

The values are the blood glucose concentration(mean+/-SEM) mg/dl

n= 6

Values considered significant at P<0.05

* significant at P<0.05

Adaramoye O.A. and Adeyemi E.O. (2006). Hypoglycemic and hypolipidemic effect of fractions from kolaviron, a biflavonoid complex from Garcinia kola in Streptozocin-induced diabetes mellitus in rats. Journal of Pharmacy and Pharmacology 58, 121-8.

Farombi E.O, Tahnteng J. G., Agboola A.O., Nwankwo J.O. and Emerolle G.O. (2000): Chemo prevention of 2-acetylation fluorine-induced heoatotoxicity and lipid peroxidation in rats by Kolaviron- A Garcinia kola seed extract. Food and Chemical Toxicology 38, 535-41

Where applicable, the authors confirm that the experiments described here conform with The Physiological Society ethical requirements.

PCD304

Effects of different sweeteners on gastric emptying, incretins release and glucose homeostasis in healthy humans

R.M. Pereira[1], M. Secaf[2] and R.B. de Oliveira[1,2]

[1]Department of Physiology, School of Medicine of Ribeirão Preto, University of São Paulo, Ribeirão Preto, São Paulo, Brazil and [2]Department of Internal Medicine, School of Medicine of Ribeirão Preto, University of São Paulo, Ribeirão Preto, São Paulo, Brazil

The global rises in the prevalence of obesity, diabetes mellitus and associated diseases, led to an increase of sweeteners consumption around the world. The presence of nutrients in the small intestine plays important roles in appetite regulation, blood glucose (BG) and gastric emptying (GE). These regulatory roles are mediated by peptides called incretins, such as glucagon-like peptide 1 (GLP-1) and glucose-dependent insulinotropic polypeptide (GIP). The release of these peptides is stimulated mainly by nutrients, whereas the effects of sweeteners, in vivo, on incretins release are not well established. Objective: To determine the effects of addition of sucrose, sorbitol, sucralose or stevia on a standard liquid test meal, on GE, on glucose homeostasis (BG and plasma insulin), as well as on GIP and GLP-1 release in humans. Design: Eleven male healthy volunteers were studied on 4 separate occasions. GE of a caloric test meal (205 kcal), containing technetium (99mTc), were determined by abdominal scintigraphy. Fifteen grams of sucrose, sorbitol, sucralose or stevia were added to the test meal, one each occasion. The GE of test meal was measured by T1/2. Blood glucose, plasma insulin and incretins were determined at t = -10 (fasting), 0, 5, 10, 15, 30, 45, 60, 90 and 120 min after the meal ingestion using a glucometer and specific immunoassay kits. Results: GE of a standard test meal prepared with sucrose was faster than when sorbitol or sucralose were added. The addition of sucrose or sweeteners in the standard meal, did not cause significant difference of BG. The insulin concentrations were significantly raised after the ingestion of sucrose as compared with sorbitol or stevia.The addition of sucrose, sorbitol, sucralose and stevia increased the GLP-1 plasma concentration equally. This increase was different, between sucrose and sucralose, only 120 min after the meal ingestion. Regarding GIP, the meal prepared with sucrose was able to increase its concentration compared with the different sweeteners. Conclusions: Our results showed that the consumption of sweeteners like sorbitol or sucralose, added in a balanced test meal (composed by carbohydrates, protein and lipids), were able to delay the GE. Moreover, the consumption of these substances added in a balanced meal, did not change the incretins release as well as the glucose homeostasis in healthy humans.

Supported by FAPESP, CAPES and CNPq.

Where applicable, the authors confirm that the experiments described here conform with The Physiological Society ethical requirements.

PCD305

Metabolic response of growing rats fed fructose from two dietary supplements

A. Ajibola[1,3], J.P. Chamunorwa[2] and K.H. Erlwanger[3]

[1]Vet Physiology & Pharmacology, University of Ilorin, Ilorin, Kwara, Nigeria, [2]Vet Anatomy & Physiology, University of Pretoria, Pretoria, Gauteng, South Africa and [3]School of Physiology, University of the Witwatersrand, Johannesburg, Gauteng, South Africa

Metabolic syndrome (MetS) is the coexistence of obesity, hyperglycaemia, hypertension and dyslipidaemia in an individual (1). The modern human diet contains high fructose level (2), which is culpable in the pathogenesis of MetS in adults (1) and children (3). We investigated the effects of two dietary sources of fructose, natural honey (NH) and cane syrup (GS) on metabolism in growing rat models (Rattus norvegicus) fed from neonatal age. Fifty-nine suckling (7-day old male (18.1±0.78g) and female (17.7±0.63g) rats were divided into five groups, namely NH Low (NHL); NH High (NHH); GS Low (GSL); GS High (GSH); and control (CRF), with replication on gender basis (n=6, except NHH female with 5rats). The rats were fed either NH or GS at low (10ml kg-1 b.wt) or high (20ml kg-1 b.wt) dose daily via stomach tube for 14 days, while the CRF was gavaged with distilled water. On weaning, NH or GS was mixed with rat feed as low (20%) or high, 50% (volume/weight, v/w) supplement, while tap water (20% v/w) was added to the control diet. The rats were euthanized at 13 weeks old to obtain visceral measurements, general health indices and growth parameters. Values are mean ± S.E.M., compared by ANOVA. NHL caused normal body weight gain (498.67±11.51g) as control (475.00±8.92g) in males, but significantly ($p<0.01$) higher than NHH, 407.17±9.75g; GSL, 426.17±9.04g, and GSH, 416.00±6.61g respectively. There was

significant (p<0.05) increase in males' long bone weight and length while there was no difference (p>0.05) in linear growth among the female rats. Dietary cane syrup significantly (p<0.0001) increased the absolute and relative weights of abdominal visceral fat (GSL, 17.70±0.73g, 3.75±0.14%; GSH, 15.48±0.85g, 3.64±0.14%) vs. NHL, 11.11±0.37g, 2.39±0.07%; NHH, 10.21±1.04g, 2.48±0.21%; and CRF, 8.56±0.50g, 1.97±0.13% in males. GS-fed males had significantly (p<0.05) increased liver weight (GSL, 14.23±0.56g; GSH, 12.57±0.30g) vs. NHL, 10.92±0.32g; NHH, 10.24±0.40g; and CRF, 11.16±0.34g. The increased visceral fat and hepatomegaly were neither observed in the NH-fed nor the female rats. The surrogate markers of liver function were normal in the NH males, unlike GS-fed male rats with significantly (p<0.05) increased AST (GSL, 75.5±4.56U/L; GSH, 86.7±8.15U/L; NHL, 58.2±4.19U/L; NHH, 69.9±2.88U/L; CRF, 67.2±2.19U/L) and ALT (GSL, 43.5±9.57U/L; GSH, 32.8±8.68U/L; NHL, 27.5±3.13U/L; NHH, 25.8±2.87U/L; CRF, 28.5±2.46U/L). The rats fed GS diets were predisposed to developing diet-induced MetS. Unlike cane syrup, feeding rats NH from an early age neither caused susceptibility to MetS, nor compromised their health status, despite the similar fructose content of NH and GS. The good metabolic health of the NH-fed rats could be due to micronutrients, antioxidants and phytochemical constituents of NH (4, 5). There are definitely nutritional and health benefits in substituting honey for refined sugars.

Ford ES & Giles WH (2003). Diabetes Care 26, 575-581.

Melanson KJ et al. (2007). Nutrition 23, 103-112.

Birch LL et al. (1989). Physiol Behavior 45, 387-395.

Ajibola A et al. (2007). J Biol Sci Res 2, 67-69.

Ajibola A et al. (2012). Nutr Metab (Lond) 9, 61.

Where applicable, the authors confirm that the experiments described here conform with The Physiological Society ethical requirements.

PCD306

Novel insights in the cross-talk of Pparα and Pparγ with the Hedgehog-Signaling Pathway

K. Arnold[1], M. Matz-Soja[1], E. Marbach[1], W. Schmidt-Heck[2], R. Guthke[2] and R. Gebhardt[1]

[1]Faculty of Medicine, Institut of Biochemistry, Leipzig, Germany and [2]Leibniz Institue for Natural Product Research and Infection Biology, Hans-Knöll Institute, Jena, Germany

As the biggest metabolic organ the liver possesses a variety of functions, including carbohydrate and lipid metabolism. The smallest functional unit thereby is displayed by the liver lobules showing a metabolic zonation. Hepatocytes can be roughly divided in periportal (PP) and pericentral (PC) cells. Numerous genes and enzymes are involved in the regulation processes of the metabolism; especially nuclear receptors like Ppars possess a coordinating role for many physiological functions. While Pparα promotes fatty acid oxidation and, thus, is controlling lipid catabolism, Pparγ promotes the storage of lipids. Transcription factors like Ppars also interact with morphogenic pathways. One example is the hedgehog (HH) signaling pathway, which is crucial for embryogenesis and organogenesis. Recent investigations showed that this pathway also plays a critical role in adult organs such as the liver but molecular mechanisms are not well characterized. Our aim was to investigate the interactions between Ppars and Gli-transcriptiption factors (TF).

C57Bl6/N mice (12 week, ♂, 20-25 g) were used to and maintained under controlled conditions (const. 12:12h LD cycle). Mice were anaesthetized with a mixture of atropine (0.1mg/kg), ketamine (100mg/kg) and rompune (5mg/kg). To examine hepatic gene expression, RNA was extracted from whole liver lysates or hepatocytes which were isolated by using collagenase perfusion technique. To receive PP and PC hepatocytes a digitonin-collagenase perfusion was performed. To investigate the functions of Pparα/γ as well as of Gli1/2/3, siRNA-mediated in vitro knockdown (KD) of those genes was performed. Alterations in gene expression of HH signaling components and lipid metabolism target genes were determined by using micro-arrays and qRT-PCR. Values are means ± S.E.M. normalized to β-actin as housekeeping gene, compared by MWUtest.

mRNA expression profiles showed a heterogeneously distribution of Pparα/γ. Pparγ is localized pericentral (PC:1±0.26 vs PP:0.17±0.12,p<0.05; n=3-4), whereas for Pparα no preferential zonated localization could be determined. Transcriptome analyses revealed that a wide variety of genes like genes for biological processes (e.g. ion transports, cell cycle) are effected by Pparγ-KD (n=3). Pparγ-KD also results in downregulation of all 3 Gli-TFs (e.g. Gli1: 0.55±0.13,p<0.05; Gli2:0.42±0.14,p<0.01; Gli3:0.05±0.03,p<0.05; n=7-8). Gli1/2/3-KD showed effects on Ppar-gene expression. Both Ppar heterologous are significantly upregulated in response to Gli3-KD (Pparα: 2.62±0.61, p<0.05; Pparγ: 1.66±0.31, p<0.05; n=4-6).

KD-experiments of Ppars and Gli-TFs and their related mRNA expression profiles indicate a putative mutual interaction between these nuclear receptors and HH signaling forming a negative feedback loop. Future experiments should investigate molecular details of this interaction.

Gebhardt,R.; Hovhannisyan,A.: Organ Patterning in the Adult Stage, Dev.Dyn,239:45-55(2010)

Yessoufou,A.; Wahli,W.: Multifaceted roles of peroxisome proliferator-activated receptors at the cellular and whole organism levels,Swiss Med Wkly,140:w13071(2010)

Where applicable, the authors confirm that the experiments described here conform with The Physiological Society ethical requirements.

PCD307

HEDGEHOG AROUND THE CLOCK: Mutual interaction between circadian rhythms of hepatic lipid metabolism and hedgehog morphogen pathway

E. Marbach[1], M. Matz-Soja[1], K. Arnold[1], W. Schmidt-Heck[2], R. Guthke[2] and R. Gebhardt[1]

[1]Institute of Biochemistry, Faculty of Medicine, Leipzig University, Leipzig, Germany and [2]Leibniz Institute for Natural Product Research and Infection Biology – Hans-Knöll-Institute, Jena, Germany

Entrained and reset by external cues, the circadian clock controls physiological processes, including liver metabolism. At the cellular level the clock is characterised by core clock genes, which modulate the fluctuating expression of central metabolic genes as transcription factors. Being an extensive biological process, the clock is linked to the elements of cell cycle control and intracellular signalling pathways. Recent analyses identified the liver clock also to be associated with the hedgehog (HH)-signalling, an evolutionary conserved cascade functioning as crucial modulator of embryogenesis and tissue dif-

ferentiation. Although there is an evidence of its role in adult liver, no exact mechanisms are known.
Our aim was, therefore, to analyse the liver specific interaction of the HH-signalling and the circadian clock, using the transgenic knock-out mice, displaying a hepatocyte specific deletion of Smo (Smo-KO), an essential transducer within the HH-signalling. Mice (male, 10-12 weeks, 19-25g) were maintained under controlled conditions (12:12 h LD-cycle, fed ad libitum) and at different time-points, animals were anesthetised with a mixture of ketamine (100mg/kg), rompune (5 mg/kg) and atropine (0.1 mg/kg). Further, the RNA was extracted either from whole livers or collagenase-perfused isolated hepatocytes. We performed gene microarray analyses, comparing KO- mice and their WT-littermates, considering the different circadian time-points of hepatocyte isolation. The data were classified according to the GO clusters and evaluated using the ANOVA statistical analyses. Generally, due to hepatic Smo deletion the results show strong alterations in the circadian expression levels of genes involved in metabolic and transport processes (e.g. Smo-WT:179 vs. Smo-KO:234 genes are up-regulated, n=3/genotype). However, these alterations seem not to provide a significant effect on the global scale (P=0.175). In contrast, especially the circadian rhythm of the lipid metabolism is significantly affected by inactive HH-pathway (e.g. Smo-WT:39 vs. Smo-KO:30 genes are up-regulated, whereby only 17 genes are common for both genotypes, P=0.001).
Verified by qRT-PCR analyses, some core clock genes exhibit strong alterations in their expression due to Smo-KO (e.g. level of Per3 is elevated at 09:00 to a factor 2.7±0.5, P=0.007; Per1 - to a factor 1.7± 0.2, P=0.5; n=6-10; values are means ±S.E.M.). A putative transcription factor binding site prediction, generated using Fantom4 database, allows us to conclude that in adult liver the HH signalling seems to be closely related to the circadian clock and, thus, might be involved in the regulation of the rhythmicity of lipid metabolic processes. However, the precise function of HH-signalling within the clock regulatory circuit still has to be evaluated, requiring further investigations.

Where applicable, the authors confirm that the experiments described here conform with The Physiological Society ethical requirements.

PCD309

Impairment of cerebrovascular reactivity is proportional to degree of insulin resistance in patients with type 2 diabetes

A. Jaryal[1], K. Prakash[1], D.S. Chandran[1], R. Khadgawat[2] and K. Deepak[1]

[1]Physiology, All India Institute of Medical Sciences, New Delhi, India and [2]Endocrinology, All India Institute of Medical Sciences, New Delhi, India

Increased risk of cerebrovascular diseases in type 2 diabetes mellitus is associated with impaired cerebrovascular reactivity (CVR) as well as the degree of insulin resistance. Recent studies in healthy human subjects have shown that CVR measured in response to hypercapneic stimulus is associated with significant rise in arterial blood pressure (ABP) and hence must be corrected for associated changes in ABP (Claasen et al, 2007). The aim of the study was to investigate the relationship between CVR and insulin resistance in the patients of type 2 diabetes mellitus after correcting for the associated ABP changes during CVR assessment. The middle cerebral artery blood flow velocity (MCAV) was measured by transcranial ultrasound technique. The non-invasive beat-to-beat blood pressure was measured from finger using technique of Penaz. The CVR was assessed by measuring the changes in MCAV and cerebrovascular conductance (CVC, calculated as MCAV / mean ABP) after breathing of 6% CO2 for 2 minutes in 34 uncomplicated type 2 diabetic patients and after breath holding for 30 second. Insulin resistance was assessed by Homeostatic model assessment of insulin resistance (HOMA-IR). The HOMA-IR of the subjects was 3.88 ± 1.84 (mean ± S.D). On breathing 6% CO2, the mean ABP increased from baseline 87.68 ± 10.52 to 101.0 ± 14.32 mmHg ($p<0.0001$), the MCAV increased from baseline 45.76±10.02 to 66.94±18.11 cm/sec ($p<0.0001$) and CVC increased from baseline 0.527 ± 0.125 to 0.669 ± 0.182 cm/s/mmHg ($p<0.0001$). On breath holding, the ABP, MCAV and CVC increased significantly as compared to baseline (101.2 ± 19.06, $p<0.0001$; 61.13 ± 16.59, $p<0.0001$ and 0.621 ± 0.186, $p<0.0001$ respectively). During 6% CO2, both MCAV and CVC were significantly correlated with HOMA-IR ($r = -0.340$, $p = 0.0491$ and $r = -0.3749$, $p = 0.0289$, respectively). However, during breath holding MCAV did not significantly correlate with HOMA-IR ($r = -0.3406$, $p = 0.0799$) while the CVC was significantly correlated ($r = -0.3746$, $p= 0.0291$). In conclusion, hypercapneic stimulus given to assess the cerebrovascular reactivity causes substantial increase in the blood pressure. The increase in blood pressure can affect the MCAV during the tests and therefore it is better to measure CVC rather than MCAV to correct for blood pressure rise during these tests. The degree of impairment of CVR is associated with severity of Insulin resistance in uncomplicated type 2 diabetes mellitus.

Claassen JAHR et al (2007). J Appl Physiol 102: 870–877.

Where applicable, the authors confirm that the experiments described here conform with The Physiological Society ethical requirements.

PCD310

Rice bran proteins inhibit effects of angiotensin and oxidative stress in murine macrophage cells

V. Kukongviriyapan[1], K. Boonloh[1], P. Pannangpetch[1], B. Kongyingyoes[1], U. Kukongviriyapan[2] and S. Thawornchinsombut[3]

[1]Department of Pharmacology, Faculty of Medicine, Khon Kaen University, Khon Kaen, Thailand, [2]Department of Physiology, Faculty of Medicine, Khon Kaen University, Khon Kaen, Thailand and [3]Department of Food Technology, Faculty of Technology, Khon Kaen University, Khon Kaen, Thailand

Rice bran contains a number of compounds which have shown to present beneficial effects on cardiovascular system. The renin-angiotensin system is suggested to play roles in insulin resistance and cardiovascular diseases. Rice bran products have been reported to ameliorate type 2 diabetes. The protein fraction from rice bran is a rich source of valuable nutrition, however, there is only few reports on its effects on angiotensin system. Rice protein hydrolysates (RBP) were prepared from defatted Hom-Mali rice cultivated in the North-East region of Thailand with controlled enzymatic hydrolysis. Murine macrophage RAW 264.7 cells were cultured in DMEM media supplemented with 10% fetal bovine serum. Exposure of RAW 264.7 cells to angiotensin-I (ANG-I) and ANG-II resulted in stimulation of superoxide formation, as detected by lucigenin-enhanced chemiluminescent assay. RBP (20-400ug/mL) concentration-dependently suppressed the oxidant formation. The suppression effect may be in part due to the inhibition of angiotensin converting enzyme (ACE) activity, as shown by an

in vitro assay using rabbit ACE and specific substrate. Thus, RBP possesses ACE inhibiting activity and Since ANG may participate in inflammatory processes in diabetes and metabolic syndrome, nitric oxide formation was measured as a marker of induction of iNOS. Rice bran protein hydrolysates (100-800 ug/mL) showed to suppress ANG-I and ANG-II-induced nitric oxide generation. This study suggests that rice bran protein hydrolysates could suppress angiotensin-mediated oxidative stress and may provide beneficial effect as food supplement in diseases with oxidative stress conditions.

This work was supported by the Agricultural Research Development Agency, Thailand.

Where applicable, the authors confirm that the experiments described here conform with The Physiological Society ethical requirements.

PCD311

Non-genomic effect of 17 β estradiol in the endothelial domination role via nitric oxide in the aorta of guinea pig: study in HUVECs culture and bioassay

R. Ratnawati[1], M.A. Widodo[2] and N. Permatasari[2]

[1]Physiology, Brawijaya University, Malang, Jawa Timur, Indonesia and [2]Pharmacology, Brawijaya University, Malang, Jawa Timur, Indonesia

Background: There were some non-linier doses, low usefulness and disadvantages resulted from epidemiological studies using Estrogen Replacement therapy as prevention or active treatment in coronary Vascular Diseases. In vitro studies also showed that the increase of the dose of Estrogen used it was not increase the diameter of the vessels. Therefore the aim of this study was to elucidate the effect of 17 β Estradiol induce NO (nitric oxide) in endothelial dysfunction of HUVEC (human umbilical vein endothelial cell) culture, and also its effect in the denuded and intact aorta of guinea pig.
Method : This study used experimental design to observe the effect of 17 β Estradiol in vasodilatation aorta ring of female guinea pigs and the concentration of NO released from normal and dysfunction endothelial of HUVECs culture. Endothelial dysfunction was done by exposed high glucose (33mM) to HUVECs culture. The study used non genomic (8 minutes) and genomic (30, 60, 120 and 240 minutes) effect of 17 β Estradiol (10-8M). To observe the vasodilatation and the concentration of NO, bioassay technique was used.
Results: The results showed that there was an increase of NO release from HUVEC culture exposed to high glucose when incubated by 17 β Estradiol (10-8M), but this increase of NO never reached the normal value. In the intact aorta was approved that 17 β Estradiol (10-8M) was more higher the ability of relaxation compare to the denuded aorta.
Conclusion: it is concluded that non genomic effect of 17 β Estradiol (10-8M) shows the domination of endothelial role to increase the activation of NO regard to the vasodilatation effect.

This study was funded partly by Hibah Pasca (Ministry of the National Higher Education of Indonesia).

Where applicable, the authors confirm that the experiments described here conform with The Physiological Society ethical requirements.

PCD312

Layer-specific dilation of cortical arteries during stimulation of the nucleus basalis of Meynert in mice

H. Hotta[1], K. Masamoto[2,3], S. Uchida[1], Y. Sekiguchi[4], H. Takuwa[2], H. Kawaguchi[2], K. Shigemoto[5], R. Sudo[4], K. Tanishita[4], H. Ito[2] and I. Kanno[2]

[1]Department of Autonomic Neuroscience, Tokyo Metropolitan Institute of Gerontology, Tokyo, Japan, [2]Molecular Imaging Center, National Institute of Radiological Sciences, Chiba, Japan, [3]Center for Frontier Science and Engineering, University of Electro-Communications, Tokyo, Japan, [4]School of Integrated Design Engineering, Keio University, Yokohama, Japan and [5]Department of Geriatric Medicine, Tokyo Metropolitan Institute of Gerontology, Tokyo, Japan

The majority of cholinergic fibers in the cerebral cortex originate in basal forebrain nuclei. Fiber terminals from basal forebrain cholinergic areas have intimate contact not only with cortical neurons, but also with cortical parenchymal blood vessels, such as penetrating arteries and microvessels (1). Stimulation of basal forebrain cholinergic nuclei such as nucleus basalis of Meynert (NBM) produces an increase in cortical parenchymal blood flow, by activating muscarinic and nicotinic cholinergic receptors (2,3). An increase in cortical blood flow during NBM stimulation is uncoupled from cortical glucose metabolism, indicating that cholinergic projection from NBM is important for vascular control in the cerebral cortex (2). However, measurements of vascular responses are limited (4). Therefore, we examined whether cortical parenchymal arteries dilate during NBM stimulation using two-photon microscopy. Imaging of cortical vasculature was performed in adult male mice (22 - 38 g, n=7) anesthetized with urethane (1.1 g/kg, i.p.) and artificially ventilated (3). The diameter of single penetrating arteries at different depths (~750 μm, layers I-V) of the frontal cortex was measured (5) and examined changes in the diameter during focal electrical stimulation of the NBM (0.5 ms at 30-50 μA and 50 Hz) (3) and hypercapnia (3% CO_2 inhalation). Values are means ± S.E.M., compared by ANOVA. At the resting condition, the diameters of 8 penetrating arteries measured ranged 10 - 28 μm over the cortical depths. The artery showed only a marginal increase in diameter at the cortical surface following stimulation of the NBM in accordance with the previous report (2). In contrast, the artery at a depth of 50 μm from the surface showed an obvious increase in diameter during stimulation of the NBM: the diameter of 15.6 ± 1.6 μm before stimulation increased to 17.6 ± 1.7 μm during NBM stimulation. A significant increase ($p<0.05$) in arterial diameter by 9 - 13% was observed throughout the different layers of the cortex, except at upper part of layer V, where the diameter of penetrating arteries increased only slightly during NBM stimulation. Hypercapnia caused obvious dilation of the penetrating arteries in all cortical layers, including the surface arteries. The diameters began to increase within 1 sec after the onset of NBM stimulation in the upper cortical layer, and later in lower layers. Our results indicate that activation of the NBM dilates cortical penetrating arteries in a layer specific manner in magnitude and latency, presumably related to the density of cholinergic nerve terminals from the NBM.

Luiten PG et al. (1987) Brain Res 413, 229-250.

Sato A et al. (1995) Alzheimer Dis Assoc Disord 9, 28-38.

Hotta H et al. (2011) J Physiol Sci 61, 201-209.

Hotta H et al. (2004) Neurosci Lett 358, 103-106.

Masamoto K et al. (2012) Neuroscience 212, 190-200.

Where applicable, the authors confirm that the experiments described here conform with The Physiological Society ethical requirements.

PCD313

Vasorelaxant mechanism of 3, 5, 7, 3', 4'-pentamethoxyflavone on isolated thoracic aorta of female rats

C. Jansakul

Physiology, Prince of Songkla University, Hat-Yai, Songkhla, Thailand

One major flavone isolated from the rhizomes of Kaempferia parviflora, is 3, 5, 7, 3', 4'-pentamethoxyflavone (PMF). Extracts from this rhizome have been used in Thai traditional medicine for many purposes including improvement of blood circulation. However there has been no scientific evidence to support this therapeutic claim. The present study aimed to establish if PMF had any effect on blood vessels and if it did what was its mode of action. Studies were performed in vitro on isolated rat thoracic aorta obtained from female rats (220-260g) after being killed by decapitation with a guillotine, and placed in oxygenated Krebs Heinseleit solution at 37oC (PSU-Ethic No. 22/52). Cumulative concentration-response (C-R) curves were recorded by a Grass Polygraph. Data are expressed as a mean ± S.E.M. (6 rats/group/each experiments) with significant differences ($p \leq 0.05$) between tests and control identified using the Student's paired t-test. PMF (0.5-50 μM) caused a concentration dependent dilatation of thoracic aortic rings preconstricted with 3 μM phenylephrine. NG-nitro-L-arginine (LNA, 300 μM), a nitric oxide synthase inhibitor, or removal of the endothelium caused a significant parallel shift of the PMF induced C-R curve to the right. In the endothelium-intact thoracic aortic ring, ODQ (soluble guanylate cyclase inhibitor, 10 μM) significantly caused a rightward shift of the PMF C-R curve. Glybenclamide (10 μM) potentiated the PMF C-R curve on the thoracic aorta that was endothelium independent. Tetraethylammonium (1 mM) had no effect on the PMF C-R curves. In normal Krebs solution with LNA and nifedipine, or in Ca2+-free Krebs solution with LNA, PMF produced a further inhibition of the Phe C-R curve on the thoracic aortic ring. With thoracic aortic rings treated with LNA and thapsigargin, PMF suppressed the C-R curve produced by Phe and a further suppression was found when nifedipine (3 μM) was also added. No further suppression was achieved with a sequential addition of SKF-96365 (100 μM). However, when Y-27632 (Rho-kinase inhibitor, 30 μM) was also added into the above incubation medium cocktail, a complete suppression of the Phe C-R curve on the thoracic aortic ring was obtained. These results indicated that PMF produced an endothelium independent dilatation of the thoracic aortic ring. The mechanism responsible for this effect would be that PMF inhibited intracellular Ca2+ mobilization, stimulated the soluble guanylate cyclase and also the release of the nitric oxide from the vascular endothelium. It is unlikely that PMF caused an opening of the Ca2+- or ATP sensitive K+ channels, neither as an L-type Ca2+ channel or store-operative Ca2+ channel blockers. These results partly support the claims that extracts from rhizomes of the K. parviflora would improve blood circulation in men.

Where applicable, the authors confirm that the experiments described here conform with The Physiological Society ethical requirements.

PCD314

Mineral imbalance and loss of contractile phenotype induce vascular smooth muscle cell calcification by promoting exosome secretion

A.N. Kapustin[1], I. Drozdov[1], D. Soong[1], M. Furmanik[1], D. Alvarez-Hernandez[1], P. Sanchis[1], R. Molls[1], R. Shroff[1], X. Yin[1], J. Skepper[2], M. Mayr[1] and C.M. Shanahan[1]

[1]Cardiology, King's College London, London, UK and [2]Anatomy, Cambridge University, Cambridge, UK

Vascular calcification is a tightly-regulated pathological process that is triggered by multiple factors ranging from extracellular mineral imbalance to pro-inflammatory cytokines and orchestrated by the osteogenic phenotypic transition of vascular smooth muscle cells (VSMCs). VSMCs secrete matrix vesicles (MVs), loaded with the calcification inhibitor fetuin-A, into the extracellular matrix and these serve as a nidus for calcification. Here we studied the mechanisms of MV secretion by VSMCs.

Fetuin-A is internalized by VSMCs and delivered to late endosomes/multivesicular bodies and secreted in MVs via the exosomal pathway. Biochemical analysis showed that MVs originate from multivesicular bodies and are enriched with exosomal markers including CD9, CD63 and Tsg101. Proteomic analysis showed that VSMC exosomes partially share proteomic composition with exosomes secreted by other cells and are enriched with proteins involved in the regulation of cell adhesion and migration. Furthermore, fetuin-A secretion and VSMC MV secretion were blocked by GW4869, an inhibitor of sphingomyelin phosphodiesterase 3 (SMPD3) which regulates exosome biogenesis.

Treatment of VSMCs in the presence of elevated extracellular calcium resulted in a significant increase in exosome secretion and this was associated with the upregulation of SMPD3 expression. Inhibition of SMPD3 prevented VSMC calcification indicating that exosome secretion is required for the initiation of VSMC calcification. Next we examined how the phenotypic transition influences exosome secretion and VSMC calcification. Heparin and TGF-β treatment markedly reduced VSMC proliferation and induced expression of VSMC contractile markers, calponin and α-smooth muscle actin. In contrast, treatment with the pro-inflammatory cytokine TNF-α induced VSMC proliferation accompanied by a reduction in contractile phenotype markers. Comparing exosome secretion revealed a significant increase in exosome secretion in the presence of TNF-α and reduced exosome production by the heparin or TGF-β treated VSMCs.

Finally, in agreement with our in vitro data, EM analysis of longitudinal sections of VSMCs in human vessel rings ex vivo revealed MVB-like structures in VSMCs. Immunohistochemical staining of normal and atherosclerotic human aortic and carotid artery samples showed no presence of exosomal marker CD63 in the normal vessel wall. However, extensive CD63 staining was observed in the atherosclerotic vasculature particularly in association with calcified VSMCs.

In conclusion, we found that fetuin-A is recycled via exosomal pathway and VSMC exosome secretion is regulated by SMPD3. Modulation of exosome secretion by mineral imbalance and phenotypic transition as well as loading with fetuin-A are novel regulatory pathways for VSMC calcification.

Supported by the British Heart Foundation

Where applicable, the authors confirm that the experiments described here conform with The Physiological Society ethical requirements.

PCD315

Prevention of macrophage-induced adhesion molecules production and endothelial permeability in SEVC endothelial cells by Sporopollenin

M. Shih[1], S. Liou[1], L. Chen[1], S. Chen[1], S. Luo[1], I. Chen[2] and L. Chen[3]

[1]Pharmacy, Chia-Nan University of Pharmacy & Science, Tainan, Taiwan, [2]Pharamcy, Taipei city Hospital, Taipei, Taiwan and [3]Health, Taipei City Government, Food and Drug Division, Taipei, Taiwan

The inflammatory response in large vessels involves the up-regulation of key vascular adhesion molecules, such as inter-cellular adhesion molecule (ICAM)-1 and vascular cell adhesion molecule (VCAM)-1, by pro-inflammatory cytokines in the development of atherosclerosis. Chlorella has been shown to possess strong anti-inflammatory effect and to suppress high fat diet-induced atherosclerosis. The aim of this study is to investigate the possible preventing role of Sporopollenin derived from Chlorella against pro-inflammatory cytokine-induced expression of vascular adhesion molecules and endothelial permeability. Endothelial SVEC cells were treated with conditioned media (normal culture media contains 50% of LPS-activated macrophage culture media, in which contained IL-6, TNF-α and MCP-1, with and without Sporopollenin (0.5 and 1 mg/mL). Indomethacin (0.25 mM) was used as a positive control. Productions and mRNA expression of ICAM-1 and VCAM-1 and endothelial permeability were monitored. ICAM-1 and VCAM-1 production and gene expression were all induced by the conditioned media. In the concentration ranges that were devoid of cytotoxicty, the inductions of ICAM-1 and VCAM-1 production and mRNA expression by conditioned media were significantly suppressed by Sporopollenin. Indomethacin was only effectively in preventing the conditioned culture media-induced VCAM-1 production. Cell permeability was also increased in the presence of conditioned culture media. The increased permeability was also inhibited by Sporopollenin but not by indomethacin. These data indicate that Sporopollenin can be a potential material in preventing chronic inflammatory-related vascular diseases.

We are grateful to Taipei City Hospital of Taiwan for providing the research funding.

Where applicable, the authors confirm that the experiments described here conform with The Physiological Society ethical requirements.

PCD316

Semaphorin 4D recruits pericytes and regulates vascular permeability through endothelial production of PDGF-B and ANGPTL4

H. Zhou and J.R. Basile

Oncology and Diagnostic Sciences, University of Maryland Dental School, Baltimore, MD, USA

Semaphorin 4D (SEMA4D) acts through its receptor Plexin-B1 to regulate axon growth cone guidance, lymphocyte activation, and bone density (Hota & Buck, 2012). It is also overexpressed by some malignancies and plays a role in tumor-induced angiogenesis, similar to vascular endothelial growth factor (VEGF) (Basile et al, 2006). We previously noted that inhibition of VEGF and SEMA4D both restricted tumor vascularity and size, but vessels forming under conditions of VEGF blockade retained association with pericytes while those arising under SEMA4D deficiency did not (Zhou et al, 2012). These findings suggested a novel approach to anti-angiogenic therapy for certain solid tumors, as tumor vessels with pericyte sheaths often exhibit resistance to anti-VEGF therapeutic intervention (Erber et al, 2004). Here we utilize ELISA-based arrays to demonstrate an approximately 2.5-fold increase in production of platelet-derived growth factor-B (PDGF-B), which attracts pericytes to endothelial cells, and angiopoietin-like 4 (ANGPTL4), a protein upregulated in some tumors that induces vascular permeability and metastasis, in human umbilical vein endothelial cells (HUVECs) incubated with SEMA4D but not VEGF (Fig. 1). Confirmation of these results by immunoblot and RT-PCR using the Rho-signaling inhibitor C3 demonstrates that this effect occurs in a Plexin-B1/ RhoA-dependent manner. Upregulation of PDGF-B from HUVECs by soluble SEMA4D leads to differentiation of C3H/10T1/2 mesenchymal stem cells into pericytes (as determined by increased RGS5 expression in an immunoblot), as well as their proliferation, migration, and co-association with HUVEC, while ANGPTL-4 enhanced permeability of a HUVEC monolayer in vivo. Pericyte effects are unlikely to be caused by SEMA4D directly, as an immunoblot analysis of the pericyte cell line hPC-PL does not demonstrate expression of Plexin-B1. We also show that malignancies may use this mechanism to regulate tumor-induced angiogenesis. SEMA4D shed from the head and neck squamous cell carcinoma line HN12 elicits similar responses, not through autocrine or paracrine production of PDGF-B and ANGPTL4 but instead by causing robust upregulation of these proteins in HUVEC, which immunofluorescence analysis shows affects association of endothelial cells with pericytes in the stroma of tumors derived from HN12 grafted subcutaneously into the flanks of athymic Foxn1nu (nude) mice. Taken together, these data show that SEMA4D-mediated induction of PDGF-B and ANGPTL4 from HUVECs influences vessel stability and permeability, possibly in developing malignancies, and suggest that targeting SEMA4D along with VEGF represents a novel anti-angiogenic therapeutic strategy for the treatment of solid tumors.

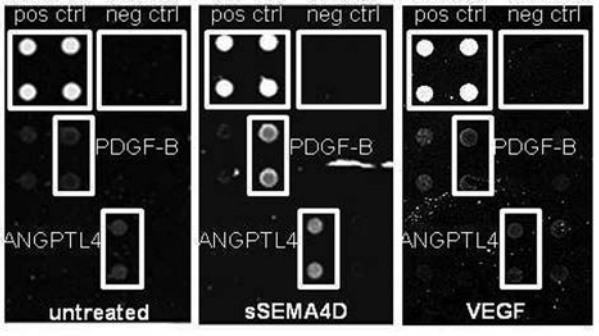

Fig. 1: An angiogenesis array reveals upregulation of PDGF-B and ANGPTL4 in HUVECs treated with

purified soluble SEMA4D, a response not observed for VEGF.

Basile JR, Castilho RM, Williams VP, Gutkind JS (2006). PNAS 103: 9017-9022

Erber R, Thurnher A, Katsen AD, Groth G, Kerger H, Hammes HP, Menger MD, Ullrich A, Vajkoczy P (2004). FASEB J 18: 338-340

Hota PK, Buck M (2012). Cell Mol Life Sci 69: 3765-3805

Zhou H, Binmadi NO, Yang YH, Proia P, Basile JR (2012). Angiogenesis

We would like to thank Dr. Snigdha Banerjee for the use of C3H/10T1/2 embryonic mesenchymal stem cells.

Where applicable, the authors confirm that the experiments described here conform with The Physiological Society ethical requirements.

PCD317

Exposure to low level of arsenic and lead in drinking water alter cardiovascular parameters and reduces vasomotion in rat aorta

J. Palacios[1], J. Vega[2] and F. Cifuentes[2]

[1]Departamento de Ciencias Químicas y Farmacéuticas, Facultad de Ciencias de la Salud, Universidad Arturo Prat, Iquique, Chile and [2]Experimental Physiology Laboratory (EPhyL), Instituto de Antofagasta, Universidad de Antofagasta, Antofagasta, Chile

The purpose of this study was to compare vascular and cardiovascular response in rats exposed to low levels of heavy metals in drinking water. Treated group was Sprague-Dawley rats exposed to drinking water from Antofagasta city, with total arsenic of 30 ppb and lead of 53 ppb for 4 months, control group was exposed to purified water by reverse osmosis. All groups drank tap water from the time of weaning. In each vascular reactivity experiment, we studied 4 to 8 adjacent aortic rings from the same animal, using the method for isometric tension measurements (Palacios et al., 2006). Animals were sacrificed by cervical dislocation. Treated group presented arsenic and lead in the hair of rats. QT interval corrected for heart rate is a sensitive biomarker for heavy metals toxicity. QT interval increased significantly in treated group compared to the control group. Treated group showed a significantly increase in systolic blood pressure, heart rate, cardiac output, and decreased the peripheral resistance, compared to the control group. Rhythmical contractions known as vasomotion occur in small resistance and larger vessels, as the aorta. This phenomenon is commonly described under pathological conditions than in physiological conditions. We hypothesize that vasomotion may contribute, in part, to regulate blood flow (Funk et al., 1983). The incubation of aortic rings with 10-7 M acetylcholine following 10-6 M phenylephrine reduced rhythmical contractions in treated group (13±3 mg maximum amplitude; $P<0.001$) compared to control group (41±6 mg maximum amplitude). However, the incubation of aortic rings with 10-8 M sodium nitroprusside (a nitric oxide donor; SNP) following 10-6 M phenylephrine increased rhythmical contractions in treated group (55±11 mg maximum amplitude; $P<0.05$) compared to control group (25±3 mg maximum amplitude). No significant differences in the relaxation properties of ACh were observed in aortic rings from treated and control groups; in both groups, the vascular relaxation was completed. Whereas, the relaxation response to SNP in treated group (121±6% of relaxation PE-induced contraction; SNP 10-7M; $P<0.05$) increased versus control group (99±6% of relaxation PE-induced contraction). In conclusion, these data suggest that exposure to low levels of arsenic and lead in drinking water could reduce rhythmical contractions in blood vessels and alter the cardiovascular parameters.

Funk W, Endrich B, Messmer K & Intaglietta M (1983). Spontaneous arteriolar vasomotion as a determinant of peripheral vascular resistance. Int J Microcirc Clin Exp 2, 11-25.

Palacios J, Espinoza F, Munita C, Cifuentes F & Michea L (2006). Na+ -K+ -2Cl- cotransporter is implicated in gender differences in the response of the rat aorta to phenylephrine. Br J Pharmacol 148, 964-972.

This work was in part supported by grants from Dirección General de Investigacion (DIRINV 1339-2007) de la Universidad de Antofagasta, Chile; FONDECYT 3120006 to J.L.V.; and Universidad Arturo Prat, Iquique, Chile.

Where applicable, the authors confirm that the experiments described here conform with The Physiological Society ethical requirements.

PCD319

Tight junction in hyaloid vessels could be induced by interaction between pericytes and endothelial cells

J. Kim[1], D. Jo[1], C. Cho[2] and J. Kim[1]

[1]Ophthalmology, Seoul National University Hospital, Seoul, Republic of Korea and [2]Pharmacology, Seoul National University, Seoul, Republic of Korea

The hyaloid vessel is a transient vascular network that nourishes the lens and the primary vitreous in the early developmental periods. In hyaloid vessels of developing C57BL6/J mouse eye devoid of the support of astrocytes, we demonstrate that tight junction proteins, zonula occludens-1 and occludin, are regularly expressed at the junction of endothelial cells. To figure out the factor influencing the formation of tight junctions in hyaloid vessels, we further progress to investigate the interactions between endothelial cells and pericytes, two representative constituent cells in hyaloid vessels. Interestingly, endothelial cells interact with pericytes in the early postnatal periods and the interaction between two cell types provokes the upregulation of TGF-β1. Further in vitro experiments demonstrate that TGF-β1 induces the activation of Smad2 and Smad3 and the formation of tight junction proteins. Taken together, in hyaloid vessels, pericytes seem to regulate the formation of tight junctions by the interaction with endothelial cells even without the support of astrocytes. Additionally, we suggest that the hyaloid vessel be a valuable system that can be utilized for the investigation of roles of cell-cell interaction in the formation of tight junctions in developing vasculatures.

Where applicable, the authors confirm that the experiments described here conform with The Physiological Society ethical requirements.

PCD320

Blood-retinal barrier breakdown of diabetic retinopathy could be attenuated by blockade of protein kinase C ζ signaling pathway

J. Kim, H. Jun and J. Kim

Ophthalmology, Seoul National University Hospital, Seoul, Republic of Korea

Vision loss in diabetic retinopathy is due to macular edema characterized by increased vascular permeability, which involves phosphorylation associated with activation of protein kinase C (PKC) isoforms. In this study, we demonstrated blockade of PKC ζ could prevent blood-retinal barrier breakdown in diabetic retinopathy. Using streptozotocin-induced diabetic mice and vascular endothelial growth factor (VEGF)-treated human retinal microvascular endothelial cells (HRMECs), effect of PKC ζ inhibition on vascular permeability and tight junction protein expression was investigated through western blotting, RT-PCR, fluorescein angiography and immunohistochemistry. Increased vascular permeability of diabetic retina is accompanied by a decrease of zonula occludens (ZO)-1 and ZO-2 expression. In diabetic retina and VEGF-treated human retinal microvascular endothelial cells, vascular leakage and loss of ZO-1 and ZO-2 on retinal vessels were effectively restored or prevented with treatment of PKC ζ inhibitor, transfection of siRNA for PKC ζ. PKC ζ activation is involved in vascular permeability in response to diabetes, and inhibition of PKC ζ effectively restores loss of tight junction proteins in retinal vessels. Therefore, we suggest that inhibition of PKC ζ could be an alternative treatment to blood-retinal barrier breakdown in diabetic retinopathy

Where applicable, the authors confirm that the experiments described here conform with The Physiological Society ethical requirements.

PCD321

Inhibitory effect of the antidepressant paroxetine on human *ether-a-go-go*-related gene (hERG) K^+ current

H. Hong, S. Jo and M. Park

Department of Physiology, School of Medicine, Kangwon National University, Chuncheon, Gangwon-do, Republic of Korea

Paroxetine is a selective serotonin reuptake inhibitor (SSRI) for psychiatric disorders that can induce QT prolongation, which may lead to torsades de pointes. We studied the effects of paroxetine on human *ether-a-go-go*-related gene (hERG) channels expressed in Xenopus oocytes and on action potential in guinea pig ventricular myocytes. The hERG encodes the pore-forming subunits of the rapidly-activating delayed rectifier K^+ channel (I_{Kr}) in the heart. Mutations in hERG reduce I_{Kr} and cause type 2 long QT syndrome (LQT2), a disorder that predisposes individuals to life-threatening arrhythmias. Paroxetine induced concentration-dependent decreases in the current amplitude at the end of the voltage steps and hERG tail currents. The inhibition was concentration-dependent and time-dependent, but voltage-independent during each voltage pulse. The S6 domain mutation Y652A did not affect the drug-induced hERG current block. In guinea-pig ventricular myocytes held at 36°C, treatment with 0.4 μM paroxetine for 5 min decreased the action potential duration at 90% of repolarization (APD_{90}) by 4.3%. Our results suggest that paroxetine is a blocker of the hERG channels, providing a molecular mechanism for the arrhythmogenic side effects during the clinical administration of paroxetine.

Where applicable, the authors confirm that the experiments described here conform with The Physiological Society ethical requirements.

PCD322

Direct inhibition of hERG K^+ channel by classic histamine H_1 receptor antagonist hydroxyzine

B. Lee, S. Jo and M. Park

Department of Physiology, School of Medicine, Kangwon National University, Chuncheon, Gangwon-do, Republic of Korea

Hydroxyzine is a potent first-generation histamine H_1 receptor antagonist that can increase action potential duration and induce QT prolongation in several animal models. Since block of cardiac human *ether-a-go-go*-related gene *(hERG)* channels is one of leading causes of acquired long QT syndrome, we investigated the acute effects of hydroxyzine on hERG channels to determine the electrophysiological basis for its proarrhythmic potential. We examined the effects of hydroxyzine on the hERG channels expressed in *Xenopus* oocytes using two-microelectrode voltage-clamp techniques. Hydroxyzine induced a concentration-dependent decrease of the current amplitude at the end of the voltage steps and hERG tail currents. The IC_{50} of hydroxyzine-dependent hERG block in *Xenopus* oocytes increased progressively relative to the degree of depolarization. Hydroxyzine affected the channels in the activated and inactivated states but not in the closed states. The S6 domain mutation Y652A attenuated the hERG current block. The IC_{50} value of hydroxyzine-dependent hERG block increased from 5.9 μM to 35.1 μM by the mutation from tyrosine to alanine at 652 amino acid of the channel. These results suggest that the H_1 antihistamine, hydroxyzine is a blocker of the hERG channels, providing a molecular mechanism for the drug-induced arrhythmogenic side effects.

Where applicable, the authors confirm that the experiments described here conform with The Physiological Society ethical requirements.

PCD323

Prelamin A accelerates vascular calcification via activation of the DNA damage response and senescence associated secretory phenotype in vascular smooth muscle cells

Y. Liu[1], I. Drozdov[1,2], R. Shroff[3], L.E. Beltran[1] and C.M. Shanahan[1]

[1]Cardiovascular Division, King's College London, London, UK, [2]Centre for Bioinformatics, King's College London, London, UK and [3]Nephrology Unit, Great Ormond Street Hospital and UCL Institute of Child Health, London, UK

Vascular calcification is prevalent in the ageing population yet little is known of the mechanisms driving age-associated vascular smooth muscle cell (VSMC) phenotypic change. Recent evidence has implicated nuclear lamina dysfunction, especially the accumulation of premature forms of lamin A, in promot-

ing premature cellular ageing, as typified in the premature ageing disorder Hutchison-Gilford Progeria Syndrome.[1, 2] Our previous data showed that Prelamin A, the unprocessed form of the nuclear lamina protein lamin A, accumulates in aged and atherosclerotic arteries and, acts as a specific hallmark of VSMC ageing, within the general population.[3] In the current study we investigated whether prelamin A accumulation plays a role in driving VSMC osteogenic differentiation.
We found that prelamin A accumulated in cacifying VSMCs both in vitro and in vivo and that overexpression of prelamin A in vitro promoted VSMC osteogenic differentiation and mineralization. During VSMC ageing in vitro prelamin A accumulation occurred concomitantly with increased p16 expression and osteogenic differentiation and was associated with increased levels of DNA damage. Microarray analysis showed that DNA damage repair pathways were significantly impaired in VSMCs expressing prelamin A and chemical inhibition or siRNA depletion of the DNA damage response (DDR) kinases ATM/ATR effectively blocked VSMC osteogenic differentiation and mineralization. In co-culture experiments, prelamin A expressing VSMCs induced alkaline phosphatase (ALP) activity in mesenchymal progenitor cells and this was abrogated by inhibition of ATM signalling suggesting DNA damage induces the secretion of pro-osteogenic factors by VSMCs. Cytokine array analysis identified a number of ATM-dependent senescence associated secretory phenotype (SASP) factors/cytokines released by prelamin A positive VSMCs including the calcification regulators BMP2, OPG and IL6, and these data were validated by quantitative PCR and ELISA.
This study demonstrates that prelamin A promotes premature VSMC calcification and ageing, in part, by inducing persistent DNA damage signalling which acts upstream of VSMC osteogenic differentiation and the SASP. Agents that target the DDR and/or prelamin A toxicity may be potential therapies for the treatment of vascular calcification.

Denecke, J., et al., A homozygous ZMPSTE24 null mutation in combination with a heterozygous mutation in the LMNA gene causes Hutchinson-Gilford progeria syndrome (HGPS): insights into the pathophysiology of HGPS. Human Mutation, 2006. 27(6): p. 524-531.

Salamat, M., et al., Aortic Calcification in a Patient With Hutchinson-Gilford Progeria Syndrome. Pediatric Cardiology, 2010. 31(6): p. 925-926.

Ragnauth, C.D., et al., Prelamin A Acts to Accelerate Smooth Muscle Cell Senescence and Is a Novel Biomarker of Human Vascular Aging. Circulation, 2010. 121(20): p. 2200-2210.

This work was supported by a British Heart Foundation Programme Grant to CMS.

Where applicable, the authors confirm that the experiments described here conform with The Physiological Society ethical requirements.

PCD324

Blockade of the renin-angiotensin system improves cerebral microcirculatory perfusion in diabetic hypertensive rats

V. Estato[1], N. Obadia[1], F. Freitas[1], M. Lessa[1], P. Reis[2], H. Castro-Faria-Neto[2], J. Carvalho-Tavares[3] and E. Tibiriçá[1]

[1]Laboratory of Cardiovascular Investigation, Oswaldo Cruz Foundation-FIOCRUZ, Rio de Janeiro, RJ, Brazil, [2]Laboratory of Immunopharmacology, Oswaldo Cruz Foundation-FIOCRUZ, Rio de Janeiro, RJ, Brazil and [3]Núcleo de Neurociências, Departamento de Fisiologia e Biofísica, UFMG, Belo Horizonte, MG, Brazil

Motivation: Hypertension often precedes the diagnosis of type 2 diabetes. It occurs twice as frequently in diabetic patients than in non-diabetic individuals, and aggravates the complications of diabetes. The high susceptibility of individuals with hypertension and diabetes to stroke depends on the sensitivity of the cerebral vasculature to increased blood pressure. It also depends on the occurrence of brain disorders such as capillary rarefaction and astrogliosis of the cerebral cortex caused by associated chronic diseases. Methods: We examined the functional and structural microcirculatory alterations in the brain, skeletal muscle and myocardium of non-diabetic spontaneously hypertensive rats (SHR) and diabetic SHR (D-SHR), as well as the effects of long-term treatment with the angiotensin AT1-receptor antagonist olmesartan (D-SHR OLM) and the angiotensin-converting enzyme inhibitor enalapril (D-SHR ENA). Diabetes was induced by a combination of a high-fat diet with a single low dose of streptozotocin (35 mg/kg, ip). D-SHR were orally administered with olmesartan (5 mg/kg/day), enalapril (10 mg/kg/day) or vehicle for 28 days, and compared with vehicle-treated non-diabetic SHR (SHR VEH) or normotensive non-diabetic Wistar–Kyoto rats (WKY VEH). The cerebral and skeletal muscle functional capillary density of pentobarbital-anesthetized rats was assessed using intravital fluorescence videomicroscopy. All experimental procedures were conducted in accordance with the Care and Use of Laboratory Animals and were approved by the FIOCRUZ Animal Welfare Committee (# LW-10/12). Chronic treatment with OLM or ENA significantly lowered blood pressure and reversed brain functional capillary rarefaction (D-SHR OLM 187 ± 10 or D-SHR ENA 220 ± 38 capillaries/mm2 vs. D-SHR VEH 94 ± 9 capillaries/mm2; $p<0.05$). Brain oxidative stress was reduced to non-diabetic control levels in animals treated with OLM or ENA. OLM or ENA treatments were able to significantly reduce the number of rolling leukocytes in (D-SHR OLM 5.9 ± 0.1 cells/min; $p<0.05$ or D-SHR ENA 4.1 ± 0.7 cells/min; $p<0.05$), when compared with the control D-SHR VEH group (10.6 ± 1.8 cells/min). Histochemical analysis showed that both OLM and ENA increased the capillary-to-fiber ratio in skeletal muscle (D-SHR OLM 2.1 ± 0.1 or D-SHR ENA 2.1 ± 0.1 vs. D-SHR VEH 1.5 ± 0.1; $p<0.001$) and in the left ventricle (D-SHR OLM 0.23 ± 0.01 or D-SHR ENA 0.30 ± 0.02 Vv[cap]/Vv[fib] ratio vs. D-SHR VEH 0.09 ± 0.01 Vv[cap]/Vv[fib] ratio; $p<0.001$). OLM or ENA also prevented collagen deposition and the increase in cardiomyocyte diameter in the left ventricle. Our results suggest that the association between hypertension and diabetes results in microvascular alterations in the brain, skeletal muscle and myocardium that can be prevented by chronic blockade of the renin-angiotensin system. Financial support: CNPq

Where applicable, the authors confirm that the experiments described here conform with The Physiological Society ethical requirements.

PCD325

Vascular reactivity and membrane potential in survivor and non-survivor rats with peritonitis-induced septic shock

S. Chen[1], C. Shih[3], C. Tsao[2] and C. Wu[3]

[1]Nursing, Kang-Ning Junior College of Medical Care and Management, Taipei, Taiwan, [2]Anaesthesiology, Taipei Veterans General Hospital, Taipei, Taiwan and [3]Pharmacology, National Defence Medical Centre, Taipei, Taiwan

Vascular hyporeactivity and hyperpolarization are important causes of circulatory failure in septic shock. However, there is no data regarding the differences of vascular reactivity and resting membrane potential in survivors and non-survivors of sepsis. Thus, the aim of this study was to examine and compare the changes of vascular reactivity and resting membrane potential in survivor and non-survivor rats after cecal ligation and puncture (CLP)-induced sepsis. Wistar rats were anaesthetised by sodium pentobarbital (30 mg/kg, i.p.), and then, subjected to CLP or sham operation after the carotid artery and vein were cannulated. The changes of hemodynamics, biochemical variables, aortic isometric tension, smooth muscle membrane potential, and aortic superoxide levels were monitored during the experimental period. The CLP surgery caused circulatory failure, multiple organ dysfunction syndrome (MODS), vascular hyporeactivity to norepinephrine (NE), and vascular hyperpolarization. Compared with survivors, non-survivor rats showed a more severe organ dysfunction and a less increase in aortic superoxide levels at 9 h. In addition, non-survivor rats manifested less decreases in vascular reactivity to NE and resting membrane potential in the aortas when compared with those in the survivors. These results demonstrate significant differences of vascular reactivity and resting membrane potential in survivor and non-survivor rats after CLP-induced sepsis. However, vascular hyporeactivity and hyperpolarization only partially contributed to the early death of septic animals, while this early death was most likely due to organ dysfunction (i.e. MODS) in this CLP-induced sepsis model.

Rittirsch D, Flierl MA, Ward PA. Harmful molecular mechanisms in sepsis. Nat Rev Immunol 2008;8:776-787.

Landry DW, Oliver JA. The pathogenesis of vasodilatory shock. N Engl J Med 2001;345:588-595.

Wichterman K, Baue A, Chaudry I. Sepsis and septic shock—a review of laboratory models and a proposal. J Surg Res 1980;29:189-201.

Chen SJ, Wu CC, Yang SN, Lin CI, Yen MH. Abnormal activation of K(+) channels in aortic smooth muscle of rats with endotoxic shock: electrophysiological and functional evidence. Br J Pharmacol 2000;131:213-222.

Shih CC, Chen SJ, Chen A, Wu JY, Liaw WJ, Wu CC. Therapeutic effects of hypertonic saline on peritonitis-induced septic shock with multiple organ dysfunction syndrome in rats. Crit Care Med 2008;36:1864-1872.

This work was supported by grants NSC 97-2320-B-016-006-MY3 and NSC 100-2320-B-016-008 from the National Science Council, R.O.C., Taiwan and C11-01 from National Defense Medical Center, R.O.C., Taiwan.

Where applicable, the authors confirm that the experiments described here conform with The Physiological Society ethical requirements.

PCD326

Molecular profile of fibrosis and elastogenesis in the vein wall of human leg varicose veins. An immunohistochemical and morphometrical study

J. Regadera[1], J.P. Velasco-Martin[1], M. Rubio[2], G. España-Caparros[2], P. Prachaney[3], P. Rodriguez-Rodriguez[4], L.M. Reparaz[5] and S.M. Arribas[4]

[1]Departament of Anatomy, Histology and Neuroscience, University Automa Madrid, Madrid, Madrid, Spain, [2]Vascular Surgery Unit, Moncloa Universitary Hospital, Madrid, Madrid, Spain, [3]Anatomy Department, Khon Kaen University, Khon Kaen, Thailand, [4]Physiology Department, University Automa Madrid, Madrid, Spain and [5]Angiology and Vascular Surgery Department, University Hospital Gregorio Marañon, Madrid, Spain

Pathological changes of chronic venous insufficiency is a common disease that appears in 20% of the world population. It is characterized by intimal and medial fibrosis of venous wall. Our aim was to link the correlation between Doppler sonography data and the degree of intimal and medial lesions in varicose saphenous veins at different locations.

Saphenous veins from ten patients were evaluated by Doppler sonography and inmunohistochemestry. Collagen I, III and IV, smooth muscular actin, laminin and vimentin were studied from normal to pathological vein lesions. Collagen fibers distribution and extracellular matrix were also studied by Red Sirius Stain. Elastogenesis was studied by confocal microscopy and orcein stain. The evaluation of each molecule was explored using almost two slides per case. Quantification of these molecules and structures were made by Image J software.

In initial lesions of varicose vein, intimal layer double their size compared to normal wall vein. Present a progressive increase of collagen I, III and IV, is also associated to an increase of extracellular matrix and myofibroblast (vimentin+ and SMA+) proliferation. At severe intimal varicose lesions, lumen of vein decreased, and Doppler sonography blood flow was lower. In this field we observed thickness in intimal wall, corresponding to significatilly increase of SMA+ cells and collagen I, III and IV deposition.

The morphometric data showed that SMA+ area at intimal layer is correlated negatively to intimal thickness. In addition, quantification of elastic fibers at intimal varicose veins is significantly high compared to normal vein. Correlation between elastics fibers area and intimal high were negative. In the intima, a deposition of elastic fibers, which were shorter and disorganized was observed. The vascular medial layer shows atrophy of smooth muscular cells and presence of fibrous tissue. The intimal and medial fibrotic changes were not related to mast cell or immunocompetent cells proliferation.

These data suggest a progressive transformation from normal to pathological varicose vein. In the eco Doppler sonography area reflux of varicose veins, we found a well established intimal and medial lesions characterized by deposition of collagen I, III and IV and extracellular matrix. These lesions are an irreversible fibrotic process in patients with leg chronic venous insufficiency.

Where applicable, the authors confirm that the experiments described here conform with The Physiological Society ethical requirements.

PCD327

Large-scale analysis and characterisation of the cardiac microvascular endothelial proteome

H. Strijdom[1], A. Genis[1], S. Van Rensburg[1] and S. Smit[2]

[1]Division of Medical Physiology, University of Stellenbosch, Tygerberg, Western Cape, South Africa and [2]Proteomics Unit, Central Analytical Facility, University of Stellenbosch, Tygerberg, Western Cape, South Africa

Vascular endothelial cells show considerable diversity, particularly when located within a specific organ such as the heart [1]. Myocardial capillaries, lined by cardiac microvascular endothelial cells (CMECs), are critical in the development of end-organ damage [2], and show adaptations in view of their close association with cardiomyocytes, whose function they tightly regulate [3]. Little is known about the total protein expression patterns in CMECs. The aim of the study was to perform a comprehensive large-scale proteomic analysis of adult rat CMECs under normoxic, baseline and hypoxic conditions in order to gain more information on their functional properties. Methods: Adult rat (Rattus norvegicus) CMECs were purchased and passaged until generation 4-7. CMECs were incubated under normoxia (21% O_2), or hypoxia (<1% O_2) for 24h. Samples were then subjected to SDS-PAGE/in-gel trypsinisation or filter-aided sample preparation (FASP) before separation of peptides by nano-LC chromatography and analysis by a LTQ Orbitrap Velos mass spectrometer. Proteins were identified with 4 different protein database search engines. Finally, protein lists were analysed for functional and pathway annotations.Results: A total of 1388 proteins were identified. The majority of proteins were expressed in the cytosol (28.3% of the proteome; $p=1.1 \times 10^{-63}$), followed by mitochondrial (22.4%; $p=1.1 \times 10^{-27}$), cytoskeletal (15.4%; $p=3.5 \times 10^{-15}$), and vesicular (11.5%; $p=2.3 \times 10^{-14}$) proteins. The top 5 biological processes represented in the CMEC proteome were: protein localisation (9.8%; $p=1.5 \times 10^{-10}$), oxidation reduction (9.6%; $p=2.7 \times 10^{-11}$), protein transport (8.8%; $p=4.9 \times 10^{-11}$), translation (8.4%; $p=2.4 \times 10^{-14}$), and vesicle-mediated transport (7.7%;$p=2.1 \times 10^{-11}$). The hypoxia protocol induced demonstrable injury (1.5-fold and 2.2-fold increase in necrosis and apoptosis respectively; $p<0.05$). 267 new proteins were expressed, whereas 32 proteins were lost in hypoxia. Five out of the 10 upregulated proteins in hypoxia were glycolytic enzymes. The cytosolic protein fraction increased to 47% of the hypoxic CMEC proteome, whereas mitochondrial proteins decreased to 16%. There was a significant presence of ribonucleoproteins (26.3%; $p= 7.8 \times 10^{-23}$), and translation (24.5%) and glycolysis (6%) were more prominent vs normoxia.Apoptotic and hypoxia response proteins were overexpressed in hypoxia (9% and 4.8% respectively).Conclusions: This is the first comprehensive characterisation of the CMEC proteome under normoxic and hypoxic conditions. Normoxic CMECs demonstrated significant mitochondrial protein expression, which decreased after hypoxia. Conversely, glycolytic proteins increased in hypoxia suggesting a metabolic switch in the cells. Vesicular and protein transport proteins were prominently expressed in the CMECs, indicative of the capillary-derived origin of the cells.

Hendrickx J *et al* (2004). *Physiol Genomics* **19**, 198-206.

Lu L *et al* (2007). *Physiol Res* **56(2)**, 159-68.

Aird WC (2007). *Circ Res* **100**, 174-190.

Where applicable, the authors confirm that the experiments described here conform with The Physiological Society ethical requirements.

PCD328

Cilostazol inhibits leukocyte-endothelial cell interaction in murine microvessels after transient bilateral common carotid artery occlusion

T. Fukuoka, T. Hayashi, H. Maruyama, H. Sano, M. Hirayama and N. Tanahashi

Saitama Medical University International Medical Center, Hidaka, Japan

Leukocyte behavior in the cerebral microvasculature following vessel occlusion has not been fully elucidated. The purpose of this study was to investigate the effects of cilostazol on leukocyte behavior (rolling and adhesion) in murine cerebral microvessels following transient bilateral carotid artery occlusion using intravital fluorescence microscopy. Three groups of mice were assigned: sham group(n=8), ischemia reperfusion(I/R) group(n=6), I/R+cilostazol (CZ) group (ischemia reperfusion after cilostazol administered orally 30 mg/kg) (n=8). Ischemia was induced of 15 min of bilateral common carotid artery (CCA) occlusion using microvascular clips. Leukocyte labeled with 0.05%acridine orange were intravenously administered and their behavior was investigated at 3 and 6 h, through a parietal lesion window made just after the ischemic period. The number of rolling or adhering leukocyte was expressed per square millimeter per 30 seconds. Numbers of rolling and adhesion leukocyte at 3 or 6 h after reperfusion in I/R group were significantly increased compared to sham group and numbers of rolling and adhesion leukocyte in the CZ group were significantly inhibited at 3 or 6 h after reperfusion compared to the I/R group in pial veins ($P<0.05$) and in pial arteries ($P<0.05$). Cilostazol inhibited leukocyte-endothelial interactions following cerebral ischemia and reperfusion.

Where applicable, the authors confirm that the experiments described here conform with The Physiological Society ethical requirements.

PCD329

Low Akt activity, decreased VEGFR-2 expression and bcl-2 suppression are associated with regressing vascular tumors in mice

P. Mabeta[1] and M.S. Pepper[2]

[1]Anatomy and Physiology, University of Pretoria, Pretoria, South Africa and [2]Immunology, University of Pretoria, Pretoria, South Africa

Angiogenesis, the process of new blood vessel formation, is a central mechanism underlying the development of hemangiomas.1,2 Hemangiomas are benign neoplasms of the vasculature frequently encountered in children. 1,2 Growth factors which mediate angiogenesis such as vascular endothelial growth factor (VEGF) and basic fibroblast growth factor (bFGF) have been implicated in the pathogenesis of hemangiomas.3 Recently we reported on the antiangiogenic effects of bleomycin in vitro in cultured human hemangioma biopsies.4 In the present study we investigated the antiangiogenic effects of bleomycin (0.6–1.2 mg/kg) in vivo in a hemangioma mouse model using C57BL6 female mice. Tumors were induced by

injecting mice on the flanks with endothelioma cells. Tumor growth was monitored every second day up to 15 days post treatment. Mice were anaesthetised using 3% Isoflurane. Tissue samples were stained with hematoxylin and eosin for light microscopy, and processed for immunohistochemistry and immunofluorescent microscopy evaluation. Blood samples were collected by cardiac puncture for the measurement of VEGF using ELISA. Analysis of tumor volumes revealed a significant reduction in tumor growth in mice treated with Bleomycin when compared with those treated with buffered saline (n = 5 per group; $p<0.05$). Low levels of the angiogenic factor VEGF were measured in samples of mice treated with bleomycin. Histological evaluation revealed a reduced microvessel density (MVD) in tumors from bleomycin-treated mice compared to those treated with saline. No tumor growth was observed in baseline mice (the group that was not injected with endothelioma cells). Tumor growth inhibition was associated with the suppression of Flk-1, bcl-2 and Akt activity. Our observations reveal a possible mechanism for the inhibitory effects of bleomycin on hemangiomagenesis, and raise the possibility that the suppression of bcl-2 in particular may provide a therapeutic target for the treatment of vascular tumors of infancy.

1. Mulliken JB, Glowacki J. Hemangiomas and vascular malformations in infants and children: a classification based on endothelial characteristics. Plast Reconstruct Surg 1982; 69:412–422.

2. Mabeta P, Pepper MS. Hemangiomas—current therapeutic strategies. Int J Dev Biol 2011; 55:431–437.

3. Takahashi K, Mulliken JB, Kozakewich HP, Rogers RA, Folkman J, Ezekowitz RA. Cellular markers that distinguish the phases of hemangioma during infancy and childhood. J Clin Invest 1994; 93:2357–2364.

4. Mabeta P, Davis PF. The mechanism of bleomycin in inducing hemangioma regression. S Afr Med J 2008; 98:538–539.

Where applicable, the authors confirm that the experiments described here conform with The Physiological Society ethical requirements.

PCD330

cAMP signalling in endothelial cells: Differential effects on angiogenesis via PKA and Epac signalling

M. Aslam[2,1], S. Rohrbach[1], R. Schulz[1], C. Hamm[2] and D. Guenduez[2]

[1]Institute of Physiology, Justus Liebig University, Giessen, Germany and [2]Cardiology and Angiology, Justus Liebig University, Giessen, UK

Background: cAMP signalling regulates several endothelial functions such as endothelial barrier integrity, nitric oxide (NO) production, and proliferation and migration in response to growth factors. cAMP mediates these effects via activation of its two well known effector proteins i.e. PKA and Epac (exchange protein directly activated by cAMP). The signalling pathways activated by PKA and Epac might be overlapping, non-overlapping, or even antagonistic. The aim of the present study was to analyse the differential signalling response of PKA and Epac on endothelial barrier, cell migration and differentiation.
Methods: The study was carried out on cultured human umbilical vein endothelial cells (HUVEC). cAMP analogues, 8-CPT-cAMP, 6-Bnz-cAMP and Forskolin (FSK) were used to activate Epac, PKA or adenylyl cyclase, respectively. Endothelial cell proliferation, migration, and sprouting were quantified by crystal violet staining, wound healing assay, and tube formation and spheroid sprouting assay, respectively. Endothelial barrier function was analysed by measuring the flux of trypan blue-labeled albumin.
Results: Specific activation of either PKA or Epac induced barrier protective response in HUVEC monolayers which was additive when both PKA and Epac were activated together. Activation of both Epac and PKA caused Akt phosphorylation at S473 which was antagonised by inhibitors of alpha and beta but not by gamma and delta isoforms of PI3K. Both Epac and PKA induced ERK phosphorylation accompanied by increased cell proliferation and migration which was abrogated by inhibition of MAPK pathway. Activation of PKA induced endothelial cell sprouting and tube formation and enhanced VEGF-mediated effect. Contrarily, activation of Epac antagonised VEGF-mediated sprouting and tube formation. Moreover, Epac activator-treated endothelial cells tend to establish monolayer on matrigels rather than forming network like structures.
Conclusion: The data of present study shows that endothelial cell functions are differentially regulated by PKA and Epac signalling. Both PKA and Epac activation stabilize endothelial barrier function, however, both have opposite effects on angiogenesis. PKA activation promotes angiogenesis while Epac activation antagonises angiogenesis.

Where applicable, the authors confirm that the experiments described here conform with The Physiological Society ethical requirements.

PCD331

The AMP-activated protein kinase (AMPK) decreases endothelial angiotensin converting enzyme (ACE) expression by phosphorylation of p53 and post-transscriptional upregulation of microRNA (miR)-143/145

K. Kohlstedt[1], C. Trouvain[1], T. Boettger[2], B. Fisslthaler[1], L. Shi[1] and I. Fleming[1]

[1]Goethe-University, Institute for Vascular Signalling, Frankfurt am Main, Germany and [2]Dept. Cardiac Development and Remodelling, Max Planck Institute for Heart and Lung Research, Bad Nauheim, Germany

High ACE levels are a risk factor for cardiovascular disease, but little is known about the molecular mechanisms regulating ACE expression in endothelial cells. Here, we determined the role of the AMPK and the miR-143/145-cluster, since they regulate ACE expression in other cell types and are activated/upregulated in response to shear stress.
Shear stress time-dependently decreased ACE expression in human endothelial cells, an effect sensitive to silencing (siRNA) of the catalytic AMPK α2 (but not the α1) subunit. The AMPK activators, AICAR and metformin also decreased ACE expression in cultured endothelial cells and endothelial cells from AMPKα2-/- (but not AMPKα1-/-) mice expressed significantly higher ACE levels. Consequently, AMPKα2-/- mice were more sensitive to the hypotensive effect of the ACE-inhibitor ramipril and demonstrated an impaired bradykinin-induced hindlimb vasodilatation. The latter response was restored by ramiprilat and was also evident in endothelial cell specific AMPKα2 knockout mice. In miR-143/145-deficient LacZ reporter gene mice, ACE was identified as target of the miR-143/145 cluster in vascular smooth muscle cells. We confirmed the suppressive effect of miR-143/145 on ACE-expression in isolated endothelial cells from these mice as well as in human endothelial cells by overexpressing miR-143/145. AMPKα2 deletion (in vitro and in vivo) decreased miR-143/145 levels and overexpression of pre-miR-143/145 decreased endothelial ACE expression. Because shear

stress increased levels of premature and mature miR-143/145, without affecting the primary transcript or miR-143/145 promoter activity, it seems that AMPKα2 regulates miR expression via a post-transcriptional rather than transcriptional mechanism. Since p53 is an AMPK target, regulates miRs at the transcriptional and post-transcriptional levels and shear-stress elicited the AMPKα2-mediated phophorylation of p53 (Ser15), we focused on validating AMPK-p53 effect on miR expression. Suppression of p53 (siRNA) decreased miR-143/145 levels, increased endothelial ACE expression and prevented its shear stress-induced downregulation. Streptozotocin-induced diabetes increased the phosphorylation of the AMPK substrates, p53 and acetyl-coenzyme A carboxylase, at the same time as increasing miR-143/145 and decreasing ACE levels.
In conclusion, the activation of AMPKα2 suppresses endothelial ACE expression via p53 activation and post-transcriptional upregulation of miR-143/145. Since dysregulation of AMPK as well as p53 plays a major role in the development of several diseases (e.g. diabetes, cancer), their effect on the regulation of miR-143/145 and thus ACE levels might explain the development of disease-associated cardiovascular disorders.

Where applicable, the authors confirm that the experiments described here conform with The Physiological Society ethical requirements.

PCD332

Tetrahydrocurcumin ameliorates vascular dysfunction and aortic remodeling in nitric oxide-deficient rats

U. Kukongviriyapan[1], O. Boonla[1], S. Nakmareong[2], P. Pakdeechote[1], V. Kukongviriyapan[3], P. Pannangpetch[3], P. Surawattanawan[4] and S.E. Greenwald[5]

[1]Department of Physiology, Faculty of Medicine, Khon Kaen University, Khon Kaen, Thailand, [2]Faculty of Associated Medical Sciences, Khon Kaen University, Khon Kaen, Thailand, [3]Department of Pharmacology, Faculty of Medicine, Khon Kaen University, Khon Kaen, Thailand, [4]Research and Development Institute, Government Pharmaceutical Organization, Bangkok, Thailand and [5]Barts & The London School of Medicine & Dentistry, Queen Mary University of London, London, UK

Nitric oxide (NO) depletion induces hypertension, oxidative stress and arterial stiffness. Previous study has shown that tetrahydrocurcumin (THU), a major antioxidant and anti-inflammatory agent, improved aortic stiffening of rats with NO-deficiency, however, the associated mechanism remains unclear. The objective of this study was to determine whether THU could attenuate vascular dysfunction and aortic remodeling in NO-deficient rats. The procedures and experimental protocols were reviewed and approved by the Institutional Animal Ethics Committee of Khon Kaen University, Thailand. Male Sprague-Dawley rats weighing 200-220 g were divided into normotensive and hypertensive groups (n=6-8/group). Hypertension was induced by administering Nω-nitro-L-arginine methyl ester (L-NAME) at a dose of 50 mg/kg/day in their drinking water for 5 weeks. After 3 weeks, hypertension had been established and was sustained in all animals. During the last two weeks, L-NAME hypertensive rats were randomly divided into three treatment groups. Group 1 was intragastrically administered with polyethylene glycol (PG), a vehicle. Group 2 and 3 were intragastrically administered with THC for 2 weeks at doses of 50 and 100 mg/kg/day, respectively. The normotensive controls were received tap water ad libitum and intragastrically administered with PG. At the end of treatment, animals were anesthetized with pentobarbital sodium (60 mg/kg body weight, i.p.), arterial blood pressure and vascular response to acetylcholine (3, 10 and 30 nmol/kg, i.v.) were determined. Thereafter, rats were sacrificed by overdose of an anesthetic drug. The thoracic aortas were excised and used for quantitative morphometric analysis of structural changes and immunohistochemistry staining of MMP-2. Values are means ± S.E.M., compared by one way ANOVA. L-NAME significantly increased blood pressure, blunted vascular response and induced aortic remodeling. THU 50 and 100 mg/kg/day significantly decreased mean arterial pressure (174 ± 2 and 165 ± 2 mmHg, respectively vs. 189 ± 2 mmHg in L-NAME control rats; $P < 0.01$), and prevented the reduction in endothelium-dependent vasodilatation. THU reduced the increases in media thickness, cross-sectional area, smooth muscle cells proliferation and collagen accumulation in the aortic wall. Increased MMP-2 expression was found in the aortas of L-NAME, and THU at test doses significantly reduced it ($P < 0.05$). Our results suggest that MMP-2 plays a role in L-NAME hypertension and its structural and functional vascular changes, which were attenuated by THU.

This study was supported by grants from the Faculty of Medicine, Khon Kaen University, the Thailand Research Fund (Grant No. DBG5380045) and the British Council PMI2 Grant (#RC53).

Where applicable, the authors confirm that the experiments described here conform with The Physiological Society ethical requirements.

PCD333

Nitric Oxide-cGMP signalling induces β-Catenin nuclear translocation and transcriptional activity

C. Warboys[1], N. Chen[1,2], Q. Zhang[1], Y. Shaifta[3], J. Ward[3] and A. Ferro[1]

[1]Cardiovascular Division, King's College London, London, UK, [2]Institute of Vascular Medicine, Peking University Third Hospital, Beijing, China and [3]Division of Allergy, Asthma and Lung Biology, King's College London, London, UK

Nitric oxide (NO) plays a key regulatory role in cardiovascular physiology due to its vasodilatory, anti-thrombotic and anti-atherogenic properties. In endothelial cells NO is synthesised by endothelial NO synthase (eNOS), which is known to associate with a number of other proteins. Our aim was to identify novel protein associations with eNOS in human umbilical vein endothelial cells (HUVEC) and to clarify the physiological role of such associations. Analysis of eNOS immunoprecipitated from lysates of HUVEC by mass spectrometry revealed a previously unrecognised association with β-catenin. This was confirmed by western blot analyses of eNOS and β-catenin immunoprecipitates, since each protein was detected in immunoprecipitates of the other (n=3). Nuclear translocation of β-catenin following eNOS activation was assessed by western blot of nuclear lysates. eNOS stimulation with adenosine, salbutamol, histamine or thrombin increased nuclear translocation of β-catenin compared to untreated controls (n=4), as did spermine NONOate or 8-bromo-cGMP (n=5). Transcriptional activity of β-catenin, a co-activator of T cell factor (TCF) / lymphoid enhancing factor (LEF) transcription factors, was assessed using a luciferase reporter assay in HUVEC transfected with TCF/LEF reporter plasmids. Spermine NONOate, 8-bromo-cGMP or sildenafil increased TCF/LEF-mediated luciferase activity relative to controls ($p<0.05$, $P<0.01$, $P<0.05$ respectively, n=6). The role of β-catenin in NO-cGMP

signalling was examined in mouse pulmonary endothelial cells (MPECs) using an *in vitro* angiogenesis assay. Stimulation of NO-cGMP signalling in wild-type (WT) MPECs using vascular endothelial growth factor (VEGF), spermine NONOate, 8-bromo-cGMP or sildenafil significantly increased tube length compared to untreated controls (respective means ± SEM 13922 ± 549, 15030 ± 605, 14445 ± 549, 14589 ± 796 *vs.* 11608 ± 971, P<0.05); these responses were not seen with MPECs lacking the β-catenin gene (β-cat$^{-/-}$) (10748 ± 473, 10424 ± 1105, 9326 ± 821, 10162 ± 1015 *vs.* 9908 ± 918). Both types of MPECs exhibited normal angiogenic responses to basic fibroblast growth factor which acts independently of NO-cGMP signalling (WT 9240 ± 518 *vs.* 7715 ± 101, P<0.05; β-cat$^{-/-}$ 10006 ± 250 *vs.* 8528 ± 83, P<0.01; n=4). Spermine NONOate, 8-bromo-cGMP or sildenafil also increased VEGF expression (which is known to be NO-dependent) relative to control in WT but not β-cat$^{-/-}$ MPECs, as determined by western blot of cell lysates (n=4). In summary, activation of the NO-cGMP pathway induces nuclear translocation of β-catenin and increased transcriptional activity, which may be facilitated by close approximation of β-catenin with eNOS in the resting state. Additionally, β-catenin plays a key role in NO-mediated angiogenesis and may be an important contributor to NO-mediated gene transcription and endothelial cell function.

Where applicable, the authors confirm that the experiments described here conform with The Physiological Society ethical requirements.

PCD334

Cytochrome P450-epoxygenase metabolites play role in vasodilation of middle cerebral arteries in response to reduced pO2 in healthy and diabetic rats that underwent hyperbaric oxygenation

S. Unfirer[1], J.R. Falck[2] and I. Drenjancevic[1]

[1]Department of Physiology and Immunology, Faculty of Medicine Osijek, University of J.J. Strossmayer Osijek, Osijek, Croatia and [2]Department of Biochemistry, University of Texas Southwestern Medical Center, Dallas, TX, USA

Introduction: Vasodilation in response to hypoxia is mainly mediated by cyclooxygenase (COX) activation and production of prostacyclin (PGI2) (1). However, there are evidences that cytochrome P450-epoxygenase metabolites contribute to vasodilation in healthy vessels (2).
Materials and Methods: Hyperbaric oxygenation (HBO2) was performed in a chamber with 100% O2 (2 bar) 2 hours/day for 4 consecutive days. Male Sprague-Dawley rats (N= 5) were divided in 4 groups; control, diabetic (DM) (DM induced by streptozocin 60mg/kg i.p.), HBO2 treated DM rats (DM+HBO2) and HBO2-control rats. On the 5th day, prior to decapitation, rats were anesthetized with ketamin-chlorid (75 mg/kg) and midazolam (0.5 mg/kg). Isolated middle cerebral arteries (MCA) were mounted on glass pipettes of DMT 110P pressure myograph system for internal diameter measurements in normoxia (21% O2 in superfusate and perfusate), and reduced pO2 (0%) conditions. To assess the role of CYP450-epoxygenases' vasodilating metabolites (EETs), the CYP450 inhibitor –MS-PPOH (10-5M) was used. To assess the role of COX metabolites, indomethacin (INDO) (10-5M) was used. The data were analyzed with One-way ANOVA and presented as mean±SEM (microns); p<0.05 was considered statistically significant. The Ethical Committee of Faculty of Medicine University of Osijek approved the study.
Results: MCA of control rats exhibit significant vasodilation (23±3) compared to DM rats which failed to dilate in response to reduced pO2 (0±3). INDO or MS-PPOH did not affect this lack of response in DM rats. Vasodilation was restored in DM+HBO2 rats (14±2). In the presence of MS-PPOH, vasodilation to reduced pO2 was diminished in control group (11±1) and more inhibited in control + HBOT group (4±1), while vasodilation was eliminated in DM+HBO2 group (-6±2) and in DM group (-6±2). INDO eliminated dilation to reduced pO2 in control (-5±4) and DM (-2±6) groups but only partly reduced it in both HBO2 groups.
Conclusion: Partially preserved vasodilation in the presence of INDO in HBO2 groups, and eliminated vasodilation in response to reduced pO2 in the presence of MS-PPOH in both HBO2 groups suggest that HBO2 affects CYP450-epoxigenase in MCAs of healthy and DM rats and shifts vasodilatory mechanisms in response to reduced pO2 towards EETs mediated pathways.
Support: This study was supported by grant of Ministry of Science, Education and Sports, Croatia, #219-2160133-2034.

Lombard JH, Liu Y, Fredricks KT, Bizub DM, Roman RJ, Rusch NJ. Electrical and mechanical responses of rat middle cerebral arteries to reduced PO2 and prostacyclin. Am J Physiol. 1999;276(2):H509-162.

Feletou M, Vanhoutte PM. EDHF: the complete story. Chapter 4: EDHF and the physiological control of blood flow. CRC Press 2006: 133-144.

Where applicable, the authors confirm that the experiments described here conform with The Physiological Society ethical requirements.

PCD338

Endothelial T-type channels (Cav3.1) are co-localized with eNOS and promote NO-formation and vasodilatation during depolarization in mesenteric resistance arteries

P.B. Hansen[1], P. Svenningsen[1], A.D. Thuesen[1], K. Andersen[1], H.S. Shin[2], B.L. Jensen[1] and O. Skott[1]

[1]Cardiovascular and Renal Research, University of Southern Denmark, Odense, Denmark and [2]Center for Neural Science, Korea Institute of Science and Technology, Seoul, Republic of Korea

Voltage-gated calcium channels are involved in the excitation-contraction mechanism of resistance vessels. However, T-type channels are also involved in relaxation of mesenteric, coronary and renal blood vessels. We investigated the mechanisms involved in the T-type channel-dependent dilatation. The secondary dilatation after potassium-induced contraction of isolated perfused mesenteric arteries was reduced significantly in Cav3.1-/- compared to Wt mice and use of eNOS -/- mice led to a significantly attenuated dilatation. Western blotting showed no difference in phosphorylated eNOS-pS1117 levels between wild type and Cav3.1-/- mice. Immunoprecipitation of Cav3.1 pulled down eNOS, and immunoprecipitation of eNOS pulled down Cav3.1 showing co-localization of Cav3.1 and eNOS. Confocal laser-scanning microscopy of mesenteric arteries labeled with antibodies against eNOS and Cav3.1 confirmed the co-localization of eNOS and Cav3.1 in endothelial cells, and showed that Cav3.1was also expressed in vascular smooth muscle cells. The basal cGMP levels in isolated aortae were not different between genotypes. We conclude that endothelial calcium-influx through Cav3.1 T-type calcium channels that are co-localized with eNOS, stimulates eNOS and NO production which, in turn, affects NO-dependent dilatation after depolarization in mesenteric resistance arteries. This

mechanism could be important for maintaining the systemic impact of NO on total peripheral resistance.

Where applicable, the authors confirm that the experiments described here conform with The Physiological Society ethical requirements.

PCD340

Properties and roles of tunneling nanotubes in vascular endothelial cells

L. McKeown[1,2] and D.J. Beech[1,2]

[1]School of Biomedical Sciences, University of Leeds, Leeds, UK and [2]Multidisciplinary Cardiovascular Research Centre, University of Leeds, Leeds, UK

Cell to cell communication plays a role in many physiological processes. A newly discovered route of communication is via Tunneling Nanotubes (TNTs) which are tubular projections that connect cells over long distances (1). TNTs have been shown to facilitate the rescue of stressed cells by allowing the transfer of cellular constituents such as organelles and Ca2+ signals (2). Using high resolution microscopy we have identified multiple types of F-actin containing intercellular connections in human umbilical vein endothelial cells. These can be classified into groups according to their diameter. Fine TNTs are less than 700nm wide. We find that the structures can permit the propagation of mechanically induced Ca2+ signals between cells over long distances (160 μm). In addition there are TNT-like structures that are similar to intercellular bridges observed in epithelial cells and which contain obvious actin bundles and have greater diameters. Staurosporine-induced TNTs were observed in situ in endothelial cells lining the murine aorta. It is concluded that TNTs exist between endothelial cells in intact blood vessels and that they can transfer Ca2+ signals from endothelial cell to endothelial cell over long distances. It is hypothesized that TNTs play important roles in endothelial repair

Rustom, A., R. Saffrich, et al. (2004). Science 303(5660): 1007-1010

Yasuda, K., H. C. Park, et al. (2010). Am J Pathol 176(4): 1685-1695

Wellcome Trust

Where applicable, the authors confirm that the experiments described here conform with The Physiological Society ethical requirements.

PCD341

Hyperglycaemia downregulates TRPV4 channels in retinal endothelial cells

K. Monaghan, J.E. McNaughten, D. Kyle, C. Kelly, M.K. McGahon, R. Hamilton, N. Scholfield, G. McGeown and T.M. Curtis

Centre for Vision and Vascular Science, Queen's University Belfast, Belfast, UK

Presently, the molecular mechanisms underlying endothelial dysfunction in diabetes are not fully understood. TRPV4 channels have been shown to play an essential role in endothelial-dependent vasodilatation in various vascular beds. In the present study, we have characterised the molecular and functional expression of TRPV4 channels in bovine retinal endothelial cells (BRECs) following culture in both normal (5mM) and high glucose (25mM) conditions (72 h incubations). (Data are presented as mean±SEM). In cells cultured in normal glucose, the TRPV4 agonist, 4α-PDD (1μM) induced a rise in $[Ca^{2+}]i$ (fura-2 microfluorimetry) (0.2±0.03 R340/380, n=8) which could be blocked by the non-selective TRPV4 antagonist, ruthenium red (10μM) (0.06±0.01 R340/380, n=6) and siRNA-mediated knockdown of TRPV4 channel expression (0.01±0.002 R340/380, n=5). The 4α-PDD response was abolished in the absence of extracellular Ca^{2+} (0.001±0.00001 R340/380, n=6) and greatly reduced following Ca^{2+} store depletion using the SERCA pump inhibitor, CPA (20μM) (0.04±0.01 R340/380, n=6). This suggests that activation of TRPV4 channels in BRECs triggers both influx of extracellular Ca^{2+} and Ca^{2+} store release. We subsequently examined the effects of high glucose on TRPV4 mRNA expression in BRECs. TRPV4 transcripts as well as protein levels were appreciably lower in cells treated with high glucose. Following pre-incubation of BRECs with CPA, the Ca^{2+} influx component of the 4α-PDD response was attenuated in cells grown under high glucose conditions (0.02±0.005 R340/380, n=8). Experiments were also performed to examine TRPV4-mediated membrane currents using the whole-cell patch clamp technique. The TRPV4 specific agonist GSK1016790A (1μM) increased membrane current amplitude at -80mV (-5.14±3.17 to -12.55±5.09 pA/pF, n=6) and this was reversed by the TRPV4 antagonist HC-067047 (1μM) (-5.53±2.80 pA/pF, n=6). The effects of GSK1016790A were abolished after culturing cells in high glucose (-0.78±0.34 pA/pF before and -1.14±0.39 pA/pF after GSK1016790A; -0.99±0.34 pA/pF after HC-067047, n=8). Osmotic control experiments were undertaken using mannitol or L-glucose (20mM + 5mM D-glucose). The gene and protein expression and functional responses of TRPV4 channels were identical to those observed under normal glucose condition. These results show that the expression and function of TRPV4 channels is downregulated in retinal endothelial cells under hyperglycaemic conditions. Changes in TRPV4 expression may contribute to endothelial cell dysfunction during diabetes, an issue that warrants further investigation.

This work is supported by funding from EFSD.

Where applicable, the authors confirm that the experiments described here conform with The Physiological Society ethical requirements.

PCD342

Elevated expression levels of microRNA-143/145 drive aberrant smooth muscle cell phenotype and function in Type 2 diabetes – evidence of metabolic memory

K. Riches[1,4], N.A. Turner[1,4], D.J. O'Regan[2,4], I.C. Wood[3] and K.E. Porter[1,4]

[1]Division of Cardiovascular and Diabetes Research, University of Leeds, Leeds, UK, [2]The Yorkshire Heart Centre, Leeds General Infirmary, Leeds, UK, [3]Faculty of Biological Sciences, University of Leeds, Leeds, UK and [4]Multidisciplinary Cardiovascular Research Centre (MCRC), University of Leeds, Leeds, UK

Individuals with Type 2 diabetes mellitus (T2DM) are at increased risk of premature atherosclerosis and coronary heart disease, and suffer poorer outcomes following surgical intervention. Smooth muscle cells (SMC) within the vessel wall play key roles in adaptation to physiological and pathological stimuli through inherent plasticity that permits phenotypic switching between quiescent, contractile and active, synthetic states. MicroRNAs (miRs) are short, non-coding RNAs that negatively regulate gene expression in a variety of pathologies and whilst roles for miRs have been associated with development of

T2DM, their influence on macrovascular complications and specifically at the level of vessel wall SMC is unknown.
SMC were cultured from saphenous vein explants of non-diabetic (ND) patients and those with established T2DM. Cell morphology was analysed using phase contrast microscopy and ImageJ software. Cytoskeletal structure (F-actin) was examined using rhodamine phalloidin fluorescence microscopy and cell proliferation was determined by direct cell counting. Expression of miRs was quantified by TaqMan real-time RT-PCR assays. Over-expression and knock-down of miRs was achieved by transfection of premiRs and antimiRs respectively.
SMC from T2DM individuals were significantly larger than ND SMC (9181 ± 926 μm2 vs. 5621 ± 431 μm2, n=15, p<0.001) with a disorganised cytoskeleton and impaired proliferation (33% reduction, n=6, p<0.01). TaqMan assays revealed a specific 1.6-fold up-regulation of miR-143 and miR-145 in SMC from multiple T2DM patients relative to ND SMC (n=10, p<0.05). Over-expression of miR-143/145 in ND cells induced an increase in spread cell area (7641 ± 863 μm2 vs 5634 ± 319 μm2 in controls, n=4, p<0.001), truncated F-actin fibres and reduced proliferation rate (35% reduction, n=6, p<0.05), similar to that observed in native T2DM SMC. Conversely, antimiR-143/145 transfection in T2DM cells reversed the phenotype towards that of native ND SMC.
In summary, SMC from T2DM patients exhibit a distinct phenotype that exhibits features of both contractile and synthetic cells. Importantly, these characteristics are maintained throughout culture and passaging, suggestive of metabolic memory. Our data support the hypothesis that aberrant expression of miR-143/145 in vascular SMC confers a persistent "T2DM phenotype". The perceived detrimental effects of miR-143/145 may impact on the functional ability of SMC to remodel the vessel wall and contribute to vascular complications in patients with T2DM. Thus, miR-143/145 may be attractive targets for therapeutic intervention.

Where applicable, the authors confirm that the experiments described here conform with The Physiological Society ethical requirements.

PCD343

Investigating a role for CGRP in the ageing cardiovascular system

R. King, S.J. Smillie and S. Brain

Cardiovascular Division, King's College London, London, UK

The sensory neuropeptide calcitonin gene-related peptide (CGRP) is a potent microvascular vasodilator (Brain et al. 1985). CGRP receptors are comprised of the seven transmembrane GPCR, the calcitonin-like receptor (CLR), a receptor activity-modifying protein 1 (RAMP1) molecule and an intracellular protein, known as the receptor component protein (RCP). Previous work in our laboratory has shown that genetic deletion of aCGRP in mice leads to increased susceptibility to elevated blood pressure and associated vascular remodeling in an Ang II model of hypertension. We now investigate the role of CGRP within the cardiovascular system of the ageing mouse.
Male and female aCGRP wild type (WT) and knockout (KO) mice were used, aged 15 months, and juveniles aged 3 months. Blood pressure measurements were taken via tail cuff (Kent Scientific) for one week following a one-week training protocol. Heart rate was determined by pulse oximetry (Kent Scientific). Mice were killed via induction of anaesthesia and subsequent cervical dislocation. We characterised potential gross organ pathology by measuring body weights and organ weights, including heart and kidney. Aortae were processed into paraffin blocks for histology (Masson's trichrome). Aortic mRNA expression of CGRP receptor constituents were analysed by RTqPCR. Raw data were normalized to reference genes and data were expressed as copies per microliter of sample. All data are expressed as mean ± SEM and data were interrogated by two-tailed unpaired t-test or one-way ANOVA, where appropriate. A level of $p < 0.05$ was deemed to be statistically significant.
Both WT and KO animals aged 15 months did not appear to display any gross organ pathology and did not differ with respect to cardiac or renal hypertrophy as determined by weight. Furthermore, we found no differences in baseline blood pressure in aged aCGRP WT and KO mice (mean arterial pressure 105.1 ± 4.1 and 104.9 ± 3.0 mm Hg, respectively, n=6). We also have shown a trend towards an increased mRNA expression of RAMP1 in KO mice (25.71 ± 21.59 vs 270.4 ± 183.9 copies/ul) and a significant increase in CLR mRNA in KO aortic tissue (1,775 ± 1,163 vs 6,732 ± 1,977 copies/ul, two tailed unpaired t-test, $P < 0.05$, n=4) was also observed. RCP expression appeared to be unchanged between groups (3,564 ± 1,404 vs 16,024 ± 10,188 copies/ul).
In conclusion, we provide new evidence showing that genetic deletion of aCGRP appears to have little effect on gross organ pathology as animals age to 15 months. Furthermore, we have shown that CGRP appears to have little role to play in the regulation of blood pressure both at baseline in juvenile animals and as age progresses. This minimal effect of CGRP deletion on haemodynamics occurs in spite of an apparent increase in CGRP receptor constituent gene expression.

Brain, S. D., Williams, T. J., Tippins, J. R., Morris, H. R. & MacIntyre, I. Calcitonin gene-related peptide is a potent vasodilator. Nature 313, 54–56 (1985).

RK is funded by a 4-year PhD studentship from The British Heart Foundation.

Where applicable, the authors confirm that the experiments described here conform with The Physiological Society ethical requirements.

PCD344

Endocannabinoid-mediated CB1 receptor activation attenuates the vasoconstrictor effect of angiotensin II and other Ca2+-mobilizing GPCR agonists in skeletal muscle resistance vasculature

M. Szekeres[1], G.L. Nádasy[2], G. Turu[1], E. Soltész-Katona[1], E. Szabó[3], Z.E. Tóth[4], Z. Takáts[3] and L. Hunyady[1,5]

[1]Department of Physiology, Semmelweis University, Budapest, Hungary, [2]Institute of Human Physiology and Clinical Experimental Research, Semmelweis University, Budapest, Hungary, [3]1st Department of Pediatrics, Semmelweis University, Budapest, Hungary, [4]Neuromorphological and Neuroendocrine Research Laboratory, Hungarian Academy of Sciences, Budapest, Hungary and [5]Laboratory of Molecular Physiology, Hungarian Academy of Sciences, Budapest, Hungary

Calcium-mobilizing G protein-coupled receptor (GPCR) agonists, such as angiotensin II (AngII), endothelin and vasopressin induce vasoconstriction. Activation of AT1 angiotensin- and other Gq/11 protein-coupled receptors leads to diacylglycerol (DAG) formation, which can be converted to 2-arachidonoylglycerol (2-AG), an important endocannabinoid by the effect of DAG lipase (1,2). Cannabinoids via CB1 cannabinoid receptors (CB1R) have peripheral hypotensive and vasodilator

actions. We tested the hypothesis that 2-AG release can modulate the vasoconstrictor action of AngII and other calcium-mobilizing hormones in rodent vascular tissue.
Male Wistar rats (300-350g), C57BL6 and CB1R knockout mice (21-25g, 3) were anaesthetised with pentobarbital (50mg kg-1 ip.). Rat skeletal muscle (gracilis) arterioles and mouse saphenous arteries were isolated, pressurized and subjected to microangiometry. Also, rats (200-250g) were anaesthetised and aorta was removed for vascular smooth muscle cell (VSMC) isolation. Vascular expression of CB1R was demonstrated with immunohistochemistry. In accordance with the functional relevance of these receptors WIN55212, a CB1R agonist caused vasodilation, which was absent in CB1R knockout mice. In gracilis arterioles dose-dependent vasoconstrictions for AngII, norepinephrine (NE), endothelin, vasopressin and prostaglandin (PG)F2α were obtained. Inhibition of CB1Rs with neutral antagonist O2050 in gracilis arterioles augmented the vasoconstriction induced by AngII, NE, endothelin and vasopressin (from 29.1±5.8% to 47.5±3.2% and from 38.8±7.6% to 76.3±4.8%, effects of 10nM AngII and 1μM NE, respectively, $p<0.05$) but did not influence the contractile effect of PGF2α (45.6±9.9% and 36.9±9.8% at 1μM, n.s.). Inhibition of CB1Rs enhanced AngII-induced vasoconstrictor action in saphenous arteries of wild type, but not of CB1R knockout mice. Inhibition of DAG lipase by tetrahydrolipstatin (THL) also augmented the vasoconstrictor effect of AngII, suggesting the role of 2-AG in CB1R activation. In VSMCs AngII-stimulated 2-AG formation was inhibited by THL but potentiated by JZL184, an inhibitor of monoacylglycerol lipase, an enzyme catalyzing degradation of 2-AG. Inhibition of CB1R also increased the sustained phase of AngII-induced calcium signal and this effect was found to be independent of nitric oxide synthase activity and of endothelial function.
These data demonstrate that vasoconstrictor effects of calcium mobilizing GPCR agonists are physiologically attenuated by agonist-induced endocannabinoid release and consequent CB1R activation. It is proposed that this effect may serve as a beneficial control mechanism by moderating the microvascular tone in high contractile states.

Szekeres M et al. Angiotensin II induces vascular endocannabinoid release, which attenuates its vasoconstrictor effect via CB1 cannabinoid receptors. J Biol Chem. 287(37):31540-50, 2012

Gyombolai P et al. Regulation of endocannabinoid release by G proteins: a paracrine mechanism of G protein-coupled receptor action. Mol Cell Endocrinol. 353(1-2):29-36, 2012

Zimmer A et al. Increased mortality, hypoactivity, and hypoalgesia in cannabinoid CB1 receptor knockout mice. Proc Natl Acad Sci U S A. 96(10):5780-5,1999

Supported by Hungarian National Science Foundation OTKA NK-100883.

Where applicable, the authors confirm that the experiments described here conform with The Physiological Society ethical requirements.

PCD345

TRPA1 mediates the cold-induced hemodynamic changes observed in the arthritic knee following exposure to low temperature

E.S. Fernandes[1,3], C. Sand[1], R. Salamon[1], J.V. Bodkin[1], A.A. Aubdool[1,2] and S.D. Brain[1,2]

[1]Vascular Biology Group - Cardiovascular Division, King's College London, London, UK, [2]Centre for Integrative Biomedicine - Cardiovascular Division, King's College London, London, UK and [3]Programa de de Pós-Graduação em Biologia Parasitária, Universidade Ceuma, Sao Luis, Brazil

Rheumatoid arthritis is a common disease, characterised by persistent synovitis, systemic inflammation and severe pain. A relationship between environmental cold exposure and increased pain in arthritic joints has been suggested (Smedslund and Hagen, 2011), although the underlying mechanisms are unknown. Changes in joint vascularization and the development of pain have been previously hypothesized to be linked in arthritis, with evidence of a correlation provided in osteoarthritis (Walsh et al., 2010; Ashraf et al., 2011). We have been studying the role of Transient Receptor Potential (TRP) channels in arthritis. We recently found by using a mono-arthritis model induced by a single injection of Complete Freund's Adjuvant (CFA; 10 ug/joint; 10 ul) in to the knee joint; that the TRP Ankyrin 1 (TRPA1), a suggested cold sensor, mediates CFA-induced secondary mechanical hyperalgesia (Fernandes et al., 2011). We have now investigated the contribution of TRPA1 activation for blood flow changes in the arthritic knee joint of mice exposed for 1h to environmental cold (10oC). We used male CD1 and TRPA1 wild-type (WT) and knockout (KO) mice (10-12 weeks of age). Blood flow was recorded by using full-field laser perfusion imager (FLPI) following cold exposure, 2 weeks after arthritis induction, in anaesthetised mice (mixture of ketamine (75 mg/kg) + medetomidine (1 mg/kg)). Briefly, after anaesthesia, the patellar ligament was carefully dissected off the knee joint to expose the synovial membrane. Changes in blood flow were then recorded for 30 min. Data obtained from the arthritic knee joint (ipsilateral knee; CFA-treated) was compared to the contralateral knee joint (saline-treated; 10 ul/joint). Naive joints were used as controls. Whilst cold exposure caused vasoconstriction in naive mice, a significant vasodilatation was observed in arthritic animals, with both saline- and CFA-treated joints exhibiting increased blood flow (1.5- and 2-fold increase, respectively). This response was not observed in mice treated systemically with the selective TRPA1 antagonist HC-030031 (100 mg/kg; 1h before blood flow recording; n=7). Similarly, vasodilatation was not present in the arthritic knee joints of TRPA1 KO mice (n=9) when compared to their WT controls (n=9). We suggest TRPA1 mediates hemodynamic changes in arthritic joints exposure to lower temperatures. This could be a potential and additional mechanism by which TRPA1 channels modulate arthritis progression and pain sensitivity.

Ashraf et al (2011). Ann Rheum Dis; 70:523-529.

Fernandes et al (2011). Arthritis Rheum; 63: 819-829.

Smedslund and Hagen (2011). Eur J Pain; 15:5-10.

Walsh et al (2010). Rheumatology; 49:1852-1861.

Work supported by the Arthritis Research UK and a BBSRC capacity building programme in mammalian biology.

Where applicable, the authors confirm that the experiments described here conform with The Physiological Society ethical requirements.

PCD346

MicroRNA-26a regulates Ca^{2+} signalling via the IP_3 pathway in retinal endothelial cells

A. O'Connor, J. Guduric-Fuchs, D.A. Simpson and T.M. Curtis

Centre for Vision and Vascular Science, Queen's University Belfast, Belfast, UK

Primary bovine retinal microvascular endothelial cells (RMECs) are widely used for angiogenesis-based studies. Ca^{2+} signalling is a fundamental part of many cellular functions including the responses of RMECs to angiogenic stimuli and this relies upon appropriate regulation of gene expression. MicroRNAs (miRNA) are endogenous, non-coding RNAs which regulate mRNA expression at the post-transcriptional level. The ability of miRNAs to target multiple genes suggests that they can potentially modulate the expression of several genes in a specific pathway. We therefore investigated the possibility that miRNAs can regulate Ca^{2+} responses in RMECs by targeting genes of the IP_3- Ca^{2+} signalling pathway. Both mRNA and miRNA expression in RMECs was quantified by high throughput, next generation sequencing (NGS) on an Illumina Genome Analyzer. Predicted target genes of the miRNAs expressed in RMECs were downloaded from the miRNA prediction algorithm TargetScan (1) and were compared with those genes in the Ca^{2+} signalling pathway which were shown to be expressed in RMECs. MiRNA-26a (miR-26a) was selected for further analysis as it was found to be within the top 20 most highly expressed miRNAs in RMECs and it was predicted to target key genes of the IP_3- Ca^{2+} signalling pathway found to be expressed in these cells (IP_3 receptor type 1 (ITPR1) and phospholipase C beta 1 (PLCB1). Overexpression (oe) of miR-26a from a plasmid vector, pSM30 (2) or knockdown (kd) with an LNA inhibitor, followed by RT-PCR, Western blotting (WB) and luciferase assays confirmed ITPR1 as a target at the protein level (3.5 fold decrease upon miR-26a oe *vs.* scrambled oe control and a 2 fold increase in miR-26a kd *vs.* scrambled kd control for WB, n=5, $p<0.05$, Student's paired t-test). Uridine triphosphate (UTP) was found to induce a transient increase in RMEC $[Ca^{2+}]_i$ that was dependent on IP_3-Ca^{2+} signalling, as determined by the use of known IP_3 receptor inhibitors, xestospongin C (3) or 2-aminoethoxydiphenyl borate (2APB) (4) and fura-2 Ca^{2+} microfluorimetry. Overexpression of miR-26a decreased the elevation in $[Ca^{2+}]_i$ observed in response to UTP and knockdown of miR-26a increased the response (0.49±0.02 change in fura-2 340/380 nm ratio in scrambled oe control decreased to 0.13±0.02 upon miR-26a oe, and increased from 0.44±0.02 in scrambled kd control to 0.69±0.04 upon miR-26a kd. Mean data ± SEM, n=12, $p<0.001$, one-way ANOVA). Taken together, our results suggest that miR-26a, can modulate the Ca^{2+} responses of RMECs by targeting the IP_3-Ca^{2+} signalling pathway. Further studies are now warranted to determine the functional significance of miR-26a in both retinal microvascular endothelial cell physiology and pathophysiology.

Lewis BP *et al.* (2005). Conserved seed pairing, often flanked by adenosines, indicates that thousands of human genes are microRNA targets. *Cell* 120:15-20.

Du G *et al.* (2006). Design of expression vectors for RNAi based on miRNAs and RNA splicing. *FEBS J* 273:5421-5427.

Gafni J *et al.* (1997). Xestospongins: potent membrane permeable blockers of the inositol 1,4,5-trisphosphate receptor. *Neuron* 19:723–733.

Maruyama T *et al.* (1997). 2APB, 2-aminoethoxydiphenyl borate, a membrane-penetrable modulator of Ins(1,4,5)P3-induced Ca2+ release. *J Biochem* 122(3):498-505.

The Department for learning and employment in Northern Ireland

Where applicable, the authors confirm that the experiments described here conform with The Physiological Society ethical requirements.

PCD347

The new NO-donor does not induce *in vitro* tolerance in rat aorta

T. Banin, L. Pernomian, R.S. da Silva and L.M. Bendhack

Physics and Chemistry, FCFRP/ USP, Ribeirão Preto, SP, Brazil

The nitrite anion (NO2-) can be the major source of intravascular and tissue storage of nitric oxide (NO), important modulator of vascular tone and blood pressure. The NO donor RUBPY synthesized by our group, releases NO inside the vascular smooth muscle cell in a tissue dependent manner. Long-term treatment with organic nitrates like nitroglycerin, leads to the development of tolerance characterized by the rapid loss of vasodilator effects. Tolerance is a multifactorial process. It may be due to endothelial dysfunction that involves increased production of vascular reactive oxygen species (ROS), decreased activity of soluble guanylyl-cyclase and increased phosphodiesterase expression and activity. This study aimed to investigate the *in vitro* tolerance to the pre-exposure of intact endothelium aorta (e+) or denuded aorta (e-) with RuBPY (EC100:10 μM). It was also evaluate if the compound releases NO in the endothelial cells in the incubation time studied. The aortic rings were isolated and used for the functional studies. Aortic rings (e+/e-) were contracted with phenylephrine, and after reaching a stable and maintained contraction, RuBPY (3 nM-5 μM) was added to the organ bath. Experiments were conducted after pre-exposure to RuBPY (tolerance) or in the absence of RuBPY (control). The maximum effect (ME) and potency (pD2) of RuBPY in inducing relaxation were evaluated. Endothelial cells were incubated with the fluorescent dye DAF-2/DA (10 μM) to quantifying the cytosolic NO and DHE (2.5 μM) to quantifying ROS. The intensity of fluorescence was detected in the absence or after exposure to RuBPY at different times (5-60min). This study was approved by the Ethical Animal Committee of the University of São Paulo (2012.1.134.53.12). The compound RuBPY induced concentration-dependent relaxation in e+ aortas (pD2:7.81±0.18; ME:101.6± 1.4%, n=7) and e- (pD2:7.54±0.13; ME:103.4±0.4%, n=6). The incubation with 10 μM RuBPY for 5 min followed by 20 min of washout did not affect the ME induced by the compound in e+ aorta (pD2:7.99±0.18; ME:98.5 ±1.6%, n=5) or in e- aortas (pD2:7.89±0.18, ME:100.0 ±0.4%, n=6). Pre-exposure for 10 min with RuBPY in e+ aortas did not alter the relaxation to RuBPY compared to respective control. However, in e- aortas the relaxing effect of RuBPY was potentiated (pD2:7.37±0.12, ME:101.5±1.0%, n=5, $P<0.05$). Pre-exposure for 30 min with RuBPY did not change the relaxation to RuBPY in e- aortas as compared to the control. RuBPY did not release NO and ROS in the endothelial cells up to 60 min incubation. Taking together, our results demonstrate that the new NO donor RuBPY does not induce tolerance in rat aorta, which is

probably due to the lack effect of RuBPY on the endothelial cells.

Supported by FAPESP and CNPq.

Where applicable, the authors confirm that the experiments described here conform with The Physiological Society ethical requirements.

PCD348

The new nitric oxide donor (RuBPY) induces tolerance only after 60 minutes exposure and it does not induce cross-tolerance with acetylcholine

M. Paulo, M.D. Grando, J.A. Vercesi, R.S. da Silva and L.M. Bendhack

Physics and Chemistry, University of São Paulo, Ribeirão Preto, SP, Brazil

Nitric oxide (NO) donors like nitroglycerin (GTN) are widely used as pharmacological tool to understand the physiological effect of NO, and in the treatment of cardiovascular diseases. The major therapeutic limitation of GTN is the tolerance that is characterized by rapid loss of its effects in long-term administration, or cross-tolerance to other vasodilator, which cause(s) is still not clear. It is endothelium-dependent and the uncoupling endothelial NO-synthase (eNOS) could contribute to the tolerance. The major clinical benefit of organic nitrates, including the GTN has been attributed to their potent venodilator effect. This study aimed to verify if the new NO donor synthesized in our laboratory (RuBPY) induces in vitro tolerance and cross-tolerance to acetylcholine and sodium nitroprusside (SNP) in rat cava vein. We compared the effects of RuBPY with GTN in relation to the maximum effect (ME) and potency (pD2). In vitro tolerance was induced by incubation for 10, 30 or 60 min with RuBPY (2 μM or 10 μM) or GTN (4 μM or 0.1mM). In vitro cross-tolerance to acetylcholine and SNP was induced by the veins pre-incubation with RuBPY (2 μM) or GTN (4 μM) for 60 min. The eNOS phosphorylated in the activation site (Ser1177) and in the inactivation site (Thr495) was accessed by Western Blotting. The cytosolic concentration of NO ([NO]c) was measured by flow cytometry and confocal microscopy. Our results demonstrated that RuBPY induced greater relaxation (ME: 92.8 ± 4.4%; n=7, P<0.05) than GTN (ME: 75.3 ± 3.7%, n=6). Both NO donors increased [NO]c in vascular smooth muscle cells. Previous exposure for 10 min with RuBPY (2 μM or 10 μM) or GTN (4 μM or 0.1mM) did not induce tolerance. However, 30 min pre-exposure did not change the relaxation to RuBPY, but it reduced the relaxation to GTN (with 4 μM, ME: 45.4 ± 2.2%, n= 6, P<0.05, and 0.1 mM, ME: 39.2 ± 1.4%, n= 6, P<0.05). Pre-exposure for 60 min with RuBPY reduced the relaxation in the concentrations of 2 μM (ME: 48.0 ± 2.3%, n= 7, P<0.05) and to 10 μM (ME: 30.1±1.2%, n= 7, P<0.05). Pre-exposure to RuBPY or GTN did not reduce the relaxation to SNP. Cross-tolerance to acetylcholine was induced only with GTN. The ME stimulated with acetylcholine was reduced from100.3 ± 5.3% to 75.1 ± 4.2% (n=7, P<0.05). Whereas RuBPY and GTN had phosphorylated eNOS in Thr495, only GTN phosphorylated eNOS-Ser1177. In conclusion, our data demonstrate that RuBPy induces tolerance in both concentrations, only after 60 min exposure. It does not induce cross-tolerance to acetylcholine and SNP. It does not interfere with the activation site of eNOs.

Supported by FAPESP and CNPq.

Where applicable, the authors confirm that the experiments described here conform with The Physiological Society ethical requirements.

PCD349

Effects of acute and long-term incubation with high D-glucose on mechanisms that induces nitric oxide and reactive oxygen species in human fetal endothelium

C. Valenzuela[1], P. Ávila[1], S. Rojas[1], R. Villalobos[1], C. Palma[1], V. Gallardo[1], L. Sobrevia[2] and M. González[1]

[1]Fisiologia, Universidad de Concepcion, Concepcion, Chile and [2]Obstetrics and Gynaecology, Medical Research Centre (CIM), Pontificia Universidad Catolica, Santiago, Chile

There is evidence that the endothelial dysfunction would be caused by an increase of reactive oxygen species (ROS) and reactive nitrogen species (RNS) induced by high extracellular concentrations of D-glucose (González et al., 2011). In human fetal endothelium, the synthesis of ROS is mediated by NADPH oxidase (Villalobos et al., 2012); meanwhile the synthesis of nitric oxide (NO) is mediated by the L-arginine uptake dependent of human cationic amino acid transporter 1 (hCAT-1)(Shin et al., 2011). Our aim is describe the mechanisms underlie the effects of high extracellular D-glucose on synthesis of NO and ROS in human umbilical vein endothelial cells (HUVEC). Biological samples were obtained from normal pregnancies (ethics committee approval and informed patient consent were obtained). HUVEC were isolated by collagenase digestion (37 celcius degree) and cultured in medium 199 (M199) supplemented with 20% newborn and fetal calf sera. HUVEC were incubated (0-30 min or 1-24 h) with M199 containing 5 mM (control) or 25 mM of D-glucose (high D-glucose) en absence or presence of apocynin (100 μM, NADPH oxidase inhibitor), N-ethylmaleimide (NEM, 200 μM, CAT inhibitor), L-NAME (200 μM, eNOS inhibitor) or insulin (1 nM, 8 h). After incubations, were determined L-arginine uptake (100 μM L-arginine, 2 μCi/mL L-[3H]arginine), NO and ROS synthesis using diaminofluorescein (DAF-2DA) and dichlorofluorescein (DCF), respectively, and hCAT-1 and NADPH oxidase expression by real time PCR and western blot. High D-glucose increased (ANOVA unpaired Student's t test, P<0.05, n=5-10) the L-arginine uptake after 10 (3±0.7-fold) and 30 (3±0.6-fold) min of incubation. These effects were blocked by pre-incubation with NEM and L-NAME. The acute incubation with high D-glucose not alter the ROS levels, but increased (P<0.05, n=3) the NO levels 2.1±04-fold and 2.8±0.6-fold after 10 and 30 min, respectively. Long term incubation with high D-glucose (24 h) increased (P<0.05, n=5-10) the L-arginine uptake (3±0.5-fold), ROS (1.8±0.1-fold) and NO (1.5±0.1-fold) levels. These effects of high D-glucose are related with increased (P<0.05, n=5-10) of mRNA (6±1-fold) and protein (2.7±0.2-fold) for hCAT-1 and mRNA for subunits of NADPH (1.5-fold). Insulin blocked the effects of high D-glucose on ROS, NO levels and hCAT-1 expression. In conclusion, the acute effect of high D-glucose is related with increases of L-arginine/NO pathway, without changes in ROS levels. Long term incubation with high D-glucose maintains the activation of this pathway but there is a concomitant activation of NADPH oxidase/ROS pathway. The endothelial dysfunction induced by high D-glucose could be prevented by insulin.

González M et al. (2011). The Molecular Basis for Origin of Fetal Congenital Abnormalities and Maternal Health: An overview of Association with Oxidative Stress 1: 98-115.

Villalobos R et al. (2012). Proc Physiol Soc 27 C30

Shin et al. (2011). Biochem Biophys Res Commun 414:660-663

Supported by FONDECYT 11100192.

Where applicable, the authors confirm that the experiments described here conform with The Physiological Society ethical requirements.

PCD350

Withdrawal of early age acute statin treatment alters RhoA pathway gene expression long term in rat mesenteric arteries

P.H. Keskivali[1], N.P. Curzen[1,2], G.F. Clough[1] and C. Torrens[1]

[1]Human Development and Health, Faculty of Medicine, University of Southampton, Southampton, Hampshire, UK and [2]Wessex Cardiothoracic Unit, Faculty of Medince, University of Southmapton, Saouthampton, Hampshire, UK

Maternal protein restriction (PR) in rats induces vascular dysfunction and though this can be ameliorated by chronic statin treatment, statin treatment and withdrawal in adolescent rats leads to a sustained increase in mesenteric artery constriction. In adult rats increase in constriction after statin withdrawal has been shown to be transient and RhoA pathway has been implicated as the mechanism. RhoA promotes constriction by activating Rho kinases (ROCK) which inhibit myosin light chain phosphatase. Statins inhibit RhoA activity but increase RhoA mRNA levels which remain elevated briefly after statin withdrawal contributing to increased RhoA activity. In this study the mRNA levels of RhoA pathway genes were investigated in the control and PR rat offspring mesenteric arteries where withdrawal of early age statin treatment lead to sustained increase in constriction.

Male and female Wistar rat offspring of dams fed 18 % protein (control) or 9 % protein restricted (PR) diet during pregnancy were given atorvastatin (10mg/kg) in drinking water from 3-5 weeks. This gave four experimental groups; control, no statin (CS: n=6 males, n=5 females), control, statin (CS: n=6 both), PR diet, no statin (PR: n=5 males, n=4 females) and PR diet, statin (PRS: n=5 both). At 16 weeks the animals were euthanised with CO2 inhalation and cervical dislocation. Segments of mesenteric arteries were frozen in liquid nitrogen. RNA extraction was carried out in Trizol and RNA was reverse transcribed into cDNA. Real time PCR was carried out with FAM/TAMRA primers and probes and gene expression was normalised against β-actin which was chosen as a stable housekeeping gene after geNorm analysis. mRNA levels of RhoA, ROCK 1 and ROCK 2 were investigated. The differences were assessed with two-way ANOVA. Results are presented as mean±SEM. Significance was accepted at $p<0.05$.

No significant differences were seen in mRNA levels of RhoA in the males ($p>0.05$) but in the females statin treatment increased RhoA mRNA expression irrespective of maternal diet (RhoA/b-actin: C 0.63±0.06; CS 0.86±0.10; PR 0.53±0.05; PRS 0.70±0.07; $p<0.05$ for statin effect; $p>0.05$ for maternal diet effect and interaction). Statin treatment increased ROCK 1 mRNA levels in the male offspring irrespective of maternal diet (ROCK1/β-actin: C 0.55±0.06; CS 0.93±0.11; PR 0.70±0.14; PRS 0.90±0.17; $p<0.05$ for statin effect; $p>0.05$ for maternal diet effect and interaction) but no significant differences were seen in the females ($p>0.05$). No significant differences were seen in the ROCK 2 mRNA levels in either males or females ($p>0.05$).

These data indicate that sustained upregulation of gene expression of RhoA pathway genes in the mesenteric arteries could contribute to the long term increase in constriction observed after withdrawal of early age statin treatment in C and PR offspring.

Where applicable, the authors confirm that the experiments described here conform with The Physiological Society ethical requirements.

PCD351

Giα-coupled β2-adrenoceptor signaling mediates oxidative stress and the endothelial dysfunction induced by isoproterenol

A.C. Davel[1], P.C. Brum[2] and L.V. Rossoni[3]

[1]Structural and Functional Biology, State University of Campinas, Campinas, Campinas, Brazil, [2]School of Physical Education and Sport, University of Sao Paulo, Sao Paulo, Sao Paulo, Brazil and [3]Physiology and Biophysics, University of Sao Paulo, Sao Paulo, Sao Paulo, Brazil

Background and aim: We have demonstrated that overactivation of β-adrenoceptors induces oxidative stress and increases vasoconstrictor responses in rat aorta. This study focusing to investigate the β-adrenoceptor subtype as well the signaling pathway involved in these vascular effects.
Methods and results: Male, 3-mo-old mice lacking β1- or β2-adrenoceptors subtypes (β1KO, β2KO, N=12-16) and wild-type (WT, N=14) were daily treated with isoproterenol (ISO, 15 mg/kg/day, s.c.) or vehicle for 7 days. ISO treatment significantly ($p<0.05$, One-Way ANOVA) enhanced the vasoconstrictor response to phenylephrine (PHE) in aorta from WT and β1KO mice as compared to vehicle (34 and 35% of increase in Emax to PHE, respectively), but not in β2KO. Nitric oxide synthase inhibitor L-NAME (100 μM) increased Emax to PHE in aorta from all groups evaluated. This effect was lesser pronounced in aorta from ISO-treated WT and β1KO mice than vehicle-treated groups, but was similar between ISO-treated and non-treated β2KO mice. Incubation with superoxide dismutase (SOD, 150 U/mL) normalized increased Emax to PHE observed in aortic rings from ISO-treated WT and β1KO mice, but did not significantly change this response in ISO-treated β2KO mice. Immunoblotting experiments revealed increased expression of Giα protein (+50%) and of phosphorylated[Thr202/Tyr204]-ERK1/2 (+90%) in aorta from ISO-treated WT compared to vehicle WT. In addition, incubation with Gi inhibitor pertussis toxin (PTx, 4 μM) normalized the enhanced Emax to PHE observed in aortic rings from ISO-treated WT mice. ISO treatment enhanced fluorescence to hydroethidine (+100%) in aortas from WT, indicating oxidative stress that was significantly reduced by SOD and PTx. These effects of ISO were abolished in β2KO mice.
Conclusions: Giα protein coupled to β2-adrenoceptor plays a pivotal role in the oxidative stress and endothelial dysfunction induced by persistent β-adrenergic activation.

FAPESP and CNPq

Where applicable, the authors confirm that the experiments described here conform with The Physiological Society ethical requirements.

PCD352

Valve defects in *Foxc2*$^{+/-}$ mice predispose lymphatic vessels to pump failure

M.J. Davis[1], A. Sabine[2], T.V. Petrova[2], N. Miura[3] and J.P. Scallan[1]

[1]Department of Medical Pharmacology and Physiology, University of Missouri, Columbia, MO, USA, [2]Division of Experimental Oncology, University of Lausanne, Lausanne, Switzerland and [3]Hamamatsu University Medical School, Hamamatsu, Japan

Lymphedema distichiasis (LD) is a form of primary lymphedema associated with mutations in the *forkhead* transcription factor gene FOXC2. Homozygous loss of *Foxc2* in the mouse is associated with agenesis of secondary lymphatic valves as well as other cardiovascular and skeletal defects that contribute to lethality between E12.5 and P1. *Foxc2*$^{+/-}$ mice are characterized by distichiasis, reduced lymphatic drainage and lymph backflow, similar to patients with LD.

We previously demonstrated a novel type of lymphatic pump dysfunction, termed valve lock, which can be experimentally induced if healthy single lymphangions or chains of lymphangions are subjected to pressure conditions that mimic those associated with the development of edema in peripheral extremities. Valve lock is due in part to a normal property of intraluminal lymphatic valves in which valve closure becomes more difficult as the vessel becomes distended (i.e. the adverse pressure gradient required for closure rises 20 fold). As we also recently reported, tests of isolated valves from *Foxc2*$^{+/-}$ mice indicate that about 50% of the valves have elevated back-leak and appear to be abnormally stiff. Here we tested whether lymphatic vessels from *Foxc2*$^{+/-}$ mice exhibit pumping deficits as a result of these valve abnormalities.

Segments of collecting lymphatic vessels, each containing two valves, were isolated from the popliteal region of anesthetized adult C57Bl/6 (WT) or *Foxc2*$^{+/-}$ mice (Nembutal, 60 mg/kg, i.p.), cannulated at each end with a micropipette. Intraluminal pressure (P_L) was measured between the valves with a servo-null micropipette, while tracking vessel diameter and monitoring the leaflet position of the output valve using video methods. A servo controller held input pressure (P_{in}) at 1 cmH_2O while output pressure (P_{out}) was slowly elevated rampwise. The pumping limit (P_{limit}) was defined as the output pressure at which the output valve first failed to open. About half of the WT vessels simply failed to eject at high P_{out} (P_{limit} ~12 cmH_2O); in the other half, valve lock occurred before this point (P_{lock}). On average *Foxc2*$^{+/-}$ vessels exhibited lower values for P_{limit} compared to WT vessels (8.0±0.8 vs 13.9±0.2 cmH_2O, respectively) and lower values for P_{lock} (10.5±0.7 vs 15.9±0.1 cmH_2O, respectively) and a higher susceptibility to valve lock (68% vs 25%).

These new methods for studying mouse lymphatic vessels under defined conditions reveal that the abnormal valves in *Foxc2*$^{+/-}$ vessels render the collecting lymphatics more susceptible to pump failure. The same susceptibility may be characteristic of lymphatic vessels in human patients with LD and contribute to the peripheral edema from which those patients suffer.

Supported by NIH HL-089784

Where applicable, the authors confirm that the experiments described here conform with The Physiological Society ethical requirements.

PCD353

Vascular endothelial growth factor-C induces angiogenesis and lymphangiogenesis in the rat mesentery culture model

R.S. Sweat and W.L. Murfee

Biomedical Engineering, Tulane University, New Orleans, LA, USA

Lymphatic and blood microvascular systems are critical for tissue function and remodeling. New insights into the coordination of both systems can be gained by better investigating the relationships between lymphangiogenesis and angiogenesis in controlled environments. Recently, our laboratory has established that in the rat mesentery culture model lymphatic and blood microvascular networks remain intact and viable (Stapor et al., 2013). The objective of this study was to determine whether the rat mesentery culture model can be used to identify temporal relationships between lymphangiogenesis and angiogenesis induced by vascular endothelial growth factor-C (VEGF-C). Adult male Wistar rats (n=4) were anaesthetized by i.m. injection of ketamine (80 mg/kg) and xylazine (8 mg/kg) and then euthanized. Mesenteric tissue windows were aseptically harvested and cultured for 3 days or 5 days in either serum-free minimum essential media (MEM) or MEM supplemented with VEGF-C (100 ng/ml) (n=10-12 tissues per group). Tissues were immunolabeled for PECAM and LYVE-1 to identify blood and lymphatic endothelial cells, respectively. Tissues selected randomly from those containing vascular networks were quantified for angiogenesis and lymphangiogenesis (n=4-6 tissues per group). Values are means ± S.E.M. and were statistically compared using Student's *t*-tests. VEGF-C treatment resulted in a significant increase in the density of blood vessel sprouting compared to MEM controls by day 3 (22.2±1.8 vs. 13.8±1.6 sprouts/mm^2, $p<0.01$). By day 5, lymphatic sprouting was significantly increased along the hierarchy of intact lymphatic networks compared to MEM controls (7.2±0.6 vs. 4.0±0.4 sprouts/mm^2, $p<0.01$). These results are consistent with *in vivo* findings that lymphangiogenesis lags angiogenesis after chronic stimulation (Sweat et al., 2012; Baluk et al., 2005) and the results establish the rat mesentery culture model as a tool to investigate the interrelationships between lymphangiogenesis and angiogenesis *ex vivo* in a multisystem environment.

Baluk P et al. (2005). *J Clin Invest* **115**, 247-257.

Stapor PC et al. (2013). *Am J Physiol Heart Circ Physiol* **304**, H235-245.

Sweat RS et al. (2012) *Lymphat Res Biol* **10**, 198-207.

Where applicable, the authors confirm that the experiments described here conform with The Physiological Society ethical requirements.

PCD354

Characterisation of cannabinoid-induced vasorelaxation in human mesenteric arteries

C.P. Stanley and S.E. O'Sullivan

University of nottingham, Derby, UK

In animal arteries cannabinoids induce vasorelaxation through mechanisms that are influenced by both the cannabinoid ligand, the artery used and species studied. In human arteries the potential vascular effects of cannabinoids have not been fully investigated. The aim of the present study was to investigate the effects of a range of cannabinoids in human mesen-

teric arteries. With ethical approval and written informed consent, human mesenteric arteries were taken from patients receiving colorectal surgery. Arteries were dissected from mesenteric tissue, mounted on a Mulvany-Halpern myograph and bathed in oxygenated physiological saline solution (PSS) at 37°C under a set tension of 90% of 100 mmHg. Arteries were contracted and concentration response curves were carried out to anandamide (AEA), 2-arachidonyl-glycerol (2-AG), Δ-9 tetrahydrocannabinol (THC), cannabidiol (CBD), CP55,940 and HU-308. In some experiments, cannabinoid mechanisms of action were probed pharmacologically. Cannabinoid maximum responses (Rmax) were derived using mean percentage vasorelaxation data that was fitted to sigmoidal slopes using GraphPad Prism software. Comparisons between Rmax values were made using 1-way ANOVA with Bonferroni post-hoc test. Comparisons between concentration response curves in the presence or absence of pharmacological inhibitors were made using 2-way ANOVA, $P<0.05$ was taken as significant. With the exception of HU-308, all cannabinoids caused significant vasorelaxation of human mesenteric arteries (Rmax: AEA≈30%, 2-AG≈40%, THC≈25%, CBD≈40%, CP55,940≈55%, n=12). CP55,940 was the most efficacious cannabinoid tested with a higher Rmax than AEA ($P<0.001$), 2-AG ($P<0.01$), THC ($P<0.001$) and CBD ($P<0.001$). 2-AG was the most efficacious endocannabinoid tested causing greater vasorelaxation than AEA ($P<0.05$). CBD was the most efficacious phytocannabinoid tested causing greater vasorelaxation than THC ($P<0.05$). 2-AG-induced vasorelaxation was inhibited by COX inhibition ($P<0.001$, n=8), prostanoid receptor antagonism (EP4 $P<0.01$, n=6 & IP $P<0.001$, n=9), in arteries that were contracted using high K+ PSS ($P<0.001$, n=8) and arteries that were bathed in Ca2+-free PSS ($P<0.01$, n=7). Experiments probing the action of CBD revealed that vasorelaxation was dependent on CB1 ($P<0.001$ n=8) and TRPV1 ($P<0.001$, n=7) receptor activation, nitric oxide production ($P<0.001$, n=6), the endothelium ($P<0.001$, n=8) and ion channel modulation ($P<0.001$, n=5). AEA-induced vasorelaxation was inhibited by CB1 receptor antagonism ($P<0.001$, n=7), endothelium removal ($P<0.01$, n=6), nitric oxide inhibition ($P<0.001$, n=6) and inhibition of a novel, as yet uncharacterised, endothelium bound cannabinoid receptor ($P<0.001$, n=6). This study shows that cannabinoids cause vasorelaxation in human mesenteric arteries and therefore suggests that the endocannabinoid system may modulate vascular tone humans.

Where applicable, the authors confirm that the experiments described here conform with The Physiological Society ethical requirements.

PCD355

Microparticles in diabetes-associated microvascular dysfunction

P. He, C.J. Stork, D. Yuan and S. Xu

Physiology and Pharmacology, West Virginia University, School of Medicine, Morgantown, WV, USA

Microparticles (MPs) are small vesicles released from cell membrane following cell activation and apoptosis. Elevated levels of circulating MPs have been reported in many cardiovascular diseases and have been proposed as clinical markers for cardiovascular risk. Released MPs carry a range of antigens depending on the type and activation state of their parental cells. Therefore, it has been suggested that MPs may play important roles in the processes of inflammation and the progression of many cardiovascular diseases. Diabetes is commonly associated with microvascular dysfunction. Our recent study found that microvessels of streptozotocin-induced diabetic rats had increased basal permeability and markedly enhanced permeability responses to inflammatory mediators. We also found that diabetic rats had a significantly increased number of circulating MPs. We hypothesized that the elevated circulating MPs in diabetic rats serve as vectors to actively disseminate inflammation to the vascular system. We used flow cytometry to quantify the numbers of MPs and their cell origins. MPs in diabetic plasma was 5.7 ± 0.9 times of that in normal rat, with 80% of these increased MPs exhibiting exposed phosphatidylserine (PS) on their surface (n=9 per group). The functional roles of MPs were examined by perfusing a matched number of MPs isolated from normal and diabetic rat plasma into individually perfused rat mesenteric venules. Each vessel was perfused with isolated MPs for 30 min followed by 10 min of resumed blood flow. When the same vessel was recannulated with BSA-Ringer perfusate, a large number of adherent leukocytes were found in the diabetic MP-perfused vessels. The adhered leukocytes were 17 ± 2.9 and 5.7 ± 0.5 per 100 μm of vessel length in vessels perfused with diabetic and normal MPs, respectively. An increase in hydraulic conductivity (7.1 ± 1.2-fold) occurred when chemoattractant fMLP (10 μM) was applied to vessels with adherent diabetic MPs. Confocal imaging showed that diabetic MPs, not normal MPs, directly adhered on microvessel walls through single vessel perfusion. Blocking PS on the surface of MPs through precoating of Annexin V prevented the adhesion of diabetic MPs to microvessel walls and also abolished MP-mediated leukocyte adhesion. Flow cytometry analysis showed that diabetic MPs had a 6.4 ± 1.1-fold higher PS exposure per MP compared to those in normal plasma MPs. These results suggest that the increased number of MPs, as well as the larger PS surface area of each diabetic MP play an essential role in their interaction with endothelium and subsequent leukocyte adhesion. These results support our hypothesis that increased MPs in diabetic rats are more than simply biomarkers of the disease, but are direct mediators of leukocyte adhesion and actively disseminate inflammation to remote regions of the vasculature.

Supported by HL56237, HL084338, F32HL114376, P20GM103434,

Where applicable, the authors confirm that the experiments described here conform with The Physiological Society ethical requirements.

PCD357

FAM3A promotes proliferation and migration of vascular smooth muscle cells via activation of Akt and ERK1/2 pathways through P2Y receptor

S. Jia, Z. Chen, Y. Guan and J. Yang

Department of Physiology and Pathophysiology, Key Laboratory of Cardiovascular Science of the Ministry of Education, Peking University Health Science Center, Beijing, China

Objective - To date, the biological function of FAM3A, a member of FAM3 gene family, remains unknown. This study aimed to determine the role of FAM3A in proliferation and migration of vascular smooth muscle cells (VSMCs).
Methods and Results – Immunohistochemical staining revealed that FAM3A protein is expressed in tunica media of rodent and human arteries. FAM3A expression is reduced in tunica media of mouse femoral artery and rat carotid artery injuried by a guidewire or balloon, and in cultured rat VSMCs stimulated by

FBS or PDGF-BB with increased expression of prostaglandin E receptor 2 (EP2). Adenoviral-mediated overexpression of FAM3A promotes proliferation and migration of VSMCs independent of FBS stimulation. FAM3A activates Akt via a PI3K-dependent manner, whereas it induces ERK1/2 activation independent of PI3K in VSMCs. FAM3A protein is located in mitochondrion of VSMCs, where it promotes ATP produce and secretion. Activation or overexpression of EP2 represses FAM3A expression with inhibited ATP produce and secretion in VSMCs. FAM3A-induced activation of Akt and ERK1/2 pathways, proliferation and migration of VSMCs is blocked by suramin, a broad-spectrum P2 receptor inhibitor, but not by PPADS, a specific P2X receptor inhibitor. Moreover, inhibition of phospholypase C (PLC) and inositol 1,4,5-triphosphate receptor (IP3R) also blocks FAM3A-induced activation of Akt and ERK1/2 pathways, and proliferation of VSMCs.
Conclusion – FAM3A promotes proliferation and migration of VSMCs via P2Y receptor-mediated activation of Akt and ERK1/2 pathways. Repression of FAM3A expression by EP2 activation might be a protective mechanism against excessive neointima formation in injuried vessles.

recipient of the travel awards for young physiologists from the Chinese Association for Physiological Sciences (CAPS)

Where applicable, the authors confirm that the experiments described here conform with The Physiological Society ethical requirements.

PCD358

Inhibition of phospholipase c and protein kinase c activity from human umbilical veins endothelial cells by aqueous extract of *Bixa orellana* leaves

Y. Yong[1], Z. Ahmad[1], J. Tan[2] and D. Israf Ali[1]

[1]Biomedical Science, Universiti Putra Malaysia, UPM Serdang, Malaysia and [2]Advance Medical and Dental Institute, Universiti Sains Malaysia, Kepala Patas, Malaysia

Phospholipase C (PLC) and protein kinase C (PKC) are known for their vital role in regulating endothelial permeability. PKC induces endothelial permeability through disassembly of adherences junctions and increased actin polymerization, whereas PLC activation triggers production of downstream signaling molecules, such as intracellular calcium, nitric oxide and cyclic guanosine monophosphate (cGMP). Previous studies showed that *Bixa orellana* leaves extract attenuated acute inflammation that caused by snake venom [1] and bradykinin [2]. Therefore, the aim of this study was to investigate the effect of aqueous extract of *B. orellana* leaves (AEBO) on PLC and PKC activities in bradykinin-induced endothelial hyperpermeability. Bradykinin-induced hyperpermeability in human umbilical veins endothelial (HUVEC) was successfully suppressed by AEBO at 0.1 – 0.4 mg/ml after 12 h pre-treatment. AEBO at 0.4 mg/ml exerted maximum inhibition with a rate of 86.7%, 70.5% and 57.5%, at 5, 15 and 30 min, respectively. Inositol phosphate production, which represent PLC activity was significantly suppressed by AEBO at 0.2 mg/ml (to 51.9 ± 0.2 nM) and 0.4 mg/ml (to 89.4 ± 1.4 nM), but notat 0.1 mg/ml, compared to untreated control. Similar inhibitory effect on PKC activity was also observed in AEBO-treated group at 0.4 mg/ml, with a maximum rate of inhibition of 44.5%. However, there was no alteration on PKC activity detected in AEBO-treated group at 0.1 mg/ml. In conclusion, AEBO possesses anti-endothelial hyperpermeability effect against bradykinin through suppression of PLC and PKC activities.

Núñez V,et al. (2004). Braz J Med Biol Res. **37** , 969-77.

Yoke Keong Y, et al. (2011). Med Princ Pract. **20** ,142-146.

Where applicable, the authors confirm that the experiments described here conform with The Physiological Society ethical requirements.

PCD359

Functional restoration of tissue perfusion by strategic recruitment of proangiogenic leukocytes to the ischemic hindlimb

E. Vågesjö[1], G. Christoffersson[1], O. Korsgren[2], M. Essand[2] and M. Phillipson[1]

[1]Medical Cell Biology, Uppsala, Sweden and [2]Immunology, Genetics and Pathology, Uppsala, Sweden

OBJECTIVE:
The importance of leukocyte subsets in angiogenesis is emerging. The aim of this project is to investigate if vascular repair during muscle ischemia can be promoted by strategic recruitment of specific leukocytes to the afflicted site as well as induce local leukocyte polarization towards a proangiogenic phenotype.
METHODS AND RESULTS:
Plasmids encoding the chemokines CCL2 and CXCL12 were constructed together with a GFP and luciferase reporter system and injected intramuscularly in wild type or CX3CR1-GFP mice. Muscle ischemia was induced immediate before plasmid delivery by excision of the femoral artery, where after restoration of functional blood flow was assessed by vascular responsiveness to heat challenge at day 1, 2, 3 and 7 post-insult in anesthetized mice using Laser Doppler flowmetry. The role of macrophages was studied by clodronate liposome-depletion two days prior to induction of ischemia. Leukocyte subsets in the injured muscle, perfused vessels and total vascular densities were quantified using confocal microscopy of ischemic tissues at 3 and 7 days post-insult.
Plasmid gene expression correlated to luminescent signal and was demonstrated to peak at day 3, but could be detected in the muscle for a period extending 4 weeks. Blood flow response to heat challenge was improved in ischemic limbs over expressing CXCL12 at 2, 3 and 7 days post induction of ischemia, and higher density of perfused capillaries was detected at days 3 and 7. Further, increased number of macrophages (F4/80+) and polarization towards the proangiogenic M2 phenotype (F4/80+/MRC1+) were observed in the ischemic muscles expressing CXCL12, while functional blood flow was not improved by CXCL12 over expression in mice depleted of macrophages. Over expression of CCL2 did not increase vascular repair as demonstrated by vascular density and blood flow recordings, and the M2 macrophage population was not amplified at the site of ischemia.
CONCLUSIONS:
Treatment of ischemic hind limbs with plasmid encoded CXCL12 partially restores a functional blood perfusion in response to heat by increasing total capillary density and perfusion, which is completely dependent on the expansion and polarization of the macrophage population into the M2 phenotype.

Where applicable, the authors confirm that the experiments described here conform with The Physiological Society ethical requirements.

PCD360

Vascular smooth muscle cell-derived exosomes isolated from human blood are enriched with fetuin-A, and may be involved in the mechanisms of vascular calcification

S.S. Kalra, A. Kapustin, A. Abbas, A. Smith, M. Waltham and C.M. Shanahan

Cardiovascular Division, King's College London, London, LONDON, UK

Vascular calcification (VC) is a highly regulated process with many similarities to developmental osteogenesis. Key features include release of vascular smooth muscle cell (VSMC) derived exosomes and dysregulated expression of physiological inhibitors of calcification such as fetuin-A (1). In vitro, fetuin-A is internalised by VSMCs and loaded into these exosomes which is thought to be a physiological mechanism to inhibit calcification. However this process becomes overwhelmed by calcification-inducing stress resulting in the loss of fetuin-A from the exosomes, thereby rendering them mineralisation competent to form the nidus for calcification (2).
In dialysis-dependent patients with chronic renal disease, lower levels of serum fetuin-A are associated with VC (3) and fetuin-A co-localises with calcified arteries (2) suggesting that a similar inhibitory mechanism exists as seen in vitro. However it is unknown if an exosome-fetuin mechanism exists in the general, non-renal failure, population.
Determine if fetuin-A enriched VSMC exosomes are found in the human circulation and if they reflect calcification stress.
Exosomes isolated from human whole blood by differential centrifugation were enriched with the exosomal marker CD63 and contained the VSMC-specific marker α-smooth muscle actin, as detected by Western Blot.
Using Western blot, fetuin-A was also detected in VSMC exosomes isolated from patients with and without clinically confirmed VC, with an observation of lower levels of fetuin-A in subjects with VC.
In a cohort (n=16) of patients with VC, we investigated the relationship between exosomal fetuin-A (as determined by ELISA), exosomal calcium (as determined by a cresolphthalein assay) and clinically quantified VC (computed tomography derived calcium score). Linear regression analysis showed a negative correlation between the exosomal fetuin-A:calcium ratio and calcium score [r^2 = -0.65; p<0.05] (see figure 1).
VSMC-derived exosomes are present in the human circulation and contain the calcification inhibitor fetuin-A. A negative correlation exists between VSMC exosomal fetuin-A and clinical calcification, confirming previous in vitro observations that fetuin-A enriched VSMC exosomes may inhibit VC and could serve as a clinical marker of VC in the general population.

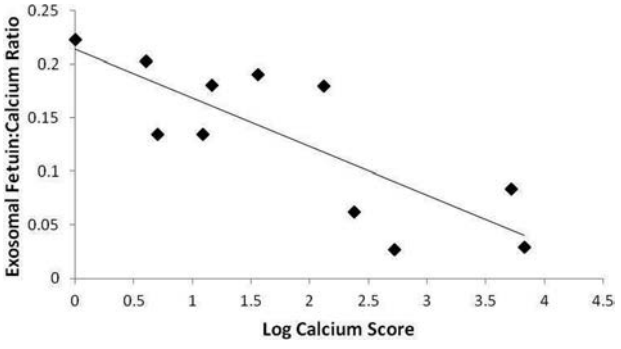

Graph showing negative correlation between exosomal fetuin-A:calcium ratio and calcium score

[r^2 = -0.65; p<0.05]

Shroff RC, Shanahan CM. Seminars in Dialysis. 2007;20(2):103-9

Reynolds JL, Skepper JN, McNair R, et al. Journal of the American Society of Nephrology. 2005;16(10):2920–30

Moe SM, Reslerova M, Ketteler M, et al. Kidney International. 2005;67(6):2295–304

SSK, AK and CMS are all funded by the British Heart Foundation

Where applicable, the authors confirm that the experiments described here conform with The Physiological Society ethical requirements.

PCD361

Effect of Nigella sativa (Blackseed) oil on inflammation and nitric oxide productionin wistar rats

A. Amin and V.B. Owoyele

Physiology, University of Ilorin, Ilorin, Kwara, Nigeria

Nigella sativa (NS) is an herbal plant commonly cultivated in many Asian countries but the products are exported to different parts of the world including Nigeria. The medicinal effects of the plant have been the subject of many scientific researches. The oil derived from its seed had been shown to possess anti-inflammatory (Mutabagani et al., 1997), and antipyretic (Ashour et al., 2006) activities among others. In this study, the effect of NS oil on inflammation and the nitric oxide (NO) system was investigated. Chronic inflammation was induced using formaldehyde as described by Owoyele et al., 2010. In this model, wistar rats (120-150g) were divided into four groups of five animals each as follows: Grp A, B, C, and D, they were administered normal saline, indomethacin (5mg/Kg), NS oil (1ml/Kg), and NS oil (2ml/Kg) orally respectively. Two models of acute inflammation, carrageenan and histamine-induced paw oedema were employed using methods described by Winter et al., 1962 and Perianayagam et al., 2006 respectively. The animals were divided into five groups of five animals each as follows: Grp A, B, C, D, and E, they were administered normal saline, indomethacin (5mg/Kg), L-NAME (100mg/Kg), NS oil (1ml/Kg), and NS oil (2ml/Kg) orally respectively. To check for the involvement of nitric oxide, the experiment was repeated (employing the acute inflammatory models) with L-arginine administered intraperitonially to all groups 1hr after inflammation induction. Change in paw circumference (oedema) after inducing inflammation was measured daily for the 10-day duration of the chronic inflammatory model and hourly for the 6-hour duration of the acute inflammatory models. Arthritis in the chronic inflammatory model was significantly reduced (P< 0.05) from 3.40 ± 0.37 to 0.80 ± 0.01mm, and 5.40 ± 0.78 to 1.00 ± 0.02mm in the groups that received indomethacin, and NS oil (2ml/Kg) respectively. In the carrageenan model, oedema reduced significantly (P< 0.05) from 1.60 ± 0.24 to 2.80 ± 0.20mm, and 1.80 ± 0.37 to 2.60 ± 0.24mm in the groups that received L-NAME, and NS (2ml/Kg) respectively. In the histamine model, oedema reduced significantly (P< 0.05) from 1.40 ± 0.22 to 3.00 ± 0.43mm, and 3.00 ± 0.19 to 4.80 ± 0.36mm in the groups that received L-NAME, and NS (2ml/Kg) respectively. Oedema further reduced significantly (P< 0.05) upon administration of L-arginine in groups that received normal saline and NS oil. The result showed that NS oil and nitric oxide worked in synergy, producing an additive effect on the anti-inflammatory activity of NS oil. It is hereby concluded the anti-inflammatory effect of NS oil may be enhanced by nitric oxide synthase

Mutabagani A. & El-Mahdy SAM. (1997). A study of the anti-inflammatory activity of Nigella sativa L. and thymoquinone in rats. Saudi Pharm. J. 5(2-3): 110-113.

Ashour MM et al. (2006). Effect of the volatile oil of Nigella sativa seeds and its components on body temperature of mice; Elucidation of the mechanisms of action. Natr. Products Sci. 12: 11-16.

Owoyele BV et al. (2010). Analgesic and anti-inflammatory effects of aqueous extract of Zea mays husk in male Wistar rats. J. Med. Food, 13(2): 343-347

Winter CA et al. (1962). Carrageenan induced oedema in hind paw of the rat as an assay for anti-inflammatory drugs. J. Proc Soc Exp Biol Med. 111: 544-547.

Perianayagam JB et al. (2006). Anti-inflammatory activity of Trichodesma indicum root extract in experimental animals. J. Ethnopharmacol. 104: 410-414.

I acknowledge the effort of the following personalities: Dr. L.A. Olayaki, Dr. L.A. Olotunji, Mrs M.T. Ayinla, Dr. L.S Ojulari and all staffs of physiology department of the University of Illorin, Nigeria

Where applicable, the authors confirm that the experiments described here conform with The Physiological Society ethical requirements.

PCD362

Blocking selectin reduced late intimal hyperplasia in vein graft in mice

C. Tseng, Y. Chang, M. Kronqvist, M. Lengquist, U. Hedin and E.E. Eriksson

Karolinska institutet, Stockholm, Sweden

Background - Venous grafts (VG) are the most used conduit in re-building arterial circulation in clinic. However, VGs degenerate easily after being implanted in the arterial circulation system. Intimal hyperplasia (IH) is the major cause of VG failure. The role of selectin-dependent leukocyte recruitment in development of IH in VG is still unclear.
Methods - VGs were studied at different time points postoperatively (Time 0, 7, 28, 63 days). VG implantation was performed by cuff fashion of the thoracic vena cava from donor mice to left carotid artery in recipients. The development of IH after VG implantation was studies by histology. Intravital microscopy was used to study interactions between leukocytes and endothelium in the native vessels and in transferred graft. VG in P- and E-selectin deficiency mice (PE-/- mice) and P-selectin deficiency mice (P-/- mice) display the effect of selectin in intimal hyperplasia. For the role of selectin-dependent leukocyte recruitment in VG, wild type mice (WT mice) transferred with VG were injected by mixture of rat anti-mouse P-selectin (100 μg, clone RB40.34) and rat anti-mouse E-selectin functional (100 μg, clone 9A9) blocking antibody through experimental time. Early single bolus of rat anti-mouse P-selectin antibody (200 μg, clone RB40.34), or early single bolus of rat anti-mouse PSGL-1 antibody (200 μg, clone 4RA10) in WT mice with VG was used to clarify the effect of P-selectin in early period after venous grafting. Immunohistochemistry showed the infiltration of leukocyte in IH of VG.
Results- Intravital microscope showed less rolling and adhesive numbers of leukocytes along venous graft endothelium in PE-/- mice during entire experimental period whereas PE-/- mice had much higher circulating leukocytes. IH developed well in VG by 28 days in WT mice. In PE-/- mice and P-/- mice, VG developed less IH compared to WT mice up to 63 days post-transfer. Moreover, P-/E-section mixture antibody injection induced reduction of IH and the number of leukocyte infiltration in WT mice VG at 28 days after transferred. Early single bolus of P-selectin antibody injection led to similar IH reduction and decreased number of leukocyte infiltration in VG IH by 28 days. At the same time, early single bolus of PSGL-1 antibody showed less IH reduction and number decreasing in leukocyte infiltration at 28 days.
Conclusions – P-/E-Selectin-dependent leukocyte recruitment is an important factor in development of intimal hyperplasia of venous graft. Functional blocking of P-and E-selectin can decrease the recruitment of leukocyte and subsequent leukocyte infiltration in IH of VG. Early single P-selectin functional blocking inhibited leukocyte recruitment and led to late IH reduction. P-selectin antagonist or combined P-/E-selectin antagonist could be a potential choice to prevent IH after VG transferred.

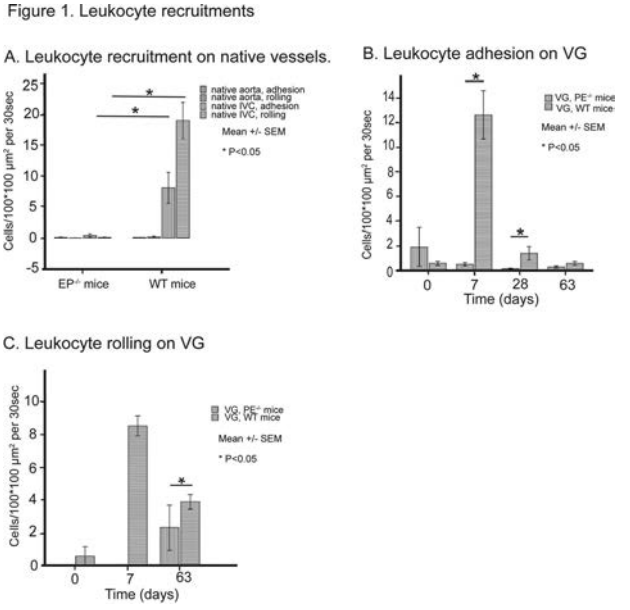

Figure 1. Leukocyte rolling and adhesion in native vessels and vascular grafts

(A) Leukocyte rolling and adhesion in native vessels in WT and in PE-/-mice. (B) Leukocyte adhesion in VGs in WT and PE-/- mice at different time points. (C) Leukocyte rolling in VGs in WT and PE-/- mice at different time points. Bars represent the number of leukocytes that were visible in a 100x100 μm square during 30 seconds. (mean±SEM, * p<0.05).

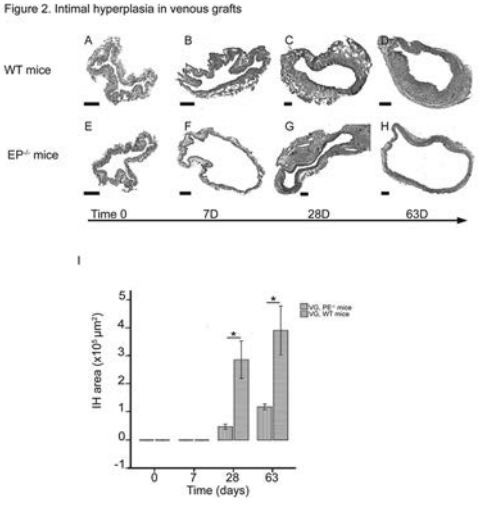

Figure 2. Intimal hyperplasia in venous grafts

Morphologic assessment of vascular grafts stained with hematoxyline and eosin. (A-D): VGs in WT mice (A: Time 0; B: 7 days; C: 28 days; D: 63 days). (E-H): VGs in PE-/- mice (E: Time 0; F: 7 days; G: 28 days; H: 63 days). Bar=100μm. (I): Intimal hyperplasia area in VGs from WT and PE-/- mice (mean±SEM, * p<0.05).

Phillips, J William (2003).*Circulation*. 2003;**107**(17):2244-9.

Hartwell, D W (1998). *Microcirculation*. 1998;**5(2-3)**:173-8.

Dong, Z M (1998). *J Clin Invest*. 1998 Jul 1;**102(1)**:145-52.

Zou, Y (1998). *Am J Pathol* . 1998 Oct;**153(4)**:1301-10.

Where applicable, the authors confirm that the experiments described here conform with The Physiological Society ethical requirements.

PCD363

Selective Estrogen Receptor Modulators benefits endothelial function by enhancing the nitric oxide via and reducing oxidative stress in ovariectomized rats

A.Z. Lamas, I. Caliman, P. Dalpiaz, P. Oliveira, A. Melo Júnior, S. Figueiredo, M. Moysés and N. Bissoli

Department of Physiological Sciences, Federal, University of Espírito Santo, Vitória, Brazil

Estrogen deficiency associated endothelial dysfunction contributes for the increased cardiovascular incidence in post-menopausal women. Because of the many complications presented by estrogen therapy, alternative therapies have emerged. The SERMs are a class of synthetic compounds that act as antagonists or agonists of the estrogen receptors. Tamoxifen (TAM) is the most widely used anti-estrogen for the management of breast cancer. Raloxifene (RAL) is used for the treatment and prevention of post-menopausal osteoporosis. This study evaluated the influence of RAL, TAM and 17-β estradiol (E) treatment on mesenteric bed (MB) vascular reactivity in rats with E deficiency. The investigation was conducted in accordance with the biomedical research guidelines for the care and use of laboratory animals, and it were approved by Ethics Committee (n°012/2008). All the surgical experiments were carried out under anesthesia (Ketamine70mg/kg+xylazine10mg/kg,i.p). Female rats were studied (n=6/group): control (SHAM); ovariectomized (OVX), OVX treated with E (0.5μg/Kg/day), RAL (2mg/Kg/day) or TAM (1mg/Kg/day), 21 days after bilateral ovariectomy. On day 35, the MB was isolated, perfused and constricted with noradrenaline. Dose response curves of ACh were obtained in absence or presence of L-NAME (NOS inhibitor) or aminoguanidine (AG iNOS inhibitor). Inducible NOS (iNOS), endothelial NOS (eNOS) and NADP(H) oxidase protein expression by western blot were analyzed. The data are reported as means±SEM, compared by ANOVA. The vasodilatation obtained in the OVX was lower compared to the SHAM Emax81±3 vs 60±3 %relaxation P<0.05. In the presence of L-NAME EmaxSHAM 31±3; OVX 21±2; E 34±9; RAL 16±2; TAM 19±4 %relaxation, decreased in all groups. In the presence of AG EmaxSHAM 76±3 vs OVX 36±3 %relaxation P<0.05; the concentration-response curve for Ach was reduced further in the OVX group and the other groups did not change when compared with non-blocking EmaxE 79±4; RAL 80±8; TAM 63±3. The levels of iNOS and NADP(H) oxidase (NOX2) protein expression in MB were elevated in OVX iNOS: SHAM 0.84±0.05; OVX 0.99±0.04 P<0.05 and NOX2: SHAM 0.76±0.10; OVX 1.12±0.13 P<0.05, while levels of eNOS were reduced in OVX when compared to SHAM eNOS: SHAM 1.07±0.10; OVX 0.71±0.10 P<0.01. All treatments were able to restore the protein expression values to those similar to control group iNOS: E 0.81±0.05; RAL 0.65±0.07; TAM 0.69±0.06; eNOS E 1.13±0.08; RAL 0.91±0.02; TAM 0.99±0.08 and NOX2 E 0.80±0.07; RAL 0.58±0.04; TAM 0.68±0.02. The treatments were able to normalize the impaired vasorelaxation of estrogen-deficient rats, indicating that despite the estrogen and SERMs present structural differences in treatment efficacy was similar to reduce a possible inflammatory and improve vascular reactivity in rats with endothelial dysfunction.

Where applicable, the authors confirm that the experiments described here conform with The Physiological Society ethical requirements.

PCD366

Decreased K^+ current in arterial myocytes of angiotensin II-induced hypertensive rats and its recovery by exercise training

E. Seo, H. Kim, C. Jin, Y. Zhang and S. Kim

Department of Physiology, Seoul National University College of medicine, Seoul, Republic of Korea

A moderate increase in extracellular K^+ induces relaxation of small arteries via augmenting inwardly rectifying K^+ current. The K^+-vasodilation is one of the mechanisms for the regional control of blood flow in response to neuronal and skeletal muscle activity. Previously we reported that exercise training (ExT) upregulates Kir current in smooth muscle cells of cerebral and skeletal arteries (CA and DFA). Here we investigated whether Kir current and K^+-vasodilation are affected in these arteries of hypertensive rats with or without ExT. To establish hypertension, rats were implanted with osmopumps delivering either Ang II (125 ng/kg/min) or saline. At 4 weeks, smooth muscle cells of CA (CASMCs) and DFA (FASMCs) were isolated and then we voltage clamped to evaluate the Ba^{2+}-sensitive Kir current and voltage-dependent K^+ current. The current density of both Kir and Kv (pA/pF) decreased in Ang II-treated hypertensive rats (AII-R). We trained rats with treadmill running for the latter two weeks (3rd and 4th weeks of Ang II application). ExT recovered Kir and Kv currents in CASMCs and FASMCs. At the same time depolarizing inward conductance (nonselective cation current) was also increased by ExT in CASMCs while not in FASMCs. This background inward current was partly inhibited by amiloride, an inhibitor for ENaC and ASIC channel. Also GTPγS, non-hydrolysable GTP analogue, induced a slowly inward current in AII-R CASMCs. And this GTPγS-activated current was further increased by ExT. The K^+-vasodilation was monitored by using video-analysis of pressurized artery. Consistent with the changes in Kir current, vasodilation by adding 2 mM KCl was weakened in both DFA and CA from AII-R. The K^+-vasodilation of DFA but not of CA was recovered in AII-R with ExT. A bath application of Ang II did not induce constriction of CAs, suggesting that the changes in K^+ channels are not directly induced by Ang II but by indirect effects of hypertension. The decreased K^+ conductance might reflect an adaptive change of resistance arteries to prevent over-perfusion of vital organs such as brain. The recovery of Kir and Kv currents by ExT might be one of the mechanisms for the beneficial effects of regular exercise on hypertension.

Where applicable, the authors confirm that the experiments described here conform with The Physiological Society ethical requirements.

PCD367

Macrophage heterogeneity in developing vulnerable atherosclerotic plaques modulated by shear stress

A.N. Seneviratne[1,2], J.E. Cole[1], M.E. Goddard[1], R. Krams[2] and C. Monaco[1]

[1]Kennedy Institute of Rheumatology, University of Oxford, London, UK and [2]Department of Bioengineering, Imperial College London, London, UK

Purpose: Atherosclerosis is a multi-factorial disease occurring in vascular sites subjected to complex flow; such as arterial bifurcations experiencing Oscillatory shear stress (OSS) and curvatures where Low shear stress (LSS) occurs. The behaviour and phenotype of macrophages, the most abundant innate immune cell in atherosclerosis, is crucial in determining the outcome of atherosclerotic plaque formation. Macrophage behaviour is conditioned by their polarisation towards a pro-inflammatory phenotype (called M1) or a regulatory one (broadly named M2). The aim of this study is to establish the activation and polarisation status of macrophages in different plaque phenotypes and shear stress conditions.
Methods: We utilised a murine model which imposes LSS to develop vulnerable plaques, and OSS to induce a stable plaque phenotype. A perivascular shear stress modifying cast was tied around a carotid artery mimicking LSS and OSS in ApoE-/- mice fed a high fat diet (HFD) from 17 weeks of age. We examined the cellular protein expression of the pan-macrophage marker CD68 and polarisation markers iNOS (M1), CD206 (M2) and HO-1 (Mox subset) in the aortic root and cast-treated carotid artery by Immunohistochemistry and Confocal Immunolocalisation at early (12 weeks), intermediate (28 weeks), and late stages of atherosclerosis (53 weeks).
Results: In the aortic roots, the majority of CD68+ cells stained positively for HO-1, reaching a maximum at 28 weeks (36.3±1.2% of lesion area; $p<0.001$ vs. 12 and 53 weeks). Immunopositivity for iNOS and CD206 were confined to a small proportion of macrophages in aortic roots (max 5.6±2.3% and 4.2±1.1% of lesional area at 20 weeks respectively). In stark contrast, the majority of macrophages in the LSS-induced carotid artery lesions express iNOS (23.6±5.1% vs. 5.4±2.7% lesion area; $p=0.006$). The expression of CD206 and HO-1 instead was not different between LSS and OSS.
Conclusions: The majority of macrophages in early and intermediate lesions of the aortic root express HO-1 (Mox phenotype). M1 or M2 polarised macrophages are present in smaller numbers at early and intermediate stages of disease but not in late disease. In atherosclerotic lesions of the carotid artery, M1 macrophages are significantly more prevalent in the low shear stress-modulated plaque. These differences suggest low shear stress promotes polarisation towards the M1 macrophage phenotype.

This work was supported by the British Heart Foundation Centre of Research Excellence, Imperial College London.

Where applicable, the authors confirm that the experiments described here conform with The Physiological Society ethical requirements.

PCD368

Endothelin-1-mediated vasoconstriction: is there therapeutic potential for intracellular sarcoplasmic reticulum calcium blockade?

Y.Y. Chan[1,3], B.J. Reddi[1,4], J.F. Beltrame[2,3], G.Y. Rychkov[1] and D.P. Wilson[1,3]

[1]School of Medical Sciences, Department of Physiology, University of Adelaide, Adelaide, SA, Australia, [2]School of Medicine, University of Adelaide, Adelaide, SA, Australia, [3]Vascular Diseases and Therapeutics Research Group, Basil Hetzel Institute, The Queen Elizabeth Hospital, Adelaide, SA, Australia and [4]Intensive Care Unit, Royal Adelaide Hospital, Adelaide, SA, Australia

Introduction: Levels of the potent vasoconstrictor, endothelin-1 (ET-1), are elevated in several pathological states, including atherosclerosis (Ivey et al., 2008), vasospasm (Clark and Pyne-Geithman, 2005), pulmonary hypertension (Barman, 2007) and coronary slow flow phenomenon. Vasoconstriction is mediated by the activation of voltage-gated calcium channels (VGCC) and intracellular sarcoplasmic reticulum (SR) calcium release, which elevates intracellular cytosolic calcium concentration. Inhibition of myosin phosphatase by protein kinase C/CPI-17 or the RhoA/Rho kinase-dependent pathways enhances calcium sensitisation, further augmenting vasoconstriction. However, recent evidence has also implicated the involvement of non-selective cation channels (NSCC) in the activation of VGCC (Wang et al., 2008).
Aims: This study aims to (1) document the role of SR calcium and calcium sensitisation in ET-1-mediated vasoconstriction, (2) identify the extent to which L-type calcium channel blockade attenuates extracellular calcium entry and vasoconstriction, and (3) identify whether NSCC are important in mediating activation of L-type calcium channels in ET-1-mediated vasoconstriction.
Methods and results: Male Sprague-Dawley rats, weighing 350g were killed by carbon dioxide inhalation. Primary smooth muscle cells from rat mesenteric arteries coupled with patch clamping analysis demonstrated that ET-1 (100nM) increased the amplitude of L-type calcium current (n=9). Using functional wire myography, pharmacological blockade of VGCC using nifedipine (10μM) significantly attenuated the ET-1-mediated vasoconstriction ($p<0.05$; n=9). Depletion of SR calcium using cyclopiazonic acid (10μM) and the IP3 receptor and NSCC blocker, 2-APB (100μM), also reduced ET-1-dependent vasoconstriction ($p<0.05$; n=9). Ionic substitution of Na+ with NMDG+ did not alter the magnitude or rate of ET-1 developed tension, suggesting that Na+ entry through NSCC was not important in ET-1-dependent contraction ($p>0.05$; n=4-5). Using an EGTA/ calcium-free solution to deplete both extra and intracellular calcium stores revealed the involvement of calcium sensitisation pathways ($p<0.05$; n=8) and was consistent with biochemical analysis, documenting an increase in the Thr855 phosphorylation state of myosin phosphatase ($p<0.05$; n=8). All data were expressed as means ± SEM and analysed using Students paired or unpaired t-test, as appropriate. Comparisons between treatment groups were analysed using one-way analysis of variance (ANOVA) followed by Bonferroni correction.
Conclusion: These data highlighted the therapeutic potential of SR calcium blockade but not NSCC blockade in mediating ET-1-dependent contraction.

Ivey ME, Osman N and Little PJ (2008). Endothelin-1 signalling in vascular smooth muscle: pathways controlling cellular functions associated with atherosclerosis. Atherosclerosis. 199(2): 237-247

Clark, JF and Pyne-Geithman G (2005). Vascular smooth muscle function: the physiology and pathology of vasoconstriction. Pathophysiology. 12(1): 35-45

Barman SA (2007). Vasoconstrictor effect of endothelin-1 on hypertensive pulmonary arterial smooth muscle involves Rho-kinase and protein kinase C. American Journal of Physiology: Lung, Cellular and Molecular Physiology. 293(2): 472-479

Wang Y, Deng X, Hewavitharana T, Soboloff J and Gill DL (2008). Stim, Orai and TRPC channels in the control of calcium entry signals in smooth muscle. Clinical and Experimental Pharmacology and Physiology. 35: 1127-1133

Where applicable, the authors confirm that the experiments described here conform with The Physiological Society ethical requirements.

PCD369

Endothelial endoglin expression and phatobiology mechanism regulation of angiogenesis in wound healing and skin angiomas

J.P. Velasco-Martin[1], L. Recio[2], J. Regadera[1], M.L. Ojeda[2], F. Leyva[3] and L.M. Botella[2]

[1]Departament of Anatomy, Histology and Neuroscience, Madrid, Spain, [2]Centro de Investigaciones Biológicas, CSIC, Madrid, Spain and [3]Service of Plastic Surgery, Hospital Clínico, Madrid, Spain

Human endothelial cells of both vascular and not vascular soft tissues tumors were all identified by using vimentin and factor VIII antibodies. However, these molecules did not allow to know the functional state of cell activity. Nowadays, experimental and human research angiogenesis can show a heterogeneous functional response of endothelial cells explored by endoglin and SMAD regulation, KLF 6, VEGF and VEGFR.
These molecules had not been quantified in cutaneous soft tissue tumours. In this report the immunochemistry and molecular expression of these endothelial epitopes in hemangiomas, dermatofibromas and lymphangiomas is evaluated, as well as in the angiogenic process found in pyogenic granuloma and granulation tissues of wound healing.
5 patients per group diagnosis of hemangioma, dermatofibromas, lymphagiomas, pyogenic granuloma and 10 patients with burned skin ulceration were examinted. The immunochemistry and molecular expression of endoglin, SMAD 1/5, SMAD 2/3, SMAD 4, KLF 6, VEGF, VEGF-R2, VEGF-R3 as well as vimentin and VIIIFG were evaluated. The evaluation of each molecule was explored using almost two slides per case.
Endothelial cells in hemangiomas express VIIIFG and vimentin and no differences were found regardless of the different types of hemangiomas. The endoglin expression of hemangiomas was observed only at endothelial proliferative cells and it seems to be higher at unicellular angiotubes. Intense endoglin expression was also seen in the lumen from proliferative new vessels that showed intense endoglin expression. However, no endoglin expression was found in endothelial cells of cavernous dilation in malformative hemangiomatosis. In hemangiomas, the endothelial cell expressed SMAD 2/3 and SMAD 4, but not SMAD 1/5.
Positive expression of Kruppel-like factor 6 was observed in all types of hemangiomas; but expression in proliferative endothelial cells was higher than in normal endothelial cells. Endothelial VEGF-R2 and VEGF-R3 inmunodetection was similar in hemangioma and normal vessels. Nevertheless, PCPH was found in higher concentrations in normal endothelial cells and quiescent hemangiomas, and their expression decrease in proliferative hemangiomas.
In conclusion, endothelial cells in angiogenic process and vascular tumours were morphology similar, but these cells express different endothelial molecules related to distinct functional endothelial activity. Tumoral angiogenic were very heterogeneous. In hemangiomas, endoglin regulation by SMAD 2/3 and SMAD 4 indicated activation of ALK 5 that signalled pathway in these tumors.

Where applicable, the authors confirm that the experiments described here conform with The Physiological Society ethical requirements.

PCD370

Differences in the signalling mechanisms underlying UTP-evoked vasoconstriction of pulmonary and systemic-like arteries

N.H. Syed[1,2], A. Tengah[1,3], S. Abdul Talip[1,3], S. Bujang[1,3] and C. Kennedy[1]

[1]SIPBS, University of Strathclyde, Glasgow, Scotland, UK, [2]University College of Pharmacy, University of the Punjab, Lahore, Punjab, Pakistan and [3]PAPRSB Institute of Health Sciences, Universiti Brunei Darussalam, Gadong, Brunei Darussalam

P2Y receptors are GPCRs that are activated by the endogenous nucleotide UTP. In the vascular system, endothelial P2Y receptors mediate vasodilation, whilst P2Y receptors located on arterial smooth muscle cells mediate vasoconstriction (Chootip et al., 2002). Previously we showed that Ca2+ influx via Cav1.2 ion channels contributes to the UTP-evoked contraction of rat intrapulmonary arteries (rIPA) (Mitchell et al., 2012). The aim was to characterise and compare the contribution of Ca2+ release and influx, rho kinase and protein kinase C (PKC) in rIPA, a low pressure, low resistance vessel and rat tail artery (rTA), a resistance-like, systemic artery.
5 mm rings of rIPA and rTA were dissected from male Sprague-Dawley rats (200-250g). The endothelium was removed and rings were mounted under isometric conditions in 1ml baths at 37°C and resting tension of 0.5-0.75g. Tension was recorded by Grass FT03 transducers connected to a Powerlab/4e system (AD Instruments). Contractions were elicited by adding UTP (300μM-rIPA; 1mM-rTA) to the bath. Data were analysed using Student's t tests.Values of $P<0.05$ were considered to be statistically significant.
UTP evoked slowly developing contractions in both tissues, which peaked within 2-3 min. Thapsigargin (1μM) depressed significantly contractions by 30-40% (rIPA-$P<0.001$, n=8; rTA-$P<0.05$, n=4), but ryanodine was ineffective (n=5). The rho kinase inhibitor, Y27632 (10μM) significantly reduced the peak amplitude of contractions by about 20% in rIPA ($P<0.01$, n=5) and by more than 80% in rTA ($P<0.01$, n=4) and the inhibition was significantly greater in rTA ($P<0.001$). The PKC inhibitor, GF109203X (10μM) also significantly reduced the peak amplitude in rIPA by over 20% ($P<0.01$, n=7) and by around 40% in rTA ($P<0.001$, n=5). Inhibition was again significantly greater in rTA ($P<0.05$). In rIPA, adding Y27632 (10μM), GF109203X (10μM), thapsigargin (1μM) and nifedipine (1μM) together abolished the UTP response (n=4). In rTA nifedipine (1μM) significantly reduced the amplitude of UTP responses by about 60% ($P<0.01$, n=6). Furthermore, contractions were abolished by Y27632 (10μM) plus thapsigargin (1μM, n=5), GF109203X (10μM, n=4) or nifedipine (1μM, n=4). Adding thapsigargin (1μM), GF109203X (10μM) and nifedipine (1μM) together abolished UTP-evoked contractions (n=4).
These results indicate that Ca2+ release from the sarcoplasmic reticulum and Ca2+ influx through Cav1.2 channels, con-

tribute to UTP-evoked vasoconstriction of rIPA and rTA. Rho kinase and protein kinase C are also involved, but more so in rTA. Thus relative importance of signalling components differs in pulmonary compared with systemic arteries.

Chootip K, Ness K, Wang J, Gurney AM & Kennedy C. (2002). Br. J. Pharmacol., 137, 637-646.

Mitchell C, Syed NH, Gurney AM & Kennedy C. (2012). Br. J. Pharmacol.,166, 1503-1512.

University College of Pharmacy, University of the Punjab, Lahore, Pakistan

PAPRSB Institute of Health Sciences, Universiti Brunei Darussalam, Jalan Tungku Link, Gadong BE1410, Brunei Darussalam

Where applicable, the authors confirm that the experiments described here conform with The Physiological Society ethical requirements.

PCD371

Synthetic or contractile, that is the question: comparing in vitro methods to modulate VSMC phenotype

J.J. Patel[1,2], M.M. Fowler[1] and R.C. Siow[2]

[1]Unilever Discover, Sharnbrook, UK and [2]Cardiovascular Division, King's College London, London, UK

Vascular smooth muscle cells (VSMCs) have the innate ability to modulate cellular phenotype in response to environmental factors such as vessel damage or disease. This phenotypic plasticity ranges between a contractile phenotype, the most common form found in vessels, to a synthetic phenotype which are unable to contract though play a vital role in vessel remodelling. Variations in VSMC phenotype are evident with changes in cell morphology, expression of SMC markers, proliferation and migratory characteristics. *In vitro* culture methods utilising calf serum and enzymatic digestion are known factors which can shift contractile VSMCs to a more synthetic phenotype. If assessing cellular contraction, changes in phenotype *in vitro* may lead to findings which may have little or no *in vivo* relevance. Numerous *in vitro* culture techniques have been suggested to maintain VSMCs in a contractile phenotype; however, no comparative study has been conducted using human aortic smooth muscle cells. In this study, VSMC gene marker expression was utilised to compare culture methods which may induce a contractile phenotype. Aortic smooth muscle cells (Lonza, Slough, UK) were cultured between passages 7 and 11 in basal medium (DMEM supplemented with 10% FCS), and compared to cells grown in DMEM with 5% FCS or Lonza medium (EBM+SmGM-2 BulletKit). In addition, cells were cultured in basal medium on plates coated with either fibrillar or monomeric collagen, or treated with heparin. Expression of mRNA for smoothelin, a contractile phenotype marker, was up-regulated at all passages in cells cultured on monomeric collagen, compared to basal medium. Expression of mRNAs for other contractile markers: caldesmon, heavy chain 11 smooth muscle and actin alpha 2 smooth muscle, was also favourable in monomeric collagen coated cultures. Cells cultured on fibrillar collagen also followed a similar pattern of mRNA expression to monomeric, though to a lesser extent. VSMCs grown in Lonza medium and DMEM supplemented with 5% FCS exhibited mRNA marker expression suggestive of a more synthetic phenotype, compared to basal medium. Further to this, VSMCs treated with heparin showed favourable mRNA expression of contractile markers, which in cases was better than that observed with monomeric collagen; however, given that heparin can effect cellular contraction, this may not be as viable a method to induce a contractile phenotype. Taken together, these findings suggest that culturing VSMCs in Lonza medium may promote the more proliferative synthetic phenotype and may serve to build up cell populations. These cells could subsequently be transferred onto cultureware coated with monomeric collagen which would induce a contractile phenotype and thus be appropriate for *in vitro* studies of cellular contraction.

Where applicable, the authors confirm that the experiments described here conform with The Physiological Society ethical requirements.

PCD372

Does oxidative stress has effect on microvascular reactivity in young healthy individuals?

A. Cosic, A. Cavka, L. Rasic and I. Drenjancevic

Department of Physiology and Immunology, Faculty of Medicine Osijek, University of J.J. Strossmayer Osijek, Osijek, Croatia

Objective: Changes in skin microcirculatory blood flow assessed by laser Doppler flowmetry (LDF) represent well systemic microvascular function (1-3). Oxidative stress appears to be the common underlying cellular mechanism for the development of endothelial dysfunction with subsequent changes in microvascular reactivity in various vascular diseases (4,5). The aim of this study was to evaluate the effect of oxidative stress on skin microcirculatory blood flow in young healthy individuals.
Materials and Methods: 40 healthy female medical students (age 20-23 yrs), volunteered to participate in this study. The study protocol and procedures conformed to the standards set by the latest revision of the Declaration of Helsinki and were approved by the Ethical Committee of the Faculty of Medicine, University of Osijek. Skin microcirculatory blood flow was assessed by LDF (MoorVMS-LDF, Axminster, UK). Changes in blood flow were measured during baseline and reactive hyperaemia following release of a 1 minute occlusion of blood flow Lipid peroxidation was measured by TBARS method (Thiobarbituric Acid Reactive Substances) and antioxidant activity by FRAP (Ferric Reducing Antioxidant Power) method in venous blood samples taken before the occlusion. Correlation analysis was calculated using Pearson's correlation coefficient at 95% confidence of interval (SigmaPlot v11.2, Systat Software, Chicago, USA).
Results: There was statistically significant negative correlation between reactive hyperaemia in skin microcirculation and lipid peroxidation (R and TBARS, Pearson r = -0.3309, R2=0.1095, P=0.037). There was no correlation between reactive hyperaemia and plasma antioxidant activity (FRAP) (R and FRAP, Pearson r=0.1404, R2=0.01973, P=0.3874).
Conclusion: The results of this study clearly suggest that the level of common oxidative stress has significant effect on microvascular reactivity in the population of young healthy individuals, and that increased oxidative stress may affect normal vascular function. This study shows that the maintaining of oxidative balance has an important role in preservation of vascular health.

Roustit M, Cracowski JL. Non-invasive assessment of skin microvascular function in humans: an insight into methods. Microcirculation. 2012 Jan;19(1):47-64.

Ghiadoni L, Versari D, Giannarelli C, Faita F, Taddei S. Non-invasive diagnostic tools for investigating endothelial dysfunction. Curr Pharm Des. 2008;14(35):3715-22.

Cracowski JL, Minson CT, Salvat-Melis M, Halliwill JR. Methodological issues in the assessment of skin microvascular endothelial function in humans. Trends Pharmacol Sci. 2006 Sep;27(9):503-8.

Han J, Shuvaev VV, Muzykantov VR.Targeted interception of signaling reactive oxygen species in the vascular endothelium. Ther Deliv. 2012 Feb;3(2):263-76.

Granger DN, Rodrigues SF, Yildirim A, Senchenkova EY. Microvascular responses to cardiovascular risk factors. Microcirculation. 2010 Apr;17(3):192-205.

Where applicable, the authors confirm that the experiments described here conform with The Physiological Society ethical requirements.

PCD373

Cutaneous microvascular regulatory response to ischaemia and association with mean oxygen saturation

D.D. Adingupu, C. Thorn, F. Casanova, S. Elyas, P.E. Gates, A.C. Shore and W.D. Strain

Diabetes and Vascular Medicine, Institute of Biomedical and Clinical Science Peninsula College of Medicine and Dentistry, Exeter, UK

Introduction: We have previously described three distinct cutaneous microvascular responses to an ischaemic stimulus using laser Doppler fluximetry (Strain et al., 2005). These are associated with a gradation of cardiovascular risk. 1) "normal response" with a controlled graded rise to peak at ~10-15 seconds, 2) "non-dominant early peak (NDEP)," with an abnormal early peak within 2 seconds of lower amplitude than the subsequent "normal" graded rise to peak, 3) "dominant early peak (DEP)" within 2 seconds of cuff release with maximum amplitude, which declines rapidly and is then followed by a lesser "normal" peak. Exact mechanism involved in abnormal peak responses are unclear, however we believe it represents a proxy for systemic microvascular (MV) regulatory disturbance.

Aims: To explore associations between microvascular regulatory responses and cutaneous blood oxygenation (SO2, %).

Methods: Post occlusive reactive hyperaemia of the microcirculation was assessed on the foot of participants with cardiovascular disease (CVD), diabetes (DM), both (DM+CVD) or neither (controls) using laser Doppler fluximetry and Oxygen to See, which measures blood oxygen saturation in the first 1mm of skin. All participants underwent basic demographic & biochemical screening.

Results: 232 participants were studied, 76 controls, 106 with CVD, 34 with DM and 16 with DM+CVD. . Results were stratified by peak response groups. In keeping with previous reports, there was an increase in CVD, diabetes and CVD risk factors across peak response groups (Table 1). Area under the curve (AUC) of oxygen saturation was incrementally lower in those with impaired autoregulation. After adjustment for CVD, diabetes, blood pressure, heart rate and BMI, this remained strongly negatively associated with abnormal peak responses, geometric mean (95% CI) normal 1459(1364-1554) vs. NDEP 1212(1132-1292) (p=0.001) vs. DEP 1142(1040-1245) (p<0.001).

Conclusion: These data suggest that the previously described abnormal peak responses have significant consequences in the delivery of oxygen as they are independently associated with reduced mean oxygen saturation post ischaemia.

Variable	Normal Peak	NDEP	DEP	Anova p
n	70	92	70	
Sex (% male)	64	65	78	0.1
Age (years)	65 ± 7.	68 ± 9	67 ± 10	0.09
Resting brachial systolic (mmHg)	128 ± 16	130 ± 17	133 ± 16	0.3
Resting brachial diastolic (mmHg)	74 ± 9	72 ± 9	74 ± 9	0.2
Heart Rate	58 ± 8	60 ± 10	64 ± 10	0.003*
BMI	26.63 ± 4.27	27.10 ± 4.51	28.80 ± 6.68	0.03*
HBA1C (mmol/mol) , geo mean (25th-75th percentiles)	41.1(38.4 - 42.5)	43.7(39.9 - 46.0)	48.0(40.1 - 55.5)	0.0004*
Total Cholesterol (mmol/l)	5.1 ± 1.2	4.6 ± 1.2	4.1 ± 0.9	<0.0001*
Cardiovascular disease (CVD) with and without Diabetes, n (%)	29 (41%)	56 (61%)	56 (53%)	<0.05*
Diabetes (%) with and without CVD, n (%)	5 (7%)	9 (10%)	36 (51%)	<0.0001*
AUC mean oxygen saturation index (SO_2) post occlusion ,mean (95% CI)	1445 (1349 - 1542)	1221 (1137 - 1305)	1141 (1038 – 1245)	<0.0001*

Table 1: Baseline characteristics and mean oxygen saturation index (SO2, %), stratified by peak response morphology. Data presented as mean ± standard deviation, except where otherwise specified, statistically significance *. AUC: area under curve, BMI: body mass index, CI: confidence interval, geo mean: geometric mean

STRAIN, W. D., CHATURVEDI, N., BULPITT, C. J., RAJKUMAR, C. & SHORE, A. C. 2005. Albumin excretion rate and cardiovascular risk: could the association be explained by early microvascular dysfunction? Diabetes, 54, 1816-22.

Where applicable, the authors confirm that the experiments described here conform with The Physiological Society ethical requirements.

PCD374

Contradictory role of apelin in vascular calcification

X. Teng[1,2], Y. Qi[3], Z. Lu[3], Y. Zhou[3], Y. Cai[3] and C. Tang[3]

[1]Department of Physiology, Hebei Medical University, Shijiazhuan, Hebei, China, [2]Hebei Key Laboratory of Laboratory Animal Science, Hebei Medical University, Shijiazhuang, Hebei, China and [3]Laboratory of Cardiovascular Bioactive Molecule, Peking University, Beijing, China

Background: Apelin is a cardiovascular peptide with multiple functions regulating homeostasis of the circulatory system and is the endogenous ligand of angiotensin receptor AT1 (APJ). The role of apelin/APJ system in vascular calcification (VC) was investigated here.

Methods: Male Sprague–Dawley (SD) rats (200±10 g) were used. A rat aorta VC model was induced by vitamin D3 plus nicotine (VDN) in vivo, and cultured vascular smooth muscle cell (VSMC) calcification of rat thoracic aortic arteries was induced in vitro by beta-glycerophosphate [1, 2]. Rats anesthetized with urethane (1 g/kg, intraperitoneally) were killed. In aortic tissure or VSMCs, von Kossa staining, calcium content and alkaline phosphatase (ALP) activity was detected [1, 2]. Immunohistochemical assessment was used to detect alpha-actin. RT-PCR was used to detect mRNA expression of apelin and APJ, and Western blot was used to detect protein expression of apelin and alpha-actin.

Results: Von Kossa staining revealed dispersed calcified nodules among the elastic fibres in calcified aortas but not in control aortas (n=6). As compared with controls, media from arteries with calcification showed significantly decreased level of alpha-actin on Western blot analysis (-18.4%, P<0.05, n=3, repeated three times). The mRNA relative level of apelin in the aorta of rats with vascular calcification was increased by 91.6% (P<0.05, n=3, reperated three times). However, the APJ mRNA expression have not significantly difference between two groups. To further investigate the effects of apelin, calcified VSMCs induced by beta-glycerophosphate were used. Compared with control group, protein expression of alpha-actin

was significantly down-regulated in calcification group (P < 0.05, n=3, repeated three times). Calcium content and ALP activity increased by 109.6% and 83.7%, resprectively in calcification VSMCs (all P<0.05, n=6). Von Kossa staining showed dispersed calcified nodules in calcification group but not in control group (n=6). 10-9 mol/L apelin could further promote calcium content, ALP activity and calcified nodules than calcification alone (all P<0.05, n=6). However, 10-7 mol/L apelin ameliorated the calcified-induced augmentation of ALP activity (P< 0.05, n=6).

Conclusions: These results suggest that apelin-APJ system might function as a regulator of VC, and could be new therapeutic targets for VC in patients.

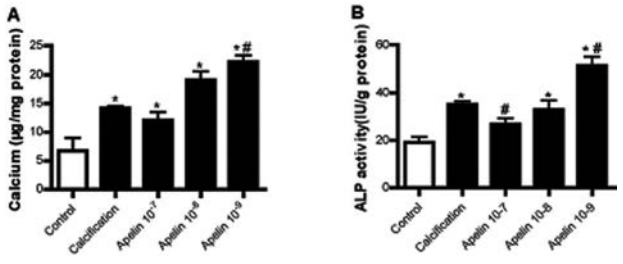

The role of different concentration Apelin on calcification VSMCs. A, calcium content; B, ALP activity. Values are expressed as mean±SD. * P < 0.05 vs control group. #P < 0.05 vs calcification group.

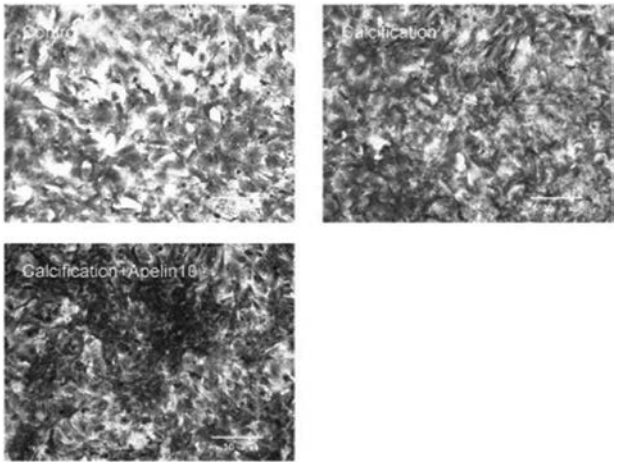

Von Kossa staining for VSMCs showed a strong positive staining of black / brown areas among VSMC (original magnification 200×). A, control group; B, calcification group; C, calcification + apelin 10-9 mol/L group.

Cai Y, Xu MJ, Teng X, Chen L, Wang X, Tang CS, Qi YF. Inhibits Vascular Calcification by Increasing the Level of Matrix {gamma}-carboxyglutamic Acid Protein. Cardiovasc Res. 2010; 85:864-73.

Cai Y, Teng X, Pan CS, Duan XH, Tang CS, Qi YF. Adrenomedullin upregulates osteopontin and attenuates vascular calcification via the cAMP/PKA signaling pathway. Acta Pharmacol Sin. 2010; 31: 1359-66.

This work was supported by the National Natural Science Foundation

of China (No.81100229), the Province Natural Science Foundation of Hebei (No. C2012206063), and the Specialized Research Fund for the Doctoral Program of Higher Education of China (No. 20111323120007).

The first author was the recipient of the travel awards for young physiologists from the Chinese Association for Physiological Sciences (CAPS)

Where applicable, the authors confirm that the experiments described here conform with The Physiological Society ethical requirements.

PCD375

Influence of hyperbaric oxygenation on gene expression in diabetic and healthy female Sprague-Dawley rats

S. Novak[1], D. Manojlovic[2], Z. Mihaljević[1] and I. Drenjancevic[1]

[1]Department of Physiology and Immunology, Medical Faculty Osijek, J.J. Strosmayer University Osijek, Osijek, Croatia and [2]Department of Surgery, General Hospital Vukovar, Vukovar, Croatia

INTRODUCTION: Our previous study demonstrated increased expression of mRNA CYP4A1 in aortas of healthy male Sprague-Dawley (SD) rats treated with hyperbaric oxygenation (HBO2) (1,2). The aim of this study was to determine the influence of HBO2 on expression of CYP4A1, CYP4A3 and thromboxane-2 synthase (TXA2) (producing vasoconstrictor 20-HETE and TXA2, respectively) and CYP2J3 and CYP4A3 genes (producing vasodilator EETs) in aorta of healthy and diabetic female SD rats.

METHODS: Female SD rats - control group, diabetic (DM) group; and control-HBO2 rats and DM-HBO2 rats that underwent HBO2 (120 minutes in duration, at 2.0 atm for 4 consecutive days, 5th day sacrified) (12 weeks-old at the time of experiment, 6 weeks DM duration) were included in the study (N=9/per group). Diabetes mellitus was induced by 1 injection of 60mg/kg i.p. streptozocin in 6 weeks old rats. Prior to decapitation, rats were anesthetized with ketamin-klorid (75 mg/kg) and midazolam (2.5 mg/kg). Aortas were collected for mRNA expression analysis by RT-PCR. Data are normalized with expression of HPRT housekeeping gene. The data are presented as mean±SEM and analyzed with t-test; p<0.05 was considered statistically significant. The Ethical Committee of Faculty of Medicine University of Osijek approved the study.

RESULTS: There is significant up-regulation of CYP2J3 gene in DM-HBO2 rats compared to all groups, and significantly higher expression of CYP2J3 in control-HBO2 compared to control group. Control group has significantly higher expression of CYP2J3 and CYP4A3 genes compared to DM group. Additionally, expression of CYP4A3 is significantly higher in control-HBO2 compared to DM-HBO2 rats. Control-HBO2 rats had significantly higher expression of TXA2 mRNA compared to DM-HBO2.

CONCLUSION: Present results demonstrated that there is a down-regulation of CYP genes in diabetic rats aortas. HBO2 led to up-regulation of CYP genes in both, control and diabetic rats, and in TXA2 expression in healthy-HBO2 rats. This finding is important in light of the role of eicosanoids produced by these enzymes in mediating various vascular responses to vasodilator stimuli, which are changed in diabetes (3).

(Support: This study was partially supported by grant of Ministry of Science, Education and Sports, Croatia, #219-2160133-2034.)

Kibel A, Cavka A, Cosic A, Falck JR, Drenjancevic I. Effects of hyperbaric oxygen treatment on vascular reactivity - responses of rat aortic rings to angiotensin II and angiotensin-(1-7).Undersea Hyperb Med. 2012; 39:1053-66.

Novak S, Ćosić A, Mihaljević Z, Kibel A, Drenjančević I. Influence of hyperbaric oxygen treatment on vascular gene expression in healthy Sprague-Dawley rat.1st International Doctoral Workshop on Natural Sciences of the University of Pécs (1st IDWoNS / UP), Book of Abstracts.Pecs, Hungary, 30-31.9.2012.

Manojlovic D, Cavka A, Drenjancevic I. Vascular relaxation to acetylcholine in female diabetic rats that underwent hyperbaric oxygenation; the role of EETs and 20-HETE. Proceedings of The Physiological Society 27. London, UK, 2012. PC180

Where applicable, the authors confirm that the experiments described here conform with The Physiological Society ethical requirements.

PCD376

Transient receptor potential vanilloid 1 in the vascular system, at baseline and in inflammation

C. Sand[1], A. Grant[2] and M. Nandi[1,3]

[1]Cardiovascular Division, King's College London, London, UK, [2]Wolfson Centre for Age-Related Diseases, King's College London, London, UK and [3]Institute of Pharmaceutical Sciences, King's College London, London, UK

Vascular inflammation greatly increases the risk of cardiovascular dysfunction, and in the setting of sepsis is an important determinant of clinical outcome. Transient receptor potential vanilloid 1 (TRPV1) is expressed in sensory neurons that contain vasoactive neuropeptides, as well as in the vasculature itself, and has been implicated in both haemodynamic regulation and inflammation (Clark *et al*, 2007; Wang *et al* 2008). We hypothesise that TRPV1 may function as a vascular regulator under inflammatory conditions, and aimed to investigate its vascular function at baseline and in inflammation. To characterise vascular TRPV1 expression, we isolated mouse aortae and cultured endothelial cells from 3 species (human, cow and mouse). Using RT-PCR we found TRPV1 mRNA expression in mouse aorta, and in all endothelial cell lines. We also investigated TRPV1 activity in isolated bovine endothelial cells by calcium fluoromtery using the selective agonist capsaicin. We found no response to 1 μM capsaicin, however, 13.75% of cells responded to 10 μM capsaicin, and the number responding to 100 μM capsaicin was significantly increased to 55.23% ($P<0.001$, compared with 1 μM capsaicin, $P<0.05$, compared with 10μM capsaicin, 1-way ANOVA with Bonferroni post-hoc test). In order to assess TRPV1 vasoactivity in resistance beds *in situ*, we developed a novel method of measuring murine mesenteric blood flow by laser speckle flowmetry. Mice were anaesthetised under 2 % isoflurane, and the small intestine was externalised through a midline incision to expose the mesenteric vasculature. Baseline mesenteric blood flow was recorded for 5 min before spray-application of 10 μM capsaicin followed by a further 5 min recording. Data are represented as mean area under the curve (flux units.time) ± SEM for baseline compared with capsaicin response. In naïve mice, capsaicin caused a significant decrease in mesenteric flow (817915 ± 34335 to 641242 ± 57640, p=0.0152, unpaired 2-tailed T-test, n=6). Conversely, in mice treated with LPS (12.5 mg/kg, 6 h or 24 h), capsaicin caused a subtle increase in blood flow at both time points (650563 ± 67794 to 711032 ± 70034 and 493428 ± 38088 to 526678 ± 25895, respectively, ns, n=3). We have demonstrated evidence of non-neuronal TRPV1 expression in vascular tissues. We hypothesise that the capsaicin-induced vasoconstriction in murine mesenteric vessels is due to TRPV1 expression in the vascular smooth muscle, and that LPS-induced endotoxaemia causes an upregulation of neuronal and/or endothelial TRPV1, generating a vasodilatory drive sufficient to overcome constriction. This may represent a protective mechanism against the lethal hypoperfusion that occurs in septic shock, though further experiments are required to confirm initial results and to understand the mechanisms involved.

Clark N *et al*. (2007). *FASEB J* **21**, 3747-3755

Wang Y *et al*. (2008). *Am J Physiol Regul Integr Comp Physiol* **294**, 1517-1523.

Dr Anna Starr

Ms Catherine Crook

Where applicable, the authors confirm that the experiments described here conform with The Physiological Society ethical requirements.

PCD377

Effects of dietary zinc and selenium on vascular responses to acetylcholine and reduced pO2 in aortic rings of male Sprague-Dawley rats

A. Cavka[1], I. Grizelj[1], A. Cosic[1], S. Novak[1], Z. Loncaric[2], B. Popovic[2] and I. Drenjancevic[1]

[1]Department of Physiology and Immunology, Faculty of Medicine Osijek, University of J.J. Strossmayer Osijek, Osijek, Croatia and [2]Desk of Plant Nutrition and Fertilization, Faculty of Agriculture Osijek, University of J.J. Strossmayer Osijek, Osijek, Croatia

Objective: Increased oxidative stress is known to decrease the bioavailability of NO, affect cyclooxygenases (COX) activity and lead to impairment of vascular function (1,2). Trace elements both zinc (Zn) and selenium (Se) are important components of antioxidative enzymes. Lack of Zn and Se in daily diet may be involved in the initiation of endothelial dysfunction (3-5). However, at the present there are no functional vascular studies to address this issue. The objective of this work was to determine if changes in dietary content of Zn and Se affect vascular responses in rat aortic rings.

Materials and Methods: Fifteen male Sprague Dawley rats were fed with 3 types of custom made rat chow (Faculty of Agriculture University of Osijek, Croatia) from weaning for 10 weeks: a) high Zn(70.81 mg/kg)-low Se(0.043 mg/kg) group (N=5); b) high Se (0.363 mg/kg)-low Zn(30.16 mg/kg) group (N=5) and c) low Zn(28.56 mg/kg)-low Se(0.030 mg/kg) group (N=5). Thoracic aortic rings were used to test dose responses to Ach (10-9-10-5 M) and response to reduced pO2 (bath gas mixture containing N2 95%, CO2 5%) after precontraction with noradrenaline (NA) for 5 minutes, in the absence/presence of the NOS inhibitor L-NAME or COX-1,2 inhibitor indomethacin (INDO) in the tissue bath. Viability of rings at the end of the hypoxic relaxation protocol was tested with their ability to contract in 95% O2-5% CO2 bath solution. To test differences among groups One-way ANOVA or t-test was used when appropriate. Statistical significance was set at $P<0.05$ (SigmaPlot v11.2).

Results: ACh induced relaxation (AchIR) was significantly reduced in low Zn-low Se group compared to both high Zn-low Se and high Se-low Zn groups ($P<0.001$ for 10-7-10-4 M Ach concentration). L-NAME blocked AChIR in all three groups of rats ($P<0.001$ for 10-7-10-4 M Ach concentration), while INDO significantly reduced AChIR only in high Se-low Zn group ($P<0.01$ for 10-7-10-4 M Ach concentration). Hypoxia induced relaxation (HIR) was significant in all study groups. However, HIR was significantly reduced in high Se-low Zn group and low Zn-low Se group compared to high Zn-low Se group ($P<0.01$). L-NAME and INDO significantly blocked HIR in high Zn-low Se and low Zn-low Se groups and INDO reduced HIR more than L-NAME. In high Se-low Zn group HIR was blocked only after INDO administration.

Conclusion: These data suggest: 1) Zn and Se deficiency affected vascular response to ACh and reduced pO2 in rat aortic rings; 2) Zn deficiency may affect vascular NO system more than Se deficiency; 3) adequate Se levels seem to have influence of the COX-dependant pathways; and 4) it seems that for

ACh dependent relaxation both microelements are equally important, while for HIR, adequate Zn level is more important.
Study was supported by grants of MZOS Croatia #219-2160133-2034 and #079-0790462-0450

Drenjancevic-Peric I, Frisbee JC, Lombard JH. Skeletal muscle arteriolar reactivity in SS.BN13 consomic rats and Dahl salt-sensitive rats. Hypertension 2003; 41(5):1012-5.

Zhu J, Drenjancevic-Peric I, McEwen S, Friesema J, Schulta D, Yu M, Roman RJ, Lombard JH. Role of superoxide and angiotensin II suppression in salt-induced changes in endothelial Ca2+ signaling and NO production in rat aorta. Am J Physiol Heart Circ Physiol 2006; 291(2):H929-38.

Brigelius-Flohe R, Banning A, Schnurr K. Selenium-dependent enzymes in endothelial function. Antioxid redox Signal 2003; 5(2):205-15.

Tomat AL, Weisstaub AR, Jauregui A, Pineiro A, Balaszuk AM, Costa MA, Arranz CT. Moderate zinc deficiency influences arterial blood pressure and vascular nitric oxide pathway in growing rats. Pediatr Res. 2005 Oct; 58(4):672-6.

Funk CD, Boubez W, Powell WS. Effects of selenium-deficient diets on the production of prostaglandins and other oxygenated metabolites of arachidonic acid and linoleic acid by rat and rabbit aortae. Biochim Biophys Acta 1987; 921(2):213-20.

Where applicable, the authors confirm that the experiments described here conform with The Physiological Society ethical requirements.

PCD378

Deficiency in endothelial cell tetrahydrobipterin reveals hydrogen peroxide mediated changes in vascular function and blood pressure in vivo

S. Chuaiphichai, E. McNeill, J.K. Bendall, G. Douglas, M.J. Crabtree, A.B. Hale, N.J. Alp and K.M. Channon

Department of Cardiovascular Medicine, University of Oxford, Oxford, UK

Nitric oxide (NO), produced by endothelial NO synthase (NOS) is a key regulator of vascular tone and blood pressure. Tetrahydrobiopterin (BH4) is an essential cofactor for endothelial NOS. When BH4 levels become limiting, eNOS produces superoxide anion rather than NO and in turn further reduces NO bioavailability, resulting in endothelial dysfunction. Endothelial cell BH4 has been hypothesized to be critical in maintaining vascular function, but to date in vivo models of BH4 deficiency have achieved only partial global depletion of BH4 synthesis. We have investigated the specific role of endothelial cell BH4 using a novel line of conditional knockout mice.
Mice homozygous for a floxed GCH1 ($GCH1^{fl/fl}$) allele (encoding for GTPCH I protein an essential enzyme in BH4 biosynthesis) were crossed with Tie2-cre transgenic mice to produce $GCH1^{fl/fl}$/Tie2-cre line, where the GCH1 gene is knocked out in endothelial cells. We have shown that the GCH1 gene is completely excised in isolated endothelial cells, with an accompanying lack of BH4 production in aortas from $GCH1^{fl/fl}$/Tie2-cre mice. To assess the effects of endothelial cell BH4 deficiency on eNOS uncoupling, superoxide production in the aorta was measured using dihydroethidium fluorescence. Endothelial-derived superoxide production was significantly 4-fold greater in $GCH1^{fl/fl}$/Tie2-cre mice compared to wild-type littermates, and was abolished by the NOS inhibitor L-NAME. Vasomotor studies demonstrated that $GCH1^{fl/fl}$/Tie2-cre aortas had enhanced vasoconstriction to phenylephrine (Emax, 97.8±7.3 vs 118.4±5.6; P<0.05) that normalised in the presence of L-NAME. Endothelium-dependent vasodilatations in response to the receptor-mediated eNOS agonist, acetylcholine were impaired in isolated aortic rings (- log ECH_{50}, 7.53±0.05 vs 7.30±0.05; P<0.01) and vasodilatations were abolished in the presence of L-NAME in both genotypes. The NOS-derived vasodilator in $GCH1^{fl/fl}$/Tie2-cre aortas was identified as H_2O_2 using the scavenger PEG-catalase, which inhibited vasodilatation only in $GCH1^{fl/fl}$/Tie2-cre aortas. *Ex vivo* supplementation of aortic rings with BH4 analogue sepiapterin restored normal endothelial function and abolished eNOS-derived H_2O_2 production in $GCH1^{fl/fl}$/Tie2-cre aortas.
Non-invasive blood pressure measurement using tail-cuff plethysmography demonstrated higher systolic blood pressure in $GCH1^{fl/fl}$/Tie2-cre mice than wild-type littermates (96.4±0.8 in WT vs 103.4±1.3 in $GCH1^{fl/fl}$/Tie2-cre) that normalised when L-NAME was given in drinking water (114.3±1.1 in WT vs 113.4±1.8 in $GCH1^{fl/fl}$/Tie2-cre). These findings demonstrate that endothelial cell BH4 plays a pivotal role in maintaining normal vascular function and determining the formation of the alternative eNOS-derived vasodilators, NO vs H_2O_2.

Where applicable, the authors confirm that the experiments described here conform with The Physiological Society ethical requirements.

PCD379

Simvastatin and lovastatin reverse functional microvascular rarefaction in the brain and skeletal muscle of spontaneously hypertensive rats

F. Freitas, V. Estato, M. Lessa and E. Tibiriçá

Physiology and Pharmacodynamic, Oswaldo Cruz Foudation, Rio de Janeiro, Rio de Janeiro, Brazil

Motivation: Microvascular rarefaction is an aggravating factor of hypertensive end-organ damage. However, the microcirculatory effects of statins in hypertension remains unknown. Thus, this study was designed to investigate the acute effects of simvastatin and lovastatin on cerebral and muscular microcirculation in Spontaneously Hypertensive Rats (SHR). Methods: Male normotensive Wistar rats (WKY) and SHR were divided into 4 groups of 6 animals each: WKY and SHR-CTL treated with 0.9% saline solution, and SHR+SIM and SHR+LOVA treated with simvastatin (SIM) and lovastatin (LOVA) 30 mg/kg/day during 3 days orally by gavage. Systolic Blood Pressure (SBP) was measured by a computerized tail-cuff plethysmography system. We investigated brain and skeletal muscle (SM; gracilis muscle) Functional Capillary Density (FCD) of pentobarbital-anesthetized rats (75 mg/kg) using intravital fluorescence videomicroscopy. Values are means ± S.E.M., compared by Two-tailed unpaired t test. All surgical procedures and protocols were approved in accordance with the internationally accepted principles for the Care and Use of Laboratory Animals (license # L-48/12). Results: SIM administration reduced SBP in SHR (SHR-CTL 203±3 vs. SHR+SIM 172±6 mmHg; p< 0.001; in contrast LOVA treatment was not able to reduce SBP (SHR+LOVA 192±3 mmHg). SHR showed a significantly lower FCD in the gracilis muscle compared to WKY (SHR-CTL 210±17 vs. WKY 338±16 capillaries/mm^2 ; p<0.01). SIM (SHR+SIM 447±20 capillaries/mm^2) and LOVA (SHR+LOVA 418±22 capillaries/mm^2) treatment reverted functional capillary rarefaction in the SM of SHR (SHR-CTL 210±17 capillaries/mm^2; p<0.001). Cerebral FCD was reduced in SHR compared with WKY (SHR-CTL 337±61 vs. WKY 421±35 capillaries/mm^2, p<0.05). The administration of SIM (SHR+SIM 530±31 capillaries/ mm^2) and LOVA (SHR+LOVA 471±37 capillaries/mm^2) during 3 days was capable to increase cerebral

FCD in SHR (SHR-CTL 337±61 capillaries/mm^2; p< 0.05). Leukocyte rolling was significantly greater in SHR when compared with WKY (SHR-CTL 6.2±0.7 vs. WKY 2.7±0.5 cells/min; p<0.05), and 3 day treatment with SIM (SHR+SIM 2.8±0.6 cells/min; p< 0.01) and LOVA (SHR+LOVA 1.8±0.5 cells/min; p< 0.001) reduced leukocyte rolling when compared with SHR (SHR-CTL 6.2±0.7 cells/min). Conclusions: Acute treatment with simvastatin and lovastatin significantly reduced brain post-capillary venules leukocyte rolling and reversed microvascular rarefaction in SHR. In addition to cholesterol-lowering effects, pleiotropic effects of statins could turn out to be a new therapeutic approach for improving microcirculatory function in hypertensive patients. However, it is necessary to further investigate the mechanisms and pathways which may additionally play important roles in statin-mediated cardiovascular protection in hypertension.

Kwok, J. M., C. C. Ma, et al. (2013). "Recent development in the effects of statins on cardiovascular disease through Rac1 and NADPH oxidase." Vascul Pharmacol 58(1-2): 21-30.

Zhang, W. B., Q. J. Du, et al. (2012). "The therapeutic effect of rosuvastatin on cardiac remodelling from hypertrophy to fibrosis during the end-stage hypertension in rats." J Cell Mol Med 16(9): 2227-2237.

Where applicable, the authors confirm that the experiments described here conform with The Physiological Society ethical requirements.

PCD381

Dynamics of neutrophil-endothelial interactions governs dissemination of local inflammation

J.V. Bodkin[1], M. Beyrau[1], A. Woodfin[1], B. Colom[1], N. McCloskey[1], M. Bianchi[2] and S. Nourshargh[1]

[1]Queen Mary University of London, London, UK and [2]San Raffaele University and Scientific Institute, Milan, Italy

Neutrophil transmigration through venular walls is an important physiological reaction to inflammatory insults. This response normally occurs in vivo in a luminal-to-abluminal direction, however neutrophil reverse transendothelial migration (rTEM) has been observed in an in vitro flow model[1]. Furthermore, we recently reported on the occurrence of directionally disrupted modes of neutrophil TEM in an in vivo mouse model of ischemia-reperfusion (I-R) injury[2]; namely "hesitant" TEM (characterised by oscillatory movements within the endothelial cell junction followed by complete transmigration) and reverse TEM (migration in an abluminal-to-luminal direction resulting in return of the neutrophil to the circulation). Of importance, the latter was causally linked with the appearance of a phenotypically distinct and pathogenic subset of neutrophils found within the lung vasculature[2]. The present study further characterises the profile and prevalence of these rare and disrupted TEM phenomena in response to a range of inflammatory agents.

Neutrophil TEM was induced in the cremaster muscle microcirculation of LysM-EGFP$^{+/-}$ mice through local application of multiple inflammatory stimuli. Dynamics of neutrophil TEM was subsequently measured under ketamine/xylazine anaesthesia by 4D confocal intravital microscopy as previously detailed [2]. Neutrophils in the blood, pulmonary vasculature and lung tissue were quantified and phenotypically analysed by flow cytometry.

TEM induced by LPS and leukotriene B_4 involved a high frequency of rTEM (~10-25% of all TEM events quantified), whereas TNF and HMGB1 caused low levels of rTEM (~0-2%), but were associated with significant levels of 'hesitant' TEM (~11-21%). In contrast, a relatively low percentage of disrupted TEM events was observed in KC and IL1-β-stimulated tissues. In all the models investigated, the frequency of rTEM was associated with the occurrence of lung inflammation alongside a sub-set of ICAM-1^{+ve} neutrophils in the pulmonary vasculature. Our findings demonstrate that inflammatory stimuli can cause distinct neutrophil TEM dynamics, which specifically contribute to the pathogenic outcome of these reactions at sites distant from the inflammatory insult.

Buckley et al., J. Leuk. Bio., 2006

Woodfin A, et al., Nat. Immunol., 2011.

Funded by The Wellcome Trust.

Where applicable, the authors confirm that the experiments described here conform with The Physiological Society ethical requirements.

PCD382

Signalling responses in cardiac endothelial cells, following treatment with high concentrations of TNF-α, with or without co-treatment with Oleanolic Acid

A. Genis, C. Westcott, M. Mudau and H. Strijdom

Biomedical Sciences, University of Stellenbosch, Cape Town, Western Cape, South Africa

Introduction: TNF-α is a pro-inflammatory cytokine and harmful circulating stimulus (1). Endothelial cells are targets of harmful TNF-α (1) and high concentrations of TNF-α can set off signalling events that can lead to endothelial injury. Oleanolic Acid (OA) is a triterpenoid found in food and plants (2) and has previously been shown to have antioxidant properties (3). Combination treatment with TNF-α and OA has not been investigated before.

Aims: Investigating the effects of TNF-α (20ng/ml, 24h), OA (40μM, 24h) or OA pre-treatment+TNF-α on the eNOS-NO biosynthesis pathway, oxidative stress and cell viability in vitro.

Methods: CMECs (*Rattus norvegicus*) were incubated with: TNF-α and/or OA-containing medium. At the end of incubation, samples were prepared for flow cytometric (FC) and western blot analyses (WB). Intracellular levels of nitric oxide (NO) and reactive oxygen species (ROS) were determined by FC analyses of DAF-2/DA and DHR-123 fluorescence. eNOS, iNOS, PKB, caveolin-1, HSP90, nitrotyrosine, p22-phox, cleaved caspase-3, cleaved PARP and Iκβα were determined by WB measurements.

Results: TNF-α resulted in decreased NO levels (77.32±0.87 *vs*. 100; p<0.05). TNF-α and TNF-α+OA resulted in reduced phospho/total ratio eNOS (0.79±0.05; 0.79±0.04 *vs*. 1; p<0.05). A reduction in caveolin-1, HSP90 and phospho/total ratio PKB was also seen in TNF-α and TNF+OA (p<0.05). Despite reduced ROS levels observed with TNF-α, p22-phox expression increased in all three groups (1.93±0.05; 1.38±0.09; 2.06±0.04 *vs*. 1; p<0.05). Reduced DHR-123-sensitive ROS corresponded with reduced nitrotyrosine in TNF-α and OA groups (p<0.05). Caspase-3 increased in TNF-α (1.12±0.02 *vs*. 1; p<0.05), whereas OA resulted in reduced caspase-3 (0.94±0.01 *vs*. 1; p<0.05). No changes were observed in cleaved PARP. Reduced Iκβα expression was observed in all treatments (p<0.05).

Discussion: The TNF-α-induced decrease in NO seemed to be associated with a decrease in phospho/total eNOS ratios, accompanied by reduced PKB ratio, HSP90 and caveolin-1. The TNF-α-induced decrease in ROS levels, contradicted the increase observed in p22-phox expression. The reduced DHR-123-sen-

sitive ROS levels corresponded with a reduction in nitrotyrosine. TNF-α seemed to be pro-apoptotic, whereas OA was anti-apoptotic. The increase in p22-phox (TNF-α, OA and TNF+OA) did not translate in increased ROS generation. In conclusion, TNF-α induced an overall adaptive response with early signs of increased NADPH-oxidase activity and apoptosis. OA seemed to be protective, though it was not able to reverse the effects seen with TNF-α.

Zhang H, Park Y, Wu J, Chen S, Lee S, Yang J, Dellsperger KC and Zhang C. Role of TNF-α in vascular dysfunction. Clin Sci (Lond). 2009: 1; 116(Pt 3): 219–230.

Pollier J and Goossens A. Oleanolic acid. Phytochemistry. 2012 May;77:10-5.

Liu J. Pharmacology of oleanolic acid and ursolic acid. Journal of Ethnopharmacology. 1995: 49 (2): 57–68.

Where applicable, the authors confirm that the experiments described here conform with The Physiological Society ethical requirements.

PCD383

Regulation of lymphatic endothelial cell migration by platelets

S.A. Langan, L. Navarro-Núñez, S.P. Watson and G.B. Nash

Centre for Cardiovascular Sciences, University of Birmingham, Birmingham, UK

Introduction: Podoplanin, a transmembrane receptor expressed on lymphatic endothelial cells (LEC), is the only known endogenous ligand for the platelet receptor CLEC-2[1]. Both of these proteins are thought to be involved in lymphatic development as mice deficient in either CLEC-2 or podoplanin develop a blood-lymphatic mixing phenotype. Work by others has also shown that podoplanin knockdown reduces LEC migration in response to vascular endothelial growth factor C (VEGF-C)[2]. Therefore, we aimed to assess whether the interaction between podoplanin and CLEC-2 on platelets regulates LEC migration, and to begin to uncover the signalling mechanism underlying this.
Methods: Transfilter assays were used to assess human LEC and human microvascular endothelial cell (HMEC)-1 migration. VEGF-C solution or normal culture medium was placed in the lower chamber of the well before endothelial cells were seeded onto the filter. After an hour, washed human platelets, antibodies or a Rho inhibitor (CT04; Cytoskeleton Inc., CO) were added to the filter. Percentage transmigration was assessed after 12 or 24 hours. A paired t-test was used to determine significance of single treatments. To compare several conditions, an ANOVA was performed, followed by post hoc Dunnett test.
Results: Platelets inhibited VEGF-C mediated increase in LEC migration in a count-dependent manner, but had no effect in the absence of VEGF-C ($P<0.05$; N=4). Similarly, platelets were able to inhibit VEGF-C mediated increase in migration of HMEC-1 cells ($P<0.05$; N=3), which are described as a microvascular endothelial cell line, but are known to express podoplanin and vascular endothelial growth factor receptor 3 (VEGFR3)[3]. Crosslinking podoplanin with an anti-human podoplanin antibody and an appropriate secondary also inhibited VEGF-C mediated LEC migration ($P<0.01$; N=3). Rho inhibitor CT04 inhibited migration but combining the inhibitor with crosslinking did not have an additive effect.
Conclusions: Platelets have a strong inhibitory effect on LEC migration in response to VEGF-C, which may be due to the interaction of CLEC-2 and podoplanin. Platelets also inhibited VEGF-C mediated migration of HMEC-1, further supporting the hypothesis that this is due to the interaction of CLEC-2 and podoplanin. Antibody-mediated crosslinking also inhibited VEGF-C mediated LEC migration, suggesting that CLEC-2 may be clustering podoplanin. Combining crosslinking with the Rho inhibitor CT04 did not have an extra inhibitory effect, suggesting that the effects of crosslinking podoplanin may involve Rho signalling.

Suzuki-Inoue K *et al.* (2006). *Blood* **107(2)**, 542-549

Navarro A *et al.* (2011). *Am. J. Physiol.-Lung Cell. Mol. Physiol.* **300(1)**, L32-L42

Nisato RE *et al.* (2004). *Am. J. Pathol.* **165**, 11-24

This work was funded by the British Heart Foundation and the Medical Research Council.

Where applicable, the authors confirm that the experiments described here conform with The Physiological Society ethical requirements.

PCD384

Targeted deletion of the extracellular calcium-sensing receptor (CaSR) from vascular smooth muscle cells reveals roles for the receptor in blood pressure regulation and protection against vascular calcification

M. Schepelmann[1], T. Davies[1], P. Yarova[1,2], S. Brennan[1], J. Graca[3], W. Chang[4], D. Bikle[4], P. Edwards[1], M. Krssak[5], D. Ward[6], A. Canfield[6], D. Edwards[7], S. Price[3], P. Kemp[1] and D. Riccardi[1]

[1]School of Biosciences, Cardiff University, Cardiff, UK, [2]Kings College, London, UK, [3]Astra Zeneca, Macclesfield, UK, [4]Department of Medicine, University of California, San Francisco, CA, USA, [5]Department of Internal Medicine III, Medical University of Vienna, Vienna, Austria, [6]Faculty of Medical and Human Sciences, University of Manchester, Manchester, UK and [7]School of Medicine, Cardiff University, Cardiff, UK

Background: The extracellular Calcium Sensing Receptor (CaSR) is expressed in the vasculature where its roles are still poorly understood. In this study, we investigate the physiopathological roles of the CaSR in the vasculature in a mouse model of vascular smooth muscle cell (VSMC) specific targeted CaSR deletion (SM22α-Cre x LoxP-CaSR) by performing *in vitro*, *ex vivo* and *in vivo* studies.
Results: Wild type (WT) and knock-out (KO) mice were identical in size, lifespan, and reproductive capability. ***In vitro*:** In the presence of calcifying concentrations of inorganic phosphate (Pi; 3 mM) and Ca^{2+} (1.8 mM), cultured VSMC from KO mouse aortae showed a significant increase in calcification compared to WT control (24.60±2.84 vs. 0.99±0.90, arbitrary units, $p<0.001$, N=6-8, Alizarin Red densitometry), while the allosteric CaSR agonist R-568 reduced Pi/Ca^{2+}-dependent calcification in WT, but not KO VSMC. ***Ex vivo*:** Wire myography on aortic rings of WT and KO mice demonstrated that aortae from KO mice had significantly narrower luminal diameters compared to those from WT control (950.2±25.6 vs. 1024.7±36.0 μm, $p<0.01$, N=5-8). Contractile force of KO aortae in response to KCl and phenylephrine (PE) was significantly impaired compared to that of WT control (3.57±0.79 vs. 5.76±1.36 mN $p<0.01$, N=5-8, 3 μM PE). ***In vivo*:** Blood pressure of 3-6 month old KO mice was significantly reduced compared to WT (106±6 vs. 134±7 mm Hg diastolic, $p<0.01$ and 157±4 vs. 180±5 mm Hg systolic, $p<0.05$; N=10-11, tail-cuff).

Cardiac MRI performed under anaesthesia showed significant heart remodelling of 14 month old KO mice compared to WT control in the form of increased left ventricular ejection fractions (74.3±1.9 vs. 59.0±2.5 %, p<0.01, N=3) and reduced diastolic and end-systolic volumes. Accordingly, heart wet-weight of 18 month old, but not 3 month old, KO mice was higher than that of age-matched WT control, suggesting that the observed heart remodelling progresses with age. (All data mean±SEM, two-tail t-test)
Conclusions: Under pathological conditions of elevated Ca^{2+} and Pi concentrations, loss of CaSR increased *in vitro* VSMC calcification while CaSR activation with a calcimimetic reduced VSMC calcification. The reduction in contractile force in aortae from KO is consistent with the observed decrease in blood pressure compared to WT control. The reduction of aortic luminal diameter and heart remodelling indicate a compensatory response to the hypotensive phenotype. Together, these data suggest that the vascular CaSR plays an important role in physiology, by influencing blood pressure regulation, and in pathology, by preventing vascular calcification.

This project is funded by the European Union through a Marie Curie Initial Training Network FP7 [264663] "Multifaceted CaSR".

Where applicable, the authors confirm that the experiments described here conform with The Physiological Society ethical requirements.

PCD385

Characterization of endothelial progenitor cell migration in vivo

J. Pircher, K. Pogoda and U. Pohl

Walter-Brendel-Centre of Experimental Medicine, Munich, Germany

Introduction: Endothelial progenitor cells (EPCs) are not only involved in physiological neovascularization but also play an important role in wound healing, tissue regeneration and remodeling (e.g. in myocardial ischemia), and tumor angiogenesis. To exert some of these functions migration of the cells within the tissue is required. However, the kinetics of migration as well as the underlying mechanisms in vivo are still poorly understood. Therefore we aimed to develop a model to investigate migration of EPCs in vivo.
Methods and Results: EPC migration in vivo was investigated in the dorsal skinfold chamber model in C57Bl/6 mice. Cultivated murine embryonic EPC (Hatzopoulos et al. 1998) were stimulated with SDF1-α (100ng/mL) to induce a migratory phenotype and labeled with Carboxyfluorescin (CFDA-SE 10μM) for 30 minutes before being detached from the culture plate using accutase. Immediately after preparation of the dorsal skinfold chamber model 10μL of the cell suspension (about 10^6 cells/mL) were injected into the dermal tissue in close apposition to a medium sized skin arteriole (diameter about 50μm) using a 30g needle. Application of the cells did not result in tissue edema or overt inflammation over an observation period of 3-4 days. According to expansion of the tissue volume covered by EPCs most cells remained intact and showed migratory activity as revealed by conventional intravital fluorescence microscopy as well as two-photon microscopy. While most cells migrated individually others formed larger aggregates within the tissue. Regular observations of migrating cells were possible by two-photon microscopy over several days.
Conclusions: We established a model which allows us to characterize behavior and migration of EPCs in the perivascular tissue of the skin for several days. By using two-photon microscopy we were able to follow small changes and movements of single cells in the deeper layers of the tissue in a three-dimensional manner. Our model constitutes a potentially useful tool to investigate mechanisms involved in homing and migration of endothelial progenitor cells in response to different migratory stimuli.

Where applicable, the authors confirm that the experiments described here conform with The Physiological Society ethical requirements.

PCD386

Targeting vulnerable *loci* in the endothelium

J. Amado-Azevedo, J. van Bezu, E.T. Valent, V. van Hinsbergh and G.P. van Nieuw Amerongen

Physiology (ICar-VU), VU University Medical Center, Amsterdam, NH, Netherlands

Despite being an extremely thin single-cell layer, the endothelium performs exceedingly well in preventing blood fluids from leaking into the surrounding tissues. However, under specific pathological conditions this cell layer can be affected, compromising the barrier's integrity. Vascular leakage is a hallmark of many cardiovascular diseases and albeit its medical importance no specialized therapies are available to prevent it or reduce it (1). Rho (Ras homology) GTPases are known as key regulators of different aspects of cell behavior, such as cell shape, migration, tension, division and contraction. The activity of Rho proteins is regulated by conformational changes induced by binding of guanine nucleotides, being GTP-bound Rho the active form and GDP-bound Rho the inactive (2). The regulators of this activation-inactivation cycle are: *ca* 70 GAPs (GTPase Activating Proteins) responsible for the inactivation process and approximately 80 GEFs (Guanine nucleotide Exchange Factors) controlling the activation. Interestingly, studies have shown that they can exert both positive and negative effects on the endothelial barrier's integrity (3). Knowledge about both the precise mechanism of this regulation and the individual contribution of these specific regulatory proteins remains fragmentary.
In order to identify suitable targets for intervention with the underlying RhoA-mediated signaling, we propose to study all known regulators of RhoGTPase activity. RNA interference screens will be carried out with small interfering RNA (siRNA) libraries targeting RhoGAPs, RhoGEFs and effectors, using human umbilical vein endothelial cells (HUVECs). With this approach we will be able to: test the effect of depletion on cellular morphology and endothelial barrier integrity using Electric Cell-Substrate Impedance Sensing (ECIS) technology and permeability assays; and also test the effect of depletion on RhoGTPase activity using an automated microscope (Cellomics Array Scan), as well as Rho G-LISAs. Positive candidates will be further studied using in-depth FRET-based biosensors in order to determine their role in regulation of RhoGTPase activity.
The outcome of this project will provide detailed information on cellular RhoGTPase activity measured in space and time, as well as valuable insight regarding both the regulatory mechanism of these important proteins and the vulnerable *loci* in the endothelium. This mechanistic understanding will unveil unanticipated pathways suitable for therapeutic intervention, through which specific molecular targets for stabilization of the endothelial barrier will be identified, limiting episodes of vascular leakage.

Goldenberg NM *et al.* (2011). *Sci Transl Med* **3**,88ps25.

Hall A (2012). *Biochem Soc Trans* **40(6)** 1378–82.

Beckers CM *et al.* (2010). *Thromb Haemost* **103(1)** 40-55.

This study is financially supported by the Dutch Heart Foundation (Grant: 2011T072).

Where applicable, the authors confirm that the experiments described here conform with The Physiological Society ethical requirements.

PCD387

Endothelial-dependent relaxation in the murine thoracic aorta is transiently increased after high fat feeding

C.J. Cobb, R.E. Walker, K.A. Farrell, D. Eisner, C.E. Austin and C.M. Holt

Institute of Cardiovascular Sciences, University of Manchester, Manchester, Greater Manchester, UK

Hypercholesterolaemia is an associated risk factor for cardiovascular disorders, including atherosclerosis and hypertension, and is thought to contribute to endothelial dysfunction. The role of cholesterol in the modulation of vascular endothelial and smooth muscle signalling has previously been demonstrated via its removal from membranes using agents such as methyl-β-cyclodextrin. However, to date there has been limited investigation into the effects of increased serum cholesterol concentration on vascular function. In this study, wire myography was employed on sections of thoracic aorta taken from the apolipoprotein-E knock-out mouse model ($ApoE^{-/-}$) of hypercholesterolaemia. The tissue was equilibrated at 5mN of resting tension for 1hr before endothelial-dependent relaxation was assessed by exposure to 10μM acetylcholine, after pre-constriction with 10μM phenylephrine. Data are expressed as means ± S.E.M., compared by one-way ANOVA, unless stated. $ApoE^{-/-}$ mice fed a normal chow diet (8 weeks), showed no change in endothelial dysfunction when compared to age and strain matched controls (42.5±10.5 vs. 45.1±4.4% relaxation, respectively). However, feeding with a high fat diet (HFD; 8 weeks) caused a significant increase in thoracic aorta endothelial-dependent relaxation in both $ApoE^{-/-}$ (69.4±3.0 vs. 45.1±4.45% relaxation; $p<0.05$, n=7,8) and control mice (75.3±4.5 vs. 45.1±4.4% relaxation; $p<0.01$, n= 7,8) compared to the chow fed controls. This augmented response was not maintained after further high fat feeding to 16 weeks (51.6±12.1 vs. 45.1±4.4% relaxation; n=4,8). The transient increase in endothelial–dependent relaxation in high fat fed control mice was preserved after incubation with a nitric oxide synthase inhibitor (LNNA (N-nitro-L-arginine) 50μM; 24.7±6.0 vs. 50.4±8.0% relaxation; chow vs HFD, post-treatment; $p<0.05$, unpaired t-test, n = 4) but was reduced after incubation with a cyclooxygenase inhibitor (indomethacin 10μM; 60.2±4.3 vs. 71.8±3.8% relaxation; chow vs HFD, post-treatment; n=4). These data suggest that high fat feeding results in a transient increase in endothelial-dependent relaxation that is mediated by cyclooxygenase signalling. It is widely known that cyclooxygenase activity is modulated by inflammation; therefore, it is possible that the response observed may represent a compensatory vascular reaction to inflammation induced by high fat feeding.

This studentship was funded by the British Heart Foundation.

Where applicable, the authors confirm that the experiments described here conform with The Physiological Society ethical requirements.

PCD388

Chronic hypoxia-enforced inhibition of vascularization; Involvement of HIF1α and HIF2α

T. Nauta[1,3], E. Weijer[1], S. Gibbs[2], R. Scheper[3], V. van Hinsberg[1] and P. Koolwijk[1]

[1]Physiology, VU University Medical Centre, Amsterdam, Netherlands, [2]Dermatology, VU Medical Centre, Amsterdam, Netherlands and [3]ASkin BV, Amsterdam, Netherlands

Motivation
Many patients with chronic open wounds need skin tissue transplantation. Transplantation with donor skin often results in rejection of the donor skin and nowadays transplantation with a tissue engineered scaffold is performed. Successful tissue transplantation and engineering requires adequate vascularization. Even though it is generally accepted that short term hypoxia stimulates angiogenesis, in chronically ischemic/hypoxic tissues and tissue-engineered scaffolds, endothelial cells have reduced angiogenic capacities. Despite the progress in knowledge on inhibiting angiogenesis, little is known about the stimulation. Exposure of endothelial cells to high concentrations of angiogenic growth factors induces chaotic and unstable vascular structures that are not adequately perfused. Therefore, it is important to understand how the induction of angiogenesis during hypoxia can be controlled. Many of the processes induced by hypoxia are mediated by the Hypoxia Inducible Factors, a family of transcription factors that directly induce the expression of many genes. Mainly HIF1α and HIF2α are involved in the regulation of genes under hypoxic conditions. Therefore, this study aims to investigate the putative role of HIF1α and HIF2α in chronic hypoxia-enforced inhibition of vascularization in vitro.
Methods
Human microvascular endothelial cells (hMVECs) were cultured at 20% oxygen or 1% oxygen for 14 days, without reoxygenation, and transfected with short interfering RNA (si-control, si-HIF1α or si-HIF-2α). The hMVECs were seeded on top of 3D fibrin matrices, and stimulated with the combination of VEGF and TNFα for 6 days to induce tube formation.
Results
hMVECs cultured at 20% oxygen formed tube-like structures in vitro, whereas those cells that were preconditioned at low (1%) oxygen did not form these structures. Surprisingly, cells transfected with si-HIF2α were able to form tube-like structures at 1% oxygen while the cells transfected with si-HIF1α or si-control did not (n=3).
Conclusion
Clearly, the formation of tube-like structures was inhibited under chronic hypoxia. However, transfection of chronic hypoxic cells with si-HIF2α restored the sprouting of endothelial cells. This indicates that counter intuitively HIF2α can impair tube formation in vitro. It is, therefore, important to further unravel its actions by using genome-wide RNA-sequence analysis and determine which transcription factor(s) and pathways downstream of HIF2α are involved.

Funded by NIRM, Netherlands Institute for Regenerative Medicine

Where applicable, the authors confirm that the experiments described here conform with The Physiological Society ethical requirements.

PCD389

Investigating the role of perivascular adipose tissue on vasoconstriction in mouse mesenteric arteries

P. Thakore[1], A.A. Aubdool[2], S.D. Brain[2] and I. McFadzean[1]

[1]Institute of Pharmaceutical Sciences, King's College London, London, UK and [2]BHF Centre of Cardiovascular Excellence and Centre of Integrative Biomedicine, King's College London, London, UK

Soltis and Cassis (1991) initially discovered that perivascular adipose tissue (PVAT) is able to regulate vascular tone. Since then a number of groups confirmed this finding, but most studies have been carried out in large conduit arteries. The aim of this study was to determine the influence of PVAT on vasoconstrictor responses in small resistance arteries. Male CD1 mice (3 months; 35-45g) were culled by cervical dislocation. First-order mesenteric arteries (either with or without associated PVAT) were mounted onto a wire myograph (Danish Myo Technology) and bathed in a modified Kreb's-Henseleit solution, gassed with 95% air/5% CO_2, warmed to 37ºC and set to a resting tension of 13.3kPa. Vasoconstrictor responses were expressed as a percentage of the increase in tension produce by 80mM KCl. Log-concentration *vs.* response curves were fitted with a 4 parameter logistic function to obtain E_{Max} (maximum response) and pEC_{50}. Results are shown as mean ± SEM and analysed by Student's unpaired *t-test*.

In the first series of experiments the effects of PVAT on responses to contractile agents was investigated. The presence of PVAT produced a significant reduction in the maximum response to phenylephrine (+PVAT E_{Max}=21.4±3.2% *vs.* -PVAT E_{Max}=47.8±4.8%, p<0.01; n=4) with a concomitant decrease in pEC_{50} (+PVAT pEC_{50}=5.1±0.1 *vs.* -PVAT pEC_{50}=5.8±0.1, p<0.05). The presence of PVAT also produced a right-ward shift in the concentration response curve to U46619 (100pM-1μM; +PVAT pEC_{50}=7.0±0.2 *vs.* -PVAT pEC_{50}=8.1±0.2, p<0.01; n=4) however this was not accompanied by a decrease in Emax (+PVAT E_{Max}=104.2±13.3% *vs.* -PVAT E_{Max}=100.8±9.2%). The presence of PVAT had no significant effect on contractile responses to KCl (n=4).

We next investigated whether PVAT releases a diffusible factor to inhibit vasoconstrictor responses. Vessels denuded of PVAT were set up in the myograph as described. The effect of a 30 minute co-incubation with PVAT collected from first order mesenteric arteries on contractile responses was then tested. The maximum response to phenylephrine was significantly reduced in the presence of PVAT (PVAT E_{Max}=19.5±2.2% *vs.* time control E_{Max}=61.8±9.5%, p<0.01; n=5). However the responses to U46619 (n=5) and KCl (n=4) were comparable in both groups.

These results suggest that PVAT releases a factor that attenuates phenylephrine-induced vasoconstrictor responses in mouse mesenteric arteries. The lack of effect of PVAT on contractions produced by raised extracellular potassium may suggest the involvement of K^+ channels in the inhibition produced by the adipose tissue.

Soltis EE & Cassis LA (1991). *Clin Exp Hypertens A* **13**, 277-96

Funded by King's College London, Graduate Teaching Assistantship Programme

Where applicable, the authors confirm that the experiments described here conform with The Physiological Society ethical requirements.

PCD390

Microcirculation disorders and inflammatory markers in patients with coronary artery decease and chronic heart failure

A. Shchendrygina, E. Privalova and Y. Belenkov

I.M. Sechenov First Moscow State Medical University, Moscow, Russian Federation

Abnormalities of microcirculation occur in multiple tissue beds in patients with cardiovascular diseases (CVDs) and lead to end-organ damage. It is known that high levels of inflammatory markers in CVDs patients were found. The purpose of our study was to estimate whether micro vascular disorders correlates with level of inflammatory markers. In patients with coronary artery disease CAD (n=37; male: 23; mean age: 62,7±6) and chronic heart failure (CHF) (n=33; male: 20; mean age: 58,2±7,5) New York Heart Association (NYHA) class II -III and 34 healthy controls (male: 17; mean age: 57,3± 7,9) digital photoplethysmography and nail fold videocapillaroscopy at resting baseline, during venous occlusion were performed. We evaluated structural changes of microcirculation in small resistance arteries (reflection index, RI) and diameters of arterial (Da) and venous (Dv) part of capillary loop. Endothelial function (occlusion index, IO) of arterioles and capillary function (percent capillary recruitment, pCR) (Cheng C et al. (2008). Ther Adv Cardiovasc Dis. 2(2), 79–88) were estimated. Inflammatory markers such as C-reactive protein (CRP), erythrocyte sedimentation rate (ESR) and fibrinogen were determined. Values are median and IQI, compared by Mann-Whitney U-test. Correlation was estimated by Spearman's Rank Correlation Coefficient (rs). In patients with CAD and CHF structural and functional of microcirculation in arterioles were found. IO in CAD and CHF patients was significantly different from controls (IO CAD: 1,6 (1,4;1,9) vs. CHF: 1,5 (1,3;1,7) vs. control: 1,8 (1,5;2,7); p<0.05). Structural changes in arterioles level (RI) were above norm (< 30%), in all groups but there was no different RI between groups (RI CAD 37,2 (22,3;47,5) vs. CHF 32,2 (25,3;47,2) vs. Control: 33,5 (29,5;47), p= 0.3). Functional disorders of capillary (pCR) in patients with CAD and CHF were found. pCR was significantly lower in CVDs groups than in controls, while there was no differences between CAD and CHF groups (pCR CAD: 90 (82;93) vs. CHF: 88 (75;95) vs. control: 93 (88;96), p<0.05). Da was significantly lower in CAD patients than controls (Da CAD: 5.2 (4.9;5.5) vs. control 7.1 (7.0;9.5), p<0.05). Dv was higher in CHF patients (Dv CHF: 13.7 (10.5;17) vs. control 2.1 (10.8;14.6), p<0.05), while there was no differences between CAD and control. Correlation between Da and CRP (rs = 0,34; p<0.05), Da and fibrinogen (rs = -0,28; p<0.05) were found. Dv correlated with ESR (rs = -0,23; p<0.05). This data show that abnormalities of microcirculation in capillary level correlate with levels of inflammatory markers in patients with coronary artery decease and chronic heart failure. It might be that micro vascular disorders are also occurs via mechanisms of inflammation.

Cheng C et al. (2008). Ther Adv Cardiovasc Dis. 2(2), 79–88

Where applicable, the authors confirm that the experiments described here conform with The Physiological Society ethical requirements.

PCD391

Responses of aortic and cardiac microvascular endothelial cells to TNF-α: Does endothelial heterogeneity matter?

M. Mudau, A. Genis, C. Westcott and H. Strijdom

Biomedical Sciences, Stellenbosch University, Tygerberg, Western Cape, South Africa

Background: Endothelial heterogeneity represents the structural and functional ability of the endothelium to cater for the diverse needs of the underlying tissues in the vascular tree [1]. TNF-α is an inflammatory cytokine which has been associated with endothelial dysfunction (ED) and hence cardiovascular disease [2].**Objectives**: To compare the *in vitro* TNF-α induced responses of two cell lines from distinct vascular sites, viz. cardiac microvascular endothelial cells (CMECs) and aortic endothelial cells (AECs).**Methods**: Adult rat (Rattus Norvegicus) CMECs and AECs were treated with 0.5, 5 and 20ng/ml TNF-α (24 and 48H). Nitric oxide (NO) and reactive oxygen species (ROS) were measured by DAF-2/DA and DHR fluorescence respectively. Cell viability was quantified by PI/Annexin-V fluorescence. The following proteins were measured by Western blotting: eNOS, PkB/Akt, heat shock protein 90 (HSP90), caveolin-1, nitrotyrosine and IkBα in cells treated with 5 and 20 ng/ml TNF-α (24h). All data are expressed as % of control (control:100%).**Results**: After 24H, AECs treated with 5ng/ml TNF-α showed significantly lower NO-production vs. control (AECs: 54±7.7% vs. Control, p<0.05). At 48h, all TNF-α concentrations significantly reduced NO-production in AECs and CMECs vs. controls; however, there were no differences in AECs vs. CMECs. TNF-α decreased DHR sensitive ROS in both cell lines vs. control, with a significantly greater reduction in CMECs vs. AECs. There were no differences in cell viability in either cell line after 24h. At 48h, CMECs showed higher % apoptosis vs. AECS, and 20ng/ml TNF-α significantly increased necrosis in CMECs (8.30±1.3%) vs. AECs (1.0±0.3%), p<0.05. At 20ng/ml TNF-α, phospho/total eNOS ratios were significantly lower in CMECs (68±5%) vs. AECs (94±10%); p <0.05. Although total PKB/Akt expression was significantly lower in CMECs vs. AECS (5ng/ml and 20ng/ml TNF-α), a significant reduction in phospho/total PKB/Akt ratio was only observed at 20ng/ml TNF-α (AECs: 94±4% vs. CMECs: 55±4%, p<0.05). HSP90 was decreased in both cell lines after TNF-α treatment vs. controls; with no differences observed in CMECs vs. AECs. IkBα expression was reduced in CMECs (5ng/ml: 70±2%; 20ng/ml: 50±10% vs. controls; p<0.05) and vs. AECs (5ng/ml:100±0.2%; 20ng/ml:75±10%; p<0.05). Caveolin -1 and nitrotyrosine levels remained unchanged.**Conclusion**: The PKB/Akt-eNOS pathway is a principal source of NO production in ECs [2]. TNF-α resulted in a downregulation of this pathway in AECs and CMECs, which was more pronounced in CMECs. The TNF-α-induced attenuation of the PKB/Akt-eNOS pathway suggested an early dysfunctional response in our cells. The reduced expression of IkBα (more pronounced in CMECs) is a reflection of NFkB-activation, a major pro-inflammatory pathway[3]. Overall, CMECs appeared to be more susceptible to the harmful effects of TNF-α than AECs.

Aird WC. Endothelial cell heterogeneity.*Cold Spring Harb Perspect Med* 2012;**2**:a006429

Mudau M, Genis A, Lochner A, Strijdom H. Endothelial dysfunction: the early predictor of atherosclerosis.*Cardiovasc J Afr* 2012;**23**:222-231.

Huang NL, Chiang SH, Hsueh CH *et al*. Metformin inhibits TNF-alpha-induced IkappaB kinase phosphorylation, IkappaB-alpha degradation and IL-6 production in endothelial cells through PI3K-dependent AMPK phosphorylation.*Int J Cardiol* 2009;**134(2)**:169-75.

Where applicable, the authors confirm that the experiments described here conform with The Physiological Society ethical requirements.

PCD392

Exchange protein activated by cAMP (Epac) inhibits human vascular smooth muscle cell migration

J.S. McKean[1], D. Shewan[1], G. Gibson[2] and G.F. Nixon[1]

[1]School of Medical Sciences, University of Aberdeen, Aberdeen, UK and [2]Department of Cardiothoracic Surgery, Aberdeen Royal Infirmary, Aberdeen, UK

Following vein grafting, endothelial damage initiates vascular smooth muscle cell (VSMC) migration to the intima leading to neointimal hyperplasia. Inhibition of VSMC migration is therefore a therapeutic target in vascular disease. Cyclic adenosine monophosphate (cAMP) inhibits VSMC migration and activation of this pathway could be used to prevent neointimal hyperplasia. Prostacyclin analogues, such as beraprost and iloprost, bind to prostanoid receptors and induce cAMP production. This project aims to characterise the effects of prostacyclin analogues in VSMC migration and determine the cAMP downstream molecules involved, specifically examining the role of protein kinase A (PKA) and exchange protein activated by cAMP (Epac). Saphenous veins were obtained from patients undergoing coronary artery bypass. VSMCs were primary cultured and migration measured using a chemotaxis chamber. Cells were seeded onto membranes with 8 μm pores and platelet-derived growth factor-BB (PDGF) (10 ng/ml) was added to the lower well of the chemotaxis chamber. Chemotactic cell migration after 4 hours at 37°C was significantly increased with PDGF in comparison to the migration towards the vehicle (PDGF - 402 ± 31 migrated cells, vehicle - 148 ± 14, n=14 each group, mean ± S.E.M, p<0.05, ANOVA). Cell migration stimulated by PDGF was significantly inhibited in the presence of iloprost (100 nM) (174 ± 13 migrated cells, n=4) or beraprost (100 nM) (130 ±11, n=4) in comparison to PDGF alone (324 ± 26, n=4, p<0.05). To examine potential mechanisms of beraprost/iloprost inhibition of PDGF-induced migration, selective agonists for direct activation of PKA (N^6-Phenyl-cAMP, 5μM) and Epac (8-CPT-2'-O-Me-cAMP, 2μM) were added to the bottom well of the chemotaxis chamber. Both the Epac agonist and PKA agonist significantly reversed migration towards PDGF in comparison to PDGF alone (PDGF - 438 ± 53 cells migrated; PDGF + Epac agonist - 275 ± 22; PDGF + PKA agonist - 313 ± 35, n=8 each group, p<0.05). As Epac and PKA agonists inhibit migration and could both be activated by prostacyclin analogues, the effects of a PKA inhibitor KT-5720 (2 μM) was examined. KT-5720 did not significantly change the inhibition of PDGF-induced migration previously observed with beraprost (PDGF + beraprost - 123 ± 23 cells migrated; PDGF + beraprost + KT-5720 - 160 ± 42, n=3 each group, not significant). This potentially indicates that prostacyclin analogues may inhibit VSMC migration via activation of Epac. To examine Epac localisation in VSMCs, labelling of cells with the Epac1 antibody was investigated. Epac1 was localised to the perinuclear region of cells and at the leading edge of migrating cells. In conclusion prostacyclin analogues inhibit VSMC migration, and activation of Epac may be sufficient for this inhibitory pathway. This may provide a new therapeutic target to prevent neointimal hyperplasia.

Where applicable, the authors confirm that the experiments described here conform with The Physiological Society ethical requirements.

PCD394

Concordant low frequency oscillations in tissue blood flux and oxygenation in human skin

K. Kuliga[1], A.J. Chipperfield[2], R. Gush[3] and G.F. Clough[1]

[1]Faculty of Medicine, University of Southampton, Southampton, Hampshire, UK, [2]Faculty of Engineering, University of Southampton, Southampton, Hampshire, UK and [3]Moor Instruments Ltd, Axminster, UK

Adequate skin microvascular blood flow and oxygenation are fundamental for tissue health. Detection of impairments in peripheral perfusion may allow for early diagnosis of microvascular dysfunction. Laser Doppler flowmetry (LDF) and white light spectroscopy are non-invasive techniques for measuring microcirculatory blood flux (BF) and tissue oxygenation (SO2). We have used frequency domain power spectral analysis (PSD) to investigate the relationship between the rhythmic low frequency variations in skin BF and SO2 associated with endothelial (0.0095-0.02Hz), neurogenic (0.02-0.06Hz), myogenic (0.06-0.15Hz), respiratory (0.15-0.4Hz) and cardiogenic (0.4-1.6Hz) activity in the skin of 19 healthy individuals (31±10y; mean±SD; 8 males) before and during maximal vasodilatation induced by local warming of the skin to 43oC for 20 min. BF (arbitrary perfusion units, PU) and SO2 (%) were recorded simultaneously at the same skin site using a combined OXY+flow+temperature probe (moorCP1T-1000, Moor Instruments, Axminster UK) and data analysed using a Fourier transform and magnitude squared coherence. The relationship between BF and SO2 was described by a one-phase association ($SO2=-22.8+104.2x(1-e^{-0.097xFlux})$) with an SO2 plateau of 81% for BF values >150 PU. At room temperature PSD of the respiratory and cardiac frequency bands in the SO2 signal was significantly lower than that in the BF signal. Low frequency BF and SO2 activities oscillated coherently (mean±SD, endothelial, 0.64±0.12; neurogenic, 0.60±0.18; myogenic, 0.32±0.14). However, the relative PSD contribution of the three low frequency bands to the BF and SO2 activities differed significantly ($P<0.0004$, paired t test) with the neurogenic component the most prominent in both BF and SO2 signals. The increase in microvascular BF and tissue SO2 during local skin warming was associated with an increase in the total spectral power of the BF signal and reduction in the total spectral power SO2 signal. The relative contribution in both BF and SO2 signals of myogenic activity was augmented and neurogenic activity reduced in vasodilated skin compared with skin at room temperature. These data demonstrate an association between a simultaneous measure of microvascular blood flux and tissue oxygenation. They suggest that there are multiple continuously varying and coherently coupled oscillations in local control mechanisms that contribute to the homeostatic regulation of skin blood flow and tissue oxygenation.

KK supported by an EPSRC CASE studentship

Where applicable, the authors confirm that the experiments described here conform with The Physiological Society ethical requirements.

PCD395

Scavenger receptors mediate uptake of modified low-density lipoprotein by circulating blood monocyte subsets: consequences for atherosclerosis

W. Jackson[1], R. Khamis[2], D. Haskard[1,2] and K. Woollard[1]

[1]Medicine, Imperial College London, London, UK and [2]NHLI, Imperial College London, London, UK

A major risk factor for cardiovascular disease (CVD) is elevated LDL-cholesterol, which can undergo oxidative modification (mLDL) (1). Experimental models show that mLDL in atherosclerotic prone vascular beds leads to increased monocyte derived macrophage foam cell formation and atherosclerosis (2). However, an increasing appreciation of blood monocyte functional heterogeneity has complicated this model and the subset specific functions of blood monocytes in atherosclerosis is unknown (3). In humans, three circulating monocyte subsets can be identified based on CD14 and CD16 expression and 2 subsets in mice based on Gr1 expression. $CD14^{high}CD16^{low}$ ($Gr1^{high}$) monocytes are well-characterized inflammatory monocytes that respond to bacterial cues, while $CD14^{low}CD16^{high}$ ($Gr1^{low}$) monocytes can crawl on the vascular endothelium in the steady state, although their role in homeostatic conditions is largely unresolved (4). $CD14^{high}CD16^{high}$ are poorly described in mice, but are shown to have increased frequency in human inflammatory disease (5). We aimed to characterise the blood monocyte subset response to mLDL by addressing the quantitation and mechanisms of uptake, subsequent functionality and how intravascular crawling monocytes may regulate mLDL endothelial deposition.

We have demonstrated differential intracellular uptake kinetics of mLDL in vitro by human monocyte subsets via quantitative imaging and flow cytometry. $CD14^{high}CD16^{high}$ monocytes showed greatest uptake after 2 hours, via the scavenger receptor CD36 (fig1). In-vivo experiments in mice showed similar uptake in monocyte subsets, peaking at 4 hours post mLDL infusion ($Gr1^{high}$: 4hrs 6.9 +/- 2.8, 24hrs 5.7 +/- 3.9; $Gr1^{low}$: 4hrs 10.3 +/- 4.4, 24hrs 4.3 +/- 2.8. Percentage cells mLDL positive, mean+/-S.E.M, n=3). Currently, we are developing whole body imaging modalities and high-resolution intravital microscopy in mice to attempt to understand the fate and function of 'LDL-loaded' blood monocytes. Preliminary data suggests LDL loaded monocytes localise to discrete tissues and that crawling $Gr1^{low}$ ($CD14^{low}$) monocytes can scavenge LDL at the endothelial interface. Further work will determine whether they transmigrate into the arterial wall, undergo differentiation or apoptosis, localise to draining lymph nodes and/or efflux lipid to anti-inflammatory HDL. In summary, these complementary approaches add to existing knowledge on the role of mLDL and blood monocytes in atherosclerosis.

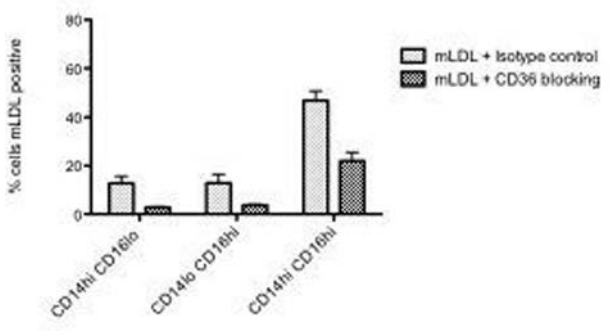

Figure 1: CD14 ^{high}CD16 ^{high} monocytes show preferential mLDL uptake via CD36. Human blood monocytes incubated for 30 minutes with a CD36 blocking antibody or isotype control (ctrl), followed by a 2-hour incubation with DiO labelled mLDL. mLDL uptake was analysed in monocyte subsets via flow cytometry. (n=3, in triplicate. Error= mean +/- SEM). P=<0.0001, Two-way ANOVA, Ctrl v CD36 Block.

Stocker R, Keaney JF, Jr. (2004) *Physiol Rev* **84**; 1381-1478.

Moore, KJ, Tabas, I. (2011) *Cell* **145**, 341-555.

Woollard, KJ and Geissmann F (2010) *Nat. Rev. Cardiol.* **7**, 77–86.

Cros J, Cagnard N, Woollard K et al. (2010) *Immunity* **33**, 375–386.

Walter GJ et al. (2013) *Arthritis Rheum.* **65**,627-638.

Where applicable, the authors confirm that the experiments described here conform with The Physiological Society ethical requirements.

PCD396

Investigating the effects of L-phenylalanine on the endogenous tetrahydrobiopterin regulatory system in spontaneously hypertensive rats

L. Heikal[1], A. Starr[2], D. Hussein[2], J. Prieto-Lloret[3], P. Aaronson[3], L. Dailey[1] and M. Nandi[2]

[1]Pharmacy, Kings College London, London, UK, [2]Pharmacology and therapeutics group, Kings College London, London, UK and [3]Asthma and lung biology, Kings College London, London, UK

Strategies to pharmacologically modulate pathways that stimulate endogenous nitric oxide (NO) bioavailability have generated considerable interest for the treatment of cardiovascular disease. Tetrahydrobiopterin (BH4) is an essential cofactor for the synthesis of nitric oxide (NO). Clinical studies have shown that intravenous administration of BH4 improves vascular function in cardiovascular disease patients, however oral BH4 appears to lack efficacy, possibly due to oxidative inactivation during absorption. BH4 is synthesised from GTP with GTP-cyclohydrolase 1 (GCH1) catalysing the first and rate limiting step of the reaction. The amino acid L-phenylalanine (L-Phe) can activate GCH-1 when it is complexed to an allosteric regulatory protein (GFRP); indeed oral administration of L-Phe increases plasma biopterin (a marker of BH4 levels) in humans. The aim of this study was to investigate the effects of exogenous L-Phe administration on BH4 levels and vascular function in wild type mice and spontaneously hypertensive rats (SHR). Wild type mice were administered with an oral L-Phe challenge (100 mg/Kg) and BH4 and NO levels measured in multiple tissues. Concentrations of nitrite, BH4 and catecholamines in tissue/plasma and superoxide levels in aorta, were measured in male SHRs and wild type normotensive rats (WKY). The effect of L-Phe on endothelium dependent vascular relaxation to acetylcholine was assessed functionally using aortic and mesenteric vessels from SHR and WKY. All tissues were collected after animals were exsanguinated under terminal anaesthesia (2% isofluorane).Oral L-Phe challenge caused a significant and temporal rise in BH4 tissue levels in wild type mice, an effect that was pronounced in aorta (n=8). Consistent with their hypertensive pathology, BH4 and nitrite levels were lower whilst catecholamines and superoxide levels were elevated in SHR compared to WKY (n=18). SHR demonstrated endothelial dysfunction compared to WKY basally in aortic and mesenteric tissues [EC50 aorta (μM): SHR0.21±0.004 vs WKY0.08±0.0005; n=12] [EC50 mesenteric (μM): SHR0.03±0.0001 vs WKY0.01±0.003; n=6]. Incubation with 500 μM L-Phe significantly improved ACh induced vasorelaxation in SHR whilst having no effect in WKY (EC50 shifted to 0.038±0.0007 μM and 0.014±0.002 μM in SHR aorta and mesenteric respectively; n=6). The L-Phe effect was found to be endothelium-dependent.

L-Phe was used as a tool to investigate the potential to activate GCH1 and enhance vascular function. Consistent with our hypothesis, oral L-Phe enhanced aortic BH4 in wild type mice and improved vascular relaxations in SHR ex vivo. Small molecules that mimic this allosteric activation of GCH1 represent a potential novel therapy for the treatment of endothelial dysfunction, circumventing the problems with administering BH4 orally.

Where applicable, the authors confirm that the experiments described here conform with The Physiological Society ethical requirements.

PCD398

Comparative morphological, temporal and pharmacological profiles of two 96-well *in vitro* kinetic angiogenesis co-culture assays

C. Szybut[1], D. McEwan[2], K. Patel[1], K. Allard[2], B. O'Clair[2], E. Endsley[2], T. Dale[1], V. Groppi[2] and D. Trezise[1]

[1]Essen BioScience, Welwyn Garden City, Hertfordshire, UK and [2]Essen BioScience, Ann Arbor, MI, USA

Angiogenesis, the sprouting of new blood vessels from pre-existing ones, is a key mechanism for solid tumour growth and survival as well as damaged tissue revascularisation. In vitro models of angiogenesis play an important role in elucidating relevant signalling pathways and identifying novel therapeutic strategies. Here we compare two co-culture assays in which fully kinetic measures of vascular tube formation are enabled using live content imaging.

Co-cultures of (1) GFP-labelled human umbilical vein endothelial cells (HUVEC) and normal human dermal fibroblasts (NHDF)[1] or (2) GFP-labelled endothelial colony forming cells (ECFC) and adipocyte derived stem cells (ADSC)[2,3] were created on 96-well assay plates. Vascular tube formation was quantified (tube length, branch points) from fluorescent images (every 6-12h) using an IncuCyte live content imaging system. Exogenous growth factors evoked time and concentration-dependent increases in both assays (e.g. VEGF; HUVEC EC_{50} 28pM, ECFC EC_{50} 54pM). In the HUVEC assay vascular structures were highly branched and formed complex tubular networks. In contrast the ECFC model exhibited more regular cord-like structures; peak cord formation occurred within the first 48h and then stabilised, whereas HUVEC tube structures continued to develop over 2 weeks. From end point antibody staining the tube and cord structures were labelled by vascular markers (CD31, VEGF-R2, n=3). In the ECFC, but not HUVEC model, stromal cells surrounding the vascular structures

stained positive for pericyte markers (αSMA and PDGFR-β, n=3).
Effects of small molecule pathway inhibitors (e.g. wortmannin, suramin, CCT108159) yielded comparable inhibitory effects across the two models albeit with different temporal profiles. Striking differences in the sensitivity of developing and established tube/cord networks to the anti-VEGF antibody bevacizumab were observed. Neo-angiogenesis was substantially inhibited by bevacizumab (e.g. maximal inhibition at 6.4μg ml^{-1}: HUVEC, 99 ± 0.4%; ECFC, 85 ± 3%) whereas established tube/cord networks were resistant to disruption (HUVEC, 60 ± 3%; ECFC, 30 ± 1%). The γ-secretase inhibitor L-685458 (1-4μM) markedly increased late stage branching in the HUVEC model.
Together these data findings further validate these kinetic co-culture models for translational angiogenesis research. The presence of pericyte-like cells in the ECFC/ADSC model may be relevant to the observed resistance of established cords to bevacizumab given that previous studies indicate a role for pericytes in vascular stabilisation. This resistance of established vascular structures to bevacizumab may represent a useful translational paradigm for addressing tumour resistance of anti-VEGF therapies.

Donovan, D *et al.* (2001). *Angiogenesis* **4**, 113-121

Merfeld-Clauss, S *et al.* (2010). *Tissue Eng* Part A, **16**, 2953-2966

Falcon *et al*., (2013). J Haemotol. 6, 31-45.

Where applicable, the authors confirm that the experiments described here conform with The Physiological Society ethical requirements.

PCD399

The adhesion of platelets to monocyte subsets in stirred whole blood in response to different platelet agonists

C.L. Box, C. Yates, M. Chimen, M. Harrison, G. Nash, S. Watson and E. Rainger

Clinical and Experimental Medicine, University of Birmningham, Birmingham, UK

Introduction: Using in vitro and in vivo models of vascular inflammation which resemble aspects of the chronic inflammatory environment in the atherosclerotic artery wall, we have recently described a paradigm where platelets recruited to intact endothelial cell monolayers formed adhesive bridges between the vessel wall and flowing leukocytes. Interestingly, monocytes, the major inflammatory leukocyte population recruited during atherogenesis, were preferentially recruited from flowing blood. In these models, platelet adhesion to endothelial cells preceded interaction with monocytes. However, the formation of platelet-monocyte aggregates in the circulating blood is well documented, as is the propensity for such heterotypic aggregation to increase in patients with cardiovascular and chronic inflammatory disease. It is unknown whether heterotypic aggregation increases the efficiency of monocyte recruitment during vascular inflammation, a phenomenon we will investigate in the near future. The aim of the current study was to determine how efficiently platelet-monocyte aggregates could form in whole blood, in particular monitoring heterotypic aggregation on monocyte subsets in response to different platelet agonists.
Methods: Whole blood was treated with the platelet agonists adenosine diphosphate (ADP; 30μM), thrombin receptor activating peptide (TRAP; 100μM), thromboxane mimetic, U46619 (10μM), rhodocytin, (100nM) or collagen related peptide (CRP-XL; 1μg/ml). Blood was placed on a rolling mixer at 37°C and aliquots were periodically taken for analysis. Heterotypic aggregation was assessed by flow cytometry using antibodies against monocyte markers (CD14 and CD16) and against platelet GPIb (CD42b). Statistical significance was determined by ANOVA and Bonfferoni.
Results: After treatment with any of the agonists there was a significant increase in heterotypic aggregate formation compared to untreated control for both $CD14^+CD16^-$ and $CD14^+CD16^+$ monocyte subsets, the incidence of aggregate formation did not vary between the subsets. Interestingly, there were significant differences between the rate and efficiency of heterotypic aggregate formation with different agonists, with CRP-XL being the weakest agonist (≈30% of $CD14^+CD16^-$ monocytes positive for GPIb) and TRAP the most potent (≈65% of $CD14^+CD16^-$ monocytes positive for GPIb) after 30 minutes of stirring.
Conclusions: Platelet-monocyte aggregates form in whole blood in response to a range of platelet agonists, although the efficiency of aggregation varies in an agonist dependent manner. Both monocyte subsets form heterotypic aggregates with equal efficiency. These data imply that the route of platelet activation may be an important arbiter of the efficiency of platelet-monocyte interaction in whole blood and could influence down stream functional outcomes such as monocyte recruitment.

MRC

Where applicable, the authors confirm that the experiments described here conform with The Physiological Society ethical requirements.

PCD400

Evaluation of the mechanisms involved in the reduced vascular contraction in aortas of diabetic female rats: role of iNOS and insulin

S.M. Sartoretto[1], R.A. Dos Santos[1], G.S. Ceravolo[1], R.C. Tostes[2], M.C. Carvalho[1], Z.B. Fortes[1] and E.H. Akamine[1]

[1]Institute of Biomedical Science, University of São Paulo, São Paulo, São Paulo, Brazil and [2]Faculty of Medicine of Ribeirão Preto, University of São Paulo, Ribeirão Preto, São Paulo, Brazil

Objective: Although hypertension can be a complication of diabetes mellitus, hypotension and reduced pressor response to vasoconstrictor agents have been observed, especially in type 1 diabetes. The mechanisms by which this reduction occurs remain unclear, but increased expression of iNOS seems to be involved at least in male rats. We previously observed reduced contractile response induced by noradrenaline (NE) in aortas of diabetic female (DF) rats, but the mechanisms were not investigated. It has been observed that estrogen receptor (ER)β activation induces expression of iNOS in vascular smooth muscle of diabetic male rats, but nothing is known in female. The objective of this study was to investigate whether the reduction of vasoconstrictor response in aortas of DF rats is due to increased expression of iNOS/ERβ and the effects of insulin. Methods and Results: Diabetes was induced in female Wistar rats (180-200g) by an injection of alloxan (40 mg/kg) and after 3 and 15 days, treatment with iNOS inhibitor L-NIL (3 mg/kg/day/30 days) and insulin (NPH, 6IU/day/15 days) began, respectively. At the end of the treatment period, we analyzed the iNOS mRNA expression, the ER-α and ER-β protein expression by immunohistochemistry, and concentration-response curves were performed in endothelium-denuded aor-

tic rings to NE and potassium chloride (KCl). The results are expressed as means ± S.E.M., compared by ANOVA followed by Bartlett's test for homogeneity of variances and Tukey-Kramer multiple comparisons test. We observed that the expression of iNOS mRNA is increased in diabetic endothelium-denuded aortas (80%) in comparison to control aortas. Treatment with insulin did not correct it. The maximum contraction to NE (Control (n=6): 3.21±0.23 g; DF (n=7): 2.19±0.16 g; $p < 0.05$) and KCl (Control (n=8): 2.70±0.13 g; DF (n=9): 2.15±0.08 g; $p < 0.05$) was reduced in diabetic endothelium-denuded aortic rings. After treatment with L-NIL and insulin only the reduced maximum contraction to NE (L-NIL (n=6): 3.03±0.23 g; insulin (n=6): 3.12±0.16 g) was corrected. We found that ER-α immunostaining was similar among the groups. On the other hand, the ER-β immunostaining was increased in aorta of DF rats. Treatment with insulin, but not with L-NIL, corrected the increased ER-β immunostaining. Conclusion: Our data suggest that the increased iNOS and/or ER-β expression are involved in the reduced NE-induced contraction in DF rats, by interfering with the adrenergic receptor pathway, and not by reducing the ability of the smooth muscle to contract. The effects of the insulin treatment are selective on the adrenergic receptor pathway and may be dependent on ER-β, but not on iNOS, reduction.

Financial support: FAPESP, CNPq and CAPES-DGU.

Where applicable, the authors confirm that the experiments described here conform with The Physiological Society ethical requirements.

PCD401

Vitronectin stabilizes neutrophil-endothelial cell interactions in the inflamed microvasculature

G. Zuchtriegel[1,2], K. Lauber[3], F. Krombach[2] and C. Reichel[1,2]

[1]Department of Otorhinolaryngology, Head and Neck Surgery, Ludwig-Maximilians-Universität München, Munich, Germany, Munich, Germany, [2]Walter Brendel Centre of Experimental Medicine, Ludwig-Maximilians-Universität München, Munich, Germany, Munich, Germany and [3]Department of Radiation Oncology, Ludwig-Maximilians-Universität München, Munich, Germany, Munich, Germany

Background: Leukocyte recruitment from the microvasculature to the site of inflammation represents a key event in the pathogenesis of inflammatory diseases. Vitronectin is a glycoprotein present in serum and extracellular matrix. Through interaction with integrins and components of the fibrinolytic system vitronectin has been implicated in cell adhesion and migration. The role of this glycoprotein in the extravasation process of leukocytes, however, remains unclear.
Methods: Using in vivo microscopy on the cremaster muscle of anesthetized (ketamine, 75 mg/kg b.w. i.p., and xylazine, 25 mg/kg b.w. i.p.) wild-type and vitronectin-deficient mice, intravascular rolling and adherence as well as transmigration of leukocytes were analyzed in postcapillary venules upon intrascrotal stimulation with the C-X-C motif chemokine CXCL1/KC or lipopolysaccharide (LPS). Phenotyping of transmigrated leukocytes was performed by immunostaining of paraffin-embedded tissue sections. For statistical analysis, the ANOVA on ranks test followed by the Student-Newman-Keuls test was used.
Results: Intrascrotal stimulation with CXCL1 or LPS induced a significant elevation in numbers of intravascularly firmly adherent (cells remaining stationary on the endothelium for > 30 s) and transmigrated leukocytes (> 90 % Ly-6G-positive neutrophils) as compared to PBS-treated controls. In vitronectin-deficient animals, this elevation was significantly diminished, while the number of leukocytes only temporarily adhering to microvascular endothelial cells (cells remaining stationary on the endothelium for < 30 s) was significantly increased. The average time leukocytes arrest on endothelial cells before detachment was less than 5 s in vitronectin-deficient animals. No significant differences were observed in numbers of intravascularly rolling leukocytes and in leukocyte rolling velocities among experimental groups.
Conclusions: Vitronectin is critically involved in the extravasation process of neutrophils by stabilizing the adherence of these phagocytes to inflamed microvascular endothelial cells.

Where applicable, the authors confirm that the experiments described here conform with The Physiological Society ethical requirements.

PCD402

TMEM16A: Do we have suitable pharmacological tools?

R. Brookfield, A. Gurney and P. Tammaro

Faculty of Life Sciences, The University of Manchester, Manchester, UK

Calcium-activated chloride channels (CaCC) are expressed in almost every cell type and are implicated in a plethora of physiological functions, spanning from smooth muscle contraction to the control of cardiac and neuronal excitability. TMEM16A was recently found to encode the major component of CaCCs. The exact role of this protein in the tissues where CaCCs have been detected remains, however, largely unexplored: this issue is currently the subject of intense investigation by the scientific community. Potent and selective channel blockers would prove invaluable as pharmacological tools for TMEM16A research. Our work explored the ability of available chloride channel blockers to inhibit cloned human TMEM16A channels. Blockers studied were niflumic acid, 4,4' diisothio-cyanatostilbene-2,2'-disulfonic acid (DIDS), tannic acid, penta-O-galloyl-β-D-glucose (PGG), epigallocatechin gallate (EGCG), flufenamic acid, mefenamic acid, meclofenamic acid, glibenclamide and $T16A_{inh}$-A01, a compound recently identified via high-throughput screening against TMEM16A. Human TMEM16A (splice variant, *abcd*) was permanently expressed in HEK-293 cells. Heterologous channel expression was verified using immunocytochemistry and whole cell patch-clamp recordings. The extent of inhibition that each compound produced on hTMEM16A mediated currents was measured in the presence of equimolar trans-membrane Cl^- and ~103 nM intracellular free Ca^{2+}. The selectivity of blockers was also explored by screening activity against 7 human cardiac ion channels (Cav1.2, Nav1.5, Kv7.1, Kv4.3, hERG, Cav3.2, Kv1.5) using IonWorks high-throughput patch clamp technique. None of the compounds tested presented complete selectivity for TMEM16A channels. Tannic acid was the least selective compound. It irreversibly inhibited TMEM16A with IC_{50}=5±2μM (n=5), but also blocked 6 of the cardiac ion channels tested with IC_{50}<100 μM. The most selective was DIDS, which reversibly inhibited TMEM16A with IC_{50}=14±3μM (n=11). Although it inhibited Nav1.5 with similar potency, it did not block the other cardiac channels. $T16A_{inh}$-A01 blocked up to 60% of hTMEM16A current with an IC_{50} of 0.26 ± 0.09 μM (n=7). It also inhibited Nav1.5 and Kv7.1, but at concentrations 2 orders of magnitude higher (IC_{50}=74 and 88 μM, respec-

tively). This difference in potency suggests $T16A_{inh}$-A01 may be a selective blocker of TMEM16A if used at sub-μM concentrations. In general though, the currently available chloride channel blockers lack selectivity and are therefore not ideal pharmacological tools for TMEM16A research. This work highlights the need for the identification and development of more potent and selective hTMEM16A blockers.

This work was supported by The BBSRC, UK.

Where applicable, the authors confirm that the experiments described here conform with The Physiological Society ethical requirements.

PCD403

Redox-dependent angiogenesis by nucleoside derivatives of deoxyribose-1-phosphate

D. Vara[1], C. Wheeler-Jones[2], H. Mellor[3] and G. Pula[1]

[1]Pharmacy & Pharmacology, University of Bath, Bath, UK, [2]Comparative Biomedical Sciences, The Royal Veterinary College, London, UK and [3]School of Biochemistry, University of Bristol, Bristol, UK

Reactive oxygen species (ROS) are associated with multiple cellular functions such as cell proliferation, differentiation and apoptosis. Signal transduction by ROS, 'redox signaling' in angiogenesis is an important and emerging topic in cardiovascular sciences. ROS mediate vascular endothelial cell (EC) proliferation and migration, but the molecular mechanism underlying this phenomenon remains largely unclear. Recently we investigated the pro-angiogenic effect of deoxyribose-1-phosphate (dRP) released by stimulated platelets, which was shown to induce an increase in EC motility in vitro and a strong angiogenic response in vivo. In this study, we investigated the role of ROS generation in the angiogenic response mediated by dRP. ROS generation was investigated in human umbilical vein endothelial cells (HUVECs) by live cell confocal imaging, which showed that the addition of exogenous dRP decisively increased ROS generation. Similarly, the dRP derivatives deoxyribose-5-phospate (dR5P), glyceraldehyde-3-phosphate (G3P), and ribose-1-phosphate (R1P) also induced ROS accumulation in HUVECs, whereas deoxyribose (dR) did not. As expected, the redox stress marker heme oxygenase-1 (HO-1) was shown to be upregulated by dRP and its derivatives. The expression of critical pro-angiogenic molecules such as vascular endothelial growth factor (VEGF), interleukin 8 (IL-8), and stromal cell-derived factor 1α (SDF-1α) in HUVECs treated with dRP was tested by immunoblot. Interestingly, integrin β3 was shown to be upregulated by HUVEC treatment with dRP and its phorphorylated derivatives (i.e. except dR), as demonstrated by immunoblot experiments in the presence of the ROS scavenger N-acetyl-cysteine (NAC) and the antioxidant apocynin. In parallel, only the phosphorylated derivatives of dRP appeared to increase HUVEC cell motility in scratch-healing assay. The causative link between integrin β3 upregulation and increased HUVEC motility was proved using integrin-specific inhibitory antbodies. In summary, this study demonstrates a link between dRP-dependent increase in endothelial ROS generation, the upregulation of integrin β3 and the increase in endothelial cell motility and angiogenic activity. The paracrine regulation of endothelial cell motility by platelet-derived dRP is likely to play an important role in the stimulation of postnatal angiogenesis and tissue repair.

Pula G et al (2010). Arterioscler Thromb Vasc Biol 30(12), 2631-2638

Pula G et al (2009). Circ Res 104(1), 32-40

The authors would like to thank Dr Adrian Churchman at the University of Bath for his assistance with the live cell imaging. The research was funded by BBSRC.

Where applicable, the authors confirm that the experiments described here conform with The Physiological Society ethical requirements.

PCD404

Hyperoxic-induced contraction in porcine pulmonary veins

A. Arnold[1], C. Hannon[1], C. Dospinescu[2], H. Widmer[1], I. Rowe[1] and S.F. Cruickshank[1]

[1]Pharmacy and Life Sciences, The Robert Gordon University, Aberdeen, UK and [2]Department of Cardiology, Aberdeen Royal Infirmary, NHS Grampian, Aberdeen, UK

Hypoxia induces a transient contractile response of the porcine pulmonary vein (PV)(1). In 3rd-4th order intrapulmonary veins, this contraction is followed by a relaxation to below baseline while subsequent exposure to hyperoxia produces a second contractile response (unpublished observations). The underlying cellular effectors of this contraction in response to high oxygen conditions remain unclear, though hyperoxia has been shown to result in medial thickening and lumen occlusion of rat PVs(2).

Porcine lungs were obtained from a local abattoir. Size-matched 3rd order superior and 4th order inferior pulmonary veins (mean external diameter 3.3± 0.4 mm, n=3-4) were dissected free and mounted in a four channel myobath. Resting tone was 1.5g. KREB's-based bath solutions were gassed with 95% O_2/5% CO_2 (hyperoxia) or 95% N_2/5% CO_2 (hypoxia). Hypoxic and hyperoxic contractions were induced in the absence of pharmacological pre-tone. PVs samples were snap frozen in liquid N_2 and K^+ channel expression identified using end point RT-PCR. Data are expressed as a % of KCl-induced contraction and presented as mean values ± S.E.M. Statistical significance was determined at $P< 0.05$ using a Students unpaired *t*-test.

Under control conditions, hyperoxia did not induce a contractile response in either superior or inferior PV rings. Hypoxia induced a transient, monophasic contractile response in 89% of PV rings. There was no significant difference in the hypoxia-induced venoconstriction between superior and inferior PVs (37±12 (n=4) and 35±15%KCl (n=3), respectively; $P>0.05$). and 76% of the veins then relaxed to below baseline tension. All PV rings tested contracted when gassing was reverted from hypoxia to hyperoxia. There was no significant difference in the maximal contractile response between superior and inferior PVs (37±16%KCl for superior (n=4) and 24±7%KCl for inferior PVs (n=3);$P>0.05$). The large conductance Ca^{2+}-activated K^+ channel (BK_{Ca}) blocker Penitrem A(1) (500nM) inhibited hypoxia-induced relaxation and pre-incubation with 2 μM ryanodine (known to inhibit SR Ca^{2+} release(3)) prevented both the hypoxia-induced relaxation and hyperoxic-induced contraction. RT-PCR and product sequencing identified a truncated BK_{Ca} Zero and STREX splice variant in PVs (n=3)(1).

Hyperoxic-induced contraction and hypoxia-induced relaxation in 3rd-4th order PVs require an intact ryanodine-sensitive Ca^{2+} source. The underlying mechanisms and regulatory pathways require clarification but may involve the activation of BK_{Ca} channels.

Dospinescu *et al.*, Am J Physiol Lung Mol Physiol 2012; 303, p476-92

Hu and Jones, Am J Pathol, 1989; 134(2), p253-262

Meissner G, J Biol Chem, 1986; 261, p6300-6306

AA is a RGU IHWR funded PhD student.

Where applicable, the authors confirm that the experiments described here conform with The Physiological Society ethical requirements.

PCD405

Induction of classically activated macrophages results in the loss of anti-contractile effect of perivascular adipose tissue

L.J. Murfitt, S.B. Withers, C.E. Bussey and A.M. Heagerty

University of Manchester, Institute of Cardiovascular Sciences, Manchester, UK

Introduction: Perivascular adipose tissue (PVAT) is now regarded as a metabolically active organ that exerts an anti-contractile effect which is lost in obesity. Here, PVAT undergoes conformational change: there is adipocyte hypertrophy and an increase in the infiltration and activation of macrophages, leading to inflammation. Lean individuals have alternatively activated macrophages (AAMs) but this polarisation shifts to classically activated macrophages (CAMs) with increasing adiposity. These CAMs produce pro-inflammatory cytokines that stimulate inflammation, abrogating the anti-contractile response of PVAT. Previously, we have shown the presence of macrophages in mediating the loss of anti-contractile effect following the induction of experimental hypoxia. (Withers *et al*. 2011). Therefore, the aim of this study was to determine whether the induction of CAMs by LPS and IFN-γ abrogated the anti-contractile effect of PVAT *in vitro*.
Method: Small segments of mesenteric arteries ±PVAT (diameter 250-300 μm) from male Sprague-Dawley rats (350 g) underwent pharmacological assessment using wire myography. All procedures were performed in accordance with Scientific Procedures Act (1986). Induction of inflammation and CAMs activation was carried out by overnight incubation in Dulbecco's Modified Eagle Medium (DMEM) containing 1 μg/ml LPS and 0.1 μg/ml IFN-γ. Cumulative noradrenaline (1 x 10^{-9} to 3 x 10^{-5} M) dose response curves were calculated as a percentage of KCl (60 mM) contraction and expressed as mean±SEM. Data were analysed by two-way ANOVA and Bonferroni post hoc test. P values <0.05 were deemed significant.
Results: PVAT exerted an anti-contractile effect compared to no PVAT which is consistent with previous work (PVAT vs. no PVAT: P<0.001, n=7). After induction of inflammation and CAMs activation, PVAT had a significant loss of anti-contractile effect compared to PVAT controls (PVAT control vs. PVAT + LPS/IFN-γ: p=0.0168, n=7). No significant difference was seen in no PVAT vessels treated with LPS and IFN-γ compared to no PVAT controls (no PVAT control vs. no PVAT + LPS/IFN-γ: p=0.7053, n=7).
Conclusions: This study indicates a major role of CAMs in the loss of PVAT function as seen in inflammation and obesity. Research is ongoing to ascertain the presence of CAMs and inflammation in LPS and IFN-γ treated ±PVAT mesenteric vessels.

Withers, S. B., Agabiti-Rosei, C., Livingstone, D. M., Little, M. C., Aslam, R., Malik, R. A. & Heagerty, A. M. (2011). Macrophage activation is responsible for loss of anticontractile function in inflamed perivascular fat. Arterioscler Thromb Vasc Biol, 31(4), 908-13.

Where applicable, the authors confirm that the experiments described here conform with The Physiological Society ethical requirements.

PCD406

β-adrenergic signalling contributes to the anticontractile action of perivascular adipose tissue through nitric oxide release

C.E. Bussey, S.B. Withers, G. Edwards and A.M. Heagerty

Cardiovascular Medicine, University of Manchester, Manchester, UK

Introduction: Perivascular adipose tissue (PVAT) exerts an anti-contractile effect. Studies using various vasoconstrictors suggest that this may be dependent on adrenergic stimulation and the subsequent release of nitric oxide. This has not previously been investigated in PVAT but β3-adrenoceptors are known to be the predominant subtype mediating lipolysis in rodent adipocytes.
Design and methods: The effects of PVAT on the contractility of isolated Wistar rat mesenteric arteries were investigated using wire myography. All procedures were performed in accordance with Scientific Procedures Act (1986). Concentration-response curves to noradrenaline ($1x10^{-5}$ - $3x10^{-9}$ mol.l^{-1}) or phenylephrine ($1x10^{-5}$ - $3x10^{-9}$mol.l^{-1}) were generated in the presence and absence of the β3-adrenergic agonist, CL-316,243 (10 μmol.l^{-1}). In addition, a Griess reagent kit was used to determine NO production from adipose tissue surrounding the mesenteric artery in response to adrenergic agonist stimulation +/- the nitric oxide synthase inhibitor, L-NMMA (100 μmol.l^{-1}).
Results and summary: The vasoconstrictor response to noradrenaline was reduced in the presence of PVAT through an endothelium-dependent mechanism involving activation of vascular smooth muscle K+ channels (endo: PVAT vs no PVAT P<0.01, n = 12, no endo: PVAT vs no PVAT P=0.54, n=12). A reduced anticontractile effect was observed in response to phenylephrine (P=0.45, n =12), which acts mainly via α-adrenergic receptors, suggesting that the anticontractile effect of PVAT is dependent on β-adrenergic stimulation. Moreover, in vessels with intact PVAT but lacking endothelium, the presence of CL-316,243 caused a reduction in the vasoconstrictor effect of phenylephrine (P<0.05, n=6) whereas the vasoconstrictor response to noradrenaline was unaltered reaffirming the role of β-adrenergic stimulation in the anticontractile effect of PVAT.
Adrenergic stimulation of adipose tissue (devoid of vessels) with noradrenaline and CL-316,243, but not phenylephrine, was associated with a significant increase in nitric oxide production (P<0.05, n=5), which was inhibited by the presence of L-NMMA. The similarity in response to noradrenaline and CL-316,243 suggests that β3-adrenoceptors are the main β-adrenergic subtype mediating this response.
Overall, this study indicates a role for β-adrenergic stimulation and subsequent nitric oxide production in the anticontractile action of PVAT.

Where applicable, the authors confirm that the experiments described here conform with The Physiological Society ethical requirements.

PCD407

Investigating tetrahydrobiopterin biosynthesis

D. Hussein, A. Starr, L. Heilkal and M. Nandi

King's College London, London, UK

Background: Tetrahydrobiopterin (BH4) is an essential cofactor for aromatic amino acid-hydroxylases and all isoforms of nitric oxide-synthase. In the cardiovascular system nitric oxide (NO) acts as a potent vasodilator and maintains endothelial function. Administration of BH4 can improve endothelial function in numerous cardiovascular pathologies, an effect that likely results from increased NO bioavailability and local antioxidant effects. GTP cyclohydrolase 1 (GCH1) is the rate-limiting enzyme for BH4 biosynthesis. GCH1 activity has been shown to be modified by both levels of phenylalanine and BH4 through allosteric regulation when bound to GCH1feedback regulatory protein (GFRP). Studies have shown that phenylalanine(L-phe) binds to and activates the GCH1-GFRP complex, whilst BH4 binding to the complex inhibits GCH1 activity. Our studies aim to investigate the significance of this protein-protein interaction on BH4 bioavailability.

Methods: Human proteins GCH1 (both the full length and truncated forms) and GFRP, were recombinantly expressed, and the binding affinities were determined using surface plasmon resonance (SPR). In addition the activity of purified recombinant enzymes has been measured by two methods; using both a kinetic micro-plate assay and high performance liquid chromatography (HPLC). In order to investigate the regulation of BH4 levels in vivo via the GCH1-GFRP axis we conducted an oral challenge of L-phe (100mg/kg) in mice (n=8) and measured levels of L-phe and biopterin (a marker of BH4) in both tissue and plasma.

Results: Soluble human truncated and full length GCH1 and GFRP have been successfully expressed (with the truncated form of GCH1 lacking the first 42 animo acids of the N-terminus). Initial SPR experiments determined a Kd of approximately 20-40nM for GCH1-GFRP. The activity of both truncated and full length GCH1 was measured by two methods and we found truncated GCH1 to be more active than full length GCH1. Oral L-phe challenge in mice (n=8) was shown to significantly increase biopterin production in both plasma and tissue $p<0.001$ ANOVA (vs. saline control).

Conclusion: The aim of this project is to investigate the protein-protein interaction between GCH1 and GFRP. Targeting BH4 bioavailability can provide a means to restore endothelial dysfunction in a range of cardiovascular disorders. Our studies suggest a regulatory role for the first 42 amino acids which may influence the interaction of GCH1 with GFRP. L-Phe oral challenge was shown to cause a rise in circulating and vascular biopterin in mice indicating the potential of pharmacological agents that can mimic the feed-forward allosteric changes to regulate BH4 levels. Further studies are required to understand the different factors that may affect the nature of the GCH1-GFRP interaction and how it may influence BH4 bioavailability.

Where applicable, the authors confirm that the experiments described here conform with The Physiological Society ethical requirements.

PCD408

Endothelial cell-mediated lipid handling in human adipose tissue

F. Volat, P. Decaunes, A. Zakaroff-Girard, J. Galitzky and A. Bouloumié

INSERM U1048 - Institut des maladies métaboliques et cardiovasculaires, Toulouse, France

Human adipose tissue (AT) is well recognized as a key player in energy homeostasis due to its storage function of circulating non-esterified free fatty acids (NEFA) as triglycerides in adipocytes. A defective extraction of plasma NEFA by adipose tissue might lead to post-prandial hyperlipidemia and thus increase the risk to develop insulin resistance. Human AT-endothelial cells (ECs) are the first cell type that modulates lipid passage from the blood compartment to the adipose tissue. However, mechanisms underlying lipid handling in human adipose tissue remain to be fully characterized in AT-ECs.

Using a fluorescent-activated cell sorter (FACS) approach, uptake of fluorescent labelled fatty acid by stroma-vascular cells from human subcutaneous AT was studied. AT-ECs (CD34+/CD31+ cells) are able to incorporate several saturated FA such as palmitic (C16:0) and lauric (C12:0) acids. FA-uptake kinetics of AT-ECs depend on the length of fatty acid chain and differ from that of progenitors cells (CD34+/CD31- cells).

Trans-endothelial transport of NEFA in human adipose tissue may occur by diffusion or may be mediated by plasma-membrane and cytoplasm proteins. Real-time PCR and FACS analyses performed on AT-ECs isolated from freshly harvested stroma-vascular fraction revealed that these cells express several fatty acid transport proteins (FATPs) and fatty acid binding proteins (FABPs) and the fatty acid translocase FAT/CD36. AT-ECs also express the transcription factor PPARγ known as the major regulator of adipocyte lipid storage and we observed that maintaining AT-ECs in culture with an adipogenic media supplemented by PPARγ agonist leads to lipid droplet formation. This effect of PPARγ agonists was only observed on endothelial cells isolated from the adipose tissue.

In agreement with lipid droplet formation, immunohistochemical approaches revealed a marked accumulation of the lipid droplet-associated protein ADRP/Adipophilin in endothelial cells of subcutaneous AT from obese patients (BMI>30) (n=8) compared to lean patient (BMI<25) (n=7).

In addition, compared to AT-ECs of non obese patients (n=4-6), AT-EC of obese patients (n=4-9) exhibited a lower expression of proteins involved in the endothelial barrier function including VE-cadherin (adherens junction), JAM2 and Claudin 5 (thight junction) and CD31.

Our results showed that endothelial cells of human adipose tissue exhibit specific properties regarding lipid handling and suggest that, during obesity, a local dysfunction of adipose tissue endothelial cells occurs. This dysfunction might be a primary event involved in the genesis of obesity-associated pathologies.

This work was supported by AstraZeneca.

Where applicable, the authors confirm that the experiments described here conform with The Physiological Society ethical requirements.

PCD409

Divergent vascular effects of hydrogen-peroxide in isolated systemic and coronary arterioles

V. Csató[1], A. Tóth[1], . Koller[2], I. Édes[1] and Z. Papp[1]

[1]Cardiology, University of Debrecen Medical and Health Science Center, Debrecen, Hungary and [2]Pathophysiology and Gerontology, University of Pécs, Pécs, Hungary

Hydrogen-peroxide (H_2O_2) has been reported to either relax or constrict blood vessels depending on species and vessel type.

Arteriolar responses (internal diameter (i.d.) and changes in $[Ca^{2+}]_i$ by Fura-2 fluorescence ratio ($F_{340/380}$)) were determined in isolated, cannulated and pressurized (80 mmHg) arterioles obtained from rat skeletal muscle (i.d.: 168±6 μm, n=50), from rat coronaries (i.d.: 120±9 μm, n=6), or from human coronaries (i.d.: 138±29 μm, n=5). Wistar rats (male, 250-350 g, n=50) were anaesthetized with an I.P. injection of pentobarbital-natrium (150 mg/kg). Human arterioles were dissected from right atrial appendages of patients (n=5) who underwent cardiac surgery. Data are shown as average diameter ± S.E.M., compared by Student's t-test or ANOVA. Arteriolar constrictions were expressed as changes in i.d. as a percentage of the baseline diameter, dilations were represented as changes in i.d. as percentage of maximal dilation.

H_2O_2 evoked biphasic responses in skeletal muscle arterioles: constriction at lower (10 μM-100 μM, 34±3% at 100 μM, $p<0.001$) and dilation at higher concentrations (1 mM-10 mM, 80±11% at 10 mM, $p<0.001$). In contrast, H_2O_2 (10 mM) caused only vasodilation in rat (96±3%, $p<0.001$) and human (94±14%, $p=0.01$) coronary arterioles. The H_2O_2 evoked constriction in skeletal muscle arterioles was not accompanied by significant changes in $F_{340/380}$ in a range of H_2O_2 concentrations between 1 μM and 100 μM, but higher concentrations of H_2O_2 elicited significant decreases in $[Ca^{2+}]_i$ (decrease in $F_{340/380}$ from 1.13±0.03 to 1.01±0.01 at 1 mM H_2O_2, $p<0.05$). In skeletal muscle arterioles 100 μM H_2O_2 induced constrictions were inhibited in the absence of endothelium (0±8% constriction, $p=0.03$). Moreover, in the presence of antagonists of: thromboxane A2 (1 μM SQ-29548), cyclooxygenase (10 μM indomethacin), or protein tyrosine phosphatase (5 μM α-Bromo-4-methoxyacetophenone) the 100 μM H_2O_2-induced constrictions were converted to dilations (44±11%; 50±17%, or 22±17%, respectively, $p<0.005$). Furthermore, antagonists of phospholypase A (100 μM 7,7-Dimethyl-(5Z,8Z)-eicosadienoic acid), protein kinase C (10 μM chelerytrine), phospholypase C (1 μM U-73122), or src kinase (1 μM Src inhibitor-1) decreased the 100 μM H_2O_2-induced constriction (9±2%, 9±4%, 4±2%, 8±3%, respectively, $p<0.005$).

Our data suggest that in skeletal muscle arterioles H_2O_2 increases the Ca^{2+} sensitivity of the contractile apparatus of arteriolar smooth muscle and activate the endothelial src kinase, phospholypase C, protein kinase C, phospholypase A, cyclooxygenase pathway leading to the synthesis of thromboxane A2 an hence generate constriction. In contrast, in coronary arterioles this pathway is not functional, suggesting differences in H_2O_2 mediated physiological responses in particular endothelium-derived hyperpolarizing factor like effects in these vessels.

Where applicable, the authors confirm that the experiments described here conform with The Physiological Society ethical requirements.

PCD410

Spironolactone but not losartan prevents enhanced contractility and oxidative stress mediated by nitric oxide synthase uncoupling in aortas from isoproterenol-treated rats

J.A. Victorio[1], L.V. Rossoni[2] and A.P. Davel[1]

[1]Structural and Functional Biology, UNICAMP, Campinas, São Paulo, Brazil and [2]Physiology and Biophysics, USP, São Paulo, São Paulo, Brazil

Overactivation of β-adrenoceptors induced by isoproterenol (ISO) treatment causes cardiac remodeling and vascular dysfunction. It is known that angiotensin II via AT1 receptor and aldosterone via mineralocorticoid receptor (MR) partially mediates the cardiac injury induced by ISO, including: myocardial hypertrophy and fibrosis, oxidative stress and inflammation. In the present study we tested the hypothesis that signaling pathways activated by AT1 and/or MR receptors are involved in the impairment of nitric oxide (NO) bioavailability induced by ISO treatment. Male Wistar rats were treated with ISO (0.3 mg/kg/day, s.c.) or vehicle (CT) and co-treated or not with the AT1 antagonist losartan (LOS, 40 mg/kg/day, p.o.) or MR antagonist spironolactone (SPI, 200 mg/kg/day, p.o.) for one week. In isolated aortic rings with endothelium (n=6-8 in each group), maximal response (Rmax) evoked by phenylephrine (Phe, 1ηM- 10μM) was enhanced in ISO-treated rats (CT= 6.8 ± 0.4 vs. ISO= 8.8 ± 0.5 mN/mm; $p<0.05$; n=6-8). LOS co-treatment did not modify this contractile hyperresponsiveness (ISO/LOS= 8.3 ± 0.2 mN/mm; n=6; $p<0.05$ vs. ISO), while SPI abolished this effect (ISO/SPI= 6.3 ± 0.3 mN/mm; n=8; $p<0.05$ vs. ISO). The NO synthase (NOS) inhibitor L-NAME (100 μM) enhanced the Rmax to Phe in aortas from all groups, abolishing differences among then. The superoxide dismutase (SOD, 150 U/mL) reduced Rmax to Phe only in ISO and ISO/LOS groups. This result suggests an enhanced participation of superoxide anion on aortic contractile response of ISO-treated rats that is normalized by SPI but not altered by LOS. Fluorescences to hydroethidine (DHE, 2 μM) and to diaminofluorescein-2 (DAF-2, 8 μM) were used to quantify reactive oxygen species and NO, respectively (n=5-6 in each group). Elevated DHE (+44%) and reduced DAF-2 (-60%) fluorescence was observed in aortas from ISO-treated rats; SPI co-treatment, but not LOS, normalized it. Incubation with L-NAME significantly reduced the fluorescence to DHE (-33%) in aortic slices of ISO group. Protein expression was evaluated in aortic homogenates (n=6-8 in each group) and no significant changes in SOD-1, -2 and -3 protein expression among groups were observed. On the other hand, eNOS protein expression was significantly enhanced by ISO treatment (+56%) whilst phosphorylation of eNOS at Ser1177 (normalized by total eNOS content) was reduced (-43%). Neither LOS nor SPI modified this ISO effect. In conclusion, data suggest that ISO treatment could enhance vascular contractility due to high superoxide anion production via uncoupled eNOS and reduced NO availability. These vascular effects seem to be mediated by MR but not by AT1 receptor.

Financial support of FAPESP-Brazil

Where applicable, the authors confirm that the experiments described here conform with The Physiological Society ethical requirements.

PCD411

Inhibitory influence of physiological levels of arterial shear stress on local proteolysis and podosome formation of endothelial cells

T. Fey, U. Pohl and A. Dendorfer

Walter-Brendel-Centre for Experimental Medicine, Ludwig Maximilians University, Munich, Germany

Vascular remodelling can often be observed as consequence of chronic changes in blood flow. Whereas arteriogenesis is thought to be induced by elevated flow, a decrease in flow may result in plaque formation or atherosclerosis. Both processes are tightly controlled by proteases and their individual inhibitors. Podosomes are actin-rich cell protrusions which are locally associated with enhanced proteolysis of the extracellular matrix. To delineate the role of podosomes for endothelial matrix degradation, we studied the gelatinolytic activity and cellular arrangement of podosomes in endothelial cells exposed to shear stress.

Human umbilical vein endothelial cells (HUVEC, passage 2 to 3) were grown on fluorescent gelatin (Oregon green-conjugated) whose structure was imaged by confocal microscopy. The cells constitutively formed podosomes that were identified via costaining of cortactin and F-actin. Gelatinolytic activity of HUVECs was quantified according to gelatin fluorescence and to the density of circular gelatin defects. Shear stress was produced by unidirectional perfusion of a parallel plate flow chamber (Ibidi).

Cells grown under static conditions expressed podosomes either in even distribution or in circular arrangements (rosettes) that were associated with corresponding structures of gelatin degradation. Rosette density and gelatin degradation were highly increased after 2 hours of protein kinase C (PKC) stimulation by PMA (phorbol-12-myristate-13-acetate, 50 ng/ml) (reduction of gelatin fluorescence to 68% of control). Inhibition of matrix metalloproteinase (MMP) activity by GM6001 (15 μM) virtually abolished the occurrence of gelatin defects in untreated and PMA-treated endothelial cells. Exposure to shear stress for 48 hours altered the density of ring-shaped gelatin defects of 5 - 30 μm in diameter. Under very low shear stress (< 1 dyn/cm^2) the amount of rosette imprints was significantly increased compared to physiological flow (10 - 20 dyn/cm^2) and medium flow conditions (2 - 4 dyn/cm^2) (high flow 45 ± 10, medium flow 43 ± 28 vs. low flow 83 ± 7 per mm^2, n = 3, means ± S.D., ANOVA). HUVECS demonstrated typical alignment under high shear stress, but no signs of altered cell density or damage.

Thus gelatinolytic activity of endothelial cells is locally upregulated at podosome rosettes under low flow conditions, as compared to physiological arterial shear stress. This effect is presumably produced by an increased number in podosome rosettes recruiting higher MMP activities. Since matrix degradation promotes cell migration and impairs vessel stability, shear stress is critically important to stabilize the structure of the vascular wall under physiological conditions through mechanisms that locally regulate proteolytic activities.

Where applicable, the authors confirm that the experiments described here conform with The Physiological Society ethical requirements.

PCD413

C-type natriuretic peptide reduces phenylephrine-induced vasoconstriction in intact endothelium aorta isolated from rats submitted by septic shock

L. Pernomian[1] and L. Bendhack[2]

[1]Pharmacology, Faculdade de Medicina de Ribeirão Preto - Universidade de São Paulo, Ribeirão Preto, SP, Brazil and [2]Physics and Chemistry, Faculty of Pharmaceutical Sciences of Ribeirão Preto - Universidade de São Paulo, Ribeirão Preto, SP, Brazil

Septic shock is systemic inflammatory condition secondary to an infectious process leading to systemic hypotension and reduced vasoconstriction to several agonists with great production of nitric oxide (NO). Plasma concentration of C-type natriuretic peptide (CNP) is increased in animal models and patients in sepsis. The present study aimed to evaluate the contractile response induced by phenylephrine (PE) and the effect of CNP on this response in the isolated aorta from rats submitted to sepsis by ligation and puncture model (CLP). All the experimental protocols used in this study are approved by the Ethics Committee of the University of São Paulo (#144/2011). Male rats (35 days old) were anaesthetized with tribromoethanol (250 mg/Kg, ip). They were submitted to catheterization of femoral artery and vein 24h before the surgery to sepsis induced by CLP (16G needle) or sham-surgery (control rats, CO). The mean arterial pressure (MAP) of the rats was measured 4h after the surgery following PE administration (10-10 a 10-8 mol/Kg or saline, iv). The aortic rings were isolated from CO and CLP rats, for in vitro experiments of vascular reactivity. It was performed cumulative concentration-effect curves to PE (10-10 a 10-5 mol/L) with (E+) or without (E-) endothelium, in the absence or in the presence of CNP (10-8 mol/L). The aortic endothelial cells were used for flow cytometry studies. The cytosolic concentration of NO ([NO]c) was measured by using DAF-2/DA (10-5 mol/L). It was evaluated the maximum effect (Emax) and potency (pD2) of the PE. The MAP was higher in CO rats (74.3±0.3 mmHg, n=13) than in CLP rats (49.5±0.8 mmHg, n=15, P<0.05) 4h after the surgery, and the heart rate was enhanced in both groups as compared to the basal levels. Intravenous administration of PE increased the MAP and reduced the heart rate in both groups. PE induced contractile response in aortic rings from CO and CLP. It was reduced in CLP E+ group (Emax: 733±63,2g/g; pD2: 6,89±0,06, n=5, P<0.05) compared to CLP E- (Emax: 1468,3±181,7g/g; pD2: 7,51±0,31, n=8, P<0.05) and CO E+(Emax: 1231,4±106,4g/g; pD2: 7,32±0,10, n=11, P<0.05). CNP presented a negatively modulation in this PE response, only in E+ (CO Emax: 723,6±154,6g/g; pD2: 6,92±0,09; CLP Emax: 284,39±9,3g/g; pD2: 6,32±0,09, n=4, P<0.05). In the endothelial cells, the increase of [NO]c was higher in CLP (2706,3±325,8U, n= 4, P<0.05) than in CO rat aortic endothelial cells (1794,8±38,5U, n=4). Taken together, the results indicate that the vasoconstriction to PE is decreased in septic rat aorta, which should be due the enhanced production of NO in the endothelial cells. PE-induced contractile response is negatively modulated by CNP in intact-endothelium CO and CLP rat aortas.

Support by FAPESP, CAPES and CNPq.

Where applicable, the authors confirm that the experiments described here conform with The Physiological Society ethical requirements.

PCD414

Cannabidiol ameliorates the increased permeability of the blood-brain barrier following oxygen-glucose deprivation, an in vitro study

W.H. Hind, T.J. England and S.E. O'Sullivan

Vascular Medicine, The University of Nottingham, Derby, UK

During stroke, blood-brain barrier (BBB) permeability increases and cannabidiol (CBD) has shown protection in animal stroke models. The aim of this study was to establish if CBD modulates BBB permeability following oxygen-glucose deprivation (OGD).

To model the BBB co-cultures of human brain microvascular endothelial cells (HBMECs) and human astrocytes were grown on inserts. BBB permeability was measured by transepithelial electrical resistance (TEER) using STX2 electrodes and an EVOM2 meter. Inserts were subjected to 4h OGD by incubation in GasPak pouches with glucose-free RPMI medium. Reperfusion was established by returning cells to normoxia and their normal medium; TEER was measured at various time-points over 28h. CBD, receptor antagonists, or vehicle were added pre or post-OGD. The effect of giving 10μM CBD 2 or 4h into reperfusion was also investigated. Lactate dehydrogenase (LDH) was measured using a kit and VCAM-1 was measured by ELISA. Levels of cytokines/chemokine's known to be altered in stroke were measured by Multiplex. HBMEC-monocultures were also grown on 6 well-plates, and IL-6 and VCAM-1 were measured by ELISA, both in the presence and absence of OGD. Statistics: Student's t-test or one-way ANOVA with Dunnett's. Exposing the BBB to 4h OGD increased its permeability ($P<0.001$). Pre-treatment with 10μM CBD attenuated this increase ($P<0.05$), and 100nM, 1 or 10μM CBD decreased barrier permeability during reperfusion ($P<0.001$-0.05, n=8-11). CBD given post-OGD decreased barrier permeability during reperfusion ($P<0.01$-0.05, n=8-16). Receptor antagonists for CB1, CB2, PPARα, adenosine-A2A, 5-HT1A and TRPV1 did not affect CBD responses (n=6-10). However, the effect of CBD was inhibited by PPARγ antagonism ($P<0.001$-0.05, n=6). Administration of the PPARγ agonist Pioglitazone post-OGD also decreased barrier resistance during reperfusion ($P<0.01$-0.05, n=6). CBD given 2h into reperfusion decreased permeability ($P<0.05$, n=8-11), but CBD given 4h into reperfusion did not (n=6-9). LDH was raised following 4h OGD and 28h reperfusion ($P<0.05$), this was inhibited by CBD ($P<0.05$) in a non-PPARγ manner (n=6-9). Detectable levels of IL-10, IL-6, MIP-1α, MIP-1β and VEGF did not differ with CBD treatment. However, VCAM-1 at the end of reperfusion was attenuated by CBD ($P<0.05$, n=6), which was insensitive to PPARγ-antagonism. VCAM-1 in medium from HBMEC-monoculture was also attenuated by CBD both in the presence ($P<0.05$, n=3) or absence ($P<0.01$, n=3) of OGD. IL-6 from HBMEC-monoculture medium was increased by OGD exposure ($P<0.001$, n=6), and this increase was even greater in CBD-treated cells ($P<0.001$, n=6). Furthermore, CBD increased IL-6 in a concentration-dependent manner in HBMEC-monocultures that had not been exposed to OGD ($P<0.05$, n=3).

In conclusion, CBD given pre- or post-OGD decreases barrier permeability.

Where applicable, the authors confirm that the experiments described here conform with The Physiological Society ethical requirements.

PCD416

The effects of endocannabinoids on permeability in a cell culture model of the blood-brain barrier

W.H. Hind, T.J. England and S.E. O'Sullivan

Vascular Medicine, The University of Nottingham, Derby, UK

The blood-brain barrier (BBB) is a selective barrier. Other groups have demonstrated the ability of various cannabinoids to attenuate damage caused to the BBB in a range of pathologies. The role that AEA, and other endocannabinoids (eCBs), play in regulating BBB permeability has yet to be investigated using human cells, therefore, the aim of the present study is to establish whether they modulate BBB permeability. To model the BBB, co-cultures of human brain microvascular endothelial cells and human astrocytes were grown to confluence on Transwell collagen-coated inserts. BBB permeability was measured by transepithelial electrical resistance (TEER) using STX2 electrodes and an EVOM2 resistance meter. Resistance readings were taken at various intervals over 96h and compared to their baseline value. AEA (100 nM, 1 or 10μM) or other eCBs (10μM), and/or antagonist were added to the endothelial cells at 0 and again at 48h when the medium was replaced. In a separate series of experiments, inserts were subjected to 4h oxygen-glucose deprivation (OGD, to model ischaemia) by incubating them in GasPak EZ Anaerobe pouches with glucose-free RPMI medium. Reperfusion was established by returning the cells to normoxia and their specialised medium, and TEER was measured at various time-points over 28h. eCBs were added either pre- or post-OGD. Statistical analysis was conducted using one-way ANOVA with Dunnett's post hoc test. Administration of AEA at 10μM only resulted in a significant, acute decrease in BBB permeability (i.e. an increase in barrier tightness) compared to baseline at 2, 50 and 52h (i.e. immediately after AEA administration; n=9; $P<0.001$-0.05). Receptor involvement was probed, and AM251 (CB1, 100nM), GW6471 (PPARα, 100nM) and GW9662 (PPARγ, 100nM) had not effect. However, the AEA-induced decrease in permeability was significantly inhibited by AM630 (CB2, 1μM) ($P<0.001$-0.05) and capsazepine (TRPV1, 1μM) ($P<0.001$-0.05). The decrease in permeability was also inhibited by URB597 (FAAH inhibitor, 1μM) ($P<0.01$-0.05) (n=6-8 for all antagonist studies). Of the other eCBs investigated, 2-AG, PEA and virodhamine did not alter permeability. However, NADA increased BBB permeability ($P<0.001$-0.01), whilst OEA decreased BBB permeability ($P<0.05$-0.001) (n=6-8). 4h OGD increased BBB permeability ($P<0.001$), but administration of AEA following OGD did not decrease permeability (n=7-12). However, AEA (100nM, 10 or 30μM) given pre-OGD promoted a more rapid decrease in permeability during reperfusion ($P<0.001$-0.05; n=5-7), as did OEA ($P<0.001$-0.05), PEA ($P<0.05$) and virodhamine ($P<0.01$-0.05) (n=5-6). 2-AG did not alter BBB permeability following OGD. In conclusion, this study demonstrates that eCBs do play a role in regulating BBB permeability in vitro using human cells.

Where applicable, the authors confirm that the experiments described here conform with The Physiological Society ethical requirements.

PCD417

Impairment of aortic structure and function in a mouse model of neurofibromatosis type 1

K. Jett[1,3], J. Cui[2,3], H. Chohan[2,3], D. Arman[2,3], A. Tehrani[2,3], J. Friedman[1,3], C. Van Breemen[2,3] and M. Esfandiarei[2,3]

[1]Medical Genetics, University of British Columbia, Vancouver, BC, Canada, [2]Pharmacology and Therapeutics, University of British Columbia, Vancouver, BC, Canada and [3]Child and Family Research Institute, Vancouver, BC, Canada

Neurofibromatosis 1 (NF1) is an autosomal dominant disorder with complete penetrance and an estimated prevalence of 1 in 3000. Clinical manifestations are extremely variable. The disease is characterized by multiple café-au-lait spots (skin pigmentation), iris harmartomas, and multiple benign and malignant nerve sheath tumors (neurofibromas) in the central and peripheral nervous systems (Jett and Friedman 2010). NF1 vasculopathy is a serious and well documented but poorly understood feature of NF1. NF1 vasculopathy may result in hypertension, cerebrovascular disease, ischemia, aneurysm, hemorrhage or death in young adults (Rasmussen et al 2001). The response to standard therapeutic interventions is often disappointing (Friedman et al 2002), so further understanding of the underlying mechanisms for vascular complications in NF1 is essential. Endothelial and vascular smooth muscle functions are altered in Nf1+/- mice in vitro (Li et al 2001, Li et al 2006, Munchhof et al 2006), however, it is unknown how these alterations affect function of the vessel.

We have compared vascular function of the thoracic aorta in Nf1+/- mice with age-matched control littermates (n=16) using a small vessel myograph (A/S Danish Myotechnology, Aarthus N, Denmark). Isometric force measurements revealed increased contraction in response to depolarization (maximal response of3.3 ± 0.32 in Nf1+/- aorta versus 2.0 ± 0.22 in controls; p= 0.005), but diminished contraction in response to phenylephrine in Nf1+/- thoracic aorta at 6 months of age (pEC50 = 5.36 ± 0.18 in Nf1+/- aorta versus 7.02 ± 0.09 in controls; maximal response, Emax = 67.28 ± 3.4 in Nf1+/- aorta versus 86.34 ± 5.7; p= 0.008). Stress-strain curves indicated that arterial stiffness was increased at 6 months of age in Nf1+/- vessels. Elastin staining revealed disorganization of elastic fibers in Nf1+/- vessels.

In conclusion, the pathogenesis of NF1 vasculopathy in the thoracic aorta increases stiffness and impairs vasomotor function.

Friedman JM, Arbiser J, Epstein JA, et al. Cardiovascular disease in neurofibromatosis 1: report of the NF1 Cardiovascular Task Force. Genet Med 2002, 4:105-11

Li J, et al. Vascular smooth muscle cells of recipient origin mediate intimal expansion after aortic allotransplantation in mice. Am J Pathol 2001; 158: 1943-7

Li, F., et al., Neurofibromin is a novel regulator of RAS-induced signals in primary vascular smooth muscle cells. Hum. Mol. Genet., 2006; 15 (11): 1921-1930

Munchhof, A.M., et al. Neurofibroma-associated growth factors activate a distinct signaling network to alter the function of neurofibromin-deficient endothelial cells. Hum Mol Genet 2006; 15: 1858-1869

Rasmussen SA, Yang Q, Friedman JM . Mortality in neurofibromatosis 1: an analysis using U.S. death certificates. Am J Hum Genet 2001; 68:1110-8

Where applicable, the authors confirm that the experiments described here conform with The Physiological Society ethical requirements.

PCD418

The role of microRNA-30c-2* as an anti-angiogenic mediator

S. Shantikumar[1], A. Caporali[1], M. Meloni[1], M. Marchetti[1], L. Howard[1], F. Martelli[2] and C. Emanueli[1]

[1]Bristol Heart Institute, Bristol, UK and [2]Department of Vascular Pathology, IDI-IRCSS, Rome, Italy

Purpose: MicroRNAs (miRs) are small noncoding RNAs which negatively regulate the expression of targeted mRNA transcripts. Some miRs are already known to modulate angiogenesis. The p75 neurotrophin receptor (p75NTR) is upregulated in endothelial cells (ECs) of diabetic models and contributes to impaired post-ischaemic reparative angiogenesis in diabetes. To elucidate the miR signature of p75NTR in ECs, human umbilical vein ECs (HUVECs) infected with Ad.p75NTR demonstrated the upregulation of miR-30c-2* on an array. We aim to characterize the impact of miR-30c-2* on EC function.

Methods: Array results were confirmed by q-PCR using validated miR primers and SnU6 as an internal reference. To mimic advanced diabetes, where hyperglycaemia is accompanied by tissue starvation, HUVECs were cultured in high D-glucose (HG, 25 mM) and low growth factors (LGF). For modulating miR expression, HUVECs were transfected with pre-miR precursor, anti-miR inhibitor or negative control. Transfected cells were prompted in proliferation (BrdU incorporation) and in vitro angiogenesis on Matrigel assays. Predicted miR target genes were searched using the databases Microcosm and TargetScan. Finally, relative miR-expression was quantified in limb muscles of type 2 diabetic db/db mice and non-diabetic controls. Statistical analyses are performed using either an unpaired t-test (two groups) or ANOVA (more than two groups).

Results: Relative expression of miR-30c-2* was upregulated (three-fold) in p75NTR–transduced HUVECs ($p<0.01$ vs. null-HUVECs) and five-fold in HG/LGF compared to culture in normal conditions ($p<0.01$). Overexpression of miR-30c-2* in HUVECs impaired both proliferation and angiogenesis (40% decrease in proliferation and 25% decrease in tube length of Matrigel network, $p<0.01$ for both). In addition, miR-30c-2* was upregulated three-fold in the adductor muscles of db/db diabetic mice ($p<0.05$ vs. non-diabetic controls). A bioinformatics analysis identified the cell cycle regulator minichromosome maintenance complex component 7 (MCM7) as a putative miR-30c-2* target, In line, MCM-7 mRNA levels were decreased in p75NTR–HUVECs (by 57% vs. Null-HUVECs, $p<0.05$) and in HUVECs cultured in HG/LGF. Overexpression of miR-30c-2* also reduced MCM7 mRNA (by 64%, $p<0.01$).

Conclusion: Our data suggest that the p75NTR-induced miRNA miR-30c-2* may act as an anti-angiogenic mediator in the context of diabetes by inhibiting the cell cycle regulator MCM7. miR-30c-2* may prove to be a novel therapeutic target for diabetes-induced impairment of post-ischaemic reparative neovascularisation.

Caporali A et al. (2008) Circulation Research;103(2):e15-26.

Caporali A et al. (2011) Circulation; 123(3):282-91

Where applicable, the authors confirm that the experiments described here conform with The Physiological Society ethical requirements.

PCD421

Non-L-type calcium channels play a role in regulating contractile responses in human mammary arteries

A.D. Thuesen[1], L. Rasmussen[1], A. Toft[2], N. Marcussen[3], S. Walther[2], B.L. Jensen[1], L.M. Rasmussen[4] and P.B. Hansen[1]

[1]Cardiovascular and Renal research Unit, Institute of Molecular Medicine, Odense, Denmark, [2]Urology, Odense University Hospital, Odense, Denmark, [3]Pathology, Odense University Hospital, Odense, Denmark and [4]Clinical biochemistry, Odense University Hospital, Odense, Denmark

Calcium channel blockers are widely used for treatment of hypertension, and L-type voltage-gated calcium channels are regarded as the subtype involved in the excitation-contraction mechanism in resistance vessels. However, both L- and P/Q-type calcium channels are of functional importance for the depolarization-induced contraction in human renal blood vessels. It was hypothesized that non-L-type channels are of general importance for vascular function in human blood vessels. In human internal mammary arteries from bypass surgery patients, PCR analysis showed expression of L-type (Cav 1.2) and T-type (Cav 3.1 and Cav 3.2) voltage-gated calcium channels and variable expression of P/Q-type (Cav 2.1) channels between patients. Immunohistochemical labeling of human mammary arteries vessels revealed signal for Cav 2.1 in both endothelium and smooth muscle cells. The T-type blocker mibefradil (10-7 M) significantly attenuated the depolarization-induced contraction (60 mM potassium) by 21±6,7% in human mammary arteries using a myograph set-up. The P/Q type antagonist, ω-agatoxin IVA (10-9 M and 10-8 M) inhibited the potassium-induced contraction with large variations between patients. In human intrarenal arteries, mibefradil had a tendency to inhibit the contraction induced by 60 mM potassium. In summary, human mammary arteries express functionally significant L-type and T-type channels with variable presence and significance of P/Q-type channels. We conclude that non-L-type channels are involved in excitation-contraction coupling in human arteries and could be involved in regulation of blood pressure.

Kenneth Andersen

Where applicable, the authors confirm that the experiments described here conform with The Physiological Society ethical requirements.

PCD422

Magnetic resonance imaging (MRI) of microvascular blood volume recruitment capacity in the rat heart

J. van Haare[1], H. Vink[1], E. Kooi[2], J. Slenter[2], G. Strijkers[3], H. Cobelens[1] and J. van Teeffelen[1]

[1]Physiology, Maastricht University, Maastricht, Netherlands, [2]Radiology, Maastrcht University Medical Centre, Maastricht, Netherlands and [3]Biomedical Engineering, Eindhoven University of Technology, Eindhoven, Netherlands

Background/Objectives
A considerable number of patients with symptoms of chest pain during exercise have no functional relevant stenosis in their coronary arteries. In these patients the angina may relate to coronary microvascular dysfunction as a consequence of glycocalyx loss; since the latter has been associated with an impaired ability of adenosine to increase microvascular blood volume, we hypothesize that non-invasive measurements of myocardial microvascular blood volume recruitment with MRI could diagnose patients with coronary glycocalyx loss. As a first step, we measured in the current study coronary microvascular blood volume using first-pass dynamic contrast-enhanced MRI to assess myocardial microvascular blood volume in healthy control rats under baseline conditions and during adenosine infusion.
Methods
Rats (male, 300-450g, n=5) were anaesthetised with isoflurane (induction chamber 4,5% isoflurane and 1% oxygen, during experiment 2% isoflurane and 0,4% oxygen). MRI was performed on a 7.0 Tesla Bruker Biospec animal scanner. A bolus of 150 μl Gadovist (Gd-DTPA) was injected in the femoral vein, while scanning continued. The method was optimized to capture the first pass of the contrast agent through the heart. Measurements were performed at baseline and during intravenous adenosine infusion (3 mg/ml; 1,5 ml/h). In the first-pass perfusion images, regions of interest (ROI) were placed in the left ventricular (LV) lumen and in the myocardium of the LV wall. Signal intensity-time curves were calculated for all ROIs and were corrected for baseline. The following semi-quantitative parameters of myocardial perfusion and volume were derived from these curves: total area under the curve (AUC), peak intensity and the upslope to the peak.
Results
Values are percentages of changes after adenosine infusion compared to baseline ± S.E.M., compared by t-test. A significant increase of 47% ± 14 in total AUC was seen in rats after intravenous adenosine infusion compared to baseline ($P<0.05$). Peak intensity increased significantly with 49% ± 36 in rat hearts during adenosine infusion compared to baseline conditions. Also a significant increase (63% ± 64) was seen for the upslope of the first-pass peak during adenosine infusion compared to baseline conditions.
Conclusion
Adenosine-induced increases in myocardial microvascular blood volume in the rat heart are reflected by increases in first-pass MRI-derived contrast intensity. Our next step is to study the effect of glycocalyx damage on myocardial microvascular blood volume recruitment in rats using pharmacological and dietary degradation of the glycocalyx.

Supported by Dutch Heart Foundation grant: NHS2009B56

Where applicable, the authors confirm that the experiments described here conform with The Physiological Society ethical requirements.

PCD423

Zebrafish caudal fin regeneration – a novel quantitative angiogenic assay in vivo

D. Brönnimann

University of Bern, Bern, Switzerland

Background: Teleost fish, including zebrafish, are able to regenerate heart, retina, spinal cord, and fins after a lesion. The tie2-eGFP zebrafish is a suitable model to study the whole vascular tree down to the capillary level. Therefore, we introduced a novel assay to quantify angiogenesis after partial amputation of the zebrafish caudal fin.
Methods: At first, the zebrafish caudal fin was partially amputated. Complete regeneration of the vasculature and the fin itself occurred within five weeks at 30°C. Remarkably, initial

size and shape of the fin as well as the vascular parameters and patterns were completely restored. Most importantly, the concept of a reference situation was therefore introduced. Alterations in the neo-angiogenesis induced by external manipulations (pharmaceutical compounds, growth factors, flow disturbance etc.) can be precisely observed and quantified using stereomicroscopic imaging. Because blood vessels run straight and planar at the site of interest, the zebrafish caudal fin is introduced as a 2D-model. Three main quantitative parameters were introduced in this angiogenic assay. First, the total area (TA) represents the area of the fin that regenerated after partial amputation. Second, the vascular projection area (VPA) represents the regenerated vascular area visualized by a stereomicroscope. Third, the contour length (CL) represents the length of the blood vessel wall visualized by a stereomicroscope. During the first seven days of regeneration, extensive angiogenic growth was observed. Therefore, we introduced the short angiogenic assay. It allows evaluation of pro- and anti-angiogenic compounds within a week using unbiased stereological methods. In addition, this novel angiogenic assay includes a multitude of investigations in parallel. By the use of confocal imaging and transmission electron microscopy, morphology is linked to observed alterations in vivo. Hemodynamic conditions and their role in the process of neo-angiogenesis are evaluated. Moreover, the interplay between the two most important modes of angiogenesis (sprouting and intussusceptive angiogenesis) is evaluated.
Conclusions: The zebrafish caudal fin regeneration assay is a promising and highly reproducible model for time-efficient quantitative evaluation of angiogenesis. It is useful to assess neo-angiogenic mechanisms and the effects of different pro- and anti-angiogenic treatments. The model has potential implications on future treatment strategies of angiogenesis related diseases such as carcinogenesis, retinopathy, macular degeneration, and wound healing, among others.

Where applicable, the authors confirm that the experiments described here conform with The Physiological Society ethical requirements.

PCD424

Uric acid prevents middle cerebral artery structural and mechanical alterations induced by focal cerebral ischemia in rats

Y. Onetti, F. Jiménez, B. Pérez and E. Vila

Farmacologia, terapeutica i toxicologia, Universitat Autonoma de Barcelona, Bellaterra (Cerdanyola del Valles), Barcelona, Spain

Oxidative stress, a major contributor to brain damage in ischemic stroke, is involved in alterations of cerebrovascular properties after an episode of ischemia/reperfusion. (Jiménez-Altayó F et al., 2009). Uric acid (UA) is an endogenous antioxidant that protects the rat brain in a model of thromboembolic (Romanos E et al., 2007) and transient focal (Yu et al., 1998) ischemic injury. Nevertheless, little is known about the mechanisms whereby UA exerts its beneficial effects. We hypothesized that UA could influence the changes on vessel properties due to ischemia/reperfusion. Male Sprague-Dawley rats (270-320g) were subjected to right middle cerebral artery (MCA) intraluminal occlusion (90 min) followed by 24 h reperfusion. Sham-operated animals underwent the same surgical procedure but the MCA was occluded for less than 1 min. Rats were anaesthetized with isoflurane (3-2.5 %) in a mixture of O2 and N2O (30:70) and divided into 4 groups: sham-operated vehicle (n=7), ischemic vehicle (IV, n=18), sham-operated UA (n=4) and ischemic UA (IUA, n=9). UA (16 mg/kg in 3 ml Locke's buffer, i.v.) or vehicle (3 ml Locke's buffer, i.v.) was infused during 20 min at 30 min reperfusion. Mean arterial pressure, rectal temperature and cortical cerebral blood flow was permanently monitored. Afterwards (24 h), rats were killed under isoflurane (4%) and the ipsilateral MCA was removed and set up in a pressure myograph under physiological conditions. Values are means ± S.E.M., compared by two-way ANOVA or Student's t-Test. Mean arterial blood pressure (IV: 94.7±1.6 mmHg, n=18; IUA: 91.3±1.0 mmHg, n=9) and rectal temperature (IV: 37.3±0.119 °C, n=18; IUA: 37.0±0.197 °C, n=9) was similar in all groups. UA reduced infarct volume (IV: 129.6±23.5 mm^3, n=18; IUA: 48.9±16.6 mm^3, n=9, $p<0.01$), neurological score (IV: 3.4±0.4, n=18; IUA: 2.0±0.3, n=9, $p<0.05$) and brain oedema (IV: 7.7±1.1, n=16; IUA: 2.9±1.4, n=7, $p<0.05$). Ischemia/reperfusion increased MCA wall thickness ($p<0.01$), cross-sectional area ($p<0.05$) and wall/lumen ratio ($p<0.05$) while decreased wall stress ($p<0.05$) and stiffness (β value SV: 7.8±0.1, n=5; β value IV: 6.8±0.2, n=17, $p<0.001$). UA prevented all MCA changes induced by ischemia/reperfusion. These results show that a single dose of UA administered early after the onset of reperfusion prevents MCA structural and mechanical alterations induced by ischemia/reperfusion. We suggest that UA might exert beneficial actions on ischemic damage through prevention of cerebrovascular remodelling. These results reinforce the involvement of the vascular response in brain damage.

Jiménez-Altayó F et al. (2009). J Pharmacol Exp Ther 331, 429-436.

Romanos E et al. (2007). J Cereb Blood Flow Metab 27, 14-20.

Yu ZF et al. (1998). Neurosci Res 53, 613-625.

Supported by SAF2010-19282, 2009SGR-890. Y.O. was supported by MEC.

Where applicable, the authors confirm that the experiments described here conform with The Physiological Society ethical requirements.

PCD425

Diltiazem prevents aortic aneurysm formation via inhibition of Interleukin-6-induced AP-1 promoter activity in macrophages

A. Mieth[1], M. Revermann[1], A. Weigert[2], B. Brüne[2] and R.P. Brandes[1]

[1]Institut für Kardiovaskuläre Physiologie, Goethe-Universität Frankfurt am Main, Frankfurt am Main, Germany and [2]Institut für Pathobiochemie, Goethe-Universität Frankfurt am Main, Frankfurt am Main, Germany

Abdominal aortic aneurysm is an important manifestation of arteriosclerosis with increasing incidence in the western world. Progressive inflammatory processes involving infiltration and differentiation of monocytes into the vessel wall, proliferation and migration of smooth muscle cells and eventually the degradation of the internal elastic lamina are causal for aneurysm formation. Since calcium channel blockers exert multiple beneficial effects in the vascular system we investigated the effect of the benzothiazepine-type calcium channel blocker diltiazem (DIL) on aneurysm formation.
Angiotensin II infusion (ATII, 4 weeks, 1.44 mg/kg bw/d) induced massive aneurysm formation in ApoE-deficient mice that was blocked by co-treatment with DIL (100 mg/kg bw/day). Additional treatment with phenylephrine (PHE, 18 mg/kg bw/d) to counteract the blood pressure-lowering effect

of DIL had no influence on its beneficial effect. Moreover DIL prevented the ATII-induced mRNA expression of pro-inflammatory cytokines in the aortic arch after 6 days of ATII treatment due to a reduction in the amount of locally infiltrating macrophages which was accompanied by attenuated systemic CCL12 serum level.
Ex vivo, DIL (10 μM) did not reduce the ATII-induced (100 nM) expression of promigratory chemokine CCL2 and proinflammatory cytokine IL-6 of vascular segments in organ culture or vascular smooth muscle cells. Moreover, DIL (30 μM) did not affect the recruitement of Ly6C+-monocyte into subcutaneously implanted matrigel plugs filled with CCL2 (600 ng/ml) in ApoE-deficient mice. In contrast, in peritoneal macrophages and RAW264.7 cells, DIL prevented the IL-6-induced (10 ng/ml) mRNA expression of IL-1β and CCL12. As underlying mechanism, DIL abrogated the IL-6 induced activation of AP-1 promoter without affecting NF-kB activity as well as phosphorylation and nuclear translocation of MAPK1 and Stat3 or intracellular calcium.
These observations indicate that DIL prevents aneurysm formation by a mechanism independent of its blood pressure and intracellular calcium lowering effects.

Where applicable, the authors confirm that the experiments described here conform with The Physiological Society ethical requirements.

A

B

C

D

E

F

G

H

I

J

K

L

M

N

O

P

Q

R

S

T

U

V

W

X

Y

Z